

# ***Chemistry of the Elements***

*Second Edition*

N. N. GREENWOOD and A. EARNSHAW


*School of Chemistry  
University of Leeds, U.K.*

**B**UTTERWORTH  
**H**EINEMANN

OXFORD AUCKLAND BOSTON JOHANNESBURG MELBOURNE NEW DELHI



Butterworth-Heinemann  
Linacre House, Jordan Hill, Oxford OX2 8DP  
225 Wildwood Avenue, Woburn, MA 01801-2041  
A division of Reed Educational and Professional Publishing Ltd

 A member of the Reed Elsevier plc group

First published by Pergamon Press plc 1984  
Reprinted with corrections 1985, 1986  
Reprinted 1989, 1990, 1993, 1994, 1995  
Second edition 1997  
Reprinted with corrections 1998

© Reed Educational and Professional Publishing Ltd 1984, 1997

All rights reserved. No part of this publication may be reproduced in any material form (including photocopying or storing in any medium by electronic means and whether or not transiently or incidentally to some other use of this publication) without the written permission of the copyright holder except in accordance with the provisions of the Copyright, Designs and Patents Act 1988 or under the terms of a licence issued by the Copyright Licensing Agency Ltd, 90 Tottenham Court Road, London, England W1P 9HE. Applications for the copyright holder's written permission to reproduce any part of this publication should be addressed to the publishers

**British Library Cataloguing in Publication Data**

A catalogue record for this book is available from the British Library

ISBN 0 7506 3365 4

**Library of Congress Cataloguing in Publication Data**

A catalogue record for this book is available from the Library of Congress

Typeset in 10/12pt Times by Laser Words, Madras, India  
Printed in Great Britain

## **Related Titles**

Brethericks Reactive Chemical Hazards, Fifth edition  
Urban

Colloid and Surface Chemistry, Fourth edition  
Shaw

Crystallization, Third edition  
Mullin

Precipitation  
Sohnel and Garside

Purification of Laboratory Chemicals, Fourth edition  
Armarego and Perrin

Molecular Geometry  
Rodger and Rodger

Radiochemistry and Nuclear Chemistry, Second edition  
Rydborg, Chopin and Liljentzen

# Preface to the Second Edition

When this book first appeared in 1984 it rapidly established itself as one of the foremost textbooks and references on the subject. It was enthusiastically adopted by both students and teachers and has already been translated into several European and Asian languages. The novel features which it adopted (see Preface to the First Edition) were clearly much appreciated and we have been pressed for some time now to bring out a second edition. Accordingly we have completely revised and updated the text and have incorporated over 2000 new literature references to work which has appeared since the first edition was published. In addition, innumerable modifications and extensions incorporating recent advances have been made throughout the text and, indeed, no single page has been left unaltered. However, by judicious editing we have ensured that all the features which made the first edition so attractive to its readers have been retained.

The main plan of the book has been left unchanged except that the general section on organometallic chemistry has been removed from Chapter 8 (Carbon) and has been incorporated, together with a summary of other aspects of coordination chemistry, in a restyled Chapter 19. However, the chemistry of even the simplest elements has been considerably enriched during the past few years, sometimes by quite dramatic advances. Thus the chemistry of the alkali metals has a complexity that was undreamt of one or two decades ago and lithium, for example, is now known in at least 20 coordination geometries having coordination numbers from 1 to 12. Compounds of alkali metal *anions* and even electrides are known. Likewise, there is expanding interest in the organometallic chemistry of the heavier congeners of magnesium, particularly those with bulky ligands. Boron continues to amaze and confound, and its cluster chemistry continues to expand, as does sulfur–nitrogen chemistry, heteropolyacid chemistry, bioinorganic aspects of the chemistry of many of the elements, lower-valent lanthanide element chemistry, and so on through each of the chapters, up to the synthesis and characterization of the heaviest trans-actinide element,  $Z = 112$ . It is salutary to reflect that there are now 49 more elements known than the 63 known to Mendeleev when he devised the periodic table of the elements.

A further indication of the rapid advances that have occurred in the chemistry of the elements during the past 15 years can be gauged from the several completely new sections which have been added to review work in what were previously both nonexistent and unsuspected areas. These include (a) coordination compounds of dihapto-dihydrogen, (b) the fullerenes and their many derivatives, (c) the metcars, and (d) high-temperature oxide superconductors.

We hope that this new edition of *Chemistry of the Elements* will continue to stimulate and inform its readers, and that they will experience something of the excitement and fascination which we ourselves feel for this burgeoning subject. We should also like to thank our many correspondents who have kept us informed of their work and the School of Chemistry in the University of Leeds for providing us with facilities.

N. N. Greenwood  
A. Earnshaw  
August, 1997

# Preface to the First Edition

IN this book we have tried to give a balanced, coherent and comprehensive account of the chemistry of the elements for both undergraduate and postgraduate students. This crucial central area of chemistry is full of ingenious experiments, intriguing compounds and exciting new discoveries. We have specifically avoided the term *inorganic chemistry* since this emphasizes an outmoded view of chemistry which is no longer appropriate in the closing decades of the 20th century. Accordingly, we deal not only with inorganic chemistry but also with those aspects which might be called analytical, theoretical, industrial, organometallic, bio-inorganic or any other of the numerous branches of the subject currently in vogue.

We make no apology for giving pride of place to the phenomena of chemistry and to the factual basis of the subject. Of course the chemistry of the elements is discussed within the context of an underlying theoretical framework that gives cohesion and structure to the text, but at all times it is the chemical chemistry that is emphasized. There are several reasons for this. First, theories change whereas facts do so less often — a greater permanency and value therefore attaches to a treatment based on a knowledge and understanding of the factual basis of the subject. We recognize, of course, that though the facts may not change dramatically, their significance frequently does. It is therefore important to learn how to assess observations and to analyse information reliably. Numerous examples are provided throughout the text. Moreover, it is scientifically unsound to present a theory and then describe experiments which purport to prove it. It is essential to distinguish between facts and theories and to recognize that, by their nature, theories are ephemeral and continually changing. Science advances by removing error, not by establishing truth, and no amount of experimentation can “prove” a theory, only that the theory is consistent with the facts as known *so far*. (At a more subtle level we also recognize that all facts are theory-laden.)

It is also important to realize that chemistry is not a static body of knowledge as defined by the contents of a textbook. Chemistry came from somewhere and is at present heading in various specific directions. It is a living self-stimulating discipline, and we have tried to transmit this sense of growth and excitement by reference to the historical development of the subject when appropriate. The chemistry of the elements is presented in a logical and academically consistent way but is interspersed with additional material which illuminates, exemplifies, extends or otherwise enhances the chemistry being discussed.

Chemistry is a human activity and its results have a substantial impact on our daily lives. However, we have not allowed ourselves to become obsessed by “relevance”. Today’s relevance is tomorrow’s obsolescence. On the other hand, it would be obtuse in the modern world not to recognize that chemistry, in addition to being academically stimulating and aesthetically satisfying, is frequently also useful. This gives added point to much of the chemistry of the elements and indeed a great deal of that chemistry has been specifically developed because of society’s needs. To many this is one of the most attractive aspects of the subject — its potential usefulness. We therefore wrote to over 500 chemically based firms throughout the world asking for information about the chemicals they manufactured or used, in what

quantities and for what purposes. This produced an immense wealth of technical information which has proved to be an invaluable resource in discussing the chemistry of the elements. Our own experience as teachers had already alerted us to the difficulty of acquiring such topical information and we have incorporated much of this material where appropriate throughout the text. We believe it is important to know whether a given compound was made perhaps once in milligram amounts, or is produced annually in tonne quantities, and for what purpose.

In a textbook devoted to the chemistry of the elements it seemed logical to begin with such questions as: where do the elements come from, how were they made, why do they have their observed terrestrial abundances, what determines their atomic weights, and so on. Such questions, though usually ignored in textbooks and certainly difficult to answer, are ones which are currently being actively pursued, and some tentative answers and suggestions are given in the opening chapter. This followed by a brief description of chemical periodicity and the periodic table before the chemistry of the individual elements and their group relationships are discussed on a systematic basis.

We have been much encouraged by the careful assessment and comments on individual chapters by numerous colleagues not only throughout the U.K. but also in Australia, Canada, Denmark, the Federal Republic of Germany, Japan, the U.S.A and several other countries. We believe that this new approach will be widely welcomed as a basis for discussing the very diverse behaviour of the chemical elements and their compounds.

It is a pleasure to record our gratitude to the staff of the Edward Boyle Library in the University of Leeds for their unfailing help over many years during the writing of this book. We should also like to express our deep appreciation to Mrs Jean Thomas for her perseverance and outstanding skill in preparing the manuscript for the publishers. Without her generous help and the understanding of our families this work could not have been completed.

N. N. GREENWOOD  
A. EARNSHAW

# Contents

<b>Preface to the second edition</b>	<b>xix</b>	
<b>Preface to the first edition</b>	<b>xxi</b>	
<b>Chapter 1</b>	<b>Origin of the Elements. Isotopes and Atomic Weights</b>	<b>1</b>
1.1	Introduction	1
1.2	Origin of the Universe	1
1.3	Abundances of the Elements in the Universe	3
1.4	Stellar Evolution and the Spectral Classes of Stars	5
1.5	Synthesis of the Elements	9
1.5.1	Hydrogen burning	9
1.5.2	Helium burning and carbon burning	10
1.5.3	The $\alpha$ -process	11
1.5.4	The e-process (equilibrium process)	12
1.5.5	The s- and r-processes (slow and rapid neutron absorption)	12
1.5.6	The p-process (proton capture)	13
1.5.7	The x-process	13
1.6	Atomic Weights	15
1.6.1	Uncertainty in atomic weights	16
1.6.2	The problem of radioactive elements	18
<b>Chapter 2</b>	<b>Chemical Periodicity and the Periodic Table</b>	<b>20</b>
2.1	Introduction	20
2.2	The Electronic Structure of Atoms	21
2.3	Periodic Trends in Properties	23
2.3.1	Trends in atomic and physical properties	23
2.3.2	Trends in chemical properties	27
2.4	Prediction of New Elements and Compounds	29
<b>Chapter 3</b>	<b>Hydrogen</b>	<b>32</b>
3.1	Introduction	32
3.2	Atomic and Physical Properties of Hydrogen	34
3.2.1	Isotopes of hydrogen	34
3.2.2	<i>Ortho</i> - and <i>para</i> -hydrogen	35
3.2.3	Ionized forms of hydrogen	36
3.3	Preparation, Production and Uses	38
3.3.1	Hydrogen	38
3.3.2	Deuterium	39
3.3.3	Tritium	41
3.4	Chemical Properties and Trends	43
3.4.1	The coordination chemistry of hydrogen	44

3.5	Protonic Acids and Bases	48
3.6	The Hydrogen Bond	52
3.6.1	Influence on properties	53
3.6.2	Influence on structure	59
3.6.3	Strength of hydrogen bonds and theoretical description	61
3.7	Hydrides of the Elements	64
<b>Chapter 4</b>	<b>Lithium, Sodium, Potassium, Rubidium, Caesium and Francium</b>	<b>68</b>
4.1	Introduction	68
4.2	The Elements	68
4.2.1	Discovery and isolation	68
4.2.2	Terrestrial abundance and distribution	69
4.2.3	Production and uses of the metals	71
4.2.4	Properties of the alkali metals	74
4.2.5	Chemical reactivity and trends	76
4.2.6	Solutions in liquid ammonia and other solvents	77
4.3	Compounds	79
4.3.1	Introduction: the ionic-bond model	79
4.3.2	Halides and hydrides	82
4.3.3	Oxides, peroxides, superoxides and suboxides	84
4.3.4	Hydroxides	86
4.3.5	Oxoacid salts and other compounds	87
4.3.6	Coordination chemistry	90
4.3.7	Imides, amides and related compounds	99
4.3.8	Organometallic compounds	102
<b>Chapter 5</b>	<b>Beryllium, Magnesium, Calcium, Strontium, Barium and Radium</b>	<b>107</b>
5.1	Introduction	107
5.2	The Elements	108
5.2.1	Terrestrial abundance and distribution	108
5.2.2	Production and uses of the metals	110
5.2.3	Properties of the elements	111
5.2.4	Chemical reactivity and trends	112
5.3	Compounds	113
5.3.1	Introduction	113
5.3.2	Hydrides and halides	115
5.3.3	Oxides and hydroxides	119
5.3.4	Oxoacid salts and coordination complexes	122
5.3.5	Organometallic compounds	127
	Beryllium	127
	Magnesium	131
	Calcium, strontium and barium	136
<b>Chapter 6</b>	<b>Boron</b>	<b>139</b>
6.1	Introduction	139
6.2	Boron	140
6.2.1	Isolation and purification of the element	140
6.2.2	Structure of crystalline boron	141
6.2.3	Atomic and physical properties of boron	144
6.2.4	Chemical properties	144
6.3	Borides	145
6.3.1	Introduction	145
6.3.2	Preparation and stoichiometry	146
6.3.3	Structures of borides	147



6.4	Boranes (Boron Hydrides)	151
6.4.1	Introduction	151
6.4.2	Bonding and topology	157
6.4.3	Preparation and properties of boranes	162
6.4.4	The chemistry of small boranes and their anions ( $B_1$ – $B_4$ )	164
6.4.5	Intermediate-sized boranes and their anions ( $B_5$ – $B_9$ )	170
6.4.6	Chemistry of <i>nido</i> -decaborane, $B_{10}H_{14}$	173
6.4.7	Chemistry of <i>closo</i> - $B_nH_n^{2-}$	178
6.5	Carboranes	181
6.6	Metallocarboranes	189
6.7	Boron Halides	195
6.7.1	Boron trihalides	195
6.7.2	Lower halides of boron	200
6.8	Boron–Oxygen Compounds	203
6.8.1	Boron oxides and oxoacids	203
6.8.2	Borates	205
6.8.3	Organic compounds containing boron–oxygen bonds	207
6.9	Boron–Nitrogen Compounds	207
6.10	Other Compounds of Boron	211
6.10.1	Compounds with bonds to P, As or Sb	211
6.10.2	Compounds with bonds to S, Se and Te	213

## Chapter 7 Aluminium, Gallium, Indium and Thallium 216

7.1	Introduction	216
7.2	The Elements	217
7.2.1	Terrestrial abundance and distribution	217
7.2.2	Preparation and uses of the metals	219
7.2.3	Properties of the elements	222
7.2.4	Chemical reactivity and trends	224
7.3	Compounds	227
7.3.1	Hydrides and related complexes	227
7.3.2	Halides and halide complexes	233
	Aluminium trihalides	233
	Trihalides of gallium, indium and thallium	237
	Lower halides of gallium, indium and thallium	240
7.3.3	Oxides and hydroxides	242
7.3.4	Ternary and more complex oxide phases	247
	Spinel and related compounds	247
	Sodium- $\beta$ -alumina and related phases	249
	Tricalcium aluminate, $Ca_3Al_2O_6$	251
7.3.5	Other inorganic compounds	252
	Chalcogenides	252
	Compounds with bonds to N, P, As, Sb or Bi	255
	Some unusual stereochemistries	256
7.3.6	Organometallic compounds	257
	Organoaluminium compounds	258
	Organometallic compounds of Ga, In and Tl	262
	Al–N heterocycles and clusters	265

## Chapter 8 Carbon 268

8.1	Introduction	268
8.2	Carbon	269
8.2.1	Terrestrial abundance and distribution	269
8.2.2	Allotropic forms	274
8.2.3	Atomic and physical properties	276
8.2.4	Fullerenes	278
	Structure of the fullerenes	280
	Other molecular allotropes of carbon	282
	Chemistry of the fullerenes	282
	Reduction of fullerenes to fullerides	285

	Addition reactions	286
	Heteroatom fullerene-type clusters	287
	Encapsulation of metal atoms by fullerene clusters	288
8.2.5	Chemical properties of carbon	289
8.3	Graphite Intercalation Compounds	293
8.4	Carbides	296
	Metallo-carbides (met-cars)	300
8.5	Hydrides, Halides and Oxohalides	301
8.6	Oxides and Carbonates	305
8.7	Chalcogenides and Related Compounds	313
8.8	Cyanides and Other Carbon-Nitrogen Compounds	319
8.9	Organometallic Compounds	326
<b>Chapter 9</b>	<b>Silicon</b>	<b>328</b>
9.1	Introduction	328
9.2	Silicon	329
9.2.1	Occurrence and distribution	329
9.2.2	Isolation, production and industrial uses	330
9.2.3	Atomic and physical properties	330
9.2.4	Chemical properties	331
9.3	Compounds	335
9.3.1	Silicides	335
9.3.2	Silicon hydrides (silanes)	337
9.3.3	Silicon halides and related complexes	340
9.3.4	Silica and silicic acids	342
9.3.5	Silicate minerals	347
	Silicates with discrete units	347
	Silicates with chain or ribbon structures	349
	Silicates with layer structures	349
	Silicates with framework structures	354
9.3.6	Other inorganic compounds of silicon	359
9.3.7	Organosilicon compounds and silicones	361
<b>Chapter 10</b>	<b>Germanium, Tin and Lead</b>	<b>367</b>
10.1	Introduction	367
10.2	The Elements	368
10.2.1	Terrestrial abundance and distribution	368
10.2.2	Production and uses of the elements	369
10.2.3	Properties of the elements	371
10.2.4	Chemical reactivity and group trends	373
10.3	Compounds	374
10.3.1	Hydrides and hydrohalides	374
10.3.2	Halides and related complexes	375
	Germanium halides	376
	Tin halides	377
	Lead halides	381
10.3.3	Oxides and hydroxides	382
10.3.4	Derivatives of oxoacids	387
10.3.5	Other inorganic compounds	389
10.3.6	Metal-metal bonds and clusters	391
10.3.7	Organometallic compounds	396
	Germanium	396
	Tin	399
	Lead	404
<b>Chapter 11</b>	<b>Nitrogen</b>	<b>406</b>
11.1	Introduction	406

11.2	The Element	407
11.2.1	Abundance and distribution	407
11.2.2	Production and uses of nitrogen	409
11.2.3	Atomic and physical properties	411
11.2.4	Chemical reactivity	412
11.3	Compounds	416
11.3.1	Nitrides, azides and nitrido complexes	417
11.3.2	Ammonia and ammonium salts	420
	Liquid ammonia as a solvent	424
11.3.3	Other hydrides of nitrogen	426
	Hydrazine	427
	Hydroxylamine	431
	Hydrogen azide	432
11.3.4	Thermodynamic relations between N-containing species	434
11.3.5	Nitrogen halides and related compounds	438
11.3.6	Oxides of nitrogen	443
	Nitrous oxide, $N_2O$	443
	Nitric oxide, $NO$	445
	Dinitrogen trioxide, $N_2O_3$	454
	Nitrogen dioxide, $NO_2$ , and dinitrogen tetroxide, $N_2O_4$	455
	Dinitrogen pentoxide, $N_2O_5$ , and nitrogen trioxide, $NO_3$	458
11.3.7	Oxoacids, oxoanions and oxoacid salts of nitrogen	459
	Hyponitrous acid and hyponitrites	459
	Nitrous acid and nitrites	461
	Nitric acid and nitrates	465
	Orthonitrates, $M_3^I NO_4$	471

## Chapter 12 Phosphorus

473

12.1	Introduction	473
12.2	The Element	475
12.2.1	Abundance and distribution	475
12.2.2	Production and uses of elemental phosphorus	479
12.2.3	Allotropes of phosphorus	479
12.2.4	Atomic and physical properties	482
12.2.5	Chemical reactivity and stereochemistry	483
12.3	Compounds	489
12.3.1	Phosphides	489
12.3.2	Phosphine and related compounds	492
12.3.3	Phosphorus halides	495
	Phosphorus trihalides	495
	Diphosphorus tetrahalides and other lower halides of phosphorus	497
	Phosphorus pentahalides	498
	Pseudohalides of phosphorus(III)	501
12.3.4	Oxohalides and thiohalides of phosphorus	501
12.3.5	Phosphorus oxides, sulfides, selenides and related compounds	503
	Oxides	503
	Sulfides	506
	Oxosulfides	510
12.3.6	Oxoacids of phosphorus and their salts	510
	Hypophosphorous acid and hypophosphites [ $H_2PO(OH)$ and $H_2PO_2^-$ ]	513
	Phosphorous acid and phosphites [ $HPO(OH)_2$ and $HPO_3^{2-}$ ]	514
	Hypophosphoric acid ( $H_4P_2O_6$ ) and hypophosphates	515
	Other lower oxoacids of phosphorus	516
	The phosphoric acids	516
	Orthophosphates	523
	Chain polyphosphates	526
	<i>Cyclo</i> -polyphosphoric acids and <i>cyclo</i> -polyphosphates	529
12.3.7	Phosphorus–nitrogen compounds	531
	Cyclophosphazanes	533
	Phosphazenes	534

	Polyphosphazenes	536
	Applications	542
12.3.8	Organophosphorus compounds	542

## Chapter 13 Arsenic, Antimony and Bismuth 547

13.1	Introduction	547
13.2	The Elements	548
13.2.1	Abundance, distribution and extraction	548
13.2.2	Atomic and physical properties	550
13.2.3	Chemical reactivity and group trends	552
13.3	Compounds of Arsenic, Antimony and Bismuth	554
13.3.1	Intermetallic compounds and alloys	554
13.3.2	Hydrides of arsenic, antimony and bismuth	557
13.3.3	Halides and related complexes	558
	Trihalides, $MX_3$	558
	Pentahalides, $MX_5$	561
	Mixed halides and lower halides	563
	Halide complexes of $M^{III}$ and $M^V$	564
	Oxide halides	570
13.3.4	Oxides and oxo compounds	572
	Oxo compounds of $M^{III}$	573
	Mixed-valence oxides	576
	Oxo compounds of $M^V$	576
13.3.5	Sulfides and related compounds	578
13.3.6	Metal-metal bonds and clusters	583
13.3.7	Other inorganic compounds	591
13.3.8	Organometallic compounds	592
	Organoarsenic(III) compounds	593
	Organoarsenic(V) compounds	594
	Physiological activity of arsenicals	596
	Organoantimony and organobismuth compounds	596

## Chapter 14 Oxygen 600

14.1	The Element	600
14.1.1	Introduction	600
14.1.2	Occurrence	602
14.1.3	Preparation	603
14.1.4	Atomic and physical properties	604
14.1.5	Other forms of oxygen	607
	Ozone	607
	Atomic oxygen	611
14.1.6	Chemical properties of dioxygen, $O_2$	612
14.2	Compounds of Oxygen	615
14.2.1	Coordination chemistry: dioxygen as a ligand	615
14.2.2	Water	620
	Introduction	620
	Distribution and availability	621
	Physical properties and structure	623
	Water of crystallization, aquo complexes and solid hydrates	625
	Chemical properties	627
	Polywater	632
14.2.3	Hydrogen peroxide	633
	Physical properties	633
	Chemical properties	634
14.2.4	Oxygen fluorides	638
14.2.5	Oxides	640
	Various methods of classification	640
	Nonstoichiometry	642

## Chapter 15 Sulfur

645

15.1	The Element	645
15.1.1	Introduction	645
15.1.2	Abundance and distribution	647
15.1.3	Production and uses of elemental sulfur	649
15.1.4	Allotropes of sulfur	652
15.1.5	Atomic and physical properties	661
15.1.6	Chemical reactivity	662
	Polyatomic sulfur cations	664
	Sulfur as a ligand	665
	Other ligands containing sulfur as donor atom	673
15.2	Compounds of Sulfur	676
15.2.1	Sulfides of the metallic elements	676
	General considerations	676
	Structural chemistry of metal sulfides	679
	Anionic polysulfides	681
15.2.2	Hydrides of sulfur (sulfanes)	682
15.2.3	Halides of sulfur	683
	Sulfur fluorides	683
	Chlorides, bromides and iodides of sulfur	689
15.2.4	Oxohalides of sulfur	693
15.2.5	Oxides of sulfur	695
	Lower oxides	695
	Sulfur dioxide, SO <sub>2</sub>	698
	Sulfur dioxide as a ligand	701
	Sulfur trioxide	703
	Higher oxides	704
15.2.6	Oxoacids of sulfur	706
	Sulfuric acid, H <sub>2</sub> SO <sub>4</sub>	710
	Peroxo-sulfuric acids, H <sub>2</sub> SO <sub>5</sub> and H <sub>2</sub> S <sub>2</sub> O <sub>8</sub>	712
	Thio-sulfuric acid, H <sub>2</sub> S <sub>2</sub> O <sub>3</sub>	714
	Dithionic acid, H <sub>2</sub> S <sub>2</sub> O <sub>6</sub>	715
	Polythionic acids, H <sub>2</sub> S <sub>n</sub> O <sub>6</sub>	716
	Sulfurous acid, H <sub>2</sub> SO <sub>3</sub>	717
	Disulfurous acid, H <sub>2</sub> S <sub>2</sub> O <sub>5</sub>	720
	Dithionous acid, H <sub>2</sub> S <sub>2</sub> O <sub>4</sub>	720
15.2.7	Sulfur–nitrogen compounds	721
	Binary sulfur nitrides	722
	Sulfur–nitrogen cations and anions	730
	Sulfur imides, S <sub>8–n</sub> (NH) <sub>n</sub>	735
	Other cyclic sulfur–nitrogen compounds	736
	Sulfur–nitrogen–halogen compounds	736
	Sulfur–nitrogen–oxygen compounds	740

## Chapter 16 Selenium, Tellurium and Polonium

747

16.1	The Elements	747
16.1.1	Introduction: history, abundance, distribution	747
16.1.2	Production and uses of the elements	748
16.1.3	Allotropy	751
16.1.4	Atomic and physical properties	753
16.1.5	Chemical reactivity and trends	754
16.1.6	Polyatomic cations, M <sub>x</sub> <sup>n+</sup>	759
16.1.7	Polyatomic anions, M <sub>x</sub> <sup>2–</sup>	762
16.2	Compounds of Selenium, Tellurium and Polonium	765
16.2.1	Selenides, tellurides and polonides	765
16.2.2	Hydrides	766
16.2.3	Halides	767
	Lower halides	768
	Tetrahalides	772

	Hexahalides	775
	Halide complexes	776
16.2.4	Oxohalides and pseudohalides	777
16.2.5	Oxides	779
16.2.6	Hydroxides and oxoacids	781
16.2.7	Other inorganic compounds	783
16.2.8	Organo-compounds	786

## Chapter 17 The Halogens: Fluorine, Chlorine, Bromine, Iodine and Astatine 789

17.1	The Elements	789
17.1.1	Introduction	789
	Fluorine	789
	Chlorine	792
	Bromine	793
	Iodine	794
	Astatine	794
17.1.2	Abundance and distribution	795
17.1.3	Production and uses of the elements	796
17.1.4	Atomic and physical properties	800
17.1.5	Chemical reactivity and trends	804
	General reactivity and stereochemistry	804
	Solutions and charge-transfer complexes	806
17.2	Compounds of Fluorine, Chlorine, Bromine and Iodine	809
17.2.1	Hydrogen halides, HX	809
	Preparation and uses	809
	Physical properties of the hydrogen halides	812
	Chemical reactivity of the hydrogen halides	813
	The hydrogen halides as nonaqueous solvents	816
17.2.2	Halides of the elements	819
	Fluorides	820
	Chlorides, bromides and iodides	821
17.2.3	Interhalogen compounds	824
	Diatomic interhalogens, XY	824
	Tetra-atomic interhalogens, XY <sub>3</sub>	828
	Hexa-atomic and octa-atomic interhalogens, XF <sub>5</sub> and IF <sub>7</sub>	832
17.2.4	Polyhalide anions	835
17.2.5	Polyhalonium cations XY <sub>2n</sub> <sup>+</sup>	839
17.2.6	Halogen cations	842
17.2.7	Oxides of chlorine, bromine and iodine	844
	Oxides of chlorine	844
	Oxides of bromine	850
	Oxides of iodine	851
17.2.8	Oxoacids and oxoacid salts	853
	General considerations	853
	Hypohalous acids, HOX, and hypohalites, XO <sup>-</sup>	856
	Halous acids, HOXO, and halites, XO <sub>2</sub> <sup>-</sup>	859
	Halic acids, HOXO <sub>2</sub> , and halates, XO <sub>3</sub> <sup>-</sup>	862
	Perhalic acid and perchalates	865
	Perchloric acid and perchlorates	865
	Perbromic acid and perbromates	871
	Periodic acids and periodates	872
17.2.9	Halogen oxide fluorides and related compounds	875
	Chlorine oxide fluorides	875
	Bromine oxide fluorides	880
	Iodine oxide fluorides	881
17.2.10	Halogen derivatives of oxoacids	883
17.3	The Chemistry of Astatine	885

<b>Chapter 18</b>	<b>The Noble Gases: Helium, Neon, Argon, Krypton, Xenon and Radon</b>	<b>888</b>
18.1	Introduction	888
18.2	The Elements	889
18.2.1	Distribution, production and uses	889
18.2.2	Atomic and physical properties of the elements	890
18.3	Chemistry of the Noble Gases	892
18.3.1	Clathrates	893
18.3.2	Compounds of xenon	893
18.3.3	Compounds of other noble gases	903
<b>Chapter 19</b>	<b>Coordination and Organometallic Compounds</b>	<b>905</b>
19.1	Introduction	905
19.2	Types of Ligand	906
19.3	Stability of Coordination Compounds	908
19.4	The Various Coordination Numbers	912
19.5	Isomerism	918
	Conformational isomerism	918
	Geometrical isomerism	919
	Optical isomerism	919
	Ionization isomerism	920
	Linkage isomerism	920
	Coordination isomerism	920
	Polymerization isomerism	921
	Ligand isomerism	921
19.6	The Coordinate Bond	921
19.7	Organometallic Compounds	924
19.7.1	Monohapto ligands	925
19.7.2	Dihapto ligands	930
19.7.3	Trihapto ligands	933
19.7.4	Tetrahapto ligands	935
19.7.5	Pentahapto ligands	937
19.7.6	Hexahapto ligands	940
19.7.7	Heptahapto and octahapto ligands	941
<b>Chapter 20</b>	<b>Scandium, Yttrium, Lanthanum and Actinium</b>	<b>944</b>
20.1	Introduction	944
20.2	The Elements	945
20.2.1	Terrestrial abundance and distribution	945
20.2.2	Preparation and uses of the metals	945
20.2.3	Properties of the elements	946
20.2.4	Chemical reactivity and trends	948
20.3	Compounds of Scandium, Yttrium, Lanthanum and Actinium	949
20.3.1	Simple compounds	949
20.3.2	Complexes	950
20.3.3	Organometallic compounds	953
<b>Chapter 21</b>	<b>Titanium, Zirconium and Hafnium</b>	<b>954</b>
21.1	Introduction	954
21.2	The Elements	955
21.2.1	Terrestrial abundance and distribution	955
21.2.2	Preparation and uses of the metals	955
21.2.3	Properties of the elements	956
21.2.4	Chemical reactivity and trends	958
21.3	Compounds of Titanium, Zirconium and Hafnium	961
21.3.1	Oxides and sulfides	961

21.3.2	Mixed (or complex) oxides	962
21.3.3	Halides	964
21.3.4	Compounds with oxoanions	966
21.3.5	Complexes	967
	Oxidation state IV ( $d^0$ )	967
	Oxidation state III ( $d^1$ )	969
	Lower oxidation states	971
21.3.6	Organometallic compounds	972

## Chapter 22 Vanadium, Niobium and Tantalum 976

22.1	Introduction	976
22.2	The Elements	977
22.2.1	Terrestrial abundance and distribution	977
22.2.2	Preparation and uses of the metals	977
22.2.3	Atomic and physical properties of the elements	978
22.2.4	Chemical reactivity and trends	979
22.3	Compounds of Vanadium, Niobium and Tantalum	981
22.3.1	Oxides	981
22.3.2	Polymetallates	983
22.3.3	Sulfides, selenides and tellurides	987
22.3.4	Halides and oxohalides	988
22.3.5	Compounds with oxoanions	993
22.3.6	Complexes	994
	Oxidation state V ( $d^0$ )	994
	Oxidation state IV ( $d^1$ )	994
	Oxidation state III ( $d^2$ )	996
	Oxidation state II ( $d^3$ )	998
22.3.7	The biochemistry of vanadium	999
22.3.8	Organometallic compounds	999

## Chapter 23 Chromium, Molybdenum and Tungsten 1002

23.1	Introduction	1002
23.2	The Elements	1003
23.2.1	Terrestrial abundance and distribution	1003
23.2.2	Preparation and uses of the metals	1003
23.2.3	Properties of the elements	1004
23.2.4	Chemical reactivity and trends	1005
23.3	Compounds of Chromium, Molybdenum and Tungsten	1007
23.3.1	Oxides	1007
23.3.2	Isopolymetallates	1009
23.3.3	Heteropolymetallates	1013
23.3.4	Tungsten and molybdenum bronzes	1016
23.3.5	Sulfides, selenides and tellurides	1017
23.3.6	Halides and oxohalides	1019
23.3.7	Complexes of chromium, molybdenum and tungsten	1023
	Oxidation state VI ( $d^0$ )	1023
	Oxidation state V ( $d^1$ )	1024
	Oxidation state IV ( $d^2$ )	1025
	Oxidation state III ( $d^3$ )	1027
	Oxidation state II ( $d^4$ )	1031
23.3.8	Biological activity and nitrogen fixation	1035
23.3.9	Organometallic compounds	1037

## Chapter 24 Manganese, Technetium and Rhenium 1040

24.1	Introduction	1040
24.2	The Elements	1041



24.2.1	Terrestrial abundance and distribution	1041
24.2.2	Preparation and uses of the metals	1041
24.2.3	Properties of the elements	1043
24.2.4	Chemical reactivity and trends	1044
24.3	Compounds of Manganese, Technetium and Rhenium	1045
24.3.1	Oxides and chalcogenides	1045
24.3.2	Oxoanions	1049
24.3.3	Halides and oxohalides	1051
24.3.4	Complexes of manganese, technetium and rhenium	1054
	Oxidation state VII ( $d^0$ )	1054
	Oxidation state VI ( $d^1$ )	1055
	Oxidation state V ( $d^2$ )	1055
	Oxidation state IV ( $d^3$ )	1056
	Oxidation state III ( $d^4$ )	1057
	Oxidation state II ( $d^5$ )	1058
	Lower oxidation states	1061
24.3.5	The biochemistry of manganese	1061
24.3.6	Organometallic compounds	1062

## Chapter 25 Iron, Ruthenium and Osmium 1070

25.1	Introduction	1070
25.2	The Elements Iron, Ruthenium and Osmium	1071
25.2.1	Terrestrial abundance and distribution	1071
25.2.2	Preparation and uses of the elements	1071
25.2.3	Properties of the elements	1074
25.2.4	Chemical reactivity and trends	1075
25.3	Compounds of Iron, Ruthenium and Osmium	1079
25.3.1	Oxides and other chalcogenides	1079
25.3.2	Mixed metal oxides and oxoanions	1081
25.3.3	Halides and oxohalides	1082
25.3.4	Complexes	1085
	Oxidation state VIII ( $d^0$ )	1085
	Oxidation state VII ( $d^1$ )	1085
	Oxidation state VI ( $d^2$ )	1085
	Oxidation state V ( $d^3$ )	1086
	Oxidation state IV ( $d^4$ )	1086
	Oxidation state III ( $d^5$ )	1088
	Oxidation state II ( $d^6$ )	1091
	Mixed valence compounds of ruthenium	1097
	Lower oxidation states	1098
25.3.5	The biochemistry of iron	1098
	Haemoglobin and myoglobin	1099
	Cytochromes	1101
	Iron-sulfur proteins	1102
25.3.6	Organometallic compounds	1104
	Carbonyls	1104
	Carbonyl hydrides and carbonylate anions	1105
	Carbonyl halides and other substituted carbonyls	1108
	Ferrocene and other cyclopentadienyls	1109

## Chapter 26 Cobalt, Rhodium and Iridium 1113

26.1	Introduction	1113
26.2	The Elements	1113
26.2.1	Terrestrial abundance and distribution	1113
26.2.2	Preparation and uses of the elements	1114
26.2.3	Properties of the elements	1115
26.2.4	Chemical reactivity and trends	1116
26.3	Compounds of Cobalt, Rhodium and Iridium	1117

26.3.1	Oxides and sulfides	1117
26.3.2	Halides	1119
26.3.3	Complexes	1121
	Oxidation state IV ( $d^5$ )	1121
	Oxidation state III ( $d^6$ )	1122
	Oxidation state II ( $d^7$ )	1129
	Oxidation state I ( $d^8$ )	1133
	Lower oxidation states	1137
26.3.4	The biochemistry of cobalt	1138
26.3.5	Organometallic compounds	1139
	Carbonyls	1140
	Cyclopentadienyls	1143

## Chapter 27 Nickel, Palladium and Platinum 1144

27.1	Introduction	1144
27.2	The Elements	1145
	27.2.1 Terrestrial abundance and distribution	1145
	27.2.2 Preparation and uses of the elements	1145
	27.2.3 Properties of the elements	1148
	27.2.4 Chemical reactivity and trends	1149
27.3	Compounds of Nickel, Palladium and Platinum	1150
	27.3.1 The Pd/H <sub>2</sub> system	1150
	27.3.2 Oxides and chalcogenides	1151
	27.3.3 Halides	1152
	27.3.4 Complexes	1154
	Oxidation state IV ( $d^6$ )	1154
	Oxidation state III ( $d^7$ )	1155
	Oxidation state II ( $d^8$ )	1156
	Oxidation state I ( $d^9$ )	1166
	Oxidation state 0 ( $d^{10}$ )	1166
	27.3.5 The biochemistry of nickel	1167
	27.3.6 Organometallic compounds	1167
	$\sigma$ -Bonded compounds	1167
	Carbonyls	1168
	Cyclopentadienyls	1170
	Alkene and alkyne complexes	1170
	$\pi$ -Allylic complexes	1171

## Chapter 28 Copper, Silver and Gold 1173

28.1	Introduction	1173
28.2	The Elements	1174
	28.2.1 Terrestrial abundance and distribution	1174
	28.2.2 Preparation and uses of the elements	1174
	28.2.3 Atomic and physical properties of the elements	1176
	28.2.4 Chemical reactivity and trends	1177
28.3	Compounds of Copper, Silver and Gold	1180
	28.3.1 Oxides and sulfides	1181
	28.3.2 High temperature superconductors	1182
	28.3.3 Halides	1183
	28.3.4 Photography	1185
	28.3.5 Complexes	1187
	Oxidation state III ( $d^8$ )	1187
	Oxidation state II ( $d^9$ )	1189
	Electronic spectra and magnetic properties of copper(II)	1193
	Oxidation state I ( $d^{10}$ )	1194
	Gold cluster compounds	1197
	28.3.6 Biochemistry of copper	1197
	28.3.7 Organometallic compounds	1199

<b>Chapter 29</b>	<b>Zinc, Cadmium and Mercury</b>	<b>1201</b>
29.1	Introduction	1201
29.2	The Elements	1202
29.2.1	Terrestrial abundance and distribution	1202
29.2.2	Preparation and uses of the elements	1202
29.2.3	Properties of the elements	1203
29.2.4	Chemical reactivity and trends	1205
29.3	Compounds of Zinc, Cadmium and Mercury	1208
29.3.1	Oxides and chalcogenides	1208
29.3.2	Halides	1211
29.3.3	Mercury(I) Polycations of mercury	1213 1214
29.3.4	Zinc(II) and cadmium(II)	1215
29.3.5	Mercury(II) Hg <sup>II</sup> -N compounds Hg <sup>II</sup> -S compounds Cluster compounds involving mercury	1217 1218 1220 1220
29.3.6	Organometallic compounds	1221
29.3.7	Biological and environmental importance	1224
<b>Chapter 30</b>	<b>The Lanthanide Elements (Z = 58–71)</b>	<b>1227</b>
30.1	Introduction	1227
30.2	The Elements	1229
30.2.1	Terrestrial abundance and distribution	1229
30.2.2	Preparation and uses of the elements	1230
30.2.3	Properties of the elements	1232
30.2.4	Chemical reactivity and trends	1235
30.3	Compounds of the Lanthanides	1238
30.3.1	Oxides and chalcogenides	1238
30.3.2	Halides	1240
30.3.3	Magnetic and spectroscopic properties	1242
30.3.4	Complexes Oxidation state IV Oxidation state III Oxidation state II	1244 1244 1245 1248
30.3.5	Organometallic compounds Cyclopentadienides and related compounds Alkyls and aryls	1248 1248 1249
<b>Chapter 31</b>	<b>The Actinide and Transactinide Elements (Z = 90–112)</b>	<b>1250</b>
31.1	Introduction	1250
	Superheavy elements	1253
31.2	The Actinide Elements	1253
31.2.1	Terrestrial abundance and distribution	1253
31.2.2	Preparation and uses of the actinide elements Nuclear reactors and atomic energy Nuclear fuel reprocessing	1255 1256 1260
31.2.3	Properties of the actinide elements	1262
31.2.4	Chemical reactivity and trends	1264
31.3	Compounds of the Actinides	1267
31.3.1	Oxides and chalcogenides of the actinides	1268
31.3.2	Mixed metal oxides	1269
31.3.3	Halides of the actinide elements	1269
31.3.4	Magnetic and spectroscopic properties	1272
31.3.5	Complexes of the actinide elements Oxidation state VII Oxidation state VI Oxidation state V Oxidation state IV	1273 1273 1273 1274 1275

	Oxidation state III	1277
	Oxidation state II	1278
	31.3.6 Organometallic compounds of the actinides	1278
31.4	The Transactinide Elements	1280
	31.4.1 Introduction	1280
	31.4.2 Element 104	1281
	31.4.3 Element 105	1282
	31.4.4 Element 106	1282
	31.4.5 Elements 107, 108 and 109	1283
	31.4.6 Elements 110, 111 and 112	1283
<b>Appendix 1</b>	<b>Atomic Orbitals</b>	<b>1285</b>
<b>Appendix 2</b>	<b>Symmetry Elements, Symmetry Operations and Point Groups</b>	<b>1290</b>
<b>Appendix 3</b>	<b>Some Non-SI Units</b>	<b>1293</b>
<b>Appendix 4</b>	<b>Abundance of Elements in Crustal Rocks</b>	<b>1294</b>
<b>Appendix 5</b>	<b>Effective Ionic Radii</b>	<b>1295</b>
<b>Appendix 6</b>	<b>Nobel Prize for Chemistry</b>	<b>1296</b>
<b>Appendix 7</b>	<b>Nobel Prize for Physics</b>	<b>1300</b>
<b>Index</b>		<b>1305</b>

																1	2										
																H	He										
3	4															5	6	7	8	9	10						
Li	Be															B	C	N	O	F	Ne						
11	12															13	14	15	16	17	18						
Na	Mg															Al	Si	P	S	Cl	Ar						
19	20	21	22	23	24	25	26	27	28	29	30	31	32	33	34	35	36										
K	Ca	Sc	Ti	V	Cr	Mn	Fe	Cu	Ni	Cu	Zn	Ga	Ge	As	Se	Br	Kr										
37	38	39	40	41	42	43	44	45	46	47	48	49	50	51	52	53	54										
Rb	Sr	Y	Zr	Nb	Mu	Tc	Ru	Rh	Pd	Ag	Cd	In	Sn	Sb	Te	I	Xe										
55	56	57	58	59	60	61	62	63	64	65	66	67	68	69	70	71	72										
Cs	Ba	La	Hf	Ta	W	Re	Os	Ir	Pt	Au	Hg	Tl	Pb	Bi	Po	At	Rn										
87	88	89	90	91	92	93	94	95	96	97	98	99	100	101	102	103	104										
Fr	Ra	Ac	Rf	Db	Sg	Bh	Hs	Mt	Uun	Uun	Uun																
88	89	90	91	92	93	94	95	96	97	98	99	100	101	102	103	104	105										
Th	Pa	U	Np	Pu	Am	Cm	Bk	Cf	Es	Fm	Md	No	Lr														

# 1

## Origin of the Elements. Isotopes and Atomic Weights

### 1.1 Introduction

This book presents a unified treatment of the chemistry of the elements. At present 112 elements are known, though not all occur in nature: of the 92 elements from hydrogen to uranium all except technetium and promethium are found on earth and technetium has been detected in some stars. To these elements a further 20 have been added by artificial nuclear syntheses in the laboratory. Why are there only 90 elements in nature? Why do they have their observed abundances and why do their individual isotopes occur with the particular relative abundances observed? Indeed, we must also ask to what extent these isotopic abundances commonly vary in nature, thus causing variability in atomic weights and possibly jeopardizing the classical means of determining chemical composition and structure by chemical analysis.

Theories abound, and it is important at all times to distinguish carefully between what has been experimentally established, what is a useful model for suggesting further experiments, and

what is a currently acceptable theory which interprets the known facts. The tentative nature of our knowledge is perhaps nowhere more evident than in the first few sections of this chapter dealing with the origin of the chemical elements and their present isotopic composition. This is not surprising, for it is only in the last few decades that progress in this enormous enterprise has been made possible by discoveries in nuclear physics, astrophysics, relativity and quantum theory.

### 1.2 Origin of the Universe

At present, the most widely accepted theory for the origin and evolution of the universe to its present form is the "hot big bang".<sup>(1)</sup> It is supposed that all the matter in the universe

<sup>1</sup> J. SILK, *The Big Bang: The Creation and Evolution of the Universe*, 2nd edn., W. H. Freeman, New York, 1989, 485 pp. J. D. BARROW and J. SILK, *The Left Hand of Creation: The Origin and Evolution of the Expanding Universe*, Heinemann, London, 1984, 256 pp. E. W. KOLB and M. S. TURNER, *The Early Universe*, Addison-Wesley, Redwood City, CA, 1990, 547 pp.

was once contained in a primeval nucleus of immense density ( $\sim 10^{96} \text{ g cm}^{-3}$ ) and temperature ( $\sim 10^{32} \text{ K}$ ) which, for some reason, exploded and distributed radiation and matter uniformly throughout space. As the universe expanded it cooled; this allowed the four main types of force to become progressively differentiated, and permitted the formation of various types of particle to occur. Nothing scientific can be said about the conditions obtaining at times shorter than the Planck time,  $t_P [(Gh/c^5)^{1/2} = 1.33 \times 10^{-43} \text{ s}]$  at which moment the forces of gravity and electromagnetism, and the weak and strong nuclear forces were all undifferentiated and equally powerful. At  $10^{-43} \text{ s}$  after the big bang ( $T = 10^{31} \text{ K}$ ) gravity separated as a distinct force, and at  $10^{-35} \text{ s}$  ( $10^{28} \text{ K}$ ) the strong nuclear force separated from the still combined electro-weak force. These are, of course, inconceivably short times and unimaginably high temperatures: for example, it takes as long as  $10^{-24} \text{ s}$  for a photon (travelling at the speed of light) to traverse a distance equal to the diameter of an atomic nucleus. When a time interval of  $10^{-10} \text{ s}$  had elapsed from the big bang the temperature is calculated to have fallen to  $10^{15} \text{ K}$  and this enabled the electromagnetic and weak nuclear forces to separate. By  $6 \times 10^{-6} \text{ s}$  ( $1.4 \times 10^{12} \text{ K}$ ) protons and neutrons had been formed from quarks, and this was followed by stabilization of electrons. One second after the big bang, after a period of extensive particle-antiparticle annihilation to form electromagnetic photons, the universe was populated by particles which sound familiar to chemists — protons, neutrons and electrons.

Shortly thereafter, the strong nuclear force ensured that large numbers of protons and neutrons rapidly combined to form deuterium nuclei ( $p + n$ ), then helium ( $2p + 2n$ ). *The process of element building had begun.* During this small niche of cosmic history, from about 10–500 s after the big bang, the entire universe is thought to have behaved as a colossal homogeneous fusion reactor converting hydrogen into helium. Previously no helium nuclei could exist — the temperature was so high that the sea

of radiation would have immediately decomposed them back to protons and neutrons. Subsequently, the continuing expansion of the universe was such that the particle density was too low for these strong (but short-range) interactions to occur. Thus, within the time slot of about eight minutes, it has been calculated that about one-quarter of the mass of the universe was converted to helium nuclei and about three-quarters remained as hydrogen. Simultaneously, a minute  $10^{-3}\%$  was converted to deuterons and about  $10^{-6}\%$  to lithium nuclei. These remarkable predictions of the big bang cosmological theory are borne out by experimental observations. Wherever one looks in the universe — the oldest stars in our own galaxy, or the “more recent” stars in remote galaxies — the universal abundance of helium is about 25%. Even more remarkably, the expected concentration of deuterium has been detected in interstellar clouds. Yet, as we shall shortly see, stars can only destroy deuterium as soon as it is formed; they cannot create any appreciable equilibrium concentration of deuterium nuclei because of the high temperature of the stellar environment. The sole source of deuterium in the universe seems to be the big bang. At present no other cosmological theory can explain this observed ratio of H:He:D.

Two other features of the universe find ready interpretation in terms of the big bang theory. First, as observed originally by E. Hubble in 1929, the light received on earth from distant galaxies is shifted increasingly towards the red end of the spectrum as the distance of the source increases. This implies that the universe is continually expanding and, on certain assumptions, extrapolation backwards in time indicates that the big bang occurred some 15 billion years ago. Estimates from several other independent lines of evidence give reassuringly similar values for the age of the universe. Secondly, the theory convincingly explains (indeed predicted) the existence of an all-pervading isotropic cosmic black-body radiation. This radiation (which corresponds to a temperature of  $2.735 \pm 0.06 \text{ K}$  according to the most recent measurements) was discovered in

1965 by A. A. Penzias and R. W. Wilson<sup>(2)</sup> and is seen as the dying remnants of the big bang. No other cosmological theory yet proposed is able to interpret all these diverse observations.

### 1.3 Abundances of the Elements in the Universe

Information on the abundances of at least some of the elements in the sun, stars, gaseous nebulae and the interstellar regions has been obtained from detailed spectroscopic analysis using various regions of the electromagnetic spectrum. This data can be supplemented by direct analysis of samples from the earth, from meteorites, and increasingly from comets, the moon, and the surfaces of other planets and satellites in the solar system. The results indicate extensive differentiation in the solar system and in some stars, but the overall picture is one of astonishing uniformity of composition. Hydrogen is by far the most abundant element in the universe, accounting for some 88.6% of all atoms (or nuclei). Helium is about eightfold less abundant (11.3%), but these two elements together account for over 99.9% of the atoms and nearly 99% of the mass of the universe. Clearly nucleosynthesis of the heavier elements from hydrogen and helium has not yet proceeded very far.

Various estimates of the universal abundances of the elements have been made and, although these sometimes differ in detail for particular elements, they rarely do so by more than a factor of 3 ( $10^{0.5}$ ) on a scale that spans more than 12 orders of magnitude. Representative values are plotted in Fig. 1.1, which shows a number of features that must be explained by any satisfactory theory of the origin of the elements. For example:

- (i) Abundances decrease approximately exponentially with increase in atomic mass number  $A$  until  $A \sim 100$  (i.e.  $Z \sim 42$ ); thereafter the decrease is more gradual and is sometimes masked by local fluctuations.
- (ii) There is a pronounced peak between  $Z = 23-28$  including V, Cr, Mn, Fe, Co and Ni, and rising to a maximum at Fe which is  $\sim 10^3$  more abundant than expected from the general trend.
- (iii) Deuterium (D), Li, Be and B are rare compared with the neighbouring H, He, C and N.
- (iv) Among the lighter nuclei (up to Sc,  $Z = 21$ ), those having an atomic mass number  $A$  divisible by 4 are more abundant than their neighbours, e.g.  $^{16}\text{O}$ ,  $^{20}\text{Ne}$ ,  $^{24}\text{Mg}$ ,  $^{28}\text{Si}$ ,  $^{32}\text{S}$ ,  $^{36}\text{Ar}$  and  $^{40}\text{Ca}$  (rule of G. Oddo, 1914).
- (v) Atoms with  $A$  even are more abundant than those with  $A$  odd. (This is seen in Fig. 1.1 as an upward displacement of the curve for  $Z$  even, the exception at beryllium being due to the non-existence of  $^8\text{Be}$ , the isotope  $^9\text{Be}$  being the stable species.)

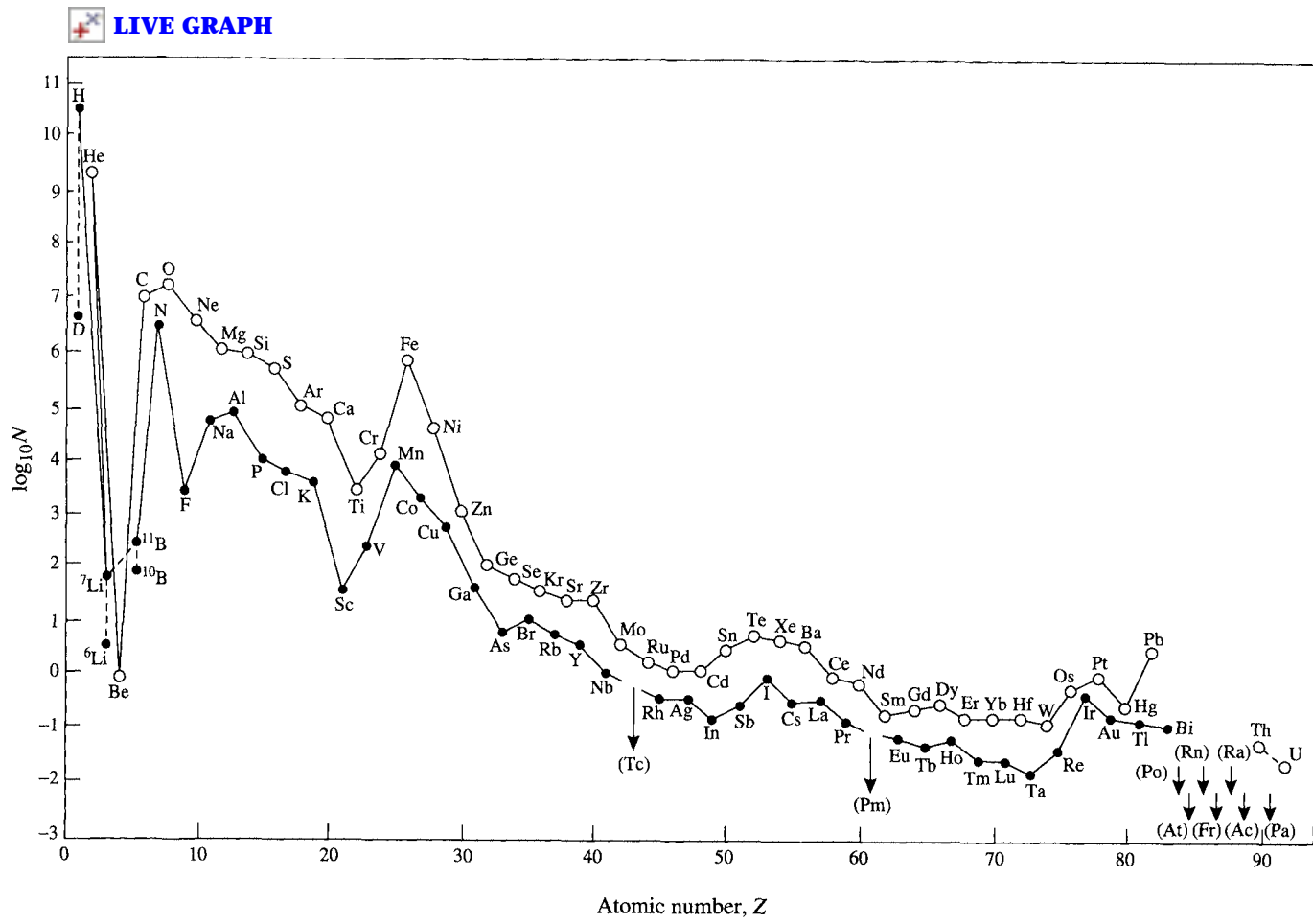
Two further features become apparent when abundances are plotted against  $A$  rather than  $Z$ :

- (vi) Atoms of heavy elements tend to be neutron rich; heavy proton-rich nuclides are rare.
- (vii) Double-peaked abundance maxima occur at  $A = 80, 90$ ;  $A = 130, 138$ ; and  $A = 196, 208$  (see Fig. 1.5 on p. 11).

It is also necessary to explain the existence of naturally occurring radioactive elements whose half-lives (or those of their precursors) are substantially less than the presumed age of the universe.

As a result of extensive studies over the past four decades it is now possible to give a detailed and convincing explanation of the experimental abundance data summarized above. The historical sequence of events which led to our present

<sup>2</sup>R. W. WILSON, The cosmic microwave background radiation, pp. 113–33 in *Les Prix Nobel 1978*, Almqvist & Wiksell International, Stockholm 1979. A. A. PENZIAS, The origin of the elements, pp. 93–106 in *Les Prix Nobel 1978* (also in *Science* **105**, 549–54 (1979)).



**Figure 1.1** Cosmic abundances of the elements as a function of atomic number  $Z$ . Abundances are expressed as numbers of atoms per  $10^6$  atoms of Si and are plotted on a logarithmic scale. (From A. G. W. Cameron, *Space Sci. Rev.* **15**, 121–46 (1973), with some updating.)



understanding is briefly summarized in the Panel. As the genesis of the elements is closely linked with theories of stellar evolution, a short description of the various types of star is given in the next section and this is then followed by a fuller discussion of the various processes by which the chemical elements are synthesized.

## 1.4 Stellar Evolution and the Spectral Classes of Stars<sup>(3,4)</sup>

In broad outline stars are thought to evolve by the following sequence of events. First, there is self-gravitational accretion from the cooled primordial

<sup>3</sup> I. S. SHKLOVSKII, *Stars: Their Birth, Life and Death* (translated by R. B. Rodman), W. H. Freeman, San Francisco, 1978, 442 pp. M. HARWIT, *Astrophysical Concepts* (2nd edn) Springer Verlag, New York, 1988, 626 pp.

<sup>4</sup> D. H. CLARK and F. R. STEPHENSON, *The Historical Supernovae*, Pergamon Press, Oxford, 1977, 233 pp.

hydrogen and helium. For a star the size and mean density of the sun (mass =  $1.991 \times 10^{30}$  kg =  $1 M_{\odot}$ ) this might take  $\sim 20$  y. This gravitational contraction releases heat energy, some of which is lost by radiation; however, the continued contraction results in a steady rise in temperature until at  $\sim 10^7$  K the core can sustain nuclear reactions. These reactions release enough additional energy to compensate for radiational losses and a temporary equilibrium or steady state is established.

When  $\sim 10\%$  of the hydrogen in the core has been consumed gravitational contraction again occurs until at a temperature of  $\sim 2 \times 10^8$  K helium burning (fusion) can occur. This is followed by a similar depletion, contraction and temperature rise until nuclear reactions involving

L. A. MARSCHALL, *The Supernova Story*, Plenum Press, New York, 1989, 276 pp. P. MURDIN, *End in Fire: The Supernova in the Large Magellanic Cloud*, Cambridge University Press, 1990, 253 pp.

### Genesis of the Elements — Historical Landmarks

1890s	First systematic studies on the terrestrial abundances of the elements	F. W. Clarke; H. S. Washington and others
1905	Special relativity theory: $E = mc^2$	A. Einstein
1911	Nuclear model of the atom	E. Rutherford
1913	First observation of isotopes in a stable element (Ne)	J. J. Thompson
1919	First artificial transmutation of an element ${}^{14}_7\text{N}(\alpha, p){}^{17}_8\text{O}$	E. Rutherford
1925–8	First abundance data on stars (spectroscopy)	Cecilia H. Payne; H. N. Russell
1929	First proposal of stellar nucleosynthesis by proton fusion to helium and heavier nuclides	R. D'E. Atkinson and F. G. Houtermans
1937	The "missing element" $Z = 43$ (technetium) synthesized by ${}^{99}_{42}\text{Mo}(d, n){}^{99}_{43}\text{Tc}$	C. Perrier and E. G. Segré
1938	Catalytic CNO process independently proposed to assist nuclear synthesis in stars	H. A. Bethe; C. F. von Weizsäcker
1938	Uranium fission discovered experimentally	O. Hahn and F. Strassmann
1940	First transuranium element ${}^{239}_{93}\text{Np}$ synthesized	E. M. McMillan and P. Abelson
1947	The last "missing element" $Z = 61$ (Pm) discovered among uranium fission products	J. A. Marinsky, L. E. Glendenin and C. D. Coryell
1948	Hot big-bang theory of expanding universe includes an (incorrect) theory of nucleogenesis	R. A. Alpher, H. A. Bethe and G. Gamow
1952–4	Helium burning as additional process for nucleogenesis	E. E. Salpeter; F. Hoyle
1954	Slow neutron absorption added to stellar reactions	A. G. W. Cameron
1955–7	Comprehensive theory of stellar synthesis of all elements in observed cosmic abundances	E. M. Burbidge, G. R. Burbidge, W. A. Fowler and F. Hoyle
1965	2.7 K radiation detected	A. P. Penzias and R. W. Wilson

still heavier nuclei ( $Z = 8-22$ ) can occur at  $\sim 10^9$  K. The time scale of these processes depends sensitively on the mass of the star, taking perhaps  $10^{12}$  y for a star of mass  $0.2 M_{\odot}$ ,  $10^{10}$  y for a star of 1 solar mass,  $10^7$  y for mass  $10 M_{\odot}$ , and only  $8 \times 10^4$  y for a star of  $50 M_{\odot}$ ; i.e. the more massive the star, the more rapidly it consumes its nuclear fuel. Further catastrophic changes may then occur which result in much of the stellar material being ejected into space, where it becomes incorporated together with further hydrogen and helium in the next generation of stars. It should be noted, however, that, as iron is at the maximum of the nuclear binding energy curve, only those elements up to iron ( $Z = 26$ ) can be produced by exothermic processes of the type just considered, which occur automatically if the temperature rises sufficiently. Beyond iron, an input of energy is required to promote further element building.

The evidence on which this theory of stellar evolution is based comes not only from known nuclear reactions and the relativistic equivalence of mass and energy, but also from the spectroscopic analysis of the light reaching us from the stars. This leads to the spectral classification of stars, which is the cornerstone of modern experimental astrophysics. The spectroscopic analysis of starlight reveals much information about the

chemical composition of stars — the identity of the elements present and their relative concentrations. In addition, the “red shift” or Doppler effect can be used to gauge the relative motions of the stars and their distance from the earth. More subtly, the surface temperature of stars can be determined from the spectral characteristics of their “blackbody” radiation, the higher the temperature the shorter the wavelength of maximum emission. Thus cooler stars appear red, and successively hotter stars appear progressively yellow, white, and blue. Differences in colour are also associated with differences in chemical composition as indicated in Table 1.1.

If the spectral classes (or temperatures) of stars are plotted against their absolute magnitudes (or luminosities) the resulting diagram shows several preferred regions into which most of the stars fall. Such diagrams were first made, independently, by E. Hertzsprung and H. N. Russell about 1913 and are now called HR diagrams (Fig. 1.2). More than 90% of all stars fall on a broad band called the main sequence, which covers the full range of spectral classes and magnitudes from the large, hot, massive O stars at the top to the small, dense, reddish M stars at the bottom. However, it should be emphasized that the terms “large” and “small” are purely relative since all stars within the main sequence are classified as dwarfs.

**Table 1.1** Spectral classes of stars

Class <sup>(a)</sup>	Colour	Surface ( $T/K$ )	Spectral characterization	Examples
O	Blue	>25 000	Lines of ionized He and other elements; H lines weak	10 Lacertae
B	Blue-white	11 000–25 000	H and He prominent	Rigel, Spica
A	White	7500–11 000	H lines very strong	Sirius, Vega
F	Yellow-white	6000–7000	H weaker; lines of ionized metals becoming prominent	Canopus, Procyon
G	Yellow	5000–6000	Lines of ionized and neutral metals prominent (especially Ca)	Sun, Capella
K	Orange	3500–5000	Lines of neutral metals and band spectra of simple radicals (e.g. CN, OH, CH)	Arcturus, Aldebaran
M	Red	2000–3500	Band spectra of many simple compounds prominent (e.g. TiO)	Betelgeuse, Antares

<sup>(a)</sup>Further division of each class into 10 subclasses is possible, e.g. . . . F8, F9, G0, G1, G2, . . . The sun is G2 with a surface temperature of 5780 K. This curious alphabetical sequence of classes arose historically and can perhaps best be remembered by the mnemonic “Oh Be A Fine Girl (Guy), Kiss Me”.

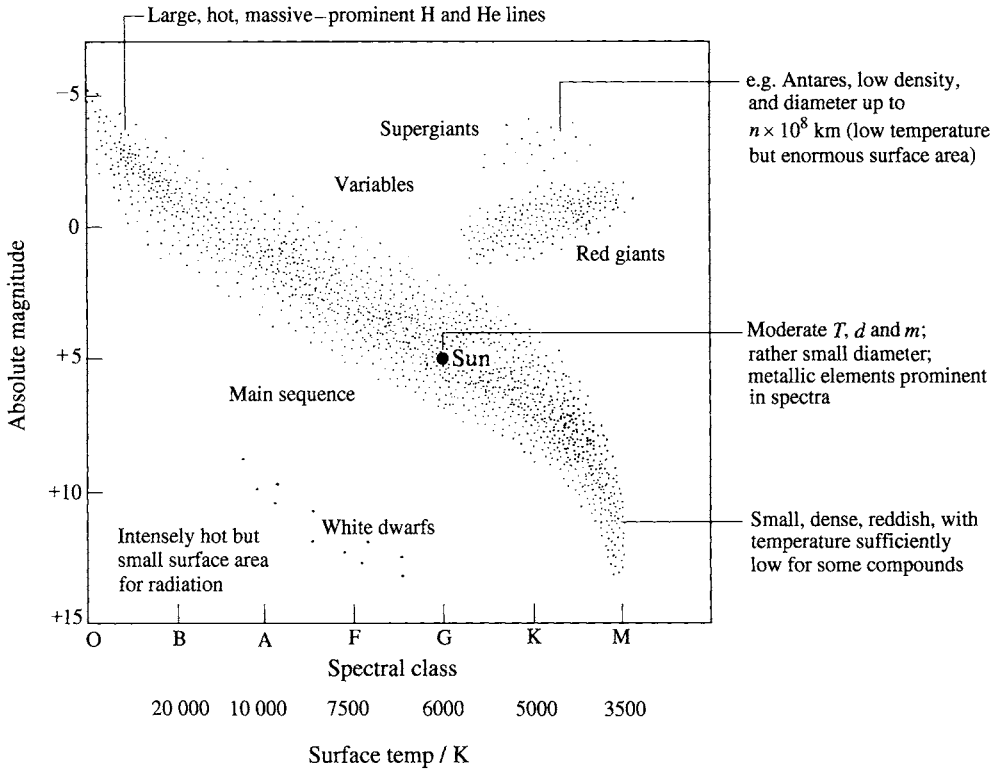


Figure 1.2 The Hertzsprung-Russell diagram for stars with known luminosities and spectra.

The next most numerous group of stars lie above and to the right of the main sequence and are called red giants. For example, Capella and the sun are both G-type stars yet Capella is 100 times more luminous than the sun; since they both have the same temperature it is concluded that Capella must have a radiating surface 100 times larger than the sun and thus has about 10 times its radius. Lying above the red giants are the supergiants such as Antares (Fig. 1.3), which has a surface temperature only half that of the sun but is 10 000 times more luminous: it is concluded that its radius is 100 times that of the sun. By contrast, the lower left-hand corner of the HR diagram is populated with relatively hot stars of low luminosity which implies that they are very small. These are the white dwarfs such as Sirius B which is only about the size of the earth though its mass is that of the sun: the implied density

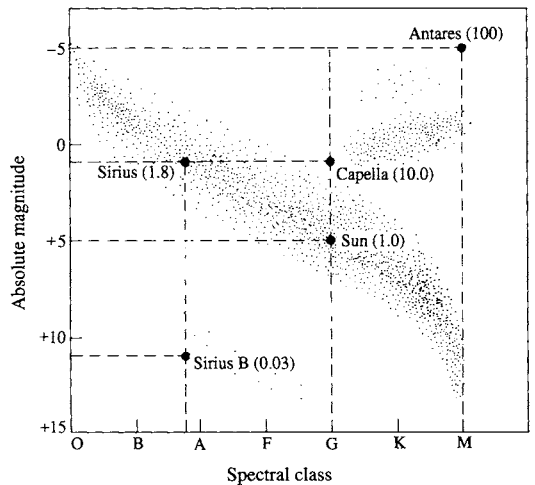


Figure 1.3 The comparison of various stars on the HR diagram. The number in parentheses indicates the approximate diameter of the star (sun = 1.0).

of  $\sim 5 \times 10^4 \text{ g cm}^{-3}$  indicates the extraordinarily compact nature of these bodies.

It is now possible to connect this description of stellar types with the discussion of the thermonuclear processes and the synthesis of the elements to be given in the next section. When a protostar begins to form by gravitational contraction from interstellar hydrogen and helium, its temperature rises until the temperature in its core can sustain proton burning (p. 9). A star of approximately the mass of the sun joins the main sequence at this point and spends perhaps 90% of its life there, losing little mass but generating colossal amounts of energy. Subsequent exhaustion of the hydrogen in the core (but not in the outer layers of the star) leads to further contraction to form a helium-burning core which forces much of the remaining hydrogen into a vast tenuous outer envelope — the star has become a red giant since its enormous radiating surface area can no longer be maintained at such a high temperature as previously despite the higher core temperature. Typical red giants have surface temperatures in the range 3500–5500 K; their luminosities are about  $10^2$ – $10^4$  times that of the sun and diameters about 10–100 times that of the sun. Carbon burning (p. 10) can follow in older red giants followed by the  $\alpha$ -process (p. 11) during its final demise to white dwarf status.

Many stars are in fact partners in a binary system of two stars revolving around each other. If, as frequently occurs, the two stars have different masses, the more massive one will evolve faster and reach the white-dwarf stage before its partner. Then, as the second star expands to become a red giant its extended atmosphere encompasses the neighbouring white dwarf and induces instabilities which result in an outburst of energy and transfer of matter to the more massive partner. During this process the luminosity of the white dwarf increases perhaps ten-thousandfold and the event is witnessed as a nova (since the preceding binary was previously invisible to the naked eye).

As we shall see in the description of the e-process and the  $\gamma$ -process (p. 12), even more spectacular instabilities can develop in larger

main sequence stars. If the initial mass is greater than about 3.5 solar masses, current theories suggest that gravitational collapse may be so catastrophic that the system implodes beyond nuclear densities to become a black hole. For main sequence stars in the mass range 1.4–3.5  $M_{\odot}$ , implosion probably halts at nuclear densities to give a rapidly rotating neutron star (density  $\sim 10^{14} \text{ g cm}^{-3}$ ) which may be observable as a pulsar emitting electromagnetic radiation over a wide range of frequencies in pulses at intervals of a fraction of a second. During this process of star implosion the sudden arrest of the collapsing core at nuclear densities yields an enormous temperature ( $\sim 10^{12} \text{ K}$ ) and high pressure which produces an outward-moving shock wave. This strikes the star's outer envelope with resulting rapid compression, a dramatic rise in temperature, the onset of many new nuclear reactions, and explosive ejection of a significant fraction of the star's mass. The overall result is a supernova up to  $10^8$  times as bright as the original star. At this point a single supernova is comparable in brightness to the whole of the rest of the galaxy in which it is formed, after which the brightness decays exponentially, often with a half-life of about two months. Supernovae, novae, and unstable variables from dying red giants are thus all candidates for the synthesis of heavier elements and their ejection into interstellar regions for subsequent processing in later generations of condensing main sequence stars such as the sun. It should be stressed, however, that these various theories of the origin of the chemical elements are all very recent and the detailed processes are by no means all fully understood. Since this is at present a very active area of research, some of the conclusions given in this chapter are correspondingly tentative, and will undoubtedly be modified and refined in the light of future experimental and theoretical studies. With this caveat we now turn to a more detailed description of the individual nuclear processes thought to be involved in the synthesis of the elements.

## 1.5 Synthesis of the Elements<sup>(5-9)</sup>

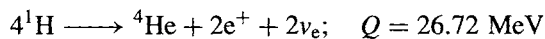
The following types of nuclear reactions have been proposed to account for the various types of stars and the observed abundances of the elements:

- (i) Exothermic processes in stellar interiors: these include (successively) hydrogen burning, helium burning, carbon burning, the  $\alpha$ -process, and the equilibrium or e-process.
- (ii) Neutron capture processes: these include the s-process (slow neutron capture) and the r-process (rapid neutron capture).
- (iii) Miscellaneous processes: these include the p-process (proton capture) and spallation within the stars, and the x-process which involves spallation (p. 14) by galactic cosmic rays in interstellar regions.

### 1.5.1 Hydrogen burning

When the temperature of a contracting mass of hydrogen and helium atoms reaches about  $10^7$  K, a sequence of thermonuclear reactions is possible of which the most important are as shown in Table 1.2.

The overall reaction thus converts 4 protons into 1 helium nucleus plus 2 positrons and 2 neutrinos:



<sup>5</sup> D. N. SCHRAMM and R. WAGONER, Element production in the early universe, *A. Rev. Nucl. Sci.* **27**, 37-74 (1977).

<sup>6</sup> E. M. BURBIDGE, G. R. BURBIDGE, W. A. FOWLER and F. HOYLE, Synthesis of the elements in stars, *Rev. Mod. Phys.* **29**, 547-650 (1957). This is the definitive review on which all later work has been based.

<sup>7</sup> L. H. ALLER, *The Abundance of the Elements*, Interscience, New York, 1961, 283 pp.

<sup>7a</sup> L. H. AHRENS (ed.), *Origin and Distribution of the Elements*, Pergamon Press, Oxford, 1979, 920 pp.

<sup>8</sup> R. J. TAYLOR, *The Origin of Chemical Elements*, Wykeham Publications, London, 1972, 169 pp.

<sup>9</sup> W. A. FOWLER, The quest for the origin of the elements (Nobel Lecture), *Angew. Chem. Int. Edn. Engl.* **23**, 645-71 (1984).

Table 1.2 Thermonuclear consumption of protons

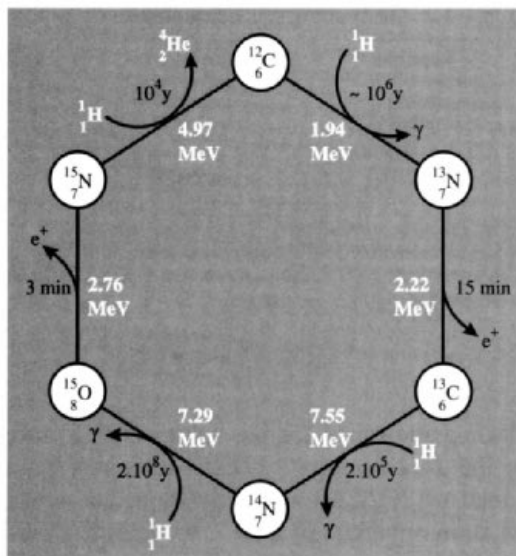
Reaction	Energy evolved, $Q$	Reaction time <sup>(a)</sup>
$^1\text{H} + ^1\text{H} \rightarrow ^2\text{H} + e^+ + \nu_e$	1.44 MeV	$1.4 \times 10^{10}$ y
$^2\text{H} + ^1\text{H} \rightarrow ^3\text{He} + \gamma$	5.49 MeV	0.6 s
$^3\text{He} + ^3\text{He} \rightarrow ^4\text{He} + 2^1\text{H}$	12.86 MeV	$10^6$ y

(a) The reaction time quoted is the time required for half the constituents involved to undergo reaction — this is sensitively dependent on both temperature and density; the figures given are appropriate for the centre of the sun, i.e.  $1.3 \times 10^7$  K and  $200 \text{ g cm}^{-3}$ .

1 MeV per atom  $\equiv 96.485 \times 10^6 \text{ kJ mol}^{-1}$ .

Making allowance for the energy carried away by the 2 neutrinos ( $2 \times 0.25 \text{ MeV}$ ) this leaves a total of 26.22 MeV for radiation, i.e.  $4.20 \text{ pJ}$  per atom of helium or  $2.53 \times 10^9 \text{ kJ mol}^{-1}$ . This vast release of energy arises mainly from the difference between the rest mass of the helium-4 nucleus and the 4 protons from which it was formed (0.028 atomic mass units). There are several other peripheral reactions between the protons, deuterons and  $^3\text{He}$  nuclei, but these need not detain us. It should be noted, however, that only 0.7% of the mass is lost during this transformation, so that the star remains approximately constant in mass. For example, in the sun during each second, some  $600 \times 10^6$  tonnes ( $600 \times 10^9 \text{ kg}$ ) of hydrogen are processed into  $595.5 \times 10^6$  tonnes of helium, the remaining  $4.5 \times 10^6$  tonnes of matter being transformed into energy. This energy is released deep in the sun's interior as high-energy  $\gamma$ -rays which interact with stellar material and are gradually transformed into photons with longer wavelengths; these work their way to the surface taking perhaps  $10^6$  y to emerge.

In fact, the sun is not a first-generation main-sequence star since spectroscopic evidence shows the presence of many heavier elements thought to be formed in other types of stars and subsequently distributed throughout the galaxy for eventual accretion into later generations of main-sequence stars. In the presence of heavier elements, particularly carbon and nitrogen, a catalytic sequence of nuclear reactions aids the fusion of protons to helium (H. A. Bethe



**Figure 1.4** Catalytic C–N–O cycle for conversion of  ${}^1\text{H}$  to  ${}^4\text{He}$ . The times quoted are the calculated half-lives for the individual steps at  $1.5 \times 10^7$  K.

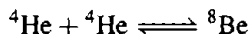
and C. F. von Weizsäcker, 1938) (Fig. 1.4). The overall reaction is precisely as before with the evolution of 26.72 MeV, but the 2 neutrinos now carry away 0.7 and 1.0 MeV respectively, leaving 25.0 MeV (4.01 pJ) per cycle for radiation. The coulombic energy barriers in the C–N–O cycle are some 6–7 times greater than for the direct proton–proton reaction and hence the catalytic cycle does not predominate until about  $1.6 \times 10^7$  K. In the sun, for example, it is estimated that about 10% of the energy comes from this process and most of the rest comes from the straightforward proton–proton reaction.

When approximately 10% of the hydrogen in a main-sequence star like the sun has been consumed in making helium, the outward thermal pressure of radiation is insufficient to counteract the gravitational attraction and a further stage of contraction ensues. During this process the helium concentrates in a dense central core ( $\rho \sim 10^5$  g cm $^{-3}$ ) and the temperature rises to perhaps  $2 \times 10^8$  K. This is sufficient to overcome the coulombic potential energy barriers surrounding the helium nuclei, and helium burning (fusion)

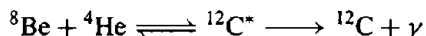
can occur. The hydrogen forms a vast tenuous envelope around this core with the result that the star evolves rapidly from the main sequence to become a red giant (p. 7). It is salutary to note that hydrogen burning in main-sequence stars has so far contributed an amount of helium to the universe which is only about 20% of that which was formed in the few minutes directly following the big bang (p. 2).

### 1.5.2 Helium burning and carbon burning

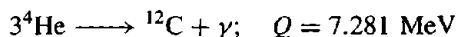
The main nuclear reactions occurring in helium burning are:



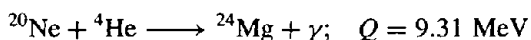
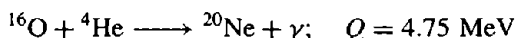
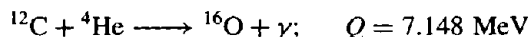
and



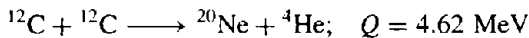
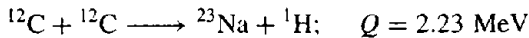
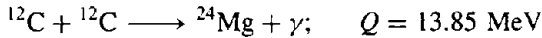
The nucleus  ${}^8\text{Be}$  is unstable to  $\alpha$ -particle emission ( $t_{1/2} \sim 2 \times 10^{-16}$  s) being 0.094 MeV less stable than its constituent helium nuclei; under the conditions obtaining in the core of a red giant the calculated equilibrium ratio of  ${}^8\text{Be}$  to  ${}^4\text{He}$  is  $\sim 10^{-9}$ . Though small, this enables the otherwise improbable 3-body collision to occur. It is noteworthy that, from consideration of stellar nucleogenesis, F. Hoyle predicted in 1954 that the nucleus of  ${}^{12}\text{C}$  would have a radioactive excited state  ${}^{12}\text{C}^*$  7.70 MeV above its ground state, some three years before this activity was observed experimentally at 7.653 MeV. Experiments also indicate that the energy difference  $Q({}^{12}\text{C}^* - 3{}^4\text{He})$  is 0.373 MeV, thus leading to the overall reaction energy



Further helium-burning reactions can now follow during which even heavier nuclei are synthesized:



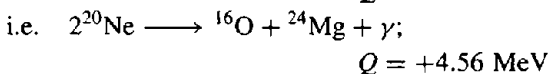
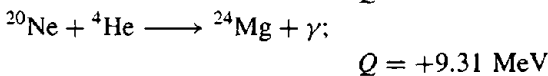
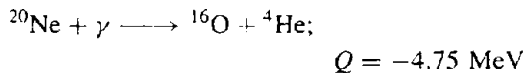
These reactions result in the exhaustion of helium previously produced in the hydrogen-burning process and an inner core of carbon, oxygen and neon develops which eventually undergoes gravitational contraction and heating as before. At a temperature of  $\sim 5 \times 10^8$  K carbon burning becomes possible in addition to other processes which must be considered. Thus, ageing red giant stars are now thought to be capable of generating a carbon-rich nuclear reactor core at densities of the order of  $10^4 \text{ g cm}^{-3}$ . Typical initial reactions would be:



The time scale of such reactions is calculated to be  $\sim 10^5$  y at  $6 \times 10^8$  K and  $\sim 1$  y at  $8.5 \times 10^8$  K. It will be noticed that hydrogen and helium nuclei are regenerated in these processes and numerous subsequent reactions become possible, generating numerous nuclides in this mass range.

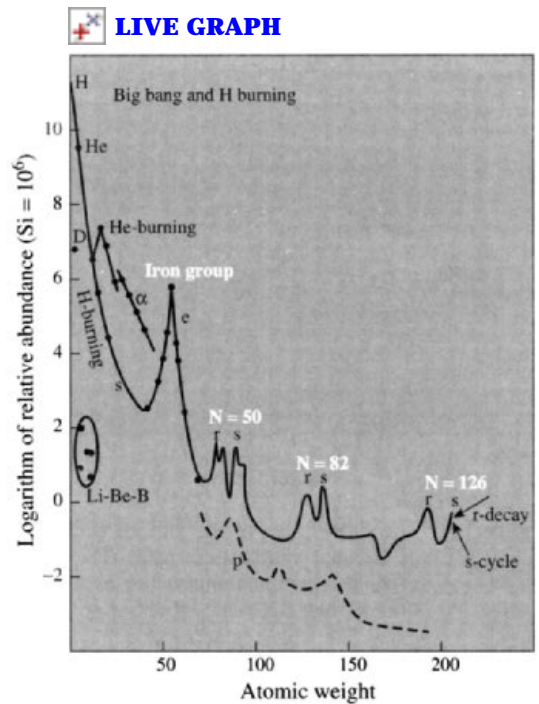
### 1.5.3 The $\alpha$ -process

The evolution of a star after it leaves the red-giant phase depends to some extent on its mass. If it is not more than about  $1.4 M_{\odot}$  it may contract appreciably again and then enter an oscillatory phase of its life before becoming a white dwarf (p. 7). When core contraction following helium and carbon depletion raises the temperature above  $\sim 10^9$  K the  $\gamma$ -rays in the stellar assembly become sufficiently energetic to promote the (endothermic) reaction  $^{20}\text{Ne}(\gamma, \alpha)^{16}\text{O}$ . The  $\alpha$ -particle released can penetrate the coulomb barrier of other neon nuclei to form  $^{24}\text{Mg}$  in a strongly exothermic reaction:



Some of the released  $\alpha$ -particles can also scour out  $^{12}\text{C}$  to give more  $^{16}\text{O}$  and the  $^{24}\text{Mg}$  formed can react further by  $^{24}\text{Mg}(\alpha, \gamma)^{28}\text{Si}$ . Likewise for  $^{32}\text{S}$ ,  $^{36}\text{Ar}$  and  $^{40}\text{Ca}$ . It is this process that is considered to be responsible for building up the decreasing proportion of these so-called  $\alpha$ -particle nuclei (Figs. 1.1 and 1.5). The relevant numerical data (including for comparison those for  $^{20}\text{Ne}$  which is produced in helium and carbon burning) are as follows:

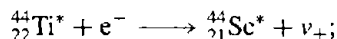
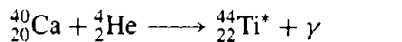
Nuclide	$^{20}\text{Ne}$	$^{24}\text{Mg}$	$^{28}\text{Si}$	$^{32}\text{S}$	$^{36}\text{Ar}$	$^{40}\text{Ca}$	$^{44}\text{Ca}$	$^{48}\text{Ti}$
$Q_{\alpha}/\text{MeV}$	(9.31)	10.00	6.94	6.66	7.04	5.28		
Relative abundance (as observed)	(8.4)	0.78	1.00	0.39	0.14	0.052	0.0011	0.0019



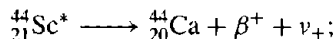
**Figure 1.5** Schematic representation of the main features of the curve of cosmic abundances shown in Fig. 1.1, labelled according to the various stellar reactions considered to be responsible for the synthesis of the elements. (After E. M. Burbidge *et al.*<sup>(6)</sup>.)

In a sense the  $\alpha$ -process resembles helium burning but is distinguished from it by the quite

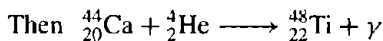
different source of the  $\alpha$ -particles consumed. The straightforward  $\alpha$ -process stops at  $^{40}\text{Ca}$  since  $^{44}\text{Ti}^*$  is unstable to electron-capture decay. Hence (and including atomic numbers  $Z$  as subscripts for clarity):



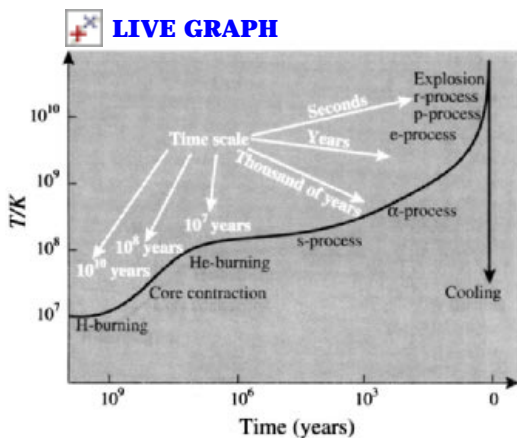
$$t_{1/2} \sim 49 \text{ y}$$



$$t_{1/2} \text{ 3.93 h}$$



The total time spent by a star in this  $\alpha$ -phase may be  $\sim 10^2 - 10^4 \text{ y}$  (Fig. 1.6).



**Figure 1.6** The time-scales of the various processes of element synthesis in stars. The curve gives the central temperature as a function of time for a star of about one solar mass. The curve is schematic.<sup>(6)</sup>

### 1.5.4 The e-process (equilibrium process)

More massive stars in the upper part of the main-sequence diagram (i.e. stars with masses in the range  $1.4 - 3.5 M_{\odot}$ ) have a somewhat different history to that considered in the preceding sections. We have seen (p. 6) that such stars consume their hydrogen much more rapidly than do smaller stars and hence spend less

time in the main sequence. Helium reactions begin in their interiors long before the hydrogen is exhausted, and in the middle part of their life they may expand only slightly. Eventually they become unstable and explode violently, emitting enormous amounts of material into interstellar space. Such explosions are seen on earth as supernovae, perhaps 10 000 times more luminous than ordinary novae. In the seconds (or minutes) preceding this catastrophic outburst, at temperatures above  $\sim 3 \times 10^9 \text{ K}$ , many types of nuclear reactions can occur in great profusion, e.g.  $(\gamma, \alpha)$ ,  $(\gamma, p)$ ,  $(\gamma, n)$ ,  $(\alpha, n)$ ,  $(p, \gamma)$ ,  $(n, \gamma)$ ,  $(p, n)$ , etc. (Fig. 1.6). This enables numerous interconversions to occur with the rapid establishment of a statistical equilibrium between the various nuclei and the free protons and neutrons. This is believed to explain the cosmic abundances of elements from  $^{22}\text{Ti}$  to  $^{29}\text{Cu}$ . Specifically, since  $^{56}_{26}\text{Fe}$  is at the peak of the nuclear binding-energy curve, this element is considerably more abundant than those further removed from the most stable state.

### 1.5.5 The s- and r-processes (slow and rapid neutron absorption)

Slow neutron capture with emission of  $\gamma$ -rays is thought to be responsible for synthesizing most of the isotopes in the mass range  $A = 63 - 209$  and also the majority of non- $\alpha$ -process nuclei in the range  $A = 23 - 46$ . These processes probably occur in pulsating red giants over a time span of  $\sim 10^7 \text{ y}$ , and production loops for individual isotopes are typically in the range  $10^2 - 10^5 \text{ y}$ . Several stellar neutron sources have been proposed, but the most likely candidates are the exothermic reactions  $^{13}\text{C}(\alpha, n)^{16}\text{O}$  (2.20 MeV) and  $^{21}\text{Ne}(\alpha, n)^{24}\text{Mg}$  (2.58 MeV). In both cases the target nuclei ( $A = 4n + 1$ ) would be produced by a  $(p, \gamma)$  reaction on the more stable  $4n$  nucleus followed by positron emission.

Because of the long time scale involved in the s-process, unstable nuclides formed by  $(n, \gamma)$  reactions have time to decay subsequently by  $\beta^-$  decay (electron emission). The crucial factor in determining the relative abundance of elements



formed by this process is thus the neutron capture cross-section of the precursor nuclide. In this way the process provides an ingenious explanation of the local peaks in abundance that occur near  $A = 90, 138$  and  $208$ , since these occur near unusually stable nuclei (neutron “magic numbers”  $50, 82$  and  $126$ ) which have very low capture cross-sections (Fig. 1.5). Their concentration therefore builds up by resisting further reaction. In this way the relatively high abundances of specific isotopes such as  $^{89}_{39}\text{Y}$  and  $^{90}_{40}\text{Zr}$ ,  $^{138}_{56}\text{Ba}$  and  $^{140}_{58}\text{Ce}$ ,  $^{208}_{82}\text{Pb}$  and  $^{209}_{83}\text{Bi}$  can be understood.

In contrast to the more leisureed processes considered in preceding paragraphs, conditions can arise (e.g. at  $\sim 10^9$  K in supernovae outbursts) where many neutrons are rapidly added successively to a nucleus before subsequent  $\beta^-$  decay becomes possible. The time scale for the *r*-process is envisaged as  $\sim 0.01$ – $10$  s, so that, for example, some 200 neutrons might be added to an iron nucleus in  $10$ – $100$  s. Only when  $\beta^-$  instability of the excessively neutron-rich product nuclei becomes extreme and the cross-section for further neutron absorption diminishes near the “magic numbers”, does a cascade of some  $8$ – $10$   $\beta^-$  emissions bring the product back into the region of stable isotopes. This gives a convincing interpretation of the local abundance peaks near  $A = 80, 130$  and  $194$ , i.e. some  $8$ – $10$  mass units below the nuclides associated with the *s*-process maxima (Fig. 1.5). It has also been suggested that neutron-rich isotopes of several of the lighter elements might also be the products of an *r*-process, e.g.  $^{36}\text{S}$ ,  $^{46}\text{Ca}$ ,  $^{48}\text{Ca}$  and perhaps  $^{47}\text{Ti}$ ,  $^{49}\text{Ti}$  and  $^{50}\text{Ti}$ . These isotopes, though not as abundant as others of these elements, nevertheless do exist as stable species and cannot be so readily synthesized by other potential routes.

The problem of the existence of the heavy elements must also be considered. The short half-lives of all isotopes of technetium and promethium adequately accounts for their absence on earth. However, no element with atomic number greater than  $83$ Bi has any stable isotope. Many of these (notably  $^{84}\text{Po}$ ,  $^{85}\text{At}$ ,  $^{86}\text{Rn}$ ,  $^{87}\text{Fr}$ ,  $^{88}\text{Ra}$ ,  $^{89}\text{Ac}$  and  $^{91}\text{Pa}$ ) can be

understood on the basis of secular equilibria with radioactive precursors, and their relative concentrations are determined by the various half-lives of the isotopes in the radioactive series which produce them. The problem then devolves on explaining the cosmic presence of thorium and uranium, the longest lived of whose isotopes are  $^{232}\text{Th}$  ( $t_{1/2} 1.4 \times 10^{10}$  y),  $^{238}\text{U}$  ( $t_{1/2} 4.5 \times 10^9$  y) and  $^{235}\text{U}$  ( $t_{1/2} 7.0 \times 10^8$  y). The half-life of thorium is commensurate with the age of the universe ( $\sim 1.5 \times 10^{10}$  y) and so causes no difficulty. If all the present terrestrial uranium was produced by an *r*-process in a single supernova event then this occurred  $6.6 \times 10^9$  y ago (p. 1257). If, as seems more probable, many supernovae contributed to this process, then such events, distributed uniformly in time, must have started  $\sim 10^{10}$  y ago. In either case the uranium appears to have been formed long before the formation of the solar system ( $4.6$ – $5.0$ )  $\times 10^9$  y ago. More recent considerations of the formation and decay of  $^{232}\text{Th}$ ,  $^{235}\text{U}$  and  $^{238}\text{U}$  suggest that our own galaxy is  $(1.2$ – $2.0) \times 10^{10}$  y old.

### 1.5.6 The *p*-process (proton capture)

Proton capture processes by heavy nuclei have already been briefly mentioned in several of the preceding sections. The  $(p, \gamma)$  reaction can also be invoked to explain the presence of a number of proton-rich isotopes of lower abundance than those of nearby normal and neutron-rich isotopes (Fig. 1.5). Such isotopes would also result from expulsion of a neutron by a  $\gamma$ -ray, i.e.  $(\gamma, n)$ . Such processes may again be associated with supernovae activity on a very short time scale. With the exceptions of  $^{113}\text{In}$  and  $^{115}\text{Sn}$ , all of the 36 isotopes thought to be produced in this way have even atomic mass numbers; the lightest is  $^{74}_{34}\text{Se}$  and the heaviest  $^{196}_{80}\text{Hg}$ .

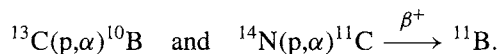
### 1.5.7 The *x*-process

One of the most obvious features of Figs. 1.1 and 1.5 is the very low cosmic abundance of the stable isotopes of lithium, beryllium and

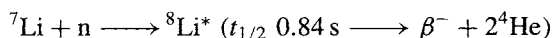
boron.<sup>10</sup> Paradoxically, the problem is not to explain why these abundances are so low but why these elements exist at all since their isotopes are bypassed by the normal chain of thermonuclear reactions described on the preceding pages. Again, deuterium and  $^3\text{He}$ , though part of the hydrogen-burning process, are also virtually completely consumed by it, so that their existence in the universe, even at relatively low abundances, is very surprising. Moreover, even if these various isotopes were produced in stars, they would not survive the intense internal heat since their bonding energies imply that deuterium would be destroyed above  $0.5 \times 10^6$  K, Li above  $2 \times 10^6$  K, Be above  $3.5 \times 10^6$  and B above  $5 \times 10^6$ . Deuterium and  $^3\text{He}$  are absent from the spectra of almost all stars and are now generally thought to have been formed by nucleosynthesis during the last few seconds of the original big bang; their main agent of destruction is stellar processing.

It now seems likely that the 5 stable isotopes  $^6\text{Li}$ ,  $^7\text{Li}$ ,  $^9\text{Be}$ ,  $^{10}\text{B}$  and  $^{11}\text{B}$  are formed predominantly by spallation reactions (i.e. fragmentation) effected by galactic cosmic-ray bombardment (the x-process). Cosmic rays consist of a wide variety of atomic particles moving through the galaxy at relativistic velocities. Nuclei ranging from hydrogen to uranium have been detected in cosmic rays though  $^1\text{H}$  and  $^4\text{He}$  are by far the most abundant components [ $^1\text{H}$ : 500;  $^4\text{He}$ : 40; all particles with atomic numbers from 3 to 9: 5; all particles with  $Z \geq 10$ :  $\sim 1$ ]. However, there is a striking deviation from stellar abundances since Li, Be and B are vastly over abundant as are Sc, Ti, V and Cr (immediately preceding the abundance peak near iron). The simplest interpretation of these facts is that the (heavier) particles comprising cosmic rays, travelling as they do great distances in the galaxy, occasionally collide with atoms of the interstellar gas (predominantly  $^1\text{H}$  and  $^4\text{He}$ ) and thereby fragment. This fragmentation, or spallation as it

is called, produces lighter nuclei from heavier ones. Conversely, high-speed  $^4\text{He}$  particles may occasionally collide with interstellar iron-group elements and other heavy nuclei, thus inducing spallation and forming Li, Be and B (and possibly even some  $^2\text{H}$  and  $^3\text{He}$ ), on the one hand, and elements in the range Sc–Cr, on the other. As we have seen, the lighter transition elements are also formed in various stellar processes, but the presence of elements in the mass range 6–12 suggest the need for a low-temperature low-density extra-stellar process. In addition to spallation, interstellar (p, $\alpha$ ) reactions in the wake of supernova shock waves may contribute to the synthesis of boron isotopes:



A further intriguing possibility has recently been mooted.<sup>11</sup> If the universe were not completely isotropic and uniform in density during the first few minutes after the big bang, then the high-density regions would have a greater concentration of protons than expected and the low-density regions would have more neutrons; this is because the diffusion of protons from high to low density regions would be inhibited by the presence of oppositely charged electrons whereas the electrically neutral neutrons can diffuse more readily. In the neutron-abundant lower-density regions certain neutron-rich species can then be synthesized. For example, in the homogeneous big bang, most of the  $^7\text{Li}$  formed is rapidly destroyed by proton bombardment ( $^7\text{Li} + p \rightarrow ^2\text{He}$ ) but in a neutron-rich region the radioactive isotope  $^8\text{Li}^*$  can be formed:

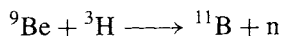
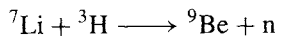


If, before it decays,  $^8\text{Li}^*$  is struck by a prevalent  $^4\text{He}$  nucleus then  $^{11}\text{B}$  can be formed ( $^8\text{Li}^* + ^4\text{He} \rightarrow ^{11}\text{B} + n$ ) and this will survive longer than in a proton-rich environment ( $^{11}\text{B} + p \rightarrow ^3\text{He}$ ). Other neutron-rich species could also be synthesized and survive in greater numbers than would

<sup>10</sup> H. REEVES, Origin of the light elements, *A. Rev. Astron. Astrophys.* **12**, 437–69 (1974).

<sup>11</sup> K. CROSSWELL, *New Scientist*, 9 Nov. 1991, 42–8.

be possible with higher concentrations of protons, e.g.:



The relative abundances of the various isotopes of the light elements Li, Be and B therefore depend to some extent on which detailed model of the big bang is adopted, and experimentally determined abundances may in time permit conclusions to be drawn as to the relative importance of these processes as compared to x-process spallation reactions.

In overall summary, using a variety of nuclear syntheses it is now possible to account for the presence of the 270 known stable isotopes of the elements up to  ${}^{209}\text{Bi}$  and to understand, at least in broad outline, their relative concentrations in the universe. The tremendous number of hypothetically possible internuclear conversions and reactions makes detailed computation extremely difficult. Energy changes are readily calculated from the known relative atomic masses of the various nuclides, but the cross-sections (probabilities) of many of the reactions are unknown and this prevents precise calculation of reaction rates and equilibrium concentrations in the extreme conditions occurring even in stable stars. Conditions and reactions occurring during supernova outbursts are even more difficult to define precisely. However, it is clear that substantial progress has been made in the last few decades in interpreting the bewildering variety of isotopic abundances which comprise the elements used by chemists. The approximate constancy of the isotopic composition of the individual elements is a fortunate result of the quasi-steady-state conditions obtaining in the universe during the time required to form the solar system. It is tempting to speculate whether chemistry could ever have emerged as a quantitative science if the elements had had widely varying isotopic composition, since gravimetric analysis would then have been impossible and the great developments of the nineteenth century could hardly have occurred. Equally, it should no longer cause surprise that the atomic weights of the

elements are not necessarily always “constants of nature”, and variations are to be expected, particularly among the lighter elements, which can have appreciable effects on physicochemical measurements and quantitative analysis.

## 1.6 Atomic Weights<sup>(12)</sup>

The concept of “atomic weight” or “mean relative atomic mass” is fundamental to the development of chemistry. Dalton originally supposed that all atoms of a given element had the same unalterable weight but, after the discovery of isotopes earlier this century, this property was transferred to them. Today the possibility of variable isotopic composition of an element (whether natural or artificially induced) precludes the possibility of defining *the* atomic weight of most elements, and the tendency nowadays is to define *an* atomic weight of an element as “the ratio of the average mass per atom of an element to one-twelfth of the mass of an atom of  ${}^{12}\text{C}$ ”. It is important to stress that atomic weights (mean relative atomic masses) of the elements are dimensionless numbers (ratios) and therefore have no units.

Because of their central importance in chemistry, atomic weights have been continually refined and improved since the first tabulations by Dalton (1803–5). By 1808 Dalton had included 20 elements in his list and these results were substantially extended and improved by Berzelius during the following decades. An illustration of the dramatic and continuing improvement in accuracy and precision during the past 100 y is given in Table 1.3. In 1874 no atomic weight was quoted to better than one part in 200, but by 1903 33 elements had values quoted to one part in  $10^3$  and 2 of these (silver and

<sup>12</sup> N. N. GREENWOOD, Atomic weights, Ch. 8 in Part I, Vol. 1, Section C, of Kolthoff and Elving's *Treatise on Analytical Chemistry*, pp. 453–78, Interscience, New York, 1978. This gives a fuller account of the history and techniques of atomic weight determinations and their significance, and incorporates a full bibliographical list of Reports on Atomic Weights.

iodine) were quoted to 1 in  $10^4$ . Today the majority of values are known to 1 in  $10^4$  and 26 elements have an accuracy exceeding 1 in  $10^6$ . This improvement was first due to improved chemical methods, particularly between 1900 and 1935 when increasing use of fused silica ware and electric furnaces reduced the possibility of contamination. More recently the use of mass spectrometry has effected a further improvement in precision. Mass spectrometric data were first used in a confirmatory role in the 1935 table of atomic weights, and by 1938 mass spectrometric values were preferred to chemical determinations for hydrogen and osmium and to gas-density values for helium. In 1959 the atomic weight values of over 50 elements were still based on classical chemical methods, but by 1973 this number had dwindled to 9 (Ti, Ge, Se, Mo, Sn, Sb, Te, Hg and Tl) or to 10 if the coulometric determination for Zn is counted as chemical. The values for a further 8 elements were based on a judicious blend of chemical and mass-spectrometric data, but the values quoted for

all other elements were based entirely on mass-spectrometric data.

Accurate atomic weight values do not automatically follow from precise measurements of relative atomic masses, however, since the relative abundance of the various isotopes must also be determined. That this can be a limiting factor is readily seen from Table 1.3: the value for praseodymium (which has only 1 stable naturally occurring isotope) has two more significant figures than the value for the neighbouring element cerium which has 4 such isotopes. In the twelve years since the first edition of this book was published the atomic weight values of no fewer than 55 elements have been improved, sometimes spectacularly, e.g. Ni from 58.69(1) to 58.6934(2).

### 1.6.1 Uncertainty in atomic weights

Numerical values for the atomic weights of the elements are now reviewed every 2 y by the Commission on Atomic Weights and Isotopic

**Table 1.3** Evolution of atomic weight values for selected elements<sup>(a)</sup>; (the dates selected were chosen for the reasons given below)

Element	1873-5	1903	1925	1959	1961	1997	
H	1	1.008	1.008	1.0080	1.00797	1.00794(7)	gmr
C	12	12.00	12.000	12.011 15	12.011 15	12.0107(8)	g r
O	16	16.00	16.000	<b>16</b>	15.9994	15.9994(3)	g r
P	31	31.0	31.027	30.975	30.9738	30.973 761(2)	
Ti	50	48.1	48.1	47.90	47.90	47.867(1)	
Zn	65	65.4	65.38	65.38	65.37	65.39(2)	
Se	79	79.2	79.2	78.96	78.96	78.96(3)	
Ag	108	107.93	107.880	107.880	107.870	107.8682(2)	g
I	127	126.85	126.932	126.91	126.9044	126.90447(3)	
Ce	92	140.0	140.25	140.13	140.12	140.116(1)	g
Pr	—	140.5	140.92	140.92	140.907	140.907 65(2)	
Re	—	—	188.7 <sup>(b)</sup>	186.22	186.22	186.207(1)	
Hg	200	200.0	200.61	200.61	200.59	200.59(2)	

<sup>(a)</sup>The annotations g, m and r appended to some values in the final column have the same meanings as those in the definitive table (facing inside front cover). The numbers in parentheses are the uncertainties in the last digit of the quoted value.

<sup>(b)</sup>The value for rhenium was first listed in 1929.

Note on dates:

1874 Foundation of the American Chemical Society (64 elements listed).

1903 First international table of atomic weights (78 elements listed).

1925 Major review of table (83 elements listed).

1959 Last table to be based on oxygen = 16 (83 elements listed).

1961 Complete reassessment of data and revision to  $^{12}\text{C} = 12$  (83 elements).

1997 Latest available IUPAC values (84 + 28 elements listed).

Abundances of IUPAC (the International Union of Pure and Applied Chemistry). Their most recent recommendations<sup>(13)</sup> are tabulated on the inside front fly sheet. From this it is clear that there is still a wide variation in the reliability of the data. The most accurately quoted value is that for fluorine which is known to better than 1 part in 38 million; the least accurate is for boron (1 part in 1500, i.e. 7 parts in  $10^4$ ). Apart from boron all values are reliable to better than 5 parts in  $10^4$  and the majority are reliable to better than 1 part in  $10^4$ . For some elements (such as boron) the rather large uncertainty arises not because of experimental error, since the use of mass-spectrometric measurements has yielded results of very high precision, but because the natural variation in the relative abundance of the 2 isotopes  $^{10}\text{B}$  and  $^{11}\text{B}$  results in a range of values of at least  $\pm 0.003$  about the quoted value of 10.811. By contrast, there is no known variation in isotopic abundances for elements such as selenium and osmium, but calibrated mass-spectrometric data are not available, and the existence of 6 and 7 stable isotopes respectively for these elements makes high precision difficult to obtain: they are thus prime candidates for improvement.

Atomic weights are known most accurately for elements which have only 1 stable isotope; the relative atomic mass of this isotope can be determined to at least 1 ppm and there is no possibility of variability in nature. There are 20 such elements: Be, F, Na, Al, P, Sc, Mn, Co, As, Y, Nb, Rh, I, Cs, Pr, Tb, Ho, Tm, Au and Bi. (Note that all of these elements except beryllium have odd atomic numbers — why?)

Elements with 1 predominant isotope can also, potentially, permit very precise atomic weight determinations since variations in isotopic composition or errors in its determination have a correspondingly small effect on the mass-spectrometrically determined value of the atomic weight. Nine elements have 1 isotope that is more than 99% abundant (H, He, N, O, Ar, V, La, Ta

and U) and carbon also approaches this category ( $^{13}\text{C}$  1.11% abundant).

Known variations in the isotopic composition of normal terrestrial material prevent a more accurate atomic weight being given for 13 elements and these carry the footnote r in the Table of Atomic Weights. For each of these elements (H, He, Li, B, C, N, O, Si, S, Ar, Cu, Sr and Pb) the accuracy attainable in an atomic weight determination on a given sample is greater than that implied by the recommended value since this must be applicable to any sample and so must embrace all known variations in isotopic composition from commercial terrestrial sources. For example, for hydrogen the present attainable accuracy of calibrated mass-spectrometric atomic weight determinations is about  $\pm 1$  in the sixth significant figure, but the recommended value of 1.00794( $\pm 7$ ) is so given because of the natural terrestrial variation in the deuterium content. The most likely value relevant to laboratory chemicals (e.g.  $\text{H}_2\text{O}$ ) is 1.00797, but it should be noted that hydrogen gas used in laboratories is often inadvertently depleted during its preparation by electrolysis, and for such samples the atomic weight is close to 1.00790. By contrast, intentional fractionation to yield heavy water (thousands of tonnes annually) or deuterated chemicals implies an atomic weight approaching 2.014, and great care should be taken to avoid contamination of "normal" samples when working with or disposing of such enriched materials.

Fascinating stories of natural variability could be told for each of the 13 elements having the footnote r and, indeed, determinations of such variations in isotopic composition are now an essential tool in unravelling the geochemical history of various ore bodies. For example, the atomic weight of sulfur obtained from virgin Texas sulfur is detectably different from that obtained from sulfate ores, and an overall range approaching  $\pm 0.01$  is found for terrestrial samples; this limits the value quoted to 32.066(6) though the accuracy of atomic weight determinations on individual samples is  $\pm 0.00015$ . Boron is even more adversely

<sup>13</sup> IUPAC Inorganic Chemistry Division, Atomic Weights of the Elements 1995, *Pure Appl. Chem.* **68**, 2339–59 (1996).

affected, as previously noted, and the actual atomic weight can vary from 10.809 to 10.812 depending on whether the mineral source is Turkey or the USA.

Even more disconcerting are the substantial deviations in atomic weight that can occur in commercially available material because of inadvertent or undisclosed changes in isotopic composition (footnote m in the Table of Atomic Weights). This situation at present obtains for 8 elements (H, Li, B, Ne, Cl, Kr, Xe and U) and may well also soon affect others (such as C, N and O). The separated or partially enriched isotopes of Li, B and U are now extensively used in nuclear reactor technology and weaponry, and the unwanted residues, depleted in the desired isotopes, are sometimes dumped on the market and sold as "normal" material. Thus lithium salts may unsuspectingly be purchased which have been severely depleted in  ${}^6\text{Li}$  (natural abundance 7.5%), and a major commercial supplier has marketed lithium containing as little as 3.75% of this isotope, thereby inducing an atomic weight change of 0.53%. For this reason practically all lithium compounds now obtainable in the USA are suspect and quantitative data obtained on them are potentially unreliable. Again, the practice of "milking" fission-product rare gases from reactor fuels and marketing these materials, produces samples with anomalous isotopic compositions. The effect, particularly on physicochemical computations, can be serious and, whilst not wishing to strike an alarmist note, the possibility of such deviations must continually be borne in mind for elements carrying the footnote m in the Table of Atomic Weights.

The related problem arising from radioactive elements is considered in the next section.

### 1.6.2 The problem of radioactive elements

Elements with radioactive nuclides amongst their naturally occurring isotopes have a built-in time variation of the relative concentration of their isotopes and hence a continually

varying atomic weight. Whether this variation is chemically significant depends on the half-life of the transition and the relative abundance of the various isotopes. Similarly, the actual concentration of stable isotopes of several elements (e.g. Ar, Ca and Pb) may be influenced by association of those elements with radioactive precursors (i.e.  ${}^{40}\text{K}$ ,  ${}^{238}\text{U}$ , etc.) which generate potentially variable amounts of the stable isotopes concerned. Again, some elements (such as technetium, promethium and the transuranium elements) are synthesized by nuclear reactions which produce a single isotope of the element. The "atomic weight" therefore depends on which particular isotope is being synthesized, and the concept of a "normal" atomic weight is irrelevant. For example, cyclotron production of technetium yields  ${}^{97}\text{Tc}$  ( $t_{1/2}$   $2.6 \times 10^6$  y) with an atomic weight of 96.9064, whereas fission product technetium is  ${}^{99}\text{Tc}$  ( $t_{1/2}$   $2.11 \times 10^5$  y), atomic weight 98.9063, and the isotope of longest half-life is  ${}^{98}\text{Tc}$  ( $t_{1/2}$   $4.2 \times 10^6$  y), atomic weight 97.9072.

At least 19 elements not usually considered to be radioactive do in fact have naturally occurring unstable isotopes. The minute traces of naturally occurring  ${}^3\text{H}$  ( $t_{1/2}$  12.33 y) and  ${}^{14}\text{C}$  ( $t_{1/2}$  5730 y) have no influence on the atomic weights of these elements though, of course, they are of crucial importance in other areas of study. The radioactivity of  ${}^{40}\text{K}$  ( $t_{1/2}$   $1.28 \times 10^9$  y) influences the atomic weights of its daughter elements argon (by electron capture) and calcium (by  $\beta^-$  emission) but fortunately does not significantly affect the atomic weight of potassium itself because of the low absolute abundance of this particular isotope (0.0117%). The half-lives of the radioactive isotopes of the 16 other "stable" elements are all greater than  $10^{10}$  y and so normally have little influence on the atomic weight of these elements even when, as in the case of  ${}^{115}\text{In}$  ( $t_{1/2}$   $4.41 \times 10^{14}$  y, 95.7% abundant) and  ${}^{187}\text{Re}$  ( $t_{1/2}$   $4.35 \times 10^{10}$  y, 62.6% abundant), they are the most abundant isotopes. Note, however, that on a geological time scale it has been possible to build up significant concentrations of  ${}^{187}\text{Os}$  in rhenium-containing

ores (by  $\beta^-$  decay of  $^{187}\text{Re}$ ), thereby generating samples of osmium with an anomalous atomic weight nearer to 187 than to the published value of 190.23(3). Lead was the first element known to be subject to such isotopic disturbances and, indeed, the discovery and interpretation of the significance of isotopes was itself hastened by the reluctant conclusion of T. W. Richards at the turn of the century that a group of lead samples of differing geological origins were identical chemically but differed in atomic weight — the possible variation is now known to span almost the complete range from 204 to 208. Such elements, for which geological specimens are known in which the element has an anomalous isotopic composition, are given the footnote g in the Table of Atomic Weights. In addition to Ar, Ca, Os and Pb just discussed, such variability affects at least 38 other elements, including Sr

(resulting from the  $\beta^-$  decay of  $^{87}\text{Rb}$ ), Ra, Th and U. A spectacular example, which affects virtually every element in the central third of the periodic table, has recently come to light with the discovery of prehistoric natural nuclear reactors at Oklo in Africa (see p. 1257). Fortunately this mine is a source of uranium ore only and so will not affect commercially available samples of the other elements involved.

In summary, as a consequence of the factors considered in this and the preceding section, the atomic weights of only the 20 mononuclidic elements can be regarded as “constants of nature”. For all other elements variability in atomic weight is potentially possible and in several instances is known to occur to an extent which affects the reliability of quantitative results of even modest precision.

																		1	2																												
																		H	He																												
3	4																	19	20																	35	36										
Li	Be																	K	Ca																	Br	Kr										
11	12																	17	18																	33	34										
Na	Mg																	Al	Si	P	S	Cl	Ar																								
19	20	21	22	23	24	25	26	27	28	29	30	31	32	37	38	39	40	41	42	43	44	45	46	47	48	49	50	51	52	53	54																
K	Ca	Sc	Ti	V	Cr	Mn	Fe	Co	Ni	Cu	Zn	Ga	Ge	As	Se	Br	Kr																														
37	38	39	40	41	42	43	44	45	46	47	48	49	50	51	52	53	54																														
Rb	Sr	Y	Zr	Nb	Mo	Tc	Ru	Rh	Pd	Ag	Cd	In	Sn	Sb	Te	I	Xe																														
55	56	57	58	59	60	61	62	63	64	65	66	67	68	69	70	71	72	73	74	75	76	77	78	79	80	81	82	83	84	85	86																
Cs	Ba	La	Hf	Ta	W	Re	Os	Ir	Pt	Au	Hg	Tl	Pb	Bi	Po	At	Rn																														
87	88	89	90	91	92	93	94	95	96	97	98	99	100	101	102	103	104	105	106	107	108	109	110	111	112	113	114	115	116	117	118																
Fr	Ra	Ac	Rf	Db	Sg	Bh	Hs	Mt	Uun	Uun	Uub																																				
																		89	90	91	92	93	94	95	96	97	98	99	100	101	102	103	104	105	106	107	108	109	110	111	112	113	114	115	116	117	118
																		Ce	Pr	Nd	Pm	Sm	Eu	Gd	Tb	Dy	Ho	Er	Tm	Yb	Lu																
																		Th	Pa	U	Np	Pu	Am	Cm	Bk	Cf	Es	Fm	Md	No	Lr																

# 2

## Chemical Periodicity and the Periodic Table

### 2.1 Introduction

The concept of chemical periodicity is central to the study of inorganic chemistry. No other generalization rivals the periodic table of the elements in its ability to systematize and rationalize known chemical facts or to predict new ones and suggest fruitful areas for further study. Chemical periodicity and the periodic table now find their natural interpretation in the detailed electronic structure of the atom; indeed, they played a major role at the turn of the century in elucidating the mysterious phenomena of radioactivity and the quantum effects which led ultimately to Bohr's theory of the hydrogen atom. Because of this central position it is perhaps not surprising that innumerable articles and books have been written on the subject since the seminal papers by Mendeleev in 1869, and some 700 forms of the periodic table (classified into 146 different types or subtypes) have been proposed.<sup>(1-3)</sup> A brief historical survey of these developments is summarized in the Panel opposite.

There is no single *best* form of the periodic table since the choice depends on the purpose for which the table is used. Some forms emphasize chemical relations and valence, whereas others stress the electronic configuration of the elements or the dependence of the periods on the shells and subshells of the atomic structure. The most convenient form for our purpose is the so-called "long form" with separate panels for the lanthanide and actinide elements (see inside front cover). There has been a lively debate during the past decade as to the best numbering system to be used for the individual

<sup>1</sup> F. P. VENABLE, *The Development of the Periodic Law*, Chemical Publishing Co., Easton, Pa., 1896. This is the first general review of periodic tables and has an almost complete collection of those published to that time. J. W. VAN SPRONSEN, *The Periodic System of the Chemical Elements*, Elsevier, Amsterdam, 1969, 368 pp. An excellent modern account of the historical developments leading up to Mendeleev's table.

<sup>2</sup> E. G. MAZURS, *Graphic Representation of the Periodic System during One Hundred Years*, University of Alabama Press, Alabama, 1974. An exhaustive topological classification of over 700 forms of the periodic table.



groups in the table; we will adopt the 1–18 numbering scheme recommended by IUPAC.<sup>(3)</sup> The following sections of this chapter summarize:

- (a) the interpretation of the periodic law in terms of the electronic structure of atoms;
- (b) the use of the periodic table and graphs to systematize trends in physical and chemical properties and to detect possible errors, anomalies, and inconsistencies;
- (c) the use of the periodic table to predict new elements and compounds, and to suggest new areas of research.

## 2.2 The Electronic Structure of Atoms<sup>(4)</sup>

The ubiquitous electron was discovered by J. J. Thompson in 1897 some 25 y after the original work on chemical periodicity by D. I. Mendeleev and Lothar Meyer; however, a further 20 y were to pass before G. N. Lewis and then I. Langmuir connected the electron with valency and chemical bonding. Refinements continued via wave mechanics and molecular orbital theory, and the symbiotic relation between experiment and theory still continues

<sup>3</sup> E. FLUCK, *Pure Appl. Chem.* **60**, 432–6 (1988); G. J. LEIGH (ed.), *Nomenclature of Inorganic Chemistry: IUPAC Recommendations 1990*, Blackwell, Oxford, 1990, 289 pp. The “Red Book”.

<sup>4</sup> N. N. GREENWOOD, *Principles of Atomic Orbitals*, revised SI edition, Monograph for Teachers, No. 8, Chemical Society, London, 1980, 48 pp.

### Mendeleev’s Periodic Table

#### *Precursors and Successors*

- 1772 L. B. G. de Morveau made the first table of “chemically simple” substances. A. L. Lavoisier used this in his *Traité Élémentaire de Chimie* published in 1789.
- 1817–29 J. W. Döbereiner discovered many triads of elements and compounds, the combining weight of the central component being the average of its partners (e.g. CaO, SrO, BaO, and NiO, CuO, ZnO).
- 1843 L. Gmelin included a V-shaped arrangement of 16 triads in the 4th edition of his *Handbuch der Chemie*.
- 1857 J. B. Dumas published a rudimentary table of 32 elements in 8 columns indicating their relationships.
- 1862 A. E. B. de Chancourtois first arranged the elements in order of increasing atomic weight; he located similar elements in this way and published a helical form in 1863.
- 1864 L. Meyer published a table of valences for 49 elements.
- 1864 W. Odling drew up an almost correct table with 17 vertical columns and including 57 elements.
- 1865 J. A. R. Newlands propounded his law of octaves after several partial classifications during the preceding 2 y; he also correctly predicted the atomic weight of the undiscovered element germanium.
- 1868–9 L. Meyer drew up an atomic volume curve and a periodic table, but this latter was not published until 1895.
- 1869 D. I. Mendeleev enunciated his periodic law that “the properties of the elements are a periodic function of their atomic weights”. He published several forms of periodic table, one containing 63 elements.
- 1871 D. I. Mendeleev modified and improved his tables and predicted the discovery of 10 elements (now known as Sc, Ga, Ge, Tc, Re, Po, Fr, Ra, Ac and Pa). He fully described with amazing prescience the properties of 4 of these (Sc, Ga, Ge, Po). Note, however, that it was not possible to predict the existence of the noble gases or the number of lanthanide elements.
- 1894–8 Lord Rayleigh, W. Ramsay and M. W. Travers detected and then isolated the noble gases (He), Ne, Ar, Kr, Xe.
- 1913 N. Bohr explained the form of the periodic table on the basis of his theory of atomic structure and showed that there could be only 14 lanthanide elements.
- 1913 H. G. J. Moseley observed regularities in the characteristic X-ray spectra of the elements; he thereby discovered atomic numbers *Z* and provided justification for the ordinal sequence of the elements.
- 1940 E. McMillan and P. Abelson synthesized the first transuranium element  ${}_{93}\text{Np}$ . Others were synthesized by G. T. Seaborg and his colleagues during the next 15 y.
- 1944 G. T. Seaborg proposed the actinide hypothesis and predicted 14 elements (up to  $Z = 103$ ) in this group.

today. It should always be remembered, however, that it is incorrect to “deduce” known chemical phenomena from theoretical models; the proper relationship is that the currently accepted theoretical models interpret the facts and suggest new experiments — they will be modified (or discarded and replaced) when new results demand it. Theories can never be proved by experiment — only refuted, the best that can be said of a theory is that it is consistent with a wide range of information which it interprets logically and that it is a fruitful source of predictions and new experiments.

Our present views on the electronic structure of atoms are based on a variety of experimental results and theoretical models which are fully discussed in many elementary texts. In summary, an atom comprises a central, massive, positively charged nucleus surrounded by a more tenuous envelope of negative electrons. The nucleus is composed of neutrons ( ${}^1_0\text{n}$ ) and protons ( ${}^1_1\text{p}$ , i.e.  ${}^1_1\text{H}^+$ ) of approximately equal mass tightly bound by the force field of mesons. The number of protons ( $Z$ ) is called the atomic number and this, together with the number of neutrons ( $N$ ), gives the atomic mass number of the nuclide ( $A = N + Z$ ). An element consists of atoms all of which have the same number of protons ( $Z$ ) and this number determines the position of the element in the periodic table (H. G. J. Moseley, 1913). Isotopes of an element all have the same value of  $Z$  but differ in the number of neutrons in their nuclei. The charge on the electron ( $e^-$ ) is equal in size but opposite in sign to that of the proton and the ratio of their masses is 1/1836.1527.

The arrangement of electrons in an atom is described by means of four quantum numbers which determine the spatial distribution, energy, and other properties, see Appendix 1 (p. 1285). The principal quantum number  $n$  defines the general energy level or “shell” to which the electron belongs. Electrons with  $n = 1, 2, 3, 4, \dots$ , are sometimes referred to as K, L, M, N,  $\dots$ , electrons. The orbital quantum number  $l$  defines both the shape of the electron charge distribution and its orbital angular

momentum. The number of possible values for  $l$  for a given electron depends on its principal quantum number  $n$ ; it can have  $n$  values running from 0 to  $n - 1$ , and electrons with  $l = 0, 1, 2, 3, \dots$ , are designated s, p, d, f,  $\dots$ , electrons. Whereas  $n$  is the prime determinant of an electron's energy this also depends to some extent on  $l$  (for atoms or ions containing more than one electron). It is found that the sequence of increasing electron energy levels in an atom follows the sequence of values  $n + l$ ; if 2 electrons have the same value of  $n + l$  then the one with smaller  $n$  is the more tightly bound.

The third quantum number  $m$  is called the magnetic quantum number for it is only in an applied magnetic field that it is possible to define a direction within the atom with respect to which the orbital can be directed. In general, the magnetic quantum number can take up  $2l + 1$  values (i.e.  $0, \pm 1, \dots, \pm l$ ); thus an s electron (which is spherically symmetrical and has zero orbital angular momentum) can have only one orientation, but a p electron can have three (frequently chosen to be the  $x, y$ , and  $z$  directions in Cartesian coordinates). Likewise there are five possibilities for d orbitals and seven for f orbitals.

The fourth quantum number  $m_s$  is called the spin angular momentum quantum number for historical reasons. In relativistic (four-dimensional) quantum mechanics this quantum number is associated with the property of symmetry of the wave function and it can take on one of two values designated as  $+\frac{1}{2}$  and  $-\frac{1}{2}$ , or simply  $\alpha$  and  $\beta$ . All electrons in atoms can be described by means of these four quantum numbers and, as first enumerated by W. Pauli in his *Exclusion Principle* (1926), each electron in an atom must have a unique set of the four quantum numbers.

It can now be seen that there is a direct and simple correspondence between this description of electronic structure and the form of the periodic table. Hydrogen, with 1 proton and 1 electron, is the first element, and, in the ground state (i.e. the state of lowest energy) it has the electronic configuration  $1s^1$  with zero orbital angular momentum. Helium,  $Z = 2$ , has the configuration  $1s^2$ , and this completes the first period since no

other unique combination of  $n = 1$ ,  $l = m = 0$ ,  $m_s = \pm \frac{1}{2}$  exists. The second period begins with lithium ( $Z = 3$ ), the least tightly bound electron having the configuration  $2s^1$ . The same situation obtains for each of the other periods in the table, the number of the period being the principal quantum number of the least tightly bound electron of the first element in the period. It will also be seen that there is a direct relation between the various blocks of elements in the periodic table and the electronic configuration of the atoms it contains; the s block is 2 elements wide, the p block 6 elements wide, the d block 10, and the f block 14, i.e.  $2(2l + 1)$ , the factor 2 appearing because of the spins.

In so far as the chemical (and physical) properties of an element derive from its electronic configuration, and especially the configuration of its least tightly bound electrons, it follows that chemical periodicity and the form of the periodic table can be elegantly interpreted in terms of electronic structure.

## 2.3 Periodic Trends in Properties<sup>(5,6)</sup>

General similarities and trends in the *chemical* properties of the elements had been noticed increasingly since the end of the eighteenth century and predated the observation of periodic variations in *physical* properties which were not noted until about 1868. However, it is more convenient to invert this order and to look at trends in atomic and physical properties first.

### 2.3.1 Trends in atomic and physical properties

Figure 2.1 shows a modern version of Lothar Meyer's atomic volume curve: the alkali metals

<sup>5</sup> R. RICH, *Periodic Correlations*, W. A. Benjamin, New York, 1965, 159 pp.

<sup>6</sup> R. T. SANDERSON, *Inorganic Chemistry*, Reinhold Publishing Corp., New York, 1967, 430 pp.

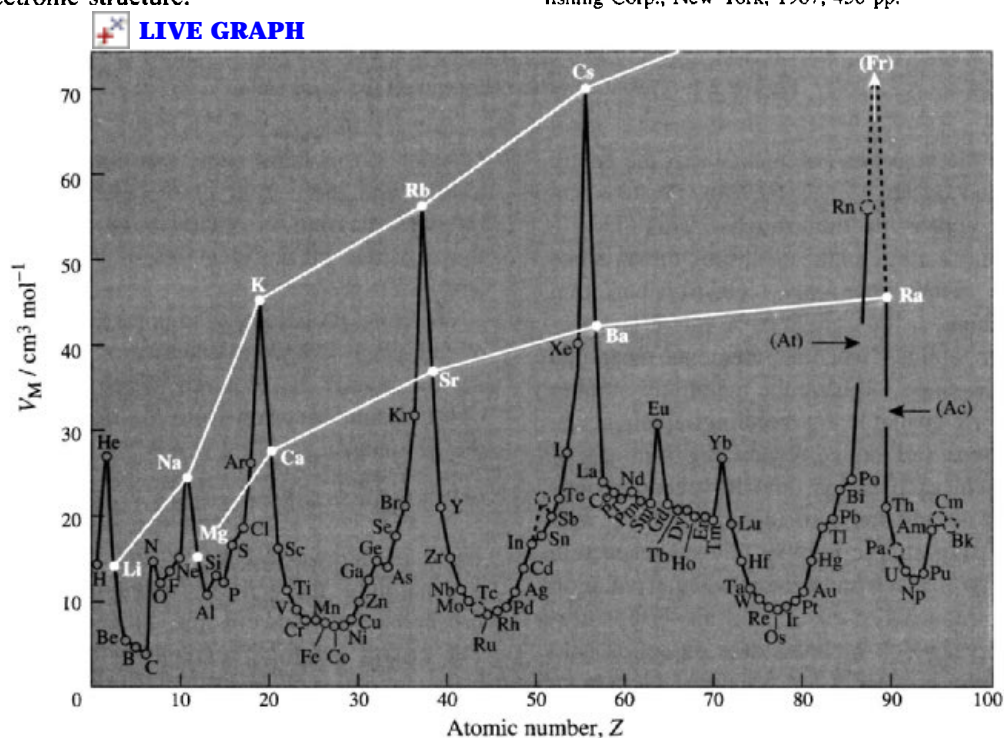


Figure 2.1 Atomic volumes (molar volumes) of the elements in the solid state.

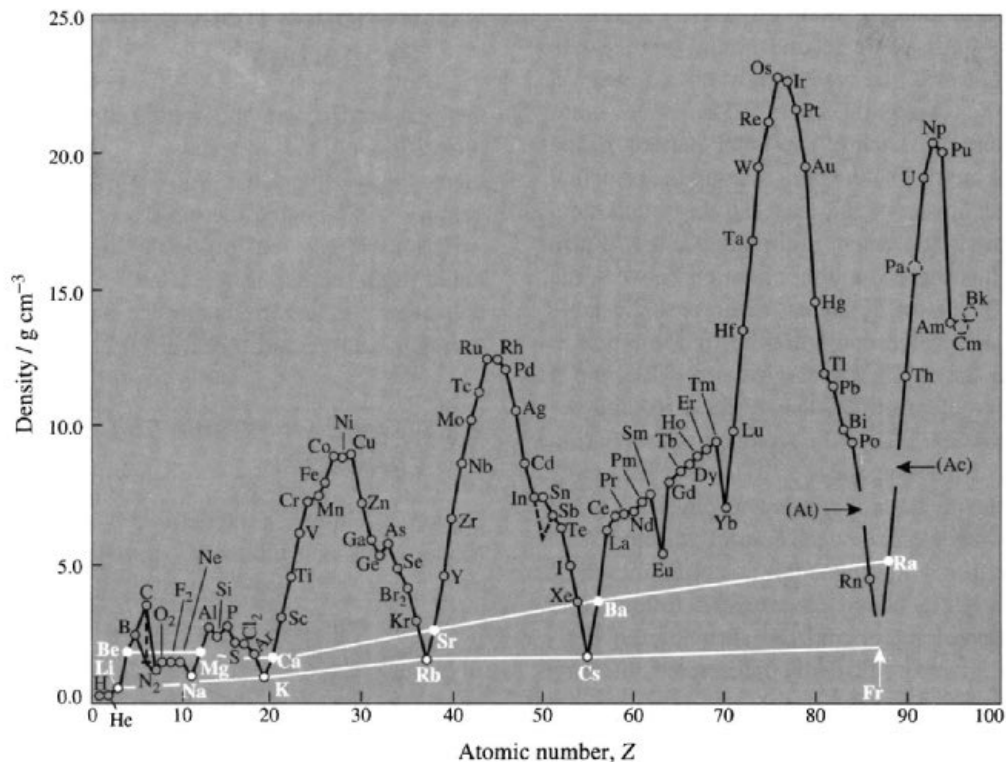
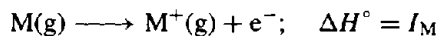


Figure 2.2 Densities of the elements in the solid state.

appear at the peaks and elements near the centre of each period (B, C; Al, Si; Mn, Fe, Co; Ru; and Os) appear in the troughs. This finds a ready interpretation on the electronic theory since the alkali metals have only 1 electron per atom to contribute to the binding of the 8 nearest-neighbour atoms, whereas elements near the centre of each period have the maximum number of electrons available for bonding. Elements in other groups fall on corresponding sections of the curve in each period, and in several groups there is a steady trend to higher volumes with the increasing atomic number. Closer inspection reveals that a much more detailed interpretation would be required to encompass all the features of the curve which includes data on solids held by very diverse types of bonding. Note also that the position of helium is anomalous (why?), and that there are local anomalies at europium and ytterbium in the lanthanide elements (see

Chapter 30). Similar plots are obtained for the atomic and ionic radii of the elements and an inverted diagram is obtained, as expected, for the densities of the elements in the solid state (Fig. 2.2).

Of more fundamental importance is the plot of first-stage ionization energies of the elements, i.e. the energy  $I_M$  required to remove the least tightly bound electron from the neutral atom in the gas phase:



These are shown in Fig. 2.3 and illustrate most convincingly the various quantum shells and subshells described in the preceding section. The energy required to remove the 1 electron from an atom of hydrogen is 13.606 eV (i.e. 1312 kJ per mole of H atoms). This rises to 2372 kJ mol<sup>-1</sup> for He (1s<sup>2</sup>) since the positive charge on the helium nucleus is twice that of the

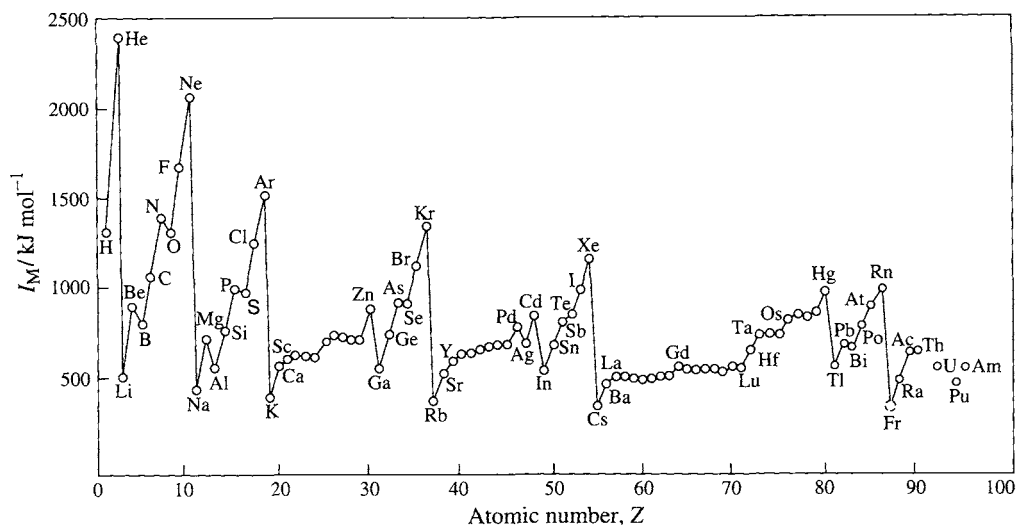


Figure 2.3 First-stage ionization energies of the elements.

proton and the additional charge is not completely shielded by the second electron. There is a large drop in ionization energy between helium and lithium ( $1s^22s^1$ ) because the principal quantum number  $n$  increases from 1 to 2, after which the ionization energy rises somewhat for beryllium ( $1s^22s^2$ ), though not to a value which is so high that beryllium would be expected to be an inert gas. The interpretation that is placed on the other values in Fig. 2.3 is as follows. The slight decrease at boron ( $1s^22s^22p^1$ ) is due to the increase in orbital quantum number  $l$  from 0 to 1 and the similar decrease between nitrogen and oxygen is due to increased interelectronic coulomb repulsion as the fourth p electron is added to the 3 already occupying  $2p_x$ ,  $2p_y$ , and  $2p_z$ . The ionization energy then continues to increase with increasing  $Z$  until the second quantum shell is filled at neon ( $2s^22p^6$ ). The process is precisely repeated from sodium ( $3s^1$ ) to argon ( $3s^23p^6$ ) which again occurs at a peak in the curve, although at this point the third quantum shell is not yet completed (3d). This is because the next added electron for the next element potassium ( $Z = 19$ ) enters the 4s shell ( $n + l = 4$ ) rather than the 3d ( $n + l = 5$ ). After calcium ( $Z = 20$ ) the 3d shell fills and then the 4p ( $n + l = 5$ , but  $n$  higher than for 3d). The

implications of this and of the subsequent filling of later s, p, d, and f levels will be elaborated in considerable detail in later chapters. Suffice it to note for the moment that the chemical inertness of the lighter noble gases correlates with their high ionization energies whereas the extreme reactivity of the alkali metals (and their prominent flame tests) finds a ready interpretation in their much lower ionization energies.

Electronegativities also show well-developed periodic trends though the concept of electronegativity itself, as introduced by L. Pauling,<sup>(7)</sup> is rather qualitative: "Electronegativity is the power of an atom *in a molecule* to attract electrons to itself." It is to be expected that the electronegativity of an element will depend to some extent not only on the other atoms to which it is bonded but also on its coordination number and oxidation state; for example, the electronegativity of a given atom increases with increase in its oxidation state. Fortunately, however, these effects do not obscure the main trends. Various measures of electronegativity have been proposed by L. Pauling, by R. S. Mulliken, by A. L. Allred

<sup>7</sup> L. PAULING, *J. Am. Chem. Soc.* **54**, 3570 (1932); *The Nature of the Chemical Bond*, 3rd edn., pp. 88–107. Cornell University Press, Ithaca, NY, 1960.

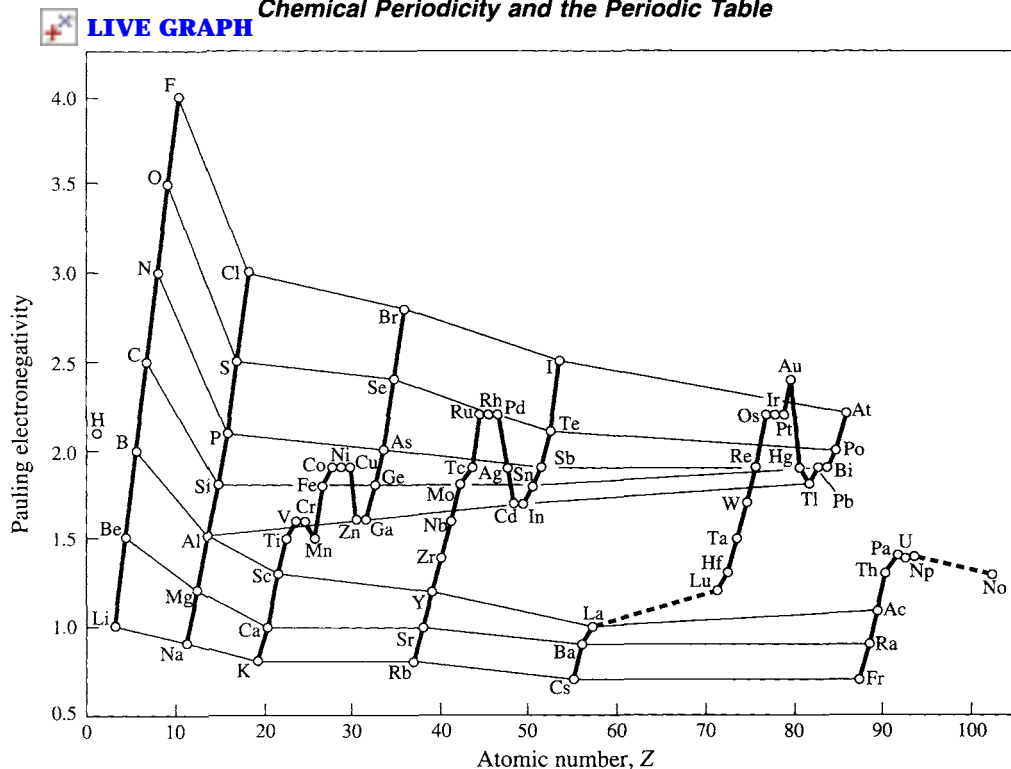


Figure 2.4 Values of electronegativity of the elements.

and E. Rochow, and by R. T. Sanderson, and all give roughly parallel scales. Figure 2.4, which incorporates Pauling's values, illustrates the trends observed; electronegativities tend to increase with increasing atomic number within a given period (e.g. Li to F, or K to Br) and to decrease with increasing atomic number within a given group (e.g. F to At, or O to Po). Numerous reviews are available.<sup>(8)</sup>

Many other properties have been found to show periodic variations and these can be displayed graphically or by circles of varying size on a periodic table, e.g. melting points of the elements, boiling points, heats of fusion, heats of vaporization, energies of atomization, etc.<sup>(6)</sup> Similarly, the properties of simple binary

compounds of the elements can be plotted, e.g. heats of formation, melting points and boiling points of hydrides, fluorides, chlorides, bromides, iodides, oxides, sulfides, etc.<sup>(6)</sup> Trends immediately become apparent, and the selection of compounds with specific values for particular properties is facilitated. Such trends also permit interpolation to give estimates of undetermined values of properties for a given compound though such a procedure can be misleading and should only be used as a first rough guide. Extrapolation has also frequently been used, and to good effect, though it too can be hazardous and unreliable particularly when new or unsuspected effects are involved. Perhaps the classic example concerns the dissociation energy of the fluorine molecule which is difficult to measure experimentally: for many years this was taken to be  $\sim 265 \text{ kJ mol}^{-1}$  by extrapolation of the values for iodine, bromine, and chlorine (151, 193, and  $243 \text{ kJ mol}^{-1}$ ), whereas the

<sup>8</sup> K. D. SEN and C. K. JØRGENSEN (eds.), *Structure and Bonding* 66 *Electronegativity*, Springer-Verlag, Berlin, 1987, 198 pp. J. Mullay, *J. Am. Chem. Soc.* **106**, 5842-7 (1984). R. T. Sanderson, *Inorg. Chem.* **25**, 1856-8 (1986). R. G. Pearson, *Inorg. Chem.* **27**, 734-40 (1988).

most recent experimental values are close to  $159 \text{ kJ mol}^{-1}$  (see Chapter 17). The detection of such anomalous data from periodic plots thus serves to identify either inaccurate experimental observations or inadequate theories (or both).

### 2.3.2 Trends in chemical properties

These, though more difficult to describe quantitatively than the trends in atomic and physical properties described in the preceding subsection, also become apparent when the elements are compared in each group and along each period. Such trends will be discussed in detail in later chapters and it is only necessary here to enumerate briefly the various types of behaviour that frequently recur.

The most characteristic chemical property of an element is its valence. There are numerous measures of valency each with its own area of usefulness and applicability. Simple definitions refer to the number of hydrogen atoms that can combine with an element in a binary hydride or to twice the number of oxygen atoms combining with an element in its oxide(s). It was noticed from the beginning that there was a close relation between the position of an element in the periodic table and the stoichiometry of its simple compounds. Hydrides of main group elements have the formula  $\text{MH}_n$  where  $n$  was related to the group number  $N$  by the equations  $n = N$  ( $N \leq 4$ ), and  $n = 18 - N$  for  $N > 14$ . By contrast, oxygen elicited an increasing valence in the highest normal oxide of each element and this was directly related to the group number, i.e.  $\text{M}_2\text{O}$ ,  $\text{MO}$ ,  $\text{M}_2\text{O}_3$ , . . . ,  $\text{M}_2\text{O}_7$ . These periodic regularities find a ready explanation in terms of the electronic configuration of the elements and simple theories of chemical bonding. In more complicated chemical formulae involving more than 2 elements, it is convenient to define the "oxidation state" of an element as the formal charge remaining on the element when all other atoms have been removed as their normal ions. For example, nitrogen has an oxidation state of  $-3$  in ammonium chloride [ $\text{NH}_4\text{Cl} - (4\text{H}^+ + \text{Cl}^-) = \text{N}^{3-}$ ] and manganese

has an oxidation state of  $+7$  in potassium permanganate {tetraoxomanganate(1-)} [ $\text{KMnO}_4 - (\text{K}^+ + 4\text{O}^{2-}) = \text{Mn}^{7+}$ ]. For a compound such as  $\text{Fe}_3\text{O}_4$  iron has an average oxidation state of  $+2.67$  [i.e.  $(4 \times 2)/3$ ] which may be thought of as comprising  $1\text{Fe}^{2+}$  and  $2\text{Fe}^{3+}$ . It should be emphasized that these charges are formal, not actual, and that the concept of oxidation state is not particularly helpful when considering predominantly covalent compounds (such as organic compounds) or highly catenated inorganic compounds such as  $\text{S}_7\text{NH}$ .

The periodicity in the oxidation state or valence shown by the elements was forcefully illustrated by Mendeleev in one of his early forms of the periodic system and this is shown in an extended form in Fig. 2.5 which incorporates more recent information. The predictive and interpolative powers of such a plot are obvious and have been a fruitful source of chemical experimentation for over a century.

Other periodic trends which occur in the chemical properties of the elements and which are discussed in more detail throughout later chapters are:

- (i) The "anomalous" properties of elements in the first short period (from lithium to fluorine) — see Chapters 4, 5, 6, 8, 11, 14 and 17.
- (ii) The "anomalies" in the post-transition element series (from gallium to bromine) related to the d-block contraction — see Chapters 7, 10, 13, 16 and 17.
- (iii) The effects of the lanthanide contraction — see Chapters 21–30.
- (iv) Diagonal relationships between lithium and magnesium, beryllium and aluminium, boron and silicon.
- (v) The so-called inert pair effect (see Chapters 7, 10 and 13) and the variation of oxidation state in the main group elements in steps of 2 (e.g.  $\text{IF}$ ,  $\text{IF}_3$ ,  $\text{IF}_5$ ,  $\text{IF}_7$ ).
- (vi) Variability in the oxidation state of transition elements in steps of 1.
- (vii) Trends in the basicity and electropositivity of elements — both vertical trends



The figure displays two periodic tables showing formal oxidation states. The top table covers elements from Hydrogen (H) to Xenon (Xe), and the bottom table covers elements from Calcium (Ca) to Berkelium (Bk). Oxidation states are indicated by numbers placed above or below the element symbols. Common oxidation states (0, ±1, ±2, ±3, ±4, ±5, ±6, ±7, ±8) are shown in white, while nonintegral values (e.g., 1/2, 2/3, 3/4) are shown in black. Arrows on the left of each table indicate the 'plus' (upward) and 'minus' (downward) directions for oxidation states.

**Figure 2.5** Formal oxidation states of the elements displayed in a format originally devised by Mendeleev in 1889. The more common oxidation states (including zero) are shown in white. Nonintegral values, as in  $B_5H_9$ ,  $C_3H_8$ ,  $HN_3$ ,  $S_8^{2+}$ , etc., are not included.



within groups and horizontal trends along periods.

- (viii) Trends in bond type with position of the elements in the table and with oxidation state for a given element.
- (ix) Trends in stability of compounds and regularities in the methods used to extract the elements from their compounds.
- (x) Trends in the stability of coordination complexes and the electron-donor power of various series of ligands.

## 2.4 Prediction of New Elements and Compounds

Newlands (1864) was the first to predict correctly the existence of a “missing element” when he calculated an atomic weight of 73 for an element between silicon and tin, close to the present value of 72.61 for germanium (discovered by C. A. Winkler in 1886). However, his method of detecting potential triads was unreliable and he predicted (non-existent) elements between

rhodium and iridium, and between palladium and platinum. Mendeleev’s predictions 1869–71 were much more extensive and reliable, as indicated in the historical panel on p. 21. The depth of his insight and the power of his method remain impressive even today, but in the state of development of the subject in 1869 they were monumental. A comparison of the properties of eka-silicon predicted by Mendeleev and those determined experimentally for germanium is shown in Table 2.1. Similarly accurate predictions were made for eka-aluminium and gallium and for eka-boron and scandium.

Of the remaining 26 undiscovered elements between hydrogen and uranium, 11 were lanthanoids which Mendeleev’s system was unable to characterize because of their great chemical similarity and the new numerical feature dictated by the filling of the 4f orbitals. Only cerium, terbium and erbium were established with certainty in 1871, and the others (except promethium, 1945) were separated and identified in the period 1879–1907. The isolation of the (unpredicted) noble gases also occurred at this time (1894–8).

Table 2.1

Mendeleev’s predictions (1871) for eka-silicon, M	Observed properties (1995) of germanium (discovered 1886)		
Atomic weight	72	Atomic weight	72.61(2)
Density/g cm <sup>-3</sup>	5.5	Density/g cm <sup>-3</sup>	5.323
Molar volume/cm <sup>3</sup> mol <sup>-1</sup>	13.1	Molar volume/cm <sup>3</sup> mol <sup>-1</sup>	13.64
MP/°C	high	MP/°C	945
Specific heat/J g <sup>-1</sup> K <sup>-1</sup>	0.305	Specific heat/J g <sup>-1</sup> K <sup>-1</sup>	0.309
Valence	4	Valence	4
Colour	dark grey	Colour	greyish-white
M will be obtained from MO <sub>2</sub> or K <sub>2</sub> MF <sub>6</sub> by reaction with Na		Ge is obtained by reaction of K <sub>2</sub> GeF <sub>6</sub> with Na	
M will be slightly attacked by acids such as HCl and will resist alkalis such as NaOH		Ge is not dissolved by HCl or dilute NaOH but reacts with hot conc HNO <sub>3</sub>	
M, on being heated, will form MO <sub>2</sub> with high mp, and <i>d</i> 4.7 g cm <sup>-3</sup>		Ge reacts with oxygen to give GeO <sub>2</sub> , mp 1086°, <i>d</i> 4.228 g cm <sup>-3</sup>	
M will give a hydrated MO <sub>2</sub> soluble in acid and easily reprecipitated		“Ge(OH) <sub>4</sub> ” dissolves in conc acid and is reprecipitated on dilution or addition of base	
MS <sub>2</sub> will be insoluble in water but soluble in ammonium sulfide		GeS <sub>2</sub> is insoluble in water and dilute acid but readily soluble in ammonium sulfide	
MCl <sub>4</sub> will be a volatile liquid with bp a little under 100°C and <i>d</i> 1.9 g cm <sup>-3</sup>		GeCl <sub>4</sub> is a volatile liquid with bp 83°C and <i>d</i> 1.8443 g cm <sup>-3</sup>	
M will form MEt <sub>4</sub> bp 160°C		GeEt <sub>4</sub> bp 185°C	

The isolation and identification of 4 radioactive elements in minute amounts took place at the turn of the century, and in each case the insight provided by the periodic classification into the predicted chemical properties of these elements proved invaluable. Marie Curie identified polonium in 1898 and, later in the same year working with Pierre Curie, isolated radium. Actinium followed in 1899 (A. Debierne) and the heaviest noble gas, radon, in 1900 (F. E. Dorn). Details will be found in later chapters which also recount the discoveries made in the present century of protactinium (O. Hahn and Lise Meitner, 1917), hafnium (D. Coster and G. von Hevesey, 1923), rhenium (W. Noddack, Ida Tacke and O. Berg, 1925), technetium (C. Perrier and E. Segré, 1937), francium (Marguerite Perey, 1939) and promethium (J. A. Marinsky, L. E. Glendenin and C. D. Coryell, 1945).

A further group of elements, the transuranium elements, has been synthesized by artificial nuclear reactions in the period from 1940 onwards; their relation to the periodic table is discussed fully in Chapter 31 and need not be repeated here. Perhaps even more striking today are the predictions, as yet unverified, for the properties of the currently non-existent superheavy elements.<sup>(9)</sup> Elements up to lawrencium ( $Z = 103$ ) are actinides (5f) and the 6d transition series starts with element 104. So far only elements 104–112 have been synthesized,<sup>(10)</sup> and, because there is as yet no agreement on trivial names for some of these elements (see pp. 1280–1), they are here referred to by their atomic numbers. A systematic naming scheme was approved by IUPAC in 1977 but is not widely used by researchers in the field. It involves the use of three-letter symbols derived directly from the atomic number by using the

following numerical roots:

0	1	2	3	4	5	6	7	8	9
nil	un	bi	tri	quad	pent	hex	sept	oct	enn

These names and symbols can be used for elements 110 and beyond until agreed trivial names have been internationally approved. Hence, 110 is un-un-nilium (Uun), 111 is un-un-unium (Uuu), and 112 is un-un-bium, (Uub). These elements are increasingly unstable with respect to  $\alpha$ -decay or spontaneous fission with half-lives of less than 1 s. It is therefore unlikely that much chemistry will ever be carried out on them though their ionization energies, mps, bps, densities, atomic and metallic radii, etc., have all been predicted. Element 112 is expected to be eka-mercury at the end of the 6d transition series, and should be, followed by the 7p and 8s configurations  $Z = 113$ –120. On the basis of present theories of nuclear structure an “island of stability” is expected near element 114 with half-lives in the region of years. Much effort is being concentrated on attempts to make these elements, and oxidation states are expected to follow the main group trends (e.g. 113: eka-thallium mainly + 1). Other physical properties have been predicted by extrapolation of known periodic trends. Still heavier elements have been postulated, though it is unlikely (on present theories) that their chemistry will ever be studied because of their very short predicted half-lives. Calculated energy levels for the range  $Z = 121$ –154 lead to the expectation of an unprecedented 5g series of 18 elements followed by fourteen 6f elements.

In addition to the prediction of new elements and their probable properties, the periodic table has proved invaluable in suggesting fruitful lines of research in the preparation of new compounds. Indeed, this mode of thinking is now so ingrained in the minds of chemists that they rarely pause to reflect how extraordinarily difficult their task would be if periodic trends were unknown. It is the ability to anticipate the effect of changing an element or a group in a compound which enables work to be planned effectively, though the prudent chemist is always alert to the possibility of

<sup>9</sup> B. FRICKE, Superheavy elements, *Structure and Bonding* **21**, 89 (1975). A full account of the predicted stabilities and chemical properties of elements with atomic numbers in the range  $Z = 104$ –184.

<sup>10</sup> R. C. BARBER, N. N. GREENWOOD, A. Z. HRYNKIEWICZ, M. LEFORT, M. SAKAI, I. ULEHLA, A. H. WAPSTRA and D. H. WILKINSON, *Progr. in Particle and Nuclear Physics*, **29**, 453–530 (1992); also published in *Pure Appl. Chem.* **65**, 1757–824 (1993). See also §31.4.

new effects or unsuspected factors which might surprisingly intervene.

Typical examples taken from the developments of the past two or three decades include:

- (i) the organometallic chemistry of lithium and thallium (Chapters 4 and 7);
- (ii) the use of boron hydrides as ligands (Chapter 6);
- (iii) solvent systems and preparative chemistry based on the interhalogens (Chapter 17);

(iv) the development of the chemistry of xenon (Chapter 18);

(v) ferrocene — leading to ruthenocene and dibenzene chromium, etc. (Chapters 19, 25 and 23 respectively);

(vi) the development of solid-state chemistry.

Indeed, the influence of Mendeleev's fruitful generalization pervades the whole modern approach to the chemistry of the elements.

																		1	2	3																					
																		H	He																						
4	5																	6	7	8	9	10																			
Li	Be																	B	C	N	O	F	Ne																		
11	12																	13	14	15	16	17	18																		
Na	Mg																	Al	Si	P	S	Cl	Ar																		
19	20	21	22	23	24	25	26	27	28	29	30	31	32	33	34	35	36																								
K	Ca	Sc	Ti	V	Cr	Mn	Fe	Cu	Ni	Cd	Zn	Ga	Ge	As	Se	Br	Kr																								
37	38	39	40	41	42	43	44	45	46	47	48	49	50	51	52	53	54																								
Rb	Sr	Y	Zr	Nb	Mo	Tc	Ru	Rh	Pd	Ag	Cd	In	Sn	Sb	Te	I	Xe																								
55	56	57	58	59	60	61	62	63	64	65	66	67	68	69	70	71	72																								
Cs	Ba	La	Hf	Ta	W	Re	Os	Ir	Pt	Au	Hg	Tl	Pb	Bi	Po	At	Rn																								
87	88	89	90	91	92	93	94	95	96	97	98	99	100	101	102	103	104																								
Fr	Ra	Ac	Th	Pa	U	Np	Pu	Am	Cm	Bk	Cf	Es	Fm	Md	No	Lr																									
																		105	106	107	108	109	110	111	112																
																		Uub	Uuq	Uuq	Uub	Uub	Uub	Uub	Uub																
																		113	114	115	116	117	118	119	120																
																		Cu	Pt	Ni	Pd	Sm	Eu	Gd	Tb	Dy	Ho	Er	Tm	Yb	Lu										
																		121	122	123	124	125	126	127	128	129	130	131	132	133	134										
																		Uut	Uuq	Uuq	Uuq	Uuq	Uuq	Uuq	Uuq	Uuq	Uuq	Uuq	Uuq	Uuq	Uuq										

# 3

## Hydrogen

### 3.1 Introduction

Hydrogen is the most abundant element in the universe and is also common on earth, being the third most abundant element (after oxygen and silicon) on the surface of the globe. Hydrogen in combined form accounts for about 15.4% of the atoms in the earth's crust and oceans and is the ninth element in order of abundance by weight (0.9%). In the crustal rocks alone it is tenth in order of abundance (0.15 wt%). The gradual recognition of hydrogen as an element during the sixteenth and seventeenth centuries forms part of the obscure and tangled web of experiments that were carried out as chemistry emerged from alchemy to become a modern science.<sup>(1)</sup> Until almost the end of the eighteenth century the element was inextricably entwined with the concept of phlogiston and H. Cavendish, who is generally regarded as having finally isolated and identified the gas in 1766, and who established conclusively that water was a compound of

oxygen and hydrogen, actually communicated his findings to the Royal Society in January 1784 in the following words: "There seems to be the utmost reason to think that dephlogisticated air is only water deprived of its phlogiston" and that "water consists of dephlogisticated air united with phlogiston".

The continued importance of hydrogen in the development of experimental and theoretical chemistry is further illustrated by some of the dates listed in the Panel on the page opposite.

Hydrogen was recognized as the essential element in acids by H. Davy after his work on the hydrohalic acids, and theories of acids and bases have played an important role ever since. The electrolytic dissociation theory of S. A. Arrhenius and W. Ostwald in the 1880s, the introduction of the pH scale for hydrogen-ion concentrations by S. P. L. Sørensen in 1909, the theory of acid-base titrations and indicators, and J. N. Brønsted's fruitful concept of acids and conjugate bases as proton donors and acceptors (1923) are other land marks (see p. 48). The discovery of *ortho*- and *para*-hydrogen in 1924, closely followed by the discovery of heavy hydrogen (deuterium) and

<sup>1</sup> J. W. MELLOR, *A Comprehensive Treatise on Inorganic and Theoretical Chemistry*, Vol. 1, Chap. 3, Longmans, Green & Co., London, 1922.

tritium in the 1930s, added a further range of phenomena that could be studied by means of this element (pp. 34–43). In more recent times, the technique of nmr spectroscopy, which was first demonstrated in 1946 using the hydrogen nucleus, has revolutionized the study of structural chemistry and permitted previously unsuspected

phenomena such as fluxionality to be studied. Simultaneously, the discovery of complex metal hydrides such as  $\text{LiAlH}_4$  has had a major impact on synthetic chemistry and enabled new classes of compound to be readily prepared in high yield (p. 229). The most important compound of hydrogen is, of course, water,

### Hydrogen — Some Significant Dates

- 1671 R. Boyle showed that dilute sulfuric acid acting on iron gave a flammable gas; several other seventeenth-century scientists made similar observations.
- 1766 H. Cavendish established the true properties of hydrogen by reacting several acids with iron, zinc and tin; he showed that it was much lighter than air.
- 1781 H. Cavendish showed quantitatively that water was formed when hydrogen was exploded with oxygen, and that water was therefore not an element as had previously been supposed.
- 1783 A. L. Lavoisier proposed the name "hydrogen" (Greek ὕδωρ γείνομαι, water former).
- 1800 W. Nicholson and A. Carlisle decomposed water electrolytically into hydrogen and oxygen which were then recombined by explosion to resynthesize water.
- 1810–15 Hydrogen recognized as the essential element in acids by H. Davy (contrary to Lavoisier who originally considered oxygen to be essential — hence Greek ὀξύς γείνομαι, acid former).
- 1866 The remarkable solubility of hydrogen in palladium discovered by T. Graham following the observation of hydrogen diffusion through red-hot platinum and iron by H. St. C. Deville and L. Troost, 1863.
- 1878 Hydrogen detected spectroscopically in the sun's chromosphere (J. N. Lockyer).
- 1895 Hydrogen first liquefied in sufficient quantity to show a meniscus (J. Dewar) following earlier observations of mists and droplets by others, 1877–85.
- 1909 The pH scale for hydrogen-ion concentration introduced by S. P. L. Sørensen.
- 1912  $\text{H}_3^+$  discovered mass-spectrometrically by J. J. Thompson.
- 1920 The concept of hydrogen bonding introduced by W. M. Latimer and W. H. Rodebush (and by M. L. Huggins, 1921).
- 1923 J. N. Brønsted defined an acid as a species that tended to lose a proton:  $\text{A} \rightleftharpoons \text{B} + \text{H}^+$ .
- 1924 *Ortho*- and *para*-hydrogen discovered spectroscopically by R. Mecke and interpreted quantum-mechanically by W. Heisenberg, 1927.
- 1929–30 Concept of quantum-mechanical tunnelling in proton-transfer reactions introduced (without experimental evidence) by several authors.
- 1931 First hydrido complex of a transition metal prepared by W. Hieber and F. Leutert.
- 1932 Deuterium discovered spectroscopically and enriched by gaseous diffusion of hydrogen and by electrolysis of water (H. C. Urey, F. G. Brickwedde and G. M. Murphy).
- 1932 Acidity function  $\text{H}_0$  proposed by L. P. Hammett for assessing the strength of very strong acids.
- 1934 Tritium first made by deuteron bombardment of  $\text{D}_3\text{PO}_4$  and  $(\text{ND}_4)_2\text{SO}_4$  (i.e.  ${}^2\text{D} + {}^2\text{D} = {}^3\text{T} + {}^1\text{H}$ ); M. L. E. Oliphant, P. Harteck and E. Rutherford.
- 1939 Tritium found to be radioactive by L. W. Alvarez and R. Cornog after a prediction by T. W. Bonner in 1938.
- 1946 Proton nmr first detected in bulk matter by E. M. Purcell, H. C. Torrey and R. V. Pound; and by F. Bloch, W. W. Hansen and M. E. Packard.
- 1947  $\text{LiAlH}_4$  first prepared and subsequently shown to be a versatile reducing agent; A. E. Finholt, A. C. Bond and H. I. Schlesinger.
- 1950 Tritium first detected in atmospheric hydrogen (V. Faltings and P. Harteck) and later shown to be present in rain water (W. F. Libby *et al.*, 1951).
- 1954 Detonation of the first hydrogen bomb on Bikini Atoll.
- 1960s "Superacids" ( $10^7$ – $10^{19}$  times stronger than sulfuric acid) studied systematically by G. A. Olah's group and by R. J. Gillespie's group.
- 1966 The term "magic acid" coined in G. A. Olah's laboratory for the non-aqueous system  $\text{HSO}_3\text{F}/\text{SbF}_5$ .
- 1976–79 Encapsulated H atom detected and located in octahedral polynuclear carbonyls such as  $[\text{HRu}_6(\text{CO})_{18}]^-$  and  $[\text{HCo}_6(\text{CO})_{15}]^-$  following A. Simon's characterization of interstitial H in  $\text{HNb}_6\text{I}_{11}$ .
- 1984 Stable transition-metal complexes of dihapto-dihydrogen ( $\eta^2\text{-H}_2$ ) discovered by G. Kubas.

and a detailed discussion of this compound is given on pp. 620–33 in the chapter on oxygen. In fact, hydrogen forms more chemical compounds than any other element, including carbon, and a survey of its chemistry therefore encompasses virtually the whole periodic table. However, before embarking on such a review in Sections 3.4–3.7 it is convenient to summarize the atomic and physical properties of the various forms of hydrogen (Section 3.2), to enumerate the various methods used for its preparation and industrial production, and to indicate some of its many applications and uses (Section 3.3).

## 3.2 Atomic and Physical Properties of Hydrogen<sup>(2)</sup>

Despite its very simple electronic configuration ( $1s^1$ ) hydrogen can, paradoxically, exist in over 50 different forms most of which have been well characterized. This multiplicity of forms arises firstly from the existence of atomic, molecular and ionized species in the gas phase: H, H<sub>2</sub>, H<sup>+</sup>, H<sup>-</sup>, H<sub>2</sub><sup>+</sup>, H<sub>3</sub><sup>+</sup> . . . , H<sub>11</sub><sup>+</sup>; secondly, from the existence of three isotopes, <sup>1</sup>H, <sup>2</sup>H(D) and <sup>3</sup>H(T), and correspondingly of D, D<sub>2</sub>, HD, DT, etc.; and, finally, from the existence of nuclear spin isomers for the homonuclear diatomic species,

<sup>2</sup> K. M. MACKAY, The element hydrogen, *Comprehensive Inorganic Chemistry*, Vol. 1, Chap. 1. K. M. MACKAY and M. F. A. DOVE, Deuterium and tritium, *ibid.*, Vol. 1, Chap. 3, Pergamon Press, Oxford, 1973.

i.e. *ortho*- and *para*-dihydrogen, -dideuterium and -ditritium.<sup>†</sup>

### 3.2.1 Isotopes of hydrogen

Hydrogen as it occurs in nature is predominantly composed of atoms in which the nucleus is a single proton. In addition, terrestrial hydrogen contains about 0.0156% of deuterium atoms in which the nucleus also contains a neutron, and this is the reason for its variable atomic weight (p. 17). Addition of a second neutron induces instability and tritium is radioactive, emitting low-energy  $\beta^-$  particles with a half-life of 12.33 y. Some characteristic properties of these 3 atoms are given in Table 3.1, and their implications for stable isotope studies, radioactive tracer studies, and nmr spectroscopy are obvious.

In the molecular form, dihydrogen is a stable, colourless, odourless, tasteless gas with a very low mp and bp. Data are in Table 3.2 from which it is clear that the values for deuterium and tritium are substantially higher.

<sup>†</sup> The term dihydrogen (like dinitrogen, dioxygen, etc.) is used when it is necessary to refer unambiguously to the molecule H<sub>2</sub> (or N<sub>2</sub>, O<sub>2</sub>, etc.) rather than to the element as a substance or to an atom of the element. Strictly, one should use "diprotium" when referring specifically to the species H<sub>2</sub> and "dihydrogen" when referring to an undifferentiated isotopic mixture such as would be obtained from materials having the natural isotopic abundances of H and D; likewise "proton" only when referring specifically to H<sup>+</sup>, but "hydron" when referring to an undifferentiated isotopic mixture.

**Table 3.1** Atomic properties of hydrogen (protium), deuterium, and tritium

Property	H	D	T
Relative atomic mass	1.007 825	2.014 102	3.016 049
Nuclear spin quantum number	$\frac{1}{2}$	1	$\frac{1}{2}$
Nuclear magnetic moment/(nuclear magnetons) <sup>(a)</sup>	2.792 70	0.857 38	2.978 8
NMR frequency (at 2.35 tesla)/MHz	100.56	15.360	104.68
NMR relative sensitivity (constant field)	1.000	0.009 64	1.21
Nuclear quadrupole moment/( $10^{-28}$ m <sup>2</sup> )	0	$2.766 \times 10^{-3}$	0
Radioactive stability	Stable	Stable	$\beta^-$ $t_{\frac{1}{2}}$ 12.33 y <sup>(b)</sup>

<sup>(a)</sup> Nuclear magneton  $\mu_N = eh/2m_p = 5.0508 \times 10^{-27}$  J T<sup>-1</sup>.

<sup>(b)</sup>  $E_{\max}$  18.6 keV;  $E_{\text{mean}}$  5.7 keV; range in air  $\sim 6$  mm; range in water  $\sim 6 \mu\text{m}$ .

Table 3.2 Physical properties of hydrogen, deuterium and tritium

Property <sup>(a)</sup>	H <sub>2</sub>	D <sub>2</sub>	T <sub>2</sub>
MP/K	13.957	18.73	20.62
BP/K	20.39	23.67	25.04
Heat of fusion/kJ mol <sup>-1</sup>	0.117	0.197	0.250
Heat of vaporization/kJ mol <sup>-1</sup>	0.904	1.226	1.393
Critical temperature/K	33.19	38.35	40.6 (calc)
Critical pressure/atm <sup>(b)</sup>	12.98	16.43	18.1 (calc)
Heat of dissociation/kJ mol <sup>-1</sup> (at 298.2 K)	435.88	443.35	446.9
Zero point energy/kJ mol <sup>-1</sup>	25.9	18.5	15.1
Internuclear distance/pm	74.14	74.14	(74.14)

<sup>(a)</sup>Data refer to H<sub>2</sub> of normal isotopic composition (i.e. containing 0.0156 atom % of deuterium, predominantly as HD). All data refer to the mixture of *ortho*- and *para*-forms that are in equilibrium at room temperature.

<sup>(b)</sup>1 atm = 101.325 kN m<sup>-2</sup> = 101.325 kPa.

For example, the mp of T<sub>2</sub> is above the bp of H<sub>2</sub>. Other forms such as HD and DT tend to have properties intermediate between those of their components. Thus HD has mp 16.60 K, bp 22.13 K,  $\Delta H_{\text{fus}}$  0.159 kJ mol<sup>-1</sup>,  $\Delta H_{\text{vap}}$  1.075 kJ mol<sup>-1</sup>,  $T_c$  35.91 K,  $P_c$  14.64 atm and  $\Delta H_{\text{dissoc}}$  439.3 kJ mol<sup>-1</sup>. The critical temperature  $T_c$  is the temperature above which a gas cannot be liquefied simply by application of pressure, and the critical pressure  $P_c$  is the pressure required for liquefaction at this point.

Table 3.2 also indicates that the heat of dissociation of the hydrogen molecule is extremely high, the H–H bond energy being larger than for almost all other single bonds. This contributes to the relative unreactivity of hydrogen at room temperature. Significant thermal decomposition into hydrogen atoms occurs only above 2000 K: the percentage of atomic H is 0.081 at this temperature, and this rises to 7.85% at 3000 K and 95.5% at 5000 K. Atomic hydrogen can, however, be conveniently prepared in low-pressure glow discharges, and the study of its reactions forms an important branch of chemical gas kinetics. The high heat of recombination of hydrogen atoms finds application in the atomic hydrogen torch — dihydrogen is dissociated in an arc and the atoms then recombine on the surface of a metal, generating temperatures in the region of 4000 K which can be used to weld very high melting metals such as tantalum and tungsten.

### 3.2.2 Ortho- and para-hydrogen

All homonuclear diatomic molecules having nuclides with non-zero spin are expected to show nuclear spin isomers. The effect was first detected in dihydrogen where it is particularly noticeable, and it has also been established for D<sub>2</sub>, T<sub>2</sub>, <sup>14</sup>N<sub>2</sub>, <sup>15</sup>N<sub>2</sub>, <sup>17</sup>O<sub>2</sub>, etc. When the two nuclear spins are parallel (*ortho*-hydrogen) the resultant nuclear spin quantum number is 1 (i.e.  $\frac{1}{2} + \frac{1}{2}$ ) and the state is threefold degenerate ( $2S + 1$ ). When the two proton spins are antiparallel, however, the resultant nuclear spin is zero and the state is non-degenerate. Conversion between the two states involves a forbidden triplet–singlet transition and is normally slow unless catalysed by interaction with solids or paramagnetic species which either break the H–H bond, weaken it, or allow magnetic perturbations. Typical catalysts are Pd, Pt, active Fe<sub>2</sub>O<sub>3</sub> and NO. *Para*-hydrogen (spins antiparallel) has the lower energy and this state is favoured at low temperatures. Above 0 K (100% *para*) the equilibrium concentration of *ortho*-hydrogen gradually increases until, above room temperature, the statistically weighted proportion of 3 *ortho*:1 *para* is obtained, i.e. 25% *para*. Typical equilibrium concentrations of *para*-hydrogen are 99.8% at 20 K, 65.4% at 60 K, 38.5% at 100 K, 25.7% at 210 K, and 25.1% at 273 K (Fig. 3.1). It follows that, whereas essentially pure *para*-hydrogen can be obtained, it is never possible to obtain a sample

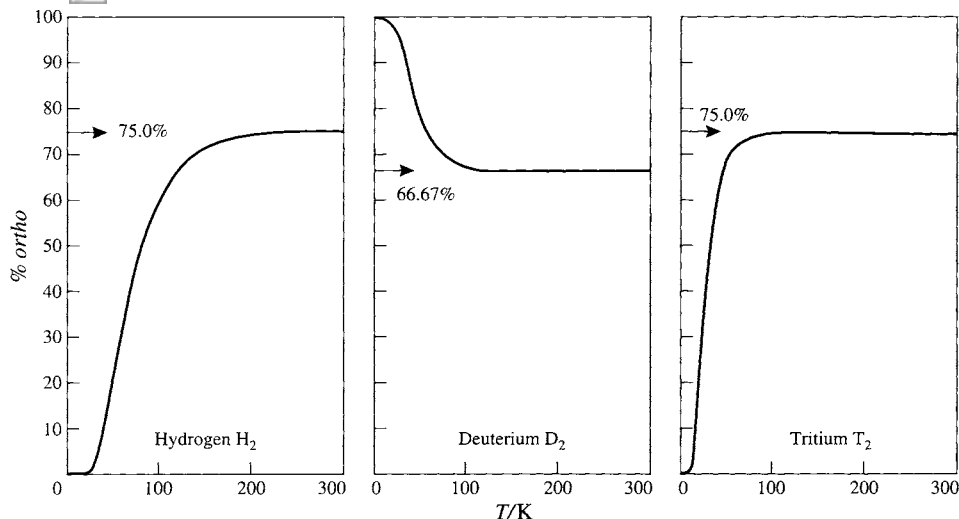


Figure 3.1 *Ortho-para* equilibria for  $\text{H}_2$ ,  $\text{D}_2$  and  $\text{T}_2$ .

containing more than 75% of *ortho*-hydrogen. Experimentally, the presence of both *o*- $\text{H}_2$  and *p*- $\text{H}_2$  is seen as an alternation in the intensities of successive rotational lines in the fine structure of the electronic band spectrum of  $\text{H}_2$ . It also explains the curious temperature dependence of the heat capacity of hydrogen gas.

Similar principles apply to *ortho*- and *para*-deuterium except that, as the nuclear spin quantum number of the deuteron is 1 rather than  $\frac{1}{2}$  as for the proton, the system is described by Bose–Einstein statistics rather than the more familiar Fermi–Dirac statistics. For this reason, the stable low-temperature form is *ortho*-deuterium and at high temperatures the statistical weights are 6 *ortho*:3 *para* leading to an upper equilibrium concentration of 33.3% *para*-deuterium above about 190 K as shown in Fig. 3.1. Tritium (spin  $\frac{1}{2}$ ) resembles  $\text{H}_2$  rather than  $\text{D}_2$ .

Most physical properties are but little affected by nuclear-spin isomerism though the thermal conductivity of *p*- $\text{H}_2$  is more than 50% greater than that of *o*- $\text{H}_2$ , and this forms a ready means of analysing mixtures. The mp of *p*- $\text{H}_2$  (containing only 0.21% *o*- $\text{H}_2$ ) is 0.15 K below that of “normal” hydrogen (containing 75% *o*- $\text{H}_2$ ), and by extrapolation the mp of (unobtainable) pure

*o*- $\text{H}_2$  is calculated to be 0.24 K above that of *p*- $\text{H}_2$ . Similar differences are found for the bps which occur at the following temperatures: normal- $\text{H}_2$  20.39 K, *o*- $\text{H}_2$  20.45 K. For deuterium the converse relation holds, *o*- $\text{D}_2$  melting some 0.03 K below “normal”- $\text{D}_2$  (66.7% *ortho*) and boiling some 0.04 K below. The effects for other elements are even smaller.

### 3.2.3 Ionized forms of hydrogen

This section briefly considers the proton  $\text{H}^+$ , the hydride ion  $\text{H}^-$ , the hydrogen molecule ion  $\text{H}_2^+$ , the triatomic 2-electron species  $\text{H}_3^+$  and the recently established cluster species  $\text{H}_n^+$ ,<sup>(3,4)</sup>

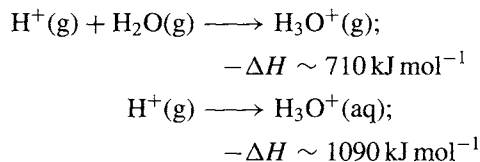
The hydrogen atom has a high ionization energy ( $1312 \text{ kJ mol}^{-1}$ ) and in this it resembles the halogens rather than the alkali metals. Removal of the 1s electron leaves a bare proton which, having a radius of only about  $1.5 \times 10^{-3} \text{ pm}$ , is not a stable chemical entity in the condensed phase. However, when bonded to other species it is well known in solution and in

<sup>3</sup> N. J. KIRCHNER and M. T. BOWERS, *J. Chem. Phys.* **86**, 1301–10 (1987).

<sup>4</sup> M. OKUMURA, L. I. YEH and Y. T. LEE, *J. Chem. Phys.* **88**, 79–91 (1988), and references cited therein.

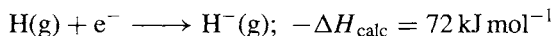


solids, e.g.  $\text{H}_3\text{O}^+$ ,  $\text{NH}_4^+$ , etc. The proton affinity of water and the enthalpy of solution of  $\text{H}^+$  in water have been estimated by several authors and typical values that are currently accepted are:



It follows that the heat of solution of the oxonium ion in water is  $\sim 380 \text{ kJ mol}^{-1}$ , intermediate between the values calculated for  $\text{Na}^+$  ( $405 \text{ kJ mol}^{-1}$ ) and  $\text{K}^+$  ( $325 \text{ kJ mol}^{-1}$ ). Reactions involving proton transfer will be considered in more detail in Section 3.5.

The hydrogen atom, like the alkali metals ( $ns^1$ ) and halogens ( $ns^2np^5$ ), has an affinity for the electron and heat is evolved in the following process:



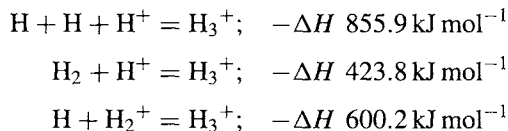
This is larger than the corresponding value for Li ( $57 \text{ kJ mol}^{-1}$ ) but substantially smaller than the value for F ( $333 \text{ kJ mol}^{-1}$ ). The hydride ion  $\text{H}^-$  has the same electron configuration as helium but is much less stable because the single positive charge on the proton must now control the 2 electrons. The hydride ion is thus readily deformable and this constitutes a characteristic feature of its structural chemistry (see p. 66).

The species  $\text{H}_2^+$  and  $\text{H}_3^+$  are important as model systems for chemical bonding theory. The hydrogen molecule ion  $\text{H}_2^+$  comprises 2 protons and 1 electron and is extremely unstable even in a low-pressure gas discharge system; the energy of dissociation and the internuclear distance (with the corresponding values for  $\text{H}_2$  in parentheses) are:

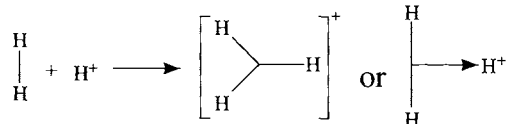
$$\begin{aligned} \Delta H_{\text{dissoc}} &255(436) \text{ kJ mol}^{-1}; \\ r(\text{H}-\text{H}) &106(74.2) \text{ pm} \end{aligned}$$

The triatomic hydrogen molecule ion  $\text{H}_3^+$  was first detected by J. J. Thomson in gas discharges and later fully characterized by mass spectrometry; its relative atomic mass, 3.0235, clearly distinguishes it from HD (3.0219) and from tritium

(3.0160). The “observed” equilateral triangular 3-centre, 2-electron structure is more stable than the hypothetical linear structure, and the comparative stability of the species is shown by the following gas-phase enthalpies:



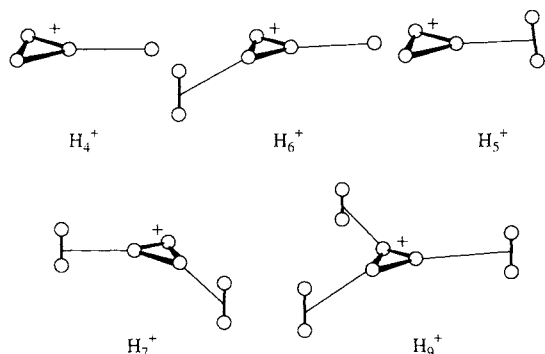
The  $\text{H}_3^+$  ion is the simplest possible example of a three-centre two-electron bond (see discussion of bonding in boranes on p. 157) and is also a model for the dihapto bonding mode of the ligand  $\eta^2\text{-H}_2$  (pp. 44–7):



A series of ions  $\text{H}_n^+$  with  $n$ -odd up to 15 and  $n$ -even up to 10 have recently been observed mass-spectrometrically and characterized for the first time.<sup>(3,4)</sup> The odd-numbered species are much more stable than the even-numbered members, as shown in the subjoined table which gives the relative intensities,  $I$ , as a function of  $n$  (in  $\text{H}_n^+$ ) obtained in a particular experiment with a high-pressure ion source, relative to  $\text{H}_3^+$ .<sup>(3)</sup>

$n$	1	2	3	4	5	6
$10^4 I$	160	50	<b>10 000</b>	4.2	4200	210
$n$	7	8	9	10	11	
$10^4 I$	3200	7.4	2600	18	34	

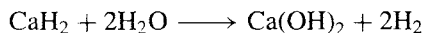
The structures of  $\text{H}_5^+$ ,  $\text{H}_7^+$  and  $\text{H}_9^+$  are related to that of  $\text{H}_3^+$  with  $\text{H}_2$  molecules added perpendicularly at the corners, whereas those of  $\text{H}_4^+$ ,  $\text{H}_6^+$  and  $\text{H}_8^+$  feature an added H atom at the first corner. Typical structures are shown below. The structures of higher members of the series, with  $n \geq 10$  are unknown but may involve further loosely bonded  $\text{H}_2$  molecules above and below the  $\text{H}_3^+$  plane. Enthalpies of dissociation are  $\Delta H_{300}^\circ (\text{H}_5^+ \rightleftharpoons \text{H}_3^+ + \text{H}_2)$   $28 \text{ kJ mol}^{-1}$  and  $\Delta H_{300}^\circ (\text{H}_7^+ \rightleftharpoons \text{H}_5^+ + \text{H}_2)$   $13 \text{ kJ mol}^{-1}$ .<sup>(4)</sup>



### 3.3 Preparation, Production and Uses<sup>(5,6)</sup>

#### 3.3.1 Hydrogen

Hydrogen can be prepared by the reaction of water or dilute acids on electropositive metals such as the alkali metals, alkaline earth metals, the metals of Groups 3, 4 and the lanthanoids. The reaction can be explosively violent. Convenient laboratory methods employ sodium amalgam or calcium with water, or zinc with hydrochloric acid. The reaction of aluminium or ferrosilicon with aqueous sodium hydroxide has also been used. For small-scale preparations the hydrolysis of metal hydrides is convenient, and this generates twice the amount of hydrogen as contained in the hydride, e.g.:

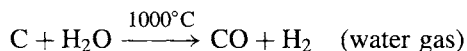
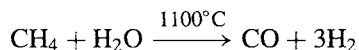


Electrolysis of acidified water using platinum electrodes is a convenient source of hydrogen (and oxygen) and, on a larger scale, very pure hydrogen (>99.95%) can be obtained from the electrolysis of warm aqueous solutions of barium hydroxide between nickel electrodes. The method is expensive but becomes economical

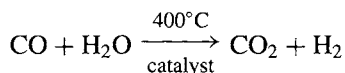
<sup>5</sup> T. A. CZUPPON, S. A. KNEZ and D. S. NEWSOME, Hydrogen, in *Kirk-Othmer Encyclopedia of Chemical Technology*, 4th edn., Vol. 13, Wiley, New York, 1995, pp. 838–94.

<sup>6</sup> P. HÄUSSINGER R. LOHMÜLLER and A. M. WATSON, Hydrogen, in *Ullmann's Encyclopedia of Industrial Chemistry*, 5th edn., Vol. A13, VCH, Weinheim, 1989, pp. 297–442.

on an industrial scale when integrated with the chloralkali industry (p. 798). Other bulk processes involve the (endothermic) reaction of steam on hydrocarbons or coke:

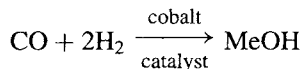


In both processes the CO can be converted to CO<sub>2</sub> by passing the gases and steam over an iron oxide or cobalt oxide catalyst at 400°C, thereby generating more hydrogen:



This is the so-called water-gas shift reaction ( $-\Delta G_{298}^\circ 19.9 \text{ kJ mol}^{-1}$ ) and it can also be effected by low-temperature homogeneous catalysts in aqueous acid solutions.<sup>(7)</sup> The extent of subsequent purification of the hydrogen depends on the use to which it will be put.

The industrial production of hydrogen is considered in more detail in the Panel. The largest single use of hydrogen is in ammonia synthesis (p. 421) but other major applications are in the catalytic hydrogenation of unsaturated liquid vegetable oils to solid, edible fats (margarine), and in the manufacture of bulk organic chemicals, particularly methanol (by the “oxo” or hydroformylation process):

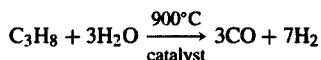


Direct reaction of hydrogen with chlorine is a major source of hydrogen chloride (p. 811), and a smaller, though still substantial use is in the manufacture of metal hydrides and complex metal hydrides (p. 64). Hydrogen is used in metallurgy to reduce oxides to metals (e.g. Mo, W) and to produce a reducing atmosphere. Direct reduction of iron ores in steelmaking is also now becoming technically and economically feasible.

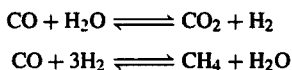
<sup>7</sup> C.-H. CHENG and R. EISENBERG, *J. Am. Chem. Soc.* **100**, 5969–70 (1978).

### Industrial Production of Hydrogen

Many reactions are available for the preparation of hydrogen and the one chosen depends on the amount needed, the purity required, and the availability of raw materials. Most (~97%) of the hydrogen produced in industry is consumed in integrated plants on site (e.g. ammonia synthesis, petrochemical works, etc.). Even so, vast amounts of the gas are produced for the general market, e.g.  $\sim 6.5 \times 10^{10} \text{ m}^3$  or 5.4 million tonnes yearly in the USA alone. Small generators may have a capacity of  $100\text{--}4000 \text{ m}^3 \text{ h}^{-1}$ , medium-sized plants  $4000\text{--}10\,000 \text{ m}^3 \text{ h}^{-1}$ , and large plants can produce  $10^4\text{--}10^5 \text{ m}^3 \text{ h}^{-1}$ . The dominant large-scale process in integrated plants is the catalytic steam-hydrocarbon reforming process using natural gas or oil-refinery feedstock. After desulfurization (to protect catalysts) the feedstock is mixed with process steam and passed over a nickel-based catalyst at  $700\text{--}1000^\circ\text{C}$  to convert it irreversibly to CO and  $\text{H}_2$ , e.g.



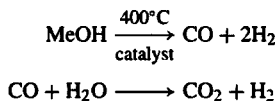
Two reversible reactions also occur to give an equilibrium mixture of  $\text{H}_2$ , CO,  $\text{CO}_2$  and  $\text{H}_2\text{O}$ :



The mixture is cooled to  $\sim 350^\circ\text{C}$  before entering a high-temperature shift convertor where the major portion of the CO is catalytically and exothermically converted to  $\text{CO}_2$  and hydrogen by reaction with  $\text{H}_2\text{O}$ . The issuing gas is further cooled to  $200^\circ$  before entering the low-temperature shift convertor which reduces the CO content to 0.2 vol%. The product is further cooled and  $\text{CO}_2$  absorbed in a liquid contactor. Further removal of residual CO and  $\text{CO}_2$  can be effected by methanation at  $350^\circ\text{C}$  to a maximum of 10 ppm. Provided that the feedstock contains no nitrogen the product purity is about 98%. Alternatively the low-temperature shift process and methanation stage can be replaced by a single pressure-swing absorption (PSA) system in which the hydrogen is purified by molecular sieves. The sieves are regenerated by adiabatic depressurization at ambient temperature (hence the name) and the product has a purity of  $\geq 99.9\%$ .

At present about 77% of the industrial hydrogen produced is from petrochemicals, 18% from coal, 4% by electrolysis of aqueous solutions and at most 1% from other sources. Thus, hydrogen is produced as a byproduct of the brine electrolysis process for the manufacture of chlorine and sodium hydroxide (p. 798). The ratio of  $\text{H}_2:\text{Cl}_2:\text{NaOH}$  is, of course, fixed by stoichiometry and this is an economic determinant since bulk transport of the byproduct hydrogen is expensive. To illustrate the scale of the problem: the total world chlorine production capacity is about 38 million tonnes per year which corresponds to 105 000 tonnes of hydrogen ( $1.3 \times 10^{10} \text{ m}^3$ ). Plants designed specifically for the electrolytic manufacture of hydrogen as the main product, use steel cells and aqueous potassium hydroxide as electrolyte. The cells may be operated at atmospheric pressure (Knowles cells) or at 30 atm (Lonza cells).

When relatively small amounts of hydrogen are required, perhaps in remote locations such as weather stations, then small transportable generators can be used which can produce  $1\text{--}17 \text{ m}^3 \text{ h}^{-1}$ . During production a 1:1 molar mixture of hydrogen and water is vaporized and passed over a "base-metal chromite" type catalyst at  $400^\circ\text{C}$  where it is cracked into hydrogen and carbon monoxide; subsequently steam reacts with the carbon monoxide to produce the dioxide and more hydrogen:



All the gases are then passed through a diffuser separator comprising a large number of small-diameter thin-walled tubes of palladium-silver alloy tightly packed in a stainless steel case. The solubility of hydrogen in palladium is well known (p. 1150) and the alloy with silver is used to prolong the life of the diffuser by avoiding troublesome changes in dimensions during the passage of hydrogen. The hydrogen which emerges is cool, pure, dry and ready for use via a metering device.

Another medium-scale use is in oxyhydrogen torches and atomic hydrogen torches for welding and cutting. Liquid hydrogen is used in bubble chambers for studying high-energy particles and as a rocket fuel (with oxygen) in the space programme. Hydrogen gas is potentially a large-scale fuel for use in internal combustion engines

and fuel cells if the notional "hydrogen economy" (see Panel on p. 40) is ever developed.

### 3.3.2 Deuterium

Deuterium is invariably prepared from heavy water,  $\text{D}_2\text{O}$ , which is itself now manufactured

### The Hydrogen Economy<sup>(6,8-11)</sup>

The growing recognition during the past decades that world reserves of coal and oil are finite and that nuclear power cannot supply all our energy requirements, particularly for small mobile units such as cars, has prompted an active search for alternatives. One solution which has many attractive features is the "hydrogen economy" whereby energy is transported and stored in the form of liquid or gaseous hydrogen. Enthusiasts point out that such a major change in the source of energy, though apparently dramatic, is not unprecedented and has in fact occurred twice during the past 100 y. In 1880 wood was overtaken by coal as the main world supplier of energy and now it accounts for only about 2% of the total. Likewise in 1960 coal was itself overtaken by oil and now accounts for only 15% of the total. (Note, however, that this does not imply a decrease in the total amount of coal used: in 1930 this was  $14.5 \times 10^6$  barrels per day of oil equivalent and was 75% of the then total energy supply whereas in 1975 coal had increased in absolute terms by 11% to  $16.2 \times 10^6$  b/d oe, but this was only 18% of the total energy supply which had itself increased 4.6-fold in the interim.) Another change may well be in the offing since nuclear power, which was effectively non-existent as an industrial source of energy in 1950, now accounts for 16% of the world supply of electricity; it has already overtaken coal as a source of energy and may well overtake oil during the next century. The aim of the "hydrogen economy" is to transmit this energy, not as electric power but in the form of hydrogen; this overcomes the great problem of electricity — that it cannot be stored — and also reduces the costs of power transmission.

The technology already exists for producing hydrogen electrically and storing it in bulk. For example huge quantities of liquid hydrogen are routinely stored in vacuum insulated cryogenic tanks for the US space programme, one such tank alone holding over  $3400 \text{ m}^3$  (900 000 US gallons). Liquid hydrogen can be transported by road or by rail tankers of  $75.7 \text{ m}^3$  capacity (20 000 US gallons). Underground storage of the type currently used for hydrogen — natural gas mixtures and transmission through large pipes is also feasible, and pipelines carrying hydrogen up to 80 km in the USA and South Africa and 200 km in Europe have been in operation for many years. Smaller storage units based on metal alloy systems have also been suggested, e.g.  $\text{LaNi}_5$  can absorb up to 7 moles of H atoms per mole of  $\text{LaNi}_5$  at room temperature and 2.5 atm, the density of contained hydrogen being twice that in the liquid element itself. Other systems include  $\text{Mg-MgH}_2$ ,  $\text{Mg}_2\text{Ni-Mg}_2\text{NiH}_4$ ,  $\text{Ti-TiH}_2$  and  $\text{TiFe-TiFeH}_{1.95}$ .

The advantages claimed for hydrogen as an automobile fuel are the greater energy release per unit weight of fuel and the absence of polluting emissions such as  $\text{CO}$ ,  $\text{CO}_2$ ,  $\text{NO}_x$ ,  $\text{SO}_2$ , hydrocarbons, aldehydes and lead compounds. The product of combustion is water with only traces of nitrogen oxides. Several conventional internal-combustion petrol engines have already been simply and effectively modified to run on hydrogen. Fuel cells for the regeneration of electric power have also been successfully operated commercially with a conversion efficiency of 70%, and test cells at higher pressures have achieved 85% efficiency.

Non-electrolytic sources of hydrogen have also been studied. The chemical problem is how to transfer the correct amount of free energy to a water molecule in order to decompose it. In the last few years about 10 000 such thermochemical water-splitting cycles have been identified, most of them with the help of computers, though it is significant that the most promising ones were discovered first by the intuition of chemists.

The stage is thus set, and further work to establish safe and economically viable sources of hydrogen for general energy usage seems destined to flourish as an active area of research for some while.

on the multitonne scale by the electrolytic enrichment of normal water.<sup>(12,13)</sup> The enrichment is expressed as a separation factor between the gaseous and liquid phases:

$$s = (\text{H/D})_g / (\text{H/D})_l$$

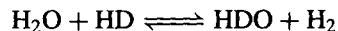
<sup>8</sup> D. P. GREGORY, *The hydrogen economy*, Chap. 23 in *Chemistry in the Environment*, Readings from *Scientific American*, 1973, pp. 219-27.

<sup>9</sup> L. B. MCGOWN and J. O'M. BOCKRIS, *How to Obtain Abundant Clean Energy*, Plenum, New York, 1980, 275 pp. L. O. WILLIAMS, *Hydrogen Power*, Pergamon Press, Oxford, 1980, 158 pp.

<sup>10</sup> C. J. WINTER and J. NITSCH (eds.), *Hydrogen as an Energy Carrier*, Springer Verlag, Berlin, 1988, 377 pp.

<sup>11</sup> B. BOGDANOVIĆ, *Angew. Chem. Int. Edn. Engl.* **24**, 262-73 (1985).

The equilibrium constant for the exchange reaction



is about 3 at room temperature and this would lead to a value of  $s = 3$  if this were the only effect. However, the choice of the metal used for the electrodes can also affect the various electrode processes, and this increases the separation still further. Using alkaline solutions  $s$  values in

<sup>12</sup> G. VASARU, D. URSU, A. MIHĂILĂ and P. SZENT-GYÖRGYI, *Deuterium and Heavy Water*, Elsevier, Amsterdam, 1975, 404 pp.

<sup>13</sup> H. K. RAE (ed.), *Separation of Hydrogen Isotopes*, ACS Symposium Series No. 68, 1978, 184 pp.

the range 5–7.6 are obtained for many metals, rising to 13.9 for platinum cathodes and even higher for gold. By operating a large number of cells in cascade, and burning the evolved H<sub>2</sub>/D<sub>2</sub> mixture to replenish the electrolyte of earlier cells in the sequence, any desired degree of enrichment can ultimately be attained. Thus, starting with normal water (0.0156% of hydrogen as deuterium) and a separation factor of 5, the deuterium content rises to 10% after the original volume has been reduced by a factor of 2400. Reduction by 66 000 is required for 90% deuterium and by 130 000 for 99% deuterium. If, however, the separation factor is 10, then 99% deuterium can be obtained by a volume reduction on electrolysis of 22 000. Prior enrichment of the electrolyte to 15% deuterium can be achieved by a chemical exchange between H<sub>2</sub>S and H<sub>2</sub>O after which a fortyfold volume reduction produces heavy water with 99% deuterium content. Other enrichment processes are now rarely used but include fractional distillation of water (which also enriches <sup>18</sup>O), thermal diffusion of gaseous hydrogen, and diffusion of H<sub>2</sub>/D<sub>2</sub> through palladium metal.

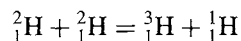
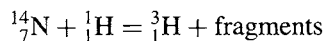
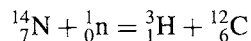
Many methods have been used to determine the deuterium content of hydrogen gas or water. For H<sub>2</sub>/D<sub>2</sub> mixtures mass spectroscopy and thermal conductivity can be used together with gas chromatography (alumina activated with manganese chloride at 77 K). For heavy water the deuterium content can be determined by density measurements, refractive index change, or infrared spectroscopy.

The main uses of deuterium are in tracer studies to follow reaction paths and in kinetic studies to determine isotope effects.<sup>(14)</sup> A good discussion with appropriate references is in *Comprehensive Inorganic Chemistry*, Vol. 1, pp. 99–116. The use of deuterated solvents is widespread in proton nmr studies to avoid interference from solvent hydrogen atoms, and deuterated compounds are also valuable in structural studies involving neutron diffraction techniques.

<sup>14</sup> L. MELANDER and W. H. SAUNDERS, *Reaction Rates of Isotopic Molecules*, Wiley, New York, 1980, 331 pp.

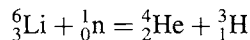
### 3.3.3 Tritium<sup>(15)</sup>

Tritium differs from the other two isotopes of hydrogen in being radioactive and this immediately indicates its potential uses and its method of detection. Tritium occurs naturally to the extent of about 1 atom per 10<sup>18</sup> hydrogen atoms as a result of nuclear reactions induced by cosmic rays in the upper atmosphere:



The concentration of tritium increased by over a hundredfold when thermonuclear weapon testing began on Bikini Atoll in March 1954 but has now subsided as a result of the ban on atmospheric weapon testing and the natural radioactivity of the isotope ( $t_{1/2}$  12.33 y).

Numerous reactions are available for the artificial production of tritium and it is now made on a large scale by neutron irradiation of enriched <sup>6</sup>Li in a nuclear reactor:



The lithium is in the form of an alloy with magnesium or aluminium which retains much of the tritium until it is released by treatment with acid. Alternatively the tritium can be produced by neutron irradiation of enriched LiF at 450° in a vacuum and then recovered from the gaseous products by diffusion through a palladium barrier. As a result of the massive production of tritium for thermonuclear devices and research into energy production by fusion reactions, tritium is available cheaply on the megacurie scale for peaceful purposes.<sup>†</sup> The most convenient way of storing the gas is to react it with finely divided uranium

<sup>15</sup> E. A. EVANS, *Tritium and its Compounds*, 2nd edn., Butterworths, London, 1974, 840 pp. E. A. EVANS, D. C. WARRELL, J. A. ELVIDGE and J. R. JONES, *Handbook of Tritium NMR Spectroscopy and Applications*, Wiley, Chichester, 1985, 249 pp.

<sup>†</sup> See also p. 18 for the influence on the atomic weight of commercially available lithium in some countries.

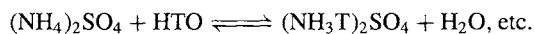
to give  $UT_3$  from which it can be released by heating above  $400^\circ\text{C}$ .

Besides being one of the least expensive radioisotopes, tritium has certain unique advantages as a tracer. Like  $^{14}\text{C}$  it is a pure low-energy  $\beta^-$  emitter with no associated  $\gamma$ -rays. The radiation is stopped by  $\sim 6$  mm of air or  $\sim 6$   $\mu\text{m}$  of material of density  $1\text{ g cm}^{-3}$  (e.g. water). As the range is inversely proportional to the density, this is reduced to only  $\sim 1$   $\mu\text{m}$  in photographic emulsion ( $\rho \sim 3.5\text{ g cm}^{-3}$ ) thus making tritium ideal for high-resolution autoradiography. Moreover, tritium has a high specific activity. The weight of tritium equal to an activity of 1 Ci is 0.103 mg and 1 mmol  $T_2$  has an activity of 58.25 Ci. [Note: 1 Ci (curie) =  $3.7 \times 10^{10}$  Bq (becquerel); 1 Bq =  $1\text{ s}^{-1}$ .] Tritium is one of the least toxic of radioisotopes and shielding is unnecessary; however, precautions must be taken against ingestion, and no work should be carried out without appropriate statutory authorization and adequate radiochemical facilities.

Tritium has been used extensively in hydrological studies to follow the movement of ground waters and to determine the age of various bodies of water. It has also been used to study the adsorption of hydrogen and the hydrogenation of ethylene on a nickel catalyst and to study the absorption of hydrogen in metals. Autoradiography has been used extensively to study the distribution of tritium in multiphase alloys, though care must be taken to correct for the photographic darkening caused by emanated tritium gas. Increasing use is also being made of tritium as a tracer for hydrogen in the study of reaction mechanisms and kinetics and in work on homogeneous catalysis.

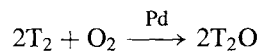
The production of tritium-labelled organic compounds was enormously facilitated by K. E. Wilzbach's discovery in 1956 that tritium could be introduced merely by storing a compound under tritium gas for a few days or weeks: the  $\beta^-$  radiation induces exchange reactions between the hydrogen atoms in the compound and the tritium gas. The excess of gas is recovered for further use and the tritiated compound is purified chromatographically. Another widely used method of

general applicability is catalytic exchange in solution using either a tritiated solution or tritium gas. This is valuable for the routine production of tritium compounds in high radiochemical yield and at high specific activity ( $> 50\text{ mCi mmol}^{-1}$ ). For example, although ammonium ions exchange relatively slowly with  $D_2O$ , tritium exchange equilibria are established virtually instantaneously: tritiated ammonium salts can therefore be readily prepared by dissolving the salt in tritiated water and then removing the water by evaporation:



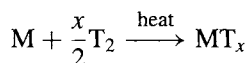
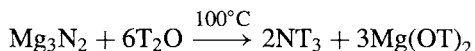
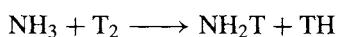
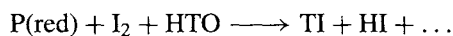
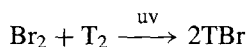
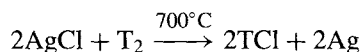
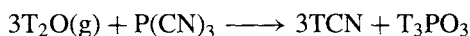
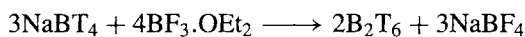
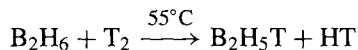
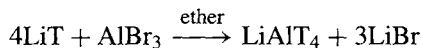
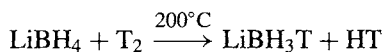
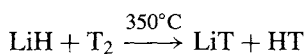
For exchange of non-labile organic hydrogen atoms, acid-base catalysis (or some other catalytic hydrogen-transfer agent such as palladium or platinum) is required. The method routinely gives tritiated products having a specific activity almost 1000 times that obtained by the Wilzbach method; shorter times are required (2–12 h) and subsequent purification is easier.

When specifically labelled compounds are required, direct chemical synthesis may be necessary. The standard techniques of preparative chemistry are used, suitably modified for small-scale work with radioactive materials. The starting material is tritium gas which can be obtained at greater than 98% isotopic abundance. Tritiated water can be made either by catalytic oxidation over palladium or by reduction of a metal oxide:



Note, however, that pure tritiated water is virtually never used since 1 ml would contain 2650 Ci; it is self-luminescent, irradiates itself at the rate of  $6 \times 10^{17}\text{ eV ml}^{-1}\text{ s}^{-1}$  ( $\sim 10^9$  rad  $\text{day}^{-1}$ ), undergoes rapid self-radiolysis, and also causes considerable radiation damage to dissolved species. In chemical syntheses or exchange reactions tritiated water of 1% tritium abundance ( $580\text{ mCi mmol}^{-1}$ ) is usually sufficient to produce compounds having a specific activity of at least  $100\text{ mCi mmol}^{-1}$ . Other useful

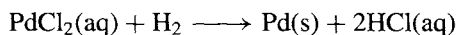
synthetic reagents are NaT, LiAlH<sub>3</sub>T, NaBH<sub>3</sub>T, NaBT<sub>4</sub>, B<sub>2</sub>T<sub>6</sub> and tritiated Grignard reagents. Typical preparations are as follows:



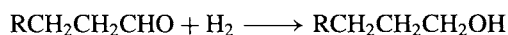
The preparation and use of LiEt<sub>3</sub>BT and LiAlT<sub>4</sub> at maximum specific activity (57.5 Ci mmol<sup>-1</sup>) has also been described.<sup>(16)</sup>

### 3.4 Chemical Properties and Trends

Hydrogen is a colourless, tasteless, odourless gas which has only low solubility in liquid solvents. It is comparatively unreactive at room temperature though it combines with fluorine even in the dark and readily reduces aqueous solutions of palladium(II) chloride:



This reaction can be used as a sensitive test for the presence of hydrogen. At higher temperatures hydrogen reacts vigorously, even explosively, with many metals and non-metals to give the corresponding hydrides. Activation can also be induced photolytically, by heterogeneous catalysts (Raney nickel, Pd, Pt, etc.), or by means of homogeneous hydrogenation catalysts. Industrially important processes include the hydrogenation of many organic compounds and the use of cobalt compounds as catalysts in the hydroformylation of olefins to aldehydes and alcohols at high temperatures and pressures (p. 1140):



An even more effective homogeneous hydrogenation catalyst is the complex [RhCl(PPh<sub>3</sub>)<sub>3</sub>] which permits rapid reduction of alkenes, alkynes and other unsaturated compounds in benzene solution at 25°C and 1 atm pressure (p. 1134). The Haber process, which uses iron metal catalysts for the direct synthesis of ammonia from nitrogen and hydrogen at high temperatures and pressures, is a further example (p. 421).

The hydrogen atom has a unique electronic configuration 1s<sup>1</sup>: accordingly it can gain an electron to give H<sup>-</sup> with the helium configuration 1s<sup>2</sup> or it can lose an electron to give the proton H<sup>+</sup> (p. 36). There are thus superficial resemblances both to the halogens which can gain an electron to give an inert-gas configuration ns<sup>2</sup>np<sup>6</sup>, and to the alkali metals which can lose an electron to give M<sup>+</sup> (ns<sup>2</sup>np<sup>6</sup>). However, because hydrogen has no other electrons in its structure there are sufficient differences from each of these two groups to justify placing hydrogen outside either. For example, the proton is so small (*r* ~ 1.5 × 10<sup>-3</sup> pm compared with normal atomic and ionic sizes of ~50–220 pm) that it cannot exist in condensed systems unless associated with other atoms or molecules. The transfer of protons between chemical species constitutes the basis of acid–base phenomena (see Section 3.5). The hydrogen atom is also frequently found in close association with 2

<sup>16</sup> H. ANDRES, H. MORIMOTO and P. G. WILLIAMS, *J. Chem. Soc., Chem. Commun.*, 627–8 (1990).



other atoms in linear array; this particularly important type of interaction is called hydrogen bonding (see Section 3.6). Again, the ability to penetrate metals to form nonstoichiometric metallic hydrides, though not unique to hydrogen, is one of its more characteristic properties as is its ability to form nonlinear hydrogen bridge bonds in many of its compounds. These properties will be further discussed during the general classification of the hydrides of the elements in section 3.7. The most important compound of hydrogen is, of course, water and a detailed discussion of this compound is given on pp. 620–33 in the chapter on oxygen.

### 3.4.1 The coordination chemistry of hydrogen

Perhaps the most exciting recent development in the chemistry of hydrogen is the discovery that, in transition metal polyhydrides, the molecule  $H_2$  can act as a dihapto ligand,  $\eta^2-H_2$  (see below). Even the H atom itself can form compounds in which its coordination number (CN) is not just 1 (as expected) but also 2, 3, 4, 5 or even 6. A rich and unexpectedly varied coordination chemistry is thus emerging. We shall deal with the H atom first and then with the  $H_2$  molecule.

By far the most common CN of hydrogen is 1, as in  $HCl$ ,  $H_2S$ ,  $PH_3$ ,  $CH_4$  and most other covalent hydrides and organic compounds. Bridging modes in which the H atom has a higher CN are shown schematically in the next column — in these structures M is typically a transition metal but, particularly in the  $\mu_2$ -mode and to some extent in the  $\mu_3$ -mode, one or more of the M can represent a main-group element such as B, Al; C, Si; N etc. Typical examples are in Table 3.3.<sup>(17–19)</sup> Fuller discussion and references, when appropriate, will be found in later chapters dealing with the individual elements concerned.

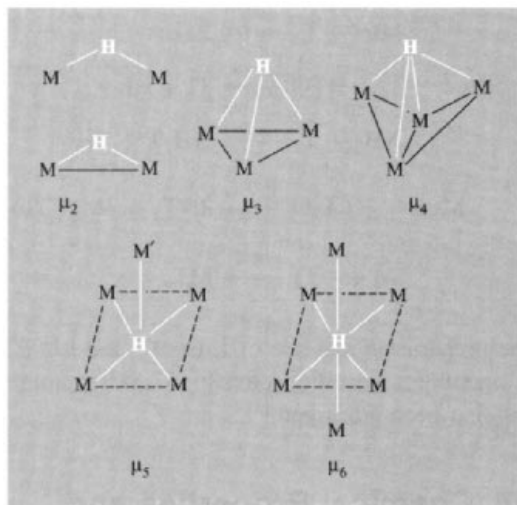
<sup>17</sup> D. S. MOORE and S. D. ROBINSON, *Chem. Soc. Revs.* **12**, 415–52 (1983).

<sup>18</sup> A. DEDIEU (ed.), *Transition Metal Hydrides*, VCH, Berlin, 1991, 416 pp.

<sup>19</sup> T. P. FEHLNER, *Polyhedron*, **9**, 1955–63 (1990).

**Table 3.3** Stereochemistry of hydrogen

CN	Examples
1	$HCl$ , $H_2S$ , $PH_3$ , $NH_4^+$ , $BH_4^-$ , etc.; $[HMn(CO)_5]$ , $[H_2Fe(CO)_4]$ , $[H_3Ta(C_5H_5)_2]$ , $[H_4Cr(dmpe)_2]$ , $[CoH_5]^+$ , $[H_6W(PR_3)_3]$ , $\{[H_7Re(PR_3)_2]_2Ag\}^+$ , $[H_8Re(PR_3)]^-$ , $[ReH_9]^{2-}$
2	$B_2H_6$ , $[Me_2NAlH_2]_3$ , $[H_3BHCu(PMePh_3)_3]$ , <i>nido</i> - $Ir(B_5H_8)(CO)(PPh_3)_2$ , $[(CO)_5WHW(CO)_5]^-$ , $[(C_5Me_5)Ir(\mu_2-H)_3Ir(C_5Me_5)]$
3	<i>closo</i> - $B_6H_6(\mu_3-H)^-$ , $[(\mu_3-H)Rh_3(C_5H_5)_4]$ , $[(\mu_3-H)_4Co_4(C_5H_5)_4]$
4	$[(\mu_4-H)Ru_8(CO)_{21}H]^{2-}$
5	$\beta$ - $Mg_2NiH_4(d_4)$ (1 “covalent” Ni–D 149 pm plus 4 “ionic” Mg–D 230 pm)
6	$[HNb_6I_{11}]$ , $[HRu_6(CO)_{18}]^-$ , $[HCo_6(CO)_{15}]^-$ , $[(\mu_6-H)_2Ni_{12}(CO)_{21}]^{2-}$ , $[(\mu_6-H)Ni_{12}(CO)_{21}]^{3-}$

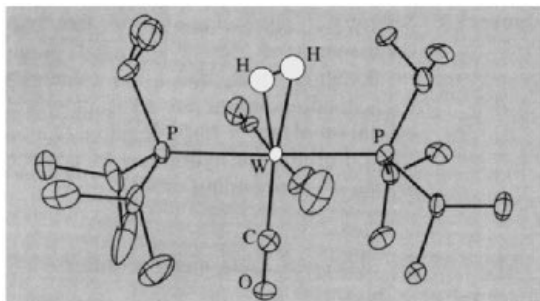


The crucial experiment suggesting that the  $H_2$  molecule might act as a dihapto ligand to transition metals was the dramatic observation<sup>(20)</sup> that toluene solutions of the deep purple coordinatively unsaturated 16-electron complexes  $[Mo(CO)_3(PCy_3)_2]$  and  $[W(CO)_3(PCy_3)_2]$  (where Cy = cyclohexyl) react readily and cleanly with  $H_2$  (1 atm) at low temperatures to precipitate yellow crystals of  $[M(CO)_3H_2(PCy_3)_2]$  in 85–95% yield. The

<sup>20</sup> G. J. KUBAS, *J. Chem. Soc., Chem. Commun.*, 61–2 (1980).



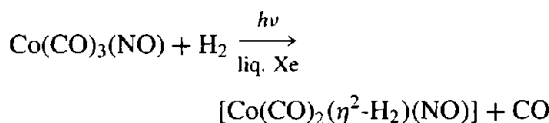
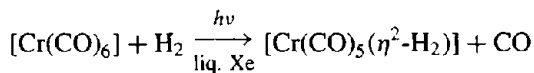
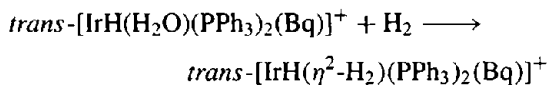
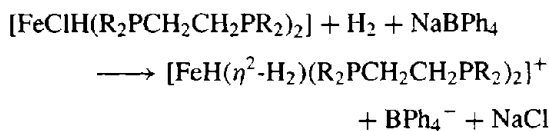
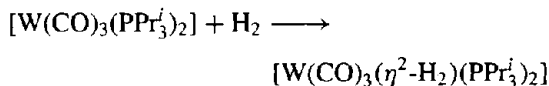
H<sub>2</sub> could be quantitatively removed at room temperature either by partial evacuation or by sparging the solution with argon. Definitive confirmation that the complexes did indeed contain  $\eta^2\text{-H}_2$  came from X-ray and neutron diffraction studies on the bis(tri *i*-propylphosphine) analogue at  $-100^\circ$ , which revealed the side-on coordination of H<sub>2</sub> as shown in Fig. 3.2.<sup>(21)</sup> During the past decade many other such compounds have been prepared and studied in great detail, and the field has been well reviewed.<sup>(22–24)</sup>



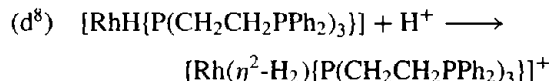
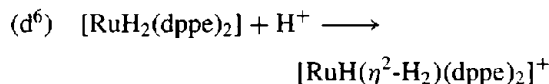
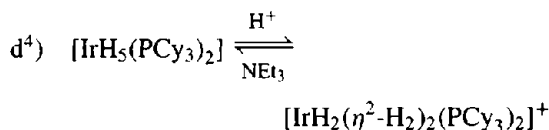
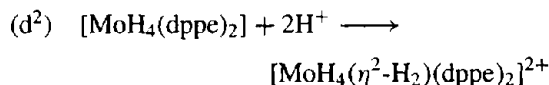
**Figure 3.2** The geometry of *mer-trans*-[W(CO)<sub>3</sub>-( $\eta^2\text{-H}_2$ )(PPR<sub>3</sub>)<sub>2</sub>] from X-ray and neutron diffraction data:  $r(\text{H-H})$  84 pm (compared with 74.14 pm for free H<sub>2</sub>),  $r(\text{W-H})$  175 pm. Infrared vibration spectroscopy gives  $\nu(\text{H-H})$  2690 cm<sup>-1</sup> compared with 4159 cm<sup>-1</sup> (Raman) for free H<sub>2</sub>.

There are two general routes to  $\eta^2\text{-H}_2$  complexes. The first involves direct addition of molecular H<sub>2</sub> either to an unoccupied coordination site in a 16-electron complex (as above) or by displacement of a ligand such as CO, Cl, H<sub>2</sub>O in the coordination sphere of an 18-electron complex; in this latter case ultraviolet irradiation may be required to assist in the

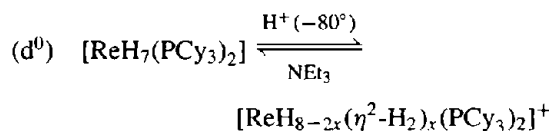
substitution reaction. Examples are:



The second general method involves the protonation of a polyhydrido complex using a strong acid such as HBF<sub>4</sub>·Et<sub>2</sub>O. Typical examples involving d<sup>2</sup>, d<sup>4</sup>, d<sup>6</sup> or d<sup>8</sup> metal centres are:



There is even a rare example involving a d<sup>0</sup> polyhydride:<sup>(25)</sup>



<sup>21</sup> G. J. KUBAS, R. R. RYAN, B. I. SWANSON, P. I. VERGAMINI and H. J. WASSERMAN, *J. Am. Chem. Soc.* **106**, 452–4 (1984).

<sup>22</sup> G. J. KUBAS, *Acc. Chem. Res.* **21**, 120–8 (1988).

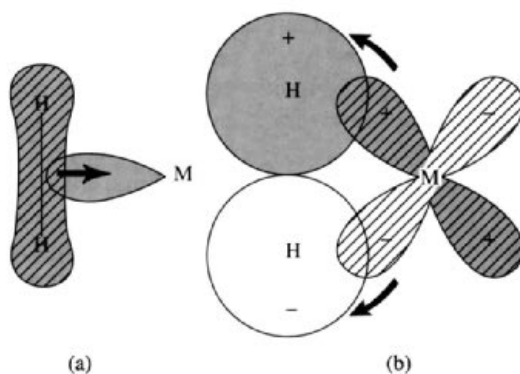
<sup>23</sup> R. H. CRABTREE and D. G. HAMILTON, *Adv. Organomet. Chem.* **28**, 299–338 (1988); R. H. CRABTREE, *Acc. Chem. Res.* **23**, 95–101 (1990).

<sup>24</sup> A. G. GINZBURG and A. A. BAGATUR'ANTS, *Organomet. Chem. in USSR* **2**, 111–26 (1989).

<sup>25</sup> X. L. R. FONTAINE, E. H. FOWLES and B. L. SHAW, *J. Chem. Soc., Chem. Commun.*, 482–3 (1988).

If deuterio acids are used then  $\eta^2$ -HD complexes are formed; these are particularly useful in establishing the retention of substantive H-H bonding in the coordinated ligand by observation of a 1:1:1 triplet in the proton nmr spectrum (the proton signal being split by coupling to deuterium with nuclear spin  $J = 1$ ).

The stability of  $\eta^2$ -H<sub>2</sub> complexes varies considerably, from those which can be observed only in low-temperature matrix-isolation experiments to those which are moderately robust even at room temperature and above. Stability depends on the electron configuration of the metal centre, the electronic and steric nature of the co-ligands, the overall charge on the complex, the state of aggregation and, of course, the temperature. Most  $\eta^2$ -H<sub>2</sub> complexes involve transition metals in Groups 6–8, in oxidation states having a formal d<sup>6</sup> electron configuration. No  $\eta^2$ -H<sub>2</sub> complexes are yet known for transition metals in Groups 3 or 4 of the periodic table, although examples involving Group 5 metals have recently been reported, e.g. the d<sup>4</sup> species [V( $\eta^5$ -C<sub>5</sub>H<sub>5</sub>)(CO)<sub>3</sub>( $\eta^2$ -H<sub>2</sub>)]<sup>(26)</sup> and [Nb( $\eta^5$ -C<sub>5</sub>H<sub>5</sub>)(CO)<sub>3</sub>( $\eta^2$ -H<sub>2</sub>)]<sup>(27)</sup>. Within a given Group, the first and second members more readily form  $\eta^2$ -H<sub>2</sub> complexes while the third member tends to form polyhydrido species, e.g. [Fe(H)<sub>2</sub>( $\eta^2$ -H<sub>2</sub>)(PEtPh<sub>2</sub>)<sub>3</sub>] and [Ru(H)<sub>2</sub>( $\eta^2$ -H<sub>2</sub>)(PPh<sub>3</sub>)<sub>3</sub>] but [Os(H)<sub>4</sub>(P(*o*-tol)<sub>3</sub>)<sub>3</sub>]<sup>(28)</sup>. Stability is also enhanced by an overall cationic charge on the complex (remember protonation as a route to  $\eta^2$ -H<sub>2</sub> complexes). In such cases, however, stability of the resulting compound depends on the presence of a non-coordinating anion such as BF<sub>4</sub><sup>-</sup>, otherwise there is a risk of decomposition by displacement of the more weakly coordinating ( $\eta^2$ -H<sub>2</sub>). Neutral complexes are also well known, but no examples of anionic  $\eta^2$ -H<sub>2</sub> complexes have been reported.



**Figure 3.3** Schematic representation of the two components of the  $\eta^2$ -H<sub>2</sub>-metal bond: (a) donation from the filled (hatched)  $\sigma$ -H<sub>2</sub> bonding orbital into a vacant hybrid orbital on M; (b)  $\pi$ -back donation from a filled d orbital (or hybrid) on M into the vacant  $\sigma^*$  antibonding orbital of H<sub>2</sub>.

Most of the observed facts can be understood in terms of a bonding scheme which envisages donation of electron density from the  $\sigma$  bond of H<sub>2</sub> into a vacant hybrid orbital on the metal, plus a certain amount of synergic back donation from an occupied d orbital on the metal into the  $\sigma^*$  antibonding orbital of H<sub>2</sub> (see Fig. 3.3). This is reminiscent of the bonding in the well known metal-alkene complexes (to be discussed in more detail on p. 931) but with two significant differences: (a) the electron density being donated from the H<sub>2</sub> ligand is in the single-bond  $\sigma$  orbital whereas for alkenes such as H<sub>2</sub>C=CH<sub>2</sub> it is in the  $\pi$  component of the double bond; and (b) the H<sub>2</sub> antibonding orbital involved in accepting back-donated electron density has  $\sigma^*$  symmetry rather than  $\pi^*$  as in alkenes. It is clear from this description that an overall positive charge on the metal centre encourages

forward donation to form the 3-centre

$$\begin{array}{c} \text{H} \\ \diagdown \quad \diagup \\ \text{H} \quad \text{M} \end{array}$$

bond, but diminishes the extent of back donation. By contrast, an overall negative charge might be expected to enhance back donation into the  $\sigma^*$  antibonding orbital and thus promote rupture of the H<sub>2</sub> single bond, with concomitant formation of two new hydrido M-H bonds.

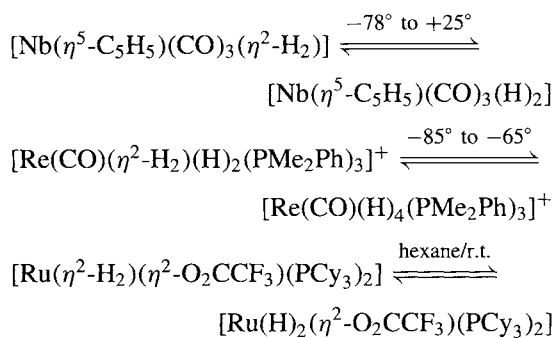
<sup>26</sup> M. T. HAWARD, M. W. GEORGE, S. M. HOWDLE and M. POLIAKOFF, *J. Chem. Soc., Chem. Commun.*, 913–5 (1990).

<sup>27</sup> M. T. HAWARD, M. W. GEORGE, P. HAMLEY and M. POLIAKOFF, *J. Chem. Soc., Chem. Commun.*, 1101–3 (1991).

<sup>28</sup> R. H. CRABTREE and D. G. HAMILTON, *J. Am. Chem. Soc.* **108** 3124–5 (1986).

The bonding scheme is also consistent with the observed lengthening of the H–H distance to about 84–90 pm in the  $\eta^2$ -H<sub>2</sub> complexes (as compared with 74 pm in free molecular H<sub>2</sub>), and with the lowering of the  $\nu(\text{H-H})$  vibration frequency from 4159 cm<sup>-1</sup> in free H<sub>2</sub> to values typically in the range 2650–3250 cm<sup>-1</sup> in the complexes.

There is evidently a very fine balance between the two options {M( $\eta^2$ -H<sub>2</sub>)} and {M(H)<sub>2</sub>}; indeed, examples of an equilibrium between the two forms have recently been discovered:<sup>(27,29,30)</sup>



In the niobium system<sup>(27)</sup> the  $\eta^2$ -H<sub>2</sub> form is marginally the more stable, with  $\Delta H = 2.0 \text{ kJ mol}^{-1}$ , whereas in the rhenium system,<sup>(29)</sup> it is the tetrahydrido form which is the more stable, with  $-\Delta G_{208} = 2.5 \text{ kJ mol}^{-1}$  and  $-\Delta H = 4.6 \text{ kJ mol}^{-1}$ .

In a sense the formation of  $\eta^2$ -H<sub>2</sub> complexes can be thought of as an intermediate stage in the oxidative addition of H<sub>2</sub> to form two M–H bonds and, as such, the complexes might serve as a model for this process and for catalytic hydrogenation reactions by metal hydrides.<sup>(31)</sup> Indeed, intermediate cases between  $\eta^2$ -H<sub>2</sub> and ( $\sigma$ -H)<sub>2</sub> coordination are occasionally observed, as in [ReH<sub>7</sub>(P(*p*-tol)<sub>3</sub>)<sub>2</sub>], where neutron-diffraction

studies<sup>(32)</sup> have revealed one H···H contact of 137.7(7) pm whereas all other H···H distances in the complex are greater than 174 pm. (This distance of 137.7 pm is seen to be intermediate between values of *ca.* 80 pm typical of  $\eta^2$ -H<sub>2</sub> complexes and values greater than *ca.* 160 pm which are found in classical hydrido complexes.) Likewise, some trihydrogen complexes, such as [Ir( $\eta^5$ -C<sub>5</sub>H<sub>5</sub>)H<sub>3</sub>(PMe<sub>3</sub>)],<sup>(33)</sup> have nmr behaviour which suggests the presence of a bent (or possibly triangular)  $\eta^3$ -H<sub>3</sub> ligand which is bonded “side-on” rather like an allylic group (pp. 933–5).

The possibility of  $\eta^1$ -H<sub>2</sub> “end-on” coordination has also been mooted. For example, deposition of Pd atoms onto a krypton matrix doped with H<sub>2</sub> at 12 K apparently yields both Pd( $\eta^1$ -H<sub>2</sub>) and Pd( $\eta^2$ -H<sub>2</sub>) species, whereas with a Xe/H<sub>2</sub> matrix only Pd( $\eta^2$ -H<sub>2</sub>) was obtained.<sup>(34)</sup> Again, the complex [ReCl(H<sub>2</sub>)(PMePh<sub>2</sub>)<sub>4</sub>] appears to feature an asymmetrically-bonded H<sub>2</sub> ligand which may well be ( $\eta^1$ -H<sub>2</sub>).<sup>(35)</sup>

Nearly one hundred  $\eta^2$ -H<sub>2</sub> complexes have so far been prepared and the crystal and molecular structure of about half a dozen have been determined by X-ray/neutron diffraction. Some are dinuclear, such as the homobimetallic [(P–N)( $\eta^2$ -H<sub>2</sub>)Ru( $\mu$ -Cl)<sub>2</sub>( $\mu$ -H)Ru(H)(PPh<sub>3</sub>)<sub>2</sub>]<sup>(36)</sup> and the heterobimetallic [(PPh<sub>3</sub>)<sub>2</sub>HRe( $\mu$ -H)( $\mu$ -Cl)<sub>2</sub>( $\mu$ -CO)Ru( $\eta^2$ -H<sub>2</sub>)(PPh<sub>3</sub>)<sub>2</sub>]<sup>(37)</sup>.

The coordination chemistry of hydrogen is still being intensively studied and new developments are continually being reported.

<sup>32</sup> L. BRAMMER, J. A. K. HOWARD, O. JOHNSON, T. F. KOETZLE, J. L. SPENCER and A. M. STRINGER, *J. Chem. Soc., Chem. Commun.*, 241–3 (1991).

<sup>33</sup> D. M. HEINEKEY, N. G. PAYNE and G. K. SCHULTE, *J. Am. Chem. Soc.* **110**, 2303–5 (1988).

<sup>34</sup> G. A. OZIN and J. GARCIA-PRIETO, *J. Am. Chem. Soc.* **108**, 3099–100 (1986).

<sup>35</sup> F. A. COTTON and R. L. LUCK, *Inorg. Chem.* **30**, 767–74 (1991).

<sup>36</sup> C. HAMPTON, W. R. CULLEN and B. R. JAMES, *J. Am. Chem. Soc.* **110**, 6918–9 (1988). In this compound, P–N is a complex substituted ferrocene ligand. See also A. M. JOSHI and B. R. JAMES, *J. Chem. Soc., Chem. Commun.*, 1785–6 (1989).

<sup>37</sup> M. CAZANOUE, Z. HE, D. NEILBECKER and R. MATHIEU, *J. Chem. Soc., Chem. Commun.*, 307–9 (1991).

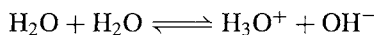
<sup>29</sup> X.-L. LUO and R. H. CRABTREE, *J. Chem. Soc., Chem. Commun.*, 189–90 (1990).

<sup>30</sup> T. ANLIGUIE and B. CHAUDRET, *J. Chem. Soc., Chem. Commun.*, 155–7 (1989).

<sup>31</sup> C. BIANCHINI, C. MEALLI, A. MELI, M. PERUZZINI and F. ZANOBINI, *J. Am. Chem. Soc.* **110**, 8725–6 (1988). See also L. D. FIELD, A. V. GEORGE, E. Y. MALOUF and D. J. YOUNG, *Chem. Soc., Chem. Commun.*, 931–3 (1990).

### 3.5 Protonic acids and bases<sup>(38)</sup>

Many compounds that contain hydrogen can donate protons to a solvent such as water and so behave as acids. Water itself undergoes ionic dissociation to a small extent by means of autoprotolysis; the process is usually represented formally by the equilibrium



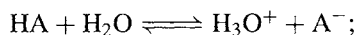
though it should be remembered that both ions are further solvated and that the time a proton spends in close association with any one water molecule is probably only about  $10^{-13}$  s. (See also pp. 630–2 for structural studies on  $[\text{H}(\text{OH}_2)_n]^+$   $n = 1-6$ .) Depending on what aspect of the process is being emphasized, the species  $\text{H}_3\text{O}^+(\text{aq})$  can be called an oxonium ion, a hydrogen ion, or simply a solvated (hydrated) proton. The equilibrium constant for autoprotolysis is

$$K_1 = [\text{H}_3\text{O}^+][\text{OH}^-]/[\text{H}_2\text{O}]^2$$

and, since the concentration of water is essentially constant, the ionic product of water can be written as

$$K_w = [\text{H}_3\text{O}^+][\text{OH}^-] \text{ mol}^2 \text{ l}^{-2}$$

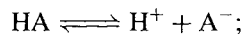
The value of  $K_w$  depends on the temperature, being  $0.69 \times 10^{-14} \text{ mol}^2 \text{ l}^{-2}$  at  $0^\circ\text{C}$ ,  $1.00 \times 10^{-14}$  at  $25^\circ\text{C}$  and  $47.6 \times 10^{-14}$  at  $100^\circ\text{C}$ . It follows that the hydrogen-ion concentration in pure water at  $25^\circ\text{C}$  is  $10^{-7} \text{ mol l}^{-1}$ . Acids increase this concentration by means of the reaction



$$K = \frac{[\text{H}_3\text{O}^+][\text{A}^-]}{[\text{HA}][\text{H}_2\text{O}]}$$

It is to be understood that all the species are in aqueous solution and the symbol HA implies only that the (aquated) species can act as a proton donor: it can be a neutral species (e.g.  $\text{H}_2\text{S}$ ), an anion (e.g.  $\text{H}_2\text{PO}_4^-$ ) or a cation such as

$[\text{Fe}(\text{H}_2\text{O})_6]^{3+}$ . The hydrogen-ion concentration is usually expressed as pH (see Panel). In dilute solution the concentration of water molecules is constant at  $25^\circ\text{C}$  ( $55.345 \text{ mol l}^{-1}$ ), and the dissociation of the acid is often rewritten as



$$K_a = [\text{H}^+][\text{A}^-]/[\text{HA}] \text{ mol l}^{-1}$$

The acid constant  $K_a$  can also be expressed by the relation

$$\text{p}K_a = -\log K_a. \quad \text{Hence, as } K_a = 55.345 K$$

$$\text{p}K_a = \text{p}K - 1.734$$

Further, as the free energy of dissociation is given by

$$\Delta G^\circ = -RT \ln K = -2.3026RT \log K,$$

the standard free energy of dissociation is

$$\begin{aligned} \Delta G_{298.15}^\circ &= 5.708 \text{ p}K \\ &= 5.708(\text{p}K_a + 1.734) \text{ kJ mol}^{-1} \end{aligned}$$

Textbooks of analytical chemistry should be consulted for further details concerning the ionization of weak acids and bases and the theory of indicators, buffer solutions, and acid-alkali titrations.<sup>(39-41)</sup>

Various trends have long been noted in the acid strengths of many binary hydrides and oxoacids.<sup>(38)</sup> Values for some simple hydrides are given in Table 3.4 from which it is clear that acid strength increases with atomic number both in any one horizontal period and in any

<sup>39</sup> A. I. VOGEL, *Quantitative Chemical Analysis*, 5th edn., Sections 2.12–2.27, pp. 31–60. Longman, London, 1989.

<sup>40</sup> A. HULANICKI, *Reactions of Acids and Bases in Analytical Chemistry*, Ellis Horwood (Wiley), Chichester, 1987, 308 pp.

<sup>41</sup> D. ROSENTHAL and P. ZUMAN, Acid-base equilibria, buffers and titrations in water, Chap. 18 in I. M. KOLTHOFF and P. J. ELVING (eds.), *Treatise on Analytical Chemistry*, 2nd edn., Vol. 2, Part 1, 1979, pp. 157–236. Succeeding chapters (pp. 237–440) deal with acid-base equilibria and titrations in non-aqueous solvents.

<sup>38</sup> R. P. BELL, *The Proton in Chemistry*, 2nd edn. Chapman & Hall, London, 1973, 223 pp.

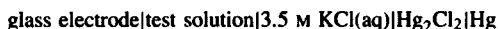
## The Concept of pH

The now universally used measure of the hydrogen-ion concentration was introduced in 1909 by the Danish biochemist S. P. L. Sørensen during his work at the Carlsberg Breweries (*Biochem. Z.* 21, 131, 1909):

$$\text{pH} = -\log[\text{H}^+]$$

The symbol pH derives from the French *puissance d'hydrogène*, referring to the exponent or "power of ten" used to express the concentration. Thus a hydrogen-ion concentration of  $10^{-7} \text{ mol l}^{-1}$  is designated pH 7, whilst acid solutions with higher hydrogen-ion concentrations have a lower pH. For example, a strong acid of concentration  $1 \text{ mmol l}^{-1}$  has pH 3, whereas a strong alkali of the same concentration has pH 11 since  $[\text{H}_3\text{O}^+] = 10^{-14}/[\text{OH}^-] = 10^{-11}$ .

Unfortunately, it is far simpler to define pH than to measure it, despite the commercial availability of instruments that purport to do this. Most instruments use an electrochemical cell such as



Assuming that the glass electrode shows an ideal hydrogen electrode response, the emf of the cell still depends on the magnitude of the liquid junction potential  $E_j$  and the activity coefficients  $\gamma$  of the ionic species:

$$E = E^\circ - \frac{RT}{F} \ln \gamma_{\text{Cl}}[\text{Cl}^-] + E_j - \frac{RT}{F} \ln \gamma_{\text{H}}[\text{H}^+]$$

For this reason, the pH as measured by any of the existing national standards is an operational quantity which has no simple fundamental significance. It is defined by the equation

$$\text{pH(X)} = \text{pH(S)} + \frac{(E_x - E_s)F}{RT \ln 10}$$

where pH(S) is the *assigned* pH of a standard buffer solution such as those supplied with pH meters.

Only in the case of dilute aqueous solutions ( $< 0.1 \text{ mol l}^{-1}$ ) which are neither strongly acid or alkaline ( $2 < \text{pH} < 12$ ) is pH(X) such that

$$\text{pH(X)} = -\log[\text{H}^+] \gamma_{\pm} \pm 0.02$$

where  $\gamma_{\pm}$ , the mean ionic activity coefficient of a typical uni-univalent electrolyte, is given by

$$-\log \gamma_{\pm} = A I^{\frac{1}{2}} (1 + I)^{-\frac{1}{2}}$$

In this expression  $I$  is the ionic strength of the solution and  $A$  is a temperature-dependent constant ( $0.511^{\frac{1}{2}} \text{ mol}^{-\frac{1}{2}}$  at  $25^\circ\text{C}$ ;  $0.501^{\frac{1}{2}} \text{ mol}^{-\frac{1}{2}}$  at  $15^\circ\text{C}$ ). It is clearly unwise to associate a pH meter reading too closely with pH unless under very controlled conditions, and still less sensible to relate the reading to the actual hydrogen-ion concentration in solution. For further discussion of pH measurements, see *Pure Appl. Chem.* 57, 531–42 (1985): Definition of pH Scales, Standard Reference Values, Measurement of pH and Related Terminology. Also *C&E News*, Oct. 20, 1997, p. 6.

**Table 3.4** Approximate values of  $\text{p}K_a$  for simple hydrides

CH <sub>4</sub>	46	NH <sub>3</sub>	35	OH <sub>2</sub>	16	FH	3
		PH <sub>3</sub>	27	SH <sub>2</sub>	7	ClH	-7
				SeH <sub>2</sub>	4	BrH	-9
				TeH <sub>2</sub>	3	IH	-10

vertical group. Several attempts have been made to interpret these trends, at least qualitatively, but the situation is complex. The trend to increasing acidity from left to right in the

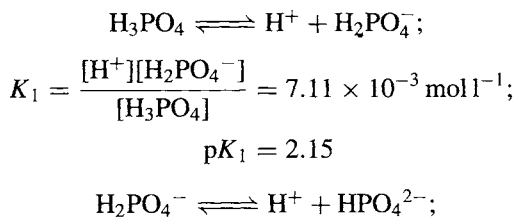
periodic table could be ascribed to the increasing electronegativity of the elements which would favour release of the proton, but this is clearly not the dominant effect within any one group since the trend there is in precisely the opposite direction. Within a group it is the diminution in bond strength with increasing atomic number that prevails, and entropies of solvation are also important. It should, perhaps, also be emphasized that thermodynamic computations do not "explain" the observed acid strengths; they merely allocate the overall values of  $\Delta G$ ,

$\Delta H$  and  $\Delta S$  to various notional subprocesses such as bond dissociation energies, ionization energies, electron affinities, heats and entropies of hydration, etc., which themselves have empirically observed values that are difficult to compute *ab initio*.

Regularities in the observed strengths of oxoacids have been formulated in terms of two rules by L. Pauling and others:

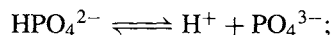
- (i) for polybasic mononuclear oxoacids, successive acid dissociation constants diminish approximately in the ratios  $1:10^{-5}:10^{-10}:\dots$ ;
- (ii) the value of the first ionization constant for acids of formula  $XO_m(OH)_n$  depends sensitively on  $m$  but is approximately independent of  $n$  and  $X$  for constant  $m$ , being  $\leq 10^{-8}$  for  $m = 0$ ,  $\sim 10^{-2}$  for  $m = 1$ ,  $\sim 10^3$  for  $m = 2$ , and  $> 10^8$  for  $m = 3$ .

Thus to illustrate the first rule:



$$K_2 = \frac{[H^+][HPO_4^{2-}]}{[H_2PO_4^-]} = 6.31 \times 10^{-8} \text{ mol l}^{-1};$$

$$pK_2 = 7.20$$



$$K_3 = \frac{[H^+][PO_4^{3-}]}{[HPO_4^{2-}]} = 4.22 \times 10^{-13} \text{ mol l}^{-1};$$

$$pK_3 = 12.37$$

Qualitatively, a reduction in  $pK_a$  for each successive stage of ionization is to be expected since the proton must separate from an anion of increasingly negative charge, though the approximately constant reduction factor of  $10^5$  is more difficult to rationalize quantitatively.

Acids which illustrate the second rule are summarized in Table 3.5. The qualitative explanation for this regularity is that, with increasing numbers of oxygen atoms the single negative charge on the anion can be spread more widely, thereby reducing the electrostatic energy attracting the proton and facilitating the ionization. On this basis one might expect an even more dramatic effect if the anion were monoatomic (e.g.  $S^{2-}$ ,  $Se^{2-}$ ,  $Te^{2-}$ ) since the attraction of these dianions for protons will be very strong and the acid dissociation constant of  $SH^-$ ,  $SeH^-$  and  $TeH^-$  correspondingly small; this is indeed observed and the ratio of

**Table 3.5** Values of  $pK_a$  for some mononuclear oxoacids  $XO_m(OH)_n$  ( $pK_a \approx 8-5n$ )

$X(OH)_n$ (very weak)		$XO(OH)_n$ (weak)		$XO_2(OH)_n$ (strong)		$XO_3(OH)_n$ (very strong)	
Cl(OH)	7.2	NO(OH)	3.3	NO <sub>2</sub> (OH)	-1.4	ClO <sub>3</sub> (OH)	(-10)
Br(OH)	8.7	ClO(OH)	2.0	ClO <sub>2</sub> (OH)	-1	MnO <sub>3</sub> (OH)	—
I(OH)	10.0	CO(OH) <sub>2</sub>	3.9 <sup>(a)</sup>	IO <sub>2</sub> (OH)	0.8		
B(OH) <sub>3</sub>	9.2	SO(OH) <sub>2</sub>	1.9	SO <sub>2</sub> (OH) <sub>2</sub>	<0		
As(OH) <sub>3</sub>	9.2	SeO(OH) <sub>2</sub>	2.6	SeO <sub>2</sub> (OH) <sub>2</sub>	<0		
Sb(OH) <sub>3</sub>	11.0	TeO(OH) <sub>2</sub>	2.7				
Si(OH) <sub>4</sub>	10.0	PO(OH) <sub>3</sub>	2.1				
Ge(OH) <sub>4</sub>	8.6	AsO(OH) <sub>3</sub>	2.3				
Te(OH) <sub>6</sub>	8.8	IO(OH) <sub>5</sub>	1.6				
		HPO(OH) <sub>2</sub>	1.8 <sup>(b)</sup>				
		H <sub>2</sub> PO(OH)	2.0 <sup>(b)</sup>				

<sup>(a)</sup>Corrected for the fact that only 0.4% of dissolved CO<sub>2</sub> is in the form of H<sub>2</sub>CO<sub>3</sub>; the conventional value is  $pK_a$  6.5.

<sup>(b)</sup>Note that the value of  $pK_a$  for hypophosphorous acid H<sub>3</sub>PO<sub>3</sub> is consistent with its (correct) formulation as HPO(OH)<sub>2</sub> rather than as P(OH)<sub>3</sub>, which would be expected to have  $pK_a > 8$ . Similarly for H<sub>3</sub>PO<sub>2</sub>, which is H<sub>2</sub>PO(OH) rather than HP(OH)<sub>2</sub>.

**Table 3.6** First and second ionization constants for H<sub>2</sub>S, H<sub>2</sub>Se and H<sub>2</sub>Te

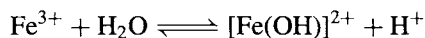
	p <i>K</i> <sub>1</sub>	p <i>K</i> <sub>2</sub>	Δp <i>K</i>
H <sub>2</sub> S	7	14	7
H <sub>2</sub> Se	4	12	8
H <sub>2</sub> Te	3	11	8

the first and second dissociation constants is  $\sim 10^8$  rather than  $10^5$  (Table 3.6).

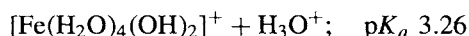
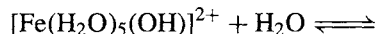
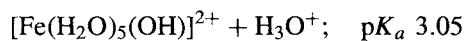
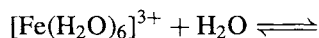
The results for dinuclear and polynuclear oxoacids are also consistent with this interpretation. Thus for phosphoric acid, H<sub>4</sub>P<sub>2</sub>O<sub>7</sub>, the successive p*K*<sub>a</sub> values are 1.5, 2.4, 6.6 and 9.2; the  $\sim 10$ -fold decrease between p*K*<sub>1</sub> and p*K*<sub>2</sub> (instead of a decrease of  $10^5$ ) is related to the fact that ionization occurs from two different PO<sub>4</sub> units. The third stage ionization, however, is  $\sim 10^5$  less than the first stage and the difference between the mean of the first two and the last two ionization constants is  $\sim 5 \times 10^5$ .

Another phenomenon that is closely associated with acid–base equilibria is the so-called hydrolysis of metal cations in aqueous solution, which is probably better considered as the protolysis of hydrated cations, e.g.:

“hydrolysis”:



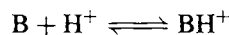
protolysis:



It is these reactions that impart the characteristic yellow to reddish-brown coloration of the hydroxoquo species to aqueous solutions of iron(III) salts, whereas the undissociated ion  $[\text{Fe}(\text{H}_2\text{O})_6]^{3+}$  is pale mauve, as seen in crystals of iron(III) alum  $\{[\text{Fe}(\text{H}_2\text{O})_6][\text{K}(\text{H}_2\text{O})_6](\text{SO}_4)_2\}$  and iron(III) nitrate  $\{[\text{Fe}(\text{H}_2\text{O})_6](\text{NO}_3)_3 \cdot 3\text{H}_2\text{O}\}$ . Such reactions may proceed to the stage where the diminished charge on the hydrated cation permits the formation of oxobridged,

or hydroxobridged polynuclear species that eventually precipitate as hydrous oxides (see discussion of the chemistry of many elements in later chapters). A useful summary is in Fig. 3.4. By contrast, extensive studies of the p*K*<sub>a</sub> values of hydrated metal ions in solution has generated a wealth of numerical data but no generalizations such as those just discussed for the hydrides and oxoacids of the non-metals.<sup>(42)</sup> Typical p*K*<sub>a</sub> values fall in the range 3–14 and, as expected, there is a general tendency for protolysis to be greater (p*K*<sub>a</sub> values to be lower) the higher the cationic charge. For example, aqueous solutions of iron(III) salts are more acidic than solutions of the corresponding iron(II) salts. However, it is difficult to discern any regularities in p*K*<sub>a</sub> for series of cations of the same ionic charge, and it is clear that specific “chemical” effects must also be considered.

Brønsted acidity is not confined to dilute aqueous solutions and the ideas developed in the preceding pages can be extended to proton donors in nonaqueous solutions.<sup>(43,44)</sup> In organic solvents and anhydrous protonic liquids the concepts of hydrogen-ion concentration and pH, if not actually meaningless, are certainly operationally inapplicable and acidity must be defined on some other scale. The one most frequently used is the Hammett acidity function *H*<sub>0</sub> which enables various acids to be compared in a given solvent and a given acid to be compared in various solvents. For the equilibrium between a base and its conjugate acid (frequently a coloured indicator)



the acidity function is defined as

$$H_0 = \text{p}K_{\text{BH}^+} - \log\{[\text{BH}^+]/[\text{B}]\}$$

In very dilute solutions

$$K_{\text{BH}^+} = [\text{B}][\text{H}^+]/[\text{BH}^+]$$

<sup>42</sup> L. G. SILLÉN, *Q. Rev. (London)* **13**, 146–68 (1969); *Pure Appl. Chem.* **17**, 55–78 (1968).

<sup>43</sup> C. H. ROCHESTER, *Acidity Functions*, Academic Press, London, 1970, 300 pp.

<sup>44</sup> G. A. OLAH, G. K. S. PRAKASH and J. SOMMER, *Superacids*, Wiley, New York, 1985, 371 pp.

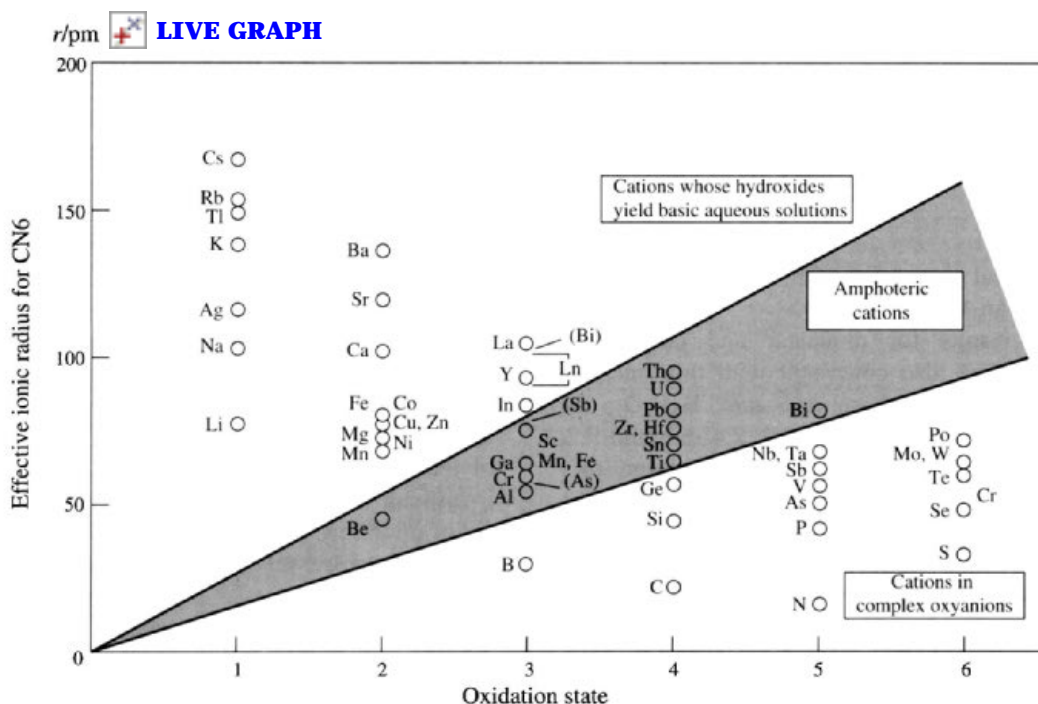


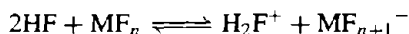
Figure 3.4 Plot of effective ionic radii versus oxidation state for various elements.

so that in water  $H_0$  becomes the same as pH. Some values for typical anhydrous acids are in Table 3.7 and these are discussed in more detail in appropriate sections of later chapters.

Table 3.7 Hammett acidity functions for some anhydrous acids

Acid	$-H_0$	Acid	$-H_0$
$\text{HSO}_3\text{F} + \text{SbF}_5$	15–27	HF	~11
HF + $\text{SbF}_5$ (1M)	20.4	$\text{H}_3\text{PO}_4$	5.0
$\text{HSO}_3\text{F}$	15.0	$\text{H}_2\text{SO}_4$ (63% in $\text{H}_2\text{O}$ )	4.9
$\text{H}_2\text{SO}_4$	12.0	$\text{HCO}_2\text{H}$	2.2

It will be noted that addition of  $\text{SbF}_5$  to HF considerably enhances its acidity and the same effect can be achieved by other fluoride acceptors such as  $\text{BF}_3$  and  $\text{TaF}_5$ :



The enhancement of the acidity of  $\text{HSO}_3\text{F}$  by the addition of  $\text{SbF}_5$  is more complex and the equilibria involved are discussed on p. 570.

### 3.6 The Hydrogen Bond<sup>(45-7)</sup>

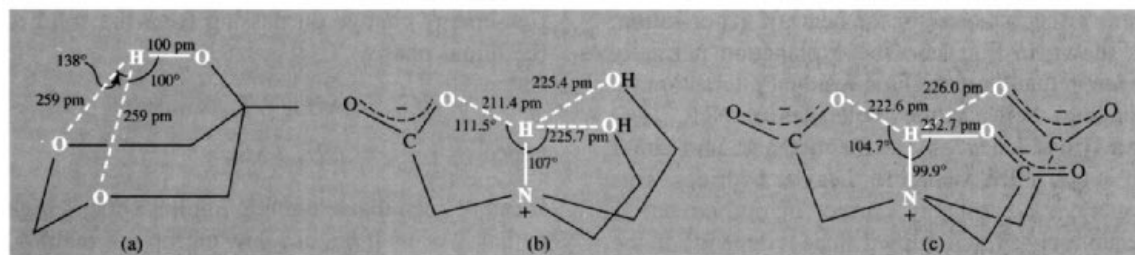
The properties of many substances suggest that, in addition to the “normal” chemical bonding between the atoms and ions, there exists some further interaction involving a hydrogen atom placed between two or more other groups of atoms. Such interaction is called hydrogen bonding and, though normally weak (10–60 kJ per mol of H-bonded H), it frequently has a decisive influence on the structure and properties of the substance. A hydrogen bond can be said to exist between 2 atoms A and B when these atoms approach more closely than would otherwise be expected in the absence of the hydrogen atom and when, as a result, the system has a lower total energy. The bond is represented

<sup>45</sup> G. C. PIMENTEL and A. L. MCCLELLAN, *The Hydrogen Bond*, W. H. Freeman, San Francisco, 1960, 475 pp.

<sup>46</sup> W. C. HAMILTON and J. A. IBERS, *Hydrogen Bonding in Solids*, W. A. Benjamin, New York, 1968, 284 pp.

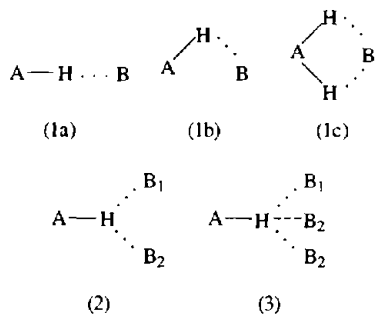
<sup>47</sup> J. EMSLEY, *Chem. Soc. Revs.* 9, 91–124 (1980).





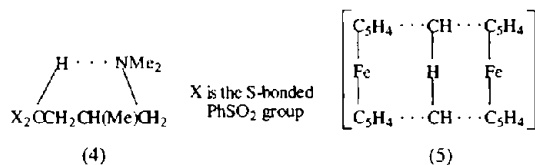
**Figure 3.5** Some examples of branched H bonds: (a) the bifurcated bond in 1,3-dioxanol-5<sup>(49)</sup>; and trifurcated bonds in (b) *N,N*-bis(2-hydroxyethyl)glycine<sup>(50)</sup> and (c) the nitrilotriacetate dianion.<sup>(51)</sup>

as  $A-H \cdots B$  and usually occurs when A is sufficiently electronegative to enhance the acidic nature of H (proton donor) and where the acceptor B has a region of high electron density (such as a lone pair of electrons) which can interact strongly with the acidic hydrogen. In fact, the H bond in  $A-H \cdots B$  can be either linear as in schematic structure (1) or significantly non-linear as in structures (1b) and (1c). H-bonds can also join three adjacent atoms (bifurcated) as in structure (2) or even four atoms (trifurcated) as in structure (3).



Thus, in a recent survey of 1509  $N-H \cdots O=C$  hydrogen bonds in organic carbonyls or carbonylates, nearly 80% (1199) were unbranched, some 20% (304) were bifurcated, but only 0.4% (6) were trifurcated.<sup>(48)</sup> Some examples are in Fig. 3.5.

It will be convenient first to indicate the range of phenomena which are influenced by H bonding and then to discuss more specifically the nature of the bond itself according to current theories. The experimental evidence suggests that strong H bonds can be formed when A is F, O or N; weaker H bonds are sometimes formed when A is C or a second row element, P, S, Cl or even Br, I. Strong H bonds are favoured when the atom B is F, O or N; the other halogens Cl, Br, I are less effective unless negatively charged and the atoms C, S and P can also sometimes act as B in weak H bonds. Recent examples of  $C-H \cdots N$  and  $C-H \cdots C$  bonds are in bis(phenylsulfonyl)trimethylbutylamine (4)<sup>(52)</sup> and the carbanion of [1.1]ferrocenophane (5).<sup>(53)</sup>



### 3.6.1 Influence on properties

It is well known that the mps and bps of  $NH_3$ ,  $H_2O$  and  $HF$  are anomalously high when compared with the mps and bps of the hydrides of other elements in Groups 15, 16 and 17, and the

<sup>48</sup> R. TAYLOR, O. KENNARD and W. VERICHEL, *J. Am. Chem. Soc.* **106**, 244–8 (1984).

<sup>49</sup> J. L. ALONSO and E. B. WILSON, *J. Am. Chem. Soc.* **102**, 1248–51 (1980).

<sup>50</sup> V. CODY, J. HAZEL and D. LANGS, *Acta Crystallogr.* **B33**, 905–7 (1977).

<sup>51</sup> S. H. WHITLOW, *Acta Crystallogr.* **B28**, 1914–9 (1972).

<sup>52</sup> R. L. HARLOW, C. LI and M. P. SAMMES, *J. Chem. Soc., Chem. Commun.*, 818–9 (1984).

<sup>53</sup> P. AHLBERG and O. DAVIDSSON, *J. Chem. Soc., Chem. Commun.*, 623–4 (1987).

same effect is noted for the heats of vaporization, as shown in Fig. 3.6. The explanation normally given is that there is some residual interaction (H bonding) between the molecules of  $\text{NH}_3$ ,  $\text{H}_2\text{O}$  and  $\text{HF}$  which is absent for methane, and either absent or much weaker for heavier hydrides. This argument is probably correct in outline but is deceptively oversimplified since it depends on the assumption that only some of the H bonds in solid  $\text{HF}$  (for example) are broken during the melting process and that others are broken on vaporization, though not all, since  $\text{HF}$  is known to be substantially polymerized even in the gas phase. The mp is the temperature at which there is zero

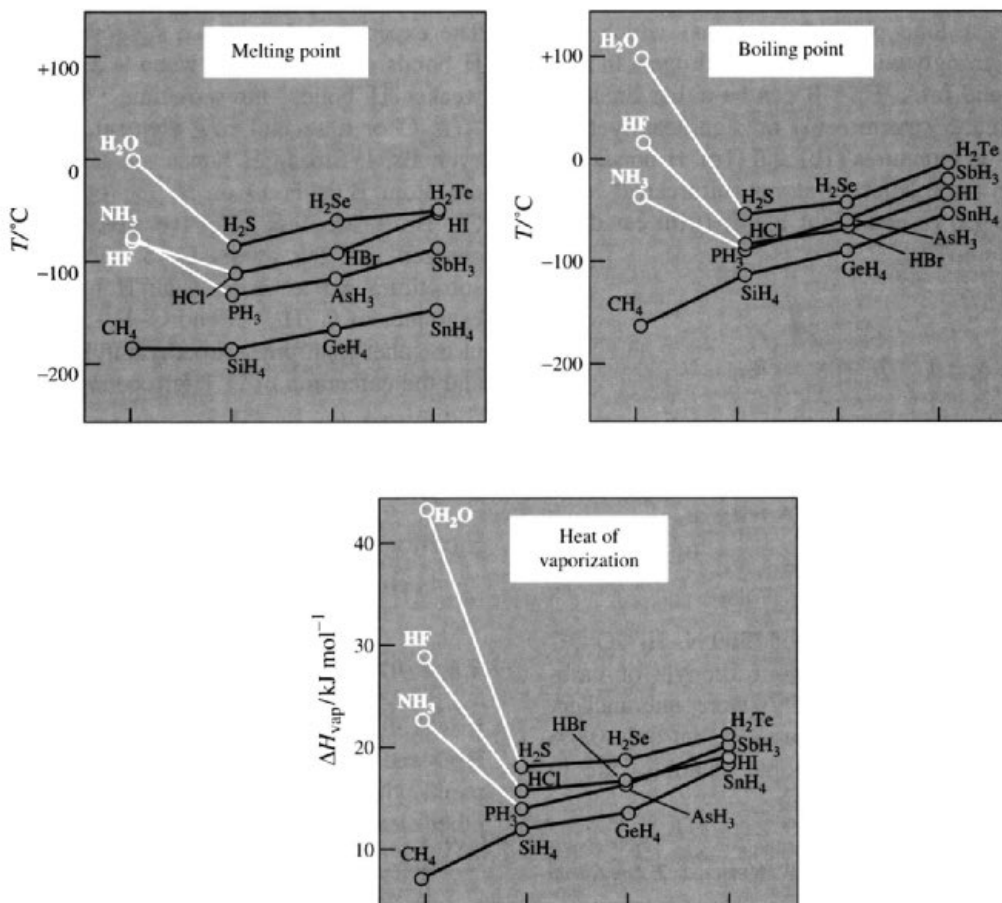
free-energy change on passing from the solid to the liquid phase:

$$\Delta G_m = \Delta H_m - T_m \Delta S_m = 0;$$

hence 
$$T_m = \Delta H_m / \Delta S_m$$

It can be seen that a high mp implies either a high enthalpy of melting, or a low entropy of melting, or both. Similar arguments apply to vaporization and the bp, and indicate the difficulties in quantifying the discussion.

Other properties that are influenced by H bonding are solubility and miscibility, heats of mixing, phase-partitioning properties, the



**Figure 3.6** Plots showing the high values of mp, bp and heat of vaporization of  $\text{NH}_3$ ,  $\text{H}_2\text{O}$  and  $\text{HF}$  when compared with other hydrides. Note also that the mp of  $\text{CH}_4$  ( $-182.5^\circ\text{C}$ ) is slightly higher than that of  $\text{SiH}_4$  ( $-185^\circ\text{C}$ ).

existence of azeotropes, and the sensitivity of chromatographic separation. Liquid crystals (or mesophases) which can be regarded as “partly melted” solids also frequently involve molecules that have H-bonded groups (e.g. cholesterol, polypeptides, etc.). Again, H bonding frequently results in liquids having a higher density and lower molar volume than would otherwise have been expected, and viscosity is also affected (e.g. glycerol, anhydrous  $\text{H}_2\text{SO}_4$ ,  $\text{H}_3\text{PO}_4$ , etc.).

Electrical properties of liquids and solids are sometimes crucially influenced by H bonding. The ionic mobility and conductance of  $\text{H}_3\text{O}^+$  and  $\text{OH}^-$  in aqueous solutions are substantially greater than those of other univalent ions due to a proton-switch mechanism in the H-bonded associated solvent, water. For example, at  $25^\circ\text{C}$  the conductance of  $\text{H}_3\text{O}^+$  and  $\text{OH}^-$  are  $350$  and  $192 \text{ ohm}^{-1} \text{ cm}^2 \text{ mol}^{-1}$ , whereas for other (viscosity-controlled) ions the values fall

mainly in the range  $50\text{--}75 \text{ ohm}^{-1} \text{ cm}^2 \text{ mol}^{-1}$ . (To convert to mobility,  $\nu \text{ cm}^2 \text{ s}^{-1} \text{ V}^{-1}$ , divide by  $96485 \text{ C mol}^{-1}$ .) It is also notable that the dielectric constant is not linearly related to molecular dipole moments for H-bonded liquids being much higher due to the orientating effect of the H bonds: large domains are able to align in an applied electric field so that the molecular dipoles reinforce one another rather than cancelling each other due to random thermal motion. Some examples are given in Fig. 3.7, which also illustrates the substantial influence of temperature on the dielectric constant of H-bonded liquids presumably due to the progressive thermal dissociation of the H bonds. Even more dramatic are the properties of ferroelectric crystals where there is a stable permanent electric polarization (see Fig. 3.8). Hydrogen bonding is one of the important ordering mechanisms

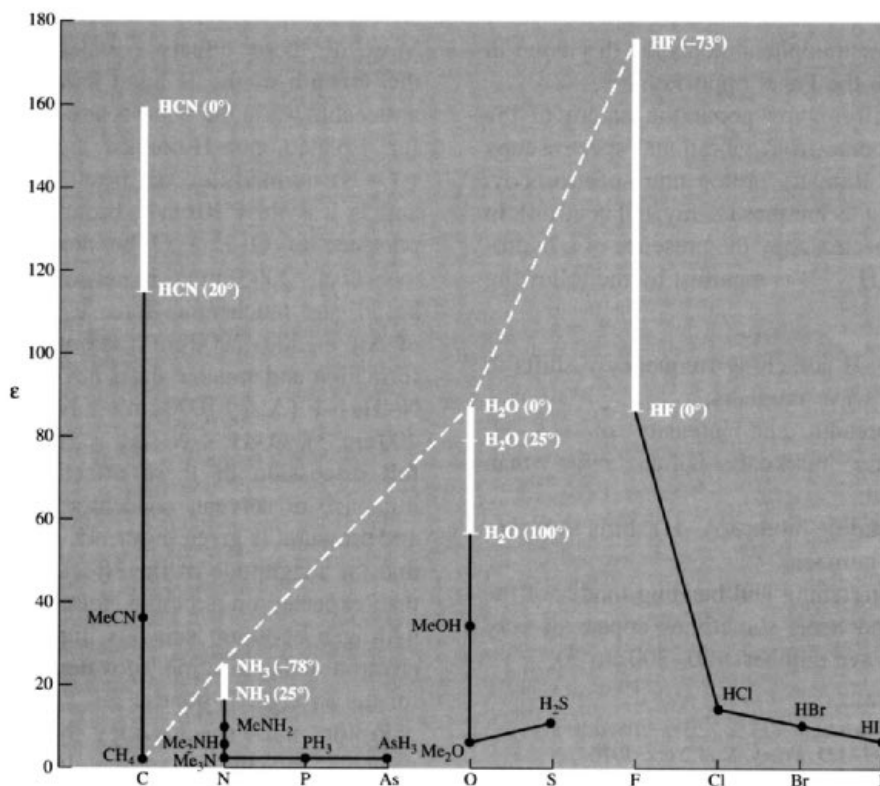
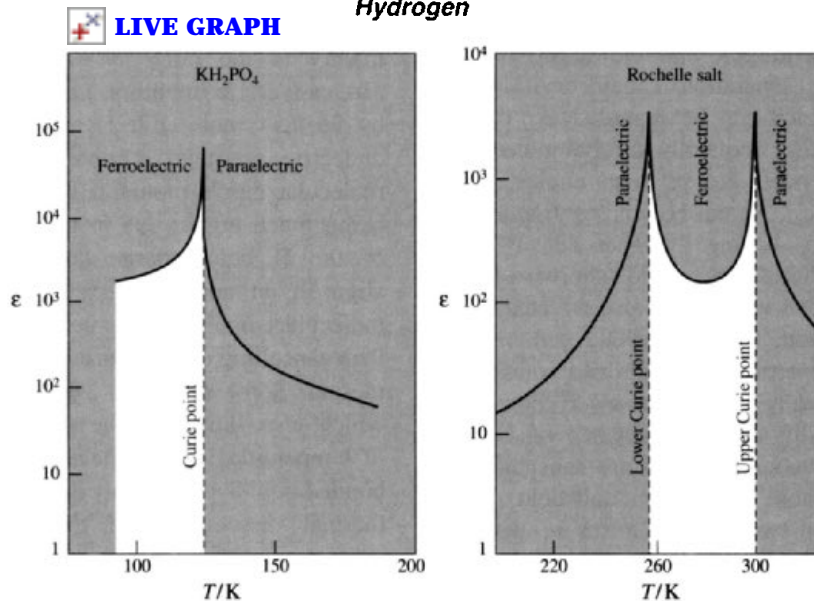


Figure 3.7 Dielectric constant of selected liquids.



**Figure 3.8** Anomalous temperature dependence of relative dielectric constant of ferroelectric crystals at the transition temperature (Curie point).

responsible for this phenomenon as discussed in more detail in the Panel opposite.<sup>(54,55)</sup>

Intimate information about the nature of the H bond has come from vibrational spectroscopy (infrared and Raman), proton nmr spectroscopy, and diffraction techniques (X-ray and neutron). In vibrational spectroscopy the presence of a hydrogen bond  $A-H \cdots B$  is manifest by the following effects:

- (i) the  $A-H$  stretching frequency  $\nu$  shifts to lower wave numbers;
- (ii) the breadth and intensity of  $\nu(A-H)$  increase markedly, often more than tenfold;
- (iii) the bending mode  $\delta(A-H)$  shifts to higher wave numbers;
- (iv) new stretching and bending modes of the H bond itself sometimes appear at very low wave numbers ( $20-200 \text{ cm}^{-1}$ ).

<sup>54</sup> C. KITTEL, *Introduction to Solid State Physics*, 5th edn., Chap. 13, pp. 399-431. Wiley, New York, 1976.

<sup>55</sup> H.-G. UNRUH, *Ferroelectrics in Ullmann's Encyclopedia of Industrial Chemistry*, Vol. A10, VCH, Weinheim, 1987, pp. 309-21, and references cited therein.

Most of these effects correlate roughly with the strength of the H bond and are particularly noticeable when the bond is strong. For example, for isolated non-H-bonded hydrogen groups,  $\nu(O-H)$  normally occurs near  $3500-3600 \text{ cm}^{-1}$  and is less than  $10 \text{ cm}^{-1}$  broad whereas in the presence of  $O-H \cdots O$  bonding  $\nu_{\text{antisym}}$  drops to  $\sim 1700-2000 \text{ cm}^{-1}$ , is several hundred  $\text{cm}^{-1}$  broad, and much more intense. A similar effect of  $\Delta\nu \sim 1500-2000 \text{ cm}^{-1}$  is noted on  $F-H \cdots F$  formation and smaller shifts have been found for  $N-H \cdots F$  ( $\Delta\nu \leq 1000 \text{ cm}^{-1}$ ),  $N-H \cdots O$  ( $\Delta\nu \leq 400 \text{ cm}^{-1}$ ),  $O-H \cdots N$  ( $\Delta\nu \leq 100 \text{ cm}^{-1}$ ), etc. A full discussion of these effects, including the influence of solvent, concentration, temperature and pressure, is given in ref. 45. Suffice it to note that the magnitude of the effect is much greater than expected on a simple electrostatic theory of hydrogen bonding, and this implies appreciable electron delocalization (covalency) particularly for the stronger H bonds.

Proton nmr spectroscopy has also proved valuable in studying H-bonded systems. As might be expected, substantial chemical shifts are observed and information can be obtained

### Ferroelectric Crystals<sup>(54,55)</sup>

A ferroelectric crystal is one that has an electric dipole moment even in the absence of an external electric field. This arises because the centre of positive charge in the crystal does not coincide with the centre of negative charge. The phenomenon was discovered in 1920 by J. Valasek in Rochelle salt, which is the H-bonded hydrated d-tartrate  $\text{NaKC}_4\text{H}_4\text{O}_6 \cdot 4\text{H}_2\text{O}$ . In such compounds the dielectric constant can rise to enormous values of  $10^3$  or more due to presence of a stable permanent electric polarization. Before considering the effect further, it will be helpful to recall various definitions and SI units:

$$\text{electric polarization } P = D - \epsilon_0 E (\text{C m}^{-2})$$

where  $D$  is the electric displacement ( $\text{C m}^{-2}$ )

$E$  is the electric field strength ( $\text{V m}^{-1}$ )

$\epsilon_0$  is the permittivity of vacuum ( $\text{F m}^{-1} = \text{A s V}^{-1} \text{m}^{-1}$ )

$$\text{dielectric constant } \epsilon = \frac{\epsilon_0 E + P}{\epsilon_0 E} = 1 + \chi \text{ (dimensionless)}$$

where  $\chi = \epsilon - 1 = P/\epsilon_0 E$  is the dielectric susceptibility.

There are two main types of ferroelectric crystal:

- those in which the polarization arises from an ordering process typically by H bonding;
- those in which the polarization arises by a displacement of one sublattice with respect to another, as in perovskite-type structures like barium titanate (p. 963).

The ferroelectricity usually disappears above a certain transition temperature (often called a Curie temperature) above which the crystal is said to be paraelectric; this is because thermal motion has destroyed the ferroelectric order. Occasionally the crystal melts or decomposes before the paraelectric state is reached. There are thus some analogies to ferromagnetic and paramagnetic compounds though it should be noted that there is no iron in ferroelectric compounds. Some typical examples, together with their transition temperatures and spontaneous permanent electric polarization  $P_s$ , are given in the Table.

**Table** Properties of some ferroelectric compounds

Compound	$T_c/\text{K}$	$P_s/\mu\text{C cm}^{-2(a)}$	(at $T/\text{K}$ )
$\text{KH}_2\text{PO}_4$	123	5.3	(96)
$\text{KD}_2\text{PO}_4$	213	4.5	—
$\text{KH}_2\text{AsO}_4$	96	3.0	(80)
$\text{KD}_2\text{AsO}_4$	162		
$\text{RbH}_2\text{PO}_4$	147	5.6	(90)
$(\text{NH}_2\text{CH}_2\text{CO}_2\text{H})_3 \cdot \text{H}_2\text{SO}_4^{(b)}$	322	2.8	(293)
$(\text{NH}_2\text{CH}_2\text{CO}_2\text{H})_3 \cdot \text{H}_2\text{SeO}_4^{(b)}$	295	3.2	(273)
$\text{BaTiO}_3$	393	26.0	(296)
$\text{KNbO}_3$	712	30.0	(523)
$\text{PbTiO}_3$	763	>50.0	(300)
$\text{LiTaO}_3$	890	23.0	(720)
$\text{LiNbO}_3$	1470	300.0	—

<sup>(a)</sup>To convert to the basic SI unit of  $\text{C m}^{-2}$  divide the tabulated values of  $P_s$  by  $10^2$ ; to convert to the CGS unit of  $\text{esu cm}^{-2}$  multiply by  $3 \times 10^3$ . For a full compilation see E. C. Subbarao, *Ferroelectrics* 5, 267 (1973).

<sup>(b)</sup>Triglycinesulfate and selenate.

In  $\text{KH}_2\text{PO}_4$  and related compounds each tetrahedral  $[\text{PO}_2(\text{OH})_2]^-$  group is joined by H bonds to neighbouring  $[\text{PO}_2(\text{OH})_2]^-$  groups; below the transition temperature all the short O–H bonds are ordered on the same side of the  $\text{PO}_4$  units, and by appropriate application of an electric field, the polarization of the H bonds can be reversed. The dramatic effect of deuterium substitution in raising the transition temperature of such compounds can be seen from the Table: this has been ascribed to a quantum-mechanical effect involving the mass dependence of the de Broglie wavelength of hydrogen. Other examples of H-bonded ferroelectrics are  $(\text{NH}_4)\text{H}_2\text{PO}_4$ ,  $(\text{NH}_4)\text{H}_2\text{AsO}_4$ ,  $\text{Ag}_2\text{H}_3\text{IO}_6$ ,  $(\text{NH}_4)\text{Al}(\text{SO}_4)_2 \cdot 6\text{H}_2\text{O}$  and  $(\text{NH}_4)_2\text{SO}_4$ . Rochelle salt is unusual in having both an upper and a lower critical temperature between which the compound is ferroelectric.

*Panel continues*

The closely related phenomenon of antiferroelectric behaviour is also known, in which there is an ordered, self-cancelling arrangement of permanent electric dipole moments below a certain transition temperature; H bonding is again implicated in the ordering mechanism for several ammonium salts of this type, e.g.  $(\text{NH}_4)\text{H}_2\text{PO}_4$  148 K,  $(\text{NH}_4)\text{D}_2\text{PO}_4$  242 K,  $(\text{NH}_4)\text{H}_2\text{AsO}_4$  216 K,  $(\text{NH}_4)\text{D}_2\text{AsO}_4$  304 K and  $(\text{NH}_4)_2\text{H}_3\text{IO}_6$  254 K. As with ferroelectrics, antiferroelectrics can also arise by a displacive mechanism in perovskite-type structures, and typical examples, with their transition temperatures, are:

$\text{PbZrO}_3$  506 K,  $\text{PbHfO}_3$  488 K,  $\text{NaNbO}_3$  793, 911 K,  $\text{WO}_3$  1010 K.

Ferroelectrics have many practical applications: they can be used as miniature ceramic capacitors because of their large capacitance, and their electro-optical characteristics enable them to modulate and deflect laser beams. The temperature dependence of spontaneous polarization induces a strong pyroelectric effect which can be exploited in thermal and infrared detection. Many applications depend on the fact that all ferroelectrics are also piezoelectrics. Piezoelectricity is the property of acquiring (or altering) an electric polarization  $P$  under external mechanical stress, or conversely, the property of changing size (or shape) when subjected to an external electric field  $E$ . Thus ferroelectrics have been used as transducers to convert mechanical pulses into electrical ones and vice versa, and find extensive application in ultrasonic generators, microphones, and gramophone pickups; they can also be used as frequency controllers, electric filters, modulating devices, frequency multipliers, and as switches, counters and other bistable elements in computer circuits. A further ingenious application is in delay lines by means of which an electric signal is transformed piezoelectrically into an acoustic signal which passes down the piezoelectric rod at the velocity of sound until, at the other end, it is reconverted into a (delayed) electric signal.

It should be noted that, whereas ferroelectrics are necessarily piezoelectrics, the converse need not apply. The necessary condition for a crystal to be piezoelectric is that it must lack a centre of inversion symmetry. Of the 32 point groups, 20 qualify for piezoelectricity on this criterion, but for ferroelectric behaviour a further criterion is required (the possession of a single non-equivalent direction) and only 10 space groups meet this additional requirement. An example of a crystal that is piezoelectric but not ferroelectric is quartz, and indeed this is a particularly important example since the use of quartz for oscillator stabilization has permitted the development of extremely accurate clocks ( $1$  in  $10^8$ ) and has also made possible the whole of modern radio and television broadcasting including mobile radio communications with aircraft and ground vehicles.

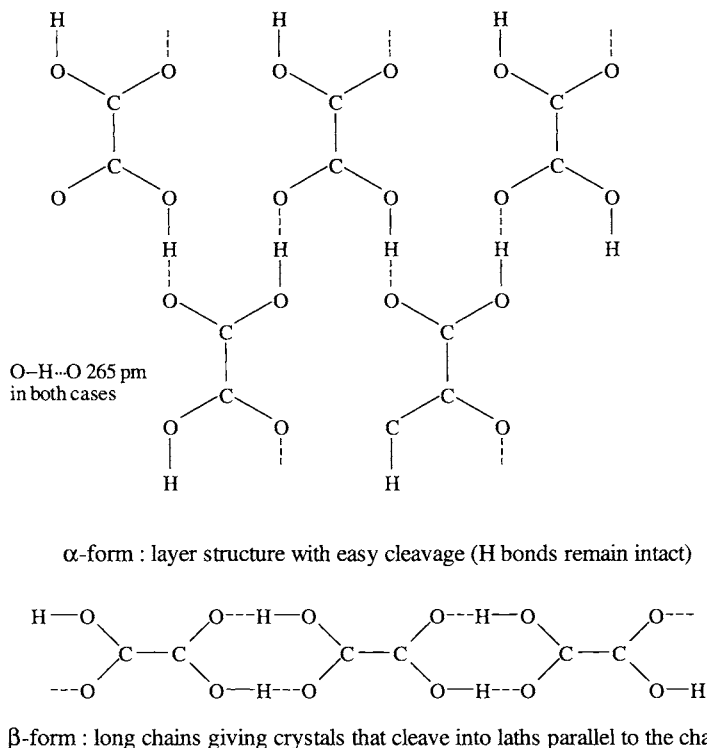
concerning H-bond dissociation, proton exchange times, and other relaxation processes. The chemical shift always occurs to low field and some typical values are tabulated below for the shifts which occur between the gas and liquid phases or on dilution in an inert solvent:

Compound	$\text{CH}_4$	$\text{C}_2\text{H}_6$	$\text{CHCl}_3$	$\text{HCN}$	$\text{NH}_3$	$\text{PH}_3$
$\delta$ ppm	0	0	0.30	1.65	1.05	0.78
Compound	$\text{H}_2\text{O}$	$\text{H}_2\text{S}$	$\text{HF}$	$\text{HCl}$	$\text{HBr}$	$\text{HI}$
$\delta$ ppm	4.58	1.50	6.65	2.05	1.78	2.55

The low-field shift is generally interpreted, at least qualitatively, in terms of a decrease in diamagnetic shielding of the proton: the formation of  $\text{A-H}\cdots\text{B}$  tends to draw H towards B and to repel the bonding electrons in  $\text{A-H}$  towards A thus reducing the electron density about H and reducing the shielding. The strong electric field due to B also inhibits the diamagnetic circulation within the H atom and this further reduces the shielding. In addition,

there is a magnetic anisotropy effect due to B; this will be positive (upfield shift) if the principal symmetry axis of B is towards the H bond, but the effect is presumably small since the overall shift is always downfield.

Ultraviolet and visible spectra are also influenced by H bonding, but the effects are more difficult to quantify and have been rather less used than ir and nmr. It has been found that the  $n \rightarrow \pi^*$  transition of the base B always moves to high frequency (blue shift) on H-bond formation, the magnitude of  $\Delta\nu$  being  $\sim 300\text{--}4000\text{ cm}^{-1}$  for bands in the region  $15\,000\text{--}35\,000\text{ cm}^{-1}$ . By contrast  $\pi \rightarrow \pi^*$  transitions on the base B usually move to lower frequencies (red shift) and shifts are in the range  $-500$  to  $-2300\text{ cm}^{-1}$  for bands in the region  $30\,000\text{--}47\,000\text{ cm}^{-1}$ . Detailed interpretations of these data are somewhat complex and obscure, but it will be noted that the shifts are approximately of the same magnitude as the enthalpy of formation of many H bonds ( $83.59\text{ cm}^{-1}$  per atom  $\equiv 1\text{ kJ mol}^{-1}$ ).



**Figure 3.9** Schematic representation of the two forms of oxalic acid,  $(-\text{CO}_2\text{H})_2$ .

### 3.6.2 Influence on structure<sup>(56,57)</sup>

The crystal structure of many compounds is dominated by the effect of H bonds, and numerous examples will emerge in ensuing chapters. Ice (p. 624) is perhaps the classic example, but the layer lattice structure of  $\text{B}(\text{OH})_3$  (p. 203) and the striking difference between the  $\alpha$ - and  $\beta$ -forms of oxalic and other dicarboxylic acids is notable (Fig. 3.9). The more subtle distortions that lead to ferroelectric phenomena in  $\text{KH}_2\text{PO}_4$  and other crystals have already been noted (p. 57). Hydrogen bonds between fluorine atoms result in the formation of infinite zigzag chains in crystalline hydrogen fluoride

with  $\text{F}-\text{H}\cdots\text{F}$  distance 249 pm and the angle  $\text{HFH}$   $120.1^\circ$ . Likewise, the crystal structure of  $\text{NH}_4\text{HF}_2$  is completely determined by H bonds, each nitrogen atom being surrounded by 8 fluorines, 4 in tetrahedral array at 280 pm due to the formation of  $\text{N}-\text{H}\cdots\text{F}$  bonds, and 4 further away at about 310 pm; the two sets of fluorine atoms are themselves bonded pairwise at 232 pm by  $\text{F}-\text{H}-\text{F}$  interactions. Ammonium azide  $\text{NH}_4\text{N}_3$  has the same structure as  $\text{NH}_4\text{HF}_2$ , with  $\text{N}-\text{H}\cdots\text{N}$  298 pm. Hydrogen bonding also leads  $\text{NH}_4\text{F}$  to crystallize with a structure different from that of the other ammonium (and alkali) halides:  $\text{NH}_4\text{Cl}$ ,  $\text{NH}_4\text{Br}$  and  $\text{NH}_4\text{I}$  each have a low-temperature CsCl-type structure and a high-temperature NaCl-type structure, but  $\text{NH}_4\text{F}$  adopts the wurtzite ( $\text{ZnS}$ ) structure in which each  $\text{NH}_4^+$  group is surrounded tetrahedrally by 4 F to which it is bonded by 4  $\text{N}-\text{H}\cdots\text{F}$  bonds at 271 pm. This is very similar to the structure

<sup>56</sup> L. PAULING, *The Nature of the Chemical Bond*, 3rd edn., Chap. 12, Cornell University Press, Ithaca, 1960.

<sup>57</sup> A. F. WELLS, *Structural Inorganic Chemistry*, 5th edn., Clarendon Press, Oxford, 1984, 1382 pp.

Table 3.8 Length of typical H bonds<sup>(46,57)</sup>

Bond	Length/pm	$\Sigma$ /pm <sup>(a)</sup>	Examples
F-H-F	227	(270)	NaHF <sub>2</sub> , KHF <sub>2</sub>
F-H...F	245-249	(270)	KH <sub>4</sub> F <sub>5</sub> , HF
O-H...F	265-287	(275)	CuF <sub>2</sub> ·2H <sub>2</sub> O, FeSiF <sub>6</sub> ·6H <sub>2</sub> O
O-H...Cl	295-310	(320)	HCl·H <sub>2</sub> O, (NH <sub>3</sub> OH)Cl, CuCl <sub>2</sub> ·2H <sub>2</sub> O
O-H...Br	320-340	(335)	NaBr·2H <sub>2</sub> O, HBr·4H <sub>2</sub> O
O-H-O	240-263	(280)	Ni dimethylglyoxime, KH maleate, HCrO <sub>2</sub> Na <sub>3</sub> H(CO <sub>3</sub> ) <sub>2</sub> ·2H <sub>2</sub> O
O-H...O	248-290	(280)	KH <sub>2</sub> PO <sub>4</sub> , NH <sub>4</sub> H <sub>2</sub> PO <sub>4</sub> , KH <sub>2</sub> AsO <sub>4</sub> , AlOOH, $\alpha$ -HIO <sub>3</sub> , numerous hydrated metal sulfates and nitrates
O-H...S	310-340	(325)	MgS <sub>2</sub> O <sub>3</sub> ·6H <sub>2</sub> O
O-H...N	268-279	(290)	N <sub>2</sub> H <sub>4</sub> ·4MeOH, N <sub>2</sub> H <sub>4</sub> ·H <sub>2</sub> O
N-H...F	262-296	(285)	NH <sub>4</sub> F, N <sub>2</sub> H <sub>6</sub> F <sub>2</sub> , (N <sub>2</sub> H <sub>6</sub> )SiF <sub>6</sub>
N-H...Cl	300-320	(330)	Me <sub>3</sub> NHCl, Me <sub>2</sub> NH <sub>2</sub> Cl, (NH <sub>3</sub> OH)Cl
N-H...I	346	(365)	Me <sub>3</sub> NHI
N-H...O	281-304	(290)	HSO <sub>3</sub> NH <sub>2</sub> , (NH <sub>4</sub> ) <sub>2</sub> SO <sub>4</sub> , NH <sub>4</sub> OOCH, CO(NH <sub>2</sub> ) <sub>2</sub>
N-H...S	323, 329	(335)	N <sub>2</sub> H <sub>5</sub> (HS)
N-H...N	294-315	(300)	NH <sub>4</sub> N <sub>3</sub> , NCNC(NH <sub>2</sub> ) <sub>2</sub> (i.e. dicyandiamide)
P-H...I	424	(405)	PH <sub>4</sub> I

<sup>(a)</sup>  $\Sigma$  = sum of van der Waals' radii (in pm) of A and B (ignoring H which has a value of ~120 pm) and using the values F 135, Cl 180, Br 195, I 215; O 140, S 185; N 150, P 190.

of ordinary ice. Typical values of A-H...B distances found in crystals are given in Table 3.8.

The precise position of the H atom in crystalline compounds containing H bonds has excited considerable experimental and theoretical interest. In situations where a symmetric H bond is possible in principle, it is frequently difficult to decide whether the proton is vibrating with a large amplitude about a single potential minimum or whether it is vibrating with a smaller amplitude but is also statistically disordered between two close sites, the potential energy barrier between the two sites being small.<sup>(46,47)</sup> It now seems well established that the F-H-F bond is symmetrical in NaHF<sub>2</sub> and KHF<sub>2</sub>, and that the O-H-O bond is symmetrical in HCrO<sub>2</sub>. Other examples are the intra-molecular H bonds in potassium hydrogen maleate, K<sup>+</sup>[*cis*- $\overline{\text{C}}\text{H}=\overline{\text{C}}\text{H}\text{C}(\text{O})\text{O}-\text{H}-\overline{\text{O}}\text{C}(\text{O})$ ]<sup>-</sup> and its monochloro derivative: Numerous other examples of H bonding will be found in later chapters.

In summary, we can see that H bonding influences crystal structure by linking atoms or groups

into larger structural units. These may be:

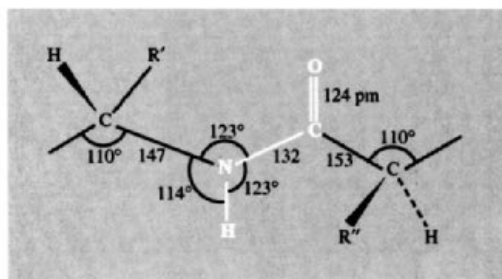
- finite groups: HF<sub>2</sub><sup>-</sup>; [O<sub>2</sub>CO-H...OCO<sub>2</sub>]<sup>3-</sup> in Na<sub>3</sub>H(CO<sub>3</sub>)<sub>2</sub>·2H<sub>2</sub>O dimers of carboxylic acids, etc.;
- infinite chains: HF, HCN, HCO<sub>3</sub><sup>-</sup>, HSO<sub>4</sub><sup>-</sup>, etc.;
- infinite layers: N<sub>2</sub>H<sub>6</sub>F<sub>2</sub>, B(OH)<sub>3</sub>, B<sub>3</sub>O<sub>3</sub>(OH)<sub>3</sub>, H<sub>2</sub>SO<sub>4</sub>, etc.;
- three-dimensional nets: NH<sub>4</sub>F, H<sub>2</sub>O, H<sub>2</sub>O<sub>2</sub>, Te(OH)<sub>6</sub>, H<sub>2</sub>PO<sub>4</sub><sup>-</sup> in KH<sub>2</sub>PO<sub>4</sub>, etc.

H bonding also vitally influences the conformation and detailed structure of the polypeptide chains of protein molecules and the complementary intertwined polynucleotide chains which form the double helix in nucleic acids.<sup>(56,58)</sup> Thus, proteins are built up from polypeptide chains of the type shown at the top of the next column.

These chains are coiled in a precise way which is determined to a large extent by N-H...O hydrogen bonds of length 279 ±

<sup>58</sup> G. A. JEFFREY and W. SAENGER, *Hydrogen Bonding in Biological Structures*, Springer Verlag, Berlin, 1991, 567 pp.





12 pm depending on the amino-acid residue involved. Each amide group is attached by such a hydrogen bond to the third amide group from it in both directions along the chain, resulting in an  $\alpha$ -helix of pitch (total rise of helix per turn) of about 538 pm, corresponding to 3.60 amino-acid residues per turn. These helical chains can, in turn, become stretched and form hydrogen bonds with neighbouring chains to generate either parallel-chain pleated sheets (repeat distances 650 pm) or antiparallel-chain pleated sheets (700 pm).

Nucleic acids, which control the synthesis of proteins in the cells of living organisms and which transfer heredity information via genes, are also dominated by H bonding. Their structure involves two polynucleotide chains intertwined to form a double helix. The complementarity in the structure of the two chains is ascribed to the formation of H bonds between the pyrimidine residue (thymine or cytosine) in one chain and the purine residue (adenine or guanine) in the other as illustrated in Fig. 3.10. Whilst there is still some uncertainty as to the precise configuration of the  $N-H \cdots O$  and  $N-H \cdots N$  hydrogen bonds in particular cases, the extraordinary fruitfulness of these basic ideas has led to a profusion

of developments of fundamental importance in biochemistry.<sup>(58)</sup>

### 3.6.3 Strength of hydrogen bonds and theoretical description<sup>(59)</sup>

Measurement of the properties of H-bonded systems over a range of temperatures leads to experimental values of  $\Delta G$ ,  $\Delta H$  and  $\Delta S$  for H-bond formation, and these data have been supplemented in recent years by increasingly reliable *ab initio* quantum-mechanical calculations.<sup>(60)</sup> Some typical values for the enthalpy of dissociation of H-bonded pairs in the gas phase are in Table 3.9.

The uncertainty in these values varies between  $\pm 1$  and  $\pm 6$  kJ mol<sup>-1</sup>. In general, H bonds of energy  $< 25$  kJ mol<sup>-1</sup> are classified as weak; those in the range 25–40 kJ mol<sup>-1</sup> are medium; and those having  $\Delta H > 40$  kJ mol<sup>-1</sup> are strong. Until recently, it was thought that the strongest H bond was that in the hydrogendifluoride ion  $[F-H-F]^-$ ; this is difficult to determine experimentally and values in the range 150–250 kJ mol<sup>-1</sup> have been reported. A recent theoretically computed value is 169 kJ mol<sup>-1</sup> which agrees well with the value of  $163 \pm 4$  kJ mol<sup>-1</sup> from ion cyclotron resonance studies.<sup>(61)</sup> In fact, it now seems that the H bond between formic acid and the fluoride ion,

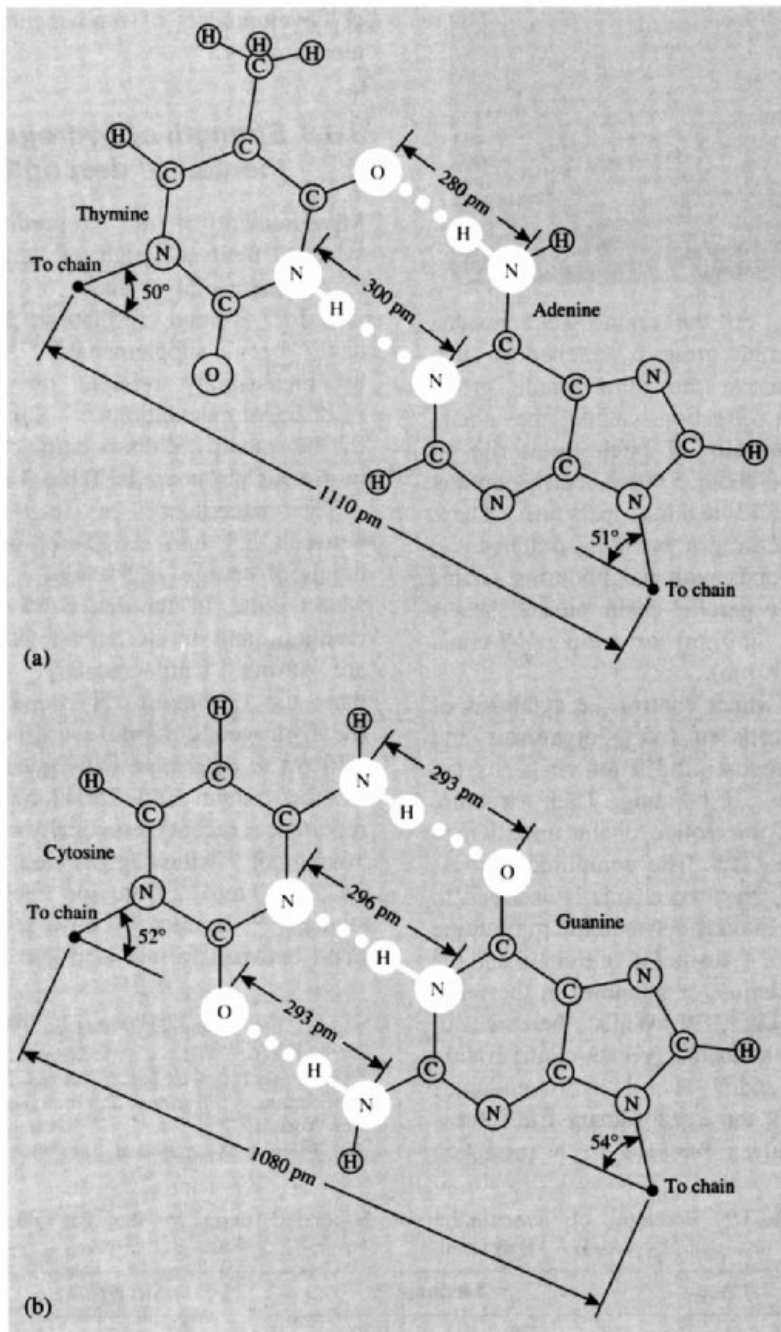
<sup>59</sup> A. C. LEGON and D. J. MILLEN, *Chem. Soc. Revs.* **21**, 71–8 (1992).

<sup>60</sup> P. A. KOLLMAN, Chap. 3 in H. F. SCHAEFFER (ed.), *Applications of Electronic Structure Theory*, Plenum Press, New York, 1977.

<sup>61</sup> J. EMSLEY, *Polyhedron* **4**, 489–90 (1985).

**Table 3.9** Enthalpy of dissociation of H-bonded pairs in the gas phase,  $\Delta H_{298}(A-H \cdots B)/\text{kJ mol}^{-1}$

Weak		Medium		Strong	
HSH $\cdots$ SH <sub>2</sub>	7	FH $\cdots$ FH	29	HOH $\cdots$ Cl <sup>-</sup>	55
NCH $\cdots$ NCH	16	ClH $\cdots$ OMe <sub>2</sub>	30	HCONH <sub>2</sub> $\cdots$ OCHNH <sub>2</sub>	59
H <sub>2</sub> NH $\cdots$ NH <sub>3</sub>	17	FH $\cdots$ OH <sub>2</sub>	38	HCOOH $\cdots$ OCHOH	59
MeOH $\cdots$ OHMe	19			HOH $\cdots$ F <sup>-</sup>	98
HOH $\cdots$ OH <sub>2</sub>	22			H <sub>2</sub> OH <sup>+</sup> $\cdots$ OH <sub>2</sub>	151
				FH $\cdots$ F <sup>-</sup>	169
				HCO <sub>2</sub> H $\cdots$ F <sup>-</sup>	~200



**Figure 3.10** Structural details of the bridging units between pairs of bases in separate strands of the double helix of DNA: (a) the thymine-adenine pair (b) the cytosine-guanine pair.

[HCO<sub>2</sub>H...F<sup>-</sup>], is some 30 kJ mol<sup>-1</sup> stronger than that calculated on the same basis for HF<sub>2</sub><sup>-</sup>.<sup>(62)</sup>

Early discussions on the nature of the hydrogen bond tended to adopt an electrostatic approach in order to avoid the implication of a covalency greater than one for hydrogen. Indeed, such calculations can reproduce the experimental H-bond energies and dipole moments, but this is not a particularly severe test because of the parametric freedom in positioning the charges. However, the purely electrostatic theory is unable to account for the substantial increase in intensity of the stretching vibration  $\nu(\text{A-H})$  on H bonding or for the lowered intensity of the bending mode  $\delta(\text{A-H})$ . More seriously, such a theory does not account for the absence of correlation between H-bond strength and dipole moment of the base, and it leaves the frequency shifts in the electronic transitions unexplained. Nonlinear A-H...B bonds would also be unexpected, though numerous examples of angles in the range 150–180° are known.<sup>(46)</sup>

Valence-bond descriptions envisage up to five contributions to the total bond wave function,<sup>(45)</sup> but these are now considered to be merely computational devices for approximating to the true wave function. Perturbation theory has also been employed and apportions the resultant bond energy between (1) the electrostatic energy of interaction between the fixed nuclei and the electron distribution of the component molecules, (2) Pauli exchange repulsion energy between electrons of like spin, (3) polarization energy resulting from the attraction between the polarizable charge cloud of one molecule and the permanent multipoles of the other molecule, (4) quantum-mechanical charge-transfer energy, and (5) dispersion energy, resulting from second-order induced dipole-induced dipole attraction. The results suggest that electrostatic effects predominate, particularly for weak bonds, but that covalency effects increase in importance as the strength of the bond increases. It is also

possible to apportion the energy obtained from *ab initio* SCF-MO calculations in this way.<sup>(63)</sup> For example, in one particular calculation for the water dimer HOH...OH<sub>2</sub>, the five energy terms enumerated above were calculated to be:  $E_{\text{elec stat}} - 26.5$ ,  $E_{\text{Pauli}} + 18$ ,  $E_{\text{polar}} - 2$ ,  $E_{\text{ch tr}} - 7.5$ ,  $E_{\text{disp}} 0 \text{ kJ mol}^{-1}$ . There was also a coupling interaction  $E_{\text{mix}} - 0.5$ , making in all a total attractive force  $\Delta E_0 = E_{\text{dimer}} - E_{\text{monomers}} = -18.5 \text{ kJ mol}^{-1}$ . To calculate the enthalpy change  $\Delta H_{298}$  as listed on p. 61, it is also necessary to consider the work of expansion and the various spectroscopic degrees of freedom:

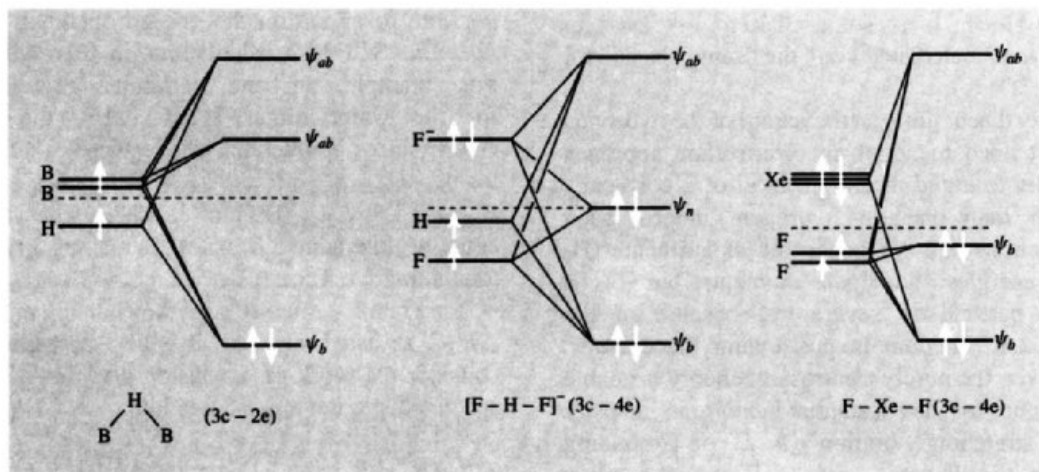
$$\Delta H_{298} = E_0 + \Delta(PV) + \Delta E_{\text{trans}} + \Delta E_{\text{vib}} + \Delta E_{\text{rot}}$$

Such calculations can also give an indication of the influence of H-bond formation on the detailed electron distribution within the interacting components. There is general agreement that in the system X-A-H...B-Y as compared with the isolated species XAH and BY, there is a net gain of electron density by X, A and B and a net loss of electrons by H and Y. There is also a small transfer of electronic charge (~0.05 electrons) from BY to XAH in moderately strong H bonds (20–40 kJ mol<sup>-1</sup>). In virtually all neutral dimers, the increase in the A-H bond length on H-bond formation is quite small (<5 pm), the one exception so far studied theoretically being ClH...NH<sub>3</sub>, where the proton position in the H bond is half-way between completely transferred to NH<sub>3</sub> and completely fixed on HCl.

It follows from the preceding discussion that the unbranched H bond can be regarded as a 3-centre 4-electron bond A-H...B in which the 2 pairs of electrons involved are the bond pair in A-H and the lone pair on B. The degree of charge separation on bond formation will depend on the nature of the proton-donor group AH and the Lewis base B. The relation between this 3-centre bond formalism and the 3-centre bond descriptions frequently used for boranes, polyhalides and compounds of xenon is particularly instructive and is elaborated in

<sup>62</sup> J. EMSLEY, O. P. A. HOYTE and R. E. OVERILL, *J. Chem. Soc., Chem. Commun.*, 225 (1977).

<sup>63</sup> H. UMEYAMA and K. MOROKUMA, *J. Am. Chem. Soc.* **99**, 1316–32 (1977).



**Figure 3.11** Schematic representation of the energy levels in various types of 3-centre bond. The B-H-B (“electron deficient”) bond is non-linear, the (“electron excess”) F-Xe-F bond is linear, and the A-H...B hydrogen bond can be either linear or non-linear depending on the compound.

Fig. 3.11. Numerous examples are also known in which hydrogen acts as a bridge between metallic elements in binary and more complex hydrides, and some of these will be mentioned in the following section which considers the general question of the hydrides of the elements.

### 3.7 Hydrides of the Elements<sup>(64-6)</sup>

Hydrogen combines with many elements to form binary hydrides  $MH_x$  (or  $M_mH_n$ ). All the main-group elements except the noble gases and perhaps indium and thallium form hydrides, as do all the lanthanoids and actinoids that have been studied. Hydrides are also formed by the more electropositive transition elements, notably Sc, Y, La, Ac; Ti, Zr, Hf; and to a lesser

extent V, Nb, Ta; Cr; Cu; and Zn. Hydrides of other transition elements are either non-existent or poorly characterized, with the spectacular exception of palladium which has been more studied than any other metal hydride system.<sup>(67)</sup> The situation is summarized in Fig. 3.12; this indicates the idealized formulae of the known hydrides though many of the d-block and f-block elements form phases of variable compositions.

It has been customary to group the binary hydrides of the elements into various classes according to the presumed nature of their bonding: ionic, metallic, covalent, polymeric, and “intermediate” or “borderline”. However, this is unsatisfactory because the nature of the bonding is but poorly understood in many cases and the classification obscures the important point that there is an almost continuous gradation in properties — and bond types(?) — between members of the various classes. It is also somewhat misleading in implying that the various bond types are mutually exclusive whereas it seems likely that more than one type of bonding is present in many cases. The situation is not unique to hydrides but is also well known for

<sup>64</sup> K. M. MACKAY, *Hydrogen Compounds of the Metallic Elements*, E. and F. N. Spon, London, 1966, 168 pp.; Hydrides, *Comprehensive Inorganic Chemistry*, Vol. 1, Chap. 2, Pergamon Press, Oxford, 1973.

<sup>65</sup> E. WIBERG and E. AMBERGER, *Hydrides of the Elements of Main Groups I-IV*, Elsevier, Amsterdam, 1971, 785 pp.

<sup>66</sup> W. M. MUELLER, J. P. BLACKLEDGE and G. G. LIBOWITZ (eds.), *Metal Hydrides*, Academic Press, New York, 1968, 791 pp.

<sup>67</sup> F. A. LEWIS, *The Palladium-Hydrogen System*, Academic Press, London, 1967, 178 pp.

		H <sub>2</sub>		He																	
LiH	BeH <sub>2</sub>															~40 boranes B <sub>n</sub> H <sub>n</sub>	lanthanide C <sub>m</sub> H <sub>m</sub> hydrides Si <sub>m</sub> H <sub>m+2</sub> etc. n = 1-8(+) m = 1-5(+)	NH <sub>3</sub> N <sub>2</sub> H <sub>4</sub> N <sub>3</sub> H	OH <sub>2</sub> O <sub>2</sub> H <sub>2</sub>	FH	Ne
NaH	MgH <sub>2</sub>															AlH <sub>3</sub>	P <sub>n</sub> H <sub>m-2</sub> n = 1-9 etc.	S <sub>n</sub> H <sub>2</sub> n = 1-8(+)	CH	Ar	
KH	CaH <sub>2</sub>	ScH <sub>2</sub>	TiH <sub>2</sub>	VH VH <sub>2</sub>	CrH	Mn	Fe	Co	(NiH)	CuH	ZnH <sub>2</sub>	GaH <sub>3</sub>	(Gr <sub>m</sub> H <sub>m+2</sub> ) m = 1-5(+)	AsH <sub>3</sub>	SeH <sub>2</sub>	BrH	Kr				
RbH	SrH <sub>2</sub>	YH <sub>2</sub> YH <sub>3</sub>	ZrH <sub>2</sub>	NbH NbH <sub>2</sub>	Mo	Tc	Ru	Rh	PdH<1	Ag	(CdH <sub>2</sub> ) ?	(InH <sub>3</sub> ) ?	SnH <sub>4</sub> Sn <sub>2</sub> H <sub>6</sub>	SbH <sub>3</sub>	TeH <sub>2</sub>	III	Xc				
CsH	BaH <sub>2</sub>	LaH <sub>2</sub> LaH <sub>3</sub>	HfH <sub>2</sub>	TaH	W	Re	Os	Ir	Pt	Au	(HgH <sub>2</sub> ) ?	(TlH <sub>3</sub> ) ?	PbH <sub>4</sub>	BiH <sub>3</sub>	(PoH <sub>2</sub> ) ?	AtH	Rn				
Fr	Ra	AcH <sub>2</sub>																			
			CeH <sub>2</sub> CeH <sub>3</sub>	PrH <sub>2</sub> PrH <sub>3</sub>	NdH <sub>2</sub> NdH <sub>3</sub>	Pm	SmH <sub>2</sub> SmH <sub>3</sub>	EuH <sub>2</sub>	GdH <sub>2</sub> GdH <sub>3</sub>	TbH <sub>2</sub> TbH <sub>3</sub>	DyH <sub>2</sub> DyH <sub>3</sub>	HoH <sub>2</sub> HoH <sub>3</sub>	ErH <sub>2</sub> ErH <sub>3</sub>	TmH <sub>2</sub> TmH <sub>3</sub>	YbH <sub>2</sub> YbH <sub>2.5</sub>	LuH <sub>2</sub> LuH <sub>3</sub>					
			ThH <sub>2</sub> Th <sub>4</sub> H <sub>15</sub>	PaH <sub>3</sub>	UH <sub>3</sub>	NpH <sub>2</sub> NpH <sub>3</sub>	PuH <sub>2</sub> PuH <sub>3</sub>	AmH <sub>2</sub> AmH <sub>3</sub>	CmH <sub>2</sub>	Bk	Cf	Es	Fm	Md	No	Lr					

Figure 3.12 The hydrides of the elements.

binary halides, oxides, sulfides, etc.: this serves to remind us that the various bond models represent grossly oversimplified limiting cases and that in most actual systems the position is more complex. For example, oxides might be classed as ionic (MgO), metallic (TiO, ReO<sub>3</sub>), covalent (CO<sub>2</sub>), polymeric (SiO<sub>2</sub>), or as intermediate between these various classes, though any adequate bonding theory would recognize the arbitrary nature of these distinctions which merely emphasize particular features of the overall assembly of molecular orbitals and electron populations.

The metals in Groups 1 and 2 of the periodic table react directly with hydrogen to form white, crystalline, stoichiometric hydrides of formula MX and MX<sub>2</sub> respectively. The salt-like character of these compounds was recognized by G. N. Lewis in 1916 and he suggested that they contained the hydride ion H<sup>-</sup>. Shortly thereafter

(1920) K. Moers showed that electrolysis of molten LiH (mp 692°C) gave the appropriate amount of hydrogen at the anode; the other hydrides tended to decompose before they could be melted. As expected, the ionic-bond model is most satisfactory for the later (larger) members of each group, and the tendency towards covalency becomes more marked for the smaller elements LiH, MgH<sub>2</sub>, and particularly BeH<sub>2</sub>, which is best described in terms of polymeric covalent bridge bonds. X-ray and neutron diffraction studies show that the alkali metal hydrides adopt the cubic NaCl structure (p. 242) whereas MgH<sub>2</sub> has the tetragonal TiO<sub>2</sub> (rutile type) structure (p. 961) and CaH<sub>2</sub>, SrH<sub>2</sub> and BaH<sub>2</sub> adopt the orthorhombic PbCl<sub>2</sub>-type structure (p. 382). The implied radius of the hydride ion H<sup>-</sup> (1s<sup>2</sup>) varies considerably with the nature of the metal because of the ready deformability of the pair of electrons surrounding a single proton. Typical values are

given below and these can be compared with  $r(\text{F}^-) \sim 133$  pm and  $r(\text{Cl}^-) \sim 184$  pm.

Compound	MgH <sub>2</sub>	LiH	NaH	KH	RbH	CsH	Free H <sup>-</sup> (calculated)
$r(\text{H}^-)/\text{pm}$	130	137	146	152	154	152	208

The closest M–M approach in these compounds is often less than for the metal itself: this should occasion no surprise since this is a common feature of many compounds in which there is substantial separation of charge. For example, the shortest Ca–Ca interatomic distance is 393 pm in calcium metal, 360 pm in CaH<sub>2</sub>, 380 pm in CaF<sub>2</sub>, and only 340 pm in CaO (why?).

The thermal stability of the alkali metal hydrides decreases from lithium to caesium, the temperature at which the reversible dissociation pressure of hydrogen reaches 10 mmHg being  $\sim 550^\circ\text{C}$  for LiH,  $\sim 210^\circ\text{C}$  for NaH and KH, and  $\sim 170^\circ\text{C}$  for RbH and CsH. The corresponding figures for the alkaline earth metal hydrides are CaH<sub>2</sub>  $885^\circ\text{C}$ , SrH<sub>2</sub>  $585^\circ\text{C}$  and BaH<sub>2</sub>  $230^\circ\text{C}$ , though for MgH<sub>2</sub> it is only  $85^\circ\text{C}$ . Chemical reactivity depends markedly on both the purity and the state of subdivision but increases from lithium to caesium and from calcium to barium with CaH<sub>2</sub> being rather less reactive than LiH. The reaction of water with these latter two compounds forms a convenient portable source of hydrogen, but with NaH the reaction is more violent than with sodium itself. RbH and CsH actually ignite spontaneously in dry air.

Turning next to Group 3, Fig. 3.12 indicates that hydrides of limiting stoichiometry MH<sub>2</sub> are also formed by Sc, Y, La, Ac and by most of the lanthanoids and actinoids. In the special case of EuH<sub>2</sub> (Eu<sup>II</sup> 4f<sup>7</sup>) and YbH<sub>2</sub> (Yb<sup>II</sup> 4f<sup>14</sup>) the hydrides are isostructural with CaH<sub>2</sub> and the ionic bonding model gives a reasonable description of the observed properties; however, YbH<sub>2</sub> can absorb more hydrogen up to about YbH<sub>2.5</sub>. The other hydrides adopt the fluorite (CaF<sub>2</sub>) crystal structure (p. 118) and the supernumerary valence electron is delocalized, thereby conferring considerable metallic conductivity. For example, LaH<sub>2</sub> is a dark-coloured, brittle compound with a conductivity of about  $10 \text{ ohm}^{-1} \text{ cm}^{-1}$  ( $\sim 1\%$  of

that of La metal). Further uptake of hydrogen progressively diminishes this conductivity to  $< 10^{-1} \text{ ohm}^{-1} \text{ cm}^{-1}$  for the cubic phase LaH<sub>3</sub> (cf.  $\sim 3 \times 10^{-5} \text{ ohm}^{-1} \text{ cm}^{-1}$  for YbH<sub>2</sub>). The other Group 3 elements and the lanthanoids and actinoids are similar.

There is a lively controversy concerning the interpretation of these and other properties, and cogent arguments have been advanced both for the presence of hydride ions H<sup>-</sup> and for the presence of protons H<sup>+</sup> in the d-block and f-block hydride phases.<sup>(64,66)</sup> These difficulties emphasize again the problems attending any classification based on presumed bond type, and a phenomenological approach which describes the observed properties is a sounder initial basis for discussion. Thus the predominantly ionic nature of a phase cannot safely be inferred either from crystal structure or from calculated lattice energies since many metallic alloys adopt the NaCl-type or CsCl-type structures (e.g. LaBi,  $\beta$ -brass) and enthalpy calculations are notoriously insensitive to bond type.

The hydrides of limiting composition MH<sub>3</sub> have complex structures and there is evidence that the third hydrogen is sometimes less strongly bound in the crystal. For the earlier (larger) lanthanoids La, Ce, Pr and Nd, hydrogen enters octahedral sites and LnH<sub>3</sub> has the cubic Li<sub>3</sub>Bi structure.<sup>(57)</sup> For Y and the smaller lanthanoids Sm, Gd, Tb, Dy, Ho, Er, Tm and Lu, as well as for the actinoids Np, Pu and Am, the hexagonal HoH<sub>3</sub> structure is adopted. This is a rather complex structure based on an extended unit cell containing 6 Ho and 18 H atoms.<sup>(68)</sup> The idealized structure has hcp Ho atoms with 12 tetrahedrally coordinated H atoms and 6 octahedrally coordinated H atoms; however, to make room for the bulky Ho atoms, close pairs of tetrahedral H atoms are slightly displaced and there is a more substantial movement of the "octahedral" H atoms towards the planes of the Ho atoms so that 2 of the H atoms are actually in the Ho planes and are trigonal 3-coordinate. The

<sup>68</sup> M. MANSMANN and W. E. WALLACE *J. de Physique* **25**, 454–9 (1964).

hydrogen atoms are thus of three types having respectively 14, 11, and 9 H neighbours for the distorted trigonal, octahedral and tetrahedral sites. Each H atom has 3 Ho neighbours at either 210 or 217 or 224–299 pm respectively, and each Ho has 11 hydrogen neighbours, 9 at 210–229 pm and 2 somewhat further away at 248 pm. The 3-coordinate hydrogen is most unusual, the only other hydride in which it occurs being the complex cubic phase  $\text{Th}_4\text{H}_{15}$ .

Uranium forms two hydrides of stoichiometric composition  $\text{UH}_3$ . The normal  $\beta$ -form has a complex cubic structure and is the only one formed when the preparation is carried out above  $200^\circ\text{C}$ . Below this temperature increasing amounts of the slightly denser cubic  $\alpha$ -form occur and this can be transformed to the  $\beta$ -phase by warming to  $250^\circ\text{C}$ . Both phases have ferromagnetic and metallic properties. Uranium hydride is commonly used as a starting material for the preparation of uranium compounds as it is finely powdered and extremely reactive. It is also used for purifying and regenerating hydrogen (or deuterium) gas.

The hydrides of Ti, Zr and Hf are characterized by considerable variability in composition and structure. When pure, the limiting phases  $\text{MH}_2$  form massive, metallic crystals of fluorite structure ( $\text{TiH}_2$ ) or body-centred tetragonal structure ( $\text{ZrH}_2$ ,  $\text{HfH}_2$ ,  $\text{ThH}_2$ ), but there are also several hydrogen-deficient phases of variable composition and complex structure in which several M–H distances occur.<sup>(57,64,66)</sup> These phases (and others based on Y, Ce and Nb) have been extensively investigated in recent years because of their potential applications as moderators, reflectors, or shield components for high-temperature, mobile nuclear reactors.

Other hydrides with interstitial or metallic properties are formed by V, Nb and Ta; they are, however, very much less stable than the compounds we have been considering and have extensive ranges of composition. Chromium also forms a hydride,  $\text{CrH}$ , though this must be prepared electrolytically rather than by direct reaction of the metal with hydrogen. It has the anti-NiAs structure (p. 555). Most other elements

in this area of the periodic table have little or no affinity for hydrogen and this has given rise to the phrase “hydrogen gap”. The notable exception is the palladium–hydrogen system which is discussed on p. 1150.

The hydrides of the later main-group elements present few problems of classification and are best discussed during the detailed treatment of the individual elements. Many of these hydrides are covalent, molecular species, though association via H bonding sometimes occurs, as already noted (p. 53). Catenation flourishes in Group 14 and the complexities of the boron hydrides merit special attention (p. 151). The hydrides of aluminium, gallium, zinc (and beryllium) tend to be more extensively associated via M–H–M bonds, but their characterization and detailed structural elucidation has proved extremely difficult.

Two further important groups of hydride compounds should be mentioned and will receive detailed attention in later chapters. One is the group of complex metal hydrides of which notable examples are  $\text{LiBH}_4$ ,  $\text{NaBH}_4$ ,  $\text{LiAlH}_4$ ,  $\text{Al}(\text{BH}_4)_3$ , etc.<sup>(69)</sup> The other is the growing number of compounds in which the hydrogen atom is a monodentate or bidentate (bridging) ligand to a transition element.<sup>(70–73)</sup> these date from the early 1930s when W. Hieber discovered  $[\text{Fe}(\text{CO})_4\text{H}_2]$  and  $[\text{Co}(\text{CO})_4\text{H}]$  and now cover an astonishing variety of structural types. The modest steric requirements of the H atom enable complexes such as  $[\text{ReH}_9]^{2-}$  to be synthesized, and bridged complexes such as the linear  $[\text{Cr}_2(\text{CO})_{10}\text{H}]^-$  and bent  $[\text{W}_2(\text{CO})_9\text{H}(\text{NO})]$ , are known. For  $\eta^2\text{-H}_2$  complexes see pp. 44–7. The role of hydrido complexes in homogeneous catalysis is also exciting considerable attention.

<sup>69</sup> A. HAJOS, *Complex Hydrides*, Elsevier, Amsterdam, 1979, 398 pp.

<sup>70</sup> J. C. GREEN and M. L. H. GREEN, *Comprehensive Inorganic Chemistry*, Vol. 4, Chap. 48, Pergamon Press, Oxford, 1973.

<sup>71</sup> H. D. KAESZ and R. B. SAILLANT, *Chem. Rev.* **72**, 231–81 (1972).

<sup>72</sup> A. P. HUMPHRIES and H. D. KAESZ, *Progr. Inorg. Chem.* **25**, 145–222 (1979).

<sup>73</sup> G. L. GEOFFROY, *Progr. Inorg. Chem.* **27**, 123–51 (1980).

																		1	2																						
																		H	He																						
3	4																	5	6	7	8	9	10	11	12																
Li	Be																	B	C	N	O	F	Ne																		
13	14	15	16	17	18												19	20	21	22	23	24	25	26																	
Na	Mg	Al	Si	P	S	Cl	Ar												K	Ca	Sc	Ti	V	Cr	Mn	Fe	Co	Ni	Cu	Zn											
27	28	29	30	31	32	33	34	35	36	37	38	39	40	41	42	43	44	45	46	47	48	49	50	51	52	53	54														
K	Ca	Sc	Ti	V	Cr	Mn	Fe	Co	Ni	Cu	Zn	Ga	Ge	As	Se	Br	Kr	Rb	Sr	Y	Zr	Nb	Mo	Tc	Ru	Rh	Pd	Ag	Cd	In	Sn	Sb	Te	I	Xe						
55	56	57	58	59	60	61	62	63	64	65	66	67	68	69	70	71	72	73	74	75	76	77	78	79	80	81	82	83	84	85	86	87	88	89	90						
Fr	Ra	Ac	Rf	Db	Sg	Bh	Hs	Mt	Uun	Uuu	Uub	Tl	Pb	Bi	Po	At	Rn	Cs	Ba	La	Hf	Ta	W	Re	Os	Ir	Pt	Au	Hg	Tl	Pb	Bi	Po	At	Rn						
91	92	93	94	95	96	97	98	99	100	101	102	103	104	105	106	107	108	109	110	111	112	113	114	115	116	117	118	119	120	121	122	123	124	125	126						
Th	Pa	U	Np	Pu	Am	Cm	Bk	Cf	Es	Fm	Md	No	Lr	Lu	Hf	Ta	W	Re	Os	Ir	Pt	Au	Hg	Tl	Pb	Bi	Po	At	Rn	Fr	Ra	Ac	Rf	Db	Sg	Bh	Hs	Mt	Uun	Uuu	Uub

# 4

## *Lithium, Sodium, Potassium, Rubidium, Caesium and Francium*

### 4.1 Introduction

The alkali metals form a homogeneous group of extremely reactive elements which illustrate well the similarities and trends to be expected from the periodic classification, as discussed in Chapter 2. Their physical and chemical properties are readily interpreted in terms of their simple electronic configuration,  $ns^1$ , and for this reason they have been extensively studied by the full range of experimental and theoretical techniques. Compounds of sodium and potassium have been known from ancient times and both elements are essential for animal life. They are also major items of trade, commerce and chemical industry. Lithium was first recognized as a separate element at the beginning of the nineteenth century but did not assume major industrial importance until about 40 y ago. Rubidium and caesium are of considerable academic interest but so far have few industrial applications. Francium, the elusive element 87, has only fleeting existence in nature due to its very short radioactive half-life, and this delayed its discovery until 1939.

### 4.2 The Elements

#### 4.2.1 *Discovery and isolation*

The spectacular success (in 1807) of Humphry Davy, then aged 29 y, in isolating metallic potassium by electrolysis of molten caustic potash (KOH) is too well known to need repeating in detail.<sup>(1)</sup> Globules of molten sodium were similarly prepared by him a few days later from molten caustic soda. Earlier experiments with aqueous solutions had been unsuccessful because of the great reactivity of these new elements. The names chosen by Davy reflect the sources of the elements.

Lithium was recognized as a new alkali metal by J. A. Arfvedson in 1817 whilst he was working as a young assistant in J. J. Berzelius's laboratory. He noted that Li compounds were similar to those of Na and K but that the carbonate and hydroxide were much less soluble

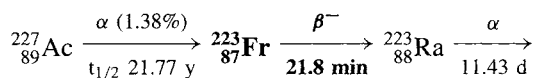
<sup>1</sup> M. E. WEEKS, *Discovery of the Elements*, Journal of Chemical Education, Easton, 6th edn., 1956, 910 pp.



in water. Lithium was first isolated from the sheet silicate mineral petalite,  $\text{LiAlSi}_4\text{O}_{10}$ , and Arfvedson also showed it was present in the pyroxene silicate spodumene,  $\text{LiAlSi}_2\text{O}_6$ , and in the mica lepidolite, which has an approximate composition  $\text{K}_2\text{Li}_3\text{Al}_4\text{Si}_7\text{O}_{21}(\text{OH},\text{F})_3$ . He chose the name lithium (Greek  $\lambda\iota\theta\omicron\varsigma$ , stone) to contrast it with the vegetable origin of Davy's sodium and potassium. Davy isolated the metal in 1818 by electrolysing molten  $\text{Li}_2\text{O}$ .

Rubidium was discovered as a minor constituent of lepidolite by R. W. Bunsen and G. R. Kirchhoff in 1861 only a few months after their discovery of caesium (1860) in mineral spa waters. These two elements were the first to be discovered by means of the spectroscope, which Bunsen and Kirchhoff had invented the previous year (1859); accordingly their names refer to the colour of the most prominent lines in their spectra (Latin *rubidus*, deepest red; *caesius*, sky blue).

Francium was first identified in 1939 by the elegant radiochemical work of Marguerite Perey who named the element in honour of her native country. It occurs in minute traces in nature as a result of the rare (1.38%) branching decay of  $^{227}\text{Ac}$  in the  $^{235}\text{U}$  series:



Its terrestrial abundance has been estimated as  $2 \times 10^{-18}$  ppm, which corresponds to a total of only 15 g in the top 1 km of the earth's crust. Other isotopes have since been produced by nuclear reactions but all have shorter half-lives than  $^{223}\text{Fr}$ , which decays by energetic  $\beta^-$  emission,  $t_{1/2}$  21.8 min. Because of this intense radioactivity it is only possible to work with tracer amounts of the element.

#### 4.2.2 Terrestrial abundance and distribution

Despite their chemical similarity, Li, Na and K are not closely associated in their occurrence, mainly because of differences in size (see

Table on p. 75). Lithium tends to occur in ferromagnesian minerals where it partly replaces magnesium; it occurs to the extent of about 18 ppm by weight in crustal rocks, and this reflects its relatively low abundance in the cosmos (Chapter 1). It is about as abundant as gallium (19 ppm) and niobium (20 ppm). The most important mineral commercially is spodumene,  $\text{LiAlSi}_2\text{O}_6$ , and large deposits occur in the USA, Canada, Brazil, Argentina, the former USSR, Spain, China, Zimbabwe and the Congo. An indication of the industrial uses of lithium and its compounds is given in the Panel. World production of lithium compounds in 1994 corresponded to some 5700 tonnes of contained lithium (equivalent to 30 000 tonnes of lithium carbonate) of which over 70% was in the USA.

Sodium, 22 700 ppm (2.27%) is the seventh most abundant element in crustal rocks and the fifth most abundant metal, after Al, Fe, Ca and Mg. Potassium (18 400 ppm) is the next most abundant element after sodium. Vast deposits of both Na and K salts occur in relatively pure form on all continents as a result of evaporation of ancient seas, and this process still continues today in the Great Salt Lake (Utah), the Dead Sea and elsewhere. Sodium occurs as rock-salt (NaCl) and as the carbonate (trona), nitrate (saltpetre), sulfate (mirabilite), borate (borax, kernite), etc. Potassium occurs principally as the simple chloride (sylvite), as the double chloride  $\text{KCl}\cdot\text{MgCl}_2\cdot 6\text{H}_2\text{O}$  (carnallite) and the anhydrous sulfate  $\text{K}_2\text{Mg}_2(\text{SO}_4)_3$  (langbeinite). There are also unlimited supplies of NaCl in natural brines and oceanic waters ( $\sim 30 \text{ kg m}^{-3}$ ). Thus, it has been calculated that rock-salt equivalent to the NaCl in the oceans of the world would occupy 19 million cubic km (i.e. 50% more than the total volume of the North American continent above sea-level). Alternatively stated, a one-km square prism would stretch from the earth to the moon 47 times. Note also that, although Na and K are almost equally abundant in the crustal rocks of the earth, Na is some 30 times as abundant as K in the oceans. This is partly because K salts with the larger anions tend to be less soluble than the Na salts and, likewise, K is more strongly bound to

### Lithium and its Compounds<sup>(2-4)</sup>

The dramatic transformation of Li from a small-scale specialist commodity to a multikilotonne industry during the past three decades is due to the many valuable properties of its compounds. About 35 compounds of Li are currently available in bulk, and a similar number again can be obtained in developmental or research quantities. A major industrial use of Li is in the form of **lithium stearate** which is used as a thickener and gelling agent to transform oils into lubricating greases. These "all-purpose" greases combine high water resistance with good low-temperature properties ( $-20^{\circ}\text{C}$ ) and excellent high-temperature stability ( $>150^{\circ}\text{C}$ ); they are readily prepared from  $\text{LiOH}\cdot\text{H}_2\text{O}$  and tallow or other natural fats and have captured nearly half the total market for automotive greases in the USA.

**Lithium carbonate** is the most important industrial compound of lithium and is the starting point for the production of most other lithium compounds. It is also used as a flux in porcelain enamel formulations and in the production of special toughened glasses (by replacement of the larger Na ions): Li can either be incorporated within the glass itself or the preformed Na-glass can be dipped in a molten-salt bath containing Li ions to effect a surface cation exchange. In another application, the use of  $\text{Li}_2\text{CO}_3$  by primary aluminium producers has risen sharply in recent years since it increases production capacity by 7–10% by lowering the mp of the cell content and permitting larger current flow; in addition, troublesome fluorine emissions are reduced by 25–50% and production costs are appreciably lowered. In 1987 the price for bulk quantities of  $\text{Li}_2\text{CO}_3$  in the USA was \$3.30 per kg.

The first commercial use of **Li metal** (in the 1920s) was as an alloying agent with lead to give toughened bearings; currently it is used to produce high-strength, low-density aluminium alloys for aircraft construction. With magnesium it forms an extremely tough low-density alloy which is used for armour plate and for aerospace components (e.g. LA 141,  $d$   $1.35\text{ g cm}^{-3}$ , contains 14% Li, 1% Al, 85% Mg). Other metallurgical applications employ **LiCl** as an invaluable brazing flux for Al automobile parts.

**LiOH** is used in the manufacture of lithium stearate greases (see above) and for  $\text{CO}_2$  absorption in closed environments such as space capsules (light weight) and submarines. **LiH** is used to generate hydrogen in military, meteorological, and other applications, and the use of **LiD** in thermonuclear weaponry and research has been mentioned (p. 18). Likewise, the important applications of  **$\text{LiAlH}_4$** ,  **$\text{Li/NH}_3$**  and **organolithium reagents** in synthetic organic chemistry are well known, though these account for only a small percentage of the lithium produced. Other specialist uses include the growing market for ferroelectrics such as  **$\text{LiTaO}_3$**  to modulate laser beams (p. 57), and increasing use of thermoluminescent **LiF** in X-ray dosimetry.

Perhaps one of the most exciting new applications stems from the discovery in 1949 that small daily doses (1–2 g) of  **$\text{Li}_2\text{CO}_3$**  taken orally provide an effective treatment for manic-depressive psychoses. The mode of action is not well understood but there appear to be no undesirable side effects. The dosage maintains the level of Li in the blood at about  $1\text{ mmol l}^{-1}$  and its action may be related to the influence of Li on the Na/K balance and (or) the Mg/Ca balance since Li is related chemically to both pairs of elements.

Looking to the future,  **$\text{Li/FeS}_x$**  battery systems are emerging as a potentially viable energy storage system for off-peak electricity and as a non-polluting silent source of power for electric cars. The battery resembles the conventional lead-acid battery in having solid electrodes ( **$\text{Li/Si}$**  alloy, negative;  **$\text{FeS}_x$**  positive) and a liquid electrolyte (molten  **$\text{LiCl/KCl}$**  at  $400^{\circ}\text{C}$ ). Other battery systems which have reached the prototype stage include the  **$\text{Li/S}$**  and  **$\text{Na/S}$**  cells (see p. 678).

the complex silicates and alumino silicates in the soils (ion exchange in clays). Again, K leached from rocks is preferentially absorbed and used by plants whereas Na can proceed to the sea. Potassium is an essential element for plant life and the growth of wild plants is often limited by the supply of K available to them.

The vital importance of NaCl in the heavy chemical industry is indicated in the Panel opposite, and information on potassium salts is given in the Panel on p. 73.

Rubidium (78 ppm, similar to Ni, Cu, Zn) and caesium (2.6 ppm, similar to Br, Hf, U) are much less abundant than Na and K and have only recently become available in quantity. No purely Rb-containing mineral is known and much of the commercially available material is obtained as a byproduct of lepidolite processing for Li. Caesium occurs as the hydrated aluminosilicate pollucite,  **$\text{Cs}_4\text{Al}_4\text{Si}_9\text{O}_{26}\cdot\text{H}_2\text{O}$** , but the world's only commercial source is at Bernic Lake,

<sup>2</sup> Kirk-Othmer *Encyclopedia of Chemical Technology*, 4th edn., 1995, Vol 15, pp. 434–63.

<sup>3</sup> J. E. LLOYD in R. THOMPSON (ed.) *Speciality Inorganic Chemicals*, Royal Society of Chemistry, London, 1981, pp. 98–122.

<sup>4</sup> W. BÜCHNER, R. SCHLIEBS, G. WINTER and K. H. BÜCHEL, *Industrial Inorganic Chemistry*, VCH, New York, 1989, pp. 215–8.

### Production and Uses of Salt<sup>(5-7)</sup>

More NaCl is used for inorganic chemical manufacture than is any other material. It is approached only by phosphate rock, and world consumption of each exceeds 150 million tonnes annually, the figure for NaCl in 1982 being 168.7 million tonnes. Production is dominated by Europe (39%), North America (34%) and Asia (20%), whilst South America and Oceania have only 3% each and Africa 1%. Rock-salt occurs as vast subterranean deposits often hundreds of metres thick and containing >90% NaCl. The Cheshire salt field (which is the principal UK source of NaCl) is typical, occupying an area of 60 km × 24 km and being some 400 m thick: this field alone corresponds to reserves of >10<sup>11</sup> tonnes. Similar deposits occur near Carlsbad New Mexico, in Saskatchewan Canada and in many other places. Production methods vary with locality and with the use to be made of the salt. For example, in the UK 82% is extracted as brine for direct use in the chemical industry and 18% is mined as rock-salt, mainly for use on roads; less than 1% is obtained by solar evaporation. By contrast, in the USA only 55% comes from brine, whereas 32% is mined as rock salt, 8% is obtained by vacuum pan evaporation, 4% by solar evaporation and 1% by the open pan process.

Major sections of the inorganic heavy chemicals industry are based on salt and, indeed, this compound was the very starting point of the chemical industry. Nicolas Leblanc (1742-1806), physician to the Duke of Orleans, devised a satisfactory process for making NaOH from NaCl in 1787 (Patent 1791) and this achieved enormous technological significance in Europe during most of the nineteenth century as the first industrial chemical process to be worked on a really large scale. It was, however, never important in the USA since it was initially cheaper to import from Europe and, by the time the US chemical industry began to develop in the last quarter of the century, the Leblanc process had been superseded by the electrolytic process. Thus in 1874 world production of NaOH was 525 000 tonnes of which 495 000 were by the Leblanc process; by 1902 production had risen to 1 800 000 tonnes, but only 150 000 tonnes of this was Leblanc. Despite its long history, there is still great scope for innovation and development in the chlor-alkali and related industries. For example, in recent years there has been a steady switch from mercury electrolysis cells to diaphragm and membrane cells for environmental and economic reasons.<sup>(7)</sup> Similarly, the ammonia-soda (Solvay) process for Na<sub>2</sub>CO<sub>3</sub> is being phased out because of the difficulty of disposing of embarrassing byproducts such as NH<sub>4</sub>Cl and CaCl<sub>2</sub>, coupled with the increasing cost of NH<sub>3</sub> and the possibility of direct mining for trona, Na<sub>2</sub>CO<sub>3</sub>·NaHCO<sub>3</sub>·2H<sub>2</sub>O. The closely interlocking chemical processes based on salt are set out in the flow sheet (Fig. 4.1). The detailed balance of the processes differs somewhat in the various industrial nations but data for the usage of salt in the USA are typical: of the 34.8 million tonnes consumed in 1982, 48% was used for chlor-alkali production and Na<sub>2</sub>CO<sub>3</sub>, 24% for the salting of roads, 6% for food and food processing, 5% for animal feeds, 5% for various industries such as paper pulp, textiles, metal manufacturing and the rubber and oil industries, 2% for all other chemical manufacturing, and the remaining 10% for a wide variety of other purposes. Further discussion on the industrial production and uses of many of these chemicals (e.g. NaOH, Na<sub>2</sub>CO<sub>3</sub>, Na<sub>2</sub>SO<sub>4</sub>) is given on p. 89.

Current industrial prices are ~\$5 per tonne for salt in brine and ~\$55 per tonne for solid salt, depending on quality.

Manitoba and Cs (like Rb) is mainly obtained as a byproduct of the Li industry. The intense interest in Li for thermonuclear purposes since about 1958, coupled with its extensive use in automotive greases (p. 70), has consequently made Rb and Cs compounds much more available than formerly: annual production is in the region of 5 tonnes for each.

### 4.2.3 Production and uses of the metals

Most commercial Li ores have 1-3% Li and this is increased by flotation to 4-6%. Spodumene, LiAlSi<sub>2</sub>O<sub>6</sub>, is heated to ~1100° to convert the α-form into the less-dense, more friable β-form, which is then washed with H<sub>2</sub>SO<sub>4</sub> at 250°C and water-leached to give Li<sub>2</sub>SO<sub>4</sub>·H<sub>2</sub>O. Successive treatment with Na<sub>2</sub>CO<sub>3</sub> and HCl gives Li<sub>2</sub>CO<sub>3</sub> (insol) and LiCl. Alternatively, the chloride can be obtained by calcining the washed ore with limestone (CaCO<sub>3</sub>) at 1000° followed by water leaching to give LiOH and then treatment with HCl. Recovery from natural brines is also extensively used in the USA (Searles Lake, California and Clayton Valley, Nevada).

<sup>5</sup> L. F. HABER, *The Chemical Industry during the Nineteenth Century*, Oxford University Press, Oxford, 1958, 292 pp. T. K. DERRY and T. I. WILLIAMS, *A Short History of Chemical Technology*, Oxford University Press, Oxford, 1960, 782 pp.

<sup>6</sup> *Kirk-Othmer Encyclopedia of Chemical Technology*, 3rd edn., 1983, Vol. 21 pp. 205-23.

<sup>7</sup> W. BÜCHNER, R. SCHLIEBS, G. WINTER and K. H. BÜCHEL, *Industrial Inorganic Chemistry*, VCH, New York, 1989, 149 ff., 218 ff.

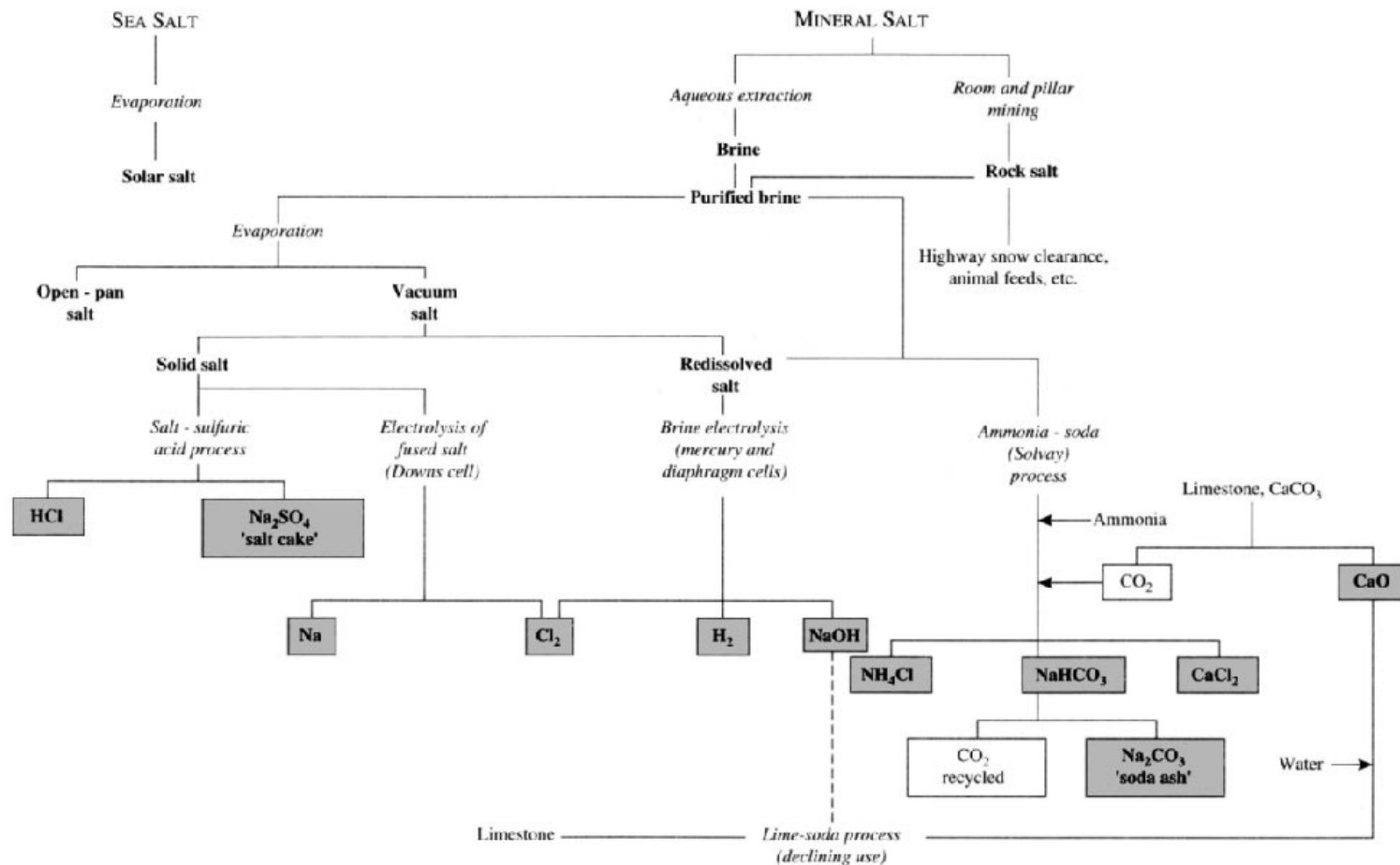


Figure 4.1 Flow sheet on chemical processes based on salt.

### Production of Potassium Salts<sup>(8-10)</sup>

Sylvite (KCl) and sylvinit (mixed NaCl, KCl) are the most important K minerals for chemical industry; carnallite is also mined. Ocean waters contain only about 0.06% KCl, though this can rise to as high as 1.5% in some inland marshes and seas such as Searle's Lake, the Great Salt Lake, or the Dead Sea, thereby making recovery economically feasible. Soluble minerals of K are generally referred to (incorrectly) as potash, and production figures are always expressed as the weight of K<sub>2</sub>O equivalent. Massive evaporite beds of soluble K salts were first discovered at Stassfurt, Germany, in 1856 and were worked there for potash and rock-salt from 1861 until 1972. World production was 28.6 million tonnes K<sub>2</sub>O equivalent in 1986 of which 35% was produced in the USSR and 24% Canada.

In the UK workable potash deposits are confined to the Cleveland-North Yorkshire bed which is ~11 m thick and has reserves of >500 million tonnes. Massive recovery is also possible from brines; e.g. Jordan has a huge plant capable of recovering up to a million tonnes pa from the Dead Sea and the annual production by this country and by Israel now matches that of the USA and France.

Potassium is a major essential element for plant growth and potassic fertilizers account for the overwhelming proportion of production (95%). Again KCl is dominant, accounting for more than 90% of the K used in fertilizers; K<sub>2</sub>SO<sub>4</sub> is also used. KNO<sub>3</sub>, though an excellent fertilizer, is now of only minor importance because of production costs. In addition to its dominant use in fertilizers, KCl is used mainly to manufacture KOH by electrolysis using the mercury and membrane processes (about 0.7 million tonnes of KOH worldwide in 1985). This in turn is used to make a variety of other compounds and materials such as those listed below (the figures referring to the percentage usage of KOH in the USA in 1984): K<sub>2</sub>CO<sub>3</sub> 25%, liquid fertilizers 15%, soaps 10%, liquid detergents (K<sub>4</sub>P<sub>2</sub>O<sub>7</sub>) 9%, synthetic rubber 5%, crop protection agents 3%, KMnO<sub>4</sub> 2%, other chemicals 26% and export 5%. The manufacture of metallic K is relatively minor, the world production in 1994 amounting only to about 500 tonnes. Prices in 1994 were \$30-40 per kg for bulk K and \$16-22 per kg for NaK (78% K).

The main industrial uses of potassium compounds other than KCl and KOH are:

K<sub>2</sub>CO<sub>3</sub> (from KOH and CO<sub>2</sub>), used chiefly in high-quality decorative glassware, in optical lenses, colour TV tubes and fluorescent lamps; it is also used in china ware, textile dyes and pigments.

KNO<sub>3</sub>, a powerful oxidizing agent now used mainly in gunpowders and pyrotechnics, and in fertilizers.

KMnO<sub>4</sub>, an oxidizer, decolorizer, bleacher and purification agent; its major application is in the manufacture of saccharin.

KO<sub>2</sub>, used in breathing apparatus (p. 74).

KClO<sub>3</sub>, used in small amounts in matches and explosives (pp. 509, 862).

KBr, used extensively in photography and as the usual source of bromine in organic syntheses; formerly used as a sedative.

It is interesting to note the effect of varying the alkali metal cation on the properties of various compounds and industrial materials. For example, a soap is an alkali metal salt formed by neutralizing a long-chain organic acid such as stearic acid, CH<sub>3</sub>(CH<sub>2</sub>)<sub>16</sub>CO<sub>2</sub>H, with MOH. Potassium soaps are soft and low melting, and are therefore used in liquid detergents. Sodium soaps have higher mp's and are the basis for the familiar domestic "hard soaps" or bar soaps. Lithium soaps have still higher mp's and are therefore used as thickening agents for high-temperature lubricating oils and greases — their job is to hold the oil in contact with the metal under conditions when the oil by itself would run off.

The metal is obtained by electrolysis of a fused mixture of 55% LiCl, 45% KCl at ~450°C, the first commercial production being by Metallgesellschaft AG, in Germany, 1923. Current world production of Li metal is about 1000 tonnes pa. Far greater tonnages of Li compounds are, of course, produced and their major commercial applications have already been noted (p. 70).

Sodium metal is produced commercially on the kilotonne scale by the electrolysis of a fused eutectic mixture of 40% NaCl, 60% CaCl<sub>2</sub> at ~580°C in a Downs cell (introduced by du Pont, Niagara Falls, 1921). Metallic Na and Ca are liberated at the cylindrical steel cathode and rise through a cooled collecting pipe which allows the calcium to solidify and fall back into the melt. Chlorine liberated at the central graphite anode is collected in a nickel dome and subsequently purified. Potassium cannot be produced in this way because it is too soluble in the molten chloride to float on top of the cell for collection and because it vaporizes readily

<sup>8</sup> Kirk-Othmer Encyclopedia of Chemical Technology, 4th edn., 1996, Vol. 19, pp. 1047-92.

<sup>9</sup> P. CROWSON, *Minerals Handbook 1988-89*, Stockton Press, New York, 1988, pp. 216-21

<sup>10</sup> Ref. 7 pp. 228-31.

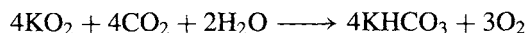
at the operating temperatures, creating hazardous conditions. Superoxide formation is an added difficulty since this reacts explosively with K metal. Consequently, commercial production of K relies on reduction of molten KCl with metallic Na at 850°C.<sup>†</sup> A similar process using Ca metal at 750°C under reduced pressure is used to produce metallic Rb and Cs.

Industrial uses of Na metal reflect its strong reducing properties. Much of the world production was used to make PbEt<sub>4</sub> (or PbMe<sub>4</sub>) for gasoline antiknocks via the high-pressure reaction of alkyl chlorides with Na/Pb alloy, though this use is declining rapidly for environmental reasons. A further major use is to produce Ti, Zr and other metals by reduction of their chlorides, and a smaller amount is used to make compounds such as NaH, NaOR and Na<sub>2</sub>O<sub>2</sub>. Sodium dispersions are also a valuable catalyst for the production of some artificial rubbers and elastomers. A growing use is as a heat-exchange liquid in fast breeder nuclear reactors where sodium's low mp, low viscosity and low neutron absorption cross-section combine with its exceptionally high heat capacity and thermal conductivity to make it (and its alloys with K) the most-favoured material.<sup>(11)</sup> The annual production of metallic Na in the USA fell steadily from 170 000 tonnes in 1974 to 86 000 tonnes in 1985 and is still falling. Potassium metal, being more difficult and expensive to produce, is manufactured on a much smaller scale. One of its main uses is to make the superoxide KO<sub>2</sub> by direct combustion; this compound is used in breathing masks as an auxiliary supply of O<sub>2</sub> in mines, submarines and space vehicles:



<sup>†</sup> This reduction of KCl by Na appears to be contrary to the normal order of reactivity (K > Na). However, at 850–880° an equilibrium is set up:  $\text{Na}(\text{g}) + \text{K}^+(\text{l}) \rightleftharpoons \text{Na}^+(\text{l}) + \text{K}(\text{g})$ . Since K is the more volatile (p. 75), it distils off more readily, thus displacing the equilibrium and allowing the reaction to proceed. By fractional distillation through a packed tower, K of 99.5% purity can be obtained but usually an Na/K mixture is drawn off because alloys with 15–55% Na are liquid at room temperature and therefore easier to transport.

<sup>11</sup> C. C. ADDISON, *The Chemistry of Liquid Alkali Metals*, Wiley, Chichester, 1984, 330 pp.



An indication of the relative cost of the alkali metals in bulk at 1980–82 prices (USA) is:

Metal	Li	Na	K	Rb	Cs
Price/\$ kg <sup>-1</sup>	36.3	1.50	34.4	827	716
Relative cost (per kg)	24	1	23	550	477
Relative cost (per mol)	7.3	1	39	2050	2760

#### 4.2.4 Properties of the alkali metals

The Group 1 elements are soft, low-melting metals which crystallize with bcc lattices. All are silvery-white except caesium which is golden yellow;<sup>(12)</sup> in fact, caesium is one of only three metallic elements which are intensely coloured, the other two being copper and gold (see also pp. 112, 1177, 1232). Lithium is harder than sodium but softer than lead. Atomic properties are summarized in Table 4.1 and general physical properties are in Table 4.2. Further physical properties of the alkali metals, together with a review of the chemical properties and industrial applications of the metals in the molten state are in ref. 11.

Lithium has a variable atomic weight (p. 18) whereas sodium and caesium, being mononucleidic, have very precisely known and invariant atomic weights. Potassium and rubidium are both radioactive but the half-lives of their radioisotopes are so long that the atomic weight does not vary significantly from this cause. The large size and low ionization energies of the alkali metals compared with all other elements have already been noted (pp. 23–5) and this confers on the elements their characteristic properties. The group usually shows smooth trends in properties, and the weak bonding of the single valence electron leads to low mp, bp and density, and low heats of sublimation, vaporization and dissociation. Conversely, the elements have large atomic and ionic radii and extremely high thermal and electrical conductivity. Lithium is the smallest element in the group and has the highest ionization energy, mp and heat

<sup>12</sup> R. J. MOOLENAAR, *Journal of Metals* 16, 21–4 (1964).

Table 4.1 Atomic properties of the alkali metals

Property	Li	Na	K	Rb	Cs	Fr
Atomic number	3	11	19	37	55	87
Number of naturally occurring isotopes	2	1	2 + 1 <sup>(a)</sup>	1 + 1 <sup>(a)</sup>	1	1 <sup>(a)</sup>
Atomic weight	6.941(2)	22.989 768(6)	39.0983(1)	85.4678(3)	132.90543(5)	(223)
Electronic configuration	[He]2s <sup>1</sup>	[Ne]3s <sup>1</sup>	[Ar]4s <sup>1</sup>	[Kr]5s <sup>1</sup>	[Xe]6s <sup>1</sup>	[Rn]7s <sup>1</sup>
Ionization energy/kJ mol <sup>-1</sup>	520.2	495.8	418.8	403.0	375.7	~375
Electron affinity/kJ mol <sup>-1</sup>	59.8	52.9	46.36	46.88	45.5	(44.0)
$\Delta H_{\text{dissoc}}/\text{kJ mol}^{-1}$ (M <sub>2</sub> )	106.5	73.6	57.3	45.6	44.77	—
Metal radius/pm	152	186	227	248	265	—
Ionic radius (6-coordinate)/pm	76	102	138	152	167	(180)
$E^\circ/\text{V}$ for $\text{M}^+(\text{aq}) + \text{e}^- \longrightarrow \text{M}(\text{s})$	-3.045	-2.714	-2.925	-2.925	-2.923	—

(a) Radioactive: <sup>40</sup>K  $t_{1/2}$  1.277 × 10<sup>9</sup> y; <sup>87</sup>Rb  $t_{1/2}$  4.75 × 10<sup>10</sup> y; <sup>223</sup>Fr  $t_{1/2}$  21.8 min.

Table 4.2 Physical properties of the alkali metals

Property	Li	Na	K	Rb	Cs
MP/°C	180.6	97.8	63.7	39.5	28.4
BP/°C	1342	883	759	688	671
Density (20°C)/g cm <sup>-3</sup>	0.534	0.968	0.856	1.532	1.90
$\Delta H_{\text{fus}}/\text{kJ mol}^{-1}$	2.93	2.64	2.39	2.20	2.09
$\Delta H_{\text{vap}}/\text{kJ mol}^{-1}$	148	99	79	76	67
$\Delta H_{\text{f}}$ (monatomic gas)/kJ mol <sup>-1</sup>	162	108	89.6	82.0	78.2
Electrical resistivity (25°C)/μohm cm	9.47	4.89	7.39	13.1	20.8

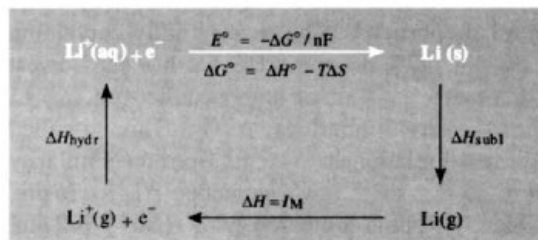
of atomization; it also has the lowest density of any solid at room temperature.

All the alkali metals have characteristic flame colorations due to the ready excitation of the outermost electron, and this is the basis of their analytical determination by flame photometry or atomic absorption spectroscopy. The colours and principal emission (or absorption) wavelengths,  $\lambda$ , are given below but it should be noted that these lines do not all refer to the same transition; for example, the Na D-line doublet at 589.0, 589.6 nm arises from the 3s<sup>1</sup> – 3p<sup>1</sup> transition in Na atoms formed by reduction of Na<sup>+</sup> in the flame, whereas the red line for lithium is associated with the short-lived species LiOH.

Element	Li	Na	K	Rb	Cs
Colour	Crimson	Yellow	Violet	Red-violet	Blue
$\lambda/\text{nm}$	670.8	589.2	766.5	780.0	455.5

The reduction potential for lithium appears at first sight to be anomalous and is one of the

few properties that does not show a smooth trend with increasing atomic number in the group. This arises from the small size and very large hydration energy of the free gaseous lithium ion. The standard reduction potential  $E^\circ$  refers to the reaction  $\text{Li}^+(\text{aq}) + \text{e}^- \longrightarrow \text{Li}(\text{s})$  and is related to the free-energy change:  $\Delta G^\circ = -nFE^\circ$ . The ionization energy  $I_M$ , which is the enthalpy change of the gas-phase reaction  $\text{Li}(\text{g}) \longrightarrow \text{Li}^+(\text{g}) + \text{e}^-$ , is only one component of this, as can be seen from the following cycle:



Estimates of the heat of hydration of Li<sup>+</sup>(g) give values near 520 kJ mol<sup>-1</sup> compared with

405 kJ mol<sup>-1</sup> for Na<sup>+</sup>(g) and only 265 kJ mol<sup>-1</sup> for Cs<sup>+</sup>(g). This factor, although opposed by the much larger entropy change for the lithium electrode reaction (due to the more severe disruption of the water structure by the lithium ion), is sufficient to reverse the position of lithium and make it the most electropositive of the alkali metals (as measured by electrode potential) despite the fact that it is the most difficult element of the group to ionize in the gas phase.

#### 4.2.5 Chemical reactivity and trends

The ease of involving the outermost  $ns^1$  electron in bonding, coupled with the very high second-stage ionization energy of the alkali metals, immediately explains both the great chemical reactivity of these elements and the fact that their oxidation state in compounds never exceeds +1. The metals have a high lustre when freshly cut but tarnish rapidly in air due to reaction with O<sub>2</sub> and moisture. Reaction with the halogens is vigorous; even explosive in some cases. All the alkali metals react with hydrogen (p. 65) and with proton donors such as alcohols, gaseous ammonia and even alkynes. They also act as powerful reducing agents towards many oxides and halides and so can be used to prepare many metallic elements or their alloys.

The small size of lithium frequently confers special properties on its compounds and for this reason the element is sometimes termed "anomalous". For example, it is miscible with Na only above 380° and is immiscible with molten K, Rb and Cs, whereas all other pairs of alkali metals are miscible with each other in all proportions. (The ternary alloy containing 12% Na, 47% K and 41% Cs has the lowest known mp, -78°C, of any metallic system.) Li shows many similarities to Mg. This so-called "diagonal relationship" stems from the similarity in ionic size of the two elements:  $r(\text{Li}^+)$  76 pm,  $r(\text{Mg}^{2+})$  72 pm, compared with  $r(\text{Na}^+)$  102 pm. Thus, as first noted by Arfvedson in establishing lithium as a new element, LiOH and Li<sub>2</sub>CO<sub>3</sub> are much less soluble than the corresponding

Na and K compounds and the carbonate (like MgCO<sub>3</sub>) decomposes more readily on being heated. Similarly, LiF (like MgF<sub>2</sub>) is much less soluble in water than are the other alkali metal fluorides because of the large lattice energy associated with the small size of both the cation and the anion. By contrast, lithium salts of large, non-polarizable anions such as ClO<sub>4</sub><sup>-</sup> are much more soluble than those of the other alkali metals, presumably because of the high energy of solvation of Li<sup>+</sup>. For the same reason many simple lithium salts are normally hydrated (p. 88) and the anhydrous salts are extremely hygroscopic: this great affinity for water forms the basis of the widespread use of LiCl and LiBr brines in dehumidifying and air-conditioning units. More subtly there is also a close structural relation between the hydrogen-bonded structures of LiClO<sub>4</sub>·3H<sub>2</sub>O and Mg(ClO<sub>4</sub>)<sub>2</sub>·6H<sub>2</sub>O in which the face-shared octahedral groups of [Li(H<sub>2</sub>O)<sub>6</sub>]<sup>+</sup> are replaced alternately by half the number of discrete [Mg(H<sub>2</sub>O)<sub>6</sub>]<sup>2+</sup> groups.<sup>(13)</sup> Lithium sulfate, unlike the other alkali metal sulfates, does not form alums [M(H<sub>2</sub>O)<sub>6</sub>]<sup>+</sup>[Al(H<sub>2</sub>O)<sub>6</sub>]<sup>3+</sup>[SO<sub>4</sub>]<sup>2-</sup> because the hydrated lithium cation is too small to fill the appropriate site in the alum structure.

Lithium is unusual in reacting directly with N<sub>2</sub> to form the nitride Li<sub>3</sub>N; no other alkali metal has this property, which lithium shares with magnesium (which readily forms Mg<sub>3</sub>N<sub>2</sub>). On the basis of size, it would be expected that Li would be tetrahedrally coordinated by N but, as pointed out by A. F. Wells,<sup>(13)</sup> this would require 12 tetrahedra to meet at a point which is a geometrical impossibility, 8 being the maximum number theoretically possible; accordingly Li<sub>3</sub>N has a unique structure (see p. 92) in which one-third of the Li have 2 N atoms as nearest neighbours (at 194 pm) and the remainder have 3 N atoms as neighbours (at 213 pm); each N is surrounded by 2 Li at 194 pm and 6 more at 213 pm.

<sup>13</sup> A. F. WELLS, *Structural Inorganic Chemistry*, 5th edn., Oxford University Press, Oxford, 1984, 1382 pp.

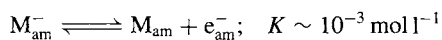
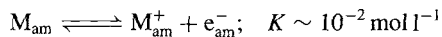


### 4.2.6 Solutions in liquid ammonia and other solvents<sup>(14)</sup>

One of the most remarkable features of the alkali metals is their ready solubility in liquid ammonia to give bright blue, metastable solutions with unusual properties. Such solutions have been extensively studied since they were first observed by T. Weyl in 1863,<sup>†</sup> and it is now known that similar solutions are formed by the heavier alkaline earth metals (Ca, Sr and Ba) and the divalent lanthanoids europium and ytterbium in liquid ammonia. Many amines share with ammonia this ability though to a much lesser extent. It is clear that solubility is favoured by low metal lattice energy, low ionization energies and high cation solvation energy. The most striking physical properties of the solutions are their colour, electrical conductivity and magnetic susceptibility. The solutions all have the same blue colour when dilute, suggesting the presence of a common coloured species, and they become bronze-coloured and metallic at higher concentrations. The conductivity of the dilute solutions is an order of magnitude higher than that of completely ionized salts in water; as the solutions become more concentrated the conductivity at first diminishes to a minimum value at about 0.04M and then increases dramatically to approach values typical of liquid metals. Dilute solutions are paramagnetic with a susceptibility appropriate to the presence of 1 free electron per metal atom; this susceptibility diminishes with increase in concentration, the

solutions becoming diamagnetic in the region of the conductivity minimum and then weakly paramagnetic again at still higher concentrations.

The interpretation of these remarkable properties has excited considerable interest: whilst there is still some uncertainty as to detail, it is now generally agreed that in dilute solution the alkali metals ionize to give a cation  $M^+$  and a quasi-free electron which is distributed over a cavity in the solvent of radius 300–340 pm formed by displacement of 2–3  $NH_3$  molecules. This species has a broad absorption band extending into the infrared with a maximum at  $\sim 1500$  nm and it is the short wavelength tail of this band which gives rise to the deep-blue colour of the solutions. The cavity model also interprets the fact that dissolution occurs with considerable expansion of volume so that the solutions have densities that are appreciably lower than that of liquid ammonia itself. The variation of properties with concentration can best be explained in terms of three equilibria between five solute species  $M$ ,  $M_2$ ,  $M^+$ ,  $M^-$  and  $e^-$ :



The subscript am indicates that the species are dissolved in liquid ammonia and may be solvated. At very low concentrations the first equilibrium predominates and the high ionic conductivity stems from the high mobility of the electron which is some 280 times that of the cation. The species  $M_{am}$  can be thought of as an ion pair in which  $M_{am}^+$  and  $e_{am}^-$  are held together by coulombic forces. As the concentration is raised the second equilibrium begins to remove mobile electrons  $e_{am}^-$  as the complex  $M_{am}^-$  and the conductivity drops. Concurrently  $M_{am}$  begins to dimerize to give  $(M_2)_{am}$  in which the interaction between the 2 electrons is sufficiently strong to lead to spin-pairing and diamagnetism. At still higher concentrations the system behaves as a molten metal in which the metal cations are ammoniated. Saturated solutions are indeed extremely concentrated as indicated by the following table:

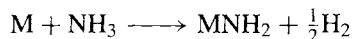
<sup>14</sup> W. L. JOLLY and C. J. HALLADA, *Liquid ammonia*, Chap. 1 in T. C. WADDINGTON (ed.), *Non-aqueous Solvent Systems*, pp. 1–45, Academic Press, London, 1965. J. C. THOMPSON, The physical properties of metal solutions in non-aqueous solvents, Chap. 6 in J. LAGOWSKI (ed.), *The Chemistry of Non-aqueous Solvents*, Vol. 2, pp. 265–317, Academic Press, New York, 1967. J. JANDER (ed.), *Chemistry in Anhydrous Liquid Ammonia*, Wiley, Interscience, New York, 1966, 561 pp.

<sup>†</sup> Actually, the first observation was probably made by Sir Humphry Davy some 55 years earlier: an unpublished observation in his Notebook for November 1807 reads "When 8 grains of potassium were heated in ammoniacal gas it assumed a beautiful metallic appearance and gradually became of a pure blue colour".

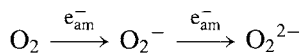
Solute	Li	Na	K	Rb	Cs
$T/^{\circ}\text{C}$	$-33.2^{\circ}$	$-33.5^{\circ}$	$-33.2^{\circ}$	-	$-50^{\circ}$
$g(\text{M})/\text{kg}(\text{NH}_3)$	108.7	251.4	463.7	-	3335
$\text{mol}(\text{NH}_3)/\text{mol}(\text{M})$	3.75	5.37	4.95	-	2.34

The lower solubility of Li on a wt/wt basis reflects its lower atomic weight and, when compared on a molar basis, it is nearly 50% more soluble than Na (15.66 mol/kg  $\text{NH}_3$  compared to 10.93 mol/kg  $\text{NH}_3$ ). Note that it requires only 2.34 mol  $\text{NH}_3$  (39.8 g) to dissolve 1 mol Cs (132.9 g).

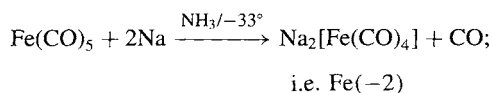
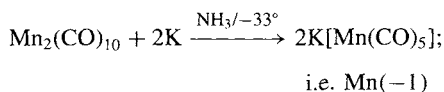
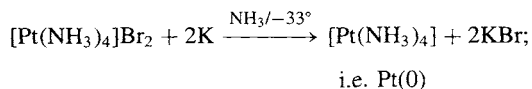
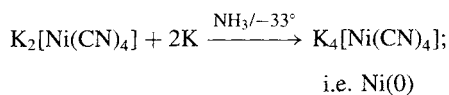
Solutions of alkali metals in liquid ammonia are valuable as powerful and selective reducing agents. The solutions are themselves unstable with respect to amide formation:



However, under anhydrous conditions and in the absence of catalytic impurities such as transition metal ions, solutions can be stored for several days with only a few per cent decomposition. Some reductions occur without bond cleavage as in the formation of alkali metal superoxides and peroxide (p. 84).

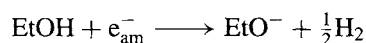
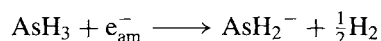
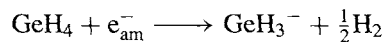


Transition metal complexes can be reduced to unusually low oxidation states either with or without bond cleavage, e.g.:

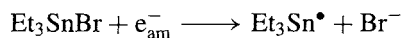
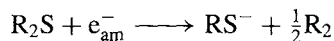


Salts of several heavy main-group elements can be reduced to form polyanions such as  $\text{Na}_4[\text{Sn}_9]$ ,  $\text{Na}_3[\text{Sb}_3]$  and  $\text{Na}_3[\text{Sb}_7]$  (p. 588).

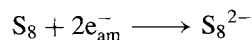
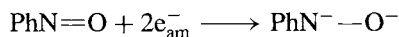
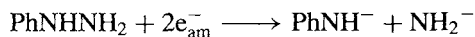
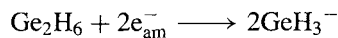
Many protonic species react with liberation of hydrogen:



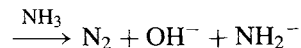
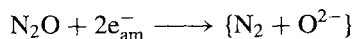
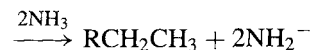
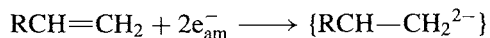
These and similar reactions have considerable synthetic utility. Other reactions which result in bond cleavage by the addition of one electron are:

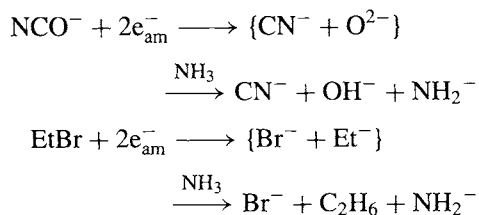


When a bond is broken by addition of 2 electrons, either 2 anions or a dianion is formed:



Subsequent ammonolysis may also occur:





Solutions of alkali metals in liquid ammonia have been developed as versatile reducing agents which effect reactions with organic compounds that are otherwise difficult or impossible.<sup>(15)</sup> Aromatic systems are reduced smoothly to cyclic mono- or di-olefins and alkynes are reduced stereospecifically to *trans*-alkenes (in contrast to Pd/H<sub>2</sub> which gives *cis*-alkenes).

The alkali metals are also soluble in aliphatic amines and hexamethylphosphoramide, P(NMe<sub>2</sub>)<sub>3</sub> to give coloured solutions which are strong reducing agents. These solutions appear to be similar in many respects to the dilute solutions in liquid ammonia though they are less stable with respect to decomposition into amide and H<sub>2</sub>. Likewise, fairly stable solutions of the larger alkali metals K, Rb and Cs have been obtained in tetrahydrofuran, ethylene glycol dimethyl ether and other polyethers. These and similar solutions have been successfully used as strong reducing agents in situations where protonic solvents would have caused solvolysis. For example, naphthalene reacts with Na in tetrahydrofuran to form deep-green solutions of the paramagnetic sodium naphthenide, NaC<sub>10</sub>H<sub>8</sub>, which can be used directly in the presence of a bis(tertiary phosphine) ligand to reduce the anhydrous chlorides VCl<sub>3</sub>, CrCl<sub>3</sub>, MoCl<sub>5</sub> and WCl<sub>6</sub> to the zerovalent octahedral complexes [M(Me<sub>2</sub>PCH<sub>2</sub>CH<sub>2</sub>PMe<sub>2</sub>)<sub>3</sub>], where M = V, Cr, Mo, W. Similarly the planar complex [Fe(Me<sub>2</sub>PCH<sub>2</sub>CH<sub>2</sub>PMe<sub>2</sub>)<sub>2</sub>] was obtained from *trans*-[Fe(Me<sub>2</sub>PCH<sub>2</sub>CH<sub>2</sub>PMe<sub>2</sub>)<sub>2</sub>Cl<sub>2</sub>], and the corresponding tetrahedral Co(0) compound from CoCl<sub>2</sub>.<sup>(16)</sup>

## 4.3 Compounds<sup>(17)</sup>

### 4.3.1 Introduction: the ionic-bond model<sup>(18)</sup>

The alkali metals form a complete range of compounds with all the common anions and have long been used to illustrate group similarities and trends. It has been customary to discuss the simple binary compounds in terms of the ionic bond model and there is little doubt that there is substantial separation of charge between the cationic and anionic components of the crystal lattice. On this model the ions are considered as hard, undeformable spheres carrying charges which are integral multiples of the electronic charge  $z_1e^+$ . Corrections can be incorporated for zero-point energies, London dispersion energies, ligand-field stabilization energies and non-spherical ions (such as NO<sub>3</sub><sup>-</sup>, etc.). The attractive simplicity of this model, and its considerable success during the past 70 y in interpreting many of the properties of simple salts, should not, however, be allowed to obscure the growing realization of its inadequacy.<sup>(18,19)</sup> In particular, as already noted, success in calculating lattice energies and hence enthalpy of formation via the Born–Haber cycle, does not establish the correctness of the model but merely indicates that it is consistent with these particular observations. For example, the ionic model is quite successful in reproducing the enthalpy of formation of BF<sub>3</sub>, SiF<sub>4</sub>, PF<sub>5</sub> and even SF<sub>6</sub> on the assumption that they are assemblies of point charges at the known interatomic distance, i.e. B<sup>3+</sup>(F<sup>-</sup>)<sub>3</sub>, etc.,<sup>(20)</sup> but this is not a sound reason

<sup>17</sup> W. A. HART and O. F. BEUMEL, Lithium and its compounds, *Comprehensive Inorganic Chemistry*, Vol. 1, Chap. 7, Pergamon Press, Oxford, 1973. T. P. WHALEY, Sodium, potassium, rubidium, caesium and francium, *ibid.*, Chap. 8.

<sup>18</sup> N. N. GREENWOOD, *Ionic Crystals, Lattice Defects and Nonstoichiometry*, Butterworths, London, 1968, 194 pp.

<sup>19</sup> D. M. ADAMS, *Inorganic Solids: An Introduction to Concepts in Solid-State Structural Chemistry*, Wiley, London, 1974, 336 pp.

<sup>20</sup> F. J. GARRICK, *Phil. Mag.* **14**, 914–37 (1932). It is instructive to repeat some of these calculations with more recent values for the constants and properties used.

<sup>15</sup> A. J. BIRCH, *Qt. Rev.* **4**, 69–93 (1950); A. J. BIRCH and H. SMITH, *Qt. Rev.* **12**, 17–33 (1958).

<sup>16</sup> J. CHATT and H. R. WATSON, Complexes of zero-valent transition metals with the ditertiary phosphine, Me<sub>2</sub>PCH<sub>2</sub>CH<sub>2</sub>PMe<sub>2</sub>, *J. Chem. Soc.* 2545–9 (1962).

for considering these molecular compounds as ionic. Likewise, the known lattice energy of lithium metal can be reproduced quite well by assuming that the observed bcc arrangement of atoms is made up from alternating ions  $\text{Li}^+\text{Li}^-$  in the CsCl structure;<sup>(21)</sup> the discrepancy is no worse than that obtained using the same model for AgCl (which has the NaCl structure). It appears that the ionic-bond model is self compensating and that the decrease in the hypothetical binding energy which accompanies the diminution of formal charges on the atoms is accompanied by an equivalent increase in binding energy which could be described as "covalent" ( $\text{BF}_3$ ) or "metallic" (Li metal).

Indeed, the inherent improbability of the ionic bond model can be appreciated when it is realized that all simple cations have a positive charge and several vacant orbitals (and are therefore potentially electron pair acceptors) whereas all simple anions have a negative charge and several lone pairs of electrons (and are therefore potentially electron pair donors). The close juxtaposition of these electron-pair donor and acceptor species is thus likely to result in the transfer of at least some charge density by coordination, thereby introducing a substantial measure of covalency into the bonding of the alkali metal halides and related compounds. A more satisfactory procedure, at least conceptually, would be to describe crystalline salts and other solid compounds in terms of molecular orbitals. Quantitative calculations are difficult to carry out but the model allows flexibility in placing "partial ionic charges" on atoms by modifying orbital coefficients and populations, and it can also incorporate metallic behaviour by modifying the extent to which partly filled individual molecular orbitals are either separated by energy gaps or overlap.

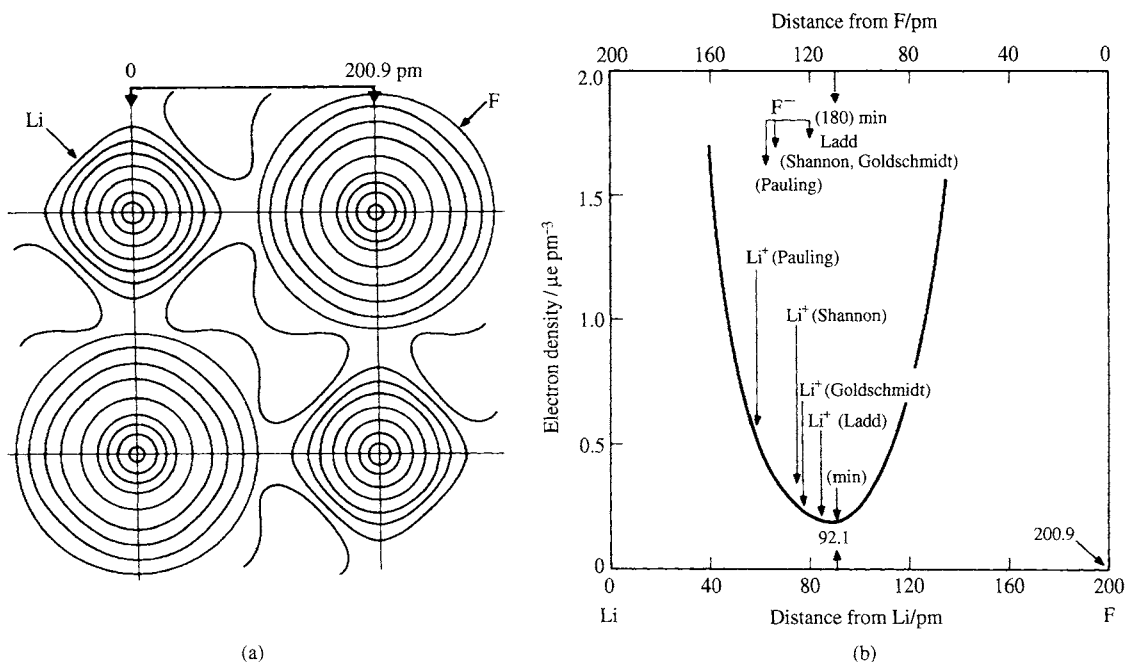
The compounds which most nearly fit the classical conception of ionic bonding are the alkali metal halides. However, even here, one must ask to what extent it is reasonable to maintain that positively charged cations  $\text{M}^+$  with favourably

directed vacant p orbitals remain uncoordinated by the surrounding anionic ligands  $\text{X}^-$  to form extended (bridged) complexes. Such interaction would be expected to increase from  $\text{Cs}^+$  to  $\text{Li}^+$  and from  $\text{F}^-$  to  $\text{I}^-$  (why?) and would place some electron density between the cation and anion. Some evidence on this comes from very precise electron density plots obtained by X-ray diffraction experiments on LiF, NaCl, KCl, MgO and  $\text{CaF}_2$ .<sup>(22)</sup> Data for LiF are shown in Fig. 4.2a from which it is clear that the  $\text{Li}^+$  ion is no longer spherical and that the electron density, while it falls to a low value between the ions, does not become zero. Even more significantly, as shown in Fig. 4.2b, the minimum does not occur at the position to be expected from the conventional ionic radii: whatever set of tabulated values is used the cation is always larger than expected and the anion smaller. This is consistent with a transfer of some electronic density from anion to cation since the smaller resultant positive charge on the cation exerts smaller coulombic attraction for the electrons and the ion expands. The opposite holds for the anion. These results also call into question the use of radius-ratio rules to calculate the coordination number of cations and leave undecided the numerical value of the ionic radii to be used (see also p. 66, hydrides). In fact, the radius-ratio rules are particularly unhelpful for the alkali halides, since they predict (incorrectly) that LiCl, LiBr and LiI should have tetrahedral coordination and that NaF, KF, KCl, RbF, RbCl, RbBr and CsF should all have the CsCl structure. It may be significant that adoption of the NaCl structure by all these compounds maximizes the p orbital overlap along the orthogonal x-, y- and z-directions, and so favours molecular orbital formation in these directions. Further information on the variation in apparent radius of the hydride, halide and other anions in compounds with the alkali metals and other cations is in ref. 23.

<sup>22</sup> H. WITTE and E. WÖLFEL, *Z. phys. Chem.* **3**, 296–329 (1955). J. KRUG, H. WITTE and E. WÖLFEL, *ibid.* **4**, 36–64 (1955). H. WITTE and E. WÖLFEL, *Rev. Mod. Phys.* **30**, 51–5 (1958).

<sup>23</sup> O. JOHNSON, *Inorg. Chem.* **12**, 780–5 (1973).

<sup>21</sup> C. S. G. PHILLIPS and R. J. P. WILLIAMS, *Inorganic Chemistry*, Vol. 1, Chap. 5, "The ionic model", pp. 142–87, Oxford University Press, Oxford, 1965.



**Figure 4.2** (a) Distribution of electron density ( $\mu\text{e}/\text{pm}^3$ ) in the  $xy$  plane of  $\text{LiF}$ , and (b) variation of electron density along the Li-F direction near the minimum. The electron density rises to  $17.99 \mu\text{e pm}^{-3}$  at Li and to  $115.63 \mu\text{e pm}^{-3}$  at F. (The unit  $\mu\text{e pm}^{-3}$  is numerically identical to  $\text{e \AA}^{-3}$ .)

Deviations from the simple ionic model are expected to increase with increasing formal charge on the cation or anion and with increasing size and ease of distortion of the anion. Again, deviations tend to be greater for smaller cations and for those (such as  $\text{Cu}^+$ ,  $\text{Ag}^+$ , etc.) which do not have an inert-gas configuration.<sup>(18)</sup> The gradual transition from predominantly ionic to covalent is illustrated by the “isoelectronic” series:



A similar transition towards metallic bonding is illustrated by the series:



Alkali metal alloys with gold have the CsCl structure and, whilst  $\text{NaAu}$  and  $\text{KAu}$  are essentially metallic,  $\text{RbAu}$  and  $\text{CsAu}$  have partial ionic bonding and are n-type semiconductors. These factors

should constantly be borne in mind during the discussion of compounds in later chapters.

The extent to which charge is transferred back from the anion towards the cation in the alkali metal halides themselves is difficult to determine precisely. Calculations indicate that it is probably only a few percent for some salts such as  $\text{NaCl}$ , whereas for others (e.g.  $\text{LiI}$ ) it may amount to more than  $0.33 e^-$  per atom. Direct experimental evidence on these matters is available for some other elements from techniques such as Mössbauer spectroscopy,<sup>(24)</sup> electron spin resonance spectroscopy,<sup>(25)</sup> and neutron scattering form factors.<sup>(26)</sup>

<sup>24</sup> N. N. GREENWOOD and T. C. GIBB, *Mössbauer Spectroscopy*, Chapman & Hall, London, 1971, 659 pp.

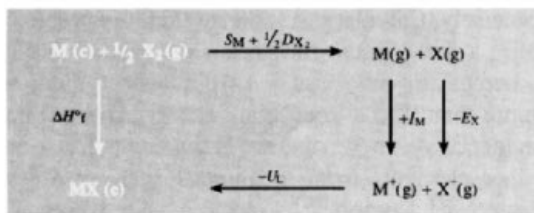
<sup>25</sup> P. B. AYSOUGH, *Electron Spin Resonance in Chemistry*, pp. 300–1, Methuen, London, 1967. P. W. ATKINS and M. C. R. SYMONS, *The Structure of Inorganic Radicals*, pp. 51–73, Elsevier, Amsterdam, 1967.

<sup>26</sup> G. E. BACON, *Neutron Diffraction*, 3rd edn., Oxford University Press, Oxford, 1975, 636 pp.

### 4.3.2 Halides and hydrides

The alkali metal halides are all high-melting, colourless crystalline solids which can be conveniently prepared by reaction of the appropriate hydroxide (MOH) or carbonate ( $M_2CO_3$ ) with aqueous hydrohalic acid (HX), followed by recrystallization. Vast quantities of NaCl and KCl are available in nature and can be purified if necessary by simple crystallization. The hydrides have already been discussed (p. 65).

Trends in the properties of MX have been much studied and typical examples are illustrated in Figs. 4.3 and 4.4. The mp and bp always follow the trend  $F > Cl > Br > I$  except perhaps for some of the Cs salts where the data are uncertain. Figure 4.3 also shows that the mp and bp of LiX are always below those of NaX and that (with the exception of the mp of KI) the values for NaX are the maximum for each series. Trends in enthalpy of formation  $\Delta H_f^\circ$  and lattice energy  $U_L$  are even more regular (Fig. 4.4) and can readily be interpreted in terms of the Born-Haber cycle, providing one assumes an invariant charge corresponding to loss or gain of one complete electron per ion,  $M^+X^-$ . The Born-Haber cycle considers two possible routes to the formation of MX and equates the corresponding enthalpy changes by applying Hess's law.<sup>(18)</sup>



Hence

$$\Delta H_f^\circ(\text{MX}) = S_M + \frac{1}{2}D_{X_2} + I_M - E_X - U_L$$

where  $S_M$  is the heat of sublimation of  $M(c)$  to a monatomic gas (Table 4.2),  $D_{X_2}$  is the dissociation energy of  $X_2(g)$  (Table 4.2),  $I_M$  is the ionization energy of  $M(g)$  (Table 4.2), and  $E_X$  the electron affinity of  $X(g)$  (Table 17.3, p. 800). The

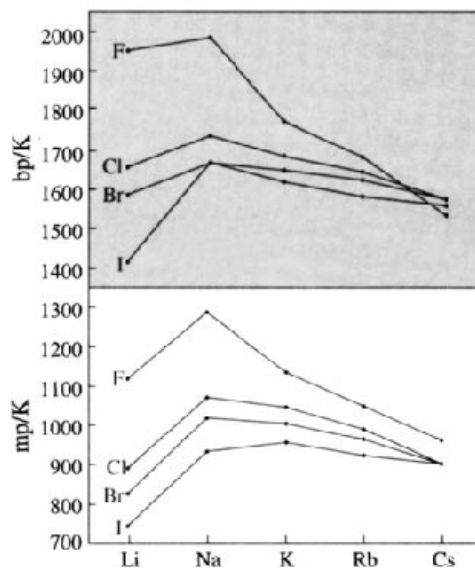


Figure 4.3 Melting point and boiling point of alkali metal halides.

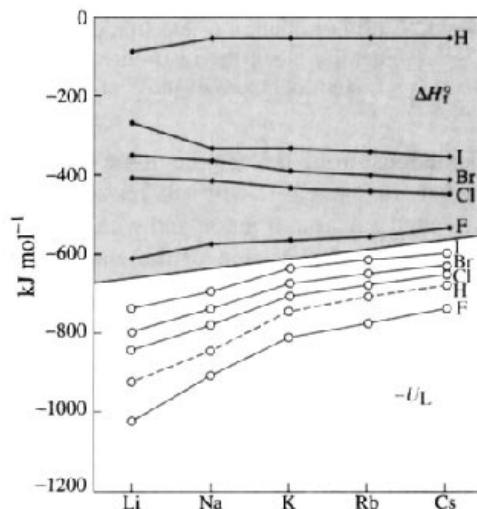


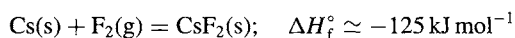
Figure 4.4 Standard enthalpies of formation ( $\Delta H_f^\circ$ ) and lattice energies (plotted as  $-U_L$ ) for alkali metal halides and hydrides.

lattice energy  $U_L$  is given approximately by the expression

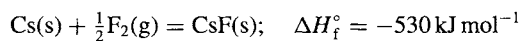
$$U_L = \frac{N_0 A e^2}{4\pi\epsilon_0 r_0} \left(1 - \frac{\rho}{r_0}\right)$$

where  $N_0$  is the Avogadro constant,  $A$  is a geometrical factor, the Madelung constant (which has the value of 1.7627 for the CsCl structure and 1.7476 for the NaCl structure),  $r_0$  is the shortest internuclear distance between  $M^+$  and  $X^-$  in the crystal, and  $\rho$  is a measure of the close-range repulsion force which resists mutual interpenetration of the ions. It is clear that the sequence of lattice energies is determined primarily by  $r_0$ , so that the lattice energy is greatest for LiF and smallest for CsI, as shown in Fig. 4.4. In the Born-Haber expression for  $\Delta H_f^\circ$  this factor predominates for the fluorides and there is a trend to smaller enthalpies of formation from LiF to CsF (Fig. 4.4). The same incipient trend is noted for the hydrides MH, though here the numerical values of  $\Delta H_f^\circ$  are all much smaller than those for MX because of the much higher heat of dissociation of  $H_2$  compared to  $X_2$ . By contrast with the fluorides, the lattice energy for the larger halides is smaller and less dominant, and the resultant trend of  $\Delta H_f^\circ$  is to larger values, thus reflecting the greater ease of subliming and ionizing the heavier alkali metals.

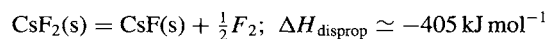
The Born-Haber cycle is also useful in examining the possibility of forming alkali-metal halides of stoichiometry  $MX_2$ . The dominant term will clearly be the very large second-stage ionization energy for the process  $M^+(g) \longrightarrow M^{2+}(g) + e^-$ ; this is  $7297 \text{ kJ mol}^{-1}$  for Li but drops to  $2255 \text{ kJ mol}^{-1}$  for Cs. The largest possible lattice energy to compensate for this would be obtained with the smallest halogen F and (making plausible assumptions on lattice structure and ionic radius) calculations indicate that  $CsF_2$  could indeed be formed exothermically from its elements:



However, the compound cannot be prepared because of the much greater enthalpy of formation of CsF which makes  $CsF_2$  unstable with respect to decomposition:



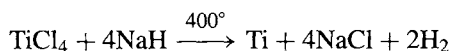
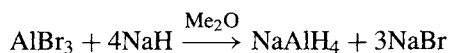
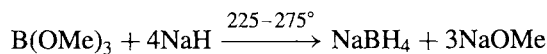
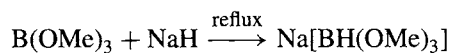
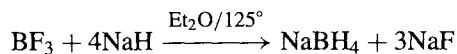
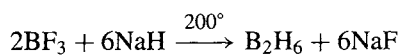
whence



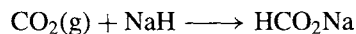
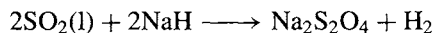
There is some evidence that  $Cs^{3+}$  can be formed by cyclic voltammetry of  $Cs^+[OTeF_5]^-$  in pure MeCN at the extremely high oxidizing potential of 3 V, and that  $Cs^{3+}$  might be stabilized by 18-crown-6 and cryptand (see pp. 96 and 97 for nomenclature).<sup>(27)</sup> However, the isolation of pure compounds containing  $Cs^{3+}$  has so far not been reported.

Ternary alkali-metal halide oxides are known and have the expected structures. Thus  $Na_3ClO$  and the yellow  $K_3BrO$  have the anti-perovskite structure (p. 963) whereas  $Na_4Br_2O$ ,  $Na_4I_2O$  and  $K_4Br_2O$  have the tetragonal anti- $K_2NiF_4$  structure.<sup>(28)</sup>

The alkali metal halides, particularly NaCl and KCl, find extensive application in industry (pp. 71 and 73). The hydrides are frequently used as reducing agents, the product being a hydride or complex metal hydride depending on the conditions used, or the free element if the hydride is unstable. Illustrative examples using NaH are:



Sulfur dioxide is uniquely reduced to dithionite (a process useful in bleaching paper pulp, p. 720).  $CO_2$  gives the formate:



Particularly reactive (pyrophoric) forms of LiH, NaH and KH can be prepared simply and in high yield by the direct hydrogenation of

<sup>27</sup> K. MOOCK and K. SEPPELT, *Angew. Chem. Int. Edn. Engl.* **28**, 1676-8 (1989).

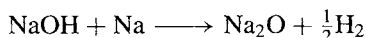
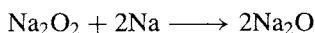
<sup>28</sup> S. SITTA, K. HIPPLER, P. VOGT and H. SABROWSKY, *Z. anorg. allg. Chem.* **597**, 197-200 (1991).

hexane solutions of  $\text{MBu}^n$  in the presence of tetramethylethylenediamine (tmeda) and these have proved extremely useful reagents for the metalation of organic compounds which have an active hydrogen site.<sup>(29)</sup>

### 4.3.3 Oxides, peroxides, superoxides and suboxides

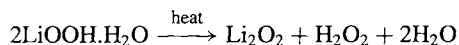
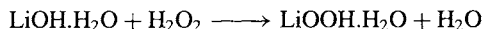
The alkali metals form a fascinating variety of binary compounds with oxygen, the most versatile being Cs which forms 9 compounds with stoichiometries ranging from  $\text{Cs}_7\text{O}$  to  $\text{CsO}_3$ . When the metals are burned in a free supply of air the predominant product depends on the metal: Li forms the oxide  $\text{Li}_2\text{O}$  (plus some  $\text{Li}_2\text{O}_2$ ), Na forms the peroxide  $\text{Na}_2\text{O}_2$  (plus some  $\text{Na}_2\text{O}$ ) whilst K, Rb and Cs form the superoxide  $\text{MO}_2$ . Under the appropriate conditions pure compounds  $\text{M}_2\text{O}$ ,  $\text{M}_2\text{O}_2$  and  $\text{MO}_2$  can be prepared for all five metals.

The "normal" oxides  $\text{M}_2\text{O}$  (Li, Na, K, Rb) have the antifluorite structure as do many of the corresponding sulfides, selenides and tellurides. This structure is related to the  $\text{CaF}_2$  structure (p. 118) but with the sites occupied by the cations and anions interchanged so that M replaces F and O replaces Ca in the structure.  $\text{Cs}_2\text{O}$  has the anti- $\text{CdCl}_2$  layer structure (p. 1211). There is a trend to increasing coloration with increasing atomic number,  $\text{Li}_2\text{O}$  and  $\text{Na}_2\text{O}$  being pure white,  $\text{K}_2\text{O}$  yellowish white,  $\text{Rb}_2\text{O}$  bright yellow and  $\text{Cs}_2\text{O}$  orange. The compounds are fairly stable towards heat, and thermal decomposition is not extensive below about  $500^\circ$ . Pure  $\text{Li}_2\text{O}$  is best prepared by thermal decomposition of  $\text{Li}_2\text{O}_2$  (see below) at  $450^\circ\text{C}$ .  $\text{Na}_2\text{O}$  is obtained by reaction of  $\text{Na}_2\text{O}_2$ ,  $\text{NaOH}$  or preferably  $\text{NaNO}_2$  with the Na metal:



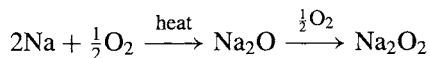
In this last reaction Na can be replaced by the azide  $\text{NaN}_3$  to give the same products. The normal oxides of the other alkali metals can be prepared similarly.

The peroxides  $\text{M}_2\text{O}_2$  contain the peroxide ion  $\text{O}_2^{2-}$  which is isoelectronic with  $\text{F}_2$ .  $\text{Li}_2\text{O}_2$  is prepared industrially by the reaction of  $\text{LiOH}\cdot\text{H}_2\text{O}$  with hydrogen peroxide, followed by dehydration of the hydroperoxide by gentle heating under reduced pressure:

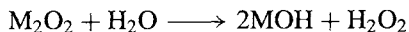
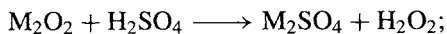


It is a thermodynamically stable, white, crystalline solid which decomposes to  $\text{Li}_2\text{O}$  on being heated above  $195^\circ\text{C}$ .

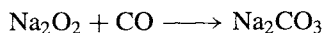
$\text{Na}_2\text{O}_2$ , is prepared as pale-yellow powder by first oxidizing Na to  $\text{Na}_2\text{O}$  in a limited supply of dry oxygen (air) and then reacting this further to give  $\text{Na}_2\text{O}_2$ :



Preparation of pure  $\text{K}_2\text{O}_2$ ,  $\text{Rb}_2\text{O}_2$  and  $\text{Cs}_2\text{O}_2$  by this route is difficult because of the ease with which they oxidize further to the superoxides  $\text{MO}_2$ . Oxidation of the metals with NO has been used but the best method is the quantitative oxidation of the metals in liquid ammonia solution (p. 78). The peroxides can be regarded as salts of the dibasic acid  $\text{H}_2\text{O}_2$ . Thus reaction with acids or water quantitatively liberates  $\text{H}_2\text{O}_2$ :

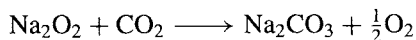


Sodium peroxide finds widespread use industrially as a bleaching agent for fabrics, paper pulp, wood, etc., and as a powerful oxidant; it explodes with powdered aluminium or charcoal, reacts with sulfur with incandescence and ignites many organic liquids. Carbon monoxide forms the carbonate, and  $\text{CO}_2$  liberates oxygen (an important application in breathing apparatus for divers, firemen, and in submarines — space capsules use the lighter  $\text{Li}_2\text{O}_2$ ):



<sup>29</sup> P. A. A. KLUSENER, L. BRANDSMA, H. D. VERKRUJSE, P. V. R. SCHLEYER, T. FRIEDL and R. PI, *Angew. Chem. Int. Edn. Engl.* **25**, 465 (1986).



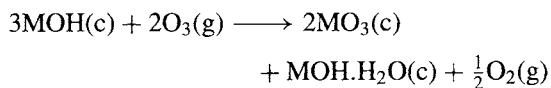


In the absence of oxygen or oxidizable material, the peroxides (except  $\text{Li}_2\text{O}_2$ ) are stable towards thermal decomposition up to quite high temperatures, e.g.  $\text{Na}_2\text{O}_2 \sim 675^\circ\text{C}$ ,  $\text{Cs}_2\text{O}_2 \sim 590^\circ\text{C}$ .

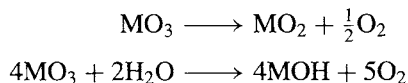
The superoxides  $\text{MO}_2$  contain the paramagnetic ion  $\text{O}_2^-$  which is stable only in the presence of large cations such as K, Rb, Cs (and Sr, Ba, etc.).  $\text{LiO}_2$  has only been prepared by matrix isolation experiments at 15 K and positive evidence for  $\text{NaO}_2$  was first obtained by reaction of  $\text{O}_2$  with Na dissolved in liquid  $\text{NH}_3$ ; it can be obtained pure by reacting Na with  $\text{O}_2$  at  $450^\circ\text{C}$  and 150 atm pressure. By contrast, the normal products of combustion of the heavier alkali metals in air are  $\text{KO}_2$  (orange), mp  $380^\circ\text{C}$ ,  $\text{RbO}_2$  (dark brown), mp  $412^\circ\text{C}$  and  $\text{CsO}_2$  (orange), mp  $432^\circ\text{C}$ .  $\text{NaO}_2$  is trimorphic, having the marcasite structure (p. 680) at low temperatures, the pyrite structure (p. 680) between  $-77^\circ$  and  $-50^\circ\text{C}$  and a pseudo- $\text{NaCl}$  structure above this, due to disordering of the  $\text{O}_2^-$  ions by rotation. The heavier congeners adopt the tetragonal  $\text{CaC}_2$  structure (p. 298) at room temperature and the pseudo- $\text{NaCl}$  structure at high temperature.

Sesquioxides " $\text{M}_2\text{O}_3$ " have been prepared as dark-coloured paramagnetic powders by careful thermal decomposition of  $\text{MO}_2$  (K, Rb, Cs). They can also be obtained by oxidation of liquid ammonia solutions of the metals or by controlled oxidation of the peroxides, and are considered to be peroxide disuperoxides  $[(\text{M}^+)_4(\text{O}_2^{2-})_2(\text{O}_2^-)_2]$ . Indeed, pure  $\text{Rb}_4\text{O}_6$ , prepared by solid-state reaction between  $\text{Rb}_2\text{O}_2$  and  $2\text{RbO}_2$ , has recently been shown to be  $[\text{Rb}_4(\text{O}_2^{2-})_2(\text{O}_2^-)_2]$  by single-crystal diffractometry, although the two types of diatomic anion could not be distinguished in the cubic unit cell even at  $-60^\circ\text{C}$ ; the compound is thermodynamically stable and melts at  $461^\circ\text{C}$ <sup>(30)</sup>

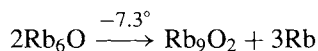
Ozonides  $\text{MO}_3$  have been prepared for Na, K, Rb and Cs by the reaction of  $\text{O}_3$  on powdered anhydrous  $\text{MOH}$  at low temperature and extraction of the red  $\text{MO}_3$  by liquid  $\text{NH}_3$ :



Under similar conditions Li gives  $[\text{Li}(\text{NH}_3)_4]\text{O}_3$  which decomposes on attempted removal of the coordinated  $\text{NH}_3$ , again emphasizing the important role of cation size in stabilizing catenated oxygen anions. Improved techniques involving the reaction of oxygen/ozone mixtures on the preformed peroxide, followed by extraction with liquid ammonia, now permit gram amounts of the pure crystalline ozonides of K, Rb and Cs to be prepared.<sup>(31)</sup> (See also p. 98, p. 610.) The ozonides, on standing, slowly decompose to oxygen and the superoxide  $\text{MO}_2$ , but on hydrolysis they appear to go directly to the hydroxide:



In addition to the above oxides  $\text{M}_2\text{O}$ ,  $\text{M}_2\text{O}_2$ ,  $\text{M}_4\text{O}_6$ ,  $\text{MO}_2$  and  $\text{MO}_3$  in which the alkali metal has the constant oxidation state +1, rubidium and caesium also form suboxides in which the formal oxidation state of the metal is considerably lower. Some of these intriguing compounds have been known since the turn of the century but only recently have their structures been elucidated by single crystal X-ray analysis.<sup>(32)</sup> Partial oxidation of Rb at low temperatures gives  $\text{Rb}_6\text{O}$  which decomposes above  $-7.3^\circ\text{C}$  to give copper-coloured metallic crystals of  $\text{Rb}_9\text{O}_2$ :

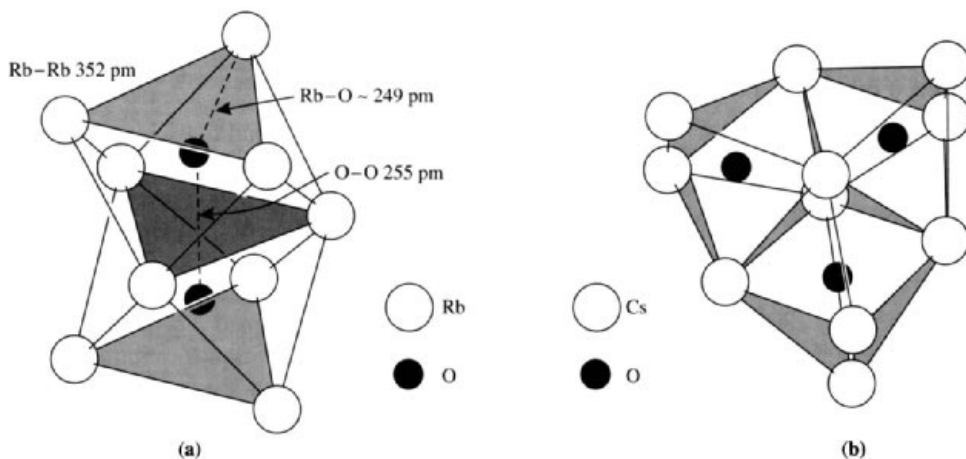


$\text{Rb}_9\text{O}_2$  inflames with  $\text{H}_2\text{O}$  and melts incongruently at  $40.2^\circ$  to give  $2\text{Rb}_2\text{O} + 5\text{Rb}$ . The structure of  $\text{Rb}_9\text{O}_2$  comprises two  $\text{ORb}_6$  octahedra sharing a common face (Fig. 4.5). It thus has the anti- $[\text{Ti}_2\text{Cl}_9]^{3-}$  structure. The Rb-Rb distance within this unit is only 352 pm (compared with 485 pm in Rb metal) and the nearest Rb-Rb distance

<sup>31</sup> W. SCHNICK and M. JANSEN, *Z. anorg. allg. Chem.* **532**, 37-46 (1986).

<sup>32</sup> A. SIMON, *Naturwiss.* **58**, 622-3 (1971); *Z. anorg. allg. Chem.* **395**, 301 (1973); *Struct. Bonding* **36**, 81-127 (1979); *Angew. Chem. Int. Edn. Engl.* **27**, 159-83 (1988).

<sup>30</sup> M. JANSEN and N. KORBER, *Z. anorg. allg. Chem.* **598/599**, 163-73 (1991).



**Figure 4.5** (a) The confacial bioctahedral  $Rb_9O_2$  group in  $Rb_9O_2$  and  $Rb_6O$ , and (b) the confacial trioctahedral  $Cs_{11}O_3$  group in  $Cs_7O$ .

between groups is 511 pm. The Rb–O distance is  $\sim 249$  pm, much less than the sum of the conventional ionic radii (289 pm) and the metallic character of the oxide comes from the excess of at least 5 electrons above that required for simple bookkeeping. Crystalline  $Rb_6O$  has a unit cell containing 4 formula units, i.e.  $Rb_{24}O_4$ , and the structure consists of alternating layers of  $Rb_9O_2$  and close-packed metal atoms parallel to (001) to give the structural formula  $[(Rb_9O_2)Rb_3]$ .

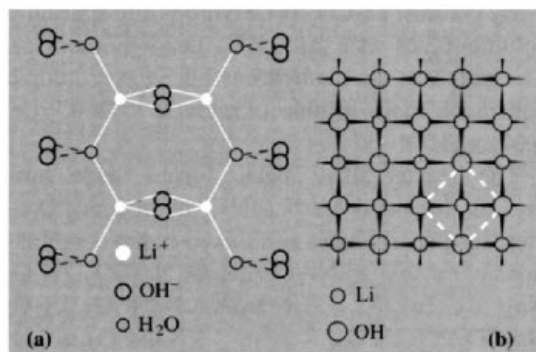
Caesium forms an even more extensive series of suboxides:<sup>(32)</sup>  $Cs_7O$ , bronze-coloured, mp  $+4.3^\circ C$ ;  $Cs_4O$ , red-violet, decomposes  $>10.5^\circ C$ ;  $Cs_{11}O_3$ , violet crystals, mp (incongruent)  $52.5^\circ C$ ; and  $Cs_{3+x}O$ , a nonstoichiometric phase up to  $Cs_4O$ , which decomposes at  $166^\circ C$ .  $Cs_7O$  reacts vigorously with  $O_2$  and  $H_2O$  and the unit cell is found to be  $Cs_{21}O_3$ , i.e.  $[(Cs_{11}O_3)Cs_{10}]$ . The unit  $Cs_{11}O_3$  comprises 3 octahedral  $OCs_6$  groups each sharing 2 adjacent faces to form the trigonal group shown in Fig. 4.5b. These groups form chains along (001) and are also surrounded by the other Cs atoms. The Cs–Cs distance within the  $Cs_{11}O_3$  group is only 376 pm, whereas between groups it is 527 pm; this latter distance is also the shortest distance between Cs in a group and the other 10 Cs atoms, and is similar to the interatomic distance in Cs metal. The structures of the other 3 suboxides are more complex

but it is salutary to realize that Cs forms at least 9 crystalline oxides whose structures can be rationalized in terms of general bonding systematics.

#### 4.3.4 Hydroxides

Evaporation of aqueous solutions of LiOH under normal conditions produces the monohydrate, and this can be readily dehydrated by heating in an inert atmosphere or under reduced pressure.  $LiOH \cdot H_2O$  has a crystal structure built up of double chains in which both Li and  $H_2O$  have 4 nearest neighbours (Fig. 4.6a); Li is tetrahedrally coordinated by 2OH and 2 $H_2O$ , and each tetrahedron shares an edge (2OH) and two corners (2 $H_2O$ ) to produce double chains which are held laterally by H bonds. Each  $H_2O$  molecule is tetrahedrally coordinated by 2Li from the same chain and 2OH from other chains. Anhydrous LiOH has a layer lattice of edge-shared  $Li(OH)_4$  tetrahedra (Fig. 4.6b) in which each Li in a plane is surrounded tetrahedrally by 4OH, and each OH has 4Li neighbours all lying on one side; neutron diffraction shows that the OH bonds are normal to the layer plane and there is no H bonding between layers.

Numerous hydrates have been prepared from aqueous solutions of the heavier alkali metal



**Figure 4.6** (a) The double-chain structure of  $\text{LiOH}\cdot\text{H}_2\text{O}$ , and (b) the layer structure of anhydrous  $\text{LiOH}$  (see text).

hydroxides (e.g.  $\text{NaOH}\cdot n\text{H}_2\text{O}$ , where  $n = 1, 2, 2.5, 3.5, 4, 5.25$  and  $7$ ) but little detailed structural information is available.<sup>(33)</sup> The anhydrous compounds all show the influence of oriented  $\text{OH}$  groups on the structure,<sup>(13)</sup> and there is evidence of weak  $\text{O}-\text{H}\cdots\text{O}$  bonding for  $\text{KOH}$  and  $\text{RbOH}$ . Melting points are substantially lower than those of the halides, decreasing from  $471^\circ\text{C}$  for  $\text{LiOH}$  to  $272^\circ$  for  $\text{CsOH}$ , and the mp of the hydrates is even lower, e.g.  $2.5^\circ\text{C}$  (incongr.) for  $\text{CsOH}\cdot 2\text{H}_2\text{O}$  and  $-5.5^\circ\text{C}$  for the trihydrate.

The alkali metal hydroxides are the most basic of all hydroxides. They react with acids to form salts and with alcohols to form alkoxides. The alkoxides are oligomeric and the degree of polymerization can vary depending on the particular metal and the state of aggregation. The *tert*-butoxides,  $\text{MOBu}'$ , ( $\text{Bu}' = \text{OCMe}_3$ ) can be considered as an example. Crystalline  $(\text{KOBu}')_4$  has a cubane-like structure and the tetramer persists in tetrahydrofuran solution and in the gas phase.<sup>(34,35)</sup> By contrast,  $(\text{NaOBu}')_4$  is exclusively tetrameric in *thf*, but is a mixture of hexamers and nonamers

in the crystalline state and of hexamers and heptamers in the vapour phase. The lithium analogue is tetrameric in *thf* but is hexameric in benzene, toluene or cyclohexane and in the gas phase. The degree of polymerization can also be influenced by the nature of the organic residue. Thus X-ray crystallography shows that lithium 2,6-di-*tert*-butyl-4-methylphenolate is dimeric whereas the closely related phenolate  $\{\text{LiOC}_6\text{H}_2(\text{CH}_2\text{NMe}_2)_2\text{-2,6-Me-4}\}_3$  provides the first example of a trimeric structure, with an essentially planar central  $\text{Li}_3\text{O}_3$  heterocyclic ring.<sup>(36)</sup> The trimer, like the dimer, features unusually short  $\text{Li}-\text{O}$  and  $\text{C}_{ipso}-\text{O}$  bonds (186.5 and 130.1 pm, respectively) perhaps suggesting quasi-aromaticity of the  $\text{Li}_3\text{O}_3$  ring, the delocalized  $\pi$ -electrons originating from the lone pairs on the oxygen atoms.

The alkali metal hydroxides are also readily absorb  $\text{CO}_2$  and  $\text{H}_2\text{S}$  to form carbonates (or hydrogencarbonates) and sulfides (or hydrogensulfides), and are extensively used to remove mercaptans from petroleum products. Amphoteric oxides such as those of  $\text{Al}$ ,  $\text{Zn}$ ,  $\text{Sn}$  and  $\text{Pb}$  react with  $\text{MOH}$  to form aluminates, zincates, stannates and plumbates, and even  $\text{SiO}_2$  (and silicate glasses) are attacked.

Production and uses of  $\text{LiOH}$  have already been discussed (p. 70). Huge tonnages of  $\text{NaOH}$  and  $\text{KOH}$  are produced by electrolysis of brine (pp. 71, 73) and the enormous industrial importance of these chemicals has already been alluded to.

### 4.3.5 Oxoacid salts and other compounds

Many binary and pseudo-binary compounds of the alkali metals are more conveniently treated within the context of the chemistry of the other element and for this reason discussion is deferred to later chapters, e.g. borides (p. 145),

<sup>33</sup> H. JACOBS and U. METZNER, *Z. anorg. allg. Chem.* **597**, 97–106 (1991). D. MOOTZ and H. RUTTER, *Z. anorg. allg. Chem.* **608**, 123–30 (1992).

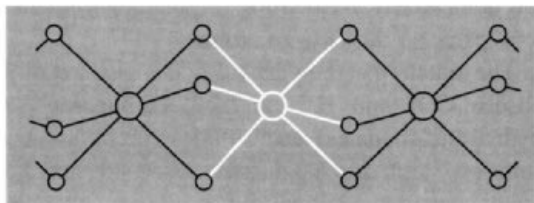
<sup>34</sup> M. H. CHISHOLM, S. R. DRAKE, A. A. NAIINI and W. E. STREIB, *Polyhedron* **10**, 337–43 (1991).

<sup>35</sup> M. BRAUN, D. WALDMÜLLER and B. MAYER, *Angew. Chem. Int. Edn. Engl.* **28**, 895–6 (1989).

<sup>36</sup> P. A. VAN DER SCHAAF, M. P. HOGERHEIDE, D. M. GROVE, A. L. SPEK and G. VAN KOTEN, *J. Chem. Soc., Chem. Commun.*, 1703–5 (1992).

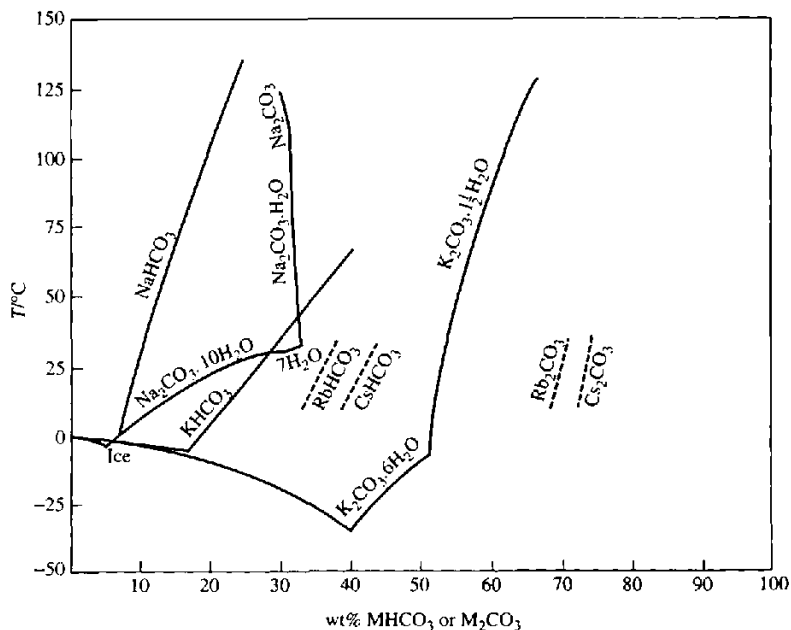
graphite intercalation compounds (p. 293), carbides, cyanides, cyanates, etc. (pp. 297, 319), silicides (p. 335), germanides (p. 393), nitrides, azides and amides (p. 417), phosphides (p. 489), arsenides (p. 554), sulfides (p. 676), selenides and tellurides (p. 765), polyhalides (p. 835), etc. Likewise, the alkali metals form stable salts with virtually all oxoacids and these are also discussed in later chapters.

Lithium salts show a great propensity to crystallize as hydrates, the trihydrates being particularly common, e.g.  $\text{LiX} \cdot 3\text{H}_2\text{O}$ ,  $\text{X} = \text{Cl}, \text{Br}, \text{I}, \text{ClO}_3, \text{ClO}_4, \text{MnO}_4, \text{NO}_3, \text{BF}_4$ , etc. In most of these Li is coordinated by  $6\text{H}_2\text{O}$  to form chains of face-sharing octahedra:



By contrast  $\text{Li}_2\text{CO}_3$  is anhydrous and sparingly soluble (1.28 wt% at  $25^\circ\text{C}$ , i.e.  $0.17 \text{ mol l}^{-1}$ ). The nitrate is also anhydrous but is hygroscopic and much more soluble (45.8 wt% at  $25^\circ\text{C}$ , i.e.  $6.64 \text{ mol l}^{-1}$ ).

The heavier alkali metals form a wide variety of hydrated carbonates, hydrogencarbonates, sesquicarbonates and mixed-metal combinations of these, e.g.  $\text{Na}_2\text{CO}_3 \cdot \text{H}_2\text{O}$ ,  $\text{Na}_2\text{CO}_3 \cdot 7\text{H}_2\text{O}$ ,  $\text{Na}_2\text{CO}_3 \cdot 10\text{H}_2\text{O}$ ,  $\text{Na}_2\text{CO}_3 \cdot \text{NaHCO}_3 \cdot 2\text{H}_2\text{O}$ ,  $\text{Na}_2\text{CO}_3 \cdot 3\text{NaHCO}_3$ ,  $\text{NaKCO}_3 \cdot n\text{H}_2\text{O}$ ,  $\text{K}_2\text{CO}_3 \cdot \text{NaHCO}_3 \cdot 2\text{H}_2\text{O}$ , etc. These systems have been studied in great detail because of their industrial and geochemical significance (see Panel). Some solubility data are in Fig. 4.7, which indicates the considerable solubility of  $\text{Rb}_2\text{CO}_3$  and  $\text{Cs}_2\text{CO}_3$  and the lower solubility of the hydrogencarbonates. The various stoichiometries reflect differing ways of achieving charge balance, preferred coordination polyhedra, and H bonding. Thus  $\text{Na}_2\text{CO}_3 \cdot \text{H}_2\text{O}$  has two types of 6-coordinate Na, half being surrounded by  $1\text{H}_2\text{O}$  plus 5 oxygen atoms from  $\text{CO}_3$  groups and half by



**Figure 4.7** Solubilities of alkali carbonates and bicarbonates (hydrogencarbonates). (H. Stephen and T. Stephen, *Solubilities of Inorganic and Organic Compounds*, Vol. 1, Part 1, Macmillan, New York.).

### Industrial Production and Uses of Sodium Carbonate, Hydroxide and Sulfate<sup>(37)</sup>

$\text{Na}_2\text{CO}_3$  (soda ash) is interchangeable with  $\text{NaOH}$  in many of its applications (e.g. paper pulping, soap, detergents) and this gives a valuable flexibility to the chlor-alkali industry. About half the  $\text{Na}_2\text{CO}_3$  produced is used in the glass industry. One developing application is in the reduction of sulfur pollution resulting from stack gases of power plants and other large furnaces: powdered  $\text{Na}_2\text{CO}_3$  is injected with the fuel and reacts with  $\text{SO}_2$  to give solids such as  $\text{Na}_2\text{SO}_3$  which can be removed by filtration or precipitation. World production of  $\text{Na}_2\text{CO}_3$  was 28.7 million tonnes in 1985: the five leading countries were the USA, the USSR, China, Bulgaria and the Federal Republic of Germany, and they accounted for over 70% of production. Most of this material was synthetic (Solvay), but the increasing use of natural carbonate (trona) is notable, particularly in the USA where it is now the sole source of  $\text{Na}_2\text{CO}_3$ , the last synthetic unit having been closed in 1985: reserves in the Green River, Wyoming, deposit alone exceed  $10^{10}$  tonnes and occur in beds up to 3 m thick over an area of 2300  $\text{km}^2$ . About one third of the world production is now from natural deposits.

Formerly  $\text{Na}_2\text{CO}_3$  found extensive use as "washing soda" but this market has now disappeared due to the domestic use of detergents. The related compound  $\text{NaHCO}_3$  is, however, still used, particularly because of its ready decomposition in the temperature range 50–100°C:



Production in the USA is ~350 000 tonnes annually of which 30% is used in baking-powder formulations, 20% in animal feedstuffs, 15% in chemicals manufacture, 11% in pharmaceuticals, 9% in fire extinguishers and the remaining 15% in the textile, leather and paper industries and in soaps, detergents and neutralizing agents.

Caustic soda ( $\text{NaOH}$ ) is industry's most important alkali. It is manufactured on a huge scale by the electrolysis of brine (p. 72) and annual production in the USA alone is over 10 million tonnes. Electrolysis is followed by concentration of the alkali in huge tandem evaporators such as those at PPG Industries' Lake Charles plant. The evaporators, which are perhaps the world's largest, are 41 m high and 12 m in diameter. About half the caustic produced is used directly in chemical production; a detailed breakdown of usage (USA, 1985) is: organic chemicals 30%, inorganic chemicals 20%, paper and pulp 20%, export 10%, soap and detergents 5%, oil industry 5%, textiles 4%, bauxite digestion 3% and miscellaneous 3%. Principal applications are in acid neutralization, the manufacture of phenol, resorcinol,  $\beta$ -naphthol, etc., and the production of sodium hypochlorite, phosphate, sulfide, aluminates, etc.

Salt cake ( $\text{Na}_2\text{SO}_4$ ) is a byproduct of  $\text{HCl}$  manufacture using  $\text{H}_2\text{SO}_4$  and is also the end-product of hundreds of industrial operations in which  $\text{H}_2\text{SO}_4$  used for processing is neutralized by  $\text{NaOH}$ . For long it had few uses, but now it is the mainstay of the paper industry, being a key chemical in the kraft process for making brown wrapping paper and corrugated boxes: digestion of wood chips or saw-mill waste in very hot alkaline solutions of  $\text{Na}_2\text{SO}_4$  dissolves the lignin (the brown resinous component of wood which cements the fibres together) and liberates the cellulose fibres as pulp which then goes to the paper-making screens. The remaining solution is evaporated until it can be burned, thereby producing steam for the plant and heat for the evaporation: the fused  $\text{Na}_2\text{SO}_4$  and  $\text{NaOH}$  survive the flames and can be reused. Total world production of  $\text{Na}_2\text{SO}_4$  (1985) was ~4.5 million tonnes (45% natural, 55% synthetic). Most of this (~70%) is used in the paper industry and smaller amounts are used in glass manufacture and detergents (~10% each). The hydrated form,  $\text{Na}_2\text{SO}_4 \cdot 10\text{H}_2\text{O}$ , Glauber's salt, is now less used than formerly. Further information on the industrial production and uses of  $\text{Na}_2\text{CO}_3$ ,  $\text{NaOH}$  and  $\text{Na}_2\text{SO}_4$  are given in *Kirk-Othmer Encyclopedia of Chemical Technology*, 4th edn., Vol. 1, 1991, pp. 1025–39 and Vol. 22, 1997, pp. 354–419.

$2\text{H}_2\text{O}$  plus 4 oxygen atoms from  $\text{CO}_3$  groups. The decahydrate has octahedral  $\text{Na}(\text{H}_2\text{O})_6$  groups associated in pairs by edge sharing to give  $[\text{Na}_2(\text{H}_2\text{O})_{10}]$ . The hydrogencarbonate  $\text{NaHCO}_3$  has infinite one-dimensional chains of  $\text{HCO}_3$  formed by unsymmetrical  $\text{O}-\text{H}\cdots\text{O}$  bonds (261 pm) which are held laterally by Na ions. The sesquicarbonates  $\text{Na}_3\text{H}(\text{CO}_3)_2 \cdot 2\text{H}_2\text{O}$  have short,

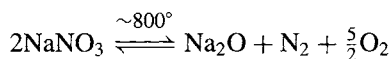
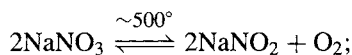
symmetrical  $\text{O}-\text{H}-\text{O}$  bonds (253 pm) which link the carbonate ions in pairs, and longer  $\text{O}-\text{H}\cdots\text{O}$  bonds (275 pm) which link these pairs to water molecules. Similar phases are known for the other alkali metals.

Alkali metal nitrates can be prepared by direct reaction of aqueous nitric acid on the appropriate hydroxide or carbonate.  $\text{LiNO}_3$  is used for scarlet flares and pyrotechnic displays. Large deposits of  $\text{NaNO}_3$  (saltpetre) are found in Chile and were probably formed by bacterial decay of small marine organisms: the  $\text{NH}_3$  initially produced

<sup>37</sup> Ref. 4, pp. 149–63 and 219–25. See also *Kirk-Othmer Encyclopedia of Chemical Technology*, 4th edn., Vol. 1, 1991, Chlorine and sodium hydroxide, pp. 938–1025. Sodium carbonate, pp. 1025–39.

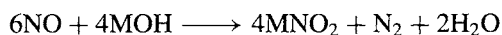
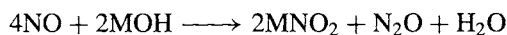
presumably oxidized to nitrous acid and nitric acid which would then react with dissolved NaCl.  $\text{KNO}_3$  was formerly prepared by metathesis of  $\text{NaNO}_3$  and  $\text{KCl}$  but is now obtained directly as part of the synthetic ammonia/nitric acid industry (p. 421).

Alkali metal nitrates are low-melting salts that decompose with evolution of oxygen above about  $500^\circ\text{C}$ , e.g.

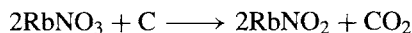
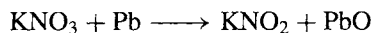


Thermal stability increases with increasing atomic weight, as expected. Nitrates have been widely used as molten salt baths and heat transfer media, e.g. the 1:1 mixture  $\text{LiNO}_3:\text{KNO}_3$  melts at  $125^\circ\text{C}$  and the ternary mixture of 40%  $\text{NaNO}_2$ , 7%  $\text{NaNO}_3$  and 53%  $\text{KNO}_3$  can be used from its mp  $142^\circ$  up to about  $600^\circ\text{C}$ .

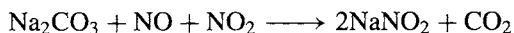
The corresponding nitrites,  $\text{MNO}_2$ , can be prepared by thermal decomposition of  $\text{MNO}_3$  as indicated above or by reaction of  $\text{NO}$  with the hydroxide:



Chemical reduction of nitrates has also been employed:



The commercial production of  $\text{NaNO}_2$  is achieved by absorbing oxides of nitrogen in aqueous  $\text{Na}_2\text{CO}_3$  solution:



Nitrites are white, crystalline hygroscopic salts that are very soluble in water. When heated in the absence of air they disproportionate:



$\text{NaNO}_2$ , in addition to its use with nitrates in heat-transfer molten-salt baths, is much used in the production of azo dyes and other organo-nitrogen compounds, as a corrosion inhibitor and in curing meats.

Other oxoacid salts of the alkali metals are discussed in later chapters, e.g. borates (p. 205), silicates (p. 347), phosphites and phosphates (p. 510), sulfites, hydrogensulfates, thiosulfates, etc. (p. 706) selenites, selenates, tellurites and tellurates (p. 781), hypohalites, halites, halates and perhalates (p. 853), etc.

### 4.3.6 Coordination chemistry <sup>(38-42)</sup>

Exciting developments have occurred in the coordination chemistry of the alkali metals during the last few years that have completely rejuvenated what appeared to be a largely predictable and worked-out area of chemistry. Conventional beliefs had reinforced the predominant impression of very weak coordinating ability, and had rationalized this in terms of the relatively large size and low charge of the cations  $\text{M}^+$ . On this view, stability of coordination complexes should diminish in the sequence  $\text{Li} > \text{Na} > \text{K} > \text{Rb} > \text{Cs}$ , and this is frequently observed, though the reverse sequence is also known for the formation constants of, for example, the weak complexes with sulfate, peroxosulfate, thiosulfate and the hexacyanoferrates in aqueous solutions.<sup>(39)</sup> It was also known that the alkali metal cations formed numerous hydrates, or aqua-complexes, as discussed in the preceding section, and there is a definite, though smaller tendency to form ammine complexes such as  $[\text{Li}(\text{NH}_3)_4]\text{I}$ . Other well-defined complexes include the extremely stable adducts  $\text{LiX}\cdot 5\text{Ph}_3\text{PO}$ ,  $\text{LiX}\cdot 4\text{Ph}_3\text{PO}$  and  $\text{NaX}\cdot 5\text{Ph}_3\text{PO}$ , where X is a large anion such as I,  $\text{NO}_3$ ,  $\text{ClO}_4$ ,  $\text{BPh}_4$ ,  $\text{SbF}_6$ ,  $\text{AuCl}_4$ , etc.; these compounds melt in the range  $200\text{--}315^\circ$  and are stable to air and water (in which they are insoluble).

<sup>38</sup> P. N. KAPOOR and R. C. MEHROTRA, *Coord. Chem. Rev.* **14**, 1-27 (1974).

<sup>39</sup> D. MIDGLEY, *Chem. Soc. Revs.* **4**, 549-68 (1975).

<sup>40</sup> N. S. POONIA and A. V. BAJAJ, *Chem. Revs.* **79**, 389-445 (1979).

<sup>41</sup> W. SETZER and P. v. R. SCHLEYER, *Adv. Organomet. Chem.* **24**, 353-451 (1985).

<sup>42</sup> C. SCHADE and P. v. R. SCHLEYER, *Adv. Organomet. Chem.* **27**, 169-278 (1987).

They probably all contain the tetrahedral ion  $[\text{Li}(\text{OPPh}_3)_4]^+$  which was established by X-ray crystallography for the compound  $\text{LiI} \cdot 5\text{Ph}_3\text{PO}$ ; the fifth molecule of  $\text{Ph}_3\text{PO}$  is uncoordinated.

In recent years this simple picture has been completely transformed and it is now recognized that the alkali metals have a rich and extremely varied coordination chemistry which frequently transcends even that of the transition metals. The efflorescence is due to several factors such as the emerging molecular chemistry of lithium in particular, the imaginative use of bulky ligands, the burgeoning numbers of metal amides, alkoxides, enolates and organometallic compounds, and the exploitation of multidentate

crown and cryptand ligands. Some of these aspects will be dealt with more fully in subsequent subsections (4.3.7 and 4.3.8).

Lithium is now known in at least 20 coordination geometries with coordination numbers ranging from 1–12. Some illustrative examples are in Table 4.3 and in the accompanying Figs. 4.8 and 4.9 which will repay close attention. The bulky ligand bis(trimethylsilyl)methyl forms a derivative in which Li is 1-coordinate in the gas phase but which polymerizes in the crystalline form to give bent 2-coordinate Li (and 5-coordinate carbon). The related ligand tris(trimethylsilyl)methyl gives an anionic complex in which Li is linear 2-coordinate, and the

Table 4.3 Stereochemistry of lithium

CN and shape	Examples	Remarks	Ref.
1	$[\text{LiCH}(\text{SiMe}_3)_2]$	Gas-phase electron diffr. Li–C 203 pm	43
2 linear	$[\text{Li}\{\text{C}(\text{SiMe}_3)_3\}_2]^-$	Li–C 216 pm, C–Li–C 180°. Cation is $[\text{Li}(\text{thf})_4]^+$	44
bent	$\text{Li}_3\text{N}$	$\text{Li}_1\text{–N}$ 194 pm. See Fig. 4.8a	45
	$\{\text{LiCH}(\text{SiMe}_3)_2\}_\infty$	Note 5-Coord $\text{C}_\alpha$ , Li–C 214, 222 pm; C–Li–C 147–152°, Li–C–Li 152°	43
3 planar	$\{[\text{Li}(\mu\text{-OCBu}_3')_2]\}$	Li–O 167.7 pm, O–Li–O 103°	46
	$\{[\text{Li}(\mu\text{-NR}_2)(\text{OEt}_2)_2]\}$	R = $\text{SiMe}_3$ ; Li–N 206 pm, Li–O 195 pm; N–Li–N 105°, N–Li–O 127.5°. See also Fig. 4.13 below	47
pyramidal angular	$[\text{Li}_5(\text{N}=\text{CPh}_2)_6(\text{O}=\text{P}(\text{NMe}_2)_3)]^-$	Cluster anion, see Fig. 4.8b	48
	$[\text{LiEt}]_4$	Cubane-like cluster, See Fig. 4.8c	49
4 tetrahedral	$[\text{Li}(\text{OCMe}_2\text{Ph})_6]$ ; $[\text{Li}(\text{c-hexyl})_6]$	Hexagonal prism, see Fig. 4.8d	50
	$[\text{Li}(\text{MeOH})_4]\text{I}$	See also $[\text{Li}(\text{thf})_4]^+$ in line 3, above, and Fig. 4.8b	51
5 trigonal-bipyramidal	$\{\text{LiAl}(\mu\text{-C}_2\text{H}_5)_4\}_\infty$		
	$[\text{LiBr}(\text{phen})_2] \cdot \text{Pr}^t\text{OH}$	Br equatorial, one N from each phen axial; N–Li–N 169°; $\text{Pr}^t\text{OH}$ uncoordinated	52
	$[\text{LiL}][\text{ClO}_4]$	L is the aza cage shown in Fig. 4.8e	53

<sup>43</sup>J. L. ATWOOD, T. FJELDBERG, M. F. LAPPERT, N. T. LUONG-THI, R. SHAKIR and A. J. THORNE, *J. Chem. Soc., Chem. Commun.*, 1163–5 (1984).

<sup>44</sup>C. EABORN, P. B. HITCHOCK, J. D. SMITH and A. C. SULLIVAN, *J. Chem. Soc., Chem. Commun.*, 827–8 (1983).

<sup>45</sup>U. v. ALPEN, *J. Solid State Chem.* **29**, 379–92 (1979), and refs. therein.

<sup>46</sup>G. BECK, P. B. HITCHOCK, M. F. LAPPERT and I. A. MACKINNON, *J. Chem. Soc., Chem. Commun.*, 1313–4 (1989); see also ref. d.

<sup>47</sup>T. FJELDBERG, P. B. HITCHOCK, M. F. LAPPERT and A. J. THORNE, *J. Chem. Soc., Chem. Commun.*, 822–4 (1984).

<sup>48</sup>D. BARR, W. CLEGG, R. E. MULVEY and R. SNAITH, *J. Chem. Soc., Chem. Commun.*, 226–7 (1984).

<sup>49</sup>H. DIETRICH, *J. Organomet. Chem.* **205**, 291–9 (1981).

<sup>50</sup>M. H. CHISHOLM, S. R. DRAKE, A. A. NAINI and W. E. STRIEB, *Polyhedron* **10**, 805–10 (1991).

<sup>51</sup>W. WEPPNER, W. WELZEL, R. KNIEP and A. RABENAU, *Angew. Chem. Int. Edn. Engl.* **25**, 1087–9 (1986).

<sup>52</sup>W. C. PATALINGHUG, C. R. WHITAKER and A. H. WHITE, *Aust. J. Chem.* **43**, 635–7 (1990).

<sup>53</sup>A. BENCINI, A. BIANCHI, A. BORSELLI, M. CIAMPOLINI, M. MICHELONI, N. NARDI, P. PAOLI, B. VALTANCOLI, S. CHIMICHI and P. DAPPORTO, *J. Chem. Soc., Chem. Commun.*, 174–5 (1990).

Table 4.3 continued

CN and shape	Examples	Remarks	Ref.
sq. pyramidal	[LiL'] [BPh <sub>4</sub> ]	L' is the aza cage shown in Fig. 4.8f	54
	[(Li(thf)) <sub>4</sub> (C <sub>4</sub> Bu' <sub>2</sub> ) <sub>2</sub> ]	Dimeric dilithiobutatriene complex, Fig. 4.8g	55
planar	[LiL''] [PF <sub>6</sub> ]	L'' is the pentadentate ligand in Fig. 4.8h	56
6 octahedral	LiX	NaCl-type, X = H, F, Cl, Br, I. Also LiIO <sub>3</sub> ; LiNO <sub>3</sub> (calcite-type); LiAlSi <sub>2</sub> O <sub>6</sub> (spodumene)	
planar	Li <sub>3</sub> N	See Fig. 4.8a. Li <sub>II</sub> has 3 Li <sub>I</sub> and 3 N at 213 pm	45
pentag. pyram.	[LiL*(MeOH)] [PF <sub>6</sub> ]	See Fig. 4.8i	57
irregular	[Li <sub>2</sub> (μ-η <sup>4</sup> , η <sup>4</sup> -C <sub>6</sub> H <sub>8</sub> (tmeda) <sub>2</sub> )]	See Fig. 4.9a	58
7 irregular	[Li(η <sup>5</sup> -C <sub>5</sub> H <sub>4</sub> SiMe <sub>3</sub> )(tmeda)]	5C at 227 pm, 2N at 215 pm. See Fig. 4.9b	59
	[Li <sub>2</sub> (μ-η <sup>5</sup> , η <sup>5</sup> -C <sub>8</sub> H <sub>6</sub> )(dme) <sub>2</sub> ]	Pentalene-dimethoxyethane complex, Fig. 4.9c	60
8 cubic	Li metal	Body-centered cubic	
	LiHg, LiTl	CsCl-type	
irregular	[Li <sub>2</sub> (μ-η <sup>6</sup> , η <sup>6</sup> -C <sub>10</sub> H <sub>8</sub> )(tmeda) <sub>2</sub> ]	Dilithionaphthalene complex, Fig. 4.9d	61
9 irregular	[Na <sub>2</sub> Ph(Et <sub>2</sub> O <sub>2</sub> (Ph <sub>2</sub> Ni) <sub>2</sub> N <sub>2</sub> Na-Li <sub>6</sub> (OEt) <sub>4</sub> (Et <sub>2</sub> O) <sub>2</sub> )]	Fig. 4.9e. 4Li are 9-coord (1, 2, 5, 6), Li(4) is 7-coord and Li(3) is 6 coord	62
12 cuboctahedron	Li metal (cold worked, ccp)	Below 78 K Li is hcp (12 coord)	
hexag. prism.	[Li <sub>2</sub> (μ-C <sub>19</sub> H <sub>12</sub> ) <sub>2</sub> ]	Lithium 7bH-indenofluorene dimer, see Fig. 4.9f	63

<sup>54</sup>A. BENCINI, A. BIANCHI, M. CIAMPOLINI, E. GARCIA-ESPANA, P. DAPPORTO, M. MICHELONI, P. PAOLI, J. A. RAMIREZ and B. VALTANCOLI, *J. Chem. Soc., Chem. Commun.*, 701-3 (1989).

<sup>55</sup>W. NEUGEBAUER, G. A. P. GEIGER, A. J. KOS, J. J. STEZOWSKI and P. v. R. SCHLEYER, *Chem. Ber.* **118**, 1504-16 (1985).

<sup>56</sup>E. C. CONSTABLE, M. J. DOYLE, J. HEALY and P. R. RAITHBY, *J. Chem. Soc., Chem. Commun.*, 1262-4 (1988).

<sup>57</sup>E. C. CONSTABLE, L.-Y. CHUNG, J. LEWIS and P. R. RAITHBY, *J. Chem. Soc., Chem. Commun.*, 1719-20 (1986).

<sup>58</sup>S. K. ARORA, R. B. BATES, W. A. BEAVERS and R. S. CUTLER, *J. Am. Chem. Soc.* **97**, 6271-2 (1975).

<sup>59</sup>M. F. LAPPERT, A. SINGH, L. M. ENGELHART and A. H. WHITE, *J. Organomet. Chem.* **262**, 271-8 (1984).

<sup>60</sup>J. J. STEZOWSKI, H. OIER, D. WILHELM, T. CLARK and P. v. R. SCHLEYER, *J. Chem. Soc., Chem. Commun.*, 1263-4 (1985).

<sup>61</sup>J. J. BROOKS, W. RHINE, G. D. STUCKY *J. Am. Chem. Soc.* **94**, 7346-51 (1972).

<sup>62</sup>K. JONAS, D. J. BRAUER, C. KRÜGER, P. J. ROBERTS and Y.-H. TSAY *J. Am. Chem. Soc.* **98**, 74-81 (1976).

<sup>63</sup>D. BLADAUSKI, H. DIETRICH, H.-J. HECHT and D. REWICKI, *Angew. Chem. Int. Edn. Engl.* **16**, 474-5 (1977).

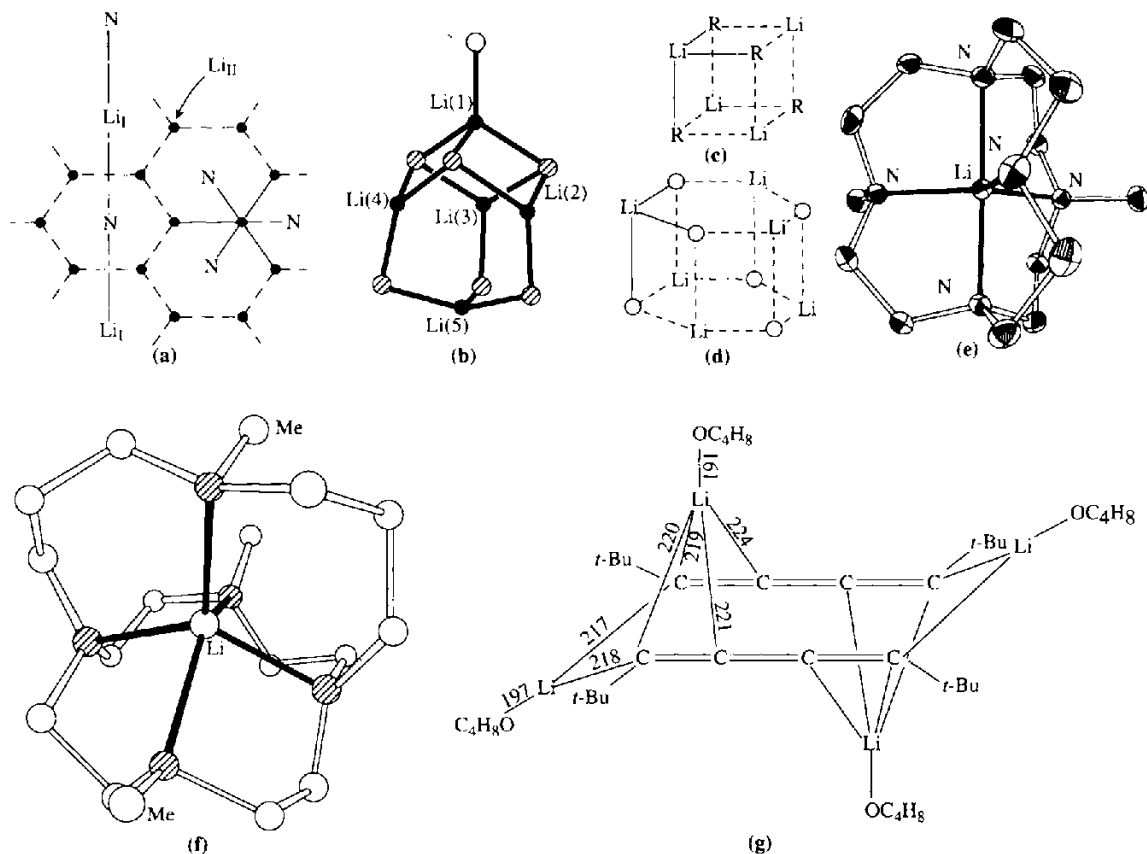
same stereochemistry is observed in the unique structure of Li<sub>3</sub>N (Fig. 4.8a) which also features the highly unusual planar 6-coordination mode; the structure comprises hexagonal sheets of overall composition Li<sub>2</sub>N stacked alternately with planes containing the 2-coordinate Li. The coordination number of N is 8 (hexagonal bipyramidal). Three-coordinate Li is known in planar, pyramidal and angular geometries, the latter two modes being illustrated in Fig. 4.8b, c and d. Numerous examples of 4-coordinate Li have already been mentioned. Five-coordinate Li can be trigonal bipyramidal as in [LiBr(phen)<sub>2</sub>]

and the aza cage cation shown in Fig. 4.8e, square pyramidal (Fig. 4.8f and g) or planar (Fig. 4.8h).

Table 4.3 indicates that octahedral coordination is a common mode for Li. Less usual is planar 6-fold coordination (Fig. 4.8a), pentagonal pyramidal coordination (Fig. 4.8i) or irregular 6-fold coordination (Fig. 4.9a). Examples of 7-fold coordination are in Fig. 4.9b and c. Lithium has cubic 8-fold coordination in the metallic form and in several of its alloys with metals of large radius. It is also 8-coordinate in the dilithionaphthalene complex shown in Fig. 4.9d; here the aromatic



hydrocarbon bonds to two lithium atoms in a bis-hexahapto bridging mode and each lithium is also coordinated by a chelating diamine. A much more complicated dimeric cluster compound, whose central ( $\text{Li}_6\text{Na}_2\text{Ni}_2$ ) core is shown schematically in Fig. 4.9e, includes 9-coordinate lithium among its many fascinating structural features.



**Figure 4.8** Structures of selected lithium compounds having coordination numbers ranging from 2 to 6. (a) The unique structure of  $\text{Li}_3\text{N}$ <sup>(45)</sup> (b) The cluster anion  $[\text{Li}_5(\text{N}=\text{CPh}_2)_6(\text{O}=\text{P}(\text{NMe}_2)_3)]^-$  showing four pyramidal and one tetrahedral  $\text{Li}^{(48)}$  [● = Li, ○ =  $(\text{Me}_2\text{N})_3\text{P}=\text{O}$ , ⊗ =  $\text{Ph}_2\text{C}=\text{N}$ ]. (c) Schematic structure of the cubane-like cluster  $[(\text{LiEt})_4]$  (rings are puckered).<sup>(49)</sup> (d) Schematic structure of the hexagonal prismatic cluster  $[(\text{LiOCMe})_2\text{Ph}_6]$  (rings puckered).<sup>(50)</sup> (e)  $\text{Li}^+$  encapsulated trigonal-bipyramidally by the cryptand trimethylpentaaza[5.5.5]heptadecane (L).<sup>(53)</sup> (f)  $\text{Li}^+$  encapsulated square-pyramidally by the cryptand trimethylpentaazabicyclo[7.5.5]nonadecane (L').<sup>(54)</sup> (g) The dimeric dilithiobutatriene complex showing square-pyramidal coordination of two Li and trigonal coordination of the other two Li.<sup>(55)</sup> (h) Coordination of  $\text{Li}^+$  by the planar pentadentate macrocycle dimethyltetraaza[6.0.0]pyridinophanediene (L'').<sup>(56)</sup> (i) Pentagonal-pyramidal coordination of  $\text{Li}^+$  by the pentadentate macrocycle (L\*) and an apical MeOH ligand.; L\* = (bis-2-hydroxyethyl)-6H,13H-tripyridoheptaazapentadecine.<sup>(57)</sup>

When Li metal is cold-worked it transforms from body-centred cubic to cubic close-packed in which each atom is surrounded by 12 others in twinned cuboctahedral coordination; below 78 K the stable crystalline modification is hexagonal close-packed in which each lithium atom has 12 nearest neighbours in the form of a cuboctahedron. This very high coordination

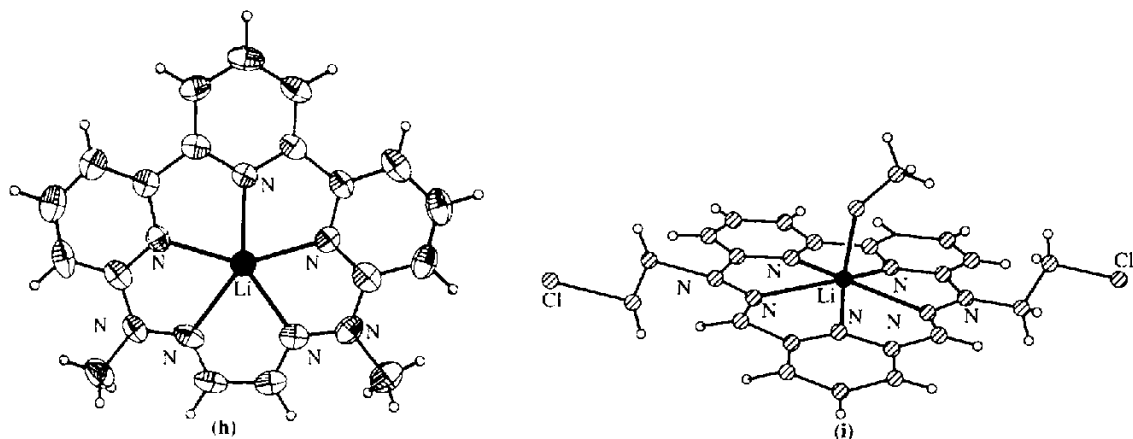
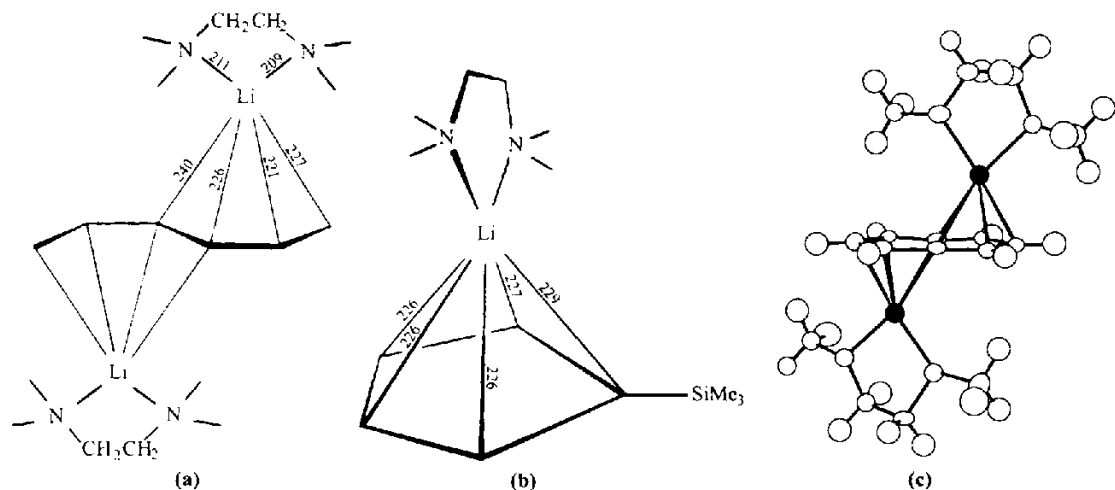


Figure 4.8 continued



**Figure 4.9** Structures of selected organolithium compounds illustrating coordination numbers ranging from 6 to 12. (a) The dilithiobis(tetramethylethylenediamine)hexatriene complex; each Li is coordinated by the bridging bistetrahapto triene and by one chelating tmeda ligand.<sup>(58)</sup> (b) The trimethylsilylcyclopentadienyllithium complex with tmeda.<sup>(59)</sup> (c) The dilithiopentalene-dimethoxyethane complex.<sup>(60)</sup> (d) The dilithionaphthalene complex with tmeda.<sup>(61)</sup> (e) The  $\text{Li}_6\text{Na}_2\text{Ni}_2$  core in the cluster  $[(\text{Na}_2\text{Ph}(\text{Et}_2\text{O})_2(\text{Ph}_2\text{Ni})_2\text{N}_2\text{NaLi}_6(\text{OEt})_4(\text{Et}_2\text{O}))_2]$  showing the four 9-coordinate Li atoms (1, 2, 5, 6), together with the 7-coordinate Li(4) and 6-coordinate Li(3) atoms.<sup>(62)</sup> (f) Hexagonal-prismatic 12-fold coordination of Li in its *H*-indenofluorene dimer.<sup>(63)</sup>

number is also found in the dimeric sandwich compound that Li forms with the extended planar hydrocarbon 7*bH*-indeno[1,2,3-*jk*]fluorene; in this case, as can be seen from Fig. 4.9f, the coordination geometry about the metal atoms is hexagonal prismatic.

Similar structural diversity has been established for the heavier alkali metals also but it is unnecessary to deal with this in detail. The structural chemistry of the organometallic compounds in particular, and of related complexes, has been well reviewed.<sup>(41,42)</sup>

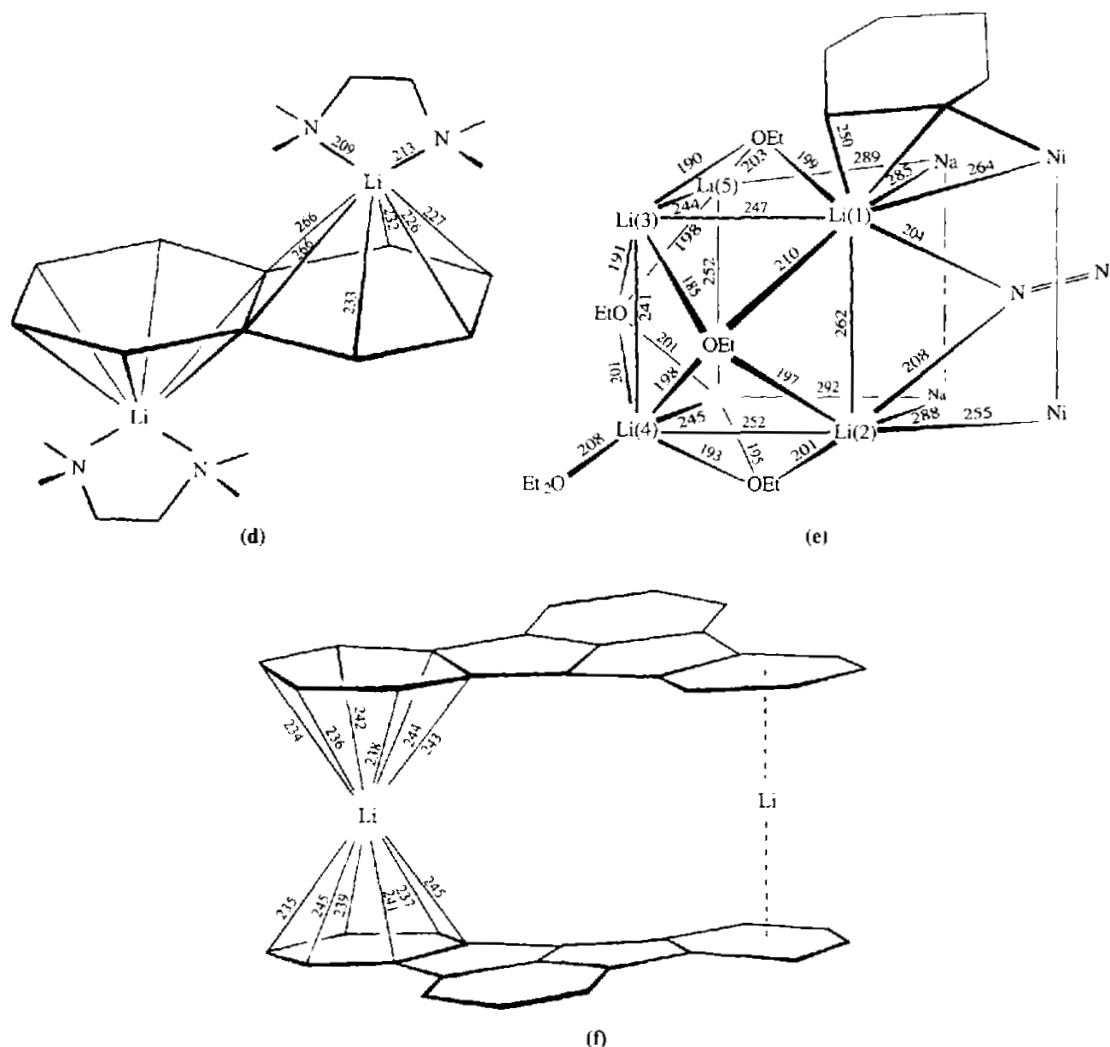


Figure 4.9 continued

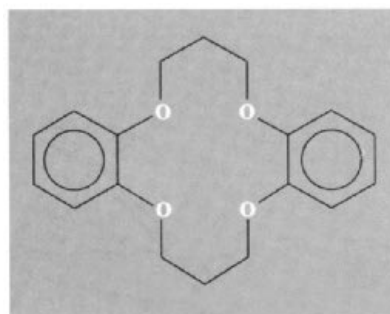
Complexes with chelating organic reagents such as salicylaldehyde and  $\beta$ -diketonates were first prepared by N. V. Sidgwick and his students in 1925, and many more have since been characterized. Stability, as measured by equilibrium formation constants, is rather low and almost invariably decreases in the sequence  $\text{Li} > \text{Na} > \text{K}$ . This situation changed dramatically in 1967 when C. J. Pedersen announced the synthesis of several macrocyclic polyethers which were shown to form stable complexes with

alkali metal and other cations.<sup>(64)</sup> The stability of the complexes was found to depend on the number and geometrical disposition of the ether oxygen atoms and in particular on the size and shape of potential coordination polyhedra relative to the size of the cation. For this reason stability could peak at any particular cation

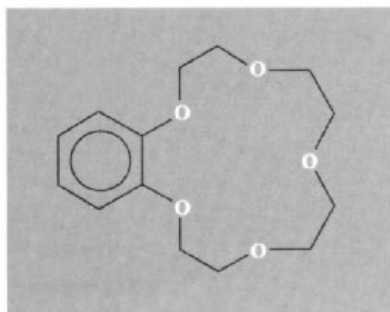
<sup>64</sup> C. J. PEDERSEN, *J. Am. Chem. Soc.* **89**, 2495, 7017–36 (1967). See also C. J. PEDERSEN and H. K. FRENDSORF, *Angew. Chem. Int. Edn. Engl.* **11**, 16–25 (1972).

and, for  $M^I$ , this was often K and sometimes Na or Rb rather than Li. Pedersen, who was awarded a Nobel Prize for these discoveries, coined the epithet “crown” for this class of macrocyclic polyethers because, as he said “the molecular structure looked like one and, with it, cations could be crowned and uncrowned without physical damage to either”.<sup>(65)</sup> Typical examples of such “crown” ethers are given in Fig. 4.10, the numerical prefix indicating the number of atoms in the heterocycle and the suffix the number of ether oxygens. The aromatic rings can be substituted, replaced by naphthalene residues, or reduced to cyclohexyl derivatives. The “hole size” for coordination depends on the number of atoms in the ring and is compared with conventional ionic diameters in Table 4.4. The best complexing agents are rings of 15–24 atoms including 5 to eight oxygen atoms. Nitrogen and sulfur can also serve as the donor atoms in analogous macroheterocycles.

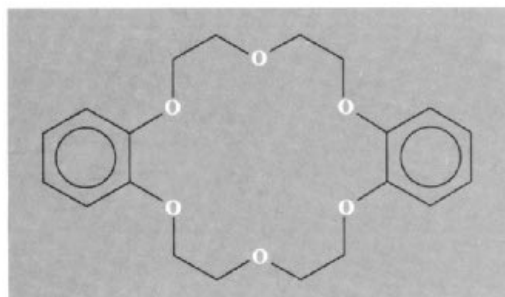
The X-ray crystal structures of many of these complexes have now been determined: representative examples are shown in Fig. 4.11 from which it is clear that, at least for the larger cations, coordinative saturation and bond directionality are far less significant factors than in many transition element complexes.<sup>(66,67)</sup> Further interest in these ligands stems from their use in biochemical modelling since they sometimes mimic the behaviour of naturally occurring, neutral, macrocyclic antibiotics such as valinomycin, monactin, nonactin, nigericin



Dibenzo-14-crown-4



Benzo-15-crown-5



Dibenzo-18-crown-6

**Figure 4.10** Schematic representation of the (non-planar) structure of some typical crown ethers.

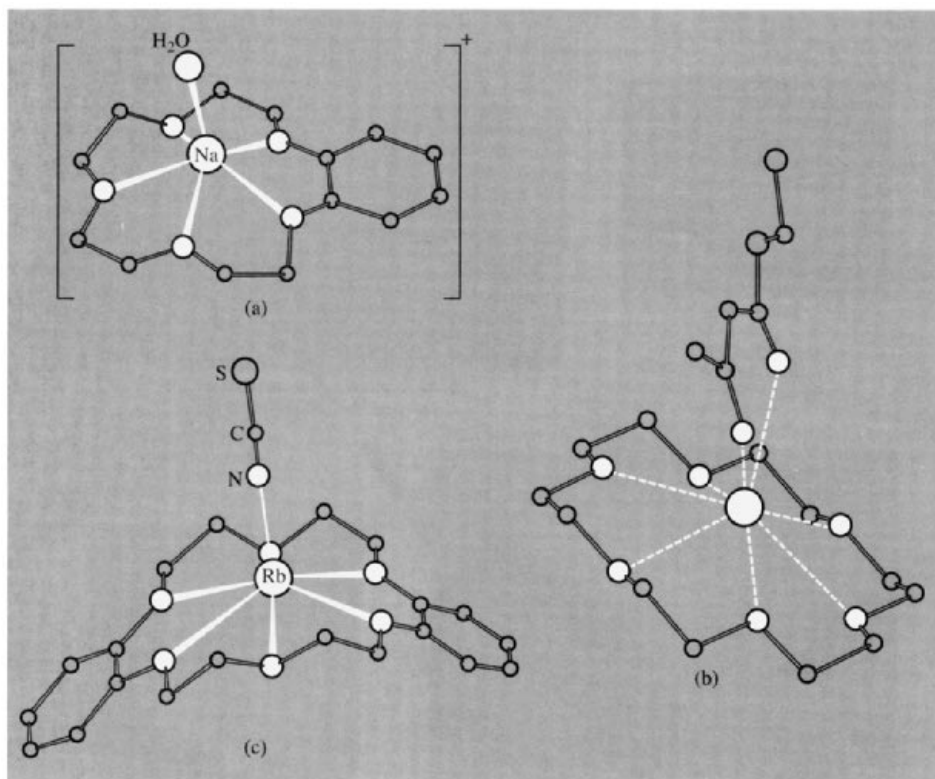
<sup>65</sup> C. J. PEDERSON, Nobel Lecture, *Angew. Chem. Int. Edn. Engl.* **27**, 1021–7 (1988).

<sup>66</sup> J.-M. LEHN, *Struct. Bonding* **16**, 1–69 (1973).

<sup>67</sup> M. R. TRUTER, *Struct. Bonding* **16**, 71–111 (1973).

**Table 4.4** Comparison of ionic diameters and crown ether “hole sizes”

Cation	Ionic diam/pm	Cation	Ionic diam/pm	Polyether ring	“Hole size”/pm
Li <sup>+</sup>	152	Mg <sup>2+</sup>	144	14-crown-4	120–150
Na <sup>+</sup>	204	Ca <sup>2+</sup>	200	15-crown-5	170–220
K <sup>+</sup>	276	Sr <sup>2+</sup>	236	18-crown-6	260–320
Rb <sup>+</sup>	304	Ba <sup>2+</sup>	270	21-crown-7	340–430
Cs <sup>+</sup>	334	Ra <sup>2+</sup>	296	—	—



**Figure 4.11** Molecular structures of typical crown-ether complexes with alkali metal cations: (a) sodium-water-benzo-15-crown-5 showing pentagonal-pyramidal coordination of Na by 6 oxygen atoms; (b) 18-crown-6-potassium-ethyl acetoacetate enolate showing unsymmetrical coordination of K by 8 oxygen atoms; and (c) the RbNCS ion pair coordinated by dibenzo-18-crown-6 to give seven-fold coordination about Rb.

and enneatin.<sup>(68,69)</sup> They may also shed some light on the perplexing and remarkably efficient selectivity between Na and K in biological systems.<sup>(68–70)</sup>

Another group of very effective ligands that have recently been employed to coordinate alkali metal cations are the macrobicyclic polydentate ligands that J.-M. Lehn has termed

“cryptands”,<sup>(71)</sup> e.g.  $N\{(CH_2CH_2O)_2CH_2CH_2\}_3N$  (Fig. 4.13a, b). This forms a complex  $[Rb(\text{crypt})]CNS.H_2O$  in which the ligand encapsulates the cation with a bicapped trigonal prismatic coordination polyhedron (Fig. 4.12c, d). Such complexes are finding increasing use in solvent extraction, phase-transfer catalysis,<sup>(72)</sup> the

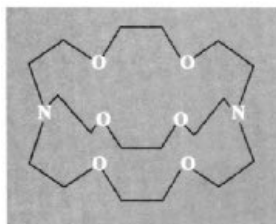
<sup>68</sup> W. SIMON, W. E. MORF and P. CH. MEIER, *Struct. Bonding* **16**, 113–60 (1973).

<sup>69</sup> D. J. CRAM, Nobel Lecture, *Angew. Chem. Int. Edn. Engl.* **27**, 1009–20 (1988). See also F. VÖGTLE (ed.) *Host Guest Complex Chemistry, I, II and III*, Springer-Verlag, *Topics in Current Chemistry* **98**, 1–197 (1981); **101**, 1–203 (1982); **121**, 1–224 (1984).

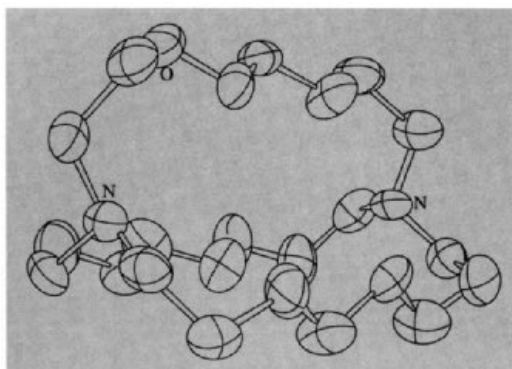
<sup>70</sup> R. M. IZATT, D. J. EATOUGH, and J. J. CHRISTENSEN, *Struct. Bonding* **16**, 161–89 (1973).

<sup>71</sup> J.-M. LEHN, Nobel Lecture, *Angew. Chem. Int. Edn. Engl.* **27**, 89–112. (1988).

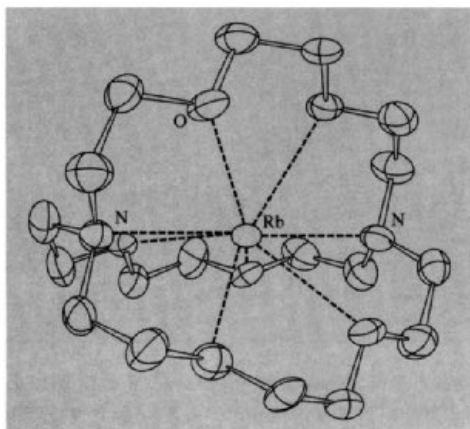
<sup>72</sup> W. P. WEBER and G. W. GOKEL, *Phase Transfer Catalysis in Organic Synthesis*, Vol. 4 of *Reactivity and Structure*, Springer-Verlag, 1977, 250 pp. C. M. STARKS and C. LIOTTA, *Phase Transfer Catalysis*, Academic Press, New York, 1978, 365 pp. F. MONTANARI, D. LANDINI and F. ROLLA, *Topics in Current Chemistry* **101**, 149–201 (1982). E. V. DEHMLOW and S. S. DEHMLOW, *Phase Transfer Catalysis* (2nd edn.), VCH Publishers, London 1983, 386 pp. T. G. SOUTHERN, *Polyhedron* **8**, 407–13 (1989).



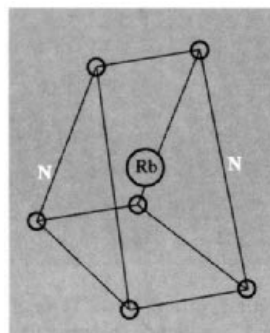
(a) Cryptand



(b) Molecular structure and conformation of the free macrobicyclic cryptand ligand



(c) Molecular structure of complex cation of RbSCN with cryptand.

(d) Schematic representation of bicapped trigonal prismatic coordination about Rb<sup>+</sup>.**Figure 4.12** A typical cryptand and its complex.

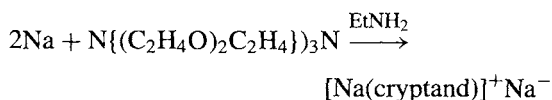
stabilization of uncommon or reactive oxidation states and the promotion of otherwise improbable reactions. Extraordinarily pronounced selectivity in complexation can be achieved by suitably designed ligands, some of the more spectacular being  $K^+/Na^+ \sim 10^5$ ,  $Cu^{2+}/Zn^{2+} \sim 10^8$ ,  $Cd^{2+}/Zn^{2+} \sim 10^9$ .

A growing application of cryptands and other macrocyclic polydentate ligands is in protecting sensitive anions from the polarizing and destabilizing effect of cationic charges, by encapsulating or crowning the cation and so preventing its close approach to the anion. For example, ozonides of K, Rb and Cs form

stable solutions in typical organic solvents (such as  $CH_2Cl_2$ , tetrahydrofuran or MeCN) when the cation is coordinated by crown ethers or cryptands, thus enabling the previously unstudied solution chemistry of  $O_3^-$  to be investigated at room temperature.<sup>(73)</sup> Slow evaporation of ammonia solutions of such complexes yields red crystalline products and an X-ray structure of  $[Rb(\eta^6-18\text{-crown-6})(\eta^2-O_3)(NH_3)]$  reveals 9-coordinate Rb, the chelating ozonide ion itself having O–O distances of 129 and 130 pm and an O–O–O angle of  $117^\circ$ .

<sup>73</sup> N. KORBBER and M. JANSEN, *J. Chem. Soc., Chem. Commun.*, 1654–5 (1990).

A particularly imaginative application of this concept has led to the isolation of compounds which contain monatomic alkali metal *anions*. For example, Na was reacted with cryptand in the presence of EtNH<sub>2</sub> to give the first example of a sodide salt of Na<sup>-</sup>.<sup>(74)</sup>



The Na<sup>-</sup> is 555 pm from the nearest N and 516 pm from the nearest O, indicating that it is a separate entity in the structure. Potas-sides, rubidides and caesides have similarly been prepared.<sup>(74)</sup> The same technique has been used to prepare solutions and even crystals of electrides, in which trapped electrons can play the role of anion. Typical examples are [K(cryptand)]<sup>+</sup>e<sup>-</sup> and [Cs(18-crown-6)]<sup>+</sup>e<sup>-</sup>.<sup>(74,75)</sup>

Macrocycles, though extremely effective as polydentate ligands, are not essential for the production of stable alkali metal complexes; additional conformational flexibility without loss of coordinating power can be achieved by synthesizing benzene derivatives with 2–6 pendant mercapto-polyether groups C<sub>6</sub>H<sub>6-n</sub>R<sub>n</sub>, where R is —SC<sub>2</sub>H<sub>4</sub>OC<sub>2</sub>H<sub>4</sub>OMe, —S(C<sub>2</sub>H<sub>4</sub>O)<sub>3</sub>Bu, etc. Such “octopus” ligands are more effective than crowns and often equally as effective as cryptands in sequestering alkali metal cations.<sup>(76)</sup> Indeed, it is not even essential to invoke organic ligands at all since an inorganic cryptate which completely surrounds Na has been identified in the heteropolytungstate (NH<sub>4</sub>)<sub>17</sub>Na[NaW<sub>21</sub>Sb<sub>9</sub>O<sub>86</sub>].14H<sub>2</sub>O; the compound was also found to have pronounced antiviral activity.<sup>(77)</sup>

<sup>74</sup> J. L. DYE, J. M. CERASE, M. T. LOK, B. L. BARNETT and F. J. TEHAN, *J. Am. Chem. Soc.* **96**, 608–9, 7203–8 (1974).  
J. L. DYE, *Angew. Chem. Int. Edn. Engl.* **18**, 587–98 (1979).

<sup>75</sup> J. L. DYE, *Prog. Inorg. Chem.* **32**, 327–441 (1984);  
J. L. DYE and R.-H. HUANG, *Chem. in Britain* March, 239–44 (1990).

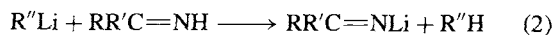
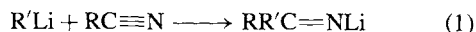
<sup>76</sup> F. VÖGTLE and E. WEBER, *Angew. Chem. Int. Edn. Engl.* **13**, 814–5 (1974).

<sup>77</sup> J. FISCHER, L. RICHARD and R. WEISS, *J. Am. Chem. Soc.* **98**, 3050–2 (1976).

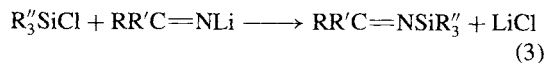
### 4.3.7 Imides, amides and related compounds<sup>(78,79)</sup>

Before discussing the organometallic compounds of the alkali metals (which contain direct M–C bonds, Section 4.3.8) it is convenient to mention another important class of compounds: those which involve M–N bonds. In this way we shall resume the sequence of compounds which started with those having M–X bonds (i.e. halides, Section 4.3.2), through those with M–O bonds (oxides, hydroxides etc., Sections 4.3.3–4.3.5) to those with M–N and finally those with M–C bonds. As we shall see, several significant perceptions have emerged in this field during the past decade. For example, it is now generally agreed that in all these classes of compound the bond from the main group element to the alkali metal is predominantly ionic. Furthermore, structural studies of compounds with Li–N bonds in particular have led to the seminal concepts of *ring-stacking* and *ring-laddering* which, in turn, have permitted the rationalization of many otherwise puzzling structural features.

Lithium imides (imidolithiums) are air-sensitive compounds of general formula (RR'C=NLi)<sub>n</sub>. They can be prepared in high yield either by the addition of an organolithium compound across the triple bond of a nitrile (equation (1)) or by lithiation of a ketimine (equation (2)).



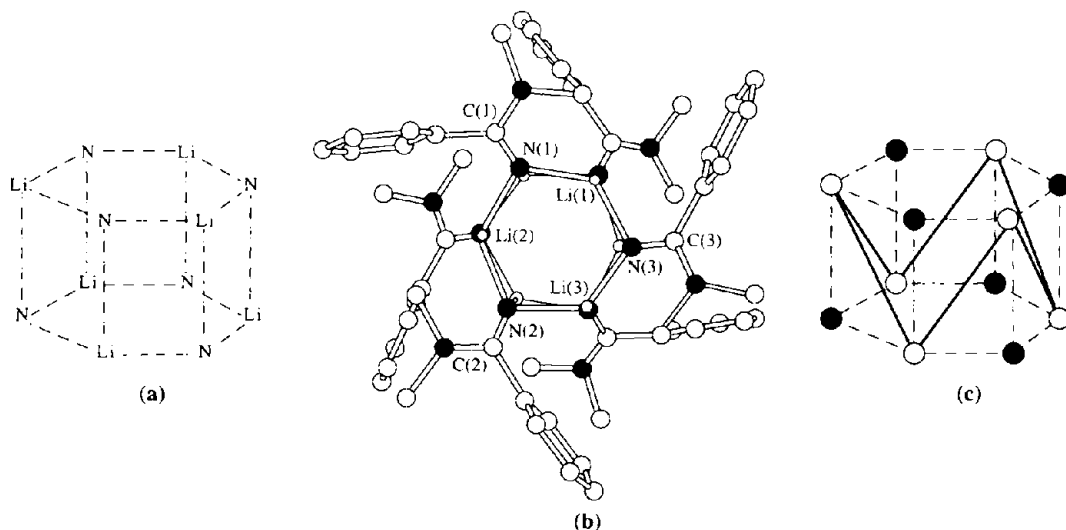
Lithium imides have proved to be useful reagents for the synthesis of imino derivatives of a wide variety of other elements, e.g. Be, B, Al, Si, P, Mo, W and Fe as in equation (3).



When R and R' are both aryl groups the resulting lithium imides are amorphous, insoluble

<sup>78</sup> R. E. MULVEY, *Chem. Soc. Rev.* **20**, 167–209 (1991).

<sup>79</sup> K. GREGORY, P. V. R. SCHLEYER and R. SNAITH, *Adv. Inorg. Chem.* **37**, 47–142 (1991).



**Figure 4.13** (a) Schematic representation of the  $\text{Li}_6\text{N}_6$  core cluster in hexameric lithium imides. (b) The X-ray structure of  $[\text{Me}_2\text{N}(\text{Ph})\text{C}=\text{NLi}]_6$  viewed from above showing the stacking of two 6-membered  $\text{Li}_3\text{N}_3$  rings. (c) Each Li atom has two nearest-neighbour Li atoms in the adjacent ring at 248 pm, shown here joined by full lines; the mean Li-N distances (broken lines) are 198 pm within each ring and 206 pm between rings.<sup>(80)</sup>

(presumably polymeric) solids, but if only one or neither of R, R' is an aryl group, soluble crystalline hexamers are obtained. The skeletal structure of these hexamers comprises an  $\text{Li}_6\text{N}_6$  cluster formed by the stacking of two slightly puckered heterocyclic  $\text{Li}_3\text{N}_3$  rings so that the Li atoms in each ring are almost directly above or below the N atoms in the adjacent ring. This is illustrated schematically in Fig. 4.13a (cf. Fig. 4.8d for the analogous hexameric alkoxide structure). An alternative view, looking down onto the open 6-membered face of the stack, is shown in Fig. 4.13b for the case of  $[\text{Me}_2\text{N}(\text{Ph})\text{C}=\text{NLi}]_6$ . Formation of such hexamers can be viewed as a stepwise process. Initially formed ion-pairs (monomers),  $\text{Li}^+[\text{N}=\text{CRR}']^-$ , with 1-coordinate  $\text{Li}^+$ , associate at first to cyclic trimers,  $(\text{LiN}=\text{CRR}')_3$ , containing 2-coordinate  $\text{Li}^+$  centres. Such rings are essentially planar systems [the planarity of the  $(\text{LiN})_3$  ring itself extending outwards through the imido C up to

and including the  $\alpha$ -atoms of R and R'] and so two such rings can come together, sharing their  $(\text{LiN})_3$  faces and so raising the  $\text{Li}^+$  coordination number to 3. Such stacking necessitates a loss in planarity of the original trimeric rings thus normally preventing more extensive stacking. A further feature of the stacked hexameric structure is the close approach of neighbouring Li atoms across the diagonals of the square faces (Fig. 4.13c), each Li atom being only 248 pm from its two nearest neighbours. This is much less than the Li-Li distance in Li metal (304 pm) or even in the necessarily covalent diatomic molecule  $\text{Li}_2$  (274 pm), but this does not imply either metallic or covalent metal-metal bonding. Such close approaches merely reflect the small size of the  $\text{Li}^+$  ion. For example, the Li-Li distance in LiF (which has the NaCl-type crystal structure) is 284 pm, which is 7% less than the Li-Li distance in Li metal itself.

The ring-stacking concept used in the preceding paragraph to explain the occurrence and structure of lithium imide hexamers can be applied more widely to Li-C, Li-N and Li-O rings and

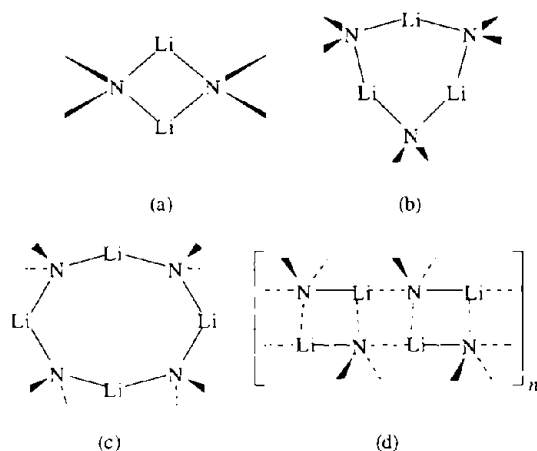
<sup>80</sup> D. BARR, W. CLEGG, R. E. MULVEY, R. SNAITH and K. WADE, *J. Chem. Soc., Chem. Commun.*, 295-7 (1986).



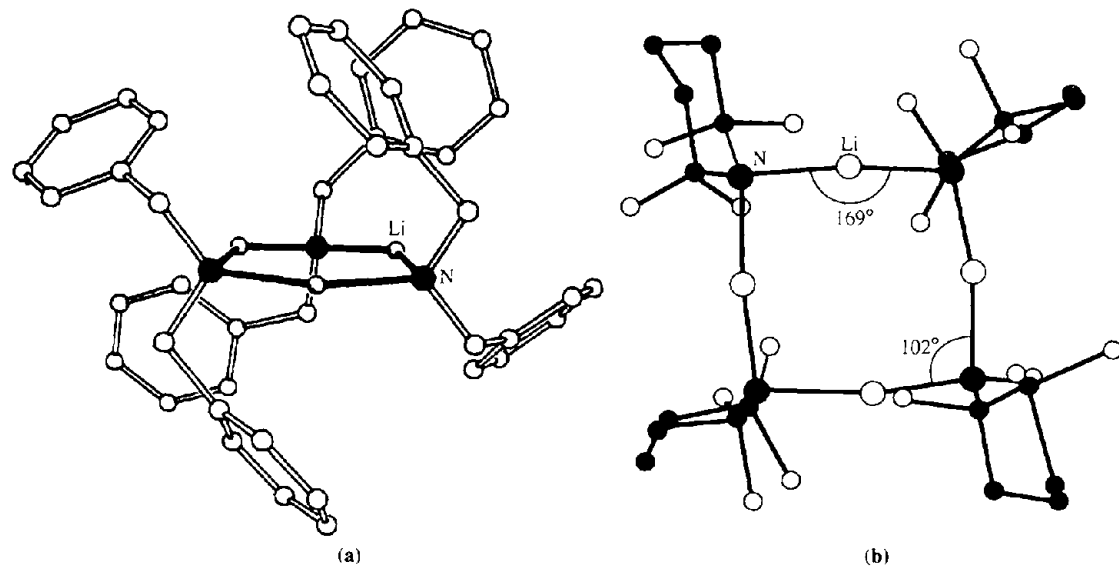
clusters of various sizes.<sup>(78,79)</sup> but the details lie outside the scope of the present treatment.

In contrast to the planar ( $sp^2$ ) nitrogen centres in lithium imides, lithium amides,  $(RR'NLi)_n$ , feature tetrahedral ( $sp^3$ ) nitrogen. The exocyclic R groups are thus above and below the  $(LiN)_n$  plane and this prevents ring stacking. Rings of varying size are known, with  $n = 2, 3$  or 4 depending on the nature of the substituents (Fig. 4.14a, b and c). In the important case of  $n = 2$ , the 4-membered  $Li_2N_2$  heterocycles can associate further by edge fusion (rather than by face fusion) to form ladder-like structures as shown schematically in Fig. 4.14d. Specific examples of amidolithium heterocycles are  $[(Me_3Si)_2NLi]_2$  (gas-phase),  $[(PhCH_2)_2NLi]_3$  (Fig. 4.15a) and the tetramethylpiperidinolithium tetramer  $[Me_2\bar{C}(CH)_2]_3CMe_2\bar{N}Li_4$  (Fig. 4.15b). By contrast, lithiation of the cyclic amine pyrrolidine

in the presence of the chelating ligand tetramethylethylenediamine (tmeda) affords the



**Figure 4.14** Schematic representation of (a) 4-membered, (b) 6-membered and (c) 8-membered  $(LiN)_n$  heterocycles showing pendant groups on N lying both above and below the plane of the ring. (d) the ladder-like structure formed by lateral bonding of two  $Li_2N_2$  units.

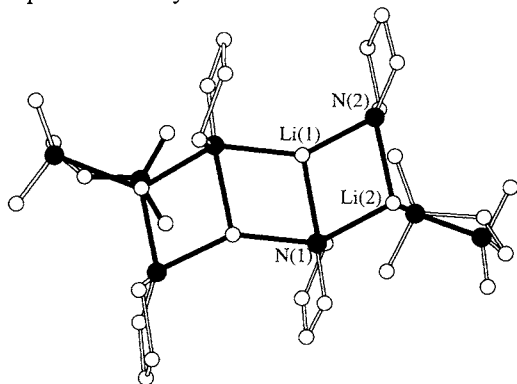


**Figure 4.15** X-ray structure of (a) dibenzylamidolithium,  $[(PhCH_2)_2NLi]_3$ <sup>(81)</sup> and (b) tetramethylpiperidinolithium,  $[Me_2\bar{C}(CH)_2]_3CMe_2\bar{N}Li_4$ .<sup>(82)</sup>

<sup>81</sup> D. R. ARMSTRONG, R. E. MULVEY, G. T. WALKER, D. BARR, R. SNAITH, W. CLEGG and D. REED, *J. Chem. Soc., Dalton Trans.*, 617–28 (1988).

<sup>82</sup> M. F. LAPPERT, M. J. SLADE, A. SINGH, J. L. ATWOOD, R. D. ROGERS and R. SHAKIR, *J. Am. Chem. Soc.* **105**, 302–3 (1983).

laddered complex  $[(\text{H}_2\overline{\text{C}}(\text{CH}_2)_3\text{NLi})_2\text{tmeda}]_2$  (Fig. 4.16). Detailed examination of the interatomic distances in this structure clearly indicate that laddering is achieved by the lateral connection of the two outer  $\text{Li}_2\text{N}_2$  rings. The Li–N bonds in all these compounds are considered to be predominantly ionic.



**Figure 4.16** X-ray structure of the laddered complex  $[(\text{H}_2\overline{\text{C}}(\text{CH}_2)_3\text{NLi})_2\text{tmeda}]_2$  where tmeda is tetramethylethylenediamine.<sup>(83)</sup>

### 4.3.8 Organometallic compounds<sup>(41,42,84,85)</sup>

Some structural aspects of the organometallic compounds of the alkali metals have already been briefly mentioned in Section 4.3.6. The diagonal relation of Li with Mg (p. 76), coupled with the known synthetic utility of Grignard reagents (pp. 132–5), suggests that Li, and perhaps the other alkali metals, might afford synthetically

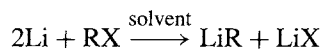
<sup>83</sup> D. R. ARMSTRONG, D. BARR, W. CLEGG, R. E. MULVEY, D. REED, R. SNAITH and K. WADE, *J. Chem. Soc., Chem. Commun.*, 869–70 (1986). D. R. ARMSTRONG, D. BARR, W. CLEGG, S. M. HODGSON, R. E. MULVEY, D. REED, R. SNAITH and D. S. WRIGHT, *J. Am. Chem. Soc.*, **111**, 4719–27 (1989).

<sup>84</sup> G. E. COATES, M. L. H. GREEN and K. WADE, *Organometallic Compounds*, Vol. 1, *The Main Group Elements*, 3rd edn., Chap. 1, The alkali metals, pp. 1–70, Methuen, London, 1967.

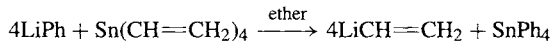
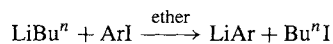
<sup>85</sup> G. WILKINSON, F. G. A. STONE and E. W. ABEL (eds.) *Comprehensive Organometallic Chemistry*, Pergamon Press, Oxford, 1982. Vol. 1, Chap. 2. J. L. WARDELL, Alkali Metals, pp. 43–120.

useful organometallic reagents. Such is found to be the case.<sup>(86)</sup>

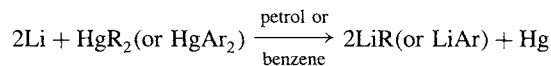
Organolithium compounds can readily be prepared from metallic Li and this is one of the major uses of the metal. Because of the great reactivity both of the reactants and the products, air and moisture must be rigorously excluded by use of an inert atmosphere. Lithium can be reacted directly with alkyl halides in light petroleum, cyclohexane, benzene or ether, the chlorides generally being preferred:



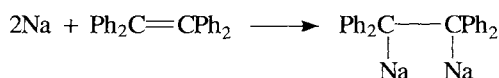
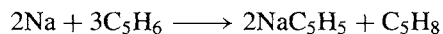
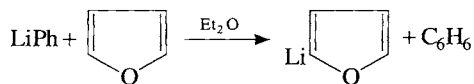
Reactivity and yields are greatly enhanced by the presence of 0.5–1% Na in the Li. The reaction is also generally available for the preparation of metal alkyls of the heavier Group 1 metals. Lithium aryls are best prepared by metal–halogen exchange using  $\text{LiBu}^n$  and an aryl iodide, and transmetalation is the most convenient route to vinyl, allyl and other unsaturated derivatives:



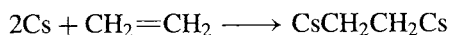
The reaction between an excess of Li and an organomercury compound is a useful alternative when isolation of the product is required, rather than its direct use in further synthetic work:



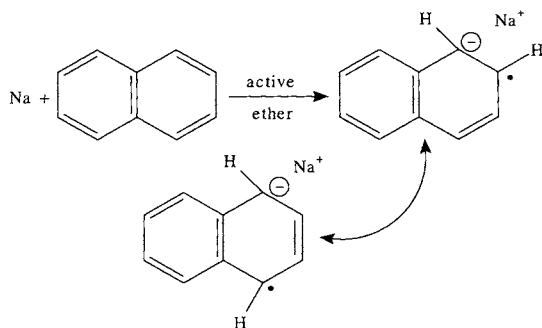
Similar reactions are available for the other alkali metals. Metalation (metal–hydrogen exchange) and metal addition to alkenes provide further routes, e.g.



<sup>86</sup> B. J. WAKEFIELD, *Organolithium Methods*, Academic Press, New York, 1988, 189 pp.

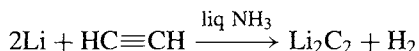
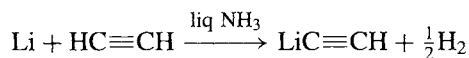


In the presence of certain ethers such as  $\text{Me}_2\text{O}$ ,  $\text{MeOCH}_2\text{CH}_2\text{OMe}$  or tetrahydrofuran, Na forms deep-green highly reactive paramagnetic adducts with polynuclear aromatic hydrocarbons such as naphthalene, phenanthrene, anthracene, etc.:

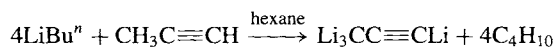


These compounds are in many ways analogous to the solutions of alkali metals in liquid ammonia (p. 77).

The most ionic of the organometallic derivatives of Group 1 elements are the acetylides and dicarbides formed by the deprotonation of alkynes in liquid ammonia solutions:



The largest industrial use of  $\text{LiC}_2\text{H}$  is in the production of vitamin A, where it effects ethynylation of methyl vinyl ketone to produce a key tertiary carbinol intermediate. The acetylides and dicarbides of the other alkali metals are prepared similarly. It is not always necessary to prepare this type of compound in liquid ammonia and, indeed, further substitution to give the bright red perliithiopropyne  $\text{Li}_4\text{C}_3$  can be effected in hexane under reflux:<sup>(87)</sup>



<sup>87</sup> R. WEST, P. A. CARNEY and I. C. MINEO, *J. Am. Chem. Soc.* **87**, 3788–9 (1965).

Organolithium compounds tend to be thermally unstable and most of them decompose to  $\text{LiH}$  and an alkene on standing at room temperature or above. Among the more stable compounds are the colourless, crystalline solids  $\text{LiMe}$  (decomp above  $200^\circ\text{C}$ ),  $\text{LiBu}^n$  and  $\text{LiBu}^t$  (which shows little decomposition over a period of days at  $100^\circ\text{C}$ ). Common lithium alkyls have unusual tetrameric or hexameric structures (see preceding sections). The physical properties of these oligomers are similar to those often associated with covalent compounds (e.g. moderately high volatility, high solubility in organic solvents and low electrical conductivity when fused). Despite this it is now generally agreed that the central  $(\text{LiC})_n$  core is held together by predominantly ionic forces, though estimates of the precise extent of charge separation vary from about 55 to 95%.<sup>(88–91)</sup> The resolution of this apparent paradox lies in the realization that continued polymerization of  $(\text{Li}^+\text{R}^-)$  monomers into infinite ionic arrays, such as are found in the alkali-metal halides, is hindered by the bulky nature of the R groups. Furthermore, these organic groups, which are covalently bonded within themselves, almost completely surround the ionic core and so dominate the bulk physical properties. Such ionic/covalent oligomers have been termed “supramolecules”.<sup>(92)</sup>

The structure and bonding in lithium methyl have been particularly fully studied. The crystal structure consists of interconnected tetrameric units  $(\text{LiMe})_4$  as shown in Fig. 4.17: the individual  $\text{Li}_4\text{C}_4$  clusters consist of a tetrahedron

<sup>88</sup> A. STREITWIESER, J. E. WILLIAMS, S. ALEXANDRATOS and J. M. MCKELVEY, *J. Am. Chem. Soc.* **98**, 4778–84 (1976). A. STREITWIESER, *Acc. Chem. Res.* **17**, 353–7 (1984).

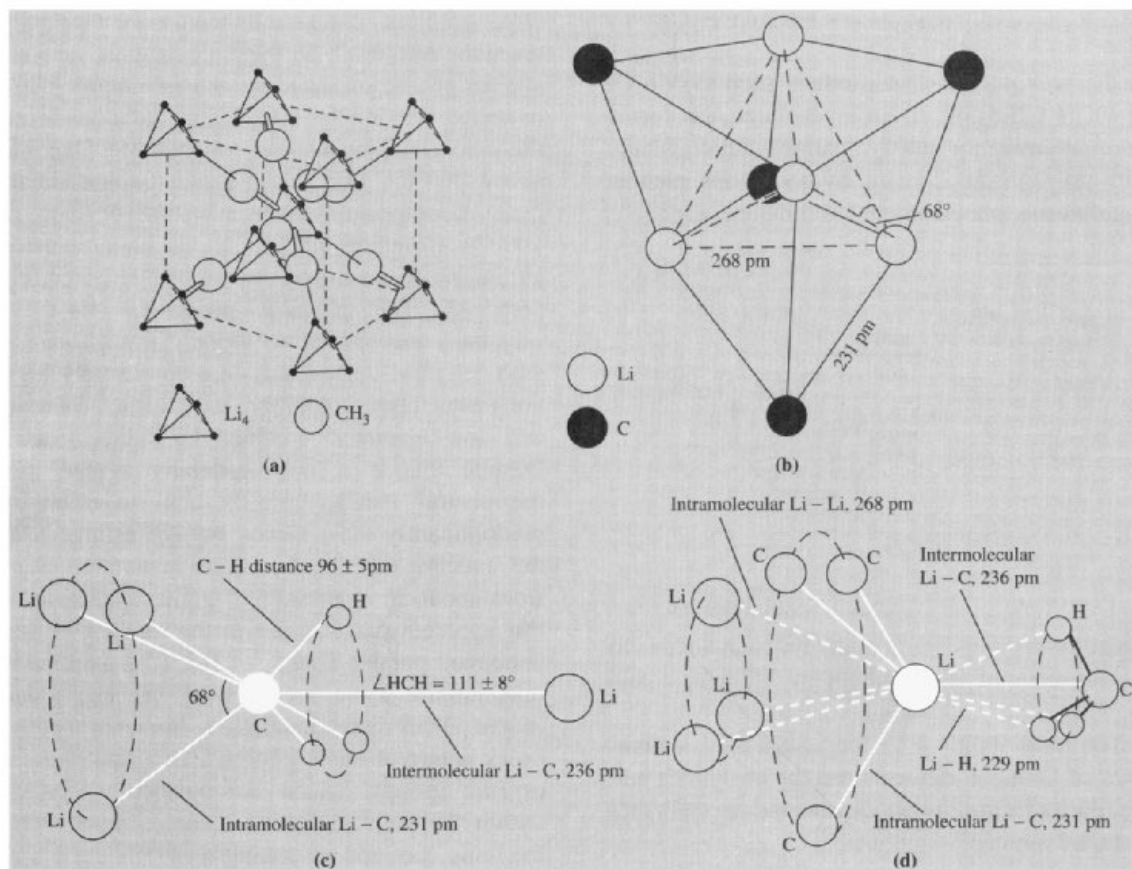
<sup>89</sup> E. D. JEMMIS, J. CHANDRASEKHAR and P. v. R. SCHLEYER, *J. Am. Chem. Soc.* **101**, 2848–56 (1979). P. v. R. SCHLEYER, *Pure Appl. Chem.* **55**, 355–62 (1983); **56**, 151–62 (1984).

<sup>90</sup> G. D. GRAHAM, D. S. MARYNICK and W. N. LIPSCOMB, *J. Am. Chem. Soc.* **102**, 4572–8 (1980).

<sup>91</sup> D. BARR, R. SNAITH, R. E. MULVEY and P. G. PERKINS, *Polyhedron* **7**, 2119–28 (1988).

<sup>92</sup> D. SEEBACH, *Angew. Chem. Int. Edn. Engl.* **27**, 1624–54 (1988).

<sup>93</sup> K. WADE, *Electron Deficient Compounds*, Nelson, London, 1971, 203 pp.



**Figure 4.17** Crystal and molecular structure of  $(\text{LiMe})_4$  showing (a) the unit cell of lithium methyl, (b) the  $\text{Li}_4\text{C}_4$  skeleton of the tetramer viewed approximately along one of the threefold axes, (c) the 7-coordinate environment of each C atom, and (d) the  $(4 + 3 + 3)$ -coordinate environment of each Li atom. After ref. 93, modified to include Li—H contacts.

of 4Li with a triply-bridging C above the centre of each face to complete a distorted cube. The clusters are interconnected along cube diagonals via the bridging  $\text{CH}_3$  groups and the intercluster Li—C distance (236 pm) is very similar to the Li—C distance within each cluster (231 pm). The carbon atoms are thus essentially 7-coordinate being bonded directly to 3H and 4Li. The Li—Li distance within the cluster is 268 pm, which is virtually identical with the value of 267.3 pm for the gaseous  $\text{Li}_2$  molecule and substantially smaller than the value of 304 pm in Li metal (where each Li has 8 nearest neighbours). Each Li atom is

therefore closely associated with three other Li atoms and three C atoms within its own cluster and with one C and three H atoms in an adjoining cluster. Detailed calculations show that the C—H $\cdots$ Li interactions make a substantial contribution to the overall bonding.<sup>(91)</sup> Such “agostic” interactions were indeed first noted in lithium methyl long before their importance in transition metal organometallic compounds was recognized. The effect is most pronounced in  $(\text{LiEt})_4$  where the  $\alpha$ -H on the ethyl group comes within 198 pm of its neighbouring Li atom;<sup>(79,91)</sup> cf. 204.3 pm in solid LiH, which has the NaCl structure (pp. 65, 82).

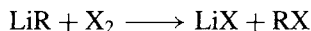
Higher alkyls of lithium adopt similar structures in which polyhedral clusters of metal atoms are bridged by alkyl groups located over the triangular faces of these clusters. For example, crystalline lithium *t*-butyl is tetrameric and the structural units  $(\text{LiBu}^t)_4$  persist in solution; by contrast lithium ethyl, which is tetrameric in the solid state, dissolves in hydrocarbons as the hexamer  $(\text{LiEt})_6$  which probably consists of octahedra of  $\text{Li}_6$  with triply bridging  $-\text{CH}_2\text{CH}_3$  groups above 6 of the 8 faces. As the atomic number of the alkali metal increases there is a gradual trend away from these oligomeric structures towards structures which are more typical of polarized ionic compounds. Thus, although  $\text{NaMe}$  is tetrameric like  $\text{LiMe}$ ,  $\text{NaEt}$  adopts a layer structure in which the  $\text{CH}_2$  groups have a trigonal pyramidal array of Na neighbours, and  $\text{KMe}$  adopts a NiAs-type structure (p. 679) in which each Me is surrounded by a trigonal prismatic array of K. The extent to which this is considered to be  $\text{K}^+\text{CH}_3^-$  is a matter for discussion though it will be noted that  $\text{CH}_3^-$  is isoelectronic with the molecule  $\text{NH}_3$ .

The structure of the organometallic complex lithium tetramethylborate  $\text{LiBMe}_4$  is discussed on pp. 127–8 alongside that of polymeric  $\text{BeMe}_2$  with which it is isoelectronic.

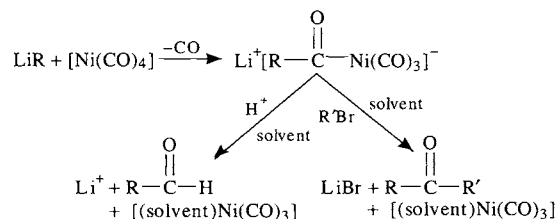
Organometallic compounds of the alkali metals (particularly  $\text{LiMe}$  and  $\text{LiBu}^n$ ) are valuable synthetic reagents and have been increasingly used in industrial and laboratory-scale organic syntheses during the past 20 y.<sup>(86,94,95)</sup> The annual production of  $\text{LiBu}^n$  alone has leapt from a few kilograms to about 1000 tonnes. Large scale applications are as a polymerization catalyst, alkylating agent and precursor to metalated organic reagents. Many of the synthetic reactions parallel those of Grignard reagents over which they sometimes have distinct advantages in terms of speed of reaction, freedom from complicating side reactions or convenience of handling. Reactions are

those to be expected for carbanions, though free-radical mechanisms occasionally occur.

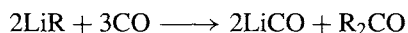
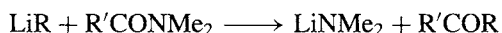
Halogens regenerate the parent alkyl (or aryl) halide and proton donors give the corresponding hydrocarbon:



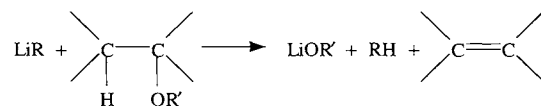
C–C bonds can be formed by reaction with alkyl iodides or more usefully by reaction with metal carbonyls to give aldehydes and ketones: e.g.  $\text{Ni}(\text{CO})_4$  reacts with  $\text{LiR}$  to form an unstable acyl nickel carbonyl complex which can be attacked by electrophiles such as  $\text{H}^+$  or  $\text{R}'\text{Br}$  to give aldehydes or ketones by solvent-induced reductive elimination:



$[\text{Fe}(\text{CO})_5]$  reacts similarly. Aldehydes and ketones can also be obtained from *N,N*-disubstituted amides, and symmetrical ketones are formed by reaction with CO:



Thermal decomposition of  $\text{LiR}$  eliminates a  $\beta$ -hydrogen atom to give an olefin and  $\text{LiH}$ , a process of industrial importance for long-chain terminal alkenes. Alkenes can also be produced by treatment of ethers, the organometallic reacting here as a very strong base (proton acceptor):

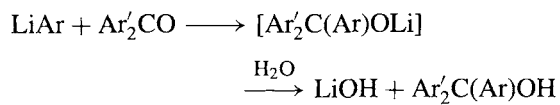
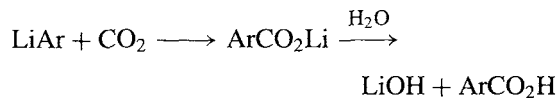


<sup>94</sup> B. J. WAKEFIELD, *The Chemistry of Organolithium Compounds*, Pergamon Press, Oxford, 1976, 337 pp.

<sup>95</sup> K. SMITH, Lithiation and organic synthesis, *Chem. in Br.* **18**(1), 29–32 (1982)

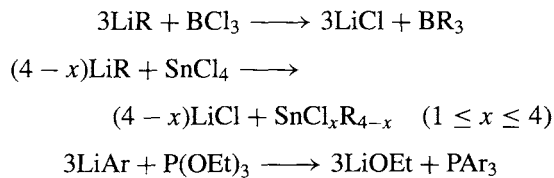
Lithium aryls react as typical carbanions in non-polar solvents giving carboxylic acids with  $\text{CO}_2$

and tertiary carbinols with aryl ketones:



Organolithium reagents are also valuable in the synthesis of other organometallic compounds via

metal-halogen exchange:



Similar reactions have been used to produce organo derivatives of As, Sb, Bi; Si, Ge and many other elements.

																H		He																																
3	4																	5	6	7	8	9	10																											
Li	Be																	B	C	N	O	F	Ne																											
11	12																	13	14	15	16	17	18																											
Na	Mg																	Al	Si	P	S	Cl	Ar																											
19	20	21	22	23	24	25	26	27	28	29	30	31	32	33	34	35	36																																	
K	Ca	Sc	Ti	V	Cr	Mn	Fe	Co	Ni	Cu	Zn	Ga	Ge	As	Se	Br	Kr																																	
37	38	39	40	41	42	43	44	45	46	47	48	49	50	51	52	53	54																																	
Rb	Sr	Y	Zr	Nb	Mo	Tc	Ru	Rh	Pd	Ag	Cd	In	Sn	Sb	Te	I	Xe																																	
55	56	57	58	59	60	61	62	63	64	65	66	67	68	69	70	71	72																																	
Cs	Ba	La	Hf	Ta	W	Re	Os	Ir	Pt	Au	Hg	Tl	Pb	Bi	Po	At	Rn																																	
87	88	89	90	91	92	93	94	95	96	97	98	99	100	101	102	103	104																																	
Fr	Ra	Ac	Rf	Db	Sg	Bh	Hs	Mt	Uu	Uu	Uu	Uu	Uu	Uu	Uu	Uu	Uu																																	
																		59	60	61	62	63	64	65	66	67	68	69	70	71																				
																		Ce	Pr	Nd	Pm	Sm	Eu	Gd	Tb	Dy	Ho	Er	Tm	Yb	Lu																			
																		89	90	91	92	93	94	95	96	97	98	99	100	101	102	103	104	105																
																		Th	Pa	U	Np	Pu	Am	Cm	Bk	Cf	Es	Fm	Md	No	Lr																			

# 5

## Beryllium, Magnesium, Calcium, Strontium, Barium and Radium

### 5.1 Introduction

The Group 2 or alkaline earth metals exemplify and continue the trends in properties noted for the alkali metals. No new principles are involved, but the ideas developed in the preceding chapter gain emphasis and clarity by their further application and extension. Indeed, there is an impressively close parallelism between the two groups as will become increasingly clear throughout the chapter.

The discovery of beryllium in 1798 followed an unusual train of events.<sup>(1)</sup> The mineralogist R.-J. Haüy had observed the remarkable similarity in external crystalline structure, hardness and density of a beryl from Limoges and an emerald from Peru, and suggested to L.-N. Vauquelin that he should analyse them to see if they were chemically identical.<sup>†</sup> As a result, Vauquelin showed

that both minerals contained not only alumina and silica as had previously been known, but also a new earth, beryllia, which closely resembled alumina but gave no alums, apparently did not dissolve in an excess of KOH (perhaps because it had been fused?) and had a sweet rather than an astringent taste. *Caution:* beryllium compounds are now known to be extremely toxic, especially as dusts or smokes;<sup>(2)</sup> it seems likely that this toxicity results from the ability of Be<sup>II</sup> to displace Mg<sup>II</sup> from Mg-activated enzymes due to its stronger coordinating ability.

Both beryl and emerald were found to be essentially Be<sub>3</sub>Al<sub>2</sub>Si<sub>6</sub>O<sub>18</sub>, the only difference between them being that emerald also contains ~2% Cr, the source of its green colour. The combining weight of Be was ~4.7 but the similarity (diagonal relation) between Be and

<sup>1</sup> M. E. WEEKS, *Discovery of the Elements*, 6th edn., Journal of Chemical Education, Easton, Pa, 1956, 910 pp.

<sup>2</sup> J. SCHUBERT, Beryllium and berylliosis, Chap. 34 (1958), in *Chemistry in the Environment*, pp. 321–7, Readings from *Scientific American*, W. H. Freeman, San Francisco, 1973.

<sup>†</sup> A similar observation had been made (with less dramatic consequences) nearly 2000 y earlier by Pliny the Elder when he wrote: "Beryls, it is thought, are of the same nature as the smaragdus (emerald), or at least closely analogous" (*Historia Naturalis*, Book 37).

Al led to considerable confusion concerning the valency and atomic weight of Be ( $2 \times 4.7$  or  $3 \times 4.7$ ); this was not resolved until Mendeleev 70 y later stated that there was no room for a trivalent element of atomic weight 14 near nitrogen in his periodic table, but that a divalent element of atomic weight 9 would fit snugly between Li and B. Beryllium metal was first prepared by F. Wöhler in 1828 (the year he carried out his celebrated synthesis of urea from  $\text{NH}_4\text{CNO}$ ); he suggested the name by allusion to the mineral (Latin *beryllus* from Greek  $\beta\eta\rho\upsilon\lambda\lambda\omicron\varsigma$ ). The metal was independently isolated in the same year by A.-B. Bussy using the same method — reduction of  $\text{BeCl}_2$  with metallic K. The first electrolytic preparation was by P. Lebeau in 1898 and the first commercial process (electrolysis of a fused mixture of  $\text{BeF}_2$  and  $\text{BaF}_2$ ) was devised by A. Stock and H. Goldschmidt in 1932. The close parallel with the development of Li technology (pp. 68–70) is notable.

Compounds of Mg and Ca, like those of their Group 1 neighbours Na and K, have been known from ancient times though nothing was known of their chemical nature until the seventeenth century. Magnesian stone (Greek  $\text{Μαγνησία λιθός}$ ) was the name given to the soft white mineral steatite (otherwise called soapstone or talc) which was found in the Magnesia district of Thessaly, whereas calcium derives from the Latin *calx*, *calcis* — lime. The Romans used a mortar prepared from sand and lime (obtained by heating limestone,  $\text{CaCO}_3$ ) because these lime mortars withstood the moist climate of Italy better than the Egyptian mortars based on partly dehydrated gypsum ( $\text{CaSO}_4 \cdot 2\text{H}_2\text{O}$ ); these had been used, for example, in the Great Pyramid of Gizeh, and all the plaster in Tutankhamun's tomb was based on gypsum. The names of the elements themselves were coined by H. Davy in 1808 when he isolated Mg and Ca, along with Sr and Ba by an electrolytic method following work by J. J. Berzelius and M. M. Pontin: the moist earth (oxide) was mixed with one-third its weight of  $\text{HgO}$  on a Pt plate which served as anode; the cathode was a Pt wire dipping into a pool of Hg and electrolysis

gave an amalgam from which the desired metal could be isolated by distilling off the Hg.

A mineral found in a lead mine near Strontian, Scotland, in 1787 was shown to be a compound of a new element by A. Crawford in 1790. This was confirmed by T. C. Hope the following year and he clearly distinguished the compounds of Ba, Sr and Ca, using amongst other things their characteristic flame colorations: Ba yellow-green, Sr bright red, Ca orange-red. Barium-containing minerals had been known since the seventeenth century but the complex process of unravelling the relation between them was not accomplished until the independent work of C. W. Scheele and J. G. Gahn between 1774 and 1779: heavy spar was found to be  $\text{BaSO}_4$  and called barite or barytes (Greek  $\beta\alpha\rho\acute{\upsilon}\varsigma$ , heavy), whence Scheele's new base baryta ( $\text{BaO}$ ) from which Davy isolated barium in 1808.

Radium, the last element in the group, was isolated in trace amounts as the chloride by P. and M. Curie in 1898 after their historic processing of tonnes of pitchblende. It was named by Mme Curie in allusion to its radioactivity, a word also coined by her (Latin *radius*, a ray); the element itself was isolated electrolytically via an amalgam by M. Curie and A. Debierne in 1910 and its compounds give a carmine-red flame test.

## 5.2 The Elements

### 5.2.1 Terrestrial abundance and distribution

Beryllium, like its neighbours Li and B, is relatively unabundant in the earth's crust; it occurs to the extent of about 2 ppm and is thus similar to Sn (2.1 ppm), Eu (2.1 ppm) and As (1.8 ppm). However, its occurrence as surface deposits of beryl in pegmatite rocks (which are the last portions of granite domes to crystallize) makes it readily accessible. Crystals as large as 1 m on edge and weighing up to 60 tonnes have been reported. World reserves in commercial deposits are about 4 million tonnes of contained Be and mined production in 1985–86 was USA



223, USSR 76 and Brazil 37 tonnes of contained Be, which together accounted for 98% of world production. The cost of Be metal was \$690/kg in 1987. By contrast, world supplies of magnesium are virtually limitless: it occurs to the extent of 0.13% in sea water, and electrolytic extraction at the present annual rate, if continued for a million years, would only reduce this to 0.12%.

Magnesium, like its heavier congeners Ca, Sr and Ba, occurs in crustal rocks mainly as the insoluble carbonates and sulfates, and (less accessibly) as silicates. Estimates of its total abundance depend sensitively on the geochemical model used, particularly on the relative weightings given to the various igneous and sedimentary rock types, and values ranging from 20 000 to 133 000 ppm are current.<sup>(3)</sup> Perhaps the most acceptable value is 27 640 ppm (2.76%), which places Mg sixth in order of abundance by weight immediately following Ca (4.66%) and preceding Na (2.27%) and K (1.84%). Large land masses such as the Dolomites in Italy consist predominantly of the magnesian limestone mineral dolomite [ $\text{MgCa}(\text{CO}_3)_2$ ], and there are substantial deposits of magnesite ( $\text{MgCO}_3$ ), epsomite ( $\text{MgSO}_4 \cdot 7\text{H}_2\text{O}$ ) and other evaporites such as carnallite ( $\text{K}_2\text{MgCl}_4 \cdot 6\text{H}_2\text{O}$ ) and langbeinite [ $\text{K}_2\text{Mg}_2(\text{SO}_4)_3$ ]. Silicates are represented by the common basaltic mineral olivine [ $(\text{Mg,Fe})_2\text{SiO}_4$ ] and by soapstone (talc) [ $\text{Mg}_3\text{Si}_4\text{O}_{10}(\text{OH})_2$ ], asbestos (chrysotile) [ $\text{Mg}_3\text{Si}_2\text{O}_5(\text{OH})_4$ ] and micas. Spinel ( $\text{MgAl}_2\text{O}_4$ ) is a metamorphic mineral and gemstone. It should also be remembered that the green leaves of plants, though not a commercial source of Mg, contain chlorophylls which are the Mg-porphine complexes primarily involved in photosynthesis.

Calcium, as noted above, is the fifth most abundant element in the earth's crust and hence the third most abundant metal after Al and Fe. Vast sedimentary deposits of  $\text{CaCO}_3$ , which represent the fossilized remains of earlier marine life, occur over large parts of the earth's surface. The deposits are of two main

types — rhombohedral calcite, which is the more common, and orthorhombic aragonite, which sometimes forms in more temperate seas. Representative minerals of the first type are limestone itself, dolomite, marble, chalk and iceland spar. Extensive beds of the aragonite form of  $\text{CaCO}_3$  make up the Bahamas, the Florida Keys and the Red Sea basin. Corals, sea shells and pearls are also mainly  $\text{CaCO}_3$ . Other important minerals are gypsum ( $\text{CaSO}_4 \cdot 2\text{H}_2\text{O}$ ), anhydrite ( $\text{CaSO}_4$ ), fluorite ( $\text{CaF}_2$ ; also blue john and fluorspar) and apatite [ $\text{Ca}_5(\text{PO}_4)_3\text{F}$ ].

Strontium (384 ppm) and barium (390 ppm) are respectively the fifteenth and fourteenth elements in order of abundance, being bracketed by S (340 ppm) and F (544 ppm). The most important mineral of Sr is celestite ( $\text{SrSO}_4$ ), and strontianite ( $\text{SrCO}_3$ ) is also mined. The largest producers are Mexico, Spain, Turkey and the UK, and the world production of these two minerals in 1985 was  $10^5$  tonnes. The main uses of Sr compounds, especially  $\text{SrCO}_3$ , are in the manufacture of special glasses for colour television and computer monitors (53%), for pyrotechnic displays (14%) and magnetic materials (11%). Strontium carbonate and sulfate are critical raw materials for the USA which is totally dependent on imports for supplies. The sulfate (barite) is also the most important mineral of Ba: it is mined commercially in over 40 countries throughout the world. Production in 1985 was 6.0 million tonnes, of which 44% was mined in the USA. The major use of  $\text{BaSO}_4$  (92%) is as a heavy mud slurry in well drilling; production of Ba chemicals accounts for only 7%.

Radium occurs only in association with uranium (Chapter 31); the observed ratio  $^{226}\text{Ra}/\text{U}$  is  $\sim 1$  mg per 3 kg, leading to a terrestrial abundance for Ra of  $\sim 10^{-6}$  ppm. As uranium ores normally contain only a few hundred ppm of U, it follows that about 10 tonnes of ore must be processed for 1 mg Ra. The total amount of Ra available worldwide is of the order of a few kilograms, but its use in cancer therapy has been superseded by the use of other isotopes, and the

<sup>3</sup> K. K. TUREKIAN, Elements, geochemical distribution of, *McGraw Hill Encyclopedia of Science and Technology*, Vol. 4, pp. 627–30, 1977.

annual production of separated Ra compounds is probably now only about 100 g. Chief suppliers are Belgium, Canada, Czechoslovakia, the UK, and the former Soviet Union.  $^{226}\text{Ra}$  decays by  $\alpha$ -emission with a half-life of 1600 y, although 3 in every  $10^{11}$  decays occur by  $^{14}\text{C}$  emission ( $^{226}_{88}\text{Ra} \longrightarrow ^{212}_{82}\text{Pb} + ^{14}_6\text{C}$ ). This exceedingly rare form of radioactivity was discovered in 1984 in the rare naturally occurring radium isotope  $^{223}\text{Ra}$  where about 1 in  $10^9$  of the atoms decays by  $^{14}\text{C}$  rather than  $\alpha$ -emission.<sup>(4)</sup>

### 5.2.2 Production and uses of the metals<sup>(5)</sup>

Beryllium is extracted from beryl by roasting the mineral with  $\text{Na}_2\text{SiF}_6$  at 700–750°C, leaching the soluble fluoride with water and then precipitating  $\text{Be}(\text{OH})_2$  at about pH 12. The metal is usually prepared by reduction of  $\text{BeF}_2$  (p. 116) with Mg at about 1300°C or by electrolysis of fused mixtures of  $\text{BeCl}_2$  and alkali metal chlorides. It is one of the lightest metals known and has one of the highest mps of the light metals. Its modulus of elasticity is one-third greater than that of steel. The largest use of Be is in high-strength alloys of Cu and Ni (see Panel below).

Magnesium is produced on a large scale (400 000 tonnes in 1985) either by electrolysis or

silicothermal reduction. The major producers are the USA (43%), the former Soviet Union (26%), and Norway (17%). The electrolytic process uses either fused anhydrous  $\text{MgCl}_2$  at 750°C or partly hydrated  $\text{MgCl}_2$  from sea water at a slightly lower temperature. The silicothermal process uses calcined dolomite and ferrosilicon alloy under reduced pressure at 1150°C:



Magnesium is industry's lightest constructional metal, having a density less than two-thirds that of Al (see Panel on the next page). The price of the metal (99.8% purity) was \$3.4/kg in 1994.

The other alkaline earth metals Ca, Sr and Ba are produced on a much smaller scale than Mg. Calcium is produced by electrolysis of fused  $\text{CaCl}_2$  (obtained either as a byproduct of the Solvay process (p. 71) or by the action of HCl or  $\text{CaCO}_3$ ). It is less reactive than Sr or Ba, forming a protective oxide-nitride coating in air which enables it to be machined in a lathe or handled by other standard metallurgical techniques. Calcium metal is used mainly as an alloying agent to strengthen Al bearings, to control graphitic C in cast-iron and to remove Bi from Pb. Chemically it is used as a scavenger in the steel industry (O, S and P), as a getter for oxygen and nitrogen, to remove  $\text{N}_2$  from argon and as a reducing agent in the production of other metals such as Cr, Zr, Th and U. Calcium also reacts directly with  $\text{H}_2$  to give  $\text{CaH}_2$ , which is a useful source of  $\text{H}_2$ . World production of

<sup>4</sup> H. J. ROSE and G. A. JONES, *Nature* **307**, 245–7 (1984).

<sup>5</sup> W. BÜCHNER, R. SCHLIEBS, G. WINTER and K. H. BÜCHEL, *Industrial Inorganic Chemistry*, VCH, New York, 1989, pp. 231–46.

### Uses of Beryllium Metal and Alloys

The ability of Be to age-harden Cu was discovered by M. G. Corson in 1926 and it is now known that ~2% of Be increases the strength of Cu sixfold. In addition, the alloys (which also usually contain 0.25% Co) have good electrical conductivity, high strength, unusual wear resistance, and resistance to anelastic behaviour (hysteresis, damping, etc.): they are non-magnetic and corrosion resistant, and find numerous applications in critical moving parts of aero-engines, key components in precision instruments, control relays and electronics. They are also non-sparking and are thus of great use for hand tools in the petroleum industry. A nickel alloy containing 2% Be is used for high-temperature springs, clips, bellows and electrical connections. Another major use for Be is in nuclear reactors since it is one of the most effective neutron moderators and reflectors known. A small, but important, use of Be is as a window material in X-ray tubes: it transmits X-rays 17 times better than Al and 8 times better than Lindemann glass. A mixture of compounds of radium and beryllium has long been used as a convenient laboratory source of neutrons and, indeed, led to the discovery of the neutron by J. Chadwick in 1932:  $^9\text{Be}(\alpha, n)^{12}\text{C}$ .

### Magnesium Metal and Alloys

The principal advantage of Mg as a structural metal is its low density ( $1.7 \text{ g cm}^{-3}$  compared with 2.70 for Al and 7.80 for steel). For equal strength, the best Mg alloy weighs only a quarter as much as steel, and the best Al alloy weighs about one-third as much as steel. In addition, Mg has excellent machinability and it can be cast or fabricated by any of the standard metallurgical methods (rolling, extruding, drawing, forging, welding, brazing or riveting). Its major use therefore is as a light-weight construction metal, not only in aircraft but also in luggage, photographic and optical equipment, etc. It is also used for cathodic protection of other metals from corrosion, as an oxygen scavenger, and as a reducing agent in the production of Be, Ti, Zr, Hf and U. World production approaches 400 000 tonnes pa.

Magnesium alloys typically contain >90% Mg together with 2–9% Al, 1–3% Zn and 0.2–1% Mn. Greatly improved retention of strength at high temperature (up to  $450^\circ\text{C}$ ) is achieved by alloying with rare-earth metals (e.g. Pr/Nd) or Th. These alloys can be used for automobile engine casings and for aeroplane fuselages and landing wheels. Other uses are in light-weight tread-plates, dock-boards, loading platforms, gravity conveyors and shovels.

Up to 5% Mg is added to most commercial Al to improve its mechanical properties, weldability and resistance to corrosion.

For further details see *Kirk-Othmer Encyclopedia of Chemical Technology*, 4th edn., 1995, Vol. 15, pp. 622–74.

the metal is about 2500 tonnes pa of which >50% was in the USA (price \$5.00–8.00/kg in 1991).

Metallic Sr and Ba are best prepared by high-temperature reduction of their oxides with Al in an evacuated retort or by small-scale electrolysis of fused chloride baths. They have limited use as getters, and a Ni–Ba alloy is used for spark-plug wire because of its high emissivity. Annual production of Ba metal is about 20–30 tonnes worldwide and the 1991 price about \$80–140/kg depending on quality.

### 5.2.3 Properties of the elements

Table 5.1 lists some of the atomic properties of the Group 2 elements. Comparison with the data for Group 1 elements (p. 75) shows the substantial increase in the ionization energies; this is related to their smaller size and higher nuclear charge, and is particularly notable for Be. Indeed, the “ionic radius” of Be is purely a notional figure since no compounds are known in which uncoordinated Be has a  $2+$  charge. In aqueous solutions the reduction potential of

**Table 5.1** Atomic properties of the alkaline earth metals

Property	Be	Mg	Ca	Sr	Ba	Ra
Atomic number	4	12	20	38	56	88
Number of naturally occurring isotopes	1	3	6	4	7	4 <sup>a</sup>
Atomic weight	9.012 182(3)	24.3050(6)	40.078(4)	87.62(1)	137.327(7)	(226.0254) <sup>b</sup>
Electronic configuration	[He]2s <sup>2</sup>	[Ne]3s <sup>2</sup>	[Ar]4s <sup>2</sup>	[Kr]5s <sup>2</sup>	[Xe]6s <sup>2</sup>	[Rn]7s <sup>2</sup>
Ionization energies/ kJ mol <sup>-1</sup>	899.4 1757.1	737.7 1450.7	589.8 1145.4	549.5 1064.2	502.9 965.2	509.3 979.0
Metal radius/pm	112	160	197	215	222	—
Ionic radius (6 coord)/pm	(27) <sup>c</sup>	72	100	118	135	148
$E^\circ/V$ for $M^{2+}(\text{aq}) + 2e^- \rightarrow M(\text{s})$	-1.97	-2.356	-2.84	-2.89	-2.92	-2.916

(<sup>a</sup>) All isotopes are radioactive: longest  $t_{1/2}$  1600 y for Ra(226).

(<sup>b</sup>) Value refers to isotope with longest half-life.

(<sup>c</sup>) Four-coordinate.

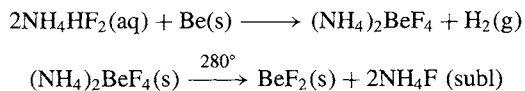
Be is much less than that of its congeners, again indicating its lower electropositivity. By contrast, Ca, Sr, Ba and Ra have reduction potentials which are almost identical with those of the heavier alkali metals; Mg occupies an intermediate position.

Be and Mg are silvery white metals whereas Ca, Sr and Ba are pale yellow (as are the divalent rare earth metals Eu and Yb) although the colour is less intense than for Cs (p. 74). All the alkaline earth metals are lustrous and relatively soft, and their physical properties (Table 5.2), when compared with those of Group 1 metals, show that they have a substantially higher mp, bp, density and enthalpies of fusion and vaporization. This can be understood in terms of the size factor mentioned in the preceding paragraph and the fact that 2 valency electrons per atom are now available for bonding. Again, Be is notable in melting more than 1100° above Li and being nearly 3.5 times as dense; its enthalpy of fusion is more than 5 times that of Li. Beryllium resembles Al in being stable in moist air due to the formation of a protective oxide layer, and highly polished specimens retain their shine indefinitely. Magnesium also resists oxidation but the heavier metals tarnish readily. Beryllium, like Mg and the high-temperature form of Ca (>450°C), crystallizes in the hcp arrangement, and this confers a marked anisotropy on its properties; Sr is fcc, Ba and Ra are bcc like the alkali metals.

### 5.2.4 Chemical reactivity and trends

Beryllium metal is relatively unreactive at room temperature, particularly in its massive form. It does not react with water or steam even

at red heat and does not oxidize in air below 600°C, though powdered Be burns brilliantly on ignition to give BeO and Be<sub>3</sub>N<sub>2</sub>. The halogens (X<sub>2</sub>) react above about 600°C to give BeX<sub>2</sub> but the chalcogens (S, Se, Te) require even higher temperatures to form BeS, etc. Ammonia reacts above 1200°C to give Be<sub>3</sub>N<sub>2</sub> and carbon forms Be<sub>2</sub>C at 1700°C. In contrast with the other Group 2 metals, Be does not react directly with hydrogen, and BeH<sub>2</sub> must be prepared indirectly (p. 115). Cold, concentrated HNO<sub>3</sub> passivates Be but the metal dissolves readily in dilute aqueous acids (HCl, H<sub>2</sub>SO<sub>4</sub>, HNO<sub>3</sub>) with evolution of hydrogen. Beryllium is sharply distinguished from the other alkaline earth metals in reacting with aqueous alkalis (NaOH, KOH) with evolution of hydrogen. It also dissolves rapidly in aqueous NH<sub>4</sub>HF<sub>2</sub> (as does Be(OH)<sub>2</sub>), a reaction of some technological importance in the preparation of anhydrous BeF<sub>2</sub> and purified Be:



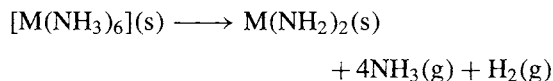
Magnesium is more electropositive than the amphoteric Be and reacts more readily with most of the non-metals. It ignites with the halogens, particularly when they are moist, to give MgX<sub>2</sub>, and burns with dazzling brilliance in air to give MgO and Mg<sub>3</sub>N<sub>2</sub>. It also reacts directly with the other elements in Groups 15 and 16 (and Group 14) when heated and even forms MgH<sub>2</sub> with hydrogen at 570° and 200 atm. Steam produces MgO (or Mg(OH)<sub>2</sub>) plus H<sub>2</sub>, and ammonia reacts at elevated temperature to give Mg<sub>3</sub>N<sub>2</sub>. Methanol reacts at 200° to give Mg(OMe)<sub>2</sub> and ethanol (when activated

**Table 5.2** Physical properties of the alkaline earth metals

Property	Be	Mg	Ca	Sr	Ba	Ra
MP/°C	1289	650	842	769	729	700
BP/°C	2472	1090	1494	1382	1805	(1700)
Density (20°C)/g cm <sup>-3</sup>	1.848	1.738	1.55	2.63	3.59	5.5
ΔH <sub>fus</sub> /kJ mol <sup>-1</sup>	15	8.9	8.6	8.2	7.8	(8.5)
ΔH <sub>vap</sub> /kJ mol <sup>-1</sup>	309	127.4	155	158	136	(113)
ΔH <sub>f</sub> (monatomic gas)/kJ mol <sup>-1</sup>	324	146	178	164	178	—
Electrical resistivity (25°C)/μohm cm	3.70	4.48	3.42	13.4	34.0	(100)

by a trace of iodine) reacts similarly at room temperature. Alkyl and aryl halides react with Mg to give Grignard reagents RMgX (pp. 132–5).

The heavier alkaline earth metals Ca, Sr, Ba (and Ra) react even more readily with non-metals, and again the direct formation of nitrides  $M_3N_2$  is notable. Other products are similar though the hydrides are more stable (p. 65) and the carbides less stable than for Be and Mg. There is also a tendency, previously noted for the alkali metals (p. 84), to form peroxides  $MO_2$  of increasing stability in addition to the normal oxides  $MO$ . Calcium, Sr and Ba dissolve in liquid  $NH_3$  to give deep blue-black solutions from which lustrous, coppery, ammoniates  $M(NH_3)_6$  can be recovered on evaporation; these ammoniates gradually decompose to the corresponding amides, especially in the presence of catalysts:



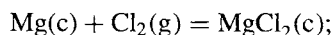
In these properties, as in many others, the heavier alkaline earth metals resemble the alkali metals rather than Mg (which has many similarities to Zn) or Be (which is analogous to Al).

## 5.3 Compounds

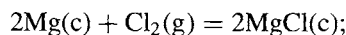
### 5.3.1 Introduction

The predominant divalence of the Group 2 metals can be interpreted in terms of their electronic configuration, ionization energies, and size (see Table 5.1). Further ionization to give simple salts of stoichiometry  $MX_3$  is precluded by the magnitude of the energies involved, the third stage ionization being  $14\,849\text{ kJ mol}^{-1}$  for Be,  $7733\text{ kJ mol}^{-1}$  for Mg and  $4912\text{ kJ mol}^{-1}$  for Ca; even for Ra the estimated value of  $3281\text{ kJ mol}^{-1}$  involves far more energy than could be recovered by additional bonding even if this were predominantly covalent. Reasons for the absence of *univalent* compounds  $MX$  are less obvious. The first-stage ionization energies for Ca, Sr, Ba and Ra are similar to that of Li (p. 75) though the larger

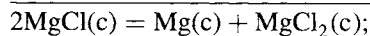
size of the hypothetical univalent Group 2 ions, when compared to Li, would reduce the lattice energy somewhat (p. 82). By making plausible assumptions about the ionic radius and structure we can estimate the approximate enthalpy of formation of such compounds and they are predicted to be stable with respect to the constituent elements; their non-existence is related to the much higher enthalpy of formation of the conventional compounds  $MX_2$ , which leads to rapid and complete disproportionation. For example, the standard enthalpy of formation of hypothetical crystalline  $MgCl$ , assuming the  $NaCl$  structure, is  $\sim -125\text{ kJ mol}^{-1}$ , which is substantially greater than for many known stable compounds and essentially the same as the experimentally observed value for  $AgCl$ :  $\Delta H_f^\circ = -127\text{ kJ mol}^{-1}$ . However, the corresponding (experimental) value for  $\Delta H_f^\circ(MgCl_2)$  is  $-642\text{ kJ mol}^{-1}$ , whence an enthalpy of disproportionation of  $-196\text{ kJ mol}^{-1}$ :



$$\Delta H_f^\circ = -642\text{ kJ/(mol of } MgCl_2)$$



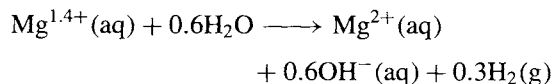
$$\Delta H_f^\circ = -250\text{ kJ/(2 mol of } MgCl)$$



$$\Delta H_{disprop}^\circ = -392\text{ kJ/(2 mol of } MgCl)$$


---

It is clear that, if synthetic routes could be devised which would mechanistically hinder disproportionation, such compounds might be preparable. Although univalent compounds of the Group 2 metals have not yet been isolated, there is some evidence for the formation of  $Mg^1$  species during electrolysis with Mg electrodes. Thus  $H_2$  is evolved at the anode when an aqueous solution of  $NaCl$  is electrolysed and the amount of Mg lost from the anode corresponds to an oxidation state of 1.3. Similarly, when aqueous  $Na_2SO_4$  is electrolysed, the amount of  $H_2$  evolved corresponds to the oxidation by water of Mg ions having an average oxidation state of 1.4:

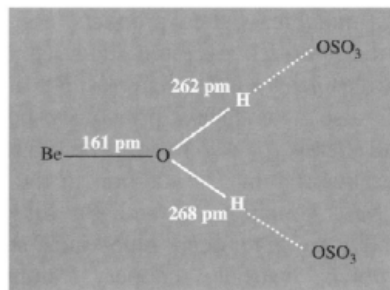


On the basis of the discussion on pp. 79–81 the elements in Group 2 would be expected to deviate further from simple ionic bonding than do the alkali metals. The charge on  $M^{2+}$  is higher and the radius for corresponding ions is smaller, thereby inducing more distortion of the surrounding anions. This is reflected in the decreased thermal stability of oxoacid salts such as nitrates, carbonates and sulfates. For example, the temperature at which the carbonate reaches a dissociation pressure of 1 atm  $CO_2$  is:  $BeCO_3$  250°,  $MgCO_3$  540°,  $CaCO_3$  900°,  $SrCO_3$  1289°,  $BaCO_3$  1360°. The tendency towards covalency is greatest with Be, and this element forms no compounds in which the bonding is predominantly ionic. For similar reasons Be (and to a lesser extent Mg) forms numerous stable coordination compounds; organometallic compounds are also well characterized, and these frequently involve multicentre (electron deficient) bonding similar to that found in analogous compounds of Li and B.

Many compounds of the Group 2 elements are much less soluble in water than their Group 1 counterparts. This is particularly true for the fluorides, carbonates and sulfates of the heavier members, and is related to their higher lattice energies. These solubility relations have had a profound influence on the mineralization of these elements as noted on p. 109. The ready solubility of  $BeF_2$  (~20 000 times that of  $CaF_2$ ) is presumably related to the very high solvation enthalpy of Be to give  $[Be(H_2O)_4]^{2+}$ .

Beryllium, because of its small size, almost invariably has a coordination number of 4. This is important in analytical chemistry since it ensures that edta, which coordinates strongly to Mg, Ca (and Al), does not chelate Be appreciably.  $BeO$  has the wurtzite ( $ZnS$ , p. 1209) structure whilst the other Be chalcogenides adopt the zinc blende modification.  $BeF_2$  has the cristobalite ( $SiO_2$ , p. 342) structure and has only a very low electrical conductivity when fused.  $Be_2C$  and  $Be_2B$  have extended lattices of the antifluorite type with 4-coordinate Be and 8-coordinate C or B.  $Be_2SiO_4$  has the phenacite structure (p. 347) in which both Be and Si

are tetrahedrally coordinated, and  $Li_2BeF_4$  has the same structure.  $[Be(H_2O)_4]SO_4$  features a tetrahedral aquo-ion which is H bonded to the surrounding sulfate groups in such a way that Be–O is 161 pm and the O–H...O are 262



and 268 pm. Further examples of tetrahedral coordination to Be are to be found in later sections. Other configurations, involving linear (two-fold) coordination (e.g.  $BeBu_2$ ) or trigonal coordination [e.g. cyclic  $(MeBeNMe_2)_2$ ] are rare and most compounds which might appear to have such coordination (e.g.  $BeMe_2$ ,  $CsBeF_3$ , etc.) achieve 4-coordination by polymerization. However  $K_2BeO_2$ ,<sup>(6)</sup>  $Y_2BeO_4$ <sup>(7)</sup> and one or two more complex structures<sup>(8)</sup> do indeed contain trigonal planar  $\{BeO_3\}$  units with Be–O ca. 155 pm, i.e. some 11 pm shorter than in tetrahedral  $\{BeO_4\}$ . Likewise,  $K_4BeE_2$  (E = P, As, Sb) feature linear anions  $[E-Be-E]^{4-}$  isoelectronic with  $BeCl_2$  molecules (p. 117).<sup>(9)</sup> (See also p. 123). Six-coordination has been observed in  $K_3Zr_6Cl_{15}Be$  and  $Be_3Zr_6Cl_{18}Be$ , in which the Be atom is encapsulated by and contributes two bonding electrons to the octahedral  $Zr_6$  cluster.<sup>(10)</sup> Trigonal-pyramidal

<sup>6</sup> P. KASTNER and R. HOPPE, *Naturwiss.* **61**, 79 (1974).

<sup>7</sup> L. A. HARRIS and H. L. YANKEL, *Acta Cryst.* **22**, 354–60 (1967).

<sup>8</sup> R. A. HOWIE and A. R. WEST, *Nature* **259**, 473 (1976).  
D. SCHULDT and R. HOPPE, *Z. anorg. allg. Chem.*, **578** 119–32 (1989), **594**, 87–94 (1991).

<sup>9</sup> M. SOMER, M. HARTWEG, K. PETERS, T. POPP and H.-G. VON SCHNERING, *Z. anorg. allg. Chem.* **595**, 217–23 (1991).

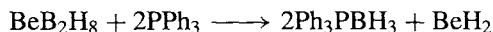
<sup>10</sup> R. P. ZIEBARTH and J. D. CORBETT, *J. Am. Chem. Soc.* **110**, 1132–9 (1988). J. ZHANG and J. D. CORBETT, *Z. anorg. allg. Chem.* **598/599**, 363–70 (1991).

6-fold coordination of Be by H is found in  $\text{Be}(\text{BH}_4)_2$  (p. 116).

The stereochemistry of Mg and the heavier alkaline earth metals is more flexible than that of Be and, in addition to occasional compounds which feature low coordination numbers (2, 3 and 4), there are many examples of 6, 8 and 12 coordination, some with 7, 9 or 10 coordination, and even some with coordination numbers as high as 22 or 24, as in  $\text{SrCd}_{11}$ ,  $\text{BaCd}_{11}$  and  $(\text{Ca}, \text{Sr} \text{ or } \text{Ba})\text{Zn}_{13}$ .<sup>(11)</sup> Strontium is 5-coordinate on the hemisolvate  $[\text{Sr}(\text{OC}_6\text{H}_2\text{Bu}_3)_2(\text{thf})_3] \cdot \frac{1}{2}\text{thf}$  which features a distorted trigonal bipyramidal structure with the two aryloxides in equatorial positions.<sup>(11a)</sup>

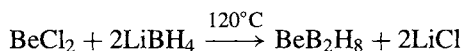
### 5.3.2 Hydrides and halides

Many features of the structure, bonding and stability of the Group 2 hydrides have already been discussed (p. 65) and it is only necessary to add some comments on  $\text{BeH}_2$ , which is the most difficult of these compounds to prepare and the least stable.  $\text{BeH}_2$  (contaminated with variable amounts of ether) was first prepared in 1951 by reduction of  $\text{BeCl}_2$  with  $\text{LiH}$  and by the reaction of  $\text{BeMe}_2$  with  $\text{LiAlH}_4$ . A purer sample can be made by pyrolysis of  $\text{BeBu}_2$  at  $210^\circ\text{C}$  and the best product is obtained by displacing  $\text{BH}_3$  from  $\text{BeB}_2\text{H}_8$  using  $\text{PPh}_3$  in a sealed tube reaction at  $180^\circ$ :

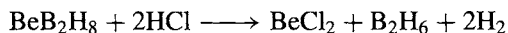


$\text{BeH}_2$  is an amorphous white solid ( $d$   $0.65 \text{ g cm}^{-3}$ ) which begins to evolve hydrogen when heated above  $250^\circ$ ; it is moderately stable in air or water but is rapidly hydrolysed by acids, liberating  $\text{H}_2$ . A hexagonal crystalline form ( $d$   $0.78 \text{ g cm}^{-3}$ ) has been prepared by compaction fusion at 6.2 kbar and  $130^\circ$  in the presence of  $\sim 1\%$  Li as catalyst.<sup>(12)</sup> In all forms  $\text{BeH}_2$  appears to be highly polymerized by means of  $\text{BeHBe}$

3-centre bonds and its structure is probably similar to that of crystalline  $\text{BeCl}_2$  and  $\text{BeMe}_2$  (see below). A related compound is the volatile mixed hydride  $\text{BeB}_2\text{H}_8$ , which is readily prepared (in the absence of solvent) by the reaction of  $\text{BeCl}_2$  with  $\text{LiBH}_4$  in a sealed tube:



$\text{BeB}_2\text{H}_8$  inflames in air, reacts almost explosively with water and reacts with dry  $\text{HCl}$  even at low temperatures:



The structure of this compound has proved particularly elusive and at least nine different structures have been proposed; it therefore affords an instructive example of the difficulties which attend the use of physical techniques for the structural determination of compounds in the gaseous, liquid or solution phases. In the gas phase it now seems likely that more than one species is present<sup>(13)</sup> and the compound certainly shows fluxional behaviour which makes all the hydrogen atoms equivalent on the nmr time scale.<sup>(14)</sup> A linear structure such as (a), with possible admixture of singly bridged  $\text{B-H-B}$  and triply bridged  $\text{BeH}_3\text{B}$  variants is now favoured, after a period in which triangular structures such as (b) had been vigorously canvassed. Even structure (c), which features planar 3-coordinate Be, had been advocated because it was thought to fit best much of the infrared and electron diffraction data and also accounted for the ready formation of adducts (d) with typical ligands such as  $\text{Et}_2\text{O}$ ,  $\text{thf}$ ,  $\text{R}_3\text{N}$ ,  $\text{R}_3\text{P}$ , etc. In the solid state the structure has recently been established with some certainty by single-crystal X-ray analysis.<sup>(15)</sup>  $\text{BeB}_2\text{H}_8$  consists of helical polymers of  $\text{BH}_4\text{Be}$

<sup>13</sup> K. BRENDHAUGEN, A. HAARLAND and D. P. NOVAK, *Acta Chem. Scand.* **A29**, 801–2 (1975).

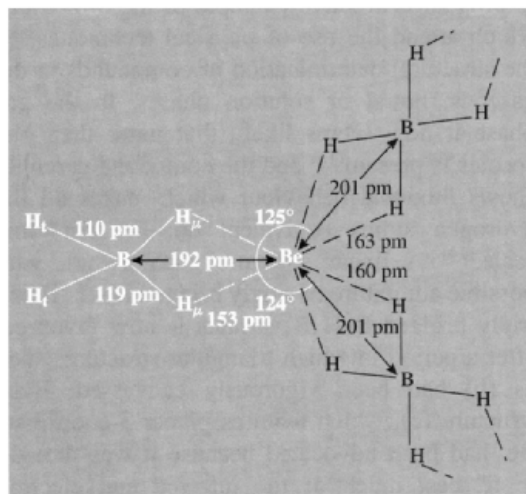
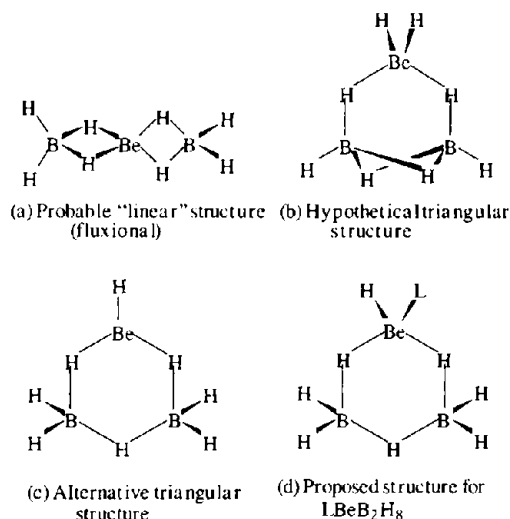
<sup>14</sup> D. F. GAINES, J. L. WALSH and D. F. HILLENBRAND, *J. Chem. Soc., Chem. Commun.*, 224–5 (1977).

<sup>15</sup> D. S. MARYNICK and W. N. LIPSCOMB, *Inorg. Chem.* **11**, 820–3 (1972). D. S. MARYNICK, *J. Am. Chem. Soc.* **101**, 6876–80 (1979). [See also J. F. STANTON, W. N. LIPSCOMB and R. J. BARTLETT, *J. Chem. Phys.* **88**, 5726–34 (1988) for results of high-level computations.]

<sup>11</sup> A. F. WELLS, *Structural Inorganic Chemistry*, 5th edn., Oxford University Press, Oxford, 1984, 1382 pp.

<sup>11a</sup> S. R. DRAKE, D. J. OTWAY, M. B. HURSTHOUSE and K. M. A. MALIK, *Polyhedron* **11**, 1995–2007 (1992).

<sup>12</sup> G. J. BRENDL, E. M. MARLETT and L. M. NIEBYLSKI, *Inorg. Chem.* **17**, 3589–92 (1978).

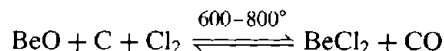


**Figure 5.1** Polymeric structure of crystalline  $Be(BH_4)_2$  showing a section of the  $\cdots(H_2BH_2)Be(H_2BH_2)\cdots$  helix and one "terminal" or non-bridging group  $\{(H)_2B(H_\mu)_2\}$ .

units linked by an equal number of bridging  $BH_4$  units (Fig. 5.1). Of the 8 H atoms only 2 are not involved in bonding to Be; the Be is thus 6-coordinate (distorted trigonal prism) though the H atoms are much closer to B ( $\sim 110$  pm) than to Be (2 at  $\sim 153$  pm and 4 at  $\sim 162$  pm). The  $Be\cdots B$  distance within the helical chain is 201 pm and in the branch is 192 pm. The relationship of this

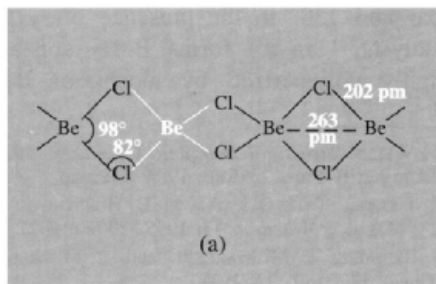
structure to those of  $Al(BH_4)_3$  and  $AlH_3$  itself (p. 227) is noteworthy.

Anhydrous beryllium halides cannot be obtained from reactions in aqueous solutions because of the formation of hydrates such as  $[Be(H_2O)_4]F_2$  and the subsequent hydrolysis which attends attempted dehydration. Thermal decomposition of  $(NH_4)_2BeF_4$  is the best route for  $BeF_2$ , and  $BeCl_2$  is conveniently made from the oxide

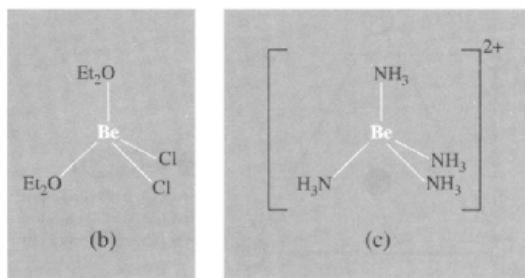


$BeCl_2$  can also be prepared by direct high-temperature chlorination of metallic Be or  $Be_2C$ , and these reactions are also used for the bromide and iodide.  $BeF_2$  is a glassy material that is difficult to crystallize; it consists of a random network of 4-coordinate F-bridged Be atoms similar to the structure of vitreous silica,  $SiO_2$ . Above  $270^\circ$ ,  $BeF_2$  spontaneously crystallizes to give the quartz modification (p. 342) and, like quartz, it exists in a low-temperature  $\alpha$ -form which transforms to the  $\beta$ -form at  $227^\circ$ ; crystalbite and tridymite forms (p. 343) have also been prepared. The structural similarities between  $BeF_2$  and  $SiO_2$  extend to fluoberyllates and silicates, and numerous parallels have been drawn: e.g. the phase diagram, compounds, and structures in the system  $NaF-BeF_2$  resemble those for  $CaO-SiO_2$ ; the system  $CaF_2-BeF_2$  resembles  $ZrO_2-SiO_2$ ; the compound  $KZnBe_3F_9$  is isostructural with benitoite,  $BaTiSi_3O_9$ , etc.

$BeCl_2$  has an unusual chain structure (a) which can be cleaved by weak ligands such as  $Et_2O$  to give 4-coordinate molecular complexes  $L_2BeCl_2$  (b); stronger donors such as  $H_2O$  or  $NH_3$  lead

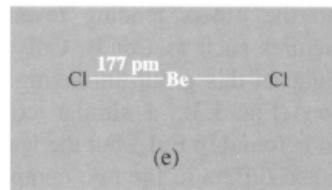
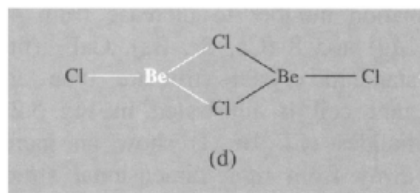






to ionic complexes  $[\text{BeL}_4]^{2+}[\text{Cl}]^{-}_2$  (c). In all these forms Be can be considered to use the  $s$ ,  $p_x$ ,  $p_y$  and  $p_z$  orbitals for bonding; the  $\text{ClBeCl}$  angle is substantially less than the tetrahedral angle of  $109^\circ$  probably because this lessens the repulsive interaction between neighbouring Be atoms in the chain by keeping them further apart and also enables a wider angle than  $71^\circ$  to be accommodated at each Cl atom, consistent with its predominant use of two  $p$  orbitals. The detailed interatomic distances and angles therefore differ significantly from those in the analogous chain structure  $\text{BeMe}_2$  (p. 128), which is best described in terms of 3-centred “electron-deficient” bonding at the Me groups, leading to a  $\text{BeCBe}$  angle of  $66^\circ$  and a much closer approach of neighbouring Be atoms (209 pm). In the vapour phase  $\text{BeCl}_2$  tends to form a bridged  $\text{sp}^2$  dimer (d) and dissociation to the linear ( $\text{sp}$ ) monomer (e) is not complete below about  $900^\circ$ ; in contrast,  $\text{BeF}_2$  is monomeric and shows little tendency to dimerize in the gas phase.

The shapes of the monomeric molecules of the Group 2 halides (gas phase or matrix isolation) pose some interesting problems for those who are content with simple theories of bonding and molecular geometry. Thus, as expected on the basis of either  $\text{sp}$  hybridization or the



VSEPR model, the dihalides of Be and Mg and the heavier halides of Ca and Sr are essentially linear. However, the other dihalides are appreciably bent, e.g.  $\text{CaF}_2 \sim 145^\circ$ ,  $\text{SrF}_2 \sim 120^\circ$ ,  $\text{BaF}_2 \sim 108^\circ$ ;  $\text{SrCl}_2 \sim 130^\circ$ ,  $\text{BaCl}_2 \sim 115^\circ$ ;  $\text{BaBr}_2 \sim 115^\circ$ ;  $\text{BaI}_2 \sim 105^\circ$ . The uncertainties on these bond angles are often quite large ( $\pm 10^\circ$ ) and the molecules are rather flexible, but there seems little doubt that the equilibrium geometry is substantially non-linear. This has been interpreted in terms of  $sd$  (rather than  $\text{sp}$ ) hybridization<sup>(16)</sup> or by a suitable *ad hoc* modification of the VSEPR theory<sup>(17)</sup>.

The *crystal* structures of the halides of the heavier Group 2 elements also show some interesting trends (Table 5.3). For the fluorides, increasing size of the metal enables its

<sup>16</sup> R.L. DEKOCK, M. A. PETERSON, L. A. TIMMER, E. J. BAERENDS and P. VERNOOUS. *Polyhedron* **9**, 1919–34 (1990) and references cited therein. D. M. HASSETT and C. J. MARSDEN, *J. Chem. Soc., Chem. Commun.*, 667–9 (1990).

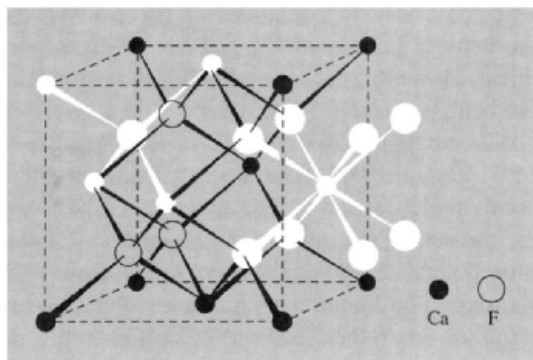
<sup>17</sup> R. J. GILLESPIE, *Chem. Soc. Revs.* **21**, 59–69 (1992).

Table 5.3 Crystal structures of alkaline earth halides<sup>(a)</sup>

	Be	Mg	Ca	Sr	Ba
F	Quartz	Rutile( $\text{TiO}_2$ )	Fluorite	Fluorite	Fluorite
Cl	Chain	$\text{CdCl}_2$	Deformed $\text{TiO}_2$	Deformed $\text{TiO}_2$	$\text{PbCl}_2$
Br	Chain	$\text{CdI}_2$	Deformed $\text{TiO}_2$	Deformed $\text{PbCl}_2$	$\text{PbCl}_2$
I	—	$\text{CdI}_2$	$\text{CdI}_2$	$\text{SrI}_2$	$\text{PbCl}_2$

<sup>(a)</sup> For description of these structures see: quartz (p. 342), rutile (p. 961),  $\text{CdCl}_2$  (p. 1212),  $\text{CdI}_2$  (p. 1212),  $\text{PbCl}_2$  (p. 382); the fluorite,  $\text{BeCl}_2$ -chain and  $\text{SrI}_2$  structures are described in this subsection.

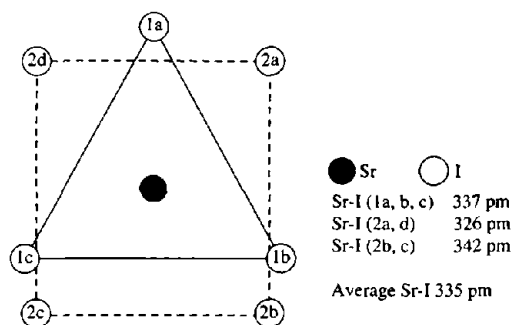
coordination number to increase from 4 (Be) to 6 (Mg) and 8 (Ca, Sr, Ba).  $\text{CaF}_2$  (fluorite) is a standard crystal structure type and its cubic unit cell is illustrated in Fig. 5.2. The other halides (Cl, Br, I) show an increasing trend away from three-dimensional structures, the Be halides forming chains (as discussed above) and the others tending towards layer-lattice structures such as  $\text{CdCl}_2$ ,  $\text{CdI}_2$  and  $\text{PbI}_2$ .  $\text{SrI}_2$  is unique in this group in having sevenfold coordination (Fig. 5.3); a similar coordination polyhedron is found in  $\text{EuI}_2$ , but the way they are interconnected differs in the two compounds.<sup>(18)</sup>



**Figure 5.2** Unit cell of  $\text{CaF}_2$  showing eightfold (cubic) coordination of Ca by 8F and fourfold (tetrahedral) coordination of F by 4Ca. The structure can be thought of as an fcc array of Ca in which all the tetrahedral interstices are occupied by F.

The most important fluoride of the alkaline earth metals is  $\text{CaF}_2$  since this mineral (fluorspar) is the only large-scale source of fluorine (p. 795). Annual world production now exceeds 5 million tonnes the principal suppliers (in 1984) being Mexico (15%), Mongolia (15%), China (14%), USSR (13%) and South Africa (7%). The largest consumer is the USA, though 85% of its needs must be imported.  $\text{CaF}_2$  is a white, high-melting ( $1418^\circ\text{C}$ ) solid whose low solubility in water permits quantitative analytical precipitation. The

<sup>18</sup> E. T. RIETSCHEL and H. BÄRNIGHAUSEN, *Z. anorg. allg. Chem.* **368**, 62–72 (1969).



**Figure 5.3** Structure of  $\text{SrI}_2$  showing sevenfold coordination of Sr by I. The planes 1 and 2 are almost parallel ( $4.5^\circ$ ) and the planes 1a2a2d and 1b2b2c1c are at an angle of  $12^\circ$  to each other.<sup>(9)</sup>

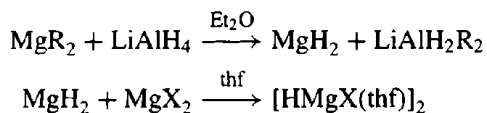
other fluorides (except  $\text{BeF}_2$ ) are also high-melting and rather insoluble. By contrast, the chlorides tend to be deliquescent and to have much lower mps ( $715\text{--}960^\circ$ ); they readily form numerous hydrates and are soluble in alcohols.  $\text{MgCl}_2$  is one of the most important salts of Mg industrially (p. 110) and its concentration in sea water is exceeded only by NaCl.  $\text{CaCl}_2$  is also of great importance, as noted earlier; its production in the US is in the megatonne region and its 1990 price was: bulk \$182/tonne, granules \$360/tonne, i.e. 36 cents/kg. Its traditional uses include:

- brine for refrigeration plants (and for filling inflated tires of tractors and earth-moving equipment to increase traction);
- control of snow and ice on highways and pavements (side walks) — the  $\text{CaCl}_2\text{--H}_2\text{O}$  eutectic at 30 wt%  $\text{CaCl}_2$  melts at  $-55^\circ\text{C}$  (compared with  $\text{NaCl--H}_2\text{O}$  at  $-18^\circ\text{C}$ );
- dust control on secondary roads, unpaved streets, and highway shoulders;
- freeze-proofing of coal and ores in shipping and stock piling;
- use in concrete mixes to give quicker initial set, higher early strength, and greater ultimate strength.

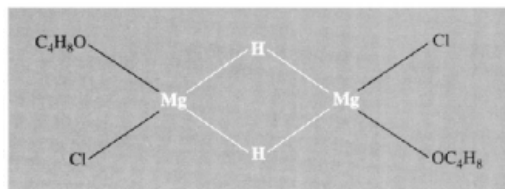
The bromides and iodides continue the trends to lower mps and higher solubilities

in water and their ready solubility in alcohols, ethers, etc., is also notable; indeed,  $\text{MgBr}_2$  forms numerous crystalline solvates such as  $\text{MgBr}_2 \cdot 6\text{ROH}$  ( $\text{R} = \text{Me}, \text{Et}, \text{Pr}$ ),  $\text{MgBr}_2 \cdot 6\text{Me}_2\text{CO}$ ,  $\text{MgBr}_2 \cdot 3\text{Et}_2\text{O}$ , in addition to numerous amines  $\text{MgBr}_2 \cdot n\text{NH}_3$  ( $n = 2-6$ ). The ability of Group 2 cations to form coordination complexes is clearly greater than that of Group 1 cations (p. 90).

Alkaline earth salts  $\text{MHX}$ , where  $\text{M} = \text{Ca}, \text{Sr}$  or  $\text{Ba}$  and  $\text{X} = \text{Cl}, \text{Br}$  or  $\text{I}$  can be prepared by fusing the hydride  $\text{MH}_2$  with the appropriate halide  $\text{MX}_2$  or by heating  $\text{M} + \text{MX}_2$  in an atmosphere of  $\text{H}_2$  at  $900^\circ$ . These hydride halides appear to have the  $\text{PbClF}$  layer lattice structure though the H atoms were not directly located. The analogous compounds of Mg have proved more elusive and the preceding preparative routes merely yield physical mixtures. However,  $\text{MgClH}$  and  $\text{MgBrH}$  can be prepared as solvated dimers by the reaction of specially activated  $\text{MgH}_2$  with  $\text{MgX}_2$  in thf:



The chloride can be crystallized but the bromide disproportionates. On the basis of mol wt and infrared spectroscopic evidence the proposed structure is:



### 5.3.3 Oxides and hydroxides<sup>(19,20)</sup>

The oxides  $\text{MO}$  are best obtained by calcining the carbonates (pp. 114 and 122); dehydration of the hydroxides at red heat offers an alternative route.  $\text{BeO}$  (like the other Be chalcogenides)

has the wurtzite structure (p. 1210) and is an excellent refractory, combining a high mp ( $2507^\circ\text{C}$ ) with negligible vapour pressure below this temperature; it has good chemical stability and a very high thermal conductivity which is greater than that of any other non-metal and even exceeds that of some metals. The other oxides in the group all have the  $\text{NaCl}$  structure and this structure is also adopted by the chalcogenides (except  $\text{MgTe}$  which has the wurtzite structure). Lattice energies and mps are again very high:  $\text{MgO}$  mp  $2832^\circ$ ,  $\text{CaO}$   $2627^\circ$ ,  $\text{SrO}$   $2665^\circ$ ,  $\text{BaO}$   $1913^\circ\text{C}$  (all  $\pm$  ca.  $30^\circ$ ). The compounds are comparatively unreactive in bulk but their reactivity increases markedly with decrease in particle size and increase in atomic weight. Notable reactions (which reverse those used to prepare the oxides) are with  $\text{CO}_2$  and with  $\text{H}_2\text{O}$ .  $\text{MgO}$  is extensively used as a refractory: like  $\text{BeO}$  it is unusual in being both an excellent thermal conductor and a good electrical insulator, thus finding widespread use as the insulating radiator in domestic heating ranges and similar appliances.  $\text{CaO}$  (lime) is produced on an enormous scale in many countries and, indeed, is one of the half-dozen largest tonnage industrial chemicals to be manufactured (see Panel on p. 120). Production in 1991 exceeded 16 million tonnes in the USA alone. Its major end uses (in descending tonnages) are as a flux in steel manufacture; in the production of Ca chemicals; in the treatment of municipal water supplies, industrial wastes and sewage; in mortars and cements; in the pulp and paper industries; and in non-ferrous metal production. Price for bulk quantities is  $\sim$  $\$45$  per tonne.

In addition to the oxides  $\text{MO}$ , peroxides  $\text{MO}_2$  are known for the heavier alkaline earth metals and there is some evidence for yellow superoxides  $\text{M}(\text{O}_2)_2$  of  $\text{Ca}$ ,  $\text{Sr}$  and  $\text{Ba}$ ; impure ozonides  $\text{Ca}(\text{O}_3)_2$  and  $\text{Ba}(\text{O}_3)_2$  have also been reported.<sup>(21)</sup> As with the alkali metals, stability

<sup>19</sup> D. A. EVEREST, Beryllium, *Comprehensive Inorganic Chemistry* Vol. 1, pp. 531-90 Pergamon Press, Oxford (1973).

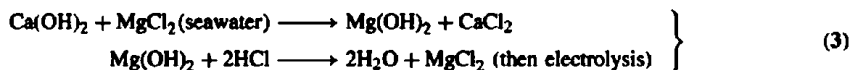
<sup>20</sup> R. D. GOODENOUGH and V. A. STENGER, Magnesium, calcium, strontium, barium and radium. *Comprehensive Inorganic Chemistry*, Vol. 1, pp. 591-664 (1973).

<sup>21</sup> N.-G. VANNERBERG, *Prog. Inorg. Chem.* 4, 125-97 (1962).

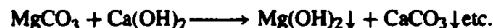
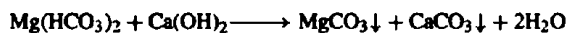
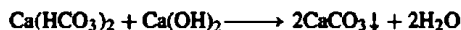
### Industrial Uses of Limestone and Lime

Limestone rock is the commonest form of calcium carbonate, which also occurs as chalk, marble, corals, calcite, aragonite, etc., and (with Mg) as dolomite. Limestone and dolomite are widely used as building materials and road aggregate and both are quarried on a vast scale worldwide.  $\text{CaCO}_3$  is also a major industrial chemical and is indispensable as the precursor of quick lime (CaO) and slaked lime,  $\text{Ca}(\text{OH})_2$ . These chemicals are crucial to large sections of the chemical, metallurgical and construction industries, as noted below, and are produced on a scale exceeded by very few other materials.<sup>(22)</sup> Thus, world production of lime exceeds 110 million tonnes, and even this is dwarfed by Portland cement (793 million tonnes in 1984) which is made by roasting limestone and sand with clay (p. 252).

Large quantities of lime are consumed in the steel industry where it is used as a flux to remove P, S, Si and to a lesser extent Mn. The basic oxygen steel process typically uses 75 kg lime per tonne of steel, or a rather larger quantity (100–300 kg) of dolomitic quick lime, which markedly extends the life of the refractory furnace linings. Lime is also used as a lubricant in steel wire drawing and in neutralizing waste sulfuric-acid-based pickling liquors. Another metallurgical application is in the production of Mg (p. 110): the ferro-silicon (Pidgeon) process (1) uses dolomitic lime and both of the Dow electrolytic methods (2), (3), also require lime.



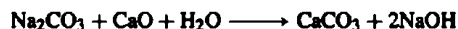
Lime is the largest tonnage chemical used in the treatment of potable and industrial water supplies. In conjunction with alum or iron salts it is used to coagulate suspended solids and remove turbidity. It is also used in water softening to remove temporary (bicarbonate) hardness. Typical reactions are:



The neutralization of acid waters (and industrial wastes) and the maintenance of optimum pH for the biological oxidation of sewage are further applications. Another major use of lime is in scrubbers to remove  $\text{SO}_2/\text{H}_2\text{S}$  from stack gases of fossil-fuel-powered generating stations and metallurgical smelters.

The chemical industry uses lime in the manufacture of calcium carbide (for acetylene, p. 297), cyanamide (p. 323), and numerous other chemicals. Glass manufacturing is also a major consumer, most common glasses having ~12% CaO in their formulation. The insecticide calcium arsenate, obtained by neutralizing arsenic acid with lime, is much used for controlling the cotton boll weevil, codling moth, tobacco worm, and Colorado potato beetle. Lime-sulfur sprays and Bordeaux mixtures [ $(\text{CuSO}_4/\text{Ca}(\text{OH})_2)$ ] are important fungicides.

The paper and pulp industries consume large quantities of  $\text{Ca}(\text{OH})_2$  and precipitated (as distinct from naturally occurring)  $\text{CaCO}_3$ . The largest application of lime in pulp manufacture is as a causticizing agent in sulfate (kraft) plants (p. 89). Here the waste  $\text{Na}_2\text{CO}_3$  solution is reacted with lime to regenerate the caustic soda used in the process:



About 95% of the  $\text{CaCO}_3$  mud is dried and recalcined in rotary kilns to recover the CaO. Calcium hypochlorite bleaching liquor (p. 860) for paper pulp is obtained by reacting lime and  $\text{Cl}_2$ .

The manufacture of high quality paper involves the extensive use of specially precipitated  $\text{CaCO}_3$ . This is formed by calcining limestone and collecting the  $\text{CO}_2$  and CaO separately; the latter is then hydrated and recarbonated to give the desired product. The type of crystals obtained, as well as their size and habit, depend on the temperature, pH, rate of mixing, concentration and presence of additives. The fine crystals (<45  $\mu\text{m}$ ) are often subsequently coated with fatty acids, resins and wetting agents to improve their flow properties. US prices (1991) range from 5–45 cents per kg depending on grade and the amounts consumed are immense, e.g. 5.9 million tonnes p.a. in the USA alone.  $\text{CaCO}_3$  adds brightness, opacity, ink receptivity and smoothness to paper and, in higher concentration, counteracts the high gloss produced by kaolin additives and produces a matte or dull finish which is particularly popular for textbooks. Such papers may contain 5–50% by weight of precipitated  $\text{CaCO}_3$ . The compound is also used as a filler in rubbers, latex, wallpaints and enamels, and in plastics (~10% by weight) to improve their heat resistance, dimensional stability, stiffness, hardness and processability.

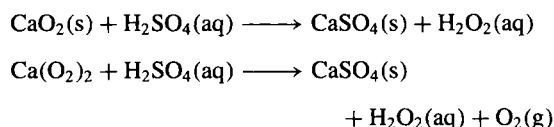
*Panel continues*

<sup>22</sup>R. S. BOYNTON, *Chemistry and Technology of Lime and Limestone*, 2nd edn., Wiley, Chichester, 1980, 579 pp.

Domestic and pharmaceutical uses of precipitated  $\text{CaCO}_3$  include its direct use as an antacid, a mild abrasive in toothpastes, a source of Ca enrichment in diets, a constituent of chewing gum and a filler in cosmetics.

In the dairy industry lime finds many uses. Lime water is often added to cream when separated from whole milk, in order to reduce its acidity prior to pasteurization and conversion to butter. The skimmed milk is then acidified to separate casein which is mixed with lime to produce calcium caseinate glue. Fermentation of the remaining skimmed milk (whey) followed by addition of lime yields calcium lactate which is used as a medicinal or to produce lactic acid on reacidification. Likewise the sugar industry relies heavily on lime: the crude sugar juice is reacted with lime to precipitate calcium sucrate which permits purification from phosphatic and organic impurities. Subsequent treatment with  $\text{CO}_2$  produces insoluble  $\text{CaCO}_3$  and purified soluble sucrose. The cycle is usually repeated several times; cane sugar normally requires  $\sim 3\text{--}5$  kg lime per tonne but beet sugar requires 100 times this amount i.e.  $\sim \frac{1}{4}$  tonne lime per tonne of sugar.

increases with electropositive character and size: no peroxide of Be is known; anhydrous  $\text{MgO}_2$  can only be made in liquid  $\text{NH}_3$  solution, aqueous reactions leading to various peroxide hydrates;  $\text{CaO}_2$  can be obtained by dehydrating  $\text{CaO}_2 \cdot 8\text{H}_2\text{O}$  but not by direct oxidation, whereas  $\text{SrO}_2$  can be synthesized directly at high oxygen pressures and  $\text{BaO}_2$  forms readily in air at  $500^\circ$ . Reactions with aqueous reagents are as expected, and the compounds can be used as oxidizing agents and bleaches:



$\text{MgO}_2$  has the pyrite structure (p. 680) and the Ca, Sr and Ba analogues have the  $\text{CaC}_2$  structure (p. 298).

The hydroxides of Group 2 elements show a smooth gradation in properties, with steadily increasing basicity, solubility, and heats of formation from the corresponding oxide.  $\text{Be}(\text{OH})_2$  is amphoteric and  $\text{Mg}(\text{OH})_2$  is a mild base which, as an aqueous suspension (milk of magnesia), is widely used as a digestive antacid. Note that, though mild,  $\text{Mg}(\text{OH})_2$  will neutralize 1.37 times as much acid as  $\text{NaOH}$ , weight for weight, and 2.85 times as much as  $\text{NaHCO}_3$ .  $\text{Ca}(\text{OH})_2$  and  $\text{Sr}(\text{OH})_2$  are moderately strong to strong bases and  $\text{Ba}(\text{OH})_2$  approaches the alkali hydroxides in strength.

Beryllium salts rapidly hydrolyse in water to give a series of hydroxo complexes of undetermined structure; the equilibria depend

sensitively on initial concentration, pH, temperature, etc., and precipitation begins when the ratio  $\text{OH}^-/\text{Be}^{2+}(\text{aq}) > 1$ . Addition of further alkali redissolves the precipitate and the properties of the resultant solution are consistent (at least qualitatively) with the presence of isopolyanions of the type  $[(\text{HO})_2\{\text{Be}(\mu\text{-OH})_2\}_n\text{Be}(\text{OH})_2]^{2-}$ . Further addition of alkali progressively depolymerizes this chain anion by hydroxyl addition until ultimately the mononuclear beryllate anion  $[\text{Be}(\text{OH})_4]^{2-}$  is formed. The analogy with  $\text{Zn}(\text{OH})_2$  and  $\text{Al}(\text{OH})_3$  is clear.

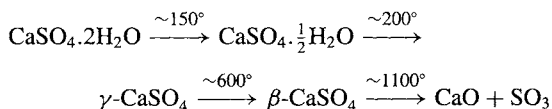
The solubility of  $\text{Be}(\text{OH})_2$  in water is only  $\sim 3 \times 10^{-4} \text{ g l}^{-1}$  at room temperature, compared with  $\sim 3 \times 10^{-2} \text{ g l}^{-1}$  for  $\text{Mg}(\text{OH})_2$  and  $\sim 1.3 \text{ g l}^{-1}$  for  $\text{Ca}(\text{OH})_2$ . Strontium and barium hydroxides have even greater solubilities (8 and  $38 \text{ g l}^{-1}$  respectively at  $20^\circ$ ).

The crystal structures of  $\text{M}(\text{OH})_2$  also follow group trends.<sup>(11)</sup>  $\text{Be}(\text{OH})_2$  crystallizes with 4-coordinate Be in the  $\text{Zn}(\text{OH})_2$  structure which can be considered as a diamond or cristobalite ( $\text{SiO}_2$ ) lattice distorted by H bonding.  $\text{Mg}(\text{OH})_2$  (brucite) and  $\text{Ca}(\text{OH})_2$  have 6-coordinate cations in a  $\text{CdI}_2$  layer lattice structure with OH bonds perpendicular to the layers and strong  $\text{O-H}\cdots\text{O}$  bonding between them. Strontium is too large for the  $\text{CdI}_2$  structure and  $\text{Sr}(\text{OH})_2$  features 7-coordinate Sr (3 + 4), the structure being built up of edge-sharing monocapped trigonal prisms with no H bonds. (The monohydrate has bicapped trigonal prismatic coordination about Sr.) The structure of  $\text{Ba}(\text{OH})_2$  is complex and has not yet been fully determined.

### 5.3.4 Oxoacid salts and coordination complexes

The chemical trends and geochemical significance of the oxoacid salts of the alkaline earth metals have already been mentioned (p. 109) and the immense industrial importance of the carbonates and sulfates in particular can hardly be over emphasized (see Panel on limestone and lime). A speciality use can also be noted: mother-of-pearl (nacre) is a material composed of thin plates of chalk (in the form of aragonite) stuck together with a protein glue. It is iridescent and highly decorative when polished and, despite being 95% chalk, is very strong.

Calcium sulfate usually occurs as the dihydrate (gypsum) though anhydrite ( $\text{CaSO}_4$ ) is also mined. Alabaster is a compact, massive, finegrained form of  $\text{CaSO}_4 \cdot 2\text{H}_2\text{O}$  resembling marble. When gypsum is calcined at 150–165°C it loses approximately three-quarters of its water of crystallization to give the hemihydrate  $\text{CaSO}_4 \cdot \frac{1}{2}\text{H}_2\text{O}$ , also known as plaster of Paris because it was originally obtained from gypsum quarried at Montmartre. Heating at higher temperatures yields various anhydrous forms:



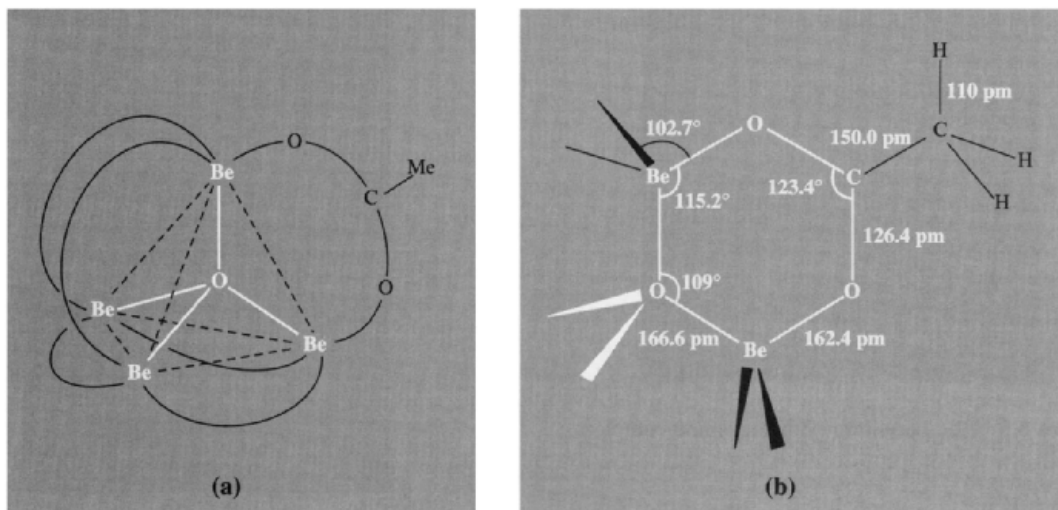
Gypsum, though not mined on the same scale as limestone, is nevertheless still a major industrial mineral. World production in 1990 was 97.7 million tonnes, the major producing countries being the USA (15.2%), Canada (8.4%), Iran (8.2%), China (8.2%), Japan (6.5%), Mexico (6.1%), Thailand (5.9%), France (5.8%) and Spain (5.1%); the remaining 30.6% (30 million tonnes) was distributed between over 20 other countries including the former Soviet Union (4.8%) and the UK (4.1%). A representative price in 1990 was \$5.5 per tonne. In the USA about 28% of the gypsum used is uncalcined and most of this is for Portland cement (p. 252) or agricultural purposes. Of calcined gypsum, virtually all (95%) is used for

prefabricated products, mainly wall board, and the rest is for industrial and building plasters. The hemihydrate expands slightly (0.2–0.3% linear) on rehydration with water and this is crucial to its use in mouldings and plasters; the expansion can be modified in the range 0.03–1.2% by the use of additives.

Other oxoacid salts and binary compounds are more conveniently discussed under the chemistry of the appropriate non-metals in later chapters.

Beryllium is unique in forming a series of stable, volatile, molecular oxide-carboxylates of general formula  $[\text{OBe}_4(\text{RCO}_2)_6]$ , where R = H, Me, Et, Pr, Ph, etc. These white crystalline compounds, of which “basic beryllium acetate” (R = Me) is typical, are readily soluble in organic solvents, including alkanes, but are insoluble in water or the lower alcohols. They are best prepared simply by refluxing the hydroxide or oxide with the carboxylic acid; mixed oxide carboxylates can be prepared by reacting a given compound with another organic acid or acid chloride. The structure (Fig. 5.4) features a central O atom tetrahedrally surrounded by 4 Be. The 6 edges of the tetrahedron so formed are bridged by the 6 acetate groups in such a way that each Be is also tetrahedrally coordinated by 4 oxygens.  $[\text{OBe}_4(\text{MeCO}_2)_6]$  melts at 285° and boils at 330°; it is stable to heat and oxidation except under drastic conditions, is only slowly hydrolysed by hot water, but is decomposed rapidly by mineral acids to give an aqueous solution of the corresponding beryllium salt and free carboxylic acid. The basic nitrate  $[\text{OBe}_4(\text{NO}_3)_6]$  appears to have a similar structure with bridging nitrate groups. The compound is formed by first dissolving  $\text{BeCl}_2$  in  $\text{N}_2\text{O}_4$ /ethyl-acetate to give the crystalline solvate  $[\text{Be}(\text{NO}_3)_2 \cdot 2\text{N}_2\text{O}_4]$ ; when heated to 50° this gives  $\text{Be}(\text{NO}_3)_2$  which decomposes suddenly at 125°C into  $\text{N}_2\text{O}_4$  and  $[\text{OBe}_4(\text{NO}_3)_6]$ .

In addition to the oxide carboxylates, beryllium forms numerous chelating and bridged complexes with ligands such as the oxalate ion  $\text{C}_2\text{O}_4^{2-}$ , alkoxides,  $\beta$ -diketonates and 1,3-diketonates.<sup>(20)</sup> These almost invariably feature 4-coordinate Be

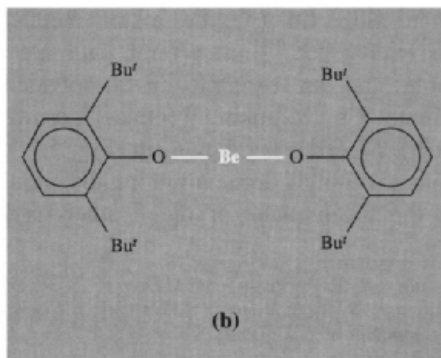
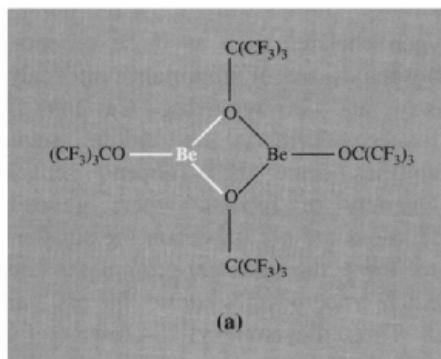


**Figure 5.4** The molecular structure of “basic beryllium acetate” showing (a) the regular tetrahedral arrangement of 4 Be about the central oxygen and the octahedral arrangement of the 6 bridging acetate groups, and (b) the detailed dimensions of one of the six non-planar 6-membered heterocycles. (The Be atoms are 24 pm above and below the plane of the acetate group.) The 2 oxygen atoms in each acetate group are equivalent. The central Be–O distances (166.6 pm) are very close to that in BeO itself (165 pm).

though severe steric crowding can reduce the coordination number to 3 or even 2; for example, the very volatile dimeric perfluoroalkoxide (a) was prepared in 1975 and the unique monomeric bis(2,6-di-*t*-butylphenoxy)beryllium (b) has been known since 1972.

Halide complexes are also well known but complexes with nitrogen-containing ligands are rare. An exception is the blue phthalocyanine complex formed by reaction of Be metal with phthalonitrile, 1,2- $C_6H_4(CN)_2$ , and this affords an unusual example of planar 4-coordinate Be (Fig. 5.5). The complex readily picks up two molecules of  $H_2O$  to form an extremely stable dihydrate, perhaps by dislodging 2 adjacent Be–N bonds and forming 2 Be–O bonds at the preferred tetrahedral angle above and below the plane of the macrocycle.

Magnesium forms few halide complexes of the type  $MX_4^{2-}$ , though  $[NEt_4]_2[MgCl_4]$  has been reported; examples of  $MX_n^{(n-2)-}$  for the heavier alkaline earths are lacking, though hydrates and



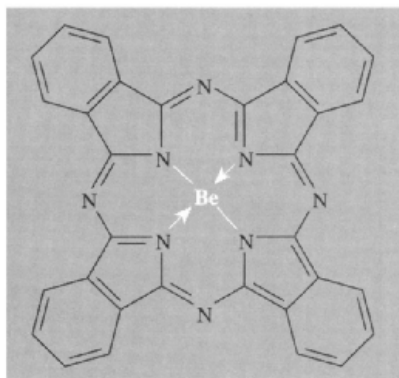


Figure 5.5 The beryllium phthalocyanine complex.

other solvates are well known. The first examples of monomeric six-coordinate (octahedral) complexes of strontium salts have recently been characterized, *viz.*  $trans\text{-}[\text{SrI}_2(\text{hmpa})_4]$  and  $cis\text{-}[\text{Sr}(\text{NCS})_2(\text{hmpa})_4]$  where hmpa is  $(\text{Me}_2\text{N})_3\text{PO}$ ; they were made as colourless crystals by refluxing a mixture of  $\text{NH}_4\text{I}$  (or  $\text{NH}_4\text{SCN}$ ) with metallic Sr and hmpa in toluene for 1 hour.<sup>(23)</sup>

Oxygen chelates such as those of edta and polyphosphates are of importance in analytical chemistry and in removing Ca ions from hard water. There is no unique sequence of stabilities since these depend sensitively on a variety of factors: where geometrical considerations are not important the smaller ions tend to form the stronger complexes but in polydentate macrocycles steric factors can be crucial. Thus dicyclohexyl-18-crown-6 (p. 96) forms much stronger complexes with Sr and Ba than with Ca (or the alkali metals) as shown in Fig. 5.6.<sup>(24)</sup> Structural data are also available and an example of a solvated 8-coordinate Ca complex  $[(\text{benzo-15-crown-5})\text{-Ca}(\text{NCS})_2.\text{MeOH}]$  is shown in Fig. 5.7. The coordination polyhedron is not regular: Ca lies above the mean plane of the 5 ether oxygens

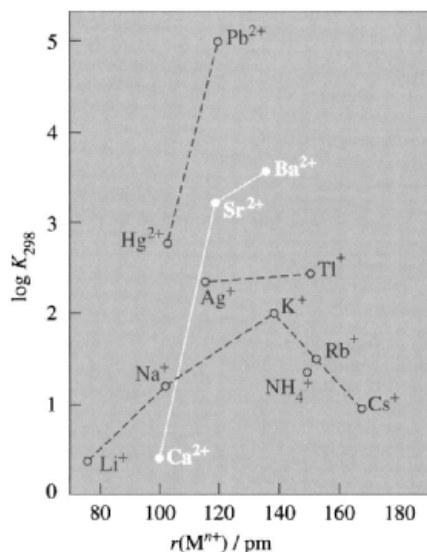


Figure 5.6 Formation constants  $K$  for complexes of dicyclohexyl-18-crown-6 ether with various cations. Note that, although the radii of  $\text{Ca}^{2+}$ ,  $\text{Na}^{+}$  and  $\text{Hg}^{2+}$  are very similar, the ratio of the formation constants is 1:6.3:225. Again,  $\text{K}^{+}$  and  $\text{Ba}^{2+}$  have similar radii but the ratio of  $K$  is 1:35 in the reverse direction (note log scale).

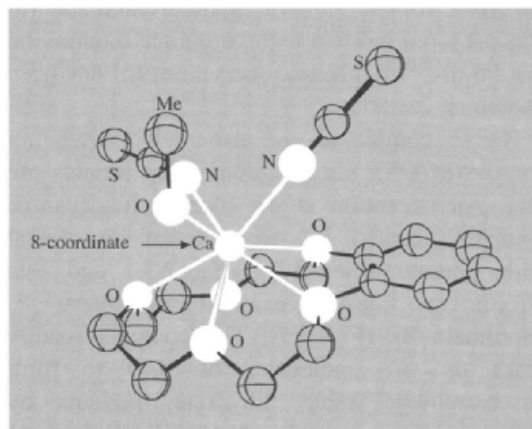


Figure 5.7 Molecular structure of benzo-15-crown-5- $\text{Ca}(\text{NCS})_2.\text{MeOH}$ .

<sup>23</sup> D. BARR, A. T. BROOKER, M. J. DOYLE, S. R. DRAKE, P. R. RAITHBY, R. SNAITH and D. S. WRIGHT, *J. Chem. Soc., Chem. Commun.*, 893–5 (1989).

<sup>24</sup> See refs. 38 and 66 of Chapter 4.

(mean Ca–O 253 pm) and is coordinated on the other side by a methanol molecule (Ca–O 239 pm) and two non-equivalent isothiocyanate



groups (Ca–N 244 pm) which make angles Ca–N–CS of 153° and 172° respectively.<sup>(25)</sup> Cryptates (pp. 97–8) are also known and usually follow the stability sequence Mg < Ca < Sr < Ba.<sup>(24)</sup> The first monomeric barium alkoxides, [Ba{O(CH<sub>2</sub>CH<sub>2</sub>O)<sub>n</sub>Me}<sub>2</sub>] (n = 2, 3), which incorporate coordinating polyether functions, were isolated in 1991; the compounds, which are unusual in being liquids at room temperature and which feature 6- and 8-coordinate Ba, respectively, were made by direct reaction of Ba metal with the oligoether alcohols in thf.<sup>(26)</sup>

Preeminent in importance among the macrocyclic complexes of Group 2 elements are the chlorophylls, which are modified porphyrin complexes of Mg. These compounds are vital to the process of photosynthesis in green plants (see Panel). Magnesium and Ca are also intimately

involved in biochemical processes in animals: Mg ions are required to trigger phosphate transfer enzymes, for nerve impulse transmissions and carbohydrate metabolism; Mg ions are also involved in muscle action, which is triggered by Ca ions. Ca is required for the formation of bones and teeth, maintaining heart rhythm, and in blood clotting.<sup>(27a–f)</sup>

<sup>27a</sup> W. E. C. WACKER, *Magnesium and Man*, Harvard University Press, London, 1980.

<sup>27b</sup> M. N. HUGHES, *The Inorganic Chemistry of Biological Processes*, Wiley, London, 1972, Chap. 8, pp. 256–82.

<sup>27c</sup> G. L. EICHHORN (ed.), *Inorganic Biochemistry*, Elsevier, Amsterdam, 1973, 2 Vols., 1263 pp.

<sup>27d</sup> B. S. COOPERMAN, Chap. 2 in H. SIGAL (ed.), *Metal Ions in Biological Systems*, Vol. 5, Dekker, New York, 1976, pp. 80–125.

<sup>27e</sup> K. S. RAJAN, R. W. COLBURN and J. M. DAVIS, Chap. 5 in H. SIGAL (ed.), *Metal Ions in Biological Systems*, Vol. 6, Dekker, New York, 1976, pp. 292–321. Also F. N. BRIGGS and R. J. SOLARO, Chap. 6, pp. 324–98 in the same volume.

<sup>27f</sup> H. SCHEER, *Chlorophylls*, CRC Press, Boca Raton, 1991.

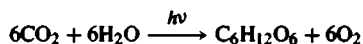
<sup>28</sup> M. CALVIN, The path of carbon in photosynthesis, *Nobel Lectures in Chemistry 1942–62*, Elsevier, Amsterdam, 1964, 618–44.

<sup>25</sup> J. D. OWEN and J. N. WINGFIELD, *J. Chem. Soc., Chem. Commun.*, 318–9 (1976).

<sup>26</sup> W. S. REES and D. A. MORENO, *J. Chem. Soc., Chem. Commun.*, 1759–60 (1991).

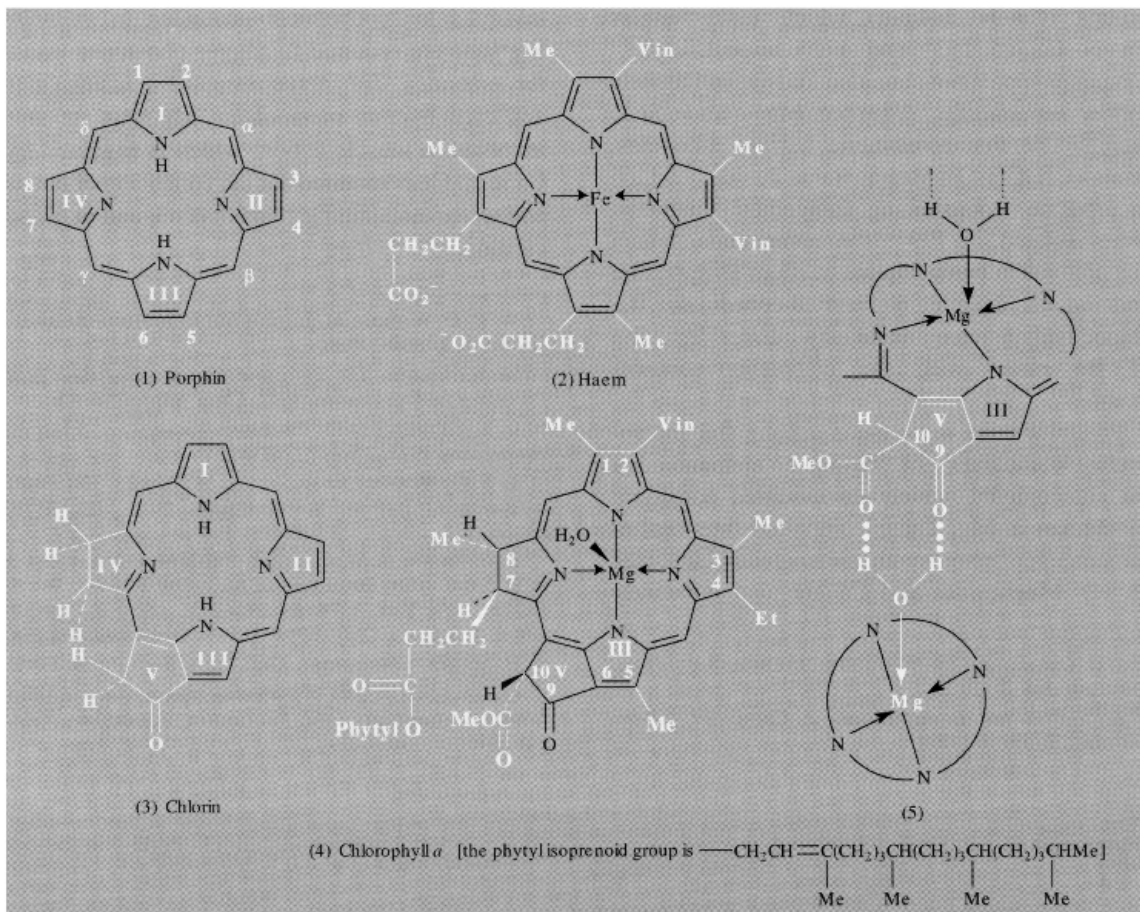
## Chlorophylls and Photosynthesis

Photosynthesis is the process by which green plants convert atmospheric CO<sub>2</sub> into carbohydrates such as glucose. The overall chemical change can be expressed as



though this is a gross and somewhat misleading over-simplification. The process is initiated in the photoreceptors of the green magnesium-containing pigments which have the generic name chlorophyll (Greek: χλωρός, *chloros* green; φύλλον, *phyllon* leaf), but many of the subsequent steps can proceed in the dark. The overall process is endothermic ( $\Delta H^\circ \sim 469$  kJ per mole of CO<sub>2</sub>) and involves more than one type of chlorophyll. It also involves a manganese complex of unknown composition, various iron-containing cytochromes and ferredoxin (p. 1102), and a copper containing plastocyanin.

Photosynthesis is essentially the conversion of radiant electromagnetic energy (light) into chemical energy in the form of adenosine triphosphate (ATP) and reduced nicotinamide adenine dinucleotide phosphate (NADP). This energy eventually permits the fixation of CO<sub>2</sub> into carbohydrates, with the liberation of O<sub>2</sub>. As such, the process is the basis for the nutrition of all living things and also provides mankind with fuel (wood, coal, petroleum), fibres (cellulose) and innumerable useful chemical compounds. About 90–95% of the dry weight of crops is derived from the CO<sub>2</sub>/H<sub>2</sub>O fixed from the air during photosynthesis — only about 5–10% comes from minerals and nitrogen taken from the soil. The detailed sequence of events is still not fully understood but tremendous advances were made from 1948 onwards by use of the then newly available radioactive <sup>14</sup>CO<sub>2</sub> and paper chromatography. With these tools and classical organic chemistry M. Calvin and his group were able to probe the biosynthetic pathways and thus laid the basis for our present understanding of the complex series of reactions. Calvin was awarded the 1961 Nobel Prize in Chemistry “for his research on the carbon dioxide assimilation in plants”.<sup>(28)</sup>



Chlorophylls are complexes of Mg with macrocyclic ligands derived from the parent tetrapyrrole molecule porphin (structure 1). They are thus related to the porphyrin (substituted porphin) complexes which occur in haem proteins<sup>†</sup> such as haemoglobin, myoglobin and the cytochromes (p. 1101). [The word haem and the prefix haemo derive directly from the Greek word *αἷμα*, blood, whereas porphyrins derive their name from the characteristic purple-red coloration which these alkaloids give when acidified (Greek *πορφύρα-ος*, *porphyros* purple).] The haem group is illustrated in structure 2. When the C=C double bond in the pyrrole-ring IV of porphin is *trans* hydrogenated and when a cyclopentanone ring is formed between ring III and the adjacent ( $\gamma$ ) methine bridge then the chlorin macrocycle (structure 3) is produced, and this is the basis for the various chlorophylls. Chlorophyll *a* (Chl *a*) is shown in structure 4; this is the most common of the chlorophylls and is found in all O<sub>2</sub>-evolving organisms. It was synthesized with complete chiral integrity by R. B. Woodward and his group in 1960 — an achievement of remarkable virtuosity. Variants of chlorophyll are:

Chlorophyll *b*, in which the 3-Me group is replaced by -CHO; this occurs in higher plants and green algae, the ratio CHI *b*:Chl *a* being ~1:3.

Chlorophyll *c*, in which position 7 is substituted by acrylic acid, -CH=CHCO<sub>2</sub>H; it occurs in diatoms and brown algae.

Chlorophyll *d*, in which 2-vinyl is replaced by -CHO.

Panel continues

<sup>†</sup>The first time that these two apparently very different but actually closely related coloured materials, chlorophyll and haemoglobin, were connected was in an extraordinarily perceptive poem written in 1612 by the English poet John Donne who mused: Why grass is green or why our blood is red/Are mysteries that none have reached unto.

It is important to note that the chlorin macrocycle is "ruffled" rather than completely planar and the Mg atom is ~30–50 pm above the plane of the 4 N atoms. In fact the Mg is not 4-coordinate but carries one (or sometimes two) other ligands, notably water molecules, which play a crucial role in interconnecting the basic chlorophyll units into stacks by H bonding to the cyclopentanone ring V of an adjacent chlorophyll molecule (see structure 5).

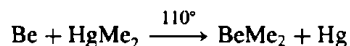
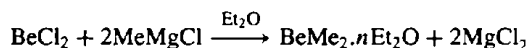
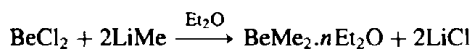
The function of the chlorophyll in the chloroplast is to absorb photons in the red part of the visible spectrum (near 680–700 nm) and to pass this energy of excitation on to other chemical intermediates in the complex reaction scheme. At least two photosystems are involved: the initiating photosystem II (P680) which absorbs at 680 nm and the subsequent photosystem I (P700). The detailed redox processes occurring, and the enzyme-catalysed synthetic pathways (dark reactions) in-so-far as they have yet been elucidated, are described in biochemical texts and fall outside our present scope. The Mg ion apparently serves several purposes: (a) it keeps the macrocycles fairly rigid so that energy is not so readily dissipated by thermal vibrations; (b) it coordinates the H<sub>2</sub>O molecules which mediate in the H bonding between adjacent molecules in the stack; and (c) it thereby enhances the rate at which the short-lived singlet excited state formed initially by absorption of a photon by the macrocycle is transformed to the corresponding longer-lived triplet state which is involved in the redox chain (since this involves the H bonded system between several individual chlorophyll units over a distance of some 1500–2000 pm). However, it is by no means clear why, of all metals, Mg is uniquely suited for this purpose.

### 5.3.5 Organometallic compounds<sup>(29–31)</sup>

Compounds containing M–C bonds are well established for Be and Mg but, as with the alkali metals, reactivity within the group increases with increasing electropositivity, and relatively few organometallic compounds of Ca, Sr or Ba have been isolated.

#### Beryllium<sup>(30)</sup>

Beryllium dialkyls (BeR<sub>2</sub>, R = Me, Et, Pr<sup>n</sup>, Pr<sup>i</sup>, Bu<sup>i</sup> etc.) can be made by reacting lithium alkyls or Grignard reagents with BeCl<sub>2</sub> in ethereal solution, but the products are difficult to free from ether and, when pure compounds rather than solutions are required, a better route is by heating Be metal with the appropriate mercury dialkyl:

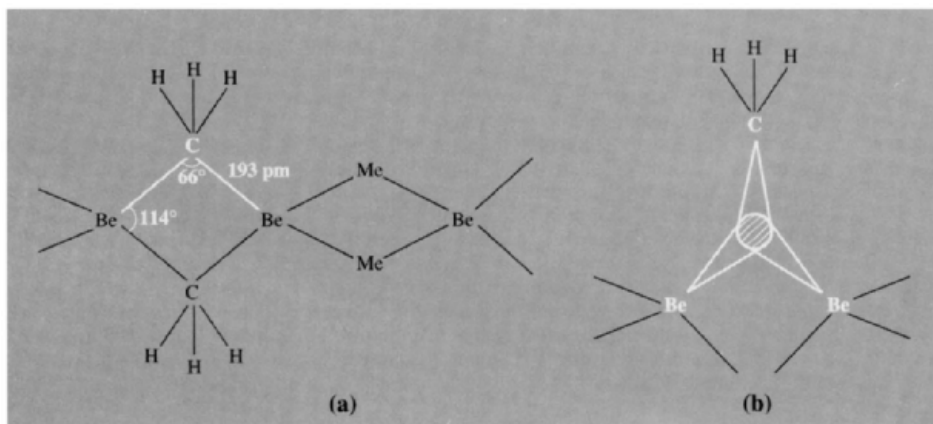


BePh<sub>2</sub> (mp 245°) can be prepared similarly, using LiPh or HgPh<sub>2</sub>; an excess of the former reagent yields Li[BePh<sub>3</sub>]. Beryllium dialkyls are colourless solids or viscous liquids which are spontaneously flammable in air and explosively hydrolysed by water. BeMe<sub>2</sub> (like MgMe<sub>2</sub>, p. 131) has been shown by X-ray analysis to have a chain structure analogous to that found in BeCl<sub>2</sub> (p. 116) though the bonding is probably best described in terms of 2-electron 3-centre bridge bonds involving •CH<sub>3</sub> groups rather than that adopted by bridging Cl atoms which each form two 2-electron 2-centre bonds involving a total of 4 electrons per Be–Cl–Be bridge (Fig. 5.8). Each C atom has a coordination number of 5 (cf. bonding in boranes, carbaboranes, etc., p. 157). Higher alkyls are progressively less highly polymerized and the sterically crowded BeBu<sub>2</sub><sup>i</sup> is monomeric. As with polymeric BeCl<sub>2</sub>, addition of strong ligands results in depolymerization and the eventual formation of monomeric adducts, e.g. [BeMe<sub>2</sub>(PMe<sub>3</sub>)<sub>2</sub>], [BeMe<sub>2</sub>(Me<sub>2</sub>NCH<sub>2</sub>CH<sub>2</sub>NMe<sub>2</sub>)], etc. Pyrolysis eliminates alkenes and leads to mixed hydrido species of variable composition (see also p. 115).

<sup>29</sup> G. E. COATES, M. L. H. GREEN and K. WADE, *Organometallic Compounds*, Vol. 1, *The Main Group Elements*, 3rd edn., Chap. II, Group II, pp. 71–121, Methuen, London, 1967.

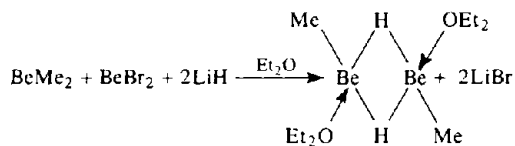
<sup>30</sup> N. A. BELL, Chap. 3, Beryllium in G. WILKINSON, F. G. A. STONE and E. W. ABEL (eds.) *Comprehensive Organometallic Chemistry*, Pergamon Press, Oxford, 1982, pp. 121–53.

<sup>31</sup> W. E. LINDSELL, Chap. 4, Mg, Ca, Sr and Ba, in G. WILKINSON, F. G. A. STONE and E. W. ABEL (eds.) *Comprehensive Organometallic Chemistry*, Pergamon Press, Oxford, 1982, pp. 155–252.

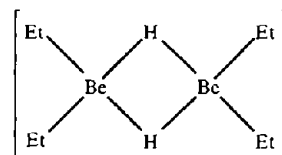


**Figure 5.8** (a) Chain structure of BeMe<sub>2</sub> showing the acute angle at the bridging methyl group; the Be...Be distance is 209 pm and the distance between the 2 C atoms across the bridge is 315 pm. (b) Pictorial representation of the 3 approximately sp<sup>3</sup> orbitals used to form one 3-centre bridge bond; this description of the bonding is consistent with the acute bridging angle at C and the close approach of adjacent Be atoms noted in (a).

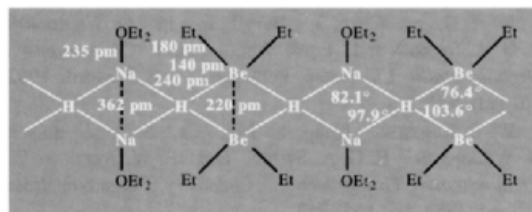
Alkylberyllium hydrides of more precise stoichiometry can be prepared by reducing BeBr<sub>2</sub> with LiH in the presence of BeR<sub>2</sub>, e.g.:



The coordinated ether molecules can be replaced by tertiary amines. Use of NaH in the absence of halide produces the related compound Na<sub>2</sub>[Me<sub>2</sub>BeH<sub>2</sub>BeMe<sub>2</sub>]; the corresponding ethyl derivative crystallizes with 1 mole of Et<sub>2</sub>O per Na but this can readily be removed under reduced pressure. The crystal structure of the etherate is shown in Fig. 5.9<sup>(32)</sup> and is important in illustrating once more (cf. p. 103) how misleading it can be to differentiate too sharply between different kinds of bonding in solids, for example: ionic [Na(OEt<sub>2</sub>)<sub>2</sub>]<sup>+</sup>[Et<sub>2</sub>BeH<sub>2</sub>BeEt<sub>2</sub>]<sup>2-</sup> or polymeric [Et<sub>2</sub>ONaHBeEt<sub>2</sub>]<sub>n</sub>. Thus in the structure shown in Fig. 5.9 each Be is surrounded tetrahedrally by 2 Et and 2 bridging H to form a subunit



In addition, each H is coordinated tetrahedrally by 2 Be and 2 Na, and each Na is directly bonded to 1 Et<sub>2</sub>O. Be-C is 180 pm and Be-H is 140 pm, close to expected values; Na-H is 240 pm, equal to that in NaH. The distance Na...Na is 362 pm which is less than in Na metal (372 pm) but greater than in NaH (345 pm), where each Na is surrounded by 6H; Be...Be is 220 pm as in Be metal. It is therefore misleading to consider the structure as being built up from the isolated ions [Na(OEt<sub>2</sub>)<sub>2</sub>]<sup>+</sup> and [Et<sub>2</sub>BeH<sub>2</sub>BeEt<sub>2</sub>]<sup>2-</sup> and it is perhaps better to regard it as a chain polymer [Et<sub>2</sub>ONaHBeEt<sub>2</sub>]<sub>n</sub> which in plane projection can be written as:



<sup>32</sup> G. W. ADAMSON and H. M. M. SHEARER, *J. Chem. Soc., Chem. Commun.*, 240 (1965).

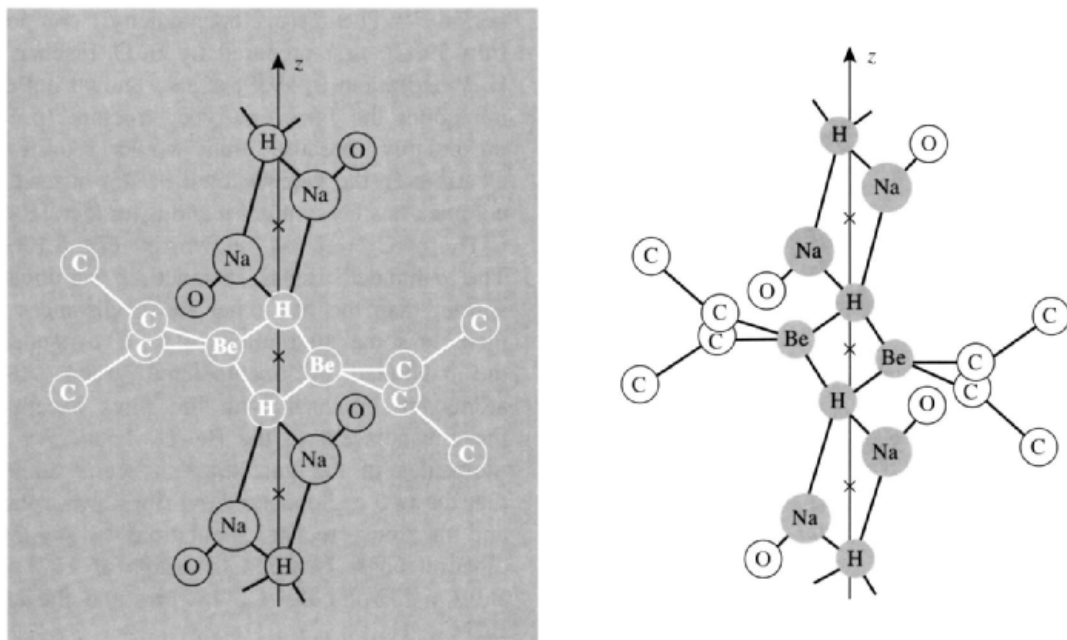
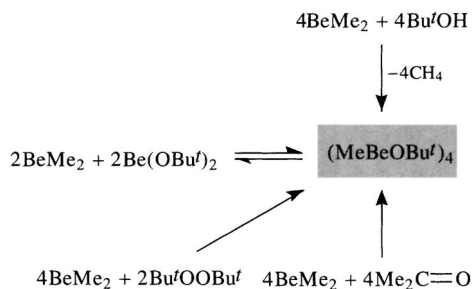
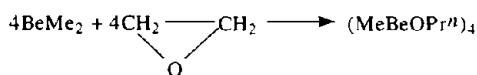


Figure 5.9 Crystal structure of the etherate of polymeric sodium hydridodiethylberyllate  $(Et_2ONaHBeEt_2)_n$ , emphasizing two features of the structure (see text).

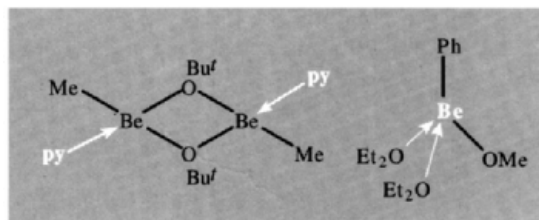
Alkylberyllium alkoxides  $(RBeOR')$  can be prepared from  $BeR_2$  by a variety of routes such as alcoholysis with  $R'OH$ , addition to carbonyls, cleavage of peroxides  $R'OOR'$  or redistribution with the appropriate dialkoxide  $Be(OR')_2$ , e.g.:



Ring opening of ethylene oxide has also been used:

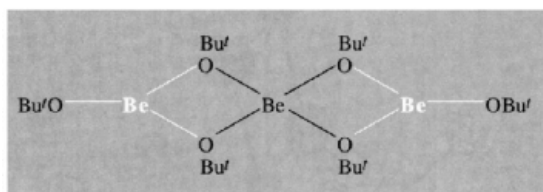


The compounds are frequently tetrameric and probably have the “cubane-like” structure established for the zinc analogue  $(MeZnOMe)_4$ . The methylberyllium alkoxides  $(MeBeOR')_4$  are reactive, low-melting solids (mp for  $R' = Me$   $25^\circ$ ,  $Et$   $30^\circ$ ,  $Pr^i$   $40^\circ$ ,  $Pr^i$   $136^\circ$ ,  $Bu^t$   $93^\circ$ ). Bulky substituents may reduce the degree of oligomerization, e.g. trimeric  $(EtBeOCeT_3)_3$ , and reaction with coordinating solvents or strong ligands can also lead to depolymerization, e.g. dimeric  $(MeBeOBu^t.py)_2$  and monomeric  $PhBeOMe \cdot 2Et_2O$ :



Reaction of beryllium dialkyls with an excess of alcohol yields the alkoxides  $Be(OR)_2$ . The methoxide and ethoxide are insoluble and

probably polymeric, whereas the *t*-butoxide (mp 112°) is readily soluble as a trimer in benzene or hexane; the proposed structure:



involves both 3- and 4-coordinate Be and is consistent with the observation of 2 proton nmr signals at  $\tau$  8.60 and 8.75 with intensities in the ratio 2:1. (A precisely analogous structure has been established by X-ray diffraction analysis for the "isoelectronic" linear trimer  $[\text{Be}(\text{NMe}_2)_2]_3$ .)<sup>(33)</sup>

Beryllium forms a series of cyclopentadienyl complexes  $[\text{Be}(\eta^5\text{-C}_5\text{H}_5\text{Y})]$  with  $\text{Y} = \text{H}, \text{Cl}, \text{Br}, \text{Me}, \text{-C}\equiv\text{CH}$  and  $\text{BH}_4$ , all of which show the expected  $C_{5v}$  symmetry (Fig. 5.10a). If the *pentahapto*-cyclopentadienyl group (p. 937) contributes 5 electrons to the bonding, then these are all 8-electron Be complexes consistent with the octet rule for elements of the first short

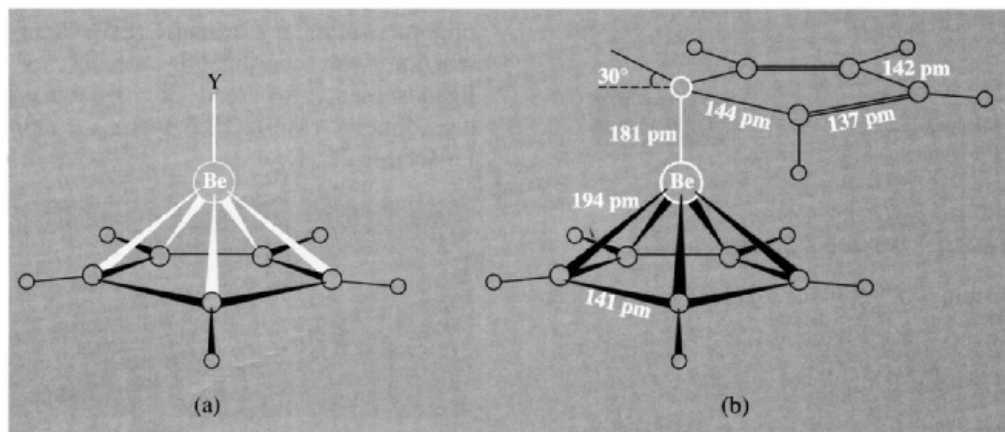
<sup>33</sup> J. L. ATWOOD and G. D. STUCKY, *Chem. Comm.* 1967, 1169-70.

period.<sup>(34)</sup> The bis(cyclopentadienyl) compound (mp 59°C), first prepared by E. O. Fischer and H. P. Hofmann in 1959, is also known but does not adopt the ferrocene-type structure (p. 937) presumably because this would require 12 electrons in the valence shell of Be. Instead, the complex has  $C_s$  symmetry and is, in fact,  $[\text{Be}(\eta^1\text{-C}_5\text{H}_5)(\eta^5\text{-C}_5\text{H}_5)]$ , as shown in Fig. 5.10b.<sup>(35)</sup> The  $\sigma$ -bonded Be-C distance is significantly shorter than the five other Be-C distances and there is some alternation of C-C distances in the  $\sigma$ -bonded cyclopentadienyl group. All H atoms are coplanar with the rings except for the one adjacent to the Be-C $_{\sigma}$  bond. For free molecules in the gas phase it seems unlikely that the two cyclopentadienyl rings are coplanar, and the most recent calculations<sup>(36)</sup> suggest a dihedral angle between the rings of 117° with Be-C $_{\sigma}$  172 pm, Be-C $_{\pi}$  187 pm, and the angle Be-C $_{\sigma}$ -H 108°.

<sup>34</sup> E. D. JEMMIS, S. ALEXANDRATOS, P. v. R. SCHLEYER, A. STREITWIESER and H. F. SCHAEFFER, *J. Am. Chem. Soc.* **100**, 5695-700 (1978).

<sup>35</sup> C.-H. WONG, T.-Y. LEE, K.-J. CHAO and S. LEE, *Acta Cryst.* **B28**, 1662-5 (1972); C. WONG, T. Y. LEE, T. J. LEE, T. W. CHANG and C. S. LIU, *Inorg. Nucl. Chem. Lett.* **9**, 667-73 (1973).

<sup>36</sup> D. S. MARYNICK, *J. Am. Chem. Soc.* **99**, 1436-41 (1977). See also J. B. COLLINS and P. v. R. SCHLEYER, *Inorg. Chem.* **16**, 152-5 (1977).

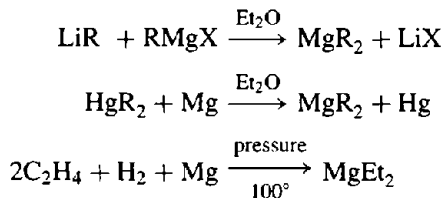


**Figure 5.10** Cyclopentadienyl derivatives of beryllium showing (a) the  $C_{5v}$  structure of  $[\text{Be}(\eta^5\text{-C}_5\text{H}_5)\text{Y}]$  and (b) the structure of crystalline  $[\text{Be}(\eta^1\text{-C}_5\text{H}_5)(\eta^5\text{-C}_5\text{H}_5)]$  at  $-120^\circ$  (see text).

Pentamethylcyclopentadienyl derivatives are also known, e.g.  $[(\eta^5\text{-C}_5\text{Me}_5)\text{BeCl}]$ ; this reacts with  $\text{LiPBu}_2$  in  $\text{Et}_2\text{O}$  at  $-78^\circ$  to give colourless crystals of  $[(\eta^5\text{-C}_5\text{Me}_5)\text{BePBu}_2]$  in high yield.<sup>(37)</sup> Here the dibutylphosphido group is acting as a 1-electron ligand to Be to form a covalent bond of length 208.3 pm almost perpendicular to the  $\text{C}_5$  plane: angle  $\text{P-Be-C}_5(\text{centroid})$   $168.3^\circ$ . Interestingly, the  $\text{Be-C}_5(\text{centroid})$  distance (148 pm) is notably shorter than that found in  $[(\eta^5\text{-C}_5\text{H}_5\text{BeMe}]$  (190.7 pm), implying stronger bonding in the pentamethyl derivative. Because the Be nucleus has a spin of  $3/2$ , the  $^{31}\text{P}\{^1\text{H}\}$  nmr signal consists of a 1:1:1:1 quartet with a coupling constant  $^1J_{\text{Be-P}}$  of 50.0 Hz; this is an order of magnitude greater than for Lewis-base (2-electron) tertiary phosphine adducts of Be.

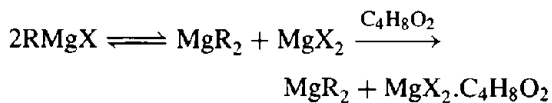
### Magnesium<sup>(31)</sup>

Magnesium dialkyls and diaryls, though well established, have been relatively little studied by comparison with the vast amount of work which has been published on the Grignard reagents  $\text{RMgX}$ . The dialkyls (and diaryls) can be conveniently made by the reaction of  $\text{LiR}$  ( $\text{LiAr}$ ) on Grignard reagents, or by the reaction of  $\text{HgR}_2$  ( $\text{HgAr}_2$ ) on Mg metal (sometimes in the presence of ether). On an industrial scale, alkenes can be reacted at  $100^\circ$  under pressure with  $\text{MgH}_2$  or with Mg in the presence of  $\text{H}_2$ :

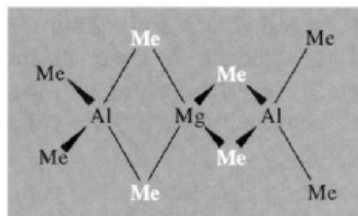


A suitable laboratory method is to shift the Schlenk equilibrium in a Grignard solution (p. 132) by adding dioxan to precipitate the

complex  $\text{MgX}_2\cdot\text{diox}$ ; this enables  $\text{MgR}_2$  to be isolated by careful removal of solvent under reduced pressure:



$\text{MgMe}_2$  is a white involatile polymeric solid which is insoluble in hydrocarbons and only slightly soluble in ether. Its structure is very similar to that of  $\text{BeMe}_2$  (p. 128) the corresponding dimensions for  $\text{MgMe}_2$  being:  $\text{Mg-C}$  224 pm,  $\text{Mg-C-Mg}$   $75^\circ$ ,  $\text{C-Mg-C}$   $105^\circ$ ,  $\text{Mg}\cdots\text{Mg}$  272 pm and  $\text{C}\cdots\text{C}$  (across the bridge) 357 pm. Precisely analogous bridging Me groups are found in dimeric  $\text{Al}_2\text{Me}_6$  (p. 259) and in the monomeric compound  $\text{Mg}(\text{AlMe}_4)_2$  which can be formed by direct reaction of  $\text{MgMe}_2$  and  $\text{Al}_2\text{Me}_6$ :



$\text{MgEt}_2$  and higher homologues are very similar to  $\text{MgMe}_2$  except that they decompose at a lower temperature ( $175\text{--}200^\circ$  instead of  $\sim 250^\circ\text{C}$ ) to give the corresponding alkene and  $\text{MgH}_2$  in a reaction which reverses their preparation.  $\text{MgPh}_2$  is similar: it is insoluble in benzene dissolves in ether to give the monomeric complex  $\text{MgPh}_2\cdot 2\text{Et}_2\text{O}$  and pyrolyses at  $280^\circ$  to give  $\text{Ph}_2$  and Mg metal. Like  $\text{BePh}_2$  it reacts with an excess of  $\text{LiPh}$  to give the colourless complex  $\text{Li}[\text{MgPh}_3]$ .

The first organosilylmagnesium compound  $[\text{Mg}(\text{SiMe}_3)_2]\cdot(\text{-CH}_2\text{OMe})_2$ , was isolated in 1977;<sup>(38)</sup> it was obtained as colourless, spontaneously flammable crystals by reaction of bis(trimethylsilyl)mercury with Mg powder in

<sup>37</sup> J. L. ATWOOD, S. G. BOTT, R. A. JONES and S. U. KOSCHMIEDER, *J. Chem. Soc., Chem. Commun.*, 692-3 (1990).

<sup>38</sup> L. RÖSCH, *Angew. Chem. Int. Edn. Engl.* **16**, 247-8 (1977).



1,2-dimethoxyethane. More recently<sup>(39)</sup> the bulkier bis{tris(trimethylsilyl)methyl} derivative,  $[\text{Mg}\{\text{C}(\text{SiMe}_3)_2\}_2]$ , was obtained as an unsolvated crystalline monomer; this was the first example of 2-coordinate (linear) Mg in the solid state, though this geometry had been established earlier by electron diffraction in the gas phase for bis(neopentyl)magnesium.<sup>(40)</sup>

Grignard reagents are the most important organometallic compounds of Mg and are probably the most extensively used of all organometallic reagents because of their easy preparation and synthetic versatility. Despite this, their constitution in solution has been a source of considerable uncertainty until recent times.<sup>(41)</sup> It now seems well established that solutions of Grignard reagents can contain a variety of chemical species interlinked by mobile equilibria whose position depends critically on at least five factors: (i) the steric and electronic nature of the alkyl (or aryl) group R, (ii) the nature of the halogen X (size, electron-donor power, etc.), (iii) the nature of the solvent ( $\text{Et}_2\text{O}$ , thf, benzene, etc.), (iv) the concentration

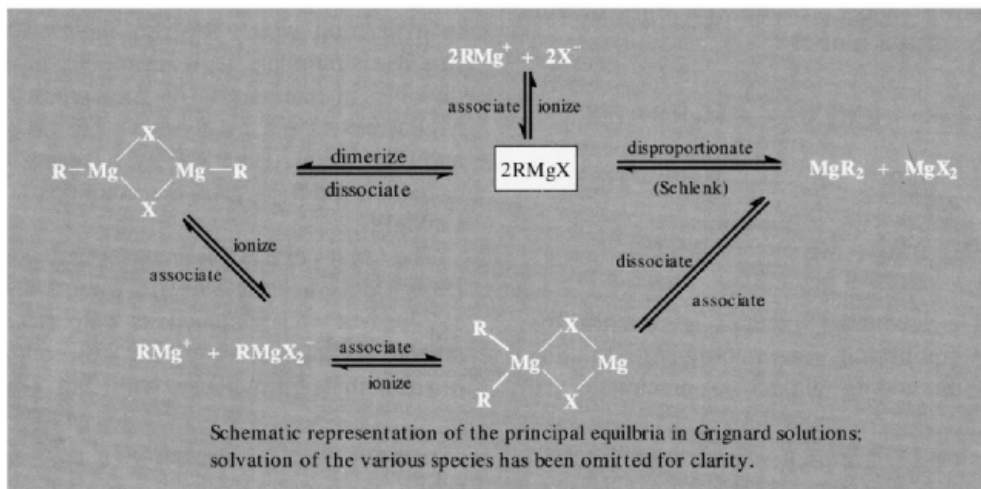
and (v) the temperature. The species present may also depend on the presence of trace impurities such as  $\text{H}_2\text{O}$  or  $\text{O}_2$ . Neglecting solvation in the first instance, the general scheme of equilibria can be set out as shown below. Thus "monomeric" (solvated)  $\text{RMgX}$  can disproportionate to  $\text{MgR}_2$  and  $\text{MgX}_2$  by the Schlenk equilibrium or can dimerize to  $\text{RMgX}_2\text{MgR}$ . Both the monomer and the dimer can ionize, and reassociation can give the alternative dimer  $\text{R}_2\text{MgX}_2\text{Mg}$ . Note that only halogen atoms X are involved in the bridging of these species.

Evidence for these species and the associated equilibria comes from a variety of techniques such as vibration spectroscopy, nmr spectroscopy, molecular-weight determinations, radioisotopic exchange using  $^{28}\text{Mg}$ , electrical conductivity, etc. In some cases equilibria can be displaced by crystallization or by the addition of complexing agents such as dioxan (p. 131) or  $\text{NEt}_3$ . The crystal structures of several pertinent adducts have recently been determined (Fig. 5.11). None call for special comment except the curious solvated dimer  $[\text{EtMg}_2\text{Cl}_3(\text{OC}_4\text{H}_8)_3]_2$  which features both 5-coordinate trigonal bipyramidal and 6-coordinate octahedral Mg groups; note also that, whilst 4 of the Cl atoms each bridge 2 Mg atoms, the remaining 2 Cl atoms are triply bridging.

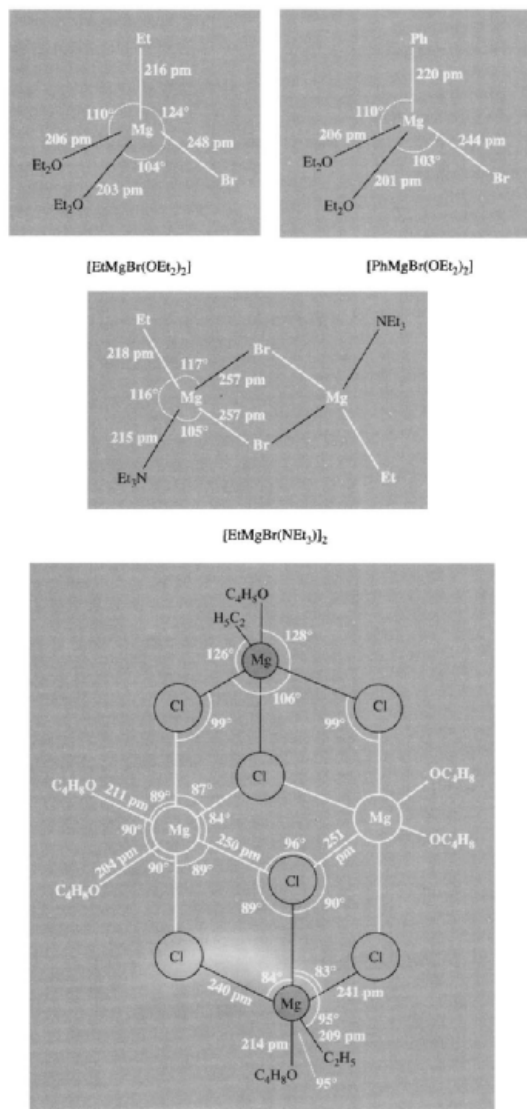
<sup>39</sup> S. S. Al-Juaid, C. Eaborn, P. B. Hitchcock, C. A. MCGEARY and J. D. SMITH, *J. Chem. Soc., Chem. Commun.*, 273-4 (1989).

<sup>40</sup> E. C. ASHBY, L. FERNHOLT, A. HAALAND, R. SEIP and R. C. SMITH, *Acta Chem. Scand., Ser. A* **34**, 213-7 (1980).

<sup>41</sup> E. C. ASHBY, *Qt. Rev.* **21**, 259-85 (1967).

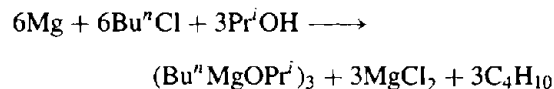
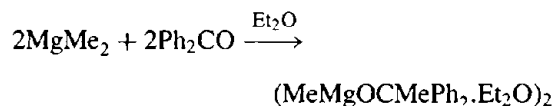
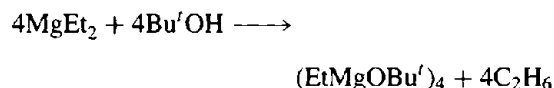






oxide (hydroxide) on the surface of the metal. The order of reactivity of RX is  $I > Br > Cl$  and  $alkyl > aryl$ . The mechanism has been much studied but is not fully understood.<sup>(42)</sup> The fluorides  $MgR_2$  ( $R = Me, Et, Bu, Ph$ ) can be prepared by reacting  $MgR_2$  with mild fluorinating agents such as  $BF_3 \cdot OEt_2$ ,  $Bu_3SnF$  or  $SiF_4$ .<sup>(43)</sup> The scope of Grignard reagents in syntheses has been greatly extended by a recently developed method for preparing very reactive Mg (by reduction of  $MgX_2$  with K in the presence of KI).<sup>(44)</sup> Grignard reagents have a wide range of application in the synthesis of alcohols, aldehydes, ketones, carboxylic acids, esters and amides, and are probably the most versatile reagents for constructing C–C bonds by carbanion (or occasionally<sup>(45)</sup> free-radical) mechanisms. Standard Grignard methods are also available for constructing C–N, C–O, C–S (Se, Te) and C–X bonds (see Panel on pp. 134–5).

A related class of compounds are the alkyl-magnesium alkoxides: these can be prepared by reaction of  $MgR_2$  with an alcohol or ketone or by reaction of Mg metal with the appropriate alcohol and alkyl chloride in methylcyclohexane solvent, e.g.:



**Figure 5.11** Crystal structures of adducts of Grignard reagents.

Grignard reagents are normally prepared by the slow addition of the organic halide to a stirred suspension of magnesium turnings in the appropriate solvent and with rigorous exclusion of air and moisture. The reaction, which usually begins slowly after an induction period, can be initiated by addition of a small crystal of iodine; this penetrates the protective layer of

<sup>42</sup> H. R. ROGERS, C. L. HILL, Y. FUJIWARA, R. J. ROGERS, H. L. MITCHELL and G. M. WHITESIDES, *J. Am. Chem. Soc.* **102**, 217–26 (1980), and the three following papers, pp. 226–43.

<sup>43</sup> E. C. ASHBY and J. NACKASHI, *J. Organometall. Chem.* **72**, 203–11 (1974).

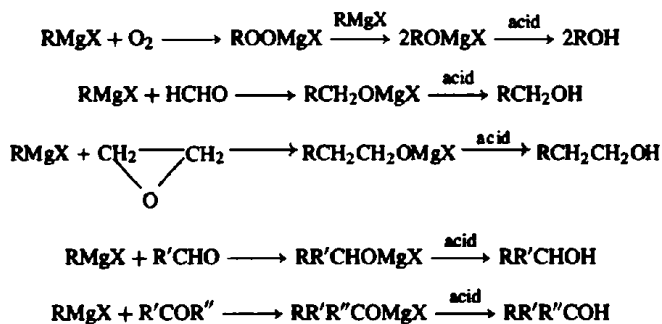
<sup>44</sup> R. D. RIEKE and S. E. BALES, *J. Am. Chem. Soc.* **96**, 1775–81 (1974).

<sup>45</sup> C. WALLING, *J. Am. Chem. Soc.* **110**, 6846–50 (1988).

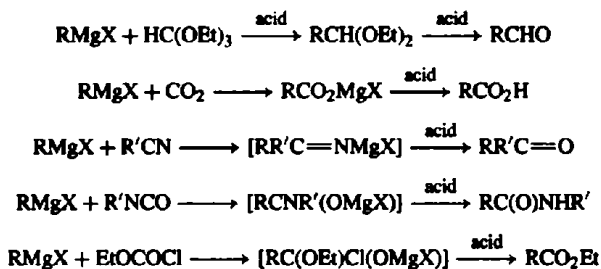
### Synthetic Uses of Grignard Reagents

Victor Grignard (1871–1935) showed in 1900 that Mg reacts with alkyl halides in dry ether at room temperature to give ether-soluble organomagnesium compounds; the use of these reagents to synthesize acids, alcohols, and hydrocarbons formed the substance of his doctorate thesis at the University of Lyon in 1901, and further studies on the synthetic utility of Grignard reagents won him the Nobel Prize for Chemistry in 1912. The range of applications is now enormous and some indication of the extraordinary versatility of organomagnesium compounds can be gauged from the following brief summary.

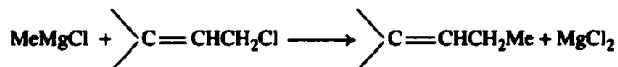
Standard procedures convert  $\text{RMgX}$  into  $\text{ROH}$ ,  $\text{RCH}_2\text{OH}$ ,  $\text{RCH}_2\text{CH}_2\text{OH}$  and an almost unlimited range of secondary and tertiary alcohols:



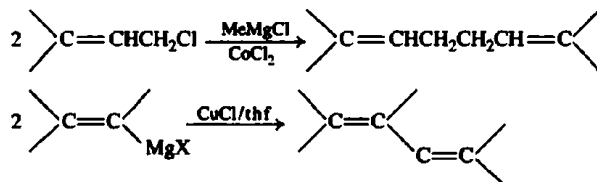
Aldehydes and carboxylic acids having 1 C atom more than R, as well as ketones, amides and esters can be prepared similarly, the reaction always proceeding in the direction predicted for potential carbanion attack on the unsaturated C atom:



Grignard reagents are rapidly hydrolysed by water or acid to give the parent hydrocarbon, RH, but this reaction is rarely of synthetic importance. Hydrocarbons can also be synthesized by nucleophilic displacement of halide ion from a reactive alkyl halide, e.g.

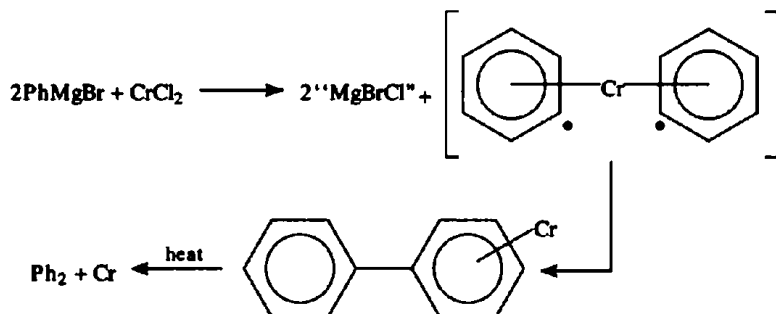


However, other products may be formed simultaneously by a free-radical process, especially in the presence of catalytic amounts of  $\text{CoCl}_2$  or  $\text{CuCl}$ :

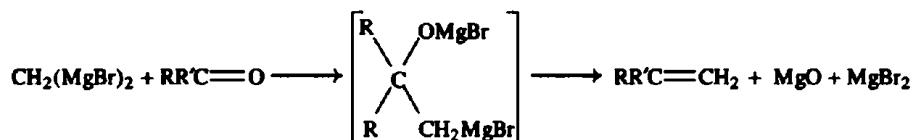


Panel continues

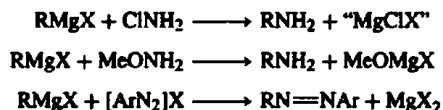
Similarly, aromatic Grignard reagents undergo free-radical self-coupling reactions when treated with  $MCl_2$  ( $M=Cr, Mn, Fe, Co, Ni$ ), e.g.:



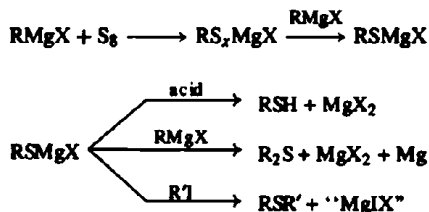
Alkenes can be synthesized from aldehydes or ketones using the Grignard reagent derived from  $CH_2Br_2$ :



The formation of C-N bonds can be achieved by using chloramine or *O*-methylhydroxylamine to yield primary amines; aryl diazonium salts yield azo-compounds:



Carbon-oxygen bonds can be made using the synthetically uninteresting conversion of  $RMgX$  into  $ROH$  (shown as the first reaction listed above); direct acid hydrolysis of the peroxy compound  $ROOMgX$  yields the hydroperoxide  $ROOH$ . Carbon-sulfur bonds can be constructed using  $S_8$  to make thiols or thioethers, and similar reactions are known for Se and Te:

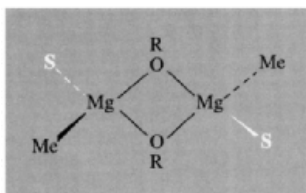


Formation of C-X bonds is not normally a problem but the Grignard route can occasionally be useful when normal halogen exchange fails. Thus iodination of  $Me_3CCH_2Cl$  cannot be achieved by reaction with  $NaI$  or similar reagents but direct iodination of the corresponding Grignard effects a smooth conversion:

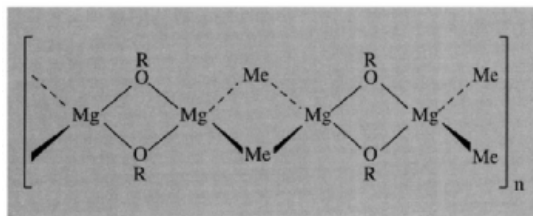


Further examples of the ingenious use of Grignard reagents will be found in many books on synthetic organic chemistry and much recent work in this area was reviewed in a special edition of *Bull. Soc. Chim. France*, 1972, 2127-86, which commemorated the centenary of Victor Grignard's birth.

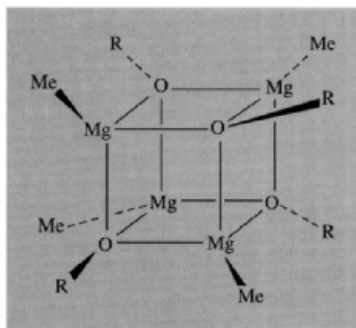
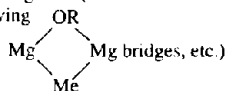
As with the Grignard reagents, the structure and degree of association of the product depend on the bulk of the organic groups, the coordinating ability of the solvent, etc. This is well illustrated by  $\text{MeMgOR}$  ( $\text{R} = \text{Pr}^n, \text{Pr}^i, \text{Bu}^i, \text{CMePh}_2$ ) in  $\text{thf}$ ,  $\text{Et}_2\text{O}$  and benzene:<sup>(46)</sup> the strongly coordinating solvent  $\text{thf}$  favours solvated dimers (A) but prevents the formation both of oligomers (B) involving the relatively weak  $\text{Me}$  bridges and of cubane structures (C) involving the relatively weak triply bonding oxygen bridges.



A. solvated dimer



B. linear oligomer (various isomers are possible e.g. involving



C. cubane tetramer (unsolvated)

By contrast, in the more weakly coordinating solvent  $\text{Et}_2\text{O}$ ,  $\text{Me}$  bridges and  $\mu_3\text{-OR}$  bridges can

form, leading to linear oligomers and cubanes, provided  $\text{OR}$  is not too bulky. Thus when  $\text{R} = \text{CMePh}_2$ , oligomerization and cubane formation are blocked and  $\text{MeMgOCMePh}_2$  exists only as a solvated dimer even in  $\text{Et}_2\text{O}$ . In benzene,  $\text{R} = \text{Bu}^i$  and  $\text{Pr}^i$  form cubane tetramers but  $\text{Pr}^n$  can form an oligomer of 7–9 monomer units. The sensitive dependence of the structure of a compound on solvation energy, lattice energy and the relative coordinating abilities of its component atoms and groups will be a recurring theme in many subsequent chapters.

Dicyclopentadienylmagnesium  $[\text{Mg}(\eta^5\text{-C}_5\text{H}_5)_2]$ , mp  $176^\circ$ , can be made in good yield by direct reaction of  $\text{Mg}$  and cyclopentadiene at  $500\text{--}600^\circ$ ; it is very reactive towards air, moisture,  $\text{CO}_2$  and  $\text{CS}_2$ , and reacts with transition-metal halides to give transition-element cyclopentadienyls. It has the staggered ( $D_{5d}$ ) "sandwich" structure (cf. ferrocene p. 1109) with  $\text{Mg-C}$  230 pm and  $\text{C-C}$  139 pm;<sup>(47)</sup> the bonding is thought to be intermediate between ionic and covalent but the actual extent of the charge separation between the central atom and the rings is still being discussed.

### Calcium, strontium and barium<sup>(31,48)</sup>

Organometallic compounds of  $\text{Ca}$ ,  $\text{Sr}$  and  $\text{Ba}$  are far more reactive than those of  $\text{Mg}$  and have been much less studied until recently. For example, although about 50 000 papers have been published on organomagnesium compounds and reagents, less than 1% of this number have appeared for the heavier triad of elements. Many of the differences in reactivity can be traced to the larger radii of the cations ( $\text{Ca}^{2+}$  100,  $\text{Sr}^{2+}$  118,  $\text{Ba}^{2+}$  135 pm) when compared to  $\text{Mg}^{2+}$  (72 pm) — i.e. the lower (charge/size) ratio enhances still further the ionic character of the bonding and thus increases the kinetic lability of the ligands. Coordinative unsaturation also plays a rôle and, indeed, the organometallic behaviour of the heavier alkali metals often resembles

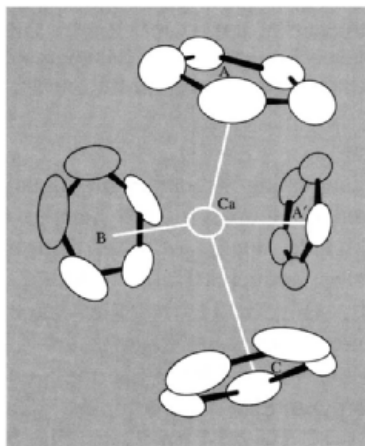
<sup>46</sup> E. C. ASHBY, J. NACKASHI and G. E. PARRIS, *J. Am. Chem. Soc.* **97**, 3162–71 (1975).

<sup>47</sup> W. BÜNDER and E. WEISS,  $[\text{Mg}(\eta^5\text{-C}_5\text{H}_5)_2]$ , *J. Organometall. Chem.* **92**, 1–6 (1975).

<sup>48</sup> T. P. HANUSA, *Polyhedron* **9**, 1345–62 (1990)

that of the similarly-sized divalent lanthanide elements ( $\text{Yb}^{2+}$  102,  $\text{Eu}^{2+}$  117,  $\text{Sm}^{2+}$  122 pm) rather than that of Mg. In these circumstances it became clear that stability would be enhanced by the use of bulky ligands. Early work showed that the reactive compounds  $\text{MR}_2$  ( $\text{M} = \text{Ca}$ ,  $\text{Sr}$ ,  $\text{Ba}$ ;  $\text{R} = \text{Me}$ ,  $\text{Et}$ , allyl,  $\text{Ph}$ ,  $\text{PhCH}_2$ , etc.) can be prepared using  $\text{HgR}_2$  under appropriate conditions, often at low temperature. Compounds of the type  $\text{RCaI}$  ( $\text{R} = \text{Bu}$ ,  $\text{Ph}$ , tolyl) have also been known for some time and can now be isolated as crystals.

Calcium (and Sr) dicyclopentadienyl can be made by direct reaction of the metal with either  $[\text{Hg}(\text{C}_5\text{H}_5)_2]$  or with cyclo- $\text{C}_5\text{H}_6$  itself; cyclopentadiene also reacts with  $\text{CaC}_2$  in liquid  $\text{NH}_3$  to form  $[\text{Ca}(\text{C}_5\text{H}_5)_2]$  and  $\text{HC}\equiv\text{CH}$ . The barium analogue  $[\text{Ba}(\text{C}_5\text{H}_5)_2]$  is best made (though still in small yield) by treating cyclo- $\text{C}_5\text{H}_6$  with  $\text{BaH}_2$ . The structure of  $[\text{Ca}(\text{C}_5\text{H}_5)_2]$  is unique.<sup>(49)</sup> Each Ca is surrounded by 4 planar cyclopentadienyl rings and the overall structure involves a complex sharing of rings which bridge the various Ca atoms. The coordination geometry about a given Ca atom is shown in Fig. 5.12:



**Figure 5.12** Coordination geometry about Ca in polymeric  $[\text{Ca}(\text{C}_5\text{H}_5)_2]$  showing  $2 \times \eta^5$ -,  $\eta^3$ - and  $\eta^1$ - bonding (see text).

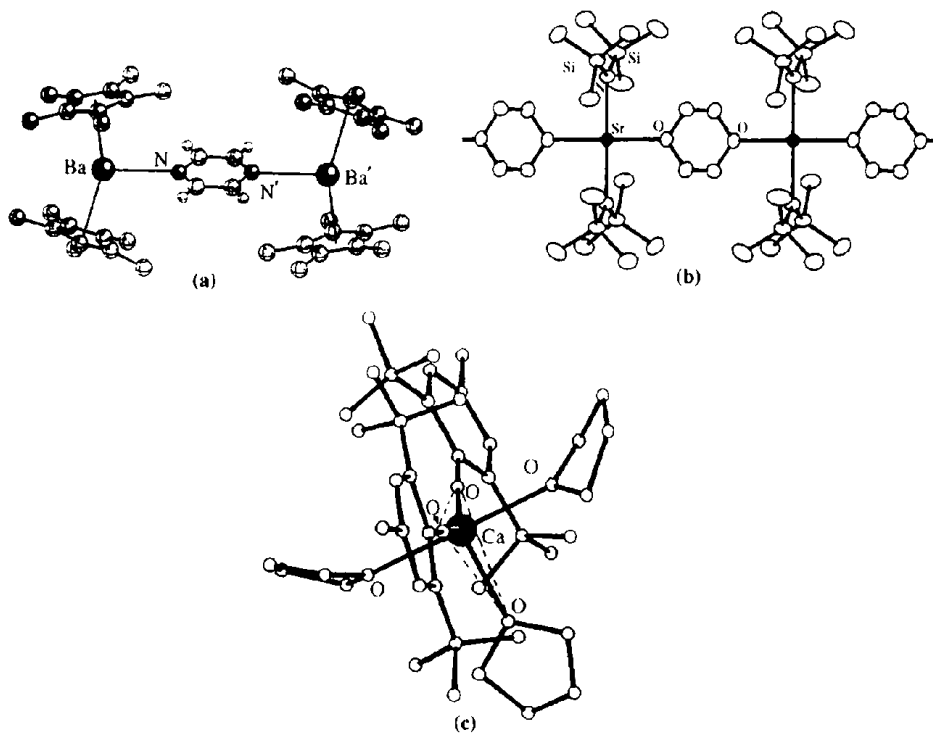
two of the rings (A, C) are  $\eta^5$ , with all Ca–C distances 275 pm. A third ring (B) is  $\eta^3$  with one Ca–C distance 270, two at 279, and two longer distances at 295 pm. These three polyhapto rings (A, B, C) are arranged so that their centroids are disposed approximately trigonally about the Ca atom. The fourth ring ( $\text{A}'$ ) is  $\eta^1$ , with only 1 Ca–C within bonding distance (310 pm) and this bond is approximately perpendicular to the plane formed by the centroids of the other 3 rings. The structure is the first example in which  $\eta^5$ -,  $\eta^3$ - and  $\eta^1$ - $\text{C}_5\text{H}_5$  groups are all present. Indeed, the structure is even more complex than this implies because of the ring-bridging between adjacent Ca atoms; for example ring A (and  $\text{A}'$ ) is simultaneously bonded  $\eta^5$  to 1 Ca (248 pm from the ring centre) and  $\eta^1$  to another on the opposite side of the ring, whereas ring C is equally associated in *pentahapto* mode with 2 Ca atoms each 260 pm from the plane of the ring.

Replacement of the ligand  $\text{C}_5\text{H}_5$  by the bulkier  $\text{C}_5\text{Me}_5$  results in improved solubility, volatility and kinetic stability of the compound, and all three complexes  $[\text{M}(\eta^5\text{-C}_5\text{Me}_5)_2]$  have been prepared in >65% yield by the reaction of  $\text{NaC}_5\text{Me}_5$  (or  $\text{KC}_5\text{Me}_5$ ) with the appropriate diiodide,  $\text{MI}_2$ , in diethyl ether or thf, followed by removal of the coordinated ether (or thf) by refluxing the product in toluene.  $[\text{Ca}(\text{C}_5\text{Me}_5)_2(\text{thf})_2]$  has also been prepared in 48% yield by the reaction of  $\text{C}_5\text{HMe}_5$  and  $\text{Ca}(\text{NH}_2)_2$  in liquid ammonia. The greater tractability of these complexes enabled the first (gas-phase) molecular structures of organo-Sr and organo-Ba compounds to be determined,<sup>(50)</sup> and also the first organo-Ba crystal structure.<sup>(51)</sup> Group comparisons show that the angle subtended by the two  $\text{C}_5\text{Me}_5$  ring centroids at the metal atom in the gas phase is almost the same (to within 1 esd) for the three metals ( $154 \pm 4^\circ$ ) but that this drops to  $131.0^\circ$  for crystalline  $[\text{Ba}(\text{C}_5\text{Me}_5)_2]$ . A theoretical rationalization for these angles, especially in the gas phase, is not obvious.<sup>(48)</sup>

<sup>50</sup> R. A. ANDERSEN, R. BLOM, C. J. BURNS and H. V. VOLDEN, *J. Chem. Soc., Chem. Commun.*, 768–9 (1987).

<sup>51</sup> R. A. WILLIAMS, T. P. HANUSA and J. C. HUFFMAN, *J. Chem. Soc., Chem. Commun.*, 1045–6 (1988).

<sup>49</sup> R. ZERGER and G. STUCKY, *J. Organometall. Chem.* **80**, 7–17 (1974).



**Figure 5.13** (a) Structure of  $[\{\text{Ba}(\eta^5\text{-C}_5\text{Me}_5)_2\}_2(\mu\text{-}1,4\text{-C}_4\text{H}_4\text{N}_2)]$  in which the pyrazine ligand bridges two bent  $\{\text{BaCp}^*\}_2$  units to give a centrosymmetric adduct with an essentially linear disposition of the four atoms BaNNBa. (b) The polymeric dioxane-bridged structure of  $[\{\text{trans-Sr}(\text{NR}_2)_2(\mu\text{-}1,4\text{-C}_4\text{H}_8\text{O}_2)\}]$  ( $\text{R} = \text{SiMe}_3$ ) showing the 4-coordinate square-planar stereochemistry of the Sr atoms. (c) The 5-coordinate trigonal-bipyramidal structure of  $[\text{Ca}(\text{OAr})_2(\text{thf})_3]$  ( $\text{Ar} = \text{C}_6\text{H}_2\text{-}2,6\text{-Bu}'_2\text{-}4\text{-Me}$ ) showing one equatorial and two axial thf ligands.

Attempts to prepare the mono(cyclopentadienyl) derivatives are sometimes frustrated by a Schlenk-type equilibrium (see p. 132), but judicious choice of ligands, solvent etc. occasionally permits the isolation of such compounds, e.g. the centrosymmetric halogen-bridged dimer  $[\{(\eta^5\text{-C}_5\text{Me}_5)\text{Ca}(\mu\text{-}1)(\text{thf})_2\}_2]$  which crystallizes from toluene solution. The complex is isostructural with the dimeric organosamarium(II) analogue.<sup>(52)</sup>

Other interesting structures of organometallic and related complexes of the heavier Group 2 metals include those of the centrosymmetric pyrazine adduct  $[\{\text{Ba}(\eta^5\text{-C}_5\text{Me}_5)_2\}_2(\mu\text{-}1,4\text{-C}_4\text{H}_4\text{N}_2)]$ , (Fig. 5.13a)<sup>(48)</sup>, the square-planar Sr complex  $[\{\text{trans-Sr}(\text{NR}_2)_2(\mu\text{-}1,4\text{-C}_4\text{H}_8\text{O}_2)\}]$  ( $\text{R} = \text{SiMe}_3$ ), Fig. 5.13b<sup>(53)</sup> and the 5-coordinate trigonal-bipyramidal Ca complex  $[\text{Ca}(\text{OAr})_2(\text{thf})_3]$  ( $\text{Ar} = \text{C}_6\text{H}_2\text{-}2,6\text{-Bu}'_2\text{-}4\text{-Me}$ ), Fig. 5.13c.<sup>(54)</sup>

<sup>53</sup> F. G. N. CLOKE, P. B. HITCHCOCK, M. F. LAPPERT, G. A. LAWLESS and B. ROYO, *J. Chem. Soc., Chem. Commun.*, 724-6 (1991).

<sup>54</sup> P. B. HITCHCOCK, M. F. LAPPERT, G. A. LAWLESS and B. ROYO, *J. Chem. Soc., Chem. Commun.*, 1141-2 (1990).

<sup>52</sup> W. J. EVANS, J. W. GRATE, H. W. CHOI, I. BLOOM, W. E. HUNTER and J. L. ATWOOD, *J. Am. Chem. Soc.* **107**, 941-6 (1985).

																1	2																																																																																																																																																																																																																																																																																																																																																																																																																																												
																H	He																																																																																																																																																																																																																																																																																																																																																																																																																																												
3	4																	5	6	7	8	9	10																																																																																																																																																																																																																																																																																																																																																																																																																																						
Li	Be																	B	C	N	O	F	Ne																																																																																																																																																																																																																																																																																																																																																																																																																																						
11	12																	13	14	15	16	17	18																																																																																																																																																																																																																																																																																																																																																																																																																																						
Na	Mg																	Al	Si	P	S	Cl	Ar																																																																																																																																																																																																																																																																																																																																																																																																																																						
19	20	21	22	23	24	25	26	27	28	29	30	31	32	33	34	35	36																																																																																																																																																																																																																																																																																																																																																																																																																																												
K	Ca	Sc	Ti	V	Cr	Mn	Fe	Co	Ni	Cu	Zn	Ga	Ge	As	Se	Br	Kr																																																																																																																																																																																																																																																																																																																																																																																																																																												
37	38	39	40	41	42	43	44	45	46	47	48	49	50	51	52	53	54																																																																																																																																																																																																																																																																																																																																																																																																																																												
Rb	Sr	Y	Zr	Nb	Mo	Tc	Ru	Rh	Pd	Ag	Cd	In	Sn	Sb	Te	I	Xe																																																																																																																																																																																																																																																																																																																																																																																																																																												
55	56	57	58	59	60	61	62	63	64	65	66	67	68	69	70	71	72																																																																																																																																																																																																																																																																																																																																																																																																																																												
Cs	Ba	La	Hf	Ta	W	Re	Os	Ir	Pt	Au	Hg	Tl	Pb	Bi	Po	At	Rn																																																																																																																																																																																																																																																																																																																																																																																																																																												
87	88	89	90	91	92	93	94	95	96	97	98	99	100	101	102	103	104																																																																																																																																																																																																																																																																																																																																																																																																																																												
Fr	Ra	Ac	Rf	Db	Sg	Bh	Hs	Mt	Uun	Uun	Uub																																																																																																																																																																																																																																																																																																																																																																																																																																																		
																		73	74	75	76	77	78	79	80	81	82	83	84	85	86	87	88	89	90	91	92	93	94	95	96	97	98	99	100	101	102	103	104	105	106	107	108	109	110	111	112	113	114	115	116	117	118	119	120	121	122	123	124	125	126	127	128	129	130	131	132	133	134	135	136	137	138	139	140	141	142	143	144	145	146	147	148	149	150	151	152	153	154	155	156	157	158	159	160	161	162	163	164	165	166	167	168	169	170	171	172	173	174	175	176	177	178	179	180	181	182	183	184	185	186	187	188	189	190	191	192	193	194	195	196	197	198	199	200	201	202	203	204	205	206	207	208	209	210	211	212	213	214	215	216	217	218	219	220	221	222	223	224	225	226	227	228	229	230	231	232	233	234	235	236	237	238	239	240	241	242	243	244	245	246	247	248	249	250	251	252	253	254	255	256	257	258	259	260	261	262	263	264	265	266	267	268	269	270	271	272	273	274	275	276	277	278	279	280	281	282	283	284	285	286	287	288	289	290	291	292	293	294	295	296	297	298	299	300	301	302	303	304	305	306	307	308	309	310	311	312	313	314	315	316	317	318	319	320	321	322	323	324	325	326	327	328	329	330	331	332	333	334	335	336	337	338	339	340	341	342	343	344	345	346	347	348	349	350	351	352	353	354	355	356	357	358	359	360	361	362	363	364	365	366	367	368	369	370	371	372	373	374	375	376	377	378	379	380	381	382	383	384	385	386	387	388	389	390	391	392	393	394	395	396	397	398	399	400	401	402	403	404	405	406	407	408	409	410	411	412	413	414	415	416	417	418	419	420	421	422	423	424	425	426	427	428	429	430	431	432	433	434	435	436	437	438	439	440	441	442	443	444	445	446	447	448	449	450	451	452	453	454	455	456	457	458	459	460	461	462	463	464	465	466	467	468	469	470	471	472	473	474	475	476	477	478	479	480	481	482	483	484	485	486	487	488	489	490	491	492	493	494	495	496	497	498	499	500

# 6

## Boron

### 6.1 Introduction

Boron is a unique and exciting element. Over the years it has proved a constant challenge and stimulus not only to preparative chemists and theoreticians, but also to industrial chemists and technologists. It is the only non-metal in Group 13 of the periodic table and shows many similarities to its neighbour, carbon, and its diagonal relative, silicon. Thus, like C and Si, it shows a marked propensity to form covalent, molecular compounds, but it differs sharply from them in having one less valence electron than the number of valence orbitals, a situation sometimes referred to as “electron deficiency”. This has a dominant effect on its chemistry.

Borax was known in the ancient world where it was used to prepare glazes and hard (borosilicate) glasses. Sporadic investigations during the eighteenth century led ultimately to the isolation of very impure boron by H. Davy and by J. L. Gay Lussac and L. J. Thénard in 1808, but it was not until 1892 that H. Moissan obtained samples of 95–98% purity by reducing  $B_2O_3$  with Mg. High-purity boron (>99%) is a product of this century, and the various crystalline forms have

been obtained only during the last few decades mainly because of the highly refractory nature of the element and its rapid reaction at high temperatures with nitrogen, oxygen and most metals. The name *boron* was proposed by Davy to indicate the source of the element and its similarity to carbon, i.e. *bor(ax + carb)on*.

Boron is comparatively un abundant in the universe (p. 14); it occurs to the extent of about 9 ppm in crustal rocks and is therefore rather less abundant than lithium (18 ppm) or lead (13 ppm) but is similar to praseodymium (9.1 ppm) and thorium (8.1 ppm). It occurs almost invariably as borate minerals or as borosilicates. Commercially valuable deposits are rare, but where they do occur, as in California or Turkey, they can be vast (see Panel). Isolated deposits are also worked in the former Soviet Union, Tibet and Argentina.

The structural complexity of borate minerals (p. 205) is surpassed only by that of silicate minerals (p. 347). Even more complex are the structures of the metal borides and the various allotropic modifications of boron itself. These factors, together with the unique structural and bonding problems of the boron hydrides, dictate that boron should be treated in a separate chapter.

## Borate Minerals

The world's major deposits of borate minerals occur in areas of former volcanic activity and appear to be associated with the waters from former hot springs. The primary mineral that first crystallized was normally ulexite,  $\text{NaCa}[\text{B}_3\text{O}_6(\text{OH})_6]\cdot 5\text{H}_2\text{O}$ , but this was frequently mixed with lesser amounts of borax,  $\text{Na}_2[\text{B}_4\text{O}_5(\text{OH})_4]\cdot 8\text{H}_2\text{O}$  (p. 206). Exposure and subsequent weathering (e.g. in the Mojave Desert, California) resulted in leaching by surface waters, leaving a residue of the less-soluble mineral colemanite,  $\text{Ca}[\text{B}_3\text{O}_4(\text{OH})_3]\cdot \text{H}_2\text{O}$  (p. 206). The leached (secondary) borax sometimes reaccumulated and sometimes underwent other changes to form other secondary minerals such as the commercially important kernite,  $\text{Na}_2[\text{B}_4\text{O}_5(\text{OH})_4]\cdot 2\text{H}_2\text{O}$ , at Boron, California: This is the world's largest single source of borates and comprises a deposit 6.5 km long, 1.5 km wide and 25–50 m thick containing material that averages 75% of hydrated sodium tetraborates (borax and kernite). World reserves (expressed as  $\text{B}_2\text{O}_3$  content) exceed 315 million tonnes (Turkey 45%, USA 21%, Kazakhstan 17%, China 8.6%, Argentina 7.3%). Annual world production of borates was 2.67 million tonnes in 1990. Production in Turkey has expanded dramatically in the last two decades and now exceeds that of the USA, the 1990 production figures being 1.20 and 1.09 Mt respectively. Smaller producers ( $10^3$  t) are: "Russia" 175, Chile 132, China 27, Argentina 26 and Peru 18. The 1991 bulk price per tonne of borax in USA was \$264 for technical grade and \$2222 for refined granules.

The main chemical products produced from these minerals are (a) boron oxides, boric acid and borates, (b) esters of boric acid, (c) refractory boron compounds (borides, etc.), (d) boron halides, (e) boranes and carbaboranes and (f) organoboranes. The main industrial and domestic uses of boron compounds in Europe (USA in parentheses) are:

Heat resistant glasses (e.g. Pyrex), glass wool, fibre glass	26% (60%)
Detergents, soaps, cleaners and cosmetics	37% ( 7%)
Porcelain enamels	16% ( 3%)
Synthetic herbicides and fertilizers	2% ( 4%)
Miscellaneous (nuclear shielding, metallurgy, corrosion control, leather tanning, flame-proofing, catalysts)	19% (26%)

The uses in the glass and ceramics industries reflect the diagonal relation between boron and silicon and the similarity of vitreous borate and silicate networks (pp. 203, 206 and 347). In the UK and continental Europe (but not in the USA or Japan) sodium perborate (p. 206) is a major constituent of washing powders since it hydrolyses to  $\text{H}_2\text{O}_2$  and acts as a bleaching agent in very hot water ( $\sim 90^\circ\text{C}$ ); in the USA domestic washing machines rarely operate above  $70^\circ$ , at which temperature perborates are ineffective as bleaches.

Details of other uses of boron compounds are noted at appropriate places in the text.

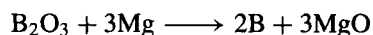
The general group trends, and a comparison with the chemistry of the metallic elements of Group 13 (Al, Ga, In and Tl), will be deferred until the next chapter.

## 6.2 Boron<sup>(1)</sup>

### 6.2.1 Isolation and purification of the element

There are four main methods of isolating boron from its compounds:

(i) Reduction by metals at high temperature, e.g. the strongly exothermic reaction



(Moissan boron, 95–98% pure)

Other electropositive elements have been used (e.g. Li, Na, K, Be, Ca, Al, Fe), but the product is generally amorphous and contaminated with refractory impurities such as metal borides. Massive crystalline boron (96%) has been prepared by reacting  $\text{BCl}_3$  with zinc in a flow system at  $900^\circ\text{C}$ .

(ii) Electrolytic reduction of fused borates or tetrafluoroborates, e.g.  $\text{KBF}_4$  in molten  $\text{KCl/KF}$  at  $800^\circ$ . The process is comparatively cheap but yields only powdered boron of 95% purity.

(iii) Reduction of volatile boron compounds by  $\text{H}_2$ , e.g. the reaction of  $\text{BBr}_3 + \text{H}_2$  on a heated

<sup>1</sup> N. N. GREENWOOD, *Boron*, Pergamon Press, Oxford, 1975, 327 pp.; also as Chap. 11 in *Comprehensive Inorganic Chemistry*, Vol. 1, Pergamon Press, Oxford, 1973.



tantalum metal filament. This method, which was introduced in 1922 and can now be operated on the kilogram scale, is undoubtedly the most effective general preparation for high purity boron (>99.9%). Crystallinity improves with increasing temperature, amorphous products being obtained below 1000°C,  $\alpha$ - and  $\beta$ -rhombohedral modifications between 1000–1200° and tetragonal crystals above this.  $\text{BCl}_3$  can be substituted for  $\text{BBr}_3$  but  $\text{BI}_3$  is unsatisfactory because it is expensive and too difficult to purify sufficiently. Free energy calculations indicate that  $\text{BF}_3$  would require impracticably high temperatures (>2000°).

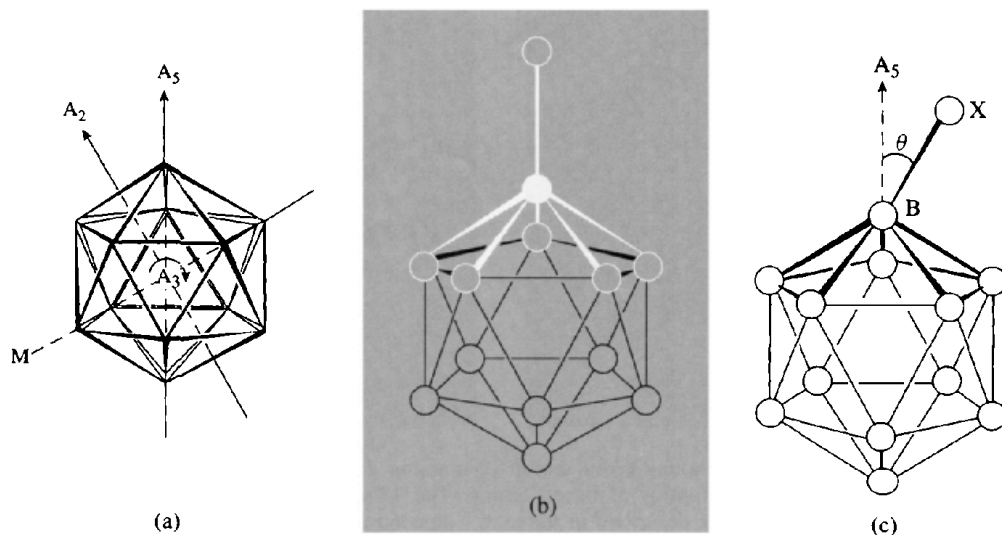
(iv) Thermal decomposition of boron hydrides and halides. Boranes decompose to amorphous boron when heated at temperatures up to 900° and crystalline products can be obtained by thermal decomposition of  $\text{BI}_3$ . Indeed, the first recognized sample of  $\alpha$ -rhombohedral B was prepared (in 1960) by decomposition of  $\text{BI}_3$  on Ta at 800–1000°, and this is still an excellent exclusive preparation of this allotrope.

## 6.2.2 Structure of crystalline boron<sup>(1-3)</sup>

Boron is unique among the elements in the structural complexity of its allotropic modifications; this reflects the variety of ways in which boron seeks to solve the problem of having fewer electrons than atomic orbitals available for bonding. Elements in this situation usually adopt metallic bonding, but the small size and high ionization energies of B (p. 222) result in covalent rather than metallic bonding. The structural unit which dominates the various allotropes of B is the  $\text{B}_{12}$  icosahedron (Fig. 6.1), and this also occurs in several metal boride structures and in certain boron hydride derivatives. Because of the fivefold rotation symmetry at the individual B atoms, the  $\text{B}_{12}$  icosahedra pack rather inefficiently and there

<sup>2</sup> V. I. MATKOVICH (ed.), *Boron and Refractory Borides*, Springer-Verlag, Berlin, 1977, 656 pp.

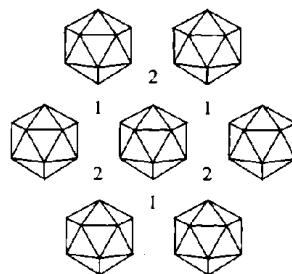
<sup>3</sup> GMELIN, *Handbook of Inorganic Chemistry, Boron, Supplement Vol. 2: Elemental Boron. Boron Carbides*, 1981, 242 pp.



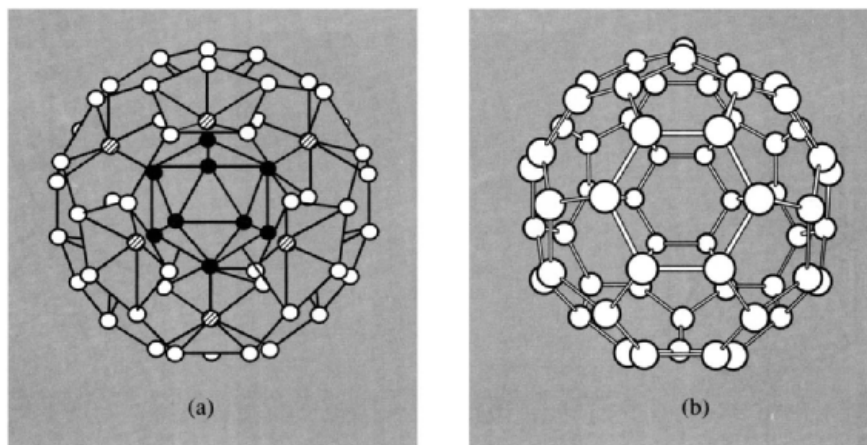
**Figure 6.1** The icosahedron and some of its symmetry elements. (a) An icosahedron has 12 vertices and 20 triangular faces defined by 30 edges. (b) The preferred pentagonal pyramidal coordination polyhedron for 6-coordinate boron in icosahedral structures; as it is not possible to generate an infinite three-dimensional lattice on the basis of fivefold symmetry, various distortions, translations and voids occur in the actual crystal structures. (c) The distortion angle  $\theta$ , which varies from 0° to 25°, for various boron atoms in crystalline boron and metal borides.

are regularly spaced voids which are large enough to accommodate additional boron (or metal) atoms. Even in the densest form of boron, the  $\alpha$ -rhombohedral modification, the percentage of space occupied by atoms is only 37% (compared with 74% for closest packing of spheres).

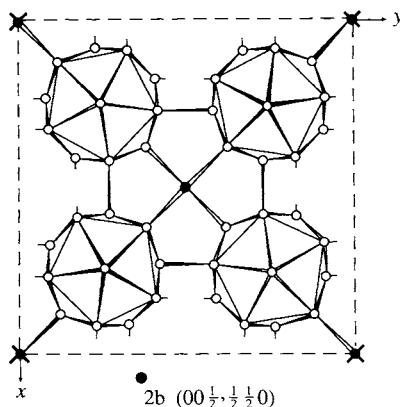
The  $\alpha$ -rhombohedral form of boron is the simplest allotropic modification and consists of nearly regular  $B_{12}$  icosahedra in slightly deformed cubic close packing. The rhombohedral unit cell (Fig. 6.2) has  $a_0$  505.7 pm,  $\alpha$  58.06° (60° for regular ccp) and contains 12 B atoms. *It is important to remember that in Fig. 6.2, as in most other structural diagrams in this chapter, the lines merely define the geometry of the clusters of boron atoms; they do not usually represent 2-centre 2-electron bonds between pairs of atoms.* In terms of the MO theory to be discussed on p. 157, the 36 valence electrons of each  $B_{12}$  unit are distributed as follows: 26 electrons just fill the 13 available bonding MOs within the icosahedron and 6 electrons share with 6 other electrons from 6 neighbouring icosahedra in adjacent planes to



**Figure 6.2** Basal plane of  $\alpha$ -rhombohedral boron showing close-packed arrangement of  $B_{12}$  icosahedra. The B-B distances within each icosahedron vary regularly between 173–179 pm. Dotted lines show the 3-centre bonds between the 6 equatorial boron atoms in each icosahedron to 6 other icosahedra in the same sheet at 202.5 pm. The sheets are stacked so that each icosahedron is bonded by six 2-centre B-B bonds at 171 pm (directed rhombohedrally, 3 above and 3 below the icosahedron).  $B_{12}$  units in the layer above are centred over 1 and those in the layer below are centred under 2.



**Figure 6.3** (a) The  $B_{84}$  unit in  $\beta$ -rhombohedral boron comprising a central  $B_{12}$  icosahedron and 12 outwardly directed pentagonal pyramids of boron atoms. The 12 outer icosahedra are completed by linking with the  $B_{10}$  subunits as described in the text. The central icosahedron (●) is almost exactly regular with B-B 176.7 pm. The shortest B-B distances (162–172 pm) are between the central icosahedron and the apices of the 12 surrounding pentagonal pyramids (⊙). The B-B distances within the 12  $B_6$  pentagonal pyramids (half-icosahedra) are somewhat longer (185 pm) and the longest B-B distances (188–192 pm) occur within the hexagonal rings surrounding the 3-fold symmetry axes of the  $B_{84}$  polyhedron. Note that if the 24 “internal” B atoms (● and ⊙) are removed from the  $B_{84}$  unit then a  $B_{60}$  unit (b) remains which has precisely the fullerene structure subsequently found some 25 years later for  $C_{60}$  (p. 279).



**Figure 6.4** Crystal structure of  $\alpha$ -tetragonal boron. This was originally thought to be  $B_{50}$  ( $4B_{12} + 2B$ ) but is now known to be either  $B_{50}C_2$  or  $B_{50}N_2$  in which the 2C (or 2N) occupy the 2(b) positions; the remaining 2B are distributed statistically at other “vacant” sites in the lattice. Note that this reformulation solves three problems which attended the description of the  $\alpha$ -tetragonal phase as a crystalline modification of pure B:

1. The lattice parameters showed considerable variation from one crystal to another with average values  $a$  875 pm,  $c$  506 pm; this is now thought to arise from variable composition depending on the precise preparative conditions used.
2. The interatomic distances involving the single 4-coordinate atoms at 2(b) were only 160 pm; this is unusually short for B–B but reasonable for B–C or B–N distances.
3. The structure requires 160 valence electrons per unit cell computed as follows: internal bonding within the 4 icosahedra ( $4 \times 26 = 104$ ); external bonds for the 4 icosahedra ( $4 \times 12 = 48$ ); bonds shared by the atoms in 2(b) positions ( $2 \times 4 = 8$ ). However, 50 B atoms have only 150 valence electrons and even with the maximum possible excess of boron in the unit cell (0.75 B) this rises to only 152 electrons. The required extra 8 or 10 electrons are now supplied by 2C or 2N though the detailed description of the bonding is more intricate than this simple numerology implies.

form the 6 rhombohedrally directed normal 2-centre 2-electron bonds; this leaves 4 electrons which is just the number required for contribution to the 6 equatorial 3-centre 2-electron bonds ( $6 \times \frac{2}{3} = 4$ ).

The thermodynamically most stable polymorph of boron is the  $\beta$ -rhombohedral modification which has a much more complex structure with 105 B atoms in the unit cell ( $a_0$  1014.5 pm,  $\alpha$  65.28°). The basic unit can be thought of as a central  $B_{12}$  icosahedron surrounded by an icosahedron of icosahedra; this can be visualized as 12 of the  $B_7$  units in Fig. 6.1b arranged so that the apex atoms form the central  $B_{12}$  surrounded by 12 radially disposed pentagonal dishes to give the  $B_{84}$  unit shown in Fig. 6.3a. The 12 half-icosahedra are then completed by means of 2 complicated  $B_{10}$  subunits per unit cell,

each comprising a central 9-coordinate B atom surrounded by 9 B atoms in the form of 4 fused pentagonal rings. This arrangement corresponds to 104 B ( $84 + 10 + 10$ ) and there is, finally, a 6-coordinate B atom at the centre of symmetry between 2 adjacent  $B_{10}$  condensed units, bringing the total to 105 B atoms in the unit cell.

The first crystalline polymorph of B to be prepared (1943) was termed  $\alpha$ -tetragonal boron and was found to have 50 B atoms in the unit cell ( $4B_{12} + 2B$ ) (Fig. 6.4). Paradoxically, however, more recent work (1974) suggests that this phase never forms in the absence of carbon or nitrogen as impurity and that it is, in reality,  $B_{50}C_2$  or  $B_{50}N_2$  depending on the preparative conditions; yields are increased considerably when the  $BBr_3/H_2$  mixture is purposely doped with a few per cent of  $CH_4$ ,  $CHBr_3$  or  $N_2$ . The

work illustrates the great difficulties attending preparative and structural studies in this area. The crystal structures of other boron polymorphs, particularly the  $\beta$ -tetragonal phase with 192 B atoms in the unit cell ( $a$  1012,  $c$  1414 pm), are even more complex and have so far defied elucidation despite extensive work by many investigators.<sup>3</sup>

### 6.2.3 Atomic and physical properties of boron

Boron has 2 stable naturally occurring isotopes and the variability of their concentration (particularly the difference between borates from California (low in  $^{10}\text{B}$ ) and Turkey (high in  $^{10}\text{B}$ ) prevents the atomic weight of boron being quoted more precisely than 10.811(7) (p. 17). Each isotope has a nuclear spin (Table 6.1) and this has proved particularly valuable in nmr spectroscopy, especially for  $^{11}\text{B}$ .<sup>(4)</sup> The great difference in neutron absorption cross-section of the 2 isotopes is also notable, and this has led to the development of viable separation processes on an industrial scale. The commercial availability of the separated isotopes has greatly assisted the solution of structural and mechanistic problems in boron chemistry and has led to the development of boron-10 neutron capture therapy for the treatment of certain types of brain tumour (see p. 179).

<sup>4</sup> J. D. KENNEDY, Chap. 8 in J. MASON (ed.), *Multinuclear NMR*, Plenum, New York, pp. 221–58 (1987). T. L. VENABLE, W. C. HUTTON and R. N. GRIMES, *J. Am. Chem. Soc.* **106**, 29–37 (1984). D. REED, *Chem. Soc. Rev.* **22**, 109–16 (1993).

Boron is the fifth element in the periodic table and its ground-state electronic configuration is  $[\text{He}]2s^22p^1$ . The first 3 ionization energies are 800.6, 2427.1 and 3659.7 kJ mol<sup>-1</sup>, all substantially larger than for the other elements in Group 13. (The values for this and other properties of B are compared with those for Al, Ga, In and Tl on p. 222). The electronegativity (p. 25) of B is 2.0, which is close to the values for H (2.1) Si (1.8) and Ge (1.8) but somewhat less than the value for C (2.5). The implied reversal of the polarity of B–H and C–H bonds is an important factor in discussing hydroboration (p. 166) and other reactions.

The determination of precise physical properties for elemental boron is bedevilled by the twin difficulties of complex polymorphism and contamination by irremovable impurities. Boron is an extremely hard refractory solid of high mp, low density and very low electrical conductivity. Crystalline forms are dark red in transmitted light and powdered forms are black. The most stable ( $\beta$ -rhombohedral) modification has mp 2092°C (exceeded only by C among the non-metals), bp  $\sim$ 4000°C,  $d$  2.35 g cm<sup>-3</sup> ( $\alpha$ -rhombohedral form 2.45 g cm<sup>-3</sup>),  $\Delta H_{\text{sublimation}}$  570 kJ per mol of B, electrical conductivity at room temperature  $1.5 \times 10^{-6}$  ohm<sup>-1</sup> cm<sup>-1</sup>.

### 6.2.4 Chemical properties

It has been argued<sup>(1)</sup> that the inorganic chemistry of boron is more diverse and complex than that of any other element in the periodic table. Indeed, it is only during the last three decades that the enormous range of structural types has begun to

**Table 6.1** Nuclear properties of boron isotopes

Property	$^{10}\text{B}$	$^{11}\text{B}$
Relative mass ( $^{12}\text{C} = 12$ )	10.012 939	11.009 305
Natural abundance/(%)	19.055–20.316	80.945–79.684
Nuclear spin (parity)	3(+)	$\frac{3}{2}$ (–)
Magnetic moment/(nuclear magnetons) <sup>(a)</sup>	+1.800 63	+2.688 57
Quadrupole moment/barns <sup>(b)</sup>	+0.074	+0.036
Cross-section for (n, $\alpha$ )/barns <sup>(b)</sup>	3835( $\pm$ 10)	0.005

<sup>(a)</sup> 1 nuclear magneton =  $5.0505 \times 10^{-27}$  A m<sup>2</sup> in SI.

<sup>(b)</sup> 1 barn =  $10^{-28}$  m<sup>2</sup> in SI; the cross-section for natural boron ( $\sim$ 20%  $^{10}\text{B}$ ) is  $\sim$ 767 barns.

be elucidated and the subtle types of bonding appreciated. The chemical nature of boron is influenced primarily by its small size and high ionization energy, and these factors, coupled with the similarity in electronegativity of B, C and H, lead to an extensive and unusual type of covalent (molecular) chemistry. The electronic configuration  $2s^2 2p^1$  is reflected in a predominant trivalence, and bond energies involving B are such that there is no tendency to form univalent compounds of the type which increasingly occur in the chemistry of Al, Ga, In and Tl. However, the availability of only 3 electrons to contribute to covalent bonding involving the 4 orbitals s,  $p_x$ ,  $p_y$  and  $p_z$  confers a further range of properties on B leading to electron-pair acceptor behaviour (Lewis acidity) and multicentre bonding (p. 157). The high affinity for oxygen is another dominant characteristic which forms the basis of the extensive chemistry of borates and related oxo complexes (p. 203). Finally, the small size of B enables many interstitial alloy-type metal borides to be prepared, and the range of these is considerably extended by the propensity of B to form branched and unbranched chains, planar networks, and three-dimensional arrays of great intrinsic stability which act as host frameworks to house metal atoms in various stoichiometric proportions.

It is thus possible to distinguish five types of boron compound, each having its own chemical systematics which can be rationalized in terms of the type of bonding involved, and each resulting in highly individualistic structures and chemical reactions:

- (i) metal borides ranging from  $M_5B$  to  $MB_{66}$  (or even  $MB_{>100}$ ) (see below);
- (ii) boron hydrides and their derivatives including carbaboranes and polyhedral borane-metal complexes (p. 151);
- (iii) boron trihalides and their adducts and derivatives (p. 195);
- (iv) oxo compounds including polyborates, borosilicates, peroxoborates, etc. (p. 203);
- (v) organoboron compounds and B–N compounds (B–N being isoelectronic with C–C) (p. 207).

The chemical reactivity of boron itself obviously depends markedly on the purity, crystallinity, state of subdivision and temperature. Boron reacts with  $F_2$  at room temperature and is superficially attacked by  $O_2$  but is otherwise inert. At higher temperatures boron reacts directly with all the non-metals except H, Ge, Te and the noble gases. It also reacts readily and directly with almost all metals at elevated temperatures, the few exceptions being the heavier members of groups 11–15 (Ag, Au; Cd, Hg; Ga, In, Tl; Sn, Pb; Sb, Bi).

The general chemical inertness of boron at lower temperatures can be gauged by the fact that it resists attack by boiling concentrated aqueous NaOH or by fused NaOH up to  $500^\circ$ , though it is dissolved by fused  $Na_2CO_3/NaNO_3$  mixtures at  $900^\circ C$ . A 2:1 mixture of hot concentrated  $H_2SO_4/HNO_3$  is also effective for dissolving elemental boron for analysis but non-oxidizing acids do not react.

## 6.3 Borides<sup>(1-3)</sup>

### 6.3.1 Introduction

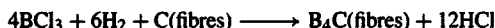
The borides comprise a group of over 200 binary compounds which show an amazing diversity of stoichiometries and structural types; e.g.  $M_5B$ ,  $M_4B$ ,  $M_3B$ ,  $M_5B_2$ ,  $M_7B_3$ ,  $M_2B$ ,  $M_5B_3$ ,  $M_3B_2$ ,  $M_{11}B_8$ ,  $MB$ ,  $M_{10}B_{11}$ ,  $M_3B_4$ ,  $M_2B_3$ ,  $M_3B_5$ ,  $MB_2$ ,  $M_2B_5$ ,  $MB_3$ ,  $MB_4$ ,  $MB_6$ ,  $M_2B_{13}$ ,  $MB_{10}$ ,  $MB_{12}$ ,  $MB_{15}$ ,  $MB_{18}$  and  $MB_{66}$ . There are also numerous nonstoichiometric phases of variable composition and many ternary and more complex phases in which more than one metal combines with boron. The rapid advance in our understanding of these compounds during the past few decades has been based mainly on X-ray diffraction analysis and the work has been stimulated not only by the inherent academic challenge implied by the existence of these unusual compounds but also by the extensive industrial interest generated by their unique combination of desirable physical and chemical properties (see Panel).

## Properties and Uses of Borides

Metal-rich borides are extremely hard, chemically inert, involatile, refractory materials with mps and electrical conductivities which often exceed those of the parent metals. Thus the highly conducting diborides of Zr, Hf, Nb and Ta all have mps > 3000°C and TiB<sub>2</sub> (mp 2980°C) has a conductivity 5 times greater than that of Ti metal. Borides are normally prepared as powders but can be fabricated into the desired form by standard techniques of powder metallurgy and ceramic technology. TiB<sub>2</sub>, ZrB<sub>2</sub> and CrB<sub>2</sub> find application as turbine blades, combustion chamber liners, rocket nozzles and ablation shields. Ability to withstand attack by molten metals, slags and salts have commended borides or boride-coated metals as high-temperature reactor vessels, vaporizing boats, crucibles, pump impellers and thermocouple sheaths. Inertness to chemical attack at high temperatures, coupled with excellent electrical conductivity, suggest application as electrodes in industrial processes.

Nuclear applications turn on the very high absorption cross-section of <sup>10</sup>B for thermal neutrons (p. 144) and the fact that this property is retained for high-energy neutrons (10<sup>4</sup>–10<sup>6</sup> eV) more effectively than for any other nuclide. Another advantage of <sup>10</sup>B is that the products of the (n,α) reaction are the stable, non-radioactive elements Li and He. Accordingly, metal borides and boron carbide have been used extensively as neutron shields and control rods since the beginning of the nuclear power industry. More dramatically, following the disaster at Chernobyl in the early hours of 26 April 1986, some 40 tonnes of boron carbide particles were dumped from helicopters onto the stricken reactor to prevent further runaway fission occurring. (In addition there were 800 tonnes of dolomite to provide a CO<sub>2</sub> gas blanket, 1800 t of clay and sand to quench the fires and filter radionuclides, plus 2400 t of lead to absorb heat by melting and to provide a liquid layer that would in time solidify and seal the top of the core of the vault.)

The principal non-nuclear industrial use of boron carbide is as an abrasive grit or powder for polishing or grinding; it is also used on brake and clutch linings. In addition, there is much current interest in its use as light-weight protective armour, and tests have indicated that boron carbide and beryllium borides offer the best choice; applications are in bullet-proof protective clothing and in protective armour for aircraft. More elegantly, boron carbide can now be produced in fibre form by reacting BCl<sub>3</sub>/H<sub>2</sub> with carbon yarn at 1600–1900°C:



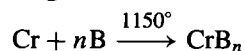
Fibre curling can be eliminated by heat treatment under tension near the mp, and the resulting fibres have a tensile strength of  $3.5 \times 10^5$  psi (1 psi = 6895 N m<sup>-2</sup>) and an elastic modulus of  $50 \times 10^6$  psi at a density of 2.35 g cm<sup>-3</sup>; the form was 1 ply, 720 filament yarn with a filament diameter of 11–12 μm. The fibres are inert to hot acid and alkali, resistant to Cl<sub>2</sub> up to 700° and air up to 800°C.

Boron itself has been used for over two decades in filament form in various composites; BCl<sub>3</sub>/H<sub>2</sub> is reacted at 1300° on the surface of a continuously moving tungsten fibre 12 μm in diameter. US production capacity is about 20 tonnes pa and the price is about \$800/kg. The primary use so far has been in military aircraft and space shuttles, but boron fibre composites are also being studied as reinforcement materials for commercial aircraft. At the domestic level they are finding increasing application in golf shafts, tennis rackets and bicycle frames.

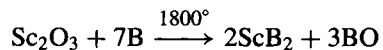
### 6.3.2 Preparation and stoichiometry

Eight general methods are available for the synthesis of borides, the first four being appropriate for small-scale laboratory preparations and the remaining four for commercial production on a scale ranging from kilogram amounts to tonne quantities. Because high temperatures are involved and the products are involatile, borides are not easy to prepare pure and subsequent purification is often difficult; precise stoichiometry is also sometimes hard to achieve because of differential volatility or high activation energies. The methods are:

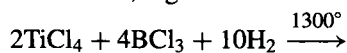
- (i) Direct combination of the elements: this is probably the most widely used technique, e.g.



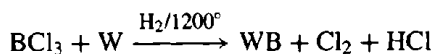
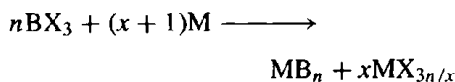
- (ii) Reduction of metal oxide with B (rather wasteful of expensive elemental B), e.g.



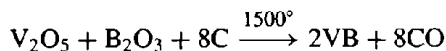
- (iii) Co-reduction of volatile mixed halides with H<sub>2</sub> using a metal filament, hot tube or plasma torch, e.g.



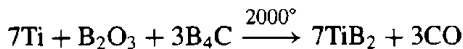
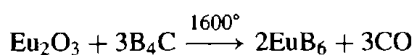
- (iv) Reduction of  $\text{BCl}_3$  (or  $\text{BX}_3$ ) with a metal (sometimes assisted by  $\text{H}_2$ ), e.g.



- (v) Electrolytic deposition from fused salts: this is particularly effective for  $\text{MB}_6$  ( $\text{M}$  = alkaline earth or rare earth metal) and for the borides of Mo, W, Fe, Co and Ni. The metal oxide and  $\text{B}_2\text{O}_3$  or borax are dissolved in a suitable, molten salt bath and electrolysed at  $700\text{--}1000^\circ$  using a graphite anode; the boride is deposited on the cathode which can be graphite or steel.
- (vi) Co-reduction of oxides with carbon at temperatures up to  $2000^\circ$ , e.g.

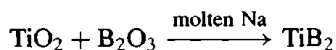


- (vii) Reduction of metal oxide (or  $\text{M} + \text{B}_2\text{O}_3$ ) with boron carbide, e.g.

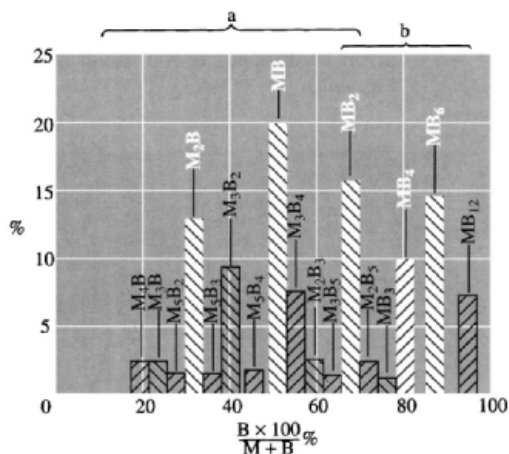


Boron carbide (p. 149) is a most useful and economic source of B and will react with most metals or their oxides. It is produced in tonnage quantities by direct reduction of  $\text{B}_2\text{O}_3$  with C at  $1600^\circ$ : a C resistor is embedded in a mixture of  $\text{B}_2\text{O}_3$  and C, and a heavy electric current passed.

- (viii) Co-reduction of mixed oxides with metals (Mg or Al) in a thermite-type reaction — this usually gives contaminated products including ternary borides, e.g.  $\text{Mo}_7\text{Al}_6\text{B}_7$ . Alternatively, alkali metals or Ca can be used as reductants, e.g.



The various stoichiometries are not equally common, as can be seen from Fig. 6.5; the most frequently occurring are  $\text{M}_2\text{B}$ ,  $\text{MB}$ ,  $\text{MB}_2$ ,  $\text{MB}_4$  and  $\text{MB}_6$ , and these five classes account for 75% of the compounds. At the other extreme  $\text{Ru}_{11}\text{B}_8$  is the only known example of this stoichiometry. Metal-rich borides tend to be formed by the transition elements whereas the boron-rich borides are characteristic of the more electropositive elements in Groups 1–3, the lanthanides and the actinides. Only the diborides  $\text{MB}_2$  are common to both classes.

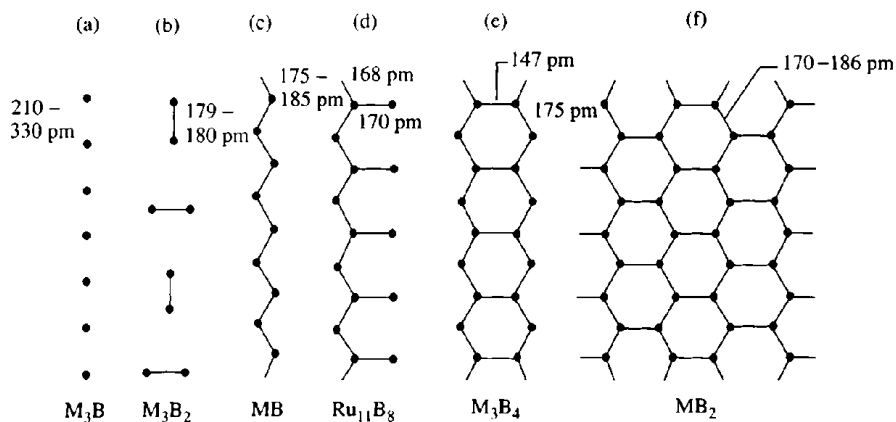


**Figure 6.5** Frequency of occurrence of various stoichiometries among boride phases: (a) field of borides of d elements, and (b) field of borides of s, p and f elements.

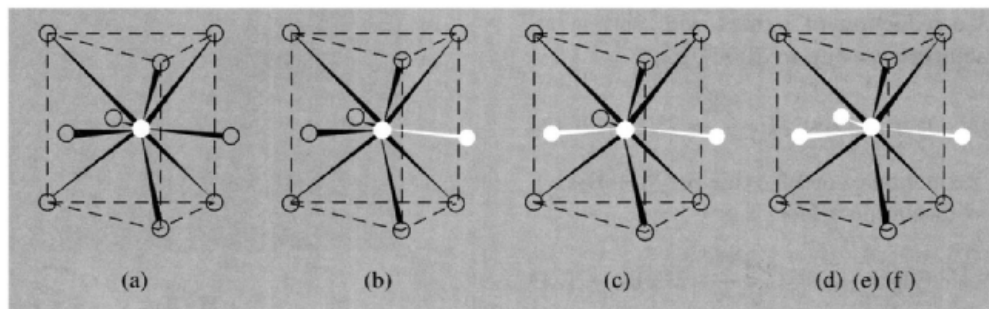
### 6.3.3 Structures of borides<sup>(1-3.5)</sup>

The structures of metal-rich borides can be systematized by the schematic arrangements shown in Fig. 6.6, which illustrates the increasing tendency of B atoms to catenate as their concentration in the boride phase increases; the B atoms are often at the centres of trigonal prisms of metal atoms (Fig. 6.7) and the various stoichiometries are accommodated as follows:

<sup>5</sup> T. LUNDSTROM, *Pure Appl. Chem.* 57, 1383–90 (1985).



**Figure 6.6** Idealized patterns of boron catenation in metal-rich borides. Examples of the structures (a)–(f) are given in the text. Boron atoms are often surrounded by trigonal prisms of M atoms as shown in Fig. 6.7.



**Figure 6.7** Idealized boron environment in metal-rich borides (see text): (a) isolated B atoms in  $M_3B$  and  $M_7B_3$ ; (b) pairs of B atoms in  $Cr_5B_3$  and  $M_3B_2$ ; (c) zigzag chains of B atoms in  $Ni_3B_4$  and  $MB$ ; (d) branched chains in  $Ru_{11}B_8$ ; and (e), (f) double chains and plane nets in  $M_3B_4$ ,  $MB_2$  and  $M_2B_5$ .

- |                                 |   |                               |  |
|---------------------------------|---|-------------------------------|--|
| (a) isolated B atoms:           | $Mn_4B$ ; $M_3B$ (Tc, Re, Co, Ni, Pd); $Pd_5B_2$ ; $M_7B_3$ (Tc, Re, Ru, Rh); $M_2B$ (Ta, Mo, W, Mn, Fe, Co, Ni); | (e) double chains of B atoms: | $M_3B_4$ (V, Nb, Ta; Cr, Mn);  |
| (b) isolated pairs $B_2$ :      | $Cr_5B_3$ ; $M_3B_2$ (V, Nb, Ta);   | (f) plane (or puckered) nets: | $MB_2$ (Mg, Al; Sc, Y; Ti, Zr, Hf; V, Nb, Ta; Cr, Mo, W; Mn, Tc, Re; Ru, Os; U, Pu); $M_2B_5$ (Ti; Mo, W). |
| (c) zigzag chains of B atoms:   | $M_3B_4$ (Ti; V, Nb, Ta; Cr, Mn, Ni); $MB$ (Ti, Hf; V, Nb, Ta; Cr, Mo, W; Mn, Fe, Co, Ni);                        |                               |  |
| (d) branched chains of B atoms: | $Ru_{11}B_8$ ;  |                               |  |

It will be noted from Fig. 6.6 that structures with isolated B atoms can have widely differing interatomic B–B distances, but all other classes involve appreciable bonding between B atoms, and the B–B distances remain almost invariant despite the extensive variation in the size of the metal atoms.



The structures of boron-rich borides (e.g.  $MB_4$ ,  $MB_6$ ,  $MB_{10}$ ,  $MB_{12}$ ,  $MB_{66}$ ) are even more effectively dominated by inter-B bonding, and the structures comprise three-dimensional networks of B atoms and clusters in which the metal atoms occupy specific voids or otherwise vacant sites. The structures are often exceedingly complicated (for the reasons given in Section 6.2.2): for example, the cubic unit cell of  $YB_{66}$  has  $a_0$  2344 pm and contains 1584 B and 24 Y atoms; the basic structural unit is the 13-icosahedron unit of 156 B atoms found in  $\beta$ -rhombohedral B (p. 142); there are 8 such units (1248 B) in the unit cell and the remaining 336 B atoms are statistically distributed in channels formed by the packing of the 13-icosahedron units.

Another compound which is even more closely related to  $\beta$ -rhombohedral boron is boron carbide, " $B_4C$ "; this is now more correctly written as  $B_{13}C_2$ ,<sup>(6)</sup> but the phase can vary over wide composition ranges which approach the stoichiometry  $B_{12}C_3$ . The structure is best thought of in terms of  $B_{84}$  polyhedra (p. 142) but these are now interconnected simply by linear C–B–C units instead of the larger  $B_{10}$ –B– $B_{10}$  units in  $\beta$ -rhombohedral B. The result is a more compact packing of the 13-icosahedron units so generated and this is reflected in the unit cell dimensions ( $a$  517.5 pm,  $\alpha$  65.74°). A notable feature of the structure (Fig. 6.8) is the presence of regular hexagonal planar rings  $B_4C_2$  (shaded). Stringent tests had to be applied to distinguish confidently between B and C atoms in this structure and to establish that it was indeed  $B_{12}$  CBC and not  $B_{12}C_3$  as had previously been thought. [This view has recently been challenged as a result of a  $^{13}C$  nmr study using magic-angle spinning, which suggests that the carbon is present only as  $C_3$  chains and that the structure is in fact still best represented as  $B_{12}C_3$  (or  $B_{12}^{2-}C_3^{2+}$ ).]<sup>(7)</sup> It is salutary to recall that boron carbide, which was first made by H. Moissan in 1899 and which has been manufactured in tonne amounts for several decades, still waits definitive

structural characterization. On one view the wide variation in stoichiometry from " $B_{6.5}C$ " to " $B_4C$ " is due to progressive vacancies in the CBC chain ( $B_{12}C_2 \equiv B_6C$ ) and/or progressive substitution of one C for B in the icosahedron [ $(B_{11}C)CBC \equiv B_4C$ ]. Related phases are  $B_{12}PBP$  and  $B_{12}X_2$  ( $X = P, As, O, S$ ). See also p. 288 for  $B_nC_{60-n}$  ( $n = 1-6$ ).

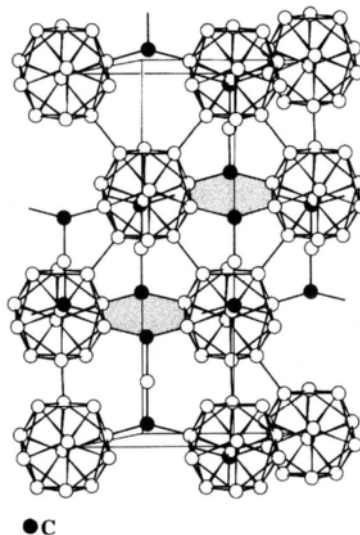
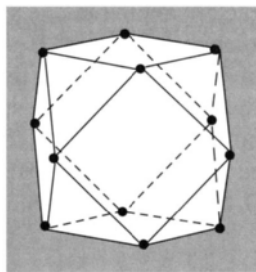


Figure 6.8 Crystal structure of  $B_{13}C_2$  showing the planar hexagonal rings connecting the  $B_{12}$  icosahedra. These rings are perpendicular to the C–B–C chains.

By contrast with the many complex structures formally related to  $\beta$ -rhombohedral boron, the structures of the large and important groups of cubic borides  $MB_{12}$  and  $MB_6$  are comparatively simple.  $MB_{12}$  is formed by many large electropositive metals (e.g. Sc, Y, Zr, lanthanides and actinides) and has an "NaCl-type" fcc structure in which M atoms alternate with  $B_{12}$  cubo-octahedral clusters (Fig. 6.9). (Note that the  $B_{12}$  cluster is not an icosahedron.) Similarly, the cubic hexaborides  $MB_6$  consist of a simple CsCl-type lattice in which the halogen is replaced by  $B_6$  octahedra (Fig. 6.10); these  $B_6$  octahedra are linked together in all 6 orthogonal directions to give a rigid but open framework which can accommodate large,

<sup>6</sup> G. WILL and K. H. KOSSOBUTZKI, *J. Less-Common Metals* **47**, 43–8 (1976).

<sup>7</sup> T. M. DUNCAN, *J. Am. Chem. Soc.* **106**, 2270–5 (1984).



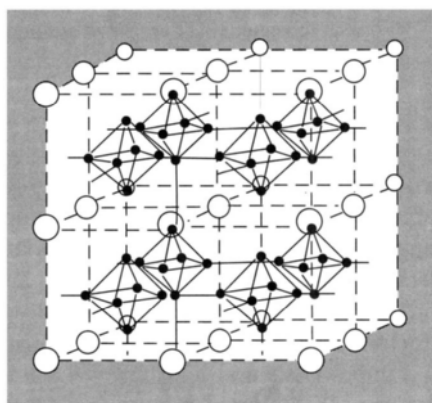
**Figure 6.9**  $B_{12}$  Cubo-octahedral cluster as found in  $MB_{12}$ . This  $B_{12}$  cluster alternates with M atoms on an fcc lattice as in NaCl, the  $B_{12}$  cluster replacing Cl.

electropositive metal atoms at the corners of the interpenetrating cubic sublattice. The rigidity of the B framework is shown by the very small linear coefficient of thermal expansion of hexaborides ( $6-8 \times 10^{-6} \text{ deg}^{-1}$ ) and by the narrow range of lattice constants of these phases which vary by only 4% (410–427 pm), whereas the diameters of the constituent metal atoms vary by 25% (355–445 pm). Bonding theory for isolated groups such as  $B_6H_6^{2-}$  (p. 160) requires the transfer of 2 electrons to the borane cluster to fill all the bonding MOs; however, complete

transfer of 2e per  $B_6$  unit is not required in a three-dimensional crystal lattice and calculations for  $MB_6$  (Ca, Sr, Ba) indicate the transfer of only 0.9–1.0e.<sup>(8)</sup> This also explains why metal-deficit phases  $M_{1-x}B_6$  remain stable and why the alkali metals (Na, K) can form hexaborides. The  $M^{II}B_6$  hexaborides (Ca, Sr, Ba, Eu, Yb) are semiconductors but  $M^{III}B_6$  and  $M^{IV}B_6$  ( $M^{III} = Y, La, \text{lanthanides}$ ;  $M^{IV} = Th$ ) have a high metallic conductivity at room temperature ( $10^4 - 10^5 \text{ ohm}^{-1} \text{ cm}^{-1}$ ).

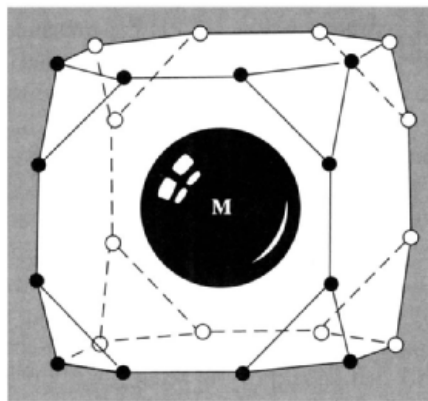
The “radius” of the 24-coordinate metal site in  $MB_6$  is too large (215–225 pm) to be comfortably occupied by the later (smaller) lanthanide elements Ho, Er, Tm and Lu, and these form  $MB_4$  instead, where the metal site has a radius of 185–200 pm. The structure of  $MB_4$  (also formed by Ca, Y, Mo and W) consists of a tetragonal lattice formed by chains of  $B_6$  octahedra linked along the  $c$ -axis and joined laterally by pairs of  $B_2$  atoms in the  $xy$  plane so as to form a 3D skeleton with tunnels along the  $c$ -axis that are filled by metal atoms (Fig. 6.11). The pairs of boron atoms are thus surrounded by trigonal prisms of

<sup>8</sup> P. G. PERKINS, pp. 31–51 in ref. 2.



○ Metal  
● Boron

(a)



● Boron  
○

(b)

**Figure 6.10** Cubic  $MB_6$  showing (a) boron octahedra (B–B in range 170–174 pm), and (b) 24-atom coordination polyhedron around each metal atom.

metal atoms and the structure represents a transition between the puckered layer structures of  $MB_2$  and the cubic  $MB_6$ .

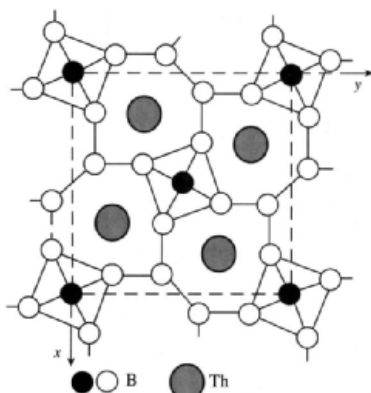


Figure 6.11 Structure of  $ThB_4$ .

The structure and properties of many borides emphasize again the inadequacy of describing bonding in inorganic compounds as either ionic, covalent or metallic. For example, in conventional terminology  $LaB_6$  would be described as a rigid, covalently bonded network of  $B_6$  clusters having multicentred bonding within each cluster and 2-centre covalent B–B bonds between the clusters; this requires the transfer of up to 2 electrons from the metal to the boron sublattice and so could be said also to involve ionic bonding ( $La^{2+}B_6^{2-}$ ) in addition to the covalent inter-boron bonding. Finally, the third valency electron on La is delocalized in a conduction band of the crystal (mainly metal based) and the electrical conductivity of the boride is actually greater than that of La metal itself so that this aspect of the bonding could be called metallic. The resulting description of the bonding is an *ad hoc* mixture of four oversimplified limiting models and should more logically be replaced by a generalized MO approach.<sup>(8)</sup> It will also be clear from the preceding paragraphs that a classification of borides according to the periodic table does not result in the usual change in stoichiometry from one group to the next; instead, a classification

in terms of the type of boron network and the size and electropositivity of the other atoms is frequently more helpful and revealing of periodic trends.

## 6.4 Boranes (Boron Hydrides)<sup>(1,9)</sup>

### 6.4.1 Introduction

Borane chemistry began in 1912 with A. Stock's classic investigations,<sup>(10)</sup> and the numerous compounds prepared by his group during the following 20 y proved to be the forerunners of an amazingly diverse and complex new area of chemistry. During the past few decades the chemistry of boranes and the related carboranes (p. 181) has been one of the major growth areas in inorganic chemistry, and interest continues unabated. The importance of boranes stems from three factors: first, the completely unsuspected structural principles involved; secondly, the growing need to extend covalent MO bond theory considerably to cope with the unusual stoichiometries; and finally, the emergence of a versatile and extremely extensive reaction chemistry which parallels but is quite distinct from that of organic and organometallic chemistry. This efflorescence of activity culminated (in the centenary year of Stock's birth) in the award of the 1976 Nobel Prize for Chemistry to W. N. Lipscomb (Harvard) "for his studies of boranes which have illuminated problems of chemical bonding".

Over 50 neutral boranes,  $B_nH_m$ , and an even larger number of borane anions  $B_nH_m^{x-}$  have been characterized;<sup>(11)</sup> these can be classified

<sup>9</sup> E. L. MUETTERTIES (ed.), *Boron Hydride Chemistry*, Academic Press, New York, 1975, 532 pp.

<sup>10</sup> A. STOCK, *Hydrides of Boron and Silicon*, Cornell University Press, Ithaca, New York, 1933, 250 pp.

<sup>11</sup> N. N. GREENWOOD, Boron Hydride Clusters, in H. W. ROESKY (ed.) *Rings, Clusters and Polymers of Main Group and Transition Elements*, Elsevier, Amsterdam, 1989, pp. 49–105.

according to structure and stoichiometry into 5 series though examples of neutral or unsubstituted boranes themselves are not known for all 5 classes:

*closo*-boranes (from Greek κλωβός, *clovos*, a cage) have complete, closed polyhedral clusters of  $n$  boron atoms;

*nido*-boranes (from Latin *nidus*, a nest) have non-closed structures in which the  $B_n$  cluster occupies  $n$  corners of an  $(n + 1)$ -cornered polyhedron;

*arachno*-boranes (from Greek ἀράχνη, *arachne*, a spider's web) have even more open clusters in which the B atoms occupy  $n$  contiguous corners of an  $(n + 2)$ -cornered polyhedron;

*hypho*-boranes (from Greek ὑφή, *hyphe*, a net) have the most open clusters in which the B atoms occupy  $n$  corners of an  $(n + 3)$ -cornered polyhedron;

*conjuncto*-boranes (from Latin *conjuncto*, I join together) have structures formed by linking two (or more) of the preceding types of cluster together.

Examples of these various series are listed below and illustrated in the accompanying structural diagrams. Their interrelations are further discussed in connection with carborane structures 51–81.

*Closo*-boranes:

$B_nH_n^{2-}$  ( $n = 6-12$ ) see structures 1–7. The neutral boranes  $B_nH_{n+2}$  are not known.

*Nido*-boranes:

$B_nH_{n+4}$ , e.g.  $B_2H_6$  (8),  $B_5H_9$  (9),  $B_6H_{10}$  (10),  $B_{10}H_{14}$  (11);  $B_8H_{12}$  also has this formula but has a rather more open structure (12) which can be visualized as being formed from  $B_{10}H_{14}$  by removal of B(9) and B(10).

$B_nH_{n+3}^-$  formed by removal of 1 bridge proton from  $B_nH_{n+4}$ , e.g.  $B_5H_8^-$ ,  $B_{10}H_{13}^-$ ; other anions in this series such as  $B_4H_7^-$  and  $B_9H_{12}^-$  are known though the parent boranes have proved too

fugitive to isolate;  $BH_4^-$  can be thought of as formed by addition of  $H^-$  to  $BH_3$ .

$B_nH_{n+2}^{2-}$ , e.g.  $B_{10}H_{12}^{2-}$ ,  $B_{11}H_{13}^{2-}$ .

*Arachno*-boranes:

$B_nH_{n+6}$ , e.g.  $B_4H_{10}$  (13),  $B_5H_{11}$  (14),  $B_6H_{12}$  (15),  $B_8H_{14}$  (16), *n*- $B_9H_{15}$  (17), *i*- $B_9H_{15}$ .

$B_nH_{n+5}^-$ , e.g.  $B_2H_7^-$  (18),  $B_3H_8^-$  (19),  $B_5H_{10}^-$ ,  $B_9H_{14}^-$  (20),  $B_{10}H_{15}^-$ .

$B_nH_{n+4}^{2-}$ , e.g.  $B_{10}H_{14}^{2-}$  (21).

*Hypho*-boranes:

$B_nH_{n+8}$ . No neutral borane has yet been definitely established in this series but the known compounds  $B_8H_{16}$  and  $B_{10}H_{18}$  may prove to be *hypho*-boranes and several adducts are known to have *hypho*-structures (pp. 171–2).

*Conjuncto*-boranes:

$B_nH_m$ . At least five different structure types of interconnected borane clusters have been identified; they have the following features:

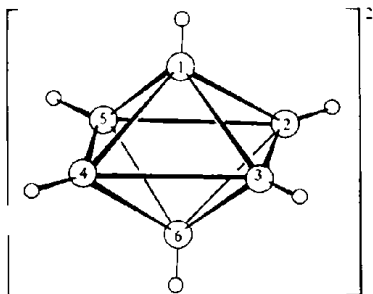
(a) fusion by sharing a single common B atom, e.g.  $B_{15}H_{23}$  (22);

(b) formation of a direct 2-centre B–B  $\sigma$  bond between 2 clusters, e.g.  $B_8H_{18}$ , i.e.  $(B_4H_9)_2$  (23),  $B_{10}H_{16}$ , i.e.  $(B_5H_8)_2$  (3 isomers) (24),  $B_{20}H_{26}$ , i.e.  $(B_{10}H_{13})_2$  (11 possible isomers of which most have been prepared and separated), (e.g. 25a, b, c); anions in this subgroup are represented by the 3 isomers of  $B_{20}H_{18}^{4-}$ , i.e.  $(B_{10}H_9^{2-})_2$  (26);

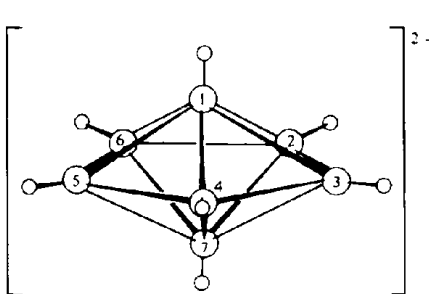
(c) fusion of 2 clusters via 2 B atoms at a common edge, e.g.  $B_{13}H_{19}$  (27),  $B_{14}H_{18}$  (28),  $B_{14}H_{20}$  (29),  $B_{16}H_{20}$  (30), *n*- $B_{18}H_{22}$  (31), *i*- $B_{18}H_{22}$  (32);

(d) fusion of two clusters via 3 B atoms at a common face: no neutral borane or borane anion is yet known with this conformation but the solvated complex  $(MeCN)_2B_{20}H_{16}$ .MeCN has this structure (33);

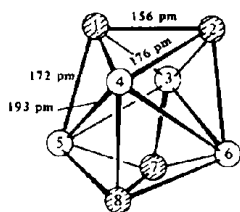
(e) more extensive fusion involving 4 B atoms in various configurations, e.g.  $B_{20}H_{16}$  (34),  $B_{20}H_{18}^{2-}$  (35).



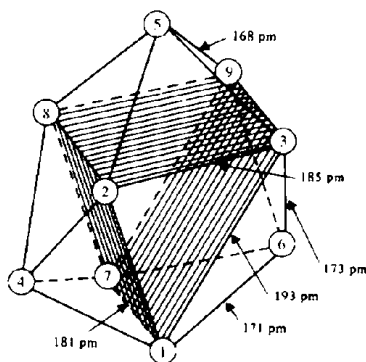
(1) The  $B_4H_6^{2-}$  anion. The relationship to the structure of the  $B_4$  network in  $CaB_4$  and the boron cluster in  $B_4H_4$  should be noted.



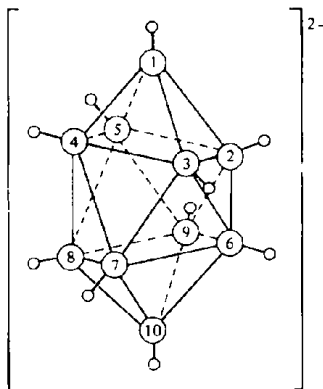
(2) Probable  $D_{3h}$  pentagonal bipyramidal structure of the anion  $B_5H_5^{2-}$  in solution.



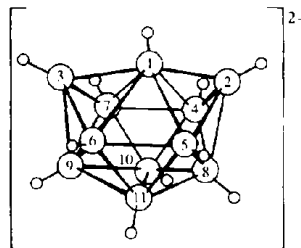
(3) The  $D_{2d}$  configuration of the boron atoms in  $B_5H_5^{2-}$  showing the two structurally non-equivalent sets of 4 boron atoms.



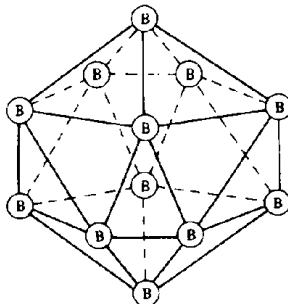
(4) Structure of the boron cluster in  $B_6H_6^{2-}$  (interatomic distances  $\pm 1.5$  pm). The four unique B-H distances are 107, 110, 127 and 144  $\pm 15$  pm.



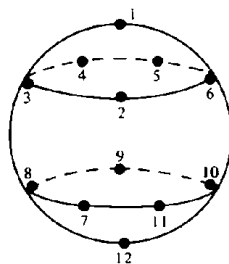
(5)  $B_{10}H_{10}^{2-}$ : decahydro-closo-decaborate (2-)

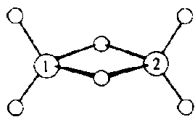
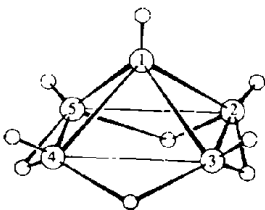
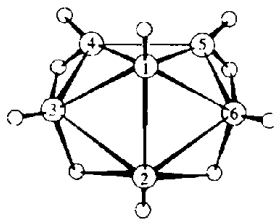
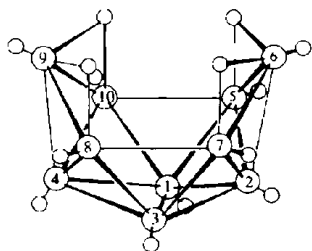
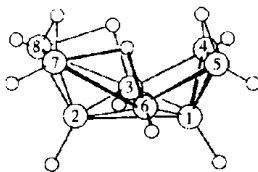
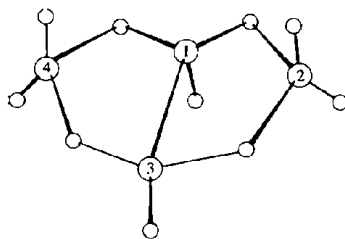
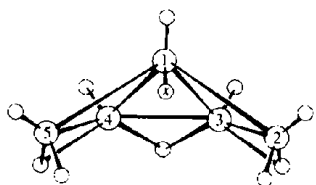
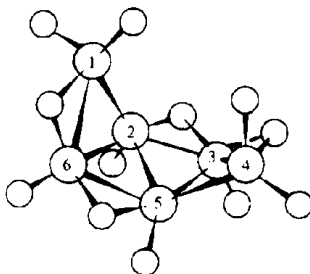
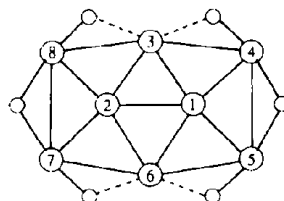
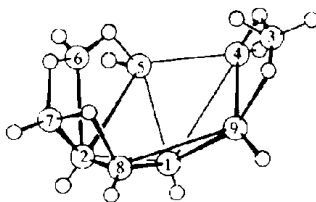
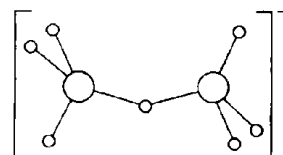
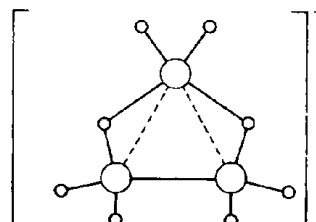
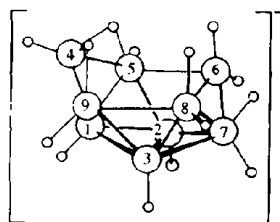
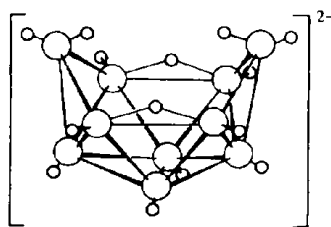


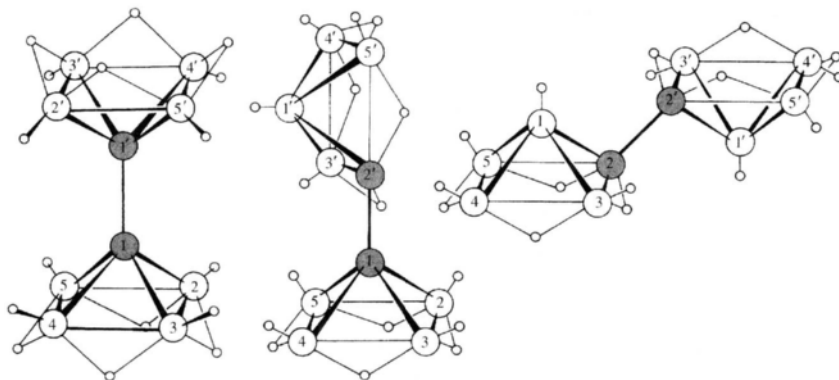
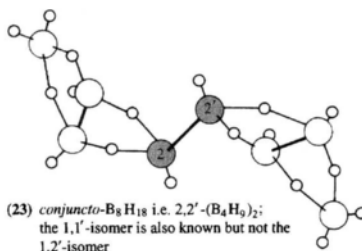
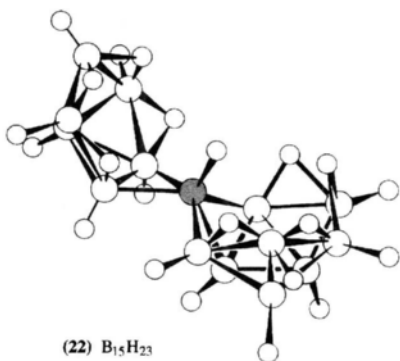
(6)  $B_{11}H_{11}^{2-}$



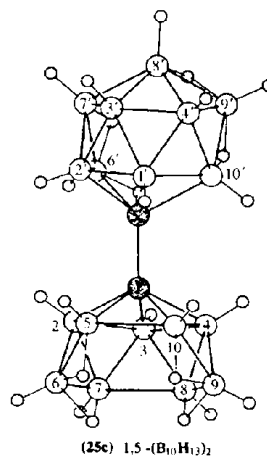
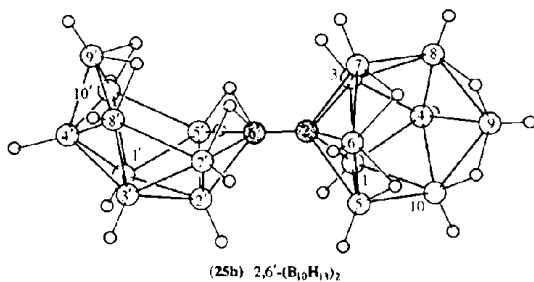
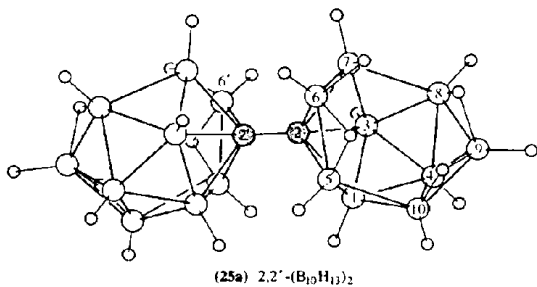
(7) Position of boron atoms and numbering system in the icosahedral borane anion  $B_{12}H_{12}^{2-}$ . The hydrogen atoms, which are attached radially to each boron atom, are omitted for clarity. There are six B-B distances of 175.5 pm and 24 of 178 pm.

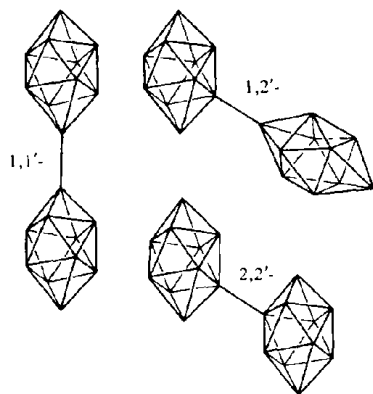


(8)  $B_2H_6$ (9)  $B_5H_9$ (10)  $B_6H_{10}$ (11)  $B_7H_{14}$ (12)  $B_8H_{12}$ (13)  $B_4H_{10}$ (14)  $B_5H_{11}$ (15)  $B_6H_{12}$ (16) Proposed structure for  $B_8H_{14}$   
(terminal H atoms omitted)(17)  $n$ - $B_5H_{15}$ (18)  $B_2H_7^-$ (19)  $B_3H_8^-$ (20)  $B_7H_{14}$ (21)  $B_{10}H_{14}^{2-}$

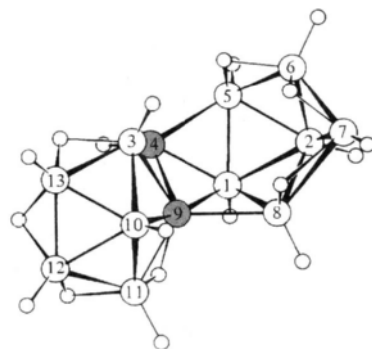


(24) Structures of the three isomers of  $B_{10}H_{16}$ . The  $1,1'$  isomer comprises two pentaborane(9) groups linked in eclipsed configuration via the apex boron atoms to give overall  $D_{2h}$  symmetry, the B-B bond distances are 174 pm for the linking bond, 176 pm for the slant edge of the pyramids, and 171 pm for the basal boron atoms

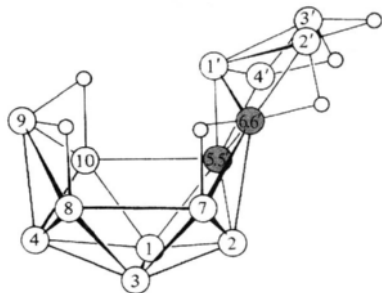




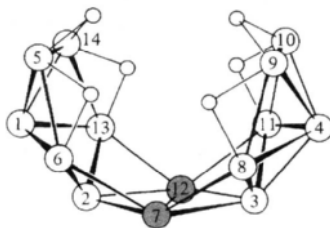
(26) Proposed structures for the three isomers of  $[B_{10}H_{10}]^{4-}$ ; terminal hydrogen atoms omitted for clarity. (See also p. 180)



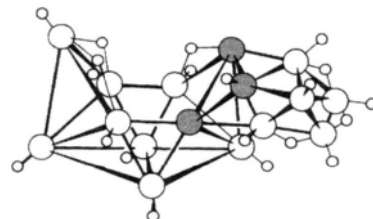
(27)  $B_{13}H_{19}$



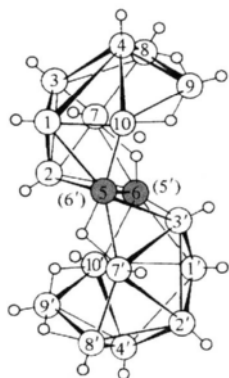
(28) Proposed structure of  $B_{14}H_{18}$ , omitting terminal hydrogen atoms for clarity



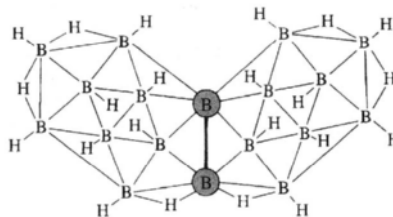
(29)  $B_{14}H_{20}$   
Terminal hydrogen atoms have been omitted for clarity



(30)  $B_{16}H_{20}$

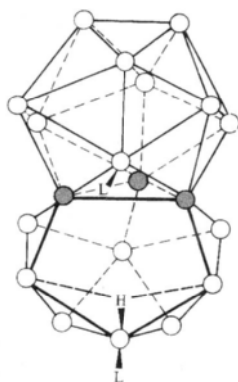


(31)  $n-B_{18}H_{22}$  (centrosymmetric)

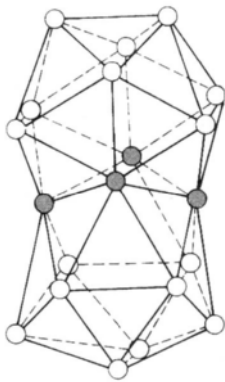


(32) Plane projection of the structure of  $i-B_{18}H_{22}$ .  
The two decaborane units are fused at the 5(7') and 6(6') positions to give a non-centrosymmetric structure with  $C_2$  symmetry

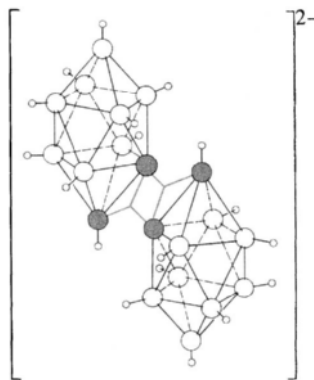




(33) Molecular structure of  $(\text{MeCN})_2\text{B}_{20}\text{H}_{16}$  as found in crystals of the solvate  $(\text{MeCN})_2\text{B}_{20}\text{H}_{16}\cdot\text{MeCN}$  (see text)



(34) The boron atom arrangement in *closo*- $\text{B}_{20}\text{H}_{16}$ . Each boron atom except the 4 "fusion borons" carries an external hydrogen atom and there are no BHB bridges



(35) Structure of the  $\text{B}_{20}\text{H}_{18}^{2-}$  ion. The two 3-centre BBB bonds joining the  $2\text{B}_{10}\text{H}_9^-$  units are shown by broad shaded lines

Boranes are usually named<sup>(12)</sup> by indicating the number of B atoms with a latin prefix and the number of H atoms by an arabic number in parentheses, e.g.  $\text{B}_5\text{H}_9$ , pentaborane(9);  $\text{B}_5\text{H}_{11}$ , pentaborane(11). Names for anions end in "ate" rather than "ane" and specify both the number of H and B atoms and the charge, e.g.  $\text{B}_5\text{H}_8^-$  octahydropentaborate(1-). Further information can be provided by the optional inclusion of the italicized descriptors *closo*-, *nido*-, *arachno*-, *hypho*- and *conjuncto*-, e.g.:

$\text{B}_{10}\text{H}_{10}^{2-}$  : decahydro-*closo*-decaborate(2-) [structure (5)]

$\text{B}_{10}\text{H}_{14}$  : *nido*-decaborane(14) [structure (11)]

$\text{B}_{10}\text{H}_{14}^{2-}$  : tetradecahydro-*arachno*-decaborate(2-) [structure (21)]

$\text{B}_{10}\text{H}_{16}$  : 1,1'-*conjuncto*-decaborane(16) [structure (24a)]  
[i.e. 1,1'-bi(*nido*-pentaboranyl)]

The detailed numbering schemes are necessarily somewhat complicated but, in all other respects, standard nomenclature practices are followed.<sup>(12)</sup>

Derivatives of the boranes include not only simple substituted compounds in which H has been replaced by halogen, OH, alkyl or aryl groups, etc., but also the much more diverse and numerous class of compounds in which one or more B atom in the cluster is replaced by another main-group element such as C, P or S, or by a wide range of metal atoms or coordinated metal groups. These will be considered in later sections.

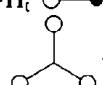
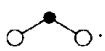
## 6.4.2 Bonding and topology

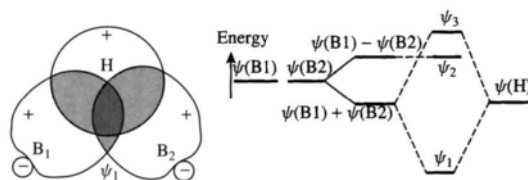
The definitive structural chemistry of the boranes began in 1948 with the X-ray crystallographic determination of the structure of decaborane(14); this showed the presence of 4 bridging H atoms and an icosahedral fragment of 10 B atoms. This was rapidly followed in 1951 by the unequivocal demonstration of the H-bridged structure of diborane(6) and by the determination of the structure of pentaborane(9). Satisfactory theories of bonding in boranes date from the introduction of the concept of the 3-centre 2-electron B-H-B bond by H. C. Longuet-Higgins in 1949; he also extended the principle of 3-centre bonding and multicentre bonding to the higher boranes. These ideas have been extensively developed and

<sup>12</sup> G. J. LEIGH (ed.), *Nomenclature of Inorganic Chemistry: Recommendations 1990* (The IUPAC "Red Book"), Blackwell, Oxford, 1990, Chap. 11, pp. 207-37.

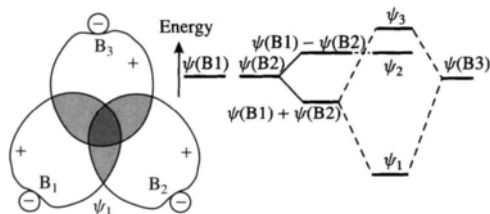
refined by W. N. Lipscomb and his group during the past four decades.<sup>(13)</sup>

In simple covalent bonding theory molecular orbitals (MOs) are formed by the linear combination of atomic orbitals (LCAO); for example, 2 AOs can combine to give 1 bonding and 1 antibonding MO and the orbital of lower energy will be occupied by a pair of electrons. This is a special case of a more general situation in which a number of AOs are combined together by the LCAO method to construct an equal number of MOs of differing energies, some of which will be bonding, some possibly nonbonding and some antibonding. In this way 2-centre, 3-centre, and multicentre orbitals can be envisaged. The three criteria that determine whether particular AOs can combine to form MOs are that the AOs must (a) be similar in energy, (b) have appreciable spatial overlap, and (c) have appropriate symmetry. In borane chemistry two types of 3-centre bond find considerable application: B–H–B bridge bonds (Fig. 6.12) and central 3-centre BBB bonds (Fig. 6.13). Open 3-centre B–B–B bonds are not now thought to occur in boranes and their anions though they are still useful in describing the bonding in carbaboranes and other heteroatom clusters (p. 194). The relation between the 3-centre bond formation for B–H–B, where the bond angle at H is  $\sim 90^\circ$  and the 3-centre bond formation for approximately linear H bonds A–H $\cdots$ B is given on pp. 63–4.

Localized 3-centre bond formalism can readily be used to rationalize the structure and bonding in most of the non-*closo*-boranes. This is illustrated for some typical *nido*- and *arachno*-boranes in the following plane-projection diagrams which use an obvious symbolism for normal 2-centre bonds: B–B  $\bigcirc$ — $\bigcirc$ , B–H<sub>t</sub>  $\bigcirc$ — $\bullet$ , (t = terminal), central 3-centre bonds , and B–H<sub>μ</sub>–B bridge bonds . It is particularly important



**Figure 6.12** Formation of a bonding 3-centre B–H–B orbital  $\psi_1$  from an  $sp^x$  hybrid orbital on each of B(1), B(2) and the H 1s orbital,  $\psi(H)$ . The 3 AOs have similar energy and appreciable spatial overlap, but only the combination  $\psi(B1) + \psi(B2)$  has the correct symmetry to combine linearly with  $\psi(H)$ .

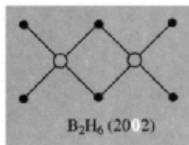


**Figure 6.13** Formation of a bonding, central 3-centre bond  $\psi_1$  and schematic representation of the relative energies of the 3 molecular orbitals  $\psi_1$ ,  $\psi_2$  and  $\psi_3$ .

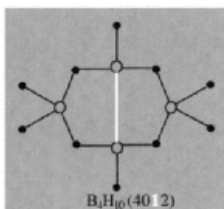
to realize that the latter two symbols each represent a single (3-centre) bond involving one pair of electrons. As each B atom has 3 valence electrons, and each B–H<sub>t</sub> bond requires 1 electron from B and one from H, it follows that each B–H<sub>t</sub> group can contribute the remaining 2 electrons on B towards the bonding of the cluster (including B–H–B bonds), and likewise each BH<sub>2</sub> group can contribute 1 electron for cluster bonding. The overall bonding is sometimes codified in a 4-digit number, the so-called *styx* number, where *s* is the number of B–H–B bonds, *t* is the number of 3-centre BBB bonds, *y* the number of 2-centre BB bonds, and *x* the number of BH<sub>2</sub> groups.<sup>(13)</sup> Examples are on p. 159.

Electron counting and orbital bookkeeping can easily be checked in these diagrams: as each B has 4 valency orbitals (*s* + 3*p*) there should be 4 lines emanating from each open circle; likewise, as each B atom contributes 3 electrons in all and each H atom contributes 1 electron, the total

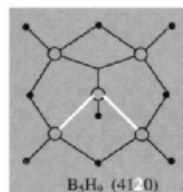
<sup>13</sup> W. N. LIPSCOMB, Chap. 2 in ref. 9, pp. 30–78. W. N. LIPSCOMB, *Boron Hydrides*, Benjamin, New York, 1963, 275 pp. W. N. LIPSCOMB, Nobel Prize Lecture, *Science* **196**, 1047–55 (1977).



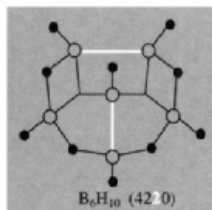
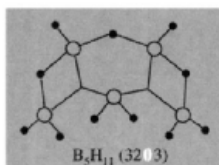
Each terminal  $BH_2$  group and each (bridging)  $H_u$  contributes 1 electron to the bridging; these 4 electrons just fill the two B-H-B bonds.



Each of the 4 B and 4  $H_u$  contribute 1 electron to the B-H-B bonds, i.e. 4 pairs of electrons for the 4 (3-centre) bonds. The 2 "hinge"  $BH_2$  groups each have 1 remaining electron and 1 orbital which interact to give the 2-centre B-B bond.



In  $B_5H_9$  the bonding can be thought of as involving the structure shown and 3 other equivalent structures in which successive pairs of adjacent basal B atoms are combined with the apex B in a 3-centre bond.

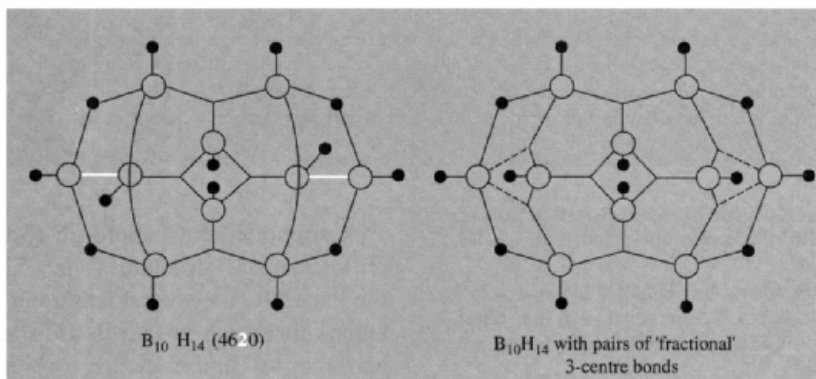


number of valence electrons for a borane of formula  $B_nH_m$  is  $(3n + m)$  and the number of bonds shown in the structure should be just half this. It follows, too, that the number of electron-pair bonds in the molecule is  $n$  plus the sum of the individual *styx* numbers (e.g. 13 for  $B_5H_{11}$ , 14 for  $B_6H_{10}$ ) and this constitutes a further check.<sup>†</sup> An appropriate number of additional electrons should be added for anionic species.

For *closo*-boranes and for the larger open-cluster boranes it becomes increasingly difficult to write a simple satisfactory localized orbital structure, and a full MO treatment is required. Intermediate cases, such as  $B_5H_9$ , require several "resonance hybrids" in the localized orbital

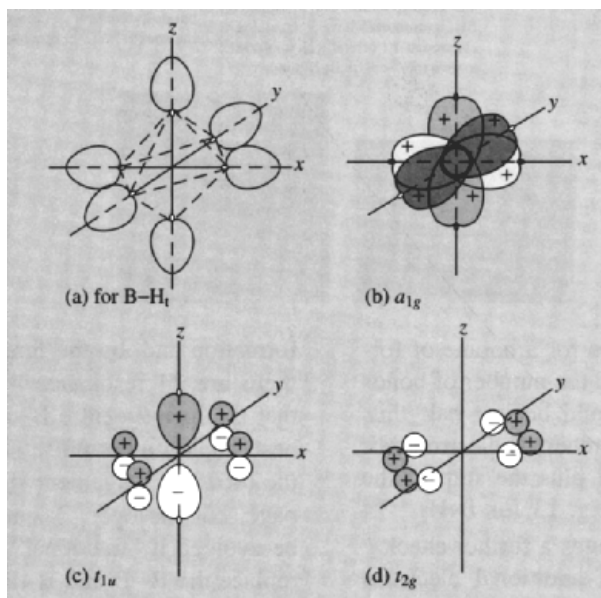
formation and, by the time  $B_{10}H_{14}$  is considered there are 24 resonance hybrids, even assuming that no open 3-centre B-B-B bonds occur. The best single compromise structure in this case is the (4620) arrangement shown at the foot of the page, but the open 3-centre B-B-B bonds can be avoided if "fractional" central 3-centre bonds replace the B-B and B-B-B bonds in pairs:

<sup>†</sup> Further checks, which can readily be verified from the equations of balance, are (a) the number of atoms in a neutral borane molecule =  $2(s + t + y + x)$ , and (b) there are as many framework electrons as there are atoms in a neutral borane  $B_nH_m$  since each BH group supplies 2 electrons and each of the  $(m - n)$  "extra" H atoms supplies 1 electron, making  $n + m$  in all.



### MO Description of Bonding in *closo*-B<sub>6</sub>H<sub>6</sub><sup>2-</sup>

*Closo* B<sub>6</sub>H<sub>6</sub><sup>2-</sup> (structure 1) has a regular octahedral cluster of 6 B atoms surrounded by a larger octahedron of 6 radially disposed H atoms. Framework MOs for the B<sub>6</sub> cluster are constructed (LCAO) using the 2s, 2p<sub>x</sub>, 2p<sub>y</sub>, and 2p<sub>z</sub> boron AOs. The symmetry of the octahedron suggests the use of sp hybrids directed radially outwards and inwards from each B along the cartesian axes (see figure) and 2 pure p orbitals at right angles to these (i.e. oriented tangentially to the B<sub>6</sub> octahedron). These sets of AOs are combined, with due regard to symmetry, to give 24 MOs as follows: the 24 AOs on the 6 B combine to give 24 MOs of which 7 (i.e. *n* + 1) are bonding framework MOs, 6 are used to form B-H<sub>i</sub> bonds, and the remaining 11 are antibonding.



Symmetry of orbitals on the B<sub>6</sub> octahedron. (a) Six outward-pointing (sp) orbitals used for  $\sigma$  bonding to 6 H<sub>i</sub>. (b) Six inward-pointing (sp) orbitals used to form the  $a_{1g}$  framework bonding molecular orbital. (c) Components for one of the  $t_{1u}$  framework bonding molecular orbitals — the other two molecular orbitals are in the *yz* and *zx* planes. (d) Components for one of the  $t_{2g}$  framework bonding molecular orbitals — the other two molecular orbitals are in the *yz* and *zx* planes.

The diagrams also indicate why neutral *closo*-boranes B<sub>*n*</sub>H<sub>*n*+2</sub> are unknown since the 2 anionic charges are effectively located in the low-lying inwardly directed  $a_{1g}$  orbital which has no overlap with protons outside the cluster (e.g. above the edges or faces of the B<sub>6</sub> octahedron). Replacement of the 6 H<sub>i</sub> by 6 further B<sub>6</sub> builds up the basic three-dimensional network of hexaborides MB<sub>6</sub> (p. 150) just as replacement of the 4 H<sub>i</sub> in CH<sub>4</sub> begins to build up the diamond lattice.

The diagrams, with minor modification, also describe the bonding in isoelectronic species such as *closo*-CB<sub>5</sub>H<sub>6</sub><sup>-</sup>, 1,2-*closo*-C<sub>2</sub>B<sub>4</sub>H<sub>6</sub>, 1,6-*closo*-C<sub>2</sub>B<sub>4</sub>H<sub>6</sub>, etc. (pp. 181–2). Similar though more complex, diagrams can be derived for all *closo*-B<sub>*n*</sub>H<sub>*n*+2</sub><sup>-</sup> (*n* = 6–12); these have the common feature of a low lying  $a_{1g}$  orbital and *n* other framework bonding MOs; in each case, therefore (*n* + 1) pairs of electrons are required to fill these orbitals as indicated in Wade's rules (p. 161). It is a triumph for MO theory that the existence of B<sub>6</sub>H<sub>6</sub><sup>2-</sup> and B<sub>12</sub>H<sub>12</sub><sup>2-</sup> were predicted by H. C. Longuet-Higgins in 1954–5,<sup>(14)</sup> a decade before B<sub>6</sub>H<sub>6</sub><sup>2-</sup> was first synthesized and some 5 y before the (accidental) preparation of B<sub>10</sub>H<sub>10</sub><sup>2-</sup> and B<sub>12</sub>H<sub>12</sub><sup>2-</sup> were reported.<sup>(15,16)</sup>

<sup>14</sup> H. C. LONGUET-HIGGINS and M. DE V. ROBERTS, *Proc. R. Soc. A*, **230**, 110–19 (1955); see also *idem ibid.* A, **224**, 336–47 (1954).

<sup>15</sup> J. L. BOONE, *J. Am. Chem. Soc.* **86**, 5036 (1964).

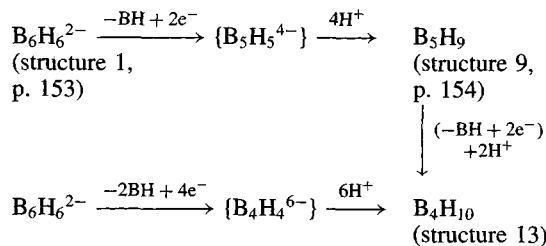
<sup>16</sup> M. F. HAWTHORNE and A. R. PITTOCHELLI, *J. Am. Chem. Soc.* **81**, 5519 (and also 5833–4) (1959); *J. Am. Chem. Soc.* **82**, 3228–9 (1960).

A simplified MO approach to the bonding in *closo*-B<sub>6</sub>H<sub>6</sub><sup>2-</sup> (structure 1, p. 153) is shown in the Panel. It is a general feature of *closo*-B<sub>*n*</sub>H<sub>*n*+2</sub><sup>-</sup> anions that there are no B-H-B or BH<sub>2</sub> groups and the 4*n* boron atomic orbitals are always

distributed as follows:

- $n$  in the  $n(\text{B}-\text{H}_t)$  bonding orbitals
- $(n + 1)$  in framework bonding MOs
- $(2n - 1)$  in nonbonding and antibonding framework MOs

As each B atom contributes 1 electron to its B-H<sub>t</sub> bond and 2 electrons to the framework MOs, the  $(n + 1)$  framework bonding MOs are just filled by the  $2n$  electrons from  $n$ B atoms and the 2 electrons from the anionic charge. Further, it is possible (conceptually) to remove a BH<sub>t</sub> group and replace it by 2 electrons to compensate for the 2 electrons contributed by the BH<sub>t</sub> group to the MOs. Electroneutrality can then be achieved by adding the appropriate number of protons; this does not alter the number of electrons in the system and hence all bonding MOs remain just filled.



The structural interrelationship of all the various *closo*-, *nido*- and *arachno*-boranes thus becomes evident; a further example is shown at the foot of the page.

These relationships were codified in 1971 by K. Wade in a set of rules which have been

extremely helpful not only in rationalizing known structures, but also in suggesting the probable structures of new species.<sup>(17)</sup> Wade's rules can be stated in extended form as follows:

*closo*-borane anions have the formula B<sub>n</sub>H<sub>n</sub><sup>2-</sup>; the B atoms occupy all  $n$  corners of an  $n$ -cornered triangulated polyhedron, and the structures require  $(n + 1)$  pairs of framework bonding electrons;

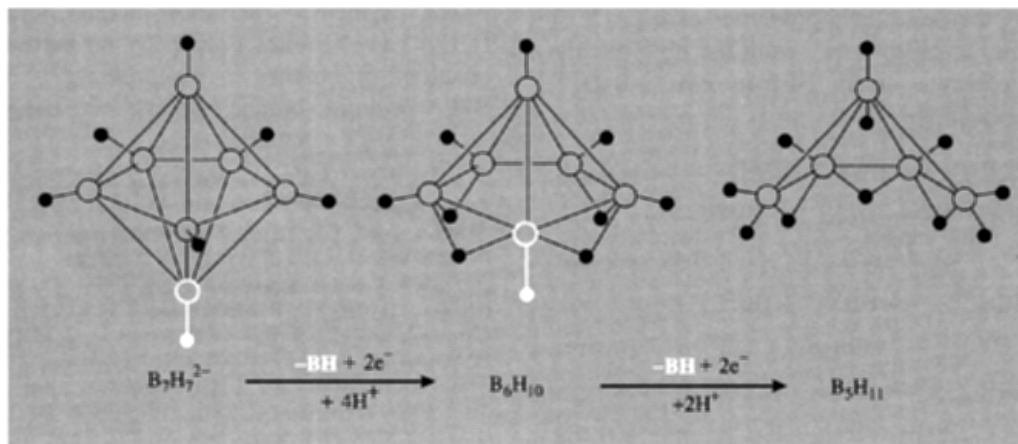
*nido*-boranes have the formula B<sub>n</sub>H<sub>n+4</sub> with B atoms at  $n$  corners of an  $(n + 1)$  cornered polyhedron; they require  $(n + 2)$  pairs of framework-bonding electrons;

*arachno*-boranes: B<sub>n</sub>H<sub>n+6</sub>,  $n$  corners of an  $(n + 2)$  cornered polyhedron, requiring  $(n + 3)$  pairs of framework-bonding electrons;

*hypho*-boranes: B<sub>n</sub>H<sub>n+8</sub>;  $n$  corners of an  $(n + 3)$  cornered polyhedron, requiring  $(n + 4)$  pairs of framework-bonding electrons.

The rules can readily be extended to isoelectronic anions and carbaboranes (BH≡B<sup>-</sup>≡C) and also to metalloboranes (p. 174), metallocarbaboranes (p. 194) and even to metal clusters themselves, though they become less reliable the further one moves away from boron in atomic size, ionization energy, electronegativity, etc.

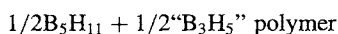
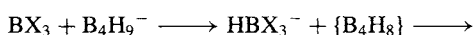
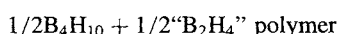
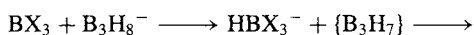
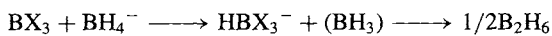
<sup>17</sup> K. WADE, *Adv. Inorg. Chem. Radiochem.* **18**, 1-66 (1976).



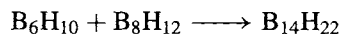
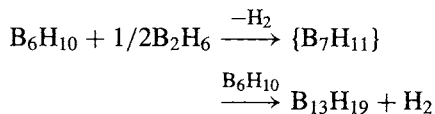
More sophisticated and refined calculations lead to orbital populations and electron charge distributions within the borane molecules and to predictions concerning the sites of electrophilic and nucleophilic attack. In general, the highest electron charge density (and the preferred site of electrophilic attack) occurs at apical B atoms which are furthest removed from open faces; conversely the lowest electron charge density (and the preferred site of nucleophilic attack) occurs on B atoms involved in B-H-B bonding. The consistency of this correlation implies that the electron distribution in the activated complex formed during reaction must follow a similar sequence to that in the ground state. Bridge H atoms tend to be more acidic than terminal H atoms and are the ones first lost during the formation of anions in acid-base reactions.

### 6.4.3 Preparation and properties of boranes

Earlier methods for preparing the boron hydrides were tedious and inefficient<sup>(10)</sup> but have now been superseded by modern high-yield routes.<sup>(11,18)</sup> The first great advance was to replace the reaction between protonic hydrogen and negative boride clusters by the reaction of hydridic species such as LiH or LiAlH<sub>4</sub> with boron halides or alkoxides which contain more positive boron centres. Subsequently, S. G. Shore and his group developed a systematic synthesis by using the Lewis acid properties of BX<sub>3</sub> (X = F, Cl, Br) to abstract H<sup>-</sup> from the now readily available borane anions such as BH<sub>4</sub><sup>-</sup>, B<sub>3</sub>H<sub>8</sub><sup>-</sup> etc. For example:<sup>(19)</sup>



The perception by R. Schaeffer that *nido*-B<sub>6</sub>H<sub>10</sub> (structure 10, pp. 154, 159) could act as a Lewis base towards reactive (vacant orbital) borane radicals has led to several new *conjuncto*-boranes, e.g.:<sup>(20)</sup>



A useful route to B-B bonded *conjuncto*-boranes involves the photolysis of parent *nido*-boranes. Thus, ultraviolet irradiation of B<sub>5</sub>H<sub>9</sub> (9) yields the three isomers of *conjuncto*-B<sub>10</sub>H<sub>16</sub> (24) and similar treatment of B<sub>10</sub>H<sub>14</sub> (11) yields a mixture of 1,2'- and 2,2'-(B<sub>10</sub>H<sub>13</sub>)<sub>2</sub> (25a). High-yield catalytic routes to specific B-B coupled *conjuncto*-boranes (using PtBr<sub>2</sub>) have been developed by L. G. Sneddon and his group<sup>(21)</sup>, e.g. B<sub>5</sub>H<sub>9</sub> gave 1,2'-(B<sub>5</sub>H<sub>8</sub>)<sub>2</sub> (24), B<sub>4</sub>H<sub>10</sub> gave 1,1'-(B<sub>4</sub>H<sub>9</sub>)<sub>2</sub> (i.e. *conjuncto*-B<sub>8</sub>H<sub>18</sub>, of which the 2,2'-isomer is shown in 23), and a mixture of B<sub>4</sub>H<sub>10</sub> and B<sub>5</sub>H<sub>9</sub> yielded 1,2'-(B<sub>4</sub>H<sub>9</sub>)(B<sub>5</sub>H<sub>8</sub>), i.e. *conjuncto*-B<sub>9</sub>H<sub>17</sub>. When applied to a mixture of B<sub>2</sub>H<sub>6</sub> and B<sub>5</sub>H<sub>9</sub> in decane at room temperature, the method gave the first authenticated neutral heptaborane, B<sub>7</sub>H<sub>13</sub>, in which one of the bridging H atoms in diborane has been replaced by a basal B atom of the B<sub>5</sub> unit, i.e. 1,2-μ(2-B<sub>5</sub>H<sub>8</sub>)B<sub>2</sub>H<sub>5</sub>.

The synthesis of *closo*-borane dianions B<sub>n</sub>H<sub>n</sub><sup>2-</sup> (1-7) relies principally on thermolysis reactions of boranes in the presence of either BH<sub>4</sub><sup>-</sup> or amino-borane adducts.<sup>(9,11)</sup> The yields

<sup>18</sup> R. W. PARRY and M. K. WALTER, in W. L. JOLLY (ed.), *Preparative Inorganic Reactions* 5, 45-102 (1968).

<sup>19</sup> M. A. TOFT, J. B. LEACH, F. L. HIMPSL and S. G. SHORE *Inorg. Chem.* 21, 1952-7 (1982).

<sup>20</sup> J. RATHKE and R. SCHAEFFER, *Inorg. Chem.* 13, 3008-11 (1974); J. RATHKE, D. C. MOODY and R. SCHAEFFER, *Inorg. Chem.* 13, 3040-2 (1974); J. C. HUFFMAN, D. C. MOODY and R. SCHAEFFER, *Inorg. Chem.* 20, 741-5 (1981).

<sup>21</sup> E. W. CORCORAN and L. G. SNEDDON, *J. Am. Chem. Soc.* 106, 7793-7800 (1984); 107, 7446-50 (1985); L. G. SNEDDON, *Pure Appl. Chem.* 59, 837-46 (1987).

Table 6.2 Properties of some boranes

Nido-boranes				Arachno-boranes			
Compound	mp	bp	$\Delta H_f^\circ/\text{kJ mol}^{-1}$	Compound	mp	bp	$\Delta H_f^\circ/\text{kJ mol}^{-1}$
B <sub>2</sub> H <sub>6</sub>	-164.9°	-92.6°	36	B <sub>4</sub> H <sub>10</sub>	-120°	18°	58
B <sub>5</sub> H <sub>9</sub>	-46.8°	60.0°	54	B <sub>5</sub> H <sub>11</sub>	-122°	65°	67 (or 93)
B <sub>6</sub> H <sub>10</sub>	-62.3°	108°	71	B <sub>6</sub> H <sub>12</sub>	-82.3°	~85° (extrap)	111
B <sub>8</sub> H <sub>12</sub>	Decomp	above -35°	—	B <sub>8</sub> H <sub>14</sub>	Decomp	above -30°	—
B <sub>10</sub> H <sub>14</sub>	99.5°	213°	32	n-B <sub>9</sub> H <sub>15</sub>	2.6°	28°/0.8 mmHg	—

are very sensitive to conditions (solvent, pressure and temperature) and mixtures are often obtained. A more recent variant is the thermolysis of Et<sub>4</sub>NBH<sub>4</sub> at 175–190°C for about 12 hours, which yields a mixture of *closo*-B<sub>9</sub>H<sub>9</sub><sup>2-</sup>, B<sub>10</sub>H<sub>10</sub><sup>2-</sup>, B<sub>12</sub>H<sub>12</sub><sup>2-</sup> and *nido*-B<sub>11</sub>H<sub>14</sub><sup>-</sup>. The smaller *closo*-dianions ( $n = 6, 7, 8$ ) can then be obtained (in smaller yield) by the oxidative (air) degradation of B<sub>9</sub>H<sub>9</sub><sup>2-</sup> salts in the presence of EtOH, thf or 1,2-dimethoxyethane.

Boranes are colourless, diamagnetic, molecular compounds of moderate to low thermal stability. The lower members are gases at room temperature but with increasing molecular weight they become volatile liquids or solids (Table 6.2); bps are approximately the same as those of hydrocarbons of similar molecular weight. The boranes are all endothermic and their free energies of formation  $\Delta G_f^\circ$  are also positive; however, their thermodynamic instability results from the exceptionally strong interatomic bonds in both elemental B and H<sub>2</sub> rather than any weakness of the B–H bond. In this the boranes resemble the hydrocarbons. Likewise, the remarkable chemical reactivity of the boranes and their ready thermolytic interconversion (p. 164) should not be taken to imply that the bonds holding the boranes together are inherently weak. Indeed, the opposite is the case; the B–B and B–H bonds are among the strongest 2-electron bonds known, and the great reactivity of the boranes is to be sought rather in the availability of alternative structures and vacant orbitals of similar energies. Some comparative data are in Table 6.3<sup>(22)</sup> which

shows that the bond enthalpies  $E$  for the 2-centre B–B bond in boranes and for the C–C bond in C<sub>2</sub>H<sub>6</sub> are essentially identical and that the value for the 3-centre 2-electron BBB bond in boranes is very similar to that for the B–C bond in BMe<sub>3</sub>.

Table 6.3 Some enthalpies of atomization ( $\Delta H_f^\circ$ , 298 K) and comparative bond-enthalpy contributions,  $E$ 

$\Delta H_f^\circ/\text{kJ mol}^{-1}$	$E/\text{kJ mol}^{-1}$	$E/\text{kJ mol}^{-1}$
H(g) 1/2 × 436	B–B (2c,2e) 332	C–C 331
B(g) 566	BBB(3c,2e) 380	B–C 372
C(g) 356	B–H (2c,2e) 381	C–H 416
	BHB(3c,2e) 441	H–H 436

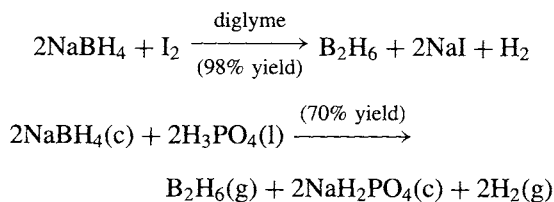
Boranes are extremely reactive compounds and several are spontaneously flammable in air. *Arachno*-boranes tend to be more reactive (and less stable to thermal decomposition) than *nido*-boranes and reactivity also diminishes with increasing mol wt. *Closo*-borane anions are exceptionally stable and their general chemical behaviour has suggested the term “three-dimensional aromaticity”.

Boron hydrides have proved to be extremely versatile chemical reagents but the very diversity of their reactions makes a general classification unduly cumbersome. For this reason, the range of behaviour will be illustrated by typical examples taken from the chemistry of the boranes and their anions, arranged approximately according to the size of the borane cluster being discussed. Nearly all boranes are highly toxic when inhaled or absorbed through the skin though they can be safely and conveniently handled with relatively minor precautions.

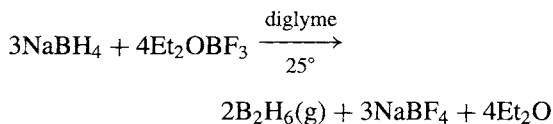
<sup>22</sup>N. N. GREENWOOD and R. GREATREX, *Pure Appl. Chem.* **59**, 857–68 (1987).

### 6.4.4 The chemistry of small boranes and their anions (B<sub>1</sub>–B<sub>4</sub>)

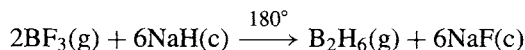
Diborane occupies a special place because all the other boranes can be prepared from it (directly or indirectly); it is also one of the most studied and synthetically useful reagents in the whole of chemistry.<sup>(1,23)</sup> B<sub>2</sub>H<sub>6</sub> gas can most conveniently be prepared in small quantities by the reaction of I<sub>2</sub> on NaBH<sub>4</sub> in diglyme [(MeOCH<sub>2</sub>CH<sub>2</sub>)<sub>2</sub>O], or by the reaction of a solid tetrahydroborate with an anhydrous acid:



When B<sub>2</sub>H<sub>6</sub> is to be used as a reaction intermediate without the need for isolation or purification, the best procedure is to add Et<sub>2</sub>OBF<sub>3</sub> to NaBH<sub>4</sub> in a polyether such as diglyme:



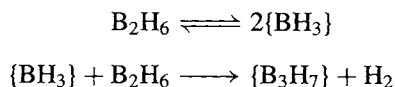
On an industrial scale gaseous BF<sub>3</sub> can be reduced directly with NaH at 180° and the product trapped out as it is formed to prevent subsequent pyrolysis:



Some 200 tonnes per annum of B<sub>2</sub>H<sub>6</sub> is produced commercially, worldwide. Care should be taken in all these reactions because B<sub>2</sub>H<sub>6</sub> is spontaneously flammable; its heat of combustion (–Δ*H*°) is higher per unit weight of fuel than for any other substance except

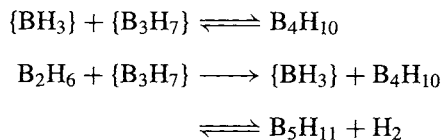
H<sub>2</sub>, BeH<sub>2</sub> and Be(BH<sub>4</sub>)<sub>2</sub>: [–Δ*H*°(B<sub>2</sub>H<sub>6</sub>) = 2165 kJ mol<sup>–1</sup> = 78.2 kJ g<sup>–1</sup>].

The pyrolysis of gaseous B<sub>2</sub>H<sub>6</sub> in sealed vessels at temperatures above 100° is exceedingly complex and has only recently been fully elucidated.<sup>(24–27)</sup> The initiating step is the unimolecular equilibrium dissociation of B<sub>2</sub>H<sub>6</sub> to give 2{BH<sub>3</sub>}, and the {BH<sub>3</sub>} then reacts with further B<sub>2</sub>H<sub>6</sub> to give {B<sub>3</sub>H<sub>7</sub>} plus H<sub>2</sub> in a concerted rate-controlling reaction via a {B<sub>3</sub>H<sub>9</sub>} transition state. This explains the observed 1.5-order of the kinetics and also successfully interprets all other aspects of the initial reaction:



In these and subsequent reactions, unstable intermediates that have but transitory existence are placed in curly brackets, {}.

The first stable intermediate, B<sub>4</sub>H<sub>10</sub>, is then formed followed by B<sub>5</sub>H<sub>11</sub>:



A complex series of further steps gives B<sub>5</sub>H<sub>9</sub>, B<sub>6</sub>H<sub>10</sub>, B<sub>6</sub>H<sub>12</sub>, and higher boranes, culminating in B<sub>10</sub>H<sub>14</sub> as the most stable end product, together with polymeric materials BH<sub>*x*</sub> and a trace of *conjuncto*-icosaboranes B<sub>20</sub>H<sub>26</sub>.

Careful control of temperature, pressure and reaction time enables the yield of the various intermediate boranes to be optimized. For example, B<sub>4</sub>H<sub>10</sub> is best prepared by storing B<sub>2</sub>H<sub>6</sub> under pressure at 25° for 10 days; this gives a 15% yield and quantitative conversion according to the

<sup>24</sup> J. F. STANTON, W. N. LIPSCOMB and R. J. BARTLETT, *J. Am. Chem. Soc.* **111**, 5165–73 (1989).

<sup>25</sup> R. GREATREX, N. N. GREENWOOD and S. M. LUCAS, *J. Am. Chem. Soc.* **111**, 8721–2 (1989).

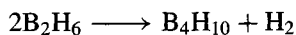
<sup>26</sup> N. N. GREENWOOD and R. GREATREX, *Pure Appl. Chem.* **59**, 857–68 (1987).

<sup>27</sup> N. N. GREENWOOD, *Chem. Soc. Revs.* **21**, 49–57 (1992).

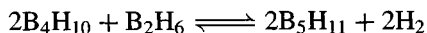
<sup>23</sup> L. H. LONG, Chap. 22 in *Mellor's Comprehensive Treatise on Inorganic and Theoretical Chemistry*, Vol. 5, Supplement 2, Part 2, pp. 52–162, Longmans, London, 1981.



overall reaction:

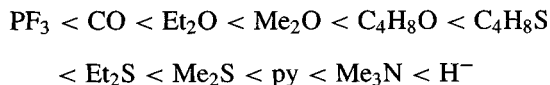


B<sub>5</sub>H<sub>11</sub> can be prepared in 70% yield by the reaction of B<sub>2</sub>H<sub>6</sub> and B<sub>4</sub>H<sub>10</sub> in a carefully dimensioned hot/cold reactor at +120°/-30°:



Alternative high-yield syntheses of these various boranes via hydride-ion abstraction from borane anions by BBr<sub>3</sub> and other Lewis acids have recently been devised<sup>(19)</sup> (see p. 162).

From the foregoing it is clear that {BH<sub>3</sub>} is a fugitive reaction species: it exists only at exceedingly low concentrations but can be isolated and studied using matrix isolation techniques. Thus it can be generated by thermal dissociation of loosely bound 1:1 adducts with Lewis bases, such as PF<sub>3</sub>.BH<sub>3</sub>, and its reactions studied.<sup>(28)</sup> The relative stability of the adducts L.BH<sub>3</sub> has been determined from thermochemical and spectroscopic data and leads to the following unusual sequence:



Note that both PF<sub>3</sub> and CO form isolable although weak adducts, and that organic sulfide

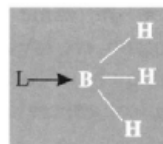
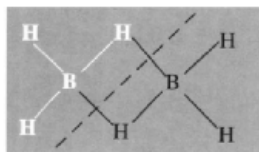
adducts are more stable than those of ethers, thereby showing that BH<sub>3</sub> has some class b acceptor ("soft acid") characteristics despite the absence of low-lying d orbitals on boron (see p. 909). The ligand H<sup>-</sup> is a special case since it gives the symmetrical tetrahedral ion BH<sub>4</sub><sup>-</sup>, isoelectronic with CH<sub>4</sub> and NH<sub>4</sub><sup>+</sup>. Many other complexes of BH<sub>3</sub> with N, P, As, O, S etc. donor atoms are also known and they are readily formed by symmetrical homolytic (cleavage of the bridge bonds in B<sub>2</sub>H<sub>6</sub>. Occasionally, however, unsymmetrical (heterolytic) cleavage products result, perhaps partly as a result of steric effects,<sup>(29)</sup> e.g. NH<sub>3</sub>, MeNH<sub>2</sub> and Me<sub>2</sub>NH give unsymmetrical cleavage products whereas Me<sub>3</sub>N gives the symmetrical cleavage product, Me<sub>3</sub>N.BH<sub>3</sub> (see scheme below).

In addition to pyrolysis and cleavage reactions, B<sub>2</sub>H<sub>6</sub> undergoes a wide variety of substitution, redistribution, and solvolytic reactions of which the following are representative. Gaseous HCl yields B<sub>2</sub>H<sub>5</sub>Cl, whereas Cl<sub>2</sub> (and F<sub>2</sub>) give BX<sub>3</sub> directly even at low temperatures and high dilution. Methylation with PbMe<sub>4</sub> yields B<sub>2</sub>H<sub>5</sub>Me, but comproportionation with BMe<sub>3</sub> affords Me<sub>n</sub>B<sub>2</sub>H<sub>6-n</sub> (n = 1-4), the two BHB bridge bonds remaining intact. Hydrolysis gives the stoichiometric amount of B(OH)<sub>3</sub>. The related alcoholysis reaction was much used in earlier times as a convenient means of total analysis

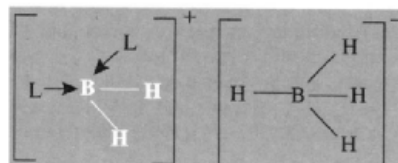
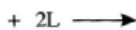
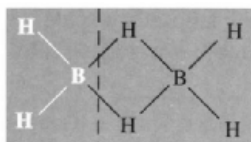
<sup>28</sup> T. P. FEHLNER, Chap. 4 in ref. 9, pp. 175-96.

<sup>29</sup> S. G. SHORE, Chap. 3 in ref. 9, pp. 79-174.

Symmetrical  
(homolytic)



Unsymmetrical  
(heterolytic)

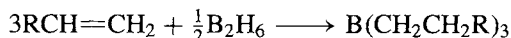


since the volatile  $B(OMe)_3$  could readily be distilled off and determined while the number of moles of  $H_2$  evolved equalled the number of H atoms in the borane molecule:



This works well for all *nido*- and *arachno*-boranes but not for the *closo*-dianions, which are much less reactive. Reactions of  $B_2H_6$  with  $NH_3$  are complex and, depending on the conditions, yield aminodiborane,  $H_2B(\mu-H)(\mu-NH_2)BH_2$ , or the diammoniate of diborane,  $[BH_2(NH_3)_2]^- [BH_4]^-$  (p. 165); at higher temperatures the benzene analogue borazine,  $(HNBH)_3$ , results (see p. 210).

The remarkably facile addition of  $B_2H_6$  to alkenes and alkynes in ether solvents at room temperatures was discovered by H. C. Brown and B. C. Subba Rao in 1956:



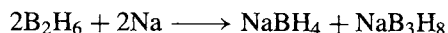
This reaction, now termed hydroboration, has opened up the quantitative preparation of organoboranes and these, in turn, have proved to be of outstanding synthetic utility.<sup>(30,31)</sup> It was for his development of this field that H. C. Brown (Purdue) was awarded the 1979 Nobel Prize in Chemistry. Hydroboration is regiospecific, the boron showing preferential attachment to the least substituted C atom (anti-Markovnikov). This finds ready interpretation in terms of electronic factors and relative bond polarities (p. 144); steric factors also work in the same direction. The addition is stereospecific *cis* (*syn*). Recent extensions of the methodology have encompassed the significant development of generalized chiral syntheses.<sup>(32)</sup>

<sup>30</sup> H. C. BROWN, *Organic Syntheses via Boranes*, Wiley, New York, 1975, 283 pp., *Boranes in Organic Chemistry*, Cornell University Press, Ithaca, New York, 1972, 462 pp.

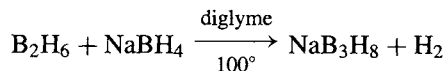
<sup>31</sup> D. J. PASTO, Solution reactions of borane and substituted boranes, Chap. 5 in ref. 7, pp. 197–222.

<sup>32</sup> H. C. BROWN and B. SINGARAM, *Pure Appl. Chem.* **59**, 879–94 (1987); H. C. BROWN and P. V. RAMACHANDRAN, *Pure Appl. Chem.* **63**, 307–16 (1991) and references cited therein.

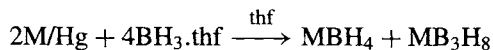
Diborane reacts slowly over a period of days with metals such as Na, K, Ca or their amalgams and more rapidly in the presence of ether:



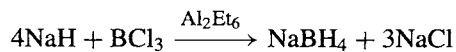
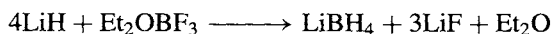
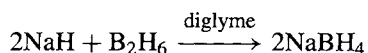
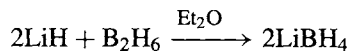
$B_3H_8^-$  prepared in this way was the first polyborane anion (1955); it is now more conveniently made by the reaction



Alternatively,  $BH_3 \cdot thf$  can be reduced by alkali metal amalgams ( $M = K, Rb, Cs$ ) to give good yields of solvent-free products:<sup>(33)</sup>



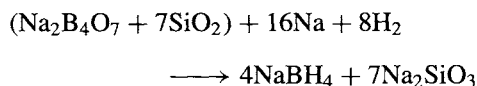
Tetrahydroborates,  $M(BH_4)_x$ , were first identified in 1940 ( $M = Li, Be, Al$ ) and since then have been widely exploited as versatile nucleophilic reducing agents which attack centres of low electron density (cf. electrophiles such as  $B_2H_6$  and  $LBH_3$  which attack electron-rich centres). The most stable are the alkali derivatives  $MBH_4$ :  $LiBH_4$  decomposes above  $\sim 380^\circ$  but the others ( $Na-Cs$ ) are stable up to  $\sim 600^\circ$ .  $MBH_4$  are readily soluble in water and many other coordinating solvents such as liquid ammonia, amines, ethers ( $LiBH_4$ ) and polyethers ( $NaBH_4$ ). They can be prepared by direct reaction of  $MH$  with either  $B_2H_6$  or  $BX_3$  at room temperature though the choice of solvent is often crucial, e.g.:



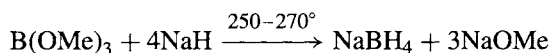
These laboratory-scale syntheses are clearly unsuitable for large-scale industrial production;

<sup>33</sup> T. G. HILL, R. A. GODFROID, J. P. WHITE and S. G. SHORE, *Inorg. Chem.* **30**, 2952–4 (1991).

here the preferred route, introduced in the early 1960s is the Bayer process which uses borax (or ulexite), quartz, Na and H<sub>2</sub> under moderate pressure at 450–500°. <sup>(34)</sup>



The resulting mixture is extracted under pressure with liquid NH<sub>3</sub> and the product obtained as a 98% pure powder (or pellets) by evaporation. An alternative route is:



The resulting mixture is hydrolysed with water and the aqueous phase extracted with Pr<sup>i</sup>NH<sub>2</sub>.

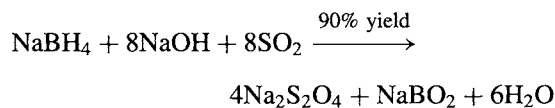
Worldwide production of NaBH<sub>4</sub> is now about 3000 tonnes per annum (1990) and the price for powdered NaBH<sub>4</sub> in 1991 was \$48.39/kg.

Reaction of MBH<sub>4</sub> with electronegative elements is also often crucially dependent on the solvent and on the temperature and stoichiometry of reagents. Thus LiBH<sub>4</sub> reacts with S at –50° in the presence of Et<sub>2</sub>O to give Li[BH<sub>3</sub>SH], whereas at room temperature the main products are Li<sub>2</sub>S, Li[B<sub>3</sub>S<sub>2</sub>H<sub>6</sub>], and H<sub>2</sub>; at 200° in the absence of solvent LiBH<sub>4</sub> reacts with S to give LiBS<sub>2</sub> and either H<sub>2</sub> or H<sub>2</sub>S depending on whether S is in excess. Similarly, MBH<sub>4</sub> react with I<sub>2</sub> in cyclohexane at room temperature to give BI<sub>3</sub>, HI and MI, whereas in diglyme B<sub>2</sub>H<sub>6</sub> is formed quantitatively (p. 164).

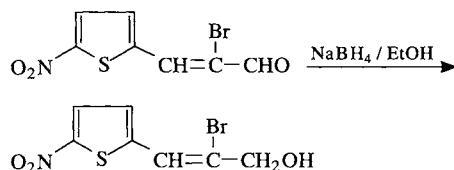
The product of reaction of BH<sub>4</sub><sup>–</sup> with element halides depends on the electropositivity of the element. Halides of the electropositive elements tend to form the corresponding M(BH<sub>4</sub>)<sub>x</sub>, e.g. M = Be, Mg, Ca, Sr, Ba; Zn, Cd; Al, Ga, Tl<sup>I</sup>; lanthanides; Ti, Zr, Hf and U<sup>IV</sup>. Halides of the less electropositive elements tend to give the hydride or a hydrido-complex since the BH<sub>4</sub> derivative is either unstable or non-existent: thus SiCl<sub>4</sub> gives SiH<sub>4</sub>;

PCl<sub>3</sub> and PCl<sub>5</sub> give PH<sub>3</sub>; Ph<sub>2</sub>AsCl gives Ph<sub>2</sub>AsH; [Fe(η<sup>5</sup>-C<sub>5</sub>H<sub>5</sub>)(CO)<sub>2</sub>Cl] gives [Fe(η<sup>5</sup>-C<sub>5</sub>H<sub>5</sub>)(CO)<sub>2</sub>H], etc.

A particularly interesting reaction (and one of considerable commercial value in the BOROL process for the *in situ* bleaching of wood pulp) is the production of dithionite, S<sub>2</sub>O<sub>4</sub><sup>2–</sup>, from SO<sub>2</sub>:



In reactions with organic compounds, LiBH<sub>4</sub> is a stronger (less selective) reducing agent than NaBH<sub>4</sub> and can be used, for example, to reduce esters to alcohols. NaBH<sub>4</sub> reduces ketones, acid chlorides and aldehydes under mild conditions but leaves other functions (such as –CN, –NO<sub>2</sub>, esters) untouched; it can be used as a solution in alcohols, ethers, dimethylsulfoxide, or even aqueous alkali (pH > 10). Perhaps the classic example of its selectivity is shown below where an aldehyde group is hydrogenated in high yield without any attack on the nitro group, the bromine atom, the olefinic bond, or the thiophene ring:



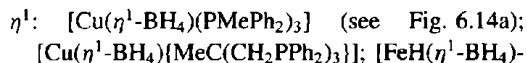
Industrial interest in LiBH<sub>4</sub>, and particularly NaBH<sub>4</sub>, stems not only from their use as versatile reducing agents for organic functional groups and their use in the bleaching of wood pulp, but also for their application in the electroless (chemical) plating of metals. Traditionally, either sodium hypophosphite, NaH<sub>2</sub>PO<sub>2</sub>, or formaldehyde have been used (as in the silvering of glass), but NaBH<sub>4</sub> was introduced on an industrial scale in the early 1960s, notably for the deposition of Ni on metal or non-metallic substrates; this gives corrosion-resistant, hard, protective coatings, and is also useful for metallizing plastics prior to

<sup>34</sup> R. WADE, in R. THOMPSON (ed.), *Speciality Inorganic Chemistry*, Royal Soc. Chem., London, 1981, pp. 25–58; see also *Kirk–Othmer Encyclopedia of Chemical Technology*, 4th edn., John Wiley, New York, 1992, Vol. 4, pp. 490–501.

further electroplating or for depositing contacts in electronics. Chemical plating also achieves a uniform thickness of deposit independent of the geometric shape, however complicated.

The  $\text{BH}_4^-$  ion is essentially non-coordinating in its alkali metal salts. However, despite the fact that it is isoelectronic with methane,  $\text{BH}_4^-$  has been found to act as a versatile ligand, forming many coordination compounds by means of 3-centre  $\text{B-H}\rightarrow\text{M}$  bonds to somewhat less electropositive metals.<sup>(35-37)</sup> Indeed,  $\text{BH}_4^-$

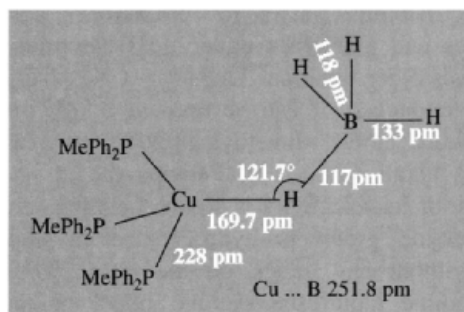
affords a rare example of a ligand that can act in at least 6 coordination modes:  $\eta^1$ ,  $\eta^2$ ,  $\eta^3$ ,  $\mu(\eta^2, \eta^2)$ ,  $\mu(\eta^3)$  and  $\mu(\eta^4)$ . Such complexes are usually readily prepared by reacting the corresponding (or closely related) halides with  $\text{BH}_4^-$  in what are essentially ligand replacement reactions. Some examples follow:



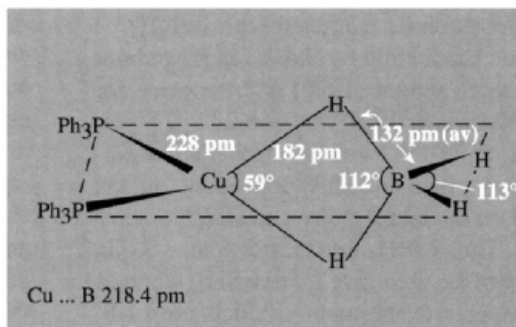
<sup>35</sup> B. D. JAMES and M. G. H. WALLBRIDGE, *Prog. Inorg. Chem.* **11**, 99-231 (1970).

<sup>36</sup> P. A. WEGNER, Chap. 12 in ref. 9, pp. 431-80.

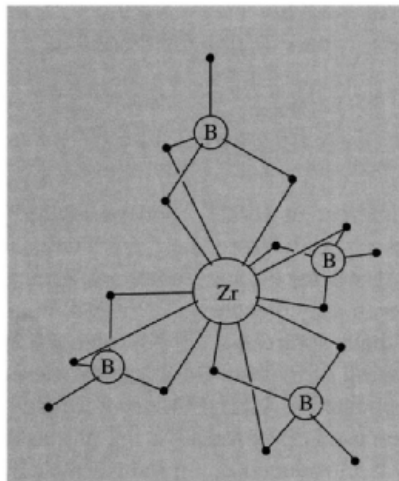
<sup>37</sup> T. J. MARKS and J. R. KOLB, *Chem. Rev.* **77**, 263-93 (1977).



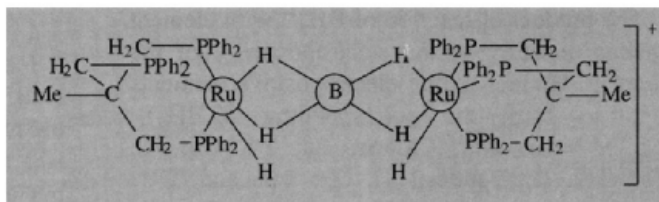
(a)  $[\text{Cu}(\eta^1\text{-BH}_4)(\text{PMePh}_2)_3]$



(b)  $[\text{Cu}(\eta^2\text{-BH}_4)(\text{PPh}_3)_2]$



(c)  $[\text{Zr}(\eta^3\text{-BH}_4)_4]$



(d)  $[\{\text{RuH}(\text{tripod})\}_2(\mu\text{:}\eta^2, \eta^2\text{-BH}_4)]^+$

**Figure 6.14** Examples of the various coordination modes of  $\text{BH}_4^-$  (continued on facing page).

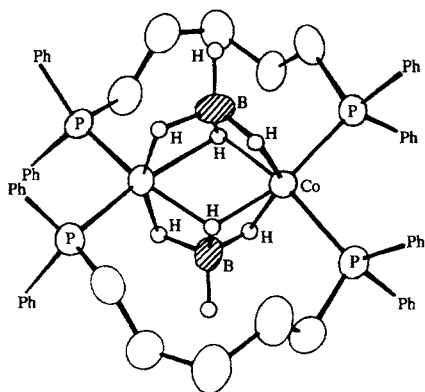
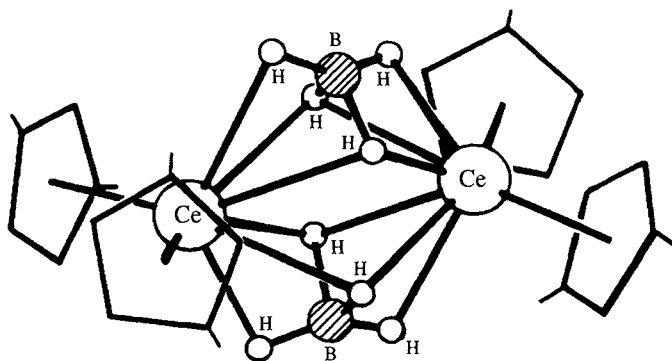
(e) [Co(μ:η<sup>3</sup>-BH<sub>4</sub>)<sub>2</sub>{(μ-Ph<sub>2</sub>P(CH<sub>2</sub>)<sub>5</sub>PPh<sub>2</sub>)<sub>2</sub>}]<sub>2</sub>(f) [Ce(μ:η<sup>4</sup>-BH<sub>4</sub>)(η<sup>5</sup>-C<sub>5</sub>H<sub>3</sub>Bu<sub>3</sub>)<sub>2</sub>]<sub>2</sub>

Figure 6.14 continued

(dmpe)] (dmpe = Me<sub>2</sub>PCH<sub>2</sub>CH<sub>2</sub>PMe<sub>2</sub>); [*trans*-V(η<sup>1</sup>-BH<sub>4</sub>)<sub>2</sub>(dmpe)<sub>2</sub>]; (also B<sub>2</sub>H<sub>7</sub><sup>-</sup>, i.e. [BH<sub>3</sub>(η<sup>1</sup>-BH<sub>4</sub>)<sup>-</sup>])

η<sup>2</sup>: [Al(η<sup>2</sup>-BH<sub>4</sub>)<sub>3</sub>] (see p. 230); [Cu(η<sup>2</sup>-BH<sub>4</sub>)(PPh<sub>3</sub>)<sub>2</sub>] (Fig. 6.14b); [Ti<sup>III</sup>(η<sup>2</sup>-BH<sub>4</sub>)<sub>3</sub>(dme)] (dme = 1,2-dimethoxyethane); [Sc(η<sup>2</sup>-BH<sub>4</sub>)(η<sup>5</sup>-Cp<sup>II</sup>)<sub>2</sub>] (Cp<sup>II</sup> = [C<sub>5</sub>H<sub>3</sub>(SiMe<sub>3</sub>)<sub>2</sub>]); [Y(η<sup>2</sup>-BH<sub>4</sub>)(η<sup>5</sup>-Cp<sup>II</sup>)<sub>2</sub>(thf)]

η<sup>3</sup>: [M(η<sup>3</sup>-BH<sub>4</sub>)<sub>4</sub>] (M = Zr, Hf, Np, Pu; see Fig. 6.14c); [Ln(η<sup>3</sup>-BH<sub>4</sub>)(η<sup>5</sup>-Cp<sup>II</sup>)<sub>2</sub>(thf)] (Ln = La, Pr, Nd, Sm); [U<sup>IV</sup>(η<sup>3</sup>-BH<sub>4</sub>)<sub>3</sub>(η<sup>5</sup>-C<sub>5</sub>H<sub>5</sub>)]

μ(η<sup>2</sup>, η<sup>2</sup>): [{RuH(tripod)}<sub>2</sub>(μ:η<sup>2</sup>, η<sup>2</sup>-BH<sub>4</sub>)<sup>+</sup>] (Fig. 6.14d)

μ(η<sup>3</sup>): [Co(μ:η<sup>3</sup>-BH<sub>4</sub>){μ-Ph<sub>2</sub>P(CH<sub>2</sub>)<sub>5</sub>PPh<sub>2</sub>}]<sub>2</sub> (Fig. 6.14e); [(tmeda)Li-μ(η<sup>3</sup>-BH<sub>4</sub>)<sub>2</sub>] (tmeda = tetramethylethylenediamine)

μ(η<sup>4</sup>): [Ce(μ:η<sup>4</sup>-BH<sub>4</sub>)(η<sup>5</sup>-C<sub>5</sub>H<sub>3</sub>Bu<sub>3</sub>)<sub>2</sub>]<sub>2</sub> (Fig. 6.14f)

Many complexes have more than one coordination mode of BH<sub>4</sub><sup>-</sup> featured in their structure, e.g. [U<sup>III</sup>(η<sup>2</sup>-BH<sub>4</sub>)(η<sup>3</sup>-BH<sub>4</sub>)<sub>2</sub>(dmpe)<sub>2</sub>]. Likewise, whereas [M(BH<sub>4</sub>)<sub>4</sub>] are monomeric 12-coordinate complexes for M = Zr, Hf, Np, Pu, they are polymeric for M = Th, Pa, U: the coordination number rises to 14 and each metal centre is coordinated by two η<sup>3</sup>-BH<sub>4</sub><sup>-</sup> and four bridging η<sup>2</sup>-BH<sub>4</sub><sup>-</sup> groups. It is clear that among the factors which determine the mode adopted are the size of the metal atom and the steric requirements of the co-ligands. Many of the complexes

are fluxional on an nmr timescale in solution; indeed, this property of fluxionality, which has been increasingly recognized to occur in many inorganic and organometallic systems, was first observed (1955) on the tris-bidentate complex [Al(η<sup>2</sup>-BH<sub>4</sub>)<sub>3</sub>].<sup>(38)</sup>

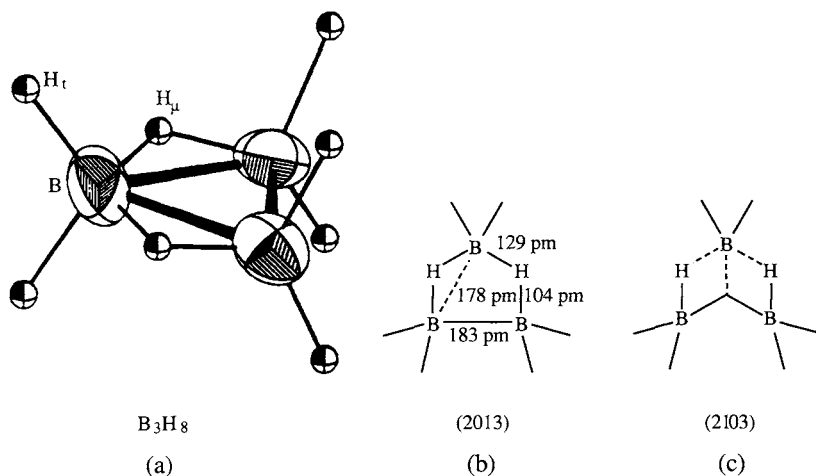
The B<sub>3</sub>H<sub>8</sub><sup>-</sup> ion (p. 166) is a triangular cluster of C<sub>s</sub> (rather than C<sub>2v</sub>) symmetry (see Fig. 6.15a);<sup>(39)</sup> the bridging H<sub>μ</sub> atoms are essentially in the B<sub>3</sub> plane with H<sub>t</sub> above and below. While it has been conventional to represent the cluster bonding in terms of two BHB and one B–B bond (Fig. 6.15b), recent high-level computations<sup>(40)</sup> suggest the presence of a 3-centre BBB bond, as depicted approximately in Fig. 6.15c.

The *arachno*-anion B<sub>3</sub>H<sub>8</sub><sup>-</sup> is the only binary triboron species that is stable at room temperature and above. It can be viewed as a ligand-stabilized {B<sub>3</sub>H<sub>7</sub>} group, i.e. (L.B<sub>3</sub>H<sub>7</sub>), in which the ligand is H<sup>-</sup> (cf. BH<sub>4</sub><sup>-</sup>). However, the ion is completely fluxional in solution, all three boron atoms (and all eight protons) being equivalent on an nmr timescale. The B<sub>3</sub>H<sub>8</sub><sup>-</sup> anion has an

<sup>38</sup> R. A. OGG and J. D. RAY, *Disc. Faraday Soc.* **19**, 239–46 (1955).

<sup>39</sup> H. J. DEISEROTH, O. SOMMER, H. BINDER, K. WOLFER and B. FREI, *Z. anorg. allg. Chem.* **571**, 21–8 (1989).

<sup>40</sup> M. SIRONI, M. RAIMONDI, D. L. COOPER and J. GERRATT, *J. Phys. Chem.* **95**, 10617–23 (1991).



**Figure 6.15** (a) Structure of  $B_3H_8^-$  showing  $C_s$  symmetry; (b) dimensions and representation of the bonding using a direct B–B bond (2013) for the longer (unbridged) B–B distance; (c) most recent (2103) description of the bonding in terms of a 3-centre BBB bond. (See p. 158 for *styx* formalism.)

extensive reaction chemistry both as a reducing agent and as a source of *arachno*- $B_4H_{10}$  (p. 162). Conversely, unsymmetrical (heterolytic) cleavage of  $B_4H_{10}$  with ligands, L, such as  $NH_3$  yield  $[L_2BH_2]^+[B_3H_8]^-$ .

The  $B_3H_8^-$  ion is also a versatile ligand and forms bidentate and even tridentate complexes with many metal centres.<sup>(41)</sup> The octahedrally coordinated 18-electron manganese(I) complex  $[Mn(\eta^2-B_3H_8)(CO)_4]$  is a particularly instructive example. As can be seen from Fig. 6.16a it has a cluster structure that is clearly related to that of  $B_4H_{10}$  (13). When heated to  $180^\circ C$  or irradiated with ultraviolet light the complex loses one of the four CO ligands and this enables a further B–H group to coordinate to give the trihapto complex *fac*- $[Mn(\eta^3-B_3H_8)(CO)_3]$  (Fig. 6.16b). Treatment of this product with an excess of CO under moderate pressure regenerates the original dihapto species by a simple ligand replacement reaction.<sup>(42)</sup>

### 6.4.5 Intermediate-sized Boranes and their Anions ( $B_5$ – $B_9$ )

Pentaborane(9), *nido*- $B_5H_9$ , is by far the most studied borane in this group. It can be prepared by passing a 1:5 mixture of  $B_2H_6$  and  $H_2$  at subatmospheric pressure through a furnace at  $250^\circ C$  with a residence time of 3 s (or at  $225^\circ C$  with a 15 s residence time); there is a 70% yield and 30% conversion. Alternatively  $B_2H_6$  can be pyrolysed for 2.5 days in a static hot/cold reactor at  $180^\circ/-80^\circ$ .  $B_5H_9$  is a colourless, volatile liquid, bp  $60.0^\circ$ ; it is thermally stable but chemically very reactive and spontaneously flammable in air. Its structure is essentially a square-based pyramid of B atoms each of which carries a terminal H atom and there are 4 bridging H atoms around the base (structure 9, p. 154). The slant edge of the pyramid, B(1)–B(2), is 168 pm and the basal interboron distances, B(2)–B(3) etc, are 178 pm; other key dimensions are B– $H_t$  122 pm, B– $H_\mu$  135 pm and B– $H_\mu$ –B  $83^\circ$ . Calculations suggest that B(1) has a slightly higher electron density than the basal borons and that  $H_\mu$  is slightly more positive than  $H_t$ . Apex-substituted derivatives 1- $XB_5H_8$  can

<sup>41</sup> D. F. GAINES and S. J. HILDEBRANDT, Chap. 3 in R. N. GRIMES (ed.), *Metal Interactions with Boron Clusters*, Plenum Press, New York, 1982, pp. 119–43.

<sup>42</sup> S. J. HILDEBRANDT, D. F. GAINES and J. C. CALABRESE, *Inorg. Chem.* **17**, 790–4 (1978).

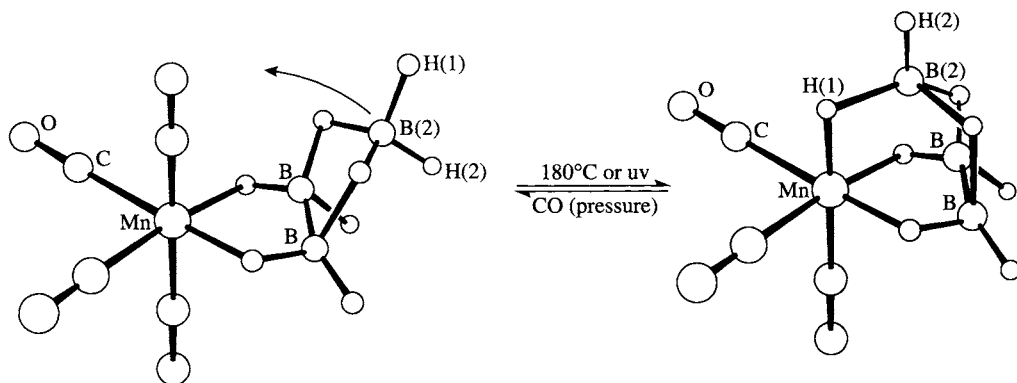
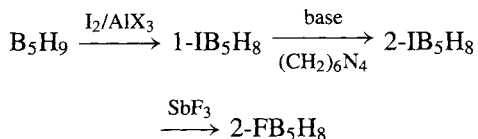
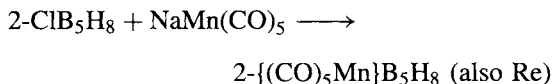


Figure 6.16 Ligand replacement reaction of  $[\text{Mn}(\eta^2\text{-B}_3\text{H}_8)(\text{CO})_4]$  (see text).

readily be prepared by electrophilic substitution (e.g. halogenation or Friedel-Crafts alkylation with  $\text{RX}$  or alkenes), whereas base-substituted derivatives  $2\text{-XB}_5\text{H}_8$  result when nucleophilic reaction is induced by amines or ethers, or when  $1\text{-XB}_5\text{H}_8$  is isomerized in the presence of a Lewis base such as hexamethylenetetramine or an ether:



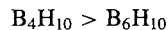
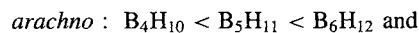
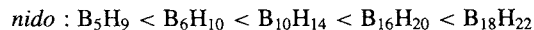
Further derivatives can be obtained by metathesis, e.g.



$\text{B}_5\text{H}_9$  reacts with Lewis bases (electron-pair donors) to form adducts, some of which have now been recognized as belonging to the new series of *hypho*-borane derivatives  $\text{B}_n\text{H}_{n+8}$  (p. 152). Thus  $\text{PMe}_3$  gives the adduct  $[\text{B}_5\text{H}_9(\text{PMe}_3)_2]$  which is formally analogous to  $[\text{B}_5\text{H}_{11}]^{2-}$  and the (unknown) borane  $\text{B}_5\text{H}_{13}$ .  $[\text{B}_5\text{H}_9(\text{PMe}_3)_2]$  has a very open structure in the form of a shallow pyramid with the ligands attached at positions 1 and 2 and with major rearrangement of the H atoms (Fig. 6.17a). Chelating phosphine ligands such as  $(\text{Ph}_2\text{P})_2\text{CH}_2$

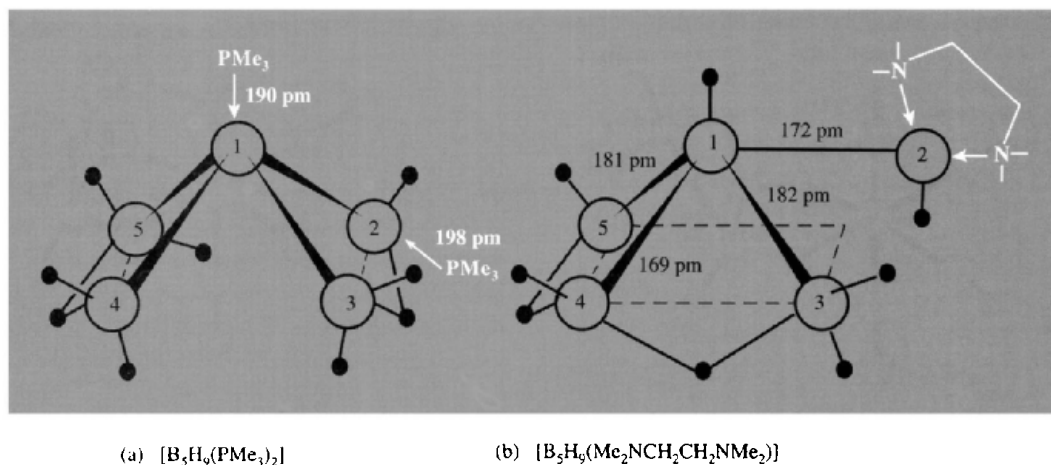
and  $(\text{Ph}_2\text{PCH}_2)_2$  have similar structures but  $[\text{B}_5\text{H}_9(\text{Me}_2\text{NCH}_2\text{CH}_2\text{NMe}_2)]$  undergoes a much more severe distortion in which the ligand chelates a single boron atom, B(2), which is joined to the rest of the molecule by a single bond to the apex B(1) (Fig. 6.17b).<sup>(43)</sup> With  $\text{NH}_3$  as ligand (at  $-78^\circ$ ) complete excision of one B atom occurs by “unsymmetrical cleavage” to give  $[(\text{NH}_3)_2\text{BH}_2]^+[\text{B}_4\text{H}_7]^-$

$\text{B}_5\text{H}_9$  also acts as a weak Brønsted acid and, from proton competition reactions with other boranes and borane anions, it has been established that acidity increases with increasing size of the borane cluster and that *arachno*-boranes are more acidic than *nido*-boranes:



Accordingly,  $\text{B}_5\text{H}_9$  can be deprotonated at low temperatures by loss of  $\text{H}_\mu$  to give  $\text{B}_5\text{H}_8^-$  providing a sufficiently strong base such as a lithium alkyl or alkali metal hydride is used. Bridge-substituted derivatives of  $\text{B}_5\text{H}_9$  can then be obtained by reacting  $\text{MB}_5\text{H}_8$  with chloro compounds such as  $\text{R}_2\text{PCl}$ ,  $\text{Me}_3\text{SiCl}$ ,  $\text{Me}_3\text{GeCl}$ ,

<sup>43</sup> N. W. ALCOCK, H. M. COLQUHOUN, G. HARAN, J. F. SAWYER and M. G. H. WALLBRIDGE, *J. Chem. Soc., Chem. Commun.*, 368–70 (1977); *J. Chem. Soc., Dalton Trans.*, 2243–55 (1982).

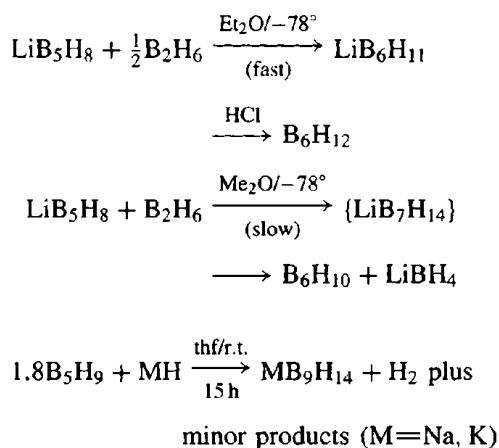


**Figure 6.17** Structure of *hypho*-borane derivatives: (a)  $[\text{B}_5\text{H}_9(\text{PMe}_3)_2]$  — the distances B(1)-B(2) and B(2)-B(3) are as in  $\text{B}_5\text{H}_9$  (p. 170) but B(3)⋯B(4) is 295 pm (cf. B⋯B 297 pm in  $\text{B}_5\text{H}_{11}$ , structure 14, p. 154), and (b)  $[\text{B}_5\text{H}_9(\text{Me}_2\text{NCH}_2\text{CH}_2\text{NMe}_2)]$  — the distances B(2)⋯B(3) and B(2)⋯B(5) are 273 and 272 pm respectively.

or even  $\text{Me}_2\text{BCl}$  to give compounds in which the 3-centre B-H<sub>μ</sub>-B bond has been replaced by a 3-centre bond between the 2 B atoms and P, Si, Ge or B respectively. Many metal-halide coordination complexes react similarly, and the products can be considered as adducts in which the  $\text{B}_5\text{H}_8^-$  anion is acting formally as a 2-electron ligand via a 3-centre B-M-B bond.<sup>(44,45)</sup> Thus  $[\text{Cu}^{\text{I}}(\text{B}_5\text{H}_8)(\text{PPh}_3)_2]$  (Fig. 6.18a) is readily formed by the low-temperature reaction of  $\text{KB}_5\text{H}_8$  with  $[\text{CuCl}(\text{PPh}_3)_3]$  and analogous 16-electron complexes have been prepared for many of the later transition elements, e.g.  $[\text{Cd}(\text{B}_5\text{H}_8)\text{Cl}(\text{PPh}_3)]$ ,  $[\text{Ag}(\text{B}_5\text{H}_8)(\text{PPh}_3)_2]$  and  $[\text{M}^{\text{II}}(\text{B}_5\text{H}_8)\text{XL}_2]$ , where  $\text{M}^{\text{II}} = \text{Ni}, \text{Pd}, \text{Pt}$ ; X = Cl, Br, I; L<sub>2</sub> = a diphosphine or related ligand. By contrast,  $[\text{Ir}^{\text{I}}(\text{CO})\text{Cl}(\text{PPh}_3)_2]$  reacts by oxidative insertion of Ir and consequent cluster expansion to give  $[(\text{IrB}_5\text{H}_8)(\text{CO})(\text{PPh}_3)_2]$  which, though superficially of similar formula, has the structure of an irida-*nido*-hexaborane

(Fig. 6.18b).<sup>(46)</sup> In this, the  $\{\text{Ir}(\text{CO})(\text{PPh}_3)_2\}$  moiety replaces a basal  $\text{BH}_\mu\text{H}_\mu$  unit in  $\text{B}_6\text{H}_{10}$  (structure 10, p. 154).

Cluster-expansion and cluster-degradation reactions are a feature of many polyhedral borane species. Examples of cluster-expansion are:<sup>(11,47)</sup>



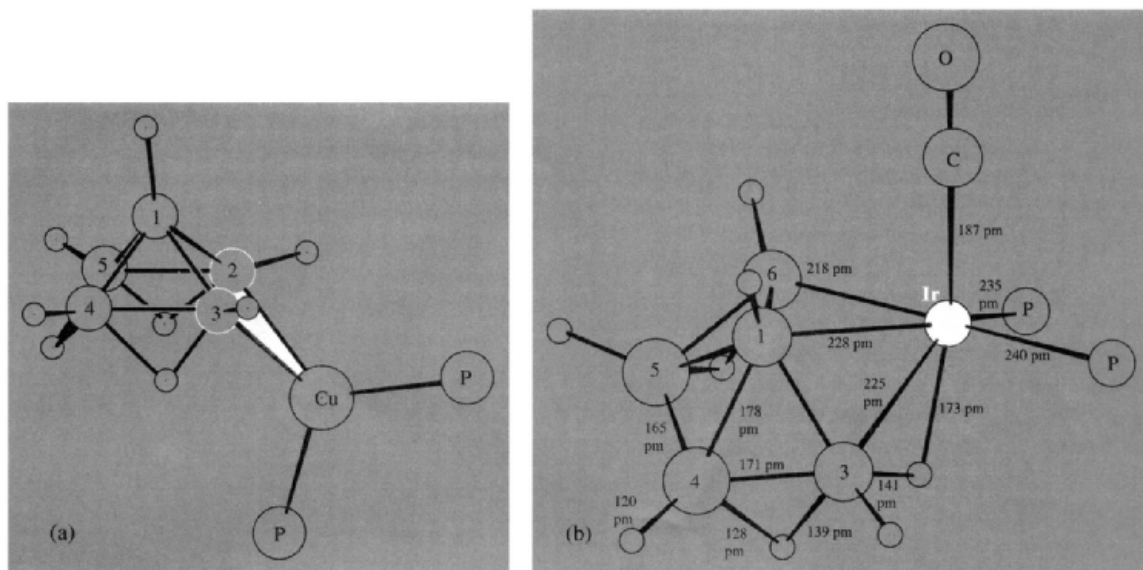
<sup>44</sup> N. N. GREENWOOD and I. M. WARD, *Chem. Soc. Revs.* **3**, 231-71 (1974).

<sup>45</sup> N. N. GREENWOOD, *Pure Appl. Chem.* **49**, 791-802 (1977).

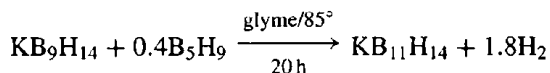
<sup>46</sup> N. N. GREENWOOD, J. D. KENNEDY, W. S. McDONALD, D. REED and J. STAVES, *J. Chem. Soc., Dalton Trans.*, 117-23 (1979).

<sup>47</sup> N. S. HOSMANE, J. R. WERMER, ZHU HONG, T. D. GETMAN and S. G. SHORE, *Inorg. Chem.* **26**, 3638-9 (1987), and references cited therein.

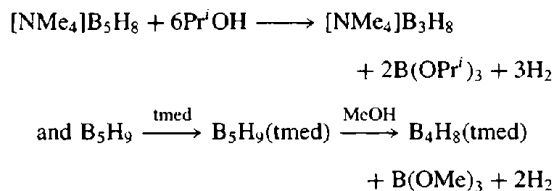




**Figure 6.18** (a) Structure of [Cu(B<sub>5</sub>H<sub>8</sub>)(PPh<sub>3</sub>)<sub>2</sub>], showing η<sup>2</sup>-bonding of B<sub>5</sub>H<sub>8</sub><sup>-</sup> (phenyl groups omitted for clarity); (b) Structure of [(IrB<sub>5</sub>H<sub>8</sub>)(CO)(PPh<sub>3</sub>)<sub>2</sub>] showing the structure about the iridium atom and the relationship of the metallaborane cluster to that of *nido*-B<sub>6</sub>H<sub>10</sub>.



Cluster degradation has already been mentioned in connection with the unsymmetrical cleavage reaction (p. 165) and other examples are:



(where Pr<sup>i</sup> is Me<sub>2</sub>CH- and tmed is Me<sub>2</sub>NCH<sub>2</sub>-CH<sub>2</sub>NMe<sub>2</sub>).

Replacement of a {BH} unit in B<sub>5</sub>H<sub>9</sub> by an “isoelectronic” organometallic group such as {Fe(CO)<sub>3</sub>} or {Co(η<sup>5</sup>-C<sub>5</sub>H<sub>5</sub>)} can also occur, and this illustrates the close interrelation between metallaboranes, metal-metal cluster

compounds, and organometallic complexes in general (see Panel).

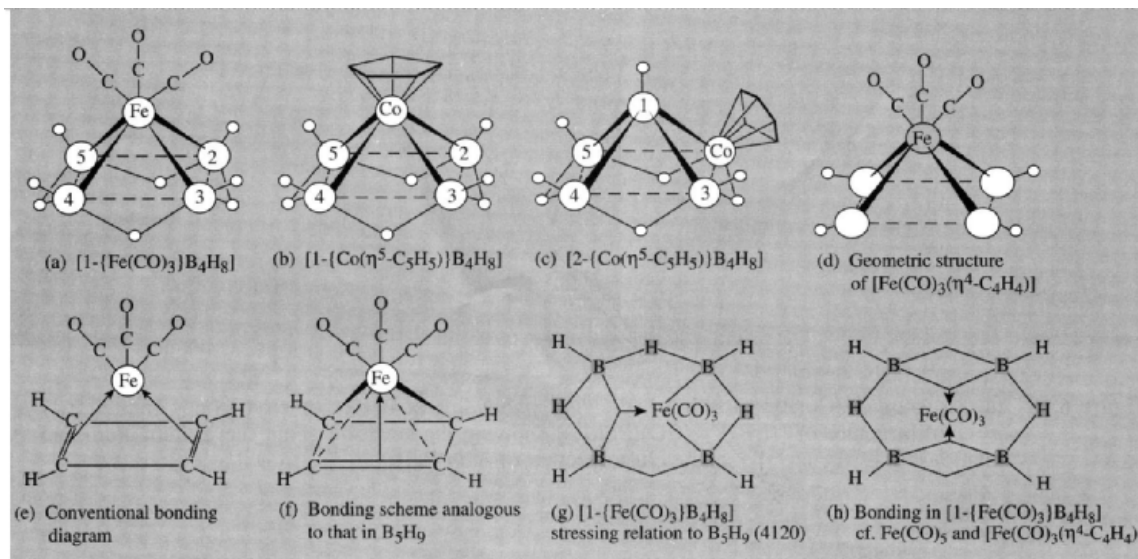
The structures of several other *nido*- and *arachno*-B<sub>5</sub>-B<sub>9</sub> boranes are given on page 154 but a detailed discussion of their chemistry is beyond the scope of this treatment. Further information is in refs. 9, 11, 27, 51 and 52.

### 6.4.6 Chemistry of *nido*-decaborane, B<sub>10</sub>H<sub>14</sub>

Decaborane is the most studied of all the polyhedral boranes and at one time (mid-1950s) was manufactured on a multitonne scale in the USA as a potential high-energy fuel. It is now obtainable in research quantities by the pyrolysis of B<sub>2</sub>H<sub>6</sub> at 100–200°C in the presence of catalytic amounts of Lewis bases such as Me<sub>2</sub>O. B<sub>10</sub>H<sub>14</sub> is a colourless, volatile, crystalline solid (see Table 6.2, p. 163) which

## Metalloboranes, Metal Clusters and Organometallic Complexes

Copyrolysis of  $B_5H_9$  and  $[Fe(CO)_5]$  in a hot/cold reactor at  $220^\circ/20^\circ$  for 3 days gives an orange liquid (mp  $5^\circ C$ ) of formula  $[1-[Fe(CO)_3]B_4H_8]$  having the structure shown in (a).<sup>(48)</sup> The isoelectronic complex  $[1-[Co(\eta^5-C_5H_5)]B_4H_8]$  (structure b) can be obtained as yellow crystals by pyrolysis at  $200^\circ$  of the corresponding basal derivative  $[2-[Co(\eta^5-C_5H_5)]B_4H_8]$  (structure (c)) which is obtained as red crystals from the reaction of  $NaB_5H_8$  and  $CoCl_2$  with  $NaC_5H_5$  in thf at  $-20^\circ$ .<sup>(49)</sup> The course of these reactions is obscure and other products are also obtained.



As  $[BH_2]$  is isoelectronic with  $[CH]$ , these metalloborane clusters are isoelectronic with the cyclobutadiene adduct  $[Fe(\eta^4-C_4H_4)(CO)_3]$ , see (d). (e) and (f). Likewise  $[Fe(CO)_3]$  or  $[Co(\eta^5-C_5H_5)]$  can replace a  $[BH]$  group in  $B_5H_9$  and two descriptions of the bonding are given in (g) and (h): the Fe atom supplies 2 electrons and 3 atomic orbitals to the cluster (as does BH), thereby enabling it to form 2 Fe-B  $\sigma$  bonds and to accept a pair of electrons from adjacent B atoms to form a 3-centre BMB bond. In this description the Fe atom is formally octahedral  $Fe^{II}$  ( $d^6$ ). Alternatively, diagram (h) emphasizes the relation between  $[1-[Fe(CO)_3]B_4H_8]$  and  $[Fe(CO)_3(\eta^4-C_4H_4)]$  or  $[Fe(CO)_5]$ : the Fe atom accepts 2 pairs of electrons to form two 3-centre BMB bonds and is formally  $Fe^0$  with a trigonal bipyramidal arrangement of bonds.

It is possible to replace more than one  $[BH]$  group in  $B_5H_9$  by a metal centre, e.g. in the dimetalla species  $[1,2-[Fe(CO)_3]_2B_3H_7]$ ;<sup>(50)</sup> it is also notable that the iron carbonyl cluster compound  $[Fe_5(CO)_{15}C]$  (p. 1108) features the same square-pyramidal cluster in which 5  $[Fe(CO)_3]$  groups have replaced the five  $[BH]$  groups in  $B_5H_9$ , and the C atom (in the centre of the base) replaces the 4 bridging H atoms by supplying the 4 electrons required to complete the bonding.

Many other equivalent groups can be envisaged and the formalism permits a unified approach to possible synthetic routes and to probable structures of a wide variety of compounds.<sup>(17,51-53)</sup>

<sup>48</sup> N. N. GREENWOOD, C. G. SAVORY, R. N. GRIMES, L. G. SNEDDON, A. DAVISON and S. S. WREFORD, *J. Chem. Soc., Chem. Commun.*, 718 (1974).

<sup>49</sup> V. R. MILLER and R. N. GRIMES, *J. Am. Chem. Soc.* **95**, 5078-80 (1973).

<sup>50</sup> K. J. HALLER, E. L. ANDERSEN and T. P. FEHLNER, *Inorg. Chem.* **20**, 309-13 (1981).

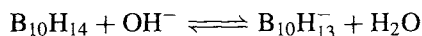
<sup>51</sup> N. N. GREENWOOD and J. D. KENNEDY, Chap. 2 in R. N. GRIMES (ed.), *Metal Interactions with Boron Clusters*, Plenum, New York, 1982, pp. 43-118.

<sup>52</sup> J. D. KENNEDY, *Prog. Inorg. Chem.* **32**, 519-679 (1984); **34**, 211-434 (1986).

<sup>53</sup> T. P. FEHLNER (ed.), *Inorganometallic Chemistry*, Plenum, New York, 1992, 401 pp.

is insoluble in H<sub>2</sub>O but readily soluble in a wide range of organic solvents. Its structure (36) can be regarded as derived from the 11 B atom cluster B<sub>11</sub>H<sub>11</sub><sup>2-</sup> (p. 153) by replacing the unique BH group with 2 electrons and appropriate addition of 4H<sub>μ</sub>. MO-calculations give the sequence of electron charge densities at the various B atoms as 2, 4 > 1, 3 > 5, 7, 8, 10 > 6, 9 though the total range of deviation from charge neutrality is less than ±0.1 electron per B atom. The chemistry of B<sub>10</sub>H<sub>14</sub> can be conveniently discussed under the headings (a) proton abstraction, (b) electron addition, (c) adduct formation, (d) cluster rearrangements, cluster expansions, and cluster degradation reactions, and (e) metalloborane and other heteroborane compounds.

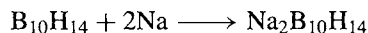
B<sub>10</sub>H<sub>14</sub> can be titrated in aqueous/alcoholic media as a monobasic acid, pK<sub>a</sub> 2.70:



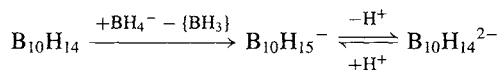
Proton abstraction can also be effected by other strong bases such as H<sup>-</sup>, OMe<sup>-</sup>, NH<sub>2</sub><sup>-</sup>, etc. The B<sub>10</sub>H<sub>13</sub><sup>-</sup> ion is formed by loss of a bridge proton, as expected, and this results

in a considerable shortening of the B(5)–B(6) distance from 179 pm in B<sub>10</sub>H<sub>14</sub> to 165 pm in B<sub>10</sub>H<sub>13</sub><sup>-</sup> (structures 36, 37). Under more forcing conditions with NaH a second H<sub>μ</sub> can be removed to give Na<sub>2</sub>B<sub>10</sub>H<sub>12</sub>; the probable structure of B<sub>10</sub>H<sub>12</sub><sup>2-</sup> is (38) and the anion acts as a formal bidentate (tetrahapto) ligand to many metals (p. 177).

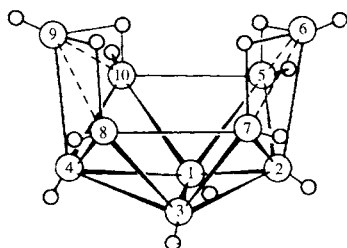
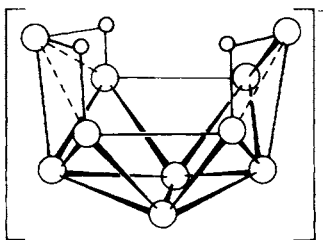
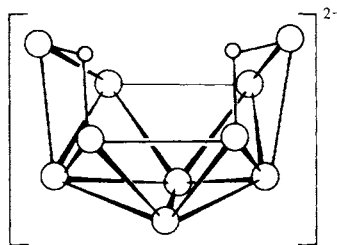
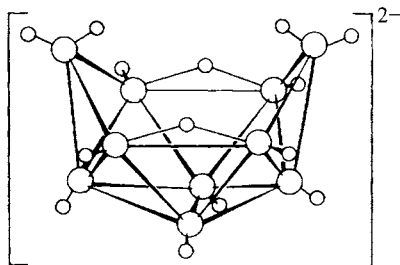
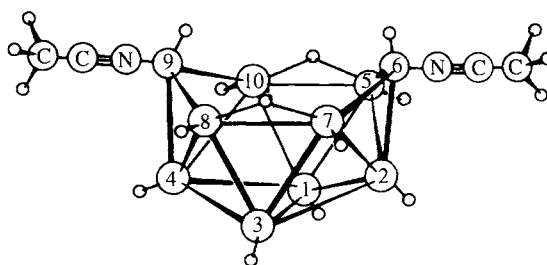
Electron addition to B<sub>10</sub>H<sub>14</sub> can be achieved by direct reaction with alkali metals in ethers, benzene or liquid NH<sub>3</sub>:



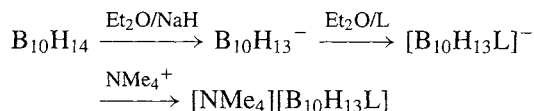
A more convenient preparation of the B<sub>10</sub>H<sub>14</sub><sup>2-</sup> anion uses the reaction of aqueous BH<sub>4</sub><sup>-</sup> in alkaline solution:



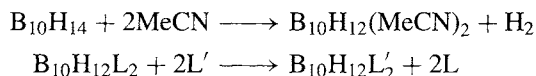
Structure (39) conforms to the predicted (2632) topology (p. 158) and shows that the 2 added electrons have relieved the electron deficiency to the extent that the 2 B–H<sub>μ</sub>–B groups have been

(36) B<sub>10</sub>H<sub>14</sub>(37) B<sub>10</sub>H<sub>13</sub><sup>-</sup>(38) B<sub>10</sub>H<sub>12</sub><sup>2-</sup>(39) B<sub>10</sub>H<sub>14</sub><sup>2-</sup>(40) B<sub>10</sub>H<sub>12</sub>(MeCN)<sub>2</sub>

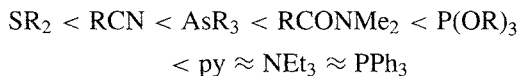
converted to B-H<sub>t</sub> with the consequent appearance of 2BH<sub>2</sub> groups in the structure. Calculations show that this conversion of a *nido*- to an *arachno*-cluster reverses the sequence of electron charge density at the 2, 4 and 6, 9 positions so that for B<sub>10</sub>H<sub>14</sub><sup>2-</sup> the sequence is 6, 9 > 1, 3 > 5, 7, 8, 10 > 2, 4; this is paralleled by changes in the chemistry. B<sub>10</sub>H<sub>14</sub><sup>2-</sup> can formally be regarded as B<sub>10</sub>H<sub>12</sub>L<sub>2</sub> for the special case of L = H<sup>-</sup>. Compounds of intermediate stoichiometry B<sub>10</sub>H<sub>13</sub>L<sup>-</sup> are formed when B<sub>10</sub>H<sub>14</sub> is deprotonated in the presence of the ligand L:



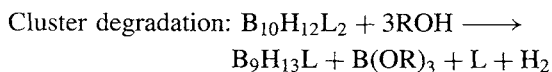
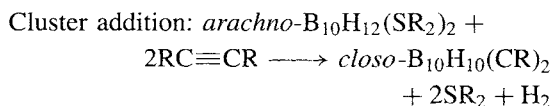
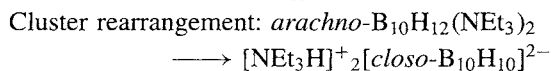
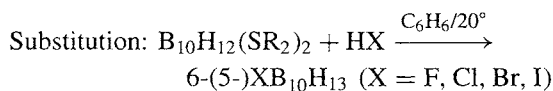
The adducts B<sub>10</sub>H<sub>12</sub>L<sub>2</sub> (structure 40) can be prepared by direct reaction of B<sub>10</sub>H<sub>14</sub> with L or by ligand replacement reactions:



Ligands L, L' can be drawn from virtually the full range of inorganic and organic neutral and anionic ligands and, indeed, the reaction severely limits the range of donor solvents in which B<sub>10</sub>H<sub>14</sub> can be dissolved. The approximate sequence of stability is:



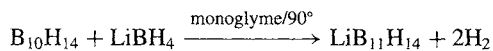
The stability of the phosphine adducts is notable as is the fact that thioethers readily form such adducts whereas ethers do not. Bis-ligand adducts of moderate stability play an important role in activating decaborane for several types of reaction to be considered in more detail in subsequent paragraphs, e.g.:



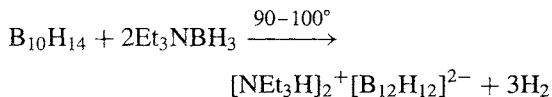
In this last reaction it is the coordinated B atom at position 9 that is solvolytically cleaved from the cluster.

Electrophilic substitution of B<sub>10</sub>H<sub>14</sub> follows the sequence of electron densities in the ground-state molecule. Thus halogenation in the presence of AlCl<sub>3</sub> leads to 1- and 2-monosubstituted derivatives and to 2,4-disubstitution. Similarly, Friedel-Crafts alkylations with RX/AlCl<sub>3</sub> (or FeCl<sub>3</sub>) yield mixtures such as 2-MeB<sub>10</sub>H<sub>13</sub>, 2,4- and 1,2-Me<sub>2</sub>B<sub>10</sub>H<sub>12</sub>, 1,2,3- and 1,2,4-Me<sub>3</sub>B<sub>10</sub>H<sub>11</sub>, and 1,2,3,4-Me<sub>4</sub>B<sub>10</sub>H<sub>10</sub>. By contrast, nucleophilic substitution (like the adduct formation with Lewis bases) occurs preferentially at the 6 (9) position; e.g., LiMe produces 6-MeB<sub>10</sub>H<sub>13</sub> as the main product with smaller amounts of 5-MeB<sub>10</sub>H<sub>13</sub>, 6,5(8)-Me<sub>2</sub>B<sub>10</sub>H<sub>12</sub> and 6,9-Me<sub>2</sub>B<sub>10</sub>H<sub>12</sub>.

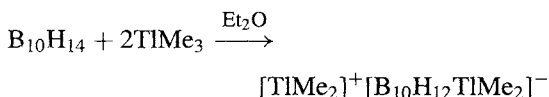
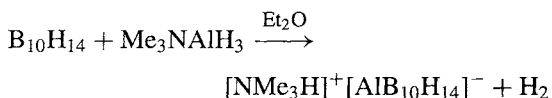
B<sub>10</sub>H<sub>14</sub> undergoes numerous cluster-addition reactions in which B or other atoms become incorporated in an expanded cluster. Thus in a reaction which differs from that on p. 175 BH<sub>4</sub><sup>-</sup> adds to B<sub>10</sub>H<sub>14</sub> with elimination of H<sub>2</sub> to form initially the *nido*-B<sub>11</sub>H<sub>14</sub><sup>-</sup> anion (structure 41, p. 178) and then the *closo*-B<sub>12</sub>H<sub>12</sub><sup>2-</sup>:



A more convenient high-yield synthesis of B<sub>12</sub>H<sub>12</sub><sup>2-</sup> is by the direct reaction of amineboranes with B<sub>10</sub>H<sub>14</sub> in the absence of solvents:



Heteroatom cluster addition reactions are exemplified by the following:



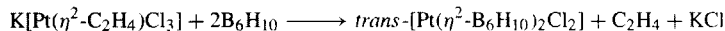
### The Concept of Boranes as Ligands

Boranes are usually regarded as being electron-deficient, in the sense that they have an insufficient number of electrons to form classical 2-centre 2-electron bonds between each contiguous pair of atoms. However, in the mid-1960s several groups began to realize that, far from being deficient in electrons, many boranes and their anions could act as very effective polyhapto ligands: that is, they could form donor-acceptor complexes (coordination compounds, Chap. 19) in which the borane cluster itself was acting as the electron donor or ligand. The application of this astonishing idea has extended enormously the range of boron hydride compounds which can be made.<sup>(54)</sup> Many aspects have already been alluded to in the preceding pages and these are briefly summarized in this Panel.

Boranes can act as ligands either by forming 3-centre, 2-electron B-H-M bonds (analogous to BHB bonds) or by forming direct B<sub>n</sub>M bonds ( $n = 1-6$ , analogous to B-B, BBB etc bonds). All hapticities from  $\eta^1-\eta^6$  and occasionally beyond are known. The various coordination modes of BH<sub>4</sub><sup>-</sup> and B<sub>3</sub>H<sub>8</sub><sup>-</sup> were discussed on pp. 168-71; these involve the conversion of B-H<sub>i</sub> bonds to B-H→M bonds. Likewise, the use of B<sub>5</sub>H<sub>8</sub><sup>-</sup> as an  $\eta^2$ -ligand was described on pp. 172-3, this involves the notional donation to a metal centre of the electron pair in a B-B bond, thus forming a BMB 3-centre bond. B<sub>5</sub>H<sub>8</sub><sup>-</sup> can also act as a notional  $\eta^1$ -donor by replacement of a terminal H atom in B<sub>5</sub>H<sub>9</sub> with a metal centre: e.g. direct reaction of B<sub>5</sub>H<sub>8</sub>Cl or B<sub>5</sub>H<sub>8</sub>Br with NaM(CO)<sub>5</sub> to give [M( $\eta^1$ -2-B<sub>5</sub>H<sub>8</sub>)(CO)<sub>5</sub>] (M = Mn, Re).

It is clear that some boranes are amphoteric Lewis acid/bases — that is they can act either as electron-pair donors as above or as electron-pair acceptors (e.g. in L.BH<sub>3</sub> and L.B<sub>3</sub>H<sub>7</sub>). It follows that a borane donor could conceivably ligate to a borane acceptor to form a borane-borane complex, i.e. a larger borane, e.g. BH<sub>4</sub><sup>-</sup> + {BH<sub>3</sub>} → B<sub>2</sub>H<sub>7</sub><sup>-</sup> (p. 154). In this sense B<sub>2</sub>H<sub>6</sub> itself could be regarded either as a coordination complex of BH<sub>4</sub><sup>-</sup> with the notional cation {BH<sub>2</sub><sup>+</sup>}, or as the mutual coordination of two monodentate {BH<sub>3</sub>} units. Replacement of these donors with stronger ligands such as NH<sub>3</sub> or NMe<sub>3</sub> would then result in either unsymmetrical or symmetrical cleavage of B<sub>2</sub>H<sub>6</sub> as discussed on p. 165. Likewise, B<sub>4</sub>H<sub>10</sub> could be regarded either as a complex between  $\eta^2$ -B<sub>3</sub>H<sub>8</sub><sup>-</sup> and {BH<sub>2</sub><sup>+</sup>} or as a mutual coordination between {B<sub>3</sub>H<sub>7</sub>} and {BH<sub>3</sub>}; reaction with stronger ligands, L, would then yield either [L<sub>2</sub>BH<sub>2</sub>]<sup>+</sup>[B<sub>3</sub>H<sub>8</sub>]<sup>-</sup> or L.B<sub>3</sub>H<sub>7</sub> and L.BH<sub>3</sub> by ligand displacement reactions (pp. 169-70).

The neutral *nido*-borane B<sub>6</sub>H<sub>10</sub> (structure 10) has a basal B-B bond (see p. 159) and this enables it to act as a ligand by displacing ethene from Zeise's salt (p. 930).



Similarly, reaction of B<sub>6</sub>H<sub>10</sub> with Fe<sub>2</sub>(CO)<sub>9</sub> (p. 1104) at room temperature results in the smooth elimination of Fe(CO)<sub>5</sub> to form [Fe( $\eta^2$ -B<sub>6</sub>H<sub>10</sub>)(CO)<sub>4</sub>] as a stable, volatile yellow solid. Use of these electron-donor properties of B<sub>6</sub>H<sub>10</sub> towards reactive (vacant orbital) borane radicals resulted in the preparation of several new *conjuncto*-boranes, e.g. B<sub>13</sub>H<sub>19</sub>, B<sub>14</sub>H<sub>22</sub> and B<sub>15</sub>H<sub>23</sub> (p. 162).

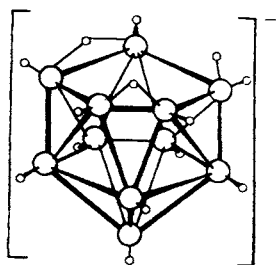
Another important concept is the notion of stabilization by means of coordination. A classic example is the stabilization of the fugitive species cyclobutadiene, {C<sub>4</sub>H<sub>4</sub>} by coordination to {Fe(CO)<sub>3</sub>} (p. 936). As the C atom is isoelectronic with {BH}, so {C<sub>4</sub>H<sub>4</sub>} is isoelectronic with the borane fragment {B<sub>4</sub>H<sub>8</sub>} which is similarly stabilized by coordination to {Fe(CO)<sub>3</sub>} or the isoelectronic {Co( $\eta^5$ -C<sub>5</sub>H<sub>5</sub>)} (see Panel on p. 174). Indeed it is a general feature of metallaborane chemistry that such clusters are often much more stable than are the parent boranes themselves.

As a result of the systematic application of coordination-chemistry principles, dozens of previously unsuspected structure types have been synthesized in which polyhedral boranes or their anions can be considered to act as ligands which donate electron density to metal centres, thereby forming novel metallaborane clusters.<sup>(36,44,45,51-54)</sup> Some 40 metals have been found to act as acceptors in this way (see also p. 178). The ideas have been particularly helpful in emphasizing the close interconnection between several previously separated branches of chemistry, notably boron hydride cluster chemistry, metallaborane and metallocarbaborane chemistry (pp. 189-95), organometallic chemistry and metal-metal cluster chemistry. All are now seen to be parts of a coherent whole.

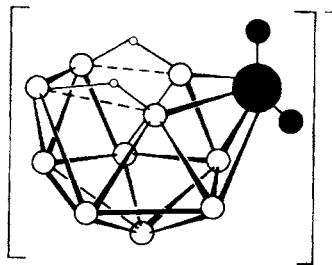
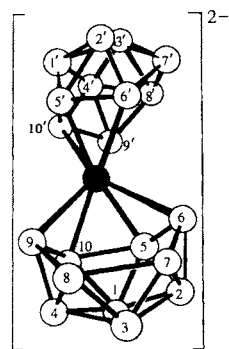
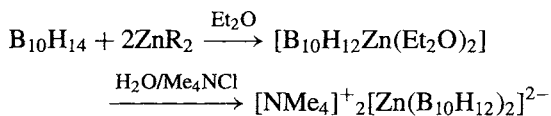
It is also noteworthy that Alfred Stock, who is universally acclaimed as the discoverer of the boron hydrides (1912),<sup>(10)</sup> was also the first to propose the use of the term "ligand" (in a lecture in Berlin on 27 November 1916).<sup>(55)</sup> Both events essentially predate the formulation by G. N. Lewis of the electronic theory of valency (1916). It is therefore felicitous that, albeit some 20 years after Stock's death in 1946, two such apparently disparate aspects of his work should be connected in the emerging concept of "boranes as ligands".

<sup>54</sup>N. N. GREENWOOD, Chap 28 in G. B. KAUFFMAN (ed.), *Coordination Chemistry: A Century of Progress* A.C.S. Symposium Series No. 565 (1994) pp. 333-45.

<sup>55</sup>A. STOCK, *Berichte* 50, 170 (1917).

(41) *nido*-B<sub>11</sub>H<sub>14</sub><sup>-</sup>

(The open face comprises a fluxional system involving the two H<sub>μ</sub> atoms and the *endo*-H<sub>1</sub> atom of the BH<sub>2</sub> group)

(42) *nido*-[B<sub>10</sub>H<sub>12</sub>TiMe<sub>2</sub>]<sup>-</sup>(43) [Zn(B<sub>10</sub>H<sub>12</sub>)<sub>2</sub>]<sup>2-</sup>

The structure of the highly reactive anion [AlB<sub>10</sub>H<sub>14</sub>]<sup>-</sup> is thought to be similar to *nido*-B<sub>11</sub>H<sub>14</sub><sup>-</sup> with one facial B atom replaced by Al. The metal alkyls react somewhat differently to give extremely stable metalloborane anions which can be thought of as complexes of the bidentate ligand B<sub>10</sub>H<sub>12</sub><sup>2-</sup> (structures 42, 43).<sup>(44,51,52)</sup> Many other complexes [M(B<sub>10</sub>H<sub>12</sub>)<sub>2</sub>]<sup>2-</sup> and [L<sub>2</sub>M(B<sub>10</sub>H<sub>12</sub>)] are known with similar structures except that, where M = Ni, Pd, Pt, the coordination about the metal is essentially square-planar rather than pseudo-tetrahedral as for Zn, Cd and Hg. Such compounds were among the first examples to be recognized of the novel and extremely fruitful perception that “electron-deficient” boranes and their anions can, in fact, act as powerful stabilizing electron-donor ligands (see Panel on p. 177).

#### 6.4.7 Chemistry of *closo*-B<sub>n</sub>H<sub>n</sub><sup>2-(1,56,57)</sup>

The structures of these anions have been indicated on p. 153. Preparative reactions are often mechanistically obscure but thermolysis under controlled conditions is the dominant

procedure (pp. 162–3). Many of the product *closo*-boranes are not degraded even when heated to 600°C. Salts of B<sub>12</sub>H<sub>12</sub><sup>2-</sup> and B<sub>10</sub>H<sub>10</sub><sup>2-</sup> are particularly stable and their reaction chemistry has been extensively studied. As expected from their charge, they are extremely stable towards nucleophiles but moderately susceptible to electrophilic attack. For B<sub>10</sub>H<sub>10</sub><sup>2-</sup> the apex positions 1,10 are substituted preferentially to the equatorial positions; reference to structure (5) shows that there are 2 geometrical isomers for monosubstituted derivatives B<sub>10</sub>H<sub>9</sub>X<sub>2</sub><sup>-</sup>, 7 isomers for B<sub>10</sub>H<sub>8</sub>X<sub>2</sub><sup>2-</sup> and 16 for B<sub>10</sub>H<sub>7</sub>X<sub>3</sub><sup>2-</sup>. Many of these isomers exist, additionally, as enantiomeric pairs. Because of its higher symmetry B<sub>12</sub>H<sub>12</sub><sup>2-</sup> has only 1 isomer for monosubstituted species B<sub>12</sub>H<sub>11</sub>X<sup>2-</sup>, 3 for B<sub>12</sub>H<sub>10</sub>X<sub>2</sub><sup>2-</sup> (sometimes referred to as *ortho*-, *meta*- and *para*-) and 5 for B<sub>12</sub>H<sub>9</sub>X<sub>3</sub><sup>2-</sup>. A particularly important derivative of B<sub>12</sub>H<sub>12</sub><sup>2-</sup> is the thiol [B<sub>12</sub>H<sub>11</sub>(SH)]<sup>2-</sup> which has found use in the treatment of brain tumours by neutron capture therapy (see Panel on next page).

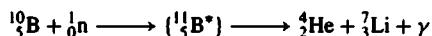
Oxidation of *closo*-B<sub>10</sub>H<sub>10</sub><sup>2-</sup> with aqueous solutions of Fe<sup>III</sup> or Ce<sup>IV</sup> (or electrochemically) yields *conjuncto*-B<sub>20</sub>H<sub>18</sub><sup>2-</sup> (44) which can be photoisomerized to *neo*-B<sub>20</sub>H<sub>18</sub><sup>2-</sup> (45). If the oxidation is carried out at 0° with Ce<sup>IV</sup>,

<sup>56</sup> E. L. MEUTTERIES and W. H. KNOTH, *Polyhedral Boranes*, Marcel Dekker, New York, 1968, 197 pp.

<sup>57</sup> R. L. MIDDAGH, Chap. 8 in ref. 9, pp. 273–300.

### Boron-10 Neutron Capture Therapy<sup>(58,59)</sup>

Every year more than 600 000 people throughout the world contract brain tumours and about 1700 die from this cause every day. Treatment by surgical excision is usually impossible because of the site of the malignant growth and the lack of a distinct boundary (gliomas). Likewise, conventional radiotherapy (X-rays, γ-rays etc.) from outside the skull is rarely effective. An ingenious approach to this problem which has given encouraging results so far is impregnation of the tumour with a suitable boron compound, followed by irradiation with thermal neutrons which readily pass harmlessly through normal tissue but are strongly absorbed by the isotope <sup>10</sup>B. As can be seen from Table 6.1 (p. 144) <sup>10</sup>B is 767 000 times more effective than <sup>11</sup>B and, in fact, has one of the highest neutron absorption cross-sections for any nuclide. The strategy is thus to synthesize cluster compounds enriched in <sup>10</sup>B, thereby enhancing the neutron absorption cross-section of the boron nearly five-fold, and then to attach these clusters to the cells comprising the brain tumour. A single injection of, say, Na<sub>2</sub>[<sup>10</sup>B<sub>12</sub>H<sub>11</sub>SH] usually suffices. Treatment with thermal neutrons from a nuclear reactor then releases huge amounts of energy right within the tumour tissue (and nowhere else) as a result of the nuclear reaction:



The recoiling α-particle (<sup>4</sup>He) and lithium nucleus (<sup>7</sup>Li) between them carry 2.4 MeV of energy and this is shed within just a few μm, the α-particle travelling about 9 μm and the Li nucleus about 5.5 μm in the opposite direction. The radiation damage is thus confined within the cancerous tissue alone.

This is a very active area of research which involves collaboration between synthetic inorganic chemists, biochemists, neurosurgeons, nuclear physicists and reactor engineers, and there is considerable scope for advance in all of these areas.<sup>(58,60,61)</sup>

or in a two-phase system with Fe<sup>III</sup> using very concentrated solutions of B<sub>10</sub>H<sub>10</sub><sup>2-</sup>, the intermediate H-bridged species B<sub>20</sub>H<sub>19</sub><sup>3-</sup> (46) can be isolated. Reduction of *conjuncto*-B<sub>20</sub>H<sub>18</sub><sup>2-</sup> with Na/NH<sub>3</sub> yields the equatorial–equatorial (ee) isomer of *conjuncto*-B<sub>20</sub>H<sub>18</sub><sup>4-</sup> (47), and this can be successively converted by acid catalyst to the ae isomer (49) and, finally, to the aa isomer (48). Careful protonation of this aa isomer yields the elusive anion [aa-B<sub>20</sub>H<sub>19</sub>]<sup>3-</sup> in which the *conjuncto* B–B bond in structure (48) is replaced by an unsupported B–H<sub>μ</sub>–B bond (angle 91(3)°, B–H<sub>μ</sub> 136(5) pm, B<sub>a</sub>···B<sub>a</sub> 193.6 pm), though the two *closo* clusters still share a common axis through their B(1)–B(10) vertices.<sup>(61a)</sup> An extensive derivative chemistry of these various

species has been developed. Another important (though mechanistically obscure) reaction of *conjuncto*-B<sub>20</sub>H<sub>18</sub><sup>2-</sup> is its degradation in high yield to *n*-B<sub>18</sub>H<sub>22</sub> by passage of an ethanolic solution through an acidic ion exchange resin; *i*-B<sub>18</sub>H<sub>22</sub> is also formed as a minor product. The relation of these 2 edge-fused decaborane clusters to the B<sub>20</sub> species is illustrated in structures (31) and (32) (p. 156).

When salts of *closo*-B<sub>10</sub>H<sub>10</sub><sup>2-</sup> and *closo*-B<sub>12</sub>H<sub>12</sub><sup>2-</sup> are passed through an acid ion exchange resin, hydrates of the strong acids H<sub>2</sub>B<sub>n</sub>H<sub>n</sub> are obtained. For example, [NEt<sub>4</sub>]<sup>+</sup><sub>2</sub>[B<sub>10</sub>H<sub>10</sub>]<sup>2-</sup> gives H<sub>2</sub>B<sub>10</sub>H<sub>10</sub>·4H<sub>2</sub>O which, on careful dehydration, yields the dihydrate, [H<sub>3</sub>O]<sup>+</sup><sub>2</sub>[B<sub>10</sub>H<sub>10</sub>]<sup>2-</sup>. Repeated low-pressure evaporation of benzene solutions of this acid at room temperature results in reductive cluster opening to give the *nido*-decaborane derivative [6,6'-(B<sub>10</sub>H<sub>13</sub>)<sub>2</sub>O] in good yield, probably via *nido*-6-B<sub>10</sub>H<sub>13</sub>(OH).<sup>(62)</sup> The structure of the readily sublimable bis(*nido*-decaboranyl) oxide,

<sup>58</sup> A. H. SOLOWAY, F. ALAM, R. F. BARTH, N. MAFUNE, B. BAPAT and D. M. ADAMS, in S. Heřmánek (ed.), *Boron Chemistry: Proc. 6th Internat. Meeting on Boron Chemistry*, World Scientific, Singapore, 1987, pp. 495–509.

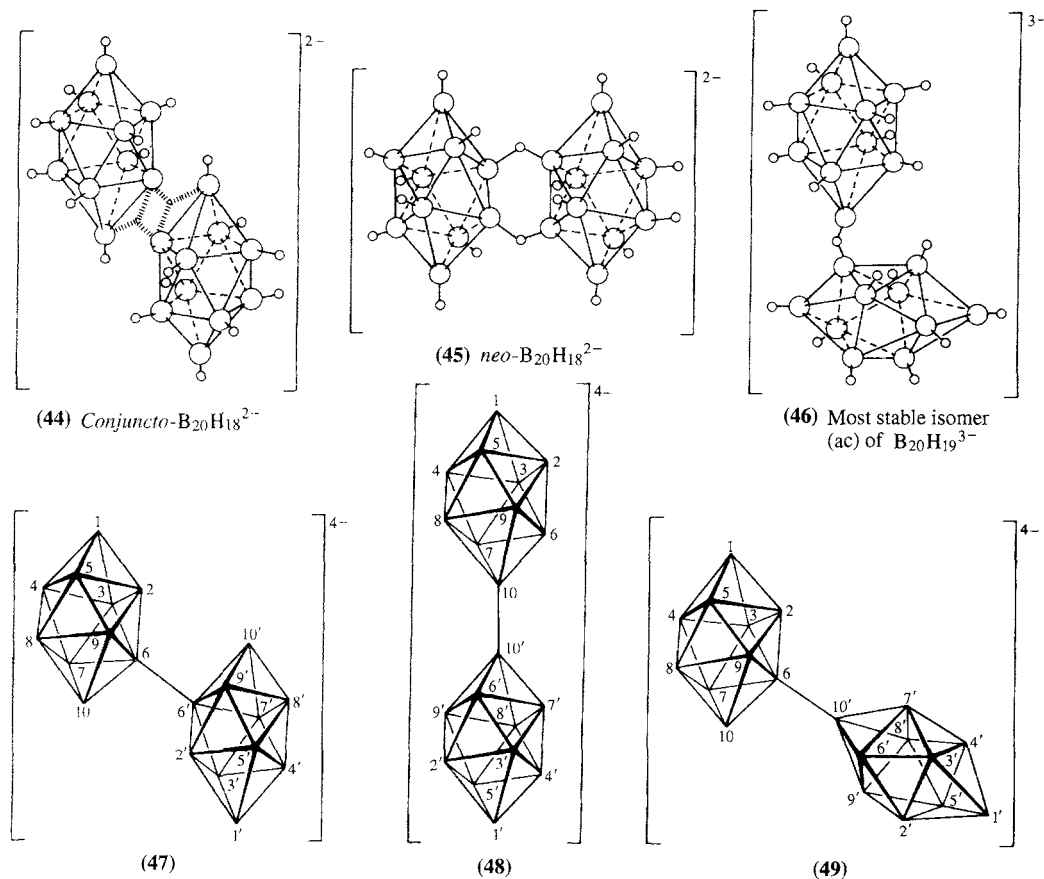
<sup>59</sup> H. HATANAKA, *Boron Neutron Capture Therapy for Tumours*, Nishimura, Niigata, Japan, 1986. R. G. FAIRCHILD, V. P. BOND and A. D. WOODHEAD (eds.), *Clinical Aspects of Neutron Capture Therapy*, Plenum, New York, 1989, 370 pp.

<sup>60</sup> M. F. HAWTHORNE, *Pure Appl. Chem.* **63**, 327–34 (1991).

<sup>61</sup> B. J. ALLEN, D. E. MOORE and B. V. HARRINGTON (eds.), *Progress in Neutron Capture Therapy for Cancer* (Proc. 4th Internat. Conf.), Plenum, New York, 1992, 668 pp.

<sup>61a</sup> R. A. WATSON-CLARK, C. B. KNOBLER and M. F. HAWTHORNE, *Inorg. Chem.* **35**, 2963–6 (1996).

<sup>62</sup> B. BONNETOT, A. TANGI, M. COLOMBIER and H. MONGEOT, *Inorg. Chem. Acta* **105**, L15–L16 (1985).

Structures of the 3 isomers of *conjuncto*- $B_{20}H_{18}^{4-}$ 

$(B_{10}H_{13})_2O$ , prepared by other routes, had previously been established by X-ray diffraction analysis<sup>(63)</sup> and by nmr spectroscopy.<sup>(64)</sup> Another interesting derivative is [*closo*-1,10- $B_{10}H_8(N_2)_2$ ] in which the apical H atoms in  $B_{10}H_{10}^{2-}$  have been replaced by end-on dinitrogen ligands (see pp. 414–6): the B–N distance is 149.9 pm and the N–N distance is 109.1 pm<sup>(65)</sup> (cf 109.8 pm in gaseous  $N_2$ ). The isoelectronic

ligand CO fulfils the same function in [*closo*-1,10- $B_{10}H_8(CO)_2$ ].<sup>(66,67)</sup> The closely related stable, volatile, icosahedral molecule [*closo*-1,12- $B_{12}H_{10}(CO)_2$ ] can be prepared by the reaction of  $H_2B_{12}H_{12} \cdot 4H_2O$  with CO at 130°C and 800–1000 atm. pressure in the presence of dicobaltoctacarbonyl as catalyst.<sup>(67)</sup> In the absence of this catalyst, approximately equal amounts of the 1,7- and 1,12-isomers are formed.

<sup>63</sup> N. N. GREENWOOD, W. S. McDONALD and T. R. SPALDING, *J. Chem. Soc., Chem. Commun.*, 1251–2 (1980).

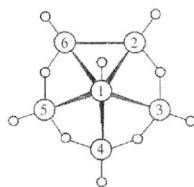
<sup>64</sup> J. D. KENNEDY and N. N. GREENWOOD, *Inorg. Chem. Acta* **38**, 93–6 (1980).

<sup>65</sup> T. WHELAN, P. BRINT, T. R. SPALDING, W. S. McDONALD and D. R. LLOYD, *J. Chem. Soc., Dalton Trans.*, 2469–73 (1982).

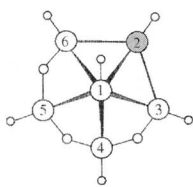
<sup>66</sup> W. H. KNOX, J. C. SAUER, H. C. MILLER and E. L. MUEITERTIES, *J. Amer. Chem. Soc.* **86**, 115–6 (1964).

<sup>67</sup> W. H. KNOX, J. C. SAUER, J. H. BALTHIS, H. C. MILLER and E. L. MUEITERTIES, *J. Amer. Chem. Soc.* **89**, 4842–50 (1967). See also P. BRINT, B. SANGCHAKR, M. MCGRATH, T. R. SPALDING and R. J. SUFFOLK, *Inorg. Chem.* **29**, 47–52 (1990) for references to more recent work.

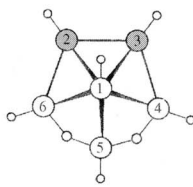




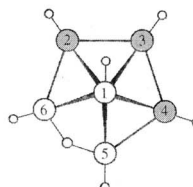
(50)  $B_6H_{10}$   
*nido*-hexaborane(10)



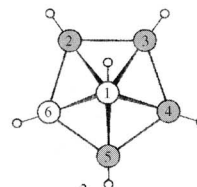
(51)  $CB_5H_9$   
2-carba-*nido*-hexaborane(9)



(52)  $C_2B_4H_8$   
2,3-dicarba-*nido*-hexaborane(8)



(53)  $C_3B_3H_7$   
2,3,4-tricarba-*nido*-hexaborane(7)



(54)  $C_4B_2H_6$   
2,3,4,5-tetracarba-*nido*-hexaborane(6)

## 6.5 Carboranes<sup>(1,17,68-71)</sup>

Carboranes burst onto the chemical scene in 1962–3 when classified work that had been done in the USA during the late 1950s was cleared for publication. The succeeding 30 y has seen a tremendous burgeoning of activity, as a result of which the carboranes and the related metallocarboranes (p. 189) now occupy a strategic position in the chemistry of the elements, since they overlap and give coherence to several other large areas including the chemistry of polyhedral boranes, transition-metal complexes, metal-cluster compounds and organometallic chemistry. The field has become so vast that it is only possible to give a few illustrative examples of the many thousands of known compounds, and to indicate the general structural features and reactivity. The vast majority of carboranes (>95%) have two C atoms in the cluster, reflecting their ready formation from alkynes (see below). A few have one C atom and there are a growing number incorporating three or even four C atoms as cluster vertices.

Carboranes (or more correctly carbaboranes) are compounds having as the basic structural unit a number of C and B atoms arranged on

the vertices of a triangulated polyhedron. Their structures are closely related to those of the isoelectronic boranes (p. 161) [ $BH \equiv B^- \equiv C$ ;  $BH_2 \equiv BH^- \equiv B.L \equiv CH$ ]. For example, *nido*- $B_6H_{10}$  (structures 10, 50) provides the basic cluster structure for the 4 carboranes  $CB_5H_9$  (51),  $C_2B_4H_8$  (52),  $C_3B_3H_7$  (53) and  $C_4B_2H_6$  (54), each successive replacement of a basal B atom by C being compensated by the removal of one  $H_\mu$ . Carboranes have the general formula  $[(CH)_a(BH)_mH_b]^{c-}$  with  $a$  CH units and  $m$  BH units at the polyhedral vertices, plus  $b$  “extra” H atoms which are either bridging ( $H_\mu$ ) or *endo* (i.e. tangential to the surface of the polyhedron as distinct from the axial  $H_t$  atoms specified in the CH and BH groups;  $H_{endo}$  occur in  $BH_2$  groups which are thus more precisely specified as  $BH_tH_{endo}$ ). It follows that the number of electrons available for skeletal bonding is  $3e$  from each CH unit,  $2e$  from each BH unit,  $1e$  from each  $H_\mu$  or  $H_{endo}$ , and  $ce$  from the anionic charge. Hence:

total number of skeletal bonding electron pairs =  $\frac{1}{2}(3a + 2m + b + c) = n + \frac{1}{2}(a + b + c)$ , where  $n (= a + m)$  is the number of occupied vertices of the polyhedron.

*closo*-structures have  $(n + 1)$  pairs of skeletal bonding electrons (i.e.  $a + b + c = 2$ ).

*nido*-structures have  $(n + 2)$  pairs of skeletal bonding electrons (i.e.  $a + b + c = 4$ ).

*arachno*-structures have  $(n + 3)$  pairs of skeletal bonding electrons (i.e.  $a + b + c = 6$ ).

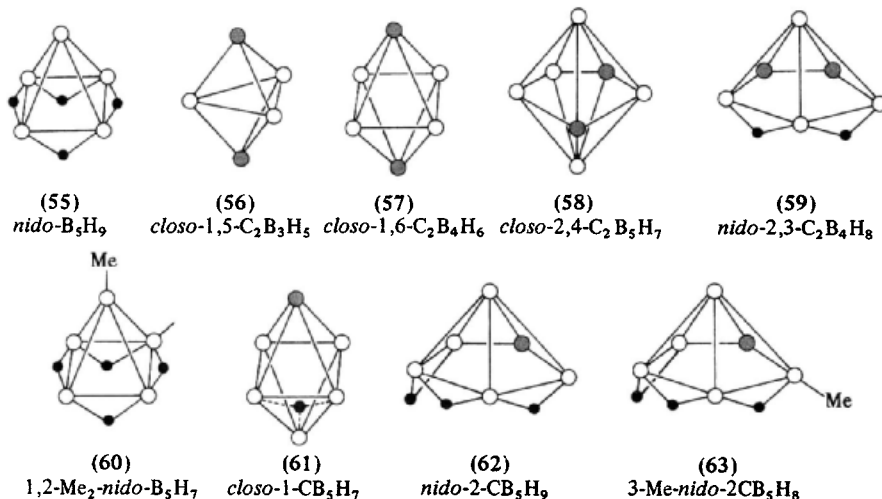
If  $a = 0$  the compound is a borane or borane anion rather than a carborane. If  $b = 0$  there are no  $H_\mu$  or  $H_{endo}$ ; this is the case for all *closo*-carboranes except for the unique octahedral

<sup>68</sup> R. N. GRIMES, *Carboranes*, Academic Press, New York, 1970, 272 pp.

<sup>69</sup> H. BEALL, Chap. 9 in ref. 9, pp. 302–47. T. ONAK, Chap. 10 in ref. 9, pp. 349–82.

<sup>70</sup> R. E. WILLIAMS, Coordination number–pattern recognition theory of carborane structures, *Adv. Inorg. Chem. Radiochem.* **18**, 67–142 (1976). R. E. WILLIAMS, Chap. 2 in G. A. OLAH, K. WADE and R. E. WILLIAMS (eds.), *Electron Deficient Boron and Carbon Clusters*, Wiley, New York, 1991, pp. 11–93.

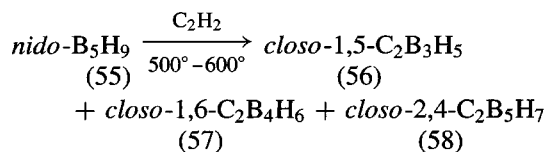
<sup>71</sup> R. N. GRIMES, *Adv. Inorg. Chem. Radiochem.* **26**, 55–117 (1983).



monocarbaborane, 1-CB<sub>5</sub>H<sub>7</sub>, which has a triply bridging H<sub>μ</sub> over one B<sub>3</sub> face of the octahedron. If *c* = 0 the compound is a neutral carborane molecule rather than an anion.

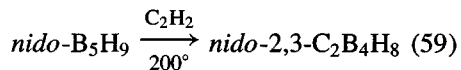
Nomenclature<sup>(12)</sup> follows the well-established oxa-aza convention of organic chemistry. Numbering begins with the apex atom of lowest coordination and successive rings or belts of polyhedral vertex atoms are numbered in a clockwise direction with C atoms being given the lowest possible numbers within these rules.†

*Closo*-carboranes are the most numerous and the most stable of the carboranes. They are colourless volatile liquids or solids (depending on mol wt.) and can be prepared from an alkyne and a borane by pyrolysis, or by reaction in a silent electric discharge. This route, which generally gives mixtures, is particularly useful for small *closo*-carboranes (*n* = 5–7) and for some intermediate *closo*-carboranes (*n* = 8–11), e.g.

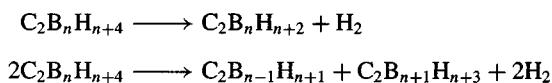


† As frequently happens in a rapidly developing field, nomenclature and numbering for the carboranes gradually evolved to cope with increasing complexity. Consequently, many systems have been used, often by the same author in successive years, and the only safe procedure is to draw a labelled diagram and convert to the preferred numbering system.

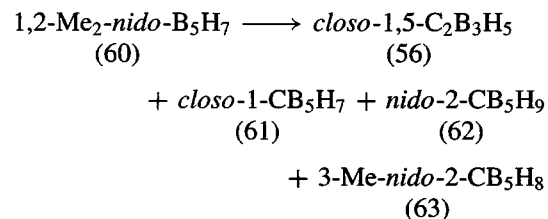
Milder conditions provide a route to *nido*-carboranes, e.g.:

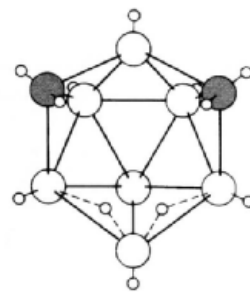
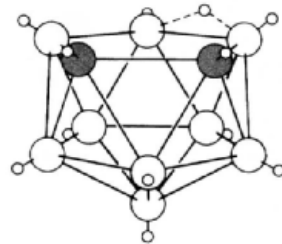
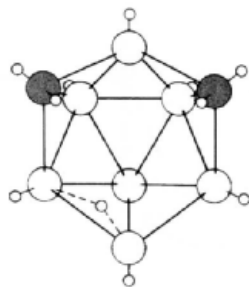
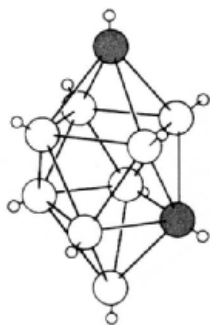


Pyrolysis of *nido*- or *arachno*-carboranes or their reaction in a silent electric discharge also leads to *closo*-species either by loss of H<sub>2</sub> or disproportionation:

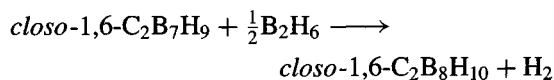
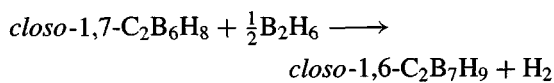


For example, pyrolysis of the previously mentioned *nido*-2,3-C<sub>2</sub>B<sub>4</sub>H<sub>8</sub> gives the 3 *closo*-species shown above, whereas under the milder conditions of photolytic closure the less-stable isomer *closo*-1,2-C<sub>2</sub>B<sub>4</sub>H<sub>6</sub> is obtained. Pyrolysis of alkyl boranes at 500–600° is a related route which is particularly useful to monocarbaboranes though the yields are often low, e.g.:

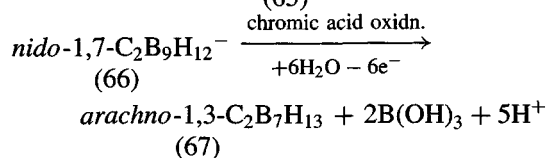
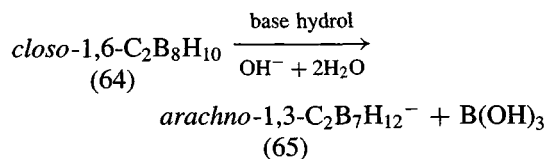


(64) *closo*-1,6-C<sub>2</sub>B<sub>8</sub>H<sub>10</sub> (65) *arachno*-1,3-C<sub>2</sub>B<sub>7</sub>H<sub>12</sub><sup>-</sup>(66) *nido*-1,7-C<sub>2</sub>B<sub>9</sub>H<sub>12</sub><sup>-</sup> (67) *arachno*-1,3-C<sub>2</sub>B<sub>7</sub>H<sub>13</sub>

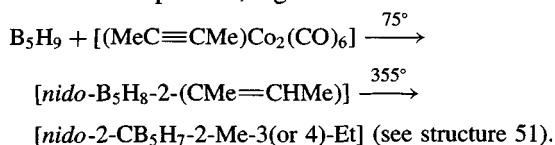
Cluster expansion reactions with diborane provide an alternative route to intermediate *closo*-carboranes, e.g.:



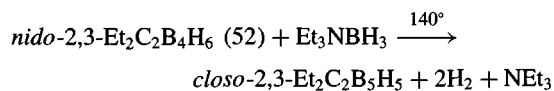
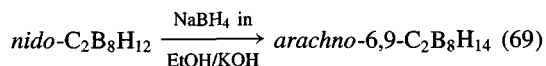
Conversely, cluster degradation reactions lead to more open structures, e.g.:



Other convenient routes to carboranes, selected from the growing number of recently reported syntheses, are as follows. Monocarbon carboranes can be prepared in good yield by the transition-metal catalysed hydroboration of alkenes followed by thermal rearrangement of the intermediate product, e.g.<sup>(72)</sup>



The two isomers are each obtained in about 30% yield. Again, the Me<sub>2</sub>S-promoted reaction of *nido*-B<sub>10</sub>H<sub>14</sub> with bis(trimethylsilyl) ethyne, Me<sub>3</sub>SiC≡CSiMe<sub>3</sub>, results in monocarbon insertion by internal hydroboration and SiMe<sub>3</sub> group migration to give [*nido*-7-CB<sub>10</sub>H<sub>11</sub>-7-((Me<sub>3</sub>Si)<sub>2</sub>CH)-9-(Me<sub>2</sub>S)] structure (68) in 28% yield.<sup>(73)</sup> New dicarbaboranes can be obtained from preformed *nido*-dicarbaboranes either by reducing them to give the corresponding *arachno* species<sup>(74)</sup> or by a capping reaction to give a *closo*-dicarbaborane,<sup>(75)</sup> e.g.



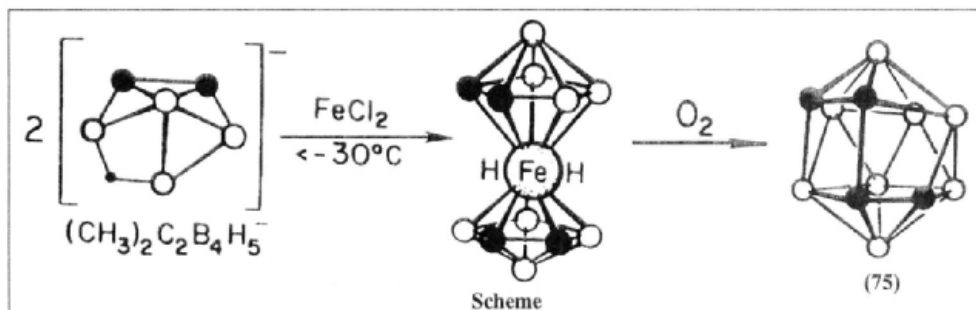
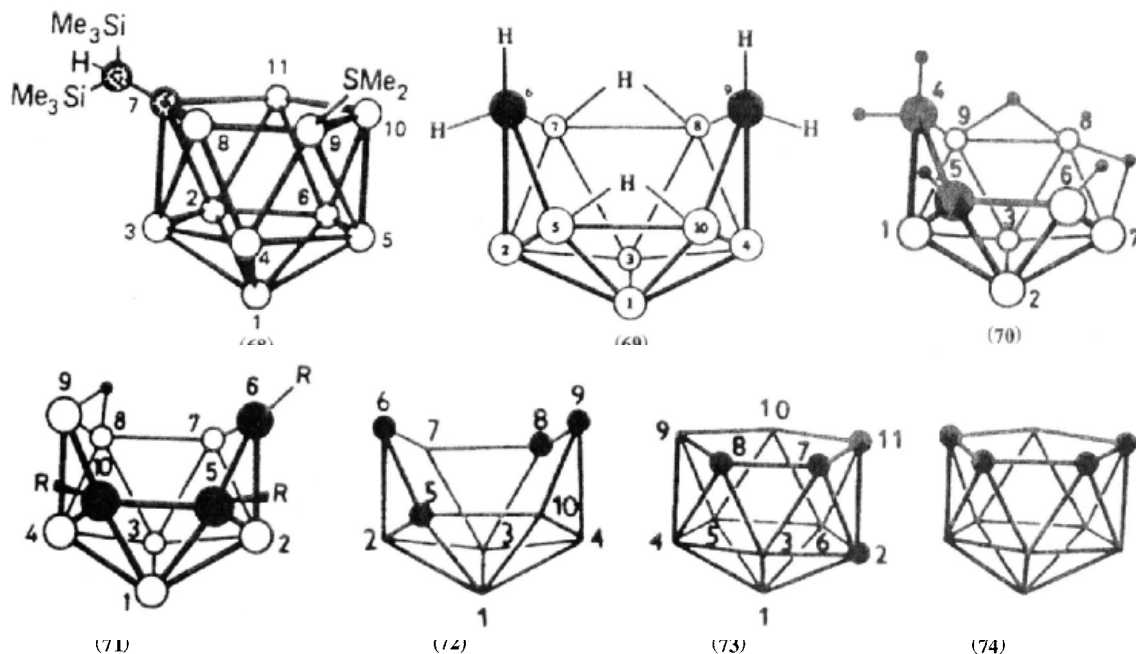
A convenient route to three-carbon carboranes is the hydroboration of an alkyne with a preformed dicarbaborane. For example,<sup>(76)</sup> reaction of ethyne (or propyne) with *arachno*-4,5-C<sub>2</sub>B<sub>7</sub>H<sub>13</sub> (70) in hexane at 120°C gives a mixture of tri- and tetra-carbaboranes, e.g. (71), (72), (73), (74) in modest yield. Access to other

<sup>72</sup> R. L. ERNEST, W. QUINTANA, R. ROSEN, P. J. CARROLL and L. G. SNEDDON, *Organometallics* **6**, 80-8 (1987).

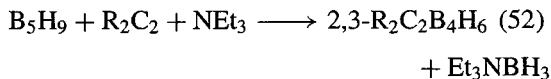
<sup>74</sup> Z. JANOUŠEK, J. PLEŠEK, S. HEŘMÁNEK and B. ŠTÍBR, *Polyhedron* **4**, 1797-8 (1985).

<sup>75</sup> J. S. BECK, A. P. KAHN and L. G. SNEDDON, *Organometallics* **5**, 2552-3 (1986).

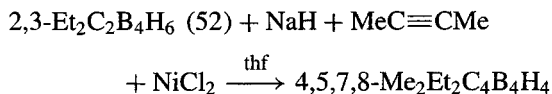
<sup>76</sup> B. ŠTÍBR, T. JELINEK, Z. JANOUŠEK, S. HEŘMÁNEK, E. DRDÁKOVÁ, Z. PLZÁK and J. PLEŠEK, *J. Chem. Soc., Chem. Commun.*, 1106-7 (1987). B. ŠTÍBR, T. JELINEK, E. DRDÁKOVÁ, S. HEŘMÁNEK and J. PLEŠEK, *Polyhedron*, **7**, 669-70 (1988).



tetracarboranes was greatly facilitated by the discovery of oxidative fusion reactions in 1974; these involve the construction of large clusters by metal-promoted face-to-face fusion of smaller clusters.<sup>(71)</sup> For example, bridge-deprotonation of 2,3- $R_2C_2B_4H_6$  (see structure 52) with alkali metal hydride, followed by treatment with  $FeCl_2$  and exposure to  $O_2$  yields the desired product  $R_4C_4B_8H_8$  (75) (see Scheme above). The starting material is available in multigram amounts via the room-temperature reaction of  $B_5H_9$  with alkynes in the presence of  $NEt_3$ :



Metal-promoted alkyne-insertion reactions afford another good method (see structure 12 for cluster geometry and numbering).<sup>(77)</sup>



<sup>77</sup> M. G. L. MIRABELLI and L. G. SNEDDON, *Organometallics* **5**, 1510-11 (1986).

### Some Further Generalizations Concerning Carboranes

1. Carbon tends to adopt the position of lowest coordination number on the polyhedron and to keep as far from other C atoms as possible (i.e. the most stable isomer has the greatest number of B-C connections).
2. Boron-boron distances in the cluster increase with increasing coordination number (as expected). Average B-B distances are: 5-coordinate B 170 pm, 6-coordinate B 177 pm, 7-coordinate B 186 pm.
3. Carbon is somewhat smaller than B and interatomic distances involving C are correspondingly shorter. Thus B-C and C-C distances are about 165 pm and 145 pm, respectively, for 5-coordinate C; the corresponding values for 6-coordinate C are 172 pm and 165 pm.
4. Negative electronic charge on B is computed to decrease in the sequence:



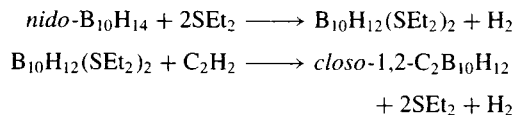
Within each group the B with lower coordination number has a greater negative charge than those with higher coordination.

5. CH groups tend to be more positive than BH groups with the same coordination number (despite the higher electronegativity of C). This presumably arises because each C contributes 3e for bonding within the cluster whereas each B contributes only 2e.
6. In *nido*- and *arachno*-carboranes  $\text{H}_\mu$  is more acidic than  $\text{H}_i$  and is the one removed on deprotonation with NaH.

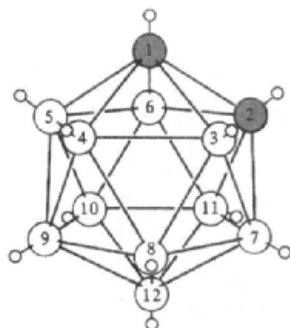
In general *nido*- (and *arachno*-) carboranes are less stable thermally than are the corresponding *closo*-compounds and they are less stable to aerial oxidation and other reactions, due to their more open structure and the presence of labile H atoms in the open face. Most *closo*-carboranes are stable to at least 400° though they may undergo rearrangement to more stable isomers in which the distance between the C atoms is increased. Some other structural and bonding generalizations are summarized in the Panel. Note, however, that kinetic control during synthesis may result in the isolation of a thermodynamically less favoured structure, with contiguous C atoms, while electronic factors in carboranes with as many as four C atoms may result in distortions or other deviations from the structures predicted on the basis

of the simple application of electron counting rules.<sup>(71)</sup>

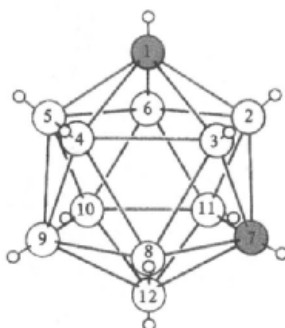
The three isomeric icosahedral carboranes (76–78) are unique both in their ease of preparation and their great stability in air, and consequently their chemistry has been the most fully studied. The 1,2-isomer in particular is available on the multikilogram scale. It is best prepared in bulk by the direct reaction of ethyne with decaborane in the presence of a Lewis base, preferably  $\text{Et}_2\text{S}$ :



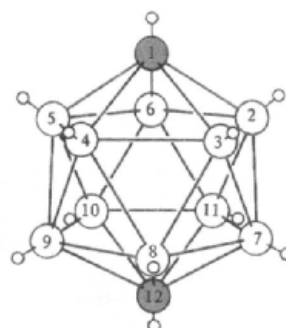
The 1,7-isomer is obtained in 90% yield by heating the 1,2-isomer in the gas phase at 470°C



(76) *ortho*-carborane,  
1,2-C<sub>2</sub>B<sub>10</sub>H<sub>12</sub> (mp 320°C)



(77) *meta*-carborane,  
1,7-C<sub>2</sub>B<sub>10</sub>H<sub>12</sub> (mp 265°C)



(78) *para*-carborane,  
1,12-C<sub>2</sub>B<sub>10</sub>H<sub>12</sub> (mp 261°C)

for several hours (or in quantitative yield by flash pyrolysis at 600° for 30 s). The 1,12-isomer is most efficiently prepared (20% yield) by heating the 1,7-isomer for a few seconds at 700°C. The mechanism of these isomerizations has been the subject of considerable speculation but definitive experiments are hard to devise. The “diamond-square-diamond” mechanism has been proposed (Fig. 6.19) for the  $1,2 \rightleftharpoons 1,7$  isomerization, but the 1,12 isomer cannot be generated by this mechanism. Moreover, the activation energy required to pass through the cubo-octahedral transition state is likely to be rather high. An alternative proposal, which could, in principle, lead to both the 1,7 and the 1,12 isomers, is the successive concerted rotation of the 3 atoms on a triangular face, and a third possible mechanism involves the concerted basal twisting of two parallel pentagonal pyramids comprising the icosahedron. Vertex extrusion to a capping position, followed by reinsertion at an adjacent site in the cluster has also been suggested. It is extremely difficult to devise experiments to test these mechanisms, but where this has been achieved (as in the case of the disubstituted derivative of (58), *closo*-5-Me-6-Cl-2,4-C<sub>2</sub>B<sub>5</sub>H<sub>6</sub>, for example) the results rule out triangular face rotation and are consistent with a “diamond-square-diamond” mechanisms.<sup>(78)</sup> It is conceivable that for other clusters the various mechanisms operate in different temperature ranges or that two (or more) mechanisms are

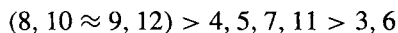
<sup>78</sup> Z. J. ABDU, G. ABDU, T. ONAK and S. LEE, *Inorg. Chem.* **25**, 2678–83 (1986).

active simultaneously. For recent definitive work on *closo*-C<sub>2</sub>B<sub>10</sub>H<sub>12</sub> see refs. 79 and 80.

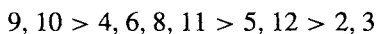
An entirely different form of isomerism, which is attracting increasing attention, is described in the Panel opposite.

An extensive derivative chemistry of the icosahedral carboranes has been developed, especially for 1,2-C<sub>2</sub>B<sub>10</sub>H<sub>12</sub>. Terminal H atoms attached to B undergo facile electrophilic substitution and the sequence of reactivity follows the sequence of negative charge density on the BH<sub>t</sub> group:<sup>(81)</sup>

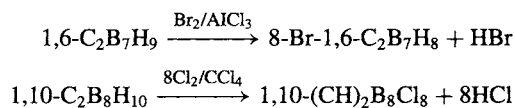
*closo*-1,2-C<sub>2</sub>B<sub>10</sub>H<sub>12</sub> :



*closo*-1,7-C<sub>2</sub>B<sub>10</sub>H<sub>12</sub> :



Similar reactions occur for other *closo*-carboranes, e.g.:

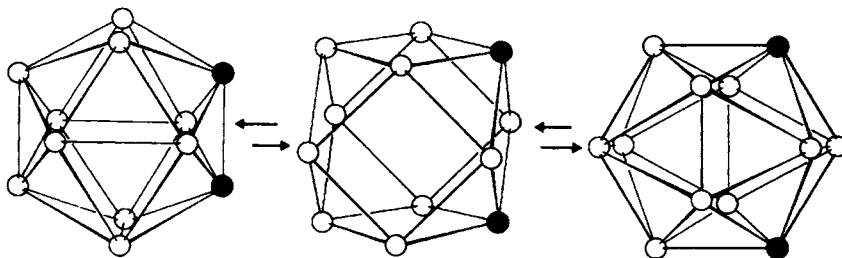


It is noteworthy that, despite the greater electronegativity of C, the CH group tends to be more

<sup>79</sup> S.-H. WU and M. JONES *J. Amer. Chem. Soc.* **111**, 5373–84 (1989).

<sup>80</sup> G. M. EDVENSON and D. F. GAINES *Inorg. Chem.* **29**, 1210–16 (1990).

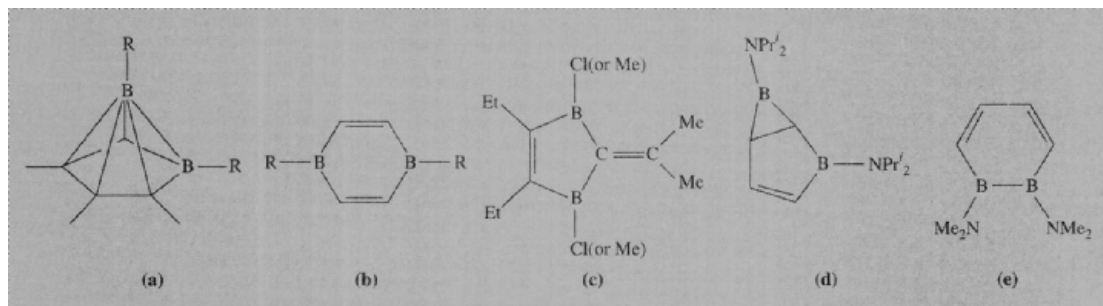
<sup>81</sup> D. A. DIXON, D. A. KLEIR, T. A. HALGREN, J. H. HALL and W. N. LIPSCOMB, *J. Am. Chem. Soc.* **99**, 6226–37 (1977).



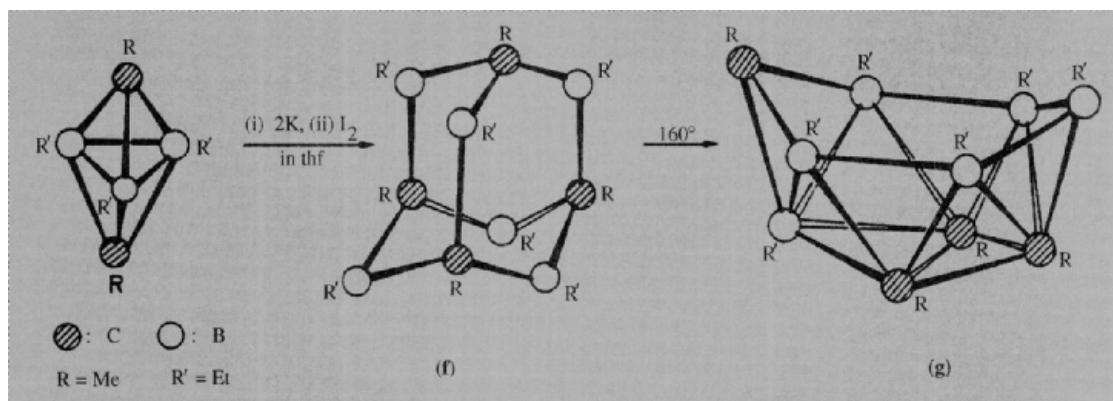
**Figure 6.19** The interconversion of 1,2- and 1,7-disubstituted icosahedral species via a proposed cubo-octahedral intermediate formed during four “diamond-square-diamond” rearrangements.

### “Classical-Nonclassical” Valence Isomerism

A novel and far-reaching type of isomerism concerns the possibility of valence isomerism between “nonclassical” (electron-deficient) clusters and “classical” organoboron structures. Thus,  $n$ -vertexed *nido*-boranes,  $B_nH_{n+4}$ , have cluster structures with  $4H_\mu$  — cf. (9), (10), (11) — whereas the precisely isoelectronic  $n$ -vertexed *nido*-tetracarboranes,  $C_4B_{n-4}H_n$ , have no bridging H atoms and can, in principle, adopt either a cluster borane structure or one of several classical organic structures. For example, derivatives of  $C_4B_2H_6$  could adopt either the *nido*-2,3,4,5-tetracarbahexaborane structure (a) — i.e. (54) — or the 1,4-dibora-2,5-cyclohexadiene structure (b). As might be expected, the 3-coordinate B atoms in (b) are stabilized by  $\pi$ -donor substituents (e.g. R = F, OMe) whereas when R = alkyl, rearrangement to the *nido*-carbaborane (a) occurs.<sup>(82)</sup> The novel diborafulvene isomer (c) has also been synthesized in good yield<sup>(82,83)</sup> and two other isomers, (d) and (e) have been stabilized as ligands in Ru- and Rh-complexes.



Similar possibilities arise for 10-atom clusters. Thus, dimerization of the *closo*- $C_2B_3$  cluster 1,5- $Me_2C_2B_3Et_3$  (56) by means of K metal then  $I_2$  in thf yields the “classical” adamantane derivative  $Me_4C_4B_6Et_6$  (f); when this is heated to  $160^\circ$  the *nido*-tetracarbadecaborane cluster (g) is obtained rapidly and quantitatively.<sup>(84)</sup> It will be noted that in (f) all four C atoms are 4-coordinate and all six B atoms are 3-coordinate, whereas in (g) the three C atoms in the  $C_3$  triangular face are 5-coordinate while the boron atoms are variously 4, 5 or 6 coordinate.



<sup>82</sup>V. SCHÄFER, H. PRITZKOW and W. SIEBERT, *Angew. Chem. Int. Edn. Engl.* **27**, 299–300 (1988) and references cited therein. See also B. WRACKMEYER and G. KEHR, *Polyhedron* **10**, 1497–506 (1991).

<sup>83</sup>G. E. HERBERICH, H. OHST and H. MAYER, *Angew. Chem. Int. Edn. Engl.* **23**, 969–70 (1984).

<sup>84</sup>R. KÖSTER, G. SEIDEL and B. WRACKMEYER, *Angew. Chem. Int. Edn. Engl.* **24**, 326–7 (1985).

positive than the BH groups and does not normally react under these conditions.

The weakly acidic  $\text{CH}_i$  group can be deprotonated by strong nucleophiles such as  $\text{LiBu}$  or  $\text{RMgX}$ ; the resulting metalated carboranes  $\text{LiCCHB}_{10}\text{H}_{10}$  and  $(\text{LiC})_2\text{B}_{10}\text{H}_{10}$  can then be used to prepare a full range of C-substituted derivatives  $-\text{R}$ ,  $-\text{X}$ ,  $-\text{SiMe}_3$ ,  $-\text{COOH}$ ,  $-\text{COCl}$ ,  $-\text{CONHR}$ , etc. The possibility of synthesizing extensive covalent C-C or siloxane networks with pendant carborane clusters is obvious and the excellent thermal stability of such polymers has already been exploited in several industrial applications.

Although *closo*-carboranes are stable to high temperatures and to most common reagents, M. F. Hawthorne showed (1964) that they can

be specifically degraded to *nido*-carborane anions by the reaction of strong bases in the presence of protonic solvents, e.g.:

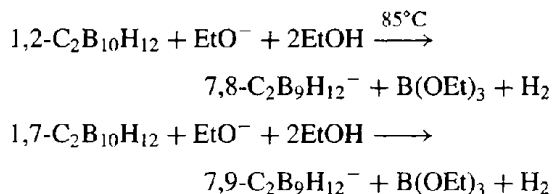


Figure 6.20 indicates that, in both cases, the BH vertex removed is the one adjacent to the two CH vertices: since the C atoms tend to remove electronic charge preferentially from contiguous B atoms, the reaction can be described as a nucleophilic attack by  $\text{EtO}^-$  on the most positive (most electron deficient) B atom in the

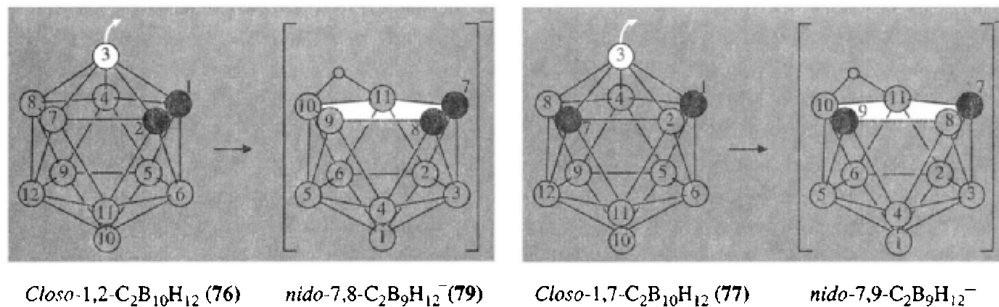


Figure 6.20 Degradation of *closo*-carboranes to the corresponding debor-*nido*-carborane anions.

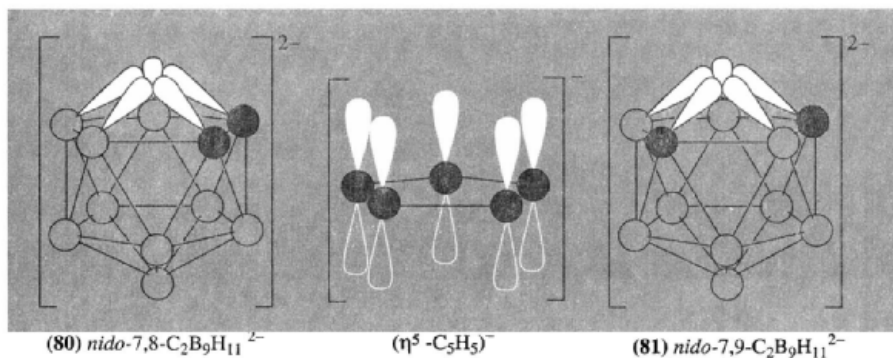


Figure 6.21 Relation between  $\text{C}_2\text{B}_9\text{H}_{11}^{2-}$  and  $\text{C}_5\text{H}_5^-$ . In this formalism the *closo*-carboranes  $\text{C}_2\text{B}_{10}\text{H}_{12}$  are considered as a coordination complex between the pentahapto 6-electron donor  $\text{C}_2\text{B}_9\text{H}_{11}^{2-}$  and the acceptor  $\text{BH}^{2+}$  (which has 3 vacant orbitals). The *closo*-structure can be regained by capping the open pentagonal face with an equivalent metal acceptor that has 3 vacant orbitals.



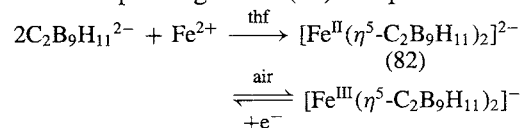
cluster. Deprotonation of the monoanions by NaH removes the bridge proton to give the *nido*-dianions  $7,8\text{-C}_2\text{B}_9\text{H}_{11}^{2-}$  (80) and  $7,9\text{-C}_2\text{B}_9\text{H}_{11}^{2-}$  (81). It was the perceptive recognition that the open pentagonal faces of these dianions were structurally and electronically equivalent to the pentahapto cyclopentadienide anion  $(\eta^5\text{-C}_5\text{H}_5)^-$  (Fig. 6.21) that led to the discovery of the metallocarboranes and the development of some of the most intriguing and far-reaching reactions of the carboranes. These are considered in the next section.

## 6.6 Metallocarboranes<sup>(1,17,85–90)</sup>

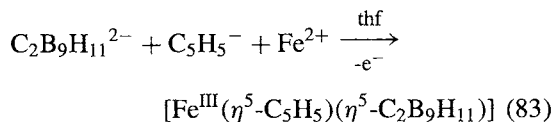
There are now at least a dozen synthetic routes to metallocarboranes including (i) coordination using *nido*-carborane anions as ligands, (ii) polyhedral expansion reactions, (iii) polyhedral contraction reactions, (iv) polyhedral subrogation and (v) thermal metal transfer reactions. These first five routes were all devised by M. F. Hawthorne and his group in the period 1965–74 and have since been extensively exploited and extended by several groups. Examples of each will be given before mentioning some of the more recent routes that have been developed. It is worth noting that the carborane dianions (80) and (81) are both more effective as ligands than is  $\eta^5\text{-C}_5\text{H}_5^-$ , perhaps because of the more favourable angles of the orbitals, the lower electronegativity of boron and the higher formal anionic charge. Thus, the carboranes form stable sandwich complexes with  $\text{Cu}^{\text{II}}$ ,  $\text{Al}^{\text{III}}$  and

$\text{Si}^{\text{IV}}$ , for example, whereas cyclopentadienyl does not.<sup>(90,91)</sup>

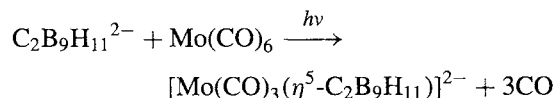
(i) *Coordination using nido-carborane anions as ligands* (1965). Reaction of  $\text{C}_2\text{B}_9\text{H}_{11}^{2-}$  with  $\text{FeCl}_2$  in tetrahydrofuran (thf) with rigorous exclusion of moisture and air gives the pink, diamagnetic bis-sandwich-type complex of  $\text{Fe}(\text{II})$  (structure 82) which can be reversibly oxidized to the corresponding red  $\text{Fe}(\text{III})$  complex:



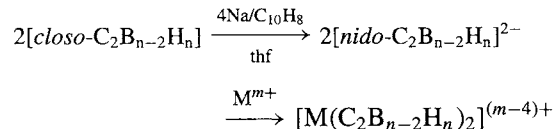
When the reaction is carried out in the presence of  $\text{NaC}_5\text{H}_5$  the purple mixed sandwich complex (83) is obtained:



The reaction is general and has been applied to many transition metals as well as lanthanides and actinides.<sup>(92)</sup> Variants use metal carbonyls and other complexes to supply the capping unit, e.g.



(ii) *Polyhedral expansion* (1970). This entails the 2-electron reduction of a *closo*-carborane with a strong reducing agent such as sodium naphthalide in thf followed by reaction with a transition-metal reagent:



The reaction, which is quite general for *closo*-carboranes, involves the reductive opening of an *n*-vertex *closo*-cluster followed by metal

<sup>85</sup> R. N. GRIMES, *Pure Appl. Chem.* **39**, 455–74 (1974).

<sup>86</sup> K. P. CALLAHAN and M. F. HAWTHORNE, *Pure Appl. Chem.* **39**, 475–95 (1974).

<sup>87</sup> G. B. DUNKS and M. F. HAWTHORNE, Chap. 11 in ref. 9, pp. 383–430.

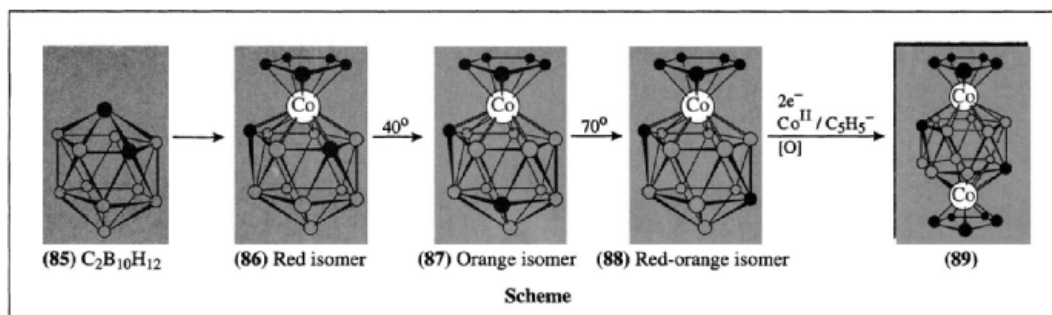
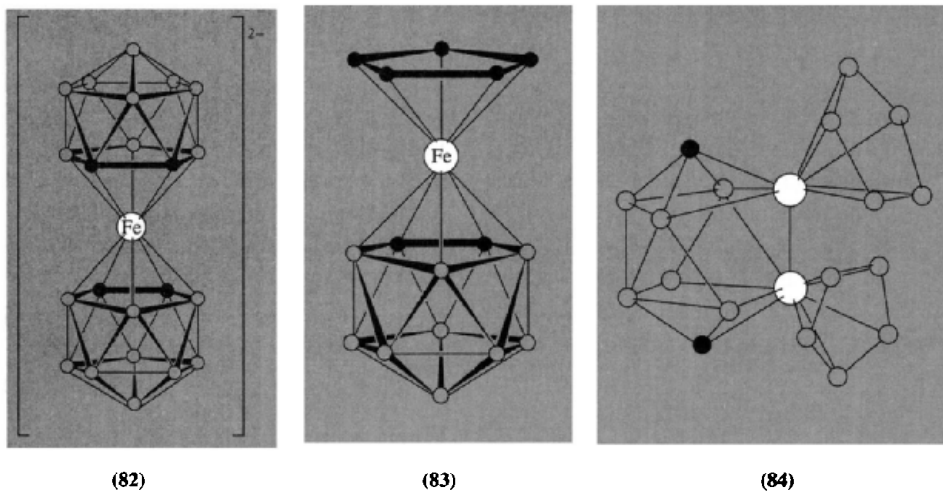
<sup>88</sup> K. P. CALLAHAN and M. F. HAWTHORNE, *Adv. Organometallic Chem.* **14**, 145–86 (1976).

<sup>89</sup> R. N. GRIMES, Chap. 2 in E. BECHER and M. TSUTSUI (eds.), *Organometallic Reactions and Syntheses* **6**, 63–221 (1977).

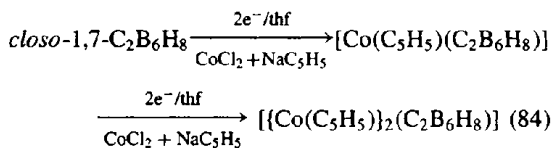
<sup>90</sup> D. M. SCHUBERT, M. A. BANDMAN, W. S. REES, C. B. KNOBLER, P. LU, W. NAM and M. F. HAWTHORNE, *Organometallics* **9**, 2046–61 (1990), and refs. cited therein.

<sup>91</sup> D. M. SCHUBERT, W. S. REES, C. B. KNOBLER and M. F. HAWTHORNE, *Organometallics* **9**, 2938–44 (1990), and refs. cited therein.

<sup>92</sup> M. J. MANNING, C. B. KNOBLER and M. F. HAWTHORNE, *J. Am. Chem. Soc.* **110**, 4458–9 (1988).



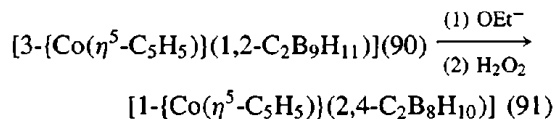
insertion to give an  $(n + 1)$ -vertex *closo*-cluster. Numerous variants are possible including the insertion of a second metal centre into an existing metalloborane, e.g.:



The structure of the bimetallic 10-vertex cluster was shown by X-ray diffraction to be (84). When the icosahedral carborane 1,2-C<sub>2</sub>B<sub>10</sub>H<sub>12</sub> was used, the reaction led to the first supraicosahedral metalloboranes with 13- and 14-vertex polyhedral structures (85)–(89). Facile isomerism of the 13-vertex monometalloboranes was observed as indicated in the scheme above (in which ● = CH and ○ = BH).

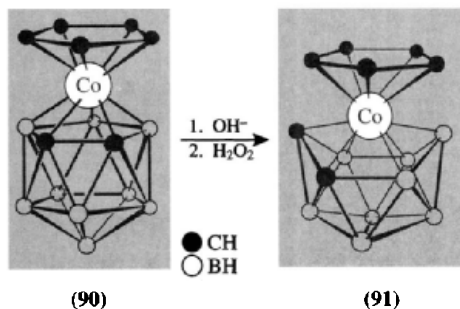
(iii) *Polyhedral contraction* (1972). This involves the clean removal of one BH group from

a *closo*-metalloborane by nucleophilic base degradation, followed by oxidative closure of the resulting *nido*-metalloborane complex to a *closo*-species with one vertex less than the original, e.g.:

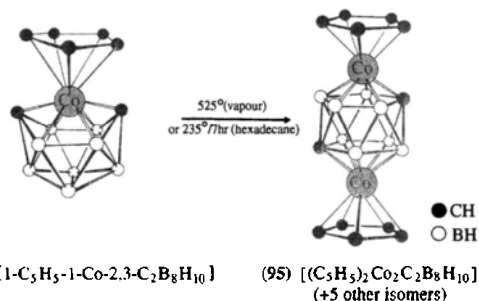


Polyhedral contraction is not so general a method of preparing metalloboranes as is polyhedral expansion since some metalloboranes degrade completely under these conditions.

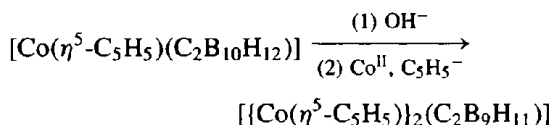
(iv) *Polyhedral subrogation* (1973). Replacement of a BH vertex by a metal vertex without changing the number of vertices in the cluster is termed polyhedral subrogation. It is an offshoot of the polyhedral contraction route in that degradative removal of the BH unit is followed by reaction with a transition metal ion rather than



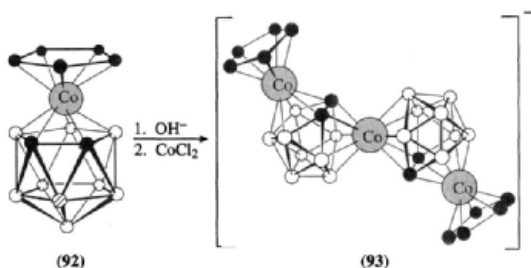
Similarly:



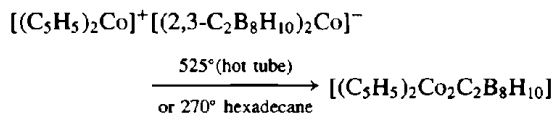
with an oxidizing agent, e.g.:



The method is clearly of potential use in preparing mixed metal clusters, e.g. (Co + Ni) or (Co + Fe), and can be extended to prepare more complicated cluster arrays as depicted below, the subrogated B atom being indicated as a shaded circle in (92).

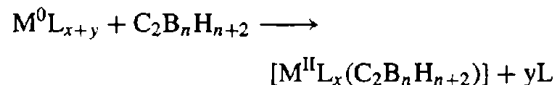


(v) *Thermal metal transfer* (1974). This method is less general and often less specific than the coordination of *nido*-anions or polyhedral expansion; it involves the pyrolysis of pre-existing metallocarboranes and consequent cluster expansion or disproportionation similar to that of the *closo*-carboranes themselves (p. 182). Mixtures of products are usually obtained, e.g.:

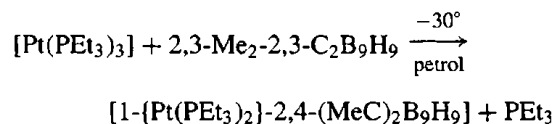


A related technique (R. N. Grimes, 1973) is direct metal insertion by gas-phase reactions at elevated temperatures; typical reactions are shown in the scheme (p. 192). The reaction with  $[Co(\eta^5-C_5H_5)(CO)_2]$  also gave the 7-vertex *closo*-bimetallocarborane (101) which can be considered as a rare example of a triple-decker sandwich compound; another isomer (102) can be made by base degradation of  $[[Co(\eta^5-C_5H_5)](C_2B_4H_6)]$  followed by deprotonation and subrogation with a second  $[Co(\eta^5-C_5H_5)]$  unit.<sup>(85)</sup> It will be noted that the central planar formal  $C_2B_3H_5^{4-}$  unit is isoelectronic with  $C_5H_5^-$ .

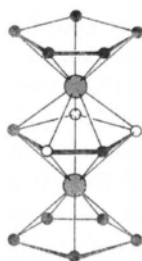
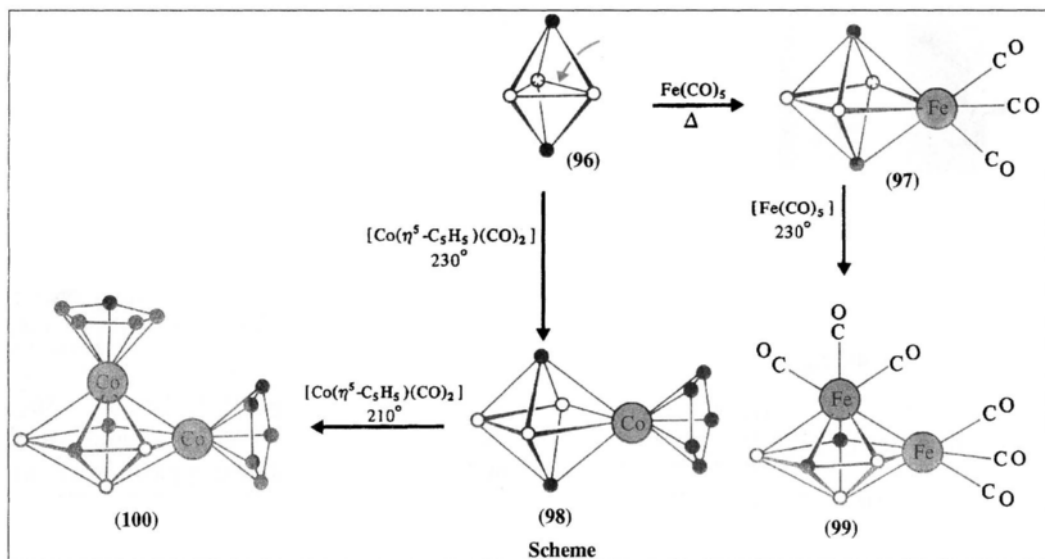
A particularly elegant route to metallocarboranes is the *direct oxidative insertion of a metal centre* into a *closo*-carborane cluster: the reaction uses zero-valent derivatives of Ni, Pd and Pt in a concerted process which involves a net transfer of electrons from the nucleophilic metal centre to the cage.<sup>(93)</sup>



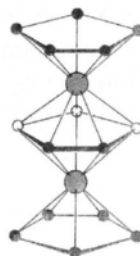
where  $L = PR_3, C_8H_{12}, RNC$ , etc. A typical reaction is



<sup>93</sup> F. G. A. STONE, *J. Organometallic Chem.* **100**, 257–71 (1975).

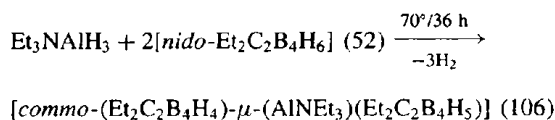
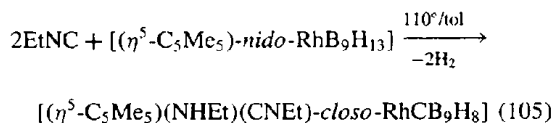
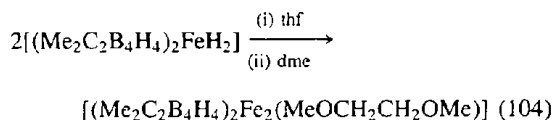
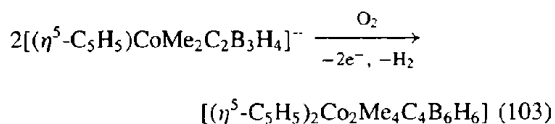


(101)



(102)

Many novel cluster compounds have now been prepared in this way, including mixed metal clusters. Further routes involve the *oxidative fusion of dicarbon metallacarborane anions* to give dimetal tetracarborane clusters such as (103) and (104);<sup>(71)</sup> the *insertion of isonitriles into metallaborane clusters* to give monocarbon metallacarboranes such as (105);<sup>(94)</sup> and the reaction of small *nido*-carboranes with alane adducts such as  $\text{Et}_3\text{NAlH}_3$  to give the *commo* species (106);<sup>(95)</sup>

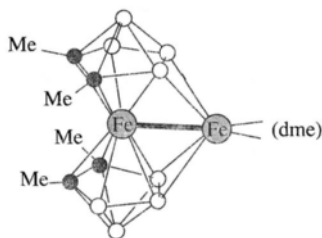


<sup>94</sup> E. J. DITZEL, X. L. R. FONTAINE, N. N. GREENWOOD, J. D. KENNEDY, Z. SISAN, B. ŠTÍBR and M. THORNTON-PETT, *J. Chem. Soc., Chem. Commun.*, 1741–3 (1990). See also N. N. GREENWOOD and J. D. KENNEDY, *Pure Appl. Chem.* **63**, 317–26 (1991) and refs. therein.

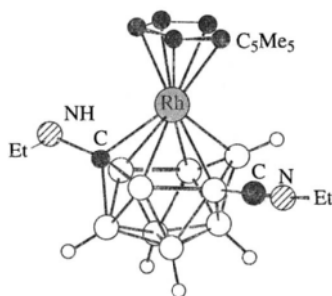
<sup>95</sup> J. S. BECK and L. G. SNEDDON, *J. Am. Chem. Soc.* **110**, 3467–72 (1988).



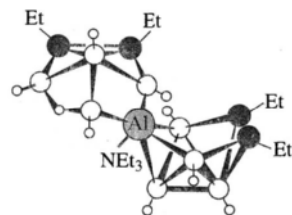
(103)



(104)



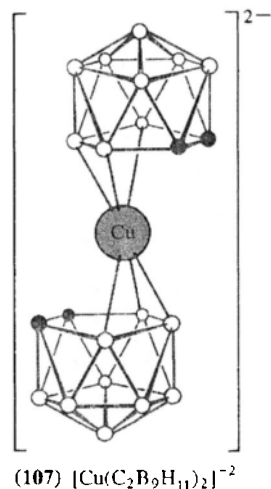
(105)



(106)

Numerous other aluminacarborane structural types have also recently been synthesized by a variety of routes<sup>(91)</sup> and, indeed, the burgeoning field of metallocarborane chemistry now encompasses the whole Periodic Table with an almost bewildering display of exotic and unprecedented structural types.

The electron-counting rules outlined for boranes (p. 161) and carboranes (p. 181) can readily be extended to the metallocarboranes (see Panel on next page). For bis-complexes of 1,2-C<sub>2</sub>B<sub>10</sub>H<sub>11</sub><sup>2-</sup> which can be regarded as a 6-electron penta-hapto ligand, it has been found that "electron-sufficient" (18-electron) systems such as those involving d<sup>6</sup> metal centres (e.g. Fe<sup>II</sup>, Co<sup>III</sup> or Ni<sup>IV</sup>) have symmetrical structures with the metal atom equidistant from the 2 C and 3 B atoms in the pentagonal face. The same is true for "electron-deficient" systems such as those involving d<sup>2</sup> Ti<sup>II</sup> (14-electron), d<sup>3</sup> Cr<sup>III</sup> (15-electron), etc., though here the metal-cluster bonds are somewhat longer. With "electron excess" complexes such as [Ni<sup>II</sup>(C<sub>2</sub>B<sub>10</sub>H<sub>11</sub>)<sub>2</sub>]<sup>2-</sup> and the corresponding complexes of Pd<sup>II</sup>, Cu<sup>III</sup> and Au<sup>III</sup> (20 electrons), so-called "slipped-sandwich" structures (107) are observed in which the metal atom is significantly closer to the 3 B atoms than to the 2 C atoms. This has been thought by some to indicate π-allylic bonding to the 3 B but is more likely to arise from an occupation of orbitals that are antibonding with respect to both the metal and the cluster thereby leading to an opening of the 12-vertex

(107) [Cu(C<sub>2</sub>B<sub>9</sub>H<sub>11</sub>)<sub>2</sub>]<sup>2-</sup>

*closo*-structure to a pseudo-*nido* structure in which the 12 atoms of the cluster occupy 12 vertices of a 13-vertex polyhedron.<sup>(96)</sup> A similar type of distortion accompanies the use of metal centres with increasing numbers of electron-pairs on the metal and it seems that these electrons may also, at least in part, contribute to the framework electron count with consequent cluster opening.<sup>(97)</sup> Thus, progressive opening of the

<sup>96</sup> D. M. P. MINGOS, M. I. FORSYTH and A. J. WELCH, *J. Chem. Soc., Chem. Commun.*, 605-7 (1977). See also G. K. BARKER, M. GREEN, F. G. A. STONE and A. J. WELCH, *J. Chem. Soc., Dalton Trans.*, 1186-99 (1980); D. M. P. MINGOS and A. J. WELCH, *ibid.* 1674-81.

<sup>97</sup> H. M. COLQUHOUN, T. J. GREENHOUGH and M. G. H. WALLBRIDGE, *J. Chem. Soc., Chem. Commun.*, 737-8 (1977); see also H. M. COLQUHOUN, T. J. GREENHOUGH

## Electron-counting Rules for Metallocarboranes and Other Heteroboranes

As indicated on pp. 161 and 174 each framework atom (except H) uses 3 atomic orbitals (AOs) in cluster bonding. For B, C, and other first-row elements this leaves one remaining AO to bond exopolyhedrally to  $-H$ ,  $-X$ ,  $-R$ , etc. In contrast, transition elements have a total of 9 valence AOs (five d, one s, three p). Hence, after contributing 3 AOs to the cluster, they have 6 remaining AOs which can be used for bonding to external ligands and for storage of nonbonding electrons. In *closo*-clusters the  $(n + 1)$  MOs require  $(2n + 2)$  electrons from the B, C and M vertex atoms. In its simplest form the electron counting scheme invokes only the total number of framework MOs and electrons, and requires no assumptions as to orbital hybridization or formal oxidation state. For example, the neutral moiety  $\{Fe(CO)_3\}$  has 8 Fe electrons and 9 Fe AOs: since 3 AOs are involved in bonding to 3 CO and 3 AOs are used in cluster bonding, there remain 3 AOs which can accommodate 6 (nonbonding) Fe electrons, leaving 2 Fe electrons to be used in cluster bonding. Neutral  $\{Fe(CO)_3\}$  is thus precisely equivalent to  $\{BH\}$ , as distinct from  $\{CH\}$ , which provides 3 electrons for the cluster. Other groups such as  $\{Co(\eta^5-C_5H_5)\}$  and  $\{Ni(CO)_2\}$  are clearly equivalent to  $\{Fe(CO)_3\}$ .

An alternative scheme that is qualitatively equivalent is to assign formal oxidation states to the metal moiety and to consider the bonding as coordination from a carborane ligand, e.g.  $\{Fe(CO)_3\}^{2+} \eta^5$ -bonded to a cyclocarborane ring as in  $\{C_2B_9H_{11}\}^{2-}$ . This is acceptable when the anionic ligand is well characterized as an independent entity, as in the case just cited, but for many metallocarboranes the "ligands" are not known as free species and the presumed anionic charge and metal oxidation state become somewhat arbitrary. It is therefore recommended that the metalborane cluster be treated as a single covalently bonded structure with no artificial separation between the metal and the rest of the cluster; electron counting can then be done unambiguously on the basis of neutral atoms and attached groups.

To the structural generalizations on carboranes (p. 185) can be added the rule that, in metallocarboranes, the M atom tends to adopt a vertex with high coordination number: M occupancy of a low CN vertex is not precluded, particularly in kinetically controlled syntheses, but isomerization to more stable configurations usually results in the migration of M to high CN vertices.

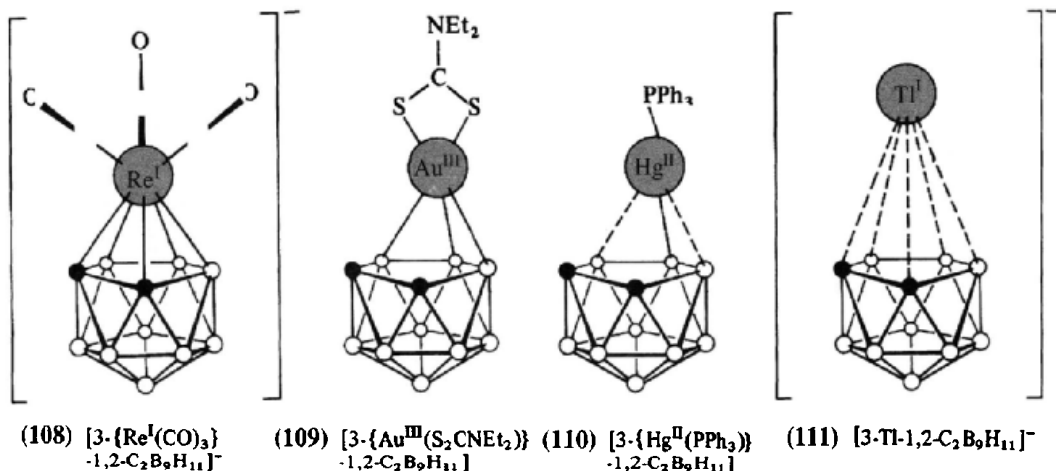
Other main-group atoms besides C can occur in heteroborane clusters and the electron-counting rules can readily be extended to them.<sup>(17)</sup> Thus, whereas each  $\{BH\}$  contributes 2 e and  $\{CH\}$  contributes 3 e to the cluster, so  $\{NH\}$  or  $\{PH\}$  contributes 4 e,  $\{SH\}$  contributes 5 e,  $\{S\}$  contributes 4 e, etc. For example, the following 10-vertex thiaboranes (and their isoelectronic equivalents) are known: *closo*-1-SB<sub>9</sub>H<sub>9</sub> ( $B_{10}H_{10}^{2-}$ ), *nido*-6-SB<sub>9</sub>H<sub>11</sub> ( $B_{10}H_{13}^-$ ) and *arachno*-6-SB<sub>9</sub>H<sub>12</sub> ( $B_{10}H_{14}^{2-}$ ). Similarly, the structures of 12-, 11- and 9-vertex thiaboranes parallel those of boranes and carbaboranes with the same skeletal electron count, the S atom in each case contributing 4 electrons to the framework plus an *exo*-polyhedral lone-pair.

cluster is noted for complexes of 1,2-C<sub>2</sub>B<sub>9</sub>H<sub>11</sub><sup>2-</sup> with Re<sup>I</sup> (d<sup>6</sup>), Au<sup>III</sup> (d<sup>8</sup>), Hg<sup>II</sup> (d<sup>10</sup>) and Tl<sup>I</sup> (d<sup>10</sup>s<sup>2</sup>) as shown in structures (108)–(111). Thus the Re<sup>I</sup> (d<sup>6</sup>) complex (108) is a symmetrically bonded 12-vertex cluster with Re–B 234 pm and Re–C 231 pm. The Au<sup>III</sup> (d<sup>8</sup>) complex (109) has the metal appreciably closer to the 3 B atoms (221 pm) than to the 2 C atoms (278 pm). With the Hg<sup>II</sup> (d<sup>10</sup>) complex (110) this distortion is even more pronounced and the metal is pseudo-σ-bonded to 1 B atom at 220 pm; there is

some additional though weak interaction with the other 2 B (252 pm) but the two Hg...C distances (290 pm) are essentially nonbonding. Finally, the Tl<sup>I</sup> (d<sup>10</sup>s<sup>2</sup>) complex (111), whilst having the Tl atom more symmetrically located above the open face, has Tl–cluster distances that exceed considerably the expected covalent Tl<sup>I</sup>–B distance of ~236 pm; the shortest Tl–B distance is 266 pm and there are two other Tl–B at 274 pm and two Tl–C at 292 pm: the species can thus be regarded formally as being closer to an ion pair  $[Tl^+(C_2B_9H_{11})^{2-}]$ .

In general, metallocarboranes are much less reactive (more stable) than the corresponding metallocenes and they tend to stabilize higher oxidation states of the later transition metals, e.g.  $[Cu^{II}(1,2-C_2B_9H_{11})_2]^{2-}$  and  $[Cu^{III}(1,2-C_2B_9H_{11})_2]^-$  are known whereas cuprocene

and M. G. H. WALLBRIDGE, *J. Chem. Soc., Chem. Commun.*, 1019–20 (1976); 737–8 (1977); *J. Chem. Soc., Dalton Trans.*, 619–28 (1979); *J. Chem. Soc., Chem. Commun.*, 192–4 (1980); G. K. BARKER, M. GREEN, F. G. A. STONE, A. J. WELCH and W. C. WOLSEY, *J. Chem. Soc., Chem. Commun.*, 627–9 (1980), K. NESTOR, B. ŠTIBR, T. JELÍNEK and J. D. KENNEDY, *J. Chem. Soc., Dalton Trans.*, 1661–3 (1993).



$[\text{Cu}^{\text{II}}(\eta^5\text{-C}_5\text{H}_5)_2]$  is not. Likewise,  $\text{Fe}^{\text{III}}$  and  $\text{Ni}^{\text{IV}}$  carborane derivatives are extremely stable. Conversely, metallocarboranes tend to stabilize lower oxidation states of early transition elements and complexes are well established for  $\text{Ti}^{\text{II}}$ ,  $\text{Zr}^{\text{II}}$ ,  $\text{Hf}^{\text{II}}$ ,  $\text{V}^{\text{II}}$ ,  $\text{Cr}^{\text{II}}$  and  $\text{Mn}^{\text{II}}$ : these do not react with  $\text{H}_2$ ,  $\text{N}_2$ ,  $\text{CO}$  or  $\text{PPh}_3$  as do cyclopentadienyl derivatives of these elements.

The chemistry of metallocarboranes of all cluster sizes is still rapidly developing and further unusual reactions and novel structures are continually appearing. Furthermore, as Si, Ge, Sn (and Pb) are in the same periodic group as C, heteroboranes containing these elements are to be expected (see p. 394). Likewise, as CC is isoelectronic with BN, the dicarbaboranes such as  $\text{C}_2\text{B}_{10}\text{H}_{12}$  can be paralleled by  $\text{NB}_{11}\text{H}_{12}$  etc. Numerous azaboranes and their metalladerivatives are known (see p. 211) as indeed are clusters incorporating P, As, Sb (and Bi) (p. 212). The incorporation of the more electronegative element O has proved to be a greater challenge but several examples are now known. Sulfur provides an extensive thia- and polythia-borane chemistry (p. 214) and this is paralleled, although to a lesser extent, by Se and Te derivatives (p. 215). Detailed discussion of these burgeoning areas of borane cluster chemistry fall outside this present treatment but the general references cited on the above mentioned pages provide a

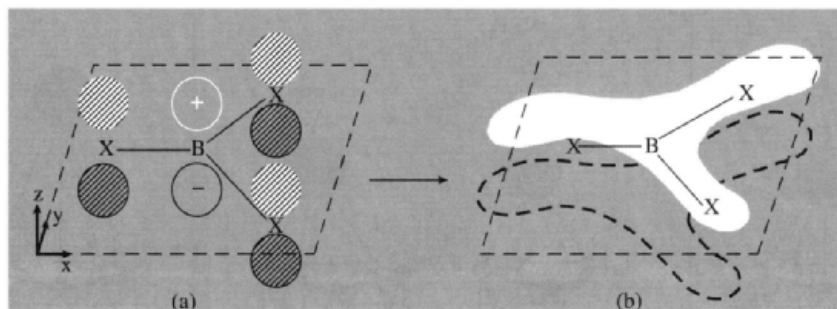
useful introduction into this important new area of chemistry.

## 6.7 Boron Halides

Boron forms numerous binary halides of which the monomeric trihalides  $\text{BX}_3$  are the most stable and most extensively studied. They can be regarded as the first members of a homologous series  $\text{B}_n\text{H}_{n+2}$ . The second members  $\text{B}_2\text{X}_4$  are also known for all 4 halogens but only F forms more highly catenated species containing  $\text{BX}_2$  groups:  $\text{B}_3\text{F}_5$ ,  $\text{B}_4\text{F}_6$ ,  $\text{B}_8\text{F}_{12}$  (p. 201). Chlorine forms a series of neutral *closo*-polyhedral compounds  $\text{B}_n\text{Cl}_n$  ( $n = 4, 8-12$ ) and several similar compounds are known for Br ( $n = 7-10$ ) and I (e.g.  $\text{B}_9\text{I}_9$ ). There are also numerous involatile subhalides, particularly of Br and I, but these are of uncertain stoichiometry and undetermined structure.

### 6.7.1 Boron trihalides

The boron trihalides are volatile, highly reactive, monomeric molecular compounds which show no detectable tendency to dimerize (except perhaps in Kr matrix-isolation experiments at 20K). In



**Figure 6.22** Schematic indication of the  $p_{\pi}-p_{\pi}$  interaction between the "vacant"  $p_z$  orbital on B and the 3 filled  $p_z$  orbitals on the 3 X atoms leading to a bonding MO of  $\pi$  symmetry.

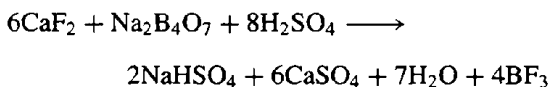
this they resemble organoboranes,  $BR_3$ , but differ sharply from diborane,  $B_2H_6$ , and the aluminium halides and alkyls,  $Al_2X_6$ ,  $Al_2R_6$  (p. 259). Some physical properties are listed in Table 6.4; mps and volatilities parallel those of the parent halogens,  $BF_3$  and  $BCl_3$  being gases at room temperature,  $BBr_3$  a volatile liquid, and  $BI_3$  a solid. All four compounds have trigonal planar molecules of  $D_{3h}$  symmetry with angle  $X-B-X$   $120^\circ$  (Fig. 6.22a). The interatomic distances  $B-X$  are substantially less than those expected for single bonds and this has been interpreted in terms of appreciable  $p_{\pi}-p_{\pi}$  interaction (Fig. 6.22b). However, there is disagreement as to whether the extent of this  $\pi$  bonding increases or diminishes with increasing atomic number of the halogen; this probably reflects the differing criteria used (extent of orbital overlap, percentage  $\pi$ -bond character, amount of  $\pi$ -charge transfer from X to B,  $\pi$ -bond energy, or reorganization energy in going from planar  $BX_3$  to tetrahedral  $LBX_3$ , etc.).<sup>(98)</sup> For example, it is quite possible for the extent of  $\pi$ -charge transfer from X to B to increase in the sequence  $F < Cl < Br < I$  but for the actual magnitude of the  $\pi$ -bond energy to be in

the reverse sequence  $BF_3 > BCl_3 > BBr_3 > BI_3$  because of the much greater bond energy of the lighter homologues. Indeed, the mean  $B-F$  bond energy in  $BF_3$  is  $646 \text{ kJ mol}^{-1}$ , which makes it the strongest known "single" bond; if  $x\%$  of this were due to  $\pi$  bonding, then even if  $2.4x\%$  of the  $B-I$  bond energy were due to  $\pi$  bonding, the  $\pi$ -bond energy in  $BI_3$  would be less than that in  $BF_3$  in absolute magnitude. The point is one of some importance since the chemistry of the trihalides is dominated by interactions involving this orbital.

**Table 6.4** Some physical properties of boron trihalides

Property	$BF_3$	$BCl_3$	$BBr_3$	$BI_3$
MP/ $^\circ\text{C}$	-127.1	-107	-46	49.9
BP/ $^\circ\text{C}$	-99.9	12.5	91.3	210
$r(B-X)/\text{pm}$	130	175	187	210
$\Delta H_f^\circ$ (298 K)/ $\text{kJ mol}^{-1}$ (gas)	-1123	-408	-208	+
$E(B-X)/\text{kJ mol}^{-1}$	646	444	368	267

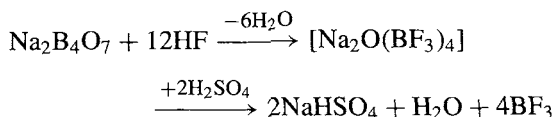
$BF_3$  is used extensively as a catalyst in various industrial processes (p. 199) and can be prepared on a large scale by the fluorination of boric oxide or borates with fluorspar and concentrated  $H_2SO_4$ :



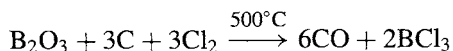
<sup>98</sup> Some key references will be found in D. R. ARMSTRONG and P. G. PERKINS, *J. Chem. Soc. (A)*, 1967, 1218-22; and in M. F. LAPPERT, M. R. LITZOW, J. B. PEDLEY, P. N. K. RILEY and A. TWEEDALE, *J. Chem. Soc. (A)*, 1968, 3105-10. Y. A. BUSLAEV, E. A. KRAVCHENKO and L. KOLDIZ, *Coord. Chem. Rev.* **82**, 9-231 (1987). V. BRANCHADELL and A. OLIVA, *J. Am. Chem. Soc.* **113**, 4132-6 (1991) and *Theochem.* **236**, 75-84 (1991).



Better yields are obtained in the more modern two-stage process:



On the laboratory scale, pure  $\text{BF}_3$  is best made by thermal decomposition of a diazonium tetrafluoroborate (e.g.  $\text{PhN}_2\text{BF}_4 \longrightarrow \text{PhF} + \text{N}_2 + \text{BF}_3$ ).  $\text{BCl}_3$  and  $\text{BBr}_3$  are prepared on an industrial scale by direct halogenation of the oxide in the presence of C, e.g.:



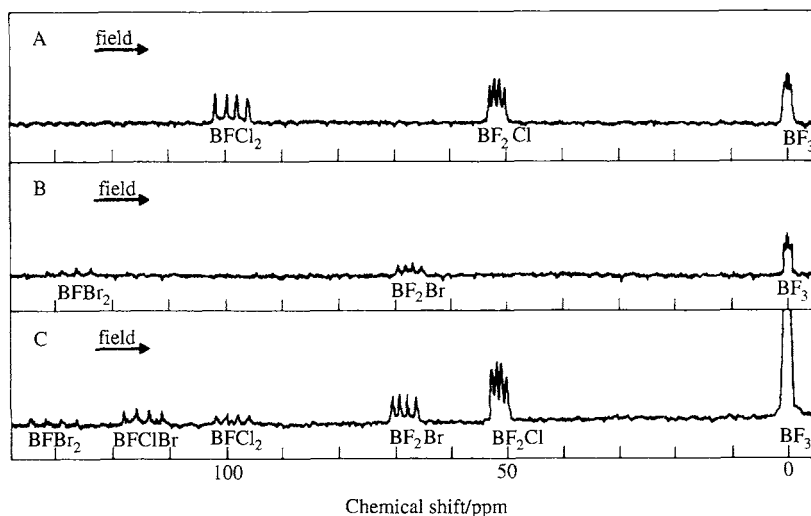
Laboratory samples of the pure compounds can be made by halogen exchange between  $\text{BF}_3$  and  $\text{Al}_2\text{X}_6$ .  $\text{BI}_3$  is made in good yield by treating  $\text{LiBH}_4$  (or  $\text{NaBH}_4$ ) with elemental  $\text{I}_2$  at  $125^\circ$  (or  $200^\circ$ ). Both  $\text{BBr}_3$  and  $\text{BI}_3$  tend to decompose with liberation of free halogen when exposed to light or heat; they can be purified by treatment with Hg or Zn/Hg.

Simple  $\text{BX}_3$  undergo rapid scrambling or redistribution reactions on being mixed and

the mixed halides  $\text{BX}_2\text{Y}$  and  $\text{BXY}_2$  have been identified by vibrational spectroscopy, mass spectrometry, or nmr spectroscopy using  $^{11}\text{B}$  or  $^{19}\text{F}$ . A good example of this last technique is shown in Fig. 6.23, where not only the species  $\text{BF}_{3-n}\text{X}_n$  ( $n = 0, 1, 2$ ) were observed but also the trihalogeno species  $\text{BFCIBr}$ .<sup>(99)</sup> The equilibrium concentration of the various species are always approximately random (equilibrium constants between 0.5 and 2.0) but it is not possible to isolate individual mixed halides because the equilibrium is too rapidly attained from either direction ( $<1$  s). The related systems  $\text{RBX}_2/\text{R}'\text{BY}_2$  (and  $\text{ArBX}_2/\text{Ar}'\text{BY}_2$ ) also exchange X and Y but not R (or Ar). The scrambling mechanism probably involves a 4-centre transition state. Consistent with this, complexes such as  $\text{Me}_2\text{OBX}_3$  or  $\text{Me}_3\text{NBX}_3$  do not scramble at room temperature, or even above, in the absence of free  $\text{BX}_3$ <sup>(100)</sup> (cf. the stability of  $\text{CFCl}_3$ ,  $\text{CF}_2\text{Cl}_2$ , etc.) and species that are

<sup>99</sup> T. D. COYLE and F. G. A. STONE, *J. Chem. Phys.* **32**, 1892-3 (1960).

<sup>100</sup> J. S. HARTMAN and J. M. MILLER, *Adv. Inorg. Chem. Radiochem.* **21**, 147-77 (1978).



**Figure 6.23** Fluorine-19 nmr spectra of mixtures of boron halides showing the presence of mixed fluorohalogenoboranes.

### Factors Affecting the Stability of Donor–Acceptor Complexes<sup>(101–103)</sup>

For a given ligand, stability of the adduct  $\text{LBX}_3$  usually increases in the sequence  $\text{BF}_3 < \text{BCl}_3 < \text{BBr}_3 < \text{BI}_3$ , probably because the loss of  $\pi$  bonding on reorganization from planar to tetrahedral geometry (p. 196) is not fully compensated for by the expected electronegativity effect. However, if the ligand has an H atom directly bonded to the donor atom, the resulting complex is susceptible to protonolysis of the B–X bond, e.g.:

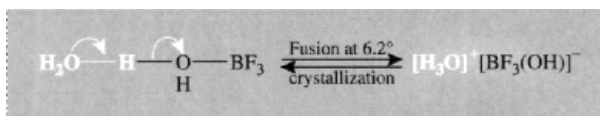


In such cases the great strength of the B–F bond ensures that the  $\text{BF}_3$  complex is more stable than the others. For example,  $\text{BF}_3$  forms stable complexes with  $\text{H}_2\text{O}$ ,  $\text{MeOH}$ ,  $\text{Me}_2\text{NH}$ , etc., whereas  $\text{BCl}_3$  reacts rapidly to give  $\text{B}(\text{OH})_3$ ,  $\text{B}(\text{OMe})_3$  and  $\text{B}(\text{NMe}_2)_3$ ; with  $\text{BBr}_3$  and  $\text{BI}_3$  such protolytic reactions are sometimes of explosive violence. Even ethers may be cleaved by  $\text{BCl}_3$  to give  $\text{RCl}$  and  $\text{ROBCl}_2$ , etc.

For a given  $\text{BX}_3$ , the stability of the complex depends on (a) the chemical nature of the donor atom, (b) the presence of polar substituents on the ligand, (c) steric effects, (d) the stoichiometric ratio of ligand to acceptor, and (e) the state of aggregation. Thus the majority of adducts have as the donor atom N, P, As; O, S; or the halide and hydride ions  $\text{X}^-$ .  $\text{BX}_3$  (but not  $\text{BH}_3$ ) can be classified as type-a acceptors, forming stronger complexes with N, O and F ligands than with P, S and Cl. However, complexes are not limited to these traditional main-group donor atoms, and, following the work of D. F. Shriver (1963), many complexes have been characterized in which the donor atom is a transition metal, e.g.  $[(\text{C}_5\text{H}_5)_2\text{H}_2\text{W}^{\text{IV}} \rightarrow \text{BF}_3]$ ,  $[(\text{Ph}_3\text{P})_2(\text{CO})\text{ClRh}^{\text{I}} \rightarrow \text{BBr}_3]$ ,  $[(\text{Ph}_2\text{PCH}_2\text{CH}_2\text{PPh}_2)_2\text{Rh}^{\text{I}}(\text{BCl}_3)_2]^+$ ,  $[(\text{Ph}_3\text{P})_2(\text{CO})\text{ClIr}^{\text{I}}(\text{BF}_3)_2]$ ,  $[(\text{Ph}_3\text{P})_2\text{Pt}^{\text{0}}(\text{BCl}_3)_2]$ , etc. Displacement studies on several such complexes indicate that  $\text{BF}_3$  is a weaker acceptor than  $\text{BCl}_3$ .

The influence of polar substituents on the ligand follows the expected sequence for electronegative groups, e.g. electron donor properties decrease in the order  $\text{NMe}_3 > \text{NMe}_2\text{Cl} > \text{NMeCl}_2 \gg \text{NCl}_3$ . Steric effects can also limit the electron-donor strength. For example, whereas pyridine,  $\text{C}_5\text{H}_5\text{N}$ , is a weaker base (proton acceptor) than 2-Me $\text{C}_5\text{H}_4\text{N}$  and 2,6-Me $_2\text{C}_5\text{H}_3\text{N}$ , the reverse is true when  $\text{BF}_3$  is the acceptor due to steric crowding of the  $\alpha$ -Me groups which prevent the close approach of  $\text{BF}_3$  to the donor atom. Steric effects also predominate in determining the decreasing stability of  $\text{BF}_3$  etherates in the sequence  $\text{C}_4\text{H}_8\text{O}(\text{thf}) > \text{Me}_2\text{O} > \text{Et}_2\text{O} > \text{Pr}_2\text{O}$ .

The influences of stoichiometry and state of aggregation are more subtle. At first sight it is not obvious why  $\text{BF}_3$ , with 1 vacant orbital should form not only  $\text{BF}_3 \cdot \text{H}_2\text{O}$  but also the more stable  $\text{BF}_3 \cdot 2\text{H}_2\text{O}$ ; similarly, the 1:2 complexes with  $\text{ROH}$  and  $\text{RCOOH}$  are always more stable than the 1:1 complexes. The second mole of ligand is held by hydrogen bonding in the solid, e.g.  $\text{BF}_3 \cdot \text{OH}_2 \dots \text{OH}_2$ ; however, above the mp  $6.2^\circ\text{C}$  the compound melts and the act of coordinate-bond formation causes sufficient change in the electron distribution within the ligand that ionization ensues and the compound is virtually completely ionized as a molten salt:<sup>(101)</sup>



The greater stability of the 1:2 complex is thus seen to be related to the formation of  $\text{H}_3\text{O}^+$ ,  $\text{ROH}_2^+$ , etc., and the lower stability of the 1:1 complexes  $\text{HBF}_3\text{OH}$ ,  $\text{HBF}_3\text{OR}$ , is paralleled by the instability of some other anhydrous oxo acids, e.g.  $\text{H}_2\text{CO}_3$ . The mp of the hydrate is essentially the transition temperature between an H-bonded molecular solid and an ionically dissociated liquid. A transition in the opposite sense occurs when crystalline  $[\text{PCl}_4]^+[\text{PCl}_6]^-$  melts to give molecular  $\text{PCl}_5$  (p. 498) and several other examples are known. The fact that coordination can substantially modify the type of bonding should occasion no surprise: the classic example (first observed by J. Priestley in 1774) was the reaction  $\text{NH}_3(\text{g}) + \text{HCl}(\text{g}) \rightarrow \text{NH}_4\text{Cl}(\text{c})$ .

expected to form stronger  $\pi$  bonds than  $\text{BX}_3$  (such as  $\text{R}_2\text{NBX}_2$ ) exchange much more slowly (days or weeks).

The boron trihalides form a great many molecular addition compounds with molecules

<sup>101</sup>N. N. GREENWOOD and R. L. MARTIN *Qt. Revs.* **8**, 1–39 (1954).

<sup>102</sup>V. GUTMANN, *The Donor-Acceptor Approach to Molecular Interactions*, Plenum, New York, 1978, 279 pp.

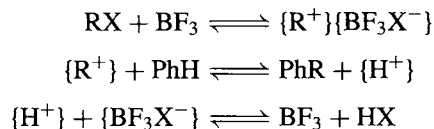
<sup>103</sup>A. HAALAND, *Angew. Chem. Int. Edn. Engl.* **28**, 992–1007 (1989).

(ligands) possessing a lone-pair of electrons (Lewis base). Such adducts have assumed considerable importance since it is possible to investigate in detail the process of making and breaking one bond, and to study the effect this has on the rest of the molecule (see Panel). The tetrahalogeno borates  $BX_4^-$  are a special case in which the ligand is  $X^-$ ; they are isoelectronic with  $BH_4^-$  (p. 165) and with  $CH_4$  and  $CX_4$ . Salts of  $BF_4^-$  are readily formed by adding a suitable metal fluoride to  $BF_3$  either in the absence of solvent or in such nonaqueous solvents as HF,  $BrF_3$ ,  $AsF_3$  or  $SO_2$ . The alkali metal salts  $MBF_4$  are stable to hydrolysis in aqueous solutions. Some molecular fluorides such as  $NO_2F$  and  $RCOF$  react similarly. There is a significant lengthening of the B–F bond from 130 pm in  $BF_3$  to 145 pm in  $BF_4^-$ . The other tetrahalogenoborates,  $BX_4^-$ , are less stable but may be prepared using large counter cations, e.g. Rb, Cs, pyridinium, tetraalkylammonium, tropenium, triphenylcarbonium, etc. The  $BF_4^-$  anion is a very weakly coordinating ligand, indeed one of the weakest,<sup>(104)</sup> however, unstable complexes are known in which it acts as an  $\eta^1$ -ligand and, in the case of  $[Ag(lut)_2(BF_4)]$  it acts as a bis(bidentate) bridging ligand  $[\mu_4-\eta^2, \eta^2-BF_4]^-$  to form a polymeric chain of 6-coordinate Ag centres<sup>(105)</sup> [lut = lutidene, i.e. 2,6-dimethylpyridine].

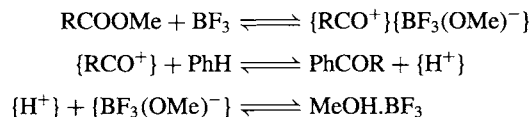
The importance of the trihalides as industrial chemicals stems partly from their use in preparing crystalline boron (p. 141) but mainly from their ability to catalyse a wide variety of organic reactions.<sup>(106)</sup>  $BF_3$  is the most widely used but  $BCl_3$  is employed in special cases. Thus,  $BF_3$  is manufactured on the multikilotonne scale whereas the production of  $BCl_3$  (USA, 1990) was 250 tonnes and  $BBr_3$  was about 23 tonnes.  $BF_3$  is shipped in steel cylinders containing 2.7 or 28 kg at a pressure of 10–12 atm, or in tube trailers

containing about 5.5 tonnes. Prices for  $BF_3$  are in the range \$4.00–5.00/kg depending on purity and quantity; corresponding prices (USA, 1991) for  $BCl_3$  and  $BBr_3$  were \$8.50–16.75/kg and \$81.50/kg, respectively.

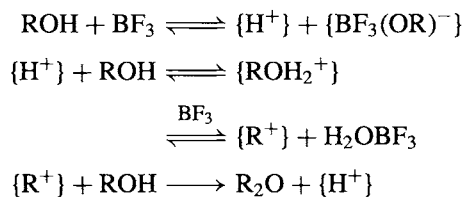
Many of the reactions of  $BF_3$  are of the Friedel–Crafts type though they are perhaps not strictly catalytic since  $BF_3$  is required in essentially equimolar quantities with the reactant. The mechanism is not always fully understood but it is generally agreed that in most cases ionic intermediates are produced by or promoted by the formation of a  $BX_3$  complex; electrophilic attack of the substrate by the cation so produced completes the process. For example, in the Friedel–Crafts-type alkylation of aromatic hydrocarbons:



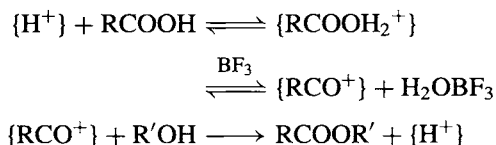
Similarly, ketones are prepared via acyl carbonium ions:



Evidence for many of these ions has been extensively documented.<sup>(101)</sup>



A similar mechanism has been proposed for the esterification of carboxylic acids:

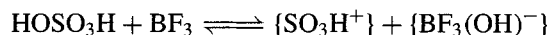
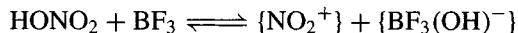


<sup>104</sup> W. BECK and K. SÜNKEL, *Chem. Rev.* **88**, 1405–21 (1988).

<sup>105</sup> E. HORM, M. R. SNOW and E. R. T. TIEKINK, *Aust. J. Chem.* **40**, 761–5 (1987).

<sup>106</sup> G. OLAH (ed.), *Friedel–Crafts and Related Reactions*, Interscience, New York, 1963 (4 vols).

Nitration and sulfonation of aromatic compounds probably occur via the formation of the nityl and sulfonyl cations:

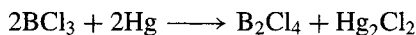


Polymerization of alkenes and the isomerization of alkanes and alkenes occur in the presence of a cocatalyst such as  $\text{H}_2\text{O}$ , whereas the cracking of hydrocarbons is best performed with  $\text{HF}$  as cocatalyst. These latter reactions are of major commercial importance in the petrochemicals industry.

### 6.7.2 Lower halides of boron

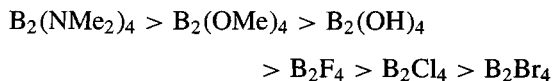
$\text{B}_2\text{F}_4$  (mp  $-56^\circ$ , bp  $-34^\circ\text{C}$ ) has a planar ( $D_{2h}$ ) structure with a rather long B–B bond; in this it resembles both the oxalate ion  $\text{C}_2\text{O}_4^{2-}$  and  $\text{N}_2\text{O}_4$  with which it is precisely isoelectronic. Crystalline  $\text{B}_2\text{Cl}_4$  (mp  $-92.6^\circ\text{C}$ ) has the same structure, but in the gas phase (bp  $65.5^\circ$ ) it adopts the staggered  $D_{2d}$  configuration (see below) with hindered rotation about the B–B bond ( $\Delta E_r$   $7.7 \text{ kJ mol}^{-1}$ ). The structure of gaseous  $\text{B}_2\text{Br}_4$  is also  $D_{2d}$  with B–B 169 pm and  $\Delta E_r$   $12.8 \text{ kJ mol}^{-1}$ .  $\text{B}_2\text{I}_4$  is presumably similar.

$\text{B}_2\text{Cl}_4$  was the first compound in this series to be prepared and is the most studied; it is best made by subjecting  $\text{BCl}_3$  vapour to an electrical discharge between mercury or copper electrodes:

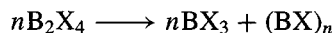


The reaction probably proceeds by formation of a  $\{\text{BCl}\}$  intermediate which then inserts into a B–Cl bond of  $\text{BCl}_3$  to give the product directly.

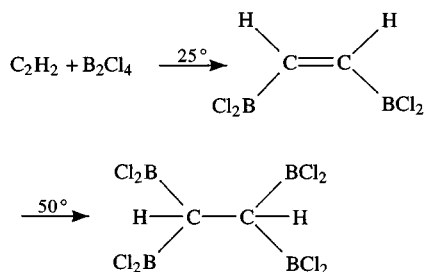
Another route is via the more stable  $\text{B}_2(\text{NMe}_2)_4$  (see reaction scheme). Thermal stabilities of these compounds parallel the expected sequence of  $p_\pi-p_\pi$  bonding between the substituent and B:



The halides are much less stable than the corresponding  $\text{BX}_3$ , the most stable member  $\text{B}_2\text{F}_4$  decomposing at the rate of about 8% per day at room temperature.  $\text{B}_2\text{Br}_4$  disproportionates so rapidly at room temperature that it is difficult to purify:

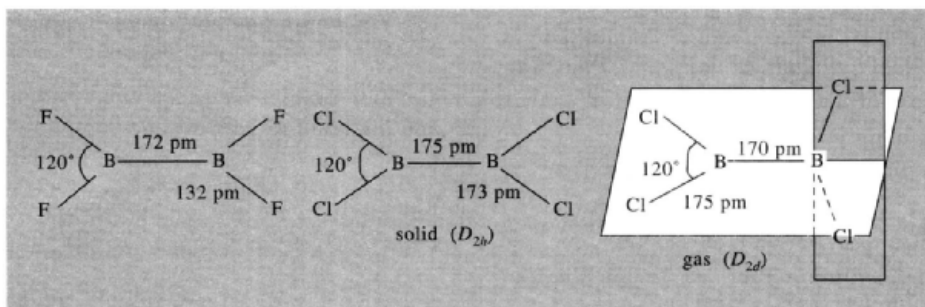


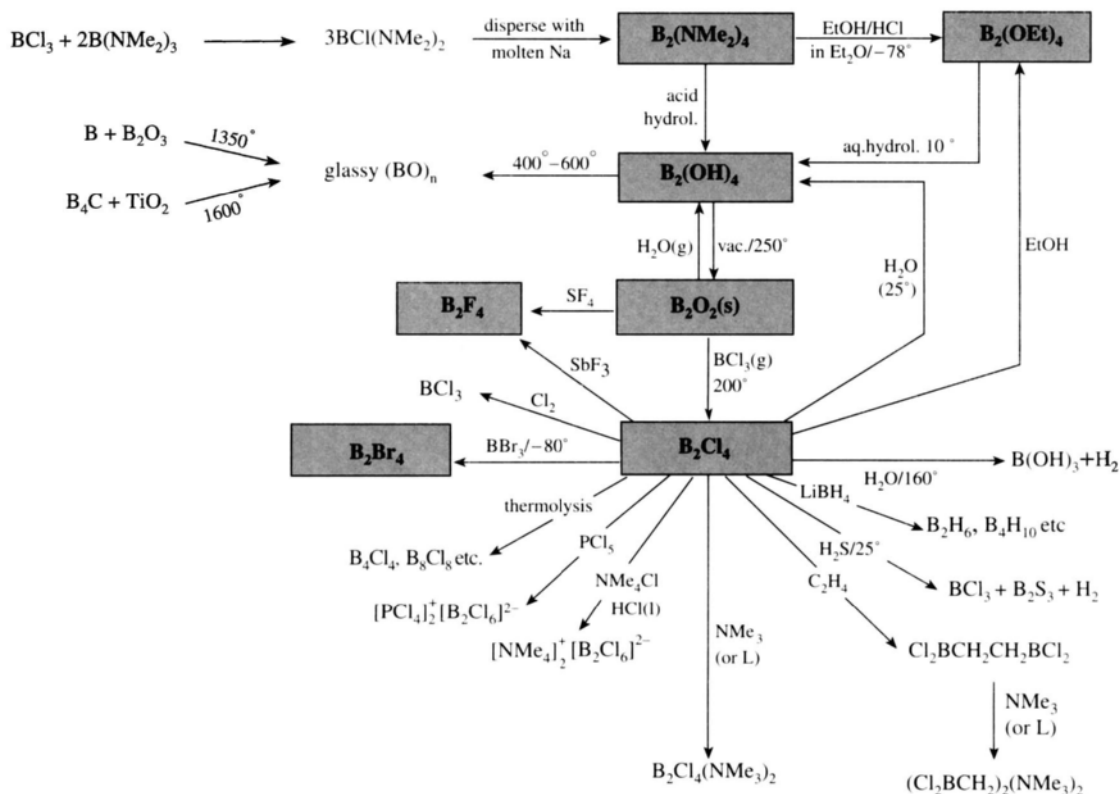
The compounds  $\text{B}_2\text{X}_4$  are spontaneously flammable in air and react with  $\text{H}_2$  to give  $\text{BHX}_2$ ,  $\text{B}_2\text{H}_6$  and related hydrohalides; they form adducts with Lewis bases ( $\text{B}_2\text{Cl}_4\text{L}_2$  more stable than  $\text{B}_2\text{F}_4\text{L}_2$ ) and add across C–C multiple bonds, e.g.



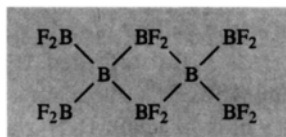
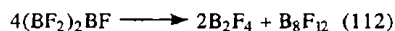
Other reactions of  $\text{B}_2\text{Cl}_4$  are shown in the scheme and many of these also occur with  $\text{B}_2\text{F}_4$ .

When  $\text{BF}_3$  is passed over crystalline B at  $1850^\circ\text{C}$  and pressures of less than 1 mmHg, the reactive gas  $\text{BF}$  is obtained in high yield and can





be condensed out at  $-196^\circ$ . Cocondensation with  $\text{BF}_3$  yields  $\text{B}_2\text{F}_4$  then  $\text{B}_3\text{F}_5$  (i.e.  $\text{F}_2\text{B}-\text{B}(\text{F})-\text{BF}_2$ ). However, this latter compound is unstable and it disproportionates above  $-50^\circ$  according to



(112)

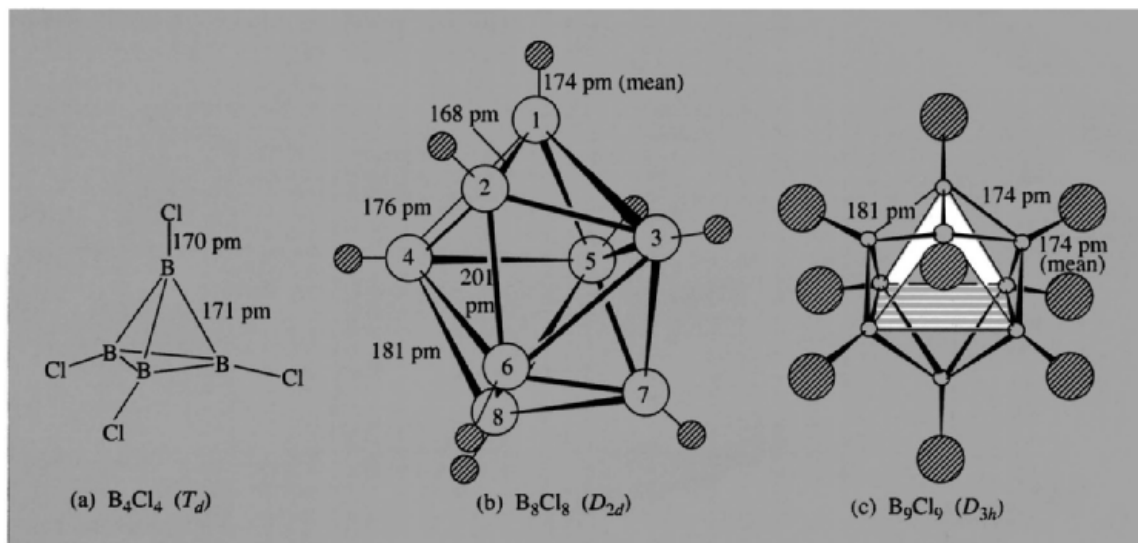
The yellow compound  $\text{B}_8\text{F}_{12}$  appears to have a diborane-like structure (112) and this readily undergoes symmetrical cleavage with a variety of ligands such as  $\text{CO}$ ,  $\text{PF}_3$ ,  $\text{PCl}_3$ ,  $\text{PH}_3$ ,  $\text{AsH}_3$  and  $\text{SMe}_2$  to give adducts  $\text{L}_2\text{B}(\text{BF}_2)_3$  which are stable at room temperature in the absence of air or moisture.

Thermolysis of  $\text{B}_2\text{Cl}_4$ <sup>(107)</sup> and  $\text{B}_2\text{Br}_4$  at moderate temperatures gives a series of *closo*-halogenoboranes  $\text{B}_n\text{X}_n$  where  $n = 4, 8-12$  for  $\text{Cl}$ , and  $n = 7-10$  for  $\text{Br}$ . Other preparative routes include the high-yield halogenation of  $\text{B}_9\text{H}_9^{2-}$  to  $\text{B}_9\text{X}_9^{2-}$  using *N*-chlorosuccinimide, *N*-bromosuccinimide or  $\text{I}_2$ .<sup>(108)</sup> The redox sequences  $\text{B}_9\text{X}_9^{2-} \rightleftharpoons \text{B}_9\text{X}_9^- \rightleftharpoons \text{B}_9\text{X}_9$  have also been established, the radical anions  $\text{B}_9\text{X}_9^-$  being isolated as air-stable coloured salts.<sup>(108)</sup>

$\text{B}_4\text{Cl}_4$ , a pale-yellow-green solid, has a regular *closo*-tetrahedral structure (Fig. 6.24a); it is hyperelectron deficient when compared with the *closo*-boranes  $\text{B}_n\text{H}_n^{2-}$  (pp. 153, 160) and the

<sup>107</sup> T. DAVAN and J. A. MORRISON, *Inorg. Chem.* **25**, 2366-72 (1986).

<sup>108</sup> E. H. WONG and R. M. KABBANI, *Inorg. Chem.* **19**, 451-5 (1980). See also E. H. WONG, *Inorg. Chem.* **20**, 1300-2 (1981); A. J. MARKWELL, A. G. MASSEY and P. J. PORTAL, *Polyhedron* **1**, 134-5 (1982).



**Figure 6.24** Molecular structures of (a) tetrahedral  $B_4Cl_4$ , (b) dodecahedral  $B_8Cl_8$ , and (c) tricapped trigonal pyramidal  $B_9Cl_9$  and  $B_9Br_9$ . In  $B_8Cl_8$  note that the shortest B-B distances are between two 5-coordinate B atoms, e.g. B(1)–B(2) 168 pm; the longest are between two 6-coordinate B atoms, e.g. B(4)–B(6) 201 pm and intermediate distances are between one 5- and one 6-coordinate B atom. A similar trend occurs in  $B_9Cl_9$ .

bonding has been discussed in terms of localized 3-centre bonds above the 4 tetrahedral faces supplemented by  $p_\pi$  interaction with p orbitals of suitable symmetry on the 4 Cl atoms: the 8 electrons available for framework bonding from the 4 {BCl} groups fill 4 bonding MOs of class  $A_1$  and  $T_2$  and there are 2 additional bonding MOs of class  $E$  which have correct symmetry to mix with the Cl  $p_\pi$  orbitals.  $B_8Cl_8$  (variously described as dark red, dark purple or green-black crystals) has an irregular dodecahedral (bisphenoid) arrangement of the *closo*- $B_8$  cluster (Fig. 6.24b) with 14 B–B distances in the range 168–184 pm and 4 substantially longer B–B distances at 193–205 pm.  $B_9Br_9$  is a particularly stable compound; it forms as dark-red crystals together with other subbromides ( $n = 7$ –10) when gaseous  $BBr_3$  is subjected to a silent electric discharge in the presence of Cu wool, and can be purified by sublimation under conditions (200°C) which rapidly decompose the other products.  $B_9Br_9$  is isostructural with  $B_9Cl_9$  (yellow-orange) (Fig. 6.24c). The photoelectron

spectra and bonding in  $B_4Cl_4$ ,  $B_8Cl_8$  and  $B_9Cl_9$  have been described in detail.<sup>(109)</sup>

Many mixed halides  $B_nBr_{n-x}Cl_x$  ( $n = 9, 10, 11$ ) have been identified by mass spectrometry and other techniques, but their separation as pure compounds has so far not been achieved. Chemical reactions of  $B_nX_n$  resemble those of  $B_2X_4$  except that alkenes do not cleave the B–B bonds in the *closo*-species. Thus,  $B_4Cl_4$  reacts with LiEt to give the yellow liquids  $B_4Cl_3Et$  and  $B_4Cl_2Et_2$ , whereas  $LiBu^t$  afforded  $B_4Bu^t_4$  as a glassy solid, mp 45°C.<sup>(110)</sup> By contrast, reaction with  $Me_3SnH$  yields *arachno*- $B_4H_{10}$  and  $LiBH_4$  yields a mixture of *nido*- $B_5H_9$  and *nido*- $B_6H_{10}$ , while  $B_2H_6$  gave *nido*- $B_6H_6Cl_4$  and a mixture of *nido*- $B_{10}H_nCl_{14-n}$  ( $n = 8$ –12).<sup>(111)</sup>

<sup>109</sup> P. R. LEBRETON, S. URANO, M. SHAHBAZ, S. L. EMERY and J. A. MORRISON, *J. Am. Chem. Soc.* **108**, 3937–46 (1986).

<sup>110</sup> T. DAVAN and J. A. MORRISON, *J. Chem. Soc., Chem. Commun.*, 250–1 (1981).

<sup>111</sup> S. L. EMERY and J. A. MORRISON, *Inorg. Chem.* **24**, 1612–13 (1985).

## 6.8 Boron–Oxygen Compounds<sup>(112)</sup>

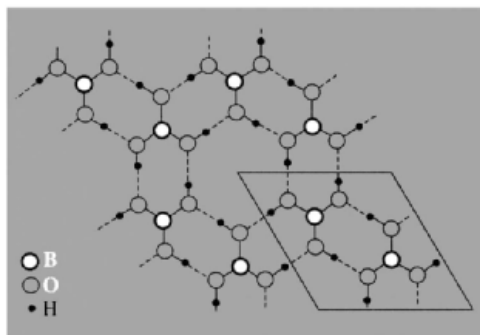
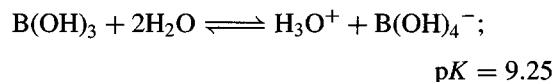
Boron (like silicon) invariably occurs in nature as oxo compounds and is never found as the element or even directly bonded to any other element than oxygen.<sup>†</sup> The structural chemistry of B–O compounds is characterized by an extraordinary complexity and diversity which rivals those of the borides (p. 145) and boranes (p. 151). In addition, vast numbers of predominantly organic compounds containing B–O are known.

### 6.8.1 Boron oxides and oxoacids<sup>(112)</sup>

The principal oxide of boron is boric oxide, B<sub>2</sub>O<sub>3</sub> (mp 450°, bp (extrap) 2250°C). It is one of the most difficult substances to crystallize and, indeed, was known only in the vitreous state until 1937. It is generally prepared by careful dehydration of boric acid B(OH)<sub>3</sub>. The normal crystalline form (*d* 2.56 g cm<sup>-3</sup>) consists of a 3D network of trigonal BO<sub>3</sub> groups joined through their O atoms, but there is also a dense form (*d* 3.11 g cm<sup>-3</sup>) formed under a pressure of 35 kbar at 525°C and built up from irregular interconnected BO<sub>4</sub> tetrahedra. In the vitreous state (*d* ≈ 1.83 g cm<sup>-3</sup>) B<sub>2</sub>O<sub>3</sub> probably consists of a network of partially ordered trigonal BO<sub>3</sub> units in which the 6-membered (BO)<sub>3</sub> ring predominates; at higher temperatures the structure becomes increasingly disordered and above 450°C polar —B=O groups are formed. Fused B<sub>2</sub>O<sub>3</sub> readily dissolves many metal oxides to give characteristically coloured borate glasses. Its major application is in the glass industry where borosilicate glasses

(e.g. Pyrex) are extensively used because of their small coefficient of thermal expansion and their easy workability. US production of B<sub>2</sub>O<sub>3</sub> exceeds 25 000 tonnes pa and the price (1990) was \$2780–2950 per tonne for 99% grade.

Orthoboric acid, B(OH)<sub>3</sub>, is the normal end product of hydrolysis of most boron compounds and is usually made (≈160 000 tonnes pa) by acidification of aqueous solutions of borax. Price depends on quality, being \$805 per tonne for technical grade and about twice that for refined material (1990). It forms flaky, white, transparent crystals in which a planar array of BO<sub>3</sub> units is joined by unsymmetrical H bonds as shown in Fig. 6.25. In contrast to the short O—H···O distance of 272 pm within the plane, the distance between consecutive layers in the crystal is 318 pm, thus accounting for the pronounced basal cleavage of the waxy, plate-like crystals, and their low density (1.48 g cm<sup>-3</sup>). B(OH)<sub>3</sub> is a very weak monobasic acid and acts exclusively by hydroxylation acceptance rather than proton donation:



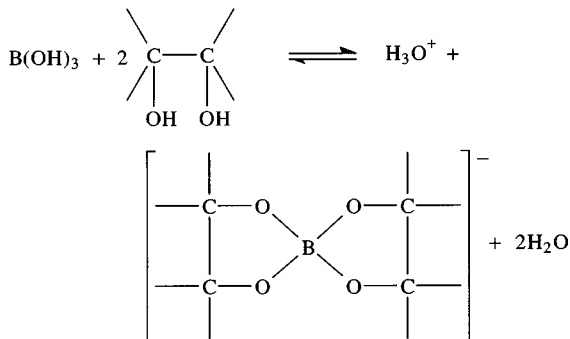
**Figure 6.25** Layer structure of B(OH)<sub>3</sub>. Interatomic distances are B–O 136 pm, O–H 97 pm, O—H···O 272 pm. Angles at B are 120° and at O 126° and 114°. The H bond is almost linear.

Its acidity is considerably enhanced by chelation with polyhydric alcohols (e.g. glycerol, mannitol) and this forms the basis of its use in analytical chemistry; e.g. with mannitol p*K* drops to 5.15,

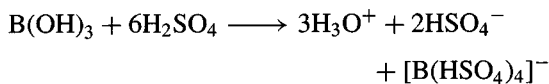
<sup>112</sup> Supplement to "Mellor's Comprehensive Treatise on Inorganic and Theoretical Chemistry", Vol. V, Boron: Part A, "Boron-Oxygen Compounds", Longman, London, 1980, 825 pp. See also J. R. BOWSER and T. P. FEHLNER, Chap. 1 in H. W. ROESKY (ed.), *Rings, Clusters and Polymers of Main Group and Transition Elements*, Elsevier, Amsterdam, 1989, pp. 1–48.

<sup>†</sup> Trivial exceptions to this sweeping generalization are NaBF<sub>4</sub> (ferrucite) and (K,Cs)BF<sub>4</sub> (avogadrite) which have been reported from Mt. Vesuvius, Italy.

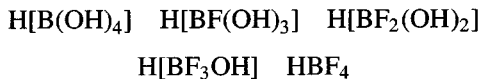
indicating an increase in the acid equilibrium constant by a factor of more than  $10^4$ .<sup>(113)</sup>



$\text{B(OH)}_3$  also acts as a strong acid in anhydrous  $\text{H}_2\text{SO}_4$ :



Other reactions include esterification with  $\text{ROH}/\text{H}_2\text{SO}_4$  to give  $\text{B(OR)}_3$ , and coordination of this with  $\text{NaH}$  in  $\text{thf}$  to give the powerful reducing agent  $\text{Na[BH(OR)}_3]$ . Reaction with  $\text{H}_2\text{O}_2$  gives peroxoboric acid solutions which probably contain the monoperoxoborate anion  $[\text{B(OH)}_3\text{OOH}]^-$ . A complete series of fluoroboric acids is also known in aqueous solution and several have been isolated as pure compounds:



The hypohalito analogues  $[\text{B(OH)}_3(\text{OX})]^-$  ( $\text{X}=\text{Cl}, \text{Br}$ ) have recently been characterized in aqueous solutions of  $\text{B(OH)}_3$  containing  $\text{NaOX}$ ; the stability constants  $\log \beta'$  at  $25^\circ\text{C}$  being 2.25(1) and 1.83(4), respectively,<sup>(114)</sup> compared with 5.39(7) for  $\text{B(OH)}_4^-$ .

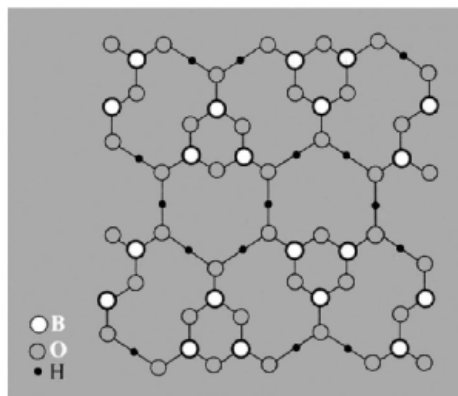
<sup>113</sup> J. M. CODDINGTON and M. J. TAYLOR, *J. Coord. Chem.* **20**, 27–38 (1989), and references cited therein, including those which describe its application to conformational analysis of carbohydrates and its use in separation and chromatographic techniques.

<sup>114</sup> A. BOUSHER, P. BRIMBLECOMBE and D. MIDGLEY, *J. Chem. Soc., Dalton Trans.*, 943–6 (1987).

Partial dehydration of  $\text{B(OH)}_3$  above  $100^\circ$  yields metaboric acid  $\text{HBO}_2$  which can exist in several crystalline modifications:

	CN of B	d/g cm <sup>-3</sup>	mp/°C
Orthorhombic $\text{HBO}_2$	3	1.784	176°
↑ rapid quench			
$\text{B(OH)}_3 \xrightarrow{140^\circ}$ monoclinic $\text{HBO}_2$	3 and 4	2.045	201°
$\xrightarrow{175^\circ}$ cubic $\text{HBO}_2$	4	2.487	236°

Orthorhombic  $\text{HBO}_2$  consists of trimeric units  $\text{B}_3\text{O}_3(\text{OH})_3$  which are linked into layers by H bonding (Fig. 6.26); all the B atoms are 3-coordinate. Monoclinic  $\text{HBO}_2$  is built of chains of composition  $[\text{B}_3\text{O}_4(\text{OH})(\text{H}_2\text{O})]$  in which some of the B atoms are now 4-coordinate, whereas cubic  $\text{HBO}_2$  has a framework structure of tetrahedral  $\text{BO}_4$  groups some of which are H bonded. The increase in CN of B is paralleled by an increase in density and mp.



**Figure 6.26** Layer structure of orthorhombic metaboric acid  $\text{HBO}_2(\text{III})$ , comprising units of formula  $\text{B}_3\text{O}_3(\text{OH})_3$  linked by  $\text{O} \cdots \text{H} \cdots \text{O}$  bonds.

Boron suboxide  $(\text{BO})_n$  and subboric acid  $\text{B}_2(\text{OH})_4$  were mentioned on p. 201.



### 6.8.2 Borates <sup>(112,115)</sup>

The phase relations, stoichiometry and structural chemistry of the metal borates have been extensively studied because of their geochemical implications and technological importance. Borates are known in which the structural unit is mononuclear (1 B atom), bi-, tri-, tetra- or pentanuclear, or in which there are polydimensional networks including glasses. The main structural principles underlying the bonding in crystalline metal borates are as follows:<sup>(116)</sup>

1. Boron can link either three oxygens to form a triangle or four oxygens to form a tetrahedron.
2. Polynuclear anions are formed by corner-sharing only of boron-oxygen triangles and tetrahedra in such a manner that a compact insular group results.
3. In the hydrated borates, protonatable oxygen atoms will be protonated in the following sequence: available protons are first assigned to free  $O^{2-}$  ions to convert these to free  $OH^-$  ions; additional protons are assigned to tetrahedral oxygens in the borate ion, and then to triangular oxygens in the borate ion; finally any remaining protons are assigned to free  $OH^-$  ions to form  $H_2O$  molecules.

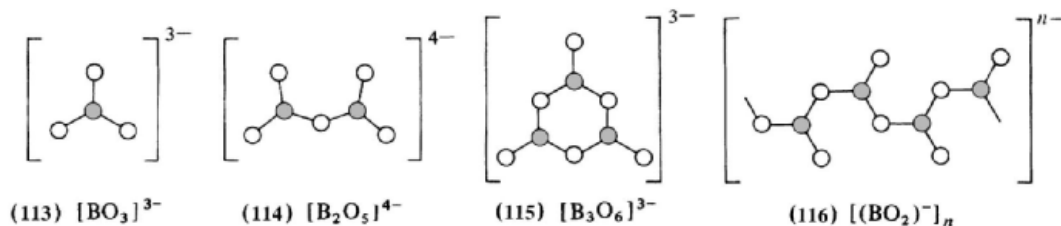
4. The hydrated insular groups may polymerize in various ways by splitting out water; this process may be accompanied by the breaking of boron-oxygen bonds within the polyanion framework.
5. Complex borate polyanions may be modified by attachment of an individual side group, such as (but not limited to) an extra borate tetrahedron, an extra borate triangle, 2 linked triangles, an arsenate tetrahedron, and so on.
6. Isolated  $B(OH)_3$  groups, or polymers of these, may exist in the presence of other anions.

Examples of minerals and compounds containing monomeric triangular,  $BO_3$  units (structure 113) are the rare-earth orthoborates  $M^{III}BO_3$  and the minerals  $CaSn^{IV}(BO_3)_2$  and  $Mg_3(BO_3)_2$ . Binuclear trigonal planar units (114) are found in the pyroborates  $Mg_2B_2O_5$ ,  $Co^{II}_2B_2O_5$  and  $Fe^{II}_2B_2O_5$ . Trinuclear cyclic units (115) occur in the metaborates  $NaBO_2$  and  $KBO_2$ , which should therefore be written as  $M_3B_3O_6$  (cf. metaboric acid, p. 204). Polynuclear linkage of  $BO_3$  units into infinite chains of stoichiometry  $BO_2$  (116) occurs in  $Ca(BO_2)_2$ , and three-dimensional linkage of planar  $BO_3$  units occurs in the borosilicate mineral tourmaline and in glassy  $B_2O_3$  (p. 203).

Monomeric tetrahedral  $BO_4$  units (117) are found in the zircon-type compound  $Ta^VBO_4$  and in the minerals  $(Ta,Nb)BO_4$  and  $Ca_2H_4BAS^VO_8$ . The related tetrahedral unit  $[B(OH)_4]^-$  (118) occurs in  $Na_2[B(OH)_4]Cl$  and  $Cu^{II}[B(OH)_4]Cl$ . Binuclear tetrahedral units (119) have been found

<sup>115</sup> G. HELLER, *Topics in Current Chemistry* No. 131 Springer-Verlag, Berlin, 1986, 39–98 (a survey of structural types with 568 refs.).

<sup>116</sup> C. L. CHRIST and J. R. CLARK, *Phys. Chem. Minerals* 2, 59–87 (1977). See also J. B. FARMER, *Adv. Inorg. Chem. Radiochem.* 25, 187–237 (1982).

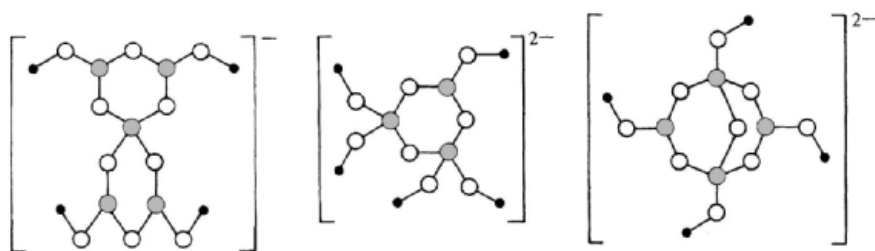


Units containing B in planar  $BO_3$  coordination only



(117)  $[\text{BO}_4]^{5-}$  (118)  $[\text{B}(\text{OH})_4]^{-}$  (119)  $[\text{B}_2\text{O}(\text{OH})_6]^{2-}$  (120)  $[\text{B}_2(\text{O}_2)_2(\text{OH})_4]^{2-}$

Units containing B in tetrahedral  $\text{BO}_2$  coordination only



(121)  $[\text{B}_5\text{O}_6(\text{OH})_4]^{-}$  (122)  $[\text{B}_3\text{O}_3(\text{OH})_5]^{2-}$  (123)  $[\text{B}_4\text{O}_5(\text{OH})_4]^{2-}$

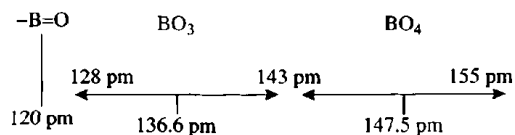
Units containing B in both  $\text{BO}_3$  and  $\text{BO}_4$  coordination

in  $\text{Mg}[\text{B}_2\text{O}(\text{OH})_6]$  and a cyclic binuclear tetrahedral structure (120) characterizes the peroxoanion  $[\text{B}_2(\text{O}_2)_2(\text{OH})_4]^{2-}$  in "sodium perborate"  $\text{NaBO}_3 \cdot 4\text{H}_2\text{O}$ , i.e.  $\text{Na}_2[\text{B}_2(\text{O}_2)_2(\text{OH})_4] \cdot 6\text{H}_2\text{O}$ . A more complex polynuclear structure comprising sheets of tetrahedrally coordinated  $\text{BO}_3(\text{OH})$  units occurs in the borosilicate mineral  $\text{CaB}(\text{OH})\text{SiO}_4$  and the fully three-dimensional polynuclear structure is found in  $\text{BPO}_4$  (cf. the isoelectronic  $\text{SiO}_2$ ),  $\text{BaSO}_4$  and the minerals  $\text{NaBSi}_3\text{O}_8$  and  $\text{Zn}_4\text{B}_6\text{O}_{13}$ .

The final degree of structural complexity occurs when the polynuclear assemblages contain both planar  $\text{BO}_3$  and tetrahedral  $\text{BO}_4$  units joined by sharing common O atoms. The structure of monoclinic  $\text{HBO}_2$  affords an example (p. 204). A structure in which the ring has but one  $\text{BO}_4$  unit is the spiroanion  $[\text{B}_5\text{O}_6(\text{OH})_4]^{-}$  (structure 121) which occurs in hydrated potassium pentaborate  $\text{KB}_5\text{O}_8 \cdot 4\text{H}_2\text{O}$ , i.e.  $\text{K}[\text{B}_5\text{O}_6(\text{OH})_4] \cdot 2\text{H}_2\text{O}$ . The anhydrous pentaborate  $\text{KB}_5\text{O}_8$  has the same structural unit but dehydration of the OH groups link the spiroanions of structure (121) sideways into ribbon-like helical chains. The mineral  $\text{CaB}_3\text{O}_3(\text{OH})_5 \cdot \text{H}_2\text{O}$  has 2  $\text{BO}_4$  units in the 6-membered heterocycle (122) and related chain elements  $[\text{B}_3\text{O}_4(\text{OH})_3]^{2-}_n$  linked by a common oxygen atom are found in the

important mineral colemanite  $\text{Ca}_2\text{B}_6\text{O}_{11} \cdot 5\text{H}_2\text{O}$ , i.e.  $[\text{CaB}_3\text{O}_4(\text{OH})_3] \cdot \text{H}_2\text{O}$ . It is clear from these examples that, without structural data, the stoichiometry of these borate minerals gives little indication of their constitution. A further illustration is afforded by borax which is normally formulated  $\text{Na}_2\text{B}_4\text{O}_7 \cdot 10\text{H}_2\text{O}$ , but which contains tetranuclear units  $[\text{B}_4\text{O}_5(\text{OH})_4]^{2-}$  formed by fusing 2  $\text{B}_3\text{O}_3$  rings which each contain 2  $\text{BO}_4$  (shared) and 1  $\text{BO}_3$  unit (123); borax should therefore be written as  $\text{Na}_2[\text{B}_4\text{O}_5(\text{OH})_4] \cdot 8\text{H}_2\text{O}$ .

There is wide variation of B–O distances in these various structures the values increasing, as expected, with increase in coordination:



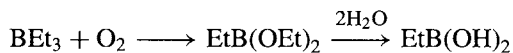
The extent to which  $\text{B}_3\text{O}_3$  rings catenate into more complex structures or hydrolyse into smaller units such as  $[\text{B}(\text{OH})_4]^{-}$  clearly depends sensitively on the activity (concentration) of water in the system, on the stoichiometric ratio of metal ions to boron and on the temperature ( $T\Delta S$ ).

Many metal borates find important industrial applications (p. 140) and annual world production exceeds 2.9 million tonnes: Turkey 1.2, USA 1.1, Argentina 0.26, the former Soviet Union 0.18, Chile 0.13 Mt. Main uses are in glass-fibre and cellular insulation, the manufacture of borosilicate glasses and enamels, and as fire retardants. Sodium perborate (for detergents) is manufactured on a 550 000 tonne pa scale.

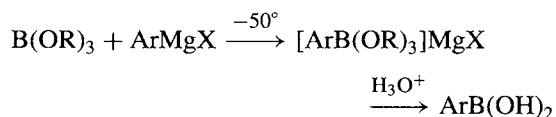
### 6.8.3 Organic compounds containing boron–oxygen bonds

Only a brief classification of this very large and important class of compounds will be given; most contain trigonal planar B though many 4-coordinate complexes have also been characterized. The orthoborates  $B(OR)_3$  can readily be prepared by direct reaction of  $BCl_3$  or  $B(OH)_3$  with ROH, while transesterification with  $R'OH$  affords a route to unsymmetrical products  $B(OR)_2(OR')$ , etc. The compounds range from colourless volatile liquids to involatile white solids depending on molecular weight. R can be a primary, secondary, tertiary, substituted or unsaturated alkyl group or an aryl group, and orthoborates of polyhydric alcohols and phenols are also numerous.

Boronic acids  $RB(OH)_2$  were first made over a century ago by the unlikely route of slow partial oxidation of the spontaneously flammable trialkyl boranes followed by hydrolysis of the ester so formed (E. Frankland, 1862):



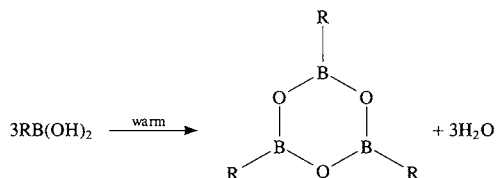
Many other routes are now available but the most used involve the reaction of Grignard reagents or lithium alkyls on orthoborates or boron trihalides:



Phenylboronic acid in particular has proved invaluable, since its complexes with *cis*-diols and -polyols have formed the basis

of chromatographic separations, asymmetric syntheses, enzyme immobilization and the preparation of polymers capable of molecular recognition.<sup>(117)</sup>

Boronic acids readily dehydrate at moderate temperatures (or over  $P_4O_{10}$  at room temperature) to give trimeric cyclic anhydrides known as trialkyl(aryl)boroxines:



The related trialkoxyboroxines  $(ROBO)_3$  can be prepared by esterifying  $B(OH)_3$ ,  $B_2O_3$  or metaboric acid  $BO(OH)$  with the appropriate mole ratio of ROH.

Endless variations have been played on these themes and the B atom can be surrounded by innumerable combinations of groups such as acyloxy (RCOO), peroxy (ROO), halogeno (X), hydrido, etc., in either open or cyclic arrays. However, no new chemical principles emerge.

## 6.9 Boron–Nitrogen Compounds

Two factors have contributed to the special interest that attaches to B–N compounds. First, the B–N unit is isoelectronic with C–C and secondly, the size and electronegativity of the 3 atoms are similar, C being the mean of B and N:

	B	C	N
Number of valence electrons	3	4	5
Covalent single-bond radius/pm	88	77	70
Electronegativity	2.0	2.5	3.0

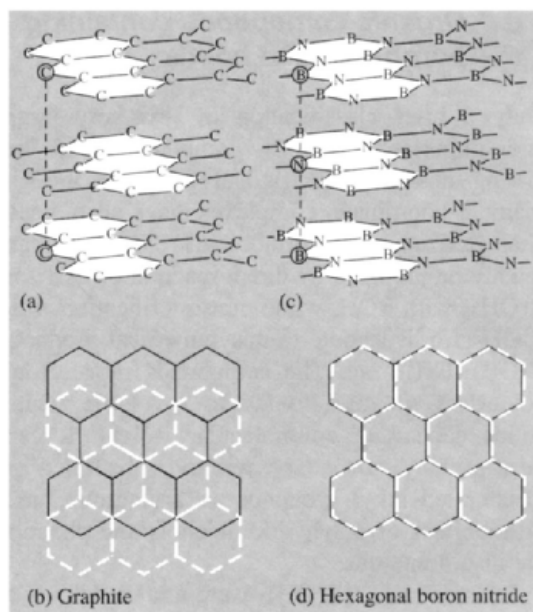
The repetition of much organic chemistry by replacing pairs of C atoms with the B–N

<sup>117</sup> C. D'SILVA and D. GREEN, *J. Chem. Soc., Chem. Commun.*, 227–9 (1991) and leading references cited therein.

grouping has led to many new classes of compound but these need not detain us.<sup>(118)</sup> By contrast, key points emerge from several other areas of B–N chemistry and, accordingly, this section deals briefly with the structure, properties and reaction chemistry of boron nitride, amine-borane adducts, aminoboranes, iminoboranes, cyclic borazines and azaborane clusters.

The synthesis of boron nitride, BN, involves considerable technical difficulty;<sup>(119)</sup> a laboratory preparation yielding relatively pure samples involves the fusion of borax with ammonium chloride, whereas technical-scale production relies on the fusion of urea with  $B(OH)_3$  in an atmosphere of  $NH_3$  at 500–950°C. Only a brave (or foolhardy) chemist would attempt to write a balanced equation for either reaction. An alternative synthesis (>99% purity) treats  $BCl_3$  with an excess of  $NH_3$  (see below) and pyrolyses the resulting mixture in an atmosphere of  $NH_3$  at 750°C. The hexagonal modification of BN has a simple layer structure (Fig. 6.27) similar to graphite but with the significant difference that the layers are packed directly on top of each other so that the B atom in one layer is located over an N atom in the next layer at a distance of 333 pm. Cell dimensions and other data for BN and graphite are compared in Table 6.5. Within each layer the B–N distance is only 145 pm; this is similar to the distance of 144 pm in borazine (p. 210) but much less than the sum of single-bond covalent radii (158 pm) and this has been taken to indicate substantial additional  $\pi$  bonding within the layer. However, unlike graphite, BN is colourless and a good insulator; it also resists

attack by most reagents though fluorine converts it quantitatively to  $BF_3$  and  $N_2$  and HF gives  $NH_4BF_4$  quantitatively. Hexagonal BN can be converted into a cubic form (zinc-blende type structure) at 1800°C and 85 000 atm pressure in the presence of an alkali or alkaline-earth metal catalyst. The lattice constant of cubic BN is 361.5 pm (cf. diamond 356.7 pm). A wurtzite-type modification (p. 1210) can be obtained at lower temperatures.



**Figure 6.27** Comparison of the hexagonal layer structures of BN and graphite. In BN the atoms of one layer are located directly above the atoms of adjacent layers with B...N contacts; in graphite the C atoms in one layer are located above interstices in the adjacent layer and are directly above atoms in alternate layers only.

Amine-borane adducts have the general formula  $R_3NBX_3$  where R = alkyl, H, etc., and

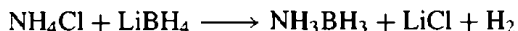
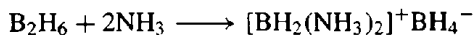
<sup>118</sup> I. ANDER, Chap. 1.21 in A. R. KATRITZKY and C. W. REES (eds.), *Comprehensive Heterocyclic Chemistry*, Pergamon, Oxford, 1984, pp. 629–63.

<sup>119</sup> R. T. PAINE and C. K. NARULA, *Chem. Rev.* **90**, 73–91 (1990).

**Table 6.5** Comparison of hexagonal BN and graphite

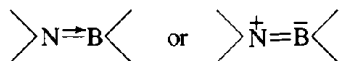
	<i>a</i> /pm	<i>c</i> /pm	<i>c/a</i>	Inter-layer spacing/pm	Intra-layer spacing/pm	<i>d</i> /g cm <sup>-3</sup>
BN (hexagonal)	250.4	666.1	2.66	333	144.6	2.29
Graphite	245.6	669.6	2.73	335	142	2.255

X = alkyl, H, halogen, etc. They are usually colourless, crystalline compounds with mp in the range 0–100° for X = H and 50–200° for X = halogen. Synthetic routes, and factors affecting the stability of the adducts have already been discussed (p. 165 and p. 198). In cases where diborane undergoes unsymmetrical cleavage (e.g. with NH<sub>3</sub>) alternative routes must be devised:

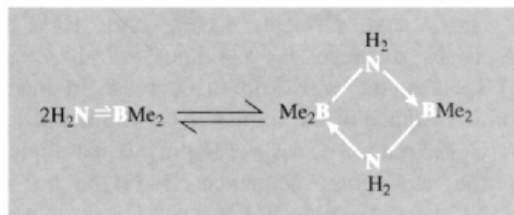


The nature of the bonding in amine-boranes and related adducts has been the subject of considerable theoretical discussion and has also been the source of some confusion. Conventional representations of the donor-acceptor (or coordinate) bond use symbols such as  $\text{R}_3\text{N} \rightarrow \text{BX}_3$  or  $\text{R}_3\overset{+}{\text{N}} - \overset{-}{\text{B}}\text{X}_3$  to indicate the origin of the bonding electrons and the direction (but not the magnitude) of charge transfer. It is important to realize that these symbols refer to the relative change in electron density with respect to the individual separate donor and acceptor molecules. Thus,  $\text{R}_3\overset{+}{\text{N}}$  in the adduct has less electron density on N than has free  $\text{R}_3\text{N}$ , and  $\overset{-}{\text{B}}\text{X}_3$  has more electron density on B in the adduct than has free  $\text{BX}_3$ ; this does not necessarily mean that N is positive with respect to B in the adduct. Indeed, several MO calculations indicate that the change in electron density on coordination merely reduces but is insufficient to reverse the initial positive charge on the B atom. Consistent with this, experiments show that electrophilic reagents always attack N in amine-borane adducts, and nucleophilic reagents attack B.

A similar situation obtains in the aminoboranes where one or more of the substituents on B is an  $\text{R}_2\text{N}$  group (R = alkyl, aryl, H), e.g.  $\text{Me}_2\text{N}-\text{BMe}_2$ . Reference to Fig. 6.22 indicates the possibility of some  $p_\pi$  interaction between the lone pair on N and the “vacant” orbital on trigonal B. This is frequently indicated as

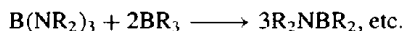
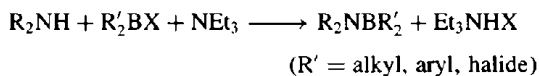
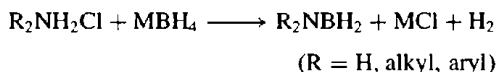


However, as with the amine-borane adducts just considered, this does not normally indicate the actual sign of the net charges on N and B because the greater electronegativity of N causes the  $\sigma$  bond to be polarized in the opposite sense. Thus, N–B bond moments in aminoboranes have been found to be negligible and MO calculations again suggest that the N atom bears a larger net negative charge than does the B atom. The partial double-bond formulation of these compounds, however, is useful in implying an analogy to the isoelectronic alkenes. Coordinative saturation in aminoboranes can be achieved not only through partial double bond formation but also by association (usually dimerization) of the monomeric units to form  $(\text{B}-\text{N})_n$  rings. For example, in the gas phase, aminodimethylborane exists as both monomer and dimer in reversible equilibrium:



The presence of bulky groups on either B or N hinders dimer formation and favours monomers, e.g.  $(\text{Me}_2\text{NBF}_2)_2$  is dimeric whereas the larger halides form monomers at least in the liquid phase. Association to form trimers (6-membered heterocycles) is less common, presumably because of even greater crowding of substituents, though triborazane  $(\text{H}_2\text{NBH}_2)_3$  and its *N*-methyl derivatives,  $(\text{MeHNBH}_2)_3$  and  $(\text{Me}_2\text{NBH}_2)_3$ , are known in which the  $\text{B}_3\text{N}_3$  ring adopts the cyclohexane chair conformation.

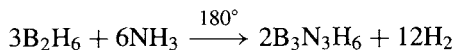
Preparative routes to these compounds are straightforward, e.g.:



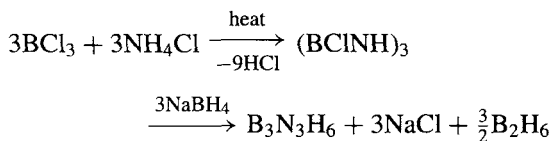
In general monomeric products are readily hydrolysed but associated species (containing 4-coordinate B) are much more stable: e.g.  $(\text{Me}_2\text{NBH}_2)_2$  does not react with  $\text{H}_2\text{O}$  at  $50^\circ$  but is rapidly hydrolysed by dilute  $\text{HCl}$  at  $110^\circ$  because at this temperature there is a significant concentration of monomer present.

Iminoboranes,  $\text{R}-\text{N}^{\equiv}\text{B}-\text{R}'$ , are isoelectronic with alkynes and contain 2-coordinate boron; their chemistry has recently been reviewed.<sup>(120,121)</sup> Likewise for amino iminoboranes,  $\text{R}_2\text{N}-\text{B}=\text{NR}'$ .<sup>(122)</sup> In both classes of compound inductive and steric effects have an important influence on stability. Another stable 2-coordinate boron species is the linear anion  $\text{BN}_2^{3-}$  (isoelectronic with  $\text{CO}_2$ ,  $\text{CNO}^-$ ,  $\text{NCO}^-$ ,  $\text{N}_2\text{O}$ ,  $\text{NO}_2^+$ ,  $\text{N}_3^-$  and  $\text{CN}_2^{2-}$ ) which occurs in  $\text{M}_3^{\text{I}}\text{BN}_2$  and  $\text{M}_3^{\text{II}}(\text{BN}_2)_2$ . For example,  $\text{Na}_3\text{BN}_2$  can be prepared as light honey-coloured crystals by heating a 2:1 mixture of  $\text{NaN}_3$  and  $\text{BN}$  at 4 GPa and  $1000^\circ\text{C}$ ; the B-N distance is 134.5 pm.<sup>(123)</sup> In neutral species, the well known decrease in interatomic distance in the sequence  $\text{C}-\text{C}$  (154 pm) >  $\text{C}=\text{C}$  (133 pm), >  $\text{C}\equiv\text{C}$  (118 pm) is paralleled by the analogous sequence  $\text{B}-\text{N}$  (158 pm) >  $\text{B}=\text{N}$  (140 pm) >  $\text{B}\equiv\text{N}$  (124 pm).

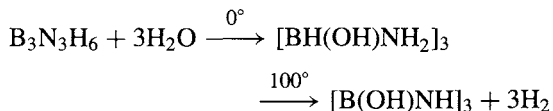
The cyclic borazine  $(-\text{BH}-\text{NH}-)_3$  and its derivatives form one of the largest classes of B-N compounds. The parent compound, also known as "inorganic benzene", was first isolated as a colourless liquid from the mixture of products obtained by reacting  $\text{B}_2\text{H}_6$  and  $\text{NH}_3$  (A. Stock and E. Pohland, 1926):



It is now best prepared by reduction of the B-trichloro derivative:



Borazine has a regular plane hexagonal ring structure and its physical properties closely resemble those of the isoelectronic compound benzene (Table 6.6). Although it is possible to write Kekulé-type structures with  $\text{N}=\text{B}$   $\pi$  bonding superimposed on the  $\sigma$  bonding, the weight of chemical evidence suggests that borazine has but little aromatic character. It reacts readily with  $\text{H}_2\text{O}$ ,  $\text{MeOH}$  and  $\text{HX}$  to yield 1:3 adducts which eliminate  $3\text{H}_2$  on being heated to  $100^\circ$ , e.g.:



**Table 6.6** Comparison of borazine and benzene

Property	$\text{B}_3\text{N}_3\text{H}_6$	$\text{C}_6\text{H}_6$
Molecular weight	80.5	78.1
MP/ $^\circ\text{C}$	-57	6
BP/ $^\circ\text{C}$	55	80
Critical temperature	252	288
Density (l at mp)/ $\text{g cm}^{-3}$	0.81	0.81
Density (s)/ $\text{g cm}^{-3}$	1.00	1.01
Surface tension at mp/ dyne $\text{cm}^{-1}$ ( <sup>a</sup> )	31.1	31.0
Interatomic distances/pm	B-N 144 B-H 120 N-H 102	C-C 142 C-H 108

(<sup>a</sup>) 1 dyne =  $10^{-5}$  newton.

Numerous other reactions have been documented, most of which are initiated by nucleophilic attack on B. There is no evidence that electrophilic substitution of the borazine ring occurs and conditions required for such reactions in benzenoid systems disrupt the borazine ring by oxidation or solvolysis. However, it is known that the less-reactive hexamethyl derivative  $\text{B}_3\text{N}_3\text{Me}_6$  (which can be heated to  $460^\circ$  for 3 h without significant decomposition)

<sup>120</sup> P. PAETZOLD, *Adv. Inorg. Chem.* **31**, 123-70 (1987).

<sup>121</sup> P. PAETZOLD, *Pure Appl. Chem.* **63**, 345-50 (1991).

<sup>122</sup> H. NÖTH, *Angew. Chem. Int. Edn. Engl.* **27**, 1603-22 (1988).

<sup>123</sup> J. EVERS, M. MÜNSTERKÖTTER, G. OEHLINGER, K. POLBORN and B. SENDLINGER, *J. Less Common Metals* **162**, L17-22 (1990). For the crystal structure of  $\text{Sr}_3(\text{BN}_2)_2$ , [B-N 135.8(6) pm, angle  $180^\circ$ ] see H. WOMELSDORF and H.-J. MEYER, *Z. anorg. allg. Chem.* **620**, 2652-5 (1994).

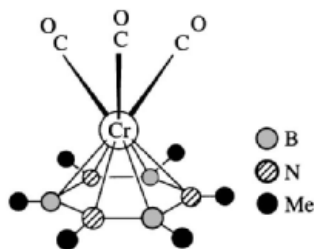
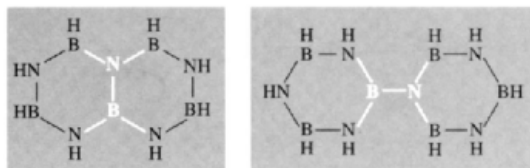


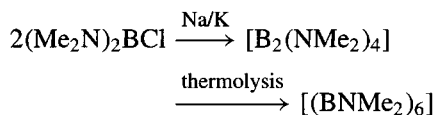
Figure 6.28 Structure of  $[\text{Cr}(\eta^6\text{-B}_3\text{N}_3\text{Me}_6)(\text{CO})_3]$ .

reacts with  $[\text{Cr}(\text{CO})_3(\text{MeCN})_3]$  to give the complex  $[\text{Cr}(\eta^6\text{-B}_3\text{N}_3\text{Me}_6)(\text{CO})_3]$  (Fig. 6.28) which closely resembles the corresponding hexamethylbenzene complex  $[\text{Cr}(\eta^6\text{-C}_6\text{Me}_6)(\text{CO})_3]$ .

*N*-substituted and *B*-substituted borazines are readily prepared by suitable choice of amine and borane starting materials or by subsequent reaction of other borazines with Grignard reagents, etc. Thermolysis of monocyclic borazines leads to polymeric materials and to polyborazine analogues of naphthalene, biphenyl, etc.:



A quite different structural motif is found in the curious cyclic hexamer  $[(\text{BNMe}_2)_6]$  which can be obtained as orange-red crystals by distilling the initial product formed by dehalogenation of  $(\text{Me}_2\text{N})_2\text{BCl}$  with Na/K alloy:<sup>(124)</sup>



The  $\text{B}_6$  ring has a chair conformation (dihedral angle  $57.6^\circ$ ) with mean B–B distances of 172 pm. All 6 B and all 6 N are trigonal planar and the 6-exocyclic  $\text{NMe}_2$  groups are each twisted at an angle of  $\sim 65^\circ$  from the adjacent  $\text{B}_3$  plane, with

B–N 140 pm. Structurally, this cyclohexaborane derivative resembles the radialenes, particularly the isoelectronic  $[\text{C}_6(=\text{CHMe})_6]$  in which the  $\text{C}_6$  ring likewise adopts the chair conformation.

Finally, the conceptual isoelectronic replacement of C–C by B–N can be applied to carboranes, thus leading (by appropriate synthetic routes) to azaboranes in which one or more of the cluster vertices of the borane is occupied by an N atom. So far, the following species have been characterized,<sup>(125)</sup> the relevant cluster geometries and numbering schemes being given by the indicated structures on pp. 153–85: *arachno*-4-NB<sub>8</sub>H<sub>13</sub> (20), *nido*-6-NB<sub>9</sub>H<sub>12</sub> (11), *closo*-1-NB<sub>9</sub>H<sub>10</sub> (5), *arachno*-6,9-N<sub>2</sub>B<sub>8</sub>H<sub>12</sub> (21), *nido*-7-NB<sub>10</sub>H<sub>13</sub> (41), *nido*-7-NB<sub>10</sub>H<sub>11</sub><sup>2-</sup> (80), *closo*-1-NB<sub>11</sub>H<sub>12</sub> (7, 76) and *anti*-9-NB<sub>17</sub>H<sub>20</sub> (31).

## 6.10 Other Compounds of Boron

### 6.10.1 Compounds with bonds to P, As or Sb

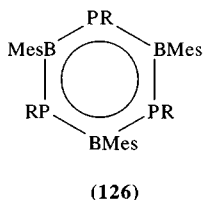
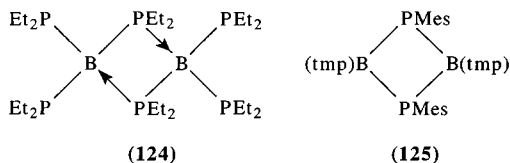
Only minor echoes of the extensive themes of B–N chemistry occur in compounds containing B–P, B–As or B–Sb bonds but there are signs that the field is now beginning to expand rapidly. Few 1:1 phosphine-borane adducts are known, although the recently characterized white crystalline complex  $(\text{C}_6\text{F}_5)_3\text{B}\cdot\text{PH}_3$ , which dissociates reversibly above room temperature, has been suggested as a useful storage material for the safe purification and generation of  $\text{PH}_3$ .<sup>(126)</sup> The interesting compound  $\text{Na}[\text{B}(\text{PH}_2)_4]$  can readily be made by reacting  $\text{BCl}_3$  with 4 moles of  $\text{NaPH}_2$ ; at moderate temperatures and in the presence of thf it rearranges to the diborate analogue  $\text{Na}[(\text{PH}_2)_3\text{B}-\text{PH}_2-\text{B}(\text{PH}_2)_3]$

<sup>124</sup> H. NÖTH and H. POMMERENING, *Angew. Chem. Int. Edn. Engl.* **19**, 482–3 (1980).

<sup>125</sup> T. JELÍNEK, J. D. KENNEDY and B. ŠTÍBR, *J. Chem. Soc., Chem. Commun.*, 677–8 (1994) and references cited therein. L. SCHNEIDER, U. ENGLERT and P. PAETZOLD, *Z. anorg. allg. Chem.* **620**, 1191–3 (1994). H.-P. HANSEN, U. E. ENGLERT and P. PAETZOLD, *Z. anorg. allg. Chem.* **621**, 719–24 (1995).  
<sup>126</sup> D. C. BRADLEY, M. B. HURSTHOUSE, M. MOTEVALLI and Z. DAO-HONG, *J. Chem. Soc., Chem. Commun.*, 7–8 (1991).

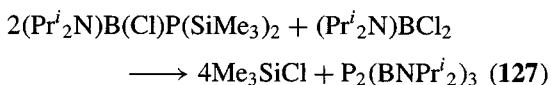
and with  $\text{BH}_3\cdot\text{thf}$  it gives the tetrakis(borane) adduct  $\text{Na}[\text{B}(\text{PH}_2\cdot\text{BH}_3)_4]$ .<sup>(127)</sup>

Phosphinoboranes, like their aminoborane analogues (p. 209), tend to oligomerize, although monomeric examples with planar B and pyramidal P atoms have recently been prepared using bulky substituents, e.g. yellow  $\text{Mes}_2\text{BPPh}_2$ ,<sup>(128)</sup> orange  $(\text{Mes}_2\text{P})_2\text{BBr}$ <sup>(129)</sup> and colourless  $(\text{Mes}_2\text{P})_2\text{BOEt}$ , mp  $163^\circ\text{C}$  <sup>130</sup> $(\text{Mes} = 2,4,6\text{-Me}_3\text{C}_6\text{H}_2\text{-})$ . By contrast,  $\text{B}(\text{PEt}_2)_3$  is a dimer with a planar  $\text{B}_2\text{P}_2$  ring of 4-coordinate B and P atoms (124).<sup>(130)</sup> A planar 4-membered ring of 3-coordinate planar B and pyramidal P atoms is featured in the diphosphadiboretane  $\{\text{MesPB}(\text{tmp})\}_2$  (125) ( $\text{tmp} = 2,2,6,6\text{-tetramethylpiperidino}$ );<sup>(131)</sup> the corresponding diarsadiboretane is also known. A phosphorus analogue of borazine (p. 210) having a planar  $\text{B}_3\text{P}_3$  ring is the pale yellow crystalline  $(\text{MesBPC}_6\text{H}_{11})_3$  (126), synthesized by reacting  $\text{MesBBR}_2$  with  $\text{C}_6\text{H}_{11}\text{PHLi}$  in hexane at room temperature;<sup>(132)</sup> the B–P distances in

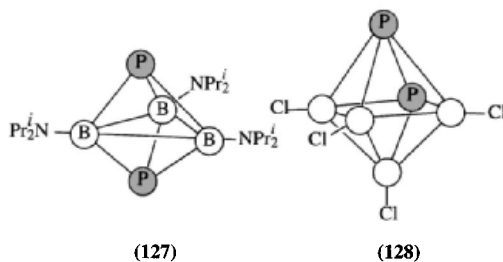


the boraphosphabenzene are all essentially equal, averaging 184 pm, which is considerably shorter than the known range of single-bond distances (192–196 pm). The cyclohexyl group,  $\text{C}_6\text{H}_{11}$ , can be replaced by Ph, Mes,  $\text{Bu}^t$ , etc.

Phosphaborane cluster compounds have also been synthesized. For example, thermolysis of a 1:2 mixture of  $(\text{Pr}_2\text{N})\text{BCl}$  and  $(\text{Pr}_2\text{N})\text{B}(\text{Cl})(\text{SiMe}_3)_2$  at  $160^\circ\text{C}$  results in the smooth elimination of  $\text{Me}_3\text{SiCl}$  to give colourless crystals of [*closo*-1,5- $\text{P}_2(\text{BNPr}_2)_3$ ] (127) in high yield:<sup>(133)</sup>



The structural analogy with the dicarbaborane  $\text{C}_2\text{B}_3\text{H}_5$  (56) is obvious. Likewise, pyrolysis of a mixture of  $\text{B}_2\text{Cl}_4$  and  $\text{PCl}_3$  yields [*closo*-1,2- $\text{P}_2\text{B}_4\text{Cl}_4$ ] (128) as hygroscopic colourless crystals.<sup>(134)</sup>



Typical borane clusters incorporating As or Sb atoms are *closo*-1,2- $\text{B}_{10}\text{H}_{10}\text{CHAs}$  and *closo*-1,2- $\text{B}_{10}\text{H}_{10}\text{CHSb}$  in which the group 15 heteroatom replaces a CH vertex in the dicarbaborane (76); they are prepared in 25 and 41% yield, respectively, by direct reaction of  $\text{Na}_3\text{B}_{10}\text{H}_{10}\text{CH}$  with  $\text{AsCl}_3$  or  $\text{SbI}_3$ , and can be isomerized in high yield below  $500^\circ\text{C}$  to the 1,7-isomers. Above  $500^\circ$  the 1,12-isomers can be obtained but this is accompanied by substantial decomposition. The diarsa derivative 1,2- $\text{B}_{10}\text{H}_{10}\text{As}_2$  is also known. Likewise, reaction of *nido*- $\text{B}_{10}\text{H}_{14}$  with  $\text{AsCl}_3$  and NaH or  $\text{NaBH}_4$  affords the 11-vertex anion 7- $\text{B}_{10}\text{H}_{12}\text{As}^-$

<sup>127</sup> M. BAUDLER, C. BLOCK, H. BUDZIKIEWICZ and H. MÜNSTER, *Z. anorg. allg. Chem.* **569**, 7–15 (1989).

<sup>128</sup> Z. FENG, M. M. OLMSTEAD and P. P. POWER, *Inorg. Chem.* **25**, 4615–6 (1986).

<sup>129</sup> H. H. KARSCH, G. HANIKA, B. HUBER, K. MEINDL, S. KÖNIG, K. KRÜGER and G. MÜLLER, *J. Chem. Soc., Chem. Commun.*, 373–5 (1989).

<sup>130</sup> H. NÖTH, *Z. anorg. allg. Chem.* **555**, 79–84 (1987).

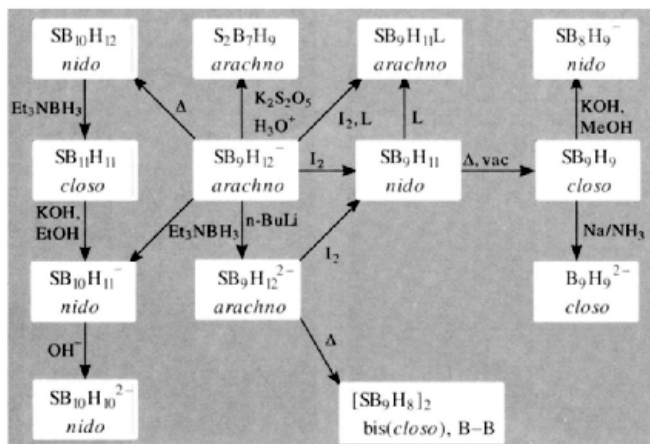
<sup>131</sup> A. M. ARIF, A. H. COWLEY, M. PAKULSKI and J. M. POWER, *J. Chem. Soc., Chem. Commun.*, 889–90 (1986).

<sup>132</sup> H. V. R. DIAS and P. P. POWER, *Angew. Chem. Int. Edn. Engl.* **26**, 1270–1 (1987); H. V. R. DIAS and P. P. POWER, *J. Am. Chem. Soc.* **111**, 144–8 (1989).

<sup>133</sup> G. L. WOOD, E. N. DUESLER, C. K. NARULA, R. T. PAINE and H. NÖTH, *J. Chem. Soc., Chem. Commun.*, 496–8 (1987).

<sup>134</sup> W. HAUBOLD, W. KELLER and G. SAWITZKI, *Angew. Chem. Int. Edn. Engl.* **27**, 925–6 (1988).





Scheme (for page 215)

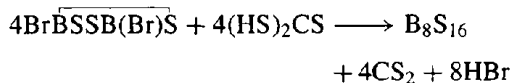
and this can be capped using  $\text{Et}_3\text{N}\cdot\text{BH}_3$  in diglyme at  $160^\circ$  to give the *closo*-icosahedral anion  $\text{B}_{11}\text{H}_{11}\text{As}^-$  in 51% yield. Other examples include  $\text{B}_{11}\text{H}_{11}\text{Sb}^-$ ,  $1,2\text{-B}_{10}\text{H}_{10}\text{Sb}_2$ ,  $1,2\text{-B}_{10}\text{H}_{10}\text{AsSb}$  and the arsenathia- and arsenaselenaboranes  $\text{B}_8\text{H}_8\text{As}_2\text{S}$  and  $\text{B}_8\text{H}_8\text{As}_2\text{Se}$ .<sup>(135)</sup>

### 6.10.2 Compounds with bonds to S, Se and Te

The vast array of B–O minerals and compounds (pp. 139–40 and 203–7) finds no parallel in B–S or B–Se chemistry though thioborates of the type  $\text{B}(\text{SR})_3$ ,  $\text{R}'\text{B}(\text{SR})_2$  and  $\text{R}'_2\text{B}(\text{SR})$  are well documented. There are also a growing number of binary boron sulfides and boron–sulfur anions which feature chains, rings and networks.  $\text{B}_2\text{S}_3$  itself has been known for many years as a pale-yellow solid which tends to form a glassy phase (cf.  $\text{B}_2\text{O}_3$  and also  $\text{B}_2\text{Se}_3$ ). This absence of a suitable crystalline sample prevented the structural characterization of this compound until as late as 1977. It has now been found that  $\text{B}_2\text{S}_3$  has a fascinating layer structure which bears no resemblance to the three-dimensionally linked  $\text{B}_2\text{O}_3$  crystal structure but is slightly reminiscent of BN. The structure (Fig. 6.29a) is made up of planar

$\text{B}_3\text{S}_3$  6-membered rings and  $\text{B}_2\text{S}_2$  4-membered rings linked by S bridges into almost planar two-dimensional layers.<sup>(136)</sup> All the boron atoms are trigonal planar with B–S distances averaging 181 pm and the perpendicular interlayer distance is almost twice this at 355 pm. More recently<sup>(137)</sup> a monomeric form of  $\text{B}_2\text{S}_3$  was prepared by matrix-isolation techniques at 10 K and shown by vibrational spectroscopy to be a planar V-shaped molecule,  $\text{S}=\text{B}-\text{S}-\text{B}=\text{S}$ , with  $C_{2v}$  symmetry, the angle subtended at the central S atom by the linear arms being about  $120^\circ$ .

Another boron sulfide, of stoichiometry  $\text{BS}_2$ , can be made by heating  $\text{B}_2\text{S}_3$  and sulfur to  $300^\circ\text{C}$  under very carefully defined conditions.<sup>(138)</sup> It is a colourless, moisture-sensitive material with a porphine-like molecular structure,  $\text{B}_8\text{S}_{16}$ , as shown in Fig. 6.29b. An alternative route to  $\text{B}_8\text{S}_{16}$  involves the reaction of dibromotrithiadiborolane with trithiocarbonic acid in an  $\text{H}_2\text{S}$  generator in dilute  $\text{CS}_2$  solution:

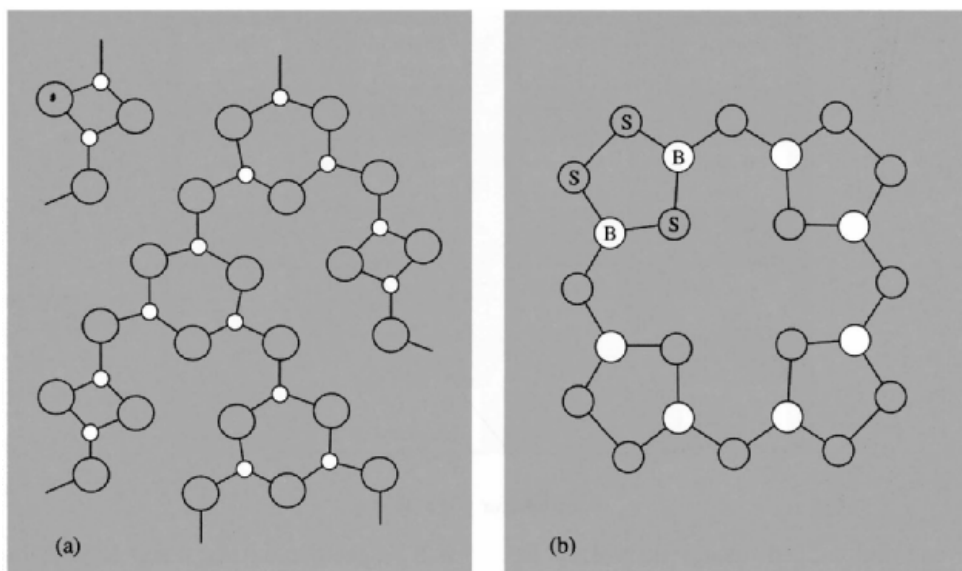


<sup>136</sup> H. DIERCKS and B. KREBS, *Angew. Chem. Int. Edn. Engl.* **16**, 313 (1977).

<sup>137</sup> I. R. BEATTIE, P. J. JONES, D. J. WILD and T. R. GILSON, *J. Chem. Soc., Dalton Trans.*, 267–9 (1987).

<sup>138</sup> B. KREBS and H. U. HURTER, *Angew. Chem. Int. Edn. Engl.* **19**, 481–2 (1980).

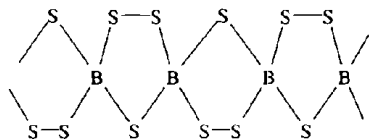
<sup>135</sup> L. J. TODD, Chap. 4 in R. N. GRIMES (ed.) *Metal Interactions with Boron Clusters*, Plenum, New York, 1982, pp. 145–71.



**Figure 6.29** (a) Part of the layer structure of  $B_2S_3$  perpendicular to the plane of the layer. (b) Porphine-like structure of the molecule  $B_8S_{16}$ .

The monomeric selenium compound  $BSe_2$  has been identified mass-spectrometrically in the vapours formed by reacting solid boron with  $Se_2$  and its thermodynamic properties evaluated.<sup>(139)</sup>

Another expanding area of B–S chemistry is the synthesis and structural characterization of anionic species. The colourless thioborate  $RbBS_3$  was formed by heating the stoichiometric amounts of  $Rb_2S$ , B and S at  $600^\circ$ . Its structure, and that of the yellow  $TlBS_3$ , features polymeric anionic chains that are spirocyclically connected via tetrahedral B atoms as shown schematically below:<sup>(140)</sup>



The sulfur-rich analogue  $Tl_3B_3S_{10}$  was likewise prepared as yellow plates from the appropriate stoichiometric mixture of  $(3Tl_2S + 6B + 17S)$  at

<sup>139</sup> M. BINNEWIES, *Z. anorg. allg. Chem.* **589**, 115–21 (1990).

<sup>140</sup> C. PUTTMANN, F. HILTMANN, W. HAMANN, C. BRENDL and B. KREBS, *Z. anorg. allg. Chem.* **619**, 109–16 (1993).

$850^\circ$  and shown to have a similar polymeric anion with the extra S atoms inserted into each third pentatomic heterocycle to make it a hexatomic unit,  $>B(S_2)_2B<$ . With the smaller cation,  $Li^+$ , similar procedures generate  $Li_5B_7S_{13}$  and  $Li_9B_{19}S_{33}$  which again have novel polymeric anions. The  $\{B_7S_{13}^{5-}\}_\infty$  polymer is formed by sharing  $B_4S_{10}$  and  $B_{10}S_{20}$  units, i.e.  $\{B_4S_6S_{4/2}^{4-}\}$  (cf.  $P_4O_{10}$ ) and  $\{B_{10}S_{16}S_{4/2}^{6-}\}$  both of which are built up from tetrahedral  $BS_4$  subunits, whereas the  $\{B_{19}S_{33}^{9-}\}_\infty$  polymer is formed from the conjoining of  $\{B_{19}S_{30}S_{6/2}^{9-}\}$  units.<sup>(141)</sup>

The structural principles and reaction chemistry of B–S compounds have recently been reviewed.<sup>(142)</sup> This includes not only electron-precise 4-, 5- and 6-membered heterocycles of the types described above, but also electron-deficient polyhedral clusters based on *closo*-,

<sup>141</sup> F. HILTMANN, P. ZUM HEBEL, A. HAMMERSCHMIDT and B. KREBS, *Z. anorg. allg. Chem.* **619**, 293–302 (1993). For other novel B/S/Se anions from B. Krebs' group see *Z. anorg. allg. Chem.* **620**, 1898–1904 (1994); **621**, 424–30, 1322–9 and 1330–7 (1995).

<sup>142</sup> J. R. BOWSER and T. P. FEHLNER, in H. W. ROESKY (ed.), *Rings, Clusters and Polymers of Main Group and Transition Elements*, Elsevier, Amsterdam, 1989, pp. 1–48.

*nido*- and *arachno*-boranes. Some typical inter-conversion reactions of thiaboranes are shown in the scheme on p. 213,<sup>(142)</sup> and further examples are in references (143) and (144). Seleno- and telluro-derivatives are also known<sup>(135,145)</sup> and, like the thiaboranes, have structures that can be rationalized by the normal electron

counting rules, taking the chalcogen atom as a 4-electron donor, e.g. *closo*-B<sub>11</sub>H<sub>11</sub>Te, *nido*-B<sub>10</sub>H<sub>12</sub>Te, *nido*-B<sub>10</sub>H<sub>11</sub>Te<sup>-</sup>, *nido*-B<sub>9</sub>H<sub>11</sub>Te, *nido*-B<sub>9</sub>H<sub>9</sub>Se<sub>2</sub>, *nido*-B<sub>9</sub>H<sub>9</sub>STe, *arachno*-B<sub>8</sub>H<sub>10</sub>Se<sub>2</sub>, [Fe( $\eta^5$ -B<sub>10</sub>H<sub>10</sub>Te)<sub>2</sub>]<sup>2-</sup> (green) and [Co( $\eta^5$ -C<sub>5</sub>H<sub>5</sub>)-( $\eta^5$ -B<sub>10</sub>H<sub>10</sub>Te)] (yellow).

There appears to be no end to the structural ingenuity of boron and, whilst it is true that many regularities can now be discerned in its stereochemistry, much more work is still needed to unravel the reaction pathways by which the compounds are formed and to elucidate the mechanisms by which they isomerize and interconvert.

<sup>143</sup> T. JELINEK, J. D. KENNEDY and B. ŠTÍBR, *J. Chem. Soc., Chem. Commun.*, 1415–6 (1994).

<sup>144</sup> S. O. KANG and L. G. SNEDDON, Chap. 8 in G. A. OLAH, K. WADE and R. E. WILLIAMS (eds.), *Electron Deficient Boron and Carbon Clusters*, Wiley, New York, 1991, pp. 195–213.

<sup>145</sup> G. D. FRIESEN, T. P. HANUSA and L. J. TODD, *Inorg. Synth.* **29**, 103–7, (1992).

																H		He																	
Li												Be																		B	C	N	O	F	Ne
11	Na	12											Mg	13	Al	14	Si	15	P	16	S	17	Cl	18	Ar										
19	K	20	Ca	21	Sc	22	Ti	23	V	24	Cr	25	Mn	26	Fe	27	Cu	28	Ni	29	Cu	30	Zn	31	Ga	32	Ge	33	As	34	Se	35	Br	36	Kr
37	Rb	38	Sr	39	Y	40	Zr	41	Nb	42	Mo	43	Tc	44	Ru	45	Rh	46	Pd	47	Ag	48	Cd	49	In	50	Sn	51	Sb	52	Te	53	I	54	Xe
55	Cs	56	Ba	57	La	58	Ce	59	Pr	60	Nd	61	Pm	62	Sm	63	Eu	64	Gd	65	Tb	66	Dy	67	Ho	68	Er	69	Tm	70	Yb	71	Lu		
87	Fr	88	Ra	89	Ac	90	Th	91	Pa	92	U	93	Np	94	Pu	95	Am	96	Cm	97	Bk	98	Cf	99	Es	100	Fm	101	Md	102	No	103	Lr		

# 7

## Aluminium, Gallium, Indium and Thallium

### 7.1 Introduction

Aluminium derives its name from alum, the double sulfate  $KAl(SO_4)_2 \cdot 12H_2O$ , which was used medicinally as an astringent in ancient Greece and Rome (Latin *alumen*, bitter salt). Humphry Davy was unable to isolate the metal but proposed the name “aluminum” and then “aluminium”; this was soon modified to aluminium and this form is used throughout the world except in North America where the ACS decided in 1925 to adopt “aluminum” in its publications. The impure metal was first isolated by the Danish scientist H. C. Oersted using the reaction of dilute potassium amalgam on  $AlCl_3$ . This method was improved in 1827 by H. Wöhler who used metallic potassium, but the first commercially successful process was devised by H. St.-C. Deville in 1854 using sodium. In the same year both he and R. W. Bunsen independently obtained metallic aluminium by electrolysis of fused  $NaAlCl_4$ . So precious was the metal at this time that it was exhibited next to the crown jewels at the Paris Exposition of 1855 and the Emperor Louis Napoleon

III used Al cutlery on state occasions. The dramatic thousand-fold drop in price which occurred before the end of the century (Table 7.1) was due first to the advent of cheap electric power following the development of the dynamo by W. von Siemens in the 1870s, and secondly to the independent development in 1886 of the electrolysis of alumina dissolved in cryolite ( $Na_3AlF_6$ ) by P. L. T. Héroult in France and C. M. Hall in the USA; both men were 22 years old at the time. World production rose quickly and in 1893 exceeded 1000 tonnes pa for the first time.

Gallium was predicted as eka-aluminium by D. I. Mendeleev in 1870 and was discovered by P. E. Lecoq de Boisbaudran in 1875 by means of the spectroscope; de Boisbaudran was, in fact, guided at the time by an independent theory of his own and had been searching for the missing element for some years. The first indications came with the observation of two new violet lines in the spark spectrum of a sample deposited on zinc, and within a month he had isolated 1 g of the metal starting from several hundred kilograms of crude zinc blende ore. The

Table 7.1 Price of aluminium metal (\$ per kg)

1852	1854	1855	1856	1857	1858	1886	
1200	600	250	75	60	25	17	
→   Introduction of St. C. Deville's Na/AlCl <sub>3</sub> process							
1888	1890	1895	1900	1950	1965	1980	1989
11.5	5.0	1.15	0.73	0.40	0.54	1.53	1.94
→   Introduction of Héroult-Hall electrolysis				↑ minimum			

Table 7.2 Comparison of predicted and observed properties of gallium

Mendeleev's predictions (1871) for eka-aluminium, M	Observed properties (1993) of gallium (discovered 1875)
Atomic weight ~68	Atomic weight 69.723
Density/g cm <sup>-3</sup> 5.9	Density/g cm <sup>-3</sup> 5.904
MP low	MP/°C 29.767
Non-volatile	Vapour pressure 10 <sup>-3</sup> mmHg at 1000°C
Valence 3	Valence 3
M will probably be discovered by spectroscopic analysis	Ga was discovered by means of the spectroscope
M will have an oxide of formula M <sub>2</sub> O <sub>3</sub> , <i>d</i> 5.5 g cm <sup>-3</sup> , soluble in acids to give MX <sub>3</sub>	Ga has an oxide Ga <sub>2</sub> O <sub>3</sub> , <i>d</i> 5.88 g cm <sup>-3</sup> , soluble in acids to give salts of the type GaX <sub>3</sub>
M should dissolve slowly in acids and alkalis and be stable in air	Ga metal dissolves slowly in acids and alkalis and is stable in air
M(OH) <sub>3</sub> should dissolve in both acids and alkalis	Ga(OH) <sub>3</sub> dissolves in both acids and alkalis
M salts will tend to form basic salts; the sulfate should form alums; M <sub>2</sub> S <sub>3</sub> should be precipitated by H <sub>2</sub> S or (NH <sub>4</sub> ) <sub>2</sub> S; anhydrous MCl <sub>3</sub> should be more volatile than ZnCl <sub>2</sub>	Ga salts readily hydrolyse and form basic salts; alums are known; Ga <sub>2</sub> S <sub>3</sub> can be precipitated under special conditions by H <sub>2</sub> S or (NH <sub>4</sub> ) <sub>2</sub> S; anhydrous GaCl <sub>3</sub> is more volatile than ZnCl <sub>2</sub>

element was named in honour of France (Latin *Gallia*) and the striking similarity of its physical and chemical properties to those predicted by Mendeleev (Table 7.2) did much to establish the general acceptance of the Periodic Law (p. 20); indeed, when de Boisbaudran first stated that the density of Ga was 4.7 g cm<sup>-3</sup> rather than the predicted 5.9 g cm<sup>-3</sup>, Mendeleev wrote to him suggesting that he redetermine the figure (the correct value is 5.904 g cm<sup>-3</sup>).

Indium and thallium were also discovered by means of the spectroscope as their names indicate. Indium was first identified in 1863 by F. Reich and H. T. Richter and named from the brilliant indigo blue line in its flame spectrum (Latin *indicum*). Thallium was discovered independently by W. Crookes and by

C. A. Lamy in the preceding year 1861/2 and named after the characteristic bright green line in its flame spectrum (Greek *θαλλός*, *thallos*, a budding shoot or twig).

## 7.2 The Elements

### 7.2.1 Terrestrial abundance and distribution

Aluminium is the most abundant metal in the earth's crust (8.3% by weight); it is exceeded in abundance only by O (45.5%) and Si (25.7%), and is approached only by Fe (6.2%) and Ca (4.6%). Aluminium is a major constituent of many common igneous minerals including

feldspars and micas. These, in turn, weather in temperate climates to give clay minerals such as kaolinite [ $\text{Al}_2(\text{OH})_4\text{Si}_2\text{O}_5$ ], montmorillonite and vermiculite (p. 349). It also occurs in many well-known though rarer minerals such as cryolite ( $\text{Na}_3\text{AlF}_6$ ), spinel ( $\text{MgAl}_2\text{O}_4$ ), garnet [ $\text{Ca}_3\text{Al}_2(\text{SiO}_4)_3$ ], beryl ( $\text{Be}_3\text{Al}_2\text{Si}_6\text{O}_{18}$ ), and turquoise [ $\text{Al}_2(\text{OH})_3\text{PO}_4\text{H}_2\text{O}/\text{Cu}$ ]. Corundum ( $\text{Al}_2\text{O}_3$ ) is one of the hardest substances known and is therefore used as an abrasive; many gemstones are impure forms of  $\text{Al}_2\text{O}_3$ , e.g. ruby (Cr), sapphire (Co), oriental emerald, etc. Commercially, the most important mineral is bauxite  $\text{AlO}_x(\text{OH})_{3-2x}$  ( $0 < x < 1$ ); this occurs in a wide belt in tropical and subtropical regions as a result of the leaching out of both silica and various metals from aluminosilicates (see Panel).

Gallium, In and Tl are very much less abundant than Al and tend to occur at low concentrations in sulfide minerals rather than as oxides, though Ga is also found associated with Al in bauxite. Ga (19 ppm) is about as abundant as N, Nb, Li and Pb; it is twice as abundant as B (9 ppm) but is more difficult to extract because of the absence of major Ga-containing ores. The highest concentrations (0.1–1%) are in the rare mineral germanite (a complex sulfide of Zn, Cu, Ge and As); concentrations in sphalerite (ZnS), bauxite or coal, are a hundredfold less. Gallium always occurs in association either with Zn or Ge, its neighbours in the periodic table, or with Al in the same group. It was formerly recovered from

flue dusts emitted during sulfide roasting or coal burning (up to 1.5% Ga) but is now obtained as a byproduct of the vast Al industry. Since bauxites contain 0.003–0.01% Ga, complete recovery would yield over 1000 tonnes pa. However, present consumption, though growing rapidly, is little more than 1% of this and production is of the order of 50 tonnes pa (1986). This can be compared with the estimate of 5 tonnes for the total of Ga metal in the 90 y following its discovery (1875–1965). Its price in 1928 was \$50 per g; in 1965 it was \$1 per g, similar to the then price of gold (\$1.1 per g), and in 1986 it was \$0.45 per g, i.e. \$450/kg for semiconductor grade metal (99.9999%).

Indium (0.24 ppm) is similar in abundance to Sb and Cd, whereas Tl (0.7 ppm) is close to Tm and somewhat less abundant than Mo, W and Tb (1.2 ppm). Both elements are chalcophiles (p. 648), indium tending to associate with the similarly sized Zn in its sulfide minerals whilst the larger Tl tends to replace Pb in galena, PbS. Thallium(I) has a similar radius to  $\text{Rb}^+$  and so also concentrates with this element in the late magmatic potassium minerals such as feldspars and micas.

Indium is now commercially recovered from the flue dusts emitted during the roasting of Zn/Pb sulfide ores and can also be recovered during the roasting of Fe and Cu sulfide ores. Before 1925 only 1 g of the element was available in the world but production now exceeds 80 000 000 g

### Bauxite

The mixed aluminium oxide hydroxide mineral bauxite was discovered by P. Berthier in 1821 near Les Baux in Provence. In temperate countries (such as Mediterranean Europe) it occurs mainly as the "monohydrate"  $\text{AlOOH}$  (boehmite and diaspore) whereas in the tropics it is generally closer to the "trihydrate"  $\text{Al}(\text{OH})_3$  (gibbsite and hydrargillite). Since  $\text{AlOOH}$  is less soluble in aqueous NaOH than is  $\text{Al}(\text{OH})_3$ , this has a major bearing on the extraction process for Al manufacture (p. 219). Typical compositions for industrially used bauxites are  $\text{Al}_2\text{O}_3$  40–60%, combined  $\text{H}_2\text{O}$  12–30%,  $\text{SiO}_2$  free and combined 1–15%,  $\text{Fe}_2\text{O}_3$  7–30%,  $\text{TiO}_2$  3–4%, F,  $\text{P}_2\text{O}_5$ ,  $\text{V}_2\text{O}_5$ , etc., 0.05–0.2%.

World production in 1989 was over 101 million tonnes and this is still increasing. Reserves are immense, being of the order of  $22 \times 10^9$  tonnes in all (Guinea 5.6, Australia 4.4, Brazil 2.8, Jamaica 2.0, India 1.0, USA 0.038 Gt). Australia is currently the largest producer of alumina with 36.6%, followed by Guinea 16.6%, Brazil 8.7%, Jamaica 8.2% the former Soviet Union 4.6%, India 3.9%, etc. Bauxite is easy to mine by open-cast methods since it occurs typically in broad layers 3–10 m thick with very little topsoil or other overburden. Apart from its preponderant use (>80%) in Al extraction, bauxite is used to manufacture refractories, high-alumina cements and aluminium compounds, and smaller amounts are used as drying agents and as catalysts in the petrochemicals industry.

(i.e. 80 tonnes) each year. Prices have fluctuated widely during the past 20 years, being \$270/kg for 99.97% purity in 1987.

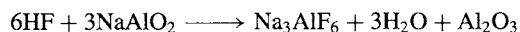
Thallium is likewise recovered from flue dusts emitted during sulfide roasting for H<sub>2</sub>SO<sub>4</sub> manufacture, and from the smelting of Zn/Pb ores. Extraction procedures are complicated because of the need to recover Cd at the same time. There are no major commercial uses for Tl metal; world production in 1983 was estimated to be 5–15 tonnes p.a. and the price ranged from \$60 to \$80 per kg depending on purity and amount purchased.

### 7.2.2 Preparation and uses of the metals <sup>(1)</sup>

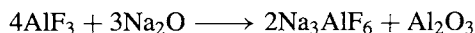
The huge difference in scale between the production of Al metal, on the one hand, and the other elements in the group is clear from the preceding section. The tremendous growth of the Al industry compared with all other non-ferrous metals is indicated in Table 7.3 and Al production is now exceeded only by that of iron and steel (p. 1072).

Production of Al metal involves two stages: (a) the extraction, purification and dehydration of bauxite, and (b) the electrolysis of Al<sub>2</sub>O<sub>3</sub> dissolved in molten cryolite Na<sub>3</sub>AlF<sub>6</sub>. Bauxite is now almost universally treated by the Bayer process; this involves dissolution in aqueous NaOH, separation from insoluble impurities (red muds), partial precipitation of the trihydrate

and calcining at 1200°. Bauxites approximating to the “monohydrate” AlOOH require higher concentrations of NaOH (200–300 g l<sup>-1</sup>) and higher temperatures and pressures (200–250°C, 35 atm) than do bauxites approximating to Al(OH)<sub>3</sub> (100–150 g l<sup>-1</sup> NaOH, 120–140°C). Electrolysis is carried out at 940–980°C in a carbon-lined steel cell (cathode) with carbon anodes. Originally Al<sub>2</sub>O<sub>3</sub> was dissolved in molten cryolite (Héroult–Hall process) but cryolite is a rather rare mineral and production from the mines in Greenland provide only about 30 000 tonnes pa, quite insufficient for world needs. Synthetic cryolite is therefore manufactured in lead-clad vessels by the reaction of HF on sodium aluminate (from the Bayer process):



No further cryolite is actually needed once the smelting process is in operation because it is produced in the reduction cells by neutralizing the Na<sub>2</sub>O brought into the cell as an impurity in the alumina using AlF<sub>3</sub>:



Thus operating cells need AlF<sub>3</sub> rather than cryolite, much of it being produced in a fluidized bed reactor from gaseous HF and activated alumina (made by partially calcining the alumina hydrate from the Bayer process). Typical electrolyte composition ranges are Na<sub>3</sub>AlF<sub>6</sub> (80–85%), CaF<sub>2</sub> (5–7%), AlF<sub>3</sub> (5–7%), Al<sub>2</sub>O<sub>3</sub> (2–8% — intermittently recharged). See also p. 70 for the beneficial use of Li<sub>2</sub>CO<sub>3</sub>. The detailed electrolysis mechanism is still imperfectly understood but typical operating conditions require up to 10<sup>5</sup> A at 4.5 V and a current density of 0.7 A cm<sup>-2</sup>. One tonne Al metal requires 1.89 tonnes Al<sub>2</sub>O<sub>3</sub>, ~0.45 tonnes C anode material, 0.07 tonnes Na<sub>3</sub>AlF<sub>6</sub> and about 15 000 kWh of electrical energy. It follows that cheap electric power is the overriding commercial consideration. World production (1988) exceeded 17 million tonnes pa, the leading producers being the USA (23%), China (21%), the former Soviet Union (14%), Canada (9%), Australia (7%),

**Table 7.3** World production of some non-ferrous metals/million tonnes pa

Metal	1900	1950	1970	1980	1988
Al	0.0057	1.52	9.78	16.04	17.30
Cu	0.50	2.79	6.38	6.08	5.96
Zn	0.48	1.96	5.10	6.15	7.22
Pb	0.88	1.75	4.00	5.40	3.37

<sup>1</sup> *Kirk–Othmer Encyclopedia of Chemical Technology*, 4th edn., Vol. 2, Aluminium and aluminium alloys, pp. 184–251; Aluminium compounds, pp. 252–345. Interscience, New York, 1992.

Brazil, Norway and Czechoslovakia (5% each). In addition to this primary production, recycling of used alloys probably adds a further 3–4 million tonnes pa to the total Al metal consumed.

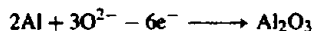
Some uses of Al and its alloys are noted in the Panel from which it will be seen that many of

the mechanical properties of pure Al are greatly improved by alloying it with Cu, Mn, Si, Mg or Zn (Table A). The example of Cu is particularly important because of the insight which it gives into the subtle solid-state diffusion processes that occur during heat treatment. At room temperature

### Some Uses of Aluminium Metal and Alloys

Pure aluminium is a silvery-white metal with many desirable properties: it is light, non-toxic, of pleasing appearance, and capable of taking a high polish. It has a high thermal and electrical conductivity, excellent corrosion resistance, is non-magnetic, non-sparking and stands second only to gold for malleability and sixth for ductility. Many of its alloys have high mechanical and tensile strength. Aluminium and its alloys can be cast, rolled, extruded, forged, drawn or machined, and they are readily obtained as pipes, tubes, rods, bars, wires, plates, sheets or foils.

Aluminium resists corrosion not because of its position in the electrochemical series but because of the rapid formation of a coherent, inert, oxide layer. Contact with graphite, Fe, Ni, Cu, Ag or Pb is disastrous for corrosion resistance; the effect of contact with steel, Zn and Cd depends on pH and exposure conditions. Protection is enhanced by anodizing the metal; this involves immersing it in 15–20% H<sub>2</sub>SO<sub>4</sub> and connecting it to the positive terminal so that it becomes coated with alumina:



A layer 10–20 μm thick gives excellent protection between pH 4.5–8.7 and is also adequate for external architectural use; thicker layers (50–100 μm) also impart abrasion resistance. The layer can be coloured by incorporating suitable organic or inorganic compounds in the bath and incorporation of photosensitive material enables photographic images to be developed. Decorative engraving using solutions of nitrate or NH<sub>4</sub>HF<sub>2</sub> gives the metal a fine silky texture.

Table A Some aluminium alloys

1000 Series:	Commercially pure Al (<1% of other elements); good properties except for limited mechanical strength. Used in chemical equipment, reflectors, heat exchangers, buildings and decorative trim.
2000 Series:	Cu alloys (~5%); excellent strength and machinability, limited corrosion resistance. Used for components requiring high strength/weight ratio, e.g. truck trailer panels, aircraft structure parts.
3000 Series:	Mn alloys (~1.2%); moderate strength, high workability. Used for cooking utensils, heat exchangers, storage tanks, awnings, furniture, highway signs, roofing, side panels, etc.
4000 Series:	Si alloys (≤12%); low mp and low coefficient of expansion. Used for castings and as filler material for brazing and welding; readily anodized to attractive grey colours.
5000 Series:	Mg alloys (0.3–5%); good strength and weldability coupled with excellent corrosion resistance in marine atmospheres. Used for ornamental and decorative trim, street light standards, ships, boats, cryogenic vessels, gun mounts and crane parts.
6000 Series:	Mg/Si alloys; good formability and high corrosion resistance. Used in buildings, transportation equipment, bridges, railings and welded construction.
7000 Series:	Zn alloys (3–8%) plus Mg; when heat treated and aged have very high strength. Used principally for aircraft structures, mobile equipment and equipment requiring high strength/weight ratio.

Many of the uses listed in Table A are a matter of everyday observation. In addition we may note that the electrical conductivity of pure Al is 63.5% of the conductivity of an equal *volume* of pure Cu; when the lower density of Al is considered its conductivity is 2.1 times that of Cu on a wt. for wt. basis. This, coupled with its corrosion resistance and ready workability makes it an ideal metal for power lines and, indeed, more than 90% of all overhead electrical transmission lines in the USA are Al alloy.

Aluminium is now extensively used in the construction and aerospace industries throughout the world although in the USA packaging has replaced the construction industry as the largest consumer of Al and its alloys. For example, 95% of beer and soft drinks is packaged in two-piece cans comprising an Al/Mn alloy body and Al/Mg alloy ends. There is also extensive use in food packaging, aerosol cans, collapsible tubes for toiletries and pharmaceuticals and as foil (typically 0.18 mm thick).



Al dissolves only about 0.1% Cu and this has little effect on its properties. The solubility rises to a maximum of 5.65% Cu at 548°C and this remains in metastable solid solution to give a soft workable alloy when the alloy is rapidly quenched to temperatures below 65°. Subsequent ageing of the shaped material at 100–150° for a few minutes hardens the alloy due to the formation of Guinier–Preston zones: these zones, independently discovered in 1938 by A. Guinier (France) and G. D. Preston (England), are minute discs of material higher in Cu content than the matrix — they are about 4 atoms thick and up to 100 atoms across; they mesh coherently with the host lattice in two directions, the (100) planes, but not in the third. The coherency strains which thereby develop in the lattice are the basis for the hardening of the alloy. Besides its immense technological importance, this phenomenon is particularly significant in being one of the first recognized examples of a single phase which nevertheless varies regularly in composition throughout its extent.

Gallium metal is now obtained as a byproduct of the Al industry. The Bayer process for obtaining alumina from bauxite gradually enriches the alkaline solutions from an initial weight ratio Ga/Al of about 1/5000 to about 1/300; electrolysis of these extracts with an Hg electrode gives further concentration, and the solution of sodium gallate is then electrolysed with a stainless steel cathode to give Ga metal. Ultra high-purity Ga for semiconductor uses is obtained by further chemical treatment with acids and O<sub>2</sub> at high temperatures followed by crystallization and zone refining. Gallium has a beautiful silvery blue appearance; it wets glass, porcelain, and most other surfaces (except quartz, graphite, and teflon) and forms a brilliant mirror when painted on to glass. Its main use is in semiconductor technology (p. 258). For example, GaAs (isoelectronic with Ge) can convert electricity directly into coherent light (laser diodes) and is employed in electroluminescent light-emitting diodes (LEDs); it is also used for doping other semiconductors and in solid-state devices such as transistors.

The compound MgGa<sub>2</sub>O<sub>4</sub>, when activated by divalent impurities such as Mn<sup>2+</sup>, is used in ultraviolet-activated powders as a brilliant green phosphor. Another very important application is to improve the sensitivity of various bands used in the spectroscopic analysis of uranium. Minor uses are as high-temperature liquid seals, manometric fluids and heat-transfer media, and for low-temperature solders.

Indium, like Ga, is normally recovered by electrolysis after prior concentration in processes leading primarily to other elements (Pb/Zn). It is a soft, silvery metal with a brilliant lustre and (like Sn) it gives out a high-pitched “cry” when bent. Formerly it was much used to protect bearings against wear and corrosion but the pattern of use has been changing in recent years and now its most important applications are in low-melting alloys and in electronic devices. Thus meltable safety devices, heat regulators, and sprinklers use alloys of In with Bi, Cd, Pb and Sn (mp 50–100°C) and In-rich solders are valuable in sealing metal-nonmetal joints in high vacuum apparatus. Indium is of particular importance in the manufacture of p–n–p transistor junctions in Ge (p. 369) and to solder semiconductor leads at low temperature; the softness of the metal also minimizes stress in the Ge during subsequent cooling. So-called III–V semiconductors like InAs and InSb are used in low-temperature transistors, thermistors and optical devices (photoconductors), and InP is used for high-temperature transistors. A further minor use, which exploits the high neutron capture cross-section of In, is as a component in control rods for certain nuclear reactors.

Technical grade Tl is purified from other flue-dust elements (Ni; Zn, Cd; In; Ge, Pb; As; Se, Te) by dissolving it in warm dilute acid, then precipitating the insoluble PbSO<sub>4</sub> and adding HCl to precipitate TlCl. Further purification is effected by electrolysing Tl<sub>2</sub>SO<sub>4</sub> in dilute H<sub>2</sub>SO<sub>4</sub> with short Pt wire electrodes, followed by fusion of the deposited Tl metal at 350–400°C under an atmosphere of H<sub>2</sub>. Both the element and its compounds are extremely toxic; skin-contact, ingestion and inhalation are all dangerous, and

the maximum allowable concentration of soluble Tl compounds in air is  $0.1 \text{ mg m}^{-3}$ . In this context the position of Tl in the periodic table will be noted — it occurs between two other poisonous heavy metals Hg and Pb.  $\text{Tl}_2\text{SO}_4$  was formerly widely used as a rodenticide and ant killer but it is both odourless and tasteless and is now banned in many countries as being too dangerous for general use. Many suggestions have been made for the use of Tl compounds in industry but none have been substantially developed. A few specialist uses have emerged in infrared technology since  $\text{TlBr}$  and  $\text{TlI}$  are transparent to long wavelengths, and there are possibilities for photosensitive diodes and infrared detectors. The very high density of aqueous solutions of Tl formate and malonate have found application in the small-scale separation of minerals and the determination of their densities; a saturated solution containing approximately equal weights of these salts (Clerici's solution) has a density of  $4.324 \text{ g cm}^{-3}$  at  $20^\circ$  and progressively lower densities can be obtained by dilution.

### 7.2.3 Properties of the elements

The atomic properties of the Group 13 elements (including boron) are compared in Table 7.4. All have odd atomic numbers and correspondingly few stable isotopes. The varying precision of

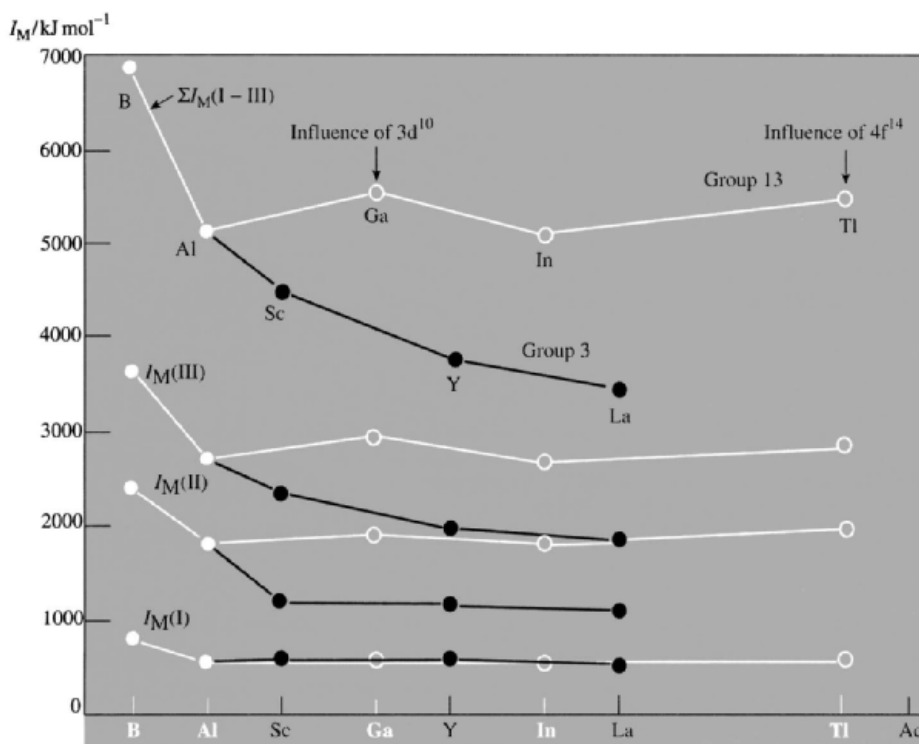
atomic weights has been discussed (p. 17). The electronic configuration is  $ns^2np^1$  in each case but the underlying core varies considerably: for B and Al it is the preceding noble gas core, for Ga and In it is noble gas plus  $d^{10}$ , and for Tl noble gas plus  $4f^{14}5d^{10}$ . This variation has a substantial influence on the trends in chemical properties of the group and is also reflected in the ionization energies of the elements. Thus, as shown in Fig. 7.1, the expected decrease from B to Al is not followed by a further decrease to Ga because of the "d-block contraction" in atomic size and the higher effective nuclear charge for this element which stems from the fact that the 10 added d electrons do not completely shield the extra 10 positive charges on the nucleus. Similarly, the decrease between Ga and In is reversed for Tl as a result of the further influence of the f block or lanthanide contraction. It is notable that these irregularities for the Group 13 elements do not occur for the Group 3 elements Sc, Y and La, which show a steady decrease in ionization energy from B and Al, all 5 elements having the same type of underlying core (noble gas). This has a decisive influence on the comparative chemistry of the two subgroups.

Boron is a covalently bonded, refractory, non-metallic insulator of great hardness and is thus not directly comparable in its physical properties with Al, Ga, In and Tl, which are all low-melting, rather soft metals having a very low electrical

Table 7.4 Atomic properties of Group 13 elements

Property	B	Al	Ga	In	Tl
Atomic number	5	13	31	49	81
No. of naturally occurring isotopes	2	1	2	2	2
Atomic weight	10.811(7)	26.981538(2)	69.723(1)	114.818(3)	204.3833(2)
Electronic configuration	$[\text{He}]2s^22p^1$	$[\text{Ne}]3s^23p^1$	$[\text{Ar}]3d^{10}4s^24p^1$	$[\text{Kr}]4d^{10}5s^25p^1$	$[\text{Xe}]4f^{14}5d^{10}6p^1$
Ionization energy/ $\text{kJ mol}^{-1}$					
I	800.6	577.5	578.8	558.3	589.4
II	2427.1	1816.7	1979.3	1820.6	1971.0
III	3659.7	2744.8	2963	2704	2878
Metal radius/pm	(80–90)	143	135 (see text)	167	170
Ionic radius/pm (6-coord.)					
III	27 <sup>(a)</sup>	53.5	62.0	80.0	88.5
I	—	—	120	140	150

<sup>(a)</sup>Nominal "ionic" radius for  $\text{B}^{\text{III}}$ .



**Figure 7.1** Trends in successive ionization energies  $I_M(\text{I})$ ,  $I_M(\text{II})$ , and  $I_M(\text{III})$ , and their sum  $\Sigma$  for elements in Groups 3 and 13.

resistivity (Table 7.5). The heats of fusion and vaporization of the metals are also much lower than those of boron and tend to decrease with increasing atomic number. In all these properties the metals resemble the neighbouring metals Zn, Cd, Hg; Sn, Pb, etc., and it is probable that in each case the properties are related to the rather small number of electrons available for metallic bonding. Some have seen this as a manifestation of the “inert-pair effect” (see p. 226). The interatomic distances in these elements are also somewhat longer than expected from general trends.

The crystal structure of Al is fcc, typical of many metals, each Al being surrounded by 12 nearest neighbours at 286 pm. Thallium also has a typical metallic structure (hcp) with 12 nearest neighbours at 340 pm. Indium has an unusual structure which is slightly distorted from a regular close-packed arrangement: the structure is face-centred tetragonal and each In has 4 neighbours

at 324 pm and 8 at the slightly greater distance of 336 pm. Gallium has a unique orthorhombic (pseudotetragonal) structure in which each Ga has 1 very close neighbour at 244 pm and 6 further neighbours, 2 each at 270, 273 and 279 pm. The structure is very similar to that of iodine and the appearance of pseudo-molecules  $\text{Ga}_2$  may result from partial pair-wise interaction on neighbouring atoms of the single p electron outside the  $[\text{Ar}]3d^{10}4s^2$  core which immediately follows the first transition series. As such it can be compared with Hg which also has a very low mp and completes the  $[\text{Xe}]4f^{14}5d^{10}6s^2$  “pseudo-noble-gas” configuration following the lanthanide elements. Note that all interatomic contacts in metallic Ga are less than those in Al, again emphasizing the presence of a “d-block contraction”. Gallium is also unusual in contracting on melting, the volume of the liquid phase being 3.4% less than that of the solid; the

Table 7.5 Physical properties of Group 13 elements

Property	B	Al	Ga	In	Tl
MP/°C	2092	660.45	29.767	156.63	303.5
BP/°C	4002	2520	2205	2073	1473
Density (20°C)/g cm <sup>-3</sup>	2.35	2.699	5.904	7.31	11.85
Hardness (Mohs)	11	2.75	1.5	1.2	1.2–1.3
$\Delta H_{\text{fus}}/\text{kJ mol}^{-1}$	50.2	10.71	5.56	3.28	4.21
$\Delta H_{\text{vap}}/\text{kJ mol}^{-1}$	480	294	254	232	166
$\Delta H_f$ (monoatomic gas)/kJ mol <sup>-1</sup>	560	329.7	286.2	243	182.2
Electrical resistivity/ $\mu\text{ohm cm}$	$6.7 \times 10^{11}$	2.655	$\sim 27^{(a)}$	8.37	18
$E^\circ(\text{M}^{3+} + 3\text{e}^- = \text{M}(\text{s}))/\text{V}$	-0.890 <sup>(b)</sup>	-1.676	-0.529	-0.338	+1.26 <sup>(c)</sup>
$E^\circ(\text{M}^+ + \text{e}^- = \text{M}(\text{s}))/\text{V}$	—	0.55	-0.79(acid) -1.39(alkali)	-0.18	-0.336
Electronegativity $\chi$	2.0	1.5	1.6	1.7	1.8

<sup>(a)</sup>The resistivity of crystalline Ga is markedly anisotropic, the values in the three orthorhombic directions being  $a$  17.5,  $b$  8.20,  $c$  55.3  $\mu\text{ohm cm}$ . The resistivity of liquid Ga at 30° is 25.8  $\mu\text{ohm cm}$ .

<sup>(b)</sup> $E^\circ$  for reaction  $\text{H}_3\text{BO}_3 + 3\text{H}^+ + 3\text{e}^- = \text{B}(\text{s}) + 3\text{H}_2\text{O}$ .

<sup>(c)</sup>This is the observed value for  $E^\circ(\text{Tl}^{3+}/\text{Tl}^+)$ , hence the calculated value for the corresponding  $E^\circ(\text{Tl}^{3+}/\text{Tl}(\text{s}))$  is +0.73 V.

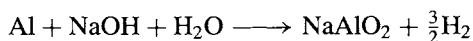
same phenomenon occurs with the next element in the periodic table Ge, and also with Sb and Bi, in addition to the well-known example of H<sub>2</sub>O. In each case, a structural feature in the solid is broken down to permit more efficient packing of atoms in the liquid state.

The standard electrode potentials of the heavier Group 13 elements reflect the decreasing stability of the +3 oxidation state in aqueous solution and the tendency, particularly of Tl, to form compounds in the +1 oxidation state (p. 226). The trend to increasing electropositivity of the group oxidation state which was noted for Groups 1 and 2 does not occur with Group 13 but is found, as expected, in Group 3 (Fig. 7.2). Similarly, the steady decrease in electronegativity in the series B > Al > Sc > Y > La > Ac is reversed in Group 13 and there is a steady increase in electronegativity from Al to Tl.

### 7.2.4 Chemical reactivity and trends

The Group 13 metals differ sharply from the non-metallic element boron both in their greater chemical reactivity at moderate temperatures and in their well-defined cationic chemistry for aqueous solutions. The absence of a range of

volatile hydrides and other cluster compounds analogous to the boranes and carboranes is also notable. Aluminium combines with most non-metallic elements when heated to give compounds such as AlN, Al<sub>2</sub>S<sub>3</sub>, AlX<sub>3</sub>, etc. It also forms intermetallic compounds with elements from all groups of the periodic table that contain metals. Because of its great affinity for oxygen it is used as a reducing agent to obtain Cr, Mn, V, etc., by means of the thermite process of J. W. Goldschmidt. Finely powdered Al metal explodes on contact with liquid O<sub>2</sub>, but for normal samples of the metal a coherent protective oxide film prevents appreciable reaction with oxygen, water or dilute acids; amalgamation with Hg or contact with solutions of salts of certain electropositive metals destroys the film and permits further reaction. Aluminium is also readily soluble in hot concentrated hydrochloric acid and in aqueous NaOH or KOH at room temperature with liberation of H<sub>2</sub>. This latter reaction is sometimes written as



though it is likely that the species in solution is the hydrated tetrahydroxaluminate anion  $[\text{Al}(\text{OH})_4]^-$ (aq) or  $[\text{Al}(\text{H}_2\text{O})_2(\text{OH})_4]^-$ .

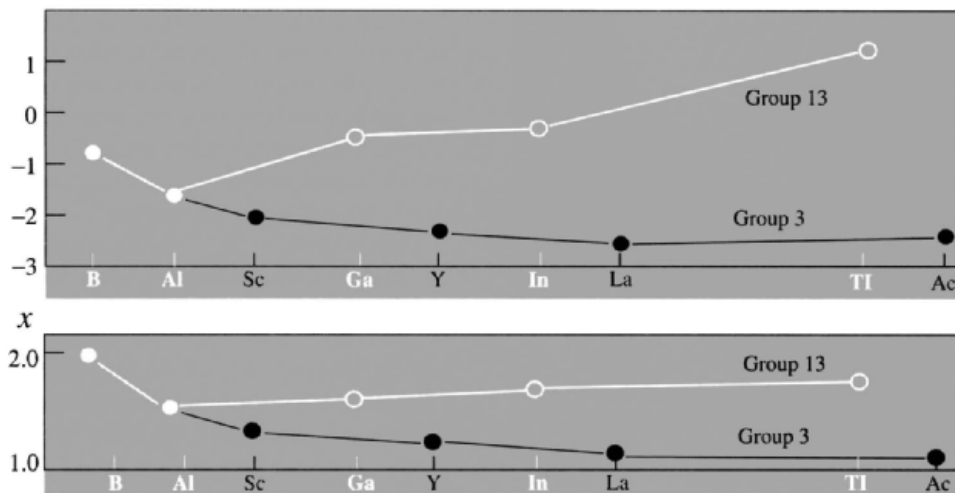
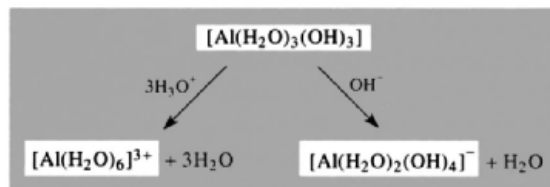
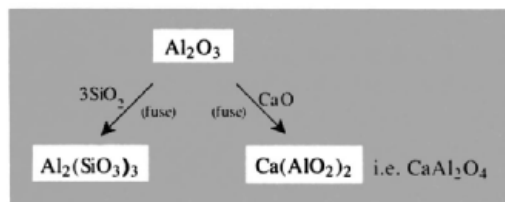
$E^\circ(M^{3+}/M)/V$ 

Figure 7.2 Trends in standard electrode potential  $E^\circ$  and electronegativity  $\chi$  for elements in Groups 3 and 13.

$Al(OH)_3$  is amphoteric, forming both salts and aluminates (Greek ἀμφοτέρως, *amphoterōs*, in both ways). Thus the freshly precipitated hydroxide is readily soluble in both acid and alkali:

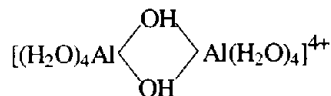


In these reactions the coordination number of Al has been assumed to be 6 throughout though direct evidence on this point is rarely available. Amphoterism is also exhibited in anhydrous reactions, e.g.:

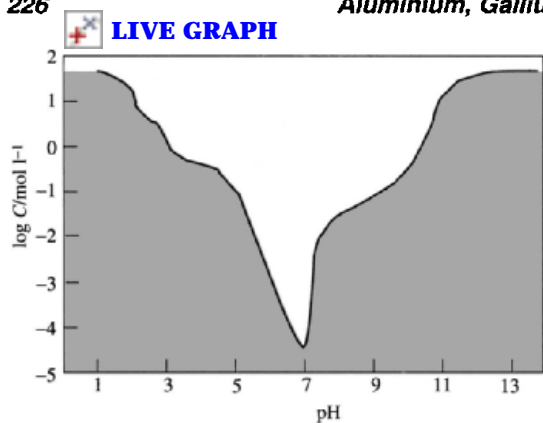


Aluminium compounds of weak acids are extensively hydrolysed to  $[Al(H_2O)_3(OH)_3]$  and the corresponding hydride, e.g.  $Al_2S_3 \longrightarrow$

$3H_2S$ ,  $AlN \longrightarrow NH_3$ , and  $Al_4C_3 \longrightarrow 3CH_4$ . Similarly, the cyanide, acetate and carbonate are unstable in aqueous solution. Hydrolysis of the halides and other salts such as the nitrate and sulfate is incomplete but aqueous solutions are acidic due to the ability of the hydrated cation  $[Al(H_2O)_6]^{3+}$  to act as proton donor giving  $[Al(H_2O)_5(OH)]^{2+}$ ,  $[Al(H_2O)_4(OH)_2]^+$ , etc. If the pH is gradually increased this deprotonation of the mononuclear species is accompanied by aggregation via OH bridges to give species such as



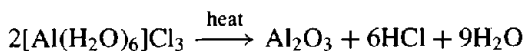
and then to precipitation of the hydrous oxide. This is of particular use in water clarification since the precipitating hydroxide nucleates on fine suspended particles which are thereby thrown out of suspension. Still further increase in pH leads to redissolution as an aluminate (Fig. 7.3). Similar behaviour is shown by  $Be^{II}$ ,  $Zn^{II}$ ,  $Ga^{III}$ ,  $Sn^{II}$ ,  $Pb^{II}$ , etc. A detailed quantitative theory of amphoterism is difficult to construct but it is known that amphoteric behaviour occurs when (a) the cation is weakly basic, (b) its hydroxide



**Figure 7.3** Schematic representation of the variation of concentration of an Al salt as a function of pH (see text).

is moderately insoluble, and (c) the hydrated species can also act as proton donors.<sup>(2)</sup>

Anhydrous Al salts cannot be prepared by heating the corresponding hydrate for reasons closely related to the amphoterism and hydrolysis of such compounds. For example,  $\text{AlCl}_3 \cdot 6\text{H}_2\text{O}$  is, in reality,  $[\text{Al}(\text{H}_2\text{O})_6]\text{Cl}_3$  and the strength of the Al–O interaction precludes the formation of Al–Cl bonds:



The amphoteric behaviour of  $\text{Ga}^{\text{III}}$  salts parallels that of  $\text{Al}^{\text{III}}$ ; indeed,  $\text{Ga}_2\text{O}_3$  is slightly more acidic than  $\text{Al}_2\text{O}_3$  and solutions of gallates tend to be more stable than aluminates. Consistent with this,  $\text{p}K_a$  for the equilibrium



is 4.95 for Al and 2.60 for Ga. Indium is more basic than Ga and is only weakly amphoteric. The metal does not dissolve in aqueous alkali whereas Ga does. This alternation in the sequence of basicity can be related to the electronic and size factors mentioned on p. 222. Thallium behaves as a moderately strong base but is not strictly

comparable with other members of the group because it normally exists as  $\text{Tl}^{\text{I}}$  in aqueous solution. Thus, Tl metal tarnishes readily and reacts with steam or moist air to give  $\text{TlOH}$ . The electrode potential data in Table 7.5 show that  $\text{Tl}^{\text{I}}$  is much more stable than  $\text{Tl}^{\text{III}}$  in aqueous solution and indicate that  $\text{Tl}^{\text{III}}$  compounds can act as strong oxidizing agents.

Compounds of  $\text{Tl}^{\text{I}}$  have many similarities to those of the alkali metals:  $\text{TlOH}$  is very soluble and is a strong base;  $\text{Tl}_2\text{CO}_3$  is also soluble and resembles the corresponding Na and K compounds;  $\text{Tl}^{\text{I}}$  forms colourless, well-crystallized salts of many oxoacids, and these tend to be anhydrous like those of the similarly sized Rb and Cs;  $\text{Tl}^{\text{I}}$  salts of weak acids have a basic reaction in aqueous solution as a result of hydrolysis;  $\text{Tl}^{\text{I}}$  forms polysulfides (e.g.  $\text{Tl}_2\text{S}_5$ ) and polyiodides, etc. In other respects  $\text{Tl}^{\text{I}}$  resembles the more highly polarizing ion  $\text{Ag}^+$ , e.g. in the colour and insolubility of its chromate, sulfide, arsenate and halides (except F), though it does not form ammine complexes in aqueous solution and its azide is not explosive.

The stability of the +1 oxidation state in Group 13 increases in the sequence  $\text{Al} < \text{Ga} < \text{In} < \text{Tl}$ , and numerous examples of  $\text{M}^{\text{I}}$  compounds will be found in the following sections. The occurrence of an oxidation state which is 2 less than the group valency is sometimes referred to as the “inert-pair effect” but it is important to recognize that this is a description not an explanation. The phenomenon is quite general among the heavier elements of the p block (i.e. the post-transition elements in Groups 13–16). For example, Sn and Pb commonly occur in both the +2 and +4 oxidation states; P, As, Sb and Bi in the +3 and +5; S, Se, Te and Po in the +2, +4, and +6 states. The term “inert-pair effect” is somewhat misleading since it implies that the energy required to involve the  $ns^2$  electrons in bonding increases in the sequence  $\text{Al} < \text{Ga} < \text{In} < \text{Tl}$ . Reference to Table 7.4 shows that this is not so (the sequence is, in fact,  $\text{In} < \text{Al} < \text{Tl} < \text{Ga}$ ). The explanation lies rather in the decrease in bond energy with increase in size from Al to Tl so that the energy required

<sup>2</sup> C. S. G. PHILLIPS and R. J. P. WILLIAMS, *Inorganic Chemistry*, Vol. 1, Chap. 14; Vol. 2, pp. 524–5, Oxford University Press, Oxford, 1966.

to involve the s electrons in bonding is not compensated by the energy released in forming the 2 additional bonds. The argument is difficult to quantify since the requisite energy terms are not known. Thus it is unrealistic to use the simple ionic bond model (p. 79) to calculate the heat of formation of  $\text{MX}_3$  because compounds like  $\text{TlCl}_3$  are not ionic, i.e.  $[\text{Tl}^{3+}(\text{Cl}^-)_3]$  — the energy for the ionization of  $\text{M}(\text{g})$  to  $\text{M}^{3+}(\text{g})$  is greater than  $5000 \text{ kJ mol}^{-1}$  for each element and substantial covalent interaction between  $\text{M}^{3+}$  and  $\text{X}^-$  would also be expected. In the absence of semi-empirical bond energy data or *ab initio* MO calculations it is only possible to note that the higher oxidation state becomes progressively less stable with respect to the lower oxidation state as atomic number increases within the group. This is seen, for example, by comparing the standard electrode potentials in aqueous solution for  $\text{M}^{\text{III}}$  and  $\text{M}^{\text{I}}$  in Table 7.5. Similarly, from the somewhat fragmentary data available, it appears that the enthalpy of formation of the anhydrous halides remains approximately constant for  $\text{MX}$  but diminishes irregularly from Al to Tl for  $\text{MX}_3$  ( $\text{X} = \text{Cl}, \text{Br}, \text{I}$ ). The overall result depends not only on the simple Born–Haber terms (p. 82) but also on a combination of several other factors including changes in structure and bond type, covalency effects, enthalpies of hydration, entropy effects, etc., and a quantitative rationalization of all the data has not yet been achieved.

Group 13 metals furnish a good example of the general rule that an element is more electropositive in its lower than in its higher oxidation state: the lower oxide and hydroxide are more basic and the higher oxide and hydroxide more acidic. The reasons for this behaviour are similar to those already discussed when comparing Group 2 with Group 1 (p. 111) and turn on the relative magnitude of ionization energies, cationic size, hydration enthalpy and entropy, etc. Again, the higher the charge on an aquo cation  $[\text{M}(\text{H}_2\text{O}_x)]^{n+}$  the more readily will it act as a proton donor (p. 51).

Other group trends will emerge in subsequent sections. However, it is worth noting here an

important vestigial structural relation of these elements to the icosahedral units in elementary boron (p. 142). Thus, the structures of both  $\beta$ -rhombohedral boron and the cubic alloy phase  $\text{Al}_5\text{CuLi}_3$  can be constructed from 60-vertex truncated icosahedra, although linked in very different ways in the 3-dimensional crystalline lattice. Likewise,  $\text{Ga}_{12}$  icosahedra have been found in intermetallic phases such as  $\text{RbGa}_7$ ,  $\text{CsGa}_7$ ,  $\text{Li}_2\text{Ga}_7$ ,  $\text{K}_3\text{Ga}_{13}$  and  $\text{Na}_{22}\text{Ga}_{39}$ . This has led to the proposal<sup>(3)</sup> that the Group 13 elements should be given the collective epithet of ‘icosagens’.

## 7.3 Compounds

### 7.3.1 Hydrides and related complexes<sup>(4–8)</sup>

The extensive covalent cluster chemistry of the boron hydrides finds no parallel with the heavier elements of Group 13.  $\text{AlH}_3$  is a colourless, involatile solid which is extensively polymerized via Al–H–Al bonds; it is thermally unstable above  $150\text{--}200^\circ$ , is a strong reducing agent and reacts violently with water and other protic reagents to liberate  $\text{H}_2$ . Several crystalline and amorphous modifications have been described and the structure of  $\alpha\text{-AlH}_3$  has been determined by X-ray and neutron diffraction:<sup>(9)</sup> each Al is octahedrally surrounded by 6 H atoms at 172 pm and the Al–H–Al angle is  $141^\circ$ . The participation of each Al in 6 bridges, and the equivalence of all

<sup>3</sup> R. B. KING, *Inorg. Chim. Acta* **181**, 217–25 (1991).

<sup>4</sup> E. WIBERG and E. AMBERGER, *Hydrides of the Elements of Main Groups I–IV*, Chaps. 5 and 6, pp. 381–461, Elsevier, Amsterdam, 1971.

<sup>5</sup> N. N. GREENWOOD Chap. 3 in E. A. V. EBSWORTH, A. G. MADDOCK, and A. G. SHARPE (eds.), *New Pathways in Inorganic Chemistry*, pp. 37–64, Cambridge University Press, Cambridge, 1968.

<sup>6</sup> A. R. BARRON and G. WILKINSON, *Polyhedron* **5**, 1897–1915 (1986).

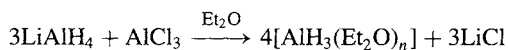
<sup>7</sup> B. M. BULYCHEV, *Polyhedron* **9**, 387–408 (1990).

<sup>8</sup> C. JONES, G. A. KOUSATONIS and C. L. RASTON, *Polyhedron* **12**, 1829–48 (1993).

<sup>9</sup> J. W. TURLEY and H. W. RINN, *Inorg. Chem.* **8**, 18–22 (1969).

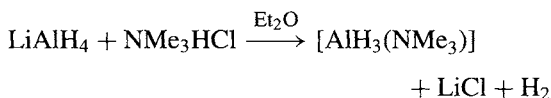
Al–H distances suggests that 3-centre 2-electron bonding occurs as in the boranes (p. 157). The closest Al...Al distance is 324 pm, which is appreciably shorter than in metallic Al (340 pm), but there is no direct metal–metal bonding and the density of AlH<sub>3</sub> (1.477 g cm<sup>-3</sup>) is markedly less than that for Al (2.699 g cm<sup>-3</sup>); this is because in Al metal all 12 nearest neighbours are at 340 pm whereas in AlH<sub>3</sub> there are 6 Al at 324 and 6 at 445 pm.

AlH<sub>3</sub> is best prepared by the reaction of ethereal solutions of LiAlH<sub>4</sub> and AlCl<sub>3</sub> under very carefully controlled conditions:<sup>(10)</sup>



The LiCl is removed and the filtrate, if left at this stage, soon deposits an intractable etherate of variable composition. To avoid this, the solution is worked up with an excess of LiAlH<sub>4</sub> and some added LiBH<sub>4</sub> in the presence of a large excess of benzene under reflux at 76–79°C. Crystals of α-AlH<sub>3</sub> soon form. Slight variations in the conditions lead to other crystalline modifications of unsolvated AlH<sub>3</sub>, 6 of which have been identified.

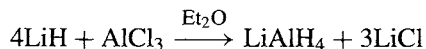
AlH<sub>3</sub> readily forms adducts with strong Lewis bases (L) but these are more conveniently prepared by reactions of the type



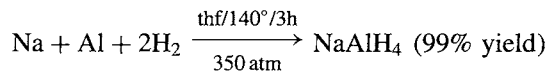
[AlH<sub>3</sub>(NMe<sub>3</sub>)] has a tetrahedral structure and can take up a further mole of ligand to give [AlH<sub>3</sub>(NMe<sub>3</sub>)<sub>2</sub>]; this was the first compound in which Al was shown to adopt a 5-coordinate trigonal bipyramidal structure<sup>(11)</sup> Such complexes are now of interest since their thermal decomposition can be used to prepare ultra-thin carbon-free Al films by chemical

vapour deposition on GaAs semiconductor devices.<sup>(12)</sup>

LiAlH<sub>4</sub> is a white crystalline solid, stable in dry air but highly reactive towards moisture, protic solvents, and many organic functional groups. It is readily soluble in ether (~29 g per 100 g at room temperature) and is normally used in this solvent. LiAlH<sub>4</sub> has proved to be an outstandingly versatile reducing agent since its discovery some 50 y ago<sup>(13,14)</sup> (see Panel opposite). It can be prepared on the laboratory (and industrial) scale by the reaction



On the industrial (multitonne) scale it can also be prepared by direct high-pressure reaction of the elements or preferably via the intermediate formation of the Na analogue.



The Li salt can then be obtained by metathesis with LiCl in Et<sub>2</sub>O. The X-ray crystal structure of LiAlH<sub>4</sub> shows the presence of tetrahedral AlH<sub>4</sub> groups (Al–H 155 pm) bridged by Li in such a way that each Li is surrounded by 4H at 188–200 pm (cf. 204 pm in LiH) and a fifth H at 216 pm. The bonding therefore deviates considerably from the simple ionic formulation Li<sup>+</sup>AlH<sub>4</sub><sup>-</sup> and there appears to be substantial covalent bonding as found in other complex hydrides (p. 67).

Other complex hydrides of Al are known including Li<sub>3</sub>AlH<sub>6</sub>, M<sup>I</sup>AlH<sub>4</sub> (M<sup>I</sup> = Li, Na, K, Cs), M<sup>II</sup>(AlH<sub>4</sub>)<sub>2</sub> (M<sup>II</sup> = Be, Mg, Ca), Ga(AlH<sub>4</sub>)<sub>3</sub>, M<sup>I</sup>(AlH<sub>3</sub>R), M<sup>I</sup>(AlH<sub>2</sub>R<sub>2</sub>), M<sup>I</sup>[AlH(OEt)<sub>3</sub>], etc. (see Panel). The important complex Al(BH<sub>4</sub>)<sub>3</sub> has already been mentioned (p. 169); it is a colourless liquid, mp –64.5°, bp +44.5°. It is best prepared

<sup>12</sup> A. T. S. WEE, A. J. MURRELL, N. K. SINGH, D. O'HARE and J. S. FORD, *J. Chem. Soc., Chem. Commun.*, 11–13 (1990).

<sup>13</sup> A. E. FINHOLD, A. C. BOND, and H. J. SCHLESINGER, *J. Am. Chem. Soc.* **9**, 1199–203 (1947).

<sup>14</sup> N. G. GAYLORD, *Reduction with Complex Metal Hydrides*, Interscience, New York, 1956, 1046 pp. J. S. PIZEY, *Lithium Aluminium Hydride*, Ellis Horwood, Ltd., Chichester, 1977, 288 pp.

<sup>10</sup> F. M. BROWER, N. E. MATZEK, P. F. REIGLER, H. W. RINN, C. B. ROBERTS, D. L. SCHMIDT, J. A. SHOVER and K. TERADA, *J. Am. Chem. Soc.* **98**, 2450–3 (1976).

<sup>11</sup> G. W. FRASER, N. N. GREENWOOD and B. P. STRAUGHAN, *J. Chem. Soc.* 3742–9 (1963). C. W. HEITSCH, C. E. NORDMAN, and R. W. PARRY, *Inorg. Chem.* **2**, 508–12 (1963).



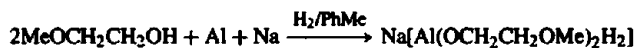
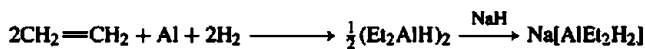
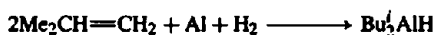
### Synthetic Reactions of $\text{LiAlH}_4$ <sup>(4,14)</sup>

$\text{LiAlH}_4$  is a versatile reducing and hydrogenating reagent for both inorganic and organic compounds. With inorganic halides the product obtained depends on the relative stabilities of the corresponding tetrahydroaluminate, hydride and element. For example,  $\text{BeCl}_2$  gives  $\text{Be}(\text{AlH}_4)_2$ , whereas  $\text{BCl}_3$  gives  $\text{B}_2\text{H}_6$  and  $\text{HgI}_2$  gives Hg metal. The halides of Cu, Ag, Au, Zn, Cd and Hg give some evidence of unstable hydrido species at low temperatures but all are reduced to the metal at room temperature. The halides of main groups 14 and 15 yield the corresponding hydrides since the  $\text{AlH}_4$  derivatives are unstable or non-existent. Thus  $\text{SiCl}_4$ ,  $\text{GeCl}_4$  and  $\text{SnCl}_4$  yield  $\text{MH}_4$  and substituted halides such as  $\text{R}_n\text{SiX}_{4-n}$  give  $\text{R}_n\text{SiH}_{4-n}$ . Similarly,  $\text{PCl}_3$  (and  $\text{PCl}_5$ ),  $\text{AsCl}_3$  and  $\text{SbCl}_3$  afford  $\text{MH}_3$  but  $\text{BiCl}_3$  is reduced to the metal.  $\text{PhAsCl}_2$  gives  $\text{PhAsH}_2$  and  $\text{Ph}_2\text{SbCl}$  gives  $\text{Ph}_2\text{SbH}$ , etc. Less work has been done on oxides but  $\text{COCl}_2$  yields  $\text{MeOH}$ ,  $\text{NO}$  yields hyponitrous acid  $\text{HON}=\text{NOH}$  (which can be isolated as the Ag salt), and  $\text{CO}_2$  gives  $\text{LiAl}(\text{OMe})_4$  or  $\text{LiAl}(\text{OCH}_2\text{O})_2$  depending on conditions.

The real importance of  $\text{LiAlH}_4$  stems from the applications in organic syntheses. Its commercial introduction dates from 1948. By 1951 the number of functional groups that were known to react was 23 and this rose to more than 60 by the 1970s. Despite this, the heyday of  $\text{LiAlH}_4$  seems to have been reached in the late 1960s and it has now been replaced in many systems by the more selective borohydrides (p. 167) or by organometallic hydrides (see below). Reaction is usually carried out in ether solution, followed by hydrolysis of the intermediate so formed when appropriate. Typical examples are listed below.

Compound	Product	Compound	Product
Reactive $>\text{C}=\text{C}<$	$>\text{CH}-\text{CH}<$	$\text{RCOSR}$	$\text{RCH}_2\text{OH}$
$\text{RCH}=\text{CH}_2$	$[\text{Al}(\text{CH}_2\text{CH}_2\text{R})_4]^-$	$\text{RCSNH}_2$	$\text{RCH}_2\text{NH}_2$
$\text{C}_2\text{H}_2$	$[\text{AlH}(\text{CH}=\text{CH}_2)_3]^-$	$\text{RSCN}$	$\text{RSH}$
$\text{RC}\equiv\text{CH}$	$\text{RCH}=\text{CH}_2$	$\text{R}_2\text{SO}$	$\text{R}_2\text{S}$
$\text{RX}$	$\text{RH}$ (not aryl)	$\text{R}_2\text{SO}_2$	$\text{R}_2\text{S}$
$\text{ROH}$	$[\text{Al}(\text{OR})_4]^-$ or $[\text{AlH}(\text{OR})_3]^-$	$\text{RSO}_2\text{X}$	$\text{RSH}$
$\text{RCHO}$	$\text{RCH}_2\text{OH}$	$\text{ROSO}_2\text{R}'$ , $(\text{ArOSO}_2\text{R}')$	$\text{RH}$ , $(\text{ArOH})$
$\text{R}_2\text{CO}$	$\text{R}_2\text{CHOH}$	$\text{RSO}_2\text{H}$	$\text{RSSR} + \text{RSH}$
Quinone	Hydroquinone	$\text{RNC}$ or $\text{RNCO}$	$\text{RNHMe}$
$\text{RCO}_2\text{H}$ or $(\text{RCO})_2\text{O}$	$\text{RCH}_2\text{OH}$	or $\text{RNCS}$	
or $\text{RCOX}$		$\text{RCN}$	$\text{RCH}_2\text{NH}_2$ or $\text{RCHO}$
$\text{RCO}_2\text{R}'$	$\text{RCH}_2\text{OH} + \text{R}'\text{OH}$	$\text{R}_2\text{C}=\text{NOH}$	$\text{R}_2\text{CHNH}_2$
Lactones, i.e. $\text{O}(\text{CH}_2)_n\text{C}=\text{O}$	Diols, i.e. $\text{HO}(\text{CH}_2)_{n+1}\text{OH}$	$\text{R}_3\text{NO}$	$\text{R}_3\text{N}$
$\text{RCONH}_2$	$\text{RCH}_2\text{NH}_2$ (also $2^\circ$ , $3^\circ$ )	$\text{R}_2\text{NNO}$	$\text{R}_2\text{NNH}_2$
Epoxides $\text{O}(\text{CR}_2)\text{CHR}$	$\text{R}_2\text{C}(\text{OH})\text{CHR}$	$\text{RNO}_2$ , $\text{RNHOH}$ or $\text{RN}_3$	$\text{RNH}_2$
$\text{SCR}_2-\text{CR}_2$	$\text{R}_2\text{C}(\text{SH})\text{CHR}_2$	$\text{ArNO}_2$	$\text{ArN}=\text{NAr}$
$\text{RSSR}$	$\text{RSH}$		

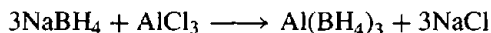
More recently,  $\text{LiAlH}_4$  has been eclipsed as an organic reducing agent by the emergence of several cheaper organo-aluminium hydrides which are also safer and easier to handle than  $\text{LiAlH}_4$ . Pre-eminent among these are  $\text{Bu}_2\text{AlH}$  and  $\text{Na}[\text{AlEt}_2\text{H}_2]$  which were introduced commercially in the early 1970s and  $\text{Na}[\text{Al}(\text{OCH}_2\text{CH}_2\text{OMe})_2\text{H}_2]$ , VTRIDE<sup>®</sup>, which became available in bulk during 1979. All three reagents can be prepared directly:



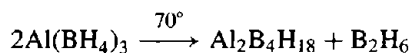
All three are substantially cheaper than  $\text{LiAlH}_4$  and are now produced on a far larger scale as indicated in the table overleaf. Data refer to US industrial use in 1980 and even larger markets are available outside the chemical industry (e.g. in polymerization catalysis).

Compound	Production/kg	Price/\$ kg <sup>-1</sup>	\$ per kg 'H'
LiAlH <sub>4</sub>	6 000	88.00	835.00
Bu <sub>2</sub> AlH	195 000	5.10	715.00
Na[AlEt <sub>2</sub> H <sub>2</sub> ]	91 000	11.00	605.00
Na[Al(OCH <sub>2</sub> CH <sub>2</sub> OMe) <sub>2</sub> H <sub>2</sub> ]	123 000	6.25	638.00

in the absence of solvent by the reaction



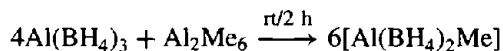
Al(BH<sub>4</sub>)<sub>3</sub> was the first fluxional compound to be recognized as such (1955) and its thermal decomposition led to a new compound which was the first to be discovered and structurally characterized by means of nmr:



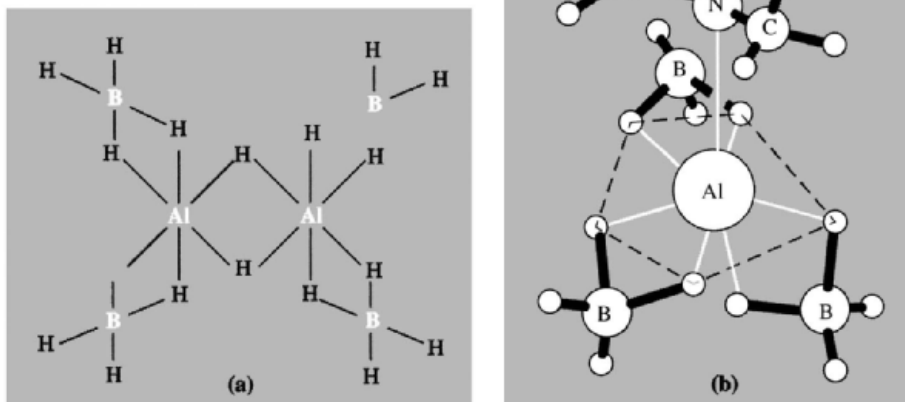
This binuclear complex is also fluxional and has the structure shown in Fig. 7.4a. Al(BH<sub>4</sub>)<sub>3</sub> reacts readily with NMe<sub>3</sub> to give a 1:1 adduct in which Al adopts the unusual pentagonal bipyramidal

bipyramidal 7-fold coordination as shown in Fig. 7.4b.<sup>(15)</sup>

At room temperature Al(BH<sub>4</sub>)<sub>3</sub> reacts quantitatively in the gas phase with Al<sub>2</sub>Me<sub>6</sub> (p. 259) to give [Al(η<sup>2</sup>-BH<sub>4</sub>)<sub>2</sub>Me] (mp -76°) in which one of the BH<sub>4</sub> groups of the parent compound has been replaced by a Me group:

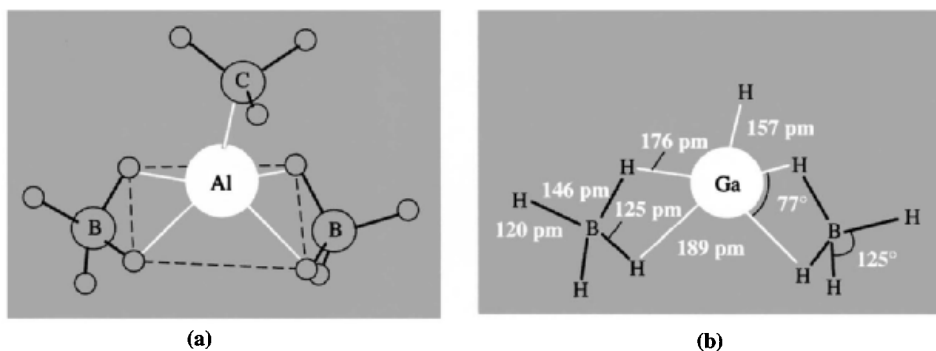


Electron diffraction studies in the gas phase reveal an unusual structure in which the 5-coordinate Al atom has square-pyramidal



**Figure 7.4** (a) Structure of Al<sub>2</sub>B<sub>4</sub>H<sub>18</sub> showing 6-coordinate Al, (b) Structure of the adduct Me<sub>3</sub>N·Al(BH<sub>4</sub>)<sub>3</sub> showing 7-coordinate pentagonal bipyramidal Al.

<sup>15</sup> N. A. BAILEY, P. H. BIRD and M. G. H. WALLBRIDGE, *Chem. Commun.*, 286-7 (1966); *Inorg. Chem.* 7, 1575-81 (1968).



**Figure 7.5** (a) Structure of  $[\text{MeAl}(\eta^2\text{-BH}_4)_2]$  as revealed by electron diffraction, and (b) structure and key dimensions of  $[\text{HGa}(\eta^2\text{-BH}_4)_2]$  as determined by low temperature X-ray diffractometry.

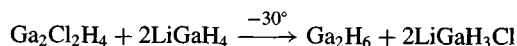
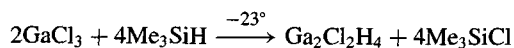
geometry (Fig. 7.5a).<sup>(16)</sup> The heavy atoms  $\text{CAIB}_2$  are coplanar and the symmetry is close to  $C_{2v}$ . A similar structure (Fig. 7.5b) has been found by X-ray diffraction for  $[\text{Ga}(\eta^2\text{-BH}_4)_2\text{H}]$ , which was prepared by the dry reaction of  $\text{LiBH}_4$  and  $\text{GaCl}_3$  at  $-45^\circ\text{C}$ ,<sup>(17)</sup> and this geometry is emerging as a notable structural feature of many  $\text{AlH}_4^-$  complexes (see next paragraph).

Many complexes in which  $\text{AlH}_4^-$  acts as a dihapto (or bridging bis-dihapto) ligand to transition metals have recently been characterized. These are usually stabilized by coligands such as tertiary phosphines or  $\eta^5$ -cyclopentadienyls and are readily prepared by treating the corresponding chloro-complexes with  $\text{LiAlH}_4$  in ether. Typical examples, frequently dimeric, are:<sup>(6)</sup>  $[\{(\text{C}_5\text{H}_5)_2\text{Y}(\text{AlH}_4\cdot\text{thf})\}_2]$ ,  $[\{(\text{C}_5\text{Me}_5)_2\text{Ti}(\text{AlH}_4)\}_2]$  (Fig. 7.6a),  $[\{(\text{C}_5\text{Me}_5)_2\text{Ta}(\text{AlH}_4)\}_2]$ ,  $[\{(\text{PMe}_3)_3\text{-H}_3\text{W}\}_2\text{-}\mu\text{-(}\eta^2, \eta^2\text{-AlH}_5\text{)}]$  (Fig. 7.6b),  $[\{(\text{dmpe})_2\text{-Mn}(\text{AlH}_4)\}_2]$  and  $[\{(\text{PPH}_3)_3\text{HRu}(\text{AlH}_4)\}_2]$ . A few transition metal tetrahydroaluminates  $[\text{M}(\text{AlH}_4)_n]$  are also known but their structures have not yet been determined by X-ray crystallography, e.g.:<sup>(6)</sup>  $[\text{Y}(\text{AlH}_4)_3]$ ,  $[\text{Ti}(\text{AlH}_4)_4]$ ,  $[\text{Nb}(\text{AlH}_4)_5]$  and  $[\text{Fe}(\text{AlH}_4)_2]$ .

<sup>16</sup> M. T. BARLOW, C. J. DAIN, A. J. DOWNS, P. D. P. THOMAS and D. W. H. RANKIN, *J. Chem. Soc., Dalton Trans.*, 1374–8 (1980). See also A. J. DOWNS and L. A. JONES, *Polyhedron* **13**, 2401–15 (1994) for a description of the polymeric Al analogue,  $[\text{Al}(\text{BH}_4)_2\text{H}]$ .

<sup>17</sup> M. T. BARLOW, C. J. DAIN, A. J. DOWNS, G. S. LAUREN-SON and D. W. H. RANKIN, *J. Chem. Soc., Dalton Trans.*, 597–602 (1982).

The synthesis and characterization of gallane, the binary hydride of gallium, has proved even more elusive than that of alane,  $\text{AlH}_3$ . Success was finally achieved<sup>(18,19)</sup> by first preparing dimeric monochlorogallane,  $\{\text{H}_2\text{Ga}(\mu\text{-Cl})\}_2$ ,<sup>(20)</sup> and then reducing a freshly prepared sample of this liquid with freshly prepared  $\text{LiGaH}_4$  under solvent-free conditions in an all-glass apparatus at  $-30^\circ\text{C}$ :

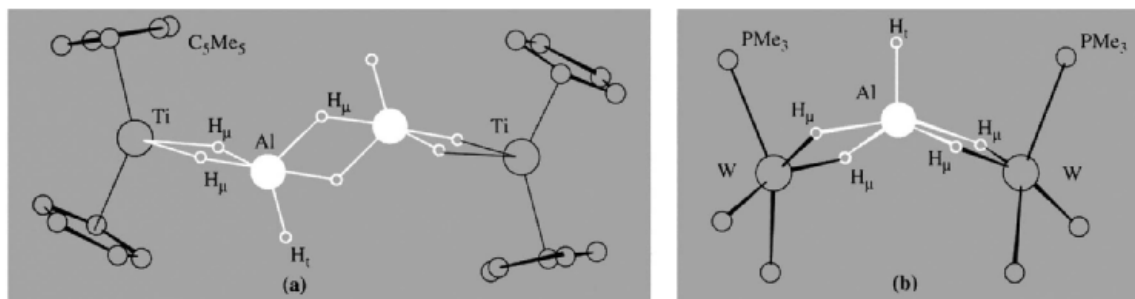


The volatile product, obtained in about 5% yield, condensed as a white solid at  $-50^\circ$  and had a vapour pressure of about 1 mmHg at  $-63^\circ$ . Gallane decomposes into its elements at ambient temperatures. In the vapour phase it has a diborane-like structure,  $\text{Ga}_2\text{H}_6$ , with  $\text{Ga-H}_t$  152 pm,  $\text{Ga-H}_\mu$  171 pm,  $\text{Ga}\cdots\text{Ga}$  258 pm and angle  $\text{GaHGa}$   $98^\circ$  (electron diffraction).<sup>(19)</sup> In the solid state gallane tends to aggregate via  $\text{Ga-H-Ga}$  bonds to give  $(\text{GaH}_3)_n$  with  $n$ , perhaps equal to 4 but, in contrast to the structure

<sup>18</sup> A. J. DOWNS, M. J. GOODE and C. R. PULHAM, *J. Am. Chem. Soc.* **111**, 1936–7 (1989).

<sup>19</sup> C. R. PULHAM, A. J. DOWNS, M. J. GOODE, D. W. H. RANKIN and H. E. ROBERTSON, *J. Am. Chem. Soc.* **113**, 5149–62 (1991).

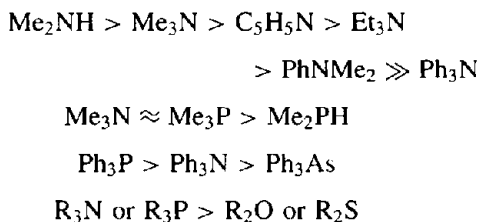
<sup>20</sup> M. J. GOODE, A. J. DOWNS, C. R. PULHAM, D. W. H. RANKIN and H. E. ROBERTSON, *J. Chem. Soc., Chem. Commun.*, 768–9 (1988).



**Figure 7.6** (a) The structure of  $[(\eta^5\text{-C}_5\text{Me}_5)_2\text{Ti}(\text{AlH}_4)_2]_2$ , i.e.  $[(\eta^5\text{-C}_5\text{Me}_5)_2\text{Ti}(\mu\text{-H})_2\text{Al}(\text{H}_t(\mu\text{-H}))_2]_2$ ; the Me groups have been omitted for clarity. (b) The structure of  $[(\text{PMe}_3)_3\text{H}_3\text{W}]_2\text{-}\mu\text{-}(\eta^2, \eta^2\text{-AlH}_5)$ ; the Me groups have been omitted for clarity and the three H atoms on each W were not located with certainty.

of  $\alpha\text{-AlH}_3$  (p. 227), some terminal Ga–H<sub>t</sub> bonds remain.

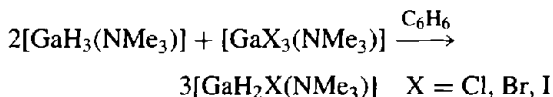
The known reactions of gallane appear mostly to parallel those of diborane (p. 165). Thus, at  $-95^\circ$ ,  $\text{NH}_3$  causes unsymmetrical cleavage to give  $[\text{H}_2\text{Ga}(\text{NH}_3)_2]^+[\text{GaH}_4]^-$  whereas  $\text{NMe}_3$  effects symmetrical cleavage to give  $\text{Me}_3\text{N}\cdot\text{GaH}_3$  or  $(\text{Me}_3\text{N})_2\text{GaH}_3$  according to the amount used.<sup>(19)</sup> These last two adducts were already well known.  $\text{Me}_3\text{N}\cdot\text{GaH}_3$  can readily be prepared as a colourless crystalline solid, mp  $70.5^\circ$ , by the reaction of ethereal solutions of  $\text{LiGaH}_4$  and  $\text{Me}_3\text{NHCl}$ .<sup>(21)</sup> It is one of the most stable complexes of  $\text{GaH}_3$  and, like its Al analogue, can take up a further mole of ligand to give the trigonal bipyramidal 2:1 complex.<sup>(22)</sup> Numerous other complexes have been prepared and the stabilities of the 1:1 adducts decrease in the following sequences:<sup>(5)</sup>



<sup>21</sup> N. N. GREENWOOD, A. STORR and M. G. H. WALLBRIDGE, *Proc. Chem. Soc.* 249 (1962).

<sup>22</sup> N. N. GREENWOOD, A. STORR and M. G. H. WALLBRIDGE, *Inorg. Chem.* 2, 1036–9 (1963). D. F. SHRIVER and R. W. PARRY, *Inorg. Chem.* 2, 1039–42 (1963).

Complexes of the type  $[\text{GaH}_2\text{X}(\text{NMe}_3)]$  and  $[\text{GaHX}_2(\text{NMe}_3)]$  are readily prepared by reaction of  $\text{HCl}$  or  $\text{HBr}$  on the  $\text{GaH}_3$  complex at low temperatures or by reactions of the type



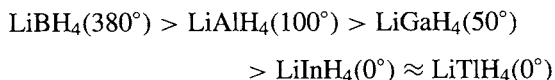
The relative stabilities of these various complexes can be rationalized in terms of the factors discussed on p. 198. A few mixed hydrides have also been characterized, e.g. galladiborane,  $\text{H}_2\text{Ga}(\mu\text{-H})_2\text{BH}_2$ ,<sup>(23)</sup> and *arachno*-2-gallatettraborane(10),  $\text{H}_2\text{GaB}_3\text{H}_8$ ,<sup>(24)</sup> as well as derivatives such as tetramethyldigallane,  $\text{Me}_2\text{Ga}(\mu\text{-H})_2\text{GaMe}_2$ .<sup>(25)</sup>

$\text{InH}_3$  and  $\text{TlH}_3$  appear to be too unstable to exist in the uncoordinated state though they may have transitory existence in ethereal solutions at low temperatures. A similar decrease in thermal stability is noted for the tetrahydro complexes; e.g. the temperature at which the Li salts decompose rapidly, follows the sequence

<sup>23</sup> C. R. PULHAM, P. T. BRAIN, A. J. DOWNS, D. W. H. RANKIN and H. E. ROBERTSON, *J. Chem. Soc., Chem. Commun.*, 177–8 (1990).

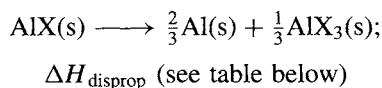
<sup>24</sup> C. R. PULHAM, A. J. DOWNS, D. W. H. RANKIN and H. E. ROBERTSON, *J. Chem. Soc., Chem. Commun.*, 1520–1 (1990). B. J. DUKE and H. F. SCHAEFER, *J. Chem. Soc., Chem. Commun.*, 123–4 (1991).

<sup>25</sup> P. L. BAXTER, A. J. DOWNS, M. J. GOODE, D. W. H. RANKIN and H. E. ROBERTSON, *J. Chem. Soc., Chem. Commun.*, 805–6 (1986).



### 7.3.2 Halides and halide complexes

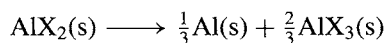
Several important points emerge in considering the wide range of Group 13 metal halides and their complexes. Monohalides are known for all 4 metals with each halogen though for Al they occur only as short-lived diatomic species in the gas phase or as cryogenically isolated solids. This may seem paradoxical, since the bond dissociation energies for Al–X are substantially greater than for the corresponding monohalides of the other elements and fall in the range 655 kJ mol<sup>-1</sup> (AlF) to 365 kJ mol<sup>-1</sup> (AlI). The corresponding values for the gaseous TlX decrease from 460 to 270 kJ mol<sup>-1</sup> yet it is these latter compounds that form stable crystalline solids. In fact, the instability of AlX in the condensed phase at normal temperatures is due not to the weakness of the Al–X bond but to the ready disproportionation of these compounds into the even more stable AlX<sub>3</sub>:



The reverse reaction to give the gaseous species AlX(g) at high temperature accounts for the enhanced volatility of AlF<sub>3</sub> when heated in the presence of Al metal, and the ready volatilization of Al metal in the presence of AlCl<sub>3</sub>. Using calculations of the type outlined on p. 82 the standard heats of formation of the crystalline monohalides AlX and their heats of disproportionation have been estimated as:

Compound (s)	AlF	AlCl	AlBr	AlI
$\Delta H_f^\circ/\text{kJ mol}^{-1}$	-393	-188	-126	-46
$\Delta H_{\text{disprop}}^\circ/\text{kJ mol}^{-1}$	-105	-46	-50	-59

The crystalline dihalides AlX<sub>2</sub> are even less stable with respect to disproportionation, value of  $\Delta H_{\text{disprop}}$  falling in the range -200 to -230 kJ mol<sup>-1</sup> for the reaction



Very recently the first AlII compound to be stable at room temperature, the tetrameric complex [{AlII(NEt<sub>3</sub>)<sub>4</sub>]<sub>4</sub>], has been prepared and shown to feature a planar Al<sub>4</sub> ring with Al–Al 265 pm, Al–I 265 pm and Al–N 207 pm.<sup>(25a)</sup>

#### Aluminium trihalides

AlF<sub>3</sub> is made by treating Al<sub>2</sub>O<sub>3</sub> with HF gas at 700° and the other trihalides are made by the direct exothermic combination of the elements. AlF<sub>3</sub> is important in the industrial production of Al metal (p. 219) and is made on a scale approaching 700 000 tonnes per annum world wide. AlCl<sub>3</sub> finds extensive use as a Friedel–Crafts catalyst (p. 236): its annual production approaches 100 000 tpa and is dominated by Western Europe, USA and Japan. The price for bulk AlCl<sub>3</sub> is about \$0.35/kg.

AlF<sub>3</sub> differs from the other trihalides of Al in being involatile and insoluble, and in having a much greater heat of formation (Table 7.6). These differences probably stem from differences in coordination number (6 for AlF<sub>3</sub>; change from 6 to 4 at mp for AlCl<sub>3</sub>; 4 for AlBr<sub>3</sub> and AlI<sub>3</sub>) and from the subtle interplay of a variety of other factors mentioned below, rather than from any discontinuous change in bond type between the fluoride and the other halides. Similar differences dictated by change in coordination number are noted for many other metal halides, e.g. SnF<sub>4</sub> and SnX<sub>4</sub> (p. 381), BiF<sub>3</sub> and BiX<sub>3</sub> (p. 559), etc., and even more dramatically for some oxides such as CO<sub>2</sub> and SiO<sub>2</sub>. In AlF<sub>3</sub> each Al is surrounded by

**Table 7.6** Properties of crystalline AlX<sub>3</sub>

Property	AlF <sub>3</sub>	AlCl <sub>3</sub>	AlBr <sub>3</sub>	AlI <sub>3</sub>
MP/°C	1290	192.4	97.8	189.4
Sublimation pt (1 atm)/°C	1272	180	256	382
$\Delta H_f^\circ/\text{kJ mol}^{-1}$	1498	707	527	310

<sup>25a</sup>A. ECKER and H.-G. SCHNÖCKEL, *Z. anorg. allg. Chem.* **622**, 149–52 (1996).

a distorted octahedron of 6 F atoms and the 1:3 stoichiometry is achieved by the corner sharing of each F between 2 octahedra. The structure is thus related to the  $\text{ReO}_3$  structure (p. 1047) but is somewhat distorted from ideal symmetry for reasons which are not understood. Maybe the detailed crystal structure data are wrong.<sup>(26)</sup> The relatively "open" lattice of  $\text{AlF}_3$  provides sites for water molecules and permits the formation of a range of nonstoichiometric hydrates. In addition, well-defined hydrates  $\text{AlF}_3 \cdot n\text{H}_2\text{O}$  ( $n = 1, 3, 9$ ) are known but, curiously, no hexahydrate corresponding to the familiar  $[\text{Al}(\text{H}_2\text{O})_6]\text{Cl}_3$ . In the gas phase at  $1000^\circ\text{C}$  the  $\text{AlF}_3$  molecule has trigonal planar symmetry ( $D_{3h}$ )<sup>(27)</sup> with Al–F 163.0(3) pm which is considerably shorter than in the solid phase 170–190 pm (for 6-coordinate Al).

The complex fluorides of  $\text{Al}^{\text{III}}$  (and  $\text{Fe}^{\text{III}}$ ) provide a good example of a family of structures with differing stoichiometries all derived by the sharing of vertices between octahedral  $\{\text{AlF}_6\}$  units;<sup>(26)</sup> edge sharing and face sharing are not observed, presumably because of the destabilizing influence of the close (repulsive) approach of 2 Al atoms each of which carries a net partial positive charge. Discrete  $\{\text{AlF}_6\}$  units occur in cryolite,  $\text{Na}_3\text{AlF}_6$ , and in the garnet structure  $\text{Li}_3\text{Na}_3\text{Al}_2\text{F}_{12}$  (i.e.  $[\text{Al}_2\text{Na}_3(\text{LiF}_4)_3]$ , see p. 348) but it is misleading to think in terms of  $[\text{AlF}_6]^{3-}$  ions since the Al–F bonds are not appreciably different from the other M–F bonds in the structure. Thus the  $\text{Na}_3\text{AlF}_6$  structure is closely related to perovskite  $\text{ABO}_3$  (p. 963) in which one-third of the Na and all the Al atoms occupy octahedral  $\{\text{MF}_6\}$  sites and the remaining two-thirds of the Na occupy the 12-coordinate sites. When two opposite vertices of  $\{\text{AlF}_6\}$  are shared the stoichiometry becomes  $\{\text{AlF}_5\}$  as in  $\text{Ti}_2^{\text{I}}\text{AlF}_5$  (and  $\text{Ti}_2^{\text{I}}\text{GaF}_5$ ). The sharing of 4 equatorial vertices of  $\{\text{AlF}_6\}$  leads to the stoichiometry  $\{\text{AlF}_4\}$  in  $\text{Ti}^{\text{I}}\text{AlF}_4$ . The same structural motif is found in each of

the "isoelectronic" 6-coordinate layer lattices of  $\text{K}_2\text{Mg}^{\text{II}}\text{F}_4$ ,  $\text{KAl}^{\text{III}}\text{F}_4$  and  $\text{Sn}^{\text{IV}}\text{F}_4$ , none of which contain tetrahedral  $\{\text{MF}_4\}$  units.

More complex patterns of sharing give intermediate stoichiometries as in  $\text{Na}_5\text{Al}_3\text{F}_{14}$  which features layers of  $\{\text{Al}_3\text{F}_{14}^{5-}\}$  built up by one-third of the  $\{\text{AlF}_6\}$  octahedra sharing 4 equatorial vertices and the remainder sharing 2 opposite vertices. Again,  $\text{Na}_2\text{MgAlF}_7$  comprises linked  $\{\text{AlF}_6\}$  and  $\{\text{MgF}_6\}$  octahedra in which 4 vertices of  $\{\text{AlF}_6\}$  and all vertices of  $\{\text{MgF}_6\}$  are shared. Likewise,  $\text{Sm}^{\text{II}}\text{AlF}_5$  features  $\{\text{Al}_2\text{F}_{10}^{4-}\}$  bioctahedra and linear chains of *trans* corner-sharing  $\{\text{AlF}_6\}$ ,<sup>(28)</sup> and  $\text{Ba}_3\text{Al}_2\text{F}_{12}$  has a tetrameric  $\{(\text{F}_4\text{AlF}_{2/2})_4^{8-}\}$  ring, i.e.  $[\text{Ba}_6\text{F}_4(\text{Al}_4\text{F}_{20})]$ ,<sup>(29)</sup> which is unique for fluorometallates, being previously encountered only in neutral molecules  $(\text{MF}_5)_4$  where M is Nb, Ta (p. 990); Mo, W (p. 1020); Ru, Os (p. 1083). In all of these structures the degree of charge separation, though considerable, is unlikely to approach the formal group charges: thus  $\text{AlF}_3$  should not be regarded as a network of alternating ions  $\text{Al}^{3+}$  and  $\text{F}^-$  nor, at the other extreme, as an alternating set of  $\text{Al}^{3+}$  and  $\text{AlF}_6^{3-}$ , and lattice energies calculated on the basis of such formal charges placed at the observed interatomic distances are bound to be of limited reliability. Equally, the structure is not well described as a covalently bonded network of Al atoms and F atoms, and detailed MO calculations would be required to assess the actual extent of charge separation, on the one hand, and of interatomic covalent bonding, on the other.

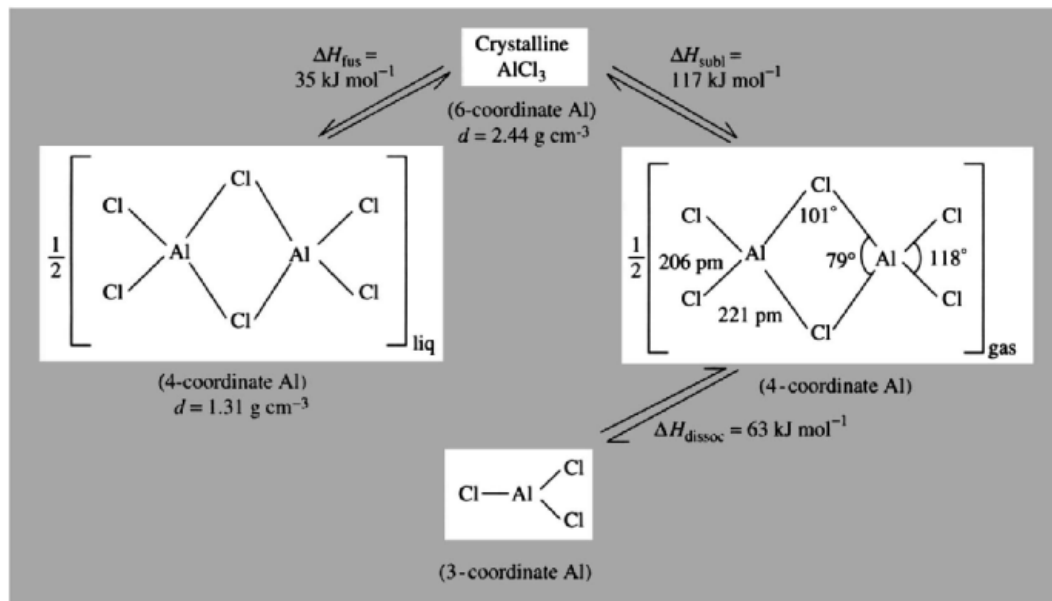
The structure of  $\text{AlCl}_3$  is similarly revealing. The crystalline solid has a layer lattice with 6-coordinate Al but at the mp  $192.4^\circ$  the structure changes to a 4-coordinate molecular dimer  $\text{Al}_2\text{Cl}_6$ ; as a result there is a dramatic increase in volume (by 85%) and an even more dramatic drop in electrical conductivity almost to zero. The mp therefore represents a substantial change in the nature of the bonding. The covalently bonded

<sup>26</sup> A. F. WELLS, *Structural Inorganic Chemistry*, 4th edn., Oxford University Press, Oxford, 1975, 1095 pp.

<sup>27</sup> M. HARGITTAI, M. KOLONITS, J. TREMMEL, J.-L. FOURQUET and G. FERREY, *Struct. Chem.* **1**, 75–8 (1989).

<sup>28</sup> J. KÖHLER, *Z. anorg. allg. Chem.* **619**, 181–8 (1993).

<sup>29</sup> R. DOMESLE and R. HOPPE, *Angew. Chem. Int. Edn. Engl.* **19**, 489–90 (1980).



molecular dimers are also the main species in the gas phase at low temperatures ( $\sim 150\text{--}200^\circ$ ) but at higher temperature there is an increasing tendency to dissociate into trigonal planar  $\text{AlCl}_3$  molecules isostructural with  $\text{BX}_3$  (p. 196).

By contrast,  $\text{Al}_2\text{Br}_6$  and  $\text{Al}_2\text{I}_6$  form dimeric molecular units in the crystalline phase as well as in the liquid and gaseous states and fusion is not attended by such extensive changes in properties. In the gas phase  $\Delta H_{\text{dissoc}} = 59 \text{ kJ mol}^{-1}$  for  $\text{AlBr}_3$  and  $50 \text{ kJ mol}^{-1}$  for  $\text{AlI}_3$ . In all these dimeric species, as in the analogous dimers  $\text{Ga}_2\text{Cl}_6$ ,  $\text{Ga}_2\text{Br}_6$ ,  $\text{Ga}_2\text{I}_6$  and  $\text{In}_2\text{I}_6$ , the  $\text{M}\text{--}\text{X}_t$  distance is  $10\text{--}20 \text{ pm}$  shorter than the  $\text{M}\text{--}\text{X}_\mu$  distance; the external angle  $\text{X}_t\text{MX}_t$  is in the range  $110\text{--}125^\circ$  whereas the internal angle  $\text{X}_\mu\text{MX}_\mu$  is in the range  $79\text{--}102^\circ$ .

The trihalides of Al form a large number of addition compounds or complexes and these have been extensively studied because of their importance in understanding the nature of Friedel–Crafts catalysis.<sup>(30,31)</sup> The adducts vary enormously in stability from weak interactions to very stable complexes, and they also vary widely in their mode of bonding, structure and

properties. Aromatic hydrocarbons and olefins interact weakly though in some cases crystalline adducts can be isolated, e.g. the clathrate-like complex  $\text{Al}_2\text{Br}_6 \cdot \text{C}_6\text{H}_6$ , mp  $37^\circ$  (decomp). With mesitylene ( $\text{C}_6\text{H}_3\text{Me}_3$ ) and the xylenes ( $\text{C}_6\text{H}_4\text{Me}_2$ ) the interaction is slightly stronger, leading to dissociation of the dimer and the formation of weak monomeric complexes  $\text{AlBr}_3\text{L}$  both in solution and in the solid state. At the other end of the stability scale  $\text{NMe}_3$  forms two crystalline complexes:  $[\text{AlCl}_3(\text{NMe}_3)]$  mp  $156.9^\circ$  which features molecular units with 4-coordinate tetrahedral Al, and  $[\text{AlCl}_3(\text{NMe}_3)_2]$  which has 5-coordinate Al with trigonal bipyramidal geometry and *trans* axial ligands. By contrast, the adduct  $\text{AlCl}_3 \cdot 3\text{NH}_3$  has been shown by X-ray diffraction analysis to consist of elongated octahedra  $[\text{AlCl}_2(\text{NH}_3)_4]^+$  and compressed octahedra  $[\text{AlCl}_4(\text{NH}_3)_2]^-$ , the

<sup>30</sup> N. N. GREENWOOD and K. WADE, Chap. 7 in G. A. OLAH (ed.), *Friedel–Crafts and Related Reactions*, Vol. 1, pp. 569–622, Interscience, New York, 1963.

<sup>31</sup> K. WADE and A. J. BANISTER, Chap. 12 in *Comprehensive Inorganic Chemistry*, Vol. 1, pp. 993–1172, Pergamon Press, Oxford, 1973.

arrangement being further stabilized by a network of N-H...Cl hydrogen bonds.<sup>(32)</sup>

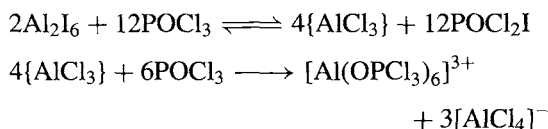
Alkyl halides interact rather weakly and vibrational spectroscopy suggests bonding of the type R-X...AlX<sub>3</sub>. However, for readily ionizable halides such as Ph<sub>3</sub>CCl the degree of charge separation is much more extensive and the complex can be formulated as Ph<sub>3</sub>C<sup>+</sup>AlCl<sub>4</sub><sup>-</sup>. Acyl halides RCOX may interact either through the carbonyl oxygen, PhC(Cl)=O→AlCl<sub>3</sub>, or through the halogen, RCOX...AlX<sub>3</sub> or RCO<sup>+</sup>AlX<sub>4</sub><sup>-</sup>. Again, vibrational spectroscopy is a sensitive, though not always reliable, diagnostic for the mode of bonding. X-ray crystal structures of several complexes have been obtained but these do not necessarily establish the predominant species in nonaqueous solvents because of the delicate balance between the various factors which determine the structure (p. 198). Even in the crystalline state the act of coordination may lead to substantial charge separation. For example, X-ray analysis has established that AlCl<sub>3</sub>ICl<sub>3</sub> comprises chains of alternating units which are best described as ICl<sub>2</sub><sup>+</sup> and AlCl<sub>4</sub><sup>-</sup> with rather weaker interactions between the ions.

Another instructive example is the ligand POCl<sub>3</sub> which forms 3 crystalline complexes AlCl<sub>3</sub>POCl<sub>3</sub> mp 186.5°, AlCl<sub>3</sub>(POCl<sub>3</sub>)<sub>2</sub> mp 164° (d), and AlCl<sub>3</sub>(POCl<sub>3</sub>)<sub>6</sub> mp 41° (d). Although the crystal structures of these adducts have not been established it is known that POCl<sub>3</sub> normally coordinates through oxygen rather than chlorine and very recently a Raman spectroscopic study of the 1:1 adduct in the gas phase suggests that it is indeed Cl<sub>3</sub>P=O→AlCl<sub>3</sub> with C<sub>s</sub> symmetry.<sup>(33)</sup> Also consistent with oxygen ligation is the observation that there is no exchange of radioactive <sup>36</sup>Cl when AlCl<sub>3</sub> containing <sup>36</sup>Cl is dissolved in inactive POCl<sub>3</sub>. However, such solutions are good electrical conductors and spectroscopy reveals AlCl<sub>4</sub><sup>-</sup> as a predominant solute species. The resolution of this apparent paradox was provided by means

of <sup>27</sup>Al nmr spectroscopy<sup>(34)</sup> which showed that ionization occurred according to the reaction

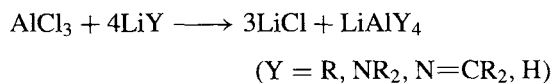
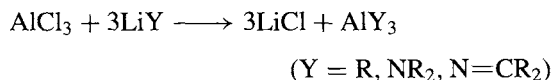


It can be seen that all the Cl atoms in [AlCl<sub>4</sub>]<sup>-</sup> come from the AlCl<sub>3</sub>. It was further shown that the same two species predominated when Al<sub>2</sub>I<sub>6</sub> was dissolved in an excess of POCl<sub>3</sub>:



No mixed Al species were found by <sup>27</sup>Al nmr in this case.

AlCl<sub>3</sub> is a convenient starting material for the synthesis of a wide range of other Al compounds, e.g.:



Similarly, NaOR reacts to give Al(OR)<sub>3</sub> and NaAl(OR)<sub>4</sub>. AlCl<sub>3</sub> also converts non-metal fluorides into the corresponding chloride, e.g.



This type of transhalogenation reaction, which is common amongst the halides of main group elements, always proceeds in the direction which pairs the most electropositive element with the most electronegative, since the greatest amount of energy is evolved with this combination.<sup>(35)</sup>

The major industrial use of AlCl<sub>3</sub> is in catalytic reactions of the type first observed in 1877 by C. Friedel and J. M. Crafts. AlCl<sub>3</sub> is now extensively used to effect alkylations (with RCl, ROH or RCH=CH<sub>2</sub>), acylations (with RCOCl), and

<sup>32</sup> H. JACOBS and B. NÖCKER, *Z. anorg. allg. Chem.* **619**, 73-6 (1993).

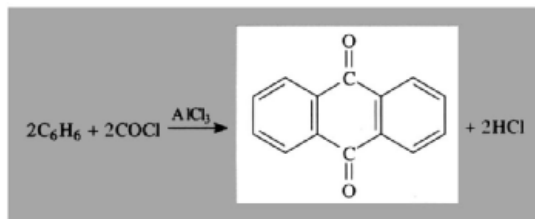
<sup>33</sup> S. BOGHOSIAN, D. A. KARYDIS and G. A. VOYIATZIS, *Polyhedron* **12**, 771-82 (1993).

<sup>34</sup> R. G. KIDD and D. R. TRUAX, *J. Chem. Soc., Chem. Commun.*, 160-1 (1969).

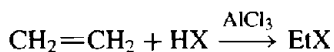
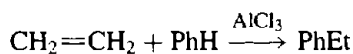
<sup>35</sup> F. SEEL, *Atomic Structure and Chemical Bonding*, 4th edn. translated and revised by N. N. GREENWOOD and H. P. STADLER, Methuen, London, 1963, pp. 83-4.



various condensation, polymerization, cyclization, and isomerization reactions.<sup>(36)</sup> The reactions are examples of the more general class of electrophilic reactions that are catalysed by metal halides and other Lewis acids (electron pair acceptors). Of the 30 000 tonnes of  $\text{AlCl}_3$  produced annually in the USA, about 15% is used in the synthesis of anthraquinones for the dyestuffs industry:



A further 15% of the  $\text{AlCl}_3$  is used in the production of ethyl benzene for styrene manufacture, and 13% in making  $\text{EtCl}$  or  $\text{EtBr}$  (for  $\text{PbEt}_4$ ):

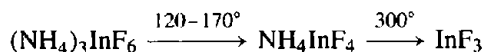


The isomerization of hydrocarbons in the petroleum industry and the production of dodecyl benzene for detergents accounts for a further 10% each of the  $\text{AlCl}_3$  used.

### *Trihalides of gallium, indium and thallium*

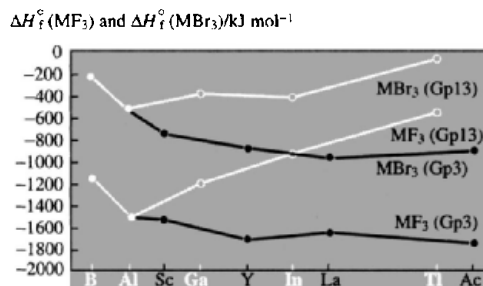
These compounds have been mentioned several times in the preceding sections. As with  $\text{AlX}_3$  (p. 233), the trifluorides are involatile and have much higher mps and heats of formation than the other trihalides;<sup>(31)</sup> e.g.  $\text{GaF}_3$  melts above  $1000^\circ$ , sublimes at  $\sim 950^\circ$  and has the 6-coordinate  $\text{FeF}_3$ -type structure, whereas  $\text{GaCl}_3$  melts at  $77.8^\circ$ , boils at  $201.2^\circ$ , and has the 4-coordinate molecular structure  $\text{Ga}_2\text{Cl}_6$ .  $\text{GaF}_3$  and

$\text{InF}_3$  are best prepared by thermal decomposition of  $(\text{NH}_4)_3\text{MF}_6$ , e.g.:



Preparations using aqueous  $\text{HF}$  on  $\text{M}(\text{OH})_3$ ,  $\text{M}_2\text{O}_3$ , or  $\text{M}$  metal give the trihydrate.  $\text{TlF}_3$  is best prepared by the direct fluorination of  $\text{Tl}_2\text{O}_3$  with  $\text{F}_2$ ,  $\text{BrF}_3$  or  $\text{SF}_4$  at  $300^\circ$ . Trends in the heats of formation of the Group 13 trihalides show the same divergence from  $\text{BX}_3$ ,  $\text{AlX}_3$  and the Group 3 trihalides as was found for trends in other properties such as  $I_M$ ,  $E^\circ$  and  $\chi$  (pp. 223–5) and for the same reasons. For example, the data for  $\Delta H_f^\circ$  for the trifluorides and tribromides are compared in Fig. 7.7 from which it is clear that the trend noted for the sequence B, Al, Sc, Y, La, Ac is not followed for the Group 13 metal trihalides which become progressively less stable from Al to Tl.

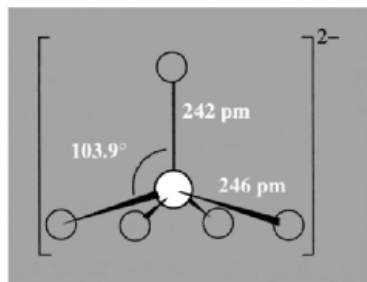
The volatile trihalides  $\text{MX}_3$  form several ranges of addition compounds  $\text{MX}_3\text{L}$ ,  $\text{MX}_3\text{L}_2$ ,  $\text{MX}_3\text{L}_3$ , and these have been extensively studied because of the insight they provide on the relative influence of the underlying  $d^{10}$  electron configuration on the structure and stability of the complexes. With halide ions  $\text{X}^-$  as ligands the stoichiometry depends sensitively on crystal lattice effects or on the nature of the solvent and the relative concentration of the species in solution. Thus X-ray studies have established the tetrahedral ions  $[\text{GaX}_4]^-$ ,  $[\text{InCl}_4]^-$ , etc., and these persist in ethereal



**Figure 7.7** Trends in the standard enthalpies of formation  $\Delta H_f^\circ$  for Groups 3 and 13 trihalides as illustrated by data for  $\text{MF}_3$  and  $\text{MB}_3$ .

<sup>36</sup> G. A. OLAH (ed.), *Friedel-Crafts and Related Reactions*, Vols. 1–4, Interscience, New York, 1963. See especially Chap. 1, Historical, by G. A. OLAH and R. E. A. DEAR, and Chap. 2, Definition and scope by G. A. OLAH.

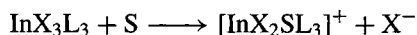
solution, though in aqueous solution  $[\text{InCl}_4]^-$  loses its  $T_d$  symmetry due to coordination of further molecules of  $\text{H}_2\text{O}$ .  $[\text{NEt}_4]_2[\text{InCl}_5]$  is remarkable in featuring a square-pyramidal ion of  $C_{4v}$  symmetry (Fig. 7.8) and was one of the first recorded examples of this geometry in nontransition element chemistry (1969), cf  $\text{SbPh}_5$  on p. 598 and the hydrido aluminate species on p. 231. The structure is apparently favoured by electrostatic packing considerations though it also persists in nonaqueous solution, possibly due to the formation of a pseudo-octahedral solvate  $[\text{InCl}_5\text{S}]^{2-}$ . It will be noted that  $[\text{InCl}_5]^{2-}$  is not isostructural with the isoelectronic species  $\text{SnCl}_5^-$  and  $\text{SbCl}_5$  which have the more common  $D_{3h}$  symmetry. Substituted 5-coordinate chloroderivatives of  $\text{In}^{\text{III}}$  and  $\text{Tl}^{\text{III}}$  often have geometries intermediate between square pyramidal and trigonal bipyramidal.<sup>(37)</sup>



**Figure 7.8** The structure of  $[\text{InCl}_5]^{2-}$  showing square-pyramidal ( $C_{4v}$ ) geometry. The  $\text{In}-\text{Cl}_{\text{apex}}$  distance is significantly shorter than the  $\text{In}-\text{Cl}_{\text{base}}$  distances and In is 59 pm above the basal plane; this leads to a  $\text{Cl}_{\text{apex}}-\text{In}-\text{Cl}_{\text{base}}$  angle of  $103.9^\circ$  which is very close to the theoretical value required to minimize  $\text{Cl}\cdots\text{Cl}$  repulsions whilst still retaining  $C_{4v}$  symmetry ( $103.6^\circ$ ) calculated on the basis of a simple inverse square law for repulsion between ligands.  $[\text{NEt}_4]_2[\text{TlCl}_5]$  is isomorphous with  $[\text{NEt}_4]_2[\text{InCl}_5]$  and presumably has a similar structure for the anion.

<sup>37</sup> R. O. DAY and R. R. HOLMES, *Inorg. Chem.* **21**, 2379–82 (1982). H. BORGHOLTE, K. DEHNICKE, H. GOESMANN and D. FENSKE, *Z. anorg. allg. Chem.* **600**, 7–14 (1991).

With neutral ligands, L,  $\text{GaX}_3$  tend to resemble  $\text{AlX}_3$  in forming predominantly  $\text{MX}_3\text{L}$  and some  $\text{MX}_3\text{L}_2$ , whereas  $\text{InX}_3$  are more varied.<sup>(38)</sup>  $\text{InX}_3\text{L}_3$  is the commonest stoichiometry for N and O donors and these are probably predominantly 6-coordinate in the solid state, though in coordinating solvents (S) partial dissociation into ions frequently occurs:



More extensive ionization occurs if, instead of the halides  $\text{X}^-$ , a less strongly coordinating anion  $\text{Y}^-$  such as  $\text{ClO}_4^-$  or  $\text{NO}_3^-$  is used; in such cases the coordinating stoichiometry tends to be 1:6, e.g.  $[\text{InL}_6]^{3+}(\text{Y}^-)_3$ ,  $\text{L} = \text{Me}_2\text{SO}$ ,  $\text{Ph}_2\text{SO}$ ,  $(\text{Me}_2\text{N})_2\text{CO}$ ,  $\text{HCO}(\text{NMe}_2)$ ,  $\text{P}(\text{OMe})_3$ , etc. Bulky ligands such as  $\text{PPh}_3$  and  $\text{AsPh}_3$  tend to give 1:4 adducts  $[\text{InL}_4]^{3+}(\text{Y}^-)_3$ . The same effect of ionic dissociation can be achieved in 1:3 complexes of the trihalides themselves by use of bidentate chelating ligands (B) such as en, bipy, or phen, e.g.  $[\text{InB}_3]^{3+}(\text{X}^-)_3$  ( $\text{X} = \text{Cl}, \text{Br}, \text{I}, \text{NCO}, \text{NCS}, \text{NCSe}$ ).  $\text{InX}_3$  complexes having 1:2 stoichiometry also have a variety of structures. Trigonal bipyramidal geometry with axial ligands is found for  $\text{InX}_3\text{L}_2$ , where  $\text{L} = \text{MNE}_3$ ,  $\text{PMe}_3$ ,  $\text{PPh}_3$ ,  $\text{Et}_2\text{O}$ , etc. By contrast, the crystal structure of the 1:2 complex of  $\text{InI}_3$  with  $\text{Me}_2\text{SO}$  shows that it is fully ionized as  $[\text{cis}-\text{InI}_2(\text{OSMe}_2)_4]^+[\text{InI}_4]^-$ , and fivefold coordination is avoided by a disproportionation into 6- and 4-coordinate species. Complexes having 1:1 stoichiometry are rare for  $\text{InX}_3$ ;  $\text{InCl}_3$  forms  $[\text{InCl}_3(\text{OPCl}_3)]$ ,  $[\text{InCl}_3(\text{OCMe}_2)]$  and  $[\text{InCl}_3(\text{OCPh}_2)]$  and py forms a 1:1 (and a 1:3) adduct with  $\text{InI}_3$ . Frequently, of course, a given donor–acceptor pair combines in more than one stoichiometric ratio.

The thermochemistry of the Group 13 trihalide complexes has been extensively studied<sup>(30,31,39)</sup> and several stability sequences have been

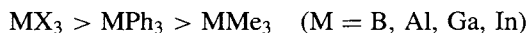
<sup>38</sup> A. J. CARTY and D. J. TUCK, *Prog. Inorg. Chem.* **19**, 243–337 (1975).

<sup>39</sup> N. N. GREENWOOD *et al.*, *Pure Appl. Chem.* **2**, 55–9 (1961); *J. Chem. Soc. A*, 267–70, 270–3, 703–6 (1966); *J. Chem. Soc. A*, 753–6 (1968); 249–53, 2876–8 (1969); *Inorg. Chem.* **9**, 86–90 (1970), and references therein. R. C. GEARHART, J. D. BECK and R. H. WOOD, *Inorg. Chem.* **14**, 2413–6 (1975).

established which can be interpreted in terms of the factors listed on p. 198. In addition, Ga and In differ from B and Al in having an underlying  $d^{10}$  configuration which can, in principle, take part in  $d_{\pi}-d_{\pi}$  back bonding with donors such as S (but not N or O); alternatively (or additionally), some of the trends can be interpreted in terms of the differing polarizabilities of B and Al, as compared to Ga and In, the former pair behaving as class-a or "hard" acceptors whereas Ga and In frequently behave as class-b or "soft" acceptors. Again, it should be emphasized that these categories tend to provide descriptions rather than explanations. Towards amines and ethers the acceptor strengths as measured by gas-phase enthalpies of formation decrease in the sequence  $MCl_3 > MBr_3 > MI_3$  for  $M = Al, Ga$  or  $In$ . Likewise, towards phosphines the acceptor strength decreases as  $GaCl_3 > GaBr_3 > GaI_3$ . However, towards the "softer" sulfur donors  $Me_2S$ ,  $Et_2S$  and  $C_4H_8S$ , whilst  $AlX_3$  retains the same sequence, the order for  $GaX_3$  and  $InX_3$  is reversed to read  $MI_3 > MBr_3 > MCl_3$ . A similar reversal is noted when the acceptor strengths of individual  $AlX_3$  are compared with those of the corresponding  $GaX_3$ : towards N and O donors the sequence is invariably  $AlX_3 > GaX_3$  but for S donors the relative acceptor strength is  $GaX_3 > AlX_3$ . These trends emphasize the variety of factors that contribute towards the strength of chemical bonds and indicate that there are no unique series of donor or acceptor strengths when the acceptor atom is varied, e.g.:

- towards  $MeCO_2Et$ :  $BCl_3 > AlCl_3 > GaCl_3 > InCl_3$   
 towards  $py$ :  $AlPh_3 > GaPh_3 > BPh_3 \approx InPh_3$   
 towards  $py$ :  $AlX_3 > BX_3 > GaX_3$  ( $X = Cl, Br$ )  
 towards  $Me_2S$ :  $GaX_3 > AlX_3 > BX_3$  ( $X = Cl, Br$ )

Regularities are more apparent when the acceptor atom remains constant and the attached groups are varied; e.g., for all ligands so far studied the acceptor strength diminishes in the sequence



It has also been found that halide-ion donors (such as  $X^-$  in  $AlX_4^-$  and  $GaX_4^-$ ) are more than

twice as strong as any neutral donor such as X in  $M_2X_6$ , or N, P, O and S donors in  $MX_3L$ .<sup>(39)</sup> Finally, the complexity of factors influencing the strength of such bonds can be gauged from the curious alternation of the gas-phase enthalpies of dissociation of the dimers  $M_2X_6$  themselves; e.g.  $\Delta H_{298}^\circ(\text{dissoc})$  for  $Al_2Cl_6$ ,  $Ga_2Cl_6$  and  $In_2Cl_6$  are respectively 126.8, 93.9 and 121.5  $\text{kJ mol}^{-1}$ .<sup>(40)</sup> The corresponding entropies of dissociation  $\Delta S_{298}^\circ$  are 152.3, 150.4 and 136.0  $\text{J mol}^{-1}$ .

The trihalides of Tl are much less stable than those of the lighter Group 13 metals and are chemically quite distinct from them.  $TlF_3$ , mp  $550^\circ$  (decomp), is a white crystalline solid isomorphous with  $\beta\text{-BiF}_3$  (p. 560); it does not form hydrates but hydrolyses rapidly to  $Tl(OH)_3$  and HF. Nor does it give  $TlF_4^-$  in aqueous solution, and the compounds  $LiTlF_4$  and  $NaTlF_4$  have structures related to fluorite,  $CaF_2$  (p. 118): in  $NaTlF_4$  the cations have very similar 8-coordinate radii (Na 116 pm, Tl 100 pm) and are disordered on the Ca sites (Ca 112 pm); in  $LiTlF_4$ , the smaller size of Li ( $\sim 83$  pm for eightfold coordination) favours a superlattice structure in which Li and Tl are ordered on the Ca sites.  $Na_3TlF_6$  has the cryolite structure (p. 234).

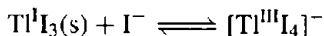
$TlCl_3$  and  $TlBr_3$  are obtained from aqueous solution as the stable tetrahydrates and  $TlCl_3 \cdot 4H_2O$  can be dehydrated with  $SOCl_2$  to give anhydrous  $TlCl_3$ , mp  $155^\circ$ ; it has the  $YCl_3$ -type structure which can be described as  $NaCl$ -type with two-thirds of the cations missing in an ordered manner.

$TlI_3$  is an intriguing compound which is isomorphous with  $NH_4I_3$  and  $CsI_3$  (p. 836); it therefore contains the linear  $I_3^-$  ion<sup>†</sup> and is a compound of  $Tl^I$  rather than  $Tl^{III}$ . It is obtained as black crystals by evaporating an equimolar solution of  $TlI$  and  $I_2$  in concentrated aqueous  $Hl$ . The formulation  $Tl^I(I_3^-)$  rather than  $Tl^{III}(I^-)_3$  is consistent with the standard reduction potentials  $E^\circ(Tl^{III}/Tl^I) + 1.26$  V and  $E^\circ(\frac{1}{2}I_2/I^-) + 0.54$  V,

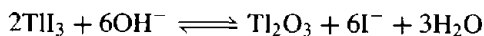
<sup>40</sup> K. KRAUSZE, H. OPPERMAN, U. BRUHN and M. BALARIN, *Z. anorg. allg. Chem.* **550**, 116–22 (1987).

<sup>†</sup> Note that this X-ray evidence by itself does not rule out the possibility that the compound is  $[I-Tl^{III}-I]^+I^-$ .

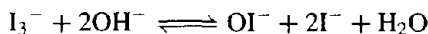
which shows that uncomplexed  $\text{Tl}^{\text{III}}$  is susceptible to rapid and complete reduction to  $\text{Tl}^{\text{I}}$  by  $\text{I}^-$  in acid solution. The same conclusion follows from a consideration of the  $\text{I}_3^-/\text{I}^-$  couple for which  $E^\circ = +0.55 \text{ V}$ . Curiously, however, in the presence of an excess of  $\text{I}^-$ , the  $\text{Tl}^{\text{III}}$  state is stabilized by complex formation



Moreover, solutions of  $\text{TlI}_3$  in MeOH do not show the visible absorption spectrum of  $\text{I}_3^-$  and, when shaken with aqueous  $\text{Na}_2\text{CO}_3$ , give a precipitate of  $\text{Tl}_2\text{O}_3$ , i.e.:



This is due partly to the great insolubility of  $\text{Tl}_2\text{O}_3$  ( $2.5 \times 10^{-10} \text{ g l}^{-1}$  at  $25^\circ$ ) and partly to the enhanced oxidizing power of iodine in alkaline solution as a result of the formation of hypoiodate:

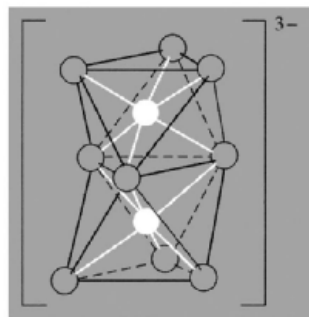


Consistent with this, even  $\text{KI}_3$  is rapidly decolorized in alkaline solution. The example is a salutary reminder of the influence of pH, solubility, and complex formation on the standard reduction potentials of many elements.

Numerous tetrahedral halogeno complexes  $[\text{Tl}^{\text{III}}\text{X}_4]^-$  ( $\text{X} = \text{Cl}, \text{Br}, \text{I}$ ) have been prepared by reaction of quaternary ammonium or arsonium halides on  $\text{TlX}_3$  in nonaqueous solution, and octahedral complexes  $[\text{Tl}^{\text{III}}\text{X}_6]^{3-}$  ( $\text{X} = \text{Cl}, \text{Br}$ ) are also well established. The binuclear complex  $\text{Cs}_3[\text{Tl}_2^{\text{III}}\text{Cl}_9]$  is an important structural type which features two  $\text{TlCl}_6$  octahedra sharing a common face of 3 bridging Cl atoms (Fig. 7.9); the same binuclear complex structure is retained when  $\text{Tl}^{\text{III}}$  is replaced by  $\text{Al}^{\text{III}}$ ,  $\text{V}^{\text{III}}$ ,  $\text{Cr}^{\text{III}}$  and  $\text{Fe}^{\text{III}}$  and also in  $\text{K}_3\text{W}_2\text{Cl}_9$  and  $\text{Cs}_3\text{Bi}_2\text{I}_9$ , etc.

### Lower halides of gallium, indium and thallium

Like  $\text{AlX}$  (p. 233),  $\text{GaF}$  and  $\text{InF}$  are known as unstable gaseous species. The other monohalides are more stable.  $\text{GaX}$  can be obtained as reactive sublimates by treating  $\text{GaX}_3$  with



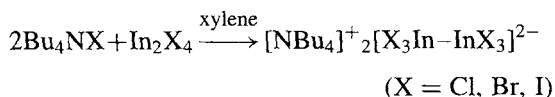
**Figure 7.9** The structure of the ion  $[\text{Tl}_2\text{Cl}_9]^{3-}$  showing two octahedral  $\text{TlCl}_6$  units sharing a common face:  $\text{Tl}-\text{Cl}$ , 254 pm,  $\text{Tl}-\text{Cl}_\mu$ , 266 pm. The  $\text{Tl}\cdots\text{Tl}$  distance is nonbonding (281 pm. cf.  $2 \times \text{Tl}^{\text{III}} = 177 \text{ pm}$ ).

$2\text{Ga}$ : stability increases with increasing size of the anion and  $\text{GaI}$  melts at  $271^\circ$ . Stability is still further enhanced by coordination of the anion with, for example,  $\text{AlX}_3$  to give  $\text{Ga}^{\text{I}}[\text{Al}^{\text{III}}\text{X}_4]$ . Likewise, the very stable "dihalides"  $\text{Ga}^{\text{I}}[\text{Ga}^{\text{III}}\text{Cl}_4]$ ,  $\text{Ga}[\text{GaBr}_4]$ , and  $\text{Ga}[\text{GaI}_4]$  can be prepared by heating equimolar amounts of  $\text{GaX}_3$  and  $\text{Ga}$ , or more conveniently by halogenation of  $\text{Ga}$  with the stoichiometric amount of  $\text{Hg}_2\text{X}_2$  or  $\text{HgX}_2$ . They form complexes of the type  $[\text{Ga}^{\text{I}}\text{L}_4]^+[\text{Ga}^{\text{III}}\text{X}_4]^-$  with a wide range of N, As, O, S and Se donors. See also p. 264 for arene complexes of the type  $[\text{Ga}^{\text{I}}(\text{ar})_n]^+[\text{Ga}^{\text{III}}\text{X}_4]^-$ . Note, however, that the complexes with dioxan  $[\text{Ga}_2\text{X}_4(\text{C}_4\text{H}_8\text{O}_2)_2]$ , do in fact contain  $\text{Ga}^{\text{II}}$  and a  $\text{Ga}-\text{Ga}$  bond, e.g. the chloro complex is a discrete molecule with  $\text{Ga}-\text{Ga}$  240.6 pm (cf. 239.0 pm in  $\text{Ga}_2\text{Cl}_6^{2-}$ );<sup>(41)</sup> the coordination about each Ga atom is essentially tetrahedral and the compound surprisingly adopts an essentially eclipsed structure rather than the staggered structure of  $\text{Ga}_2\text{Cl}_6^{2-}$ . Likewise  $[\text{Ga}_2\text{I}_4 \cdot 2\text{L}]$ , where L is a wide range of organic ligands with N, P, O or S donor atoms, have been shown by vibration spectroscopy to have a  $\text{Ga}-\text{Ga}$  bond.<sup>(42)</sup>

<sup>41</sup> J. C. BEAMISH, R. W. H. SMALL and I. J. WORRALL, *Inorg. Chem.* **18**, 220-3 (1979).

<sup>42</sup> J. C. BEAMISH, A. BOARDMAN and I. J. WORRALL, *Polyhedron* **10**, 95-9 (1991).

Indium monohalides,  $\text{InX}$ , can be prepared as red crystals either directly from the elements or by heating  $\text{In}$  metal with  $\text{HgX}_2$  at  $320\text{--}350^\circ$ . They have a TII-type structure (p. 242) with  $[1 + 4 + 2]$  rather than 6-fold coordination of  $\text{In}$  by  $\text{X}$ , leading to rather close  $\text{In}^{\text{I}} \dots \text{In}^{\text{I}}$  contacts of 362, 356 and 357 pm respectively for  $\text{X} = \text{Cl}$ ,  $\text{Br}$  and  $\text{I}$ .<sup>(43)</sup> Again,  $\text{InI}$  is the most stable, and mixed halides of the type  $\text{In}^{\text{I}}[\text{Al}^{\text{III}}\text{Cl}_4]$ ,  $\text{In}^{\text{I}}[\text{Ga}^{\text{III}}\text{Cl}_4]$  and  $\text{Tl}^{\text{I}}[\text{In}^{\text{III}}\text{Cl}_4]$  are known. Numerous intermediate halides have also been reported and structural assignments of varying degrees of reliability have been suggested, e.g.  $\text{In}^{\text{I}}[\text{In}^{\text{III}}\text{X}_4]$  for  $\text{InX}_2$  ( $\text{Cl}$ ,  $\text{Br}$ ,  $\text{I}$ ); and  $\text{In}_3^{\text{I}}[\text{In}^{\text{III}}\text{Cl}_6]$  for  $\text{In}_2\text{Cl}_3$ . In contrast to the chloride,  $\text{In}_2\text{Br}_3$  has the unexpected structure  $[(\text{In}^+)_2(\text{In}_2^{\text{II}}\text{Br}_6)^{2-}]$ .<sup>(44)</sup> The compounds  $\text{In}_4\text{X}_7$  and  $\text{In}_5\text{X}_7$  ( $\text{Cl}$ ,  $\text{Br}$ ) and  $\text{In}_7\text{Br}_9$  are also known. In all of these halides the observed stoichiometry is achieved by varying the ratio of  $\text{In}^{\text{I}}$  to  $\text{In}^{\text{II}}$  or  $\text{In}^{\text{III}}$ , e.g.  $[(\text{In}^+)_5(\text{InBr}_4^-)_2(\text{InBr}_6^{3-})]$ ,  $[(\text{In}^+)_3(\text{In}_2\text{Br}_6^{2-})\text{Br}^-]$  and  $[(\text{In}^+)_6(\text{InBr}_6^{3-})(\text{Br}^-)_3]$ .<sup>(45,46)</sup> Compounds containing  $\text{In}^{\text{II}}$  were unknown until 1976 when the  $[\text{In}_2\text{X}_6]^{2-}$  dianions having an ethane-like structure were prepared:<sup>(47)</sup>



The analogous  $\text{Ga}$  compounds, e.g.  $[\text{NET}_4]_2[\text{Cl}_3\text{-Ga-GaCl}_3]$ , have been known for rather longer (1965). Oxidation of  $\text{In}_2\text{X}_6^{2-}$  with halogens  $\text{Y}_2$  yields the mononuclear mixed halide complexes  $\text{InX}_3\text{Y}^-$  and  $\text{InX}_2\text{Y}_2^-$  ( $\text{X} \neq \text{Y} = \text{Cl}$ ,  $\text{Br}$ ,  $\text{I}$ ).<sup>(48)</sup>

Thallium(I) is the stable oxidation state for the halides of this element (p. 226) and some physical properties are in Table 7.7.  $\text{TlF}$  is readily obtained by the action of aqueous  $\text{HF}$  on  $\text{Tl}_2\text{CO}_3$ ; it is very soluble in water (in contrast to the other  $\text{TlX}$ ) and has a distorted  $\text{NaCl}$  structure in which there are 3 pairs of  $\text{Tl-F}$  distances at 259, 275 and 304 pm.  $\text{TlCl}$ ,  $\text{TlBr}$  and  $\text{TlI}$  are all prepared by addition of the appropriate halide ion to acidified solutions of soluble  $\text{Tl}^{\text{I}}$  salts (e.g. perchlorate, sulfate, nitrate).  $\text{TlCl}$  and  $\text{TlBr}$  have the  $\text{CsCl}$  structure (p. 80) as befits the large  $\text{Tl}^{\text{I}}$  cation and both salts (and  $\text{TlI}$ ) are photosensitive (like  $\text{AgX}$ ). Yellow  $\text{TlI}$  has a curious orthorhombic layer structure related to  $\text{NaCl}$  (Fig. 7.10), and this transforms at  $175^\circ$  or at 4.7 kbar to a metastable red cubic form with 8-iodine neighbours at 364 pm ( $\text{CsCl}$  type). This transformation is accompanied by 3% reduction in volume. Further application of pressure steadily reduces the volume and at pressures above about 160 kbar, when the volume has decreased by about 35%, the compound becomes a metallic conductor with a resistivity of the order of  $10^{-4}$  ohm cm at room temperature and a positive temperature coefficient.  $\text{TlCl}$  and  $\text{TlBr}$  behave similarly. All three compounds are excellent insulators at normal pressures with negligible conductivity and an energy gap between the valence band and conduction band

<sup>43</sup> G. MEYER and T. STAFFEL, *Z. anorg. allg. Chem.* **574**, 114–8 (1989).

<sup>44</sup> T. STAFFEL and G. MEYER, *Z. anorg. allg. Chem.* **552**, 113–22 (1987).

<sup>45</sup> J. E. DAVIES, L. G. WATERWORTH and I. J. WORRALL, *J. Inorg. Nucl. Chem.* **36**, 805–7 (1974).

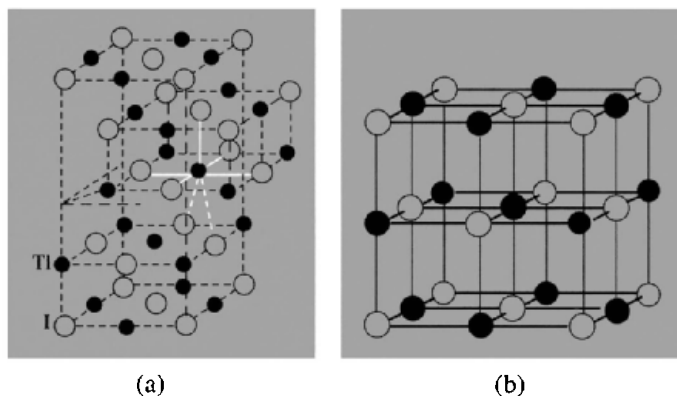
<sup>46</sup> T. STAFFEL and G. MEYER, *Z. anorg. allg. Chem.* **563** 27–37 (1988). See also correction in R. E. MARSH and G. MEYER, *Z. anorg. allg. Chem.* **582**, 128–30 (1990).

<sup>47</sup> B. H. FREELAND, J. L. HENCHER, D. G. TUCK and J. G. CONTRERAS, *Inorg. Chem.* **15**, 2144–6 (1976). See also D. G. TUCK, *Polyhedron* **9**, 377–86 (1990).

<sup>48</sup> J. E. DRAKE, J. L. HENCHER, L. N. KHASROU, D. G. TUCK and L. VICTORIANO, *Inorg. Chem.* **19**, 34–8 (1980).

**Table 7.7** Some properties of  $\text{TlX}$

Property	TlF	TlCl	TlBr	TlI
MP/ $^\circ\text{C}$	322	431	460	442
BP/ $^\circ\text{C}$	826	720	815	823
Colour	White	White	Pale yellow	Yellow
Crystal structure	Distorted $\text{NaCl}$	$\text{CsCl}$	$\text{CsCl}$	See text
Solubility/g per 100 g $\text{H}_2\text{O}$ ( $^\circ\text{C}$ )	80 ( $15^\circ$ )	0.33 ( $20^\circ$ )	0.058 ( $25^\circ$ )	0.006 ( $20^\circ$ )
$\Delta H_f^\circ/\text{kJ mol}^{-1}$	–326	–204	–173	–124



**Figure 7.10** Structure of yellow TlI (a) showing its relation to NaCl (b). Tl has 5 nearest-neighbour I atoms at 5 of the vertices of an octahedron and then 2I + 2Tl as next-nearest neighbours; there is one I at 336 pm, 4 at 349 pm, and 2 at 387 pm, and the 2 close Tl–Tl approaches, one at 383 pm. InX (X = Cl, Br, I) have similar structures in their red forms.<sup>(43)</sup>

of about 3 eV ( $\sim 300 \text{ kJ mol}^{-1}$ ), and the onset of metallic conduction is presumably due to the spreading and eventual overlap of the two bands as the atoms are forced closer together.<sup>(49)</sup>

Several other lower halides of Tl are known:  $\text{TlCl}_2$  and  $\text{TlBr}_2$  are  $\text{Tl}^{\text{I}}[\text{Tl}^{\text{III}}\text{X}_4]$ ,  $\text{Tl}_2\text{Cl}_3$  and  $\text{Tl}_2\text{Br}_3$  are  $\text{Tl}_3^{\text{I}}[\text{Tl}^{\text{III}}\text{X}_6]$ . In addition there is  $\text{Tl}_3\text{I}_4$ , which is formed as an intermediate in the preparation of  $\text{Tl}^{\text{I}}\text{I}_3$  from TlI and  $\text{I}_2$  (p. 239).

### 7.3.3 Oxides and hydroxides

The structural relations between the many crystalline forms of aluminium oxide and hydroxide are exceedingly complex but they are of exceptional scientific interest and immense technological importance. The principal structural types are listed in Table 7.8 and many intermediate and related structures are also known.  $\text{Al}_2\text{O}_3$  occurs as the mineral corundum ( $\alpha\text{-Al}_2\text{O}_3$ ,  $d$  4.0  $\text{g cm}^{-3}$ ) and as emery, a granular form of corundum contaminated with iron oxide and silica. Because of its great hardness (Mohs 9),<sup>†</sup> high mp (2045°C), involatility ( $10^{-6}$  atm at 1950°), chemical inertness and good electrical

insulating properties, it finds many applications in abrasives (including toothpaste), refractories, and ceramics, in addition to its major use in the electrolytic production of Al metal (p. 219). Larger crystals, when coloured with metal-ion impurities, are prized as gemstones, e.g. ruby ( $\text{Cr}^{\text{III}}$  red), sapphire ( $\text{Fe}^{\text{II/III}}$ ,  $\text{Ti}^{\text{IV}}$  blue), oriental emerald (? $\text{Cr}^{\text{III}}$ / $\text{V}^{\text{III}}$  green), oriental amethyst ( $\text{Cr}^{\text{III}}$ / $\text{Ti}^{\text{IV}}$  violet) and oriental topaz ( $\text{Fe}^{\text{III}}$ , yellow). Many of these gems are also made industrially on a large scale by the fusion process first developed at the turn of the century by A. Verneuil. Pure  $\alpha\text{-Al}_2\text{O}_3$  is made industrially by igniting  $\text{Al}(\text{OH})_3$  or  $\text{AlO}(\text{OH})$  at high temperatures ( $\sim 1200^\circ$ ); it is also formed by the combustion of Al and by calcination of various Al salts. It has a rhombohedral crystal structure comprising a hcp array of oxide ions with Al ordered on two-thirds of the octahedral interstices as shown in Fig. 7.11.<sup>(26)</sup> The same  $\alpha\text{-M}_2\text{O}_3$  structure is adopted by several other elements with small  $\text{M}^{\text{III}}$  ( $r$  62–67 pm), e.g. Ga, Ti, V, Cr, Fe and Rh.<sup>‡</sup>

<sup>†</sup> On the Mohs scale diamond is 10 and quartz 7. An alternative measure is the Knoop hardness ( $\text{kg mm}^{-2}$ ) as measured with a 100-g load: typical values on this scale are diamond 7000, boron carbide 2750, corundum 2100, topaz 1340, quartz 820, hardened tool steel 740.

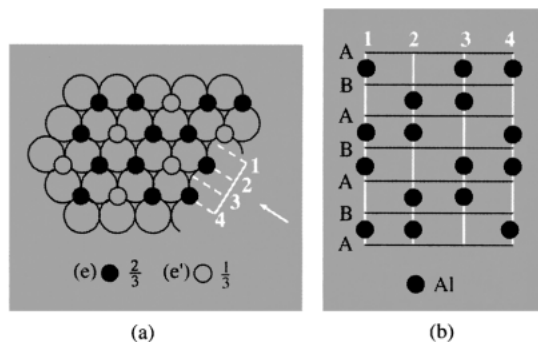
<sup>‡</sup> For somewhat larger cations ( $r$  70–96 pm) the C-type rare-earth  $\text{M}_2\text{O}_3$  structure (p. 1238) is adopted, e.g. for In,

<sup>49</sup> G. A. SAMARA and H. G. DRICKAMER, *J. Chem. Phys.* **37**, 408–10 (1962); see also E. A. PEREZ-ALBUERNE and H. G. DRICKAMER, *J. Chem. Phys.* **43**, 1381–7 (1965).

**Table 7.8** The main structural types of aluminium oxides and hydroxides<sup>(a)</sup>

Formula	Mineral name	Idealized structure
$\alpha\text{-Al}_2\text{O}_3$	Corundum	hcp O with Al in two-thirds of the octahedral sites
$\alpha\text{-AlO(OH)}$	Diaspore	hcp O (OH) with chains of octahedra stacked in layers interconnected with H bonds, and Al in certain octahedral sites
$\alpha\text{-Al(OH)}_3$	Bayerite	hcp (OH) with Al in two-thirds of the octahedral sites
$\gamma\text{-Al}_2\text{O}_3$	—	ccp O defect spinel with Al in $21\frac{1}{3}$ of the 16 octahedral and 8 tetrahedral sites
$\gamma\text{-AlO(OH)}$	Boehmite	ccp O (OH) within layers; details uncertain
$\gamma\text{-Al(OH)}_3$	Gibbsite (Hydrargillite)	ccp OH within layers of edge-shared $\text{Al(OH)}_6$ ; octahedra stacked vertically via H bonds

<sup>(a)</sup>The Greek prefixes  $\alpha$ - and  $\gamma$ - are not used consistently in the literature, e.g. bayerite is sometimes designated as  $\beta\text{-Al(OH)}_3$  and gibbsite as  $\alpha\text{-Al(OH)}_3$ . The UK usage adopted here is consistent with Wells<sup>(26)</sup> and emphasizes the structural relations between the hcp  $\alpha$ -series and the ccp  $\gamma$ -series. Numerous other intermediate crystalline phases have been characterized during partial dehydration and designated as  $\gamma'$ ,  $\delta$ ,  $\zeta$ ,  $\eta$ ,  $\theta$ ,  $\kappa$ ,  $\kappa'$ ,  $\rho$ ,  $\chi$ , etc.



**Figure 7.11** Schematic representation of the structure of  $\alpha\text{-Al}_2\text{O}_3$ . (a) pattern of occupancy by Al (●) of the octahedral sites between hcp layers of oxide ion (○), and (b) stacking sequence of successive planes of Al atoms viewed in the direction of the arrow in (a).

The second modification of alumina is the less compact cubic  $\gamma\text{-Al}_2\text{O}_3$  ( $d$  3.4 g cm<sup>-3</sup>); it is formed by the low-temperature dehydration (<450°) of gibbsite,  $\gamma\text{-Al(OH)}_3$ , or boehmite,  $\gamma\text{-AlO(OH)}$ . It has a defect spinel-type structure (p. 248) comprising a face-centred cubic (fcc) arrangement of 32 oxide ions and a random occupation of  $21\frac{1}{3}$  of the 24 available cation

sites (16 octahedral, 8 tetrahedral). This structure forms the basis of the so-called “activated aluminas” and progressive dehydration in the  $\gamma$ -series leads to open-structured materials of great value as catalysts, catalyst-supports, ion exchangers and chromatographic media. Calcination of  $\gamma\text{-Al}_2\text{O}_3$  above 1000° converts it irreversibly to the more stable and compact  $\alpha$ -form ( $\Delta H_{\text{trans}} - 20 \text{ kJ mol}^{-1}$ ). Yet another form of  $\text{Al}_2\text{O}_3$  occurs as the protective surface layer on the metal: it has a defect NaCl-type structure with Al occupying two-thirds of the octahedral (Na) interstices in the fcc oxide lattice. Perhaps the most ingenious and sophisticated development in aluminium technology has been the recent production of  $\text{Al}_2\text{O}_3$  fibres which can be fabricated into a variety of textile forms, blankets, papers, and boards. Some idea of the many possibilities of such high-temperature inert fabrics is indicated in the Panel on p. 244.

Diaspore,  $\alpha\text{-AlO(OH)}$  occurs in some types of clay and bauxite; it is stable in the range 280–450° and can be made by hydrothermal treatment of boehmite,  $\gamma\text{-AlO(OH)}$ , in 0.4% aqueous NaOH at 380° and 500 atm. Crystalline boehmite is readily prepared by warming the amorphous, gelatinous white precipitate which first forms when aqueous  $\text{NH}_3$  is added to cold solutions of Al salts. In  $\alpha\text{-AlO(OH)}$  the O atoms are arranged in hcp; continuous chains of edge-shared octahedra are stacked in layers

Tl, Sc, Y, Sm and the subsequent lanthanoids, and perhaps surprisingly for  $\text{Mn}^{\text{III}}$  ( $r$  65 pm); the largest lanthanoids La, Ce, Pr and Nd ( $r$  106–100 pm) adopt the A-type rare-earth  $\text{M}_2\text{O}_3$  structure (p. 1238).

### Fibrous Alumina and Zirconia<sup>(50,51)</sup>

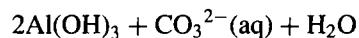
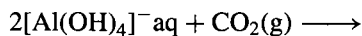
A new family of lightweight inorganic fibres made its commercial debut in 1974 when ICI announced the production of "Saffil", fibrous  $\text{Al}_2\text{O}_3$  and  $\text{ZrO}_2$  on an initial scale of 100 tonnes pa. Du Pont also has a process for  $\alpha$ - $\text{Al}_2\text{O}_3$  fibres and the current world production of fibrous  $\text{Al}_2\text{O}_3$  is of the order of 1000 tonnes per annum. The price is about \$60/kg (1986). The fibres, which have no demonstrable toxic effects (cf. asbestos), have a diameter of  $\sim 3 \mu\text{m}$  (cf. human hair  $\sim 70 \mu\text{m}$ ), and each fibre is extremely uniform along its length (2–5 cm). The fibres are microcrystalline (5–50  $\mu\text{m}$  diam) and are both flexible and resilient with a high tensile strength. They have a soft, silky feel and can be made into rope, yarn, cloth, blankets, fibre matts, paper of various thickness, semi-rigid and rigid boards, and vacuum-formed objects of any required shape. The surface area of Saffil alumina is 100–150  $\text{m}^2 \text{g}^{-1}$  due to the presence of small pores 2–10  $\mu\text{m}$  diameter between the microcrystals, and this enhances its properties as an insulator, filtration medium, and catalyst support. The fibres withstand extended heating to 1400° ( $\text{Al}_2\text{O}_3$ ) or 1600°C ( $\text{ZrO}_2$ ) and are impervious to attack by hot concentrated alkalis and most hot acids except conc  $\text{H}_2\text{SO}_4$ , conc  $\text{H}_3\text{PO}_4$  and aq HF. This unique combination of properties provides the basis for their use in high-temperature insulation, heat shields, thermal barriers, and expansion joints and seals. Fibrous alumina and zirconia are also valuable in thermocouple protection, electric-cable sheathing, and heating-element supports in addition to their use in the high-temperature filtration of corrosive liquids. Both oxides are stabilized by incorporation of small amounts of other inorganic oxides which inhibit disruptive transformation to other crystalline forms.

Alumina fibres can also be used to strengthen metals. Molten metals (e.g. Al, Mg, Pb) or their alloys are forced into moulds containing up to 70% by volume of  $\alpha$ - $\text{Al}_2\text{O}_3$  fibre. For example, fibre-reinforced Al containing 55% fibre by volume is 4–6 times stiffer than unreinforced Al even up to 370°C and has 2–4 times the fatigue strength. Potential applications for which high structural stiffness, heat resistance, and low weight are required include helicopter housings, automotive and jet engines, aerospace structures and lead-acid batteries. For example, fibre reinforced composites of Al or Mg could eventually replace much of the steel used in car bodies without decreasing safety, since the composite has the stiffness of steel but only one-third of its density.

In addition to the production of stabilized  $\text{Al}_2\text{O}_3$  fibres there is also a huge production of melt-spun glassy fibres containing approximately equal proportions by weight of  $\text{Al}_2\text{O}_3$  and  $\text{SiO}_2$ . This is used mainly for thermal insulation at temperatures up to 1400°C and current world production exceeds 20 000 tonnes per annum.

and are further interconnected by H bonds. The underlying hcp structure ensures that diaspore dehydrates directly to  $\alpha$ - $\text{Al}_2\text{O}_3$  (corundum) which has the same basic hcp arrangement of O atoms. The structure is also adopted by several other  $\alpha$ - $\text{MO}(\text{OH})$  ( $\text{M} = \text{Ga}, \text{V}, \text{Mn}$  and  $\text{Fe}$ ); this contrasts with the structure of boehmite,  $\gamma$ - $\text{AlO}(\text{OH})$ , which as a whole is not close-packed, though within each layer the O atoms are arranged in cubic close packing. Dehydration at temperatures up to 450° proceeds via a succession of phases to the cubic  $\gamma$ - $\text{Al}_2\text{O}_3$  and the  $\alpha$  (hexagonal) structure cannot be attained without much more reconstruction of the lattice at 1100–1200° as noted above [and of  $\gamma$ - $\text{ScO}(\text{OH})$  and  $\gamma$ - $\text{FeO}(\text{OH})$ ].

Bayerite,  $\alpha$ - $\text{Al}(\text{OH})_3$ , does not occur in nature but can be made by rapid precipitation from alkaline solutions in the cold:

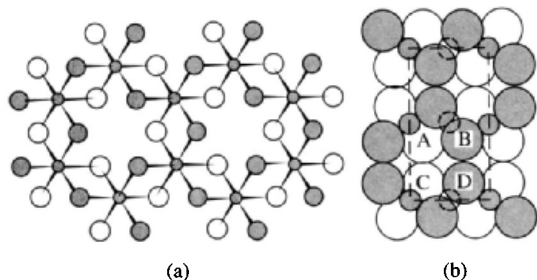


Gibbsite (or hydrargillite),  $\gamma$ - $\text{Al}(\text{OH})_3$ , is a more stable form and can be prepared by slow precipitation from warm alkaline solutions or by digesting the  $\alpha$ -form in aqueous sodium aluminate solution at 80°. In both bayerite ( $\alpha$ ) and gibbsite ( $\gamma$ ) there are layers of composition  $\text{Al}(\text{OH})_3$  built up by the edge sharing of  $\text{Al}(\text{OH})_6$  octahedra to give a pair of approximately close-packed OH layers with Al atoms in two-thirds of the octahedral interstices (Fig. 7.12a). The two crystalline modifications differ in the way this layer is stacked: it is approximately hcp in  $\alpha$ - $\text{Al}(\text{OH})_3$  but in the  $\gamma$ -form the OH groups on the under side of one layer rest directly above the OH groups of the layer below as shown in Fig. 7.12b. A third form of  $\text{Al}(\text{OH})_3$ , nordstrandite, is obtained from the gelatinous

<sup>50</sup> J. D. BIRCHALL, J. A. A. BRADBURY and J. DINWOODIE, Chap IV in W. WATT and B. V. PEROV (eds.), *Handbook of Composites, Vol. 1, Strong Fibres*, Elsevier, Amsterdam, 1985, pp. 115–54. J. D. BIRCHALL, in M. B. BEVER (ed.) *Encyclopedia of Materials Science and Engineering*, Pergamon Press, Oxford, 1986, pp. 2333–5.

<sup>51</sup> W. BÜCHNER, R. SCHLIEBS, G. WINTER and K. H. BÜCHEL, *Industrial Inorganic Chemistry*, VCH, Weinheim, 1989, pp. 362–4.





**Figure 7.12** (a) Part of a layer of  $\text{Al}(\text{OH})_3$  (idealized); the heavy and light open circles represent OH groups above and below the plane of the Al atoms. In  $\alpha\text{-Al}(\text{OH})_3$  the layers are stacked to give approximately hcp. (b) Structure of  $\gamma\text{-Al}(\text{OH})_3$  viewed in a direction parallel to the layers; the OH groups labelled C and D are stacked directly beneath A and B. The six OH groups A, B, C, D and B', D' (behind B and D), form a distorted H-bonded trigonal prism.

hydroxide by ageing it in the presence of a chelating agent such as ethylenediamine, ethylene glycol, or edta; this aligns the OH to give a stacking arrangement which is intermediate between those of the  $\alpha$ - and  $\gamma$ -forms.

As expected from the foregoing structural discussion, gibbsite can be dehydrated to boehmite at  $100^\circ$  and to anhydrous  $\gamma\text{-Al}_2\text{O}_3$  at  $150^\circ$ , but ignition above  $800^\circ$  is required to form  $\alpha\text{-Al}_2\text{O}_3$ . Numerous recipes have been devised for preparing catalysts of differing reactivity and absorptive power, based on the partial dehydration and progressive reconstitution of the Al/O/OH system.<sup>(1)</sup> In addition to pore size, surface area and general reactivity, the basic character of the surface diminishes (and its acidic character increases) in the following series as indicated by the pH of the isoelectric point:

(amorph. Al oxide hydrate)	$>\gamma\text{-AlO}(\text{OH})$	$>\alpha\text{-Al}(\text{OH})_3$	$>\gamma\text{-Al}(\text{OH})_3$	$>\gamma\text{-Al}_2\text{O}_3$
	boehmite	bayerite	gibbsite	
pH: 9.45	9.45–9.40	9.20	–	8.00
(isoelec. pt.)				

The aqueous solution chemistry of Al and the other group 13 metals is rather complicated. The aquo ions are acidic with

$\text{p}K_{\text{A}} \approx 10^{-5}, 10^{-3}, 10^{-4}$  and  $10^{-1}$ , respectively, for  $[\text{M}(\text{H}_2\text{O})_6]^{3+} \rightleftharpoons [\text{M}(\text{OH})(\text{H}_2\text{O})_5]^{2+} + \text{H}^+$  ( $\text{M} = \text{Al}, \text{Ga}, \text{In}, \text{Tl}$ ). The solution chemistry of Al in particular has been extensively investigated because of its industrial importance in water treatment plants, its use in many toiletry formulations, its possible implication in both Alzheimer's disease and the deleterious effects of acid rain, and the ubiquity of Al cooking utensils.<sup>(52–54)</sup> For example, hydrated aluminium sulphate ( $10\text{--}30 \text{ g m}^{-3}$ ) can be added to turbid water supplies at pH 6.5–7.5 to flocculate the colloids, some 3 million tonnes per annum being used worldwide for this application alone. Likewise kilotonne amounts of “ $\text{Al}(\text{OH})_{2.5}\text{Cl}_{0.5}$ ” in concentrated (6M) aqueous solution are used in the manufacture of deodorants and antiperspirants.

The use of  $^{27}\text{Al}$  nmr (see Panel) has been particularly valuable in characterizing the species present in aqueous solution of Al salts.<sup>(55)</sup> These depend very much on both concentration and pH and include the mononuclear ions  $[\text{Al}(\text{OH})_4]^-$ ,  $[\text{Al}(\text{H}_2\text{O}_6)]^{3+}$  and  $[\text{Al}(\text{OH})(\text{H}_2\text{O})_5]^{2+}$ . This latter species can deprotonate further to  $[\text{Al}(\text{OH})_2(\text{H}_2\text{O})_4]^+$  and readily dimerizes via hydroxyl bridges to  $[(\text{H}_2\text{O})_4\text{Al}(\mu\text{-OH})_2\text{Al}(\text{H}_2\text{O})_4]^{4+}$ , i.e.  $[\text{H}_{18}\text{Al}_2\text{O}_{10}]^{4+}$ , which has also been found in several crystalline salts. Higher oligomers probably include appropriately hydrated forms of  $[\text{Al}_3(\text{OH})_{11}]^{2-}$ ,  $[\text{Al}_6(\text{OH})_{15}]^{3+}$  and  $[\text{Al}_8(\text{OH})_{22}]^{2+}$ . A particularly important species is the well-characterized tridecameric cation  $[\text{Al}_{13}\text{O}_4(\text{OH})_{24}(\text{H}_2\text{O})_{12}]^{7+}$  which has the well-known Keggin structure (p. 1014),

<sup>52</sup> H. SIGEL and A. SIGEL (eds), *Metal Ions in Biological Systems*, Vol. 24, *Aluminium and its Role in Biology*, Marcel Dekker, New York, 1988, 440 pp.

<sup>53</sup> R. C. MASSEY and D. TAYLOR (eds.), *Aluminium in Food and the Environment*. Royal Society of Chemistry (London) Special Publ. No. 73, 1989, 116 pp.

<sup>54</sup> G. H. ROBINSON (ed.), *Coordination Chemistry of Aluminium*, VCH, Cambridge, 1993, 234 pp.

<sup>55</sup> J. W. AKITT, *Prog. NMR Spectroscopy* **21**, 1–149 (1989). See also J. W. AKITT, Chap 9 in J. MASON (ed.), *Multinuclear NMR*, Plenum Press, New York, 1987, pp. 259–92, which also includes nmr of Ga, In and Tl isotopes.

### <sup>27</sup>Al in Nuclear Magnetic Resonance Spectroscopy

Aluminium is a very convenient element for nmr spectroscopy because <sup>27</sup>Al is 100% abundant and has a high nmr sensitivity, its receptivity being 0.206 when compared to <sup>1</sup>H and 1170 when compared to <sup>13</sup>C. It also has a high operating frequency (26.077 MHz when scaled to 100 MHz for <sup>1</sup>H) and a wide range of chemical shifts,  $\delta$  (>300 ppm). The nuclear spin quantum number is 5/2 and the magnetogyric ratio  $\gamma$  is 6.9763 rad s<sup>-1</sup>T<sup>-1</sup>. The only disadvantage is the presence of a nuclear quadrupole moment ( $Q = 0.149 \times 10^{-28}$  m<sup>2</sup>) which leads to substantial line broadening for many species. The narrowest lines ( $\omega_{1/2} \sim 2$  Hz) are obtained for highly symmetrical species such as [Al(H<sub>2</sub>O)<sub>6</sub>]<sup>3+</sup> and [Al(OH)<sub>4</sub>]<sup>-</sup>, but line widths of 1000 Hz or more are not uncommon and the use of special curve-analysis techniques is needed to extract the required parameters.

As expected, chemical shifts depend on coordination number (CN) and also on the nature of the atoms directly bonded to Al. Organometallic species, i.e. those with Al-C bonds, resonate at low field (high frequency): those with CN 3 have  $\delta$  in the range 275–220 ppm, those with CN 4 have  $\delta$  220–140 ppm and those with CN 5 have  $\delta$  140–110 ppm. Tetrahalogenoaluminates, AlX<sub>4</sub><sup>-</sup>, AlX<sub>n</sub>Y<sub>4-n</sub><sup>-</sup>, and 4-coordinate ligand adducts in general have  $\delta$  in the range 120–50 ppm with the curious exception of AlI<sub>4</sub><sup>-</sup> which shows a resonance at a higher field than for any other Al species so far,  $\delta$  being –26.7 ppm. Five-coordinate adducts have  $\delta$  in the range 65–25 ppm and octahedral species have  $\delta$  in the range +40 to –25 ppm. Typical parameters for some of the species mentioned in the main text are:

Species	[Al(OH) <sub>4</sub> ] <sup>-</sup>	[Al(H <sub>2</sub> O) <sub>6</sub> ] <sup>3+</sup>	[Al <sub>2</sub> (OH) <sub>2</sub> (H <sub>2</sub> O) <sub>8</sub> ] <sup>4+</sup>	[Al <sub>13</sub> O <sub>4</sub> (OH) <sub>24</sub> (H <sub>2</sub> O) <sub>12</sub> ] <sup>7+</sup>
$\delta$ /ppm	80	0.00 (std)	4	12Al @ ~12, 1Al @ 625
$\omega_{1/2}$ /Hz	10	2	500	8000, 25

These values show some dependence on concentration, pH and temperature. Note also the much smaller linewidth for the central, symmetrically 4-coordinated Al atom of the tridecameric Al<sub>13</sub> species when compared with that of the twelve less symmetrically coordinated octahedral Al atoms, and the possibility of extracting a reasonably precise value of  $\delta$  for this latter resonance which has a linewidth of some 8000 Hz.

Solid-state <sup>27</sup>Al nmr spectroscopy has been much used in recent years to study the composition and structure of aluminosilicates (pp. 351–9) and other crystalline or amorphous Al compounds. The technique of magic angle spinning (MAS) must be used in such cases.<sup>(55)</sup>

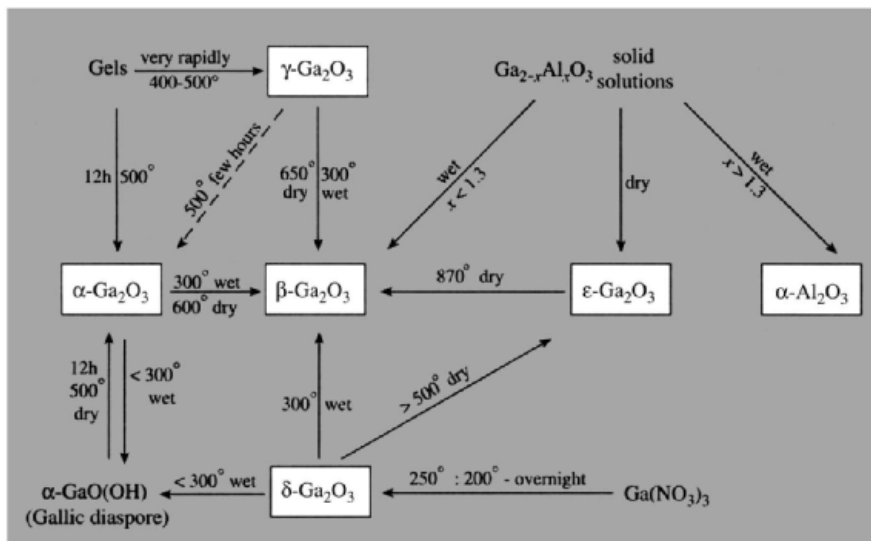
[AlO<sub>4</sub>{Al(OH)<sub>2</sub>(H<sub>2</sub>O)}<sub>12</sub>]<sup>7+</sup>, in which the central tetrahedral AlO<sub>4</sub> group is surrounded by corner- and edge-shared AlO<sub>6</sub> octahedra. The ion, which is almost spherical, has been further characterized by an X-ray diffraction study of crystalline Na[Al<sub>13</sub>O<sub>4</sub>(OH)<sub>24</sub>(H<sub>2</sub>O)<sub>12</sub>](SO<sub>4</sub>)<sub>4</sub>·13H<sub>2</sub>O.

The binary oxides and hydroxides of Ga, In and Tl have been much less extensively studied. The Ga system is somewhat similar to the Al system and a diagram summarizing the transformations in the systems is in Fig. 7.13. In general the  $\alpha$ - and  $\gamma$ -series have the same structure as their Al counterparts.  $\beta$ -Ga<sub>2</sub>O<sub>3</sub> is the most stable crystalline modification (mp 1740°); it has a unique crystal structure with the oxide ions in distorted ccp and Ga<sup>III</sup> in distorted tetrahedral and octahedral sites. The structure appears to owe its stability to these distortions and, because of the lower coordination of half the Ga<sup>III</sup>, the density is ~10% less than for the  $\alpha$ - (corundum-type) form. This preference of Ga<sup>III</sup>

for fourfold coordination despite the fact that it is larger than Al<sup>III</sup> may again indicate the polarizing influence of the d<sup>10</sup> core; a similar tetrahedral site preference is observed for Fe<sup>III</sup>.

In<sub>2</sub>O<sub>3</sub> has the C-type M<sub>2</sub>O<sub>3</sub> structure (p. 1238) and InO(OH) (prepared hydrothermally from In(OH)<sub>3</sub> at 250–400°C and 100–1500 atm) has a deformed rutile structure (p. 961) rather than the layer lattice structure of AlO(OH) and GaO(OH). Crystalline In(OH)<sub>3</sub> is best prepared by addition of NH<sub>3</sub> to aqueous InCl<sub>3</sub> at 100° and ageing the precipitate for a few hours at this temperature; it has the simple ReO<sub>3</sub>-type structure distorted somewhat by multiple H bonds.<sup>(26)</sup>

Thallium is notably different. Tl<sub>2</sub>O forms as black platelets when Tl<sub>2</sub>CO<sub>3</sub> is heated in N<sub>2</sub> at 700° (mp 596°,  $d$  10.36 g cm<sup>-3</sup>); it is hygroscopic and gives TlOH with water. Tl<sub>2</sub><sup>III</sup>O<sub>3</sub> is brown-black (mp 716°,  $d$  10.04 g cm<sup>-3</sup>) and can be made by oxidation of aqueous TlNO<sub>3</sub> with Cl<sub>2</sub> or Br<sub>2</sub> followed by precipitation



**Figure 7.13** Chart illustrating transformation relationships among the forms of gallium oxide and its hydrates. Conversion (wet) of the phase designated as  $\text{Ga}_{2-x}\text{Al}_x\text{O}_3$  to  $\beta\text{-Ga}_2\text{O}_3$  occurs only where  $x < 1.3$ ; where  $x > 1.3$  an  $\alpha\text{-Al}_2\text{O}_3$  structure forms.

of the hydrated oxide  $\text{Tl}_2\text{O}_3 \cdot 1\frac{1}{2}\text{H}_2\text{O}$  and desiccation; single crystals have a very low electrical resistivity (e.g.  $7 \times 10^{-5}$  ohm cm at room temperature). A mixed oxide  $\text{Tl}_4\text{O}_3$  (black) is known and also a violet peroxide  $\text{Tl}^{\text{I}}\text{O}_2$  made by electrolysis of an aqueous solution of  $\text{Tl}_2\text{SO}_4$  and oxalic acid between Pt electrodes.  $\text{TlOH}$  has been mentioned previously (p. 226).

### 7.3.4 Ternary and more complex oxide phases

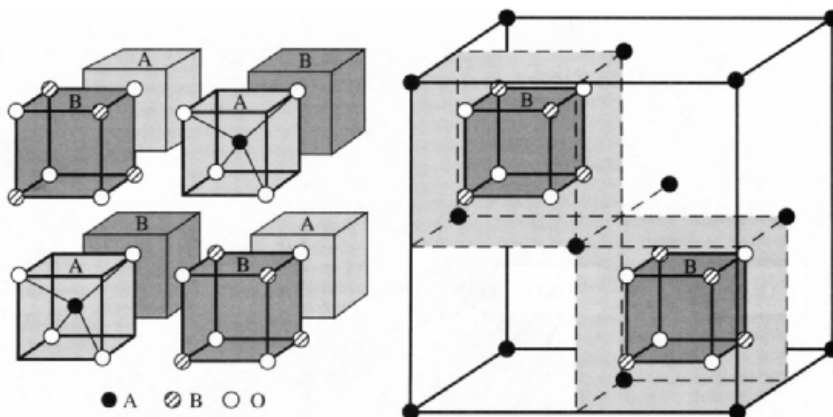
This section considers a number of extremely important structure types in which Al combines with one or more other metals to form a mixed oxide phase. The most significant of these from both a theoretical and an industrial viewpoint are spinel ( $\text{MgAl}_2\text{O}_4$ ) and related compounds, Na- $\beta$ -alumina ( $\text{NaAl}_{11}\text{O}_{17}$ ) and related phases, and tricalcium aluminate ( $\text{Ca}_3\text{Al}_2\text{O}_6$ ) which is a major constituent of Portland cement. Each of these compounds raises points of fundamental importance in solid-state chemistry and each possesses properties of crucial significance to

modern technology. For aluminosilicates see p. 351 and for aluminophosphates see p. 526.

#### Spinel and related compounds<sup>(56)</sup>

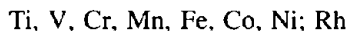
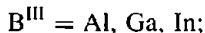
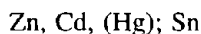
Spinel form a large class of compounds whose crystal structure is related to that of the mineral spinel itself,  $\text{MgAl}_2\text{O}_4$ . The general formula is  $\text{AB}_2\text{X}_4$  and the unit cell contains 32 oxygen atoms in almost perfect ccp array, i.e.  $\text{A}_8\text{B}_{16}\text{O}_{32}$ . In the normal spinel structure (Fig. 7.14) 8 metal atoms (A) occupy tetrahedral sites and 16 metal atoms (B) occupy octahedral sites, and the structure can be regarded as being built up of alternating cubelets of ZnS-type and NaCl-type structures. The two factors that determine which combinations of atoms can form a spinel-type structure are (a) the total formal cation charge, and (b) the relative sizes of the 2 cations with respect both to each other and to the

<sup>56</sup> N. N. GREENWOOD, *Ionic Crystals, Lattice Defects and Nonstoichiometry*, Butterworths, London, 1968, 194 pp. See also J. K. BURDETT, G. D. PRICE and S. L. PRICE, *J. Am. Chem. Soc.* **104**, 92-5 (1982).



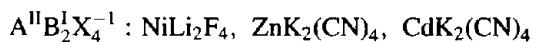
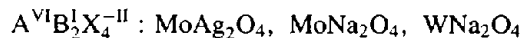
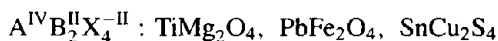
**Figure 7.14** Spinel structure AB<sub>2</sub>O<sub>4</sub>. The structure can be thought of as 8 octants of alternating AO<sub>4</sub> tetrahedra and B<sub>4</sub>O<sub>4</sub> cubes as shown in the left-hand diagram; the 4O have the same orientation in all 8 octants and so build up into a fcc lattice of 32 ions which coordinate A tetrahedrally and B octahedrally. The 4 A octants contain 4 A ions and the 4 B octants contain 16 B ions. The unit cell is completed by an encompassing fcc of A ions (●) as shown in the right-hand diagram; this is shared with adjacent unit cells and comprises the remaining 4 A ions in the complete unit cell A<sub>8</sub>B<sub>16</sub>O<sub>32</sub>. The location of two of the B<sub>4</sub>O<sub>4</sub> cubes is shown for orientation.

anion. For oxides of formula AB<sub>2</sub>O<sub>4</sub> charge balance can be achieved by three combinations of cation oxidation state: A<sup>II</sup>B<sup>III</sup><sub>2</sub>O<sub>4</sub>, A<sup>IV</sup>B<sup>II</sup><sub>2</sub>O<sub>4</sub>, and A<sup>VI</sup>B<sup>I</sup><sub>2</sub>O<sub>4</sub>. The first combination is the most numerous and examples are known with



The anion can be O, S, Se or Te. Most of the A<sup>II</sup> cations have radii (6-coordinate) in the range 65–95 pm and larger cations such as Ca<sup>II</sup> (100 pm) and Hg<sup>II</sup> (102 pm) do not form oxide spinels. The radii of B<sup>III</sup> fall predominantly in the range 60–70 pm though Al<sup>III</sup> (53 pm) is smaller, and In<sup>III</sup> (80 pm) normally forms sulfide spinels only.

Examples of spinels with other combinations of oxidation state are:



Many of the spinel-type compounds mentioned above do not have the normal structure in which A are in tetrahedral sites (t) and B are in octahedral sites (o); instead they adopt the inverse spinel structure in which half the B cations occupy the tetrahedral sites whilst the other half of the B cations and all the A cations are distributed on the octahedral sites, i.e. (B)<sub>t</sub>[AB]<sub>o</sub>O<sub>4</sub>. The occupancy of the octahedral sites may be random or ordered. Several factors influence whether a given spinel will adopt the normal or inverse structure, including (a) the relative sizes of A and B, (b) the Madelung constants for the normal and inverse structures, (c) ligand-field stabilization energies (p. 1131) of cations on tetrahedral and octahedral sites, and (d) polarization or covalency effects.<sup>(56)</sup>

Thus, if size alone were important it might be expected that the smaller cation would occupy the site of lower coordination number, i.e. A<sub>t</sub>[MgAl]<sub>o</sub>O<sub>4</sub>; however, in spinel itself this is outweighed by the greater lattice energy achieved by having the cation of higher charge, (Al<sup>III</sup>) on the site of higher coordination and

the normal structure is adopted:  $(\text{Mg})_t[\text{Al}_2]_o\text{O}_4$ . An additional factor must be considered in a spinel such as  $\text{NiAl}_2\text{O}_4$  since the crystal field stabilization energy of  $\text{Ni}^{\text{II}}$  is greater in octahedral than tetrahedral coordination; this redresses the balance, making the normal and inverse structures almost equal in energy and there is almost complete randomization of all the cations on all the available sites:  $(\text{Al}_{0.75}\text{Ni}_{0.25})_t[\text{Ni}_{0.75}\text{Al}_{1.25}]_o\text{O}_4$ .

Inverse and disordered spinels are said to have a defect structure because all crystallographically identical sites within the unit cell are not occupied by the same cation. A related type of defect structure occurs in valency disordered spinels where, for example, the divalent  $\text{A}^{\text{II}}$  cations in  $\text{AB}_2\text{O}_4$  are replaced by equal numbers of  $\text{M}^{\text{I}}$  and  $\text{M}^{\text{III}}$  of appropriate size. Thus, in spinel itself, which can be written  $\text{Mg}_8\text{Al}_{16}\text{O}_{32}$ , the  $8\text{Mg}^{\text{II}}$  (72 pm) can be replaced by  $4\text{Li}^{\text{I}}$  (76 pm) and  $4\text{Al}^{\text{III}}$  (53 pm) to give  $\text{Li}_4\text{Al}_{20}\text{O}_{32}$ , i.e.  $\text{LiAl}_5\text{O}_8$ . This has a defect spinel structure in which two-fifths of the Al occupy all the tetrahedral sites:  $(\text{Al}_2^{\text{III}})_t[\text{Li}^{\text{I}}\text{Al}_3^{\text{III}}]_o\text{O}_8$ . Other compounds having this cation-disordered spinel structure are  $\text{LiGa}_5\text{O}_8$  and  $\text{LiFe}_5\text{O}_8$ . Disordering on the tetrahedral sites occurs in  $\text{CuAl}_5\text{S}_8$ ,  $\text{CuIn}_5\text{S}_8$ ,  $\text{AgAl}_5\text{S}_8$  and  $\text{AgIn}_5\text{S}_8$ , i.e.  $(\text{Cu}^{\text{I}}\text{Al}^{\text{III}})_t[\text{Al}_4^{\text{III}}]_o\text{S}_8$ , etc. Valency disordering can also be achieved by replacing  $\text{A}^{\text{II}}$  completely by  $\text{M}^{\text{I}}$ , thus necessitating replacement of half the  $\text{B}^{\text{III}}$  by  $\text{M}^{\text{IV}}$ , e.g.  $(\text{Li}^{\text{I}})_t[\text{Al}^{\text{III}}\text{Ti}^{\text{IV}}]_o\text{O}_4$ . Even more extensive substitution of cations has been achieved in many cubic spinel phases, e.g.  $\text{Li}_5\text{Zn}^{\text{II}}\text{Al}_5^{\text{III}}\text{Ge}_9^{\text{IV}}\text{O}_{36}$  (and the  $\text{Ga}^{\text{III}}$  and  $\text{Fe}^{\text{III}}$  analogues), and the possibilities are virtually limitless.

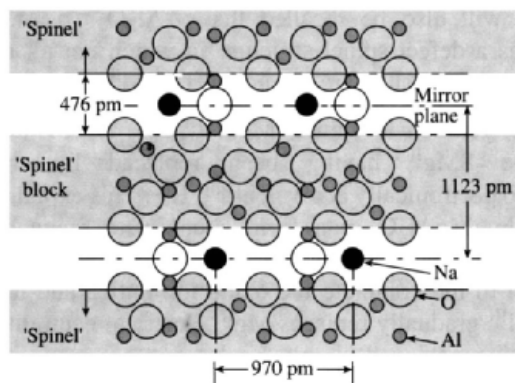
The sensitive dependence of the electrical and magnetic properties of spinel-type compounds on composition, temperature, and detailed cation arrangement has proved a powerful incentive for the extensive study of these compounds in connection with the solid-state electronics industry. Perhaps the best-known examples are the ferrites, including the extraordinary compound magnetite  $\text{Fe}_3\text{O}_4$  (p. 1080) which has an inverse spinel structure  $(\text{Fe}^{\text{III}})_t[\text{Fe}^{\text{II}}\text{Fe}^{\text{III}}]_o\text{O}_4$ .

It will also be recalled that  $\gamma\text{-Al}_2\text{O}_3$  (p. 243) has a defect spinel structure in which not all of the cation sites are occupied, i.e.  $\text{Al}_{21\frac{1}{3}}^{\text{III}}\square_{2\frac{2}{3}}\text{O}_{32}$ : the relation to spinel  $(\text{Mg}_8^{\text{II}}\text{Al}_{16}^{\text{III}}\text{O}_{32})$  is obvious, the  $8\text{Mg}^{\text{II}}$  having been replaced by the isoelectronically equivalent  $5\frac{1}{3}\text{Al}^{\text{III}}$ . This explains why  $\text{MgAl}_2\text{O}_4$  can form a complete range of solid solutions with  $\gamma\text{-Al}_2\text{O}_3$ : the oxygen builds on to the complete fcc oxide ion lattice and the  $\text{Al}^{\text{III}}$  gradually replaces  $\text{Mg}^{\text{II}}$ , electrical neutrality being achieved simply by leaving 1 cation site vacant for each  $3\text{Mg}^{\text{II}}$  replaced by  $2\text{Al}^{\text{III}}$ .

### Sodium- $\beta$ -alumina and related phases<sup>(57)</sup>

Sodium- $\beta$ -alumina has assumed tremendous importance as a solid-state electrolyte since its very high electrical conductivity was discovered at the Ford Motor Company by J. T. Kummer and N. Weber in 1967. The compound, which has the idealized formula  $\text{NaAl}_{11}\text{O}_{17}(\text{Na}_2\text{O}\cdot 11\text{Al}_2\text{O}_3)$  was originally thought to be a form of  $\text{Al}_2\text{O}_3$  and hence called  $\beta$ -alumina (1916); the presence of Na, which was at first either undetected or ignored, is now known to be essential for stability. X-ray analysis shows that the structure is closely related to that of spinel, no fewer than 50 of the 58 atoms in the unit cell being arranged exactly as in spinel. The large Na atoms are situated exclusively in loosely packed planes together with an equal number of O atoms as shown in Fig. 7.15; these planes are 1123 pm apart, being separated by the "spinel blocks". The close-packed oxygen layers above and below the Na planes are mirror images of each other 476 pm apart and they are bound together not only by the Na atoms but by an equal number of Al–O–Al bonds. There are several other sites in the mirror plane which can physically accommodate Na and this permits rapid two-dimensional diffusion of Na within the basal

<sup>57</sup> J. T. KUMMER, *Prog. Solid State Chem.* **7**, 141–75 (1972).  
J. H. KENNEDY, *Topics in Applied Physics* **21**, 105–41 (1977).



**Figure 7.15** Crystal structure of Na- $\beta$ -alumina (see text). This section, which is a plane parallel to the  $c$ -axis, does not show the closest Na–Na distance.

plane; it also explains the very low resistivity of the order of 30 ohm cm. The structure can also accommodate supernumerary Na ions, and the compound, even in the form of single crystals, is massively defective, having typically 20–30% more Na than indicated by the idealized formula; this is probably compensated by additional Al vacancies in the “spinel blocks” adjacent to the mirror planes, e.g.  $\text{Na}_{2.58}\text{Al}_{21.8}\text{O}_{34}$ .

Sodium- $\beta$ -alumina can be prepared by heating  $\text{Na}_2\text{CO}_3$  (or  $\text{NaNO}_3$  or  $\text{NaOH}$ ) with any modification of  $\text{Al}_2\text{O}_3$  or its hydrates to  $\sim 1500^\circ$  in a Pt vessel suitably sealed to avoid loss of  $\text{Na}_2\text{O}$  (as  $\text{Na} + \text{O}_2$ ). In the presence of  $\text{NaF}$  or  $\text{AlF}_3$  a temperature of  $1000^\circ$  suffices. Na- $\beta$ -alumina melts at  $\sim 2000^\circ$  (probably incongruently) and has  $d$  3.25  $\text{g cm}^{-3}$ . The Na can be replaced by Li, K, Rb,  $\text{Cu}^I$ ,  $\text{Ag}^I$ ,  $\text{Ga}^I$ ,  $\text{In}^I$  or  $\text{Tl}^I$  by heating with a suitable molten salt, and  $\text{Ag}^I$  can be replaced by  $\text{NO}^+$  by treatment with molten  $\text{NOCl/AlCl}_3$ . The ammonium compound is also known and  $\text{H}_3\text{O}^+$ - $\beta$ -alumina can be prepared by reduction of the Ag compound. Similarly,  $\text{Al}^{III}$  can be replaced by  $\text{Ga}^{III}$  or  $\text{Fe}^{III}$  in the preparation, leading to compounds of (idealized) formulae  $\text{Na}_2\text{O} \cdot 11\text{Ga}_2\text{O}_3$ ,  $\text{Na}_2\text{O} \cdot 11\text{Fe}_2\text{O}_3$ ,  $\text{K}_2\text{O} \cdot 11\text{Fe}_2\text{O}_3$ , etc. Altrivalent substitution is also possible, e.g. in Na- $\beta''$ -alumina,  $\text{Na}_{1+x}\text{M}_x\text{Al}_{1-x}\text{O}_{17}$ , in which M is a

divalent cation such as Mg, Ni or Zn. A typical composition is  $\text{Na}_{1.67}\text{Mg}_{0.67}\text{Al}_{10.33}\text{O}_{17}$  and the excess Na charge is compensated for by substituting the divalent or univalent cation into the lattice sites normally occupied by Al.<sup>(58)</sup>

Apart from the intriguing structural implications of these fast-ion solid-state conductors, Na- $\beta$ -alumina and related phases have been extensively used as permeable membranes in the Na/S battery system (p. 678): this requires an air-stable membrane that is readily permeable to Na ions but not to Na atoms or S, that is non-reactive with molten Na and S, and that is not an electronic conductor. Not surprisingly, few compounds have been found to compete with Na- $\beta$ -alumina in this field, although Na- $\beta''$ -alumina has the remarkable additional property of enabling the rapid diffusion of a large proportion of cations in the periodic table (whereas Na- $\beta$ -alumina itself is restricted mainly to univalent cations). Indeed, the  $\beta''$ -aluminas are the first family of high conductivity solid electrolytes which permit fast ion transport of multivalent cations in solids.<sup>(58)</sup>

Unrelated to the  $\beta$ - and  $\beta''$ -aluminas are a group of white, hygroscopic sodium-rich aluminates which have recently been prepared by heating  $\text{Na}_2\text{O}$  and  $\text{Al}_2\text{O}_3$  in appropriate stoichiometric ratios at  $700^\circ\text{C}$  for 18–24 hours.<sup>(59)</sup>  $\text{Na}_5\text{AlO}_4$ , which is isostructural with  $\text{Na}_5\text{FeO}_4$ , contains isolated  $[\text{AlO}_4]$  tetrahedra with Al–O 176–179 pm.  $\text{Na}_7\text{Al}_3\text{O}_8$  features a novel ring structure made up of six  $\text{AlO}_4$  tetrahedra sharing corners to form a non-planar 12-membered ring which is then joined by pairs of oxygen atom bridges to adjacent rings, thus generating an infinite chain of alternating 12- and 8-membered rings with Al– $\text{O}_\mu$  175–179 pm and Al– $\text{O}_t$  173–4 pm. Finally,  $\text{Na}_{17}\text{Al}_5\text{O}_{16}$  has discrete chains composed of five  $\text{AlO}_4$  tetrahedra sharing corners with almost linear angles ( $160^\circ$  and  $173^\circ$ ) at the bridging O atoms and with

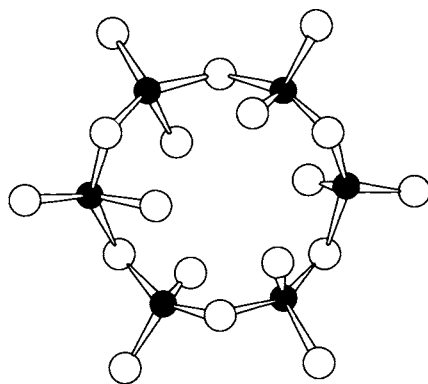
<sup>58</sup> D. F. SHRIVER and G. C. FARRINGTON, *Chem. and Eng. News*, May 20, 42–57 (1985), and references cited therein.

<sup>59</sup> M. G. BARKER, P. G. GADD and M. J. BEGLEY, *J. Chem. Soc., Chem. Commun.*, 379–81 (1981). M. G. BARKER, P. G. GADD and S. C. WALLWORK, *J. Chem. Soc., Chem. Commun.*, 516–7 (1982).

the various Al–O distances again falling in the range 170–180 pm. Note that the unusual formula  $\text{Na}_{17}\text{Al}_5\text{O}_{16}$  (i.e.  $\text{Na}_{3.4}\text{AlO}_{3.2}$ ) is nearly the same as  $\text{Na}_3\text{AlO}_3$  which would have been the stoichiometry if the chains of  $\text{AlO}_4$  tetrahedra had been infinite.

### Tricalcium aluminate, $\text{Ca}_3\text{Al}_2\text{O}_6$

Tricalcium aluminate is an important component of Portland cement yet, despite numerous attempts dating back over the preceding 50 y, its structure remained unsolved until 1975.<sup>(60)</sup> The basic unit is now known to be a 12-membered ring of 6 fused  $\{\text{AlO}_4\}$  tetrahedra  $[\text{Al}_6\text{O}_{18}]^{18-}$  as shown in Fig. 7.16; there are 8 such rings per unit cell surrounding holes of radius 147 pm, and the rings are held together by Ca ions in distorted sixfold coordination to give the structural formula  $\text{Ca}_9\text{Al}_6\text{O}_{18}$ . The rather short Ca–O distance (226 pm) and the observed compression of the  $\{\text{CaO}_6\}$  octahedra may indicate some strain and this, together with the large holes in the lattice, facilitate the rapid reaction with water. The products of hydration depend sensitively on the temperature. Above 21°  $\text{Ca}_3\text{Al}_2\text{O}_6$  gives the hexahydrate  $\text{Ca}_3\text{Al}_2\text{O}_6 \cdot 6\text{H}_2\text{O}$ , but below this temperature hydrated di- and tetra-calcium aluminates are formed of empirical composition  $2\text{CaO} \cdot \text{Al}_2\text{O}_3 \cdot 5-9\text{H}_2\text{O}$  and  $4\text{CaO} \cdot \text{Al}_2\text{O}_3 \cdot 12-14\text{H}_2\text{O}$ . This is of great importance in cement technology (see Panel) since, in the absence of a retarder, cement reacts rapidly with water giving a sharp rise in temperature and a “flash set” during which the various calcium aluminate hydrates precipitate and congeal into an unmanageable mass. This can be avoided by grinding in 2–5% of gypsum ( $\text{CaSO}_4 \cdot 2\text{H}_2\text{O}$ ) with the cement clinker; this reacts rapidly with dissolved aluminates in the presence of  $\text{Ca}(\text{OH})_2$  to give the calcium sulfatoaluminate,  $3\text{CaO} \cdot \text{Al}_2\text{O}_3 \cdot 3\text{CaSO}_4 \cdot 31\text{H}_2\text{O}$ , which is much less soluble than the hydrated calcium aluminates and



**Figure 7.16** Structure of the  $[\text{Al}_6\text{O}_{18}]^{18-}$  unit in  $\text{Ca}_3\text{Al}_2\text{O}_6$  (i.e.  $\text{Ca}_9\text{Al}_6\text{O}_{18}$ ). The Al–O distances are all in the range  $175 \pm 2$  pm.

therefore preferentially precipitates and prevents the premature congealing.

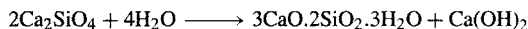
Another important calcium aluminate system occurs in high-alumina cement (*ciment fondu*). This is not a Portland cement but is made by fusing limestone and bauxite with small amounts of  $\text{SiO}_2$  and  $\text{TiO}_2$  in an open-hearth furnace at 1425–1500°; rotary kilns with tap-holes for the molten cement can also be used. Typical analytical compositions for a high-alumina cement are ~40% each of  $\text{Al}_2\text{O}_3$  and  $\text{CaO}$  and about 10% each of  $\text{Fe}_2\text{O}_3$  and  $\text{SiO}_2$ ; the most important compounds in the cement are  $\text{CaAl}_2\text{O}_4$ ,  $\text{Ca}_2\text{Al}_2\text{SiO}_7$  and  $\text{Ca}_6\text{Al}_8\text{FeSiO}_{21}$ . Setting and hardening of high-alumina cement are probably due to the formation of calcium aluminate gels such as  $\text{CaO} \cdot \text{Al}_2\text{O}_3 \cdot 10\text{H}_2\text{O}$ , and the more basic  $2\text{CaO} \cdot \text{Al}_2\text{O}_3 \cdot 8\text{H}_2\text{O}$ ,  $3\text{CaO} \cdot \text{Al}_2\text{O}_3 \cdot 6\text{H}_2\text{O}$  and  $4\text{CaO} \cdot \text{Al}_2\text{O}_3 \cdot 13\text{H}_2\text{O}$ , though these empirical formulae give no indication of the structural units involved. The most notable property of high-alumina cement is that it develops very high strength at a very early stage (within 1 day). Long exposure to warm, moist conditions may lead to failure but resistance to corrosion by sea water and sulfate brines, or by weak mineral acids, is outstanding. It has also been much used as a refractory cement to withstand temperatures up to 1500°.

<sup>60</sup> P. MONDAL and J. W. JEFFREY, *Acta Cryst.* **B31**, 689–97 (1975).

### Portland Cement<sup>(61)</sup>

The name "Portland cement" was first used by J. Aspdin in a patent (1824) because, when mixed with water and sand the powder hardened into a block that resembled the natural limestone quarried in the Isle of Portland, England. The two crucial discoveries which led to the production of strong, durable, hydraulic cement that did not disintegrate in water, were made in the eighteenth and nineteenth centuries. In 1756 John Smeaton, carrying out experiments in connection with building the Eddystone Lighthouse (UK), recognized the importance of using limes which contained admixed clays or shales (i.e. aluminosilicates), and by the early 1800s it was realized that firing must be carried out at sintering temperatures in order to produce a clinker now known to contain calcium silicates and aluminates. The first major engineering work to use Portland cement was in the tunnel constructed beneath the Thames in 1828. The first truly high-temperature cement (1450–1600°C) was made in 1854, and the technology was revolutionized in 1899 by the introduction of rotary kilns.

The important compounds in Portland cement are dicalcium silicate (Ca<sub>2</sub>SiO<sub>4</sub>) 26%, tricalcium silicate (Ca<sub>3</sub>SiO<sub>5</sub>) 51%, tricalcium aluminate (Ca<sub>3</sub>Al<sub>2</sub>O<sub>6</sub>) 11% and the tetracalcium species Ca<sub>4</sub>Al<sub>2</sub>Fe<sub>2</sub><sup>III</sup>O<sub>10</sub> (1%). The principal constituent of moistened cement paste is a tobermorite gel which can be represented schematically by the following idealized equations:



The adhesion of the tobermorite particles to each other and to the embedded aggregates is responsible for the strength of the cement which is due, ultimately, to the formation of –Si–O–Si–O bonds.

Portland cement is made by heating a mixture of limestone (or chalk, shells, etc.) with aluminosilicates (derived from sand, shales, and clays) in carefully controlled amounts so as to give the approximate composition CaO ~70%, SiO<sub>2</sub> ~20%, Al<sub>2</sub>O<sub>3</sub> ~5%, Fe<sub>2</sub>O<sub>3</sub> ~3%. The presence of Na<sub>2</sub>O, K<sub>2</sub>O, MgO and P<sub>2</sub>O<sub>5</sub> are detrimental and must be limited. The raw materials are ground to pass 200-mesh sieves and then heated in a rotary kiln to ~1500° to give a sintered clinker; this is reground to 325-mesh and mixed with 2–5% of gypsum. An average-sized kiln can produce 1000–3000 tonnes of cement per day and the world's largest plants can produce up to 8000 tonnes per day. The vast scale of the industry can be gauged from the US production figures in the table below. Price (1990) was \$45–55 per tonne for bulk supplies. In the same year China emerged as the world's largest cement producer (200 million tonnes per annum). Total world production continues to grow dramatically, from 590 Mtpa in 1970 and 881 Mtpa in 1980 to nearly 1200 Mtpa in 1990, of which Europe (including the European parts of the former Soviet Union) accounted for some 40%.

*Production of Portland Cement in the USA/million tonnes (Mt)*

1890	1900	1910	1920	1930	1940	1950	1960	1970	1980	1990
0.057	1.45	13.1	17.1	27.5	22.2	38.5	56.0	66.4	68.2	70.0

### 7.3.5 Other inorganic compounds

#### Chalcogenides

At normal temperatures the only stable chalcogenides of Al are Al<sub>2</sub>S<sub>3</sub> (white), Al<sub>2</sub>Se<sub>3</sub> (grey) and Al<sub>2</sub>Te<sub>3</sub> (dark grey). They can be prepared by direct reaction of the elements at ~1000° and all hydrolyse rapidly and completely in aqueous solution to give Al(OH)<sub>3</sub> and H<sub>2</sub>X (X = S, Se, Te). The small size of Al relative to the chalcogens dictates tetrahedral coordination and the various polymorphs are related to wurtzite (hexagonal ZnS, p. 1210), two-thirds of the available

metal sites being occupied in either an ordered (α) or a random (β) fashion. Al<sub>2</sub>S<sub>3</sub> also has a γ-form related to γ-Al<sub>2</sub>O<sub>3</sub> (p. 243), and very recently a novel high-temperature hexagonal modification of Al<sub>2</sub>S<sub>3</sub> containing 5-coordinate Al has been obtained by annealing α-Al<sub>2</sub>S<sub>3</sub> at 550°C;<sup>(62)</sup> in this new form half the Al atoms are tetrahedrally coordinated (Al–S<sub>223</sub>–227 pm) whereas the other half are in trigonal bipyramidal coordination with Al–S<sub>eq</sub> 227–232 pm and Al–S<sub>ax</sub> 250–252 pm.

The chalcogenides of Ga, In and Tl are much more numerous and at least a dozen different structure types have been established by X-ray

<sup>61</sup> Kirk–Othmer *Encyclopedia of Chemical Technology*, 4th edn., Vol. 5, Interscience, New York, 564–98 (1993).

<sup>62</sup> B. KREBS, A. SCHIEMANN and M. LAGE, *Z. anorg. allg. Chem.* **619**, 983–8 (1993).



crystallography.<sup>(63)</sup> The compounds have been extensively studied not only because of their intriguing stoichiometries, but also because many of them are semiconductors, semi-metals, photoconductors or light emitters, and  $Tl_5Te_3$  has been found to be a superconductor at low temperatures. (See p. 1182 for high-temperature superconductors, including  $Tl_2Ca_2Ba_2Cu_3O_{10+x}$  which has one of the highest known superconducting transition temperatures,  $T_c = 125$  K.) The chalcogenides, as expected from their position in the

periodic table, are far from ionic, but formal oxidation states remain a useful device for electron counting and for checking the overall charge balance. Well-established compounds are summarized in Table 7.9. The following points are noteworthy. The hexagonal  $\alpha$ - and  $\beta$ -forms of  $Ga_2S_3$  are isostructural with the Al analogues and an additional form,  $\gamma$ - $Ga_2S_3$ , adopts the related defect sphalerite structure derived from cubic ZnS (zinc blende, p. 1210). The same structure is found for  $Ga_2Se_3$  and  $Ga_2Te_3$  but for the larger  $In^{III}$  atom octahedral coordination also becomes possible. The corresponding  $Tl^{III}$  sesquichalcogenides  $Tl_2X_3$  are either

<sup>63</sup> L. I. MAN, R. M. IMANOV and S. A. SEMILETOV, *Sov. Phys. Crystallogr.* **21**, 255–63 (1976).

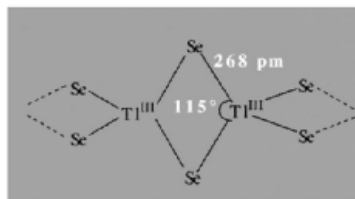
**Table 7.9** Stoichiometries and structures of the crystalline chalcogenides of Group 13 elements

$Ga_2S$	$Ga_2Se$	
$GaS$ (yellow) layer structure with Ga–Ga bonds	$GaSe$ (like $GaS$ )	$GaTe$ (like $GaS$ )
$Ga_4S_5$		$(Ga_3Te_2)$
$\alpha$ - $Ga_2S_3$ (yellow) ordered defect wurtzite (hexagonal ZnS)		
$\beta$ - $Ga_2S_3$ defect wurtzite		
$\gamma$ - $Ga_2S_3$ defect sphalerite (cubic ZnS)	$Ga_2Se_3$ defect sphalerite	$Ga_2Te_3$ defect sphalerite
		$Ga_2Te_5$ chains of linked $\{GaTe_4\}$ plus single Te atoms
	$In_4Se_3$ contains $[(In^{III})_3]^V$ groups: $In^I[In_3^{III}]Se_3$	$In_4Te_3$ like $In_4Se_3$
$InS$ (red) like $GaS$	$InSe$ distorted NaCl, somewhat like $GaS$	$InTe$ like $TlSe$ (cubes and tetrahedra)
$In_6S_7$ see text	$In_6Se_7$ like $In_6S_7$	$In_3Te_4$
$\alpha$ - $In_2S_3$ (yellow) cubic $\gamma'$ - $Al_2O_3$	$\alpha$ - $In_2Se_3$ defect wurtzite, but $\frac{1}{16}$ of In octahedral	$\alpha$ - $In_2Te_3$ defect sphalerite (cubic ZnS)
$\beta$ - $In_2S_3$ (red) defect spinel, $\gamma$ - $Al_2O_3$	$\beta$ - $In_2Se_3$ ordered defect wurtzite (hexagonal ZnS)	$\beta$ - $In_2Te_3$
$In_6S_7$ see text		$In_3Te_5$ $In_2Te_5$
$Tl_2S$ (black) distorted $CdI_2$ layer lattice ( $Tl^I$ in threefold coordination)		
$Tl_4S_3$ chains of linked $\{Tl^{III}S_4\}$ tetrahedra $(Tl^I)_3[Tl^{III}S_3]$	$Tl_5Se_3$ complex $Cr_5B_3$ -type structure	$Tl_5Te_3$ $Cr_5B_3$ layer structure, CN of Tl varies up to 9 and Te up to 10
$TlS$ (black) like $TlSe$ , $Tl^I[Tl^{III}S_2]$	$TlSe$ (black) chains of edgeshared $\{Tl^{III}Se_4\}$ tetrahedra $Tl^I[Tl^{III}Se_2]$	$TlTe$ variant of $W_5Si_3$ (complex)
[No $Tl_2S_3$ known]	$Tl_2Se_3$	$(Tl_2Te_3)$
$TlS_2$ $Tl^I$ polysulfide		
$Tl_2S_5$ (red and black forms) $Tl^I$ polysulfide		
$Tl_2S_9$ $Tl^I$ polysulfide		

non-existent or of dubious authenticity, perhaps because of the ready reduction to  $Tl^I$  (see  $TlI_3$ , p. 239).

$GaS$  (yellow, mp  $970^\circ$ ) has a hexagonal layer structure with  $Ga-Ga$  bonds (248 pm); each  $Ga$  is coordinated by 3S and 1Ga, and the sequence of layers along the  $c$ -axis is  $\cdots SGaGaS, SGaGaS \cdots$ ; the compound can therefore be considered as an example of  $Ga^{II}$ . The structures of  $GaSe$ ,  $GaTe$ , red  $InS$  and  $InSe$  are similar. By contrast,  $InTe$ ,  $TlS$  (black) and  $TlSe$  (black, metallic) have a structure which can be formalized as  $M^I[M^{III}X_2]$ ; each  $Tl^{III}$  is tetrahedrally coordinated by 4 Se at 268 pm and the tetrahedra are linked into infinite chains by edge sharing along the  $c$ -axis (see structure), whereas each  $Tl^I$  lies between these chains and is surrounded by a distorted cube of 8 Se at 342 pm. This explains the marked anisotropy of properties, especially the metallic conductivity in the (001) plane and the semiconductivity along the  $c$ -axis. Similar edge-linked  $\{GeSe_4\}$  tetrahedra are found in  $Cs_{10}Ga_6Se_{14}$  which was obtained as transparent pale-yellow crystals by heating an equimolar mixture of  $GaSe$  and  $Cs$  in a carefully controlled temperature programme; the compound features the unprecedented finite complex anion  $[Se_2Ga(\mu-Se_2Ga)_5Se_2]^{10-}$  which is 1900 pm long.<sup>(64)</sup>

<sup>64</sup> H. J. DEISEROTH and HAN FU-SON, *Angew. Chem. Int. Edn. Engl.* **20**, 962-3 (1981).



$In_6S_7$  (and the isostructural  $In_6Se_7$ ) have a curious structure comprising two separate blocks of almost ccp S which are rotated about the  $b$ -axis by  $61^\circ$  with respect to each other; the In is in octahedral coordination. The compound can be formulated as  $In^I(In_2^{III})^{IV}In_3^{III}S_7^{-II}$ . There are also numerous ternary  $In/Tl$  sulfides in which  $In^I$  has been replaced by  $Tl^I$ , e.g.:  $Tl^IIn_3^{III}S_8$ ,  $Tl^IIn_3^{III}S_5$ ,  $Tl^IIn^{III}S_2$ ,  $Tl_3In^{III}S_3$ ,  $Tl^I(In_2^{III})_2^{IV}In^{III}S_6$ ,  $Tl_3^IIn^IIn_4^{III}S_8$  and  $Tl^I(In_2^{III})^{IV}In_3^{III}S_7$ .<sup>(64a)</sup>

The crystal structures of  $In_4Se_3$  and  $In_4Te_3$  show that they can be regarded to a first approximation as  $In^I[In_3]^V(X^{-II})_3$  but the compound does not really comprise discrete ions. The triatomic unit  $[In^{III}-In^{III}-In^{III}]$  is bent, the angle at the central atom being  $158^\circ$  and the In-In distances 279 pm (cf. 324-326 pm in metallic In). However, it is also possible to discern non-planar 5-membered heterocycles in the structure formed by joining 2 In from 1  $\{In_3\}$  to the terminal In of an adjacent  $\{In_3\}$  via 2 bridging Se (or Te) atoms so that the structure can be represented schematically as in Fig. 7.17. The  $In^{III}-Se$  distances average

<sup>64a</sup> H. J. DEISEROTH and R. WALTHER, *Z. anorg. allg. Chem.* **622**, 611-16 (1996).

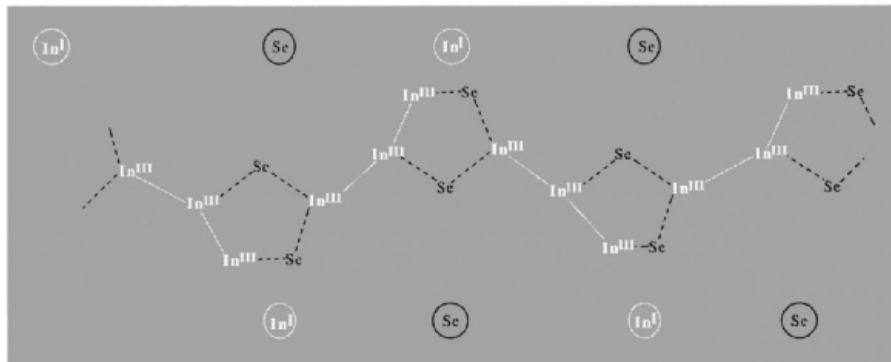


Figure 7.17 Schematic structure of  $In_4Se_3$ .

269 pm compared with the closest In<sup>I</sup>–Se contact of 297 pm. The [In<sup>III</sup>]<sup>V</sup> unit can be compared with the isoelectronic species [Hg<sub>3</sub><sup>II</sup>]<sup>II</sup>. The compound Tl<sub>4</sub>S<sub>3</sub>, which has the same stoichiometry as In<sub>4</sub>X<sub>3</sub>, has a different structure in which chains of corner-shared {Tl<sup>III</sup>S<sub>4</sub>} tetrahedra of overall stoichiometry [TlS<sub>3</sub>] are bound together by Tl<sup>I</sup>; within the chains the Tl<sup>III</sup>–S distance is 254 pm whereas the Tl<sup>I</sup>–S distances vary between 290–336 pm. A comparison of the formal designation of the two structures In<sup>I</sup>[(In<sup>III</sup>)]<sup>V</sup>(Se<sup>-II</sup>)<sub>3</sub> and (Tl<sup>I</sup>)<sub>3</sub>[Tl<sup>III</sup>S<sub>3</sub>]<sup>-III</sup> again illustrates the increasing preference of the heavier metal for the +1 oxidation state. The trend continues with the polysulfides Tl<sup>I</sup>S<sub>2</sub>, Tl<sup>I</sup>S<sub>5</sub> and Tl<sup>I</sup>S<sub>9</sub>, already alluded to on p. 253.

#### Compounds with bonds to N, P, As, Sb or Bi

The binary compounds of the Group 13 metals with the elements of Group 15 (N, P, As, Sb, Bi) are structurally less diverse than the chalcogenides just considered but they have achieved considerable technological application as III–V semiconductors isoelectronic with Si and Ge (cf. BN isoelectronic with C, p. 207). Their structures are summarized in Table 7.10: all adopt the cubic ZnS structure except the nitrides of Al, Ga and In which are probably more ionic (less covalent or metallic) than the others. Thallium does not form simple compounds

**Table 7.10** Structures of III–V compounds MX<sup>(a)</sup>

X ↓	M →	B	Al	Ga	In
N		L, S	W	W	W
P		S	S	S	S
As		S	S	S	S
Sb		—	S	S	S

<sup>(a)</sup>L = BN layer lattice (p. 208).

S = sphalerite (zinc blende), cubic ZnS (p. 1210).

W = wurtzite, hexagonal ZnS structure (p. 1210).

M<sup>III</sup>X<sup>V</sup>: the explosive black nitride Tl<sub>3</sub>N is known, and the azides Tl<sup>I</sup>N<sub>3</sub> and Tl<sup>I</sup>[Tl<sup>III</sup>(N<sub>3</sub>)<sub>4</sub>]; the phosphides Tl<sub>3</sub>P, TlP<sub>3</sub> and TlP<sub>5</sub> have been reported but are not well characterized. With As, Sb and Bi thallium forms alloys and intermetallic compounds Tl<sub>3</sub>X, Tl<sub>7</sub>Bi<sub>2</sub> and TlBi<sub>2</sub>.

The III–V semiconductors can all be made by direct reaction of the elements at high temperature and under high pressure when necessary. Some properties of the Al compounds are in Table 7.11 from which it is clear that there are trends to lower mp and energy band-gap  $E_g$  with increasing atomic number.

Analogous compounds of Ga and In are grey or semi-metallic in appearance and show similar trends (Table 7.12). These data should be compared with those for Si, Ge, Sn and Pb on p. 373 and for the isoelectronic II–VI semiconductors of Zn, Cd and Hg with S, Se and Te (p. 1210). In addition, GaN is obtained by reacting Ga and NH<sub>3</sub> at 1050° and InN by reducing and nitriding In<sub>2</sub>O<sub>3</sub> with NH<sub>3</sub> at 630°. The

**Table 7.11** Some properties of Al III–V compounds

Property	AlN	AlP	AlAs	AlSb
Colour	Pale yellow	Yellow	Orange	—
MP/°C	>2200 decomp	2000	1740	1060
$E_g$ /kJ mol <sup>-1(a)</sup>	411	236	208	145

<sup>(a)</sup>Energy gap between top of (filled) valence band and bottom of (empty) conduction band (p. 332). To convert from kJ mol<sup>-1</sup> to eV atom<sup>-1</sup> divide by 96.485.

**Table 7.12** Comparison of some III–V semiconductors

Property	GaP	GaAs	GaSb	InP	InAs	InSb
MP/°C	1465	1238	712	1070	942	525
$E_g$ /kJ mol <sup>-1(a)</sup>	218	138	69	130	34	17

<sup>(a)</sup>See note to Table 7.11.

nitrides show increasing susceptibility to chemical attack, AlN being inert to both acids and alkalis, GaN being decomposed by alkali, but not acid, and InN being decomposed by both acids and alkalis. Most of the other III–V compounds decompose slowly in moist air, e.g. AlP gives Al(OH)<sub>3</sub> and PH<sub>3</sub>. As a consequence, semiconductor devices must be completely encapsulated to prevent reaction with the atmosphere. The great value of III–V semiconductors is that they extend the range of properties of Si and Ge and by judicious mixing in ternary phases they permit a continuous interpolation of energy band gaps, current-carrier mobilities and other characteristic properties. Some of their uses are summarized in the Panel on p. 258.

Other compounds containing Al–N or Ga–N bonds, including heterocyclic compounds and cluster organometallic compounds, are considered in section 7.3.6.

### Some unusual stereochemistries

While it remains true that tetrahedral and octahedral coordination modes are the predominant stereochemistries adopted by the group 13 metals, nevertheless increasing diversity is being achieved by carefully selecting appropriate electronic and geometric features to enhance the stabilization of unusual stereochemistries. Some representative examples follow.

Trigonal planar Al is found in the [AlSb<sub>3</sub>]<sup>6-</sup> “anions” in [Cs<sub>6</sub>K<sub>3</sub>Sb(AlSb<sub>3</sub>)], which is formed by heating a stoichiometric mixture of 6Cs, 3KSb and AlSb in a sealed Nb ampoule at 677°C.<sup>(65)</sup> The Ga analogue was prepared similarly. The planar anions are embedded between columns of condensed icosahedra (Cs<sub>6</sub>K<sub>6/2</sub>)<sup>9+</sup> which in turn are centred by the remaining unique monatomic Sb<sup>3-</sup> anion.

The indium molybdate In<sub>11</sub>Mo<sub>40</sub>O<sub>62</sub>, prepared by heating the appropriate mixture of In, Mo and MoO<sub>2</sub> at 1100°C, features novel quasi-linear chain cations. In<sub>5</sub><sup>7+</sup> and In<sub>6</sub><sup>8+</sup> in channels

between condensed clusters of Mo<sub>6</sub> octahedra.<sup>(66)</sup> The intrachain distances are 262–266 pm in In<sub>5</sub><sup>7+</sup> and 265–269 pm in In<sub>6</sub><sup>8+</sup>, which are the shortest known In–In interatomic distances cf. 325 and 337 pm in In metal itself, and 333 pm for the closest distances between In atoms in neighbouring chains in the molybdate. Interatomic angles within the chains are 158° and 163° respectively and, when the coordination around each In atom by contiguous In and O atoms is considered, the chains can be formulated as [In<sup>2+</sup>(In<sup>+</sup>)<sub>n</sub>In<sup>2+</sup>], *n* = 3, 4.

Square-pyramidal 5-coordinate In<sup>III</sup> occurs in certain organoindium compounds such as the bis(2-methylaminopyridino-) adduct [MeIn{MeNC(CH<sub>3</sub>)<sub>4</sub>N}]<sub>2</sub><sup>(67)</sup> — cf. InCl<sub>5</sub><sup>2-</sup> (p. 238). The less familiar pentagonal planar coordination has been established for the InMn<sub>5</sub> group in the dianion [(μ<sub>5</sub>-In){Mn(CO)<sub>4</sub>]<sub>5</sub>]<sup>2-</sup> which is readily prepared by treatment of InCl<sub>3</sub> with the manganese carbonyl cluster compound K<sub>3</sub>[Mn<sub>3</sub>(μ-CO)<sub>2</sub>(CO)<sub>10</sub>].<sup>(68)</sup> The mean Mn–Mn distance in the encircling plane-pentagonal “ligand” {Mn(CO)<sub>4</sub>]<sub>5</sub> is 317 pm; the mean In–Mn distance is 265 pm, and the In atom is only 4.6 pm from the best plane of the five Mn atoms. Note also that the ligand is isolobal with cyclopentadienyl, C<sub>5</sub>H<sub>5</sub>.

Seven-coordinate pentagonal-bipyramidal In<sup>III</sup> has been found in the chloroindium complex of 1,4,7-triazacyclononanetriacetic acid [{"-(CH<sub>2</sub>)<sub>2</sub>N(CH<sub>2</sub>CO<sub>2</sub>H)}]<sub>3</sub>}, (LH<sub>3</sub>).<sup>(69)</sup> The neutral, monoprotinated 7-coordinate complex [InCl(LH)] features Cl and one N in axial positions (angle Cl–In–N 168°) with the other two N atoms and three carboxylate O atoms in the pentagonal plane. Interest in such compounds stems

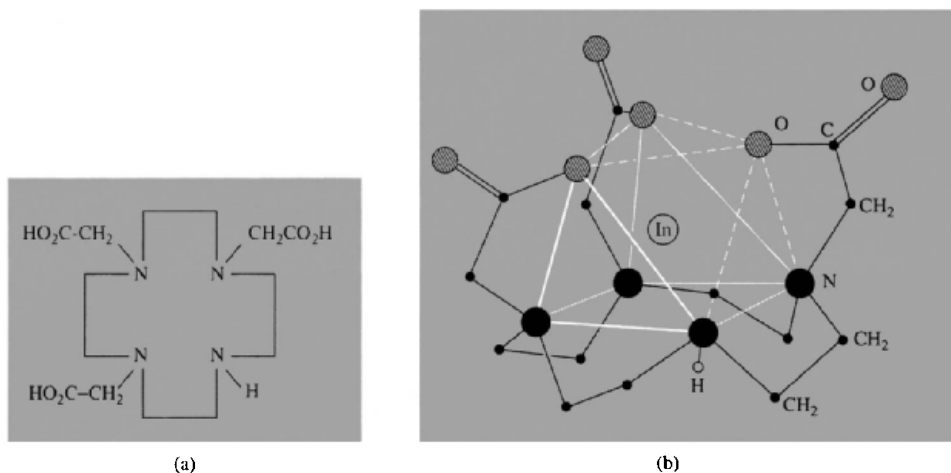
<sup>66</sup> H. MATTAUSCH, A. SIMON and E.-M. PETERS, *Inorg. Chem.* **25**, 3428–33 (1986).

<sup>67</sup> A. M. ARIA, D. C. BRADLEY, D. M. FRIGO, M. B. HURSTHOUSE and B. HUSSAIN, *J. Chem. Soc., Chem. Commun.*, 783–4 (1985).

<sup>68</sup> M. SCHOLLENBERGER, B. NUBER and M. L. ZIEGLER, *Angew. Chem. Int. Edn. Engl.* **31**, 350–1 (1992).

<sup>69</sup> A. S. CRAIG, I. M. HELPS, D. PARKER, H. ADAMS, N. A. BAILEY, M. G. WILLIAMS, J. M. A. SMITH and G. FERGUSON, *Polyhedron* **8**, 2481–4 (1989).

<sup>65</sup> M. SOMER, K. PETERS, T. POPP and H. G. VON SCHNERING, *Z. anorg. allg. Chem.* **597**, 201–8 (1991).



**Figure 7.18** (a) 1,4,7,10-tetraazacyclododecane triacetic acid, (LH<sub>3</sub>). (b) Structure of the 7-coordinate complex [InL]; the coordination polyhedron (shown in white) comprises a trigonal prism of 4N and 2O capped on one of its quadrilateral faces by the third O atom.

from the use of the  $\gamma$ -active <sup>111</sup>In isotope ( $E_{\gamma}$  173, 247 keV,  $t_{1/2}$  2.81 d) in radio-labelled monoclonal antibodies to detect tumours. Interestingly, the 7-coordinate crystalline complex reverts to a stable neutral hexacoordinate species in aqueous solution. Other 7-coordinate macrocyclic In<sup>III</sup> complexes of potential relevance in radio-pharmaceutical applications have been prepared, including [InL] where L is the triacetate of the tetraaza macrocycle shown in Fig. 7.18(a).<sup>(70)</sup> In this case the coordination polyhedron is a trigonal prism with one of its quadrilateral faces capped by a carboxylate O atom as shown schematically in Fig. 7.18(b).

Indium clusters have also recently been characterized, notably in intermetallic compounds. Thus, the Zintl phase, Rb<sub>2</sub>In<sub>3</sub>, (prepared by direct reaction between the two metals at 1530°C) has layers of octahedral *closo*-In<sub>6</sub> clusters joined into sheets through exo bonds at four coplanar vertices.<sup>(71)</sup> These four In atoms are therefore each bonded to five neighbouring In atoms at the corners of a square-based pyramid, whereas the remaining two (*trans*) In atoms in the In<sub>6</sub> cluster

show pyramidal 4-fold bonding only, to contiguous In atoms in the same cluster. Cs<sub>2</sub>In<sub>3</sub> is isostructural. The intermetallic compound K<sub>3</sub>Na<sub>26</sub>In<sub>48</sub> (synthesized from the elements in sealed Nb ampoules at 600°C) has a more complicated structure in which the In forms both *closo* icosahedral In<sub>12</sub> clusters and hexagonal antiprismatic In<sub>12</sub> clusters.<sup>(72)</sup> All the various In<sub>12</sub> clusters are interconnected by 12 exo bonds forming a covalent 3D network (In–In 291–315 pm) and the In<sub>12</sub> hexagonal antiprisms are additionally centred by single Na atoms. The phase contains several other interesting structural features and the original paper (in English) makes rewarding reading.

### 7.3.6 Organometallic compounds

Many organoaluminium compounds are known which contain 1, 2, 3 or 4 Al–C bonds per Al atom and, as these have an extensive reaction chemistry of considerable industrial importance, they will be considered before the organometallic compounds of Ga, In and Tl are discussed.

<sup>70</sup> A. RIESEN, T. A. KADEN, W. RITTER and H. A. MACKE, *J. Chem. Soc., Chem. Commun.*, 460–2 (1989).

<sup>71</sup> S. C. SEVEOV and J. D. CORBETT, *Z. anorg. allg. Chem.* **619**, 128–32 (1993).

<sup>72</sup> W. CARRILLO-CABRERA, N. CAROCA-CANALES, K. PETERS and H. G. VON SCHNERING, *Z. anorg. allg. Chem.* **619**, 1556–63 (1993).

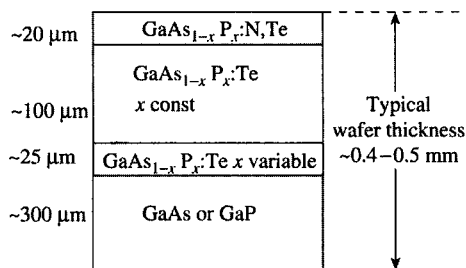
### Organoaluminium Compounds

Aluminium trialkyls and triaryls are highly reactive, colourless, volatile liquids or low-melting solids which ignite spontaneously in air and react violently with water; they should therefore be handled circumspectly and with

suitable precautions. Unlike the boron trialkyls and triaryls they are often dimeric, though with branched-chain alkyls such as  $\text{Pr}^i$ ,  $\text{Bu}^i$  and  $\text{Me}_3\text{CCH}_2$  this tendency is less marked.  $\text{Al}_2\text{Me}_6$  (mp  $15^\circ$ , bp  $126^\circ$ ) has the methyl-bridged structure shown and the same dimeric structure is found for  $\text{Al}_2\text{Ph}_6$  (mp  $225^\circ$ ).

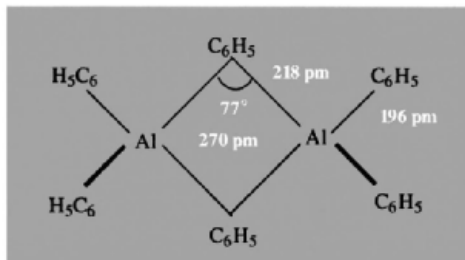
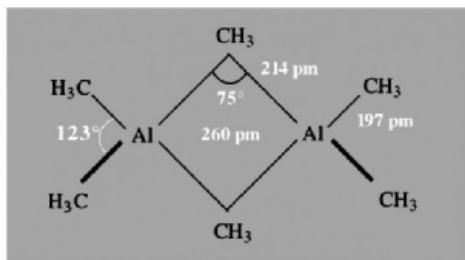
### Applications of III-V Semiconductors

The 9 compounds that Al, Ga and In form with P, As and Sb have been extensively studied because of their many applications in the electronics industry, particularly those centred on the interconversion of electrical and optical (light) energy. For example, they are produced commercially as light-emitting diodes (LEDs) familiar in pocket calculators, wrist watches and the alpha-numeric output displays of many instruments; they are also used in infrared-emitting diodes, injection lasers, infrared detectors, photocathodes and photomultiplier tubes. An extremely elegant chemical solid-state technology has evolved in which crystals of the required properties are deposited, etched and modified to form the appropriate electrical circuits. The ternary system  $\text{GaAs}_{1-x}\text{P}_x$  now dominates the LED market for  $\alpha$ -numeric and graphic displays following the first report of this activity in 1961.  $\text{GaAs}_{1-x}\text{P}_x$  is grown epitaxially on a single-crystal substrate of GaAs or GaP by chemical vapour deposition and crystal wafers as large as  $20\text{ cm}^2$  have been produced commercially. The colour of the emitted radiation is determined by the energy band gap  $E_g$ ; for GaAs itself  $E_g$  is  $138\text{ kJ mol}^{-1}$  corresponding to an infrared emission ( $\lambda$  870 nm), but this increases to  $184\text{ kJ mol}^{-1}$  for  $x \sim 0.4$  corresponding to red emission ( $\lambda$  650 nm). For  $x > 0.4$   $E_g$  continues to increase until it is  $218\text{ kJ mol}^{-1}$  for GaP (green,  $\lambda$  550 nm). Commercial yellow and green LEDs contain the added isoelectronic impurity N to improve the conversion efficiency. A schematic cross-section of a typical  $\text{GaAs}_{1-x}\text{P}_x$  epitaxial wafer doped with Te and N is shown in the diagram: Te (which has one more valence electron per atom than As or P) is the most widely used dopant to give  $n$ -type impurities in this system at concentrations of  $10^{16}$ – $10^{18}$  atoms  $\text{cm}^{-3}$  (0.5–50 ppm). The  $p$ - $n$  junction is then formed by diffusing Zn (1 less electron than Ga) into the crystal to a similar concentration.



An even more recent application is the construction of semiconductor lasers. In normal optical lasers light is absorbed by an electronic transition to a broad band which lies above the upper laser level and the electron then drops into this level by a non-radiative transition. By contrast the radiation in a semiconductor laser originates in the region of a  $p$ - $n$  junction and is due to the transitions of injected electrons and holes between the low-lying levels of the conduction band and the uppermost levels of the valence band. (Impurity levels may also be involved.) The efficiency of these semiconductor injection lasers is very much higher than those of optically pumped lasers and the devices are much smaller; they are also easily adaptable to modulation. As implied by the band gaps on p. 255, emission wavelengths are in the visible and near infrared. A heterostructure laser based on the system  $\text{GaAs}-\text{Al}_x\text{Ga}_{1-x}\text{As}$  was the first junction laser to run continuously at 3000 K and above (1970).

In the two types of device just considered, namely light emitting diodes and injection lasers, electrical energy is converted into optical energy. The reverse process of converting optical energy into electrical energy (photoconductivity and photovoltaic effects) has also been successfully achieved by III-V semiconductor systems. For example, the small band-gap compound InSb is valuable as a photoconductive infrared detector, and several compounds are being actively studied for use in solar cells to convert sunlight into useful sources of electrical power. The maximum photon flux in sunlight occurs at  $75$ – $95\text{ kJ mol}^{-1}$  and GaAs shows promise, though other factors make  $\text{Cu}_2\text{S}-\text{CdS}$  cells more attractive commercially at the present time.

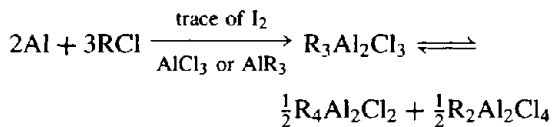


In each case  $\text{Al}-\text{C}_\mu$  is about 10% longer than  $\text{Al}-\text{C}_t$  (cf.  $\text{Al}_2\text{X}_6$ , p. 235;  $\text{B}_2\text{H}_6$ , p. 157). The enthalpy of dissociation of  $\text{Al}_2\text{Me}_6$  into monomers is  $84 \text{ kJ mol}^{-1}$ .  $\text{Al}_2\text{Et}_6$  (mp  $-53^\circ$ ) and  $\text{Al}_2\text{Pr}_6$  (mp  $-107^\circ$ ) are also dimeric at room temperature but crystalline trimesitylaluminium (mesityl = 2,4,5-trimethylphenyl) is monomeric with planar 3-coordinate Al; the mesityl groups adopt a propeller-like configuration with a dihedral angle of  $56^\circ$  between the aromatic ring and the  $\text{AlC}_3$  plane and with  $\text{Al}-\text{C}$  199.5 pm.<sup>(73)</sup>

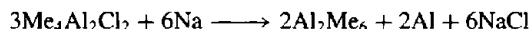
As with  $\text{Al}(\text{BH}_4)_3$  and related compounds (p. 230), solutions of  $\text{Al}_2\text{Me}_6$  show only one proton nmr signal at room temperature due to the rapid interchange of bridging and terminal Me groups; at  $-75^\circ$  this process is sufficiently slow for separate resonances to be observed.

$\text{Al}_2\text{Me}_6$  can be prepared on a laboratory scale by the reaction of  $\text{HgMe}_2$  on Al at  $\sim 90^\circ\text{C}$ .  $\text{Al}_2\text{Ph}_6$  can be prepared similarly using  $\text{HgPh}_2$  in boiling toluene or by the reaction of  $\text{LiPh}$  on  $\text{Al}_2\text{Cl}_6$ . On the industrial (kilotonne) scale Al is alkylated by means of  $\text{RX}$  or by alkenes plus  $\text{H}_2$ . In the first method the sesquichloride  $\text{R}_3\text{Al}_2\text{Cl}_3$  is formed in equilibrium with its disproportionation

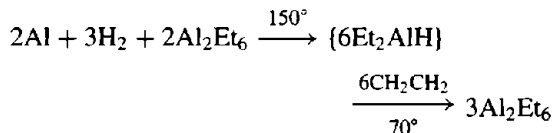
products:<sup>†</sup>



Addition of NaCl removes  $\text{R}_2\text{Al}_2\text{Cl}_4$  as the complex  $(2\text{NaAlCl}_3\text{R})$  and enables  $\text{R}_4\text{Al}_2\text{Cl}_2$  to be distilled from the mixture. Reaction with Na yields the trialkyl, e.g.:



Higher trialkyls are more readily prepared on an industrial scale by the alkene route (K. Ziegler *et al.*, 1960) in which  $\text{H}_2$  adds to Al in the presence of preformed  $\text{AlR}_3$  to give a dialkylaluminium hydride which then readily adds to the alkene:



Similarly, Al,  $\text{H}_2$  and  $\text{Me}_2\text{C}=\text{CH}_2$  react at  $100^\circ$  and 200 atm to give  $\text{AlBu}_3^i$  in a single-stage process, provided a small amount of this compound is present at the start; this is required because Al does not react directly with  $\text{H}_2$  to form  $\text{AlH}_3$  prior to alkylation under these conditions. Alkene exchange reactions can be used to transform  $\text{AlBu}_3^i$  into numerous other trialkyls.  $\text{AlBu}_3^i$  can also be reduced by potassium metal in hexane at room temperature to give the novel brown compound  $\text{K}_2\text{Al}_2\text{Bu}_6^i$  (mp  $40^\circ$ ) which is notable in providing a rare example of an Al-Al bond in the diamagnetic anion  $[\text{Bu}_3^i\text{AlAlBu}_3^i]^{2-}$ .<sup>(74)</sup>

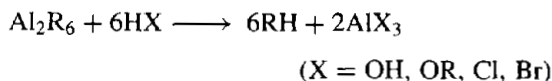
$\text{Al}_2\text{R}_6$  (or  $\text{AlR}_3$ ) react readily with ligands to form adducts,  $\text{LAlR}_3$ . They are stronger Lewis acids than are organoboron compounds,  $\text{BR}_3$ , and can be considered as 'hard' (or class a)

<sup>†</sup> It is interesting to note that the reaction of  $\text{EtI}$  with Al metal to give the sesqui-iodide "Et<sub>3</sub>Al<sub>2</sub>I<sub>3</sub>" was the first recorded preparation of an organoaluminium compound (W. Hallwachs and A. Schafarik, 1859).

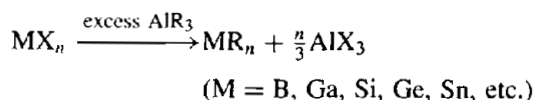
<sup>74</sup> H. HOBERG and S. KRAUSE, *Angew. Chem. Int. Edn. Engl.* **17**, 949-50 (1979).

<sup>73</sup> J. J. JERIUS, J. M. HAHN, A. F. M. M. RAHMAN, O. MOLS, W. H. ISLEY and J. P. OLIVER, *Organometallics* **5**, 1812-14 (1986).

acids; for example, the stability of the adducts  $\text{AlMe}_3$  decreases in the following sequence of L:  $\text{Me}_3\text{N} > \text{Me}_3\text{P} > \text{Me}_3\text{As} > \text{Me}_2\text{O} > \text{Me}_2\text{S} > \text{Me}_2\text{Se}$ . With protonic reagents they react to liberate alkanes:

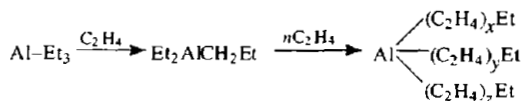


Reaction with halides or alkoxides of elements less electropositive than Al affords a useful route to other organometallics:



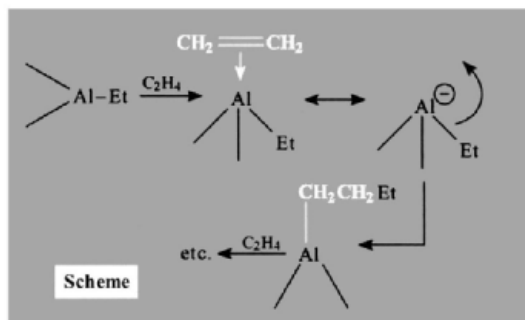
The main importance of organoaluminium compounds stems from the crucial discovery of alkene insertion reactions by K. Ziegler,<sup>(75)</sup> and an industry of immense proportions based on these reactions has developed during the past 40 y. Two main processes must be distinguished: (a) "growth reactions" to synthesize unbranched long-chain primary alcohols and alkenes (K. Ziegler *et al.*, 1955), and (b) low-pressure polymerization of ethene and propene in the presence of organometallic mixed catalysts (1955) for which K. Ziegler (Germany) and G. Natta (Italy) were jointly awarded the Nobel Prize for Chemistry in 1963.

In the first process alkenes insert into the Al-C bonds of monomeric  $\text{AlR}_3$  at  $\sim 150^\circ$  and 100 atm to give long-chain derivatives whose composition can be closely controlled by the temperature, pressure and contact time:

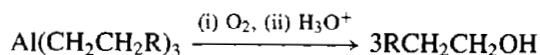


The reaction is thought to occur by repeated  $\eta^2$ -coordination of ethene molecules to Al followed by migration of an alkyl group from Al to the alkene carbon atom (see Scheme).

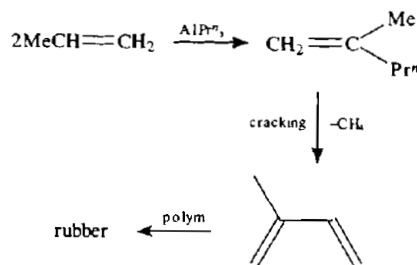
Unbranched chains up to  $\text{C}_{200}$  can be made, but prime importance attaches to chains of 14–20 C



atoms which are synthesized industrially in this way and then converted to unbranched aliphatic alcohols for use in the synthesis of biodegradable detergents:



Alternatively, thermolysis yields the terminal alkene  $\text{RCH}=\text{CH}_2$ . Note that, if propene or higher alkenes are used instead of ethene, then only single insertion into Al-C occurs. This has been commercially exploited in the catalytic dimerization of propene to 2-methylpentene-1, which can then be cracked to isoprene for the production of synthetic rubber (*cis*-1,4-polyisoprene):



Even more important is the stereoregular catalytic polymerization of ethene and other alkenes to give high-density polyethene ("polythene") and other plastics. A typical Ziegler-Natta catalyst can be made by mixing  $\text{TiCl}_4$  and  $\text{Al}_2\text{Et}_6$  in heptane: partial reduction to  $\text{Ti}^{\text{III}}$  and alkyl transfer occur, and a brown suspension forms which rapidly absorbs and polymerizes ethene even at room temperature and atmospheric pressure. Typical industrial conditions are 50–150°C and 10 atm. Polyethene

<sup>75</sup> K. ZIEGLER, *Adv. Organometallic Chem.* 6, 1–17 (1968).



produced at the surface of such a catalyst is 85–95% crystalline and has a density of 0.95–0.98 g cm<sup>-3</sup> (compared with low-density polymer 0.92 g cm<sup>-3</sup>); the product is stiffer, stronger, has a higher resistance to penetration by gases and liquids, and has a higher softening temperature (140–150°). Polyethene is produced in megatonne quantities and used mainly in the form of thin film for packaging or as molded articles, containers and bottles; electrical insulation is another major application. Stereoregular (isotactic) polypropene and many copolymers of ethene are also manufactured. Much work has been done in an attempt to elucidate the chemical nature of the catalysts and the mechanism of their action; the active site may differ in detail from system to system but there is now general agreement that polymerization is initiated by  $\eta^2$  coordination of ethene to the partly alkylated lower-valent transition-metal atom (e.g. Ti<sup>III</sup>) followed by migration of the attached alkyl group from transition-metal to carbon (the Cossee mechanism, see Scheme below). An alternative suggestion involves a metal–carbene species generated by  $\alpha$ -hydrogen transfer from carbon to the transition metal.<sup>(76)</sup>

Coordination of the ethene or propene to Ti<sup>III</sup> polarizes the C–C bond and allows ready migration of the alkyl group with its bonding electron-pair. This occurs as a concerted

process, and transforms the  $\eta^2$ -alkene into a  $\sigma$ -bonded alkyl group. As much as 1 tonne of polypropylene can be obtained from as little as 5 g Ti in the catalyst.

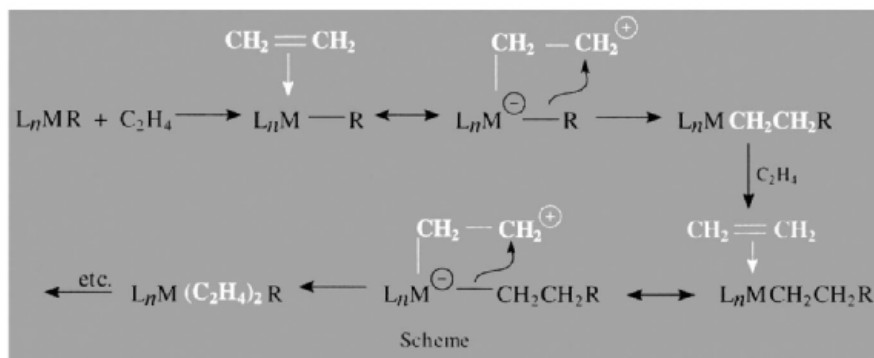
Finally, in this subsection, we mention a few recent examples of the use of specific ligands to stabilize particular coordination geometries about the organoaluminium atom (see also p. 256). Trigonal planar stereochemistry has been achieved in R<sub>2</sub>AlCH<sub>2</sub>AlR<sub>2</sub> {R = (Me<sub>3</sub>Si)<sub>2</sub>CH–}, which was prepared as colourless crystals by reacting CH<sub>2</sub>(AlCl<sub>2</sub>)<sub>2</sub> with 4 moles of LiCH(SiMe<sub>3</sub>)<sub>2</sub> in pentane.<sup>(77)</sup> It is also noteworthy that the bulky R groups permit the isolation for the first time of a molecule having the AlCH<sub>2</sub>Al grouping, by preventing the dismutation which spontaneously occurs with the Me and Et derivatives.

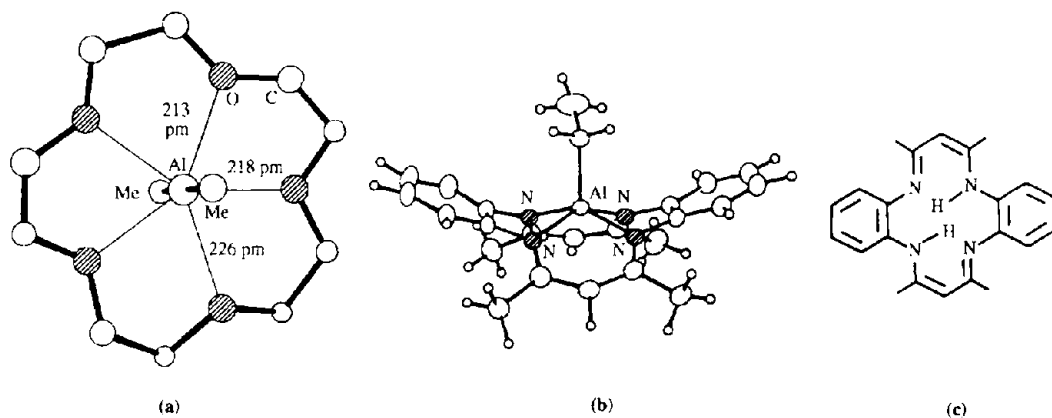
The linear cation [AlMe<sub>2</sub>]<sup>+</sup> has been stabilized by use of crown ethers (p. 96).<sup>(78)</sup> For example, 15-crown-5 gives overall pentagonal bipyramidal 7-fold coordination around Al with axial Me groups having Al–C 200 pm and angle Me–Al–Me 178° (see Fig. 7.19a). With the larger ligand 18-crown-6, the Al atom is bonded to only three of the six O atoms to give unsymmetrical 5-fold coordination with Al–C 193 pm and angle Me–Al–Me 141°. Symmetrical (square-pyramidal) 5-coordinate Al is found

<sup>76</sup> M. L. H. GREEN, *Pure Appl. Chem.* **50**, 27–35 (1978). K. J. IVIN, J. J. ROONEY, C. D. STEWART, M. L. H. GREEN and R. MAHTAB, *J. Chem. Soc., Chem. Commun.*, 604–6 (1978).

<sup>77</sup> M. LAYH and W. UHL, *Polyhedron* **9**, 277–82 (1990).

<sup>78</sup> S. G. BOTT, A. ALVANIPOUR, S. D. MORLEY, D. A. ATWOOD, C. M. MEANS, A. W. COLEMAN and J. L. ATWOOD, *Angew. Chem. Int. Edn. Engl.* **26**, 485–6 (1987).





**Figure 7.19** (a) Structure of the cation in  $[\text{AlMe}_2(15\text{-crown-5})]^+[\text{AlMe}_2\text{Cl}_2]^-$  showing pentagonal bipyramidal coordination of Al with axial Me groups. (b) Structure of  $[\text{AlEtL}]$  where L is the bis(deprotonated) form of the macrocycle  $\text{H}_2[\text{C}_{22}\text{H}_{22}\text{N}_4]$  shown in (c).

in the complex  $[\text{AlEtL}]$  (Fig. 7.19b) formed by reacting  $\text{Al}_2\text{Et}_6$  in hexane solution with  $\text{H}_2[\text{C}_{22}\text{H}_{22}\text{N}_4]$ , i.e.  $\text{H}_2\text{L}$ , shown in Fig. 7.19c.<sup>(79)</sup> The average Al–N distance is 196.7 pm, Al–C is 197.6 pm (close to the value for the terminal Al–C in  $\text{Al}_2\text{Me}_6$ , p. 259) and the Al atom is 57 pm above the  $\text{N}_4$  plane. A further notable feature is the great stability of the Al–C bond: the compound can be recrystallized unchanged from hydroxylic or water-containing solvents and does not decompose even when heated to 300°C in an inert atmosphere.

Heterocyclic and cluster organoaluminium compounds containing various sequences of Al–N bonds are discussed on p. 265.

### Organometallic compounds of Ga, In and Tl

Organometallic compounds of Ga, In and Tl have been less studied than their Al analogues. The trialkyls do not dimerize and there is a general tendency to diminishing thermal stability with increasing atomic weight of M. There is also

a general decrease of chemical reactivity of the M–C bond in the sequence  $\text{Al} > \text{Ga} \approx \text{In} > \text{Tl}$ , and this is particularly noticeable for compounds of the type  $\text{R}_2\text{MX}$ ; indeed, Tl gives air-stable non-hydrolysing ionic derivatives of the type  $[\text{TlR}_2]\text{X}$ , where  $\text{X} = \text{halogen, CN, NO}_3, \frac{1}{2}\text{SO}_4$ , etc. For example, the ion  $[\text{TlMe}_2]^+$  is stable in aqueous solution, and is linear like the isoelectronic  $\text{HgMe}_2$  and  $[\text{PbMe}_2]^{2+}$ .

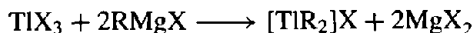
$\text{GaR}_3$  can be prepared by alkylating Ga with  $\text{HgR}_2$  or by the action of  $\text{RMgBr}$  or  $\text{AlR}_3$  on  $\text{GaCl}_3$ . They are low-melting, mobile, flammable liquids. The corresponding In and Tl compounds are similar but tend to have higher mps and bps; e.g.

Compound	$\text{GaMe}_3$	$\text{InMe}_3$	$\text{TlMe}_3$
MP	–16°	88.4°	38.5°
BP	56°	136°	147° (extrap)
Compound	$\text{GaEt}_3$	$\text{InEt}_3$	$\text{TlEt}_3$
MP	–82°	–	–63°
BP	143°	84°/12 mmHg	192° (extrap)

The triphenyl analogues are also monomeric in solution but tend to associate into chain structures in the crystalline state as a result of weak intermolecular  $\text{M} \cdots \text{C}$  interactions:  $\text{GaPh}_3$  mp

<sup>79</sup> V. L. GOEDKEN, H. ITO and T. ITO, *J. Chem. Soc., Chem. Commun.*, 1453–5 (1984).

166°, InPh<sub>3</sub> mp 208°, TlPh<sub>3</sub> mp 170°. For Ga and In compounds the primary M–C bonds can be cleaved by HX, X<sub>2</sub> or MX<sub>3</sub> to give reactive halogen-bridged dimers (R<sub>2</sub>MX)<sub>2</sub>. This contrasts with the unreactive ionic compounds of Tl mentioned above, which can be prepared by suitable Grignard reactions:



As in the case of organoaluminium compounds, unusual stereochemistries can be imposed by suitable design of ligands. Thus, reaction of GaCl<sub>3</sub> with 3,3',3''-nitriлотris(propylmagnesium chloride),  $[\text{N}\{\overline{(\text{CH}_2)_3\text{MgCl}}\}_3]$ , yields colourless crystals of  $[\text{Ga}(\text{CH}_2)_3\text{N}]$  in which intramolecular N→Ga coordination stabilizes a planar trigonal monopyramidal geometry about Ga as shown schematically in Fig. 7.20(a).<sup>(80)</sup> Because of steric constraints, the Ga–N distance of 209.5 pm is about 7% longer than the sum of the covalent radii (195 pm), although not so long as in Me<sub>3</sub>GaNMe<sub>3</sub> (220 pm). Long bonds are also a feature of the unique 6-coordinate complex of InMe<sub>3</sub> with the heterocyclic triazine ligand (Pr<sup>i</sup>NCH<sub>2</sub>)<sub>3</sub>. The air-sensitive adduct,  $[\text{Me}_3\text{In}\{\eta^3\text{-(Pr}^i\text{NCH}_2)_3\}]$ , can be prepared by

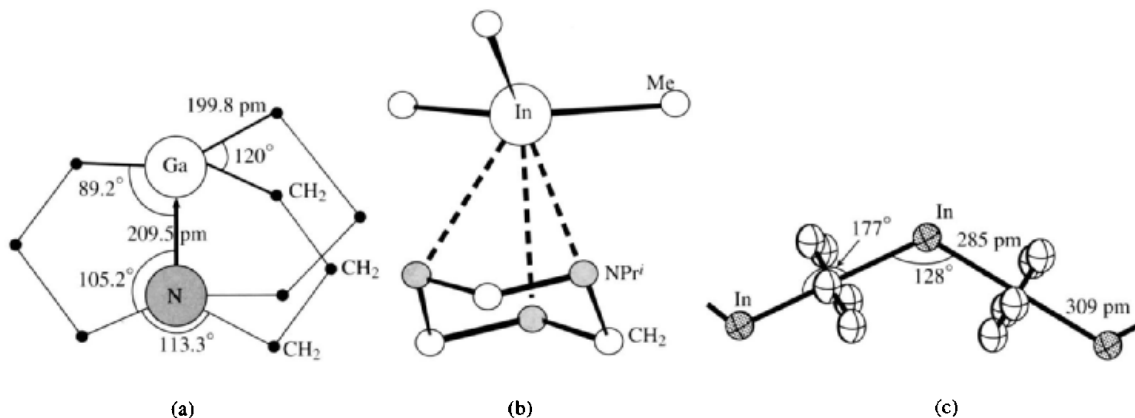
<sup>80</sup> H. SCHUMANN, U. HARTMANN, A. DIETRICH and J. PICKARDT, *Angew. Chem. Int. Edn. Engl.* **27**, 1077–8 (1988).

direct reaction of the donor and acceptor in ether solution, and is the first example of a tridentate cyclotriazine complex; it is also the first example of InMe<sub>3</sub> accepting three lone pairs of electrons rather than the more usual one or two.<sup>(81)</sup> The structure (Fig. 7.20b) features a shallow InC<sub>3</sub> pyramid with C–In–C angles of 114°–117° and extremely acute N–In–N angles (48.6°) associated with the long In–N bonds (278 pm). The three Pr<sup>i</sup> groups are all in equatorial positions.

Cyclopentadienyl and arene complexes of Ga, In and Tl have likewise attracted increasing attention during the past decade and provide a rich variety of structural types and of chemical diversity.  $[\text{Ga}(\text{C}_5\text{H}_5)_3]$ , prepared directly from GaCl<sub>3</sub> and an excess of LiC<sub>5</sub>H<sub>5</sub> in Et<sub>2</sub>O, was found to have simple trigonal planar Ga bonded to three η<sup>1</sup>-C<sub>5</sub>H<sub>5</sub> groups. The more elusive C<sub>5</sub>Me<sub>5</sub> derivative was finally prepared from GaCl<sub>3</sub> and an excess of the more reactive NaC<sub>5</sub>Me<sub>5</sub> in thf solution, or by reduction of Ga(C<sub>5</sub>Me<sub>5</sub>)<sub>n</sub>Cl<sub>3–n</sub> (n = 1, 2) with sodium naphthalene in thf.<sup>(82)</sup>  $[\text{Ga}(\text{C}_5\text{Me}_5)_3]$

<sup>81</sup> D. C. BRADLEY, D. M. FRIGO, I. S. HARDING, M. B. HURSTHOUSE and M. MOTEVALLI, *J. Chem. Soc., Chem. Commun.*, 577–8 (1992).

<sup>82</sup> O. T. BEACHLEY and R. B. HALLOCK, *Organometallics* **6**, 170–2 (1987).



**Figure 7.20** (a) Structure of  $[\text{Ga}(\text{CH}_2)_3\text{N}]$  showing trigonal planar monopyramidal 4-fold coordination about Ga and tetrahedral coordination about N. (b) Structure of  $[\text{Me}_3\text{In}\{\eta^3\text{-(Pr}^i\text{NCH}_2)_3\}]$  — see text for dimensions. (c) Structure of polymeric  $[\text{In}(\eta^5\text{-C}_5\text{H}_5)]$ .

is a colourless, sublimable, crystalline solid, mp 168°, and appears to be a very weak Lewis acid.

As distinct from the cyclopentadienyls of Ga<sup>III</sup>, those of In and Tl involve the +1 oxidation state of the metal and pentahapto bonding of the ligand. [In( $\eta^5$ -C<sub>5</sub>H<sub>5</sub>)] is best prepared by metathesis between LiC<sub>5</sub>H<sub>5</sub> and a slurry of InCl in Et<sub>2</sub>O.<sup>(83)</sup> It is monomeric in the gas phase with a 'half-sandwich' structure, the In-C<sub>5</sub>(centroid) distance being 232 pm, but in the solid state it is a zig-zag polymer with significantly larger In-C<sub>5</sub>(centroid) distances as shown in Fig. 7.20c.<sup>(84)</sup> The crystalline pentamethyl derivative, by contrast, is hexameric and features an octahedral In<sub>6</sub> cluster each vertex of which is  $\eta^5$ -coordinated by C<sub>5</sub>Me<sub>5</sub>.<sup>(85)</sup> [Tl( $\eta^5$ -C<sub>5</sub>H<sub>5</sub>)] precipitates as air-stable yellow crystals when aqueous TlOH is shaken with cyclopentadiene. In the gas phase the compound is monomeric with C<sub>5v</sub> symmetry, the Tl atom being 241 pm above the plane of the ring (microwave), whereas in the crystalline phase there are zig-zag chains of equispaced alternating

C<sub>5</sub>H<sub>5</sub> rings and Tl atoms similar to the In homologue.

Hexahapto ( $\eta^6$ -arene) complexes of Ga<sup>I</sup> and In<sup>I</sup> can be obtained from solutions of the lower halides (p. 240) in aromatic solvents, and some of these have surprisingly complex structures.<sup>(86)</sup> With bulky ligands such as C<sub>6</sub>Me<sub>6</sub> simple adducts crystallize in which the cations [M( $\eta^6$ -C<sub>6</sub>Me<sub>6</sub>)]<sup>+</sup> have the C<sub>6v</sub> 'half-sandwich' structure shown in Fig. 7.21a, e.g. [Ga( $\eta^6$ -C<sub>6</sub>Me<sub>6</sub>)] [GaCl<sub>4</sub>] mp 168° and [Ga( $\eta^6$ -C<sub>6</sub>Me<sub>6</sub>)] [GaBr<sub>4</sub>] mp 146°.<sup>(87)</sup> With less bulky ligands such as mesitylene (1,3,5-C<sub>6</sub>H<sub>3</sub>Me<sub>3</sub>), a 2:1 stoichiometry is possible to give cations [M( $\eta^6$ -C<sub>6</sub>H<sub>3</sub>Me<sub>3</sub>)<sub>2</sub>]<sup>+</sup> shown schematically in Fig. 7.21b, although further ligation from the anion may also occur; e.g. [In( $\eta^6$ -C<sub>6</sub>H<sub>3</sub>Me<sub>3</sub>)<sub>2</sub>] [InBr<sub>4</sub>] features polymeric helical chains in which bridging [ $\mu$ - $\eta^1, \eta^2$ -InBr<sub>4</sub>] units connect the cations as shown in Fig. 7.21c.<sup>(88)</sup> With still less bulky ligands such as benzene itself, discrete dimers can be formed as in the solvated complex [Ga( $\eta^6$ -C<sub>6</sub>H<sub>6</sub>)<sub>2</sub>] [GaCl<sub>4</sub>].3C<sub>6</sub>H<sub>6</sub>. This features tilted bis(arene)Ga<sup>I</sup> units linked through bridging GaCl<sub>4</sub> units to form the dimeric structure shown in Fig. 7.22a.<sup>(86)</sup> Mixed adducts can also be prepared. Thus, when

<sup>83</sup> C. PEPPE, D. G. TUCK and L. VICTORIANO, *J. Chem. Soc., Dalton Trans.*, 2592 (1981).

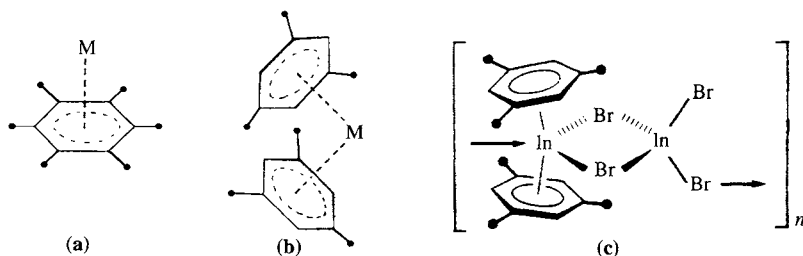
<sup>84</sup> O. T. BEACHLEY, J. C. PAZIK, T. E. GLASSMAN, M. R. CHURCHILL, J. C. FETTINGER and R. BLOM, *Organometallics* **7**, 1051-9 (1988).

<sup>85</sup> O. T. BEACHLEY, M. R. CHURCHILL, J. C. FETTINGER, J. C. PAZIK and L. VICTORIANO, *J. Am. Chem. Soc.* **108**, 4666-8 (1986).

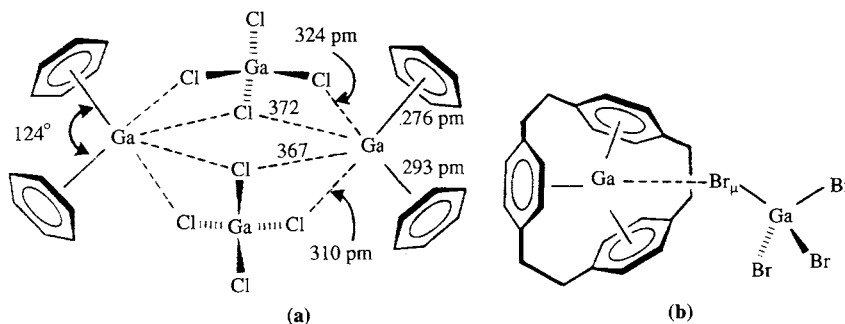
<sup>86</sup> H. SCHMIDBAUR, *Angew. Chem. Int. Edn. Engl.* **24**, 893-904 (1985).

<sup>87</sup> H. SCHMIDBAUR, U. THEWALT and T. ZAFIROPOULOS, *Angew. Chem. Int. Edn. Engl.* **23**, 76-7 (1984).

<sup>88</sup> J. EBENHÖCH, G. MÜLLER, J. RIEDE and H. SCHMIDBAUR, *Angew. Chem. Int. Edn. Engl.* **23**, 386-8 (1984).



**Figure 7.21** (a) The 'half-sandwich' C<sub>6v</sub> structure characteristic of [Ga( $\eta^6$ -C<sub>6</sub>Me<sub>6</sub>)]<sup>+</sup>. (b) The 'bent-sandwich' structure found in ions of the type [In( $\eta^6$ -C<sub>6</sub>H<sub>3</sub>Me<sub>3</sub>)<sub>2</sub>]<sup>+</sup>. (c) A section of the helical chain in [In( $\eta^6$ -mes)<sub>2</sub>] [InBr<sub>4</sub>] showing the [ $\mu$ - $\eta^1, \eta^2$ -InBr<sub>4</sub>] unit bridging ions of the type shown in (b); the tilting angle is 133° and the ring-centres of the two arene ligands are almost equidistant from In (283 and 289 pm).



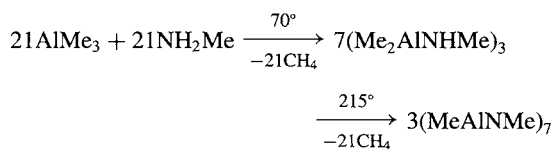
**Figure 7.22** (a) Structure of the dimeric unit in the solvated complex  $[\text{Ga}(\eta^6\text{-C}_6\text{H}_6)_2][\text{GaCl}_4] \cdot 3\text{C}_6\text{H}_6$  indicating the principal dimensions; the six benzene molecules of solvation per dimer lie outside the coordination spheres of the gallium atoms. (b) Structure of the ion-pair  $[\text{Ga}(\eta^{18}\text{-[2.2.2]paracyclophane})][\text{GaBr}_4]$ ; the four Ga-Br distances within the tetrahedral anion are in the range 230.5–233.3 pm, the distance for Ga-Br<sub>μ</sub> being 231.9 pm; the Ga<sup>I</sup>...Br<sub>μ</sub> distance is 338.8 pm.

dilute toluene solutions of  $\text{Ga}_2\text{Cl}_4$  and durene (1,2,4,5- $\text{C}_6\text{H}_2\text{Me}_4$ ) are cooled to 0°, crystals containing the centrosymmetric dimer  $[\{\text{Ga}(\eta^6\text{-dur})(\eta^6\text{-tol})\}\text{GaCl}_4]_2$  are obtained.<sup>(89)</sup> The structure resembles that in Fig. 7.22a, with each Ga<sup>I</sup> centre  $\eta^6$ -bonded to one durene molecule at 264 pm and one toluene molecule at 304 pm. These bent-sandwich moieties are then linked into dimeric units via three of the four Cl atoms of each of the two  $\text{GaCl}_4$  tetrahedra.

An even more remarkable structure emerges for the monomeric complex of  $\text{Ga}_2\text{Br}_4$  with the tris(arene) ligand [2.2.2]paracyclophane (Fig. 7.22b):<sup>(90)</sup> the Ga<sup>I</sup> centre is encapsulated in a unique  $\eta^{18}$  environment which has no parallels even in transition-metal coordination chemistry. The Ga<sup>+</sup> cation is almost equidistant from the three ring centres (265 pm) but is displaced away from the ligand centre by 43 pm towards the  $\text{GaBr}_4^-$  counter anion. The complex was prepared by dissolving the dimeric benzene complex  $[\{(\text{C}_6\text{H}_6)_2\text{Ga} \cdot \text{GaBr}_4\}_2]$  (cf. Fig. 7.22a) in benzene and adding the cyclophane.

### Al-N heterocycles and clusters

Finally, in this chapter, attention should be drawn to a remarkable range of heterocyclic and cluster organoaluminium compounds containing various sequences of Al-N bonds<sup>(91)</sup> (cf. B-N compounds, p. 207). Thus the adduct  $[\text{AlMe}_3(\text{NH}_2\text{Me})]$  decomposes at 70°C with loss of methane to give the cyclic amido trimers *cis*- and *trans*- $[\text{Me}_2\text{AlNHMe}]_3$  (structures 2 and 3) and at 215° to give the oligomeric imido cluster compounds  $(\text{MeAlNMe})_7$  (structure 6) and  $(\text{MeAlNMe})_8$  (structure 7), e.g.:



Similar reactions lead to other oligomers depending on the size of the R groups and the conditions of the reaction, e.g. *cyclo*- $(\text{Me}_2\text{AlNMe}_2)_2$  (structure 1) and the imido-clusters  $(\text{PhAlNPh})_4$ ,  $(\text{HAlNPr}^i)_4$  or 6,

<sup>89</sup> H. SCHMIDBAUR, R. NOWAK, B. HUBER and G. MÜLLER, *Polyhedron* **9**, 283–7 (1990).

<sup>90</sup> H. SCHMIDBAUR, R. HAGER, B. HUBER and G. MÜLLER, *Angew. Chem. Int. Edn. Engl.* **26**, 338–40 (1987). See also H. SCHMIDBAUR, W. BUBLAK, B. HUBER and G. MÜLLER, *Organometallics* **5**, 1647–51 (1986).

<sup>91</sup> S. AMIRKHALILI, P. B. HITCHCOCK and J. D. SMITH, *J. Chem. Soc., Dalton Trans.*, 1206–12 (1979); and references 1–9 therein. See also P. P. POWER, *J. Organometallic Chem.* **400**, 49–69 (1990); K. M. WAGGONER, M. M. OLMSTEAD and P. P. POWER, *Polyhedron* **9**, 257–63 (1990); A. J. DOWNS, D. DUCKWORTH, J. C. MACHELL and C. R. PULHAM, *Polyhedron* **11**, 1295–304 (1992).

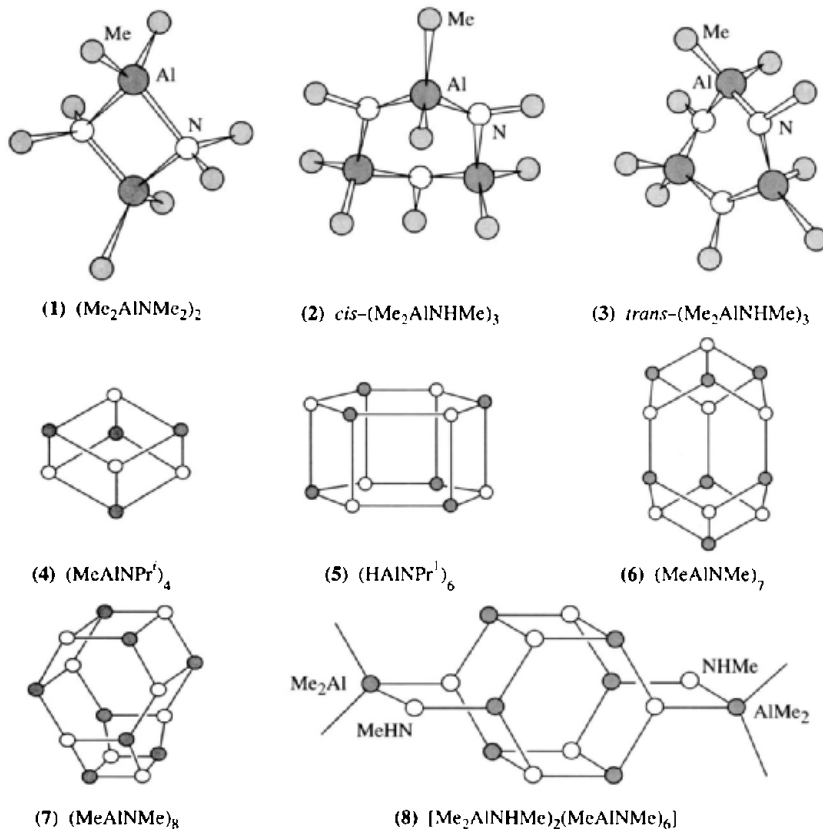
(HAINPr<sup>n</sup>)<sub>6</sub> or 8, (HAINBu<sup>t</sup>)<sub>4</sub>, and (MeAlNPr<sup>t</sup>)<sub>4</sub> or 6 (see structures 4, 5, 7). Intermediate amido-imido compounds have also been isolated from the reaction, e.g. [Me<sub>2</sub>AlNHMe]<sub>2</sub> (MeAlNMe)<sub>6</sub> (structure 8). Oligomers up to (RAINR')<sub>16</sub> have been obtained although not necessarily structurally characterized. The known structures are all built up from varying numbers of fused 4-membered and 6-membered AlN heterocycles.

Until recently tetramers such as (4) were the smallest oligomers involving alternating Al and N atoms. It will be noted, however, that the hexamer (5) comprises a hexagonal prism formed by conjoining two plane six-membered rings. By increasing the size of the exocyclic groups it has proved possible to isolate a planar trimer, (MeAlNAr)<sub>3</sub>, which is isoelectronic with borazine (p. 210). Thus, thermolysis of a mixture of AlMe<sub>3</sub> and ArNH<sub>2</sub>

(Ar = 2, 6-Pr<sup>t</sup><sub>2</sub>C<sub>6</sub>H<sub>3</sub>) in toluene at 110° results in the smooth elimination of CH<sub>4</sub> to give the dimer, (Me<sub>2</sub>AlNAr)<sub>2</sub>, which, when heated to 170°, loses more methane to give a high yield of the trimer, (MeAlNAr)<sub>3</sub>, as colourless, air- and moisture-sensitive crystals.<sup>(92)</sup> The six *ipso*-C atoms are coplanar with the planar 6-membered Al<sub>3</sub>N<sub>3</sub> ring and the Al-N distance of 178 pm is significantly shorter than in the higher (4-coordinate) oligomers (189–196 pm). Comparison with other 3-coordinate Al and N centres is difficult because of the paucity of examples but the homoleptic monomer [Al{N(SiMe<sub>3</sub>)<sub>2</sub>}<sub>3</sub>] has also been reported to have Al-N distances of 178 pm.

Several analogous gallium compounds are also known, e.g. [(Me<sub>2</sub>GaNHMe)<sub>2</sub>(MeGaNMe)<sub>6</sub>]

<sup>92</sup> K. M. WAGGONER, H. HOPE and P. P. POWER, *Angew. Chem. Int. Edn. Engl.* **27**, 1699–700 (1988).



(structure 8).<sup>(91)</sup> Likewise,  $(R_2GaPBU'_2)_2$  and  $(R_2GaAsBu'_2)_2$  ( $R = Me, Bu^t$ ) have structures analogous to (1).<sup>(93)</sup> A more complex 12-membered  $Ga_5As_7$  cluster has been characterized in  $[(PhAsH)(R_2Ga)(PhAs)_6(RGa)_4]$  ( $R = Me_3SiCH_2$ ).<sup>(94)</sup> The cyclic trimer,  $[\{(triph)GaP(chex)\}_3]$ , (where triph = 2,4,6- $Ph_3C_6H_2$  and chex = cyclo- $C_6H_{11}$ ) is of interest in being the first well characterized heterocycle consisting entirely of heavier main-group elements. It is obtained as pale yellow crystals by reacting

---

<sup>93</sup> A. M. ARIF, B. L. BENAC, A. H. COWLEY, R. GEERTS, R. A. JONES, K. B. KIDD, J. M. POWER and S. T. SCHWAB, *J. Chem. Soc., Chem. Commun.*, 1543–5 (1986).

<sup>94</sup> R. L. WELLS, A. P. PURDY, A. T. MCPHAIL and C. G. PITT, *J. Chem. Soc., Chem. Commun.*, 487–8 (1986).

(triph)GaCl<sub>2</sub> with Li<sub>2</sub>P(chex) and is formally iso-electronic with borazine (p. 210). Indeed, it has short Ga–P distances (mean 229.7 pm) but the ring is markedly non-planar and there is a slight, statistically significant alternation in Ga–P distances with three averaging at 228.5(4) pm and three at 230.8(4) pm.<sup>(95)</sup> Much of the burgeoning interest in this area of volatile compounds of Group 13 elements has come from attempts to devise effective routes to thin films of III–V semiconductors such as GaP, GaAs, etc. via MOCVD (metal-organic chemical vapour deposition).

---

<sup>95</sup> H. HOPE, D. C. PESTANA and P. P. POWER, *Angew. Chem. Int. Edn. Engl.* **30**, 691–3 (1991).

																		1	2																
																		3	4	5	6	7	8	9	10	11	12								
1	2																	13	14	15	16	17	18												
3	4	5	6	7	8	9	10	11	12	13	14	15	16	17	18																				
19	20	21	22	23	24	25	26	27	28	29	30	31	32	33	34	35	36																		
37	38	39	40	41	42	43	44	45	46	47	48	49	50	51	52	53	54																		
55	56	57	58	59	60	61	62	63	64	65	66	67	68	69	70	71	72																		
73	74	75	76	77	78	79	80	81	82	83	84	85	86	87	88	89	90																		
91	92	93	94	95	96	97	98	99	100	101	102	103	104	105	106	107	108																		
109	110	111	112																																
																		109	110	111	112														
109	110	111	112																																
109	110	111	112																																

# 8

## Carbon

### 8.1 Introduction

One thing is absolutely certain — it is quite impossible to do justice to the chemistry of carbon in a single chapter; or, indeed, a single book. The areas of chemistry traditionally thought of as organic chemistry will largely be omitted except where they illuminate the general chemistry of the element. The field of organometallic chemistry is discussed in Section 19.7: this has been one of the most rapidly developing areas of the subject during the past 40 y and has led to major advances in our understanding of the structure, bonding and reactivity of molecular compounds. In fact, the unifying concepts emerging from organometallic chemistry emphasize the dangers of erecting too rigid a barrier between various branches of the subject, and nowhere is the boundary between inorganic and organic chemistry more arbitrary and less helpful than here. The present chapter gives a general account of the chemistry of carbon and its compounds; a more detailed discussion of specific organometallic systems will be found under the individual elements. Discussion of Group trends and the comparative chemistry of the Group 14 elements C, Si, Ge, Sn and Pb is deferred until Chapter 10.

Carbon was known as a substance in prehistory (charcoal, soot) though its recognition as an element came much later, being the culmination of several experiments in the eighteenth century.<sup>(1)</sup> Diamond and graphite were known to be different forms of the element by the close of the eighteenth century, and the relationship between carbon, carbonates, carbon dioxide, photosynthesis in plants, and respiration in animals was also clearly delineated by this time (see Panel). The great upsurge in synthetic organic chemistry began in the 1830s and various structural theories developed following the introduction of the concept of valency in the 1850s. Outstanding achievements in this area were F. A. Kekulé's use of structural formulae for organic compounds and his concept of the benzene ring, L. Pasteur's work on optical activity and the concept of tetrahedral carbon (J. H. van't Hoff).<sup>†</sup>

<sup>1</sup> M. E. WEEKS, *Discovery of the Elements*, Chaps. 1 and 2, pp. 58–89. J. Chem. Educ. Publ., 1956.

<sup>†</sup> J. A. Le Bel, whose name is often also associated with this concept, did indeed independently suggest a 3-dimensional model for the 4-coordinate C atom, but vigorously opposed the tetrahedral stereochemistry of van't Hoff for many years and favoured an alternative square pyramidal arrangement of the bonds.



## Early History of Carbon and Carbon Dioxide

	Carbon known as a substance in prehistory (charcoal, soot) but not recognized as an element until the second half of the eighteenth century.
BC	"Indian inks" made from soot used in the oldest Egyptian hieroglyphs on papyrus.
AD 1273	Ordinance prohibiting use of coal in London as prejudicial to health — the earliest known attempt to reduce smoke pollution in Britain.
~1564	Lead pencils first manufactured commercially during Queen Elizabeth's reign, using Cumberland graphite.
1752/4	CO <sub>2</sub> ("fixed air"), prepared by Joseph Black (aged 24–26), was the first gas other than air to be characterized: (i) chalk when heated lost weight and evolved CO <sub>2</sub> (genesis of quantitative gravimetric analysis), and (ii) action of acids on carbonates liberates CO <sub>2</sub> .
1757	J. Black showed that CO <sub>2</sub> was produced by fermentation of vegetables, by burning charcoal and by animals (humans) when breathing; turns lime water turbid.
1771	J. Priestley established that green plants use CO <sub>2</sub> and "purify air" when growing. He later showed that the "purification" was due to the new gas oxygen (1774).
1779	Elements of photosynthesis elucidated by J. Ingenhousz: green plants in daylight use CO <sub>2</sub> and evolve oxygen; in the dark they liberate CO <sub>2</sub> .
1789	The word "carbon" (Fr. <i>carbone</i> ) coined by A. L. Lavoisier from the Latin <i>carbo</i> , charcoal. The name "graphite" was proposed by A. G. Werner and D. L. G. Harsten in the same year: Greek <i>γραφήν</i> ( <i>graphein</i> ), to write. The name "diamond" is probably a blend of Greek <i>διαφανής</i> ( <i>diaphanes</i> ), transparent, and <i>αδάμας</i> ( <i>adamas</i> ), indomitable or invincible, in reference to its extreme hardness.
1796	Diamond shown to be a form of carbon by S. Tennant who burned it and weighed the CO <sub>2</sub> produced; graphite had earlier been shown to be carbon by C. W. Scheele (1779); carbon recognized as essential for converting iron to steel (R.-A.-F de Réaumur and others in the late eighteenth century).
1805	Humphry Davy showed carbon particles are the source of luminosity in flames (lamp black).

The first metal carbonyl compounds Ni(CO)<sub>4</sub> and Fe(CO)<sub>5</sub> were prepared and characterized by L. Mond and his group in 1889–91 and this work has burgeoned into the huge field of metal carbonyl cluster compounds which is still producing results of fundamental importance. Even more extensive is the field of organometallic chemistry which developed rapidly after the seminal papers on the "sandwich" structure of ferrocene (E. O. Fischer and W. Pfab, 1952; G. Wilkinson, M. Rosenblum, M. C. Whiting and R. B. Woodward, 1952) and the "π bonding" of ethylene complexes (M. J. S. Dewar 1951, J. Chatt, and L. A. Duncanson, 1953). The constricting influence of classical covalent-bond theory was finally overcome when it was realized that carbon in many of its compounds can be 5-coordinate (Al<sub>2</sub>Me<sub>6</sub>, p. 258), 6-coordinate (C<sub>2</sub>B<sub>10</sub>H<sub>12</sub>, p. 185) or even 7-coordinate (Li<sub>4</sub>Me<sub>4</sub>, p. 104). A compound featuring an 8-coordinate carbon atom is shown on p. 1142. In parallel with these developments in synthetic chemistry and bonding theory have been technical and instrumental advances of great significance; foremost amongst these have

been the development of <sup>14</sup>C radioactive dating techniques (W. F. Libby, 1949), the commercial availability of <sup>13</sup>C nmr instruments in the early 1970s, and the industrial production of artificial diamonds (General Electric Company, 1955). These and other notable dates in carbon chemistry are summarized in the Panel on p. 270.

The most exciting recent development in the chemistry of carbon has been the intriguing discovery of a whole new range of soluble molecular forms of elemental carbon, the fullerenes, of which C<sub>60</sub> and C<sub>70</sub> are the most prominent members. This was recognized by the 1996 Nobel Prize for Chemistry and has stimulated an enormous amount of research which is discussed in Section 8.2.4 (p. 279).

## 8.2 Carbon

### 8.2.1 Terrestrial abundance and distribution

Carbon occurs both as the free element (graphite, diamond) and in combined form (mainly as the

### Some Notable Dates in Carbon Chemistry

- 1807 J. J. Berzelius classified compounds as "organic" or "inorganic" according to their origin in living matter or inanimate material.
- 1825-7 W. C. Zeise prepared  $K[Pt(C_2H_4)Cl_3]$  and related compounds; though of unknown structure at the time they later proved to be the first organometallic compounds.
- 1828 The vitalist theory of Berzelius challenged by F. Wöhler (aged 28) who synthesized urea,  $(NH_2)_2CO$ , from  $NH_4(OCN)$ .
- 1830+ Rise of synthetic organic chemistry.
- 1848 L. Pasteur (aged 26) began work on optically active sodium ammonium tartrate.
- 1849 First metal alkyls, e.g.  $ZnEt_2$ , made by E. Frankland (aged 24); he also first propounded the theory of valency (1852).
- 1858 F. A. Kekulé's structural formulae for organic compounds; ring structure of benzene 1865.
- 1874 Tetrahedral, 4-coordinate carbon proposed by J. H. van't Hoff (aged 22) see also footnote to p. 268.
- 1890 First paper on metal carbonyls  $[Ni(CO)_4]$  by L. Mond, C. Langer and F. Quincke.
- 1891 Carborundum, SiC, made by E. G. Acheson.
- 1900 First paper by V. Grignard (aged 29) on  $RMgX$  syntheses. Nobel Prize 1912.
- 1924 Solid  $CO_2$  introduced commercially as a refrigerant.
- 1926  $C_8K$  prepared — the first alkali metal-graphite intercalation compound.
- 1929 Isotopes of C ( $^{12}C$  and  $^{13}C$ ) discovered by A. S. King and R. T. Birge in the band spectrum of  $C_2$ , CO and CN (previously undetected by mass spectrometry).
- 1932 First metal halide-graphite intercalation compound made with  $FeCl_3$ .
- 1936 Radiocarbon  $^{14}C^*$  established as the product of an (n,p) reaction on  $^{14}N$  by W. E. Burcham and M. Goldhaber.
- 1940 Chemically significant amounts of  $^{14}C$  synthesized by S. Ruben and M. D. Kamen.
- 1947-9 Concept and feasibility of  $^{14}C$  dating established by W. F. Libby (awarded Nobel Prize in 1960).
- 1952 Structure of ferrocene elucidated; organometallic chemistry burgeons: Nobel Prize awarded jointly to E. O. Fischer and G. Wilkinson 1973.
- 1953 First authentic production of artificial diamonds by ASEA. Sweden: commercial production achieved by General Electric (USA) in 1955.
- 1955 Stereoregular polymerization of ethene and propene by catalysts developed by K. Ziegler and by G. Natta (shared Nobel Prize 1963).
- 1956 Cyclobutadiene-transition metal complexes predicted by H. C. Longuet-Higgins and L. E. Orgel 3 y before they were first synthesized.
- 1960  $\pi$ -allylic metal complexes first recognized.
- 1961  $^{12}C = 12$  internationally adopted as the unified atomic weight standard by both chemists and physicists.
- 1964 6-coordinate carbon established in various carboranes by W. N. Lipscomb and others. (Nobel Prize 1976 for structure and bonding of boranes).
- 1965 Mass spectrometric observation of  $CH_5^+$  by F. H. Field and M. S. B. Munson, and subsequent extensive study of hypercoordinate C compounds by G. A. Olah *et al.*
- 1966  $CS_2$  complexes such as  $[Pt(CS_2)(PPh_3)_2]$  first prepared in G. Wilkinson's laboratory.
- 1971  $^{13}C$  fourier-transform nmr commercially available following first observation of  $^{13}C$  nmr signal by P. C. Lauterbur and by C. H. Holm in 1957.
- 1976 8-coordinate carbon established in  $[Co_8C(CO)_{18}]^{2-}$  by V. G. Albano, P. Chini *et al.* (Cubic coordination of C in the antifluorite structure of  $Be_2C$  known since 1948.)
- 1985 Discovery of  $C_{60}$  and  $C_{70}$  molecules (fullerenes) by H. Kroto, R. E. Smalley and their colleagues.
- 1989 Large-scale synthesis of  $C_{60}$  and  $C_{70}$  by D. Huffman and W. Krätschmer.
- 1994 Nobel Prize to G. A. Olah for contributions to carbocation chemistry.
- 1996 Nobel Prize to R. Curl, H. Kroto and R. E. Smalley for discovery of the fullerenes.

carbonates of Ca, Mg and other electropositive elements). It also occurs as  $CO_2$  a minor but crucially important constituent of the atmosphere. Estimates of the overall abundance of carbon in crustal rocks vary considerably, but a value of 180 ppm can be taken as typical; this places the element seventeenth in order of abundance after Ba, Sr and S but before Zr, V, Cl and Cr.

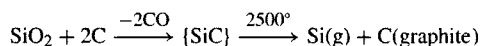
Graphite is widely distributed throughout the world though much of it is of little economic importance. Large crystals or "flake" occur in metamorphosed sedimentary silicate rocks such as quartz, mica schists and gneisses; crystal size varies from <1 mm up to about 6 mm (average ~4 mm) and the deposits form lenses up to 30m thick stretching several

### Production and Uses of Graphite<sup>(2)</sup>

There is a world shortage of natural graphite which is particularly marked in North America and Europe. As a result, prices have risen steeply; they vary widely in the range \$500–1500 per tonne (1989) depending on crystalline quality: “amorphous” graphite is \$220–440 per tonne. The annual world production of 649 ktonnes was distributed as follows in 1988: China 200 kt, South Korea 108, the former Soviet Union 84, India 52, Mexico 42, Brazil 32, North Korea 25, Czechoslovakia 25, Others 81 kt.

The USA used 37 ktonnes of natural graphite in 1989, nearly all imported; in addition, over 300 ktonnes of graphite was manufactured. Natural graphite is used in refractories (27%), lubricants (17%), foundries (14%), brake linings (12%), pencils (5.3%), crucibles, retorts, stoppers, sleeves and nozzles (4.0%) etc.

Artificial graphite was first manufactured on a large scale by A. G. Acheson in 1896. In this process coke is heated with silica at ~2500°C for 25–35 h:



In the USA artificial graphite is now made on a scale exceeding 300 kilotonnes pa (1989), and is used mainly for electrodes, crucibles and vessels, and various unmachined shapes; specialist uses include motor brushes and contacts and refractories of various sorts.

Carbon (graphite) fibres are also being manufactured on an increasing scale: The global market (1990) is of the order of 6 million kg per annum and prices range from \$20–2000/kg depending on specifications (diameter, strength, stiffness, etc.). The two main production methods are the oxidative thermolysis of polyacrylonitrile fibres at 200–300°C under tension or the thermolysis of pitch at 370° followed by die-extrusion and stretching to give filaments which are then heated progressively in dry air to 2500°. Ultra-high-purity graphite is made on a substantial scale for use as a neutron moderator in nuclear reactors. Carbon whiskers grown from highly purified graphite are finding increasing use in high-strength composites; the whiskers are manufactured by striking a carbon arc at 3600°C under 90 atm Ar — the maximum length is ~50 mm and the average diameter 5 μm.

kilometres across country. Average carbon content is 25% but can rise as high as 60% (Malagasy). Beneficiation is by flotation followed by treatment with HF and HCl, and then by heating to 1500°C *in vacuo*. Microcrystalline graphite (sometimes referred to as “amorphous”) occurs in carbon-rich metamorphosed sediments and some deposits in Mexico contain up to 95% C. World production has remained fairly constant for the past few years and was 649 ktonnes in 1988 (see Panel above).

Diamonds are found in ancient volcanic pipes embedded in a relatively soft, dark coloured basic rock called “blue ground” or “kimberlite”, from the South African town of Kimberley where such pipes were first discovered in 1870. Diamonds

are also found in alluvial gravels and marine terraces to which they have been transported over geological ages by the weathering and erosion of pipes. The original mode of formation of the diamond crystals is still a subject of active investigation. The diamond content of a typical kimberlite pipe is extremely low, of the order of 1 part in 15 million, and the mineral must be isolated mechanically by crushing, sluicing and passing the material over greased belts to which the diamonds stick. This, in part, accounts for the very high price of gem-quality diamonds which is about 1 million times the price of flake graphite. The pattern of world production has changed dramatically over the past few decades as indicated in the Panel on p. 272.

Three other forms of carbon are manufactured on a vast scale and used extensively in industry: coke, carbon black, and activated carbon. The production and uses of these impure forms of carbon are briefly discussed in the Panel on p. 274.

In addition to its natural occurrence as the free element, carbon is widely distributed in the

<sup>2</sup> Kirk–Othmer *Encyclopedia of Chemical Technology*, 4th edn., Interscience, New York, 1992, Vol. 4: Carbon and artificial graphite, pp. 949–1015; Activated carbon, pp. 1015–37; Carbon black, pp. 1037–74; Diamond, natural and synthetic, pp. 1074–96; Natural graphite, pp. 1097–117; Carbon and graphite fibres, vol 5, pp. 1–19 (1993). See also H. O. PIERSON, *Handbook of Carbon, Graphite, Diamond and Fullerenes: Properties, Processing and Applications*, Noyes Publications, Park Ridge, N.J., 1993, 399 pp.

### Production and Uses of Diamond<sup>(2,2a)</sup>

Gemstone diamonds have been greatly prized in eastern countries for over 2000 y though their introduction and recognition in Europe is more recent. The only sources were from India and Borneo until they were also found in Brazil in 1729. In South Africa diamonds were discovered in alluvial deposits in 1867 and the first kimberlite pipe was identified in 1870 with dramatic consequences. Many other finds of economic importance were made in Africa during the first half of this century: most notably in Tanzania where large-scale production began in 1940 following the discovery of the enormous Williamson pipe — still the largest in the world and covering an area of 1.4 km<sup>2</sup>. During the 1950s 99% of the world output of diamonds was from Africa but then the USSR began to emerge as a major producer following the discovery of alluvial diamonds in Siberia in 1948 and the first kimberlite-type pipe at Yakutia later the same year. Within a decade more than 20 pipes had been located in the great basin of the Vilyui River 4000 km east of the Urals, and Siberia was established as a major producer of both gem-quality and industrial diamonds. However, year-round production in Siberian conditions posed severe developmental problems, and production is now supplemented by newer finds in the Urals near Sverdlovsk. Impressive finds of kimberlite pipes have also been made in North-western Australia since 1978 and this area is now one of the world's largest producers of industrial diamonds.

Diamond is the hardest and least perishable of all minerals, and these qualities, coupled with its brilliant sparkle, which derives from its transparency and high refractive index, make it the most prized of gemstones. By far the largest natural diamond ever found (25 January 1905) was the Cullinan; it weighed 3106 carats (621.2 g) and measured  $\sim 10 \times 6.5 \times 5 \text{ cm}^3$  (the size of a man's clenched fist). Other famous stones are in the range 100–800 carats though specimens larger than 50 carats are only rarely encountered. Most naturally occurring diamonds, however, are of industrial rather than gem-stone quality. They are used as single-point tools for engraving or cutting, and for surgical knives, bearings and wire dies, as well as for industrial abrasives for grinding and polishing. Other uses are as thermistors and radiation detectors, and as optical windows for lasers, etc.

Since the late 1950s the supply of natural diamonds has been progressively augmented by diamonds synthesized at high pressures and temperatures (p. 278) and this source now accounts for 90% of all industrial diamonds. The price for such diamond grit is relatively low, about \$5–25 per g, the higher prices being for the largest crystals (0.3–1 mm on edge). Total world production (1990) approached 100 tonnes (500 megacarats) and was worth about \$10<sup>9</sup>. In 1985, Sumitomo Electric (Japan) began commercial production of diamond crystals of up to 2 carats (as large as 8 mm in length) and de Beer's (South Africa) have made single crystals up to 17 mm long. Such diamonds, which are pale yellow due to nitrogen inclusions, are used as heat sinks in the electronics industry because of the very high thermal conductivity of diamond. The synthetic stones are machined and laser cut to about  $3 \times 3 \times 1 \text{ mm}^3$  and are commercially available for \$150 a piece. Synthetic industrial diamonds are manufactured in 16 countries, the major producers being in USA, Japan, China and Russia.

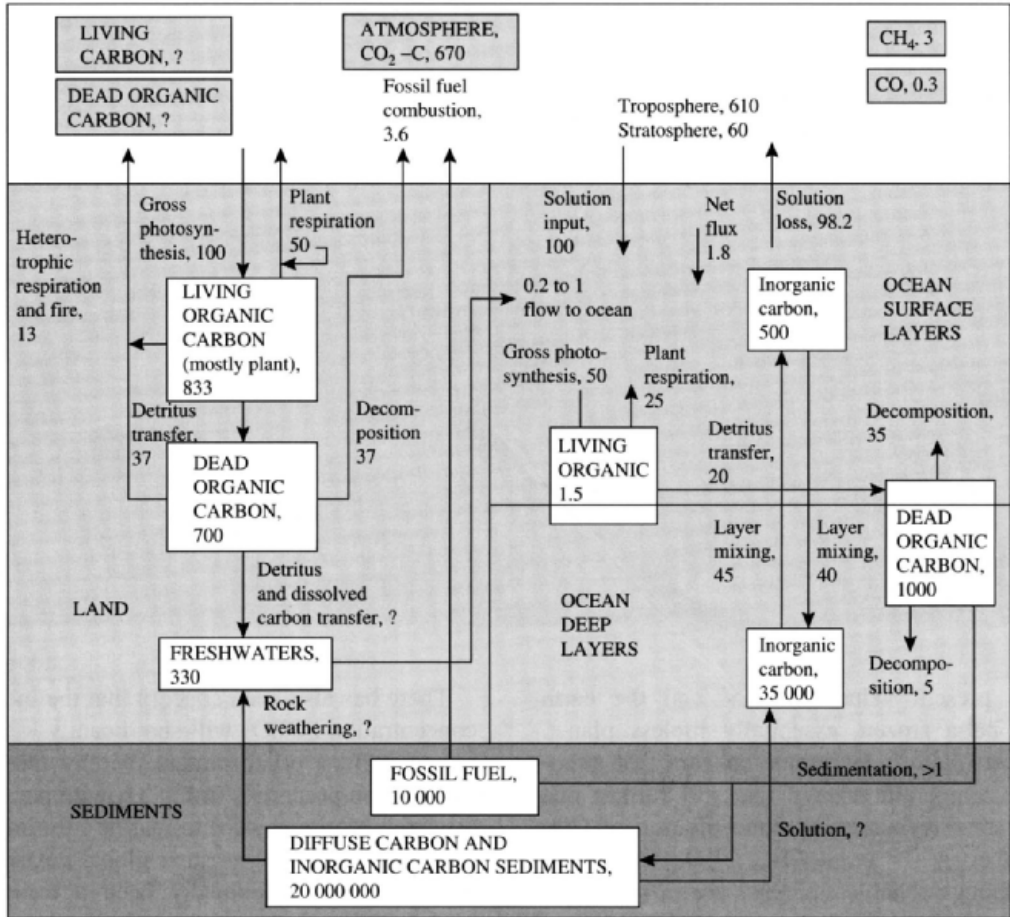
Exciting developments are also occurring in the emerging technology of large-area thin films of synthetic diamond. Such films are of interest as heat sinks for components in the electronics industry and, when bonded to inexpensive non-diamond surfaces, can also provide the unexcelled hardness, wear resistance and chemical inertness of diamond at lower cost than that of the bulk element. The films are made by low pressure (50 mbar) chemical vapour deposition of metastable diamond at 1000°C, the crucial feature of the method being the simultaneous presence of a plasma of atomic H to prevent the concurrent deposition of graphite from the decomposing organic vapours (see p. 278).

form of coal and petroleum, and as carbonates of the more electropositive<sup>†</sup> elements (e.g. Group 1, p. 88, Group 2, pp. 109, 122). The great bulk of carbon is immobilized in the form of coal, limestone, chalk, dolomite and other deposits, but there is also a dynamic equilibrium as a result of the numerous natural processes which constitute the so-called carbon cycle. The various

reservoirs of carbon and the flow between them are illustrated in Fig. 8.1 from which it is clear that there are two distinct cycles — one on land and one in the sea, dynamically inter-connected by the atmosphere. CO<sub>2</sub> in the atmosphere ( $\sim 6.7 \times 10^{11}$  tonnes) accounts for only 0.003% of carbon in the earth's crust ( $\sim 2 \times 10^{16}$  tonnes). It is in rapid circulation with the biosphere being removed by plant photosynthesis and added to by plant and animal respiration, and the decomposition of dead organic matter; it is also produced by the activities of man, notably the combustion of fossil fuels for energy and the calcination of limestone for cement. These last

<sup>2a</sup> R. M. HAZEN, *The New Alchemists: Breaking Through the Barriers of High Pressure*, Times Books, New York, 1994, 286 pp. P. W. MAY, *Endeavour* **19**, 101–6 (1995).

<sup>†</sup> Note that the *weight* of diamonds is usually quoted in carats (1 carat = 0.200 g); this unit is quite different from the carat used to describe the *quality* of gold (p. 1176).



**Figure 8.1** Diagrammatic model of the global carbon cycle. Questions marks indicate that no estimates are available. Figures are in units of  $10^9$  tonnes of contained carbon but estimates from various sources sometimes differ by factors of 3 or more. The diagram is based on one by B. Bolin<sup>(3)</sup> modified to include more recent data.<sup>(4)</sup>

two activities have increased dramatically in recent years and give some cause for concern. Interchange on a similar scale occurs between the atmosphere and ocean waters, and the total residence time of  $\text{CO}_2$  in the atmosphere is  $\sim 10\text{--}15$  y (as measured by  $^{14}\text{C}$  experiments).

An increase in the concentration of atmospheric  $\text{CO}_2$  has been thought by some to expose the planet to the dangers of a “greenhouse

effect” whereby the temperature is raised due to the trapping of the earth’s thermal radiation by infrared absorption in the  $\text{CO}_2$  molecules. In fact, the greenhouse gases, especially water vapour and  $\text{CO}_2$ , play a crucial role in regulating the temperature of the earth and its atmosphere. In the absence of these gases the average surface temperature would be  $-18^\circ\text{C}$  instead

<sup>3</sup>B. BOLIN, The carbon cycle, *Scientific American*, September 1970, reprinted in *Chemistry in the Environment*, pp. 53–61, W. H. Freeman, San Francisco, 1973.

<sup>4</sup>SCOPE Report 10 on Environmental Issues, Carbon, pp. 55–8, Wiley, New York, 1977. SCOPE is the Scientific Committee on Problems of the Environment; it reports to ICSU, the International Council of Scientific Unions.

## Production and Uses of Coke, Carbon Black and Activated Carbon<sup>(2)</sup>

The high-temperature carbonization of coal yields metallurgical coke, a poorly graphitized form of carbon; most of this (92%) is used in blast furnaces for steel manufacture (p. 1072). World production of coke is of the order of 400 million tonnes per annum and was dominated, as expected, by the large industrial nations. Carbon black (soot) is made by the incomplete combustion of liquid hydrocarbons or natural gas; the scale of operations is enormous, world production in 1992 being nearly 7 million tonnes. The particle size of carbon black is exceedingly small (0.02–0.30  $\mu\text{m}$ ) and its principal application (90%) is in the rubber industry where it is used to strengthen and reinforce the rubber in a way that is not completely understood. For example, each car tyre uses 3 kg carbon black and each truck tyre  $\sim 9$  kg. Its other main uses are as a pigment in plastics (4.4%) in printing inks (3.6%) and paints (0.7%).

Activated carbons, being highly specialized products, are produced on a correspondingly smaller scale. World production capacity in 1990 being some 400 kilotonnes (USA 146, Western Europe 108, Japan 72 kt). They are distinguished by their enormous surface area which is typically in the range 300–2000  $\text{m}^2 \text{g}^{-1}$ . Activated carbon can be made either by chemical or by gas activation. In chemical activation the carbonaceous material (sawdust, peat, etc.) is mixed or impregnated with materials which oxidize and dehydrate the organic substrate when heated to 500–900°, e.g. alkali metal hydroxides, carbonates or sulfates, alkaline earth metal chlorides, carbonates or sulfates,  $\text{ZnCl}_2$ ,  $\text{H}_2\text{SO}_4$  or  $\text{H}_3\text{PO}_4$ . In gas activation, the carbonaceous matter is heated with air at low temperature or with steam,  $\text{CO}_2$  or flue gas at high temperature (800–1000°).

Activated carbon is used extensively in the sugar industry as a decolorizing agent and this accounts for some 20% of the output; related applications are in the purification of chemicals and gases including air pollution (15%), and in water and waste water treatment (50%). Notable catalytic uses are the aerial oxidation in aqueous solutions of  $\text{Fe}^{\text{II}}$ ,  $[\text{Fe}^{\text{II}}(\text{CN})_6]^{4-}$ ,  $[\text{As}^{\text{III}}\text{O}_3]^{3-}$  and  $[\text{N}^{\text{III}}\text{O}_2]^-$ , the manufacture of  $\text{COCl}_2$  from  $\text{CO}$  and  $\text{Cl}_2$ , and the production of  $\text{SO}_2\text{Cl}_2$  from  $\text{SO}_2$  and  $\text{Cl}_2$ . The cost of activated carbon (USA, 1990) was \$0.70–5.50 per kg depending on the grade.

of the present value of +15° and the earth would be a frozen, essentially lifeless planet. However, there is legitimate concern that atmospheric temperatures may rise still further due to the steadily increasing concentration of  $\text{CO}_2$  and other gases (e.g.  $\text{CH}_4$ ,  $\text{N}_2\text{O}$ , CFCs and  $\text{O}_3$ ) although reliable estimates are extraordinarily difficult to obtain and depend sensitively on the computer modelling of the many interacting effects.<sup>(5)</sup> Perhaps the most reliable estimate is that there will be a temperature rise from the greenhouse effect of  $1.5 \pm 1.0^\circ\text{C}$  and a resulting average rise in sea level of  $20 \pm 14$  cm by the year AD 2030, though even this assumes that other unrelated effects of potentially similar magnitude will not occur. The best estimates of all the various counterbalancing effects leads to the conclusion that the change in sea level will probably not exceed  $\pm 10$  cm during the next century.

<sup>5</sup> THE ROYAL SOCIETY (LONDON), *The Greenhouse Effect: the scientific basis for policy*, Submission to the House of Lords Select Committee, 40 pp. (1989). See also *Global Climate Change*, Information Pamphlet (12 pp.) issued by the American Chemical Society (1990); B. HILEMAN, *Global Warming*, *Chem. & Eng. News*, April 27, 7–19 (1992); and references cited therein.

There has also been concern that the increased concentration of  $\text{CO}_2$  will significantly lower the pH of surface ocean waters thereby modifying the solution properties of  $\text{CaCO}_3$  with potentially disastrous consequences to marine life. Informed opinion now discounts such global catastrophes but there has undoubtedly been a measurable perturbation of the carbon cycle in the last few decades, and the prudent course is to conserve resources, minimize wasteful practices and improve efficiency, whilst simultaneously collecting reliable data on the magnitude of the various carbon-containing reservoirs and the rates of transfer between them.<sup>(6)</sup>

### 8.2.2 Allotropic forms

Carbon can exist in at least 6 crystalline forms in addition to the many newly prepared fullerenes described in Section 8.2.4:  $\alpha$ - and  $\beta$ -graphite, diamond, Lonsdaleite (hexagonal

<sup>6</sup> B. BOLIN, B. R. DÖÖS, J. JÄGER and R. A. WARRICK (eds.), *SCOPE 29, The Greenhouse Effect, Climatic Change and Ecosystems*, 2nd edn., 1989, 574 pp.

diamond), chaoite, and carbon(VI). Of these,  $\alpha$ - (or hexagonal) graphite is thermodynamically the most stable form at normal temperatures and pressures. The various modifications differ either in the coordination environment of the carbon atoms or in the sequence of stacking of layers in the crystal. These differences have a profound effect on both the physical and the chemical properties of the element.

Graphite is composed of planar hexagonal nets of carbon atoms as shown in Fig. 8.2. In normal  $\alpha$ - (or hexagonal) graphite the layers are arranged in the sequence  $\dots ABAB\dots$  with carbon atoms in alternate layers vertically above each other, whereas in  $\beta$ - (or rhombohedral) graphite the stacking sequence is  $\dots ABCABC\dots$ . In both forms the C–C distance within the layer is 141.5 pm and the interlayer spacing is much greater, 335.4 pm. The two forms are interconvertible by grinding ( $\alpha \rightarrow \beta$ ) or heating above 1025°C ( $\beta \rightarrow \alpha$ ), and partial conversion

leads to an increase in the average spacing between layers; this reaches a maximum of 344 pm for turbostratic graphite in which the stacking sequence of the parallel layers is completely random. The enthalpy difference between  $\alpha$ - and  $\beta$ -graphite is only  $0.59 \pm 0.17 \text{ kJ mol}^{-1}$ .

In diamond, each C atom is tetrahedrally surrounded by 4 equidistant neighbours at 154.45 pm, and the tetrahedra are arranged to give a cubic unit cell with  $a_0$  356.68 pm as in Fig. 8.3. Note that, although the diamond structure itself is not close-packed, it is built up of 2 interpenetrating fcc lattices which are off-set along the body diagonal of the unit cell by one-quarter of its length. Nearly all naturally occurring diamonds ( $\sim 98\%$ ) are of this type but contain, in addition, a small amount of nitrogen atoms (0.05–0.25%) in platelets of approximate composition  $\text{C}_3\text{N}$  (type Ia) or, very occasionally ( $\sim 1\%$ ), dispersed throughout the

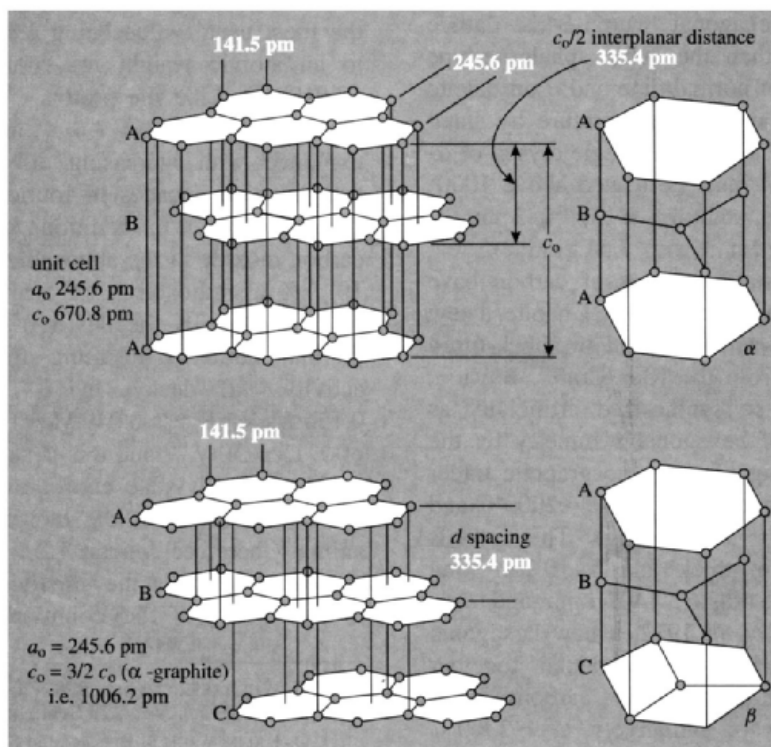
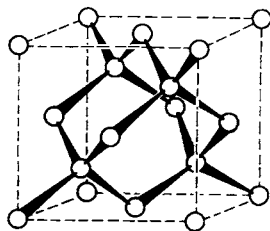


Figure 8.2 Structure of the  $\alpha$  (hexagonal) and  $\beta$  (rhombohedral) forms of graphite.



**Figure 8.3** Structure of diamond showing the tetrahedral coordination of C; the dashed lines indicate the cubic unit cell containing 8 C atoms.

crystal (type Ib). A small minority of natural diamonds contain no significant amount of N (type IIa) and a very small percentage of these (including the highly valued blue diamonds, type IIb), contain Al. The exceedingly rare hexagonal modification of diamond, Lonsdaleite, was first found in the Canyon Diablo Meteorite, Arizona, in 1967: each C atom is tetrahedrally coordinated but the tetrahedra are stacked so as to give a hexagonal wurtzite-like lattice (p. 1210) rather than the cubic sphalerite-type lattice (p. 1210) of normal diamond. Lonsdaleite can be prepared at room temperature by static pressure along the  $c$ -axis of a single crystal of  $\alpha$ -graphite, though it must be heated above  $1000^\circ$  under pressure to stabilize it ( $a_o$  252 pm,  $c_o$  412 pm,  $d_{\text{obs}}$   $3.3 \text{ g cm}^{-3}$ ,  $d_{\text{calc}}$   $3.51 \text{ g cm}^{-3}$ ).

Two other crystalline forms of carbon have been discovered in the recent past. Chaoite, a new white allotrope, was first found in shock-fused graphitic gneiss from the Ries Crater, Bavaria, in 1968; it can be synthesized artificially as white dendrites of hexagonal symmetry by the sublimation etching of pyrolytic graphite under free vaporization conditions above  $\sim 2000^\circ\text{C}$  and at low pressure ( $\sim 10^{-4}$  mmHg). The crystals were only  $0.5 \mu\text{m}$  thick and  $5\text{--}10 \mu\text{m}$  long and had  $a_o$  894.5 pm,  $c_o$  1407.1 pm and  $d_{\text{calc}}$   $3.43 \text{ g cm}^{-3}$ . Finally, in 1972, a new hexagonal allotrope, carbon(VI), was obtained together with chaoite when graphitic carbons were heated resistively or radiatively at  $\sim 2300^\circ\text{C}$  under any pressure of argon in the range  $10^{-4}$  mmHg to 1 atm; laser heating was even

more effective ( $a_o$  533 pm,  $c_o$  1224 pm,  $d > 2.9 \text{ g cm}^{-3}$ ). The detailed crystal structures of chaoite and carbon(VI) have not yet been determined but they appear to be based on a carbyne-type motif  $\text{—C}\equiv\text{C—C}\equiv\text{C}$ ; <sup>(7)</sup> both are much more resistant to oxidation and reduction than graphite is and their properties are closer to those of diamond. Indeed, it now seems possible that there is a sequence of at least 6 stable carbyne allotropes in the region between stable graphite and the mp of carbon.

The structural differences between graphite and diamond are reflected in their differing physical and chemical properties, as outlined in the following sections.

### 8.2.3 Atomic and physical properties

Carbon occurs predominantly as the isotope  $^{12}\text{C}$  but there also is a small amount of  $^{13}\text{C}$ ; the concentration of  $^{13}\text{C}$  varies slightly from 0.99 to 1.15% depending on the source of the element, the most usual value being 1.10% which leads to an atomic weight for “normal” carbon of 12.0107(8). Like the proton,  $^{13}\text{C}$  has a nuclear spin quantum number  $I = \frac{1}{2}$ , and this has been exploited with increasing effectiveness during the past two decades in fourier transform nmr spectroscopy. <sup>(8)</sup> In addition to  $^{12}\text{C}$  and  $^{13}\text{C}$ , carbon dioxide in the atmosphere contains  $1.2 \times 10^{-10}\%$  of radioactive  $^{14}\text{C}$  which is continually being formed by the  $^{14}\text{N}(\text{n,p})^{14}\text{C}$  reaction with thermal neutrons resulting from cosmic ray activity.  $^{14}\text{C}$  decays by  $\beta^-$  emission ( $E_{\text{max}}$  0.156 MeV,  $E_{\text{mean}}$  0.049 MeV) with a half-life of  $5715 \pm 30 \text{ y}$ , <sup>(9)</sup> and this is sufficiently long to enable a steady-state equilibrium concentration to be established in the biosphere. Plants and animals therefore contain  $1.2 \times 10^{-10}\%$  of their carbon as  $^{14}\text{C}$  whilst they are living, and this leads to a  $\beta^-$ -activity of 15.3 counts per min per gram

<sup>7</sup> A. G. WHITTAKER, *Science* **200**, 763–4 (1978). See also Anon, *Chem. & Eng. News*, 29 Sept., p. 12 (1980).

<sup>8</sup> H.-O. KALINOWSKI, S. BERGER and S. BRAUN, *Carbon-13 NMR Spectroscopy*, Wiley, Chichester, 1988.

<sup>9</sup> N.E. HOLDEN, *Pure Appl. Chem.* **62**, 941–58 (1990).



of contained C. However, after death the dynamic interchange with the environment ceases and the  $^{14}\text{C}$  concentration decreases exponentially. This is the basis of W. F. Libby's elegant radio-carbon dating technique for which he was awarded the Nobel Prize for Chemistry in 1960. It is particularly valuable for archeological dating.<sup>(10)</sup> (A modern variant is to count the number of  $^{14}\text{C}$  atoms directly in a mass spectrometer.) The practical limit is about 50 000 y since by this time the  $^{14}\text{C}$  activity has fallen to about 0.2% of its original valuable and becomes submerged in the background counts.  $^{14}\text{C}$  is also extremely valuable as a radioactive tracer for mechanistic studies using labelled compounds, and many such compounds, particularly organic ones, are commercially available (p. 310).

Carbon is the sixth element in the periodic table and its ground-state electronic configuration is  $[\text{He}]2s^22p^2$ . The first 4 ionization energies of C are 1086.5, 2352.6, 4620.5 and 6222.7  $\text{kJ mol}^{-1}$ , all much higher than those for the other Group 14 elements Si, Ge, Sn and Pb (p. 372). Excitation energies from the ground-state to various low-lying electron configurations of importance in valence theory are also well established:

Configuration	$2s^22p^2$	$2s^22p^2$	$2s^22p^2$
Term symbol	$^3P$	$^1D$	$^1S$
Energy/ $\text{kJ mol}^{-1}$	0.000	121.5	258.2
Configuration	$2s^12p^3$	$2s^12p^3$	
Term symbol	$^5S^o$	$^5S_{\text{valence state}}$	
Energy/ $\text{kJ mol}^{-1}$	402.3	$\sim 632$	

Of these, all are experimentally observable except the  $^5S_{\text{valence state}}$  level which is a calculated value for a carbon atom with 4 unpaired and uncorrelated electron spins; this is a hypothetical state, not amenable to experimental observation, but is helpful in some discussions of bond energies and covalent bonding theory.

The electronegativity of C is 2.5, which is fairly close to the values for other members of the

group (1.8–1.9) and for several other elements: B, As (2.0); H, P (2.1); Se (2.4); S, I (2.5); many of the second- and third-row transition metals also have electronegativities in the range 1.9–2.4.

The “single-bond covalent radius” of C can be taken as half the interatomic distance in diamond, i.e.  $r(\text{C}) = 77.2 \text{ pm}$ . The corresponding values for “doubly-bonded” and “triply-bonded” carbon atoms are usually taken to be 66.7 and 60.3 pm respectively though variations occur, depending on details of the bonding and the nature of the attached atom (see also p. 292). Despite these smaller perturbations the underlying trend is clear: the covalent radius of the carbon atom becomes smaller the lower the coordination number and the higher the formal bond order.

Some properties of  $\alpha$ -graphite and diamond are compared in Table 8.1. As expected from its structure, graphite is less dense than diamond and many of its properties are markedly anisotropic. It shows ready cleavage parallel to the basal plane, and this accounts for its flaky appearance, softness, and use as a lubricant although this latter property is due not so much to weak interplanar forces on an atomic scale as to the presence of adsorbed gases, since the coefficient of friction of graphite increases 5-fold at high altitudes and by a factor of 8 in a vacuum. By contrast, diamond can be cleaved in many directions, thus enabling many facets to be cut in gem-stones, but it is extremely hard and involatile because of the strong C–C bonding throughout the crystal. Interestingly, diamond has the highest thermal conductivity of any known substance (more than 5 times that of Cu) and for this reason the points of diamond cutting tools do not become overheated. Diamond also has one of the lowest known coefficients of thermal expansion:  $1.06 \times 10^{-6}$  at room temperature.

The optical and electrical properties of the two forms of carbon likewise reflect their differing structures. Graphite is a black, highly reflecting semi-metal with a resistivity  $\rho \sim 10^{-4} \text{ ohm cm}$  within the basal plane though this increases by a factor of  $\sim 5000$  along the  $c$ -axis. Diamond, on the other hand, is transparent and has a high refractive index; there is a band energy gap of

<sup>10</sup> J. M. MICHELS, *Dating Methods in Archeology*, Seminar Press, New York, 1973, 230 pp., S. FLEMING, *Dating in Archeology: A Guide to Scientific Techniques*, Dent, London, 1976, 272 pp.

**Table 8.1** Some properties of  $\alpha$ -graphite and diamond

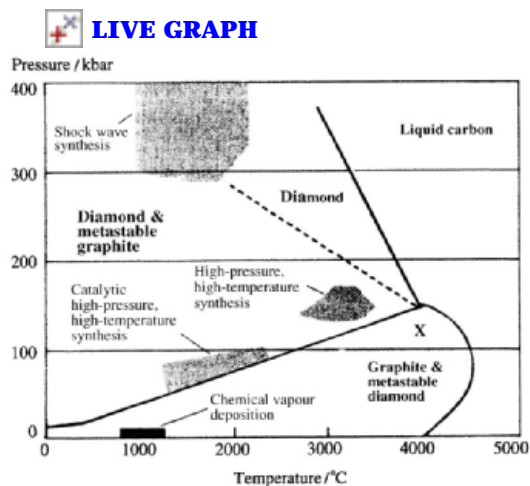
Property	$\alpha$ -Graphite	Diamond
Density/g cm <sup>-3</sup>	2.266 (ideal) varies from 2.23 (petroleum coke) to 1.48 (activated C)	3.514
Hardness/Mohs	<1	10
MP/K	4100 $\pm$ 100 (at 9 kbar)	4100 $\pm$ 200 (at 125 kbar)
$\Delta H_{\text{subl}}/\text{kJ mol}^{-1}$	715 <sup>(a)</sup>	$\sim$ 710 <sup>(a)</sup>
Refractive index, $n$ (at 546 nm)	2.15 (basal) 1.81 ( $c$ -axis)	2.41
Band gap $E_g/\text{kJ mol}^{-1}$	—	$\sim$ 580
$\rho/\text{ohm cm}$	(0.4–5.0) $\times 10^{-4}$ (basal) 0.2–1.0 ( $c$ -axis)	10 <sup>14</sup> –10 <sup>16</sup>
$\Delta H_{\text{combustion}}/\text{kJ mol}^{-1}$	393.51	395.41
$\Delta H_f^\circ/\text{kJ mol}^{-1}$	0.00 (standard state)	1.90

<sup>(a)</sup>Sublimation to monatomic C(g).

$\sim 580 \text{ kJ mol}^{-1}$  so that diamond has a negligible electrical conductivity, the specific resistivity being of the order  $10^{14}$ – $10^{16}$  ohm cm. (For other properties and industrial applications of diamond, see ref. 11.)

As may be seen from the heats of combustion,  $\alpha$ -graphite is more stable than diamond at room temperature, the heat of transformation being about  $1.9 \text{ kJ mol}^{-1}$ . However, as the molar volume of diamond ( $3.418 \text{ cm}^3$ ) is much smaller than that of graphite ( $5.301 \text{ cm}^3$ ), it follows that diamond can be made from graphite by application of a suitably high pressure, provided that the temperature is also sufficiently high to permit movement of the atoms. Such transformations were first successfully achieved in 1953–5, using pressures up to 100 kbar and temperatures in the range 1200–2800 K;<sup>(2a)</sup> the presence of molten-metal catalysts such as Cr, Fe, or Ni was also found to be necessary, suggesting that the transformation may proceed via the formation of unstable metal carbide intermediates. Very recently red phosphorus has also been shown to catalyse the conversion of graphite to diamond at 77 kbar and 1800°C.<sup>(12)</sup> The use of kinetically controlled non-equilibrium processes to deposit thin films of crystalline

diamond has already been mentioned (p. 272). The relationship between the conditions for these various processes is summarized in Fig. 8.4 which shows the phase diagram of carbon near its triple point.<sup>(13)</sup> This schematic representation does not explicitly include the several carbyne-like carbon phases<sup>(7)</sup> which have been identified at very low pressures ( $10^{-4}$ – $10^{-8}$  kbar) in the region marked X.

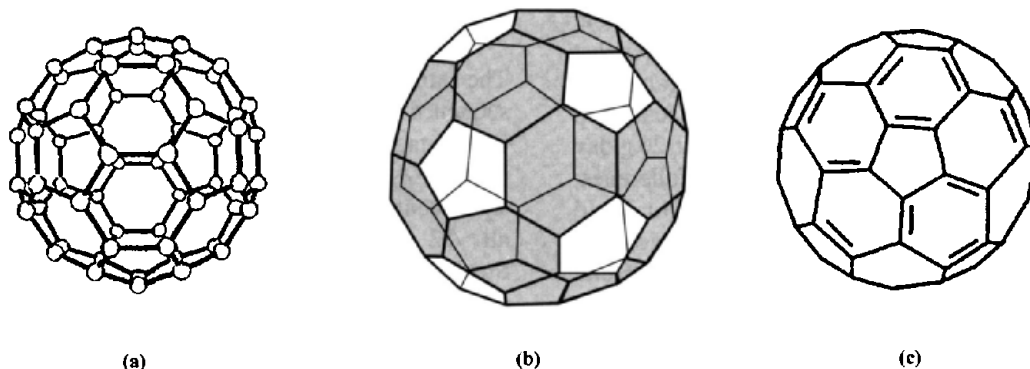


**Figure 8.4** Phase diagram of carbon showing regions of importance for the production of synthetic diamond.<sup>(13)</sup>

<sup>11</sup> J. E. FIELD (ed.), *The Properties of Diamond*, Academic Press, London, 1979, 660 pp.

<sup>12</sup> M. AKAISHI, H. KANDA and S. YAMAOKA, *Science* **259**, 1592–3 (1993).

<sup>13</sup> P. K. BACHMANN and R. MESSLER, *Chem. & Eng. News*, May 15, 24–39 (1989).



**Figure 8.5** Three representations of the structure of  $C_{60}$ . (a) normal “ball-and-stick” model; (b) the polyhedron derived by truncating the 12 vertices of an icosahedron to form 12 symmetrically separated pentagonal faces; (c) a conventional bonding model.

### 8.2.4 Fullerenes

One of the most exciting and challenging developments in recent chemistry has been the synthesis and characterization of many new, soluble, *molecular* modifications of carbon. As a result, the number of identified allotropes of this element has increased enormously and their intriguing chemistry is gradually being elucidated. The new allotropes form an extensive series of polyhedral cluster molecules,  $C_n$  ( $n$  even), comprising fused pentagonal and hexagonal rings of C atoms. The first member to be characterized was  $C_{60}$  which features 12 pentagons separated by 20 fused hexagons as shown in Fig. 8.5. It has full icosahedral symmetry (p. 141) and was given the name buckminsterfullerene in honour of the architect R. Buckminster Fuller whose buildings popularized the geodesic dome, which uses the same tectonic principle. Other fullerenes which have been isolated and characterized include  $C_{70}$ ,  $C_{76}$  (chiral),  $C_{78}$  (3 isomers),  $C_{84}$  (3 isomers),  $C_{90}$  and  $C_{94}$ , but there is mass spectrometric evidence for all even  $C_n$  from  $C_{30}$  to  $C_{>600}$ , (m.wt. 7206.6).

The fullerene story began in September 1985 when a group lead by H. W. Kroto (Sussex, UK) and R. E. Smalley (Rice, Texas) laser-blasted graphite at  $T > 10^4$  °C and showed mass spectrometrically that the product contained a series of molecules with even numbers of atoms

from  $C_{44}$  to  $C_{90}$ .<sup>(14)</sup> Concentrations of the individual molecules varied with conditions but the peak for  $C_{60}$  was always by far the strongest, followed by  $C_{70}$ . This experiment showed the existence of new molecular forms of carbon but was not a bulk preparation. However, in a brilliant flash of insight it was conjectured that the stability of  $C_{60}$  might result from the football-like “spherical” structure of a truncated icosahedron, the most symmetrical of all possible structures in 3-dimensional space (Nobel Prize, 1996, see p. 270).

Three years later two astrophysicists, W. Krätschmer (Heidelberg, Germany) and D. R. Huffman (Tucson, Arizona), remembered an unusual and unexpected UV spectrum they had obtained in 1983 from soot obtained by striking an arc between graphite electrodes at about 3500°C under a low pressure of helium gas. They re-examined the material mass-spectrometrically and found it contained high concentrations of  $C_{60}$  and  $C_{70}$  which were soluble in aromatic hydrocarbon solvents such as benzene and toluene.<sup>(15)</sup> Here was a stunningly simple preparation of fullerenes in bulk, although separation of individual members proved to

<sup>14</sup> H. W. KROTO, J. R. HEATH, S. C. O'BRIEN and R. E. SMALLEY, *Nature* **318**, 162–4 (1985).

<sup>15</sup> W. KRÄTSCHMER, L. D. LAMB, K. FOSTIROPOULOS and D. R. HUFFMAN, *Nature* **347**, 354–8 (1990).

be more difficult. Pure  $C_{60}$  and  $C_{70}$  were obtained for the first time on 22 August 1990 by chromatographic separation (alumina, hexane).<sup>(16)</sup> The process can easily be scaled up using multi-rod apparatus to give about 20 g/day of soot containing up to 10% of fullerenes; this can be extracted with toluene to yield about 15 g/week of mixed fullerenes which can be further separated if required. Commercial availability has also assisted progress, typical prices (1994) being £150/g for  $C_{60}$  (99.9%) and £2000/g for  $C_{70}$  (98%).

Other routes to  $C_{60}$  and  $C_{70}$  are being developed, e.g. (i) heating naphthalene vapour ( $C_{10}H_8$ ) in argon at about 1000°C followed by extraction with  $CS_2$ ; (ii) burning soot in a benzene/oxygen flame at about 1500°C with argon as a diluent.  $C_{60}$  and  $C_{70}$  have also been detected in several naturally occurring minerals, e.g. in carbon-rich semi-anthracite deposits from the Yarrabee mine in Queensland, Australia;<sup>(17a)</sup> in shungite, a highly metamorphosed meta-anthracite from Shunga, Karelia, Russia;<sup>(17b)</sup> and in a Colorado, USA fulgurite (a glassy mineral which can be formed when lightning strikes the ground).<sup>(17c)</sup> Most recently, significant finds of naturally occurring fullerenes have been made in Sudbury (Canada) and New Zealand.<sup>(17d)</sup>

The purified fullerenes have very attractive colours. Thin films of  $C_{60}$  are mustard-coloured (dark brown in bulk) and solutions in aromatic hydrocarbons are a beautiful magenta. Thin films of  $C_{70}$  are reddish brown (greyish black in bulk) and solutions are port-wine red.  $C_{76}$ ,  $C_{78}$  and  $C_{84}$  are yellow.<sup>(16)</sup>

<sup>16</sup> R. TAYLOR, J. P. HARE, A. K. ABDUL-SADA and H. W. KROTO, *J. Chem. Soc., Chem. Commun.*, 1423–5 (1990).

R. TAYLOR (and 12 others), *Pure Appl. Chem.* **65**, 135–42 (1993).

<sup>17a</sup> M. A. WILSON, L. S. K. PANG and A. M. VASSALLO, *Nature* **355**, 117–8 (1992).

<sup>17b</sup> P. R. BUSEK, S. J. TSIPURSKI and R. HETTICH, *Science* **257**, 215–17 (1992).

<sup>17c</sup> T. K. DALY, P. R. BUSECK, P. W. WILLIAMS and C. F. LEWIS, *Science* **259**, 1599–601 (1993).

<sup>17d</sup> R. DAGANI, *Chem. & Eng. News*, Aug. 1, 1994, pp. 4,5. See also L. BECKER, R. J. POREDA and J. L. BADA, *Science* **272**, 249–52 (1996).

## Structure of the fullerenes

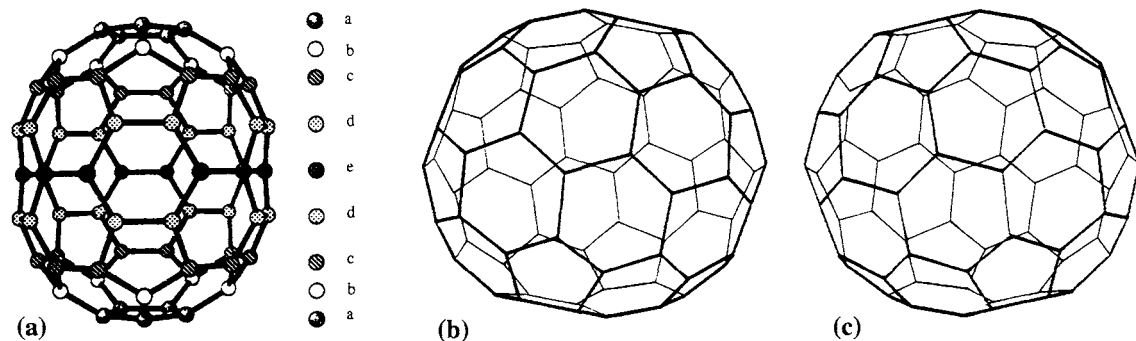
The structural motif of the fullerenes is a sequence of polyhedral clusters,  $C_n$ , each with 12 pentagonal faces and  $(\frac{1}{2}n - 10)$  hexagonal faces.  $C_{60}$  itself has 20 hexagonal faces and, significantly, is the first member for which all 12 pentagonal faces are non-adjacent. Smaller homologues have increasing numbers of contiguous pentagonal faces; e.g.  $C_{32}$  is expected to have only 6 hexagonal faces. As can be seen from Fig. 8.5, all C atoms in  $C_{60}$  are structurally identical and, consistent with this, only one signal is observed in the  $^{13}C$  nmr spectrum (at 142.68 ppm). However, there are two geometrically distinct types of C–C bond: those at an edge shared between two fused hexagons, and those at an edge between a hexagon and a pentagon.

By contrast,  $C_{70}$  has 25 hexagonal faces and  $D_{5h}$  symmetry (Fig. 8.6a) with 5 types of C atom (a, b, c, d, e) and 8 types of C–C bond. Five  $^{13}C$  nmr signals are therefore expected, with intensities in the ratio 10:10:20:20:10, and these are observed in the range 150.77–130.28 ppm.<sup>(16)</sup> Again, a  $^{13}C$  nmr study of chromatographically isolated  $C_{76}$  showed it to have 28 hexagonal faces and a fascinating chiral structure of  $D_2$  symmetry, consisting of a spiralling double helical arrangement of edge-sharing pentagons and hexagons (Fig. 8.6b and c) uniquely consistent with the observed 19  $^{13}C$  nmr signals in the range 150.03–129.56 ppm, and each of equal intensity ( $19 \times 4 = 76$ ).<sup>(18)</sup>

The total potential number of geometric isomers increases enormously with increase in cluster size, being, for example, three for  $C_{30}$ , 40 for  $C_{40}$ , 271 for  $C_{50}$  and no fewer than 1812 for  $C_{60}$ .<sup>(19)</sup> However, the number becomes much more manageable if one considers only those isomers that have no contiguous pentagons. The theoretical justifications for this

<sup>18</sup> R. EITL, I. CHAO, F. DIEDERICH and R. L. WHETTEN, *Nature* **353**, 149–53 (1991). D. E. MANOLOPOULOS, *J. Chem. Soc., Faraday Trans.*, **87**, 2861–2 (1991).

<sup>19</sup> D. E. MANOLOPOULOS and P. W. FOWLER, *J. Chem. Phys.* **96**, 7603–14 (1991).



**Figure 8.6** (a) The  $D_{5h}$  structure of  $C_{70}$  with the 5-fold rotation axis vertical; the five sets of geometrically distinct C atoms are labelled a-e (see text). (b), (c) Line drawings of the two enantiomers of  $C_{76}$  viewed along the short  $C_2$  rotation axis and illustrating the chiral  $D_2$  symmetry of the molecule.

restriction would be (a) that isomers with fused pentagons are expected to have greater  $\sigma$ -bonding strain energy and (b) that, since two fused pentagons have an 8-cycle around their periphery, there would be a further Hückel antiaromatic destabilizing effect on the overall  $\pi$  electron system. In fact, in the range  $C_{20}$ – $C_{70}$  this restriction of isolated pentagons eliminates all structures except the observed  $C_{60}(I_h)$  and  $C_{70}(D_{5h})$ . From mass-spectrometric evidence other oligomers clearly exist, though not yet in isolable concentrations. Above  $C_{70}$  the number of distinct geometric isomers ( $i$ ) with isolated pentagons increases rather rapidly with  $n$  as indicated below:<sup>(19)</sup>

$n$	72	74	76	78	80	82	84	86
$i$	1	1	2	5	7	9	24	19
$n$	88	90	92	94	96	98	100	
$i$	35	46	86	134	187	259	450	

Numerous other fullerenes have been isolated by the same techniques and their structures elucidated by <sup>13</sup>C nmr spectroscopy, e.g.  $C_{76}$  (see above);  $C_{78}$  [3 isomers:  $C_{2v}\{18(4C) + 3(2C)\}$  nmr lines],  $D_3\{13(6C)\}$  and  $C_{2v}\{17(4C) + 5(2C)\}$ ];  $C_{82}$  [3 isomers:  $C_2\{41(2C)\}$ ,  $C_{2v}\{17(4C) + 7(2C)\}$  and  $C_{3v}\{12(6C) + 3(3C) + 1(1C)\}$ ]; and  $C_{84}$  [2 isomers:  $D_2\{21(4C)\}$  and  $D_{2d}\{10(8C)$

+ 1(4C)]].<sup>(20)</sup> A copiously illustrated atlas of fullerenes elaborating and enumerating the numbers and structures of all possible fullerenes and fullerene isomers  $C_n$  as a function of  $n$  up to high  $n$  has recently been published.<sup>(20a)</sup>

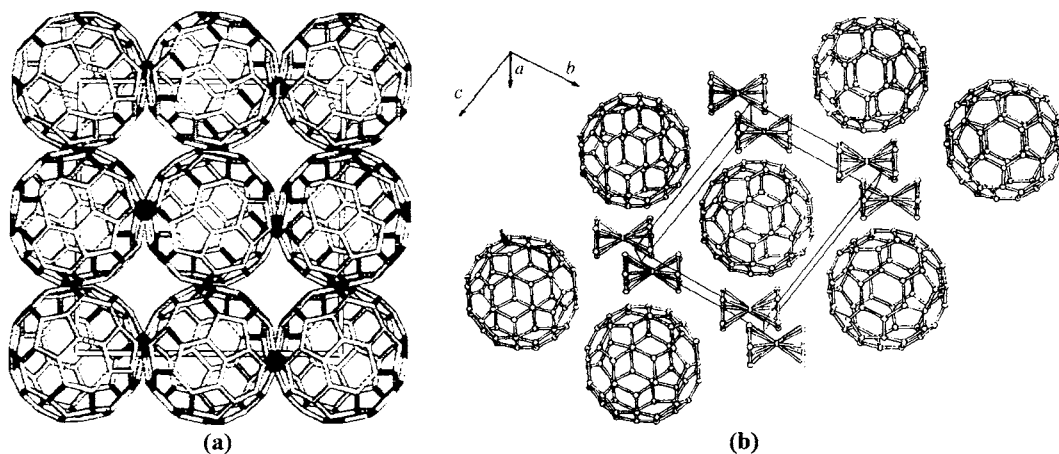
Except for  $C_{60}$ ,<sup>†</sup> lack of sufficient quantities of pure material has prevented more detailed structural characterization of the fullerenes by X-ray diffraction analysis, and even for  $C_{60}$  problems of orientational disorder of the quasi-spherical molecules in the lattice have exacerbated the situation. At room temperature  $C_{60}$  crystallizes in a face-centred cubic lattice ( $Fm\bar{3}$ ) but below 249 K the molecules become orientationally ordered and a simple cubic lattice ( $Pa\bar{3}$ ) results. A neutron diffraction analysis of the ordered phase at 5 K led to the structure shown in Fig. 8.7a;<sup>(21)</sup> this reveals that the ordering results from the fact that

<sup>20</sup> F. DIEDERICH, R. L. WHETTEN, C. THILGEN, R. EITL, I. CHAO and M. M. ALVAREZ, *Science* **254**, 1768–70 (1991). R. TAYLOR, G. J. LANGLEY, T. J. S. DENNIS, H. W. KROTO and D. R. M. WALTON, *J. Chem. Soc., Chem. Commun.*, 1043–6 (1992). K. KIKUCHI, Y. ACHIBA (and eight others) *Nature* **357**, 142–5 (1992).

<sup>20a</sup> P. W. FOWLER and D. E. MANOLOPOULOS, *An Atlas of Fullerenes*, Clarendon Press, Oxford, 1995, 392 pp.

<sup>†</sup> Gram amounts of purified  $C_{70}$  can now also be obtained by column chromatography (see *J. Am. Chem. Soc.* **116**, 6939 (1994)) and are available commercially.

<sup>21</sup> W. I. F. DAVID, R. M. IBERSON, J. C. MATHEWMAN, K. PRASSIDES, T. J. S. DENNIS, J. P. HARE, H. W. KROTO, R. TAYLOR and D. R. M. WALTON, *Nature* **353**, 147–9 (1992).



**Figure 8.7** (a) The low-temperature, ordered, simple cubic arrangement of  $C_{60}$  molecules as revealed by neutron diffraction at 5 K; above 249 K the molecules become orientationally disordered and the lattice becomes fcc. (b) The packing arrangement for  $[C_{60}(\text{ferrocene})_2]$  in the  $bc$  plane.

the electron-rich short bonds *between* pentagons ( $139.1 \pm 1.8$  pm) are positioned directly above the electron-poor pentagon face-centres of adjacent  $C_{60}$  units. The bonds *within* a given pentagon are somewhat longer ( $145.5 \pm 1.2$  pm).

The structures of the black crystalline benzene solvate  $C_{60} \cdot 4C_6H_6$ ,<sup>(22)</sup> the black charge-transfer complex with bis(ethylenedithio)tetrathiafulvene,  $[C_{60}(\text{BEDT-TTF})_2]$ ,<sup>(23)</sup> and the black ferrocene adduct  $[C_{60}\{\text{Fe}(\text{Cp})_2\}_2]$  (Fig. 8.7b)<sup>(24)</sup> have also been solved and all feature the packing of  $C_{60}$  clusters.

### Other molecular allotropes of carbon

Quite apart from the fullerene cluster molecules, numerous other molecular allotropes of carbon,  $C_n$ , have been discovered in the gases formed by the laser vaporization/supersonic expansion of graphite. The products are detected by mass

spectrometry after separation into identifiable series by gas-ion chromatography.<sup>(25)</sup> The technique suggests that linear oligomers exist from  $n = 3-10$  and an overlapping series of monocyclic planar ring isomers from  $n = 7-36$ . Planar bicyclic rings appear for  $n = 21-44$  and yet other series of condensed rings occur in the ranges  $n = 37-54$  and  $55-61$ . Three-dimensional fused ring clusters form a series with  $n = 28-35$ , and the fullerenes from  $C_{30}-C_{70}$  were seen as a quite distinct series. For each value of  $n$  from 29-41 there are at least three isomers: e.g.  $C_{32}^+$  comprises 23% monocyclic ring, 71% bicyclic ring, 2.4% open 3D cluster and 3.2% fullerene. The structural assignments are tentative.

### Chemistry of the fullerenes

The tremendous burst of excitement which attended the initial isolation in 1990 of weighable amounts of separated fullerenes has been followed by an unparalleled and sustained surge of activity as chemists throughout the world rushed to investigate the chemical reactivity of these novel molecular forms of carbon.

<sup>22</sup> M. F. MEIDINE, P. B. HITCHCOCK, H. W. KROTO, R. TAYLOR and D. R. M. WALTON, *J. Chem. Soc., Chem. Commun.*, 1534-7 (1992).

<sup>23</sup> A. IZUOKA, T. TACHIKAWA, T. SUGAWARA, Y. SUZUKI, M. KONO, Y. SAITO and H. SINOHARA, *J. Chem. Soc., Chem. Commun.*, 1472-3 (1992).

<sup>24</sup> J. D. CRANE, P. B. HITCHCOCK, H. W. KROTO, R. TAYLOR and D. R. M. WALTON, *J. Chem. Soc., Chem. Commun.*, 1764-5 (1992).

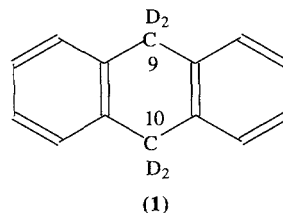
<sup>25</sup> G. VON HELDEN, M.-T. HSU, P. R. KEMPER and M. T. BOWERS, *J. Chem. Phys.* **95**, 3835-7 (1991).

Considerable attention has been paid to possible mechanisms of formation<sup>(26,27)</sup> since a firm understanding of this aspect could lead to the development of more effective synthetic routes to the individual fullerenes. It is also known that, when thin films of C<sub>60</sub> and C<sub>70</sub> are laser-vaporized into a rapid stream of an inert gas, individual molecules of C<sub>60</sub> or C<sub>70</sub> can themselves coalesce to form stable larger fullerenes such as C<sub>120</sub> or C<sub>140</sub>, and higher multiples. Even more dramatically, when a sample of C<sub>60</sub> is subjected to a pressure of 20 GPa (i.e. 200 kbar), it apparently immediately transforms into polycrystalline diamond.

Most solvents will only dissolve a few mg/l of the fullerenes. Solubility in benzene, toluene or CS<sub>2</sub> is somewhat higher but even so the acquisition of <sup>13</sup>C nmr data is still a lengthy and tedious business. By far the best solvents to date for C<sub>60</sub> at 25°C are *o*-dichlorobenzene (25 mg cm<sup>-3</sup>), 1-methylnaphthalene (33 mg cm<sup>-3</sup>) and 1-Br-2-Me-naphthalene (35 mg cm<sup>-3</sup>).<sup>(28)</sup> Colours in a range of some 30 solvents are variously pink, magenta, magenta-brown, brown-yellow, brown-green and brown, no doubt reflecting the varying interaction of the solute with the solvent (cf. I<sub>2</sub>, p. 807).

**Hydrogenation** — One of the first chemical reactions of C<sub>60</sub> to be studied was its Birch reduction. In a typical procedure, Li metal was added under an argon atmosphere to a suspension of C<sub>60</sub> in liquid NH<sub>3</sub>/thf, followed after 30 min by addition of Bu<sup>t</sup>OH. Initially the off-white product was thought to be C<sub>60</sub>H<sub>36</sub> but subsequent work using a variety of techniques<sup>(29)</sup> has shown that the product at low temperatures is a mixture of polyhydrofullerenes ranging from C<sub>60</sub>H<sub>18</sub> to C<sub>60</sub>H<sub>36</sub> with C<sub>60</sub>H<sub>32</sub> being the

predominant species. This mixture is thermally labile and in the mass spectrometer probe (>250°C) C<sub>60</sub>H<sub>36</sub> predominates, consistent with a molecule in which the 12 isolated pentagons of the C<sub>60</sub> cluster each retain one double bond, i.e. [(C<sub>2</sub>)<sub>12</sub>(CH)<sub>36</sub>]. A cleaner route to pure, white C<sub>60</sub>H<sub>36</sub> is by using a 120-fold molar excess of 9,10-dihydroanthracene (1) as a H-transfer reagent at 350°C for 30 min. Prolonging the reaction time to 24 h produces C<sub>60</sub>H<sub>18</sub> as a second product and the method has the added advantage that it permits the ready synthesis of C<sub>60</sub>D<sub>36</sub>, by use of 9,9',10,10'[D<sub>4</sub>]dihydroanthracene.<sup>(30)</sup>



**Oxidation reactions** — Direct fluorination of solid C<sub>60</sub> with F<sub>2</sub> gas at 70° proceeds slowly in a stepwise manner *via* several coloured partially fluorinated materials to give, after a period of several days, the colourless fully fluorinated product C<sub>60</sub>F<sub>60</sub>.<sup>(31)</sup> Rapid fluorination under more forcing conditions (F<sub>2</sub> gas/UV irradiation/250°) yields C<sub>60</sub>F<sub>48</sub> as the main product, plus an intractable mixture of other fluorides C<sub>60</sub>F<sub>2n</sub> including some hyperfluorinated materials (2n > 60) which would require the opening of some skeletal C–C bonds.<sup>(32)</sup> C<sub>60</sub>F<sub>48</sub> itself has over 20 million possible isomers but, astonishingly, the high-yield synthesis of just one of these has recently been achieved by heating a mixture of C<sub>60</sub> and NaF under F<sub>2</sub> at 275° for several days.<sup>(33)</sup> Actually a racemic mixture of the two

<sup>26</sup> R. F. CURL, *Phil. Trans. Roy. Soc.* **343**, 119–32 (1993).

<sup>27</sup> H. SCHWARZ, *Angew. Chem. Int. Edn. Engl.* **32**, 1412–5 (1993). R. M. BAUM, *Chem. & Eng. News*, May 17, 32–4 (1993) and references cited therein.

<sup>28</sup> W. A. SCRIVENS and J. M. TOUR, *J. Chem. Soc., Chem. Commun.*, 1207–9 (1993).

<sup>29</sup> M. R. BANKS (and 14 others), *J. Chem. Soc., Chem. Commun.*, 1149–52 (1993).

<sup>30</sup> C. RÜCHARDT (and 8 others), *Angew. Chem. Int. Edn. Engl.* **32**, 584–6 (1993).

<sup>31</sup> J. H. HOLLOWAY (and 8 others), *J. Chem. Soc., Chem. Commun.*, 966–9 (1991).

<sup>32</sup> A. A. TUINMAN, A. A. GAKH, J. L. ADCKOCK and R. N. COMPTON, *J. Am. Chem. Soc.* **115**, 5885–6 (1993).

<sup>33</sup> A. A. GAKH, A. A. TUINMAN, J. L. ADCKOCK, R. A. SACHLEBEN and R. N. COMPTON, *J. Am. Chem. Soc.* **116**, 819–20 (1994).

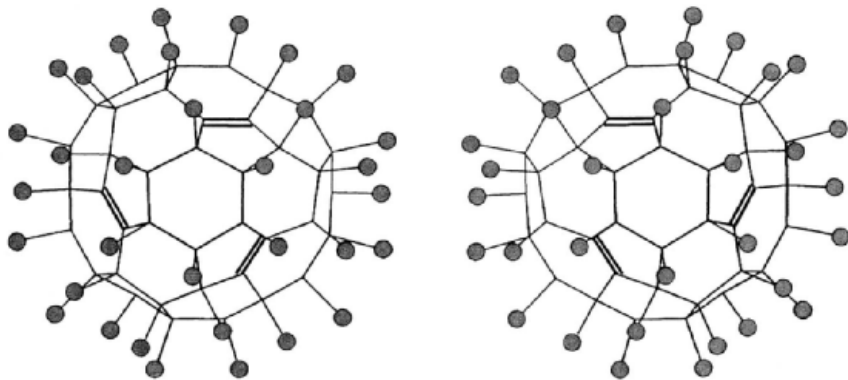


Figure 8.8 The enantiomeric pair of isomers of  $C_{60}F_{48}$ .<sup>(33)</sup>

chiral enantiomers shown in Fig. 8.8 is obtained. Shorter reaction times give complex mixtures of  $C_{60}F_{46}$  and  $C_{60}F_{48}$  isomers.

Direct chlorination of  $C_{60}$  with  $Cl_2$  gas at 250–400°C led to an intractable pale orange mixture of polychlorinated species having on average about 24 Cl atoms per cluster molecule, but milder conditions using  $Cl_2$  at various temperatures in a range of chloro organic solvents produced no detectable reaction.<sup>(34)</sup> By contrast, treatment of  $C_{60}$  with an excess of  $ICl$  in benzene or toluene at room temperature gave a quantitative yield of deep orange  $C_{60}Cl_6$ <sup>(35)</sup> which is isostructural with  $C_{60}Br_6$  (see below).

Bromination of  $C_{60}$  in solution gives  $C_{60}Br_6$  (magenta plates) and  $C_{60}Br_8$  (dark brown prisms). The former has a structure involving one monobrominated pentagon with a long C–Br bond (203 pm) itself adjacent to five other monobrominated pentagons (C–Br 196 pm) as shown in Fig. 8.9a. It disproportionates on being warmed to give  $C_{60}$  and  $C_{60}Br_8$  which has a  $C_{2v}$  structure with pairs of Br atoms arranged *meta* on four 6-membered rings (Fig. 8.9b).<sup>(36)</sup>

Bromination with liquid  $Br_2$  yields the somewhat more stable  $C_{60}Br_{24}$  which has  $T_h$  symmetry (Fig. 8.9c) with 12 hexagons disubstituted *para* and in pairs with boat conformation but mutually *meta* on the other 8 hexagons which have the chair conformation. The structure has 18 C=C arranged one per pentagon (12) and one at each 6:6 bond (6).<sup>(37)</sup> All three bromides can be completely dehalogenated on strong heating, as can the polychlorides. Iodine appears not to add directly to  $C_{60}$  but forms an intercalation product.

Fullerene epoxide,  $C_{60}O$ , is formed by the UV irradiation of an oxygenated benzene solution of  $C_{60}$ .<sup>(38)</sup> The O atom bridges a 6:6 bond of the closed fullerene structure. The same compound is also formed as one of the products of the reaction of  $C_{60}$  with dimethyldioxirane,  $Me_2\overline{COO}$  (see later).<sup>(39)</sup>

Fullerols,  $C_{60}(OH)_n$  ( $n = 24–26$ ), can be synthesized directly by aerobic oxidation of a benzene solution of  $C_{60}$  using an aqueous solution of NaOH containing a few drops of  $Bu_4NOH$  as the most efficient catalyst: the deep violet benzene solution rapidly decolorizes and a brown sludge precipitates; further reaction with more water over a period of 10 h gives a clear red-brown solution from which the

<sup>34</sup> G. A. OLAH, I. BUSCI, C. LAMBERT, R. ANISFELD, N. J. TRIVEDI, D. K. SENSHARMA and G. K. S. PRAKASH, *J. Am. Chem. Soc.* **113**, 9385–7 (1991).

<sup>35</sup> P. R. BIRKETT, A. G. AVENT, A. D. DARWISH, H. W. KROTO, R. TAYLOR and D. R. M. WALTON, *J. Chem. Soc., Chem. Commun.*, 1230–2 (1993).

<sup>36</sup> P. R. BIRKETT, P. B. HITCHCOCK, H. W. KROTO, R. TAYLOR and D. R. M. WALTON, *Nature* **357**, 479–81 (1992).

<sup>37</sup> F. N. TEBBE (and 8 others), *Science* **256**, 822–5 (1992).

<sup>38</sup> K. M. CREEGAN (and 10 others), *J. Am. Chem. Soc.* **114**, 1103–5 (1992).

<sup>39</sup> Y. ELEMES (and 6 others), *Angew. Chem. Int. Edn. Engl.* **31**, 351–3 (1992).



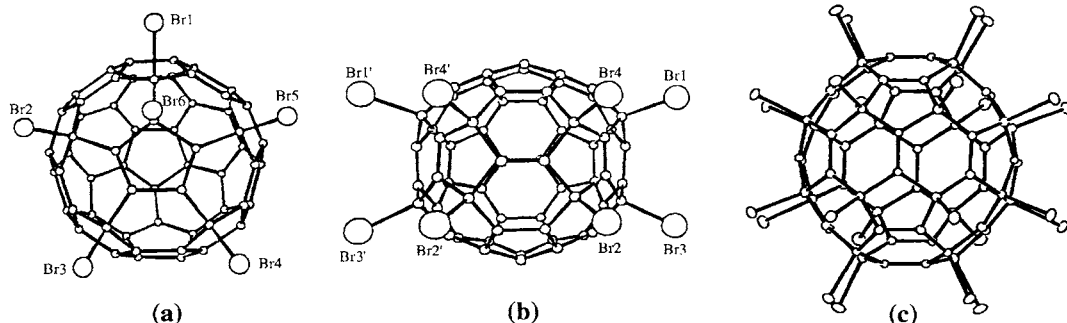


Figure 8.9 Structures of (a)  $C_{60}Br_6$ ; (b)  $C_{60}Br_8$ ; (c)  $C_{60}Br_{24}$ .

brown solid product is obtained by vacuum evaporation.<sup>(40)</sup> Hydroboration of  $C_{60}$  followed by treatment either with glacial acetic acid or aqueous  $NaOH/H_2O_2$  affords another route to water-soluble fullerols, suggesting that C–H bonds on the fullerene cluster are readily oxidized to C–OH groups.<sup>(41)</sup>

*Reduction of fullerenes to fullerides* – Reversible electrochemical reduction of  $C_{60}$  in anhydrous dimethylformamide/toluene mixtures at low temperatures leads to the air-sensitive coloured anions  $C_{60}^{n-}$ , ( $n = 1-6$ ). The successive mid-point reduction potentials,  $E_{1/2}$ , at  $-60^\circ C$  are  $-0.82$ ,  $-1.26$ ,  $-1.82$ ,  $-2.33$ ,  $-2.89$  and  $-3.34$  V, respectively.<sup>(42)</sup> Liquid  $NH_3$  solutions can also be used.<sup>(43)</sup>  $C_{60}$  is thus a very strong oxidizing agent, its first reduction potential being at least 1 V more positive than those of polycyclic aromatic hydrocarbons.  $C_{70}$  can also be reversibly reduced and various ions up to  $C_{70}^{6-}$  have been detected.

Chemical reduction by alkali metals leads to solid fullerides which are sometimes solvated.

Thus, fullerides  $M_nC_{60}$  are known for  $n = 1$  when  $M = Rb, Cs$  and for  $n = 2, 3, 4$  and  $6$  when  $M = Na, K, Rb$  and  $Cs$ . An important alternative route treats  $C_{60}$  in toluene with a solution of  $Na[Mn(\eta^5-C_5Me_5)_2]$  in thf to give an 80% yield of the dark-purple, air- and moisture-sensitive crystalline solvate  $NaC_{60} \cdot 5thf$ .<sup>(44)</sup>

Interest in the unsolvated compounds  $M_nC_{60}$  increased dramatically when several were found to be good electrical conductors.  $C_{60}$  films when doped with alkali metal vapour become organic metals, some of which show superconductivity at low temperatures. For example,  $K_3C_{60}$ , prepared from stoichiometric amounts of solid  $C_{60}$  and potassium vapour, has  $T_c$  19.3 K: it has an fcc structure derived from that of  $C_{60}$  itself by incorporating K ions into all the octahedral and tetrahedral interstices of the host lattice as shown in Fig. 8.10.<sup>(45)</sup>  $Rb_3C_{60}$  has an even higher superconducting critical temperature,  $T_c \sim 28$  K. It seems that, when electrons are added to  $C_{60}$  from an alkali metal, they enter a conduction band composed of the triply degenerate  $t_{1u}$   $\pi$  orbitals of the individual  $C_{60}$  molecules. Maximum conductivity is observed when this band is half-filled (at  $C_{60}^{3-}$ ) after which the conductivity gradually decreases until the composition  $M_6C_{60}$  when it is full, consistent

<sup>40</sup> J. LI, A. TAKEUCHI, M. OZAWA, X. LI, K. SAIGO and K. KITAZAWA, *J. Chem. Soc., Chem. Commun.*, 1784–5 (1993) and references cited therein.

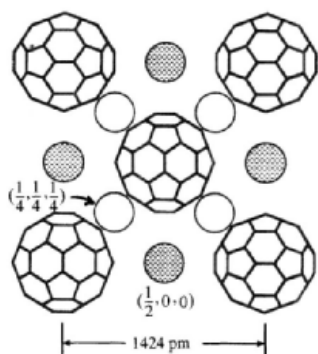
<sup>41</sup> N. S. SCHNEIDER, A. D. DARWISH, H. W. KROTO, R. TAYLOR and D. R. M. WALTON, *J. Chem. Soc., Chem. Commun.*, 463–4 (1994).

<sup>42</sup> Y. OSHAWA and T. SAJI, *J. Chem. Soc., Chem. Commun.*, 781–2 (1992).

<sup>43</sup> W. K. FULLAGAR, I. R. GENTLE, G. A. HEATH and J. W. WHITE, *J. Chem. Soc., Chem. Commun.*, 525–7 (1993).

<sup>44</sup> R. H. DOUTHWAITE, A. R. BROUGH and M. L. H. GREEN, *J. Chem. Soc., Chem. Commun.*, 267–8 (1994).

<sup>45</sup> P. W. STEPHENS (and 7 others), *Nature* **351**, 632–4 (1991). See also H. H. WANG (and 13 others), *Inorg. Chem.* **30**, 2838–9 (1991).

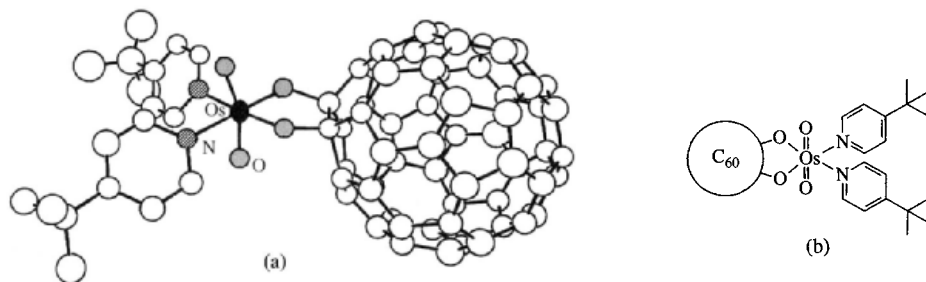


**Figure 8.10** The fcc structure of  $K_3C_{60}$ , showing potassium ions occupying the tetrahedral (○) and octahedral (●) sites. The shortest K–K distance is 617 pm (much larger than in metallic K) and the diameter of  $C_{60}^{3-}$  is 708 pm.

with the observation that  $K_6C_{60}$  (bcc lattice) is an insulator.<sup>(46)</sup>

**Addition reactions** – The fullerenes  $C_{60}$  and  $C_{70}$  react as electron-poor olefins with fairly localized double bonds. Addition occurs preferentially at a double bond common to two annelated 6-membered rings (a 6:6 bond) and a second addition, when it occurs is generally in the opposite hemisphere. The first characterizable mono adduct was  $[C_{60}OsO_4(NC_5H_4Bu^t)_2]$ , formed by reacting  $C_{60}$  with an excess of  $OsO_4$  in 4-butylpyridine. The structure is shown in

<sup>46</sup> R. C. HADDON, *Pure Appl. Chem.* **65**, 11–15 (1993) and refs. cited therein.



**Figure 8.11** (a) Structure of  $C_{60}OsO_4(NC_5H_4Bu^t)_2$  as determined by X-ray diffraction analysis.<sup>(47)</sup> (b) A schematic representation of the structure.

Fig. 8.11 and was, in fact, the first definitive X-ray structural determination of a fullerene derivative.<sup>(47)</sup>

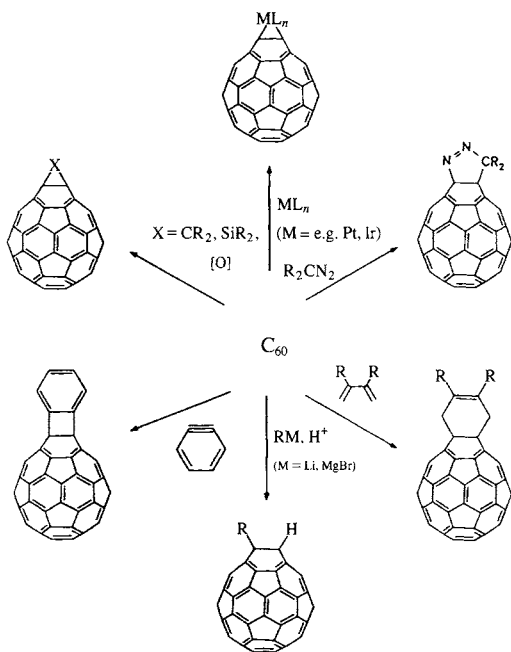
Other addition reactions are shown in the scheme.<sup>(48)</sup> Thus,  $C_{60}$  reacts as an olefin towards  $[Pt^0(PPh_3)_2]$  to give the  $\eta^2$  adduct  $[Pt(\eta^2-C_{60})(PPh_3)_2]$ . Indeed six  $M^0$  centres can simultaneously be coordinated by a single fullerene cluster to give  $[C_{60}\{M(PEt_3)_2\}_6]$ , ( $M = Ni, Pd, Pt$ ), with the 6M arranged octahedrally about the  $(\eta^2)_6-C_{60}$  core.<sup>(49)</sup> Likewise, reaction of  $C_{60}$  with  $[Ir(CO)Cl(PMe_2Ph)_2]$  provides two conformational isomers of  $[(\eta^2, \eta^2-C_{60})\{Ir(CO)Cl(PMe_2Ph)_2\}_2]$  in both of which the Ir atoms are ligated by 6:6 double bonds at diametrically opposite sides of the fullerene. Similarly,<sup>(50)</sup>  $C_{70}$  reacts with  $[Ir(CO)Cl(PPh_3)_2]$  in benzene solution to give brown crystals of  $[Ir(\eta^2-C_{70})(CO)Cl(PPh_3)_2]$ , ligation occurring from a 6:6 double bond near one of the poles (i.e. an a–b bond in Fig. 8.6), and the bis-adduct  $[(\eta^2, \eta^2-C_{70})\{Ir(CO)Cl(PPh_3)_2\}_2]$  involves a–b bonds at opposite poles. Very recently, in addition to  $\eta^2$  dihapto and

<sup>47</sup> J. M. HAWKINS, A. MEYER, T. LEWIS, S. LOREN and F. J. HOLLANDER, *Science* **252**, 312–4 (1991).

<sup>48</sup> A. HIRSCH, *Angew. Chem. Int. Edn. Engl.* **32**, 1138–41 (1993) and references cited therein.

<sup>49</sup> P. J. FAGAN, J. C. CALABRESE and B. MALONE, *J. Am. Chem. Soc.* **113**, 9408–9 (1991). P. J. FAGAN, J. C. CALABRESE and B. MALONE, *Acc. Chem. Res.* **25**, 134–42 (1992).

<sup>50</sup> A. L. BALCH, V. J. CATALANO, J. W. LEE, M. M. OLMSTEAD and S. R. PARKIN, *J. Am. Chem. Soc.* **113**, 8953–5 (1991).



Scheme Syntheses of exohedral fullerene derivatives. For clarity only the front sides of the fullerenes are shown.<sup>(48)</sup>

$\eta^2, \eta^2$  tetrahapto ligation of  $C_{60}$ , an example of  $\eta^2, \eta^2, \eta^2$  hexahapto coordination has been identified in the red crystalline complex  $[Ru_3[\mu_3-\eta^2, \eta^2, \eta^2-C_{60}](CO)_9]$ , formed by heating  $C_{60}$  with  $Ru_3(CO)_{12}$  in *n*-hexane, the three C=C bonds from one hexagonal face displacing one CO from each Ru atom in the cluster.<sup>(50a)(50b)</sup> Extensive cluster opening can also occur, as in the cobalt(I) cyclopentadienyl adduct of the purple  $C_{60}$ /butadiene fulleroid,  $[Co(\eta^5-C_5H_5)(\eta^2, \eta^2-C_{60}C_4H_4)]$ , which features an unprecedented fifteen-membered “trimethano[15]annulene” opening within the  $C_{60}$  framework.

Returning now to the reactions in the scheme it can be seen that carbenes and silenes

yield the derivatives  $C_{60}CR_2$  and  $C_{60}SiR_2$ . The structurally related epoxide  $C_{60}O$  has already been mentioned (p. 284). Bzzyne yields a [2 + 2] adduct as shown, since the [4 + 2] adduct would require the formation of an energetically unfavourable 5:6 double bond. Nucleophilic reactions with Grignard reagents and Li alkyls yield intermediates which, after protonolysis, afford 1,9- $C_{60}RH$  derivatives, whereas hydroboration (not shown) yields  $C_{60}H(BH_2)$  which on protonolysis gives the parent 1,9-dihydrofullerene,  $C_{60}H_2$ . Diels–Alder reactions give highly regiospecific addition products which can be isolated in high yield. By contrast, diphenyldiazomethane and related diazoalkanes and diazoacetates give substituted dihydropyrazole intermediates (via a [3 + 2] cycloaddition reaction) which then lose  $N_2$  to form the thermally stable final products; these may be *opened*  $\pi$  homoaromatic structures bridged at either a 5:6 or a 6:6 ring junction (Fig. 8.12a,b), or a *closed*  $\sigma$  homoaromatic fullerene bridged at a 6:6 ring junction (Fig. 8.12c). In the special case of diazomethane,  $C_{60}(CH_2N_2)$  is formed as a thermally unstable brown solution in toluene; this loses  $N_2$  when heated under reflux and  $C_{61}H_2$  can be isolated as a dark powder from the now purple solution.<sup>51</sup> Structure type a (Fig. 8.12) in which the  $CH_2$  group bridges an opened 5:6 junction is assigned on the basis of spectroscopic evidence. The opened azafulleroids  $C_{60}NR$  (Fig. 8.12d) can be

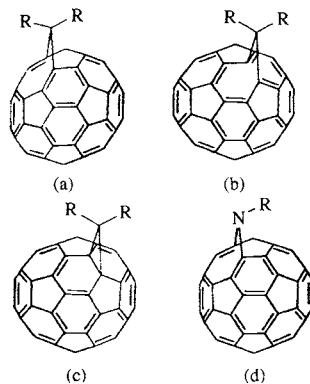


Figure 8.12 Structures (a), (b), (c) and (d); see text.

<sup>50a</sup> H.-F. HSU and J. R. SHAPLEY, *J. Am. Chem. Soc.* **118**, 9192–3 (1996).

<sup>50b</sup> M.-J. ARCE, A. L. VIADO, Y.-Z. AN, S. I. KHAN and Y. RUBIN, *J. Am. Chem. Soc.* **118**, 3775–6 (1996).

<sup>51</sup> T. SUZUKI, Q. C. LI, K. C. KHEMANI and F. WUDL, *J. Am. Chem. Soc.* **114**, 7301–2 (1992).

obtained from  $C_{60}$  and organic azides,  $RN_3$ , by  $[3 + 2]$  cycloaddition and subsequent loss of  $N_2$ .

*Heteroatom fullerene-type clusters* — The possibility of incorporation of hetero atoms into  $C_n$  clusters has excited the attention of both theoreticians and experimentalists since the earliest days of fullerene chemistry, particularly in view of the known stability and ubiquity of organic heterocycles. The structural relationship between  $C_{60}$  and  $\beta$ -rhombohedral boron has already been alluded to (p. 142).

Laser vaporization of a composite pressed disc of graphite and BN using He as carrier gas, followed by mass spectrometric analysis, gave a range of clusters with even numbers of atoms from less than 50 to well above 72:<sup>(52)</sup> the peak with 60 atoms was the most abundant and, in a typical run, was shown to be a mixture of clusters:  $C_{60}$  (22%),  $C_{59}B$  (21%),  $C_{58}B_2$  (24%),  $C_{57}B_3$  (18%),  $C_{56}B_4$  (9%),  $C_{55}B_5$  (4%) and  $C_{54}B_6$  (2%). Brief exposure of this mixture of 60-atom clusters to  $NH_3$  at 1  $\mu$ torr for 2 s led, typically, to the formation of  $C_{60-x}\{B.NH_3\}_x$  ( $x = 0-4$ ).

Preliminary experiments with contact-arc vaporization of graphite in a stream of He containing  $N_2$  or  $NH_3$  yielded nitrogen-containing products tentatively assigned to species such as  $C_{70}N_2$  and  $C_{59}N_x$  ( $x = 2, 4, 6$ ) of as yet undetermined structure.

The possibility of the isoelectronic replacement of pairs of C atoms by contiguous BN groups (p. 207) in fullerenes is particularly intriguing, e.g.  $C_{58}BN$ ,  $C_{60-2x}(BN)_x$ . Because each fullerene,  $C_n$ , contains 12 pentagonal faces, the limit of such substitution of  $C_2$  by alternating BN would seem to be at  $C_{12}B_{24}N_{24}$ , since there is a structural frustration at the odd (fifth) C atom of each pentagon.<sup>(54)</sup>

*Encapsulation of metal atoms by fullerene clusters* — It is readily apparent that there is sufficient space inside fullerene clusters to accommodate several other atoms: the trick has been in learning how to synthesize such species. When a composite rod of graphite/ $La_2O_3$  was vaporized at 1200°C in argon and the resulting “soot” extracted with pyridine, the products included not only  $C_{60}$  and  $C_{70}$  but also  $LaC_{60}$ ,  $LaC_{70}$ ,  $LaC_{74}$  and  $LaC_{82}$ .<sup>(55)</sup> Photo fragmentation by laser irradiation can then strip off C atoms pairwise to “shrink wrap” the metal with ever smaller clusters down to about  $LaC_{44}$ . In each of these compounds the La is encapsulated by  $C_n$ , i.e. it is an *endo* compound, in contradistinction to the alkali metal fullerenes discussed on p. 285. The accepted symbolism for this novel type of compound is  $[La@C_{60}]$  etc., and esr shows that the correct electronic formulation is  $[La^{3+}@C_{60}^{3-}]$ . The smallest endohedral metallafullerene so far is  $[U@C_{28}]$ .<sup>(56)</sup> It is notable that  $C_{28}$  would have its 12 pentagons as 4 sets of 3, plus 4 hexagons, all arranged tetrahedrally to give  $T_d$  symmetry. MO calculations suggest that neutral  $C_{28}$  lacks 4e<sup>-</sup> to fill completely its bonding MOs and these are supplied by M in  $[M^{4+}@C_{28}^{4-}]$ , (M = U, Ti, Zr, Hf).

The first dimetalla analogue to be characterized was  $[La_2@C_{60}]$ , and mixed metal and trimetalla compounds are also known, e.g.  $[YLa@C_{80}]$ <sup>(57)</sup> and  $[Sc_3@C_{82}]$ .<sup>(58)</sup> Other known compounds include the monometalla species  $[M@C_{82}]$  for M = La, Ce, Nd, Sm, Eu, Gd, Tb, Dy, Ho and Er,<sup>(59)</sup> the dimetalla compounds  $[Ce_2@C_{80}]$ ,  $[Tb_2@C_{80}]$ ,  $[Sc_2@C_{82}]$ ,  $[Y_2@C_{82}]$ ,  $[La_2@C_{82}]$  and  $[Sc_2@C_{84}]$ , and the trimetalla species  $[La_3@C_{106}]$  and  $[La_3@C_{112}]$ . The products

<sup>55</sup> R. E. SMALLLEY (and 8 others), *J. Phys. Chem.* **95**, 7564–8 (1991).

<sup>56</sup> R. E. SMALLLEY (and 9 others), *Science* **257**, 1661–4 (1992).

<sup>57</sup> M. M. ROSS, H. H. NELSON, J. H. CALLAHAN and S. W. McELVANEY, *J. Phys. Chem.* **96**, 5231–4 (1992).

<sup>58</sup> H. SHINOHARA (and 7 others), *Nature* **357**, 52–4 (1992).

<sup>59</sup> E. G. GILLAN, C. YERETZIAN, K. S. MIN, M. M. ALVAREZ, R. L. WHETTEN and R. B. KANER, *J. Phys. Chem.* **96**, 6869–71 (1992).

<sup>52</sup> T. GUO, C. JIN and R. E. SMALLLEY, *J. Phys. Chem.* **95**, 4948–50 (1991).

<sup>53</sup> T. PRADEEP, V. VIJAYAKRISHNAN, A. K. SANTRA and C. N. R. RAO, *J. Phys. Chem.* **95**, 10564–5 (1991).

<sup>54</sup> J. R. BOWSER, D. A. JELSKI and T. F. GEORGE, *Inorg. Chem.* **31**, 156–7 (1992).

obtained depend sensitively on the relative concentrations of metal oxide and carbon in the electrode material.<sup>(59)</sup> Note also that only metals from the left-hand side of the periodic table have so far been encapsulated and there are no substantiated examples with  $M = \text{Fe, Cu, Ag, Au, etc.}$

Some recent books and general reviews on the preparation, properties and chemical reactions of the fullerenes and their derivatives are in ref. 60.

The endohedral metallofullerenes just described (and the alkali metal fullerides described on p. 285) are all formally examples of metal carbides,  $M_xC_y$ , but they have entirely different structure motifs and properties from the classical metal carbides and the more recently discovered metallacarbohedrenes (metcars) on the one hand (both to be considered in Section 8.4) and the graphite intercalation compounds to be discussed in Section 8.3. Before that, however, we must complete this present section on the various forms of the element carbon by describing and comparing the chemical properties of the two most familiar forms of the element, diamond and graphite.

### 8.2.5 Chemical properties of carbon

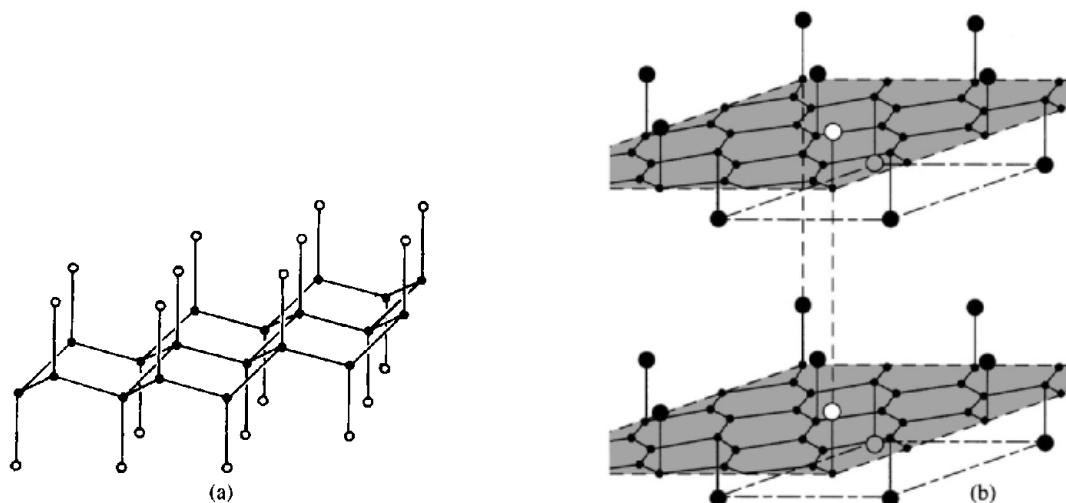
Carbon in the form of diamond is extremely unreactive at room temperature. Graphite, although thermodynamically more stable than diamond under normal conditions, tends to react more readily due to its more vulnerable

layer structure. For example, it is oxidized by hot concentrated  $\text{HNO}_3$  to mellitic acid,  $\text{C}_6(\text{CO}_2\text{H})_6$ , in which planar-hexagonal  $\text{C}_{12}$  units are preserved. Graphite reacts with a suspension of  $\text{KClO}_4$  in a 1:2 mixture (by volume) of conc  $\text{HNO}_3/\text{H}_2\text{SO}_4$  to give "graphite oxide" an unstable, pale lemon-coloured product of variable stoichiometry and structure. Similar products can be prepared by anodic oxidation of graphite or by reaction with  $\text{NaNO}_3/\text{KMnO}_4/\text{conc H}_2\text{SO}_4$ . Graphite oxide decomposes slowly at  $70^\circ\text{C}$ , and at  $200^\circ$  it undergoes a spectacular deflagration with the formation of  $\text{CO}$ ,  $\text{CO}_2$ ,  $\text{H}_2\text{O}$  and soot. Infrared and X-ray evidence suggest that the structure-motif is a puckered hexagonal network of  $\text{C}_6$  rings predominantly in the "chair" conformation but with a few remaining  $\text{C}=\text{C}$  bonds; in addition there are terminal and bridging O atoms and pendant OH groups; keto-enol tautomerism is implied and the empirical formula can be represented as  $\text{C}_6\text{O}_x(\text{OH})_y$ , with  $x \sim 1.0-1.7$  and  $y \sim 2.25-1.7$ .

Graphite reacts with an atmosphere of  $\text{F}_2$  at temperatures between  $400-500^\circ\text{C}$  to give "graphite monofluoride"  $\text{CF}_x$  ( $x \sim 0.68-0.99$ ). The reaction is catalysed by HF and can then occur at much lower temperatures (leading, on occasion, to the destruction of graphite electrodes during the preparation of  $\text{F}_2$  by the electrolysis of  $\text{KF}/\text{HF}$  melts, p. 797). At  $\sim 600^\circ$  the reaction proceeds with explosive violence to give a mixture of  $\text{CF}_4$ ,  $\text{C}_2\text{F}_6$ , and  $\text{C}_5\text{F}_{12}$ . The colour of  $\text{CF}_x$  depends on the reaction temperature and on the fluorine content, becoming progressively lighter from black ( $x \sim 0.7$ ) to grey ( $x \sim 0.8$ ), silver ( $x \sim 0.9$ ) and transparent white ( $x > 0.98$ ).<sup>(61)</sup> The structure has not been definitely established but the idealized layer lattice shown in Fig. 8.13a accounts for the observed interplanar spacings, infrared data, colour, and lack of electrical conductivity ( $\rho > 3000 \text{ ohm cm}$ ).  $\text{CF}$  is very unreactive, but when heated slowly between

<sup>60</sup> J. BAGGOTT, *Perfect Symmetry* (the discovery of buckminsterfullerene), Oxford University Press, Oxford, 1994, 300 pp. H. ALDERSLEY-WILLIAMS, *The Most Beautiful Molecule*, Aurum Press, London, 1995, 340 pp. T. BRAUN, A. SCHUBERT, H. MACZELKA and L. VASVÁRI, *Fullerene Research 1985-1993* (A computer-generated cross-indexed bibliography of the Journal literature), World Scientific Singapore, 1995, 480 pp. R. TAYLOR, *The Chemistry of the Fullerenes* (vol. 4 in *Advanced Series in Fullerenes*), World Scientific, Singapore, 1995, 260 pp. T. BRAUN (ed.) *Fullerene Science and Technology*, [now a regular Journal, vol. 3 (1995)], Marcel Dekker, New York, W. E. BILLUPS, and W. E. CIUFOLINI (eds.) *Buckminsterfullerenes*, VCH, New York, 1993, 308 pp. H. W. KROTO, J. E. FISCHER and D. E. COX (eds.), *The Fullerenes*, Pergamon Press, Oxford, 1993, 318 pp.

<sup>61</sup> Y. KITA, N. WATANABE and Y. FUJII, *J. Am. Chem. Soc.* **101**, 3832-41 (1979) and refs cited therein. See also H. TOUHARA, K. KADONO, Y. FUJII and N. WATANABE, *Z. anorg. allg. Chem.* **544**, 7-20 (1987) for structure of  $(\text{C}_2\text{F})_n$ .



**Figure 8.13** (a) Idealized structure of CF showing puckerred layer lattice of fused  $C_6$  rings in "chair" conformation and axial F atoms. The spacing between successive C layers is  $\sim 817$  pm (cf. graphite 335.4 pm) and the density  $2.43$  g  $cm^{-3}$ . (b) Proposed structure for  $C_4F$  showing retention of the planar graphite sheets but with regularly spaced F atoms above and below each layer. The spacing between successive C layers is  $\sim 534$  pm and the density is  $2.077$  g  $cm^{-3}$ .

600–1000° it gradually liberates fluorocarbons,  $C_nF_{2n+2}$ .

When gaseous mixtures of  $F_2/HF$  are allowed to react with finely powdered graphite at room temperature an inert bluish-black compound with a velvety appearance is formed with a composition which varies in the range  $C_4F$  to  $C_{3.57}F$ . The in-plane C–C distance remains as in graphite but the interlayer spacing increases to 534–550 pm depending on the F content. The infrared and X-ray data are best interpreted in terms of the structure shown in Fig. 8.13b. The electrical conductivity, though less than that of graphite, is still appreciable, the resistivity being  $\sim 2$ –4 ohm cm. Other chemical and electrochemical routes to  $C_xF$  ( $x < 2$ ) and  $C_{14}F(HF)_y$ , have also been explored.<sup>(62)</sup>

At high temperatures, C reacts with many elements including H (in the presence of a finely

divided Ni catalyst), F (but not the other halogens), O, S, Si (p. 334), B (p. 149) and many metals (p. 297). It is an active reducing agent and reacts readily with many oxides to liberate the element or form a carbide. These reactions, which reflect the high enthalpy of formation of CO and  $CO_2$ , are of great industrial importance (p. 307).

Carbon is known with all coordination numbers from 0 to 8 though compounds in which it is 3- or 4-coordinate are the most numerous. Some typical examples are summarized in the Panel (p. 291). Particular mention should also be made of hypercoordinate "non-classical" carbonium ions such as 5-coordinate  $CH_5^+$ , square pyramidal  $C_5H_5^+$  (cf. the isoelectronic cluster  $B_5H_9$ , p. 154), pentagonal pyramidal  $C_6Me_6^{2+}$  (cf. iso-electronic  $B_6H_{10}$ , p. 154) and the bicyclic cation 2-norbornyl,  $C_7H_{11}^+$ .<sup>(63)</sup>

<sup>62</sup> R. HAGIWARA, M. LERNER and N. BARTLETT, *J. Chem. Soc., Chem. Commun.*, 573–4 (1989); H. TAKENAKA, M. KAWAGUCHI, M. LERNER and N. BARTLETT, *J. Chem. Soc., Chem. Commun.*, 1431–2 (1987).

<sup>63</sup> G. A. OLAH, *J. Am. Chem. Soc.* **94**, 808–20 (1972); G. A. OLAH, G. K. S. PRAKASH, R. E. WILLIAMS, L. D. FIELD and K. WADE, *Hypercarbon Chemistry*, Wiley, New York, 1987, 311 pp.

## Coordination Numbers of Carbon

CN	Examples	Comments
0	C atoms	High-temp. low-press. gas phase
1	CO CH <sup>•</sup> (carbynes)	Stable gas Reactive free-radical intermediates
2 (linear)	CO <sub>2</sub> , CS <sub>2</sub> HCN, HC≡CH, NCO <sup>-</sup> , NCS <sup>-</sup> M(CO) <sub>n</sub> RP=C=PR (R = 2,4,6-Bu <sub>3</sub> C <sub>6</sub> H <sub>2</sub> )	Stable gas, liquid The ions are isoelectronic with CO <sub>2</sub> and COS respectively Terminal M-CO groups sometimes <180° Angle PCP 172.6° <sup>(63)</sup>
2 (bent)	Ph <sub>3</sub> P:C:PPh <sub>3</sub> :CH <sub>2</sub> , :CX <sub>2</sub> (carbenes)	A bis(ylide) with angle PCP 130.1° (and 143.8°) <sup>(64)</sup> Reactive intermediates with 1 lone-pair and 1 vacant orbital; (carbenes are bent for X = H, F, OH, OMe, NH <sub>2</sub> , but linear if X is less electronegative, e.g. BH <sub>2</sub> , BeH, Li) <sup>(65)</sup> Reactive intermediates with 2 unpaired electrons
3 (planar)	•CH <sub>2</sub> •, •CPh <sub>2</sub> • (methylenes) COXY (X = H, hal, OH, O <sup>-</sup> R, Ar)  [C(N=PCL <sub>3</sub> ) <sub>3</sub> ] <sup>+</sup> [SbCl <sub>6</sub> ] <sup>-</sup>  M <sub>n</sub> (CO) <sub>n</sub>  [PhC(OMe)M(CO) <sub>5</sub> ] CH <sub>3</sub> <sup>+</sup> (carbonium ions)	Stable oxohalides, carbonates, carboxylic acids, aldehydes, ketones, etc. Colourless crystals prepared from [C(N <sub>3</sub> ) <sub>3</sub> ] <sup>+</sup> + PCl <sub>3</sub> <sup>(66)</sup> Metal carbonyl clusters with bridging CO groups M-C(O)-M Stable metal-carbene complexes. e.g. M = Cr, W Unstable reaction intermediates with 1 vacant orbital <sup>(67)</sup>
3 (pyramidal)	CH <sub>3</sub> <sup>-</sup> , CPh <sub>3</sub> <sup>-</sup> (carbanions), RMgX Ph <sub>3</sub> C <sup>•</sup> , R <sub>3</sub> C <sup>•</sup> (free radicals)	Unstable reaction intermediates with 1 lone pair of electrons Paramagnetic species of varying stability
3 (T-shaped)	[Ta(=CHCMe <sub>3</sub> ) <sub>2</sub> (2,4,6-Me <sub>3</sub> C <sub>6</sub> H <sub>2</sub> )(PMe <sub>3</sub> ) <sub>2</sub> ]	The unique H is equatorial and angle Ta=C-CMe <sub>3</sub> is 169° <sup>(68)</sup>
4 (tetrahedral)	CX <sub>4</sub> , etc. M <sub>n</sub> (CO) <sub>n</sub>	4-coord covalent compds such as CF <sub>4</sub> , C <sub>2</sub> H <sub>6</sub> , CHXYZ, etc. Metal carbonyl clusters with triply bridging CO groups (p. 928)
4 (see-saw, C <sub>2v</sub> )	[Fe <sub>4</sub> C(CO) <sub>13</sub> ]	The μ <sub>4</sub> -carbido C caps Fe <sub>4</sub> "butterfly" <sup>(69)</sup>
5	Al <sub>2</sub> Me <sub>6</sub>  C <sub>2</sub> B <sub>3</sub> H <sub>6</sub> , etc. [(η <sup>5</sup> -C <sub>5</sub> H <sub>5</sub> )NiRu <sub>3</sub> (CO) <sub>9</sub> CCHBu <sup>+</sup> ] [Os <sub>5</sub> C(CO) <sub>13</sub> HL <sub>2</sub> ] [C{AuPPh <sub>3</sub> } <sub>5</sub> ] <sup>+</sup> BF <sub>4</sub> <sup>-</sup>	Alkyl-bridged organometallics involving 3c-2e, bonds (pp. 259, etc.) Several stable carboranes (p. 183) The C atom bonds to CHBu <sup>+</sup> and to M <sub>4</sub> "butterfly" <sup>(70)</sup> The μ <sub>5</sub> -carbido C bonds to all 5 Os <sub>5</sub> <sup>(71)</sup> trigonal bipyramidal cation <sup>(72)</sup>
6	C <sub>2</sub> B <sub>10</sub> H <sub>12</sub> , etc. [C{AuPPh <sub>3</sub> } <sub>6</sub> ] <sup>2+</sup> [BF <sub>3</sub> (OMe)] <sub>2</sub> <sup>-</sup>	Several stable carboranes (p. 185) octahedral dication <sup>(73)</sup>
7	(LiMe) <sub>4</sub> crystals	See structure, p. 104
8	Be <sub>2</sub> C (antifluorite), [Co <sub>8</sub> C(CO) <sub>18</sub> ] <sup>2-</sup>	See structure, p. 118 See structure, p. 1142

<sup>(64)</sup>A. T. VINCENT and P. J. WHEATLEY, *J. Chem. Soc., Dalton Trans.*, 617-22 (1972). G. E. HARDY, J. I. ZINK, W. C. KASKA and J. C. BALDWIN, *J. Am. Chem. Soc.* **100**, 8001-2 (1978). see also E. FLUCK, B. NEUMÜLLER, R. BRAUN, G. HECKMANN, A. SIMON and H. BORRMANN, *Z. anorg. allg. Chem.* **567**, 23-38 (1988) and the many references cited therein.

<sup>(65)</sup>W. W. SCHOELLER, *J. Chem. Soc., Chem. Commun.*, 124-5 (1980).

<sup>(66)</sup>U. MÜLLER, I. LORENZ, and F. SCHMOCK, *Angew. Chem. Int. Edn. Engl.* **18**, 693-4 (1979).

<sup>(67)</sup>Note, however, that an X-ray structure analysis of the stable, crystalline carbocation 3,5,7-trimethyladamantyl showed the 3-coordinate C(1) atom as a considerably flattened pyramid 21 pm above the plane of the 3 adjacent C atoms and with bond angles 120°, 118° and 116° (Σ = 354°). T. Laube, *Angew. Chem. Int. Edn. Engl.* **25**, 349-51 (1986).

<sup>(68)</sup>M. R. CHURCHILL and W. J. YOUNGS, *J. Chem. Soc., Chem. Commun.*, 1048-9 (1978).

<sup>(69)</sup>J. S. BRADLEY, G. B. ANSELL, M. E. LEONOWICZ and E. W. HILL, *J. Am. Chem. Soc.* **103**, 4968-70 (1981).

<sup>(70)</sup>E. SAPPA, A. TIRIPICCHIO and M. T. CAMELLINI, *J. Chem. Soc., Chem. Commun.*, 154 (1979).

<sup>(71)</sup>J. M. FERNANDEZ, B. F. G. JOHNSON, J. LEWIS and P. RAITBY, *J. Chem. Soc., Dalton Trans.*, 2250-7 (1981).

<sup>(72)</sup>F. SCHERBAUM, A. GROHMANN, G. MÜLLER and H. SCHMIDBAUR, *Angew. Chem. Int. Edn. Engl.* **28**, 463-5 (1989).

<sup>(73)</sup>F. SCHERBAUM, A. GROHMANN, B. HÜBER, C. KRÜGER and H. SCHMIDBAUR, *Angew. Chem. Int. Edn. Engl.* **27**, 1544-6 (1988).

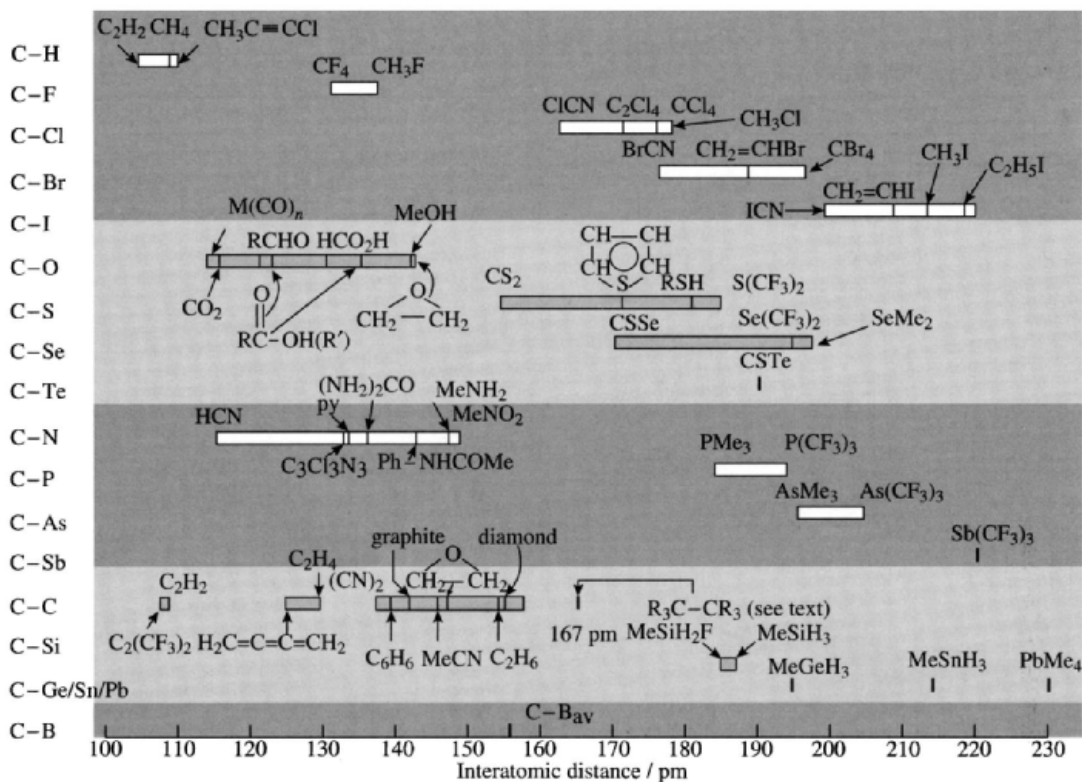


Figure 8.14 Some interatomic distances involving carbon.

Interatomic distances vary with the type of bond and the nature of the other atoms or groups attached to the bonded atoms. For example, the formally single-bonded C-C distance varies from 146 pm in  $Me-CN$  to 163.8 pm in  $Bu_2^nPhC-CPhBu_2^{(74)}$  and 167 pm in  $3,5-Bu_2^i-C_6H_3)_2C-C(C_6H_3-3,5-Bu_2^i)_3$  and  $(CF_3)_2(4-FC_6H_4)C-C(C_6H_4-4-F)(CF_3)_2$ .<sup>(75)</sup> Some typical examples are in Fig. 8.14. Note that because of the breadth of some of these ranges the interatomic distance between quite different pairs of atoms can be identical. For example, the value 133 pm includes C-F, C-O, C-N and C-C; likewise the value of 185 pm includes C-Br, C-S, C-Se, C-P and C-Si. The conventional

classification into single, double and triple bonds is adopted for simplicity, but bonding is frequently more subtle and more extended than these localized descriptions imply. Bond energies are listed on p. 374, where they are compared with those for other elements of Group 14. It should perhaps be emphasized that interatomic distances are experimentally observable, whereas bond orders depend on theoretical models and the estimation of bond energies in polyatomic molecules depends additionally on various assumptions as to how the total energy is apportioned. Nevertheless, taken together, the data indicate that an increase in the order of a bond between 2 atoms is accompanied both by a decrease in bond length and by an increase in bond energy. Similarly, for a given bond order between C and a series of other elements (e.g. C-X), the bond energy increases as the bond length decreases.

<sup>74</sup> W. LITTFE and U. DRÜCK, *Angew. Chem. Int. Edn. Engl.* **18**, 406-7 (1979).

<sup>75</sup> B. KAHR, D. VAN EUGEN and K. MISLOW, *J. Am. Chem. Soc.* **108**, 8305-7 (1986), and references cited therein.



## 8.3 Graphite Intercalation Compounds<sup>(76)</sup>

The large interlayer distance between the parallel planes of C atoms in graphite implies that the interlayer bonding is relatively weak. This accounts for the ready cleavage along the basal plane and the remarkable softness of the crystals. It also enables a wide range of substances to intercalate between the planes under mild conditions to give lamellar compounds of variable composition. These reactions are often reversible (unlike those with O and F discussed above) and the graphitic nature of the host lattice is retained. The compounds have quite different structures and properties from those previously encountered in this book and so will be described in some detail. They may be compared with the materials formed by intercalation into certain sheet silicates (p. 349).

The first alkali-metal graphite compound was reported in 1926: bronze-coloured  $C_8K$  was formed by direct reaction of graphite with K vapour at  $300^\circ\text{C}$ . Rubidium and Cs behave similarly. When heated at  $\sim 360^\circ$  under reduced pressure the metal is removed in stages to give a series of intercalation compounds  $C_8M$  (bronze-red),  $C_{24}M$  (steel-blue),  $C_{36}M$  (dark blue),  $C_{48}M$  (black) and  $C_{60}M$  (black). The compounds can also be prepared by electrolysis of fused melts with graphite electrodes, by reaction of graphite with solutions of M in liquid ammonia or amines, and by exchange reactions using M/aromatic radical anions. Intercalation is more difficult to achieve with Li and Na though direct reaction with highly purified graphite at  $500^\circ$  yields  $C_6\text{Li}$  (brass coloured),  $C_{12}\text{Li}$  (copper), and  $C_{18}\text{Li}$  (steel), and reaction with Li/naphthalene in thf yields  $C_{16}\text{Li}$  and  $C_{40}\text{Li}$ . Corresponding reaction of graphite and molten Na at  $450^\circ$  gives  $C_{64}\text{Na}$  (deep violet) whereas Na/naphthalene gives  $C_{32}\text{Na}$  and  $C_{120}\text{Na}$ .

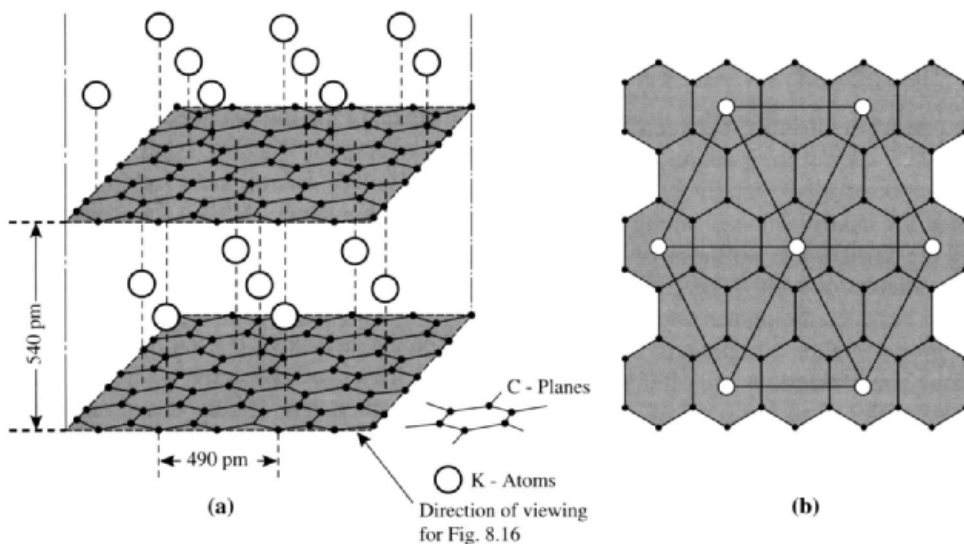
The crystal structure of  $C_8K$  is shown in Fig. 8.15(a); the graphite layers remain intact but are stacked vertically above each other instead of in the sequence  $\cdots\text{ABAB}\cdots$  found in  $\alpha$ -graphite itself. Each graphite layer is interleaved by a layer of K atoms having a commensurate lattice in which the spacing between each K is twice the spacing between the centres of the graphite hexagons (Fig. 8.15(b)). The stoichiometries of the other stages can then be achieved by varying the frequency of occurrence of the intercalated M layers in the host lattice. An idealized representation of this model is shown in Fig. 8.16. Difficulties are encountered in devising a plausible mechanistic route to the formation of these compounds since the direct preparation of one stage from an adjacent stage apparently requires both the complete emptying and the complete filling of inserted layers. It may be that the situation is more complex, with distributions of stages rather than a single uniform arrangement for each stoichiometry. Very recently a new metal-rich phase has been prepared by reacting graphite with molten potassium; the composition is very close to  $C_4K$  and the structure comprises double planes of K atoms intercalated between each graphite sheet, with a consequent increase in the interplanar spacing to 850 pm.<sup>(77)</sup>

The electrical resistance of graphite intercalation compounds is even lower than for graphite itself, resistance along the  $a$ -axis dropping by a factor of  $\sim 10$  and that along the  $c$ -axis by  $\sim 100$ ; moreover, in contrast to graphite, which is diamagnetic, the compounds have a temperature-independent (Pauli) paramagnetism and also behave as true metals in having a resistivity that increases with increase in temperature. This is illustrated by the comparative data shown in Table 8.2.

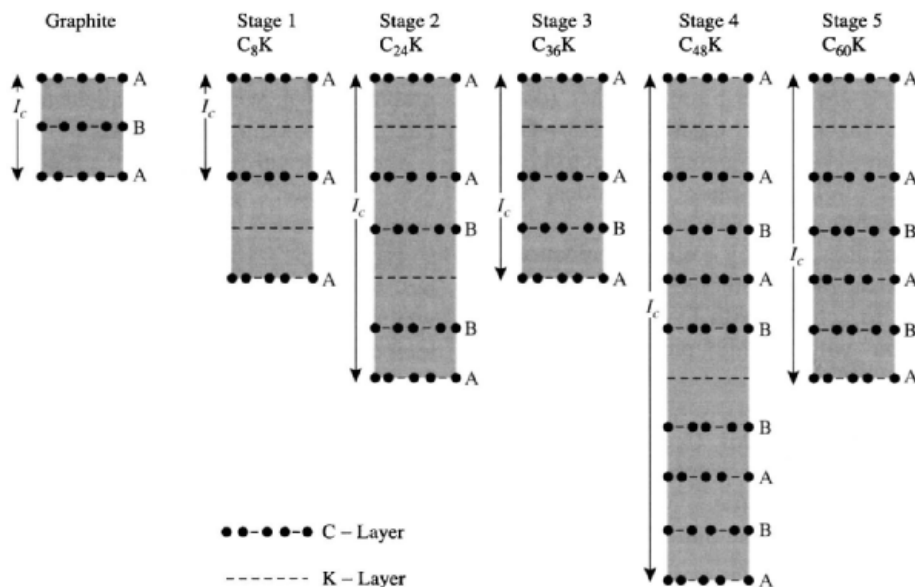
These data, and the other properties of  $C_nM$ , suggest that bonding occurs by transfer of electrons from the alkali metal atoms to the conduction band of the host graphite. Consistent with

<sup>76</sup> L. B. EBERT, *A. Rev. Materials Sci.* **6**, 181–211 (1976). A. HÉROLD, in F. LEVY (ed.), *Intercalated Layered Materials*, pp. 323–421, Reidel, 1979. H. SELIG and L. B. EBERT, *Adv. Inorg. Chem. Radiochem.* **23**, 281–327 (1980); a review with  $\sim 350$  references.

<sup>77</sup> M. EL GADI, C. HÉROLD and P. LAGRANGE, *Compt. Rend. Acad. Sci. Paris* **316**, 763–9 (1993).



**Figure 8.15** (a) Crystal lattice of  $C_8K$  showing the vertical packing of graphitic layers. The C-C distance within layers almost identical to that in graphite itself but the interplanar spacing (540 pm) is much larger than for graphite (335 pm) due to the presence of K atoms. The spacing increases still further to 561 pm for  $C_8Rb$  and to 595 pm for  $C_8Cs$ . (b) Triangular location of K atoms in  $C_8K$  showing the relation to the host graphite layers. In the other alkali-metal graphite compounds  $C_{12n}M$  the central M atom is missing, leading to a stoichiometry of  $C_{12}M$  if every alternate layer is M,  $C_{24}M$  if each third layer is M, etc.



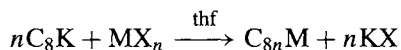
**Figure 8.16** Layer-plane sequence along the  $c$ -axis for graphite in various stage 1-5 of alkali-metal graphite intercalation compounds. Comparison with Fig. 8.15 shows that the horizontal planes are being viewed diagonally across the figure.  $I_c$  is the interlayer repeat distance along the  $c$ -axis.

**Table 8.2** Resistivity of graphite and its intercalates

Material	$\rho$ (90 K)/ohm cm	$\rho$ (285 K)/ohm cm	$\rho_{90}/\rho_{285}$
$\alpha$ -graphite	37.7	28.4	1.33
C <sub>8</sub> K	0.768	1.02	0.75
C <sub>12</sub> K	0.932	1.15	0.81

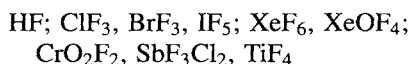
this, direct metal intercalation has only been observed with the most electropositive elements (Group 1) though Ba, with a first-stage ionization energy intermediate between those of Li and Na, was recently (1974) found to give C<sub>6</sub>Ba.

Alkali-metal graphites are extremely reactive in air and may explode with water. In general, reactivity decreases with ease of ionization of M in the sequence Li > Na > K > Rb > Cs. Under controlled conditions H<sub>2</sub>O or ROH produce only H<sub>2</sub>, MOH and graphite, unlike the alkali-metal carbides M<sub>2</sub>C<sub>2</sub> (p. 297) which produce hydrocarbons such as acetylene. In an important new reaction C<sub>8</sub>K has been found to react smoothly with transition metal salts in tetrahydrofuran at room temperature to give the corresponding transition metal lamellar compounds:<sup>(78)</sup>



Examples include reaction of Ti(OPr<sup>i</sup>)<sub>4</sub>, MnCl<sub>2</sub>·4H<sub>2</sub>O, FeCl<sub>3</sub>, CoCl<sub>2</sub>·6H<sub>2</sub>O, CuCl<sub>2</sub>·2H<sub>2</sub>O, and ZnCl<sub>2</sub> to give C<sub>32</sub>Ti, C<sub>16</sub>Mn, C<sub>24</sub>Fe, C<sub>16</sub>Co, C<sub>16</sub>Cu and C<sub>16</sub>Zn, respectively.

A quite different sort of graphite intercalation compound is formed by the halides of many elements, particularly those halides which themselves have layer structures or weak intermolecular binding. The first such compound (1932) was with FeCl<sub>3</sub>; chlorides, in general, have been the most studied, but fluoride and bromide intercalates are also known. Halides which have been reported to intercalate include the following:



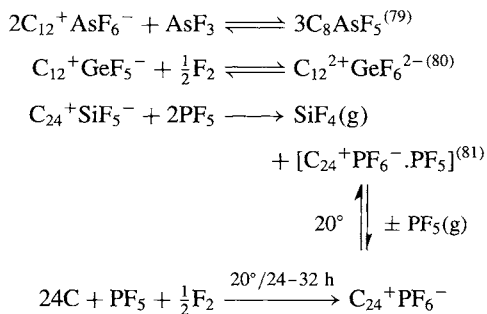
MF<sub>5</sub> (M = As, Sb, Nb, Ta); UF<sub>6</sub>  
 MCl<sub>2</sub>: M = Be; Mn, Co, Ni, Cu; Zn, Cd, Hg  
 MCl<sub>3</sub>: M = B, Al, Ga, In, Tl; Y; Sm, Eu,  
 Gd, Tb, Dy; Cr, Fe, Co; Ru, Rh, Au; I  
 MCl<sub>4</sub>: M = Zr, Hf; Re, Ir; Pd, Pt  
 MCl<sub>5</sub>: M = Sb; Mo; U  
 MCl<sub>6</sub>: M = W, U; also CrO<sub>2</sub>Cl<sub>2</sub>, UO<sub>2</sub>Cl<sub>2</sub>  
 Mixtures of AlCl<sub>3</sub> plus Br<sub>2</sub>, I<sub>2</sub>, ICl<sub>3</sub>,  
 FeCl<sub>3</sub>, WCl<sub>6</sub>  
 Bromides: CuBr<sub>2</sub>; AlBr<sub>3</sub>, GaBr<sub>3</sub>; AuBr<sub>3</sub>

The intercalates are usually prepared by heating a mixture of the reactants though sometimes the presence of free Cl<sub>2</sub> is also necessary, particularly for "non-oxidizing" chlorides such as MnCl<sub>2</sub>, NiCl<sub>2</sub>, ZnCl<sub>2</sub>, AlCl<sub>3</sub>, etc. Many of the compounds appear to show various stages of intercalation, the first stage usually exhibiting a typical blue colour. A common feature of many of the intercalated halides is their ability to act as electron-pair acceptors (Lewis acids). Low heat of sublimation is a further characteristic of most of the intercalating compounds. It may be that an important feature is an ability of the guest molecule to form a layer lattice commensurate with the host graphite. For example, in C<sub>6,69</sub>FeCl<sub>3</sub> the intercalated FeCl<sub>3</sub> has a layer structure similar to that in FeCl<sub>3</sub> itself with Cl in approximately close-packed arrangement though with some distortion, and with extensive stacking disorder. The "first-stage" compound varies in composition in the range C<sub>~6-7</sub>FeCl<sub>3</sub>; in addition a "second-stage" compound corresponding to C<sub>~12</sub>FeCl<sub>3</sub> is known, and also a "third-stage" with composition in the range C<sub>~24-30</sub>FeCl<sub>3</sub>. Another well-characterized phase occurs with MoCl<sub>5</sub>: layers of close-packed Mo<sub>2</sub>Cl<sub>10</sub> molecules alternate with sets of 4 graphite layers along the *c*-axis.

There appears to be a small but definite transfer of electron charge from the graphite to the guest species and this has led to formulations such as C<sub>70</sub><sup>+</sup>Cl<sup>-</sup>.FeCl<sub>2</sub>.5FeCl<sub>3</sub>. Similarly, the intercalate of AlCl<sub>3</sub> (which is formed in the presence of free Cl<sub>2</sub>) has been formulated as C<sub>27</sub><sup>+</sup>Cl<sup>-</sup>.3AlCl<sub>3</sub> or C<sub>27</sub><sup>+</sup>AlCl<sub>4</sub><sup>-</sup>.2AlCl<sub>3</sub>. This would explain the enhanced conductivity of the graphite-metal

<sup>78</sup> D. BRAGA, A. RIPAMONTI, D. SAVOIA, C. TROMBINI and A. UMANI-RONCHI, *J. Chem. Soc., Dalton Trans.*, 2026-8 (1979).

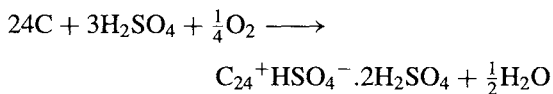
halide compounds, due to the formation of positive holes near the top of the valence band. However, despite extensive work using a variety of techniques, many structural problems remain unresolved and there is still no consensus on the detailed description of the bonding. Recent work includes studies on intercalation and staging in main-group element fluoride systems, e.g. (using ionic formulations)



The halogens themselves show a curious alternation of behaviour towards graphite.  $\text{F}_2$  gives the compounds  $\text{CF}$ ,  $\text{C}_2\text{F}$  and  $\text{C}_4\text{F}$  (p. 289) whereas liquid  $\text{Cl}_2$  reacts slowly to give  $\text{C}_8\text{Cl}$ , and  $\text{I}_2$  appears not to intercalate at all. By contrast,  $\text{Br}_2$  readily intercalates in several stages to give compounds of formula  $\text{C}_8\text{Br}$ ,  $\text{C}_{12}\text{Br}$ ,  $\text{C}_{16}\text{Br}$  and  $\text{C}_{20}\text{Br}$ ; the compounds  $\text{C}_{14}\text{Br}$  and  $\text{C}_{28}\text{Br}$  have also been well-characterized crystallographically but may be metastable phases. A notable feature of the  $\text{Br}_2$  intercalation reaction is that it is completely prevented by prior coating of the *basal* plane of the sample of graphite with a layer impervious to  $\text{Br}_2$ . The lamellar character of blue  $\text{C}_8\text{Br}$  has been confirmed by X-ray diffraction and the intercalation of bromine, is accompanied by a marked decrease in the resistivity of the graphite — more than tenfold along the *a*-axis and twofold along the *c*-axis.  $\text{C}_8\text{ICl}$  and  $\text{C}_{36}\text{ICl}$  have also been prepared.

Numerous oxides, sulfides and oxoacids have been found to intercalate into graphite. For example, lamellar compounds with  $\text{SO}_3$ ,  $\text{N}_2\text{O}_5$  and  $\text{Cl}_2\text{O}_7$  are known (but not with  $\text{SO}_2$ ,  $\text{NO}$  or  $\text{NO}_2$ ).  $\text{CrO}_3$  and  $\text{MoO}_3$  readily intercalate as do several sulfides such as  $\text{V}_2\text{S}_3$ ,  $\text{Cr}_2\text{S}_3(+\text{S})$ ,  $\text{WS}_2$ ,  $\text{PdS}(+\text{S})$  and  $\text{Sb}_2\text{S}_5$ . Metal nitrates and oxonitrates can also form intercalates, e.g.  $\text{Cu}(\text{NO}_3)_2$ ,  $\text{Zn}(\text{NO}_3)_2$ ,  $\text{Zr}(\text{NO}_3)_4$ ,  $\text{CrO}_2(\text{NO}_3)_2$ ,  $\text{NbO}(\text{NO}_3)_3$  and  $\text{TaO}(\text{NO}_3)_3$ . A recent example is  $[\text{C}_{28}\text{MoO}_2(\text{NO}_3)_2\cdot 0.3\text{N}_2\text{O}_5]^{(82)}$

The reversible intercalation of various oxoacids under oxidizing conditions leads to lamellar graphite “salts” some of which have been known for over a century and are now particularly well characterized structurally. For example, the formation of the blue, “first-stage” compound with conc  $\text{H}_2\text{SO}_4$  can be expressed by the idealized equation



The overall stoichiometry is thus close to  $\text{C}_8\text{H}_2\text{SO}_4$  and the structure is very similar to that of  $\text{C}_8\text{K}$  (p. 293) except for the detail of vertical alignment of the carbon atoms in the *c* direction which is  $\dots\text{ABAB}\dots$ . Several later stages (2, 3, 4, 5, 11) have been established and their properties studied. Intercalation is accompanied by a marked decrease in electrical resistance. A series of graphite nitrates can be prepared similarly, e.g.  $\text{C}_{24}^+\text{NO}_3^-\cdot 2\text{HNO}_3$  (blue),  $\text{C}_{48}^+\text{NO}_3^-\cdot 3\text{HNO}_3$  (black), etc. Other oxoacids which intercalate (particularly under electrolytic conditions) include  $\text{HClO}_4$ ,  $\text{HSO}_3\text{F}$ ,  $\text{HSO}_3\text{Cl}$ ,  $\text{H}_2\text{SeO}_4$ ,  $\text{H}_3\text{PO}_4$ ,  $\text{H}_4\text{P}_2\text{O}_7$ ,  $\text{H}_3\text{AsO}_4$ ,  $\text{CF}_3\text{CO}_2\text{H}$ ,  $\text{CCl}_3\text{CO}_2\text{H}$ , etc. The extent of intercalation depends both on the strength of the acid and its concentration, and the reactions are of considerable technological importance because they can lead to the swelling and eventual destruction of the graphite electrodes used in many electrochemical processes.

<sup>79</sup> E. M. McCARRON and N. BARTLETT, *J. Chem. Soc., Chem. Commun.*, 404–6 (1980).

<sup>80</sup> E. M. McCARRON, J. GRANNEC and N. BARTLETT, *J. Chem. Soc., Chem. Commun.*, 890–1 (1980).

<sup>81</sup> G. L. ROSENTHAL, T. E. MALLOUK and N. BARTLETT, *Synthetic Metals* **9**, 433–40 (1984).

<sup>82</sup> E. STUMPP and H. GRIEBEL, *Z. anorg. allg. Chem.* **579**, 205–10 (1989).

## 8.4 Carbides

Carbon forms binary compounds with most elements: those with metals are considered in this section whilst those with H, the halogens, O, and the chalcogens are discussed in subsequent sections. Alkali metal fullerides and encapsulated (endohedral) metallafullerenes have already been considered (pp. 285, 288 respectively) and metallocarbohedrenes (metcars) will be dealt with later in this section (p. 300). Silicon carbide is discussed on p. 334. General methods of preparation of metal carbides are:<sup>(83)</sup>

- (1) Direct combination of the elements above  $\sim 2000^\circ\text{C}$ .
- (2) Reaction of the metal oxide with carbon at high temperature.
- (3) Reaction of the heated metal with gaseous hydrocarbon.
- (4) Reaction of acetylene with electropositive metals in liquid ammonia.

Attempts to classify carbides according to structure or bond type meet the same difficulties as were encountered with hydrides (p. 64) and borides (p. 145) and for the same reasons. The general trends in properties of the three groups of compounds are, however, broadly similar, being most polar (ionic) for the electropositive metals, most covalent (molecular) for the electronegative non-metals and somewhat complex (interstitial) for the elements in the centre of the d block. There are also several elements with poorly characterized, unstable, or non-existent carbides, namely the later transition elements (Groups 11 and 12), the platinum metals, and the post transition-metal elements in Group 13.

Salt-like carbides containing individual C "anions" are sometimes called "methanides" since they yield predominantly  $\text{CH}_4$  on hydrolysis.  $\text{Be}_2\text{C}$  and  $\text{Al}_4\text{C}_3$  are the best-characterized examples, indicating the importance of small

compact cations.  $\text{Be}_2\text{C}$  is prepared from  $\text{BeO}$  and C at  $1900\text{--}2000^\circ\text{C}$ ; it is brick-red, has the antifluorite structure (p. 118), and decomposes to graphite when heated above  $2100^\circ$ . *Ab initio* calculations suggest that the structure is predominantly ionic with charges close to the nominal  $\text{Be}^{2+}_2\text{C}^{4-}$ .<sup>(84)</sup>  $\text{Al}_4\text{C}_3$ , prepared by direct union of the elements in an electric furnace, forms pale-yellow crystals, mp  $2200^\circ\text{C}$ . It has a complex structure in which  $\{\text{AlC}_4\}$  tetrahedra of two types are linked to form a layer lattice: this defines two types of C atom, one surrounded by a deformed octahedron of 6 Al at 217 pm and the other surrounded by 4 Al at 190–194 pm and a fifth Al at 221 pm. The closest C...C approach is at the nonbonding distance of 316 pm. Although it is formally possible to describe the structure as ionic,  $(\text{Al}^{3+})_4(\text{C}^{4-})_3$ , such a gross separation of charges is unlikely to occur over the observed interatomic distances.

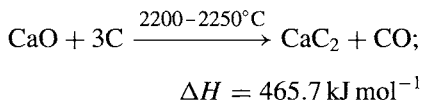
Carbides containing a  $\text{C}_2$  unit are well known; they are exemplified by the acetylides (ethynides) of the alkali metals,  $\text{M}_2^{\text{I}}\text{C}_2$ , alkaline earth metals,  $\text{M}^{\text{II}}\text{C}_2$ , and the lanthanoids  $\text{LnC}_2$  and  $\text{Ln}_2\text{C}_3$  i.e.  $\text{Ln}_4(\text{C}_2)_3$ . The corresponding compounds of Group 11 (Cu, Ag, Au) are explosive and those of Group 12 (Zn, Cd, Hg) are poorly characterized.  $\text{M}_2^{\text{I}}\text{C}_2$  are best prepared by the action of  $\text{C}_2\text{H}_2$  on a solution of alkali metal in liquid  $\text{NH}_3$ ; they are colourless crystalline compounds which react violently with water and oxidize to the carbonate on being heated in air.  $\text{M}^{\text{II}}\text{C}_2$  can be prepared by heating the alkaline earth metal with ethyne above  $500^\circ\text{C}$ . By far the most important compound in this group is  $\text{CaC}_2$  — it is manufactured on a huge scale, 6.4 million tonnes worldwide in 1982 and is used as a major source of ethyne for the chemical industry and for oxyacetylene welding. US production peaked at 1.03 Mt in 1964 but then declined substantially as ethyne became available from petrochemical feedstocks, from the thermal cracking of hydrocarbons and as a byproduct of  $\text{C}_2\text{H}_4$  manufacture. US production of  $\text{CaC}_2$

<sup>83</sup> Reference 2, pp. 841–911: Carbides (p. 841); Cemented carbides (p. 848); Industrial hard carbides (p. 861); Calcium carbide (p. 878); Silicon carbide (p. 891).

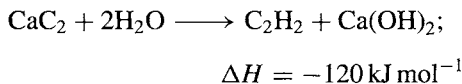
<sup>84</sup> P. W. FOWLER and P. TOLE, *J. Chem. Soc., Chem. Commun.*, 1652–4 (1989).

has been below 250 000 tonnes per annum for the past 20 years and was 236 000 tonnes in 1990 (price \$515/t). Europe (3.25 Mtpa) and Asia/Australia (2.42 Mtpa) are currently the major producers.

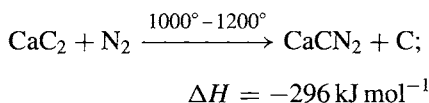
Industrially,  $\text{CaC}_2$  is produced by the endothermic reaction of lime and coke:



Subsequent hydrolysis is highly exothermic and must be carefully controlled:

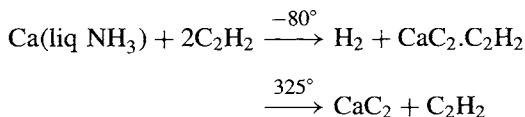


Another industrially important reaction of  $\text{CaC}_2$  is its ability to fix  $\text{N}_2$  from the air by formation of calcium cyanamide:

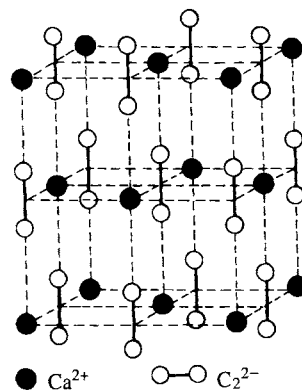


$\text{CaCN}_2$  is widely used as a fertilizer because of its ready hydrolysis to cyanamide,  $\text{H}_2\text{NCN}$  (p. 323).

Pure  $\text{CaC}_2$  is a colourless solid, mp  $2300^\circ\text{C}$ . It can be prepared on the laboratory scale by passing ethyne into a solution of Ca in liquid  $\text{NH}_3$ , followed by decomposition of the complex so formed, under reduced pressure at  $\sim 325^\circ$ :



It exists in at least four crystalline forms, the one stable at room temperature being a tetragonally distorted NaCl-type structure (Fig. 8.17) in which the  $\text{C}_2$  units are aligned along the  $c$ -axis. The ethynides of Mg, Sr and Ba have the same structure and also hydrolyse to give ethyne. In addition,  $\text{BaC}_2$  absorbs  $\text{N}_2$  from the atmosphere to give  $\text{Ba}(\text{CN})_2$  (cf.  $\text{CaC}_2$  above).



**Figure 8.17** Crystal structure of tetragonal  $\text{CaC}_2$  showing the resemblance to NaCl (p. 242). Above  $450^\circ\text{C}$  the parallel alignment of the  $\text{C}_2$  units breaks down and the structure becomes cubic.

Carbides containing the essentially linear  $\text{C}_3^{4-}$  unit are known, e.g.  $\text{Li}_4\text{C}_3$ ,  $\text{Mg}_2\text{C}_3$ , and the recently characterized  $\text{Ca}_3\text{C}_3\text{Cl}_2$  and  $\text{Sc}_3\text{C}_4$ .<sup>(85)</sup> Thus  $\text{Ca}_3\text{C}_3\text{Cl}_2$  forms as transparent red crystals when  $\text{CaCl}_2$  is heated with graphite in sealed Ta capsules at  $900^\circ\text{C}$  for 1 day (C–C 134.6 pm, angle  $169.0^\circ$ ). By contrast  $\text{Sc}_3\text{C}_4$  is a grey-black metallic substance with Pauli paramagnetism: it contains  $\text{C}^{4-}$  and  $\text{C}_2^{2-}$  ions, and supernumerary electrons  $e^-$  in addition to  $\text{C}_3^{4-}$  (C–C 134.2 pm, angle  $175.8^\circ$ ). It can best be represented as  $10\text{Sc}_3\text{C}_4 \equiv [(\text{Sc}^{3+})_{30}(\text{C}^{4-})_{12}(\text{C}_2^{2-})_2(\text{C}_3^{4-})_8(e^-)_6]$ .<sup>(85)</sup>

The carbides of the lanthanoids and actinoids can be prepared by heating  $\text{M}_2\text{O}_3$  with C in an electric furnace or by arc-melting compressed pellets of the elements in an inert atmosphere. They contain the  $\text{C}_2$  unit and have a stoichiometry  $\text{MC}_2$  or  $\text{M}_4(\text{C}_2)_3$ .  $\text{MC}_2$  have the  $\text{CaC}_2$  structure or a related one of lower symmetry in which the  $\text{C}_2$  units lie at right-angles to the  $c$ -axis of an orthogonal NaCl-type cell.<sup>(86)</sup> They are more reactive than the alkaline-earth metal

<sup>85</sup> R. HOFFMANN and H.-J. MEYER, *Z. anorg. allg. Chem.* **607**, 57–71 (1992).

<sup>86</sup> A. F. WELLS, *Structural Inorganic Chemistry*, 5th edn., Oxford University Press, Oxford, 1984, 1382 pp.

carbides, combining readily with atmospheric oxygen and hydrolysing to a complex mixture of hydrocarbons. This derives from their more complicated electronic structure and, indeed,  $\text{LnC}_2$  are metallic conductors (not insulators like  $\text{CaC}_2$ ); they are best regarded as ethynides of  $\text{Ln}^{\text{III}}$  with the supernumerary electron partly delocalized in a conduction band of the crystal. This would explain the evolution of  $\text{H}_2$  as well as  $\text{C}_2\text{H}_2$  on hydrolysis, and the simultaneous production of the reduced species  $\text{C}_2\text{H}_4$  and  $\text{C}_2\text{H}_6$  together with various other hydrocarbons up to  $\text{C}_6\text{H}_{10}$ :



An interesting feature of the ethynides  $\text{MC}_2$  and  $\text{M}_4(\text{C}_2)_3$  is the variation in the C–C distance as measured by neutron diffraction. Typical values (in pm) are:

$\text{CaC}_2$	$\text{YC}_2$	$\text{CeC}_2$	$\text{LaC}_2$	$\text{UC}_2$
119.2	127.5	128.3	130.3	135.0
$\text{La}_4(\text{C}_2)_3$	$\text{Ce}_4(\text{C}_2)_3$	$\text{U}_4(\text{C}_2)_3$		
123.6	127.6	129.5		

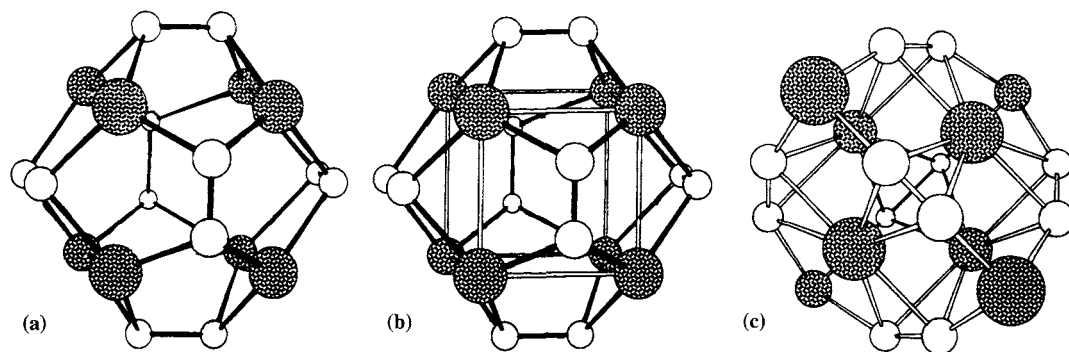
The C–C distance in  $\text{CaC}_2$  is close to that in ethyne (120.5 pm) and it has been suggested that the observed increase in the lanthanoid and actinoid carbides results from a partial localization of the supernumerary electron in the antibonding orbital of the ethynide ion  $[\text{C}\equiv\text{C}]^{2-}$  (see p. 932). The effect is noticeably less in the sesquicarbides than in the dicarbides. The compounds  $\text{EuC}_2$  and  $\text{YbC}_2$  differ in their lattice parameters and hydrolysis behaviour from the other  $\text{LnC}_2$  and this may be related to the relative stability of  $\text{Eu}^{\text{II}}$  and  $\text{Yb}^{\text{II}}$  (p. 1237).

The lanthanoids also form metal-rich carbides of stoichiometry  $\text{M}_3\text{C}$  in which individual C atoms occupy at random one-third of the octahedral Cl sites in a NaCl-like structure. Several of the actinoids (e.g. Th, U, Pu) form monocarbides,  $\text{MC}$ , in which all the octahedral Cl sites in the NaCl structure are occupied and this stoichiometry is also observed for several other carbides of the early transition elements, e.g.  $\text{M} = \text{Ti}, \text{Zr}, \text{Hf}; \text{V}, \text{Nb}, \text{Ta}; \text{Mo}, \text{W}$ . These

are best considered as interstitial carbides and in this sense the lanthanoids and actinoids occupy an intermediate position in the classification of the carbides, as they did with the hydrides (p. 66).

Interstitial carbides are infusible, extremely hard, refractory materials that retain many of the characteristic properties of metals (lustre, metallic conductivity).<sup>(87)</sup> Reported mps are frequently in the range 3000–4000°C. Interstitial carbides derive their name from the fact that the C atoms occupy octahedral interstices in a close-packed lattice of metal atoms, though the arrangement of metal atoms is not always the same as in the metal itself. The size of the metal atoms must be large enough to generate a site of sufficient size to accommodate C, and the critical radius of M seems to be  $\sim 135$  pm: thus the transition metals mentioned in the preceding paragraph all have 12-coordinate radii  $> 135$  pm, whereas metals with smaller radii (e.g. Cr, Mn, Fe, Co, Ni) do not form MC and their interstitial carbides have a more complex structure (see below). If the close-packed arrangement of M atoms is hexagonal (h) rather than cubic (c) then the 2 octahedral interstices on either side of a close-packed M layer are located directly above one another and only one of these is ever occupied. This gives a stoichiometry  $\text{M}_2\text{C}$  as in  $\text{V}_2\text{C}$ ,  $\text{Nb}_2\text{C}$ ,  $\text{Ta}_2\text{C}$  and  $\text{W}_2\text{C}$ . Intermediate stoichiometries are encountered when the M atom stacking sequence alternates, e.g.  $\text{Mo}_3\text{C}_2$  (hcc) and  $\text{V}_4\text{C}_3$  (hhcc). Ordered defect NaCl-type structures are also known, e.g.  $\text{V}_8\text{C}_7$  and  $\text{V}_6\text{C}_5$ , thus illustrating the wide range of stoichiometries which occur among interstitial carbides. Unlike the “ionic” carbides, interstitial carbides do not react with water and are generally very inert, though some do react with air when heated above 1000° and most are degraded by conc  $\text{HNO}_3$  or HF. The extreme hardness and inertness of WC and TaC have led to their extensive use as high-speed cutting tools.

<sup>87</sup> H. H. JOHANSEN, *Survey of Progress in Chemistry* **8**, 57–81 (1977). See also A. COTTRELL, *Chemical Bonding in Transition Metal Carbides*, Inst. of Materials, London, 1995, 99 pp.



**Figure 8.18** (a) Proposed pentagonal dodecahedral structure of  $Ti_8C_{12}$ . (b) The same structure viewed as a  $Ti_8$  cube with each face capped by a  $C_2$  group. (c) An alternative  $T_h$  structure (see text).

**Table 8.3** Stoichiometries of some transition element carbides

$V_2C$ , $V_4C_3$	$Cr_{23}C_6$	$Mn_{23}C_6$ , $Mn_{15}C_4$	$Fe_3C$ , $Fe_7C_3$	$Co_3C$	$Ni_3C$
$V_6C_5$ , $V_8C_7$	$Cr_7C_3$	$Mn_3C$ , $Mn_5C_2$	$Fe_2C$	$Co_2C$	
$VC$	$Cr_3C_2$	$Mn_7C_3$			

The carbides of Cr, Mn, Fe, Co and Ni are profuse in number, complicated in structure, and of great importance industrially. Cementite,  $Fe_3C$ , is an important constituent of steel (p. 1075). Typical stoichiometries are listed in Table 8.3 though it should be noted that several of the phases can exist over a range of composition.

The structures, particularly of the most metal-rich phases, are frequently related to those of the corresponding metal-rich borides (and silicides, germanides, phosphides, arsenides, sulfides and selenides), in which the non-metal is surrounded by a trigonal prism of M atoms with 0, 1, 2, or 3 additional neighbours beyond the quadrilateral prism faces (p. 148). e.g.  $Fe_3C$  (cementite),  $Mn_3C$  and  $Co_3B$ ;  $Mn_5C_2$  and  $Pd_5B_2$ ;  $Cr_7C_3$  and  $Re_7B_3$ . Numerous ternary carbides, carbonitrides, and oxocarbides are also known.

The carbides of Cr, Mn, Fe, Co and Ni are much more reactive than the interstitial carbides of the earlier transition metals. They are rapidly hydrolysed by dilute acid and sometimes even by water to give  $H_2$  and a mixture of hydrocarbons. For example,  $M_3C$  give  $H_2$  (75%),  $CH_4$  (15%)

and  $C_2H_6$  (8%) together with small amounts of higher hydrocarbons.

### Metallo-carbohedrenes (met-cars)

An entirely novel group of binary metal carbides, reminiscent of the fullerenes (p. 279), were discovered by accident in 1992.<sup>(88)</sup> When Ti metal is vaporized in a laser plasma reactor in the presence of He gas containing a hydrocarbon such as methane, ethene, ethyne or benzene, the mass spectrum of the emerging beam contains a single dominant peak at 528 corresponding to  $Ti_8C_{12}$  [isotope  $^{48}Ti$  73.8% abundant:  $(8 \times 48) + (12 \times 12) = 528$ ]. Detailed isotope distribution studies confirmed the molecular formula. The proposed structure, shown in Fig. 8.18a, is a pentagonal dodecahedron of  $T_h$  symmetry comprising 12 mutually fused  $Ti_2C_3$  pentagons.

<sup>88</sup> B. C. GUO, K. P. KERNS and A. W. CASTLEMAN, *Science* **255**, 1411–3 (1992). B. C. GUO, S. WEI, J. PURNELL, S. BUZZA and A. W. CASTLEMAN, *Science* **256**, 515–6 and 818–20 (1992), *J. Chem. Phys.* **96**, 4166–8 (1992).



Table 8.4 Some properties of methane and CX<sub>4</sub>

Property	CH <sub>4</sub>	CF <sub>4</sub>	CCl <sub>4</sub>	CBr <sub>4</sub>	CI <sub>4</sub>
MP/°C	-182.5	-183.5	-22.9	90.1	171 (d)
BP/°C	-161.5	-128.5	76.7	189.5	~130 (subl)
Density/g cm <sup>-3</sup> (at T°C)	0.424 (-164°)	1.96 (-184°)	1.594 (20°)	2.961 (100°)	4.32 (20°) (s)
-ΔH <sub>f</sub> <sup>o</sup> /kJ mol <sup>-1</sup>	74.87	679.9	106.7 (g) 139.3 (l)	160 (l)	—
D(X <sub>3</sub> C-X)/kJ mol <sup>-1</sup>	435	515	295	235	—

Each Ti bonds to 3C via  $\sigma$  bonds and each C bonds to 2Ti and one C. The all-carbon analogue, C<sub>20</sub>, is not expected to be stable because of severe internal strain; (it would be the smallest possible fullerene, p. 280). Note, however, that dodecahedrane, C<sub>20</sub>H<sub>20</sub>, is known.<sup>(89)</sup> An alternative description of the structure (Fig. 8.18b) would be as a weakly bonded cube, Ti<sub>8</sub>, each face of which is capped by a C<sub>2</sub> unit. The calculated distances<sup>(90)</sup> are Ti...Ti 302 pm, Ti-C 199 pm and C-C 140 pm (implying some multiple bonding; cf. 140 pm in benzene). An alternative *T<sub>h</sub>* structure for Ti<sub>8</sub>C<sub>12</sub>, which is calculated to have a lower energy, has also been proposed.<sup>(90)</sup> In this, the Ti<sub>8</sub> array is a tetracapped tetrahedron containing six Ti<sub>4</sub> faces in butterfly conformation; each of these Ti<sub>4</sub> faces can then accommodate a C<sub>2</sub> unit as shown in Fig. 8.18c.

Other met-cars that have been detected mass spectrometrically are M<sub>8</sub>C<sub>12</sub> (M = V, Zr, Hf) and there is some evidence for higher members such as Zr<sub>13</sub>C<sub>22</sub>, Zr<sub>14</sub>C<sub>23</sub>, Zr<sub>18</sub>C<sub>29</sub> and Zr<sub>23</sub>C<sub>32</sub> which may feature fused clusters of clusters. The possibility of a super-pentagonal cluster, M<sub>30</sub>C<sub>45</sub>, of *D<sub>5h</sub>* symmetry has also been mooted.<sup>(91)</sup>

As with the fullerenes, further detailed studies will depend on the discovery of viable bulk preparations of the met-cars. Macroscopic

amounts of Ti<sub>8</sub>C<sub>12</sub> and V<sub>8</sub>C<sub>12</sub> have indeed been made by DC arc discharge techniques using electrodes of compacted metal and graphite powders and He as the quenching carrier gas.<sup>(92)</sup> The resulting soot contains about 1% of air-stable M<sub>8</sub>C<sub>12</sub> plus some C<sub>60</sub> (unstable in air). Solution studies have not yet been reported but there is mass spectrometric evidence for Ti<sub>8</sub>C<sub>12</sub>L<sub>8</sub> (L = NH<sub>3</sub>, ND<sub>3</sub>, H<sub>2</sub>O) as well as for Ti<sub>8</sub>C<sub>12</sub>(MeOH)<sub>4</sub>.

## 8.5 Hydrides, Halides and Oxohalides

The ability of C to catenate (i.e. to form bonds to itself in compounds) is nowhere better illustrated than in the compounds it forms with H. Hydrocarbons occur in great variety in petroleum deposits and elsewhere, and form various homologous series in which the C atoms are linked into chains, branched chains and rings. The study of these compounds and their derivatives forms the subject of organic chemistry and is fully discussed in the many textbooks and treatises on that subject. The matter is further considered on p. 374 in relation to the much smaller ability of other Group 14 elements to form such catenated compounds. Methane, CH<sub>4</sub>, is the archetype of tetrahedral coordination in molecular compounds; some of its properties are listed in Table 8.4 where they are compared with those of the

<sup>89</sup> R. J. TERNANSKY, D. W. BALOGH and L. A. PAQUETTE, *J. Am. Chem. Soc.* **104**, 4503-4 (1982). J. C. GALLUCCI, C. W. DOECKE and L. A. PAQUETTE *J. Am. Chem. Soc.* **108**, 1343-4 (1986).

<sup>90</sup> I. G. DANCE, *J. Chem. Soc., Chem. Commun.*, 1779-80 (1992).

<sup>91</sup> I. G. DANCE, *Aust. J. Chem.* **46**, 727-30 (1993).

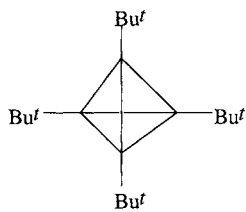
<sup>92</sup> S. F. CARTIER, Z. Y. CHEN, G. J. WALDER and A. W. CASTLEMAN, *Science* **260**, 195-6 (1993).

corresponding halides. Unsaturated hydrocarbons such as ethene ( $C_2H_4$ ), ethyne ( $C_2H_2$ ), benzene ( $C_6H_6$ ), cyclooctatetraene ( $C_8H_8$ ) and homocyclic radicals such as cyclopentadienyl ( $C_5H_5$ ) and cycloheptatrienyl ( $C_7H_7$ ) are effective ligands to metals and form many organometallic complexes (pp. 930–43).

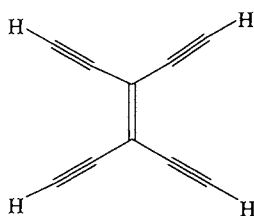
Methane is unique among hydrocarbons in being thermodynamically stable with respect to its elements. It follows that pyrolytic reactions to convert it to other hydrocarbons are energetically unfavourable and will be strongly equilibrium-limited. This is in marked contrast to the boranes where mild thermolysis of  $B_2H_6$  or  $B_4H_{10}$ , for example, readily yields mixtures of the higher boranes (p. 164). Vast natural reserves of  $CH_4$  gas exist but much is wasted

by flaring (direct burning off at the petroleum production site) because of the uneconomical cost of transport. However, in convenient locations such as the North Sea, natural gas is piped ashore for use as domestic or industrial fuel or as chemical feedstock. After  $CO_2$ , methane is the most important “greenhouse gas” (p. 273) accounting for an estimated 15–20% of the atmospheric global warming ( $CO_2 > 50\%$ ). The major sources of atmospheric  $CH_4$  are natural wetlands (25%), rice cultivation (22%), animals (mainly domestic ruminants) (17%) and the mining of fossil fuels (16%), the total “production” being some 460 million tonnes per annum.

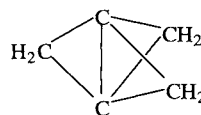
Notable recent advances in the chemistry of hydrocarbons include the synthesis and



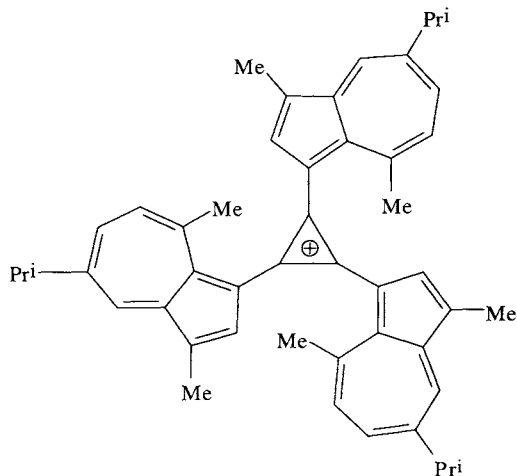
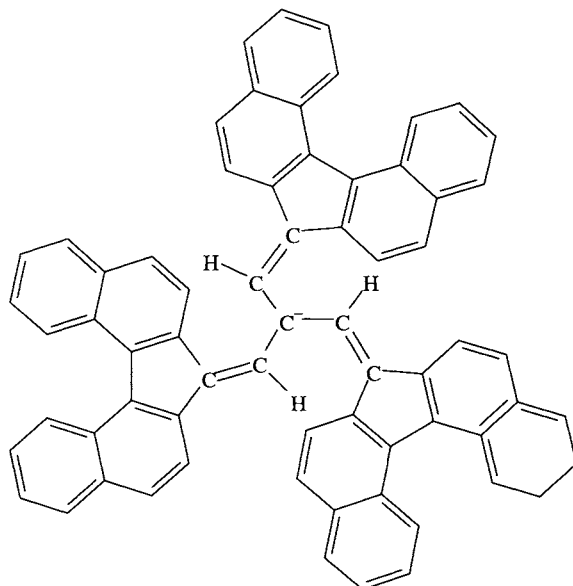
(1)

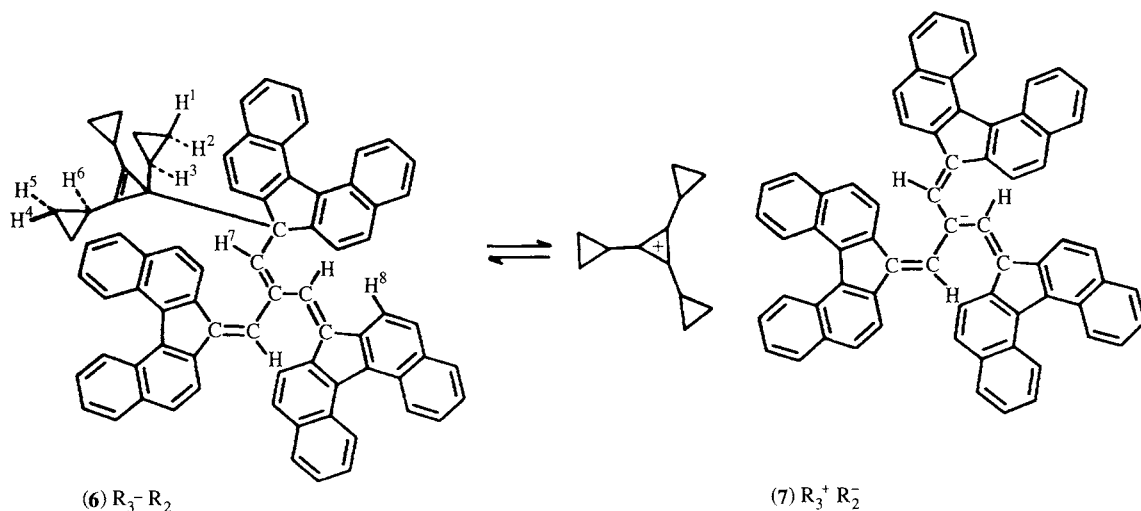


(2)



(3)

(4)  $R_1^+$ (5)  $R_2^-$



molecular structure determination of the tetrahydride derivative,  $C_4Bu_4^+$  (1),<sup>(93)</sup> the carbon-rich molecules tetraethynylmethane,  $C(C\equiv CH)_4$  i.e.  $C_9H_4$ <sup>(94)</sup> and tetraethynylethene,  $C_2(C\equiv CH)_4$  i.e.  $C_{10}H_4$ <sup>(95)</sup> the highly strained [1.1.1]propellane (3)<sup>(96)</sup> and the preparation of the largest discrete hydrocarbon molecules yet synthesized, the polyphenylethyne dendrimers  $C_{1134}H_{1146}$  and  $C_{1398}H_{1278}$  (mol wts 14 777.6 and 18 079.6).<sup>(97)</sup> There is also increasing interest in hydrocarbon salts  $R_1^+R_2^-$ . The first example was the stable, greenish-black crystalline compound  $C_{48}H_{51}^+C_{61}H_{39}^-$  (mp 230°C decomp.) obtained by mixing the solutions of Agranat's carbocation (4) and Kuhn's carbanion (5).<sup>(98)</sup> Of special interest is the covalent molecular hydrocarbon

$R_3-R_2$  (6) which exists in chloroform solution but which crystallizes on evaporation or cooling to give the ionic salt  $R_3^+R_2^-$  (7).<sup>(99)</sup> This reversible ionic-covalent equilibrium is reminiscent of similar behaviour in certain halides such as  $AlCl_3$  (p. 234),  $PCl_5$  (p. 499) and  $TeCl_4$  (p. 772), etc.

Fullerene derivatives such as  $C_{60}H_n$  (p. 283),  $C_{60}H_2$  (p. 287), and  $C_{61}H_2$  (p. 287), and hypercoordinated non-classical carbonium ions (p. 290) have already been briefly mentioned.

Turning next to the simple halides of carbon: tetrafluoromethane ( $CF_4$ ) is an exceptionally stable gas with mp close to that of  $CH_4$  (see Table 8.4). It can be prepared on a laboratory scale by reacting  $SiC$  with  $F_2$  or by fluorinating  $CO_2$ ,  $CO$  or  $COCl_2$  with  $SF_4$ . Industrially it is prepared by the aggressive reaction of  $F_2$  on  $CF_2Cl_2$  or  $CF_3Cl$ , or by electrolysis of  $MF$  or  $MF_2$  using a  $C$  anode.  $CF_4$  was first obtained pure in 1926;  $C_2F_6$  was isolated in 1930 and  $C_2F_4$  in 1933; but it was not until 1937 that the various homologous series of fluorocarbons were isolated and identified. Replacement of  $H$  by  $F$  greatly increases both thermal stability and chemical inertness because of the great strength of the  $C-F$

<sup>93</sup> H. IRNGARTINGER, A. GOLDMANN, R. JAHN, M. NIXDORF, H. RODEWALD, G. MAIER, K.-D. MALSCH and R. EMRICH, *Angew. Chem. Int. Edn. Engl.* **23**, 993–4 (1984).

<sup>94</sup> K. S. FELDMAN and C. M. KRAEBEL, *J. Am. Chem. Soc.* **115**, 3846–7 (1993).

<sup>95</sup> Y. RUBIN, C. B. KNOBLER and F. DIEDERICH, *Angew. Chem. Int. Edn. Engl.* **30**, 698–700 (1991).

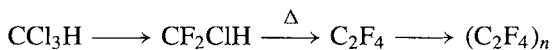
<sup>96</sup> J. E. JACKSON and L. C. ALLEN, *J. Am. Chem. Soc.* **106**, 591–9 (1984).

<sup>97</sup> Z. XU and J. S. MOORE, *Angew. Chem. Int. Edn. Engl.* **32**, 246–8 (1993), and *Abstracts*, ACS Denver Meeting, April 1993.

<sup>98</sup> K. OKAMOTO, T. KITAGAWA, K. TAKEUCHI, K. KOMATSU and K. TAKAHASHI, *J. Chem. Soc., Chem. Commun.*, 173–4 (1985).

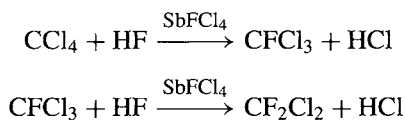
<sup>99</sup> K. OKAMOTO, T. KITAGAWA, K. TAKEUCHI, K. KOMATSU and A. MIYABO, *J. Chem. Soc., Chem. Commun.*, 923–4 (1988).

bond (Table 8.4). Accordingly, fluorocarbons are resistant to attack by acids, alkalis, oxidizing agents, reducing agents and most chemicals up to 600°. They are immiscible with both water and hydrocarbon solvents, and when combined with other groups they confer water-repellance and stain-resistance to paper, textiles and fabrics.<sup>(100)</sup> Tetrafluoroethene (C<sub>2</sub>F<sub>4</sub>) can be polymerized to a chemically inert, thermosetting plastic PTFE (polytetrafluoroethene); this has an extremely low coefficient of friction and is finding increasing use as a protective coating in non-stick kitchen utensils, razor blades and bearings. PTFE is made by partial fluorination of chloroform using HF in the presence of SbFCl<sub>4</sub> as catalyst, followed by thermolysis to C<sub>2</sub>F<sub>4</sub> and subsequent polymerization:



As a ligand towards metals, C<sub>2</sub>F<sub>4</sub> and other unsaturated fluorocarbons differ markedly from alkenes (p. 931).

CCl<sub>4</sub> is a common laboratory and industrial solvent with a distinctive smell, usually prepared by reaction of CS<sub>2</sub> or CH<sub>4</sub> with Cl<sub>2</sub>. Its use as a solvent has declined somewhat because of its toxicity, but CCl<sub>4</sub> is still extensively used as an intermediate in preparing "Freons" such as CFCl<sub>3</sub>, CF<sub>2</sub>Cl<sub>2</sub> and CF<sub>3</sub>Cl:<sup>(100)</sup>

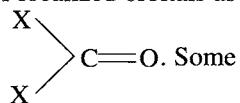


The catalyst is formed by reaction of HF on SbCl<sub>5</sub>. The Freons have a unique combination of properties which make them ideally suited for use as refrigerants and aerosol propellants. They have low bp, low viscosity, low surface tension and high density, and are non-toxic, non-flammable, odourless, chemically inert and thermally stable. The most commonly used is CF<sub>2</sub>Cl<sub>2</sub>, bp, -29.8°. The market for Freons

and other fluorocarbons expanded rapidly in the sixties: production in the USA alone exceeded 200 000 tonnes in 1964 (417 000 tonnes in 1990) and global production was about three times this amount. Already in 1977 there was an annual production of 2.4 × 10<sup>9</sup> spray-cans. However, there has been growing concern that chlorofluorocarbons from spray-cans gradually work their way into the upper atmosphere where they may, through a complex chemical reaction, deplete the earth's ozone layer (p. 608). For this reason there was an enforced progressive elimination of this particular application in the USA starting 15 October 1978 and production of CFCs will effectively be completely phased out following the Montreal Protocol of September 1981.

CBr<sub>4</sub> is a pale-yellow solid which is markedly less stable than the lighter tetrahalides. Preparation involves bromination of CH<sub>4</sub> with HBr or Br<sub>2</sub> or, more conveniently, reaction of CCl<sub>4</sub> with Al<sub>2</sub>Br<sub>6</sub> at 100°. The trend to diminishing thermal stability continues to Cl<sub>4</sub> which is a bright-red crystalline solid with a smell reminiscent of I<sub>2</sub>. It is prepared by the AlCl<sub>3</sub>-catalysed halogen exchange reaction between CCl<sub>4</sub> and EtI.

Carbon oxohalides are reactive gases or volatile liquids which feature planar molecules of C<sub>2v</sub> symmetry; they are isoelectronic with BX<sub>3</sub> (p. 196) and the bonding is best described in terms of molecular orbitals spanning all 4 atoms rather than in terms of localized orbitals as

implied by the formulation  C=O. Some

physical properties and molecular dimensions are in Table 8.5. The values call for little comment except to note that the XCX angle is significantly less (as expected) than the value of 120° found for the more symmetrical isoelectronic species BX<sub>3</sub> and CO<sub>3</sub><sup>2-</sup>. The C-Br distance is unusually long; it comes from a very early diffraction measurement and could profitably be checked.

Mixed oxohalides are also known and their volatilities are intermediate between those of the

<sup>100</sup> Kirk-Othmer Encyclopedia of Chemical Technology, 4th edn., Vol 11, 1994, pp. 467-729.

Table 8.5 Some physical properties and molecular dimensions of COX<sub>2</sub>

Property	COF <sub>2</sub>	COCl <sub>2</sub>	COBr <sub>2</sub>
MP/°C	-114°	-127.8°	—
BP/°C	-83.1°	7.6°	64.5°
Density (T°C)/g cm <sup>-3</sup>	1.139(-144°)	1.392(19°)	—
Distance (C-O)/pm	117.4	116.6	113
Distance (C-X)/pm	131.2	174.6	(205)
Angle X-C-X	108.0°	111.3°	110 ± 5°
Angle X-C-O	126.0°	124.3°	~125°

parent species, e.g. COFCl (bp -42°), COFBr (bp -20.6°). COI<sub>2</sub> is unknown but COFI has been prepared (mp -90°, bp 23.4°). Synthetic routes are as follows: COFCl from COCl<sub>2</sub>/HF; COFBr from CO/BrF<sub>3</sub>; COFI from CO/IF<sub>3</sub>; and COClBr from CCl<sub>3</sub>Br/H<sub>2</sub>SO<sub>4</sub>.

COF<sub>2</sub> can be made by fluorinating COCl<sub>2</sub> with standard fluorinating agents such as NaF/MeCN or SbF<sub>5</sub>/SbF<sub>3</sub>; direct fluorination of CO with AgF<sub>2</sub> affords an alternative route. COF<sub>2</sub> is rapidly hydrolysed by water to CO<sub>2</sub> and HX, as are all the other COX<sub>2</sub>. It is a useful laboratory reagent for producing a wide range of fluoroorganic compounds and the heavier alkali metal fluorides react in MeCN to give trifluoromethoxides MOCF<sub>3</sub>.

COCl<sub>2</sub> (phosgene) is highly toxic and should be handled with great caution. It was first made in 1812 by John Davy (Sir Humphry Davy's brother) by the action of sunlight on CO + Cl<sub>2</sub>, whence its otherwise surprising name (Greek φως *phos*, light; -γενής, *-genes*, born of). It is now a major industrial chemical and is made on the kilotonne scale by combining the two gases catalytically over activated C (p. 274). It was used briefly and rather ineffectively as a chemical warfare gas in 1916 but is now principally used to prepare isocyanates as intermediates to polyurethanes. It also acts as a ligand (Lewis base) towards AlCl<sub>3</sub>, SnCl<sub>4</sub>, SbCl<sub>5</sub>, etc., forming adducts Cl<sub>2</sub>CO→MCl<sub>n</sub>, and is a useful chlorinating agent, converting metal oxides into highly pure chlorides. It reacts with NH<sub>3</sub> to form mainly urea, CO(NH<sub>2</sub>)<sub>2</sub>, together with more highly condensed products such as guanidine,

C(NH)(NH<sub>2</sub>)<sub>2</sub>; biuret, NH<sub>2</sub>CONHCONH<sub>2</sub>; and cyanuric acid, i.e. *cyclo*-[CO(NH)]<sub>3</sub> (p. 323).

COBr<sub>2</sub> has recently been shown to be a useful general brominating reagent for the preparation of d- and f-block bromides and oxide bromides.<sup>(101)</sup> Thus, when V<sub>2</sub>O<sub>5</sub> is heated with an excess of COBr<sub>2</sub> in a sealed Curious tube at 125°C for 10 days, a quantitative yield of VOBr<sub>2</sub> is obtained by a reaction that is driven thermodynamically by the formation of CO<sub>2</sub>: [V<sub>2</sub>O<sub>5</sub> + 3COBr<sub>2</sub> → 2VOBr<sub>2</sub> + 3CO<sub>2</sub> + Br<sub>2</sub>]. Similarly, MoO<sub>2</sub>, Re<sub>2</sub>O<sub>7</sub>, Sm<sub>2</sub>O<sub>3</sub> and UO<sub>3</sub> were smoothly converted to MoO<sub>2</sub>Br<sub>2</sub>, ReOBr<sub>4</sub>, SmBr<sub>3</sub> and UOBr<sub>3</sub>, respectively.

## 8.6 Oxides and Carbonates

Carbon forms 2 extremely stable oxides, CO and CO<sub>2</sub>, 3 oxides of considerably lower stability, C<sub>3</sub>O<sub>2</sub>, C<sub>5</sub>O<sub>2</sub> and C<sub>12</sub>O<sub>9</sub>, and a number of unstable or poorly characterized oxides including C<sub>2</sub>O, C<sub>2</sub>O<sub>3</sub> and the nonstoichiometric graphite oxide (p. 289). Of these, CO and CO<sub>2</sub> are of outstanding importance and their chemistry will be discussed in subsequent paragraphs after a few brief remarks about some of the others.

Tricarbon dioxide, C<sub>3</sub>O<sub>2</sub>, often called "carbon suboxide" and ponderously referred to in *Chemical Abstracts* as 1,2-propadiene-1,3-dione, is a foul-smelling gas obtained by dehydrating malonic acid, CH<sub>2</sub>(CO<sub>2</sub>H)<sub>2</sub>, at

<sup>101</sup> J. S. YADAV and V. R. GADGIL, *J. Chem. Soc., Chem. Commun.*, 1824-5 (1989).

Table 8.6 Some properties of CO, CO<sub>2</sub> and C<sub>3</sub>O<sub>2</sub>

Property	CO	CO <sub>2</sub>	C <sub>3</sub> O <sub>2</sub>
MP/°C	-205.1	-56.6(5.2 atm)	-112.5
BP/°C	-191.5	-78.5 (subl)	6.7
$\Delta H_f^\circ/\text{kJ mol}^{-1}$	-110.5	-393.7	+97.8
Distance (C-O)/pm	112.8	116.3	116
Distance (C-C)/pm	—	—	128
$D(\text{C-O})/\text{kJ mol}^{-1}$	1070.3	531.4	—

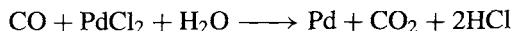
reduced pressure over P<sub>4</sub>O<sub>10</sub> at 140°, or by thermolysis of bis(trimethylsilyl) malonate, CH<sub>2</sub>(CO<sub>2</sub>SiMe<sub>3</sub>)<sub>2</sub>.<sup>(102)</sup> It has mp -112.5°, bp 6.7°, is stable at -78°, and polymerizes at room temperature to a yellow solid. C<sub>3</sub>O<sub>2</sub> forms linear molecules (*D*<sub>∞h</sub> symmetry) which can be written as O=C=C=C=O, consistent with the short interatomic distances C-C 128 pm and C-O 116 pm. Above 100°, polymerization yields a ruby-red solid; at 400° the product is violet and at 500° the polymer decomposes to C. The basic structure of all the polymers appears to be a polycyclic 6-membered lactone. C<sub>3</sub>O<sub>2</sub> readily rehydrates to malonic acid, and reacts with NH<sub>3</sub> and HCl to give respectively the corresponding amide and acid chloride: CH<sub>2</sub>(CONH<sub>2</sub>)<sub>2</sub> and CH<sub>2</sub>(COCl)<sub>2</sub>. Thermolysis of C<sub>3</sub>O<sub>2</sub> in a flow system has been reported to give a liquid product C<sub>5</sub>O<sub>2</sub> though a better preparation is the photolysis or thermolysis of the tris(diazo)ketone, cyclo-1,3,5-C<sub>6</sub>O<sub>3</sub>(N<sub>2</sub>)<sub>3</sub>.<sup>(103)</sup> C<sub>5</sub>O<sub>2</sub> is a yellow solid which decomposes above -90°; in solution it apparently remains unchanged for several days even at room temperature. Note that C<sub>5</sub>O<sub>2</sub> is the next member after CO<sub>2</sub> and C<sub>3</sub>O<sub>2</sub> of the linear catenated series OC<sub>*n*</sub>O with *n* odd as required by simple  $\pi$ -bond theory. The other moderately stable lower oxide is C<sub>12</sub>O<sub>9</sub>, a white sublimable solid which is the anhydride of mellitic acid, C<sub>6</sub>(COOH)<sub>6</sub>.

Direct oxidation of C in a limited supply of oxygen or air yields CO; in a free supply CO<sub>2</sub>

results. Some properties of these familiar gases and of C<sub>3</sub>O<sub>2</sub> are in Table 8.6. The great strength of the C-O bond confers considerable thermal stability on these molecules but the compounds are also quite reactive chemically, and many of the reactions are of major industrial importance. Some of these are discussed more fully in the Panel.

The nature of the bonding, particularly in CO, has excited much attention because of the unusual coordination number (1) and oxidation state (+2) of carbon: it is discussed on p. 926 in connection with the formation of metal-carbonyl complexes.

Pure CO can be made on a laboratory scale by dehydrating formic acid (HCOOH) with conc H<sub>2</sub>SO<sub>4</sub> at ~140°. CO is a colourless, odourless, flammable gas; it has a relatively high toxicity due to its ability to form a complex with haemoglobin that is some 300 times more stable than the oxygen-haemoglobin complex (p. 1099): the oxygen-transport function of the red corpuscles in the blood is thereby impeded. This can result in unconsciousness or death, though recovery from mild poisoning is rapid and complete in fresh air and the effects are not cumulative. CO can be detected by its ability to reduce an aqueous solution of PdCl<sub>2</sub> to metallic Pd:



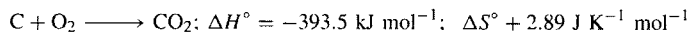
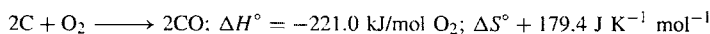
Quantitative estimation relies on the liberation of I<sub>2</sub> from I<sub>2</sub>O<sub>5</sub> or (in the absence of C<sub>2</sub>H<sub>2</sub>) on absorption in an acid solution of CuCl to form the adduct [Cu(CO)Cl(H<sub>2</sub>O)<sub>2</sub>].

<sup>102</sup> L. BIRKOFER and P. SOMMER, *Chem. Ber.* **109**, 1701-7 (1976).

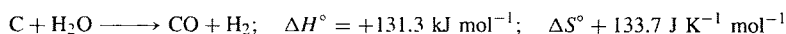
<sup>103</sup> G. MAIER, H. P. REISENAUER, U. SCHÄFER and H. BALLI, *Angew. Chem. Int. Edn. Engl.* **27**, 566-8 (1988).

### Industrially Important Reactions of Oxygen and Oxides with Carbon

Carbon monoxide is widely used as a fuel in the form of producer gas or water gas and is also formed during the isolation of many metals from their oxides by reduction with coke. Producer gas is obtained by blowing air through incandescent coke and consists of about 25% CO, 4% CO<sub>2</sub> and 70% N<sub>2</sub>, together with traces of H<sub>2</sub>, CH<sub>4</sub> and O<sub>2</sub>. The reactions occurring during production are:

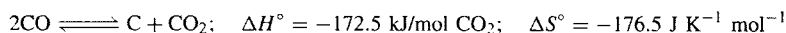


Water gas is made by blowing steam through incandescent coke: it consists of about 50% H<sub>2</sub>, 40% CO, 5% CO<sub>2</sub> and 5% N<sub>2</sub> + CH<sub>4</sub>. The oxidation of C by H<sub>2</sub>O is strongly endothermic:



Consequently, the coke cools down and the steam must be intermittently replaced by a flow of air to reheat the coke.

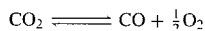
At high temperatures, particularly in the presence of metal catalysts, CO undergoes reversible disproportionation:<sup>†</sup>



The equilibrium concentration of CO is 10% at 550°C and 99% at 1000°. As the forward reaction involves a reduction in the number of gaseous molecules it is accompanied by a large decrease in entropy. Remembering that  $\Delta G = \Delta H - T\Delta S$  this implies that the reverse reaction becomes progressively more favoured at higher temperatures. The thermodynamic data for the formation of CO and CO<sub>2</sub> can be represented diagrammatically on an Ellingham diagram (Fig. 19) which plots standard free energy changes per mol of O<sub>2</sub> as a function of the absolute temperature. The oxidation of C to CO results in an increase in the number of gaseous molecules; it is therefore accompanied by a large increase in entropy and is favoured at high temperature. By contrast, oxidation to CO<sub>2</sub> leaves the number of gaseous molecules unchanged; there is little change in entropy ( $\Delta S^\circ 2.93 \text{ J K}^{-1} \text{ mol}^{-1}$ ), and the free energy is almost independent of temperature. The two lines (and that for the oxidation of CO to CO<sub>2</sub>) intersect at 983 K; it follows that  $\Delta G$  for the disproportionation reaction is zero at this temperature. The diagram also includes the plots of  $\Delta G$  (per mole of O<sub>2</sub>) for the oxidation of several representative metals. On the left of the diagram (at  $T = 0 \text{ K}$ )  $\Delta G = \Delta H$  and the sequence of elements is approximately that of the electrochemical series. The slope of most of the lines is similar and corresponds to the loss of 1 mol of gaseous O<sub>2</sub>; small changes of slope occur at the temperature of phase changes or the mp of the metal, and a more dramatic increase in slope signals the bp of the metal. For example, for MgO(s), the slope increases about three-fold at the bp of Mg since, above this temperature, reaction removes three gaseous species (2Mg + O<sub>2</sub>) rather than one (O<sub>2</sub>).

Such diagrams are of great value in codifying a mass of information of use in extractive metallurgy.<sup>(105)</sup> For example, it is clear that below 710°C (983 K) carbon is a stronger reducing agent when it is converted into CO<sub>2</sub> rather than CO, whereas above this temperature the reverse is true. Again, as reduction of metal oxides with C will occur when the accompanying  $\Delta G$  is negative, such reduction becomes progressively more feasible the higher the temperature: Zn (and Cd) can be reduced at relatively low temperatures but MgO can only be reduced at temperatures approaching 2000 K. Caution should be exercised, however, in predicting the outcome of such reactions since a number of otherwise reasonable reductions cannot be used because the metal forms a carbide (e.g. Cr, Ti). The temperature at which the oxygen dissociation pressure of the various metal oxides reaches a given value can also be obtained from the diagram: as  $-\Delta G = RT \ln K_p [= 2.303RT \log\{p(\text{O}_2)/\text{atm}\}]$  for the reactions considered] it follows that the line drawn from the point  $\odot$  ( $\Delta G = 0, T = 0$ ) to the appropriate scale mark on the right-hand side of the diagram intercepts the free-energy line for the element concerned at the required temperature. (Establish to your own satisfaction that this statement is approximately true — what assumptions does it embody?)

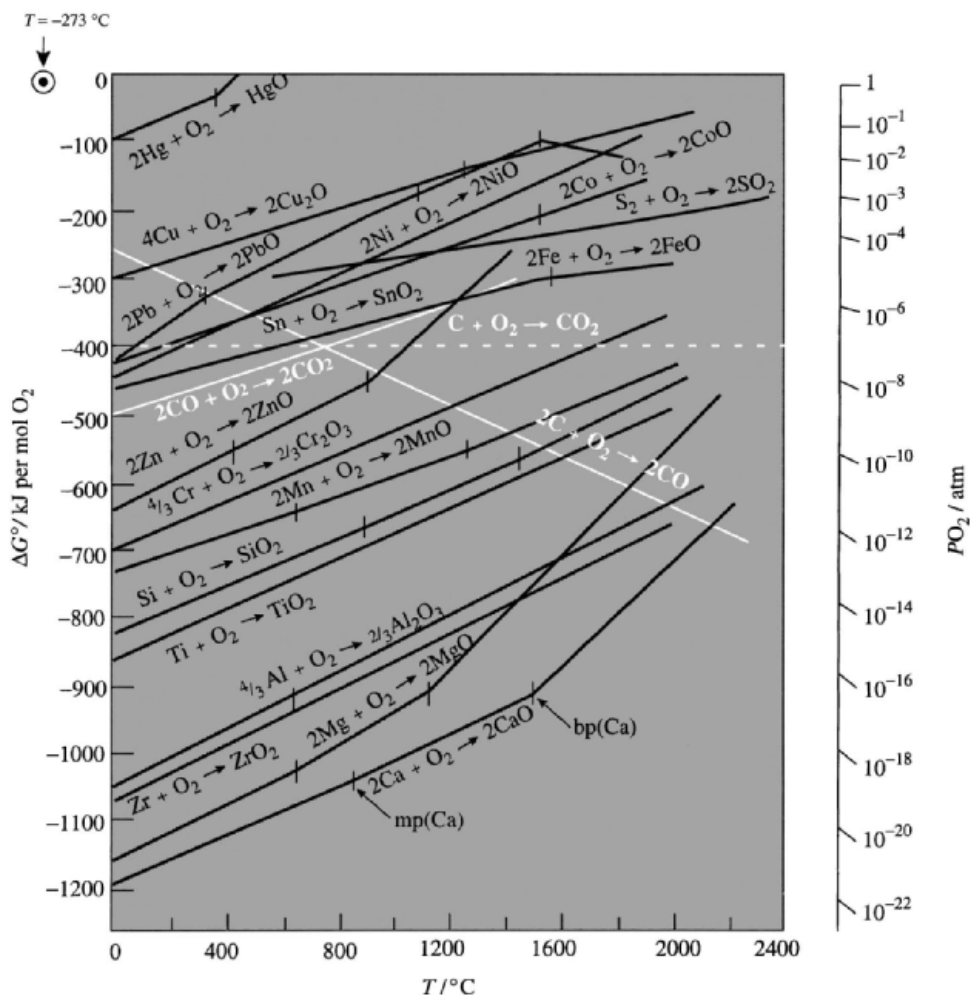
<sup>†</sup> Note however that, at all pressures, there is a fairly wide range of temperatures in which CO<sub>2</sub> dissociates directly into CO and O<sub>2</sub> without precipitation of carbon.<sup>(104)</sup>



For example, the temperature range is 250–370°C at 10<sup>-2</sup> atm, 320–480°C at 1 atm, and 405–630°C at 100 atm. At higher temperatures in each case, C is also formed, but always in the presence of some O<sub>2</sub>.

<sup>104</sup>M. H. LIETZKE and C. MULLINS, *J. Inorg. Nucl. Chem.* **43**, 1769–71 (1981).

<sup>105</sup>C. B. ALCOCK, *Principles of Pyrometallurgy*, Academic Press, London, 1976, 348 pp.



**Figure 8.19** Ellingham diagram for the free energy of formation of metallic oxides. (After F. D. Richardson and J. H. E. Jeffes, *J. Iron Steel Inst.* **160**, 261 (1948).) The oxygen dissociation pressure of a given M-MO system at a given temperature is obtained by joining  $\odot$  on the top left hand to the appropriate point on the M-MO free-energy line, and extrapolating to the scale on the right hand ordinate for  $p_{\text{O}_2}$  (atm).

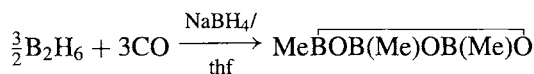
CO reacts at elevated temperatures to give formates with alkali hydroxides, and acetates with methoxides:



Reaction with alkali metals in liquid  $\text{NH}_3$  leads to reductive coupling to give colourless crystals of

the salt  $\text{Na}_2\text{C}_2\text{O}_2$  which contains linear groups  $\text{NaOC}\equiv\text{CONa}$  packed in chains. CO reacts with  $\text{Cl}_2$  and  $\text{Br}_2$  to give  $\text{COX}_2$  (p. 305) and with liquid S to give COS. It cleaves  $\text{B}_2\text{H}_6$  at high pressures to give the “symmetrical” adduct  $\text{BH}_3\text{CO}$  (p. 165), but in the presence of  $\text{NaBH}_4/\text{thf}$  the reaction takes a different course to yield the cyclic *B*-trimethylboroxine:





With  $\text{BR}_3$ , CO inserts in successive stages to give, ultimately, the corresponding trialkylmethylboroxine  $(\text{R}_3\text{CBO})_3$ . Alternative products are obtained in the presence of other reagents, e.g. aqueous alkali yields  $\text{R}_3\text{COH}$ ; water followed by alkaline peroxide yields  $\text{R}_2\text{CO}$ ; and alkaline  $\text{NaBH}_4$  yields  $\text{RCH}_2\text{OH}$  (p. 167). CO can also insert into M-C bonds (M = Mo, W; Mn, Fe, Co; Ni, Pd, Pt):

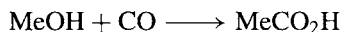


A detailed discussion of CO as a ligand and the chemistry of metal carbonyls is on pp. 926–9. CO is a key intermediate in the catalytic production of a wide variety of organic compounds on an industrial scale. These include:<sup>(106,107)</sup>

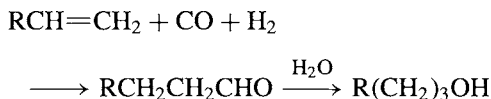
1. Catalytic reduction to methanol (230–400°C, 50–100 atm):



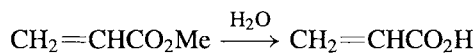
2. Homogeneous methanol carboxylation with  $\text{I}^-/\text{Rh}$  catalyst (175–195°C, 30 atm), this is now a leading route to acetic acid:



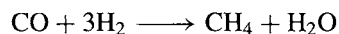
3. Hydroformylation of olefins to alcohols (the oxo process):<sup>(108)</sup>



4. The Reppe synthesis of methyl acrylate and acrylic acid (100–190°C, 30 atm, Ni catalyst: or 40°C and 1 atm using  $\text{Ni}(\text{CO})_4$  as both the source of CO and the catalyst):



5. Sabatier methanation (230–450°C, 1–100 atm, Ni catalyst):



6. Fischer-Tropsch hydrogenation to a mixture of straight chain aliphatic, olefinic and oxygenated hydrocarbons.<sup>(109)</sup> Despite an enormous amount of research during the past two decades, this is still not an economically viable process except in special circumstances, such as in South Africa.<sup>(110)</sup>

Most industrial CO is produced and used on site. Prices for commercial supplies vary enormously depending on volume and purity required.<sup>(106)</sup> For large volumes (~28 000 m<sup>3</sup>/day), “over the fence” prices can be as low as \$0.30/m<sup>3</sup> whereas for tube-trailer loads (1500–3000 m<sup>3</sup>) prices are nearer \$1.40/m<sup>3</sup>. For CO supplied in high-pressure cylinders current prices (1993) are \$15.00–35.00/m<sup>3</sup> for commercial grade (98–99% purity), \$63/m<sup>3</sup> for ultra high purity grade (99.8%) and \$68–1580/m<sup>3</sup> for research grades (99.97–99.98%).

Further reactions of CO of potential industrial or research significance are continually being explored. Recent examples include:

1. Amination with ammonia over zeolite catalysts at 350–400°C to give methylamine (and some dimethylamine):<sup>(111)</sup>

<sup>106</sup> Kirk-Othmer *Encyclopedia of Chemical Technology*, 4th ed., Wiley, New York, 5, 97–122 (1993).

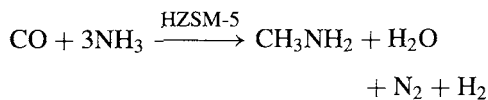
<sup>107</sup> W. KEIM, in H. GRÜNEWALD (ed.), *Chemistry for the Future* (Proc. 29th IUPAC Congress, Cologne, Germany, 5–10 June 1983) Pergamon Press, Oxford, 1984, pp. 53–62.

<sup>108</sup> R. L. PRUETT, *Adv. Organometallic Chem.* **17**, 1–60 (1979). See also G. P. COOLES and R. DAVIS, *Educ. in Chem.*, 48–50, March 1982.

<sup>109</sup> C. MASTERS, *Adv. Organometallic Chem.* **17**, 61–103 (1979). R. B. ANDERSON, *The Fischer-Tropsch Synthesis*, Academic Press, London, 1984, 320 pp.

<sup>110</sup> R. C. EVERSON and D. T. THOMPSON, *Platinum Metals Review* **25**, 50–6 (1981).

<sup>111</sup> M. SUBRAHMANYAM, S. J. KULKARNI and A. V. RAMA RAO, *J. Chem. Soc., Chem. Commun.*, 607–8 (1992).



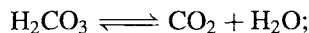
2. Reductive coupling of two CO ligands to form a coordinated alkyne derivative, e.g. treatment of the Ta<sup>I</sup> complex [Ta(CO)<sub>2</sub>(dmpe)<sub>2</sub>Cl] with activated Zn dust in thf and then with Me<sub>3</sub>SiCl gave a 25% yield of [Ta(Me<sub>3</sub>SiOC≡COSiMe<sub>3</sub>)(dmpe)<sub>2</sub>Cl] which can in turn be hydrolysed to the corresponding complex of the novel dihydroxyacetylene, HOC=COH.<sup>(112)</sup>

CO<sub>2</sub> is much less volatile than CO (p. 306). It is a major industrial chemical but its uses, though occasionally chemical, more frequently depend on its properties as a refrigerant, as an inert atmosphere, or as a carbonating (gasifying) agent in drinks and foam plastic (see Panel).<sup>(113)</sup> Of more chemical interest is the synthesis of radioactive <sup>14</sup>C compounds from <sup>14</sup>CO<sub>2</sub> which is conveniently stored as a carbonate. <sup>14</sup>C is generated by an (n,p) reaction on a nitride or nitrate in a nuclear reactor (see p. 1256). More than 500 compounds specifically labelled with <sup>14</sup>C are now available commercially, the starting point of many of the syntheses being one of the following reactions:

1.  $\text{NaH}^{14}\text{CO}_3 + \text{H}_2/\text{Pd/C} \longrightarrow \text{H}^{14}\text{CO}_2\text{H}$
2.  $^{14}\text{CO}_2 + \text{RMgX} \longrightarrow \text{R}^{14}\text{CO}_2\text{H}$
3.  $^{14}\text{CO}_2 + \text{LiAlH}_4 \longrightarrow ^{14}\text{CH}_3\text{OH}$
4.  $\text{Ba}^{14}\text{CO}_3 + \text{Ba} \longrightarrow \text{Ba}^{14}\text{C}_2 \xrightarrow{\text{H}_2\text{O}} ^{14}\text{C}_2\text{H}_2$
5.  $\text{Ba}^{14}\text{CO}_3 + \text{NH}_3 \longrightarrow \text{Ba}^{14}\text{CN}_2 \longrightarrow ^{14}\text{C/N compounds}$

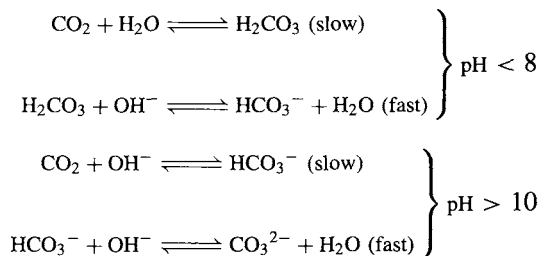
When CO<sub>2</sub> dissolves in water at 25° it is only partly hydrated to carbonic acid according to the

equilibrium



$$K = [\text{CO}_2]/[\text{H}_2\text{CO}_3] \approx 600$$

Interpretation of acid–base behaviour in this system is further complicated by the slowness of some of the reactions and their dependence on pH. The main reactions are:



In the range pH 8–10 both sets of equilibria are important. The apparent dissociation constant of carbonic acid is

$$K_1 = \frac{[\text{H}^+][\text{HCO}_3^-]}{[\text{CO}_2 + \text{H}_2\text{CO}_3]} = 4.45 \times 10^{-7} \text{ mol l}^{-1}$$

As  $[\text{CO}_2]/[\text{H}_2\text{CO}_3] = K \approx 600$ , it follows that the true dissociation constant is:

$$K_a = \frac{[\text{H}^+][\text{HCO}_3^-]}{[\text{H}_2\text{CO}_3]} = K_1(1 + K) \approx 2.5 \times 10^{-4} \text{ mol l}^{-1}$$

This value is in the range expected from an acid of structure (HO)<sub>2</sub>CO (p. 50). The second dissociation constant is given by

$$K_2 = \frac{[\text{H}^+][\text{CO}_3^{2-}]}{[\text{HCO}_3^-]} = 4.84 \times 10^{-11} \text{ mol l}^{-1}$$

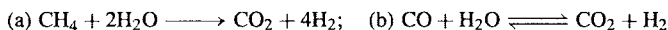
A hydrate CO<sub>2</sub>·8H<sub>2</sub>O can be crystallized from aqueous solutions at 0° and  $p(\text{CO}_2) \sim 45$  atm. There is also evidence for a hydrogen-bonded sesquicarbonate ion, H<sub>3</sub>C<sub>2</sub>O<sub>6</sub><sup>−</sup>; this was originally suggested to have the sandwich

<sup>112</sup> P. A. BIANCONI, I. D. WILLIAMS, M. P. ENGELER and S. J. LIPPARD, *J. Am. Chem. Soc.* **108**, 311–3 (1986). R. N. VRTIS, C. P. RAO, S. G. BOTT and S. J. LIPPARD, *J. Am. Chem. Soc.* **110**, 7564–6 (1988).

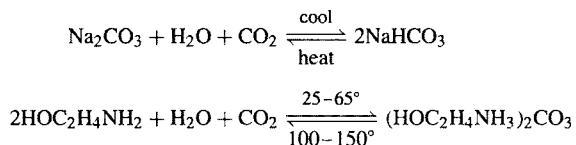
<sup>113</sup> Ref. 106, pp. 35–53. See also W. M. AYERS, (ed.) *Catalytic Activation of Carbon Dioxide*, ACS Symposium 363, Washington, DC (1988), 212 pp.

### Production and Uses of CO<sub>2</sub>

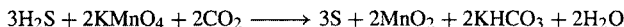
CO<sub>2</sub> can be readily obtained in small amounts by the action of acids on carbonates. On an industrial scale the main source is as a byproduct of the synthetic ammonia process in which the H<sub>2</sub> required is generated either by the catalytic reaction (a) or by the water-gas shift reaction (b):



CO<sub>2</sub> is also recovered economically from the flue gases resulting from combustion of carbonaceous fuels, from fermentation of sugars and from the calcination of limestone: recovery is by reversible absorption either in aqueous Na<sub>2</sub>CO<sub>3</sub> or aqueous ethanolamine (Girbotol process).



In certain places CO<sub>2</sub> can be obtained from natural gas wells. H<sub>2</sub>S impurity is removed by oxidation using a buffered alkaline solution saturated with KMnO<sub>4</sub>:



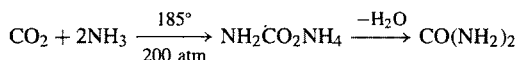
The scale of production has increased rapidly in recent years and in 1980 exceeded 33 million tonnes in the USA alone though much of this is used in integrated plants, on site.

The most extensive application of CO<sub>2</sub> is as a refrigerant, some 52% of production being consumed in this way. CO<sub>2</sub> can be liquefied at any temperature between its triple point  $-56.6^\circ$  (5.11 atm) and its critical point  $+31.1^\circ$  (72.9 atm). The gas can either be pressurized to 75 atm and then water-cooled to room temperature, or precooled to about  $-15^\circ$  ( $\pm 5^\circ$ ) and then pressurized to 15.25 atm. Solid CO<sub>2</sub> is obtained by expanding liquid CO<sub>2</sub> from cylinders to give a "snow" which is then mechanically compressed into blocks of convenient size. Until about 40 y ago the bulk of CO<sub>2</sub> refrigerant was in the form of solid CO<sub>2</sub>, but since 1960 production of liquid CO<sub>2</sub> has overtaken the solid form because of lower production costs and ease of transporting and metering the material. Some typical production figures are shown in the Table. Supercritical CO<sub>2</sub> is also finding increasing use as a versatile solvent for chemical reactions.<sup>(113a)</sup>

USA production of CO <sub>2</sub>					
CO <sub>2</sub> production/kilotonnes	1955	1960	1962	1977	1987
Solid	520	426	406	340	310
Liquid and gas	185	432	522	1660	7310
Total	705	858	928	2000	7620

Solid CO<sub>2</sub> is used as a refrigerant for ice-cream, meat and frozen foods, and as a convenient laboratory cooling agent and refrigerant. Liquid CO<sub>2</sub> is extensively used to improve the grindability of low-melting metals (and hamburger meat), and for the rapid cooling of loaded trucks and rail cars; it is also used for inflating life rafts, in fire extinguishers, and in blasting shells for coal mining. A related application of growing importance is as a replacement for chlorofluorocarbon aerosol propellants (p. 304) though this application will never consume large amounts of the gas since the amount in each tin is extremely small.

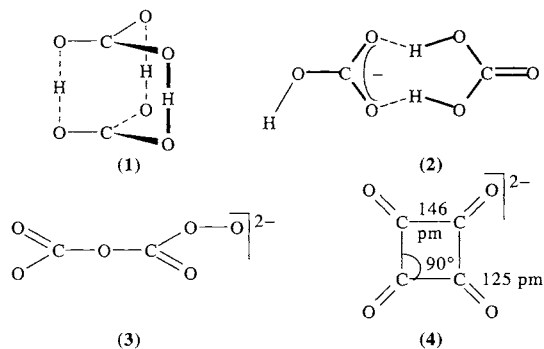
Gaseous CO<sub>2</sub> is extensively used to carbonate soft drinks and this use alone accounts for 20% of production. Other quasi-chemical applications are its use as a gas purge, as an inert protective gas for welding, and for the neutralization of caustic and alkaline waste waters. Small amounts are also used in the manufacture of sodium salicylate, basic lead carbonate ("white lead"), and various carbonates such as M<sub>2</sub>CO<sub>3</sub> and M<sup>1</sup>HCO<sub>3</sub> (M<sup>1</sup> = Na, K, NH<sub>4</sub>, etc.). One of the most important uses of CO<sub>2</sub> is to manufacture urea via ammonium carbamate:



Urea is used to make urea-formaldehyde plastics and resins and, increasingly, as a nitrogenous fertilizer (46.7% N). World production of urea was 23 million tonnes in 1984.

<sup>113a</sup>M. POLIAKOFF and S. HOWDLE, *Chem in Brit.*, February 1995, pp. 118–21, and references cited therein.

structure (1)<sup>(114)</sup> though later *ab initio* calculations favour the all-planar structure (2).<sup>(115)</sup> Solid alkali-metal peroxocarbonates  $\text{Li}_2\text{CO}_4$ ,  $\text{MHCO}_4$  and  $\text{M}_2\text{C}_2\text{O}_6$  ( $\text{M} = \text{Na}, \text{K}, \text{Rb}, \text{Cs}$ ) are known and the anion  $\text{HCO}_4^-$  ( $\text{CO}_4^{2-}$  at high pH) can be prepared in solution by reaction of  $\text{HCO}_3^-$  with aqueous  $\text{H}_2\text{O}_2$ .<sup>(116)</sup> The peroxodianion,  $\text{C}_2\text{O}_6^{2-}$  (3), can be prepared in aprotic solvents such as MeCN, dmf and dmsO, via nucleophilic oxidation of  $\text{CO}_2$  by the superoxide ion  $\text{O}_2^-$ :  $[\text{2CO}_2 + \text{2O}_2^- \rightarrow \text{C}_2\text{O}_6^{2-} + \text{O}_2]$ .<sup>(117)</sup> The amusing all-planar squarate ion,  $\text{C}_4\text{O}_4^{2-}$  (4), although chemically unrelated to the preceding species, may be mentioned here as a further well-characterized binary C/O anion.<sup>(118,119)</sup> The short C–C and C–O distances have been interpreted in terms of  $\pi$ -electron delocalization.



The coordination chemistry of  $\text{CO}_2$  is by no means as extensive as that of  $\text{CO}$  (p. 926) but some exciting developments have recently been published.<sup>(120)</sup> The first transition metal complexes with  $\text{CO}_2$  were claimed by

<sup>114</sup> A. K. COVINGTON, *Chem. Soc. Rev.* **14**, 265–81 (1985).

<sup>115</sup> N. V. RIGGS, *J. Chem. Soc., Chem. Commun.*, 137–8 (1987).

<sup>116</sup> J. FLANAGAN, D. P. JONES, W. P. GRIFFITH, A. C. SKAPSKI and A. P. WEST, *J. Chem. Soc., Chem. Commun.*, 20–1 (1986).

<sup>117</sup> J. L. ROBERTS, T. S. CALDERWOOD and D. T. SAWYER, *J. Am. Chem. Soc.* **106**, 4667–70 (1984).

<sup>118</sup> C. ROBL, V. GNUTZMANN and A. WEISS, *Z. anorg. allg. Chem.* **549**, 187–94 (1987), and references cited therein.

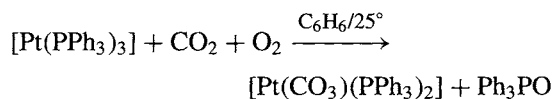
<sup>119</sup> R. SOULIS, F. DAHAN, J.-P. LAURENT and P. CASTAN, *J. Chem. Soc., Dalton Trans.*, 587–90 (1988).

<sup>120</sup> M. E. VOLPIN and I. S. KOLOMNIKOV, *Organometallic Reactions* **5**, 313–86 (1975). Further references to isolable  $\text{CO}_2$ -transition metal adducts are given in R. L. HARLOW,

M. E. Volpin's group in 1969: tertiary phosphine or  $\text{N}_2$  ligands were displaced from Rh and Ni complexes to give binuclear products whose definitive structure has not yet been established.  $\text{CO}_2$  also displaced  $\text{N}_2$  from  $[\text{Co}(\text{N}_2)(\text{PPh}_3)_3]$  to give  $[\text{Co}(\text{CO}_2)(\text{PPh}_3)_3]$ . The  $\text{Ni}^0$  complexes  $[\text{Ni}(\text{PET}_3)_4]$  (violet) and  $[\text{Ni}(\text{PBU}_3)_4]$  (red) react in toluene at room temperature with  $\text{CO}_2$  (1 atm) to give the yellow complexes  $[\text{Ni}(\text{CO}_2)_3\text{L}_3]$ . The structure of the analogous complex with  $\text{P}(\text{C}_6\text{H}_{11})_3$  was established by X-ray diffraction analysis; it features a pseudo-3-coordinate Ni atom  $\mu$ -bonded to a bent  $\text{CO}_2$  ligand as in Fig. 8.20a. The isoelectronic  $\text{Rh}^1$  appears to form two types of complex: an orange-red series  $[\text{Rh}(\text{CO}_2)\text{ClL}_2]$  ( $\text{L} =$  tertiary phosphine) with a  $\mu$ -bonded bent  $\text{CO}_2$  as in Fig. 8.20a and a somewhat less-stable yellow series  $[\text{Rh}(\text{CO}_2)\text{ClL}_3]$  which is thought to contain

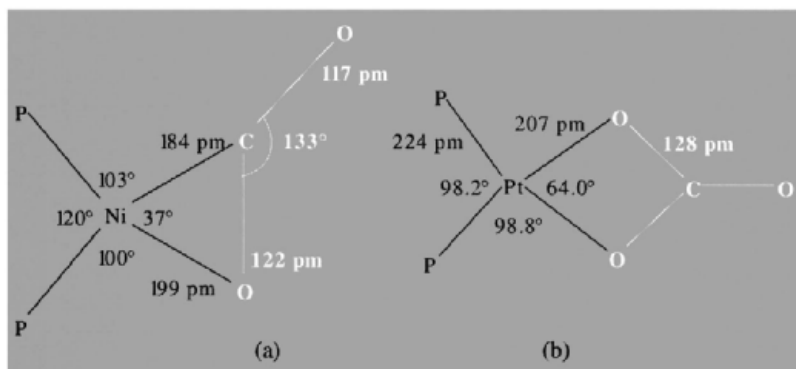
the ligand configuration  $\text{Rh}-\text{C} \begin{matrix} \diagup \text{O} \\ \diagdown \text{O} \end{matrix}$ . A Pt

compound which had earlier (1965) been thought to contain  $\text{CO}_2$  as a ligand was subsequently found to require the presence of  $\text{O}_2$  for its formation and to be, in fact, a novel bidentate carbonato complex (Fig. 8.20b).



If the starting material contains M–H or M–C bonds a further complication can arise due to the possibility of a  $\text{CO}_2$  insertion reaction. Thus, both  $[\text{Ru}(\text{H})_2(\text{N}_2)(\text{PPh}_3)_3]$  and  $[\text{Ru}(\text{H})_2(\text{PPh}_3)_4]$  react to give the formate  $[\text{Ru}(\text{H})(\text{OOCH})(\text{PPh}_3)_3]$ , and similar  $\text{CO}_2$  insertions into M–H are known for  $\text{M} = \text{Co}, \text{Fe}, \text{Os}, \text{Ir}, \text{Pt}$ . These “normal” insertion reactions are consistent with the expected bond polarities  $\text{M}^{\delta+}-\text{H}^{\delta-}$  and  $\text{O}^{\delta-}=\text{C}^{\delta+}=\text{O}$ , but occasionally “abnormal” insertion occurs to give metal carboxylic acids

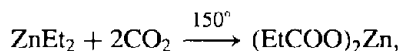
J. B. KINNEY, and T. HERSKOVITZ, *J. Chem. Soc., Chem. Commun.*, 813–4. (1980). G. S. BRISTOW, P. B. HITCHCOCK and M. F. LAPPERT, *J. Chem. Soc., Chem. Commun.*, 1145–6 (1981).



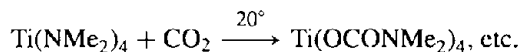
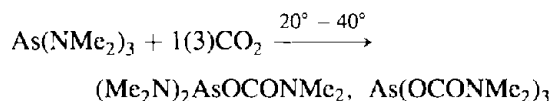
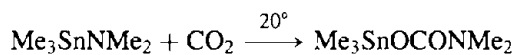
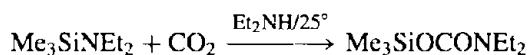
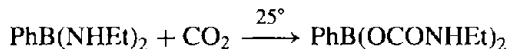
**Figure 8.20** (a) Coordination about the Ni atom in the complex  $[\text{Ni}(\text{CO}_2)\{\text{P}(\text{C}_6\text{H}_{11})_3\}_2] \cdot 0.75\text{C}_6\text{H}_5\text{Me}$ . (b) Coordination about the Pt atom in the complex  $[\text{Pt}(\text{CO}_3)(\text{PPh}_3)_2] \cdot \text{C}_6\text{H}_6$ .

$\text{M}-\text{COOH}$ . Likewise, normal insertion into  $\text{M}-\text{C}$  yields alkyl carboxylates  $\text{M}-\text{OOCR}$ , though metalloacid esters  $\text{M}-\text{COOR}$  are sometimes obtained. The reactions have obvious catalytic implications and are being actively studied at the present time by several groups.<sup>(121)</sup>

$\text{CO}_2$  insertion into  $\text{M}-\text{C}$  bonds has, of course, been known since the first papers of V. Grignard in 1901 (p. 134). Organo-Li (and other  $\text{M}^{\text{I}}$  and  $\text{M}^{\text{II}}$ ) also react extremely vigorously to give salts of carboxylic acids,  $\text{RCO}_2\text{Li}$ ,  $(\text{RCO}_2)_2\text{Be}$ , etc. Zinc dialkyls are much less reactive towards  $\text{CO}_2$ , e.g.



and organo-Cd and -Hg compounds are even less reactive. With  $\text{AlR}_3$ , one  $\text{CO}_2$  inserts at room temperature and a second at  $220^\circ$  under pressure to give  $\text{R}_2\text{Al}(\text{OOCR})$  and  $\text{RAl}(\text{OOCR})_2$  respectively. B-C, Si-C, Ge-C, and Sn-C are rather inert to  $\text{CO}_2$  but insertion readily occurs into bonds between these elements and N. A few examples are:



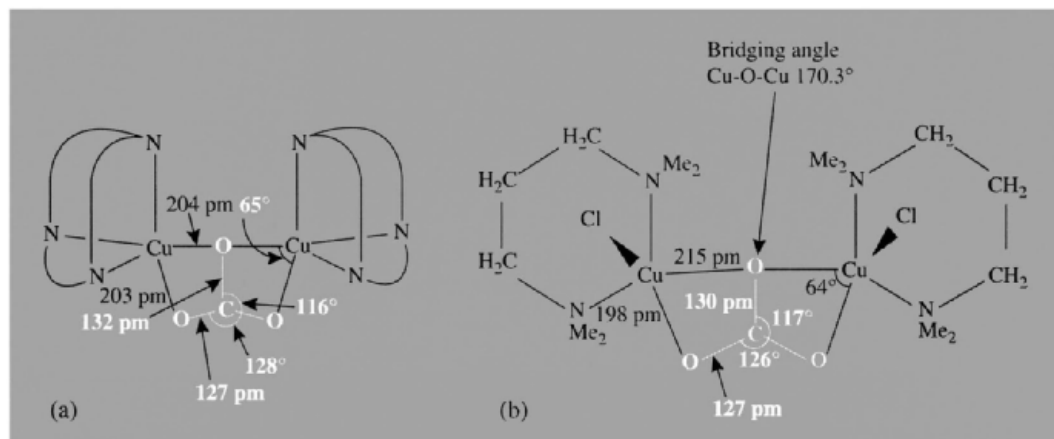
Returning briefly to  $\text{CO}_2$  as a ligand: in addition to the various mono- $\text{CO}_2$  complexes referred to above, several bis( $\eta^2\text{-CO}_2$ ) transition-metal adducts are known, e.g. *trans*- $[\text{Mo}(\eta^2\text{-CO}_2)_2(\text{PMe}_3)_4]$  (5) and *trans,mer*- $[\text{Mo}(\eta^2\text{-CO}_2)_2(\text{PMe}_3)_3(\text{CNPr}^i)]$ .<sup>(122)</sup> The first homo-bimetallic bridging- $\text{CO}_2$  complex has also been structurally characterized by X-ray analysis, *viz.*  $[(\text{dppp})(\text{CO})_2\text{Re}(\mu, \eta^2\text{-O}, \text{O}':\eta^1\text{-C})\text{Re}(\text{CO})_3(\text{dppp})]$  (6) [dppp = 1,3-bis(diphenylphosphino)propane].<sup>(123)</sup>

The carbonate ion,  $\text{CO}_3^{2-}$ , by contrast, is a classic Werner ligand which forms innumerable complexes as a monohapto, dihapto or bridging donor. Examples of this latter mode

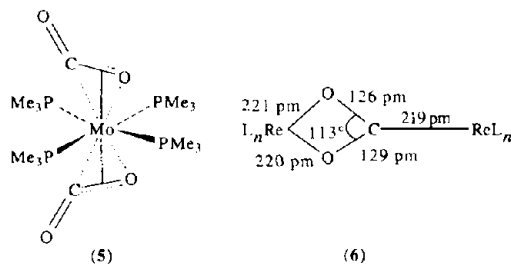
<sup>121</sup> A. BEHR, *Carbon Dioxide Activation by Metal Complexes*, VCH, Weinheim, 1988, 161 pp. See also J. D. MILLER in P. S. BRATERMAN (ed.), *Reactions of Coordinated Ligands*, Vol. 2., Plenum Press, New York, pp. 1-52 (1989) and J. L. GRANT, K. GOSWAMI, L. O. SPREER, J. W. OTVOS and M. CALVIN, *J. Chem. Soc., Dalton Trans.*, 2105-9 (1987) and references cited therein.

<sup>122</sup> R. ALVAREZ, E. CARMONA, M. L. POVEDA and R. SÁNCHEZ-DELGADO, *J. Am. Chem. Soc.* **106**, 2731-2 (1984). R. ALVAREZ, E. CARMONA, E. GUTIERREZ-PUEBLA, J. M. MARIN, A. MONGE and M. L. POVEDA, *J. Chem. Soc., Chem. Commun.*, 1326-7 (1984).

<sup>123</sup> S. K. MANDAL, J. A. KRAUSE and M. ORCHIN, *Polyhedron* **12**, 1423-5 (1993).



**Figure 8.21** (a) The complex cation  $[\text{Cu}(\text{L})_2(\mu\text{-}\eta^2, \eta^2\text{-CO}_3)]^{2+}$ . (b) The binuclear complex  $[[\text{CuCl}(\text{Me}_2\text{N-CH}_2\text{CH}_2\text{CH}_2\text{NMe}_2)]_2(\mu\text{-}\eta^2, \eta^2\text{-CO}_3)]$ .



are the complex cation  $[(\text{CuL})_2(\mu\text{-CO}_3)]^{2+}$ , where L is a tridentate macrocyclic triaza ligand (Fig. 8.21a),<sup>(124)</sup> and in the binuclear molecular complex molecule  $[[\text{CuCl}(\text{Me}_2\text{NCH}_2\text{CH}_2\text{-CH}_2\text{NMe}_2)]_2(\mu\text{-CO}_3)]$  (Fig. 8.21b).<sup>(125)</sup> This mode of coordination confers some unusual properties including diamagnetism on these  $\text{Cu}^{\text{II}}$  complexes. Even more extensive ligation occurs in the deep violet hexanuclear vanadium (IV) complex  $(\text{NH}_4)_5[(\text{VO})_6(\text{CO}_3)_4(\text{OH})_9] \cdot 10\text{H}_2\text{O}$  which was made by reacting  $\text{VOCl}_2$  with aqueous  $\text{NH}_4\text{HCO}_3$  under  $\text{CO}_2$ .<sup>(126)</sup> The novel anion

(Fig. 8.22) features a unique tris(bidentate) sextuply bridging carbonate ligand as well as three bidentate  $\mu_2$ -carbonato ligands. Other chelating and bridging coordination modes are also known.<sup>(126a)</sup>

## 8.7 Chalcogenides and Related Compounds

Carbon forms a great many sulfides in addition to the well known  $\text{CS}_2$ .  $\text{CS}$  (unlike  $\text{CO}$ ) is an unstable reactive radical even at  $-196^\circ$ : it reacts with the other chalcogens and with halogens to give  $\text{CSSe}$ ,  $\text{CSTe}$ , and  $\text{CSX}_2$ . It is formed by action of a high-frequency discharge on  $\text{CS}_2$  vapour. (See p. 319 for complexes of  $\text{CS}$ .) Passage of an electric discharge or arc through liquid or gaseous  $\text{CS}_2$  yields  $\text{C}_3\text{S}_2$ , a red liquid mp  $-5^\circ$ ; it has a linear molecular structure,  $\text{S}=\text{C}=\text{C}=\text{S}$ , which polymerizes slowly at room temperature (cf.  $\text{C}_3\text{O}_2$ ).<sup>(127)</sup>

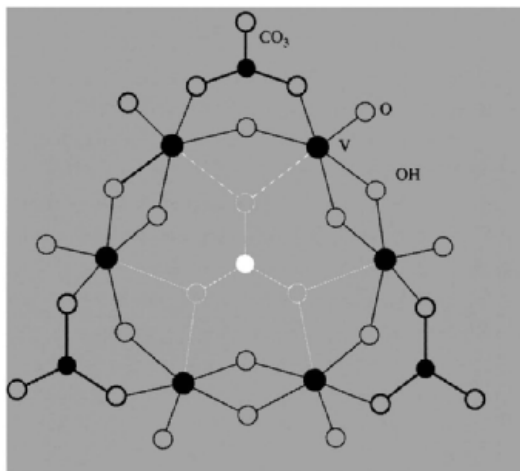
<sup>124</sup> A. R. DAVIS, F. W. P. EINSTEIN, N. F. CURTIS and J. W. L. MARTIN, *J. Am. Chem. Soc.* **100**, 6258-60 (1978).

<sup>125</sup> M. R. CHURCHILL, G. DAVIES, M. A. EL-SAYED, M. F. EL-SHAZLY, J. P. HUTCHINSON, M. RUPICH and K. O. WATKINS, *Inorg. Chem.* **18**, 2296-300 (1979).

<sup>126</sup> T. C. W. MAK, P. L. C. ZHENG and K. HUANG, *J. Chem. Soc., Chem. Commun.*, 1597-8 (1986).

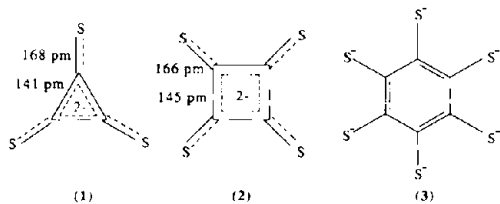
<sup>126a</sup> F. W. B. EINSTEIN and A. C. WILLIS, *Inorg. Chem.* **20**, 609-14 (1981). A. J. LINDSAY, M. MOTEVALLI, M. B. HURSTHOUSE and G. WILKINSON, *J. Chem. Soc., Chem. Commun.*, 433-4 (1986).

<sup>127</sup> M. T. BECH and G. B. KAUFFMAN, *Polyhedron* **5**, 775-81 (1985) and references cited therein. (This paper also gives an accessible account of the history of the discovery and applications of  $\text{COS}$ , i.e.  $\text{O}=\text{C}=\text{S}$ .)



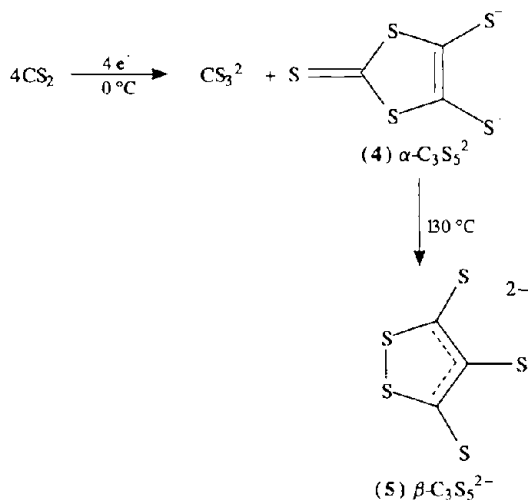
**Figure 8.22** Perspective view of the hexanuclear anion  $[(VO)_6(\mu_6-\eta^2,\eta^2-CO_3)(\mu-CO_3)_3-(\mu-OH)_9]^{5-}$ . Averaged interatomic distances: vanadyl  $V=O$  161.6 pm,  $V-OH(syn)$  195.6 pm,  $V-OH(anti)$  201.2 pm,  $V-O$  ( $\mu_2-CO_3$ ) 200.2 pm,  $V-O$  ( $\mu_6-CO_3$ ) 228.7 pm,  $C-O(\mu)$  129.1 pm,  $C-O(exo)$  126.6 pm.<sup>(126)</sup>

During the past decade there has been an astonishing proliferation of further binary carbon-sulfur species, both anionic and neutral.<sup>(128)</sup> Of the anions, the beige coloured dianion  $C_3S_3^{2-}$  (made from tetrachlorocyclopropene) has the  $D_{3h}$  structure (1) and the yellow  $C_4S_4^{2-}$  (made from squaric acid, p. 312) has the  $D_{4h}$  structure (2). The off-white  $C_6S_6^{6-}$ , (3), (made from



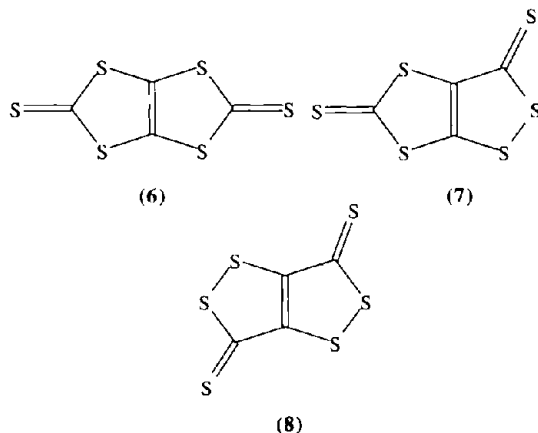
<sup>128</sup> C. P. GALLOWAY, T. B. RAUCHFUSS and X. YANG, in R. STEUDEL (ed.) *The Chemistry of Inorganic Ring Systems*, Studies in Inorganic Chemistry, Vol. 14, Elsevier, Amsterdam, 1992, pp. 25-34. See also X. YANG, T. B. RAUCHFUSS and S. R. WILSON, *J. Am. Chem. Soc.* **111**, 3465-6 (1989) and *J. Chem. Soc., Chem. Commun.*, 34-5 (1990).

$C_6Cl_6$ ) is air-sensitive but can readily be protonated to give the more stable hexathiol  $C_6(SH)_6$ . Reduction of  $CS_2$  either electrochemically or by alkali metals yields  $C_3S_5^{2-}$  which can exist in two isomeric forms, (4) and (5):

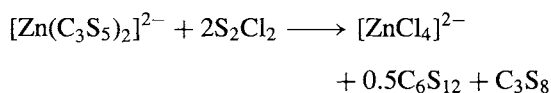


Treatment of the primary product with a zinc salt leads to separation of  $\alpha-C_3S_5^{2-}$  from its coproduct  $CS_3^{2-}$ , and multigram amounts of its complexes  $[NR_4]_2[Zn(\alpha-C_3S_5)_2]$  and of the corresponding  $\beta$ -isomer's complexes afford convenient starting points for the synthesis of *molecular* binary sulfides as indicated below.

The sulfide  $C_4S_6$  is known in three isomeric forms (6), (7) and (8).<sup>(128)</sup> The yellow-orange  $D_{2h}$  isomer (6) is readily prepared

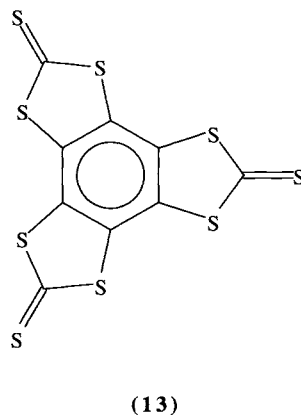
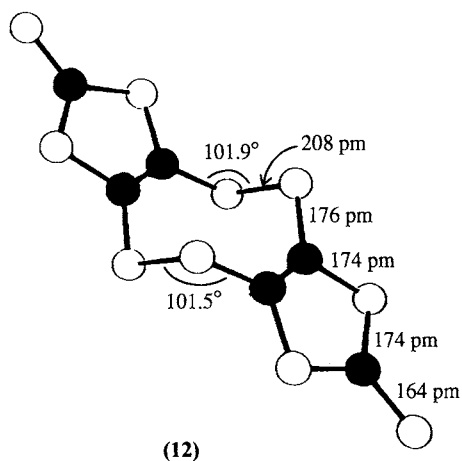
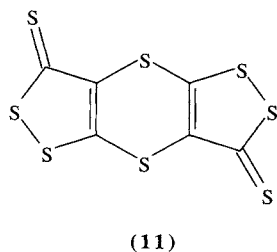
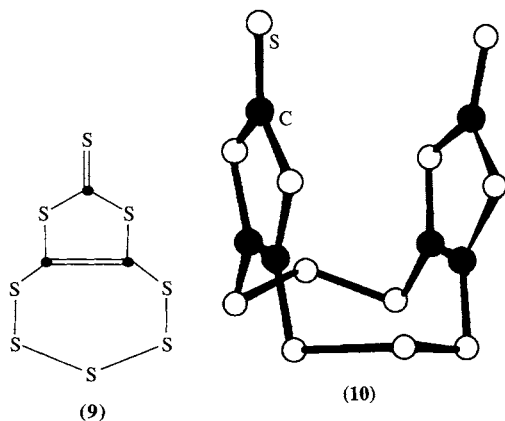


by the reaction of  $\text{CSCl}_2$  with  $\alpha\text{-C}_3\text{S}_5^{2-}$ , whilst the  $\text{C}_1$  isomer (7) results from the corresponding reaction with  $\beta\text{-C}_3\text{S}_5^{2-}$ . The  $\text{C}_{2h}$  isomer (8) is less well characterized but is said to result from the reaction of hexachlorobutadiene,  $\text{CCl}_2=\text{CCl}-\text{CCl}=\text{CCl}_2$ , with polysulfide anions. The treatment of  $\text{S}_2\text{Cl}_2$  with  $[\text{NBu}_4]_2[\text{Zn}(\alpha\text{-C}_3\text{S}_5)_2]$  yields a mixture of  $\text{C}_3\text{S}_8$  and  $\text{C}_6\text{S}_{12}$  which can be separated by fractional crystallization from  $\text{CS}_2$ :



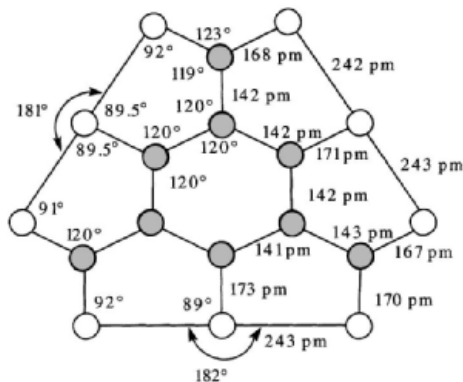
$\text{C}_3\text{S}_8$  is a bicyclic species composed of the  $\alpha\text{-C}_3\text{S}_5$  unit capped by a polysulfide linkage (9), whereas  $\text{C}_6\text{S}_{12}$  features two cisoid eclipsed planar  $\alpha\text{-C}_3\text{S}_5$  units conjoined by further sulfur linkages to form a third ring (10); note that, if each of the two  $\text{C}_2$  groups in this 10-membered ring are notionally replaced by an S atom, the conformation of the resulting  $\text{S}_8$  ring is reminiscent of the familiar crown

configuration for this species (p. 655). Oxidation of  $[\text{NEt}_4]_2[\text{Zn}(\beta\text{-C}_3\text{S}_5)_2]$  with  $\text{SOCl}_2$  affords small amounts of the yellow  $\text{C}_6\text{S}_8$  (11) which features an almost planar molecule with  $\text{S}\cdots\text{S}$  fold angles  $<3.8^\circ$ . By contrast, oxidation of  $[\text{NBu}_4]_2[\text{Zn}(\alpha\text{-C}_3\text{S}_8)_2]$  with  $\text{SO}_2\text{Cl}_2$  yields the orange dimer  $\text{C}_6\text{S}_{10}$  (12) in which the two planar  $\text{C}_3\text{S}_5$  groups are interconnected by a pair of transoid  $\text{S}_2$  linkages to give an overall chair configuration. Finally we should mention the two known isomers of  $\text{C}_9\text{S}_9$ . The simpler, formed by the reaction of  $\text{C}_6\text{S}_6^{6-}$  (3) with  $\text{CSCl}_2$ , is the tris(trithiocarbonate) (13) which sublimates at  $310^\circ$  and can be recrystallized from 1,2- $\text{C}_6\text{H}_4\text{Cl}_2$ . The second  $\text{C}_9\text{S}_9$  isomer is synthesized by



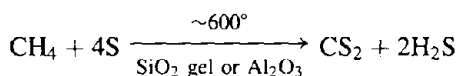


reaction of the benzene derivative 1,3,5-C<sub>6</sub>Cl<sub>3</sub>-2,4,6-(CH<sub>2</sub>NMe<sub>2</sub>)<sub>3</sub> with sulfur and H<sub>2</sub>S in boiling quinoline; it forms red crystals of the planar D<sub>3h</sub> molecule (14) which has a non-classical structure with three 3-coordinate S atoms. Both isomers are formally also oligomeric isomers of the diatomic monomer CS (p. 314).



(14)

By far the most important sulfide is CS<sub>2</sub>, a colourless, volatile, flammable liquid (mp -111.6°, bp 46.25°, flash point -30°, auto-ignition temperature 100°, explosion limits in air 1.25–50%). Impure samples have a fetid almost nauseating stench due to organic impurities but the purified liquid has a rather pleasant ethereal smell; it is very poisonous and can have disastrous effects on the nervous system and brain. CS<sub>2</sub> was formerly manufactured by direct reaction of S vapour and coke in Fe or steel retorts at 750–1000°C but, since the early 1950s, the preferred synthesis has been the catalysed reaction between sulfur and natural gas:



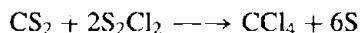
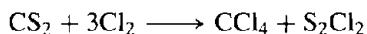
World production in 1991 was about 1 million tonnes the principal industrial uses being in the manufacture of viscose rayon (35–50%), cellophane films (15%) (see below), and CCl<sub>4</sub> (15–30%) depending on country. Indeed the CCl<sub>4</sub> application dropped to zero in USA in 1991 because of environmental concerns (p. 304).

CS<sub>2</sub> reacts with aqueous alkali to give a mixture of M<sub>2</sub>CO<sub>3</sub> and the trithiocarbonate M<sub>2</sub>CS<sub>3</sub>. NH<sub>3</sub> gives ammonium dithiocarbamate NH<sub>4</sub>[H<sub>2</sub>NCS<sub>2</sub>]; under more forcing conditions in the presence of Al<sub>2</sub>O<sub>3</sub> the product is NH<sub>4</sub>CNS and this can be isomerized at 160° to thiourea, (NH<sub>2</sub>)<sub>2</sub>CS. Water itself reacts only reluctantly, yielding COS at 200° and H<sub>2</sub>S + CO<sub>2</sub> at higher temperatures; many other oxocompounds also convert CS<sub>2</sub> to COS, e.g. MgO, SO<sub>3</sub>, HSO<sub>3</sub>Cl and urea. With aqueous NaOH/EtOH carbon disulfide yields sodium ethyl dithiocarbonate (xanthate):



When ethanol is replaced by cellulose, sodium cellulose xanthate is obtained; this dissolves in aqueous alkali to give a viscous solution (viscose) from which either viscose rayon or cellophane can be obtained by adding acid to regenerate the (reconstituted) cellulose. Trithiocarbonates (CS<sub>3</sub><sup>2-</sup>), dithiocarbonates (COS<sub>2</sub><sup>2-</sup>), xanthates (CS<sub>2</sub>OR<sup>-</sup>), dithiocarbamates (CS<sub>2</sub>NR<sub>2</sub><sup>-</sup>) and 1,2-dithiolates have an extensive coordination chemistry which has been reviewed.<sup>(129)</sup>

Chlorination of CS<sub>2</sub>, when catalysed by Fe/FeCl<sub>3</sub>, proceeds in two steps:



With I<sub>2</sub> as catalyst the main product is perchloromethylthiol (Cl<sub>3</sub>CSCI). Reaction products with F<sub>2</sub> depend on the conditions used, typical products being SF<sub>4</sub>, SF<sub>6</sub>, S<sub>2</sub>F<sub>10</sub>, F<sub>2</sub>C(SF<sub>3</sub>)<sub>2</sub>, F<sub>2</sub>C(SF<sub>5</sub>)<sub>2</sub>, F<sub>3</sub>CSF<sub>5</sub> and F<sub>3</sub>SCF<sub>2</sub>SF<sub>5</sub>.

CS<sub>2</sub> is rather more reactive than CO<sub>2</sub> in forming complexes and in undergoing insertion reactions. The field was opened up by G. Wilkinson and his group in 1966 when they showed that [Pt(PPh<sub>3</sub>)<sub>3</sub>] reacts rapidly and

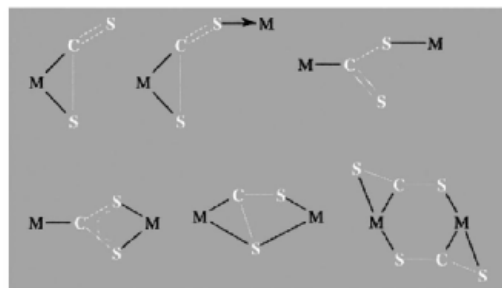
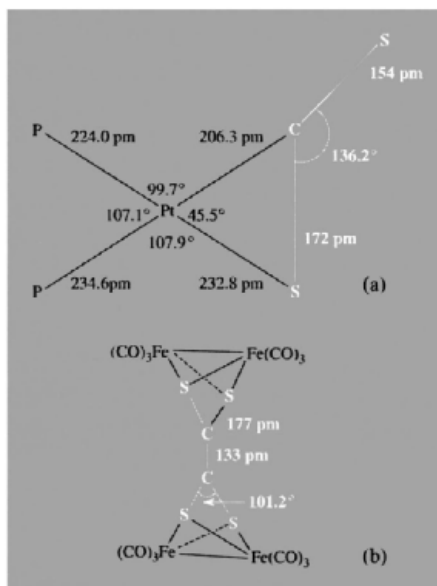
<sup>129</sup> G. D. THORN and R. A. LUDWIG, *The Dithiocarbonates and Related Compounds*, Elsevier 1962, 298 pp. J. A. MCCLEVERTY, *Prog. Inorg. Chem.* **10**, 49–221 (1968) (188 refs.). D. COUCOUANIS, *Prog. Inorg. Chem.* **11**, 233–71 (1970) (516 refs.). R. E. EISENBERG, *Prog. Inorg. Chem.* **12**, 295–369 (1971) (173 refs.).

quantitatively with  $\text{CS}_2$  at room temperature to give orange needles of  $[\text{Pt}(\text{CS}_2)(\text{PPh}_3)_2]$ , mp  $170^\circ$ . X-ray crystal diffraction analysis revealed the structure shown diagrammatically in Fig. 8.23(a). The geometry of the bent  $\text{CS}_2$  ligand is similar to that in the first excited state of the molecule and the  $\text{CS}_2$  is almost coplanar with  $\text{PtP}_2$  (dihedral angle  $6^\circ$ ). Bonding is considered to involve a 1-electron transfer via the intermediary of Pt from the highest filled  $\pi$  MO of the ligand to its lowest antibonding MO, and the Pt can be thought of as being oxidized from  $\text{Pt}^0$  to  $\text{Pt}^{\text{II}}$ . However, the substantial difference between the two Pt-P distances and the wide deviation of the angles of Pt from  $90^\circ$  emphasize the inadequacy of describing the bonding of such complicated species in terms of simple localized bonding theory. The orange complex  $[\text{Pd}(\text{CS}_2)(\text{PPh}_3)_2]$  is isostructural and further work yielded deep-green  $[\text{V}(\eta^5\text{-C}_5\text{H}_5)_2(\text{CS}_2)]$ , dimeric  $[(\text{Ph}_3\text{P})\text{Ni}(\mu\text{-CS}_2)_2\text{Ni}(\text{PPh}_3)]$  and various  $\text{CS}_2$  complexes of Fe, Ru, Rh and Ir. The deep-red complex  $[\text{Rh}(\text{CS}_2)_2\text{Cl}(\text{PPh}_3)_2]$  probably involves pseudo-octahedral  $\text{Rh}^{\text{III}}$  with one of the  $\text{CS}_2$  ligands  $\eta^2$ -bonded as above and the other one  $\sigma$ -bonded via a single S atom. By contrast, reaction of  $[\text{Fe}_3(\text{CO})_{12}]$  with an excess of  $\text{CS}_2$  in hexane for several hours at  $80^\circ\text{C}$  under a 10 atm pressure of  $\text{CO}/\text{Ar}$  gave the orange complex  $[\{\text{Fe}_2(\text{CO})_6\}_2(\mu_4\text{-C}_2\text{S}_4)]$  as one of the products (1–2%). As can be seen from Fig. 8.23(b), the structure has two  $\{\text{Fe}_2(\text{CO})_6\}$  units bridged by a planar  $\{\text{S}_2\text{C}=\text{CS}_2\}$  group, which can in turn be regarded as an ethenetetrathiol moiety formed by the C-C coupling of two  $\text{CS}_2$  molecules.<sup>(130)</sup>

The numerous  $\eta^1$ ,  $\eta^2$ , and bridging modes of coordination now known for  $\text{CS}_2$  are indicated schematically below:<sup>(131)</sup>

<sup>130</sup> P. V. BROADHURST, B. F. G. JOHNSON, J. LEWIS and P. R. RAITBY, *J. Chem. Soc., Chem. Commun.*, 140–1 (1982).

<sup>131</sup> T. G. SOUTHERN, U. OEHMICHEN, J. Y. LE MAROUILLE, H. LE BOZEC, D. GRANDJEAN and P. H. DIXNEUF, *Inorg. Chem.* **19**, 2976–80 (1980). Other key papers in this burgeoning field are: G. FACHINETTI, C. FLORIANI, A. CHIESI-VILLA and C. GUESTINI, *J. Chem. Soc., Dalton Trans.*, 1612–17 (1979). P. CONWAY, S. M. GRANT and A. R. MANNING, *J. Chem. Soc., Dalton Trans.*, 1920–4



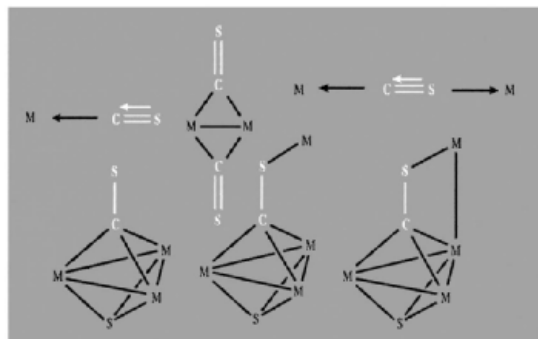
Insertion reactions of  $\text{CS}_2$  are known for all the elements which undergo  $\text{CO}_2$  insertion

(1979). P. J. VERGAMINI and P. G. ELLER, *Inorg. Chim. Acta* **34**, L291–2 (1979). C. BIANCHINI, A. MELI, A. ORLANDINI and L. SACCONI, *Inorg. Chim. Acta* **35**, L375–6 (1979). C. BIANCHINI, C. MEALLI, A. MELI, A. ORLANDINI and L. SACCONI, *Angew. Chem. Int. Edn. Engl.*, **18**, 673–4 (1979). C. BIANCHINI, C. MEALLI, A. MELI, A. ORLANDINI and L. SACCONI, *Inorg. Chem.* **19**, 2968–75 (1980). W. P. FEHLHAMMER and H. STOLZENBERG, *Inorg. Chim. Acta* **44**, L151–2 (1980). C. BIANCHINI, C. A. GHILARDI, A. MELI, S. MIDOLLINI and A. ORLANDINI, *J. Chem. Soc., Chem. Commun.*, 753–4 (1983). D. H. FARRAR, R. R. GUKATHASAN and S. A. MORRIS, *Inorg. Chem.* **23**, 3258–61 (1984).

(p. 312) and also for M–N bonds involving  $\text{Sb}^{\text{III}}$ ,  $\text{Zr}^{\text{IV}}$ ,  $\text{Nb}^{\text{V}}$ ,  $\text{Ta}^{\text{V}}$ , etc. Reaction of  $\text{CS}_2$  with  $\text{Au}_2\text{Cl}_6$  results in its novel insertion into Au–Cl bonds to form orange crystals of the chlorodithioformate complex  $[\text{AuCl}_2(\eta^2\text{-S}_2\text{CCl})]$ .<sup>(132)</sup> The parent dithioformate ligand,  $\text{HCS}_2^-$ , has been prepared by insertion of  $\text{CS}_2$  into the Ru–H bond of  $[\text{RuH}(\text{CO})\text{Cl}(\text{PPh}_3)_2(4\text{-vinyl pyridine})]$  to form the yellow complex  $[\text{Ru}(\text{CO})\text{Cl}(\text{PPh}_3)_2(\eta^2\text{-S}_2\text{CH})]\cdot\text{thf}$ .<sup>(133)</sup> Perhaps even more intriguingly, treatment of the orange *nido* 11-vertex metallathiorborane cluster  $[\text{8,8-(PPh}_3)_2\text{-8,7-nido-RhSB}_9\text{H}_{10}]$  (cf. structure (42), p. 178) with  $\text{CS}_2$  under reflux gives a 37% yield of the pale orange *nido* cluster  $[\text{8,8-(PPh}_3)_2\text{-}\mu\text{-8,9-(}\eta^2\text{-S}_2\text{CH)-8,7-RhSB}_9\text{H}_9]$  which features a unique dithioformate bridge between Rh(8)–B(9), perhaps by addition of  $\text{B-H}_f(9)$  across a C–S bond.<sup>(134)</sup>

Stable thiocarbonyl complexes containing the elusive CS ligand are also now well established and known coordination modes, which include terminal, bridging and polyhapto, are as shown at the top of the next column.<sup>(135)</sup>

Likewise complexes of CSe and CTe have been characterized.<sup>(136)</sup> The structure and reactivity of



CS complexes has been well reviewed<sup>(137)</sup> and exciting work in this area continues.<sup>(138)</sup>

## 8.8 Cyanides and Other Carbon–Nitrogen Compounds

The chemistry of compounds containing the CN group is both extensive and varied. The types of compound to be discussed are listed in Table 8.7, which also summarizes some basic structural information. The names cyanide, cyanogen, etc., refer to the property of forming deep-blue pigments such as Prussian blue (p. 1094) with iron salts (Greek *κύανος*, *cyanos*, dark blue).

A useful theme for cohering much of the chemistry of compounds containing the CN group is the concept of pseudohalogens, a term introduced in 1925 for certain strongly bound, univalent radicals such as CN, OCN, SCN, SeCN, (and  $\text{N}_3$ , etc.). These groups can form anions  $\text{X}^-$ , hydric acids  $\text{HX}$ , and sometimes neutral species  $\text{X}_2$ .

<sup>132</sup> D. JENTSCH, P. G. JONES, C. THONE and E. SCHWARZMANN, *J. Chem. Soc., Chem. Commun.*, 1495–6 (1989).

<sup>133</sup> V. G. PURANIK, S. S. TAVALE and T. N. G. ROW, *Polyhedron* **6**, 1859–61 (1987).

<sup>134</sup> G. FERGUSON, M. C. JENNINGS, A. L. LOUGH, S. COUGHLAN, T. R. SPALDING, J. D. KENNEDY, X. L. R. FONTAINE and B. ŠTÍBR, *J. Chem. Soc., Chem. Commun.*, 891–4 (1990).

<sup>135</sup> I. S. BUTLER, *Acc. Chem. Res.* **10**, 359–65 (1977). P. V. YANIEFF, *Coord. Chem. Rev.* **23**, 183–220 (1977) (includes  $\text{CS}_2$  complexes also). H. WERNER and K. LEONHARD, *Angew. Chem. Int. Edn. Engl.* **18**, 627–8 (1979). H. HERBERHOLD and P. H. SMITH, *Angew. Chem. Int. Edn. Engl.* **18**, 631–2 (1979). W. W. GREAVES, R. J. ANGELICI, B. J. HELLAND, R. KLIMA and R. A. JACOBSON, *J. Am. Chem. Soc.* **101**, 7618–20 (1979). F. FARONE, G. TRESOLDI, and G. A. LOPRETE, *J. Chem. Soc., Dalton Trans.*, 933–7 (1979); *J. Chem. Soc., Dalton Trans.*, 1053–6 (1979). P. V. BROADHURST, B. F. G. JOHNSON, J. LEWIS and P. R. RAITHY, *J. Chem. Soc., Chem. Commun.*, 812–13 (1980); *J. Am. Chem. Soc.* **103**, 3198–200 (1981).

<sup>136</sup> G. R. CLARK, K. MARSDEN, W. R. ROPER and L. J. WRIGHT, *J. Am. Chem. Soc.* **102**, 1206–7 (1981). J.-P. BATTIONI, D. MANSUY and J.-C. CHOTTARD, *Inorg. Chem.* **19**, 791–2 (1980).

<sup>137</sup> P. V. BROADHURST, *Polyhedron* **4**, 1801–46 (1985).

<sup>138</sup> K. J. KLABUNDE, M. P. KRAMER, A. SENNING and E. K. MOLTZEN, *J. Am. Chem. Soc.* **106**, 263–4 (1984). L. Busetto, V. Zanotti, V. G. Albano, D. Braga and M. Monari, *J. Chem. Soc., Dalton Trans.*, 1791–4 (1986) and 1133–3 (1987). S. Lotz, R. R. Pille and P. H. van Rooyen, *Inorg. Chem.* **25**, 3053–7 (1986). G. Gervasio, R. Rosselli, P. L. Stanghellini and G. Bor, *J. Chem. Soc., Dalton Trans.*, 1707–11 (1987). A. R. Manning, L. O'Dwyer, P. A. McArdle and D. Cunningham, *J. Chem. Soc., Chem. Commun.*, 897–8 (1992).

Table 8.7 Some compounds containing the CN group

Name	Conventional formula	$r(\text{C-N})/\text{pm}$	Remarks <sup>(a)</sup>
Cyanogen	$\text{N}\equiv\text{C}-\text{C}\equiv\text{N}$	115	Linear; $r(\text{C}-\text{C})$ 138 pm (short)
Paracyanogen	$(\text{CN})_x$	—	Involatile polymer, see text
diisocyanogen	$\text{CN}-\text{NC}$	118 (calc.)	Linear, symmetric, unstable <sup>(140)</sup>
isocyanogen	$\text{CN}-\text{CN}$	118&116 (calc.)	Zig-zag, unsymmetric, stable <sup>(140)</sup>
Hydrogen cyanide	$\text{H}-\text{C}\equiv\text{N}$	115.6	Linear; $r(\text{C}-\text{H})$ 106.5 pm
Cyanide ion	$(\text{C}\equiv\text{N})^-$	116	$r_{\text{eff}}$ 192 pm when "freely rotating" in MCN
Cyanides (nitriles)	$\text{M}-\text{C}\equiv\text{N}$ $(\text{R}-\text{C}\equiv\text{N})$	115.8	Linear; $r(\text{C}-\text{C})$ 146.0 pm (for MeCN)
Isocyanides	$\text{R}-\text{N}\equiv\text{C}$	116.7	Linear, $r(\text{H}_3\text{C}-\text{N})$ 142.6 pm (for MeNC). Coordinated isocyanides are slightly bent, e.g. $[\text{M}(\leftarrow\text{C}=\text{N}-\text{C}_6\text{H}_5)_6]$ angle CNC 173°. $r(\text{C}=\text{N})$ 117.6 pm: bridging modes are also known, e.g. structure (1), p. 321
Cyanogen halides (halogen cyanides)	$\text{X}-\text{C}\equiv\text{N}$	116	Linear
Cyanamide	$\text{H}_2\text{N}-\text{C}\equiv\text{N}$	115	Linear NCN; $r(\text{C}-\text{NH}_2)$ 131 pm
Dicyandiamide	$\text{N}\equiv\text{C}-\text{N}=\text{C}(\text{NH}_2)_2$	122-136	See structure (2), p. 321
Cyanuric compounds	$\{-\text{C}(\text{X})=\text{N}-\}_3$	134	Cyclic trimers; X = halogen, OH, NH <sub>2</sub>
Cyanate ion	$(\text{O}-\text{C}\equiv\text{N})^-$	~121	Linear
Isocyanates	$\text{R}-\text{N}=\text{C}=\text{O}$	120	Linear NCO; $\angle\text{RNC} \sim 126^\circ$
Fulminate ion	$>(\text{C}=\text{N}-\text{O})^-$	109	Linear; another form of AgCNO has $r(\text{C}-\text{N})$ 112 pm
Thiocyanate ion	$(\text{S}-\text{C}\equiv\text{N})^-$	115	Linear
Thiocyanates	$\text{R}-\text{S}-\text{C}\equiv\text{N}$ $(\text{M}-\text{S}-\text{C}\equiv\text{N})$	116	Linear NCS; $\angle\text{RSC}$ 100° in MeSCN; $\angle\text{MSC}$ variable (80-107°)
Isothiocyanates	$\text{R}-\text{N}=\text{C}=\text{S}$	122	Linear NCS; $\angle\text{HNC}$ 135° in HNCS; $\angle\text{MNC}$ variable (111-180°)
Selenocyanate ion	$(\text{Se}-\text{C}\equiv\text{N})^-$	~112	Linear NCSe

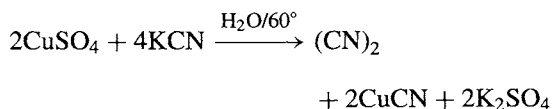
<sup>(a)</sup>Several groups can also act as bridging ligands in metal complexes, e.g.  $-\text{CN}-$ ,  $>\text{NCO}$ ,  $-\text{SCN}-$

XY, etc. It is also helpful to recognize that  $\text{CN}^-$  is isoelectronic with  $\text{C}_2^{2-}$  (p. 299) and with several notable ligands such as CO, N<sub>2</sub> and NO<sup>+</sup>. Similarly, the cyanate ion  $\text{OCN}^-$  is isoelectronic with CO<sub>2</sub>, N<sub>3</sub><sup>-</sup>, fulminate ( $\text{CNO}^-$ ), etc.<sup>(139)</sup>

Cyanogen,  $(\text{CN})_2$ , is a colourless poisonous gas (like HCN) mp  $-27.9^\circ$ , bp  $-21.2^\circ$  (cf. Cl<sub>2</sub>, Br<sub>2</sub>). When pure it possesses considerable

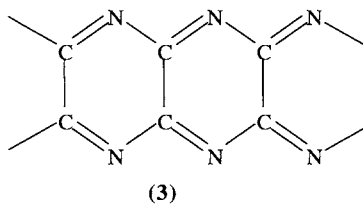
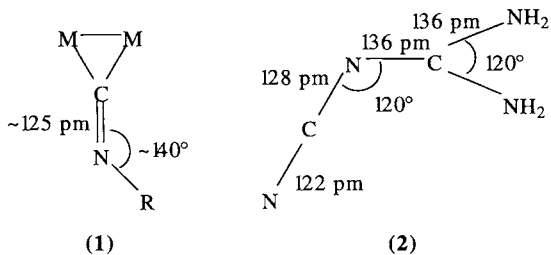
thermal stability (800°C) but trace impurities normally facilitate polymerization at 300-500° to paracyanogen a dark-coloured solid which may have a condensed polycyclic structure (3).

The polymer reverts to  $(\text{CN})_2$  above 800° and to CN radicals above 850°.  $(\text{CN})_2$  can be prepared in 80% yield by mild oxidation of  $\text{CN}^-$  with aqueous Cu<sup>II</sup>; the reaction is complex but can be idealized as

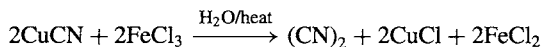


<sup>139</sup>A. M. GOLUB, H. KÖHLER and V. V. SKOPENKO (eds.), *Chemistry of Pseudohalides*, Elsevier, Amsterdam, 1986, 479 pp., 4217 refs.

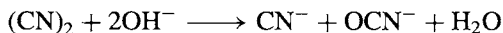
<sup>140</sup>L. S. CEDERBAUM, F. TARANTELLI, H. G. WEIKERT, M. SCHELLER and H. KÖPPEL, *Angew. Chem. Int. Edn. Engl.* **28**, 761-2 (1989).



CO<sub>2</sub> which is also formed (20%) can be removed by passage of the product gas over solid NaOH and the byproduct CuCN can be further oxidized with hot aqueous Fe<sup>III</sup> to complete the conversion:



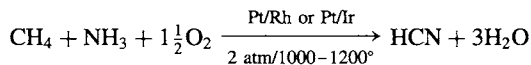
Industrially it is now made by direct gas-phase oxidation of HCN with O<sub>2</sub> (over a silver catalyst), or with Cl<sub>2</sub> (over activated charcoal), or NO<sub>2</sub> (over CaO glass). (CN)<sub>2</sub> is fairly stable in H<sub>2</sub>O, EtOH and Et<sub>2</sub>O but slowly decomposes in solution to give HCN, HNCO, (H<sub>2</sub>N)<sub>2</sub>CO and H<sub>2</sub>NC(O)C(O)NH<sub>2</sub> (oxamide). Alkaline solutions yield CN<sup>-</sup> and (OCN)<sup>-</sup> (cf. halogens).



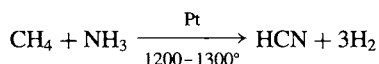
Hydrogen cyanide, mp -13.3° bp 25.7°, is an extremely poisonous compound of very high dielectric constant (p. 55). It is miscible with H<sub>2</sub>O, EtOH and Et<sub>2</sub>O. In aqueous solution it is an even weaker acid than HF, the dissociation constant *K<sub>a</sub>* being 7.2 × 10<sup>-10</sup> at 25°C. It was formerly produced industrially by acidifying NaCN or Ca(CN)<sub>2</sub> but the most modern catalytic processes are based on direct reaction between

CH<sub>4</sub> and NH<sub>3</sub>, e.g.:<sup>(141)</sup>

Andrussow process:

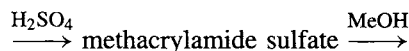


Degussa process:



Both processes rely on a fast flow system and the rapid quenching of product gases; yields of up to 90% can be attained. It is salutary to note that US production of this highly toxic compound is 600 000 tonnes pa (1992) and world production exceeds one million tonnes pa. Of this, 41% is used to manufacture adiponitrile for nylon and 28% for acrylic plastics:

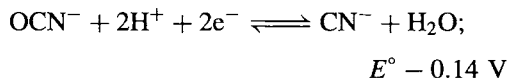
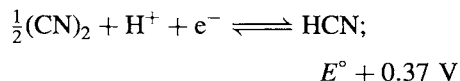
HCN + Me<sub>2</sub>CO → acetone cyanohydrin



methyl methacrylate

HCN is now also used to make (ClCN)<sub>3</sub> for pesticides (9%), NaCN for gold recovery (13%), and chelating agents such as edta (4%), etc.

As noted above, CN<sup>-</sup>(aq) is fairly easily oxidized to (CN)<sub>2</sub> or OCN<sup>-</sup>; *E*<sup>o</sup> values calculated from free energy data (p. 435) are:

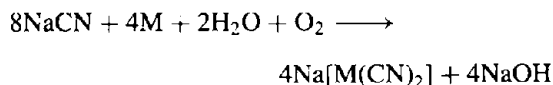


HCN can also be reduced to MeNH<sub>2</sub> by powerful reducing agents such as Pd/H<sub>2</sub> at 140°.

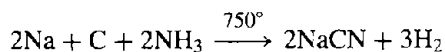
The alkali metal cyanides M<sup>I</sup>CN are produced by direct neutralization of HCN; they crystallize

<sup>141</sup> Ref. 2, Vol. 7 (1993), Cyanides (including HCN, M<sup>I</sup>CN, and M<sup>II</sup>(CN)<sub>2</sub>, pp. 753–82; Cyanamides including CaNCN, H<sub>2</sub>NCN, dicyandiamide, and melamine), pp. 736–52; cyanuric and isocyanuric acids, pp. 834–51.

with the NaCl structure ( $M = \text{Na}, \text{K}, \text{Rb}$ ) or the CsCl structure ( $M = \text{Cs}, \text{Tl}$ ) consistent with "free" rotation of the  $\text{CN}^-$  group. The effective radius is  $\sim 190$  pm, intermediate between those of  $\text{Cl}^-$  and  $\text{Br}^-$ . At lower temperatures the structures transform to lower symmetries as a result of alignment of the  $\text{CN}^-$  ions. LiCN differs in having a loosely packed 4-coordinate arrangement and this explains its low density ( $1.025 \text{ g cm}^{-3}$ ) and unusually low mp ( $160^\circ$ , cf. NaCN  $564^\circ$ , KCN  $634^\circ\text{C}$ ). World production of alkali metal cyanides was  $\sim 340\,000$  tonnes in 1989. NaCN readily complexes metallic Ag and Au under mildly oxidizing conditions and is much used in the extraction of these metals from their low-grade ores (first patented in 1888 by R. W. Forrest, W. Forrest and J. S. McArthur):



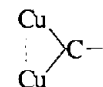
Until the 1960s, when HCN became widely available, NaCN was made by the Castner process via sodamide and sodium cyanamide:



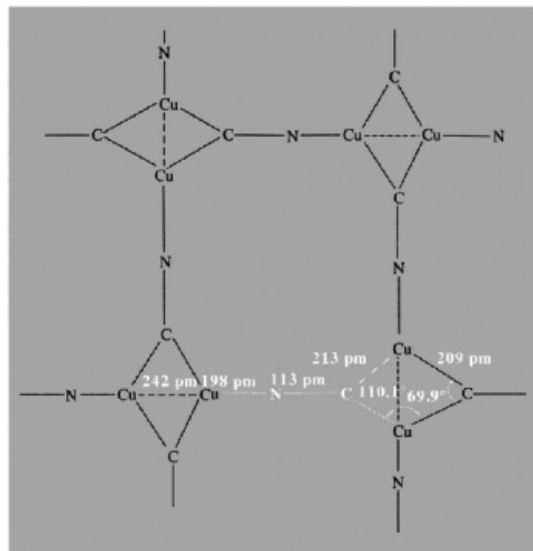
The  $\text{CN}^-$  ion can act either as a monodentate or bidentate ligand.<sup>(142)</sup> Because of the similarity of electron density at C and N it is not usually possible to decide from X-ray data whether C or N is the donor atom in monodentate complexes, but in those cases where the matter has been established by neutron diffraction C is always found to be the donor atom (as with CO). Very frequently  $\text{CN}^-$  acts as a bridging ligand -CN- as in AgCN, and AuCN (both of which are infinite linear chain polymers), and in Prussian-blue type compounds (p. 1094). The same tendency for a coordinated M-CN group to form a further donor-acceptor bond using the lone-pair of electrons on the N atom is illustrated by the mononuclear  $\text{BF}_3$  complexes

with tetracyanonickelates and hexacyanoferrates, e.g.  $\text{K}_2[\text{Ni}(\text{CN}.\text{BF}_3)_4]$  and  $\text{K}_4[\text{Fe}(\text{CN}.\text{BF}_3)_6]$ .

The complex  $\text{CuCN}.\text{NH}_3$  provides an unusual example of CN acting as a bridging ligand at C, a mode which is common in  $\mu\text{-CO}$  complexes (p. 928); indeed, the complex is unique in featuring tridentate CN groups which link the metal atoms into plane nets via the

grouping  as shown in Fig. 8.24.

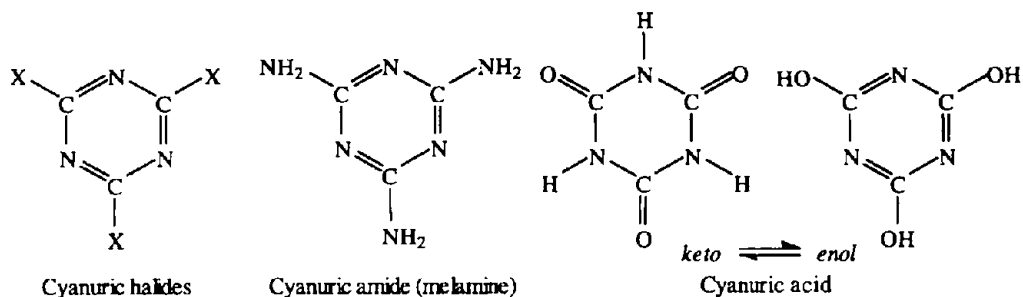
Other cyanide complexes are discussed under the appropriate metals. In organic chemistry, both nitriles  $\text{R-CN}$  and isocyanides (isocyanides)  $\text{R-NC}$  are known. Isocyanides have been extensively studied as ligands (p. 926).<sup>(143)</sup> More



**Figure 8.24** Schematic diagram of the layer structure of  $\text{CuCN}.\text{NH}_3$  showing the tridentate CN groups; each Cu is also bonded to 1  $\text{NH}_3$  molecule at 207 pm. Note also the unusual 5-coordination of Cu including one near neighbour Cu at 242 pm (13 pm closer than Cu-Cu in the metal). The lines in the diagram delineate the geometry and do not represent pairs of electrons.

<sup>142</sup> A. G. SHARPE, *The Chemistry of Cyano Complexes of the Transition Metals*, Academic Press, London, 1976, 302 pp.

<sup>143</sup> L. MALATESTA and F. BONATI, *Isocyanide Complexes of Metals*, Wiley, London, 1969, 199 pp.



**Figure 8.25** The planar structure of various cyanuric compounds: all 6 C–N distances within the ring are equal.

complex coordination modes are now also well documented for  $\text{CN}^-$ ,  $\text{RCN}$  and  $\text{RNC}$ .<sup>(144)</sup>

Cyanogen halides,  $\text{X}\cdot\text{CN}$ , are colourless, volatile, reactive compounds which can be regarded as pseudohalogen analogues of the interhalogen compounds,  $\text{XY}$  (p. 824) (Table 8.8). All tend to trimerize to give cyclic cyanuric halides (Fig. 8.25) especially in the presence of free  $\text{HX}$ .  $\text{FCN}$  is prepared by pyrolysis of  $(\text{FCN})_3$  which in turn is made by fluorinating  $(\text{ClCN})_3$  with  $\text{NaF}$  in tetramethylene sulfone.  $\text{ClCN}$  and  $\text{BrCN}$  are prepared by direct reaction of  $\text{X}_2$  on  $\text{MCN}$  in water or  $\text{CCl}_4$ , and  $\text{ICN}$  is prepared by a dry route from  $\text{Hg}(\text{CN})_2$  and  $\text{I}_2$ . Similarly, colourless crystals of cyanamide ( $\text{H}_2\text{NCN}$  mp  $46^\circ$ ) result from the reaction of  $\text{NH}_3$  on  $\text{ClCN}$  and trimerize to melamine at  $150^\circ$  (Fig. 8.25). The industrial preparation is by acidifying  $\text{CaNCN}$  (see Panel). The “dimer”,

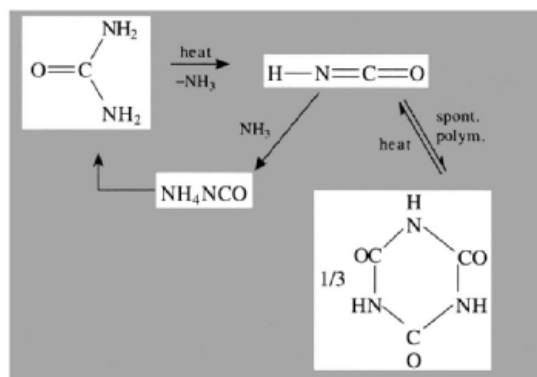
dicyandiamide,  $\text{CNC}(\text{NH}_2)_2$ , can be made by boiling calcium cyanamide with water: the colourless crystals are composed of nonlinear molecules which feature three different C–N distances (see Table 8.7).

The hydroxyl derivative of  $\text{X}\cdot\text{CN}$  is cyanic acid  $\text{HO}\cdot\text{CN}$ : it cannot be prepared pure due to rapid decomposition but it is probably present to the extent of about 3% when its tautomer, isocyanic acid ( $\text{HNCO}$ ) is prepared from sodium cyanate and  $\text{HCl}$ .  $\text{HNCO}$  rapidly trimerizes to cyanuric acid (Fig. 8.25) from which it can be regenerated by pyrolysis. It is a fairly strong acid ( $K_a$   $1.2 \times 10^{-4}$  at  $0^\circ$ ) freezing at  $-86.8^\circ$  and boiling at  $23.5^\circ\text{C}$ . Thermolysis of urea is an alternative route to  $\text{HNCO}$  and  $(\text{HNCO})_3$ ; the reverse reaction, involving the isomerization of ammonium cyanate, is the classic synthesis of urea by F. Wöhler (1828).<sup>(145)</sup>

**Table 8.8** Cyanogen halides

Property	$\text{FCN}$	$\text{ClCN}$	$\text{BrCN}$	$\text{ICN}$
MP/ $^\circ\text{C}$	-82	-6.9	51.3	146
BP/ $^\circ\text{C}$	-46	13.0	61.3	146 (subl)

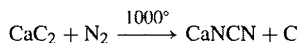
<sup>144</sup> Some typical examples will be found in the following references. M. A. ANDREWS, C. B. KNOBLER and H. D. KAESZ, *J. Am. Chem. Soc.* **101**, 7260–4 (1979). M. I. BRUCE, T. W. HAMBLEY and B. K. NICHOLSON, *J. Chem. Soc., Chem. Commun.*, 353–5 (1982). V. CHEBOLU, R. R. WHITTLE and A. SEN, *Inorg. Chem.* **24**, 3082–5 (1985). T. C. WRIGHT, G. WILKINSON, M. MOTEVALLI and M. B. HURSTHOUSE, *J. Chem. Soc., Dalton Trans.*, 2017–9 (1986). K. S. RATLIFF, P. E. FANWICK and C. P. KUBIAK, *Polyhedron* **9**, 1487–9 (1990).



<sup>145</sup> J. SHORTER, *Chem. Soc. Revs.* **7**, 1–14 (1978).

### The Cyanamide Industry<sup>(141)</sup>

The basic chemical of the cyanamide industry is calcium cyanamide  $\text{CaNCN}$ , mp  $1340^\circ$ , obtained by nitrogenation of  $\text{CaC}_2$ .



$\text{CaNCN}$  is used as a direct application fertilizer, weed killer, and cotton defoliant; it is also used for producing cyanamide, dicyandiamide and melamine plastics. Production formerly exceeded 1.3 million tonnes pa, but this has fallen considerably in the last few years, particularly in the USA where the use of  $\text{CaNCN}$  as a nitrogenous fertilizer has been replaced by other materials. In 1990 most of the world's supply was made in Japan, Germany and Canada.

Acidification of  $\text{CaNCN}$  yields free cyanamide,  $\text{H}_2\text{NCN}$ , which reacts further to give differing products depending on pH: at  $\text{pH} \leq 2$  or  $> 12$  urea is formed, but at  $\text{pH} 7-9$  dimerization to dicyandiamide  $\text{NCNC}(\text{NH}_2)_2$  occurs. Solutions are most stable at  $\text{pH} \sim 5$ ; accordingly commercial preparation of  $\text{H}_2\text{NCN}$  is by continuous carbonation of an aqueous slurry of  $\text{CaNCN}$  in the presence of graphite: the overall reaction can be represented

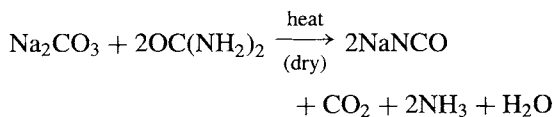


Reaction of  $\text{H}_2\text{NCN}$  with  $\text{H}_2\text{S}$  gives thiourea,  $\text{SC}(\text{NH}_2)_2$ .

Dicyandiamide forms white, non-hygroscopic crystals which melt with decomposition at  $209^\circ$ . Its most important reaction is conversion to melamine (Fig. 8.25) by pyrolysis above the mp under a pressure of  $\text{NH}_3$  to counteract the tendency to deamination. Melamine is mainly used for melamine-formaldehyde plastics. Total annual production of both  $\text{H}_2\text{NCN}$  and  $\text{NCNC}(\text{NH}_2)_2$  is on the 30 000 tonne scale.

Several of these compounds and their derivatives are commercially and industrially important. Urea has already been mentioned on p. 311. Again, world production of chloroisocyanurates,  $(\text{CINC}=\text{O})_3$ , in 1987 was ca. 80 000 tonnes (50 000 tonnes in USA alone, of which 75% went for swimming pool disinfection and most of the rest for scouring powders, household bleaches and dishwashing powder formulations).<sup>(141)</sup>

Alkali metal cyanates are stable and readily obtained by mild oxidation of aqueous cyanide solutions using oxides of  $\text{Pb}^{\text{II}}$  or  $\text{Pb}^{\text{IV}}$ . The commercial preparation of  $\text{NaNCO}$  is by reaction of urea with  $\text{Na}_2\text{CO}_3$ .



The pseudohalogen concept (p. 319) might lead one to expect the existence of a cyanate analogue of cyanogen but there is little evidence for  $\text{NCO}-\text{OCN}$ , consistent with the known reluctance of oxygen to catenate. By contrast,

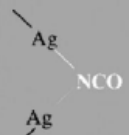


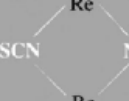

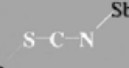
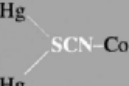
thiocyanogen  $(\text{SCN})_2$  is moderately stable; it can be prepared as white crystals by suspending  $\text{AgSCN}$  in  $\text{Et}_2\text{O}$  or  $\text{SO}_2$  and oxidizing the anion at low temperatures with  $\text{Br}_2$  or  $\text{I}_2$ .  $(\text{SCN})_2$  melts at  $\sim -7^\circ$  to an unstable orange suspension which rapidly polymerizes to the brick-red solid parathiocyanogen  $(\text{SCN})_x$ .<sup>(146)</sup> This ready polymerization hampers structural studies but it is probable that the molecular structure is  $\text{N}\equiv\text{C}-\text{S}-\text{S}-\text{C}\equiv\text{N}$  with a nonlinear central  $\text{C}-\text{S}-\text{S}-\text{C}$  group.  $(\text{SeCN})_2$  can be prepared similarly as a yellow powder which polymerizes to a red solid.

Thiocyanates and selenocyanates can be made by fusing the corresponding cyanide with S or Se. The  $\text{SCN}^-$  and  $\text{SeCN}^-$  ions are both linear, like  $\text{OCN}^-$ . (See p. 779 for  $\text{TeCN}^-$ ) Treatment of  $\text{KSCN}$  with dry  $\text{KHSO}_4$  produces free isothiocyanic acid  $\text{HNCS}$ , a white crystalline solid which is stable below  $0^\circ$  but which decomposes rapidly at room temperatures to  $\text{HCN}$  and a yellow solid  $\text{H}_2\text{C}_2\text{N}_2\text{S}_3$ . Thiocyanic acid,  $\text{HSCN}$ , (like  $\text{HOCN}$ ) has not been prepared

<sup>146</sup> F. CATALDO, *Polyhedron* **11**, 79-83 (1992).



Table 8.9 Modes of bonding established by X-ray crystallography

Mode	Example	Comment
Ag–NCO	[AsPh <sub>4</sub> ] [Ag(NCO) <sub>2</sub> ]	Linear anion
Mo–OCN	[Mo(OCN) <sub>6</sub> ] <sup>3-</sup> , [Rh(OCN)(PPh <sub>3</sub> ) <sub>3</sub> ]	Based on infrared data only
	AgNCO	Cf. fulminate in Table 8.7
	[Ni <sub>2</sub> (NCO) <sub>2</sub> {N(CH <sub>2</sub> CH <sub>2</sub> NH <sub>2</sub> ) <sub>3</sub> ] <sub>2</sub> ] [BPh <sub>4</sub> ] <sub>2</sub>	Note bent Ni–N–C
Co–NCS	[Co(NH <sub>3</sub> ) <sub>5</sub> (NCS)]Cl <sub>2</sub> } [Co(NH <sub>3</sub> ) <sub>5</sub> (SCN)]Cl <sub>2</sub> }	Linkage isomerism
Co–SCN		
Pd–NCS	[Pd(NCS)(SCN){Ph <sub>2</sub> P(CH <sub>2</sub> ) <sub>3</sub> PPh <sub>2</sub> }]	Both <i>N</i> and <i>S</i> monodentate in a single crystal
SCN		
	K <sub>2</sub> [Pd(SCN) <sub>4</sub> ]	Weak <i>S</i> bridging to a second Pd
	[NBu <sub>4</sub> <sup>n</sup> ] <sub>3</sub> [Re <sub>2</sub> (NCS) <sub>10</sub> ]	<i>N</i> -bonded bridging (and terminal) <sup>(154)</sup>
Co–NCS–Hg	[Co(NCS) <sub>4</sub> Hg]	Bidentate, different metals
	[Pt <sub>2</sub> (Cl) <sub>2</sub> (PPr <sub>3</sub> ) <sub>2</sub> (SCN) <sub>2</sub> ]	Bidentate, same metal
	Ph <sub>2</sub> SbSCN	Spiral chain polymer <sup>(149)</sup>
	[Co(NCS) <sub>6</sub> Hg <sub>2</sub> ]·C <sub>6</sub> H <sub>6</sub>	Tridentate
Ni–NCSe	[Ni(HCONMe <sub>2</sub> ) <sub>4</sub> (NCSe) <sub>2</sub> ]	<i>N</i> donor
Co–SeCN	K[Co(Me <sub>2</sub> glyoxime) <sub>2</sub> (SeCN) <sub>2</sub> ]	<i>Se</i> donor

pure but compounds such as MeSCN and  $\text{Se}(\text{SCN})_2$  are known.

The thiocyanate ion has been much studied as an ambidentate ligand (in which either S or N is the donor atom); it can also act as a bidentate bridging ligand  $-\text{SCN}-$ , and even as a tridentate ligand  $>\text{SCN}-$ .<sup>(147,148,149)</sup> The ligands  $\text{OCN}^-$  and  $\text{SeCN}^-$  have been less studied but appear to be generally similar. A preliminary indication of the mode of coordination can sometimes be obtained from vibrational spectroscopy since *N* coordination raises both  $\nu(\text{CN})$  and  $\nu(\text{CS})$  relative to the values of the uncoordinated ion, whereas *S* coordination leaves  $\nu(\text{CN})$  unchanged and increases  $\nu(\text{CS})$  only somewhat. The bridging mode tends to increase both  $\nu(\text{CN})$  and  $\nu(\text{CS})$ . Similar trends are noted for  $\text{OCN}^-$  and  $\text{SeCN}^-$  complexes. However, these "group vibrations" are in reality appreciably mixed with other modes both in the ligand itself and in the complex as a whole, and vibrational spectroscopy is therefore not always a reliable criterion. Increasing use is being made of  $^{14}\text{N}$  and  $^{13}\text{C}$  nmr data<sup>(150)</sup> but the most reliable data, at least for crystalline complexes, come from X-ray diffraction studies.<sup>(151)</sup> The variety of coordination modes so revealed is illustrated in Table 8.9, which is based on one by A. H. Norbury.<sup>(147)</sup> Phenomenologically it is observed that class a metals tend to be *N*-bonded whereas class b tend to be *S*-bonded (see below), though it should be stressed that kinetic and solubility factors as well as relative thermodynamic stability are sometimes

implicated, and so-called 'linkage isomerism' is well established, e.g.  $[\text{Co}(\text{NH}_3)_5(\text{NCS})]\text{Cl}_2$  and  $[\text{Co}(\text{NH}_3)_5(\text{SCN})]\text{Cl}_2$ . In terms of the a and b (or "hard" and "soft") classification of ligands and acceptors it is noted that metals in Groups 3–8 together with the lanthanoids and actinoids tend to form  $-\text{NCS}$  complexes; in the later transition groups Co, Ni, Cu and Zn also tend to form  $-\text{NCS}$  complexes whereas their heavier congeners Rh, Ir; Pd, Pt; Au; and Hg are predominantly *S*-bonded. Ag and Cd are intermediate and readily form both types of complex. See also refs. 152, 153. The interpretation to be placed on these observations is less certain. Steric influences have been mentioned (*N* bonding, which is usually linear, requires less space than the bent  $\text{M}-\text{S}-\text{CN}$  mode). Electronic factors also play a role, though the detailed nature of the bonding is still a matter of debate and devotees of the various types of electronic influence have numerous interpretations to select from. Solvent effects (dielectric constant  $\epsilon$ , coordinating power, etc.) have also been invoked and it is clear that these various explanations are not mutually exclusive but simply tend to emphasize differing aspects of an extremely complicated and delicately balanced situation. The interrelation of these various interpretations is summarized in Table 8.10.

**Table 8.10** Mode of bonding in thiocyanate complexes

Metal type <sup>(a)</sup>	$\sigma$ -Donor ligand	High- $\epsilon$ solvent	Low- $\epsilon$ solvent	$\pi$ -Acceptor ligand
Class a	$-\text{NCS}$	$-\text{NCS}$	$-\text{SCN}$	$-\text{SCN}$
Class b	$-\text{SCN}$	$-\text{SCN}$	$-\text{NCS}$	$-\text{NCS}$

<sup>(a)</sup>Sometimes discussed in terms of "hard" and "soft" acids and bases.

Fewer data are available for  $\text{SeCN}^-$  complexes but similar generalizations seem to hold. By contrast,  $\text{OCN}^-$  complexes are not so readily discussed in these terms: in fact, very few cyanato

<sup>147</sup> A. H. NORBURY, *Adv. Inorg. Chem. Radiochem.* **17**, 231–402 (1975) (825 refs.).

<sup>148</sup> A. A. NEWMAN (ed.), *Chemistry and Biochemistry of Thiocyanic Acid and its Derivatives*, Academic Press, London, 1975, 351 pp.

<sup>149</sup> G. E. FORSTER, I. G. SOUTHERINGTON, M. J. BEGLEY and D. B. SOWERBY, *J. Chem. Soc., Chem. Commun.*, 54–5 (1991).

<sup>150</sup> J. A. KARGOL, R. W. CRECELY and J. L. BURMEISTER, *Inorg. Chim. Acta* **25**, L109–L110 (1977), and references therein.

<sup>151</sup> S. J. ANDERSON, D. S. BROWN and K. J. FINNEY, *J. Chem. Soc., Dalton Trans.*, 152–4 (1979). (The compounds, originally thought to be *O*-bonded on the basis of infrared and  $^{14}\text{N}$  nmr spectroscopy, now shown by X-ray analysis to be *N*-bonded.) See also ref. 154.

<sup>152</sup> W. KELM and W. PREETZ, *Z. anorg. allg. Chem.* **568**, 106–16 (1989).

<sup>153</sup> M. KAKOTI, S. CHAUDHURY, A. K. DEB and S. GOSWAMI, *Polyhedron* **12**, 783–9 (1993).

(-OCN) complexes have been characterized and the ligand is usually *N*-bonded (isocyanato).<sup>(151)</sup>

## 8.9 Organometallic Compounds

Compounds which contain direct M-C bonds comprise a vast field which spans the traditional branches of inorganic and organic chemistry. A general overview is given in Section 19.7

<sup>154</sup> F. A. COTTON, A. DAVISON, W. H. ISLEY and H. S. TROP, *Inorg. Chem.* **18**, 2719-23 (1979).

<sup>155</sup> A. W. PARKINS and R. C. POLLER, *An Introduction to Organometallic Chemistry*, Macmillan, Basingstoke, 1986, 252 pp.

<sup>156</sup> J. S. THAYER, *Organometallic Chemistry: An Overview*, VCH Publishers (UK), 1988, 250 pp.

(p. 924) and specific aspects are treated separately under the chemistry of each individual element, e.g. alkali metals (pp. 102-6), alkaline earth metals (pp. 127-38), Group 13 metals (pp. 257-67) etc. In addition to the references cited on p. 924, useful general accounts can be found in refs. 155-160.

<sup>157</sup> R. H. CRABTREE *The Organometallic Chemistry of the Transition Metals*, Wiley, New York, 1988, 440 pp.

<sup>158</sup> Ch. ELSCHENBROICH and A. SALZER, *Organometallics*, VCH Publishers (NY), 1989, 479 pp.

<sup>159</sup> T. J. MARKS (ed.) *Bonding Energetics in Organometallic Compounds*, ACS Symposium Series No. 428, Washington DC, 1990, 320 pp.

<sup>160</sup> E. W. ABEL, F. G. A. STONE and G. WILKINSON (eds.), *Comprehensive Organometallic Chemistry II: A review of the literature 1982-1994* in 14 volumes, Pergamon, Oxford, 1995, approx 8750 pp.

																1	2																																				
																H	He																																				
3	4																	5	6	7	8	9	10																														
Li	Be																	B	C	N	O	F	Ne																														
11	12																	13	14	15	16	17	18																														
Na	Mg																	Al	Si	P	S	Cl	Ar																														
19	20	21	22	23	24	25	26	27	28	29	30	31	32	33	34	35	36																																				
K	Ca	Sc	Ti	V	Cr	Mn	Fe	Co	Ni	Cu	Zn	Ga	Ge	As	Se	Br	Kr																																				
37	38	39	40	41	42	43	44	45	46	47	48	49	50	51	52	53	54																																				
Rb	Sr	Y	Zr	Nb	Mo	Tc	Ru	Rh	Pd	Ag	Cd	In	Sn	Sb	Te	I	Xe																																				
55	56	57	58	59	60	61	62	63	64	65	66	67	68	69	70	71	72																																				
Cs	Ba	La	Hf	Ta	W	Re	Os	Ir	Pt	Au	Hg	Tl	Pb	Bi	Po	At	Rn																																				
87	88	89	90	91	92	93	94	95	96	97	98	99	100	101	102	103	104																																				
Fr	Ra	Ac	Rf	Db	Sg	Bh	Hs	Mt	Uu	Uu	Uu	Uu	Uu	Uu	Uu	Uu	Uu																																				
																		73	74	75	76	77	78	79	80	81	82	83	84	85	86	87	88	89	90	91																	
																		Ce	Pr	Nd	Pm	Sm	Eu	Gd	Tb	Dy	Ho	Er	Tm	Yb	Lu																						
																		92	93	94	95	96	97	98	99	100	101	102	103	104	105	106	107	108	109	110	111																
																		Th	Pa	U	Np	Pu	Am	Cm	Bk	Cf	Es	Fm	Md	No	Lr																						

# 9

## Silicon

### 9.1 Introduction

Silicon shows a rich variety of chemical properties and it lies at the heart of much modern technology.<sup>(1)</sup> Indeed, it ranges from such bulk commodities as concrete, clays and ceramics, through more chemically modified systems such as soluble silicates, glasses and glazes to the recent industries based on silicone polymers and solid-state electronics devices. The refined technology of ultrapure silicon itself is perhaps the most elegant example of the close relation between chemistry and solid-state physics and has led to numerous developments such as the transistor, printed circuits and microelectronics (p. 332).

In its chemistry, silicon is clearly a member of Group 14 of the periodic classification but there are notable differences from carbon, on the one hand, and the heavier metals of the group on the other (p. 371). Perhaps the most

obvious questions to be considered are why the vast covalent chemistry of carbon and its organic compounds finds such pallid reflection in the chemistry of silicon, and why the intricate and complex structural chemistry of the mineral silicates is not mirrored in the chemistry of carbon-oxygen compounds.<sup>†</sup>

Silica (SiO<sub>2</sub>) and silicates have been intimately connected with the evolution of mankind from prehistoric times: the names derive from the Latin *silex*, gen. *silicis*, flint, and serve as a reminder of the simple tools developed in paleolithic times (~500 000 years ago) and the shaped flint knives and arrowheads of the neolithic age which began some 20 000 years ago. The name of the element, silicon, was proposed by Thomas Thomson in

<sup>†</sup> Throughout this chapter we will notice important differences between the chemical behaviour of carbon and silicon, and one is reminded of Grant Urry's memorable words: "It is perhaps appropriate to chide the polysilane chemist for milking the horse and riding the cow in attempting to adapt the success of organic chemistry in the study of polysilanes. A valid argument can be made for the point of view that the most effective chemistry of silicon arises from the differences with the chemistry of carbon compounds rather than the similarities" (see ref. 35 on p. 342).

<sup>1</sup> *Kirk-Othmer Encyclopedia of Chemical Technology*, 3rd edn., Vol. 20, pp. 748-973 (1982) (Silica, silicon and silicon alloys; Silicon compounds); 4th edn., Vol. 5 (1993) Cement pp. 564-98; Ceramics, pp. 599-697; Ceramics as electrical materials, pp. 698-728; Clays, Vol. 6, pp. 381-423 (1993).

1831, the ending *on* being intended to stress the analogy with carbon and boron.

The great affinity of silicon for oxygen delayed its isolation as the free element until 1823 when J. J. Berzelius succeeded in reducing  $K_2SiF_6$  with molten potassium. He first made  $SiCl_4$  in the same year,  $SiF_4$  having previously been made in 1771 by C. W. Scheele who dissolved  $SiO_2$  in hydrofluoric acid. The first volatile hydrides were discovered by F. Wöhler who synthesized  $SiHCl_3$  in 1857 and  $SiH_4$  in 1858, but major advances in the chemistry of the silanes awaited the work of A. Stock during the first third of the twentieth century. Likewise, the first organosilicon compound  $SiEt_4$  was synthesized by C. Friedel and J. M. Crafts in 1863, but the extensive development of the field was due to F. S. Kipping in the first decades of this century.<sup>(2)</sup> The unique properties and industrial potential of siloxanes escaped attention at that time and the dramatic development of silicone polymers, elastomers, and resins has occurred during the past 50 years (p. 365).

The solid-state chemistry of silicon has shown similar phases. The bizarre compositions derived by analytical chemistry for the silicates only became intelligible following the pioneering X-ray structural work of W. L. Bragg in the 1920s<sup>(3)</sup> and the concurrent development of the principles of crystal chemistry by L. Pauling<sup>(4)</sup> and of geochemistry by V. M. Goldschmidt.<sup>(5)</sup> More recently the complex crystal chemistry of the silicides has been elucidated and the solid-state chemistry of doped semiconductors has been developed to a level of sophistication that was undreamt of even in the 1960s.

<sup>2</sup> E. G. ROCHOW, Silicon, Chap. 15 in *Comprehensive Inorganic Chemistry*, Vol. 1, pp. 1323–467, Pergamon Press, Oxford, 1973. See also E. G. ROCHOW, *Silicon and Silicones*, Springer-Verlag, Newark, N.J., 1987, 181 pp.

<sup>3</sup> W. L. BRAGG, *The Atomic Structure of Minerals*, Oxford University Press, 1937, 292 pp.

<sup>4</sup> L. PAULING, *The Nature of the Chemical Bond*, 3rd edn., pp. 543–62, Cornell University Press, 1960, and references cited therein.

<sup>5</sup> V. M. GOLDSCHMIDT, *Trans. Faraday Soc.* **25**, 253–83 (1929); *Geochemistry*, Oxford University Press, Oxford, 1954, 730 pp.

## 9.2 Silicon

### 9.2.1 Occurrence and distribution

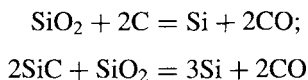
Silicon (27.2 wt%) is the most abundant element in the earth's crust after oxygen (45.5%), and together these 2 elements comprise 4 out of every 5 atoms available near the surface of the globe. This implies that there has been a substantial fractionation of the elements during the formation of the solar system since, in the universe as a whole, silicon is only seventh in order of abundance after H, He, C, N, O and Ne (p. 4). Further fractionation must have occurred within the earth itself: the core, which has 31.5% of the earth's mass, is commonly considered to have a composition close to  $Fe_{25}Ni_2Co_{0.1}S_3$ ; the mantle (68.1% of the mass) probably consists of dense oxides and silicates such as olivine  $(Mg,Fe)_2SiO_4$ , whereas the crust (0.4% of the mass) accumulates the lighter siliceous minerals which "float" to the surface. The crystallization of igneous rocks from magma (molten rock, e.g. lava) depends on several factors such as the overall composition, the lattice energy, mp and crystalline complexity of individual minerals, the rate of cooling, etc. This has been summarized by N. L. Bowen in a reaction series which gives the approximate sequence of appearance of crystalline minerals as the magma is cooled: olivine  $[M_2^{II}SiO_4]$ , pyroxene  $[M_2^{II}Si_2O_6]$ , amphibole  $[M_7^{II}\{(Al,Si)_4O_{11}\}(OH)_2]$ , biotite mica  $[(K,H)_2(Mg,Fe)_2(Al,Fe)_2(SiO_4)_3]$ , orthoclase feldspar  $[KAlSi_3O_8]$ , muscovite mica  $[KAl_2(AlSi_3O_{10})(OH)_2]$ , quartz  $[SiO_2]$ , zeolites and hydrothermal minerals. The structure of these mineral types is discussed later (p. 347), but it is clear that the reaction series leads to progressively more complex silicate structural units and that the later part of the series is characterized by the introduction of OH (and F) into the structures. Extensive isomorphous substitution among the metals is also possible. Subsequent weathering, transport and deposition leads to sedimentary rocks such as clays, shales and sandstones. Metamorphism at high temperatures and pressures can effect further

changes during which the presence or absence of water plays a vital role.<sup>(6,7)</sup>

Silicon never occurs free: it invariably occurs combined with oxygen and, with trivial exceptions, is always 4-coordinate in nature. The {SiO<sub>4</sub>} unit may occur as an individual group or be linked into chains, ribbons, rings, sheets or three-dimensional frameworks (pp. 347–59).

### 9.2.2 Isolation, production and industrial uses

Silicon (96–99% pure) is now invariably made by the reduction of quartzite or sand with high purity coke in an electric arc furnace; the SiO<sub>2</sub> is kept in excess to prevent the accumulation of SiC (p. 334):



The reaction is frequently carried out in the presence of scrap iron (with low P and S content) to produce ferrosilicon alloys: these are used in the metallurgical industry to deoxidize steel, to manufacture high-Si corrosion-resistant Fe, and Si/steel laminations for electric motors. The scale of operations can be gauged from the 1980 world production figures which were in excess of 5 megatonnes. Consumption of high purity (semiconductor grade) Si leapt from less than 10 tonnes in 1955 to 2800 tonnes in 1980.

Silicon for the chemical industry is usually purified to ~98.5% by leaching the powdered 96–97% material with water. Very pure Si for semiconductor applications is obtained either from SiCl<sub>4</sub> (made from the chlorination of scrap Si) or from SiHCl<sub>3</sub> (a byproduct of the silicone industry, p. 338). These volatile compounds are

<sup>6</sup> B. MASON, *Principles of Geochemistry*, 3rd edn., Wiley, New York, 1966, 329 pp. P. HENDERSON, *Inorganic Geochemistry*, Pergamon Press, Oxford, 1982, 372 pp. S. R. ASTON (ed.), *Silicon Geochemistry and Biogeochemistry*, Academic Press, 1983, 272 pp.

<sup>7</sup> D. K. BAILEY and R. MACDONALD (eds.), *The Evolution of the Crystalline Rocks*, Academic Press, London, 1976, 484 pp.

purified by exhaustive fractional distillation and then reduced with exceedingly pure Zn or Mg; the resulting spongy Si is melted, grown into cylindrical single crystals, and then purified by zone refining. Alternative routes are the thermal decomposition of SiL<sub>4</sub>/H<sub>2</sub> on a hot tungsten filament (cf. boron, p. 140), or the epitaxial growth of a single-crystal layer by thermal decomposition of SiH<sub>4</sub>. A one-step process has also been developed to produce high-purity Si for solar cells at one-tenth of the cost of rival methods. In this process Na<sub>2</sub>SiF<sub>6</sub> (which is a plentiful waste product from the phosphate fertilizer industry) is reduced by metallic Na; the reaction is highly exothermic and is self-sustaining without the need for external fuel.

Hyperfine Si is one of the purest materials ever made on an industrial scale: the production of transistors (p. 332) requires the routine preparation of crystals with impurity levels below 1 atom in 10<sup>10</sup>, and levels below 1 atom in 10<sup>12</sup> can be attained in special cases.

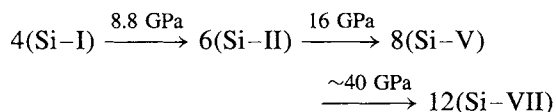
### 9.2.3 Atomic and physical properties

Silicon consists predominantly of <sup>28</sup>Si (92.23%) together with 4.67% <sup>29</sup>Si and 3.10% <sup>30</sup>Si. No other isotopes are stable. The <sup>29</sup>Si isotope (like the proton) has a nuclear spin  $I = \frac{1}{2}$ , and is being increasingly used in nmr spectroscopy.<sup>(8)</sup> <sup>31</sup>Si, formed by neutron irradiation of <sup>30</sup>Si, has  $t_{\frac{1}{2}}$  2.62 h; it can be detected by its characteristic β<sup>-</sup> activity ( $E_{\text{max}}$  1.48 MeV) and is very useful for the quantitative analysis of Si by neutron activation. The radioisotope with the longest half-life (~172 y) is the soft β<sup>-</sup> emitter <sup>32</sup>Si ( $E_{\text{max}}$  0.2 MeV).

In its ground state, the free atom Si has the electronic configuration [Ne]3s<sup>2</sup>3p<sup>2</sup>. Ionization energies and other properties are compared with those of the other members of Group 14 on p. 372. Silicon crystallizes in the diamond

<sup>8</sup> J.-P. KINTZINGER and H. MARSMANN, *Oxygen-17 and Silicon-29 NMR*, Vol. 17 of *NMR Basic Principles and Progress* (P. DIEHL, E. FLUCK and R. KOSFIELD, eds.), Springer-Verlag, Berlin, 1980, 250 pp.

lattice (p. 275) with  $a_0$  543.10204 pm at 25°, corresponding to an Si–Si distance of 235.17 pm and a covalent atomic radius of 117.59 pm. The density and lattice constant of pure single-crystal Si are now known sufficiently accurately to give a direct value of the Avogadro constant ( $N_A = 6.022\,1363 \times 10^{23} \text{ mol}^{-1}$ ) which is as precise as the best currently accepted value ( $6.022\,1367 \times 10^{23} \text{ mol}^{-1}$ ).<sup>(9)</sup> There appear to be no allotropes of Si at ambient pressure but the 4-coordinate diamond lattice of Si–I transforms to several other modifications at higher pressures, of which distorted-diamond Si–II, primitive hexagonal Si–V and eventually hexagonal close packed Si–VII may be mentioned; the structural sequence corresponds to a systematic increase in coordination number:<sup>(10)</sup>



[1 GPa = 10 kbar  $\approx$  9869 atm.]

Physical properties are summarized in Table 9.1 (see also p. 373). Silicon is notably more volatile than C and has a substantially lower energy of vaporization, thus reflecting the smaller

**Table 9.1** Some physical properties of silicon

MP/°C	1420
BP/°C	$\sim$ 3280
Density (20°C)/g cm <sup>-3</sup>	2.53259
$\Delta H_{\text{fus}}/\text{kJ mol}^{-1}$	$50.6 \pm 1.7$
$\Delta H_{\text{vap}}/\text{kJ mol}^{-1}$	$383 \pm 10$
$\Delta H_f$ (monatomic gas)/kJ mol <sup>-1</sup>	$454 \pm 12$
$a_0/\text{pm}$	543.10204
$r$ (covalent)/pm	117.59
$r$ ("ionic")/pm	26 <sup>(a)</sup>
Pauling electronegativity	1.8

<sup>(a)</sup> This is the "effective ionic radius" for 4-coordinate Si<sup>IV</sup> in silicates, obtained by subtracting  $r(\text{O}^{2-}) = 140$  pm from the observed Si–O distance. The value for 6-coordinate Si<sup>IV</sup> is 40 pm. [R. D. Shannon, *Acta Cryst.* **A32**, 751–67 (1976).]

<sup>9</sup> P. SEYFRIED and 13 others, *Z. Phys. B-Condensed Matter* **87**, 289–98 (1992).

<sup>10</sup> H. OLJNYK, S. K. SIKKA and W. B. HOLZAPFEL, *Phys. Lett.* **103A**, 137–40 (1984).

Si–Si bond energy. The element is a semiconductor with a distinct shiny, blue–grey metallic lustre; the resistivity decreases with increase of temperature, as expected for a semiconductor. The actual value of the resistivity depends markedly on purity but is  $\sim$ 40 ohm cm at 25° for very pure material.

The immense importance of Si in transistor technology stems from the chance discovery of the effect in Ge at Bell Telephone Laboratories, New Jersey, in 1947, and the brilliant theoretical and practical development of the device by J. Bardeen, W. H. Brattain and W. Shockley for which they were awarded the 1956 Nobel Prize for Physics. A brief description of the physics and chemistry underlying transistor action in Si is given in the Panel (p. 332).

## 9.2.4 Chemical properties

Silicon in the massive, crystalline form is relatively unreactive except at high temperatures. Oxygen, water and steam all have little effect probably because of the formation of a very thin, continuous, protective surface layer of SiO<sub>2</sub> a few atoms thick (cf. Al, p. 224). Oxidation in air is not measurable below 900°; between 950° and 1160° the rate of formation of vitreous SiO<sub>2</sub> rapidly increases and at 1400° the N<sub>2</sub> in the air also reacts to give SiN and Si<sub>3</sub>N<sub>4</sub>. Sulfur vapour reacts at 600° and P vapour at 1000°. Silicon is also unreactive towards aqueous acids, though the aggressive mixture of conc HNO<sub>3</sub>/HF oxidizes and fluorinates the element. Silicon dissolves readily in hot aqueous alkali due to reactions of the type  $\text{Si} + 4\text{OH}^- = \text{SiO}_4^{4-} + 2\text{H}_2$ . Likewise, the thin film of SiO<sub>2</sub> is no barrier to attack by halogens, F<sub>2</sub> reacting vigorously at room temperature, Cl<sub>2</sub> at  $\sim$ 300°, and Br<sub>2</sub>, I<sub>2</sub> at  $\sim$ 500°. Even alkyl halides will react at elevated temperatures and, in the presence of Cu catalysts, this constitutes the preferred "direct" synthesis of organosilicon chlorides for the manufacture of silicones (p. 364).

In contrast to the relative inertness of solid Si to gaseous and liquid reagents, molten Si is an extremely reactive material: it forms alloys or

## The Physics and Chemistry of Transistors

In ultrapure semiconductor grade Si there is an energy gap  $E_g$  between the highest occupied energy levels (the valence band) and the lowest unoccupied energy levels (the conduction band). This is shown diagrammatically in Fig. a: the valence band is completely filled, the conduction band is empty, the Fermi level ( $E_F$ ), which is the energy at which the chance of a state being occupied by an electron is  $\frac{1}{2}$ , lies approximately midway between these, and the material is an insulator at room temperature. If the Si is doped with a Group 15 element such as P, As or Sb, each atom of dopant introduces a supernumerary electron and the impurity levels can act as a source of electrons which can be thermally or photolytically excited into the conduction band (Fig. b): the material is an n-type semiconductor with an activation energy  $\Delta E_n$  (where n indicates negative current carriers, i.e. electrons). Conversely, doping with a Group 13 element such as B, Al or Ga introduces acceptor levels that can act as traps for electrons excited from the filled valence band (Fig. c): the material is a p-type semiconductor and the current is carried by the positive holes in the valence band.

When an n-type sample of Si is joined to a p-type sample, a p-n junction is formed having a common Fermi level as in Fig. d: electrons will flow from n to p and holes from p to n thereby producing a voltage drop  $V_0$  across the space charge region. A p-n junction can thus act as a diode for rectifying alternating current, the current passing more easily in one direction than the other. In practise a large p-n junction might cover  $10\text{ mm}^2$ , whereas in integrated circuits such a device might cover no more than  $10^{-4}\text{ mm}^2$  (i.e. a square of side  $10\text{ }\mu\text{m}$ ).

A transistor, or n-p-n junction, is built up of two n-type regions of Si separated by a thin layer of weakly p-type (Fig. e). When the emitter is biased by a small voltage in the forward direction and the collector by a larger voltage in the reverse direction, this device acts as a triode amplifier. The relevant energy level diagram is shown schematically in Fig. f.

The large-scale reproducible manufacture of minute, electronically-stable, single-crystal transistor junctions is a triumph of the elegant techniques of solid-state chemical synthesis. The sequence of steps is illustrated in diagrams (i)-(v).

- (i) A small wafer of single-crystal n-type Si is oxidized by heating it in  $\text{O}_2$  or  $\text{H}_2\text{O}$  vapour to form a thin surface layer of  $\text{SiO}_2$ .
- (ii) The oxide coating is covered by a photosensitive film called "photoresist".
- (iii) A mask is placed over the photoresist to confine the exposure to the desired pattern and the chip is exposed to ultraviolet light; the exposed photoresist is then removed by treatment with acid, leaving a tough protective layer over the parts of the oxide coating that are to be retained.
- (iv) The unprotected areas of Si are etched away with hydrofluoric acid and the remaining photoresist is also removed.
- (v) The surface is exposed to the vapour of a Group 13 element and the impurity atoms diffuse into the unprotected area to form a layer of p-type Si.
- (vi) Steps (i)-(v) are repeated, with a different mask, and then the newly exposed areas are treated with the vapour of a Group 15 element to produce a patterned layer of n-type Si.
- (vii) Finally, again with a different mask, the surface is reoxidized and then re-etched to produce openings into which metal is deposited so as to connect the n- and p-regions into an integrated circuit.

Each individual p-n diode or n-p-n transistor can be made almost unbelievably minute by these techniques; for example computer memory units storing over  $10^5$  bits of information on a single small chip are routinely used. Further information can be obtained from textbooks of solid-state physics or electronic engineering.

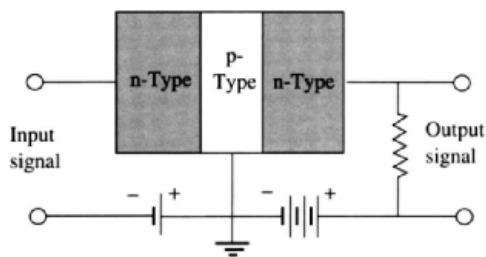
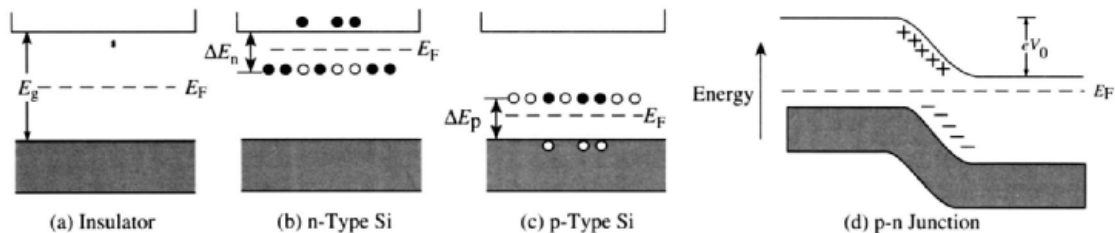
silicides with most metals (see below) and rapidly reduces most metal oxides because of the very large heat of formation of  $\text{SiO}_2$  ( $\sim 900\text{ kJ mol}^{-1}$ ). This presents problems of containment when working with molten Si, and crucibles must be made of refractories such as  $\text{ZrO}_2$  or the borides of transition metals in Groups 4-6 (p. 146).

Chemical trends within Group 14 are discussed on p. 373. Silicon does not form binary compounds with the heavier members of the group (Ge, Sn, Pb) but its compound with carbon, SiC,

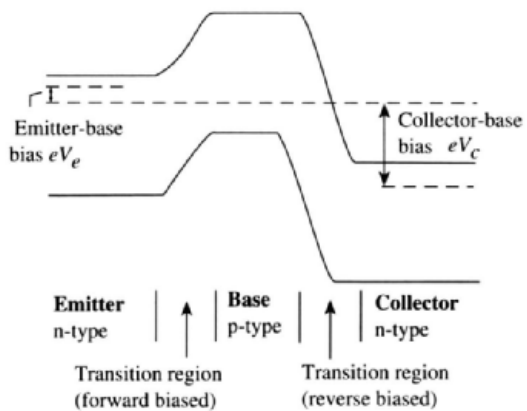
is of outstanding academic and practical interest, and is manufactured on a huge scale industrially (see Panel on p. 334).

In the vast majority of its compounds Si is tetrahedrally coordinated but sixfold coordination also occurs, and occasional examples of other coordination geometries are known as indicated in Table 9.2 (p. 335). Unstable 2-coordinate Si has been known for many years but in 1994 the stable, colourless, crystalline silylene  $[\text{:SiNBu}^t\text{CH}=\text{CHNBu}^t]$ , structure (1), p. 336, was



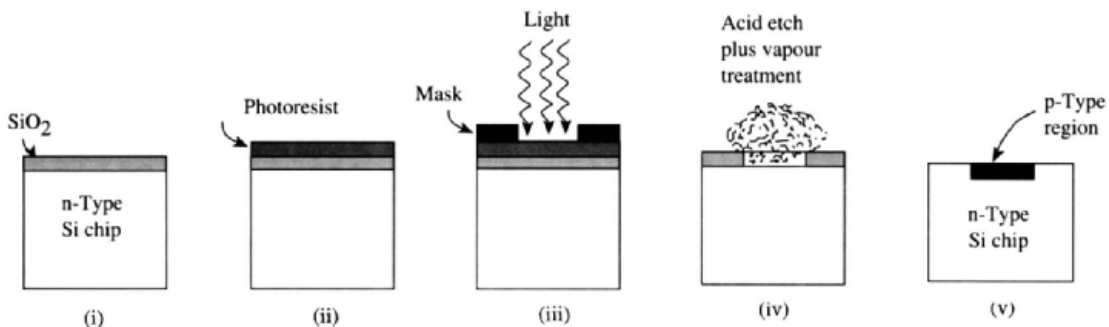


(e) An n-p-n transistor junction with the left n-p junction forward biased and the right p-n junction reverse biased



(f) Energy level diagram

Figs. (a)-(f) mentioned in Panel opposite.

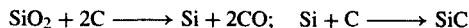


Steps (i)-(v) mentioned in Panel opposite.

### Silicon Carbide, SiC<sup>(11,12)</sup>

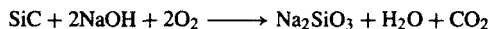
Silicon carbide was made accidentally by E. G. Acheson in 1891; he recognized its abrasive power and coined the name "carborundum" from carbo(n) and (co)rundum (Al<sub>2</sub>O<sub>3</sub>) to indicate that its hardness on the Mohs scale (9.5) was intermediate between that of diamond (10) and Al<sub>2</sub>O<sub>3</sub> (9). Within months he had formed the Carborundum Co. for its manufacture, and current world production approaches 1 million tonnes annually.

Despite its simple formula, SiC exists in at least 200 crystalline modifications based on hexagonal  $\alpha$ -SiC (wurtzite-type ZnS, p. 1210) or cubic  $\beta$ -SiC (diamond or zincblende-type, p. 1210). The complexity arises from the numerous stacking sequences of the *a* and *b* "layers" in the crystal.<sup>(13)</sup> The  $\alpha$ -form is marginally the more stable thermodynamically. Industrially,  $\alpha$ -SiC is obtained as black, dark green or purplish iridescent crystals by reducing high-grade quartz sand with a slight excess of coke or anthracite in an electric furnace at 2000–2500°C:



The dark colour is caused by impurities such as iron, and the iridescence is due to a very thin layer of SiO<sub>2</sub> formed by surface oxidation. Purer samples are pale yellow or colourless. Even higher temperatures (and vacuum conditions) are required to produce the  $\beta$ -form. Alternatively, very pure  $\beta$ -SiC can be obtained by heating grains of ultrapure Si with graphite at 1500° or by gas-phase plasma decomposition of Me<sub>2</sub>SiCl<sub>2</sub>, MeSiCl<sub>3</sub> or SiCl<sub>4</sub>/CH<sub>4</sub> mixtures. Fibres of SiC are made by the progressive pyrolysis of organosilicon polymers such as -CH<sub>2</sub>SiHMe- or -CH<sub>2</sub>SiMe<sub>2</sub>-. Lattice constants for  $\alpha$ -SiC are *a* 307.39 pm, *c* 1006.1 pm, *c/a* 3.273; for cubic  $\beta$ -SiC, *a*<sub>0</sub> 435.02 pm (cf. diamond 356.68, Si 543.10, mean 449.89 pm).

SiC has greater thermal stability than any other binary compound of Si and decomposition by loss of Si only becomes appreciable at ~2700°. It resists attack by most aqueous acids (including HF but not H<sub>3</sub>PO<sub>4</sub>) and is oxidized in air only above 1000° because of the protective layer of SiO<sub>2</sub>; this can be removed by molten hydroxides or carbonates and oxidation is much more rapid under these conditions, e.g.:



Cl<sub>2</sub> attacks SiC vigorously, yielding SiCl<sub>4</sub> + C at 100° and SiCl<sub>4</sub> + CCl<sub>4</sub> at 1000°.

Technical interest in SiC originally stemmed from its excellence as an abrasive powder; this derives not only from the great intrinsic hardness of the compound but also from its peculiar fracture to give sharp cutting edges. As a refractory,  $\alpha$ -SiC combines great strength and chemical stability, with an extremely low thermal expansion coefficient ( $\sim 6 \times 10^{-6}$ ) which shows no sudden discontinuities due to phase transitions. Pure  $\alpha$ -SiC is an intrinsic semiconductor with an energy band gap sufficiently large ( $1.90 \pm 0.10$  eV) to make it a very poor electrical conductor ( $\sim 10^{-13}$  ohm<sup>-1</sup> cm<sup>-1</sup>). However, the presence of controlled amounts of impurities makes it a valuable extrinsic semiconductor ( $10^{-2} - 3$  ohm<sup>-1</sup> cm<sup>-1</sup>) with a positive temperature coefficient. This, combined with its mechanical and chemical stability, accounts for its extensive use in electrical heating elements. In recent years pure  $\beta$ -SiC has received much attention as a high-temperature semiconductor with applications in transistors, diode rectifiers, electroluminescent diodes, etc. (see p. 332). In fact, these various electrical and refractory uses account for only about 2% of the vast tonnages of SiC manufactured each year. About 43% is still used for its original application as an abrasive, and the remaining 55% is used in metallurgical processes, especially as a refining agent in the casting of iron and steel: the SiC reacts with free oxygen and with metal oxides to form CO and a siliceous slag.

isolated;<sup>(14)</sup> it distils without change at 85°C/0.1 torr and can be kept in solution in a sealed tube for several months at 150°C without

apparent change. A recent example of pyramidal 3-coordinate Si is the Si<sub>4</sub><sup>4-</sup> anion (isoelectronic with the tetrahedral P<sub>4</sub> molecule, p. 479), which has been shown to occur in the long-known red silicide CsSi.<sup>(17)</sup> There has been much discussion about the possibility of planar 4-coordinate Si in orthosilicate esters of pyrocatechol (2) but this is

<sup>11</sup> Kirk-Othmer *Encyclopedia of Chemical Technology*, 4th edn., Vol. 4, Silicon Carbide, 1992, pp. 891–911.

<sup>12</sup> *Silicon Carbide*, World Business Publications, Ltd., 2nd edn., 1988, 340 pp.

<sup>13</sup> *Gmelin Handbook of Inorganic Chemistry*, 8th edn., Springer-Verlag, Berlin, *Silicon Suppl. B2*, 1984, 312 pp. See also *Suppl. B1*, 1986, 545 pp. for further information on occurrence of SiC in nature, its manufacture, chemical reactions, applications, etc.

<sup>14</sup> M. DENK and 8 others, *J. Am. Chem. Soc.* **116**, 2691–2 (1994).

<sup>15</sup> T. J. BARTON and G. T. BURNS, *J. Am. Chem. Soc.* **100**, 5246 (1978).

<sup>16</sup> C. L. KREIL, O. L. CHAPMAN, G. T. BURNS and T. J. BARTON, *J. Am. Chem. Soc.* **102**, 841–2 (1980).

<sup>17</sup> G. KLICHE, M. SCHWARZ and H. G. VON SCHNERING, *Angew. Chem. Int. Edn. Engl.* **26**, 349–51 (1987).

Table 9.2 Coordination geometries of silicon

Coordination number	Examples
2 (bent)	SiF <sub>2</sub> (g), SiMe <sub>2</sub> (matrix, 77 K), [ $\overline{\text{SiNBu}^+\text{CH}=\text{CHNBu}^+}$ ] (1) <sup>(14)</sup>
3 (planar)	Silabenzene, SiC <sub>5</sub> H <sub>6</sub> , <sup>(15)</sup> silatoluene, C <sub>5</sub> H <sub>5</sub> SiMe <sup>(16)</sup>
3 (pyramidal)	Si <sub>4</sub> <sup>4-</sup> , (?)SiH <sub>3</sub> <sup>-</sup> in KSiH <sub>3</sub> (NaCl structure)
4 (tetrahedral)	SiH <sub>4</sub> , SiX <sub>4</sub> , SiX <sub>n</sub> Y <sub>4-n</sub> , SiO <sub>2</sub> , silicates, etc.
4 (planar)	(see text) <sup>(18)</sup> (2)
4 (see-saw, C <sub>2v</sub> )	SiLi <sub>4</sub> (3) <sup>(19)</sup>
5 (trigonal bipyramidal)	SiX <sub>5</sub> <sup>-</sup> , cyclo-[Me <sub>2</sub> NSiH <sub>3</sub> ] <sub>5</sub> , [Si(O <sub>2</sub> C <sub>6</sub> H <sub>4</sub> ) <sub>2</sub> (OPPh <sub>3</sub> )] (4) <sup>(20)</sup>
5 (square pyramidal)	[Si(O <sub>2</sub> C <sub>6</sub> H <sub>4</sub> ) <sub>2</sub> {OP(NC <sub>5</sub> H <sub>10</sub> )}] (5), <sup>(20)</sup> [SiF(O <sub>2</sub> C <sub>6</sub> H <sub>4</sub> ) <sub>2</sub> ] <sup>(21)</sup>
6 (octahedral)	SiF <sub>6</sub> <sup>2-</sup> , [Si(acac) <sub>3</sub> ] <sup>+</sup> , [L <sub>2</sub> SiX <sub>4</sub> ], SiO <sub>2</sub> (stishovite), SiP <sub>2</sub> O
7 (capped trig. antiprism)	[(2-(Me <sub>2</sub> NCH <sub>2</sub> )C <sub>6</sub> H <sub>4</sub> ) <sub>3</sub> SiH] (6) <sup>(22)</sup>
8 (cubic)	Mg <sub>2</sub> Si (antifluorite)
9 (capped square antiprism)	[μ <sub>8</sub> -SiCo <sub>9</sub> (CO) <sub>21</sub> ] <sup>2-</sup> (7) <sup>(23)</sup>
10 (various)	TiSi <sub>2</sub> , CrSi <sub>2</sub> , MoSi <sub>2</sub> , <sup>(24)</sup> [Si(η <sup>5</sup> -C <sub>5</sub> Me <sub>5</sub> ) <sub>2</sub> ] (8) <sup>(25)</sup>

still far from being unequivocally established.<sup>(18)</sup> However, a 'one-sided' C<sub>2v</sub> geometry for SiLi<sub>4</sub> (3) seems probable.<sup>(19)</sup> Five-coordinate Si can be either trigonal bipyramidal or square pyramidal, e.g. (4), (5), etc.<sup>(20,21)</sup> Numerous examples of octahedral 6-coordination are known. A single example of 7-coordinate Si has been identified, (6)<sup>(22)</sup> and there are occasional examples of higher coordination numbers. Thus, Si has cubic 8-fold coordination in Mg<sub>2</sub>Si which has the antifluorite structure, Si occupying the Ca sites and Mg the F sites of the fluorite lattice (p. 118). The capped square antiprismatic structure of the anion [SiCo<sub>9</sub>(CO)<sub>21</sub>]<sup>2-</sup> has essentially 9-fold coordination about the encapsulated Si atom (7), with Si-Co<sub>base</sub> 231 pm, Si-Co<sub>upper</sub> 228 pm and Si-Co<sub>cap</sub> 252.7 pm; each of the four basal Co atoms has two terminal CO ligands, each of the

other five Co atoms has one, and there are eight bridging CO groups.<sup>(23)</sup> The coordination number 10 is found in the structures of several transition metal silicides<sup>(24)</sup> and in decamethylsilicocene (8). The crystal structure of this latter compound reveals two types of molecular geometry; one-third of the molecules have the two rings parallel and staggered as in [Fe(C<sub>5</sub>Me<sub>5</sub>)<sub>2</sub>] with Si-C 242 pm whereas the other two-thirds have non-parallel rings, implying a stereochemically active lone pair of electrons on the Si atom.<sup>(25)</sup> The bent (C<sub>s</sub>) structure persists in the gas phase, the angle between the two C<sub>5</sub> planes being 22°.

## 9.3 Compounds

### 9.3.1 Silicides<sup>(26,27)</sup>

As with borides (p. 145) and carbides (p. 297) the formulae of metal silicides cannot be rationalized by the application of simple valency rules, and

<sup>18</sup> W. HÖNLE, U. DETTLAUF-WEGLIKOWSKA, L. WALZ and H. G. VON SCHNERING, *Angew. Chem. Int. Edn. Engl.* **28**, 623-4 (1989), and references cited therein.

<sup>19</sup> P. VON RAGUÉ SCHLEYER and A. E. REED, *J. Am. Chem. Soc.* **110**, 4453-4 (1988).

<sup>20</sup> E. HEY-HAWKINS, U. DETTLAUF-WEGLIKOWSKA, D. THIERY and H. G. VON SCHNERING, *Polyhedron* **11**, 1789-94 (1992). See also T. VAN DEN ANKER, B. S. JOLLY, M. F. LAPPERT, C. L. RASTON, B. W. SKELTON and A. H. WHITE, *J. Chem. Soc., Chem. Commun.*, 1006-8 (1990).

<sup>21</sup> J. J. HARLAND, R. O. DAY, J. F. VOLLANO, A. C. SAU and R. R. HOLMES, *J. Am. Chem. Soc.* **103**, 5269-70 (1981).

<sup>22</sup> C. BRELLIERE, F. CARRÉ, R. J. P. CORRIU and G. ROYO, *Organometallics* **7**, 1006-8 (1988).

<sup>23</sup> K. M. MACKAY, B. K. NICHOLSON, W. T. ROBINSON and A. W. SIMS, *J. Chem. Soc., Chem. Commun.*, 1276-7 (1984).

<sup>24</sup> A. F. WELLS, *Structural Inorganic Chemistry*, 5th edn., Oxford University Press, Oxford, pp. 987-91 (1984).

<sup>25</sup> P. JUTZI, U. HOLTSMANN, D. KANNE, C. KRÜGER, R. BLOM, R. GLEITER and I. HYLA-KRYSPIK *Chem. Ber.* **122**, 1629-39 (1989).

<sup>26</sup> A. S. BEREZHAI, *Silicon and its Binary Systems*, Consultants Bureau, New York, 1960, 275 pp.

<sup>27</sup> B. ARONSSON, T. LUNDSTRÖM and S. RUNDQVIST, *Borides, Silicides, and Phosphides*, Methuen, London, 1965, 120 pp.

Table 9.2 Coordination geometries of silicon

Coordination number	Examples
2 (bent)	SiF <sub>2</sub> (g), SiMe <sub>2</sub> (matrix, 77 K), [ $\overline{\text{SiNBu}^+\text{CH}=\text{CHNBu}^+}$ ] (1) <sup>(14)</sup>
3 (planar)	Silabenzene, SiC <sub>5</sub> H <sub>6</sub> , <sup>(15)</sup> silatoluene, C <sub>5</sub> H <sub>5</sub> SiMe <sup>(16)</sup>
3 (pyramidal)	Si <sub>4</sub> <sup>4-</sup> , (?)SiH <sub>3</sub> <sup>-</sup> in KSiH <sub>3</sub> (NaCl structure)
4 (tetrahedral)	SiH <sub>4</sub> , SiX <sub>4</sub> , SiX <sub>n</sub> Y <sub>4-n</sub> , SiO <sub>2</sub> , silicates, etc.
4 (planar)	(see text) <sup>(18)</sup> (2)
4 (see-saw, C <sub>2v</sub> )	SiLi <sub>4</sub> (3) <sup>(19)</sup>
5 (trigonal bipyramidal)	SiX <sub>5</sub> <sup>-</sup> , <i>cyclo</i> -[Me <sub>2</sub> NSiH <sub>3</sub> ] <sub>5</sub> , [Si(O <sub>2</sub> C <sub>6</sub> H <sub>4</sub> ) <sub>2</sub> (OPPh <sub>3</sub> )] (4) <sup>(20)</sup>
5 (square pyramidal)	[Si(O <sub>2</sub> C <sub>6</sub> H <sub>4</sub> ) <sub>2</sub> {OP(NC <sub>5</sub> H <sub>10</sub> )}] (5), <sup>(20)</sup> [SiF(O <sub>2</sub> C <sub>6</sub> H <sub>4</sub> ) <sub>2</sub> ] <sup>-(21)</sup>
6 (octahedral)	SiF <sub>6</sub> <sup>2-</sup> , [Si(acac) <sub>3</sub> ] <sup>+</sup> , [L <sub>2</sub> SiX <sub>4</sub> ], SiO <sub>2</sub> (stishovite), SiP <sub>2</sub> O
7 (capped trig. antiprism)	[(2-(Me <sub>2</sub> NCH <sub>2</sub> )C <sub>6</sub> H <sub>4</sub> ) <sub>3</sub> SiH] (6) <sup>(22)</sup>
8 (cubic)	Mg <sub>2</sub> Si (antifluorite)
9 (capped square antiprism)	[μ <sub>8</sub> -SiCo <sub>9</sub> (CO) <sub>21</sub> ] <sup>2-</sup> (7) <sup>(23)</sup>
10 (various)	TiSi <sub>2</sub> , CrSi <sub>2</sub> , MoSi <sub>2</sub> , <sup>(24)</sup> [Si(η <sup>5</sup> -C <sub>5</sub> Me <sub>5</sub> ) <sub>2</sub> ] (8) <sup>(25)</sup>

still far from being unequivocally established.<sup>(18)</sup> However, a 'one-sided' C<sub>2v</sub> geometry for SiLi<sub>4</sub> (3) seems probable.<sup>(19)</sup> Five-coordinate Si can be either trigonal bipyramidal or square pyramidal, e.g. (4), (5), etc.<sup>(20,21)</sup> Numerous examples of octahedral 6-coordination are known. A single example of 7-coordinate Si has been identified, (6)<sup>(22)</sup> and there are occasional examples of higher coordination numbers. Thus, Si has cubic 8-fold coordination in Mg<sub>2</sub>Si which has the antifluorite structure, Si occupying the Ca sites and Mg the F sites of the fluorite lattice (p. 118). The capped square antiprismatic structure of the anion [SiCo<sub>9</sub>(CO)<sub>21</sub>]<sup>2-</sup> has essentially 9-fold coordination about the encapsulated Si atom (7), with Si-Co<sub>base</sub> 231 pm, Si-Co<sub>upper</sub> 228 pm and Si-Co<sub>cap</sub> 252.7 pm; each of the four basal Co atoms has two terminal CO ligands, each of the

other five Co atoms has one, and there are eight bridging CO groups.<sup>(23)</sup> The coordination number 10 is found in the structures of several transition metal silicides<sup>(24)</sup> and in decamethylsilicocene (8). The crystal structure of this latter compound reveals two types of molecular geometry; one-third of the molecules have the two rings parallel and staggered as in [Fe(C<sub>5</sub>Me<sub>5</sub>)<sub>2</sub>] with Si-C 242 pm whereas the other two-thirds have non-parallel rings, implying a stereochemically active lone pair of electrons on the Si atom.<sup>(25)</sup> The bent (C<sub>s</sub>) structure persists in the gas phase, the angle between the two C<sub>5</sub> planes being 22°.

## 9.3 Compounds

### 9.3.1 Silicides<sup>(26,27)</sup>

As with borides (p. 145) and carbides (p. 297) the formulae of metal silicides cannot be rationalized by the application of simple valency rules, and

<sup>18</sup> W. HÖNLE, U. DETTLAUF-WEGLIKOWSKA, L. WALZ and H. G. VON SCHNERING, *Angew. Chem. Int. Edn. Engl.* **28**, 623-4 (1989), and references cited therein.

<sup>19</sup> P. VON RAGUÉ SCHLEYER and A. E. REED, *J. Am. Chem. Soc.* **110**, 4453-4 (1988).

<sup>20</sup> E. HEY-HAWKINS, U. DETTLAUF-WEGLIKOWSKA, D. THIERY and H. G. VON SCHNERING, *Polyhedron* **11**, 1789-94 (1992). See also T. VAN DEN ANKER, B. S. JOLLY, M. F. LAPPERT, C. L. RASTON, B. W. SKELTON and A. H. WHITE, *J. Chem. Soc., Chem. Commun.*, 1006-8 (1990).

<sup>21</sup> J. J. HARLAND, R. O. DAY, J. F. VOLLANO, A. C. SAU and R. R. HOLMES, *J. Am. Chem. Soc.* **103**, 5269-70 (1981).

<sup>22</sup> C. BRELLIERE, F. CARRÉ, R. J. P. CORRIU and G. ROYO, *Organometallics* **7**, 1006-8 (1988).

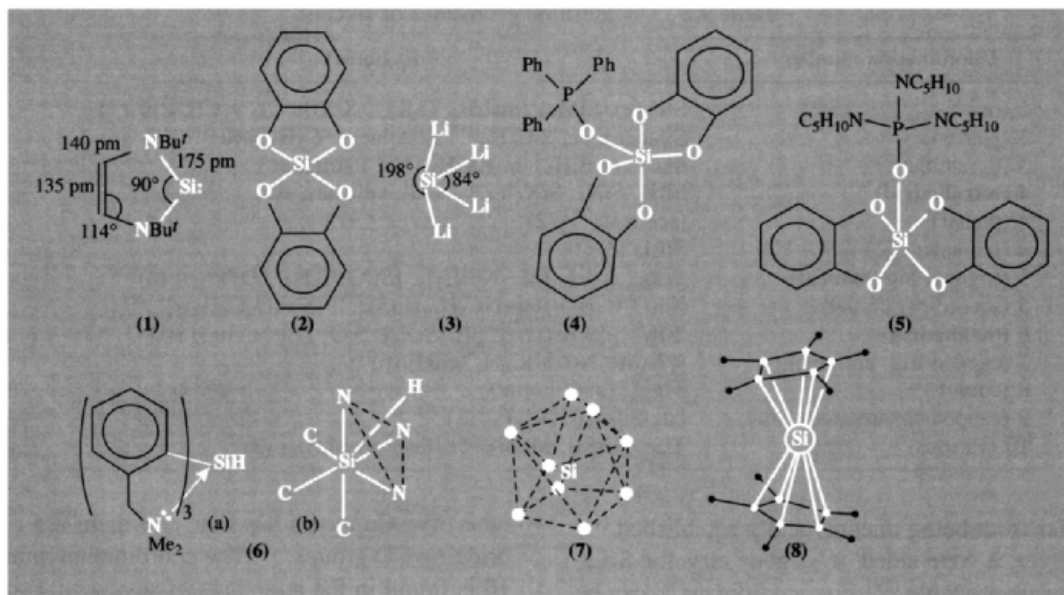
<sup>23</sup> K. M. MACKAY, B. K. NICHOLSON, W. T. ROBINSON and A. W. SIMS, *J. Chem. Soc., Chem. Commun.*, 1276-7 (1984).

<sup>24</sup> A. F. WELLS, *Structural Inorganic Chemistry*, 5th edn., Oxford University Press, Oxford, pp. 987-91 (1984).

<sup>25</sup> P. JUTZI, U. HOLTSMANN, D. KANNE, C. KRÜGER, R. BLOM, R. GLEITER and I. HYLAKRYSPIKIN *Chem. Ber.* **122**, 1629-39 (1989).

<sup>26</sup> A. S. BEREZHOL, *Silicon and its Binary Systems*, Consultants Bureau, New York, 1960, 275 pp.

<sup>27</sup> B. ARONSSON, T. LUNDSTRÖM and S. RUNDQVIST, *Borides, Silicides, and Phosphides*, Methuen, London, 1965, 120 pp.

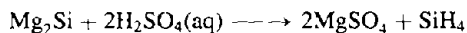
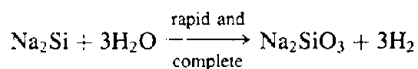


the bonding varies from essentially metallic to ionic and covalent. Observed stoichiometries include  $M_6Si$ ,  $M_5Si$ ,  $M_4Si$ ,  $M_{15}Si_4$ ,  $M_3Si$ ,  $M_5Si_2$ ,  $M_2Si$ ,  $M_5Si_3$ ,  $M_3Si_2$ ,  $MSi$ ,  $M_2Si_3$ ,  $MSi_2$ ,  $MSi_3$  and  $MSi_6$ . Silicon, like boron, is more electropositive than carbon, and structurally the silicides are more closely related to the borides than the carbides (cf. diagonal relation, p. 27). However, the covalent radius of Si (118 pm) is appreciably larger than for B (88 pm) and few silicides are actually isostructural with the corresponding borides. Silicides have been reported for virtually all elements in Groups 1–10 except Be, the greatest range of stoichiometries being shown by the transition metals in Groups 4–10 and uranium. No silicides are known for the metals in Groups 11–15 except Cu; most form simple eutectic mixtures, but the heaviest post-transition metals Hg, Tl, Pb and Bi are completely immiscible with molten Si.

Some metal-rich silicides have isolated Si atoms and these occur either in typical metal-like structures or in more polar structures. With increasing Si content, there is an increasing tendency to catenate into isolated  $Si_2$  or  $Si_4$ , or into chains, layers or 3D networks of Si atoms. Examples are in Table 9.3 and further structural details are in refs. 24, 26 and 27.

Silicides are usually prepared by direct fusion of the elements but coreduction of  $SiO_2$  and a metal oxide with C or Al is sometimes used. Heats of formation are similar to those of borides and carbides but mps are substantially lower; e.g. TiC 3140°,  $TiB_2$  2980°,  $TiSi_2$  1540°; and TaC 3800°,  $TaB_2$  3100°,  $TaSi_2$  1560°C. Few silicides melt as high as 2000–2500°, and above this temperature only SiC is solid (decomp  $\sim$ 2700°C).

Silicides of groups 1 and 2 are generally much more reactive than those of the transition elements (cf. borides and carbides). Hydrogen and/or silanes are typical products; e.g.:



Products also depend on stoichiometry (i.e. structural type). For example, the polar, non-conducting  $Ca_2Si$  (anti- $PbCl_2$  structure with isolated Si atoms) reacts with water to give  $Ca(OH)_2$ ,  $SiO_2$  (hydrated), and  $H_2$ , whereas  $CaSi$  (which features zigzag Si chains) gives silanes and the polymeric  $SiH_2$ . By contrast  $CaSi_2$ , which has puckered layers of Si atoms, does not react with pure water, but with dilute hydrochloric acid it yields a yellow polymeric solid of overall composition  $Si_2H_2O$ . Transition metal silicides

Table 9.3 Structural units in metal silicides

Unit	Examples	
Isolated Si	Cu <sub>5</sub> Si ( $\beta$ -Mn structure)	} Metal structures (good electrical conductors)
	M <sub>3</sub> Si ( $\beta$ -W structure) M = V, Cr, Mo	
	Fe <sub>3</sub> Si (Fe <sub>3</sub> Al superstructure)	} Non-metal structures (non-conductors)
	Mn <sub>3</sub> Si (random bcc)	
	M <sub>2</sub> Si (anti-CaF <sub>2</sub> ); M = Mg, Ge, Sn, Pb	}
	M <sub>2</sub> Si (anti-PbCl <sub>2</sub> ); M = Ca, Ru, Ce, Rh, Ir, Ni	
Si <sub>2</sub> pairs	U <sub>3</sub> Si <sub>2</sub> (Si-Si 230 pm), also for Hf and Th	
Si <sub>4</sub> tetrahedra	KS <sub>2</sub> Si (Si-Si 243 pm), i.e. [M <sup>+</sup> ] <sub>4</sub> [Si <sub>4</sub> ] <sup>4-</sup> cf. isoelectronic P <sub>4</sub> (M = Li, K, Rb, Cs; also for M <sub>4</sub> Ge <sub>4</sub> )	
Si chains	USi (FeB structure) (Si-Si 236 pm); also for Ti, Zr, Hf, Th, Ce, Pu CaSi (CrB structure) (Si-Si 247 pm); also for Sr, Y	
Plane hexagonal Si nets	$\beta$ -USi <sub>2</sub> (AlB <sub>2</sub> structure) (Si-Si 222-236 pm); also for other actinoids and lanthanoids	
Puckered hexagonal Si nets	CaSi <sub>2</sub> (Si-Si 248 pm) — as in "puckered graphite" layer	
Open 3D Si frameworks	SrSi <sub>2</sub> , $\alpha$ -ThSi <sub>2</sub> (Si-Si 239 pm; closely related to AlB <sub>2</sub> ), $\alpha$ -USi <sub>2</sub>	

are usually inert to aqueous reagents except HF, but yield to more aggressive reagents such as molten KOH, or F<sub>2</sub> (Cl<sub>2</sub>) at red heat.

### 9.3.2 Silicon hydrides (silanes)

The great development which occurred in synthetic organic chemistry from the 1830s onward encouraged early speculations that a similar extensive chemistry might be generated based on Si. The first silanes were made in 1857 by F. Wöhler and H. Buff who reacted Al/Si alloys with aqueous HCl; the compounds prepared were shown to be SiH<sub>4</sub> and SiHCl<sub>3</sub> by C. Friedel and A. Ladenburg in 1867 but it was not until 1902 that the first homologue, Si<sub>2</sub>H<sub>6</sub>, was prepared by H. Moissan and S. Smiles from the protonolysis of magnesium silicide. The thermal instability and great chemical reactivity of the compounds precluded further advances until A. Stock developed his greaseless vacuum techniques and first began to study them as contaminants of his boron hydrides in 1916. He proposed the names silanes and boranes (p. 151) by analogy with the alkanes.

Silanes Si<sub>n</sub>H<sub>2n+2</sub> are now known as unbranched and branched chains (up to n = 8) and as cyclic compounds Si<sub>n</sub>H<sub>2n</sub> (n = 5, 6). Silanes are colourless gases or volatile liquids; they

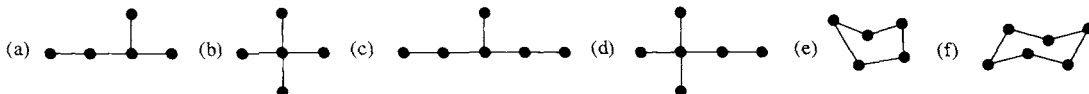
are extremely reactive and spontaneously ignite or explode in air. Thermal stability decreases with increasing chain length and only SiH<sub>4</sub> is stable indefinitely at room temperature; Si<sub>2</sub>H<sub>6</sub> decomposes very slowly (2.5% in 8 months), Si<sub>3</sub>H<sub>8</sub> slowly and the tetrasilanes more rapidly, at room temperature. Some physical properties are in Table 9.4 from which it can be seen that silanes are less volatile than both the alkanes and boranes (p. 163) of similar formula, but more volatile than the corresponding germanes (p. 375).

There are three general types of preparative route to the silanes and their derivatives. Early methods (pre-1945) treated materials such as metal silicides which contained negatively charged Si<sup>δ-</sup> with a protonic reagent such as an aqueous acid. Concurrent hydrolysis of the products limited the yield but considerable improvement resulted from the use of nonaqueous systems such as NH<sub>4</sub>Br/liq NH<sub>3</sub> (1934). The second general preparative route involves treatment of compounds such as SiX<sub>4</sub> (Si<sup>δ+</sup>) with hydridic reagents such as LiH, NaH, LiAlH<sub>4</sub>, etc., in ether solvents at low temperatures. This is now the preferred route: e.g. reaction of Si<sub>n</sub>Cl<sub>2n+2</sub> (n = 1, 2, 3) with LiAlH<sub>4</sub> gives essentially quantitative

<sup>28</sup> Ref. 13, Suppl. B1, 1982, 259 pp. (Si-H) and references cited therein.

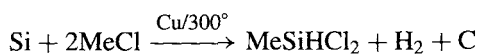
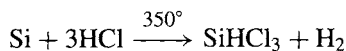
Table 9.4 Some properties of silanes<sup>(28)</sup>

Property	MP/°C	BP(extrap)/°C	$d(20^\circ)/\text{g cm}^{-3}$	Property	MP/°C	BP(extrap)/°C	$d(20^\circ)/\text{g cm}^{-3}$
SiH <sub>4</sub>	-184.7°	-111.8°	0.68 (-185°)	<i>neo</i> -Si <sub>5</sub> H <sub>12</sub> <sup>(b)</sup>	-57.8°	130°	—
Si <sub>2</sub> H <sub>6</sub>	-132.5°	-14.3°	0.686 (-25°)	<i>n</i> -Si <sub>6</sub> H <sub>14</sub>	-44.7°	193.6°	0.847
Si <sub>3</sub> H <sub>8</sub>	-117.4°	+53.1°	0.739	Si <sub>6</sub> H <sub>14</sub> <sup>(c)</sup>	-78.4°	185.2°	0.840
<i>n</i> -Si <sub>4</sub> H <sub>10</sub>	-89.9°	108.1°	0.792	Si <sub>6</sub> H <sub>14</sub> <sup>(d)</sup>	-57.8°	134.3°	0.815
<i>i</i> -Si <sub>4</sub> H <sub>10</sub>	-99.4°	101.7°	0.793	<i>n</i> -Si <sub>7</sub> H <sub>14</sub>	-30.1°	226.8°	0.859
<i>n</i> -Si <sub>5</sub> H <sub>12</sub>	-72.8°	153.2°	0.827	<i>cyclo</i> -Si <sub>5</sub> H <sub>10</sub> <sup>(e)</sup>	-10.5°	194.3°	0.963
<i>i</i> -Si <sub>5</sub> H <sub>12</sub> <sup>(a)</sup>	-109.8°	146.2°	0.820	<i>cyclo</i> -Si <sub>6</sub> H <sub>12</sub> <sup>(f)</sup>	+16.5°	226°	—

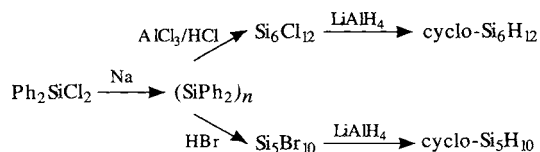
Table 9.5 Some typical bond energies/kJ mol<sup>-1</sup>

X	=	C	Si	H	F	Cl	Br	I	O-	N<
C-X		368	360	435	453	351	293	216	~360	~305
Si-X		360	340	393	565	381	310	234	452	322

yields of SiH<sub>4</sub>, Si<sub>2</sub>H<sub>6</sub>, and Si<sub>3</sub>H<sub>8</sub>. Organosilanes can be prepared similarly, e.g. Me<sub>2</sub>SiCl<sub>2</sub> gives Me<sub>2</sub>SiH<sub>2</sub>. The third general method for preparing Si-H compounds involves direct reaction of HX or RX with Si or a ferrosilicon alloy in the presence of a catalyst such as Cu when necessary (p. 364), e.g.:



Combination of these various methods has led to a vast number of derivatives in which H is progressively replaced by one or more monofunctional group such as F, Cl, Br, I, CN, R, Ar, OR, SH, SR, NH<sub>2</sub>, NR<sub>2</sub>, etc.<sup>(1)</sup> The cyclic silanes Si<sub>5</sub>H<sub>10</sub> and Si<sub>6</sub>H<sub>12</sub> were prepared in the late 1970s<sup>(29)</sup> via (SiPh)<sub>n</sub> which were themselves the first known homocyclic silane derivatives (F. S. Kipping, 1921):



Silanes are much more reactive than the corresponding C compounds.<sup>(1,2,30)</sup> This has been ascribed to several factors including: (a) the larger radius of Si which would facilitate attack by nucleophiles, (b) the great polarity of Si-X bonds, and (c) the presence of low-lying d orbitals which permit the formation of 1:1 and 1:2 adducts, thereby lowering the activation energy of the reaction. The relative magnitude of the various bond energies is also an important factor in deciding which bonds will survive and which will be formed. Thus, it can be seen in Table 9.5, Si-Si < Si-C < C-C and Si-H < C-H, whereas for bonds for the other elements the energy C-X < Si-X. These data should

<sup>29</sup> E. HENGGE and G. BAUER, *Monatshefte für Chemie* **106**, 503-12 (1975). E. HENGGE and D. KOVAR, *Z. anorg. allg. Chem.* **459**, 123-30 (1979).

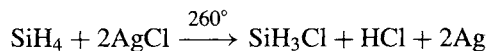
<sup>30</sup> E. WIBERG and E. AMBERGER, *Hydrides of the Elements of Main Groups I-IV*, Chap. 7, pp. 462-638, Elsevier, Amsterdam, 1971. A comprehensive review of compounds containing Si-H bonds; over 700 references.

be used only for broad comparisons since the estimated bond energies depend markedly on the particular compounds being studied and also on the experimental technique employed and the method of computation.

The pyrolysis of silanes leads to polymeric species and ultimately to Si and H<sub>2</sub>; indeed, pyrolysis of SiH<sub>4</sub> is a commercial route to ultrapure Si. The reactions occurring have been less studied than those of alkanes (and boranes, p. 164), but it is clear that there are significant differences. Thus the initial step in the thermal decomposition of alkanes is the cleavage of a C–H or C–C bond with formation of radical intermediates R<sub>3</sub>C•. However, studies using deuterium-substituted compounds suggest that the initial step in the decomposition of polysilanes is the elimination of silenes :SiH<sub>2</sub> or :SiHR.<sup>(31)</sup> Activation energies for this process (~210 kJ mol<sup>-1</sup>) are substantially less than Si–Si and Si–H bond energies and the reaction appears to involve a 1,2-H shift with a 5-coordinate transition state.

<sup>31</sup> I. M. T. DAVIDSON and A. V. HOWARD, *J. Chem. Soc., Faraday I*, **71**, 69–77 (1975) and references therein. C. H. HAAS and M. A. RING, *Inorg. Chem.* **14**, 2253–6 (1975). A. J. VANDERWIELEN, M. A. RING and H. E. O'NEAL, *J. Am. Chem. Soc.* **97**, 993–8 (1975).

Pure silanes do not react with pure water or dilute acids in silica vessels, but even traces of alkali dissolved out of glass apparatus catalyse the hydrolysis which is then rapid and complete (SiO<sub>2</sub>.nH<sub>2</sub>O + 4H<sub>2</sub>). Solvolysis with MeOH can be controlled to give several products SiH<sub>4-n</sub>-(OMe)<sub>n</sub> (n = 2, 3, 4). Si–H adds (with difficulty) to alkenes though the reaction occurs more readily with substituted silanes. Similarly, SiH<sub>4</sub> adds to Me<sub>2</sub>CO at 450° to give C<sub>3</sub>H<sub>7</sub>OSiH<sub>3</sub>, and it ring-opens ethylene oxide at the same temperature to give EtOSiH<sub>3</sub> and other products. Silanes explode in the presence of Cl<sub>2</sub> or Br<sub>2</sub> but the reaction with Br<sub>2</sub> can be moderated at –80° to give good yields of SiH<sub>3</sub>Br and SiH<sub>2</sub>Br<sub>2</sub>. More conveniently, halogenosilanes SiH<sub>3</sub>X can be made by the catalysed reaction of SiH<sub>4</sub> and HX in the presence of Al<sub>2</sub>X<sub>6</sub>, or by the reaction with solid AgX in a heated flow reactor, e.g.:



SiH<sub>3</sub>I in particular is a valuable synthetic intermediate and some of its reactions are summarized in Table 9.6. SiH<sub>3</sub>I is a dense, colourless, mobile liquid, mp –57.0°, bp +45.4°, *d*(15°) 2.035 g cm<sup>-3</sup>.

Another valuable reagent is KSiH<sub>3</sub>, a colourless crystalline compound with NaCl-type

**Table 9.6** Some reactions of SiH<sub>3</sub>I<sup>(a)</sup>

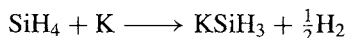
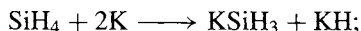
Reagent	Major Si product	Reagent	Major Si product
Na/Hg	Si <sub>2</sub> H <sub>6</sub>	N <sub>2</sub> H <sub>4</sub>	(SiH <sub>3</sub> ) <sub>2</sub> NN(SiH <sub>3</sub> ) <sub>2</sub>
H <sub>2</sub> O	O(SiH <sub>3</sub> ) <sub>2</sub>	LiN(SiCl <sub>3</sub> ) <sub>2</sub>	SiH <sub>3</sub> N(SiCl <sub>3</sub> ) <sub>2</sub>
HgS	S(SiH <sub>3</sub> ) <sub>2</sub>	P <sub>4</sub>	(SiH <sub>3</sub> ) <sub>n</sub> PI <sub>3-n</sub> (n = 1, 2, 3)
Ag <sub>2</sub> Se	Se(SiH <sub>3</sub> ) <sub>2</sub>	AgXCN (N <sub>2</sub> atm)	SiH <sub>3</sub> NCX (X = O, Se)
Li <sub>2</sub> Te	Te(SiH <sub>3</sub> ) <sub>2</sub>	AgSCN	SiH <sub>3</sub> NCS
Si <sub>2</sub> H <sub>5</sub> Br + H <sub>2</sub> O	SiH <sub>3</sub> OSi <sub>2</sub> H <sub>5</sub>	AgCN	SiH <sub>3</sub> CN
Hg(SCF <sub>3</sub> ) <sub>2</sub>	SiH <sub>3</sub> SCF <sub>3</sub>	Ag <sub>2</sub> NCN	(SiH <sub>3</sub> ) <sub>2</sub> NCN
Hg(SeCF <sub>3</sub> ) <sub>2</sub>	SiH <sub>3</sub> SeCF <sub>3</sub>	HC≡CMgBr	SiH <sub>3</sub> C≡CH
NH <sub>3</sub>	N(SiH <sub>3</sub> ) <sub>3</sub>	NaMn(CO) <sub>5</sub>	[Mn(CO) <sub>5</sub> (SiH <sub>3</sub> )]
R <sub>2</sub> NH	SiH <sub>3</sub> NR <sub>2</sub>	Na <sub>2</sub> Fe(CO) <sub>4</sub>	[Fe(CO) <sub>4</sub> (SiH <sub>3</sub> ) <sub>2</sub> ]
NMe <sub>3</sub> <sup>(b)</sup>	SiH <sub>3</sub> I.NMe <sub>3</sub> and SiH <sub>3</sub> I.2NMe <sub>3</sub>	[Co(CO) <sub>4</sub> ] <sup>-</sup>	[Co(CO) <sub>4</sub> (SiH <sub>3</sub> )]

<sup>(a)</sup>Detailed references to conditions, yields and other minor products are given in ref. 1 [2nd edn. Vol. 18, pp. 172–215 (1969)] which also summarizes the extensive reaction chemistry of O(SiH<sub>3</sub>)<sub>2</sub>, S(SiH<sub>3</sub>)<sub>2</sub>, and N(SiH<sub>3</sub>)<sub>3</sub>.

<sup>(b)</sup>Many other ligands (L) also give 1:1 and 1:2 adducts.



structure; it is stable up to  $\sim 200^\circ$  and is prepared by direct reaction of potassium on silane in monoglyme or diglyme:



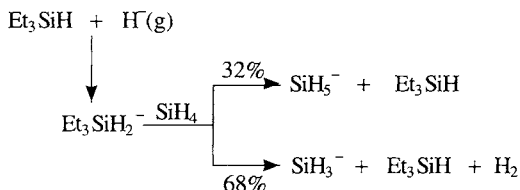
**Table 9.7** Some reactions of  $\text{KSiH}_3$ <sup>(a)</sup>

Reagent	Major Si product	Reagent	Major Si product
$\text{H}_2\text{O}$	$\text{SiO}_2 \cdot n\text{H}_2\text{O}$	$\text{Me}_3\text{SiCl}$	$[\text{SiMe}_3(\text{SiH}_3)]$
$\text{MeOH}$	$\text{Si}(\text{OMe})_4$	$\text{Me}_3\text{GeBr}$	$[\text{GeMe}_3(\text{SiH}_3)]$
$\text{HCl}$	$\text{SiH}_4$	$\text{Me}_3\text{SnBr}$	$[\text{SnMe}_3(\text{SiH}_3)]$
$\text{MeI}$	$\text{SiH}_3\text{Me}$	$\text{GeH}_3\text{Cl}$	$\text{GeH}_3\text{SiH}_3$
$\text{SiH}_3\text{Br}$	$\text{Si}_2\text{H}_6, \text{SiH}_4$	$\text{MeOCH}_2\text{Cl}$	$\text{SiH}_3(\text{CH}_2\text{OMe})$
$\text{Si}_2\text{H}_5\text{Br}$	$\text{Si}_3\text{H}_8, \text{Si}_2\text{H}_6$		

<sup>(a)</sup>See footnote (a) to Table 9.6.

When hexamethylphosphoramide,  $(\text{NMe}_2)_3\text{PO}$ , is used as solvent only the second reaction occurs. The synthetic utility of  $\text{KSiH}_3$  can be gauged from Table 9.7 which summarizes some of its reactions. In addition,  $\text{PCl}_3$  gives polymeric  $(\text{PH})_x$ ,  $\text{CO}_2$  gives  $\text{CO}$  plus  $\text{HCO}_2\text{K}$  (formate), and  $\text{N}_2\text{O}$  gives  $\text{N}_2 + \text{H}_2$  (plus) some  $\text{SiH}_4$  in each case.<sup>(32)</sup>

The hypervalent silicon hydride anion,  $\text{SiH}_5^-$  (cf.  $\text{SiF}_5^-$  below), has been synthesized as a reactive species in a low-pressure flow reactor:<sup>(33)</sup>



### 9.3.3 Silicon halides and related complexes

Silicon and silicon carbide both react readily with all the halogens to form colourless

volatile reactive products  $\text{SiX}_4$ .  $\text{SiCl}_4$  is particularly important and is manufactured on the multikilotonne scale for producing boron-free transistor grade Si, fumed silica (p. 345), and various silicon esters. When two different tetrahalides are heated together they equilibrate to form an approximately random distribution of silicon halides which, on cooling, can be separated and characterized:



Mixed halides can also be made by halogen exchange reaction, e.g. by use of  $\text{SbF}_3$  to successively fluorinate  $\text{SiCl}_4$  or  $\text{SiBr}_4$ . The mps and bps of these numerous species are compared with those of the parent hydride and halides in Fig. 9.1. While there is a clear trend to higher mps and bps with increase in molecular weight, this is by no means always regular. More notable is the enormous drop in mp (bp) which occurs for the halides of Si when compared with Al and earlier elements in the same row of the periodic table, e.g.:

Compound	NaF	MgF <sub>2</sub>	AlF <sub>3</sub>	SiF <sub>4</sub>	PF <sub>5</sub>	SF <sub>6</sub>
MP/°C	988	1266	1291	-90	-94	-50
				(subl)		

This is sometimes erroneously ascribed to a discontinuous change from "ionic" to "covalent" bonding, but the electronegativity and other bonding parameters of Al are fairly similar to those of Si and the difference is more convincingly seen merely as a consequence of the change from an infinite lattice structure (in which each Al is surrounded by 6 F) to a lattice of discrete  $\text{SiF}_4$  molecules as dictated by stoichiometry and size. Several other examples of this effect will be noticed amongst compounds of the Group 14 elements. Another instructive trend is in the Si-F interatomic distance in binary Si/F species: in tetrahedral  $\text{SiF}_4(\text{c})$  it is 154.0 pm; in trigonal bipyramidal  $\text{SiF}_5^-$  it is 159.4 and 164.6 pm, respectively, for equatorial and axial bonds, and in  $\text{SiF}_6^{2-}$  it is 168.5 pm. The trend is to longer distances with increase in coordination number, presumably reflecting a gradual decrease in bond order. The 3.3% increase in going from

<sup>32</sup> V. A. WILLIAMS and D. M. RITTER, *Inorg. Chem.* **24**, 3278-80 (1985).

<sup>33</sup> D. J. HAJDASZ and R. R. SQUIRES, *J. Am. Chem. Soc.* **108**, 3139-40 (1986).

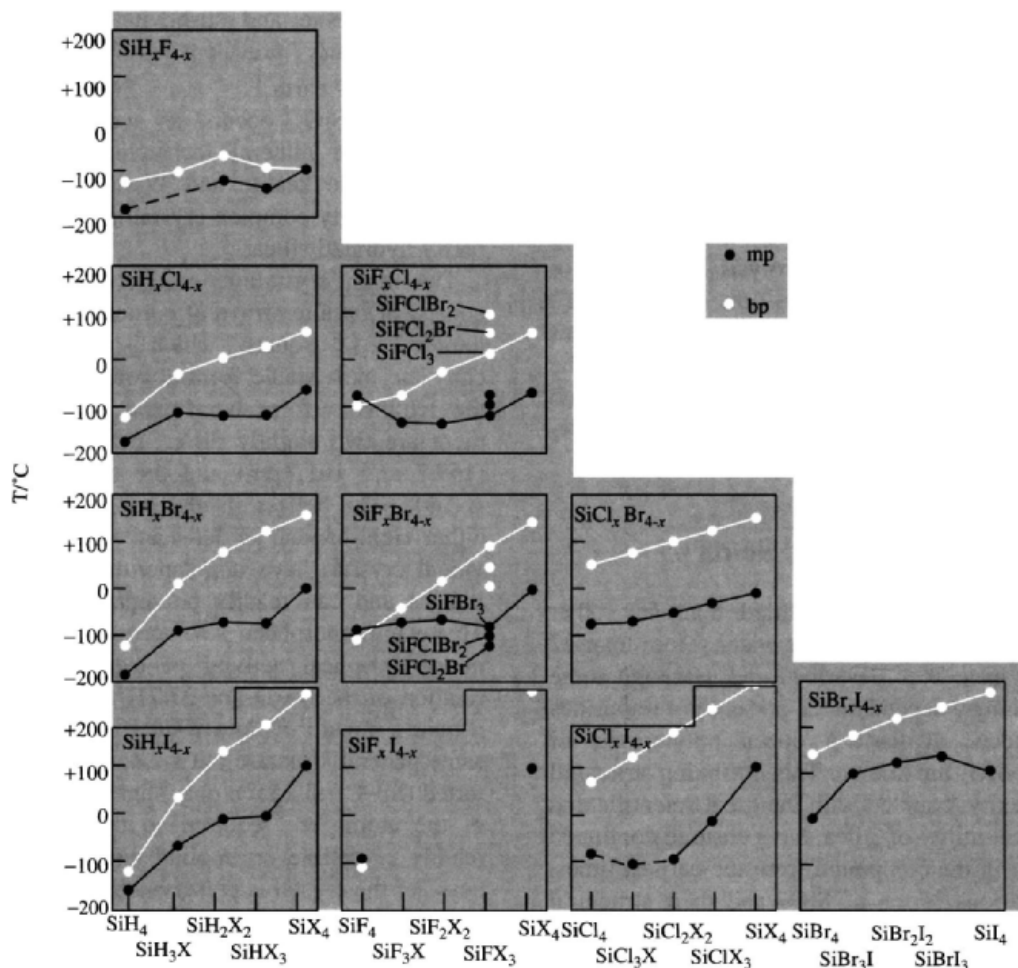


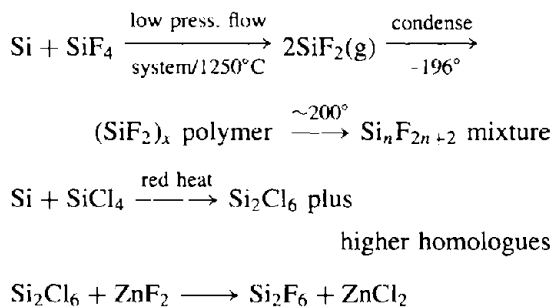
Figure 9.1 Trends in the mp and bp of silicon hydride halides and mixed halides.

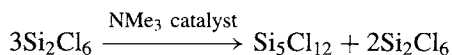
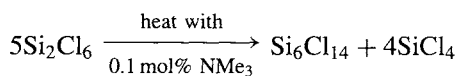
equatorial to axial bonding in  $\text{SiF}_5^-$  is also in the usual direction.

The reactions of  $\text{SiX}_4$  are straightforward and call for little comment.<sup>(1,2)</sup>

Higher homologues  $\text{Si}_n\text{X}_{2n+2}$  are volatile liquids or solids and, contrary to the situation in carbon chemistry, catenation in Si compounds reaches its maximum in the halides rather than the hydrides. This has been ascribed to additional back-bonding from filled halogen  $p_\pi$  orbitals into the Si  $d_\pi$  orbitals which thus synergically compensates for electron loss from Si via  $\sigma$  bonding to the electronegative halogens (cf. CO, pp. 926–8). Fluoropolysilanes up to  $\text{Si}_{14}\text{F}_{30}$  and

other series up to at least  $\text{Si}_6\text{Cl}_{14}$  and  $\text{Si}_4\text{Br}_{10}$  are known. Preparative routes are exemplified by the following reactions:





These compounds show many unusual reactions and reviews of their chemistry make fascinating reading.<sup>(34,35)</sup> Partial hydrolysis of  $\text{SiCl}_4$  (or the reaction of  $\text{Cl}_2 + \text{O}_2$  on Si at  $700^\circ$ ) leads to a series of volatile chlorosiloxanes  $\text{Cl}_3\text{Si}(\text{OSiCl}_2)_n\text{OSiCl}_3$  ( $n = 0-5$ ) and to the cyclic  $(\text{SiOCl}_2)_4$ . The corresponding bromo compounds are prepared similarly, using  $\text{Br}_2$  and  $\text{O}_2$ .

### 9.3.4 Silica and silicic acids

Silica has been more studied than any other chemical compound except water. More than 22 phases have been described and, although some of these may depend on the presence of impurities or defects, at least a dozen polymorphs of "pure"  $\text{SiO}_2$  are known. This intriguing structural complexity, coupled with the great scientific and technical utility of silica, have ensured continued interest in the compound from the earliest times. The various forms of  $\text{SiO}_2$  and their structural inter relations will be described in the following paragraphs. By far the most commonly occurring form of  $\text{SiO}_2$  is  $\alpha$ -quartz which is a major mineral constituent of many rocks such as granite and sandstone; it also occurs alone as rock crystal and in impure forms as rose quartz, smoky quartz (red brown), morion (dark brown), amethyst (violet) and citrine (yellow). Poorly crystalline forms of quartz include chalcedony (various colours), chrysoprase (leek green), carnelian (deep red), agate (banded), onyx (banded), jasper (various), heliotrope (bloodstone) and flint (often black due to inclusions of carbon). Less-common crystalline modifications of  $\text{SiO}_2$  are tridymite, cristobalite and the extremely rare

minerals coesite and stishovite. Earthy forms are particularly prevalent as kieselguhr and diatomaceous earth.<sup>†</sup>

Vitreous  $\text{SiO}_2$  occurs as tectites, obsidian and the rare mineral lechatelierite. Synthetic forms include keatite and W-silica. Opals are an exceedingly complex crystalline aggregate of partly hydrated silica.

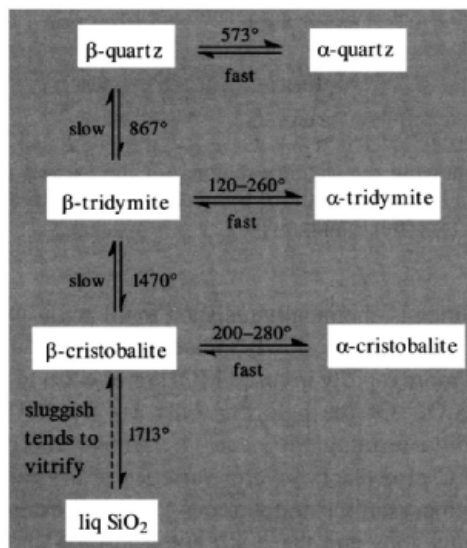
The main crystalline modifications of  $\text{SiO}_2$  consist of infinite arrays of corner-shared  $\{\text{SiO}_4\}$  tetrahedra. In  $\alpha$ -quartz, which is thermodynamically the most stable form at room temperature, the tetrahedra form interlinked helical chains; there are two slightly different Si-O distances (159.7 and 161.7 pm) and the angle Si-O-Si is  $144^\circ$ . The helices in any one crystal can be either right-handed or left-handed so that individual crystals have non-superimposable mirror images and can readily be separated by hand. This enantiomorphism also accounts for the pronounced optical activity of  $\alpha$ -quartz (specific rotation of the Na D-line  $27.71^\circ/\text{mm}$ ). At  $573^\circ\text{C}$   $\alpha$ -quartz transforms into  $\beta$ -quartz which has the same general structure but is somewhat less distorted (Si-O-Si  $155^\circ$ ): only slight displacements of the atoms are required so the transition is readily reversible on cooling and the "handedness" of the crystal is preserved throughout. This is called a non-reconstructive transformation. A more drastic structural change occurs at  $867^\circ$  when  $\beta$ -quartz transforms into  $\beta$ -tridymite. This is a reconstructive transformation which requires the breaking of Si-O bonds to enable the  $\{\text{SiO}_4\}$

<sup>†</sup> The names of minerals often give a clue to their properties or discovery. Coesite, stishovite, and keatite are named after their discoverers (p. 343). Quartz derives from *kwardy*, a West Slav dialectal equivalent of the Polish *twardy*, hard. Tridymite was recognized as a new polymorph by von Rath in 1861 because of its typical occurrence as trillings or groups of 3 crystals (Greek *τριδυμος*, *tridyomos*, threefold). Cristobalite was discovered by von Rath in 1884 on the slopes of Mt San Cristobal, Mexico, where tridymite had also first been discovered. Kieselguhr is a combination of the German *Kiesel*, flint, and *Guhr*, earthy deposit. Diatomaceous earth refers to its origin as the remains of minute unicellular algae called diatoms: these marine organisms (0.01–0.1 mm diam) have the astonishing property of accreting silica on their cell walls and this preserves the shape of the organism after death — enormous deposits occur in many places (see p. 345).

<sup>34</sup> J. L. MARGRAVE and P. W. WILSON, *Acc. Chem. Res.* **4**, 145–52 (1971).

<sup>35</sup> G. URRY, *Acc. Chem. Res.* **3**, 306–12 (1970).

tetrahedra to be rearranged into a simpler, more open hexagonal structure of lower density. For this reason the change is often sluggish and this enables tridymite to occur as a (metastable) mineral phase below the transition temperature. When  $\beta$ -tridymite is cooled to  $\sim 120^\circ$  it undergoes a fast, reversible, non-reconstructive transition to (metastable)  $\alpha$ -tridymite by slight displacements of the atoms. Conversely, when  $\beta$ -tridymite is heated to  $1470^\circ$  it undergoes a sluggish reconstructive transformation into  $\beta$ -cristobalite and this, in turn, can retain its structure as a metastable phase when cooled below the transition temperature; further slight displacements occur rapidly and reversibly in the temperature range  $200\text{--}280^\circ$  to give  $\alpha$ -cristobalite (Si-O 161 pm, Si-O-Si  $147^\circ$ ). These transitions are summarized below.

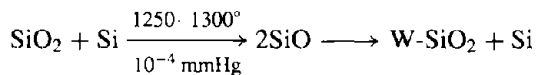


The  $\alpha$ -form of each of the three minerals can thus be obtained at room temperature and, because of the sluggishness of the reconstructive interconversions of the  $\beta$ -forms, it is even possible to melt  $\beta$ -quartz ( $1550^\circ$ ) and  $\beta$ -tridymite ( $1703^\circ$ ) if they are heated sufficiently rapidly. The bp of  $\text{SiO}_2$  is not accurately known but is about  $2800^\circ\text{C}$ .

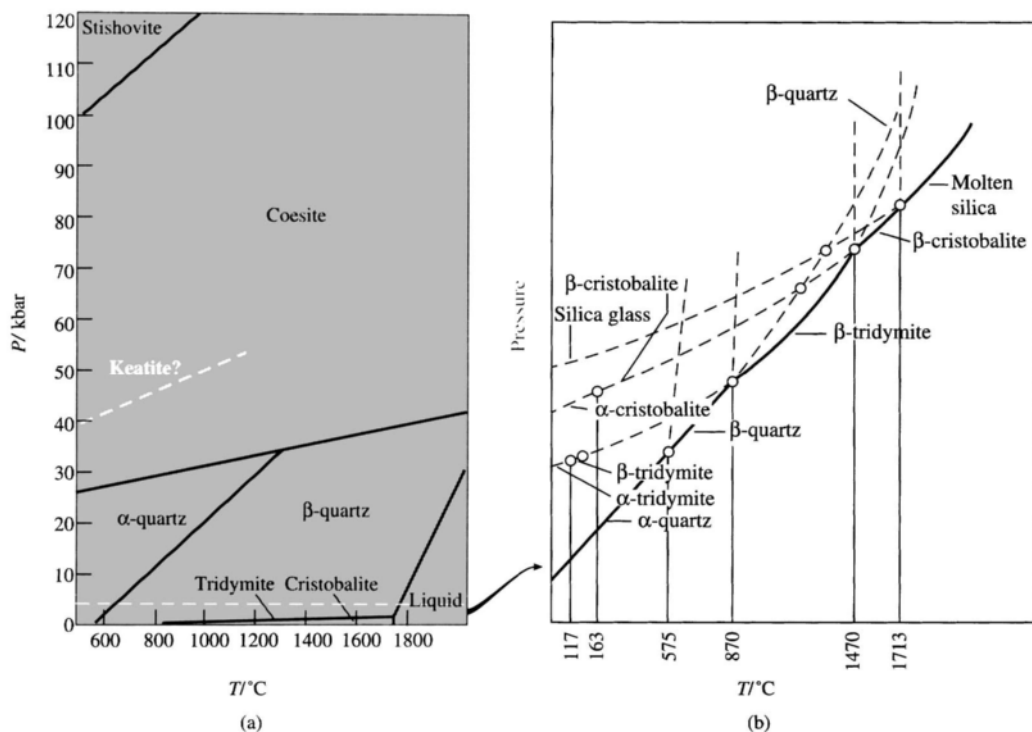
Other forms of  $\text{SiO}_2$  can be made at high pressure (Fig. 9.2). Coesite was first made

by L. Coes in 1953 by heating dry  $\text{Na}_2\text{SiO}_3$  and  $(\text{NH}_4)_2\text{HPO}_4$  at  $700^\circ$  and 40 kbar, and was subsequently found in nature at Meteor Crater, Arizona (1960). Its structure consists of 4-connected networks of  $\{\text{SiO}_4\}$  in which the smallest rings are 4- and 8-membered, and this compact structure explains its high density (Table 9.8). On being heated it rapidly converts to tridymite or cristobalite. At still higher pressures (40–120 kbar,  $380\text{--}585^\circ$ ) keatite is formed under hydrothermal conditions from amorphous silica and dilute alkali (P. P. Keat, 1959); the  $\{\text{SiO}_4\}$  are connected into 5-, 7-, and 8-membered rings as in ice(III) (p. 624). The highest density form of  $\text{SiO}_2$  was predicted in 1952 by J. B. Thompson who visualized 6-coordinate Si in a rutile structure (p. 961). It was first synthesized in S. M. Stishov's laboratory (1961) at  $1200\text{--}1400^\circ$  and 160–180 kbar, and found to have the predicted structure. It was discovered in association with coesite at Meteor Crater in 1962: presumably both minerals were formed under transient shock pressures following meteorite impact and then preserved by rapid quenching from high temperature. The rapid melting and cooling of pre-existing silica phases also occurs during lightning strikes, and this leads to the formation of lechatelierite, a glassy or vitreous silica mineral.

Finally, a very low-density form of fibrous silica, W- $\text{SiO}_2$  has been made by the disproportionation of (metastable) crystalline  $\text{SiO}$ :



W- $\text{SiO}_2$  features  $\{\text{SiO}_4\}$  tetrahedra linked by sharing opposite edges to form infinite parallel chains analogous to  $\text{SiS}_2$  and  $\text{SiSe}_2$ ; this edge-sharing of pairs of O atoms between pairs of Si atoms is not observed elsewhere in Si-O chemistry where linking is by corner sharing of single O atoms. The configuration is unstable, and fibrous  $\text{SiO}_2$  rapidly reverts to amorphous  $\text{SiO}_2$  on heating or in the presence of traces of moisture. It has also recently been shown that reaction of  $(\text{SiO})_2$  and  $\text{O}_2$  in an argon matrix results in the formation of dimeric molecules



**Figure 9.2** (a) Pressure-temperature phase diagram for  $\text{SiO}_2$  showing the stability regions for the various polymorphs. The low-pressure segment below the broken line is shown in (b) using an (arbitrary) expanded scale to illustrate the relationships described in the preceding paragraphs.

of silica,  $\text{O}=\text{Si}(\mu\text{-O})_2\text{Si}=\text{O}$ .<sup>(36)</sup> Interaction of molecular  $\text{SiO}$  with  $\text{Ag}$  atoms in an argon matrix gives cyclic  $\overline{\text{AgSiO}}$  with the angle at  $\text{Si}$  being  $\leq 90^\circ$ .<sup>(37)</sup>

**Table 9.8** Density of the main forms of  $\text{SiO}_2$  (room temperature)

	$d/\text{g cm}^{-3}$		$d/\text{g cm}^{-3}$
W (fibrous)	1.97	$\beta$ -quartz ( $600^\circ$ )	2.533
Lechatelierite	2.19	$\alpha$ -quartz	2.648
Vitreous	2.196	Coesite	2.911
Tridymite	2.265	Keatite	3.010
Cristobalite	2.334	Stishovite	4.287

<sup>36</sup> T. MEHNER, H. J. GÖCKE, S. SCHUNCK and H. SCHNOCKEL, *Z. anorg. allg. Chem.* **580**, 121–30 (1990).

<sup>37</sup> T. MEHNER, H. SCHNOCKEL, M. J. ALMOND and A. J. DOWNS, *J. Chem. Soc., Chem. Commun.*, 117–9 (1988).

Silica is chemically resistant to all acids except  $\text{HF}$  but dissolves slowly in hot concentrated alkali and more rapidly in fused  $\text{MOH}$  or  $\text{M}_2\text{CO}_3$  to give  $\text{M}_2\text{SiO}_3$ . Of the halogens only  $\text{F}_2$  attacks  $\text{SiO}_2$  readily, forming  $\text{SiF}_4$  and  $\text{O}_2$ . Above  $1000^\circ$   $\text{H}_2$  and  $\text{C}$  also react. Several varieties of crystalline, cryptocrystalline and vitreous  $\text{SiO}_2$  find extensive applications and these are noted in the Panel. In vitreous silica  $\{\text{SiO}_4\}$  tetrahedra are again linked by sharing corners with each  $\text{O}$  linked to  $2\text{Si}$  but the extended three-dimensional network lacks the symmetry and periodicity of the crystalline forms. The  $\text{Si}-\text{O}$  distances are similar to those in other forms of  $\text{SiO}_2$  (158–162 pm) but the  $\text{Si}-\text{O}-\text{Si}$  angles vary by as much as  $15-20^\circ$  on either side of the mean value of  $153^\circ$ .

The detailed reactions of  $\text{SiO}_2$  with the oxides of the metals and semi-metals are of great importance in glass technology and ceramics

but will not be treated here.<sup>(1,2,38)</sup> Suffice it to say that, in addition to innumerable crystalline compounds and vitreous phases, many water-soluble compositions are known and many of these find extensive commercial application.

<sup>38</sup> S. FRANK, *Glass and Archaeology*, Academic Press, London, 1982, 156 pp. O. V. MAZURIN, M. V. STRELTINA and T. P. SHVAIKO-SHVAIKOVSKAYA, *Handbook of Glass Data*, Elsevier, Amsterdam, Part A, 1983, 670 pp; B, 1985, 806 pp; C, 1987, 1110 pp; D, 1991, 992 pp; E, Supplements, to be published.

Perhaps the best known are the soluble sodium (and potassium) silicates which are made by fusing sand with the appropriate carbonate in a glass-making furnace at  $\sim 1400^\circ$ . The resulting soluble glass is dissolved in hot water under pressure and any insoluble glass or unreacted sand filtered off. The ternary phase diagram for  $\text{Na}_2\text{O}-\text{SiO}_2-\text{H}_2\text{O}$  (Fig. 9.3) indicates that only certain limited regions are of commercial interest, e.g. the stable liquid materials (area 9) in the composition range

### Some Uses of Silica<sup>1</sup>

The main types of  $\text{SiO}_2$  used in industry are high-purity  $\alpha$ -quartz, vitreous silica, silica gel, fumed silica and diatomaceous earth. The most important application of quartz is as a piezoelectric material (p. 58); it is used in crystal oscillators and filters for frequency control and modulation, and in electromechanical devices such as transducers and pickups: tens of millions of such devices are made each year. There is insufficient natural quartz of adequate purity so it must be synthesized by hydrothermal growth of a seed crystal using dilute aqueous  $\text{NaOH}$  and vitreous  $\text{SiO}_2$  at  $400^\circ\text{C}$  and 1.7 kbar. The technique was first successfully employed by G. R. Spezia in 1905. (Crystal growth from molten  $\text{SiO}_2$  cannot be used — why?)

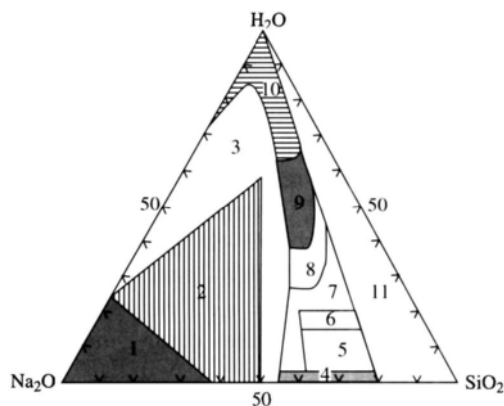
Vitreous silica combines exceptionally low thermal expansion<sup>†</sup> and high thermal shock resistance with high transparency to ultraviolet light, good refractory properties, and general chemical inertness. As a glass it is hard to work because of its very high softening point, high viscosity, short liquid range and high volatility at forming temperatures. It is familiar in high-quality laboratory glassware, particularly for photolysis experiments and as sample cells in ultraviolet/visible spectroscopy; it is also much used as a protective sheath in the form of tubing or as thin films deposited from the vapour.

Silica gel is an amorphous form of  $\text{SiO}_2$  with a very porous structure, formed by acidification of aqueous solutions of sodium silicate; the gelatinous precipitate is washed free of electrolytes and then dehydrated either by roasting or spray drying. The properties of the resulting microporous material depend critically on the conditions of preparation, but typical samples have a pore diameter of 2200–2600 pm, a surface area of  $750\text{--}800\text{ m}^2\text{ g}^{-1}$ , and an apparent bulk density of  $0.67\text{--}0.75\text{ g cm}^{-3}$ . Such material finds extensive use as a desiccant, selective absorbant, chromatographic support, catalyst substrate and insulator (thermal and sound). It can absorb more than 40% of its own weight of water and, when stained with cobalt salts such as the nitrate or  $(\text{NH}_4)_2\text{CoCl}_4$ , is familiar as a self-indicating desiccant that can readily be regenerated by heating (anhydrous, blue; hydrated, pink). It is chemically inert, non-toxic and dimensionally stable, and finds a growing application in the food industry as an anticaking agent in cocoa, fruit juice powders,  $\text{NaHCO}_3$  and powdered sugar and spices. It is also used as a flattening agent to produce an attractive matte finish on lacquers, varnishes and paints, and on the surface of vinyl plastics and synthetic fabrics.

Another manufactured form of ultrafine powdered  $\text{SiO}_2$  is pyrogenic or fumed silica, formed by the high-temperature hydrolysis of  $\text{SiCl}_4$  in an oxyhydrogen flame in specially designed burners; the  $\text{SiO}_2$  is formed as a very fine white smoke which is collected on cooled rotating rollers. The bulk density is only  $0.03\text{--}0.06\text{ g cm}^{-3}$  and the surface area  $150\text{--}500\text{ m}^2\text{ g}^{-1}$ . Its main use is as a thixotropic thickening agent in the processing of epoxy and polyester resins and plastics, and as a reinforcing filler in silicone rubbers where, in contrast to carbon black fillers (p. 271), its chemical inertness does not interfere with the peroxide initiated cure (p. 365).

Diatomaceous earth or kieselguhr (p. 342) is mined by open-cast methods on a very substantial scale, particularly in Europe and North America, which respectively account for 59% and 39% of the world production (1.8 million tonnes in 1977). The principal use is in filtration plants, and this accounts for about 60% of the supply; a further 20% is used in abrasives, fillers, light-weight aggregates and insulation material, and the remainder is used as an inert carrier, coating agent or in the manufacture of pozzolan.

<sup>†</sup> The linear coefficient of thermal expansion of vitreous silica is  $\sim 0.25 \times 10^{-6}$ . This can be compared with a value of  $\sim 100 \times 10^{-6}$  for ordinary soda-lime glasses ( $\sim 79\% \text{ SiO}_2$ ,  $\sim 12.5\% \text{ Na}_2\text{O}$ ,  $\sim 8.5\% \text{ CaO}$ ). Addition of  $\text{B}_2\text{O}_3$  (as in Pyrex) sharply reduces this value to  $3 \times 10^{-6}$  (typical laboratory glassware has a composition 83.9%  $\text{SiO}_2$ , 10.6%  $\text{B}_2\text{O}_3$ , 1.2%  $\text{Al}_2\text{O}_3$ , 3.9%  $\text{Na}_2\text{O}$ , 0.4%  $\text{K}_2\text{O}$ ).



**Figure 9.3** Simplified schematic ternary phase diagram for the system  $\text{Na}_2\text{O}-\text{SiO}_2-\text{H}_2\text{O}$ . Commercially important areas are shaded. (1) anhydrous " $\text{Na}_4\text{SiO}_4$ ," and its granular mixtures with  $\text{NaOH}$ ; (2) granular crystalline alkaline silicates such as  $\text{Na}_2\text{SiO}_3$  and its hydrates; (3) uneconomic partially crystallized mixtures; (4) glasses; (5) uneconomic hydrated glasses; (6) dehydrated liquids; (7) uneconomic semi-solids and gels; (8) uneconomic, unstable viscous liquids; (9) ordinary commercial liquids; (10) dilute liquids; (11) unstable liquids and gels. (From J. G. Vail, *Soluble Silicates*, Reinhold, New York, 1952.)

30–40%  $\text{SiO}_2$ , 10–20%  $\text{Na}_2\text{O}$ , 60–40%  $\text{H}_2\text{O}$ , i.e.  $\sim\text{Na}_2\text{Si}_2\text{O}_5 \cdot 6\text{H}_2\text{O}$ . These find extensive use in industrial and domestic liquid detergents because they maintain high pH by means of their buffering ability and can saponify animal and vegetable oils and fats; they also emulsify mineral oils, deflocculate dirt particles, and prevent redeposition of suspended dirt and soil. The more dilute solutions (area 10) are used in production of silica gels by acidification (pp. 345 and below). There are numerous other uses of soluble silicates including adhesives, glues and binders, especially for corrugated cardboard boxes, and as refractory acid-resistant cements and sealants. World production in 1981 was  $\sim 3.0$  million tonnes of which the sodium silicates formed the major part. Price range from \$220–450/tonne depending on composition.

Potassium silicate solutions are equally complex; for example, an aqueous solution prepared from  $\text{KOH}$  and  $\text{SiO}_2$  in which the ratio  $\text{K}:\text{Si}$  is 1:1 contains 22 different discrete silicate anions as identified by  $^{29}\text{Si}$  COSY nmr studies.<sup>(39)</sup>

The system  $\text{SiO}_2-\text{H}_2\text{O}$ , even in the absence of metal oxides, is particularly complex and of immense geochemical and industrial importance.<sup>(40)</sup> The mp of pure  $\text{SiO}_2$  decreases dramatically by as much as  $800^\circ$  on addition of 1–2%  $\text{H}_2\text{O}$  (at high pressure), presumably as a result of the structure-breaking effect of replacing  $\text{Si}-\text{O}-\text{Si}$  links by "terminal"  $\text{Si}-\text{OH}$  groups. With increasing concentrations of  $\text{H}_2\text{O}$  one obtains hydrated silica gels and colloidal dispersions of silica; there are also numerous hydrates and distinct silicic acids in very dilute aqueous solutions, but these tend to be rather insoluble and rapidly precipitate with further condensation when aqueous solutions of soluble silicates are acidified. Structural information is sparse, particularly for the solid state, but in solution evidence has been claimed for at least 5 species (Table 9.9). It is unlikely that any of these species exist in the solid state since precipitation is accompanied by further condensation and cross-linking to form "polysilicic acids" of indefinite and variable composition  $[\text{SiO}_x(\text{OH})_{4-2x}]_n$  (cf B, Al, Fe, etc.). However, the crystal structure of  $\{(\text{C}-\text{C}_6\text{H}_{11})_7\text{Si}_7\text{O}_9\{\text{O}_3\text{W}(\text{NMe}_2)_3\}_3\}$  has been

**Table 9.9** Silicic acids in solution

Formula	$n^{(a)}$	Name	Sol. ( $\text{H}_2\text{O}$ , $20^\circ$ ) $\text{mol l}^{-1}$
$\text{H}_{10}\text{Si}_2\text{O}_9$	2.5	Pentahydrosilicic acid	$2.9 \times 10^{-4}$
$\text{H}_4\text{SiO}_4$	2	Orthosilicic acid	$7 \times 10^{-4}$
$\text{H}_6\text{Si}_2\text{O}_7$	1.5	Pyrosilicic acid	$9.6 \times 10^{-4}$
$\text{H}_2\text{SiO}_3$	1	Metasilicic acid	$10 \times 10^{-4}$
$\text{H}_2\text{Si}_2\text{O}_5$	0.5	Disilicic acid	$20 \times 10^{-4}$

<sup>(a)</sup> Number of mols  $\text{H}_2\text{O}$  per mol  $\text{SiO}_2$ , i.e.  $\text{SiO}_2 \cdot n\text{H}_2\text{O}$ .

<sup>39</sup> C. T. G. KNIGHT, *J. Chem. Soc., Dalton Trans.*, 1457–60 (1988).

<sup>40</sup> R. K. ILER, *The Chemistry of Silica: Solubility, Polymerization, Colloid and Surface Properties, and Biochemistry*, Wiley, New York, 1979, 866 pp.

determined<sup>(41)</sup> and various crystalline methyl and ethyl esters of cyclic silicic acids have been isolated.<sup>(42)</sup>

### 9.3.5 Silicate minerals<sup>(24,43,44)</sup>

The earth's crustal rocks and their breakdown products — the various soils, clays and sands — are composed almost entirely (~95%) of silicate minerals and silica. This predominance of silicates and aluminosilicates is reflected in the abundance of O, Si and Al, which are the commonest elements in the crust (p. 329). Despite the great profusion of structural types and the widely varying stoichiometries which are unmatched elsewhere in chemistry, it is possible to classify these structures on the basis of a few simple principles. Almost invariably Si is coordinated tetrahedrally by 4 oxygen atoms and these {SiO<sub>4</sub>} units can exist either as discrete structural entities or can combine by corner sharing of O atoms into larger units. The resulting O lattice is frequently close-packed, or approximately so, and charge balance is achieved by the presence of further cations in tetrahedral, octahedral, or other sites depending on their size. Typical examples are as follows (radii in pm):<sup>†</sup>

CN 4 : Li<sup>I</sup> (59) Be<sup>II</sup> (27) Al<sup>III</sup> (39) Si<sup>IV</sup> (26)  
 CN 6 : Na<sup>I</sup> (102) Mg<sup>II</sup> (72) Al<sup>III</sup> (54) Ti<sup>IV</sup> (61) Fe<sup>II</sup> (78)  
 CN 8 : K<sup>I</sup> (151) Ca<sup>II</sup> (112)  
 CN 12: K<sup>I</sup> (164)

The quoted radii, which in turn depend on the CN, are the empirical “effective ionic radii” deduced by R. D. Shannon (and C. T. Prewitt)<sup>(45)</sup> and do not imply full charge separation such as {Si<sup>4+</sup>(O<sup>2-</sup>)<sub>4</sub>}, etc. Note that Al<sup>III</sup> can occupy either 4- or 6-coordinate sites so that it can replace either Si or M in the lattice — this is particularly important in discussing the structures of the aluminosilicates. Several other cations can occupy sites of differing CN, e.g. Li (4 and 6), Na (6 and 8), K (6–12), though they are most commonly observed in the CN shown.

As with the borates (p. 205) and to a lesser extent the phosphates (p. 526), the {SiO<sub>4</sub>} units can build up into chains, multiple chains (or ribbons), rings, sheets and three-dimensional networks as summarized below and elaborated in the following paragraphs.

<i>Neso</i> -silicates	discrete {SiO <sub>4</sub> }	no O atoms shared
<i>soro</i> -silicates	discrete {Si <sub>2</sub> O <sub>7</sub> }	1 O atom shared
<i>cyclo</i> -silicates	closed ring structures continuous chains or ribbons	} 2 O atoms shared
<i>ino</i> -silicates		
<i>phyllo</i> -silicates	continuous sheets	3 O atoms shared
<i>tecto</i> -silicates	continuous 3D frameworks	all 4 O atoms shared

#### Silicates with discrete units

Discrete {SiO<sub>4</sub>} units occur in the orthosilicates M<sub>2</sub>SiO<sub>4</sub> (M = Be, Mg, Mn, Fe and Zn) and in ZrSiO<sub>4</sub> as well as in the synthetic orthosilicates Na<sub>4</sub>SiO<sub>4</sub> and K<sub>4</sub>SiO<sub>4</sub>.<sup>(46)</sup> In phenacite, Be<sub>2</sub>SiO<sub>4</sub>, both Be and Si occupy sites of CN 4 and the structure could equally well be described as a 3D network M<sub>3</sub>O<sub>4</sub>. When octahedral sites are occupied, isomorphous replacement of M<sup>II</sup> is often extensive as in olivine, (Mg,Fe,Mn)<sub>2</sub>SiO<sub>4</sub> which derives its name from its olive-green colour (Fe<sup>II</sup>). In zircon, ZrSiO<sub>4</sub>, the stoichiometry

<sup>45</sup> R. D. SHANNON, *Acta Cryst.* **A32**, 751–67 (1976).

<sup>46</sup> M. G. BARKER and P. G. GOOD, *J. Chem. Research (S)*, 1981, 274, and references cited therein.

<sup>41</sup> M. H. CHISHOLM, T. A. BUDZICHOWSKI, F. J. FEHER and J. W. ZILLER, *Polyhedron* **11**, 1575–9 (1992).

<sup>42</sup> H. C. MARSMANN and E. MEYER, *Z. anorg. allg. Chem.* **548**, 193–203 (1987).

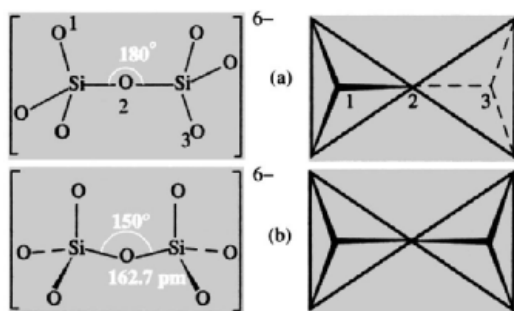
<sup>43</sup> W. A. DEER, R. A. HOWIE and J. ZUSSMAN, *An Introduction to the Rock-forming Minerals*, Longmans, London, 1966, 528 pp. B. MASON and L. G. BERRY, *Elements of Mineralogy*, W. H. Freeman, San Francisco, 1968, 550 pp.

<sup>44</sup> F. LIEBAU, Silicon, element 14, in K. H. WEDEPOHL (ed.), *Handbook of Geochemistry*, Vol. II–2, Chap. 14, Springer-Verlag, Berlin, 1978. F. LIEBAU, *Structural Chemistry of Silicates*, Springer-Verlag, Berlin, 1985, 347 pp.

<sup>†</sup> The metals which form silicate and aluminosilicate minerals are the more electropositive metals, i.e. those in Groups 1, 2 and the 3d transition series (except Co), together with Y, La and the lanthanoids, Zr, Hf, Th, U and to a much lesser extent the post-transition elements Sn<sup>II</sup>, Pb<sup>II</sup>, and Bi<sup>III</sup>.



of the crystal and the larger radius of Zr (84 pm) dictate eightfold coordination of the cation. Another important group of orthosilicates is the garnets,  $[M_3^{II}M_2^{III}(\text{SiO}_4)_3]$ , in which  $M^{II}$  are 8-coordinate (e.g. Ca, Mg, Fe) and  $M^{III}$  are 6-coordinate (e.g. Al, Cr, Fe).<sup>(47)</sup> Orthosilicates are also vital components of Portland cement (p. 252):  $\beta$ - $\text{Ca}_2\text{SiO}_4$  has discrete  $\{\text{SiO}_4\}$  groups with rather irregularly coordinated Ca in sixfold and eightfold environments (the  $\alpha$ -form has the  $\text{K}_2\text{SO}_4$  structure and the  $\gamma$ -form has the olivine structure). Again alite,  $\text{Ca}_3\text{SiO}_5$ , which is intimately involved in the “setting” process, has individual Ca,  $\{\text{SiO}_4\}$  and O as the structural units.



**Figure 9.4** (a) Two representations of the  $\{\text{Si}_2\text{O}_7\}$  unit in  $\text{Sc}_2\text{Si}_2\text{O}_7$ , showing the linear Si–O–Si link between the two tetrahedra and the  $D_{3d}$  (staggered) conformation, and (b) eclipsed ( $C_{2v}$ ) conformation of the  $\{\text{Si}_2\text{O}_7\}$  unit in hemimorphite,  $[\text{Zn}_4\text{Si}_2\text{O}_7(\text{OH})_2]\cdot\text{H}_2\text{O}$ .

Disilicates, containing the discrete  $\{\text{Si}_2\text{O}_7^{6-}\}$  unit, are rare. One example is the mineral thortveitite,  $\text{Sc}_2\text{Si}_2\text{O}_7$ , which features octahedral  $\text{Sc}^{III}$  ( $r$  75 pm) and a linear Si–O–Si bond between staggered tetrahedra (Fig. 9.4a). There is also a series of lanthanoid disilicates  $\text{Ln}_2\text{Si}_2\text{O}_7$  in which the Si–O–Si angle decreases progressively

from  $180^\circ$  to  $133^\circ$  and the CN of Ln increases from 6 through 7 to 8 as the size of Ln increases from 6-coordinated  $\text{Lu}^{III}$  (86 pm) to 8-coordinated  $\text{Nd}^{III}$  (111 pm). In the Zn mineral hemimorphite the angle is  $150^\circ$  but the conformation of the 2 tetrahedra is eclipsed ( $C_{2v}$ ) rather than staggered (Fig. 9.4b); the mineral was originally formulated as  $\text{Zn}_2\text{SiO}_4\cdot\text{H}_2\text{O}$  or  $\text{H}_2\text{Zn}_2\text{SiO}_5$ , but X-ray studies showed that the correct formula was  $[\text{Zn}_4(\text{OH})_2\text{Si}_2\text{O}_7]\cdot\text{H}_2\text{O}$ , i.e. “ $2\text{H}_2\text{Zn}_2\text{SiO}_5$ ”. Two further features of importance also emerged. The first was that there was no significant difference between the Si–O distances to “bridging” and “terminal” O atoms as would be expected for isolated  $\{\text{Si}_2\text{O}_7^{6-}\}$  groups, and the structure is best considered as a 3D framework of  $\{\text{ZnO}_3(\text{OH})\}$  and  $\{\text{SiO}_4\}$  tetrahedra linked in threes to form 6-atom rings  $\text{Zn}-\text{O}-\text{Si}-\text{O}-\text{Zn}-\text{OH}$ . The rings are linked into infinite sheets in the (010) planes which are themselves linked via  $\text{Zn}-\text{O}(\text{H})-\text{Zn}$  or  $\text{Si}-\text{O}-\text{Si}$  bonds. The 3D framework so generated leaves large channels which open into large cavities that accommodate the removable  $\text{H}_2\text{O}$  molecules. The structure is thus very similar in principle to that of the framework aluminosilicates (p. 354) and its conventional description in terms of discrete  $\text{Si}_2\text{O}_7^{6-}$  ions is rather misleading and uninformative.

Structures having triple tetrahedral units are extremely rare but they exist in aminoffite,  $\text{Ca}_3(\text{BeOH})_2(\text{Si}_3\text{O}_{10})$ , and kinoite,  $\text{Cu}_2\text{Ca}_2(\text{Si}_3\text{O}_{10})\cdot 2\text{H}_2\text{O}$ . The first chain-tetrasilicate,  $[\text{O}_3\text{Si}(\text{OSiO}_2)_2\text{OSiO}_3]^{10-}$ , was synthesized as recently as 1979.<sup>(48)</sup>  $\text{Ag}_{10}\text{Si}_4\text{O}_{13}$  was prepared as stable vermilion crystals by heating  $\text{Ag}_2\text{O}$  and  $\text{SiO}_2$  for 1–3 days at  $500\text{--}600^\circ\text{C}$  under a pressure of 2–4.5 kbar of  $\text{O}_2$ . At lower temperatures ( $<470^\circ\text{C}$ ) the bright red mixed silicate  $[\text{Ag}_{18}(\text{SiO}_4)_2(\text{Si}_4\text{O}_{13})]$  crystallizes.<sup>(49)</sup>

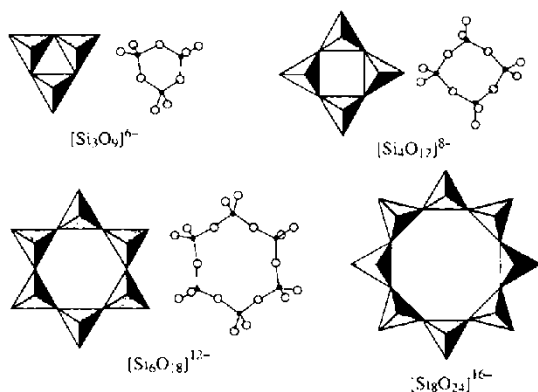
When every  $\{\text{SiO}_4\}$  shares 2 O with contiguous tetrahedra, metasilicates of empirical

<sup>47</sup> See p. 500 of ref. 24 for a description of the garnet structure which is also adopted by many synthetic and non-silicate compounds; these have been much studied recently because of their important optical and magnetic properties, e.g. ferrimagnetic yttrium iron garnet (YIG),  $\text{Y}_3^{III}\text{Fe}_2^{II}(\text{Al}^{III}\text{O}_4)_3$ .

<sup>48</sup> M. JANSEN and H.-L. KELLER, *Angew. Chem. Int. Edn. Engl.* **18**, 464 (1979).

<sup>49</sup> K. HEIDEBRECHT and M. JANSEN, *Z. anorg. allg. Chem.* **597**, 79–86 (1991).

formula  $\text{SiO}_3^{2-}$  are formed. Cyclic metasilicates  $\{(\text{SiO}_3)_n\}^{2n-}$  having 3, 4, 6 or 8 linked tetrahedra are known, though 3 and 6 are the most common. These anions are shown schematically in Fig. 9.5 and are exemplified by the mineral benitoite  $[\text{BaTi}\{\text{Si}_3\text{O}_9\}]$ , the synthetic compound  $[\text{K}_4\{\text{Si}_4\text{O}_8(\text{OH})_4\}]$ , and by beryl  $[\text{Be}_3\text{Al}_2\{\text{Si}_6\text{O}_{18}\}]$  (p. 107) and murite  $[\text{Ba}_{10}(\text{Ca}, \text{Mn}, \text{Ti})_4\{\text{Si}_8\text{O}_{24}\}(\text{Cl}, \text{OH}, \text{O})_{12}]\cdot 4\text{H}_2\text{O}$ .



**Figure 9.5** Schematic representations of the structures of cyclic metasilicate anions with  $n = 3, 4, 6,$  and  $8$ .

### Silicates with chain or ribbon structures

Chain metasilicates  $\{\text{SiO}_3^{2-}\}_\infty$  formed by corner-sharing of  $\{\text{SiO}_4\}$  tetrahedra are particularly prevalent in nature and many important minerals have this basic structural unit (cf. polyphosphates, p. 528). Despite the apparent simplicity of their structure motif and stoichiometry considerable structural diversity is encountered because of the differing conformations that can be adopted by the linked tetrahedra. As a result, the repeat distance along the  $c$ -axis can be (1), 2, 3, ..., 7, 9 or 12 tetrahedra (T), as illustrated schematically in Fig. 9.6. The most common conformation for metasilicates is a repeat after every second tetrahedron (2T) with the chains stacked parallel so as to provide sites of 6- or 8-coordination for the cations; e.g. the pyroxene minerals enstatite  $[\text{Mg}_2\text{Si}_2\text{O}_6]$ ,

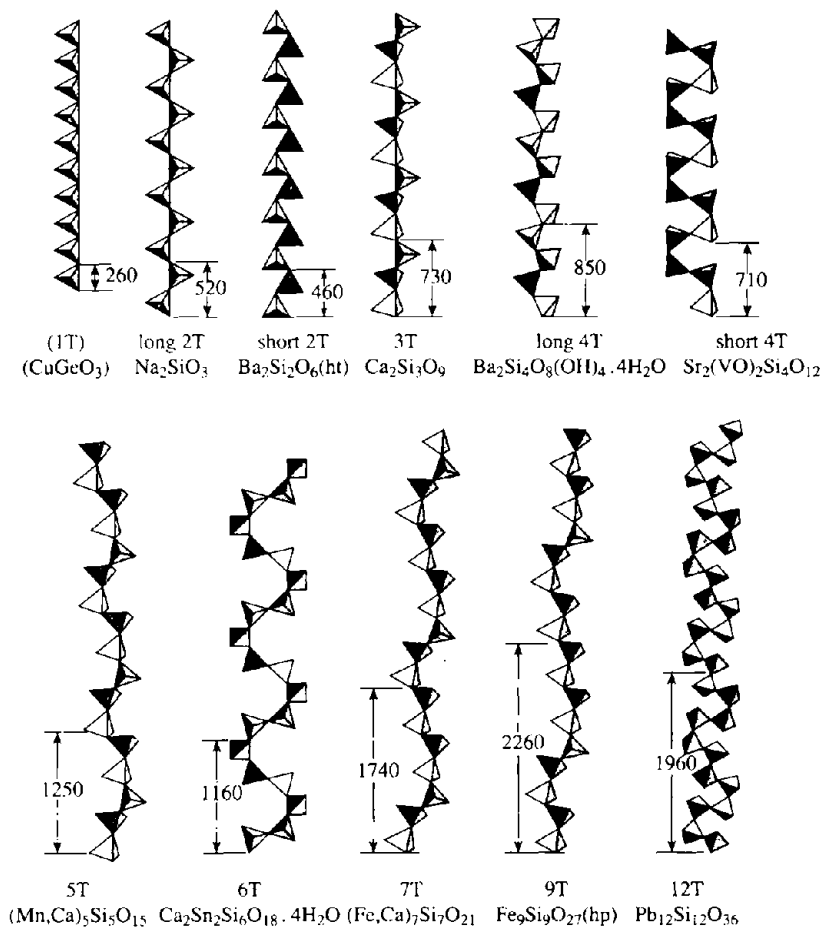
diopside  $[\text{CaMgSi}_2\text{O}_6]$ , jadeite  $[\text{NaAlSi}_2\text{O}_6]$ , and spodumene  $[\text{LiAlSi}_2\text{O}_6]$  (p. 69). The synthetic metasilicates  $\text{Li}_2\text{SiO}_3$  and  $\text{Na}_2\text{SiO}_3$  are similar; for the latter compound Si-O-Si is  $134^\circ$  and the Si-O distance is 167 pm within the chain and 159 pm for the other two O. The minerals wollastonite  $[\text{Ca}_3\text{Si}_3\text{O}_9]$  and pectolite  $[\text{Ca}_2\text{NaHSi}_3\text{O}_9]$  have a 3T repeat unit, haradaite  $[\text{Sr}_2(\text{VO})\text{Si}_4\text{O}_{12}]$  is 4T, rhodonite  $[\text{CaMn}_4\text{Si}_5\text{O}_{15}]$  has a 5T repeat, etc.<sup>(24,44)</sup>

In the next stage of structural complexity the single  $\{\text{SiO}_3^{2-}\}_\infty$  chains can link laterally to form double chains or ribbons whose stoichiometry depends on the repeat unit of the single chain (Fig. 9.7). By far the most numerous are the amphiboles or asbestos minerals which adopt the  $\{\text{Si}_4\text{O}_{11}^{6-}\}$  double chain, e.g. tremolite  $[\text{Ca}_2\text{Mg}_5(\text{Si}_4\text{O}_{11})_2(\text{OH})_2]$ ; the structure of this compound is very similar to that of diopside (above) except that the length of the  $b$ -axis of the unit cell is doubled. The fibrous nature of the asbestos minerals thus finds a ready interpretation on the basis of their crystal structures (see Panel on p. 351). In addition to these well-established double chains of linked  $\{\text{SiO}_4\}$  tetrahedra, examples of infinite one-dimensional structures consisting of linked triple, quadruple and even sextuple chains have been discovered in nephrite jade by means of electron microscopy,<sup>(50)</sup> and these form a satisfying link between the pyroxenes and amphiboles, on the one hand, and the sheet silicates (to be described in the next paragraph), on the other.

### Silicates with layer structures

Silicates with layer structures include some of the most familiar and important minerals known to man, particularly the clay minerals [such as kaolinite (china clay), montmorillonite (bentonite, fuller's earth), and vermiculite], the micas (e.g. muscovite, phlogopite, and biotite), and others such as chrysotile (white asbestos),

<sup>50</sup> L. G. MALLINSON, J. L. HUTCHINSON, D. A. JEFFERSON and J. M. THOMAS, *J. Chem. Soc., Chem. Commun.*, 910-11 (1977).



**Figure 9.6** Schematic representation and examples of various chain metasilicates  $\{\text{SiO}_3^{2-}\}_\infty$  with repeat distances (in pm) after 1, 2, ..., 7, 9 or 12 tetrahedra (T), [(ht) high-temperature form; (hp) high-pressure form].

talc, soapstone, and pyrophyllite. The physical and chemical properties of these minerals, which have made many of them so valued for domestic and industrial use for several milleniums (p. 328), can be directly related to the details of their crystal structure. The simplest silicate layer structure can be thought of as being formed either by the horizontal cross-linking of the 2T metasilicate chain  $\{\text{Si}_2\text{O}_6^{4-}\}$  in Fig. 9.6 or by the planar condensation of the  $\{\text{Si}_6\text{O}_{18}^{12-}\}$  unit in Fig. 9.5 to give a 6T network of composition  $\{\text{Si}_2\text{O}_5^{2-}\}$  in which 3 of the 4 O atoms in each tetrahedron are shared; this is shown in both plan and elevation in Fig. 9.8. In fact, such a

structure with a completely planar arrangement is extremely rare though closely related puckered 6T networks are found in  $\text{M}_2\text{Si}_2\text{O}_5$  ( $\text{M}=\text{Li, Na, Ag, H}$ ) and in petalite ( $\text{LiAlSi}_4\text{O}_{10}$ , p. 69). More complex arrangements are also found in which the 6T rings forming the network are replaced by alternate 4T and 8T rings, or by equal numbers of 4T, 6T, and 8T rings, or even by a network of 4T, 6T and 12T rings.<sup>(24,44)</sup>

Double layers can be generated by sharing the fourth (apical) O atom between pairs of tetrahedra as in Fig. 9.9(a). This would give a stoichiometry  $\text{SiO}_2$  (since each O atom is shared between 2 Si atoms) but if half the  $\text{Si}^{\text{IV}}$  were replaced by

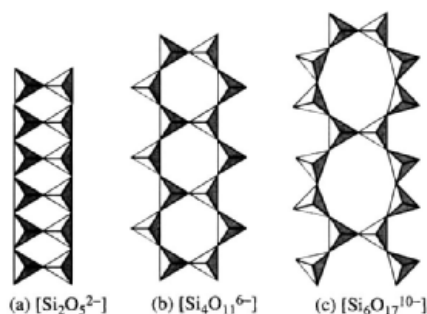
### Production and Uses of Asbestos

The fibrous silicate minerals known collectively as asbestos (Greek *ἀσβεστος*, unquenchable) have been used both in Europe and the Far East for thousands of years. In ancient Rome the wicks of the lamps of the vestal virgins were woven from asbestos, and Charlemagne astounded his barbarian guests by throwing the festive table cloth into the fire whence, being woven asbestos, it emerged cleansed and unburnt. Its use has accelerated during the past 100 y and it is now an important ingredient in over 3000 different products. Its desirable characteristics are high tensile strength, great flexibility, resistance both to heat and flame and also to corrosion by acids or alkalis, good thermal insulation properties and low cost.

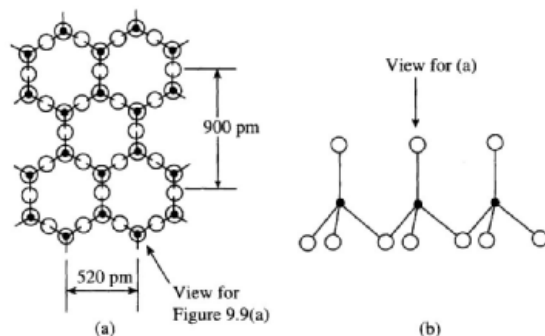
Asbestos is derived from two large groups of rock-forming minerals — the serpentines and the amphiboles. Chrysotile, or white asbestos  $[\text{Mg}_3(\text{Si}_2\text{O}_5)(\text{OH})_4]$ , is the sole representative of the serpentine layer silicate group (p. 352) but is by far the most abundant kind of asbestos and constitutes more than 98% of world production. The amphibole group includes the blue asbestos mineral crocidolite  $[\text{Na}_2\text{Fe}_3^{\text{II}}\text{Fe}_2^{\text{III}}\text{Si}_8\text{O}_{22}(\text{OH})_2]$  (<1% of world production) and the grey-brown mineral amosite  $[(\text{Mg},\text{Fe})_7\text{Si}_8\text{O}_{22}(\text{OH})_2]$  (<1%). Annual production in 1989 was 4.3 million tonnes having fallen from a maximum of 5 Mt in 1979.<sup>(51)</sup> The main producing countries are Russia (55%), Canada (20%), South Africa (4.7%) and Zimbabwe, China, Italy and Brazil (3–4% each).

Asbestos-reinforced cements (~12.5% asbestos) absorb nearly two-thirds of the world's annual production of chrysotile: it is used in corrugated and flat roofing sheets, pressure pipes and ducts, and many other hard-wearing, weather-proof, long-lasting products. About 8% is used in asbestos papers and a further 7% is used for making vinyl floor tiles. Other important uses include composites for brake linings, clutch facings, and other friction products. Long-fibred chrysotile (fibre length >20 μm) is woven into asbestos textiles for fire-fighting garments and numerous fire-proofing and insulating applications.

Prolonged exposure to airborne suspensions of asbestos fibre dust can be very dangerous and there has been increasing concern at the incidence of asbestosis (non-malignant scarring of lung tissue) and lung carcinoma among certain workers in the industry. Unfortunately, there is an extended latent period (typically 20–30 y) before these diseases are manifest. Stringent precautions are now enforced in many countries and the incidence of the disease appears to be falling steadily. There is also general (though not universal) agreement that white asbestos (chrysotile), which is the overwhelmingly predominant type of asbestos in use, is not implicated in the incidence of asbestosis and lung carcinoma which seems to be confined mainly (perhaps exclusively) to the blue crocidolite and brown amosite amphibole varieties. Asbestosis is dose-related and the best form of control is to reduce the level of dust exposure in places where the mineral is mined, processed or fabricated.



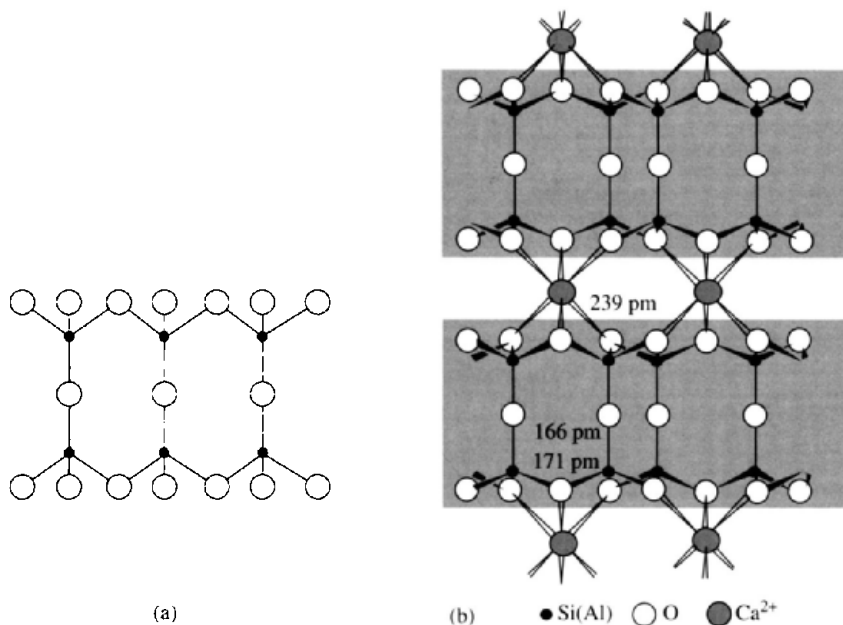
**Figure 9.7** Double chains of  $\{\text{SiO}_4\}$  tetrahedra: (a) the double chain based on the 1T metasilicate structure, stoichiometry  $[\text{Si}_2\text{O}_5]^{2-}$  — it is found in the aluminosilicate sillimanite  $[\text{Al}(\text{AlSiO}_5)]$ ; (b)  $[\text{Si}_4\text{O}_{11}]^{6-}$  chain based on the 2T metasilicate occurs in the amphiboles (see text); and (c) the rare 3T double chain  $\text{Si}_6\text{O}_{17}^{10-}$  occurs in xonotlite  $[\text{Ca}_6\text{Si}_6\text{O}_{17}(\text{OH})_2]$ . More complex 3T, 4T and 6T double chains are also known.<sup>(44)</sup>



**Figure 9.8** Planar network formed by extended 2D condensation of rings of 6  $\{\text{SiO}_4\}$  tetrahedra to give  $[\text{Si}_2\text{O}_5]^{2-}$ . (a) Plan as seen looking down the O–Si direction, and (b) side elevation.

$\text{Al}^{\text{III}}$  then the composition would be  $[\text{Al}_2\text{Si}_2\text{O}_8]^{2-}$  as found in  $\text{Ca}_2\text{Al}_2\text{Si}_2\text{O}_8$  and  $\text{Ba}_2\text{Al}_2\text{Si}_2\text{O}_8$  (Fig. 9.9b). Another way of building up double layers involves the interleaving of layers of the

<sup>51</sup> Reference 1, 4th edn., Asbestos 3, 659–88 (1992).

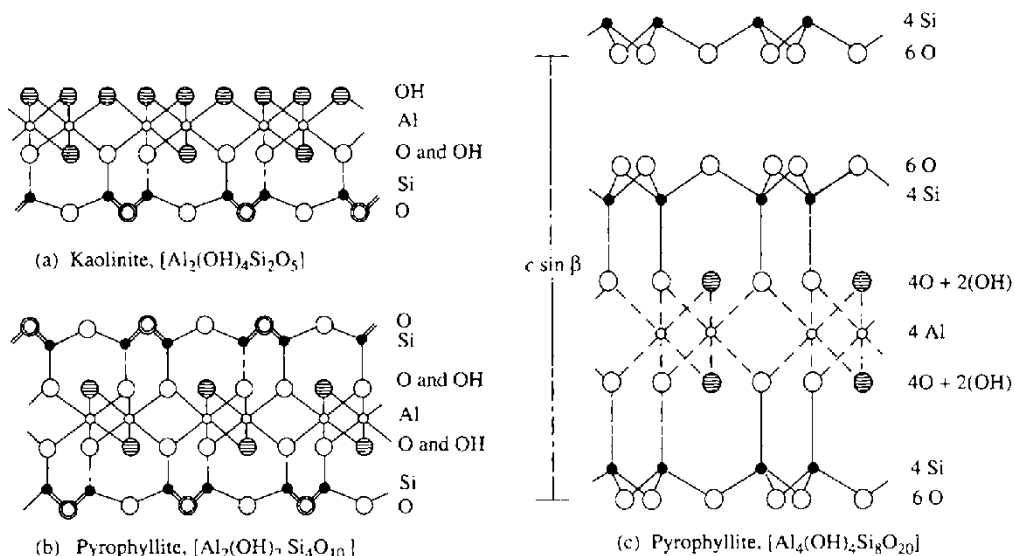


**Figure 9.9** (a) Side elevation of double layers of formula  $\{\text{Al}_2\text{Si}_2\text{O}_8^{2-}\}$  formed by sharing the fourth (apical) O in Fig. 9.9(b). Sites marked ● are occupied by equal numbers of Al and Si atoms. (b) Structure of  $\text{Ca}_2\text{Al}_2\text{Si}_2\text{O}_8$  formed by interleaving 6-coordinated  $\text{Ca}^{II}$  atoms between the double layers depicted in (a).

gibbsite  $\text{Al}(\text{OH})_3$  or brucite  $\text{Mg}(\text{OH})_2$  structure (pp. 243–5, 121) which happen to have closely similar dimensions and can thus share O atoms with the silicate network. This leads to the china-clay mineral kaolinite  $[\text{Al}_2(\text{OH})_4\text{Si}_2\text{O}_5]$  illustrated in Figs. 9.10(a) and 9.11(a). [The mineral was so-named in 1867 from “kaolin”, a corruption of the Chinese *kauling*, or high-ridge, the name of the hill where this china clay was found some 300 miles north of Hong Kong.]

Repetition of the process on the other side of the Al/O layer leads to the structure of pyrophyllite  $[\text{Al}_2(\text{OH})_2\text{Si}_4\text{O}_{10}]$  (Fig. 9.10b,c). Replacement of  $2\text{Al}^{III}$  by  $3\text{Mg}^{II}$  in kaolinite  $[\text{Al}_2(\text{OH})_4\text{Si}_2\text{O}_5]$  gives the serpentine asbestos mineral chrysotile  $[\text{Mg}_3(\text{OH})_4\text{Si}_2\text{O}_5]$  and a similar replacement in pyrophyllite gives talc  $[\text{Mg}_3(\text{OH})_2\text{Si}_4\text{O}_{10}]$ . The gibbsite series is sometimes called dioctahedral and the brucite series trioctahedral in obvious reference to the number of octahedral sites occupied in the “non-silicate” layer.

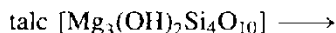
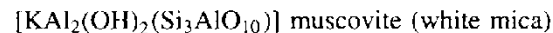
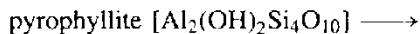
Alternative representations of the structures are given in Fig. 9.11, and it is well worth while looking carefully at these various diagrams since they have the pleasing property of becoming simpler and easier to understand the longer they are contemplated. It should be stressed that the formulae given are ideal limiting compositions and that  $\text{Al}^{III}$  or  $\text{Mg}^{II}$  can be replaced by several other cations of appropriate size. The stoichiometry is further complicated by the possibility that  $\text{Si}^{IV}$  can be partly replaced by  $\text{Al}^{III}$  in the tetrahedral sites thereby giving rise to charged layers. These layers can be interleaved with  $\text{M}^I$  or  $\text{M}^{II}$  cations to give the micas or by layers of hydrated cations to give montmorillonite. Alternatively, charge balance can be achieved by interleaving positively charged  $(\text{Mg},\text{Al})(\text{OH})_2$  layers as in the chlorites. These possibilities are shown schematically in Figs. 9.12 and 9.13 (p. 355) and elaborated in the following paragraphs.



**Figure 9.10** (a) Schematic representation of the structure of kaolinite (side elevation) showing  $[\text{SiO}_3\text{O}]$  tetrahedra (bottom) sharing common O atoms with  $[\text{Al}(\text{OH})_2\text{O}]$  to give a composite layer of formula  $[\text{Al}_2(\text{OH})_4\text{Si}_2\text{O}_5]$ . The double lines and double circles in the tetrahedra indicate bonds to 2 O atoms (one in front and one behind). (b) Similar representation of the structure of pyrophyllite, showing shared  $[\text{SiO}_3\text{O}]$  tetrahedra above and below the  $[\text{Al}(\text{OH})_2\text{O}]$  layer to give a composite layer of formula  $[\text{Al}_2(\text{OH})_2\text{Si}_4\text{O}_{10}]$ . (c) Alternative representation of pyrophyllite to be compared with (b), and showing the stoichiometry of each layer.

The technological importance of the clay minerals is outlined in the Panel on p. 356.

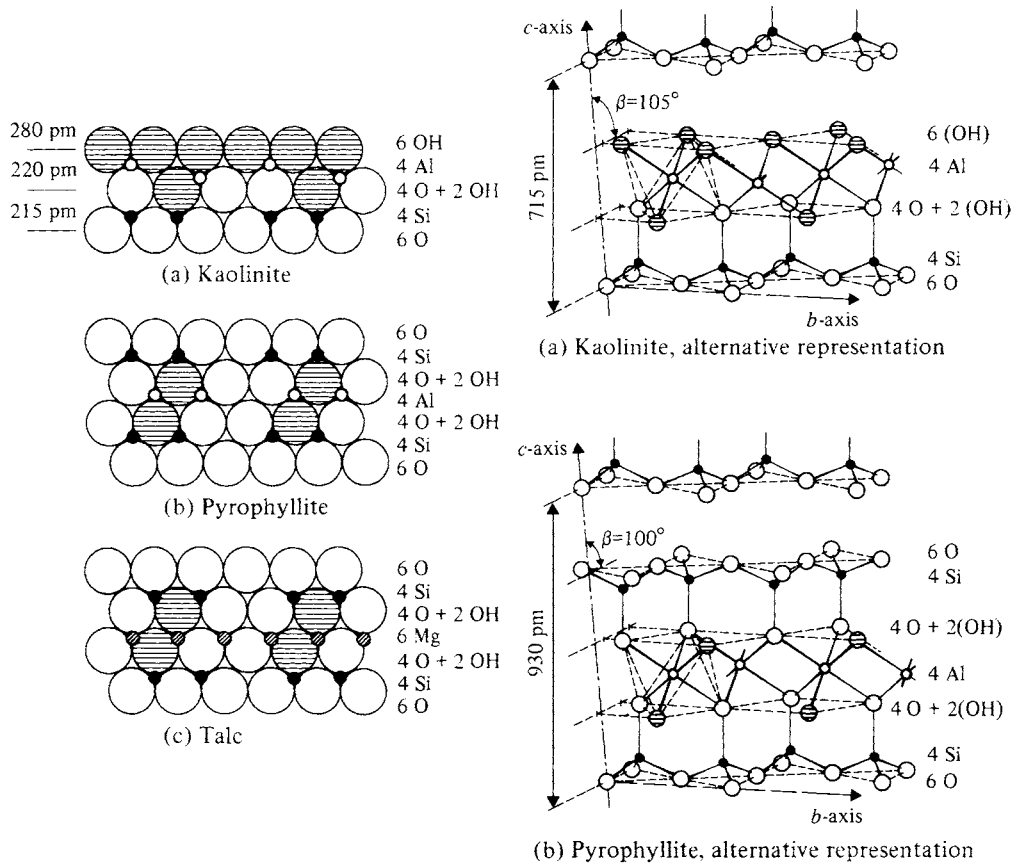
Micas are formed when one-quarter of the  $\text{Si}^{\text{IV}}$  in pyrophyllite and talc are replaced by  $\text{Al}^{\text{III}}$  and the resulting negative charge is balanced by  $\text{K}^{\text{I}}$ :



The OH can be partly replaced by F and, in phlogopite, partial replacement of  $\text{Mg}^{\text{II}}$  by  $\text{Fe}^{\text{II}}$  gives biotite (black mica)  $[\text{K}(\text{Mg},\text{Fe})_3(\text{OH},\text{F})_2(\text{Si}_3\text{AlO}_{10})]$ . The presence of  $\text{K}^{\text{I}}$  between the layers makes the micas appreciably harder than pyrophyllite and talc but the layers are still a source of weakness and micas show perfect cleavage parallel to the layers. With further

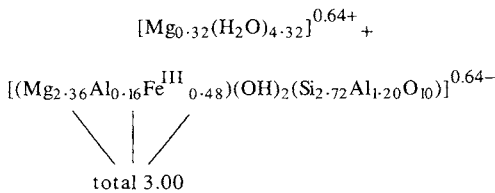
substitution of up to half the Si by Al charge balance can be restored by the more highly charged  $\text{Ca}^{\text{II}}$  and brittle micas result, such as margarite  $[\text{CaAl}_2(\text{OH})_2(\text{Si}_2\text{Al}_2\text{O}_{10})]$  which is even harder than muscovite.

Another set of minerals, the montmorillonites, result if, instead of replacing tetrahedral  $\text{Si}^{\text{IV}}$  by  $\text{Al}^{\text{III}}$  in phlogopite, the octahedral  $\text{Al}^{\text{III}}$  is *partially* replaced by  $\text{Mg}^{\text{II}}$  (not *completely* as in talc). The resulting partial negative charge per unit formula can be balanced by incorporating hydrated  $\text{M}^{\text{I}}$  or  $\text{M}^{\text{II}}$  between the layers; this leads to the characteristic swelling, cation exchange and thixotropy of these minerals (see Panel, p. 356). A typical sodium montmorillonite might be formulated  $\text{Na}_{0.33}[\text{Mg}_{0.33}\text{Al}_{1.67}(\text{OH})_2(\text{Si}_4\text{O}_{10})].n\text{H}_2\text{O}$ , but more generally they can be written as  $\text{M}_x[(\text{Mg},\text{Al},\text{Fe})_2(\text{OH})_2(\text{Si}_4\text{O}_{10})].n\text{H}_2\text{O}$  where  $\text{M} = \text{H}, \text{Na}, \text{K}, \frac{1}{2}\text{Mg}$  or  $\frac{1}{2}\text{Ca}$ . Simultaneous aliovalent substitution in both the octahedral and tetrahedral sites in talc leads to the vermiculites



**Figure 9.11** Alternative representations of the layer structures of (a) kaolinite, (b) pyrophyllite, and (c) talc. (After H. J. Emeléus and J. S. Anderson, 1960 and B. Mason and L. G. Berry, 1968.)

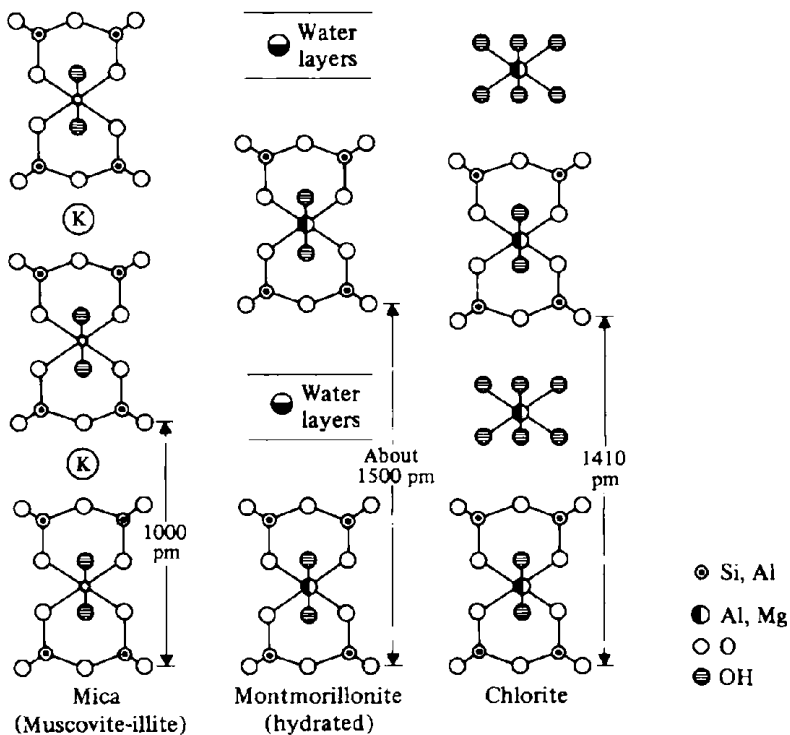
of which a typical formula is



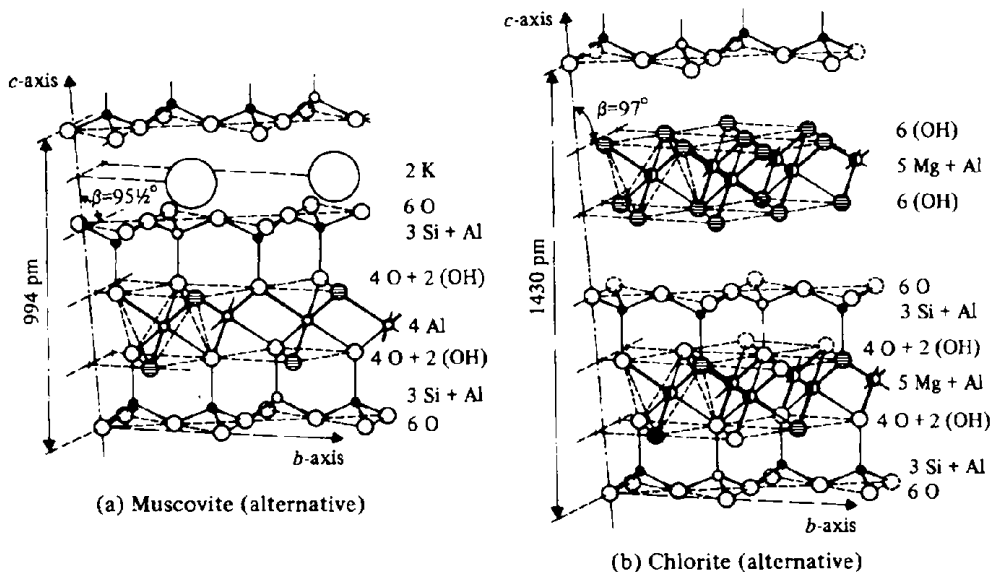
When these minerals are heated they dehydrate in a remarkable way by extruding little worm-like structures as indicated by their name (Latin *vermiculus*, little worm); the resulting porous light-weight mass is much used for packing and insulation. The relationship between the various layer silicates is summarized with idealized formulae in Table 9.10 (on page 357).

### Silicates with framework structures

The structural complexity of the 3D framework aluminosilicates precludes a detailed treatment here, but many of the minerals are of paramount importance. The group includes the feldspars (which are the most abundant of all minerals, and comprise ~60% of the earth's crust), the zeolites (which find major applications as molecular sieves, desiccants, ion exchangers and water softeners), and the ultramarines which, as their name implies, often have an intense blue colour. All are constructed from SiO<sub>4</sub> units in which each O atom is shared by 2 tetrahedra (as in the various forms of SiO<sub>2</sub> itself), but up to one-half of the Si



**Figure 9.12** Schematic representation of the structures of muscovite mica,  $[K_2Al_4(Si_6Al_2)O_{20}(OH)_4]$ , hydrated montmorillonite,  $[Al_4Si_8O_{20}(OH)_4] \cdot xH_2O$  and chlorite,  $[Mg_{10}Al_2(Si_6Al_2)O_{20}(OH)_{16}]$ , see text.

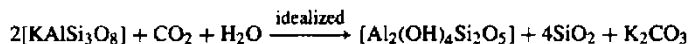


**Figure 9.13** Alternative representations of muscovite and chlorite (after B. Mason and L. G. Berry<sup>(43)</sup>).



### Clay Minerals and Related Aluminosilicates<sup>(1,52)</sup>

Clays are an essential component of soils, to which we owe our survival, and they are also the raw materials for some of mankind's most ancient and essential artefacts: pottery, bricks, tiles, etc. Clays are formed by the weathering and decomposition of igneous rocks and occur typically as very fine particles: e.g. kaolinite is formed as hexagonal plates of edge  $\sim 0.1\text{--}3\ \mu\text{m}$  by the weathering of alkaline feldspar:



When mixed with water, clays become soft, plastic and mouldable; the water of plasticity can be removed at  $\sim 100^\circ$  and the clay then becomes rigid and brittle. Further heating ( $\sim 500^\circ$ ) removes structural water of crystallization and results in the oxidation of any carbonaceous material or  $\text{Fe}^{\text{II}}$  ( $600\text{--}900^\circ$ ). Above about  $950^\circ$  mullite ( $\text{Al}_6\text{Si}_2\text{O}_{13}$ ) begins to form and glassy phases appear. Common clay is mined on a huge scale (28 million tonnes in USA alone in 1991) and is used principally in the manufacture of bricks (12 Mt), portland cement (10 Mt) and concrete (2.4 Mt), as well as for paper filling and coating (3.7 Mt).

China clay or kaolin, which is predominantly kaolinite, is particularly valuable because it is essentially free from iron impurities (and therefore colourless). World production in 1991 was 24.7 Mt (USA 39%, UK 13%, Colombia, Korea and USSR  $\sim 7\%$  each). In the USA over half of this vast tonnage is used for paper filling or paper coating and only 130 000 tonnes was used for china, crockery, and earthenware, which is now usually made from ball clay, a particularly fine-grained, highly plastic material which is predominantly kaolinite together with clay-mica and quartz. Some 800 000 tonnes of ball clay is used annually in the USA for white ware, table ware, wall and floor tiles, sanitary ware, and electrical porcelain.

Fuller's earth is a montmorillonite in which the principal exchangeable cation is calcium. It has a high absorbance and adsorptive capacity, and pronounced cation exchange properties which enable it to be converted to sodium-montmorillonite (bentonite). Nomenclature is confusing and, in American usage, the fibrous hydrated magnesium aluminosilicate attapulgite is also called fuller's earth. World production (1991) was 4.0 million tonnes (USA 68%, Germany 19%, UK 5%). Of the 2.74 Mt produced in the USA, two-thirds was used for what government statisticians coyly call "pet absorbant" and about one-eighth was for oil and grease absorbance.

Bentonite (sodium-montmorillonite) is extensively used as a drilling mud, but this apparently mundane application is based on the astonishing thixotropic properties of its aqueous suspensions. Thus, replacement of Ca by Na in the montmorillonite greatly enhances its ability to swell in one dimension by the reversible uptake of water; this effectively cleaves the clay particles causing a separation of the lamellar units to give a suspension of very finely divided, exceedingly thin plates. These plate-like particles have negative charges on the surface and positive charges on the edges and, even in a suspension of quite low solid content, the particles orient themselves negative to positive to give a jelly-like mass or gel; on agitation, however, the weak electrical bonds are broken and the dispersion becomes a fluid whose viscosity diminishes with the extent of agitation. This indefinitely reversible property is called thixotropy and is widely used in civil engineering applications, in oil-well drilling, and in non-drip paints. The plasticity of bentonite is also used in mortars, putties, and adhesives, in the pelletizing of iron ore and in foundry sands. World production was 9.3 Mt in 1991 (USA 37%, USSR 26% Greece 11%).

Micas occur as a late crystallization phase in igneous rocks. Usually the crystals are 1–5 mm on edge but in pegmatites (p. 108) they may considerably exceed this to give the valuable block mica. Uses of muscovite mica depend on its perfect basal cleavage, toughness, elasticity, transparency, high dielectric strength, chemical inertness and thermal stability to  $500^\circ$ . Phlogopite (Mg-mica) is less used except when stability to  $850\text{--}1000^\circ$  is required. Sheet mica is used for furnace windows, for electrical insulation (condensers, heating elements, etc.) and in vacuum tubes. Ground mica is used as a filler for rubber, plastics and insulating board, for silver glitter paints, etc. World production (excluding China) was  $\sim 240\ 000$  tonnes in 1974 (USA 53%, India 20%, USSR 17%).

Talc, unlike the micas, consists of electrically neutral layers without the interleaving cations. It is valued for its softness, smoothness and dry lubricating properties, and for its whiteness, chemical inertness and foliated structure. Its most important applications are in ceramics, insecticides, paints and paper manufacture. The more familiar use in cosmetics and toilet preparations accounts for only 3% of world production which is about 5 Mt per annum. Half of this comes from Japan and the USA, and other major producers are Korea, the former Soviet Union, France and China. Talc and its more massive mineral form soapstone or steatite are widely distributed throughout the world and many countries produce it for domestic consumption either by open-cast or underground mining.

atoms have been replaced by Al, thus requiring the addition of further cations for charge-balance.

Most feldspars can be classified chemically as members of the ternary system  $\text{NaAlSi}_3\text{O}_8\text{--KAlSi}_3\text{O}_8\text{--CaAl}_2\text{Si}_2\text{O}_8$ . This is illustrated in Fig. 9.14, which also indicates the names of the mineral phases. Particularly notable

<sup>52</sup> *Minerals Yearbook Vol. 1, 1991*, US Dept of the Interior, Bureau of Mines, Washington DC, pp. 403–45 (1991).

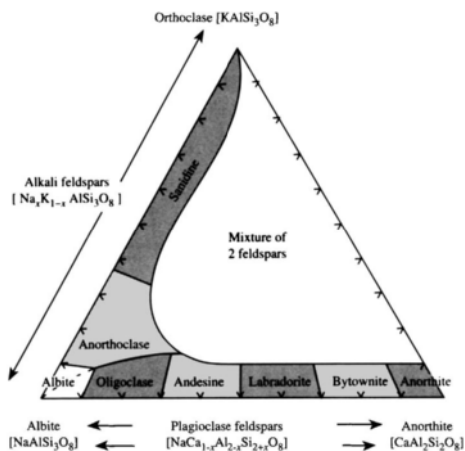
**Table 9.10** Summary of layer silicate structures (idealized formulae)<sup>(44)</sup>

Di octahedral (with gibbsite-type layers)	Tri octahedral (with brucite-type layers)
<i>Two-layer structures</i>	
Kaolinite, nacrite, dickite [Al <sub>4</sub> (OH) <sub>8</sub> (Si <sub>4</sub> O <sub>10</sub> )]	Antigorite (platy serpentine) [Mg <sub>6</sub> (OH) <sub>8</sub> (Si <sub>4</sub> O <sub>10</sub> )]
Halloysite [Al <sub>4</sub> (OH) <sub>8</sub> (Si <sub>4</sub> O <sub>10</sub> )]	Chrysotile (fibrous serpentine) [Mg <sub>6</sub> (OH) <sub>8</sub> (Si <sub>4</sub> O <sub>10</sub> )]
<i>Three-layer structures</i>	
Pyrophyllite [Al <sub>2</sub> (OH) <sub>2</sub> (Si <sub>4</sub> O <sub>10</sub> )]	Talc [Mg <sub>3</sub> (OH) <sub>2</sub> (Si <sub>4</sub> O <sub>10</sub> )]
Montmorillonite [Al <sub>2</sub> (OH) <sub>2</sub> (Si <sub>4</sub> O <sub>10</sub> ).xH <sub>2</sub> O <sup>(a)</sup> ]	Vermiculite [Mg <sub>3</sub> (OH) <sub>2</sub> (Si <sub>4</sub> O <sub>10</sub> ).xH <sub>2</sub> O <sup>(b)</sup> ]
Muscovite (mica) [KAl <sub>2</sub> (OH) <sub>2</sub> (AlSi <sub>3</sub> O <sub>10</sub> )]	Phlogopite (mica) [KMg <sub>3</sub> (OH) <sub>2</sub> (AlSi <sub>3</sub> O <sub>10</sub> )]
Margarite (brittle mica) [CaAl <sub>2</sub> (OH) <sub>2</sub> (Al <sub>2</sub> Si <sub>2</sub> O <sub>10</sub> )]	Clintonite [CaMg <sub>3</sub> (OH) <sub>2</sub> (Al <sub>2</sub> Si <sub>2</sub> O <sub>10</sub> )]
	Chlorite [Mg <sub>5</sub> Al(OH) <sub>8</sub> (AlSi <sub>3</sub> O <sub>10</sub> )] <sup>(c)</sup>

(a) With partial replacement of octahedral Al by Mg and with adsorbed cations.

(b) With partial replacement of octahedral Mg by Al and with adsorbed cations.

(c) That is, regularly alternating talc-like and brucite-like sheets.



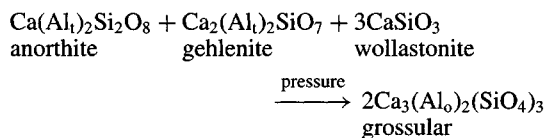
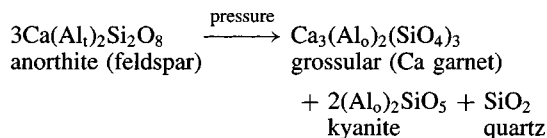
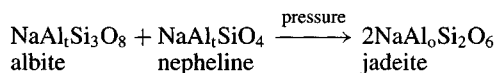
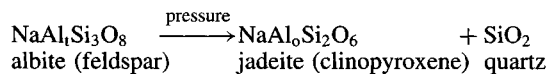
**Figure 9.14** Ternary phase diagram for feldspars. The precise positions of the various phase boundaries depend on the temperature of formation.

is the continuous plagioclase series in which Na<sup>I</sup> (102 pm) is replaced by Ca<sup>II</sup> (100 pm) on octahedral sites, the charge-balance being maintained by a simultaneous substitution of Al<sup>III</sup> for Si<sup>IV</sup> on the tetrahedral sites. K<sup>I</sup> (138 pm)

is too disparate in size to substitute for Ca<sup>II</sup> and 2-phase mixtures result, though orthoclase does form a continuous series of solid solutions with the Ba feldspar celsian [BaAl<sub>2</sub>Si<sub>2</sub>O<sub>8</sub>] (Ba<sup>II</sup> 136 pm). Likewise, most of the alkaline feldspars are not homogeneous but tend to contain separate K-rich and Na-rich phases unless they have crystallized rapidly from solid solutions at high temperatures (above ~600°). Feldspars have tightly constructed aluminosilicate frameworks that generate large interstices in which the large M<sup>I</sup> or M<sup>II</sup> are accommodated in irregular coordination.<sup>(43)</sup> Smaller cations, which are common in the chain and sheet silicates (e.g. Li<sup>I</sup>, Mg<sup>II</sup>, Fe<sup>III</sup>), do not occur as major constituents in feldspars presumably because they are unable to fill the interstices adequately.

Pressure is another important variable in the formation of feldspars and at sufficiently high pressures there is a tendency for Al to increase its coordination number from 4 to 6 with consequent destruction of the feldspar lattice.<sup>†</sup> For example:

<sup>†</sup> In some compounds of course, octahedrally coordinated Al is stable at normal atmospheric pressure, e.g. in Al<sub>2</sub>O<sub>3</sub>,



Such reactions marking the disappearance of plagioclase feldspars may be responsible for the Mohorovicic discontinuity between the earth's crust and mantle: this implies that the crust and mantle are isocompositional, the crustal rocks above having phases characteristic of gabbro rock (olivine, pyroxene, plagioclase) whilst the mantle rocks below are an eclogite-containing garnet, Al-rich pyroxene and quartz. Not all geochemists agree, however.

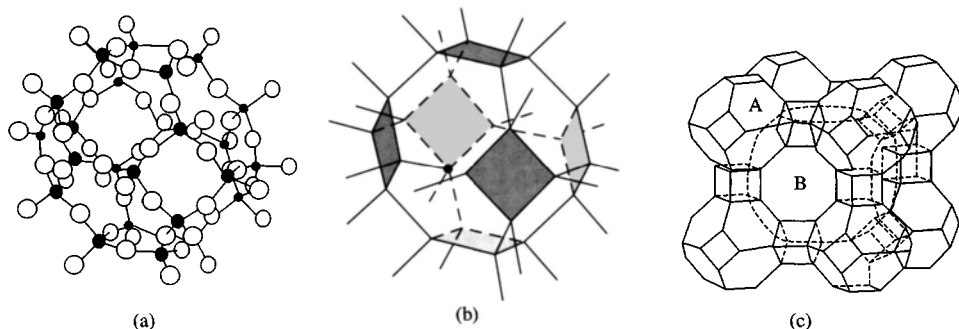
Zeolites have much more open aluminosilicate frameworks than feldspars and this enables them to take up loosely bound water or other small molecules in their structure. Indeed, the name zeolite was coined by the mineralogist

$\text{Al}(\text{OH})_3$ , and spinels such as  $\text{MgAl}_2\text{O}_4$ . Much higher pressures still are required to transform 4-coordinated Si to 6-coordinated (p. 343).

A. F. Cronstedt in 1756 ( $\zeta\epsilon\text{iv}$  *zein*, to boil;  $\lambda\text{it}\theta\sigma\varsigma$  *lithos*, stone) because the mineral appeared to boil when heated in the blow-pipe flame. Zeolite structures are characterized by the presence of tunnels or systems of interconnected cavities; these can be linked either in one direction giving fibrous crystals, or more usually in two or three directions to give lamellar and 3D structures respectively. Figure 9.15a shows the construction of a single cavity from 24 linked  $\{\text{SiO}_4\}$  tetrahedra and Fig. 9.15b shows how this can be conventionally represented by a truncated cubo-octahedron formed by joining the Si atom positions. Several other types of polyhedron have also been observed. These are then linked in three dimensions to build the aluminosilicate framework. A typical structure is shown in Fig. 9.15c for the synthetic zeolite "Linde A" which has the formula  $[\text{Na}_{12}(\text{Al}_{12}\text{Si}_{12}\text{O}_{48})]\cdot 27\text{H}_2\text{O}$ .<sup>(53)</sup> Other cavity frameworks are found in other zeolites such as faujasite, which has the idealized formula  $[\text{NaCa}_{0.5}(\text{Al}_2\text{Si}_5\text{O}_{14})]\cdot 10\text{H}_2\text{O}$ , and chabazite  $[\text{Ca}(\text{Al}_2\text{Si}_4\text{O}_{12})]\cdot 6\text{H}_2\text{O}$ . There is great current interest in this field since it offers scope for the reproducible synthesis of structures having cavities, tunnels and pores of precisely defined dimensions on the atomic scale.<sup>(54)</sup> By

<sup>53</sup> J. M. THOMAS, L. A. BURSILL, E. A. LODGE, A. K. CHEETHAM and C. A. FYFE, *J. Chem. Soc., Chem. Commun.*, 276-7 (1981).

<sup>54</sup> G. GOTTARD and E. GALLI, *Natural Zeolites*, Springer-Verlag, Berlin, 1985, 400 pp. P. A. JACOBS and



**Figure 9.15** (a) 24  $\{\text{SiO}_4\}$  tetrahedra linked by corner sharing to form a framework surrounding a truncated cubo-octahedral cavity; (b) conventional representation of the polyhedron in (a); and (c) space-filling arrangement of the polyhedra A which also generates larger cavities B.

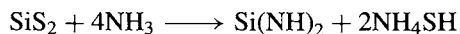
appropriate design such molecular sieves can be used to selectively remove water or other small molecules, to separate normal from branched-chain paraffins, to generate highly dispersed metal catalysts, and to promote specific size-dependent chemical reactions.<sup>(55)</sup> Zeolites are made commercially by crystallizing aqueous gels of mixed alkaline silicates and aluminates at 60–100°. Zeolite-A is being increasingly used as a detergent builder to replace sodium tripolyphosphate (p. 528).

The final group of framework aluminosilicates are the ultramarines which have alternate Si and Al atoms at the corners of the polyhedra shown in Fig. 9.15a and b and, in addition, contain substantial concentrations of anions such as  $\text{Cl}^-$ ,  $\text{SO}_4^{2-}$  or  $\text{S}_2^{2-}$ . These minerals tend to be anhydrous, like the feldspars, and in contrast to the even more open zeolites. Examples are sodalite  $[\text{Na}_8\text{Cl}_2(\text{Al}_6\text{Si}_6\text{O}_{24})]$ , noselite  $[\text{Na}_8(\text{SO}_4)(\text{Al}_6\text{Si}_6\text{O}_{24})]$  and ultramarine  $[\text{Na}_8(\text{S}_2)(\text{Al}_6\text{Si}_6\text{O}_{24})]$ . Sodalite is colourless if the supernumerary anions are all chloride, but partial replacement by sulfide gives the brilliant blue mineral lapis lazuli. Further replacement gives ultramarine which is now manufactured synthetically as an important blue pigment for oil-based paints and porcelain, and as a “blueing” agent to mask yellow tints in domestic washing,

paper making, starch, etc.<sup>†</sup> The colour is due to the presence of the sulfur radical anions  $\text{S}_2^-$  and  $\text{S}_3^-$  and shifts from green to blue as the ratio  $\text{S}_3^-/\text{S}_2^-$  increases; in ultramarine red the predominant species may be the neutral  $\text{S}_4$  molecule though  $\text{S}_3^-$  and  $\text{S}_2^-$  are also present.<sup>(56)</sup>

### 9.3.6 Other inorganic compounds of silicon

This section briefly considers compounds in which Si is bonded to elements other than hydrogen, the halogens or oxygen, especially compounds in which Si is bonded to S, N or P. Silicon burns in S vapour at 100° to give  $\text{SiS}_2$  which can be sublimed in a stream of  $\text{N}_2$  to give long, white, flexible, asbestos-like fibres, mp 1090°, sublimation 1250°C. The structure consists of infinite chains of edge-shared tetrahedra (like W-silica, p. 343) and these transform at high temperature and pressure to a (corner-shared) cristobalite modification. The structural complexity of  $\text{SiO}_2$  is not repeated, however.  $\text{SiS}_2$  hydrolyses rapidly to  $\text{SiO}_2$  and  $\text{H}_2\text{S}$  and is completely ammonolysed by liquid  $\text{NH}_3$  to the imide



Sulfides of Na, Mg, Al and Fe convert  $\text{SiS}_2$  into metal thiosilicates, and ethanol yields “ethylsilicate”  $\text{Si}(\text{OEt})_4$  and  $\text{H}_2\text{S}$ .<sup>‡</sup> Volatile

J. A. MARTENS, *Synthesis of High-Silica Aluminosilicate Zeolites*, Elsevier, Amsterdam, 1987, 390 pp. M. L. OCCELLI and H. E. ROBSON (eds.), *Zeolite Synthesis*, ACS Symposium Series No. 398, 1989, 664 pp. J. KLINOWSKI and P. J. BARRIE (eds.) *Recent Advances in Zeolite Science*, Elsevier, Amsterdam, 1990, 310 pp. G. V. TSITSISHVILI, T. G. ANDRONIKASHVILI, G. M. KIROV and L. D. FILIZOVA, *Natural Zeolites*, Ellis Horwood, Chichester, 1990, 274 pp.

<sup>55</sup> D. W. BRECK, *Zeolite Molecular Sieves (Structure, Chemistry, and Uses)*, Wiley, New York, 1974, 771 pp. K. SEFF, *Acc. Chem. Res.* **9**, 121–8 (1976). R. M. BARRER, *Zeolites and Clay Minerals as Sorbents and Molecular Sieves*, Academic Press, London, 1978, 496 pp. W. HÖLDERICH, M. HESSE and F. NÄUMANN, *Angew. Chem. Int. Edn. Engl.* **27**, 226–46 (1988). G. A. OZIN, A. KUPEMAN and A. STEIN, *Angew. Chem. Int. Edn. Engl.* **28**, 359–76 (1989). See also K. B. YOON and J. K. KOCHI, *J. Chem. Soc., Chem. Commun.*, 510–11 (1988) for the novel synthesis of ionic clusters  $[\text{Na}_5^{3+}]$ , and P. A. ANDERSON, R. J. SINGER and P. P. EDWARDS, *J. Chem. Soc., Chem. Commun.*, 914–5 (1991) for the synthesis of  $[\text{Na}_5^{4+}]$ ,  $[\text{Na}_6^{5+}]$  and  $[\text{K}_3^{2+}]$  by reaction of alkali metal vapours with zeolites.

<sup>†</sup> According to H. Remy the artificial production of ultramarine was first suggested by J. W. von Goethe in his *Italian Journey* (1786–8); it was first accomplished by L. Gmelin in 1828 and developed industrially by the Meissen porcelain works in the following year. It can be made by firing kaolin and sulfur with sodium carbonate; various treatments yield greens, reds and violets, as well as the deep blue, the colours being reminiscent of the highly coloured species obtained in nonaqueous solutions of S, Se and Te (pp. 664, 759).

<sup>56</sup> R. J. H. CLARK and D. G. COBBOLD, *Inorg. Chem.* **17**, 3169–74 (1978).

<sup>‡</sup>  $\text{Si}(\text{OEt})_4$  is an important industrial chemical that is made on the kilotonne scale by the action of EtOH on  $\text{SiCl}_4$ . It has mp  $-77^\circ$ , bp  $168.5^\circ$ , and  $d_{20} 0.9346 \text{ g cm}^{-3}$ . Almost all uses depend on its controlled hydrolysis to produce silica in an adhesive or film-producing form. It is also a source of

thiohalides have been reported from the reaction of  $\text{SiX}_4$  with  $\text{H}_2\text{S}$  at red heat; e.g.  $\text{SiCl}_4$  yields  $\text{S}(\text{SiCl}_3)_2$ , cyclic  $\text{Cl}_2\text{Si}(\mu\text{-S})_2\text{SiCl}_2$  and crystalline  $(\text{SiSCl}_2)_4$ . The first normal thiocyanate derivative of Si,  $\text{RMe}_2\text{Si-SCN}$ , [ $\text{R} = -\text{C}(\text{SiMe}_3)_2\{\text{SiMe}_2(\text{OMe})\}$ ] was prepared from the corresponding chloride by treatment with  $\text{AgSCN}$ ; it is more readily solvolysed than its isothiocyanate isomer,  $\text{RMe}_2\text{Si-NCS}$ .<sup>(57)</sup>

The elusive  $\text{Si}=\text{S}$  grouping has been synthesized by reaction between solid Si and  $\text{H}_2\text{S}$  at  $1200^\circ\text{C}$  to give monomeric  $\text{SiS}$ ; this high-temperature molecule can itself be reacted with  $\text{Cl}_2$  or  $\text{HCl}$  in an argon matrix to yield monomeric  $\text{S}=\text{SiCl}_2$  and  $\text{S}=\text{SiHCl}$ .<sup>(58)</sup> Synthesis of stable organosilanethiones,  $\text{RR}'\text{Si}=\text{S}$  has been achieved by using the stratagem of imparting additional stabilization through intramolecular coordination via an amine function; e.g. [ $(\alpha\text{-naphthyl})(8\text{-Me}_2\text{NCH}_2\text{C}_{10}\text{H}_8)\text{Si}=\text{S}$ ] was prepared by heating the corresponding silane  $\text{RR}'\text{SiH}_2$  with  $\text{S}_8$ ; the  $\text{Si}=\text{S}$  distance of 201.3 pm was noticeably shorter than the normal single bond  $\text{Si-S}$  distance of 216 pm.<sup>(59)</sup>

The most important nitride of Si is  $\text{Si}_3\text{N}_4$ ; this is formed by direct reaction of the elements above  $1300^\circ$  or more economically by heating  $\text{SiO}_2$  and coke in a stream of  $\text{N}_2/\text{H}_2$  at  $1500^\circ$ . The compound is of considerable interest as an engineering material since it is almost completely inert chemically, and retains its strength, shape and resistance to corrosion and wear even above  $1000^\circ$ .<sup>(60)</sup> Its great hardness (Mohs 9), high

metal-free silica for use in phosphors in fluorescent lamps and TV tubes. In partly hydrolysed form it is used as a paint vehicle, a protective coating for porous stone, and as a vehicle for zinc-containing galvanic corrosion-preventing coatings. Many other orthoesters  $\text{Si}(\text{OR})_4$  are known but none are commercially important.

<sup>57</sup> C. EABORN and M. N. ROMANELLI, *J. Chem. Soc., Chem. Commun.*, 1616-7 (1984).

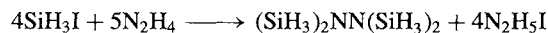
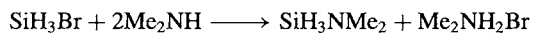
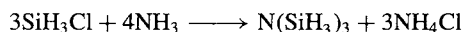
<sup>58</sup> H. SCHNÖCKEL, H. J. GÖCKE and R. KÖPPE, *Z. anorg. allg. Chem.* **578**, 159-65 (1989). R. KÖPPE and H. SCHNÖCKEL, *Z. anorg. allg. Chem.* **607**, 41-4 (1992).

<sup>59</sup> P. ARYA, J. BOYER, F. CARRÉ, R. CORRIU, G. LANNEAU, J. LAPASSET, M. PERROT and C. PRIOU, *Angew. Chem. Int. Edn. Engl.* **28**, 1016-7 (1989).

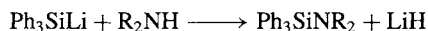
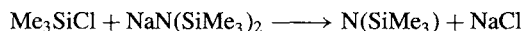
<sup>60</sup> *Silicon Nitride and the SiALONS* World Business Publications Ltd., (two vols.), 1989, 285 pp.

dissociation temperature ( $1900^\circ$ , 1 atm) and high density ( $3.185\text{ g cm}^{-3}$ ) can all be related to its compact structure which resembles that of phenacite ( $\text{Be}_2\text{SiO}_4$ , p. 347). It is an insulator with a resistivity at room temperature  $\sim 6.6 \times 10^{10}$  ohm cm. Another refractory,  $\text{Si}_2\text{N}_2\text{O}$ , is formed when Si +  $\text{SiO}_2$  are heated to  $1450^\circ$  in a stream of Ar containing 5%  $\text{N}_2$ . The structure comprises puckered hexagonal nets of alternating Si and N atoms interlinked by nonlinear  $\text{Si-O-Si}$  bonds to similar nets on either side; the Si atoms are thus each 4-coordinate and the N atoms 3-coordinate.

Volatile silylamides are readily prepared by reacting a silyl halide with  $\text{NH}_3$ ,  $\text{RNH}_2$  or  $\text{R}_2\text{NH}$  in the vapour phase or in  $\text{Et}_2\text{O}$ , e.g.:

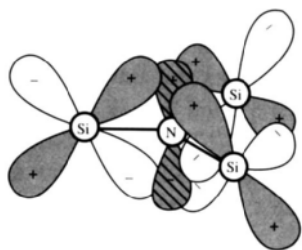


Silicon-substituted derivatives may require the use of lithio or sodio reagents, e.g.:



The N atom is always tertiary in these compounds and no species containing the  $\text{SiH-NH}$  group is stable at room temperature. Apart from this restriction, innumerable such compounds have been prepared including cyclic and polymeric analogues, e.g. [cyclo- $\{\text{Me}_2\text{SiN}(\text{SiMe}_3)_2\}$ ] and [cyclo- $(\text{Me}_2\text{SiNH})_4$ ]. Interest has focused on the stereochemistry of the N atom which is often planar, or nearly so.<sup>(61)</sup> Thus  $\text{N}(\text{SiH}_3)_3$  features a planar N atom and this has been ascribed to  $p_\pi\text{-d}_\pi$  interaction between the "nonbonding" pair of electrons on N and the "vacant"  $d_\pi$  orbitals on Si as shown schematically in Fig. 9.16. Consistent with this trisilylamines are notably weaker ligands than their tertiary amine analogues though replacement of one or two  $\text{SiH}_3$  by  $\text{CH}_3$  enhances the donor power again; e.g.  $\text{N}(\text{SiH}_3)_3$  forms no adduct with  $\text{BH}_3$  even at low temperature;

<sup>61</sup> E. A. V. EBSWORTH, *Volatile Silicon Compounds*, Pergamon Press, Oxford, 1963, 179 pp.



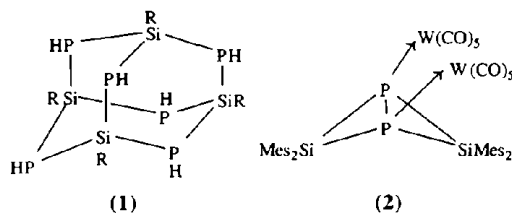
**Figure 9.16** Symmetry relation between  $p_\pi$  orbital on N and  $d_\pi$  orbitals on the 3 Si atoms in planar  $[\text{NSi}_3]$  compounds such as  $\text{N}(\text{SiH}_3)_3$ .

$\text{MeN}(\text{SiH}_3)_2$  forms a 1:1 adduct with  $\text{BH}_3$  at  $-80^\circ$  but this decomposes when warmed;  $\text{Me}_2\text{N}(\text{SiH}_3)$  gives a similar adduct which decomposes at room temperature into  $\text{Me}_2\text{NBH}_2$  and  $\text{SiH}_4$  (cf. the stability of  $\text{Me}_3\text{NBH}_3$ , p. 165). The linear skeleton of  $\text{H}_3\text{SiNCO}$  and  $\text{H}_3\text{SiNCS}$  has also been interpreted in terms of  $p_\pi-d_\pi$   $\text{N}=\text{Si}$  bonding.

Compounds containing an  $\text{Si}=\text{N}$  double bond are of very recent provenance. The first stable silanimine,  $\text{Bu}'_2\text{Si}=\text{N}-\text{SiBu}'_3$ , was prepared in 1986 as pale yellow crystals, mp  $85^\circ$  (decomp.);<sup>(62)</sup> it features a short  $\text{Si}=\text{N}$  distance (156.8 pm, cf.  $\text{Si}-\text{N}$  169.5 pm) and almost linear coordination about the N atom ( $177.8^\circ$ ), suggesting some electronic delocalization as described above. The compound was made by reacting the azidosilane  $\text{Bu}'_2\text{SiCl}(\text{N}_3)$  with  $\text{NaSiBu}'_3$  in  $\text{Bu}_2\text{O}$  at  $-78^\circ$ . The related compound  $\text{Pr}'_2\text{Si}=\text{NR}$  ( $\text{R} = 2,4,6\text{-Bu}'_3\text{C}_6\text{H}_2^-$ ) forms stable orange crystals, mp  $98^\circ$ .<sup>(63)</sup>

Unusual Si/P compounds are also beginning to appear, for example, the tetrasilahexaphosphadamantane derivative  $[(\text{Pr}'\text{Si})_4(\text{PH})_6]$  (1), which is made by reacting  $\text{Pr}'\text{SiCl}_3$  with  $\text{Li}[\text{Al}(\text{PH}_2)_4]$ .<sup>(64)</sup> Again, reaction of white phosphorus,  $\text{P}_4$ , with tetramesityldisilene,  $\text{Mes}_2\text{Si}=\text{SiMes}_2$ , in toluene

at  $40^\circ$  gives an 87% yield of the yellow bicyclo  $(\text{Mes}_2\text{Si})_2\text{P}_2$ : this has a “butterfly” structure in which the “hinge” P atoms retain electron donor properties to give adducts such as the bis- $\text{W}(\text{CO})_5$  complex (2) ( $\text{P}-\text{P}$  234.2 pm;  $\text{Si}-\text{P}$  224.4, 226.7 pm;  $\text{P}-\text{W}$  256.0 pm;  $\text{Si}\cdots\text{Si}$  324.4 pm; angle  $\text{Si}-\text{P}-\text{Si}$   $91.9^\circ$ ).<sup>(65)</sup> The now extensive field of phosphorus-rich silaphosphanes has been reviewed.<sup>(66)</sup> Silaphosphenes,  $\text{RR}'\text{Si}=\text{PAR}$  are also known.<sup>(67)</sup>



### 9.3.7 Organosilicon compounds and silicones

Well over 100 000 organosilicon compounds have been synthesized. Of these, during the past few decades, silicone oils, elastomers and resins have become major industrial products. Many organosilicon compounds have considerable thermal stability and chemical inertness; e.g.  $\text{SiPh}_4$  can be distilled in air at its bp  $428^\circ$ , as can  $\text{Ph}_3\text{SiCl}$  (bp  $378^\circ$ ) and  $\text{Ph}_2\text{SiCl}_2$  (bp  $305^\circ$ ). These, and innumerable similar compounds, reflect the considerable strength of the  $\text{Si}-\text{C}$  bond which is, indeed, comparable with that of the  $\text{C}-\text{C}$  bond (p. 338). A further illustration is the compound  $\text{SiC}$  which closely resembles diamond in its properties (p. 334). Catenation and the formation of multiple bonds are further similarities with carbon chemistry, though these features are less prominent in organosilicon chemistry and much of the work in these areas is of recent

<sup>62</sup> N. WIBERG, K. SCHURZ, G. REBER and G. MÜLLER, *J. Chem. Soc., Chem. Commun.*, 591-2 (1986).

<sup>63</sup> M. HESSE and U. KLINGEBIEL, *Angew. Chem. Int. Edn. Engl.* **25**, 649-50 (1986).

<sup>64</sup> M. BAUDLER, W. OELERT and K.-F. TEBBE, *Z. anorg. allg. Chem.* **598/599**, 9-23 (1991).

<sup>65</sup> M. DRIESS, A. D. FANTA, D. R. POWELL and R. WEST, *Angew. Chem. Int. Edn. Engl.* **28**, 1038-40 (1989).

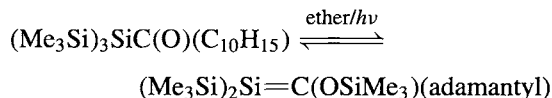
<sup>66</sup> G. FRITZ *Advances in Inorg. Chem.* **31**, 171-214 (1987).

<sup>67</sup> N. C. NORMAN, *Polyhedron* **12**, 2431-46 (1993) and references cited therein. M. DRIESS, *Adv. Organomet. Chem.* **39**, 193-229 (1996) — also deals with sila-arsenes containing  $\text{Si}=\text{As}$  bonds.

origin (e.g. pp. 338 and below). For example, although the word "silicone" was coined by F. S. Kipping in 1901 to indicate the similarity in *formula* of  $\text{Ph}_2\text{SiO}$  with that of the ketone benzophenone,  $\text{Ph}_2\text{CO}$ , he stressed that there was no chemical resemblance between them and that  $\text{Ph}_2\text{SiO}$  was polymeric.<sup>(68)</sup> It is now recognized that the great thermal and chemical stability of the silicones derives from the strength both of the Si-C bonds and of the Si-O-Si linkages. Many general reviews of the vast subject of organosilicon chemistry are available (e.g. refs 1, 2, 69-74) and only some of the salient or topical features will be touched on here. An interesting subset comprises the carbosilanes, that is compounds with a skeleton of alternating C and Si atoms.<sup>(75)</sup> These include chains, rings and polycyclic compounds, many of which can be made on a multigram or even larger scale by controlled thermolysis or by standard organometallic syntheses.

Transient reaction species containing  $\text{Si}=\text{C}$  bonds have been known since about 1966 and can be generated thermally, photolytically, or even chemically. A decade later  $\text{Me}_2\text{Si}=\text{CHMe}$

was isolated in low-temperature matrices<sup>(76)</sup> but, despite concerted and well-planned attempts over many years, it was not until 1981 that a stable silene was reported.<sup>(77)</sup> A. G. Brook and his group prepared 2-adamantyl-2-trimethylsiloxy-1,1-bis(trimethylsilyl)-1-silaethene as very pale yellow needles, mp 92°:



The solid silaethene was stable indefinitely at room temperature in the absence of air or other reagents but in solution it slowly reverted (over several days) to the isomeric acylsilane starting material. An X-ray analysis confirmed the structure and revealed a short  $>\text{Si}=\text{C}<$  bond (176.4 pm, cf. 187-191 pm for single-bonded Si-C) and a planar disposition of *ipso* atoms, the two planes being slightly twisted with respect to each other (14.6°). The use of bulky groups to enhance the stability of the silaethene is also notable, though this is not a necessary feature, at least at the Si centre, since  $\text{Me}_2\text{Si}=\text{C}(\text{SiMe}_3)(\text{SiMeBu}^t_2)$  is stable as colourless crystals at room temperature ( $>\text{Si}=\text{C}<$  distance 170.2 pm, Si-C 189.0 pm and a planar  $\text{C}_2\text{Si}=\text{CSi}_2$  skeleton).<sup>(78)</sup> The not unrelated planar heterocyclic compounds silabenzene,  $\text{C}_5\text{SiH}_6$ ,<sup>(15)</sup> and silatoluene,  $\text{C}_5\text{H}_5\text{SiMe}$ ,<sup>(16)</sup> should also be recalled.

Disilenes, containing the grouping  $>\text{Si}=\text{Si}<$ , can be isolated as thermally stable yellow or orange crystalline compounds provided that the substituents are sufficiently large to prevent

<sup>68</sup> F. S. KIPPING and L. L. LLOYD, *J. Chem. Soc. (Transactions)* **79**, 449-59 (1901).

<sup>69</sup> G. WILKINSON, F. G. A. STONE and E. W. ABEL (eds.), *Comprehensive Organometallic Chemistry*, Pergamon Press, Oxford, Vol. 2 (1982): D. A. ARMATAGE, Organosilanes, pp. 1-203; T. J. BARTON, Carbocyclic Silanes, pp. 205-303; F. O. STARK, J. R. FALENDER and A. P. WRIGHT, Silicones, pp. 305-63; R. WEST, Organopolysilanes, pp. 365-97.

<sup>70</sup> S. PAWLENKO, *Organosilicon Chemistry*, de Gruyter, Berlin, 1986, 186 pp.

<sup>71</sup> J. Y. COREY, E. J. COREY and P. P. GASPER (eds.), *Silicon Chemistry*, Ellis Horwood, Chichester, 1988, 565 pp.

<sup>72</sup> M. ZELDIN, K. J. WYNNE and H. R. ALCOCK (eds.), *Inorganic and Organometallic Polymers*, ACS Symposium Series **360** (1988) 512 pp.

<sup>73</sup> S. PATAI and Z. RAPPOPORT (eds.), *The Chemistry of Organic Silicon Compounds* (2 vols.), Wiley, Chichester, 1989, 892 pp. and 1668 pp.

<sup>74</sup> N. AUNER, W. ZICHE and R. WEST, *Heteroatom Chemistry* **2**, 335-55 (1991). This is a very readable account of current work, and includes an update of ref. 73 with a further 222 references.

<sup>75</sup> G. FRITZ, *Angew. Chem. Int. Edn. Engl.* **26**, 1111-32 (1987).

<sup>76</sup> O. L. CHAPMAN, C.-C. CHANG, J. KOLE, M. E. JUNG, J. A. LOWE, T. J. BARTON and M. L. TUMEY, *J. Am. Chem. Soc.* **98**, 7844-6 (1976). M. R. CHEDEKEL, M. SKOGLUND, R. L. KREGER and H. SHECHTER, *ibid.*, 7846-8 (1976).

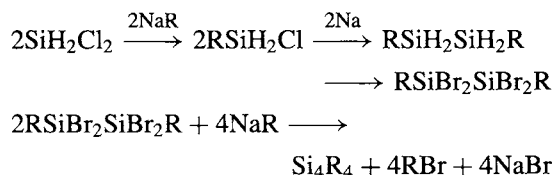
<sup>77</sup> A. G. BROOK, F. ABDESAKEN, B. GUTERKUNST, G. GUTERKUNST and R. K. KALLURY, *J. Chem. Soc., Chem. Commun.*, 191-2 (1981). A. G. BROOK and 8 others, *J. Am. Chem. Soc.*, **104**, 5667-72 (1982). For the most recent review of the chemistry of silenes see A. G. BROOK and M. A. BROOK, *Adv. Organomet. Chem.*, **39**, 71-158 (1996).

<sup>78</sup> N. WIBERG, G. WAGNER and G. MÜLLER, *Angew. Chem. Int. Edn. Engl.* **24**, 229-31 (1985). See also N. WIBERG *et al.*, *Organometallics* **6**, 32-5 and 35-41 (1987).

polymerization (e.g. mesityl, *t*-butyl, etc.).<sup>(79)</sup> The first such compound, Si<sub>2</sub>Mes<sub>4</sub>, was isolated in 1981 as orange crystals, mp 176°, following photolysis of the trisilane SiMes<sub>2</sub>(SiMe<sub>3</sub>)<sub>2</sub>.<sup>(80)</sup> The Si=Si distance in several such compounds falls in the range 214–216 pm, which is about 10% shorter than the normal single-bonded Si–Si distance. Disilenes are chemically very reactive. Halogens and HX molecules give 1,2-addition products, e.g. Mes<sub>2</sub>Si(Cl)Si(Cl)Mes<sub>2</sub>, whilst aldehydes and ketones undergo [2 + 2] cyclo-addition reactions to give 1,2,3-oxadisilenes,  $\overline{\text{OSi}}(\text{Mes})_2\overline{\text{Si}}(\text{Mes})_2\overline{\text{CHR}}$ . Controlled oxidation gives predominantly the 1,2-dioxetane  $\overline{\text{OSiR}_2\text{SiR}_2\text{O}}$  (80%), plus the 1,3-cyclodisiloxane  $\overline{\text{OSiR}_2\text{OSiR}_2}$  as a minor product. Numerous other novel heterocycles have been prepared by controlled reactions of disilenes with chalcogens, N<sub>2</sub>O, P<sub>4</sub> and organic nitro-, nitroso-, azo- and azido-compounds.<sup>(81)</sup> Transition metal complexes can give  $\eta^2$ -disilene adducts such as [Pt(PR<sub>3</sub>)<sub>2</sub>]( $\eta^2$ -Si<sub>2</sub>Mes<sub>4</sub>).<sup>(79,82)</sup>

Another fertile area of current interest is the synthesis of stable homocyclic polysilane derivatives.<sup>(83)</sup> Typical examples are cyclo-(SiMe<sub>2</sub>)<sub>7</sub>,<sup>(84)</sup> (cyclo-Si<sub>5</sub>Me<sub>9</sub>)-(SiMe<sub>2</sub>)<sub>*n*</sub>-(cyclo-Si<sub>5</sub>Me<sub>9</sub>), *n* = 2–5,<sup>(85)</sup> and several new permethylated polycyclic silanes such as the colourless crystalline compounds bicyclo[3.2.1]-Si<sub>8</sub>Me<sub>14</sub> (mp 245°), bicyclo[3.3.1]-Si<sub>9</sub>Me<sub>16</sub> (mp ≥330°) and

bicyclo[4.4.0]-Si<sub>10</sub>Me<sub>18</sub> (mp 165°).<sup>(86)</sup> Analogues of cubane and tetrahedrane have also been synthesized. Thus, the one-step condensation of Br<sub>2</sub>RSiSiRBr<sub>2</sub> or even RSiBr<sub>3</sub> with Na in toluene at 90° gave yields of up to 72% of the cubane (SiR)<sub>8</sub> (R = SiMe<sub>2</sub>Bu<sup>t</sup>) as bright yellow, air-sensitive crystals which are stable up to at least 400°C.<sup>(87)</sup> The synthesis of a molecular tetrasilatetrahedrane has also finally been achieved by the following ingenious route (R = SiBu<sup>t</sup>)<sup>(88)</sup>



The product, Si<sub>4</sub>(SiBu<sup>t</sup>)<sub>4</sub>, forms intensely orange crystals that are stable to heat, light, water and air, and do not melt below 350°. The Si–Si distances within the *closo*-Si<sub>4</sub> cluster are 232–234 pm and the *exo* Si–Si distances are slightly longer, 235–237 pm (cf. Si–Si 235.17 in crystalline Si). Comparison with the *closo*-anion Si<sub>4</sub><sup>4-</sup>, which occurs in several metal silicides (p. 337) and is isoelectronic with the P<sub>4</sub> molecule, is also appropriate.

There are three general methods for forming Si–C bonds. The most convenient laboratory method for small-scale preparations is by the reaction of SiCl<sub>4</sub> with organolithium, Grignard or organoaluminium reagents. A second attractive route is the hydrosilylation of alkenes, i.e. the catalytic addition of Si–H across C=C double bonds; this is widely applicable except for the crucially important methyl and phenyl silanes. Industrially, organosilanes are made by the direct reaction of RX or ArX with a fluidized bed of Si in the presence of about 10% by weight of metallic Cu as catalyst (cf. the direct preparation of organo compounds of

<sup>79</sup> R. WEST, *Angew. Chem. Int. Edn. Engl.* **26** 1201–11 (1987). R. OKAZAKI and R. WEST, *Adv. Organomet. Chem.* **39**, 232–73 (1996).

<sup>80</sup> R. WEST, M. J. FINK and J. MICHL, *Science* **214**, 1343–4 (1981). See also B. D. SHEPHERD, C. F. CAMPANA and R. WEST, *Heteroatom Chemistry*, **1**, 1–7 (1990).

<sup>81</sup> R. WEST, in R. STEUDEL (ed.), *The Chemistry of Inorganic Ring Systems*, Elsevier, Amsterdam, 1992, pp. 35–50. See also M. WEIDENBRUCH, *ibid.*, pp. 51–74.

<sup>82</sup> C. ZYBILL, *Topics in Current Chemistry* **160**, 1–45 (1992).

<sup>83</sup> E. HENGGE and H. STÜGER, in H. W. ROESKY (ed.), *Rings, Clusters and Polymers of Main Group and Transition Metals*, Elsevier, Amsterdam, 1989, pp. 107–38.

<sup>84</sup> F. SHAFIEE, J. R. DAMEWOOD, K. J. HALLER and R. WEST, *J. Am. Chem. Soc.* **107**, 6950–6 (1985).

<sup>85</sup> E. HENGGE and P. K. JENKNER, *Z. anorg. allg. Chem.* **560**, 27–34 (1988).

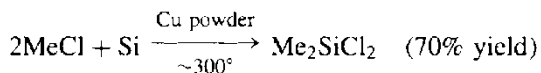
<sup>86</sup> E. HENGGE and P. K. JENKNER, *Z. anorg. allg. Chem.* **606**, 97–104 (1991).

<sup>87</sup> H. MATSUMOTO, K. HIGUCHI, Y. HOSHINO, H. KOIKE, Y. NAOI and Y. NAGAI, *J. Chem. Soc., Chem. Commun.*, 1083–4 (1988).

<sup>88</sup> N. WIBERG, C. M. M. FINGER and K. POLBORN, *Angew. Chem. Int. Edn. Engl.* **32**, 1054–6 (1993).

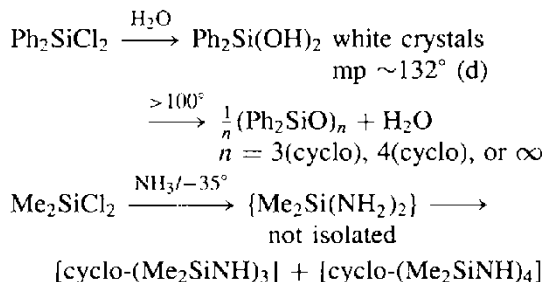


Ge, Sn, and Pb, pp. 396ff). The method was patented by E. G. Rochow in 1945 and ensured the commercial viability of the now extensive silicone industry.<sup>(2,69,72)</sup>



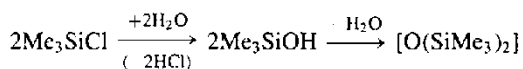
By-products are  $\text{MeSiCl}_3$  (12%) and  $\text{Me}_3\text{SiCl}$  (5%) together with 1–2% each of  $\text{SiCl}_4$ ,  $\text{SiMe}_4$ ,  $\text{MeSiHCl}_2$ , etc. Relative yields can readily be altered by modifying the reaction conditions or by adding HCl (which increases  $\text{MeSiHCl}_2$  and drastically reduces  $\text{Me}_2\text{SiCl}_2$ ). The overall reaction is exothermic and heat must be removed from the fluidized bed. Because of their very similar bps, careful fractionation is necessary if pure products are required:  $\text{Me}_3\text{SiCl}$  57.7°,  $\text{Me}_2\text{SiCl}_2$  69.6°,  $\text{MeSiCl}_3$  66.4°. Mixtures of ethylchlorosilanes or phenylchlorosilanes (or their bromo analogues) can be made similarly. All these compounds are mobile, volatile liquids (except  $\text{Ph}_3\text{SiCl}$ , mp 89°, bp 378°).

Innumerable derivatives have been prepared by the standard techniques of organic chemistry.<sup>(2,69–75)</sup> The organosilanes tend to be much more reactive than their carbon analogues, particularly towards hydrolysis, ammonolysis, and alcoholysis. Further condensation to cyclic oligomers or linear polymers generally ensues, e.g.:

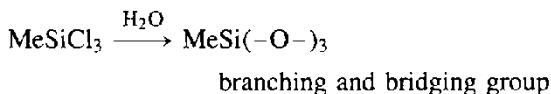
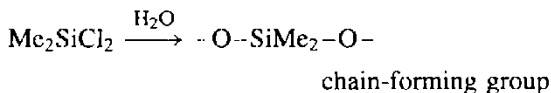
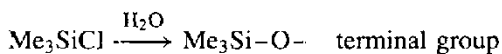


For both economic and technical reasons, commercial production of such polymers is almost entirely restricted to the methyl derivatives (and to a lesser extent the phenyl derivatives) and hydrolysis of the various methylchlorosilanes has, accordingly, been much studied. Hydrolysis of  $\text{Me}_3\text{SiCl}$  yields trimethylsilanol as a volatile liquid (bp 99°); it is noticeably more acidic than

the corresponding  $\text{Bu}'\text{OH}$  and can be converted to its Na salt by aqueous NaOH (12M). Condensation gives hexamethyldisiloxane which has a very similar bp (100.8°):



Hydrolysis of  $\text{Me}_2\text{SiCl}_2$  usually gives high polymers, but under carefully controlled conditions leads to cyclic dimethylsiloxanes  $[(\text{Me}_2\text{SiO})_n]$  ( $n = 3, 4, 5, 6$ ). Linear siloxanes have also been made by hydrolysing  $\text{Me}_2\text{SiCl}_2$  in the presence of varying amounts of  $\text{Me}_3\text{SiCl}$  as a “chain-stopping” group, i.e.  $[\text{Me}_3\text{SiO}(\text{Me}_2\text{SiO})_x\text{SiMe}_3]$  ( $x = 0, 1, 2, 3, 4$ ), etc. Cross-linking is achieved by hydrolysis and condensation in the presence of  $\text{MeSiCl}_3$  since this generates a third Si–O function in addition to the two required for polymerization:



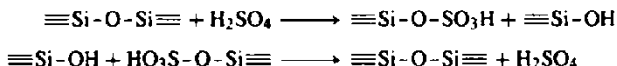
Comparison with the mineral silicates is instructive since there is a 1:1 correspondence between the two sets of compounds, the methyl groups in the silicones being replaced by the formally isoelectronic  $\text{O}^-$  in the silicates (see p. 366). This reminds us of the essentially covalent nature of the Si–O–Si linkage, but the analogy should not be taken to imply identity of structures in detail, particularly for the more highly condensed polymers. Some aspects of the technology of silicones are summarized in the concluding Panel.

While siloxanes and silicones are generally regarded as being unreactive, it is well to remember that they do indeed react with fluorinating agents and with concentrated hydroxide solutions. In certain cases they can even be employed as mild selective reagents for specific syntheses. For example,  $(\text{Me}_3\text{Si})_2\text{O}$  is a useful reagent for the convenient high-yield

### Silicone Polymers<sup>(1,2)</sup>

Silicones have good thermal and oxidative stability, valuable resistance to high and low temperatures, excellent water repellency, good dielectric properties, desirable antistick and antifoam properties, chemical inertness, prolonged resistance to ultraviolet irradiation and weathering, and complete physiological inertness. They can be made as fluids (oils), greases, emulsions, elastomers (rubbers) and resins.

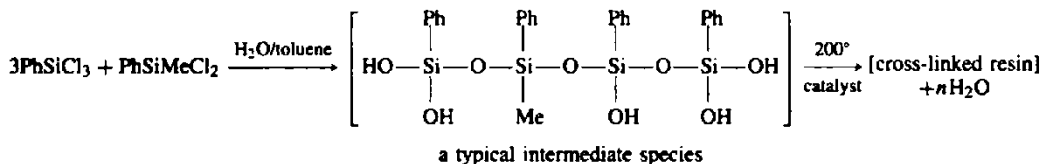
**Silicone oils** are made by shaking suitable proportions of  $[O(SiMe_3)_2]$  and  $[cyclo-(Me_2SiO)_4]$  with a small quantity of 100%  $H_2SO_4$ ; this randomizes the siloxane links by repeatedly cleaving the Si-O bonds to form  $HSO_4$  esters and then reforming new Si-O bonds by hydrolysing the ester group:



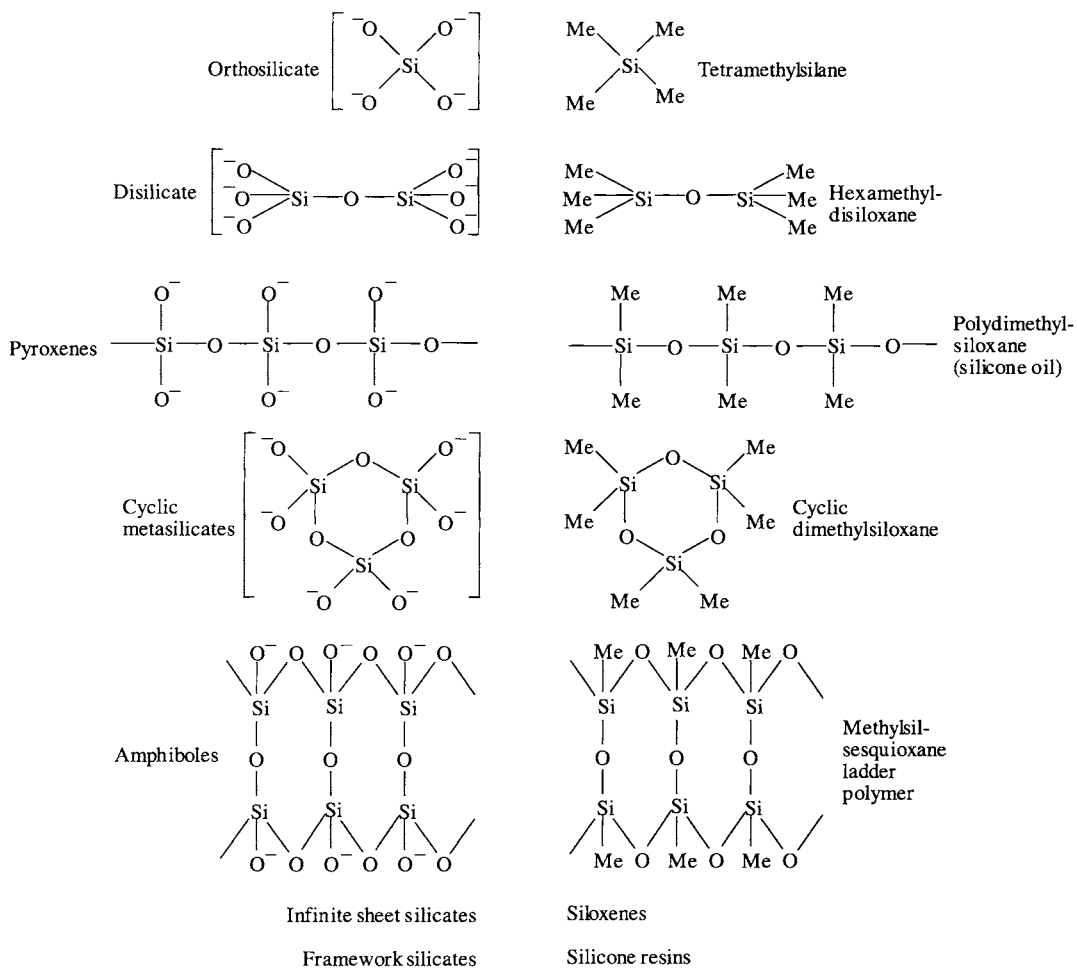
The molecular weight of the resulting polymer depends only on the initial proportion of the chain-ending groups ( $Me_3SiO-$  and  $Me_3Si-$ ) and the chain-building groups ( $-Me_2SiO-$ ) from the two components. Viscosity at room temperature is typically in the range 50–300 000 times that of water and it changes only slowly with temperature. These liquids are used as dielectric insulating media, hydraulic oils and compressible fluids for liquid springs. Pure methylsilicone oils are good lubricants at light loads but cannot be used for heavy-duty steel gears and shafts since they contain no polar film-forming groups and so are too readily exuded under high pressure. The introduction of some phenyl groups improves performance, and satisfactory greases can be made by thickening methyl phenyl silicone oil with Li soaps. Other uses are as heat transfer media in heating baths and as components in car polish, sun-tan lotion, lipstick and other cosmetic formulations. Their low surface tension leads to their extensive use as antifoams in textile dyeing, fermentation processes and sewage disposal: about  $10^{-2}$  to  $10^{-4}\%$  is sufficient for these applications. Likewise their complete non-toxicity allows them to be used to prevent frothing in cooking oils, the processing of fruit juices and the production of potato crisps.

**Silicone elastomers** (rubbers) are reinforced linear dimethylpolysiloxanes of exceedingly high molecular weight ( $5 \times 10^5 - 10^7$ ). The reinforcing agent, without which the viscous gum is useless, is usually fumed silica (p. 345). Polymerization can be acid-catalysed but KOH produces a rubber with superior physical properties; in either case scrupulous care must be taken to avoid the presence of precursors of chain-blocking groups  $[Me_3Si-O-]$  or cross-linking groups  $[MeSi(-O-)_3]$ . The reinforced silicone rubber composition can be "vulcanized" by oxidative cross-linking using 1–3% of benzoyl peroxide or similar reagents; the mixture is heated to  $150^\circ$  for 10 min at the time of pressing or moulding and then cured for 1–10 h at  $250^\circ$ . Alternatively, and more elegantly, the process can be achieved at room temperature or slightly above by incorporating a small controlled concentration of Si-H groups which can be catalytically added across pre-introduced Si-CH=CH<sub>2</sub> groups in adjacent chains. Again, the cross-linking of 1-component silicone rubbers containing acetoxy groups can be readily effected at room temperature by exposure to moisture: Such rubbers generally have 1 cross-link for every 100–1000 Si atoms and are unmatched by any other synthetic or natural rubbers in retaining their inertness, flexibility, elasticity and strength up to  $250^\circ$  and down to  $-100^\circ$ . They find use in cable-insulation sleeving, static and rotary seals, gaskets, belting, rollers, diaphragms, industrial sealants and adhesives, electrical tape insulation, plug-and-socket connectors, oxygen masks, medical tubing, space suits, fabrication of heart-valve implants, etc. They are also much used for making accurate moulds and to give rapid, accurate and flexible impressions for dentures and inlays.

**Silicone resins** are prepared by hydrolysing phenyl substituted dichloro- and trichloro-silanes in toluene. The Ph groups increase the heat stability, flexibility, and processability of the resins. The hydrolysed mixture is washed with water to remove HCl and then partly polymerized or "bodied" to a carefully controlled stage at which the resin is still soluble. It is in this form that the resins are normally applied, after which the final cross-linking to a 3D siloxane network is effected by heating to  $200^\circ$  in the presence of a heavy metal or quaternary ammonium catalyst to condense the silanol groups, e.g.:



Silicone resins are used in the insulation of electrical equipment and machinery, and in electronics as laminates for printed circuit boards; they are also used for the encapsulation of components such as resistors and integrated circuits by means of transfer moulding. Non-electrical uses include high-temperature paints and the resinous release coatings familiar on domestic cooking ware and industrial tyre moulds. When one recalls the very small quantities of silicones needed in many of these individual applications, the global production figures are particularly impressive: they have grown from a few tonnes in the mid-1940s to over 100 000 tonnes in 1969 and an estimated production of 350 000 tonnes in 1982. About half of this is in the USA, distributed so that some 65–70% is as fluid silicones, 25–30% as elastomers, and 5–10% as resins. Over 1000 different silicone products are commercially available.



preparation of oxyhalide derivatives of Mo and W.<sup>(89)</sup> Thus, in  $\text{CH}_2\text{Cl}_2$  solution,  $(\text{Me}_3\text{Si})_2\text{O}$  converts a suspension of  $\text{WCl}_6$  quantitatively to red crystals of  $\text{W}(\text{O})\text{Cl}_4$  in less than 1 h at room temperature, and  $\text{W}(\text{O})\text{Cl}_4$  can then itself be converted to yellow  $\text{W}(\text{O})_2\text{Cl}_2$  in 95% yield (light petroleum,  $100^\circ$ , overnight). Likewise,

<sup>89</sup>V. C. GIBSON, T. P. KEE and A. SHAW, *Polyhedron* **7**, 579–80 (1988).

$\text{Mo}(\text{O})\text{Cl}_4$  when treated with  $(\text{Me}_3\text{Si})_2\text{O}$  in  $\text{CH}_2\text{Cl}_2$  gives  $\text{Mo}(\text{O})_2\text{Cl}_2$  in 97% yield at r.t. Even silicone high-vacuum grease has been found unexpectedly to react with the potassium salt of an organoindium hydride to give crystals of the pseudo-crown ether complex  $[\text{cyclo}-(\text{Me}_2\text{SiO})_7\text{K}^+](\text{K}^+)_3[\text{HIn}(\text{CH}_2\text{CMe}_3)_3^-]_4$ .<sup>(90)</sup>

<sup>90</sup>M. R. CHURCHILL, C. H. LAKE, S.-H. L. CHAO and O. T. BEACHLEY, *J. Chem. Soc., Chem. Commun.*, 1577–8 (1993).

1																		2																																																																							
H																		He																																																																							
3	4											5	6	7	8	9	10																																																																								
Li	Be											B	C	N	O	F	Ne																																																																								
11	12											13	14	15	16	17	18																																																																								
Na	Mg											Al	Si	P	S	Cl	Ar																																																																								
19	20	21	22	23	24	25	26	27	28	29	30	31	32	33	34	35	36																																																																								
K	Ca	Sc	Ti	V	Cr	Mn	Fe	Co	Ni	Cu	Zn	Ga	Ge	As	Se	Br	Kr																																																																								
37	38	39	40	41	42	43	44	45	46	47	48	49	50	51	52	53	54																																																																								
Rb	Sr	Y	Zr	Nb	Mo	Tc	Ru	Rh	Pd	Ag	Cd	In	Sn	Sb	Te	I	Xe																																																																								
55	56	57	58	59	60	61	62	63	64	65	66	67	68	69	70	71	72																																																																								
Cs	Ba	La	Hf	Ta	W	Re	Os	Ir	Pt	Au	Hg	Tl	Pb	Bi	Po	At	Rn																																																																								
87	88	89	90	91	92	93	94	95	96	97	98	99	100	101	102	103	104																																																																								
Fr	Ra	Ac	Rf	Db	Sg	Bh	Hs	Mt	Dub	Dub	Dub																																																																														
<table border="1"> <tr> <td>73</td><td>74</td><td>75</td><td>76</td><td>77</td><td>78</td><td>79</td><td>80</td><td>81</td><td>82</td><td>83</td><td>84</td><td>85</td><td>86</td><td>87</td><td>88</td><td>89</td><td>90</td> </tr> <tr> <td>Ce</td><td>Pr</td><td>Nd</td><td>Pm</td><td>Sm</td><td>Eu</td><td>Gd</td><td>Tb</td><td>Dy</td><td>Ho</td><td>Er</td><td>Tm</td><td>Yb</td><td>Lu</td><td colspan="4"></td> </tr> <tr> <td>93</td><td>94</td><td>95</td><td>96</td><td>97</td><td>98</td><td>99</td><td>100</td><td>101</td><td>102</td><td>103</td><td>104</td><td>105</td><td>106</td><td>107</td><td>108</td><td>109</td><td>110</td> </tr> <tr> <td>Th</td><td>Pa</td><td>U</td><td>Np</td><td>Pu</td><td>Am</td><td>Cm</td><td>Bk</td><td>Cf</td><td>Es</td><td>Fm</td><td>Md</td><td>No</td><td>Lr</td><td colspan="4"></td> </tr> </table>																		73	74	75	76	77	78	79	80	81	82	83	84	85	86	87	88	89	90	Ce	Pr	Nd	Pm	Sm	Eu	Gd	Tb	Dy	Ho	Er	Tm	Yb	Lu					93	94	95	96	97	98	99	100	101	102	103	104	105	106	107	108	109	110	Th	Pa	U	Np	Pu	Am	Cm	Bk	Cf	Es	Fm	Md	No	Lr				
73	74	75	76	77	78	79	80	81	82	83	84	85	86	87	88	89	90																																																																								
Ce	Pr	Nd	Pm	Sm	Eu	Gd	Tb	Dy	Ho	Er	Tm	Yb	Lu																																																																												
93	94	95	96	97	98	99	100	101	102	103	104	105	106	107	108	109	110																																																																								
Th	Pa	U	Np	Pu	Am	Cm	Bk	Cf	Es	Fm	Md	No	Lr																																																																												

# 10

## Germanium, Tin and Lead

### 10.1 Introduction

Germanium was predicted as the missing element of a triad between silicon and tin by J. A. R. Newlands in 1864, and in 1871 D. I. Mendeleev specified the properties that “ekasilicon” would have (p. 29). The new element was discovered by C. A. Winkler in 1886 during the analysis of a new and rare mineral argyrodite,  $\text{Ag}_8\text{GeS}_6$ ;<sup>(1)</sup> he named it in honour of his country, Germany.<sup>†</sup> By contrast, tin and lead are two of the oldest metals known

to man and both are mentioned in early books of the Old Testament. The chemical symbols for the elements come from their Latin names *stannum* and *plumbum*. Lead was used in ancient Egypt for glazing pottery (7000–5000 BC); the Hanging Gardens of Babylon were floored with sheet lead to retain moisture and the Romans used lead extensively for water-pipes and plumbing; they extracted some 6–8 million tonnes in four centuries with a peak annual production of 60 000 tonnes. Production of tin, though equally influential, has been on a more modest scale and dates back to 3500–3200 BC. Bronze weapons and tools containing 10–15% Sn alloyed with Cu have been found at Ur, and Pliny described solder as an alloy of Sn and Pb in AD 79.

Germanium and Sn are non-toxic (like C and Si). Lead is now recognized as a heavy-metal poison;<sup>(2)</sup> it acts by complexing with oxo-groups

<sup>1</sup> M. E. WEEKS, *Discovery of the Elements*, 6th edn., Journal of Chemical Education Publ. 1956, 910 pp. Germanium, pp. 683–93; Tin and lead, pp. 41–7.

<sup>†</sup> The astonishing correspondence between the predicted and observed properties of Ge (p. 29) has tempted later writers to overlook the fact that Winkler thought he had discovered a metalloid like As and Sb and he originally identified Ge with Mendeleev’s (incorrectly) predicted “eka-stibium” between Sb and Bi; Mendeleev himself thought it was “eka-cadmium”, which he had (again incorrectly) predicted as a missing element between Cd and Hg. H. T. von Richter thought it was “eka-silicon”; so did Lothar Meyer, and they proved to be correct. This illustrates the great difficulties encountered by chemists working only 100 y ago, yet three decades before the rationale which stemmed from the work of Moseley and Bohr.

<sup>2</sup> J. J. CHISHOLM, Lead poisoning, *Scientific American* 224, 15–23 (1971). Reprinted as Chap. 36 in *Chemistry in the Environment*, Readings from *Scientific American*, pp. 335–43. W. H. Freeman, San Francisco, 1973. See also R. M. HARRISON and D. P. H. LAXEN, *Lead Pollution*, Chapman and Hall, London, 1981, 175 pp; T. C. HUTCHINSON and K. N. MEEMA (eds.), *Lead, Mercury, Cadmium and (ctd.)*

in enzymes and affects virtually all steps in the process of haem synthesis and porphyrin metabolism. It also inhibits acetylcholinesterase, acid phosphatase, ATPase, carbonic anhydrase, etc. and inhibits protein synthesis probably by modifying transfer-RNA. In addition to O complexation (in which it resembles  $Tl^I$ ,  $Ba^{II}$  and  $Ln^{III}$ ),  $Pb^{II}$  also inhibits SH enzymes (though less strongly than  $Cd^{II}$  and  $Hg^{II}$ ), especially by interaction with cysteine residues in proteins. Typical symptoms of lead poisoning are cholic, anaemia, headaches, convulsions, chronic nephritis of the kidneys, brain damage and central nervous-system disorders. Treatment is by complexing and sequestering the Pb using a strong chelating agent such as edta,  $\{-CH_2N(CH_2CO_2H)_2\}_2$ , or BAL i.e. British anti-Lewisite,  $HSCH_2CH(SH)CH_2OH$ .

## 10.2 The Elements

### 10.2.1 Terrestrial abundance and distribution

Germanium and Sn appear about half-way down the list of elements in order of abundance in crustal rocks, together with several other elements in the region of 1–2 ppm:

Element	Br	U	<b>Sn</b>	Eu	Be	As
PPM	2.5	2.3	<b>2.1</b>	2.1	2	1.8
Order	46	47	<b>48</b>	=48	50	51
Element	Ta	<b>Ge</b>	Ho	Mo	W	Tb
PPM	1.7	<b>1.5</b>	1.4	1.2	1.2	1.2
Order	52	<b>53</b>	54	55	=55	=55

Germanium minerals are extremely rare but the element is widely distributed in trace amounts (like its neighbour Ga). Recovery has been achieved from coal ash but is now normally from the flue dusts of smelters processing Zn ores.

Tin occurs mainly as cassiterite,  $SnO_2$ , and this has been the only important source of the element from earliest times. Julius Caesar recorded the presence of tin in Britain, and Cornwall remained the predominant supplier for European needs until the present century (apart from a minor flourish from Bohemia between 1400 and 1550).<sup>(3)</sup> Today (1990s) world production approaches 200 000 tonnes per annum (see next section), of which the UK contributes less than 1%.<sup>(4)</sup>

Lead (13 ppm) is by far the most abundant of the heavy elements, being approached amongst these only by thallium (8.1 ppm) and uranium (2.3 ppm). This abundance is related to the fact that 3 of the 4 naturally occurring isotopes of lead (206, 207 and 208) arise primarily as the stable end products of the natural radioactive series. Only  $^{204}Pb$  (1.4%) is non-radiogenic in origin. The variation in isotopic composition of Pb with its origin also accounts for the variability of atomic weight and the limited precision with which it can be quoted (p. 19). The most important Pb ore is the heavy black mineral galena,  $PbS$ . Other ore minerals are anglesite ( $PbSO_4$ ), cerussite ( $PbCO_3$ ), pyromorphite ( $Pb_5(PO_4)_3Cl$ ) and mimetosite ( $Pb_5(AsO_4)_3Cl$ ). Some 25 other minerals are known but are not economically important; all contain  $Pb^{II}$  in contrast to tin minerals which are invariably  $Sn^{IV}$  compounds. Lead ores are widely distributed and commercial deposits are worked in over fifty countries. Primary production (from mines) was 3.3 million tonnes (as Pb) in 1991 of which four-fifths came from the half dozen main producers: Australia 17.4%, USA 14.3%, the former Soviet Union 13.8%, China 9.6%, Canada 8.3% and Peru 6.0%.<sup>(4)</sup> Secondary production (from the remelting of scrap) produces a further 5.6 Mtpa i.e. nearly two-thirds of the world's supply in 1991. The average price in 1992 was £306.4/tonne (\$542/t).

<sup>3</sup> R. D. PENHALLURICK, *Tin in Antiquity*, Institute of Metals Publication, 1986, 271 pp.

<sup>4</sup> A. MACMILLAN (ed.) *Base Metals Handbook*, Woodhead Publ., Cambridge, 1993 (loose leaf). See also refs. 6 and 9.

### 10.2.2 Production and uses of the elements

Recovery of Ge from flue dusts is complicated, not only because of the small concentration of Ge but also because its amphoteric properties are similar to those of Zn from which it is being separated.<sup>(5)</sup> Leaching with  $\text{H}_2\text{SO}_4$ , followed by addition of aqueous NaOH, results in the coprecipitation of the 2 elements at pH  $\sim 5$  and enrichment of Ge from  $\sim 2$  to 10%:  $\text{GeO}_2$  begins to precipitate at pH 2.4, is 90% precipitated at pH 3, and 98% precipitated at pH 5.  $\text{Zn}(\text{OH})_2$  begins to precipitate at pH 4 and is completely precipitated at pH 5.5. The concentrate is heated with  $\text{HCl}/\text{Cl}_2$  to drive off  $\text{GeCl}_4$ , bp  $83.1^\circ$  (cf.  $\text{ZnCl}_2$ , bp  $756^\circ$ ). After further fractionation of  $\text{GeCl}_4$ , hydrolysis affords purified  $\text{GeO}_2$ , which can be slowly reduced to the element by  $\text{H}_2$  at  $\sim 530^\circ$ . Final purification for semiconductor-grade Ge is effected by zone refining. World production of Ge in 1991 was 80 000 kg (80 tonnes), about 10% less than a decade earlier. The largest use is in transistor technology and, indeed, transistor action was first discovered in this element (p. 331). This use is now diminishing somewhat whilst that in optics is growing — Ge is transparent in the infrared and is used in infrared windows, prisms and lenses. Magnesium germanate is a useful phosphor, and other small-scale applications are in special alloys, strain gauges and superconductors. Despite its spectacular increase in availability during the past few decades from a laboratory rarity to a general article of commerce Ge and its compounds are still relatively expensive. Zone-refined Ge was quoted at \$850 per kg in 1991 and  $\text{GeO}_2$  at \$500 per kg.

The ready reduction of  $\text{SnO}_2$  by glowing coals accounts for the knowledge of Sn and its alloys in the ancient world. Modern technology uses a reverberatory furnace at  $1200\text{--}1300^\circ$ .<sup>(6)</sup> The main chemical problem in reducing  $\text{SnO}_2$  comes

from the presence of Fe in the ores which leads to a hard product with unacceptable properties. Reference to Ellingham-type diagrams of the sort shown on p. 308 shows that  $-\Delta G(\text{SnO}_2)$  is very close to that for  $\text{FeO}/\text{Fe}_3\text{O}_4$  and only about  $80\text{ kJ mol}^{-1}$  above the line for reducing  $\text{FeO}$  to Fe at  $1000\text{--}2000^\circ$ . It is therefore essential to reduce cassiterite/iron oxide ores at an oxygen pressure sufficiently high to prevent extensive reduction to Fe. This is achieved in a two-stage process, the impure molten Sn from the initial carbon reduction being stirred vigorously in contact with atmospheric  $\text{O}_2$  to oxidize the iron — a process that can be effected by “poling” with long billets of green wood — or, alternatively, by use of steam or compressed air. The price of tin was formerly regulated by The International Tin Council, but the market became progressively less stable and the suspension of buffer stock interventions in October 1985 precipitated on immediate collapse in the market from which it has not yet recovered. The ITC was superseded by The Association of Tin Producing Countries which attempts to limit production by the member countries. In 1991 there was an excess of tin on the world market for the 11th successive year and primary production was limited to 95 850 tonnes (Malaysia 29.8%, Indonesia 29.6%, Thailand 17.9%, Bolivia 13.2%, Australia 7.2%, Zaire 1.4%, Nigeria 0.9%). Additional production by China (43 000 t), the former USSR (13 500 t) and other countries brought the primary production of Sn in concentrates in 1991 to 196 700 tonnes. Prices hovered around \$5700 per tonne, about half that of a few years earlier.<sup>(7,8)</sup> The many uses of metallic tin and its alloys are summarized in the Panel overleaf.

Lead is normally obtained from  $\text{PbS}$ . This is first concentrated from low-grade ores by froth flotation then roasted in a limited supply of air

<sup>6</sup> Kirk-Othmer *Encyclopedia of Chemical Technology* 3rd edn. 23, 18–42 (1983), Tin and tin alloys; 42–77, Tin compounds.

<sup>7</sup> *Minerals year book, Vol. 1: Metals and Minerals*, 1991, US Dept. of the Interior, Bureau of Mines. Ge pp. 649–54; Sn pp. 1591–612, Pb pp. 873–910.

<sup>8</sup> R. WOLFF, *Tin Market Report*, Metal Bulletin Books Ltd., Worcester Park, Surrey, 1991.

<sup>5</sup> Kirk-Othmer *Encyclopedia of Chemical Technology* 4th edn. 12, 540–55 (1994). Germanium and germanium compounds.

### Uses of Metallic Tin and Its Alloys

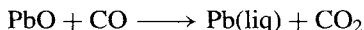
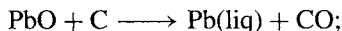
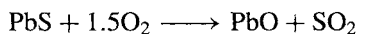
Because of its low strength and high cost, Sn is seldom used by itself but its use as a coating, and as alloys, is familiar in a variety of domestic and technological applications. Tin-plate accounts for almost 27% of tin used — it provides a non-toxic corrosion-resistant cover for sheet steel and can be applied either by hot dipping in molten Sn or more elegantly and controllably by electrolytic tinning. The layer is typically 0.4–25 μm thick. In addition to extensive use in food packaging, tin-plate is used increasingly for distributing beer and other drinks. In the USA alone 35 000 million of the 130 000 million drink cans sold annually are tin-plate, the rest being Al: this is a staggering per capita consumption of 500 pa.

The main alloys of tin together with an indication of the percentage of total Sn production for these alloys in the USA (1991) are:

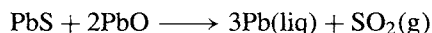
- Solder (37%)** (Sn/Pb) typically containing 33% Sn by weight but varying between 2–63% depending on use; sometimes Cd, Ga, In or Bi are added for increased fusibility.
- Bronze (7%)** (Cu/Sn) typically 5–10% Sn often with added P or Zn to aid casting and impart superior elasticity and strain resistance. Gun metal is ~85% Cu, 5% Sn, 5% Zn and 5% Pb. Coinage metal and brass also often contain small amounts of Sn. World production of bronzes approaches 500 000 tonnes pa.
- Babbitt (2%)** (heavy duty bearing metal introduced by I. Babbitt in 1839). The two main compositions are 80–90% Sn, 0–5% Pb, 5% Cu; and 75% Pb, 12% Sn, 13% Sb, 0–1% Cu. They have the characteristics of a hard compound embedded in a soft matrix and are used mainly in railway wagons, diesel locomotives, etc.
- Pewter (3%)** (90–95% Sn, 1–8% Sb, 0.5–3% Cu); a decorative and servicable alloy that can be cast, bent, spun or formed into any shape; it is much used for coffee and tea services, trays, plates, jugs, tankards, candelabra, bowls and trophies. A related alloy of 90–95% Sn with Pb and other elements is highly prized and much used for organ pipes because of its tonal qualities, e.g. the Royal Albert Hall organ in London has 10 000 pipes containing some 150 tonnes Sn.

Other specialized uses of Sn and its alloys are as type metal, as the molten-metal bath in the manufacture of float glass and as the alloy Nb<sub>3</sub>Sn in superconducting magnets. The many industrial and domestic uses of tin compounds are discussed in later sections; these compounds account for about 15% of the tin produced worldwide.

to give PbO which is then mixed with coke and a flux such as limestone and reduced in a blast furnace:<sup>(9)</sup>



Alternatively, the carbon reduction can be replaced by reduction of the roasted ore with fresh galena:



In either case the Pb contains numerous undesirable metal impurities, notably Cu, Ag, Au, Zn, Sn, As and Sb, some of which are clearly valuable in themselves. Copper is first removed by liquation: the Pb bullion is melted and held just above its freezing point when Cu rises to the surface as an insoluble solid which is skimmed off. Tin, As and Sb are next removed by preferential oxidation in a reverberatory furnace and skimming off the oxides; alternatively, the molten bullion is churned with an oxidizing flux of molten NaOH/NaNO<sub>3</sub> (Harris process). The softened Pb may still contain Ag, Au and perhaps Bi. Removal of the first two depends on their preferential solubility in Zn: the mixed metals are cooled slowly from 480° to below 420° when the Zn (now containing nearly all the Ag and Au) solidifies as a crust which is skimmed off; the

<sup>9</sup> Kirk-Othmer Encyclopedia of Chemical Technology 4th edn. 15, 69–113 (1995), Lead; 113–32, Lead alloys; 132–58, Lead compounds.

### Uses of Lead Alloys and Chemicals

Although much lead is used as an inert material in cast, rolled or extruded form, a far greater tonnage is consumed as alloys. Its major application is in storage batteries where an alloy of 91% Pb, 9% Sb forms the supporting grid for the oxidizing agent ( $\text{PbO}_2$ ) and the reducing agent (spongy Pb).<sup>(10)</sup> Over 70% of this Pb is recovered and recycled. In addition, its use (with Sn) in solders, fusible alloys, bearing metals (babbitt) and type metals has been summarized on p. 370. Other mechanical as distinct from chemical applications are in ammunition, lead shot, lead weights and ballast.

The pattern of chemical usage of Pb compounds in a particular country depends very much on whether organolead compounds are allowed as antiknock additives in petrol for cars (gasoline for automobiles). In a growing number of developed countries such additives are considered to be wasteful, dangerous and unnecessary and environmental legislation is gradually achieving the elimination of  $\text{PbEt}_4$  and  $\text{PbMe}_4$  as antiknocks.<sup>(2)</sup> The presence of Pb additives in petrol also interferes with the catalytic converters that are being developed to reduce or eliminate CO,  $\text{NO}_x$  and hydrocarbons from exhaust fumes, and this has likewise encouraged the change to other antiknocks.

World production of mined lead was 3 331 000 tonnes in 1991 and a further 5 558 000 tonnes was refined by reprocessing. In the same year US consumption of Pb in metal products was 1 125 000 tonnes (including 967 000 tonnes in storage batteries). In addition, some 57 250 tonnes of other oxides and 29 750 tonnes of miscellaneous Pb-containing products were consumed. The US market price of Pb dropped from \$1.05/kg in 1990 to \$0.40/kg in 1993 due in part to the collapse in use of  $\text{PbEt}_4$  in petrol.

Lead pigments are widely used as rust-inhibiting priming paints for iron and steel. Red lead ( $\text{Pb}_3\text{O}_4$ ) is the traditional primer but  $\text{Ca}_2\text{PbO}_4$  is finding increasing use, particularly for galvanized steel. Lead chromate,  $\text{PbCrO}_4$ , is a strong yellow pigment extensively used in yellow paints for road markings and as an ingredient (with iron blues) in many green paints and coloured plastics. Other pigments include  $\text{PbMoO}_4$  (red-orange), litharge  $\text{PbO}$  (canary yellow), and white lead,  $\sim 2\text{PbCO}_3 \cdot \text{Pb}(\text{OH})_2$ . Lead compounds are also used for ceramic glazes, e.g.  $\text{PbSi}_2\text{O}_5$  (colourless), in crown glass manufacture, and as polyvinylchloride plastic stabilizers, e.g. "tribasic lead sulfate",  $3\text{PbO} \cdot \text{PbSO}_4 \cdot \text{H}_2\text{O}$ . See also p. 386.

excess of dissolved Zn is then removed either by oxidation in a reverberatory furnace, or by preferential reaction with gaseous  $\text{Cl}_2$ , or by vacuum distillation. Final purification (which also removes any Bi) is by electrolysis using massive cast Pb anodes and an electrolyte of acid  $\text{PbSiF}_6$  or a sulfamate;<sup>(10)</sup> this yields a cathode deposit of 99.99% Pb which can be further purified by zone refining to <1 ppm impurity if required. Total world production figures and the current price were given at the end of the preceding section, and the various uses for lead alloys and chemicals are summarized in the Panel.

### 10.2.3 Properties of the elements

The atomic properties of Ge, Sn and Pb are compared with those of C and Si in Table 10.1. Trends noted in previous groups are again apparent. The pairwise similarity in the ionization energies of Si and Ge (which can be related to the filling of the  $3d^{10}$  shell) and of Sn and Pb

(which is likewise related to the filling of the  $4f^{14}$  shell) are notable (Fig. 10.1). Tin has more stable isotopes than any other element (why?) and one of these,  $^{119}\text{Sn}$  (nuclear spin  $\frac{1}{2}$ ), is particularly valuable both for nmr experiments<sup>(11)</sup> and for Mössbauer spectroscopy.<sup>(12)</sup>

Some physical properties of the elements are compared in Table 10.2. Germanium forms brittle, grey-white lustrous crystals with the diamond structure; it is a metalloid with a similar electrical resistivity to Si at room temperature but with a substantially smaller band gap. Its mp, bp and associated enthalpy changes are also lower than for Si and this trend continues for Sn and Pb which are both very soft, low-melting metals.

Tin has two allotropes: at room temperature the stable modification is white, tetragonal

<sup>11</sup> J. D. KENNEDY and W. MCFARLANE, in J. MASON (ed), *Multinuclear NMR*, Plenum Press, New York, 1987, Chap. 11, Si, Ge, Sn and Pb, pp. 305–33. See also B. WRACKMEYER, *Ann. Rept. NMR Spectrosc.* **16**, 73–186 (1985).

<sup>12</sup> N. N. GREENWOOD and T. C. GIBB, *Mössbauer Spectroscopy*, Chapman & Hall, London, 1971, 659 pp. T. C. GIBB, *Principles of Mössbauer Spectroscopy*, Chapman & Hall, London, 1976, 254 pp.

<sup>10</sup> A. T. KUHN (ed.), *The Electrochemistry of Lead*, Academic Press, London, 1977, 467 pp. H. BODE, *Lead-Acid Batteries*, Wiley, New York, 1977, 408 pp.



Table 10.1 Atomic properties of Group 14 elements

Property	C	Si	Ge	Sn	Pb	
Atomic number	6	14	32	50	82	
Electronic structure	[He]2s <sup>2</sup> 2p <sup>2</sup>	[Ne]3s <sup>2</sup> 3p <sup>2</sup>	[Ar]3d <sup>10</sup> 4s <sup>2</sup> 4p <sup>2</sup>	[Kr]4d <sup>10</sup> 5s <sup>2</sup> 5p <sup>2</sup>	[Xe]4f <sup>14</sup> 5d <sup>10</sup> 6s <sup>2</sup> 6p <sup>2</sup>	
Number of naturally occurring isotopes	2 + 1	3	5	10	4	
Atomic weight	12.0107(8)	28.0855(3)	72.61(2)	118.710(7)	207.2(1)	
Ionization energy/kJ mol <sup>-1</sup>	I	1086.1	786.3	761.2	708.4	715.4
	II	2351.9	1576.5	1537.0	1411.4	1450.0
	III	4618.8	3228.3	3301.2	2942.2	3080.7
	IV	6221.0	4354.4	4409.4	3929.3	4082.3
r <sup>IV</sup> (covalent)/pm	77.2	117.6	122.3	140.5	146	
r <sup>IV</sup> ("ionic"; 6-coordinate)/pm	(15) (CN 4)	40	53	69	78	
r <sup>II</sup> ("ionic", 6-coordinate)/pm	—	—	73	118	119	
Pauling electronegativity	2.5	1.8	1.8	1.8	1.9	

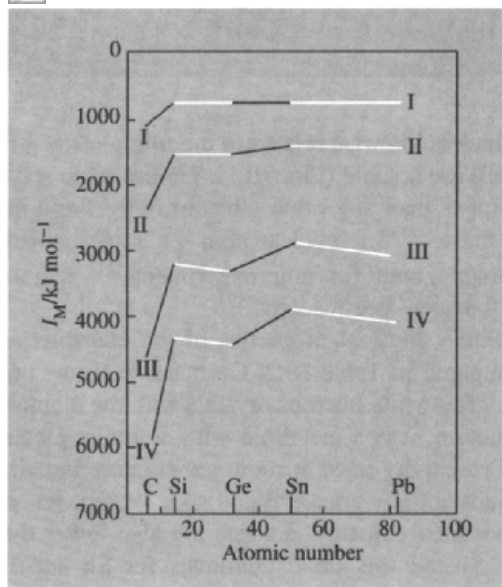
 LIVE GRAPH


Figure 10.1 Successive ionization energies for Group 14 elements showing the influence of the 3d<sup>10</sup> shell between Si and Ge and the 4f<sup>14</sup> shell between Sn and Pb.

$\beta$ -Sn, but at low temperatures this transforms into grey  $\alpha$ -Sn which has the cubic diamond structure. The transition temperature is 13.2° but the transformation usually requires prolonged exposure at temperatures well below this.

The reverse transition from  $\alpha \rightarrow \beta$  involves a structural distortion along the  $c$ -axis and is remarkable for the fact that the density increases by 26% in the high-temperature form. This arises because, although the Sn–Sn distances increase in the  $\alpha \rightarrow \beta$  transition, the CN increases from 4 to 6 and the distortion also permits a closer approach of the 12 next-nearest neighbours:

Modification	$\alpha$ (grey, diamond)	$\beta$ (white, tetragonal)
Bond angles	6 at 109.5°	$\left\{ \begin{array}{l} 4 \text{ at } 94^\circ \\ 2 \text{ at } 149.6^\circ \end{array} \right.$
Nearest neighbours	4 at 280 pm	$\left\{ \begin{array}{l} 4 \text{ at } 302 \text{ pm} \\ 2 \text{ at } 318 \text{ pm} \end{array} \right.$
Next nearest neighbours	12 at 459 pm	$\left\{ \begin{array}{l} 4 \text{ at } 377 \text{ pm} \\ 8 \text{ at } 441 \text{ pm} \end{array} \right.$

A similar transformation to a metallic, tetragonal  $\beta$ -form can be effected in Si and Ge by subjecting them to pressures of  $\sim 200$  and  $\sim 120$  kbar respectively along the  $c$ -axis, and again the density increases by  $\sim 25\%$  from the value at atmospheric pressure. Lead is familiar as a blue-grey, malleable metal with a fairly high density (nearly 5 times that of Si and twice those of Ge and Sn, but only half that of Os and Ir).

Table 10.2 Some physical properties of Group 14 elements

Property	C	Si	Ge	Sn	Pb
MP/°C	4100	1420	945	232	327
BP/°C	—	~3280	2850	2623	1751
Density (20°C)/g cm <sup>-3</sup>	3.514	2.336	5.323	$\alpha$ 5.769	11.342
$a_0$ /pm	356.68 <sup>(c)</sup>	( $\beta$ 2.905) <sup>(a)</sup>	( $\beta$ 6.71) <sup>(a)</sup>	$\beta$ 7.265 <sup>(b)</sup>	494.9 <sup>(d)</sup>
$\Delta H_{\text{fus}}/\text{kJ mol}^{-1}$	—	50.6	36.8	7.07	4.81
$\Delta H_{\text{vap}}/\text{kJ mol}^{-1}$	—	383	328	296	178
$\Delta H_f$ (monatomic gas)/kJ mol <sup>-1</sup>	716.7	454	283	300.7	195.0
Electrical resistivity (20°)/ohm cm	10 <sup>14</sup> –10 <sup>16</sup>	~48	~47	$\beta$ 11 $\times$ 10 <sup>-6</sup>	20 $\times$ 10 <sup>-6</sup>
Band gap $E_g$ /kJ mol <sup>-1</sup>	~580	106.8	64.2	$\alpha$ 7.7, $\beta$ 0	0

<sup>(a)</sup>See text. <sup>(b)</sup> $\beta$ -form (stable at room temperature) is tetragonal  $a_0$  583.1 pm,  $c_0$  318.1 pm.

<sup>(c)</sup>Diamond structure. <sup>(d)</sup>Face-centred cubic.

### 10.2.4 Chemical reactivity and group trends

Germanium is somewhat more reactive and more electropositive than Si: it dissolves slowly in hot concentrated H<sub>2</sub>SO<sub>4</sub> and HNO<sub>3</sub> but does not react with water or with dilute acids or alkalis unless an oxidizing agent such as H<sub>2</sub>O<sub>2</sub> or NaOCl is present; fused alkalis react with incandescence to give germanates. Germanium is oxidized to GeO<sub>2</sub> in air at red heat and both H<sub>2</sub>S and gaseous S yield GeS<sub>2</sub>; Cl<sub>2</sub> and Br<sub>2</sub> yield GeX<sub>4</sub> on moderate heating and HCl gives both GeCl<sub>4</sub> and GeHCl<sub>3</sub>. Alkyl halides react with heated Ge (as with Si) to give the corresponding organogermanium halides.

Tin<sup>(13)</sup> is notably more reactive and electropositive than Ge though it is still markedly amphoteric in its aqueous chemistry. It is stable towards both water and air at ordinary temperatures but reacts with steam to give SnO<sub>2</sub> plus H<sub>2</sub> and with air or oxygen on heating to give SnO<sub>2</sub>. Dilute HCl and H<sub>2</sub>SO<sub>4</sub> show little, if any, reaction but dilute HNO<sub>3</sub> produces Sn(NO<sub>3</sub>)<sub>2</sub> and NH<sub>4</sub>NO<sub>3</sub>. Hot concentrated HCl yields SnCl<sub>2</sub> and H<sub>2</sub> whereas hot concentrated H<sub>2</sub>SO<sub>4</sub> forms SnSO<sub>4</sub> and SO<sub>2</sub>. The occurrence of Sn<sup>II</sup> compounds in these reactions is notable. By contrast, the action of hot aqueous alkali yields

hydroxostannate(IV) compounds, e.g.:



Tin reacts readily with Cl<sub>2</sub> and Br<sub>2</sub> in the cold and with F<sub>2</sub> and I<sub>2</sub> on warming to give SnX<sub>4</sub>. It reacts vigorously with heated S and Se, to form Sn<sup>II</sup> and Sn<sup>IV</sup> chalcogenides depending on the proportions used, and with Te to form SnTe.

Finely divided Pb powder is pyrophoric but the reactivity of the metal is usually greatly diminished by the formation of a thin, coherent, protective layer of insoluble product such as oxide, oxocarbonate, sulfate or chloride. This inertness has been exploited as one of the main assets of the metal since early times: e.g. a temperature of 600–800° is needed to form PbO in air and Pb is widely used for handling hot concentrated H<sub>2</sub>SO<sub>4</sub>. Aqueous HCl does, in fact, react slowly to give the sparingly soluble PbCl<sub>2</sub> (<1% at room temperature) and nitric acid reacts quite rapidly to liberate oxides of nitrogen and form the very soluble Pb(NO<sub>3</sub>)<sub>2</sub> (~50 g per 100 cm<sup>3</sup>, i.e. 1.5 M). Organic acids such as acetic acid also dissolve Pb in the presence of air to give Pb(OAc)<sub>2</sub>, etc.; this precludes contact with the metal when processing or storing wine, fruit juices and other drinks. The familiar soft metal protective caps covering the cork on quality wines is Pb-foil laminated between thin outer layers of non-toxic Sn metal to which coloured decorative finishes can be applied. Fluorine reacts at room temperatures to give PbF<sub>2</sub> and Cl<sub>2</sub> gives PbCl<sub>2</sub> on heating.

<sup>13</sup> P. G. HARRISON (ed.), *Chemistry of Tin*, Blackie, Glasgow, 1989, 461 pp.

Molten Pb reacts with the chalcogens to give PbS, PbSe and PbTe.

The steady trend towards increasing stability of  $M^{II}$  rather than  $M^{IV}$  compounds in the sequence Ge, Sn, Pb is an example of the so-called "inert-pair effect" which is well established for the heavier post-transition metals. The discussion on p. 226 is relevant here. A notable exception is the organometallic chemistry of Sn and Pb which is almost entirely confined to the  $M^{IV}$  state (pp. 399–405).

Catenation is also an important feature of the chemistry of Ge, Sn and Pb though less so than for C and Si. The discussion on p. 341 can be extended by reference to the bond energies in Table 10.3 from which it can be seen that there is a steady decrease in the M–M bond strength. In general, with the exception of M–H bonds, the strength of other M–X bonds diminishes less noticeably, though the absence of Ge analogues of silicone polymers speaks for the lower stability of the Ge–O–Ge linkage.

The structural chemistry of the Group 14 elements affords abundant illustrations of the trends to be expected from increasing atomic size, increasing electropositivity and increasing tendency to form  $M^{II}$  compounds, and these will become clear during the more detailed treatment of the chemistry in the succeeding sections. The often complicated stereochemistry of  $M^{II}$  compounds (which arises from the presence of a nonbonding electron-pair on the metal) is

particularly revealing as also is the propensity of  $Sn^{IV}$  to become 5- and 6-coordinate.<sup>(14)</sup> The ability of both Sn and Pb to form polyatomic cluster anions of very low formal oxidation state, (e.g.  $M_5^{2-}$ ,  $M_9^{4-}$ , etc.) reflects the now well-established tendency of the heavier post-transition elements to form chain, ring or cluster homopolyatomic ions:<sup>(18)</sup> this was first established for the polyhalide anions and for  $Hg_2^{2+}$  but is also prevalent in Groups 14, 15 and 16, e.g.  $Pb_9^{4-}$  is isoelectronic with  $Bi_9^{5+}$  (see Section 10.3.6, p. 391).

## 10.3 Compounds

### 10.3.1 Hydrides and hydrohalides

Germanes of general formula  $Ge_nH_{2n+2}$  are known as colourless gases or volatile liquids for  $n = 1-5$  and their preparation, physical properties, and chemical reactions are very similar to those of silanes (p. 337). Thus  $GeH_4$  was formerly made by the inefficient hydrolysis of Mg/Ge alloys with aqueous acids but is now generally made by the reaction of  $GeCl_4$  with  $LiAlH_4$  in ether or even more conveniently by the reaction of  $GeO_2$  with aqueous solutions of  $NaBH_4$ . The higher germanes are prepared by the action of a silent electric discharge on  $GeH_4$ ; mixed hydrides such as  $SiH_3GeH_3$  can be prepared similarly by circulating a mixture of  $SiH_4$  and  $GeH_4$  but no cyclic or unsaturated hydrides have yet been prepared. The germanes are all less volatile than the corresponding silanes (see Table) and, perhaps surprisingly,

**Table 10.3** Approximate average bond energies/ $\text{kJ mol}^{-1(a)}$

M–	–M	–C	–H	–F	–Cl	–Br	–I
C	356	356	416	490	325	279	216
Si	226	360	323	596	400	325	248
Ge	188	255	289	471	339	281	216
Sn	151	226	253	—	315	261	187
Pb	98	130	205	411	308	—	—

<sup>(a)</sup>These values often vary widely (by as much as  $50-100 \text{ kJ mol}^{-1}$ ) depending on the particular compound considered and the method of computation used. Individual values are thus less significant than general trends. The data represent a collation of values for typical compounds gleaned from refs 15–17.

<sup>14</sup> J. A. ZUBIETA and J. J. ZUCKERMAN, Structural tin chemistry, *Prog. Inorg. Chem.* **24**, 251–475 (1978). An excellent comprehensive review with full structural diagrams and data, and more than 750 references.

<sup>15</sup> J. A. KERR, Bond strengths in polyatomic molecules, *CRC Handbook of Chemistry and Physics*, 73rd edn., 1992–3, pp. 9.138–9.145.

<sup>16</sup> W. E. DASENT, *Inorganic Energetics*, 2nd edn., Cambridge Univ. Press, 1982, 185 pp.

<sup>17</sup> C. F. SHAW and A. L. ALLRED, *Organometallic Chem. Rev.* **5A**, 95–142 (1970).

<sup>18</sup> J. D. CORBETT, *Prog. Inorg. Chem.* **21**, 129–55 (1976).

Property	GeH <sub>4</sub>	Ge <sub>2</sub> H <sub>6</sub>
MP/°C	-164.8	-109
BP/°C	-88.1	29
Density (T°C)/g cm <sup>-3</sup>	1.52 (-142°)	1.98 (-109°)

Property	Ge <sub>3</sub> H <sub>8</sub>	Ge <sub>4</sub> H <sub>10</sub>	Ge <sub>5</sub> H <sub>12</sub>
MP/°C	-105.6	-	-
BP/°C	110.5	176.9	234
Density (T°C)/g cm <sup>-3</sup>	2.20 (-105°)	-	-

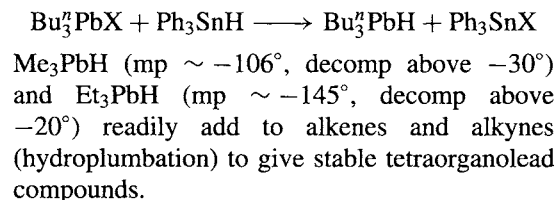
noticeably less reactive. Thus, in contrast to SiH<sub>4</sub> and SnH<sub>4</sub>, GeH<sub>4</sub> does not ignite in contact with air and is unaffected by aqueous acid or 30% aqueous NaOH. It acts as an acid in liquid NH<sub>3</sub> forming NH<sub>4</sub><sup>+</sup> and GeH<sub>3</sub><sup>-</sup> ions and reacts with alkali metals in this solvent (or in MeOC<sub>2</sub>H<sub>4</sub>-OMe) to give MGeH<sub>3</sub>. Like the corresponding MSiH<sub>3</sub>, these are white, crystalline compounds of considerable synthetic utility. X-ray diffraction analysis shows that KGeH<sub>3</sub> and RbGeH<sub>3</sub> have the NaCl-type structure, implying free rotation of GeH<sub>3</sub><sup>-</sup>, and CsGeH<sub>3</sub> has the rare TII structure (p. 242). The derived "ionic radius" of 229 pm emphasizes the similarity to SiH<sub>3</sub><sup>-</sup> (226 pm) and this is reinforced by the bond angles deduced from broad-line nmr experiments: SiH<sub>3</sub><sup>-</sup> 94 ± 4° (cf. isoelectronic PH<sub>3</sub>, 93.5°); GeH<sub>3</sub><sup>-</sup> 92.5 ± 4° (cf. isoelectronic AsH<sub>3</sub>, 91.8°).<sup>(19)</sup>

The germanium hydrohalides GeH<sub>x</sub>X<sub>4-x</sub> (X = Cl, Br, I; x = 1, 2, 3) are colourless, volatile, reactive liquids. Preparative routes include reaction of Ge, GeX<sub>2</sub> or GeH<sub>4</sub> with HX. The compounds are valuable synthetic intermediates (cf. SiH<sub>3</sub>I). For example, hydrolysis of GeH<sub>3</sub>Cl yields O(GeH<sub>3</sub>)<sub>2</sub>, and various metatheses can be effected by use of the appropriate Ag salts or, more effectively, Pb<sup>II</sup> salts, e.g. GeH<sub>3</sub>Br with PbO, Pb(OAc)<sub>2</sub>, and Pb(NCS)<sub>2</sub> affords O(GeH<sub>3</sub>)<sub>2</sub>, GeH<sub>3</sub>(OAc), and GeH<sub>3</sub>(SCN). Treatment of this latter compound with MeSH or [Mn(CO)<sub>5</sub>H] yields GeH<sub>3</sub>SMe

and [Mn(CO)<sub>5</sub>(GeH<sub>3</sub>)] respectively. An extensive phosphinogermane chemistry is also known, e.g. R<sub>n</sub>Ge(PH<sub>2</sub>)<sub>4-n</sub>, R = alkyl or H. The novel germimine CF<sub>3</sub>N=GeH<sub>2</sub> has been obtained as a colourless gas by reacting a 1:1 mixture of GeH<sub>4</sub> and CF<sub>3</sub>NO in a sealed tube at 120° (the other product being H<sub>2</sub>O). Addition of HI to the Ge=N double bond gave CF<sub>3</sub>NHGeH<sub>2</sub>I.<sup>(20)</sup>

Binary Sn hydrides are much less stable. Reduction of SnCl<sub>4</sub> with ethereal LiAlH<sub>4</sub> gives SnH<sub>4</sub> in 80–90% yield; SnCl<sub>2</sub> reacts similarly with aqueous NaBH<sub>4</sub>. SnH<sub>4</sub> (mp -146°, bp -52.5°) decomposes slowly to Sn and H<sub>2</sub> at room temperature; it is unattacked by dilute aqueous acids or alkalis but is decomposed by more concentrated solutions. It is a potent reducing agent. Sn<sub>2</sub>H<sub>6</sub> is even less stable, and higher homologues have not been obtained. By contrast, organotin hydrides are more stable, and catenation up to H(SnPh<sub>2</sub>)<sub>6</sub>H has been achieved by thermolysis of Ph<sub>2</sub>SnH<sub>2</sub>. Preparation of R<sub>n</sub>SnH<sub>4-n</sub> is usually by LiAlH<sub>4</sub> reduction of the corresponding organotin chloride.

PbH<sub>4</sub> is the least well-characterized Group 14 hydride and it is unlikely that it has ever been prepared except perhaps in trace amounts at high dilution; methods which successfully yield MH<sub>4</sub> for the other Group 14 elements all fail even at low temperatures. The alkyl derivatives R<sub>2</sub>PbH<sub>2</sub> and R<sub>3</sub>PbH can be prepared from the corresponding halides and LiAlH<sub>4</sub> at -78° or by exchange reactions with Ph<sub>3</sub>SnH, e.g.:



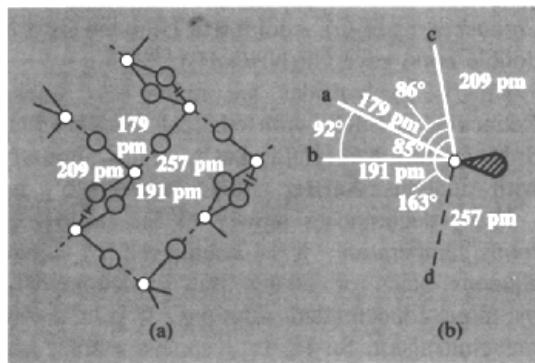
### 10.3.2 Halides and related complexes

Germanium, Sn and Pb form two series of halides: MX<sub>2</sub> and MX<sub>4</sub>. PbX<sub>2</sub> are more stable than PbX<sub>4</sub>, whereas the reverse is

<sup>19</sup> G. THIRASE, E. WEISS, H. J. HENNING and H. LECHERT, *Z. anorg. allg. Chem.* **417**, 221–8 (1975).

<sup>20</sup> H. G. ANG and F. KLEE, *J. Chem. Soc., Chem. Commun.*, 310–12 (1989).

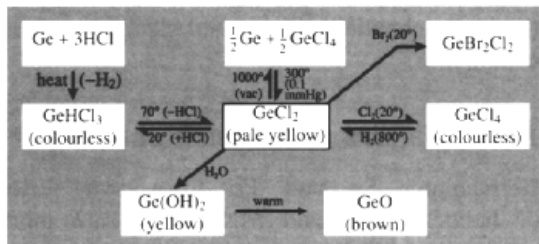
true for Ge, consistent with the steady increase in stability of the dihalides in the sequence  $CX_2 \ll SiX_2 < GeX_2 < SnX_2 < PbX_2$ . Numerous complex halides are also known for both oxidation states.



**Figure 10.2** Crystal structure of  $GeF_2$ : (a) projection along the chains, and (b) environment of Ge (pseudo trigonal bipyramidal). The bond to the unshared F is appreciably shorter (179 pm) than those in the chain and there is a weaker interaction (257 pm) linking the chains into a 3D structure.

### Germanium halides

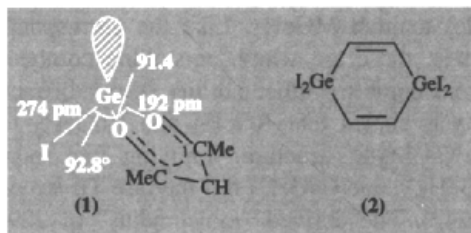
$GeF_2$  is formed as a volatile white solid (mp  $110^\circ$ ) by the action of  $GeF_4$  on powdered Ge at  $150$ – $300^\circ$ ; it has a unique structure in which trigonal pyramidal  $\{GeF_3\}$  units share 2 F atoms to form infinite spiral chains (Fig. 10.2). Pale-yellow  $GeCl_2$  can be prepared similarly at  $300^\circ$  or by thermal decomposition of  $GeHCl_3$  at  $70^\circ$ . Typical reactions are summarized in the scheme:



$GeBr_2$  is made by reduction of  $GeBr_4$  or  $GeHBr_3$  with Zn, or by the action of HBr on an excess of Ge at  $400^\circ$ ; it is a yellow solid, mp  $122^\circ$ ,

which disproportionates to Ge and  $GeBr_4$  at  $150^\circ$ , adds HBr at  $40^\circ$ , and hydrolyses to the unstable yellow  $Ge(OH)_2$ .  $GeI_2$  is best prepared by reduction of  $GeI_4$  with aqueous  $H_3PO_2$  in the presence of HI to prevent hydrolysis; it sublimes to give bright orange-yellow crystals, is stable in dry air and disproportionates only when heated above  $\sim 550^\circ$ . The structure of the lemon-yellow, monomeric, pyramidal 3-coordinate  $Ge^{II}$  complex  $[Ge(acac)I]$  (1) has been determined.<sup>(21)</sup>  $GeI_2$  is oxidized to  $GeI_4$  in aqueous KI/HCl; it forms numerous adducts with nitrogen ligands, and reacts with  $C_2H_2$  at  $140^\circ$  to give a compound that was originally formulated as a

3-membered heterocycle  $\begin{array}{c} CH \\ || \\ CH \end{array} \rangle GeI_2$  but which was subsequently shown by mass spectroscopy to have the unusual dimeric structure (2).



The ternary  $Ge^{II}$  halides,  $MGeX_3$  ( $M = Rb, Cs; X = Cl, Br, I$ ) are polymorphic with various distorted perovskite-like (p. 963) structures which reflect the influence of the “non-bonding” pair of electrons on the  $Ge^{II}$  centre.<sup>(22)</sup> Thus, at room temperature, rhombohedral  $CsGeI_3$  has three Ge–I at 275 pm and three at 327 pm whereas in the high-temperature cubic form (above  $277^\circ C$ ) there are six Ge–I distances at 320 pm as a result of position changes of the Ge atoms (reversible order–disorder transition). Again,  $RbGeI_3$  has a lemon-yellow, orthorhombic form below  $-92^\circ$ ; an intermediate, bordeaux-red orthorhombic perovskite form ( $-92^\circ$  to  $-52^\circ$ ); a black rhombohedral form ( $-52^\circ$  to  $-29^\circ$ ); and

<sup>21</sup> S. R. STOBART, M. R. CHURCHILL, F. J. HOLLANDER and W. J. YOUNGS, *J. Chem. Soc., Chem. Commun.*, 911–12 (1979).

<sup>22</sup> G. THIELE, H. W. ROTTER and K. D. SCHMIDT, *Z. anorg. allg. Chem.* **545**, 148–56 (1987); **571**, 60–8 (1989).

a black, cubic perovskite form between  $-29^\circ$  and the decomposition temperature,  $+61^\circ$ . In the yellow form there is one Ge–I at 281 pm, four at 306 pm and one at 327 pm, whereas in the red form there are three Ge–I at 287 pm and three at 324 pm. All the compounds are readily made simply by heating  $\text{Ge}(\text{OH})_2$  with MX in aqueous HX solutions.

Germanium tetrahalides are readily prepared by direct action of the elements or via the action of aqueous HX on  $\text{GeO}_2$ . The lighter members are colourless, volatile liquids, but  $\text{GeI}_4$  is an orange solid (cf.  $\text{CX}_4$ ,  $\text{SiX}_4$ ). All hydrolyse readily and  $\text{GeCl}_4$  in particular is an important intermediate in the preparation of organogermanium compounds via LiR or  $\text{RMgX}$  reagents. Many mixed halides and hydrohalides are also known, as are complexes of the type  $\text{GeF}_6^{2-}$ ,  $\text{GeCl}_6^{2-}$ , *trans*- $\text{L}_2\text{GeCl}_4$  and  $\text{L}_4\text{GeCl}_4$  (L = tertiary amine or pyridine). The curious mixed-valency complex  $\text{Ge}_3\text{F}_{12}$ , i.e.  $[(\text{GeF}_2)_4\text{GeF}_4]$  has been shown to feature distorted square pyramids of  $\{\text{:Ge}^{\text{II}}\text{F}_4\}$  with the “lone-pair” of electrons pointing away from the 4 basal F atoms which are at 181, 195, 220, and 245 pm from the apical  $\text{Ge}^{\text{II}}$ ; the  $\text{Ge}^{\text{IV}}$  atom is at the centre of a slightly distorted octahedron ( $\text{Ge}^{\text{IV}}\text{–F}$  171–180 pm, angle F–Ge–F  $87.5\text{--}92.5^\circ$ ) and the whole structure is held together by F bridges.<sup>(23)</sup>

Property	$\text{GeF}_4$	$\text{GeCl}_4$
MP/ $^\circ\text{C}$	$-15$ (4 atm)	$-49.5$
BP/ $^\circ\text{C}$	$-36.5$ (subl)	83.1
Density ( $T^\circ\text{C}$ )/ $\text{g cm}^{-3}$	2.126 ( $0^\circ$ )	1.844 ( $30^\circ$ )
Property	$\text{GeBr}_4$	$\text{GeI}_4$
MP/ $^\circ\text{C}$	26	146
BP/ $^\circ\text{C}$	186	$\sim 400$
Density ( $T^\circ\text{C}$ )/ $\text{g cm}^{-3}$	2.100 ( $30^\circ$ )	4.322 ( $26^\circ$ )

### Tin halides

The structural chemistry of  $\text{Sn}^{\text{II}}$  halides is particularly complex, partly because of the

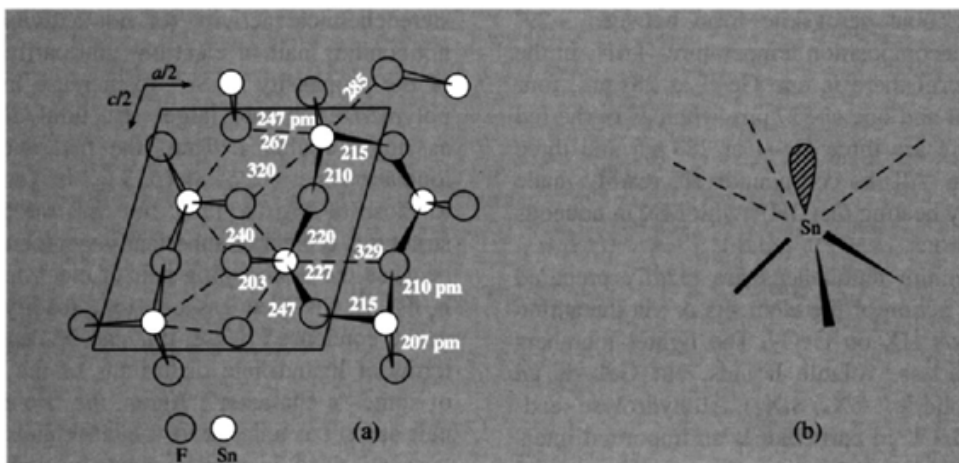
stereochemical activity (or non-activity) of the nonbonding pair of electrons and partly because of the propensity of  $\text{Sn}^{\text{II}}$  to increase its CN by polymerization into larger structural units such as rings or chains. Thus, the first and second ionization energies of Sn (p. 372) are very similar to those of Mg (p. 111), but  $\text{Sn}^{\text{II}}$  rarely adopts structures typical of spherically symmetrical ions because the nonbonding pair of electrons, which is  $5s^2$  in the free gaseous ion, readily distorts in the condensed phase; this can be described in terms of ligand-field distortions or the adoption of some “p character”. Again, the “nonbonding” pair can act as a donor to vacant orbitals, and the “vacant” third 5p orbital and 5d orbitals can act as acceptors in forming further covalent bonds. A good example of this occurs with the adducts  $[\text{SnX}_2(\text{NMe}_3)]$  (X = Cl, Br, I): the  $\text{Sn}^{\text{II}}$  atom, which has accepted a pair of electrons from the ligand  $\text{NMe}_3$ , can itself donate its own lone-pair to a strong Lewis acid to form a double adduct of the type  $[\text{BF}_3\{\leftarrow\text{SnX}_2(\leftarrow\text{NMe}_3)\}]$  (X = Cl, Br, I).<sup>(24)</sup> Further examples, including more complicated interactions, are described later in this subsection.

$\text{SnF}_2$  (which is obtained as colourless monoclinic crystals by evaporation of a solution of SnO in 40% aqueous HF) is composed of  $\text{Sn}_4\text{F}_8$  tetramers interlinked by weaker Sn–F interactions;<sup>(25)</sup> the tetramers are puckered 8-membered rings of alternating Sn and F as shown in Fig. 10.3 and each Sn is surrounded by a highly distorted octahedron of F (1 Sn– $\text{F}_t$  at  $\sim 205$  pm, 2 Sn– $\text{F}_\mu$  at  $\sim 218$  pm, and 3 much longer Sn $\cdots$ F in the range 240–329 pm, presumably due to the influence of the nonbonding pair of electrons. In aqueous solutions containing  $\text{F}^-$  the predominant species is the very stable pyramidal complex  $\text{SnF}_3^-$  but crystallization is attended by further condensation. For example, crystallization of  $\text{SnF}_2$  from aqueous solutions containing NaF does not give  $\text{NaSnF}_3$  as previously supposed but

<sup>24</sup> C. C. HSU and R. A. GEANANGEL, *Inorg. Chem.* **19**, 110–9 (1980).

<sup>25</sup> R. C. McDONALD, H. HO-KUEN HAU and K. ERIKS, *Inorg. Chem.* **15**, 762–5 (1976).

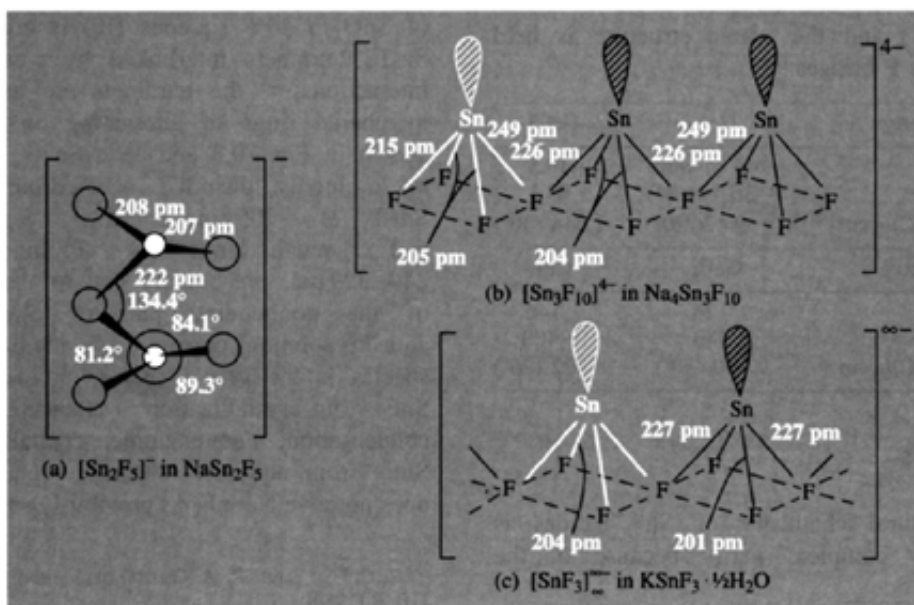
<sup>23</sup> J. C. TAYLOR and P. W. WILSON, *J. Am. Chem. Soc.* **95**, 1834–8 (1973).



**Figure 10.3** Structure of  $SnF_2$  showing (a) interconnected rings of  $\{Sn_4F_4(F_4)\}$ , and (b) the unsymmetrical 3 + 3 coordination around Sn.

$NaSn_2F_5$  or  $Na_4Sn_3F_{10}$  depending on conditions. The  $\{Sn_2F_5\}$  unit in the first compound can be thought of as a discrete ion  $[Sn_2F_5]^-$  or as an  $F^-$  ion coordinating to 2  $SnF_2$  molecules (Fig. 10.4a): each Sn is trigonal pyramidal with two close  $F_1$ , one intermediate  $F_\mu$ , and 3 more distant F at 253, 298, and

301 pm. By contrast the compound  $Na_4Sn_3F_{10}$  features 3 corner-shared square-pyramidal  $\{SnF_4\}$  units (Fig. 10.4b) though the wide range of Sn–F distances could be taken to indicate incipient formation of a central  $SnF_4^{2-}$  weakly bridged to two terminal  $SnF_3^-$  groups. In the corresponding system with KF the compound



**Figure 10.4** Structure of some fluoro-complexes of  $Sn^{II}$ .



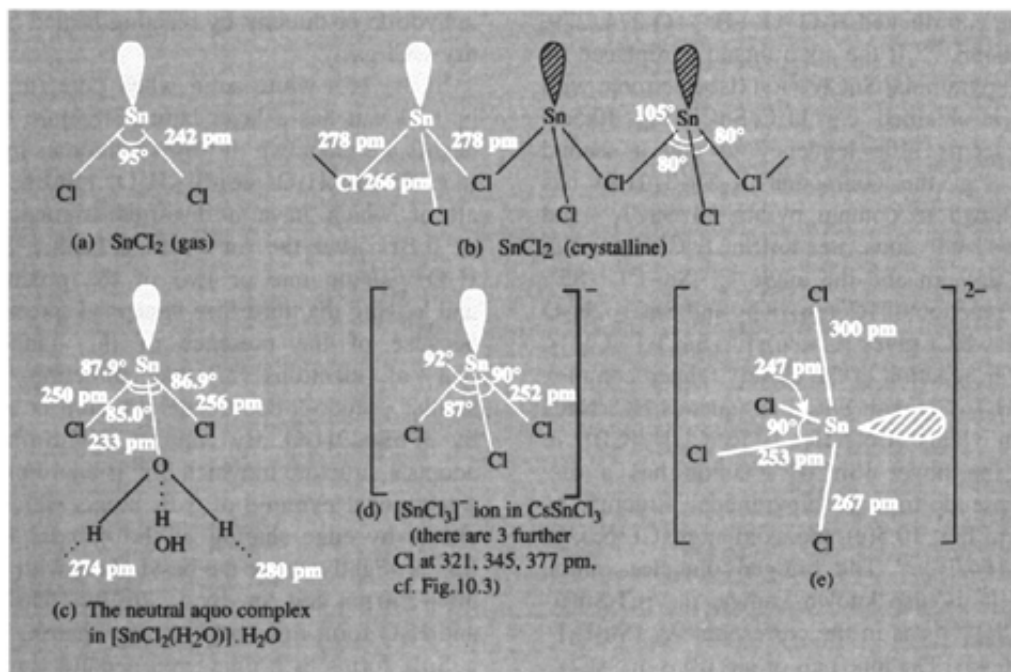


Figure 10.5 Structure of  $\text{SnCl}_2$  and some chloro complexes of  $\text{Sn}^{\text{II}}$ .

that crystallizes is  $\text{KSnF}_3 \cdot \frac{1}{2}\text{H}_2\text{O}$  in which the bridging of square pyramids is extended to give infinite chain polymers (Fig. 10.4c). (The main commercial application of  $\text{SnF}_2$  is in toothpaste and dental preparations where it is used to prevent demineralization of teeth and to lessen the development of dental caries.)

$\text{SnF}_4$  is described on p. 381. There are also some intriguing mixed valence compounds such as  $\text{Sn}_3\text{F}_8$  (i.e.  $\text{Sn}_2^{\text{II}}\text{Sn}^{\text{IV}}\text{F}_8$ ) which is formed when solutions of  $\text{SnF}_2$  in anhydrous  $\text{HF}$  are oxidized at room temperature with  $\text{F}_2$ ,  $\text{O}_2$  or even  $\text{SO}_2$ ; the structure features nearly regular  $\{\text{Sn}^{\text{IV}}\text{F}_6\}$  octahedra *trans*-bridged to  $\{\text{Sn}^{\text{II}}\text{F}_3\}$  pyramids which themselves form polymeric  $\text{Sn}^{\text{II}}\text{F}$  chains:  $\text{Sn}^{\text{IV}}\text{-F}$  196 pm and  $\text{Sn}^{\text{II}}\text{-F}$  210, 217, 225 pm with weaker  $\text{Sn}^{\text{II}}\cdots\text{F}$  interactions in the range 255–265 pm.<sup>(26)</sup> Another example is  $\alpha\text{-Sn}_2\text{F}_6$  (i.e.  $\text{Sn}^{\text{II}}\text{Sn}^{\text{IV}}\text{F}_6$ ) which transforms to  $\beta\text{-Sn}_2\text{F}_6$  at  $112^\circ$  and to  $\gamma\text{-Sn}_2\text{F}_6$  at  $197^\circ$ .

High-temperature neutron diffraction studies<sup>(27)</sup> have shown that this latter phase has the cubic ordered  $\text{ReO}_3$ -type structure (p. 1047) with octahedral coordination of both types of Sn atoms by F ( $\text{Sn}^{\text{II}}\text{-F}$  229 pm,  $\text{Sn}^{\text{IV}}\text{-F}$  186 pm). The  $\beta$ -phase also features octahedral coordination in a structure closely related to that of rhombohedral  $\text{LiSbF}_6$ .

Tin(II) chlorides are similarly complex (Fig. 10.5). In the gas phase,  $\text{SnCl}_2$  forms bent molecules, but the crystalline material (mp  $246^\circ$ , bp  $623^\circ$ ) has a layer structure with chains of corner-shared trigonal pyramidal  $\{\text{SnCl}_3\}$  groups. The dihydrate also has a 3-coordinated structure with only 1 of the  $\text{H}_2\text{O}$  molecules directly bonded to the  $\text{Sn}^{\text{II}}$  (Fig. 10.5c); the neutral aquo complexes are arranged in double layers with the second  $\text{H}_2\text{O}$  molecules interleaved between them to form a two-dimensional H-bonded network

<sup>26</sup> M. F. A. DOVE, R. KING and T. J. KING, *J. Chem. Soc., Chem. Commun.*, 944–5 (1973).

<sup>27</sup> M. RUCHAUD, C. MIRAMBET, L. FOURNES, J. GRANNEC and J. L. SOUBEYROUX, *Z. anorg. allg. Chem.* **590**, 173–80 (1990).



with the coordinated  $\text{H}_2\text{O}$  ( $\text{O}-\text{H}\cdots\text{O}$  274, 279, and 280 pm.<sup>(28)</sup> If the aquo ligand is replaced by  $\text{Cl}^-$  the pyramidal  $\text{SnCl}_3^-$  ion (isoelectronic with  $\text{SbCl}_3$ ) is obtained, e.g. in  $\text{CsSnCl}_3$  Fig. 10.5d). There seems little tendency to add a second ligand: e.g. the compound  $\text{K}_2\text{SnCl}_4\cdot\text{H}_2\text{O}$  has been shown to contain pyramidal  $\text{SnCl}_3^-$  and "isolated"  $\text{Cl}^-$  ions, i.e.  $\text{K}_2[\text{SnCl}_3]\text{Cl}\cdot\text{H}_2\text{O}$  with  $\text{Sn}-\text{Cl}$  259 pm and the angle  $\text{Cl}-\text{Sn}-\text{Cl} \sim 85^\circ$ . Again, reaction of  $[\text{Co}(\text{en})_3]\text{Cl}_3$  and  $\text{SnCl}_2\cdot 2\text{H}_2\text{O}$  in excess  $\text{HCl}$  gives  $[\text{Co}(\text{en})_3]^{3+}[\text{SnCl}_3]^- (\text{Cl}^-)_2$ . However, reaction of the closely related complex  $[\text{Co}(\text{NH}_3)_6]\text{Cl}_3$  with  $\text{SnCl}_2$  in aqueous  $\text{HCl}/\text{NaCl}$  solution yields  $[\text{Co}(\text{NH}_3)_6]^{3+}[\text{SnCl}_4]^{2-} (\text{Cl}^-)$  in which the novel  $[\text{SnCl}_4]^{2-}$  anion has a distorted pseudo-trigonal bipyramidal structure as shown in Fig. 10.5(e), the axial angle  $\text{Cl}-\text{Sn}-\text{Cl}$  being  $164.7^\circ$ .<sup>(29)</sup> The bridged dinuclear anion  $[\text{Sn}_2\text{Cl}_5]^-$  is also known, i.e.  $[\text{Cl}_2\text{Sn}(\mu\text{-Cl})\text{SnCl}_2]^-$ <sup>(30)</sup> as in the corresponding  $[\text{Sn}_2\text{F}_5]^-$  (Fig. 10.4a). The lone pair of electrons in  $\text{SnCl}_3^-$  can itself act as a ligating bond: for example,  $\text{SnCl}_3^-$  can replace  $\text{PPh}_3$  from the central Au atom in the cluster cation  $[\text{Au}_8(\text{PPh}_3)_8]^{2+}$  to give  $[\text{Au}_8(\text{PPh}_3)_7(\text{SnCl}_3)]^+$ .<sup>(31)</sup> Another interesting system involves crown complexes (p. 96) such as  $[\text{Sn}(18\text{-crown-6})\text{Cl}]^+[\text{SnCl}_3]^-$  in which the cation features 7-coordinate hexagonal-pyramidal  $\text{Sn}^{\text{II}}$ .<sup>(32)</sup>

Apart from its structural interest,  $\text{SnCl}_2$  is important as a widely used mild reducing agent in acid solution. The dihydrate is commercially available for use in electrolytic tin-plating baths, as a sensitizer in silvering mirrors and in the plating of plastics, and as a perfume stabilizer in toilet soaps. The anhydrous material can be obtained either by dehydration using acetic

anhydride or directly by reacting heated Sn with dry  $\text{HCl}$  gas.

$\text{SnBr}_2$  is a white solid when pure (mp  $216^\circ$ , bp  $620^\circ$ ); it has a layer-lattice structure but the details are unknown. It forms numerous hydrates (e.g.  $3\text{SnBr}_2\cdot\text{H}_2\text{O}$ ,  $2\text{SnBr}_2\cdot\text{H}_2\text{O}$ ,  $6\text{SnBr}_2\cdot 5\text{H}_2\text{O}$ ) all of which have a distorted trigonal prism of 6 Br about the  $\text{Sn}^{\text{II}}$  with a further Br and  $\text{H}_2\text{O}$  capping one or two of the prism faces and leaving the third face uncapped (presumably because of the presence of the nonbonding pair of electrons in that direction).<sup>(33)</sup> A similar pseudo-9-coordinate structure is adopted by  $3\text{PbBr}_2\cdot 2\text{H}_2\text{O}$ . By contrast,  $\text{NH}_4\text{SnBr}_3\cdot\text{H}_2\text{O}$  adopts a structure in which  $\text{Sn}^{\text{II}}$  is coordinated by a tetragonal pyramid of 5 Br atoms which form chains by edge sharing of the 4 basal Br; the  $\text{Sn}^{\text{II}}$  is slightly above the basal plane with  $\text{Sn}-\text{Br}$  304–350 pm and  $\text{Sn}-\text{Br}_{\text{apex}}$  269 pm. The  $\text{NH}_4^+$  and  $\text{H}_2\text{O}$  form rows between the chains.

$\text{SnI}_2$  forms as brilliant red needles (mp  $316^\circ$ , bp  $720^\circ$ ) when Sn is heated with  $\text{I}_2$  in 2 M hydrochloric acid. It has a unique structure in which one-third of the Sn atoms are in almost perfect octahedral coordination in rutile-like chains (2 Sn–I 314.7 pm, 4 Sn–I 317.4 pm, and no significant distortions of angles from  $90^\circ$ ); these chains are in turn cross-linked by double chains containing the remaining Sn atoms which are themselves 7-coordinate (5 Sn–I all on one side at 300.4–325.1 and 2 more-distant I at 371.8 pm).<sup>(34)</sup> There is an indication here of reduced distortion in the octahedral site and this has been observed more generally for compounds with the heavier halides and chalcogenides in which the nonbonding electron pair on  $\text{Sn}^{\text{II}}$  can delocalize into a low-lying band of the crystal. Accordingly,  $\text{SnTe}$  is a metalloid with cubic NaCl structure. Likewise,  $\text{CsSn}^{\text{II}}\text{Br}_3$  has the ideal cubic perovskite structure (p. 963);<sup>(35)</sup> the compound forms black lustrous crystals with a semi-metallic

<sup>28</sup> H. KIRIYAMA, K. KITAHAMA, O. NAKAMURA and R. KIRIYAMA, *Bull. Chem. Soc. Japan* **46**, 1389–95 (1973).

<sup>29</sup> H. J. HAUPT, F. HUBER and H. PREUT, *Z. anorg. allg. Chem.* **422**, 97–103 (1976).

<sup>30</sup> M. VEITH, B. GÜDICKE and V. HUCH, *Z. anorg. allg. Chem.* **579**, 99–110 (1989).

<sup>31</sup> Z. DEMIDOWICZ, R. L. JOHNSTON, J. C. MACHELL, D. M. P. MINGOS and I. D. WILLIAMS, *J. Chem. Soc., Dalton Trans.*, 1751–6 (1988).

<sup>32</sup> M. G. B. DREW and D. G. NICHOLSON, *J. Chem. Soc., Dalton Trans.*, 1543–9 (1986).

<sup>33</sup> J. ANDERSON, *Acta Chem. Scand.* **26**, 1730, 2543, 3813 (1973).

<sup>34</sup> R. A. HOWIE, W. MOSER and I. C. TREVENA, *Acta Cryst.* **B28**, 2965–71 (1972).

<sup>35</sup> J. D. DONALDSON, J. SILVER, S. HADJIMINOLIS and S. D. ROSS, *J. Chem. Soc., Dalton Trans.*, 1500–6 (1975) and

conductivity of  $\sim 10^3 \text{ ohm}^{-1} \text{ cm}^{-1}$  at room temperature due, it is thought, to the population of a low-lying conduction band formed by the overlap of "empty"  $t_2$  5d orbitals on Br. In this connection it is noteworthy that  $\text{Cs}_2\text{Sn}^{\text{IV}}\text{Br}_6$  has a very similar structure to  $\text{CsSn}^{\text{II}}\text{Br}_3$  (i.e.  $\text{Cs}_2\text{Sn}_2^{\text{II}}\text{Br}_6$ ) but with only half the Sn sites occupied — it is white and non-conducting since there are no high-energy nonbonding electrons to populate the conduction band which must be present. Similarly, yellow  $\text{CsSn}^{\text{II}}\text{I}_3$ ,  $\text{CsSn}_2^{\text{II}}\text{Br}_5$ ,  $\text{Cs}_4\text{Sn}^{\text{II}}\text{Br}_6$  and compositions in the system  $\text{CsSn}_2^{\text{II}}\text{X}_5$  ( $\text{X} = \text{Cl}, \text{Br}$ ) all transform to black metalloids on being warmed, and even yellow monoclinic  $\text{CsSnCl}_3$  (Fig. 10.5d) transforms at  $90^\circ$  to a dark-coloured cubic perovskite structure. In solutions of  $\text{SnX}_2$  in aqueous  $\text{HX}$ , however, the pyramidal  $\text{SnX}_3^-$  ions are formed and, by suitable mixtures of halides followed by extraction into  $\text{Et}_2\text{O}$ , all ten trihalogenostannate(II) anions  $[\text{SnCl}_x\text{Br}_y\text{I}_z]^-$  ( $x + y + z = 3$ ) have been observed and characterized by  $^{119}\text{Sn}$  nmr spectroscopy.<sup>(36)</sup>

Tin(IV) halides are more straightforward.  $\text{SnF}_4$  (prepared by the action of anhydrous  $\text{HF}$  on  $\text{SnCl}_4$ ) is an extremely hygroscopic, white crystalline compound which sublimes above  $700^\circ$ . The structure (unlike that of  $\text{CF}_4$ ,  $\text{SiF}_4$  and  $\text{GeF}_4$ ) is polymeric with octahedral coordination

Property	$\text{SnF}_4$	$\text{SnCl}_4$
Colour	White	Colourless
MP/ $^\circ\text{C}$	—	-33.3
BP/ $^\circ\text{C}$	$\sim 705$ (subl)	114
Density ( $T^\circ\text{C}$ )/ $\text{g cm}^{-3}$	4.78 (20°)	2.234(20°)
Sn-X/pm	188, 202	231
Property	$\text{SnBr}_4$	$\text{SnI}_4$
Colour	Colourless	Brown
MP/ $^\circ\text{C}$	31	144
BP/ $^\circ\text{C}$	205	348
Density ( $T^\circ\text{C}$ )/ $\text{g cm}^{-3}$	3.340(35°)	4.56(20°)
Sn-X/pm	244	264

about Sn: the  $\{\text{SnF}_6\}$  units are joined into planar layers by edge-sharing of 4 equatorial F atoms ( $\text{Sn}-\text{F}_\mu$  202 pm) leaving 2 further (terminal) F in *trans* positions above and below each Sn ( $\text{Sn}-\text{F}_t$  188 pm). The other  $\text{SnX}_4$  can be made by direct action of the elements and are unremarkable volatile liquids or solids comprising tetrahedral molecules. Similarities with the tetrahalides of Si and Ge are obvious. The compounds hydrolyse readily but definite hydrates can also be isolated from acid solution, e.g.  $\text{SnCl}_4 \cdot 5\text{H}_2\text{O}$ ,  $\text{SnBr}_4 \cdot 4\text{H}_2\text{O}$ . Complexes with a wide range of organic and inorganic ligands are known, particularly the 6-coordinate *cis*- and *trans*- $\text{L}_2\text{SnX}_4$  and occasionally the 1:1 complexes  $\text{LSnX}_4$ . Stereochemistry has been deduced by infrared and Mössbauer spectroscopy and, when possible, by X-ray crystallography. The octahedral complexes  $\text{SnX}_6^{2-}$  ( $\text{X} = \text{Cl}, \text{Br}, \text{I}$ ) are also well characterized for numerous cations. Five-coordinate trigonal bipyramidal complexes are less common but have been established for  $\text{SnCl}_5^-$  and  $\text{Me}_2\text{SnCl}_3^-$ . A novel rectangular pyramidal geometry for  $\text{Sn}^{\text{IV}}$  has been revealed by X-ray analysis of the spirocyclic dithiolato complex anion  $[(\text{MeC}_6\text{H}_3\text{S}_2)_2\text{SnCl}]^-$ : the Cl atom occupies the apical position and the Sn atom is slightly above the plane of the 4 S atoms (mean angle  $\text{Cl}-\text{Sn}-\text{Cl}$   $103^\circ$ ).<sup>(37)</sup> A similar stereochemistry has also been established for  $\text{Si}^{\text{IV}}$  (p. 335) and for  $\text{Ge}^{\text{IV}}$  in  $[(\text{C}_6\text{H}_4\text{O}_2)_2\text{GeCl}]^-$ .

### Lead halides

Lead continues the trends outlined in preceding sections,  $\text{PbX}_2$  being much more stable thermally and chemically than  $\text{PbX}_4$ . Indeed, the only stable tetrahalide is the yellow  $\text{PbF}_4$  (mp  $600^\circ$ );  $\text{PbCl}_4$  is a yellow oil (mp  $-15^\circ$ ) stable below  $0^\circ$  but decomposing to  $\text{PbCl}_2$  and  $\text{Cl}_2$  above  $50^\circ$ ;  $\text{PbBr}_4$  is even less stable and  $\text{PbI}_4$  is of doubtful existence (cf. discussion on  $\text{TlI}_3$ , p. 239). Stability can be markedly increased by coordination: e.g.

1980-3 (1975); see also J. D. DONALDSON and J. SILVER, *J. Chem. Soc., Dalton Trans.*, 666-9 (1973).

<sup>36</sup> J. M. CODDINGTON and M. J. TAYLOR, *J. Chem. Soc., Dalton Trans.*, 2223-7 (1989).

<sup>37</sup> A. C. SAU, R. O. DAY and R. R. HOLMES, *Inorg. Chem.* **20**, 3076-81 (1981); *J. Am. Chem. Soc.* **102**, 7972-3 (1980).

direct chlorination of  $\text{PbCl}_2$  in aqueous  $\text{HCl}$  followed by addition of an alkali metal chloride gives stable yellow salts  $\text{M}_2\text{PbCl}_6$  ( $\text{M} = \text{Na}, \text{K}, \text{Rb}, \text{Cs}, \text{NH}_4$ ) which can serve as a useful source of  $\text{Pb}^{\text{IV}}$ . By contrast,  $\text{PbX}_2$  are stable crystalline compounds which can readily be prepared by treating any water-soluble  $\text{Pb}^{\text{II}}$  salt with  $\text{HX}$  or halide ions to precipitate the insoluble  $\text{PbX}_2$ . As with  $\text{Sn}$ , the first two ionization energies of  $\text{Pb}$  are very similar to those of  $\text{Mg}$ ; moreover, the 6-coordinate radius of  $\text{Pb}^{\text{II}}$  (119 pm) is virtually identical with that of  $\text{Sr}^{\text{II}}$  (118 pm) and there is less evidence of the structurally distorting influence of the nonbonding pair of electrons. Thus  $\alpha$ - $\text{PbF}_2$ ,  $\text{PbCl}_2$ , and  $\text{PbBr}_2$  all form colourless orthorhombic crystals in which  $\text{Pb}^{\text{II}}$  is surrounded by 9 X at the corners of a tricapped trigonal prism. There are, in fact, never 9 equidistant X neighbours but a range of distances in which one can discern 7 closer and 2 more distant neighbours. This (7 + 2)-coordination is also a feature of the structures of  $\text{BaX}_2$  ( $\text{X} = \text{Cl}, \text{Br}, \text{I}$ ),  $\text{EuCl}_2$ ,  $\text{CaH}_2$ , etc.; see also hydrated tin(II) bromides, p. 380.

The high-temperature  $\beta$ -form of  $\text{PbF}_2$  has the cubic fluorite ( $\text{CaF}_2$ ) structure with 8-coordinated  $\text{Pb}^{\text{II}}$ .  $\text{PbI}_2$  (yellow) has the  $\text{CdI}_2$  hexagonal layer lattice structure. Like many other heavy-metal halides,  $\text{PbCl}_2$  and  $\text{PbBr}_2$  are photo-sensitive and deposit metallic  $\text{Pb}$  on irradiation with ultraviolet or visible light.  $\text{PbI}_2$  is a photoconductor and decomposes on exposure to green light ( $\lambda_{\text{max}}$  494.9 nm). Many mixed halides have also been characterized, e.g.  $\text{PbFCl}$ ,  $\text{PbFBr}$ ,  $\text{PbFI}$ ,  $\text{PbX}_2 \cdot 4\text{PbF}_2$ , etc. Of these  $\text{PbFCl}$  is an important tetragonal layer-lattice structure type frequently adopted by large cations in the presence of 2 anions of differing size;<sup>(38)</sup> its sparing solubility in water (37 mg per 100  $\text{cm}^3$  at 25°C) forms the basis of a gravimetric method of determining F. It is also interesting to note that  $\text{PbF}_2$  was the first ionically conducting crystalline compound to be discovered (Michael Faraday, 1838).

Property	$\text{PbF}_2$	$\text{PbCl}_2$
MP/°C	818	500
BP/°C	1290	953
Density/g $\text{cm}^{-3}$	8.24 ( $\alpha$ ), 7.77 ( $\beta$ )	5.85
Solubility in		
$\text{H}_2\text{O}$ (T°C)/	64 (20°)	670 (0°)
mg per 100 $\text{cm}^3$		3200 (100°)
Property	$\text{PbBr}_2$	$\text{PbI}_2$
MP/°C	367	400
BP/°C	916	860–950 (decomp)
Density/g $\text{cm}^{-3}$	6.66	6.2
Solubility in		
$\text{H}_2\text{O}$ (T°C)/	455 (0°)	44 (0°)
mg per 100 $\text{cm}^3$	4710 (100°)	410 (100°)

$\text{Pb}^{\text{II}}$  apparently forms complexes with an astonishing range of stoichiometries,<sup>(39)</sup> but structural information is frequently lacking.  $\text{Cs}_4\text{PbX}_6$  ( $\text{X} = \text{Cl}, \text{Br}, \text{I}$ ) have the  $\text{K}_4\text{CdCl}_6$  structure with discrete  $[\text{Pb}^{\text{II}}\text{X}_6]^{4-}$  units.  $\text{CsPb}^{\text{II}}\text{X}_3$  also feature octahedral coordination (in perovskite-like structures, cf. p. 963) but there is sometimes appreciable distortion as in the yellow, low-temperature form of  $\text{CsPbI}_3$  which adopts the  $\text{NH}_4\text{CdCl}_3$  structure with three  $\text{Pb}$ – $\text{I}$  distances, 301, 325, and 342 pm. Note also the orange-yellow crystalline compound of overall composition  $[\text{Co}(\text{en})_3\text{PbCl}_5 \cdot 1.5\text{H}_2\text{O}]$  which in fact features a novel chain anion  $[\text{Pb}_2\text{Cl}_9]_n^{5n-}$  and should be formulated  $[\text{Co}(\text{en})_3]_2[\text{Pb}_2\text{Cl}_9]\text{Cl} \cdot 3\text{H}_2\text{O}$ .<sup>(40)</sup> There are also many ternary solid state compounds, e.g.  $\text{Pb}_{13}^{\text{II}}\text{O}_{10}\text{Br}_6$ .<sup>(41)</sup>

### 10.3.3 Oxides and hydroxides

$\text{GeO}$  is obtained as a yellow sublimate when powdered  $\text{Ge}$  and  $\text{GeO}_2$  are heated to 1000°, and dark-brown crystalline  $\text{GeO}$  is obtained on further heating at 650°. The compound can also be obtained by dehydrating  $\text{Ge}(\text{OH})_2$

<sup>39</sup> E. W. ABEL, Lead, Chap. 18 in *Comprehensive Inorganic Chemistry*, Vol. 2, pp. 105–46, Pergamon Press, Oxford, 1973.

<sup>40</sup> A. AQUILINO, M. CANNAS, A. CHRISTINI and G. MARONGIU, *J. Chem. Soc., Chem. Commun.*, 347–8 (1978).

<sup>41</sup> H.-J. RIEBE and H.-L. KELLER, *Z. anorg. allg. Chem.* **571**, 139–47 (1989).

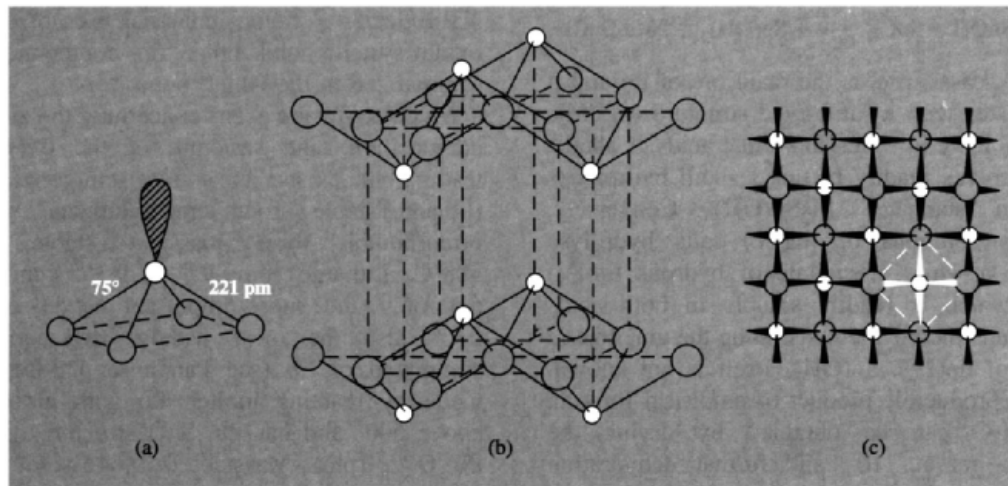
<sup>38</sup> N. N. GREENWOOD, *Ionic Crystals, Lattice Defects, and Nonstoichiometry*, pp. 59–60, Butterworths, London 1968.

(p. 376) but neither compound is particularly well characterized. Both are reducing agents and GeO disproportionates rapidly to Ge and GeO<sub>2</sub> above 700°. Much more is known about GeO<sub>2</sub> and there is an impressive resemblance between the oxide chemistry of Ge<sup>IV</sup> and Si<sup>IV</sup>. Thus hexagonal GeO<sub>2</sub> has the 4-coordinated  $\beta$ -quartz structure (p. 342), tetragonal GeO<sub>2</sub> has the 6-coordinated rutile-like structure of stishovite (p. 343), and vitreous GeO<sub>2</sub> resembles fused silica. Similarly, Ge analogues of all the major types of silicates and aluminosilicates (pp. 347–59) have been prepared. Be<sub>2</sub>GeO<sub>4</sub> and Zn<sub>2</sub>GeO<sub>4</sub> have the phenacite and willemite structures with “isolated” {GeO<sub>4</sub>} units; Sc<sub>2</sub>Ge<sub>2</sub>O<sub>7</sub> has the thortveitite structure; BaTiGe<sub>3</sub>O<sub>9</sub> has the same type of cyclic ion as benitoite, and CaMgGe<sub>2</sub>O<sub>6</sub> has a chain structure similar to diopside. Further, the two crystalline forms of Ca<sub>2</sub>GeO<sub>4</sub> are isostructural with two forms of Ca<sub>2</sub>SiO<sub>4</sub>, and Ca<sub>3</sub>GeO<sub>5</sub> crystallizes in no fewer than 4 of the known structures of Ca<sub>3</sub>SiO<sub>5</sub>. The reaction chemistry of the two sets of compounds is also very similar.

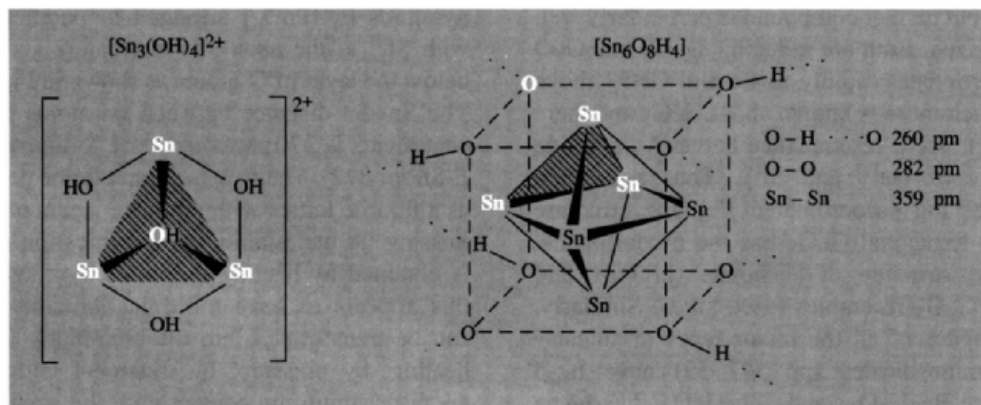
SnO exists in several modifications. The commonest is the blue-black tetragonal modification formed by the alkaline hydrolysis of Sn<sup>II</sup> salts to the hydrous oxide and subsequent dehydration in the absence of air. The structure features square

pyramids of {SnO<sub>4</sub>} arranged in parallel layers with Sn<sup>II</sup> at the apex and alternately above and below the layer of O atoms as shown in Fig. 10.6. The Sn–Sn distance between tin atoms in adjacent layers is 370 pm, very close to the values in  $\beta$ -Sn (p. 372). The structure can also be described as a fluorite lattice with alternate layers of anions missing. A metastable, red modification of SnO is obtained by heating the white hydrous oxide; this appears to have a similar structure and it can be transformed into the blue-black form by heating, by pressure, by treatment with strong alkali or simply by contact with the stable form. Both forms oxidize to SnO<sub>2</sub> with incandescence when heated in air to ~300° but when heated in the absence of O<sub>2</sub>, the compound disproportionates like GeO. Various mixed-valence oxides have also been reported of which the best characterized is Sn<sub>3</sub>O<sub>4</sub>, i.e. Sn<sup>II</sup>Sn<sup>IV</sup>O<sub>4</sub>.

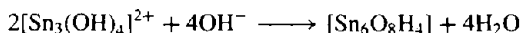
SnO and hydrous tin(II) oxide are amphoteric, dissolving readily in aqueous acids to give Sn<sup>II</sup> or its complexes, and in alkalis to give the pyramidal Sn(OH)<sub>3</sub><sup>-</sup>; at intermediate values of pH, condensed basic oxide–hydroxide species form, e.g. [(OH)<sub>2</sub>SnOSn(OH)<sub>2</sub>]<sup>2-</sup> and [Sn<sub>3</sub>(OH)<sub>4</sub>]<sup>2+</sup>, etc. Analytically, the hydrous oxide frequently has a composition close to 3SnO·H<sub>2</sub>O and an X-ray study shows it to



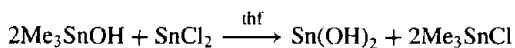
**Figure 10.6** Structure of tetragonal SnO (and PbO) showing (a) a single square-based pyramid {SnO<sub>4</sub>}, (b) the arrangement of the pyramids in layers, and (c) a plane view of a single layer.



contain pseudo-cubic Sn<sub>6</sub>O<sub>8</sub> clusters resembling Mo<sub>6</sub>Cl<sub>8</sub><sup>4+</sup> (p. 1022) with 8 oxygen atoms centred above the faces of an Sn<sub>6</sub> octahedron and joined in infinite array by H bonds, i.e. Sn<sub>6</sub>O<sub>8</sub>H<sub>4</sub>; the compound can be thought of as being formed by the deprotonation and condensation of 2[Sn<sub>3</sub>(OH)<sub>4</sub>]<sup>2+</sup> units as the pH is raised:



(Hydrolysis of Pb<sup>II</sup> salts leads to different structures, p. 395.) It seems unlikely that pure Sn(OH)<sub>2</sub> itself has ever been prepared from aqueous solutions but it can be obtained as a white, amorphous solid by an anhydrous organometallic method:<sup>(42)</sup>



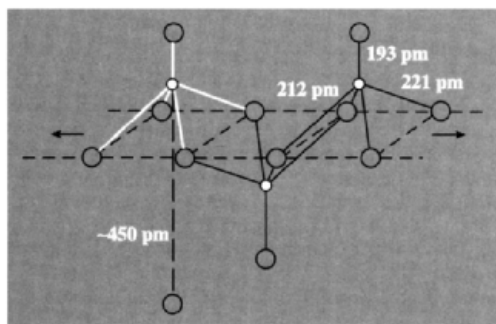
SnO<sub>2</sub>, cassiterite, is the main ore of tin and it crystallizes with a rutile-type structure (p. 961): It is insoluble in water and dilute acids or alkalis but dissolves readily in fused alkali hydroxides to form "stannates" M<sub>2</sub>Sn(OH)<sub>6</sub>. Conversely, aqueous solutions of tin(IV) salts hydrolyse to give a white precipitate of hydrous tin(IV) oxide which is readily soluble in both acids and alkalis thereby demonstrating the amphoteric nature of tin(IV). Sn(OH)<sub>4</sub> itself is not known, but a reproducible product of empirical formula SnO<sub>2</sub>·H<sub>2</sub>O can be obtained by drying the hydrous gel at 110°, and further dehydration

at temperatures up to 600° eventually yields crystalline SnO<sub>2</sub>. Similarly, thermal dehydration of K<sub>2</sub>[Sn(OH)<sub>6</sub>], i.e. "K<sub>2</sub>SnO<sub>3</sub>·3H<sub>2</sub>O", yields successively K<sub>2</sub>SnO<sub>3</sub>·H<sub>2</sub>O, 3K<sub>2</sub>SnO<sub>3</sub>·2H<sub>2</sub>O and, finally, anhydrous K<sub>2</sub>SnO<sub>3</sub>; this latter compound also results when K<sub>2</sub>O is heated directly with SnO<sub>2</sub>, and variations in the ratio of the two reactants yield K<sub>4</sub>SnO<sub>4</sub> and K<sub>2</sub>Sn<sub>3</sub>O<sub>7</sub>. The structure of K<sub>2</sub>SnO<sub>3</sub> does not have 6-coordinate Sn<sup>IV</sup> but chains of 5-coordinate Sn<sup>IV</sup> of composition {SnO<sub>3</sub>} formed by the edge sharing of tetragonal pyramids of {SnO<sub>5</sub>} as shown in Fig. 10.7. The colourless compound RbNa<sub>3</sub>SnO<sub>4</sub>, formed by heating RbSn and Na<sub>2</sub>O<sub>2</sub> at 750° has tetrahedral SnO<sub>4</sub><sup>4-</sup> units (Sn-O 196 pm); it is isotypic with NaLi<sub>3</sub>SiO<sub>4</sub> and NaLi<sub>3</sub>GeO<sub>4</sub>.<sup>(43)</sup> Some industrial uses of tin(IV) oxide systems and other tin compounds are summarized in the Panel (opposite).

Much confusion exists concerning the number, composition, and structure of the oxides of lead. PbO exists as a red tetragonal form (litharge) stable at room temperature and a yellow orthorhombic form (massicot) stable above 488°C. Litharge (mp 897°, *d* 9.355 g cm<sup>-3</sup>) is not only the most important oxide of Pb, it is also the most widely used inorganic compound of Pb (see Panel on p. 386); it is made by reacting molten Pb with air or O<sub>2</sub> above 600° and has the SnO structure (p. 383, Pb-O 230 pm). Massicot (*d* 9.642 g cm<sup>-3</sup>) has

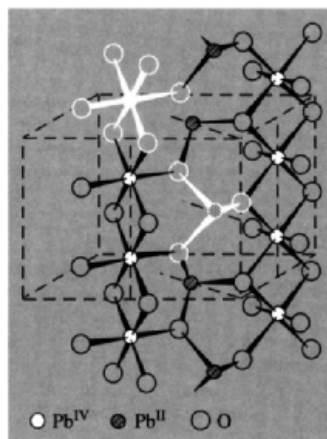
<sup>42</sup> W. D. HONNICK and J. J. ZUCKERMAN, *Inorg. Chem.* **15**, 3034-7 (1976).

<sup>43</sup> K. BERNET and R. HOPPE, *Z. anorg. allg. Chem.* **571**, 101-12 (1989).



**Figure 10.7**  $\{\text{SnO}_3\}$  chain in the structure of  $\text{K}_2\text{SnO}_3$  (and  $\text{K}_2\text{PbO}_3$ ).

a distorted version of the same structure. The mixed-valency oxide  $\text{Pb}_3\text{O}_4$  (red lead, minium,  $d$   $8.924 \text{ g cm}^{-3}$ ) is made by heating  $\text{PbO}$  in air in a reverberatory furnace at  $450\text{--}500^\circ$  and is important commercially as a pigment and primer (see Panel on p. 386). Its structure (Fig. 10.8) consists of chains of  $\text{Pb}^{\text{IV}}\text{O}_6$  octahedra ( $\text{Pb}\text{--O}$



**Figure 10.8** Portion of the crystal structure of  $\text{Pb}_3\text{O}_4$  showing chains of edge-shared  $\text{Pb}^{\text{IV}}\text{O}_6$  octahedra joined by pyramids of  $\text{Pb}^{\text{II}}\text{O}_3$ ; the mean  $\text{O}\text{--Pb}^{\text{II}}\text{--O}$  angle is  $76^\circ$  as in  $\text{PbO}$ .

$214 \text{ pm}$ ) sharing opposite edges, these chains being linked by the  $\text{Pb}^{\text{II}}$  atoms which themselves

### Some Industrial Uses of Tin Compounds

Tin(IV) oxide is much used in the ceramics industry as an opacifier for glazes and enamels. Because of its insolubility (or, rather, slow solubility) in glasses and glazes it also serves as a base for pigments, e.g.  $\text{SnO}_2/\text{V}_2\text{O}_5$  yellows,  $\text{SnO}_2/\text{Sb}_2\text{O}_5$  blue-greys and  $\text{SnO}_2/\text{Cr}_2\text{O}_3$  pinks. These latter, which can vary from a delicate pale pink to a dark maroon, probably involve substitutional incorporation of  $\text{Cr}^{\text{III}}$  for  $\text{Sn}^{\text{IV}}$  with concomitant oxide-ion vacancies, i.e.  $[\text{Sn}^{\text{IV}}_{1-2x}\text{Cr}^{\text{III}}_x\text{O}_{2-x}^{\text{II}}] (\square^-)_x$ . The vanadium- and antimony-tin glazes, on the other hand, probably involve reductive substitution without vacant sites, e.g.  $[\text{Sn}^{\text{IV}}_{1-3x}\text{Sn}^{\text{II}}\text{Sb}_x\text{O}_{2-x}^{\text{II}}]$ . Some 3500 tonnes of  $\text{SnO}_2$  are consumed annually for ceramic glazes.

A related application is the use of  $\text{SnCl}_4$  vapour to toughen freshly fabricated glass bottles by deposition of an invisible transparent film of  $\text{SnO}_2$  ( $<0.1 \mu\text{m}$ ) which is then incorporated in the surface structure of the glass. This increases the strength of the glass and improves its abrasion resistance so that bottles so treated can be made considerably lighter without loss of robustness. When the thickness of the  $\text{SnO}_2$  film is similar to the wavelength of visible light ( $0.1\text{--}1.0 \mu\text{m}$ ), then thin-film interference effects occur and the glass acquires an attractive iridescence. Still thicker films give electrically conducting layers which, after suitable doping with Sb or F ions, can be used as electrodes, electro-luminescent devices (for low-intensity light panels and display signs, in aircraft, cinemas, etc.), fluorescent lamps, antistatic cover-glasses, transparent tube furnaces, deiceable windcreens (especially for aircraft), etc. Another property of these thicker films is their ability to reflect a high proportion of infrared (heat) radiation whilst remaining transparent to visible radiation — the application to heat insulation of windows is obvious.

Attention should be drawn to the use of tin oxide systems as heterogeneous catalysts. The oldest and most extensively patented systems are the mixed tin–vanadium oxide catalysts for the oxidation of aromatic compounds such as benzene, toluene, xylenes and naphthalene in the synthesis of organic acids and acid anhydrides. More recently mixed tin–antimony oxides have been applied to the selective oxidation and ammoxidation of propylene to acrolein, acrylic acid and acrylonitrile.

Homogeneous catalysis by tin compounds is also of great industrial importance. The use of  $\text{SnCl}_4$  as a Friedel–Crafts catalyst for homogeneous acylation, alkylation and cyclization reactions has been known for many decades. The most commonly used industrial homogeneous tin catalysts, however, are the Sn(II) salts of organic acids (e.g. acetate, oxalate, oleate, stearate and octoate) for the curing of silicone elastomers and, more importantly, for the production of polyurethane foams. World consumption of tin catalysts for these last applications alone is over 1000 tonnes pa.

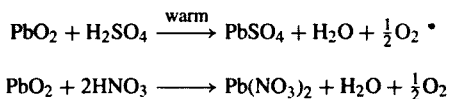
For uses of organotin compounds (i.e. compounds having at least one Sn–C bond), see p. 400.

### The Oxides of Lead<sup>(9,10)</sup>

PbO (red, orange or yellow depending on the method of preparation) is amphoteric and dissolves readily in both acids and alkalis. It is much used in glass manufacture since a high Pb content leads to greater density, lower thermal conductivity, higher refractive index (greater brilliance), and greater stability and toughness. The replacement of the very mobile alkali ions by Pb also leads to high electrical capacities, comparable with mica. PbO is also used to form stable ceramic glazes and vitreous enamels (see SnO<sub>2</sub>, p. 385). Electric storage batteries are the other major user of PbO (either as litharge or as "black oxide", i.e. PbO + Pb). The plates of the battery consist of an inactive grid or support onto which is applied a paste of PbO/H<sub>2</sub>SO<sub>4</sub>. The positive plates are activated by oxidizing PbO to PbO<sub>2</sub> and the negative plates by reducing PbO to Pb. Another use of PbO is in the production of pigments (p. 371).

Red lead (Pb<sub>3</sub>O<sub>4</sub>) is manufactured on the 20000-tonne scale annually and is used primarily as a surface coating to prevent corrosion of iron and steel (check oxidation-reduction potentials). It is also used in the production of leaded glasses and ceramic glazes and, very substantially, as an activator, vulcanizing agent and pigment in natural and artificial rubbers and plastics.

PbO<sub>2</sub> is a strong oxidizing agent and, in addition to its *in situ* production in storage batteries, it is independently manufactured for use as an oxidant in the manufacture of chemicals, dyes, matches and pyrotechnics. It is also used in considerable quantity as a curing agent for sulfide polymers and in high-voltage lightning arresters. Because of the instability of Pb<sup>IV</sup>, PbO<sub>2</sub> tends to give salts of Pb<sup>II</sup> with liberation of O<sub>2</sub> when treated with acids, e.g.

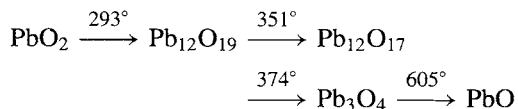


Warm HCl reacts similarly but in the cold PbCl<sub>4</sub> is obtained. PbO<sub>2</sub> is produced commercially by the oxidation of Pb<sub>3</sub>O<sub>4</sub> in alkaline slurry with Cl<sub>2</sub> and the technical product is marketed in 90-kg drums.

Mixed oxides of Pb<sup>IV</sup> with other metals find numerous applications in technology and industry. They are usually made by heating PbO<sub>2</sub> (or PbO) in air with the appropriate oxide, hydroxide or oxoacid salt, the product formed being dependent on the stoichiometry used, e.g. M<sup>II</sup>Pb<sup>IV</sup>O<sub>3</sub>, M<sup>II</sup>Pb<sup>IV</sup>O<sub>4</sub> (M<sup>II</sup> = Ca, Sr, Ba). CaPbO<sub>3</sub> in particular is increasingly replacing Pb<sub>3</sub>O<sub>4</sub> as a priming pigment to protect steel against corrosion by salt water. Mixed oxides of Pb<sup>II</sup> are also important. Ferrimagnetic oxides of general formula PbO.*n*Fe<sub>2</sub>O<sub>3</sub> (*n* = 6, 5, 2.5, 1, 0.5) can be prepared by direct reaction but have not proved to be as attractive, commercially, as the hard ferrite BaFe<sub>12</sub>O<sub>19</sub>. By contrast, the ferroelectric behaviour (p. 57) of several mixed oxides with Pb<sup>II</sup> has excited considerable interest. Many of these compounds have a distorted perovskite-type structure (p. 963); e.g. yellow PbTiO<sub>3</sub> (ferroelectric below 490°C), colourless PbZrO<sub>3</sub> (230°), and PbHfO<sub>3</sub> (215°, antiferroelectric). Others have a tetragonal tungsten-bronze-type structure (p. 1016), e.g. PbNb<sub>2</sub>O<sub>6</sub> (ferroelectric up to 560°C), PbTi<sub>2</sub>O<sub>6</sub> (~215°). The mode of action and uses of hard ferroelectrics has been discussed on p. 58, and the high Curie temperature of many Pb<sup>II</sup> ferroelectrics makes them particularly useful for high-temperature applications.

are pyramidally coordinated by 3 oxygen atoms (2 at 218 pm and 1 at 213 pm). The dioxide normally occurs as the maroon-coloured PbO<sub>2</sub>(I) which has the tetragonal, rutile structure (Pb<sup>IV</sup>-O 218 pm, *d* 9.643 g cm<sup>-3</sup>), but there is also a high-pressure, black, orthorhombic polymorph, PbO<sub>2</sub>(II) (*d* 9.773 g cm<sup>-3</sup>).

When PbO<sub>2</sub> is heated in air it decomposes as follows:<sup>(44)</sup>



In addition, a sesquioxide Pb<sub>2</sub>O<sub>3</sub> can be obtained as vitreous black monoclinic crystals (*d* 10.046 g cm<sup>-3</sup>) by decomposing PbO<sub>2</sub> (or PbO) at 580–620° under an oxygen pressure of 1.4 kbar: in this compound the Pb<sup>II</sup> atoms are situated between layers of distorted Pb<sup>IV</sup>O<sub>6</sub> octahedra (mean Pb<sup>IV</sup>-O 218 pm) with 3 Pb<sup>II</sup>-O in the range 231–246 pm and 3 in the range 264–300 pm. The monoclinic compound Pb<sub>12</sub>O<sub>19</sub> (i.e. PbO<sub>1.583</sub>) forms dark-brown or black crystals which have a pseudocubic defect-fluorite structure with 10 ordered anion vacancies according to the formulation [Pb<sub>24</sub>O<sub>38</sub>(□<sub>-</sub>)<sub>10</sub>] and no detectable variability of composition. It will be recalled that PbO can be considered as a defect fluorite structure in which each alternate layer

<sup>44</sup> W. B. WHITE and R. RAY, *J. Am. Ceram. Soc.* **47**, 242–7 (1964) and references therein.

of O atoms in the (001) direction is missing (p. 383), i.e.  $[\text{Pb}_{24}\text{O}_{24}(\square)_{24}]$ ; it therefore seems reasonable to suppose that the anion vacancies in  $[\text{Pb}_{24}\text{O}_{38}(\square)_{10}]$  are also confined to alternate layers, though it is not clear why this structure should show no variability in composition. Further heating above  $350^\circ$  (or careful oxidation of PbO) yields  $\text{Pb}_{12}\text{O}_{17}$  (i.e.  $\text{PbO}_{1.417}$ ) which is also a stoichiometric ordered defect fluorite structure  $[\text{Pb}_{24}\text{O}_{34}(\square)_{14}]$ . However, oxidation of this phase under increasing oxygen pressure leads to a nonstoichiometric phase of variable composition between  $\text{PbO}_{1.42}$  and  $\text{PbO}_{1.57}$  in which there appears to be a quasi-random array of anion vacancies.<sup>(45)</sup>

Lead does not appear to form a simple hydroxide,  $\text{Pb}(\text{OH})_2$ , [cf.  $\text{Sn}(\text{OH})_2$ , p. 384]. Instead, increasing the pH of solutions of  $\text{Pb}^{\text{II}}$  salts leads to hydrolysis and condensation, see  $[\text{Pb}_6\text{O}(\text{OH})_6]^{4+}$  (p. 395).

### 10.3.4 Derivatives of oxoacids

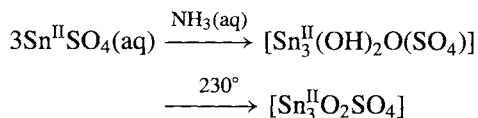
Oxoacid salts of Ge are usually unstable, generally uninteresting, and commercially unimportant. The tetraacetate  $\text{Ge}(\text{OAc})_4$  separates as white needles, mp  $156^\circ$ , when  $\text{GeCl}_4$  is treated with  $\text{TIOAc}$  in acetic anhydride and the resulting solution is concentrated at low pressure and cooled. An unstable sulfate  $\text{Ge}(\text{SO}_4)_2$  is formed in a curious reaction when  $\text{GeCl}_4$  is heated with  $\text{SO}_3$  in a sealed tube at  $160^\circ$ :



Numerous oxoacid salts of  $\text{Sn}^{\text{II}}$  and  $\text{Sn}^{\text{IV}}$  have been reported and several basic salts are also known. Anhydrous  $\text{Sn}(\text{NO}_3)_2$  has not been prepared but the basic salt  $\text{Sn}_3(\text{OH})_4(\text{NO}_3)_2$  can be made by reacting a paste of hydrous tin(II) oxide with aqueous  $\text{HNO}_3$ ; the compound may well contain the oligomeric cation  $[\text{Sn}_3(\text{OH})_4]^{2+}$  illustrated on p. 384.  $\text{Sn}(\text{NO}_3)_4$  can be obtained in anhydrous reactions of

$\text{SnCl}_4$  with  $\text{N}_2\text{O}_5$ ,  $\text{ClNO}_3$  or  $\text{BrNO}_3$ ; the compound readily oxidizes or nitrates organic compounds, probably by releasing reactive  $\text{NO}_3$  radicals. Many phosphates and phosphato complexes have been described: typical examples for  $\text{Sn}^{\text{II}}$  are  $\text{Sn}_3(\text{PO}_4)_2$ ,  $\text{SnHPO}_4$ ,  $\text{Sn}(\text{H}_2\text{PO}_4)_2$ ,  $\text{Sn}_2\text{P}_2\text{O}_7$  and  $\text{Sn}(\text{PO}_3)_2$ . Examples with  $\text{Sn}^{\text{IV}}$  are  $\text{Sn}_2\text{O}(\text{PO}_4)_2$ ,  $\text{Sn}_2\text{O}(\text{PO}_4)_2 \cdot 10\text{H}_2\text{O}$ ,  $\text{SnP}_4\text{O}_7$ ,  $\text{KSn}(\text{PO}_4)_3$ ,  $\text{KSnOPO}_4$  and  $\text{Na}_2\text{Sn}(\text{PO}_4)_2$ . One remarkable compound is tin(IV) hypophosphite,  $\text{Sn}(\text{H}_2\text{PO}_2)_4$  since it contains  $\text{Sn}^{\text{IV}}$  in the presence of the strongly reducing hypophosphorous anion; it has been suggested that the isolation of  $\text{Sn}(\text{H}_2\text{PO}_2)_4$  (colourless crystals) by bubbling  $\text{O}_2$  through a solution of  $\text{SnO}$  in hypophosphorous acid,  $[\text{H}_2\text{PO}(\text{OH})]$ , may be due to a combination of kinetic effects and the low solubility of the product.

Treatment of  $\text{SnO}_2$  with hot dilute  $\text{H}_2\text{SO}_4$  yields the hygroscopic dihydrate  $\text{Sn}(\text{SO}_4)_2 \cdot 2\text{H}_2\text{O}$ . In the  $\text{Sn}^{\text{II}}$  series  $\text{SnSO}_4$  is a stable, colourless compound which is probably the most convenient laboratory source of  $\text{Sn}^{\text{II}}$  uncontaminated with  $\text{Sn}^{\text{IV}}$ ; it is readily prepared by using metallic Sn to displace Cu from aqueous solutions of  $\text{CuSO}_4$ .  $\text{SnSO}_4$  was at one time thought to be isostructural with  $\text{BaSO}_4$  but this seemed unlikely in view of the very different sizes of the cations and the known propensity of  $\text{Sn}^{\text{II}}$  to form distorted structures; it is now known to consist of  $\{\text{SO}_4\}$  groups linked into a framework by O–Sn–O bonds in such a way that Sn is pyramidally coordinated by 3 O atoms at 226 pm (O–Sn–O angles  $77$ – $79^\circ$ ); other Sn–O distances are much larger and fall in the range 295–334 pm.<sup>(46)</sup> A basic sulfate and oxosulfate are also known:



The crystal structures of the oxalates  $\text{SnC}_2\text{O}_4$  and  $\text{K}_2\text{Sn}(\text{C}_2\text{O}_4)_2 \cdot \text{H}_2\text{O}$  show interesting features<sup>(47)</sup>

<sup>46</sup> J. D. DONALDSON and D. C. PUXLEY, *Acta Cryst.* **28B**, 864–7 (1972).

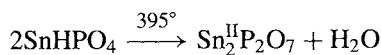
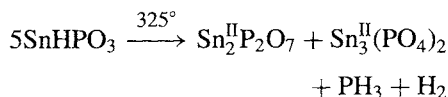
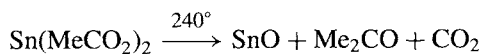
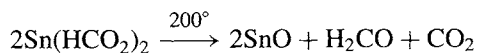
<sup>47</sup> A. D. CHRISTIE, R. A. HOWIE and W. MOSER, *Inorg. Chim. Acta.* **36**, L447–L448 (1979).

<sup>45</sup> J. S. ANDERSON and M. STERNS, *J. Inorg. Nucl. Chem.* **11**, 272–85 (1959).

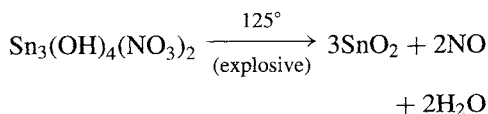
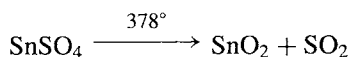
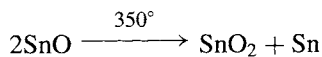


reminiscent of tetragonal SnO (Fig. 10.6). The organotin(IV) sulfate  $(\text{Me}_3\text{Sn})_2\text{SO}_4 \cdot 2\text{H}_2\text{O}$  has trigonal bipyramidal Sn with *trans*- $\text{O}_2\text{SnMe}_3$  stereochemistry, i.e.  $[\text{H}_2\text{O}-\text{SnMe}_3-(\mu-\text{OSO}_2\text{O})-\text{SnMe}_3-\text{OH}_2]$ ; H-bonding between the two non-bridging O-atoms of the sulfate group and water molecules in neighbouring units produces a three-dimensional network.<sup>(48)</sup> In general, the product obtained by the thermal decomposition of  $\text{Sn}^{\text{II}}$  oxoacid salts depends on the coordinating strength of the oxoacid anion. For strong ligands such as formate, acetate and phosphite, other  $\text{Sn}^{\text{II}}$  compounds are formed (often SnO), whereas for less-strongly coordinating ligands such as the sulfate or nitrate internal oxidation to  $\text{SnO}_2$  occurs, e.g.:

*Strong ligands:*



*Weak ligands:*



Most oxoacid derivatives of lead are  $\text{Pb}^{\text{II}}$  compounds, though  $\text{Pb}(\text{OAc})_4$  is well known and is extensively used as a selective oxidizing agent in organic chemistry.<sup>(49)</sup> It can be obtained as

colourless, moisture-sensitive crystals by treating  $\text{Pb}_3\text{O}_4$  with glacial acetic acid.  $\text{Pb}(\text{SO}_4)_2$  is also stable when dry and can be made by the action of conc  $\text{H}_2\text{SO}_4$  on  $\text{Pb}(\text{OAc})_4$  or by electrolysis of strong  $\text{H}_2\text{SO}_4$  between Pb electrodes.  $\text{PbSO}_4$  is familiar as a precipitate for the gravimetric determination of sulfate (solubility 4.25 mg per 100  $\text{cm}^3$  at 25°C);  $\text{PbSeO}_4$  is likewise insoluble. By contrast  $\text{Pb}(\text{NO}_3)_2$  is very soluble in water (37.7 g per 100  $\text{cm}^3$  at 0°, 127 g at 100°). The diacetate is similarly soluble (19.7 and 221 g per 100  $\text{cm}^3$  at 0° and 50° respectively). Both compounds find wide use in the preparation of Pb chemicals by wet methods and are made simply by dissolving PbO in the appropriate aqueous acid. A large number of basic nitrates and acetates is also known. The thermal decomposition of anhydrous  $\text{Pb}(\text{NO}_3)_2$  above 400° affords a convenient source of  $\text{N}_2\text{O}_4$  (see p. 456).

Other important  $\text{Pb}^{\text{II}}$  salts are the carbonate, basic carbonate, silicates, phosphates and perchlorate, but little new chemistry is involved.  $\text{PbCO}_3$  occurs as cerussite; the compound is made as a dense white precipitate by treating the nitrate or acetate with  $\text{CO}_2$  in the presence of  $(\text{NH}_4)_2\text{CO}_3$  or  $\text{Na}_2\text{CO}_3$ , care being taken to keep the temperature low to avoid formation of the basic carbonate  $\sim 2\text{Pb}(\text{CO}_3) \cdot \text{Pb}(\text{OH})_2$ . These compounds were formerly much used as pigments (white lead) but are now largely replaced by other white pigments such as  $\text{TiO}_2$  which has higher covering power and lower toxicity. The highly soluble perchlorate [and even more the tetrafluoroborate  $\text{Pb}(\text{BF}_4)_2$ ] are much used as electrolytic plating baths for the deposition of Pb to impart corrosion resistance or lubricating properties to various metal parts. Throughout the chemistry of the oxoacid salts of  $\text{Pb}^{\text{II}}$  the close correlation between anionic charge and aqueous solubility is apparent.

The complex coordination chemistry of  $\text{Pb}^{\text{II}}$  is also beginning to be actively explored and some unusual stereochemistries are emerging. Thus, the mononuclear  $(\eta^2\text{-nitrato})\text{bis}(\text{phenanthroline})(N\text{-thiocyanato})$  complex  $[\text{Pb}(\text{phen})_2(\text{NCS})(\eta^2\text{-NO}_3)]$  has 7-coordinate  $\text{Pb}^{\text{II}}$  with a large vacancy

<sup>48</sup> K. C. MOLLOY, K. QUILL, D. CUNNINGHAM, P. MCARDLE and T. HIGGINS, *J. Chem. Soc., Dalton Trans.*, 267–73 (1989).

<sup>49</sup> R. N. BUTLER, in J. S. PIZEY (ed.), *Synthetic Reagents*, Vol. 3, pp. 278–419, Wiley Chichester, 1977.

in the coordination sphere, possibly indicating a stereochemically active lone pair.<sup>(50)</sup> Again,  $[\text{Pb}(\text{phen})_4(\text{OCIO}_3)]\text{ClO}_4$  features 9-fold, capped square antiprismatic coordination about Pb,<sup>(51)</sup> whereas in  $[\text{Pb}(\text{tpy})_3][\text{ClO}_4]_2$  (tpy = 2, 2':6', 2''-terpyridine) there is an unusual  $D_3$  9-coordinate environment around the  $\text{Pb}^{\text{II}}$  centre.<sup>(52)</sup>

### 10.3.5 Other inorganic compounds

Few of the many other inorganic compounds of Ge, Sn and Pb call for special comment. Many pseudo-halogen derivatives of  $\text{Sn}^{\text{IV}}$ ,  $\text{Pb}^{\text{IV}}$  and  $\text{Pb}^{\text{II}}$  have been reported, e.g. cyanides, azides, isocyanates, isothiocyanates, isoselenocyanates and alkoxides.<sup>(39,53)</sup>

All 9 chalcogenides  $\text{MX}$  are known ( $X = \text{S}, \text{Se}, \text{Te}$ ).  $\text{GeS}$  and  $\text{SnS}$  are interesting in having layer structures similar to that of the isoelectronic black-P (p. 482). The former is prepared by reducing a fresh precipitate of  $\text{GeS}_2$  with excess  $\text{H}_3\text{PO}_2$  and purifying the resulting amorphous red-brown powder by vacuum sublimation.  $\text{SnS}$  is usually made by sulfide precipitation from  $\text{Sn}^{\text{II}}$  salts.  $\text{PbS}$  occurs widely as the black opaque mineral galena, which is the principal ore of Pb (p. 368). In common with  $\text{PbSe}$ ,  $\text{PbTe}$  and  $\text{SnTe}$ , it has the cubic  $\text{NaCl}$ -type structure. Pure  $\text{PbS}$  can be made by direct reaction of the elements or by reaction of  $\text{Pb}(\text{OAc})_2$  with thiourea; the pure compound is an intrinsic semiconductor which, in the presence of impurities or stoichiometric imbalance, can develop either  $n$ -type or  $p$ -type semiconducting properties (p. 332). It is also a photoconductor (like  $\text{PbSe}$  and  $\text{PbTe}$ )

and is one of the most sensitive detectors of infrared radiation; the photovoltaic effect in these compounds is also widely used in photoelectric cells, e.g.  $\text{PbS}$  in photographic exposure meters. The three compounds are also unusual in that their colour diminishes with increasing molecular weight:  $\text{PbS}$  is black,  $\text{PbSe}$  grey, and  $\text{PbTe}$  white.

Of the selenides,  $\text{GeSe}$  (mp  $667^\circ$ ) forms as a dark-brown precipitate when  $\text{H}_2\text{Se}$  is passed into an aqueous solution of  $\text{GeCl}_2$ .  $\text{SnSe}$  (mp  $861^\circ$ ) is a grey-blue solid made by direct reaction of the elements above  $350^\circ$ .  $\text{PbSe}$  (mp  $1075^\circ$ ) can be obtained by volatilizing  $\text{PbCl}_2$  with  $\text{H}_2\text{Se}$ , by reacting  $\text{PbEt}_4$  with  $\text{H}_2\text{Se}$  in organic solvents, or by reducing  $\text{PbSeO}_4$  with  $\text{H}_2$  or  $\text{C}$  in an electric furnace; thin films for semiconductor devices are generally made by the reaction of  $\text{Pb}(\text{OAc})_2$  with selenourea,  $(\text{NH}_2)_2\text{CSe}$ . The tellurides are best made by heating Ge, Sn or Pb with the stoichiometric amount of Te.

Other chalcogenides that have been described include  $\text{GeS}_2$ ,  $\text{GeSe}_2$ ,  $\text{Sn}_2\text{S}_3$  and  $\text{SnSe}_2$ , but these introduce no novel chemistry or structural principles. Of more interest, perhaps, is the polymeric anion  $[\text{Sn}_5\text{S}_{12}^{4-}]_\infty$  (1) which occurs in  $\text{Cs}_4\text{Sn}_5\text{S}_{12} \cdot 2\text{H}_2\text{O}$  and which contains both trigonal bipyramidal and octahedral  $\text{Sn}^{\text{IV}}$ .<sup>(54)</sup> The compound was prepared by hydrothermal reaction of  $\text{Cs}_2\text{CO}_3$  with  $\text{SnS}_2$  at  $150^\circ\text{C}$ . A similar reaction between  $\text{Rb}_2\text{CO}_3$  and  $\text{SnS}_2$  in saturated aqueous  $\text{H}_2\text{S}$  solution at  $190^\circ\text{C}$  afforded  $\text{Rb}_2\text{Sn}_3\text{S}_7 \cdot 2\text{H}_2\text{O}$  in which the polymeric  $[\text{Sn}_3\text{S}_7^{2-}]_\infty$  anion (2) features both  $\text{SnS}_4$  tetrahedra and  $\text{SnS}_6$  octahedra.<sup>(55)</sup> Another new structural form, in which a *commo*-Sn atom joins a double cube, is found in the discrete  $\{\text{Sn}_7\text{S}_6\text{O}_2\}$  cluster core (3) of  $[\{\text{Bu}^t\text{Sn}(\text{S})\text{L}\}_3]_2\text{Sn}$ ; the diphosphinate ligand  $\text{L} = \mu\text{-}\eta^2\text{-O}_2\text{PPh}_2$  bridges the three non-*commo* Sn atoms in each of the cubes.<sup>(56)</sup> Examples of

<sup>50</sup> L. M. ENGELHARDT, J. M. PATRICK and A. H. WHITE, *Aust. J. Chem.* **42**, 335–8 (1989). See also L. M. ENGELHARDT, B. M. FURPHY, J. MCB. HARROWFIELD, J. M. PATRICK, B. W. SKELTON and A. H. WHITE, *J. Chem. Soc., Dalton Trans.*, 595–9 (1989).

<sup>51</sup> L. M. ENGELHARDT, D. L. KEPERT, J. M. PATRICK and A. H. WHITE, *Aust. J. Chem.* **42**, 329–34 (1989).

<sup>52</sup> D. L. KEPERT, J. M. PATRICK, B. W. SKELTON and A. H. WHITE, *Aust. J. Chem.* **41**, 157–8 (1988).

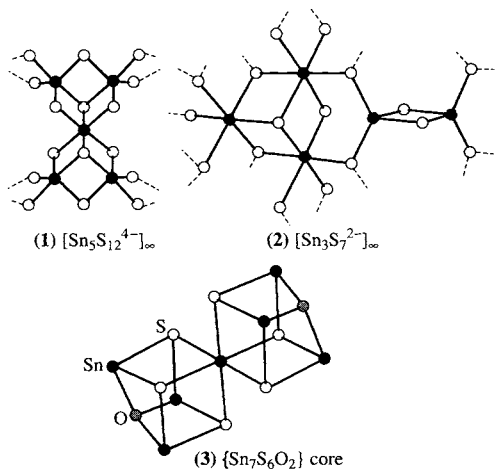
<sup>53</sup> E. W. ABEL, Tin, Chap. 17 in *Comprehensive Inorganic Chemistry*, Vol. 2, pp. 43–104, Pergamon Press, Oxford, 1973.

<sup>54</sup> W. S. SHELDRIK Z. *anorg. allg. Chem.* **562**, 23–30 (1988).

<sup>55</sup> W. S. SHELDRIK and B. SCHAFF, Z. *anorg. allg. Chem.* **620**, 1041–5 (1994).

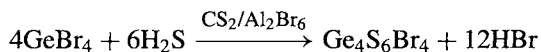
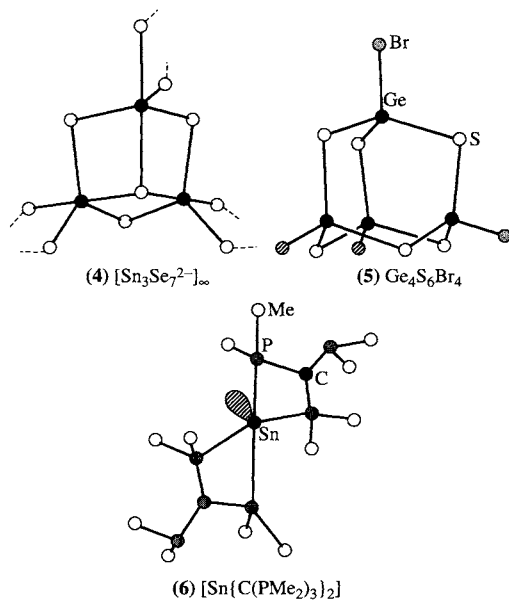
<sup>56</sup> K. C. K. SWAMY, R. O. DAY and R. R. HOLMES, *J. Am. Chem. Soc.* **110**, 7543–4 (1988).

square-pyramidal 5-coordinate  $\text{Sn}^{\text{IV}}$  (57,58) and pentagonal bipyramidal 7-coordinate  $\text{Sn}^{\text{IV}}$  (59) have also been recently established in various thio-organotin complexes.



The discrete anions  $[\text{Sn}_2\text{Se}_6]^{4-}$  and  $[\text{Sn}_2\text{Te}_6]^{4-}$  have the  $\text{B}_2\text{H}_6$ -type structure (p. 154) and are known in  $\text{Rb}_4(\text{Sn}_2\text{Se}_6)$ ,<sup>(55)</sup>  $[\text{enH}_2]_2[\text{Sn}_2\text{Se}_6]$ <sup>(60)</sup> and  $[\text{NMe}_4]_4[\text{Sn}_2\text{Te}_6]$ .<sup>(61)</sup> By contrast,  $[\text{enH}_2]_2[\text{Sn}_3\text{Se}_7] \cdot \frac{1}{2}\text{en}$  features a sheet polymeric anion  $[\text{Sn}_3\text{Se}_7]^{2-}_\infty$  (4) in which the basic elements are  $\text{SnSe}_5$  trigonal bipyramids.<sup>(60)</sup> The adamantane-like anion  $[\text{Ge}_4\text{Te}_{10}]^{4-}$  was identified by X-ray diffraction analysis of the black crystalline salt  $[\text{NEt}_4]_4[\text{Ge}_4\text{Te}_{10}]$ , prepared in 72% yield by extraction of the alloy of composition  $\text{K}_4\text{Ge}_4\text{Te}_{10}$  with ethylene diamine in the presence of  $\text{Et}_4\text{NBr}$ <sup>(61a)</sup>

The first sulfide halide of Ge was made by the apparently straightforward reaction:



The unexpectedly complex product was isolated as an almost colourless air-stable powder, and a single-crystal X-ray analysis showed that it had the molecular adamantane-like structure (5).<sup>(62)</sup> This is very similar to the structure of the “iso-electronic” compound  $\text{P}_4\text{O}_{10}$  (p. 504).

There has been growing interest in the detailed structure and reaction chemistry of monomeric forms of two-coordinate derivatives of  $\text{Ge}^{\text{II}}$ ,  $\text{Sn}^{\text{II}}$  and  $\text{Pb}^{\text{II}}$  since the first examples were unequivocally established in 1980.<sup>(63,64)</sup> Thus, treatment of the corresponding chlorides  $\text{MCl}_2$  with lithium di-*tert*-butyl phenoxide derivatives in thf affords a series of yellow ( $\text{Ge}^{\text{II}}$ ,  $\text{Sn}^{\text{II}}$ ) and red ( $\text{Pb}^{\text{II}}$ ) compounds  $\text{M}(\text{OAr})_2$  in high yield.<sup>(63)</sup> The O–M–O bond angle in  $\text{M}(\text{OC}_6\text{H}_2\text{Me-4-Bu}_2\text{-2,6})_2$  was  $92^\circ$  for Ge and  $89^\circ$  for Sn. Similar reactions

<sup>57</sup> A. C. SAU, R. O. DAY and R. R. HOLMES, *J. Am. Chem. Soc.* **103**, 1264–5 (1981) and *Inorg. Chem.* **20**, 3076–81 (1981).

<sup>58</sup> S. W. NG, C. WEI, V. G. K. DAS and T. C. W. MAK, *J. Organometallic Chem.* **334**, 283–93 (1987).

<sup>59</sup> S. W. NG, C. WEI, V. G. K. DAS, G. B. JAMESON and R. J. BUTCHER, *J. Organometallic Chem.* **365**, 75–82 (1989).  
<sup>60</sup> W. S. SHELDRIK and H. G. BRAUNBECK, *Z. anorg. allg. Chem.* **619**, 1300–6 (1993).

<sup>61</sup> J. C. HUFFMAN, J. P. HAUSHALTER, A. M. UMARI, G. K. SHENOY and R. C. HAUSHALTER, *Inorg. Chem.* **23**, 2312–15 (1984).

<sup>61a</sup> S. S. DHINGRA and R. C. HAUSHALTER, *Polyhedron* **13**, 2775–9 (1994).

<sup>62</sup> S. POHL, *Angew. Chem. Int. Edn. Engl.* **15**, 162 (1976).

<sup>63</sup> B. CETINKAYA, I. GÜMRÜKÇÜ, M. F. LAPPERT, J. L. ATWOOD, R. D. ROGERS and M. J. ZAWOROTKO, *J. Am. Chem. Soc.* **102**, 2088–9 (1980). See also T. FJELDBERG, P. B. HITCHCOCK, M. F. LAPPERT, S. J. SMITH and A. J. THORNE, *J. Chem. Soc., Chem. Commun.*, 939–41 (1985).

<sup>64</sup> M. F. LAPPERT, M. J. SLADE, J. L. ATWOOD and M. J. ZAWOROTKO, *J. Chem. Soc., Chem. Commun.*, 621–2 (1980).

of  $MCl_2$  with  $LiNBu_2^t$  yielded the (less stable) monomeric di-*tert*-butylamide,  $Ge(NBu_2^t)_2$  (orange), and  $Sn(NBu_2^t)_2$  (maroon);<sup>(64)</sup> the more stable related bis(tetramethylpiperidino) compound  $[Ge\{N[NCMe_2(CH_2)_3CMe_2]\}_2]$  was found to have a somewhat larger bond angle at Ge ( $N-Ge-N = 111^\circ$ ) and a rather long Ge–N bond (189 pm). More recent examples are  $[Ge\{N(SiMe_3)_2\}_2]$ <sup>(65)</sup> and  $[GeN(Bu^t)CH=CHN(Bu^t)]$ .<sup>(66)</sup> The first monomeric prochiral  $Sn^{II}$  complexes,  $[Sn\{N(SiMe_3)_2\}X]$ , have also been reported, where X is a bulky substituted phenoxy group or a tetramethylpiperidino moiety.<sup>(67)</sup> These are but illustrative examples of a large and burgeoning field.<sup>(68)</sup>

Turning finally to compounds with bonds from the heavier Group 14 elements to heavier Group 15 elements we may note compounds such as  $[Sn\{C(PMe_2)_3\}_2]$  which has the pseudo trigonal bipyramidal structure (6). This complex, which has Sn bonded exclusively to four P atoms, is formed as yellow crystals by the

<sup>65</sup> S. M. HAWKINS, P. B. HITCHCOCK, M. F. LAPPERT and A. K. RAI, *J. Chem. Soc., Chem. Commun.*, 1689–90 (1986) and references cited therein; C. GLIDEWELL, D. LLOYD, K. W. LUMBARD and J. S. MCKECHNIE, *J. Chem. Soc., Dalton Trans.*, 2981–7 (1987).

<sup>66</sup> W. A. HERRMANN, M. DENK, J. BEHM, W. SCHERER, F. R. KLINGAN, H. BOCK, B. SOLOUKI and M. WAGNER, *Angew. Chem. Int. Edn. Engl.* **31**, 1485–8 (1992).

<sup>67</sup> H. BRAUNSCHWEIG, R. W. CHORLEY, P. B. HITCHCOCK and M. F. LAPPERT, *J. Chem. Soc., Chem. Commun.*, 1311–13 (1992).

<sup>68</sup> M. VEITH and W. FRANK, *Angew. Chem. Int. Edn. Engl.* **24**, 223–4 (1985), C. GLIDEWELL, D. LLOYD and K. W. LUMBARD, *J. Chem. Soc., Dalton Trans.*, 501–8 (1987), J. KOCHER, M. LEHNIG and W. P. NEUMANN, *Organometallics* **7**, 1201–7 (1988), M. VEITH, L. STAHL and V. HUCH, *J. Chem. Soc., Chem. Commun.*, 359–61 (1990), P. B. HITCHCOCK, M. F. LAPPERT and A. J. THORNE, *J. Chem. Soc., Chem. Commun.*, 1587–9 (1990), A. MELLER, G. OSSIG, W. MARINGGELE, D. STALKE, R. HERBST-IRMER, S. FREITAG and G. M. SHELDRIK, *J. Chem. Soc., Chem. Commun.*, 1123–4 (1991), R. W. CHORLEY, P. B. HITCHCOCK, B. S. JOLLY, M. F. LAPPERT and G. A. LAWLESS, *J. Chem. Soc., Chem. Commun.*, 1302–3 (1991), R. W. CHORLEY, P. B. HITCHCOCK and M. F. LAPPERT, *J. Chem. Soc., Chem. Commun.*, 525–6 (1992), M. VEITH, M. NOTZEL, L. STAHL and V. HUCH, *Z. anorg. allg. Chem.* **620**, 1264–70 (1994). See also Polyhedra Symposia-in-Print No. 12, M. J. HAMPDEN-SMITH (ed.), *Polyhedron* **10**, 1147–309 (1991).

reaction of  $SnCl_2$  with  $2Li\{C(PMe_2)_3\}$  in  $Et_2O$  at  $-78^\circ C$ .<sup>(69)</sup> A notable feature of the structure is the substantial difference between the equatorial and axial Sn–P distances (260 pm vs 279 and 284 pm, respectively) and the small chelate bite angle of  $62.9^\circ$  at the Sn atom. The compound is fluxional in solution even at  $-90^\circ C$  due to pseudorotation (p. 499) which equilibrates the axial and equatorial positions. Several similar compounds are known.<sup>(69)</sup> Germanium analogues of (6) such as the stable crystalline complexes  $[Ge\{C(PMe_2)_3\}_2]$  and  $[Ge\{C(PMe_2)_2(SiMe_3)\}_2]$  can be made by similar procedures, starting from  $GeCl_2$ .dioxane:<sup>(70)</sup> see also next section.

A range of shiny metallic compounds featuring trigonal planar anions  $SnX_3^{5-}$  ( $X = As, Sb, Bi$ ) have been characterized with composition  $M_6(SnX_3)O_{0.5}$  ( $M = Rb, Cs$ ); the Sn and X atoms in  $SnX_3^{5-}$  (isostructural with  $CO_3^{2-}$ ) are coordinated by trigonal prisms of  $6M^+$ , and the  $O^{2-}$  ions occupy octahedral sites in the  $M^+$  lattice.<sup>(70a)</sup>

Rather different is the X-ray structural characterization of the ‘bare’  $Sn^{2+}$  ion in  $[Sn^{2+}][SbF_6^-]_2 \cdot 2AsF_3$  (prepared by treating the product of the direct reaction between  $SnF_2$  and  $SbF_5$  with  $AsF_3$ ).<sup>(71)</sup> The crystal packing is such that each  $Sn^{2+}$  is surrounded by nine F atoms (tricapped trigonal prism) and the average Sn–F distance is 257 pm (cf. the sum of the ionic radii, 251 pm). The Mössbauer spectrum (p. 371) shows zero quadrupole splitting and the highest known chemical shift for any tin(II) species, consistent with the ‘bare ion’ formulation.

### 10.3.6 Metal–metal bonds and clusters

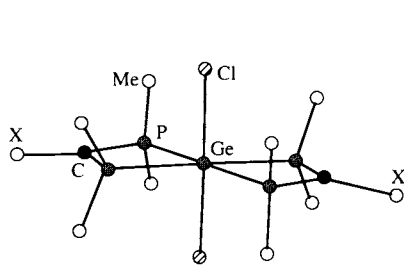
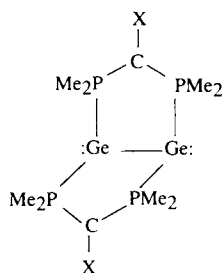
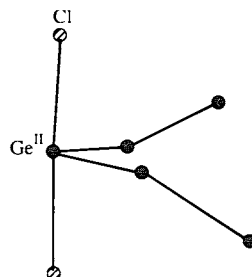
The catenation of Group 14 elements has been discussed on pp. 337–42 and 374–5,

<sup>69</sup> H. H. KARSCH, A. APPELT and G. MÜLLER, *Organometallics* **5**, 1664–70 (1986) and references cited therein.

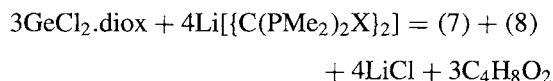
<sup>70</sup> H. H. KARSCH, B. DEUBELLY, J. REIDE and G. MÜLLER, *Angew. Chem. Int. Edn. Engl.* **26**, 673–4 (1987).

<sup>70a</sup> M. ASBRAND and B. EISENMANN, *Z. anorg. allg. Chem.* **620**, 1837–43 (1994).

<sup>71</sup> A. J. EDWARDS and K. L. KHALLOW, *J. Chem. Soc., Chem. Commun.*, 50–1 (1984).

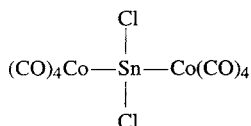
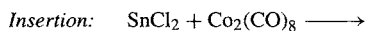
(7)  $[\text{Ge}^{\text{IV}}\{\text{C}(\text{PMe}_2)_2\text{X}\}_2\text{Cl}_2]$ (8)  $[\text{Ge}^{\text{I}}_2\{\text{C}(\text{PMe}_2)_2\text{X}\}_2]$ (9)  $[\text{Ge}^{\text{I}}_2\{\mu\text{-(PMe}_2)_2\text{CX}\}_2]_2\text{Ge}^{\text{II}}\text{Cl}_2(\text{core})$ 

and further examples are in Section 10.3.7. In addition, when the reaction of  $\text{GeCl}_2$ .dioxane with  $2\text{Li}[\text{C}\{\text{PMe}_2\}_2\text{X}]_2$  (mentioned above<sup>(70)</sup>) is varied by using a higher proportion of  $\text{GeCl}_2$ , concurrent redox disproportionation occurs to yield a mixture of  $[\text{Ge}^{\text{IV}}\{\text{C}(\text{PMe}_2)_2\text{X}\}_2\text{Cl}_2]$  (7) and  $[\text{Ge}^{\text{I}}_2\{\text{C}(\text{PMe}_2)_2\text{X}\}_2]$  (8) according to the optimized stoichiometry:<sup>(72)</sup>

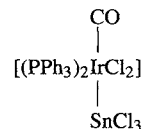
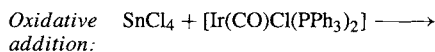
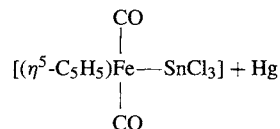
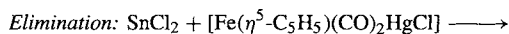
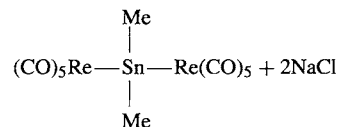
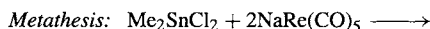


where  $\text{X} = \text{SiMe}_3$  (or  $\text{PMe}_2$ ). The Ge–Ge distance in (8) is 254 pm, i.e. about 10 pm longer than in polygermanes. The stereochemically active lone pairs of electrons on  $\text{Ge}^{\text{I}}$  in (8) can be used as electron-pair donors to a further  $\text{GeCl}_2$  moiety to form the homonuclear (germanediyl donor)–(germanediyl acceptor) complex  $[\text{Ge}_2\{\mu\text{-(PMe}_2)_2\text{CX}\}_2]_2\text{GeCl}_2$  which features a mixed-valent  $\text{Ge}_5$  chain as shown schematically in (9). The Ge–Ge distances along the  $\text{Ge}^{\text{I}}\text{--Ge}^{\text{I}}\text{--Ge}^{\text{II}}\text{--Ge}^{\text{I}}\text{--Ge}^{\text{I}}$  chain are 249.2, 255.4, 256.2 and 248.5 pm, respectively.

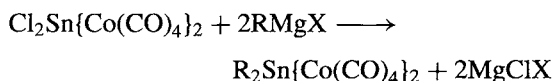
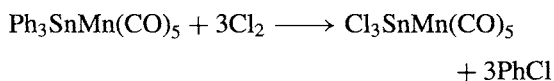
Heteroatomic metal-metal bonds can be formed by a variety of synthetic routes as illustrated below for tin:



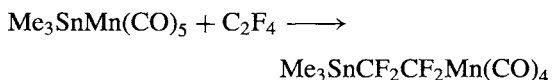
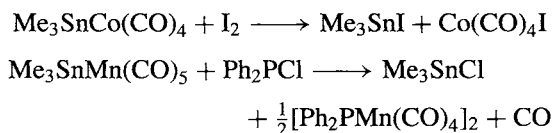
<sup>72</sup> H. H. KARSCH, B. DEUBELLY, J. REIDE and G. MÜLLER, *Angew. Chem. Int. Edn. Engl.* **26**, 674–6 (1987).



Some representative examples, all featuring tetrahedral Sn, are in Fig. 10.9.<sup>(53)</sup> Several reactions are known in which the Sn–M bond remains intact, e.g.:



Others result in cleavage, e.g.:



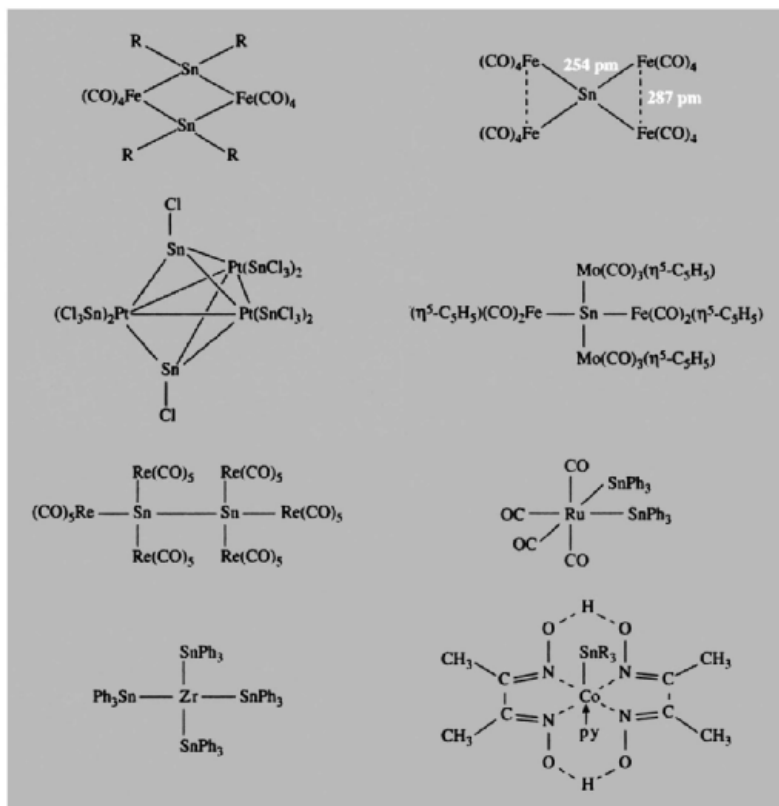


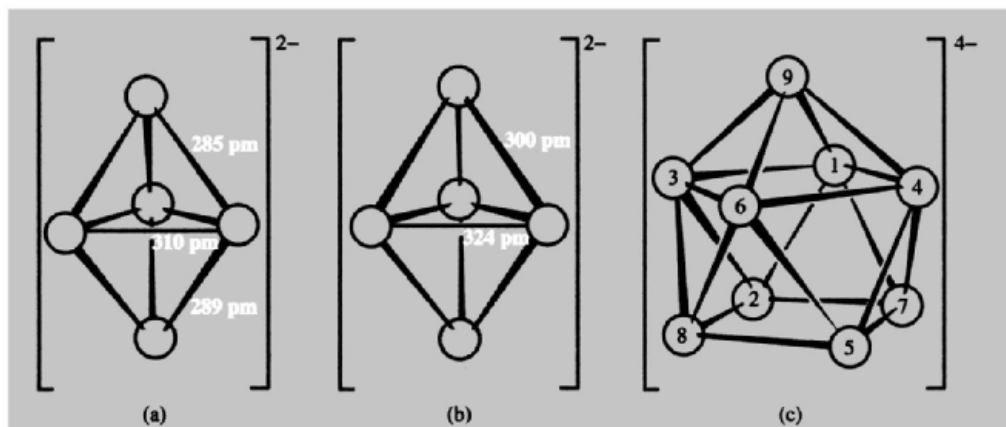
Figure 10.9 Some examples of metal sequences and metal clusters containing tin-transition metal bonds.

A similar though less extensive range of Pb-M compounds has been established;<sup>(39)</sup> e.g.  $[\text{Ph}_2\text{Pb}\{\text{Mn}(\text{CO})_5\}_2]$ ,  $[\text{Ph}_3\text{PbRe}(\text{CO})_5]$ ,  $[\text{Ph}_2\text{Pb}\{\text{Co}(\text{CO})_4\}_2]$ ,  $[(\text{PPh}_3)_2\text{Pt}(\text{PbPh}_3)_2]$ ,  $[(\text{CO})_3\text{Fe}(\text{PbEt}_3)_2]$ , and the cyclic dimer  $[(\text{CO})_4\text{Fe}-\text{PbEt}_2]_2$ . Reaction of these compounds with halogens results in fission of the Pb-M bonds. In the unique case of  $[\text{Pb}\{\text{Mn}(\eta^5\text{-C}_5\text{H}_5)(\text{CO})_2\}_2]$  the linear central MnPbMn core ( $177.2^\circ$ ) and short Mn-Pb distance (246.3 pm) suggest that this is the first example of multiple bonding between Pb and a transition metal,  $\text{Mn}=\text{Pb}=\text{Mn}$ .<sup>(73)</sup> The compound is obtained in 20% yield as air-stable reddish-brown crystals by the reaction of  $\text{PbCl}_2$  with the substitutionally labile complex  $[\text{Mn}(\eta^5\text{-C}_5\text{H}_5)(\text{CO})_2(\text{thf})]$ .

It has been known since the early 1930s that reduction of Ge, Sn and Pb by Na in liquid ammonia gives polyatomic Group 14 metal anions, and crystalline compounds can be isolated using ethylenediamine, e.g.  $[\text{Na}_4(\text{en})_5\text{Ge}_9]$  and  $[\text{Na}_4(\text{en})_7\text{Sn}_9]$ . A dramatic advance was achieved<sup>(74)</sup> in the 1970s by means of the polydentate cryptand ligand  $[\text{N}(\text{C}_2\text{H}_4)\text{O}(\text{C}_2\text{H}_4)\text{O}(\text{C}_2\text{H}_4)_3\text{N}]$  (p. 98). Thus, reaction of cryptand in ethylenediamine with the alloys  $\text{NaSn}_{1-1.7}$  and  $\text{NaPb}_{1.7-2}$  gave red crystalline salts  $[\text{Na}(\text{crypt})]_2^+[\text{Sn}_5]^{2-}$  and  $[\text{Na}(\text{crypt})]_2^+[\text{Pb}_5]^{2-}$  containing the  $D_{3h}$  cluster anions illustrated in Fig. 10.10. If each Sn or Pb atom is thought to have 1 nonbonding pair of electrons then the

<sup>73</sup> W. A. HERRMANN, H.-J. KNEUPER and E. HERDTWECK, *Angew. Chem. Int. Edn. Engl.* **24**, 1062-3 (1985).

<sup>74</sup> P. A. EDWARDS and J. D. CORBETT, *Inorg. Chem.* **16**, 903-7 (1977). J. D. CORBETT and P. A. EDWARDS, *J. Am. Chem. Soc.* **99**, 3313-7 (1977).



**Figure 10.10** The structure of polystannide and polyplumbide anions: (a) the slightly distorted  $D_{3h}$  structure of  $[\text{Sn}_5]^{2-}$ , (b) the  $D_{3h}$  structure of  $[\text{Pb}_5]^{2-}$ , and (c) the unique  $C_{4v}$  structure of  $[\text{Sn}_9]^{4-}$ : all Sn-Sn distances are in the range 295–302 pm except those in the slightly longer upper square (1,3,6,4) which are in the range 319–331 pm; the angles within the two parallel squares are all  $90^\circ (\pm 0.8^\circ)$ .

$\text{M}_5^{2-}$  clusters have 12 framework bonding electrons as has  $[\text{B}_5\text{H}_5]^{2-}$  (p. 161); the anions are also isoelectronic with the well-known cation  $[\text{Bi}_5]^{3+}$ . Similarly, the alloy  $\text{NaSn}_{\sim 2.25}$  reacts with cryptand in ethylenediamine to give dark-red crystals of  $[\text{Na}(\text{crypt})]_4^+[\text{Sn}_9]^{4-}$ ; the anion is the first example of a  $C_{4v}$  uncapped Archimedean antiprism (Fig. 10.10c) and differs from the  $D_{3h}$  structure of the isoelectronic cation  $[\text{Bi}_9]^{5+}$  which, in the salt  $\text{Bi}^+[\text{Bi}_9]^{5+}[\text{HfCl}_6]_3^{2-}$  (p. 591), features a tricapped trigonal prism, as in  $[\text{B}_9\text{H}_9]^{2-}$  (p. 153). The emerald green species  $[\text{Pb}_9]^{4-}$ , which is stable in liquid  $\text{NH}_3$  solution, has not so far proved amenable to isolation via cryptand-complexed cations.

The influence of electron-count on cluster geometry has been very elegantly shown by a crystallographic study of the deep-red compound  $[\text{K}(\text{crypt})]_6^+[\text{Ge}_9]^{2-}[\text{Ge}_9]^{4-} \cdot 2.5\text{en}$ , prepared by the reaction of KGe with cryptand in ethylenediamine.  $[\text{Ge}_9]^{4-}$  has the  $C_{4v}$  uncapped square-antiprismatic structure (10.10c) whereas  $[\text{Ge}_9]^{2-}$ , with 2 less electrons, adopts a distorted  $D_{3h}$  structure which clearly derives from the tricapped trigonal prism (p. 153).<sup>(75)</sup> The field is one of

great interest and activity, as evidenced by papers describing the synthesis of and structural studies on tetrahedral  $\text{Ge}_4^{2-}$  and  $\text{Sn}_4^{2-}$ ,<sup>(76)</sup> tricapped trigonal-prismatic  $\text{TlSn}_8^{3-}$ ,<sup>(77)</sup> bicapped square-antiprismatic  $\text{TlSn}_9^{3-}$ ,<sup>(77)</sup> and the two *nido*-series  $\text{Sn}_{9-x}\text{Ge}_x^{4-}$  ( $x = 0-9$ ) and  $\text{Sn}_{9-x}\text{Pb}_x^{4-}$  ( $x = 0-9$ ).<sup>(78)</sup> Other theoretical studies on many of these polymetallic-cluster anions have also been published.<sup>(79)</sup> Recent synthetic and structural work includes the characterization of the octahedral *closo*- $[\text{Ge}_2\text{Co}_4]$  grouping in  $[\text{1,6-}\{(\text{CO})_4\text{COGe}\}_2\text{Co}_4(\text{CO})_{11}]$ ,<sup>(80)</sup>

<sup>76</sup> S. C. CRITCHLOW and J. D. CORBETT, *J. Chem. Soc., Chem. Commun.*, 236–7 (1981). M. J. ROTHMAN, L. S. BARTLETT and L. L. LOHR, *J. Am. Chem. Soc.* **103**, 2482–3 (1981).

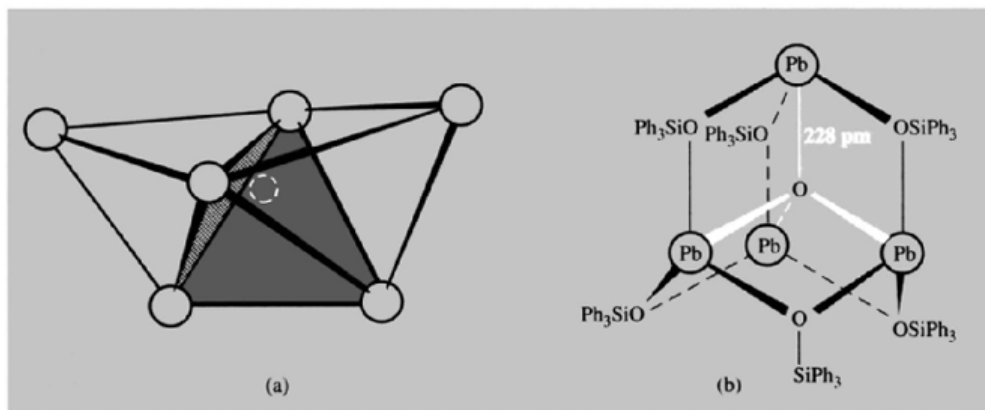
<sup>77</sup> R. C. BURNS and J. D. CORBETT, *J. Am. Chem. Soc.* **104**, 2804–10 (1982). See also *Inorg. Chem.* **24**, 1489–92 (1985) for  $[\text{KSn}_9^{3-}]$ .

<sup>78</sup> R. W. RUDOLPH, W. L. WILSON and R. C. TAYLOR *J. Am. Chem. Soc.* **103**, 2480–1 (1981), and references therein. See also W. L. WILSON, R. W. RUDOLPH, L. L. LOHR, R. C. TAYLOR and P. PYYKKÖ, *Inorg. Chem.* **25**, 1535–41 (1985).

<sup>79</sup> L. L. LOHR, *Inorg. Chem.* **20**, 4229–35 (1981); R. C. BURNS, R. J. GILLESPIE, J. A. BARNES and M. J. MCGLINCHAY, *Inorg. Chem.* **31**, 799–807 (1982). G. KLICHE, H. G. VON SCHNERING and M. SCHWARZ, *Z. anorg. allg. Chem.* **608**, 131–4 (1992).

<sup>80</sup> S. P. FOSTER, K. M. MACKAY and B. K. NICHOLSON, *Inorg. Chem.* **24**, 909–13 (1985).

<sup>75</sup> C. H. E. BELIN, J. D. CORBETT and A. CISAR, *J. Am. Chem. Soc.* **99**, 7163–9 (1977).



**Figure 10.11** (a) The three face-sharing tetrahedra of Pb atoms in the  $\text{Pb}_6\text{O}(\text{OH})_6^{4+}$  cluster; only the unique 4-coordinate O atom at the centre of the central tetrahedron is shown (in white). (b) The adamantane-like structure of  $[\text{Pb}_4\text{O}(\text{OSiPh}_3)_6]$  showing the fourfold coordination about the central O atom.

the *closo*-10 vertex cluster  $[\text{Sn}_9\text{Cr}(\text{CO})_3]^{4-}$ <sup>(81)</sup> and encapsulated Ge and Sn atoms (E) in species such as  $[\text{Ni}_{12}(\mu_{12}\text{-E})(\text{CO})_{22}]^{2-}$  and  $[\text{Ni}(\mu_{10}\text{-Ge})(\text{CO})_{20}]^{2-}$ .<sup>(82)</sup>

The polymeric cluster compound  $[\text{Sn}_6\text{O}_4(\text{OH})_4]$  formed by hydrolysis of  $\text{Sn}^{\text{II}}$  compounds has been mentioned on p. 384. Hydrolysis of  $\text{Pb}^{\text{II}}$  compounds also leads to polymerized species; e.g. dissolution of PbO in aqueous  $\text{HClO}_4$  followed by careful addition of base leads to  $[\text{Pb}_6\text{O}(\text{OH})_6]^{4+}[\text{ClO}_4]_4 \cdot \text{H}_2\text{O}$ . The cluster cation (Fig. 10.11a) consists of 3 tetrahedra of Pb sharing faces; the central tetrahedron encompasses the unique O atom and the 6 OH groups lie on the faces of the 2 end tetrahedra.<sup>(83)</sup> The extent of direct Pb–Pb interaction within the overall cluster has not been established but it is noted that the distance between “adjacent” Pb atoms falls in the range 344–409 pm (average 381 pm) which is appreciably larger than in the  $\text{Pb}_5^{2-}$  anion. The distance from the central O

to the 4 surrounding Pb atoms is 222–235 pm and the other Pb–O(H) distances are in the range 218–267 pm. The structure should be compared with the  $[\text{Sn}_6\text{O}_4(\text{OH})_4]$  cluster (p. 384), which also has larger Sn–Sn distances than in the polystannide anions in Fig. 10.10.

Another polycyclic structure in which a unique O atom is surrounded tetrahedrally by 4  $\text{Pb}^{\text{II}}$  atoms is the colourless adamantane-like complex  $[\text{Pb}_4\text{O}(\text{OSiPh}_3)_6]$ , obtained as a 1:1 benzene solvate by reaction of  $\text{Ph}_3\text{SiOH}$  with  $[\text{Pb}(\text{C}_5\text{H}_5)_2]$  (p. 404). The local geometry about  $\text{Pb}^{\text{II}}$  is also noteworthy: it comprises pseudo-trigonal bipyramidal coordination in which the bridging  $\text{OSiPh}_3$  groups occupy the equatorial sites whilst the apical sites are occupied by the unique O atom and axially directed lone pairs of electrons.<sup>(84)</sup> The first heterometallic oxoalkoxide,  $[\text{Pb}_6\text{Nb}_4\text{O}_4(\text{OEt})_{24}]$ , has also been prepared, by reacting  $[\text{Pb}_4\text{O}(\text{OEt})_6]$  and  $[\text{Nb}_2(\text{OEt})_{10}]$  in ethanol at room temperature.<sup>(85)</sup> X-ray structural analysis shows an octahedral  $\text{Pb}_6$  framework, four of whose faces are capped by a  $\mu_4$ -oxo ligand connected to 3Pb atoms and an  $\{\text{Nb}(\text{OEt})_5\}$  moiety; the remaining

<sup>81</sup> B. W. EICHHORN, R. C. HAUSHALTER and W. T. PENNINGTON, *J. Am. Chem. Soc.* **110**, 8704–6 (1988). B. W. EICHHORN and R. C. HAUSHALTER, *J. Chem. Soc., Chem. Commun.*, 937–8 (1990).

<sup>82</sup> A. CERIOTTI, F. DEMARTIN, B. T. HEATON, P. INGALLINA, G. LONGONI, M. MANASSERO, M. MARCHIONNA and N. MASCIOCCHI, *J. Chem. Soc., Chem. Commun.*, 786–7 (1989).

<sup>83</sup> T. G. SPIRO, D. H. TEMPLETON and A. ZALKIN, *Inorg. Chem.* **8**, 856–61 (1969).

<sup>84</sup> C. GAFFNEY, P. G. HARRISON, and T. J. KING, *J. Chem. Soc., Chem. Commun.*, 1251–2 (1980).

<sup>85</sup> R. PAPIERNIK, L. G. HUBERT-PFALZGRAF, J.-C. DARAN and Y. JEANNIN, *J. Chem. Soc., Chem. Commun.*, 695–7 (1990).

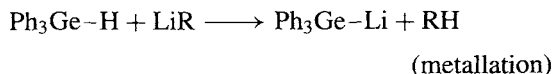
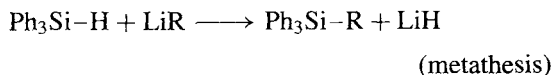


four faces of the  $\text{Pb}_6$  octahedron are capped by  $(\mu_3\text{-OEt})$  groups. This leads, to the overall detailed formulation of the compound as  $[\text{Pb}_6(\mu_4\text{-O})_4\{\text{Nb}(\text{OEt})_2\}_4(\mu_3\text{-OEt})_4(\mu_2\text{-OEt})_{12}]$ . Alternatively the complex can be described as a tetradentate oxo ligand donating to  $4\{\text{Nb}(\text{OEt})_2(\mu_2\text{-OEt})_3\}$  groups i.e.  $[\text{Pb}_6\text{O}_4(\text{OEt})_4\{\text{Nb}(\text{OEt})_5\}_4]$ .

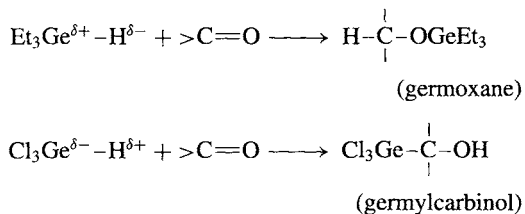
### 10.3.7 Organometallic compounds<sup>(86)</sup>

#### Germanium<sup>(87)</sup>

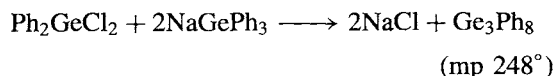
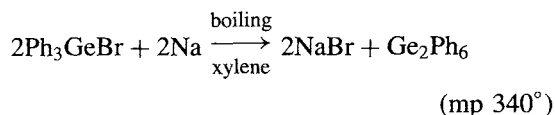
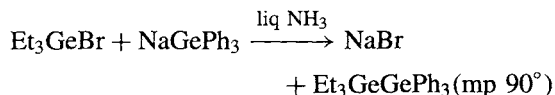
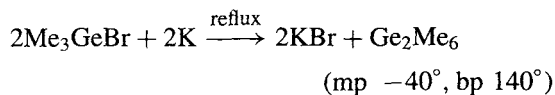
Organogermanium chemistry closely resembles that of Si though the Ge compounds tend to be somewhat less thermally stable. They are also often rather more chemically reactive than their Si counterparts, e.g. in ligand scrambling reactions, Ge–C bond cleavage and hydrogermylation. However,  $\text{GeR}_4$  compounds themselves are rather inert chemically and  $\text{R}_n\text{GeX}_{4-n}$  tend to be less prone to hydrolysis and condensation reactions than their Si analogues. Again, following expected group trends, germynes ( $\text{R}_2\text{Ge:}$ ) are more stable than silylenes. The table of comparative bond energies on p. 374 indicates that the Ge–C and Ge–H bonds are weaker than the corresponding bonds involving Si but are nevertheless quite strong; Ge–Ge is noticeably weaker. The electronegativity of both Si and Ge are similar to that of H, though the reactivity pattern towards organolithium reagents suggests a slight hydridic character ( $\text{H}^{\delta-}$ ) for  $\text{Ph}_3\text{SiH}$  and some protic character ( $\text{H}^{\delta+}$ ) for  $\text{Ph}_3\text{GeH}$ :



In fact, the polarity of the Ge–H bond can readily be reversed (umpolung) by an appropriate choice of constituents, e.g.:



Preparative routes to organogermanium compounds parallel those for organosilicon compounds (p. 363) and most of the several thousand known organogermans can be considered as derivatives of  $\text{R}_n\text{GeX}_{4-n}$  or  $\text{Ar}_n\text{GeX}_{4-n}$  where X = hydrogen, halogen, pseudohalogen, OR, etc. The compounds are colourless, volatile liquids, or solids. Attempts to prepare  $(-\text{R}_2\text{GeO}-)_x$  analogues of the silicones (p. 364) show that the system is different: hydrolysis of  $\text{Me}_2\text{GeCl}_2$  is reversible and incomplete, but extraction of aqueous solutions of  $\text{Me}_2\text{GeCl}_2$  with petrol leads to the cyclic tetramer  $[\text{Me}_2\text{GeO}]_4$ , mp  $92^\circ$ ; the compound is monomeric in water. Organodigermans and -polygermans have also been made by standard routes, e.g.:



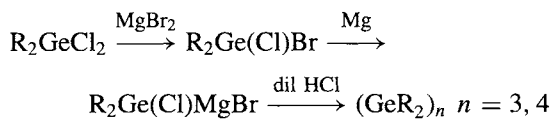
In general, the Ge–Ge bond is readily cleaved by  $\text{Br}_2$  either at ambient or elevated temperatures but the compounds are stable to thermal cleavage at moderate temperatures.  $\text{Ge}_2\text{R}_6$  compounds can even be distilled unchanged in air (like  $\text{Si}_2\text{R}_6$  but unlike the more reactive  $\text{Sn}_2\text{R}_6$ ) and are stable towards hydrolysis and ammonolysis.

<sup>86</sup> C. ELSCHENBROICH and A. SALZER, *Organometallics*, VCH, Weinheim, 1989, pp. 115–46.

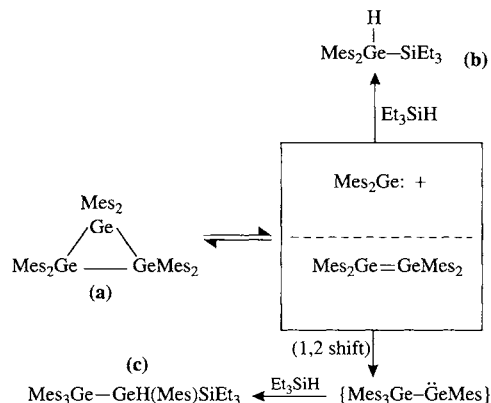
<sup>87</sup> P. RIVIÈRE, M. RIVIÈRE-BAUDET and J. SATGÈ, Chap. 10 in G. WILKINSON, F. G. A. STONE and E. W. ABEL (eds.) *Comprehensive Organometallic Chemistry*, Pergamon Press, Oxford, Vol. 2, pp. 399–518 (1982) (716 refs.).

Considerable recent attention has focused on the preparation, structure and stability of germenes ( $>Ge=C<$ ), germynes ( $R_2Ge\cdot$ ), cyclo and polyhedral oligopolygermanes, and  $Ge^{II}$  species with coordination numbers greater than 4 (especially 5 and 10). Thus, evidence for fugitive germene species has been known for some 20 years<sup>(88)</sup> but stable germenes,  $R_2Ge=CR'_2$ , were first reported only in 1987,<sup>(89,90)</sup> the stabilization being achieved by use of bulky groups both on Ge [e.g.  $R =$  mesityl or  $-N(SiMe_3)_2$ ] and on C [e.g.  $R'_2 = -B(Bu^t)C(SiMe_3)_2B(Bu^t)-$  or  $CR'_2 =$  fluorenylidene]. Numerous other stable germenes have since been characterized.<sup>(90)</sup>

The first germylene,  $R_2Ge$ : [ $R = (SiMe_3)_2CH-$ ], was reported in 1976. It can now be conveniently prepared from  $GeCl_2$ , diox and Grignard-type derivatives of the bulky bis(trimethylsilyl)methyl R group in  $Et_2O$  (e.g. ether complexes of  $RMgCl$  or  $MgR_2$ ); gas-phase electron diffraction at  $155^\circ C$  shows it to be a V-shaped monomer with the angle  $CGeC$   $107^\circ$ .<sup>(91)</sup> In the solid phase the compound forms bright yellow crystals (mp  $182^\circ C$ ) of the centrosymmetric dimer  $Ge_2R_4$  which has a *trans*-folded framework (see structure on p. 403) with a fold angle  $\theta$  of  $32^\circ$  and a Ge-Ge distance of 235 pm.<sup>(92)</sup> By contrast, reductive coupling reactions of  $R_2GeX_2$  with a mixture of  $Mg/MgBr_2$  in thf affords colourless crystals of cyclotrigermanes or cyclotetragermanes in moderate or good yield.<sup>(93)</sup>



Bulky R groups such as mesityl, xylyl or 2,6-diethylphenyl lead to  $Ge_3$  rings whereas sterically less demanding groups such as Pr, Ph or  $Me_3SiCH_2$  yield  $Ge_4$  rings. Note that the compounds  $(GeR_2)_n$  feature Ge with the coordination number 2, 3 or 4 depending on whether  $n = 1, 2,$  or  $\geq 3$ , respectively. Mixed derivatives can also be made: e.g., reductive coupling of  $Mes(Bu)GeCl_2$  at room temperature affords  $\{[Ge(Mes)Bu]_3\}$ , mp  $201^\circ$ . Thermolysis of  $\{[Ge(Mes)_2]_3\}$ , (a) in the presence of  $Et_3SiH$  at  $105^\circ$  yields a mixture of dimesityl(triethylsilyl)germane (b) and tetramesityl(triethylsilyl)digermane (c) according to the subjoined scheme:<sup>(94)</sup>



Polyhedral oligogermanes of varying complexity can be made by careful choice of the organo R group and the metal reductive coupling agent.<sup>(95)</sup> Thus, treatment of  $\{(Me_3Si)_2CH\}GeCl_3$  with Li metal in thf gave thermochroic yellow-orange crystals of the hexamer  $[Ge_6\{CH(SiMe_3)_2\}_6]$  which were unexpectedly stable to atmospheric

<sup>88</sup> T. J. BARTON, E. A. KLINE and P. M. GARVEY, *J. Am. Chem. Soc.* **95**, 3078 (1973). J. BARRAU, J. ESCUDIE and J. SATGÉ, *Chem. Rev.* **90**, 283-319 (1990) and references cited therein.

<sup>89</sup> C. COURET, J. ESCUDIE, J. SATGÉ and M. LAZRAQ, *J. Am. Chem. Soc.* **109**, 4411-12 (1987).

<sup>90</sup> M. LAZRAQ, C. COURET, J. ESCUDIE, J. SATGÉ and M. SOUFAOUI, *Polyhedron* **10**, 1153-61 (1991) and references cited therein.

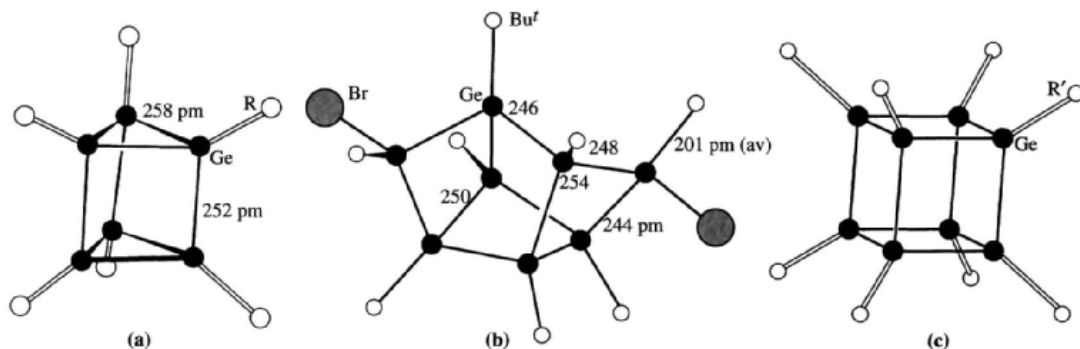
<sup>91</sup> T. FIELDBERG, A. HAALAND, B. E. R. SCHILLING, M. F. LAPPERT and A. J. THORNE, *J. Chem. Soc., Dalton Trans.*, 1551-6 (1986).

<sup>92</sup> D. E. GOLDBERG, P. B. HITCHCOCK, M. F. LAPPERT, K. M. THOMAS and A. J. THORNE, *J. Chem. Soc., Dalton Trans.*, 2387-94 (1986).

<sup>93</sup> W. ANDO and T. TSUMURAYA, *J. Chem. Soc., Chem. Commun.*, 1514-5 (1987).

<sup>94</sup> K. M. BAINES, J. A. COOKE and J. J. VITTAL, *J. Chem. Soc., Chem. Commun.*, 1484-5 (1992).

<sup>95</sup> A. SEKIGUCHI and H. SAKURAI, Chap. 7 in R. STEUDEL (ed.), *The Chemistry of Inorganic Ring Systems*, Elsevier, Amsterdam, pp. 101-24 (1992).



**Figure 10.12** (a) Prismane structure of  $[\text{Ge}_6[\text{CH}(\text{SiMe}_3)_2]_6]$  (for clarity only the *ipso* C atoms of the R groups are shown). (b) The tetracyclo structure of  $[\text{Ge}_8\text{Bu}_8^t\text{Br}_2]$  with only the *ipso* C atoms of the  $\text{Bu}^t$  groups shown. (c) The cubane structure of  $[\text{Ge}_8(\text{CMeEt}_2)_8]$  again with only the *ipso* C atoms of the *t*-hexyl groups shown.

$\text{O}_2$  and moisture.<sup>(96)</sup> X-ray analysis revealed a prismane structure (Fig. 10.12a) rather than a monocyclic benzenoid structure. The Ge–Ge distances within the two triangular faces (258 pm) are, perhaps surprisingly, longer than those in the prism quadrilateral edges (252 pm) and all the Ge–Ge distances are significantly longer than in other polygermanes (237–247 pm). Again, treatment of  $\text{GeBr}_4$  with  $\text{LiBu}^t$  yields a mixture of  $\text{Bu}_2^t\text{GeBr}_2$  and  $\text{Bu}^t\text{Br}_2\text{Ge}-\text{GeBr}_2\text{Bu}^t$ , and treatment of this latter with an excess of Li/naphthalene afforded the polycyclic octagermane.  $\text{Ge}_8\text{Bu}_8^t\text{Br}_2$ , in 50% yield.<sup>(97)</sup> As shown in Fig 10.12b, the molecule is chiral with  $C_2$  skeletal symmetry. The octagermacubane  $[\text{Ge}_8(\text{CHMeEt}_2)_8]$  (Fig. 10.12c) was obtained as yellow crystals (mp > 215°) by a simple coupling reaction of  $\text{R}_3\text{GeCl}$  with  $\text{Mg}/\text{MgBr}_2$ , and numerous other cyclic, ladder and cluster polygermanes have been described.<sup>(95)</sup>

The coordination number of Ge in organogermanes is not limited to 2, 3 or 4, and higher coordination numbers are well documented. Examples are 5-coordinate  $\text{Ge}^{\text{II}}$  in the cation of  $[\text{Ge}(\eta^5\text{-C}_5\text{Me}_5)]^+[\text{BF}_4]^-$  (10),<sup>(98)</sup>

6-coordinate  $\text{Ge}^{\text{II}}$  in the corresponding chloride  $[(\eta^5\text{-C}_5\text{Me}_5)\text{GeCl}]$  (11)<sup>(98)</sup> and 10-coordinate  $\text{Ge}^{\text{II}}$  in  $[\text{Ge}(\eta^5\text{-C}_5\text{H}_5)_2]$  (12)<sup>(99)</sup> and its  $(\eta^5\text{-C}_5\text{R}_5)$  analogues.<sup>(98)</sup> These species can now readily be prepared by standard reactions, and structural details are in the leading references cited. Thus, reaction of  $\text{NaC}_5\text{H}_5$  with  $\text{GeCl}_2$ .diox in thf gives a 60% yield of (12) as colourless crystals, mp 78°C. The angle of aperture between the two  $\text{C}_5\text{H}_5$  planes in (12) is 50.4° compared with 45.9° or 48.4° for stannocene.<sup>(99)</sup> By contrast, 5-coordinate  $\text{Ge}^{\text{IV}}$  adopts a structure midway between trigonal bipyramidal and rectangular pyramidal in phenyl-substituted anionic germanates such as  $[\text{PhGe}(\eta^2\text{-C}_6\text{H}_4\text{O}_2)_2]^-$  (13), the precise geometry being dictated by the co-cation, e.g.  $[\text{NEt}_4]^+$ ,  $[\text{N}(\text{Et})_3\text{H}]^+$  or  $[\text{AsPh}_4]^+$ .<sup>(100)</sup>

Finally, brief mention should be made of the growing range of heterocyclic organogermanium compounds. Compounds with 3–13(+) atoms in the ring have recently been reviewed.<sup>(101)</sup> Cyclic organogermapolyasilanes are also known, e.g.

<sup>99</sup> M. GRENZ, E. HAHN, W.-W. DU MONT and J. PICKARDT, *Angew. Chem. Int. Edn. Engl.* **23**, 61–3 (1984).

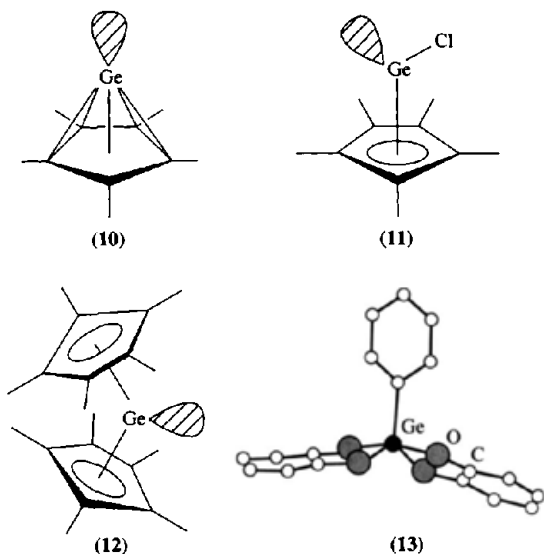
<sup>100</sup> R. R. HOLMES, R. O. DAY, A. C. SAU, C. A. POUTASSE and J. M. HOLMES, *Inorg. Chem.* **25**, 607–11 (1986) and references cited therein.

<sup>101</sup> P. MAZEROLLES, pp. 139–93 in H. W. ROESKY (ed.), *Rings, Clusters and Polymers of Main Group and Transition Elements*, Elsevier, Amsterdam (1989).

<sup>96</sup> A. SEKIGUCHI, C. KABUTO and H. SAKURAI, *Angew. Chem. Int. Edn. Engl.* **28**, 55–6 (1989).

<sup>97</sup> M. WEIDENBRUCH, F.-T. GRIMM, S. POHL and W. SAAK, *Angew. Chem. Int. Edn. Engl.* **28**, 198–9 (1989).

<sup>98</sup> P. JUTZI, B. HAMPEL, M. B. HURSTHOUSE and A. J. HOWES, *Organometallics* **5**, 1944–8 (1986).



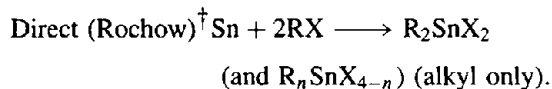
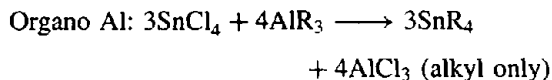
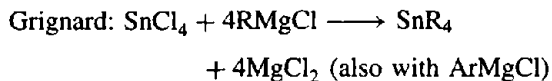
peralkyl-1-germa-2,3,4-trisilacyclobutanes.<sup>(102)</sup>

Other variants include the novel telluradigermiranes,  $\text{Ar}_2\text{Ge}-\text{Te}-\text{GeAr}_2$ ,<sup>(103)</sup> a yellow phosphagermirene  $\text{Bu}'\text{C}=\text{P}-\text{GeR}_2$  [mp.  $89^\circ$  for  $\text{R} = (\text{Me}_3\text{Si})_2\text{CH}-$ ],<sup>(104)</sup> and a germaphosphetene featuring a  $\text{GeCCP}$  ring system.<sup>(105)</sup> The possibilities are clearly limitless.

### Tin<sup>(106,107)</sup>

Organotin compounds have been much more extensively investigated than those of Ge and, as described in the Panel, many have important

industrial applications.<sup>(108)</sup> Syntheses are by standard techniques (pp. 134, 259, 363) of which the following are typical:



All three routes are used on an industrial scale and the Grignard route (or the equivalent organo-Li reagent) is convenient for laboratory scale. Rather less used is the modified Wurtz-type reaction ( $\text{SnCl}_4 + 4\text{RCl} \xrightarrow{8\text{Na}} \text{SnR}_4 + 8\text{NaCl}$ ). Conversion of  $\text{SnR}_4$  to the partially halogenated species is readily achieved by scrambling reactions with  $\text{SnCl}_4$ . Reduction of  $\text{R}_n\text{SnX}_{4-n}$  with  $\text{LiAlH}_4$  affords the corresponding hydrides and hydrostannation (addition of  $\text{Sn}-\text{H}$ ) to C-C double and triple bonds is an attractive route to unsymmetrical or heterocyclic organotin compounds.

Most organotin compounds can be regarded as derivatives of  $\text{R}_n\text{Sn}^{\text{IV}}\text{X}_{4-n}$  ( $n = 1-4$ ) and even compounds such as  $\text{SnR}_2$  or  $\text{SnAr}_2$  are in fact cyclic oligomers  $(\text{Sn}^{\text{IV}}\text{R}_2)_x$  (p. 402). The physical properties of tetraorganostannanes closely resemble those of the corresponding hydrocarbons or tetraorganosilanes but with higher densities, refractive indices, etc. They are colourless, monomeric, volatile liquids or solids. Chemically they resist hydrolysis or oxidation under normal conditions though when

<sup>102</sup> H. SUZUKI, K. OKABE, N. SATO, Y. FUKUDA and H. WATANABE, *J. Chem. Soc., Chem. Commun.*, 1298-300 (1991).

<sup>103</sup> T. T. SUMURAYA, Y. KABE and W. ANDO, *J. Chem. Soc., Chem. Commun.*, 1159-60 (1990).

<sup>104</sup> A. H. COWLEY, S. W. HALL, C. M. NUNN and J. M. POWER, *J. Chem. Soc., Chem. Commun.*, 753-4 (1988).

<sup>105</sup> M. ANDRIANARISON, C. COURET, J.-P. DECLERCQ, A. DUBOURG, J. ESCUDIE and J. SATGÉ, *J. Chem. Soc., Chem. Commun.*, 921-3 (1987).

<sup>106</sup> A. G. DAVIES and P. J. SMITH, Chap. 11 in G. WILKINSON, F. G. A. STONE and E. W. ABEL (eds.) *Comprehensive Organometallic Chemistry*, Pergamon Press, Oxford, Vol. 2, pp 519-627 (1982), (722 refs.).

<sup>107</sup> I. OMAE, *Organotin Chemistry*, Elsevier, Amsterdam, 1989, 355 pp.

<sup>108</sup> C. J. EVANS and S. KARPEL, *Organotin Compounds in Modern Technology*, Journal of Organometallic Chemistry Library, 16 Elsevier, Amsterdam, 1985, 280 pp. S. J. BLUNDEN, P. A. CUSACK and R. HILL, *The Industrial Uses of Tin Chemicals*, Royal Society of Chemistry, London, 1985, 346 pp. K. DAS, S. W. NG and M. GIELEN, *Chemistry and Technology of Silicon and Tin*, Oxford University Press, Oxford, 1992, 608 pp.

<sup>†</sup> For example, with  $\text{MeCl}$  at  $175^\circ$  in the presence of catalytic amounts of  $\text{CH}_3\text{I}$  and  $\text{NEt}_3$ , the yields were  $\text{Me}_2\text{SnCl}_2$  (39%),  $\text{MeSnCl}_3$  (6.6%),  $\text{Me}_3\text{SnCl}$  (4.6%).

### Uses of Organotin Compounds

Tin is unsurpassed by any other metal in the multiplicity of applications of its organometallic compounds. The first organotin compound was made in 1849 but large-scale applications have developed only recently; indeed, world production figures for organotin compounds increased more than 700-fold between 1950 and 1980:

Year	1950	1960	1965	1970	1975	1980
Tonnes pa	<50	2000	5000	15 000	25 000	35 000

The largest application for organotin compounds (75% by weight) is as stabilizers for PVC plastics; in their absence halogenated polymers are rapidly degraded by heat, light or oxygen to give discoloured, brittle products. The most effective stabilizers are  $R_2SnX_2$ , where R is an alkyl residue (typically *n*-octyl) and X is laurate, maleate, etc. For food packaging the *cis*-butenedioate polymer,  $[Oct_2Sn-OC(O)CH=CHC(O)O]_n$ , and the *S,S'*-bis-(*iso*-octyl mercaptoethanoate),  $Oct_2Sn[SCH_2C(O)OOct]_2$  have been approved and are used when colourless non-toxic materials with high transparency are required. The compounds are thought to be such effective stabilizers because (i) they inhibit the onset of dehydrochlorination by exchanging their anionic groups X with reactive Cl sites in the polymer, (ii) they react with and hence scavenge the HCl which is produced and which would otherwise catalyse further elimination, and (iii) they act as antioxidants and thereby prevent breakdown of the polymer initiated by atmospheric  $O_2$ .

Another major use of organotin compounds is as curing agents for the room temperature "vulcanization" of silicones; the 3 most commonly used compounds are  $Bu_2SnX_2$ , where X is acetate, 2-ethylhexanoate or laurate. The same compounds are also used to catalyse the addition of alcohols to isocyanates to produce polyurethanes.

The next major use of organotin compounds (15–20%) is as agricultural biocides and here triorganotins are the most active materials; the importance of this application can readily be appreciated since, at present, over one-third of the world's food crops are lost annually to pests such as fungi, bacteria, insects or weeds. The great advantage of organotin compounds in these applications is that their toxic action is selective and there is little danger to higher (mammalian) life; furthermore, their inorganic degradation products are completely non-toxic.  $Bu_3SnOH$  and  $Ph_3SnOAc$  control fungal growths such as potato blight and related infections of sugar-beet, peanuts, and rice. They also eradicate red spider mite from apples and pears. Other  $R_3SnX$  are effective in controlling insects, either by acting as chemosterilants or by killing the larvae. Again,  $O(SnBu_3)_2$  is an excellent wood preserver, and derivatives of  $Ph_3Sn-$  and (cyclohexyl) $_3Sn-$  are also used for this. Related applications are as marine antifouling agents for timber-hulled boats; paints containing  $Bu_3Sn-$  or  $Ph_3Sn-$  derivatives slowly release these groups and provide long-term protection against attachment of barnacles or attack by *Teredo* woodworm borers. Cellulose and woollen fabrics are likewise protected against fungal attack or destruction by moths.  $R_3SnX$  are also used as bacteriostats to control slime in paper and wood-pulp manufacture.

$Me_2SnCl_2$  is now used as an alternative to  $SnCl_4$  for coating glass with a thin film of  $SnO_2$  since it is a non-corrosive solid which is easier to handle. The glass (or ceramic) surface is treated with  $Me_2SnCl_2$  vapour at temperatures above  $450^\circ$  and, depending on the thickness of the oxide film produced, the glass is toughened and the surface can be rendered scratch-resistant, lustrous, or electroconductive (p. 385).

Organotin reagents and intermediates are finding increasing use in organic syntheses.<sup>(109)</sup>

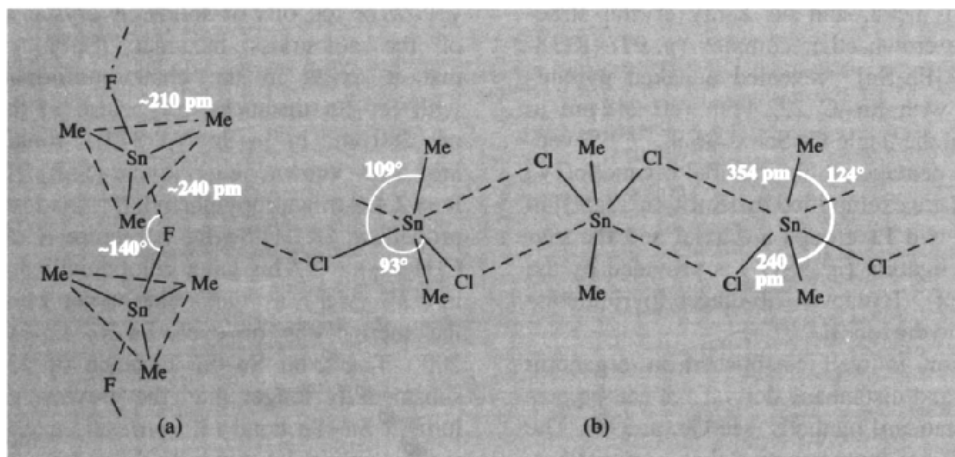
ignited they burn to  $SnO_2$ ,  $CO_2$  and  $H_2O$ . Ease of  $Sn-C$  cleavage by halogens or other reagents varies considerably with the nature of the organic group and generally increases in the sequence Bu (most stable) < Pr < Et < Me < vinyl < Ph < Bz < allyl <  $CH_2CN$  <  $CH_2CO_2R$  (least stable). The lability of  $Sn-C$  bonds and the ease of redistribution in mixed organostannane systems frustrated early attempts to prepare optically active tin compounds and

the first synthesis of a 4-coordinate Sn compound in which the metal is the sole chiral centre was only achieved in 1971 with the isolation and resolution of  $[MeSn(4-anisyl)(1-naphthyl)-\{CH_2CH_2C(OH)Me_2\}]$ .<sup>(110)</sup>

The association of  $SnR_4$  via bridging alkyl groups (which is such a notable feature of many organometallic compounds of Groups 1, 2 and 13) is not observed at all. However, many compounds of general formula  $R_3SnX$  or  $R_2SnX_2$  are strongly associated via bridging X-groups

<sup>109</sup> M. PÉREYÉ, J.-P. QUINTARD and A. RAHM, *Tin in Organic Synthesis*, Butterworths, London, 1987, 342 pp. J. K. STILLE, *Angew. Chem. Int. Edn. Engl.* **25**, 508–24 (1986).

<sup>110</sup> M. GIELEN, *Acc. Chem. Res.* **6**, 198–202 (1973).



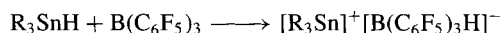
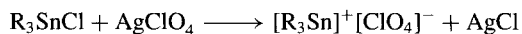
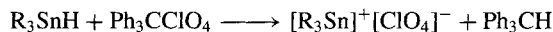
**Figure 10.13** Crystal structure of (a)  $\text{Me}_3\text{SnF}$ , and (b)  $\text{Me}_2\text{SnCl}_2$ , showing tendency to polymerize via  $\text{Sn}-\text{X}\cdots\text{Sn}$  bonds.

which thereby raise the coordination number of Sn to 5, 6 or even 7. As expected, F is more effective in this role than the other halogens (why?). For example,  $\text{Ph}_3\text{SnF}$  is a strictly linear polymer with 5-coordinate trigonal bipyramidal geometry about Sn; the angles  $\text{Sn}-\text{F}-\text{Sn}$  and  $\text{F}-\text{Sn}-\text{F}$  are both  $180^\circ$  and the  $\text{Sn}-\text{F}$  distances in the chain are identical (214.6 pm).<sup>(111)</sup> By contrast,  $\text{Me}_3\text{SnF}$  has a zig-zag chain structure (Fig. 10.13a) with unequal  $\text{Sn}-\text{F}$  distances and a pronounced bend at F ( $\sim 140^\circ$ ). The volatile chlorine analogue ( $\text{Me}_3\text{SnCl}$ : mp  $39.5^\circ$ , bp  $154^\circ$ ) also has a zig-zag chain structure with angle  $\text{Sn}-\text{Cl}-\text{Sn}$   $151^\circ$  and essentially linear  $\text{Cl}-\text{Sn}-\text{Cl}$  ( $177^\circ$ ); The two  $\text{Sn}-\text{Cl}$  distances in the chain are 243 and 326 pm but even this longer distance is substantially shorter than the sum of the van der Waals radii (385 pm).<sup>(112)</sup> On the other hand crystalline  $\text{Ph}_3\text{SnCl}$  and  $\text{Ph}_3\text{SnBr}$  feature monomeric molecules with 4-coordinate Sn atoms.

$\text{Me}_2\text{SnF}_2$  has a layer structure with octahedral Sn and *trans*-Me groups above and below the F-bridged layers as in  $\text{SnF}_4$  (p. 381). The

weaker Cl bridging in  $\text{Me}_2\text{SnCl}_2$  leads to the more distorted structure shown in Fig. 10.13b. The O atom is an even more effective ligand than F and, amongst the numerous compounds  $\text{R}_3\text{SnOR}'$  and  $\text{R}_2\text{Sn}(\text{OR}')_2$  that have been studied by X-ray crystallography, the only ones with 4-coordinate tin (presumably because of the bulky ligands) are 1,4- $(\text{Et}_3\text{SnO})_2\text{C}_6\text{Cl}_4$  and  $[\text{Mn}(\text{CO})_3\{\eta^5\text{-C}_5\text{Ph}_4(\text{OSnPh}_3)\}]$ .

The converse of polymerization is heterolytic bond scission leading either to  $\text{R}_3\text{Sn}^+$  or  $\text{R}_3\text{Sn}^-$  species. Tricoordinate organotin(IV) cations can readily be synthesized at room temperature by hydride or halide abstraction reactions in benzene or other solvents.<sup>(113)</sup> For example, with R = Me, Bu or Ph:



The highly ionic nature of these (presumably planar) species is revealed by cryoscopy, electrical conductance and the diagnostically large downfield  $^{119}\text{Sn}$  nmr chemical shift. Salts of the corresponding anionic species  $\text{Ph}_3\text{Sn}^-$  are easily generated by heating either  $\text{Ph}_3\text{SnH}$  or  $\text{Sn}_2\text{Ph}_6$

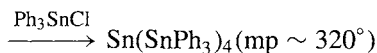
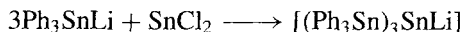
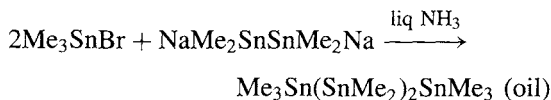
<sup>111</sup> D. TUDELA, E. GUTIÉRREZ-PUEBLA and A. MONGE, *J. Chem. Soc., Dalton Trans.*, 1069–71 (1992).

<sup>112</sup> M. B. HOSSAIN, J. L. LEFFERTS, K. C. MOLLOY, D. VAN DER HELM and J. J. ZUCKERMAN, *Inorg. Chim. Acta* **36**, L409–L410 (1979).

<sup>113</sup> J. B. LAMBERT and B. KUHLMANN, *J. Chem. Soc., Chem. Commun.*, 931–2 (1992).

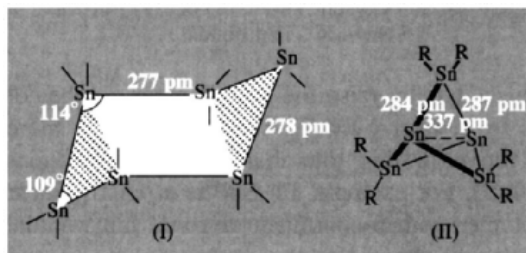
with alkali metal, and an X-ray crystal structure of the crown ether complex (p. 97)  $[\text{K}(\text{18-crown-6})]^+[\text{Ph}_3\text{Sn}]^-$  revealed a naked pyramidal anion with Sn–C 222.4 pm (cf. 212 pm in  $\text{SnPh}_4$ ) and the angle C–Sn–C  $96.9^\circ$ .<sup>(114)</sup> Seven-coordinate pentagonal bipyramidal organotin(IV) complexes are exemplified by  $[\text{SnEt}_2(\eta^5\text{-dapt})]$  in which the two Et groups are axial and the planar 5-fold ligation ( $\eta^5\text{-N}_3\text{O}_2$ ) is provided by the ligand (dapt), ( $\text{H}_2\text{dapt} = 2,6\text{-diacetylpyridinebis}(2\text{-thenoylhydrazone})$ ).<sup>(115)</sup>

Catenation is well established in organotin chemistry and distannane derivatives can be prepared by standard methods (see Ge, p. 396). The compounds are more reactive than organodigermanes; e.g.  $\text{Sn}_2\text{Me}_6$  (mp  $23^\circ$ ) inflames in air at its bp ( $182^\circ$ ) and absorbs oxygen slowly at room temperature to give  $(\text{Me}_2\text{Sn})_2\text{O}$ . Typical routes to higher polystannanes are:



Unbranched chains up to at least  $\text{Sn}_6$  are known, e.g.  $\text{Ph}_3\text{Sn}(\text{Bu}_2\text{Sn})_n\text{SnPh}_3$  ( $n = 0\text{--}4$ ).<sup>(116)</sup> Cyclo-dialkyl stannanes(IV) can also be readily prepared, e.g. reaction of  $\text{Me}_2\text{SnCl}_2$  with  $\text{Na/liq NH}_3$  yields  $\text{cyclo}(\text{SnMe}_2)_6$  together with acyclic  $\text{X}(\text{SnMe}_2)_n\text{X}$  ( $n = 12\text{--}20$ ). Yellow crystalline  $\text{cyclo}(\text{SnEt}_2)_9$  is obtained almost quantitatively when  $\text{Et}_2\text{SnH}_2$ , dissolved in toluene/pyridine, is catalytically dehydrogenated at  $100^\circ$  in the presence of a small amount of  $\text{Et}_2\text{SnCl}_2$ . Similarly, under differing conditions, the following have been prepared:<sup>(34)</sup>  $(\text{SnEt}_2)_6$ ,  $(\text{SnEt}_2)_7$ ,  $(\text{SnBu}_2)_4$ ,  $(\text{SnBu}_2)_5$ ,  $(\text{SnBu}_2)_6$ , and  $(\text{SnPh}_2)_5$ . The compounds are highly reactive

yellow or red oils or solids. A crystal structure of the colourless hexamer  $(\text{SnPh}_2)_6$  shows that it exists in the chair conformation (I) with Sn–Sn distances very close to the value of 280 pm in  $\alpha\text{-Sn}$  (p. 372). Small rings are also known, e.g.  $[\text{cyclo}(\text{SnR}_2)_3]$  where  $\text{R} = 2,4,6\text{-triisopropylphenyl}$ ,<sup>(117)</sup> and even the propellane  $[1.1.1]\text{-Sn}_5\text{R}_6$  (structure II,  $\text{R} = 2,6\text{-C}_6\text{H}_3\text{Et}_2$ ).<sup>(118)</sup> This latter compound was formed in 13% yield as dark blue-violet crystals by the thermolysis of  $\text{cyclo-Sn}_3\text{R}_6$  in xylene at  $200^\circ$ . The axial Sn–Sn distance of 337 pm is substantially longer than the previously known longest Sn–Sn bond (305 pm) and may indicate significant singlet diradical character).



True monomeric organotin(II) compounds have proved rather elusive. The cyclopentadienyl compound  $[\text{Sn}(\eta^5\text{-C}_5\text{H}_5)_2]$  (which is obtained as white crystals mp  $105^\circ$  from the reaction of  $\text{NaC}_5\text{H}_5$  and  $\text{SnCl}_2$  in thf) has a structure similar to that of germanocene (12 pp. 398–9) with the angle subtended at Sn by the midpoints of the  $\text{C}_5$  rings  $143.7^\circ$  and  $148.0^\circ$  in the two independent molecules.<sup>(119)</sup> Interestingly, the mean value of  $146^\circ$  is  $1^\circ$  larger than the value for  $[\text{Sn}(\eta^5\text{-C}_5\text{Me}_5)_2]$ , suggesting that the angle is governed predominantly by electronic rather than steric factors. However, with the much more demanding  $\eta^5\text{-C}_5\text{Ph}_5$  ligand, the two planar  $\text{C}_5$  rings are exactly parallel and staggered, the opposed canting of the phenyl rings with respect to the  $\text{C}_5$  rings giving overall

<sup>114</sup> T. BIRCHALL and J. A. VETRONE, *J. Chem. Soc., Chem. Commun.*, 877–9 (1988).

<sup>115</sup> C. CARINI, G. PELIZZI, P. TARASCONI, C. PELIZZI, K. C. MOLLOY and P. C. WATERFIELD, *J. Chem. Soc., Dalton Trans.*, 289–93 (1989).

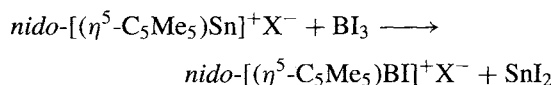
<sup>116</sup> S. ADAMS and M. DRÄGER *Angew. Chem. Int. Edn. Engl.* **26**, 1255–6 (1987).

<sup>117</sup> S. MASAMUNE and L. R. SITA, *J. Am. Chem. Soc.* **107** 6390–1 (1985).

<sup>118</sup> L. R. SITA and R. D. BICKERSTAFF, *J. Am. Chem. Soc.* **111** 6454–6 (1989).

<sup>119</sup> J. L. ATWOOD and W. E. HUNTER, *J. Chem. Soc., Chem. Commun.*, 925–7 (1981).

$S_{10}$  symmetry.<sup>(120)</sup> Heterostannocenes such as the pyrrole analogue,  $[\text{Sn}(\eta^5\text{-C}_4\text{Bu}_2\text{H}_2\text{N})_2]$ , (in which a CH group has been replaced by the isoelectronic N atom) have also been reported, the angle subtended by the ring centres at Sn being  $142.5^\circ$  in this case.<sup>(121)</sup> The related “half-sandwich” cation, *nido*- $[(\eta^5\text{-C}_5\text{Me}_5)\text{Sn}]^+$ , which is isostructural with *nido*- $\text{B}_6\text{H}_{10}$  (p. 154), can be made in moderate yield by treating  $[\text{Sn}(\eta^5\text{-C}_5\text{Me}_5)_2]$  with an ethereal solution of  $\text{HBF}_4$ . The product,  $[(\eta^5\text{-C}_5\text{Me}_5)\text{Sn}]\text{BF}_4$ , forms colourless crystals which are somewhat sensitive to air and moisture.<sup>(122)</sup> As its trifluoromethanesulfonate salt ( $\text{X}^- = \text{CF}_3\text{SO}_3^-$ ), the cation undergoes a remarkable reaction with  $\text{BI}_3$  which results in replacement of the apical Sn atom with the [BI] group to give a pentacarba analogue of *nido*- $\text{B}_6\text{H}_{10}$ .<sup>(123)</sup>



The stabilization of  $\sigma$ -bonded dialkyltin(II) compounds,  $\text{R}_2\text{Sn}$ , (and also those of Ge and Pb) can be achieved by the use of bulky R groups. The first such compound,  $[\text{Sn}\{\text{CH}(\text{SiMe}_3)_2\}_2]$ , was prepared by direct reaction of  $\text{LiCH}(\text{SiMe}_3)_2$  with  $\text{SnCl}_2$  or  $[\text{Sn}\{\text{N}(\text{SiMe}_3)_2\}_2]$  in ether, and was obtained as air-sensitive red crystals (mp  $136^\circ$ ).<sup>(124,125)</sup> It is monomeric in the gas phase and in benzene solution, and behaves chemically as a “stannylene”, displacing CO from  $\text{M}(\text{CO})_6$  to give orange  $[\text{Cr}(\text{CO})_5(\text{SnR}_2)]$  and yellow  $[\text{Mo}(\text{CO})_5(\text{SnR}_2)]$ .<sup>(124,126)</sup> However,

<sup>120</sup> M. J. HEEG, C. JANIÁK and J. J. ZUCKERMAN, *J. Am. Chem. Soc.* **106**, 4259–61 (1984).

<sup>121</sup> N. KUHN, G. HENKEL and S. STUBENRAUCH, *J. Chem. Soc., Chem. Commun.*, 760–1 (1992).

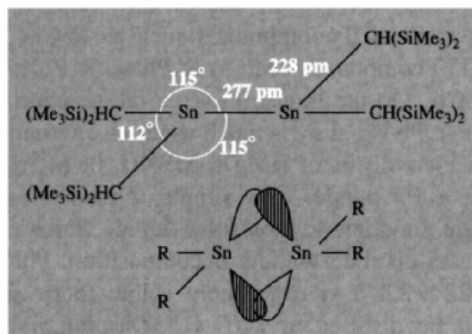
<sup>122</sup> P. JUTZI, F. KOHL and C. KRÜGER, *Angew. Chem. Int. Edn. Engl.* **18**, 59–61 (1979).

<sup>123</sup> F. KOHL and P. JUTZI, *Angew. Chem. Int. Edn. Engl.* **22**, 56 (1983).

<sup>124</sup> P. J. DAVIDSON and M. F. LAPPERT, *J. Chem. Soc., Chem. Commun.*, 317 (1973).

<sup>125</sup> D. E. GOLDBERG, D. H. HARRIS, M. F. LAPPERT and K. M. THOMAS, *J. Chem. Soc., Chem. Commun.*, 261–2 (1976).

a crystal structure determination showed that the compound dimerizes in the solid state, perhaps by donation of the lone-pair of electrons on each Sn centre into the “vacant” orbital of its neighbour, to give a weak bent double bond as indicated schematically below,<sup>(125,127)</sup> this would interpret the orientation of the four  $\{-\text{CH}(\text{SiMe}_3)_2\}$  groups.



A synthetic strategy which ensures retention of the monomeric form of  $\text{SnR}_2$  even in the crystalline state is to use functionalized R groups which contain a chelating substituent, e.g. by replacing the H atom in  $\{-\text{CH}(\text{SiMe}_3)_2\}$  with a 2-pyridyl group.<sup>(128)</sup>

Stable stannaethenes,  $>\text{C}=\text{Sn}<$ ,<sup>(129)</sup> and stannaphosphenes,  $>\text{Sn}=\text{P}<$ ,<sup>(130)</sup> have been reported and these, again, exploit the use of bulky groups to prevent oligomerization.

<sup>126</sup> J. D. COTTON, P. J. DAVIDSON, D. E. GOLDBERG, M. F. LAPPERT and K. M. THOMAS, *J. Chem. Soc., Chem. Commun.*, 893–5 (1974).

<sup>127</sup> P. J. DAVIDSON, D. H. HARRIS and M. F. LAPPERT, *J. Chem. Soc., Dalton Trans.*, 2268–74 (1976). D. E. GOLDBERG, P. B. HITCHCOCK, M. F. LAPPERT, K. M. THOMAS, A. J. THORNE, T. FIELDBERG, A. HAALAND and B. E. R. SCHILLING, *J. Chem. Soc., Dalton Trans.*, 2387–94 (1986). See also U. Lay, H. PRITZKOW and H. GRÜTZMANN, *J. Chem. Soc., Chem. Commun.*, 260–2 (1992) for isomeric structures of crystalline  $[\text{Sn}\{\text{C}_6\text{H}_2(\text{CF}_3)_3\text{-2,4,6}\}_2]$ , viz. a yellow monomeric form (mp  $76^\circ$ ) and a bright red form (mp  $66^\circ$ ) which features a weakly associated dimer with a very long Sn–Sn interaction (364 pm).

<sup>128</sup> L. M. ENGELHARDT, B. S. JOLLY, M. F. LAPPERT, C. L. RASTON and A. H. WHITE, *J. Chem. Soc., Chem. Commun.*, 336–8 (1988).

<sup>129</sup> H. MEYER, G. BAUM, W. MASSA, S. BERGER and A. BERNDT, *Angew. Chem. Int. Edn. Engl.* **26**, 546–8 (1987).

<sup>130</sup> H. RANAIVONJATOVO, J. ESCUDIE, C. COURET and J. SATGÉ, *J. Chem. Soc., Chem. Commun.*, 1047–8 (1992).



Lead<sup>(131)</sup>

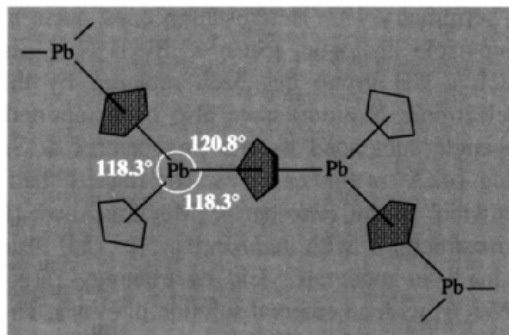
The organic chemistry of Pb is much less extensive than that of Sn, though over 2000 organolead compounds are known and PbEt<sub>4</sub> has been produced on a larger tonnage than any other single organometallic compound (p. 371). The most useful laboratory-scale routes to organoleads involve the use of LiR, RMgX, or AlR<sub>3</sub> on lead(II) compounds such as PbCl<sub>2</sub>, or lead(IV) compounds such as R<sub>2</sub>PbX<sub>2</sub>, R<sub>3</sub>PbX, or K<sub>2</sub>PbCl<sub>6</sub>. On the industrial scale the reaction of RX on a Pb/Na alloy is much used; an alternative is the electrolysis of RMgX, M<sup>I</sup>BR<sub>4</sub>, or M<sup>I</sup>AlR<sub>4</sub> using a Pb anode. The simple tetraalkyls are volatile, monomeric molecular liquids which can be steam-distilled without decomposition; PbPh<sub>4</sub> (mp 227–228°) is even more stable thermally: it can be distilled at 240° (15–20 mmHg) but decomposes above 270°. Diplumbanes Pb<sub>2</sub>R<sub>6</sub> are much less stable and higher polyplumbanes are unknown except for the thermally unstable, reactive red solid, Pb(PbPh<sub>3</sub>)<sub>4</sub>.

The decreasing thermal stability of Group 14 organometallics with increasing atomic number of M reflects the decreasing M–C and M–M bond energies. This in turn is related to the increasing size of M and the consequent increasing interatomic distance (see table).

M	C	Si	Ge	Sn	Pb
M–C distance in MR <sub>4</sub> /pm	154	194	199	217	227

Parallel with these trends and related to them is the increase in chemical reactivity which is further enhanced by the increasing bond polarity and the increasing availability of low-lying vacant orbitals for energetically favourable reaction pathways.

It is notable that the preparation of alkyl and aryl derivatives from Pb<sup>II</sup> starting materials always results in Pb<sup>IV</sup> organometallic compounds. The only well-defined examples of Pb<sup>II</sup>

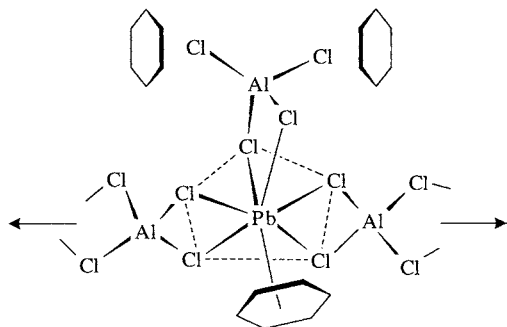


**Figure 10.14** Schematic diagram of the chain structure of orthorhombic Pb( $\eta^5$ -C<sub>5</sub>H<sub>5</sub>)<sub>2</sub>. For the doubly coordinated C<sub>5</sub>H<sub>5</sub> ring (shaded) Pb–C<sub>av</sub> is 306 pm, and for the “terminal” C<sub>5</sub>H<sub>5</sub> ring Pb–C<sub>av</sub> is 276 pm; the Pb ⋯ Pb distance within the chain is 564 pm.

organometallics are purple compound Pb[CH-(SiMe<sub>3</sub>)<sub>2</sub>]<sub>2</sub> (see refs on p. 403) and the cyclopentadienyl compound Pb( $\eta^5$ -C<sub>5</sub>H<sub>5</sub>)<sub>2</sub> and its ring-methyl derivative. Like the Sn analogue (p. 402) Pb( $\eta^5$ -C<sub>5</sub>H<sub>5</sub>)<sub>2</sub> features non-parallel cyclopentadienyl rings in the gas phase, the angle subtended at Pb being 135 ± 15°. Two crystalline forms are known and the orthorhombic polymorph has the unusual chain-like structure shown in Fig. 10.14:<sup>(132)</sup> one C<sub>5</sub>H<sub>5</sub> is between 2 Pb and perpendicular to the Pb–Pb vector whilst the other C<sub>5</sub>H<sub>5</sub> is bonded (more closely) to only 1 Pb. The chain polymer can be thought to arise as a result of the interaction of the lone-pair of electrons on a given Pb atom with a neighbouring (chain) C<sub>5</sub>H<sub>5</sub> ring; a 3-centre bond is constructed by overlapping 2 opposite sp<sup>2</sup> hybrids on 2 successive Pb atoms in the chain with the  $\sigma$ MO (A<sub>2</sub>'') of the C<sub>5</sub>H<sub>5</sub> group: this forms one bonding, one nonbonding, and one antibonding MO of which the first 2 are filled and the third empty. By contrast, the deep red crystalline compound [Pb( $\eta^5$ -C<sub>5</sub>Me<sub>5</sub>)<sub>2</sub>] (mp 100–105°) is monomeric;<sup>(119)</sup> the angle subtended by the ring centres at Pb is 151° (i.e. even larger than in the Sn analogue) and there is a slight ring slippage

<sup>131</sup> P. G. HARRISON, Chap. 12 in G. WILKINSON, F. G. A. STONE and E. W. ABEL (eds.), *Comprehensive Organometallic Chemistry*, Pergamon Press, Oxford, Vol. 2, pp. 629–80 (1982), 419 refs.

<sup>132</sup> C. PANATTONI, G. BOMBIERI, and U. CROATO, *Acta Cryst.* **21**, 823–6 (1966).



**Figure 10.15** Schematic diagram of the chain structure of  $[\text{Pb}^{\text{II}}(\text{AlCl}_4)_2(\eta^6\text{-C}_6\text{H}_6)]\cdot\text{C}_6\text{H}_6$ : Pb–Cl varies from 285–322 pm, Pb–C<sub>av</sub> (bound) 311 pm, Pb–centre of C<sub>6</sub>H<sub>6</sub> (bound) 277 pm.

which leads to a range of Pb–C distances (269–290 pm) to the pentahapto rings.

Another unusual organo-Pb<sup>II</sup> compound is the  $\eta^6$ -benzene complex  $[\text{Pb}^{\text{II}}(\text{AlCl}_4)_2(\eta^6\text{-C}_6\text{H}_6)]\cdot$

C<sub>6</sub>H<sub>6</sub> in which Pb<sup>II</sup> is in a distorted pentagonal bipyramidal site with 1 axial Cl and the other axial site occupied by the centre of the benzene ring (Fig. 10.15). The other C<sub>6</sub>H<sub>6</sub> is a molecule of solvation far removed from the metal. One {AlCl<sub>4</sub>} group chelates the Pb in an axial-equatorial configuration and the other {AlCl<sub>4</sub>} chelates and bridges neighbouring Pb atoms to form a chain. There is a similar Sn<sup>II</sup> compound with the same structure. The original paper should be consulted for a discussion of the bonding.<sup>(133)</sup>

The coordination chemistry of Pb<sup>II</sup> with conventional ligands from groups 14–16 and with macrocyclic ligands has recently been reviewed.<sup>(134)</sup>

<sup>133</sup> A. G. GASH, P. F. RODESILER and E. L. AMMA, *Inorg. Chem.* **13**, 2429–4 (1974). See also J. L. LEFFERTS, M. B. HOSSAIN, K. C. MOLLOY, D. VAN DER HELM and J. J. ZUCKERMAN, *Angew. Chem. Int. Edn. Engl.* **19**, 309–10 (1980).

<sup>134</sup> J. PARR, *Polyhedron* **16**, 551–66 (1997).

																		1		2																			
3		4																5		6		7		8		9		10											
11		12																13		14		15		16		17		18											
19		20		21		22		23		24		25		26		27		28		29		30		31		32		33		34		35		36					
37		38		39		40		41		42		43		44		45		46		47		48		49		50		51		52		53		54					
55		56		57		58		59		60		61		62		63		64		65		66		67		68		69		70		71		72					
73		74		75		76		77		78		79		80		81		82		83		84		85		86		87		88		89							
91		92		93		94		95		96		97		98		99		100		101		102		103		104		105		106		107							
109		110		111		112		113		114		115		116		117		118		119		120		121		122		123		124		125							

# 11

## Nitrogen

### 11.1 Introduction

Nitrogen is the most abundant uncombined element accessible to man. It comprises 78.1% by volume of the atmosphere (i.e. 78.3 atom% or 75.5 wt%) and is produced industrially from this source on the multimegatonne scale annually. In combined form it is essential to all forms of life, and constitutes, on average, about 15% by weight of proteins. The industrial fixation of nitrogen for agricultural fertilizers and other chemical products is now carried out on a vast scale in many countries, and the number of moles of anhydrous ammonia manufactured exceeds that of any other compound. Indeed, of the top fifteen "high-volume" industrial chemicals produced in the USA, five contain nitrogen (Fig. 11.1).<sup>(1)</sup> This has important consequences, predominantly beneficial but occasionally detrimental, since of all man's recent interventions in the cycles of nature the industrial fixation of nitrogen is by far the most extensive. These aspects will be discussed further in later sections.

The "discovery" of nitrogen in 1772 is generally credited to Daniel Rutherford, though the gas was also isolated independently about the same time by both C. W. Scheele and H. Cavendish.<sup>(2)</sup> Rutherford (at the suggestion of his teacher Joseph Black who had earlier discovered CO<sub>2</sub>, p. 269) was studying the properties of the residual "air" left after carbonaceous substances were burned in a limited supply of air; he removed the CO<sub>2</sub> by means of KOH and so obtained nitrogen which he thought was ordinary air that had taken up phlogiston from the combusted material. The elementary nature of nitrogen was disputed by some even as late as 1840 despite the work of A. L. Lavoisier. The name "nitrogen" was suggested by Jean-Antoine-Claude Chaptal in 1790 when it was realized that the element was a constituent of nitric acid and nitrates (Greek *νίτρον*, nitron; *γεννάω*, to form). Lavoisier preferred *azote* (Greek *ἄζωτικός*, no life) because

<sup>2</sup> M. E. WEEKS, in H. M. LEICESTER (ed.), *Discovery of the Elements*, 6th edn., Journal of Chemical Education Publication, 1956: Nitrogen, pp. 205-8; Rutherford, discoverer of nitrogen, pp. 235-51; Old compounds of nitrogen, pp. 188-95.

<sup>1</sup> Facts and Figures, *Chem. & Eng. News*, 23 June, 1997, pp. 40-1.

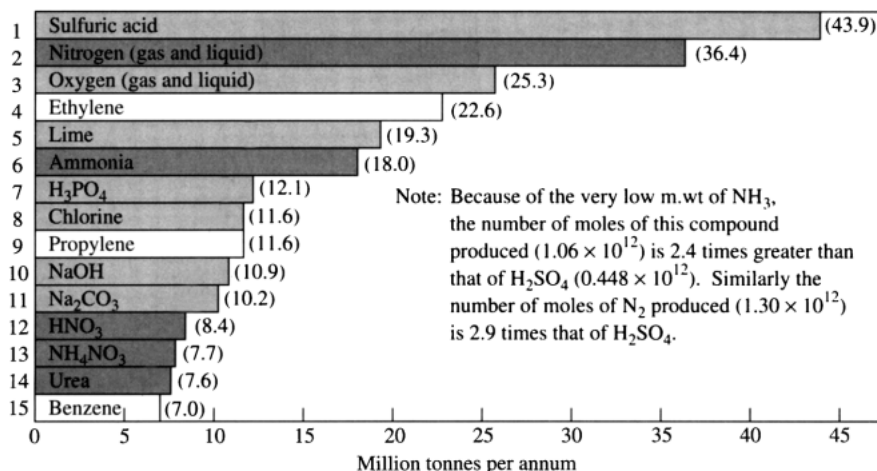


Figure 11.1 US production of the top 15 industrial chemicals (1996).

of the asphyxiating properties of the gas, and this name is still used in the French language and in such forms as azo, diazo, azide, etc. The German name *Stickstoff* refers to the same property (*sticken*, to choke or suffocate).

Compounds of nitrogen have an impressive history. Ammonium chloride was first mentioned in the *Historia* of Herodotus (fifth century BC)<sup>†</sup> and ammonium salts, together with nitrates, nitric acid and aqua regia, were well known to the early alchemists.<sup>(2)</sup> Some important dates in the subsequent development of the chemistry of nitrogen are given in the Panel on p. 408. Exciting discoveries are still being made at the present time and, indeed, the detailed mechanisms by which bacteria fix nitrogen at

ambient temperatures and pressures is still an active area of research. Several recent reviews, monographs, and proceedings of symposia have been published.<sup>(3-6)</sup>

## 11.2 The Element

### 11.2.1 Abundance and distribution

Despite its ready availability in the atmosphere, nitrogen is relatively un abundant in the crustal rocks and soils of the earth. At 19 ppm it is equal 33rd with Ga in the order of abundance, and similar to Nb (20 ppm) and Li (18 ppm). The only major minerals are KNO<sub>3</sub> (nitre, saltpetre) and NaNO<sub>3</sub> (sodanitre, Chile saltpetre). Both occur widespread, usually in small amounts as evaporites in arid regions, often as an efflorescence on soils or in caverns. NaNO<sub>3</sub> is isomorphous with calcite (p. 109) whereas KNO<sub>3</sub> is isomorphous with aragonite (p. 109), thus reflecting the similar size of NO<sub>3</sub><sup>-</sup> and CO<sub>3</sub><sup>2-</sup>, and the fact that K<sup>+</sup> is considerably larger than Na<sup>+</sup> and Ca<sup>2+</sup>. Major deposits of KNO<sub>3</sub> occur in India and there are smaller amounts in Bolivia, Italy, Spain and the former Soviet Union. There are vast deposits of NaNO<sub>3</sub> in the desert regions of northern Chile where it occurs with other evaporites such as NaCl, Na<sub>2</sub>SO<sub>4</sub> and

<sup>†</sup> "There are pieces of salt in large lumps on the hills of Libya and the Ammonians who live there worship the god Ammon in a temple resembling that of the Theban Jupiter." (Greek Ἀμμων, the name of the Egyptian diety Amun, whence *sal ammoniac* from ἄμμωνιακόν, belonging to Ammon.)

<sup>3</sup> R. W. F. HARDY, F. BOTTOMLEY and R. C. BURNS (eds.), *A Treatise on Dinitrogen Fixation*, Sections 1 and 2, Wiley, New York 1979, 812 pp.

<sup>4</sup> J. CHATT, L. M. DA C. PINA and R. L. RICHARDS, *New Trends in the Chemistry of Nitrogen Fixation*, Academic Press, London, 1980, 284 pp.

<sup>5</sup> J. CHATT, J. R. DILWORTH and R. L. RICHARDS, *Chem. Rev.* **78**, 589-625 (1978).

<sup>6</sup> A. E. SHILOV, *Pure Appl. Chem.* **64**, 1409-20 (1992).

### Time Chart for Nitrogen Chemistry

- 1772 N<sub>2</sub> gas isolated by D. Rutherford (also by C. W. Scheele and H. Cavendish).  
 1772 N<sub>2</sub>O prepared by J. Priestley who also showed it supported combustion  
 1774 NH<sub>3</sub> gas isolated by Priestley using mercury in a pneumatic trough.  
 1809 First donor-acceptor adduct (coordination compound) NH<sub>3</sub>.BF<sub>3</sub> prepared by J. L. Gay Lussac (A. Werner's theory, 1891-5).  
 1811 NCl<sub>3</sub> prepared by P. L. Dulong who lost an eye and three fingers studying its properties.  
 1828 Urea made from NH<sub>4</sub>CNO by F. Wöhler.  
 1832 Phosphonitrilic chloride (NPCl<sub>2</sub>)<sub>x</sub> prepared by J. von Liebig by heating NH<sub>3</sub> or NH<sub>4</sub>Cl with PCl<sub>5</sub>.  
 1835 S<sub>4</sub>N<sub>4</sub> first prepared by M. Gregory.  
 1862 Importance of N in soil for agriculture recognized (despite von Liebig having incorrectly maintained, in the face of fierce opposition, that it came from the atmosphere directly).  
 1864 Ability of liquid NH<sub>3</sub> to dissolve metals giving coloured solutions reported by W. Weyl.  
 1886 Atmospheric N<sub>2</sub> shown to be "fixed" by organisms in certain root nodules.  
 1887 Hydrazine, N<sub>2</sub>H<sub>4</sub>, first isolated by T. Curtius; he also first made HN<sub>3</sub> (from N<sub>2</sub>H<sub>4</sub>) in 1890.  
 1895 First industrial process involving atmospheric N<sub>2</sub> — the Frank-Caro process for calcium cyanamide.  
 1900 Birkeland-Eyde industrial oxidation of N<sub>2</sub> to NO and hence HNO<sub>3</sub> (now obsolete).  
 1906 Crystalline sulfamic acid, H<sub>3</sub>NSO<sub>3</sub>, first obtained by F. Raschig.  
 1907 Raschig's industrial oxidation of NH<sub>3</sub> to N<sub>2</sub>H<sub>4</sub> using hypochlorite.  
 1908 Catalytic oxidation of NH<sub>3</sub> to HNO<sub>3</sub> (1901) developed on an industrial scale by W. Ostwald (awarded the 1909 Nobel Prize in Chemistry for his work on catalysis).  
 1909 F. Haber's catalytic synthesis of NH<sub>3</sub> developed in collaboration with C. Bosch into a large-scale industrial process by 1913. (Haber was awarded the 1918 Nobel Prize in Chemistry "for the synthesis of ammonia from its elements"; Bosch shared the 1931 Nobel Prize for "contributions to the invention and development of chemical high-pressure methods", the Haber synthesis of NH<sub>3</sub> being the first high-pressure industrial process.)  
 1926 Borazine, (HBNH)<sub>3</sub>, analogous to benzene prepared by A. Stock and E. Pohland.  
 1928 NF<sub>3</sub> first prepared by O. Ruff and E. Hanke, 117 y after NCl<sub>3</sub>.  
 1925-35 Spectrum of atomic N gradually analysed.  
 1929 Discovery of a nitrogen isotope <sup>15</sup>N by S. M. Naudé following the discovery of isotopes of O and C by others earlier in the same year.  
 1934 Microwave absorption in NH<sub>3</sub> (due to molecular inversion) first observed — this marks the start of microwave spectroscopy.  
 1950 Nuclear magnetic resonance in compounds, containing <sup>14</sup>N and <sup>15</sup>N first observed by W. E. Proctor and F. C. Yu.  
 1957 N<sub>2</sub>F<sub>4</sub> first made by C. B. Colburn and A. Kennedy and later (1961) shown to be in dissociative equilibrium with paramagnetic NF<sub>2</sub> above 100°C.  
 1958 NH<sub>3</sub>.BH<sub>3</sub> isoelectronic with ethane prepared by S. G. Shore and R. W. Parry (direct reaction of NH<sub>3</sub> and B<sub>2</sub>H<sub>6</sub> gives [BH<sub>2</sub>(NH<sub>3</sub>)<sub>2</sub>]<sup>+</sup>[BH<sub>4</sub>]<sup>-</sup>).  
 1962 First "bent" NO complex encountered, viz. [Co(NO)(S<sub>2</sub>CNMe<sub>2</sub>)<sub>2</sub>] (P. R. H. Alderman, P. G. Owston and J. M. Rowe).  
 1965 First N<sub>2</sub> ligand complex prepared by A. D. Allan and C. V. Senoff.  
 1966 ONF<sub>3</sub> (isoelectronic with CF<sub>4</sub>) discovered independently by two groups.  
 1968 N<sub>2</sub> recognized as a bridging ligand in [(NH<sub>3</sub>)<sub>5</sub>RuN<sub>2</sub>Ru(NH<sub>3</sub>)<sub>5</sub>]<sup>4+</sup> by D. F. Harrison, E. Weissberger, and H. Taube. (H. Taube, 1983 Nobel Prize for chemistry "for his work on the mechanisms of electron transfer reactions especially in metal complexes").  
 1974 First thionitrosyl (NS) complex isolated by J. Chatt and J. R. Dilworth.  
 1975 (SN)<sub>x</sub> polymer, known since 1910, found to be metallic (and a superconductor at temperatures below 0.33 K).  
 1979 Trigonal prismatic 6-fold coordination of N (Table 11.1, p. 413).  
 1980-90 Square pyramidal and trigonal bipyramidal 5-fold coordination of N (Table 11.1).

KNO<sub>3</sub> on the eastern slopes of the coastal ranges at an elevation of 1200-2500 m. Because of the development of the synthetic ammonia and nitric acid industries these large deposits are no longer a major source of nitrates, though they played an important role in agriculture until the 1920s (as also did guano, the massive deposits of bird excreta on certain islands).

The continuous interchange of nitrogen between the atmosphere and the biosphere is called the nitrogen cycle. Global estimates are difficult to obtain and there are frequently regional and local impacts which vary greatly from the mean. However, some indication of the size of the various "reservoirs" of nitrogen in the atmosphere, on land, and in the seas is

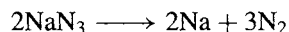
given in Fig. 11.2 together with the estimated annual rate of transfer between these various pools.<sup>(7,8)</sup> Estimates frequently vary by a factor of 3 or more. Atmospheric nitrogen is fixed by biological action (p. 1035), industrial processes (p. 421), and to a significant extent by fires, lightning and other atmospheric discharges which produce NO<sub>x</sub>. There is also a minute production (on the global scale) of NO<sub>x</sub> from internal combustion engines and from coal-burning, though the local concentration in some urban environments can be very high and extremely unpleasant.<sup>(9-11)</sup> Absorption of fixed nitrogen by both terrestrial and aquatic plants leads to protein synthesis followed by death, decay, oxidation and denitrification by bacterial and other action which eventually returns the nitrogen to the seas and the atmosphere as N<sub>2</sub>. An alternative sequence involves the digestion of plants by animals, the synthesis of animal proteins, excretion of nitrogenous material, and, again, ultimate death, decay and denitrification. Figure 11.2 indicates that the greatest anthropogenic impact on the cycle arises from the industrial fixation of nitrogen by the Haber and other processes. Much of this is used beneficially as fertilizers but the leaching of excess nitrogenous material can lead to eutrophication in freshwater systems, and the increased nitrate concentration in waters used for human consumption can pose a health hazard. Nevertheless, there is no doubt that the high yields of agriculture necessary to maintain even the present human population of the world cannot be achieved without the judicious application of manufactured nitrogenous fertilizers. Concern has also been expressed that increasing levels

of N<sub>2</sub>O following denitrification may eventually impoverish the ozone layer in the stratosphere. Much more data are required and the subject is being actively pursued by several international agencies as well as by national and local governments and individual scientists.

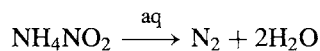
### 11.2.2 Production and uses of nitrogen

The only important large-scale process for producing N<sub>2</sub> is the liquefaction and fractional distillation of air<sup>(12)</sup> (see Panel on p. 411). Production has grown remarkably during the past few years, partly as a result of the increasing demand for its coproduct O<sub>2</sub> for steelmaking. For example, US domestic production has increased 250-fold in the past 25 y from 0.12 million tonnes in 1955 to 30 million tonnes in 1980. In 1991 world production was 56 million tonnes (USA 47%; Europe 35%; Asia 15%). Commercial N<sub>2</sub> is a highly purified product, typically containing less than 20 ppm O<sub>2</sub>. Specially purified "oxygen-free" N<sub>2</sub>, containing less than 2 ppm, is available commercially, and "ultrapure" N<sub>2</sub> (99.999%) containing less than 10 ppm Ar is also produced on the multitonne per day scale.

Laboratory routes to highly purified N<sub>2</sub> are seldom required. Thermal decomposition of sodium azide at 300°C under carefully controlled conditions is one possibility:



Hot aqueous solutions of ammonium nitrite also decompose to give nitrogen though small amounts of NO and HNO<sub>3</sub> are also formed (p. 434) and must be removed by suitable absorbents such as dichromate in aqueous sulfuric acid:



Other routes are the thermal decomposition of (NH<sub>4</sub>)<sub>2</sub>Cr<sub>2</sub>O<sub>7</sub>, the reaction of NH<sub>3</sub> with bromine water, or the high-temperature reaction of NH<sub>3</sub>

<sup>7</sup> C. C. DELWICHE, The nitrogen cycle, Chap. 5 in C. L. HAMILTON (ed.), *Chemistry in the Environment*, Readings from Scientific American, W. H. Freeman, San Francisco, 1973.

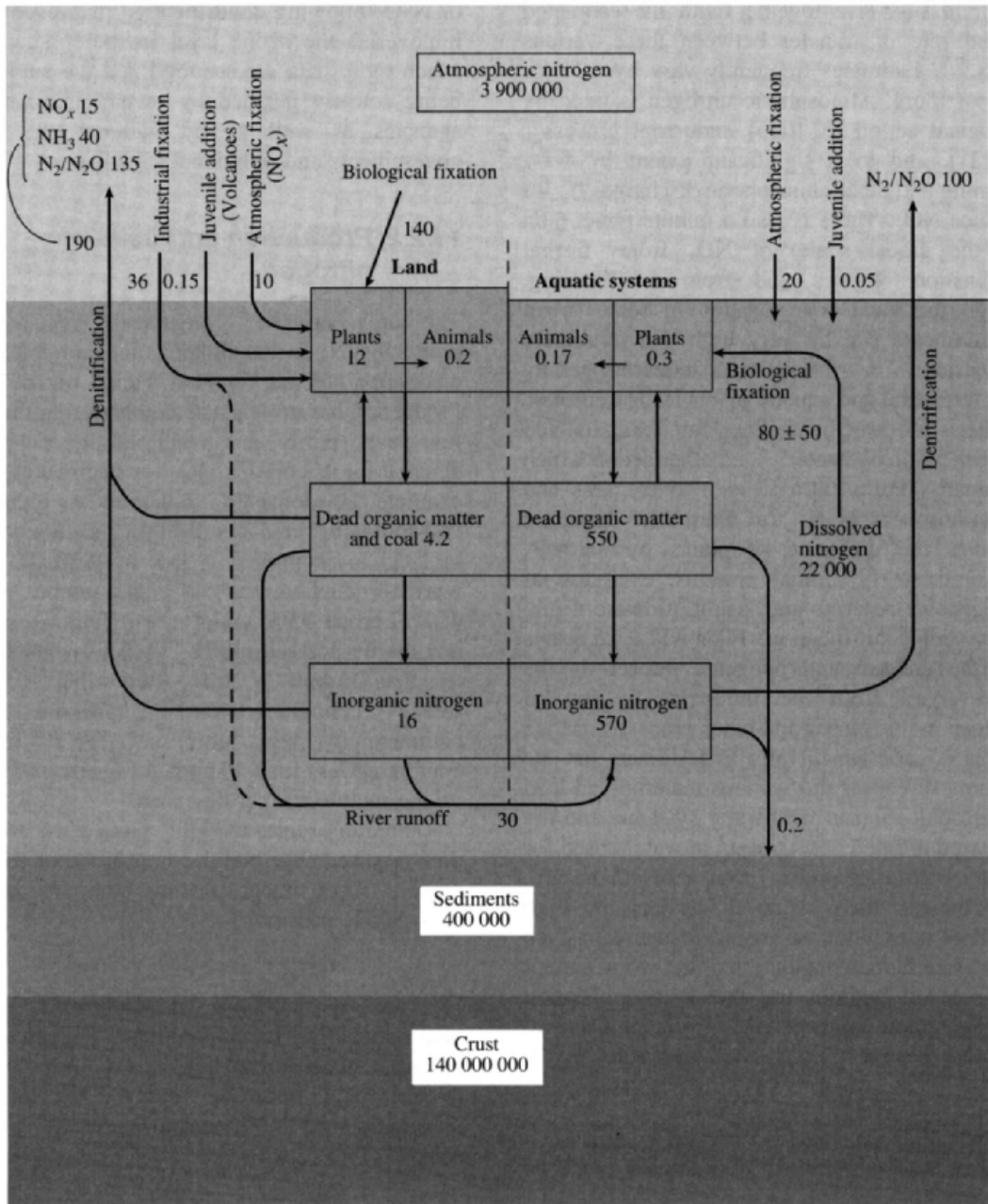
<sup>8</sup> SCOPE Report No. 10, *Environmental Issues*, Wiley, New York, 1977, 220 pp.

<sup>9</sup> J. HEICKLEN, *Atmospheric Chemistry*, Academic Press, 1976, 406 pp.

<sup>10</sup> I. M. CAMPBELL, *Energy and the Atmosphere*, 2nd edn. Wiley, London, 1986, Nitrogen cycles, pp 169-81.

<sup>11</sup> U. S. OZKAN, S. K. AGARWAL and G. MARCELIN (eds.), *Reduction of Nitrogen Oxide Emissions*, ACS Symposium Series No. 587, 1995, 260 pp.

<sup>12</sup> W. J. GRANT and S. L. REDFEARN, Industrial gases, in R. THOMPSON (ed.), *The Modern Inorganic Chemicals Industry*, Chem. Soc. Special Publ. 31, 273-301 (1977).



**Figure 11.2** Distribution of nitrogen in the biosphere and annual transfer rates can be estimated only within broad limits. The two quantities known with high confidence are the amount of nitrogen in the atmosphere and the rate of industrial fixation. The inventories (within the boxes) are expressed in terms of  $10^9$  tonnes of N; the transfers (indicated by arrows) are in  $10^6$  tonnes of N. Taken from ref. 7 with some adjustments for more recent data.

### Industrial Gases from Air

Air is the source of six industrial gases, N<sub>2</sub>, O<sub>2</sub>, Ne, Ar, Kr and Xe. As the mass of the earth's atmosphere is approximately  $5 \times 10^9$  million tonnes, the supply is unlimited and the annual industrial production, though vast, is insignificant by comparison. The composition of air at low altitudes is remarkably constant, the main variable component being water vapour which ranges from ~4% by volume in tropical jungles to very low values in cold or arid climates. Other minor local variations result from volcanism or human activity. The main invariant part of the air has the following composition (% by volume, bp in parentheses):

N <sub>2</sub>	78.03 (77.2 K)	CO <sub>2</sub>	0.033 (194.7 K)	He	0.0005 (4.2 K)
O <sub>2</sub>	20.99 (90.1 K)	Ne	0.0015 (27.2 K)	Kr	0.0001 (119.6 K)
Ar	0.93 (87.2 K)	H <sub>2</sub>	0.0010 (20.2 K)	Xe	0.000008 (165.1 K)

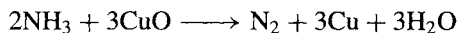
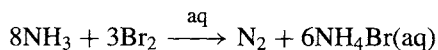
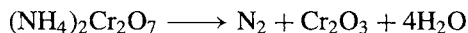
Details of the production and uses of O<sub>2</sub> (p. 604) and the noble gases (p. 889) are in later chapters.

About two-thirds of the N<sub>2</sub> produced industrially is supplied as a gas, mainly in pipes but also in cylinders under pressure. The remaining one-third is supplied as liquid N<sub>2</sub> since this is also a very convenient source of the dry gas. The main use is as an inert atmosphere in the iron and steel industry and in many other metallurgical and chemical processes where the presence of air would involve fire or explosion hazards or unacceptable oxidation of products. Thus, it is extensively used as a purge in petrochemical reactors and other chemical equipment, as an inert diluent for chemicals, and in the float glass process to prevent oxidation of the molten tin (p. 370). It is also used as a blanketing gas in the electronics industry, in the packaging of processed foods and pharmaceuticals, and to pressurize electric cables, telephone wires, and inflatable rubber tyres, etc.

About 10% of the N<sub>2</sub> produced is used as a refrigerant. Typical of such applications are (a) freeze grinding of normally soft or rubbery materials, (b) low-temperature machining of rubbers, (c) shrink fitting and assembly of engineering components, (d) the preservation of biological specimens such as blood, semen, etc., and (e) as a constant low-temperature bath (-196°C). Liquid N<sub>2</sub> is also frequently used for convenience in applications where a very low temperature is not essential such as (a) food freezing (and hamburger meat grinding), (b) in-transit refrigeration, (c) freeze branding of cattle, (d) pipe-freezing for stopping flow in the absence of valves, and (e) soil-freezing for consolidating unstable ground in tunnelling or excavation.

The cost of N<sub>2</sub>, like that of O<sub>2</sub>, is particularly dependent on electricity costs, though plant maintenance and transport costs also obtrude. Typical prices in 1992 for N<sub>2</sub> in the USA were about \$32 per tonne for bulk liquid (exclusive of transportation and handling charges). Costs for small-scale users of N<sub>2</sub> from gas cylinders are proportionately much higher.

with CuO; overall equations can be written as:



### 11.2.3 Atomic and physical properties

Nitrogen has two stable isotopes <sup>14</sup>N (relative atomic mass 14.003 07, abundance 99.634%) and <sup>15</sup>N (15.000 11, 0.366%); their relative abundance (272:1) is almost invariant in terrestrial sources and corresponds to an atomic weight of 14.006 74(7). Both isotopes have a nuclear spin and can be used in nmr experiments.<sup>(13)</sup> though

the sensitivity at constant field is only one-thousandth that of <sup>1</sup>H. The <sup>14</sup>N nucleus has a spin quantum number of 1 and, in consequence, the spectra are broadened by quadrupole effects. The <sup>15</sup>N nucleus with spin  $\frac{1}{2}$  does not have this difficulty though its low abundance poses problems.<sup>(14)</sup> Interestingly, the first chemical shift ever to be observed in nmr spectroscopy ("as an annoying ambiguity in the magnetic moment of <sup>14</sup>N") was in 1950 in an aqueous solution of NH<sub>4</sub>NO<sub>3</sub>.<sup>(15)</sup> Nowadays <sup>14</sup>N and <sup>15</sup>N nmr chemical shifts are widely used to probe the

1981, 382 pp. J. MASON, Nitrogen, in J. MASON (ed.), *Multinuclear NMR*, Plenum Press, New York, pp. 335-67 (1987).

<sup>14</sup> G. C. LEVY and R. L. LICHTER, *Nitrogen-15 Nuclear Magnetic Resonance Spectroscopy*, Wiley, New York, 1979, 221 pp. W. VON PHILIPSBORN and R. MÜLLER, *Angew. Chem. Int. Edn. Engl.* **25**, 383-413 (1986).

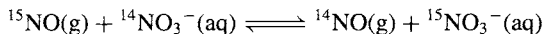
<sup>15</sup> W. G. PROCTOR and F. C. YU, *Phys. Rev.* **77**, 717 (1950).

<sup>13</sup> G. J. MARTIN, M. L. MARTIN and J.-P. GOUESNARD, *NMR Volume 18: <sup>15</sup>N NMR Spectroscopy*, Springer-Verlag, Berlin,

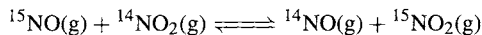


nature of bonding in N-containing compounds, to study structural features (e.g. linear, bent, encapsulated N), to determine the site of coordination or protonation, to follow kinetically the course of chemical reactions and to detect new species.

Isotopic enrichment of  $^{15}\text{N}$  is usually effected by chemical exchange, and samples containing up to 99.5%  $^{15}\text{N}$  have been obtained from the 2-phase equilibrium



Other exchange reactions that have been used are:



Fractional distillation of NO provides another effective route and, as the heavier isotope of oxygen is simultaneously enriched, the product has a high concentration of  $^{15}\text{N}^{18}\text{O}$ . Many key nitrogen compounds are now commercially available with  $^{15}\text{N}$  enriched to 5%, 30% or 95%, e.g.  $\text{N}_2$ , NO,  $\text{NO}_2$ ,  $\text{NH}_3$ ,  $\text{HNO}_3$  and several ammonium salts and nitrates. Fortunately the use of these compounds in tracer experiments is simplified by the absence of exchange with atmospheric  $\text{N}_2$  under normal conditions, in marked contrast with labelled H, C and O compounds where contact with atmospheric moisture and  $\text{CO}_2$  must be avoided.

The ground state electronic configuration of the N atom is  $1s^2 2s^2 2p_x^1 2p_y^1 2p_z^1$  with three unpaired electrons ( $^4S$ ). The electronegativity of N ( $\sim 3.0$ ) is exceeded only by those of F and O. Its "single-bond" covalent radius ( $\sim 70$  pm) is slightly smaller than those of B and C, as expected; the nitride ion,  $\text{N}^{3-}$ , is much larger and has been assigned a radius in the range 140–170 pm. Ionization energies and other properties are compared with those of the other Group 15 elements (P, As, Sb and Bi) on p. 550.

Molecular  $\text{N}_2$ , i.e. dinitrogen (see p. 34), (mp  $-210^\circ\text{C}$ , bp  $-195.8^\circ\text{C}$ ) is a colourless, odourless, tasteless, diamagnetic gas. The short interatomic distance (109.76 pm) and very high dissociation energy ( $945.41 \text{ kJ mol}^{-1}$ ) are both

consistent with multiple bonding. The free-energy change for the equilibrium  $\text{N}_2 \rightleftharpoons 2\text{N}$  is  $\Delta G = 911.13 \text{ kJ mol}^{-1}$  from which it is clear that the dissociation constant  $K_p = [\text{N}]^2/[\text{N}_2]$  atm is negligible under normal conditions; it is  $1.6 \times 10^{-24}$  atm at 2000 K and still only  $1.3 \times 10^{-12}$  atm at 4000 K. Detailed tabulations of other physical properties of nitrogen are available.<sup>(16)</sup>

### 11.2.4 Chemical reactivity

Gaseous  $\text{N}_2$  is rather inert at room temperature presumably because of the great strength of the  $\text{N}\equiv\text{N}$  bond and the large energy gap between the highest occupied molecular orbitals (HOMO) and the lowest unoccupied molecular orbitals (LUMO). Further contributory factors are the very symmetrical electron distribution in the molecule and the absence of bond polarity — when these are modified, as in the isoelectronic analogues CO,  $\text{CN}^-$  and  $\text{NO}^+$ , the reactivity is considerably enhanced. Nitrogen reacts readily with Li at room temperature (p. 76) and with several transition-element complexes (p. 414).

Reactivity increases rapidly with rising temperature and the element combines directly with Be, the alkaline earth metals, and B, Al, Si and Ge to give nitrides (p. 417); hydrogen yields ammonia (p. 421), and coke yields cyanogen,  $(\text{CN})_2$ , when heated to incandescence (p. 320). Many finely divided transition metals also react directly at elevated temperatures to give nitrides of general formula  $\text{MN}$  ( $\text{M} = \text{Sc}, \text{Y}, \text{lanthanoids}; \text{Zr}, \text{Hf}; \text{V}; \text{Cr}, \text{Mo}, \text{W}; \text{Th}, \text{U}, \text{Pu}$ ). Although not always directly preparable from  $\text{N}_2(\text{g})$ , many other nitrides are known (p. 417) and, indeed, nitrides as a class include some of the most stable compounds in the whole of chemistry. Nitrogen forms bonds with almost all elements in the periodic table, the only exceptions apparently being the noble gases (other than Xe and Kr, pp. 902, 904). A wide range of stereochemistries is observed and

<sup>16</sup> B. R. BROWN, Physical properties of nitrogen, in *Mellor's Comprehensive Treatise on Inorganic and Theoretical Chemistry*, Vol. 8, Suppl. 1, *Nitrogen*, Part 1, pp. 27–149, Longmans, London, 1964.

Table 11.1 Stereochemistry of nitrogen<sup>(a)</sup>

CN	Examples
0	N(g) in "active nitrogen"
1	N <sub>2</sub> , NO, NNO, [N <sub>3</sub> N] <sup>-</sup> , HN <sub>3</sub> , RC≡N, XC≡N (X = Hal), [OsO <sub>3</sub> N] <sup>-</sup>
2	<i>Linear:</i> [NO <sub>2</sub> ] <sup>+</sup> , NNO, [N <sub>3</sub> N] <sup>-</sup> , HN <sub>3</sub> ; η <sup>1</sup> -N <sub>2</sub> complexes, e.g. [Ru(N <sub>2</sub> )(NH <sub>3</sub> ) <sub>5</sub> ] <sup>2+</sup> ; η <sup>1</sup> -NO complexes, e.g. [Fe(CN) <sub>5</sub> (NO)] <sup>2-</sup> ; μ <sub>2</sub> -N complexes, e.g. [(H <sub>2</sub> O)Cl <sub>4</sub> RuNRuCl <sub>4</sub> (OH <sub>2</sub> )] <sup>3-</sup> and [Cl <sub>5</sub> WNWCl <sub>5</sub> ] <sup>2-</sup> (ref. 18)
	<i>Bent:</i> NO <sub>2</sub> , [NO <sub>2</sub> ] <sup>-</sup> , [NH <sub>2</sub> ] <sup>-</sup> , HN <sub>3</sub> , HNCO, RNCO, XNCO, N <sub>2</sub> F <sub>2</sub> , <i>cyclo</i> - $\overline{\text{CH}_2\text{NN}}$ , <i>cyclo</i> -[NSF(O)] <sub>3</sub> [W(CO) <sub>5</sub> OPPh <sub>2</sub> NPPPh <sub>3</sub> ] (ref. 19)
3	<i>Planar:</i> [NO <sub>3</sub> ] <sup>-</sup> , N <sub>2</sub> O <sub>4</sub> , XNO <sub>2</sub> , (HO)NO <sub>2</sub> , K[ON(NO)(SO <sub>3</sub> )], K <sub>2</sub> [ON(SO <sub>3</sub> ) <sub>2</sub> ] (Fremy's salt), N(SiH <sub>3</sub> ) <sub>3</sub> , NMe(SiMe <sub>3</sub> ) <sub>2</sub> (ref. 20), N(GeH <sub>3</sub> ) <sub>3</sub> , N(PF <sub>2</sub> ) <sub>3</sub> , Si <sub>3</sub> N <sub>4</sub> , and Ge <sub>3</sub> N <sub>4</sub> (Be <sub>2</sub> SiO <sub>4</sub> structure, p. 347), μ <sub>3</sub> -N complexes, e.g. [(H <sub>2</sub> O(SO <sub>4</sub> ) <sub>2</sub> Ir) <sub>3</sub> N] <sup>4-</sup>
	<i>Pyramidal:</i> NH <sub>3</sub> , NF <sub>3</sub> , NH <sub>2</sub> F, NHF <sub>2</sub> , (HO)NH <sub>2</sub> , N <sub>2</sub> H <sub>4</sub> , N <sub>2</sub> F <sub>4</sub> , [N <sub>4</sub> (CH <sub>2</sub> ) <sub>6</sub> ]
	<i>T-shaped:</i> [Mo <sub>3</sub> (μ <sub>3</sub> -N)O(η <sup>5</sup> -C <sub>5</sub> H <sub>5</sub> ) <sub>3</sub> (CO) <sub>4</sub> ] (ref. 21)
4	<i>Tetrahedral:</i> [NH <sub>4</sub> ] <sup>+</sup> , [NH <sub>3</sub> (OH)] <sup>+</sup> , [NF <sub>4</sub> ] <sup>+</sup> , H <sub>3</sub> NBF <sub>3</sub> and innumerable other coordination complexes of NH <sub>3</sub> , NR <sub>3</sub> , en, edta, etc., including Me <sub>3</sub> NO and sulfamic acid (H <sub>3</sub> NSO <sub>3</sub> ). BN (layer structure and Zn blende-type), AlN (wurtzite-type), [PhAlNPh] <sub>4</sub> (cubane-type)
	<i>See-saw:</i> [{Fe(CO) <sub>3</sub> ] <sub>4</sub> (μ <sub>4</sub> -N)] <sup>-</sup> (refs. 22, 23)
5	<i>Square-pyramidal:</i> [Fe <sub>5</sub> (CO) <sub>14</sub> H(μ <sub>5</sub> -N)] (ref. 23), [(η <sup>5</sup> -C <sub>5</sub> Me <sub>5</sub> ) <sub>2</sub> Mo <sub>2</sub> Co <sub>3</sub> (CO) <sub>10</sub> (μ <sub>5</sub> -N)] (ref. 24), <i>closo</i> -NB <sub>9</sub> H <sub>10</sub> (p. 211)
	<i>Trig. bipyramidal:</i> [N(AuPPh <sub>3</sub> ) <sub>5</sub> ] <sup>2+</sup> (ref. 25)
6	<i>Octahedral:</i> MN (interstitial nitrides with NaCl or hcp structure, e.g. M = Sc, La; Ce, Pr, Nd; Ti, Zr, Hf; V, Nb, Ta; Cr, Mo, W; Th, U), Ti <sub>2</sub> N (anti-rutile TiO <sub>2</sub> -type), Cu <sub>3</sub> N (ReO <sub>3</sub> -type), Ca <sub>3</sub> N <sub>2</sub> (anti-Mn <sub>2</sub> O <sub>3</sub> )
	<i>Trigonal prism:</i> [NC <sub>6</sub> (CO) <sub>15</sub> ] <sup>-</sup> (ref. 26), [Rh <sub>12</sub> H(N) <sub>2</sub> (CO) <sub>23</sub> ] <sup>3-</sup> (ref. 27)
	<i>Pentagonal prism:</i> <i>closo</i> -NB <sub>11</sub> H <sub>12</sub> (p. 211)
8	<i>Cubic:</i> Ternary nitrides with anti-CaF <sub>2</sub> structure, e.g. BeLiN, AlLi <sub>3</sub> N <sub>2</sub> , TiLi <sub>5</sub> N <sub>3</sub> , NbLi <sub>7</sub> N <sub>4</sub> , and CrLi <sub>9</sub> N <sub>5</sub>
	<i>Square antiprism:</i> [Rh <sub>12</sub> H(N) <sub>2</sub> (CO) <sub>23</sub> ] <sup>3-</sup> (ref. 27)

<sup>(a)</sup>For coordination numbers 1, 2, and 3 the CN is sometimes increased in the condensed phase as a result of H bonding (p. 52), e.g. HCN, NH<sub>2</sub><sup>-</sup>, NH<sub>3</sub>, N<sub>2</sub>H<sub>4</sub>, NH<sub>2</sub>(OH), NO<sub>2</sub>(OH).

typical examples of coordination numbers 0, 1, 2, 3, 4, 5, 6, and 8 are given in Table 11.1.

A particularly reactive form of nitrogen can be obtained by passing an electric discharge through N<sub>2</sub>(g) at a pressure of 0.1–2 mmHg.<sup>(16,17)</sup> Atomic

N is formed, and the process is accompanied by a peach-yellow emission which persists as an after-glow, often for several minutes after the discharge

<sup>21</sup> N. D. FEASEY, S. A. R. KNOX and A. G. ORPEN, *J. Chem. Soc., Chem. Commun.*, 75–6 (1982).

<sup>22</sup> D. FJARE and W. L. GLADFELTER, *J. Am. Chem. Soc.* **103**, 1572–4 (1981); **106**, 4799–4810 (1984).

<sup>23</sup> M. TACHIKAWA, J. STEIN, E. L. MUEHTERTIES, R. G. TELLER, M. A. BENO, E. GEBERT and J. M. WILLIAMS, *J. Am. Chem. Soc.* **102**, 6648–9 (1980).

<sup>24</sup> C. P. GIBSON and L. F. DAHL, *Organometallics* **7**, 543–52 (1988).

<sup>25</sup> A. GROHMANN, J. RIEDE and H. SCHMIDBAUR, *Nature* **345**, 140–2 (1990).

<sup>26</sup> S. MARTINENGO, G. CIANI, A. SIRONI, B. T. HEATON and J. MASON, *J. Am. Chem. Soc.* **101**, 7095–7 (1979).

<sup>27</sup> S. MARTINENGO, G. CIANI and A. SIRONI, *J. Chem. Soc., Chem. Commun.*, 1742–4 (1986).

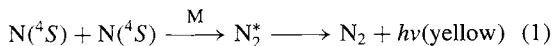
<sup>17</sup> A. N. WRIGHT and C. A. WINKLER, *Active Nitrogen*, Academic Press, New York, 1968.

<sup>18</sup> F. WELLER, W. LIEBELT and K. DEHNICKE, *Angew. Chem. Int. Edn. Engl.* **19**, 220 (1980). [The W–N–W linkage is linear and the interatomic distances are 166 pm (W<sup>VI</sup>-N) and 207 pm (W<sup>V</sup>-N).

<sup>19</sup> D. J. DARENSBOURG, M. PALA, D. SIMMONS and A. L. RHEINGOLD, *Inorg. Chem.* **25**, 2537–41 (1986). See also H. G. ANG, Y. M. CAI, L. L. KOH and W. L. KWIK, *J. Chem. Soc., Chem. Commun.*, 850–2 (1991).

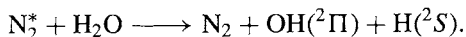
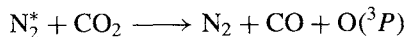
<sup>20</sup> D. W. H. RANKIN and H. E. ROBERTSON, *J. Chem. Soc., Dalton Trans.*, 785–8 (1987).

has been stopped. Atoms of N in their ground state ( $^4S$ ) have a relatively long lifetime since recombination involves either a 3-body collision on the surface of the vessel (first-order reaction in N at pressures below  $\sim 3$  mmHg) or a termolecular homogeneous association reaction (second order in N at pressures above  $\sim 3$  mmHg):



The molecules of  $N_2^*$  so formed are in an excited state ( $B^3\Pi_g$ ) and give rise to the emission of the first positive band system of the spectrum of molecular  $N_2$  in returning to the ground state ( $A^3\Sigma_u^+$ ).

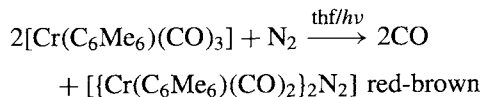
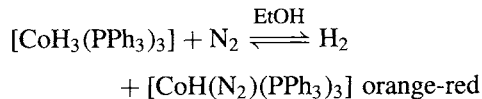
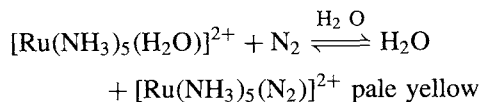
Several elements react with the N atoms in active nitrogen to form nitrides. The excited  $N_2$  molecules are also highly reactive and can cause the dissociation of molecules that are normally stable to attack either by ordinary  $N_2$  or even N atoms, e.g.:



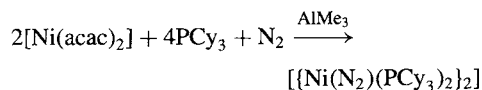
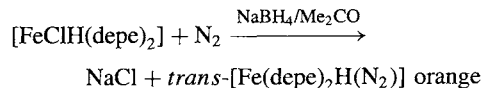
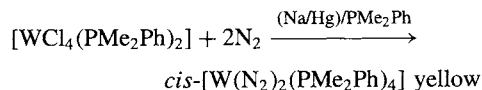
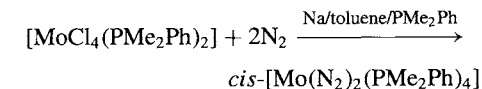
One of the most dramatic developments in the chemistry of  $N_2$  during the past 30 years was the discovery by A. D. Allen and C. V. Senoff in 1965 that dinitrogen complexes such as  $[Ru(NH_3)_5(N_2)]^{2+}$  could readily be prepared from aqueous  $RuCl_3$  using hydrazine hydrate in aqueous solution.<sup>(28)</sup> Since that time virtually all transition metals have been found to give dinitrogen complexes and several hundred such compounds are now characterized.<sup>(5,29,30)</sup> Three general preparative methods are available:

(a) Direct replacement of labile ligands in metal complexes by  $N_2$ : such reactions

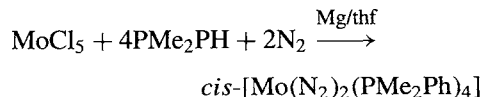
proceed under mild conditions and are often reversible, e.g.:



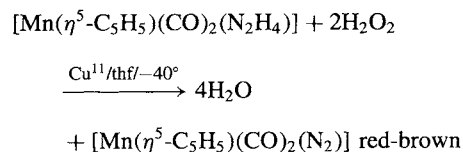
(b) Reduction of a metal complex in the presence of an excess of a suitable coligand under  $N_2$ , e.g.:



where *depe* is  $Et_2PCH_2CH_2PET_2$ , *acac* is 3,5-pentanedionate, and  $PCy_3$  is tris(cyclohexyl)phosphine. In some systems  $Mg/thf$  is a better reducing agent than Na, e.g.:



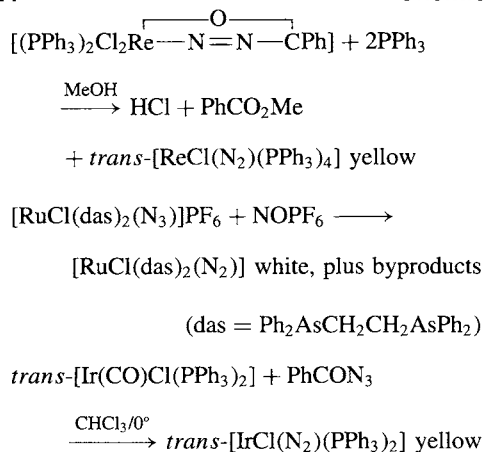
(c) Conversion of a ligand with N–N bonds into  $N_2$ ; in the early development of  $N_2$  complex chemistry this was the most successful and widely used route, e.g.:



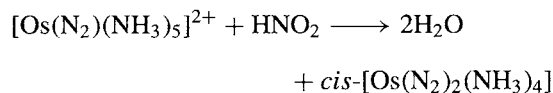
<sup>28</sup> A. D. ALLEN and C. V. SENOFF, *Chem. Commun.*, 1965, 621–2. The unprecedented nature of the reaction can be gauged from the fact that this paper was rejected for publication by *J. Am. Chem. Soc.* on the grounds that it was impossible, before being accepted by *Chem. Commun.*. See also H. TAUBE, The researches of A. D. Allen — an appreciation, *Coord. Chem. Rev.* **26**, 1–5 (1978).

<sup>29</sup> A. D. ALLEN, R. O. HARRIS, B. R. LOESCHER, J. R. STEVENS and R. N. WHITELEY, *Chem. Revs.* **73**, 11–20 (1973).

<sup>30</sup> D. SELLMANN, *Angew. Chem. Int. Edn. Engl.* **13**, 639–49 (1974).

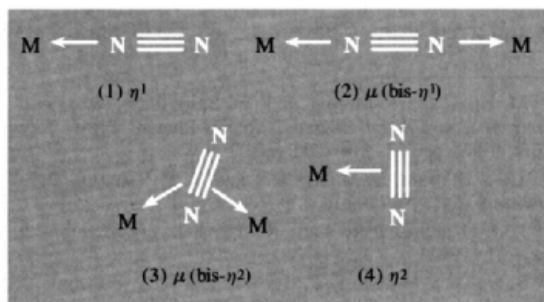


A related example is the reaction of  $\text{NbCl}_5$  and  $\text{thf}$  with  $(\text{Me}_3\text{Si})_2\text{NN}(\text{SiMe}_3)_2$  in  $\text{CH}_2\text{Cl}_2$  to give an 80% yield of  $[(\mu\text{-N}_2)\{\text{NbCl}_3(\text{thf})_2\}_2]$ .<sup>(31)</sup> Occasionally an  $\text{N}\equiv\text{N}$  triple bond can be formed within a metal complex, e.g. by reaction of coordinated  $\text{NH}_3$  with  $\text{HNO}_2$ , but this method is of limited application, e.g.:



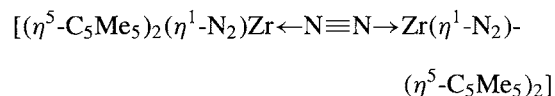
Frequently dinitrogen complexes have colours in the range white-yellow-orange-red-brown but other colours are known, e.g.  $[\{\text{Ti}(\eta^5\text{-C}_5\text{H}_5)_2\}_2\text{-}(\text{N}_2)]$  is blue.

Dinitrogen might coordinate to metals in at least 4 ways,<sup>(32)</sup> but only the end-on modes, structures (1) and (2), are well established as common bonding modes by numerous well-defined examples:



The side-on structure (3) has been established in two dinickel complexes which have very complicated structures involving lithium atoms also in association with the bridging  $\text{N}_2$ .<sup>(33)</sup> It also occurs in the first fully characterized  $\text{N}_2$  complex of a lanthanide element,  $[(\mu\text{-}\eta^2\text{:}\eta^2\text{-N}_2)\{\text{Sm}(\eta^5\text{-C}_5\text{Me}_5)_2\}_2]$ .<sup>(34)</sup> The “side-on”  $\eta^2$  mode (structure 4) was at one time thought to be exemplified by the rhodium(I) complex  $[\text{RhCl}(\text{N}_2)(\text{PPr}_3)_2]$  but a reinvestigation of the X-ray structure by another group<sup>(35)</sup> showed conclusively that the  $\text{N}_2$  ligand was coordinated in the “end-on” mode (1) — an instructive example of mistaken conclusions that can initially be drawn from this technique. The side on structure (4) has been postulated for the zirconium(III) complex  $[\text{Zr}(\eta^5\text{-C}_5\text{H}_5)(\text{N}_2)\text{R}]$  on the basis of its  $^{15}\text{N}$  nmr spectrum.<sup>(36)</sup> A unique triply-coordinated bridging mode ( $\mu_3\text{-N}_2$ ) has also recently been established by X-ray crystallography.<sup>(37)</sup>

Complexes are known which feature more than one  $\text{N}_2$  ligand, e.g.  $\textit{cis}\text{-}[\text{W}(\text{N}_2)_2(\text{PMe}_2\text{Ph})_4]$  and  $\textit{trans}\text{-}[\text{W}(\text{N}_2)_2(\text{diphos})_2]$  (where  $\text{diphos} = \text{Ph}_2\text{PCH}_2\text{CH}_2\text{PPh}_2$ ) and some complexes feature more than one bonding mode, e.g.:<sup>(38)</sup>



<sup>31</sup> J. R. DILWORTH, S. J. HARRISON, R. A. HENDERSON and D. R. M. WALTON, *J. Chem. Soc., Chem. Commun.*, 176–7 (1984).

<sup>32</sup> K. JONAS, D. J. BRAUER, C. KRÜGER, P. J. ROBERTS and Y.-H. TSAY, *J. Am. Chem. Soc.* **98**, 74–81 (1976). P. R. HOFFMAN, T. YOSHIDA, T. OKANO, S. OTSUKA and J. IBERS, *Inorg. Chem.* **15**, 2462–6 (1976).

<sup>33</sup> K. KRÜGER and Y.-H. TSAY, *Angew. Chem. Int. Edn. Engl.* **12**, 998–9 (1973).

<sup>34</sup> W. J. EVANS, T. A. ULIBARRI and J. W. ZILLER, *J. Am. Chem. Soc.* **110**, 6877–9 (1988).

<sup>35</sup> D. L. THORN, T. H. TULIP and J. A. IBERS, *J. Chem. Soc., Dalton Trans.*, 2022–5 (1979).

<sup>36</sup> M. J. S. GYNANE, J. JEFFREY and M. F. LAPPERT, *J. Chem. Soc., Chem. Commun.*, 34–6 (1978).

<sup>37</sup> G. P. PEZ, P. APGAR and R. K. CRISSEY, *J. Am. Chem. Soc.* **104**, 482–90 (1982).

<sup>38</sup> R. D. SANNER, J. M. MANRIQUEZ, R. E. MARSH and J. E. BERCAW, *J. Am. Chem. Soc.* **98**, 8351–7 (1976).

The first example of a tris-N<sub>2</sub> complex is the yellow crystalline compound *mer*-[Mo( $\eta^1$ -N<sub>2</sub>)<sub>3</sub>(PPt<sub>2</sub>Ph)<sub>3</sub>].<sup>(39)</sup>

X-ray structural studies have shown that for N<sub>2</sub> complexes with structure (1), the M–N–N group is linear or nearly so (172–180°); the N–N internuclear distance is usually in the range 110–113 pm, only slightly longer than in gaseous N<sub>2</sub> (109.8 pm). Such complexes have a strong sharp, infrared absorption in the range 1900–2200 cm<sup>-1</sup>, corresponding to the Raman-active band at 2331 cm<sup>-1</sup> in free N<sub>2</sub>. Similarly, in complexes with structure (2), when both transition metals have a closed d-shell, the N–N distance falls in the range 112–120 pm and  $\nu$ (N–N) often occurs near 2100 cm<sup>-1</sup>, i.e. little altered from that of the corresponding complexes of structure (1). On the other hand, if one of the M is a transition metal with a closed d-shell and the other is either a main-group metal such as Al in AlMe<sub>3</sub> or an open-shell transition metal such as Mo in MoCl<sub>4</sub>, then the N–N bond is greatly lengthened and the N–N stretching frequency is lowered even to 1600 cm<sup>-1</sup>. Compounds with structure (3) have N–N ~134–136 pm, and this very substantial lengthening has been attributed to interaction with the Li atoms in the structure.<sup>(33)</sup>

As implied above, N<sub>2</sub> is isoelectronic with both CO and C<sub>2</sub>H<sub>2</sub>, and the detailed description of the bonding in structures 1–4 follows closely along the lines indicated on pp. 927 and 932 though there are some differences in the detailed sequences of orbital energies. Crystallographic and vibrational spectroscopic data have been taken to indicate that N<sub>2</sub> is weaker than CO in both its  $\sigma$ -donor and  $\pi$ -acceptor functions. Theoretical studies suggest that  $\sigma$  donation is more important for the formation of the M–N bond than is  $\pi$  back-donation, which mainly contributes to the weakening of the N–N bond, and end-on ( $\eta^1$ ) donation is more favourable than side-on ( $\eta^2$ ).<sup>(40)</sup>

The chemical reactivity of coordinated N<sub>2</sub> has been extensively studied because of its potential relevance to the catalytic and biological fixation of N<sub>2</sub> to NH<sub>3</sub> (p. 1035). For other recent work on the reactions of coordinated dinitrogen see refs. 41–44

To conclude this section on the chemical reactivity of nitrogen it will be helpful to compare the element briefly with its horizontal neighbours C and O, and also with the heavier elements in Group 15, P, As, Sb and Bi. The diagonal relationship with S is vestigial. Nitrogen resembles oxygen in its high electronegativity and in its ability to form H bonds (p. 52) and coordination complexes (p. 198) by use of its lone-pair of electrons. Catenation is more limited than for carbon, the longest chain so far reported being the N<sub>8</sub> unit in PhN=N–N(Ph)—N=N–N(Ph)—N=NPh.

Nitrogen shares with C and O the propensity for multiple bonding via  $p_\pi$ – $p_\pi$  interactions both with another N atom or with a C or O atom. In this it differs sharply from its Group 15 congeners which have no analogues of the oxides of nitrogen, nitrites, nitrates, nitro-, nitroso-, azo- and diazo-compounds, azides, cyanates, thiocyanates or imino-derivatives. Conversely, there are no nitrogen analogues of the various oxoacids of phosphorus (p. 510).

## 11.3 Compounds

This section deals with the binary compounds that nitrogen forms with metals, and then describes the extensive chemistry of the hydrides, halides, pseudohalides, oxides and oxoacids of the element. The chemistry of P–N compounds is deferred until Chapter 12 (p. 531) and S–N

<sup>41</sup> M. HIDAI and Y. MIZOBE, in P. S. BRATERMAN (ed.) *Reactions of Coordinated Ligands*, Vol. 2, Plenum Press, New York, 1989, pp. 53–114 (202 refs.)

<sup>42</sup> T. A. GEORGE, L. M. KOCZON and R. C. TISDALE, *Polyhedron* **9**, 545–51 (1990).

<sup>43</sup> J. O. DZIEGIELEWSKI and R. GRZYBEK, *Polyhedron* **9**, 645–51 (1990).

<sup>44</sup> S. NIELSON-MARSH, R. J. CROWTE and P. G. EDWARDS, *J. Chem. Soc., Chem. Commun.*, 699–700 (1992).

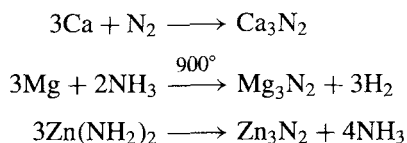
<sup>39</sup> S. N. ANDERSON, D. L. HUGHES and R. L. RICHARDS, *J. Chem. Soc., Chem. Commun.*, 958–9 (1984).

<sup>40</sup> T. YAMABE, K. HORI, T. MINATO and K. FUKUI, *Inorg. Chem.* **19**, 2154–9 (1980).

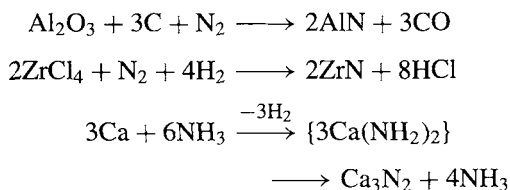
compounds are discussed in Chapter 15 (p. 721). Compounds with B (p. 207) and C (p. 319) have already been treated.

### 11.3.1 Nitrides, azides and nitrido complexes

Nitrogen forms binary compounds with almost all elements of the periodic table and for many elements several stoichiometries are observed, e.g. MnN, Mn<sub>6</sub>N<sub>5</sub>, Mn<sub>3</sub>N<sub>2</sub>, Mn<sub>2</sub>N, Mn<sub>4</sub>N and Mn<sub>x</sub>N (9.2 < x < 25.3). Nitrides are frequently classified into 4 groups: "salt-like", covalent, "diamond-like" and metallic (or "interstitial"). The remarks on p. 64 concerning the limitations of such classifications are relevant here. The two main methods of preparation are by direct reaction of the metal with N<sub>2</sub> or NH<sub>3</sub> (often at high temperatures) and the thermal decomposition of metal amides, e.g.:



Common variants include reduction of a metal oxide or halide in the presence of N<sub>2</sub> and the formation of a metal amide as an intermediate in reactions in liquid NH<sub>3</sub>:



Metal nitrides have also been prepared by adding KNH<sub>2</sub> to liquid-ammonia solutions of the appropriate metal salts in order to precipitate the nitride, e.g. Cu<sub>3</sub>N, Hg<sub>3</sub>N<sub>2</sub>, AlN, Tl<sub>3</sub>N and BiN.

"Salt-like" nitrides are exemplified by Li<sub>3</sub>N (mp 548°C, decomp) and M<sub>3</sub>N<sub>2</sub> (M = Be, Mg, Ca, Sr, Ba). It is possible to write ionic formulations of these compounds using the species N<sup>3-</sup> though charge separation is

unlikely to be complete, particularly for the corresponding compounds of Groups 11 and 12, i.e. Cu<sub>3</sub>N, Ag<sub>3</sub>N, and M<sub>3</sub>N<sub>2</sub> (M = Zn, Cd, Hg). The N<sup>3-</sup> ion has been assigned a radius of 146 pm, slightly larger than the value for the isoelectronic ions O<sup>2-</sup> (140 pm) and F<sup>-</sup> (133 pm), as expected. Stability varies widely; e.g. Be<sub>3</sub>N<sub>2</sub> melts at 2200°C whereas Mg<sub>3</sub>N<sub>2</sub> decomposes above 271°C. The existence of Na<sub>3</sub>N is doubtful and the heavier alkali metals appear not to form analogous compounds, perhaps for steric reasons (p. 76). However the azides NaN<sub>3</sub> and KN<sub>3</sub> are well characterized as colourless crystalline salts which can be melted with little decomposition; they feature the symmetrical linear N<sub>3</sub><sup>-</sup> group as do Sr(N<sub>3</sub>)<sub>2</sub> and Ba(N<sub>3</sub>)<sub>2</sub>. The corresponding "B subgroup" metal azides such as AgN<sub>3</sub>, Cu(N<sub>3</sub>)<sub>2</sub>, and Pb(N<sub>3</sub>)<sub>2</sub> are shock-sensitive and detonate readily; they are far less ionic and have more complex structures. Further discussion of azides is on p. 433. Other stoichiometries are also known, e.g. Ca<sub>2</sub>N (anti-CdCl<sub>2</sub> layer structure), Ca<sub>3</sub>N<sub>4</sub>, and Ca<sub>11</sub>N<sub>8</sub>.

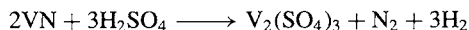
The covalent binary nitrides are more conveniently treated under the appropriate element. Examples include cyanogen (CN)<sub>2</sub> (p. 320), P<sub>3</sub>N<sub>5</sub> (p. 531), S<sub>2</sub>N<sub>2</sub> (p. 725) and S<sub>4</sub>N<sub>4</sub> (p. 722). The Group 13 nitrides MN (M = B, Al, Ga, In, Tl) are a special case since they are isoelectronic with graphite, diamond, SiC, etc., to which they are structurally related (p. 255). Their physical properties suggest a gradation of bond-type from covalent, through partially ionic, to essentially metallic as the atomic number increases. Si<sub>3</sub>N<sub>4</sub> and Ge<sub>3</sub>N<sub>4</sub> are also known and have the phenacite (Be<sub>2</sub>SiO<sub>4</sub>)-type structure. Si<sub>3</sub>N<sub>4</sub>, in particular, has excited considerable interest in recent years as a ceramic material with extremely desirable properties: high strength and wear resistance, high decomposition temperature and oxidation resistance, excellent thermal-shock properties and resistance to corrosive environments, low coefficient of friction, etc. Unfortunately it is extremely difficult to fabricate and sinter suitably shaped components, and considerable efforts have therefore been spent on developing related nitrogen ceramics by forming

solid solutions between  $\text{Si}_3\text{N}_4$  and  $\text{Al}_2\text{O}_3$  to give the "sialons" ( $\text{SiAlON}$ ) of general formula  $\text{Si}_{6-0.75x}\text{Al}_{0.67x}\text{O}_x\text{N}_{8-x}$  ( $0 < x < 6$ ).<sup>(45)</sup>

The most extensive group of nitrides are the metallic nitrides of general formulae  $\text{MN}$ ,  $\text{M}_2\text{N}$ , and  $\text{M}_4\text{N}$  in which N atoms occupy some or all of the interstices in cubic or hcp metal lattices (examples are in Table 11.1, p. 413). These compounds are usually opaque, very hard, chemically inert, refractory materials with metallic lustre and conductivity and sometimes having variable composition. Similarities with borides (p. 145) and carbides (p. 297) are notable. Typical mps ( $^\circ\text{C}$ ) are:

TiN	ZrN	HfN	VN	NbN	TaN
2950	2980	2700	2050	2300	3090
CrN	ThN	UN			
d1770	2630	2800			

Hardness on the Mohs scale is often above 8 and sometimes approaches 10 (diamond). These properties commend nitrides for use as crucibles, high-temperature reaction vessels, thermocouple sheaths and related applications. Several metal nitrides are also used as heterogeneous catalysts, notably the iron nitrides in the Fischer-Tropsch hydriding of carbonyls. Few chemical reactions of metal nitrides have been studied; the most characteristic (often extremely slow but occasionally rapid) is hydrolysis to give ammonia or nitrogen:

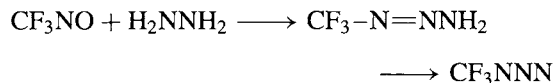


The crystal chemistry of metal nitrides has been reviewed<sup>(45a)</sup> and there have recently been some intriguing developments in our understanding of the stoichiometries and structures of ternary and quaternary metal nitrides.<sup>(45b)</sup>

The nitride ion  $\text{N}^{3-}$  is an excellent ligand, particularly towards second- and third-row

transition metals.<sup>(46)</sup> It is considered to be by far the strongest  $\pi$  donor known, the next strongest being the isoelectronic species  $\text{O}^{2-}$ . Nitrido complexes are usually prepared by the thermal decomposition of azides (e.g. those of phosphine complexes of  $\text{V}^{\text{V}}$ ,  $\text{Mo}^{\text{VI}}$ ,  $\text{W}^{\text{VI}}$ ,  $\text{Ru}^{\text{VI}}$ ,  $\text{Re}^{\text{V}}$ ) or by deprotonation of  $\text{NH}_3$  (e.g.  $[\text{OsO}_4 \rightarrow \text{OsO}_3\text{N}]^-$ ). Most involve a terminal  $\{\equiv\text{N}\}^{3-}$  group as in  $[\text{VCl}_3\text{N}]^-$ ,  $[\text{MoO}_3\text{N}]^-$ ,  $[\text{WCl}_5\text{N}]^{2-}$ ,  $[\text{ReN}(\text{PR}_3)_3\text{X}_2]$  and  $[\text{RuN}(\text{OH}_2)\text{X}_4]^-$ . The M–N distance is much shorter (by 40–50 pm) than the "normal"  $\sigma$ -(M–N) distance, consistent with strong multiple bonding. Other bonding modes feature linear symmetrical bridging as in  $[(\text{H}_2\text{O})\text{Cl}_4\text{Ru}-\text{N}-\text{RuCl}_4(\text{OH}_2)]^{3-}$ , trigonal planar  $\mu_3$  bridging as in  $[(\text{H}_2\text{O})(\text{SO}_4)_2\text{Ir}_3\text{N}]^{4-}$ , and tetrahedral coordination as in  $[(\text{MeHg})_4\text{N}]^+$  (Fig. 11.3). The nitrido ligand has a strong *trans* influence, e.g. in  $[\text{Os}^{\text{VI}}\text{NCl}_5]^{2-}$  (p. 1085); likewise, in the octahedral complex,  $[\text{Tc}^{\text{V}}\text{NCl}_2(\text{PMe}_2\text{Ph})_3]$ , the Tc–Cl distance *trans* to N is 266.5 pm whereas that *cis* to N is only 244.1 pm.<sup>(47)</sup>

Azidotrifluoromethylmethane,  $\text{CF}_3\text{N}_3$ , (mp  $-152^\circ$ , bp  $-285^\circ$ ) is a colourless gas which is thermally stable at room temperature. It can be prepared in 90% yield by reacting  $\text{CF}_3\text{NO}$  with hydrazine in MeOH at  $-78^\circ$  and then treating the product with HCl gas.<sup>(48)</sup>



The molecule has an almost linear  $\text{N}_3$  group and an angle C–N–N of  $112.4^\circ$  (Fig. 11.4a).<sup>(49)</sup> The (linear) azide ion,  $\text{N}_3^-$ , is isoelectronic with  $\text{N}_2\text{O}$ ,  $\text{CO}_2$ ,  $\text{OCN}^-$ , etc. and forms numerous coordination complexes by standard ligand replacement reactions. Various coordination modes have been established, including end-on  $\eta^1$ , bridging

<sup>46</sup> W. P. GRIFFITH, *Coord. Chem. Revs.* **8**, 369–96 (1972).

<sup>47</sup> A. S. BATSANOV, YU. T. STRUCHKOV, B. LORENZ and B. OLK, *Z. anorg. allg. Chem.* **564**, 129–34 (1988).

<sup>48</sup> K. O. CHRISTE, and C. J. SCHACK, *Inorg. Chem.* **20**, 2566–70 (1981).

<sup>49</sup> K. O. CHRISTE, D. CHRISTEN, H. OBERHAMMER and C. J. SCHACK, *Inorg. Chem.* **23**, 4283–8 (1984).

<sup>45</sup> K. H. JACK, *Trans. J. Br. Ceram. Soc.* **72**, 376–84 (1973). F. L. RILEY (ed.), *Nitrogen Ceramics*, Noordhoff-Leyden, 1977, 694 pp.

<sup>45a</sup> N. E. BRESE and M. O'KEEFE, *Structure and Bonding*, **79**, 307–78 (1992).

<sup>45b</sup> R. KNIEP, *Pure Appl. Chem.* **69**, 185–91 (1997).

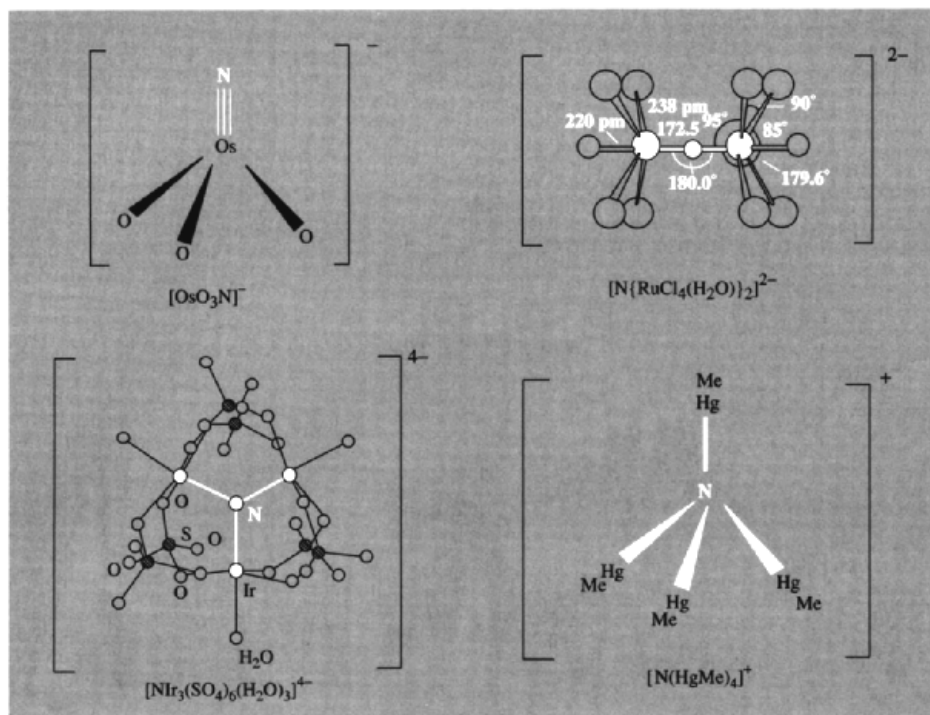
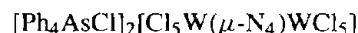
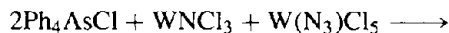


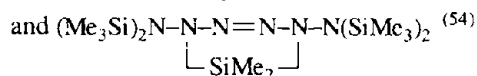
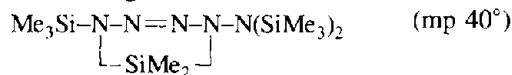
Figure 11.3 Structures of some nitrido complexes.<sup>(24)</sup>

$\mu, \eta^1$  and bridging  $\mu, \eta^1: \eta^1$  (Fig. 11.4).<sup>(50,51)</sup> The binuclear complex  $[\text{Mo}_2\text{Cl}_2\text{N}_{20}]^{2-}$  features a terminal nitrido ligand,  $\text{N}\equiv$ , as well as terminal and bridging azido ligands, i.e.  $[\{(\text{MoCl}(\text{N})(\eta^1\text{-N}_3)_2(\mu, \eta^1\text{-N}_3)_2\}_2]^{2-}$ .<sup>(52)</sup>

Concatenations larger than  $\text{N}_3$  are rare. The planar bridging  $\text{N}_4^{4-}$  occurs in the binuclear  $\text{W}^{\text{VI}}$  dianion,  $[\text{Cl}_5\text{W}(\mu, \eta^1: \eta^1\text{-N}_4)\text{WCl}_5]^{2-}$ ; this is formed during the thermolytic interconversion of  $[\text{W}(\text{N}_3)\text{Cl}_5]$  to the corresponding nitrido complex  $\text{WCl}_3$  in the presence of  $\text{Ph}_4\text{AsCl}$ , the nitride reacting as it is formed with unreacted azide still present according to the simple stoichiometry:<sup>(53)</sup>



It will be noted that  $\text{N}_4^{4-}$  is isosteric with the tetradeprotonated urea molecule,  $(\text{H}_2\text{N})_2\text{C}=\text{O}$ , and is also isoelectronic and isostructural with  $\text{CO}_3^{2-}$  and  $\text{NO}_3^-$ . An X-ray analysis of the red single crystals shows that  $\text{N}(\text{central})\text{-N}_\mu$  is long (149 pm) and that  $\text{N}(\text{central})\text{-N}_i$  is short (123 pm). Unbranched N-catenation is observed in 2-tetrazenes such as  $(\text{Me}_3\text{Si})_2\text{N}-\text{N}=\text{N}-\text{N}(\text{SiMe}_3)_2$  (mp  $46^\circ$ ) and its derivatives, e.g.



<sup>50</sup> D. FENSKE, K. STEINER and K. DEHNICKE, *Z. anorg. allg. Chem.* **553**, 57–63 (1987).

<sup>51</sup> P. CHAUDHURI, M. GUTTMANN, D. VENTUR, K. WIEG HAROT, B. NUBER and J. WEISS, *J. Chem. Soc., Chem. Commun.* 1618–20 (1985).

<sup>52</sup> K. JANSEN, J. SCHMITTE and K. DEHNICKE, *Z. anorg. allg. Chem.* **552**, 201–9 (1987).

<sup>53</sup> W. MASSA, R. KUJANEK, G. BAUM and K. DEHNICKE, *Angew. Chem. Int. Edn. Engl.* **23**, 149 (1984).

<sup>54</sup> N. WIBERG and G. ZIEGLER, *Chem. Ber.* **111**, 2123–9 (1978).



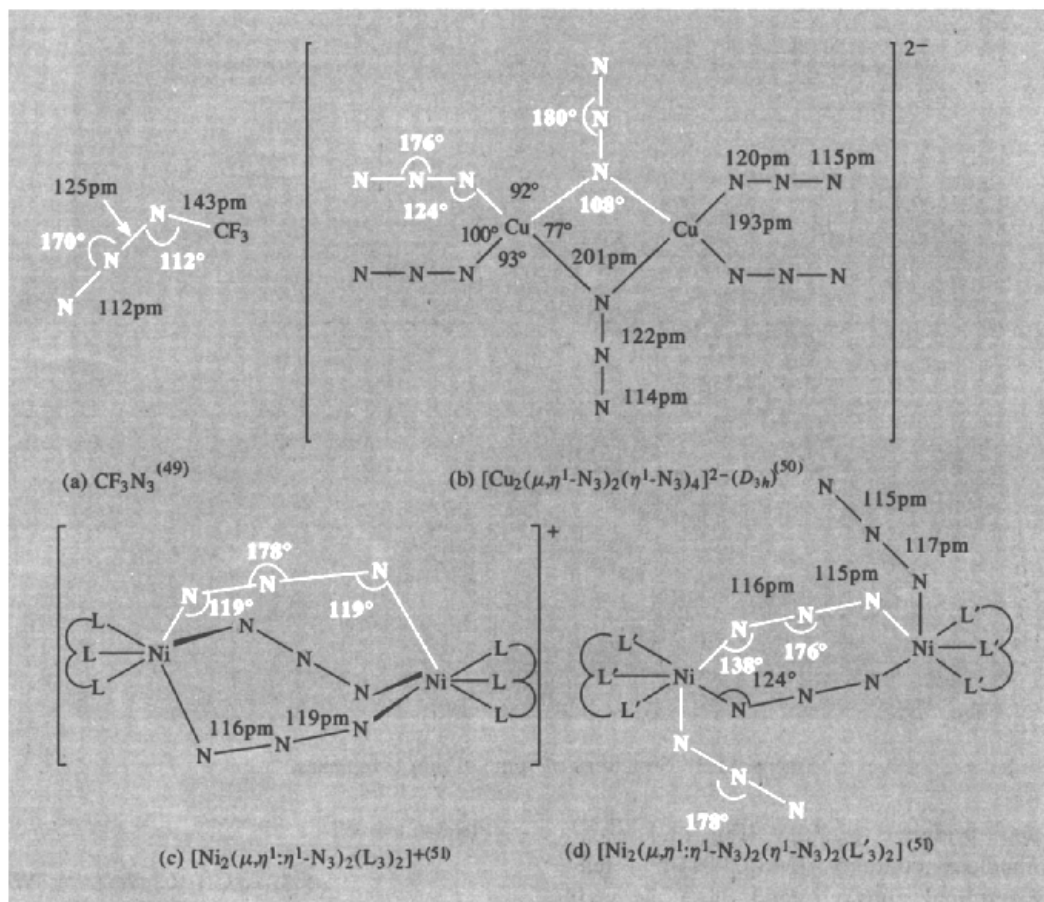


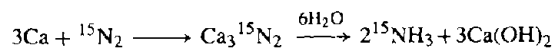
Figure 11.4 Structures of some azido complexes.

### 11.3.2 Ammonia and ammonium salts

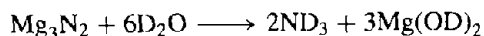
$\text{NH}_3$  is a colourless, alkaline gas with a unique, penetrating odour that is first perceptible at concentrations of about 20–50 ppm. Noticeable irritation to eyes and the nasal passages begins at about 100–200 ppm, and higher concentrations can be dangerous.<sup>(55)</sup>  $\text{NH}_3$  is prepared industrially in larger amounts (number of moles) than any other single compound (p. 407) and the production of synthetic ammonia is of major importance for several industries (see Panel).

<sup>55</sup> T. A. CZUPPON, S. A. KNEZ and J. M. ROVNER, *Ammonia, Kirk-Othmer Encyclopedia of Chemical Technology*, 4th edn., Vol. 2, pp. 638–91, Wiley, New York, 1992

In the laboratory  $\text{NH}_3$  is usually obtained from cylinders unless isotopically enriched species such as  $^{15}\text{NH}_3$  or  $\text{ND}_3$  are required. Pure dry  $^{15}\text{NH}_3$  can be prepared by treating an enriched  $^{15}\text{NH}_4^+$  salt with an excess of  $\text{KOH}$  and drying the product gas over metallic  $\text{Na}$ . Reduction of  $^{15}\text{NO}_3^-$  or  $^{15}\text{NO}_2^-$  with Devarda's alloy (50%  $\text{Cu}$ , 45%  $\text{Al}$ , 5%  $\text{Zn}$ ) in alkaline solution provides an alternative route as does the hydrolysis of a nitride, e.g.:



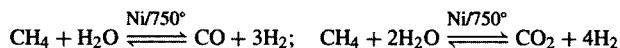
$\text{ND}_3$  can be prepared similarly using  $\text{D}_2\text{O}$ , e.g.:



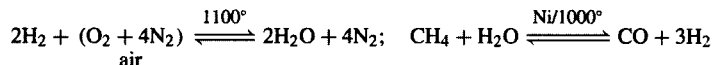
### Industrial Production of Synthetic Ammonia<sup>(55-57)</sup>

The first industrial production of  $\text{NH}_3$  began in 1913 at the BASF works in Ludwigshaven-Oppau, Germany. The plant, which had a design capacity of 30 tonnes per day, involved an entirely new concept in process technology; it was based on the Haber-Bosch high-pressure catalytic reduction of  $\text{N}_2$  with  $\text{H}_2$  obtained by electrolysis of water. Modern methods employ the same principles for the final synthesis but differ markedly in the source of hydrogen, the efficiency of the catalysts, and the scale of operations, many plants now having a capacity of 1650 tonnes per day or more. Great ingenuity has been shown not only in plant development but also in the application of fundamental thermodynamics to the selection of feasible chemical processes. Except where electricity is unusually cheap, reduction by electrolytic hydrogen has now been replaced either by coke/ $\text{H}_2\text{O}$  or, more recently, by natural gas (essentially  $\text{CH}_4$ ) or naphtha (a volatile aliphatic petrol-like fraction of crude oil). The great advantages of modern hydrocarbon reduction methods over coal-based processes are that, comparing plant of similar capital costs, they occupy one-third the land area, use half the energy, and require one-tenth the manpower, yet produce 4 times the annual tonnage of  $\text{NH}_3$ .

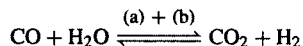
The operation of a large synthetic ammonia plant based on natural gas involves a delicately balanced sequence of reactions. The gas is first *desulfurized* to remove compounds which will poison the metal catalysts, then compressed to ~30 atm and reacted with steam over a nickel catalyst at  $750^\circ\text{C}$  in the *primary steam reformer* to produce  $\text{H}_2$  and oxides of carbon:



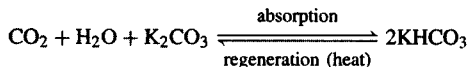
Under these conditions the issuing gases contain some 9% of unreacted methane; sufficient air is injected via a compressor to give a final composition of 1 : 3  $\text{N}_2$  :  $\text{H}_2$  and the air burns in the hydrogen thereby heating the gas to  $\sim 1100^\circ\text{C}$  in the *secondary reformer*:



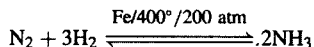
The emerging gas, now containing only 0.25%  $\text{CH}_4$ , is cooled in heat exchangers which generate high-pressure steam for use first in the turbine compressors and then as a reactant in the primary steam reformer. Next, the  $\text{CO}$  is converted to  $\text{CO}_2$  by the *shift reaction* which also produces more  $\text{H}_2$ :



Maximum conversion occurs by equilibration at the lowest possible temperature so the reaction is carried out sequentially on two beds of catalyst: (a) iron oxide ( $400^\circ\text{C}$ ) which reduces the  $\text{CO}$  concentration from 11% to 3%; (b) a copper catalyst ( $200^\circ$ ) which reduces the  $\text{CO}$  content to 0.3%. Removal of  $\text{CO}_2$  (~18%) is effected in a *scrubber* containing either a concentrated alkaline solution of  $\text{K}_2\text{CO}_3$  or an amine such as ethanolamine:



Remaining trace quantities of  $\text{CO}$  (which would poison the iron catalyst during ammonia synthesis) are converted back to  $\text{CH}_4$  by passing the damp gas from the scrubbers over a *Ni methanation catalyst* at  $325^\circ$ :  $\text{CO} + 3\text{H}_2 \rightleftharpoons \text{CH}_4 + \text{H}_2\text{O}$ . This reaction is the reverse of that occurring in the primary steam reformer. The *synthesis gas* now emerging has the approximate composition  $\text{H}_2$  74.3%,  $\text{N}_2$  24.7%,  $\text{CH}_4$  0.8%,  $\text{Ar}$  0.3%,  $\text{CO}$  1–2 ppm. It is *compressed* in three stages from 25 atm to ~200 atm and then passed over a *promoted iron catalyst* at  $380\text{--}450^\circ\text{C}$ :



The gas leaving the catalyst beds contains about 15%  $\text{NH}_3$ ; this is condensed by refrigeration and the remaining gas mixed with more incoming synthesis gas and recycled. Variables in the final reaction are the synthesis pressure,

*Panel continues*

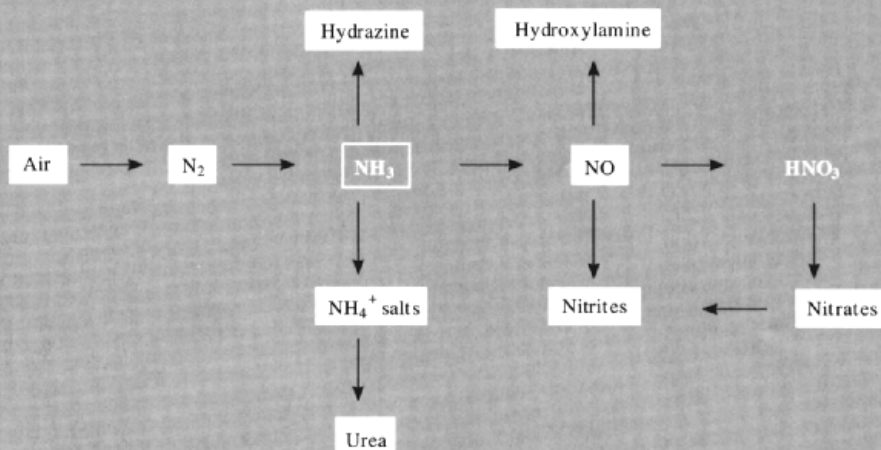
<sup>56</sup>S. P. S. ANDREW, in R. THOMPSON (ed.), *The Modern Inorganic Chemicals Industry*, pp. 201–31, The Chemical Society, London, 1977.

<sup>57</sup>S. D. LYON, *Chem. Ind.* 731–9 (1975).

synthesis temperature, gas composition, gas flow rate<sup>†</sup> and catalyst composition and particle size. Since the earliest days the "promoted" Fe catalysts have been prepared by fusing magnetite ( $\text{Fe}_3\text{O}_4$ ) on a table with KOH in the presence of a small amount of mixed refractory oxides such as MgO,  $\text{Al}_2\text{O}_3$  and  $\text{SiO}_2$ ; the solidified sheet is broken up into chunks 5–10 mm in size. These chunks are then reduced inside the ammonia synthesis converter to give the active catalyst which consists of Fe crystallites separated by the amorphous refractory oxides and partly covered by the alkali promoter which increases its activity by at least an order of magnitude.

World production of synthetic ammonia has increased dramatically particularly during the period 1950–80. Production in 1950 was little more than 1 million tonnes; though this was huge when compared with the production of most other compounds, it is dwarfed by today's rate of production which exceeds 120 million tonnes pa. In 1990 world production capacity was 119.6 million tonnes distributed as follows: Asia 35.4%, the former Soviet Union 21.5%, North America 13.8%, Western Europe 11.3%, Eastern Europe 9.7% Latin America 5.3%, Africa 3.0%, The price of  $\text{NH}_3$  (FOB Gulf Coast plants, USA) was \$107/tonne in 1990.

The applications of  $\text{NH}_3$  are dominated (over 85%) by its use in various forms as a fertilizer. Of these, direct application is the most common (28.7%), followed by urea (22.4%),  $\text{NH}_4\text{NO}_3$  (15.8%), ammonium phosphates (14.6%), and  $(\text{NH}_4)_2\text{SO}_4$  (3.4%). Industrial uses include (a) commercial explosives — such as  $\text{NH}_4\text{NO}_3$ , nitroglycerine, TNT and nitrocellulose, which are produced from  $\text{NH}_3$  via  $\text{HNO}_3$  — and (b) fibres/plastics e.g. in the manufacture of caprolactam for nylon-6, hexamethylenediamine for nylon-6,6, polyamides, rayon and polyurethanes. Other uses include a wide variety of applications in refrigeration, wood pulping, detinning of scrap-metal and corrosion inhibition; it is also used as a rubber stabilizer, pH controller, in the manufacture of household detergents, in the food and beverage industry, pharmaceuticals, water purification and the manufacture of numerous organic and inorganic chemicals. Indeed, synthetic ammonia is the key to the industrial production of most inorganic nitrogen compounds, as indicated in the subjoined Scheme.



<sup>†</sup>Flow rate is usually quoted as "space velocity", i.e. the ratio of volumetric rate of gas at STP to volume of catalyst; typical values are in the range 8000–60000  $\text{h}^{-1}$ .

The chemical fixation of  $\text{N}_2$  to  $\text{NH}_3$  under less extreme conditions than those used industrially is a continuing area of active research and considerable progress has been made in elucidating mechanisms involving  $\text{N}_2$  coordinated to Mo, W, V and other centres.<sup>(5,6,58–63)</sup>

Some physical and molecular properties of  $\text{NH}_3$  are in Table 11.2. The influence of H

<sup>59</sup> K. ALKA, *Angew. Chem. Int. Edn. Engl.* **25**, 558–9 (1986).

<sup>60</sup> R. L. RICHARDS, *Chem. in Britain*, Feb. 1988, pp. 133–6.

<sup>61</sup> M. Y. MOHAMMED and C. J. PICKETT, *J. Chem. Soc., Chem. Commun.*, 1119–21 (1988).

<sup>62</sup> R. R. EADY, *Polyhedron* **8**, 1695–1700 (1989).

<sup>63</sup> G. J. LEIGH, R. PRIETO-ALCÓN and J. R. SANDERS, *J. Chem. Soc., Chem. Commun.*, 921–2 (1991).

<sup>58</sup> T. A. GEORGE and R. C. TISDALE, *J. Am. Chem. Soc.* **107**, 5157–9 (1985).

Table 11.2 Some properties of ammonia, NH<sub>3</sub>

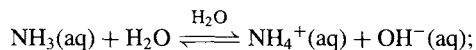
Physical properties		Molecular properties	
MP/K	195.42	Symmetry	C <sub>3v</sub> (pyramidal)
BP/K	239.74	Distance (N–H)/pm	101.7
Density(l; 239 K)/g cm <sup>-3</sup>	0.6826	Angle H–N–H	107.8°
Density(g; rel. air = 1)	0.5963	Pyramid height/pm	36.7
η(239.5 K)/centipoise <sup>(a)</sup>	0.254	μ/Debye <sup>(b)</sup>	1.46
Dielectric constant ε(239 K)	22	Inversion barrier kJ mol <sup>-1</sup>	24.7
κ(234.3 K)/ohm <sup>-1</sup> cm <sup>-1</sup>	1.97 × 10 <sup>-7</sup>	Inversion frequency/GHz <sup>(c)</sup>	23.79
ΔH <sub>f</sub> <sup>o</sup> (298 K)/kJ mol <sup>-1</sup>	-46.1	D(H–NH <sub>2</sub> )/kJ mol <sup>-1</sup>	435
ΔG <sub>f</sub> <sup>o</sup> (298 K)/kJ mol <sup>-1</sup>	-16.5	Ionization energy/kJ mol <sup>-1</sup>	979.7
S <sup>o</sup> (298 K)/J K <sup>-1</sup> mol <sup>-1</sup>	192.3	Proton affinity (gas)/kJ mol <sup>-1</sup>	841

<sup>(a)</sup>1 centipoise = 10<sup>-3</sup> kg m<sup>-1</sup> s<sup>-1</sup>. <sup>(b)</sup>1 Debye = 10<sup>-18</sup> esu = 3.335 64 × 10<sup>-30</sup> C m. <sup>(c)</sup>1 GHz = 10<sup>9</sup> s<sup>-1</sup>.

bonding on the bp and other properties has already been noted (p. 53). It has been estimated that 26% of the H bonding in NH<sub>3</sub> breaks down on melting, 7% on warming from the mp to the bp, and the final 67% on transfer to the gas phase at the bp. The low density, viscosity and electrical conductivity, and the high dielectric constant of liquid ammonia are also notable. Liquid NH<sub>3</sub> is an excellent solvent and a valuable medium for chemical reactions (p. 424); its high heat of vaporization (23.35 kJ mol<sup>-1</sup> at the bp) makes it relatively easy to handle in simple vacuum flasks. The molecular properties call for little comment except to note that the rapid inversion frequency with which the N atom moves through the plane of the 3 H atoms has a marked effect on the vibrational spectrum of the molecule. The inversion itself occurs in the microwave region of the spectrum at 23.79 GHz (corresponding to a wavelength of 1.260 cm) and was, in fact, the first microwave absorption spectrum to be detected (C. E. Cleeton and N. H. Williams, 1934). The associated energy ( $hc\bar{\nu}$ ) is 0.7935 cm<sup>-1</sup> i.e. 9.49 J mol<sup>-1</sup>. Inversion also occurs in ND<sub>3</sub> at a frequency of 1.591 GHz, i.e. less than for NH<sub>3</sub> by a factor of 14.95. The inversion can be stopped in NH<sub>3</sub> by increasing the pressure to ~2 atm. The corresponding figure for ND<sub>3</sub> is ~90 mmHg (i.e. again a factor of about 15).

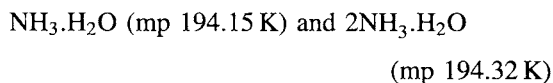
Ammonia is readily absorbed by H<sub>2</sub>O with considerable evolution of heat (~37.1 kJ per mol of NH<sub>3</sub> gas). Aqueous solutions are weakly basic

due to the equilibrium



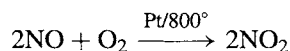
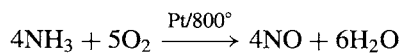
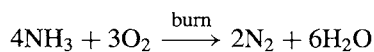
$$K_{298.2} = [\text{NH}_4^+][\text{OH}^-]/[\text{NH}_3] = 1.81 \times 10^{-5} \text{ mol l}^{-1}$$

The equilibrium constant at room temperature corresponds to  $\text{p}K_b = 4.74$  and implies that a 1 molar aqueous solution of NH<sub>3</sub> contains only 4.25 mmol l<sup>-1</sup> of NH<sub>4</sub><sup>+</sup> (or OH<sup>-</sup>). Such solutions do not contain the undissociated “molecule” NH<sub>4</sub>OH, though weakly bonded hydrates have been isolated at low temperature:



These hydrates are not ionically dissociated but contain chains of H<sub>2</sub>O molecules cross-linked by NH<sub>3</sub> molecules into a three-dimensional H-bonded network.

Ammonia burns in air with difficulty, the flammable limits being 16–25 vol%. Normal combustion yields nitrogen but, in the presence of a Pt or Pt/Rh catalyst at 750–900°C, the reaction proceeds further to give the thermodynamically less-favoured products NO and NO<sub>2</sub>:



These reactions are very important industrially in the production of  $\text{HNO}_3$  (p. 466). See also the industrial production of  $\text{HCN}$  by the Andrussov process (p. 321):  $2\text{NH}_3 + 3\text{O}_2 + 2\text{CH}_4 \longrightarrow 2\text{HCN} + 6\text{H}_2\text{O}$ .

Gaseous  $\text{NH}_3$  burns with a greenish-yellow flame in  $\text{F}_2$  (or  $\text{ClF}_3$ ) to produce  $\text{NF}_3$  (p. 439). Chlorine yields several products depending on conditions:  $\text{NH}_4\text{Cl}$ ,  $\text{NH}_2\text{Cl}$ ,  $\text{NHCl}_2$ ,  $\text{NCl}_3$ ,  $\text{NCl}_3 \cdot \text{NH}_3$ ,  $\text{N}_2$  and even small amounts of  $\text{N}_2\text{H}_4$ . The reaction to give chloramine,  $\text{NH}_2\text{Cl}$ , is important in urban and domestic water purification systems. Reactions with other non-metals and their halides or oxides are equally complex and lead to a variety of compounds, many of which are treated elsewhere (pp. 497, 501, 506, 535, 723, etc.). At red heat carbon reacts with  $\text{NH}_3$  to give  $\text{NH}_4\text{CN} + \text{H}_2$ , whereas phosphorus yields  $\text{PH}_3$  and  $\text{N}_2$ , and sulfur gives  $\text{H}_2\text{S}$  and  $\text{N}_4\text{S}_4$ . Metals frequently react at higher temperature to give nitrides (p. 417). Of particular importance is the attack on Cu in the presence of oxygen (air) at room temperature since this precludes the use of this metal and its alloys in piping and valves for handling either liquid or gaseous  $\text{NH}_3$ . Corrosion of Cu and brass by moist  $\text{NH}_3$ /air mixtures and by air-saturated aqueous solutions of  $\text{NH}_3$  is also rapid. Contact with Ni and with polyvinylchloride plastics should be avoided for the same reason.

### Liquid ammonia as a solvent<sup>(64-67)</sup>

Liquid ammonia is the best-known and most widely studied non-aqueous ionizing solvent. Its most conspicuous property is its ability to

dissolve alkali metals to form highly coloured, electrically conducting solutions containing solvated electrons, and the intriguing physical properties and synthetic utility of these solutions have already been discussed (p. 77). Apart from these remarkable solutions, much of the chemistry in liquid ammonia can be classified by analogy with related reactions in aqueous solutions. Accordingly, we briefly consider in turn, solubility relationships, metathesis reactions, acid-base reactions, amphoterism, solvates and solvolysis, redox reactions and the preparation of compounds in unusual oxidation states. Comparison of the physical properties of liquid  $\text{NH}_3$  (p. 423) with those of water (p. 623) shows that  $\text{NH}_3$  has the lower mp, bp, density, viscosity, dielectric constant and electrical conductivity; this is due at least in part to the weaker H bonding in  $\text{NH}_3$  and the fact that such bonding cannot form cross-linked networks since each  $\text{NH}_3$  molecule has only 1 lone-pair of electrons compared with 2 for each  $\text{H}_2\text{O}$  molecule. The ionic self-dissociation constant of liquid  $\text{NH}_3$  at  $-50^\circ\text{C}$  is  $\sim 10^{-33} \text{ mol}^2 \text{ l}^{-2}$ .

Most ammonium salts are freely soluble in liquid  $\text{NH}_3$  as are many nitrates, nitrites, cyanides and thiocyanates. The solubilities of halides tend to increase from the fluoride to the iodide; solubilities of salts of multivalent ions are generally low suggesting that (as in aqueous systems) lattice-energy and entropy effects outweigh solvation energies. The possibility of H-bond formation also influences solubility and, in the case of  $\text{NH}_4\text{I}$ , an X-ray single-crystal analysis of the monosolvate shows the presence of an H-bonded cation  $\text{N}_2\text{H}_7^+$  with an N-H...N distance of  $269 \pm 5 \text{ pm}$ .<sup>(68)</sup> Some typical solubilities at  $25^\circ\text{C}$  expressed as g per 100 g solvent are:  $\text{NH}_4\text{OAc}$  253.2,  $\text{NH}_4\text{NO}_3$  389.6,  $\text{LiNO}_3$  243.7,  $\text{NaNO}_3$  97.6,  $\text{KNO}_3$  10.4,  $\text{NaF}$  0.35,  $\text{NaCl}$  3.0,  $\text{NaBr}$  138.0,  $\text{NaI}$  161.9,  $\text{NaSCN}$  205.5. Some of these solubilities are astonishingly high, particularly when expressed as the number of moles of solute per 10 mol

<sup>64</sup> W. L. JOLLY and C. J. HALLADA, Chap. 1 in T. C. WAD-DINGTON (ed.), *Non-Aqueous Solvent Systems*, pp. 1-45, Academic Press, London, 1965.

<sup>65</sup> G. W. A. FOWLES, Chap. 7, in C. B. COLBURN (ed.), *Developments in Inorganic Nitrogen Chemistry*, pp. 522-76, Elsevier, Amsterdam, 1966.

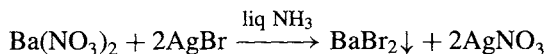
<sup>66</sup> J. J. LAGOWSKI and G. A. MOCZYGEMBA, Chap. 7 in J. J. LAGOWSKI (ed.), *The Chemistry of Non-aqueous Solvents*, Vol. 2, pp. 320-71, Academic Press, 1967.

<sup>67</sup> D. NICHOLLS, *Inorganic Chemistry in Liquid Ammonia: Topics in Inorganic and General Chemistry*, Monograph 17, Elsevier, Amsterdam, 1979, 238 pp.

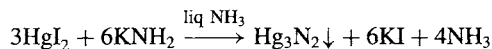
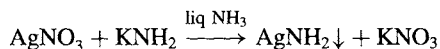
<sup>68</sup> H. J. BERTHOLD, W. PREIBSCH and E. VONHOLDT, *Angew. Chem. Int. Edn. Engl.* **27**, 1524-5 (1988).

NH<sub>3</sub>, e.g.: NH<sub>4</sub>NO<sub>3</sub> 8.3, LiNO<sub>3</sub> 6.1, NaSCN 4.3. Further data at 25° and other temperatures are in ref. 69.

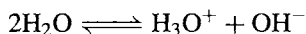
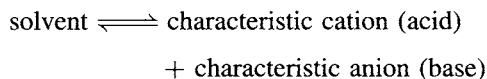
Metathesis reactions are sometimes the reverse of those in aqueous systems because of the differing solubility relations. For example because AgBr forms the complex ion [Ag(NH<sub>3</sub>)<sub>2</sub>]<sup>+</sup> in liquid NH<sub>3</sub> it is readily soluble, whereas BaBr<sub>2</sub> is not, and can be precipitated:



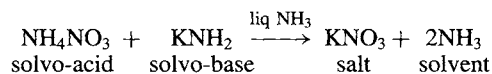
Reactions analogous to the precipitation of AgOH and of insoluble oxides from aqueous solution are:



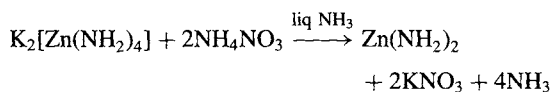
Acid-base reactions in many solvent systems can be thought of in terms of the characteristic cations and anions of the solvent (see also p. 831)



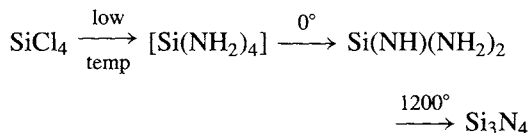
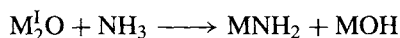
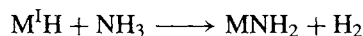
On this basis NH<sub>4</sub><sup>+</sup> salts can be considered as solvo-acids in liquid NH<sub>3</sub> and amides as solvo-bases. Neutralization reactions can be followed conductimetrically, potentiometrically or even with coloured indicators such as phenolphthalein:



Likewise, amphoteric behaviour can be observed. For example Zn(NH<sub>2</sub>)<sub>2</sub> is insoluble in liquid NH<sub>3</sub> (as is Zn(OH)<sub>2</sub> in H<sub>2</sub>O), but it dissolves on addition of the solvo-base KNH<sub>2</sub> due to the formation of K<sub>2</sub>[Zn(NH<sub>2</sub>)<sub>4</sub>]; this in turn is decomposed by NH<sub>4</sub><sup>+</sup> salts (solvo-acids) with reprecipitation of the amide:



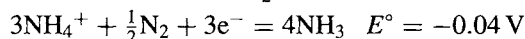
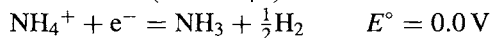
Solvates are perhaps less prevalent in compounds prepared from liquid ammonia solutions than are hydrates precipitated from aqueous systems, but large numbers of amines are known, and their study formed the basis of Werner's theory of coordination compounds (1891–5). Frequently, however, solvolysis (ammonolysis) occurs (cf. hydrolysis).<sup>(65)</sup> Examples are:



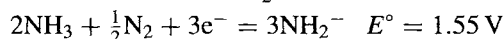
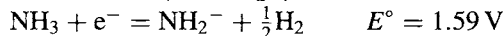
Amides are one of the most prolific classes of ligand and the subject of metal and metalloid amides has been extensively reviewed.<sup>(70)</sup>

Redox reactions are particularly instructive. If all thermodynamically allowed reactions in liquid NH<sub>3</sub> were kinetically rapid, then no oxidizing agent more powerful than N<sub>2</sub> and no reducing agent more powerful than H<sub>2</sub> could exist in this solvent. Using data for solutions at 25°:<sup>(64)</sup>

*Acid solutions* (1 M NH<sub>4</sub><sup>+</sup>)



*Basic solutions* (1 M NH<sub>2</sub><sup>-</sup>)

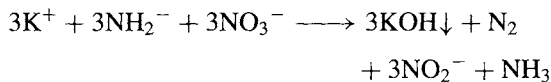


Obviously, with a range of only 0.04 V available very few species are thermodynamically stable. However, both the hydrogen couple and the nitrogen couple usually exhibit "overvoltages" of ~1 V, so that in acid solutions the practical range of potentials for solutes is from +1.0 to -1.0 V. Similarly in basic solutions the practical range

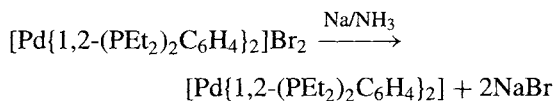
<sup>69</sup> K. JONES, Nitrogen, Chap. 19 in *Comprehensive Inorganic Chemistry* Vol. 2, pp. 147–388, Pergamon Press, Oxford, 1973.

<sup>70</sup> M. F. LAPPERT, P. P. POWER, A. R. SANGER and R. C. SRIVASTAVA, *Metal and Metalloid Amides*, Ellis Horwood Ltd., Chichester, 1980, 847 pp. (approximately 3000 references).

extends from 2.6 to 0.6 V. It is thus possible to work in liquid ammonia with species which are extremely strong reducing agents (e.g. alkali metals) and also with extremely strong oxidizing agents (e.g. permanganates, superoxides and ozonides; p. 609). For similar reasons the  $\text{NO}_3^-$  ion is effectively inert towards  $\text{NH}_3$  in acid solution but in alkaline solutions  $\text{N}_2$  is slowly evolved:

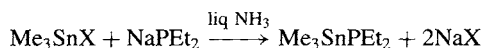
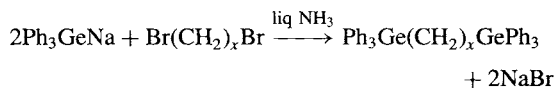


The use of liquid  $\text{NH}_3$  to prepare compounds of elements in unusual (low) oxidation states is exemplified by the successive reduction of  $\text{K}_2[\text{Ni}(\text{CN})_4]$  with  $\text{Na}/\text{Hg}$  in the presence of an excess of  $\text{CN}^-$ : the dark-red dimeric  $\text{Ni}^{\text{I}}$  complex  $\text{K}_4[\text{Ni}_2(\text{CN})_6]$  is first formed and this can be further reduced to the yellow  $\text{Ni}^0$  complex  $\text{K}_4[\text{Ni}(\text{CN})_4]$ . The corresponding complexes  $[\text{Pd}(\text{CN})_4]^{4-}$  and  $[\text{Pt}(\text{CN})_4]^{4-}$  can be prepared similarly, though there is no evidence in these latter systems for the formation of the  $\text{M}^{\text{I}}$  dimer. A ditertiaryphosphine complex of  $\text{Pd}^0$  has also been prepared:



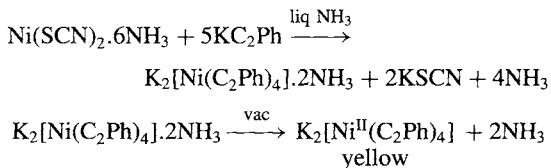
$[\text{Co}^{\text{III}}(\text{CN})_6]^{3-}$  yields the pale-yellow complex  $[\text{Co}^{\text{I}}(\text{CN})_4]^{3-}$  and the brown-violet complex  $[\text{Co}_2^0(\text{CN})_8]^{8-}$  (cf. the dimeric carbonyl  $[\text{Co}_2(\text{CO})_8]$ ).

Liquid  $\text{NH}_3$  is also extensively used as a preparative medium for compounds which are unstable in aqueous solutions, e.g.:



Alkali metal acetylides  $\text{M}_2\text{C}_2$ ,  $\text{MCCH}$  and  $\text{MCCR}$  can readily be prepared by passing  $\text{C}_2\text{H}_2$  or  $\text{C}_2\text{HR}$  into solutions of the alkali metal in liquid  $\text{NH}_3$ , and these can be used to synthesize a wide range of transition-element

acetylides,<sup>(71)</sup> e.g.:



Other examples are orange-red  $\text{K}_3[\text{Cr}^{\text{III}}(\text{C}_2\text{H})_6]$ , rose-pink  $\text{Na}_2[\text{Mn}^{\text{II}}(\text{C}_2\text{Me})_4]$ , dark-green  $\text{Na}_4[\text{Co}^{\text{II}}(\text{C}_2\text{Me})_6]$ , orange  $\text{K}_4[\text{Ni}^0(\text{C}_2\text{H})_4]$ , yellow  $\text{K}_6[\text{Ni}_2^{\text{I}}(\text{C}_2\text{Ph})_6]$ . Such compounds are often explosive, though the analogues of  $\text{Cu}^{\text{I}}$  and  $\text{Zn}^{\text{II}}$  are not, e.g. yellow  $\text{Na}[\text{Cu}(\text{C}_2\text{Me})_2]$ , colourless  $\text{K}_2[\text{Cu}(\text{C}_2\text{H})_3]$ , and colourless  $\text{K}_2[\text{Zn}(\text{C}_2\text{H})_4]$ .

Ammonium halides have been used as versatile reagents in low-temperature solid-state redox and acid-base reactions.<sup>(72)</sup> For example, direct reaction with the appropriate metal at 270–300° yields the ammonium salts of  $\text{ZnCl}_4^{2-}$ ,  $\text{LaCl}_5^{2-}$ ,  $\text{YCl}_6^{3-}$ ,  $\text{YBr}_6^{3-}$ ,  $\text{CuCl}_3^{2-}$ , etc., whereas  $\text{Y}_2\text{O}_3$  yields either  $(\text{NH}_4)_3\text{YBr}_6$  or  $\text{YOBr}$  depending on the stoichiometric ratio of the reagents. Solid-state reactions of ammonium sulfate, nitrate, phosphates and carbonate have also been studied.

### 11.3.3 Other hydrides of nitrogen

Nitrogen forms more than 20 binary compounds with hydrogen<sup>(73)</sup> of which ammonia ( $\text{NH}_3$ , p. 420), hydrazine ( $\text{N}_2\text{H}_4$ , p. 427) and hydrogen azide ( $\text{N}_3\text{H}$ , p. 432) are by far the most important. Hydroxylamine,  $\text{NH}_2(\text{OH})$ , is closely related in structure and properties to both ammonia,  $\text{NH}_2(\text{H})$ , and hydrazine,  $\text{NH}_2(\text{NH}_2)$  and it will be convenient to discuss this compound in the present section also (p. 431). Several protonated cationic species such as  $\text{NH}_4^+$ ,  $\text{N}_2\text{H}_5^+$ , etc., and deprotonated anionic species such as  $\text{NH}_2^-$ ,  $\text{N}_2\text{H}_3^-$ , etc. also exist but ammonium hydride,  $\text{NH}_5$ , is unknown. Among

<sup>71</sup> R. NAST and coworkers; for summary of results and detailed refs., see pp. 568–71 of ref. 65.

<sup>72</sup> G. MEYER, T. STAFFEL, S. DÖTSCH and T. SCHLEID, *Inorg. Chem.* **24**, 3504–5 (1985).

<sup>73</sup> *Gmelin Handbook of Inorganic and Organometallic Chemistry*, 8th Edition, Nitrogen, Supplement B1, 280 pp., Supplement B2, 188 pp., Springer Verlag, Berlin, 1993.

Table 11.3 Some physical and thermochemical properties of hydrazine

MP/°C	2.0	Dielectric constant $\epsilon(25^\circ)$	51.7
BP/°C	113.5	$\kappa(25^\circ)/\text{ohm}^{-1} \text{ cm}^{-1}$	$\sim 2.5 \times 10^{-6}$
Density/(solid at $-5^\circ$ )/g cm <sup>-3</sup>	1.146	$\Delta H_{\text{combustion}}/\text{kJ mol}^{-1}$	621.5
Density (liquid at $25^\circ$ )/g cm <sup>-3</sup>	1.00	$\Delta H_f^\circ(25^\circ)/\text{kJ mol}^{-1}$	50.6
$\eta(25^\circ)/\text{centipoise}^{(a)}$	0.9	$\Delta G_f^\circ(25^\circ)/\text{kJ mol}^{-1}$	149.2
Refractive index $n_D^{25}$	1.470	$S^\circ(25^\circ)/\text{J K}^{-1} \text{ mol}^{-1}$	121.2

<sup>(a)</sup>1 centipoise =  $10^{-3} \text{ kg m}^{-1} \text{ s}^{-1}$ .

the less familiar (and less stable) neutral radicals which have been well characterized are the imidogen (NH), amidogen (NH<sub>2</sub>), diazenyl (N<sub>2</sub>H) and hydrazyl (N<sub>2</sub>H<sub>3</sub>) radicals. Such species are important in atmospheric chemistry and in combustion reactions. Of the neutral compounds the following can be mentioned:<sup>(73)</sup>

N<sub>2</sub>H<sub>2</sub>: *trans*-diazene, HN=NH (yellow), and its 1:1 isomer, H<sub>2</sub>N=N

N<sub>3</sub>H: hydrogen azide (p. 432) and cyclo-triazene (triazairine).  $\bar{N}=\text{N}-\bar{N}\text{H}$

N<sub>3</sub>H<sub>3</sub>: triazene, HN=N-NH<sub>2</sub> and cyclo-triazane (triaziridene) c-(NH)<sub>3</sub>

N<sub>3</sub>H<sub>5</sub>: triazane (aminohydrazine), H<sub>2</sub>NN(H)-NH<sub>2</sub>

N<sub>4</sub>H<sub>4</sub>: *trans*-2-tetrazene, H<sub>2</sub>N-N=N-NH<sub>2</sub>, (colourless, low-melting crystals, N-N 143 pm, N=N 121 pm). and ammonium azide, NH<sub>4</sub>N<sub>3</sub> (white crystals, subl. 133°C, *d* 1.350 g cm<sup>-3</sup>)

N<sub>4</sub>H<sub>6</sub>: tetrazane, H<sub>2</sub>NN(H)N(H)NH<sub>2</sub>, (bright yellow solid)

N<sub>5</sub>H<sub>5</sub>: hydrazinium azide, N<sub>2</sub>H<sub>5</sub>N<sub>3</sub>, (explosive white crystals)

N<sub>6</sub>H<sub>2</sub>: Probably a cyclic dimer of N<sub>3</sub>H

N<sub>7</sub>H<sub>9</sub>: hydrazinium azide monohydrazinate, N<sub>2</sub>H<sub>5</sub>N<sub>3</sub>.N<sub>2</sub>H<sub>4</sub>

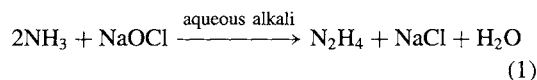
N<sub>9</sub>H<sub>3</sub>: cyclic trimer of N<sub>3</sub>H, i.e. 1,3,5-N<sub>6</sub>(NH)<sub>3</sub>

### Hydrazine<sup>(74)</sup>

Anhydrous N<sub>2</sub>H<sub>4</sub> is a fuming, colourless liquid with a faint ammoniacal odour which is first

detectable at a concentration of 70–80 ppm. Many of its physical properties (Table 11.3) are remarkably similar to those of water (p. 623); comparisons with NH<sub>3</sub> (p. 423) H<sub>2</sub>O<sub>2</sub> (p. 634) are also instructive, and the influence of H bonding is apparent. In the gas phase four conformational isomers are conceivable (Fig. 11.5) but the large dipole (1.85 D) clearly eliminates the staggered *trans*-conformation; electron diffraction data (and infrared) indicate the *gauche*-conformation with an angle of rotation of 90–95° from the eclipsed position.

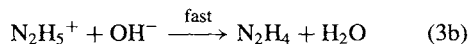
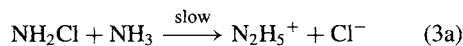
The most effective preparative routes to hydrazine are still based on the process introduced by F. Raschig in 1907: this involves the reaction of ammonia with an alkaline solution of sodium hypochlorite in the presence of gelatin or glue. The overall reaction can be written as



but it proceeds in two main steps. First there is a rapid formation of chloramine which proceeds to completion even in the cold:

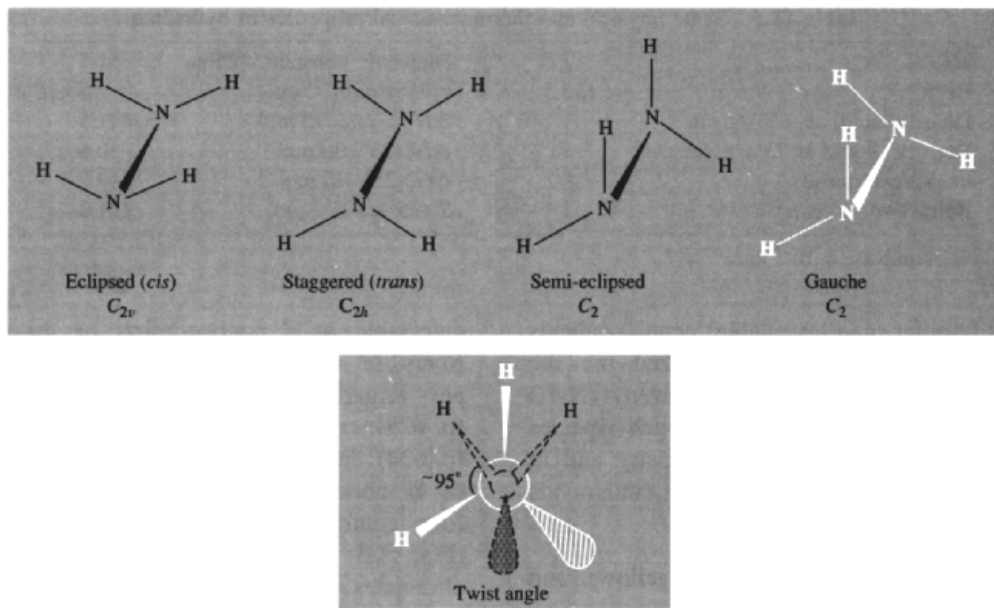


The chloramine then reacts further to produce N<sub>2</sub>H<sub>4</sub> either by slow nucleophilic attack of NH<sub>3</sub> (3a) and subsequent rapid neutralization (3b), or by preliminary rapid formation of the chloramide ion (4a) followed by slow nucleophilic attack of NH<sub>3</sub> (4b):

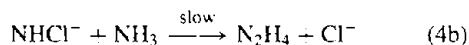
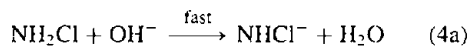


<sup>74</sup>E. W. SCHMIDT, *Hydrazine and its Derivatives, Preparation, Properties, Application* Wiley, Chichester, 1984, 1059 pp. (over 4400 references).

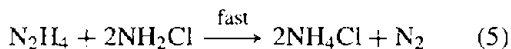




**Figure 11.5** Possible conformations of  $\text{N}_2\text{H}_4$  with pyramidal N. Hydrazine adopts the gauche  $C_2$  form with N-N 145 pm, H-N-H  $108^\circ$ , and a twist angle of  $95^\circ$  as shown in the lower diagram.

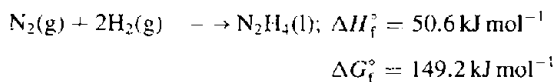


In addition there is a further rapid but undesirable reaction with chloramine which destroys the  $\text{N}_2\text{H}_4$  produced:



This reaction is catalysed by traces of heavy metal ions such as  $\text{Cu}^{\text{II}}$  and the purpose of the gelatin is to suppress reaction (5) by sequestering the metal ions; it is probable that gelatin also assists the hydrazine-forming reactions between ammonia and chloramine in a way that is not fully understood. The industrial preparation and uses of  $\text{N}_2\text{H}_4$  are summarized in the Panel.

At room temperature, pure  $\text{N}_2\text{H}_4$  and its aqueous solutions are kinetically stable with respect to decomposition despite the endothermic nature of the compound and its positive free energy of formation:



When ignited,  $\text{N}_2\text{H}_4$  burns rapidly and completely in air with considerable evolution of heat (see Panel):



$$\Delta H = -621.5 \text{ kJ mol}^{-1}$$

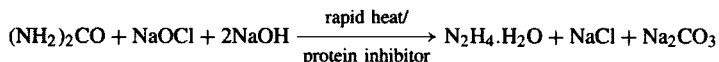
In solution,  $\text{N}_2\text{H}_4$  is oxidized by a wide variety of oxidizing agents (including  $\text{O}_2$ ) and it finds use as a versatile reducing agent because of the variety of reactions it can undergo. Thus the thermodynamic reducing strength of  $\text{N}_2\text{H}_4$  depends on whether it undergoes a 1-, 2-, or 4-electron oxidation and whether this is in acid or alkaline solution. Typical examples in acid solution are as follows:<sup>†</sup>

1-electron change (e.g. using  $\text{Fe}^{\text{III}}$ ,  $\text{Ce}^{\text{IV}}$ , or  $\text{MnO}_4^-$ ):

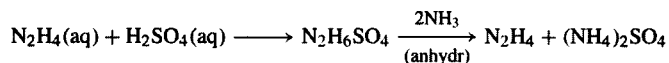
<sup>†</sup> See p. 435 for discussion of standard electrode potentials and their use. It is conventional to write the half-reactions as (oxidized form) +  $ne^-$  = (reduced form). Since  $\Delta G = -nE^\circ F$  at unit activities, it follows that the reactions will occur spontaneously in the reverse direction to that written when  $E^\circ$  is negative, i.e. hydrazine is oxidized by the reagents listed.

### Industrial Production and Uses of Hydrazine<sup>(75)</sup>

Hydrazine is usually prepared in a continuous process based on the Raschig reaction. Solutions of ammonia and sodium hypochlorite (30:1) are mixed in the cold with a gelatin solution and then passed rapidly under pressure through a reactor at 150° (residence time 1 s). This results in a 60% conversion based on hypochlorite and produces a solution of ~0.5% by weight of N<sub>2</sub>H<sub>4</sub>. The excess of NH<sub>3</sub> and steam are stripped off in stages and the solution finally distilled to give pure hydrazine hydrate N<sub>2</sub>H<sub>4</sub>·H<sub>2</sub>O (mp -51.7°, bp 118.5°, *d* 1.0305 g cm<sup>-3</sup> at 21°). In the Olin Mathieson variation of this process, NH<sub>2</sub>Cl is preformed from NH<sub>3</sub> + NaOCl (3:1) and then anhydrous NH<sub>3</sub> is injected to a ratio of ~30:1; this simultaneously raises the temperature and pressure in the reactor. An alternative industrial route, which is economical only for smaller plants, uses urea instead of ammonia in a process very similar to Raschig's:



Hydrazine hydrate contains 64.0% by weight of N<sub>2</sub>H<sub>4</sub> and is frequently preferred to the pure compound not only because it is cheaper but also because its much lower mp avoids problems of solidification. Anhydrous N<sub>2</sub>H<sub>4</sub> can be obtained from concentrated aqueous solutions by distillation in the presence of dehydrating agents such as solid NaOH or KOH. Alternatively, hydrazine sulfate can be precipitated from dilute aqueous solutions using dilute H<sub>2</sub>SO<sub>4</sub> and the precipitate treated with liquid NH<sub>3</sub> to liberate the hydrazine:



World production capacity of hydrazine solutions in 1995 (expressed as N<sub>2</sub>H<sub>4</sub>) was about 40 000 tonnes, predominantly in USA 16 500 t, Germany 6400 t, Japan 6600 t and France 6100 t. In addition some 3200 t of anhydrous N<sub>2</sub>H<sub>4</sub> was manufactured in USA for rocket fuels.

The major use (non-commercial) of anhydrous N<sub>2</sub>H<sub>4</sub> and its methyl derivatives MeNHNH<sub>2</sub> and Me<sub>2</sub>NNH<sub>2</sub> is as a rocket fuel in guided missiles, space shuttles, lunar missions, etc. For example the Apollo lunar modules were decelerated on landing and powered on blast-off for the return journey by the oxidation of a 1:1 mixture of MeNHNH<sub>2</sub> and Me<sub>2</sub>NNH<sub>2</sub> with liquid N<sub>2</sub>O<sub>4</sub>; the landing required some 3 tonnes of fuel and 4.5 tonnes of oxidizer, and the relaunching about one-third of this amount. Other oxidants used are O<sub>2</sub>, H<sub>2</sub>O<sub>2</sub>, HNO<sub>3</sub>, or even F<sub>2</sub>. Space vehicles propelled by anhydrous N<sub>2</sub>H<sub>4</sub> itself include the Viking Lander on Mars, the Pioneer and Voyager interplanetary probes and the Giotto space probe to Halley's comet.

The major commercial applications of hydrazine solutions are as blowing agents (~40%), agricultural chemicals (~25%), medicinals (~5%), and — increasingly — in boiler water treatment now as much as 20%. The detailed pattern of usage, of course, depends to some extent on the country concerned.

Aqueous solutions of N<sub>2</sub>H<sub>4</sub> are versatile and attractive reducing agents. They have long been used to prepare silver (and copper) mirrors, to precipitate many elements (such as the platinum metals) from solutions of their compounds, and in other analytical applications. A major application as noted above is now in the treatment of high-pressure boiler water: this was first introduced in about 1945 and has the following advantages over the previously favoured Na<sub>2</sub>SO<sub>3</sub>:

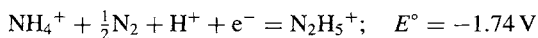
- N<sub>2</sub>H<sub>4</sub> is completely miscible with H<sub>2</sub>O and reacts with dissolved O<sub>2</sub> to give merely N<sub>2</sub> and H<sub>2</sub>O:  

$$\text{N}_2\text{H}_4 + \text{O}_2 \longrightarrow \text{N}_2 + 2\text{H}_2\text{O}$$
- N<sub>2</sub>H<sub>4</sub> does not increase the dissolved solids (cf. Na<sub>2</sub>SO<sub>3</sub>) since N<sub>2</sub>H<sub>4</sub> itself and all its reaction and decomposition products are volatile.
- These products are either alkaline (like N<sub>2</sub>H<sub>4</sub>) or neutral, but never acidic.
- N<sub>2</sub>H<sub>4</sub> is also a corrosion inhibitor (by reducing Fe<sub>2</sub>O<sub>3</sub> to hard, coherent Fe<sub>3</sub>O<sub>4</sub>) and it is therefore useful for stand-by and idle boilers.

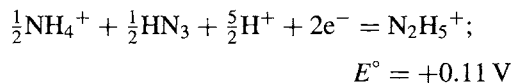
The usual concentration of O<sub>2</sub> in boiler feed water is ~0.01 ppm so that, even allowing for a twofold excess, 1 kg N<sub>2</sub>H<sub>4</sub> is sufficient to treat 50 000 tonnes of feed water (say ~4 days' supply at the rate of 500 tonnes per hour).

Hydrazine and its derivatives find considerable use in the synthesis of biologically active materials, dyestuff intermediates and other organic derivatives. Reactions of aldehydes to form hydrazides (RCH=NNH<sub>2</sub>) and azines (RCH=NN=CHR) are well known in organic chemistry, as is the use of hydrazine and its derivatives in the synthesis of heterocyclic compounds.

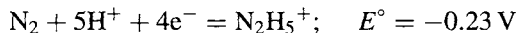
<sup>75</sup>Hydrazine and its derivatives, *Kirk-Othmer Encyclopedia of Chemical Technology*, 4th edn., Vol. 13, pp. 560–606 (1995).



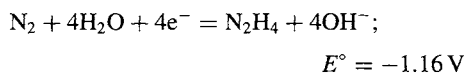
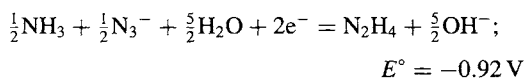
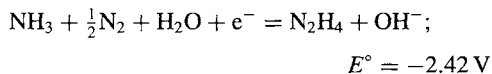
2-electron change (e.g. using  $\text{H}_2\text{O}_2$  or  $\text{HNO}_2$ ):



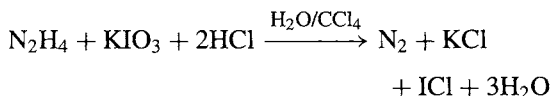
4-electron change (e.g. using  $\text{IO}_3^-$  or  $\text{I}_2$ ):



For basic solutions the corresponding reduction potentials are:

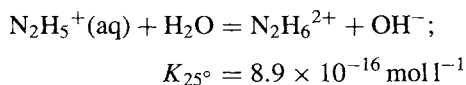
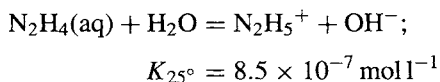


In the 4-electron oxidation of acidified  $\text{N}_2\text{H}_4$  to  $\text{N}_2$ , it has been shown by the use of  $\text{N}_2\text{H}_4$  isotopically enriched in  $^{15}\text{N}$  that both the N atoms of each molecule of  $\text{N}_2$  originated in the same molecule of  $\text{N}_2\text{H}_4$ . This reaction is also the basis for the most commonly used method for the analytical determination of  $\text{N}_2\text{H}_4$  in dilute aqueous solution:



The  $\text{IO}_3^-$  is first reduced to  $\text{I}_2$  which is subsequently oxidized to  $\text{ICl}$  by additional  $\text{IO}_3^-$ ; the end-point is detected by the complete discharge of the iodine colour from the  $\text{CCl}_4$  phase.

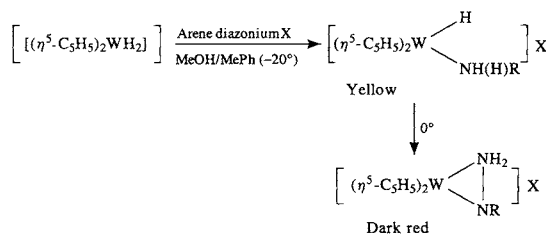
As expected,  $\text{N}_2\text{H}_4$  in aqueous solutions is somewhat weaker as a base than is ammonia (p. 423):



The hydrate  $\text{N}_2\text{H}_4 \cdot \text{H}_2\text{O}$  is an H-bonded molecular adduct and is not ionically dissociated. Two series

of salts are known, e.g.  $\text{N}_2\text{H}_5\text{Cl}$  and  $\text{N}_2\text{H}_6\text{Cl}_2$ . (It will be noticed that  $\text{N}_2\text{H}_6^{2+}$  is isoelectronic with ethane.) H bonding frequently influences the crystal structure and this is particularly noticeable in  $\text{N}_2\text{H}_6\text{F}_2$  which features a layer lattice similar to  $\text{CdI}_2$  though the structure is more open and the fluoride ions are not close packed. Sulfuric acid forms three salts,  $\text{N}_2\text{H}_4 \cdot n\text{H}_2\text{SO}_4$  ( $n = \frac{1}{2}, 1, 2$ ), i.e.  $[\text{N}_2\text{H}_5]\text{SO}_4$ ,  $[\text{N}_2\text{H}_6]\text{SO}_4$  and  $[\text{N}_2\text{H}_6][\text{HSO}_4]_2$ .

Hydrazido(2-)-complexes of Mo and W have been prepared by protonating dinitrogen complexes with concentrated solutions of  $\text{HX}$  and by ligand exchange.<sup>(76)</sup> For example several dozen complexes of general formulae  $[\text{MX}_2(\text{NNH}_2)\text{L}_3]$  and *trans*- $[\text{MX}(\text{NNH}_2)\text{L}_4]$  have been characterized for  $\text{M} = \text{Mo}$ ;  $\text{X} = \text{halogen}$ ;  $\text{L} = \text{phosphine}$  or heterocyclic-N donor. Similarly, *cis*- $[\text{W}(\text{N}_2)_2(\text{PMe}_2\text{Ph})_4]$  afforded *trans*- $[\text{WF}(\text{NNH}_2)(\text{PMe}_2\text{Ph})_4][\text{BF}_4]$  when treated with  $\text{HF}/\text{MeOH}$  in a borosilicate glass vessel. Side-on coordination of a phenylhydrazido(1-) ligand has also been established in compounds such as the dark-red  $[\text{W}(\eta^5\text{-C}_5\text{H}_5)_2(\eta^2\text{-H}_2\text{NNPh})][\text{BF}_4]$ ;<sup>(77)</sup> these are synthesized by the ready isomerization of the first-formed yellow  $\eta^1$ -arylhydrazido(2-) tungsten hydride complex above  $-20^\circ$  ( $\text{X} = \text{BF}_4, \text{PF}_6$ ):



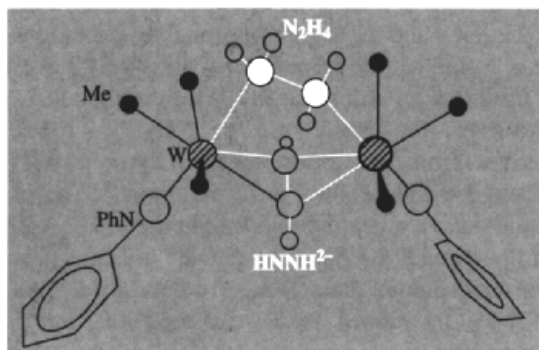
In these reactions  $\text{R} = \text{Ph}$ , *p*- $\text{MeOC}_6\text{H}_4$ , *p*- $\text{MeC}_6\text{H}_4$  or *p*- $\text{FC}_6\text{H}_4$ . Further bonding modes are as an isodiazene (i.e.  $\text{M} \leftarrow \text{N} = \text{NMe}_2$  rather than  $\text{M} = \text{N} - \text{NMe}_2$ )<sup>(78)</sup> and as a bridging diimido

<sup>76</sup> J. CHATT, A. J. PEARMAN and R. L. RICHARDS, *J. Chem. Soc., Dalton Trans.*, 1766-76 (1978).

<sup>77</sup> J. A. CARROLL, D. SUTTON, M. COWIE and M. D. GAUTHIER, *J. Chem. Soc., Chem. Commun.*, 1058-9 (1979).

<sup>78</sup> J. R. DILWORTH, J. ZUBIETA and J. R. HYDE, *J. Am. Chem. Soc.* **104**, 365-7 (1982).

group (M...N=N=M).<sup>(79)</sup> Both hydrazine itself and its dianion,  $\text{HNNH}^{2-}$ , act as bridging ligands in the pale yellow dinuclear tungsten(VI) complex shown in Fig. 11.6.<sup>(80)</sup> A selection of further recent work on the various coordination modes of substituted hydrazido, diazenido and related ligands is appended.<sup>(81)</sup>

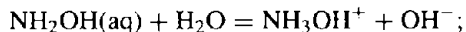


**Figure 11.6** Structure of  $[\{\text{W}(\text{NPh})\text{Me}_3\}_2(\mu\text{-}\eta^1, \eta^1\text{-NH}_2\text{NH}_2)(\mu\text{-}\eta^2, \eta^2\text{-NHNH})]$ .

### Hydroxylamine

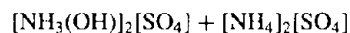
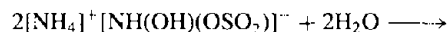
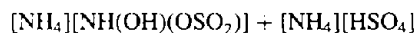
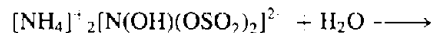
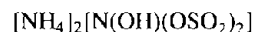
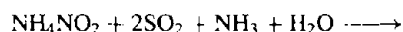
Anhydrous  $\text{NH}_2\text{OH}$  is a colourless, thermally unstable hygroscopic compound which is usually handled as an aqueous solution or in the form of one of its salts. The pure compound (mp  $32.05^\circ\text{C}$ ,  $d$   $1.204\text{ g cm}^{-3}$  at  $33^\circ\text{C}$ ) has a very high dielectric constant (77.63–77.85) and a vapour pressure of 10 mmHg at  $47.2^\circ$ . It can be regarded as water in which 1 H has been replaced by the more electronegative  $\text{NH}_2$  group or as  $\text{NH}_3$  in which

1 H has been replaced by OH. Aqueous solutions are less basic than either ammonia or hydrazine:



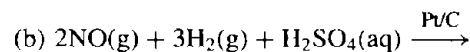
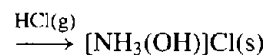
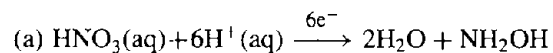
$$K_{25^\circ} = 6.6 \times 10^{-9} \text{ mol l}^{-1}$$

Hydroxylamine can be prepared by a variety of reactions involving the reduction of nitrites, nitric acid or NO, or by the acid hydrolysis of nitroalkanes. In the conventional Raschig synthesis, an aqueous solution of  $\text{NH}_4\text{NO}_2$  is reduced with  $\text{HSO}_4^-/\text{SO}_2$  at  $0^\circ$  to give the hydroxylamido-*N,N*-disulfate anion which is then hydrolysed stepwise to hydroxylammonium sulfate:



Aqueous solutions of  $\text{NH}_2\text{OH}$  can then be obtained by ion exchange, or the free compound can be prepared by ammonolysis with liquid  $\text{NH}_3$ ; insoluble ammonium sulfate is filtered off and the excess of  $\text{NH}_3$  removed under reduced pressure to leave solid  $\text{NH}_2\text{OH}$ .

Alternatively, hydroxylammonium salts can be made either (a) by the electrolytic reduction of aqueous nitric acid between amalgamated lead electrodes in the presence of  $\text{H}_2\text{SO}_4/\text{HCl}$ , or (b) by the hydrogenation of nitric oxide in acid solutions over a Pt/charcoal catalyst:



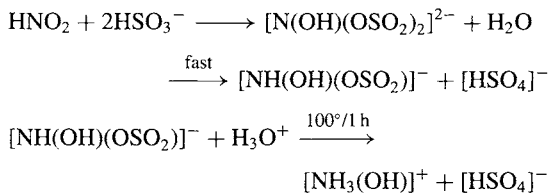
A convenient laboratory route involves the reduction of an aqueous solution of nitrous acid or potassium nitrite with bisulfite under carefully

<sup>79</sup> M. R. CHURCHILL and H. J. WASSERMAN, *Inorg. Chem.* **20**, 2899–904 (1981).

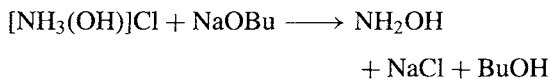
<sup>80</sup> L. BLUM, I. D. WILLIAMS and R. R. SCHROCK, *J. Am. Chem. Soc.* **106**, 8316–7 (1984).

<sup>81</sup> M. D. FITZROY, J. M. FREDERIKSEN, K. S. MURRAY and M. R. SNOW, *Inorg. Chem.* **24**, 3265–70 (1985). J. BULTITUDE, I. F. LARKWORTHY, D. C. POVEY, G. W. SMITH, J. R. DILWORTH and G. J. LEIGH, *J. Chem. Soc., Chem. Commun.*, 1748–50 (1986). J. R. DILWORTH, R. A. HENDERSON, P. DAHLSTROM, T. NICHOLSON and J. S. ZUBIETA, *J. Chem. Soc., Dalton Trans.*, 529–40 (1987). T. NICHOLSON and J. ZUBIETA, *Polyhedron* **7**, 171–85 (1988). F. W. EINSTEIN, X. YAN and D. SUTTON, *J. Chem. Soc., Chem. Commun.*, 1466–7 (1990).

controlled conditions: The hydroxylamidodisulfate first formed, though stable in alkaline solution, rapidly hydrolyses to the monosulfate in acid solution and this can then subsequently be hydrolysed to the hydroxylammonium ion by treatment with aqueous HCl at 100° for 1 h:



Anhydrous  $\text{NH}_2\text{OH}$  can be prepared by treating a suspension of hydroxylammonium chloride in butanol with NaOBu:



The NaCl is removed by filtration and the  $\text{NH}_2\text{OH}$  precipitated by addition of  $\text{Et}_2\text{O}$  and cooling.

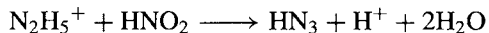
$\text{NH}_2\text{OH}$  can exist as 2 configurational isomers (*cis* and *trans*) and in numerous intermediate *gauche* conformations as shown in Fig. 11.7. In the crystalline form, H bonding appears to favour packing in the *trans* conformation. The N–O distance is 147 pm consistent with its formulation as a single bond. Above room temperature the compound decomposes (sometimes explosively) by internal oxidation-reduction reactions into a complex mixture of  $\text{N}_2$ ,  $\text{NH}_3$ ,  $\text{N}_2\text{O}$  and  $\text{H}_2\text{O}$ . Aqueous solutions are much more stable, particularly acid solutions in which the compound

is protonated,  $[\text{NH}_3(\text{OH})]^+$ . Such solutions can act as oxidizing agents particularly when acidified but are more generally used as reducing agents, e.g. as antioxidants in photographic developers, stabilizers of monomers, and for reducing  $\text{Cu}^{\text{II}}$  to  $\text{Cu}^{\text{I}}$  in the dyeing of acrylic fibres. Comparisons with the redox chemistry of  $\text{H}_2\text{O}_2$  and  $\text{N}_2\text{H}_4$  are also instructive (see, for example, pp. 272–3 of ref. 69). The ability of  $\text{NH}_2\text{OH}$  to react with  $\text{N}_2\text{O}$ ,  $\text{NO}$  and  $\text{N}_2\text{O}_4$  under suitable conditions (e.g. as the sulfate adsorbed on silica gel) makes it useful as an absorbent in combustion analysis. However, the major use of  $\text{NH}_2\text{OH}$ , which derives from its ability to form oximes with aldehydes and ketones, is in the manufacture of caprolactam, a key intermediate in the production of polyamide-6 fibres such as nylon. This consumes more than 97% of world production of  $\text{NH}_2\text{OH}$ , which is at least 650 000 tonnes per annum.

The extensive chemistry of the hydroxylamides of sulfuric acid is discussed later in the context of other H–N–O–S compounds (pp. 740–6).

### Hydrogen azide

Aqueous solutions of  $\text{HN}_3$  were first prepared in 1890 by T. Curtius who oxidized aqueous hydrazine with nitrous acid:



Other oxidizing agents that can be used include nitric acid, hydrogen peroxide, peroxydisulfate, chlorate and the pervanadyl ion. The anhydrous

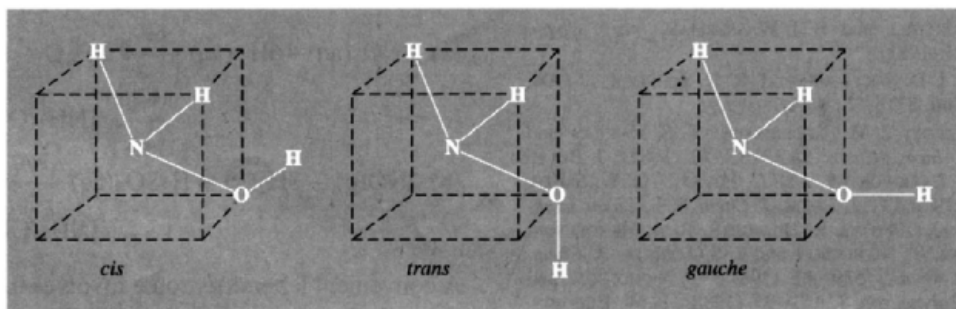
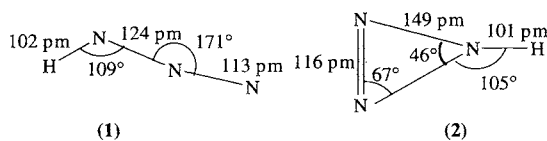


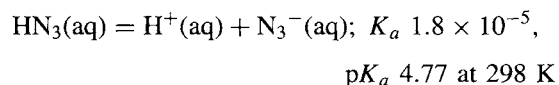
Figure 11.7 Configurations of  $\text{NH}_2\text{OH}$ .

compound is extremely explosive and even dilute solutions should be treated as potentially hazardous. Pure  $\text{HN}_3$  is best prepared by careful addition of  $\text{H}_2\text{SO}_4$  to  $\text{NaN}_3$ ; it is a colourless liquid or gas (mp  $\sim -80^\circ$ , estimated bp  $35.7^\circ$ ,  $d$   $1.126 \text{ g cm}^{-3}$  at  $0^\circ$ ). Its large positive enthalpy and free energy of formation emphasize its inherent instability:  $\Delta H_f^\circ(1, 298 \text{ K})$   $269.5$ ,  $\Delta G_f^\circ(1, 298 \text{ K})$   $327.2 \text{ kJ mol}^{-1}$ . It has a repulsive, intensely irritating odour and is a deadly (though non-cumulative) poison; even at concentrations less than 1 ppm in air it can be dangerous. In the gas phase the 3 N atoms are (almost) colinear, as expected for a 16 valence-electron species, and the angle HNN is  $109^\circ$ ; the two N–N distances are appreciably different, as shown in structure (1). The structure and dimensions of the isomeric molecule cyclotriazene are given in (2) for comparison; the N–H bond is tilted out of the plane of the  $\text{N}_3$  ring by  $74^\circ$ .



Similar differences are found for organic azides (e.g.  $\text{MeN}_3$ ). In ionic azides (p. 417) the  $\text{N}_3^-$  ion is both linear and symmetrical (both N–N distances being 116 pm) as befits a 16-electron species isoelectronic with  $\text{CO}_2$  (cf. also the cyanamide ion  $\text{NCN}^{2-}$ , the cyanate ion  $\text{NCO}^-$ , the fulminate ion  $\text{CNO}^-$  and the nitronium ion  $\text{NO}_2^+$ ).

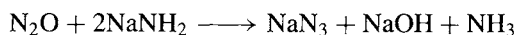
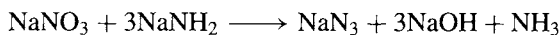
Aqueous solutions of  $\text{HN}_3$  are about as strongly acidic as acetic acid:



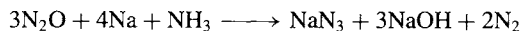
Numerous metal azides have been characterized (p. 417) and covalent derivatives of non-metals are also readily preparable by simple metathesis using either  $\text{NaN}_3$  or aqueous solutions of

$\text{HN}_3$ <sup>(82,83)</sup>. In these compounds the  $\text{N}_3$  group behaves as a pseudohalogen (p. 319) and, indeed, the unstable compounds  $\text{FN}_3$ ,  $\text{ClN}_3$ ,  $\text{BrN}_3$ ,  $\text{IN}_3$  and  $\text{NCN}_3$  are known, though potential allotropes of nitrogen such as  $\text{N}_3\text{--N}_3$  (analogous to  $\text{Cl}_2$ ) and  $\text{N}(\text{N}_3)_3$  (analogous to  $\text{NCl}_3$ ) have not been isolated. More complex heterocyclic compounds are, however, well established, e.g. cyanuric azide  $\{-\text{NC}(\text{N}_3)-\}_3$ , *B,B,B*-triazidoborazine  $\{-\text{NB}(\text{N}_3)-\}_3$  and even the azidophosphazene derivative  $\{-\text{NP}(\text{N}_3)_2-\}_3$ .

Most preparative routes to  $\text{HN}_3$  and its derivatives involve the use of  $\text{NaN}_3$  since this is reasonably stable and commercially available.  $\text{NaN}_3$  can be made by adding powdered  $\text{NaNO}_3$  to fused  $\text{NaNH}_2$  at  $175^\circ$  or by passing  $\text{N}_2\text{O}$  into the same molten amide at  $190^\circ$ :



The latter reaction is carried out on an industrial scale using liquid  $\text{NH}_3$  as solvent; a variant uses  $\text{Na/NH}_3$  without isolation of the  $\text{NaNH}_2$ :



A remarkable new covalent azide is the pale yellow nitrosyl  $\text{NNNNO}$ , prepared by reacting gaseous  $\text{NOCl}$  (p. 441) with solid  $\text{NaN}_3$  at low temperature.<sup>(84)</sup>  $\text{NNNN}(\text{SO}_2\text{F})_2$  has also very recently been made by a similar route from  $(\text{SO}_2\text{F})_2\text{NCl}$ ; it is a volatile yellow liquid which sometimes decomposes explosively.<sup>(84a)</sup>

The major use of inorganic azides exploits the explosive nature of heavy metal azides.  $\text{Pb}(\text{N}_3)_2$  in particular is extensively used in detonators because of its reliability, especially in damp conditions; it is prepared by metathesis between  $\text{Pb}(\text{NO}_3)_2$  and  $\text{NaN}_3$  in aqueous solution.

<sup>82</sup> Pp. 276–93 of ref. 69.

<sup>83</sup> A. D. YOFFE, Chap. 2 in C. B. COLBURN (ed.), *Developments in Inorganic Nitrogen Chemistry*, Vol. 1, pp. 72–149, Elsevier, Amsterdam, 1966.

<sup>84</sup> A. SCHULZ, I. C. TORNIERTH-OETTING and T. M. KLAPÖTKE, *Angew. Chem. Int. Edn. Engl.* **32**, 1610–12 (1993).

<sup>84a</sup> H. HOLFTER, T. M. KLAPÖTKE and A. SCHULZ, *Polyhedron* **15**, 1405–7 (1996).

### 11.3.4 Thermodynamic relations between N-containing species

The ability of N to exist in its compounds in at least 10 different oxidation states from  $-3$  to  $+5$  poses certain thermodynamic and mechanistic problems that invite systematic treatment. Thus, in several compounds N exists in more than one oxidation state, e.g.  $[\text{N}^{-\text{III}}\text{H}_4]^+[\text{N}^{\text{III}}\text{O}_2]^-$ ,  $[\text{N}^{-\text{III}}\text{H}_4]^+[\text{N}^{\text{V}}\text{O}_3]^-$ ,  $[\text{N}^{-\text{II}}\text{H}_5]^+[\text{N}^{\text{V}}\text{O}_3]^-$ ,  $[\text{N}^{-\text{III}}\text{H}_4]^+[\text{N}^{-\frac{1}{3}}\text{H}_3]^-$ , etc. Furthermore, we have seen (p. 423) that, under appropriate conditions,  $\text{NH}_3$  can be oxidized by  $\text{O}_2$  to yield  $\text{N}_2$ ,  $\text{NO}$  or  $\text{NO}_2$ , whereas oxidation by  $\text{OCI}^-$  yields  $\text{N}_2\text{H}_4$  (p. 427). Likewise, using appropriate reagents,  $\text{N}_2\text{H}_4$  can be oxidized either to  $\text{N}_2$  or to  $\text{HN}_3$  (in which the “average” oxidation number of N is  $-\frac{1}{3}$ ). The thermodynamic relations between these various hydrido and oxo species containing N can be elegantly codified by means of their

standard reduction potentials, and these can be displayed pictorially using the concept of the “volt equivalent” of each species (see Panel).

The standard reduction potentials in acidic aqueous solution are given in Table 11.4; these are shown diagrammatically in Fig. 11.8 (p. 437) which also includes the corresponding data for alkaline solutions. The reduction potentials are readily converted to volt equivalents (by multiplying by the appropriate oxidation state) and these are plotted against oxidation state in Fig. 11.9. This latter diagram is particularly valuable in giving a visual representation of the redox chemistry of the element. Thus, it follows from the definition of “volt equivalent” that the reduction potential of any couple is the *slope* of the line joining the two points: the greater the positive slope the stronger the oxidizing potential and the greater the negative slope the stronger the reducing power. Any pair of points can be joined. For example in acid solution  $\text{N}_2\text{H}_4$  is a

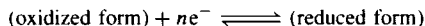
**Table 11.4** Standard reduction potentials for nitrogen species<sup>(a)</sup> in acidic aqueous solution (pH 0, 25°C)

Couple	$E^\circ/V$	Corresponding half-reaction
$\text{N}_2/\text{HN}_3$	-3.09	$\frac{3}{2}\text{N}_2 + \text{H}^+(\text{aq}) + \text{e}^- \longrightarrow \text{HN}_3(\text{aq})$
$\text{N}_2/\text{N}_2\text{H}_5^+$	-0.23	$\text{N}_2 + 5\text{H}^+ + 4\text{e}^- \longrightarrow \text{N}_2\text{H}_5^+$
$\text{H}_2\text{N}_2\text{O}_2/\text{NH}_3\text{OH}^+$	+0.387	$\text{H}_2\text{N}_2\text{O}_2 + 6\text{H}^+ + 4\text{e}^- \longrightarrow 2\text{NH}_3\text{OH}^+$
$\text{HN}_3/\text{NH}_4^+$	+0.695	$\text{HN}_3 + 11\text{H}^+ + 8\text{e}^- \longrightarrow 3\text{NH}_4^+$
$\text{NO}/\text{H}_2\text{N}_2\text{O}_2$	+0.712	$2\text{NO} + 2\text{H}^+ + 2\text{e}^- \longrightarrow \text{H}_2\text{N}_2\text{O}_2$
$\text{NO}_3^-/\text{N}_2\text{O}_4$	+0.803	$2\text{NO}_3^- + 4\text{H}^+ + 2\text{e}^- \longrightarrow \text{N}_2\text{O}_4 + 2\text{H}_2\text{O}$
$\text{HNO}_2/\text{H}_2\text{N}_2\text{O}_2$	+0.86	$2\text{HNO}_2 + 4\text{H}^+ + 4\text{e}^- \longrightarrow \text{H}_2\text{N}_2\text{O}_2 + 2\text{H}_2\text{O}$
$\text{NO}_3^-/\text{HNO}_2$	+0.94	$\text{NO}_3^- + 3\text{H}^+ + 2\text{e}^- \longrightarrow \text{HNO}_2 + \text{H}_2\text{O}$
$\text{NO}_3^-/\text{NO}$	+0.957	$\text{NO}_3^- + 4\text{H}^+ + 3\text{e}^- \longrightarrow \text{NO} + 2\text{H}_2\text{O}$
$\text{HNO}_2/\text{NO}$	+0.983	$\text{HNO}_2 + \text{H}^+ + \text{e}^- \longrightarrow \text{NO} + \text{H}_2\text{O}$
$\text{N}_2\text{O}_4/\text{NO}$	+1.035	$\text{N}_2\text{O}_4 + 4\text{H}^+ + 4\text{e}^- \longrightarrow 2\text{NO} + 2\text{H}_2\text{O}$
$\text{N}_2\text{O}_4/\text{HNO}_2$	+1.065	$\text{N}_2\text{O}_4 + 2\text{H}^+ + 2\text{e}^- \longrightarrow 2\text{HNO}_2$
$\text{N}_2\text{H}_5^+/\text{NH}_4^+$	+1.275	$\text{N}_2\text{H}_5^+ + 3\text{H}^+ + 2\text{e}^- \longrightarrow 2\text{NH}_4^+$
$\text{HNO}_2/\text{N}_2\text{O}$	+1.29	$2\text{HNO}_2 + 4\text{H}^+ + 4\text{e}^- \longrightarrow \text{N}_2\text{O} + 3\text{H}_2\text{O}$
$\text{NH}_3\text{OH}^+/\text{NH}_4^+$	+1.35	$\text{NH}_3\text{OH}^+ + 2\text{H}^+ + 2\text{e}^- \longrightarrow \text{NH}_4^+ + \text{H}_2\text{O}$
$\text{NH}_3\text{OH}^+/\text{N}_2\text{H}_5^+$	+1.42	$2\text{NH}_3\text{OH}^+ + \text{H}^+ + 2\text{e}^- \longrightarrow \text{N}_2\text{H}_5^+ + 2\text{H}_2\text{O}$
$\text{HN}_3/\text{NH}_4^+$	+1.96	$\text{HN}_3 + 3\text{H}^+ + 2\text{e}^- \longrightarrow \text{NH}_4^+ + \text{N}_2$
$\text{H}_2\text{N}_2\text{O}_2/\text{N}_2$	+2.65	$\text{H}_2\text{N}_2\text{O}_2 + 2\text{H}^+ + 2\text{e}^- \longrightarrow \text{N}_2 + 2\text{H}_2\text{O}$

<sup>(a)</sup>All the half-reactions listed in this table have only (Ox),  $\text{H}^+$  and  $\text{e}^-$  on the left-hand side of the half-reaction. Others, such as  $\text{N}_2/\text{NH}_3\text{OH}^+ - 1.87$  (i.e.  $\text{N}_2 + 2\text{H}_2\text{O} + 4\text{H}^+ + 2\text{e}^- \longrightarrow 2\text{NH}_3\text{OH}^+$ ) can readily be calculated by appropriate combinations (in this case, for example,  $\text{N}_2/\text{N}_2\text{H}_5^+ - \text{NH}_3\text{OH}^+/\text{N}_2\text{H}_5^+$ ). There are also simple electron addition reactions, e.g.  $\text{NO}^+/\text{NO}$ ,  $E^\circ + 1.46$  V (i.e.  $\text{NO}^+ + \text{e}^- \longrightarrow \text{NO}$ ) and more complex electron additions, e.g.  $\text{NO}_3^-/\text{NO}/\text{NO}_2^-$ ,  $E^\circ + 0.49$  V (i.e.  $\text{NO}_3^- + \text{NO} + \text{e}^- \longrightarrow 2\text{NO}_2^-$ ), etc.

### Standard Reduction Potentials and Volt Equivalents

Chemical reactions can often formally be expressed as the sum of two or more “half-reactions” in which electrons are transferred from one chemical species to another. Conventionally these are now almost always represented as equilibria in which the forward reaction is a reduction (addition of electrons):



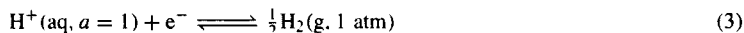
The electrochemical reduction potential ( $E$  volts) of such an equilibrium is given by

$$E = E^\circ - \frac{2.3026RT}{nF} \log_{10} \frac{a(\text{red})}{a(\text{ox})} \quad (1)$$

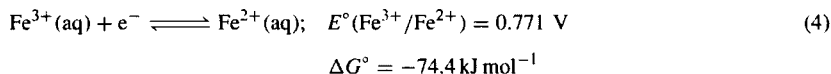
where  $E^\circ$  is the “standard reduction potential” at unit activity  $a$ ,  $R$  is the gas constant ( $8.3144 \text{ J mol}^{-1} \text{ K}^{-1}$ ),  $T$  is the absolute temperature,  $F$  is the Faraday constant ( $96485 \text{ C mol}^{-1}$ ) and 2.3026 is the constant  $\ln_e 10$  required to convert from natural to decadic logarithms. At 298.15 K ( $25^\circ \text{C}$ ) the factor  $2.3026RT/F$  has the value  $0.05916 \text{ V}$  and, replacing activities by concentrations, one obtains the approximate expression

$$E \approx E^\circ - \frac{0.05916}{n} \log_{10} \frac{[\text{red}]}{[\text{ox}]} \quad (2)$$

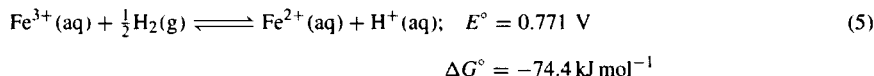
By convention,  $E^\circ$  for the half-reaction (3) is taken as zero, i.e.  $E^\circ(\text{H}^+/\frac{1}{2}\text{H}_2) = 0.0 \text{ V}$ :



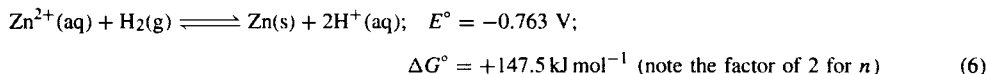
Remembering that  $\Delta G = -nEF$ , it follows that the standard free energy change for the half reaction is  $\Delta G^\circ = -nE^\circ F$ , e.g.:



Coupling the half-reactions (3) and (4) gives the reaction (5) [i.e.(4) – (3)] which, because  $\Delta G$  is negative, proceeds spontaneously from left to right as written:



Again,  $E^\circ(\text{Zn}^{2+}/\text{Zn}) = -0.763 \text{ V}$ , hence reaction (6) occurs spontaneously in the reverse direction:



In summary, at pH 0 a reaction is spontaneous from left to right if  $E^\circ > 0$  and spontaneous in the reverse direction if  $E^\circ < 0$ . At other H-ion concentrations eqn. (2) indicates that the potential of the H electrode (3) will be

$$E = -0.05916 \log \frac{\{P_{\text{H}_2}/\text{atm}\}^{\frac{1}{2}}}{\{[\text{H}^+(\text{aq})]/\text{mol l}^{-1}\}} \text{ V}$$

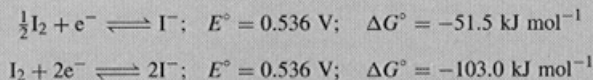
and, in general, the potential of any half-reaction changes with the concentration of the species involved according to the Nernst equation (7):

$$E = E^\circ - \frac{0.05916}{n} \log Q \quad (7)$$

where  $Q$  has the same form as the equilibrium constant but is a function of the actual activities of the reactants and products rather than those of the equilibrium state. Note also that the potential is independent of the coefficients of the half-reaction whereas the free energy is directly proportional to these, e.g.:

*Panel continues*

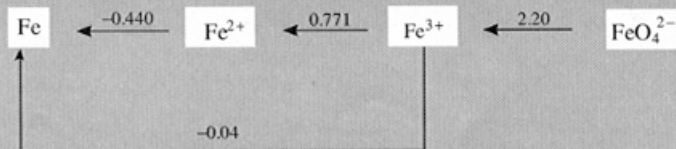




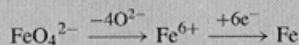
It is vital to remember that, when half-reactions are added or subtracted, one should not add or subtract the corresponding  $E^\circ$  values but rather  $nE^\circ$ . (We shall return to this point later.)

Lists of standard reduction potentials are given in many books<sup>(85)</sup> and are extensively quoted throughout this text. Almost all lists now use the IUPAC sign conventions employed above, though some earlier American books (including, unfortunately, the classic early text on the subject<sup>(86)</sup>) use the opposite sign convention. When standard reduction potentials are listed in sequence from the most negative to the most positive the strongest reducing agents are at the top of the list and a reducing agent should, in principle, be capable of reducing all oxidizing agents lying below it in the table. Conversely, the oxidizing agents are listed in order of increasing strength and a given oxidizing agent should be able to oxidize all reducing agents lying above it in the table. Such lists are an extremely compact way of summarizing a great deal of predictive information. For example a list of 100 independent reduction potentials enables the free energy change for  $100 \times 99/2 = 4950$  reactions to be calculated and indicates the direction in which a hypothetical reaction would occur under appropriate conditions (which might involve the use of a catalyst).

When an element can exist in several oxidation states it is sometimes convenient to display the various reduction potentials diagrammatically, the corresponding half-reactions under standard conditions being implied. Thus, in acidic aqueous solutions



Note that the value of  $E^\circ(\text{Fe}^{3+}/\text{Fe}) = -0.04 \text{ V}$  is equivalent to  $\{(2 \times -0.44) + 0.77\}/3$ . Because the quantity  $nE^\circ$  is used in these calculations (rather than  $E^\circ$ ) it is convenient to define the "volt equivalent" of a species; the volt equivalent of a compound or ion is the reduction potential of the species relative to the element in its standard state multiplied by the oxidation state of the element in the compound (including its sign). The oxidation state is the number of electrons that must be added to an atom of an element to regain electroneutrality when all other atoms in the compound (ion) have been removed as their "normal" ions. For example the oxidation state of Fe is +6 in  $\text{FeO}_4^{2-}$ :



It follows that, in the above example, the volt equivalents of  $\text{Fe}^{2+}$  and  $\text{Fe}^{3+}$  are  $-0.88$  and  $-0.11$  respectively and that of  $\text{FeO}_4^{2-}$  is  $+6.49$  [i.e.  $(2 \times -0.44) + 0.77 + (3 \times 2.20)$ ]. This leads to  $E^\circ(\text{FeO}_4^{2-}/\text{Fe}) = +1.08 \text{ V}$ .

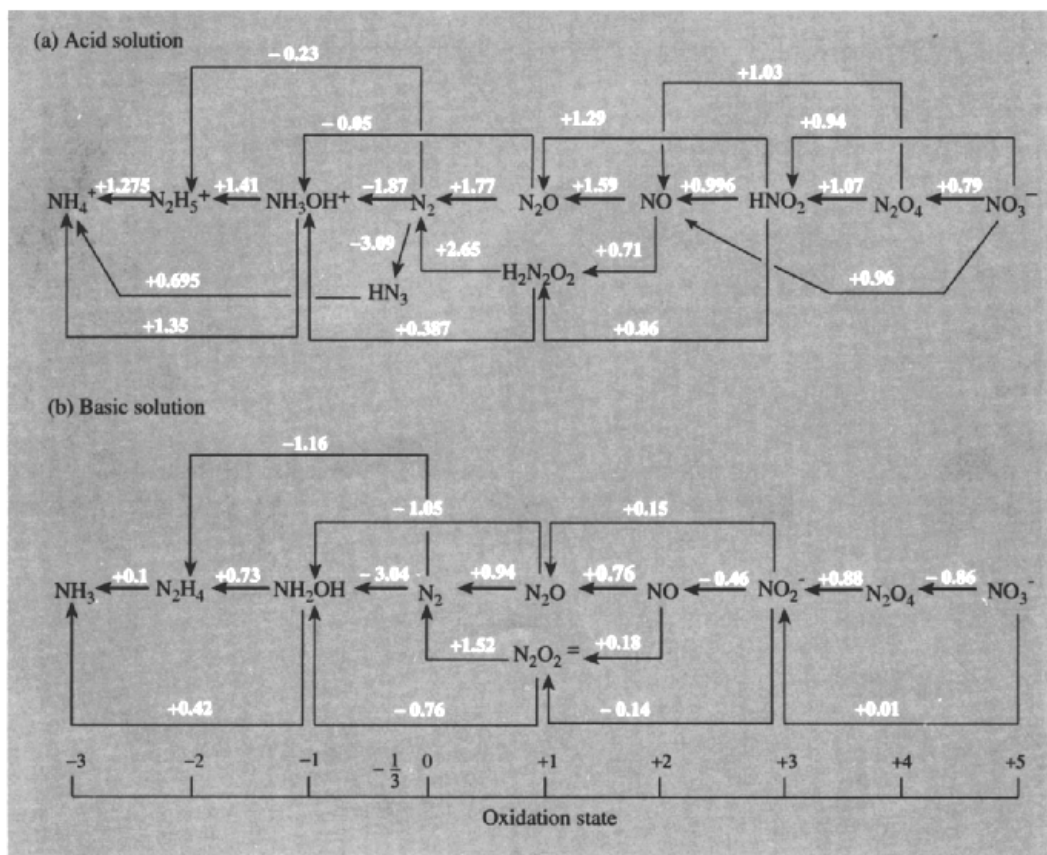
The power of these various concepts in codifying and rationalizing the redox chemistry of the elements is illustrated for the case of nitrogen in the present section. Standard reduction potentials and plots of volt equivalents against oxidation state for other elements are presented in later chapters.

stronger reducing agent than  $\text{H}_2$  (slope of tie-line  $-0.23 \text{ V}$ ) and  $\text{NH}_2\text{OH}$  is even stronger (slope  $-1.87 \text{ V}$ ). By contrast, the couple  $\text{N}_2\text{O}/\text{NH}_3\text{OH}^+$  has virtually the same reducing power as  $\text{H}_2$  (slope  $-0.05 \text{ V}$ ).

<sup>85</sup> A. J. BARD, R. PARSONS and J. JORDAN *Standard Potentials in Aqueous Solution*, Marcel Dekker, New York, 1985, 834 pp. G. MILAZZO and S. CAROLI, *Tables of Standard Electrode Potentials*, Wiley, New York, 1978, 421 pp.

<sup>86</sup> W. M. LATIMER, *The Oxidation States of the Elements and their Potentials in Aqueous Solutions*, 2nd edn., Prentice-Hall, New York, 1952, 392 pp.

It also follows that, when three (or more) oxidation states lie approximately on a straight line in the volt-equivalent diagram, they tend to form an equilibrium mixture rather than a reaction going to completion (provided that the attainment of thermodynamic equilibrium is not hindered kinetically). This is because the slopes joining the several points are almost the same, so that  $E^\circ$  for the various couples (and hence  $\Delta G^\circ$ ) are the same; there is consequently approximately zero change in free energy and a balanced

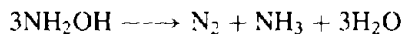
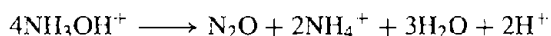


**Figure 11.8** Oxidation states of nitrogen showing standard reduction potentials in volts: (a) in acid solution at pH 0, and (b) in basic solution at pH 14.

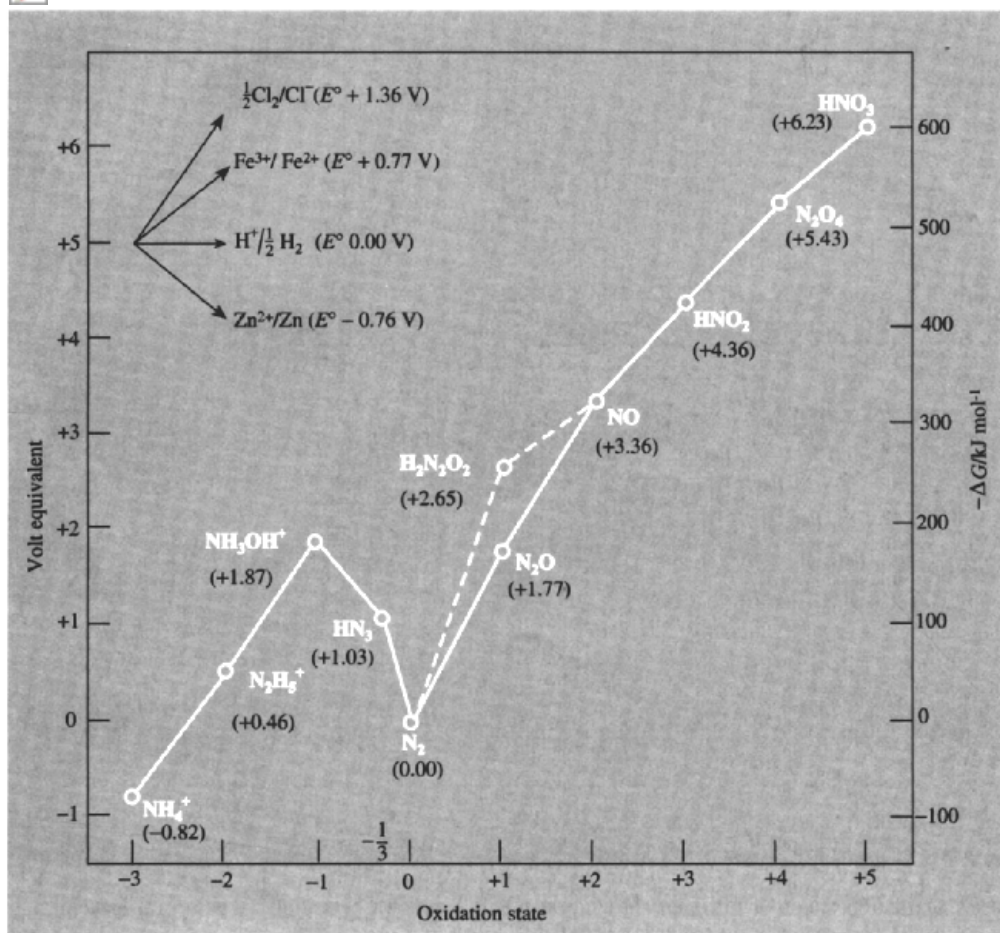
equilibrium is maintained between the several species. Indeed, the volt-equivalent diagram is essentially a plot of free energy versus oxidation state (as indicated by the right-hand ordinate of Fig. 11.9).

Two further points follow from these general considerations:

(a) a compound will tend to disproportionate into a higher and a lower oxidation state if it lies above the line joining the 2 compounds in these oxidation states, i.e. disproportionation is accompanied by a decrease in free energy and will tend to occur spontaneously if not kinetically hindered. Examples are the disproportionation of hydroxylamine in acidic solutions (slow) and alkaline solutions (fast):

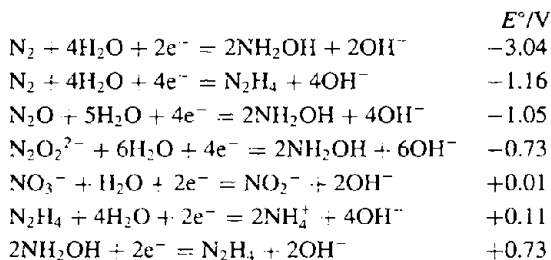


(b) Conversely, a compound can be formed by conproportionation of compounds in which the element has a higher and lower oxidation state if it lies below the line joining these two states. A particularly important example is the synthesis of  $\text{HN}_3$  by reacting  $\text{N}_2^{II}\text{H}_5^+$  and  $\text{HN}^{III}\text{O}_2$  (p. 432). It will be noted that the reduction potential of  $\text{HN}_3$  (-3.09 V) is more negative than that of any other reducing agent in acidic aqueous solution so it is thermodynamically impossible to synthesize  $\text{HN}_3$  by reduction of  $\text{N}_2$  or any of its compounds in such media unless the reducing agent itself contains N (as does hydrazine).



**Figure 11.9** Plot of volt equivalent against oxidation state for various compounds or ions containing N in acidic aqueous solution. Note that values of  $-\Delta G$  refer to N<sub>2</sub> as standard (zero) but are quoted per mol of N atoms and per mol of N<sub>2</sub>; they refer to reactions in the direction (ox) +  $ne^- \rightarrow$  (red). Slopes corresponding to some common oxidizing and reducing agents are included for comparison.

In basic solutions a different set of redox equilibria obtain and a different set of reduction potentials must be used. For example:



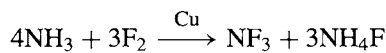
A more complete compilation is summarized in Fig. 11.8. It is instructive to use these data to derive a plot of volt equivalent versus oxidation state in basic solution and to compare this with Fig. 11.9 which refers to acidic solutions.

### 11.3.5 Nitrogen halides and related compounds<sup>(69)</sup>

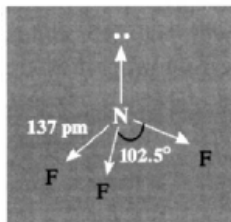
It is a curious paradox that NF<sub>3</sub>, the most stable binary halide of N, was not prepared until 1928, more than 115 y after the highly unstable

$\text{NCl}_3$  was prepared in 1811 by P. L. Dulong (who lost three fingers and an eye studying its properties). Pure  $\text{NBr}_3$  explodes even at  $-100^\circ$  and was not isolated until 1975<sup>(87)</sup> and  $\text{NI}_3$  has not been prepared, though the explosive adduct  $\text{NI}_3 \cdot \text{NH}_3$  was first made by B. Courtois in 1813 and several other amines are known. In all, there are now 5 binary fluorides of nitrogen ( $\text{NF}_3$ ,  $\text{N}_2\text{F}_4$ , *cis*- and *trans*- $\text{N}_2\text{F}_2$  and  $\text{N}_3\text{F}$ ) and these, together with the cations  $\text{NF}_4^+$  and  $\text{N}_2\text{F}_3^+$  and various mixed halides, hydride halides and oxohalides are discussed in this section.

$\text{NF}_3$  was first prepared by Otto Ruff's group in Germany by the electrolysis of molten  $\text{NH}_4\text{F}/\text{HF}$  and this process is still used commercially. An alternative is the controlled fluorination of  $\text{NH}_3$  over a Cu metal catalyst.

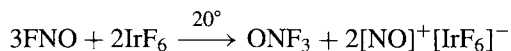
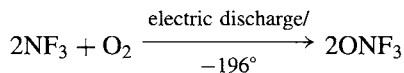
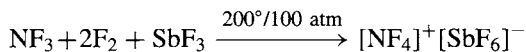


$\text{NF}_3$  is a colourless, odourless, thermodynamically stable gas (mp  $-206.8^\circ$ , bp  $-129.0^\circ$ ,  $\Delta G_{298}^\circ - 83.3 \text{ kJ mol}^{-1}$ ). The molecule is pyramidal with an F–N–F angle of  $102.5^\circ$ , but the dipole moment (0.234 D) is only one-sixth of that of  $\text{NH}_3$  (1.47 D) presumably because the N–F bond moments act in the opposite direction to that of the lone-pair moment:



The gas is remarkably unreactive (like  $\text{CF}_4$ ) being unaffected by water or dilute aqueous acid or alkali; at elevated temperatures it acts as a fluorinating agent and with Cu, As, Sb or Bi in a flow reactor it yields  $\text{N}_2\text{F}_4$  ( $2\text{NF}_3 + 2\text{Cu} \rightarrow \text{N}_2\text{F}_4 + 2\text{CuF}$ ). As perhaps expected (p. 198)  $\text{NF}_3$  shows little tendency to act as a

ligand, though  $\text{NF}_4^+$  is known<sup>(88)</sup> and also the surprisingly stable isoelectronic species  $\text{ONF}_3$  (mp  $-160^\circ$ , bp  $-87.6^\circ$ ):



$\text{ONF}_3$  was discovered independently by two groups in 1966.<sup>(89)</sup> Although isoelectronic with  $\text{BF}_4^-$ ,  $\text{CF}_4$  and  $\text{NF}_4^+$  it has excited interest because of the short N–O distance (115.8 pm), which implies some multiple bonding, and the correspondingly long N–F distances (143.1 pm). Similar partial double bonding to O and highly polar bonds to F have also been postulated for the analogous ion  $[\text{OCF}_3]^-$  in  $\text{Cs}[\text{OCF}_3]$ .<sup>(90)</sup>

$\text{FN}_3$  is one of the most explosive and thermally unstable covalent azides known. It can be prepared by reacting  $\text{HN}_3$  with  $\text{F}_2$  and is best handled as a gas at low pressure.<sup>(91)</sup> The molecular parameters (microwave) are N–F 144.4 pm,  $\text{N}_\alpha\text{--N}_\beta$  125.3 pm,  $\text{N}_\alpha\text{--N}_\omega$  113.2 pm, and angles FNN  $103.8^\circ$ , NNN  $170.9^\circ$  (cf  $\text{HN}_3$  p. 433) The species  $\text{NF}$  is known only as a ligand, in the octahedral complex  $[\text{ReF}_5(\text{NF})]$ <sup>(92)</sup> the complex is made by treating  $\text{ReF}_4\text{N}$  or  $\text{ReF}_3\text{N}$  with  $\text{XeF}_2$  and X-ray structural analysis revealed a linear Re–N–F group ( $178^\circ$ ) with N–F 126 pm.

Dinitrogen tetrafluoride,  $\text{N}_2\text{F}_4$ , is the fluorine analogue of hydrazine and exists in both the staggered (*trans*)  $C_{2h}$  and *gauche*  $C_2$  conformations

<sup>88</sup> K. O. CHRISTE, C. H. SCHACK and R. D. WILSON, *Inorg. Chem.* **16**, 849–54 (1977), and references therein. See also K. O. CHRISTE, R. D. WILSON and I. R. GOLDBERG, *Inorg. Chem.* **18**, 2572–7 (1979). K. O. CHRISTE, R. D. WILSON and C. J. SCHACK, *Inorg. Chem.* **19**, 3046–9 (1980).

<sup>89</sup> See S. A. KINREAD and J. M. SHREEVE, *Inorg. Chem.* **23** 3109–12, 4174–7 (1984) for useful references to preparation and reactions of  $\text{ONF}_3$ .

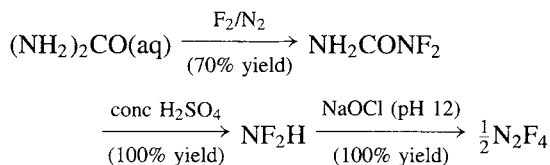
<sup>90</sup> K. O. CHRISTE, E. C. CURTIS and C. J. SCHACK, *Spectrochim. Acta* **31A**, 1035–8 (1975).

<sup>91</sup> D. CHRISTEN, H. G. MACK, G. SCHATTE and H. WILLNER, *J. Am. Chem. Soc.* **110**, 707–12 (1988).

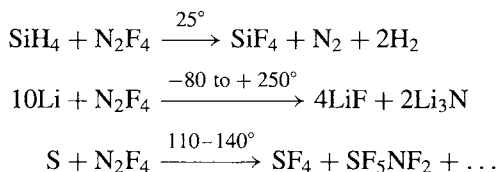
<sup>92</sup> J. FAWCETT, R. D. PEACOCK and D. R. RUSSELL, *J. Chem. Soc., Dalton Trans.*, 567–71 (1987).

<sup>87</sup> J. LANDER, J. KNACKMUSS and K.-U. THIEDEMANN, *Z. Naturforsch.* **B30**, 464–5 (1975).

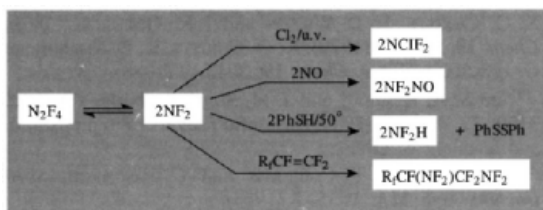
(p. 428). It was discovered in 1957 and is now made either by partial defluorination of  $\text{NF}_3$  (see above) or by quantitative oxidation of  $\text{NF}_2\text{H}$  with alkaline hypochlorite:



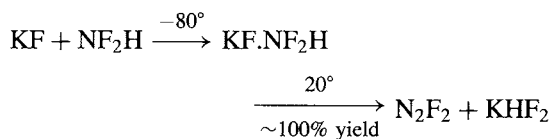
$\text{N}_2\text{F}_4$  is a colourless reactive gas (mp  $-164.5^\circ$ , bp  $-73^\circ$ ,  $\Delta G_{298}^\circ + 81.2 \text{ kJ mol}^{-1}$ ) which acts as a strong fluorinating agent towards many substances, e.g.:



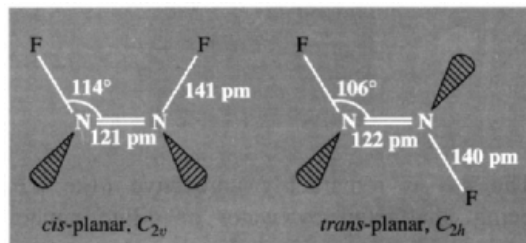
It forms adducts with strong fluoride-ion acceptors such as  $\text{AsF}_5$  which can be formulated as salts, e.g.  $[\text{N}_2\text{F}_3]^+[\text{AsF}_6]^-$ . However, its most intriguing property is an ability to dissociate at room temperature and above to give the free radical  $\text{NF}_2$ . Thus, when  $\text{N}_2\text{F}_4$  is frozen out from the warm gas at relatively low pressures the solid is dark blue whereas when it is frozen out from the cold gas at moderate pressures it is colourless. At  $150^\circ\text{C}$  the equilibrium constant for the dissociation  $\text{N}_2\text{F}_4 \rightleftharpoons 2\text{NF}_2$  is  $K = 0.03 \text{ atm}$  and the enthalpy of dissociation is  $83.2 \text{ kJ mol}^{-1}$ .<sup>(93)</sup> Such a dissociation, which interprets much of the reaction chemistry of  $\text{N}_2\text{F}_4$ ,<sup>(94)</sup> is reminiscent of the behaviour of  $\text{N}_2\text{O}_4$  (p. 455) but is not paralleled in the chemistry of  $\text{N}_2\text{H}_4$ :



Dinitrogen difluoride,  $\text{N}_2\text{F}_2$ , was first identified in 1952 as a thermal decomposition product of the azide  $\text{N}_3\text{F}$  and it also occurs in small yield during the electrolysis of  $\text{NH}_4\text{F}/\text{HF}$  (p. 439), and in the reactions of  $\text{NF}_3$  with  $\text{Hg}$  or with  $\text{NF}_3$  in a  $\text{Cu}$  reactor (p. 439). Fluorination of  $\text{NaN}_3$  gives good yields on a small scale but the compound is best prepared by the following reaction sequence:



All these methods give mixtures of the *cis*- and *trans*-isomers; these are thermally interconvertible but can be separated by low-temperature fractionation. The *trans*-form is thermodynamically more unstable than the *cis*-form but it can be stored in glass vessels whereas the *cis*-form reacts completely within 2 weeks to give  $\text{SiF}_4$  and  $\text{N}_2\text{O}$ . *Trans*- $\text{N}_2\text{F}_2$  can be prepared free of the *cis*-form by the low-temperature reaction of  $\text{N}_2\text{F}_4$  with  $\text{AlCl}_3$  or  $\text{MCl}_2$  ( $\text{M} = \text{Mn, Fe, Co, Ni, Sn}$ ); thermal isomerization of *trans*- $\text{N}_2\text{F}_2$  at  $70-100^\circ$  yields an equilibrium mixture containing  $\sim 90\%$  *cis*- $\text{N}_2\text{F}_2$  ( $\Delta H_{\text{isom}} 12.5 \text{ kJ mol}^{-1}$ ). Pure *cis*- $\text{N}_2\text{F}_2$  can be obtained by selective complexation with  $\text{AsF}_5$ ; only the *cis*-form reacts at room temperature to give  $[\text{N}_2\text{F}]^+[\text{AsF}_6]^-$  and this, when treated with  $\text{NaF}/\text{HF}$ , yields pure *cis*- $\text{N}_2\text{F}_2$ . Some characteristic properties are listed below.



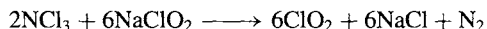
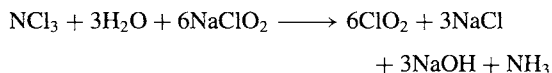
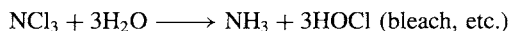
Isomer	MP/ $^\circ\text{C}$	BP/ $^\circ\text{C}$	$\Delta H_f^\circ/\text{kJ mol}^{-1}$	$\mu/\text{Debye}$
<i>cis</i> - $\text{N}_2\text{F}_2$	$< -195$	$-105.7$	69.5	0.18
<i>trans</i> - $\text{N}_2\text{F}_2$	$-172$	$-111.4$	82.0	0.00

<sup>93</sup> F. H. JOHNSON and C. B. COLBURN, *J. Am. Chem. Soc.* **83**, 3043-7 (1961).

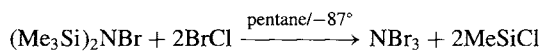
<sup>94</sup> C. L. BAUMGARDNER and E. L. LAWTON, *Acc. Chem. Res.* **7**, 14-20 (1974).

Several mixed halides and hydrohalides of nitrogen are known but they tend to be unstable, difficult to isolate pure, and of little interest. Examples are<sup>(69)</sup>  $\text{NClF}_2$ ,  $\text{NCl}_2\text{F}$ ,  $\text{NBrF}_2$ ,  $\text{NF}_2\text{H}$ ,  $\text{NCl}_2\text{H}$  and  $\text{NClH}_2$ . The cation  $\text{NH}_2\text{F}_2^+$  has also been prepared as its salts with  $\text{AsF}_6^-$  and  $\text{SbF}_6^-$ .<sup>(95)</sup>

The well known compound  $\text{NCl}_3$  is a dense, volatile, highly explosive liquid (mp  $-40^\circ$ , bp  $+71^\circ$ ,  $d(20^\circ)$   $1.65 \text{ g cm}^{-3}$ ,  $\mu$   $0.6 \text{ D}$ ) with physical properties which often closely resemble those of  $\text{CCl}_4$  (p. 301). It is much less hazardous as a dilute gas and, indeed, is used industrially on a large scale for the bleaching and sterilizing of flour; for this purpose it is prepared by electrolysis of an acidic solution of  $\text{NH}_4\text{Cl}$  at pH 4 and the product gas is swept out of the cell by means of a flow of air for immediate use.  $\text{NCl}_3$  is rapidly hydrolysed by moisture and in alkaline solution can be used to prepare  $\text{ClO}_2$ :



The elusive  $\text{NBr}_3$  was finally prepared as a deep-red, very temperature-sensitive, volatile solid by the low-temperature bromination of bistrimethylsilylbromamine with  $\text{BrCl}$ :

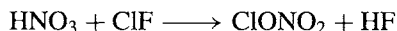
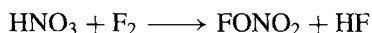


It reacts instantly with  $\text{NH}_3$  in  $\text{CH}_2\text{Cl}_2$  solution at  $-87^\circ$  to give the dark-violet solid  $\text{NBrH}_2$ ; under similar conditions  $\text{I}_2$  yields the red-brown solid  $\text{NBr}_2\text{I}$ . The ligands  $\text{NCl}$  and  $\text{NBr}$  have been characterized in the purple complexes  $[\text{ReF}_5(\text{NCl})]$  (mp  $\sim 80^\circ$ ,  $\text{N}-\text{Cl}$   $156 \text{ pm}$ , angle  $\text{Re}-\text{N}-\text{Cl}$   $177^\circ$ ) and  $[\text{ReF}_5(\text{NBr})]$  (mp  $\sim 140^\circ$ ); The preparation parallels that of  $[\text{ReF}_5(\text{NF})]$  (p. 439), the reagent  $\text{XeF}_2$  being replaced by  $\text{ClF}_3$  and  $\text{BrF}_3$ , respectively.<sup>(92)</sup> The complexes

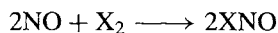
$[\text{VCl}_3(\text{NX})]$  ( $\text{X} = \text{Cl}, \text{Br}, \text{I}$ ) have also been characterized.<sup>(96)</sup>

Pure  $\text{NI}_3$  has not been isolated, but the structure of its well-known extremely shock-sensitive adduct with  $\text{NH}_3$  has been elucidated — a feat of considerable technical virtuosity.<sup>(97)</sup> Unlike the volatile, soluble, molecular solid  $\text{NCl}_3$ , the involatile, insoluble compound  $[\text{NI}_3 \cdot \text{NH}_3]_n$  has a polymeric structure in which tetrahedral  $\text{NI}_4$  units are corner-linked into infinite chains of  $-\text{N}-\text{I}-\text{N}-\text{I}-$  ( $215$  and  $230 \text{ pm}$ ) which in turn are linked into sheets by  $\text{I}-\text{I}$  interactions ( $336 \text{ pm}$ ) in the  $c$ -direction; in addition, one  $\text{I}$  of each  $\text{NI}_4$  unit is also loosely attached to an  $\text{NH}_3$  ( $253 \text{ pm}$ ) that projects into the space between the sheets of tetrahedra. The structure resembles that of the linked  $\text{SiO}_4$  units in chain metasilicates (p. 349). A further interesting feature is the presence of linear or almost linear  $\text{N}-\text{I}-\text{N}$  groupings which suggest the presence of 3-centre, 4-electron bonds (pp. 63, 64) characteristic of polyhalides and xenon halides (pp. 835–8, 897).

Nitrogen forms two series of oxohalides — the nitrosyl halides  $\text{XNO}$  and the nitryl halides  $\text{XNO}_2$ . There are also two halogen nitrates  $\text{FONO}_2$  (bp  $-46^\circ$ ) and  $\text{ClONO}_2$  (bp  $22.3^\circ$ ), but these do not contain  $\text{N}-\text{X}$  bonds and can be considered as highly reactive derivatives of nitric acid, from which they can be prepared by direct halogenation:



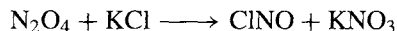
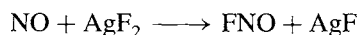
The nitrosyl halides are reactive gases that feature bent molecules; they can be made by direct halogenation of  $\text{NO}$  with  $\text{X}_2$ , though fluorination of  $\text{NO}$  with  $\text{AgF}_2$  has also been used and  $\text{ClNO}$  can be more conveniently made by passing  $\text{N}_2\text{O}_4$  over moist  $\text{KCl}$ :



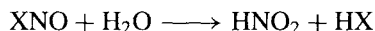
<sup>96</sup> J. STRÄHLE and K. DEHNICKE, *Z. anorg. allg. Chem.* **338**, 287–98 (1965). K. DEHNICKE and W. LIEBETT, *Z. anorg. allg. Chem.* **453**, 9–13 (1979).

<sup>97</sup> J. JANDER, Recent chemistry and structure investigation of  $\text{NI}_3$ ,  $\text{NBr}_3$ ,  $\text{NCl}_3$  and related compounds, *Adv. Inorg. Chem. Radiochem.* **19**, 1–63 (1976).

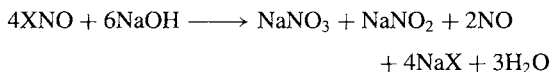
<sup>95</sup> K. O. CHRISTE, *Inorg. Chem.* **14**, 2821–4 (1975).



Some physical properties are in Table 11.5. FNO is colourless, ClNO orange-yellow and BrNO red. The compounds, though generally less reactive than the parent halogens, are nevertheless extremely vigorous reagents. Thus FNO fluorinates many metals ( $n\text{FNO} + \text{M} \rightarrow \text{MF}_n + n\text{NO}$ ) and also reacts with many fluorides to form salt-like adducts such as  $\text{NOAsF}_6$ ,  $\text{NOVF}_6$ , and  $\text{NOBF}_4$ . ClNO acts similarly and has been used as an ionizing solvent to prepare complexes such as  $\text{NOAlCl}_4$ ,  $\text{NOFeCl}_4$ ,  $\text{NOSbCl}_6$ , and  $(\text{NO})_2\text{SnCl}_6$ .<sup>(98)</sup> Aqueous solutions of XNO are particularly potent solvents for metals (like aqua regia,  $\text{HNO}_3/\text{HCl}$ ) since the  $\text{HNO}_2$  formed initially, reacts to give  $\text{HNO}_3$ :



Alkaline solutions contain a similar mixture:



With alcohols, however, the reaction stops at the nitrite stage:



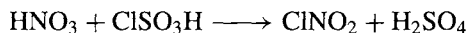
Nitryl fluoride and chloride,  $\text{XNO}_2$ , like their nitrosyl analogues, are reactive gases; they feature planar molecules, analogous to the

**Table 11.5** Some physical properties of  $\text{XNO}^{(a)}$

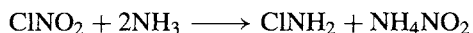
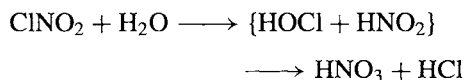
Property	FNO	ClNO	BrNO
MP/°C	-132.5	-59.6	-56
BP/°C	-59.9	-6.4	~0
$\Delta H_f^\circ(298\text{K})/\text{kJ mol}^{-1}$	-66.5	+51.7	+82.2
$\Delta G_f^\circ(298\text{K})/\text{kJ mol}^{-1}$	-51.1	+66.0	+82.4
Angle X-N-O	110°	113°	117°
Distance N-O/pm	113	114	115
Distance N-X/pm	152	198	214
$\mu/\text{D}$	1.81	0.42	--

<sup>(a)</sup>BrNO dissociates reversibly into NO and Br, the extent of dissociation being ~7% at room temperature and 1 atm pressure. A similar reversible dissociation occurs with ClNO at higher temperatures.

isoelectronic nitrate anion,  $\text{NO}_3^-$ . Some physical properties are in Table 11.6.  $\text{FNO}_2$  can be prepared by direct reaction of  $\text{F}_2$  with  $\text{NO}_2$  or  $\text{NaNO}_2$  or by fluorination of  $\text{NO}_2$  using  $\text{CoF}_3$  at 300°.  $\text{ClNO}_2$  can not be made by direct chlorination of  $\text{NO}_2$  but is conveniently synthesized in high yield by reacting anhydrous nitric acid with chlorosulfuric acid at 0°C:



Reactions of  $\text{XNO}_2$  often parallel those of XNO; e.g.  $\text{FNO}_2$  readily fluorinates many metals and reacts with the fluorides of non-metals to give nitryl "salts" such as  $\text{NO}_2\text{BF}_4$ ,  $\text{NO}_2\text{PF}_6$ , etc. Likewise,  $\text{ClNO}_2$  reacts with many chlorides in liquid  $\text{Cl}_2$  to give complexes such as  $\text{NO}_2\text{SbCl}_6$ . Hydrolysis yields aqueous solutions of nitric and hydrochloric acids, whereas ammonolysis in liquid ammonia yields chloramine and ammonium nitrite:



<sup>98</sup> V. GUTMANN (ed.), in *Halogen Chemistry*, Vol. 2, p. 399, Academic Press, London, 1967; and V. GUTMANN, *Coordination Chemistry in Nonaqueous Solutions*, Springer-Verlag, New York, 1968.

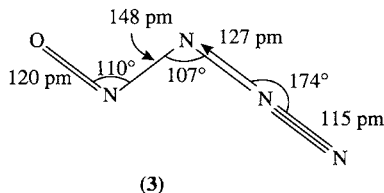
**Table 11.6** Some physical properties of  $\text{XNO}_2$

Property	$\text{FNO}_2$	$\text{ClNO}_2$	Property	$\text{FNO}_2$	$\text{ClNO}_2$
MP/°C	-166	-145	Angle X-N-O	118°	115°
BP/°C	-72.5	-15.9	Distance (N-O)/pm	123	120
$\Delta H_f^\circ(298\text{K})/\text{kJ mol}^{-1}$	-80	+13	Distance (N-X)/pm	135	184
$\Delta G_f^\circ(298\text{K})/\text{kJ mol}^{-1}$	-37.2	+54.4	$\mu/\text{D}$	0.47	0.42



### 11.3.6 Oxides of nitrogen

Nitrogen is unique among the elements in forming no fewer than 8 molecular oxides, 3 of which are paramagnetic and all of which are thermodynamically unstable with respect to decomposition into  $N_2$  and  $O_2$ . In addition there is evidence for fugitive species such as nitryl azide,  $N_3NO_2$ , but this decomposes rapidly below room temperature<sup>(99)</sup> and will not be considered further. Three of the oxides ( $N_2O$ ,  $NO$  and  $NO_2$ ) have been known for over 200 y and were, in fact, amongst the very first gaseous compounds to be isolated and identified (J. Priestley and others in the 1770s). The most recent addition, nitrosyl azide  $N_4O$  (p. 433), was isolated in 1993 as a pale yellow solid whose vibration spectrum at  $-110^\circ$  is consistent with the optimized computed structure (3).<sup>(84)</sup>



The physiological effects of  $N_2O$  (laughing gas, anaesthetic) and  $NO_2$  (acid, corrosive fumes) have been known from the earliest days, and the environmental problems of “ $NO_x$ ” from automobile exhaust fumes and as a component in photochemical smog are well known in all industrial countries.<sup>(100,101)</sup>

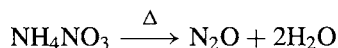
$NO$  is now recognized as a key neuro transmitter in humans and other animals and its biologically triggered synthesis is implicated in cardiovascular pharmacology, hypertension, impotence, immunology and other vital functions.<sup>(102)</sup>  $NO$  and  $NO_2$  are important in

the commercial production of nitric acid (p. 466) and nitrate fertilizers and  $N_2O_4$  has been used extensively as the oxidizer in rocket fuels for space missions (p. 429).

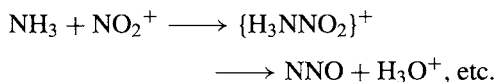
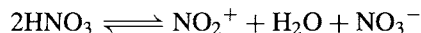
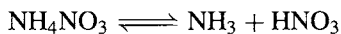
The oxides of nitrogen played an important role in exemplifying Dalton’s law of multiple proportions which led up to the formulation of his atomic theory (1803–8), and they still pose some fascinating problems in bonding theory. Their formulae, molecular structure, and physical appearance are briefly summarized in Table 11.7 and each compound is discussed in turn in the following sections.

#### Nitrous oxide (Dinitrogen monoxide), $N_2O$

Nitrous oxide can be made by the careful thermal decomposition of molten  $NH_4NO_3$  at about  $250^\circ C$ :



Although the reaction has the overall stoichiometry of a dehydration it is more complex than this and involves a mutual redox reaction between  $N^{-III}$  and  $N^V$ . This is at once explicable in terms of the volt-equivalent diagram in Fig. 11.9 which also interprets why  $NO$  and  $N_2$  are formed simultaneously as byproducts. It is probable that the mechanism involves dissociation of  $NH_4NO_3$  into  $NH_3$  and  $HNO_3$ , followed by autoprotolysis of  $HNO_3$  to give  $NO_2^+$ , which is the key intermediate:



Consistent with this  $^{15}NNO$  can be made from  $^{15}NH_4NO_3$ , and  $N^{15}NO$  from  $NH_4^{15}NO_3$ . Alternative preparative routes (Fig. 11.9) are the reduction of aqueous nitrous acid with either hydroxylamine or hydrogen azide:

and D. J. STUEHR, *Chem. and Eng. News*, 26–38, 20 December 1993. C. R. TIGGLE, *Pharmaceutical News* 1 (3), 9–14 (1994).

<sup>99</sup> M. P. DOYLE, J. J. MACIEJKO and S. C. BUSMAN, *J. Am. Chem. Soc.* **95**, 952–3 (1973).

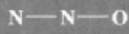

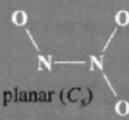
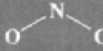
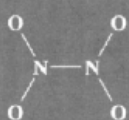
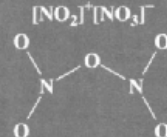
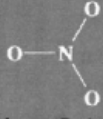
<sup>100</sup> S. D. LEE (ed.), *Nitrogen Oxides and their Effects on Health*, Ann Arbor Publishers, Michigan, 1980, 382 pp.

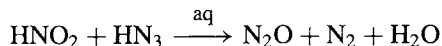
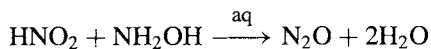
<sup>101</sup> H. BOSCH and F. J. J. JANSSEN, *Catalytic Reduction of Nitrogen Oxides*, Elsevier, Amsterdam, 1988, 164 pp.

<sup>102</sup> K. CULOTTA and D. E. KOSHLAND, *Science* **258**, 1862–5 (1992). J. S. STAMLER, D. J. SINGEL and J. S. LOSCALZO, *Science* **258**, 1898–901 (1992). P. L. FELDMAN, O. W. GRIFFITH



**Table 11.7** The oxides of nitrogen (See also structure 3, p. 443)

Formula	Name	Structure	Description
N <sub>2</sub> O	Dinitrogen monoxide (nitrous oxide)	 linear (C <sub>∞v</sub> )	Colourless gas (bp -88.5°) (cf. isoelectronic CO <sub>2</sub> , NO <sub>2</sub> <sup>+</sup> , N <sub>3</sub> <sup>-</sup> )
NO	(Mono) nitrogen monoxide		Colourless paramagnetic gas (bp -151.8°); liquid and solid are also colourless when pure
N <sub>2</sub> O <sub>3</sub>	Dinitrogen trioxide	 planar (C <sub>s</sub> )	Blue solid (mp -100.7°), dissociates reversibly in gas phase into NO and NO <sub>2</sub>
NO <sub>2</sub>	Nitrogen dioxide	 bent (C <sub>2v</sub> )	Brown paramagnetic gas, dimerizes reversibly to N <sub>2</sub> O <sub>4</sub>
N <sub>2</sub> O <sub>4</sub>	Dinitrogen tetroxide	 planar D <sub>2h</sub>	Colourless liquid (mp -11.2°) dissociates reversibly in gas phase to NO <sub>2</sub>
N <sub>2</sub> O <sub>5</sub>	Dinitrogen pentoxide	 planar C <sub>2v</sub> (~D <sub>2h</sub> )	Colourless ionic solid; sublimes at 32.4° to unstable molecular gas (angle N—O—N ~180°)
NO <sub>3</sub>	Nitrogen trioxide	 planar (D <sub>3h</sub> )	Unstable paramagnetic radical



Thermal decomposition of nitramide, H<sub>2</sub>NNO<sub>2</sub>, or hyponitrous acid H<sub>2</sub>N<sub>2</sub>O<sub>2</sub> (both of which have the empirical formula N<sub>2</sub>O.H<sub>2</sub>O) have also been used. The mechanisms of these and other reactions involving simple inorganic compounds of N have been reviewed.<sup>(103)</sup>

<sup>103</sup> G. STEDMAN, *Adv. Inorg. Chem. Radiochem.* **22**, 114–70 (1979). See also F. T. BONNER and N.-Y. WANG, *Inorg. Chem.* **25**, 1858–62 (1986).

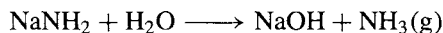
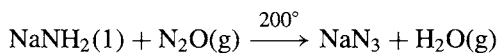
However, though N<sub>2</sub>O can be made in this way it is not to be regarded as the anhydride of hyponitrous acid since H<sub>2</sub>N<sub>2</sub>O<sub>2</sub> is not formed when N<sub>2</sub>O is dissolved in H<sub>2</sub>O (a similar relation exists between CO and formic acid).

Nitrous oxide is a moderately unreactive gas comprised of linear unsymmetrical molecules, as expected for a 16-electron triatomic species (p. 433). The symmetrical structure N—O—N is precluded on the basis of orbital energetics. Some physical properties are in Table 11.8: it will be seen that the N—N and N—O distances are

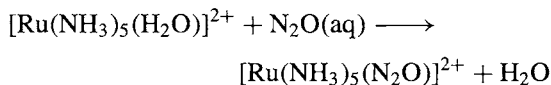
Table 11.8 Some physical properties of N<sub>2</sub>O

MP/°C	-90.86	μ/D	0.166
BP/°C	-88.48	Distance (N-N)/pm	112.6
ΔH <sub>f</sub> <sup>o</sup> (298 K)/kJ mol <sup>-1</sup>	82.0	Distance (N-O)/pm	118.6
ΔG <sub>f</sub> <sup>o</sup> (298 K)/kJ mol <sup>-1</sup>	104.2		

both short and calculations<sup>(104)</sup> give the bond orders as N-N 2.73 and N-O 1.61. N<sub>2</sub>O is thermodynamically unstable and when heated above ~600°C it dissociates by fission of the weaker bond (N<sub>2</sub>O → N<sub>2</sub> +  $\frac{1}{2}$ O<sub>2</sub>). However, the reaction is much more complex than this simple equation might imply and the process involves a "forbidden" singlet-triplet transition in which electron spin is not conserved.<sup>(105)</sup> The activation energy for the process is high (~250 kJ mol<sup>-1</sup>) and at room temperature N<sub>2</sub>O is relatively inert: e.g. it does not react with the halogens, the alkali metals or even ozone. At higher temperatures reactivity increases markedly: H<sub>2</sub> gives N<sub>2</sub> and H<sub>2</sub>O; many other non-metals (and some metals) react to form oxides, and the gas supports combustion. Perhaps its most remarkable reaction is with molten alkali metal amides to yield azides, the reaction with NaNH<sub>2</sub> being the commercial route to NaN<sub>3</sub> and hence all other azides (p. 433):



It is also notable that N<sub>2</sub>O (like N<sub>2</sub> itself) can act as a ligand by displacing H<sub>2</sub>O from the aquo complex [Ru(NH<sub>3</sub>)<sub>5</sub>(H<sub>2</sub>O)]<sup>2+</sup>:<sup>(106)</sup>



The formation constant *K* is 7.0 mol<sup>-1</sup> l for N<sub>2</sub>O and 3.3 × 10<sup>4</sup> mol<sup>-1</sup> l for N<sub>2</sub>.

<sup>104</sup> K. JUG, *J. Am. Chem. Soc.* **100**, 6581–6 (1978).

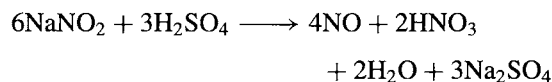
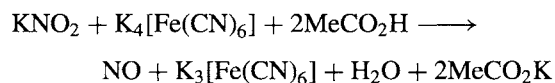
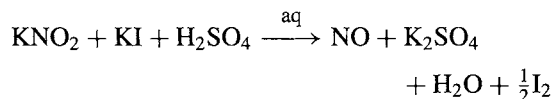
<sup>105</sup> I. R. BEATTIE, Nitrous Oxide, Section 24 in *Mellor's Comprehensive Treatise on Inorganic and Theoretical Chemistry*, Vol. 8, pp. 189–215, Supplement 2, Nitrogen (Part 2), Longmans, London, 1967.

<sup>106</sup> J. N. ARMOR and H. TAUBE, *J. Am. Chem. Soc.* **91**, 6874–6 (1969). A. A. DIAMANTIS and G. J. SPARROW, *J. Chem. Soc., Chem. Commun.*, 819–20 (1970). J. N. ARMOR and H. TAUBE, *J. Chem. Soc., Chem. Commun.*, 287–8 (1971).

Notwithstanding the fascinating reaction chemistry of N<sub>2</sub>O it is salutary to remember that its largest commercial use is as a propellant and aerating agent for "whipped" ice-cream — this depends on its solubility under pressure in vegetable fats coupled with its non-toxicity in small concentrations and its absence of taste. It was also formerly much used as an anaesthetic.

### Nitric oxide (Nitrogen monoxide), NO

Nitric oxide is the simplest thermally stable odd-electron molecule known and, accordingly, its electronic structure and reaction chemistry have been very extensively studied.<sup>(107)</sup> The compound is an intermediate in the production of nitric acid and is prepared industrially by the catalytic oxidation of ammonia (p. 466). On the laboratory scale it can be synthesized from aqueous solution by the mild reduction of acidified nitrites with iodide or ferrocyanide or by the disproportionation of nitrous acid in the presence of dilute sulfuric acid:



The dry gas has been made by direct reduction of a solid mixture of nitrite and nitrate with chromium(III) oxide (3KNO<sub>2</sub> + KNO<sub>3</sub> + Cr<sub>2</sub>O<sub>3</sub> → 4NO + 2K<sub>2</sub>CrO<sub>4</sub>) but is now more conveniently obtained from a cylinder.

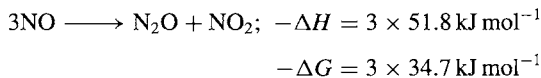
Nitric oxide is a colourless, monomeric, paramagnetic gas with a low mp and bp (Table 11.9). It is thermodynamically unstable and decomposes into its elements at elevated temperatures (1100–1200°C), a fact which militates against its direct synthesis from N<sub>2</sub> and O<sub>2</sub>. At high pressures and moderate temperatures

<sup>107</sup> pp. 323–5 of ref. 69.

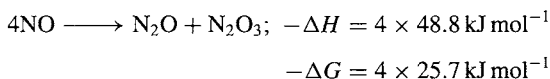
**Table 11.9** Some physical properties of NO

MP/°C	-163.6	$\mu/D$	0.15
BP/°C	-151.8	Distance (N-O)/pm	115
$\Delta H_f^\circ$ (298 K)/ kJ mol <sup>-1</sup>	90.2	Ionization energy/eV	9.23
$\Delta G_f^\circ$ (298 K)/ kJ mol <sup>-1</sup>	86.6	Ionization energy/ kJ mol <sup>-1</sup>	890.6

( $\sim 50^\circ$ ) it rapidly disproportionates:

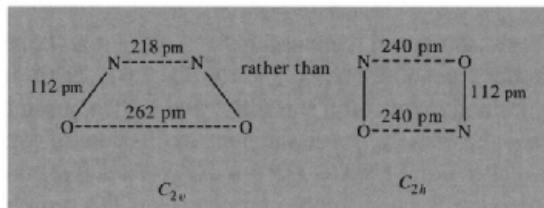


However, when the gas is occluded by zeolites the disproportionation takes a different course:



The molecular orbital description of the bonding in NO is similar to that in N<sub>2</sub> or CO (p. 927) but with an extra electron in one of the  $\pi^*$  antibonding orbitals. This effectively reduces the bond order from 3 to  $\sim 2.5$  and accounts for the fact that the interatomic N-O distance (115 pm) is intermediate between that in the triple-bonded NO<sup>+</sup> (106 pm) and values typical of double-bonded NO species ( $\sim 120$  pm). It also interprets the very low ionization energy of the molecule (9.25 eV, compared with 15.6 eV for N<sub>2</sub>, 14.0 eV for CO, and 12.1 eV for O<sub>2</sub>). Similarly, the notable reluctance of NO to dimerize can be related both to the geometrical distribution of the unpaired electron over the entire molecule and to the fact that dimerization to O=N-N=O leaves the total bond order unchanged ( $2 \times 2.5 = 5$ ). When NO condenses to a liquid, partial dimerization occurs, the *cis*-form being more stable than the *trans*-. The pure liquid is colourless, not blue as sometimes stated: blue samples owe their colour to traces of the intensely coloured N<sub>2</sub>O<sub>3</sub>.<sup>(108)</sup> Crystalline nitric oxide is also colourless (not blue) when pure,<sup>(108)</sup> and X-ray diffraction data are best interpreted in terms of weak association into

dimeric units. It seems probable that the dimers adopt the *cis*-(C<sub>2v</sub>) structure<sup>(109)</sup> rather than the rectangular C<sub>2h</sub> structure which was at one time favoured,<sup>(110)</sup> i.e.:



In either case each dimer has two possible orientations, and random disorder between these accounts for the residual entropy of the crystal (6.3 J mol<sup>-1</sup> of dimer). More recently<sup>(111)</sup> an asymmetric dimer  $\text{O}=\text{N}-\text{O}=\text{N}$  has been

characterized; this forms as a red species when NO is condensed in the presence of polar molecules such as HCl or SO<sub>2</sub>, or Lewis acids such as BX<sub>3</sub>, SiF<sub>4</sub>, SnCl<sub>4</sub> or TiCl<sub>4</sub>. Reaction of NO with either [Pt(PPh<sub>3</sub>)<sub>3</sub>] or [Pt(PPh<sub>3</sub>)<sub>4</sub>] yields [Pt(NO)<sub>2</sub>(PPh<sub>3</sub>)<sub>2</sub>] which has been shown by X-ray diffraction analysis to be an unstable planar *cis*-hyponitrite complex, [(PPh<sub>3</sub>)<sub>2</sub>Pt-ON=NO], with an N=N distance of 121 pm and N-O 132 and 139 pm.<sup>(112)</sup>

The reactivity of NO towards atoms, free radicals, and other paramagnetic species has been much studied, and the chemiluminescent reactions with atomic N and O are important in assaying atomic N (p. 414). NO reacts rapidly with molecular O<sub>2</sub> to give brown NO<sub>2</sub>, and this gas is the normal product of reactions which produce NO if these are carried out in air. The oxidation is unusual in following third-order reaction kinetics and, indeed, is the classic

<sup>109</sup> W. N. LIPSCOMB, F. E. WANG, W. R. MAY and E. L. LIPPERT, *Acta Cryst.* **14**, 1100-01 (1961).

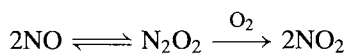
<sup>110</sup> W. J. DULMAGE, E. A. MEYERS and W. N. LIPSCOMB, *Acta Cryst.* **6**, 760-4 (1953).

<sup>111</sup> J. R. OLSEN and J. LAANE, *J. Am. Chem. Soc.* **100**, 6948-55 (1978).

<sup>112</sup> S. BHADURI, B. F. G. JOHNSON, A. PICKARD, P. R. RAITHBY, G. M. SHELDRIK and C. I. ZUCCARO, *J. Chem. Soc., Chem. Commun.*, 354-5 (1977).

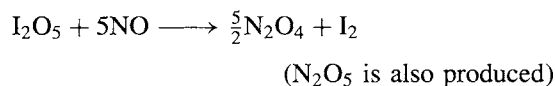
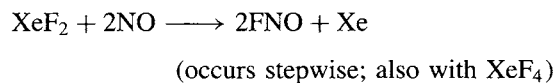
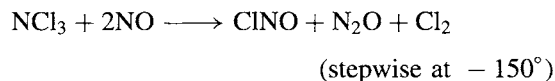
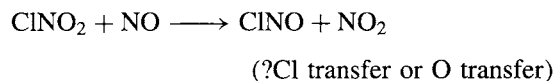
<sup>108</sup> J. MASON, *J. Chem. Educ.* **52**, 445-7 (1975).

example of such a reaction (M. Bodenstein, 1918). The reaction is also unusual in having a negative temperature coefficient, i.e. the rate becomes progressively slower at higher temperatures. For example the rate drops by a factor of 2 between room temperature and 200°. This can be accounted for by postulating that the mechanism involves the initial equilibrium formation of an unstable dimer which then reacts with oxygen:

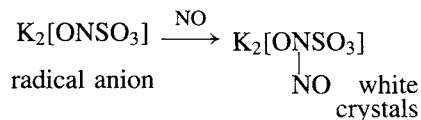
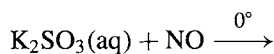
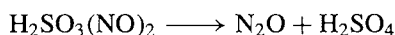
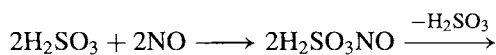
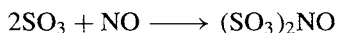
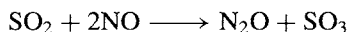


As the equilibrium concentration of  $\text{N}_2\text{O}_2$  decreases rapidly with increase in temperature the decrease in rate is explained. However alternative mechanisms have also been suggested.<sup>(107)</sup>

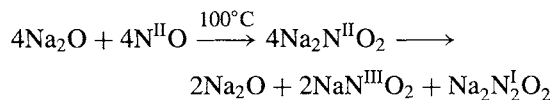
Nitric oxide reacts with the halogens to give  $\text{XNO}$  (p. 441). Some other facile reactions are listed below:



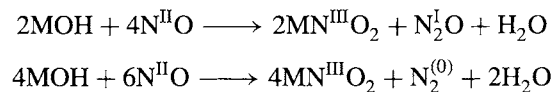
Reactions with sulfides, polysulfides, sulfur oxides and the oxoacids of sulfur are complex and the products depend markedly on reaction conditions (see also p. 745 for blue crystals in chamber acid). Some examples are:



Under alkaline conditions disproportionation reactions predominate. Thus with  $\text{Na}_2\text{O}$  the dioxonitrate(II) first formed, disproportionates into the corresponding nitrite(III) and dioxodinitrate( $N-N$ )(I) :



With alkali metal hydroxides, both  $\text{N}_2\text{O}$  and  $\text{N}_2$  are formed in addition to the nitrite:



*Nitric oxide complexes.* NO readily reacts with many transition metal compounds to give nitrosyl complexes and these are also frequently formed in reactions involving other oxo-nitrogen species. Classic examples are the "brown-ring" complex  $[\text{Fe}(\text{H}_2\text{O})_5\text{NO}]^{2+}$  formed during the qualitative test for nitrates, Roussin's red and black salts (p. 1094), and sodium nitroprusside,  $\text{Na}_2[\text{Fe}(\text{CN})_5\text{NO}]\cdot 2\text{H}_2\text{O}$ . The field has been extensively reviewed<sup>(113-115)</sup> and only the salient features need be summarized here. A variety of preparative routes is available (see Panel). Most nitrosyl complexes are highly coloured — deep reds, browns, purples, or even black. Apart from the intrinsic interest in the structure and bonding of these compounds there

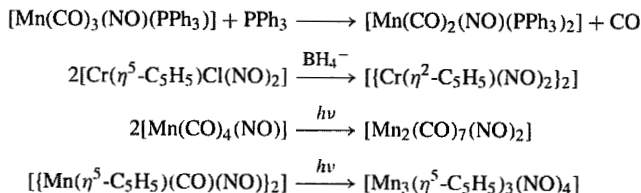
<sup>113</sup> B. F. G. JOHNSON and J. A. McCLEVERTY, *Progr. Inorg. Chem.* **7**, 277-359 (1966). W. P. GRIFFITH, *Adv. Organometallic Chem.* **7**, 211-39 (1968). J. H. ENEMARK and R. D. FELTHAM, *Coord. Chem. Revs.* **13**, 339-406 (1974).

<sup>114</sup> K. G. CAULTON, *Coord. Chem. Revs.* **14**, 317-55 (1975). J. A. McCLEVERTY, *Chem. Rev.* **79**, 53-76 (1979).

<sup>115</sup> R. EISENBERG and C. D. MEYER, *Acc. Chem. Res.* **8**, 26-34 (1975).

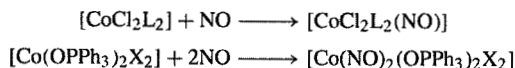
### Synthetic Routes to NO Complexes<sup>(114)</sup>

The coordination chemistry of NO is often compared to that of CO but, whereas carbonyls are frequently prepared by reactions involving CO at high pressures and temperatures, this route is less viable for nitrosyls because of the thermodynamic instability of NO and its propensity to disproportionate or decompose under such conditions (p. 446). Nitrosyl complexes can sometimes be made by transformations involving pre-existing NO complexes, e.g. by ligand replacement, oxidative addition, reductive elimination or condensation reactions (reductive, thermal or photolytic). Typical examples are:



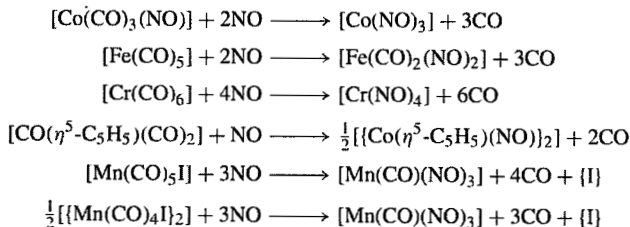
Syntheses which *increase* the number of coordinated NO molecules can be classified into more than a dozen types, of which only the first three use free NO gas.

1. *Addition of NO to coordinatively unsaturated complexes:*

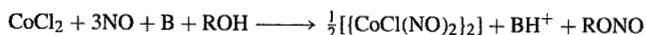


2. *Substitution (ligand replacement)*

Very frequently in these reactions 2NO replace 3CO. Alternatively, 1NO can replace 2CO with simultaneous formation of a metal-metal bond, or 1NO can replace CO + a halogen atom:



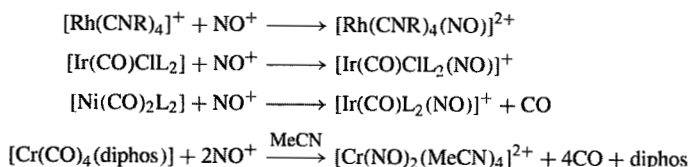
3. *Reductive nitrosylation* (cf.  $\text{MF}_6 + \text{NO} \rightarrow \text{NO}^+\text{MF}_6^-$  for Mo, Tc, Re, Ru, Os, Ir, Pt)



where B is a proton acceptor such as an alkoxide or amine.

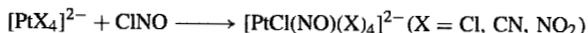
4. *Addition of or substitution by NO<sup>+</sup>*

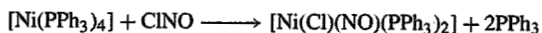
This method uses NOBF<sub>4</sub>, NOPF<sub>6</sub>, or NO[HSO<sub>4</sub>] in MeOH or MeCN, e.g.:



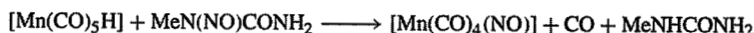
5. *Oxidative addition of XNO*

The reaction may occur with either coordinatively unsaturated or saturated complexes, e.g.:

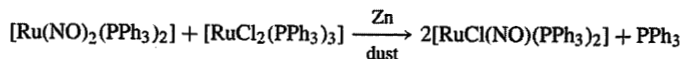




6. Reaction of metal hydride complexes with *N*-nitrosoamides, e.g. *N*-methyl-*N*-nitrosourea:

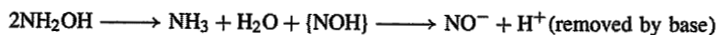


7. Transfer of coordinated NO (especially from dimethylglyoximate complexes)

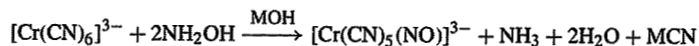


8. Use of  $\text{NH}_2\text{OH}$  in basic solution (especially for cyano complexes)

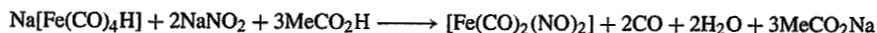
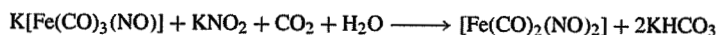
The net transformation can be considered as the replacement of  $\text{CN}^-$  (or  $\text{X}^-$ ) by  $\text{NO}^-$  and the reaction can be formally represented as



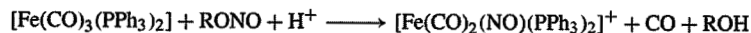
Examples are:



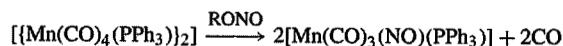
9. Use of acidified nitrites (i.e.  $\text{NO}_2^- + 2\text{H}^+ \longrightarrow \text{NO}^+ + \text{H}_2\text{O}$ ), e.g.:



10. Use of (acidified) nitrites *RONO* (i.e.  $\text{RONO} + \text{H}^+ \rightleftharpoons \text{NO}^+ + \text{ROH}$ ) e.g.:

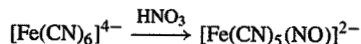
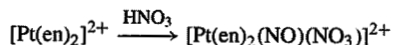


Alternatively in aprotic solvents such as benzene:

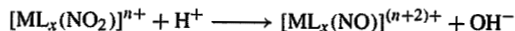


11. Use of concentrated nitric acid (i.e.  $2\text{HNO}_3 \rightleftharpoons \text{NO}^+ + \text{NO}_3^- + \text{H}_2\text{O}$ )

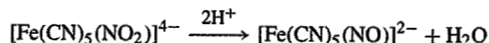
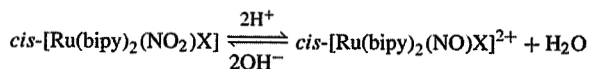
Some of these reactions result, essentially, in the oxidative addition of  $\text{NO}^+\text{NO}_3^-$  to coordinatively unsaturated metal centres whereas in others ligand replacement by  $\text{NO}^+$  occurs — this is a favoured route for producing “nitroprusside”, i.e. nitrosylpentacyanoferrate(II):



12. Oxide ion abstraction from coordinated  $\text{NO}_2$ , i.e.



e.g.



13. Oxygen atom abstraction



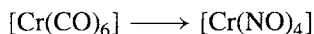
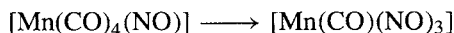
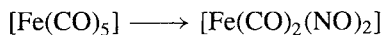
Many variations on these synthetic routes have been devised and the field is still being actively developed. The reactions of NO coordinated to transition metals have been extensively reviewed.<sup>(114)</sup>

is much current interest in their potential use as homogeneous catalysts for a variety of chemical reactions.<sup>(115)</sup> See also p. 443.<sup>(102)</sup>

NO shows a wide variety of coordination geometries (linear, bent, doubly bridging, triply bridging and quadruply bridging — see p. 453) and sometimes adopts more than one mode within the same complex. NO has one more electron than CO and often acts as a 3-electron donor — this is well illustrated by the following isoelectronic series of compounds in which successive replacement of CO by NO is compensated by a matching decrease in atomic number of the metal centre:

[Ni(CO) <sub>4</sub> ] mp -25° (colourless)	[Co(CO) <sub>3</sub> (NO)] -11° (red)	[Fe(CO) <sub>2</sub> (NO) <sub>2</sub> ] +18.4° (deep red)
[Mn(CO)(NO) <sub>3</sub> ] +27° (dark green)	[Cr(NO) <sub>4</sub> ] decomp > rt (red-black)	

For the same reason 3CO can be replaced by 2NO; e.g.:



In these and analogous compounds the M–N–O group is linear or nearly so, the M–N and N–O distances are short, and the N–O infrared stretching modes usually occur in the range 1650–1900 cm<sup>-1</sup>. The bonding in such compounds is sometimes discussed in terms of the preliminary transfer of 1 electron from NO to the metal and the coordination of NO<sup>+</sup> to the reduced metal centre as a “2-electron  $\sigma$  donor, 2-electron  $\pi$  acceptor” analogous to CO (p. 926). This formal scheme, though useful in emphasizing similarities and trends in the coordination behaviour of NO<sup>+</sup>, CO and CN<sup>-</sup>, is unnecessary even for the purpose of “book-keeping” of electrons; it is also misleading in implying an unacceptably large separation of electronic charge in these covalent complexes and in leading to uncomfortably low

oxidation states for many metals. e.g. Cr(–IV) in [Cr(NO)<sub>4</sub>], Mn(–III) in [Mn(CO)(NO)<sub>3</sub>], etc. Many physical techniques (such as ESCA, Mössbauer spectroscopy, etc.) suggest a much more even distribution of charge and there is accordingly a growing trend to consider linear NO complexes in terms of molecular orbital energy level schemes in which an almost neutral NO contributes 3 electrons to the bonding system via orbitals of  $\sigma$  and  $\pi$  symmetry.<sup>(116)</sup> Nitrogen-15 nmr spectroscopy has also been developed as a powerful tool for characterizing and distinguishing between linear and bent nitrosyl complexes and, where appropriate for studying their interconversion.<sup>(117)</sup>

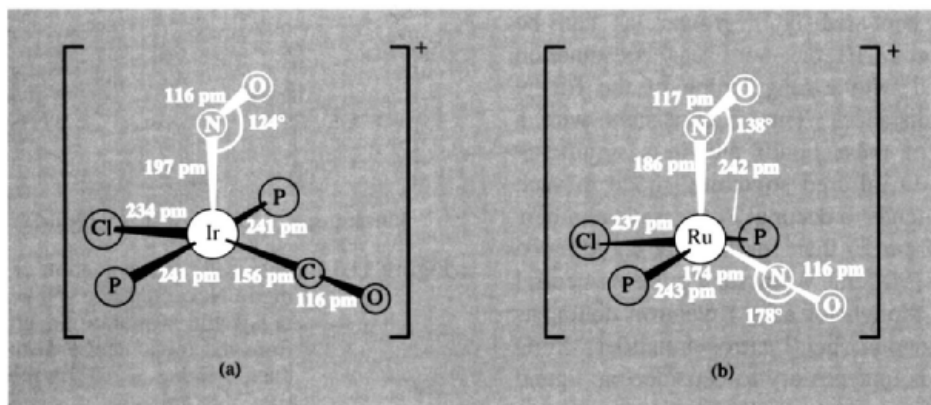
Compounds in which the {M–N–O} group is nominally linear often feature a slightly bent coordination geometry and M–N–O bond angles in the range 165–180° are frequently encountered. However, another group of compounds is known in which the angle M–N–O is close to 120°. The first example, [Co(NO)(S<sub>2</sub>CNMe)<sub>2</sub>], appeared in 1962<sup>(118)</sup> though there were problems in refining the structure, and a second example was found in 1968<sup>(119)</sup> when the cationic complex [Ir(CO)Cl(NO)(PPh<sub>3</sub>)<sub>2</sub>]<sup>+</sup> was found to have a bond angle of 124° (Fig. 11.10); values in the range 120–140° have since been observed in several other compounds (Table 11.10). The related complex [RuCl(NO)<sub>2</sub>(PPh<sub>3</sub>)<sub>2</sub>]<sup>+</sup>, in which the CO ligand has been replaced by a second NO molecule, is interesting in having both

<sup>116</sup> H. W. CHEN and W. L. JOLLY, *Inorg. Chem.* **18**, 2548–51 (1979).

<sup>117</sup> L. K. BELL, D. M. P. MINGOS, D. G. TEW, L. F. LARKWORTHY, B. SANDELL, D. C. POVEY and J. MASON, *J. Chem. Soc., Chem. Commun.*, 125–6 (1983). L. K. BELL, J. MASON, D. M. P. MINGOS, D. G. TEW, *Inorg. Chem.* **22**, 3497–502 (1983). J. MASON, D. M. P. MINGOS, D. SHERMAN and R. W. M. WARDLE, *J. Chem. Soc., Chem. Commun.*, 1223–5 (1984). J. MASON, D. M. P. MINGOS, J. SCHAEFER, D. SHERMAN and E. O. STEJSKAL, *J. Chem. Soc., Chem. Commun.*, 444–6 (1985). J. BULTITUDE, L. F. LARKWORTHY, J. MASON, D. C. POVEY and B. SANDELL, *Inorg. Chem.* **23**, 3629–33 (1984).

<sup>118</sup> P. R. H. ALDERMAN, P. G. OWSTON and J. M. ROWE, *J. Chem. Soc.* 668–73 (1962).

<sup>119</sup> D. J. HODGSON and J. A. IBERS, *Inorg. Chem.* **7**, 2345–52 (1968); see also *J. Am. Chem. Soc.* **90**, 4486–8 (1968).



**Figure 11.10** Complexes containing bent NO groups: (a)  $[\text{Ir}(\text{CO})\text{Cl}(\text{NO})(\text{PPh}_3)_2]^+$ , and (b)  $[\text{RuCl}(\text{NO})_2(\text{PPh}_3)_2]^+$ . This latter complex also has a linearly coordinated NO group. The diagrams show only the coordination geometry around the metal (the phenyl groups being omitted for clarity).

**Table 11.10** Some examples of “linear” and “bent” coordination of nitric oxide

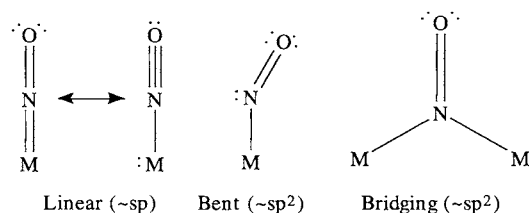
Compound	Angle M–N–O	$\nu$ (N–O)/ $\text{cm}^{-1}$
<i>Linear</i>		
$[\text{Co}(\text{en})_3][\text{Cr}(\text{CN})_5(\text{NO})] \cdot 2\text{H}_2\text{O}$	176°	1630
$[\text{Cr}(\eta^5\text{-C}_5\text{H}_5)\text{Cl}(\text{NO})_2]$	171°, 166°	1823, 1715
$\text{K}_3[\text{Mn}(\text{CN})_5(\text{NO})] \cdot 2\text{H}_2\text{O}$	174°	1700
$[\text{Mn}(\text{CO})_2(\text{NO})(\text{PPh}_3)_2]$	178°	1661
$[\text{Fe}(\text{NO})(\text{mnt})_2]^-$	180°	1867
$[\text{Fe}(\text{NO})(\text{mnt})_2]^{2-}$	165°	1645
$[\text{Fe}(\text{NO})(\text{S}_2\text{CNMe}_2)_2]$	170°	1690
$\text{Na}_2[\text{Fe}(\text{CN})_5(\text{NO})] \cdot 2\text{H}_2\text{O}$	178°	1935
$[\text{Co}(\text{diars})(\text{NO})]^{2+}$	179°	1852
$[\text{Co}(\text{Cl})_2(\text{NO})(\text{PMePh}_2)_2]$	165°	1735, 1630
$\text{Na}_2[\text{Ru}(\text{NO})(\text{NO})_2(\text{OH})] \cdot 2\text{H}_2\text{O}$	180°	1893
$[\text{RuH}(\text{NO})(\text{PPh}_3)_3]$	176°	1645
$[\text{Ru}(\text{diphos})_2(\text{NO})]^+$	174°	1673
$[\text{Os}(\text{CO})_2(\text{NO})(\text{PPh}_3)_2]^+$	177°	1750
$[\text{IrH}(\text{NO})(\text{PPh}_3)_3]^+$	175°	1715
<i>Bent</i>		
$[\text{CoCl}(\text{en})_2(\text{NO})]\text{ClO}_4$	124°	1611
$[\text{Co}(\text{NH}_3)_5\text{NO}]^{2+}$	119°	1610
$[\text{Co}(\text{NO})(\text{S}_2\text{CNMe}_2)_2]^{(a)}$	~135°	1626
$[\text{Rh}(\text{Cl})_2(\text{NO})(\text{PPh}_3)_2]$	125°	1620
$[\text{Ir}(\text{Cl})_2(\text{NO})(\text{PPh}_3)_2]$	123°	1560
$[\text{Ir}(\text{CO})\text{Cl}(\text{NO})(\text{PPh}_3)_2]\text{BF}_4$	124°	1680
$[\text{Ir}(\text{CO})\text{I}(\text{NO})(\text{PPh}_3)_2]\text{BF}_4 \cdot \text{C}_6\text{H}_6$	124°	1720
$[\text{Ir}(\text{CH}_3)\text{I}(\text{NO})(\text{PPh}_3)_2]$	120°	1525
<i>Both</i>		
$[\text{RuCl}(\text{NO})_2(\text{PPh}_3)_2]^+$	178°, 138°	1845, 1687
$[\text{Os}(\text{NO})_2(\text{OH})(\text{PPh}_3)_2]^+$	~180°, 127°	1842, 1632
$[\text{Ir}(\eta^3\text{-C}_3\text{H}_5)(\text{NO})(\text{PPh}_3)_2]^+$ (see text)	~180°, 129°	1763, 1631

mnt = maleonitriedithiolate. diars = 1,2-bis(dimethylarsino)benzene. diphos =  $\text{Ph}_2\text{PCH}_2\text{CH}_2\text{PPh}_2$ .

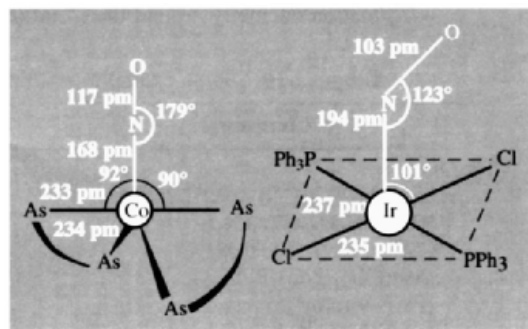
<sup>(a)</sup> Value imprecise because of crystal twinning (see ref. 118).



linear and bent  $\{M-NO\}$  groups: as can be seen in Fig. 11.10 the nonlinear coordination is associated with a lengthening of the Ru–N and N–O distances. This is consistent with a weakening of these bonds and it is significant that the N–O infrared stretching mode in such compounds tends to occur at lower wave numbers ( $1525\text{--}1690\text{ cm}^{-1}$ ) than for linearly coordinated NO ( $1650\text{--}1900\text{ cm}^{-1}$ ). In such systems neutral NO can be thought of as a 1-electron donor, as in the analogous (bent) nitrosyl halides, XNO (p. 442); it is unnecessary to consider the ligand as an  $NO^-$  2-electron donor. The implication is that the other pair of electrons on NO is placed in an essentially non-bonding orbital on N (which is thus approximately described as an  $sp^2$  hybrid) rather than being donated to the metal as in the linear, 3-electron-donor mode (Fig. 11.11). Consistent with this, non-linear coordination is generally observed with the later transition elements in which the low-lying orbitals on the metal are already filled, whereas linear coordination tends to occur with earlier transition elements which can more readily accommodate the larger number of electrons supplied by the ligand. However, the energetics are frequently finely balanced and other factors must also be considered — a good example is supplied by the two “isoelectronic” complexes shown in Fig. 11.12:  $[Co(diars)_2(NO)]^{2+}$  has a linear NO equatorially coordinated to a trigonal bipyramidal cobalt atoms whereas  $[IrCl_2(NO)(PPh_3)_2]$  has a bent NO axially coordinated to a square-pyramidal iridium atom, even though both Co and Ir are in the same group in the periodic table. Indeed, the complex cation  $[Ir(\eta^3-C_3H_5)(NO)(PPh_3)_2]^+$  shows a facile equilibrium (in  $CH_2Cl_2$  or MeCN solutions) between the linear and the bent NO modes of coordination and, with appropriate counter anions, either the linear  $\text{--NO}$  (light brown) or bent  $\text{--NO}$  (red-brown) isomer can be crystallized.<sup>(120)</sup> Some further examples of the two coordination geometries are in Table 11.10.



**Figure 11.11** Schematic representation of the bonding in NO complexes. Note that bending would withdraw an electron-pair from the metal centre to the N atom thus creating a vacant coordination site: this may be a significant factor in the catalytic activity of such complexes.<sup>(115,121)</sup>

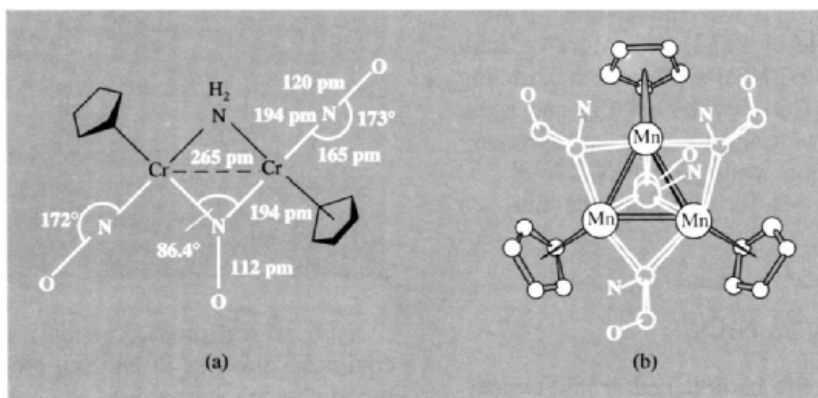


**Figure 11.12** Comparison of the coordination geometries of  $[Co(diars)_2(NO)]^{2+}$  and  $[IrCl_2(NO)(PPh_3)_2]$ ; diars = 1,2-bis(dimethylarsino)benzene.

Like CO, nitric oxide can also act as a bridging ligand between 2 or 3 metals. Examples are the Cr and Mn complexes in Fig. 11.13. In  $[\{Cr(\eta^5-C_5H_5)(NO)(\mu_2-NO)\}_2]$  the linear terminal NO has an infrared band at  $1672\text{ cm}^{-1}$  whereas for the doubly bridging NO the vibration drops to  $1505\text{ cm}^{-1}$ . In both geometries NO can be considered as a 3-electron donor and there is also a Cr–Cr bond thereby completing an 18-electron configuration around each Cr atom. In  $[Mn_3(\eta^5-C_5H_5)_3(\mu_2-NO)_3(\mu_3-NO)]$  the 3 Mn

<sup>121</sup> J. P. COLLIMAN, N. W. HOFFMAN and D. E. MORRIS, *J. Am. Chem. Soc.* **91**, 5659–60 (1969). See also F. BOTTOMLEY in P. S. BRATERMAN, *Reactions of Coordinated Ligands*, Vol 2, Plenum Press, New York, 1989, pp. 115–222.

<sup>120</sup> M. W. SCHOONOVER, E. C. BAKER and R. EISENBERG, *J. Am. Chem. Soc.* **101**, 1880–2 (1979).

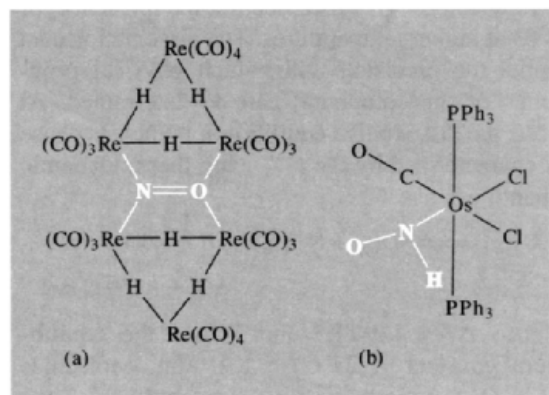


**Figure 11.13** Structures of polynuclear nitrosyl complexes: (a)  $[\text{Cr}(\eta^5\text{-C}_5\text{H}_5)(\text{NO})]_2(\mu_2\text{-NH}_2)(\mu_2\text{-NO})$  showing linear-terminal and doubly bridging NO; and (b)  $[\text{Mn}_3(\eta^5\text{-C}_5\text{H}_5)_3(\mu_2\text{-NO})_3(\mu_3\text{-NO})]$  showing double- and triply-bridging NO; the molecule has virtual  $C_{3v}$  symmetry and the average Mn–Mn distance is 250 pm (range 247–257 pm).

form an equilateral triangle each edge of which is bridged by an NO group ( $\nu$  1543, 1481  $\text{cm}^{-1}$ ); the fourth NO is normal to the  $\text{Mn}_3$  plane and bridges all 3 Mn to form a triangular pyramid; the N–O stretching vibration moves to even lower wave numbers (1328  $\text{cm}^{-1}$ ). Again, each metal is associated with 18 valency electrons if each forms Mn–Mn bonds with its 2 neighbours and each NO is a 3-electron donor.

An unprecedented quadruply bridging mode for NO has been established in the violet cluster anion  $[\{\text{Re}_3(\mu\text{-H})_3(\text{CO})_{10}\}_2(\mu_4\text{-}\eta^2\text{-NO})]^-$  (see Fig. 11.14a).<sup>(122)</sup> The complex was isolated as its  $[\text{NEt}_4]^+$  salt after its formation by reaction of  $\text{NOBF}_4$  with the trinuclear hydrido anion  $[\text{Re}_3(\mu\text{-H})_4(\text{CO})_{10}]^-$ . The rather long N–O distance (132–135 pm) is consistent with its formulation as  $\text{NO}^-$ . Another novel complex is  $[\text{Os}(\text{CO})\text{Cl}_2(\text{HNO})(\text{PPh}_3)_2]$  (Fig. 11.14b) which is formed by direct reaction of HCl with  $[\text{Os}(\text{CO})(\text{NO})(\text{PPh}_3)_2]$ .<sup>(123)</sup> The complex is the first to contain the HNO ligand which is itself thermally unstable as a free molecule. The ligand is *N*-coordinated and coplanar with the

$[\text{Os}(\text{Co})\text{Cl}_2]$  moiety and has H–N 94 pm, N–O 119 pm and angle HNO 99°.



**Figure 11.14** (a) Quadruply bridging NO in the anion  $[\{\text{Re}_3(\mu\text{-H})_3(\text{CO})_{10}\}_2(\mu_4\text{-}\eta^2\text{-NO})]^-$ . (b) The neutral complex  $[\text{Os}(\text{CO})\text{Cl}_2(\text{HNO})(\text{PPh}_3)_2]$ .

In contrast to the numerous complexes of NO which have been prepared and characterized, complexes of the thionitrosyl ligand (NS) are virtually unknown, as is the free ligand itself. The first such complex  $[\text{Mo}(\text{NS})(\text{S}_2\text{CNMe}_2)_3]$  was obtained as orange-red air-stable crystals by treating  $[\text{MoN}(\text{S}_2\text{CNMe}_2)_3]$  with sulfur in

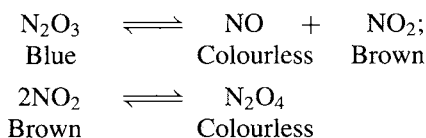
<sup>122</sup> T. BERINGHELLI, G. CIANI, G. D'ALFONSO, H. MOLINARI, A. SIRONI and M. FRENI, *J. Chem. Soc., Chem. Commun.*, 1327–9 (1984).

<sup>123</sup> R. D. WILSON and J. A. IBERS, *Inorg. Chem.* **18**, 336–43 (1979).

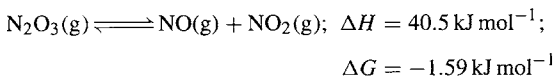
refluxing MeCN, and was shown later to have an M–N–S angle of  $172.1^\circ$ .<sup>(124)</sup> More recently  $[\text{Cr}(\eta^5\text{-C}_5\text{H}_5)(\text{CO})_2(\text{NS})]$  was made by reacting  $\text{Na}[\text{Cr}(\eta^5\text{-C}_5\text{H}_5)(\text{CO})_3]$  with  $\text{S}_3\text{N}_3\text{Cl}_3$  and again the NS group was found to adopt an essentially linear coordination with Cr–N–S  $176.8^\circ$ .<sup>(125)</sup> See also pp. 721–46 for other sulphur–nitrogen species.

### Dinitrogen trioxide, $\text{N}_2\text{O}_3$

Pure  $\text{N}_2\text{O}_3$  can only be obtained at low temperatures because, above its mp ( $-100.1^\circ\text{C}$ ), it dissociates increasingly according to the equilibria:

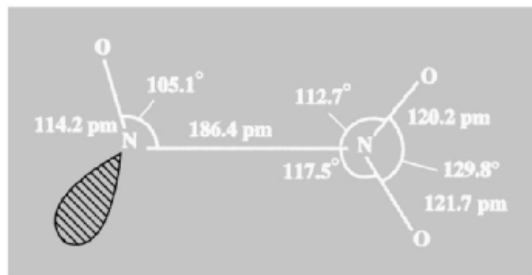


The solid is pale blue; the liquid is an intense blue at low temperatures but the colour fades and becomes greenish due to the presence of  $\text{NO}_2$  at higher temperatures. The dissociation also limits the precision with which physical properties of the compound can be determined. At  $25^\circ\text{C}$  the dissociative equilibrium in the gas phase is characterized by the following thermodynamic quantities:

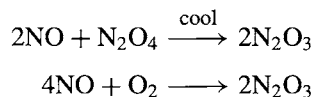


Hence  $\Delta S = 139 \text{ J K}^{-1} \text{ mol}^{-1}$  and the equilibrium constant  $K(25^\circ\text{C}) = 1.91 \text{ atm}$ . Molecules of  $\text{N}_2\text{O}_3$  are planar with  $C_s$  symmetry.

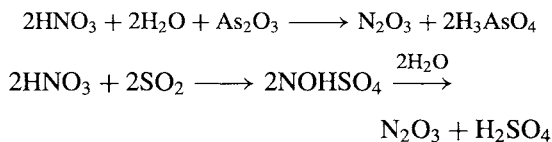
Structural data are in the diagram; these data were obtained from the microwave spectrum of the gas at low temperatures. The long (weak) N–N bond is notable (cf. 145 pm in hydrazine, p. 428). In this  $\text{N}_2\text{O}_3$  resembles  $\text{N}_2\text{O}_4$  (p. 455).



$\text{N}_2\text{O}_3$  is best prepared simply by condensing equimolar amounts of  $\text{NO}$  and  $\text{NO}_2$  at  $-20^\circ\text{C}$  or by adding the appropriate amount of  $\text{O}_2$  to  $\text{NO}$  in order to generate the  $\text{NO}_2$  *in situ*:

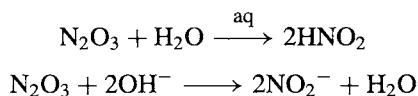


Alternative preparations involve the reduction of 1:1 nitric acid by  $\text{As}_2\text{O}_3$  at  $70^\circ$ , or the reduction of fuming  $\text{HNO}_3$  with  $\text{SO}_2$  followed by hydrolysis:

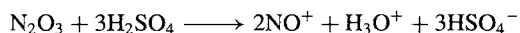


However, these methods do not yield a completely anhydrous product and dehydration can prove difficult.

Studies of the chemical reactivity of  $\text{N}_2\text{O}_3$  are complicated by its extensive dissociation into  $\text{NO}$  and  $\text{NO}_2$  which are themselves reactive species. With water  $\text{N}_2\text{O}_3$  acts as the formal anhydride of nitrous acid and in alkaline solution it is converted essentially quantitatively to nitrite:



Reaction with concentrated acids provides a preparative route to nitrosyl salts such as  $\text{NO}[\text{HSO}_4]$ ,  $\text{NO}[\text{HSeO}_4]$ ,  $\text{NO}[\text{ClO}_4]$ , and  $\text{NO}[\text{BF}_4]$ , e.g.:



<sup>124</sup> J. CHATT and J. R. DILWORTH, *J. Chem. Soc., Chem. Commun.*, 508 (1974); crystal structure by M. B. HURSTHOUSE and M. MONTEVALLI quoted by J. CHATT in *Pure Appl. Chem.* **49**, 815–26 (1977). See also M. W. BISHOP, J. CHATT and J. R. DILWORTH, *J. Chem. Soc., Dalton Trans.*, 1–5 (1979).

<sup>125</sup> T. J. GREENOUGH, B. W. S. KOLTHAMMER, P. LEGZDINS and J. TROTTER, *J. Chem. Soc., Chem. Commun.*, 1036–7 (1978).

### Nitrogen dioxide, NO<sub>2</sub>, and dinitrogen tetroxide, N<sub>2</sub>O<sub>4</sub>

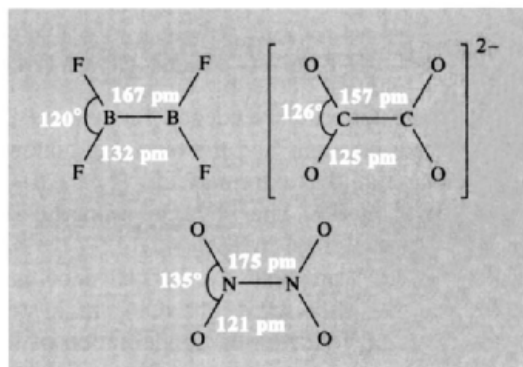
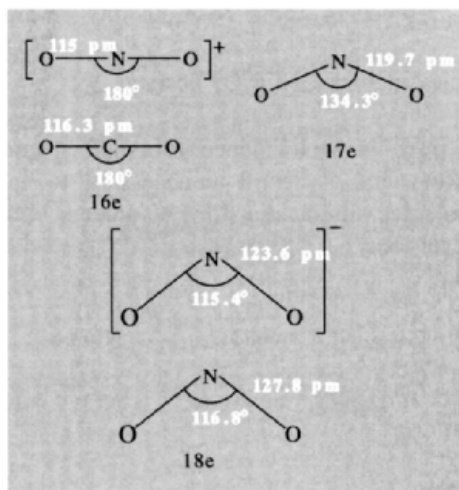
The facile equilibrium  $\text{N}_2\text{O}_4 \rightleftharpoons 2\text{NO}_2$  makes it impossible to study the pure individual compounds in the temperature range  $-10^\circ$  to  $+140^\circ$  though the *molecular* properties of each species in the equilibrium mixture can often be determined. At all temperatures below the freezing point ( $-11.2^\circ$ ) the solid consists entirely of N<sub>2</sub>O<sub>4</sub> molecules but the liquid at this temperature has 0.01% NO<sub>2</sub>. At the bp ( $21.5^\circ\text{C}$ ) the liquid contains 0.1% NO<sub>2</sub> but the gas is more extensively dissociated and contains 15.9% NO<sub>2</sub> at this temperature and 99% NO<sub>2</sub> at  $135^\circ$ . The increasing dissociation can readily be followed by a deepening of the brown colour due to NO<sub>2</sub> and an increase in the paramagnetism; the thermodynamic data for the dissociation of N<sub>2</sub>O<sub>4</sub>(g) at  $25^\circ\text{C}$  are:

$$\Delta H^\circ 57.20 \text{ kJ mol}^{-1}; \Delta G^\circ 4.77 \text{ kJ mol}^{-1};$$

$$\Delta S^\circ 175.7 \text{ J K}^{-1} \text{ mol}^{-1}$$

The unpaired electron in NO<sub>2</sub> appears to be more localized on the N atom than it is in NO and this may explain the ready dimerization. NO<sub>2</sub> is also readily ionized either by loss of an electron (9.91 eV) to give the nitryl cation NO<sub>2</sub><sup>+</sup> (isoelectronic with CO<sub>2</sub>) or by gain of an electron to give the nitrite ion NO<sub>2</sub><sup>-</sup> (isoelectronic with O<sub>3</sub>). These changes are accompanied by a dramatic diminution in bond angle and an increase in N–O distance as the number of valence electrons increases from 16 to 18 (top diagram).

The structure of N<sub>2</sub>O<sub>4</sub> in the gas phase is planar (*D*<sub>2h</sub>) with a remarkably long N–N bond, and these features persist in both the monoclinic crystalline form near the mp and the more stable low-temperature cubic form. Data for the monoclinic form are in the lower diagram<sup>†</sup> together with those for the isoelectronic species B<sub>2</sub>F<sub>4</sub> and



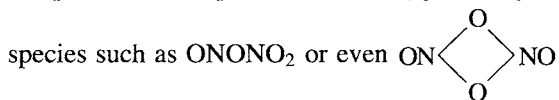
the oxalate ion C<sub>2</sub>O<sub>4</sub><sup>2-</sup>. The trends in bond angles and terminal bond distances are clear but the long central bond in N<sub>2</sub>O<sub>4</sub> is not paralleled in the other 2 molecules where the B–B distance (p. 148) and C–C distance (p. 292) are normal. However, the B–B bond in B<sub>2</sub>Cl<sub>4</sub> is also long (175 pm).

In addition to the normal homolytic dissociation of N<sub>2</sub>O<sub>4</sub> into 2NO<sub>2</sub>, the molecule sometimes reacts as if by heterolytic fission: thus in media of high dielectric constant the compound often reacts as though dissociated according to the equilibrium  $\text{N}_2\text{O}_4 \rightleftharpoons \text{NO}^+ + \text{NO}_3^-$  (see p. 457). This has sometimes been taken to imply

(non-planar) molecule O<sub>2</sub>N–NO<sub>2</sub>, and similar experiments at liquid helium temperature ( $-269^\circ\text{C}$ ) have been interpreted in terms of the unstable oxygen-bridged species ONONO<sub>2</sub>.

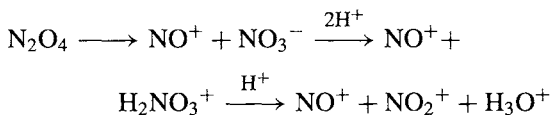
<sup>†</sup> Values for the gas phase are similar but there is a noticeable contraction in the cubic crystalline form (in parentheses). N–N 175 pm (164 pm), N–O 118 pm (117 pm), angle O–N–O 133.7° (126°). In addition, infrared studies on N<sub>2</sub>O<sub>4</sub> isolated in a low-temperature matrix at liquid nitrogen temperature ( $-196^\circ\text{C}$ ) have been interpreted in terms of a twisted

the presence in liquid  $N_2O_4$  of oxygen-bridged

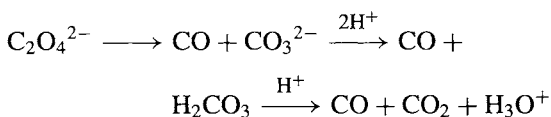


but there is no evidence for such species in solution and it seems unnecessary to invoke them since similar reactions also occur with the oxalate ion:

Thus

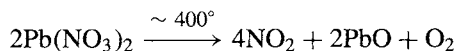


Compare

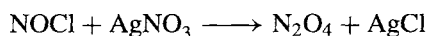
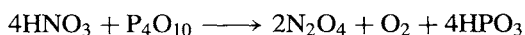
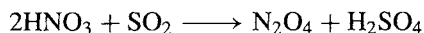


There is no noticeable tendency for pure  $N_2O_4$  to dissociate into ions and the electrical conductivity of the liquid is extremely low ( $1.3 \times 10^{-13} \text{ ohm}^{-1} \text{ cm}^{-1}$  at  $0^\circ$ ). The physical properties of  $N_2O_4$  are summarized in Table 11.11.

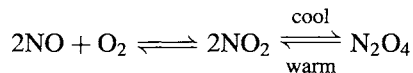
$N_2O_4$  is best prepared by thermal decomposition of rigorously dried  $Pb(NO_3)_2$  in a steel reaction vessel, followed by condensation of the effluent gases and fractional distillation:



Other methods (which are either more tedious or more expensive) include the reaction of nitric acid with  $SO_2$  or  $P_4O_{10}$  and the reaction of nitrosyl chloride with  $AgNO_3$ :

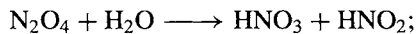


The compound is also formed when  $NO$  reacts with oxygen:

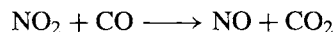
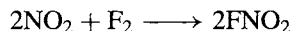
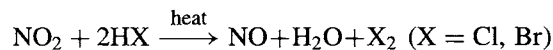


These equilibria limit the temperature range in which reactions of  $N_2O_4$  and  $NO_2$  can be studied since dissociation of  $N_2O_4$  into  $NO_2$  is extensive above room temperature and is virtually complete by  $140^\circ$  whereas decomposition of  $NO_2$  into  $NO$  and  $O_2$  becomes significant above  $150^\circ$  and is complete at about  $600^\circ$ .

$N_2O_4/NO_2$  react with water to form nitric acid (p. 466) and the moist gases are therefore highly corrosive:



The oxidizing action of  $NO_2$  is illustrated by the following:



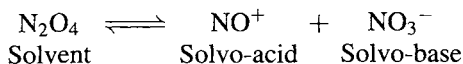
$N_2O_4$  has been extensively studied as a nonaqueous solvent system<sup>(126)</sup> and it is uniquely useful for preparing anhydrous metal nitrates and nitrate complexes (p. 468). Much of the chemistry can be rationalized in terms of a self-ionization equilibrium similar to that observed for

<sup>126</sup> C. C. ADDISON, in G. JANDER, H. SPANAU and C. C. ADDISON (eds.), *Chemistry in Non-aqueous Ionizing Solvents*, Vol. 3, Part 1, pp. 1–78, Pergamon Press, London, 1967. C. C. ADDISON, *Chem. Rev.* **80**, 21–39 (1980).

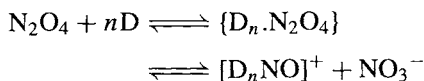
**Table 11.11** Some physical properties of  $N_2O_4$

MP/ $^\circ\text{C}$	−11.2	Density(−195 $^\circ\text{C}$ )/g cm <sup>−3</sup>	1.979 (s)
BP/ $^\circ\text{C}$	+21.15	Density(0 $^\circ\text{C}$ )/g cm <sup>−3</sup>	1.4927 (l)
$\Delta H_f^\circ(298 \text{ K})/\text{kJ mol}^{-1}$	9.16	$\eta(0^\circ\text{C})/\text{poise}$	0.527
$\Delta G_f^\circ(298 \text{ K})/\text{kJ mol}^{-1}$	97.83	$\kappa(0^\circ\text{C})/\text{ohm}^{-1} \text{ cm}^{-1}$	$1.3 \times 10^{-13}$
$S^\circ(298 \text{ K})/\text{J K}^{-1} \text{ mol}^{-1}$	304.2	Dielectric constant $\epsilon$	2.42

liquid ammonia (p. 425):

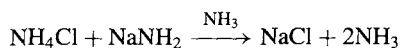
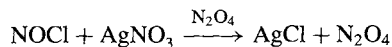


As noted above, there is no physical evidence for this equilibrium in pure  $\text{N}_2\text{O}_4$ , but the electrical conductivity is considerably enhanced when the liquid is mixed with a solvent of high dielectric constant such as nitromethane ( $\epsilon \approx 37$ ), or with donor solvents (D) such as  $\text{MeCO}_2\text{Et}$ ,  $\text{Et}_2\text{O}$ ,  $\text{Me}_2\text{SO}$ , or  $\text{Et}_2\text{NNO}$  (diethylnitrosamine):

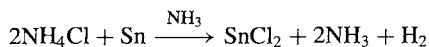
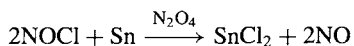


Typical solvent system reactions are summarized below together with the analogous reactions from the liquid ammonia solvent system:

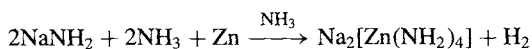
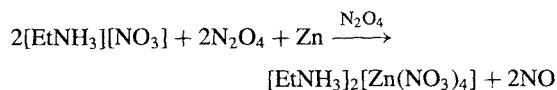
“Neutralization”



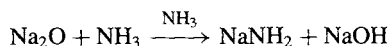
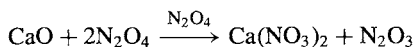
“Acid”



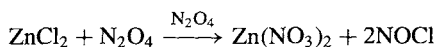
“Base/amphoterism”



“Solvolysis”



Similarly :

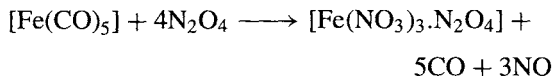
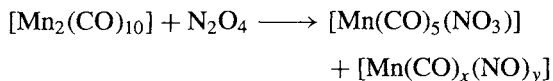


Such reactions provide an excellent route to anhydrous metal nitrates, particularly when metal bromides or iodides are used, since then the nitrosyl halide decomposes and this prevents the possible

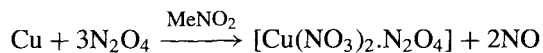
formation of nitrosyl compounds, e.g.:



Many carbonyls react similarly, e.g.:



Solvates are frequently formed in these various reactions, e.g.:



Some of these may contain undissociated solvent molecules  $\text{N}_2\text{O}_4$  but structural studies have revealed that often such “solvates” are actually nitrosonium nitrate-complexes. For example it has been shown<sup>(127)</sup> that  $[\text{Sc}(\text{NO}_3)_3 \cdot 2\text{N}_2\text{O}_4]$  is, in fact,  $[\text{NO}]_2^+[\text{Sc}(\text{NO}_3)_5]^{2-}$ . Similarly, X-ray crystallography revealed<sup>(128)</sup> that  $[\text{Fe}(\text{NO}_3)_3 \cdot 1\frac{1}{2}\text{N}_2\text{O}_4]$  is  $[\text{NO}]^+[\text{Fe}(\text{NO}_3)_4]^{2-}[\text{NO}_3]^-$ , in which there is a fairly close approach of 3  $\text{NO}^+$  groups to the “uncoordinated” nitrate ion to give a structural unit of stoichiometry  $[\text{N}_4\text{O}_6]^{2+}$  (see also p. 472).

In contrast to the wealth of reactions in which  $\text{N}_2\text{O}_4$  tends to behave as  $\text{NO}^+\text{NO}_3^-$ , there is no evidence for reactions based on the alternative heterolytic dissociation  $\text{NO}_2^+\text{NO}_2^-$ .<sup>(129)</sup> Earlier claims<sup>(129a)</sup> to have identified  $\text{BF}_3$  adducts such as  $[\text{NO}_2]^+[\text{ON}(\text{OBF}_3)]^-$  have been shown to be incorrect and the predominant products of the reaction of  $\text{BF}_3$  with  $\text{N}_2\text{O}_4$  (and also with  $\text{N}_2\text{O}_3$  and with  $\text{N}_2\text{O}_5$ ) are, in fact,  $\text{NO}^+\text{BF}_4^-$  and  $\text{NO}_2^+\text{BF}_4^-$ .<sup>(129b)</sup> This latter compound had

<sup>127</sup> C. C. ADDISON, A. J. GREENWOOD, M. J. HALEY and N. LOGAN, *J. Chem. Soc., Chem. Commun.*, 580–1 (1978).

<sup>128</sup> L. J. BLACKWELL, E. K. NUNN and S. C. WALLWORK, *J. Chem. Soc., Dalton Trans.*, 2068–72 (1975).

<sup>129</sup> C. C. ADDISON, S. ARROWSMITH, M. F. A. DOVE, B. F. G. JOHNSON, N. LOGAN and S. A. WOOD, *Polyhedron* **15**, 781–4 (1996).

<sup>129a</sup> R. W. SPRAGUE, A. B. GARRETT and H. H. SISLER, *J. Am. Chem. Soc.* **82**, 1059–64 (1960).

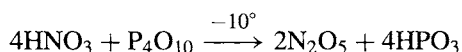
<sup>129b</sup> J. C. EVANS, H. W. RINN, S. J. KUHN and G. A. OLAH, *Inorg. Chem.* **3**, 857–61 (1964).

earlier (1956) been introduced by G. A. Olah as a powerful, stable nitrating agent in organic chemistry and it has been widely used since then.<sup>(130)</sup>

N<sub>2</sub>O<sub>4</sub> has also been used extensively as a hypogolic oxidizer for hydrazine-based fuels in spacecraft. For example, the Apollo manned lunar landing modules (1969–72) used 5.0 tonnes of liquid N<sub>2</sub>O<sub>4</sub> during descent to the lunar surface and 1.5 tonnes during the return ascent, the fuel being a 1:1 mixture of MeNHNH<sub>2</sub> and Me<sub>2</sub>NNH<sub>2</sub>.

### Dinitrogen pentoxide, N<sub>2</sub>O<sub>5</sub>, and nitrogen trioxide, NO<sub>3</sub>

N<sub>2</sub>O<sub>5</sub> is the anhydride of nitric acid and is obtained as a highly reactive deliquescent, light-sensitive, colourless, crystalline solid by carefully dehydrating the concentrated acid with P<sub>4</sub>O<sub>10</sub> at low temperatures:



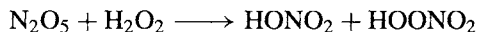
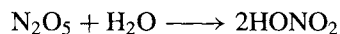
The solid has a vapour pressure of 100 mmHg at 7.5°C and sublimes (1 atm) at 32.4°C, but is thermally unstable both as a solid and as a gas above room temperature. Thermodynamic data at 25°C are:

	$\Delta H_f^\circ/\text{kJ mol}^{-1}$	$\Delta G_f^\circ/\text{kJ mol}^{-1}$	$S^\circ/\text{J K}^{-1} \text{ mol}^{-1}$
N <sub>2</sub> O <sub>5</sub> (cryst)	-43.1	113.8	178.2
N <sub>2</sub> O <sub>5</sub> (g)	11.3	115.1	355.6

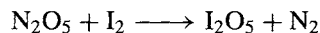
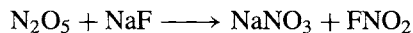
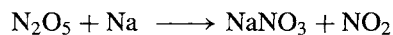
X-ray diffraction studies show that solid N<sub>2</sub>O<sub>5</sub> consists of an ionic array of linear NO<sub>2</sub><sup>+</sup> (N–O 115.4 pm) and planar NO<sub>3</sub><sup>−</sup> (N–O 124 pm). In the gas phase and in solution (CCl<sub>4</sub>, CHCl<sub>3</sub>, OPCl<sub>3</sub>) the compound is molecular; the structure is not well established but may be O<sub>2</sub>N–O–NO<sub>2</sub> with a central N–O–N angle close to 180°. The molecular form can also be obtained in the solid phase by rapidly quenching the gas to −180°, but it rapidly reverts to the more stable ionic form

on being warmed to −70°. [cf. ionic and covalent forms of BF<sub>3</sub>·2H<sub>2</sub>O (p. 198), AlCl<sub>3</sub> (p. 234), PCl<sub>5</sub> (p. 498), etc.]

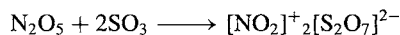
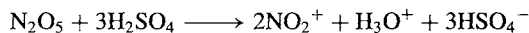
N<sub>2</sub>O<sub>5</sub> is readily hydrated to nitric acid and reacts with H<sub>2</sub>O<sub>2</sub> to give pernitric acid as a coproduct:



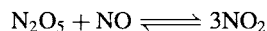
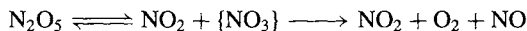
It reacts violently as an oxidizing agent towards many metals, non-metals and organic substances, e.g.:



Like N<sub>2</sub>O<sub>4</sub> (p. 457) it dissociates ionically in strong anhydrous acids such as HNO<sub>3</sub>, H<sub>3</sub>PO<sub>4</sub>, H<sub>2</sub>SO<sub>4</sub>, HSO<sub>3</sub>F and HClO<sub>4</sub>, and this affords a convenient source of nitronium ions and hence a route to nitronium salts, e.g.:



In the gas phase, N<sub>2</sub>O<sub>5</sub> decomposes according to a first-order rate law which can be explained by a dissociative equilibrium followed by rapid reaction according to the scheme



The fugitive, paramagnetic species {NO<sub>3</sub>} is also implicated in several other gas-phase reactions involving the oxides of nitrogen and, in the N<sub>2</sub>O<sub>5</sub>-catalysed decomposition of ozone, its concentration is sufficiently high for its absorption spectrum to be recorded, thereby establishing its integrity as an independent chemical species. Such reactions are the subject of considerable current interest for environmental reasons. NO<sub>3</sub> probably has a symmetrical planar structure (like NO<sub>3</sub><sup>−</sup>) but it has not been isolated as a pure compound.

<sup>130</sup> G. A. OLAH, R. MALHOTRA and S. C. NARANG, *Nitration: Methods and Mechanisms* VCH Publishers, New York, 1989.

### 11.3.7 Oxoacids, oxoanions and oxoacid salts of nitrogen

Nitrogen forms numerous oxoacids, though several are unstable in the free state and are known only in aqueous solution or as their salts. The principal species are summarized in Table 11.12; of these by far the most stable is nitric acid and this compound, together with

its salts the nitrates, are major products of the chemical industry (p. 466).

#### Hyponitrous acid and hyponitrites<sup>(131)</sup>

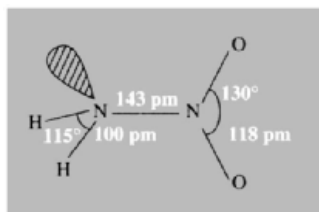
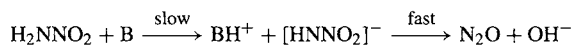
Hyponitrous acid crystallizes from ether solutions as colourless crystals which readily decompose

<sup>131</sup> M. N. HUGHES, *Q. Rev.* **22**, 1–13 (1968).

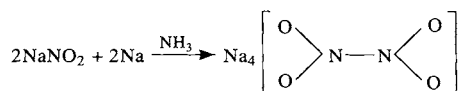
**Table 11.12** Oxoacids of nitrogen and related species

Formula	Name	Remarks
H <sub>2</sub> N <sub>2</sub> O <sub>2</sub>	Hyponitrous acid	Weak acid HON=NOH, isomeric with nitramide, H <sub>2</sub> N–NO <sub>2</sub> ; <sup>(a)</sup> salts are known (p. 460)
{HNO}	Nitroxyl	Reactive intermediate (p. 461), salts are known (see also p. 453).
H <sub>2</sub> N <sub>2</sub> O <sub>3</sub>	Hyponitric acid [trioxodinitric(II) acid]	Known in solution and as salts, e.g. Angeli's salt Na <sub>2</sub> [ON=NO <sub>2</sub> ] (p. 460)
H <sub>4</sub> N <sub>2</sub> O <sub>4</sub>	Nitroxylic (hydronitrous) acid	Explosive; sodium salt known Na <sub>4</sub> [O <sub>2</sub> NNO <sub>2</sub> ] <sup>(b)</sup>
HNO <sub>2</sub>	Nitrous acid	Unstable weak acid, HONO (p. 461); stable salts (nitrites) are known
HOONO	Peroxonitrous acid	Unstable, isomeric with nitric acid; some salts are more stable <sup>(c)</sup>
HNO <sub>3</sub>	Nitric acid	Stable strong acid HONO <sub>2</sub> ; many stable salts (nitrates) are known (p. 465)
HNO <sub>4</sub>	Peroxonitric acid	Unstable, explosive crystals, HOONO <sub>2</sub> ; no solid salts known. (For "orthonitrates", NO <sub>4</sub> <sup>3-</sup> , i.e. salts of the unknown orthonitric acid H <sub>3</sub> NO <sub>4</sub> , see p. 471–2)

<sup>(a)</sup>The structure of nitramide is as shown, the dihedral angle between NH<sub>2</sub> and NNO<sub>2</sub> is 52°. Nitramide is a weak acid pK<sub>1</sub> 6.6 (K<sub>1</sub> 2.6 × 10<sup>-7</sup>) and it decomposes into N<sub>2</sub>O and H<sub>2</sub>O by a base-catalysed mechanism:



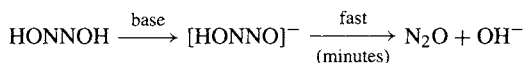
<sup>(b)</sup>Sodium nitroxylate can be prepared as a yellow solid by reduction of sodium nitrite with Na/NH<sub>3</sub>(liq.):



<sup>(c)</sup>Peroxonitrous acid is formed as an unstable intermediate during the oxidation of acidified aqueous solutions of nitrites to nitrates using H<sub>2</sub>O<sub>2</sub>; such solutions are orange-red and are more highly oxidizing than either H<sub>2</sub>O<sub>2</sub> or HNO<sub>3</sub> alone (e.g. they liberate Br<sub>2</sub> from Br<sup>-</sup>). Alkaline solutions are more stable but the yellow peroxonitrites M[OONO] have not been isolated pure. The chemistry of peroxonitrites has recently been reviewed J. O. EDWARDS and R. C. PLUMB, in K. D. KARLIN (ed). *Progr. Inorg. Chem.* **41**, 599–635 (1994).

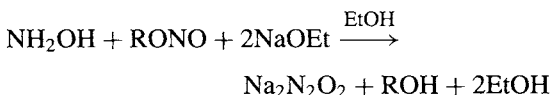
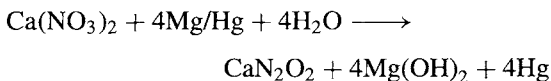
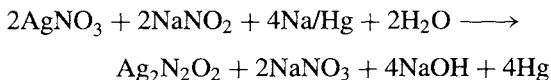
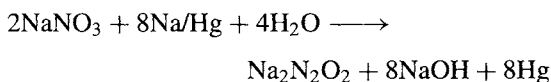


(explosively when heated). Its structure has not been determined but the molecular weight indicates a double formula  $\text{H}_2\text{N}_2\text{O}_2$ , i.e.  $\text{HON}=\text{NOH}$ ; consistent with this the compound yields  $\text{N}_2\text{O}$  when decomposed by  $\text{H}_2\text{SO}_4$ , and hydrazine when reduced. The free acid is obtained by treating  $\text{Ag}_2\text{N}_2\text{O}_2$  with anhydrous  $\text{HCl}$  in ethereal solution. It is a weak dibasic acid:  $\text{p}K_1$  6.9,  $\text{p}K_2$  11.6. Aqueous solutions are unstable between pH 4–14 due to base catalysed decomposition via the hydrogen-hyponitrite ion:



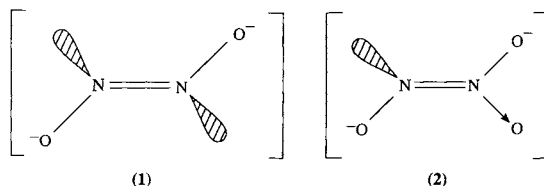
At higher acidities (lower pH) decomposition is slower ( $t_{1/2}$  days or weeks) and the pathways are more complex. The stoichiometry, kinetics and mechanisms of several other reactions of  $\text{H}_2\text{N}_2\text{O}_2$  with, for example,  $\text{NO}$  and with  $\text{HNO}_2$  have also been studied.<sup>(132)</sup>

Hyponitrites can be prepared in variable (low) yields by several routes of which the commonest are reduction of aqueous nitrite solutions using sodium (or magnesium) amalgam, and condensation of organic nitrites with hydroxylamine in  $\text{NaOEt}/\text{EtOH}$ :

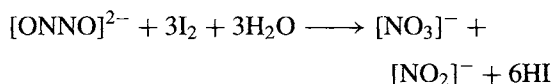


Vibrational spectroscopy indicates that the hyponitrite ion has the *trans*- ( $C_{2h}$ ) configuration (1) in the above salts.

As implied by the preparative methods employed, hyponitrites are usually stable towards

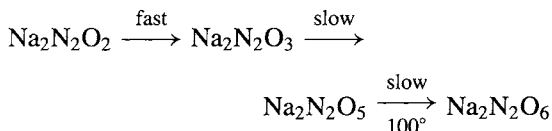


reducing agents though under some conditions they can be reduced (p. 434). More frequently they themselves act as reducing agents and are thereby oxidized, e.g. the analytically useful reaction with iodine:



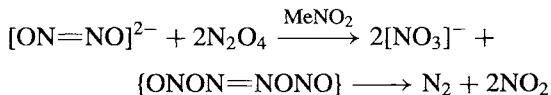
There is also considerable current environmental interest in hyponitrite oxidation because it is implicated in the oxidation of ammonia to nitrite, an important step in the nitrogen cycle (p. 410). Specifically, it seems likely that the oxidation proceeds from ammonia through hydroxylamine and hyponitrous acid to nitrite (or  $\text{N}_2\text{O}$ ).

With liquid  $\text{N}_2\text{O}_4$  stepwise oxidation of hyponitrites occurs to give  $\text{Na}_2\text{N}_2\text{O}_x$  ( $x = 3-6$ ):



Angeli's salt  $\text{Na}_2\text{N}_2\text{O}_3$  has been shown by vibration spectroscopy to contain the trioxodinitrate(II) anion structure (2). Its decomposition and reactions in aqueous solutions have been extensively studied by  $^{15}\text{N}$  nmr spectroscopy and other techniques.<sup>(133)</sup>

In contrast to the stepwise oxidation of sodium hyponitrite in liquid  $\text{N}_2\text{O}_4$ , the oxidation goes rapidly to the nitrate ion in an inert solvent of high dielectric constant such as nitromethane:



<sup>132</sup> M. N. HUGHES *et al.*, *Inorg. Chem.* **24**, 1934–5 (1985); *J. Chem. Soc., Dalton Trans.*, 527–32 and 533–7 (1989).

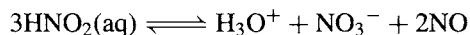
<sup>133</sup> M. J. AKHTAR, C. A. LUTZ and F. T. BONNER, *Inorg. Chem.* **18**, 2369–75 (1979). F. T. BONNER, H. DEGANI and M. J. AKHTAR, *J. Am. Chem. Soc.* **103**, 3739–42 (1981). D. A. BAZYLINSKI and T. C. HOLLOCHER, *Inorg. Chem.* **24**, 4285–8 (1985).

More recently it has been found that the hyponitrite ion can act as a bidentate ligand in either a bridging or a chelating mode. Thus, the controversy about the nature of the black and red isomers of nitrosyl pentammine cobalt(III) complexes has been resolved by X-ray crystallographic studies which show that the black chloride  $[\text{Co}(\text{NH}_3)_5\text{NO}]\text{Cl}_2$  contains a mononuclear octahedral  $\text{Co}^{\text{III}}$  cation with a linear  $\text{Co}-\text{N}-\text{O}$  group whereas the red isomer, in the form of a mixed nitrate-bromide, is dinuclear with a bridging *cis*-hyponitrite- $(\text{N},\text{O})$  group as shown in Fig. 11.15.<sup>(134)</sup> The *cis*-configuration is probably adopted for steric reasons since this is the only configuration that allows the bridging of two  $\{\text{Co}(\text{NH}_3)_5\}$  groups by an ONNO group without steric interference between them. The *cis*-chelating mode  $(\text{O},\text{O})$  was found in the air-sensitive yellow crystalline complex  $[\text{Pt}(\text{O}_2\text{N}_2)(\text{PPh}_3)_2]$  which has already been mentioned on p. 446. The presence of the *cis*-configuration in this complex invites speculation as to whether *cis*- $[\text{ON}-\text{NO}]^{2-}$  can also exist in simple hyponitrites. Likely candidates appear to be the "alkali metal nitrosyls"  $\text{MNO}$  prepared by the action of  $\text{NO}$  on  $\text{Na}/\text{NH}_3$ ; infrared data suggest they are not  $\text{M}^+[\text{NO}]^-$  and might indeed contain the *cis*-hyponitrite ion. They would therefore not be salts

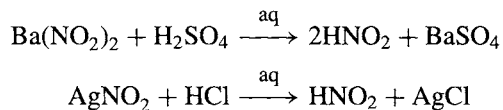
of nitroxyl  $\text{HNO}$  which has often been postulated as an intermediate in reactions which give  $\text{N}_2\text{O}$  and which is well known in the gas phase. Nitroxyl can be prepared by the action of atomic  $\text{H}$  or  $\text{HI}$  on  $\text{NO}$  and decomposes to  $\text{N}_2\text{O}$  and  $\text{H}_2\text{O}$ . As expected, the molecule is bent (angle  $\text{H}-\text{N}=\text{O}$   $109^\circ$ ). See also Fig. 11.14(b), p. 453.

### Nitrous acid and nitrites

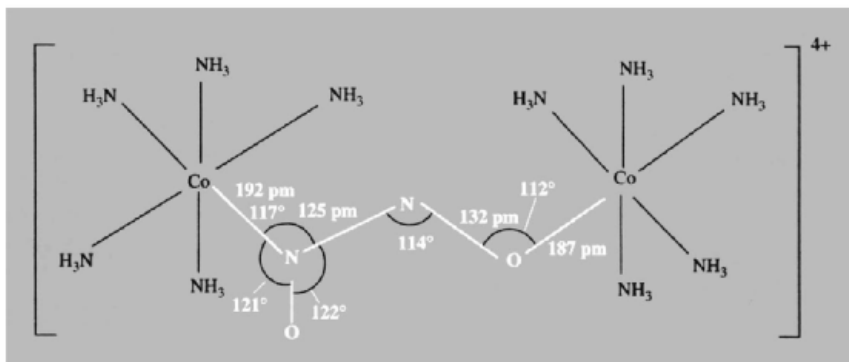
Nitrous acid,  $\text{HNO}_2$ , has not been isolated as a pure compound but it is a well known and important reagent in aqueous solutions and has also been studied as a component in gas-phase equilibria. Solutions of the free acid can readily be obtained by acidification of cooled aqueous nitrite solutions but even at room temperature disproportionation is noticeable:



It is a fairly weak acid with  $\text{p}K_a$  3.35 at  $18^\circ\text{C}$ , i.e. intermediate in strength between acetic (4.75) and chloroacetic (2.85) acids at  $25^\circ$ , and very similar to formic (3.75) and sulfanilic (3.23) acids. Salt-free aqueous solutions can be made by choosing combinations of reagents which give insoluble salts, e.g.:



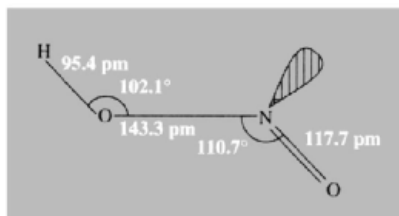
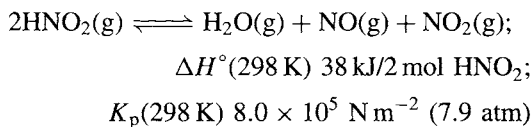
<sup>134</sup> B. F. HOSKINS, F. D. WHILLANS, D. H. DALE and D. C. HODGKIN, *J. Chem. Soc., Chem. Commun.*, 69–70 (1969).



**Figure 11.15** Structure of the dinuclear cation in the red isomer  $[\{\text{Co}(\text{NH}_3)_5\text{NO}\}_2](\text{Br})_{2.5}(\text{NO}_3)_{1.5} \cdot 2\text{H}_2\text{O}$ ; (mean  $\text{Co}-\text{NH}_3$   $194 \pm 2$  pm, mean angle  $90 \pm 4^\circ$ ).

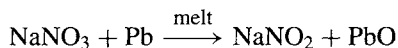
When the presence of salts in solution is unimportant, the more usual procedure is simply to acidify  $\text{NaNO}_2$  with hydrochloric acid below  $0^\circ$ .

In the gas phase, an equilibrium reaction producing  $\text{HNO}_2$  can be established by mixing equimolar amounts of  $\text{H}_2\text{O}$ ,  $\text{NO}$  and  $\text{NO}_2$ :

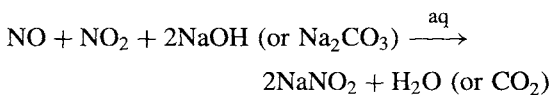


Microwave spectroscopy shows that the gaseous compound is predominantly in the *trans*-planar ( $C_s$ ) configuration with the dimensions shown. The differences between the two N–O distances is notable. Despite the formal single-bond character of the central bond the barrier to rotation is  $45.2 \text{ kJ mol}^{-1}$ . Infrared data suggest that the *trans*-form is  $\sim 2.3 \text{ kJ mol}^{-1}$  more stable ( $\Delta G^\circ$ ) than the *cis*-form at room temperature.

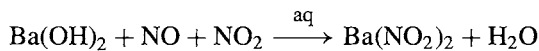
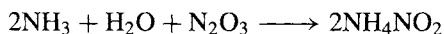
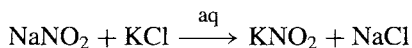
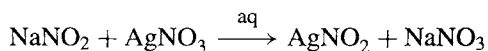
Nitrites are usually obtained by the mild reduction of nitrates, using C, Fe or Pb at moderately elevated temperatures, e.g.:



On the industrial scale, impure  $\text{NaNO}_2$  is made by absorbing “nitrous fumes” in aqueous alkali or carbonate solutions and then recrystallizing the product:

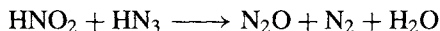
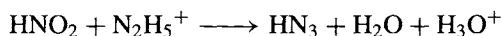


The sparingly soluble  $\text{AgNO}_2$  can be obtained by metathesis, and simple variants yield the other stable nitrites, e.g.:

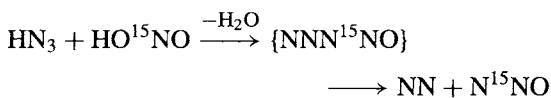


Many stable metal nitrites (Li, Na, K, Cs, Ag,  $\text{Tl}^I$ ,  $\text{NH}_4$ , Ba) contain the bent  $[\text{O}-\text{N}-\text{O}]^-$  anion (p. 413) with N–O in the range 113–123 pm and the angle  $116\text{--}132^\circ$ . Nitrites of less basic metals such as Co(II), Ni(II) and Hg(II) are often highly coloured and are probably essentially covalent assemblages. Solubility (g per 100 g  $\text{H}_2\text{O}$  at  $25^\circ$ ) varies considerably, e.g.  $\text{AgNO}_2$  0.41,  $\text{NaNO}_2$  (hygroscopic) 85.5,  $\text{KNO}_2$  (deliquescent) 314. Thermal stability also varies widely: e.g. the alkali metal nitrites can be fused without decomposition (mp  $\text{NaNO}_2$   $284^\circ$ ,  $\text{KNO}_2$   $441^\circ\text{C}$ ), whereas  $\text{Ba}(\text{NO}_2)_2$  decomposes when heated above  $220^\circ$ ,  $\text{AgNO}_2$  above  $140^\circ$  and  $\text{Hg}(\text{NO}_2)_2$  above  $75^\circ$ . Such trends are a general feature of oxoacid salts (pp. 469, 863, 868).  $\text{NH}_4\text{NO}_2$  can decompose explosively.

The aqueous solution chemistry of nitrous acid and nitrites has been extensively studied. Some reduction potentials involving these species are given in Table 11.4 (p. 434) and these form a useful summary of their redox reactions. Nitrites are quantitatively oxidized to nitrate by permanganate and this reaction is used in titrimetric analysis. Nitrites (and  $\text{HNO}_2$ ) are readily reduced to  $\text{NO}$  and  $\text{N}_2\text{O}$  with  $\text{SO}_2$ , to  $\text{H}_2\text{N}_2\text{O}_2$  with  $\text{Sn}(\text{II})$ , and to  $\text{NH}_3$  with  $\text{H}_2\text{S}$ . Hydrazinium salts yield azides (p. 432) which can then react with further  $\text{HNO}_2$ :

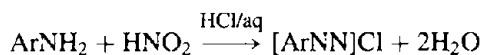


This latter reaction is most unusual in that it simultaneously involves an element (N) in four different oxidation states. Use of  $^{15}\text{N}$ -enriched reagents shows that all the N from  $\text{HNO}_2$  goes quantitatively to the internal N of  $\text{N}_2\text{O}$ .<sup>(135)</sup>

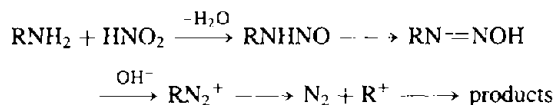


<sup>135</sup> K. CLUSIUS and H. KNOFF, *Chem. Ber.* **89**, 681–5 (1956).

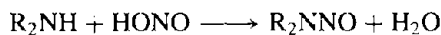
$\text{NaNO}_2$  is mildly toxic (tolerance limit  $\sim 100$  mg/kg body weight per day, i.e. 4–8 g/day for humans).  $\text{NaNO}_2$  (or a precursor such as  $\text{NaNO}_3$ , which is itself harmless) has been much used for curing meat and for treating preserved foods stuffs to prevent bacterial spoilage and consequent poisoning by the (often deadly) toxins produced by *Clostridium botulinum* etc., (normal dietary intake of  $\text{NO}_2^-$  10–15  $\mu\text{g}$  per day).  $\text{NaNO}_2$  is used industrially on a large scale for the synthesis of hydroxylamine (p. 431), and in acid solution for the diazotization of primary aromatic amines:



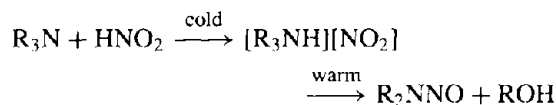
The resulting diazo reagents undergo a wide variety of reactions including those of interest in the manufacture of azo dyes and pharmaceuticals. With primary *aliphatic* amines the course of the reaction is different:  $\text{N}_2$  is quantitatively evolved and alcohols usually result:



The reaction is generally thought to involve carbonium-ion intermediates but several puzzling features remain.<sup>(136)</sup> Secondary aliphatic amines give nitrosamines without evolution of  $\text{N}_2$ :

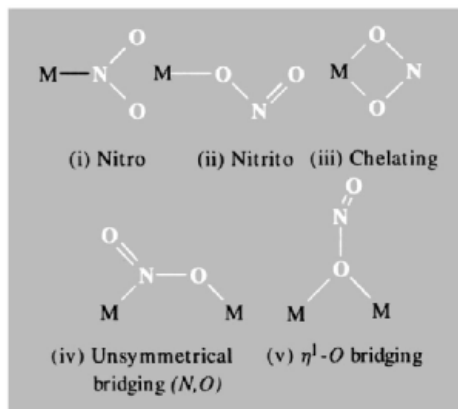


Tertiary aliphatic amines react in the cold to give nitrite salts and these decompose on warming to give nitrosamines and alcohols:



In addition to their general use in synthetic organic chemistry, these various reactions afford the major route for introducing  $^{15}\text{N}$  into organic compounds by use of  $\text{Na}^{15}\text{NO}_2$ .

The nitrite ion,  $\text{NO}_2^-$ , is a versatile ligand and can coordinate in at least five different ways (i)–(v):



Nitro-nitrito isomerism (i), (ii), was discovered by S. M. Jørgensen in 1894–9 and was extensively studied during the classic experiments of A. Werner (p. 912); the isomers usually have quite different colours, e.g.  $[\text{Co}(\text{NH}_3)_5(\text{NO}_2)]^{2+}$ , yellow, and  $[\text{Co}(\text{NH}_3)_5(\text{ONO})]^{2+}$ , red. The nitrito form is usually less stable and tends to isomerize to the nitro form. The change can also be effected by increase in pressure since the nitro form has the higher density. For example application of 20 kbar pressure converts the violet nitrito complex  $[\text{Ni}(\text{en})_2(\text{ONO})_2]$  to the red nitro complex  $[\text{Ni}(\text{en})_2(\text{NO}_2)_2]$  at 126°C, thereby reversing the change from nitro to nitrito which occurs on heating the complex from room temperature at atmospheric pressure.<sup>(137)</sup> An X-ray study of the thermally induced nitrito  $\rightarrow$  nitro isomerization and the photochemically induced nitro  $\rightarrow$  nitrito isomerization of Co(III) complexes has shown that both occur intra-molecularly by rotation of the  $\text{NO}_2$  group in its own plane, probably via a 7-coordinated cobalt intermediate.<sup>(138)</sup> Similarly, the base-catalysed nitrito  $\rightarrow$  nitro isomerization of  $[\text{M}^{\text{III}}(\text{NH}_3)_5(\text{ONO})]^{2+}$  ( $\text{M} = \text{Co}$ ,

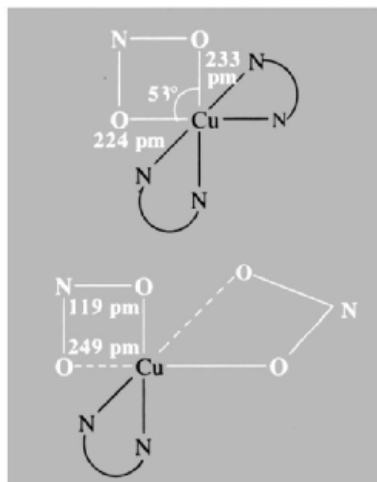
<sup>137</sup> J. R. FERRARO and L. FABBRIZZI, *Inorg. Chim. Acta* **26**, L15–L17 (1978).

<sup>138</sup> I. GRENTHE and E. NORDIN, *Inorg. Chem.* **18**, 1109–16 and 1869–74 (1979).

<sup>136</sup> C. J. COLLINS, *Acc. Chem. Res.* **4**, 315–22 (1971).

Rh, Ir) is intramolecular and occurs without  $^{18}\text{O}$  exchange of the coordinated  $\text{ONO}^-$  with  $\text{H}_2^{18}\text{O}$ ,  $^{18}\text{OH}^-$  or "free"  $\text{N}^{18}\text{O}_2^-$ .<sup>(139)</sup> However, an elegant  $^{17}\text{O}$  nmr study using specifically labelled  $[\text{Co}(\text{NH}_3)_5(^{17}\text{ONO})]^{2+}$  and  $[\text{Co}(\text{NH}_3)_5(\text{ON}^{17}\text{O})]^{2+}$  established that spontaneous intramolecular O-to-O exchange in the nitrite ligand occurs at a rate comparable to that of the spontaneous O-to-N isomerization.<sup>(140)</sup>

A typical value for the N-O distance in nitro complexes is 124 pm whereas in nitrito complexes the terminal N-O (121 pm) is shorter than the internal N-O(M)  $\sim 129$  pm. In the bidentate chelating mode (iii) the 2 M-O distances may be fairly similar as in  $[\text{Cu}(\text{bipy})_2(\text{O}_2\text{N})]\text{NO}_3$  or quite different as in  $[\text{Cu}(\text{bipy})(\text{O}_2\text{N})_2]$ :



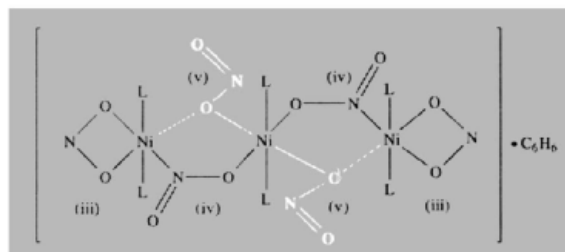
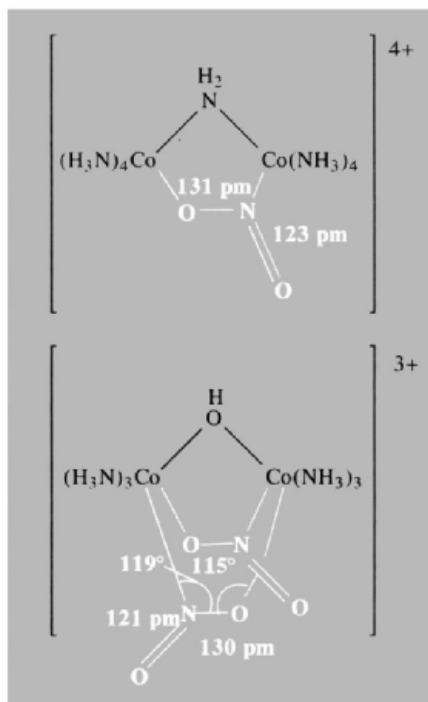
Examples of the unsymmetrical bridging mode (iv) are shown in the top diagram.

The oxygen-bridging mode (v) is less common but occurs together with modes (iii) and (iv) in the following centrosymmetrical trimeric Ni complex and related compounds.<sup>(141)</sup>

<sup>139</sup> W. G. JACKSON, G. A. LAWRENCE, P. A. LAY and A. M. SARGESON, *Inorg. Chem.* **19**, 904-10 (1980).

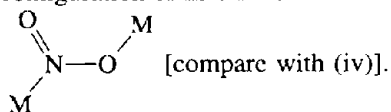
<sup>140</sup> W. G. JACKSON, G. A. LAWRENCE, P. A. LAY and A. M. SARGESON, *J. Chem. Soc., Chem. Commun.*, 70-2 (1982).

<sup>141</sup> D. M. L. GOODGAME, M. A. HITCHMAN, D. F. MARSHAM, P. PHAVANANTHA and D. ROGERS, *Chem. Commun.*, 1383-4 (1969); see also *J. Chem. Soc. A*, 259-64 (1971).



It is possible that a sixth (symmetrical bridging) mode  $\text{M}-\text{O}-\text{N}-\text{O}-\text{M}$  occurs in

some complexes such as  $\text{Rb}_3\text{Ni}(\text{NO}_2)_5$  but this has not definitely been established; an unsymmetrical bridging mode with a *trans*-configuration of metal atoms is also possible, i.e.



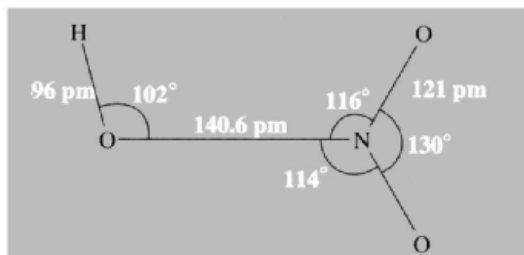
The familiar problem of misleading stoichiometries, and the frequent impossibility of deducing the correct structural formula from the empirical composition is well illustrated by the

recent synthesis of the novel alkali metal oxide nitrites  $\text{Na}_4\text{N}_2\text{O}_5$  (yellow) and  $\text{K}_4\text{N}_2\text{O}_5$  (red).<sup>(142)</sup> These compounds are made by heating powdered mixtures of  $\text{M}_2\text{O}$  and  $\text{MNO}_2$  at  $340^\circ$  for 8 days in a silver crucible and have an anti- $\text{K}_2\text{NiF}_4$  type structure,  $[(\text{NO}_2)_2\text{OM}_4]$ , i.e.  $\text{M}_4\text{O}(\text{NO}_2)_2$ , with N–O 122.1 pm, angle O–N–O  $114.5^\circ$  and octahedrally coordinated  $\text{O}^{2-}$  (i.e.  $\text{OM}_6$  with K–O 260 pm.

### Nitric acid and nitrates

Nitric acid is one of the three major acids of the modern chemical industry and has been known as a corrosive solvent for metals since alchemical times in the thirteenth century.<sup>(143,144)</sup> It is now invariably made by the catalytic oxidation of ammonia under conditions which promote the formation of NO rather than the thermodynamically more favoured products  $\text{N}_2$  or  $\text{N}_2\text{O}$  (p. 423). The NO is then further oxidized to  $\text{NO}_2$  and the gases absorbed in water to yield a concentrated aqueous solution of the acid. The vast scale of production requires the optimization of all the reaction conditions and present-day operations are based on the intricate interaction of fundamental thermodynamics, modern catalyst technology, advanced reactor design, and chemical engineering aspects of process control (see Panel). Production in the USA alone now exceeds 7 million tonnes annually, of which the greater part is used to produce nitrates for fertilizers, explosives and other purposes (see Panel).

Anhydrous  $\text{HNO}_3$  can be obtained by low-pressure distillation of concentrated aqueous nitric acid in the presence of  $\text{P}_4\text{O}_{10}$  or anhydrous  $\text{H}_2\text{SO}_4$  in an all-glass, grease-free apparatus in the dark. The molecule is planar in the gas phase



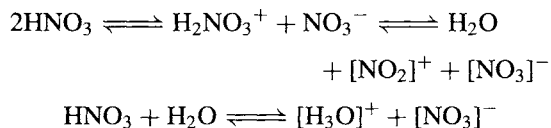
with the dimensions shown (microwave). The difference in N–O distances, the slight but real tilt of the  $\text{NO}_2$  group away from the H atom by  $2^\circ$ , and the absence of free rotation are notable features. The same general structure obtains in the solid state but detailed data are less reliable. Physical properties are shown in Table 11.13. Despite its great thermodynamic stability (with respect to the elements) pure  $\text{HNO}_3$  can only be obtained in the solid state; in the gas and liquid phases the compound decomposes spontaneously to  $\text{NO}_2$  and this occurs more rapidly in daylight (thereby accounting for the brownish colour which develops in the acid on standing):



**Table 11.13** Some physical properties of anhydrous liquid  $\text{HNO}_3$  at  $25^\circ\text{C}$

MP/ $^\circ\text{C}$	−41.6	Vapour pressure/mmHg	57
BP/ $^\circ\text{C}$	82.6	Density/g $\text{cm}^{-3}$	1.504
$\Delta H_f^\circ/\text{kJ mol}^{-1}$	−174.1	$\eta/\text{centipoise}$	7.46
$\Delta G_f^\circ/\text{kJ mol}^{-1}$	−80.8	$\kappa/\text{ohm}^{-1}\text{cm}^{-1}$ ( $20^\circ$ )	$3.72 \times 10^{-2}$
$S^\circ/\text{J K}^{-1}\text{ mol}^{-1}$	155.6	Dielectric constant $\epsilon$ ( $14^\circ$ )	$50 \pm 10$

In addition, the liquid undergoes self-ionic dissociation to a greater extent than any other nominally covalent pure liquid (cf.  $\text{BF}_3 \cdot 2\text{H}_2\text{O}$ , p. 198); initial autoprotolysis is followed by rapid loss of water which can then react with a further molecule of  $\text{HNO}_3$ :



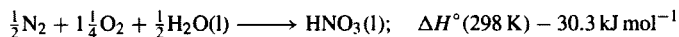
<sup>142</sup> W. MULLER and M. JANSEN, *Z. anorg. allg. Chem.* **610**, 28–32 (1992).

<sup>143</sup> J. W. MELLOR, *A Comprehensive Treatise on Inorganic and Theoretical Chemistry*, Vol. 8, pp. 555–8, Longmans, Green, London, 1928.

<sup>144</sup> T. K. DERRY and T. I. WILLIAMS, *A Short History of Technology from the Earliest Times to AD 1900*, Oxford University Press, Oxford, 1960, 782 pp.

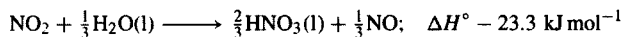
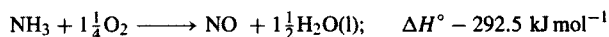
### Production and Uses of Nitric Acid<sup>(56,145,146)</sup>

Before 1900 the large-scale production of nitric acid was based entirely on the reaction of concentrated sulfuric acid with  $\text{NaNO}_3$  and  $\text{KNO}_3$  (p. 407). The first successful process for making nitric acid directly from  $\text{N}_2$  and  $\text{O}_2$  was devised in 1903 by E. Birkeland and S. Eyde in Norway and represented the first industrial fixation of nitrogen:

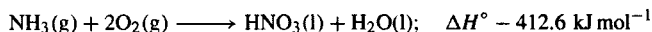


The overall reaction is exothermic but required the use of an electric arc furnace which, even with relatively cheap hydroelectricity, made the process very expensive. The severe activation energy barrier, though economically regrettable, is in fact essential to life since, in its absence, all the oxygen in the air would be rapidly consumed and the oceans would be a dilute solution of nitric acid and its salts. [Dilution of  $\text{HNO}_3(\text{l})$  to  $\text{HNO}_3(\text{aq})$  evolves a further  $33.3 \text{ kJ mol}^{-1}$  at  $25^\circ\text{C}$ .]

The modern process for manufacturing nitric acid depends on the catalytic oxidation of  $\text{NH}_3$  over heated Pt to give NO in preference to other thermodynamically more favoured products (p. 423). The reaction was first systematically studied in 1901 by W. Ostwald (Nobel Prize 1909) and by 1908 a commercial plant near Bochum, Germany, was producing 3 tonnes/day. However, significant expansion in production depended on the economical availability of synthetic ammonia by the Haber–Bosch process (p. 421). The reactions occurring, and the enthalpy changes per mole of N atoms at  $25^\circ\text{C}$  are:

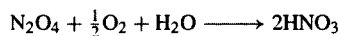


Whence, multiplying the second and third reactions by  $\frac{3}{2}$  and adding:



In a typical industrial unit a mixture of air with 10% by volume of  $\text{NH}_3$  is passed very rapidly over a series of gauzes (Pt, 5–10% Rh) at  $\sim 850^\circ\text{C}$  and 5 atm pressure; contact time with the catalyst is restricted to  $\leq 1$  ms in order to minimize unwanted side reactions. Conversion efficiency is  $\sim 96\%$  (one of the most efficient industrial catalytic reactions known) and the effluent gases are passed through an absorption column to yield 60% aqueous nitric acid at about  $40^\circ\text{C}$ . Loss of platinum metal from the catalyst under operating conditions is reduced by alloying with Rh but tends to increase with pressure from about 50–100 mg/tonne of  $\text{HNO}_3$  produced at atmospheric pressure to about 250 mg/tonne at 10 atm; though this is not a major part of the cost, the scale of operations means that about 0.5 tonne of Pt metals is lost annually in the UK from this cause and more than twice this amount in the USA.

Concentration by distillation of the 60% aqueous nitric acid produced in most modern ammonia-burning plants is limited by the formation of a maximum-boiling azeotrope ( $122^\circ$ ) at 68.5% by weight; further concentration to 98–99% can be effected by countercurrent dehydration using concentrated  $\text{H}_2\text{SO}_4$ , or by distillation from concentrated  $\text{Mg}(\text{NO}_3)_2$  solutions. Alternatively 99% pure  $\text{HNO}_3$  can be obtained directly from ammonia oxidation by incorporating a final oxidation of  $\text{N}_2\text{O}_4$  with the theoretical amounts of air and water at  $70^\circ\text{C}$  and 50 atm over a period of 4 h:



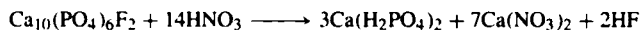
The largest use of nitric acid ( $\sim 75\%$ ) is in the manufacture of  $\text{NH}_4\text{NO}_3$  and of this, about 75% is used for fertilizer production. Many plants have a capacity of 2000 tonnes/day or more and great care must be taken to produce the  $\text{NH}_4\text{NO}_3$  in a readily handleable form (e.g. prills of about 3 mm diameter); about 1% of a “conditioner” is usually added to improve storage and handling properties.  $\text{NH}_4\text{NO}_3$  is thermally unstable (p. 469) and decomposition can become explosive. For this reason a temperature limit of  $140^\circ\text{C}$  is imposed on the neutralization step and pH is strictly controlled. The decomposition is catalysed by many inorganic materials including chloride, chromates, hypophosphites, thiosulfates and powdered metals (e.g. Cu, Zn, Hg). Organic materials (oil, paper, string, sawdust, etc.) must also be rigorously excluded during neutralization since their oxidation releases additional heat. Indeed, since the mid-1950s  $\text{NH}_4\text{NO}_3$  prills mixed with fuel oil have been extensively used as a direct explosive in mining and quarrying operations (p. 469) and this use now accounts for up to 15% of the  $\text{NH}_4\text{NO}_3$  produced.

*Panel continues*

<sup>145</sup>C. KELETI (ed), *Nitric Acid and Fertilizer Nitrates*, Marcel Dekker, N.Y. 1985, 392 pp.

<sup>146</sup>S. I. CLARKE and W. J. MAZZAFRO Nitric acid, in *Kirk–Othmer Encyclopedia of Chemical Technology*, 4th edn., Vol. 17, pp. 80–107 (1996).

Some 8–9% of  $\text{HNO}_3$  goes to make cyclohexanone, the raw material for adipic acid and  $\epsilon$ -caprolactam, which are the monomers for nylon-6,6 and nylon-6 respectively. A further 7–10% is used in other organic nitration reactions to give nitroglycerine, nitrocellulose, trinitrotoluene and numerous other organic intermediates. Minor uses (which still consume large quantities of the acid) include the pickling of stainless steel, the etching of metals, and its use as the oxidizer in rocket fuels. In Europe nitric acid is sometimes used to replace sulfuric acid in the treatment of phosphate rock to give nitrophosphate fertilizers according to the idealized equation:



Another minority use is in the manufacture of nitrates (other than  $\text{NH}_4\text{NO}_3$ ) for use in explosives, propellants, and pyrotechnics generally; typical examples are:

explosives: gun powder,  $\text{KNO}_3/\text{S}/\text{powdered C}$  (often reinforced with powdered Si)

white smokes:  $\text{ZnO}/\text{CaSi}_2/\text{KNO}_3/\text{C}_2\text{Cl}_6$

incendiary agents:  $\text{Al}/\text{NaNO}_3/\text{methylmethacrylate}/\text{benzene}$

local heat sources:  $\text{Al}/\text{Fe}_3\text{O}_4/\text{Ba}(\text{NO}_3)_2$ ;  $\text{Mg}/\text{Sr}(\text{NO}_3)_2/\text{SrC}_2\text{O}_4/\text{thiokol polysulfide}$

photoflashes:  $\text{Mg}/\text{NaNO}_3$

flares (up to 10 min):  $\text{Mg}/\text{NaNO}_3/\text{CaC}_2\text{O}_4/\text{polyvinyl chloride}/\text{varnish}$ ;  $\text{Ti}/\text{NaNO}_3/\text{boiled linseed oil}$

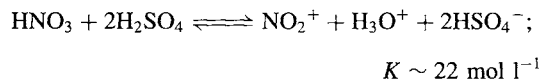
coloured flares:  $\text{Mg}/\text{Sr}(\text{NO}_3)_2/\text{chlorinated rubber (red)}$ ;  $\text{Mg}(\text{Ba}(\text{NO}_3)_2)/\text{chlorinated rubber (green)}$ .

These equilibria effect a rapid exchange of N atoms between the various species and only a single  $^{15}\text{N}$  nmr signal is seen at the weighted average position of  $\text{HNO}_3$ ,  $[\text{NO}_2]^+$  and  $[\text{NO}_3]^-$ . They also account for the high electrical conductivity of the “pure” (stoichiometric) liquid (Table 11.13), and are an important factor in the chemical reactions of nitric acid and its non-aqueous solutions see below.

The phase diagram  $\text{HNO}_3\text{--H}_2\text{O}$  shows the presence of two hydrates,  $\text{HNO}_3\cdot\text{H}_2\text{O}$  mp  $-37.68^\circ$ , and  $\text{HNO}_3\cdot 3\text{H}_2\text{O}$  mp  $-18.47^\circ$ . A further hemihydrate,  $2\text{HNO}_3\cdot\text{H}_2\text{O}$ , can be extracted into benzene or toluene from 6 to 16 M aqueous solutions of nitric acid, and a dimer hydrate,  $2\text{HNO}_3\cdot 3\text{H}_2\text{O}$ , is also known, though neither can be crystallized. The structure of the two crystalline hydrates is dominated by hydrogen bonding as expected; e.g. the monohydrate is  $[\text{H}_3\text{O}]^+[\text{NO}_3]^-$  in which there are puckered layers comprising pyramidal  $[\text{H}_3\text{O}]^+$  hydrogen bonded to planar  $[\text{NO}_3]^-$  so that there are 3 H bonds per ion. The trihydrate forms a more complex three-dimensional H-bonded framework. (See also p. 468 for the structure of hydrogen-nitrates.)

The solution chemistry of nitric acid is extremely varied. Redox data are summarized in Table 11.4 and Fig. 11.9 (pp. 434–8). In

dilute aqueous solutions (<2 M) nitric acid is extensively dissociated into ions and behaves as a typical strong acid in its reactions with metals, oxides, carbonates, etc. More concentrated aqueous solutions are strongly oxidizing and attack most metals except Au, Pt, Rh and Ir, though some metals which react at lower concentrations are rendered passive, probably because of the formation of an oxide film (e.g. Al, Cr, Fe, Cu). Aqua regia (a mixture of concentrated hydrochloric and nitric acids in the ratio of  $\sim 3:1$  by volume) is even more aggressive, due to the formation of free  $\text{Cl}_2$  and  $\text{ClNO}$  and the superior complexing ability of the chloride ion; it has long been known to “dissolve” both gold and the platinum metals, hence its name. In concentrated  $\text{H}_2\text{SO}_4$  the chemistry of nitric acid is dominated by the presence of the nitronium ion (pp. 458, 465):



Such solutions are extensively used in aromatic nitration reactions in the heavy organic chemicals industry. See also pp. 457–8.

Anhydrous nitric acid has been studied as a nonaqueous ionizing solvent, though salts tend to be rather insoluble unless they produce  $\text{NO}_2^+$  or



$\text{NO}_3^-$  ions.<sup>(147)</sup> Addition of water to nitric acid at first diminishes its electrical conductivity by repressing the autoprotolysis reactions mentioned above. For example, at  $-10^\circ$  the conductivity decreases from  $3.67 \times 10^{-2} \text{ ohm}^{-1} \text{ cm}^{-1}$  to a minimum of  $1.08 \times 10^{-2} \text{ ohm}^{-1} \text{ cm}^{-1}$  at 1.75 molal  $\text{H}_2\text{O}$  (82.8%  $\text{N}_2\text{O}_5$ ) before rising again due to the increasing formation of the hydroxonium ion according to the acid-base equilibrium



By contrast, Raman spectroscopy and conductivity measurements show that  $\text{N}_2\text{O}_4$  ionizes almost completely in anhydrous  $\text{HNO}_3$  to give  $\text{NO}^+$  and  $\text{NO}_3^-$  and such solutions show no evidence for the species  $\text{N}_2\text{O}_4$ ,  $\text{NO}_2^+$  or  $\text{NO}_2^-$ .<sup>(126)</sup>  $\text{N}_2\text{O}_5$  is also extremely soluble in anhydrous nitric acid in which it is completely ionized as  $\text{NO}_2^+ \text{NO}_3^-$ .

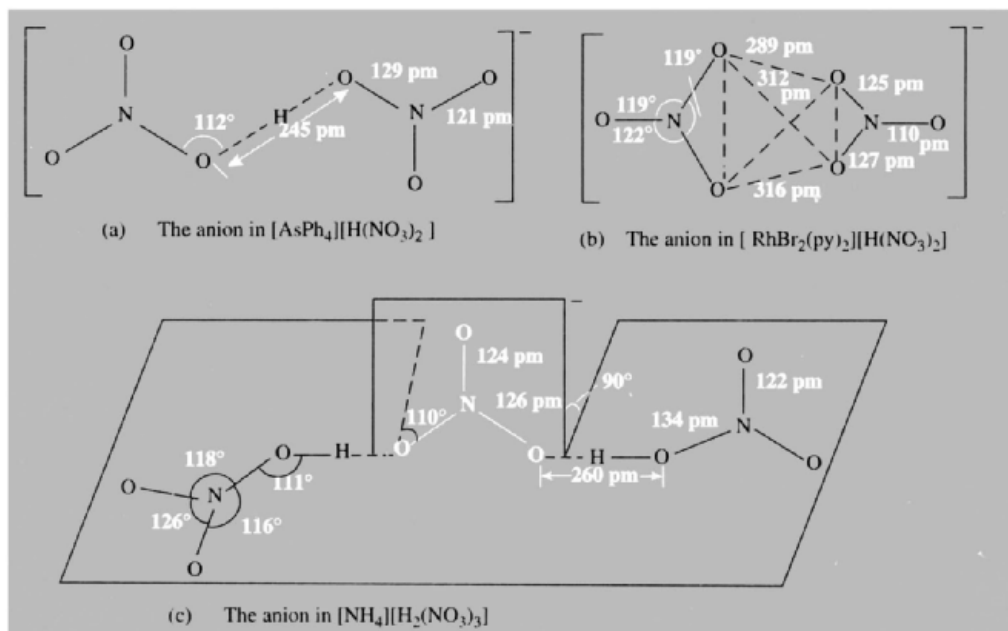
Nitrates, the salts of nitric acid, can readily be made by appropriate neutralization of the acid, though sometimes it is the hydrate which crystallizes from aqueous solution. Anhydrous

nitrates and nitrate complexes are often best prepared by use of donor solvents containing  $\text{N}_2\text{O}_4$  (p. 456). The reaction of liquid  $\text{N}_2\text{O}_5$  with metal oxides and chlorides affords an alternative route, e.g.:



Many nitrates are major items of commerce and are dealt with under the appropriate metal (e.g.  $\text{NaNO}_3$ ,  $\text{KNO}_3$ ,  $\text{NH}_4\text{NO}_3$ , etc.). In addition, various hydrogen dinitrates and dihydrogen trinitrates are known of formula  $\text{M}[\text{H}(\text{NO}_3)_2]$  and  $\text{M}[\text{H}_2(\text{NO}_3)_3]$  where M is a large cation such as K, Rb, Cs,  $\text{NH}_4$  or  $\text{AsPh}_4$ . In  $[\text{AsPh}_4][\text{H}(\text{NO}_3)_2]$  2 coplanar  $\text{NO}_3^-$  ions are linked by a short H bond as shown in (a) whereas  $[\text{trans-RhBr}_2(\text{py})_4][\text{H}(\text{NO}_3)_2]$  features a slightly distorted tetrahedral group of 4 oxygen atoms in which the position of the H atom is not obvious [structure (b)]. In  $[\text{NH}_4][\text{H}_2(\text{NO}_3)_3]$  there is a more extended system of H bonds in which 2 coplanar molecules of  $\text{HNO}_3$  are symmetrically bridged by an  $\text{NO}_3^-$  ion at right angles as shown in (c).

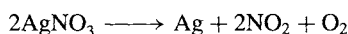
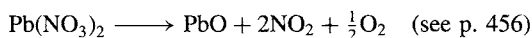
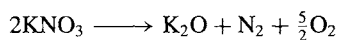
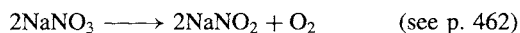
<sup>147</sup> W. H. LEE, in J. J. LAGOWSKI (ed.), *The Chemistry of Non-aqueous Solvents*, Vol. 2, pp. 151–89, Academic Press, New York, 1967.



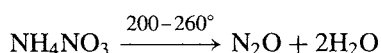
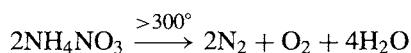
As with the salts of other oxoacids, the thermal stability of nitrates varies markedly with the basicity of the metal, and the products of decomposition are equally varied.<sup>(148)</sup> Thus the nitrates of Group 1 and 2 metals find use as molten salt baths because of their thermal stability and low mp (especially as mixtures). Representative values of mp and the temperature ( $T_d$ ) at which the decomposition pressure of  $O_2$  reaches 1 atm are:

M	Li	Na	K	Rb	Cs	Ag	Tl
MP of $MNO_3/^\circ C$	255	307	333	310	414	212	206
$T_d/^\circ C$	474	525	533	548	584	-	-

The product of thermolysis is the nitrite or, if this is unstable at the temperature employed, the oxide (or even the metal if the oxide is also unstable):<sup>(149)</sup>



As indicated in earlier sections,  $NH_4NO_3$  can be exploded violently at high temperatures or by use of detonators (p. 466), but slow controlled thermolysis yields  $N_2O$  (p. 443):



The presence of organic matter or other reducible material also markedly affects the thermal stability of nitrates and the use of  $KNO_3$  in gunpowder has been known for centuries (p. 645).

The nitrate group, like the nitrite group, is a versatile ligand and numerous modes of coordination have been found in nitrate complexes.<sup>(150)</sup> The "uncoordinated"  $NO_3^-$  ion (isoelectronic with  $BF_3$ ,  $BO_3^{3-}$ ,  $CO_3^{2-}$ , etc.) is planar with N-O near 122 pm; this value

increases to 126 pm in  $AgNO_3$  and 127 pm in  $Pb(NO_3)_2$ . The most common mode of coordination is the symmetric bidentate mode Fig. 11.16a, though unsymmetrical bidentate coordination (b) also occurs and, in the limit, unidentate coordination (c). Bridging modes include the *syn-syn* conformation (d) (and the *anti-anti* analogue), and also geometries in which a single O atom bridges 2 or even 3 metal atoms (e), (f). Sometimes more than one mode occurs in the same compound.

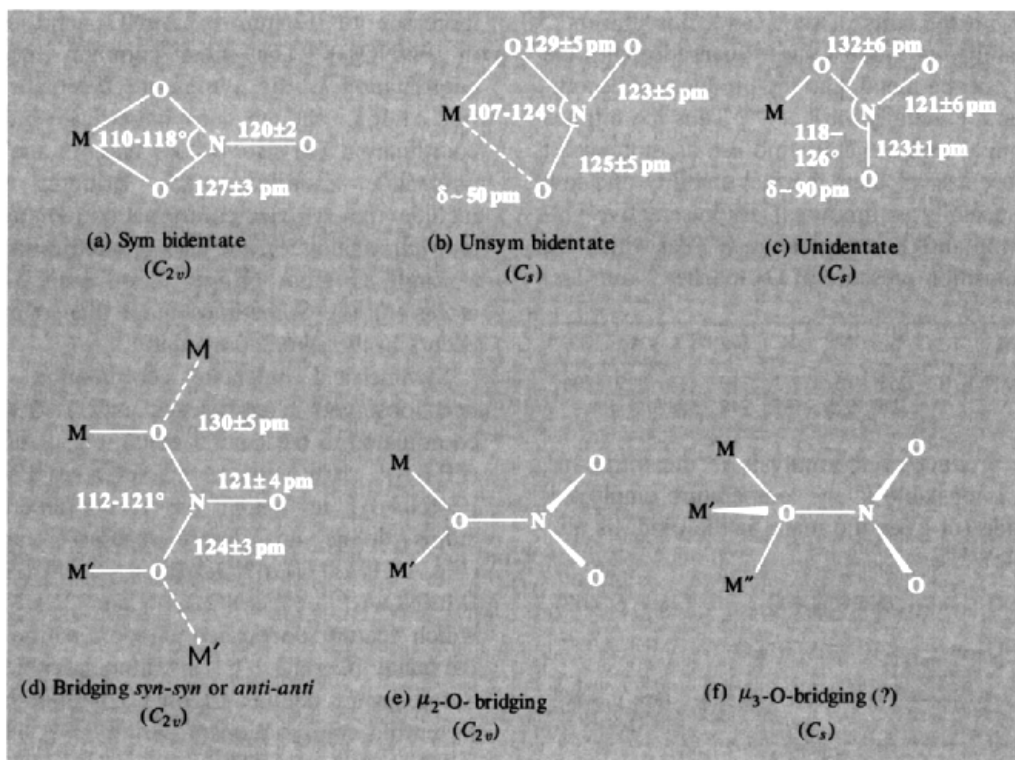
Symmetrical bidentate coordination (a) has been observed in complexes with 1-6 nitrates coordinated to the central metal, e.g.  $[Cu(NO_3)_2(PPh_3)_2]$ ;  $[Cu(NO_3)_2]$ ,  $[Co(NO_3)_2(OPMe_3)_2]$ ;  $[Co(NO_3)_3]$  in which the 6 coordinating O atoms define an almost regular octahedron (Fig. 11.17a),  $[La(NO_3)_3(bipy)_2]$ ;  $[Ti(NO_3)_4]$ ,  $[Mn(NO_3)_4]^{2-}$ ,  $[Fe(NO_3)_4]^-$  and  $[Sn(NO_3)_4]$ , which feature dodecahedral coordination about the metal;  $[Ce(NO_3)_5]^{2-}$  in which the 5 bidentate nitrate groups define a trigonal bipyramid leading to tenfold coordination of cerium (Fig. 11.17b);  $[Ce(NO_3)_6]^{2-}$  and  $[Th(NO_3)_6]^{2-}$ , which feature nearly regular icosahedral (p. 141) coordination of the metal by 12 O atoms; and many lanthanide and uranyl  $[UO_2]^{2+}$  complexes. It seems, therefore, that the size of the metal centre is not necessarily a dominant factor.

Unsymmetrical bidentate coordination (Fig. 11.16b) is observed in the high-spin  $d^7$  complex  $[Co(NO_3)_4]^{2-}$  (Fig. 11.17c), in  $[SnMe_2(NO_3)_2]$  and also in several  $Cu^{II}$  complexes of formula  $[CuL_2(NO_3)_2]$ , where L is MeCN,  $H_2O$ , py or 2-MeC<sub>5</sub>H<sub>4</sub>N ( $\alpha$ -picoline). An example of unidentate coordination is furnished by  $K[Au(NO_3)_4]$  as shown in Fig. 11.18(a), and further examples are in *cis*- $[Pd(NO_3)_2(OSMe_2)_2]$ ,  $[Re(CO)_5(NO_3)]$ ,  $[Ni(NO_3)_2(H_2O)_4]$ ,  $[Zn(NO_3)_2(H_2O)_4]$  and several  $Cu^{II}$  complexes such as  $[CuL_2(NO_3)_2]$  where L is pyridine *N*-oxide or 1,4-diazacycloheptane. It appears that a combination of steric effects and the limited availability of coordination sites in these already highly coordinated late-transition-metal complexes restricts each nitrate group to one coordination site. When more

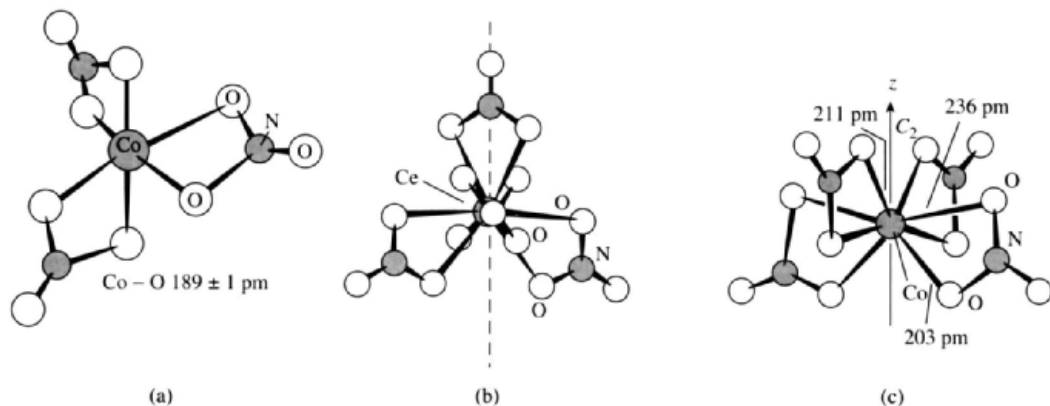
<sup>148</sup> B. O. FIELD and C. J. HARDY, *Q. Rev.* **18**, 361-88 (1964).

<sup>149</sup> K. J. MYSELS, *J. Chem. Educ.* **36** 303-4 (1959).

<sup>150</sup> C. C. ADDISON, N. LOGAN, S. C. WALLWORK and C. D. GARNER, *Q. Rev.* **25**, 289-322 (1971).



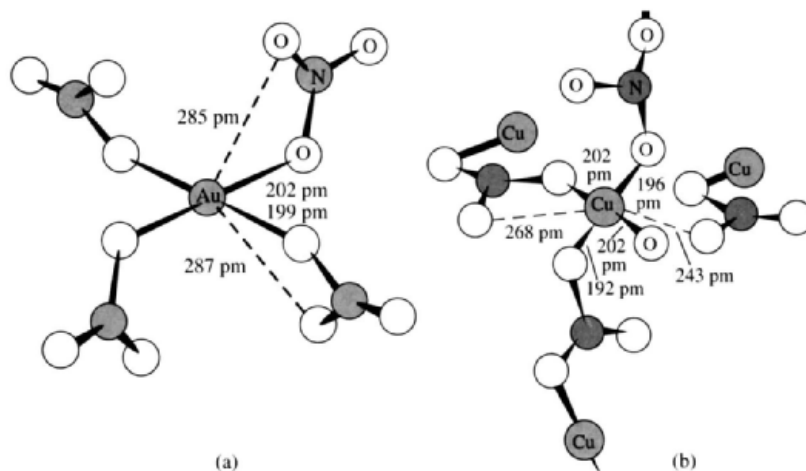
**Figure 11.16** Coordination geometries of the nitrate group showing typical values for the interatomic distances and angles. Further structural details are in ref. 150.



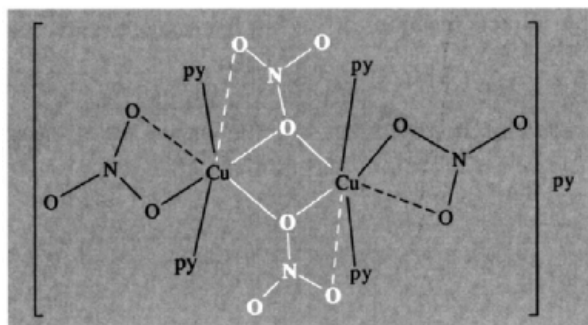
**Figure 11.17** Structures of (a)  $\text{Co}(\text{NO}_3)_3$ , (b)  $[\text{Ce}(\text{NO}_3)_5]^{2-}$  and (c)  $[\text{Co}(\text{NO}_3)_4]^{2-}$

sites become available, as in  $[\text{Ni}(\text{NO}_3)_2(\text{H}_2\text{O})_2]$  and  $[\text{Zn}(\text{NO}_3)_2(\text{H}_2\text{O})_2]$ , or when the co-ligands are less bulky, as in  $[\text{CuL}_2(\text{NO}_3)_2]$ , where L is  $\text{H}_2\text{O}$ ,  $\text{MeCN}$  or  $\text{MeNO}_2$ , then the nitrate

groups become bidentate bridging (mode d in Fig. 11.16) and a further example of this is seen in  $[\alpha\text{-Cu}(\text{NO}_3)_2]$ , which forms a more extensive network of bridging nitrate groups, as



**Figure 11.18** (a) Structure of  $[\text{Au}(\text{NO}_3)_4]^-$ . (b)  $\alpha\text{-Cu}(\text{NO}_3)_2$ .



**Figure 11.19** Schematic diagram of the centrosymmetric dimer in  $[\text{Cu}_2(\text{NO}_3)_4(\text{py})_4]\text{py}$  showing the two bridging nitrate groups each coordinated to the 2 Cu atoms by a single O atom; the dimer also has an unsymmetrical bidentate nitrate group on each Cu.

shown in Fig. 11.18(b). The single oxygen atom bridging mode (e) occurs in  $[\text{Cu}(\text{NO}_3)_2(\text{py})_2]_2\text{py}$  (Fig. 11.19) and the triple-bridge (f) may occur in  $[\text{Cu}_4(\text{NO}_3)_2(\text{OH})_6]$  though there is some uncertainty about this structure and further refinement would be desirable. Finally, the structure of the unique yellow solvate of formula  $[\text{Fe}(\text{NO}_3)_3 \cdot 1\frac{1}{2}\text{N}_2\text{O}_4]$  (p. 457) has been shown<sup>(128)</sup> to be  $[\text{N}_4\text{O}_6]^{2+}[\text{Fe}(\text{NO}_3)_4]^{-2}$ . Each anion has 4 symmetrically bidentate  $\text{NO}_3$  groups in which the coordinating O atoms lie at the corners of a trigonal dodecahedron, as is commonly found in tetranitrate species (N-O, 120 pm, N-O(Fe) 127 pm, angles O-N-O 113.4° and O-Fe-O

60.0°). The  $[\text{N}_4\text{O}_6]^{2+}$  cation comprises a central planar nitrate group (N-O 123 pm) surrounded by 3 NO groups at distances which vary from 241 to 278 pm (Fig. 11.20); the interatomic distance in the NO groups is very short (90–99 pm) implying  $\text{NO}^+$  and the distances of these to the central  $\text{NO}_3$  group are slightly less than the sum of the van der Waals radii for N and O.

### Orthonitrates, $\text{M}_3\text{NO}_4$

There is no free acid  $\text{H}_3\text{NO}_4$  analogous to orthophosphoric acid  $\text{H}_3\text{PO}_4$  (p. 516), but the alkali metal orthonitrates  $\text{Na}_3\text{NO}_4$  and  $\text{K}_3\text{NO}_4$

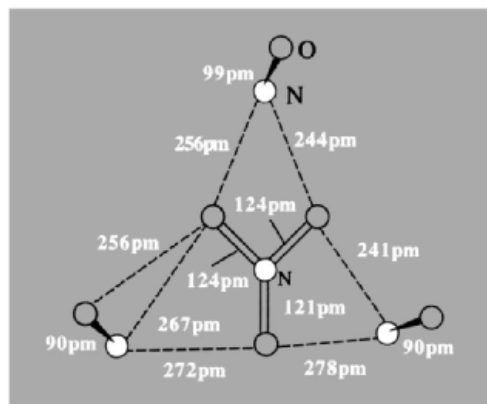
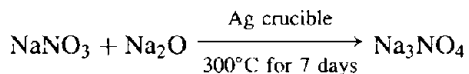


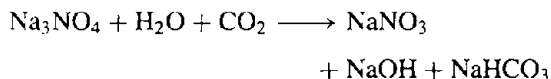
Figure 11.20 The  $\{N_4O_6\}^{2+}$  cation.

have been synthesized by direct reaction at elevated temperatures, e.g.:<sup>(151,152)</sup>

<sup>151</sup> M. JANSEN, *Angew. Chem. Int. Edn. Engl.* **16**, 534 (1977); **18**, 698 (1979).



The compound forms white crystals that are very sensitive to atmospheric moisture and  $\text{CO}_2$ :



X-ray structural analyses have shown that the  $\text{NO}_4^{3-}$  ion has regular  $T_d$  symmetry with the unexpectedly small N-O distance of 139 pm. This suggests that substantial polar interactions are superimposed on the N-O single bonds since the  $d_\pi$  orbitals on N are too high in energy to contribute significantly to multiple covalent bonding. It further implies that  $d_\pi-p_\pi$  interactions need not necessarily be invoked to explain the observed short interatomic distance in the isoelectronic oxoanions  $\text{PO}_4^{3-}$ ,  $\text{SO}_4^{2-}$  and  $\text{ClO}_4^-$ .

<sup>152</sup> T. BREMM and M. JANSEN, *Z. anorg. allg. Chem.* **608**, 56-9 (1992).

		1 H		2 He												3 B						4 C						5 N						6 O						7 F						8 Ne					
9 Li		10 Be														13 Al		14 Si		15 P		16 S		17 Cl		18 Ar																									
19 K		20 Ca		21 Sc		22 Ti		23 V		24 Cr		25 Mn		26 Fe		27 Co		28 Ni		29 Cu		30 Zn		31 Ga		32 Ge		33 As		34 Se		35 Br		36 Kr																	
37 Rb		38 Sr		39 Y		40 Zr		41 Nb		42 Mo		43 Tc		44 Ru		45 Rh		46 Pd		47 Ag		48 Cd		49 In		50 Sn		51 Sb		52 Te		53 I		54 Xe																	
55 Cs		56 Ba		57 La		58 Hf		59 Ta		60 W		61 Re		62 Os		63 Ir		64 Pt		65 Au		66 Hg		67 Tl		68 Pb		69 Bi		70 Po		71 At		72 Rn																	
87 Fr		88 Ra		89 Ac		90 Th		91 Pa		92 U		93 Np		94 Pu		95 Am		96 Cm		97 Bk		98 Cf		99 Es		100 Fm		101 Md		102 No		103 Lr																			

# 12

## Phosphorus

### 12.1 Introduction

Phosphorus has an extensive and varied chemistry which transcends the traditional boundaries of inorganic chemistry not only because of its propensity to form innumerable covalent “organophosphorus” compounds, but also because of the numerous and crucial roles it plays in the biochemistry of all living things. It was first isolated by the alchemist Hennig Brandt in 1669 by the unsavoury process of allowing urine to putrify for several days before boiling it down to a paste which was then reductively distilled at high temperatures; the vapours were condensed under water to give the element as a white waxy substance that glowed in the dark when exposed to air.<sup>(1)</sup> Robert Boyle improved the process (1680) and in subsequent years made the oxide and phosphoric acid; he referred to the element as “aerial noctiluca”, but the name phosphorus soon became generally accepted (Greek  $\phi\omega\varsigma$  *phos*, light; Greek  $\phi\omicron\rho\omicron\varsigma$  *phoros*, bringing).

As shown in the Panel on the next page, phosphorus is probably unique among the elements in being isolated first from animal (human) excreta, then from plants, and only a century later being recognized in a mineral.

6	C	7	N	8	O
14	Si	15	P	16	S
32	Ge	33	As	34	Se

In much of its chemistry phosphorus stands in relation to nitrogen as sulfur does to oxygen. For example, whereas  $N_2$  and  $O_2$  are diatomic gases, P and S have many allotropic modifications which reflect the various modes of catenation adopted. Again, the ability of P and S to form multiple bonds to C, N and O, though it exists, is less highly developed than for N (p. 416), whereas the ability to form extended networks of  $-P-O-P-O-$  and  $-S-O-S-O-$  bonds is greater; this is well illustrated by comparing the oxides and oxoanions of N

<sup>1</sup> M. E. WEEKS, *Discovery of the Elements*, Journal of Chemical Education Publ., Easton, Pa., 1956; Phosphorus, pp. 109–39.

## Time Chart for Phosphorus Chemistry

- 1669 Phosphorus isolated from urine by H. Brandt.
- 1680 R. Boyle improved the process and showed air was necessary for the phosphorescence of P.
- 1688 Phosphorus first detected in the vegetable kingdom (by B. Albino).
- 1694  $P_4O_{10}$  and  $H_3PO_4$  first made by R. Boyle.
- 1769 Phosphorus shown by J. G. Gahn and C. W. Scheele to be an essential constituent in the bones of man and animals, thereby revealing a plentiful source of fertilizers.
- 1779 Phosphorus first discovered in a mineral by J. G. Gahn (pyromorphite, a lead phosphate); subsequently found in the much more abundant apatite by T. Bergman and J. L. Proust.
- 1783  $PH_3$  first prepared by P. Gengembre (and independently in 1786 by R. Kirwan).
- 1808  $PCl_3$  and  $PCl_5$  made by J. L. Gay Lussac and L. J. Thenard (and by H. Davy).
- 1811 N. L. Vauquelin isolated the first organic P compound (lethicin) from brain fat; it was characterized as a phospholipid by Gobbley in 1850.
- 1816 P. L. Dulong first clearly demonstrated the existence of two oxides of P.
- 1820 First synthesis of an organo-P compound by J. L. Lassaigne who made alkyl phosphites from  $H_3PO_4 + ROH$ .
- 1833 T. Graham (who later became the first President of the Chemical Society) classified phosphates as ortho, pyro or meta, following J. J. Berzelius's preparation of pyrophosphoric acid by heat.
- 1834  $(PNCl_2)_n$  made by F. Wöhler and J. von Liebig (originally formulated as  $P_3N_2Cl_5$ ).
- 1843 J. Murray patented his production of "superphosphate" fertilizer (a name coined by him for the product of  $H_2SO_4$  on phosphate rock).
- 1844 A. Albright started the manufacture of elemental P in England (for matches); 0.75 tonne in 1844. 26.5 tonnes in 1851.
- 1845 Polyphosphoric acids made by T. Fleitmann and W. Henneberg.
- 1848 Red (amorphous) P discovered by A. Schrötter.
- 1850 First commercial production of "wet process" phosphoric acid.
- 1868 E. F. Hoppe-Seyler and F. Miescher isolated "nuclein", the first nucleic acid, from pus.
- 1880 Modern cyclic formulation of tetrametaphosphate anion suggested by A. Glatzel. (Ring structure of metaphosphate definitely established by L. Pauling and J. Sherman 1937.)
- 1888 Electrothermal process for manufacturing P introduced by J. B. Readman (Edinburgh).
- 1898 "Strike-anywhere" matches devised by H. Sévène and E. D. Cahen in France; previously the brothers Lundström had exhibited "safety matches" in 1855, and the first P-containing striking match had been invented by F. Dérosne in 1812.
- 1929 C. H. Fiske and Y. Subbarow discovered adenosine triphosphate (ATP) in muscle fibre; it was synthesized some 20 y later by A. Todd *et al.* (Nobel Prize 1957).
- 1932 Elucidation of the glycolysis process (by G. Embden and by O. Meyerhof) followed by the glucose oxidation process (H. A. Krebs, 1937) established the intimate involvement of P compounds in many biochemical reactions.
- 1935 Radioactive  $^{32}P$  made by  $(n,\gamma)$  reaction on  $^{31}P$ .
- ~1940 Highly polymeric phosphate esters (nucleic acids) present in all cells and recognized as essential constituents of chromosomes.
- 1951 First  $^{31}P$  nmr chemical shifts measured by W. C. Dickinson (for  $POCl_3$ ,  $PCl_3$ , etc. relative to aq.  $H_3PO_4$ ).
- 1952 Detergents (using polyphosphates) overtake soap as main washing agent in the USA. (Heavy duty liquid detergents with polyphosphates introduced in 1955.)
- 1953 F. H. C. Crick, J. B. Watson and M. H. F. Wilkins (with Rosalind Franklin) establish the double helix structure of nucleic acids (Nobel Prize 1962).
- 1960 Concept of "pseudorotation" introduced by R. S. Berry to interpret the stereochemical non-rigidity of trigonal bipyramidal  $PF_5$  (and  $SF_4$ ,  $ClF_3$ ); the 5 F atoms are equivalent (1953) due to interconversion via a square pyramidal intermediate.
- 1961 First 2-coordinate compound of P prepared by A. B. Burg ( $Me_3P=PCF_3$ ). First 1-coordinate P compound ( $HC\equiv P$ ) made by T. E. Gier.
- 1966 First heterocyclic aromatic analogue of pyridine ( $Ph_3C_5H_2P$ ) prepared by G. Märkl, followed by the parent compound  $C_5H_5P$  in 1971 (A. J. Ashe).
- 1977+  $P_4$  as an  $\eta^1$ ,  $\eta^2$ , etc. ligand (see Fig. 12.9, p. 488).
- 1979 G. Wittig shared the Chemistry Nobel Prize for his development of the Wittig reaction (first published with G. Geissler in 1953).
- 1981 First stable phospho-alkyne,  $Bu^iC\equiv P$  (cf. RCN).
- 1983+ Characterization of extended *conjuncto*-polyphosphide clusters (p. 491) and polyphosphanes (p. 492).

and P. "Valency expansion" is another point of difference between the elements of the first and second periods of the periodic table for, although compounds in which N has a formal oxidation state of +5 are known, no simple "single-bonded" species such as  $\text{NF}_5$  or  $\text{NCl}_6^-$  have been prepared, analogous to  $\text{PF}_5$  and  $\text{PCl}_6^-$ . This finds interpretation in the availability of 3d orbitals for bonding in P (and S) but not for N (or O). The extremely important Wittig reaction for olefin synthesis (p. 545) is another manifestation of this property. Discussion of more extensive group trends in which N and P are compared with the other Group 15 elements As, Sb and Bi, is deferred until the next chapter (pp. 550–4).

Because of the great importance of phosphorus and its compounds in the chemical industry, several books and reviews on their preparation and uses are available.<sup>(2–10)</sup> Some of these applications reflect the fact that P is a vital element for the growth and development of all plants and animals and is therefore an important constituent in many fertilizers. Phosphorus compounds are involved in energy transfer

processes (such as photosynthesis (p. 126), metabolism, nerve function and muscle action), in heredity (via DNA), and in the production of bones and teeth.<sup>(11–14)</sup> Topics in phosphorus chemistry are regularly reviewed.<sup>(15)</sup>

## 12.2 The Element

### 12.2.1 Abundance and distribution

Phosphorus is the eleventh element in order of abundance in crustal rocks of the earth and it occurs there to the extent of ~1120 ppm (cf. H ~1520 ppm, Mn ~1060 ppm). All its known terrestrial minerals are orthophosphates though the reduced phosphide mineral schriebersite  $(\text{Fe,Ni})_3\text{P}$  occurs in most iron meteorites. Some 200 crystalline phosphate minerals have been described, but by far the major amount of P occurs in a single mineral family, the apatites, and these are the only ones of industrial importance, the others being rare curiosities.<sup>(16)</sup> Apatites (p. 523) have the idealized general formula  $3\text{Ca}_3(\text{PO}_4)_2 \cdot \text{CaX}_2$ , that is  $\text{Ca}_{10}(\text{PO}_4)_6\text{X}_2$ , and common members are fluorapatite  $\text{Ca}_5(\text{PO}_4)_3\text{F}$ , chloroapatite  $\text{Ca}_5(\text{PO}_4)_3\text{Cl}$ , and hydroxyapatite  $\text{Ca}_5(\text{PO}_4)_3(\text{OH})$ . In addition, there are vast deposits of amorphous phosphate rock, phosphorite, which approximates in composition to fluoroapatite.<sup>(11,17)</sup> These deposits are widely

<sup>2</sup> J. EMSLEY and D. HALL, *The Chemistry of Phosphorus*, Harper & Row, London 1976, 534 pp.

<sup>3</sup> A. F. CHILDS, Phosphorus, phosphoric acid and inorganic phosphates, in *The Modern Inorganic Chemicals Industry*, (R. THOMPSON, ed.), pp. 375–401, The Chemical Society, London, 1977.

<sup>4</sup> *Proceedings of the First International Congress on Phosphorus Compounds and their Non-fertilizer Applications, 17–21 October 1977 Rabat, Morocco*, IMPHOS (Institut Mondial du Phosphat), Rabat, 1978, 767 pp.

<sup>5</sup> L. D. QUIN and J. D. VERKADE (eds.), *Phosphorus Chemistry: Proceedings of the 1981 International Conference*, ACS Symposium Series No. 171, 1981, 640 pp.

<sup>6</sup> H. GOLDWHITE, *Introduction to Phosphorus Chemistry*, Cambridge University Press, Cambridge, 1981, 113 pp.

<sup>7</sup> E. C. ALYEA and D. W. MEEK (eds.), *Catalytic Aspects of Metal Phosphine Complexes*, ACS Symposium Series No. 196, 1982, 421 pp.

<sup>8</sup> D. E. C. CORBRIDGE, *Phosphorus: An Outline of its Chemistry, Biochemistry and Technology*, 5th edn. Elsevier, Amsterdam, 1995, 1208 pp.

<sup>9</sup> A. D. F. TOY and E. N. WALSH, *Phosphorus Chemistry in Everyday Living*, (2nd edn). Washington, ACS, 1987, 362 pp.

<sup>10</sup> E. N. WALSH, E. J. GRIFFITH, R. W. PARRY and L. D. QUIN (eds.), *Phosphorus Chemistry: Developments in American Science*, ACS Symposium Series No. 486, 1992, 288 pp.

<sup>11</sup> J. R. VAN WAZER (ed.), *Phosphorus and its Compounds*, Vol. 2, *Technology, Biological Functions and Applications*, Interscience, New York, 1961, 2046 pp.

<sup>12</sup> F. H. PORTUGAL and J. S. COHEN, *A Century of DNA. A History of the Discovery of the Structure and Function of the Genetic Substance*, MIT Press, Littleton, Mass., 1977, 384 pp.

<sup>13</sup> R. L. RAWIS, *Chem. and Eng. News*, Dec. 21, 1987, pp. 26–39.

<sup>14</sup> J. K. BARTON, *Chem. and Eng. News*, Sept. 26, 1988, pp. 30–42.

<sup>15</sup> *Topics in Phosphorus Chemistry*, Wiley, New York, Vol. 1 (1964)–Vol. 11 (1983).

<sup>16</sup> J. O. NRIAGU and P. B. MOORE (eds.), *Phosphate Minerals*, Springer Verlag, Berlin, 1984, 442 pp.

<sup>17</sup> W. BÜCHNER, R. SCHLIEBS, G. WINTER and K. H. BÜCHEL, *Industrial Inorganic Chemistry*, (transl. D. R. TERRELL), VCH, Weinheim, 1989, Phosphorus, pp. 68–105.



**Table 12.1** Estimated reserves of phosphate rock (in gigatonnes of contained P)

Continent	Main areas	Reserves/10 <sup>9</sup> tonnes P
Africa	Morocco, Senegal, Tunisia, Algeria, Sahara, Egypt, Togo, Angola, South Africa	4.6
North America	USA (Florida, Georgia, Carolina, Tennessee, Idaho, Montana, Utah, Wyoming), Mexico	1.6
South America	Peru, Brazil, Chile, Columbia	0.4
Europe	Western and Eastern	0.7
Asia/Middle East	Kola Peninsula, Kazakhstan, Siberia, Jordan, Israel, Saudi Arabia, India, Turkey	1.4
Australasia	Queensland, Nauru, Makatea	0.4
Total		9.1

spread throughout the world as indicated in Table 12.1 and reserves (1982 estimates) are adequate for several centuries with present technology. The phosphate content of commercial phosphate rock generally falls in the range (72 ± 10)% BPL [i.e. "bone phosphate of lime", Ca<sub>3</sub>(PO<sub>4</sub>)<sub>2</sub>] corresponding to (33 ± 5)% P<sub>4</sub>O<sub>10</sub> or 12–17% P. The USA is the principal producer, having produced one-third of the total world output in 1985, and Morocco is the largest exporter, mainly to the UK and continental Europe. World production is a staggering 151 million tonnes of phosphate rock per annum (1985), equivalent to some 20 million tonnes of contained phosphorus (p. 480).

Phosphorus also occurs in all living things and the phosphate cycle, including the massive use of phosphatic fertilizers, is of great current interest.<sup>(18–20)</sup> The movement of phosphorus through the environment differs from that of the other non-metals essential to life (H, C, N, O and S) because it has no volatile compounds that can circulate via the atmosphere. Instead, it circulates via two rapid biological

cycles on land and sea (weeks and years) superimposed on a much slower primary geological inorganic cycle (millions of years). In the inorganic cycle, phosphates are slowly leached from the igneous or sedimentary rocks by weathering, and transported by rivers to the lakes and seas where they are precipitated as insoluble metal phosphates or incorporated into the aquatic food chain. The solubility of metal phosphates clearly depends on pH, salinity, temperature, etc., but in neutral solution Ca<sub>3</sub>(PO<sub>4</sub>)<sub>2</sub> (solubility product ~10<sup>-29</sup> mol<sup>5</sup> l<sup>-5</sup>) may first precipitate and then gradually transform into the less soluble hydroxyapatite [Ca<sub>5</sub>(PO<sub>4</sub>)<sub>3</sub>(OH)], and, finally, into the least-soluble member, fluorapatite (solubility product ~10<sup>-60</sup> mol<sup>9</sup> l<sup>-9</sup>). Sedimentation follows and eventually, on a geological time scale, uplift to form a new land mass. Some idea of actual concentrations of ions involved may be obtained from the fact that in sea water there is one phosphate group per million water molecules; at a salinity of 3.3%, pH 8 and 20°C, 87% of the inorganic phosphate exist as [HPO<sub>4</sub>]<sup>2-</sup>, 12% as [PO<sub>4</sub>]<sup>3-</sup> and 1% as [H<sub>2</sub>PO<sub>4</sub>]<sup>-</sup>. Of the [PO<sub>4</sub>]<sup>3-</sup> species, 99.6% is complexed with cations other than Na<sup>+</sup>.<sup>(21)</sup>

The secondary biological cycles stem from the crucial roles that phosphates and particularly organophosphates play in all life processes. Thus organophosphates are incorporated into the backbone structures of DNA and RNA which regulate the reproductive processes of cells, and they

<sup>18</sup> B. H. SVENSSON and R. SÖDERLUND (eds.), *Nitrogen, Phosphorus, and Sulfur—Global Biogeochemical Cycles*, SCOPE Report, No. 7, Sweden 1976, 170 pp.; also SCOPE Report No. 10, Wiley, New York, 1977, 220 pp. and SCOPE Newsletter 47, Jan. 1995, pp. 1–4.

<sup>19</sup> E. J. GRIFFITH, A. BEETON, J. M. SPENCER, and D. T. MITCHELL (eds.), *Environmental Phosphorus Handbook*, Wiley, New York, 1973, 718 pp.

<sup>20</sup> Ciba Foundation Symposium 57 (New Series), *Phosphorus in the Environment: Its Chemistry and Biochemistry*, Elsevier, Amsterdam, 1978, 320 pp.

<sup>21</sup> E. T. DEGENS, *Topics in Current Chem.* **64**, 1–112 (1976).

are also involved in many metabolic and energy-transfer processes either as adenosine triphosphate (ATP) (p. 528) or other such compounds. Another role, restricted to higher forms of life, is the structural use of calcium phosphates as bones and teeth. Tooth enamel is nearly pure hydroxyapatite and its resistance to dental caries is enhanced by replacement of  $\text{OH}^-$  by  $\text{F}^-$  (fluoridation) to give the tougher, less soluble  $[\text{Ca}_5(\text{PO}_4)_3\text{F}]$ . It is also commonly believed that the main inorganic phases in bone are hydroxyapatite and an amorphous phosphate, though many crystallographers favour an isomorphous solution of hydroxyapatite and the carbonate-apatite mineral dahllite,  $[(\text{Na},\text{Ca})_5(\text{PO}_4,\text{CO}_3)_3(\text{OH})]$ , as the main crystalline phase with little or no amorphous material. Young bones also contain brushite,  $[\text{CaHPO}_4 \cdot 2\text{H}_2\text{O}]$ , and the hydrated octacalcium phosphate  $[\text{Ca}_8\text{H}_2(\text{PO}_4)_6 \cdot 5\text{H}_2\text{O}]$  which

is composed, essentially, of alternate layers of apatite and water oriented parallel to (001).<sup>(21)</sup>

The land-based phosphate cycle is shown in Fig. 12.1.<sup>(22)</sup> The amount of phosphate in untilled soil is normally quite small and remains fairly stable because it is present as the insoluble salts of  $\text{Ca}^{\text{II}}$ ,  $\text{Fe}^{\text{III}}$  and  $\text{Al}^{\text{III}}$ . To be used by plants, the phosphate must be released as the soluble  $[\text{H}_2\text{PO}_4]^-$  anion, in which form it can be taken up by plant roots. Although acidic soil conditions will facilitate phosphate absorption, phosphorus is the nutrient which is often in shortest supply for the growing plant. Most mined phosphate is thus destined for use in fertilizers and this accounts for up to 75% of phosphate rock in technologically advanced countries and over 90% in less advanced (more

<sup>22</sup> J. EMSLEY, *Chem. Br.* 13, 459–63 (1977).

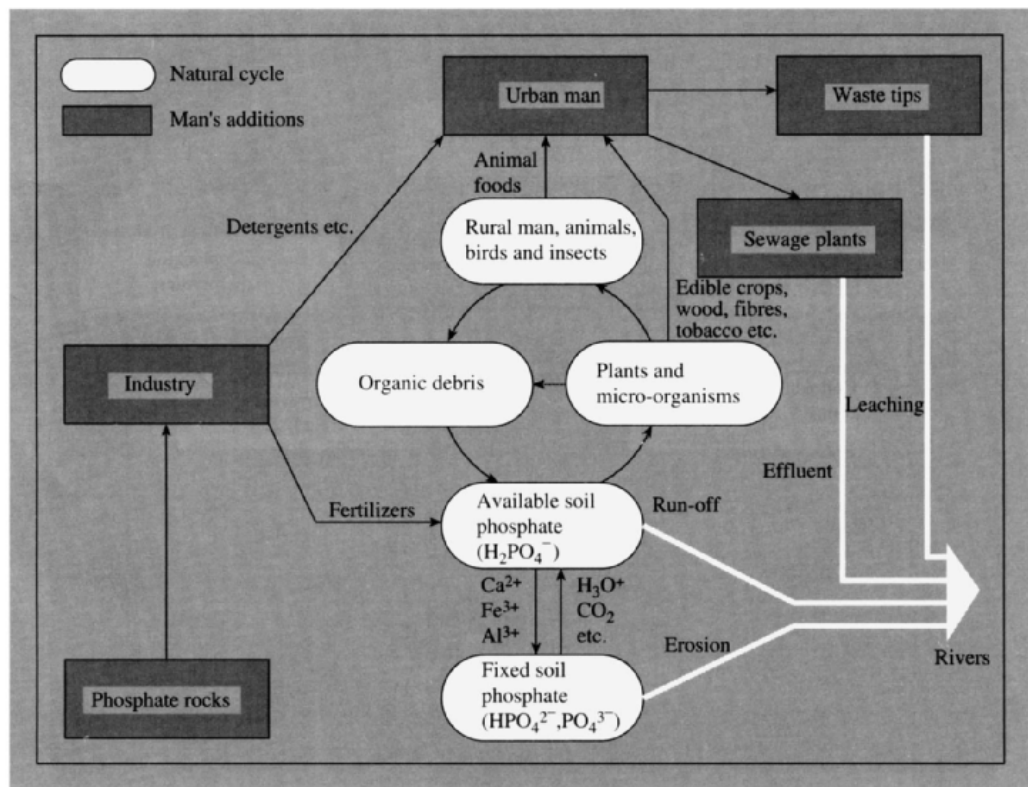


Figure 12.1 The land-based phosphate cycle.

agriculturally based) countries. Moderation in all things, however: excessive fertilization of natural waters due to detergents and untreated sewage in run-off water can lead to heavy overgrowth of algae and higher plants, thus starving the water of dissolved oxygen, killing fish and other aquatic life, and preventing the use of lakes for recreation, etc. This unintended over-fertilization and its consequences has been termed eutrophication (Greek  $\epsilon\upsilon$ , *eu*, well;  $\tau\rho\acute{\epsilon}\phi\epsilon\iota\nu$ , *trephein*, to nourish) and is the subject of active environmental legislation in several countries. Reclamation of eutrophied lakes can best be effected by addition of soluble  $Al^{III}$  salts to precipitate the phosphates.

As just implied, the land-based phosphorus cycle is connected to the water-based cycle via the rivers and sewers. It has been estimated that, on a global scale, about 2 million

tonnes of phosphate are washed into the seas annually from natural processes and rather more than this amount is dumped from human activities. For example in the UK some 200 000 tonnes of phosphate enters the sewers each year: 100 000 tonnes from detergents (now decreasing), 75 000 from human excreta, and 25 000 tonnes from industrial processes. Details of the subsequent water-based phosphate cycle are shown schematically in Fig. 12.2. The water-based cycle is the most rapid of the three phosphate cycles and can be completed within weeks (or even days). The first members of the food chain are the algae and experiments with radioactive  $^{32}P$  (p. 482) have shown that, within minutes of entering an aquatic environment, inorganic phosphate is absorbed by algae and bacteria (50% uptake in 1 min. 80% in 3 min). In the seas and oceans the various phosphate anions

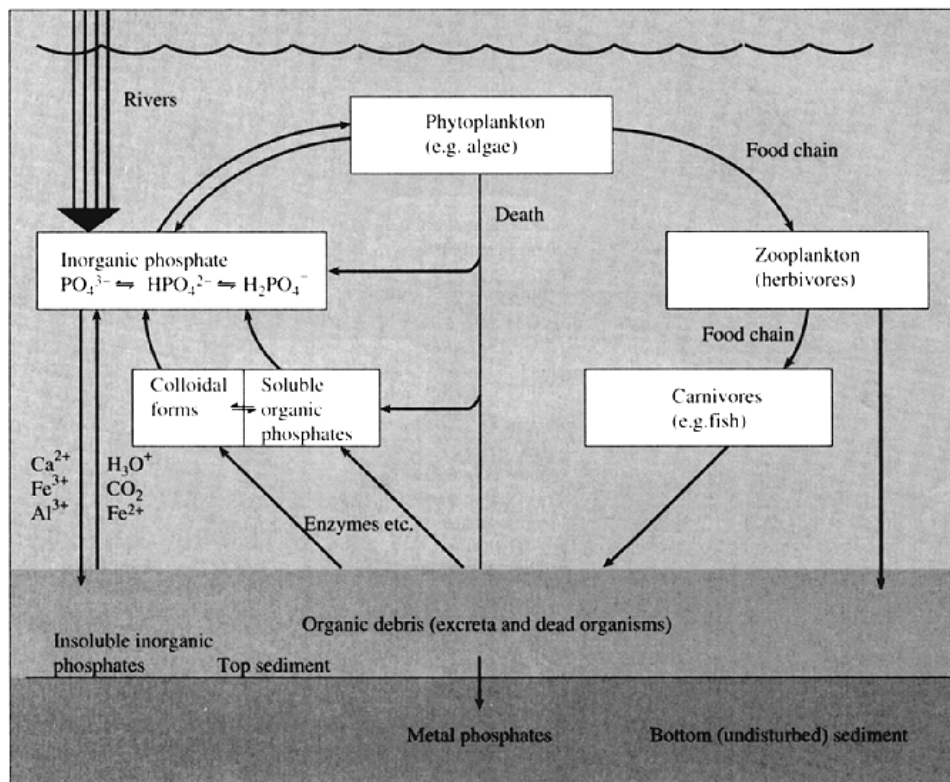
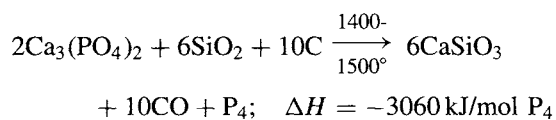


Figure 12.2 The water-based phosphate cycle.<sup>(22)</sup>

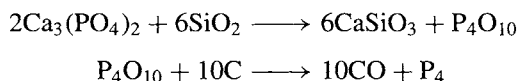
form insoluble inorganic phosphates which gradually sink to the sea bed. The concentration of phosphate therefore increases with depth (down to about 1000 m, below which it remains fairly constant); by contrast the sunlight, which is necessary for the primary photosynthesis in the food chain, is greatest at the surface and rapidly diminishes with depth. It is significant that those regions of the sea where the deeper phosphate-rich waters come welling up to the surface support by far the greatest concentration of the world's fish population; such regions, which occur in the mid-Pacific, the Pacific coast of the Americas, Arabia and Antarctica, account for only 0.1% of the sea's surface but support 50% of the world's fish population.

### 12.2.2 Production and uses of elemental phosphorus

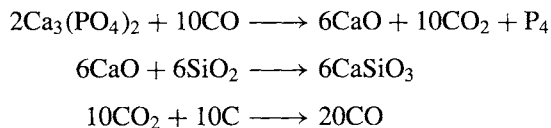
For a century after its discovery the only source of phosphorus was urine. The present process of heating phosphate rock with sand and coke was proposed by E. Aubertin and L. Boblique in 1867 and improved by J. B. Readman who introduced the use of an electric furnace. The reactions occurring are still not fully understood, but the overall process can be represented by the idealized equation:



The presence of silica to form slag which is vital to large-scale production was perceptively introduced by Robert Boyle in his very early experiments. Two apparently acceptable mechanisms have been proposed and it is possible that both may be occurring. In the first, the rock is thought to react with molten silica to form slag and  $\text{P}_4\text{O}_{10}$  which is then reduced by the carbon:



In the second possible mechanism, the rock is considered to be directly reduced by CO and the CaO so formed then reacts with the silica to form slag:



Whatever the details, the process is clearly energy intensive and, even at 90% efficiency, requires ~15 MWh per tonne of phosphorus (see Panel).

### 12.2.3 Allotropes of phosphorus<sup>(23)</sup>

Phosphorus (like C and S) exists in many allotropic modifications which reflect the variety of ways of achieving catenation. At least five crystalline polymorphs are known and there are also several "amorphous" or vitreous forms (see Fig. 12.3). All forms, however, melt to give the same liquid which consists of symmetrical  $\text{P}_4$  tetrahedral molecules, P–P 225 pm. The same molecular form exists in the gas phase (P–P 221 pm), but at high temperatures (above ~800°C) and low pressures  $\text{P}_4$  is in equilibrium with the diatomic form  $\text{P}\equiv\text{P}$  (189.5 pm). At atmospheric pressure, dissociation of  $\text{P}_4$  into  $2\text{P}_2$  reaches 50% at ~1800°C and dissociation of  $\text{P}_2$  into  $2\text{P}$  reaches 50% at ~2800°.

The commonest form of phosphorus, and the one which is usually formed by condensation from the gaseous or liquid states, is the waxy, cubic, white form  $\alpha\text{-P}_4$  ( $d$  1.8232 g cm<sup>-3</sup> at 20°C). This, paradoxically, is also the most volatile and reactive solid form and thermodynamically the least stable. It is the slow phosphorescent oxidation of the vapour above these crystals that gives white phosphorus its most characteristic property. Indeed, the emission of yellow-green light from the oxidation of  $\text{P}_4$  is one of the earliest recorded examples of chemiluminescence, though the details of the reaction

<sup>23</sup> D. E. C. CORBRIDGE, *The Structural Chemistry of Phosphorus*, Elsevier, Amsterdam, 1974, 542 pp.

### Production of White Phosphorus<sup>(3,11,17)</sup>

A typical modern phosphorus furnace (12 m diameter) can produce some 4 tonnes per hour and is rated at 60–70 MW (i.e. 140 000 A at 500 V). Three electrodes, each weighing 60 tonnes, lead in the current. The amounts of raw material required to make 1 tonne of white phosphorus depend on their purity but are typically 8 tonnes of phosphate rock, 2 tonnes of silica, 1.5 tonnes of coke, and 0.4 tonnes of electrode carbon. The phosphorus vapour is driven off from the top of the furnace together with the CO and some H<sub>2</sub>; it is passed through a hot electrostatic precipitator to remove dust and then condensed by water sprays at about 70° (P<sub>4</sub> melts at 44.1°). The byproduct CO is used for supplementary heating.

As most phosphate rock approximates in composition to fluoroapatite, [Ca<sub>5</sub>(PO<sub>4</sub>)<sub>3</sub>F], it contains 3–4 wt% F. This reacts to give the toxic and corrosive gas SiF<sub>4</sub> which must be removed from the effluent. The stoichiometry of phosphate rock might suggest that about 1 mole of SiF<sub>4</sub> is formed for each 3 moles of P<sub>4</sub>, but only about 20% of the fluorine reacts in this way, the rest being retained in the slag. Nevertheless, since a typical furnace can produce over 30 000 tonnes of phosphorus per year this represents a substantial waste of a potentially useful byproduct (~5000 tonnes SiF<sub>4</sub> yearly per furnace). In some plants the SiF<sub>4</sub> is recovered by treatment with water and soda ash (Na<sub>2</sub>CO<sub>3</sub>) to give Na<sub>2</sub>SiF<sub>6</sub> which can be used in the fluoridation of drinking water.

Another troublesome impurity in phosphate rock (1–5%) is Fe<sub>2</sub>O<sub>3</sub> which is reduced in the furnace to "ferrophosphorus", an impure form of Fe<sub>2</sub>P. This is a dense liquid at the reaction temperature; it sinks beneath the slag and can be drained away at intervals. As every tonne of ferrophosphorus contains ~0.25 tonne of P, this is a major loss, but is unavoidable since the Fe<sub>2</sub>O<sub>3</sub> cannot economically be removed beforehand. The few uses of ferrophosphorus depend on its high density (~6.6 g cm<sup>-3</sup>). It can be mixed with dynamite for blasting or used as a filler in high-density concrete and in radiation shields for nuclear reactors. It is also used in the manufacture of special steels and cast-irons, especially for non-sparking railway brake-shoes. The other substantial byproduct, CaSiO<sub>3</sub> slag, has little economic use and is sold as hard core for road-fill or concrete aggregate; about 7–9 tonnes are formed per tonne of P produced.

World capacity for the production of elemental P is ~1.5 million tonnes per year. Some figures for 1984 are as follows:

Country	USSR	USA	Germany	Netherlands	Canada	France
ktonne/y	615	412	95	90	90	39
Country	China	Japan	Mexico	India	South Africa	
ktonne/y	35	20	10	10	6	

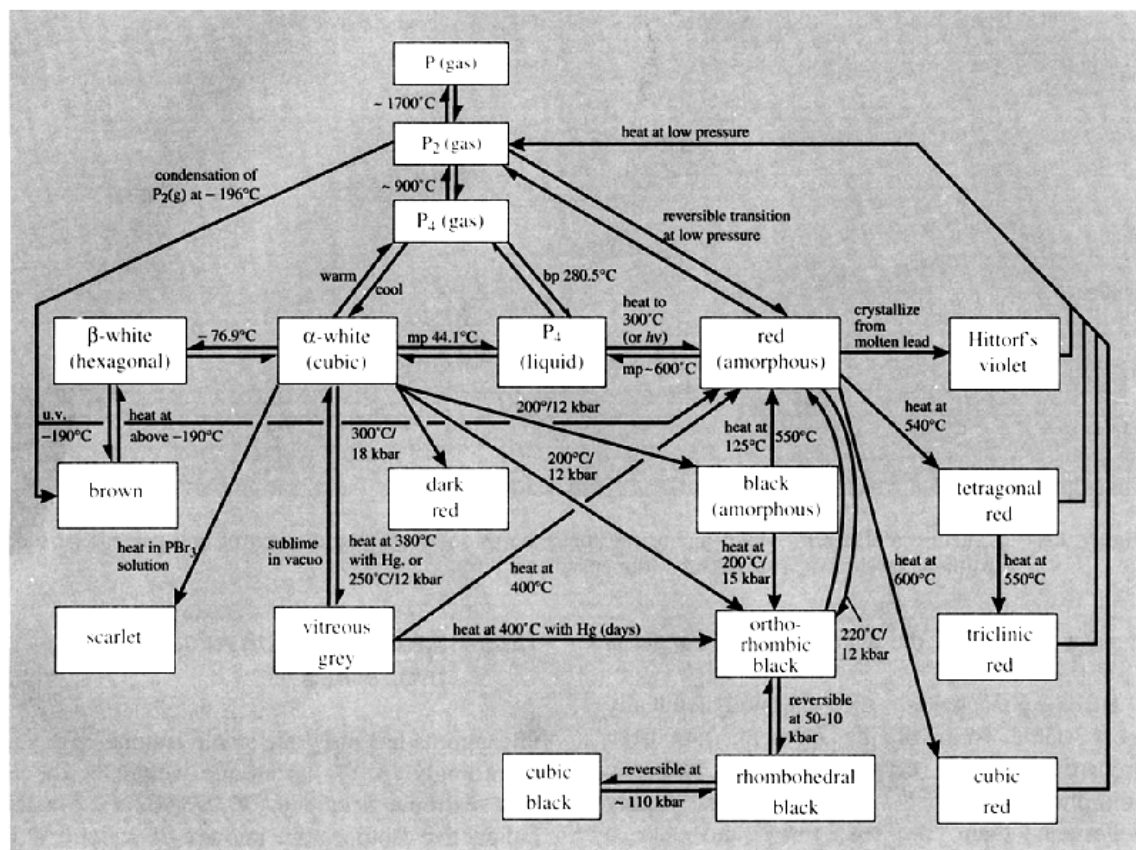
About 80–90% of the elemental P produced is reoxidized to (pure) phosphoric acid (p. 521). The rest is used to make phosphorus oxides (p. 503), sulfides (p. 506), phosphorus chlorides and oxochloride (p. 496), and organic P compounds. A small amount is converted to red phosphorus (see below) for use in the striking surface of matches for pyrotechnics and as a flame retarding agent (in polyamides). Bulk price for P<sub>4</sub> is ~\$2.00/kg.

mechanism are still not fully understood: the primary emitting species in the visible region of the spectrum are probably (PO)<sub>2</sub> and HPO; ultraviolet emission from excited states of PO also occurs.<sup>(24)</sup> At -76.9° and atmospheric pressure the α-form of P<sub>4</sub> converts to the very similar white hexagonal β-form (*d* 1.88 g cm<sup>-3</sup>), possibly by loss of rotational disorder; Δ*H*(α→β) = 15.9 kJ (mol P<sub>4</sub>)<sup>-1</sup>. White phosphorus is insoluble in water but exceedingly soluble (as P<sub>4</sub>) in CS<sub>2</sub> (~880 g per 100 g CS<sub>2</sub> at 10°C). It is also very soluble in PCl<sub>3</sub>, POCl<sub>3</sub>, liquid SO<sub>2</sub>, liquid

NH<sub>3</sub> and benzene, and somewhat less soluble in numerous other organic solvents. The β-form can be maintained as a solid up to 64.4°C under a pressure of 11 600 atm, whereas the α-form melts at 44.1°C. White phosphorus is highly toxic and ingestion, inhalation or even contact with skin must be avoided; the fatal dose when taken internally is about 50 mg.

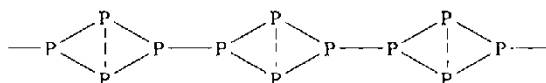
Amorphous red phosphorus was first obtained in 1848 by heating white P<sub>4</sub> out of contact with air for several days, and is now made on a commercial scale by a similar process at 270°–300°C. It is denser than white P<sub>4</sub> (~2.16 g cm<sup>-3</sup>), has a much higher m.p.

<sup>24</sup> R. J. VAN ZEE and A. U. KHAN, *J. Am. Chem. Soc.* **96**, 6805–6 (1974).



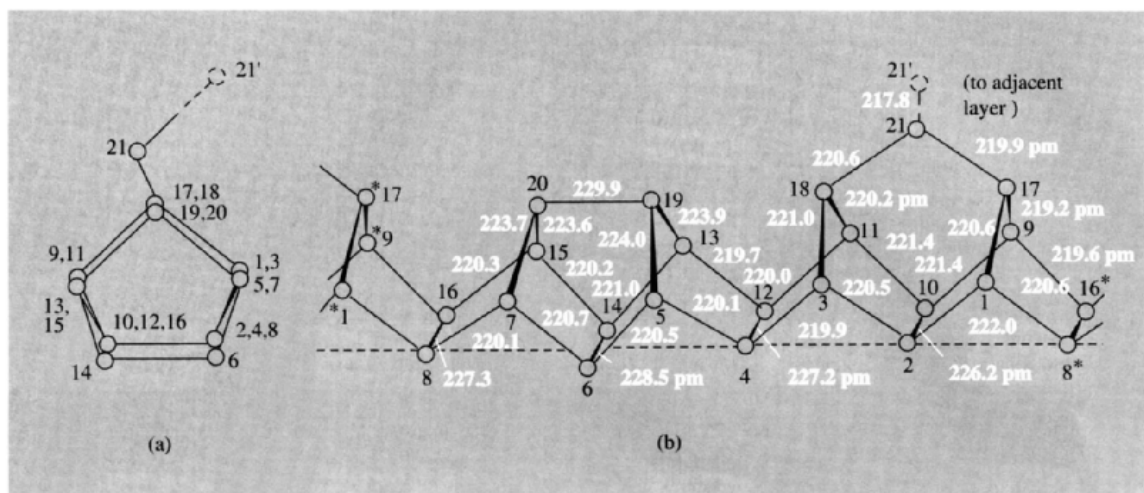
**Figure 12.3** Interconversion of the various forms of elemental phosphorus (1 kbar =  $10^8$  Pa = 987.2 atm).

(~600°C), and is much less reactive; it is therefore safer and easier to handle, and is essentially non-toxic. The amorphous material can be transformed into various crystalline red modifications by suitable heat treatment, as summarized on the right hand side of Fig. 12.3. It seems likely that all are highly polymeric and contain three-dimensional networks formed by breaking one P–P bond in each P<sub>4</sub> tetrahedron and then linking the remaining P<sub>4</sub> units into chains or rings of P atoms each of which is pyramidal and 3 coordinate as shown schematically below:



This is well illustrated by the crystal structure of Hittrorf's violet monoclinic allotrope ( $d$  2.35 g cm<sup>-3</sup>) which was first made in 1865 by crystallizing phosphorus in molten lead. The structure is exceedingly complex<sup>(25)</sup> and consists of P<sub>8</sub> and P<sub>9</sub> groups linked alternately by pairs of P atoms to form tubes of pentagonal cross-section and with a repeat unit of 21P (Fig. 12.4). These tubes, or complex chains, are stacked (without direct covalent bonding) to form sheets and are linked by P–P bonds to similar chains which lie at right angles to the first set in an adjacent parallel layer. These pairs of composite parallel sheets are then stacked to form the crystal. The average P–P distance is 222 pm (essentially the

<sup>25</sup> VON H. THURN and H. KREBS. *Acta Cryst.* **B25**, 125–35 (1969).



**Figure 12.4** Structure of Hittorf's violet monoclinic phosphorus showing (a) end view of one pentagonal tube, (b) the side view of a single tube (dimensions in pm).

same as in  $P_4$ ) but the average P-P-P angle is  $101^\circ$  (instead of  $60^\circ$ ).

Black phosphorus, the thermodynamically most stable form of the element, has been prepared in three crystalline forms and one amorphous form. It is even more highly polymeric than the red form and has a correspondingly higher density (orthorhombic 2.69, rhombohedral 3.56, cubic  $3.88 \text{ g cm}^{-3}$ ). Black phosphorus (orthorhombic) was originally made by heating white  $P_4$  to  $200^\circ$  under a pressure of 12 000 atm (P. W. Bridgman, 1916). Higher pressures convert it successively to the rhombohedral and cubic forms (Fig. 12.3). Orthorhombic black P (mp  $\sim 610^\circ$ ) has a layer structure which is based on a puckered hexagonal net of 3-coordinate P atoms with 2 interatomic angles of  $102^\circ$  and 1 of  $96.5^\circ$  (P-P 223 pm). The relation of this form to the rhombohedral and cubic forms is shown in Fig. 12.5. Comparison with the rhombohedral forms of As, Sb and Bi is also instructive in showing the increasing tendency towards octahedral coordination and metallic properties (p. 551). Black P is semiconducting but its electrical properties are probably significantly affected by impurities introduced during its preparation.

### 12.2.4 Atomic and physical properties<sup>(26)</sup>

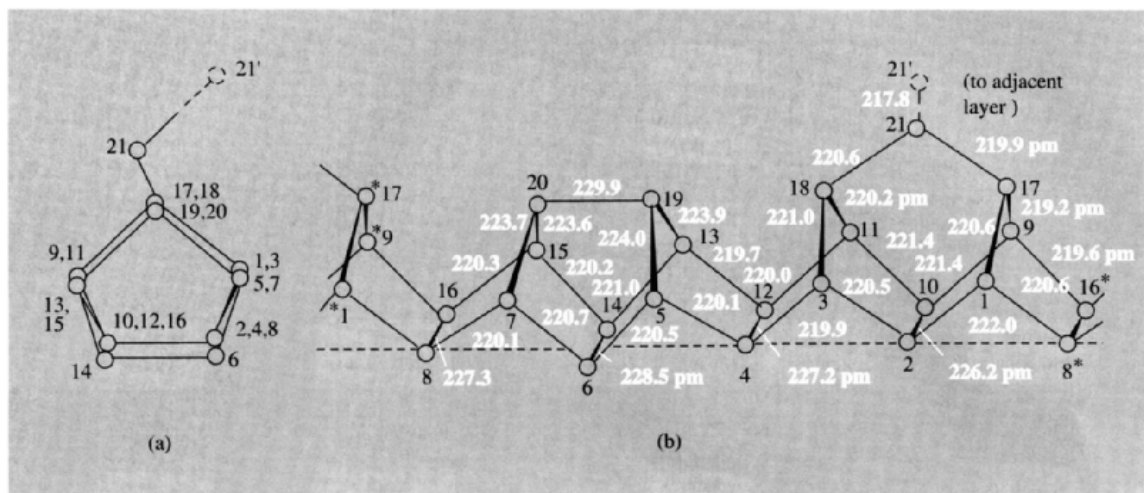
Phosphorus has only one stable isotope,  $^{31}\text{P}$ , and accordingly (p. 17) its atomic weight is known with extreme accuracy, 30.973 762(4). Sixteen radioactive isotopes are known, of which  $^{32}\text{P}$  is by far the most important; it is made on the multikilogram scale by the neutron irradiation of  $^{32}\text{S}(n,p)$  or  $^{31}\text{P}(n,\gamma)$  in a nuclear reactor, and is a pure  $\beta$ -emitter of half life 14.26 days,  $E_{\text{max}}$  1.709 MeV,  $E_{\text{mean}}$  0.69 MeV. It finds extensive use in tracer and mechanistic studies. The stable isotope  $^{31}\text{P}$  has a nuclear spin quantum number of  $\frac{1}{2}$  and this is much used in nmr spectroscopy.<sup>(27)</sup> Chemical shifts and coupling constants can both be used diagnostically to determine structural information.

In the ground state, P has the electronic configuration  $[\text{Ne}]3s^2 3p_x^1 3p_y^1 3p_z^1$  with 3 unpaired

<sup>26</sup> Mellor's *Comprehensive Treatise on Inorganic and Theoretical Chemistry*, Vol. 8, Suppl. 3, *Phosphorus*, Longman, London, 1971, 1467 pp.

<sup>27</sup> D. G. GORENSTEIN (ed.) *Phosphorus-31 NMR; Principles and Applications* Academic Press, London, 1984, 604 pp. J. G. VERKADE and L. D. QUIN (eds.), *Phosphorus-31 NMR Spectroscopy in Stereochemical Analysis*, VCH Publishers, Weinheim, 1987, 717 pp.





**Figure 12.4** Structure of Hittorf's violet monoclinic phosphorus showing (a) end view of one pentagonal tube, (b) the side view of a single tube (dimensions in pm).

same as in  $P_4$ ) but the average P-P-P angle is  $101^\circ$  (instead of  $60^\circ$ ).

Black phosphorus, the thermodynamically most stable form of the element, has been prepared in three crystalline forms and one amorphous form. It is even more highly polymeric than the red form and has a correspondingly higher density (orthorhombic  $2.69$ , rhombohedral  $3.56$ , cubic  $3.88 \text{ g cm}^{-3}$ ). Black phosphorus (orthorhombic) was originally made by heating white  $P_4$  to  $200^\circ$  under a pressure of  $12\,000 \text{ atm}$  (P. W. Bridgman, 1916). Higher pressures convert it successively to the rhombohedral and cubic forms (Fig. 12.3). Orthorhombic black P (mp  $\sim 610^\circ$ ) has a layer structure which is based on a puckered hexagonal net of 3-coordinate P atoms with 2 interatomic angles of  $102^\circ$  and 1 of  $96.5^\circ$  (P-P  $223 \text{ pm}$ ). The relation of this form to the rhombohedral and cubic forms is shown in Fig. 12.5. Comparison with the rhombohedral forms of As, Sb and Bi is also instructive in showing the increasing tendency towards octahedral coordination and metallic properties (p. 551). Black P is semiconducting but its electrical properties are probably significantly affected by impurities introduced during its preparation.

### 12.2.4 Atomic and physical properties<sup>(26)</sup>

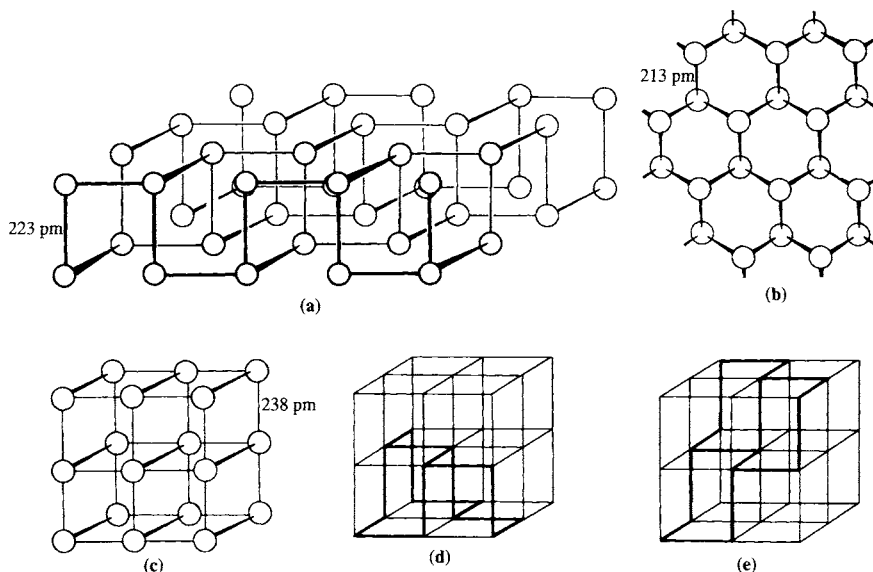
Phosphorus has only one stable isotope,  $^{31}_{15}\text{P}$ , and accordingly (p. 17) its atomic weight is known with extreme accuracy,  $30.973\,762(4)$ . Sixteen radioactive isotopes are known, of which  $^{32}\text{P}$  is by far the most important; it is made on the multikilogram scale by the neutron irradiation of  $^{32}\text{S}(n,p)$  or  $^{31}\text{P}(n,\gamma)$  in a nuclear reactor, and is a pure  $\beta$ -emitter of half life  $14.26 \text{ days}$ ,  $E_{\text{max}} 1.709 \text{ MeV}$ ,  $E_{\text{mean}} 0.69 \text{ MeV}$ . It finds extensive use in tracer and mechanistic studies. The stable isotope  $^{31}\text{P}$  has a nuclear spin quantum number of  $\frac{1}{2}$  and this is much used in nmr spectroscopy.<sup>(27)</sup> Chemical shifts and coupling constants can both be used diagnostically to determine structural information.

In the ground state, P has the electronic configuration  $[\text{Ne}]3s^2 3p_x^1 3p_y^1 3p_z^1$  with 3 unpaired

<sup>26</sup> Mellor's *Comprehensive Treatise on Inorganic and Theoretical Chemistry*, Vol. 8, Suppl. 3, *Phosphorus*, Longman, London, 1971, 1467 pp.

<sup>27</sup> D. G. GORENSTEIN (ed.) *Phosphorus-31 NMR; Principles and Applications* Academic Press, London, 1984, 604 pp. J. G. VERKADE and L. D. QUIN (eds.), *Phosphorus-31 NMR Spectroscopy in Stereochemical Analysis*, VCH Publishers, Weinheim, 1987, 717 pp.





**Figure 12.5** The structures of black phosphorus: (a) portion of one layer of orthorhombic P (idealized), (b) rhombohedral form, portion of one hexagonal layer, (c) cubic form, 4 unit cells, (d) distortion of (a) to the cubic form, and (e) distortion of (b) to the cubic form.

electrons; this, together with the availability of low-lying vacant 3d orbitals, accounts for the predominant oxidation states III and V in phosphorus chemistry. Ionization energies, electronegativity, and atomic radii are compared with those of N, As, Sb and Bi on p. 550. White phosphorus ( $\alpha$ -P<sub>4</sub>) has mp 44.1° (or 44.25° when ultrapure), bp 280.5° and a vapour pressure of 0.122 mmHg at 40°C. It is an insulator with an electrical resistivity of  $\sim 10^{11}$  ohm cm at 11°C, a dielectric constant of 4.1 (at 20°) and a refractive index  $n_D$  (29.2°) 1.8244. The heat of combustion of P<sub>4</sub> to P<sub>4</sub>O<sub>10</sub> is  $-2971 \text{ kJ mol}^{-1}$  and the heat of transition to amorphous red phosphorus is  $-29 \text{ kJ (mol P}_4\text{)}^{-1}$ .

### 12.2.5 Chemical reactivity and stereochemistry

The spontaneous chemiluminescent reaction of white phosphorus with moist air was the first property of the element to be observed and was the origin of its name (p. 473); its spontaneous ignition temperature in air is  $\sim 35^\circ$ . We have already seen (p. 481) that the reactivity

of phosphorus depends markedly upon which allotrope is being studied and that increasing catenation of the polymeric red and black forms notably diminishes both reactivity and solubility. The preference of phosphorus for these forms rather than for the gaseous form P<sub>2</sub>, which is its most obvious distinction from nitrogen, can be rationalized in terms of the relative strengths of the triple and single bonds for the 2 elements. Reliable values are hard to obtain but generally accepted values are as follows:

$E(\text{N}\equiv\text{N})/\text{kJ}$		$E(\text{P}\equiv\text{P})/\text{kJ}$	
per mol of N	946	per mol of P	490
$E(>\text{N}-\text{N}<)/\text{kJ}$	159	$E(>\text{P}-\text{P}<)/\text{kJ}$	
per mol of N	(or 296)	per mol of P	200
Ratio	5.95	Ratio	2.45
	(or 3.20)		

It is clear that, for nitrogen, the triple bond is preferred since it has more than 3 times the energy of a single bond, whereas for phosphorus the triple-bond energy is less than 3 times the single-bond energy and so allotropes having 3 single bonds per P atom are more stable than that with a triple bond.

Table 12.2 Stereochemistry of phosphorus

CN	Geometry	Examples
0	—	P(g) — in equilibrium with P <sub>2</sub> (g) above 2200°C
1	—	P <sub>2</sub> (g) — in equilibrium with P <sub>4</sub> (g) above 800°C; HC≡P; FC≡P; MeC≡P (p. 544)
2	Bent <sup>(28)</sup>	HP=CH <sub>2</sub> , <sup>(29)</sup> [P(CN) <sub>2</sub> ] <sup>-</sup> , <sup>(30)</sup> [(C <sub>6</sub> H <sub>4</sub> S(NR)C) <sub>2</sub> P] <sup>+X<sup>-</sup></sup> (p. 544), cyclo-C <sub>5</sub> H <sub>5</sub> P, 2,4,6-Ph <sub>3</sub> C <sub>5</sub> H <sub>2</sub> P; Me <sub>3</sub> P=PCF <sub>3</sub> ; P <sub>7</sub> <sup>3-</sup> anion <sup>(31)</sup> (isoelectronic with P <sub>4</sub> S <sub>3</sub> ) in Sr <sub>3</sub> P <sub>14</sub> ; P <sub>11</sub> <sup>3-</sup> anion in Na <sub>3</sub> P <sub>11</sub> ; diazaphospholes <sup>(32)</sup>
3	Planar	[PhP{Mn(η <sup>5</sup> -C <sub>5</sub> H <sub>5</sub> )(CO) <sub>2</sub> }] <sub>2</sub> <sup>(33)</sup> , [(fluorenyl)=P{=C(SiMe <sub>3</sub> ) <sub>2</sub> }] <sup>-(33a)</sup>
4	Pyramidal Tetrahedral	P <sub>4</sub> , PH <sub>3</sub> , PX <sub>3</sub> , P <sub>4</sub> O <sub>6</sub> , [PhP{Co(CO) <sub>4</sub> }] <sub>2</sub> <sup>(34)</sup> PH <sub>4</sub> <sup>+</sup> , Cl <sub>3</sub> PO, P <sub>4</sub> O <sub>10</sub> , PO <sub>4</sub> <sup>3-</sup> , polyphosphates, MP (zinc-blende type, M = B, Al, Ga, In), [Co <sub>3</sub> (CO) <sub>9</sub> (μ <sub>3</sub> -PPh)] <sub>2</sub> <sup>(35)</sup> , [(P <sub>4</sub> )Ni{(Ph <sub>2</sub> PCH <sub>2</sub> CH <sub>2</sub> ) <sub>3</sub> N}] <sub>2</sub> <sup>(36)</sup> many complexes of PR <sub>3</sub> etc., with metal centres
5	Local C <sub>2v</sub> Trigonal bipyramidal	PBr <sub>4</sub> <sup>-</sup> , [PBr <sub>2</sub> (CN) <sub>2</sub> ] <sup>-</sup> . <sup>(37)</sup> [μ(η <sup>3</sup> -P <sub>3</sub> ){Ni(triphos)} <sub>2</sub> ] <sup>2+</sup> <sup>(38)</sup> PF <sub>5</sub> , PPh <sub>5</sub>
6	Square pyramidal Octahedral Trigonal prismatic	[Co <sub>4</sub> (CO) <sub>8</sub> (μ-CO) <sub>2</sub> (μ <sub>4</sub> -PPh) <sub>2</sub> ], [Os <sub>5</sub> (CO) <sub>15</sub> (μ <sub>4</sub> -POMe)] <sup>(39)</sup> PF <sub>6</sub> <sup>-</sup> , PCl <sub>6</sub> <sup>-</sup> , MP (NaCl-type, M = La, Sm, Th, U etc.) Rh <sub>4</sub> P <sub>3</sub> , Hf <sub>3</sub> P <sub>2</sub> (also contains seven- and eight-fold coordination of P by M), [(μ <sub>6</sub> -P){Os(CO) <sub>3</sub> }] <sub>6</sub> <sup>-(40)</sup>
7	Irregular (4 + 2) Capped trigonal prismatic	[Co <sub>6</sub> (CO) <sub>14</sub> (μ-CO) <sub>2</sub> P] <sup>-</sup> Ta <sub>2</sub> P, Hf <sub>2</sub> P (contains P in seven-, eight-, and nine-fold coordination by M)
8	Cubic Bicapped trigonal prismatic	M <sub>2</sub> P (antifluorite type (p. 118), M = Ir, Rh) Hf <sub>2</sub> P
9	Tricapped trigonal prismatic Monocapped square antiprismatic	M <sub>3</sub> P (M = Ti, V, Cr, Mn, Fe, Ni, Zr, Nb, Ta) M <sub>2</sub> P (PbCl <sub>2</sub> -type, M = Fe, Co, Ru) [Rh <sub>9</sub> (CO) <sub>21</sub> P] <sub>2</sub> <sup>-(41)</sup>

<sup>28</sup>E. FLUCK, *Topics in Phosphorus Chemistry* **10**, 193–284 (1980).

<sup>29</sup>H. W. KROTO, J. F. NIXON, K. OHNO and N. P. C. SIMMONS, *J. Chem. Soc., Chem. Commun.*, 709 (1980).

<sup>30</sup>W. S. SHELDRIK, J. KRONER, F. ZWASCHKA and A. SCHMIDPETER, *Angew. Chem. Int. Edn. Engl.* **18**, 934–5 (1979).

<sup>31</sup>W. DAHLMANN and H. G. VON SCHNERING, *Naturwissenschaften* **59**, 420 (1972). W. WICHELHAUS and H. G. VON SCHNERING, *ibid.* **60**, 104 (1973).

<sup>32</sup>J. H. WEINMAIER, A. SCHMIDPETER, *et al.*, *Angew. Chem. Int. Edn. Engl.* **18**, 412 (1979); *Chem. Ber.* **113**, 2278–90 (1980); *J. Organometallic Chem.* **185**, 53–68 (1980).

<sup>33</sup>G. HUTTNER, H.-D. MÜLLER, A. FRANK, and H. LORENZ, *Angew. Chem. Int. Edn. Engl.* **14**, 705–6 (1975).

<sup>33a</sup>R. APPEL, E. GAITZSCH and F. KNOCH, *Angew. Chem. Int. Edn. Engl.* **24**, 589–90 (1985).

<sup>34</sup>J. C. BURT and G. SCHMID, *J. Chem. Soc., Dalton Trans.*, 1385–7 (1978).

<sup>35</sup>L. MARKÓ and B. MARKÓ, *Inorg. Chim. Acta* **14**, L39 (1975).

<sup>36</sup>P. DAPPORIO, S. MIDOLLINI and L. SACCONI, *Angew. Chem. Int. Edn. Engl.* **18**, 469 (1979).

<sup>37</sup>W. S. SHELDRIK, A. SCHMIDPETER, F. ZWASCHKA, K. B. DILLON, A. W. G. PLAIT and T. C. WADDINGTON, *J. Chem. Soc., Dalton Trans.*, 413–8 (1981) see also *Angew. Chem. Int. Edn. Engl.* **18**, 935–6 (1979).

<sup>38</sup>M. DI VAIRA, S. MIDOLLINI and L. SACCONI, *J. Am. Chem. Soc.* **101**, 1757–63 (1979). For analogous complexes in which μ-(η<sup>3</sup>-P<sub>3</sub>) bridges RhCo, RhNi, IrCo, and RhRh, see C. BIANCHINI, M. DI VAIRA, A. MELI and L. SACCONI, *Angew. Chem. Int. Edn. Engl.* **19**, 405–6 (1980).

<sup>39</sup>J. M. FERNANDEZ, B. F. G. JOHNSON, J. LEWIS and P. R. RAITHY, *J. Chem. Soc., Chem. Commun.*, 1015–6 (1978).

<sup>40</sup>S. B. COLBRAN, C. M. HAY, B. F. G. JOHNSON, F. J. LAHOZ, J. LEWIS and P. R. RAITHY, *J. Chem. Soc., Chem. Commun.*, 1766–8 (1986).

<sup>41</sup>J. L. VIDAL, W. E. WALKER, R. L. PRUETT and R. C. SCHOENING, [Rh<sub>9</sub>P(CO)<sub>21</sub>]<sub>2</sub><sup>2-</sup>. *Inorg. Chem.* **18**, 129–36 (1979).

Phosphorus forms binary compounds with all elements except Sb, Bi and the noble gases. It reacts spontaneously with O<sub>2</sub> and the halogens at room temperature, the mixtures rapidly reaching incandescence. Sulfur and the alkali metals also react vigorously with phosphorus on warming, and the element combines directly with all metals (except Bi, Hg, Pb) frequently with incandescence (e.g. Fe, Ni, Cu, Pt). White phosphorus (but not red) also reacts readily with heated aqueous solutions to give a variety of products (pp. 493 and 513ff), and with many other aqueous and nonaqueous reagents.

The stereochemistry and bonding of P are very varied as will become apparent in later sections: the element is known in at least 14 coordination geometries with CN up to 9, though the most frequently met have CN 3, 4, 5 and 6. Some typical coordination geometries are summarized in Table 12.2 and illustrated in Fig. 12.6. Many of these compounds will be more fully discussed in later sections.

The great propensity of P atoms to catenate into chains, rings and clusters, P<sub>n</sub>, has already been noted during the discussion on allotropy (pp. 479–83). These groupings and other similar ones also feature in the structures of metal phosphides (p. 489), polyphosphanes (p. 492) and organopolyphosphanes (p. 542). Moreover, neutral or charged groupings, P<sub>n</sub>, (*n* = 2–6, 10) can also serve as ligands<sup>(42–44)</sup>, as can isolated P atoms in anions such as [(μ<sub>6</sub>-P){Os(CO)<sub>3</sub>]<sub>6</sub>]<sup>-</sup><sup>(40)</sup> and other structures shown at the foot of Fig. 12.6. Two decades ago virtually nothing was known about this aspect of phosphorus chemistry, but it is now a burgeoning field, and the substantial progress which has been made in recent years now permits a general overview to be given.

<sup>42</sup> M. DI VAIRA and P. STOPPIONI, *Polyhedron* **6**, 351–82 (1987). (Review)

<sup>43</sup> O. J. SCHERER, *Angew. Chem. Int. Edn. Engl.* **24**, 924–43 (1985); **29** 1104–22 (1990). (Reviews)

<sup>44</sup> O. J. SCHERER (and 9 others), in R. STEUDEL (ed.), *The Chemistry of Inorganic Ring Systems*, Elsevier, Amsterdam, 1992, pp. 193–208.

The P<sub>2</sub> group is isoelectronic with ethyne (p. 932) and with N<sub>2</sub> (pp. 414–6) and As<sub>2</sub>. It has emerged as a versatile ligand with several well characterized coordination modes as shown schematically in Fig 12.7. The first compound containing the P<sub>2</sub> ligand, [(Co(CO)<sub>3</sub>]<sub>2</sub>(μ,η<sup>2</sup>-P<sub>2</sub>)], was isolated as a red oil in 1973 and was clearly similar to the already known alkyne and As<sub>2</sub> complexes [{Co(CO)<sub>3</sub>]<sub>2</sub>(μ,η<sup>2</sup>-(CR)<sub>2</sub>)] and [{Co(CO)<sub>3</sub>]<sub>2</sub>(μ,η<sup>2</sup>-As<sub>2</sub>)]. It was formed by reaction of Na[Co(CO)<sub>4</sub>] with PCl<sub>3</sub> or PBr<sub>3</sub> in thf. The tetrahedrane-like core (Fig. 12.7a) was confirmed by X-ray analysis on the related PPh<sub>3</sub> derivative [Co<sub>2</sub>(CO)<sub>5</sub>(PPh<sub>3</sub>)(μ,η<sup>2</sup>-P<sub>2</sub>)].<sup>(45)</sup> Direct action of P<sub>4</sub> with appropriate carbonyl, cyclopentadienyl or alkoxide derivatives of Cr, Mo, W, etc. has yielded a wide range of such compounds of P<sub>2</sub> acting as a 4e-donor, in all of which the two ML<sub>n</sub> vertices can be considered as 15e-acceptors (i.e. d<sup>10</sup> + 5e, “isoelectronic” with P in Group 15) e.g., {Cr(Cp)(CO)<sub>2</sub>},<sup>(46)</sup> {Mo(Cp)(CO)<sub>2</sub>}, {W(py)(OPr<sup>t</sup>)<sub>2</sub>(μ-OPr<sup>t</sup>)},<sup>(47)</sup> etc., where Cp is (η<sup>5</sup>-C<sub>5</sub>H<sub>5</sub>) or one of its derivatives. With 14e or 16e metal-vertex acceptors the core adopts the more open “butterfly” configuration (Fig 12.7b) without direct M–M bonding, e.g. [{Ni(Et<sub>2</sub>PCH<sub>2</sub>CH<sub>2</sub>PEt<sub>2</sub>)<sub>2</sub>(μ,η<sup>2</sup>-P<sub>2</sub>)}]<sup>(48)</sup> and its {Ni(PEt<sub>3</sub>)<sub>2</sub>} and [Pt(PEt<sub>3</sub>)<sub>2</sub>] analogues. Further electron-pair donation from one or both of the P atoms can also occur to give compounds such as [Cr<sub>2</sub>(η<sup>5</sup>-C<sub>5</sub>H<sub>5</sub>)<sub>2</sub>(CO)<sub>4</sub>(μ,η<sup>2</sup>-P<sub>2</sub>)[M(CO)<sub>5</sub>]<sub>1 or 2</sub> (M = Cr, Mo, W) (see Figs. 12.7 c, d).<sup>(49)</sup> In these, the P<sub>2</sub> group acts as a 6e or 8e donor, and bridges 3 or 4 M atoms respectively. See below — p. 488 — for examples cf. bis-P<sub>2</sub>, i.e. pseudo-P<sub>4</sub> complexes.)

<sup>45</sup> C. F. CAMPANA, A. VIZI-OROSZ, G. PÄLYI, L. MARKÒ and L. F. DAHL, *Inorg. Chem.* **18**, 3054–9 (1979).

<sup>46</sup> L. Y. GOH, C. K. CHU, R. C. S. WONG and T. W. HAMBLEY, *J. Chem. Soc., Chem. Commun.*, 1951–6 (1979).

<sup>47</sup> M. H. CHISHOLM, K. FOLTING, J. C. HUFFMAN and J. J. KOH, *Polyhedron* **4**, 893–5 (1985).

<sup>48</sup> H. SCHÄFFER, D. BINDER and D. FENSKE, *Angew. Chem. Int. Edn. Engl.* **24**, 522–4 (1985).

<sup>49</sup> L. Y. GOH, R. C. S. WONG and T. C. W. MAK, *J. Organometallic Chem.* **364**, 363–71 (1989) and **373**, 71–6 (1989).

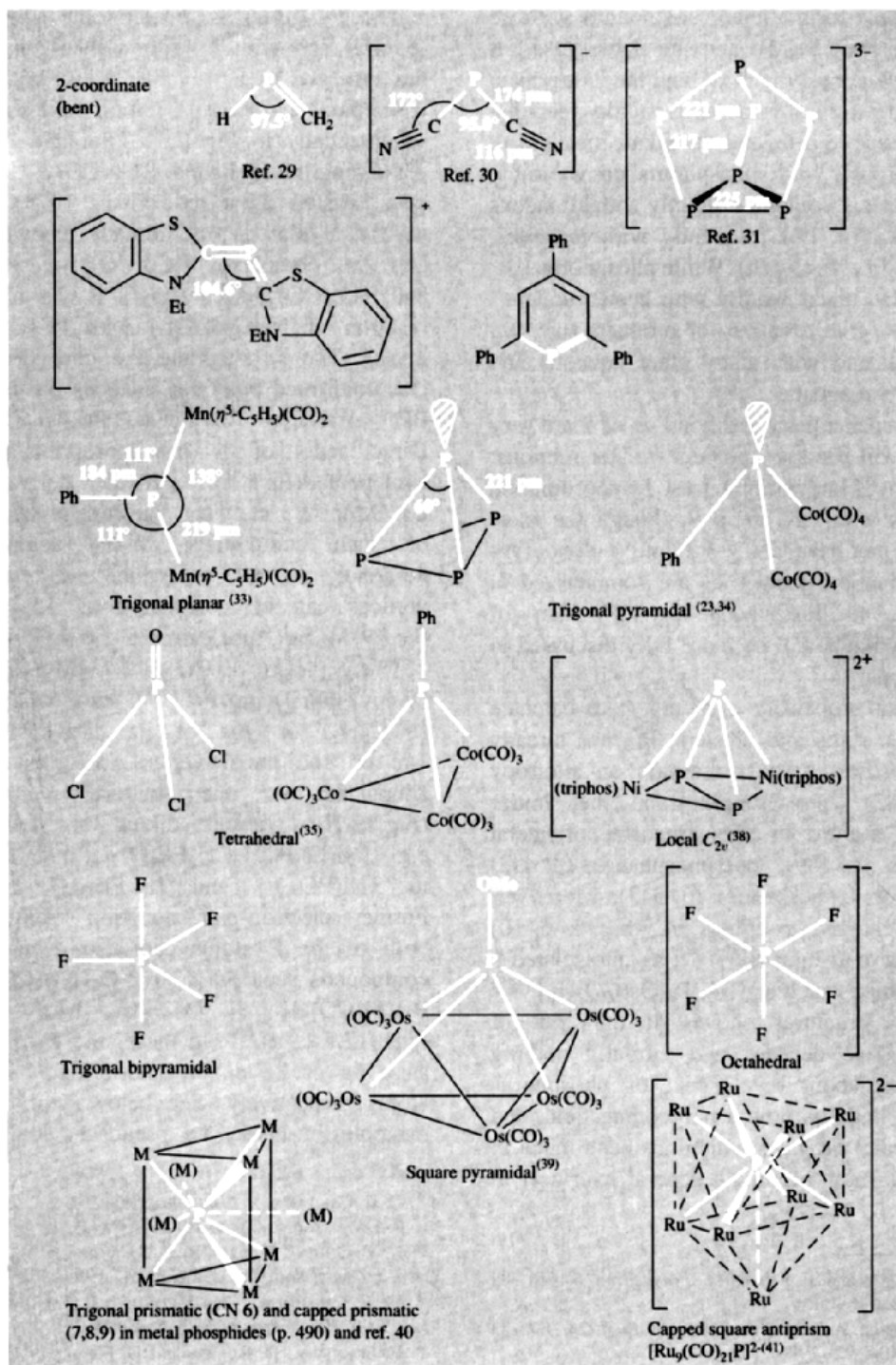
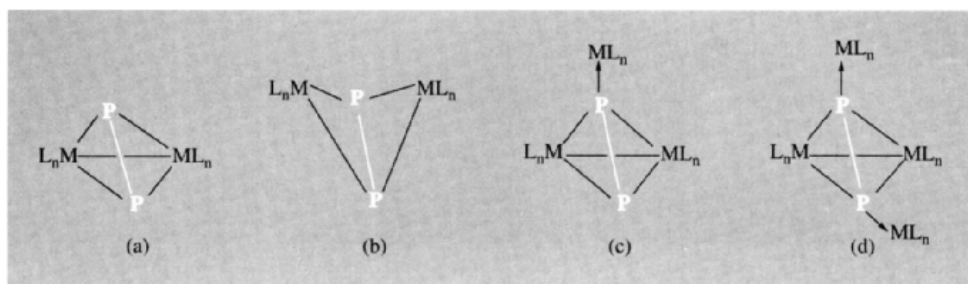
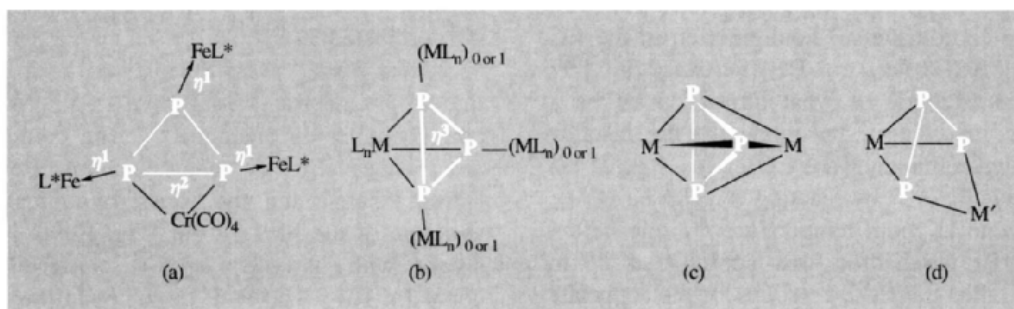


Figure 12.6 Schematic representation of some of the coordination geometries of phosphorus.



**Figure 12.7** (a)  $(\mu_2, \eta^2\text{-P}_2)$  4e-donor to 15e  $\text{ML}_n$  vertices. (b)  $(\mu_3, \eta^2\text{-P}_2)$  4e-donor to 14e or 16e  $\text{ML}_n$ . (c) Triply bridging  $(\mu_3, \eta^2\text{-P}_2)$ , a formal 6e-donor. (d) Quadruply bridging  $(\mu_4, \eta^2\text{-P}_2)$  8e-donor.



**Figure 12.8** (a) *Cyclo-P*<sub>3</sub> as an  $\eta^1$  and  $\eta^2$  donor (see text). (b) *Cyclo-P*<sub>3</sub> as an  $\eta^3$  donor; addition of  $\eta^1$  donation to 1, 2 or 3 further metal centres is possible. (c) Bis- $\eta^3$  ligation of *cyclo-P*<sub>3</sub> to coordinated metal centres  $\text{M}(\text{L}_n)$ . (d) More open  $\eta^2, \eta^3$  coordination of  $\text{P}_3$  to different metal centres, e.g.  $\text{M} = \{\text{Ni}(\text{triphos})\}^+$ ,  $\text{M}' = \{\text{Pt}(\text{PPh}_3)_2\}$  (see text).

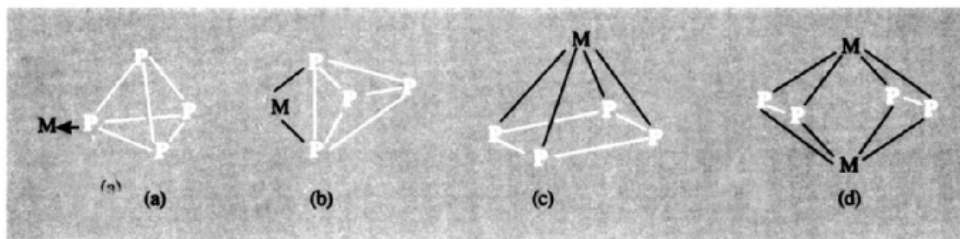
The *cyclo-P*<sub>3</sub> ligand can act in either the  $\eta^1, \eta^2$  or  $\eta^3$  mode as shown schematically in Fig. 12.8(a)–(c).<sup>(42,50)</sup> Each of the three P atoms in 8(b) can also have a further pendant  $\text{ML}_n$  group attached thereby making the *cyclo-P*<sub>3</sub> ligand  $\mu_2, \mu_3$  or  $\mu_4$ . In addition, the more open structure 8(d) is known in the binuclear cation  $[(\text{triphos})\text{Ni}\{\text{P}_3\text{Pt}(\text{PPh}_3)_2\}]^+$ , where triphos is 1,1,1-tris(diphenylphosphinomethyl)ethane,  $\{\text{CH}_3\text{C}(\text{CH}_2\text{PPh}_2)_3\}$ .<sup>(42)</sup> The  $\eta^1$  and  $\eta^2$  modes in Fig. 12.8(a) have only recently been established (in  $[(\eta^5\text{-C}_5\text{Me}_5)(\text{CO})_2\text{Fe}(\text{P})_3\text{-Cr}(\text{CO})_4]$ )<sup>(50)</sup> but the  $\eta^3$  mode in Fig. 12.8(b) has been known since 1976 when it was found that one of the main products of the reaction between  $\text{P}_4$  and  $[\text{Co}_2(\text{CO})_8]$  was the reactive

pale-yellow solid  $[\text{Co}(\text{CO})_3(\eta^3\text{-P}_3)]$ .<sup>(51)</sup> Numerous other examples featuring Co, Rh and Ir, and the isoelectronic cationic metal centres with Ni, Pd and Pt are now known. Metals in earlier groups require more electron donation from pendant ligands to achieve the 15-electron vertex configuration isolobal with the subrogated P atom in  $\text{P}_4$ , e.g.  $\{\text{Mo}(\eta^5\text{-C}_5\text{Me}_5)(\text{CO})_2\}$ . The binuclear  $\eta^3, \eta^3$  mode of *cyclo-P*<sub>3</sub> (Fig. 12.8c) and its  $\text{As}_3$  homologues were extensively studied by L. Sacconi and others in the early 1980s.<sup>(38,42,43)</sup>

As a ligand,  $\text{P}_4$  can adopt various geometries,<sup>(42,43)</sup> including the  $\text{P}_4$  tetrahedron, planar *cyclo-P*<sub>4</sub> (both square and trapezoidal), and a planar zig-zag chain. In principle, the tetrahedral cluster  $\text{P}_4$  could ligate in  $\eta^1, \eta^2$  and  $\eta^3$  modes,

<sup>50</sup> L. WEBER, U. SONNENBERG, H.-G. STAMMLER and B. NEUMANN, *Z. anorg. allg. Chem.* **605**, 87–99 (1991).

<sup>51</sup> A. VIZI-OROSZ *J. Organomet. Chem.* **111**, 61–4 (1976).



**Figure 12.9** Schematic representation of various coordination modes: (a)  $\eta^1$ -P<sub>4</sub>; (b)  $\eta^2$ -P<sub>4</sub>; (c)  $\eta^4$ -cyclo-P<sub>4</sub>; (d)  $(\mu, \eta^2$ -P<sub>2</sub>)<sub>2</sub> (see text).

though only the first two have so far been established (Fig. 12.9 (a), (b)). [Note, however, the face-coordinated  $\eta^3$  configuration in the Bi<sub>4</sub> complex [(CO)<sub>4</sub>Fe( $\mu_4, \eta^3$ -Bi<sub>4</sub>){Fe(CO)<sub>3</sub>}<sub>3</sub>]<sup>2-</sup>.]<sup>(52)</sup> The first example of what turned out to be a complex involving the  $\eta^1$  mode was the unstable red-brown compound [(Fe(CO)<sub>4</sub>)<sub>3</sub>( $\mu_3$ -P<sub>4</sub>)] which was made in 1977 by reacting P<sub>4</sub> with Fe<sub>2</sub>(CO)<sub>9</sub> in benzene at room temperature.<sup>(53)</sup> One vertex of the P<sub>4</sub> tetrahedron was coordinated  $\eta^1$  to one of the {Fe(CO)<sub>4</sub>} groups while opposite edges of the P<sub>4</sub> cluster were bonded  $\eta^2$  to the other two {Fe(CO)<sub>4</sub>} groups. The first  $\eta^1$ -P<sub>4</sub> complex to be characterized by X-ray structural analysis was [( $\eta^3$ -np<sub>3</sub>)Ni( $\eta^1$ -P<sub>4</sub>)],<sup>(54)</sup> formed by direct reaction of white P<sub>4</sub> with the Ni<sup>0</sup> complex [Ni( $\eta^4$ -np<sub>3</sub>)] in thf at 0°C where np<sub>3</sub> is N(CH<sub>2</sub>CH<sub>2</sub>PPh<sub>2</sub>)<sub>3</sub>. Coordination results in a slight elongation of the tetrahedron with P<sub>basal</sub>-P<sub>apical</sub> 220 pm and P<sub>basal</sub>-P<sub>basal</sub> 209 pm (cf. 221 pm in  $\alpha$ -P<sub>4</sub>). The  $\eta^2$ -P<sub>4</sub> mode of coordination is featured in many complexes with Rh, Ir, etc., for example [RhCl( $\eta^2$ -P<sub>4</sub>)(PPh<sub>3</sub>)<sub>2</sub>],<sup>(55)</sup> formed by direct reaction of P<sub>4</sub> with [RhCl(PPh<sub>3</sub>)<sub>3</sub>] in CH<sub>2</sub>Cl<sub>2</sub> at -78°C. The coordinated edge is almost perpendicular to the {RhClL<sub>2</sub>} plane and is lengthened by

about 25 pm to 246.2 pm, whereas the other P-P distances are essentially unchanged from those in uncoordinated P<sub>4</sub>.<sup>(56)</sup>

Square planar *cyclo*-P<sub>4</sub> features as a ligand in [Nb( $\eta^5$ -C<sub>5</sub>H<sub>3</sub>Bu<sub>2</sub><sup>-1,3</sup>)(CO)<sub>2</sub>( $\eta^4$ -P<sub>4</sub>)]<sup>(57)</sup> and the corresponding Ta analogue.<sup>(58)</sup> The compounds are formed by uv photolysis of P<sub>4</sub> with [M(cp\*)(CO)<sub>4</sub>] and the square-pyramidal *nido* structure of the MP<sub>4</sub> cluster (Fig. 12.9c) is consistent with its 14e (2n + 4) cluster-electron count (p. 161). The P-P distances in the coplanar P<sub>4</sub> ligand are in the range 214–218 pm for the Nb complex, with Nb-P<sub>4</sub>(centre) being 142 pm and the basal PPP angles being 92.6° and 88.4°. In the Ta complex, the P-P distances are 215–217 pm. A co-product of the photolysis reaction is the related bis-(P<sub>2</sub>) complex [Ta(C<sub>5</sub>H<sub>3</sub>Bu<sub>2</sub><sup>-1,3</sup>)(CO)( $\mu, \eta^2$ -P<sub>2</sub>)<sub>2</sub>], Fig. 12.9d, in which the P-P distance is 212 pm within each P<sub>2</sub> ligand and 357 pm between the coplanar P<sub>2</sub> ligands. Several similar binuclear bis-(P<sub>2</sub>) complexes are known, including Rh/Rh, and mixed metal species involving Nb/Ta and Ta/Co.<sup>(58)</sup>

A still more open configuration occurs in the zig-zag P<sub>4</sub> chain shown in Fig. 12.10(a).<sup>(59)</sup> This was found in the dianion of the deep

<sup>52</sup> K. H. WHITMIRE, T. A. ALBRIGHT, S. K. KANG, M. R. CHURCHILL and J. C. FETTINGER, *Inorg. Chem.* **25**, 2799–805 (1986).

<sup>53</sup> G. SCHMID and H. P. KEMPENY, *Z. anorg. allg. Chem.* **432**, 160–6 (1977).

<sup>54</sup> P. DAPPORTO, S. MIDOLLINI and L. SACCONI, *Angew. Chem. Int. Edn. Engl.* **18**, 469 (1979).

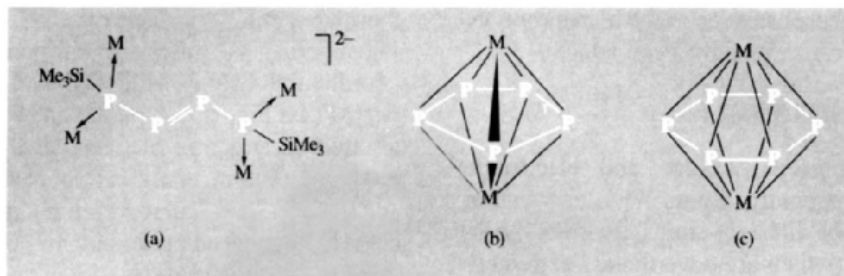
<sup>55</sup> W. E. LINDSELL, K. J. MCCULLOUGH and A. J. WELCH, *J. Am. Chem. Soc.* **105**, 4487–9 (1983).

<sup>56</sup> A. P. GINSBERG, W. E. LINDSELL, K. J. MCCULLOUGH, C. R. SPRINKLE and A. J. WELCH, *J. Am. Chem. Soc.* **108**, 403–16 (1986).

<sup>57</sup> O. J. SCHERER, J. VONDUNG and G. WOLMERSHÄUSER, *Angew. Chem. Int. Edn. Engl.* **28**, 1355–7 (1989).

<sup>58</sup> O. J. SCHERER, R. WINTER and G. WOLMERSHÄUSER, *Z. anorg. allg. Chem.* **619**, 827–35 (1993).

<sup>59</sup> G. FRITZ, E. LAYHER, H. KRAUTSCHEID, B. MAYER, E. MATERN, W. HÖNLE and H. G. VON SCHNERING, *Z. anorg. allg. Chem.* **611**, 56–60 (1992).



**Figure 12.10** (a) Zig-zag  $P_4$  chain,  $M = \{Cr(CO)_5\}$ ; (b)  $\eta^5$ -*cyclo*- $P_5$ ,  $M$  various; (c)  $\eta^6$ -*cyclo*- $P_6$ ,  $M$  various (see text).

red crystalline compound  $[Li(dme)_3]^+{}_2[(SiMe_3)-\{Cr(CO)_5\}_2P=P=P\{Cr(CO)_5\}_2(SiMe_3)]^{2-}$  which was obtained by reacting  $Li[P(SiMe_3)_2-\{Cr(CO)_5\}]$  with  $BrCH_2CH_2Br$  in 1,2-dimethoxyethane (dme). The interatomic distances  $P-P$  221.9 pm and  $P=P$  202.5 pm reflect the bond orders indicated.

Because *cyclo*- $P_5$  and *cyclo*- $P_6$  can be considered as isoelectronic with  $C_5H_5$  and  $C_6H_6$  their appearance as ligands is not entirely unexpected, but the recent synthesis and characterization of such complexes was nevertheless a noteworthy achievement.<sup>(43)</sup> Typical examples are  $[(Mn(CO)_3(\eta^5-P_5))]^{(60)}$  (formed by the direct action of  $KP_5$  on  $[Mn(CO)_5Br]$  in dmf at  $155^\circ C$ ) and  $[Fe(\eta^5-C_5H_5)(\mu:\eta^5,\eta^5-P_5)Fe(\eta^5-C_5Me_4R)]^{(43)}$  (Fig. 12.10(b)) for *cyclo*- $P_5$ ; and  $[\{Mo(\eta^5-C_5Me_5)\}_2(\mu:\eta^5,\eta^5-P_6)]^{(43)}$  (Fig. 12.10(c)) for planar *cyclo*- $P_6$ . Several *cyclo*- $As_5$  and *-As*<sub>6</sub> analogues are also known. The complex  $[\{Ti(\eta^5-C_5Me_5)\}_2(\mu:\eta^3,\eta^3-P_6)]$  features a puckered  $P_6$  ring in the chair conformation, so that the overall cluster core has a distorted cubane geometry.<sup>(61)</sup>

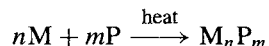
The most complex  $P_n$  ligand so far characterized is the astonishing  $\mu_5$  hexadentate  $P_{10}$  unit in  $[\{Cr(\eta^5-C_5H_5)(CO)_2\}_5P_{10}]$  (see ref. 62 for details).

## 12.3 Compounds

### 12.3.1 Phosphides<sup>(63-65)</sup>

Phosphorus forms stable binary compounds with almost every element in the periodic table and those with metals are called phosphides. Like borides (p. 145) they are known in a bewilderingly large number of stoichiometries, and typical formulae are  $M_4P$ ,  $M_3P$ ,  $M_{12}P_5$ ,  $M_7P_3$ ,  $M_2P$ ,  $M_7P_4$ ,  $M_5P_3$ ,  $M_3P_2$ ,  $M_4P_3$ ,  $M_5P_4$ ,  $M_6P_5$ ,  $MP$ ,  $M_3P_4$ ,  $M_2P_3$ ,  $MP_2$ ,  $M_3P_7$ ,  $M_2P_5$ ,  $MP_3$ ,  $M_3P_{11}$ ,  $M_3P_{14}$ ,  $MP_5$ ,  $M_3P_{16}$ ,  $M_4P_{26}$ ,  $MP_7$ ,  $M_2P_{16}$  and  $MP_{15}$ . Many metals (e.g. Ti, Ta, W, Rh) form as many as 5 or 6 phosphides and Ni has at least 8 ( $Ni_3P$ ,  $Ni_5P_2$ ,  $Ni_{12}P_5$ ,  $NiP_2$ ,  $Ni_5P_4$ ,  $NiP$ ,  $NiP_2$  and  $NiP_3$ ). Ternary and more complex metal phosphides are also known.

The most general preparative route to phosphides (Faraday's method) is to heat the metal with the appropriate amount of red P at high temperature in an inert atmosphere or an evacuated sealed tube:



An alternative route (Andrieux's method) is the electrolysis of fused salts such as molten

<sup>60</sup> M. BAUDLER and T. ETZBACH, *Angew. Chem. Int. Edn. Engl.* **30**, 580-2 (1991).

<sup>61</sup> O. J. SCHERER, H. SWAROWSKY, G. WOLMERSHÄUSER, W. KAIM and S. KOHLMANN, *Angew. Chem. Int. Edn. Engl.* **26**, 1153-5 (1987).

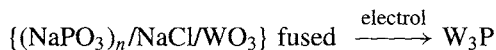
<sup>62</sup> L. Y. GOH, R. C. S. WONG and E. SINN, *Organometallics* **12**, 888-94 (1993).

<sup>63</sup> A. WILSON, *The metal phosphides*, Chap. 3 (pp. 289-363) in ref. 23, see also p. 256.

<sup>64</sup> A. D. F. TOY, in *Comprehensive Inorganic Chemistry*, Vol. 2, Pergamon Press, Oxford, 1973 (Section 20.2, Phosphides, pp. 406-14).

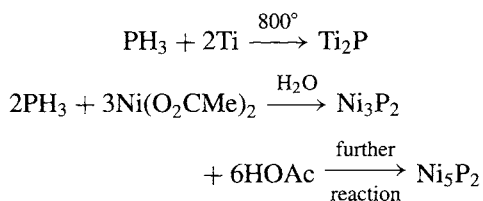
<sup>65</sup> D. E. C. CORBRIDGE, *Phosphorus* (3rd edn.), Elsevier, Amsterdam, 1985, Section 2.2 Metallic Phosphides, pp. 56-69. (See also 5th edn. 1995.)

alkali-metal phosphates to which appropriate metal oxides or halides have been added:

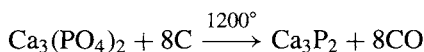


Variation in current, voltage and electrolyte composition frequently results in the formation of phosphides of different stoichiometries. Less-general routes (which are nevertheless extremely valuable in specific instances) include:

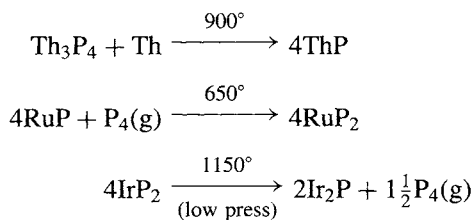
- (a) Reaction of  $\text{PH}_3$  with a metal, metal halide or sulfide, e.g.:



- (b) Reduction of a phosphate such as apatite with C at high temperature, e.g.:



- (c) Reaction of a metal phosphide with further metal or phosphorus to give a product of different stoichiometry, e.g.:



Phosphides resemble in many ways the metal borides (p. 145), carbides (p. 297), and nitrides (p. 417), and there are the same difficulties in classification and description of bonding. Perhaps the least-contentious procedure is to classify according to stoichiometry, i.e. (a) metal-rich phosphides ( $M/P > 1$ ), (b) monophosphides ( $M/P = 1$ ), and (c) phosphorus-rich phosphides ( $M/P < 1$ ):

(a) *Metal-rich phosphides* are usually hard, brittle, refractory materials with metallic lustre, high thermal and electrical conductivity, great

thermal stability and general chemical inertness. Phosphorus is often in trigonal prismatic coordination being surrounded by 6 M, or by 7, 8 or 9 M (see Fig. 6.7 on p. 148 and Fig. 12.6). The antifluorite structure of many  $\text{M}_2\text{P}$  also features eightfold (cubic) coordination of P by M. The details of the particular structure adopted in each case are influenced predominantly by size effects.

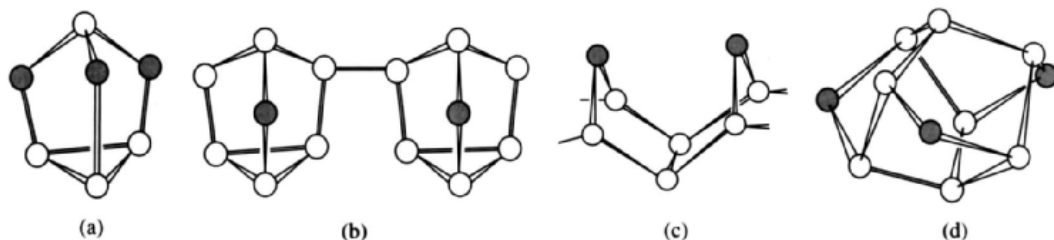
(b) *Monophosphides* adopt a variety of structures which appear to be influenced by both size and electronic effects. Thus the Group 3 phosphides MP adopt the zinc-blende structure (p. 1210) with tetrahedral coordination of P, whereas SnP has the NaCl-type structure (p. 242) with octahedral coordination of P, VP has the hexagonal NiAs-type structure (p. 556) with trigonal prismatic coordination of isolated P atoms by V, and MoP has the hexagonal WC-type structure (p. 299) in which both Mo and P have a trigonal prismatic coordination by atoms of the other kind. More complicated arrangements are also encountered, e.g..<sup>(65)</sup>

TiP, ZrP, HfP: half the P trigonal prismatic and half octahedral;

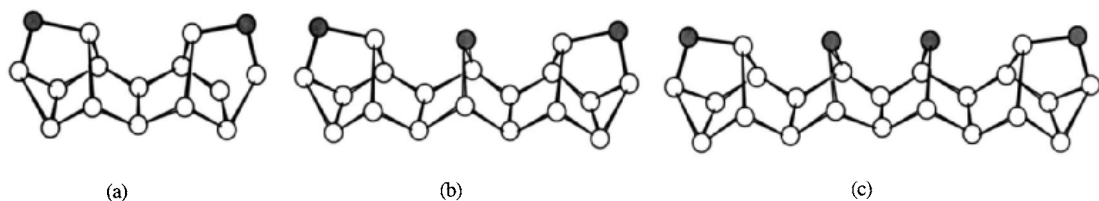
MP (M = Cr, Mn, Fe, Co, Ru, W): distorted trigonal prismatic coordination of P by M plus two rather short contacts to P atoms in adjacent trigonal prisms, thus building up a continuous chain of P atoms; NiP is a distortion of this in which the P atoms are grouped in pairs rather than in chains (or isolated as in VP).

(c) *Phosphorus-rich phosphides* are typified by lower mps and much lower thermal stabilities when compared with monophosphides or metallic phosphides. They are often semiconductors rather than metallic conductors and feature increasing catenation of the P atoms (cf. boron rich borides, p. 148).  $\text{P}_2$  units occur in  $\text{FeP}_2$ ,  $\text{RuP}_2$  and  $\text{OsP}_2$  (marcasite-type, p. 680) and in  $\text{PtP}_2$  (pyrites type, p. 680) with P–P 217 pm. Planar  $\text{P}_4$  rings (square or rectangular) occur in several  $\text{MP}_3$  (M = Co, Ni, Rh, Pd, Ir) with P–P typically 223 pm in the square ring of  $\text{RhP}_3$ . Structures are also known in which the P atoms form chains ( $\text{PdP}_2$ ,  $\text{NiP}_2$ ,  $\text{CdP}_2$ ,  $\text{BaP}_3$ ),





**Figure 12.11** Schematic representation of the structures of polycyclic polyphosphide anions (open circles P, shaded circles P<sup>-</sup>) (a) P<sub>7</sub><sup>3-</sup>, (b) {P<sub>7</sub><sup>-</sup>}<sub>x</sub>, (c) ≡P<sub>8</sub><sup>2-</sup>≡<sub>x</sub>, (d) P<sub>11</sub><sup>3-</sup>.



**Figure 12.12** Schematic representation of the structures of (a) P<sub>16</sub><sup>2-</sup>, (b) P<sub>21</sub><sup>3-</sup>, (c) P<sub>26</sub><sup>4-</sup>, (open circles P, shaded circles P<sup>-</sup>)

double chains (ZnPbP<sub>14</sub>, CdPbP<sub>14</sub>, HgPbP<sub>14</sub>), or layers (CuP<sub>2</sub>, AgP<sub>2</sub>, CdP<sub>4</sub>); in the last 3 phosphides the layers are made up by a regular fusion of puckered 10-membered rings of P atoms with the metal atoms in the interstices. The double-chained structure of MPbP<sub>14</sub> is closely related to that of violet phosphorus (p. 482).

In addition, phosphides of the electropositive elements in Groups 1, 2 and the lanthanoids form phosphides with some degree of ionic bonding. The compounds Na<sub>3</sub>P<sub>11</sub> and Sr<sub>3</sub>P<sub>14</sub> have already been mentioned (p. 484) and other somewhat ionic phosphides are M<sub>3</sub>P (M = Li, Na), M<sub>3</sub>P<sub>2</sub> (M = Be, Mg, Zn, Cd), MP (M = La, Ce) and Th<sub>3</sub>P<sub>4</sub>. However, it would be misleading to consider these as fully ionized compounds of P<sup>3-</sup> and there is extensive metallic or covalent interaction in the solids. Such compounds are characterized by their ready hydrolysis by water or dilute acid to give PH<sub>3</sub>.

Recent extensive structural studies by X-ray crystallography and by <sup>31</sup>P nmr spectroscopy have revealed an astonishing variety of *conjuncto*-polyphosphides with quasi-ionic

cluster structures.<sup>(66,67)</sup> Thus, the yellow compound Li<sub>3</sub>P<sub>7</sub> (which has been known since 1912) and its Na–Cs analogues have been found to contain the P<sub>7</sub><sup>3-</sup> cluster shown schematically in Fig. 12.11(a). The cluster can be regarded as being related to the P<sub>4</sub> tetrahedron (p. 479) by the notional insertion of three 2-connected P<sup>-</sup> atoms (cf. the structure of P<sub>4</sub>S<sub>3</sub>, p. 507, with which it is precisely isoelectronic). Substitution of P by As leads to a series of closely related anions [P<sub>7-x</sub>As<sub>x</sub>]<sup>3-</sup> x = 1–5, (?6),<sup>(68)</sup> and As<sub>7</sub><sup>3-</sup> is also known for Na, Rb, Cs). Catenation of the P<sub>7</sub><sup>3-</sup> unit, as shown in Fig. 12.11(b), leads to the stoichiometry M<sup>+</sup>P<sub>7</sub><sup>-</sup>. The repeating unit =P<sub>8</sub>=, which is clearly related to a segment in the structure of Hittorf's allotrope (p. 482), is shown in Fig. 12.11(c). A more complex

<sup>66</sup> H. G. VON SCHNERING, in A. H. COWLEY (ed.) *Rings, Clusters and Polymers of the Main Group Elements*, ACS Symposium Series No. 232, Washington D. C. 1983, pp. 69–80.

<sup>67</sup> M. BAUDLER, *Angew. Chem. Int. Edn. Engl.* **21**, 492–512 (1982); **26**, 419–41 (1987).

<sup>68</sup> W. HÖNLE and H. G. VON SCHNERING, *Angew. Chem. Int. Edn. Engl.* **25**, 352–3 (1986).

cluster occurs in the yellow/orange compounds  $M_3^+P_{11}^{3-}$  (Fig. 12.11d):  $P_{11}^{3-}$  can be thought of as comprising two axial  $PP_3$  tetrahedra joined by a central belt of three 2-connected  $P^-$  atoms, so that the sequence of cluster planes contains 1,3,(3),3,1 P atoms, respectively.

Even more complex *conjuncto*-polyphosphide anions can be constructed, such as those of stoichiometry  $P_{16}^{2-}$ ,  $P_{21}^{3-}$  and  $P_{26}^{4-}$ , Fig. 12.12(a)(b)(c).<sup>(66,67)</sup> These bear an obvious structural relationship to  $=P_8=$  (Fig. 12.11c) and to Hittorf's phosphorus (Fig. 12.4) and can be viewed as ladders of P atoms with alternate P–P and  $P(P^-)P$  rungs, terminated at each end by a ring-closing  $P(P^-)$  unit. The P–P distances and PPP angles in these various species are much as expected. These cluster anions, and those mentioned in the preceding paragraphs, can be partially or completely protonated (see next subsection) and they also occur in neutral organopolyphosphanes (p. 495).

A completely different structural motif has very recently been found in the red-brown phosphide  $Ca_5P_8$ , formed by direct fusion of Ca metal and red P in the correct atom ratio in a corundum crucible at  $1000^\circ C$ .<sup>(69)</sup> The structure comprises  $Ca^{2+}$  cations and  $P_8^{10-}$  anions, the latter adopting a staggered ethane conformation. (Note that  $P^+$  is isolobal with C and  $P^{2-}$  with H so that  $C_2H_6 = [(P^+)_2(P^{2-})_6] = P_8^{10-}$ .) The internal P–P distance is 230.1 pm and the terminal P–P distances 214.9–216.9 pm, while the internal PPP angles are  $104.2$ – $106.4^\circ$  and the outer angles are  $103.4$ – $103.7^\circ$ .

Few industrial uses have so far been found for phosphides. "Ferrophosphorus" is produced on a large scale as a byproduct of  $P_4$  manufacture, and its uses have been noted (p. 480). Phosphorus is also much used as an alloying element in iron and steel, and for improving the workability of Cu. Group 3 monophosphides are valuable semiconductors (p. 255) and  $Ca_3P_2$  is an important ingredient in some navy sea-flares since its reaction with water releases spontaneously flammable

phosphines. By contrast the phosphides of Nb, Ta and W are valued for their chemical inertness, particularly their resistance to oxidation at very high temperatures, though they are susceptible to attack by oxidizing acids or peroxides.

### 12.3.2 Phosphine and related compounds

The most stable hydride of P is phosphine (phosphane),  $PH_3$ . It is the first of a homologous open-chain series  $P_nH_{n+2}$  ( $n = 1$ – $9$ ) the members of which rapidly diminish in thermal stability, though  $P_2H_4$  and  $P_3H_5$  have been isolated pure. There are ten other (unstable) homologous series:  $P_nH_n$  ( $n = 3$ – $10$ ),  $P_nH_{n-2}$  ( $n = 4$ – $12$ ), and  $P_nH_{n-4}$  ( $n = 5$ – $13$ ) and so on up to  $P_nH_{n-18}$  ( $n = 19$ – $22$ )<sup>(67)</sup>; in all of these there is a tendency to form cyclic and condensed polyphosphanes at the expense of open-chain structures. Some 85 phosphanes have so far been identified and structurally characterized by nmr spectroscopy and other techniques, although few have been obtained pure because of problems involving thermal instability, ready disproportionation, light-sensitivity and great chemical reactivity.<sup>(67,70,71)</sup> Phosphorane,  $PH_5$ , has not been prepared or even detected, despite numerous attempts, although  $HPF_4$ ,  $H_2PF_3$  and  $H_3PF_2$  have recently been well characterized.<sup>(72,73)</sup>

$PH_3$  is an extremely poisonous, highly reactive, colourless gas which has a faint garlic odour at concentrations above about 2 ppm by volume. It is intermediate in thermal stability between  $NH_3$  (p. 421) and  $AsH_3$  (p. 557). Several convenient routes are available for its preparation:

1. Hydrolysis of a metal phosphide such as  $AlP$  or  $Ca_3P_2$ ; the method is useful even

<sup>69</sup> M. BAUDLER and K. GLINKA, *Chem. Rev.* **93**, 1623–67 (1993).

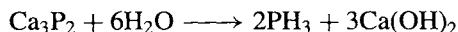
<sup>71</sup> M. BAUDLER and K. GLINKA, *Chem. Rev.* **94**, 1273–97 (1994). See also *Z. anorg. allg. Chem.* **621**, 1133–9 (1995).

<sup>72</sup> A. J. DOWNS, G. S. MCGRADY, E. A. BARNFIELD and D. W. H. RANKIN, *J. Chem. Soc., Dalton Trans.*, 545–50 (1989).

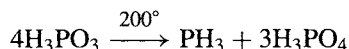
<sup>73</sup> A. BECHERS, *Z. anorg. allg. Chem.* **619**, 1869–79 (1993).

<sup>69</sup> C. HADENFELDT and F. BARTELS, *Z. anorg. allg. Chem.* **620**, 1247–52 (1994).

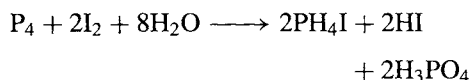
up to the 10-mole scale and can be made almost quantitative



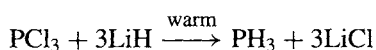
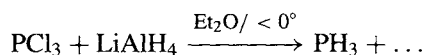
2. Pyrolysis of phosphorous acid at 205–210°; under these conditions the yield of PH<sub>3</sub> is 97% though at higher temperatures the reaction can be more complex (p. 512)



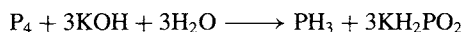
3. Alkaline hydrolysis of PH<sub>4</sub>I (for very pure phosphine):



4. Reduction of PCl<sub>3</sub> with LiAlH<sub>4</sub> or LiH:



5. Alkaline hydrolysis of white P<sub>4</sub> (industrial process):



Phosphine has a pyramidal structure, as expected, with P–H 142 pm and the H–P–H angle 93.6° (see p. 557). Other physical properties are mp –133.5°, bp –87.7°, dipole moment 0.58 D, heat of formation  $\Delta H_f^\circ$  –9.6 kJ mol<sup>–1</sup> (uncertain) and mean P–H bond energy 320 kJ mol<sup>–1</sup>. The free energy change (at 25°C) for the reaction  $\frac{1}{4}\text{P}_4(\alpha\text{-white}) + \frac{3}{2}\text{H}_2(\text{g}) = \text{PH}_3(\text{g})$  is –13.1 kJ mol<sup>–1</sup>, implying a tendency for the elements to combine, though there is negligible reaction unless H<sub>2</sub> is energized photolytically or by a high-current arc. The inversion frequency of PH<sub>3</sub> is about 4000 times less than for NH<sub>3</sub> (p. 423); this reflects the substantially higher energy barrier to inversion for PH<sub>3</sub> which is calculated to be ~155 kJ mol<sup>–1</sup> rather than 24.7 kJ mol<sup>–1</sup> for NH<sub>3</sub>.

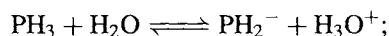
Phosphine is rather insoluble in water at atmospheric pressure but is more soluble in

organic liquids, and particularly so in CS<sub>2</sub> and CCl<sub>3</sub>CO<sub>2</sub>H. Some typical values are:

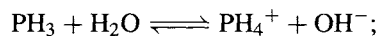
Solvent (T°C)	H <sub>2</sub> O (17°)	CH <sub>3</sub> CO <sub>2</sub> H (20°)	C <sub>6</sub> H <sub>6</sub> (22°)
Solubility/ml PH <sub>3</sub> (g) per 100 ml solvent	26	319	726
Solvent (T°C)	CS <sub>2</sub> (21°)	CCl <sub>3</sub> CO <sub>2</sub> H	
Solubility/ml PH <sub>3</sub> (g) per 100 ml solvent	1025	1590	

[Note: 1 ml PH<sub>3</sub>(g) ≈ 1.5 mg]

Aqueous solutions are neutral and there is little tendency for PH<sub>3</sub> to protonate or deprotonate:



$$K_A = 1.6 \times 10^{-29}$$

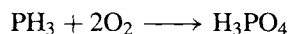


$$K_B = 4 \times 10^{-28}$$

In liquid ammonia, however, phosphine dissolves to give NH<sub>4</sub><sup>+</sup>PH<sub>2</sub><sup>–</sup> and with potassium gives KPH<sub>2</sub> in the same solvent. Again, phosphine reacts with liquid HCl to give the sparingly soluble PH<sub>4</sub><sup>+</sup>Cl<sup>–</sup> and this reacts further with BCl<sub>3</sub> to give PH<sub>4</sub>BCl<sub>4</sub>. The corresponding bromides and PH<sub>4</sub>I are also known.

More generally, phosphine readily acts as a ligand to numerous Lewis acids and typical coordination complexes are [BH<sub>3</sub>(PH<sub>3</sub>)], [BF<sub>3</sub>(PH<sub>3</sub>)], [AlCl<sub>3</sub>(PH<sub>3</sub>)], [Cr(CO)<sub>2</sub>(PH<sub>3</sub>)<sub>4</sub>], [Cr(CO)<sub>3</sub>–(PH<sub>3</sub>)<sub>3</sub>], [Co(CO)<sub>2</sub>(NO)(PH<sub>3</sub>)], [Ni(PF<sub>3</sub>)<sub>2</sub>(PH<sub>3</sub>)<sub>2</sub>] and [CuCl(PH<sub>3</sub>)]. Further details are in the Panel and other aspects of the chemistry of PH<sub>3</sub> have been extensively reviewed.<sup>(74)</sup>

Phosphine is also a strong reducing agent: many metal salts are reduced to the metal and PCl<sub>5</sub> yields PCl<sub>3</sub>. The pure gas ignites in air at about 150° but when contaminated with traces of P<sub>2</sub>H<sub>4</sub> it is spontaneously flammable:



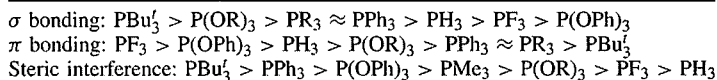
When heated with sulfur, PH<sub>3</sub> yields H<sub>2</sub>S and a mixture of phosphorus sulfides. Probably the most important reaction industrially is

<sup>74</sup> E. FLUCK, Chemistry of phosphine, *Topics in Current Chem.* **35**, 1–64 (1973). A review with 493 references.

### Phosphine and its Derivatives as Ligands<sup>(7,75-78)</sup>

A wide variety of 3-coordinate phosphorus(III) compounds are known and these have been extensively studied as ligands because of their significance in improving our understanding of the stability and reactivity of many coordination complexes. Among the most studied of these ligands are  $\text{PH}_3$ ,  $\text{PF}_3$  (p. 495),  $\text{PCl}_3$  (p. 496),  $\text{PR}_3$  ( $\text{R} = \text{alkyl}$ ),  $\text{PPh}_3$  and  $\text{P(OR)}_3$ , together with a large number of "mixed" ligands such as  $\text{Me}_2\text{NPF}_2$ ,  $\text{PMePh}_2$ , etc., and many multidentate (chelating) ligands such as  $\text{Ph}_2\text{PCH}_2\text{CH}_2\text{PPh}_2$ , etc.

In many of their complexes  $\text{PF}_3$  and  $\text{PPh}_3$  (for example) resemble  $\text{CO}$  (p. 926) and this at one time encouraged the belief that their bonding capabilities were influenced not only by the factors (p. 198) which affect the stability of the  $\sigma \text{P} \rightarrow \text{M}$  interaction which uses the lone-pair of electrons on  $\text{P}^{\text{III}}$  and a vacant orbital on  $\text{M}$ , but also by the possibility of synergic  $\pi$  back-donation from a "nonbonding"  $d_\pi$  pair of electrons on the metal into a "vacant"  $3d_\pi$  orbital on  $\text{P}$ . It is, however, not clear to what extent, if any, the  $\sigma$  and  $\pi$  bonds reinforce each other, and more recent descriptions are based on an MO approach which uses all ( $\sigma$  and  $\pi$ ) orbitals of appropriate symmetry on both the phosphine and the metal-containing moiety. To the extent that  $\sigma$  and  $\pi$  bonding effects on the stability of metal-phosphorus bonds can be isolated from each other and from steric factors (see below) the accepted sequence of effects is as follows:

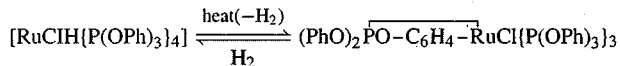


Steric factors are frequently dominant, particularly with bulky ligands, and their influence on the course of many reactions is crucial. One measure of the "size" of a ligand in so far as it affects bond formation is C. A. Tolman's cone angle (1970) which is the angle at the metal atom of the cone swept out by the van der Waals radii of the groups attached to  $\text{P}$ . This will, of course, be dependent on the actual interatomic distance between  $\text{M}$  and  $\text{P}$ . For the particular case of  $\text{Ni}$ , for which a standard value of 228 pm was adopted for  $\text{Ni}-\text{P}$ , the calculated values for the cone angle are:

Ligand	$\text{PH}_3$	$\text{PF}_3$	$\text{P(OMe)}_3$	$\text{P(OEt)}_3$	$\text{PMe}_3$	$\text{P(OPh)}_3$	$\text{PCl}_3$
Cone angle	$87^\circ$	$104^\circ$	$107^\circ$	$109^\circ$	$118^\circ$	$121^\circ$	$125^\circ$
Ligand	$\text{PEt}_3$	$\text{PPh}_3$	$\text{PPr}_3^i$	$\text{PBu}_3'$	$\text{P}(o\text{-tol})_3$	$\text{P}(\text{mesityl})_3$	
Cone angle	$132^\circ$	$145^\circ$	$160^\circ$	$182^\circ$	$195^\circ$	$212^\circ$	

Bulky tertiary phosphine ligands exert both steric and electronic influences when they form complexes (since an increase in bulkiness of a substituent on  $\text{P}$  increases the inter-bond angles and this in turn can be thought of as an increase in "p-character" of the lone-pair of electrons on  $\text{P}$ ). For example, the sterically demanding di-*t*-butylphosphines,  $\text{PBu}_2\text{R}$  ( $\text{R} = \text{alkyl}$  or  $\text{aryl}$ ), promote spatially less-demanding features such as hydride formation, coordinative unsaturation at the metal centre, and even the stabilization of unusual oxidation states, such as  $\text{Ir}^{\text{II}}$ . They also favour internal  $\text{C}-$  or  $\text{O}-$  metallation reactions for the same reasons. Indeed, the metallation of  $\text{C}-\text{H}$  and  $\text{C}-\text{P}$  bonds of coordinated tertiary phosphines can be considered as examples of intramolecular oxidative addition, and these have important mechanistic implications for homogeneous and heterogeneous catalysis.<sup>(79)</sup>

Other notable examples are the orthometallation (orthophenylation) reactions of many complexes of aryl phosphines ( $\text{PAR}_3$ ) and aryl phosphites  $\text{P(OAr)}_3$  with platinum metals in particular, e.g.:



<sup>75</sup> Chapter 5 in ref. 2, Phosphorus(III) ligands in transition-metal complexes, pp. 177-207.

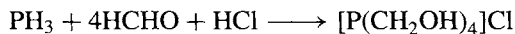
<sup>76</sup> C. A. MCAULIFFE and W. LEVASON, *Phosphine, Arsine and Stibine Complexes of the Transition Elements*, Elsevier, Amsterdam, 1979, 546 pp. A review with over 2700 references. See also C. A. MCAULIFFE (ed.), *Transition-Metal Complexes of Phosphorus, Arsenic and Antimony Donor Ligands*, Macmillan, London, 1972.

<sup>77</sup> O. STELZER, *Topics in Phosphorus Chemistry* **9**, 1-229 (1977). An extensive review with over 1700 references arranged by element and by technique but with no assessment or generalizations.

<sup>78</sup> R. MASON and D. W. MEEK, *Angew. Chem. Int. Edn. Engl.* **17**, 183-94 (1978).

<sup>79</sup> G. PARSHALL, Homogeneous catalytic activation of  $\text{C}-\text{H}$  bonds, *Acc. Chem. Res.* **8**, 113-7 (1975).

its hydrophosphorylation of formaldehyde in aqueous hydrochloric acid solution:



The tetrakis(hydroxymethyl)phosphonium chloride so formed is the major ingredient with urea-formaldehyde or melamine-formaldehyde resins for the permanent flame-proofing of cotton cloth.

Of the many other hydrides of phosphorus, diphosphane (diphosphine),  $\text{P}_2\text{H}_4$ , is the most studied. It is best made<sup>(71)</sup> by treating CaP with cold oxygen-free water. Passage of  $\text{PH}_3$  through an electric discharge at 5–10 kV is an alternative method for small amounts.  $\text{P}_2\text{H}_4$  is a colourless, volatile liquid (mp  $-99^\circ$ ) which is thermally unstable even below room temperature and is decomposed slowly by water. Its vapour pressure at  $0^\circ\text{C}$  is 70.2 mmHg but partial decomposition precludes precise determination of the bp ( $63.5^\circ$  extrap);  $d \simeq 1.014 \text{ g cm}^{-3}$  at  $20^\circ\text{C}$ . Electron-diffraction measurements on the gas establish the *gauche*- $\text{C}_2$  configuration (p. 428) with P–P 222 pm, P–H 145 pm, and the angle H–P–H  $91.3^\circ$ , though vibration spectroscopy suggests a *trans*- $\text{C}_{2h}$  configuration in the solid phase. These results can be compared with those for the halides  $\text{P}_2\text{X}_4$  on p. 498.

The next member of the open-chain series  $\text{P}_n\text{H}_{n+2}$  is  $\text{P}_3\text{H}_5$ , i.e.  $\text{PH}_2\text{P}(\text{PH})_2$ , a colourless liquid that can be stored in the dark at  $-80^\circ$  for several days.<sup>(67,71)</sup> It can be made by disproportionation ( $2\text{P}_2\text{H}_4 \longrightarrow \text{P}_3\text{H}_5 + \text{PH}_3$ ) but it is difficult to purify because of its own fairly ready disproportionation and reactivity, e.g.  $2\text{P}_3\text{H}_5 \longrightarrow \text{P}_4\text{H}_6 + \text{P}_2\text{H}_4$ ; and  $\text{P}_3\text{H}_5 + \text{P}_2\text{H}_4 \longrightarrow \text{P}_4\text{H}_6 + \text{PH}_3$ . Tetraphosphane(6),  $\text{P}_4\text{H}_6$ , exists as an equilibrium mixture of the two structural isomers  $\text{H}_2\text{P}(\text{PH})_2\text{PH}_2$  (*n*) and  $\text{P}(\text{PH}_2)_3$  (*i*), and itself reacts with  $\text{P}_3\text{H}_5$  at  $-20^\circ$  according to the idealized stoichiometry  $\text{P}_4\text{H}_6 + \text{P}_3\text{H}_5 \longrightarrow 2\text{PH}_3 + \text{P}_5\text{H}_5$ , i.e. *cyclo*-(PH)<sub>5</sub>. All members of the series *cyclo*- $\text{P}_n\text{H}_n$  ( $n = 3-10$ ) have been detected mass spectrometrically in the thermolysis products from  $\text{P}_2\text{H}_4$ .<sup>(70)</sup>

Polycyclic polyphosphanes are often best prepared by direct protonation of the corresponding polyphosphide anions (Figs. 12.11 and 12.12)

with HX, though other routes are also available. Thus, treatment of  $\text{P}_7^{3-}$  yields  $\text{P}_7\text{H}^{2-}$ ,  $\text{P}_7\text{H}_2^-$  and  $\text{P}_7\text{H}_3$  by successive protonation of the three 2-connected  $\text{P}^-$  sites. The alkyl derivatives are more stable than the parent polycyclic phosphanes and provide many examples of the elegant solution of complex conformational problems by the use of nmr spectroscopy.<sup>(67,70)</sup>

### 12.3.3 Phosphorus halides

Phosphorus forms three series of halides  $\text{P}_2\text{X}_4$ ,  $\text{PX}_3$  and  $\text{PX}_5$ . All 12 compounds may exist, although there is considerable doubt about  $\text{PI}_5$ .<sup>(80)</sup> Numerous mixed halides  $\text{PX}_2\text{Y}$  and  $\text{PX}_2\text{Y}_3$  are also known as well as various pseudohalides such as  $\text{P}(\text{CN})_3$ ,  $\text{P}(\text{CNO})_3$ ,  $\text{P}(\text{CNS})_3$  and their mixed halogeno-counterparts. The compounds form an extremely useful extended series with which to follow the effect of progressive substitution on various properties, and the pentahalides are particularly significant in spanning the “ionic-covalent” border, so that they exist in various structural forms depending on the nature of the halogen, the phase of aggregation, or the polarity of the solvent. Some subhalides such as  $\text{P}_4\text{X}_2$  and  $\text{P}_7\text{X}_3$ , and some curious polyhalides such as  $\text{PBr}_7$  and  $\text{PBr}_{11}$  have also been characterized. Physical properties of the binary halides are summarized in Table 12.3 (on the next page). Ternary (mixed) halides tend to have properties intermediate between those of the parent binary halides.

### Phosphorus trihalides

All 4 trihalides are volatile reactive compounds which feature pyramidal molecules. The fluoride is best made by the action of  $\text{CaF}_2$ ,  $\text{ZnF}_2$  or  $\text{AsF}_3$  on  $\text{PCl}_3$ , but the others are formed by direct halogenation of the element.  $\text{PF}_3$  is colourless, odourless and does not fume in air, but is very hazardous due to the formation of a complex with blood haemoglobin (cf.

<sup>80</sup> I. TORNIÉPORTH-OETTING and T. KLAPÖTKE, *J. Chem. Soc., Chem. Commun.*, 132–3 (1990).

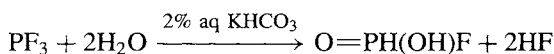
Table 12.3 Some physical properties of the binary phosphorus halides

Compound	Physical State at 25°C	MP/°C	BP/°C	P-X/pm	Angle X-P-X
PF <sub>3</sub>	Colourless gas	-151.5	-101.8	156	96.3°
PCl <sub>3</sub>	Colourless liquid	-93.6	76.1	204	100°
PBr <sub>3</sub>	Colourless liquid	-41.5	173.2	222	101°
PI <sub>3</sub>	Red hexagonal crystals	61.2	decomp > 200	243	102°
P <sub>2</sub> F <sub>4</sub>	Colourless gas	-86.5	-6.2	159 (P-P 228)	99.1° (F-P-P 95.4°)
P <sub>2</sub> Cl <sub>4</sub>	Colourless oily liquid	-28	~180 (d)	—	—
P <sub>2</sub> Br <sub>4</sub>	?	—	—	—	—
P <sub>2</sub> I <sub>4</sub>	Red triclinic needles	125.5	decomp	248 (P-P 221)	102.3° (I-P-P 94.0°)
PF <sub>5</sub>	Colourless gas	-93.7	-84.5	153 (eq) 158 (ax)	120° (eq-eq) 90° (eq-ax)
PCl <sub>5</sub>	Off-white tetragonal crystals	167	160 (subl)	—	See text
PBr <sub>5</sub>	Reddish-yellow rhombohedral crystals	<100 (d)	106 (d)	—	See text
PI <sub>5</sub> ?	Brown-black crystals	41	—	—	However, see ref. 80

CO, p. 1101). It is about as toxic as COCl<sub>2</sub>. The similarity of PF<sub>3</sub> and CO as ligands was first noted by J. Chatt<sup>(81)</sup> and many complexes with transition elements are now known,<sup>(82)</sup> e.g. [Ni(CO)<sub>n</sub>(PF<sub>3</sub>)<sub>4-n</sub>] (*n* = 0-4), [Pd(PF<sub>3</sub>)<sub>4</sub>], [Pt(PF<sub>3</sub>)<sub>4</sub>], [CoH(PF<sub>3</sub>)<sub>4</sub>], [Co<sub>2</sub>(μ-PF<sub>2</sub>)<sub>2</sub>(PF<sub>3</sub>)<sub>6</sub>], etc. Such complexes can be prepared by ligand replacement reactions, by fluorination of PCl<sub>3</sub> complexes, by direct reaction of PF<sub>3</sub> with metal salts or even by direct reaction of PF<sub>3</sub> with metals at elevated temperatures and pressures.

PF<sub>3</sub>, unlike the other trihalides of phosphorus, hydrolyses only slowly with water, the products being phosphorous acid and HF: PF<sub>3</sub> + 3H<sub>2</sub>O → H<sub>3</sub>PO<sub>3</sub> + 3HF.

The reaction is much more rapid in alkaline solutions, and in dilute aqueous KHCO<sub>3</sub> solutions the intermediate monofluorophosphorous acid is formed:



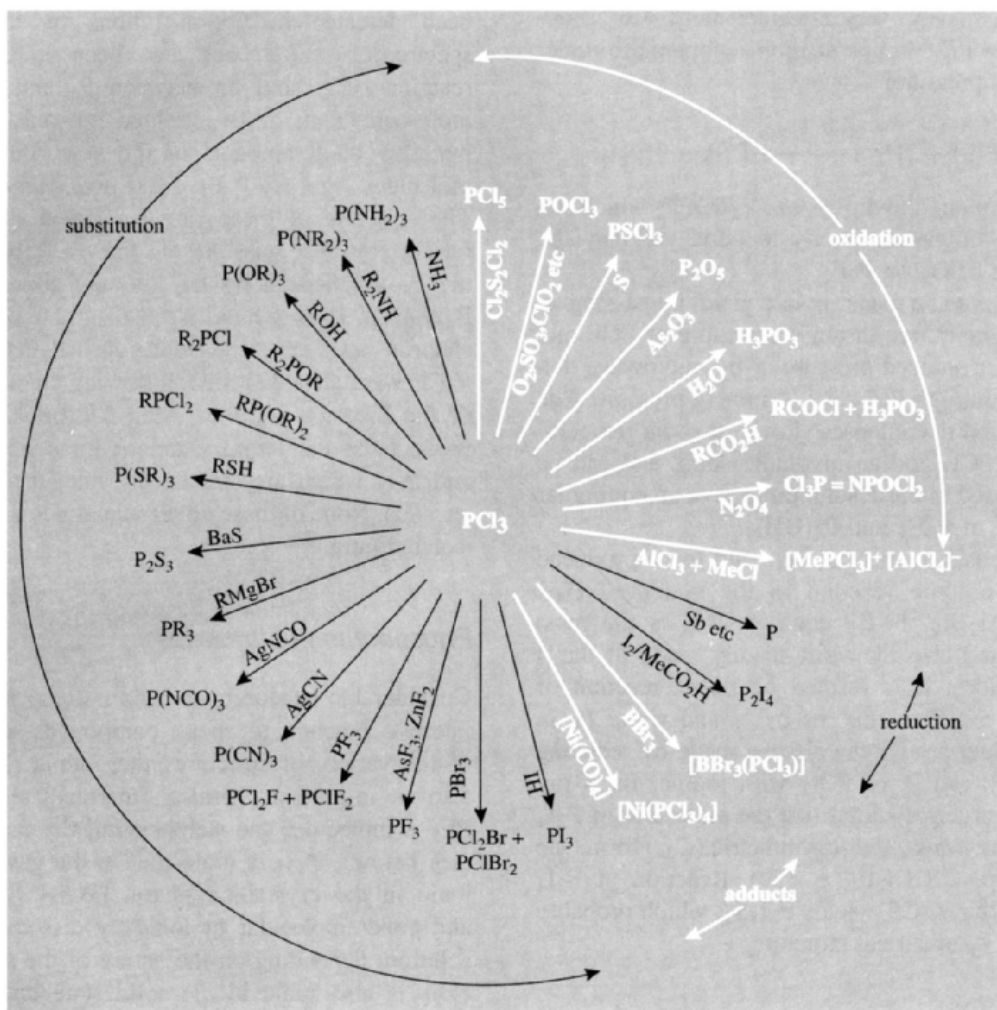
<sup>81</sup> J. CHATT, *Nature* **165**, 637-8 (1950); J. CHATT and A. A. WILLIAMS, *J. Chem. Soc.* 3061-7 (1951).

<sup>82</sup> T. KRUCK, *Angew. Chem. Int. Edn. Engl.* **6**, 53-67 (1967); J. F. NIXON, *Adv. Inorg. Chem. Radiochem.* **13**, 363-469 (1970); R. J. CLARKE and M. A. BUSCH, *Acc. Chem. Res.* **6**, 246-52 (1973).

PCl<sub>3</sub> is the most important compound of the group and is made industrially on a large scale<sup>†</sup> by direct chlorination of phosphorus suspended in a precharge of PCl<sub>3</sub> — the reaction is carried out under reflux with continuous take-off of the PCl<sub>3</sub> formed. PCl<sub>3</sub> undergoes many substitution reactions, as shown in the diagram, and is the main source of organophosphorus compounds. Particularly notable are PR<sub>3</sub>, PR<sub>*n*</sub>Cl<sub>3-*n*</sub>, PR<sub>*n*</sub>(OR)<sub>3-*n*</sub>, (PhO)<sub>3</sub>PO, and (RO)<sub>3</sub>PS. Many of these compounds are made on the 1000-tonne scale pa, and the major uses are as oil additives, plasticizers, flame retardants, fuel additives and intermediates in the manufacture of insecticides.<sup>(83)</sup> PCl<sub>3</sub> is also readily oxidized to the important phosphorus(V) derivatives PCl<sub>5</sub>, POCl<sub>3</sub> and PSCl<sub>3</sub>. It is oxidized by As<sub>2</sub>O<sub>3</sub> to P<sub>2</sub>O<sub>5</sub> though this is not the commercial route to this compound (p. 505). It fumes in moist air and is more readily hydrolysed (and oxidized) by water than is PF<sub>3</sub>. With cold N<sub>2</sub>O<sub>4</sub> (-10°) it undergoes a curious oxidative coupling reaction to give Cl<sub>3</sub>P=N-POCl<sub>2</sub>,

<sup>†</sup> World production exceeds one third of a million tonnes pa; of this USA produces ~155 000 tonnes, Western Europe ~115 000 and Japan ~35 000 tonnes pa.

<sup>83</sup> D. H. CHADWICK and R. S. WATT, Chap. 19 in ref. 11, pp. 1221-79.



mp  $35.5^\circ$ ; (note the presence of two different 4-coordinate  $\text{P}^{\text{V}}$  atoms).<sup>(84)</sup> Other notable reactions of  $\text{PCl}_3$  are its extensive use to convert alcohols to  $\text{RCl}$  and carboxylic acids to  $\text{RCOCl}$ , its reduction to  $\text{P}_2\text{I}_4$  by iodine, and its ability to form coordination complexes with Lewis acids such as  $\text{BX}_3$  and  $\text{Ni}^0$ .

$\text{PI}_3$  is emerging as a powerful and versatile deoxygenating agent.<sup>(85)</sup> For example solutions of  $\text{PI}_3$  in  $\text{CH}_2\text{Cl}_2$  at or below room temperature

convert sulfoxides ( $\text{RR}'\text{SO}$ ) into diorganosulfides, selenoxides ( $\text{RR}'\text{SeO}$ ) into selenides, aldehyde oximes ( $\text{RCH}=\text{NOH}$ ) into nitriles, and primary nitroalkanes ( $\text{RCH}_2\text{NO}_2$ ) into nitriles, all in high yield (75–95%). The formation of nitriles,  $\text{RCN}$ , in the last two reactions requires the presence of triethylamine in addition to the  $\text{PI}_3$ .

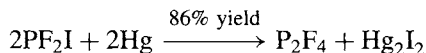
### Diphosphorus tetrahalides and other lower halides of phosphorus

The physical properties of  $\text{P}_2\text{X}_4$ , in so far as they are known, are summarized in Table 12.3.  $\text{P}_2\text{F}_4$  was first made in other than trace amounts in

<sup>84</sup> M. BECKE-GOEHRING, A. DEBO, E. FLUCK and W. GOETZE, *Chem. Ber.* **94**, 1383–7 (1961).

<sup>85</sup> J. N. DENIS and A. KRIEF, *J. Chem. Soc., Chem. Commun.*, 544–5 (1980).

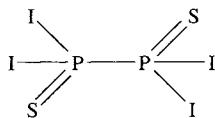
1966, using the very effective method of coupling two PF<sub>2</sub> groups at room temperature under reduced pressure:



The compound hydrolyses to F<sub>2</sub>POPf<sub>2</sub> which can also be prepared directly in good yield by the reaction of O<sub>2</sub> on P<sub>2</sub>F<sub>4</sub>.

P<sub>2</sub>Cl<sub>4</sub> can be made (in low yield) by passing an electric discharge through a mixture of PCl<sub>3</sub> and H<sub>2</sub> under reduced pressure or by microwave discharge through PCl<sub>3</sub> at 1–5 mmHg pressure. The compound decomposes slowly at room temperature to PCl<sub>3</sub> and an involatile solid, and can be hydrolysed in basic solution to give an equimolar mixture of P<sub>2</sub>H<sub>4</sub> and P<sub>2</sub>(OH)<sub>4</sub>.

Little is known of P<sub>2</sub>Br<sub>4</sub>, said to be produced by an obscure reaction in the system C<sub>2</sub>H<sub>4</sub>–PBr<sub>3</sub>–Al<sub>2</sub>Br<sub>6</sub>.<sup>(86)</sup> By contrast, P<sub>2</sub>I<sub>4</sub> is the most stable and also the most readily made of the 4 tetrahalides; it is formed by direct reaction of I<sub>2</sub> and red P at 180° or by I<sub>2</sub> and white P<sub>4</sub> in CS<sub>2</sub> solution, and can also be made by reducing PI<sub>3</sub> with red P, or PCl<sub>3</sub> with iodine. Its X-ray crystal structure shows that the molecules of P<sub>2</sub>I<sub>4</sub> adopt the *trans*-, centrosymmetric (C<sub>2h</sub>) form (see N<sub>2</sub>H<sub>4</sub>, p. 428, N<sub>2</sub>F<sub>4</sub>, p. 439). Reaction of P<sub>2</sub>I<sub>4</sub> with sulfur in CS<sub>2</sub> yields P<sub>2</sub>I<sub>4</sub>S<sub>2</sub>, which probably has the symmetrical structure



but most reactions of P<sub>2</sub>I<sub>4</sub> result in cleavage of the P–P bond, e.g. Br<sub>2</sub> gives PBrI<sub>2</sub> in 90% yield. Hydrolysis yields various phosphines and oxoacids of P, together with a small amount of hypophosphoric acid, (HO)<sub>2</sub>(O)PP(O)(OH)<sub>2</sub>.

Several ternary diphosphorus tetrahalides, P<sub>2</sub>X<sub>n</sub>Y<sub>4–n</sub>, (X, Y = Cl, Br, I) have recently

been detected in CS<sub>2</sub> solutions by <sup>31</sup>P nmr spectroscopy.<sup>(87)</sup> It has also been found that reactions CS<sub>2</sub> solution between P<sub>4</sub> and half a mole-equivalent of Br<sub>2</sub> yielded not only P<sub>2</sub>Br<sub>4</sub> but also small amounts of the new “butterfly” molecules *exo,exo*-P<sub>4</sub>Br<sub>2</sub> and *exo,endo*-P<sub>4</sub>Br<sub>2</sub>. The structure of these can be viewed as being formed by the scission of one P–P bond in the P<sub>4</sub> tetrahedron by Br<sub>2</sub> (cf. the structure of B<sub>4</sub>H<sub>10</sub>, p. 154) which is also a 22 valence-electron species). The molecules P<sub>4</sub>BrCl and P<sub>4</sub>Cl<sub>2</sub> were also identified, following chlorination of the bromide solution using Me<sub>3</sub>SnCl. Other products of the initial reactions included P<sub>7</sub>Br<sub>3</sub> and P<sub>7</sub>I<sub>3</sub> which are structurally related to P<sub>7</sub>H<sub>3</sub> (p. 495). None of these novel subhalides has been isolated pure.<sup>(87)</sup>

### Phosphorus pentahalides

Considerable theoretical and stereochemical interest attaches to these compounds because of the variety of structures they adopt; PCl<sub>5</sub> is also an important chemical intermediate. Thus, PF<sub>5</sub> is molecular and stereochemically non-rigid (see below), PCl<sub>5</sub> is molecular in the gas phase, ionic in the crystalline phase, [PCl<sub>4</sub>]<sup>+</sup>[PCl<sub>6</sub>]<sup>–</sup>, and either molecular or ionically dissociated in solution, depending on the nature of the solvent. PBr<sub>5</sub> is also ionic in the solid state but exists as [PBr<sub>4</sub>]<sup>+</sup>[Br]<sup>–</sup> rather than [PBr<sub>4</sub>]<sup>+</sup>[PBr<sub>6</sub>]<sup>–</sup>. The pentaiodide does not exist<sup>(80)</sup> (except perhaps as PI<sub>3</sub>.I<sub>2</sub>, but certainly not as PI<sub>4</sub><sup>+</sup>I<sup>–</sup> as originally claimed<sup>(88)</sup>).

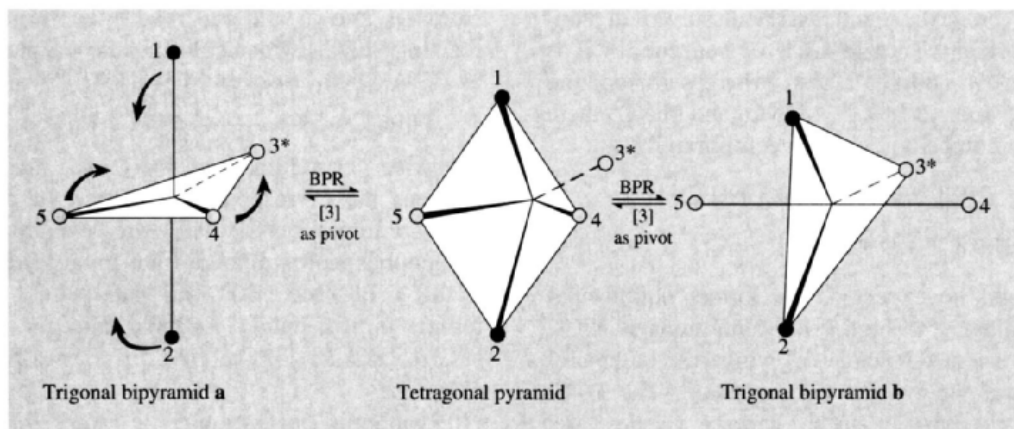
PF<sub>5</sub> is a thermally stable, chemically reactive gas which can be made either by fluorinating PCl<sub>5</sub> with AsF<sub>3</sub> (or CaF<sub>2</sub>), or by thermal decomposition of NaPF<sub>6</sub>, Ba(PF<sub>6</sub>)<sub>2</sub> or the corresponding diazonium salts. Single-crystal X-ray analysis (at –164°C) indicates a trigonal bipyramidal structure with P–F<sub>ax</sub> (158.0 pm) being

<sup>86</sup> R. I. PYRKIN, YA. A. LEVIN and E. I. GOLDFARB, *J. Gen. Chem. USSR* **43**, 1690–6 (1973). See also A. HINKE, W. KUCHEN and J. KUTTER, *Angew. Chem. Int. Edn. Engl.* **20**, 1060 (1981).

<sup>87</sup> B. W. TATTERSHALL and N. L. KENDALL, *Polyhedron* **13**, 1517–21 (1994).

<sup>88</sup> N. G. FESHCHENKO V. G. KOSTINA and A. V. KIRSANOV, *J. Gen. Chem. USSR* **48**, 195–6 (1978).





**Figure 12.13** Interchange of axial and equatorial positions by Berry pseudorotation (BPR).

significantly longer than  $\text{P-F}_{eq}$  (152.2 pm).<sup>(89)</sup> This confirms the deductions from a gas phase electron-diffraction study ( $D_{3h}$ :  $\text{P-F}_{ax}$  158 pm,  $\text{P-F}_{eq}$  153 pm). However, the  $^{19}\text{F}$  nmr spectrum, as recorded down to  $-100^\circ\text{C}$ , shows only a single fluorine resonance peak (split into a doublet by  $^{31}\text{P}$ - $^{19}\text{F}$  coupling) implying that on this longer time scale (milliseconds, as distinct from “instantaneous” for electron diffraction) all 5 F atoms are equivalent. This can be explained if the axial and equatorial F atoms interchange their positions more rapidly than this, a process termed “pseudorotation” by R. S. Berry (1960); indeed,  $\text{PF}_5$  was the first compound to show this effect.<sup>(90)</sup> The proposed mechanism is illustrated in Fig. 12.13 and is discussed more fully in ref. 91; the barrier to notation has been calculated as  $16 \pm 2 \text{ kJ mol}^{-1}$ .<sup>(92)</sup>

The mixed chlorofluorides  $\text{PCl}_4\text{F}$  (mp  $-59^\circ$ , bp  $+67^\circ$ ) and  $\text{PCl}_3\text{F}_2$  (mp  $-63^\circ$ ) are also trigonal bipyramidal with axial F atoms; likewise  $\text{PCl}_2\text{F}_3$  (mp  $-125^\circ$ , bp  $+7.1^\circ$ ) has 2 axial and 1 equatorial F atoms and  $\text{PClF}_4$  (mp  $-132^\circ$ ,

bp  $-43.4^\circ$ ) has both axial positions occupied by F atoms.<sup>(93)</sup> These compounds are obtained by addition of halogen to the appropriate phosphorus(III) chlorofluoride, but if  $\text{PCl}_5$  is fluorinated in a polar solvent, ionic isomers are formed, e.g.  $[\text{PCl}_4]^+[\text{PCl}_4\text{F}_2]^-$  (colourless crystals, subl  $175^\circ$ ) and  $[\text{PCl}_4]^+[\text{PF}_6]^-$  (white crystals, subl  $135^\circ$  with decomposition). The crystalline hemifluoride  $[\text{PCl}_4]^+[\text{PCl}_5\text{F}]^-$  has also been identified. The analogous parallel series of covalent and ionic bromofluorides is less well characterized but  $\text{PBr}_2\text{F}_3$  is known both as an unstable molecular liquid (decomp  $15^\circ$ ) and as a white crystalline powder  $[\text{PBr}_4]^+[\text{PF}_6]^-$  (subl  $135^\circ$  decomp). It can be noted that  $\text{PF}_3(\text{NH}_2)_2$  is a trigonal bipyramidal molecule with  $C_{2v}$  symmetry (i.e. equatorial  $\text{NH}_2$  groups),<sup>(94)</sup> whereas the most stable form of tetra-arylfuorophosphoranes is ionic,  $[\text{PR}_4]^+\text{F}^-$ , although molecular monomers  $\text{R}_4\text{PF}$  and an ionic dimer  $[\text{PR}_4]^+[\text{PR}_4\text{F}_2]^-$  also exist.<sup>(95)</sup>

$\text{PCl}_5$  is even closer to the ionic-covalent borderline than is  $\text{PF}_5$ , the ionic solid  $[\text{PCl}_4]^+[\text{PCl}_6]^-$  melting (or subliming) to give a covalent molecular

<sup>89</sup> D. MOOTZ and M. WIEBCKE, *Z. anorg. allg. Chem.* **545**, 39–42 (1987).

<sup>90</sup> R. S. BERRY, *J. Chem. Phys.* **32**, 933–8 (1960).

<sup>91</sup> R. LUCKENBACH, *Dynamic Stereochemistry of Pentacoordinate Phosphorus and Related Elements*, G. THIEME, Stuttgart, 1973, 259 pp.

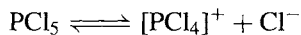
<sup>92</sup> C. J. MARSDEN, *J. Chem. Soc., Chem. Commun.*, 401–2 (1984).

<sup>93</sup> C. MACHO, R. MINKWITZ, J. ROHMAN, B. STEGER, W. WÖLFEL and H. OBERHAMMER, *Inorg. Chem.* **25**, 2828–35 (1986), and references cited therein.

<sup>94</sup> C. J. MARSDEN, K. HEDBERG, J. M. SHREEVE and K. D. GUPTA, *Inorg. Chem.* **23**, 3659–62 (1984).

<sup>95</sup> S. J. BROWN, J. H. CLARK and D. J. MACQUARRIE, *J. Chem. Soc., Dalton Trans.*, 277–80 (1988).

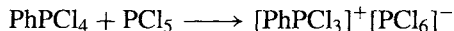
liquid (or gas). Again, when dissolved in non-polar solvents such as  $\text{CCl}_4$  or benzene,  $\text{PCl}_5$  is monomeric and molecular, whereas in ionizing solvents such as  $\text{MeCN}$ ,  $\text{MeNO}_2$  and  $\text{PhNO}_2$  there are two competing ionizing equilibria.<sup>(96)</sup>



As might be expected, the former equilibrium predominates at higher concentrations of  $\text{PCl}_5$  (above about  $0.03 \text{ mol l}^{-1}$ ) whilst the latter predominates below this concentration. The P-Cl distances (pm) in these various species are:  $\text{PCl}_5$  214 (axial), 202 (equatorial);  $[\text{PCl}_4]^+$  197;  $[\text{PCl}_6]^-$  208 pm. Ionic isomerism is also known and, in addition to  $[\text{PCl}_4]^+[\text{PCl}_6]^-$ , another (metastable) crystalline phase of constitution  $[\text{PCl}_4]_2^+[\text{PCl}_6]_2^-\text{Cl}^-$  can be formed either by application of high pressure or by crystallizing  $\text{PCl}_5$  from solutions of dichloromethane containing  $\text{Br}_2$  or  $\text{SCl}_2$ .<sup>(97)</sup> When gaseous  $\text{PCl}_5$  (in equilibrium with  $\text{PCl}_3 + \text{Cl}_2$ ) is quenched to 15 K the trigonal-bipyramidal molecular structure is retained; this forms an ordered molecular crystalline lattice on warming to  $\sim 130 \text{ K}$ , but further warming towards room temperature results in chloride-ion transfer to give  $[\text{PCl}_4]^+[\text{PCl}_6]^-$ .<sup>(98)</sup> The first alkali metal salt of  $[\text{PCl}_6]^-$ ,  $\text{CsPCl}_6$ , has only recently been made.<sup>(99)</sup>

The delicate balance between ionic and covalent forms is influenced not only by the state of aggregation (solid, liquid, gas) or the nature of the solvent, but also by the effect of substituents. Thus  $\text{PhPCl}_4$  is molecular with Ph equatorial whereas the corresponding methyl derivative is ionic,  $[\text{MePCl}_3]^+\text{Cl}^-$ . Despite this the  $[\text{PhPCl}_3]^+$

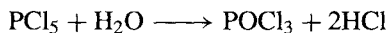
cation is known and can readily be formed by reacting  $\text{PhPCl}_4$  with a chlorine ion acceptor such as  $\text{BCl}_3$ ,  $\text{SbCl}_5$ , or even  $\text{PCl}_5$  itself:<sup>(100)</sup>



Likewise crystalline  $\text{Ph}_2\text{PCl}_3$  is molecular whereas the corresponding Me and Et derivatives are ionic  $[\text{R}_2\text{PCl}_2]^+\text{Cl}^-$ . However, all 3 triorganophosphorus dihalides are ionic  $[\text{R}_3\text{PCl}]^+\text{Cl}^-$  (R = Ph, Me, Et). The pale-yellow, crystalline mixed halide  $\text{P}_2\text{BrCl}_9$  appears to be  $[\text{PCl}_4]_6^+[\text{PCl}_3\text{Br}]_2^+[\text{PCl}_6]_4^-[ \text{Br} ]_4^-$  (i.e.  $\text{P}_{12}\text{Br}_6\text{Cl}_{54}$ ).<sup>(101)</sup>

Phosphorus pentabromide is rather different. The crystalline solid is  $[\text{PBr}_4]^+\text{Br}^-$  but this appears to dissociate completely to  $\text{PBr}_3$  and  $\text{Br}_2$  in the vapour phase; rapid cooling of this vapour to 15 K results in the formation of a disordered lattice of  $\text{PBr}_3$  and  $\text{PBr}_7$  (i.e.  $[\text{PBr}_4]^+[\text{Br}_3]^-$ ) and this mixture reverts to  $[\text{PBr}_4]^+\text{Br}^-$  on being warmed to 180 K.<sup>(98)</sup> The corresponding trichloride,  $[\text{PBr}_4]^+[\text{Cl}_3]^-$  is also known.<sup>(102)</sup>  $[\text{PI}_4]^+$  has been identified only as its salt  $[\text{PI}_4]^+[\text{AsF}_6]^-$ .<sup>(80)</sup>

$\text{PCl}_5$  is made on an industrial scale by the reaction of  $\text{Cl}_2$  on  $\text{PCl}_3$  dissolved in an equal volume of  $\text{CCl}_4$ . World production probably exceeds 20 000 tonnes pa. On the laboratory scale  $\text{Cl}_2$  gas (or liquid) can be passed directly into  $\text{PCl}_3$ .  $\text{PCl}_5$  reacts violently with water to give  $\text{HCl}$  and  $\text{H}_3\text{PO}_4$  but in equimolar amounts the reaction can be moderated to give  $\text{POCl}_3$ :



$\text{PCl}_5$  chlorinates alcohols to alkyl halides and carboxylic acids to the corresponding  $\text{RCOCl}$ . When heated with  $\text{NH}_4\text{Cl}$  the phosphonitric chlorides are obtained (p. 536). These and other reactions are summarized in the diagram.<sup>(8)</sup>

<sup>96</sup> R. W. SUTER, H. C. KNACHEL, V. P. PETRO, J. H. HOWATSON and S. G. SHORE, *J. Am. Chem. Soc.* **95**, 1474-9 (1973).

<sup>97</sup> A. FINCH, P. N. GATES, H. D. B. JENKINS and K. P. THAKUR, *J. Chem. Soc., Chem. Commun.*, 579-80 (1980). See also H. D. B. JENKINS, L. SHARMAN, A. FINCH and P. N. GATES, *Polyhedron* **13**, 1481-2 (1994) and references cited therein.

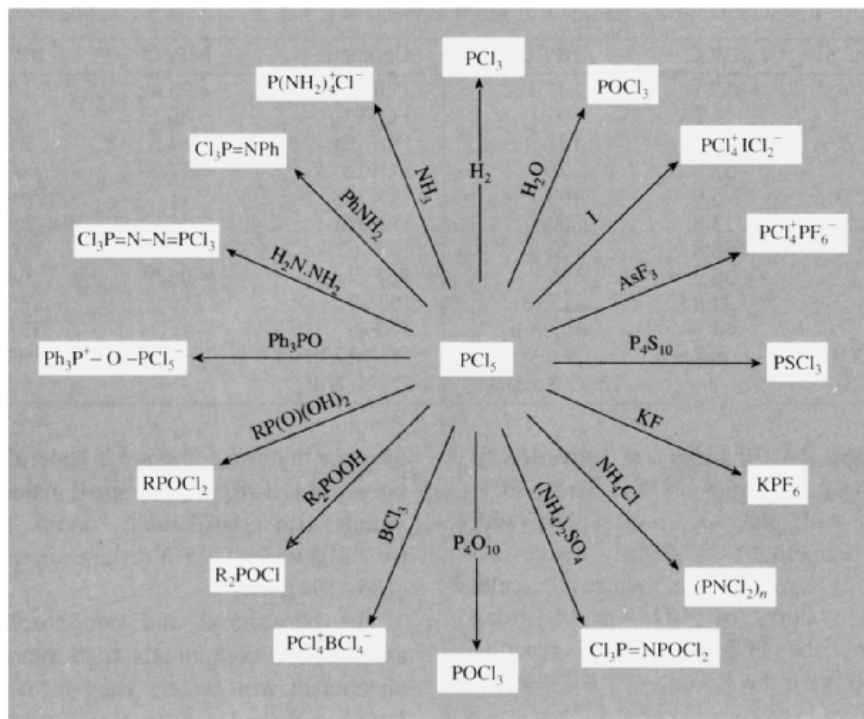
<sup>98</sup> A. FINCH, P. N. GATES and A. S. MUIR, *J. Chem. Soc., Chem. Commun.*, 812-4 (1981). See also H. D. B. JENKINS, K. P. THAKUR, A. FINCH and P. N. GATES, *Inorg. Chem.* **21**, 423-6 (1982).

<sup>99</sup> A. S. MUIR, *Polyhedron* **10**, 2217-9 (1991).

<sup>100</sup> K. B. DILLON, R. J. LYNCH, R. N. REEVE and T. C. WADDINGTON, *J. Chem. Soc., Dalton Trans.*, 1243-8 (1976). See also M. A. H. A. AL-JUBOORI, P. N. GATES and A. S. MUIR, *J. Chem. Soc., Chem. Commun.*, 1270-1 (1991).

<sup>101</sup> F. F. BENTLEY, A. FINCH, P. N. GATES, F. J. RYAN and K. B. DILLON, *J. Inorg. Nucl. Chem.* **36**, 457-9 (1974). See also *J. Chem. Soc., Dalton Trans.*, 1863-6 (1973).

<sup>102</sup> K. B. DILLON, M. P. NISBET and R. N. REEVE, *Polyhedron* **7**, 1725-6 (1988). See also H. D. B. JENKINS, *Polyhedron* **15**, 2831-4 (1996).



The chlorination of phosphonic and phosphinic acids and esters are of considerable importance.  $\text{PCl}_5$  can also act as a Lewis acid to give 6-coordinate P complexes, e.g.  $\text{pyPCl}_5$ , and  $\text{pyz-PCl}_5$ , where  $\text{py} = \text{C}_5\text{H}_5\text{N}$  (pyridine) and  $\text{pyz} = \text{cyclo-1,4-C}_4\text{H}_4\text{N}_2$  (pyrazine).<sup>(103)</sup>

### Pseudohalides of phosphorus(III)

Paralleling the various phosphorus trihalides are numerous pseudohalides and mixed pseudohalide-halides of which the various isocyanates and isothiocyanates are perhaps the best known. Most are volatile liquids, e.g.

Compound	$\text{P}(\text{NCO})_3$	$\text{PF}(\text{NCO})_2$	$\text{PF}_2(\text{NCO})$
MP/°C	-2	-55	~ -108
BP/°C	169.3	98.7	12.3

Compound	$\text{PCl}(\text{NCO})_2$	$\text{PCl}_2(\text{NCO})$	$\text{P}(\text{NCS})_3$
MP/°C	-50	-99	-4
BP/°C	134.6	104.5	~120/1 mmHg

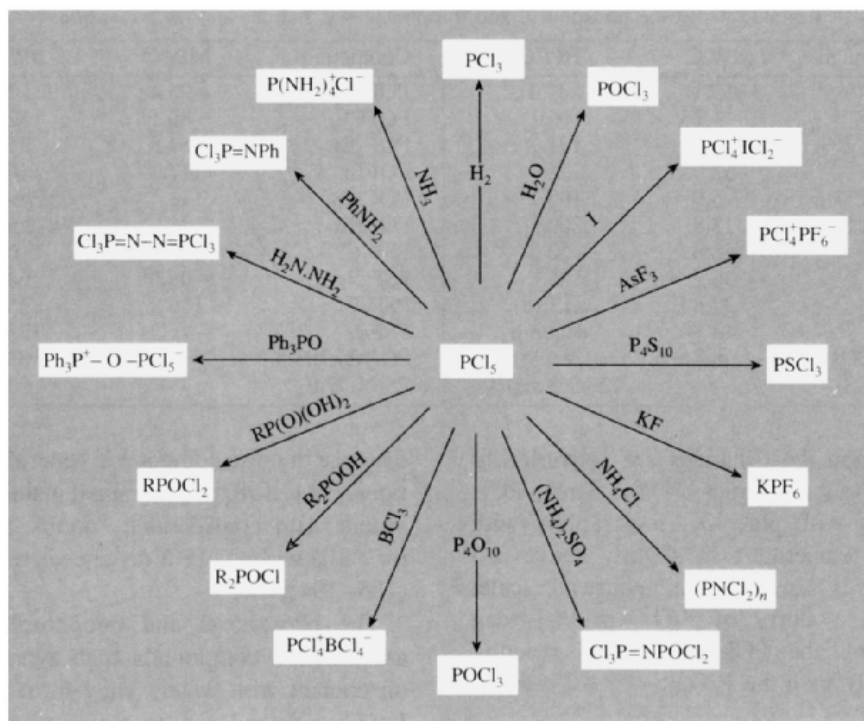
Compound	$\text{PF}_2(\text{NCS})$	$\text{PCl}_2(\text{NCS})$
MP/°C	-95	-76
BP/°C	90.3	148(decomp)

The corresponding phosphoryl and thiophosphoryl pseudohalides are also known, i.e.  $\text{PO}(\text{NCO})_3$ ,  $\text{PS}(\text{NCO})_3$ , etc. Preparations are by standard procedures such as those on the diagram for  $\text{PCl}_3$  (p. 497). As indicated there,  $\text{P}(\text{CN})_3$  has also been made: it is a highly reactive white crystalline solid mp  $203^\circ$  which reacts violently with water to give mainly phosphorous acid and  $\text{HCN}$ .

### 12.3.4 Oxohalides and thiohalides of phosphorus

The propensity of phosphorus(III) compounds to oxidize to phosphorus(V) by formation of an additional  $\text{P}=\text{O}$  bond is well illustrated by the

<sup>103</sup> B. N. MEYER, J. N. ISHLEY, A. V. FRATINI and H. C. KNACHEL, *Inorg. Chem.* **19**, 2324-7 (1980) and references therein.



The chlorination of phosphonic and phosphinic acids and esters are of considerable importance.  $\text{PCl}_5$  can also act as a Lewis acid to give 6-coordinate P complexes, e.g.  $\text{pyPCl}_5$ , and  $\text{pyz-PCl}_5$ , where  $\text{py} = \text{C}_5\text{H}_5\text{N}$  (pyridine) and  $\text{pyz} = \text{cyclo-1,4-C}_4\text{H}_4\text{N}_2$  (pyrazine).<sup>(103)</sup>

### Pseudohalides of phosphorus(III)

Paralleling the various phosphorus trihalides are numerous pseudohalides and mixed pseudohalide-halides of which the various isocyanates and isothiocyanates are perhaps the best known. Most are volatile liquids, e.g.

Compound	$\text{P}(\text{NCO})_3$	$\text{PF}(\text{NCO})_2$	$\text{PF}_2(\text{NCO})$
MP/°C	-2	-55	~ -108
BP/°C	169.3	98.7	12.3

Compound	$\text{PCl}(\text{NCO})_2$	$\text{PCl}_2(\text{NCO})$	$\text{P}(\text{NCS})_3$
MP/°C	-50	-99	-4
BP/°C	134.6	104.5	~120/1 mmHg

Compound	$\text{PF}_2(\text{NCS})$	$\text{PCl}_2(\text{NCS})$
MP/°C	-95	-76
BP/°C	90.3	148(decomp)

The corresponding phosphoryl and thiophosphoryl pseudohalides are also known, i.e.  $\text{PO}(\text{NCO})_3$ ,  $\text{PS}(\text{NCO})_3$ , etc. Preparations are by standard procedures such as those on the diagram for  $\text{PCl}_3$  (p. 497). As indicated there,  $\text{P}(\text{CN})_3$  has also been made: it is a highly reactive white crystalline solid mp  $203^\circ$  which reacts violently with water to give mainly phosphorous acid and HCN.

### 12.3.4 Oxohalides and thiohalides of phosphorus

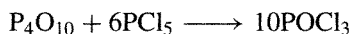
The propensity of phosphorus(III) compounds to oxidize to phosphorus(V) by formation of an additional  $\text{P}=\text{O}$  bond is well illustrated by the

<sup>103</sup> B. N. MEYER, J. N. ISHLEY, A. V. FRATINI and H. C. KNACHEL, *Inorg. Chem.* **19**, 2324-7 (1980) and references therein.

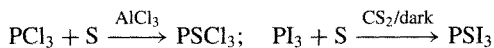
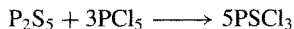
**Table 12.4** Some phosphoryl and thiophosphoryl halides and pseudohalides

Compound	MP/°C	BP/°C	Compound	MP/°C	BP/°C
POF <sub>3</sub>	-39.1	-39.7	POF <sub>2</sub> Cl	-96.4	3.1
POCl <sub>3</sub>	1.25	105.1	POFCl <sub>2</sub>	-80.1	52.9
POBr <sub>3</sub>	55	191.7	POF <sub>2</sub> Br	-84.8	31.6
POI <sub>3</sub>	53	—	POFBr <sub>2</sub>	-117.2	110.1
PO(NCO) <sub>3</sub>	5.0	193.1	POCl <sub>2</sub> Br	11	52/3 mmHg
PO(NCS) <sub>3</sub>	13.8	300.1	POClBr <sub>2</sub>	31	49/12 mmHg
PSF <sub>3</sub>	-148.8	-52.2	PSF <sub>2</sub> Cl	-155.2	6.3
PSCl <sub>3</sub>	-35	-125	PSFCl <sub>2</sub>	-96.0	64.7
PSBr <sub>3</sub>	37.8	212 (d)	PSF <sub>2</sub> Br	-136.9	35.5
PSI <sub>3</sub>	48	decomp	PSFBr <sub>2</sub>	-75.2	125.3
PS(NCO) <sub>3</sub>	8.8	215	PO(NCO)FCl	—	103
PS(NCS) <sub>3</sub>	—	123/0.3 mmHg	PS(NCS) <sub>2</sub>	—	90

ease with which the trihalides are converted to their phosphoryl analogues POX<sub>3</sub>. Thus, PCl<sub>3</sub> reacts rapidly with pure O<sub>2</sub> (less rapidly with air) at room temperature or slightly above and this reaction is used on an industrial scale. Alternatively, a slurry of P<sub>4</sub>O<sub>10</sub> in PCl<sub>3</sub> can be chlorinated, the PCl<sub>5</sub> so formed reacting instantaneously with the P<sub>4</sub>O<sub>10</sub>:



POBr<sub>3</sub> can be made by similar methods, but POF<sub>3</sub> is usually made by fluorination of POCl<sub>3</sub> using a metal fluoride (e.g. M = Na, Mg, Zn, Pb, Ag, etc.). POI<sub>3</sub> was first made in 1973 by iodinating POCl<sub>3</sub> with LiI, or by reacting ROPI<sub>2</sub> with iodine (ROPI<sub>2</sub> + I<sub>2</sub> → RI + POI<sub>3</sub>).<sup>(104)</sup> Mixed phosphoryl halides, POX<sub>n</sub>Y<sub>3-n</sub>, and pseudohalides (e.g. X = NCO, NCS) are known, as also are the thiophosphoryl halides PSX<sub>3</sub>, e.g.:



Most of the phosphoryl and thiophosphoryl compounds are colourless gases or volatile liquids though PSBr<sub>3</sub> forms yellow crystals, mp 37.8°, POI<sub>3</sub> is dark violet, mp 53°, and PSI<sub>3</sub> is red-brown, mp 48°. All are monomeric tetrahedral (C<sub>3v</sub>) or pseudotetrahedral. Some physical properties are in Table 12.4. The P–O interatomic

distance in these compounds generally falls in the range 154–158 pm, the small value being consistent with considerable “double-bond character”. Likewise the P–S distance is relatively short (185–194 pm).

The phosphoryl and thiophosphoryl halides are reactive compounds that hydrolyse readily on contact with water. They form adducts with Lewis acids and undergo a variety of substitution reactions to form numerous organophosphorus derivatives and phosphate esters. Thus, alcohols give successively (RO)POCl<sub>2</sub>, (RO)<sub>2</sub>POCl and (RO)<sub>3</sub>PO; phenols react similarly but more slowly. Likewise, amines yield (RNH)POCl<sub>2</sub>, (RNH)<sub>2</sub>POCl and (RNH)<sub>3</sub>PO whereas Grignard reagents yield R<sub>n</sub>POCl<sub>3-n</sub> (n = 1–3). Many of these compounds find extensive use as oil additives, insecticides, plasticizers, surfactants or flame retardants, and are manufactured on the multikilotonne scale.

In addition to the monophosphorus phosphoryl and thiophosphoryl compounds discussed above, several poly-phosphoryl and -thiophosphoryl halides have been characterized. Pyrophosphoryl fluoride, O=PF<sub>2</sub>–O–P(=O)F<sub>2</sub> (mp –0.1°, bp 72° extrap) and the white crystalline cyclic tetramer [O=P(F)–O]<sub>4</sub> were

obtained by subjecting equimolar mixtures of PF<sub>3</sub> and O<sub>2</sub> to a silent electric discharge at –70°. Pyrophosphoryl chloride, O=PCl<sub>2</sub>–O–P(=O)Cl<sub>2</sub> is conveniently prepared by passing Cl<sub>2</sub> into a boiling suspension

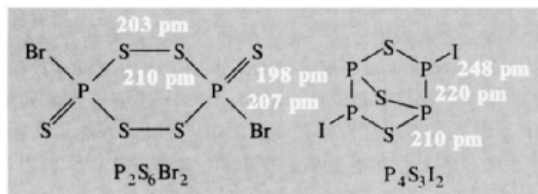
<sup>104</sup> A. V. KIRSANOV, ZH. K. GORBATENKO and N. G. FESHCHENKO, *Pure Appl. Chem.* **44**, 125–39 (1975).

of  $P_4O_{10}$  in  $PCl_3$  diluted with  $CCl_4$ :



It is a colourless, odourless, non-fuming, oily liquid, mp  $-16.5^\circ$ , bp  $215^\circ$  (decomp), with reactions similar to those of  $POCl_3$ . Sealed-tube reactions between  $P_4O_{10}$  and  $POCl_3$  at  $200-230^\circ$  give more highly condensed cyclic and open-chain polyphosphoryl chlorides. A rather different structural motif occurs in  $P_2S_4F_4$ ; this compound is obtained by fluorinating  $P_4S_{10}$  with an alkali-metal fluoride to give the anion  $[S_2PF_2]^-$  which is then oxidized by bromine to  $P_2S_4F_4$  (bp  $60^\circ$  at 10 mmHg). Vibrational and nmr spectra are consistent with the structure  $F_2(S)PSSP(S)F_2$ .

Bromination of  $P_4S_7$  in cold  $CS_2$  yields, in addition to  $PBr_3$  and  $PSBr_3$ , two further thiobromides  $P_2S_6Br_2$  (mp  $118^\circ$  decomp) and  $P_2S_5Br_4$  (mp  $90^\circ$  decomp). The first of these has the cyclic structure shown in which the ring adopts a skew-boat configuration. An even more complex, bicyclic arrangement is found in the orange-yellow compound  $P_4S_3I_2$  (mp  $120^\circ$  decomp) which is formed (together with several other products) when equiatomic amounts of P, S and I are allowed to react. The P and S atoms are arranged in two 5-membered rings having a common P-S-P group as shown; in each there is a P-P group and the I atoms are bonded in *cis*-configuration to the P atoms not common to the two rings. The orange compound  $P_2S_2I_4$  (mp  $94^\circ$ ) was mentioned on p. 498.



By contrast to the plethora of simple oxohalides and thiohalides of  $P^V$ , the corresponding derivatives of  $P^{III}$  are fugitive species that require matrix isolation techniques for preparation and characterization.<sup>(105)</sup>  $CIPO$ ,  $BrPO$ ,  $FPS$  and  $BrPS$  all form non-linear triatomic molecules, as expected. The corresponding oxosulfide,  $BrP(O)S$ ,<sup>(106)</sup> and its thio-analogue,  $FP(S)S$ ,<sup>(107)</sup> have also recently been isolated.

### 12.3.5 Phosphorus oxides, sulfides, selenides and related compounds

The oxides and sulfides of phosphorus are amongst the most important compounds of the element. At least 6 binary oxides and 9 well-defined sulfides are known, together with a similar number of selenides and several oxosulfides. It will be convenient to discuss first the preparation and structure of each group of compounds and then to mention the chemical reactions of the more important members in so far as they are known. It is notable that, in contrast to the ubiquitous  $NO$  and its many complexes (pp. 445 ff), little is known about its analogue,  $PO$  (see p. 506), although it is probably the most abundant P-containing molecule in interstellar clouds.<sup>(108)</sup> The first complex with a  $PO$  ligand was first synthesized as recently as 1991, when dark green crystals of the square-based pyramidal hetero-atom cluster  $[W(CO)_4\{Ni(\eta^5-C_5HPr_4^i)\}_2(\mu:\eta^2,\eta^2-P_2)]$  was oxidized with bis(trimethylsilyl) peroxide,  $(Me_3Si)_2O_2$ , to yield black crystals of the corresponding  $[W(CO)_4\{Ni(\eta^5-C_5HPr_4^i)\}_2(\mu:\eta^2,\eta^2-PO)_2]$ .<sup>(108)</sup>

#### Oxides

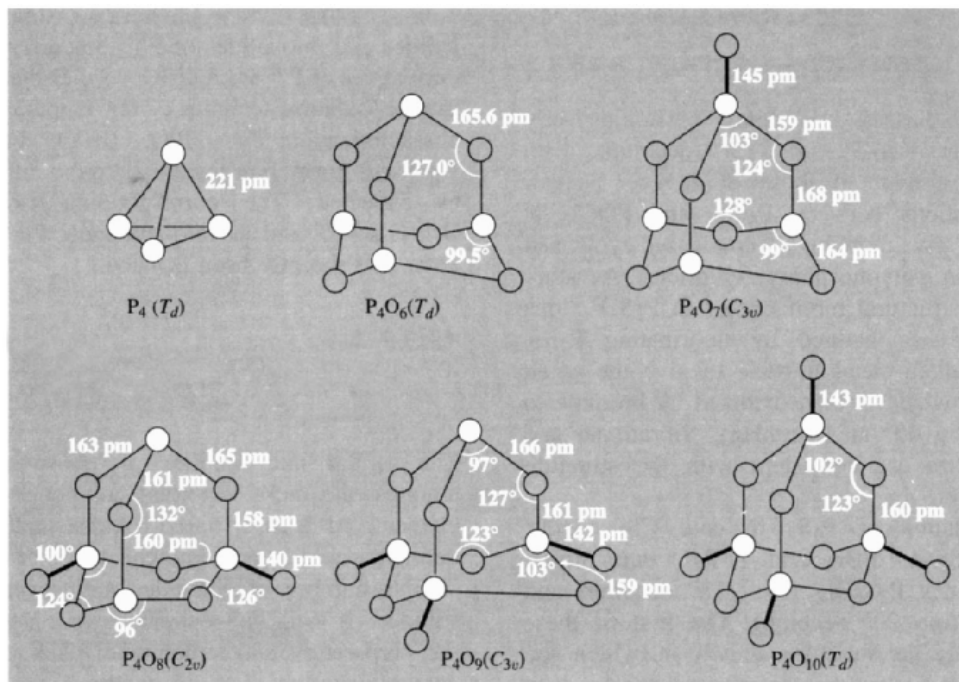
$P_4O_6$  is obtained by controlled oxidation of  $P_4$  in an atmosphere of 75%  $O_2$  and 25%  $N_2$  at  $90$  mmHg and  $\sim 50^\circ$  followed by distillation of the product from the mixture. Careful

<sup>105</sup> H. SCHNÖCKEL and S. SCHUNCK, *Z. anorg. allg. Chem.* **548**, 161-4 (1987); **552**, 155-62 and 63-70 (1987). M. BINNEWIES and H. BORRMANN, *ibid.* **552**, 147-54 (1987).

<sup>106</sup> S. SCHUNCK, H.-J. GÖCKE and H. SCHNÖCKEL, *Z. anorg. allg. Chem.* **583**, 78-84 (1990).

<sup>107</sup> H. BOK, M. KREMER, B. SOLOUKI, M. BINNEWIES and M. MEISEL, *J. Chem. Soc., Chem. Commun.*, 9-11 (1992).

<sup>108</sup> O. J. SCHERER, J. BRAUN, P. WALTHER, G. HECKMANN and G. WOLMERSHÄUSER, *Angew. Chem. Int. Edn. Engl.* **30**, 852-4. (1991).



**Figure 12.14** Molecular structures, symmetries and dimensions of the 5 oxides  $P_4O_{6+n}$  ( $n = 0-4$ ) compared with  $\alpha$ - $P_4$ . The  $P \cdots P$  distances in the oxides are  $\sim 280-290$  pm, i.e. essentially nonbonding.

precautions are necessary if good yields are to be obtained.<sup>(109)</sup> It forms soft white crystals, mp  $23.8^\circ$ , bp  $175.4^\circ$ , and is soluble in many organic solvents. The molecular structure has tetrahedral symmetry and comprises 4 fused 6-membered  $P_3O_3$  heterocycles each with the chair conformation as shown in Fig. 12.14.<sup>(110)</sup> When  $P_4O_6$  is heated to  $200-400^\circ$  in a sealed, evacuated tube it disproportionates into red phosphorus and a solid-solution series of composition  $P_4O_n$  depending on conditions. The  $\alpha$ -phase has a composition in the range  $P_4O_{8.1}-P_4O_{9.2}$  and comprises a solid solution of oxides in which one or two of the "external" O atoms in  $P_4O_{10}$  have been removed. The  $\beta$ -phase has a composition range  $P_4O_{8.0}-P_4O_{7.7}$

and appears to be a solid solution of  $P_4O_8$  and  $P_4O_7$ , the latter compound having only one O atom external to the  $P_4O_6$  cluster ( $C_{3v}$  symmetry).  $P_4O_7$  is now best prepared from  $P_4O_6$  dissolved in thf, using  $Ph_3PO$  as a catalyst (not an oxidant) at room temperature. The molecular structure and dimensions of  $P_4O_7$  are given in Fig. 12.14 from which it is apparent that there is a gradual lengthening of P-O distances in the sequence  $P^V-O_t < P^V-O_\mu < P^{III}-O_\mu$ . Similar trends are apparent in the dimensions of the other members of the series  $P_4O_{6+n}$  shown in Fig. 12.14.<sup>(110)</sup> In addition, ring angles at P ( $96-103^\circ$ ) are always less than those at O ( $122-132^\circ$ ), as expected.

$P_4O_6$  hydrolyses in cold water to give  $H_3PO_3$  i.e.  $HP(O)(OH)_2$ ; this is interesting in view of the structure of  $P_4O_6$  and implies an oxidative rearrangement of  $\{P-OH\}$  to  $\{H-P=O\}$  (p. 514). The oxide itself ignites and burns when heated in air; the progress of the reaction depends very much on the

<sup>109</sup> D. HEINZE, *Pure Appl. Chem.* **44**, 141-72 (1975).

<sup>110</sup> M. JANSEN and M. VOSS, *Angew. Chem. Int. Edn. Engl.* **20**, 100-1, 965 (1981), and references therein to crystal structure determinations on the other members of the series  $P_4O_{6+n}$ . See also M. JANSEN and M. MOEBES, *Inorg. Chem.* **23**, 4486-8 (1984).

Table 12.5 Some properties of crystalline polymorphs of P<sub>2</sub>O<sub>5</sub>

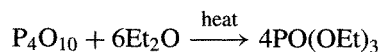
Polymorph	Density/g cm <sup>-3</sup>	MP/°C	Pressure at triple pt/mmHg	$\Delta H_{\text{subl}}/\text{kJ (mol P}_4\text{O}_{10})^{-1}$
H: hexagonal P <sub>4</sub> O <sub>10</sub>	2.30	420	3600	95
O: metastable (P <sub>2</sub> O <sub>5</sub> ) <sub>n</sub>	2.72	562	437	152
O': stable (P <sub>2</sub> O <sub>5</sub> ) <sub>n</sub>	2.74–3.05	580	555	142

purity of the oxide and the conditions employed, and, when traces of elemental phosphorus are present in the oxide, the reaction is spontaneous even at room temperature. P<sub>4</sub>O<sub>6</sub> reacts readily (often violently) with many simple inorganic and organic compounds but well-characterized products have rarely been isolated until recently.<sup>(109)</sup> It behaves as a ligand and successively displaces CO from [Ni(CO)<sub>4</sub>] to give compounds such as [P<sub>4</sub>O<sub>6</sub>{Ni(CO)<sub>3</sub>}<sub>4</sub>], [Ni(CO)<sub>2</sub>(P<sub>4</sub>O<sub>6</sub>)<sub>2</sub>] and [Ni(CO)(P<sub>4</sub>O<sub>6</sub>)<sub>3</sub>]. With diborane adducts of formula [P<sub>4</sub>O<sub>6</sub>(BH<sub>3</sub>)<sub>n</sub>] (*n* = 1–3) are obtained.

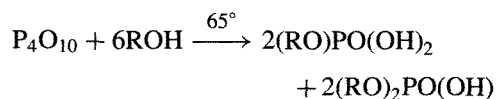
“Phosphorus pentoxide”, P<sub>4</sub>O<sub>10</sub>, is the commonest and most important oxide of phosphorus. It is formed as a fine white smoke or powder when phosphorus burns in air and, when condensed rapidly from the vapour phase in this way, is obtained in the H (hexagonal) form comprising tetrahedral molecules as shown in Fig. 12.14. This compound and the other phosphorus oxides are the first we have considered that feature the {PO<sub>4</sub>} group as a structural unit; this group dominates most of phosphate chemistry and will recur repeatedly during the rest of this chapter. The common hexagonal form of P<sub>4</sub>O<sub>10</sub> is, in fact, metastable and can be transformed into several other modifications by suitable thermal or high-pressure treatment. A metastable orthorhombic (O) form is obtained by heating H for 2 h at 400° and the stable orthorhombic (O') form is obtained after 24 h at 450°. Both consist of extensive sheet polymers of interlocking heterocyclic rings composed of fused {PO<sub>4</sub>} groups. There is also a high-pressure form and a glass, which probably consists of an irregular three-dimensional network of linked {PO<sub>4</sub>} tetrahedra. These polymeric forms are hard and brittle because of the P–O–P bonds throughout the lattice and, as

expected, they are much less volatile and reactive than the less-dense molecular H form. For example, whilst the common H form hydrolyses violently, almost explosively, with evolution of much heat, the polymeric forms react only slowly with water to give, finally, H<sub>3</sub>PO<sub>4</sub>. Some properties of the various polymorphs are compared in Table 12.5. The limp liquid obtained by rapidly heating the H form contains P<sub>4</sub>O<sub>10</sub> molecules but these rapidly polymerize and rearrange to layer or three-dimensional polymeric forms with a concomitant drop in the vapour pressure and an increase in the viscosity and mp.

Because of its avidity for water, P<sub>4</sub>O<sub>10</sub> is widely used as a dehydrating agent, but its efficacy as a desiccant is greatly impaired by the formation of a crusty surface film of hydrolysis products unless it is finely dispersed on glass wool. Its largest use is in the industrial production of ortho- and poly-phosphoric acids (p. 520) but it is also an intermediate in the production of phosphate esters. Thus, triethylphosphate is made by reacting P<sub>4</sub>O<sub>10</sub> with diethyl ether to form ethylpolyphosphates which, on subsequent pyrolysis and distillation, yield the required product:



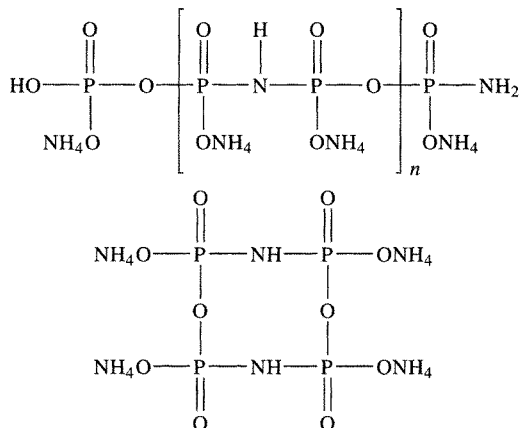
Direct reaction with alcohols gives mixed mono- and di-alkyl phosphoric acids by cleavage of the P–O–P bonds:



Under less-controlled conditions P<sub>4</sub>O<sub>10</sub> dehydrates ethanol to ethene and methylarylcarbinols to the corresponding styrenes. H<sub>2</sub>SO<sub>4</sub> is dehydrated to SO<sub>3</sub>, HNO<sub>3</sub> gives N<sub>2</sub>O<sub>5</sub> and amides

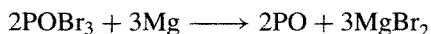


(RCONH<sub>2</sub>) yield nitriles (RCN). In each of these reactions metaphosphoric acid HPO<sub>3</sub> is the main P-containing product. P<sub>4</sub>O<sub>10</sub> reacts vigorously with both wet and dry NH<sub>3</sub> to form a range of amorphous polymeric powdery materials which are used industrially for water softening because of their ability to sequester Ca ions; composition depends markedly on the preparative conditions employed but most of the commercial products appear to be condensed linear or cyclic amidopolyphosphates which can be represented by formulae such as:



The annual production/consumption of P<sub>4</sub>O<sub>10</sub> in USA and Western Europe totals about 15 000 tonnes.

Other oxides of phosphorus are less well characterized though the suboxide PO and the peroxide P<sub>2</sub>O<sub>6</sub> seem to be definite compounds. PO was obtained as a brown cathodic deposit when a saturated solution of Et<sub>3</sub>NHCl in anhydrous POCl<sub>3</sub> was electrolysed between Pt electrodes at 0°. Alternatively it can be made by the slow reaction of POBr<sub>3</sub> with Mg in Et<sub>2</sub>O under reflux:



Its structure is unknown but is presumably based on a polymeric network of P–O–P links. It reacts with water to give PH<sub>3</sub> and is quantitatively oxidized to P<sub>2</sub>O<sub>5</sub> by oxygen at 300°. The peroxide P<sub>2</sub>O<sub>6</sub> is thought to be the active ingredient in the violet solid obtained when P<sub>4</sub>O<sub>10</sub> and O<sub>2</sub> are passed through a heated

discharge tube at low pressure. The compound has not been obtained pure but liberates I<sub>2</sub> from aqueous KI, hydrolyses to a peroxophosphoric acid, and liberates O<sub>2</sub> when heated to 130° under reduced pressure. Its structure may be (O=)<sub>2</sub>P–O–O–P(=O)<sub>2</sub> or, in view of the variable composition of the product, it may be a mixture of P<sub>4</sub>O<sub>11</sub> and P<sub>4</sub>O<sub>12</sub> obtained by replacing P–O–P links by P–O–O–P in P<sub>4</sub>O<sub>10</sub>.

### Sulfides<sup>(111)</sup>

The sulfides of phosphorus form an intriguing series of compounds which continue to present puzzling structural features. The compounds P<sub>4</sub>S<sub>10</sub>, P<sub>4</sub>S<sub>9</sub>, P<sub>4</sub>S<sub>7</sub>, α-P<sub>4</sub>S<sub>5</sub>, β-P<sub>4</sub>S<sub>5</sub>, α-P<sub>4</sub>S<sub>4</sub>, β-P<sub>4</sub>S<sub>4</sub>, P<sub>4</sub>S<sub>3</sub> and P<sub>4</sub>S<sub>2</sub> are all based on the P<sub>4</sub> tetrahedron but only P<sub>4</sub>S<sub>10</sub> (and possibly P<sub>4</sub>S<sub>9</sub>) is structurally analogous to the oxide. P<sub>4</sub>S<sub>6</sub> is conspicuous by its absence. Structural data are summarized in Fig. 12.15 and some physical properties are in Table 12.6.

P<sub>4</sub>S<sub>3</sub> is the most stable compound in the series and can be prepared by heating the required amounts of red P and sulfur above 180° in an inert atmosphere and then purifying the product by distillation at 420° or by recrystallization from toluene. The retention of a P<sub>3</sub> ring in the structure is notable. Its reactions and commercial application in match manufacture are discussed on p. 509.

The curious phase relations between phosphorus, sulfur and their binary compounds are worth noting. Because both P<sub>4</sub> and S<sub>8</sub> are stable molecules the phase diagram, if studied below 100°, shows only solid solutions with a simple eutectic at 10° (75 atom % P). By contrast, when the mixtures are heated above 200° the elements react and an entirely different phase diagram is obtained; however, as only the most stable compounds P<sub>4</sub>S<sub>3</sub>, P<sub>4</sub>S<sub>7</sub> and P<sub>4</sub>S<sub>10</sub>

<sup>111</sup> H. HOFFMANN and M. BECKE-GOEHRING, *Topics in Phosphorus Chemistry* **8**, 193–271 (1976); J. G. RIESS in A. H. COWLEY (ed.), *Rings, Clusters and Polymers of the Main Group Elements*, ACS Symposium Series No. **232**, 17–47 (1983).

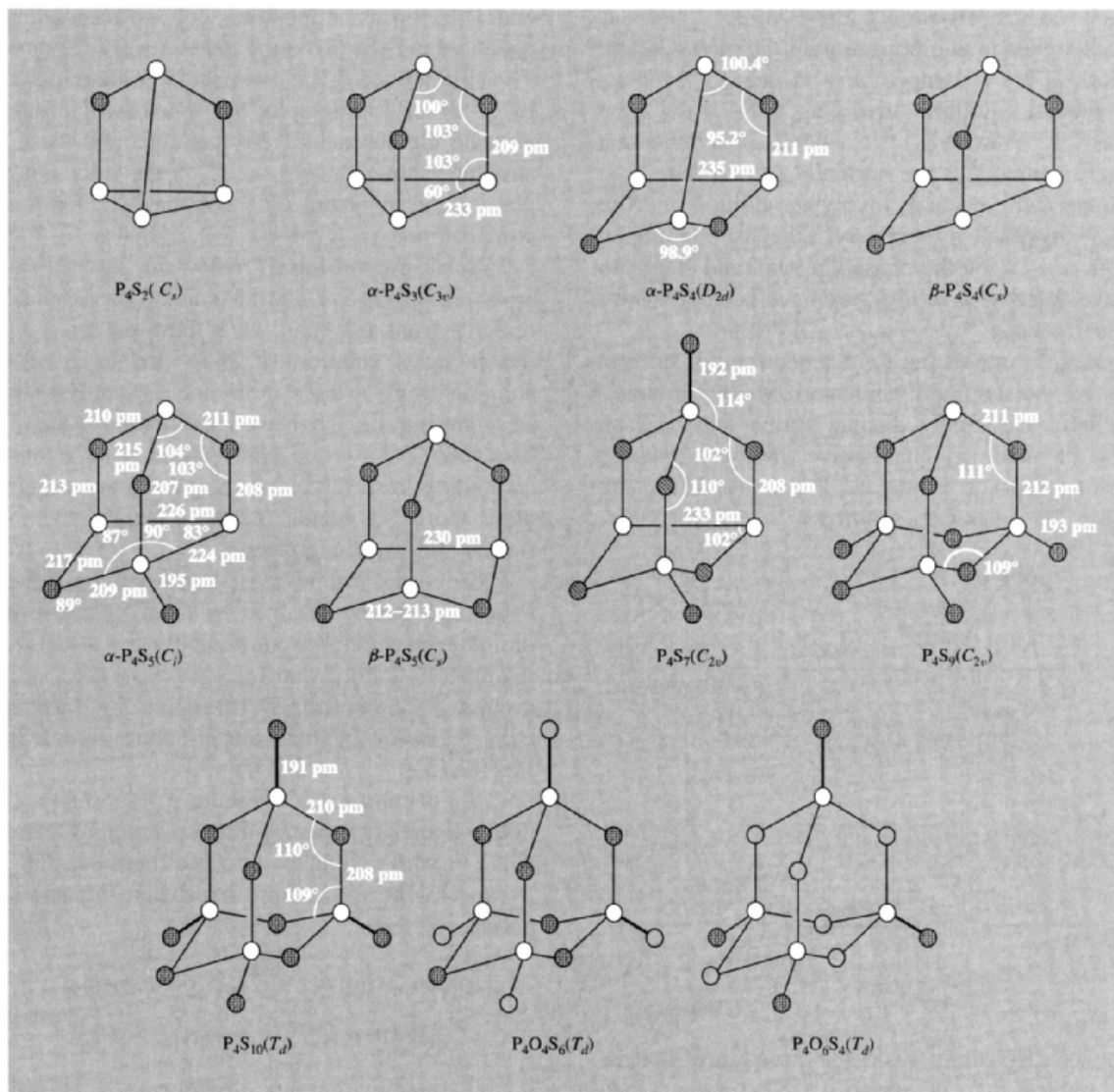


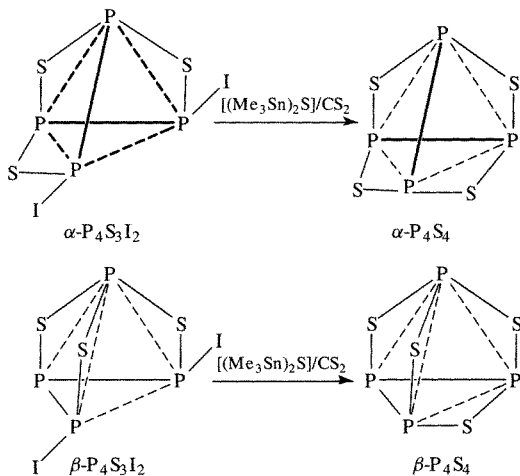
Figure 12.15 Structures of phosphorus sulfides and oxosulfides (schematic).

Table 12.6 Physical properties of some phosphorus sulfides

Property	$\alpha$ - $P_4S_3$	$\alpha$ - $P_4S_4$	$\alpha$ - $P_4S_5$	$P_4S_7$	$P_4S_{10}$
Colour	Yellow green	Pale yellow	Bright yellow	Very pale yellow	Yellow
MP/°C	174	230 (d)	170–220 (d)	308	288
BP/°C	408	—	—	523	514
Density/g cm <sup>-3</sup>	2.03	2.22	2.17	2.19	2.09
Solubility in CS <sub>2</sub> (17°)/ g per 100 g CS <sub>2</sub>	100	sol	0.5	0.029	0.222

melt congruently, only these three appear as compounds in equilibrium with the melt. Careful work at lower temperatures is needed to detect peritectic equilibria involving  $P_4S_9$ ,  $P_4S_5$  (and possibly even  $P_4S_2$ ),<sup>(112)</sup> and it is notable that these compounds are normally prepared by low-temperature reactions involving addition of 2S to  $P_4S_7$  and  $P_4S_3$  respectively. Likewise there is no sign of  $P_4S_4$  on the phase diagram, and claims to have detected it in this way have been shown to be erroneous.<sup>(113)</sup>

$P_4S_4$  is one of the most recent binary sulfides to be isolated and characterized and it exists in two structurally distinct forms.<sup>(113,114)</sup> Each can be made in quantitative yield by reacting the appropriate isomer of  $P_4S_3I_2$  (p. 503) with  $[(Me_3Sn)_2S]$  in  $CS_2$  solution:



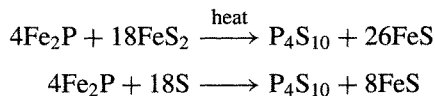
As seen from Fig. 12.15 the structure of  $\alpha\text{-P}_4\text{S}_4$  resembles that of  $As_4S_4$  (p. 579) rather than  $N_4S_4$  (p. 723). The 4 P atoms are in tetrahedral array and the 4 S atoms form a slightly distorted square. The 2 P–P bonds are long (as also in  $P_4S_3$

and  $P_4S_7$ ) when compared with corresponding distances in  $P_4S_5$  (225 pm) and  $P_4$  itself (221 pm). The structure of  $\beta\text{-P}_4\text{S}_4$  has not been determined by X-ray crystallography but spectroscopic data indicate the absence of P=S groups and the  $C_s$  structure shown in Fig. 12.15 is the only other possible arrangement of 3 coordinate P for this composition.

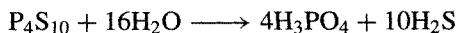
$P_4S_5$  disproportionates below its mp ( $2P_4S_5 \rightleftharpoons P_4S_3 + P_4S_7$ ) and so cannot be obtained directly from the melt. It is best prepared by irradiating a solution of  $P_4S_3$  and S in  $CS_2$  solution using a trace of iodine as catalyst. Its structure is quite unexpected and features a single exocyclic P=S group and 3 fused heterocycles containing, respectively, 4, 5 and 6 atoms; there are 2 short P–P bonds and the 4-membered  $P_3S$  ring is almost square planar.

$P_4S_7$  is the second most stable sulfide (after  $P_4S_3$ ) and can be obtained by direct reaction of the elements. Perhaps surprisingly the structure retains a P–P bond and has two exocyclic P=S groups.  $P_4S_9$  is formed reversibly by heating  $P_4S_7 + 2P_4S_{10}$  and has the structure shown in Fig. 12.15.

$P_4S_{10}$  is commercially the most important sulfide of P and is formed by direct reaction of liquid white  $P_4$  with a slight excess of sulfur above  $300^\circ$ . It can also be made from byproduct ferrophosphorus (p. 480).



It has essentially the same structure as the H form of  $P_4O_{10}$  and hydrolyses mainly according to the overall equation



Presumably intermediate thiophosphoric acids are first formed and, indeed, when the hydrolysis is carried out in aqueous NaOH solution at  $100^\circ$ , substantial amounts of the mono- and di-thiophosphates are obtained. P–S bonds are also retained during reaction of  $P_4S_{10}$  with alcohols or phenols and the products formed are used extensively in industry for a wide variety of

<sup>112</sup> H. VINCENT, *Bull. Soc. Chim. France* 1972, 4517–21; R. FÖRTHMANN and A. SCHNEIDER, *Z. Phys. Chem. (NF)* **49**, 22–37 (1966).

<sup>113</sup> A. M. GRIFFIN, P. C. MINSHALL and G. M. SHEDRICK, *J. Chem. Soc., Chem. Commun.*, 809–10 (1976).

<sup>114</sup> C.-C. CHANG, R. C. HALTIWANGER and A. D. NORMAN, *Inorg. Chem.* **17**, 2056–62 (1978). See also B. W. TATTERSHALL *J. Chem. Soc., Dalton Trans.*, 1515–20 (1987); B. W. TATTERSHALL and N. L. KENDALL, *Polyhedron* **13**, 2629–37 (1994).

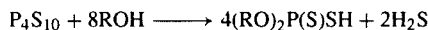
### Phosphorus Sulfides in Industry

The two compounds of importance are  $P_4S_3$  and  $P_4S_{10}$ . The former is made on a large scale for use in "strike anywhere" matches according to a formula evolved by Sévène and Cahen in France in 1898. The ignition results from the violent reaction between  $P_4S_3$  and  $KClO_3$  which is initiated by friction of the match against glass paper (on the side of the box) or other abrasive material. A typical formulation for the match head is:

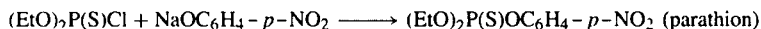
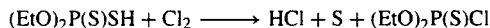
Reactants		Fillers (moderators)			Adhesives	
$KClO_3$	$P_4S_3$	Ground glass	$Fe_2O_3$	ZnO	Glue	Water
20%	9%	14%	11%	7%	10%	29%

Formulations of this type have completely replaced earlier "strike anywhere" matches based on (poisonous) white  $P_4$ , sulfur, and  $KClO_3$ , though "safety matches" still use a match head which is predominantly  $KClO_3$  struck against the side of the match-box which has been covered with a paste of (non-toxic) red P (49.5%), antimony sulfide (27.6%),  $Fe_2O_3$  (1.2%) and gum arabic (21.7%). About  $10^{11}$  matches are used annually in the UK alone.

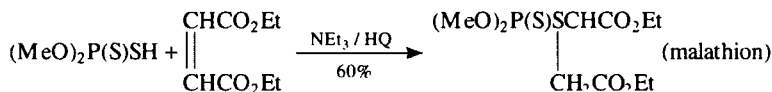
$P_4S_{10}$  is made on an even larger scale than  $P_4S_3$  and is the primary source of a very wide range of organic P-S compounds. World production of  $P_4S_{10}$  exceeds 250 000 tonnes annually of which about half is made in the USA, one-third in the UK/Europe, and the remaining 30 000 tonnes elsewhere (Japan, Romania, the former Soviet Union, Mexico, etc.). The most important reaction of  $P_4S_{10}$  is with alcohols or phenols to give dialkyl or diaryl dithiophosphoric acids:



The zinc salts of these acids are extensively used as additives to lubricating oils to improve their extreme-pressure properties. The compounds also act as antioxidants, corrosion inhibitors and detergents. Short-chain dialkyl dithiophosphates and their sodium and ammonium salts are used as flotation agents for zinc and lead sulfide ores. The methyl and ethyl derivatives  $(RO)_2P(S)SH$  and  $(RO)_2P(S)Cl$  are of particular interest in the large-scale manufacture of pesticides such as parathion, malathion, dimethylparathion, etc.<sup>(83)</sup> For example parathion, which first went into production as an insecticide in Germany in 1947, is made by the following reaction sequence:



Methylparathion is the corresponding dimethyl derivative. Later (1952) malathion found favour because of its decreased toxicity to mammals; it is readily made in 90% yield by the addition of dimethyldithiophosphate to diethylmaleate in the presence of  $NEt_3$  as a catalyst and hydroquinone as a polymerization inhibitor:



The scale of manufacture of these organophosphorus pesticides can be gauged from data referring to the USA annual production in 1975 (tonnes): methylparathion 46 000, parathion 36 000 and malathion 16 000. In addition, some 15 other thioorganophosphorus insecticides are manufactured in the USA on a scale exceeding 2000 tonnes pa each.<sup>(4)</sup> They act by inhibiting cholinesterase, thus preventing the natural hydrolysis of the neurotransmitter acetylcholine in the insect.<sup>(20)</sup>

applications (see Panel).  $P_4S_{10}$  is also widely used to replace O by S in organic compounds to form, e.g., thioamides  $RC(S)NH_2$ , thioaldehydes  $RCHS$  and thioketones  $R_2CS$ . Methanolysis yields  $(MeO)_2P(S)SH$  plus  $H_2S$ ,<sup>(115)</sup> and the related anions  $(RO)_2PS_2^-$  are known as versatile

ligands with a remarkable variety of coordination modes.<sup>(116)</sup>

A rather different series of cyclic thiophosphate(III) anions  $[(PS_2)_n]^{n-}$  is emerging from a study of the reaction of elemental phosphorus with polysulfidic sulfur. Anhydrous compounds

<sup>115</sup> P. BURDAUDUCQ and M. C. DÉMARCO, *J. Chem. Soc., Dalton Trans.*, 1897-900 (1987).

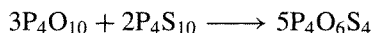
<sup>116</sup> M. G. B. DREW, R. J. HOBSON, P. P. E. M. MUMBA and D. A. RICE, *J. Chem. Soc., Dalton Trans.*, 1569-71 (1987).

$M_5^I[\text{cyclo-P}_5\text{S}_{10}]$  and  $M_6^I[\text{cyclo-P}_6\text{S}_{12}]$  were obtained using red phosphorus, whereas white  $\text{P}_4$  yielded  $[\text{NH}_4]_4[\text{cyclo-P}_4\text{S}_8] \cdot 2\text{H}_2\text{O}$  as shiny platelets. This unique  $\text{P}_4\text{S}_8^{4-}$  anion is the first known homocycle of 4 tetracoordinated P atoms and X-ray studies reveal that the P atoms form a square with rather long P–P distances (228 pm).<sup>(117)</sup>

The new planar anion  $\text{PS}_3^-$  (cf. the nitrate ion,  $\text{NO}_3^-$ ) has been isolated as its tetraphenylarsonium salt, mp  $183^\circ$ , following a surprising reaction of  $\text{P}_4\text{S}_{10}$  with  $\text{KCN}/\text{H}_2\text{S}$  in MeCN, in which the coproduct was the known dianion  $[(\text{NC})\text{P}(\text{S})_2-\text{S}-\text{P}(\text{S})_2(\text{CN})]^{2-}$ <sup>(118)</sup> The first sulfido heptaphosphane cluster anions,  $[\text{P}_7(\text{S})_3]^{3-}$  and  $[\text{HP}_7(\text{S})_2]^{2-}$  (cf.  $\text{P}_7^{3-}$ , p. 491), have also recently been characterized.<sup>(119)</sup>

### Oxosulfides

When  $\text{P}_4\text{O}_{10}$  and  $\text{P}_4\text{S}_{10}$  are heated in appropriate proportions above  $400^\circ$ ,  $\text{P}_4\text{O}_6\text{S}_4$  is obtained as colourless hygroscopic crystals, mp  $102^\circ$ .



The structure is shown in Fig. 12.15. The related compound  $\text{P}_4\text{O}_4\text{S}_6$  is said to be formed by the reaction of  $\text{H}_2\text{S}$  with  $\text{POCl}_3$  at  $0^\circ$  (A. Besson, 1897) but has not been recently investigated. An amorphous yellow material of composition  $\text{P}_4\text{O}_4\text{S}_3$  is obtained when a solution of  $\text{P}_4\text{S}_3$  in  $\text{CS}_2$  or organic solvents is oxidized by dry air or oxygen. Other oxosulfides of uncertain authenticity such as  $\text{P}_6\text{O}_{10}\text{S}_5$  have been reported but their structural integrity has not been established and they may be mixtures. However, the following series can be prepared by appropriate redistribution reactions:  $\text{P}_4\text{O}_6\text{S}_n$  ( $n = 1-4$ ),  $\text{P}_4\text{O}_6\text{Se}_n$  ( $n = 1-3$ ),  $\text{P}_4\text{O}_6\text{SSe}$ ,  $\text{P}_4\text{O}_7\text{S}_n$

<sup>117</sup> H. FALIUS, W. KRAUSE and W. S. SHELDRICK, *Angew. Chem. Int. Edn. Engl.* **20**, 103–4 (1981).

<sup>118</sup> H. W. ROESKY, R. AHLRICH and S. BRODE, *Angew. Chem. Int. Edn. Engl.* **25**, 82–3 (1986)

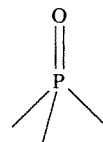
<sup>119</sup> M. BAUDLER and A. FLORUSS, *Z. anorg. allg. Chem.* **620**, 2070–6 (1994).

( $n = 1-3$ ),  $\text{P}_4\text{O}_7\text{Se}$ ,  $\text{P}_4\text{O}_8\text{S}_n$  ( $n = 1, 2$ ).<sup>(120)</sup> The crystal and molecular structures of  $\text{P}_4\text{O}_6\text{S}_2$  and  $\text{P}_4\text{O}_6\text{S}_3$  have recently been determined.<sup>(121)</sup> Two isomers each of  $\beta\text{-P}_4\text{S}_2\text{SeI}_2$  and  $\beta\text{-P}_4\text{SSe}_2\text{I}_2$ , prepared by reaction of  $\text{P}_4\text{S}_{3-n}\text{Se}_n$  with  $\text{I}_2$  in  $\text{CS}_2$  have been structurally identified by  $^{31}\text{P}$  nmr spectroscopy.<sup>(122)</sup>

### 12.3.6 Oxoacids of phosphorus and their salts

The oxoacids of P are more numerous than those of any other element, and the number of oxoanions and oxo-salts is probably exceeded only by those of Si. Many are of great importance technologically and their derivatives are vitally involved in many biological processes (p. 528). Fortunately, the structural principles covering this extensive array of compounds are very simple and can be stated as follows:<sup>†</sup>

- (i) All P atoms in the oxoacids and oxoanions are 4-coordinate and contain at least one P–O unit (1).



(1)

- (ii) All P atoms in the oxoacids have at least one P–OH group (2a) and this often occurs in the anions also; all such groups are ionizable as proton donors (2b).

<sup>120</sup> M. L. WALKER, D. E. PECKENPAUGH and J. L. MILLS, *Inorg. Chem.* **18**, 2792–6 (1979).

<sup>121</sup> F. FRICK and M. JANSEN, *Z. anorg. allg. Chem.* **619**, 281–6 (1993). See M. JANSEN and S. STROJEK, *Z. anorg. allg. Chem.* **621**, 479–83 (1995) for X-ray structures of  $\text{P}_4\text{O}_7\text{S}$ , i.e.  $\text{P}_4\text{O}_6(\text{O})_t(\text{S})_t$ .

<sup>122</sup> P. LÖNNECKE and R. BLACHNIK, *Z. anorg. allg. Chem.* **619**, 1257–61 (1993). See also M. RUCK, *ibid.* **620**, 1832–6 (1994) R. BLACHNIK, A. HEPP, P. LÖNNECKE, J. A. DONKIN and B. W. TATTERSHALL, *ibid.* **620**, 1925–31 (1994).

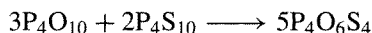
<sup>†</sup> Heteropolyacids containing P fall outside this classification and are treated, together with the isopolyacids and their salts, on pp. 1010–16. Organic esters such as  $\text{P}(\text{OR})_3$  are also excluded.

$M_3^I[\text{cyclo-P}_5\text{S}_{10}]$  and  $M_6^I[\text{cyclo-P}_6\text{S}_{12}]$  were obtained using red phosphorus, whereas white  $\text{P}_4$  yielded  $[\text{NH}_4]_4[\text{cyclo-P}_4\text{S}_8] \cdot 2\text{H}_2\text{O}$  as shiny platelets. This unique  $\text{P}_4\text{S}_8^{4-}$  anion is the first known homocycle of 4 tetracoordinated P atoms and X-ray studies reveal that the P atoms form a square with rather long P–P distances (228 pm).<sup>(117)</sup>

The new planar anion  $\text{PS}_3^-$  (cf. the nitrate ion,  $\text{NO}_3^-$ ) has been isolated as its tetraphenylarsonium salt, mp  $183^\circ$ , following a surprising reaction of  $\text{P}_4\text{S}_{10}$  with  $\text{KCN}/\text{H}_2\text{S}$  in MeCN, in which the coproduct was the known dianion  $[(\text{NC})\text{P}(\text{S})_2-\text{S}-\text{P}(\text{S})_2(\text{CN})]^{2-}$ <sup>(118)</sup> The first sulfido heptaphosphane cluster anions,  $[\text{P}_7(\text{S})_3]^{3-}$  and  $[\text{HP}_7(\text{S})_2]^{2-}$  (cf.  $\text{P}_7^{3-}$ , p. 491), have also recently been characterized.<sup>(119)</sup>

### Oxosulfides

When  $\text{P}_4\text{O}_{10}$  and  $\text{P}_4\text{S}_{10}$  are heated in appropriate proportions above  $400^\circ$ ,  $\text{P}_4\text{O}_6\text{S}_4$  is obtained as colourless hygroscopic crystals, mp  $102^\circ$ .



The structure is shown in Fig. 12.15. The related compound  $\text{P}_4\text{O}_4\text{S}_6$  is said to be formed by the reaction of  $\text{H}_2\text{S}$  with  $\text{POCl}_3$  at  $0^\circ$  (A. Besson, 1897) but has not been recently investigated. An amorphous yellow material of composition  $\text{P}_4\text{O}_4\text{S}_3$  is obtained when a solution of  $\text{P}_4\text{S}_3$  in  $\text{CS}_2$  or organic solvents is oxidized by dry air or oxygen. Other oxosulfides of uncertain authenticity such as  $\text{P}_6\text{O}_{10}\text{S}_5$  have been reported but their structural integrity has not been established and they may be mixtures. However, the following series can be prepared by appropriate redistribution reactions:  $\text{P}_4\text{O}_6\text{S}_n$  ( $n = 1-4$ ),  $\text{P}_4\text{O}_6\text{Se}_n$  ( $n = 1-3$ ),  $\text{P}_4\text{O}_6\text{SSe}$ ,  $\text{P}_4\text{O}_7\text{S}_n$

<sup>117</sup> H. FALIUS, W. KRAUSE and W. S. SHELDRICK, *Angew. Chem. Int. Edn. Engl.* **20**, 103–4 (1981).

<sup>118</sup> H. W. ROESKY, R. AHLRICH and S. BRODE, *Angew. Chem. Int. Edn. Engl.* **25**, 82–3 (1986)

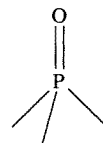
<sup>119</sup> M. BAUDLER and A. FLORUSS, *Z. anorg. allg. Chem.* **620**, 2070–6 (1994).

( $n = 1-3$ ),  $\text{P}_4\text{O}_7\text{Se}$ ,  $\text{P}_4\text{O}_8\text{S}_n$  ( $n = 1, 2$ ).<sup>(120)</sup> The crystal and molecular structures of  $\text{P}_4\text{O}_6\text{S}_2$  and  $\text{P}_4\text{O}_6\text{S}_3$  have recently been determined.<sup>(121)</sup> Two isomers each of  $\beta\text{-P}_4\text{S}_2\text{SeI}_2$  and  $\beta\text{-P}_4\text{SSe}_2\text{I}_2$ , prepared by reaction of  $\text{P}_4\text{S}_{3-n}\text{Se}_n$  with  $\text{I}_2$  in  $\text{CS}_2$  have been structurally identified by  $^{31}\text{P}$  nmr spectroscopy.<sup>(122)</sup>

### 12.3.6 Oxoacids of phosphorus and their salts

The oxoacids of P are more numerous than those of any other element, and the number of oxoanions and oxo-salts is probably exceeded only by those of Si. Many are of great importance technologically and their derivatives are vitally involved in many biological processes (p. 528). Fortunately, the structural principles covering this extensive array of compounds are very simple and can be stated as follows:<sup>†</sup>

- (i) All P atoms in the oxoacids and oxoanions are 4-coordinate and contain at least one P–O unit (1).



(1)

- (ii) All P atoms in the oxoacids have at least one P–OH group (2a) and this often occurs in the anions also; all such groups are ionizable as proton donors (2b).

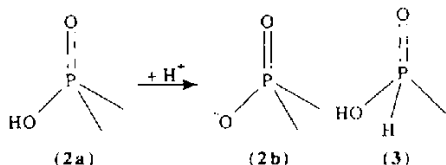
<sup>120</sup> M. L. WALKER, D. E. PECKENPAUGH and J. L. MILLS, *Inorg. Chem.* **18**, 2792–6 (1979).

<sup>121</sup> F. FRICK and M. JANSEN, *Z. anorg. allg. Chem.* **619**, 281–6 (1993). See M. JANSEN and S. STROJEK, *Z. anorg. allg. Chem.* **621**, 479–83 (1995) for X-ray structures of  $\text{P}_4\text{O}_7\text{S}$ , i.e.  $\text{P}_4\text{O}_6(\text{O})_t(\text{S})_t$ .

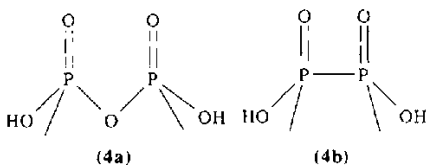
<sup>122</sup> P. LÖNNECKE and R. BLACHNIK, *Z. anorg. allg. Chem.* **619**, 1257–61 (1993). See also M. RUCK, *ibid.* **620**, 1832–6 (1994) R. BLACHNIK, A. HEPP, P. LÖNNECKE, J. A. DONKIN and B. W. TAITERSHALL, *ibid.* **620**, 1925–31 (1994).

<sup>†</sup> Heteropolyacids containing P fall outside this classification and are treated, together with the isopolyacids and their salts, on pp. 1010–16. Organic esters such as  $\text{P}(\text{OR})_3$  are also excluded.

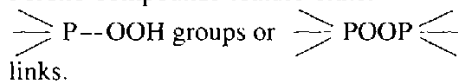
- (iii) Some species also have one (or more) P-H group (3); such directly bonded H atoms are not ionizable.



- (iv) Catenation is by P-O-P links (4a) or via direct P-P bonds (4b); with the former both open chain ("linear") and cyclic species are known but only corner sharing of tetrahedra occurs, never edge- or face-sharing.



- (v) Peroxo compounds feature either



It follows from these structural principles that each P atom is 5-covalent. However, the oxidation state of P is 5 only when it is directly bound to 4 O atoms; the oxidation state is reduced by 1 each time a P-OH is replaced by a P-P bond and by 2 each time a P-OH is replaced by

a P-H. Some examples of phosphorus oxoacids are listed in Table 12.7 together with their recommended and common names. It will be seen that the numerous structural types and the variability of oxidation state pose several problems of nomenclature which offer a rich source of confusion in the literature.

The oxoacids of P are clearly very different structurally from those of N (p. 459) and this difference is accentuated when the standard reduction potentials (p. 434) and oxidation-state diagrams (p. 437) for the two sets of compounds are compared. Some reduction potentials ( $E^\circ/V$ ) in acid solution are in Table 12.8<sup>(123)</sup> (p. 513) and these are shown schematically below, together with the corresponding data for alkaline solutions.

The alternative presentation as an oxidation state diagram is in Fig. 12.16 which shows the dramatic difference to N (p. 438).

The fact that the element readily dissolves in aqueous media with disproportionation into  $\text{PH}_3$  and an oxoacid is immediately clear from the fact that P lies above the line joining  $\text{PH}_3$  and either  $\text{H}_3\text{PO}_2$  (hypophosphorous acid),  $\text{H}_3\text{PO}_3$  (phosphorous acid) or  $\text{H}_3\text{PO}_4$  (orthophosphoric acid). The reaction is even

<sup>123</sup> G. MILAZZO and S. CAROLI, *Tables of Standard Electrode Potentials*, Wiley, New York, 1978, 421 pp. A. J. BARD, R. PARSONS and J. JORDAN, *Standard Potentials in Aqueous Solution*, Marcel Dekker, New York, 1985, 834 pp.

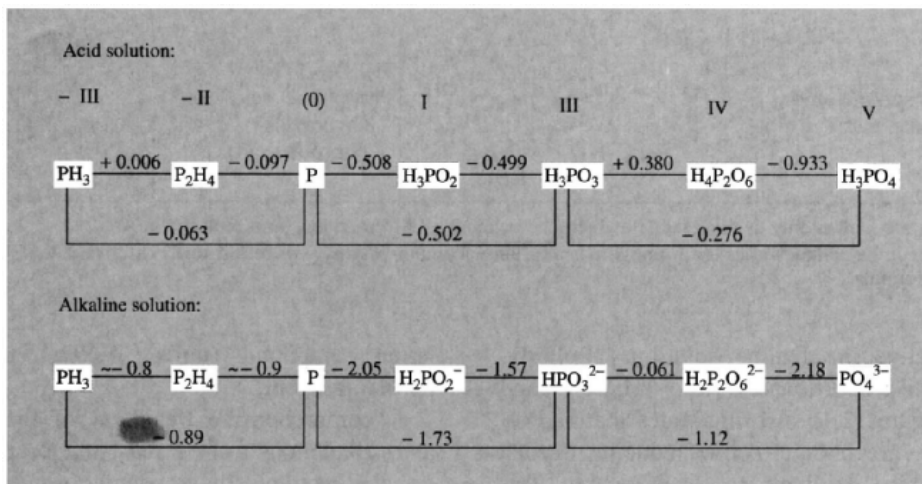


Table 12.7 Some phosphorus oxoacids<sup>(a)</sup>

Formula/Name	Structure <sup>(a)</sup>	Formula/Name	Structure <sup>(a)</sup>
H <sub>3</sub> PO <sub>4</sub> (Ortho)phosphoric acid		H <sub>3</sub> PO <sub>5</sub> Peroxomonophosphoric acid	
H <sub>4</sub> P <sub>2</sub> O <sub>7</sub> Diphosphoric acid (pyrophosphoric acid)		H <sub>4</sub> P <sub>2</sub> O <sub>8</sub> Peroxdiphosphoric acid	
H <sub>5</sub> P <sub>3</sub> O <sub>10</sub> Triphosphoric acid		H <sub>4</sub> P <sub>2</sub> O <sub>6</sub> Hypophosphoric acid [diphosphoric(IV) acid]	
H <sub>n+2</sub> P <sub>n</sub> O <sub>3n+1</sub> Polyphosphoric acid (n up to 17 isolated)		H <sub>4</sub> P <sub>2</sub> O <sub>6</sub> Isohypophosphoric acid [diphosphoric(III,V) acid]	
(HPO <sub>3</sub> ) <sub>3</sub> Cyclo-trimetaphosphoric acid		H <sub>3</sub> PO <sub>3</sub> (2) <sup>(b)</sup> Phosphonic acid (phosphorous acid)	
(HPO <sub>3</sub> ) <sub>4</sub> Cyclo-tetrametaphosphoric acid (anions known in both "boat" and "chair" forms)		H <sub>4</sub> P <sub>2</sub> O <sub>5</sub> (2) <sup>(b)</sup> Diphosphonic acid (diphosphorous or pyrophosphorous acid)	
(HPO <sub>3</sub> ) <sub>n</sub> Polymetaphosphoric acid (see text for salts)		H <sub>3</sub> PO <sub>2</sub> (1) <sup>(b)</sup> Phosphinic acid (hypophosphorous acid)	

<sup>(a)</sup>Some acids are known only as their salts in which one or more -OH group has been replaced by O<sup>-</sup>

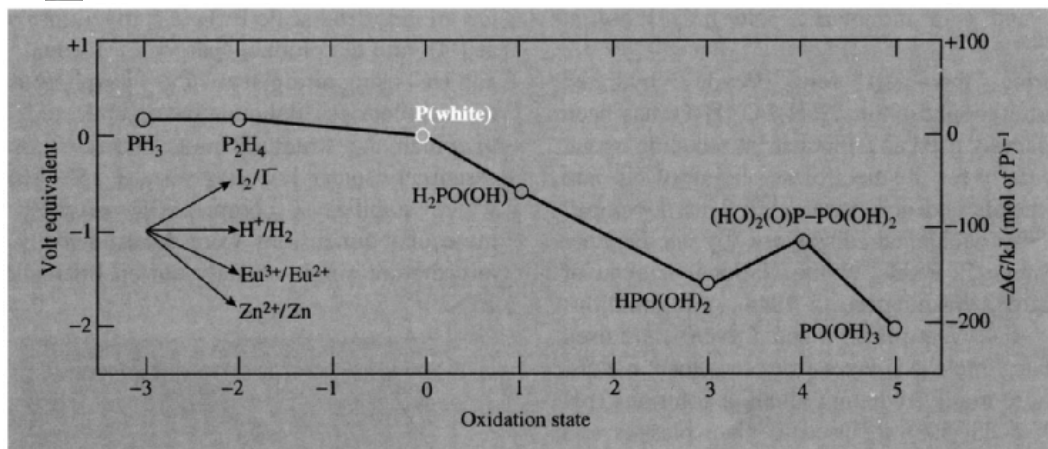
<sup>(b)</sup>The number in parentheses after the formula indicates the maximum basicity, where this differs from the total number of H atoms in the formula.

more effective in alkaline solution. Similarly, H<sub>4</sub>P<sub>2</sub>O<sub>6</sub> disproportionates into H<sub>3</sub>PO<sub>3</sub> and H<sub>3</sub>PO<sub>4</sub>. Figure 12.16 also illustrates that H<sub>3</sub>PO<sub>2</sub> and H<sub>3</sub>PO<sub>3</sub> are both effective reducing agents, being readily oxidized to H<sub>3</sub>PO<sub>4</sub>, but this

latter compound (unlike HNO<sub>3</sub>) is not an oxidizing agent.

A comprehensive treatment of the oxoacids and oxoanions of P is inappropriate but selected examples have been chosen to illustrate



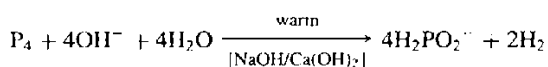


**Figure 12.16** Oxidation state diagram for phosphorus. (Note that all the oxoacids have a phosphorus covalency of 5.)

interesting points of stereochemistry, reaction chemistry or technological applications. The treatment begins with the lower oxoacids and their salts (in which P has an oxidation state less than +5) and then considers phosphoric acid, phosphates and polyphosphates. The peroxyacids  $\text{H}_3\text{PO}_5$  and  $\text{H}_4\text{P}_2\text{O}_8$  and their salts will not be treated further<sup>(124)</sup> (except peripherally) nor will the peroxohydrates of orthophosphates, which are obtained from aqueous  $\text{H}_2\text{O}_2$  solutions.<sup>(64)</sup>

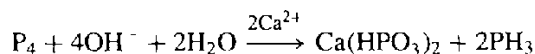
#### Hypophosphorous acid and hypophosphites [ $\text{H}_2\text{PO}(\text{OH})$ and $\text{H}_2\text{PO}_2^-$ ]

The recommended names for these compounds (phosphinic acid and phosphinates) have not yet gained wide acceptance for inorganic compounds but are generally used for organophosphorus derivatives. Hypophosphites can be made by heating white phosphorus in aqueous alkali:



Phosphite and phosphine are obtained as byproducts (p. 493) and the former can be removed via

its insoluble calcium salt:



**Table 12.8** Some reduction potentials in acid solution (pH 0)<sup>(a)</sup>

Reaction	$E^\circ/\text{V}$
$\text{P} + 3\text{H}^+ + 3\text{e}^- \rightleftharpoons \text{PH}_3(\text{g})$	-0.063
$\text{P} + 2\text{H}^+ + 2\text{e}^- \rightleftharpoons \frac{1}{2}\text{P}_2\text{H}_4(\text{g})$	-0.097
$\frac{1}{2}\text{P}_2\text{H}_4 + \text{H}^+ + \text{e}^- \rightleftharpoons \text{PH}_3$	+0.006
$\text{H}_3\text{PO}_2 + \text{H}^+ + \text{e}^- \rightleftharpoons \text{P} + 2\text{H}_2\text{O}$	-0.508
$\text{H}_3\text{PO}_3 + 3\text{H}^+ + 3\text{e}^- \rightleftharpoons \text{P} + 3\text{H}_2\text{O}$	-0.502
$\text{H}_3\text{PO}_4 + 5\text{H}^+ + 5\text{e}^- \rightleftharpoons \text{P} + 4\text{H}_2\text{O}$	-0.411
$\text{H}_3\text{PO}_3 + 2\text{H}^+ + 2\text{e}^- \rightleftharpoons \text{H}_3\text{PO}_2 + \text{H}_2\text{O}$	-0.499
$\text{H}_3\text{PO}_4 + 2\text{H}^+ + 2\text{e}^- \rightleftharpoons \text{H}_3\text{PO}_3 + \text{H}_2\text{O}$	-0.276
$\text{H}_3\text{PO}_4 + \text{H}^+ + \text{e}^- \rightleftharpoons \frac{1}{2}\text{H}_4\text{P}_2\text{O}_6 + \text{H}_2\text{O}$	-0.933
$\frac{1}{2}\text{H}_4\text{P}_2\text{O}_6 + \text{H}^+ + \text{e}^- \rightleftharpoons \text{H}_3\text{PO}_3$	+0.380

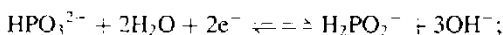
<sup>(a)</sup>P refers to white phosphorus.  $\frac{1}{4}\text{P}_4(\text{s})$ .

Free hypophosphorous acid is obtained by acidifying aqueous solutions of hypophosphites but the pure acid cannot be isolated simply by evaporating such solutions because of its ready oxidation to phosphorous and phosphoric acids and disproportionation to phosphine and phosphorous acid (Fig. 12.16). Pure  $\text{H}_3\text{PO}_2$  is obtained by continuous extraction from aqueous solutions into  $\text{Et}_2\text{O}$ ; it forms white crystals mp

<sup>124</sup> J. I. CREASER and J. O. EDWARDS, *Topics in Phosphorus Chemistry* 7, 379–435 (1972).

26.5° and is a monobasic acid  $pK_a$  1.244 at 25°.<sup>(125)</sup>

During the past few decades hydrated sodium hypophosphite,  $\text{NaH}_2\text{PO}_2 \cdot \text{H}_2\text{O}$ , has been increasingly used as an industrial reducing agent, particularly for the electroless plating of Ni onto both metals and non-metals.<sup>(126)</sup> This developed from an accidental discovery by A. Brenner and Grace E. Riddell at the National Bureau of Standards, Washington, in 1944. Acid solutions ( $E \sim -0.40$  V at pH 4–6 and  $T > 90^\circ$ ) are used to plate thick Ni layers on to other metals, but more highly reducing alkaline solutions (pH 7–10;  $T$  25–50°) are used to plate plastics and other non-conducting materials:



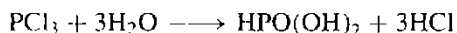
$$E \sim -1.57 \text{ V}$$

Typical plating solutions contain 10–30 g/l of nickel chloride or sulfate and 10–50 g/l  $\text{NaH}_2\text{PO}_2$ ; with suitable pump capacities it is possible to plate up to 10 kg Ni per hour from such a bath (i.e. 45 m<sup>2</sup> surface to a thickness of 25  $\mu\text{m}$ ). Chemical plating is more expensive than normal electrolytic plating but is competitive when intricate shapes are being plated and is essential for non-conducting substrates. (See also the use of  $\text{BH}_4^-$  in this connection, p. 167.)

### Phosphorous acid and phosphites

$[\text{HPO}(\text{OH})_2$  and  $\text{HPO}_3^{2-}]$

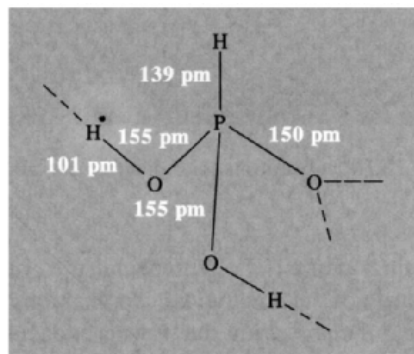
Again, the recommended names (phosphonic acid and phosphonates) have found more general acceptance for organic derivatives such as  $\text{RPO}_3^{2-}$ , and purely inorganic salts are still usually called phosphites. The free acid is readily made by direct hydrolysis of  $\text{PCl}_3$  in cold  $\text{CCl}_4$  solution:



<sup>125</sup> J. W. LARSON and M. PIPPIN, *Polyhedron* **8**, 527–30 (1989).

<sup>126</sup> H. NIEDERPRÜM, *Angew. Chem. Int. Edn. Engl.* **14**, 614–20 (1975); G. A. KRULIK, *Kirk-Othmer Encyclopedia of Chemical Technology*, 4th edn., Vol. 9, pp. 198–218, Wiley, New York, 1994.

On an industrial scale  $\text{PCl}_3$  is sprayed into steam at 190° and the product sparged of residual water and HCl using nitrogen at 165°. Phosphorous acid forms colourless, deliquescent crystals, mp 70.1°, in which the structural units shown form four essentially linear H bonds (O··H 155–160 pm) which stabilize a complex 3D network. The molecular dimensions were determined by low-temperature single-crystal neutron diffraction at 15 K.<sup>(127)</sup>



In aqueous solutions phosphorous acid is dibasic ( $pK_1$  1.257,  $pK_2$  6.7)<sup>(125)</sup> and forms two series of salts: phosphites and hydrogen phosphites (acid phosphites), e.g.

“normal”:  $[\text{NH}_4]_2[\text{HPO}_3] \cdot \text{H}_2\text{O}$ ,  $\text{Li}_2[\text{HPO}_3]$ ,  
 $\text{Na}_2[\text{HPO}_3] \cdot 5\text{H}_2\text{O}$ ,  $\text{K}_2[\text{HPO}_3]$

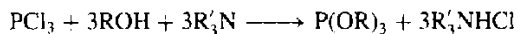
“acid”:  $[\text{NH}_4][\text{HPO}_2(\text{OH})]$ ,  $\text{Li}[\text{HPO}_2(\text{OH})]$ ,  
 $\text{Na}[\text{HPO}_2(\text{OH})] \cdot 2\frac{1}{2}\text{H}_2\text{O}$ ,  $\text{K}[\text{HPO}_2(\text{OH})]$   
and  $\text{M}[\text{HPO}_2(\text{OH})]_2$  ( $\text{M} = \text{Mg}, \text{Ca}, \text{Sr}$ ).

Dehydration of these acid phosphites by warming under reduced pressure leads to the corresponding pyrophosphites  $\text{M}_2^I[\text{HP}(\text{O})_2-\text{O}-\text{P}(\text{O})_2\text{H}]$  and  $\text{M}^{II}[\text{HP}(\text{O})_2-\text{O}-\text{P}(\text{O})_2\text{H}]$ .

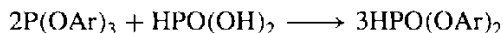
Organic derivatives fall into 4 classes  $\text{RPO}(\text{OH})_2$ ,  $\text{HPO}(\text{OR})_2$ ,  $\text{R}'\text{PO}(\text{OR})_2$  and the phosphite esters  $\text{P}(\text{OR})_3$ ; this latter class has no purely inorganic analogues, though it is, of course, closely related to  $\text{PCl}_3$ . Some preparative routes have already been indicated. Reactions with alcohols depend on conditions:



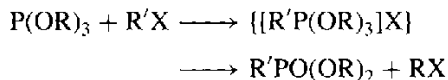
<sup>127</sup> G. BECKER, H.-D. HAUSEN, O. MUNDT, W. SCHWARZ, C. T. WAGNER and T. VOGT, *Z. anorg. allg. Chem.* **591**, 17–31 (1990).



Phenols give triaryl phosphites  $\text{P(OAr)}_3$  directly at  $\sim 160^\circ$  and these react with phosphorous acid to give diaryl phosphonates:



Trimethyl phosphite  $\text{P(OMe)}_3$  spontaneously isomerizes to methyl dimethylphosphonate  $\text{MePO(OMe)}_2$ , whereas other trialkyl phosphites undergo the Michaelis-Arbusov reaction with alkyl halides via a phosphonium intermediate:



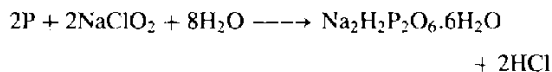
Further discussion of these fascinating series of reactions falls outside our present scope.<sup>(2)</sup>

### Hypophosphoric acid ( $\text{H}_4\text{P}_2\text{O}_6$ ) and hypophosphates

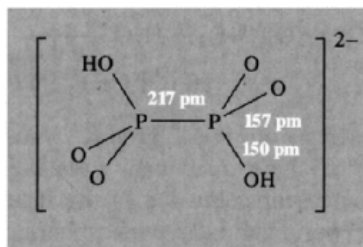
There has been much confusion over the structure of these compounds but their diamagnetism has long ruled out a monomeric formulation,  $\text{H}_2\text{PO}_3$ . In fact, as shown in Table 12.7, isomeric forms are known: (a) hypophosphoric acid and hypophosphates in which both P atoms are identical and there is a direct P-P bond; (b) isohypophosphoric acid and isohypophosphates in which 1 P has a direct P-H bond

and the 2 different P atoms are joined by a  $\text{p}^{\text{III}}-\text{O}-\text{p}^{\text{V}}$  link.<sup>(23)</sup>

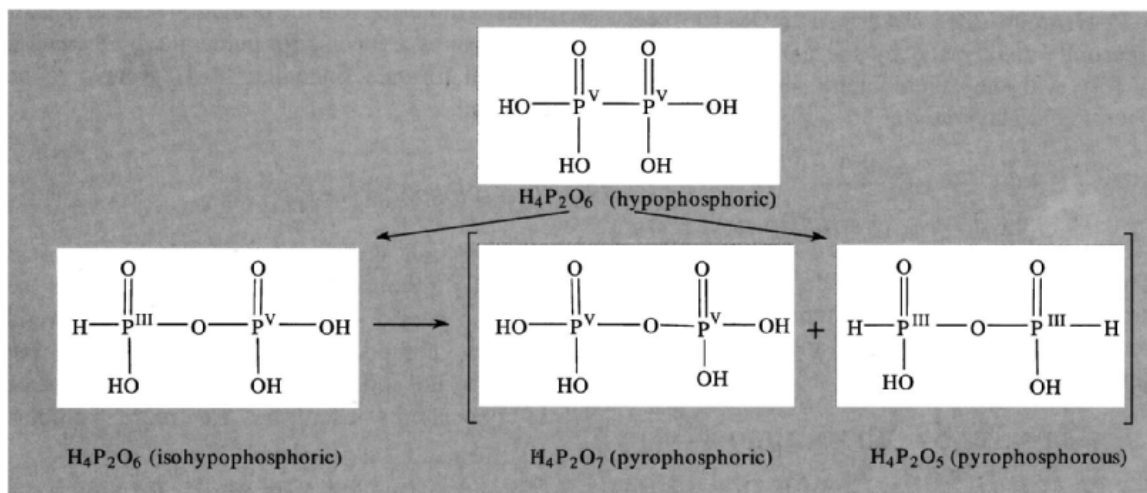
Hypophosphoric acid,  $(\text{HO})_2\text{P(O)}-\text{P(O)}(\text{OH})_2$ , is usually prepared by the controlled oxidation of red P with sodium chlorite solution at room temperature: the tetrasodium salt,  $\text{Na}_4\text{P}_2\text{O}_6 \cdot 10\text{H}_2\text{O}$ , crystallizes at pH 10 and the disodium salt at pH 5.2:



Ion exchange on an acid column yields the crystalline "dihydrate"  $\text{H}_4\text{P}_2\text{O}_6 \cdot 2\text{H}_2\text{O}$  which is actually the hydroxonium salt of the dihydrogen hypophosphate anion  $[\text{H}_3\text{O}]_2^+[(\text{HO})\text{P(O)}_2-\text{P(O)}_2(\text{OH})]^{2-}$ ; it is isostructural with the corresponding ammonium salt for which X-ray diffraction studies establish the staggered structure shown.

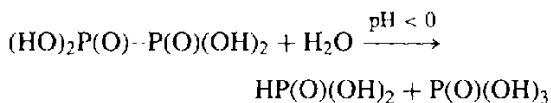


The anhydrous acid is obtained either by the vacuum dehydration of the dihydrate over  $\text{P}_4\text{O}_{10}$



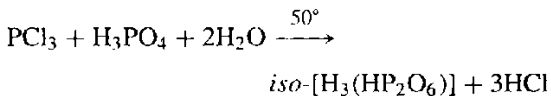
or by the action of  $\text{H}_2\text{S}$  on the insoluble lead salt  $\text{Pb}_2\text{P}_2\text{O}_6$ . As implied above, the first proton on each  $-\text{PO}(\text{OH})_2$  unit is more readily removed than the second and the successive dissociation constants at  $25^\circ$  are  $\text{p}K_1$  2.2,  $\text{p}K_2$  2.8,  $\text{p}K_3$  7.3,  $\text{p}K_4$  10.0. Both  $\text{H}_4\text{P}_2\text{O}_6$  and its dihydrate are stable at  $0^\circ$  in the absence of moisture. The acid begins to melt (with decomposition) at  $73^\circ$  but even at room temperature it undergoes rearrangement and disproportionation to give a mixture of isohypophosphoric, pyrophosphoric, and pyrophosphorous acids as represented schematically on the previous page.

Hypophosphoric acid is very stable towards alkali and does not decompose even when heated with 80%  $\text{NaOH}$  at  $200^\circ$ . However, in acid solution it is less stable and even at  $25^\circ$  hydrolyses at a rate dependent on pH (e.g.  $t_{1/2}$  180 days in 1 M  $\text{HCl}$ ,  $t_{1/2} < 1$  h in 4 M  $\text{HCl}$ ):

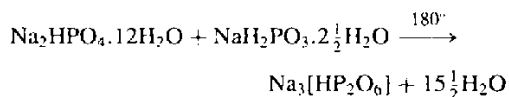


The presence of P-H groups amongst the products of these reactions was one of the earlier sources of confusion in the structures of hypophosphoric and isohypophosphoric acids.

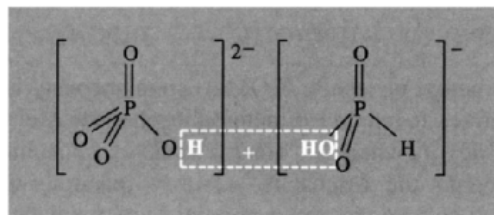
The structure of isohypophosphoric acid and its salts can be deduced from  $^{31}\text{P}$  nmr which shows the presence of 2 different 4-coordinate P atoms, the absence of a P-P bond and the presence of a P-H group (also confirmed by Raman spectroscopy). It is made by the careful hydrolysis of  $\text{PCl}_3$  with the stoichiometric amounts of phosphoric acid and water at  $50^\circ$ :



The trisodium salt is best made by careful dehydration of an equimolar mixture of hydrated disodium hydrogen phosphate and sodium hydrogen phosphite at  $180^\circ$ :



The structural relation between the reacting anions and the product is shown schematically below:



### Other lower oxoacids of phosphorus

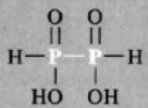
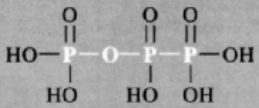
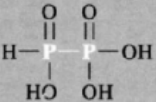
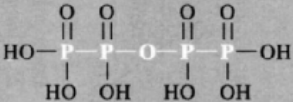
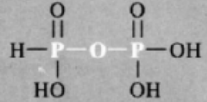
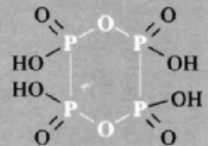
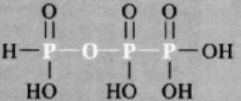
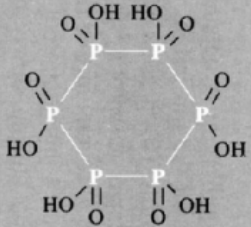
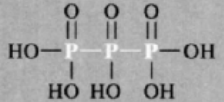
The possibility of P-H and P-P bonds in phosphorus oxoacids, coupled with the ease of polymerization via P-O-P linkages enables innumerable acids and their salts to be synthesized. Frequently mixtures are obtained and these can be separated by paper chromatography, paper electrophoresis, thin-layer chromatography, ion exchange or gel chromatography.<sup>(128)</sup> Much ingenuity has been expended in designing appropriate syntheses but no new principles emerge. A few examples are listed in Table 12.9 to illustrate both the range of compounds available and also the abbreviated notation, which proves to be more convenient than formal systematic nomenclature in this area. In this notation the sequence of P-P and P-O-P links is indicated and the oxidation state of each P is shown as a superscript numeral which enables the full formula (including P-H groups) to be deduced.

### The phosphoric acids

This section deals with orthophosphoric acid ( $\text{H}_3\text{PO}_4$ ), pyrophosphoric acid ( $\text{H}_4\text{P}_2\text{O}_7$ ) and the polyphosphoric acids ( $\text{H}_{n+2}\text{P}_n\text{O}_{3n+1}$ ). Several of these compounds can be isolated pure but their facile interconversion renders this area of phosphorus chemistry far more complex

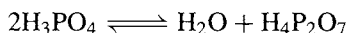
<sup>128</sup> S. OHASHI, *Pure Appl. Chem.* **44**, 415-38 (1975).

**Table 12.9** Some lower oxoacids of phosphorus (Superscript numerals in the abbreviated notation indicate oxidation states)

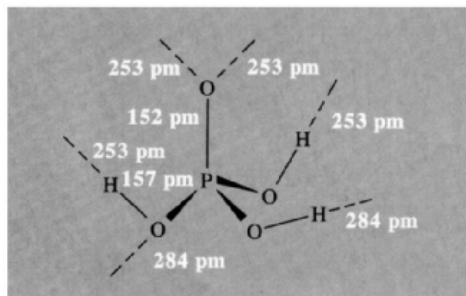
Formula (basicity)	Structure	Abbreviated notation	Formula (basicity)	Structure	Abbreviated notation
$\text{H}_4\text{P}_2\text{O}_4$ (2)		$\overset{2}{\text{P}}-\overset{2}{\text{P}}$	$\text{H}_5\text{P}_3\text{O}_9$ (5)		$\overset{5}{\text{P}}-\overset{4}{\text{P}}-\overset{4}{\text{P}}$
$\text{H}_4\text{P}_2\text{O}_5$ (3)		$\overset{2}{\text{P}}-\overset{4}{\text{P}}$	$\text{H}_6\text{P}_4\text{O}_{11}$ (6)		$\overset{4}{\text{P}}-\overset{4}{\text{P}}-\overset{4}{\text{P}}-\overset{4}{\text{P}}$
$\text{H}_4\text{P}_2\text{O}_6$ (3)		$\overset{3}{\text{P}}-\overset{5}{\text{P}}$	$\text{H}_4\text{P}_4\text{O}_{10}$ (10)		$(\overset{4}{\text{P}}-\overset{4}{\text{P}}-\text{O})_2$ ring
$\text{H}_5\text{P}_3\text{O}_7$ (4)		$\overset{3}{\text{P}}-\overset{4}{\text{P}}-\overset{4}{\text{P}}$	$\text{H}_6\text{P}_6\text{O}_{12}$ (6)		$(\overset{3}{\text{P}})_6$ ring
$\text{H}_5\text{P}_3\text{O}_8$ (5)		$\overset{4}{\text{P}}-\overset{3}{\text{P}}-\overset{4}{\text{P}}$			

than might otherwise appear. The corresponding phosphate salts are discussed in subsequent sections as also are the cyclic metaphosphoric acids  $(\text{HPO}_3)_n$ , the polymetaphosphoric acids  $(\text{HPO}_3)_n$ , and their salts.

Orthophosphoric acid is a remarkable substance: it can only be obtained pure in the crystalline state (mp  $42.35^\circ\text{C}$ ) and when fused it slowly undergoes partial self-dehydration to diphosphoric acid:



The sluggish equilibrium is obtained only after several weeks near the mp but is more rapid at higher temperatures. This process is accompanied by extremely rapid autoprotolysis (see below) which gives rise to several further (ionic) species in the melt. As the concentration of these various species builds up the mp slowly drops until at equilibrium it is  $34.6^\circ$ , corresponding to about 6.5 mole% of diphosphate.<sup>(129)</sup> Slow crystallization of stoichiometric molecular  $\text{H}_3\text{PO}_4$  from this isocompositional melt gradually reverses the equilibria and the mp eventually rises again to the initial value. Crystalline  $\text{H}_3\text{PO}_4$  has a hydrogen-bonded layer structure in which each  $\text{PO}(\text{OH})_3$  molecule is linked to 6 others by H bonds which are of two lengths, 253 and 284 pm. The shorter bonds link OH and O=P groups whereas the longer H bonds are between 2 OH groups on adjacent molecules.

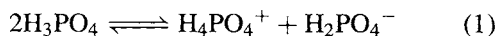


Extensive H bonding persists on fusion and phosphoric acid is a viscous syrupy liquid that

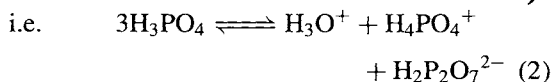
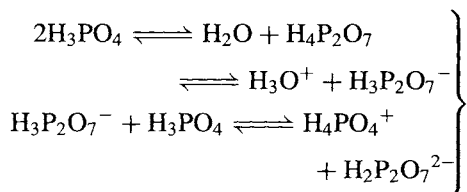
readily supercools. At  $45^\circ\text{C}$  (just above the mp) the viscosity is 76.5 centipoise (cP) and this increases to 177.7 cP at  $25^\circ$ . These values can be compared with 1.00 cP for  $\text{H}_2\text{O}$  at  $20^\circ$  and 24.5 cP for anhydrous  $\text{H}_2\text{SO}_4$  at  $25^\circ$ . As shown in the Table<sup>(129)</sup> trideuterophosphoric acid has an even higher viscosity and deuteration also raises the mp and density.

Property	$\text{H}_3\text{PO}_4$	$\text{D}_3\text{PO}_4$
MP/ $^\circ\text{C}$	42.35	46.0
Density ( $25^\circ\text{C}$ ); supercooled/ $\text{g cm}^{-3}$	1.8683	1.9083
$\eta$ ( $25^\circ\text{C}$ )/centipoise	177.5	231.8
$\kappa/\text{ohm}^{-1} \text{cm}^{-1}$	$4.68 \times 10^{-2}$	$2.82 \times 10^{-2}$
Property	$\text{H}_3\text{PO}_4 \cdot \frac{1}{2}\text{H}_2\text{O}$	
MP/ $^\circ\text{C}$	29.30	
Density ( $25^\circ\text{C}$ ); supercooled/ $\text{g cm}^{-3}$	1.7548	
$\eta$ ( $25^\circ\text{C}$ )/centipoise	70.64	
$\kappa/\text{ohm}^{-1} \text{cm}^{-1}$	$7.01 \times 10^{-2}$	

Despite this enormous viscosity, fused  $\text{H}_3\text{PO}_4$  (and  $\text{D}_3\text{PO}_4$ ) conduct electricity extremely well and this has been shown to arise from extensive self-ionization (autoprotolysis) coupled with a proton-switch conduction mechanism for the  $\text{H}_2\text{PO}_4^-$  ion:<sup>(129,130)</sup>



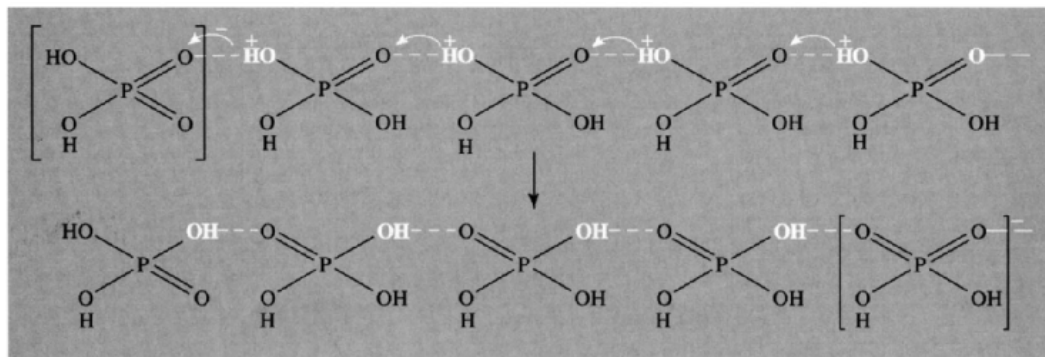
In addition, the diphosphate group is also deprotonated:



At equilibrium, the concentration of  $\text{H}_3\text{O}^+$  and  $\text{H}_2\text{P}_2\text{O}_7^{2-}$  are each  $\sim 0.28$  molal and  $\text{H}_2\text{PO}_4^-$  is  $\sim 0.26$  molal, thereby implying a

<sup>129</sup> N. N. GREENWOOD and A. THOMPSON, *J. Chem. Soc.* 3485-92 and 3864-7 (1959).

<sup>130</sup> R. A. MUNSON, *J. Phys. Chem.* **68**, 3374-7 (1964).



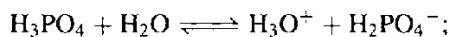
**Figure 12.17** Schematic representation of proton-switch conduction mechanism involving  $[\text{H}_2\text{PO}_4]^-$  in molten phosphoric acid.

concentration of 0.54 molal for  $\text{H}_4\text{PO}_4^+$ . These values are about 20–30 times greater than the concentrations of ions in molten  $\text{H}_2\text{SO}_4$ , namely  $[\text{HSO}_4^-]$  0.0178 molal,  $[\text{H}_3\text{SO}_4^+]$  0.0135 molal and  $[\text{HS}_2\text{O}_7^-]$  0.0088 molal (see p. 711). Because of the very high viscosity of molten  $\text{H}_3\text{PO}_4$  electrical conduction by normal ionic migration is negligible and the high conductivity is due almost entirely to a rapid proton-switch followed by a relatively slow reorientation involving the  $\text{H}_2\text{PO}_4^-$  ion, H-bonded to the solvent structure (Fig. 12.17).<sup>(129)</sup> Note that the tetrahedral  $\text{H}_4\text{PO}_4^+$  ion, i.e.  $[\text{P}(\text{OH})_4]^+$ , like the  $\text{NH}_4^+$  ion in liquid  $\text{NH}_3$ , does not contribute to the proton-switch conduction mechanism in  $\text{H}_3\text{PO}_4$  because, having no dipole moment, it does not orient preferentially in the applied electric field; accordingly any proton switching will occur randomly in all directions independently of the applied field and therefore will not contribute to the electrical conduction.

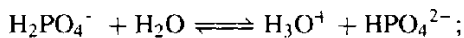
Addition of the appropriate amount of water to anhydrous  $\text{H}_3\text{PO}_4$ , or crystallization from a concentrated aqueous solution of syrupy phosphoric acid, yields the hemihydrate  $2\text{H}_3\text{PO}_4 \cdot \text{H}_2\text{O}$  as a congruently melting compound (mp  $29.3^\circ$ ). The crystal structure<sup>(131)</sup> shows the presence of 2 similar  $\text{H}_3\text{PO}_4$  molecules which, together with the  $\text{H}_2\text{O}$  molecule, are linked into

a three-dimensional H-bonded network: each of the nine O atoms participates in at least 1 relatively strong  $\text{O}-\text{H} \cdots \text{O}$  bond (255–272 pm) and the interatomic distances  $\text{P}=\text{O}$  (149 pm) and  $\text{P}-\text{OH}$  (155 pm) are both slightly shorter than the corresponding distances in  $\text{H}_3\text{PO}_4$ . Hydrogen bonding persists in the molten compound, and the proton-switch conductivity is even higher than in the anhydrous acid (See Table on p. 518).

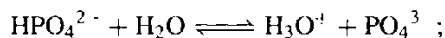
In dilute aqueous solutions  $\text{H}_3\text{PO}_4$  behaves as a strong acid but only one of the hydrogens is readily ionizable, the second and third ionization constants decreasing successively by factors of  $\sim 10^5$  (see p. 50). Thus, at  $25^\circ$ :



$$K_1 = 7.11 \times 10^{-3}; \quad \text{p}K_1 = 2.15$$



$$K_2 = 6.31 \times 10^{-8}; \quad \text{p}K_2 = 7.20$$



$$K_3 = 4.22 \times 10^{-13}; \quad \text{p}K_3 = 12.37$$

Accordingly, the acid gives three series of salts, e.g.  $\text{NaH}_2\text{PO}_4$ ,  $\text{Na}_2\text{HPO}_4$ , and  $\text{Na}_3\text{PO}_4$  (p. 523). A typical titration curve in this system is shown in Fig. 12.18: there are three steps with two inflexions at pH 4.5 and 9.5. The first inflexion, corresponding to the formation of  $\text{NaH}_2\text{PO}_4$ , can be detected by an indicator such as methyl

<sup>131</sup> A. D. MIGHELL, J. P. SMITH, and W. E. BROWN, *Acta Cryst.* **B25**, 776–81 (1969).

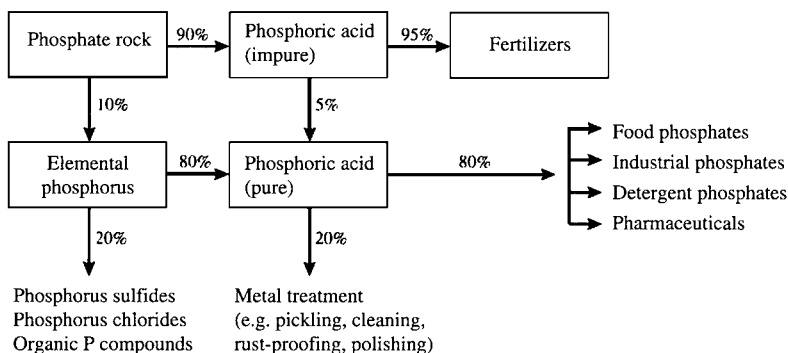
### Industrial production and uses of $\text{H}_3\text{PO}_4$ <sup>(3-5.8.9.11.132)</sup>

Phosphoric acid<sup>(132)</sup> is manufactured on a vast scale and is produced in a wide variety of concentrations and purities. It is therefore convenient to express production figures in terms of the amount of contained  $\text{P}_4\text{O}_{10}$  (the figures based on the equivalent amount of contained anhydrous  $\text{H}_3\text{PO}_4$  can be obtained by multiplying by the factor 1.380, though these may be misleading if they are taken to imply that it is the anhydrous acid that is being produced). World production capacity in 1986 exceeded 43 million tonnes of contained  $\text{P}_4\text{O}_{10}$  and was distributed as follows:

Production capacity of phosphoric acid (million tonnes/year of contained  $\text{P}_4\text{O}_{10}$ )

Region	North America	USSR & East.Eur.	Africa	Western Europe	Asia and Australasia	Central/S. America	Middle East
" $\text{P}_4\text{O}_{10}$ "/Mtpa	13.1	10.6	6.1	5.0	3.9	2.4	1.5

Production is still increasing steadily in many countries "Thermal" acid (made by oxidation of phosphorus in the presence of water vapour) is about 3 times as expensive as "wet" acid (made by treating rock phosphate with sulfuric acid). The present approximate pattern of production and uses is shown in the following scheme:



Many of these uses have already been discussed, or will be in later sections (pp. 524, 527).

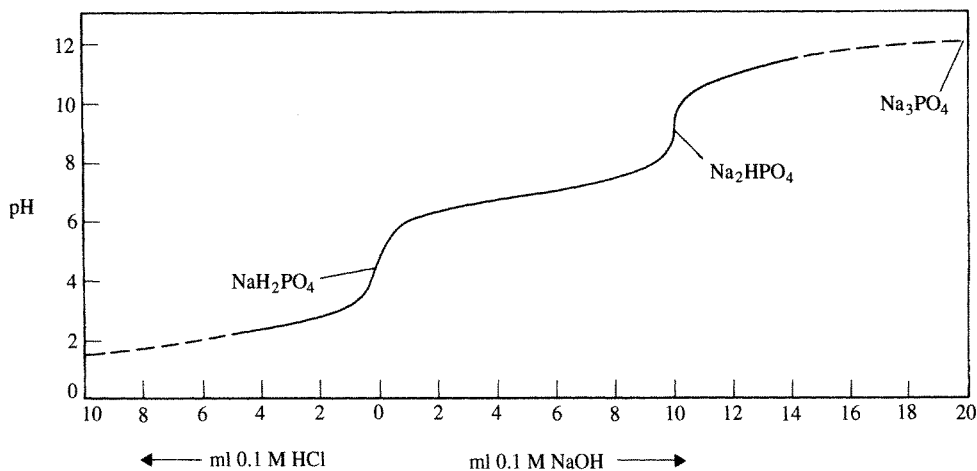
Applications of phosphoric acid in metal treatment date from 1869 when a British patent was granted for the prevention of rusting of corset stays by damp air or perspiration. Improvements followed the incorporation of certain metal ions in the phosphatizing solution (notably Mn, Fe and Zn), and today corrosion resistance is imparted in this way to innumerable metal objects such as nuts, bolts, screws, tools, car-engine parts, gears, etc. In addition, car-bodies, refrigerators, washing machines and other electrical appliances with painted or enamelled surfaces all use phosphatized undercoatings to prevent the paint from blistering or peeling. The simple immersion process may take up to 2 h at 90°C but can be accelerated 25-fold by adding small amounts of oxidizing agent such as  $\text{NaNO}_3$  and  $\text{Cu}(\text{NO}_3)_2$ . A zinc phosphatized coating is usually about  $0.6\ \mu\text{m}$  thick (i.e.  $2.2\ \text{g m}^{-2}$ ). Another important process is "bright dip" or chemical polishing of Al metal which has replaced chrome plating for car trims and other uses: the metal is immersed at 91–99°C in a solution containing 95 parts by weight of 85%  $\text{H}_3\text{PO}_4$ , 4 parts of 68%  $\text{HNO}_3$ , and 0.01%  $\text{Cu}(\text{NO}_3)_2$ , followed by electrolytic anodization to give the mirror-like surface a protective coating of transparent  $\text{Al}_2\text{O}_3$ .

Polyphosphoric acid supported on diatomaceous earth (p. 342) is a petrochemicals catalyst for the polymerization, alkylation, dehydrogenation, and low-temperature isomerization of hydrocarbons. Phosphoric acid is also used in the production of activated carbon (p. 274). In addition to its massive use in the fertilizer industry (p. 524) free phosphoric acid can be used as a stabilizer for clay soils: small additions of  $\text{H}_3\text{PO}_4$  under moist conditions gradually leach out Al and Fe from the clay and these form polymeric phosphates which bind the clay particles together. An allied, though more refined use is in the setting of dental cements.

By far the greatest consumption of pure aqueous phosphoric acid is in the preparation of various salts for use in the food, detergent and tooth-paste industries (p. 524). When highly diluted the free acid is non-toxic and devoid of odour, and is extensively used to impart the sour or tart taste to many soft drinks ("carbonated beverages") such as the various colas ( $\sim 0.05\% \text{H}_3\text{PO}_4$ , pH 2.3), root beers ( $\sim 0.01\% \text{H}_3\text{PO}_4$ , pH 5.0), and sarsaparilla ( $\sim 0.01\% \text{H}_3\text{PO}_4$ , pH  $\sim 4.5$ ).

<sup>132</sup>P. BECKER, *Phosphates and Phosphoric Acid*, Marcel Dekker, New York, 1988, 760 pp.





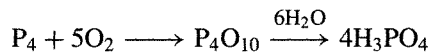
**Figure 12.18** Neutralization curve for aqueous orthophosphoric acid. For technical reasons the curve shown refers to 10 cm<sup>3</sup> of 0.1 M NaH<sub>2</sub>PO<sub>4</sub> titrated (to the left) with 0.1 M aqueous HCl and (to the right) with 0.1 M NaOH solutions. Extrapolations to points corresponding to 0.1 M H<sub>3</sub>PO<sub>4</sub> (pH 1.5) and 0.1 M Na<sub>3</sub>PO<sub>4</sub> (pH 12.0) are also shown.

orange ( $pK_i$  3.5) and the second, corresponding to Na<sub>2</sub>HPO<sub>4</sub>, is indicated by the phenolphthalein end point ( $pK_i$  9.5). The third equivalence point cannot be detected directly by means of a coloured indicator. Between the two inflexions the pH changes relatively slowly with addition of NaOH and this is an example of buffer action.<sup>†</sup> Indeed, one of the standard buffer solutions used in analytical chemistry comprises an equimolar mixture of Na<sub>2</sub>HPO<sub>4</sub> and KH<sub>2</sub>PO<sub>4</sub>. Another important buffer, which has been designed to have a pH close to that of blood, consists of 0.030 43 M Na<sub>2</sub>HPO<sub>4</sub> and 0.008 695 M KH<sub>2</sub>PO<sub>4</sub>, i.e. a mole ratio of 3.5:1 (pH 7.413 at 25°).

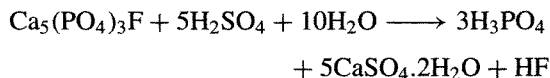
Concentrated H<sub>3</sub>PO<sub>4</sub> is one of the major acids of the chemical industry and is manufactured on

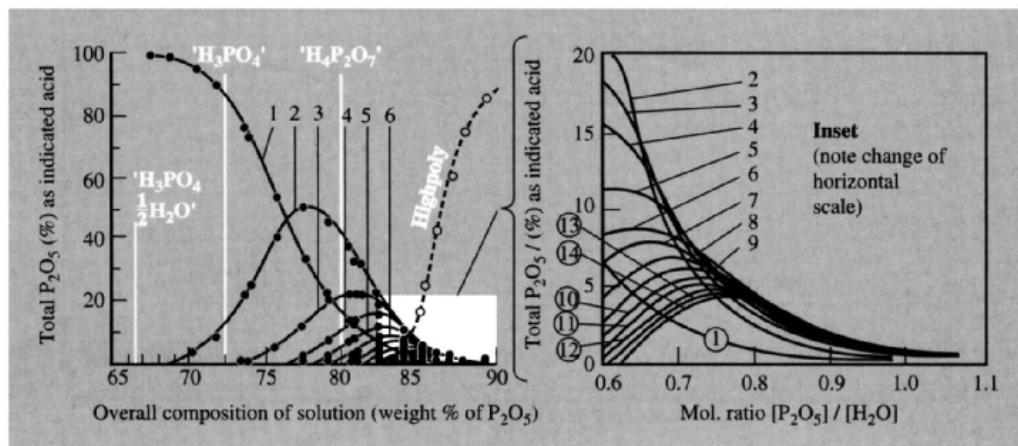
<sup>†</sup> A buffer solution is one that resists changes in pH on dilution or on addition of acid or alkali. It consists of a solution of a weak acid (e.g. H<sub>2</sub>PO<sub>4</sub><sup>-</sup>) and its conjugate base (HPO<sub>4</sub><sup>2-</sup>) and is most effective when the concentration of the two species are the same. For example at 25° an equimolar mixture of Na<sub>2</sub>HPO<sub>4</sub> and KH<sub>2</sub>PO<sub>4</sub> has pH 6.654 when each is 0.2 M and pH 6.888 when each is 0.01 M. The central section of Fig. 12.18 shows the variation in pH of an equimolar buffer of Na<sub>2</sub>HPO<sub>4</sub> and NaH<sub>2</sub>PO<sub>4</sub> at a concentration of 0.033 M (you should check this statement). Further discussion of buffer solutions is given in standard textbooks of volumetric analysis.

the multimillion-tonne scale for the production of phosphate fertilizers and for many other purposes (see Panel). Two main processes (the so-called “thermal” and “wet” processes) are used depending on the purity required. The “thermal” (or “furnace”) process yields concentrated acid essentially free from impurities and is used in applications involving products destined for human consumption (see also p. 524); in this process a spray of molten phosphorus is burned in a mixture of air and steam in a stainless steel combustion chamber:



Acid of any concentration up to 84 wt% P<sub>4</sub>O<sub>10</sub> can be prepared by this method (72.42% P<sub>4</sub>O<sub>10</sub> corresponds to anhydrous H<sub>3</sub>PO<sub>4</sub>) but the usual commercial grades are 75–85% (expressed as anhydrous H<sub>3</sub>PO<sub>4</sub>). The hemihydrate (p. 518) corresponds to 91.58% H<sub>3</sub>PO<sub>4</sub> (66.33% P<sub>4</sub>O<sub>10</sub>). The somewhat older “wet” (or “gypsum”) process involves the treatment of rock phosphate (p. 476) with sulfuric acid, the idealized stoichiometry being:





**Figure 12.19** The composition of the strong phosphoric acids shown as the weight per cent of  $P_2O_5$  present in the form of each acid plotted against the overall stoichiometric composition of the mixture. The overall stoichiometries corresponding to the three congruently melting species  $H_3PO_4 \cdot \frac{1}{2}H_2O$ ,  $H_3PO_4$  and  $H_4P_2O_7$  are indicated. Compositions above 82 wt  $P_2O_5$  are shown on an expanded scale in the inset using the mole ratio  $[P_2O_5]/[H_2O]$  as the measure of stoichiometry. (For comparison,  $H_4P_2O_7$  corresponds to a mole ratio of 0.500,  $H_5P_3O_{10}$  to a ratio 0.600,  $H_6P_4O_{13}$  to 0.667, etc.). In both diagrams the curves labelled 1,2,3, ... refer to ortho-, di-, tri- ... phosphoric acids, and "highpoly" refers to highly polymeric material hydrolysed from the column.

The gypsum is filtered off together with other insoluble matter such as silica, and the fluorine is removed as insoluble  $Na_2SiF_6$ . The dilute phosphoric acid so obtained (containing 35–70%  $H_3PO_4$  depending on the plant used) is then concentrated by evaporation. It is usually dark green or brown in colour and contains many metal impurities (c.g. Na, Mg, Ca, Al, Fe, etc.) as well as residual sulfate and fluoride, but is suitable for the manufacture of phosphatic fertilizers, metallurgical applications, etc. (see Panel on p. 520).

Diphosphoric acid  $H_4P_2O_7$  becomes an increasingly prevalent species as the system  $P_4O_{10}/H_2O$  becomes increasingly concentrated: indeed, the phase diagram shows that, in addition to the hemihydrate (mp 29.30°) and orthophosphoric acid (mp 42.35°) the only other congruently melting phase in the system is  $H_4P_2O_7$ . The compound is dimorphic with a metastable modification mp 54.3° and a stable form mp 71.5°, but in the molten state it comprises an isocompositional mixture of various polyphosphoric acids and their autoprotolysis

products. Equilibrium is reached only sluggishly and the actual constitution of the melt depends sensitively both on the precise stoichiometry and the temperature (Fig. 12.19)<sup>(133)</sup> For the nominal stoichiometry corresponding to  $H_4P_2O_7$  typical concentrations of the species  $H_{n+2}P_nO_{3n+1}$  from  $n = 1$  (i.e.  $H_3PO_4$ ) to  $n = 8$  are as follows:

$n$	1	2	3	4	5	6	7	8
mole%	35.0	42.6	14.6	5.0	1.8	0.7	0.3	0.1

Thus, although  $H_4P_2O_7$  is marginally the most abundant species present, there are substantial amounts of  $H_3PO_4$ ,  $H_5P_3O_{10}$ ,  $H_6P_4O_{13}$  and higher polyphosphoric acids. Note that the table indicates mole% of each molecular species present whereas the graphs in Fig. 12.19 plot weight percentage of  $P_2O_5$  present as each acid shown.

In dilute aqueous solution  $H_4P_2O_7$  is a somewhat stronger acid than  $H_3PO_4$ : the 4 dissociation constants at 25° are:  $K_1 \sim 10^{-1}$ ,

<sup>133</sup> R. F. JAMESON, *J. Chem. Soc.* 752-9 (1959).

Table 12.10 Factors affecting the rate of polyphosphate degradation

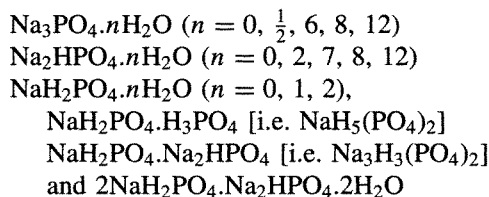
Factor	Effect on rate	Factor	Effect on rate
Temperature	$10^5$ – $10^6$ faster from $0^\circ$ to $100^\circ$	Complexing cations	Often much faster
pH	$10^3$ – $10^4$ faster from base to acid	Concentration	Roughly proportional
Enzymes	Up to $10^5$ – $10^6$ faster	Ionic environment in solution	Several-fold change
Colloidal gels	Up to $10^4$ – $10^5$ faster		

$K_2 \sim 1.5 \times 10^{-2}$ ,  $K_3 \sim 2.7 \times 10^{-7}$  and  $K_4 \sim 2.4 \times 10^{-10}$ , and the corresponding negative logarithms are:  $pK_1 \sim 1.0$ ,  $pK_2 \sim 1.8$ ,  $pK_3 \sim 6.57$  and  $pK_4 \sim 9.62$ . The P—O—P linkage is kinetically stable towards hydrolysis in dilute neutral solutions at room temperature and the reaction half-life can be of the order of years. Such hydrolytic breakdown of polyphosphate is of considerable importance in certain biological systems and has been much studied. Some factors which affect the rate of degradation of polyphosphates are shown in Table 12.10.

### Orthophosphates<sup>(23,64)</sup>

Phosphoric acid forms several series of salts in which the acidic H atoms are successively replaced by various cations; there is considerable commercial application for many of these compounds.

Lithium orthophosphates are unimportant and differ from the other alkali metal phosphates in being insoluble. At least 10 crystalline hydrated or anhydrous sodium orthophosphates are known and these can be grouped into three series:



Likewise, there are at least 10 well-characterized potassium orthophosphates and several ammonium analogues. The presence of extensive H bonding in many of these compounds leads to considerable structural complexity and frequently confers important properties (see later). The

mono- and di-sodium phosphates are prepared industrially by neutralization of aqueous  $\text{H}_3\text{PO}_4$  with soda ash (anhydrous  $\text{Na}_2\text{CO}_3$ , p. 89). However, preparation of the trisodium salts requires the use of the more expensive NaOH to replace the third H atom. Careful control of concentration and temperature are needed to avoid the simultaneous formation of pyrophosphates (diphosphates). Some indication of the structural complexity can be gained from the compound  $\text{Na}_3\text{PO}_4 \cdot 12\text{H}_2\text{O}$  which actually crystallizes with variable amounts of NaOH up to the limiting composition  $4(\text{Na}_3\text{PO}_4 \cdot 12\text{H}_2\text{O}) \cdot \text{NaOH}$ . The structure is built from octahedral  $[\text{Na}(\text{H}_2\text{O})_6]$  units which join to form "hexagonal" rings of 6 octahedra which in turn form a continuous two-dimensional network of overall composition  $\{\text{Na}(\text{H}_2\text{O})_4\}$ ; between the sheets lie  $\{\text{PO}_4\}$  connected to them by H bonds.<sup>(134)</sup> Some industrial, domestic, and scientific applications of Na, K and  $\text{NH}_4$  orthophosphates are given in the Panel.

Calcium orthophosphates are particularly important in fertilizer technology, in the chemistry of bones and teeth, and in innumerable industrial and domestic applications (see Panel). They are also the main source of phosphorus and phosphorus chemicals and occur in vast deposits as apatites and rock phosphate (p. 475). The main compounds occurring in the  $\text{CaO}-\text{H}_2\text{O}-\text{P}_2\text{O}_5$  phase diagram are:  $\text{Ca}(\text{H}_2\text{PO}_4)_2$ ,  $\text{Ca}(\text{H}_2\text{PO}_4)_2 \cdot \text{H}_2\text{O}$ ,  $\text{Ca}(\text{HPO}_4) \cdot n\text{H}_2\text{O}$  ( $n = 0, \frac{1}{2}, 2$ ),  $\text{Ca}_3(\text{PO}_4)_2$ ,  $\text{Ca}_2\text{PO}_4(\text{OH}) \cdot 2\text{H}_2\text{O}$ ,  $\text{Ca}_5(\text{PO}_4)_3\text{OH}$  (i.e. apatite),  $\text{Ca}_4\text{P}_2\text{O}_9$  [probably  $\text{Ca}_3(\text{PO}_4)_2 \cdot \text{CaO}$ ] and  $\text{Ca}_8\text{H}_2(\text{PO}_4)_6 \cdot 5\text{H}_2\text{O}$ .

In all of these alkali-metal and alkaline earth-metal orthophosphates there are discrete, approximately regular tetrahedral  $\text{PO}_4$  units in

<sup>134</sup> E. TILLMANN and W. H. BAUR, *Inorg. Chem.* **9**, 1957–8 (1970).

### Uses of Orthophosphates<sup>(9)</sup>

Phosphates are used in an astonishing variety of domestic and industrial applications but their ubiquitous presence and their substantial impact on everyday life is frequently overlooked. It will be convenient first to indicate the specific uses of individual compounds and the properties on which they are based, then to conclude with a brief summary of many different types of application and their interrelation. The most widely used compounds are the various phosphate salts of Na, K, NH<sub>4</sub> and Ca. The uses of di-, tri- and poly-phosphates are mentioned on pp. 527-29.

Na<sub>3</sub>PO<sub>4</sub> is strongly alkaline in aqueous solution and is thus a valuable constituent of scouring powders, paint strippers and grease saponifiers. Its complex with NaOCl [(Na<sub>3</sub>PO<sub>4</sub>.11H<sub>2</sub>O)<sub>4</sub>.NaOCl] is also strongly alkaline (a 1% solution has pH 11.8) and, in addition, it releases active chlorine when wetted; this combination of scouring, bleaching and bacteriocidal action makes the adduct valuable in formulations of automatic dishwashing powders.

Na<sub>2</sub>HPO<sub>4</sub> is widely used as a buffer component (p. 521). The use of the dihydrate (~2% concentration) as an emulsifier in the manufacture of pasteurized processed cheese was patented by J. L. Kraft in 1916 and is still used, together with insoluble sodium metaphosphate or the mixed phosphate Na<sub>15</sub>Al<sub>3</sub>(PO<sub>4</sub>)<sub>8</sub>, to process cheese on the multikilotonne scale daily. Despite much study, the reason why phosphate salts act as emulsifiers is still not well understood in detail. Na<sub>2</sub>HPO<sub>4</sub> is also added (~0.1%) to evaporated milk to maintain the correct Ca/PO<sub>4</sub> balance and to prevent gelation of the milk powder to a mush. Its addition at the 5% level to brine (15-20% NaCl solution) for the pickling of ham makes the product more tender and juicy by preventing the exudation of juices during subsequent cooking. Another major use in the food industry is as a starch modifier: small additions enhance the ability to form stable cold-water gels (e.g. instant pudding mixes), and the addition of 1% to farinaceous products raises the pH to slightly above 7 and provides "quick-cooking" breakfast cereals.

NaH<sub>2</sub>PO<sub>4</sub> is a solid water-soluble acid, and this property finds use (with NaHCO<sub>3</sub>) in effervescent laxative tablets and in the pH adjustment of boiler waters. It is also used as a mild phosphatizing agent for steel surfaces and as a constituent in the undercoat for metal paints.

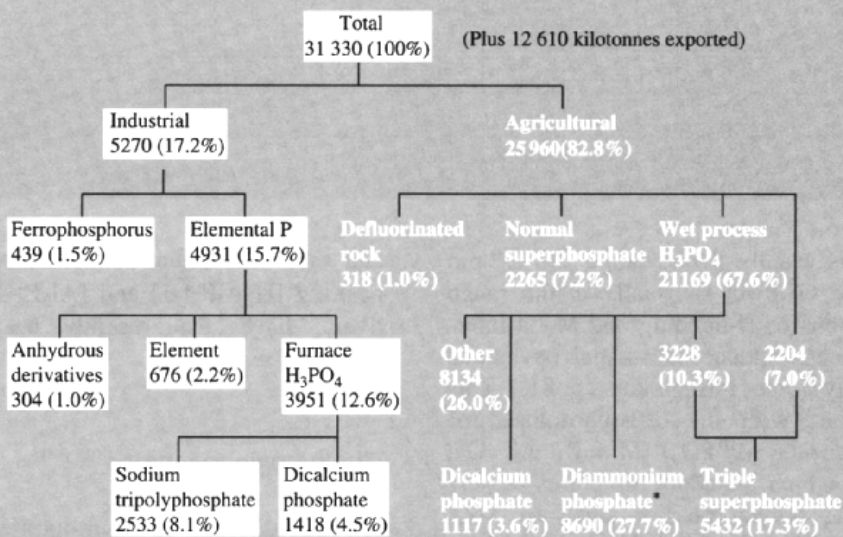
K<sub>3</sub>PO<sub>4</sub> (like Na<sub>3</sub>PO<sub>4</sub>) is strongly alkaline in aqueous solution and is used to absorb H<sub>2</sub>S from gas streams; the solution can be regenerated simply by heating. K<sub>3</sub>PO<sub>4</sub> is also used as a regulating electrolyte to control the stability of synthetic latex during the polymerization of styrenebutadiene rubbers. The buffering action of K<sub>2</sub>HPO<sub>4</sub> has already been mentioned (p. 521) and this is the reason for its addition as a corrosion inhibitor to car-radiator coolants which otherwise tend to become acidic due to slow oxidation of the glycol antifreeze. KH<sub>2</sub>PO<sub>4</sub> is a piezoelectric (p. 57) and finds use in submarine sonar systems. For many applications, however, the cheaper sodium salts are preferred unless there is a specific advantage for the potassium salt; one example is the specialist balanced commercial fertilizer formulation [KH<sub>2</sub>PO<sub>4</sub>.(NH<sub>4</sub>)<sub>2</sub>HPO<sub>4</sub>] which contains 10.5% N, 53% P<sub>2</sub>O<sub>5</sub> and 17.2% K<sub>2</sub>O (i.e. N-P-K 10-53-17).

(NH<sub>4</sub>)<sub>2</sub>HPO<sub>4</sub> and (NH<sub>4</sub>)H<sub>2</sub>PO<sub>4</sub> can be used interchangeably as specialist fertilizers and nutrients in fermentation broths; though expensive, their high concentration of active ingredients ameliorate this, particularly in localities where transportation costs are high. Indeed, (NH<sub>4</sub>)<sub>2</sub>HPO<sub>4</sub> in granulated or liquid form consumes more phosphate rock than any other single end-product (over 8 million tonnes pa in the USA alone in 1974). Ammonium phosphates are also much used as flame retardants for cellulose materials, about 3-5% gain in dry weight being the optimum treatment. Their action probably depends on their ready dissociation into NH<sub>3</sub> and H<sub>3</sub>PO<sub>4</sub> on heating; the H<sub>3</sub>PO<sub>4</sub> then catalyses the decomposition of cellulose to a slow-burning char (carbon) and this, together with the suppression of flammable volatiles, smothers the flame. As the ammonium phosphates are soluble, they are used mainly for curtains, theatre scenery and disposable paper dresses and costumes. The related compound urea phosphate (NH<sub>2</sub>CONH<sub>2</sub>.H<sub>3</sub>PO<sub>4</sub>) has also been used to flameproof cotton fabrics: the material is soaked in a concentrated aqueous solution, dried (15% weight gain) and cured at 160° to bond the retardant to the cellulose fibre. The advantage is that the retardant does not wash out, but the strength of the fabric is somewhat reduced by the process.

Calcium phosphates have a broad range of applications both in the food industry and as bulk fertilizers. The vast scale of the phosphate rock industry has already been indicated (p. 476) and this is further elaborated for the particular case of the USA in the Scheme on the page opposite (kilotonnes pa and %, 1974).

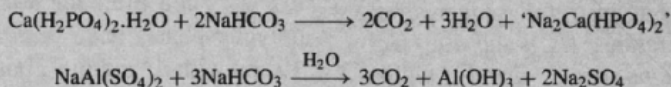
The crucial importance of Ca and PO<sub>4</sub> as nutrient supplements for the healthy growth of bones, teeth, muscle and nerve cells has long been recognized. The non-cellular bone structure of an average adult human consists of ~60% of some form of "tricalcium phosphate" [Ca<sub>3</sub>(PO<sub>4</sub>)<sub>3</sub>OH]; teeth likewise comprise ~70% and average persons carry 3.5 kg of this material in their bodies. Phosphates in the body are replenished by a continuous cycle, and used P is carried by the blood to the kidneys and then excreted in urine, mainly as Na(NH<sub>4</sub>)HPO<sub>4</sub>. An average adult eliminates 3-4 g of PO<sub>4</sub> equivalent daily (cf. the discovery of P in urine by Brandt, p. 473).

Calcium phosphates are used in baking acids, toothpastes, mineral supplements and stock feeds. Ca(H<sub>2</sub>PO<sub>4</sub>)<sub>2</sub> was introduced as a leavening acid in the late nineteenth century (to replace "cream of tartar" KHC<sub>4</sub>H<sub>4</sub>O<sub>6</sub>) but the monohydrate (introduced in the 1930s) finds more use today. "Straight baking powder", a mixture of Ca(H<sub>2</sub>PO<sub>4</sub>)<sub>2</sub>.H<sub>2</sub>O and NaHCO<sub>3</sub> with some 40% starch coating, tends to produce CO<sub>2</sub> 100 quickly during dough mixing and so "combination baking



\* Note that ammoniation of  $\text{H}_3\text{PO}_4$  to give granulated or liquid ammonium phosphates consumes more phosphate rock in the USA than any other single end product.

powder", which also incorporates a slow-acting acid such as  $\text{NaAl}(\text{SO}_4)_2$ , is preferred. Nearly 90% of all US household baking powders now use such combinations, e.g.:



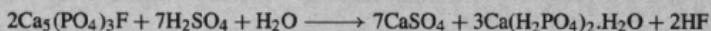
A typical powder contains 28%  $\text{NaHCO}_3$ , 10.7%  $\text{Ca}(\text{H}_2\text{PO}_4)_2 \cdot \text{H}_2\text{O}$ , 21.4%  $\text{NaAl}(\text{SO}_4)_2$  and 39.9% starch and the scale of manufacture approaches  $10^5$  tonnes pa.

In toothpastes,  $\text{CaHPO}_4 \cdot 2\text{H}_2\text{O}$  was first used to replace chalk as a mild abrasive and polishing agent in the early 1930s. It is still widely used provided the toothpaste does not also contain fluoride, since this would precipitate as  $\text{CaF}_2$  and effectively eliminate the desired anion. Some 25 000 tonnes of  $\text{CaHPO}_4 \cdot \text{H}_2\text{O}$  are used in this way annually in the USA and the compound typically comprises 50% by weight of the paste. The first important fluoride toothpaste contained 39% of the diphosphate  $\text{Ca}_2\text{P}_2\text{O}_7$  which is the most insoluble and inert of all calcium phosphates. It is made by careful dehydration of  $\text{CaHPO}_4 \cdot 2\text{H}_2\text{O}$  at  $150^\circ$  and then above  $400^\circ$ . It was first used in Procter and Gamble's "Crest" which also contained 0.4%  $\text{SnF}_2$  and 1%  $\text{Sn}_2\text{P}_2\text{O}_7$ .

Synthetic  $\text{Ca}_5(\text{PO}_4)_3\text{OH}$  is added to table salt (1–2%) to impart free-flowing properties and it is likewise added to granulated sugar, baking powders and even fertilizers. It is prepared by adding  $\text{H}_3\text{PO}_4$  to a slurry of hydrated lime — this is the reverse order of addition to that used for making  $\text{Ca}(\text{H}_2\text{PO}_4)_2$  and  $\text{CaHPO}_4$  since the aim is to deprotonate all three OH groups. The compound is extremely insoluble and precipitates as very fine particles ( $\sim 0.5\text{--}3\ \mu\text{m}$  diameter).

The idea of converting insoluble "tricalcium phosphate" or phosphate rock into soluble "monocalcium phosphate"  $\text{Ca}(\text{H}_2\text{PO}_4)_2$  dates back to the 1830s when J. von Liebig observed that acidulated bones made good fertilizer. The limited supply of bones (including those from old battlefields!) was soon replaced by Suffolk coprolites and apatites, though the vast North African deposits were still unknown. The phosphate fertilizer industry originated in England (Lawes, 1843); it grew rapidly as shown by the dramatic increase in world production of phosphate rock, which leapt from 500 tonnes in 1847 to 500 kilotonnes in 1880, 3.1 million tonnes in 1900, and now exceeds 150 Mt (p. 476). This unprecedented demand for phosphatic fertilizers is, of course, closely related to the demand for food from an exploding world population of humans which reached 1 billion ( $10^9$ ) in 1830, 2 billion in 1930, 3 billion in 1960, 4 billion in 1974 and will be over 8 billion by the end of the century.

"Superphosphate" is now made by the (highly exothermic) addition of  $\text{H}_2\text{SO}_4$  to fine-ground phosphate rock:



The  $\text{CaSO}_4$  or its hydrate (gypsum) acts only as an unwanted diluent. Its presence can be avoided by using  $\text{H}_3\text{PO}_4$  instead of  $\text{H}_2\text{SO}_4$  for the acidulation, thus giving rise to "triple superphosphate"



Commercial triple superphosphate contains almost 3 times the amount of available (soluble)  $\text{P}_2\text{O}_5$  as ordinary superphosphate, hence its name (45–50 wt% vs. 18–20 wt%).

which P–O is usually in the range  $153 \pm 3$  pm and the angle O–P–O is usually in the range  $109 \pm 5^\circ$ . Extensive H-bonding and M–O interactions frequently induce substantial deviations from a purely ionic formulation (p. 81). This trend continues with the orthophosphates of trivalent elements  $\text{M}^{\text{III}}\text{PO}_4$  (M = B, Al, Ga, Cr, Mn, Fe) which all adopt structures closely related to the polymorphs of silica (p. 342).  $\text{NaBePO}_4$  is similar, and  $\text{YPO}_4$  adopts the zircon ( $\text{ZrSiO}_4$ ) structure. The most elaborate analogy so far revealed is for  $\text{AlPO}_4$  which can adopt each of the 6 main polymorphs of silica as indicated in the scheme below. The analogy covers not only the structural relations between the phases but also the sequence of transformation temperatures ( $^\circ\text{C}$ ) and the fact that the  $\alpha$ – $\beta$ -transitions occur readily whilst the others are sluggish (p. 343). Similarly, the orthophosphates of B, Ga and Mn are known in the  $\beta$ -quartz and the  $\alpha$ - and  $\beta$ -cristobalite forms whereas  $\text{FePO}_4$  adopts either the  $\alpha$ - or  $\beta$ -quartz structure. Numerous hydrated forms are also known. The Al– $\text{PO}_4$ – $\text{H}_2\text{O}$  system is used industrially as the basis for many adhesives, binders and cements.<sup>(135)</sup> Novel chain

and sheet aluminium phosphate anions of composition  $[\text{H}_2\text{AlP}_2\text{O}_8]$  and  $[\text{Al}_5\text{P}_4\text{O}_{16}]^{3-}$ , respectively, have also recently been structurally characterized.<sup>(136)</sup>

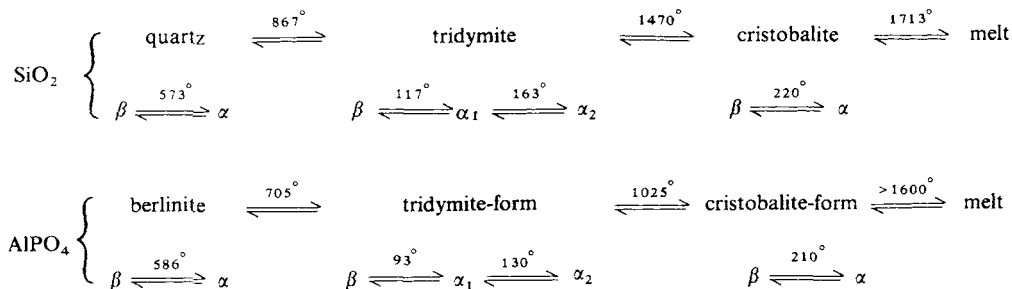
### Chain polyphosphates<sup>(23,64)</sup>

A rather different structure-motif is observed in the chain polyphosphates: these feature corner-shared  $\{\text{PO}_4\}$  tetrahedra as in the polyphosphoric acids (p. 522). The general formula for such anions is  $[\text{P}_n\text{O}_{3n+1}]^{(n+2)-}$ , of which the diphosphates,  $\text{P}_2\text{O}_7^{4-}$ , and tripolyphosphates,  $\text{P}_3\text{O}_{10}^{5-}$ , constitute the first two members. Chain polyphosphates have been isolated with  $n$  up to 10 and with  $n$  "infinite", but those of intermediate chain length ( $10 < n < 50$ ) can only be obtained as glassy or amorphous mixtures. As the chain length increases, the ratio  $(3n + 1)/n$  approaches 3.00 and the formula approaches that of the polymetaphosphates  $[\text{PO}_3^-]_\infty$ .

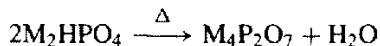
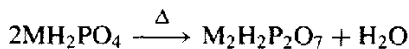
Diphosphates (pyrophosphates) are usually prepared by thermal condensation of dihydrogen

<sup>135</sup> J. H. MORRIS, P. G. PERKINS, A. E. A. ROSE and W. E. SMITH, *Chem. Soc. Revs.* **6**, 173–94 (1977).

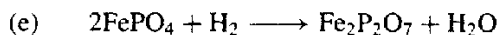
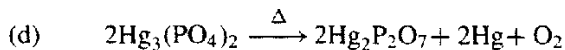
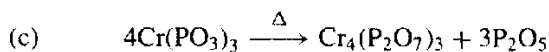
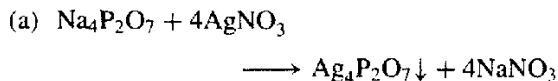
<sup>136</sup> J. M. THOMAS *et al.*, *J. Chem. Soc., Chem. Commun.*, 1170–2 (1992), 929–31 and 1266–8 (1992). See also R. KNIEP, *Angew. Chem. Int. Edn. Engl.* **25**, 525–34 (1986).



phosphates or hydrogen phosphates:



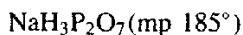
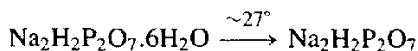
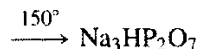
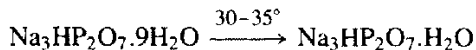
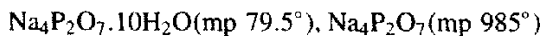
They can also be prepared in specialized cases by (a) metathesis, (b) the action of  $\text{H}_3\text{PO}_4$  on an oxide, (c) thermolysis of a metaphosphate, (d) thermolysis of an orthophosphate, or (e) reductive thermolysis, e.g.:



Many diphosphates of formula  $\text{M}^{\text{IV}}\text{P}_2\text{O}_7$ ,  $\text{M}_2^{\text{II}}\text{P}_2\text{O}_7$  and hydrated  $\text{M}_4^{\text{I}}\text{P}_2\text{O}_7$  are known and there has been considerable interest in the relative orientation of the two linked  $\{\text{PO}_4\}$  groups and in the P–O–P angle between them.<sup>(137)</sup> For small cations the 2  $\{\text{PO}_4\}$  are approximately staggered whereas for larger cations they tend to be nearly eclipsed. The P–O–P angle is large and variable, ranging from  $130^\circ$  in  $\text{Na}_4\text{P}_2\text{O}_7 \cdot 10\text{H}_2\text{O}$  to  $156^\circ$  in  $\alpha\text{-Mg}_2\text{P}_2\text{O}_7$ . The apparent colinearity in the higher-temperature ( $\beta$ ) form of many diphosphates, which was previously ascribed to a P–O–P angle of  $180^\circ$ , is now generally attributed to positional disorder. Bridging P–O distances are invariably longer than terminal P–O distances, typical values (for  $\text{Na}_4\text{P}_2\text{O}_7 \cdot 10\text{H}_2\text{O}$ ) being P–O <sub>$\mu$</sub>  161 pm, P–O <sub>$t$</sub>  152 pm. Note that bridging can also be via a peroxo group as in ammonium peroxodiphosphate<sup>(138)</sup> which features the zig-zag anion  $[\text{O}_3\text{P}-\text{O}-\text{O}-\text{PO}_3]^{4-}$  with P–O <sub>$\mu$</sub>  165.8 pm, P–O <sub>$t$</sub>  150.8 pm and O–O

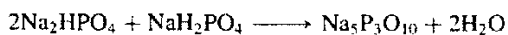
150.1 pm (cf. 145.3 pm in  $\text{H}_2\text{O}_2$  and 148–150 pm in  $\text{S}_2\text{O}_5^{2-}$ ).

As diphosphoric acid is tetrabasic, four series of salts are possible though not all are always known, even for simple cations. The most studied are those of Na, K,  $\text{NH}_4$  and Ca, e.g.:



Before the advent of synthetic detergents,  $\text{Na}_4\text{P}_2\text{O}_7$  was much used as a dispersant for lime soap scum which formed in hard water, but it has since been replaced by the tripolyphosphate (see below). However, the ability of diphosphate ions to form a gel with soluble calcium salts has made  $\text{Na}_4\text{P}_2\text{O}_7$  a useful ingredient for starch-type instant pudding which requires no cooking. The main application of  $\text{Na}_2\text{H}_2\text{P}_2\text{O}_7$  is as a leavening acid in baking: it does not react with  $\text{NaHCO}_3$  until heated, and so large batches of dough or batter can be made up and stored.  $\text{Ca}_2\text{P}_2\text{O}_7$ , because of its insolubility, inertness, and abrasive properties, is used as a toothpaste additive compatible with  $\text{Sn}^{\text{II}}$  and fluoride ions (see Panel on p. 525).

Of the tripolyphosphates only the sodium salt need be mentioned. It was introduced in the mid-1940s as a “builder” for synthetic detergents, and its production for this purpose is now measured in megatonnes per annum (see Panel on the next page). On the industrial scale  $\text{Na}_5\text{P}_3\text{O}_{10}$  is usually made by heating an intimate mixture of powdered  $\text{Na}_2\text{HPO}_4$  and  $\text{NaH}_2\text{PO}_4$  of the required stoichiometry under carefully controlled conditions:



The low-temperature form (I) converts to the high-temperature form (II) above  $417^\circ\text{C}$  and both forms react with water to give the crystalline hexahydrate. All three materials contain the

<sup>137</sup> G. M. CLARK and R. MORLEY, *Chem. Soc. Revs.* **5**, 269–95 (1976).

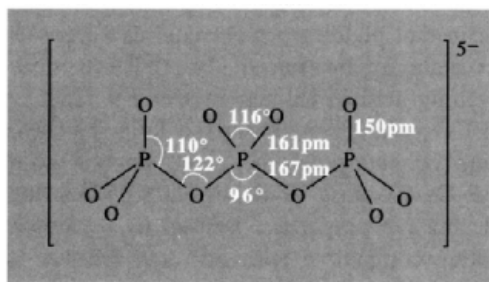
<sup>138</sup> W. P. GRIFFITH, R. D. POWELL and A. C. SKAPSKI, *Polyhedron* **7**, 1305–10 (1988).

## Uses of Sodium Tripolyphosphate

Many synthetic detergents contain 25–45%  $\text{Na}_5\text{P}_3\text{O}_{10}$  though the amount is lower in the USA than in Europe because of the problems of eutrophication in some areas (p. 478). It acts mainly as a water softener, by chelating and sequestering the  $\text{Mg}^{2+}$  and  $\text{Ca}^{2+}$  in hard water. Indeed, the formation constants of its complexes with these ions are nearly one million-fold greater than with  $\text{Na}^+$ : ( $\text{NaP}_3\text{O}_{10}^{4-}$   $\text{p}K \sim 2.8$ ;  $\text{MgP}_3\text{O}_{10}^{3-}$   $\text{p}K \sim 8.6$ ;  $\text{CaP}_3\text{O}_{10}^{3-}$   $\text{p}K \sim 8.1$ ). In addition,  $\text{Na}_5\text{P}_3\text{O}_{10}$  increases the efficiency of the surfactant by lowering the critical micelle concentration, and by its ability to suspend and peptize dirt particles by building up a large negative charge on the particles by adsorption; it also furnishes a suitable alkalinity for cleansing action without irritating eyes or skin and it provides effective buffering action at these pHs. The dramatic growth of synthetic detergent powders during the 1950s was accompanied by an equally dramatic drop in the use of soap powders.<sup>(11)</sup>

$\text{Na}_5\text{P}_3\text{O}_{10}$  is also used as a dispersing agent in clay suspensions used in oil-well drilling. Again, addition of  $<1\%$   $\text{Na}_5\text{P}_3\text{O}_{10}$  to the slurries used in manufacturing cement and bricks enables much less water to be used to attain workability, and thus less to be removed during the setting or calcining processes.

tripolyphosphate ion  $\text{P}_3\text{O}_{10}^{5-}$  with a *trans*-configuration of adjacent tetrahedra and a twofold symmetry axis; forms (I) and (II) differ mainly in the coordination of the sodium ions and the slight differences in the dimensions of the ion in the three crystals are probably within experimental error. Typical values are:



The complicated solubility relations, rates of hydrolysis, self-disproportionation and interconversion with other phosphates depends sensitively on pH, concentration, temperature and the presence of impurities.<sup>(139)</sup> Though of great interest academically and of paramount importance industrially these aspects will not be further considered here.<sup>(11,23,64,140)</sup> Triphosphates such as adenosine triphosphate (ATP) are also of vital importance in living organisms (see text books on biochemistry, and also ref. 141).

The stoichiometric formula of a chain-polyphosphate can sometimes be an unreliable guide to its structure. For example, the crystalline compound “ $\text{CaNb}_2\text{P}_6\text{O}_{21}$ ” has been shown by X-ray crystal structure analysis to contain equal numbers of oxide(2-), diphosphate(4-) and tetraphosphate(6-) anions, i.e.  $\text{CaNb}_2\text{O}[\text{P}_2\text{O}_7][\text{P}_4\text{O}_{13}]$ .<sup>(142)</sup> By contrast,  $\text{CsM}_2\text{P}_5\text{O}_{16}$  ( $\text{M} = \text{V}, \text{Fe}$ ) does contain the anticipated homologous *catena*-pentaphosphate  $[\text{P}_n\text{O}_{3n+1}]^{(n+2)-}$  anion (p. 512) with  $n = 5$ .<sup>(143)</sup>

Long-chain polyphosphates,  $\text{M}_{n+2}^1\text{P}_n\text{O}_{3n+1}$ , approach the limiting composition  $\text{M}^1\text{PO}_3$  as  $n \rightarrow \infty$  and are sometimes called linear metaphosphates to distinguish them from the cyclic metaphosphates of the same composition (p. 529). Their history extends back over 150 y to the time when Thomas Graham described the formation of a glassy sodium polyphosphate mixture now known as Graham’s salt. Various heat treatments converted this to crystalline compounds known as Kurrol’s salt, Maddrell’s salt, etc., and it is now appreciated, as a result of X-ray crystallographic studies, that these and many related substances all feature unbranched chains of corner-shared  $\{\text{PO}_4\}$  units which differ only in the mutual orientations and

<sup>139</sup> G. P. HAIGHT, T. W. HAMBLEY, P. HENDRY, G. A. LAWRENCE and A. M. SARGESON, *J. Chem. Soc., Chem. Commun.*, 488–91 (1985), and references cited therein

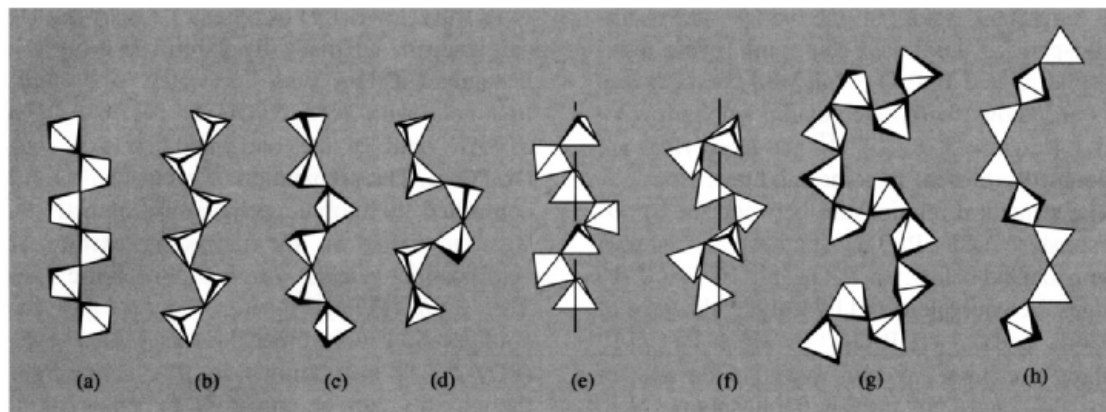
<sup>140</sup> E. J. GRIFFITH, *Pure Appl. Chem.* **44**, 173–200 (1975).

<sup>141</sup> I. S. KULAEV, *The Biochemistry of Inorganic Polyphosphates*, Wiley, Chichester, 1980, 225 pp.

<sup>142</sup> M.-T. AVERBUCH-POUCHOT, *Z. anorg. allg. Chem.* **545**, 118–24 (1987).

<sup>143</sup> B. KLINKERT and M. JANSEN, *Z. anorg. allg. Chem.* **567**, 87–94 (1988).





**Figure 12.20** Types of polyphosphate chain configuration. The diagrams indicate the relative orientations of adjacent  $PO_4$  tetrahedra, extended along the chain axes. (a)  $(RbPO_3)_n$  and  $(CsPO_3)_n$ , (b)  $(LiPO_3)_n$  low temp, and  $(KPO_3)_n$ , (c)  $(NaPO_3)_n$  high-temperature Maddrell salt and  $[Na_2H(PO_3)_3]_n$ , (d)  $[Ca(PO_3)_2]_n$  and  $[Pb(PO_3)_2]_n$ , (e)  $(NaPO_3)_n$ , Kurrol A and  $(AgPO_3)_n$ , (f)  $(NaPO_3)_n$ , Kurrol B, (g)  $[CuNH_4(PO_3)_3]_n$  and isomorphous salts, (h)  $[CuK_2(PO_3)_4]_n$  and isomorphous salts. Each crystalline form of Kurrol salt contains equal numbers of right-handed and left-handed spiralling chains.

repeat units of the constituent tetrahedra.<sup>(144)</sup> These, in turn, are dictated by the size and coordination requirements of the counter cations present (including H). Some examples are shown schematically in Fig. 12.20 and the geometric resemblance between these and many of the chain metasilicates (p. 350) should be noted. In most of these polyphosphates  $P-O_\mu$  is  $161 \pm 5$  pm,  $P-O_t$   $150 \pm 2$  pm,  $P-O_\mu-P$   $125-135^\circ$  and  $O_t-P-O_t$   $115-120^\circ$  (i.e. very similar to the dimensions and angles in the tripolyphosphate ion, p. 528).

The complex preparative interrelationships occurring in the sodium polyphosphate system are summarized in Fig. 12.21 (p. 531). Thus anhydrous  $NaH_2PO_4$ , when heated to  $170^\circ$  under conditions which allow the escape of water vapour, forms the diphosphate  $Na_2H_2P_2O_7$ , and further dehydration at  $250^\circ$  yields either Maddrell's salt (closed system) or the cyclic trimetaphosphate (water vapour pressure kept low). Maddrell's salt converts from the low-temperature to the high-temperature form above  $300^\circ$ , and above  $400^\circ$  reverts to the cyclic

trimetaphosphate. The high-temperature form can also be obtained (via Graham's and Kurrol's salts) by fusing the cyclic trimetaphosphate (mp  $526^\circ C$ ) and then quenching it from  $625^\circ$  (or from  $580^\circ$  to give Kurrol's salt directly). All these linear polyphosphates of sodium revert to the cyclic trimetaphosphate on prolonged annealing at  $\sim 400^\circ C$ .

Fuller treatments of the phase relations and structures of polyphosphates, and their uses as glasses, ceramics, refractories, cements, plasters and abrasives, are available.<sup>(144,145)</sup>

### Cyclo-polyphosphoric acids and cyclo-polyphosphates<sup>(146)</sup>

These compounds were formerly called metaphosphoric acids and metaphosphates but the IUPAC *cyclo-* nomenclature is preferred as being structurally more informative. The only

<sup>144</sup> J. MALING and F. HANIC, *Topics in Phosphorus Chemistry* 10, 341-502 (1980).

<sup>145</sup> A. E. R. WESTMAN, *Topics in Phosphorus Chemistry* 9, 231-405, 1977. A comprehensive account with 963 references.

<sup>146</sup> S. Y. KALLINEY, *Topics in Phosphorus Chemistry* 7, 255-309, 1972.

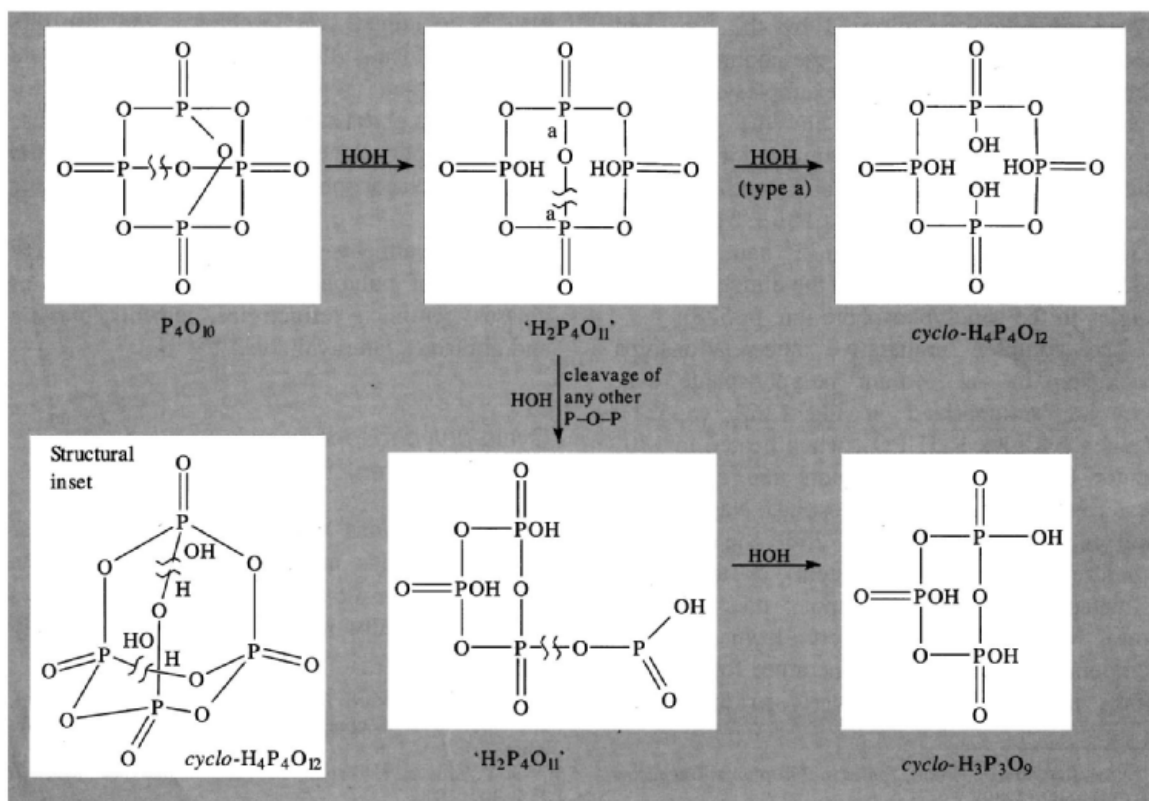
two important acids in the series are *cyclo*-triphosphoric acid  $H_3P_3O_9$  and *cyclo*-tetraphosphoric acid  $H_4P_4O_{12}$ , but well-characterized salts are known with heterocyclic anions [*cyclo*-( $PO_3$ ) $_n$ ] $^{n-}$  ( $n = 3-8, 10$ ),<sup>(147)</sup> and larger rings are undoubtedly present in some mixtures.

The structural relationship between the *cyclo*-phosphates and  $P_4O_{10}$  (p. 504) is shown schematically below. In  $P_4O_{10}$  all 10 P-O(-P) bridges are equivalent and hydrolytic cleavage of any one leads to " $H_2P_4O_{11}$ " in which P-O(-P) bridges are now of two types. Cleavage of "type a" leads to *cyclo*-tetraphosphoric acid or its salts (as shown in the upper line of the scheme), whereas cleavage of any of the other bridges leads to a *cyclo*-triphosphate ring with a pendant -OP(O)OH group which can subsequently be hydrolysed off to leave  $(HPO_3)_3$

or its salts (lower line of scheme). *Cyclo*-( $HPO_3$ ) $_4$  can, indeed, be made by careful hydrolysis of hexagonal  $P_4O_{10}$  with ice-water, and similar treatment with iced NaOH or  $NaHCO_3$  gives a 75% yield of the corresponding salt *cyclo*-( $NaPO_3$ ) $_4$ . The preparation of *cyclo*-( $NaPO_3$ ) $_3$  by controlled thermolytic dehydration of  $NaH_2PO_4$  was mentioned in the preceding section and acidification yields *cyclo*-triphosphoric acid. The *cyclo*-( $PO_3$ ) $_3^{3-}$  anion adopts the chair configuration with dimensions as shown; *cyclo*-( $PO_3$ ) $_4^{4-}$  is also known in this configuration though this can be modified by changing the cation.

The crystal structure of the *cyclo*-hexaphosphate anion in  $Na_6P_6O_{18} \cdot 6H_2O$  shows that all 6P atoms are coplanar and that bond lengths are similar to those in the  $P_3O_9^{3-}$  and  $P_4O_{12}^{4-}$  anions. See ref. 147 for the structure of the hydrated *cyclo*-decaphosphate  $K_{10}P_{10}O_{30} \cdot 4H_2O$ . Higher *cyclo*-metaphosphates can be isolated by

<sup>147</sup> U. SCHULKE, M. T. AVERBUCH-POUCHOT and A. DURIF, *Z. anorg. allg. Chem.* **612**, 107-12 (1992).



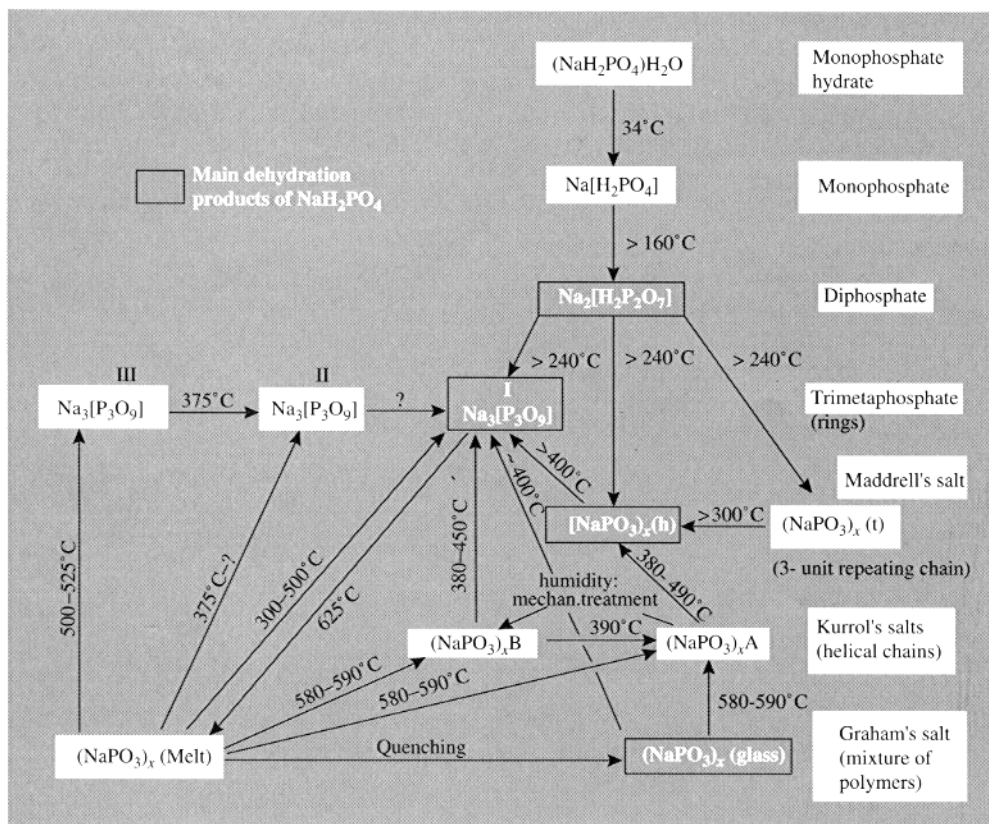
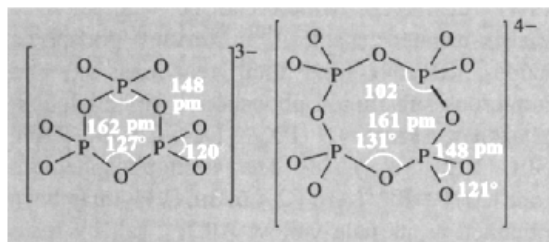


Figure 12.21 Interrelationship of metaphosphates. (From CIC, Vol. 2, p. 521.)



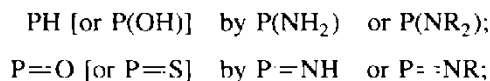
chromatographic separation from Graham's salt in which they are present to the extent of ~1%.

### 12.3.7 Phosphorus–nitrogen compounds

The P–N bond is one of the most intriguing in chemistry and many of its more subtle aspects

still elude a detailed and satisfactory description. It occurs in innumerable compounds, frequently of great stability, and in many of these the strength of the bond and the shortness of the interatomic distance have been interpreted in terms of "partial double-bond character". In fact, the conventional symbols P–N and P=N are more an aid to electron counting than a description of the bond in any given compound (see p. 538).

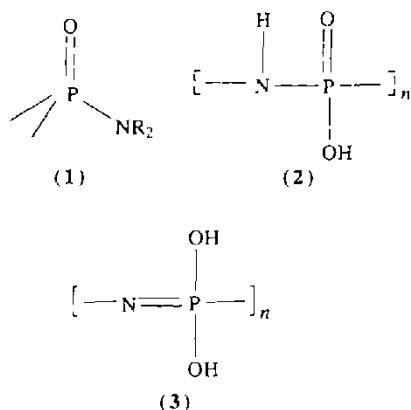
Many compounds containing the P–N link can be considered formally as derivatives of the oxoacids of phosphorus and their salts (pp. 510–31) in which there has been isoelectronic replacement of:



P—O—P by P—NH—P or P—NR—P.

etc.<sup>(148,149)</sup>

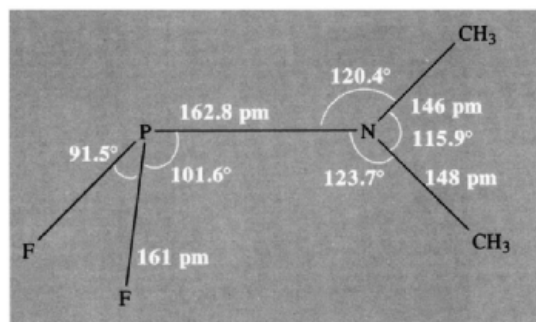
Examples are phosphoramidic acid,  $\text{H}_2\text{NP}(\text{O})\text{-(OH)}_2$ ; phosphordiamidic acid,  $(\text{H}_2\text{N})_2\text{P}(\text{O})(\text{OH})$ ; phosphoric triamide,  $(\text{H}_2\text{N})_3\text{PO}$ ; and their derivatives. There are an enormous number of compounds featuring the 4-coordinate group shown in structure (1) including the versatile nonaqueous solvent hexamethylphosphoramide  $(\text{Me}_2\text{N})_3\text{PO}$ ; this is readily made by reacting  $\text{POCl}_3$  with  $6\text{Me}_2\text{NH}$ , and dissolves metallic Na to give paramagnetic blue solutions similar to those in liquid  $\text{NH}_3$  (p. 77).



Another series includes the *cyclo*-metaphosphimic acids, which are tautomers of the *cyclo*-polyphosphazene hydroxides (p. 541). Similarly, halogen atoms in  $\text{PX}_3$  or other P—X compounds can be successively replaced by the isoelectronic groups  $-\text{NH}_2$ ,  $-\text{NHR}$ ,  $-\text{NR}_2$ , etc., and sometimes a pair of halogens can be replaced by  $=\text{NH}$  or  $=\text{NR}$ . These, in turn, can be used to prepare a large number of other derivatives as indicated schematically opposite for  $\text{P}(\text{NMe}_2)_3$ <sup>(2)</sup>.

Although such compounds all formally contain P—N single bonds, they frequently display properties consistent with more extensive bonding. A particularly clear example is  $\text{PF}_2(\text{NMe}_2)$

which features a short interatomic P—N distance and a *planar* N atom as indicated in the diagram below. (In the absence of this additional  $\pi$  bonding the P<sup>III</sup>—N single-bond distance is close to 177 pm.) Again, the proton nmr of such compounds sometimes reveals restricted rotation about P—N at low temperatures and typical energy barriers to rotation (and coalescence temperatures of the non-equivalent methyl proton signals) are  $\text{PCl}_2(\text{NMe}_2)$  35 kJ mol<sup>-1</sup> (−120°),  $\text{P}(\text{CF}_3)_2(\text{NMe}_2)$  38 kJ mol<sup>-1</sup> (−120°),  $\text{PClPh}(\text{NMe}_2)$  50 kJ mol<sup>-1</sup> (−50°).



Other unusual P/N systems which have recently been investigated include the crystalline compound  $\text{HPN}_2$ , i.e.  $\text{PN}(\text{NH})$ , which is formed by ammonolysis of  $\text{P}_3\text{N}_5$  at 580°C and which has a  $\beta$ -cristobalite ( $\text{SiO}_2$ ) type structure;<sup>(150)</sup>  $\text{PNO}$  (cf.  $\text{N}_2\text{O}$ ), which can be studied as a matrix-isolated species;<sup>(151)</sup> various phosphine azides,  $\text{RR}'\text{PN}_3$ , and their reactions;<sup>(152)</sup> and numerous substituted phosphonyl triphenylphosphazenes,  $\text{Ph}_3\text{P}=\text{N}-\text{PX}_2$ , ( $\text{X}=\text{Cl}$ ,  $\text{F}$ ,  $\text{OPh}$ ,  $\text{SEt}$ ,  $\text{NEt}_2$ , etc.).<sup>(153)</sup> The iminophosphonium ion,  $[\text{ArN}=\text{P}]^+$  ( $\text{Ar} = 2,4,6\text{-Bu}_3\text{C}_6\text{H}_2$ ) has been obtained as its pale yellow  $\text{AlCl}_4^-$  salt by reaction of the corresponding covalently bonded chloride,  $\text{ArN}=\text{PCl}$ , with  $\text{AlCl}_3$ ; the ion is notable

<sup>150</sup> W. SCHNICK and J. LÜCKE, *Z. anorg. allg. Chem.* **610**, 121–6 (1992).

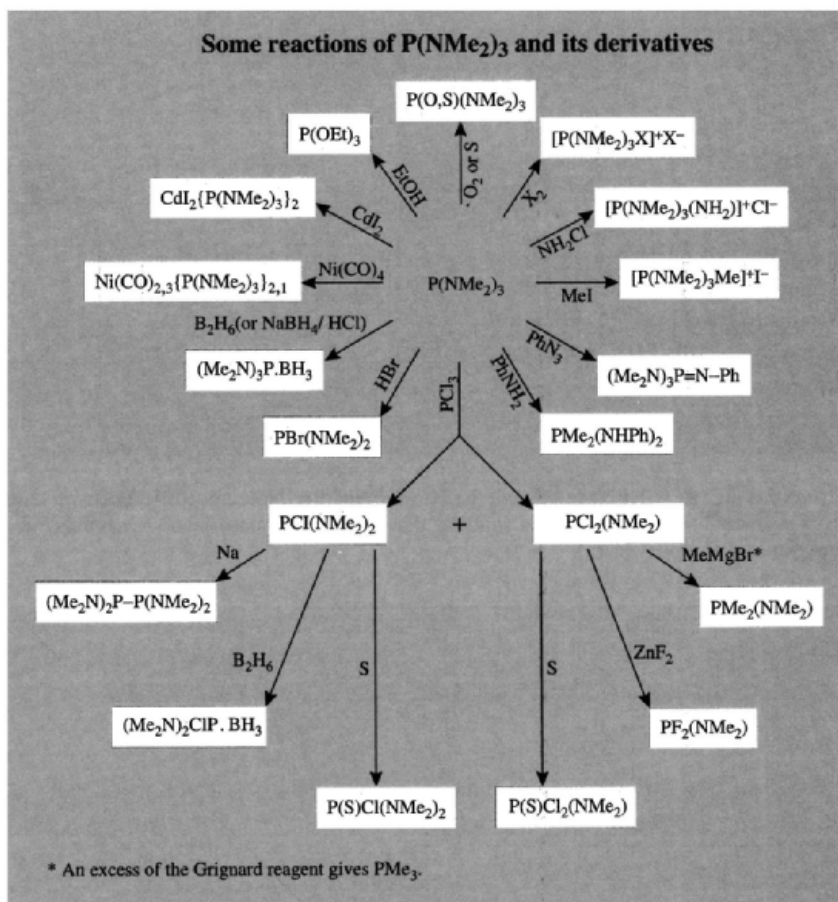
<sup>151</sup> R. AHLRICH, S. SCHUNK and H.-G. SCHNOCKEL, *Angew. Chem. Int. Edn. Engl.* **27**, 421–2 (1988).

<sup>152</sup> J. BOSKE, E. NIECKE, E. OCANDO-MAVEREZ, J.-P. MAJORAL and G. BERTAND, *Inorg. Chem.* **25**, 2695–8 (1986).

<sup>153</sup> L. RIESEL and R. FRIEBE, *Z. anorg. allg. Chem.* **604**, 85–91 (1991).

<sup>148</sup> D. A. PALGRAVE, Section 28, pp. 760–815, in ref. 26

<sup>149</sup> M. L. NIELSEN, Chap. 5 in C. B. COLBURN (ed.), *Developments in Inorganic Nitrogen Chemistry*, Vol. 1, pp. 307–469, Elsevier, Amsterdam, 1966.



as the first stable species having a  $P\equiv N$  triple bond ( $P-N$  148 pm, angle  $C-N-P$  177°).<sup>(154)</sup> The coordination chemistry of phosphorane iminato complexes (containing the  $R_3PN^-$  ligand) of transition metals has been reviewed.<sup>(155)</sup>

### Cyclophosphazanes

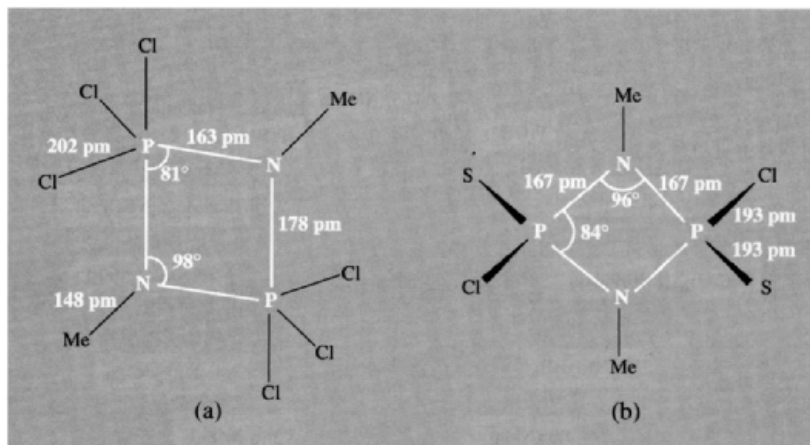
Many heterocyclic compounds contain formally single-bonded  $P-N$  groups, the simplest being the *cyclo*-diphosphazanes  $(X_3PNR)_2$  and  $\{X(O,S)PNR\}_2$ . These contain  $P^V$  and have the structures shown in Fig. 12.22. A few

phosph(III)azane dimers are also known, e.g.  $(RPNR')_2$ . A more complex example, containing fused heterocycles of alternating  $P^{III}$  and  $N$  atoms, is the interesting hexamethyl derivative  $P_4(NMe)_6$  mp 122°. This stable compound (Fig. 12.23a) is readily obtained by reacting  $PCl_3$  with  $6MeNH_2$ ; it is isoelectronic with and isostructural with  $P_4O_6$  (p. 504) and undergoes many similar reactions. The stoichiometrically similar compound  $P_4(NPr^t)_6$  can be prepared in the non-adamantane-type structure shown in Fig. 12.23b, though it converts to structure-type a on being heated at 157° for 12 days.<sup>(156)</sup> A different sequence of atoms occurs in  $P_2(NMe)_6$

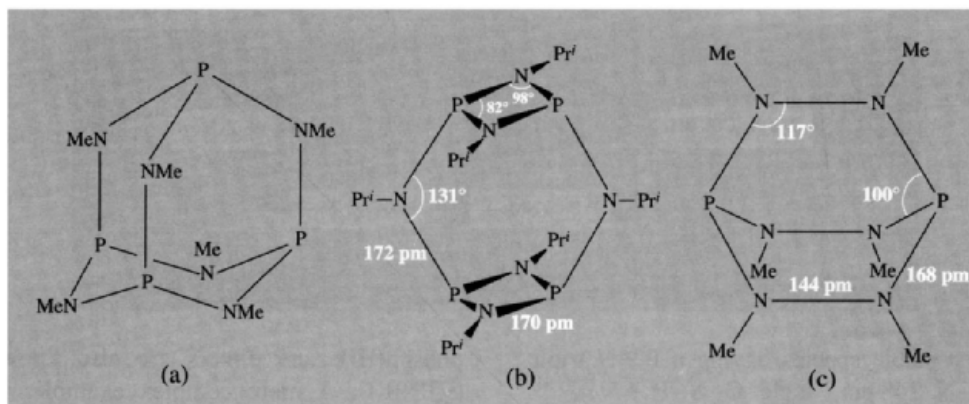
<sup>154</sup> E. NIECKF, M. NIEGER and F. REICHERT *Angew. Chem. Int. Edn. Engl.* **27**, 1715–6 (1988).

<sup>155</sup> K. DEHNICKE and J. STRÄHLE, *Polyhedron* **8**, 707–26 (1989).

<sup>156</sup> O. J. SCHERER, K. ANDRES, C. KRÜGER, Y.-H. TSAY and G. WOLMERSHÄUSER, *Angew. Chem. Int. Edn. Engl.* **19**, 571–2 (1980).

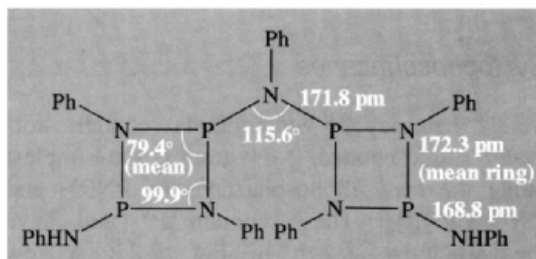


**Figure 12.22** Structures of (a)  $(\text{Cl}_3\text{PNMe})_2$ , and (b)  $[\text{Cl}(\text{S})\text{PNMe}]_2$ . Note the difference in length of the axial P-N and equatorial P-N bonds (and of the axial and equatorial P-Cl bonds) about the trigonal bipyramidal P atoms in (a).



**Figure 12.23** Structures of (a)  $\text{P}_4(\text{NMe})_6$ , (b)  $\text{P}_4(\text{NPr}^i)_6$ , and (c)  $\text{P}_2(\text{NMe})_6$  (see text).

(Fig. 12.23c) and many other “saturated” heterocycles featuring either  $\text{P}^{\text{III}}$  or  $\text{P}^{\text{V}}$  have been made. A typical example, made by slow addition of  $\text{PCl}_3$  to  $\text{PhNH}_2$  in toluene at  $0^\circ$ , is  $[\text{PhNHP}_2(\text{NPh})_2]_2\text{NPh}$ ; the crystal structure of the 1:1 solvate of this compound with  $\text{CH}_2\text{Cl}_2$  (mp  $250^\circ$ ) reveals that all N atoms are essentially planar with distances to P as indicated in the following diagram.<sup>(157)</sup>

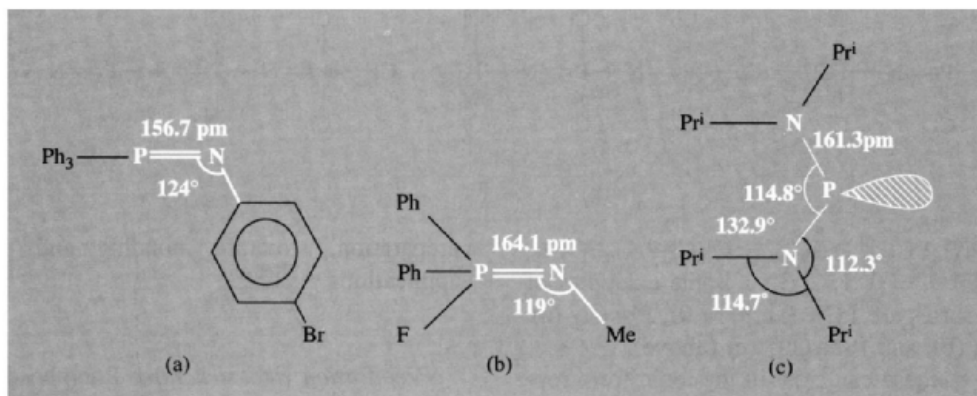


### Phosphazenes

Formally “unsaturated” PN compounds are called phosphazenes and contain  $\text{P}^{\text{V}}$  in the

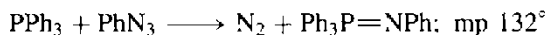
<sup>157</sup> M. L. THOMPSON, R. C. HALTIWANGER, and A. D. NORMAN, *J. Chem. Soc., Chem. Commun.*, 647-8 (1979).



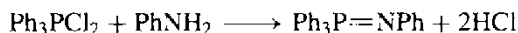


grouping  $\text{>P}=\text{N}-$ . A few phosph(III)azenes are also known. Phosphazenes can be classified into monophosphazenes (e.g.  $\text{X}_3\text{P}=\text{NR}$ ), diphosphazenes (e.g.  $\text{X}_3\text{P}=\text{N}-\text{P}(\text{O})\text{X}_2$ ), polyphosphazenes containing 2,3,4,...  $\infty$  -  $\text{X}_2\text{P}=\text{N}-$  units, and the *cyclo*-polyphosphazenes  $[-\text{X}_2\text{P}=\text{N}-]_n$ ,  $n = 3,4,5 \dots 17$ .

Monophosphazenes, particularly those with organic substituents,  $\text{R}_3\text{P}=\text{NR}'$ , derive great interest from being the N analogues of phosphorus ylides  $\text{R}_3\text{P}=\text{CR}_2$  (p. 545). They were first made by H. Staudinger in 1919 by reacting an organic azide such as  $\text{PhN}_3$  with  $\text{PR}_3$  ( $\text{R}=\text{Cl}, \text{OR}, \text{NR}_2, \text{Ar}, \text{etc.}$ ), e.g.:

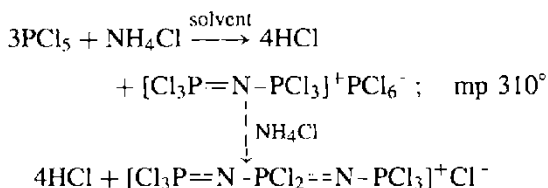


More recently they have been made via a reaction associated with the name of A. V. Kirsanov (1962), e.g.:



As expected, the P–N distance is short and the angle at N is  $\sim 120^\circ$ , e.g. (a) and (b) above. Over 600 such compounds are now known, especially those with the  $\text{Cl}_3\text{P}=\text{N}-$  group.<sup>(158)</sup>

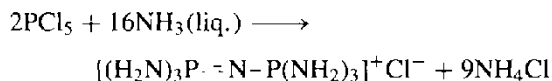
Diphosphazenes can be made by reacting  $\text{PCl}_5$  with  $\text{NH}_4\text{Cl}$  in a chlorohydrocarbon solvent under mild conditions:



The inverse of these compounds are the phosphadiazene cations, prepared by halide ion abstraction from diaminohalophosphoranes in  $\text{CH}_2\text{Cl}_2$  or  $\text{SO}_2$  solution, e.g.:



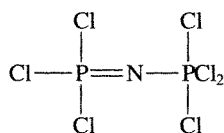
An X-ray crystal structure of the  $\text{Pr}^i_2\text{N}$ -derivative shows the presence of a bent, 2-coordinate P atom, equal P–N distances, and accurately planar 3-coordinate N atoms as in (c) above.<sup>(159)</sup> In liquid ammonia ammonolysis also occurs:



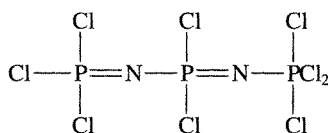
The P–N and P–N bonds are equivalent in these compounds and they could perhaps better be written as  $[\text{X}_3\text{P}=\text{N}=\text{N}=\text{PX}_3]^+$ , etc. Like the parent phosphorus pentahalides (p. 498), these diphosphazenes can often exist in ionic and covalent forms and they are part of a more extended group of compounds which can be classified into several general series  $\text{Cl}(\text{Cl}_2\text{PN})_n\text{PCl}_4$ ,  $[\text{Cl}(\text{Cl}_2\text{PN})_n\text{PCl}_3]^+\text{Cl}^-$ ,

<sup>158</sup> M. BERMAN, *Topics in Phosphorus Chemistry* 7, 311–78, 1972.

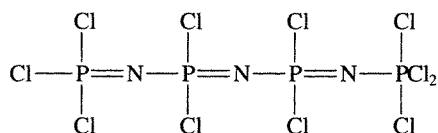
<sup>159</sup> A. H. COWLEY, M. C. CASHNER and J. S. SZOBOTA, *J. Am. Chem. Soc.* 100, 7784–6 (1978).



(a)



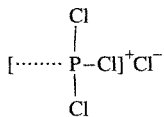
(b)



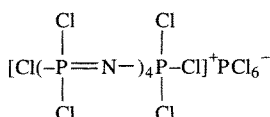
(c)

$[\text{Cl}(\text{Cl}_2\text{PN})_n\text{PCl}_3]^+\text{PCl}_6^-$ ,  $\text{Cl}(\text{Cl}_2\text{PN})_n\text{POCl}_2$ , etc., where  $n = 0, 1, 2, 3, \dots$ . Some examples of the first series are  $\text{PCl}_5$  (i.e.  $n = 0$ ),  $\text{P}_2\text{NCl}_7$  (a),  $\text{P}_3\text{N}_2\text{Cl}_9$  (b), and  $\text{P}_4\text{N}_3\text{Cl}_{11}$  (c) (above).

Some of these can exist in the ionic form represented by the second series (d):



(d)

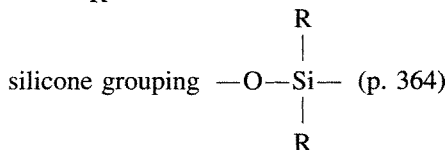
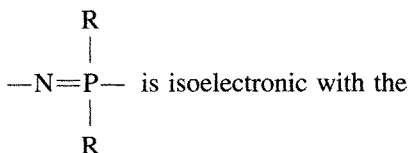


(e)

Likewise, the third series runs from  $n = 0$  (i.e.  $\text{PCl}_4^+\text{PCl}_6^-$ ) through  $\text{P}_3\text{NCl}_{12}$ ,  $\text{P}_4\text{N}_2\text{Cl}_{14}$ , and  $\text{P}_5\text{N}_3\text{Cl}_{16}$  to  $\text{P}_6\text{N}_4\text{Cl}_{18}$  (e). In the limit, polymeric phosphazene dichlorides are formed  $(-\text{NPCl}_2-)_n$ , where  $n$  can exceed  $10^4$  and these polyphosphazenes and their *cyclo*-analogues form by far the most extensive range PN compounds.

### Polyphosphazenes

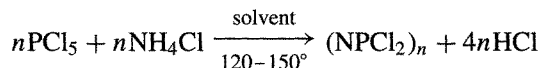
The grouping



and, after the silicones, the polyphosphazenes form the most extensive series of covalently bonded polymers with a non-carbon skeleton. This section will describe their

preparation, structure, bonding and potential applications.<sup>(2,8,160,161)</sup>

*Preparation and structure.* Polyphosphazenes have a venerable history.  $(\text{NPCl}_2)_n$  oligomers were first made in 1834 by J. von Liebig and F. Wöhler who reacted  $\text{PCl}_5$  with  $\text{NH}_3$ , but their stoichiometry and structure were not elucidated until much later. The fluoro analogues  $(\text{NPF}_2)_n$  were first made in 1956 and the bromo compounds  $(\text{NPBr}_2)_n$  in 1960. The synthesis of  $(\text{NPCl}_2)_n$  was much improved by R. Schenk and G. Römer in 1924 and their method remains the basis for present-day production on both the laboratory and industrial scales:



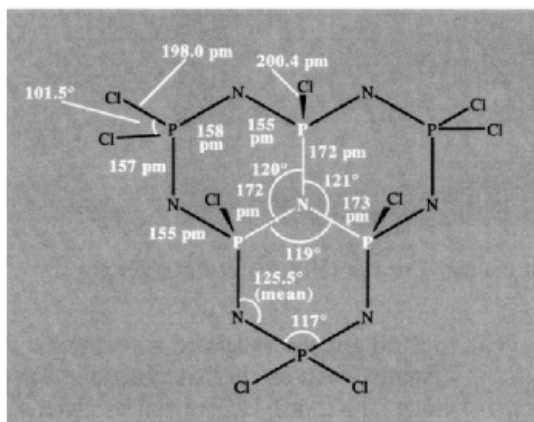
Appropriate solvents are 1,1,2,2-tetrachloroethane (bp  $146^\circ$ ),  $\text{PhCl}$  (bp  $132^\circ$ ) and 1,2-dichlorobenzene (bp  $179^\circ$ ). By varying the conditions, yields of the cyclic trimer or tetramer and other oligomers can be optimized and the compounds then separated by fractionation. Highly polymeric  $(\text{NPCl}_2)_\infty$  can be made by heating *cyclo*- $(\text{NPCl}_2)_3$  to  $150-300^\circ$ , though heating to  $350^\circ$  induces depolymerization. Polycyclic compounds are rarely obtained in

<sup>160</sup> H. R. ALLCOCK, *Phosphorus Nitrogen Compounds*, Academic Press, New York, 1972, 498 pp.; H. R. ALLCOCK, *Chem. Rev.* **72**, 315-56 (1972) (475 refs.). H. R. ALLCOCK, Chap. 3 in A. H. COWLEY (ed.) *Rings, Clusters and Polymers of the Main Group Elements*, ACS Symposium Series No. **282**, Washington, DC, 49-67 (1982). H. R. ALLCOCK in J. E. MARK, R. WEST and H. R. ALLCOCK, *Inorganic Polymers*, Prentice Hall, 1991, 304 pp. H. R. ALLCOCK, Chap. 9 in R. STEUDEL (ed.) *The Chemistry of Inorganic Ring Systems*, Elsevier, Amsterdam, 145-69 (1992).

<sup>161</sup> S. S. KRISNAMURTHY, A. C. SAU and M. WOODS, *Adv. Inorg. Chem. Radiochem.* **21**, 41-112 (1978) (499 refs.).



these preparations, one exception being  $N_7P_6Cl_9$ , mp  $237.5^\circ$ , which can be obtained in modest yields from the direct thermolytic reaction of  $PCl_5$  and  $NH_4Cl$ . The tricyclic structure is strongly distorted from planarity though the central  $NP_3$  group features an accurately planar 3-coordinate N atom with much longer N–P bonds than those in the peripheral macrocycle. The 2 sorts of P–Cl bonds are also noticeably different in length and the 3 central Cl atoms are all on one side of the  $NP_3$  plane with  $\angle NPCl$   $104^\circ$ .

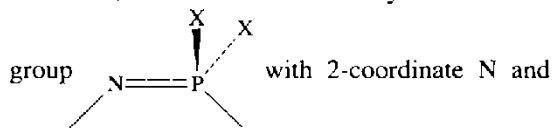


Many details of the preparative reaction mechanism remain unclear but it is thought that  $NH_4Cl$  partly dissociates into  $NH_3$  and  $HCl$ , and that  $PCl_5$  reacts in its ionic form  $PCl_4^+PCl_6^-$  (p. 499). Nucleophilic attack by  $NH_3$  on  $PCl_4^+$  then occurs with elimination of  $HCl$  and the  $\{HN=P-Cl_3\}$  attacks a second  $PCl_4^+$  to give  $[Cl_3P=N-PCl_3]^+$  and  $HCl$ . After 1 h the major (insoluble) intermediate product is  $[Cl_3P=N-PCl_3]^+PCl_6^-$  (i.e.  $P_3NCl_{12}$ , p. 536) and this then slowly reacts with more  $NH_3$  to give  $HCl$  and  $\{Cl_3P=N-PCl_2=NH\}$ , etc. It is probable that  $NH_4Br$  and  $PBr_4^+Br^-$  react similarly to give  $(NPBr_2)_n$  but  $NH_4F$  fluorinates  $PCl_5$  to  $NH_4PF_4$  and the fluoroanalogues  $(NPF_2)_n$  are best prepared by fluorinating  $(NPCl_2)_n$  with  $KSO_2F/SO_2$  (i.e.  $KF$  in liquid  $SO_2$ ). Similarly, standard substitution reactions lead to many derivatives in which all (or some) of the Cl atoms are replaced by  $OMe$ ,  $OEt$ ,  $OCH_2CF_3$ ,  $Oph$ ,  $NHPh$ ,  $NMe_2$ ,  $NR_2$ ,  $R$ ,  $Ar$ , etc. Partial

replacement leads to geminal derivatives (in which both Cl atoms on 1 P atom are replaced) and to non-geminal derivatives which, in turn, can exist as *cis*- or *trans*- isomers.

The cyclic trimer  $(NPF_2)_3$ , mp  $28^\circ$ , has an accurately planar 6-membered ring ( $D_{3h}$  symmetry) in which all 6 P–N distances are equal (156 pm) and the angles NPN and PNP are all  $120 \pm 1^\circ$ . Most other trimers are also more-or-less planar with equal P–N distances: for example,  $(NPCl_2)_3$  is almost planar (pseudo-chair with P–N 158 pm, P–Cl 197 pm,  $\angle NPN$   $118.4^\circ$ ,  $\angle PNP$   $121.4^\circ$ ,  $\angle ClPCl$   $102^\circ$ ). Perhaps surprisingly, the cyclic tetramer  $(NPF_2)_4$ , mp  $30.4^\circ$ , is also a planar heterocycle ( $D_{4h}$  symmetry) with even shorter P–N bonds (151 pm) and with ring angles of  $122.7^\circ$  and  $147.4^\circ$  at P and N respectively. However, other conformations are found in other derivatives, e.g. chair ( $C_{2h}$ ), saddle ( $D_{2d}$ ), boat ( $S_4$ ), crown tetrameric ( $C_{4v}$ ) and hybrid. Thus  $(NPCl_2)_4$  exists in the metastable **K** form (in which it has the boat conformation) and the stable **T** form (chair configuration) as shown in Fig. 12.24. The remarkable diversity of molecular conformations observed for the 8-membered heterocycle  $\{P_4N_4\}$  suggests that the particular structure adopted in each case results from a delicate balance of intra- and intermolecular forces including the details of skeletal bonding, the orientation of substituents and their polar and steric nature, crystal-packing effects, etc. The mps for various series of *cyclo*-( $NPX_2$ ) $_n$  frequently show an alternation, with values for  $n$  even being greater than those for adjacent  $n$  odd. Some examples are in Fig. 12.25. The crystal structures of the four compounds  $(NPMe_2)_{9-12}$  have recently been determined.<sup>(162)</sup>

**Bonding.** All phosphazenes, whether cyclic or chain, contain the formally unsaturated



<sup>162</sup> R. T. OAKLEY, S. J. RETTIG, N. L. PADDOCK and J. TROTTER, *J. Am. Chem. Soc.* **107**, 6923–36 (1985).

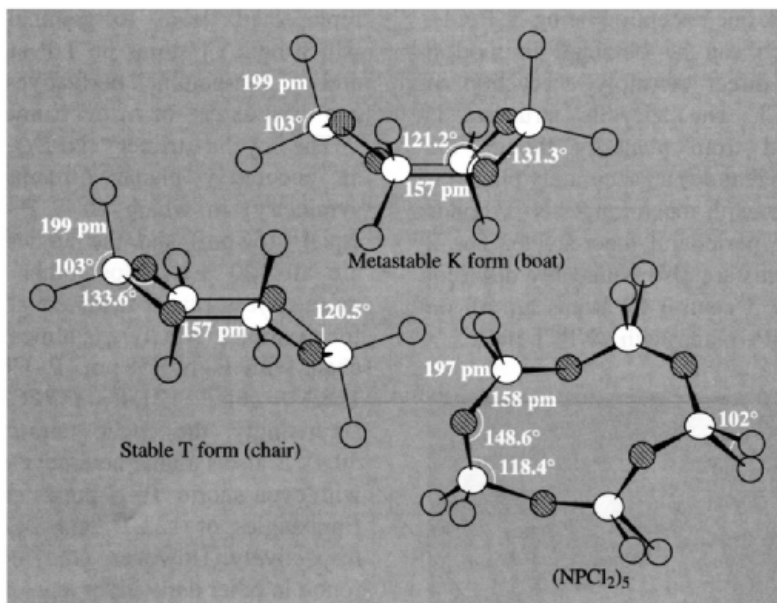


Figure 12.24 Molecular structure and dimensions of the two forms of  $(\text{NPCl}_2)_4$  and of  $(\text{NPCl}_2)_5$ .

4-coordinate P. The experimental facts that have to be interpreted by any acceptable theory of bonding are:

- (i) the rings and chains are very stable;
- (ii) the skeletal interatomic distances are equal around the ring (or along the chain) unless there is differing substitution at the various P atoms;
- (iii) the P-N distances are shorter than expected for a covalent single bond ( $\sim 177$  pm) and are usually in the range  $158 \pm 2$  pm (though bonds as short as 147 pm occur in some compounds);
- (iv) the N-P-N angles are usually in the range  $120 \pm 2^\circ$  but the P-N-P angles in various compounds span the range from 120- 148.6°;
- (v) skeletal N atoms are weakly basic and can be protonated or form coordination complexes, especially when there are electron-releasing groups on P;
- (vi) unlike many aromatic systems the phosphazene skeleton is hard to reduce electrochemically;
- (vii) spectral effects associated with organic  $\pi$ -systems (such as the bathochromic ultra-violet shift that accompanies increased electron delocalization) are not found.

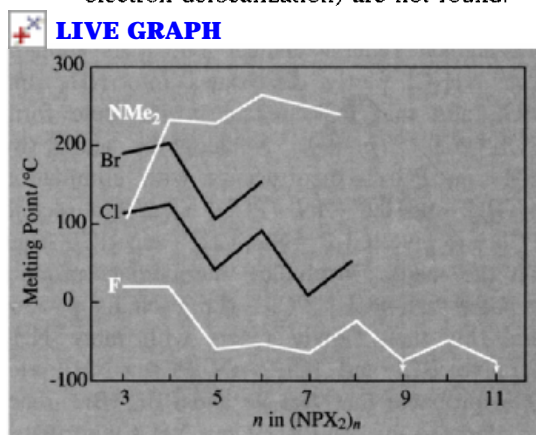
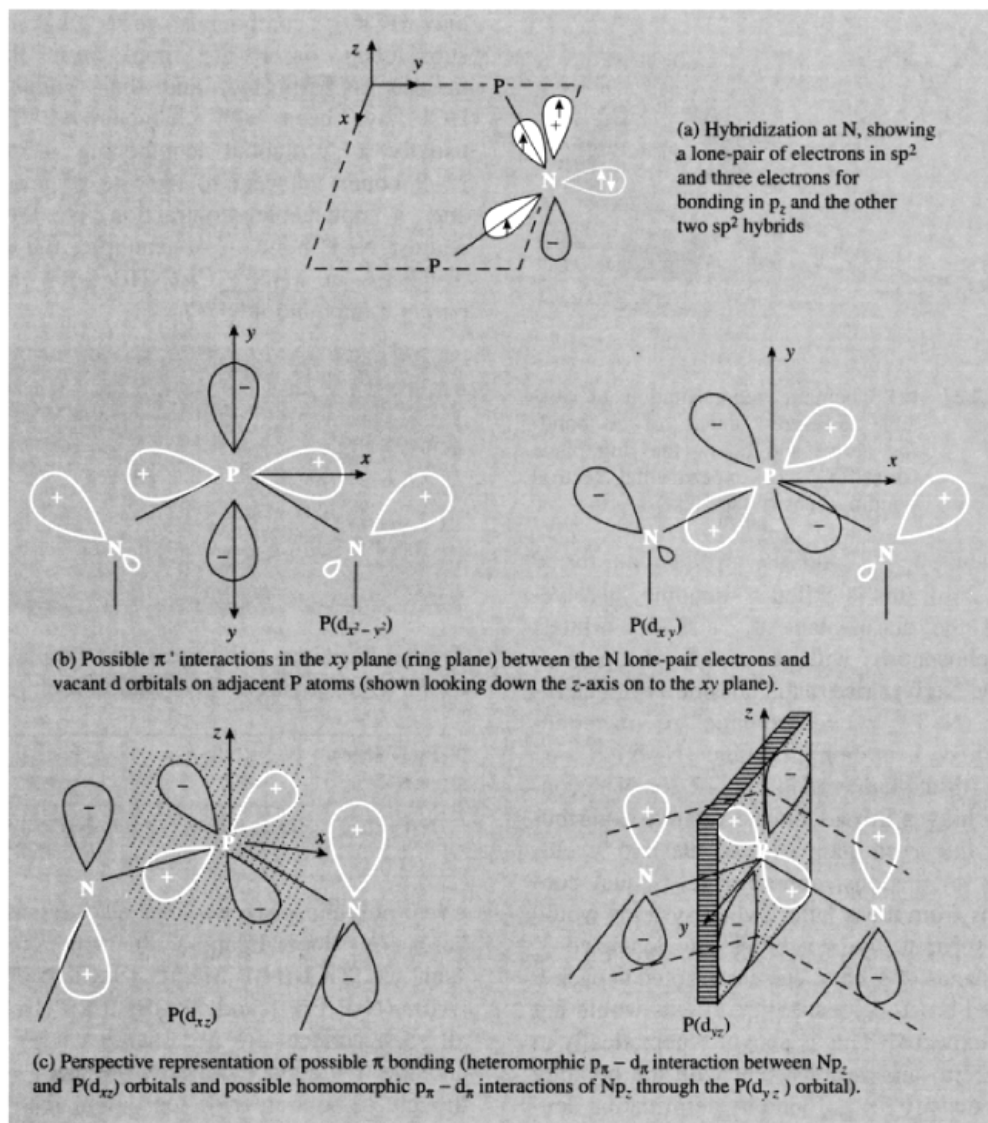


Figure 12.25 Melting points of various series of *cyclo*-polyphosphazenes  $(\text{NPX}_2)_n$  showing the higher values for  $n$  even.

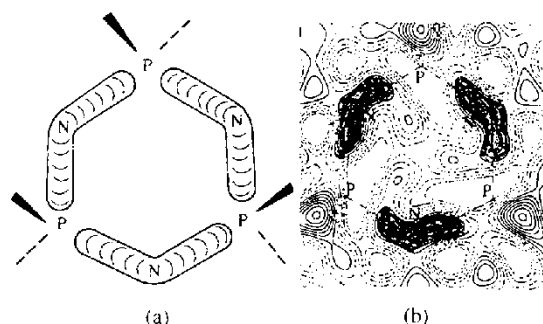
In short, the bonding in phosphazenes is not adequately represented by a sequence of alternating double and single bonds  $-\text{N}=\text{P}-\text{N}=\text{P}-$  yet it



**Figure 12.26** A possible description of bonding in phosphazenes.

differs from aromatic  $\sigma-\pi$  system in which there is extensive electron delocalization via  $p_\pi-p_\pi$  bonding. The possibility of  $p_\pi-d_\pi$  bonding in N–P systems has been considered by many authors since the mid-1950s but there is still no consensus, and for nearly every argument that can be mounted in favour of P(3d)-orbital contributions another can be raised against it. It seems generally agreed that 2 electrons on

N occupy an  $sp^2$  lone-pair in the plane of the ring (or the plane of the local PNP triangle) as in Fig. 12.26a. The situation at P is less clear mainly because of uncertainties concerning the d-orbital energies and the radial extent (size) of these orbitals in the *bonding situation* (as distinct from the free atom). In so far as symmetry is concerned, the  $sp^2$  lone-pair on each N can be involved in coordinate bonding in the  $xy$  plane

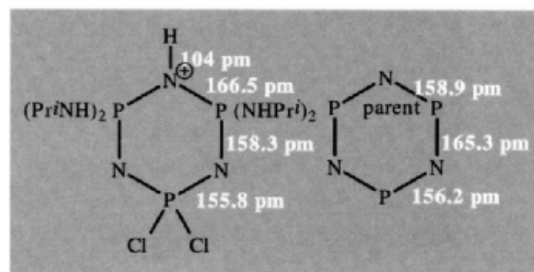


**Figure 12.27** (a) Schematic representation of possible 3-centre islands of  $\pi$  bonding above and below the ring plane for  $(NPX_2)_3$ . (b) experimental electron bonding density (see text).

to "vacant"  $d_{x^2-y^2}$  and  $d_{xy}$  orbitals on the P (Fig. 12.26b); this is called  $\pi'$ -bonding. Involvement of the out-of-plane  $d_{xz}$  and  $d_{yz}$  orbitals on the phosphorus with the singly occupied  $p_z$  orbital on N gives rise to the possibility of heteromorphic (N-P) "pseudoaromatic"  $p_\pi-d_\pi$  bonding (with  $d_{xz}$ ), or homomorphic (N-N)  $p_\pi-p_\pi$  bonding (through  $d_{yz}$ ) as in Fig. 12.26c. The controversy hinges in part on the relative contributions of the  $\pi'$  in-plane and of the two  $\pi$  out-of-plane interactions; approximately equal contributions from these latter two  $\pi$  systems would tend to separate the  $\pi$  orbitals into localized 3-centre islands of  $\pi$  character interrupted at each P atom, and broad delocalization effects would not then be expected. This is shown schematically in Fig. 12.27(a) and is consistent with the bonding electron density (b) as found by deformation density studies on the benzene clathrate of hexa(1-aziridinyl)cyclotriphosphazene,  $2(\text{CH}_2\text{CH}_2\text{N})_6\text{-P}_3\text{N}_3\cdot\text{C}_6\text{H}_6$ .<sup>(163)</sup> The possibility of exocyclic  $\pi$  bonding between P( $d_{z^2}$ ) and appropriate orbitals on the substituents X has also been envisaged.

**Reactions.** The N atom in *cyclo*-polyphosphazenes can act as a weak Brønsted base (proton acceptor) towards such strong acids as HF

and  $\text{HClO}_4$ ; compounds with alkyl or  $\text{NR}_2$  substituents on P are more basic than the halides, as expected, and their adducts with HCl have been well characterized. There is usually a substantial lengthening of the two N-P bonds adjacent to the site of protonation and a noticeable contraction of the next-nearest N-P bonds. For example, the relevant distances in  $[\text{HN}_3\text{P}_3\text{Cl}_2(\text{NHP}^i)_4]\text{Cl}$  and the parent compound are:<sup>(164)</sup>



Typical basicities ( $\text{p}K'_a$  measured against  $\text{HClO}_4$  in  $\text{PhNO}_2$ ) for ring-N protonation are:

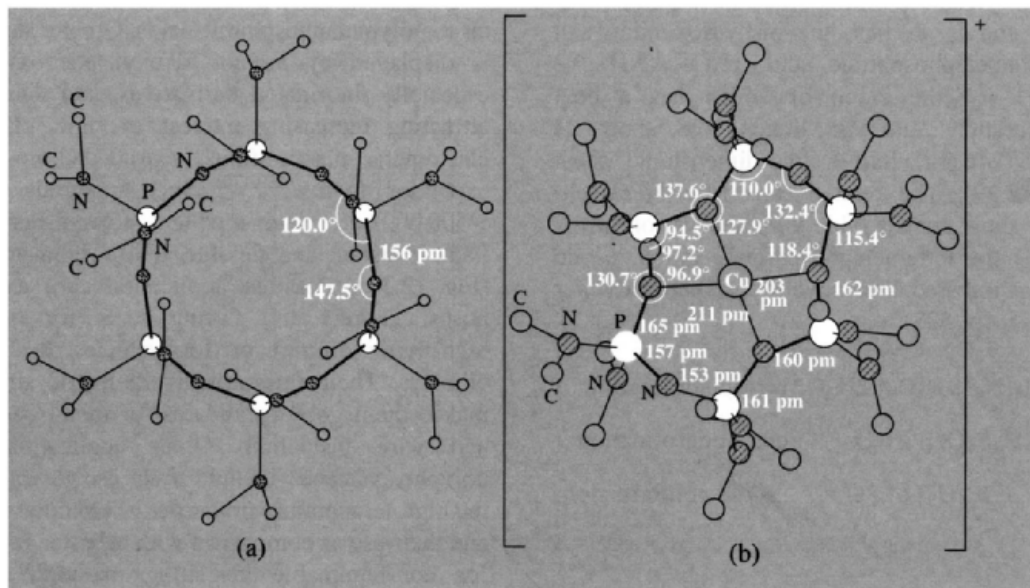
$\text{N}_3\text{P}_3(\text{NHMe})_6$	$\text{N}_3\text{P}_3(\text{NEt}_2)_6$	$\text{N}_3\text{P}_3\text{Et}_6$
8.2	8.2	6.4
$\text{N}_3\text{P}_3\text{Ph}_6$	$\text{N}_3\text{P}_3(\text{OEt})_6$	<i>trans</i> - $\text{N}_3\text{P}_3\text{Cl}_3(\text{NMe}_2)_3$
1.5	-0.2	-5.4

*Cyclo*-polyphosphazenes can also act as Lewis bases (N donor-ligands) to form complexes such as  $[\text{TiCl}_4(\text{N}_3\text{P}_3\text{Me}_6)]$ ,  $[\text{SnCl}_4(\text{N}_3\text{P}_3\text{Me}_6)]$ ,  $[\text{AlBr}_3(\text{N}_3\text{P}_3\text{Br}_6)]$  and  $[2\text{AlBr}_3\cdot(\text{N}_3\text{P}_3\text{Br}_6)]$ . Not all such adducts are necessarily ring-N donors and the 1:1 adduct of  $(\text{NPCl}_2)_3$  with  $\text{AlCl}_3$  is thought to be a chloride ion donor,  $[\text{N}_3\text{P}_3\text{Cl}_5]^+[\text{AlCl}_4]^-$ . By contrast, the complex  $[\text{Pt}^{\text{II}}\text{Cl}_2(\eta^2\text{-N}_4\text{P}_4\text{Me}_8)]\cdot\text{MeCN}$  features transannular bridging of 2 N atoms by the  $\text{PtCl}_2$  moiety.<sup>(165)</sup> An intriguing example of a *cyclo*-polyphosphazene acting as a multidentate macrocyclic ligand occurs in the bright orange complex formed when  $\text{N}_6\text{P}_6(\text{NMe}_2)_{12}$  reacts with equal amounts of  $\text{CuCl}_2$  and  $\text{CuCl}$ . The crystal structure of

<sup>164</sup> N. V. MANI and A. J. WAGNER, *Acta Cryst.* **27B**, 51-8 (1971).

<sup>165</sup> J. P. O'BRIEN, R. W. ALLEN and H. R. ALLCOCK, *Inorg. Chem.* **18**, 2230-5 (1979).

<sup>163</sup> T. S. CAMERON and B. BORECKA, *Phosphorus, Sulfur, Silicon and Related Elements*, **64**, 121-8 (1992).



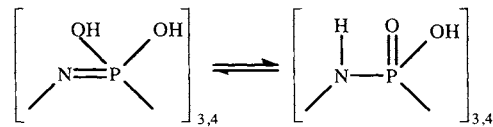
**Figure 12.28** Structure of (a) the free ligand  $N_6P_6(NMe_2)_{12}$ , and (b) the  $\eta^4$  complex cation  $[CuCl\{N_6P_6(NMe_2)_{12}\}]^+$  showing changes in conformation and interatomic distances in the phosphazene macrocycle. The Cl is obscured beneath the Cu and can be regarded as occupying either the apical position of a square pyramid or, since  $\angle N(1)-Cu-N(1')$  is large ( $160.9^\circ$ ), an equatorial position of a distorted trigonal bipyramid. Note that coordination tightens the ring, already somewhat crowded in the uncomplexed state, the mean angles at P being reduced from  $120.0^\circ$  to  $107.5^\circ$ , and the mean angles at N being reduced from  $147.5^\circ$  to  $133.6^\circ$ . The lengthening of the 8 P–N bonds contiguous to the 4 donor N atoms from 156 to 162 pm is significant, the other P–N distances (mean 156 pm) remaining similar to those in the free ligand.

the resulting  $[N_6P_6(NMe_2)_{12}CuCl]^+[CuCl_2]^-$  has been determined (Fig. 12.28b) and detailed comparison with the conformation and interatomic distances in the parent heterocycle (Fig. 12.28a) gives important clues as to the relative importance of the various  $\pi$  and  $\pi'$  bonding interactions involving N (and P) atoms.<sup>(166)</sup> Incidentally, the compound also affords the first example of the linear 2-coordinate  $Cu^I$  complex  $[CuCl_2]^-$ . The related (and more extensive) organometallic chemistry of the phosphazenes has been reviewed.<sup>(167)</sup>

As P is isoelectronic with N, it has been found possible to prepare 8-membered diazahexaphos-

phocins such as  $\overline{NPPh_2PPPPh_2NPPPh_2PPPh_2}$ , analogous to  $(NPPPh_2)_4$ .<sup>(168)</sup> The two subrogated **P** atoms can chelate to  $PdCl_2$  to form a square planar complex.<sup>(169)</sup>

Many of the cyclic and chain dichloro derivatives  $(NPhCl_2)_n$  can be hydrolysed to  $n$ -basic acids and the lower members form well-defined salts frequently in the tautomeric metaphosphimic-acid form, e.g.:



<sup>166</sup> W. C. MARSH, N. L. PADDOCK, C. J. STEWART and J. TROTTER, *J. Chem. Soc., Chem. Commun.*, 1190–1 (1970).

<sup>167</sup> H. R. ALLCOCK, J. L. DESORCIE and G. H. RIDING, *Polyhedron* **6**, 119–57 (1987).

<sup>168</sup> A. SCHMIDPETER and G. BURGET, *Angew. Chem. Int. Edn. Engl.* **24**, 580–1 (1985).

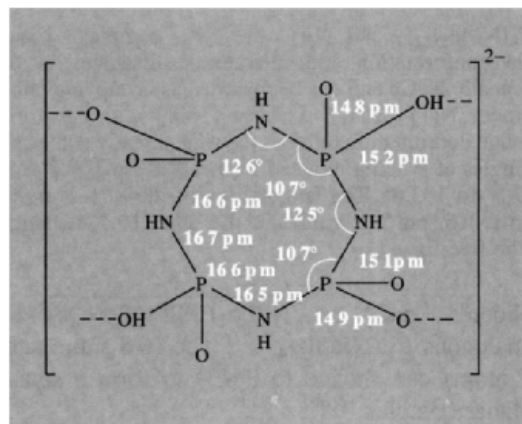
<sup>169</sup> A. SCHMIDPETER, F. STEINMÜLLER and W. S. SHELDRIK, *Z. anorg. allg. Chem.* **579**, 158–72 (1989).

The dihydrate of the tetramer is particularly stable and is, in fact, the bishydroxonium salt of tetrametaphosphimic acid  $[\text{H}_3\text{O}]_2^+[(\text{NH})_4\text{P}_4\text{O}_6(\text{OH})_2]^{2-}$  the anion of which has a boat configuration and is linked by short H bonds (246 pm) into a two-dimensional sheet (Fig. 12.29). The related salts  $\text{M}_4^+[\text{NHPO}_2]_4 \cdot n\text{H}_2\text{O}$  show considerable variation in conformation of the tetrametaphosphimate anion, as do the 8-membered heterocyclic tetraphosphazenes  $(\text{NPX}_2)_4$  (p. 537), e.g.

$[\text{NH}_4]_4[\text{N}_4\text{H}_4\text{P}_4\text{O}_8] \cdot 2\text{H}_2\text{O}$  boat conformation

$\text{K}_4[\text{N}_4\text{H}_4\text{P}_4\text{O}_8] \cdot 4\text{H}_2\text{O}$  chair conformation

$\text{Cs}_4[\text{N}_4\text{H}_4\text{P}_4\text{O}_8] \cdot 6\text{H}_2\text{O}$  saddle conformation.



**Figure 12.29** Schematic representation of the boat-shaped anion  $[(\text{NH})_4\text{P}_4\text{O}_6(\text{OH})_2]^{2-}$  showing important dimensions and the positions of H bonds.

*Applications.* Many applications have been proposed for polyphosphazenes, particularly the non-cyclic polymers of high molecular weight, but those with the most desirable properties are extremely expensive and costs will have to drop considerably before they gain widespread use (cf. silicones, p. 365). The cheapest compounds are the chloro series

$(\text{NPCl}_2)_n$  but these readily hydrolyse in moist air to polymetaphosphimic acids. Greater stability is displayed by amino, alkoxy, phenoxy and especially fluorinated derivatives, and these are attracting increasing interest as rigid plastics, elastomers, plastic films, extruded fibres and expanded foams.<sup>(160,170)</sup> Such materials (MW > 500 000) are water-repellent, solvent-resistant, flame-resistant and flexible at low temperatures (Fig. 12.30). Possible applications are as fuel hoses, gaskets and O-ring seals for use in high-flying aircraft or for vehicles in Arctic climates. Their extraordinary dielectric strength makes them good candidates for metal coatings and wire insulation. Other applications of polyphosphazenes include their use to improve the high-temperature properties of phenolic resins and their use as composites with asbestos or glass for non-flammable insulating material. Some of the more reactive derivatives have been proposed as pesticides and even as ultra-high capacity fertilizers.

### 12.3.8 Organophosphorus compounds

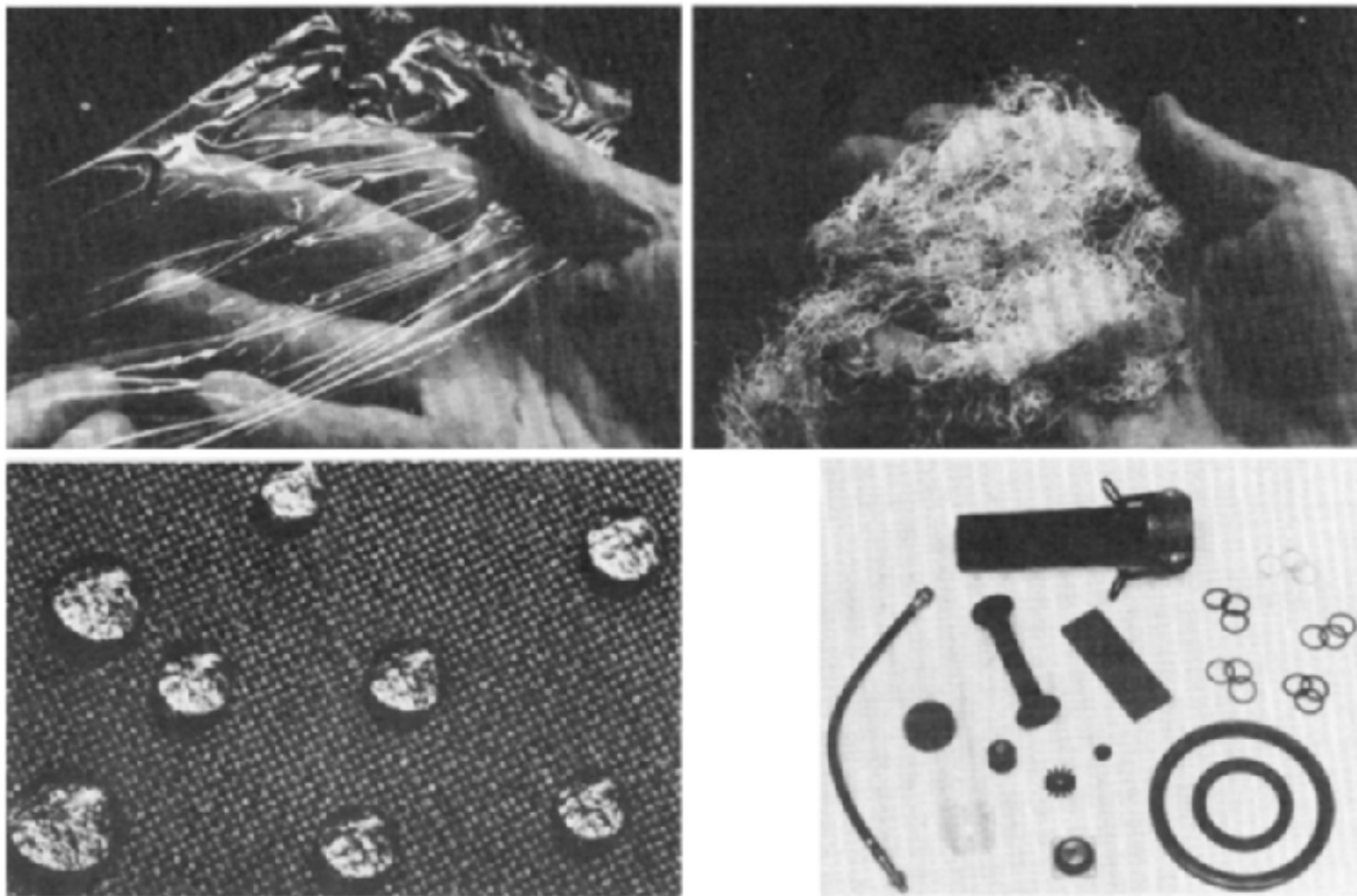
A general treatment of the vast domain of organic compounds of phosphorus<sup>(171)</sup> falls outside the scope of this book though several important classes of compound have already been briefly mentioned, e.g. tertiary phosphine ligands (p. 494), alkoxyphosphines and their derivatives (p. 496), organophosphorus halides (p. 500), phosphate esters in life processes (p. 528) and organic derivatives of PN compounds (preceding section). There are also innumerable organic derivatives of the poly-cyclic polyphosphanes (p. 495),<sup>(67,70,172)</sup> and vast numbers of heterocyclic organophosphorus

<sup>170</sup> H. R. ALLCOCK, *Sci. Progr. Oxf.* **66**, 355–69 (1980).

<sup>171</sup> R. S. EDMONDSON (ed.) *Dictionary of Organophosphorus Compounds*, Chapman and Hall, New York, 1988, 1347 pp.

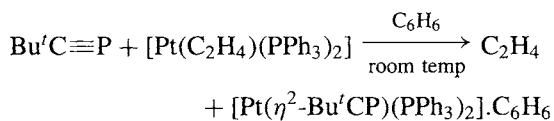
<sup>172</sup> G. FRITZ, H.-G. VON SCHERING *et al.*, *Z. anorg. allg. Chem.* **552**, 34–49 (1987); **584** 21–50, 51–70 (1990); **585**, 51–64 (1990); **595**, 67–94 (1991); and references cited therein.





**Figure 12.30** Potential uses of polyphosphazenes: (a) A thin film of a poly(aminophosphazene); such materials are of interest for biomedical applications. (b) Fibres of poly[bis(trifluoroethoxy)phosphazene]; these fibres are water-repellant, resistant to hydrolysis or strong sunlight, and do not burn. (c) Cotton cloth treated with a poly(fluoroalkoxyphosphazene) showing the water repellancy conferred by the phosphazene. (d) Polyphosphazene elastomers are now being manufactured for use in fuel lines, gaskets, O-rings, shock absorbers, and carburettor components; they are impervious to oils and fuels, do not burn, and remain flexible at very low temperatures. Photographs by courtesy of H. R. Allcock (Pennsylvania State University) and the Firestone Tire and Rubber Company.

compounds.<sup>(173,174)</sup> Within the general realm of organic compounds of phosphorus it is convenient to distinguish organophosphorus compounds as a particular group, i.e. those which contain one or more direct P–C bond. In such compounds the coordination number of P can be 1, 2, 3, 4, 5 or 6 (p. 484). Examples of coordination number 1 were initially restricted to the relatively unstable compounds HCP, FCP and MeCP (cf. HCN, FCN and MeCN).  $\text{HC}\equiv\text{P}$  was first made in 1961 by subjecting  $\text{PH}_3$  gas at 40 mmHg pressure to a low-intensity rotating arc struck between graphite electrodes;<sup>(175)</sup> it is a colourless, reactive gas, stable only below its triple point of  $-124^\circ$  (30 mmHg). Monomeric HCP slowly polymerizes at  $-130^\circ$  (more rapidly at  $-78^\circ$ ) to a black solid, and adds  $2\text{HCl}$  at  $-110^\circ$  to give  $\text{MePCL}_2$  as the sole product. Both monomer and polymer are pyrophoric in air even at room temperature. More recently<sup>(176)</sup> MeCP was made by pyrolysing  $\text{MeCH}_2\text{PCL}_2$  at  $930^\circ$  in a low-pressure flow reactor and trapping the products at  $-78^\circ$ . Dramatic stabilization of a phospho-alkyne has been achieved by  $\eta^2$ -complexation to a metal centre:<sup>(177)</sup>



The translucent, cream-coloured benzene solvate was characterized by single-crystal X-ray analysis and by  $^{31}\text{P}$  nmr spectroscopy. The first free phospho-alkyne stable to polymerization

<sup>173</sup> E. FLUCK and B. NEUMÜLLER, in H. W. ROESKY (ed.), *Rings, Clusters and Polymers of Main Group and Transition Metals*, Elsevier, Amsterdam, 1989, pp. 193–5.

<sup>174</sup> A. SCHMIDPETER and K. KARAGHIOSSOFF, in H. W. ROESKY (ed.), *Rings, Clusters and Polymers of Main Group and Transition Metals*, Elsevier, Amsterdam, 1989, pp. 307–43.

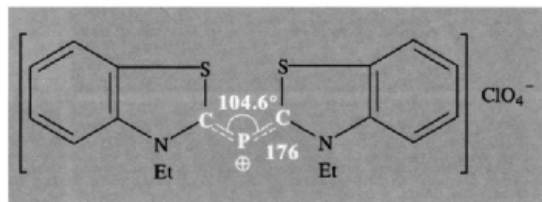
<sup>175</sup> T. E. GIER, *J. Am. Chem. Soc.* **83**, 1769–70 (1961).

<sup>176</sup> N. P. C. WESTWOOD, H. W. KROTO, J. F. NIXON and N. P. C. SIMMONS, *J. Chem. Soc., Dalton Trans.*, 1405–8 (1979).

<sup>177</sup> J. C. T. R. BURKETT-ST. LAURENT, P. B. HITCHCOCK, H. W. KROTO and J. F. NIXON, *J. Chem. Soc., Chem. Commun.*, 1141–3 (1981).

was  $\text{Bu}'\text{C}\equiv\text{P}$ ,<sup>(178)</sup> and its chemistry has been extensively investigated.<sup>(179,180)</sup> The similarly bulky  $\text{ArC}\equiv\text{P}$  ( $\text{Ar} = 2,4,6\text{-Bu}'_3\text{C}_6\text{H}_2$ ) has been studied by X-ray crystallography<sup>(182)</sup> and the C–P distance found to be 152 pm, similar to the short C–P distance of 154 pm deduced from the microwave spectrum of HCP and MeCP. The most studied reactions of phospho-alkynes are cyclo-additions to give organo-P heterocycles,<sup>(179–181)</sup> and reactions with nucleophiles to give phospho-alkenes and 1,3-diphosphabutadienes.<sup>(182)</sup>

As with coordination number 1, the first 2-coordinate P compound also appeared in 1961:<sup>(183)</sup>  $\text{Me}_3\text{P}=\text{PCF}_3$  was made as a white solid by cleaving *cyclo*- $[\text{P}(\text{CF}_3)]_4$  or  $5$  with  $\text{PMe}_3$ ; it is stable at low temperatures but readily dissociates into the starting materials above room temperature. More stable is the bent 2-coordinate phosphocation occurring in the orange salt<sup>(184)</sup>



The aromatic heterocycle phosphabenzene  $\text{C}_5\text{H}_5\text{P}$  (analogous to pyridine) was reported in 1971,<sup>(185)</sup> some years after its triphenyl derivative  $2,4,6\text{-Ph}_3\text{C}_5\text{H}_2\text{P}$ . See also  $\text{HP}=\text{CH}_2$ <sup>(29)</sup> and  $[\text{P}(\text{CN})_2]^-$ <sup>(30)</sup> (p. 484). The burgeoning field of heterocyclic phosphorus compounds featuring

<sup>178</sup> G. BECKER, G. GRESSER and W. UHL, *Z. Naturforsch., Teil B* **36**, 16 (1981).

<sup>179</sup> J. F. NIXON, *Chem. Rev.* **88**, 1327–62 (1988).

<sup>180</sup> M. REGITZ, *Chem. Rev.* **90**, 191–213 (1990). See also M. REGITZ and O. J. SCHERRER, *Multiple Bonds and Low Coordination in Phosphorus Chemistry*, Georg Thieme Verlag, Stuttgart, (1990).

<sup>181</sup> R. BARTSCH and J. F. NIXON, *Polyhedron*, **8**, 2407 (1989).

<sup>182</sup> A. M. ARIF, A. F. BARRON, A. H. COWLEY and S. W. HALL, *J. Chem. Soc., Chem. Commun.*, 171–2 (1988).

<sup>183</sup> A. BURG and W. MAHLER, *J. Am. Chem. Soc.* **83**, 2388–9 (1961).

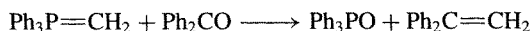
<sup>184</sup> K. DIMROTH and P. HOFFMANN, *Chem. Ber.* **99**, 1325–31 (1966); R. ALLMANN, *Chem. Ber.* **99**, 1332–40 (1966).

<sup>185</sup> A. J. ASHE, *J. Am. Chem. Soc.* **93**, 3293–5 (1971).

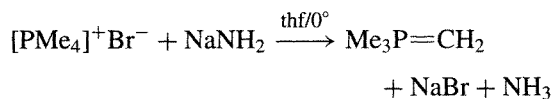
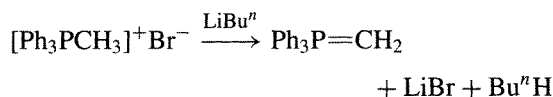


2-coordinate and 3-coordinate P has been fully reviewed,<sup>(173,174)</sup> as has the equally active field of phospho-alkenes ( $\text{>P=C}<$ ) and diphosphenes ( $\text{-P=P-}$ ).<sup>(179,180,186,187)</sup>

The most common coordination numbers for organophosphorus compounds are 3 and 4 as represented by tertiary phosphines and their complexes, and quaternary species such as  $[\text{PMe}_4]^+$  and  $[\text{PPh}_4]^+$ . Also of great significance are the 4-coordinate P ylides<sup>†</sup>  $\text{R}_3\text{P}=\text{CH}_2$ ; indeed, few papers have created so much activity as the report by G. Wittig and G. Geissler in 1953 that methylene triphenylphosphorane reacts with benzophenone to give  $\text{Ph}_3\text{PO}$  and 1,1-diphenylethylene in excellent yield.<sup>(188)</sup>



The ylide  $\text{Ph}_3\text{P}=\text{CH}_2$  can readily be made by deprotonating a quaternary phosphonium halide with *n*-butyllithium and many such ylides are now known:

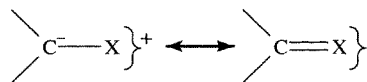


The enormous scope of the Wittig reaction and its variants in affording a smooth, high-yield synthesis of C=C double bonds, etc., has been amply delineated by the work of Wittig

<sup>186</sup> R. APPEL, F. KNOLL and I. RUPPERT, *Angew. Chem. Int. Edn. Engl.* **20**, 731–44 (1981).

<sup>187</sup> N. C. NORMAN, *Polyhedron* **12**, 2431–6 (1993).

<sup>†</sup> An ylide can be defined as a compound in which a carbanion is attached directly to a heteroatom carrying a high degree of positive charge:

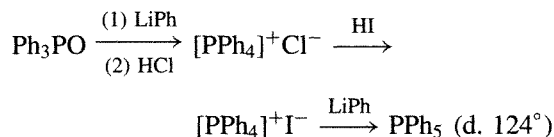


Thus  $\text{Ph}_3\text{P}=\text{CH}_2$  is triphenylphosphonium methyllide (see pp. 274–304 of reference 2, or textbooks of organic chemistry for a fuller treatment of the Wittig reaction).

<sup>188</sup> G. WITTIG and G. GEISLER, *Annalen* **580**, 44–57 (1953).

and others and culminated in the award of the 1979 Nobel Prize for Chemistry (jointly with H. C. Brown for hydroboration, p. 166). The reaction of P ylides with many inorganic compounds has also led to some fascinating new chemistry.<sup>(189)</sup> The curious yellow compound  $\text{Ph}_3\text{P}=\text{C}=\text{PPh}_3$  should also be noted.<sup>(190)</sup> Unlike allene,  $\text{H}_2\text{C}=\text{C}=\text{CH}_2$ , which has a linear central carbon atom, the molecules are bent and the structure is strikingly unusual in having 2 crystallographically independent molecules in the unit cell which have substantially differing bond angles,  $130.1^\circ$  and  $143.8^\circ$ . The short P=C distances (163 pm as compared with 183.5 pm for P–C(Ph)) suggest double bonding, but the nonlinear P=C=P unit and especially the two values of the angle, are hard to rationalize (cf. the isoelectronic cation  $[\text{Ph}_3\text{P}=\text{N}=\text{PPh}_3]^+$  which has various angles in different compounds).

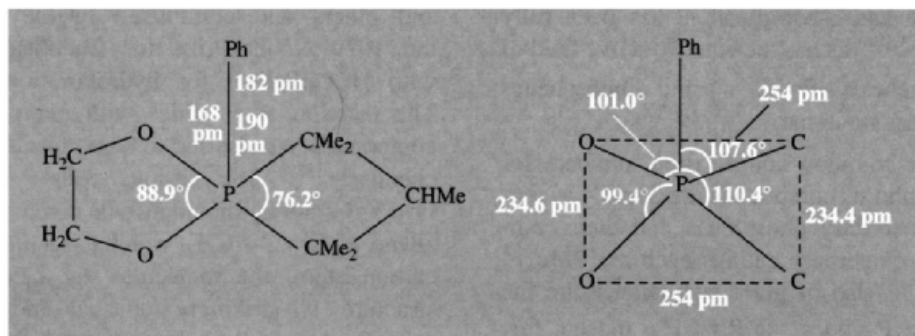
Pentaorgano derivatives of P are rare. The first to be made (by G. Wittig and M. Rieber in 1948) was  $\text{PPh}_5$ :



Unlike  $\text{SbPh}_5$  (which has a square-pyramidal structure p. 598),  $\text{PPh}_5$  adopts a trigonal bipyramidal coordination with the axial P–C distances (199 pm) being appreciably longer than the equatorial P–C distances (185 pm). More recently (1976)  $\text{P}(\text{CF}_3)_3\text{Me}_2$  and  $\text{P}(\text{CF}_3)_2\text{Me}_3$  were obtained by methylating the corresponding chlorides with  $\text{PbMe}_4$ . There are also many examples of 5-coordinate P in which not all the directly bonded atoms are carbon. One such is the dioxaphenylspiro-phosphorane shown in Fig. 12.31; the local symmetry about P is essentially square pyramidal, and the factors which affect the choice between this geometry and trigonal bipyramidal is a topic of active

<sup>189</sup> H. SCHMIDBAUR, *Acc. Chem. Res.* **8**, 62–70 (1975).

<sup>190</sup> A. T. VINCENT and P. J. WHEATLEY, *J. Chem. Soc. (D), Chem. Commun.*, 592 (1971).



**Figure 12.31** Schematic representation of the molecular structure of  $[P(C_3HMe_5)(O_2C_2H_4)Ph]$  showing the rectangular-based pyramidal disposition of the 5 atoms bonded to P; the P atom is 44 pm above the  $C_2O_2$  plane.

current interest.<sup>(39,191)</sup> It should also be noted that the compounds,  $Ph_3PBr_2$  and  $Ph_3PI_2$ , which might have been thought to involve 5-coordinate P, feature instead 4-coordinate P and an unusual end-on bonding of the dihalogen moiety, i.e.  $Ph_3P-Br-Br$ ,<sup>(192)</sup> and  $Ph_3P-I-I$ .<sup>(193)</sup>

<sup>191</sup> W. ALTHOFF, R. O. DAY, R. K. BROWN and R. R. HOLMES, *Inorg. Chem.* **17**, 3265–70 (1978); see also the immediately following two papers, pp. 3270–6 and 3276–85.

<sup>192</sup> N. BRICKLEBANK, S. M. GODFREY, A. G. MACKIE, C. A. MCAULIFFE and R. G. PRITCHARD, *J. Chem. Soc., Chem. Commun.*, 355–6 (1992).

<sup>193</sup> S. M. GODFREY, D. G. KELLY, C. S. MCAULIFFE, A. G. MACKIE, R. G. PRITCHARD and S. M. WATSON, *J. Chem. Soc., Chem. Commun.*, 1163–4 (1991).

The corresponding interhalogen adducts  $Ph_3PIX$  ( $X = Cl, Br$ ) appear to be 4-coordinate but ionic, i.e.  $[Ph_3PI]^+X^-$ .<sup>(194)</sup>

Many organophosphorus compounds are highly toxic and frequently lethal. They have been actively developed for herbicides, pesticides and more sinister purposes such as nerve gases which disorient, harass, paralyse or kill.<sup>(9)</sup>

<sup>194</sup> K. B. DILLON and J. LINCOLN, *Polyhedron*, **8**, 1445–6 (1989).

																H		He																															
3	4																	5	6	7	8	9	10																										
Li	Be																	B	C	N	O	F	Ne																										
11	12																	13	14	15	16	17	18																										
Na	Mg																	Al	Si	P	S	Cl	Ar																										
19	20	21	22	23	24	25	26	27	28	29	30	31	32	33	34	35	36																																
K	Ca	Sc	Ti	V	Cr	Mn	Fe	Co	Ni	Cu	Zn	Ga	Ge	As	Se	Br	Kr																																
37	38	39	40	41	42	43	44	45	46	47	48	49	50	51	52	53	54																																
Rb	Sr	Y	Zr	Nb	Mo	Tc	Ru	Rh	Pd	Ag	Cd	In	Sn	Sb	Te	I	Xe																																
55	56	57	58	59	60	61	62	63	64	65	66	67	68	69	70	71	72																																
Cs	Ba	La	Hf	Ta	W	Re	Os	Ir	Pt	Au	Hg	Tl	Pb	Bi	Po	At	Rn																																
87	88	89	90	91	92	93	94	95	96	97	98	99	100	101	102	103	104																																
Fr	Ra	Ac	Rf	Db	Sg	Bh	Hs	Mt	Uun	Uun	Uub																																						
																		59	60	61	62	63	64	65	66	67	68	69	70	71																			
																		Ce	Pr	Nd	Pm	Sm	Eu	Gd	Tb	Dy	Ho	Er	Tm	Yb	Lu																		
																		89	90	91	92	93	94	95	96	97	98	99	100	101	102	103	104																
																		Th	Pa	U	Np	Pu	Am	Cm	Bk	Cf	Es	Fm	Md	No	Lr																		

# 13

## Arsenic, Antimony and Bismuth

### 13.1 Introduction

The three elements arsenic, antimony and bismuth, which complete Group 15 of the periodic table, were amongst the earliest elements to be isolated and all were known before either nitrogen (1772) or phosphorus (1669) had been obtained as the free elements. The properties of arsenic sulfide and related compounds have been known to physicians and professional poisoners since the fifth century BC though their use is no longer recommended by either group of practitioners. Isolation of the element is sometimes credited to Albertus Magnus (AD 1193–1280) who heated orpiment ( $\text{As}_2\text{S}_3$ ) with soap, and its name reflects its ancient lineage. [Arsenic, Latin *arsenicum* from Greek *ἀρσενικόν* (*arsenicon*) which was itself derived (with addition of *όν*) from Persian *az-zarnīkh*, yellow orpiment (*zar* = gold).] Antimony compounds were also known to the ancients and the black sulfide, stibnite, was used in early biblical times as a cosmetic to darken and beautify women's eyebrows; a rare Chaldean vase of cast antimony dates from 4000 BC and antimony-coated copper articles were used in Egypt 2500–2200 BC. Pliny (~AD 50) gave it

the name *stibium* and writings attributed to Jabir (~AD 800) used the form *antimonium*; indeed, both names were used for both the element and its sulfide until the end of the eighteenth century (Lavoisier). The history of the element, like that of arsenic, is much obscured by the intentionally vague and misleading descriptions of the alchemists, though the elusive Benedictine monk Basil Valentine may have prepared it in 1492 (about the time of Columbus). N. Lémery published his famous *Treatise on Antimony* in 1707. Bismuth was known as the metal at least by 1480 though its previous history in the Middle Ages is difficult to unravel because the element was sometimes confused with Pb, Sn, Sb or even Ag. The Gutenberg printing presses (1440 onwards) used type that had been cut from brass or cast from Pb, Sn or Cu, but about 1450 a secret method of casting type from Bi alloys came into use and this particular use is still an important application of the element (p. 549). The name derives from the German *Wismut* (possibly white metal or meadow mines) and this was latinized to *bisemutum* by the sixteenth-century German scientist G. Bauer (Agricola) about 1530. Despite the difficulty of

assigning precise dates to discoveries made by alchemists, miners and metal workers (or indeed even discerning what those discoveries actually were), it seems clear that As, Sb and Bi became increasingly recognized in their free form during the thirteenth to fifteenth centuries; they are therefore contemporary with Zn and Co, and predate all other elements except the 7 metals and 2 non-metallic elements known from ancient times (Au, Ag, Cu, Fe, Hg, Pb, Sn; C and S).<sup>(1)</sup>

Arsenic and antimony are classed as metalloids or semi-metals and bismuth is a typical B sub-group (post-transition-element) metal like tin and lead.

## 13.2 The Elements

### 13.2.1 Abundance, distribution and extraction

None of the three elements is particularly abundant in the earth's crust though several minerals contain them as major constituents. As can be seen from Table 13.1, arsenic occurs about half-way down the elements in order of abundance, grouped with several others near 2 ppm. Antimony has only one-tenth of this abundance and Bi, down by a further factor of 20 or more, is about as unabundant as several of the commoner platinum metals and gold. In common with all the post-transition-element metals, As, Sb and Bi are chalcophiles, i.e. they occur in association with the chalcogens S, Se and Te rather than as oxides and silicates.

Arsenic minerals are widely distributed throughout the world and small amounts of the free element have also been found. Common

minerals include the two sulfides realgar ( $\text{As}_4\text{S}_4$ ) and orpiment ( $\text{As}_2\text{S}_3$ ) and the oxidized form arsenolite ( $\text{As}_2\text{O}_3$ ). The arsenides of Fe, Co and Ni and the mixed sulfides with these metals form another set of minerals, e.g. loellingite ( $\text{FeAs}_2$ ), saffrolite ( $\text{CoAs}$ ), niccolite ( $\text{NiAs}$ ), rammelsbergite ( $\text{NiAs}_2$ ), arsenopyrite ( $\text{FeAsS}$ ), cobaltite ( $\text{CoAsS}$ ), enargite ( $\text{Cu}_3\text{AsS}_4$ ), gersdorffite ( $\text{NiAsS}$ ) and the quaternary sulfide glaucodot [ $(\text{Co,Fe})\text{AsS}$ ]. Elemental As is obtained on an industrial scale by smelting  $\text{FeAs}_2$  or  $\text{FeAsS}$  at 650–700°C in the absence of air and condensing the sublimed element:  $\text{FeAsS} \longrightarrow \text{FeS} + \text{As(g)} \longrightarrow \text{As(s)}$ . Residual As trapped in the sulfide residues can be released by roasting them in air and trapping the sublimed  $\text{As}_2\text{O}_3$  in the flue system. The oxide can then either be used directly for chemical products or reduced with charcoal at 700–800° to give more As.  $\text{As}_2\text{O}_3$  is also obtained in large quantities as flue dust from the smelting of Cu and Pb concentrates; because of the huge scale of these operations (pp. 1174, 371) this represents the most important industrial source of As. Some production figures and major uses of As and its compounds are listed in the Panel.

Stibnite,  $\text{Sb}_2\text{S}_3$ , is the most important ore of antimony and it occurs in large quantities in China, South Africa, Mexico, Bolivia and Chile. Other sulfide ores include ullmanite ( $\text{NiSbS}$ ), livingstonite ( $\text{HgSb}_4\text{S}_8$ ), tetrahedrite ( $\text{Cu}_3\text{SbS}_3$ ), wolfsbergite ( $\text{CuSbS}_2$ ) and jamesonite ( $\text{FePb}_4\text{Sb}_6\text{S}_{14}$ ). Indeed, complex ores containing Pb, Cu, Ag and Hg are an important industrial source of Sb. Small amounts of oxide minerals formed by weathering are also known, e.g. valentinite ( $\text{Sb}_2\text{O}_3$ ), cervantite ( $\text{Sb}_2\text{O}_4$ ), and stibiconite ( $\text{Sb}_2\text{O}_4 \cdot \text{H}_2\text{O}$ ), and minor finds of native Sb have occasionally been reported. Commercial ores have 5–60% Sb, and recovery methods depend on the

<sup>1</sup> M. E. WEEKS, *Discovery of the Elements*, Chap. 3, pp. 91–119, Journal of Chemical Education, Easton, Pa, 1956.

Table 13.1 Abundances of elements in crustal rocks (g tonne<sup>-1</sup>)

Element	Sn	Eu	Be	As	Ta	Ge	In	Sb	Cd	Pd	Pt	Bi	Os	Au
PPM	2.1	2.1	2.0	<b>1.8</b>	1.7	1.5	0.24	<b>0.2</b>	0.16	0.015	0.01	<b>0.008</b>	0.005	0.004
Order	48 =	48 =	50	<b>51</b>	52	53	61	<b>62</b>	63	67	68	<b>69</b>	70	71

### Production and Uses of Arsenic, Antimony and Bismuth<sup>(2)</sup>

Until the late 1980s the USA was the principal supplier of "white arsenic" (i.e.  $\text{As}_2\text{O}_3$ ) but it now relies entirely on imports. World production has been steady for many years at about 52 000 tonnes pa and the main producers are France (10 000 tpa), Sweden (10 000 tpa), Russia (8 000 tpa) and Chile (7 000 tpa). The price of refined oxide was about \$480 per tonne in 1989 and commercial grade As metal (99%+) was about \$2.20/kg in 1990. High purity As (99.99%+) was \$45.00/kg and zone-refined semiconductor grade even more expensive.

The main use of elemental As is in alloys with Pb and to a lesser extent Cu. Addition of small concentrations of As improves the properties of Pb/Sb for storage batteries (see below), up to 0.75% improves the hardness and castability of type metal, and 0.5–2.0% improves the sphericity of Pb ammunition. Automotive body solder is Pb (92%), Sb (5.0%), Sn (2.5%) and As (0.5%). Intermetallic compounds with Al, Ga and In give the III–V semiconductors (p. 255) of which GaAs and InAs are of particular value for light-emitting diodes (LEDs), tunnel diodes, infrared emitters, laser windows and Hall-effect devices (p. 258).

The use of As compounds as herbicides and pest controls in agriculture is now considerably restricted because of environmental considerations though arsenic acid itself,  $\text{AsO}(\text{OH})_3$ , is still used in the formulation of wood preservatives. The oxide is widely used to decolorize glass.

World production capacity for antimony and its compounds (as contained Sb) was 116 000 tonnes in 1988, plus a similar amount of secondary (recycled) Sb obtained by smelting. However, actual production was somewhat below this. Typical prices (1988) were \$3.50/kg for high-grade  $\text{Sb}_2\text{O}_3$  and \$2.30/kg for 99.5%+ Sb metal (\$1.80/kg in 1990). Lead storage batteries use alloys containing 2.5–3% Sb and a trace of As, to minimize self-discharge, gassing and poisoning of the negative electrode. Other typical uses of Sb alloys in the USA, 1975 (tonnes of contained Sb), are shown in the Table.

Use	Sb/Pb batteries	Bearings	Ammuni- tion	Solder	Type metal	Sheet pipe	Other metal	Non- metal products
Sb/tonnes	4143	365	216	121	68	55	144	6657
Percentage	35.2	3.5	1.8	1.0	0.6	0.5	1.2	56.5

As with arsenic, semiconductor grade Sb is prepared by chemical reduction of highly purified compounds. AlSb, GaSb and InSb have applications in infrared devices, diodes and Hall-effect devices. ZnSb has good thermoelectric properties. Applications of various *compounds* of Sb will be mentioned when the compounds themselves are discussed.

World annual production of bismuth and its compounds has hovered around 4000 tonnes of contained Bi for many years and a similar amount of secondary (refinery) Bi is also produced. Production has been dominated by China, Japan, Peru, Bolivia, Mexico, Canada, USA and Australia which, between them, account for almost of all supplies. Prices for the free element have fluctuated wildly since the 1970s, from <\$4.00/kg to >\$44.00/kg; at the end of 1990 it was \$6.30/kg. Consumption of the metal and its compounds has also been unusual, usage in the USA dropping by a factor of 2 from 1973 to 1975, for example. The main uses are in pharmaceuticals, fusible alloys (including type metal, p. 547), and metallurgical additives.

No industrial poisoning by Bi metal has ever been reported but ingestion of compounds and inhalation of dust should be avoided.

grade. Low-grade sulfide ores (5–25% Sb) are volatilized as the oxide (any  $\text{As}_2\text{O}_3$  being readily removed first by virtue of its greater volatility). The oxide can be reduced to the metal by heating it in a reverberatory furnace with charcoal in the presence of an alkali metal carbonate

or sulfate as flux. Intermediate ores (25–40%) are smelted in a blast furnace and the oxide recovered from the flue system. Ores containing 40–60% Sb are liquated at 550–600° under reducing conditions to give  $\text{Sb}_2\text{S}_3$  and then treated with scrap iron to remove the sulfide:  $\text{Sb}_2\text{S}_3 + 3\text{Fe} \longrightarrow 2\text{Sb} + 3\text{FeS}$ . Some complex sulfide ores are treated by leaching and electro-winning, e.g. the electrolysis of alkaline solutions of the thioantimonate  $\text{Na}_3\text{SbS}_4$ , and the element is also recovered from the flue dusts of Pb smelters. Impure Sb contains Pb, As, S, Fe and

<sup>2</sup> *Kirk-Othmer Encyclopedia of Chemical Technology*, 4th edn., Vol. 3, Wiley, New York, 1992; Arsenic and arsenic alloys (pp. 624–33); Arsenic compounds (633–59); Antimony and antimony alloys (367–81); Antimony compounds (382–412); Bismuth and bismuth alloys (Vol. 4, 1992 (pp. 237–45); Bismuth compounds (246–70).

Cu; the latter two can be removed by stibnite treatment or heating with charcoal/ $\text{Na}_2\text{SO}_4$  flux; the As and S can be removed by an oxidizing flux of  $\text{NaNO}_3$  and  $\text{NaOH}$  (or  $\text{Na}_2\text{CO}_3$ ); Pb is hard to remove but this is unnecessary if the Sb is to be used in Pb alloys (see below). Electrolysis yields >99.9% purity and remaining impurities can be reduced to the ppm level by zone refining. The scale of production and the various uses of Sb and its compounds are summarized in the Panel.

Bismuth occurs mainly as bismite ( $\alpha\text{-Bi}_2\text{O}_3$ ), bismuthinite ( $\text{Bi}_2\text{S}_3$ ) and bismutite [ $(\text{BiO})_2\text{CO}_3$ ]; very occasionally it occurs native, in association with Pb, Ag or Co ores. The main commercial source of the element is as a byproduct from Pb/Zn and Cu plants, from which it is obtained by special processes dependent on the nature of the main product.<sup>(2)</sup> Sulfide ores are roasted to the oxide and then reduced by iron or charcoal. Because of its low mp, very low solubility in Fe, and fairly high oxidative stability in air, Bi can be melted and cast (like Pb) in iron and steel vessels. Like Sb, the metal is too brittle to roll, draw, or extrude at room temperature, but above 225°C Bi can be worked quite well.

### 13.2.2 Atomic and physical properties

Arsenic and Bi (like P) each have only 1 stable isotope and this occurs with 100% abundance in

all natural sources of the elements. Accordingly (p. 17) their atomic weights are known with great precision (Table 13.2). Antimony has 2 stable isotopes (like N); however, unlike N, which has 1 predominantly abundant isotope, the 2 isotopes of Sb are approximately equal in abundance ( $^{121}\text{Sb}$  57.21%,  $^{123}\text{Sb}$  42.79%) and consequently (p. 17) the atomic weight is known with somewhat less accuracy. It is also noteworthy that  $^{209}\text{Bi}$  is the heaviest stable isotope of any element; all nuclides beyond  $^{209}\text{Bi}$  are radioactive.

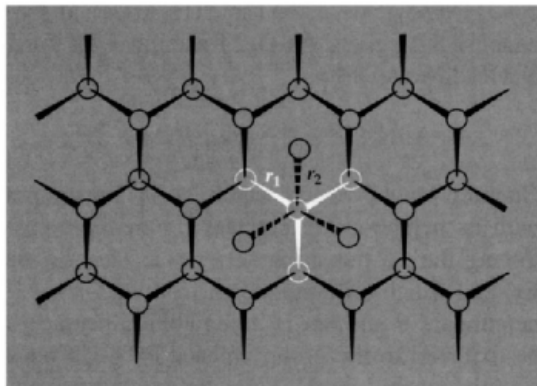
The ground-state electronic configuration of each element in the group is  $ns^2np^3$  with an unpaired electron in each of the three p orbitals, and much of the chemistry of the group can be interpreted directly on this basis. However, smooth trends are sometimes modified (or even absent altogether), firstly, because of the lack of low-lying empty d orbitals in N, which differentiates it from its heavier congeners, and, secondly, because of the countervailing influence of the underlying filled d and f orbitals in As, Sb and Bi. Such perturbations are apparent when the various ionization energies in Table 13.2 are plotted as a function of atomic number. Table 13.2 also contains approximate data on the conventional covalent single-bond radii for threefold coordination though these values vary by about  $\pm 4$  pm in various tabulations and should only be used as a rough guide. The 6-coordinate "effective ionic radii" for the +3 and +5

Table 13.2 Atomic properties of Group 15 elements

Property	N	P	As	Sb	Bi
Atomic number	7	15	33	51	83
Atomic weight (1997)	14.00674(7)	30.973762(4)	74.92160(2)	121.760(1)	208.98038(2)
Electronic configuration	[He]2s <sup>2</sup> 2p <sup>3</sup>	[Ne]3s <sup>2</sup> 3p <sup>3</sup>	[Ar]3d <sup>10</sup> 4s <sup>2</sup> 4p <sup>3</sup>	[Kr]4d <sup>10</sup> 5s <sup>2</sup> 5p <sup>3</sup>	[Xe]4f <sup>14</sup> 5d <sup>10</sup> -6s <sup>2</sup> 6p <sup>3</sup>
Ionization energies/MJ mol <sup>-1</sup> (I)	1.402	1.012	0.947	0.834	0.703
(II)	2.856	1.903	1.798	1.595	1.610
(III)	4.577	2.910	2.736	2.443	2.466
Sum (I+II+III)/MJ mol <sup>-1</sup>	8.835	5.825	5.481	4.872	4.779
Sum (IV+V)/MJ mol <sup>-1</sup>	16.920	11.220	10.880	9.636	9.776
Electronegativity $\chi$	3.0	2.1	2.0	1.9	1.9
$r_{\text{cov}}$ (M <sup>III</sup> single bond)/pm	70	110	120	140	150
$r_{\text{ionic}}$ (6-coordinate) (M <sup>III</sup> )/pm	(16)	44	58	76	103
(6-coordinate) (M <sup>V</sup> )/pm	(13)	38	46	60	76

oxidation states are taken from R. D. Shannon's tabulation,<sup>(3)</sup> but should not be taken to imply the presence of  $M^{3+}$  and  $M^{5+}$  cations in many of the compounds of these elements.

Arsenic, Sb and Bi each exist in several allotropic forms<sup>(4,5)</sup> though the allotropy is not so extensive as in P (p. 481). There are three crystalline forms of As, of which the ordinary, grey, "metallic", rhombohedral,  $\alpha$ -form is the most stable at room temperature. It consists of puckered sheets of covalently bonded As stacked in layers perpendicular to the hexagonal  $c$ -axis as shown in Fig. 13.1. Within each layer each As has 3 nearest neighbours at 251.7 pm and the angle As-As-As is  $96.7^\circ$ ; each As also has a further 3 neighbours at 312 pm in an adjacent layer. The  $\alpha$ -forms of Sb and Bi are isostructural with  $\alpha$ -As and have the dimensions shown in Table 13.3. It can be seen that there is a progressive diminution in the difference between intra-layer and inter-layer distances though the inter-bond angles remain almost constant.



**Figure 13.1** Puckered layer structure of As showing pyramidal coordination of each As to 3 neighbours at a distance  $r_1$  (252 pm). The disposition of As atoms in the next layer ( $r_2$  312 pm) is shown by dashed lines.

**Table 13.3** Comparison of black P and  $\alpha$ -rhombohedral As, Sb and Bi

	$r_1$ /pm	$r_2$ /pm	$r_2/r_1$	$\angle M-M-M$
Black P	223.1 (av)	332.4 (av)	1.490	2 at $96.3^\circ$ (1 at $102.1^\circ$ )
$\alpha$ -As	251.7	312.0	1.240	$96.7^\circ$
$\alpha$ -Sb	290.8	335.5	1.153	$96.6^\circ$
$\alpha$ -Bi	307.2	352.9	1.149	$95.5^\circ$

In the vapour phase As is known to exist as tetrahedral  $As_4$  molecules with (As-As 243.5 pm) and when the element is sublimed, a yellow, cubic modification is obtained which probably also contains  $As_4$  units though the structure has not yet been determined because the crystals decompose in the X-ray beam. The mineral arsenolamprite is another polymorph,  $\epsilon$ -As; it is possibly isostructural with "metallic" orthorhombic P.

Antimony exists in 5 forms in addition to the ordinary  $\alpha$ -form which has been discussed above. The yellow form is unstable above  $-90^\circ$ ; a black form can be obtained by cooling gaseous Sb, and an explosive (impure?) form can be made electrolytically. The two remaining crystalline forms are made by high-pressure techniques: Form I has a primitive cubic lattice with  $a_0$  296.6 pm: it is obtained from  $\alpha$ -Sb at 50 kbar (5GPa, i.e.  $5 \times 10^9 \text{ N m}^{-2}$ ) by increasing the rhombohedral angle from  $57.1^\circ$  to  $60.0^\circ$  together with small shifts in atomic position so that each Sb has 6 equidistant neighbours. Further increase in pressure to 90 kbar yields Form II which is hcp with an interatomic distance of 328 pm for the 12 nearest neighbours.

Several polymorphs of Bi have been described but there is as yet no general agreement on their structures except for  $\alpha$ -Bi (above) and  $\zeta$ -Bi which forms at 90 kbar and has a bcc structure with 8 nearest neighbours at 329.1 pm.

The physical properties of the  $\alpha$ -rhombohedral form of As, Sb and Bi are summarized in Table 13.4. Data for  $N_2$  and  $P_4$  are included for comparison. Crystalline As is rather volatile and the vapour pressure of the solid reaches 1 atm at  $615^\circ$  some  $200^\circ$  below its mp of  $816^\circ\text{C}$  (at 38.6 atm, i.e. 3.91 MPa). Antimony and Bi are

<sup>3</sup> R. D. SHANNON, *Acta Cryst.* **A32**, 751-67 (1976).

<sup>4</sup> J. DONOHUE, *The Structure of the Elements*, Wiley, 1974, 436 pp.

<sup>5</sup> H. G. VON SCHNERING, *Angew. Chem. Int. Edn. Engl.* **20**, 33-51 (1981).

Table 13.4 Some physical properties of Group 15 elements

Property	N <sub>2</sub>	P <sub>4</sub>	$\alpha$ -As	$\alpha$ -Sb	$\alpha$ -Bi
MP/°C	-210.0	44.1	816 (38.6 atm)	630.7	271.4
BP/°C	-195.8	280.5	615 (subl)	1753	1564
Density (25°C)/g cm <sup>-3</sup>	0.879 (-210°)	1.823	5.778 <sup>(a)</sup>	6.684	9.808
Hardness (Mohs)	—	—	3.5	3-3.5	2.5
Electrical resistivity (20°C)/ $\mu$ ohm cm	—	—	33.3	41.7	120
Contraction on freezing/%	—	—	10	0.8	-3.32

<sup>(a)</sup>Yellow As<sub>4</sub> has  $d_{25}$  1.97 g cm<sup>-3</sup>; cf. difference between the density of rhombohedral black P (3.56 g cm<sup>-3</sup>) and white P<sub>4</sub> (1.823 g cm<sup>-3</sup>) (p. 479).

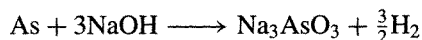
much less volatile and also have appreciably lower mps than As, so that both have quite long liquid ranges at atmospheric pressure.

Arsenic forms brittle steel-grey crystals of metallic appearance. However, its lack of ductility and comparatively high electrical resistivity (33.3  $\mu$ ohm cm), coupled with its amphoterism and intermediate chemical nature between that of metals and non-metals, have led to its being classified as a metalloid rather than a "true" metal. Antimony is also very brittle and forms bluish-white, flaky, lustrous crystals of high electrical resistivity (41.7  $\mu$ ohm cm). These values of resistivity can be compared with those for "good" metals such as Ag (1.59), Cu (1.72), and Al (2.82  $\mu$ ohm cm), and with "poor" metals such as Sn (11.5) and Pb (22  $\mu$ ohm cm). Bismuth has a still higher resistivity (120  $\mu$ ohm cm) which even exceeds that of commercial resistors such as Nichrome alloy (100  $\mu$ ohm cm). Bismuth is a brittle, white, crystalline metal with a pinkish tinge. It is the most diamagnetic of all metals (mass susceptibility  $17.0 \times 10^{-9}$  m<sup>3</sup> kg<sup>-1</sup> — to convert this SI value to cgs multiply by  $10^3/4\pi$ , i.e.  $1.35 \times 10^{-6}$  cm<sup>3</sup> g<sup>-1</sup>). It also has the highest Hall effect coefficient of any metal and is unusual in expanding on solidifying from the melt, a property which it holds uniquely with Ga and Ge among the elements.

### 13.2.3 Chemical reactivity and group trends

Arsenic is stable in dry air but the surface oxidizes in moist air to give a superficial golden

bronze tarnish which deepens to a black surface coating on further exposure. When heated in air it sublimes and oxidizes to As<sub>4</sub>O<sub>6</sub> with a garlic like odour (poisonous). Above 250–300° the reaction is accompanied by phosphorescence (cf. P<sub>4</sub>, p. 473). When ignited in oxygen, As burns brilliantly to give As<sub>4</sub>O<sub>6</sub> and As<sub>4</sub>O<sub>10</sub>. Metals give arsenides (p. 554), fluorine enflames to give AsF<sub>5</sub> (p. 561), and the other halogens yield AsX<sub>3</sub> (p. 559). Arsenic is not readily attacked by water, alkaline solutions or non-oxidizing acids, but dilute HNO<sub>3</sub> gives arsenious acid (H<sub>3</sub>AsO<sub>3</sub>), hot conc HNO<sub>3</sub> yields arsenic acid (H<sub>3</sub>AsO<sub>4</sub>), and hot conc H<sub>2</sub>SO<sub>4</sub> gives As<sub>4</sub>O<sub>6</sub>. Reaction with fused NaOH liberates H<sub>2</sub>:



One important property which As has in common with its neighbouring elements immediately following the 3d transition series (i.e. Ge, As, Se, Br) and which differentiates it from its Group 15 neighbours P and Sb, is its notable reluctance to be oxidized to the group valence of +5. Consequently As<sub>4</sub>O<sub>10</sub> and H<sub>3</sub>AsO<sub>4</sub> are oxidizing agents and arsenates are used for this purpose in titrimetric analysis (p. 577).

The ground-state electronic structure of As, as with all Group 15 elements features 3 unpaired electrons  $ns^2np^3$ ; there is a substantial electron affinity for the acquisition of 1 electron but further additions must be effected against considerable coulombic repulsion, and the formation of As<sup>3-</sup> is highly endothermic. Consistent with this there are no "ionic" compounds containing the arsenide ion and



compounds such as  $\text{Na}_3\text{As}$  are intermetallic or alloy-like. However, despite the metalloidal character of the free element, the ionization energies and electronegativity of As are similar to those of P (Table 13.2) and the element readily forms strong covalent bonds to most non-metals. Thus  $\text{AsX}_3$  ( $X = \text{H, hal, R, Ar}$  etc.) are covalent molecules like  $\text{PX}_3$  and the tertiary arsines have been widely used as ligands to b-class transition elements (p. 909).<sup>(6)</sup> Similarly,  $\text{As}_4\text{O}_6$  and  $\text{As}_4\text{O}_{10}$  resemble their P analogues in structure; the sulfides are also covalent heterocyclic molecules though their stoichiometry and structure differ from those of P.

Antimony is in many ways similar to As, but it is somewhat less reactive. It is stable to air and moisture at room temperature, oxidizes on being heated under controlled conditions to give  $\text{Sb}_2\text{O}_3$ ,  $\text{Sb}_2\text{O}_4$  or  $\text{Sb}_2\text{O}_5$ , reacts vigorously with  $\text{Cl}_2$  and more sedately with  $\text{Br}_2$  and  $\text{I}_2$  to give  $\text{SbX}_3$ , and also combines with S on being heated.  $\text{H}_2$  is without direct reaction and  $\text{SbH}_3$  (p. 557) is both very poisonous and thermally very unstable. Dilute acids have no effect on Sb; concentrated oxidizing acids react readily, e.g. conc  $\text{HNO}_3$  gives hydrated  $\text{Sb}_2\text{O}_5$ , aqua regia gives a solution of  $\text{SbCl}_5$ , and hot conc  $\text{H}_2\text{SO}_4$  gives the salt  $\text{Sb}_2(\text{SO}_4)_3$ .

Bismuth continues the trend to electropositive behaviour and  $\text{Bi}_2\text{O}_3$  is definitely basic, compared with the amphoteric oxides of Sb and As and the acidic oxides of P and N. There is also a growing tendency to form salts of oxoacids by reaction of either the metal or its oxide with the acid, e.g.  $\text{Bi}_2(\text{SO}_4)_3$  and  $\text{Bi}(\text{NO}_3)_3$ . Direct reaction of Bi with  $\text{O}_2$ , S and  $\text{X}_2$  at elevated temperatures yields  $\text{Bi}_2\text{O}_3$ ,  $\text{Bi}_2\text{S}_3$  and  $\text{BiX}_3$  respectively, but the increasing size of the metal atom results in a steady decrease in the strength of covalent linkages in the sequence  $\text{P} > \text{As} > \text{Sb} > \text{Bi}$ . This is most noticeable in the instability of  $\text{BiH}_3$  and of many organobismuth compounds (p. 599).

Most of the trends are qualitatively understandable in terms of the general atomic properties in Table 13.2 though they are not readily deducible from them in any quantitative sense. Again, the +5 oxidation state in Bi is less stable than in Sb for the reasons discussed on p. 226; not only is the sum of the 4th and 5th ionization energies for Bi greater than for Sb (9.78 vs. 9.63  $\text{MJ mol}^{-1}$ ) but the promotion energies of one of the  $ns^2$  electrons to a vacant  $nd$  orbital is also greater for Bi (and As) than for Sb. The discussions on redox properties (p. 577) and the role of d orbitals (p. 222) are also relevant. Finally, Bi shows an interesting resemblance to La in the crystal structures of the chloride oxide,  $\text{MOCl}$ , and in the isomorphism of the sulfates and double nitrates; this undoubtedly stems from the very similar ionic radii of the 2 cations:  $\text{Bi}^{3+}$  103,  $\text{La}^{3+}$  103.2 pm.

All coordination numbers from 1–10 (and 12) are known for the sub-group, though 3, 4, 5 and 6 are by far the most frequently met. CN 1 is exemplified by  $\text{RC}\equiv\text{As}^{(7)}$  ( $\text{R} = 2,4,6\text{-Bu}^t_3\text{C}_6\text{H}_2$ ; cf  $\text{RC}\equiv\text{P}$ , p. 544) and by the isolated tetrahedral anions  $\text{SiAs}_4^{8-}$  and  $\text{GeAs}_4^{8-}$  (isoelectronic with  $\text{SiO}_4^{4-}$  and  $\text{GeO}_4^{4-}$ ) which occur in the lustrous dark metallic Zintl phases  $\text{Ba}_4\text{MAS}_4$ .<sup>(8)</sup> CN 2 (bent) is quite common in heterocyclic organic compounds (p. 592) and in cluster anions such as  $\text{As}_7^{3-}$ ,  $\text{Sb}_7^{3-}$  and  $\text{As}_{11}^{3-}$  and their derivatives (p. 588). A rare example of linear 2-coordinate As was recently established in the bis(manganese) complex  $[(\eta^5\text{-C}_5\text{H}_4\text{Me})(\text{CO})_2\text{Mn}=\text{As}=\text{Mn}(\text{CO})_2(\eta^5\text{-C}_5\text{H}_4\text{Me})]^+$ , isolated as its dark brown salt with  $\text{CF}_3\text{SO}_3^-$ : the angle at As was found to be  $176.3^\circ$  and the As–Mn distance was 215 pm.<sup>(9)</sup> Likewise, examples of pyramidal 3-coordinate As, Sb and Bi are endemic, but planar CN 3 is extremely rare; examples occur in

<sup>7</sup> G. MÄRKL and H. SEJPKA, *Angew. Chem. Int. Edn. Engl.* **25**, 264 (1986).

<sup>8</sup> B. EISENMANN, H. JORDAN and H. SCHÄFER, *Angew. Chem. Int. Edn. Engl.* **20**, 197–8 (1981).

<sup>9</sup> A. STRUBE, G. HUTTNER and L. ZSOLNAI, *Angew. Chem. Int. Edn. Engl.* **27**, 1529–30 (1988).

<sup>6</sup> C. A. MCAULIFFE (ed.), *Transition Metal Complexes of Phosphorus, Arsenic and Antimony Ligands*, Macmillan, London, 1973, 428 pp.

compounds such as  $[\text{PhAs}(\text{Cr}(\text{CO})_5)_2]$  and  $[\text{PhSb}(\text{Mn}(\eta^5\text{-C}_5\text{H}_5)(\text{CO})_2)_2]$  (p. 597) See later, also, for examples of CN 4 (tetrahedral, flattened tetrahedral and see-saw), CN 5 (trigonal bipyramidal and square pyramidal) and CN 6 (octahedral, 3 + 3, and pentagonal pyramidal).

Higher coordination numbers are less common and are mainly confined to Bi. CN 7 has been found in the tetradentate crown-ether bismuth complex  $[\text{BiCl}_3(12\text{-crown-4})]^{(10)}$  and in the bismuth complex,  $[\text{BiL}]$ , of the novel heptadentate anionic ligand of 'saltren',  $(\text{H}_3\text{L})$ , i.e.  $(\text{N}(\text{CH}_2\text{CH}_2\text{N}=\text{CHC}_6\text{H}_4\text{OH})_3)$ .<sup>(11)</sup> The first example of CN 8 was found in the colourless 2:1 adduct  $[\text{2BiCl}_3, 18\text{-crown-6}]$  which was shown by X-ray analysis to involve an unexpected ionic structure featuring 8-coordinate Bi cations, viz.  $[\text{BiCl}_2(18\text{-crown-6})]^{+}_2[\text{Bi}_2\text{Cl}_8]^{2-}$ .<sup>(10)</sup> CN 9 is represented by the discrete tris(tridentate) complex  $[\text{Bi}(-\text{O}-\text{C}(\text{Bu}')=\text{C}-\text{N}=\text{C}-\text{C}(\text{Bu}')=\text{O}\rightarrow)_3]$  in which Bi has a face-capped, slightly-twisted trigonal-prismatic coordination environment.<sup>(12)</sup> Still higher coordination numbers are exemplified by encapsulated As and Sb atoms in rhodium carbonyl cluster anions: for example As is surrounded by a bicapped square antiprism of 10 Rh atoms in  $[\text{Rh}_{10}\text{As}(\text{CO})_{22}]^{3-}$ ,<sup>(13)</sup> and Sb is surrounded by an icosahedron of 12 Rh in  $[\text{Rh}_{12}\text{Sb}(\text{CO})_{27}]^{3-}$ .<sup>(14)</sup> In each case the anion is the first example of a complex in which As or Sb acts as a 5-electron donor (cf. P as a 5-electron donor in  $[\text{Rh}_9\text{P}(\text{CO})_{21}]^{3-}$ ): all these clusters then have precisely the appropriate number of valence electrons for *closo* structures on the basis of Wade's rules (pp. 161, 174).

<sup>10</sup> N. W. ALCOCK, M. RAVINDRAN and G. R. WILLEY, *J. Chem. Soc., Chem. Commun.*, 1063–5 (1989).

<sup>11</sup> P. K. BHARADWAI, A. M. LEE, S. MANDAL, B. W. SKELTON and A. H. WHITE, *Aust. J. Chem.* **47**, 1799–803 (1994).

<sup>12</sup> C. A. STEWART, J. C. CALABRESE and A. J. ARDUENGO, *J. Am. Chem. Soc.* **107**, 3397–8 (1985).

<sup>13</sup> J. L. VIDAL *Inorg. Chem.* **20**, 243–9 (1981).

<sup>14</sup> J. L. VIDAL and J. M. TROUP, *J. Organometallic Chem.* **213**, 351–63 (1981).

## 13.3 Compounds of Arsenic, Antimony and Bismuth<sup>(15)</sup>

### 13.3.1 Intermetallic compounds and alloys<sup>(16,17)</sup>

Most metals form arsenides, antimonides and bismuthides, and many of these command attention because of their interesting structures or valuable physical properties. Like the borides (p. 145), carbides (p. 297), silicides (p. 335), nitrides (p. 417) and phosphides (p. 489), classification is difficult because of the multitude of stoichiometries, the complexities of the structures and the intermediate nature of the bonding. The compounds are usually prepared by direct reaction of the elements in the required proportions and typical compositions are  $\text{M}_9\text{As}$ ,  $\text{M}_5\text{As}$ ,  $\text{M}_4\text{As}$ ,  $\text{M}_3\text{As}$ ,  $\text{M}_5\text{As}_2$ ,  $\text{M}_2\text{As}$ ,  $\text{M}_5\text{As}_3$ ,  $\text{M}_3\text{As}_2$ ,  $\text{M}_4\text{As}_3$ ,  $\text{M}_5\text{As}_4$ ,  $\text{MAs}$ ,  $\text{M}_3\text{As}_4$ ,  $\text{M}_2\text{As}_3$ ,  $\text{MAs}_2$  and  $\text{M}_3\text{As}_7$ . Antimony and bismuth are similar. Many of these intermetallic compounds exist over a range of composition, and nonstoichiometry is rife.

The (electropositive) alkali metals of Group 1 form compounds  $\text{M}_3\text{E}$  ( $\text{E} = \text{As, Sb, Bi}$ ) and the metals of Groups 2 and 12 likewise form  $\text{M}_3\text{E}_2$ . These can formally be written as  $\text{M}^{+}_3\text{E}^{3-}$  and  $\text{M}^{2+}_3\text{E}^{3-}_2$  but the compounds are even less ionic than  $\text{Li}_3\text{N}$  (p. 76) and have many metallic properties. Moreover, other stoichiometries are found (e.g.  $\text{LiBi}$ ,  $\text{KBi}_2$ ,  $\text{CaBi}_3$ ) which are not readily accounted for by the ionic model and, conversely, compounds  $\text{M}_3\text{E}$  are formed by many metals that are not usually thought of as univalent, e.g. Ti, Zr, Hf; V, Nb, Ta; Mn. There are clearly also strong additional interactions between unlike atoms as indicated by the structures adopted and the high mp of many of the compounds, e.g.  $\text{Na}_3\text{Bi}$  melts

<sup>15</sup> C. A. MCAULIFFE and A. G. MACKIE *Chemistry of Arsenic, Antimony and Bismuth*, Ellis Horwood, Chichester, 1990, 350 pp.

<sup>16</sup> J. D. SMITH, Chap. 21 in *Comprehensive Inorganic Chemistry*, Vol. 2, pp. 547–683, Pergamon Press, Oxford, 1973.

<sup>17</sup> F. HULLIGER, *Struct. Bond.* **4**, 83–229 (1968). A comprehensive review with 532 references.

at 840°, compared with Na 98° and Bi 271°C. Many of the  $M_3E$  compounds have the hexagonal  $Na_3As$  (anti- $LaF_3$ ) structure in which equal numbers of Na and As form hexagonal nets as in boron nitride and the remaining Na atoms are arranged in layers on either side of these nets. Each As has 5 Na neighbours at the corners of a trigonal bipyramid (3 at 294 and 2 at 299) and 6 other Na atoms at 330 pm form a trigonal prism (i.e. 11-coordinate). The Na atoms are of two sorts, both of high mixed CN to As and Na, and all the Na–Na distances (328–330 pm) are less than in Na metal (371.6 pm). The compounds show either metallic conductivity or are semiconductors. An even more compact metal structure (cubic) is adopted by  $\beta$ - $Li_3Bi$ ,  $\beta$ - $Li_3Sb$ , and by  $M_3E$ , where  $M = Rb, Cs$ , and  $E = Sb, Bi$ .

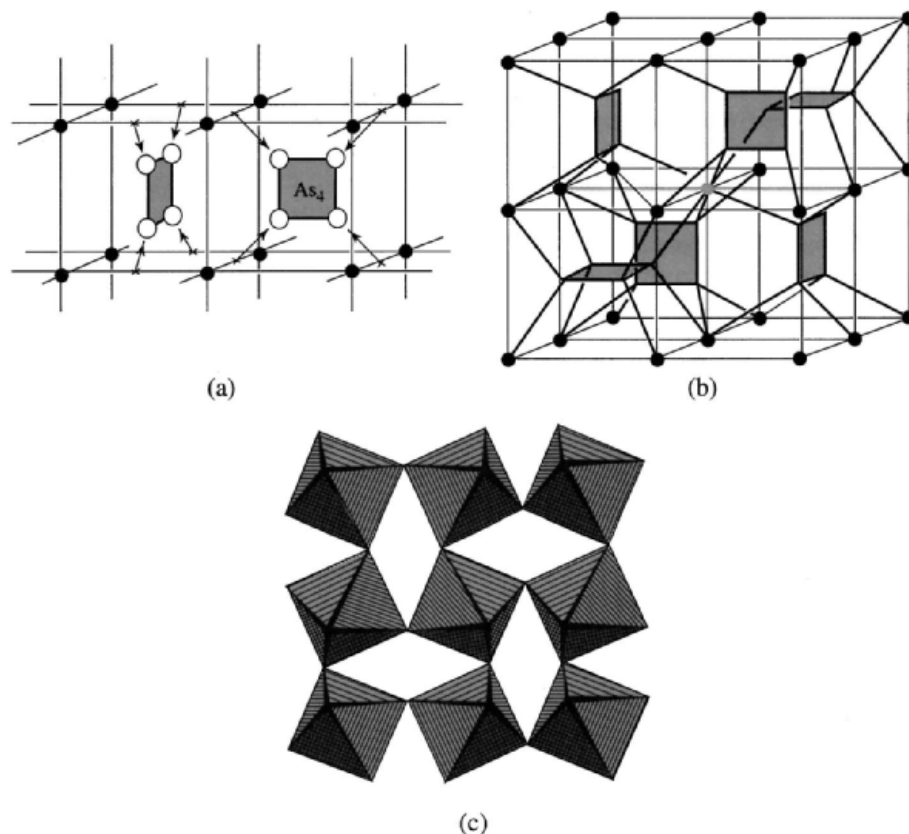
Some of the alkali metal–group 15 element systems give compounds of stoichiometry  $ME$ . Of these,  $LiBi$  and  $NaBi$  have typical alloy structures and are superconductors below 2.47 K and 2.22 K respectively. Others, like  $LiAs$ ,  $NaSb$  and  $KSb$ , have parallel infinite spirals of As or Sb atoms, and it is tempting to formulate them as  $M^+_n(E_n)^{n-}$  in which the  $(E_n)^{n-}$  spirals are iso-electronic with those of covalently catenated Se and Te (p. 752); however, their metallic lustre and electrical conductivity indicate at least some metallic bonding. Within the spiral chains As–As is 246 pm (cf. 252 pm in the element) and Sb–Sb is ~285 pm (cf. 291 pm in the element).

Compounds with Sc, Y, lanthanoids and actinoids are of three types. Those with composition  $ME$  have the (6-coordinated) NaCl structure, whereas  $M_3E_4$  (and sometimes  $M_4E_3$ ) adopt the body-centred thorium phosphide structure ( $Th_3P_4$ ) with 8-coordinated M, and  $ME_2$  are like  $ThAs_2$  in which each Th has 9 As neighbours. Most of these compounds are metallic and those of uranium are magnetically ordered. Full details of the structures and properties of the several hundred other transition metal–Group 15 element compounds fall outside the scope of this treatment, but three particularly important structure types should be mentioned because of their widespread occurrence and relation to other structure types, namely  $CoAs_3$ ,

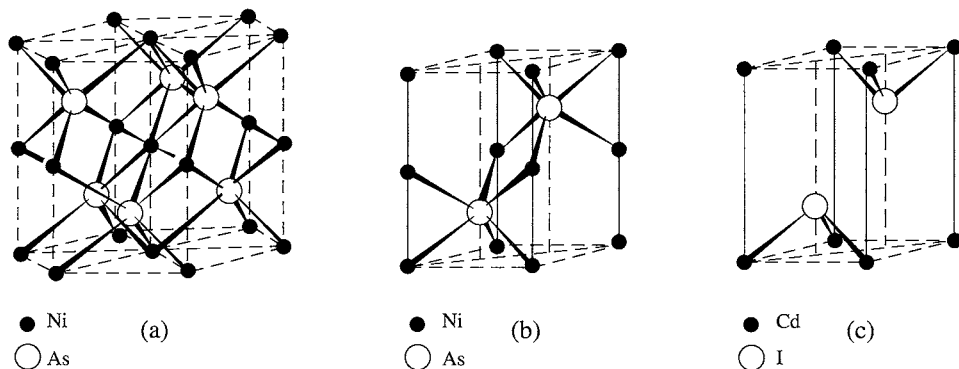
$NiAs$  and structures related to those adopted by  $FeS_2$  (marcasite, pyrites, loellingite, etc.).

$CoAs_3$  occurs in the mineral skutterudite; it is a diamagnetic semiconductor and has a cubic structure related to that of  $ReO_3$  (p. 1047) but with a systematic distortion which results in the generation of well-defined *planar* rings of  $As_4$ . The same structure motif is found in  $MP_3$  ( $M = Co, Ni, Rh, Pd$ ),  $MAs_3$  ( $M = Co, Rh, Ir$ ) and  $MSb_3$  ( $M = Co, Rh, Ir$ ). The unit cell (Fig. 13.2) contains 8Co and 24As (i.e.  $6As_4$ ), and it follows from the directions in which the various sets of atoms move, that 2 of the 8 original  $ReO_3$  cells do not contain an  $As_4$  group. Each As has a nearly regular tetrahedral arrangement of 2 Co and 2 As neighbours and each Co has a slightly distorted octahedral coordination group of 6 As. The planar  $As_4$  groups are not quite square, the sides of the rectangle being 246 and 257 pm (cf. 244 pm in the tetrahedral  $As_4$  molecule). The distortions from the  $ReO_3$  structure (in which each As would have had 8 equidistant neighbours at about 330 pm) thus permit the closer approach of the As atoms in groups of 4 though this does not proceed so far as to form 6 equidistant As–As links as in the tetrahedral  $As_4$  molecule. The P–P distances in the  $P_4$  rectangles of the isostructural phosphides are 223 and 231 pm (cf. 225 pm in the tetrahedral  $P_4$  molecule).

The  $NiAs$  structure is one of the commonest MX structure types, the number of compounds adopting it being exceeded only by those with the NaCl structure. It is peculiar to compounds formed by the transition elements with either As, Sb, Bi, the chalcogens (p. 748) or occasionally Sn. Examples with the Group 15 elements are  $Ti(As, Sb)$ ,  $V(P, Sb)$ ,  $CrSb$ ,  $Mn(As, Sb, Bi)$ ,  $FeSb$ ,  $Co(As, Sb)$ ,  $Ni(As, Sb, Bi)$ ,  $RhBi$ ,  $Ir(Sb, Bi)$ ,  $PdSb$ ,  $Pt(Sb, Bi)$ . The structure is illustrated in Fig. 13.3a: each Ni is 8-coordinate, being surrounded by 6 As and by 2 Ni (which are coplanar with 4 of the As); the As atoms form a hcp lattice in which the interstices are occupied by Ni atoms in such a way that each As is surrounded by a trigonal prism of 6 Ni. Another important feature of the  $NiAs$  structure is the close approach of Ni atoms



**Figure 13.2** The cubic structure of skutterudite ( $\text{CoAs}_3$ ). (a) Relation to the  $\text{ReO}_3$  structure; (b) unit cell (only sufficient Co-As bonds are drawn to show that there is a square group of As atoms in only 6 of the 8 octants of the cubic unit cell, the complete 6-coordination group of Co is shown only for the atom at the body-centre of the cell); and (c) section of the unit cell showing  $\{\text{CoAs}_6\}$  octahedra corner-linked to form  $\text{As}_4$  squares.



**Figure 13.3** Structure of nickel arsenide showing (a) 3 unit cells, (b) a single unit cell  $\text{Ni}_2\text{As}_2$  and its relation to (c) the unit cell of the layer lattice compound  $\text{CdI}_2$  (see text).

in chains along the (vertical) *c*-axis. The unit cell (Fig. 13.3b) contains  $\text{Ni}_2\text{As}_2$ , and if the central layer of Ni atoms is omitted the  $\text{CdI}_2$  structure is obtained (Fig. 13.3c). This structural relationship accounts for the extensive ranges of composition frequently observed in compounds with this structure, since partial filling of the intermediate layer gives compositions in the range  $\text{M}_{1+x}\text{X}_2$  ( $0 < x < 1$ ). With the chalcogens the range sometimes extends the whole way from ME to  $\text{ME}_2$  but for As, Sb and Bi it never reaches  $\text{ME}_2$  and intermetallic compounds of this composition usually have either the marcasite or pyrites structures of  $\text{FeS}_2$  (p. 680) or the compressed marcasite (loellingite) structure of  $\text{FeAs}_2$ . All three structure types contain the  $\text{E}_2$  group. Examples are:

marcasite type:	$\text{NiAs}_2$ , $\text{NiSb}_2$
pyrites type:	$\text{PdAs}_2$ , $\text{PdSb}_2$ , $\text{PtAs}_2$ , $\text{PtSb}_2$ , $\text{PtBi}_2$ , $\text{AuSb}_2$
loellingite type:	$\text{CrSb}_2$ , $\text{FeP}_2$ , $\text{FeAs}_2$ , $\text{FeSb}_2$ , $\text{RuP}_2$ , $\text{RuAs}_2$ , $\text{RuSb}_2$ , $\text{OsP}_2$ , $\text{OsAs}_2$ , $\text{OsSb}_2$
ternary compounds:	$\text{CoAsS}$ (i.e. "pyrites" $\text{Co}_2\text{As}_2\text{S}_2$ ), $\text{NiSbS}$ {i.e. "pyrites" $\text{Ni}(\text{Sb-S})$ }, $\text{NiAsS}$ (i.e. pyrites with random As and S on the S positions)

Compounds of As, Sb and Bi with the metals in Group 13 (Al, Ga, In, Tl) comprise the important III–V semiconductors whose structures, properties, and extensive applications have already been discussed (pp. 255–8). Group 14 elements also readily form compounds of which the following serve as examples:  $\text{GeAs}$  mp  $737^\circ\text{C}$ ,  $\text{GeAs}_2$  mp  $732^\circ\text{C}$ ,  $\text{SnAs}$

(NaCl structure, superconductor below 3.5 K),  $\text{Sn}_4\text{As}_3$  (defect NaCl structure, superconductor below 1.2 K). The many important industrial applications of dilute alloys of As, Sb and Bi with tin and lead were mentioned on pp. 370 and 371.

### 13.3.2 Hydrides of arsenic, antimony and bismuth

$\text{AsH}_3$ ,  $\text{SbH}_3$  and  $\text{BiH}_3$  are exceedingly poisonous, thermally unstable, colourless gases whose physical properties are compared with those of  $\text{NH}_3$  (p. 423) and  $\text{PH}_3$  (p. 492) in Table 13.5. The absence of H bonding is apparent; in addition, the proton affinity is very low and there is little tendency to form the onium ions  $\text{MH}_4^+$  analogous to  $\text{NH}_4^+$ . However, very recently the thermally unstable salts  $[\text{AsH}_4]^+[\text{SbF}_6]^-$  (decomp.  $-40^\circ\text{C}$ ),  $[\text{AsH}_4]^+[\text{AsF}_6]^-$  (d.  $-75^\circ$ ) and  $[\text{SbH}_4]^+[\text{SbF}_6]^-$  (d.  $-70^\circ$ ), have been isolated as colourless air- and moisture-sensitive crystals by protonation of the hydrides  $\text{MH}_3$  with the appropriate superacids.  $\text{HF}/\text{MF}_5$  ( $\text{M} = \text{As}, \text{Sb}$ ).<sup>(18)</sup> The gradually increasing densities of the liquids near their bp is expected, as is the increase in M–H distance. There is a small diminution in the angle H–M–H with increasing molecular weight though the difference for  $\text{AsH}_3$  and  $\text{SbH}_3$  is similar to the experimental uncertainty. The rapid diminution in thermal stability is reflected in the standard heats of formation  $\Delta H_f^\circ$ ;  $\text{AsH}_3$  decomposes to the elements on being warmed to  $250\text{--}300^\circ$ ,  $\text{SbH}_3$  decomposes steadily

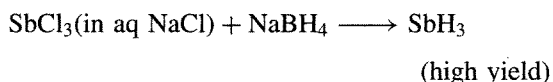
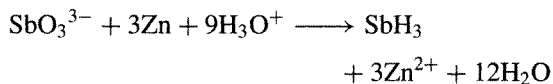
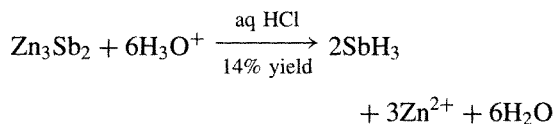
<sup>18</sup> R. MINKWITZ, A. KORNATH, W. SAWODNY and H. HÄRTNER, *Z. anorg. allg. Chem.* **620** 753–6 (1994).

**Table 13.5** Comparison of the physical properties of  $\text{AsH}_3$ ,  $\text{SbH}_3$  and  $\text{BiH}_3$  with those of  $\text{NH}_3$  and  $\text{PH}_3$

Property	$\text{NH}_3$	$\text{PH}_3$	$\text{AsH}_3$	$\text{SbH}_3$	$\text{BiH}_3$
MP/ $^\circ\text{C}$	–77.8	–133.5	–116.3	–88	–
BP/ $^\circ\text{C}$	–34.5	–87.5	–62.4	–18.4	+16.8 (extrap)
Density/g $\text{cm}^{-3}$ ( $T^\circ\text{C}$ )	0.683 (–34 $^\circ$ )	0.746 (–90 $^\circ$ )	1.640 (–64 $^\circ$ )	2.204 (–18 $^\circ$ )	–
$\Delta H_f^\circ/\text{kJ mol}^{-1}$	–46.1	–9.6(?)	66.4	145.1	277.8
Distance (M–H)/pm	101.7	141.9	151.9	170.7	–
Angle H–M–H	107.8 $^\circ$	93.6 $^\circ$	91.8 $^\circ$	91.3 $^\circ$	–

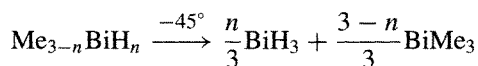
at room temperature, and  $\text{BiH}_3$ , cannot be kept above  $-45^\circ$ .

Arsine,  $\text{AsH}_3$ , is formed when many As-containing compounds are reduced with nascent hydrogen and its decomposition on a heated glass surface to form a metallic mirror formed the basis of Marsh's test for the element. The low-temperature reduction of  $\text{AsCl}_3$  with  $\text{LiAlH}_4$  in diethyl ether solution gives good yields of the gas as does the dilute acid hydrolysis of many arsenides of electropositive elements (Na, Mg, Zn, etc.). Similar reactions yield stibine, e.g.:



Both  $\text{AsH}_3$  and  $\text{SbH}_3$  oxidize readily to the trioxide and water, and similar reactions occur with S and Se.  $\text{AsH}_3$  and  $\text{SbH}_3$  form arsenides and antimonides when heated with metals and this reaction also finds application in semiconductor technology; e.g. highly purified  $\text{SbH}_3$  is used as a gaseous *n*-type dopant for Si (p. 332).

Bismuthine,  $\text{BiH}_3$ , is extremely unstable and was first detected in minute traces by F. Paneth using a radiochemical technique involving  $^{212}\text{Bi}_2\text{Mg}_3$ . These experiments, carried out in 1918, were one of the earliest applications of radiochemical tracer experiments in chemistry. Later work using  $\text{BH}_4^-$  to reduce  $\text{BiCl}_3$  was unsuccessful in producing macroscopic amounts of the gas and the best preparation (1961) is the disproportionation of  $\text{MeBiH}_2$  at  $-45^\circ$  for several hours;  $\text{Me}_2\text{BiH}$  can also be used:



Lower hydrides such as  $\text{As}_2\text{H}_4$  have occasionally been reported as fugitive species but little is known of their properties (see p. 583;

cf. also  $\text{N}_2\text{H}_4$ , p. 427;  $\text{P}_2\text{H}_4$ , p. 495). Recent fully optimized *ab initio* calculations (including relativistic core potentials) suggest that the double-bonded species  $\text{HM}=\text{MH}$  ( $\text{M} = \text{P}, \text{As}, \text{Sb}, \text{Bi}$ ) should all exist as *trans* planar ( $C_{2v}$ ) molecules;<sup>(19)</sup> close agreement with experimental interatomic distances in known organic diphosphenes (p. 544) and diarsenes adds confidence to the computed distances for  $-\text{Sb}=\text{Sb}-$  (260.8 pm) and  $-\text{Bi}=\text{Bi}-$  (271.9 pm) which are both about 9% shorter than the corresponding single-bond distances (cf. also  $-\text{P}=\text{P}-$  200.5 pm and  $-\text{As}=\text{As}-$  222.7 pm). The computed bond angles  $\text{H}-\text{M}-\text{M}$  in  $\text{M}_2\text{H}_2$  ( $\text{M} = \text{P}, \text{As}, \text{Sb}, \text{Bi}$ ) are  $96.2^\circ$ ,  $94.4^\circ$ ,  $93.0^\circ$  and  $91.8^\circ$ , respectively.

### 13.3.3 Halides and related complexes

The numerous halides of As, Sb and Bi show highly significant gradations in physical properties, structure, bonding and chemical reactivity. Distinctions between ionic, coordinate and covalent (molecular) structures in the halides and their complexes frequently depend on purely arbitrary demarcations and are often more a hindrance than a help in discerning the underlying structural and bonding principles. Alternations in the stability of the +5 oxidation state are also illuminating. It will be convenient to divide the discussion into five subsections dealing in turn with the trihalides  $\text{MX}_3$ , the pentahalides  $\text{MX}_5$ , other halides, halide complexes of  $\text{M}^{\text{III}}$  and  $\text{M}^{\text{V}}$ , and oxohalides.

#### Trihalides, $\text{MX}_3$

All 12 compounds are well known and are available commercially; their physical properties are summarized in Table 13.6 Comparisons with the corresponding data for  $\text{NX}_3$  (p. 438) and  $\text{PX}_3$  (p. 496) are also instructive. Trends in mp, bp and density are far from regular and reflect the differing structures and bond types.

<sup>19</sup> S. NAGASE, S. SUSUKI and T. KURAKAKE, *J. Chem. Soc., Chem. Commun.*, 1724–6 (1990).

Table 13.6 Some physical properties of the trihalides of arsenic, antimony and bismuth

Compound	Colour and state at 25°C	MP/°C	BP/°C	$d/g\text{ cm}^{-3}$ (T°C)	$\Delta H_f^\circ/kJ\text{ mol}^{-1}$
AsF <sub>3</sub>	Colourless liquid	-6.0	62.8	2.666 (0°)	-956.5
AsCl <sub>3</sub>	Colourless liquid	-16.2	130.2	2.205 (0°)	-305.0
AsBr <sub>3</sub>	Pale-yellow crystals	+31.2	221	3.66 (15°)	-197.0
AsI <sub>3</sub>	Red crystals	140.4	~400	4.39 (15°)	-58.2
SbF <sub>3</sub>	Colourless crystals	290	~345	4.38 (25°)	-915.5
SbCl <sub>3</sub>	White, deliquescent crystals	73.4	223	3.14 (20°)	-382.2
SbBr <sub>3</sub>	White, deliquescent crystals	96.0	288	4.15 (25°)	-259.4
SbI <sub>3</sub>	Red crystals	170.5	401	4.92 (22°)	-100.4
BiF <sub>3</sub>	Grey-white powder	649 <sup>(a)</sup>	900	~5.3	-900
BiCl <sub>3</sub>	White, deliquescent crystals	233.5	441	4.75	-379
BiBr <sub>3</sub>	Golden, deliquescent crystals	219	462	5.72	-276
BiI <sub>3</sub>	Green-black crystals	408.6	~542	5.64	-150

(extrap)

<sup>(a)</sup>BiF<sub>3</sub> is sometimes said to be "infusible" or to have mp at varying temperatures in the range 725–770°, but such materials are probably contaminated with the oxofluoride BiOF (p. 572).

Thus AsF<sub>3</sub>, AsCl<sub>3</sub>, AsBr<sub>3</sub>, SbCl<sub>3</sub> and SbBr<sub>3</sub> are clearly volatile molecular species, whereas AsI<sub>3</sub>, SbF<sub>3</sub> and BiX<sub>3</sub> have more extended interactions in the solid state. Trends in the heats of formation from the elements are more regular being *ca.* -925 kJ mol<sup>-1</sup> for MF<sub>3</sub>, *ca.* -350 kJ mol<sup>-1</sup> for MCl<sub>3</sub>, *ca.* -245 kJ mol<sup>-1</sup> for MBr<sub>3</sub> and *ca.* -100 kJ mol for MI<sub>3</sub>. Within these average values, however, AsF<sub>3</sub> is noticeably more exothermic than SbF<sub>3</sub> and BiF<sub>3</sub>, whereas the reverse is true for the chlorides; there is also a regular trend towards increasing stability in the sequence As < Sb < Bi for the bromides and for the iodides of these elements.

The trifluorides are all readily prepared by the action of HF on the oxide M<sub>2</sub>O<sub>3</sub> (direct fluorination of M or M<sub>2</sub>O<sub>3</sub> with F<sub>2</sub> gives MF<sub>5</sub>, p. 561). Because AsF<sub>3</sub> hydrolyses readily, the reaction is best done under anhydrous conditions using H<sub>2</sub>SO<sub>4</sub>/CaF<sub>2</sub> or HSO<sub>3</sub>F/CaF<sub>2</sub>, but aqueous HF can be used for the others. The trichlorides, tribromides and triiodides of As and Sb can all be prepared by direct reaction of X<sub>2</sub> with M or M<sub>2</sub>O<sub>3</sub>, whereas the less readily hydrolysed BiX<sub>3</sub> can be obtained by treating Bi<sub>2</sub>O<sub>3</sub> with the aqueous HX. Many variants of these reactions are possible: e.g., AsCl<sub>3</sub> can be made by chlorination of As<sub>2</sub>O<sub>3</sub> with Cl<sub>2</sub>, S<sub>2</sub>Cl<sub>2</sub>, conc HCl or H<sub>2</sub>SO<sub>4</sub>/MCl.

The trihalides of As are all pyramidal molecular species in the gas phase with angle X-As-X in the range 96–100°. This structure persists in the solid state, and with AsI<sub>3</sub> the packing is such that each As is surrounded by an octahedron of six I with 3 short and 3 long As-I distances (256 and 350 pm; ratio 1.37, mean 303 pm). The I atoms form a regular hcp lattice. A similar layer structure is adopted by SbI<sub>3</sub> and BiI<sub>3</sub> but with the metal atoms progressively nearer to the centre of the I<sub>6</sub> octahedra:

3 Sb-I at 287 pm and 3 at 332 pm; ratio 1.16, mean 310 pm  
all 6Bi-I at 310 pm; "ratio" 1.00

This is sometimes described as a trend from covalent, molecular AsI<sub>3</sub> through intermediate SbI<sub>3</sub> to ionic BiI<sub>3</sub>, but this exaggerates the difference in bond-type. Arsenic, Sb and Bi have very similar electronegativities (p. 550) and it seems likely that the structural trend reflects more the way in which the octahedral interstices in the hcp iodine lattice are filled by atoms of gradually increasing size. The size of these interstices is about constant (see mean M-X distance) but only Bi is sufficiently large to fill them symmetrically.

Discrete molecules are apparent in the crystal structure of the higher trihalides of Sb, and,

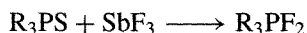
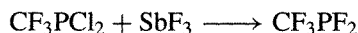
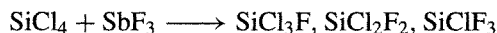
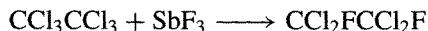
Table 13.7 Structural data for antimony trihalides

	SbF <sub>3</sub>	SbCl <sub>3</sub>	α-SbBr <sub>3</sub>	β-SbBr <sub>3</sub>	SbI <sub>3</sub>
Sb-X in gas molecule/pm	?	233	251	251	272
Three short Sb-X in crystal/pm	192	236	250	249	287
Three long Sb-X in crystal/pm	261	≥350	≥375	≥360	332
Ratio (long/short)	1.36	≥1.48	≥1.50	≥1.44	1.16
Angle X-Sb-X in crystal	87°	95°	96°	95°	96°

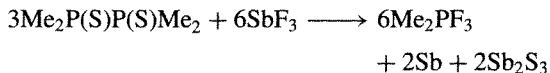
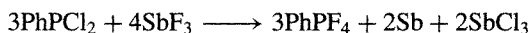
again, these pack to give 3 longer and 3 shorter interatomic distances (Table 13.7).

The structure of BiF<sub>3</sub> is quite different: β-BiF<sub>3</sub> has the "ionic" YF<sub>3</sub> structure with tricapped trigonal prismatic coordination of Bi by 9 F. BiCl<sub>3</sub> has an essentially molecular structure (like SbX<sub>3</sub>) but there is a significant distortion within the molecule itself, and the packing gives 5 (not 3) further Cl at 322–345 pm to complete a bicapped trigonal prism. As a consequence of this structure BiCl<sub>3</sub> has smaller unit cell dimensions than SbCl<sub>3</sub> despite the longer Bi–Cl bond (250 pm, as against 236 pm for Sb–Cl). The eightfold coordination has been rationalized by postulating that the ninth position is occupied by the stereochemically active lone-pair of electrons on Bi<sup>III</sup>. On this basis, the 3 long and 3 short M–X distances in octahedrally coordinated structures can also be understood, the lone-pair being directed towards the centre of the more distant triangle of 3X. However, it is hard to quantify this suggestion, particularly as the X–M–X angles are fairly constant at 97 ± 2° (rather than 109.5° for sp<sup>3</sup> hybrids), implying little variation in hybridization and a lone-pair with substantial s<sup>2</sup> character. The effect is less apparent in SbI<sub>3</sub> and absent BiI<sub>3</sub> (see above) and this parallels the diminishing steric influence of the lone-pair in some of the complexes of the heavier halides with Sn<sup>II</sup> (p. 380) and Te<sup>IV</sup> (p. 757).

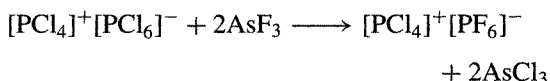
Many of the trihalides of As, Sb and Bi hydrolyse readily but can be handled without great difficulty under anhydrous conditions. AsF<sub>3</sub> and SbF<sub>3</sub> are important reagents for converting non-metal chlorides to fluorides. SbF<sub>3</sub> in particular is valuable for preparing organofluorine compounds (the Swarts reaction):



Sometimes the reagents simultaneously act as mild oxidants:



AsF<sub>3</sub>, though a weaker fluorinating agent than SbF<sub>3</sub>, is preferred for the preparation of high-boiling fluorides since AsCl<sub>3</sub> (bp 130°) can be distilled off. SbF<sub>3</sub> is preferred for low-boiling fluorides, which can be readily fractionated from SbCl<sub>3</sub> (bp 223°). Selective fluorinations are also possible, e.g.:



AsCl<sub>3</sub> and SbCl<sub>3</sub> have been used as non-aqueous solvent systems for a variety of reactions.<sup>(20,21)</sup> They are readily available, have convenient liquid ranges (p. 559), are fairly easy to handle, have low viscosities η, moderately high dielectric constants ε and good solvent properties (Table 13.8).

<sup>20</sup> D. S. PAYNE, Chap. 8 in T. C. WADDINGTON (ed.), *Nonaqueous Solvent Systems*, pp. 301–25, Academic Press, London, 1965.

<sup>21</sup> E. C. BAUGHAN, Chap. 5 in J. J. LAGOWSKI (ed.), *The Chemistry of Nonaqueous Solvents*, Vol. 4, pp. 129–65, Academic Press, London, 1976.



**Table 13.8** Some properties of liquid AsCl<sub>3</sub> and SbCl<sub>3</sub>

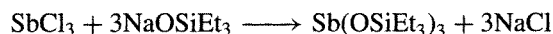
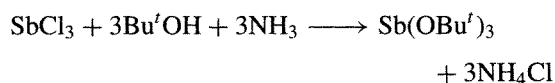
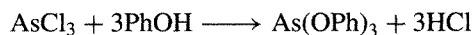
	$\eta$ /centipoise	$\epsilon$	$\kappa/\text{ohm}^{-1} \text{ cm}^{-1}$
AsCl <sub>3</sub> at 20°C	1.23	12.8	$1.4 \times 10^{-7}$
SbCl <sub>3</sub> at 75°C	2.58	33.2	$1.4 \times 10^{-6}$

The low conductivities imply almost negligible self-ionization according to the formal scheme:

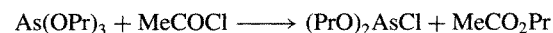
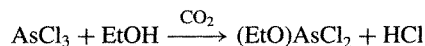
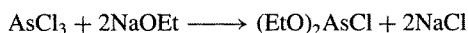


Despite this, they are good solvents for chloride-ion transfer reactions, and solvo-acid-solvo-base reactions (p. 827) can be followed conductimetrically, voltametrically or by use of coloured indicators. As expected from their constitution, the trihalides of As and Sb are only feeble electron-pair donors (p. 198) but they have marked acceptor properties, particularly towards halide ions (p. 564) and amines.

AsX<sub>3</sub> and SbX<sub>3</sub> react with alcohols (especially in the presence of bases) and with sodium alkoxide to give arsenite and antimonite esters, M(OR)<sub>3</sub> (cf. phosphorus, (p. 515):

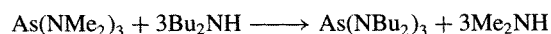
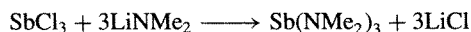
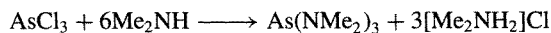


Halide esters (RO)<sub>2</sub>MX and (RO)MX<sub>2</sub> can be made similarly:



Amino derivatives are obtained by standard reactions with secondary amines, lithium amides or

by transaminations:



As with phosphorus (p. 533) there is an extensive derivative chemistry of these and related compounds.<sup>(15,16)</sup>

### Pentahalides, MX<sub>5</sub>

Until fairly recently only the pentafluorides and SbCl<sub>5</sub> were known, but the exceedingly elusive AsCl<sub>5</sub> was finally prepared in 1976 by ultraviolet irradiation of AsCl<sub>3</sub> in liquid Cl<sub>2</sub> at -105°C.<sup>(22)</sup> Some properties of the 5 pentahalides are given in Table 13.9.

The pentafluorides are prepared by direct reaction of F<sub>2</sub> with the elements (As, Bi) or their oxides (As<sub>2</sub>O<sub>3</sub>, Sb<sub>2</sub>O<sub>3</sub>). AsCl<sub>5</sub>, as noted above, has only a fugitive existence and decomposes to AsCl<sub>3</sub> and Cl<sub>2</sub> at about -50°. SbCl<sub>5</sub> is more stable and is made by reaction of Cl<sub>2</sub> on SbCl<sub>3</sub>. No pentabromides or pentaiodides have been characterized, presumably because M<sup>V</sup> is too highly oxidizing for these heavier halogens (cf. TlI<sub>3</sub>, p. 239). The relative instability of AsCl<sub>5</sub> when compared with PCl<sub>5</sub> and SbCl<sub>5</sub> is a further example of the instability of the highest valency state of p-block elements following the completion of the first (3d) transition series (p. 552). This can be understood in terms of incomplete shielding of the nucleus which leads to a "d-block contraction" and a consequent lowering of the energy of the 4s orbital in As and AsCl<sub>3</sub>, thereby making it more difficult to promote one of the 4s<sup>2</sup> electrons

<sup>22</sup> K. SEPPPELT, *Angew. Chem. Int. Edn. Engl.* **15**, 377-8 (1976).

**Table 13.9** Some properties of the known pentahalides

Property	AsF <sub>5</sub>	SbF <sub>5</sub>	BiF <sub>5</sub>	AsCl <sub>5</sub>	SbCl <sub>5</sub>
MP/°C	-79.8	8.3	154.4	~ -50 (d)	4
BP/°C	-52.8	141	230	—	140 (d)
Density (T°C)/g cm <sup>-3</sup>	2.33 (-53°)	3.11 (25°)	5.40 (25°)	—	2.35 (21°)

for the formation of  $\text{AsCl}_5$ . There is no evidence that the As–Cl bond strength itself, in  $\text{AsCl}_5$ , is unduly weak. The non-existence of  $\text{BiCl}_5$  likewise suggests that it is probably less stable than  $\text{SbCl}_5$ , due the analogous “f-block contraction” following the lanthanide elements (p. 1232).

Evidence from vibration spectroscopy suggests that gaseous  $\text{AsF}_5$ , solid  $\text{AsCl}_5$  and liquid  $\text{SbCl}_5$  are trigonal bipyramidal molecules like  $\text{PF}_5$  ( $D_{3h}$ ), and this is confirmed for  $\text{AsF}_5$  by a low-temperature X-ray crystal structure which also indicates that the As–F(axial) distances (171.9 pm) are slightly longer than the As–F (equatorial) distances (166.8 pm).<sup>(23)</sup> By contrast  $\text{SbF}_5$  is an extremely viscous, syrupy liquid with a viscosity approaching 850 centipoise at 20°: the liquid features polymeric chains of *cis*-bridged  $\{\text{SbF}_6\}$  octahedra in which the 3 different types of F atom (a, b, c) can be distinguished by low-temperature  $^{19}\text{F}$  nmr spectroscopy.<sup>(24)</sup> As shown in Fig. 13.4(a),  $F_a$  are the bridging atoms and are *cis* to each other in any one octahedron;  $F_b$  are

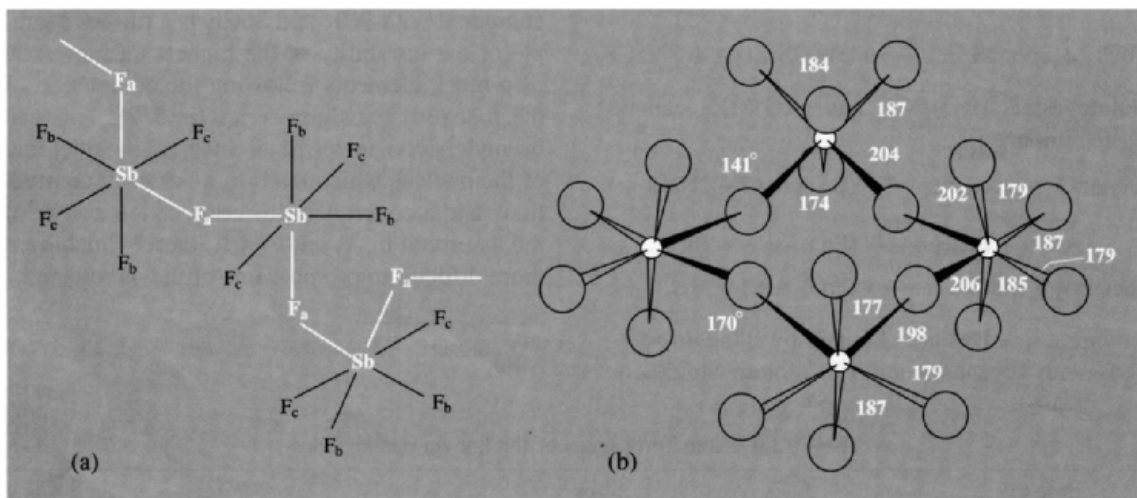
also *cis* to each other and are, in addition, *cis* to 1  $F_a$  and *trans* to the other, whereas  $F_c$  are *trans* to each other and *cis* to both  $F_a$ . In the crystalline state the *cis* bridging persists but the structure has tetrameric molecular units (Fig. 13.4(b)) rather than high polymers.<sup>(25)</sup> There are two different Sb–F–Sb bridging angles, 141° and 170°, and the terminal Sb– $F_l$  distances (mean  $182 \pm 5$  pm) are noticeably less than the bridging Sb– $F_\mu$  distances (mean  $203 \pm 5$  pm). (See p. 569 for the ionic structures of  $\text{Sb}_8\text{F}_{30}$ , i.e.  $\text{Sb}^{\text{V}}_3\text{Sb}^{\text{III}}_5\text{F}_{30}$ .) Yet another structure motif is adopted in  $\text{BiF}_5$ ; this crystallizes in long white needles and has the  $\alpha\text{-UF}_5$  structure in which infinite linear chains of *trans*-bridged  $\{\text{BiF}_6\}$  octahedra are stacked parallel to each other. The Bi–F–Bi bridging angle between adjacent octahedra in the chain is 180°.

The pentafluorides are extremely powerful fluorinating and oxidizing agents and they also have a strong tendency to form complexes with electron-pair donors. This latter property has already been presaged by the propensity of  $\text{SbF}_5$  to polymerize and is discussed more fully on p. 569.

<sup>23</sup> J. KOHLER, A. SIMON and R. HOPPE, *Z. anorg. allg. Chem.* 575, 55–60 (1989).

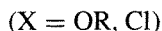
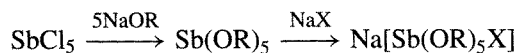
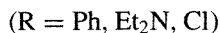
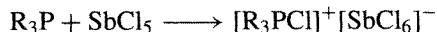
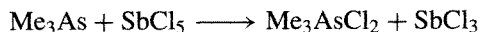
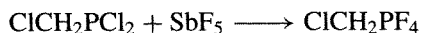
<sup>24</sup> T. K. DAVIES and K. C. MOSS, *J. Chem. Soc. (A)*, 1054–8 (1970).

<sup>25</sup> A. J. EDWARDS and P. TAYLOR, *J. Chem. Soc., Chem. Commun.*, 1376–7 (1971).



**Figure 13.4** (a) The *cis*-bridged polymeric structure of liquid  $\text{SbF}_5$  (schematic) showing the three sorts of F atom.<sup>(24)</sup> (b) Structure of the tetrameric molecular unit in crystalline  $(\text{SbF}_5)_4$  showing the *cis*-bridging of 4  $\{\text{SbF}_6\}$  octahedra (distances in pm).<sup>(25)</sup>

See also "superacids" on p. 570. Some typical reactions of  $\text{SbF}_5$  and  $\text{SbCl}_5$  are as follows:



Perhaps the most reactive compound of the group is  $\text{BiF}_5$ . It reacts extremely vigorously with  $\text{H}_2\text{O}$  to form  $\text{O}_3$ ,  $\text{OF}_2$  and a voluminous brown precipitate which is probably a hydrated bismuth(V) oxide fluoride. At room temperature  $\text{BiF}_5$  reacts vigorously with iodine or sulfur; above  $50^\circ$  it converts paraffin oil to fluorocarbons; at  $150^\circ$  it fluorinates  $\text{UF}_4$  to  $\text{UF}_6$ ; and at  $180^\circ$  it converts  $\text{Br}_2$  to  $\text{BrF}_3$  and  $\text{BrF}_5$ , and  $\text{Cl}_2$  to  $\text{ClF}$ .

### Mixed halides and lower halides

Unlike phosphorus, which forms a large number of readily isolable mixed halides of both  $\text{P}^{\text{III}}$  and  $\text{P}^{\text{V}}$ , there is apparently less tendency to form such compounds with As, Sb and Bi, and few mixed halides have so far been characterized.  $\text{AsF}_3$  and  $\text{AsCl}_3$  are immiscible below  $19^\circ\text{C}$ , but at room temperature  $^{19}\text{F}$  nmr indicates some halogen exchange; however equilibrium constants for the formation of  $\text{AsF}_2\text{Cl}$  and  $\text{AsFCl}_2$  are rather small. Likewise, Raman spectra show the presence of  $\text{AsCl}_2\text{Br}$  and  $\text{AsClBr}_2$  in mixtures of the parent trihalides, though rapid equilibration prevents isolation of the mixed halides. It is said that  $\text{SbBrI}_2$  (mp  $88^\circ$ ) can be obtained by eliminating  $\text{EtBr}$  from  $\text{EtSbI}_2\text{Br}_2$ .

Mixed pentahalides are more readily isolated and are of at least three types: ionic, tetrameric, and less stable molecular trigonal-bipyramidal monomers. Thus, chlorination of a mixture of  $\text{AsF}_3/\text{AsCl}_3$  with  $\text{Cl}_2$ , or fluorination of  $\text{AsCl}_3$  with  $\text{ClF}_3$  (p. 828) gives  $[\text{AsCl}_4]^+[\text{AsF}_6]^-$  [mp  $130^\circ(\text{d})$ ] whose X-ray

crystal structure has recently been redetermined.<sup>(26)</sup> Similarly,  $\text{AsCl}_3 + \text{SbCl}_5 + \text{Cl}_2 \rightarrow [\text{AsCl}_4]^+[\text{SbCl}_6]^-$ . It also appears that all members of the monomeric molecular series  $\text{AsCl}_{5-n}\text{F}_n$  ( $n = 1 - 4$ ) can be made either by thermolysis of  $[\text{AsCl}_4]^+[\text{AsF}_6]^-$  or, in the case of  $\text{AsCl}_3\text{F}_2$  ( $D_{3h}$ ), by gas-solid reaction of  $\text{AsCl}_2\text{F}_3$  (g) with  $\text{CaCl}_2$  (s); the compounds were characterized as trigonal-bipyramidal molecules by low-temperature matrix ir and Raman spectra.<sup>(27)</sup> The mixed bromofluoride  $[\text{AsBr}_4]^+[\text{AsF}_6]^-$ , made by reaction of  $\text{AsBr}_3$ ,  $\text{Br}_2$  and  $\text{AsF}_5$  at low temperature was also characterized by Raman spectroscopy.<sup>(28)</sup>

Antimony chloride fluorides have been known since the turn of the century but the complexity of the system, the tendency to form mixtures of compounds, and their great reactivity have conspired against structural characterization until fairly recently.<sup>(29)</sup> It is now clear that fluorination of  $\text{SbCl}_5$  depends crucially on the nature of the fluorinating agent. Thus, with  $\text{AsF}_3$  it gives  $\text{SbCl}_4\text{F}$  (mp  $83^\circ$ ) which is a *cis*-F-bridged tetramer as in Fig. 13.4(b) with the terminal F atoms replaced by Cl. Fluorination of  $\text{SbCl}_5$  with HF also gives this compound but, in addition,  $\text{SbCl}_3\text{F}_2$  mp  $68^\circ$  (*cis*-F-bridged tetramer) and  $\text{SbCl}_2\text{F}_3$  mp  $62^\circ$ , which turns out to be  $[\text{SbCl}_4]^+[\text{Sb}_2\text{Cl}_2\text{F}_6]^-$ . The anion is F-bridged, i.e.  $[\text{ClF}_4\text{Sb}-\text{F}-\text{SbF}_4\text{Cl}]^-$  with angle  $\text{Sb}-\text{F}-\text{Sb}$   $163^\circ$ . Even more extensive fluorination occurs when  $\text{SbCl}_5$  is reacted with  $\text{SbF}_5$  and the product is  $[\text{SbCl}_4]^+[\text{Sb}_2\text{F}_{11}]^-$ . By contrast, fluorination of  $(\text{SbCl}_4\text{F})_4$  with  $\text{SbF}_5$  in liquid  $\text{SO}_2$  yields  $\text{Sb}_4\text{Cl}_{13}\text{F}_7$  (mp  $\sim 50^\circ$ ) which is a *cis*-F-bridged tetramer of  $\text{SbCl}_3\text{F}_2$  with two of the Sb atoms having a Cl atom partially replaced by F, i.e.  $(\text{Sb}_2\text{Cl}_{6.5}\text{F}_{3.5})_2$  and bridge angles  $\text{Sb}-\text{F}-\text{Sb}$  of  $166-168^\circ$ .

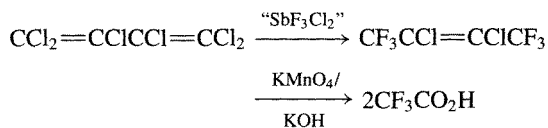
<sup>26</sup> R. MINKWITZ, J. NOWICKI and H. BORRMANN, *Z. anorg. allg. Chem.* **596**, 93-8 (1991).

<sup>27</sup> R. MINKWITZ and H. PRENZEL, *Z. anorg. allg. Chem.* **548**, 103-7 (1987).

<sup>28</sup> T. KLAPOÛTKE, J. PASSMORE and E. G. AWERE, *J. Chem. Soc., Chem. Commun.*, 1426-7 (1988).

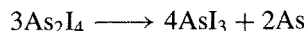
<sup>29</sup> J. G. BALLARD, T. BIRCHALL and D. R. SLIM, *J. Chem. Soc., Dalton Trans.*, 62-5 (1979), and references therein.

The attention which has been paid to the mixed chloride fluorides of  $\text{Sb}^{\text{V}}$  is due not only to the intellectual problem of their structures but also to their importance as industrial fluorinating agents (Swarts reaction). Addition of small amounts of  $\text{SbCl}_5$  to  $\text{SbF}_5$  results in a dramatic decrease in viscosity (due to the breaking of  $\text{Sb-F-Sb}$  links) and a substantial increase in electrical conductivity (due to the formation of fluoro-complex ions). Such mixed halides are often more effective fluorinating agents than  $\text{SbF}_3$ , provided that yields are not lowered by oxidation, e.g.  $\text{SOCl}_2$  gives  $\text{SOF}_2$ ;  $\text{POCl}_3$  gives  $\text{POFCl}_2$ ; and hexachlorobutadiene is partially fluorinated and oxidized to give  $\text{CF}_3\text{CCl}=\text{CClCF}_3$  which can then be further oxidized to  $\text{CF}_3\text{CO}_2\text{H}$ :



The use of  $\text{SbF}_5$  in the preparation of "superacids" such as ( $\text{HSO}_3\text{F} + \text{SbF}_5 + \text{SO}_3$ ) is described in the following subsection (p. 570).

The only well-established lower halide of As is  $\text{As}_2\text{I}_4$  which is formed as red crystals (mp  $137^\circ$ ) when stoichiometric amounts of the 2 elements are heated to  $260^\circ$  in a sealed tube in the presence of octahydrophenanthrene. The compound hydrolyses and oxidizes readily and disproportionates in warm  $\text{CS}_2$  solution but is stable up to  $150^\circ$  in an inert atmosphere. Disproportionation is quantitative at  $400^\circ$ :



$\text{Sb}_2\text{I}_4$  is much less stable: it has been detected by emf or vapour pressure measurements on solutions of Sb in  $\text{SbI}_3$  at  $230^\circ$  but has not been isolated as a pure compound.

The lower halides of Bi are rather different. The diatomic species  $\text{BiX}$  ( $\text{X} = \text{Cl}, \text{Br}, \text{I}$ ) occur in the equilibrium vapour above heated  $\text{Bi-BiX}_3$  mixtures. A black crystalline lower chloride of composition  $\text{BiCl}_{1.167}$  is obtained by heating  $\text{Bi-BiCl}_3$  mixtures to  $325^\circ$  and cooling them during 1–2 weeks to  $270^\circ$  before removing excess  $\text{BiCl}_3$  by sublimation or extraction into

benzene. The compound is diamagnetic and has an astonishing structure which involves cationic clusters of bismuth and 2 different chloro-complex anions:<sup>(30)</sup>  $[(\text{Bi}_9^{5+})_2(\text{BiCl}_5^{2-})_4(\text{Bi}_2\text{Cl}_8^{2-})]$ , i.e.  $\text{Bi}_{24}\text{Cl}_{28}$  or  $\text{Bi}_6\text{Cl}_7$ . The  $\text{Bi}_9^{5+}$  cluster is a tricapped trigonal prism (p. 591); the anion  $\text{BiCl}_5^{2-}$  has square pyramidal coordination of the 5 Cl atoms around Bi with the sixth octahedral position presumably occupied by the lone-pair of electrons, and  $\text{Bi}_2\text{Cl}_8^{2-}$  has two such pyramids *trans*-fused at a basal edge (p. 565). The compound is stable in vacuum below  $200^\circ$  but disproportionates at higher temperatures. It also disproportionates in the presence of ligands which coordinate strongly to  $\text{BiCl}_3$  and hydrolyses readily to the oxide chloride.

Bismuth also forms an intriguing family of subiodides,  $\text{Bi}_4\text{I}_4$ ,  $\text{Bi}_{14}\text{I}_4$  and  $\text{Bi}_{18}\text{I}_4$ , which comprise a series of infinite one-dimensional quasi-molecular ribbons of Bi atoms  $[\text{Bi}_m\text{I}_4]_\infty$  of different width ( $m = 4, 14, 18$ ). There are two sorts of Bi atom in these structures: "internal" atoms ( $\text{Bi}_m$ ) surrounded by three other Bi atoms only, at 300–312 pm (cf. 307 pm in Bi metal), and "external"  $\text{Bi}_{\text{ex}}$ , connected to differing numbers of Bi and I atoms depending on  $m$ .<sup>(31)</sup>  $\text{Bi}_4\text{Br}_4$  has a similar structure. The first unambiguous identification of  $\text{Bi}^+$  in the solid state came in 1971 when the structure of the complex halide  $\text{Bi}_{10}\text{Hf}_3\text{Cl}_{18}$  was shown by X-ray diffraction analysis<sup>(32)</sup> to be  $(\text{Bi}^+)(\text{Bi}_9^{5+})(\text{HfCl}_6^{2-})_3$ . The compound was made by the oxidation of Bi with  $\text{HfCl}_4/\text{BiCl}_3$ .

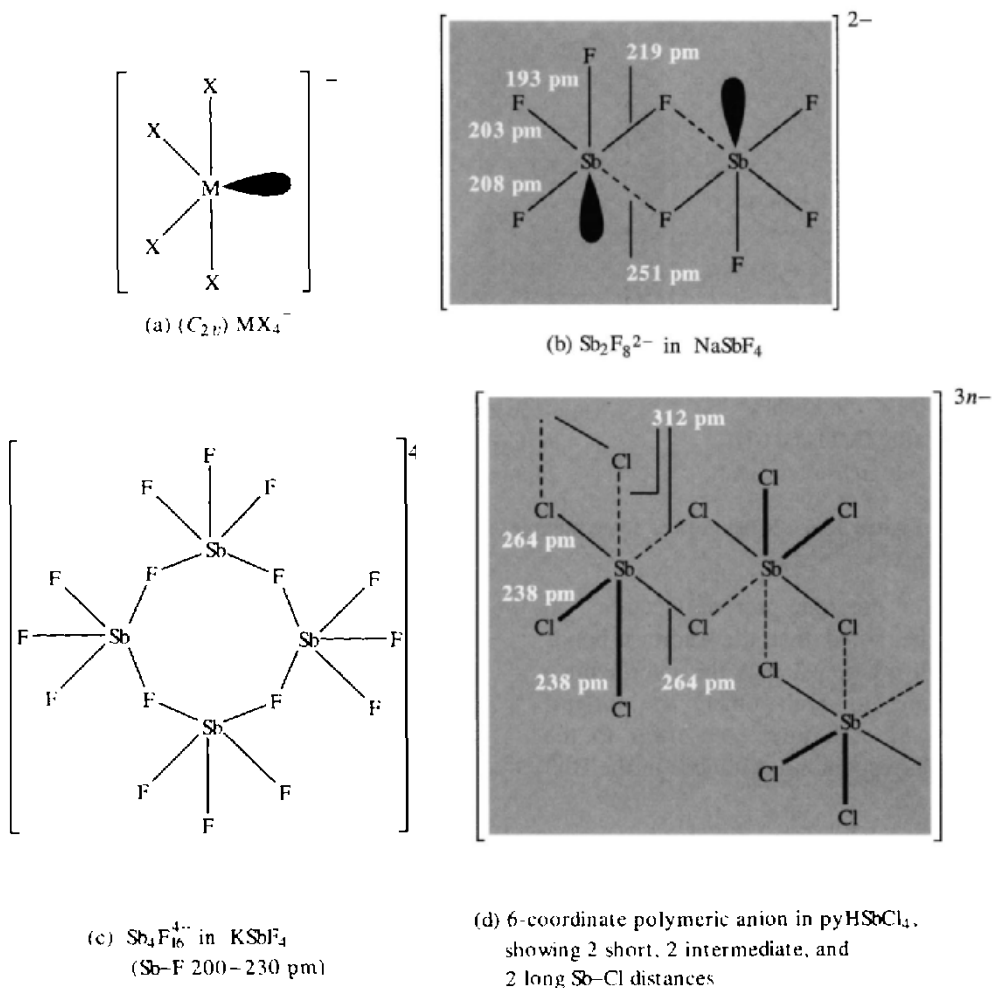
### Halide complexes of $\text{M}^{\text{III}}$ and $\text{M}^{\text{V}}$

The trihalides of As, Sb and Bi are strong halide-ion acceptors and numerous complexes have been isolated with a wide variety of compositions. They are usually prepared by direct reaction of the trihalide with the appropriate

<sup>30</sup> A. HERSHAFT and J. D. CORBETT, *Inorg. Chem.* **2**, 979–85 (1963).

<sup>31</sup> E. V. DIKAREV, B. A. POPOVKIN and A. V. SHEVELKOV, *Z. anorg. allg. Chem.* **612** 118–22 (1992).

<sup>32</sup> R. M. FRIEDMAN and J. D. CORBETT, *J. Chem. Soc., Chem. Commun.*, 422–3 (1971).

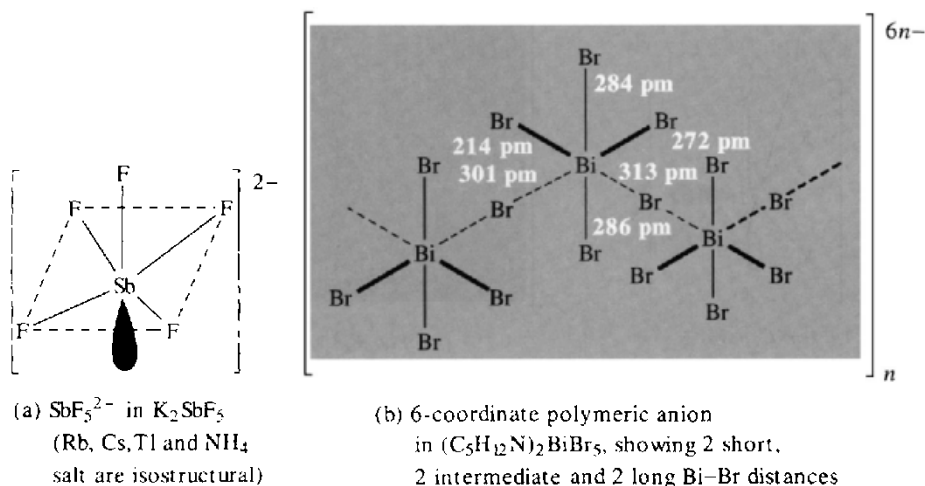


**Figure 13.5** Structures of some complex halide anions of stoichiometry  $MX_4^-$

halide-ion donor. However, stoichiometry is not always a reliable guide to structure because of the possibility of oligomerization which depends both on the nature of M and X, and often also on the nature of the counter cation.<sup>(16,33)</sup> Thus the tetra-alkylammonium salts of  $MCl_4^-$ ,  $MBr_4^-$ , and  $MI_4^-$  may contain the monomeric  $C_{2v}$  ion as shown in Fig. 13.5a (cf. isoelectronic  $SeF_4$ , p. 773), whereas in  $NaSbF_4$

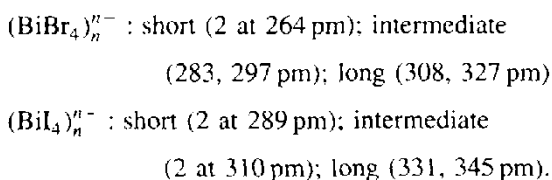
there is a tendency to dimerize by formation of subsidiary  $F \cdots Sb$  interactions (Fig. 13.5b) cf.  $Bi_2Cl_8^{2-}$  in the preceding subsection. With  $KSbF_4$  association proceeds even further to give tetrameric cyclic anions (Fig. 13.5c). In both  $NaSbF_4$  and  $KSbF_4$  the Sb atoms are 5-coordinate but coordination rises to 6 in the polymeric chain anions of the pyridinium and 2-methylpyridinium salts  $pyHSbCl_4$ ,  $(2-MeC_5H_4NH)BiBr_4$  and  $(2-MeC_5H_4NH)BiI_4$ . The structure of  $(SbCl_4)_n^{n-}$  is shown schematically in Fig. 13.5d and the three differing Sb-Cl distances reflect, in part,

<sup>33</sup> A. F. WELLS, *Structural Inorganic Chemistry*, 5th edn., pp. 879–88 and 894–9, Oxford University Press, Oxford, 1984.



**Figure 13.6** Structures of some complex halide anions of stoichiometry  $\text{MX}_5^{2-}$

the influence of the lone-pair of electrons on  $\text{Sb}^{\text{III}}$ . It will be noted that the shortest bonds are *cis* to each other, whereas the intermediate bonds are *trans* to each other; the longest bonds are *cis* to each other and *trans* to the short bonds. Corresponding distances in the  $\text{Bi}^{\text{III}}$  analogues are:

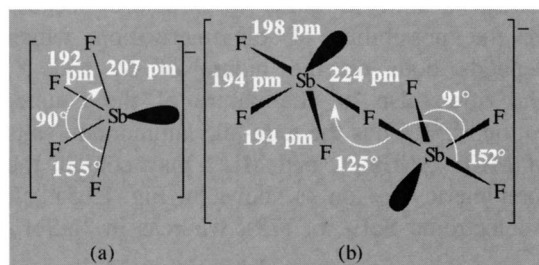


Complexes of stoichiometry  $\text{MX}_5^{2-}$  can feature either discrete 5-coordinate anions as in  $\text{K}_2\text{SbF}_5$  and  $(\text{NH}_4)_2\text{SbCl}_5$  (Fig. 13.6a), or 6-coordinate polymeric anions as in the piperidinium salt  $(\text{C}_5\text{H}_{10}\text{NH}_2)_2\text{BiBr}_5$  (Fig. 13.6b). In the discrete anion  $\text{SbCl}_5^{2-}$  the  $\text{Sb}-\text{Cl}_{\text{apex}}$  distance (236 pm) is shorter than the  $\text{Sb}-\text{Cl}_{\text{base}}$  distances (2 at 258 and 2 at 269 pm) and the Sb atom is slightly below the basal plane (by 22 pm). The same structure is observed in  $\text{K}_2\text{SbCl}_5$ .

In addition to the various complex fluoroantimonate(III) salts  $\text{M}^1\text{SbF}_4$  and  $\text{M}_2^1\text{SbF}_5$  mentioned above, the alkali metals form complexes of stoichiometry  $\text{M}^1\text{Sb}_2\text{F}_7$ ,  $\text{M}^1\text{Sb}_3\text{F}_{10}$  and  $\text{M}^1\text{Sb}_4\text{F}_{13}$ , i.e.  $[\text{SbF}_4^-(\text{SbF}_3)_n]^-$  ( $n = 1, 2, 3$ )

but the mononuclear complexes  $\text{M}_3^1\text{SbF}_6$  have not been found. The structure of  $\text{M}^1\text{Sb}_2\text{F}_7$  depends on the strength of the  $\text{Sb}-\text{F}\cdots\text{Sb}$  bridge between the 2 units and this, in turn is influenced by the cation. Thus, in  $\text{KSb}_2\text{F}_7$  there are distorted trigonal-bipyramidal  $\text{SbF}_4^-$  ions (Fig. 13.7a) and discrete pyramidal  $\text{SbF}_3$  molecules ( $\text{Sb}-\text{F}$  194 pm) with 2 (rather than 3) contacts between these and neighbouring  $\text{SbF}_4^-$  units of 241 and 257 pm (cf.  $\text{SbF}_3$  itself, p. 560). By contrast  $\text{CsSb}_2\text{F}_7$  has well-defined  $\text{Sb}_2\text{F}_7^-$  anions (Fig. 13.7b) formed from 2 distorted trigonal bipyramidal  $\{\text{SbF}_4\}$  groups sharing a common axial F atom with long bridge bonds.

Similar structural diversity characterizes the heavier halide complexes of the group. The



**Figure 13.7** Structures of  $\text{SbF}_4^-$  and  $\text{Sb}_2\text{F}_7^-$  ions in  $\text{KSbF}_4(\text{SbF}_3)$  and  $\text{CsSb}_2\text{F}_7$  respectively.

$[MX_6]^{3-}$  group occurs in several compounds, and these frequently have a regular octahedral structure like the isoelectronic  $[Te^{IV}X_6]^{2-}$  ions (p. 776), despite the formal 14-electron configuration on the central atom. For example the jet-black compound  $(NH_4)_2SbBr_6$  is actually  $[(NH_4^+)_4(Sb^{III}Br_6)^{3-}(Sb^VBr_6)^-]$  with alternating octahedral  $Sb^{III}$  and  $Sb^V$  ions. The undistorted nature of the  $SbBr_6^{3-}$  octahedra suggests that the lone-pair is predominantly  $5s^2$  but there is a sense in which this is still stereochemically active since the  $Sb-Br$  distance in  $[Sb^{III}Br_6]^{3-}$  (279.5 pm) is substantially longer than in  $[Sb^VBr_6]^-$  (256.4 pm). Similar dimensional changes are found in  $(pyH)_6Sb_4Br_{24}$  which is  $[(pyH^+)_6(Sb^{III}Br_6)^{3-}(Sb^VBr_6)^-]_3$ . In  $(Me_2NH_2)_3BiBr_6$  the  $(Bi^{III}Br_6)^{3-}$  octahedron is only slightly distorted. Sixfold coordination also occurs in compounds such as  $Cs_3Bi_2I_9$  and  $[(pyH^+)_5(Sb_2Br_9)^{3-}(Br^-)_2]$  in which  $M_2X_9^{3-}$  has the confacial bioctahedral structure of  $Tl_2Cl_9^{3-}$  (p. 240) (Fig. 13.8). In  $\beta$ - $Cs_3Sb_2Cl_9$  and  $Cs_3Bi_2Cl_9$ , however, there are close-packed  $Cs^+$  and  $Cl^-$  with  $Sb^{III}$  (or  $Bi^{III}$ ) in octahedral interstices. In  $Cs_3As_2Cl_9$  the  $\{AsCl_6\}$  groups are highly distorted so that there are discrete  $AsCl_3$  molecules ( $As-Cl$  225 pm) embedded between  $Cs^+$  and  $Cl^-$  ions ( $As-Cl^-$  275 pm).

Irregular 6- and 7-fold coordination of Sb occurs in the complexes of  $SbCl_3$  with crown thioethers,<sup>(34)</sup> and 8-fold coordination has been established in its complex with the  $\eta^5$ -ether

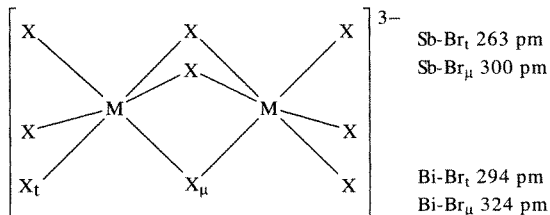
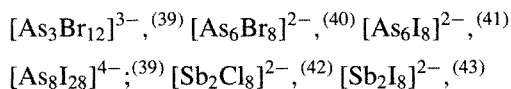


Figure 13.8 Structure of  $M_2X_9^{3-}$

ligand 15-crown-5.<sup>(35)</sup> Crown ethers have also been used to stabilize the first complexed (9-coordinate) trications of  $Sb^{III}$  and  $Bi^{III}$ , viz.  $[Sb(12-crown-4)_2(MeCN)]^{3+}[SbCl_6]_3^-$  and  $[Bi(12-crown-4)_2(MeCN)]^{3+}[SbCl_6]_3^-$ .<sup>(36)</sup> The complicated 9- and 10-fold coordination around  $Bi^{III}$  in the novel 1:1 and 1:2 arene complexes of  $BiCl_3$  with 1,3,5- $Me_3C_6H_3$  (i.e. mesitylene) and  $C_6Me_6$ , respectively, should also be noted, viz.  $[(\eta^6-mes)_2Bi_2Cl_6]$  in which each Bi is coordinated by  $6C + 3Cl + (2Cl)$ , and  $[(\mu: \eta^6, \eta^6-ar)_2Bi_4Cl_{12}]$  in which each Bi is coordinated by  $6C + 2Cl + 2Cl + (2Cl)$  and each  $C_6Me_6$  ligand bridges two Bi atoms.<sup>(37)</sup> A planar 6-membered  $[Bi_3Cl_3]$  ring occurs in  $[(Fe(\eta^5-C_5H_4Me)(CO)_2)_2BiCl]_3$ .<sup>(38)</sup>

A fascinating variety of discrete (or occasionally polymeric) polynuclear halogeno complexes of  $As^{III}$ ,  $Sb^{III}$  and Bi have recently been characterized. A detailed discussion would be inappropriate here, but structural motifs include face-shared and edge-shared distorted  $\{MX_6\}$  octahedral units fused into cubane-like and other related clusters or cluster fragments. Examples (see also preceding paragraph) are:



<sup>35</sup> E. HOUGH, D. G. NICHOLSON and A. K. VASUDEVAN, *J. Chem. Soc., Dalton Trans.*, 427–30 (1987).

<sup>36</sup> R. GARBE, B. VOLLMER, B. NEUMÜLLER, J. PEBLER and K. DENICKE, *Z. anorg. allg. Chem.* **619**, 272–6 (1993).

<sup>37</sup> A. SCHIER, J. M. WALLIS, G. MÜLLER and H. SCHMIDBAUR, *Angew. Chem. Int. Edn. Engl.* **25**, 757–9 (1986).

<sup>38</sup> W. CLEGG, N. A. COMPTON, R. J. ERRINGTON and N. C. NORMAN, *Polyhedron* **6**, 2031–3 (1987). See also W. CLEGG, N. A. COMPTON, R. J. ERRINGTON, G. A. FISHER, C. R. HOCKLESS, N. C. NORMAN and A. G. ORPEN, *Polyhedron* **10**, 123–6 (1991).

<sup>39</sup> W. S. SHELDRIK and H.-J. HÄUSLER, *Angew. Chem. Int. Edn. Engl.* **26**, 1172–4 (1987).

<sup>40</sup> U. MÜLLER and H. SINNO, *ibid.* **28**, 185–6 (1989).

<sup>41</sup> C. A. GHILARDI, S. MIDOLLINI, S. MONETI and A. ORLANDINI, *J. Chem. Soc., Chem. Commun.*, 1241–2 (1988).

<sup>42</sup> M. G. B. DREW, P. P. K. CLAIRE and G. R. WILLEY, *J. Chem. Soc., Dalton Trans.*, 215–8 (1988).

<sup>43</sup> S. POHL, W. SAAK and D. HASSE, *Angew. Chem. Int. Edn. Engl.* **26**, 467–8 (1987).

<sup>34</sup> G. R. WILLEY, M. T. LAKIN, M. RAVINDRAN and N. W. ALCOCK, *J. Chem. Soc., Chem. Commun.*, 271–2 (1991).

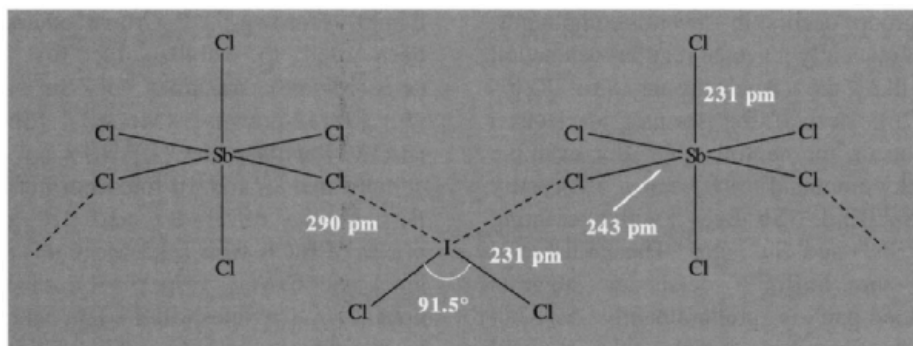
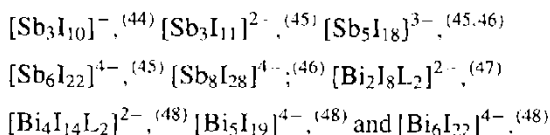


Figure 13.9 Schematic representation of the structure of  $\text{ISbCl}_8$  (see text).



The detailed coordination geometry about As, Sb or Bi in these clusters varies substantially, and is of considerable significance in describing the nature of the bonding in these species.

No completely general and quantitative theory of the stereochemical activity of the lone-pair of electrons in complex halides of trivalent As, Sb and Bi has been developed but certain trends are discernible. The lone-pair becomes less decisive in modifying the stereochemistry (a) with increase in the coordination number of the central atom from 4 through 5 to 6, (b) with increase in the atomic weight of the central atom ( $\text{As} > \text{Sb} > \text{Bi}$ ), and (c) with increase in the atomic weight of the halogen ( $\text{F} > \text{Cl} > \text{Br} > \text{I}$ ). The relative energies of the various valence-level orbitals may also be an important factor: the  $\text{F}(\sigma)$  orbital of F lies well below both the s and the p valence

orbitals of Sb (for example) whereas the  $\sigma$  orbital energies of Cl, Br and I lie between these two levels, at least in the free atoms. It follows that the lone pair is likely to be in a (stereochemically active) metal-based  $\text{sp}^f$  hybrid orbital in fluoro complexes of Sb but in a (stereochemically inactive) metal-based  $a_1$  orbital for the heavier halogens.<sup>(49)</sup>

In the +5 oxidation state, halide complexes of As, Sb and Bi are also well established and the powerful acceptor properties of  $\text{SbF}_5$  in particular have already been noted (p. 562). Such complexes are usually made by direct reaction of the pentahalide with the appropriate ligand. Thus  $\text{KAsF}_6$  and  $\text{NOAsF}_6$  have octahedral  $\text{AsF}_6^-$  groups and salts of  $\text{SbF}_6^-$  and  $\text{SbCl}_6^-$  (as well as  $[\text{Sb}(\text{OH})_6]^-$ ) are also known. Frequently, however, there is strong residual interaction between the "cation" and the "complex anion" and the structure is better thought of as an extended three-dimensional network. For example the adduct  $\text{SbCl}_5 \cdot \text{ICl}_3$  (i.e.  $\text{ISbCl}_8$ ) comprises distorted octahedra of  $\{\text{SbCl}_6\}$  and angular  $\{\text{ICl}_2\}$  groups but, as shown in Fig. 13.9, there is additional interaction between the groups which links them into chains and the structure is intermediate between  $[\text{ICl}_2]^+[\text{SbCl}_6]^-$  and  $[\text{SbCl}_4]^+[\text{ICl}_4]^-$ . Complexes are also formed by a variety of oxygen-donors, e.g.  $[\text{SbCl}_5(\text{OPCl}_3)]$  and  $[\text{SbF}_5(\text{OSO})]$  as

<sup>44</sup> S. POHL, W. SAAK, P. MAYER and A. SCHMIDPETER, *Angew. Chem. Int. Edn. Engl.*, **25**, 825 (1986).

<sup>45</sup> S. POHL, R. LOTZ, W. SAAK and D. HAASE, *ibid.* **28**, 344-5 (1989).

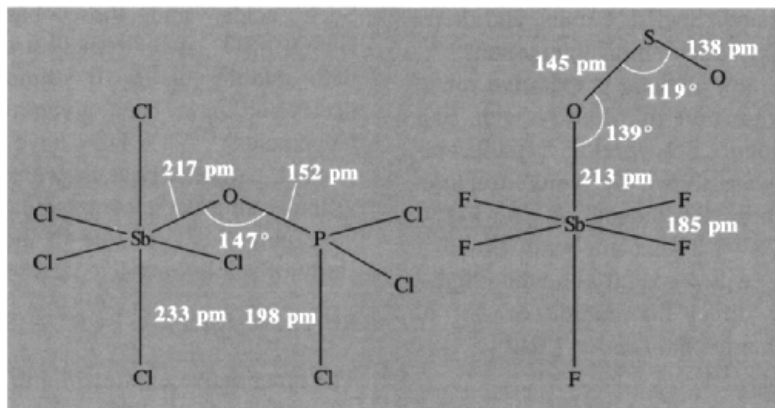
<sup>46</sup> C. J. CAMALT, N. C. NORMAN and L. J. FARRUGIA, *Polyhedron* **12**, 2081-90 (1993).

<sup>47</sup> W. CLEGG, N. C. NORMAN and N. L. PICKETT, *ibid.* **12**, 1251-2 (1993).

<sup>48</sup> H. KRAUTSCHIED, *Z. anorg. allg. Chem.* **620**, 1559-64 (1994).

<sup>49</sup> E. SHUSTOROVICH and P. A. DOBOSH, *J. Am. Chem. Soc.* **101**, 4090-5 (1979). B. M. GIMARC, *Molecular Structure and Bonding*, Academic Press, New York, 1979, 240 pp.





**Figure 13.10** Schematic representation of the pseudo-octahedral structures of  $[\text{SbCl}_5(\text{OPCl}_3)]$  and  $[\text{SbF}_5(\text{OSO})]$ .

shown in Fig. 13.10. Fluoro-complexes in particular are favoured by large non-polarizing cations, and polynuclear complex anions sometimes then result as a consequence of fluorine bridging. For example irradiation of a mixture of  $\text{SbF}_5$ ,  $\text{F}_2$  and  $\text{O}_2$  yields white crystals of  $\text{O}_2\text{Sb}_2\text{F}_{11}$  which can be formulated<sup>(50)</sup> as  $\text{O}_2^+[\text{Sb}_2\text{F}_{11}]^-$ , and this complex, when heated under reduced pressure at  $110^\circ$ , loses  $\text{SbF}_5$  to give  $\text{O}_2^+\text{SbF}_6^-$ . The dinuclear anion probably has a linear Sb-F-Sb bridge as in  $[\text{BrF}_4]^+[\text{Sb}_2\text{F}_{11}]^-$  (p. 834), but in  $[\text{XeF}]^+[\text{Sb}_2\text{F}_{11}]^-$  and  $[\text{XeF}_3]^+[\text{Sb}_2\text{F}_{11}]^-$  (p. 898) the bridging angle is reduced to  $150^\circ$  and  $155^\circ$  respectively. Even more extended coordination occurs in the 1:3 adduct  $\text{PF}_5 \cdot 3\text{SbF}_5$  which has been formulated as  $[\text{PF}_4]^+[\text{Sb}_3\text{F}_{16}]^-$  on the basis of vibrational spectroscopy.<sup>(51)</sup> The same anion occurs in the scarlet paramagnetic complex  $[\text{Br}_2]^+[\text{Sb}_3\text{F}_{16}]^-$  for which X-ray crystallography has established the *trans*-bridged octahedral structure  $[\text{F}_5\text{SbF}_5\text{Sb}(\text{F}_4)\text{FSbF}_5]^-$  with a bridging angle  $\text{SbF}_\mu\text{Sb}$  of  $148^\circ$ ; the Sb-F<sub>1</sub> distances (181–184 pm) are significantly less than the asymmetrical Sb-F<sub>μ</sub> distances (197 and 210 pm 4 pm).<sup>(52)</sup> The compound (mp  $69^\circ$ ) was prepared

by adding a small amount of  $\text{BrF}_5$  to a mixture of  $\text{Br}_2$  and  $\text{SbF}_5$ . The structure of the compound  $\text{AsF}_3 \cdot \text{SbF}_5$  can be described either as a molecular adduct,  $\text{F}_2\text{AsF} \rightarrow \text{SbF}_5$ , or as an ionic complex,  $[\text{AsF}_2]^+[\text{SbF}_6]^-$ ; in both descriptions the alternating As and Sb units are joined into an infinite network by further F bonding.<sup>(53)</sup>

The 1:1 adduct  $\text{SbF}_3 \cdot \text{SbF}_5$  has the pseudo-ionic structure  $[\text{Sb}_2^{\text{III}}\text{F}_4]^{2+}[\text{Sb}_2^{\text{V}}\text{F}_6]^{2-}$ ; however, the  $[\text{F}_2\text{Sb}-\text{F} \cdots \text{SbF}]^{2+}$  cation features 5 different Sb-F distances (185, 187, 199, 201 and 215 pm) and can be regarded either as an  $\text{SbF}^{2+}$  cation coordinated by  $\text{SbF}_3$ , or as a fluorine-bridged dinuclear cation  $[\text{F}_2\text{Sb}-\text{F}-\text{SbF}]^{2+}$ , or even as part of an infinite three-dimensional polymer  $[(\text{SbF}_4)_4]_n$  when still longer  $\text{Sb}^{\text{III}}-\text{F}$  contacts are considered.<sup>(54)</sup> Several other “adducts” have been prepared leading to the binary fluorides  $\text{Sb}_3\text{F}_{11}$ ,  $\text{Sb}_4\text{F}_{14}$ ,  $\text{Sb}_7\text{F}_{29}$ ,  $\text{Sb}_8\text{F}_{30}$  and  $\text{Sb}_{11}\text{F}_{43}$ . The fluoride  $\text{Sb}_8\text{F}_{30}$  (i.e.  $5\text{SbF}_3 \cdot 3\text{SbF}_5$ ) is unusual in having more than one structure, depending on its method of preparation. Reduction of  $\text{SbF}_3 \cdot \text{SbF}_5$  or of  $\text{SbF}_5$  itself with a stoichiometric amount of  $\text{PF}_3$  in  $\text{AsF}_3$  solutions yields crystals of  $\alpha\text{-Sb}_8\text{F}_{30}$  comprised of a 3D cross-linked polymeric cation,  $[\text{Sb}_5\text{F}_{12}^{3+}]_\infty$ , and  $[\text{SbF}_6]^-$  anions. The polymeric cation can be viewed as strongly interacting

<sup>50</sup> D. E. MCKEE and N. BARTLETT, *Inorg. Chem.* **12**, 2738–40 (1973).

<sup>51</sup> G. S. H. CHEN and J. PASSMORE, *J. Chem. Soc., Chem. Commun.*, 559 (1973).

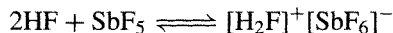
<sup>52</sup> A. J. EDWARDS and G. R. JONES, *J. Chem. Soc. A* 2318–20 (1971).

<sup>53</sup> A. J. EDWARDS and R. J. C. STILLS, *J. Chem. Soc. A* 942–5 (1971).

<sup>54</sup> R. J. GILLESPIE, D. R. SLIM and J. E. VEKRIS, *J. Chem. Soc., Dalton Trans.*, 971–4 (1977).

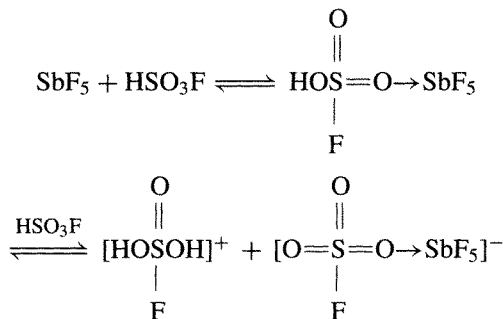
{Sb<sub>2</sub>F<sub>5</sub>}<sup>+</sup>, {SbF<sub>3</sub>} and {Sb<sub>2</sub>F<sub>3</sub>}<sup>3+</sup> units, and there are also significant cation-anion interactions.<sup>(55)</sup> Alternatively, the less obvious preparative route of oxidative bromination of MeSCN with Br<sub>2</sub> and SbF<sub>5</sub> in liquid SO<sub>2</sub> yields crystals of β-Sb<sub>8</sub>F<sub>30</sub> which were shown by X-ray structure analysis to be best formulated as [Sb<sub>2</sub>F<sub>5</sub>]<sup>+</sup>-[Sb<sub>3</sub>F<sub>7</sub>]<sup>2+</sup>[SbF<sub>6</sub>]<sub>3</sub><sup>-</sup>.<sup>(56)</sup> The compound Sb<sub>11</sub>F<sub>43</sub> (i.e. 6SbF<sub>3</sub>·5SbF<sub>5</sub>) was prepared as a white high-melting solid by direct fluorination of Sb; it contains the polymeric chain cation [Sb<sub>6</sub>F<sub>13</sub>]<sup>5+</sup><sub>∞</sub> and [SbF<sub>6</sub>]<sup>-</sup> anions.<sup>(57)</sup>

The great electron-pair acceptor capacity (Lewis acidity) of SbF<sub>5</sub> has been utilized in the production of extremely strong proton donors (Brønsted acids, p. 48). Thus the acidity of anhydrous HF is substantially increased in the presence of SbF<sub>5</sub>:



Crystalline compounds isolated from such solutions at -20° to -30°C have been shown by X-ray analysis to be the fluoronium salts [H<sub>3</sub>F<sub>2</sub>]<sup>+</sup>[Sb<sub>2</sub>F<sub>11</sub>]<sup>-</sup> and [H<sub>2</sub>F]<sup>+</sup>[Sb<sub>2</sub>F<sub>11</sub>]<sup>-</sup>.<sup>(58)</sup>

An even stronger acid ("Magic Acid") results from the interaction of SbF<sub>5</sub> with an oxygen atom in fluorosulfuric acid HSO<sub>3</sub>F (i.e. HF/SO<sub>3</sub>):



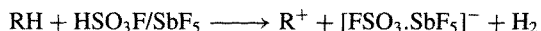
<sup>55</sup> W. A. S. NANDANA, J. PASSMORE, P. S. WHITE and C.-M. WONG, *J. Chem. Soc., Dalton Trans.*, 1989-98 (1987).

<sup>56</sup> R. MINKWITZ, J. NOWICKI and H. BORRMANN, *Z. anorg. allg. Chem.* **605**, 109-16 (1991).

<sup>57</sup> A. J. EDWARDS and D. R. SLIM, *J. Chem. Soc., Chem. Commun.*, 178-9 (1974).

<sup>58</sup> D. MOOTZ and K. BARTMANN, *Angew. Chem. Int. Edn. Engl.* **27**, 391-2 (1988).

Such acids, and those based on oleums, H<sub>2</sub>SO<sub>4</sub>·nSO<sub>3</sub>, are extremely strong proton donors with acidities up to 10<sup>12</sup> times that of H<sub>2</sub>SO<sub>4</sub> itself, and have been given the generic name 'superacids'.<sup>(59-63)</sup> They have been extensively studied, particularly as they are able to protonate virtually all organic compounds. In addition, they have played a vital rôle in the preparation and study of stable long-lived carbocations:



The imaginative exploitation of these and related reactions by G. A. Olah and his group<sup>(60-62,64,65)</sup> have had an enormous impact on our understanding of organic catalytic processes and on their industrial application, as recognized by the award to Olah of the 1994 Nobel Prize for Chemistry.<sup>(66)</sup>

### Oxide halides

The stable molecular nitrosyl halides NOX (p. 442) and phosphoryl halides POX<sub>3</sub> (p. 501) find few counterparts in the chemistry of As, Sb and Bi. AsOF has been reported as a product of the reaction of As<sub>4</sub>O<sub>6</sub> with AsF<sub>3</sub> in a sealed tube at 320° but has not been fully characterized. AsOF<sub>3</sub> is known only as a polymer. Again, just as AsCl<sub>5</sub> eluded preparation for over 140 y after Liebig's first attempt to make it in 1834, so

<sup>59</sup> R. J. GILLESPIE, *Acc. Chem. Res.* **1**, 202-9 (1968).

<sup>60</sup> G. A. OLAH, A. M. WHITE and D. H. O'BRIEN, *Chem. Rev.* **70**, 561-91 (1970).

<sup>61</sup> G. A. OLAH, G. K. S. PRAKASH and J. SOMMER, *Science* **206**, 13-20 (1979).

<sup>62</sup> G. A. OLAH, G. K. S. PRAKASH, and J. SOMMER, *Superacids*, Wiley, New York, 1985, 371 pp.

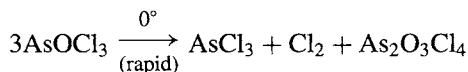
<sup>63</sup> T. A. O'DONNELL, *Superacids and Acidic Melts as Inorganic Chemical Reaction Media*, VCH, New York, 1992, 243 pp.

<sup>64</sup> G. A. OLAH, *Aldrichimica Acta* **6**, 7-16 (1973).

<sup>65</sup> G. A. OLAH, D. G. PARKER and Y. YONEDA, *Angew. Chem. Int. Edn. Engl.* **17**, 909-31 (1978). See also Chapters 1 and 7 in G. A. OLAH, G. K. S. PRAKASH, R. E. WILLIAMS L. D. FIELD and K. WADE, *Hypercarbon Chemistry*, Wiley, New York, 1987, 311 pp.

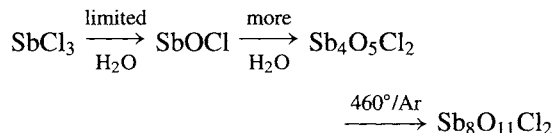
<sup>66</sup> G. A. OLAH, *Angew. Chem. Int. Edn. Engl.*, **34**, 1393-405. (Nobel Lecture.)

AsOCl<sub>3</sub> defied synthesis until 1976 when it was made by ozonization of AsCl<sub>3</sub> in CFCl<sub>3</sub>/CH<sub>2</sub>Cl<sub>2</sub> at -78°: it is a white, monomeric, crystalline solid and is one of the few compounds that can be said to contain a “real” As=O double bond.<sup>(67)</sup> AsOCl<sub>3</sub> is thermally more stable than AsCl<sub>5</sub> (p. 561) but decomposes slowly at -25° to give As<sub>2</sub>O<sub>3</sub>Cl<sub>4</sub>:

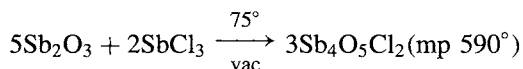


The compound As<sub>2</sub>O<sub>3</sub>Cl<sub>4</sub> is polymeric and is thus not isostructural with Cl<sub>2</sub>P(O)OP(O)Cl<sub>2</sub>.

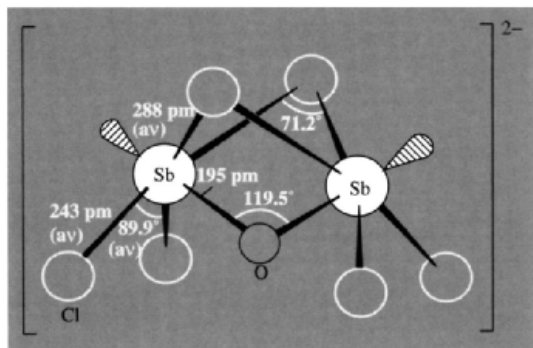
SbOF and SbOCl can be obtained as polymeric solids by controlled hydrolysis of SbX<sub>3</sub>. Several other oxide chlorides can be obtained by varying the conditions, e.g.:



An alternative dry-way preparation which permits the growth of large, colourless, single crystals suitable for ferroelectric studies (pp. 55–8) has been devised.<sup>(68)</sup>



The compounds Sb<sub>4</sub>O<sub>3</sub>(OH)<sub>3</sub>Cl<sub>2</sub> and Sb<sub>8</sub>OCl<sub>22</sub> have also been reported. SbOCl itself comprises polymeric sheets of composition [Sb<sub>6</sub>O<sub>6</sub>Cl<sub>4</sub>]<sup>2+</sup> (formed by linking Sb atoms via O and Cl bridges) interleaved with layers of chloride ions. In addition to polymeric species, finite heterocyclic complexes can also be obtained. For example partial hydrolysis of the polymeric [pyH]<sub>3</sub>[Sb<sub>2</sub><sup>III</sup>Cl<sub>9</sub>] in ethanol leads to [pyH<sup>+</sup>]<sub>2</sub>[Sb<sub>2</sub><sup>III</sup>OCl<sub>6</sub>]<sup>2-</sup> in which the anion contains 2 pseudo-octahedral {SbOCl<sub>4</sub>} units sharing a common face {μ<sub>3</sub>-OCl<sub>2</sub>} with the lone-pairs *trans* to the bridging oxygen atom



**Figure 13.11** Structure of the binuclear anion [Sb<sub>2</sub><sup>III</sup>OCl<sub>6</sub>]<sup>2-</sup> showing the bridging oxygen and chlorine atoms and the pseudo-octahedral coordination about Sb; the O atom is at the common apex of the face-shared square pyramids and the lone-pairs are *trans*- to this below the {SbCl<sub>4</sub>} bases. The bridging distances Sb-Cl<sub>μ</sub> are substantially longer than the terminal distances Sb-Cl<sub>t</sub>.

(Fig. 13.11).<sup>(69)</sup> Another novel polynuclear antimony oxide halide anion has been established in the dark-blue ferrocenium complex {[Fe(η<sup>5</sup>-C<sub>5</sub>H<sub>5</sub>)]<sub>2</sub>[Sb<sub>4</sub>Cl<sub>12</sub>O]}<sub>2</sub>·2C<sub>6</sub>H<sub>6</sub> which was made by photolysis of benzene solutions of ferrocene (p. 1109) and SbCl<sub>3</sub> in the presence of oxygen:<sup>(70)</sup> the anion (Fig. 13.12) contains 2 square-pyramidal {Sb<sup>III</sup>Cl<sub>5</sub>} units sharing a common edge and joined via a unique quadruply bridging Cl atom to 2 pseudo trigonal bipyramidal {Sb<sup>III</sup>Cl<sub>3</sub>O} units which share a common bridging O atom and the unique Cl atom. The structure implies the presence of a lone-pair of electrons beneath the basal plane of the first 2 Sb atoms and in the equatorial plane (with O<sub>μ</sub> and Cl<sub>t</sub>) of the second 2 Sb atoms.

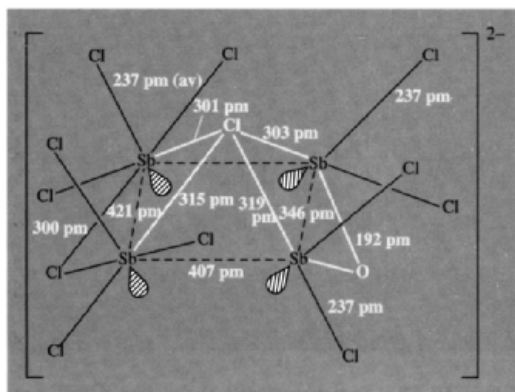
Other finite-complex anions occur in the oxyfluorides. For example the hydrated salts K<sub>2</sub>[As<sub>2</sub>F<sub>10</sub>O]·H<sub>2</sub>O and Rb<sub>2</sub>[As<sub>2</sub>F<sub>10</sub>O]·H<sub>2</sub>O

<sup>67</sup> K. SEPPELT, *Angew. Chem. Int. Edn. Engl.* **15**, 766–7 (1976).

<sup>68</sup> YA. P. KUTSENKO, *Kristallografiya* (Engl. transl.) **24**, 349–51 (1979).

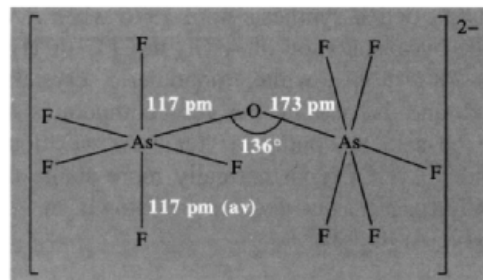
<sup>69</sup> M. HALL and D. B. SOWERBY, *J. Chem. Soc., Chem. Commun.*, 1134–5 (1979).

<sup>70</sup> A. L. RHEINGOLD, A. G. LANDERS, P. DAHLSTROM and J. ZUBIETA, *J. Chem. Soc., Chem. Commun.*, 143–4 (1979).



**Figure 13.12** Schematic representation of the structure of the complex anion  $[\text{Sb}_4\text{Cl}_{12}\text{O}]^{2-}$  showing the two different coordination geometries about Sb and the unique quadruply bridging Cl atom.

contain the oxo-bridged binuclear anion  $[\text{F}_5\text{As}-\text{OAsF}_5]^{2-}$  as shown in Fig. 13.13<sup>(71)</sup> and the anhydrous salt  $\text{Rb}_2[\text{Sb}_2\text{F}_{10}\text{O}]$  contains a similar anion with angle  $\text{Sb}-\text{O}-\text{Sb}$   $133^\circ$ ,  $\text{Sb}-\text{F}$  188 pm, and  $\text{Sb}-\text{O}$  191 pm.<sup>(72)</sup> The compound of empirical formula  $\text{CsSbF}_4\text{O}$  is, in fact, trimeric with a 6-membered heterocyclic anion in the boat configuration, i.e.  $\text{Cs}_3[\text{Sb}_3\text{F}_{12}\text{O}_3]$ ,<sup>(73)</sup> whereas the corresponding arsenic compound<sup>(74)</sup> has a dimeric



**Figure 13.13** Schematic representation of the anion structure in  $\text{M}_2[\text{As}_2\text{F}_{10}\text{O}]\cdot\text{H}_2\text{O}$ .

anion  $[\text{As}_2\text{F}_8\text{O}_2]^{2-}$  (Fig. 13.14). In both cases the Group 15 element is octahedrally coordinated by 4 F and 2 O atoms in the *cis*-configuration.

Bismuth oxide halides  $\text{BiOX}$  are readily formed as insoluble precipitates by the partial hydrolysis of the trihalides (e.g. by dilution of solutions in concentrated aqueous  $\text{HX}$ ).  $\text{BiOF}$  and  $\text{BiOI}$  can also be made by heating the corresponding  $\text{BiX}_3$  in air.  $\text{BiOI}$ , which itself decomposes above  $300^\circ$ , is brick-red in colour; the other 3  $\text{BiOX}$  are white. All have complex layer-lattice structures.<sup>(33)</sup> When  $\text{BiOCl}$  or  $\text{BiOBr}$  are heated above  $600^\circ$  oxide halides of composition  $\text{Bi}_{24}\text{O}_{31}\text{X}_{10}$  are formed, i.e. replacement of 5 O atoms by 10 X in  $\text{Bi}_{24}\text{O}_{36}$ , ( $\text{Bi}_2\text{O}_3$ ).

### 13.3.4 Oxides and oxo compounds

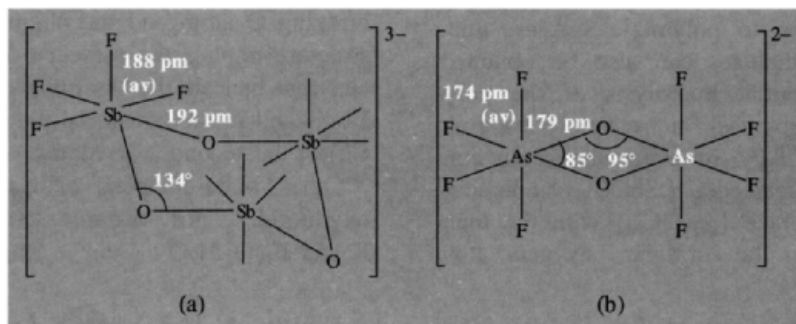
The amphoteric nature of  $\text{As}_2\text{O}_3$  and the trends in properties of several of the oxides and oxoacids

<sup>71</sup> W. HAASE, *Acta Cryst.* **B30**, 1722-7 (1974).

<sup>72</sup> W. HAASE, *Acta Cryst.* **B30**, 2508-10 (1974).

<sup>73</sup> W. HAASE, *Acta Cryst.* **B30**, 2465-9 (1974).

<sup>74</sup> W. HAASE, *Chem. Ber.* **107**, 1009-18 (1974).



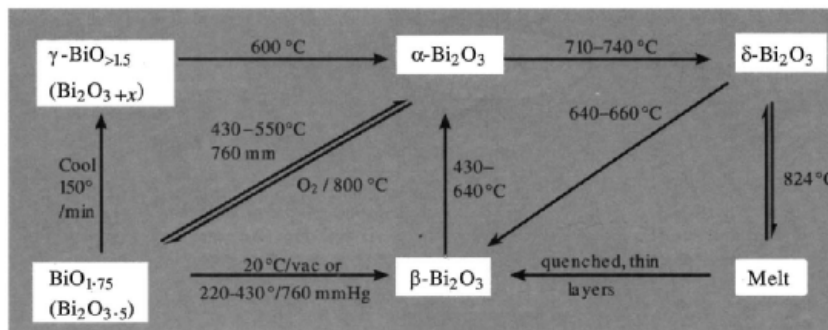
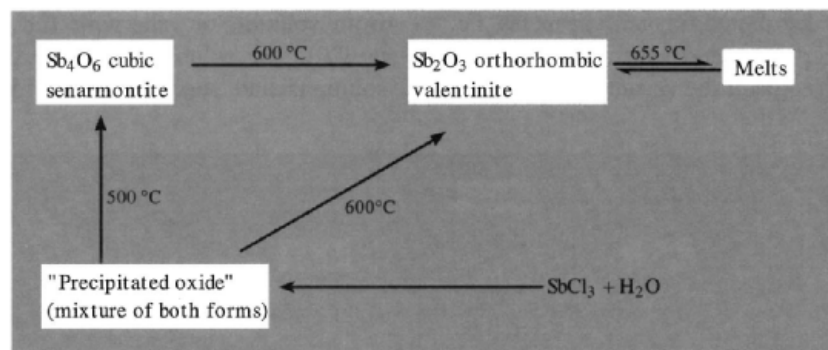
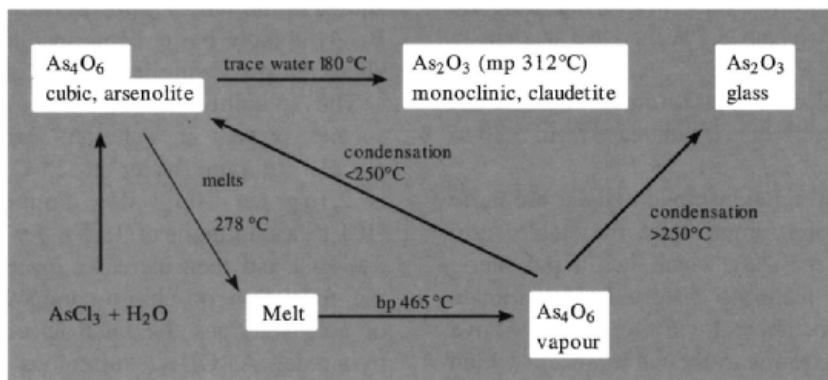
**Figure 13.14** Schematic representation of the structure of (a) the trimeric anion  $[\text{Sb}_3\text{F}_{12}\text{O}_3]^{3-}$ , and (b) the dimeric anion  $[\text{As}_2\text{F}_8\text{O}_2]^{2-}$ .

of As, Sb and Bi have already been mentioned briefly on pp. 552–3. Because of the trend towards greater basicity in the sequence  $\text{As} < \text{Sb} < \text{Bi}$  and the trend towards greater acidity in the sequence  $\text{M}^{\text{III}} < \text{M}^{\text{V}}$ , coupled with the difficulty of isolating some of the oxides from their “hydrated” forms, it is not convenient to have separate sections on oxides, hydrous oxides, hydroxides, acids, oxoacid salts, polyacid salts and mixed oxides. Accordingly, all these types of compound will be considered in the present

section;  $\text{M}^{\text{III}}$  compounds will be discussed first then intermediate  $\text{M}^{\text{III}}/\text{M}^{\text{V}}$  systems and, finally,  $\text{M}^{\text{V}}$  oxo- compounds.

### Oxo compounds of $\text{M}^{\text{III}}$

$\text{As}_2\text{O}_3$  (diarsenic trioxide) is the most important compound of As (Panel, p. 549). It is made (a) by burning As in air, (b) by hydrolysis of  $\text{AsCl}_3$  or (c) industrially, by roasting sulfide



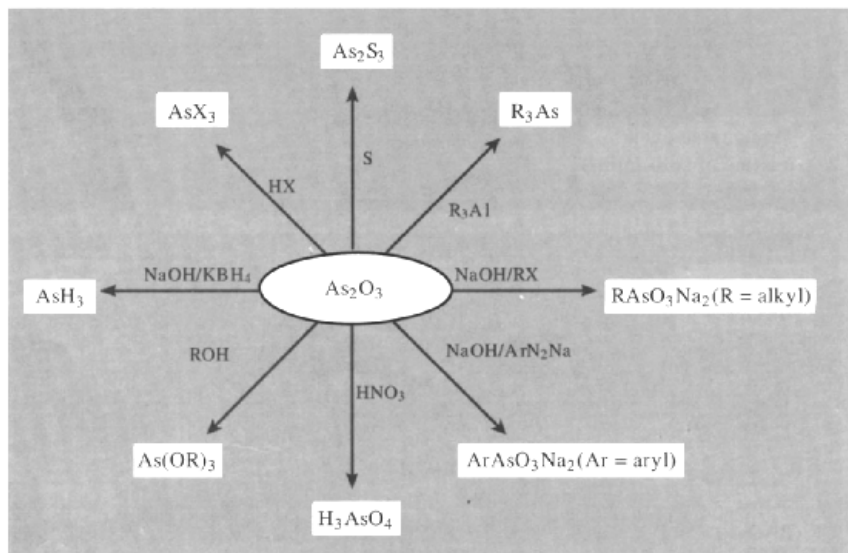
ores such as arsenopyrite,  $\text{FeAsS}$ ,  $\text{Sb}_2\text{O}_3$  and  $\text{Bi}_2\text{O}_3$  are made similarly. All 3 oxides exist in several modifications as shown in the schemes on p. 573.<sup>(16)</sup> In the vapour phase  $\text{As}_2\text{O}_3$  exists as  $\text{As}_4\text{O}_6$  molecules isostructural with  $\text{P}_4\text{O}_6$  (p. 504), and this unit also occurs in the cubic crystalline form. Above  $800^\circ$  gaseous  $\text{As}_4\text{O}_6$  partially dissociates to an equilibrium mixture containing both  $\text{As}_4\text{O}_6$  and  $\text{As}_2\text{O}_3$  molecules. The less-volatile monoclinic form of  $\text{As}_2\text{O}_3$  has a sheet-like structure of pyramidal  $\{\text{AsO}_3\}$  groups sharing common O atoms. This transformation from molecular  $\text{As}_4\text{O}_6$  units to polymeric  $\text{As}_2\text{O}_3$  is accompanied by an 8.7% increase in density from  $3.89$  to  $4.23 \text{ g cm}^{-3}$ . A similar change from cubic, molecular  $\text{Sb}_4\text{O}_6$  to polymeric  $\text{Sb}_2\text{O}_3$  results in an 11.3% density increase from  $5.20$  to  $5.79 \text{ g cm}^{-3}$ .

The structural relationships in  $\text{Bi}_2\text{O}_3$  are more complex. At room temperature the stable form is monoclinic  $\alpha\text{-Bi}_2\text{O}_3$  which has a polymeric layer structure featuring distorted, 5-coordinate Bi in pseudo-octahedral  $\{\text{BiO}_5\}$  units. Above  $717^\circ\text{C}$  this transforms to the cubic  $\delta$ -form which has a defect fluorite structure ( $\text{CaF}_2$ , p. 118) with randomly distributed oxygen vacancies, i.e.  $[\text{Bi}_2\text{O}_3\Box]$ . The  $\beta$ -form and several oxygen-rich forms (in which some of the vacant sites are filled

by  $\text{O}^{2-}$  with concomitant oxidation of some  $\text{Bi}^{\text{III}}$  to  $\text{Bi}^{\text{V}}$ ) are related to the  $\delta\text{-Bi}_2\text{O}_3$  structure. There are also numerous double oxides  $p\text{MO}_n.q\text{Bi}_2\text{O}_3$ , e.g.  $\text{Bi}_{12}\text{GeO}_{20}$  (i.e.  $\text{GeO}_2.6\text{Bi}_2\text{O}_3$ ), and other mixed oxides can be made by fusing  $\text{Bi}_2\text{O}_3$  with oxides of Ca, Sr, Ba, Cd or Pb; these latter have  $(\text{BiO})_n$  layers as in the oxide halides, interleaved with  $\text{M}^{\text{II}}$  cations.  $\text{Bi}_2\text{Sr}_2\text{CaCu}_2\text{O}_8$  is a superconductor with  $T_c = 85 \text{ K}$  (cf. p. 1182).

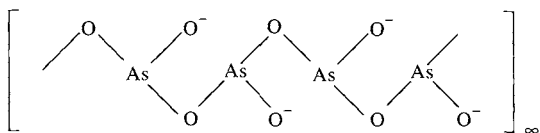
The oxides  $\text{M}_2\text{O}_3$  are convenient starting points for the synthesis of many other compounds of As, Sb and Bi. Some reactions of  $\text{As}_2\text{O}_3$  are shown in the scheme;  $\text{Sb}_2\text{O}_3$  reacts similarly, but  $\text{Bi}_2\text{O}_3$  is more basic, being insoluble in aqueous alkali but dissolving in acids to give  $\text{Bi}^{\text{III}}$  salts.

The solubility of  $\text{As}_2\text{O}_3$  in water, and the species present in solution, depend markedly on pH. In pure water at  $25^\circ\text{C}$  the solubility is  $2.16 \text{ g}$  per  $100 \text{ g}$ ; this diminishes in dilute HCl to a minimum of  $1.56 \text{ g}$  per  $100 \text{ g}$  at about  $3 \text{ M HCl}$  and then increases, presumably due to the formation of chloro-complexes. In neutral or acid solutions the main species is probably pyramidal  $\text{As}(\text{OH})_3$ , "arsenious acid", though this compound has never been isolated either from solution or otherwise (cf. carbonic acid, p. 310). The solubility is much greater in basic solutions and spectroscopic evidence points to



the presence of such anions as  $[\text{AsO}(\text{OH})_2]^-$ ,  $[\text{AsO}_2(\text{OH})]^{2-}$  and  $[\text{AsO}_3]^{3-}$ , corresponding to successive deprotonation of  $\text{H}_3\text{AsO}_3$ . The first stage dissociation constant at  $25^\circ$  is  $K_a = [\text{AsO}(\text{OH})_2^-][\text{H}^+]/[\text{H}_3\text{AsO}_3] \simeq 6 \times 10^{-10}$ ,  $\text{p}K_a$  9.2; ortho-arsenious acid is therefore a very weak acid (as expected from Pauling's rules, p. 50) and is comparable in strength to boric acid (p. 203). Dissociation as a base is even weaker:  $K_b = [\text{As}(\text{OH})_2^+][\text{OH}^-]/[\text{As}(\text{OH})_3] \simeq 10^{-14}$ . There now seems to be less evidence for other species that were formerly considered to be present in solution, e.g. the monomeric meta-acid  $\text{HAsO}_2$ , i.e.  $[\text{AsO}(\text{OH})]$  (by loss of 1  $\text{H}_2\text{O}$ ) and the hexahydroxoacid  $\text{H}_3[\text{As}(\text{OH})_6]$  or its hydrate.

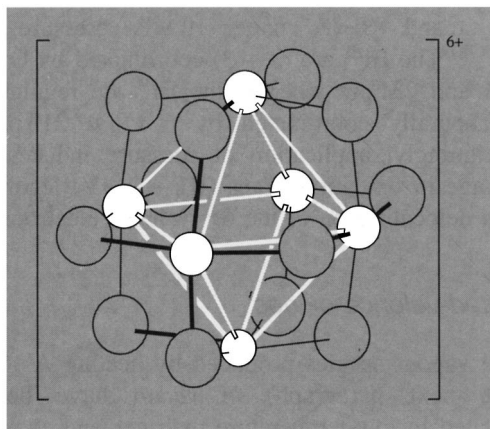
Arsenites of the alkali metals are very soluble in water, those of the alkaline earth metals less so, and those of the heavy metals are virtually insoluble. Many of the salts are obtained as meta-arsenites, e.g.  $\text{NaAsO}_2$ , which comprises polymeric chain anions formed by corner linkage of pyramidal  $\{\text{AsO}_3\}$  groups and held together by Na ions:



The sparingly soluble yellow  $\text{Ag}_3\text{AsO}_3$  is an example of an orthoarsenite. Copper(II) arsenites were formerly used as fine green pigments, e.g. Paris green, which is an acetate arsenite  $[\text{Cu}_2(\text{MeCO}_2)(\text{AsO}_3)]$ , and Scheele's green, which approximates to the hydrogen arsenite  $\text{CuHAsO}_3$  or the dehydrated composition  $\text{Cu}_2\text{As}_2\text{O}_5$ .

Antimonious acid  $\text{H}_3\text{SbO}_3$  and its salts are less well characterized but a few meta-antimonites and polyantimonites are known, e.g.  $\text{NaSbO}_2$ ,  $\text{NaSb}_3\text{O}_5 \cdot \text{H}_2\text{O}$  and  $\text{Na}_2\text{Sb}_4\text{O}_7$ . The oxide itself finds extensive use as a flame retardant in fabrics, paper, paints, plastics, epoxy resins, adhesives and rubbers. The scale of industrial use can be gauged from the US statistics which indicate an annual consumption of  $\text{Sb}_2\text{O}_3$  of some 10 000 tonnes in that country.

The corresponding Bi compound  $\text{Bi}(\text{OH})_3$  is definitely basic rather than acidic. It dissolves readily in acid giving solutions of  $\text{Bi}^{\text{III}}$  ions but an increase in pH causes precipitation of oxo-salts. Before precipitation, however, polymeric oxocations can be detected in solution of which the best characterized is  $[\text{Bi}_6(\text{OH})_{12}]^{6+}$  in perchlorate solution. The species (Fig. 13.15) resembles  $[\text{Ta}_6\text{Cl}_{12}]^{2+}$  and has 6 Bi at the corners of an octahedron with bridging OH groups above each of the 12 edges. The shortest Bi–O distance is 233 pm and the (nonbonding) Bi  $\cdots$  Bi distance is 370 pm (307 and 353 in Bi metal). This contrasts with the bicapped tetrahedral distribution of metal atoms in  $[\text{Pb}_6\text{O}(\text{OH})_6]^{4+}$  (p. 395) where there is an O atom at the centre of the central tetrahedron and OH groups above the faces of the capping tetrahedra. A different arrangement of oxygen atoms around the  $\text{Bi}_6$  octahedron has been found by X-ray and neutron diffraction studies on  $[\text{Bi}_6\text{O}_4(\text{OH})_4]^{6+}[\text{ClO}_4]^{-6} \cdot 7\text{H}_2\text{O}$ , which can be crystallized from solutions prepared by dissolving  $\text{Bi}_2\text{O}_3$  in 3 M  $\text{HClO}_4$ .<sup>(75)</sup> The eight oxygen atoms (4 O and 4 OH) are disposed, respectively, on two tetrahedra above the eight triangular faces of the octahedron, thus giving the cluster overall



**Figure 13.15** The structure of the oxocation  $[\text{Bi}_6(\text{OH})_{12}]^{6+}$ ; the white lines indicate geometry but do not imply Bi–Bi bonds (see text).

<sup>75</sup> B. SUNDVALL. *Inorg. Chem.* **22**, 1906–12 (1983).

$T_d$  symmetry and with average distances Bi–O 215 pm, Bi–O(H) 240 pm and Bi···Bi 368 pm.

The tendency of  $\text{Bi}^{\text{III}}$  oxo-groups to aggregate is also found in  $\text{Li}_3\text{BiO}_3$ , which is formed as colourless crystals by heating a mixture of  $\text{Li}_2\text{O}$  and  $\text{Bi}_2\text{O}_3$  (in a 3.1:1 mole ratio) in Ag capsules (bombs!) at  $750^\circ\text{C}$  for 20 days.<sup>(76)</sup> The “isolated” pyramidal  $\text{BiO}_3^{3-}$  ions are arranged in apparently electrostatically unfavourable groups of eight with the 8 Bi atoms at the corners of a cube, all 24 O atoms pointing outwards and the eight lone pairs of electrons pointing inwards; Bi–O 205 pm (av), Bi···Bi 368 pm (av); cf. Bi–Bi 307.2 and 352.9 pm in Bi metal (p. 551). Likewise, colourless crystals of  $\text{Ag}_3\text{BiO}_3$  and of  $\text{Ag}_5\text{BiO}_4$ , prepared by heating  $\text{Ag}_2\text{O}$  and  $\text{Bi}_2\text{O}_3$  at  $500^\circ\text{--}530^\circ\text{C}$  under 100 MPa (1 kbar) of  $\text{O}_2$  or hydrothermally at  $350^\circ\text{C}$  and 10 MPa of  $\text{O}_2$ , both feature  $\text{Bi}_2\text{O}_8^{10-}$  units. In  $\text{Ag}_5\text{BiO}_4$  (i.e.  $\text{Ag}_{10}\text{Bi}_2\text{O}_8$ ) the units are “isolated” and comprise two square-based pyramidal  $\{\text{BiO}_5\}$  groups *transfused* at a common basal edge and with Bi–O<sub>b</sub> 231 pm (av), Bi–O<sub>a</sub> 214 pm, Bi···Bi 379 pm. In  $\text{Ag}_3\text{BiO}_3$  these  $\{\text{Bi}_2\text{O}_8\}$  groups are further linked by the remaining terminal basal O atoms to form a 3D network.<sup>(77)</sup> A fascinating mixed valence bismuthate  $\text{Ag}_{25}\text{Bi}_3\text{O}_{18}$  (i.e.  $\text{Bi}_2^{\text{III}}\text{Bi}^{\text{V}}$ ) has been prepared as black crystals by heating  $\text{Ag}_2\text{O}$  and ‘ $\text{Bi}_2\text{O}_5$ ’ under 10 MPa pressure of  $\text{O}_2$ .<sup>(78)</sup> The  $\text{Bi}^{\text{III}}$  are (3 + 3)-coordinated by O at 221 and 231 pm whereas the  $\text{Bi}^{\text{V}}$  are regularly octahedrally coordinated by 6 O at 213 pm. Intriguingly, application of pressure induces a change in oxidation states (III  $\longrightarrow$  V) leading to a delocalization of the  $6s^2$  valence electrons.

### Mixed-valence oxides

The vapour species produced by heating  $\text{As}_2\text{O}_5$  (see next paragraph) *in vacuo* have been isolated in low-temperature matrices and shown

by vibration spectroscopy to comprise the complete series of stable molecules  $\text{As}_4\text{O}_n$  ( $n = 6\text{--}10$ ),<sup>(79)</sup> analogous in structures to the phosphorus series (p. 504). The intermediate diamagnetic oxide  $\alpha\text{-Sb}_2\text{O}_4$  (i.e.  $\text{Sb}^{\text{III}}\text{Sb}^{\text{V}}\text{O}_4$ ) has long been known as the massive, fine-grained, yellow, orthorhombic mineral cervantite and more recently a monoclinic  $\beta$ -form has been recognized.  $\alpha\text{-Sb}_2\text{O}_4$  can also be obtained by heating  $\text{Sb}_2\text{O}_3$  in dry air at  $460\text{--}540^\circ\text{C}$ , and further heating in air or oxygen at  $1130^\circ$  produces  $\beta\text{-Sb}_2\text{O}_4$ . Both forms have similar structures with equal numbers of  $\text{Sb}^{\text{III}}$  and  $\text{Sb}^{\text{V}}$ .  $\alpha\text{-Sb}_2\text{O}_4$  is isostructural with  $\text{SbNbO}_4$  and  $\text{SbTaO}_4$  and consists of corrugated sheets of slightly distorted  $\{\text{Sb}^{\text{V}}\text{O}_6\}$  octahedra sharing all their vertices (as in the plane layer in  $\text{K}_2\text{NiF}_4$ ); the  $\text{Sb}^{\text{III}}$  lie between the layers in positions of irregular pyramidal fourfold coordination, all four O atoms lying on the same side of the  $\text{Sb}^{\text{III}}$ . Further oxidation to anhydrous  $\text{Sb}_2\text{O}_5$  has not been achieved (see below). For oxygen-rich  $\text{Bi}_2\text{O}_{3+x}$  see pp. 573–4 and also the preceding paragraph.

### Oxo compounds of $M^{\text{V}}$

Arsenic(V) oxide,  $\text{As}_2\text{O}_5$ , is one of the oldest-known oxides, but structural analysis has been thwarted until recently because of poor thermal stability, ease of hydrolysis and the difficulty of growing a single crystal. It is now known to consist of equal numbers of  $\{\text{AsO}_6\}$  octahedra and  $\{\text{AsO}_4\}$  tetrahedra completely linked by corner sharing to give cross-linked strands which define tubular cavities (cf. the corner sharing in  $\text{ReO}_3$  octahedra, p. 1047, and  $\text{SiO}_2$  tetrahedra, p. 343).<sup>(80)</sup> The structure accounts for the reluctance of the compound to crystallize and also for the observation that only half the As atoms can be replaced by Sb (6-coordinate) and P (4-coordinate) respectively.  $\text{As}_2\text{O}_5$  can be prepared either by heating As (or  $\text{As}_2\text{O}_3$ ) with  $\text{O}_2$  under pressure or by dehydrating crystalline

<sup>76</sup> R. HOPPE and R. HÜBENTHAL, *Z. anorg. allg. Chem.* **576**, 159–78 (1989).

<sup>77</sup> M. BORTZ and M. JANSEN, *Z. anorg. allg. Chem.* **619**, 1446–54 (1993).

<sup>78</sup> M. BORTZ and M. JANSEN, *Z. anorg. allg. Chem.* **612**, 113–7 (1992).

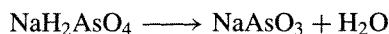
<sup>79</sup> A. K. BRISDON, R. A. GOMME and J. S. OGDEN, *J. Chem. Soc., Dalton Trans.*, 2725–30 (1986).

<sup>80</sup> M. JANSEN, *Angew. Chem. Int. Edn. Engl.* **16**, 214 (1977).



$\text{H}_3\text{AsO}_4$  at about  $200^\circ\text{C}$ . It is deliquescent, exceedingly soluble in water (230 g per 100 g  $\text{H}_2\text{O}$  at  $20^\circ$ ), thermally unstable (losing  $\text{O}_2$  near the mp, *ca.*  $300^\circ\text{C}$ ) and a strong oxidizing agent (liberating  $\text{Cl}_2$  from  $\text{HCl}$ ).

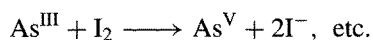
Arsenic acid,  $\text{H}_3\text{AsO}_4$ , can be obtained in aqueous solution by oxidizing  $\text{As}_2\text{O}_3$  with concentrated  $\text{HNO}_3$  or by dissolving  $\text{As}_2\text{O}_5$  in water. Crystallization below  $30^\circ$  yields  $2\text{H}_3\text{AsO}_4 \cdot \text{H}_2\text{O}$  (cf. phosphoric acid hemihydrate, p. 519), whereas crystallization at  $100^\circ\text{C}$  or above results in loss of water and the formation of  $\text{As}_2\text{O}_5 \cdot \frac{5}{3}\text{H}_2\text{O}$ , i.e. ribbon-like polymeric ( $\text{H}_5\text{As}_3\text{O}_{10}$ ) $_n$ . All these materials are strongly H-bonded. Arsenic acid, like  $\text{H}_3\text{PO}_4$  (p. 519), is tribasic with  $\text{p}K_1$  2.2,  $\text{p}K_2$  6.9,  $\text{p}K_3$  11.5 at  $25^\circ$ .  $\text{M}^1\text{H}_2\text{AsO}_4$  ( $\text{M} = \text{K}, \text{Rb}, \text{Cs}, \text{NH}_4$ ) are ferroelectric (p. 57). The corresponding sodium salt readily dehydrates to give meta-arsenate  $\text{NaAs}^{\text{V}}\text{O}_3$ :



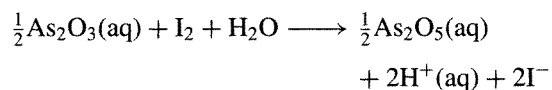
$\text{NaAsO}_3$  has an infinite polymeric chain anion similar to that in diopside (pp. 349, 529) but with a trimeric repeat unit;  $\text{LiAsO}_3$  is similar but with a dimeric repeat unit whereas  $\beta\text{-KAsO}_3$  appears to have a cyclic trimeric anion  $\text{As}_3\text{O}_9^{3-}$  which resembles the *cyclo*-trimetaphosphates (p. 530). There is thus a certain structural similarity between arsenates and phosphates, though arsenic acid and the arsenates show less tendency to catenation (p. 526). The tetrahedral  $\{\text{As}^{\text{V}}\text{O}_4\}$  group also resembles  $\{\text{PO}_4\}$  in forming the central unit in several heteropolyacid anions (p. 1014).

One striking difference between arsenates and phosphates is the appreciable oxidizing tendency of the former. This is clear from the oxidation state diagram for the Group V elements shown in Fig. 13.16, which summarizes a great deal of relevant information (p. 435). Antimony is seen to resemble arsenic quite closely but  $\text{Bi}^{\text{V}}\text{-Bi}^{\text{III}}$  is a much more strongly oxidizing couple and, indeed (as is clear from Fig. 13.16), it is able to oxidize water to oxygen. It is also clear that the +3 oxidation states of As, Sb and Bi do

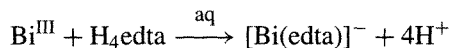
not disproportionate in solution. Nor do the elements themselves, so there are no reactions comparable to that of  $\text{P}_4$  with alkali to give phosphine and hypophosphite (p. 513). Redox reactions have proved a useful volumetric method of analysis for both As and Sb. For example  $\text{As}^{\text{III}}$  is quantitatively oxidized in aqueous solution by  $\text{I}_2$ , or by potassium bromate, iodate or permanganate. Such reactions can be formally represented as follows:



Thus, in an acid buffer such as borax-boric acid or  $\text{Na}_2\text{HPO}_4\text{-NaH}_2\text{PO}_4$  (p. 521):

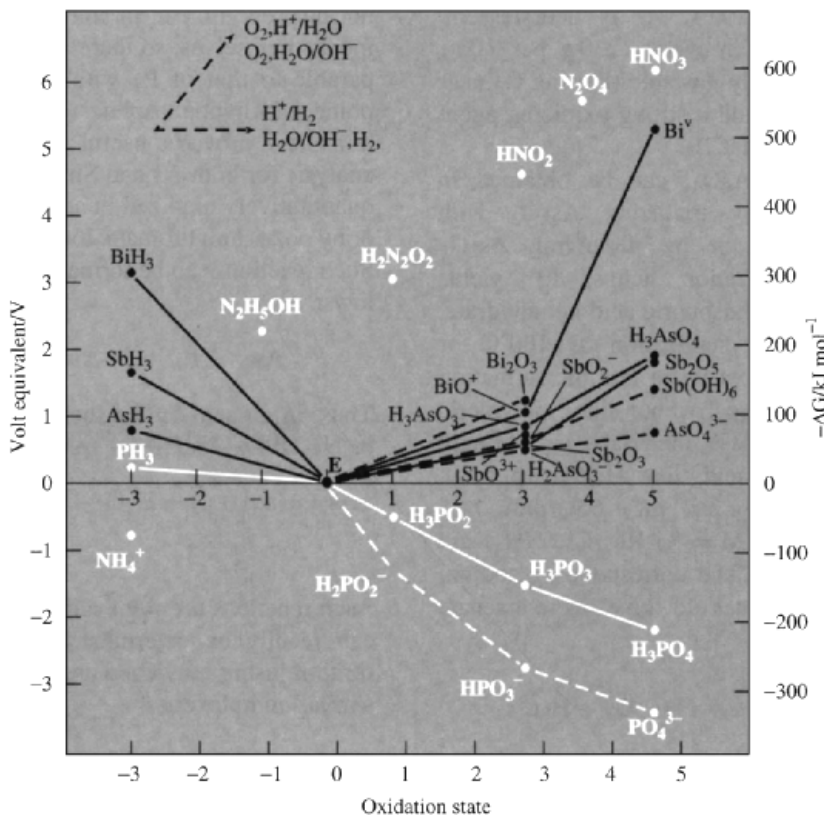


Such reactions are not available for  $\text{Bi}^{\text{III}}$  but this can readily be determined by complexometric titration using ethylenediaminetetraacetic acid or similar complexones:



Antimony(V) oxide has been obtained as a poorly characterized pale-yellow powder of ill-defined stoichiometry by hydrolysing  $\text{SbCl}_5$  with aqueous ammonia solution and dehydrating the product at  $275^\circ$ . Antimonates generally feature pseudooctahedral  $\{\text{SbO}_6\}$  units but polymerization by corner, edge or face sharing is rife. Some compounds which have been structurally characterized are  $\text{NaSb}(\text{OH})_6$ ,  $\text{LiSbO}_3$  (edge-shared),  $\text{Li}_3\text{SbO}_4$  ( $\text{NaCl}$  superstructure with isolated lozenges of  $\{\text{Sb}_4\text{O}_{16}\}^{12-}$ ),  $\text{NaSbO}_3$  (ilmenite, p. 963),  $\text{MgSb}_2\text{O}_6$  (trirutile, p. 961),  $\text{AlSbO}_4$  (rutile,  $2\text{MO}_2$  with random occupancy) and  $\text{Zn}_7\text{Sb}_2\text{O}_{12}$  (defect spinel, i.e.  $3\text{AB}_2\text{O}_4$ , p. 248).

Bismuth(V) oxide and bismuthates are even less well established though a recent important development has been the synthesis and structural characterization of  $\text{Li}_3\text{BiO}_5$ , prepared by heating an intimate mixture of  $\text{Li}_2\text{O}$  and  $\alpha\text{-Bi}_2\text{O}_3$  at  $650^\circ$  for 24 h in dry  $\text{O}_2$ . The structure is of the defect rock-salt type with an ordering of



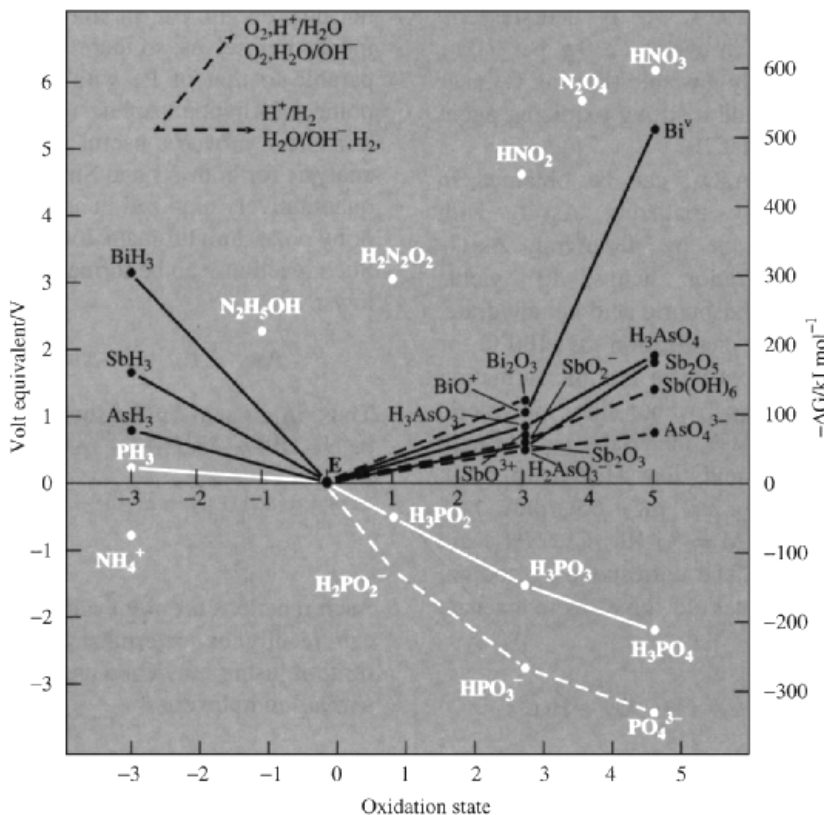
**Figure 13.16** Oxidation state diagram for As, Sb and Bi in acid and alkaline solutions, together with selected data on N and P for comparison.

cations and anion vacancies similar to that found in the ordered low-temperature phase of TiO (p. 962).<sup>(81)</sup> Note that the nominal ionic radii of  $\text{Li}^+$  and  $\text{Bi}^{5+}$  are equal (76 pm). Strong oxidizing agents give brown or black precipitates with alkaline solutions of  $\text{Bi}^{\text{III}}$ , which may be an impure higher oxide, and  $\text{NaBi}^{\text{V}}\text{O}_3$  can be made by heating  $\text{Na}_2\text{O}$  and  $\text{Bi}_2\text{O}_3$  in  $\text{O}_2$ . Such bismuthates of alkali and alkaline earth metals, though often poorly characterized, can be used as strong oxidizing agents in acid solution. Thus Mn in steel can be quantitatively determined by oxidizing it directly to permanganate and estimating the concentration colorimetrically.

<sup>81</sup> C. GREAVES and S. M. A. KATIB, *J. Chem. Soc., Chem. Commun.*, 1828–9 (1987).

### 13.3.5 Sulfides and related compounds

Despite the venerable history of the yellow mineral orpiment,  $\text{As}_2\text{S}_3$ , and the orange-red mineral realgar,  $\text{As}_4\text{S}_4$  (p. 547), it is only during the past two or three decades that the structural interrelation of the numerous arsenic sulfides has emerged.  $\text{As}_2\text{S}_3$  has a layer-structure analogous to  $\text{As}_2\text{O}_3$  (p. 574) with each As bonded pyramidally to 3 S atoms at 224 pm and angle S–As–S 99°. It can be made by heating  $\text{As}_2\text{O}_3$  with S or by passing  $\text{H}_2\text{S}$  into an acidified solution of the oxide. It sublimes readily, even below its mp of 320°, and the vapour has been shown by electron diffraction studies to comprise  $\text{As}_4\text{S}_6$  molecules isostructural with  $\text{P}_4\text{O}_6$  (p. 504). The structure can be thought



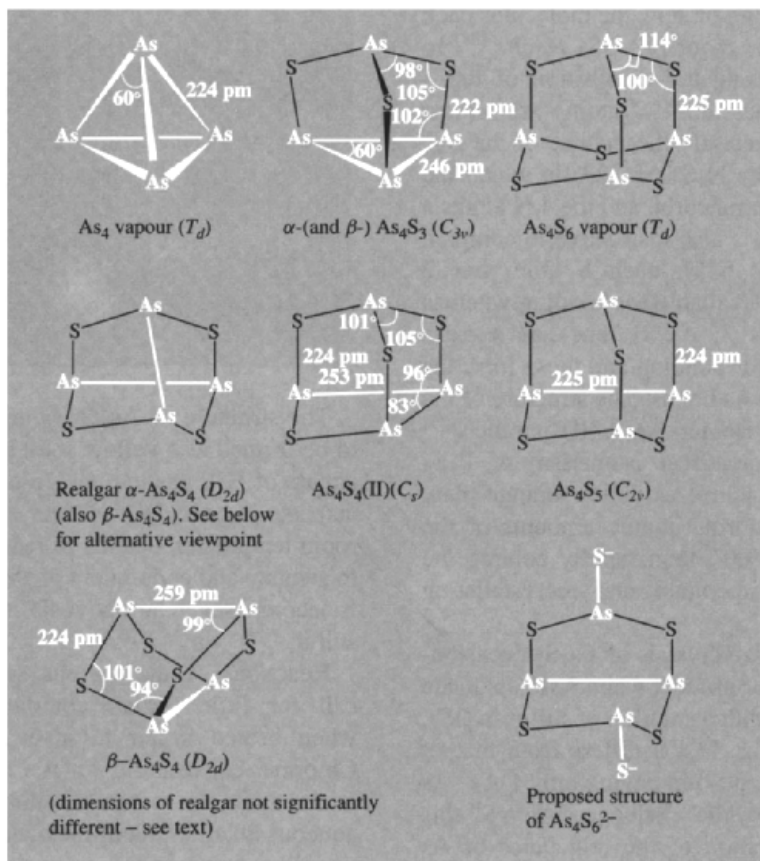
**Figure 13.16** Oxidation state diagram for As, Sb and Bi in acid and alkaline solutions, together with selected data on N and P for comparison.

cations and anion vacancies similar to that found in the ordered low-temperature phase of TiO (p. 962).<sup>(81)</sup> Note that the nominal ionic radii of  $Li^+$  and  $Bi^{5+}$  are equal (76 pm). Strong oxidizing agents give brown or black precipitates with alkaline solutions of  $Bi^{III}$ , which may be an impure higher oxide, and  $NaBi^V O_3$  can be made by heating  $Na_2O$  and  $Bi_2O_3$  in  $O_2$ . Such bismuthates of alkali and alkaline earth metals, though often poorly characterized, can be used as strong oxidizing agents in acid solution. Thus Mn in steel can be quantitatively determined by oxidizing it directly to permanganate and estimating the concentration colorimetrically.

### 13.3.5 Sulfides and related compounds

Despite the venerable history of the yellow mineral orpiment,  $As_2S_3$ , and the orange-red mineral realgar,  $As_4S_4$  (p. 547), it is only during the past two or three decades that the structural interrelation of the numerous arsenic sulfides has emerged.  $As_2S_3$  has a layer-structure analogous to  $As_2O_3$  (p. 574) with each As bonded pyramidally to 3 S atoms at 224 pm and angle S–As–S 99°. It can be made by heating  $As_2O_3$  with S or by passing  $H_2S$  into an acidified solution of the oxide. It sublimes readily, even below its mp of 320°, and the vapour has been shown by electron diffraction studies to comprise  $As_4S_6$  molecules isostructural with  $P_4O_6$  (p. 504). The structure can be thought

<sup>81</sup> C. GREAVES and S. M. A. KATIB, *J. Chem. Soc., Chem. Commun.*, 1828–9 (1987).



**Figure 13.17** Molecular structure of some sulfides of arsenic, stressing the relationship to the As<sub>4</sub> tetrahedron (point group symmetry in parentheses).

of as being derived from the As<sub>4</sub> tetrahedron by placing a bridging S atom above each edge thereby extending the As...As distance to a nonbonding value of ~290 pm. If instead of 6 As–S–As bridges there are 3, 4 or 5, then, as illustrated in Fig. 13.17, the compounds As<sub>4</sub>S<sub>3</sub>, As<sub>4</sub>S<sub>4</sub> (2 isomers) and As<sub>4</sub>S<sub>5</sub> are obtained. The molecule As<sub>4</sub>S<sub>3</sub> is seen to be isostructural with P<sub>4</sub>S<sub>3</sub> and P<sub>4</sub>Se<sub>3</sub> (p. 507); it occurs in both the α- and the β-form of the orange-yellow mineral dimorphite (literally “two forms”, discovered by A. Scacchi in volcanic fumaroles in Italy in 1849), the two forms differing only in the arrangement of the molecular units.<sup>(82)</sup> The

compound can be synthesized by heating As and S in the required proportions and purifying the product by sublimation, the β-form being the stable modification at room temperature and the α-form above 130°. The same molecular form occurs in the recently synthesized isoelectronic cationic clusters As<sub>3</sub>S<sub>4</sub><sup>+</sup> (yellow) and As<sub>3</sub>Se<sub>4</sub><sup>+</sup> (orange)<sup>(83)</sup> and in the isoelectronic clusters P<sub>7</sub><sup>3-</sup>, As<sub>7</sub><sup>3-</sup> and Sb<sub>7</sub><sup>3-</sup> (p. 588).

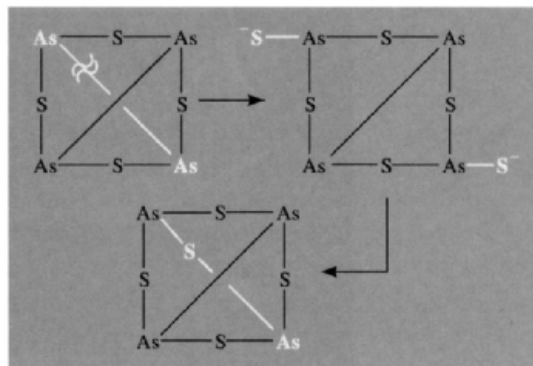
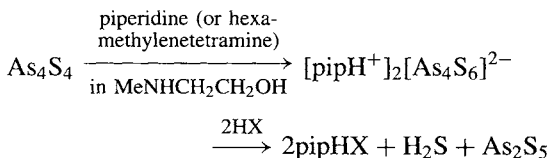
With As<sub>4</sub>S<sub>4</sub> there are two possible geometrical isomers of the molecule depending on whether the 2 As–As bonds are skew or adjacent, as shown in Fig. 13.17. Realgar (mp 307°) adopts the more symmetric *D<sub>2d</sub>* form with skew As–As

<sup>82</sup> H. J. WHITFIELD, *J. Chem. Soc. (A)*, 1800–3 (1970); 1737–8 (1973).

<sup>83</sup> B. H. CHRISTIAN, R. J. GILLESPIE and J. F. SAWYER, *Inorg. Chem.* **20**, 3410–20 (1981).

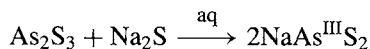
bonds and, depending on how the molecules pack in the crystal, either  $\alpha$ - or  $\beta$ -As<sub>4</sub>S<sub>4</sub> results.<sup>(84)</sup> In addition to the tetrahedral disposition of the 4 As atoms, note that the 4 S atoms are almost coplanar; this is precisely the inverse of the *D*<sub>2d</sub> structure adopted by N<sub>4</sub>S<sub>4</sub> (p. 723) in which the 4 S atoms form a tetrahedron and the 4 N atoms a coplanar square. It is also instructive to compare As<sub>4</sub>S<sub>4</sub> with S<sub>8</sub> (p. 655): each S atom has 2 unpaired electrons available for bonding whereas each As atom has 3; As<sub>4</sub>S<sub>4</sub> thus has 4 extra valency electrons for bonding and these form the 2 transannular As–As bonds. The structure of the second molecular isomer As<sub>4</sub>S<sub>4</sub>(II) parallels<sup>(85)</sup> the analogous geometrical isomerism of P<sub>4</sub>S<sub>4</sub> (p. 507). It was obtained as yellow-orange platy crystals by heating equi-atomic amounts of the elements to 500–600°, then rapidly cooling the melt to room temperature and recrystallizing from CS<sub>2</sub>.

Orange needle-like crystals of As<sub>4</sub>S<sub>5</sub> occasionally form as a minor product when As<sub>4</sub>S<sub>4</sub> is made by heating As<sub>4</sub>S<sub>3</sub> with a solution of sulfur in CS<sub>2</sub>. Its structure<sup>(86)</sup> (Fig. 13.17) differs from that of P<sub>4</sub>S<sub>5</sub> and P<sub>4</sub>Se<sub>5</sub> (p. 507) in having only 1 As–As bond and no exocyclic chalcogen As=S; this is a further illustration of the reluctance of As to oxidize beyond As<sup>III</sup> (p. 552). The compound can also be made by heterolytic cleavage of the As<sub>4</sub>S<sub>6</sub><sup>2-</sup> anion. This anion, which is itself made by base cleavage of one of the As–As bonds in realgar, probably has the structure shown in Fig. 13.17 and this would certainly explain the observed sequence of reactions:<sup>(87)</sup>

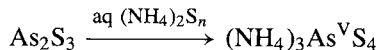


The structure of As<sub>2</sub><sup>V</sup>S<sub>5</sub> is unknown. It is said to be formed as a yellow solid by passing a rapid stream of H<sub>2</sub>S gas into an ice-cold solution of an arsenate in conc HCl; slower passage of H<sub>2</sub>S at room temperature results in reduction of arsenate to arsenite and consequent precipitation of As<sub>2</sub>S<sub>3</sub>. It decomposes in air above 95° to give As<sub>2</sub>S<sub>3</sub> and sulfur.

Reactions of the various sulfides of arsenic call for little further comment. As<sub>2</sub>S<sub>3</sub> burns when heated in air to give As<sub>2</sub>O<sub>3</sub> and SO<sub>2</sub>. Chlorine converts it to AsCl<sub>3</sub> and S<sub>2</sub>Cl<sub>2</sub>. It is insoluble in water but dissolves readily in aqueous alkali or alkali-metal sulfide solutions to give thioarsenites:



Reacidification reprecipitates As<sub>2</sub>S<sub>3</sub> quantitatively. With alkali metal or ammonium polysulfides thioarsenates are formed which are virtually insoluble even in hot conc HCl:



When As<sub>2</sub>S<sub>3</sub> is treated with boiling sodium carbonate solution it is converted to As<sub>4</sub>S<sub>4</sub>; this latter compound can also be made by fusing As<sub>2</sub>O<sub>3</sub> with sulfur or (industrially) by heating iron pyrites with arsenical pyrites. As<sub>4</sub>S<sub>4</sub> is scarcely attacked by water, inflames in Cl<sub>2</sub>, and is used in pyrotechny as it violently enflames when heated with KNO<sub>3</sub>. Above about 550° As<sub>4</sub>S<sub>4</sub> begins to dissociate reversibly and at 1000° the molecular weight corresponds to As<sub>2</sub>S<sub>2</sub> (of unknown structure).

<sup>84</sup> E. J. PORTER and G. M. SHELDRIK, *J. Chem. Soc., Dalton Trans.*, 1347–9 (1972).

<sup>85</sup> A. KUTOGLU, *Z. anorg. allg. Chem.* **419**, 176–84 (1976).

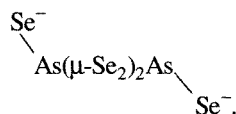
<sup>86</sup> H. J. WHITFIELD, *J. Chem. Soc., Dalton Trans.*, 1740–2 (1973).

<sup>87</sup> W. LAUER, M. BECKE-GOEHRING and K. SOMMER *Z. anorg allg. Chem.* **371**, 193–200 (1969).

$\text{As}_2\text{S}_3$  and  $\text{As}_4\text{S}_4$  have also provided a wealth of new ligands for transition-metal complexes, e.g.  $\text{AsS}$ ,  $\text{AsS}_3$ ,  $\text{As}_2\text{S}$  and, more recently, the geometrically novel bridging  $\eta^2, \eta^2$ - $\text{SAsSAsS}$  ligand.<sup>(88)</sup> Further diversity is emerging with the synthesis and structural characterization of a range of (halogenated)polythiopolyarsenate(III) ions such as cyclo- $[\text{As}_3\text{S}_3\text{X}_4]^-$ , (i.e. cyclo- $[(\text{XAs})_3\text{S}_3(\mu_3\text{-X})]^-$ ;  $\text{X} = \text{Cl}, \text{Br}, \text{I}$ ), cyclo- $[\text{S}=\text{AsS}_5]^-$ , bicyclo- $[\text{Br}_2\text{As}(\text{S})_2\text{As}_2(\text{S})_2(\text{CH}_2)]^-$  and  $[\text{As}_2\text{SBr}_6]^{2-}$  [i.e. *fac*- $[\text{Br}_2\text{As}(\mu\text{-S}, \text{Br}, \text{Br})\text{AsBr}_2]^{2-}$ ], all isolated as their  $[\text{PPh}_4]^+$  salts.<sup>(89)</sup>

Three selenides of arsenic are known:  $\text{As}_2\text{Se}_3$ ,  $\text{As}_4\text{Se}_3$  and  $\text{As}_4\text{Se}_4$ ; each can be made by direct heating of the elements in appropriate proportions at about  $500^\circ$  followed by annealing at temperatures between  $220$ – $280^\circ$ .  $\text{As}_2\text{Se}_3$  is a stable, brown, semiconducting glass which crystallizes when annealed at  $280^\circ$ ; it melts at  $380^\circ$  and is isomorphous with  $\text{As}_2\text{S}_3$ .  $\alpha\text{-As}_4\text{Se}_3$  forms fine, dark-red crystals isostructural with  $\alpha\text{-As}_4\text{S}_3(\text{C}_{3v})$  and the lighter-coloured  $\beta$ -form almost certainly contains the same molecular units.<sup>(90)</sup> Similarly,  $\text{As}_4\text{Se}_4$  is isostructural with realgar,  $\alpha\text{-As}_4\text{S}_4$ , and the directly linked  $\text{As}$ – $\text{As}$  distances are very similar in the 2 molecules (257 and 259 pm respectively);<sup>(91)</sup> other dimensions are  $\text{As}$ – $\text{Se}(\text{av})$  239 pm, angle  $\text{Se}$ – $\text{As}$ – $\text{Se}$   $95^\circ$ , angle  $\text{As}$ – $\text{Se}$ – $\text{As}$   $97^\circ$  and angle  $\text{As}$ – $\text{As}$ – $\text{Se}$   $102^\circ$  (cf. Fig. 13.17). The cationic cluster  $\text{As}_3\text{Se}_4^+$  was mentioned on p. 579, and the heterocyclic anion  $\text{As}_2\text{Se}_6^{2-}$  has been isolated as its orange  $[\text{Na}(\text{crypt})]^+$  salt:<sup>(92)</sup> the anion comprises a 6-membered heterocycle  $\{\text{As}_2\text{Se}_4\}$  in the chair conformation and each  $\text{As}$  carries a further exocyclic  $\text{Se}$  atom to give overall  $\text{C}_{2h}$

symmetry, i.e.



Methanolothermal reactions of  $\text{As}_2\text{Se}_3$  with alkali metal carbonates at  $130^\circ$  yield polymeta-selenoarsenites,  $\text{MAsSe}_2$  ( $\text{M} = \text{K}, \text{Rb}, \text{Cs}$ ), in which the polymeric anions consist of tetrahedral  $\{\text{AsSe}_3\}$  units linked by corner sharing into infinite chains.<sup>(93)</sup> Complexes of the triangulo- $\eta^3$  ligands  $\text{As}_2\text{Se}^-$  and  $\text{As}_2\text{Te}^-$ , such as  $[(\text{triphos})\text{Co}(\text{As}_2\text{E})]^+$ , can be made by reacting  $[\text{Co}(\text{H}_2\text{O})_6]^{2+}[\text{BF}_4]_2^-$  with the appropriate arsenic chalcogenide in the presence of the tridentate ligand  $\text{CH}_3\text{C}(\text{CH}_2\text{PPh}_3)_3$ , (triphos).<sup>(94)</sup>

The binary chalcogenides of  $\text{Sb}$  and  $\text{Bi}$  are also readily prepared by direct reaction of the elements at  $500$ – $900^\circ$ . They have rather complex ribbon or layer-lattice structures and have been much studied because of their semiconductor properties. Both  $n$ -type and  $p$ -type materials can be obtained by appropriate doping (pp. 258, 332) and for the compounds  $\text{M}_2\text{X}_3$  the intrinsic band gap decreases in the sequence  $\text{As} > \text{Sb} > \text{Bi}$  for a given chalcogen, and in the sequence  $\text{S} > \text{Se} > \text{Te}$  for a given Group 15 element. Some typical properties of these highly coloured compounds are in Table 13.10, but it should be mentioned that mp, density and even colour are often dependent on crystalline form and purity. The large thermoelectric effect of the selenides and tellurides of  $\text{Sb}$  and  $\text{Bi}$  finds use in solid-state refrigerators.  $\text{Sb}_2\text{S}_3$  occurs as the black or steely grey mineral stibnite and is made industrially on a moderately large scale for use in the manufacture of safety matches, military ammunition, explosives and pyrotechnic products, and in the production of ruby-coloured glass. It reacts vigorously when heated with oxidizing agents but is also useful as a pigment in plastics such as

<sup>88</sup> H. BRUNNER, H. KAUFMANN, B. NUBER, J. WACHTER and M. L. ZIEGLER, *Angew. Chem. Int. Edn. Engl.* **25**, 557–8 (1986) and references cited therein.

<sup>89</sup> U. MÜLLER and coworkers, *Z. anorg. allg. Chem.* **557**, 91–7 (1987); **566**, 18–24 (1988); **568**, 49–54 (1989); **609**, 82–8 (1992).

<sup>90</sup> T. J. BASTOW and H. J. WHITFIELD, *J. Chem. Soc., Dalton Trans.*, 959–61 (1977).

<sup>91</sup> T. J. BASTOW and H. J. WHITFIELD, *J. Chem. Soc., Dalton Trans.*, 1739–40 (1973).

<sup>92</sup> C. H. E. BELIN and M. M. CHARBONNEL, *Inorg. Chem.* **21**, 2504–6 (1982).

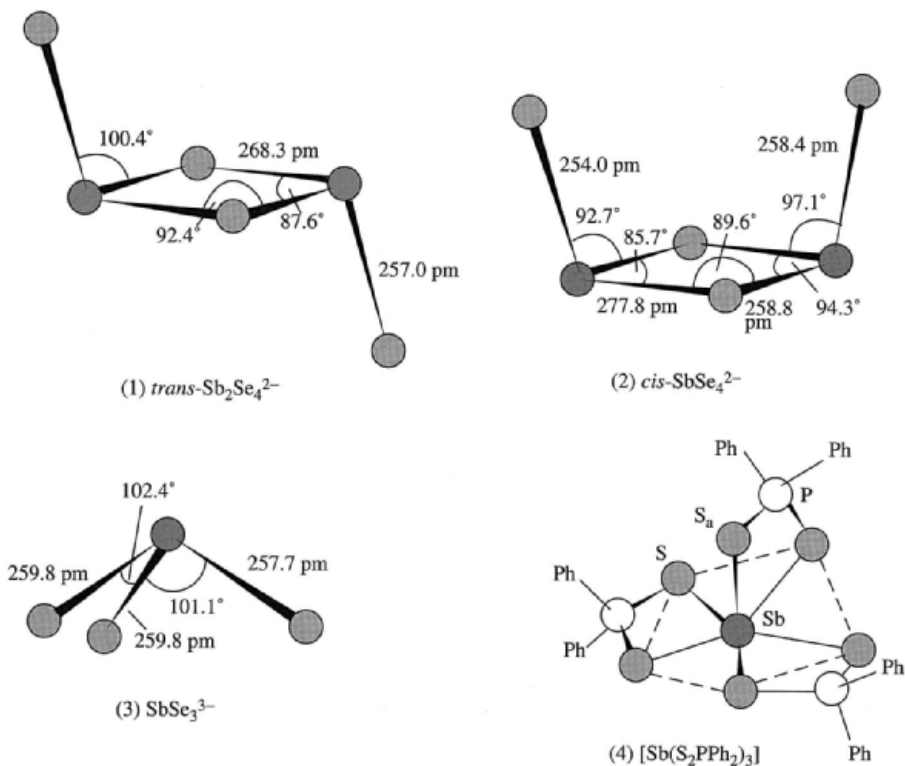
<sup>93</sup> W. S. SHELDRIK and H.-J. HÄUSLER, *Z. anorg. allg. Chem.* **561**, 139–48 (1988). See also pp. 149–56 for the similarly prepared  $\text{Cs}_3\text{Sb}_5\text{S}_9$  and  $\text{Cs}_3\text{Sb}_5\text{Se}_9$ .

<sup>94</sup> M. DI VAIRA, M. PERUZZINI and P. STOPPIONI, *Polyhedron* **5**, 945–50 (1986).

Table 13.10 Some properties of Group 15 chalcogenides  $M_2X_3$ 

Property	As <sub>2</sub> S <sub>3</sub>	Sb <sub>2</sub> S <sub>3</sub>	Bi <sub>2</sub> S <sub>3</sub>	As <sub>2</sub> Se <sub>3</sub>	Sb <sub>2</sub> Se <sub>3</sub>	Bi <sub>2</sub> Se <sub>3</sub>	As <sub>2</sub> Te <sub>3</sub>	Sb <sub>2</sub> Te <sub>3</sub>	Bi <sub>2</sub> Te <sub>3</sub>
Colour	Yellow	Black	Brown-black	Brown	Grey	Black	Grey	Grey	Grey
MP/°C	320	546	850	380	612	706	360	620	580
Density/g cm <sup>-3</sup>	3.49	4.61	6.78	4.80	5.81	7.50	6.25	6.50	7.74
$E_g$ /eV <sup>(a)</sup>	2.5	1.7	1.3	2.1	1.3	0.35	~1	0.3	0.15

<sup>(a)</sup>1 eV per atom = 96.485 kJ mol<sup>-1</sup>.



polythene or polyvinylchloride because of its flame-retarding properties. Golden and crimson antimony sulfides (which comprise mixtures of Sb<sub>2</sub>S<sub>3</sub>, Sb<sub>2</sub>S<sub>4</sub> and Sb<sub>2</sub>OS<sub>3</sub>) are likewise used as flame-retarding pigments in plastics and rubbers. A poorly characterized higher sulfide, sometimes said to be Sb<sub>2</sub>S<sub>5</sub>, can be obtained as a red solid by methods similar to those outlined for As<sub>2</sub>S<sub>5</sub> (p. 580). It is used in fireworks, as a pigment, and to vulcanize red rubber.

Of the more complex chalcogenide derivatives of the Group 15 elements two examples must suffice to indicate the great structural versatility of these elements, particularly

in the +3 oxidation state where the nonbonding electron pair can play an important stereochemical role. Thus, the compound of unusual stoichiometry Ba<sub>4</sub>Sb<sub>4</sub><sup>III</sup>Se<sub>11</sub> was found to contain within 1 unit cell: one *trans*-[Sb<sub>2</sub>Se<sub>4</sub>]<sup>2-</sup> (1), two *cis*-[Sb<sub>2</sub>Se<sub>4</sub>]<sup>2-</sup> (2), two pyramidal [SbSe<sub>3</sub>]<sup>3-</sup> (3), and two Se<sub>2</sub><sup>2-</sup> ions (Se–Se 236.7 pm) together with the requisite 8 Ba<sup>2+</sup> cations.<sup>(95)</sup> Conversely, the apparently simple 6-coordinate tris(dithiophosphate), [Sb(η<sup>2</sup>-S<sub>2</sub>PPh<sub>2</sub>)<sub>3</sub>] (4), features pentagonal pyramidal coordination

<sup>95</sup> G. CORDIER, R. COOK and H. SCHÄFER, *Angew. Chem. Int. Edn. Engl.* **19**, 324–5 (1980).

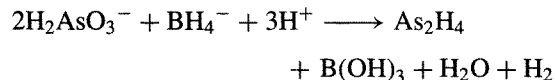
geometry, which is most unusual for a main-group element and may result from the comparatively 'small bite' of the ligand, the lone pair of electrons presumably occupying the seventh coordination position below the pentagonal plane.<sup>(96)</sup> The tris(oxalato) anion,  $[\text{Sb}^{\text{III}}(\text{C}_2\text{O}_4)_3]^{3-}$ , is perhaps the only other example of this geometry.<sup>(97)</sup>

### 13.3.6 Metal-metal bonds and clusters

The somewhat limited tendency of N and P to catenate into homonuclear chains has already been noted. The ability to form long chains is even less with As, Sb and Bi, though numerous compounds containing one M-M bond are known and many stable ring and cluster compounds featuring  $M_n$  groups have been emerging in recent years. The Group 15 elements therefore differ only qualitatively from C and the other Group 14 elements, on the one hand (p. 374), and S and the Group 16 elements, on the other (p. 751). The elements As, Sb and Bi (like P, p. 487) form well-defined sets of *triangulo*- $M_3$  and *tetrahedro*- $M_4$  compounds, whilst Bi in particular has a propensity to form cluster cations  $\text{Bi}_m^{n+}$  reminiscent of Sn and Pb clusters (p. 394) and *closo*-borane anions (p. 153). Before discussing these various classes of compound, however, it is convenient to recall that a particular grouping of atoms may well have strong interatomic bonds yet still be unstable because of disproportionation into even more stable groupings. A pertinent example concerns the bond dissociation energies of the diatomic molecules of the Group 15 elements themselves in the gas phase. Thus, the ground state electronic configuration of the atoms ( $ns^2np^3$ ) allows the possibility of triple bonding between pairs of atoms  $M_2(\text{g})$ , and it is notable that the bond dissociation energy of each of the Group 15 diatomic molecules

is much greater than for those of neighbouring molecules in the same period (Fig. 13.18). Despite this, only  $\text{N}_2$  is stable in the condensed phase because of the even greater stability of  $M_4$  or  $M_{\text{metal}}$  for the heavier congeners (p. 551). A notable advance has, however, been signalled in the isolation and X-ray structural characterization of Sb homologues of  $\text{N}_2$  and azobenzene as complex ligands: the red compounds  $[(\mu_3\eta^2\text{-Sb}\equiv\text{Sb})\{\text{W}(\text{CO})_5\}_3]$  and  $[(\eta^1, \eta^1, (\mu, \eta^2)\text{-PhSb}\equiv\text{SbPh})\{\text{W}(\text{CO})_5\}_3]$  are both stable at room temperature, even on exposure to air.<sup>(98)</sup> The dihapto distibene complex  $[\text{Fe}(\text{CO})_4(\eta^2\text{-RSb}=\text{SbR})]$   $\{\text{R}=(\text{Me}_3\text{Si})_2\text{CH}\}$  has also been characterized.<sup>(99)</sup>

Diarsane,  $\text{As}_2\text{H}_4$ , is obtained in small yield as a byproduct of the formation of  $\text{AsH}_3$  when an alkaline solution of arsenite is reduced by  $\text{BH}_4^-$  upon acidification:



Diarsane is a thermally unstable liquid with an extrapolated bp  $\sim 100^\circ$ ; it readily decomposes at room temperature to a mixture of  $\text{AsH}_3$  and a polymeric hydride of approximate composition  $(\text{As}_2\text{H})_x$ .  $\text{Sb}_2\text{H}_4$  ( $\text{SbCl}_3 + \text{NaBH}_4/\text{dil HCl}$ ) is even less stable. Both compounds can also be prepared by passing a silent electric discharge through  $\text{MH}_3$  gas in an ozonizer at low temperature. Mass spectrometric measurements give the thermochemical bond energy  $E_{298}^\circ$  (M-M) as  $128 \text{ kJ mol}^{-1}$  for  $\text{Sb}_2\text{H}_4$  and  $167 \text{ kJ mol}^{-1}$  for  $\text{As}_2\text{H}_4$ , compared with  $183 \text{ kJ mol}^{-1}$  for  $\text{P}_2\text{H}_4$ . Of the halides,  $\text{As}_2\text{I}_4$  is known (p. 564) but no corresponding compounds of Sb or Bi have yet been isolated (cf.  $\text{P}_2\text{X}_4$ , p. 497).

Organometallic derivatives  $M_2R_4$  are rather more stable than the hydrides and, indeed, dicacodyl,  $\text{Me}_2\text{AsAsMe}_2$ , was one of the very first organometallic compounds to be made

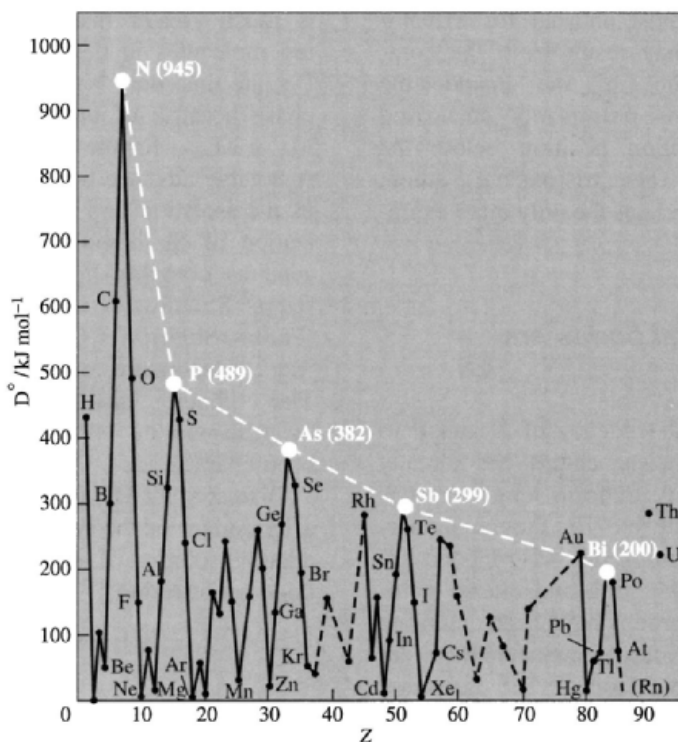
<sup>96</sup> M. J. BEGLEY, D. B. SOWERBY and I. HAIDUC, *J. Chem. Soc., Chem. Commun.*, 64-5 (1980).

<sup>97</sup> M. D. POORE and D. R. RUSSELL, *J. Chem. Soc., Chem. Commun.*, 18-9 (1971).

<sup>98</sup> G. HUTTNER, U. WEBER, B. SIGWARTH and O. SCHEIDSTEGE, *Angew. Chem. Int. Edn. Engl.* **21**, 215-6 (1982).

<sup>99</sup> A. H. COWLEY, N. C. NORMAN, M. PAKULSKI, D. L. BRICKER and D. H. RUSSELL, *J. Am. Chem. Soc.* **107**, 8211-18 (1985).

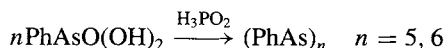
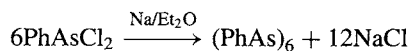




**Figure 13.18** Bond dissociation energies for gaseous, homonuclear diatomic molecules (from J. A. Kerr in *Handbook of Chemistry and Physics*, 73rd edn., 1992–3, CRC Press, Boca Raton, Florida), pp. 9.129–9.137.

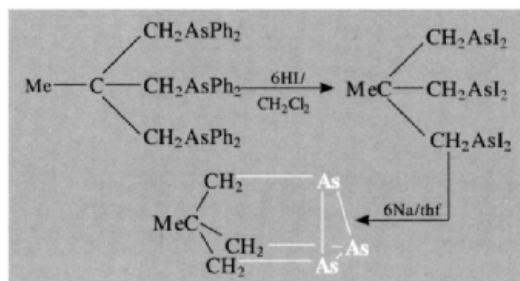
(L. C. Cadet, 1760; R. Bunsen, 1837): it has mp  $-1^\circ$ , bp  $78^\circ$ , is extremely poisonous, and has a revolting smell, as indicated by its name (Greek *κακωδία*, *cacodia*, stink). It is now readily made by the reaction of Li metal on  $\text{Me}_2\text{AsI}$  in thf. Other preparative routes to  $\text{As}_2\text{R}_4$  include reaction of  $\text{R}_2\text{AsH}$  with either  $\text{R}_2\text{AsX}$  or  $\text{R}_2\text{AsNH}_2$ , and the reaction of  $\text{R}_2\text{AsCl}$  with  $\text{MASR}_2$  ( $\text{M} = \text{Li}, \text{Na}, \text{K}$ ). In addition to alkyl derivatives numerous other compounds are known, e.g.  $\text{As}_2\text{Ph}_4$  mp  $127^\circ$ .  $\text{As}_2(\text{CF}_3)_4$  bp  $106^\circ$  has the *trans* ( $\text{C}_{2h}$ ) structure whereas  $\text{As}_2\text{Me}_4$  has a temperature-dependent mixture of *trans* and *gauche* isomers (p. 428). Corresponding Sb compounds are of more recent lineage, the first to be made (1931) being the yellow crystalline  $\text{Sb}_2\text{Ph}_4$  mp  $122^\circ$ . Other derivatives have  $\text{R} = \text{Me}, \text{Bu}^t, \text{CF}_3, \text{cyclohexyl}, p\text{-tolyl}, \text{cyclopentadienyl}$ , etc. Little is known of organodibismuthanes  $\text{Bi}_2\text{R}_4$  despite sporadic attempts to prepare them.

More extensive catenation occurs in the *cyclo*-polyarsanes  $(\text{RAs})_n$  which can readily be prepared from organoarsenic dihalides or from arsonic acids as follows:



In addition to the 6-membered ring in  $(\text{PhAs})_6$ , 5-membered rings have been obtained with  $\text{R} = \text{Me}, \text{Et}, \text{Pr}, \text{Ph}, \text{CF}_3, \text{SiH}_3, \text{GeH}_3$  and 4-membered rings occur with  $\text{R} = \text{CF}_3, \text{Ph}$ . A 3-membered  $\text{As}_3$  ring has also been made and is the first *all-cis* organocyclotriarsane to be characterized.<sup>(100)</sup>

<sup>100</sup> J. ELLERMANN and H. SCHÖSSNER, *Angew. Chem. Int. Edn. Engl.* **13**, 601–2 (1974).



The factors influencing ring size and conformation have not yet become clear. Thus, the yellow  $(\text{MeAs})_5$  has a puckered  $\text{As}_5$  ring with  $\text{As}-\text{As}$  243 pm and angle  $\text{As}-\text{As}-\text{As}$   $102^\circ$ ; there is also a more stable red form.  $(\text{PhAs})_6$  has a puckered  $\text{As}_6$  (chair form) with  $\text{As}-\text{As}$  246 pm and angle  $\text{As}-\text{As}-\text{As}$   $91^\circ$ . Numerous polycyclic compounds  $\text{As}_n\text{R}_m$  have also been characterized, for example the bright-yellow crystalline *tricyclo*- $\text{As}_{12}\text{Bu}_8^t$ .<sup>(100a)</sup>

In view of the excellent donor properties of tertiary arsines, it is of interest to inquire whether these *cyclo*-polyarsanes can also act as ligands. Indeed,  $(\text{MeAs})_5$  can displace CO from metal carbonyls to form complexes in which it behaves as a uni-, bi- or tridentate ligand. For example, direct reaction of  $(\text{MeAs})_5$  with  $\text{M}(\text{CO})_6$  in benzene at  $170^\circ$  ( $\text{M} = \text{Cr}, \text{Mo}, \text{W}$ ) yielded red crystalline compounds  $[\text{M}(\text{CO})_3(\eta^3\text{-As}_5\text{Me}_5)]$  for which the structure

<sup>100a</sup> M. BAUDLER and S. WIETFELDT-HALTENHOFF, *Angew. Chem. Int. Edn. Engl.* **24**, 991–2 (1985).

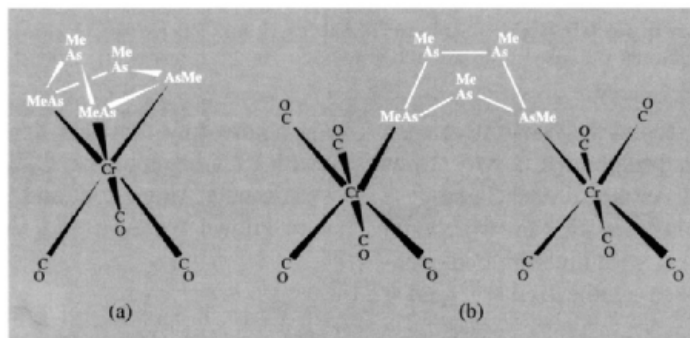
in Fig. 13.19a has been proposed,<sup>(101)</sup> whereas reaction at room temperature with the ethanol derivative  $[\text{M}(\text{CO})_5(\text{EtOH})]$  gave the yellow dinuclear product  $[\{\text{M}(\text{CO})_5\}_2\text{-}\mu\text{-}(\eta^1\eta^1\text{-As}_5\text{Me}_5)]$  for which a possible structure is given in Fig. 13.19b. Reaction can also lead to ring degradation; e.g. reaction with  $\text{Fe}(\text{CO})_5$  cleaves the ring to give dark-orange crystals of the *catena*-tetraarsane  $[\{\text{Fe}(\text{CO})_3\}_2(\text{As}_4\text{Me}_4)]$  whose structure (Fig. 13.20a) has been established by X-ray crystallography.<sup>(102)</sup> Even further degradation of the *cyclo*-polyarsane occurs when  $(\text{C}_6\text{F}_5\text{As})_4$  reacts with  $\text{Fe}(\text{CO})_5$  in benzene at  $120^\circ$  to give yellow plates of  $[\text{Fe}(\text{CO})_4\{\text{AsC}_6\text{F}_5\}_2]$  mp  $150^\circ$  (Fig. 13.20b).<sup>(103)</sup> In other reactions homoatomic ring expansion or chain extension can occur. For example  $(\text{AsMe})_5$  when heated with  $\text{Cr}(\text{CO})_6$  in benzene at  $150^\circ$  gives crystals of  $[\text{Cr}_2(\text{CO})_6\text{-}\mu\text{-}\{\eta^6\text{-cyclo}(\text{AsMe})_9\}]$ , whereas  $(\text{AsPr}^n)_5$  and  $\text{Mo}(\text{CO})_6$  under similar conditions yield crystals of  $[\text{Mo}_2(\text{CO})_6\text{-}\mu\text{-}\{\eta^4\text{-catena}(\text{AsPr}^n)_8\}]$ . The molecular structures were determined by X-ray analysis and are shown in Fig. 13.21.<sup>(104)</sup> In the first, each Cr is 6-coordinate and the  $\text{As}_9$  ring is hexahapto, donating 3 pairs of electrons to

<sup>101</sup> P. S. ELMES and B. O. WEST, *Coord. Chem. Rev.* **3**, 279–91 (1968).

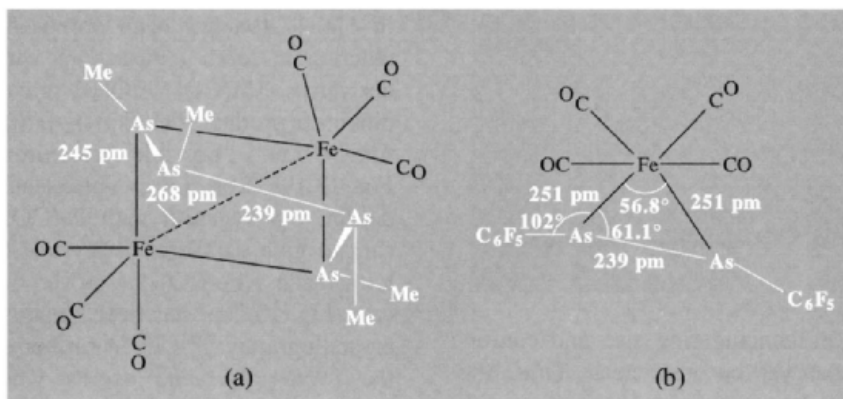
<sup>102</sup> B. M. GATEHOUSE, *J. Chem. Soc., Chem. Commun.*, 948–9 (1969).

<sup>103</sup> P. S. ELMES, P. LEVERET and B. O. WEST, *J. Chem. Soc., Chem. Commun.*, 747–8 (1971).

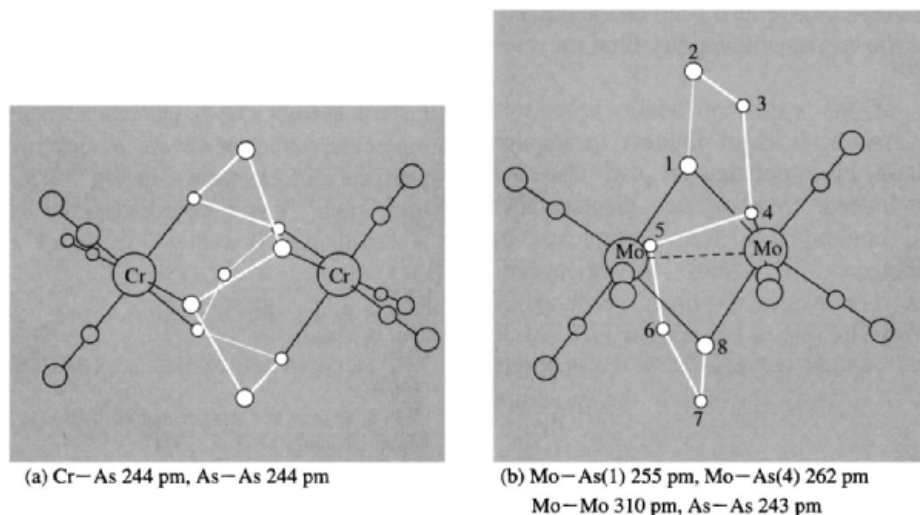
<sup>104</sup> P. S. ELMES, B. M. GATEHOUSE, D. J. LLOYD and B. O. WEST, *J. Chem. Soc., Chem. Commun.*, 953–4 (1974).



**Figure 13.19** Proposed structures for (a) the tridentate *cyclo*-polyarsane complex  $[\text{Cr}(\text{CO})_3(\text{As}_5\text{Me}_5)]$ , and (b) the bisonodentate binuclear complex  $[\{\text{Cr}(\text{CO})_5\}_2(\text{As}_5\text{Me}_5)]$ .



**Figure 13.20** Crystal structures of (a)  $[\{\text{Fe}(\text{CO})_3\}_2\{(\text{AsMe})_4\}]$ , and (b)  $[\text{Fe}(\text{CO})_4\{(\text{AsC}_6\text{F}_5)_2\}]$ . In (a) the distance between the 2 terminal As atoms is 189 pm, suggesting some “residual interaction” but no direct  $\sigma$  bond.



**Figure 13.21** Structures of (a)  $[\text{Cr}_2(\text{CO})_6-\mu-\{\eta^6\text{-cyclo}(\text{AsMe})_9\}]$ , and (b)  $[\text{Mo}_2(\text{CO})_6-\mu-\{\eta^4\text{-catena}(\text{AsPr})_8\}]$ . In both structures the alkyl group attached to each As atom has been omitted for clarity.

each Cr atom. In the second the As atom at each end of the  $\text{As}_8$  chain bridges the 2 Mo atoms whereas the 2 central As atoms each bond to 1 Mo atom only and there is an Mo–Mo bond. Complexes of *cyclo-As*<sub>8</sub> with niobium cyclopentadienyls have also been synthesized,<sup>(105)</sup> and it

is noteworthy that this ligand is “isoelectronic” with cyclooctatetraene,  $\text{C}_8\text{H}_8$ . The analogy holds for smaller rings, too, and *cyclo-As*<sub>*n*</sub> complexes are known for  $\text{As}_3$ ,  $\text{As}_4$ ,  $\text{As}_5^-$ ,  $\text{As}_6^-$  and  $\text{As}_7^-$ ,

<sup>105</sup> O. J. SCHERER, R. WINTER, G. HECKMANN and G. WOLMERSHÄUSER, *Angew. Chem. Int. Edn. Engl.* **30**, 850–2 (1991). See also H.-G. VON SCHNERING, J. WOLF,

D. WEBER, R. RAMIREZ and T. MEYER, *Angew. Chem. Int. Edn. Engl.* **25**, 353–4 (1986) for the first example of this octahapto *cyclo-As*<sub>8</sub><sup>8-</sup> ligand in the deep red complex  $[\text{Rb}(\text{crypt})]^{+}_2[\text{Rb}[\text{Nb}^{\text{V}}\text{As}_8]]^{2-}$  (Nb–As 261–9 pm, As–As 2434 pm, angle AsAsAs 93.7°.

(norbornadiene analogue) as well as for *cyclo*-As<sub>8</sub><sup>8-</sup> (crown-shaped S<sub>8</sub> analogue).

Some of the compounds mentioned in the preceding paragraph can be thought of as heteronuclear cluster compounds and it is convenient to consider here other such heteronuclear cluster species before discussing compounds in which there are homonuclear clusters of Group 15 atoms. Compounds structurally related to the As<sub>4</sub> cluster include the complete series [As<sub>4-n</sub>{Co(CO)<sub>3</sub>}]<sub>n</sub> n = 0, 1, 2, 3, 4. It will be noted that the atom As and the group {Co(CO)<sub>3</sub>} are “isoelectronic” in the sense that each requires 3 additional electrons to achieve a stable 8- or 18-electron configuration respectively. Yellow crystals of [As<sub>3</sub>Co(CO)<sub>3</sub>] are obtained by heating (MeAs)<sub>5</sub> with Co<sub>2</sub>(CO)<sub>8</sub> in hexane at 200° under a high pressure of CO.<sup>(106)</sup> The red air-sensitive liquid [As<sub>2</sub>{Co(CO)<sub>3</sub>}]<sub>2</sub> mp -10° is obtained by the milder reaction of AsCl<sub>3</sub> with Co<sub>2</sub>(CO)<sub>8</sub> in thf.<sup>(107)</sup> Substitution of some carbonyls by tertiary phosphines is also possible under ultraviolet irradiation. Typical structural details are in Fig. 13.22. In the first compound the η<sup>3</sup>-triangulo-As<sub>3</sub> group can be thought of as a 3-electron donor to the cobalt atom; in the second, the very short As-As bond suggests multiple bonding and the structure closely resembles

that of the “isoelectronic” acetylene complex [{Co(CO)<sub>3</sub>}]<sub>2</sub>PhC≡CPh] (p. 933). Phosphorus analogues are also known, e.g. the sand-coloured or colourless complexes [M(η<sup>3</sup>-P<sub>3</sub>)L\*], where M = Co, Rh or Ir and L\* is the tripod-like tris(tertiary phosphine) ligand MeC(CH<sub>2</sub>-PPh<sub>2</sub>)<sub>3</sub>.<sup>(108)</sup> Likewise the first example of an η<sup>2</sup>-P<sub>2</sub> ligand symmetrically bonded to 2 metal atoms to give a tetrahedral {P<sub>2</sub>Co<sub>2</sub>} cluster was established by the X-ray structure determination of [(μ-P<sub>2</sub>){Co(CO)<sub>3</sub>}{Co(CO)<sub>2</sub>(PPh<sub>3</sub>)}].<sup>(109)</sup> If the μ-P<sub>2</sub> (or μ-As<sub>2</sub>) ligand is replaced by μ-S<sub>2</sub> (or μ-Se<sub>2</sub>), then isoelectronic and isostructural clusters can be obtained by replacing Co by Fe, as in [(μ-S<sub>2</sub>){Fe(CO)<sub>3</sub>}]<sub>2</sub> and [(μ-Se<sub>2</sub>){Fe(CO)<sub>3</sub>}]<sub>2</sub> (p. 758).

Even more intriguing are the “double sandwich” complexes which feature {η<sup>3</sup>-P<sub>3</sub>} and {η<sup>3</sup>-As<sub>3</sub>} as symmetrically bridging 3-electron donors. Thus As<sub>4</sub> reacts smoothly with Co<sup>II</sup> or Ni<sup>II</sup> aquo ions and the triphosphane ligand L\* = MeC(CH<sub>2</sub>PPh<sub>2</sub>)<sub>3</sub> in thf/ethanol/acetone mixtures to give the exceptionally air-stable dark-green paramagnetic cation [L\*Co-μ-(η<sup>3</sup>-As<sub>3</sub>)CoL\*]<sup>2+</sup> with the dimensions shown in Fig. 13.23.<sup>(110)</sup> The structure of the related P<sub>3</sub> complex [L\*-μ-(η<sup>3</sup>-P<sub>3</sub>)-NiL\*]<sup>2+</sup> (prepared in the same way using white

<sup>106</sup> A. S. FOUST, M. F. FOSTER and L. F. DAHL, *J. Am. Chem. Soc.* **91**, 5631-3 and 5633-5 (1969).

<sup>107</sup> A. S. FOUST, C. F. CAMPANA, J. D. SINCLAIR and L. F. DAHL, *Inorg. Chem.* **18**, 3047-54 (1979).

<sup>108</sup> C. BIANCHINI, C. MEALLI, A. MELI and L. SACCONI, *Inorg. Chim. Acta* **37**, L543-L544 (1979).

<sup>109</sup> C. F. CAMPANA, A. VIZI-OROSZ, G. PALYI, L. MARKÓ and L. F. DAHL, *Inorg. Chem.* **18**, 3054-9 (1979).

<sup>110</sup> M. DI VAIRA, S. MIDOLLINI, L. SACCONI and F. ZANOBINI, *Angew. Chem. Int. Edn. Engl.* **17**, 676-7 (1978).

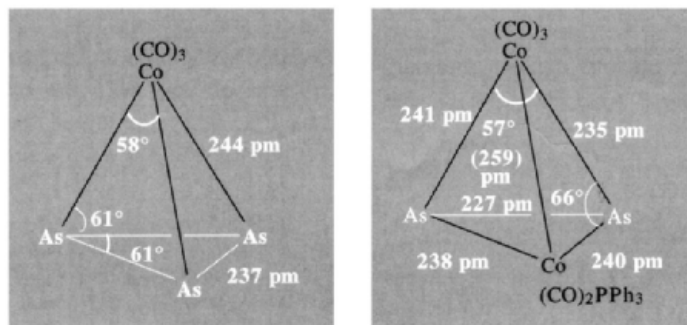


Figure 13.22 Structures of [As<sub>3</sub>Co(CO)<sub>3</sub>] and [As<sub>2</sub>{Co(CO)<sub>3</sub>}{Co(CO)<sub>2</sub>(PPh<sub>3</sub>)}].

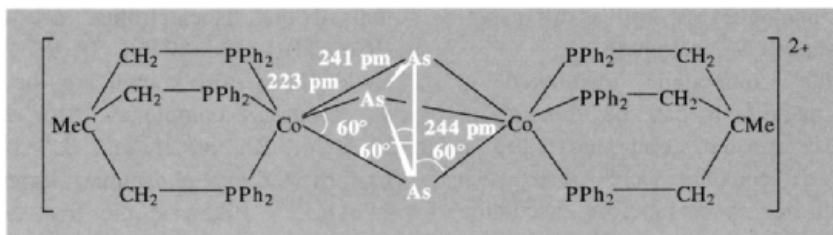


Figure 13.23 Structure of the cation  $[L^*Co-\mu-(\eta^3-As_3)CoL^*]^{2+}$ .

Table 13.11 Electronic configurations of the isostructural series of complexes containing bridging  $\eta^3-P_3$  and  $\eta^3-As_3$  ligands  $\{L^*$  is the tridentate tertiary phosphine  $MeC(CH_2PPh_2)_3\}$

$(\eta^3-P_3)$ complex	Colour	Valence electrons	Unpaired electrons	Electrons in highest (e) orbital	Colour	$(\eta^3-As_3)$ complex
$[L^*_2Co_2(P_3)]^{3+}$	Bright green	30	0	0		$[L^*_2Co_2(As_3)]^{3+}$
$[L^*_2Co_2(P_3)]^{2+}$		31	1	1	Dark green	$[L^*_2Co_2(As_3)]^{2+}$
$[L^*_2Co_2(P_3)]^+$		32	2	2		$[L^*_2Co_2(As_3)]^+$
$[L^*_2CoNi(P_3)]^{2+}$	Red-brown	32	2	2		—
$[L^*_2Ni_2(P_3)]^{2+}$		33	1	3		$[L^*_2Ni_2(As_3)]^{2+}$
$[L^*_2Ni_2(P_3)]^+$	Dark	34	0	4		$[L^*_2Ni_2(As_3)]^+$

$P_4$ ) is closely similar<sup>(111)</sup> with P–P distances of 216 pm (smaller than for  $P_4$  itself, 221 pm). Indeed, a whole series of complexes has now been established with the same structure-motif and differing only in the number of valency electrons in the cluster; some of these are summarized in Table 13.11.<sup>(111,112)</sup> The number of valence electrons in all these complexes falls in the range 30–34 as predicted by R. Hoffmann and his colleagues.<sup>(113)</sup> Many other cluster types incorporating differing numbers of Group 15 and transition metal atoms are now known and have been fully reviewed.<sup>(114,115)</sup>

With Sb even larger clusters can be obtained. For example reaction of  $Co(OAc)_2 \cdot 4H_2O$  and

$SbCl_3$  in pentane at  $150^\circ$  under a pressure of  $H_2/CO$  gave black crystals of  $[Sb_4\{Co(CO)_3\}_4]$  which was found to have a cubane like structure with Sb and Co at alternate vertices of a grossly distorted cube (Fig. 13.24).<sup>(116)</sup>

In addition to the heteronuclear clusters considered in the preceding paragraphs, As, Sb and Bi also form homonuclear clusters. We have already seen that alkaline earth phosphides  $M_3^{II}P_{14}$  contain the  $[P_7]^{3-}$  cluster isoelectronic and isostructural with  $P_4S_3$ , and the analogous clusters  $[As_7]^{3-}$  and  $[Sb_7]^{3-}$  have also been synthesized. Thus, when As was heated with metallic Ba at  $800^\circ C$ , black lustrous prisms of  $Ba_3As_{14}$  were obtained, isotypic with  $Ba_3P_{14}$ ; these contained the  $[As_7]^{3-}$  anion with dimensions as shown in Fig. 13.25(a).<sup>(117)</sup> Again,

<sup>111</sup> M. DI VAIRA, S. MIDOLLINI and L. SACCONI, *J. Am. Chem. Soc.* **101**, 1757–63 (1979).

<sup>112</sup> F. FABBRIZZI and L. SACCONI, *Inorg. Chim. Acta*, **36**, L407–L408 (1979).

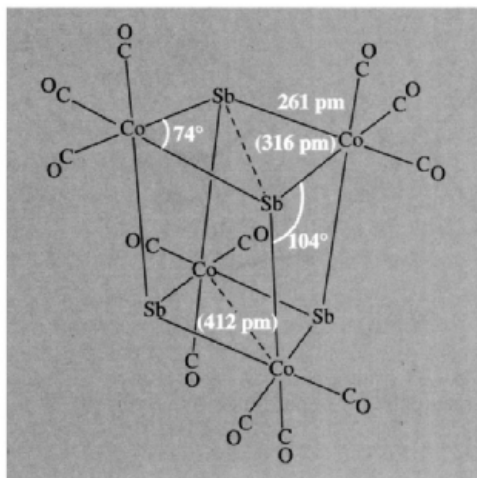
<sup>113</sup> J. W. LAUHER, M. ELIAN, R. H. SUMMERVILLE and R. HOFFMANN, *J. Am. Chem. Soc.* **98**, 3219–24 (1976).

<sup>114</sup> O. J. SCHERER (and 9 others), in R. STEUDEL (ed.), *The Chemistry of Inorganic Ring Systems*, Elsevier, Amsterdam, 1992 pp. 193–208.

<sup>115</sup> K. H. WHITMIRE, in H. W. ROESKY (ed.), *Rings, Clusters and Polymers of Main Group and Transition Elements*, Elsevier, Amsterdam, 1989, pp. 503–41.

<sup>116</sup> A. S. FOUST and L. F. DAHL, *J. Am. Chem. Soc.* **92**, 7337–41 (1970).

<sup>117</sup> W. SCHMETTOW and H. G. VON SCHNERING, *Angew. Chem. Int. Edn. Engl.* **16**, 857 (1977).



**Figure 13.24** Structure of the cubane-like mixed metal-metal cluster  $[\text{Sb}_4\text{-Co}(\text{CO})_3]_4$ .

when powdered NaSb or NaSb<sub>3</sub> were treated with crypt,  $[\text{N}(\text{C}_2\text{H}_4\text{OC}_2\text{H}_4\text{OC}_2\text{H}_4)_3\text{N}]$  (p. 98) in dry ethylenediamine, a deep-brown solution was obtained from which brown needles of  $[\text{Na}(\text{crypt})^+]_3[\text{Sb}_7]^{3-}$  were isolated with a  $C_{3v}$  anion like  $[\text{As}_7]^{3-}$  and Sb-Sb distances 286 pm (base), 270 pm (side) and 278 pm (cap).<sup>(118)</sup>

<sup>118</sup> J. D. CORBETT, D. G. ADOLPHSON, D. J. MERRIMAN, P. A. EDWARDS and F. J. ARMATIS, *J. Am. Chem. Soc.* **97**, 6267-8 (1975). S. C. CRITCHLOW and J. D. CORBETT, *Inorg.*

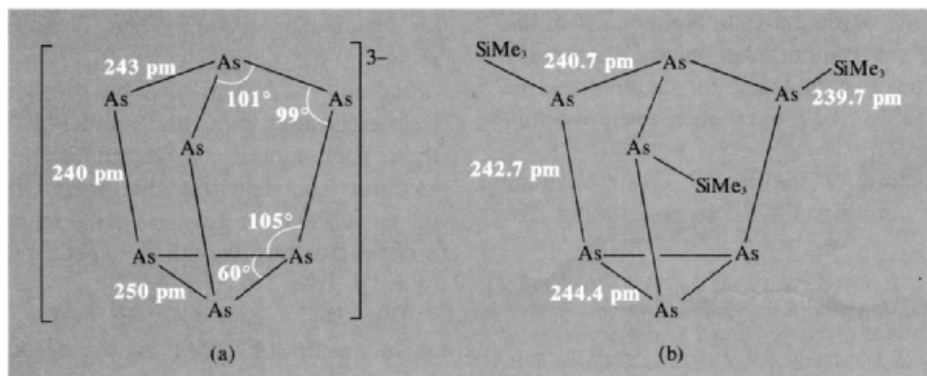
Isostructural, neutral molecular clusters can be obtained by replacing the 3 S or 3 Se atoms in P<sub>4</sub>S<sub>3</sub> or As<sub>4</sub>Se<sub>3</sub> by PR or AsR rather than by P<sup>-</sup> or As<sup>-</sup>. For example reaction of Na/K alloy with white P<sub>4</sub> and Me<sub>3</sub>SiCl in monoglyme gave P<sub>7</sub>R<sub>3</sub>, P<sub>14</sub>R<sub>4</sub> and P<sub>13</sub>R<sub>5</sub>. Similarly, Cs<sub>3</sub>P<sub>11</sub> and Rb<sub>3</sub>As<sub>7</sub> react with Me<sub>3</sub>SiCl in toluene to give good yields of the bright-yellow crystalline compounds P<sub>11</sub>(SiMe<sub>3</sub>)<sub>3</sub> and As<sub>7</sub>(SiMe<sub>3</sub>)<sub>3</sub>. This latter compound is stable to air and moisture for several hours and has the structure shown in Fig. 13.25b.<sup>(119)</sup> Other examples include As<sub>11</sub><sup>3-</sup><sup>(120)</sup> and Sb<sub>11</sub><sup>3-</sup><sup>(121)</sup> which both have the structure indicated in Fig. 13.26(a). This is very similar to the structure of P<sub>11</sub><sup>3-</sup> [Fig. 12.11(d)] and has approximately D<sub>3</sub> symmetry with eight 3-coordinate As(Sb) atoms forming a bicapped twisted triangular prism with a “waist” of three 2-coordinate bridging atoms. The related As<sub>22</sub><sup>4-</sup> anion comprises two such {As<sub>11</sub>} units conjoined by linking two of these equatorial “waist”

*Chem.* **23**, 770-4 (1994); this also describes the synthesis and structure of  $[\text{K}(\text{crypt})^+]_2[\text{Sb}_4]^{2-}$  which features the square planar  $[\text{Sb}_4]^{2-}$  anion with Sb-Sb 275 pm.

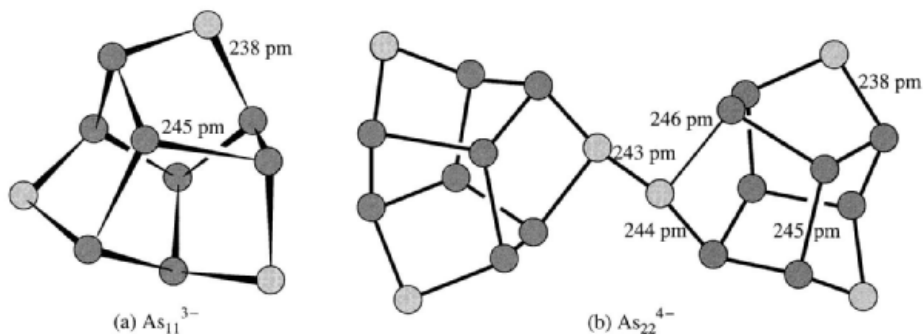
<sup>119</sup> H. G. VON SCHNERING, D. FENSKE, W. HÖNLE, M. BINNEWIES and K. PETERS, *Angew. Chem. Int. Edn. Engl.* **18**, 679 (1979).

<sup>120</sup> C. H. E. BELIN, *J. Am. Chem. Soc.* **102**, 6036-40 (1980).

<sup>121</sup> U. BOLLE and W. TREMEL, *J. Chem. Soc., Chem. Commun.*, 91-3 (1992).



**Figure 13.25** (a) Structure of the anion  $[\text{As}_7]^{3-}$ , isoelectronic with As<sub>4</sub>Se<sub>3</sub> (p. 581). The sequence of As-As distances (base>cap>side) is typical for such cluster anions but this alters to the sequence base>side>cap for neutral species such as As<sub>7</sub>(SiMe<sub>3</sub>)<sub>3</sub> shown in (b).



**Figure 13.26** (a) Structure of the anion  $As_{11}^{3-}$ ; note that the As–As distances involving the three 2-coordinate As atoms are significantly shorter than those between pairs of 3-coordinate As atoms. (b) Structure of the anion  $As_{22}^{4-}$  i.e.  $[As_{11}-As_{11}]^{4-}$  (see text).

atoms as shown in Fig. 13.26(b)<sup>(122)</sup>. Many other homonuclear and heteronuclear clusters have also been prepared, of which  $[As_7Se_4]^{3-}$ <sup>(123)</sup>,  $[As_{10}Te_3]^{2-}$ <sup>(124)</sup> and  $[As_{11}Te]^{3-}$ <sup>(125)</sup> can serve as examples. They were made, respectively, by reduction of  $As_4Se_4$  with  $K/C_2H_4(NH_2)_2$  in the presence of  $[Ph_4P]Br$ , the oxidation of polyarsenides with Te (or reduction of  $As_2Te_3$  with K), and the reaction of the alloy  $K_{1.6}As_{1.6}Te$  with a cryptand ligand in ethylenediamine.

In all the cluster compounds discussed above there are sufficient electrons to form 2-centre 2-electron bonds between each pair of adjacent atoms. Such is not the case, however, for the cationic bismuth species now to be discussed and these must be considered as “electron deficient”. The unparalleled ability of Bi/ $BiCl_3$  to form numerous low oxidation-state compounds in the presence of suitable complex anions has already been mentioned (p. 564) and the cationic species shown in Table 13.12 have been unequivocally identified.

The structure of the last 3 cluster cations are shown in Fig. 13.27. In discussing the

structure and bonding of these clusters it will be noted that  $Bi^+(6s^26p^2)$  can contribute 2p electrons to the framework bonding just as  $\{BH\}$  contributes 2 electrons to the cluster bonding in boranes (p. 158). Hence, using the theory developed for the boranes, it can be seen that  $[B_nH_n]^{2-}$  is electronically equivalent to  $(Bi^+)_n^{2-}$  i.e.  $[Bi_n]^{n-2}$ . This would account for the stoichiometries  $Bi_3^+$  and  $Bi_5^{3+}$  but would also lead one to expect  $Bi_8^{6+}$  and  $Bi_9^{7+}$  for the larger clusters. However, these charges are very large and it seems likely that the lowest-lying nonbonding orbital would also be occupied in  $(Bi^+)_n^{2-}$ . For  $(Bi^+)_8^{2-}$  this is an  $e_1$  orbital which can accommodate 4 electrons, thereby reducing the charge from  $Bi_8^{6+}$  to  $Bi_8^{2+}$  as observed. In  $(Bi^+)_9^{2-}$  the lowest nonbonding orbital is  $a_2''$  which can accommodate 2 electrons, thus reducing the charge from  $Bi_9^{7+}$  to  $Bi_9^{5+}$  as observed.<sup>(126)</sup> It will also be noted that  $Bi_5^{3+}$  is isoelectronic with  $Sn_5^{2-}$  and  $Pb_5^{2-}$  (p. 394); these penta-atomic species all have 12 valence electrons (not counting the “inert”  $s^2$  electrons on each atom), i.e.  $n+1$  pairs ( $n=5$ ) hence a *closo*-structure would be expected by Wade’s rules (p. 161).

The  $Bi_9^{5+}$  ion was discovered in 1963 as a result of work by A. Herschaft and J. D. Corbett on the structure of the black subhalide “ $BiCl$ ” (p. 564) and subsequently was

<sup>122</sup> R. C. HAUSHALTER, B. W. EICHHORN, A. L. RHEINGOLD and S. J. GIBB, *J. Chem. Soc., Chem. Commun.*, 1027–8 (1988).

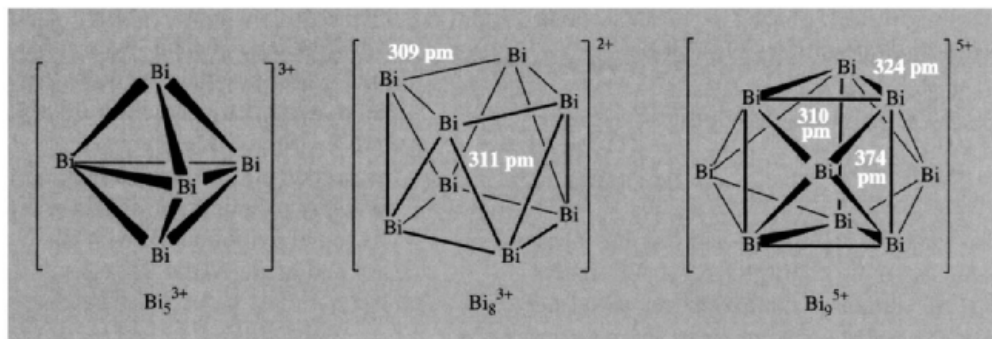
<sup>123</sup> V. ANGILELLA H. MERCIA and C. BELIN, *J. Chem. Soc., Chem. Commun.*, 1654–5 (1989).

<sup>124</sup> R. C. HAUSHALTER, *J. Chem. Soc., Chem. Commun.*, 196–7 (1987).

<sup>125</sup> C. BELIN and H. MERCIER, *J. Chem. Soc., Chem. Commun.*, 190–1 (1987).

<sup>126</sup> J. D. CORBETT, *Prog. Inorg. Chem.* **21**, 129–58 (1976).



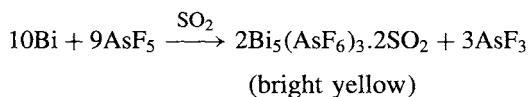


**Figure 13.27** The structures of cationic clusters of  $\text{Bi}_m^{n+}$ . The dimensions cited for  $\text{Bi}_9^{5+}$  were obtained from an X-ray study on  $[(\text{Bi}_9^{5+})(\text{Bi}^+)(\text{HfCl}_6^{2-})_3]$ ; the corresponding average distances for  $\text{Bi}_9^{5+}$  in  $\text{BiCl}_{1.167}$  i.e.  $[(\text{Bi}_9^{5+})_2(\text{BiCl}_5^{2-})_4(\text{Bi}_2\text{Cl}_8^{2-})]$  are 310, 320 and 380 pm respectively. The square antiprismatic structure of  $\text{Bi}_8^{2+}$  was established by an X-ray study of  $\text{Bi}_8[\text{AlCl}_4]_2$ .<sup>(127)</sup>

**Table 13.12** Cationic bismuth clusters

Cation	Formal oxidation state	Cluster structure	Point group symmetry
$\text{Bi}^+$	1.00	—	—
$\text{Bi}_3^+$	0.33	Triangle	$D_{3h}$
$\text{Bi}_5^{3+}$	0.60	Trigonal bipyramid	$D_{3h}$
$\text{Bi}_8^{2+}$	0.25	Square antiprism	$D_{4h}$
$\text{Bi}_9^{5+}$	0.56	Tricapped trigonal prism	$C_{3h}(\sim D_{3h})$

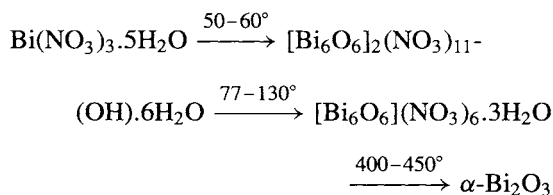
also found in  $\text{Bi}_{10}\text{HfCl}_{18}$ .<sup>(32)</sup> The diamagnetic compound  $\text{Bi}_5(\text{AlCl}_4)_3$  was prepared by reaction of  $\text{BiCl}_3/\text{AlCl}_3$  with the stoichiometric amount of Bi in fused  $\text{NaAlCl}_4$  (mp  $151^\circ$ ).<sup>(128)</sup> With an excess of Bi under the same conditions  $\text{Bi}_8(\text{AlCl}_4)_2$  was obtained. More recently it has been found that  $\text{AsF}_5$  and other pentafluorides oxidize Bi in liquid  $\text{SO}_2$  first to  $\text{Bi}_8^{2+}$  and then to  $\text{Bi}_5^{3+}$ .<sup>(129)</sup>



### 13.3.7 Other inorganic compounds

The ability to form stable oxoacid salts such as sulfates, nitrates, perchlorates, etc., increases in the order  $\text{As} \ll \text{Sb} < \text{Bi}$ .  $\text{As}^{\text{III}}$  is insufficiently basic to enable oxoacid salts to be isolated though species such as  $[\text{As}(\text{OH})(\text{HSO}_4)_2]$  and  $[\text{As}(\text{OH})(\text{HSO}_4)]^+$  have been postulated in anhydrous  $\text{H}_2\text{SO}_4$  solutions of  $\text{As}_2\text{O}_3$ . In oleum, species such as  $[\text{As}(\text{HSO}_4)_3]$ ,  $[\{(\text{HSO}_4)_2\text{As}\}_2\text{O}]$  and  $[\{(\text{HSO}_4)_2\text{As}\}_2\text{SO}_4]$  may be present. By contrast,  $\text{Sb}_2(\text{SO}_4)_3$  can be isolated, as can the hydrates  $\text{Bi}_2(\text{SO}_4)_3 \cdot n\text{H}_2\text{O}$  and the double sulfate  $\text{KBi}(\text{SO}_4)_2$ , though all are readily hydrolysed to basic salts.

The pentahydrate  $\text{Bi}(\text{NO}_3)_3 \cdot 5\text{H}_2\text{O}$  can be crystallized from solutions of  $\text{Bi}^{\text{III}}$  oxide or carbonate in conc  $\text{HNO}_3$ . Dilution causes the basic salt  $\text{BiO}(\text{NO}_3)$  to precipitate. Attempts at thermal dehydration yield complex oxocations by reactions which have been formulated as follows:



The  $[\text{Bi}_6\text{O}_6]^{6+}$  ion is the dehydrated form of  $[\text{Bi}_6(\text{OH})_{12}]^{6+}$  (p. 575). Treatment of the

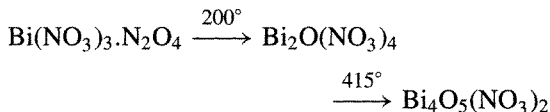
<sup>127</sup> B. KREBS, M. HUCKE and C. J. BRENDEL, *Angew. Chem. Int. Edn. Engl.* **21**, 445–6 (1982).

<sup>128</sup> J. D. CORBETT, *Inorg. Chem.* **7**, 198–208 (1968).

<sup>129</sup> R. C. BURNS, R. J. GILLESPIE and WOON-CHUNG LUK, *Inorg. Chem.* **17**, 3596–604 (1978).

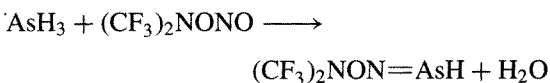


pentahydrate with  $N_2O_4$  yields an adduct which decomposes to oxide nitrates on heating:



$N_2O_5$  also yields a 1:1 adduct and this has been formulated as  $[\text{NO}_2]^+[\text{Bi}(\text{NO}_3)_4]^-$ . Bi reacts with  $\text{NO}_2$  in dimethyl sulfoxide to give the solvate  $\text{Bi}(\text{NO}_3)_3 \cdot 3\text{Me}_2\text{SO}$ , whereas Sb gives the basic salt  $\text{SbO}(\text{NO}_3) \cdot \text{Me}_2\text{SO}$ .  $\text{Bi}(\text{ClO}_4)_3 \cdot 5\text{H}_2\text{O}$  dissolves in water to give complex polymeric oxocations such as  $[\text{Bi}_6(\text{OH})_{12}]^{6+}$  (p. 575).

The first stable arsazene [dark red  $\text{ArN}(\text{H})-\text{As}=\text{NAr}$ , mp  $173^\circ\text{C}$ ,  $\text{Ar} = \text{C}_6\text{H}_2\text{Bu}'_{3-2,4,6}$ ] and its orange P analogue (mp  $203^\circ\text{C}$ ) have been prepared by treating  $\text{AsCl}_3$  (or  $\text{PCl}_3$ ) with  $\text{Li}[\text{NHAr}]$ ; an X-ray study found  $\text{As}-\text{N}$  175 pm,  $\text{As}=\text{N}$  171 pm and the angle  $\text{NAsN}$   $98.9^\circ$  (compared with 163 pm, 157 pm and  $103.8^\circ$  for the  $\text{N}-\text{P}=\text{N}$  system.<sup>(130)</sup> The first 2-coordinate iminoarsine (containing an  $\text{As}=\text{N}$  double bond) was prepared by reacting  $\text{AsH}_3$  with *O*-nitrosobis(trifluoromethyl)hydroxylamine at room temperature, and isolated as a volatile white solid at  $-86^\circ$ .<sup>(131)</sup>



Numerous Sb-N and Bi-N containing species are also beginning to appear in the literature, for example:

- (a) the Sb-subrogated *cyclo*-triphosphazene,  $\text{NPX}_2\text{NPX}_2\text{NSb}(\text{OOCMe})_2$ , which was obtained as a white moisture-sensitive solid, the 4-coordinate Sb being pseudo trigonal bipyramidal with the lone pair of electrons in the  $\text{N}_2\text{Sb}$  plane;<sup>(132)</sup>

- (b) the azastibacubane cluster compound,  $(\text{MeNSbCl}_3)_4$ , which was obtained in good yield as pale yellow crystals by the stoichiometric reaction of  $\text{SbCl}_5$  with  $\text{MeNR}_2$  ( $\text{R} = \text{SiMe}_3$ );<sup>(133)</sup>
- (c) the homoleptic bismuth amide  $\text{Bi}(\text{NPh}_2)_3$ ; an X-ray examination of the orange crystals found pyramidal Bi with Bi-N 220 pm (av) and angle  $\text{NBiN}$   $97^\circ$  (av).<sup>(134)</sup>

### 13.3.8 Organometallic compounds<sup>(2,6,15,16,135-139)</sup>

All 3 elements form a wide range of organometallic compounds in both the +3 and the +5 state, those of As being generally more stable and those of Bi less stable than their Sb analogues. For example, the mean bond dissociation energies  $\bar{D}(\text{M}-\text{Me})/\text{kJ mol}^{-1}$  are 238 for  $\text{AsMe}_3$ , 224 for  $\text{SbMe}_3$  and 140 for  $\text{BiMe}_3$ . For the corresponding  $\text{MPH}_3$ , the values are 280, 267, and  $200 \text{ kJ mol}^{-1}$  respectively, showing again that the M-C bond becomes progressively weaker in the sequence  $\text{As} > \text{Sb} > \text{Bi}$ . Comparison with organophosphorus compounds (p. 542) is also apposite. In most of the compounds the metals are 3, 4, 5 or 6 coordinate though a few multiply-bonded compounds are known in which they have a coordination number of 2. In view of the vast range of compounds which have been studied, only a representative selection of structure types will be given in this section.

<sup>133</sup> W. NEUBERT, H. PRITZKOW and H. P. LATSCHA *Angew. Chem. Int. Edn. Engl.* **27**, 287-8 (1988).

<sup>134</sup> W. CLEGG, N. A. COMPTON R. J. ERRINGTON, N. C. NORMAN and N. WISHART, *Polyhedron* **8**, 1579-80 (1989).

<sup>135</sup> G. E. COATES and K. WADE, *Organometallic Compounds*, Vol. 1, *The Main Group Elements*, 3rd edn., pp. 510-44, Methuen, London, 1967.

<sup>136</sup> B. J. AYLETT, *Organometallic Compounds*, 4th edn., Vol. 1, *The Main Group Elements*, Part 2, pp. 387-521, Chapman & Hall, London, 1979.

<sup>137</sup> G. E. COATES, M. L. H. GREEN, P. POWELL and K. WADE, *Principles of Organometallic Chemistry*, pp. 143-9, Methuen, London, 1968.

<sup>138</sup> F. G. MANN, *The Heterocyclic Derivatives of P, As, Sb and Bi*, 2nd edn., Wiley, New York, 1970, 716 pp.

<sup>139</sup> S. PATAI (ed.) *The Chemistry of Organic As, Sb and Bi Compounds*, Wiley, Chichester, 1994, 962 pp.

<sup>130</sup> P. B. HITCHCOCK, M. F. LAPPERT, A. K. RAI and H. D. WILLIAMS, *J. Chem. Soc., Chem. Commun.*, 1633-4 (1986).

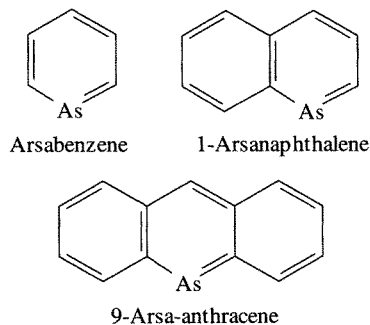
<sup>131</sup> H. G. ANG and F. K. LEE, *Polyhedron* **8**, 1461-2 (1989).

<sup>132</sup> S. K. PANDEY, R. HASSELBRING, A. STEINER, D. STALKE and H. W. ROESKY, *Polyhedron* **12**, 2941-5 (1993).

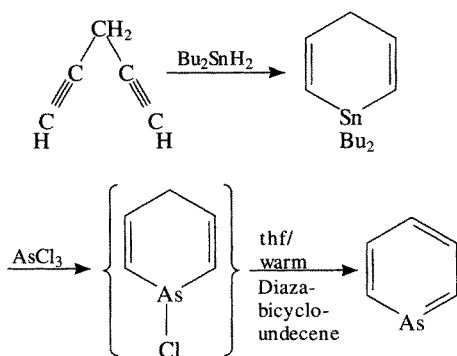
### Organoarsenic(III) compounds

The first 1-coordinate organoarsenic(III) compound,  $\text{RC}\equiv\text{As}$ , ( $\text{R} = 2,4,6\text{-tri-}t\text{-butylphenyl}$ ) was isolated in 1986 as pale yellow crystals, mp.  $114^\circ\text{C}$ .<sup>(7)</sup>

Some examples of 2-coordinate organoarsenic(III) compounds are:



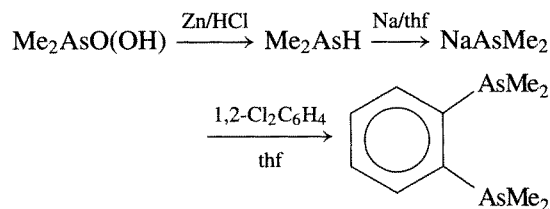
The first such compound to be prepared was the deep-yellow unstable compound 9-arsa-anthracene<sup>(140)</sup> but the thermally stable colourless arsenabenzene (arsenin) can now conveniently be made by a general route from 1,4-pentadiyne.<sup>(141)</sup>



$\text{AsC}_5\text{H}_5$  is somewhat air sensitive but is distillable and stable to hydrolysis by mild acid or base. Using the same route,  $\text{PBr}_3$  gave  $\text{PC}_5\text{H}_5$  as a colourless volatile liquid (p. 544),  $\text{SbCl}_3$  gave  $\text{SbC}_5\text{H}_5$  as an isolable though rather

labile substance which rapidly polymerized at room temperature, and  $\text{BiCl}_3$  gave the even less-stable  $\text{BiC}_5\text{H}_5$  which could only be detected spectroscopically by chemical trapping.<sup>(141,142)</sup> Arsanaphthalene is an air-sensitive yellow oil.<sup>(143)</sup> Complexes of some of these heterocycles are also known, e.g.  $[\text{Cr}(\eta^6\text{-C}_5\text{H}_5\text{As})_2]$ ,<sup>(144)</sup>  $[\text{Mo}(\eta^6\text{-C}_5\text{H}_5\text{As})(\text{CO})_3]$ ,<sup>(145)</sup> and  $[\text{Fe}(\eta^5\text{-C}_4\text{H}_4\text{As})_2]$ , i.e. diarsaferrocene.<sup>(146)</sup>

Most organoarsenic(III) compounds are readily prepared by standard methods (p. 497) such as the treatment of  $\text{AsCl}_3$  with Grignard reagents, organolithium reagents, organoaluminium compounds, or by sodium-alkyl halide (Wurtz) reactions.  $\text{As}_2\text{O}_3$  can also be used as starting material as indicated in the scheme on p. 595.  $\text{AsR}_3$  and  $\text{AsAr}_3$  are widely used as ligands in coordination chemistry.<sup>(6)</sup> Common examples are the 4 compounds  $\text{AsMe}_{3-n}\text{Ph}_n$  ( $n = 0, 1, 2, 3$ ). Multidentate ligands have also been extensively studied particularly the chelating ligand and “*o*-phenylenebis(dimethylarsine)” i.e. 1,2-bis(dimethylarseno)benzene which can be prepared from cacodylic acid (dimethylarsinic acid)  $\text{Me}_2\text{AsO}(\text{OH})$  (itself prepared as indicated in the general scheme on p. 595):



Arsine complexes are especially stable for b-class metals such as Rh, Pd and Pt, and such complexes have found considerable industrial use in hydrogenation or hydroformylation of alkenes,

<sup>142</sup> A. J. ASHE, *Acc. Chem. Res.* **11**, 153–7 (1978).

<sup>143</sup> A. J. ASHE, D. L. BELLVILLE and H. S. FRIEDMAN, *J. Chem. Soc., Chem. Commun.*, 880–1 (1979).

<sup>144</sup> C. ELSCHENBROICH, J. KROKER, W. MASSA, M. WÜNSCH and A. J. ASHE, *Angew. Chem. Int. Edn. Engl.* **25**, 571–2 (1986).

<sup>145</sup> A. J. ASHE and J. C. COLBURN, *J. Am. Chem. Soc.* **99**, 8099–100 (1977).

<sup>146</sup> A. J. ASHE, S. MAHMOUD, C. ELSCHENBROICH and M. WÜNSCH, *Angew. Chem. Int. Edn. Engl.* **26**, 229–30 (1987), and references cited therein.

<sup>140</sup> P. JUZI and K. DEUCHERT, *Angew. Chem. Int. Edn. Engl.* **8**, 991 (1969). H. VERMEER and F. BICKELHAUPT, *ibid.* 992.

<sup>141</sup> A. J. ASHE, *J. Am. Chem. Soc.* **93**, 3293–5 (1971).

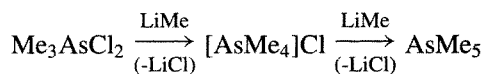
oligomerization of isoprene, carbonylation of  $\alpha$ -olefins, etc.

Halogenoarsines  $R_2AsX$  and dihalogenoarsines  $RAsX_2$  are best prepared by reducing the corresponding arsenic acids  $R_2AsO(OH)$  or arsonic acid  $RAsO(OH)_2$  with  $SO_2$  in the presence of  $HCl$  or  $HBr$  and a trace of  $KI$ . The actual reducing agent is  $I^-$  and the resulting  $I_2$  is in turn reduced by the  $SO_2$ . Fluoro compounds are best prepared by metathesis of the chloro derivative with a metal fluoride, e.g.  $AgF$ . Interestingly, the compound  $Ph_3AsI_2$  has been shown by X-ray analysis to contain 4-coordinate As and an almost linear  $As-I-I$  group with  $As-I$  264 pm,  $I-I$  300.5 pm and angle  $As-I-I$   $174.8^\circ$ .<sup>(147)</sup>

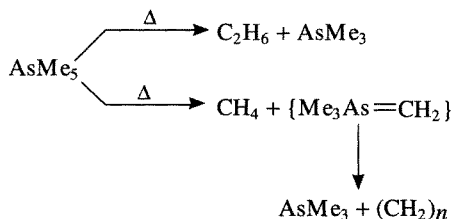
Hydrolysis of  $R_2AsX$  yields arsinous acids  $R_2AsOH$  or their anhydrides  $(R_2As)_2O$ . An alternative route employs a Grignard reagent and  $As_2O_3$ , e.g.  $PhMgBr$  affords  $(Ph_2As)_2O$ . Hydrolysis of  $RAsX_2$  yields either arsonous acids  $RAs(OH)_2$  or their anhydrides  $(RAsO)_n$ . These latter are not arsenoso compounds  $RAs=O$  analogous to nitroso compounds (p. 416) but are polymeric. Indeed, all these  $As^{III}$  compounds feature pyramidal 3-coordinate As as do the formally  $As^I$  compounds  $(RAs)_n$  discussed on p. 584. A series of *planar* 3-coordinate arsenic(I) compounds have also been prepared and these are discussed on p. 597.

### Organoarsenic(V) compounds

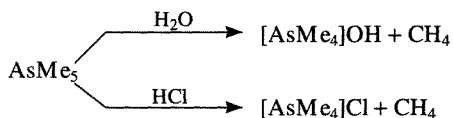
Among the compounds of  $As^V$  can be noted the complete series  $R_{5-n}AsX_n$  ( $n = 0-5$ ) where R can be alkyl or aryl. Thus  $AsPh_5$  (mp  $150^\circ$ ) can be prepared by direct reaction of  $LiPh$  on either  $[AsPh_4]I$ ,  $Ph_3AsCl_2$  or  $Ph_3As=O$ . Similarly,  $AsMe_5$  has been prepared as a colourless, volatile, mobile liquid (mp  $-6^\circ$ ):<sup>(148)</sup>



The preparation is carried out in  $Me_2O$  at  $-60^\circ$  to avoid formation of the ylide  $Me_3As=CH_2$  (mp  $35^\circ$ ) by elimination of  $CH_4$ .  $AsMe_5$  decomposes above  $100^\circ$  by one of two routes:

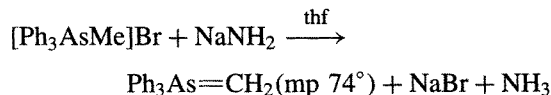


It is stable in air and hydrolyses only slowly:

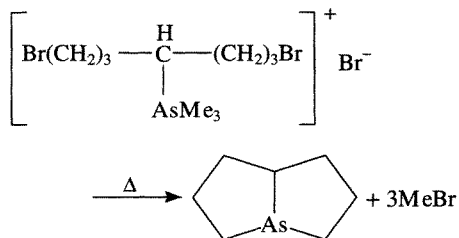


The aryl analogues are rather more stable.

Of the quaternary arsonium compounds, methyltriaryl derivatives are important as precursors of arsonium ylides, e.g.

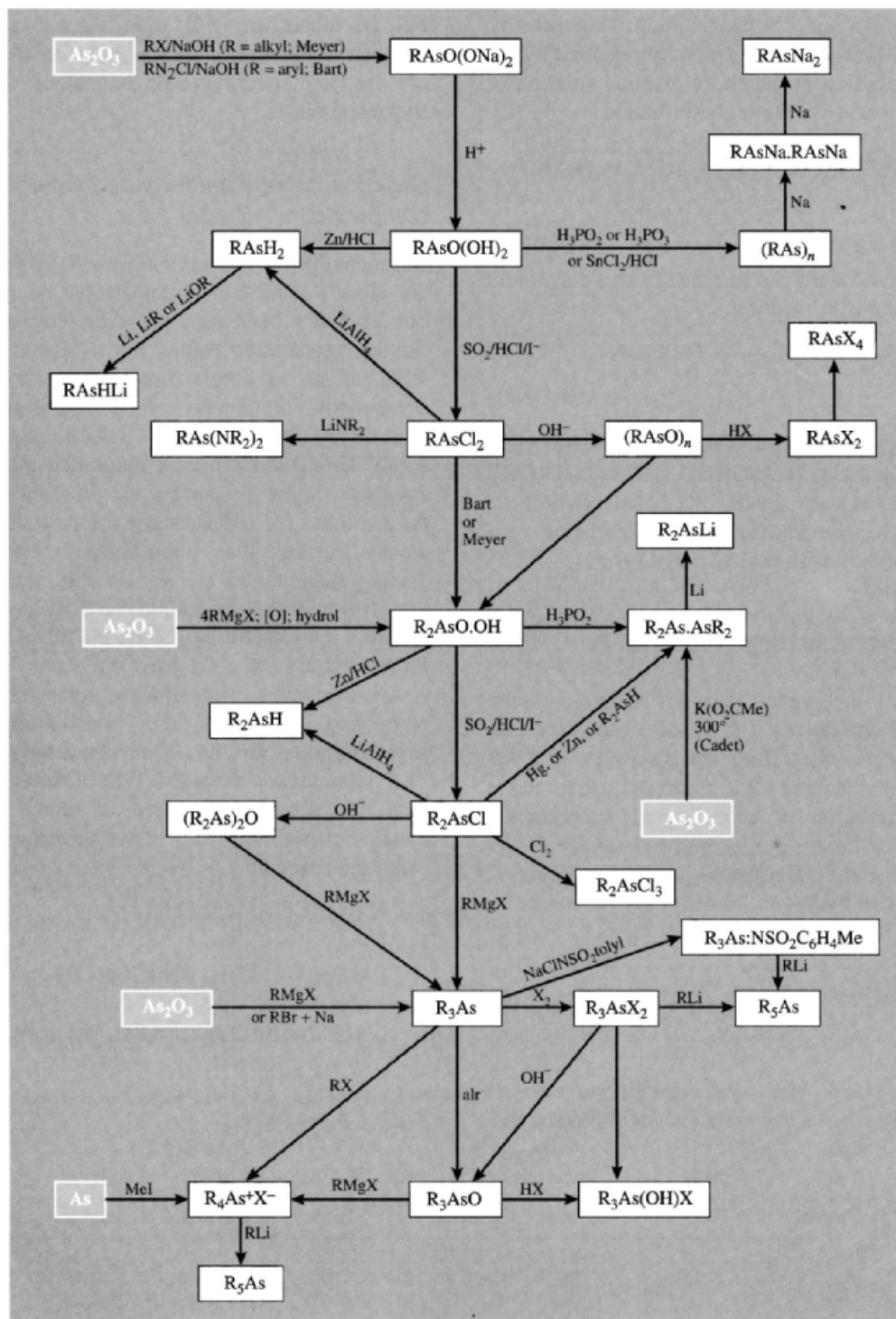


Such ylides are unstable and react with carbonyl compounds to give both the Wittig product (p. 545) as well as  $AsPh_3$  and an epoxide. However, this very reactivity is sometimes an advantage since As ylides often react with carbonyl compounds that are unresponsive to P ylides. Substituted quaternary arsonium compounds are also a useful source of heterocyclic organoarsanes, e.g. thermolysis of 4-(1,7-dibromoheptyl)trimethylarsonium bromide to 1-arsabicyclo[3.3.0]octane:

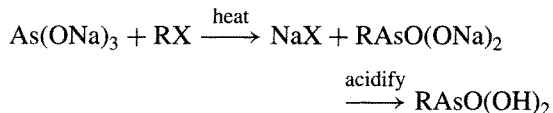


<sup>147</sup> C. A. MCAULIFFE, B. BEAGLEY, G. A. GOTT, A. G. MACKIE, P. M. MACRORY, and R. G. PRITCHARD, *Angew. Chem. Int. Edn. Engl.* **26**, 264-5 (1987).

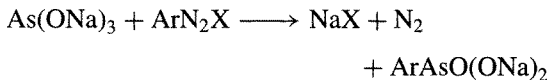
<sup>148</sup> K.-H. MITSCHKE and H. SCHMIDBAUR, *Chem. Ber.* **106**, 3645-51 (1973).

Some routes to organoarsenic compounds<sup>(137)</sup>

Arsonic acids  $\text{RAsO}(\text{OH})_2$  are amongst the most important organoarsonium compounds. Alkyl arsonic acids are generally prepared by the Meyer reaction in which an alkaline solution of  $\text{As}_2\text{O}_3$  is heated with an alkyl halide:



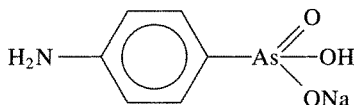
Aryl arsonic acids can be made from a diazonium salt by the Bart reaction:



Similar reactions on alkyl or aryl arsonites yield the arsinic acids  $\text{R}_2\text{AsO}(\text{OH})$  and  $\text{Ar}_2\text{AsO}(\text{OH})$ . Arsine oxides are made by alkaline hydrolysis of  $\text{R}_3\text{AsX}_2$  (or  $\text{Ar}_3\text{AsX}_2$ ) or by oxidation of a tertiary arsine with  $\text{KMnO}_4$ ,  $\text{H}_2\text{O}_2$  or  $\text{I}_2$ .

### Physiological activity of arsenicals

In general  $\text{As}^{\text{III}}$  organic derivatives are more toxic than  $\text{As}^{\text{V}}$  derivatives. The use of organoarsenicals in medicine dates from the discovery in 1905 by H. W. Thomas that "atoxyl" (first made by A. Béchamp in 1863) cured experimental trypanosomiasis (e.g. sleeping sickness). In 1907 P. Erlich and A. Bertheim showed that "atoxyl" was sodium hydrogen 4-aminophenylarsonate



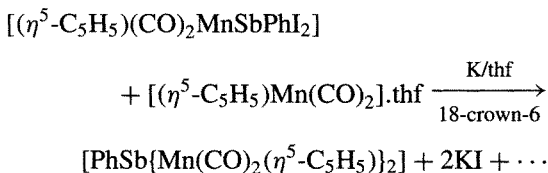
and the field was systematically developed especially when some arsenicals proved effective

against syphilis. Today such treatment is obsolete but arsenicals are still used against amoebic dysentery and are indispensable for treatment of the late neurological stages of African trypanosomiasis.

### Organoantimony and organobismuth compounds

Organoantimony and organobismuth compounds are closely related to organoarsenic compounds but have not been so extensively investigated. Similar preparative routes are available and it will suffice to single out a few individual compounds for comment or comparison.  $\text{MR}_3$  (and  $\text{MAR}_3$ ) are colourless, volatile liquids or solids having the expected pyramidal molecular structure. Some properties are in Table 13.13. As expected (p. 198) tertiary stibines are much weaker ligands than phosphines or arsines.<sup>(6)</sup> Tertiary bismuthines are weaker still: among the very few coordination complexes that have been reported are  $[\text{Ag}(\text{BiPh}_3)]\text{ClO}_4$ ,  $\text{Ph}_3\text{BiNbCl}_5$ , and  $\text{Ph}_3\text{BiM}(\text{CO})_5$  ( $\text{M} = \text{Cr}, \text{Mo}, \text{W}$ ).

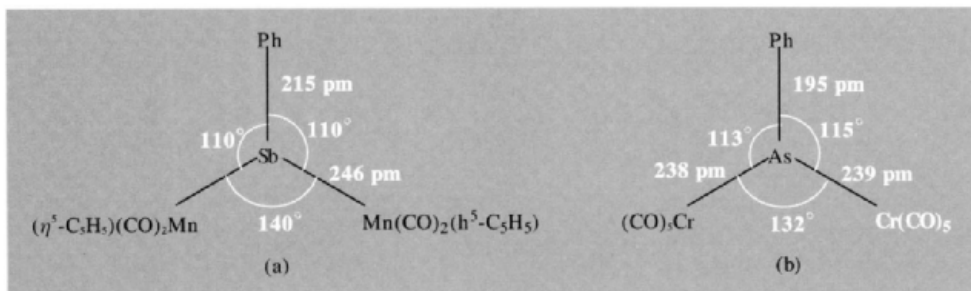
An intriguing 3-coordinate organoantimony compound, which is the first example of trigonal-planar  $\text{Sb}^{\text{I}}$ , has been characterized.<sup>(149)</sup> The stibinidene complex  $[\text{PhSb}\{\text{Mn}(\text{CO})_2(\eta^5\text{-C}_5\text{H}_5)\}_2]$  has been isolated as shiny golden metallic crystals (mp  $128^\circ$ ) from the crown-ether catalysed reaction:



<sup>149</sup> J. VON SEYERL and G. HUTTNER, *Angew. Chem. Int. Edn. Engl.* **17**, 843-4 (1978).

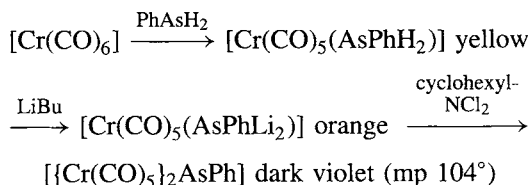
**Table 13.13** Some physical properties of  $\text{MMe}_3$  and  $\text{MPh}_3$

Property	$\text{AsMe}_3$	$\text{SbMe}_3$	$\text{BiMe}_3$	$\text{AsPh}_3$	$\text{SbPh}_3$	$\text{BiPh}_3$
MP/ $^\circ\text{C}$	-87	-62	-86	61	55	78
BP/ $^\circ\text{C}$	50	80	109	—	—	—
Bond angle at M	$96^\circ$	—	$97^\circ$	$102^\circ$	—	$94^\circ$
Mean M-C bond energy/kJ mol <sup>-1</sup>	229	215	143	267	244	177



**Figure 13.28** Planar structure of (a)  $[\text{PhSb}\{\text{Mn}(\text{CO})_2(\eta^5\text{-C}_5\text{H}_5)_2\}]$ , and (b)  $[\text{PhAs}\{\text{Cr}(\text{CO})_5\}_2]$ . Note the relatively short Sb–Mn and As–Cr bonds.

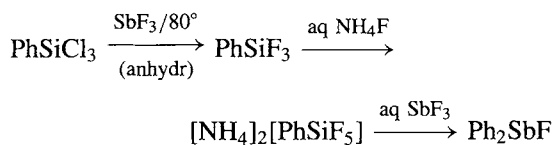
The structure is shown in Fig. 13.28a: the interatomic angles and distances suggest that the bridging  $\{\text{PhSb}^1\}$  group is stabilized by Sb–Mn  $\pi$  interactions. A similar route leads to 3-coordinate planar organoarsinidine complexes which can also be prepared by the following reaction sequence:



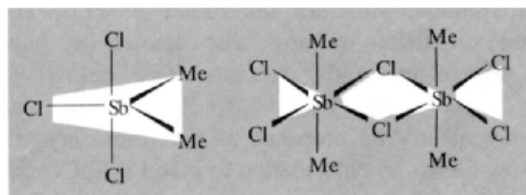
The chloro-derivative  $[\text{ClAs}\{\text{Mn}(\text{CO})_2(\eta^5\text{-C}_5\text{H}_5)\}_2]$  (shiny black crystals, mp  $124^\circ$ ) can now be much more readily obtained by direct reaction of  $\text{AsCl}_3$  with  $[\text{Mn}(\text{CO})_2(\eta^5\text{-C}_5\text{H}_5)]\cdot\text{thf}$ .<sup>(150)</sup>

Halogenostibines  $\text{R}_2\text{SbX}$  and dihalogenostibines  $\text{RSbX}_2$  (R = alkyl, aryl) can be prepared by standard methods. The former hydrolyse to the corresponding covalent molecular oxides  $(\text{R}_2\text{Sb})_2\text{O}$ , whereas  $\text{RSbX}_2$  yield highly polymeric “stiboso” compounds  $(\text{RSbO})_n$ . The stibonic acids,  $\text{RSbO}(\text{OH})_2$ , and stibinic acids,  $\text{R}_2\text{SbO}(\text{OH})$ , differ in structure from phosphonic and phosphinic acids (p. 512) or arsonic and arsenic acids (p. 594) in being high molecular weight materials of unknown structure. They are probably best considered as oxide hydroxides

of organoantimony(V) cations. Indeed, throughout its organometallic chemistry Sb shows a propensity to increase its coordination number by dimerization or polymerization. Thus  $\text{Ph}_2\text{SbF}$  consists of infinite chains of F-bridged pseudo trigonalbipyramidal units as shown in Fig. 13.29.<sup>(151)</sup> The compound could not be prepared by the normal methods of fluorinating  $\text{Ph}_2\text{SbCl}$  or phenylating  $\text{SbF}_3$  but can be obtained as a white, air-stable, crystalline solid mp  $154^\circ$  by the following sequence of steps:



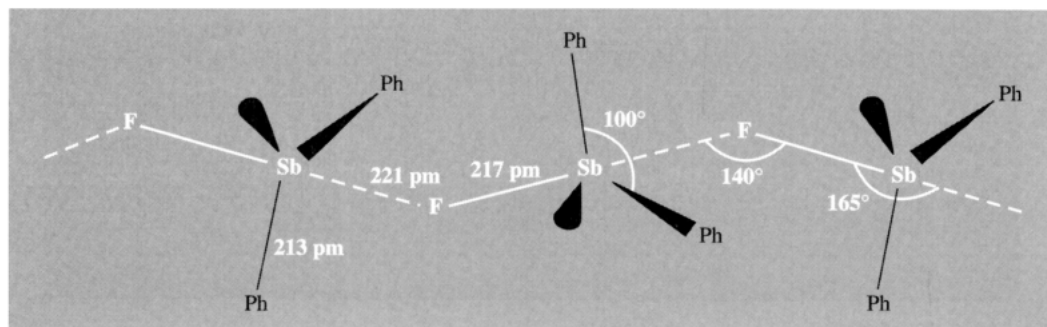
Again,  $\text{Me}_2\text{SbCl}_3$  is monomeric with equatorial methyl groups ( $C_{2v}$ ) in solution ( $\text{CH}_2\text{Cl}_2$ ,  $\text{CHCl}_3$  or  $\text{C}_6\text{H}_6$ ) but forms Cl-bridged dimers with *trans* methyl groups ( $D_{2h}$ ) in the solid:<sup>(152)</sup>



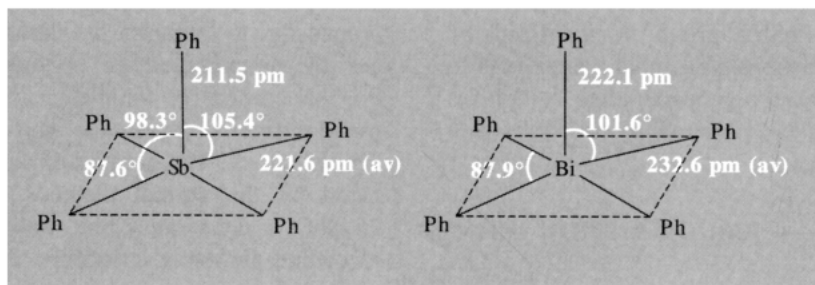
<sup>151</sup> S. P. BONE and D. B. SOWERBY, *J. Chem. Soc., Dalton Trans.*, 1430–3 (1979).

<sup>152</sup> N. BERTAZZI, T. C. GIBB and N. N. GREENWOOD, *J. Chem. Soc., Dalton Trans.*, 1153–7 (1976) K. DEHNICKE and H. G. NADLER, *Chem. Ber.* **109**, 3034–8 (1976).

<sup>150</sup> J. VON SEYERL, U. MOERING, A. WAGNER, A. FRANK and G. HUTTNER, *Angew Chem. Int. Edn. Engl.* **17**, 844–5 (1978).



**Figure 13.29** Structure of  $\text{Ph}_2\text{SbF}_2$  showing polymeric chains of apex-shared pseudo trigonal bipyramidal units  $[\text{Ph}_2\text{FSb}\dots\text{F}]$ .

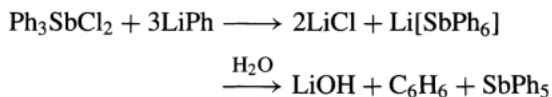


**Figure 13.30** (a) Molecular geometry of  $\text{SbPh}_5$  showing the slightly distorted square-pyramidal structure.<sup>(155)</sup> (b) Similar data obtained at  $-96^\circ$  for the slightly more regular square-pyramidal  $\text{BiPh}_5$ .<sup>(159)</sup>

A similar Cl-bridged dimeric structure was established by X-ray analysis for  $\text{Ph}_2\text{SbCl}_3$ .<sup>(153)</sup>

Pentaphenylantimony,  $\text{SbPh}_5$  (mp  $171^\circ$ ), has attracted much attention as the first known example of a 10-valence-electron molecule of a main group element that has a square pyramidal structure<sup>(154,155)</sup> rather than the usual trigonal bipyramidal structure (as found in  $\text{PPh}_5$  and  $\text{AsPh}_5$ ).  $\text{BiPh}_5$  is now also known to have a square pyramidal structure (see below) as does the anion  $\text{InCl}_5^{2-}$  (p. 238).  $\text{SbPh}_5$  can conveniently be prepared as colourless crystals from  $\text{SbPh}_3$  by chlorination to give  $\text{Ph}_3\text{SbCl}_2$  and

then reaction with  $\text{LiPh}$ :



The structure, shown in Fig. 13.30(a), is based on a slightly distorted square-pyramidal coordination around the Sb atom ( $C_{2v}$  instead of  $C_{4v}$ ), the *ipso*- $\text{C}_{\text{ax}}$ - $\text{Sb}$ - $\text{C}_{\text{e}}$  angles being alternately  $98.3^\circ$  and  $105.4^\circ$ .<sup>(155)</sup> Vibrational spectroscopy suggests that the molecule retains its square-pyramidal structure even in solution, so the structure is not an artefact of crystal packing forces. The yellow cyclopropyl analogue,  $\text{Sb}(\text{C}_3\text{H}_5)_5$ , apparently has the same geometry,<sup>(156)</sup> while the solvate  $\text{SbPh}_5 \cdot \frac{1}{2}\text{C}_6\text{H}_{12}$

<sup>153</sup> J. BORDNER, G. O. DOAK and J. R. PETERS, *J. Am. Chem. Soc.* **96**, 6763–5 (1974).

<sup>154</sup> P. J. WHEATLEY, *J. Chem. Soc.* 3718–23 (1964).

<sup>155</sup> A. L. BEAUCHAMP, M. J. BENNETT and F. A. COTTON, *J. Am. Chem. Soc.* **90**, 6675–80 (1968).

<sup>156</sup> A. H. COWLEY, J. L. MILLS, T. M. LOEHR and T. V. LONG, *J. Am. Chem. Soc.* **93**, 2150–3 (1971).

and the *p*-tolyl derivative  $\text{Sb}(4\text{-MeC}_6\text{H}_4)_5$  have almost undistorted trigonal bipyramidal structures.<sup>(157)</sup>

$\text{BiPh}_5$  is even more remarkable. Not only is it square pyramidal (Fig. 13.30b) but it is also highly coloured. It can be prepared as violet crystals by the direct reaction of  $\text{Ph}_3\text{BiCl}_2$  with two moles of  $\text{LiPh}$  in ether at  $-75^\circ$ .<sup>(158)</sup> The colour is retained in solution, and is due to a weak broad absorption in the green-yellow region ( $\lambda_{\text{max}}$  532 nm,  $\log \epsilon$  2.4).<sup>(159)</sup> Substitution on the phenyl rings modifies the colour and may also alter the structure, e.g.:<sup>(160)</sup>  $[\text{BiPh}_3(2\text{-FC}_6\text{H}_4)_2]$ , which is square pyramidal with the *o*-fluorophenyl groups *trans*-basal, forms violet crystals but is reddish in solution, whereas  $[\text{Bi}(4\text{-Me-C}_6\text{H}_4)_3(2\text{-F-C}_6\text{H}_4)_2]$  is trigonal bipyramidal with axial fluorophenyl groups; it forms yellow crystals but again gives reddish solutions. The structures and colours have been interpreted in terms of relativistic effects

which lower the energy of the  $a_1$  LUMO in the  $C_{4v}$  structure.<sup>(161)</sup>

The pentamethyl compound,  $\text{SbMe}_5$ , is surprisingly stable in view of the difficulty of obtaining  $\text{AsMe}_5$  and  $\text{BiMe}_5$ ; it melts at  $-19^\circ$ , boils at  $127^\circ$ , and does not inflame in air, though it oxidizes quickly and is hydrolysed by water. It resembles  $\text{SbPh}_5$  in reacting with  $\text{LiMe}$  ( $\text{LiPh}$ ) to give  $\text{Li}^+[\text{SbR}_6]^-$  and in reacting with  $\text{BPh}_3$  to give  $[\text{SbR}_4]^+[\text{RBPh}_3]^-$ .

Organobismuth(V) compounds are in general similar to their As and Sb analogues but are less stable and there are few examples known; e.g.  $[\text{BiR}_4]\text{X}$  and  $\text{R}_3\text{BiX}_2$  are known but not  $\text{R}_2\text{BiX}_3$  or  $\text{RBiX}_4$ , whereas all 4 classes of compound are known for P, As and Sb. Similarly, no pentaalkylbismuth compound is known, though as noted above  $\text{BiPh}_5$  and its derivatives have been prepared. It decomposes spontaneously over a period of days at room temperature and reacts readily with  $\text{HX}$ ,  $\text{X}_2$  or even  $\text{BPh}_3$  by cleaving 1 phenyl to form quaternary bismuth compounds  $[\text{BiPh}_4]\text{X}$  and  $[\text{BiPh}_4][\text{BPh}_4]$ ; this latter compound (mp  $228^\circ$ ) is the most stable bismuthonium salt yet known.

<sup>157</sup> C. BRABANT, J. HUBERT and A. L. BEAUCHAMP, *Can. J. Chem.* **51**, 2952–7 (1973).

<sup>158</sup> G. WITTIG and K. CLAUSS, *Liebig's Ann. Chem.* **578**, 136–46 (1952).

<sup>159</sup> A. SCHMUCK, J. BUSCHMANN, J. FUCHS and K. SEPPELT, *Angew. Chem. Int. Edn. Engl.* **26**, 1180–2 (1987).

<sup>160</sup> A. SCHMUCK, P. PYYKKÖ and K. SEPPELT, *Angew. Chem. Int. Edn. Engl.* **29**, 213–5 (1990).

<sup>161</sup> B. D. EL-ISSA, P. PYYKKÖ and H. M. ZANATI, *Inorg. Chem.* **30**, 2781–7 (1991).



																1	2																								
																H	He																								
3	4											5	6	7	8	9	10																								
Li	Be											B	C	N	O	F	Ne																								
11	12											13	14	15	16	17	18																								
Na	Mg											Al	Si	P	S	Cl	Ar																								
19	20	21	22	23	24	25	26	27	28	29	30	31	32	33	34	35	36																								
K	Ca	Sc	Ti	V	Cr	Mn	Fe	Co	Ni	Cu	Zn	Ga	Ge	As	Se	Br	Kr																								
37	38	39	40	41	42	43	44	45	46	47	48	49	50	51	52	53	54																								
Rb	Sr	Y	Zr	Nb	Mo	Tc	Ru	Rh	Pd	Ag	Cd	In	Sn	Sb	Te	I	Xe																								
55	56	57	72	73	74	75	76	77	78	79	80	81	82	83	84	85	86																								
Cs	Ba	La	Hf	Ta	W	Re	Os	Ir	Pt	Au	Hg	Tl	Pb	Bi	Po	At	Rn																								
87	88	89	104	105	106	107	108	109	110	111	112																														
Fr	Ra	Ac	Rf	Db	Sg	Bh	Hs	Mt	Uun	Uub	Uub																														
																		58	59	60	61	62	63	64	65	66	67	68	69	70	71										
																		Ce	Pr	Nd	Pm	Sm	Eu	Gd	Tb	Dy	Ho	Er	Tm	Yb	Lu										
																		90	91	92	93	94	95	96	97	98	99	100	101	102	103										
																		Th	Pa	U	Np	Pu	Am	Cm	Bk	Cf	Es	Fm	Md	No	Lr										

# 14

## Oxygen

### 14.1 The Element

#### 14.1.1 Introduction

Oxygen is the most abundant element on the earth's surface: it occurs both as the free element and combined in innumerable compounds, and comprises 23% of the atmosphere by weight, 46% of the lithosphere and more than 85% of the hydrosphere (~85.8% of the oceans and 88.81% of pure water). It is also, perhaps paradoxically, by far the most abundant element on the surface of the moon where, on average, 3 out of every 5 atoms are oxygen (44.6% by weight).

The "discovery" of oxygen is generally credited to C. W. Scheele and J. Priestley (independently) in 1773–4, though several earlier investigators had made pertinent observations without actually isolating and characterizing the gas.<sup>(1–4)</sup> Indeed, it is difficult to ascribe a precise meaning to the word "discovery" when applied to a substance so ubiquitously present

as oxygen; particularly when (a) experiments on combustion and respiration were interpreted in terms of the phlogiston theory, (b) there was no clear consensus on what constituted "an element", and (c) the birth of Dalton's atomic theory was still far in the future. Moreover, the technical difficulties before the mid-eighteenth century of isolating and manipulating gases compounded the problem still further, and it seems certain that several investigators had previously prepared oxygen without actually collecting it or recognizing it as a constituent of "common air". Scheele, a pharmacist in Uppsala, Sweden, prepared oxygen at various times between 1771–3 by heating  $\text{KNO}_3$ ,  $\text{Mg}(\text{NO}_3)_2$ ,  $\text{Ag}_2\text{CO}_3$ ,  $\text{HgO}$  and a mixture of  $\text{H}_3\text{AsO}_4$  and

<sup>2</sup> M. E. Weeks, *Discovery of the Elements*, 6th edn., pp. 209–23, Journal of Chemical Education, Easton, Pa, 1956. (Oxygen.)

<sup>3</sup> J. R. PARTINGTON, *A History of Chemistry*, Vol. 3, Macmillan, London, 1962; Scheele and the discovery of oxygen (pp. 219–22); Priestley and the discovery of oxygen (pp. 256–63); Lavoisier and the rediscovery of oxygen (pp. 402–10).

<sup>4</sup> *Gmelin's Handbuch der Anorganischen Chemie*, 8th edn., pp. 1–82. "Sauerstoff" System No. 3, Vol. 1, Verlag Chemie, 1943. (Historical.)

<sup>1</sup> J. W. MELLOR, *A Comprehensive Treatise on Inorganic and Theoretical Chemistry*, Vol. 1, pp. 344–51, Longmans, Green, 1922. History of the discovery of oxygen.

MnO<sub>2</sub>. He called the gas “vitriol air” and reported that it was colourless, odourless and tasteless, and supported combustion better than common air, but the results did not appear until 1777 because of his publisher’s negligence. Priestley’s classic experiment of using a “burning glass” to calcine HgO confined in a cylinder inverted over liquid mercury was first performed in Colne, England, on 1 August 1774; he related this to A. L. Lavoisier and others at a dinner party

in Paris in October 1774 and published the results in 1775 after he had shown that the gas was different from nitrous oxide. Priestley’s ingenious experiments undoubtedly established oxygen as a separate substance (“dephlogisticated air”) but it was Lavoisier’s deep insight which recognized the new gas as an element and as the key to our present understanding of the nature of combustion. This led to the overthrow of the phlogiston theory and laid the foundations

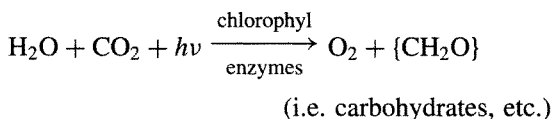
### Oxygen: Some Important Dates

- 15th century Leonardo da Vinci noted that air has several constituents, one of which supports combustion.
- 1773–4 C. W. Scheele and J. Priestley independently discovered oxygen, prepared it by several routes, and studied its properties.
- 1775–7 A. L. Lavoisier recognized oxygen as an element, developed the modern theory of combustion, and demolished the phlogiston theory.
- 1777 A. L. Lavoisier coined the name “oxygen” (acid former).
- 1781 Composition of water as a compound of oxygen and hydrogen established by H. Cavendish.
- 1800 W. Nicholson and A. Carlisle decomposed water electrolytically into hydrogen and oxygen which they then recombined by explosion to resynthesize water.
- 1818 Hydrogen peroxide discovered by L.-J. Thenard.
- 1840 C. F. Schönbein detected and named ozone from its smell (see 1857).
- 1848 M. Faraday noted that oxygen was paramagnetic, correctly ascribed to the triplet  $^3\Sigma_g^-$  ground state by R. S. Mulliken (in 1928).
- 1857 W. Siemens constructed the first machine to use the ozonator-discharge principle to generate ozone.
- 1877 Oxygen first liquefied by L. Cailletet and R. Pictet (independently).
- 1881 Oxygen gas first produced industrially (from BaO<sub>2</sub>) by A. Brin and L. W. Brin’s Oxygen Company.
- 1896 First production of liquid oxygen on a technical scale (C. von Linde).
- 1903 Ozonolysis of alkenes discovered and developed by C. D. Harries.
- 1921–3 The water molecule, previously thought to be linear, shown to be bent.
- 1929 Isotopes <sup>17</sup>O and <sup>18</sup>O discovered by W. F. Giauque and H. L. Johnston (see 1961).
- 1931 Singlet state of O<sub>2</sub>,  $^1\Sigma_g^+$ , discovered by W. H. J. Childe and R. Mecke.
- 1934 A lower lying singlet state  $^1\Delta_g$  discovered by G. Herzberg.
- 1931–9 H. Kautsky showed the significance of singlet O<sub>2</sub> in organic reactions; his views were discounted at the time but the great importance of singlet O<sub>2</sub> was rediscovered in 1964 by (a) C. S. Foote and S. Wexler, and (b) E. J. Corey and W. C. Taylor.
- 1941 <sup>18</sup>O-tracer experiments by S. Ruben and M. D. Kamen showed that the oxygen atoms in photosynthetically produced O<sub>2</sub> both come from H<sub>2</sub>O and not CO<sub>2</sub>; confirmed in 1975 by A. Stemler.
- 1951 First detection of <sup>17</sup>O nmr signal by H. E. Weaver, B. M. Tolbert and R. C. La Force.
- 1952 Introduction (in Austria) of the “basic oxygen process”, now by far the most common process for making steel.
- 1961 Dual atomic-weight scales based on oxygen = 16 (chemical) and <sup>16</sup>O = 16 (physical) abandoned in favour of the present unified scale based on <sup>12</sup>C = 12.
- 1963 First successful launch of a rocket propelled by liquid H<sub>2</sub>/liquid O<sub>2</sub> (Cape Kennedy, USA).
- 1963 Reversible formation of a dioxygen complex by direct reaction of O<sub>2</sub> with *trans*-[Ir(CO)Cl(PPh<sub>3</sub>)<sub>2</sub>] discovered by L. Vaska.
- 1967 Many crown ethers synthesized by C. J. Pederson (Nobel Prize for Chemistry, 1987) who also studied their use as complexing agents for alkali metal and other cations.
- 1974 F. S. Rowland and M. Molina showed that man-made chlorofluorocarbons, CFCs, could catalytically destroy ozone in the stratosphere (Nobel Prize for Chemistry, with P. Crutzen, 1995).
- 1985 J. C. Farman discovered the “ozone hole” (substantial seasonal depletion of ozone) over Halley Bay, Antarctica.

of modern chemistry.<sup>(5)</sup> Lavoisier named the element "oxygène" in 1777 in the erroneous belief that it was an essential constituent of all acids (Greek ὀξύς, *oxys*, sharp, sour; γείνῶμαι, *geinomai*, I produce; i.e. acid forming). Some other important dates in oxygen chemistry are in the Panel.

### 14.1.2 Occurrence

Oxygen occurs in the atmosphere in vast quantities as the free element O<sub>2</sub> (and O<sub>3</sub>, p. 607) and there are also substantial amounts dissolved in the oceans and surface waters of the world. Virtually all of this oxygen is of biological origin having been generated by green-plant photosynthesis from water (and carbon dioxide).<sup>(6,7)</sup> The net reaction can be represented by:



However, this is misleading since isotope-tracer experiments using <sup>18</sup>O have shown that both of the oxygen atoms in O<sub>2</sub> originate from H<sub>2</sub>O, whereas those in the carbohydrates come from CO<sub>2</sub>. The process is a complex multistage reaction involving many other species,<sup>(8)</sup> and requires 469 kJ mol<sup>-1</sup> of energy (supplied by the light). The reverse process, combustion of organic materials with oxygen, releases this energy again. Indeed, except for very small amounts of energy generated from wind or water power, or from nuclear reactors, all the

energy used by man comes ultimately from the combustion of wood or fossil fuels such as coal, peat, natural gas and oil. Photosynthesis thus converts inorganic compounds into organic material, generates atmospheric oxygen, and converts light energy (from the sun) into chemical energy. The 1.5 × 10<sup>9</sup> km<sup>3</sup> of water on the earth is split by photosynthesis and reconstituted by respiration and combustion once every 2 million years or so.<sup>(9)</sup> The photosynthetically generated gas temporarily enters the atmosphere and is recycled about once every 2000 years at present rates. The carbon dioxide is partly recycled in the atmosphere and oceans after an average residence time of 300 years and is partly fixed by precipitation of CaCO<sub>3</sub>, etc. (p. 273).

There was very little, if any, oxygen in the atmosphere 3000 million years ago. Green-plant photosynthesis probably began about 2500 My ago and O<sub>2</sub> first appeared in the atmosphere in geochemically significant amounts about 2000 My ago (this is signalled by the appearance of red beds of iron-containing minerals that have been weathered in an oxygen-containing atmosphere).<sup>(6-8)</sup> The O<sub>2</sub> content of the atmosphere reached ~2% of the present level some 800 My ago and ~20% of the present level about 580 My ago. This can be compared with the era of rapid sea-floor spreading to give the separated continents which occurred 110–85 My ago. The concentration of O<sub>2</sub> in the atmosphere has probably remained fairly constant for the past 50 My, a period of time which is still extensive when compared with the presence of *homo sapiens*, <1 My. The composition of the present atmosphere (excluding water vapour which is present in variable amounts depending on locality, season of the year, etc., is given in Table 14.1.<sup>(6)</sup> The oxygen content corresponds to 21.04 atom% and 23.15 wt% (see also ref. 10). The question of atmospheric ozone and pollution of the stratosphere is discussed on p. 608.

<sup>5</sup> A. L. LAVOISIER, *La Traité Élémentaire de Chimie*, Paris, 1789, translated by R. Kerr, *Elements of Chemistry*, London, 1790; facsimile reprint by Dover Publications, Inc., New York, 1965.

<sup>6</sup> J. C. G. WALKER, *Evolution of the Atmosphere*, pp. 318, Macmillan, New York, 1977.

<sup>7</sup> R. P. WAYNE, *Chemistry of Atmospheres*, 2nd edn. Oxford Univ. Press, Oxford, 1991, 456 pp (See especially Chap. 9).

<sup>8</sup> R. Govindjee, Photosynthesis, *McGraw Hill Encyclopedia of Science and Technology*, 4th edn., Vol. 10, pp. 200–10, 1977.

<sup>9</sup> P. CLOUD and A. GIBOR, The oxygen cycle, Article 4 in *Chemistry in the Environment*, pp. 31–41, Readings from Scientific American, W. H. Freeman, San Francisco, 1973.

<sup>10</sup> P. BRIMBLECOMBE, *Air Composition and Chemistry*, Cambridge Univ. Press, Cambridge, 1986, 224 pp.

**Table 14.1** Composition of the atmosphere<sup>(a)</sup> (excluding H<sub>2</sub>O, variable)

Constituent	Vol%	Total mass/tonnes	Constituent	Vol%	Total mass/tonnes
Dry air	100.0	$5.119(8) \times 10^{15}$	CH <sub>4</sub>	$\sim 1.5 \times 10^{-4}$	$\sim 4.3 \times 10^9$
N <sub>2</sub>	78.084(4)	$3.866(6) \times 10^{15}$	H <sub>2</sub>	$\sim 5 \times 10^{-5}$	$\sim 1.8 \times 10^8$
O <sub>2</sub>	<b>20.948(2)</b>	<b><math>1.185(2) \times 10^{15}</math></b>	N <sub>2</sub> O	$\sim 3 \times 10^{-5}$	$\sim 2.3 \times 10^9$
Ar	0.934(1)	$6.59(1) \times 10^{13}$	CO	$\sim 1.2 \times 10^{-5}$	$\sim 5.9 \times 10^8$
CO <sub>2</sub>	0.0315(10)	$2.45(8) \times 10^{12}$	NH <sub>3</sub>	$\sim 1 \times 10^{-6}$	$\sim 3 \times 10^7$
Ne	$1.818(4) \times 10^{-3}$	$6.48(2) \times 10^{10}$	NO <sub>2</sub>	$\sim 1 \times 10^{-7}$	$\sim 8 \times 10^6$
He	$5.24(5) \times 10^{-4}$	$3.71(4) \times 10^9$	SO <sub>2</sub>	$\sim 1 \times 10^{-8}$	$\sim 2 \times 10^6$
Kr	$1.14(1) \times 10^{-4}$	$1.69(2) \times 10^{10}$	H <sub>2</sub> S	$\sim 1 \times 10^{-8}$	$\sim 1 \times 10^6$
Xe	$8.7(1) \times 10^{-6}$	$2.02(2) \times 10^9$	O <sub>3</sub>	<b>Variable</b>	<b><math>\sim 3.3 \times 10^9</math></b>

<sup>(a)</sup>Total mass:  $5.136(7) \times 10^{15}$  tonnes; H<sub>2</sub>O  $0.017(1) \times 10^{15}$  tonnes; dry atmosphere  $5.119(8) \times 10^{15}$  tonnes. Figures in parentheses denote estimated uncertainty in last significant digit.

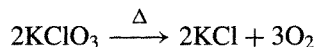
In addition to its presence as the free element in the atmosphere and dissolved in surface waters, oxygen occurs in combined form both as water, and a constituent of most rocks, minerals, and soils. The estimated abundance of oxygen in the crustal rocks of the earth is 455 000 ppm (i.e. 45.5% by weight); see silicates, p. 347; aluminosilicates, p. 347; carbonates, p. 109; phosphates, p. 475, etc.

### 14.1.3 Preparation

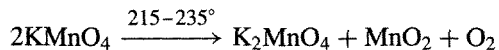
Oxygen is now separated from air on a vast scale (see below) and is conveniently obtained for most laboratory purposes from high-pressure stainless steel cylinders. Small traces of N<sub>2</sub> and the rare gases, particularly argon, are the most persistent impurities. Occasionally, small-scale laboratory preparations are required and the method chosen depends on the amount and purity required and the availability of services. Electrolysis of degassed aqueous electrolytes produces wet O<sub>2</sub>, the purest gas being obtained from 30% potassium hydroxide solution using nickel electrodes. Another source is the catalytic decomposition of 30% aqueous hydrogen peroxide on a platinumized nickel foil.

Many oxoacid salts decompose to give oxygen when heated (p. 864). A convenient source is KClO<sub>3</sub> which evolves oxygen when heated to

400–500° according to the simplified equation



The decomposition temperature is reduced to 150° in the presence of MnO<sub>2</sub> but then the product is contaminated with up to 3% of ClO<sub>2</sub> (p. 847). Small amounts of breathable oxygen for use in emergencies (e.g. failure of normal supply in aircraft or submarines) can be generated by decomposition of NaClO<sub>3</sub> in “oxygen candles”. The best method for the controlled preparation of very pure O<sub>2</sub> is the thermal decomposition of recrystallized, predried, degassed KMnO<sub>4</sub> in a vacuum line. Mn<sup>VI</sup> and Mn<sup>IV</sup> are both formed and the reaction can formally be represented as:



Oxygen gas and liquid oxygen are manufactured on a huge scale by the fractional distillation of liquid air at temperatures near –183°C. Although world production exceeds 100 million tonnes pa this is still less than one ten-millionth part of the oxygen in the atmosphere; moreover, the oxygen is continuously being replenished by photosynthesis. Further information on the industrial production and uses of oxygen are in the Panel.

## Industrial Production and Uses of Oxygen<sup>(11)</sup>

Air can be cooled and eventually liquified by compressing it isothermally and then allowing it to expand adiabatically to obtain cooling by the Joule-Thompson effect. Although this process was developed by C. von Linde (Germany) and W. Hampson (UK) at the end of the last century, it is thermodynamically inefficient and costly in energy. Most large industrial plants now use the method developed by G. Claude (France) in which air is expanded isentropically in an engine from which mechanical work can be obtained; this produces a much greater cooling effect than that obtained by the Joule-Thompson effect alone. Because N<sub>2</sub> (bp -195.8°C) is more volatile than O<sub>2</sub> (bp -183.0°C) there is a higher concentration of N<sub>2</sub> in the vapour phase above boiling liquid air than in the liquid phase, whilst O<sub>2</sub> becomes progressively enriched in the liquid phase. Fractional distillation of the liquefied air is usually effected in an ingeniously designed double-column dual-pressure still which uses product oxygen from the upper column at a lower pressure (lower bp) to condense vapour for reflux at a higher pressure in the lower column. The most volatile constituents of air (He, H<sub>2</sub>, Ne) do not condense but accumulate as a high-pressure gaseous mixture with N<sub>2</sub> at the top of the lower column. Argon, which has a volatility between those of O<sub>2</sub> and N<sub>2</sub>, concentrates in the upper column from which it can be withdrawn for further purification in a separate column, whilst the least-volatile constituents (Kr, Xe) accumulate in the oxygen boiler at the foot of the upper column. Typical operating pressures are 5 atm at the top of the lower column and 0.5 atm at the bottom of the upper column. A large plant might produce 1700 tonnes per day of separated products. A rather different design is used if liquid (rather than gaseous) N<sub>2</sub> is required in addition to the liquid and/or gaseous O<sub>2</sub>.

From modest beginnings at the turn of the century, oxygen has now become the third largest volume chemical produced in the USA (after H<sub>2</sub>SO<sub>4</sub> and N<sub>2</sub> and ahead of ethylene, lime and NH<sub>3</sub>, see p. 407). Production in 1995 was 23.3 million tonnes (USA), over 3 Mt (UK), and 100 Mt worldwide. About 20% of the USA production is as liquid O<sub>2</sub>. This phenomenal growth derived mainly from the growing use of O<sub>2</sub> in steelmaking; the use of O<sub>2</sub> rather than air in the Bessemer process was introduced in the late 1950s and greatly increased the productivity by hastening the reactions. In many of the major industrial countries this use alone now accounts for 65–85% of the oxygen produced. Much of this is manufactured on site and is simply piped from the air-separation plant to the steel converter.

Oxygen is also used to an increasing extent in iron blast furnaces since enrichment of the blast enables heavy fuel oil to replace some of the more expensive metallurgical coke. Other furnace applications are in ferrous and non-ferrous metal smelting and in glass manufacture, where considerable benefits accrue from higher temperatures, greater productivity, and longer furnace life. Related, though smaller-scale applications, include steel cutting, oxy-gas welding, and oxygen lancing (concrete drilling).

In the chemical industry oxygen is used on a large scale in the production of TiO<sub>2</sub> by the chloride process (p. 959), in the direct oxidation of ethene to ethylene oxide, and in the manufacture of synthesis gas (H<sub>2</sub> + CO), propylene oxide, vinyl chloride, vinyl acetate, etc. Environmental and biomedical uses embrace sewage treatment, river revival, paper-pulp bleaching, fish farming, artificial atmospheres for diving and submarine work, oxygen tents in hospitals, etc. Much of the oxygen for these applications is transported either in bulk liquid carriers or in high-pressure steel cylinders.

A final, somewhat variable outlet for large-scale liquid oxygen is as oxidant in rocket fuels for space exploration, satellite launching and space shuttles. For example, in the Apollo mission to the moon (1979), each Saturn 5 launch rocket used 1270 m<sup>3</sup> (i.e. 1.25 million litres or 1450 tonnes) of liquid oxygen in Stage 1, where it oxidized the kerosene fuel (195 000 l, or about 550 tonnes) in the almost unbelievably short time of 2.5 min. Stages 2 and 3 had 315 and 76.3 m<sup>3</sup> of liquid O<sub>2</sub> respectively, and the fuel was liquid H<sub>2</sub>.

### 14.1.4 Atomic and physical properties

Oxygen has 3 stable isotopes of which <sup>16</sup>O (relative atomic mass 15.994 915) is by far the most abundant (99.762 atom%). Of the others, <sup>17</sup>O (16.999 134) has an abundance of only 0.038% and <sup>18</sup>O (17.999 160) is 0.200% abundant. These values vary slightly in differing natural sources (the ranges being

0.0350–0.0407% for <sup>17</sup>O and 0.188–0.215% for <sup>18</sup>O) and this variability prevents the atomic weight of oxygen being quoted more precisely than 15.9994 ± 0.0003 (see p. 17). Artificial enrichment of <sup>17</sup>O and <sup>18</sup>O can be achieved by several physical or chemical processes such as the fractional distillation of water, the electrolysis of water, and the thermal diffusion of oxygen gas. Heavy water enriched to 20 atom% <sup>17</sup>O or 98% <sup>18</sup>O is available commercially, as is oxygen gas enriched to 95% in <sup>17</sup>O or 99% in <sup>18</sup>O. The <sup>18</sup>O isotope has been much used in kinetic and

<sup>11</sup> W. J. GRANT and S. L. REDFERN, *Industrial Gases*, in R. Thompson (ed.), *The Modern Inorganic Chemicals Industry*, pp. 273–301. Chem. Soc. Special Publ. No. 31, 1978.

mechanistic studies.<sup>(12)</sup> Ten radioactive isotopes are also known but their very short half-lives make them unsuitable for tracer work. The longest lived,  $^{15}\text{O}$ , decays by positron emission with  $t_{1/2}$  122.2 s; it can be made by bombarding  $^{16}\text{O}$  with  $^3\text{He}$  particles:  $^{16}\text{O}(^3\text{He},\alpha)^{15}\text{O}$ .

The isotope  $^{17}\text{O}$  is important in having a nuclear spin ( $I = \frac{5}{2}$ ) and this enables it to be used in nmr studies.<sup>(13)</sup> The nuclear magnetic moment is  $-1.8930$  nuclear magnetons (very similar to the value for the free neutron,  $-1.9132$  NM) and the relative sensitivity for equal numbers of nuclei is 0.0291, compared with  $^1\text{H}$  1.00,  $^{11}\text{B}$  0.17,  $^{13}\text{C}$  0.016,  $^{31}\text{P}$  0.066, etc. In addition to this low sensitivity, measurements are made more difficult because the quadrupolar nucleus leads to very broad resonances, typically  $10^2$ – $10^3$  times those for  $^1\text{H}$ . The observing frequency is  $\sim 0.136$  times that for proton nmr. The resonance was first observed in 1951<sup>(14)</sup> and the range of chemical shifts extended in 1955.<sup>(15)</sup> The technique has proved particularly valuable for studying aqueous solutions and the solvation equilibria of electrolytes. Thus the hydration numbers for the diamagnetic cations  $\text{Be}^{\text{II}}$ ,  $\text{Al}^{\text{III}}$ , and  $\text{Ga}^{\text{III}}$  have been directly measured as 4, 6 and 6 respectively, and several exchange reactions between “bound” and “free” water have been investigated. Chemical shifts for  $^{17}\text{O}$  in a wide range of oxoanions  $[\text{XO}_n]^{m-}$  have been studied and it has been found that the shifts for terminal and bridging O atoms in  $[\text{Cr}_2\text{O}_7]^{2-}$  differ by as much as 760 ppm. The technique is proving increasingly valuable in the structure determination of complex polyanions in solution; for example all seven different types of O atoms

in  $[\text{V}_{10}\text{O}_{28}]^{6-}$  (p. 986) have been detected.<sup>(16)</sup> The exchange of  $^{17}\text{O}$  between  $\text{H}_2^{17}\text{O}$  and various oxoanions has also been studied. Less work has been done so far on transition metal complexes of CO and NO though advances in techniques are now beginning to yield valuable structural and kinetic data.<sup>(17)</sup>

The electronic configuration of the free O atom is  $1s^2 2s^2 2p^4$ , leading to a  $^3P_2$  ground state. The ionization energy of O is  $1313.5 \text{ kJ mol}^{-1}$  (cf. S on p. 662 and the other Group 16 elements on p. 754). The electronegativity of O is 3.5; this is exceeded only by F and the high value is reflected in much of the chemistry of oxygen and the oxides. The single-bond atomic radius of O is usually quoted as 73–74 pm, i.e. slightly smaller than for C and N, and slightly larger than for F, as expected. The ionic radius of  $\text{O}^{2-}$  is assigned the standard value of 140 pm and all other ionic radii are derived from this.<sup>(18)</sup>

Molecular oxygen,  $\text{O}_2$ , is unique among gaseous diatomic species with an even number of electrons in being paramagnetic. This property, first observed by M. Faraday in 1848, receives a satisfying explanation in terms of molecular orbital theory. The schematic energy-level diagram is shown in Fig. 14.1; this indicates that the 2 least-strongly bound electrons in  $\text{O}_2$  occupy degenerate orbitals of  $\pi$  symmetry and have parallel spins. This leads to a triplet ground state,  $^3\Sigma_g^-$ . As there are 4 more electrons in bonding MOs than in antibonding MOs,  $\text{O}_2$  can be formally said to contain a double bond. If the 2 electrons, whilst remaining unpaired in separate orbitals, have opposite spin, then a singlet excited state of zero resultant spin results,  $^1\Delta_g$ . A singlet state also results if the 2 electrons occupy a single  $\pi^*$  orbital with opposed spins,  $^1\Sigma_g^+$ . These 2 singlet states lie 94.72 and 157.85  $\text{kJ mol}^{-1}$  above the ground state and are extremely important in gas-phase oxidation reactions (p. 614). The excitation is

<sup>12</sup> I. D. DOSTROVSKY and D. SAMUEL, in R. H. HERBER (ed.), *Inorganic Isotopic Syntheses*, Chap. 5, pp. 119–42, Benjamin, New York, 1962.

<sup>13</sup> C. ROGER, N. SHEPPARD, C. MCFARLANE and W. MCFARLANE, Chap. 12A in R. H. HARRIS and B. E. MANN (eds.), *NMR and the Periodic Table*, pp. 383–400, Academic Press, London, 1978. H. C. E. MCFARLANE and W. MCFARLANE, in J. MASON (ed.), *Multinuclear NMR*, Plenum Press, New York, 1987, pp. 403–16.

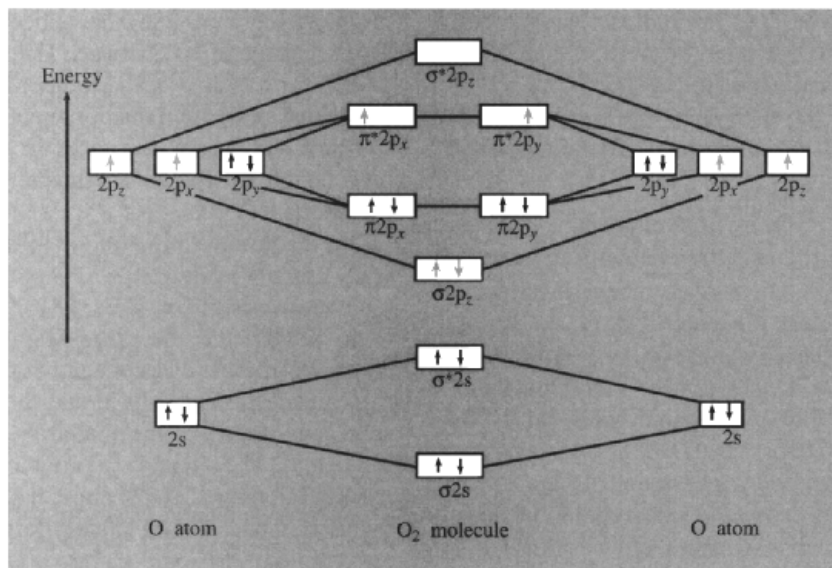
<sup>14</sup> F. ALDER and F. C. YU, *Phys. Rev.* **81**, 1067–8 (1951).

<sup>15</sup> H. E. WEAVER, B. M. TOLBERT and R. C. LAFORCE, *J. Chem. Phys.* **23**, 1956–7 (1955).

<sup>16</sup> W. G. KLEMPERER and W. SHUM, *J. Am. Chem. Soc.* **99**, 3544–5 (1977).

<sup>17</sup> R. L. KUMP and L. J. TODD, *J. Chem. Soc., Chem. Commun.*, 292–3 (1980).

<sup>18</sup> R. D. SHANNON, *Acta Cryst.* **A32**, 751–67 (1976).



**Figure 14.1** Schematic molecular-orbital energy level diagram for the molecule  $\text{O}_2$  in its ground state,  $^3\Sigma_g^-$ . The internuclear vector is along the  $z$ -axis.

accompanied by a slight but definite increase in the internuclear distance from 120.74 pm in the ground state to 121.55 and 122.77 pm in the excited states. The bond dissociation energy of  $\text{O}_2$  is  $493.4(2) \text{ kJ mol}^{-1}$ ; this is substantially less than for the triply bonded species  $\text{N}_2$  ( $945.4 \text{ kJ mol}^{-1}$ ) but is much greater than for  $\text{F}_2$  ( $158.8 \text{ kJ mol}^{-1}$ ). See also the discussion on p. 616.

Oxygen is a colourless, odourless, tasteless highly reactive gas. It dissolves to the extent of  $3.08 \text{ cm}^3$  (gas at STP) in  $100 \text{ cm}^3 \text{ H}_2\text{O}$  at  $20^\circ$  and this drops to  $2.08 \text{ cm}^3$  at  $50^\circ$ . Solubility in salt water is slightly less but is still sufficient for the vital support of marine and aquatic life. Solubility in many organic solvents is about 10 times that in water and necessitates careful degassing if these solvents are to be used in the preparation and handling of oxygen-sensitive compounds. Typical solubilities (expressed as gas volumes dissolved in  $100 \text{ cm}^3$  of solvent at  $25^\circ\text{C}$  and 1 atm pressure) are  $\text{Et}_2\text{O}$  45.0,  $\text{CCl}_4$  30.2,  $\text{Me}_2\text{CO}$  28.0 and  $\text{C}_6\text{H}_6$   $22.3 \text{ cm}^3$ .

Oxygen condenses to a pale blue, mobile paramagnetic liquid (bp  $-183.0^\circ\text{C}$  at 1 atm).

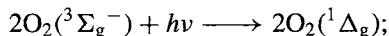
The viscosity (0.199 centipoise at  $-183.5^\circ$  and 10.6 atm) is about one-fifth that of water at room temperature. The critical temperature, above which oxygen cannot be liquefied by application of pressure alone, is  $-118.4^\circ\text{C}$  and the critical pressure is 50.15 atm. Solid oxygen (pale blue, mp  $-218.8^\circ\text{C}$ ) also comprises paramagnetic  $\text{O}_2$  molecules but, in the cubic  $\gamma$ -phase just below the mp, these are rotationally disordered and the solid is soft, transparent, and only slightly more dense than the liquid. There is a much greater increase in density when the solid transforms to the rhombohedral  $\beta$ -phase at  $-229.4^\circ$  and there is a further phase change to the monoclinic  $\alpha$ -form at  $-249.3^\circ\text{C}$ ; these various changes and the accompanying changes in molar volume  $\Delta V_M$  are summarized in Table 14.2.

The blue colour of oxygen in the liquid and solid phases is due to electronic transitions by which molecules in the triplet ground state are excited to the singlet states. These transitions are normally forbidden in pure gaseous oxygen and, in any case, they occur in the infrared region of the spectrum at  $7918 \text{ cm}^{-1}$  ( $^1\Delta_g$ ) and  $13\,195 \text{ cm}^{-1}$  ( $^1\Sigma_g^+$ ). However, in the condensed phases a

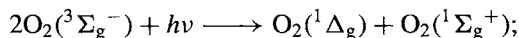
Table 14.2 Densities and molar volumes of liquid and solid O<sub>2</sub>

Transition	bp/1 (atm)	mp (triple pt)	$\gamma \longleftrightarrow \beta$	$\beta \longleftrightarrow \alpha$	
<i>T</i> /K	90.18	54.35	43.80	23.89	
<i>d</i> /g cm <sup>-3</sup>	1.1407(1)	1.3215(1)	1.334( $\gamma$ )	1.495( $\beta$ )	1.53( $\alpha$ )
$\Delta V_M$ /cm <sup>3</sup> mol <sup>-1</sup>					
		3.84	0.23	2.58	0.49

single photon can elevate 2 colliding molecules simultaneously to excited states, thereby requiring absorption of energy in the visible (red-yellow-green) regions of the spectrum.<sup>(19)</sup> For example:



$$\bar{\nu} = 15\,800\text{ cm}^{-1}, \text{ i.e. } \lambda = 631.2\text{ nm}$$



$$\bar{\nu} \sim 21\,100\text{ cm}^{-1}, \text{ i.e. } \lambda = 473.7\text{ nm}$$

The blue colour of the sky is, of course, due to Rayleigh scattering and not to electronic absorption by O<sub>2</sub> molecules.

### 14.1.5 Other forms of oxygen

#### Ozone<sup>(20)</sup>

Ozone, O<sub>3</sub>, is the triatomic allotrope of oxygen. It is an unstable, blue diamagnetic gas with a characteristic pungent odour: indeed, it was first detected by means of its smell, as reflected by its name (Greek *ὄζειν*, *ozein*, to smell) coined by C. F. Schönbein in 1840. Ozone can be detected by its smell in concentrations as low as 0.01 ppm; the maximum permissible concentration for continuous exposure is 0.1 ppm but levels as high as 1 ppm are considered non-toxic if breathed for less than 10 min.

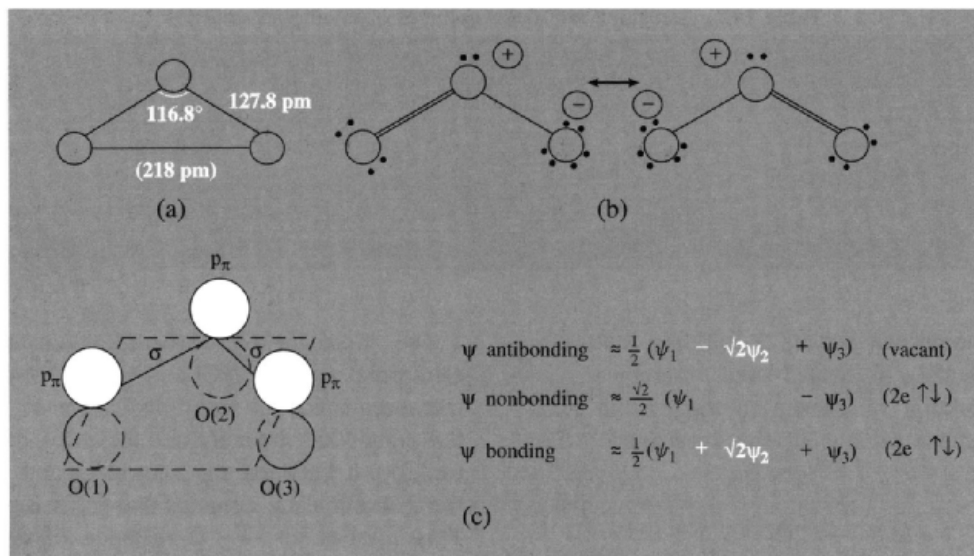
The molecule O<sub>3</sub> is bent, as are the iso-electronic species ONCl and ONO<sup>-</sup>. Microwave measurements lead to a bond angle of  $116.8 \pm 0.5^\circ$  and an interatomic distance of  $127.8 (\pm 0.3)$  pm between the central O and each of the 2 terminal O atoms as shown in Fig. 14.2a. This implies an O···O distance of only 218 pm between the 2 terminal O atoms, compared with the normal van der Waals O···O distance of 280 pm. A valence-bond description of the molecule is given by the resonance hybrids in Fig. 14.2b and a MO description of the bonding is indicated in Fig. 14.2c: in this, each O atom forms a  $\sigma$  bond to its neighbour using an sp<sup>2</sup>-type orbital, and the 3 atomic p <sub>$\pi$</sub>  orbitals can combine to give the 3 MOs shown. There are just sufficient electrons to fill the bonding and nonbonding MOs so that the  $\pi$  system can be termed a 4electron 3-centre bond. The total bond order for each O–O bond is therefore approximately 1.5 (1  $\sigma$  bond and half of 1  $\pi$ -bonding MO). It is instructive to note that SO<sub>2</sub> has a similar structure (angle O–S–O  $120^\circ$ ): the much greater stability of this molecule when compared with O<sub>3</sub> has been ascribed, in part, to the possible involvement of d <sub>$\pi$</sub>  orbitals on the S atom which would allow the filled nonbonding orbital in O<sub>3</sub> to become bonding in SO<sub>2</sub> (see also p. 700). Other comparisons of O–O bond orders, interatomic distances and bond energies are in Table 14.4 (p. 616).

Ozone condenses to a deep blue liquid (bp  $-111.9^\circ\text{C}$ ) and to a violet-black solid (mp  $-192.5^\circ\text{C}$ ). The colour is due to an intense absorption band in the red region of the spectrum between 500–700 nm ( $\lambda_{\text{max}}$  557.4 and 601.9 nm). Both the liquid and the solid are explosive

<sup>19</sup> E. A. OGRYZLO, Why liquid oxygen is blue, *J. Chem. Educ.* **42**, 647–8 (1965).

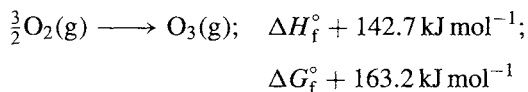
<sup>20</sup> M. HORVATH, L. BILITZKY and J. HÜTTNER (eds.), *Ozone*, Elsevier, Amsterdam, 1985, 350 pp.





**Figure 14.2** (a) Geometry of the  $O_3$  molecule, (b) valence-bond resonance description of the bonding in  $O_3$ , and (c) orbitals used in the MO description of the bonding in  $O_3$ , where  $\psi_1$  is the  $2p_\pi$  orbital of O(1), etc.

due to decomposition into gaseous  $O_2$ . Gaseous ozone is also thermodynamically unstable with respect to decomposition into dioxygen though it decomposes only slowly, even at 200°, in the absence of catalysts or ultraviolet light:



Other properties of ozone (which can be compared with those of dioxygen on p. 606) are: density at  $-119.4^\circ\text{C}$   $1.354 \text{ g cm}^{-3}$  (liquid), density at  $-195.8^\circ\text{C}$   $1.728 \text{ g cm}^{-3}$  (solid), viscosity at  $-183^\circ\text{C}$  1.57 centipoise, dipole moment 0.54 D. Liquid ozone is miscible in all proportions with  $CH_4$ ,  $CCl_2F_2$ ,  $CClF_3$ ,  $CO$ ,  $NF_3$ ,  $OF_2$  and  $F_2$  but forms two layers with liquid Ar,  $N_2$ ,  $O_2$  and  $CF_4$ .

A particularly important property of ozone is its strong absorption in the ultraviolet region of the spectrum between 220–290 nm ( $\lambda_{\text{max}} 255.3 \text{ nm}$ ); this protects the surface of the earth and its inhabitants from the intense ultraviolet radiation of the sun. Indeed, it is this absorption of energy, and the consequent rise in temperature, which is the main cause for the existence of the stratosphere in the first place.

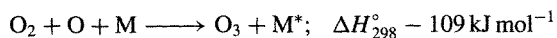
Thus, the mean temperature of the atmosphere, which is about  $20^\circ\text{C}$  at sea level, falls steadily to about  $-55^\circ$  at an altitude of 10 km and then rises to almost  $0^\circ\text{C}$  at 50 km before dropping steadily again to about  $-90^\circ$  at 90 km. Concern was expressed in 1974<sup>(21)</sup> that interaction of ozone with man-made chlorofluorocarbons would deplete the equilibrium concentration of ozone with potentially disastrous consequences, and this was dramatically confirmed by the discovery of a seasonally recurring “ozone hole” above Antarctica in 1985.<sup>(22)</sup> A less prominent ozone hole was subsequently detected above the Arctic Ocean. The detailed physical and chemical conditions required to generate these large seasonal depletions of ozone are extremely complex but the main features have now been elucidated (see p. 848). Several accounts of various aspects of the emerging story, and of the consequent international governmental actions to

<sup>21</sup> M. J. MOLINA and F. S. ROWLAND, *Nature* **249**, 810–12 (1974). (Shared 1995 Nobel Prize for Chemistry with P. Crutzen.)

<sup>22</sup> J. C. FARMAN, B. G. GARDINER and J. D. SHANKLIN, *Nature* **315**, 207–10 (1985).

ameliorate or reverse the depletion have been published.<sup>(7,23-27)</sup>

Ozone is best prepared by flowing O<sub>2</sub> at 1 atm and 25° through concentric metallized glass tubes to which low-frequency power at 50–500 Hz and 10–20 kV is applied to maintain a silent electric discharge (see also p. 611). The ozonizer tube, which becomes heated by dielectric loss, should be kept cooled to room temperature and the effluent gas, which contains up to 10% O<sub>3</sub> at moderate flow rates, can be used directly or fractionated if higher concentrations are required. Reaction proceeds via O atoms at the surface M, via excited O<sub>2</sub>\* molecules, and by dissociative ion recombination:



However, the reverse reaction of ozone with atomic oxygen is highly exothermic and must be suppressed by trapping out the ozone if good yields are to be obtained:



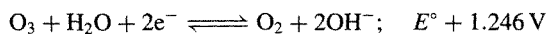
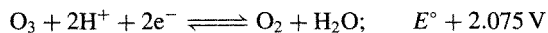
An alternative route to O<sub>3</sub> is by ultraviolet irradiation of O<sub>2</sub>: this is useful for producing low concentrations of O<sub>3</sub> for sterilization of foodstuffs and disinfection, and also occurs during the generation of photochemical smog. The electrolysis of cold aqueous H<sub>2</sub>SO<sub>4</sub> (or HClO<sub>4</sub>) at very high anode current densities also affords modest concentrations of O<sub>3</sub>, together with O<sub>2</sub> and H<sub>2</sub>S<sub>2</sub>O<sub>8</sub>

(p. 712) as byproducts. Other reactions in which O<sub>3</sub> is formed are the reaction of elementary F<sub>2</sub> with H<sub>2</sub>O (p. 804) and the thermal decomposition of periodic acid at 130° (p. 872).

The concentration of ozone in O<sub>2</sub>/O<sub>3</sub> mixtures can be determined by catalytic decomposition to O<sub>2</sub> in the gas phase and measurement of the expansion in volume. More conveniently it can be determined iodometrically by passing the gas mixture into an alkaline boric-acid-buffered aqueous solution of KI and determining the I<sub>2</sub> so formed by titration with sodium thiosulfate in acidified solution:

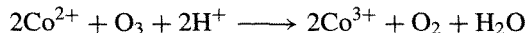
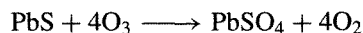
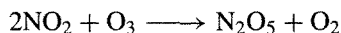
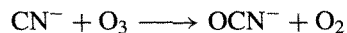


The reaction illustrates the two most characteristic chemical properties of ozone: its strongly oxidizing nature and its tendency to transfer an O atom with coproduction of O<sub>2</sub>. Standard reduction potentials in acid and in alkaline solution are:



The acid potential is exceeded only by fluorine (p. 804), perxenate (p. 901), atomic O, the OH radical, and a few other such potent oxidants. Decomposition is rapid in acid solutions but the allotrope is much more stable in alkaline solution. At 25° the half-life of O<sub>3</sub> in 1 M NaOH is ~2 min; corresponding times for 5 M and 20 M NaOH are 40 min and 83 h respectively.

The highly reactive nature of O<sub>3</sub> is further typified by the following reactions:



An important reaction of ozone is the formation of ozonides MO<sub>3</sub>. The formation of a red coloration when O<sub>3</sub> is passed into concentrated aqueous alkali was first noted by C. F. Schönbein in 1866, but the presence

<sup>23</sup> D. G. COGAN, *Stones in a Glass House: CFCs and Ozone Depletion, Investor Responsibility Research Center Inc., Washington, DC, 1988, 147 pp.*

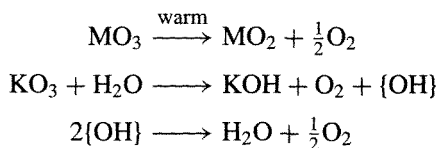
<sup>24</sup> ARJUN MAKHIJANI, ANNIE MAKHIJANI and A. BICKEL, *Saving our Skins: Technical Potential and Policies for the Elimination of Ozone-Depleting Compounds*, Environmental Policy Institute and Institute for Energy and Environmental Research, Washington, DC, 1988, 167 pp.

<sup>25</sup> R. P. WAYNE, *Proc. Royal Institution* **61**, 13–49 (1989).

<sup>26</sup> M. J. MOLINA and L. T. MOLINA, Chap. 2 in D. A. DUNNETTE and R. J. O'BRIEN (eds.), *The Science of Global Change: The Impact of Human Activities on the Environment*, ACS Symposium Series, Am. Chem. Soc., Washington, DC, 1992, pp. 24–35.

<sup>27</sup> P. S. ZURER, *Chem. and Eng. News*, May 24, 1993, pp. 8–18.

of  $O_3^-$  was not established until 1949.<sup>(28)</sup> The compounds are best prepared by action of gaseous  $O_3$  on dry, powdered MOH below  $-10^\circ$  (or  $O_3/O_2$  mixtures on  $CsO_2$ ) followed by extraction with liquid ammonia (which may also catalyse their formation). The compounds are red-brown paramagnetic solids ( $\mu = 1.74-1.80$  BM)<sup>(29)</sup> and they decrease in stability in the sequence  $Cs > Rb > K > Na$ ; unsolvated  $LiO_3$  has not been prepared but the ammine  $LiO_3 \cdot 4NH_3$  is known. Likewise the stability of  $M^{II}(O_3)_2$  decreases in the sequence  $Ba > Sr > Ca$ . Above room temperature  $MO_3$  decomposes to the superoxide  $MO_2$  (p. 616) and the compounds are also hydrolytically unstable:



The ozonide ion  $O_3^-$  has the expected  $C_{2v}$  symmetry like  $O_3$  itself and the isoelectronic, paramagnetic molecule  $ClO_2$  (p. 845). Early attempts at X-ray structural analysis were frustrated by the thermal instability of the compounds, their great reactivity, the difficulty of growing single crystals and the tendency to rotational disorder.<sup>(30)</sup> However, it is now clear that the  $O_3^-$  ion is indeed bent, the most accurate data being obtained on crystals of the surprisingly stable red compound  $[NMe_4]O_3$  (decomp.  $75^\circ$ , cf.  $CsO_3$   $53^\circ$ ):<sup>(31)</sup> the angle  $O-O-O$  is  $119.5(5)^\circ$ , only slightly larger than for  $O_3$  itself, and the  $O-O$  and  $O \cdots O$  distances

<sup>28</sup> I. A. KAZAROVSKII, G. P. NIKOL'SKII and T. A. ABLETSOVA, *Dokl. Akad. Nauk SSSR* **64**, 69-72 (1949).

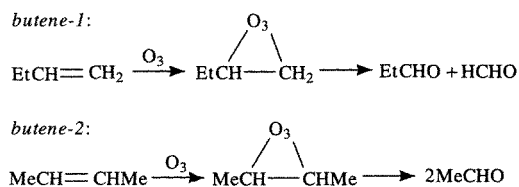
<sup>29</sup> H. LUEKEN, M. DEUSSEN, M. JANSEN, W. HESSE and W. SCHNICK, *Z. anorg. allg. Chem.* **553**, 179-86 (1981).

<sup>30</sup> L. V. AZÁROV and I. CORVIN, *Proc. Natl. Acad. Sci. (US)* **49**, 1-5 (1963). M. JANSEN and W. HESSE, *Z. anorg. allg. Chem.* **560**, 47-54 (1988).

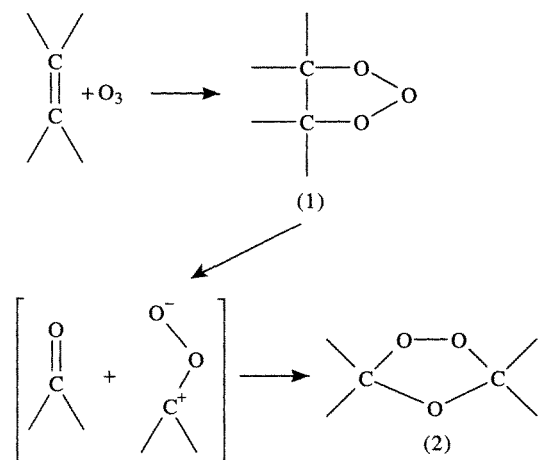
<sup>31</sup> W. HESSE and M. JANSEN, *Angew. Chem. Int. Edn. Engl.* **27**, 1341-2 (1988). See also W. ASSENMACHER and M. JANSEN, *Z. anorg. allg. Chem.* **621**, 431-4 (1995) for information on the newest ionic ozonides,  $[PMe_4]O_3$  and  $[AsMe_4]O_3$ .

are 126.4(4) and 222.2(4) pm, respectively (cf. Fig. 14.2).

Ozone adds readily to unsaturated organic compounds<sup>(32)</sup> and can cause unwanted cross-linking in rubbers and other polymers with residual unsaturation, thereby leading to brittleness and fracture. Addition to alkenes yields "ozonides" which can be reductively cleaved by  $Zn/H_2O$  (or  $I^-/MeOH$ , etc.) to yield aldehydes or ketones. This smooth reaction, discovered by C. D. Harries in 1903, has long been used to determine the position of double bonds in organic molecules, e.g.:



Ozonide formation occurs by a three-step mechanism along the lines first proposed in 1951 by R. Criegee:<sup>(33,34)</sup>

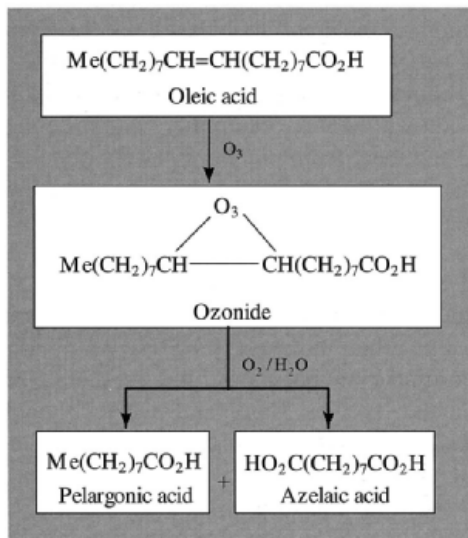


<sup>32</sup> P. S. BAILEY, *Ozonation in Organic Chemistry*, Vol. 1, Olefinic Compounds, Academic Press, New York, 1978, 272 pp.; Vol. 2, Nonolefinic Compounds, 1982, 496 pp. S. D. RAZUMOVSKI and G. E. ZAIKOV, *Ozone and Its Reactions with Organic Compounds*, Elsevier, Amsterdam, 1984, 404 pp.

<sup>33</sup> R. CRIEGEE, *Rec. Chem. Prog.* **18**, 111-20 (1957). *Angew. Chem. Int. Edn. Engl.* **14**, 745-52 (1975).

<sup>34</sup> R. L. KUCZKOWSKI, *Chem. Soc. Revs.* **21**, 79-83 (1992).

The primary ozonides (1), which are 1,2,3-trioxolanes, are formed by a concerted 1,3-dipolar cycloaddition between ozone and the alkene and are detectable only at very low temperatures. For example, at  $-175^{\circ}\text{C}$  ethene gives  $\text{CH}_2\text{CH}_2\text{OOO}$  which was shown by microwave spectroscopy to be non-planar with  $\text{O}-\text{O}$  145 pm, angle  $\text{O}-\text{O}-\text{O}$   $100^{\circ}$  and a dihedral angle between the  $\text{C}_2\text{O}_2$  and  $\text{O}_3$  planes of  $51^{\circ}$ .<sup>(35)</sup> At higher temperatures the primary ozonides spontaneously rearrange to secondary ozonides: these have a 1,2,4-trioxolane structure (2) and can be studied by a variety of techniques including  $^{17}\text{O}$  nmr spectroscopy.<sup>(36)</sup> Normally, however, the ozonide is not isolated but is reductively cleaved to aldehydes and ketones in solution. Oxidative cleavage (air or  $\text{O}_2$ ) yields carboxylic acids and, indeed, the first large-scale application of the reaction was the commercial production of pelargonic and azelaic acids from oleic acid:



Esters of these acids are used as plasticizers for PVC (polyvinylchloride) and other plastics.

Because of the reactivity, instability and hazardous nature of  $\text{O}_3$  it is always generated on

site. Typical industrial ozone generators operate at 1 or 2 atm, 15–20 kV, and 50 or 500 Hz. The concentration of  $\text{O}_3$  in the effluent gas depends on the industrial use envisaged but yields of up to 10 kg per hour or 150 kg per day from a single apparatus are not uncommon and some plants yield over 1 tonne per day. In addition to pelargonic and azelaic acid production,  $\text{O}_3$  is used to make peroxyacetic acid from acetaldehyde and for various inorganic oxidations. At low concentrations it is used (particularly in Europe) to purify drinking water, since this avoids the undesirable taste and smell of chlorinated water, and residual ozone decomposes to  $\text{O}_2$  soon after treatment.<sup>(37)</sup> Of the 1039 plants operating in 1977 all but 40 were in Europe, with the greatest numbers in France (593), Switzerland (150), Germany (136), and Austria (42). Other industrial uses include the preservation of goods in cold storage, the treatment of industrial waste and the deodorizing of air and sewage gases.<sup>(38)</sup>

### Atomic oxygen

Atomic oxygen is an extremely reactive, fugitive species which cannot be isolated free from other substances. Many methods of preparing oxygen atoms also yield other reactive or electronically excited species, and this somewhat complicates the study of their properties. Passage of a microwave or electric discharge through purified  $\text{O}_2$  gas diluted with argon produces  $\text{O}$  atoms in the  $^3\text{P}$  ground state (2 unpaired electrons). Mercury-sensitized photolysis of  $\text{N}_2\text{O}$  is perhaps a more convenient route to ground state  $\text{O}$  atoms (plus inert  $\text{N}_2$  molecules) though they can also be made by photolysis of  $\text{O}_2$  or  $\text{NO}_2$ . Photolysis of  $\text{N}_2\text{O}$  in the absence of  $\text{Hg}$  gives  $\text{O}$  atoms in the spin-paired  $^1\text{D}$  excited state, and this species can also be obtained by photolysis of  $\text{O}_3$  or  $\text{CO}_2$ .

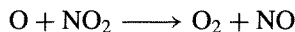
<sup>35</sup> J. Z. GILLIES, C. W. GILLIES, R. D. SUENRAM and F. J. LOVAS, *J. Am. Chem. Soc.* **110**, 1991–9 (1988).

<sup>36</sup> J. LAUTERWEIN, K. GRIESBAUM, P. KRIEGER-BECK, V. BALL and K. SCHLINDWEIN, *J. Chem. Soc., Chem. Commun.*, 816–7 (1991).

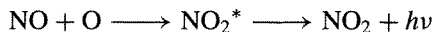
<sup>37</sup> J. KATZ (ed.), *Ozone and Chlorine Dioxide Technology for Disinfection of Drinking Water*, Noyes Data Corp., Park Ridge, New Jersey, 1980, 659 pp. R. G. RICE and M. E. BROWNING, *Ozone Treatment of Industrial Wastewater*, Noyes Data Corp., Park Ridge, New Jersey, 1981, 371 pp.

<sup>38</sup> J. A. WOJTCWICZ, *Ozone*, *Kirk-Othmer Encyclopedia of Chemical Technology*, 4th edn. **17**, 953–95. Wiley, New York, 1996.

The best method for determining the concentration of O atoms is by their extremely rapid reaction with NO<sub>2</sub> in a flow system:

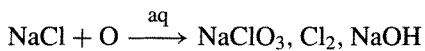
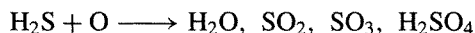
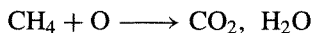
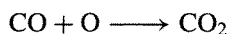
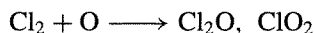
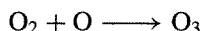
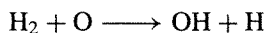


The NO thus formed reacts more slowly with any excess of O atoms to reform NO<sub>2</sub> and this reaction emits a yellow-green glow.



The system is thus titrated with NO<sub>2</sub> until the glow is sharply extinguished.

As expected, atomic O is a strong oxidizing agent and it is an important reactant in the chemistry of the upper atmosphere.<sup>(17,18)</sup> Typical reactions are:



Many of these reactions are explosive and/or chemiluminescent.

### 14.1.6 Chemical properties of dioxygen, O<sub>2</sub>

Oxygen is an extremely reactive gas which vigorously oxidizes many elements directly, either at room temperature or above. Despite the high bond dissociation energy of O<sub>2</sub> (493.4 kJ mol<sup>-1</sup>) these reactions are frequently highly exothermic and, once initiated, can continue spontaneously (combustion) or even explosively. Familiar examples are its reactions with carbon (charcoal) and hydrogen. Some elements do not combine with oxygen *directly*, e.g. certain refractory or noble metals such as

W, Pt, Au and the noble gases, though oxo compounds of all elements are known except for He, Ne, Ar and possibly Kr. This great range of compounds was one of the reasons why Mendeleev chose oxides to exemplify his periodic law (p. 20) and why oxygen was chosen as the standard element for the atomic weight scale in the early days when atomic weights were determined mainly by chemical stoichiometry (p. 16).

Many inorganic compounds and all organic compounds also react directly with O<sub>2</sub> under appropriate conditions. Reaction may be spontaneous, or may require initiation by heat, light, electric discharge, chemisorption or various catalytic means. Oxygen is normally considered to be divalent, though the oxidation state can vary widely and includes the values of + $\frac{1}{2}$ , 0, - $\frac{1}{3}$ , - $\frac{1}{2}$ , -1 and -2 in isolable compounds of such species as O<sub>2</sub><sup>+</sup>, O<sub>3</sub>, O<sub>3</sub><sup>-</sup>, O<sub>2</sub><sup>-</sup>, O<sub>2</sub><sup>2-</sup> and O<sup>2-</sup> respectively. The coordination number of oxygen in its compounds also varies widely, as illustrated in Table 14.3 and numerous examples of stable compounds are known which exemplify each coordination number from 1 to 8 (with the possible exception of 7, for which unambiguous examples are more difficult to find). Most of these examples are straightforward and structural details will be found at appropriate points in the text. Linear 2-coordinate O occurs in the silyl ether molecule [O(SiPh<sub>3</sub>)<sub>2</sub>].<sup>(39)</sup> Planar 3-coordinate O occurs in the neutral gaseous molecular species OLi<sub>3</sub> and ONa<sub>3</sub><sup>(40)</sup> and in both cationic and anionic complexes (Fig. 14.3a, b). It also occurs in two-dimensional layer lattices such as tunellite, [OB<sub>6</sub>O<sub>8</sub>(OH)<sub>2</sub>]<sup>2n-</sup> (cf. Fig. 14.3b) and in the three-dimensional rutile structure (p. 961).

Planar 4-coordinate O occurs uniquely in NbO which can be considered as a defect-NaCl-type structure with O and Nb vacancies at (000) and ( $\frac{1}{2}$   $\frac{1}{2}$   $\frac{1}{2}$ ) respectively, thereby having only 3

<sup>39</sup> C. GLIDEWELL and D. C. LILES, *J. Chem. Soc., Chem. Commun.*, 682 (1977).

<sup>40</sup> E.-U. WÜRTHWEIN, P. VON R. SCHLEYER and J. A. POPLE, *J. Am. Chem. Soc.*, **106**, 6973-8 (1984).

Table 14.3 Coordination geometry of oxygen

CN	Geometry	Examples
0	—	Atomic O
1	—	O <sub>2</sub> , CO, CO <sub>2</sub> , NO, NO <sub>2</sub> , SO <sub>3</sub> (g), OsO <sub>4</sub> ; terminal O <sub>i</sub> in P <sub>4</sub> O <sub>10</sub> , [VO(acac) <sub>2</sub> ], and many oxoanions [MO <sub>n</sub> ] <sup>m-</sup> (M = C, N, P, As, S, Se, Cl, Br, Cr, Mn, etc.)
2	Linear	Some silicates, e.g. [O <sub>3</sub> Si-O-SiO <sub>3</sub> ] <sup>6-</sup> in Sc <sub>2</sub> Si <sub>2</sub> O <sub>7</sub> ; [Cl <sub>5</sub> Ru-O-RuCl <sub>5</sub> ] <sup>4-</sup> ; ReO <sub>3</sub> (WO <sub>3</sub> )-type structures; coesite (SiO <sub>2</sub> ); [O(SiPh <sub>3</sub> ) <sub>2</sub> ] <sup>(39)</sup>
2	Bent	O <sub>3</sub> , H <sub>2</sub> O, H <sub>2</sub> O <sub>2</sub> , F <sub>2</sub> O; silica structures, GeO <sub>2</sub> ; P <sub>4</sub> O <sub>6</sub> and many heterocyclic compounds with O <sub>μ</sub> ; complexes of ligands which have O <sub>i</sub> as donor atom, e.g. [BF <sub>3</sub> (OSMe <sub>2</sub> )], [SnCl <sub>4</sub> (OSeCl <sub>2</sub> ) <sub>2</sub> ], [(TiCl <sub>4</sub> (OPCl <sub>3</sub> ) <sub>2</sub> )], [HgCl <sub>2</sub> (OAsPh <sub>3</sub> ) <sub>2</sub> ]; complexes of O <sub>2</sub> , e.g. [Pt(O <sub>2</sub> )(PPh <sub>3</sub> ) <sub>2</sub> ]
3	Planar	OLi <sub>3</sub> , ONa <sub>3</sub> ; <sup>(40)</sup> [O(HgCl) <sub>3</sub> ] <sup>+</sup> Cl <sup>-</sup> , Mg[OB <sub>6</sub> O <sub>6</sub> (OH) <sub>6</sub> ].4½H <sub>2</sub> O (macallisterite); Sr[OB <sub>6</sub> O <sub>8</sub> (OH) <sub>2</sub> ].3H <sub>2</sub> O, (tunnellite); rutile-type structures, e.g. MO <sub>2</sub> (M = Ti; V, Nb, Ta; Cr, Mo, W; Mn, Tc, Re; Ru, Os; Rh, Ir; Pt; Ge, Sn, Pb; Te)
3	Pyramidal	[H <sub>3</sub> O] <sup>+</sup> ; hydrato-complexes, e.g. [M(H <sub>2</sub> O) <sub>6</sub> ] <sup>n+</sup> ; complexes of R <sub>2</sub> O and crown ethers; organometallic clusters such as [(η-C <sub>5</sub> H <sub>5</sub> ) <sub>5</sub> (O)V <sub>6</sub> (μ <sub>3</sub> -O) <sub>8</sub> ] <sup>(41)</sup>
4	Square planar	NbO (see text)
4	Tetrahedral	[OB <sub>e</sub> <sub>4</sub> (O <sub>2</sub> CMe) <sub>6</sub> ]; CuO, AgO, PdO; wurtzite structures, e.g. BeO, ZnO; corundum structures, e.g. M <sub>2</sub> O <sub>3</sub> (M = Al, Ga, Ti, V, Cr, Fe, Rh); fluorite structures, e.g. MO <sub>2</sub> (M = Zr, Hf; Ce, Pr, Tb; Th, U, Np, Pu, Am, Cm; Po)
4	See-saw	[Fe <sub>3</sub> Mn(CO) <sub>12</sub> (μ <sub>4</sub> -O)] <sup>-</sup> <sup>(42)</sup>
5	Square pyram.	[LCu <sub>4</sub> (OH)] <sup>3+</sup> <sup>(43)</sup> , [(InOPr <sup>i</sup> ) <sub>5</sub> (μ <sub>5</sub> -O)(μ <sub>2</sub> -OPr <sup>i</sup> ) <sub>4</sub> (μ <sub>3</sub> -OPr <sup>i</sup> ) <sub>4</sub> ] <sup>(44)</sup>
6	Octahedral	Central O in [Mo <sub>6</sub> O <sub>19</sub> ] <sup>2-</sup> ; many oxides with NaCl-type structure, e.g. MO (M = Mg, Ca, Sr, Ba; Mn, Fe, Co, Ni; Cd; Eu)
7	—	—
8	Cubic	Anti-fluorite-type structure, e.g. M <sub>2</sub> O (M = Li, Na, K, Rb)

NbO (rather than 4) per unit cell (see p. 983). Tetrahedral, 4-coordinate O is featured in "basic beryllium acetate" (p. 122) and in many binary oxides as mentioned in Table 14.3. The detailed structure depends both on the stoichiometry and on the coordination geometry of the metal, which is planar in CuO, AgO and PdO, tetrahedral in BeO and ZnO, octahedral in M<sub>2</sub>O<sub>3</sub> and cubic in MO<sub>2</sub>. Tetrahedral coordination of O also occurs in the unusual species ONa<sub>4</sub> and HONa<sub>3</sub>.<sup>(40)</sup> The less common see-saw (C<sub>2v</sub>) coordination mode occurs in the "butterfly" oxo cluster anion [Fe<sub>3</sub>Mn(CO)<sub>12</sub>(μ<sub>4</sub>-O)]<sup>-</sup>, in which the O atom bridges the [Mn(CO)<sub>3</sub>] and {Fe(CO)<sub>3</sub>} wingtips and the two [Fe(CO)<sub>3</sub>] hinge groups.<sup>(42)</sup>

Five-fold coordination of O has only recently been established, in the μ<sub>4</sub>-hydroxo bridged Cu<sub>4</sub><sup>II</sup> cluster, [Cu<sub>4</sub>(μ<sub>4</sub>-OH)(η<sup>8</sup>-L\*)], in which the central planar OCu<sub>4</sub> group is supported by a circumannular octadentate macrocyclic ligand, L\*, with the H atom of the OH group vertically above (or below) this plane.<sup>(43)</sup> Square pyramidal coordination of O also occurs in the indium *iso*-propoxide cluster [(InOPr<sup>i</sup>)<sub>5</sub>(μ<sub>5</sub>-O)(μ<sub>2</sub>-OPr<sup>i</sup>)<sub>4</sub>(μ<sub>3</sub>-OPr<sup>i</sup>)<sub>4</sub>]<sup>(44)</sup> and in some complicated [Ba<sub>5</sub>(μ<sub>5</sub>-O)] oxobarium clusters supported by μ<sub>2</sub> and μ<sub>3</sub> phenoxide of *t*-butoxide ligands.<sup>(45)</sup>

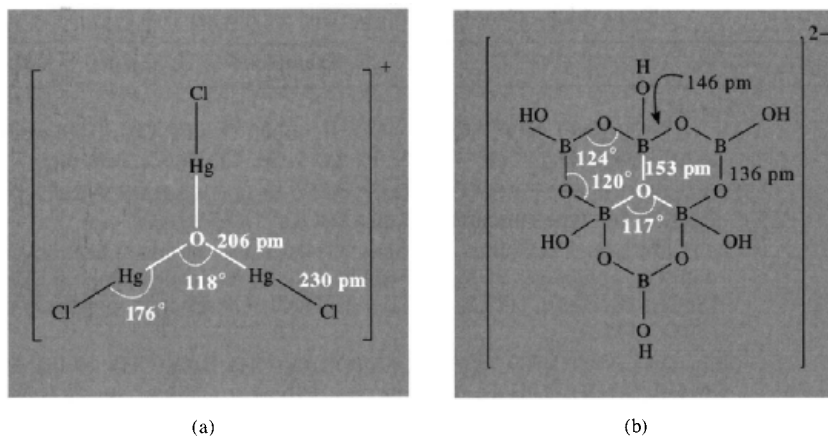
<sup>43</sup> V. MCKEE and S. S. TANDON, *J. Chem. Soc., Chem. Commun.*, 385-7 (1988). See also K. P. MCKILLOP, S. M. NELSON, J. NELSON and V. MCKEE, *ibid.*, 387-9 (1988).

<sup>44</sup> D. C. BRADLEY, H. CHUDZYNSKA, D. M. FRIGO, M. B. HURSTHOUSE and M. A. MAZID, *J. Chem. Soc., Chem. Commun.*, 1258-9 (1988).

<sup>45</sup> K. G. CAULTON, M. H. CHISHOLM, S. R. DRAKE and K. FOLTING, *J. Chem. Soc., Chem. Commun.*, 1349-51 (1990).

<sup>41</sup> F. BOTTOMLEY, D. F. DRUMMOND, D. E. PAEZ and P. S. WHITE, *J. Chem. Soc., Chem. Commun.*, 1752-3 (1986).

<sup>42</sup> C. K. SCHAUER and D. F. SHRIVER, *Angew. Chem. Int. Edn. Engl.* 26, 255-6 (1987).



**Figure 14.3** Examples of planar 3-coordinate O: (a) the cation in  $[O(HgCl)_3]Cl$ , (b) the central O atom in the discrete borate anion  $[OB_6O_6(OH)_6]^{2-}$  in macallisterite — the three heterocycles are coplanar but the 6 pendant OH groups lie out of the plane.

A recent addition to the many examples of octahedral coordination of O (Table 14.3) is the unusual volatile, hydrocarbon-soluble, crystalline oxo-alkoxide of barium  $[H_4Ba_6(\mu_6-O)(OCH_2CH_2OMe)_{14}]$ , which forms rapidly when Ba granules are reacted with  $MeOCH_2CH_2OH$  in toluene suspension.<sup>(46)</sup>

Much of the chemistry of oxygen can be rationalized in terms of its electronic structure ( $2s^2 2p^4$ ), high electronegativity (3.5) and small size. Thus, oxygen shows many similarities to nitrogen (p. 412) in its covalent chemistry, and its propensity to form H bonds (p. 52) and  $p_\pi$  double bonds (p. 416), though the anionic chemistry of  $O^{2-}$  and  $OH^-$  is much more extensive than for the isoelectronic ions  $N^{3-}$ ,  $NH^{2-}$  and  $NH_2^-$ . Similarities to fluorine and fluorides are also notable. Comparisons with the chemical properties of sulfur (p. 662) and the heavier chalcogens (p. 754) are deferred to Chapters 15 and 16.

One of the most important reactions of dioxygen is that with the protein haemoglobin which forms the basis of oxygen transport in blood (p. 1099).<sup>(47)</sup> Other coordination

complexes of  $O_2$  are discussed in the following section (p. 615).

Another particularly important aspect of the chemical reactivity of  $O_2$  concerns the photochemical reaction of singlet  $O_2$  (p. 605) with unsaturated or aromatic organic compounds.<sup>(48–51)</sup> The pioneering work was done in 1931–9 by H. Kautsky who noticed that oxygen could quench the fluorescence of certain irradiated dyes by excitation to the singlet state, and that such excited  $O_2$  molecules could oxidize compounds which did not react with oxygen in its triplet ground state. Although Kautsky gave essentially the correct explanation of his observations, his views were not accepted at the time and the work remained unnoticed by organic chemists for 25 years until the reactivity of singlet oxygen was rediscovered independently by two other groups in 1964 (p. 601). With the wisdom of hindsight it seems remarkable that Kautsky's elegant experiments

<sup>48</sup> B. RANBY and J. F. RABEK (eds.) *Singlet Oxygen: Reactions with Organic Compounds and Polymers*, Wiley, Chichester, 1978, 331 pp.

<sup>49</sup> A. A. FRIMER, *Chem. Rev.* **79**, 359–87 (1979).

<sup>50</sup> H. H. WASSERMAN and R. W. MURRAY (eds.), *Singlet Oxygen*, Academic Press, New York, 1979, 688 pp.

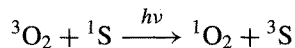
<sup>51</sup> A. A. FRIMER (ed.), *Singlet  $O_2$* , Vol. 1, 236 pp., Vol. 2, 284 pp.; Vol. 3, 269 pp.; Vol. 4, 208 pp.; CRC Press, Boca Raton, Florida, 1985.

<sup>46</sup> K. G. CAULTON, M. H. CHISHOLM, S. R. DRAKE and J. C. HUFFMAN, *J. Chem. Soc., Chem. Commun.*, 1498–9 (1990).

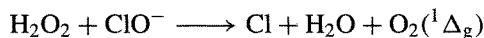
<sup>47</sup> T. G. SPIRO (ed.), *Metal Ion Activation of Dioxygen*, Wiley, New York, 1980, 247 pp.

and careful reasoning failed to convince his contemporaries.

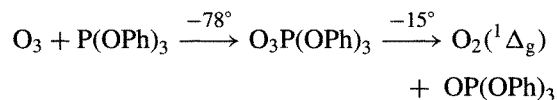
Singlet oxygen,  $^1\text{O}_2$ , can readily be generated by irradiating normal triplet oxygen,  $^3\text{O}_2$  in the presence of a sensitizer, S, which is usually a fluorescein-type dye, a polycyclic hydrocarbon or other strong absorber of light. A spin-allowed transition then occurs:



Provided that the energy gap in the sensitizer is greater than  $94.7 \text{ kJ mol}^{-1}$ , the  $^1\Delta_g$  singlet state of  $\text{O}_2$  is generated (p. 605). Above  $157.8 \text{ kJ mol}^{-1}$  some  $^1\Sigma_g^+\text{O}_2$  is also produced and this species predominates above  $200 \text{ kJ mol}^{-1}$ . The  $^1\Delta_g$  singlet state can also be conveniently generated chemically in alcoholic solution by the reaction



Another chemical route is by decomposition of solid adducts of ozone with triaryl and other phosphites at subambient temperatures:



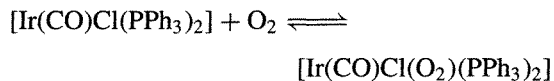
Reactions of  $^1\text{O}_2$  can be classified into three types: 1,2 addition, 1,3 addition and 1,4 addition (see refs. 48–51 for details). In addition to its great importance in synthetic organic chemistry, singlet oxygen plays an important role in autoxidation (i.e. the photodegradation of polymers in air), and methods of improving the stability of commercial polymers and vulcanized rubbers to oxidation are of considerable industrial significance. Reactions of singlet oxygen also feature in the chemistry of the upper atmosphere.

## 14.2 Compounds of Oxygen

### 14.2.1 Coordination chemistry: dioxygen as a ligand

Few discoveries in synthetic chemistry during the past three decades have caused more excitement

or had more influence on the direction of subsequent work than L. Vaska's observation in 1963 that the planar 16-electron complex *trans*- $[\text{Ir}(\text{CO})\text{Cl}(\text{PPh}_3)_2]$  can act as a reversible oxygen carrier by means of the equilibrium<sup>(52)</sup>



Not only were the structures, stabilities and range of metals that could form such complexes of theoretical interest, but there were manifest implications for an understanding of the biochemistry of the oxygen-carrying metalloproteins haemoglobin, myoglobin, haemerythrin and haemocyanin. Such complexes were also seen as potential keys to an understanding of the interactions occurring during homogeneous catalytic oxidations, heterogeneous catalysis and the action of metalloenzymes. Several excellent reviews are available.<sup>(47,53–64)</sup>

Dioxygen–metal complexes in which there is a 1:1 stoichiometry of  $\text{O}_2:\text{M}$  are of two main types, usually designated Ia (or superoxo) and IIa (or

<sup>52</sup> L. VASKA, *Science* **140**, 809–10 (1963).

<sup>53</sup> J. A. CONNOR and E. A. V. EBSWORTH, *Adv. Inorg. Chem. Radiochem.* **6**, 279–381 (1964).

<sup>54</sup> V. J. CHOY and C. J. O'CONNOR, *Coord. Chem. Rev.* **9**, 145–70 (1972/3).

<sup>55</sup> J. S. VALENTINE, *Chem. Revs.* **73**, 235–45 (1973).

<sup>56</sup> M. J. NOLTE, E. SINGLETON and M. LAING, *J. Am. Chem. Soc.* **97**, 6396–400 (1975). An important paper showing how errors can arise even in careful single crystal X-ray studies, leading to incorrect inferences.

<sup>57</sup> R. W. ERSKINE and B. O. FIELD, Reversible oxygenation, *Struct. Bond.* **28**, 1–50 (1976).

<sup>58</sup> J. P. COLLMAN, *Acc. Chem. Res.* **10**, 265–72 (1977).

<sup>59</sup> A. B. P. LEVER and H. B. GRAY, *Acc. Chem. Res.* **11**, 348–55 (1978).

<sup>60</sup> R. D. JONES, D. A. SUMMERVILLE and F. BASOLO, *Chem. Revs.* **79**, 139–79 (1979).

<sup>61</sup> A. B. P. LEVER, G. A. OZIN and H. B. GRAY, *Inorg. Chem.* **19**, 1823–4 (1980).

<sup>62</sup> T. G. SPIRO (ed.), *Metal Ion Activation of Dioxygen*, Wiley-Interscience, New York, 1980, 247 pp.

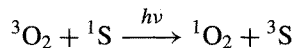
<sup>63</sup> A. E. MARTELL and D. T. SAWYER (eds.), *Oxygen Complexes and Oxygen Activation by Transition Metals*, Plenum, New York, 1988, 341 pp.

<sup>64</sup> T. VÄNNGÅRD (ed.), *Biophysical Chemistry of Dioxygen Reactions in Respiration and Photosynthesis*, Cambridge Univ. Press, New York, 1988, 131 pp.

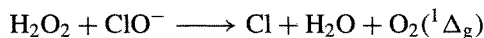


and careful reasoning failed to convince his contemporaries.

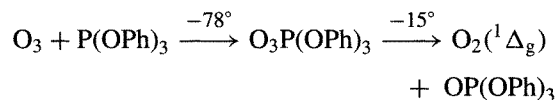
Singlet oxygen,  $^1\text{O}_2$ , can readily be generated by irradiating normal triplet oxygen,  $^3\text{O}_2$  in the presence of a sensitizer, S, which is usually a fluorescein-type dye, a polycyclic hydrocarbon or other strong absorber of light. A spin-allowed transition then occurs:



Provided that the energy gap in the sensitizer is greater than  $94.7 \text{ kJ mol}^{-1}$ , the  $^1\Delta_g$  singlet state of  $\text{O}_2$  is generated (p. 605). Above  $157.8 \text{ kJ mol}^{-1}$  some  $^1\Sigma_g^+\text{O}_2$  is also produced and this species predominates above  $200 \text{ kJ mol}^{-1}$ . The  $^1\Delta_g$  singlet state can also be conveniently generated chemically in alcoholic solution by the reaction



Another chemical route is by decomposition of solid adducts of ozone with triaryl and other phosphites at subambient temperatures:



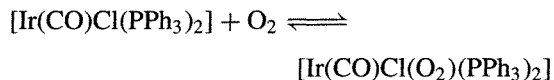
Reactions of  $^1\text{O}_2$  can be classified into three types: 1,2 addition, 1,3 addition and 1,4 addition (see refs. 48–51 for details). In addition to its great importance in synthetic organic chemistry, singlet oxygen plays an important role in autoxidation (i.e. the photodegradation of polymers in air), and methods of improving the stability of commercial polymers and vulcanized rubbers to oxidation are of considerable industrial significance. Reactions of singlet oxygen also feature in the chemistry of the upper atmosphere.

## 14.2 Compounds of Oxygen

### 14.2.1 Coordination chemistry: dioxygen as a ligand

Few discoveries in synthetic chemistry during the past three decades have caused more excitement

or had more influence on the direction of subsequent work than L. Vaska's observation in 1963 that the planar 16-electron complex *trans*- $[\text{Ir}(\text{CO})\text{Cl}(\text{PPh}_3)_2]$  can act as a reversible oxygen carrier by means of the equilibrium<sup>(52)</sup>



Not only were the structures, stabilities and range of metals that could form such complexes of theoretical interest, but there were manifest implications for an understanding of the biochemistry of the oxygen-carrying metalloproteins haemoglobin, myoglobin, haemerythrin and haemocyanin. Such complexes were also seen as potential keys to an understanding of the interactions occurring during homogeneous catalytic oxidations, heterogeneous catalysis and the action of metalloenzymes. Several excellent reviews are available.<sup>(47,53–64)</sup>

Dioxygen–metal complexes in which there is a 1:1 stoichiometry of  $\text{O}_2:\text{M}$  are of two main types, usually designated Ia (or superoxo) and IIa (or

<sup>52</sup> L. VASKA, *Science* **140**, 809–10 (1963).

<sup>53</sup> J. A. CONNOR and E. A. V. EBSWORTH, *Adv. Inorg. Chem. Radiochem.* **6**, 279–381 (1964).

<sup>54</sup> V. J. CHOY and C. J. O'CONNOR, *Coord. Chem. Rev.* **9**, 145–70 (1972/3).

<sup>55</sup> J. S. VALENTINE, *Chem. Revs.* **73**, 235–45 (1973).

<sup>56</sup> M. J. NOLTE, E. SINGLETON and M. LAING, *J. Am. Chem. Soc.* **97**, 6396–400 (1975). An important paper showing how errors can arise even in careful single crystal X-ray studies, leading to incorrect inferences.

<sup>57</sup> R. W. ERSKINE and B. O. FIELD, Reversible oxygenation, *Struct. Bond.* **28**, 1–50 (1976).

<sup>58</sup> J. P. COLLMAN, *Acc. Chem. Res.* **10**, 265–72 (1977).

<sup>59</sup> A. B. P. LEVER and H. B. GRAY, *Acc. Chem. Res.* **11**, 348–55 (1978).

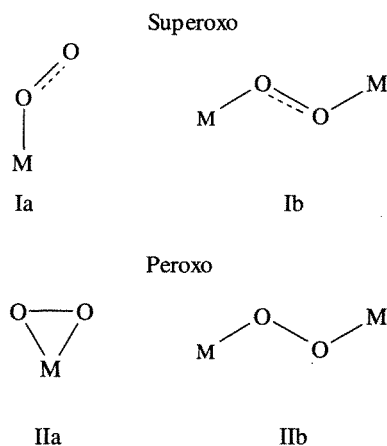
<sup>60</sup> R. D. JONES, D. A. SUMMERVILLE and F. BASOLO, *Chem. Revs.* **79**, 139–79 (1979).

<sup>61</sup> A. B. P. LEVER, G. A. OZIN and H. B. GRAY, *Inorg. Chem.* **19**, 1823–4 (1980).

<sup>62</sup> T. G. SPIRO (ed.), *Metal Ion Activation of Dioxygen*, Wiley-Interscience, New York, 1980, 247 pp.

<sup>63</sup> A. E. MARTELL and D. T. SAWYER (eds.), *Oxygen Complexes and Oxygen Activation by Transition Metals*, Plenum, New York, 1988, 341 pp.

<sup>64</sup> T. VÄNNGÅRD (ed.), *Biophysical Chemistry of Dioxygen Reactions in Respiration and Photosynthesis*, Cambridge Univ. Press, New York, 1988, 131 pp.



**Figure 14.4** The four main types of  $O_2$ -M geometry. The bridging modes Ib and IIb appear superficially similar but differ markedly in dihedral angles and other bonding properties. See also footnote to Table 14.5 for the recently established unique  $\mu, \eta^1$ -superoxide bridging mode.

peroxo) for reasons which will shortly become apparent (Fig. 14.4). Dioxygen can also form 1:2 complexes in which  $O_2$  adopts a bidentate bridging geometry, labelled Ib and IIb in Fig. 14.4. Of these four classes of complex, the Vaska-type IIa peroxo complexes, are by far the most widespread amongst the transition metals, though many are not reversible oxygen carriers and some are formed by deprotonation of  $H_2O_2$  (p. 636) rather than coordination of molecular  $O_2$ . By contrast, the bridging superoxo type Ib is known only for the green cobalt complexes formed by 1-electron oxidation of the corresponding IIb peroxo compounds. In all cases complex formation

is accompanied by a significant increase in the O-O interatomic distances and a considerable decrease in the  $\nu(O-O)$  vibrational stretching frequency. Both effects are more marked for the peroxo (type II) complexes than for the superoxo (type I) complexes and have been interpreted in terms of a transfer of electrons from M into the antibonding orbitals of  $O_2$  (p. 606) thereby weakening the O-O bond. The magnitude of the effects to be expected can be gauged from Table 14.4.<sup>(60)</sup> Note that the O-O bond in  $O_2^+$  is stronger than in  $O_2$  but this does not mean that  $O_2^+$  is more stable than  $O_2$  since energy must be supplied to remove an electron from  $O_2$  and this energy is greater than that released in forming the stronger bond: it is important not to confuse bond energy with stability. Comparative data for a wide range of dioxygen-metal complexes is in Table 14.5.<sup>(60,65)</sup> It will be noted also that the O-O distances and vibrational frequencies are rather insensitive to the nature of the metal or its other attached ligands, or, indeed, as to whether the  $O_2$  is coordinated to 1 or 2 metal centres. Both classes of superoxo complex, however, have  $d(O-O)$  and  $\nu(O-O)$  close to the values for the superoxide ion, whereas both classes of peroxo complex have values close to those for the peroxide ion. (However, see footnote to Table 14.5 for an important caveat to this generalization.)

Superoxo complexes having a nonlinear M-O-O configuration are known at present only for Fe, Co, Rh and perhaps a few other transition metals, whereas the Vaska-type (IIa) complexes are known for almost all the transition metals

<sup>65</sup> L. VASKA, *Acc. Chem. Res.* **9**, 175-83 (1976).

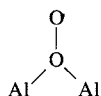
**Table 14.4** Effect of electron configuration and charge on the bond properties of dioxygen species

Species	Bond order	Compound	$d(O-O)/pm$	Bond energy/ kJ mol <sup>-1</sup>	$\nu(O-O)/cm^{-1}$
$O_2^+$	2.5	$O_2[AsF_6]$	112.3	625.1	1858
$O_2(^3\Sigma_g^-)$	2	$O_2(g)$	120.7	490.4	1554.7
$O_2(^1\Delta_g)$	2	$O_2(g)$	121.6	396.2	1483.5
$O_2^-(superoxide)$	1.5	$K[O_2]$	128	—	1145
$O_2^{2-}(peroxide)$	1	$Na_2[O_2]$	149	204.2	842
-OO-	1	$H_2O_2$ (cryst)	145.3	213	882

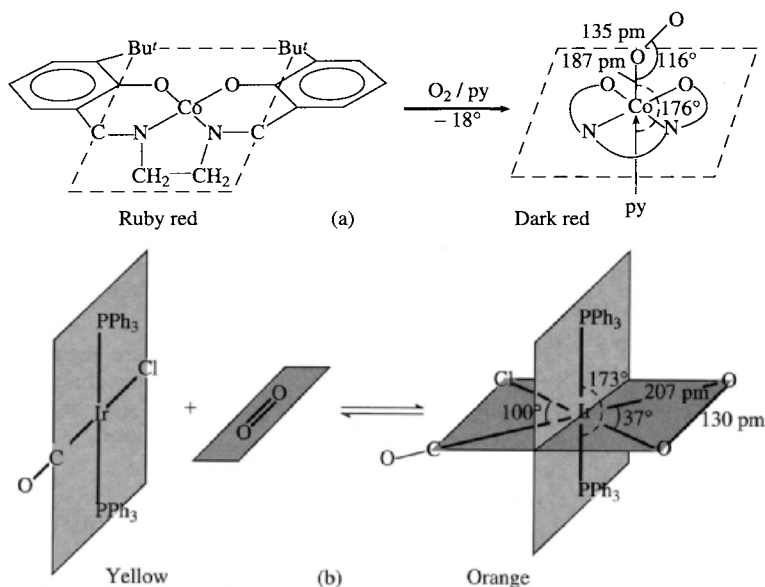
Table 14.5 Summary of properties of known dioxygen-metal complexes<sup>(a)</sup>

Complex type	O <sub>2</sub> :M ratio	Structure	<i>d</i> (O–O)/pm (normal range)	$\nu$ (O–O)/cm <sup>-1</sup> (normal range)
superoxo Ia	1:1		125–135	1130–1195
superoxo Ib	1:2		126–136	1075–1122
peroxo IIa	1:1		130–155	800–932
peroxo IIb	1:1		144–149	790–884

<sup>(a)</sup> Reaction of K<sub>2</sub>O with Al<sub>2</sub>Me<sub>6</sub> in the presence of dibenzo-18-crown-6 (p. 96) yields the surprisingly stable anion [( $\mu,\eta^1$ -O<sub>2</sub>)(AlMe<sub>3</sub>)<sub>2</sub>]<sup>-</sup> in which one O of the superoxo ion bridges the 2 Al atoms (angle Al–O–Al 128°):



In this new type of coordination mode *d*(O–O) is long (147 pm) and the weakness of the O–O linkage is also shown by the very low value of 851 cm<sup>-1</sup> for  $\nu$ (O–O), both values being more characteristic of peroxo than of superoxo complexes.<sup>(66)</sup>

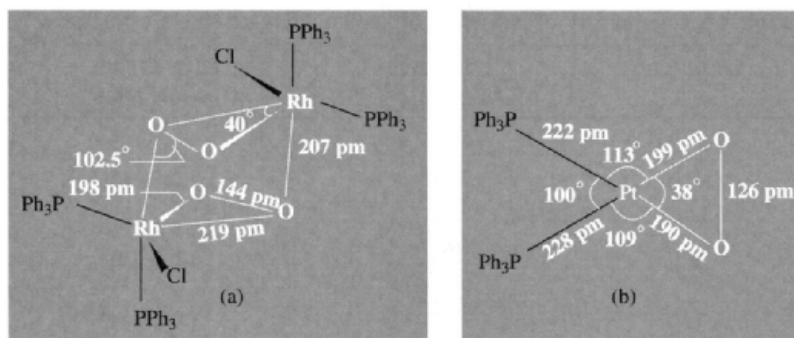


**Figure 14.5** (a) Reaction of *N,N'*-ethylenebis(3-Bu<sup>t</sup>-salicylideneiminato)cobalt(II) with dioxygen and pyridine to form the superoxo complex [Co(3-Bu<sup>t</sup>Salen)<sub>2</sub>(O<sub>2</sub>)py]; the py ligand is almost coplanar with the Co–O–O plane, the angle between the two being 18°.<sup>(67)</sup> (b) Reversible formation of the peroxo complex [Ir(CO)Cl(O<sub>2</sub>)(PPh<sub>3</sub>)<sub>2</sub>]. The more densely shaded part of the complex is accurately coplanar.<sup>(68)</sup>

<sup>66</sup>D. C. HRNCIR, R. D. ROGERS and J. L. ATWOOD, *J. Am. Chem. Soc.* **103**, 4277–8 (1981). see also P. FANTUCCI and G. PACCHIONI, *J. Chem. Soc., Dalton Trans.*, 355–60 (1987).

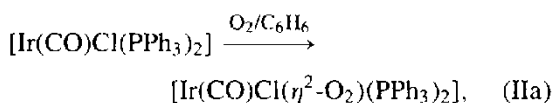
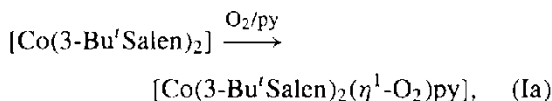
<sup>67</sup>W. P. SCHAEFFER, B. T. HUIE, M. G. KURILLA and S. E. EALICK, *Inorg. Chem.* **19**, 340–4 (1980).

<sup>68</sup>S. J. LAPLACA and J. A. IBERS, *J. Am. Chem. Soc.* **87**, 2581–6 (1965).

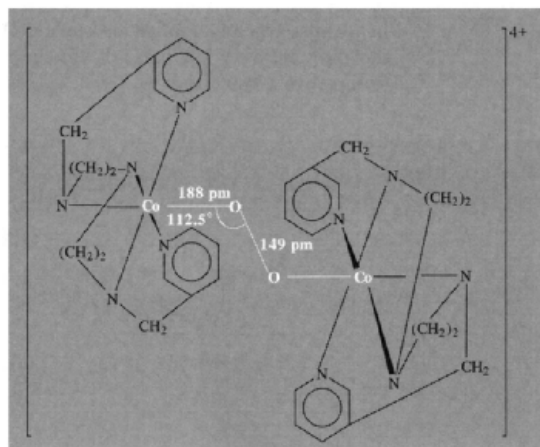


**Figure 14.6** Structure and key dimensions of (a) the complex  $[(\text{Ph}_3\text{P})_2\text{RhCl}(\mu\text{-O}_2)]_2$  and (b) the complex  $[\text{Pt}(\text{O}_2)(\text{PPh}_3)_2]$ . The data in (b) are of poor quality because of the difficulty of growing suitable crystals and their instability in the X-ray beam (distances  $\pm 5$  pm angles  $\pm 2^\circ$ ).

except those in the Sc and Zn groups and possibly Mn, Cr and Fe. The two modes of formation are illustrated in Fig. 14.5 for the two reactions:



The sensitivity of the reaction type to the detailed nature of the bonding in the metal complex can be gauged from the fact that neither the  $\text{PMe}_3$  analogue of Vaska's iridium complex, nor the corresponding rhodium complex  $[\text{Rh}(\text{CO})\text{Cl}(\text{PPh}_3)_2]$  react with dioxygen in this way. By contrast, the closely related red complex  $[\text{RhCl}(\text{PPh}_3)_3]$  reacts readily with  $\text{O}_2$  in  $\text{CH}_2\text{Cl}_2$  solution with elimination of  $\text{PPh}_3$  to give the brown dinuclear doubly bridging complex  $[(\text{Ph}_3\text{P})_2\text{RhCl}(\mu\text{-O}_2)]_2 \cdot \text{CH}_2\text{Cl}_2$  the structure of which is shown in Fig. 14.6a.<sup>(69)</sup> With  $[\text{Pt}(\text{PPh}_3)_4]$  reaction also occurs with elimination of  $\text{PPh}_3$  but the product is the yellow, planar, mononuclear complex  $[\text{Pt}(\eta^2\text{-O}_2)(\text{PPh}_3)_2]$  (Fig. 14.6b).<sup>(70)</sup>



**Figure 14.7** Schematic representation of the structure of the dinuclear cation in  $[\{\text{Co}(\text{pydien})_2\}_2\text{O}_2]^{4+}$  showing some important dimensions.

An example of a singly-bridging peroxo complex is the dinuclear cation  $[\{\text{Co}(\text{pydien})_2\}_2\text{O}_2]^{4+}$  where pydien is the pentadentate ligand 1,9-bis(2-pyridyl)-2,5,8-triazanonane,  $\text{NC}_5\text{H}_4\text{-CH}_2\text{N}(\text{CH}_2\text{CH}_2\text{N})_2\text{CH}_2\text{C}_5\text{H}_4\text{N}$ . The complex is readily formed by mixing ethanolic solutions of  $\text{CoCl}_2 \cdot 6\text{H}_2\text{O}$ ,  $\text{NaI}$  and the ligand, and then exposing the resulting solution to oxygen.<sup>(71)</sup> Some structural details are in Fig. 14.7. Such

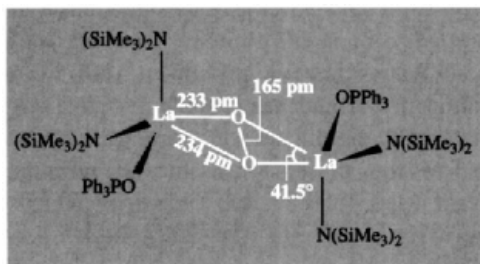
<sup>69</sup> M. J. BENNETT and P. B. DONALDSON, *J. Am. Chem. Soc.* **93**, 3307-8 (1971).

<sup>70</sup> C. D. COOK, P.-T. CHENG and S. C. NYBURG, *J. Am. Chem. Soc.* **91**, 2123 (1969).

<sup>71</sup> J. H. TIMMONS, R. H. NISWANDER, A. CLEARFIELD and A. E. MARTELL, *Inorg. Chem.* **18**, 2977-82 (1979).

$\mu$ -O<sub>2</sub> complexes are formed generally among the "Group VIII" metals (Fe), Ru, Os; Co, Rh, Ir; Ni, Pd, Pt. A unique example from main-group element chemistry is in the doubly-bridged R<sub>2</sub>Sn( $\mu$ -O)( $\mu$ : $\eta^1, \eta^1$ -O<sub>2</sub>)SnR<sub>2</sub>, (R = CH(SiMe<sub>3</sub>)<sub>2</sub>), in which O–O is 154 pm, Sn–O<sub>2</sub> 201 pm, angle Sn–O–O 103.3°; Sn–O 198 pm angle Sn–O–Sn 110.3°.<sup>(72)</sup>

Many mono- and di-nuclear peroxo-type dioxygen complexes can also be made by an alternative route involving direct reaction of transition metal compounds with H<sub>2</sub>O<sub>2</sub> and it is, in fact, quite arbitrary to distinguish these complexes from those made directly from O<sub>2</sub>. Many such compounds are discussed further on p. 637 and under the chemistry of individual transition metals, but one example calls for special mention since it was the first structurally characterized peroxo derivative to feature a symmetrical, doubly bidentate (side on) bridge linking two metal centres.<sup>(73)</sup> The local coordination geometry and dimensions of the central planar {LaO<sub>2</sub>La} group are shown in Fig. 14.8; the very long O–O distance is particularly notable, being substantially longer than in the O<sub>2</sub><sup>2-</sup> ion itself (p. 616). The compound [La{N(SiMe<sub>3</sub>)<sub>2</sub>}<sub>2</sub>(OPPh<sub>3</sub>)<sub>2</sub>O<sub>2</sub>, which is colourless, was made by treating [La{N(SiMe<sub>3</sub>)<sub>2</sub>}<sub>3</sub>]



**Figure 14.8** Schematic representation of the planar central portion of the  $\mu$ -peroxo complex [La{N(SiMe<sub>3</sub>)<sub>2</sub>}<sub>2</sub>(OPPh<sub>3</sub>)<sub>2</sub>O<sub>2</sub>.

with Ph<sub>3</sub>PO, but the origin of the peroxo group remains obscure. Similar complexes of Pr (which is also, surprisingly, colourless), Sm (pale yellow), Eu (orange-red) and Lu (colourless), were obtained in good yield either by a similar reaction or by treating [Ln{N(SiMe<sub>3</sub>)<sub>2</sub>}<sub>3</sub>] with a half-molar proportion of (Ph<sub>3</sub>PO)<sub>2</sub>·H<sub>2</sub>O<sub>2</sub>.

The nature of the metal–oxygen bonding in the various types of dioxygen complex has been the subject of much discussion.<sup>(56,58,59,60,65,74)</sup> The electronic structure of the O<sub>2</sub> molecule (p. 606) makes it unlikely that coordination would be by the usual donation of an "onium" lone-pair (from O<sub>2</sub> to the metal centre) which forms an important component of most other donor–acceptor adducts (p. 198). Most discussion has centred on the extent of electron transfer from the metal into the partly occupied antibonding orbitals of O<sub>2</sub>. There now seems general agreement that there is substantial transfer of electron density from the metal d<sub>z<sup>2</sup></sub> orbital into the  $\pi^*$  antibonding orbitals of O<sub>2</sub> with concomitant increase in the formal oxidation state of the metal, e.g. {Co<sup>II</sup>} + O<sub>2</sub> → {Co<sup>III</sup>(O<sub>2</sub><sup>-</sup>)}. Whether the resulting bonding between dioxygen and the metal atom is predominantly ionic or partly covalent may well depend to some extent on the nature of the metal centre and is largely a semantic problem which gradually disappears the more precisely one can define the detailed MOs or the actual electron distribution,<sup>(75)</sup> cf. the discussion on p. 79.

A dramatic discovery in this area was made in 1996 when a dicopper–dioxygen adduct was found to have two isomeric forms which featured either a side-on bridging unit {Cu( $\mu$ : $\eta^2, \eta^2$ -O<sub>2</sub>)-Cu}<sup>2+</sup> or a cyclic {Cu( $\mu$ -O)<sub>2</sub>Cu}<sup>2+</sup> core depending on whether it was crystallized from CH<sub>2</sub>Cl<sub>2</sub> or thf, respectively. The two forms could be readily interconverted by reversible O–O bond cleavage and reformation, the O–O distance being ~141 pm and 229 pm in the two isomers.<sup>(75a)</sup> The

<sup>72</sup> C. J. CARDIN, D. J. CARDIN, M. M. DEVEREUX and MAIRE A. CONVERY, *J. Chem. Soc., Chem. Commun.*, 1461–2 (1990).

<sup>73</sup> D. C. BRADLEY, J. S. GHOTRA, F. A. HART, M. B. HURSTHOUSE and P. R. RAITHBY, *J. Chem. Soc., Dalton Trans.*, 1166–72 (1977).

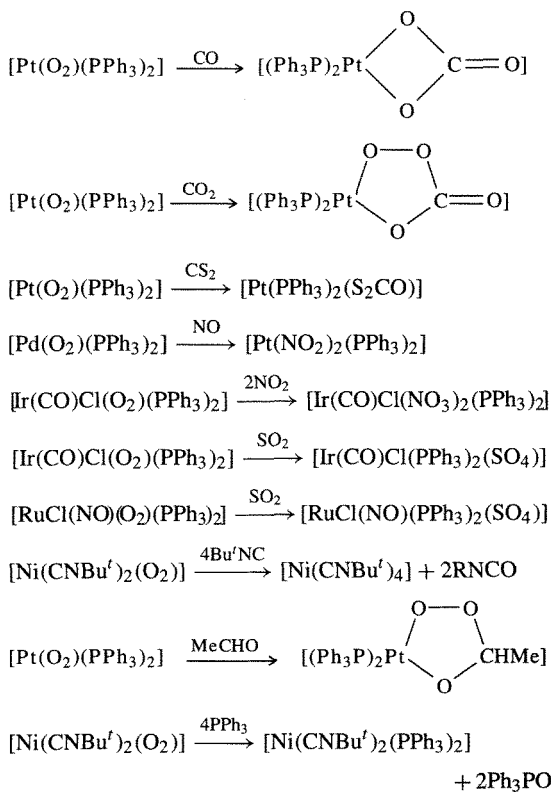
<sup>74</sup> R. S. DRAGO, T. BEUGELSDIJK, J. A. BREESE and J. P. CANNADY *J. Am. Chem. Soc.* **100**, 5374–82 (1978).

<sup>75</sup> S. SAKAKI, K. HORI and A. OHYOSHI, *Inorg. Chem.* **17**, 3183–8 (1978).

<sup>75a</sup> W. B. TOLMAN and 7 others, *Science* **271**, 1397–400 (1996).

biochemical implications for reductive cleavage of O<sub>2</sub> by metalloenzymes and for O<sub>2</sub> evolution during photosynthesis are particularly exciting.

In addition to their great importance for structural and bonding studies, dioxygen complexes undergo many reactions. As already indicated, some of these reactions are of unique importance in biological chemistry<sup>(76)</sup> and in catalytic systems. Some of the simpler inorganic reactions can be summarized as follows: aqueous acids yield H<sub>2</sub>O<sub>2</sub> and reducing agents give coordinatively unsaturated complexes. Frequently the dioxygen complex can oxidize species that do not readily react directly with free molecular O<sub>2</sub>, e.g. CO, CO<sub>2</sub>, CS<sub>2</sub>, NO, NO<sub>2</sub>, SO<sub>2</sub>, RNC, RCHO, R<sub>2</sub>CO, PPh<sub>3</sub>, etc. Illustrative examples of these reactions are:



<sup>76</sup> E.-I. OCHIAI, *J. Inorg. Nucl. Chem.* **37**, 1503-9 (1975). See also *Oxygen and Life: Second BOC Priestley Conference*, Roy. Soc. Chem. Special Publ. No. 39, London, 1981, 224 pp.

Explanations that have been advanced to explain the enhanced reactivity of coordinated dioxygen include:

- (1) The diamagnetic nature of most O<sub>2</sub> complexes might facilitate reactions to form diamagnetic products which would otherwise be hindered by the requirement of spin conservation;
- (2) the metal may hold O<sub>2</sub> and the reactant in *cis* positions thereby lowering the activation energy for oxidation, particularly with coordinatively unsaturated complexes;
- (3) coordinated O<sub>2</sub> is usually partially reduced (towards O<sub>2</sub><sup>-</sup> or O<sub>2</sub><sup>2-</sup>) and this increased electron density might activate it.

Detailed kinetic and mechanistic studies will be required to assess the relative importance of these and other possible factors in specific instances.

## 14.2.2 Water

### Introduction

Water is without doubt the most abundant, the most accessible and the most studied of all chemical compounds. Its omnipresence, its crucial importance for man's survival and its ability to transform so readily from the liquid to the solid and gaseous states has ensured its prominence in man's thinking from the earliest times. Water plays a prominent role in most creation myths and has a symbolic purifying or regenerating significance in many great religions even to the present day. In the religion of ancient Mesopotamia, the oldest of which we have written records (*ca.* 2000 BC), Nammu, goddess of the primeval sea, was "the mother who gave birth to heaven and earth"; she was also the mother of the god of water, Enki, one of the four main gods controlling the major realms of the universe. In the Judaic-Christian tradition<sup>(77)</sup> "the Spirit of God moved upon the face of the waters" and creation proceeded via "a firmament in the midst of the waters" to divide heaven from

<sup>77</sup> Holy Bible, Genesis, Chap. 1, verses 1-10.

earth. Again, the Flood figures prominently<sup>(78)</sup> as it does in the legends of many other peoples. The activities of John the Baptist<sup>(79)</sup> and the obligatory washing practised by Muslims before prayers are further manifestations of the deep ritual significance of water.

Secular philosophers also perceived the unique nature of water. Thus, Thales of Miletus, who is generally regarded as the initiator of the Greek classical tradition of philosophy, ca. 585 BC, considered water to be the sole fundamental principle in nature. His celebrated dictum maintains: "It is water that, in taking different forms, constitutes the earth, atmosphere, sky, mountains, gods and men, beasts and birds, grass and trees, and animals down to worms, flies and ants. All these are but different forms of water. Meditate on water!" Though this may sound quaint or even perverse to modern ears, we should reflect that some marine invertebrates are, indeed, 96–97% water, and the human embryo during its first month is 93% water by weight. Aristotle considered water to be one of the four elements, alongside earth, air and fire, and this belief in the fundamental and elementary nature of water persisted until the epoch-making experiments of H. Cavendish and others in the second half of the eighteenth century (pp. 32, 601) showed water to be a compound of hydrogen and oxygen.<sup>(80)</sup>

### Distribution and availability

Water is distributed very unevenly and with very variable purity over the surface of the earth (Table 14.6). Desert regions have little rainfall and no permanent surface waters, whereas oceans, containing many dissolved salts, cover vast tracts of the globe; they comprise 97% of the available water and cover an area of  $3.61 \times 10^8 \text{ km}^2$  (i.e. 70.8% of the surface of the

**Table 14.6** Estimated world water supply

Source	Volume/ $10^3 \text{ km}^3$	% of total
Salt water		
Oceans	1 348 000	97.33
Saline lakes and inland seas	105 <sup>(a)</sup>	0.008
Fresh water		
Polar ice and glaciers	28 200	2.04
Ground water	8 450	0.61
Lakes	125 <sup>(b)</sup>	0.009
Soil moisture	69	0.005
Atmospheric water vapour	13.5	0.001
Rivers	1.5	0.0001
Total	1 385 000	100.0

(a) The Caspian Sea accounts for 75% of this.

(b) More than half of this is in the four largest lakes: Baikal 26 000; Tanganyika 20 000; Nyassa 13 000; and Superior 12 000  $\text{km}^3$ .

earth). Less than 2.7% of the total surface water is fresh and most of this is locked up in the Antarctic ice cap and to a much lesser extent the Arctic. The Antarctic ice cap covers some  $1.5 \times 10^7 \text{ km}^2$ , i.e. larger than Continental Europe to the Urals ( $1.01 \times 10^7 \text{ km}^2$ ), the USA including Alaska and Hawaii ( $0.94 \times 10^7 \text{ km}^2$ ), or Australia ( $0.77 \times 10^7 \text{ km}^2$ ); it comprises some  $2.5\text{--}2.9 \times 10^7 \text{ km}^3$  of fresh water which, if melted, would supply all the rivers of the earth for more than 800 years. Every year some 5000 icebergs, totalling  $10^{12} \text{ m}^3$  of ice (i.e.  $10^{12}$  tonnes), are calved from the glaciers and ice shelves of Antarctica. Each iceberg consists (on average) of  $\sim 200$  Mtonnes of pure fresh water and, if towed at  $1\text{--}2 \text{ km h}^{-1}$ , could arrive 30% intact in Australia to provide water at one-tenth of the cost of current desalination procedures.<sup>(81)</sup> Transportation of crushed ice by ship from the polar regions is an alternative that was used intermittently towards the end of the last century.

Surface freshwater lakes contain  $1.25 \times 10^5 \text{ km}^3$  of water, more than half of which

<sup>78</sup> Holy Bible, Genesis, Chaps. 6–8.

<sup>79</sup> Holy Bible, Gospels according to St. Matthew, Chap. 3; St. Mark, Chap. 1; St. Luke, Chap. 3, St. John, Chap. 1.

<sup>80</sup> J. W. MELLOR, *A Comprehensive Treatise on Inorganic and Theoretical Chemistry*, Vol. 1, Chap. 3. pp. 122–46, Longmans Green, London, 1922.

<sup>81</sup> F. FRANKS, *Introduction — Water, the Unique Chemical*, Vol. 1, Chap. 1, of F. FRANKS (ed.), *Water, a Comprehensive Treatise in 7 Volumes*, Plenum Press, New York, 1972–82. Continued as F. FRANKS (ed.) *Water Science Reviews* published by Cambridge University Press: Vol. 1, 1985 etc.

is in the four largest lakes. Though these huge lacustrine sources dwarf the innumerable smaller lakes, springs and rivers of the earth, human habitation depends more on these widely distributed smaller sources which, in total, still far exceed the needs of man and the animal and plant kingdoms. Despite this, severe local problems can arise due to prolonged drought, the pollution of surface waters, or the extension of settlements into more arid regions. Indeed, droughts have been endemic since ancient times, and even pollution of local sources has been a cause of concern and the subject of legislation since at least 1847 (UK). Fortunately, it now appears that the quality of water supplies and amenities is rising steadily in most communities since the nadir of some 40 years ago, and public concern is now increasingly ensuring that funds are available on an appropriate scale to deal with the massive problems of water pollution.<sup>(82-85)</sup> (See also p. 478.)

Water purification and recycling is now a major industry.<sup>(86)</sup> The method of treatment depends on the source of the water, the use envisaged and the volume required. Luckily the human body is very tolerant to changes in the composition of drinking water, and in many communities this may contain  $0.5 \text{ g l}^{-1}$  or more of dissolved solids (Table 14.7). Prior treatment may consist of coagulation (by addition of alum or chlorinated  $\text{FeSO}_4$  to produce flocs of  $\text{Al}(\text{OH})_3$  or  $\text{Fe}(\text{OH})_3$ ), filtration, softening (removal of

**Table 14.7** World Health Organization standards for drinking water

Material	Maximum desirable conc/mg $\text{l}^{-1}$	Maximum permissible conc/mg $\text{l}^{-1}$
Total dissolved solids	500	1500
Mg	30	150
Ca	75	200
Chlorides	20	60
Sulfates	200	400

$\text{Mg}^{\text{II}}$  and  $\text{Ca}^{\text{II}}$  by ion exchange) and disinfection (by chlorination, p. 793, or addition of ozone, p. 611). In most developed countries industrial needs for water are at least 10 times the volume used domestically. Moreover, some industrial processes require much purer water than that for human consumption, and for high-pressure boiler feedwater in particular the purity standard is 99.999 998%, i.e. no more than 0.02 ppm impurities. This is far purer than for reactor grade uranium, the finest refined gold or the best analytical reagents, and is probably exceeded only by semiconductor grade germanium and silicon. In contrast to Ge and Si, however, water is processed on a megatonne-per-day scale at a cost of only about £1 per tonne.

The beneficiation of sea water and other saline sources to produce fresh water is also of increasing importance. Normal freshwater supplies from precipitation cannot meet the needs of the increasing world population, particularly in the semi-arid regions of the world, and desalination is being used increasingly to augment normal water supplies, or even to provide all the fresh water in some places such as the arid parts of the Arabian Peninsula. The most commonly used methods are distillation (e.g. multistage flash distillation processes) and ion-exchange techniques, including electro dialysis and reverse osmosis (hyperfiltration). The enormous importance of the field can be gauged from the fact that Gmelin's volume on *Water Desalting*,<sup>(87)</sup> which reviewed 14 000 papers published up to 1973/4, has already

<sup>82</sup> H. B. N. HYNES, *The Biology of Polluted Waters*, Liverpool Univ. Press, 4th impression 1973, 202 pp.

<sup>83</sup> A. D. MCKNIGHT, P. K. MARSTRAND and T. C. SINCLAIR (eds.), *Environmental Pollution Control*, Chap. 5: Pollution of inland waters; Chap. 6: The Law relating to pollution of inland waters; George, Allen and Unwin, London, 1974.

<sup>84</sup> C. E. WARREN, *Biology and Water Pollution Control*, Saunders, Philadelphia, 1971, 434 pp.

<sup>85</sup> B. COMMONER, The killing of a great lake, in *The 1968 World Book Year Book*, Field Enterprises Educ. Corp., 1968; Lake Erie water, Chap. 5 in *The Closing Circle*, London, Jonathan Cape, 1972. See also A. NISBETT *New Scientist*, 23 March 1972, pp. 650-2, who argues that B. Commoner's views are unfounded: Lake Erie is not dead but it is damaged.

<sup>86</sup> T. V. ARDEN, in R. THOMPSON (ed.), *The Modern Inorganic Chemicals Industry*, pp. 69-105, Chemical Society Special Publication, No. 31, 1977.

<sup>87</sup> *Gmelin Handbook of Inorganic Chemistry*, 8th edn. (in English), O: *Water Desalting*, 1974, 339 pp.



**Table 14.8** Some physical properties of H<sub>2</sub>O, D<sub>2</sub>O and T<sub>2</sub>O (at 25°C unless otherwise stated)<sup>(a)</sup>

Property	H <sub>2</sub> O	D <sub>2</sub> O	T <sub>2</sub> O
Molecular weight	18.0151	20.0276	22.0315
MP/°C	0.00	3.81	4.48
BP/°C	100.00	101.42	101.51
Temperature of maximum density/°C	3.98	11.23	13.4
Maximum density/g cm <sup>-3</sup>	1.0000	1.1059	1.2150
Density(25°)/g cm <sup>-3</sup>	0.997 01	1.1044	1.2138
Vapour pressure/mmHg	23.75	20.51	~19.8
Viscosity/centipoise	0.8903	1.107	—
Dielectric constant $\epsilon$	78.39	78.06	—
Electrical conductivity(20°C)/ohm <sup>-1</sup> cm <sup>-1</sup>	$5.7 \times 10^{-8}$	—	—
Ionization constant [H <sup>+</sup> ][OH <sup>-</sup> ]/mol <sup>2</sup> l <sup>-2</sup>	$1.008 \times 10^{-14}$	$1.95 \times 10^{-15}$	$\sim 6 \times 10^{-16}$
Ionic dissociation constant $K =$ [H <sup>+</sup> ][OH <sup>-</sup> ]/[H <sub>2</sub> O]/mol l <sup>-1</sup>	$1.821 \times 10^{-16}$	$3.54 \times 10^{-17}$	$\sim 1.1 \times 10^{-17}$
Heat of ionization/kJ mol <sup>-1</sup>	56.27	60.33	—
$\Delta H_f^\circ$ /kJ mol <sup>-1</sup>	-285.85	-294.6	—
$\Delta G_f^\circ$ /kJ mol <sup>-1</sup>	-237.19	-243.5	—

<sup>(a)</sup> Heavy water (p. 39) is now manufactured on the multikilotonne scale for use both as a coolant and neutron-moderator in nuclear reactors: its absorption cross-section for neutrons is much less than for normal water:  $\sigma_H$  332,  $\sigma_D$  0.46 mb (1 millibarn =  $10^{-21}$  cm<sup>2</sup>)

had to be supplemented by a further 360-page volume<sup>(88)</sup> dealing with the 4000 papers appearing during the following 4 years. A far cry from the first recorded use of desalination techniques in biblical times.<sup>(89)</sup>

### Physical properties and structure

Water is a volatile, mobile liquid with many curious properties, most of which can be ascribed to extensive H bonding (p. 52). In the gas phase the H<sub>2</sub>O molecule has a bond angle of 104.5° (close to tetrahedral) and an interatomic distance of 95.7 pm. The dipole moment is 1.84 D. Some properties of liquid water are summarized in Table 14.8 together with those of heavy water

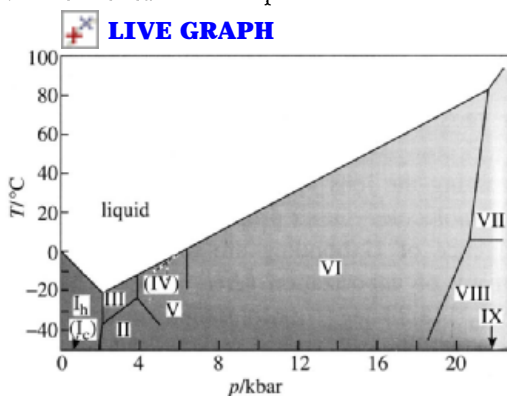
D<sub>2</sub>O and the tritium analogue T<sub>2</sub>O (p. 41). The high bp is notable (cf. H<sub>2</sub>S, etc.) as is the temperature of maximum density and its marked dependence on the isotopic composition of water. The high dielectric constant and measurable ionic dissociation equilibrium are also unusual and important properties. The ionic mobilities of [H<sub>3</sub>O]<sup>+</sup> and [OH]<sup>-</sup> in water are abnormally high ( $350 \times 10^{-4}$  and  $192 \times 10^{-4}$  cm s<sup>-1</sup> per V cm<sup>-1</sup> at 25° compared with  $50\text{--}75 \times 10^{-4}$  cm<sup>2</sup> V<sup>-1</sup> s<sup>-1</sup> for most other ions). This has been ascribed to a proton switch and reorientation mechanism involving the ions and chains of H-bonded solvent molecules. Other properties which show the influence of H bonding are the high heat and entropy of vaporization ( $\Delta H_{\text{vap}}$  44.02 kJ mol<sup>-1</sup>,  $\Delta S_{\text{vap}}$  118.8 J deg<sup>-1</sup> mol<sup>-1</sup>), high surface tension (71.97 dyne cm<sup>-1</sup>, i.e. 71.97 mN m<sup>-1</sup>) and relatively high viscosity. The strength of the H bonds has been variously estimated at between 5–50 kJ per mol of H bonds and is most probably close to 20 kJ mol<sup>-1</sup>. The structured nature of liquid water in which the molecules are linked to a small number of neighbours (2–3) by H bonds also accounts for its anomalously low density compared with a value of  $\sim 1.84$  g cm<sup>-3</sup> calculated for

<sup>88</sup> Gmelin *Handbook of Inorganic Chemistry*, 8th edn., O: Water Desalting, Supplement Vol. 1, 1979, 360 pp.

<sup>89</sup> Holy Bible, Exodus, Chap. 15, verses 22–25: "... so Moses brought the sons of Israel from the Red Sea and they went into the desert of Sur. And they marched three days in the wilderness and found no water to drink. And then they arrived at Merra and they could not drink from the waters of Merra because they were bitter. ... And the people murmured against Moses saying: What shall we drink? And Moses cried unto the Lord. And the Lord showed him a wood and he put it into the water and the water became sweet".

a normal close-packed liquid with molecules of similar size and mass. Details of the structure of liquid water have been probed for more than six decades since the classic paper of J. D. Bernal and R. H. Fowler proposed the first plausible model.<sup>(90)</sup> Despite extensive work by X-ray and neutron diffraction, Raman and infrared spectroscopy, and the theoretical calculation of thermodynamic properties based on various models, details are still controversial and there does not even appear to be general agreement on whether water consists of a mixture of two or more species of varying degrees of polymerization or whether it is better described on a continuous model of highly bent H-bond configurations.<sup>(91)</sup>

When water freezes the crystalline form adopted depends upon the detailed conditions employed. At least nine structurally distinct forms of ice are known and the phase relations between them are summarized in Fig. 14.9. Thus, when liquid or gaseous water crystallizes at atmospheric pressure normal hexagonal ice  $I_h$  forms, but at very low temperatures ( $-120^\circ$  to  $-140^\circ$ ) the vapour condenses to the cubic form, ice  $I_c$ . The relation between these structures is the same as that between the tridymite and cristobalite forms of  $\text{SiO}_2$  (p. 342), though in both forms of ice the protons are disordered.



**Figure 14.9** Partial phase diagram for ice (metastable equilibrium shown by broken lines).

<sup>90</sup> J. D. BERNAL and R. H. FOWLER, *J. Chem. Phys.* **1**, 515–48 (1933).

<sup>91</sup> P. KRINDEL and I. ELIEZER, *Coord. Chem. Rev.* **6**, 217–46 (1971).

Many of the high-pressure forms of ice are also based on silica structures (Table 14.9) and in ice II, VIII and IX the protons are ordered, the last 2 being low-temperature forms of ice VII and III respectively in which the protons are disordered. Note also that the high-pressure polymorphs VI and VII can exist at temperatures as high as  $80^\circ\text{C}$  and that, as expected, the high-pressure forms have substantially greater densities than that for ice I. A vitreous form of ice can be obtained by condensing water vapour at temperatures of  $-160^\circ\text{C}$  or below.

In “normal” hexagonal ice  $I_h$  each O is surrounded by a nearly regular tetrahedral arrangement of 4 other O atoms (3 at 276.5 pm and 1, along the  $c$ -axis, at 275.2 pm). The O–O–O angles are all close to  $109.5^\circ$  and neutron diffraction shows that the angle H–O–H is close to  $105^\circ$ , implying that the H atoms lie slightly off the O–O vectors. The detailed description of the disordered H atom positions is complex. In the proton-ordered phases II and IX neutron diffraction again indicates an angle H–O–H close to  $105^\circ$  but the O–O–O angles are now  $88^\circ$  and  $99^\circ$  respectively. More details are in the papers mentioned in ref. 92.

**Table 14.9** Structural relations in the polymorphs of ice<sup>(92)</sup>

Polymorph	Analogous silica polymorph	$d/(\text{g cm}^{-3})$	Ordered (O) or disordered (D) positions
$I_h$	Tridymite	0.92	D
$I_c$	Cristobalite	0.92	D
II	—	1.17	O
III	Keatite	1.16	D
IX	Keatite	—	O
IV	See footnote <sup>(a)</sup>	—	—
V	No obvious analogue	1.23	D
VI	Edingtonite <sup>(b,c)</sup>	1.31	D
VII	Cristobalite <sup>(c)</sup>	1.50	D
VIII	Cristobalite <sup>(c)</sup>	—	O

<sup>(a)</sup>Metastable for  $\text{H}_2\text{O}$ , but firmly established for  $\text{D}_2\text{O}$ .

<sup>(b)</sup>Edingtonite is  $\text{BaAl}_2\text{Si}_3\text{O}_{10}\cdot 4\text{H}_2\text{O}$  (see p. 1037 of ref. 93).

<sup>(c)</sup>Structure consists of two interpenetrating frameworks.

<sup>92</sup> A. F. WELLS, Water and hydrates, Chap. 15 in *Structural Inorganic Chemistry*, 5th edn., pp. 653–98, Oxford University Press, Oxford, 1984.

As indicated in Tables 14.8 and 14.9, ice  $I_h$  is unusual in having a density less than that of the liquid phase with which it is in equilibrium (a property which is of crucial significance for the preservation of aquatic life). When ice  $I_h$  melts some of the H bonds (possibly about 1 in 4) in the fully H-bonded lattice of 4-coordinate O atoms begin to break, and this process continues as the liquid is warmed, thereby enabling the molecules to pack progressively more closely with a consequent *increase* in density. This effect is opposed by the thermal motion of the molecules which tends to expand the liquid, and the net result is a maximum in the density at 3.98°C. Further heating reduces the density, though only slowly, presumably because the effects of thermal motion begin to outweigh the countervailing influence of breaking more H bonds. Again the qualitative explanation is clear but quantitative calculations of the density, viscosity, dielectric constant, etc., of  $H_2O$ ,  $D_2O$  and their mixtures remain formidable.

It was previously thought that pure ice had a low but measurable electrical conductivity of about  $1 \times 10^{-10} \text{ ohm}^{-1} \text{ cm}^{-1}$  at  $-10^\circ\text{C}$ . However, this conductivity is now thought to arise almost exclusively from surface defects, and when these have been removed ice is essentially an insulator with an immeasurably small conductivity.<sup>(93)</sup>

### *Water of crystallization, aquo complexes and solid hydrates*

Many salts crystallize from aqueous solution not as the anhydrous compound but as a well-defined hydrate. Still other solid phases have variable quantities of water associated with them, and there is an almost continuous gradation in the degree of association or "bonding" between the molecules of water and the other components of the crystal. It is convenient to recognise five limiting types of interaction though the boundaries between them are vague

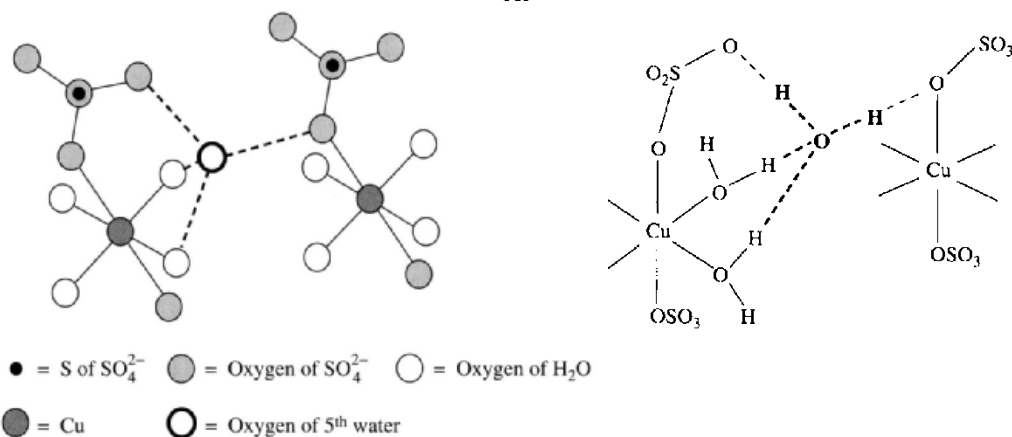
and undefined and many compounds incorporate more than one type.

(a) *H<sub>2</sub>O coordinated in a cationic complex.* This is perhaps the most familiar class and can be exemplified by complexes such as  $[\text{Be}(\text{OH}_2)_4]\text{SO}_4$ ,  $[\text{Mg}(\text{OH}_2)_6]\text{Cl}_2$ ,  $[\text{Ni}(\text{OH}_2)_6](\text{NO}_3)_2$ , etc.; the metal ion is frequently in the +2 or +3 oxidation state and tends to be small and with high coordination power. Sometimes there is further interaction via H bonding between the aquocation and the anion, particularly if this derives from an oxoacid, e.g. the alums  $\{[\text{M}(\text{OH}_2)_6]^+[\text{Al}(\text{OH}_2)_6]^{3+}[\text{SO}_4]_2^{2-}\}$  and related salts of  $\text{Cr}^{3+}$ ,  $\text{Fe}^{3+}$ , etc. The species  $\text{H}_3\text{O}^+$ ,  $\text{H}_5\text{O}_2^+$ ,  $\text{H}_7\text{O}_3^+$  and  $\text{H}_9\text{O}_4^+$  are a special case in which the cation is a proton, i.e.  $[\text{H}(\text{OH}_2)_n]^+$ , and are discussed on p. 630.

(b) *H<sub>2</sub>O coordinated by H bonding to oxoanions.* This mode is relatively uncommon but occurs in the classic case of  $\text{CuSO}_4 \cdot 5\text{H}_2\text{O}$  and probably also in  $\text{ZnSO}_4 \cdot 7\text{H}_2\text{O}$ . Thus, in hydrated copper sulfate, 1 of the  $\text{H}_2\text{O}$  molecules is held much more tenaciously than the other 4 (which can all be removed over  $\text{P}_4\text{O}_{10}$  or by warming under reduced pressure); the fifth can only be removed by heating the compound above  $350^\circ\text{C}$  (or to  $250^\circ$  *in vacuo*). The crystal structure shows that each Cu atom is coordinated by 4  $\text{H}_2\text{O}$  and 2  $\text{SO}_4$  groups in a *trans* octahedral configuration (Fig. 14.10) and that the fifth  $\text{H}_2\text{O}$  molecule is not bound to Cu but forms H (donor) bonds to 2  $\text{SO}_4$  groups on neighbouring Cu atoms and 2 further H (acceptor) bonds with *cis*- $\text{H}_2\text{O}$  molecules on 1 of the Cu atoms. It therefore plays a cohesive role in binding the various units of the structure into a continuous lattice.

(c) *Lattice water.* Sometimes hydration of either the cation or the anion is required to improve the size compatibility of the units comprising the lattice, and sometimes voids in the lattice so formed can be filled by additional molecules of water. Thus, although LiF and NaF are anhydrous, the larger alkali metal fluorides can form definite hydrates  $\text{MF} \cdot n\text{H}_2\text{O}$  ( $n = 2$  and 4 for K;  $1\frac{1}{2}$  for Rb;  $\frac{2}{3}$  and  $1\frac{1}{2}$  for Cs). Conversely, for the chlorides: KCl, RbCl and CsCl are always anhydrous whereas LiCl can form hydrates with

<sup>93</sup> A. VON HIPPEL, *Mat. Res. Bull.* **14**, 273–99 (1979).

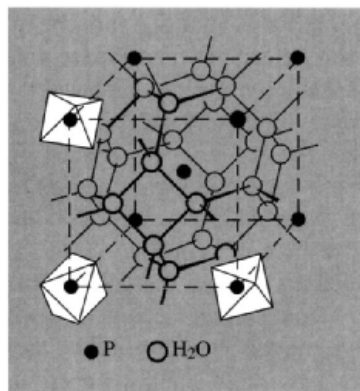


**Figure 14.10** Two representations of the repeating structural unit in  $\text{CuSO}_4 \cdot 5\text{H}_2\text{O}$  showing the geometrical distribution of ligands about Cu and the connectivity of the unique  $\text{H}_2\text{O}$  molecule.

1, 2, 3 and  $5\text{H}_2\text{O}$ , and  $\text{NaCl} \cdot 2\text{H}_2\text{O}$  is also known. The space-filling role of water molecules is even more evident with very large anions such as those of the heteropoly acids (p. 1013), e.g.  $\text{H}_3[\text{PW}_{12}\text{O}_{40}] \cdot 29\text{H}_2\text{O}$ .

(d) *Zeolitic water*. The large cavities of the framework silicates (p. 354) can readily accommodate water molecules, and the lack of specific strong interactions enables the “degree of hydration” to vary continuously over very wide ranges. The swelling of ion-exchange resins and clay minerals (p. 353) are further examples of non-specific hydrates of variable composition.

(e) *Clathrate hydrates*.<sup>(94)</sup> The structure motif of zeolite “hosts” accommodating “guest” molecules of water can be inverted in an intriguing way: just as the various forms of ice (p. 624) are formally related to those of silica (p. 342), so  $(\text{H}_2\text{O})_n$  can be induced to generate various cage-like structures with large cavities, thereby enabling the water structure itself to act as host to various guest molecules. Thus, polyhedral frameworks, sometimes with cavities of more than one size, can be generated from unit cells containing  $12\text{H}_2\text{O}$ ,  $46\text{H}_2\text{O}$ ,  $136\text{H}_2\text{O}$ , etc. In



**Figure 14.11** Crystal structure of  $\text{HPF}_6 \cdot 6\text{H}_2\text{O}$  showing the cavity formed by 24  $\text{H}_2\text{O}$  molecules disposed with their O atoms at the vertices of a truncated octahedron. The  $\text{PF}_6$  octahedra occupy centre and corners of the cubic unit cell, i.e. one  $\text{PF}_6$  at the centre of each cavity.<sup>(92)</sup>

the first of these (Fig. 14.11) there is a cubic array of 24-cornered cavities, each cavity being a truncated octahedron with square faces of O atoms and each  $\text{H}_2\text{O}$  being common to 2 adjacent cavities (i.e.  $24/2 = 12\text{H}_2\text{O}$ ). There is space for a guest molecule G at the centre of each cavity, i.e. at the centre of the cube and at each corner resulting in a stoichiometry  $\text{G}(8\text{G})_{1/8} \cdot 12\text{H}_2\text{O}$ , i.e.  $\text{G} \cdot 6\text{H}_2\text{O}$  as in  $\text{HPF}_6 \cdot 6\text{H}_2\text{O}$ . The structure should

<sup>94</sup> E. BERECZ and M. BALLA-ACHS, *Gas Hydrates*, Elsevier, Amsterdam, 1983, 343 pp.

be compared with the aluminosilicate framework in ultramarine (p. 358).

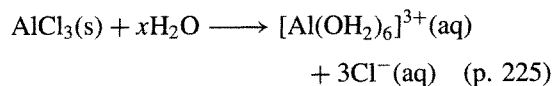
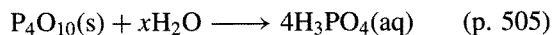
With the more complicated framework of  $46\text{H}_2\text{O}$  there are 6 cavities of one size and 2 slightly smaller. If all are filled one has  $46/8\text{H}_2\text{O}$  per guest molecule, i.e.  $G.5\frac{3}{4}\text{H}_2\text{O}$  as in the high-pressure clathrates with  $G = \text{Ar}, \text{Kr}, \text{CH}_4$  and  $\text{H}_2\text{S}$ . If only the larger cavities are filled, the stoichiometry rises to  $G.7\frac{2}{3}\text{H}_2\text{O}$ : this is approximated by the classic chlorine hydrate phase discovered by Humphry Davy and studied by Michael Faraday. The compound is now known to be  $\text{Cl}_2.7\frac{1}{4}\text{H}_2\text{O}$ , implying that up to 20% of the smaller guest sites are also occupied.

With the  $136\text{H}_2\text{O}$  polyhedron there are 8 larger and 16 smaller voids. If only the former are filled, then  $G.17\text{H}_2\text{O}$  results ( $17 = 136/8$ ) as in  $\text{CHCl}_3.17\text{H}_2\text{O}$  and  $\text{CHI}_3.17\text{H}_2\text{O}$ , whereas if both sets are filled with molecules of different sizes, compounds such as  $\text{CHCl}_3.2\text{H}_2\text{S}.17\text{H}_2\text{O}$  result. Many more complicated arrays are possible, resulting from partial filling of the voids or partial replacement of  $\text{H}_2\text{O}$  in the framework by other species capable of being H-bonded into the network, e.g.  $[\text{NMe}_4]\text{F}.4\text{H}_2\text{O}$ ,  $[\text{NMe}_4]\text{OH}.5\text{H}_2\text{O}$ ,  $\text{Bu}_3^+\text{SF}.20\text{H}_2\text{O}$  and  $[\text{N}(i\text{-C}_5\text{H}_{11})_4]\text{F}.38\text{H}_2\text{O}$ . Further structural details are in ref. 92, and industrial applications are discussed in the comprehensive ref. 94.

### Chemical properties

Water is an excellent solvent because of its high dielectric constant and very strong solvating power. Many compounds, whether hydrated or anhydrous, dissolve to give electrolytic solutions of hydrated cations and anions. However, detailed treatments of solubility relations, free energies and enthalpies of ionic hydration, temperature dependence of solubility and the influence of dissolved ions on the H-bonded structure of the solvent, fall outside the scope of the present treatment. Even predominantly covalent compounds such as  $\text{EtOH}$ ,  $\text{MeCO}_2\text{H}$ ,  $\text{Me}_2\text{CO}$ ,  $(\text{CH}_2)_4\text{O}$ , etc. can have high solubility or even complete miscibility with water due to H-bonded interaction with the solvent. Again, covalent

compounds such as  $\text{HCl}$  can dissolve to give ionic solutions by heterolytic cleavage (e.g. to aquated  $\text{H}_3\text{O}^+\text{Cl}^-$ ), and the process of dissolution sometimes also results in ionic cleavage of the solvent itself, e.g.  $[\text{H}_3\text{O}]^+[\text{BF}_3(\text{OH})]^-$  (p. 198). Because of the great affinity that many elements have for oxygen, solvolytic cleavage (hydrolysis) of "covalent" or "ionic" bonds frequently ensues, e.g.:



Such reactions are discussed at appropriate points throughout the book as each individual compound is being considered. A particularly important set of reactions in this category is the synthesis of element hydrides by hydrolysis of certain sulfides (to give  $\text{H}_2\text{S}$ ), nitrides (to give  $\text{NH}_3$ ), phosphides ( $\text{PH}_3$ ), carbides ( $\text{C}_n\text{H}_m$ ), borides ( $\text{B}_n\text{H}_m$ ), etc. Useful reviews are available on hydrometallurgy (the recovery of metals by use of aqueous solutions at relatively low temperatures),<sup>(94a)</sup> hydrothermal syntheses<sup>(94b)</sup> and the use of supercritical water as a reaction medium for chemistry.<sup>(94c)</sup>

Another important reaction (between  $\text{H}_2\text{O}$ ,  $\text{I}_2$  and  $\text{SO}_2$ ) forms the basis of the quantitative determination of water when present in small amounts. The reaction, originally investigated by R. Bunsen in 1835, was introduced in 1935 as an analytical reagent by Karl Fischer who believed, incorrectly, that each mole of  $\text{I}_2$  was equivalent to 2 moles of  $\text{H}_2\text{O}$ :



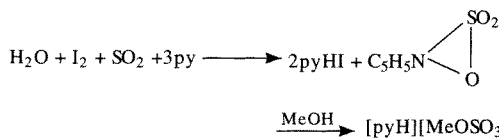
In fact, the reaction is only quantitative in the presence of pyridine, and the methanol solvent

<sup>94a</sup> F. HABASHI, *Chem. and Eng. News*, 8 Feb. 1982, pp. 46–58.

<sup>94b</sup> A. RABENAU, *Angew. Chem. Int. Edn. Engl.* **24**, 1026–40 (1985).

<sup>94c</sup> R. W. SHAW, T. B. BRILL, A. A. CLIFFORD, C. A. ECKERT and E. U. FRANCK, *Chem. and Eng. News*, 23 Dec. 1991, pp. 26–39.

is also involved leading to a 1:1 stoichiometry between  $I_2$  and  $H_2O$ :



The stability of the reagent is much improved by replacing MeOH with  $MeOCH_2CH_2OH$ , and this forms the basis of the present-day Karl Fischer reagent.<sup>(95)</sup>

In addition to simple dissolution, ionic dissociation and solvolysis, two further classes of reaction are of pre-eminent importance in aqueous solution chemistry, namely acid-base reactions (p. 48) and oxidation-reduction reactions. In water, the oxygen atom is in its lowest oxidation state (-2). Standard reduction potentials (p. 435) of oxygen in acid and alkaline solution are listed in Table 14.10<sup>(96)</sup> and shown diagrammatically in the scheme opposite. It is important to remember that if  $H^+$  or  $OH^-$  appear in the electrode half-reaction, then the electrode potential will change markedly with the pH. Thus for the first reaction in Table 14.10:  $O_2 + 4H^+ + 4e^- \rightleftharpoons 2H_2O$ , although  $E^\circ = 1.229$  V, the actual potential at 25°C will be given by

$$E/\text{volt} = 1.229 + 0.05916 \log\{[H^+]/\text{mol l}^{-1}\} \times \{P_{O_2}/\text{atm}\}^{\frac{1}{4}}$$

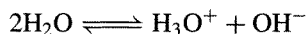
which diminishes to 0.401 V at pH 14 (Fig. 14.12). Likewise, for the half-reaction

$H^+ + e^- \rightleftharpoons \frac{1}{2}H_2$ ,  $E^\circ$  is zero by definition at pH 0, whereas at other concentrations

$$E/\text{volt} = -0.05916 \log\{P_{H_2}/\text{atm}\}^{\frac{1}{2}} / \{[H^+]/\text{mol l}^{-1}\}$$

and the value falls to -0.828 at pH 14. Theoretically no oxidizing agent whose reduction potential lies above the  $O_2/H_2O$  line and no reducing agent whose reduction potential falls below the  $H^+/H_2$  line can exist in thermodynamically stable aqueous solutions. However, for kinetic reasons associated with the existence of over-potentials, these lines can be extended by about 0.5 V as shown by the dotted lines in Fig. 14.12, and these are a more realistic estimate of the region of stability of oxidizing and reducing agents in aqueous solution. Outside these limits more strongly oxidizing species (e.g.  $F_2$ ,  $E^\circ$  2.866 V) oxidize water to  $O_2$  and more strongly reducing agents (e.g.  $K_{\text{metal}}$ ,  $E^\circ$  -2.931 V) liberate  $H_2$ . Sometimes even greater activation energies have to be overcome and reaction only proceeds at elevated temperatures (e.g.  $C + H_2O \rightarrow CO + H_2$ ; p. 307).

The acid-base behaviour of aqueous solutions has already been discussed (p. 48). The ionic self-dissociation of water is well established (Table 14.8) and can be formally represented as



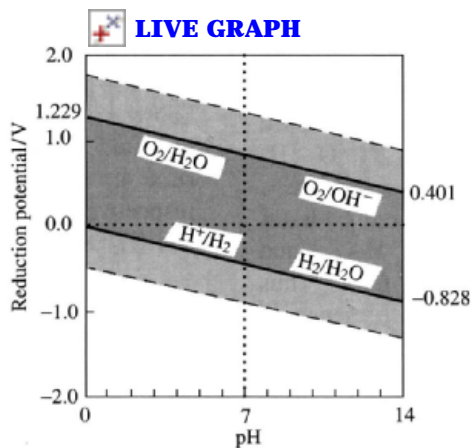
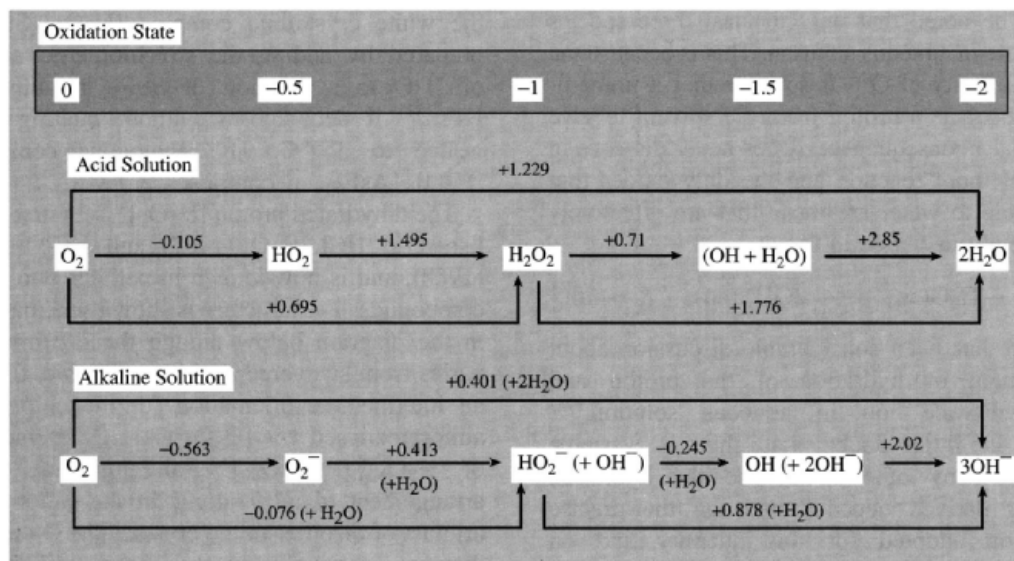
On the Brønsted theory (p. 51), solutions with concentrations of  $H_3O^+$  greater than that in pure water are acids (proton donors), and solutions rich in  $OH^-$  are bases (proton acceptors). The same classifications follow from the solvent-system theory of acids and bases

<sup>95</sup> E. SCHOLZ, *Karl Fischer Titration Determination of Water*, Springer Verlag, Berlin, 1984, 150 pp.

<sup>96</sup> G. MILAZZO and S. CAROLI, *Tables of Standard Electrode Potentials*, p. 229, Wiley-Interscience, New York, 1978.

**Table 14.10** Standard reduction potentials of oxygen

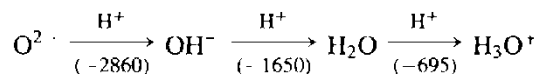
Acid solution (pH 0)	$E^\circ/V$	Alkaline solution (pH 14)	$E^\circ/V$
$O_2 + 4H^+ + 4e^- \rightleftharpoons 2H_2O$	1.229	$O_2 + 2H_2O + 4e^- \rightleftharpoons 4OH^-$	0.401
$O_2 + 2H^+ + 2e^- \rightleftharpoons H_2O_2$	0.695	$O_2 + H_2O + 2e^- \rightleftharpoons HO_2^- + OH^-$	-0.076
$O_2 + H^+ + e^- \rightleftharpoons HO_2$	-0.105	$O_2 + e^- \rightleftharpoons O_2^-$	-0.563
$HO_2 + H^+ + e^- \rightleftharpoons H_2O_2$	1.495	$O_2^- + H_2O + e^- \rightleftharpoons HO_2^- + OH^-$	0.413
$H_2O_2 + 2H^+ + 2e^- \rightleftharpoons 2H_2O$	1.776	$HO_2^- + H_2O + 2e^- \rightleftharpoons 3OH^-$	0.878
$H_2O_2 + H^+ + e^- \rightleftharpoons OH + H_2O$	0.71	$HO_2^- + H_2O + e^- \rightleftharpoons OH + 2OH^-$	-0.245
$OH + H^+ + e^- \rightleftharpoons H_2O$	2.85	$OH + e^- \rightleftharpoons OH^-$	2.02



**Figure 14.12** Variation of the reduction potentials of the couples  $\text{O}_2/\text{H}_2\text{O}$  and  $\text{H}^+/\text{H}_2$  (or  $\text{O}_2/\text{OH}^-$  and  $\text{H}_2/\text{H}_2\text{O}$ ) as a function of pH (full lines). The broken lines lie 0.5 V above and below these full lines and give the approximate practical limits of oxidants and reductants in aqueous solution beyond which the solvent itself is oxidized to  $\text{O}_2(\text{g})$  or reduced to  $\text{H}_2(\text{g})$ .

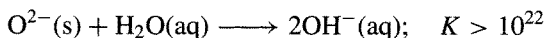
since compounds enhancing the concentrations of the characteristic solvent cation ( $\text{H}_3\text{O}^+$ ) and anion ( $\text{OH}^-$ ) are solvo-acids and solvo-bases (p. 425). On the Lewis theory,  $\text{H}^+$  is an electro-pair acceptor (acid) and  $\text{OH}^-$  an electron-pair donor (base, or ligand) (p. 198). The various definitions tend to diverge only in other systems (either nonaqueous or solvent-free), particularly when aprotic media are being considered (e.g.  $\text{N}_2\text{O}_4$ , p. 456;  $\text{BrF}_3$ , p. 831; etc.).

In considering the following isoelectronic sequence (8 valence electrons) and the corresponding gas-phase proton affinities ( $A_{\text{H}^+}/\text{kJ mol}^{-1}$ ):<sup>(97)</sup>



<sup>97</sup> R. E. KARI and I. G. CSIZMADIA, *J. Am. Chem. Soc.* **99**, 4539-45 (1977).

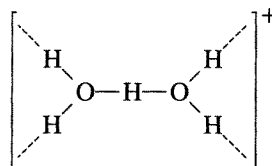
it will be noted that only the last three species are stable in aqueous solution. This is because the proton affinity of  $O^{2-}$  is so huge that it immediately abstracts a proton from the solvent to give  $OH^-$ ; as a consequence, oxides never dissolve in water without reaction and the only oxides that are stable to water are those that are effectively completely insoluble in it:



There has been considerable discussion about the extent of hydration of the proton and the hydroxide ion in aqueous solution.<sup>(98)</sup> There is little doubt that this is variable (as for many other ions) and the hydration number derived depends both on the precise definition adopted for this quantity and on the experimental method used to determine it.  $H_3O^+$  has definitely been detected by vibration spectroscopy, and by  $^{17}O$  nmr spectroscopy on a solution of  $HF/SbF_5/H_2^{17}O$  in  $SO_2$ ; a quartet was observed at  $-15^\circ$  which collapsed to a singlet on proton decoupling,  $J(^{17}O-^1H)$  106 Hz.<sup>(99)</sup> In crystalline hydrates there are a growing number of well-characterized hydrates of the series  $H_3O^+$ ,  $H_5O_2^+$ ,  $H_7O_3^+$ ,  $H_9O_4^+$  and  $H_{13}O_6^+$ , i.e.  $[H(OH_2)_n]^+$   $n = 1-4, 6$ .<sup>(100)</sup> Thus X-ray studies have established the presence of  $H_3O^+$  in the monohydrates of  $HCl$ ,  $HNO_3$  and  $HClO_4$ , and in the mono- and di-hydrates of sulfuric acid,  $[H_3O][HSO_4]$  and  $[H_3O]_2[SO_4]$ . As expected,  $H_3O^+$  is pyramidal like the isoelectronic molecule  $NH_3$ , but the values of the angles  $H-O-H$  vary considerably due to extensive H bonding throughout the crystal, e.g.  $117^\circ$  in the chloride,  $112^\circ$  in the nitrate, and  $101^\circ$ ,  $106^\circ$  and  $126^\circ$  in  $[H_3O][HSO_4]$ .<sup>(92)</sup> Likewise the H-bonded distance  $O-H \cdots O$  varies: it is 266 pm in the nitrate, 254–265 in  $[H_3O][HSO_4]$  and 252–259 in  $[H_3O]_2[SO_4]$ . The most stable hydroxonium salt yet known is

the white crystalline complex  $[H_3O]^+[SbF_6]^-$ , prepared by adding the stoichiometric amount of  $H_2O$  to a solution of  $SbF_5$  in anhydrous  $HF$ ;<sup>(101)</sup> it decomposes without melting when heated to  $357^\circ C$ . The analogous compound  $[H_3O]^+[AsF_6]^-$  decomposes at  $193^\circ C$ .

The dihydrated proton  $[H_5O_2]^+$  was first established in  $HCl \cdot 2H_2O$  (1967) and  $HClO_4 \cdot 2H_2O$  (1968), and is now known in perhaps two dozen compounds. The structure is shown schematically in the diagram below though the conformation varies from staggered in the perchlorate, through an intermediate orientation for the chloride to almost eclipsed for  $[H_5O_2]Cl \cdot H_2O$ . In the case of  $[H_5O_2]_3^+[PW_{12}O_{40}]^{3-}$ , an apparently planar arrangement of all 7 atoms in the cation is an artefact of disorder in the crystal. The  $O-H \cdots O$  distance is usually in the range 240–245 pm though in the deep-yellow crystalline compound  $[NEt_4]_3[H_5O_2][Mo_2Cl_8H][MoCl_4O(OH_2)]$  it is only 234 pm, one of the shortest  $O-H \cdots O$  bonds known.<sup>(102)</sup> The detailed crystal structures of the hydrated hexafluorosilicic acids,  $H_2SiF_6 \cdot nH_2O$  ( $n = 4, 6, 9.5$ ) have shown them to be, respectively,  $[H_5O_2]_2SiF_6$ ,  $[H_5O_2]_2SiF_6 \cdot 2H_2O$  and  $[H_5O_2][H_7O_3]SiF_6 \cdot 4.5H_2O$ .<sup>(103)</sup>



The ions  $[H_7O_3]^+$  and  $[H_9O_4]^+$  are both featured in the compound  $HBr \cdot 4H_2O$  which has the unexpectedly complicated formulation  $[H_9O_4]^+[H_7O_3]^+[Br]^- \cdot 2H_2O$ . The structures of the cations are shown schematically in Fig. 14.13

<sup>101</sup> K. O. CHRISTE, C. J. SCHACK and R. D. WILSON, *Inorg. Chem.* **14**, 2224–30 (1975). See also K. O. CHRISTE, P. CHARPIN, E. SOULIE, R. BOUGON, J. FAWCETT and D. R. RUSSELL, *Inorg. Chem.* **23**, 3756–66 (1984).

<sup>102</sup> A. BINO and F. A. COTTON, *J. Am. Chem. Soc.* **101**, 4150–4 (1979). See also G. J. KEARLEY, H. A. PRESSMAN and R. C. T. SLADE, *J. Chem. Soc., Chem. Commun.*, 1801–2 (1986).

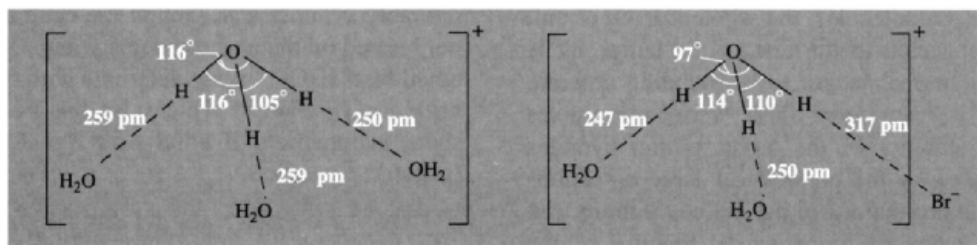
<sup>103</sup> D. MOOTZ and E.-J. OELLERS, *Z. anorg. allg. Chem.* **559**, 27–39 (1988).

<sup>98</sup> P. A. GIGUÈRE, *J. Chem. Educ.* **56**, 571–5 (1979).

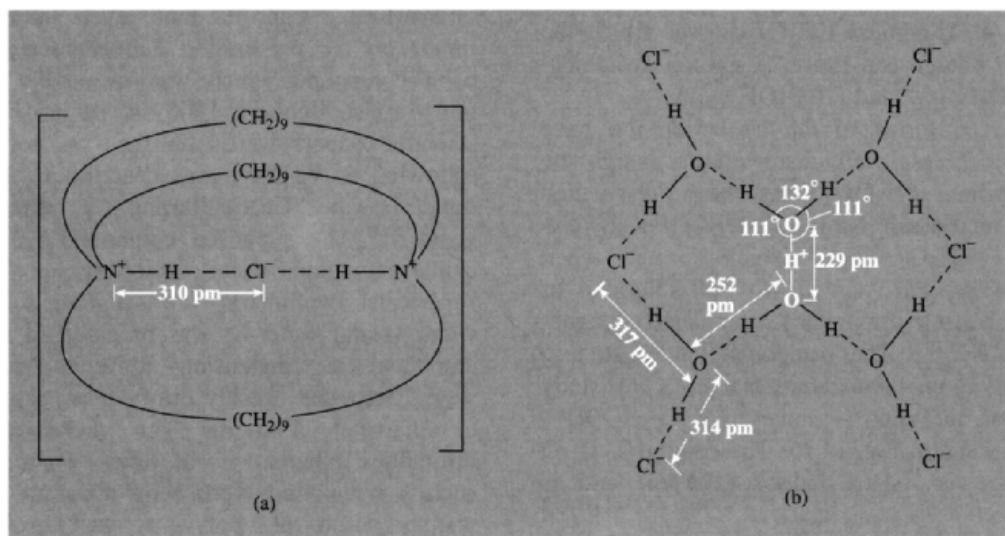
<sup>99</sup> G. D. METEESCU and G. M. BENEDIKT, *J. Am. Chem. Soc.* **101**, 3959–60 (1979). See also G. A. OLAH, G. K. S. PRAKASH, M. BARZAGHI, K. LAMMERTSMA, P. VON R. SCHLEYER and J. A. POPLÉ, *J. Am. Chem. Soc.* **108**, 1032–5 (1986).

<sup>100</sup> E. KOCHANSKI, *J. Am. Chem. Soc.* **107**, 7869–73 (1985).





**Figure 14.13** Schematic representation of the structures of the  $[\text{H}_9\text{O}_4]^+$  and  $[\text{H}_7\text{O}_3]^+ \cdots \text{Br}^-$  units in  $\text{HBr} \cdot 4\text{H}_2\text{O}$ , showing bond angles and  $\text{O}-\text{H} \cdots \text{O}$  ( $\text{O}-\text{H} \cdots \text{Br}$ ) distances.



**Figure 14.14** (a) Schematic representation of the structure of the cage cation  $[(\text{C}_9\text{H}_{18})_3(\text{NH})_2\text{Cl}]^+$ , and (b) detailed structure of the  $[\text{H}_{13}\text{O}_6]^+$  ion showing its H bonding to surrounding  $\text{Cl}^-$  anions. The ion has  $C_{2h}$  symmetry with the very short central  $\text{O}-\text{H}-\text{O}$  lying across the centre of symmetry.

which indicates that a bromide ion has essentially displaced the fourth water molecule of the second cation to give an effectively neutral H-bonded unit  $[(\text{H}_3\text{O})_2\text{H}^+\text{Br}^-]$ . The discrete  $[\text{H}_7\text{O}_3]^+$  ion is now known in about a dozen complexes of which a good example is the deep-green complex  $[\text{NEt}_4]_2[\text{H}_7\text{O}_3]_2[\text{Ru}_3\text{Cl}_{12}]$  in which the 2  $\text{O}-\text{H} \cdots \text{O}$  distances are 245 and 255 pm and the  $\text{O}-\text{O} \cdots \text{O}$  angle is  $115.9^\circ$ .<sup>(104)</sup> Similar dimensions were found in the hexafluorosilicate.<sup>(103)</sup>

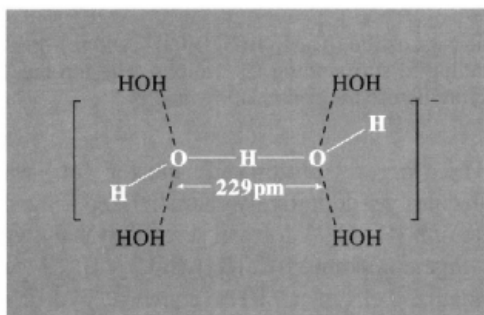
<sup>104</sup> A. BINO and F. A. COTTON, *J. Am. Chem. Soc.* **102**, 608–11 (1980).

The largest protonated cluster of water molecules yet definitively characterized is the discrete unit  $[\text{H}_{13}\text{O}_6]^+$  formed serendipitously when the cage compound  $[(\text{C}_9\text{H}_{18})_3(\text{NH})_2\text{Cl}]^+\text{Cl}^-$  was crystallized from a 10% aqueous hydrochloric acid solution.<sup>(105)</sup> The structure of the cage cation is shown in Fig. 14.14 and the unit cell contains  $4\{[(\text{C}_9\text{H}_{18})_3(\text{NH})_2\text{Cl}][\text{Cl}][\text{H}_{13}\text{O}_6]\text{Cl}\}$ . The hydrated proton features a short symmetrical  $\text{O}-\text{H}-\text{O}$  bond at the centre of symmetry and 4 longer unsymmetrical  $\text{O}-\text{H} \cdots \text{O}$  bonds to 4

<sup>105</sup> R. A. BELL, G. G. CHRISTOPH, F. R. FRONCZEK and R. E. MARSH, *Science* **190**, 151–2 (1975).

further  $\text{H}_2\text{O}$  molecules, the whole  $[\text{H}_{13}\text{O}_6]^+$  unit being connected to the rest of the lattice by H bonds of normal length to surrounding chloride ions. It is clear from these various examples that the stability of the larger proton hydrates is enhanced by the presence of large co-cations and/or counter-anions in the lattice. Stability can also be enhanced by structural features of the cluster cation itself, as beautifully exemplified by the species  $[\text{H}_{41}\text{O}_{20}]^+$  and  $[\text{H}_{43}\text{O}_{21}]^+$ .<sup>(106)</sup> These stable groupings comprise a central {H} or  $\{\text{H}_3\text{O}\}$  bonded to an encapsulating pentagonal dodecahedron of H-bonded  $\{(\text{H}_2\text{O})_{20}\}$  over which the positive charge can move by proton switching, i.e.  $[\text{H}(\text{OH}_2)_{20}]^+$  and  $[\text{H}_3\text{O}(\text{OH}_2)_{20}]^+$ .

Hydrated forms of the hydroxide ion have been much less well characterized though the monohydrate  $[\text{H}_3\text{O}_2]^-$  has been discovered in the mixed salt  $\text{Na}_2[\text{NET}_3\text{Me}][\text{Cr}\{\text{PhC}(\text{S})=\text{N}(\text{O})\}_3] \cdot \frac{1}{2}\text{NaH}_3\text{O}_2 \cdot 18\text{H}_2\text{O}$  which formed when  $[\text{NET}_3\text{Me}]\text{I}$  was added to a solution of tris(thiobenzohydroximato)chromate(III) in aqueous  $\text{NaOH}$ .<sup>(107)</sup> The compound tended to lose water at room temperature but an X-ray study identified the centro-symmetric  $[\text{HO}-\text{H}-\text{OH}]^-$  anion shown in Fig. 14.15. The central O-H-O bond is very short indeed (229 pm) and is



**Figure 14.15** Structure of the centrosymmetric  $[\text{H}_3\text{O}_2]^-$  ion showing the disposition of longer H bonds to neighbouring water molecules.

probably symmetrical, though the central H was not located on the electron density map. It will be noted that  $[\text{H}_3\text{O}_2]^-$  is isoelectronic with the bifluoride ion  $[\text{F}-\text{H}-\text{F}]^-$  which also features a very short, symmetrical H bond with  $\text{F} \cdots \text{F}$  227 pm (p. 60).

### Polywater

The saga of polywater forms a fascinating and informative case history of the massive amount of work that can be done, even in modern times, on the preparation and characterization of a compound which was eventually found not to exist. Between 1966 and 1973 over 500 scientific papers were published on polywater following B. V. Deryagin's description of work done in the USSR during the preceding years.<sup>(108)</sup> The supposed compound, variously called anomalous water, orthowater, polywater, superwater, cyclimetric water, superdense water, water II and water-X, was prepared in minute amounts by condensing purified "ordinary water" into fine, freshly drawn glass capillaries of diameter 1–3  $\mu\text{m}$ . The thermodynamic difficulties inherent in the very existence of such a compound were soon apparent and it was proposed that polywater was, in fact, a dispersion of a silica gel leached from the glass capillaries,<sup>(109)</sup> despite the specific rejection of this possibility by several groups of earlier workers. The full panoply of physicochemical techniques was brought to bear on the problem, and it was finally conceded that the anomalous properties were caused by a mixture of colloidal silicic acid and dissolved compounds of Na, K, Ca, B, Si, N (nitrate), O (sulfate) and Cl leached from the glass by the aggressive action of freshly condensed water.<sup>(110)</sup> A very informative annotated bibliography is available

<sup>108</sup> B. V. DERYAGIN, *Discussions Faraday Soc.* **42**, 109–19 (1966).

<sup>109</sup> A. CHERKIN, *Nature* **224**, 1293 (1969). (See also *Nature* **222**, 159–61 (1969)).

<sup>110</sup> B. V. DERYAGIN and N. V. CHURAEV, *Nature* **244**, 430–1 (1973); B. V. DERYAGIN, *Recent Advances in Adhesion*, 1973, 23–31.

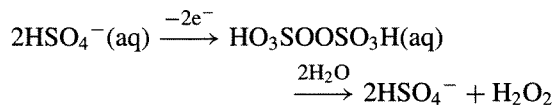
<sup>106</sup> S. WEI, Z. SHI and A. W. CASTLEMAN, *J. Chem. Phys.* **94**, 3268–70 (1991).

<sup>107</sup> J. ABU-DARI, K. N. RAYMOND and D. P. FREYBERG, *J. Am. Chem. Soc.* **101**, 3688–9 (1979).

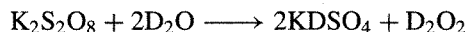
which traces the course of this controversy and analyses the reasons why it took so long to resolve.<sup>(111)</sup>

### 14.2.3 Hydrogen peroxide

Hydrogen peroxide was first made in 1818 by J. L. Thenard who acidified barium peroxide (p. 121) and then removed excess H<sub>2</sub>O by evaporation under reduced pressure. Later the compound was prepared by hydrolysis of peroxodisulfates obtained by electrolytic oxidation of acidified sulfate solutions at high current densities:



Such processes are now no longer used except in the laboratory preparation of D<sub>2</sub>O<sub>2</sub>, e.g.:



On an industrial scale H<sub>2</sub>O<sub>2</sub> is now almost exclusively prepared by the autoxidation of 2-alkylantraquinols (see Panel on next page).

#### Physical properties

Hydrogen peroxide, when pure, is an almost colourless (very pale blue) liquid, less volatile than water and somewhat more dense and viscous. Its more important physical properties are in Table 14.11 (cf. H<sub>2</sub>O, p. 623). The compound is miscible with water in all proportions and forms a hydrate H<sub>2</sub>O<sub>2</sub>·H<sub>2</sub>O, mp  $-52^\circ$ . Addition of water increases the already high dielectric constant of H<sub>2</sub>O<sub>2</sub> (70.7) to a maximum value of 121 at ~35% H<sub>2</sub>O<sub>2</sub>, i.e. substantially higher than the value of water itself (78.4 at 25°).

In the gas phase the molecule adopts a skew configuration with a dihedral angle of 111.5° as

**Table 14.11** Some physical properties of hydrogen peroxide<sup>(a)</sup>

Property	Value
MP/°C	-0.41
BP/°C (extrap)	150.2
Vapour pressure(25°)/mmHg	1.9
Density (solid at $-4.5^\circ$ )/g cm <sup>-3</sup>	1.6434
Density (liquid at 25°)/g cm <sup>-3</sup>	1.4425
Viscosity(20°)/centipoise	1.245
Dielectric constant $\epsilon(25^\circ)$	70.7
Electric conductivity(25°)/ $\Omega^{-1}$ cm <sup>-1</sup>	$5.1 \times 10^{-8}$
$\Delta H_f^\circ/\text{kJ mol}^{-1}$	-187.6
$\Delta G_f^\circ/\text{kJ mol}^{-1}$	-118.0

<sup>(a)</sup>For D<sub>2</sub>O<sub>2</sub>: mp  $+1.5^\circ$ ;  $d_{20}$  1.5348 g cm<sup>-3</sup>;  $\eta_{20}$  1.358 centipoise.

shown in Fig. 14.16a. This is due to repulsive interaction of the O–H bonds with the lone-pairs of electrons on each O atom. Indeed, H<sub>2</sub>O<sub>2</sub> is the smallest molecule known to show hindered rotation about a single bond, the rotational barriers being 4.62 and 29.45 kJ mol<sup>-1</sup> for the *trans* and *cis* conformations respectively. The skew form persists in the liquid phase, no doubt modified by H bonding, and in the crystalline state at  $-163^\circ\text{C}$  a neutron diffraction study<sup>(112)</sup> gives the dimensions shown in Fig. 14.16b. The dihedral angle is particularly sensitive to H bonding, decreasing from 111.5° in the gas phase to 90.2° in crystalline H<sub>2</sub>O<sub>2</sub>; in fact, values spanning the complete range from 90° to 180° (i.e. *trans* planar) are known for various solid phases containing molecular H<sub>2</sub>O<sub>2</sub> (Table 14.12). The O–O distance in H<sub>2</sub>O<sub>2</sub> corresponds to the value expected for a single bond (p. 616).

#### Chemical properties

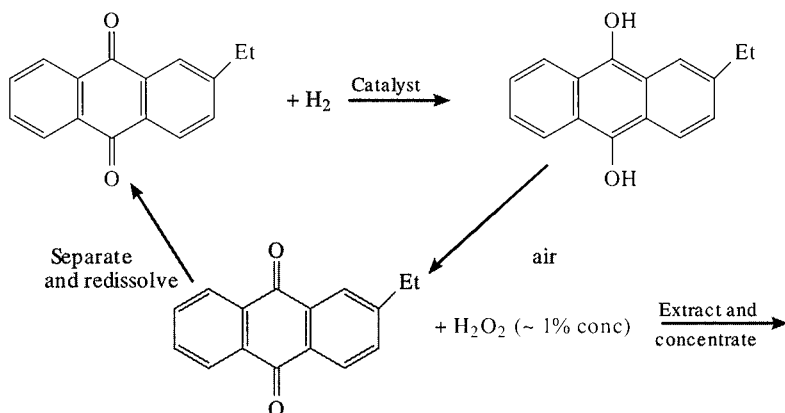
In H<sub>2</sub>O<sub>2</sub> the oxidation state of oxygen is  $-1$ , intermediate between the values for O<sub>2</sub> and H<sub>2</sub>O, and, as indicated by the reduction potentials on p. 628, aqueous solutions of H<sub>2</sub>O<sub>2</sub> should spontaneously disproportionate. For the pure

<sup>111</sup> F. PERCIVAL and A. H. JOHNSTONE, *Polywater — A Library Exercise for Chemistry Degree Students*, The Chemical Society, London, 1978, 24 pp. [See also B. F. POWELL, *J. Chem. Educ.* **48**, 663–7 (1971). H. FREIZER, *J. Chem. Educ.* **49**, 445 (1972). F. FRANKS, *Polywater*, MIT Press, Cambridge, Mass., 1981, 208 pp.]

<sup>112</sup> J.-M. SAVARIAULT and M. S. LEHMANN, *J. Am. Chem. Soc.* **102**, 1298–303 (1980).

### Preparation and Uses of Hydrogen Peroxide<sup>(113)</sup>

Hydrogen peroxide is a major industrial chemical manufactured on a multikilotonne scale by an ingenious cycle of reactions introduced by I. G. Farbenindustrie about 60 years ago. Since the value of the solvents and organic substrates used are several hundred times that of the  $\text{H}_2\text{O}_2$  produced, the economic viability of the process depends on keeping losses very small indeed. The basic process consists of dissolving 2-ethylanthraquinone in a mixed ester/hydrocarbon or alcohol/hydrocarbon solvent and reducing it by a Raney nickel or supported palladium catalyst to the corresponding quinol. The catalyst is then separated and the quinol non-catalytically reoxidized in a stream of air:



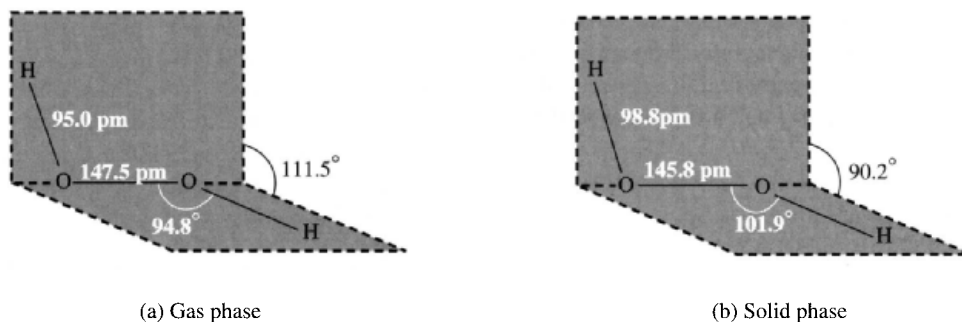
The  $\text{H}_2\text{O}_2$  is extracted by water and concentrated to ~30% (by weight) by distillation under reduced pressure. Further low-pressure distillation to concentrations up to 85% are not uncommon.

World production expressed as 100%  $\text{H}_2\text{O}_2$  approached 1.9 million tonnes in 1994 of which half was in Europe and one-fifth in the USA. The earliest and still the largest industrial use for  $\text{H}_2\text{O}_2$  is as a bleach for textiles, paper pulp, straw, leather, oils and fats, etc. Domestic use as a hair bleach and a mild disinfectant has diminished somewhat. Hydrogen peroxide is also extensively used to manufacture chemicals, notably sodium perborate (p. 206) and percarbonate, which are major constituents of most domestic detergents at least in the UK and Europe. Normal formulations include 15–25% of such peroxyacid salts, though the practice is much less widespread in the USA, and the concentrations, when included at all, are usually less than 10%.

In the organic chemicals industry,  $\text{H}_2\text{O}_2$  is used in the production of epoxides, propylene oxide, and caprolactones for PVC stabilizers and polyurethanes, in the manufacture of organic peroxy compounds for use as polymerization initiators and curing agents, and in the synthesis of fine chemicals such as hydroquinone, pharmaceuticals (e.g. cephalosporin) and food products (e.g. tartaric acid).

One of the rapidly growing uses of  $\text{H}_2\text{O}_2$  is in environmental applications such as control of pollution by treatment of domestic and industrial effluents, e.g. oxidation of cyanides and obnoxious malodorous sulfides, and the restoration of aerobic conditions to sewage waters. Its production in the USA for these and related purposes has trebled during the past decade (from 126 kt in 1984 to 360 kt in 1994) and it has substantially replaced chlorine as an industrial bleach because it yields only  $\text{H}_2\text{O}$  and  $\text{O}_2$  on decomposition. An indication of the proportion of  $\text{H}_2\text{O}_2$  production used for various applications in North America (1991) is: pulp and paper treatment 49%, chemicals manufacture 15%, environmental uses 15%, textiles 8%, all other uses 13%. The price per kg for technical grade aqueous  $\text{H}_2\text{O}_2$  in tank-car lots (1994) is \$0.54 (30%), \$0.75 (50%) and \$1.05 (70%), i.e. essentially a constant price of \$1.50 per kg on a "100% basis."

<sup>113</sup>W. T. HESS, Hydrogen Peroxide in *Kirk-Othmer Encyclopedia of Chemical Technology*, 4th Edn., Wiley, New York, Vol. 13, 961–95 (1995).



**Figure 14.16** Structure of the  $\text{H}_2\text{O}_2$  molecule (a) in the gas phase, and (b) in the crystalline state.

**Table 14.12** Dihedral angle of  $\text{H}_2\text{O}_2$  in some crystalline phases

Compound	Dihedral angle	Compound	Dihedral angle
$\text{H}_2\text{O}_2(\text{s})$	$90.2^\circ$	$\text{Li}_2\text{C}_2\text{O}_4 \cdot \text{H}_2\text{O}_2$	$180^\circ$
$\text{K}_2\text{C}_2\text{O}_4 \cdot \text{H}_2\text{O}_2$	$101.6^\circ$	$\text{Na}_2\text{C}_2\text{O}_4 \cdot \text{H}_2\text{O}_2$	$180^\circ$
$\text{Rb}_2\text{C}_2\text{O}_4 \cdot \text{H}_2\text{O}_2$	$103.4^\circ$	$\text{NH}_4\text{F} \cdot \text{H}_2\text{O}_2^{(114)}$	$180^\circ$
$\text{H}_2\text{O}_2 \cdot 2\text{H}_2\text{O}$	$129^\circ$		

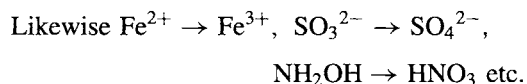
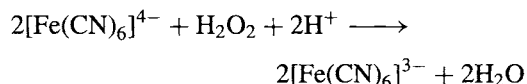
liquid:  $\text{H}_2\text{O}_2(\text{l}) \longrightarrow \text{H}_2\text{O}(\text{l}) + \frac{1}{2}\text{O}_2(\text{g}); \Delta H^\circ = -98.2 \text{ kJ mol}^{-1}$ ,  $\Delta G^\circ = -119.2 \text{ kJ mol}^{-1}$ . In fact, in the absence of catalysts, the compound decomposes negligibly slowly but the reaction is strongly catalysed by metal surfaces (Pt, Ag), by  $\text{MnO}_2$  or by traces of alkali (dissolved from glass), and for this reason  $\text{H}_2\text{O}_2$  is generally stored in wax-coated or plastic vessels with stabilizers such as urea; even a speck of dust can initiate explosive decomposition and all handling of the anhydrous compound or its concentrated solutions must be carried out in dust-free conditions and in the absence of metal ions. A useful "carrier" for  $\text{H}_2\text{O}_2$  in some reactions is the adduct  $(\text{Ph}_3\text{PO})_2 \cdot \text{H}_2\text{O}_2$ .

Hydrogen peroxide has a rich and varied chemistry which arises from (i) its ability to act either as an oxidizing or a reducing agent in both acid and alkaline solution, (ii) its ability to undergo proton acid/base reactions to form

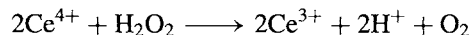
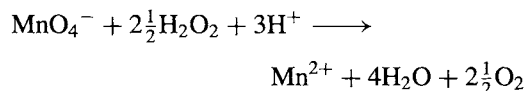
peroxonium salts  $(\text{H}_2\text{OOH})^+$ , hydroperoxides  $(\text{OOH})^-$  and peroxides  $(\text{O}_2)^{2-}$ , and (iii) its reactions to give peroxometal complexes and peroxyacid anions.

The ability of  $\text{H}_2\text{O}_2$  to act both as an oxidizing and a reducing agent is well known in analytical chemistry. Typical examples (not necessarily of analytical utility) are:

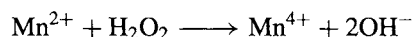
*Oxidizing agent in acid solution:*



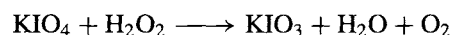
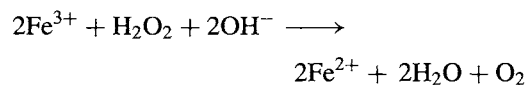
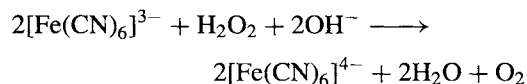
*Reducing agent in acid solution:*



*Oxidizing agent in alkaline solution:*



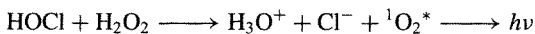
*Reducing agent in alkaline solution:*



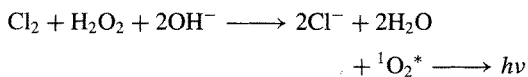
<sup>114</sup> V. A. SARIN, V. YA. DUDAREV, T. A. DOBRYNINA and V. E. ZAVODNIK, *Soviet Phys. Crystallogr.* **24**, 472-3 (1979), and references therein.

It will be noted that  $O_2$  is always evolved when  $H_2O_2$  acts as a reducing agent, and sometimes this gives rise to a red chemiluminescence if the dioxygen molecule is produced in a singlet state (p. 605), e.g.:

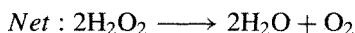
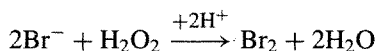
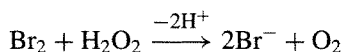
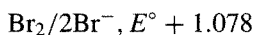
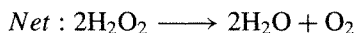
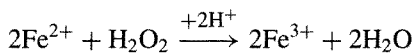
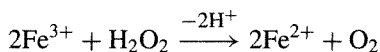
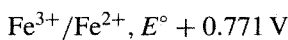
*Acid solution:*



*Alkaline solution:*



The catalytic decomposition of aqueous solutions  $H_2O_2$  alluded to on p. 635 can also be viewed as an oxidation–reduction process and, indeed, most homogeneous catalysts for this reaction are oxidation–reduction couples of which the oxidizing agent can oxidize (be reduced by)  $H_2O_2$  and the reducing agent can reduce (be oxidized by)  $H_2O_2$ . Thus, using the data on p. 628, any complex with a reduction potential between +0.695 and +1.776 V in acid solution should catalyse the reaction. For example:



In many such reactions, experiments using  $^{18}O$  show negligible exchange between  $H_2O_2$  and  $H_2O$ , and all the  $O_2$  formed when  $H_2O_2$  is used as a reducing agent comes from the  $H_2O_2$ , implying that oxidizing agents do not break the O–O bond but simply remove electrons. Not all reactions are heterolytic, however, and free radicals are sometimes involved, e.g.  $Ti^{3+}/H_2O_2$  and Fenton's

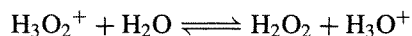
reagent ( $Fe^{2+}/H_2O_2$ ). The most important free radicals are OH and  $O_2H$ .

Hydrogen peroxide is a somewhat stronger acid than water, and in dilute aqueous solutions has  $pK_a(25^\circ) = 11.65 \pm 0.02$ , i.e. comparable with the third dissociation constant of  $H_3PO_4$  (p. 519):

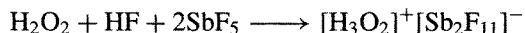
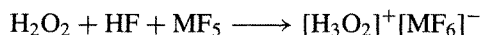


$$K_a = \frac{[H_3O^+][OOH^-]}{[H_2O_2]} = 2.24 \times 10^{-12} \text{ mol l}^{-1}$$

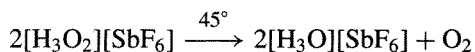
Conversely,  $H_2O_2$  is a much weaker base than  $H_2O$  (perhaps by a factor of  $10^6$ ), and the following equilibrium lies far to the right:



As a consequence, salts of  $H_3O_2^+$  cannot be prepared from aqueous solutions but they have been obtained as white solids from the strongly acid solvent systems anhydrous  $HF/SbF_5$  and  $HF/AsF_5$ , e.g.:<sup>(115)</sup>



The salts decompose quantitatively at or slightly above room temperature, e.g.:

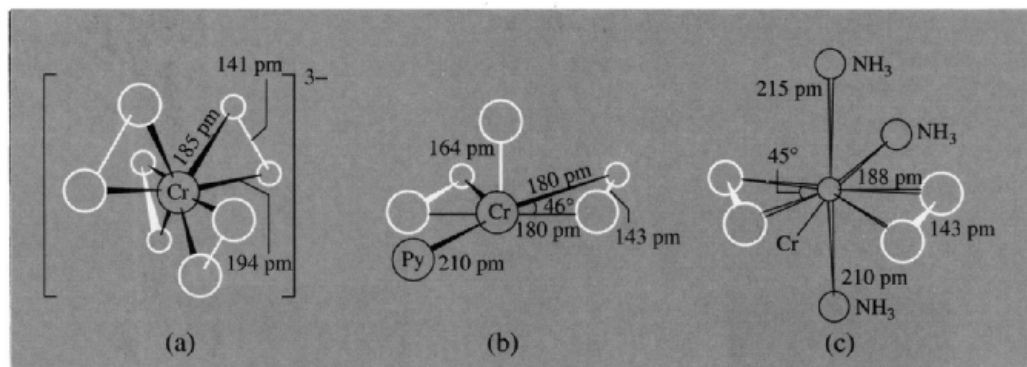


The ion  $[H_2OOH]^+$  is isoelectronic with  $H_2NOH$  and vibrational spectroscopy shows it to have the same ( $C_s$ ) symmetry.

Deprotonation of  $H_2O_2$  yields  $OOH^-$ , and hydroperoxides of the alkali metals are known in solution. Liquid ammonia can also effect deprotonation and  $NH_4OOH$  is a white solid, mp  $25^\circ$ ; infrared spectroscopy shows the presence of  $NH_4^+$  and  $OOH^-$  ions in the solid phase but the melt appears to contain only the H-bonded species  $NH_3$  and  $H_2O_2$ .<sup>(116)</sup> Double deprotonation yields the peroxide ion  $O_2^{2-}$ , and this is a standard route to transition metal peroxides.<sup>(53)</sup>

<sup>115</sup> K. O. CHRISTE, W. W. WILSON and E. C. CURTIS, *Inorg. Chem.* **18**, 2578–86 (1979).

<sup>116</sup> O. KNOP and P. A. GIGUERE, *Canad. J. Chem.* **37**, 1794–7 (1959).



**Figure 14.17** Structures of (a) the tetraperoxochromate(V) ion  $[\text{Cr}^{\text{V}}(\text{O}_2)_4]^{3-}$ , (b) the pyridine oxodiperoxochromium(VI) complex  $[\text{Cr}^{\text{VI}}\text{O}(\text{O}_2)_2\text{py}]$ , and (c) the triamminodiperoxochromium(IV) complex  $[\text{Cr}^{\text{IV}}(\text{NH}_3)_3(\text{O}_2)_2]$  showing important interatomic distances and angles. (This last compound was originally described as a chromium(II) superoxo complex  $[\text{Cr}^{\text{II}}(\text{NH}_3)_3(\text{O}_2)_2]$  on the basis of an apparent O–O distance of 131 pm,<sup>(117)</sup> and is a salutary example of the factual and interpretative errors that can arise even in X-ray diffraction studies.<sup>(118)</sup>)

Many such compounds are discussed under the individual transition elements and it is only necessary here to note that the chemical identity of the products obtained is often very sensitive to the conditions employed because of the combination of acid-base and redox reactions in the system. For example, treatment of alkaline aqueous solutions of chromate(VI) with  $\text{H}_2\text{O}_2$  yields the stable red paramagnetic tetraperoxochromate(V) compounds  $[\text{Cr}^{\text{V}}(\text{O}_2)_4]^{3-}$  ( $\mu$  1.80 BM), whereas treatment of chromate(VI) with  $\text{H}_2\text{O}_2$  in acid solution followed by extraction with ether and coordination with pyridine yields the neutral peroxochromate(VI) complex  $[\text{CrO}(\text{O}_2)_2\text{py}]$  which has a small temperature-independent paramagnetism of about 0.5 BM. The structure of these two species is in Fig. 14.17 which also includes the structure of the brown diperoxochromium(IV) complex  $[\text{Cr}^{\text{IV}}(\text{NH}_3)_3(\text{O}_2)_2]$  ( $\mu$  2.8 BM) prepared by treating either of the other two complexes with an excess of aqueous ammonia or more directly by treating an aqueous ammoniacal solution of  $[\text{NH}_4]_2[\text{Cr}_2\text{O}_7]$  with  $\text{H}_2\text{O}_2$ . Besides deprotonation of  $\text{H}_2\text{O}_2$ , other routes to metal

peroxides include the direct reduction of  $\text{O}_2$  by combustion of the electropositive alkali and alkaline earth metals in oxygen (pp. 84, 119) or by reaction of  $\text{O}_2$  with transition metal complexes in solution (p. 616).<sup>(119)</sup> Very recently  $\text{K}_2\text{O}_2$  has been obtained as a colourless crystalline biproduct of the synthesis of the orthonitrate  $\text{K}_3\text{NO}_4$  (p. 472) by prolonged heating of  $\text{KNO}_3$  and  $\text{K}_2\text{O}$  in a silver crucible at temperatures up to  $400^\circ\text{C}$ .<sup>(120)</sup> The O–O distance was found to be 154.1(6) pm, significantly longer than the values of  $\sim 150$  pm previously obtained for alkali metal peroxides (Table 14.4, p. 616).

Another recent development is the production of  $\text{HOOOH}$  (the ozone analogue of  $\text{H}_2\text{O}_2$ ) in 40% yield by the simple expedient of replacing  $\text{O}_2$  by  $\text{O}_3$  in the standard synthesis via 2-ethylanthraquinone at  $-78^\circ$  (cf. p. 634);  $\text{H}_2\text{O}_3$  begins to decompose appreciably around  $-40^\circ$  to give single oxygen,  $\Delta^1\text{O}_2$ , but is much more stable (up to  $+20^\circ$ ) in  $\text{MeOBU}^t$  and similar solvents.<sup>(121)</sup>

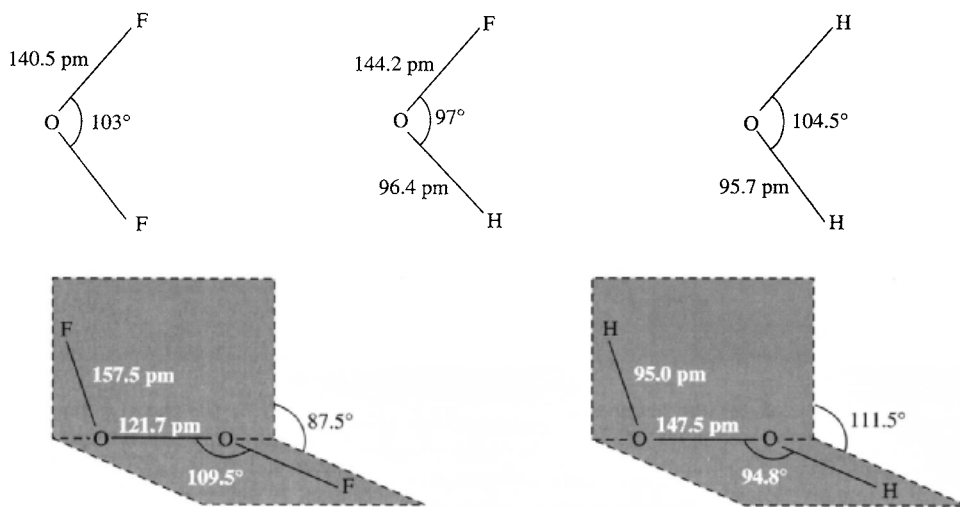
<sup>119</sup> N.-G. VANNERBERG, *Prog. Inorg. Chem.* **4**, 125–97 (1962).

<sup>120</sup> T. BREMM and M. JANSEN, *Z. anorg. allg. Chem.* **610**, 64–6 (1992).

<sup>121</sup> J. CERKOVNIK and B. PLESNIČAR, *J. Am. Chem. Soc.* **115**, 12169–70 (1993).

<sup>117</sup> E. H. McLAREN and L. HELMHOLZ, *J. Chem. Phys.* **63**, 1279–83 (1959).

<sup>118</sup> R. STROMBERG, *Arkiv Kemi* **22**, 49–64 (1974).

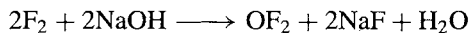


**Figure 14.18** Comparison of the molecular dimensions of various gaseous molecules having O-F and O-H bonds.

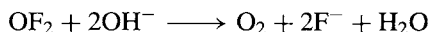
Peroxoanions are described under the appropriate element, e.g. peroxoborates (p. 206), peroxonitrates (p. 459), peroxophosphates (p. 512), peroxosulfates (p. 712), and peroxodisulfates (p. 713).

#### 14.2.4 Oxygen fluorides<sup>(122)</sup>

Oxygen forms several binary fluorides of which the most stable is  $\text{OF}_2$ . This was first made in 1929 by the electrolysis of slightly moist molten  $\text{KF}/\text{HF}$  but is now generally made by reacting  $\text{F}_2$  gas with 2% aqueous  $\text{NaOH}$  solution:



Conditions must be controlled so as to minimize loss of the product by the secondary reaction:



Oxygen fluoride is a colourless, very poisonous gas that condenses to a pale-yellow liquid (mp

$-223.8^\circ$ , bp  $-145.3^\circ\text{C}$ ). When pure it is stable to  $200^\circ$  in glass vessels but above this temperature it decomposes by a radical mechanism to the elements. Molecular dimensions (microwave) are in Fig. 14.18, where they are compared with those of related molecules. The heat of formation has been given as  $\Delta H_f^\circ$   $24.5 \text{ kJ mol}^{-1}$ , leading to an average O-F bond energy of  $187 \text{ kJ mol}^{-1}$ . Though less reactive than elementary fluorine,  $\text{OF}_2$  is a powerful oxidizing and fluorinating agent. Many metals give oxides and fluorides, phosphorus yields  $\text{PF}_5$  plus  $\text{POF}_3$ , sulfur  $\text{SO}_2$  plus  $\text{SF}_4$ , and xenon gives  $\text{XeF}_4$  and oxofluorides (p. 900).  $\text{H}_2\text{S}$  explodes on being mixed with  $\text{OF}_2$  at room temperature.  $\text{OF}_2$  is formally the anhydride of hypofluorous acid,  $\text{HOF}$ , but there is no evidence that it reacts with water to form this compound. Indeed,  $\text{HOF}$  had been sought for many decades but has only relatively recently been prepared and fully characterized.<sup>(123)</sup>

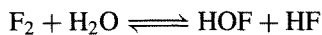
$\text{HOF}$  was first identified by P. N. Noble and G. C. Pimentel in 1968 using matrix isolation techniques:  $\text{F}_2/\text{H}_2\text{O}$  mixtures were frozen in solid

<sup>122</sup> E. A. V. EBSWORTH, J. A. CONNOR and J. J. TURNER, in J. C. BAILAR, H. J. EMELÉUS, R. S. NYHOLM and A. F. TROTMAN-DICKENSON (eds.), *Comprehensive Inorganic Chemistry*, Vol. 2, Chap. 22, Section 5, pp. 747–71. Pergamon Press, Oxford, 1973.

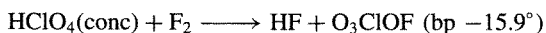
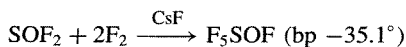
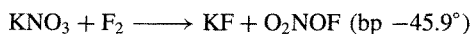
<sup>123</sup> E. H. APPELMAN, Nonexistent compounds: two case histories, *Acc. Chem. Res.* **6**, 113–7 (1973).



N<sub>2</sub> and photolysed at 14–20 K:



A more convenient larger-scale preparation was devised in 1971 by M. H. Studier and E. H. Appleman, who circulated F<sub>2</sub> rapidly through a Kel-F U-tube filled with Räschtig rings of polytetrafluoroethylene (Teflon) which had been moistened with water and cooled to –40°. An essential further condition was the presence of traps at –50° and –79° to remove H<sub>2</sub>O and HF (both of which react with HOF), and the product was retained in a trap at –183°. HOF is a white solid, melting at –117° to a pale yellow liquid which boils below room temperature. Molecular dimensions are in Fig. 14.18; the small bond angle is particularly notable, being the smallest yet recorded for 2-coordinate O in an open chain. HOF is stable with respect to its elements:  $\Delta H_f^\circ(298) = -98.2$ ,  $\Delta G_f^\circ(298) = -85.7 \text{ kJ mol}^{-1}$ . However, HOF decomposes fairly rapidly to HF and O<sub>2</sub> at room temperature ( $t_{1/2} \sim 30 \text{ min}$  at 100 mmHg in Kel-F or Teflon). Decomposition is accelerated by light and by the presence of F<sub>2</sub> or metal surfaces. HOF reacts rapidly with water to produce HF, H<sub>2</sub>O<sub>2</sub> and O<sub>2</sub>; with acid solutions H<sub>2</sub>O is oxidized primarily to H<sub>2</sub>O<sub>2</sub>, whereas in alkaline solutions O<sub>2</sub> is the principal oxygen-containing product. Ag<sup>I</sup> is oxidized to Ag<sup>II</sup> and, in alkaline solution, BrO<sub>3</sub><sup>–</sup> yields the elusive perbromate ion BrO<sub>4</sub><sup>–</sup> (p. 871). All these reactions parallel closely those of F<sub>2</sub> in water, and it may well be that HOF is the reactive species produced when F<sub>2</sub> reacts with water (p. 856). No ionic salts of hypofluorous acid have been isolated but covalent hypofluorites have been known for several decades as highly reactive (sometimes explosive) gases, e.g.:



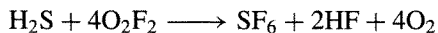
Dioxygen difluoride, O<sub>2</sub>F<sub>2</sub>, is best prepared by passing a silent electric discharge through a low-pressure mixture of F<sub>2</sub> and O<sub>2</sub>: the products obtained depend markedly on conditions, and the

yield of O<sub>2</sub>F<sub>2</sub> is optimized by using a 1:1 mixture at 7–17 mmHg and a discharge of 25–30 mA at 2.1–2.4 kV. Alternatively, pure O<sub>2</sub>F<sub>2</sub> can be synthesized by subjecting a mixture of liquid O<sub>2</sub> and F<sub>2</sub> in a stainless steel reactor at –196° to 3 MeV bremsstrahlung radiation for 1–4 h. O<sub>2</sub>F<sub>2</sub> is a yellow solid and liquid, mp –154°, bp –57° (extrapolated). It is much less stable than OF<sub>2</sub> and even at –160° decomposes at a rate of some 4% per day. Decomposition by a radical mechanism is rapid above –100°. The structure of O<sub>2</sub>F<sub>2</sub> (Fig. 14.18) resembles that of H<sub>2</sub>O<sub>2</sub> but the remarkably short O–O distance is a notable difference in detail (cf. O<sub>2</sub> gas 120.7 pm). Conversely, the O–F distance is unusually long when compared to those in OF<sub>2</sub> and HOF (Fig. 14.18). These features are paralleled by the bond dissociation energies:

$$D(\text{FO}–\text{OF}) \text{ 430 kJ mol}^{-1},$$

$$D(\text{F}–\text{OOF}) \sim 75 \text{ kJ mol}^{-1}.$$

Consistent with this, mass spectrometric, infrared and electron spin resonance studies confirm dissociation into F and OOF radicals, and low-temperature studies have also established the presence of the dimer O<sub>4</sub>F<sub>2</sub>, which is a dark red-brown solid, mp –191°C. Impure O<sub>4</sub>F<sub>2</sub> can also be prepared by silent electric discharge but the material previously thought to be O<sub>3</sub>F<sub>2</sub> is probably a mixture of O<sub>4</sub>F<sub>2</sub> and O<sub>2</sub>F<sub>2</sub>. Dioxygen difluoride, as expected, is a very vigorous and powerful oxidizing and fluorinating agent even at very low temperatures (–150°). It converts ClF to ClF<sub>3</sub>, BrF<sub>3</sub> to BrF<sub>5</sub>, and SF<sub>4</sub> to SF<sub>6</sub>. Similar products are obtained from HCl, HBr and H<sub>2</sub>S, e.g.:

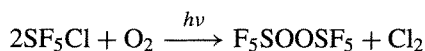
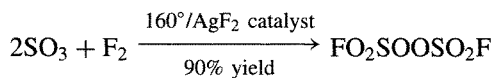


Interest in the production of high-energy oxidizers for use in rocket motors has stimulated the study of peroxy compounds bound to highly electronegative groups during the past few decades. Although such applications have not yet materialized, numerous new compounds of this type

Table 14.13 Properties of some fluorinated peroxides

Compound	MP/°C	BP/°C	Compound	MP/°C	BP/°C
FO <sub>2</sub> SOOSO <sub>2</sub> F	-55.4	67.1	F <sub>3</sub> COONO <sub>2</sub>	—	0.7
FO <sub>2</sub> SOOF	—	0	F <sub>3</sub> COOP(O)F <sub>2</sub>	-88.6	15.5
FO <sub>2</sub> SOOSF <sub>5</sub>	—	54.1	F <sub>3</sub> COOCl	-132	-22
F <sub>5</sub> SOOSF <sub>5</sub>	-95.4	49.4	(F <sub>3</sub> C) <sub>3</sub> COOC(CF <sub>3</sub> ) <sub>3</sub>	12	98.6
F <sub>5</sub> SOOCF <sub>3</sub>	-136	7.7	F <sub>3</sub> COOOCF <sub>3</sub>	-138	-16

have been synthesized and characterized, e.g.:



Such compounds are volatile liquids or gases (Table 14.13) and their extensive reaction chemistry has been very fully reviewed.<sup>(124)</sup>

## 14.2.5 Oxides

### Various methods of classification

Oxides are known for all elements of the periodic table except the lighter noble gases and, indeed, most elements form more than one binary compound with oxygen. Their properties span the full range of volatility from difficultly condensable gases such as CO (bp -191.5°C) to refractory oxides such as ZrO<sub>2</sub> (mp 3265°C, bp ~4850°C). Likewise, their electrical properties vary from being excellent insulators (e.g. MgO), through semi-conductors (e.g. NiO), to good metallic conductors (e.g. ReO<sub>3</sub>). They may be precisely stoichiometric or show stoichiometric variability over a narrow or a wide range of composition. They may be thermodynamically stable or unstable with respect to their elements, thermally stable or unstable, highly reactive to common reagents or almost completely inert even at very high temperatures. With such a vast array

of compounds and such a broad spectrum of properties any classification of oxides is likely to be either too simplified to be reliable or too complicated to be useful. One classification that is both convenient and helpful at an elementary level stresses the acid-base properties of oxides; this can be complemented and supplemented by classifications which stress the structural relationships between oxides. General classifications based on redox properties or on presumed bonding models have proved to be less helpful, though they are sometimes of use when a more restricted group of compounds is being considered.

The acid-base classification<sup>(125)</sup> turns essentially on the thermodynamic properties of hydroxides in aqueous solution, since oxides themselves are not soluble as such (p. 630). Oxides may be:

*acidic*: e.g. most oxides of non-metallic elements (CO<sub>2</sub>, NO<sub>2</sub>, P<sub>4</sub>O<sub>10</sub>, SO<sub>3</sub>, etc.);

*basic*: e.g. oxides of electropositive elements (Na<sub>2</sub>O, CaO, Ti<sub>2</sub>O, La<sub>2</sub>O<sub>3</sub>, etc.);

*amphoteric*: oxides of less electropositive elements (BeO, Al<sub>2</sub>O<sub>3</sub>, Bi<sub>2</sub>O<sub>3</sub>, ZnO, etc.);

*neutral*: oxides that do not interact with water or aqueous acids or bases (CO, NO, etc.).

Periodic trends in these properties are well documented (p. 27). Thus, in a given period, oxides progress from strongly basic, through weakly basic, amphoteric, and weakly acidic, to strongly acidic (e.g. Na<sub>2</sub>O, MgO, Al<sub>2</sub>O<sub>3</sub>, SiO<sub>2</sub>, P<sub>4</sub>O<sub>10</sub>, SO<sub>3</sub>, ClO<sub>2</sub>). Acidity also increases with increasing oxidation state (e.g. MnO < Mn<sub>2</sub>O<sub>3</sub> < MnO<sub>2</sub> < Mn<sub>2</sub>O<sub>7</sub>). A similar trend is

<sup>124</sup> R. A. DE MARCO and J. M. SHREEVE, *Adv. Inorg. Chem. Radiochem.*, **16**, 109-76 (1974); J. M. SHREEVE, *Endeavour* xxxv, No. 125, 79-82 (1976).

<sup>125</sup> C. S. G. PHILLIPS and R. J. P. WILLIAMS, *Inorganic Chemistry*, Vol. 1, Oxford University Press, Oxford, 1965; Section 14.1, see also pp. 722-9 of ref. 122.

the decrease in basicity of the lanthanide oxides with increase in atomic number from La to Lu. In the main groups, basicity of the oxides increases with increase in atomic number down a group (e.g.  $\text{BeO} < \text{MgO} < \text{CaO} < \text{SrO} < \text{BaO}$ ), though the reverse tends to occur in the later transition element groups. Acid–base interactions can also be used to classify reaction types of (a) oxides with each other (eg.  $\text{CaO}$  with  $\text{SiO}_2$ ), (b) oxides with oxysalts (eg.  $\text{CaO}$  with  $\text{CaSiO}_3$ ), and (c) oxysalts with each other (eg.  $\text{Ca}_2\text{SiO}_4$  and  $\text{Ca}_3(\text{PO}_4)_2$ ), and to predict the products of such reactions.<sup>(126)</sup>

The thermodynamic and other physical properties of binary oxides (e.g.  $\Delta H_f^\circ$ ,  $\Delta G_f^\circ$ , mp, etc.) show characteristic trends and variations when plotted as a function of atomic number, and the preparation of such plots using readily available compilations of data<sup>(127)</sup> can be a revealing and rewarding exercise.<sup>(128)</sup>

Structural classifications of oxides recognize discrete molecular species and structures which are polymeric in one or more dimensions leading to chains, layers, and ultimately, to three-dimensional networks. Some typical examples are in Table 14.14; structural details are given elsewhere under each individual element. The type of structure adopted in any particular case depends (obviously) not only on the

stoichiometry but also on the relative sizes of the atoms involved and the propensity to form  $p_\pi$  double bonds to oxygen. In structures which are conventionally described as “ionic”, the 6-coordinate radius of  $\text{O}^{2-}$  (140 pm) is larger than all 6-coordinate cation radii except for  $\text{Rb}^I$ ,  $\text{Cs}^I$ ,  $\text{Fr}^I$ ,  $\text{Ra}^{II}$ , and  $\text{Tl}^I$  though it is approached by  $\text{K}^I$  (138 pm) and  $\text{Ba}^{II}$  (135 pm).<sup>(129)</sup> Accordingly, many oxides are found to adopt structures in which there is a close-packed oxygen lattice with cations in the interstices (frequently octahedral). For “cations”, which have very small effective ionic radii (say  $< 50$  pm), particularly if they carry a high formal charge, the structure type and bonding are usually better described in covalent terms, particularly when  $\pi$  interactions enhance the stability of terminal  $\text{M}=\text{O}$  bonds ( $\text{M} = \text{C}, \text{N}, \text{P}^V, \text{S}^{VI}$ , etc.). Thus, for oxides of formula  $\text{MO}$ , a coordination number of 1 (molecular) is found for  $\text{CO}$  and  $\text{NO}$ , though the latter tends towards a coordination number of 2 (dimers, p. 446). With the somewhat larger  $\text{Be}^{II}$  and  $\text{Zn}^{II}$  the wurtzite (4:4) structure is adopted, whereas monoxides of still larger divalent cations tend to adopt the sodium chloride (6:6) structure (e.g.  $\text{M}^{II} = \text{Mg}, \text{Ca}, \text{Sr}, \text{Ba}, \text{Co}, \text{Ni}, \text{Cd}, \text{Eu}$ , etc.).

A similar trend is observed for oxides of  $\text{M}^{IV}\text{O}_2$  in Group 14 of the periodic table. The small C atom, with its propensity to form  $p_\pi$ – $p_\pi$  bonds to oxygen, adopts a linear, molecular structure  $\text{O}=\text{C}=\text{O}$ . Silicon, being somewhat larger and less prone to double bonding (p. 361), is surrounded by 4 essentially single-bonded O in most forms of  $\text{SiO}_2$  (p. 342) and the coordination geometry is thus 4:2. Similarly,  $\text{GeO}_2$  adopts the quartz structure; in addition a rutile form (p. 961) is known in which the coordination is 6:3.  $\text{SnO}_2$  and  $\text{PbO}_2$  also have rutile structures as has  $\text{TiO}_2$ , but the largest Group 4 cations Zr and Hf adopt the fluorite (8:4) structure (p. 118) in their dioxides. Other large cations with a fluorite structure for  $\text{MO}_2$  are Po; Ce, Pr, Tb; Th, U, Np, Pu, Am and Cm. Conversely, the antifluorite structure is found for

**Table 14.14** Structure types for binary oxides in the solid state

Structure type	Examples
Molecular structures	$\text{CO}, \text{CO}_2, \text{OsO}_4, \text{Tc}_2\text{O}_7,$ $\text{Sb}_2\text{O}_6, \text{P}_4\text{O}_{10}$
Chain structures	$\text{HgO}, \text{SeO}_2, \text{CrO}_3, \text{Sb}_2\text{O}_3$
Layer structures	$\text{SnO}, \text{MoO}_3, \text{As}_2\text{O}_3, \text{Re}_2\text{O}_7$
Three-dimensional structures	See text

<sup>126</sup> L. S. DENT-GLASSER and J. A. DUFFER, *J. Chem. Soc., Dalton Trans.*, 2323–8 (1987).

<sup>127</sup> M. C. BALL and A. H. NORBURY, *Physical Data for Inorganic Chemists*, Longmans, London, 1974, 175 pp. G. H. AYLWARD and T. J. V. FINDLAY, *SI Chemical Data*, 2nd edn., Wiley, Sydney, 1975, 136 pp.

<sup>128</sup> R. V. PARISH, *The Metallic Elements*, Longmans, London 1977, 254 pp. (see particularly pp. 25–8, 40–44, 66–74, 128–33, 148–50, 168–77, 188–98).

<sup>129</sup> R. D. SHANNON, *Acta Cryst.* **A32**, 751–67 (1976).

the alkali metal monoxides  $M_2O$  (p. 84). Such simple ideas are capable of considerable further elaboration.<sup>(130)</sup>

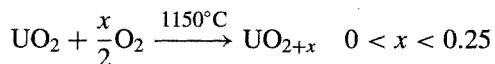
### Nonstoichiometry

Transition elements, for which variable valency is energetically feasible, frequently show nonstoichiometric behaviour (variable composition) in their oxides, sulfides and related binary compounds. For small deviations from stoichiometry a thermodynamic approach is instructive, but for larger deviations structural considerations super-vene, and the possibility of thermodynamically unstable but kinetically isolable phases must be considered. These ideas will be expanded in the following paragraphs but more detailed treatment must be sought elsewhere.<sup>(131-134)</sup>

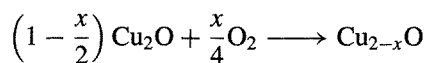
Any crystal in contact with the vapour of one of its constituents is potentially a nonstoichiometric compound since, for true thermodynamic equilibrium, the composition of the solid phase must depend on the concentration (pressure) of this constituent in the vapour phase. If the solid and vapour are in equilibrium with each other ( $\Delta G = 0$ ) at a given temperature and pressure, then a change in this pressure will lead to a change (however minute) in the composition of the solid, provided that the activation energy for the reaction is not too high at the temperature being used. Such deviations from ideal stoichiometry imply a change in valency of at least some of the ions in the crystal and

are readily detected for many oxides using a range of techniques such as pressure-composition isotherms, X-ray diffraction, neutron diffraction, electrical conductivity (semi-conductivity), visible and ultraviolet absorption spectroscopy (colour centres)<sup>(131)</sup> and Mössbauer ( $\gamma$ -ray resonance) spectroscopy.<sup>(135)</sup>

If the pressure of  $O_2$  above a crystalline oxide is increased, the oxide-ion activity in the solid can be increased by placing the supernumerary  $O^{2-}$  ions in the interstitial positions, e.g.:

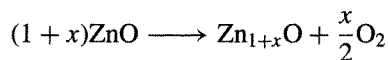


The electrons required to reduce  $\frac{1}{2}O_2$  to  $O^{2-}$  come from individual cations which are thereby oxidized to a higher oxidation state. Alternatively, if suitable interstitial sites are not available, the excess  $O^{2-}$  ions can build on to normal lattice sites thereby creating cation vacancies which diffuse into the crystal, e.g.:

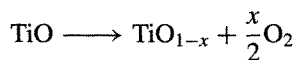


In this case the requisite electrons are provided by  $2Cu^I$  becoming oxidized to  $2Cu^{II}$ .

Conversely, if the pressure of  $O_2$  above a crystalline oxide is decreased below the equilibrium value appropriate for the stoichiometric composition, oxygen "boils out" of the lattice leaving supernumerary metal atoms or lower-valent ions in interstitial positions, e.g.:



The absorption spectrum of this nonstoichiometric phase forms the basis for the formerly much-used qualitative test for zinc oxide: "yellow when hot, white when cold". Alternatively, anion sites can be left vacant, e.g.:



In both cases the average oxidation state of the metal is reduced. It is important to appreciate that,

<sup>130</sup> A. F. WELLS, *Structural Inorganic Chemistry*, 5th edn., Oxford University Press, Oxford, 1984; Chap. 12, Binary metal oxides, pp. 531-74; Chap. 13, Complex oxides, pp. 575-625.

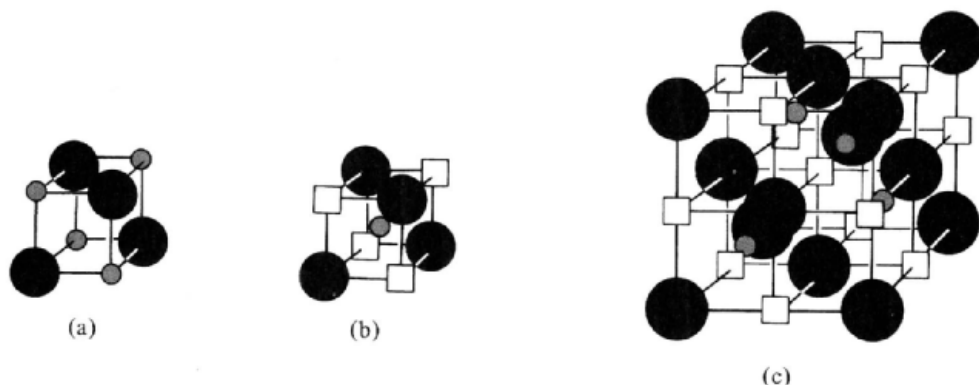
<sup>131</sup> N. N. GREENWOOD, *Ionic Crystals, Lattice Defects, and Nonstoichiometry*, Chaps. 6 and 7, pp. 111-81, Butterworths, London, 1968.

<sup>132</sup> D. J. M. BEVAN, Chap. 49 in J. C. BAILAR, H. J. EMELÉUS, R. S. NYHOLM and A. F. TROTMAN-DICKENSON (eds.), *Comprehensive Inorganic Chemistry*, Vol. 4, pp. 453-40, Pergamon Press, Oxford, 1973.

<sup>133</sup> T. SØRENSEN, *Nonstoichiometric Oxides*, Academic Press, New York, 1981, 441 pp.

<sup>134</sup> S. TRASATTI, *Electrodes of Conductive Metallic Oxides*, Elsevier, Amsterdam, Part A, 1980, 366 pp.; Part B, 1981, 336 pp.

<sup>135</sup> N. N. GREENWOOD and T. C. GIBB, *Mössbauer Spectroscopy*, Chapman & Hall, London, 1971, 659 pp.



**Figure 14.19** Schematic representation of defect clusters in  $\text{Fe}_{1-x}\text{O}$ . The normal NaCl-type structure (a) has  $\text{Fe}^{\text{II}}$  (small open circles) and  $\text{O}^{2-}$  (large dark circles) at alternate corners of the cube. In the 4:1 cluster (b), four octahedral  $\text{Fe}^{\text{II}}$  sites are left vacant and an  $\text{Fe}^{\text{III}}$  ion (grey) occupies the cube centre, thus being tetrahedrally coordinated by the  $4\text{O}^{2-}$ . In (c) a more extended 13:4 cluster is shown in which, again, all anion sites are occupied but the 13 octahedral  $\text{Fe}^{\text{II}}$  sites are vacant and four  $\text{Fe}^{\text{III}}$  occupy a tetrahedral array of cube centres.

in all such examples, the resulting nonstoichiometric compound is a homogeneous phase which is thermodynamically stable under the prevailing ambient conditions.

Sometimes the lattice defects form clusters amongst themselves rather than being randomly distributed throughout the lattice. A classic example is “ferrous oxide”, which is unstable as  $\text{FeO}$  at room temperature but exists as  $\text{Fe}_{1-x}\text{O}$  ( $0.05 < x < 0.12$ ): the NaCl-type lattice has a substantial number of vacant  $\text{Fe}^{\text{II}}$  sites and these tend to cluster so that  $\text{Fe}^{\text{III}}$  can occupy tetrahedral sites within the lattice as shown schematically in Fig. 14.19. Such clustering can sometimes nucleate a new phase in which “vacant sites” are eliminated by being ordered in a new structure type. For example,  $\text{PrO}_{2-x}$  forms a disordered nonstoichiometric phase ( $0 < x < 0.25$ ) at  $1000^\circ\text{C}$  but at lower temperatures ( $400\text{--}700^\circ\text{C}$ ) this is replaced by a succession of intermediate phases with only very narrow (and non-overlapping) composition ranges of general formula  $\text{Pr}_n\text{O}_{2n-2}$  with  $n = 4, 7, 9, 10, 11, 12$  and  $\infty$  as shown in Fig. 14.20 and Table 14.15. There is now compelling evidence that oxide-ion vacancies,  $\square$ , in these and other such fluorite-related lattices do not exist in

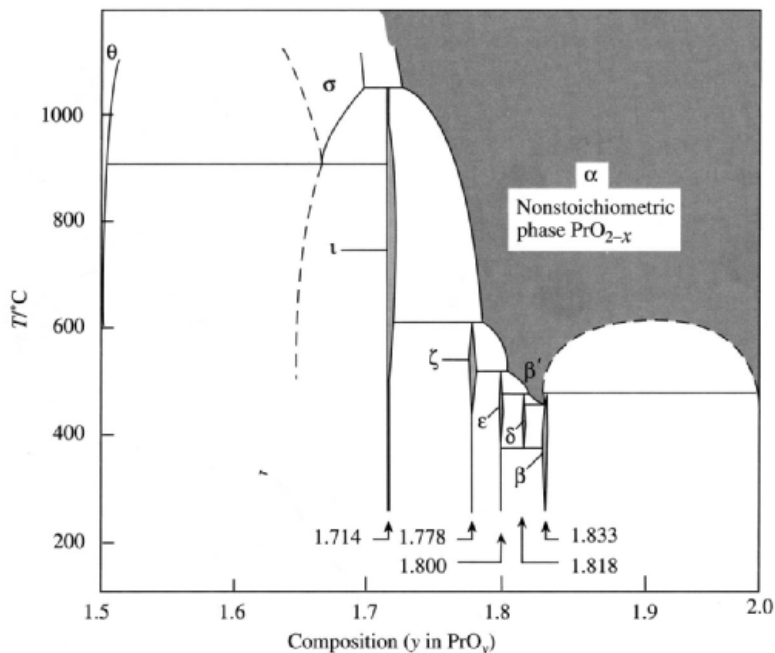
isolation but occur as octahedral ‘coordination defects’ of composition  $\{\text{M}_2^{\text{III}}\text{M}_{1.5}^{\text{IV}}\square\text{O}_6\}$ . The structure-forming topology of these coordination defects and their role in generating more extensive defects has recently been brilliantly expounded.<sup>(136)</sup>

**Table 14.15** Intermediate phases formed by ordering of defects in the praseodymium–oxygen system

$n$	Formula $\text{Pr}_n\text{O}_{2n-2}$	$y$ in $\text{PrO}_y$	Nonstoichiometric limits of $x$ at $T^\circ\text{C}$	$T^\circ\text{C}$
4	$\text{Pr}_2\text{O}_3$	1.500	1.500–1.503	1000
7	$\text{Pr}_7\text{O}_{12}$	1.714	1.713–1.719	700
9	$\text{Pr}_9\text{O}_{16}$	1.778	1.776–1.778	500
10	$\text{Pr}_{10}\text{O}_{18}$	1.800	1.799–1.801	450
11	$\text{Pr}_{11}\text{O}_{20}$	1.818	1.817–1.820	430
12	$\text{Pr}_{12}\text{O}_{22}$	1.833	1.831–1.836	400
$\infty$	$\text{PrO}_2$	2.000	1.999–2.000	400
			1.75–2.00	1000

Oxygen (oxide ions) in crystal lattices can be progressively removed by systematically

<sup>136</sup> B. F. HOSKINS and R. L. MARTIN, *Aust. J. Chem.* **48**, 709–39 (1995). R. L. MARTIN, *J. Chem. Soc., Dalton Trans.*, 3659–70 (1997).



**Figure 14.20** Part of the Pr–O phase diagram showing the extended nonstoichiometric  $\alpha$  phase  $\text{PrO}_{2-x}$  at high temperatures (shaded) and the succession of phases  $\text{Pr}_n\text{O}_{2n-2}$  at lower temperatures.

replacing corner-shared  $\{\text{MO}_6\}$  octahedra with edge-shared octahedra. The geometrical principles involved in the conceptual generation of such successions of phases (chemical-shear structures) are now well understood, but many mechanistic details of their formation remain unresolved. Typical examples are the rutile series  $\text{Ti}_n\text{O}_{2n-1}$  ( $n = 4, 5, 6, 7, 8, 9, 10, \infty$ ) between  $\text{TiO}_{1.75}$  and  $\text{TiO}_2$  and the  $\text{ReO}_3$  series  $\text{M}_n\text{O}_{3n-1}$  which leads to a succession of 6 phases with  $n = 8, 9, 10, 11, 12$  and 14 in the narrow composition range  $\text{MO}_{2.875}$  to  $\text{MO}_{2.929}$  ( $M = \text{Mo}$  or  $\text{W}$ ).

Nonstoichiometric oxide phases are of great importance in semiconductor devices, in heterogeneous catalysis and in understanding photoelectric, thermoelectric, magnetic and diffusional properties of solids. They have been used in thermistors, photoelectric cells, rectifiers, transistors, phosphors, luminescent materials and computer components (ferrites, etc.). They are crucially implicated in reactions at electrode surfaces, the performance of batteries, the tarnishing and corrosion of metals, and many other reactions of significance in catalysis.<sup>(131–134)</sup>

		1 H		2 He												3 B										4 C										5 N										6 O										7 F										8 Ne																											
9 Li		10 Be												11 Na										12 Mg										13 Al										14 Si										15 P										16 S										17 Cl										18 Ar									
19 K		20 Ca		21 Sc		22 Ti		23 V		24 Cr		25 Mn		26 Fe		27 Co		28 Ni		29 Cu		30 Zn		31 Ga		32 Ge		33 As		34 Se		35 Br		36 Kr																																																											
37 Rb		38 Sr		39 Y		40 Zr		41 Nb		42 Mo		43 Tc		44 Ru		45 Rh		46 Pd		47 Ag		48 Cd		49 In		50 Sn		51 Sb		52 Te		53 I		54 Xe																																																											
55 Cs		56 Ba		57 La		58 Ce		59 Pr		60 Nd		61 Pm		62 Sm		63 Eu		64 Gd		65 Tb		66 Dy		67 Ho		68 Er		69 Tm		70 Yb		71 Lu																																																													
73 Fr		74 Ra		75 Ac		76 Th		77 Pa		78 U		79 Np		80 Pu		81 Am		82 Cm		83 Bk		84 Cf		85 Es		86 Fm		87 Md		88 No		89 Lr																																																													

# 15

## Sulfur

### 15.1 The Element

#### 15.1.1 Introduction

Sulfur occurs uncombined in many parts of the world and has therefore been known since pre-historic times. Indeed, sulfur and carbon were the only two non-metallic elements known to the ancients. References to sulfur occur throughout recorded history from the legendary destruction of Sodom and Gomorrah by brimstone<sup>(1)</sup> to its recent discovery (together with H<sub>2</sub>SO<sub>4</sub>) as a major component in the atmosphere of the planet Venus. The element was certainly known to the Egyptians as far back as the sixteenth century BC and Homer refers to its use as a fumigant.<sup>(2)</sup> Pliny the Elder<sup>(3)</sup> mentioned the occurrence of sulfur

in volcanic islands and other Mediterranean locations, spoke of its use in religious ceremonies and in the fumigation of houses, described its use by fullers, cotton-bleachers, and match-makers, and indicated fourteen supposed medicinal virtues of the element.

Gunpowder, which revolutionized military tactics in the thirteenth century, was the sole known propellant for ammunition until the mid-nineteenth century when smokeless powders based on guncotton (1846), nitroglycerine (1846), and cordite (1889) were discovered. Gunpowder, an intimate mixture of saltpeter (KNO<sub>3</sub>), powdered charcoal and sulfur in the approximate ratios 75:15:10 by weight, was discovered by Chinese alchemists more than 1000 years ago:<sup>(4)</sup> The earliest known recipe for explosive gunpowder (as distinct from incendiary mixtures and fireworks) appeared in a Chinese military manual of AD 1044 and its use in a gun (bombard) dates from at least as early as 1128. Arab and European formulae and technology were derived from this. The first use of gunpowder

<sup>1</sup> Genesis 19, 24: "Then the Lord rained upon Sodom and Gomorrah brimstone and fire from the Lord out of heaven." Other biblical references to brimstone are in Deuteronomy 29, 23; Job 18, 15; Psalm 11, 6; Isaiah 30, 33; Ezekiel 38, 22; Revelation 19, 20; etc.

<sup>2</sup> HOMER, *Odyssey*, Book 22, 481: "Bring me sulfur, old nurse, that cleanses all pollution and bring me fire, that I may purify the house with sulfur."

<sup>3</sup> G. PLINY (the Elder), AD 23–79, mentions sulfur in several of the many books of his posthumously published major work, *Naturalis Historia*.

<sup>4</sup> A. R. BUTLER, *Chem. in Britain*, 1119–21 (1988); and research by Joseph Needham, Cambridge, UK.

### Developments in the Chemistry of Sulfur

- Prehistory Sulfur (brimstone) mentioned frequently in the Bible.<sup>(1)</sup>  
 ~800 BC Fumigating power of burning S mentioned by Homer.<sup>(2)</sup>  
 ~ AD 79 Occurrence and many uses of S recorded by G. Pliny.<sup>(3)</sup>  
 AD 940 Sulfuric acid mentioned by Persian writer Abu Bekr al Rases.  
 1044 Earliest known (Chinese) recipe for explosive gunpowder.<sup>(4)</sup>  
 1128 Gunpowder used by Chinese military in a bombard.  
 ~1245 Gunpowder "discovered" independently in Europe by Roger Bacon (England) and Berthold Swartz.  
 1661 Effects of SO<sub>2</sub> pollution in London dramatically described to Charles II by John Evelyn (p. 698).  
 1746 Lead chamber process for H<sub>2</sub>SO<sub>4</sub> introduced by John Roebuck (Birmingham, UK); this immediately superseded the cumbersome small-scale glass bell-jar process (p. 708).  
 1777 Elemental character of S proposed by A.-L. Lavoisier though even in 1809 experiments (presumably on impure samples) led Humphry Davy to contend that oxygen and hydrogen were also essential constituents of S.  
 1781 Sulfur compounds first detected in plants by N. Deyeux (roots of the dock, horse-radish, and cochlearia).  
 1809 Sulfur firmly established as an element by J. L. Gay Lussac and L. J. Thenard.  
 1813 Sulfur detected in the bile and blood of animals by H. A. Vogel.  
 1822 Xanthates (e.g. EtOCSK) discovered by W. C. Zeise who also prepared the first mercaptan (EtSH) in 1834 (see also p. 930).  
 1831 Contact process for SO<sub>3</sub>/H<sub>2</sub>SO<sub>4</sub> patented by P. Philips of Bristol, UK (the original platinum catalyst was subsequently replaced by ones based on V<sub>2</sub>O<sub>5</sub>).  
 1835 S<sub>4</sub>N<sub>4</sub> first made by M. Gregory (S<sub>2</sub>Cl<sub>2</sub> + NH<sub>3</sub>); X-ray structure by M. J. Bueger, 1936.  
 1839 Vulcanization of natural rubber latex by heating it with S discovered by Charles Goodyear (USA).  
 1865 Prospectors boring for petroleum in Louisiana discovered a great S deposit beneath a 150-m thick layer of quicksand.  
 1891-4 H. Frasch developed commercial recovery of S by superheated water process.  
 1912 E. Beckmann showed that rhombohedral sulfur was S<sub>8</sub> by cryoscopy in molten iodine.  
 1923 V. B. Goldschmid's geochemical classification includes "chalcophiles" (p. 648).  
 1926 Isotopes <sup>33</sup>S and <sup>34</sup>S discovered by F. W. Aston who previously (1920) had only detected <sup>32</sup>S in his mass spectrometer.  
 1935 Molecular structure of *cyclo*-S<sub>8</sub> established by X-ray methods (B. E. Warren and J. T. Burwell).  
 1944 Sulfur first produced from sour natural gas; by 1971 this source, together with crude oil, accounted for nearly one-third of world production.  
 1950 SF<sub>4</sub> first isolated by G. A. Silvery and G. H. Cady.  
 1951 Sulfur nmr signals (from <sup>33</sup>S) first detected by S. S. Dharmatti and H. E. Weaver.  
 1972 Sulfur and H<sub>2</sub>SO<sub>4</sub> detected in the atmosphere of the planet Venus by USSR Venera 8 (subsequently confirmed in 1978 by US Venus Pioneer 2).  
 1973 S<sub>18</sub> and S<sub>20</sub> synthesized and characterized by M. Schmidt, A. Kutoglu, and their coworkers.  
 1975 The metallic and superconducting properties of polymeric (SN)<sub>x</sub> discovered independently by two groups in the USA (p. 727).

in a major campaign in the West was at the Battle of Crécy (26 August 1346), but the guns lacked all power of manoeuvre and the devastating victory of Edward III was due chiefly to the long-bow men whom the French were also encountering for the first time. By 1415, however, gunpowder was decisive in Henry V's siege of Harfleur, and its increasing use in mobile field guns, naval artillery, and hand-held firearms was a dominant feature of world history for the next 500 y. Parallel with these activities, but largely independent of them, was the European development of the alchemy and chemistry of sulfur, and the growth of the emerging chemical

industry based on sulfuric acid (p. 708). Some of the key points in this story are summarized in the Panel and a fuller treatment can be found in standard references.<sup>(5-8)</sup>

<sup>5</sup> J. W. MELLOR, *A Comprehensive Treatise on Inorganic and Theoretical Chemistry*, Vol. 10, Chap. 57, pp. 1-692, Longmans, Green, London, 1930.

<sup>6</sup> *Gmelins Handbuch der Anorganischen Chemie*, System Number 9A *Schwefel*, pp. 1-60, Verlag Chemie, Weinheim/Bergstrasse, 1953.

<sup>7</sup> M. E. WEEKS, *Discovery of the Elements*, Sulfur, pp. 52-73, Journal of Chemical Education, Easton, 1956.

<sup>8</sup> T. K. DERRY and T. I. WILLIAMS, *A Short History of Technology*, Oxford University Press, Oxford, 1960 (consult index).



### 15.1.2 Abundance and distribution

Sulfur occurs, mainly in combined form, to the extent of about 340 ppm in the crustal rocks of the earth. It is the sixteenth element in order of abundance, closely following barium (390 ppm) and strontium (384 ppm), and being about twice as abundant as the next element carbon (180 ppm). Earlier estimates placed its global abundance in the range 300–1000 ppm. Sulfur is widely distributed in nature but only rarely is it sufficiently concentrated to justify economic mining. Its ubiquity is probably related to its occurrence in nature in both inorganic and organic compounds, and to the fact that it can occur in at least five oxidation states:  $-2$  (sulfides,  $H_2S$  and organosulfur compounds),  $-1$  (disulfides,  $S_2^{2-}$ ),  $0$  (elemental S),  $+4$  ( $SO_2$ ) and  $+6$  (sulfates). The three most important commercial sources are:

- (1) elemental sulfur in the caprock salt domes in the USA and Mexico, and the sedimentary evaporite deposits in south-eastern Poland;
- (2)  $H_2S$  in natural gas and crude oil, and organosulfur compounds in tar sands, oil shales and coal (the latter two also contain pyrites inclusions);
- (3) pyrites ( $FeS_2$ ) and other metal-sulfide minerals.

Volcanic sources of the free element are also widespread; they have been of great economic importance until this century but are now little used. They occur throughout the mountain ranges bordering the Pacific Ocean, and also in Iceland and the Mediterranean region, notably in Turkey, Italy and formerly also in Sicily and Spain.

Elemental sulfur in the caprock of salt domes was almost certainly produced by the anaerobic bacterial reduction of sedimentary sulfate deposits (mainly anhydrite or gypsum, p. 648). The strata are also associated with hydrocarbons; these are consumed as a source of energy by the anaerobic bacteria, which use sulfur instead of  $O_2$  as a hydrogen acceptor to produce  $CaCO_3$ ,  $H_2O$  and  $H_2S$ . The  $H_2S$

may then be oxidized to colloidal sulfur, or may form calcium hydrosulfide and polysulfide, which reacts with  $CO_2$  generated by the bacteria to precipitate crystalline sulfur and secondary calcite. Alternatively,  $H_2S$  may escape from the system and the limestone caprock will then be free of sulfur. Indeed, of over 400 salt-dome structures known to exist in the coastal and offshore area of the Gulf of Mexico, only about 12 contain commercial deposits of sulfur (5 in Louisiana, 5 in Texas and 2 in Mexico). The mining operations are described in the Section 15.1.3.

The great evaporite basin deposits of elemental sulfur in Poland were discovered only in 1953 but have since had a dramatic impact on the economy of that country which, by 1985, was one of the world's leading producers (p. 649). The sulfur occurs in association with secondary limestone, gypsum and anhydrite, and is believed to be derived from hydrocarbon reduction of sulfates assisted by bacterial action. The  $H_2S$  so formed is consumed by other bacteria to produce sulfur as waste — this accumulates in the bodies of the bacteria until death, when the sulfur remains.

The next great natural occurrence of sulfur is as  $H_2S$  in sour natural gas and as organosulfur compounds in crude oil. Again, distribution is widespread. Although commercial production of elemental sulfur from such sources was first effected only in 1944 (in the USA) it now represents a major source of the element in the USA, Canada and France, and this growth has been one of the most significant trends in world sulfur production during the past few decades. Sulfur, of course, also occurs in many plant and animal proteins, and three of the principal amino-acid residues contain sulfur: cysteine,  $HSCH_2CH(NH_2)CO_2H$ ; cystine  $\{-SCH_2CH(NH_2)CO_2H\}_2$ ; and methionine,  $MeSCH_2CH_2CH(NH_2)CO_2H$ .

Oil shales represent a further source of sulfur though here (unlike the tar sands which yield crude oil and  $H_2S$ ) the sulfur is predominantly in the form of pyrites. US oil shales contain about 0.7% S of which about 80% is pyritic; other

major reserves are in Brazil, the former USSR, China and Africa, though these do not at present seem to be used as an industrial source of sulfur. Coal also contains about 1–2% S and is thus as huge a potential source of the element as it is an actual present source of air pollution (p. 698). From over  $3 \times 10^9$  tonnes of coal mined annually, only some 500 000 tonnes of sulfur are recovered (as  $\text{H}_2\text{SO}_4$ ) from a potential 50 million tonnes.

The third great source of sulfur and its compounds is from the mineral sulfides. V. M. Goldschmid's geochemical classification of the elements (1923), which has formed the basis of all subsequent developments in the field, proposed four main groups of elements: chalcophile, siderophile, lithophile and atmophile.<sup>(9)</sup> Of these the chalcophiles (Greek χαλκος, *chalcos*, copper; φιλος, *philos*, loving) are associated with copper, specifically as sulfides. Elements which occur mainly as sulfide minerals are predominantly from Groups 11–16 of the periodic table (together with iron, molybdenum and, to a lesser extent, some of the platinum metals as shown in Fig. 15.1. Some

examples of the more important sulfide minerals are listed in Table 15.1, and a further discussion of the structural chemistry and reactivity of metal sulfides is on p. 676. Pyrites (fool's gold,  $\text{FeS}_2$ ) is one of the most abundant of all sulfur minerals and is a major source of the element (see above). It often occurs in massive lenses but may also appear in veins or in disseminated zones. The largest commercial deposits extend from Seville (Spain) westward into Portugal and, at the Rio Tinto mines in Huelva Province, one of the lenses is 1.5 km long and 240 m wide with a sulfur content of 48% (pure  $\text{FeS}_2$  has 53.4% S). Other major deposits are in the former USSR, Japan, Italy, Cyprus and Scandinavia. The most important non-ferrous metal sulfides are those of Cu, Ni, Zn, Pb and As.

Finally, sulfur occurs in many localities as the sulfates of electropositive elements (see Chapters 4 and 5) and to a lesser extent as sulfates of Al, Fe, Cu and Pb, etc. Gypsum ( $\text{CaSO}_4 \cdot 2\text{H}_2\text{O}$ ) and anhydrite ( $\text{CaSO}_4$ ) are particularly notable but are little used as a source of sulfur because of high capital and operating costs. Similarly, by far the largest untapped source of sulfur is in the oceans as the dissolved sulfates of Mg, Ca and K. It has been estimated that there are some  $1.5 \times 10^9$  cubic km of water in the oceans of the world and that 1 cubic km of sea-water contains approximately 1 million tonnes of sulfur combined as sulfate.

<sup>9</sup> R. W. FAIRBRIDGE, *Encyclopedia of Geochemistry and Environmental Sciences*, Van Nostrand, New York, 1972. See sections on Geochemical Classification of the Elements; Sulfates; Sulfate Reduction–Microbial; Sulfides; Sulfosalts; Sulfur; Sulfur Cycle; Sulfur Isotope Fractionation in Biological Processes, etc., pp. 1123–58.


**Figure 15.1** Position of the chalcophilic elements in the periodic table: these elements (particularly those in white) tend to occur in nature as sulfide minerals; the tendency is much less pronounced for the elements in normal black type.

**Table 15.1** Some sulfide minerals (those in bold are the more prevalent or important)

Name	Idealized formula	Name	Idealized formula
<b>Molybdenite</b>	<b>MoS<sub>2</sub></b>	<b>Galena (Pb glance)</b>	<b>PbS</b>
Tungstenite	WS <sub>2</sub>	<b>Realgar</b>	<b>As<sub>4</sub>S<sub>4</sub></b>
Alabandite	MnS	<b>Orpiment</b>	<b>As<sub>2</sub>S<sub>3</sub></b>
<b>Pyrite (fool's gold)</b>	<b>FeS<sub>2</sub></b>	Dimorphite	As <sub>4</sub> S <sub>3</sub>
<b>Marcasite</b>	<b>FeS<sub>2</sub></b>	<b>Stibnite</b>	<b>Sb<sub>2</sub>S<sub>3</sub></b>
<b>Pyrrhotite</b>	<b>Fe<sub>1-x</sub>S</b>	Bismuthinite	Bi <sub>2</sub> S <sub>3</sub>
Laurite	RuS <sub>2</sub>	Pentlandite	(Fe,Ni) <sub>9</sub> S <sub>8</sub>
Linnaeite	Co <sub>3</sub> S <sub>4</sub>	<b>Chalcopyrite</b>	<b>CuFeS<sub>2</sub></b>
Millerite	NiS	<b>Bornite</b>	<b>Cu<sub>3</sub>FeS<sub>4</sub></b>
Cooperite	PtS	<b>Arsenopyrite</b>	<b>FeAsS</b>
<b>Chalcocite (Cu glance)</b>	<b>Cu<sub>2</sub>S</b>	Cobaltite	CoAsS
Argentite (Ag glance)	Ag <sub>2</sub> S	Enargite	Cu <sub>3</sub> AsS <sub>4</sub>
<b>Sphalerite (Zn blende)</b>	<b>ZnS</b>	Bournoite	CuPbSbS <sub>3</sub>
Wurtzite	ZnS	Proustite	Ag <sub>3</sub> AsS <sub>3</sub>
Greenockite	CdS	Pyrrargyrite	Ag <sub>3</sub> SbS <sub>3</sub>
<b>Cinnabar (vermillion)</b>	<b>HgS</b>	<b>Tetrahedrite<sup>(a)</sup></b>	<b>Cu<sub>12</sub>As<sub>4</sub>S<sub>13</sub><sup>(a)</sup></b>

<sup>(a)</sup>There is a second series in which As is replaced by Sb; in both series Cu is often substituted in part by Fe, Ag, Zn, Hg or Pb.

The global geochemical sulfur cycle has been extensively studied in recent years for both commercial and environmental reasons.<sup>(10–17)</sup>

### 15.1.3 Production and uses of elemental sulfur

Sulfur is produced commercially from one or more sources in over seventy countries of

<sup>10</sup> M. V. IVANOV and J. R. FRENET (eds.), *The Global Biogeochemical Sulfur Cycle*, SCOPE Report 19, Wiley, Chichester, 1983, 495 pp.

<sup>11</sup> A. MÜLLER and B. KREBS (eds.), *Sulfur: Its Significance for Chemistry, for the Geo-, Bio-, and Cosmo-sphere and Technology*, Elsevier, Amsterdam, 1984, 512 pp.

<sup>12</sup> P. BRIMBLECOMBE and A. Y. LEIN (eds.), *Evolution of the Global Biogeochemical Sulfur Cycle*, SCOPE Report 39, Wiley, Chichester, 1989, 276 pp.

<sup>13</sup> E. S. SALZMAN and W. J. COOPER (eds.), *Biogenic Sulfur in the Environment*, ACS Symposium Series No. 393, Amer. Chem. Soc., Washington, DC, 1989, 584 pp.

<sup>14</sup> W. L. ORR and C. M. WHITE (eds.), *Geochemistry of Sulfur in Fossil Fuels*, ACS Symposium Series, No. 429, Amer. Chem. Soc., Washington, DC, 1990, 720 pp.

<sup>15</sup> H. R. KROUSE and V. A. GRINENKO (eds.), *Stable Isotopes; Natural and Anthropogenic Sulfur in the Environment*, SCOPE Report 43, Wiley, Chichester, 1991, 466 pp.

<sup>16</sup> R. W. HOWARTH, J. W. B. STEWART and M. V. IVANOV (eds.), *Sulfur Cycling on the Continents*, SCOPE Report 48, Wiley, Chichester, 1992, 372 pp.

**Table 15.2** Main producers of sulfur in 1985 (in megatonnes)<sup>(18)</sup>

World	USA	USSR	Canada	Poland	China	Japan	Others
54.0	11.4	9.7	6.7	5.1	2.9	2.5	15.7

the world, and production of all forms in 1985 amounted to 54.0 million tonnes. The main producers are shown in Table 15.2. Until the beginning of this century, sulfur was obtained mainly by mining volcanic deposits of the element, but this now accounts for less than 5% of the total. During the first half of this century the prime method of production was the process developed by H. Frasch in 1891–4. This involves forcing superheated water into submerged sulfur-bearing strata and then forcing the molten element to the surface by compressed air (see Panel). This is the method used to obtain sulfur from the caprock of salt domes in the

<sup>17</sup> D. A. DUNNETTE and R. J. O'BRIEN (eds.), *The Science of Global Change: The Impact of Human Activities on the Environment*, ACS Symposium Series No. 483, Amer. Chem. Soc., Washington, DC, 1992, 498 pp.

<sup>18</sup> W. BÜCHNER, R. SCHLIEBS, G. WINTER and K. H. BÜCHEL, (transl. by D. R. TERRELL), *Industrial Inorganic Chemistry*, VCH, Weinheim, 1989, pp. 105–8.

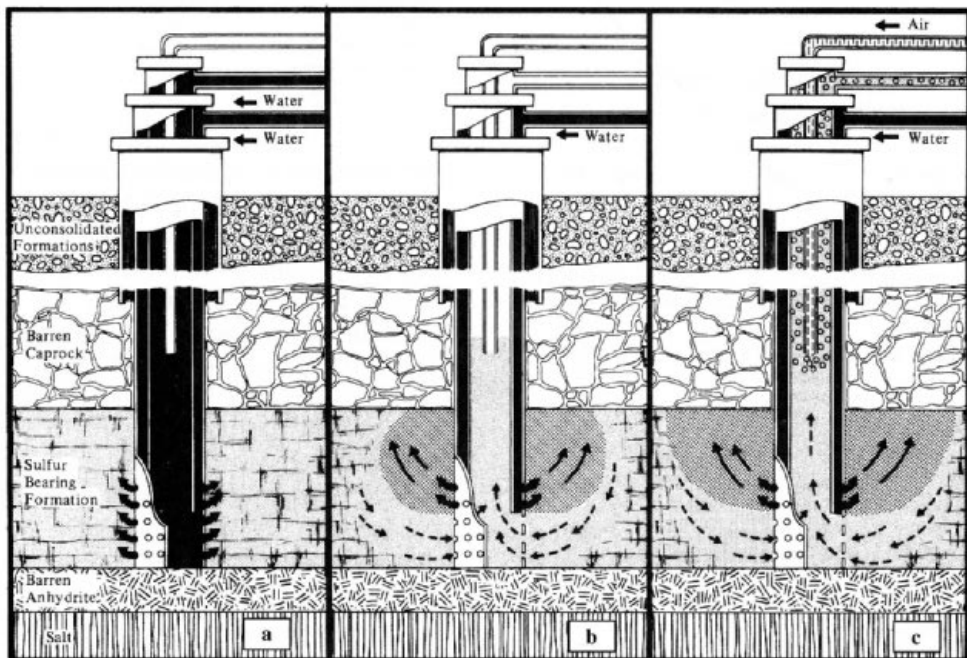
### The Frasch Process for Mining Elemental Sulfur<sup>19</sup>

The ingenious process of melting subterranean sulfur with superheated water and forcing it to the surface with compressed air was devised and perfected by Herman Frasch in the period 1891–4. Originally designed to overcome the problems of recovering sulfur from the caprock of salt domes far below the swamps and quicksands of Louisiana, the method is now also extensively used elsewhere to extract native sulfur.

The caprock typically occurs some 150–750 m beneath the surface and the sulfur-bearing zone is typically about 30 m thick and contains 20–40% S. Using oil-well drilling techniques a cased 200 mm (8-inch) pipe is sunk through the caprock to the bottom of the S-bearing layer. Its lower end is perforated with small holes. Inside this pipe a 100 mm (4-inch) pipe is lowered to within a short distance of the bottom and, finally, a concentric 25-mm (1-inch) compressed-air pipe is lowered to a point rather more than half-way down to the bottom of the well as shown in Fig. a. Superheated water at 165°C is forced down the two outer pipes and melts the surrounding sulfur (mp 119°C). As liquid sulfur is about twice as dense as water under these conditions, it flows to the bottom of the well; the pumping of water down the 100-mm pipe is discontinued, but the static pressure of the hot water being pumped down the outer 200-mm pipe forces the liquid sulfur some 100 m up the 100-mm pipe as shown in Fig. b. Compressed air is then forced down the central 25-mm pipe to aerate the molten sulfur and carry it to the surface where it emerges from the 100-mm annulus Fig. (c). One well can extract sulfur (~35 000 tonnes) from an area of about 2000 m<sup>2</sup> (0.5 acre) and new wells must continually be sunk. Bleed-water wells must also be sunk to remove the excess of water pumped into the strata.

A Frasch mine can produce as much as 2.5 million tonnes of sulfur per annum. Such massive operations clearly require huge quantities of mining water (up to 5 million gallons daily) and abundant power supplies for the drilling, pumping and superheating operations.

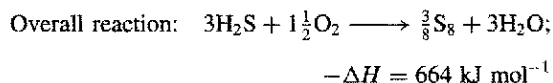
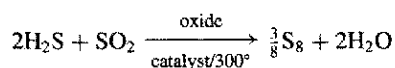
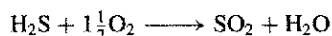
The sulfur can be piped long distances in liquid form or transported molten in ships, barges or rail cars. Alternatively it can be prilled or handled as nuggets or chunks. Despite the vast bulk of liquid sulfur mined by the Frasch process it is obtained in very pure form. There is virtually no selenium, tellurium or arsenic impurity, and the product is usually 99.5–99.9% pure.



<sup>19</sup>W. HAYNES, *Brimstone: The Stone that Burns*, Van Nostrand, Princeton, 1959, 308 pp. (The story of the Frasch sulfur industry.)

Gulf Coast region of the USA and Mexico, and from the evaporite basin deposits in west Texas, Poland, the former USSR and Iran.

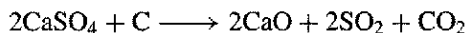
Recovery from sour natural gas and from crude oil was first developed in the USA in 1944, and by 1970 these sources exceeded the total volume of Frasch-mined sulfur for the first time. Canada (Alberta) and France are the principal producers from sour natural gas, which contains 15–20% H<sub>2</sub>S. The USA and Japan are the largest producers from petroleum refineries. The phenomenal growth of these sources is clear from the following figures (in 10<sup>6</sup> tonnes): <0.5 (1950); 2.5 (1960); 15 (1972); >25 (1985). Recovery from sour natural gas involves first separating out the H<sub>2</sub>S by absorption in mono-ethanolamine and then converting it to sulfur by a process first developed by C. F. Claus in Germany about 1880. In this process one-third of the H<sub>2</sub>S is burned to produce SO<sub>2</sub>, water vapour, and sulfur vapour; the SO<sub>2</sub> then reacts with the remaining H<sub>2</sub>S in the presence of oxide catalysts such as Fe<sub>2</sub>O<sub>3</sub> or Al<sub>2</sub>O<sub>3</sub> to produce more H<sub>2</sub>O and S vapour:



Multiple reactors achieve 95–96% conversion and recovery, and stringent air pollution legislation has now pushed this to 99%. A similar sequence of reactions is used for sulfur production from crude oil except that the organosulfur compounds must first be removed from the refinery feed and converted to H<sub>2</sub>S by a hydrogenation process before the sulfur can be recovered.

The third major source of sulfur is pyrite and related sulfide minerals. The ore is roasted to secure SO<sub>2</sub> gas which is then usually used directly for the manufacture of H<sub>2</sub>SO<sub>4</sub> (p. 708). Again air pollution by SO<sub>2</sub> gas emissions has been the subject of increasing legislation and control during the past three decades (p. 698).

The proportion of sulfur and S-containing compounds recovered by these various methods has been changing rapidly and frequently depends on the nature of local sources available. The comparative figures for 1985 are: sour natural gas 38%, Frasch S 28%, pyrites 18%, miscellaneous 16% (includes metallurgy, crude oil, coal, gypsum, tar sands and flue gases). Estimated reserves on the basis of present technology and prices are summarized in Table 15.3; these can increase more than tenfold if coal, gypsum, anhydrite and sea-water are included. At present these latter sources are economic only under special conditions though, as we have already seen (p. 648), vast quantities of SO<sub>2</sub> are lost from industrial coal each year. Recovery of useful sulfur compounds from anhydrite (and gypsum) can be achieved by two main routes. The Müller–Kühne process used in the UK and Austria involves the roasting of anhydrite with clay, sand and coke in a rotary kiln at 1200–1400°:



The emergent SO<sub>2</sub> is then fed into a contact process for H<sub>2</sub>SO<sub>4</sub> (p. 708). Alternatively, ammonia and CO<sub>2</sub> can be passed into a gypsum slurry to give ammonium sulfate for use in fertilizers:



This double decomposition route was developed in Germany and has been used in the UK since 1971.

The pattern of uses of sulfur and its compounds in the chemical industry is illustrated in the

**Table 15.3** Estimated world reserves of sulfur

Source	Natural gas	Petroleum	Native ore	Pyrite	Sulfide ore	Dome	Total
S/10 <sup>6</sup> tonne	690	450	560	380	270	150	2500

flow chart below. Most sulfur is converted via  $\text{SO}_2/\text{SO}_3$  into sulfuric acid which accounts, for example, for some 88% of the contained sulfur used in the USA. The proportion of sulfur used in making the extensive number of end products is shown in Fig. 15.2. Indeed, the uses of sulfur and its principal compounds are so widely spread throughout industry that a nation's consumption of sulfur is often used as a reliable measure of its economic development. Thus, the USA, the former USSR, Japan and Germany lead the world in industrial production and rank similarly in the consumption of sulfur. Further details of industrial uses will be found in subsequent sections dealing with specific compounds of sulfur, and various review books are available.<sup>(20-22)</sup>

<sup>20</sup> J. R. WEST (ed.), *New Uses of Sulfur*, Advances in Chemistry Series No. 140, Am. Chem. Soc., Washington, DC, 1975, 230 pp.

<sup>21</sup> D. J. BOURNE (ed.), *New Uses of Sulfur — II*, Advances in Chemistry Series No. 165, Am. Chem. Soc., Washington, DC 1978, 282 pp.

<sup>22</sup> U. H. F. SANDER, H. FISCHER, U. ROTHE and R. KOLA, (Engl. edn. prepared by A. I. MORE), *Sulfur, Sulfur Dioxide, Sulfuric Acid: Industrial Chemistry and Technology*, British Sulfur Corporation, London, 1984, 428 pp.

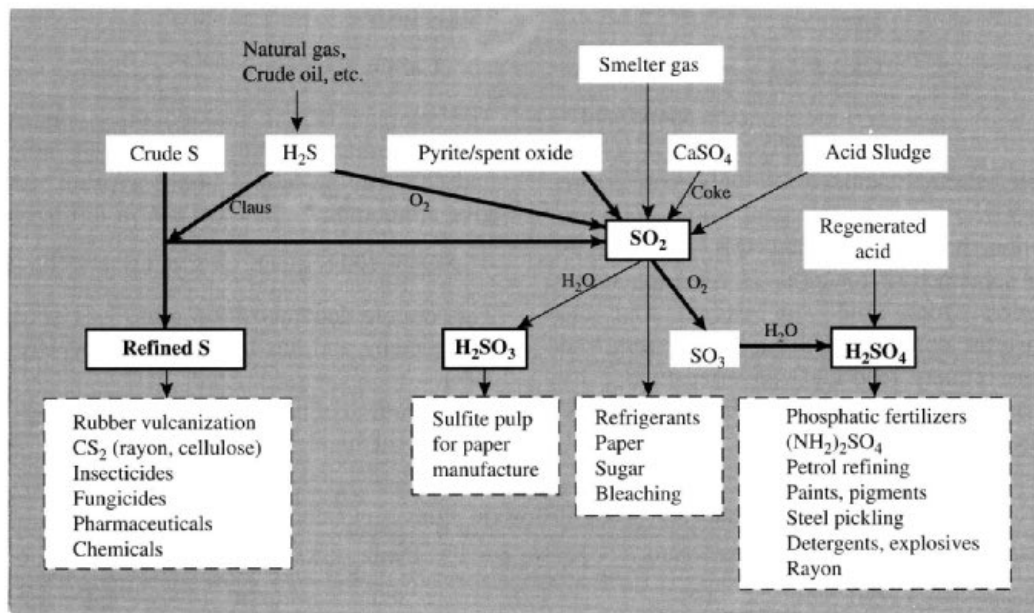
### 15.1.4 Allotropes of sulfur<sup>(23-25)</sup>

The allotropy of sulfur is far more extensive and complex than for any other element (except perhaps carbon, after the synthesis of the innumerable fullerene clusters, p. 279). This arises partly because of the great variety of molecular forms that can be achieved by  $-\text{S}-\text{S}-$  catenation and partly because of the numerous ways in which the molecules so formed can be arranged within the crystal. In fact,  $\text{S}-\text{S}$  bonds are very variable and flexible: interatomic distances cover an enormous range, 180–260 pm (depending to some extent on the amount of multiple bonding), whilst bond angles  $\text{S}-\text{S}-\text{S}$  vary from  $90^\circ$  to  $180^\circ$  and dihedral angles  $\text{S}-\text{S}-\text{S}-\text{S}$  from  $0^\circ$  to  $180^\circ$  (Fig. 15.3). Estimated  $\text{S}-\text{S}$  bond energies may be as high as  $430 \text{ kJ mol}^{-1}$  and the unrestrained  $-\text{S}-\text{S}-$  single-bond energy of  $265 \text{ kJ mol}^{-1}$  is exceeded amongst homonuclear single bonds only by those of  $\text{H}_2$  ( $435 \text{ kJ mol}^{-1}$ ) and  $\text{C}-\text{C}$

<sup>23</sup> J. DONOHUE, *The Structures of the Elements*, Sulfur, pp. 324–69, Wiley, New York, 1974.

<sup>24</sup> B. MEYER, *Chem. Revs.* **76**, 367–88, (1976).

<sup>25</sup> M. SCHMIDT, Chap. 1, pp. 1–12, in ref. 21.



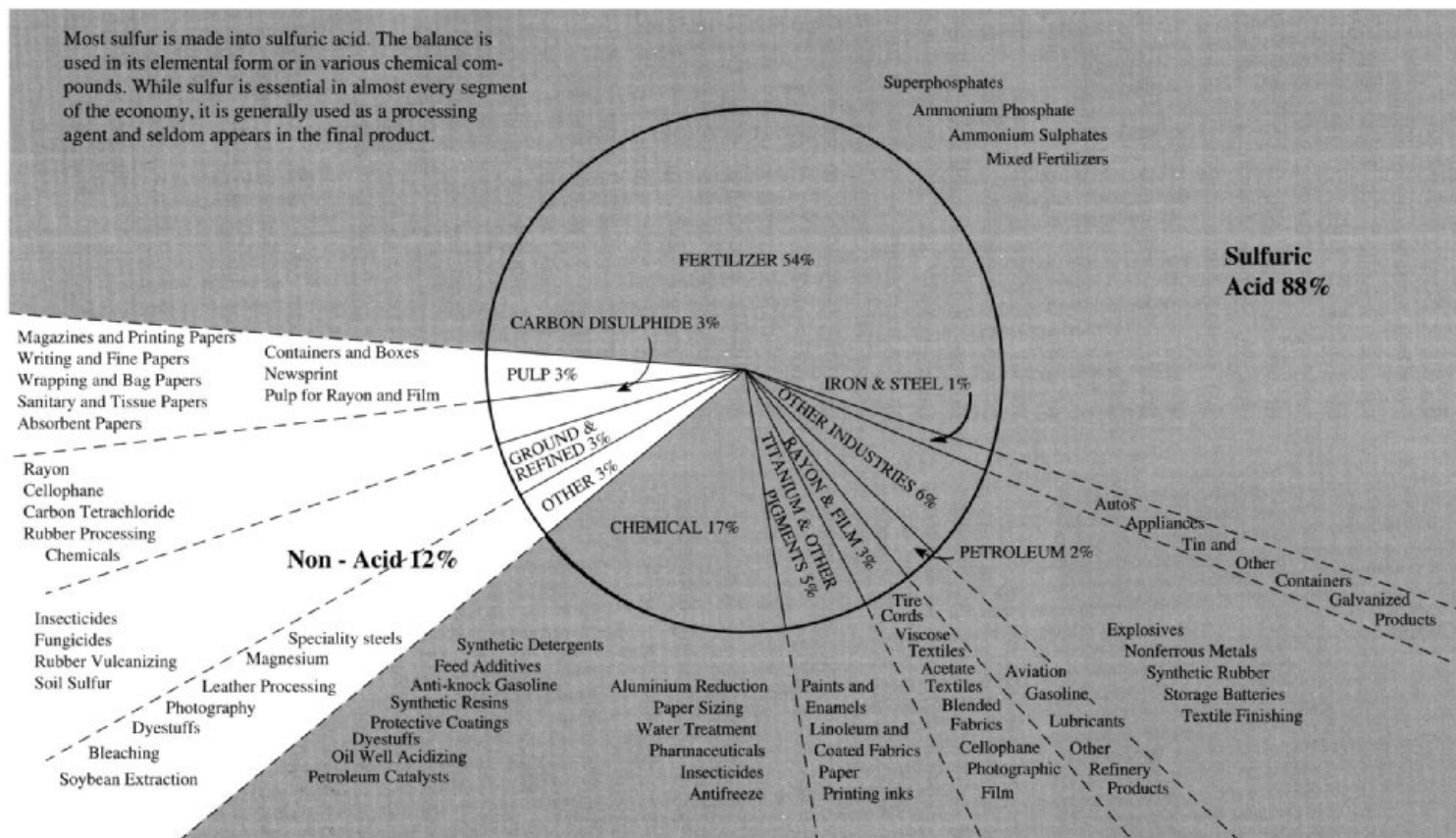
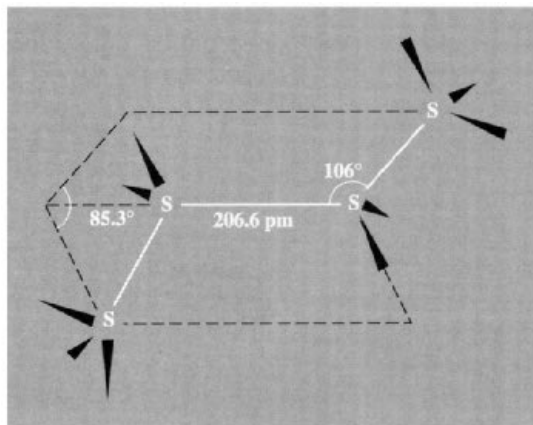


Figure 15.2 Sulfur's uses as acid and as non-acid.



**Figure 15.3** Portion of an unrestrained- $S_n$ -chain showing typical values for the S-S-S bond angle ( $106^\circ$ ) and S-S-S-S dihedral angle ( $85.3^\circ$ ). Possible alternative orientations of the bonds from the 2 inner S atoms, and possible directions for extensions of the chain from the 2 outer S atoms are indicated by the black lines. (See also p. 656.)

( $330 \text{ kJ mol}^{-1}$ ). Again, the amazing temperature dependence of the properties of liquid sulfur have attracted attention for over a century since the rapid and reversible gelation of liquid sulfur was first observed in the temperature range  $160\text{--}195^\circ\text{C}$ . Major advances have been achieved during the past 25 y in our knowledge of the molecular structure of many of the crystalline allotropes of sulfur and of the complex molecular equilibria occurring in the liquid and gaseous states. Sulfur is also unique in the extent to which new allotropes can now be purposefully synthesized using kinetically controlled reactions that rely on the great strength of the S-S bond once it is formed, and over

a dozen new elemental sulfur rings, *cyclo-S<sub>n</sub>*, have been synthesized. Fortunately, several excellent reviews are available,<sup>(23–25)</sup> and these can be consulted for fuller details and further references. It will be convenient to start with some of the classic allotropes (now known to contain *cyclo-S<sub>8</sub>* molecules), and then to consider in turn other cyclic oligomers (*cyclo-S<sub>n</sub>*) various chain polymers (*catena-S<sub>n</sub>*), certain unstable small molecules  $S_n$  ( $n = 2\text{--}5$ ) and, finally, the properties of liquid and gaseous sulfur.

The commonest (and most stable) allotrope of sulfur is the yellow, orthorhombic  $\alpha$ -form to which all other modifications eventually revert at room temperature. Commercial roll sulfur, flowers of sulfur (sublimed) and milk of sulfur (precipitated) are all of this form. It was shown to contain  $S_8$  molecules by cryoscopy in iodine (E. Beckmann, 1912) and was amongst the first substances to be examined by X-ray crystallography (W. H. Bragg, 1914), but the now familiar crown structure of *cyclo-S<sub>8</sub>* was not finally established until 1935.<sup>(23)</sup> Various representations of the idealized  $D_{4d}$  molecular structure are given in Fig. 15.4. The packing of the molecules within the crystal has been likened to a crankshaft arrangement extending in two different directions and leads to a structure which is very complex.<sup>(23)</sup> Orthorhombic  $\alpha$ - $S_8$  has a density of  $2.069 \text{ g cm}^{-3}$ , is a good electrical insulator when pure, and is an excellent thermal insulator, the extremely low thermal conductivity being similar to those of the very best insulators such as mica (p. 356) and wood. Some solubilities in common solvents are in Table 15.4.

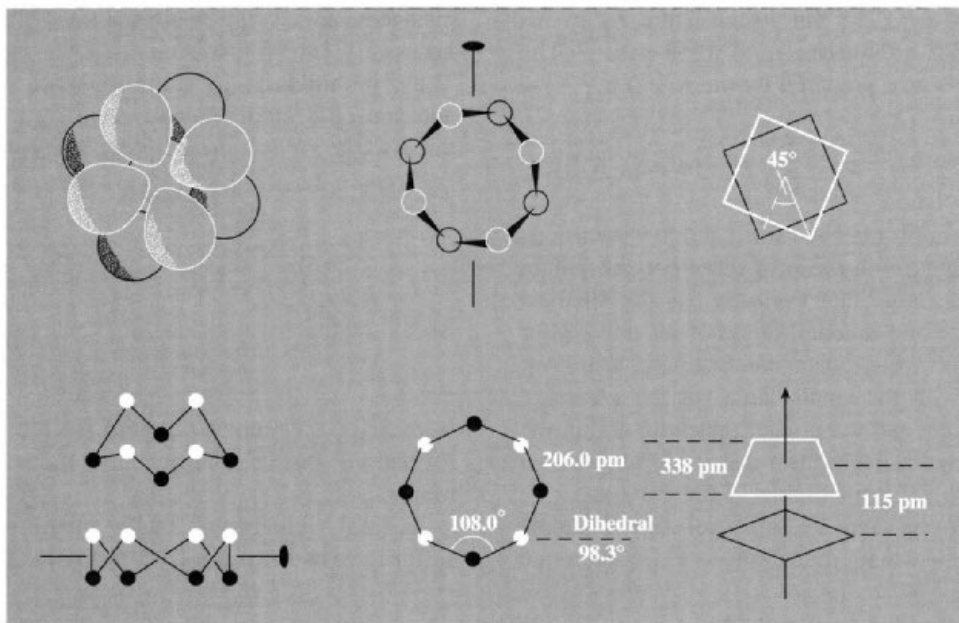
At about  $95.3^\circ$   $\alpha$ - $S_8$  becomes unstable with respect to  $\beta$ -monoclinic sulfur in which the packing of the  $S_8$  molecules is altered and their

**Table 15.4** Solubilities of  $\alpha$ -orthorhombic sulfur (at  $25^\circ\text{C}$  unless otherwise stated)

Solvent	$\text{CS}_2$	$\text{S}_2\text{Cl}_2$	$\text{Me}_2\text{CO}$	$\text{C}_6\text{H}_6$	$\text{CCl}_4$	$\text{Et}_2\text{O}$	$\text{C}_6\text{H}_{14}$	$\text{EtOH}$
g S per 100 g solvent ( $T^\circ\text{C}$ )	35.5 <sup>(a)</sup>	17 <sup>(b)</sup> ( $21^\circ$ )	2.5	2.1	0.86 <sup>(c)</sup>	0.283 ( $23^\circ$ )	0.25 ( $20^\circ$ )	0.065

<sup>(a)</sup>55.6 at  $60^\circ$ . <sup>(b)</sup>97 at  $110^\circ$ . <sup>(c)</sup>1.94 at  $60^\circ$ .





**Figure 15.4** Various representations of the molecule  $\text{cyclo-S}_8$  found in  $\alpha$ -orthorhombic,  $\beta$ -monoclinic, and  $\gamma$ -monoclinic sulfur.

orientation becomes partly disordered.<sup>(26)</sup> This results in a lower density ( $1.94\text{--}2.01\text{ g cm}^{-3}$ ), but the dimensions of the  $\text{S}_8$  rings in the two allotropes are very similar. The transition is somewhat sluggish even above  $100^\circ$ , and this enables a mp of metastable single crystals of  $\alpha\text{-S}_8$  to be obtained: a value of  $112.8^\circ$  is often quoted but microcrystals may melt as high as  $115.1^\circ$ . Monoclinic  $\beta\text{-S}_8$  has a “mp” which is usually quoted as  $119.6^\circ$  but this can rise to  $120.4^\circ$  in microcrystals or may be as low as  $114.6^\circ$ . The uncertainty arises because the  $\text{S}_8$  ring is unstable above  $\sim 119^\circ$  and begins to form other species which progressively depress the mp. The situation is reminiscent of the equilibria accompanying the melting of anhydrous phosphoric acid (p. 518). Monoclinic  $\beta\text{-S}_8$  is best prepared by crystallizing liquid sulfur at about  $100^\circ$  and then cooling it rapidly to room temperature to retard the formation of orthorhombic  $\alpha\text{-S}_8$ ; under these conditions

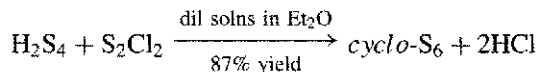
$\beta\text{-S}_8$  can be kept for several weeks at room temperature before reverting to the more stable  $\alpha$ -form.

A third crystalline modification,  $\gamma$ -monoclinic sulfur, was first obtained by W. Muthmann in 1890. It is also called nacreous or mother-of-pearl sulfur and can be made by slowly cooling a sulfur melt that has been heated above  $150^\circ$ , or by chilling hot concentrated solutions of sulfur in EtOH,  $\text{CS}_2$  or hydrocarbons. However, it is best prepared as pale-yellow needles by the mechanistically obscure reaction of pyridine with copper(I) ethyl xanthate,  $\text{CuSSCOEt}$ . Like  $\alpha$ - and  $\beta$ -sulfur,  $\gamma$ -monoclinic sulfur comprises  $\text{cyclo-S}_8$  molecules but the packing is more efficient and leads to a higher density ( $2.19\text{ g cm}^{-3}$ ). It reverts slowly to  $\alpha\text{-S}_8$  at room temperature but rapid heating leads to a mp of  $106.8^\circ$ .

We now consider other homocyclic polymorphs of sulfur containing 6–20 S atoms per ring. A rhombohedral form,  $\epsilon$ -sulfur, was first prepared by M. R. Engel in 1891 by the reaction of concentrated HCl on a saturated solution of thiosulfate  $\text{HS}_2\text{O}_3^-$  at  $0^\circ$ . It was shown to be

<sup>26</sup> L. K. TEMPLETON, D. H. TEMPLETON and A. ZALKIN, *Inorg. Chem.* **15**, 1999–2001 (1976).

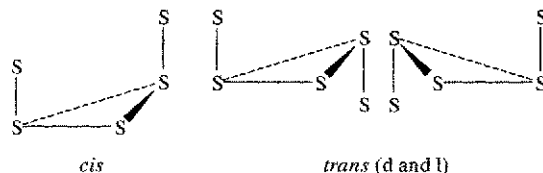
hexameric in 1914 but its structure as *cyclo-S*<sub>6</sub> was not established until 1958–61.<sup>(23)</sup> The allotrope is best prepared by the reaction



The ring adopts the chair form and its dimensions are compared with those of other polymorphs in Table 15.5. Note that *cyclo-S*<sub>6</sub> has the smallest bond angle and dihedral angle of all poly-sulfur species for which data are available and this, together with the small "hole" at the centre of the molecule and the efficient packing within the crystal, lead to the highest density of any known polymorph of sulfur (Table 15.6).

In *cyclo-S*<sub>6</sub> and *cyclo-S*<sub>8</sub> all the S atoms are equivalent with essentially equal interatomic

distances, angles and conformations. This is not necessarily so for all homocyclic molecules. Thus, in building up cumulated  $-\text{S}_n-$  bonds, addition of S atoms to an *S*<sub>3</sub> unit can occur in three ways: *cis* (c), *d-trans* (dt), and *l-trans* (lt):



Both *S*<sub>6</sub> (chair) and *S*<sub>8</sub> (crown) are all *-cis* conformations, but larger rings have more complex motifs.

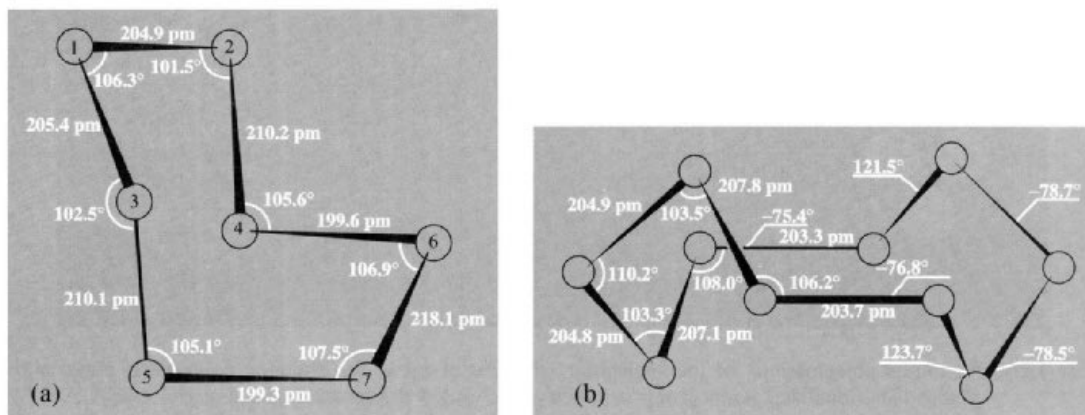
At least eight further cyclic modifications of sulfur have been synthesized during the past 25 y

**Table 15.5** Dimensions of some sulfur molecules. Average values are given except for *S*<sub>7</sub> where deviations from the mean are more substantial (see text)

Molecule	Interatomic distance/pm	Bond angle	Dihedral angle
<i>S</i> <sub>2</sub> (matrix at 20 K)	188.9	—	—
<i>cyclo-S</i> <sub>6</sub>	205.7	102.2°	74.5°
<i>cyclo-S</i> <sub>7</sub>	199.3–218.1	101.5°–107.5°	0.3°–107.6°
<i>cyclo-S</i> <sub>8</sub> (α)	203.7	107.8°	98.3°
<i>cyclo-S</i> <sub>8</sub> (β)	204.5	107.9°	—
<i>cyclo-S</i> <sub>10</sub>	205.6	106.2°	–77° and +123°
<i>cyclo-S</i> <sub>12</sub>	205.3	106.5°	86.1°
<i>cyclo-S</i> <sub>18</sub>	205.9	106.3°	84.4°
<i>cyclo-S</i> <sub>20</sub>	204.7	106.5°	83.0°
<i>catena-S</i> <sub>x</sub>	206.6	106.0°	85.3°

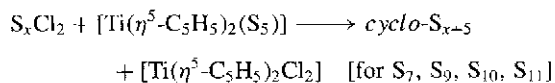
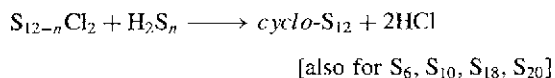
**Table 15.6** Some properties of sulfur allotropes

Allotrope	Colour	Density/g cm <sup>-3</sup>	Mp or decomp. point/°C
<i>S</i> <sub>2</sub> (g) or matrix at 20 K	Blue-violet	—	Very stable at high temp
<i>S</i> <sub>3</sub> (g)	Cherry red	—	Stable at high temp
<i>S</i> <sub>6</sub>	Orange red	2.209	<i>d</i> > 50°
<i>S</i> <sub>7</sub>	Yellow	2.182 (–110°)	<i>d</i> 39°
α- <i>S</i> <sub>8</sub>	Yellow	2.069	112.8° (see text)
β- <i>S</i> <sub>8</sub>	Yellow	1.94–2.01	119.6° (see text)
γ- <i>S</i> <sub>8</sub>	Light yellow	2.19	106.8° (see text)
<i>S</i> <sub>9</sub>	Intense yellow	—	Stable below rt
<i>S</i> <sub>10</sub>	Pale yellow green	2.103 (–110°C)	<i>d</i> > 0°
<i>S</i> <sub>11</sub>	—	—	—
<i>S</i> <sub>12</sub>	Pale yellow	2.036	148°
<i>S</i> <sub>18</sub>	Lemon yellow	2.090	m 128°(d)
<i>S</i> <sub>20</sub>	Pale yellow	2.016	m 124°(d)
<i>S</i> <sub>∞</sub>	Yellow	2.01	104°(d)

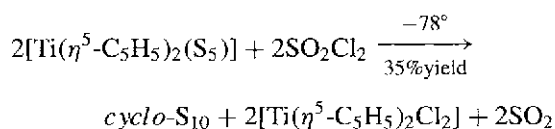


**Figure 15.5** (a) Molecular structure of *cyclo-S*<sub>7</sub> showing the large distance S(6)–(7) and alternating interatomic distances away from this bond; the point group symmetry is approximately *C*<sub>s</sub>. (b) Molecular structure of *cyclo-S*<sub>10</sub> showing interatomic distances, bond angles and dihedral angles; the distance between the 2 “horizontal” bonds is 541 pm.

by the elegant work of M. Schmidt and his group. The method is to couple two compounds which have the desired combined number of S atoms and appropriate terminal groups, e.g.:



A variant is the ligand displacement and coupling reaction:



The preparation and structures of the reactants are on p. 683 (*H*<sub>2</sub>*S*<sub>*n*</sub>), p. 689 (*S*<sub>*x*</sub>*Cl*<sub>2</sub>), and p. 670 [*Ti*(*η*<sup>5</sup>-*C*<sub>5</sub>*H*<sub>5</sub>)<sub>2</sub>(*S*<sub>5</sub>)].

*S*<sub>7</sub> is known in four crystalline modifications; one of these, obtained by crystallization from *CS*<sub>2</sub> at  $-78^\circ$ , rapidly disintegrates to a powder at room temperature, but an X-ray study at  $-110^\circ$  showed it to consist of *cyclo-S*<sub>7</sub> molecules with

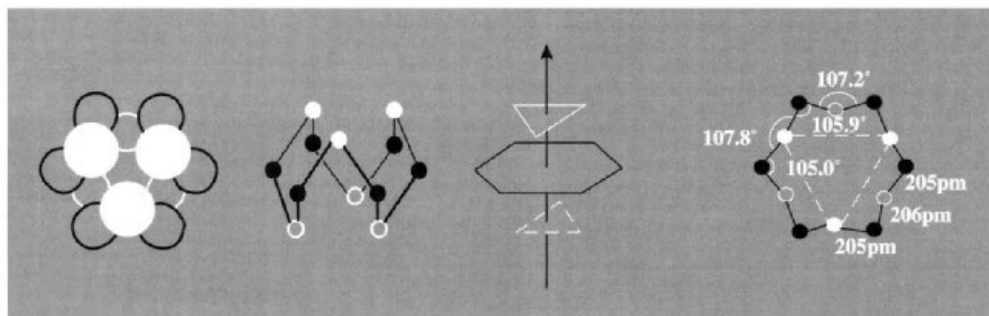
the dimensions shown in Fig. 15.5(a).<sup>(27)</sup> Notable features are the very large interatomic distance S(6)–S(7) (218.1 pm) which probably arises from the almost zero dihedral angle between the virtually coplanar atoms S(4) S(6) S(7) S(5), thus leading to maximum repulsion between nonbonding lone-pairs of electrons on adjacent S atoms. As a result of this weakening of S(6)–S(7), the adjacent bonds are strengthened (199.5 pm) and there are further alternations of bond lengths (210.2 and 205.2 pm) throughout the molecule.

The structure of *cyclo-S*<sub>10</sub> is shown in Fig. 15.5(b).<sup>(28)</sup> The molecule belongs to the very rare point group symmetry *D*<sub>2</sub> (three orthogonal twofold axes of rotation as the only symmetry elements). The mean interatomic distance and bond angle are close to those in *cyclo-S*<sub>12</sub> (Table 15.5) and the molecule can be regarded as composed of two identical *S*<sub>5</sub> units obtained from the *S*<sub>12</sub> molecule (Fig. 15.6).

*Cyclo-S*<sub>12</sub> occupies an important place amongst the cyclic oligomers of sulfur. In a

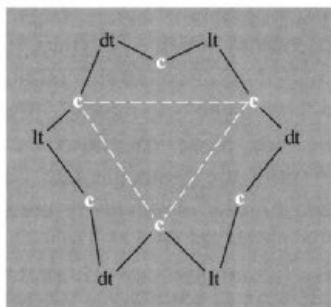
<sup>27</sup> R. STEUDEL, R. REINHARDT and F. SCHUSTER, *Angew. Chem. Int. Edn. Engl.* **16**, 715 (1977).

<sup>28</sup> R. REINHARDT, R. STEUDEL and F. SCHUSTER, *Angew. Chem. Int. Edn. Engl.* **17**, 57–8 (1978).



**Figure 15.6** Various representations of the molecular structure of *cyclo-S*<sub>12</sub> showing S atoms in three parallel planes. The idealized point group symmetry is  $D_{3d}$  and the mean dihedral angle is  $86.1 \pm 5.5^\circ$ . In the crystal the symmetry is slightly distorted to  $C_{2h}$  and the central group of 6 S atoms deviate from coplanarity by  $\pm 14$  pm.

classic paper by L. Pauling<sup>(29)</sup> the molecule had been predicted to be unstable, though subsequent synthesis showed it to be second only to *cyclo-S*<sub>8</sub> in stability. In fact, the basic principles underlying Pauling's prediction remain valid but he erroneously applied them to two sets of S atoms in two parallel planes whereas the configuration adopted has S atoms in three parallel planes. Several representations of the structure are in Fig. 15.6. Using the nomenclature of p. 656 it can be seen that, unlike *S*<sub>6</sub> and *S*<sub>8</sub>, the conformation of all S atoms is not *cis*: the S atoms in upper and lower planes do indeed have this conformation but the 6 atoms in the central plane are alternately *d-trans* and *l-trans* leading to the sequence:

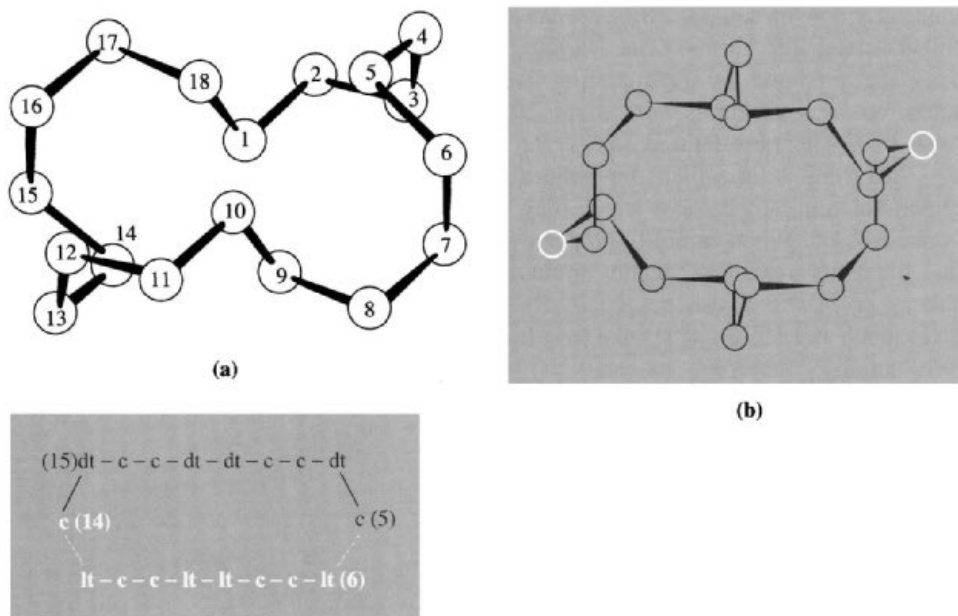


*Cyclo-S*<sub>12</sub> was first prepared in 1966 in 3% yield by reacting *H*<sub>2</sub>*S*<sub>4</sub> with *S*<sub>2</sub>*Cl*<sub>2</sub> but a better

route is the reaction between dilute solutions of *H*<sub>2</sub>*S*<sub>8</sub> and *S*<sub>4</sub>*Cl*<sub>2</sub> in *Et*<sub>2</sub>*O* (18% yield). It can also be extracted from liquid sulfur. The stability of the allotrope can be gauged from its mp (148°), which is higher than that of any other allotrope and nearly 30° above the temperature at which the *S*<sub>8</sub> ring begins to decompose.

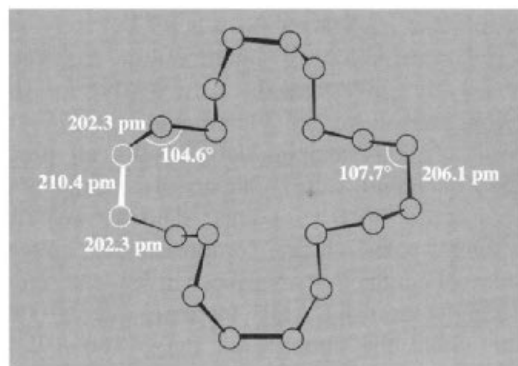
Two allotropes of *cyclo-S*<sub>18</sub> are known. The structure of the first is shown in Fig. 15.7(a): if we take 3 successive atoms out of the *S*<sub>12</sub> ring then the 9-atom fragment combines with a second one to generate the structure. Alternatively, the structure can be viewed as two parallel 9-atom helices (see below), one right-handed and one left-handed, mutually joined at each end by the *cis* atoms *S*(5) and *S*(14). Interatomic distances vary between 204–211 pm (mean 206 pm), bond angles between 103.7–108.3° (mean 106.3°), and dihedral angles between 79.1–90.0° (mean 84.5°). This form of *cyclo-S*<sub>18</sub> is formed by the reaction between *H*<sub>2</sub>*S*<sub>8</sub> and *S*<sub>10</sub>*Cl*<sub>2</sub> and forms lemon-coloured crystals, mp 128°, which can be stored in the dark for several days without apparent change. The second form of *cyclo-S*<sub>18</sub> has the molecular structure shown in Fig. 15.7(b): this has twice the 8-atom repeat motif *cis-cis-trans-cis-trans-cis-trans-cis* (one with *d-trans* and the other with *l-trans*) joined at each end by further bridging single *trans*-sulfur atoms which constitute the 2 extreme atoms of the elongated ring.

<sup>29</sup> L. PAULING, *Proc. Natl. Acad. Sci. USA* **35**, 495–9 (1949).



**Figure 15.7** (a) The molecular structure of one form of *cyclo-S*<sub>18</sub>, together with the conformational sequence of the two helical subunits.<sup>(30)</sup> (b) The molecular structure of the second form of *cyclo-S*<sub>18</sub> showing the *trans*-configuration of the S atoms at the extreme ends of the elongated rings.<sup>(25)</sup>

Pale yellow crystals of *cyclo-S*<sub>20</sub>, mp 124° (decomp),  $d$  2.016 g cm<sup>-3</sup>, have been made by the reaction of H<sub>2</sub>S<sub>10</sub> and S<sub>10</sub>Cl<sub>2</sub>. The molecular structure is shown in Fig. 15.8<sup>(31)</sup> The interatomic S-S distances vary between 202.3–210.4 pm (mean 204.2 pm), the angles S-S-S between 104.6–107.7° (mean 106.4°), and the dihedral angles between 66.3–89.9° (mean 84.7°). In this case the conformation motif is -c-It-It-It-c- repeated 4 times and the abnormally long bond required to achieve ring closure is notable; it is also this section of the molecule which has the smallest dihedral angles thereby incurring increased repulsion between adjacent nonbonding lone-pairs of electrons. Consistent with this the adjacent bonds are the shortest in the molecule.



**Figure 15.8** Molecular structure of *cyclo-S*<sub>20</sub> viewed along the [001] direction.<sup>(31)</sup> The 2 adjacent S atoms with the longest interatomic distance are shown in white.

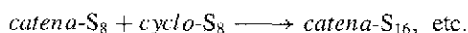
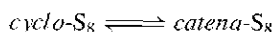
Solid polycatenasulfur comes in many forms: it is present in rubbery S, plastic ( $\chi$ )S, lamina S, fibrous ( $\psi, \phi$ ), polymeric ( $\mu$ ) and insoluble ( $\omega$ )S, supersublimation S, white S and the commercial product Crystex. All these are metastable mixtures of allotropes containing more or less

<sup>30</sup> T. DEBAERDEMAEKER and A. KUTOGLU, *Naturwissenschaften* **60**, 49 (1973).

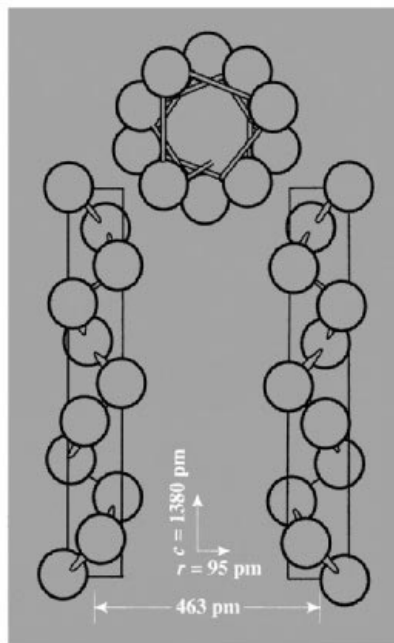
<sup>31</sup> T. DEBAERDEMAEKER, E. HELLNER, A. KUTOGLU, M. SCHMIDT and E. WILHELM, *Naturwissenschaften* **60**, 300 (1973).

defined concentrations of helices ( $S_{\infty}$ ), *cyclo*- $S_8$ , and other molecular forms. The various modifications are prepared by precipitating S from solution or by quenching *hot* liquid S (say from 400°C). The best-defined forms are fibrous ( $d \sim 2.01 \text{ g cm}^{-3}$ ) in which the helices are mainly parallel, and lamella S in which they are partly criss-crossed. When carefully prepared by drawing filaments from hot liquid sulfur, fibrous rubbery or plastic S can be repeatedly stretched to as much as 15 times its normal length without substantially impairing its elasticity. All these forms revert to *cyclo*- $S_8(\alpha)$  at room temperature and this has caused considerable difficulty in obtaining their X-ray structures.<sup>(23)</sup> However, it is now established that fibrous S consists of infinite chains of S atoms arranged in parallel helices whose axes are arranged on a close-packed (hexagonal) net 463 pm apart. The structure contains both left-handed and right-handed helices of radius 95 pm and features a repeat distance of 1380 pm comprising 10 S atoms in three turns as shown in Fig. 15.9. Within each helix the interatomic distance S–S is 206.6 pm, the bond angle S–S–S is 106.0°, and the dihedral angle S–S–S–S is 85.3°.

The constitution of liquid sulfur has been extensively investigated, particularly in the region just above the remarkable transition at 159.4°. At this temperature virtually all properties of liquid sulfur change discontinuously, e.g. specific heat ( $\lambda$  point), density, velocity of sound, polarizability, compressibility, colour, electrical conductivity, surface tension and, most strikingly, viscosity, which increases over 10 000-fold within the temperature range 160–195°C before gradually decreasing again. The phenomena can now be interpreted at least semi-quantitatively by a 2-step polymerization theory involving initiation and propagation:



The polymerization is photosensitive, involves diradicals and leads to chain lengths that exceed 200 000 S atoms at  $\sim 180^\circ\text{C}$  before dropping slowly to  $\sim 1000$  S at  $400^\circ$  and  $\sim 100$  S at  $600^\circ$ .



**Figure 15.9** The structure of right-handed and left-handed  $S_{\infty}$  helices in fibrous sulfur (see text).

Polymeric  $S_{\infty}$  is dark yellow with an absorption edge at 350 nm (cf.  $\text{H}_2\text{S}_n$ , p. 683) but the colour is often obscured either by the presence of trace organic impurities or, in pure S, by the presence of other highly coloured species such as the dark cherry-red trimer  $S_3$  or the deeper-coloured diradicals  $S_4$  and  $S_5$ .

The saturated vapour pressure above solid and liquid sulfur is given in Table 15.7. The molecular composition of the vapour has long been in contention but, mainly as a result of the work of J. Birkowitz and others<sup>(24)</sup> is now known to contain all molecules  $S_n$  with  $2 \leq n \leq 10$  including odd-numbered species. The actual concentration

**Table 15.7** Vapour pressure of crystalline *cyclo*- $S_8(\alpha)$  and liquid sulfur

$p/\text{mmHg}^{(a)}$	$10^{-5}$	$10^{-3}$	$10^{-1}$	1	10	100	760
$T/^\circ\text{C}$	39.0	81.1	141	186	244.9	328	444.61
$p/\text{atm}^{(a)}$	1	2	5	10	50	100	200
$T/^\circ\text{C}$	444.61	495	574	644	833	936	1035

<sup>(a)</sup> 1 mmHg  $\approx$  133.322 Pa; 1 atm = 101 325 Pa

of each species depends on both temperature and pressure. In the saturated vapour up to 600°C S<sub>8</sub> is the most common species followed by S<sub>6</sub> and S<sub>7</sub>, and the vapour is green. Between 620–720°C S<sub>7</sub> and S<sub>6</sub> are slightly more prevalent than S<sub>8</sub> but the concentration of all three species falls rapidly with respect to those of S<sub>2</sub>, S<sub>3</sub> and S<sub>4</sub>, and above 720°C S<sub>2</sub> is the predominant species. At lower pressures S<sub>2</sub> is even more prominent, accounting for more than 80% of all vapour species at 530°C and 100 mmHg, and 99% at 730°C and 1 mmHg. This vapour is violet. The vapour above FeS<sub>2</sub> at 850°C is also S<sub>2</sub>.

The best conditions for observing S<sub>3</sub> are 440°C and 10 mmHg when 10–20% of vapour species comprise this deep cherry-red bent triatomic species; like ozone, p. 607, it has a singlet ground state. The best conditions for S<sub>4</sub> are 450°C and 20 mmHg (concentration ~20%) but the structure is still not definitely established and may, in fact be a strained ring, an unbranched diradical chain, or a branched-chain isostructural with SO<sub>3</sub>(g) (p. 703).

The great stability of S<sub>2</sub> in the gas phase at high temperature is presumably due to the essentially double-bond character of the molecule and to the increase in entropy ( $T\Delta S$ ) consequent on the breaking up of the single-bonded S<sub>n</sub> oligomers. As with O<sub>2</sub> (p. 606) the ground state is a triplet level  $^3\Sigma_g^-$  but the splitting within the triplet state is far larger than with O<sub>2</sub> and the violet colour is due to the transition  $B^3\Sigma_u^- \leftarrow X^3\Sigma_g^-$  at 31 689 cm<sup>-1</sup>. The corresponding B→X emission is observed whenever S compounds are burned in a reducing flame and the transition can be used for the quantitative analytical determination of the concentration of S compounds. There is also a singlet  $^1\Delta$  excited state as for O<sub>2</sub>. The dissociation energy  $D_0^\circ(S_2)$  is 421.3 kJ mol<sup>-1</sup>, and the interatomic distance in the gas phase 188.7 pm (cf. Table 15.5).

### 15.1.5 Atomic and physical properties

Several physical properties of sulfur have been mentioned in the preceding section; they vary

markedly with the particular allotrope and its physical state.

Sulfur ( $Z = 16$ ) has 4 stable isotopes of which <sup>32</sup>S is by far the most abundant in nature (95.02%). The others are <sup>33</sup>S (0.75%), <sup>34</sup>S (4.21%), and <sup>36</sup>S (0.02%). These abundances vary somewhat depending on the source of the sulfur, and this prevents the atomic weight of sulfur being quoted for general use more precisely than 32.066(6) (p. 17). The variability is a valuable geochemical indication of the source of the sulfur and the isotope ratios of sulfur-containing impurities can even be used to identify the probable source of petroleum samples.<sup>(15,32)</sup> In such work it is convenient to define the abundance ratio of the 2 most abundant isotopes ( $R = ^{32}\text{S}/^{34}\text{S}$ ) and to take as standard the value of 22.22 for meteoritic troilite (FeS). Deviations from this standard ratio are then expressed in parts per thousand (sometimes confusingly called "per mil" or ‰):

$$\delta^{34}\text{S} = 1000(R_{\text{sample}} - R_{\text{std}})/R_{\text{std}}$$

On this definition,  $\delta^{34}\text{S}$  is zero for meteoritic troilite; dissolved sulfate in ocean water is enriched +20‰ in <sup>34</sup>S, as are contemporary evaporite sulfates, whereas sedimentary sulfides are depleted in <sup>34</sup>S by as much as -50‰ due to fractionation during bacterial reduction to H<sub>2</sub>S.

In addition to the 4 stable isotopes sulfur has at least 9 radioactive isotopes, the one with the longest half-life being <sup>35</sup>S which decays by  $\beta^-$  activity ( $E_{\text{max}}$  0.167 MeV,  $t_{1/2}$  87.5 d). <sup>35</sup>S can be prepared by <sup>35</sup>Cl(n,p), <sup>34</sup>S(n, $\gamma$ ) or <sup>34</sup>S(d,p) and is commercially available as S<sub>element</sub>, H<sub>2</sub>S, SOCl<sub>2</sub> and KSCN. The  $\beta^-$  radiation has a similar energy to that of <sup>14</sup>C ( $E_{\text{max}}$  0.155 MeV) and similar counting techniques can be used (p. 276). The maximum range is 300 mm in air and 0.28 mm in water, and effective shielding is provided by a perspex screen 3–10 mm thick. The preparation of many <sup>35</sup>S-containing compounds has been

<sup>32</sup> H. NIELSEN, Sulfur isotopes, in E. JÄGER and J. C. HUNZIKER (eds.), *Lectures in Isotope Geology*, pp. 283–312, Springer-Verlag, Berlin, 1979.

reviewed<sup>(33)</sup> and many of these have been used for mechanistic studies, e.g. the reactions of the specifically labelled thiosulfate ions  $^{35}\text{SSO}_3^{2-}$  and  $\text{S}^{35}\text{SO}_3^{2-}$ . Another ingenious application, which won Barbara B. Askins the US Inventor of the Year award for 1978, is the use of  $^{35}\text{S}$  for intensifying under-exposed photographic images: prints or films are immersed in dilute aqueous alkaline solutions of  $^{35}\text{S}$ -thiourea, which complexes all the silver in the image (including invisibly small amounts), and the alkaline medium converts this to immobile, insoluble  $\text{Ag}^{35}\text{S}$ ; the film so treated is then overlaid with unexposed film which reproduces the image with heightened intensity as a result of exposure to the  $\beta^-$  activity.

The isotope  $^{33}\text{S}$  has a nuclear spin quantum number  $I = \frac{3}{2}$  and so is potentially useful in nmr experiments (receptivity to nmr detection  $17 \times 10^{-6}$  that of the proton). The resonance was first observed in 1951 but the low natural abundance of  $^{33}\text{S}$  (0.75%) and the quadrupolar broadening of many of the signals has so far restricted the amount of chemically significant work appearing on this resonance.<sup>(34)</sup> However, more results are expected now that pulsed fourier-transform techniques have become generally available.

The S atom in the ground state has the electronic configuration  $[\text{Ne}]3s^23p^4$  with 2 unpaired p electrons ( $^3P_1$ ). Other atomic properties are: ionization energy  $999.30 \text{ kJ mol}^{-1}$ , electron affinities  $+200$  and  $-414 \text{ kJ mol}^{-1}$  for the addition of the first and second electrons respectively, electronegativity (Pauling) 2.5, covalent radius 103 pm and ionic radius of  $\text{S}^{2-}$  184 pm. These properties can be compared with those of the other elements in Group 16 on p. 754.

<sup>33</sup> R. H. HERBER, Sulfur-35, in R. H. HERBER (ed.), *Inorganic Isotopic Syntheses*, pp. 193–214, Benjamin, New York, 1962.

<sup>34</sup> C. RODGER, N. SHEPPARD, C. MCFARLANE and W. MCFARLANE, in R. H. HARRIS and B. E. MANN (eds.), *NMR and the Periodic Table*, pp. 401–2, Academic Press, London, 1978. H. C. E. MCFARLANE and W. MCFARLANE, in J. MASON (ed.) *Multinuclear NMR*, Plenum Press, New York, 1987, pp. 417–35.

### 15.1.6 Chemical reactivity

Sulfur is a very reactive element especially at slightly elevated temperatures (which presumably facilitates cleavage of S–S bonds). It unites directly with all elements except the noble gases, nitrogen, tellurium, iodine, iridium, platinum and gold, though even here compounds containing S bonded directly to N, Te, I, Ir, Pt and Au are known. Sulfur reacts slowly with  $\text{H}_2$  at  $120^\circ$ , more rapidly above  $200^\circ$ , and is in reversible thermodynamic equilibrium with  $\text{H}_2$  and  $\text{H}_2\text{S}$  at higher temperatures. It ignites in  $\text{F}_2$  and burns with a livid flame to give  $\text{SF}_6$ ; reaction with chlorine is more sedate at room temperature but rapidly accelerates above this to give (initially)  $\text{S}_2\text{Cl}_2$  (p. 689). Sulfur dissolves in liquid  $\text{Br}_2$  to form  $\text{S}_2\text{Br}_2$ , which readily dissociates into its elements; iodine has been used as a cryoscopic solvent for sulfur (p. 654) and no binary compound is formed (directly) even at elevated temperature (see, however, p. 691). Oxidation of sulfur by (moist?) air is very slow at room temperature though traces of  $\text{SO}_2$  are formed; the ignition temperature of S in air is  $250\text{--}260^\circ$ . Pure dry  $\text{O}_2$  does not react at room temperature though  $\text{O}_3$  does. Likewise direct reaction with  $\text{N}_2$  has not been observed but, in a discharge tube, activated N reacts. All other non-metals (B, C, Si, Ge; P, As, Sb; Se) react at elevated temperatures. Of the metals, sulfur reacts in the cold with all the main group representatives of Groups 1, 2, 13, Sn, Pb and Bi, and also Cu, Ag and Hg (which even tarnishes at liquid-air temperatures). The transition metals (except Ir, Pt and Au) and the lanthanides and actinides react more or less vigorously on being heated with sulfur to form binary metal sulfides (p. 676).

The reactivity of sulfur clearly depends sensitively on the molecular complexity of the reacting species. Little systematic work has been done. *Cyclo-S*<sub>8</sub> is obviously less reactive than the diradical *catena-S*<sub>8</sub>, and smaller oligomers in the liquid or vapour phase also complicate the picture. In the limit atomic sulfur, which can readily be generated photolytically, is an extremely reactive species. As with atomic oxygen and the various



reviewed<sup>(33)</sup> and many of these have been used for mechanistic studies, e.g. the reactions of the specifically labelled thiosulfate ions  $^{35}\text{SSO}_3^{2-}$  and  $\text{S}^{35}\text{SO}_3^{2-}$ . Another ingenious application, which won Barbara B. Askins the US Inventor of the Year award for 1978, is the use of  $^{35}\text{S}$  for intensifying under-exposed photographic images: prints or films are immersed in dilute aqueous alkaline solutions of  $^{35}\text{S}$ -thiourea, which complexes all the silver in the image (including invisibly small amounts), and the alkaline medium converts this to immobile, insoluble  $\text{Ag}^{35}\text{S}$ ; the film so treated is then overlaid with unexposed film which reproduces the image with heightened intensity as a result of exposure to the  $\beta^-$  activity.

The isotope  $^{33}\text{S}$  has a nuclear spin quantum number  $I = \frac{3}{2}$  and so is potentially useful in nmr experiments (receptivity to nmr detection  $17 \times 10^{-6}$  that of the proton). The resonance was first observed in 1951 but the low natural abundance of  $^{33}\text{S}$  (0.75%) and the quadrupolar broadening of many of the signals has so far restricted the amount of chemically significant work appearing on this resonance.<sup>(34)</sup> However, more results are expected now that pulsed fourier-transform techniques have become generally available.

The S atom in the ground state has the electronic configuration  $[\text{Ne}]3s^23p^4$  with 2 unpaired p electrons ( $^3P_1$ ). Other atomic properties are: ionization energy  $999.30 \text{ kJ mol}^{-1}$ , electron affinities  $+200$  and  $-414 \text{ kJ mol}^{-1}$  for the addition of the first and second electrons respectively, electronegativity (Pauling) 2.5, covalent radius 103 pm and ionic radius of  $\text{S}^{2-}$  184 pm. These properties can be compared with those of the other elements in Group 16 on p. 754.

<sup>33</sup> R. H. HERBER, Sulfur-35, in R. H. HERBER (ed.), *Inorganic Isotopic Syntheses*, pp. 193–214, Benjamin, New York, 1962.

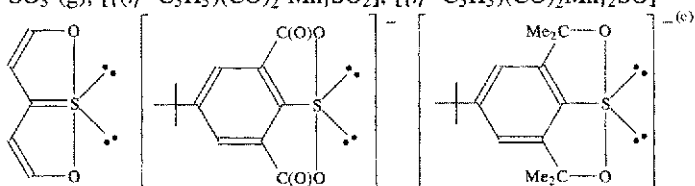
<sup>34</sup> C. RODGER, N. SHEPPARD, C. MCFARLANE and W. MCFARLANE, in R. H. HARRIS and B. E. MANN (eds.), *NMR and the Periodic Table*, pp. 401–2, Academic Press, London, 1978. H. C. E. MCFARLANE and W. MCFARLANE, in J. MASON (ed.) *Multinuclear NMR*, Plenum Press, New York, 1987, pp. 417–35.

### 15.1.6 Chemical reactivity

Sulfur is a very reactive element especially at slightly elevated temperatures (which presumably facilitates cleavage of S–S bonds). It unites directly with all elements except the noble gases, nitrogen, tellurium, iodine, iridium, platinum and gold, though even here compounds containing S bonded directly to N, Te, I, Ir, Pt and Au are known. Sulfur reacts slowly with  $\text{H}_2$  at  $120^\circ$ , more rapidly above  $200^\circ$ , and is in reversible thermodynamic equilibrium with  $\text{H}_2$  and  $\text{H}_2\text{S}$  at higher temperatures. It ignites in  $\text{F}_2$  and burns with a livid flame to give  $\text{SF}_6$ ; reaction with chlorine is more sedate at room temperature but rapidly accelerates above this to give (initially)  $\text{S}_2\text{Cl}_2$  (p. 689). Sulfur dissolves in liquid  $\text{Br}_2$  to form  $\text{S}_2\text{Br}_2$ , which readily dissociates into its elements; iodine has been used as a cryoscopic solvent for sulfur (p. 654) and no binary compound is formed (directly) even at elevated temperature (see, however, p. 691). Oxidation of sulfur by (moist?) air is very slow at room temperature though traces of  $\text{SO}_2$  are formed; the ignition temperature of S in air is  $250\text{--}260^\circ$ . Pure dry  $\text{O}_2$  does not react at room temperature though  $\text{O}_3$  does. Likewise direct reaction with  $\text{N}_2$  has not been observed but, in a discharge tube, activated N reacts. All other non-metals (B, C, Si, Ge; P, As, Sb; Se) react at elevated temperatures. Of the metals, sulfur reacts in the cold with all the main group representatives of Groups 1, 2, 13, Sn, Pb and Bi, and also Cu, Ag and Hg (which even tarnishes at liquid-air temperatures). The transition metals (except Ir, Pt and Au) and the lanthanides and actinides react more or less vigorously on being heated with sulfur to form binary metal sulfides (p. 676).

The reactivity of sulfur clearly depends sensitively on the molecular complexity of the reacting species. Little systematic work has been done. *Cyclo-S*<sub>8</sub> is obviously less reactive than the diradical *catena-S*<sub>8</sub>, and smaller oligomers in the liquid or vapour phase also complicate the picture. In the limit atomic sulfur, which can readily be generated photolytically, is an extremely reactive species. As with atomic oxygen and the various

Table 15.8 Coordination geometries of sulfur

CN	Examples
1	S <sub>2</sub> (g), CS <sub>2</sub> , HNCS, K[SCN] and "covalent" isothiocyanates, P <sub>4</sub> O <sub>6</sub> S <sub>4</sub> , P <sub>4</sub> S <sub>n</sub> (terminal S), SSF <sub>2</sub> , SSO <sub>3</sub> <sup>2-</sup> , Na <sub>3</sub> SbS <sub>4</sub> ·9H <sub>2</sub> O, Tl <sub>3</sub> VS <sub>4</sub> , M <sub>2</sub> MoS <sub>4</sub> , (NH <sub>4</sub> ) <sub>2</sub> WS <sub>4</sub> , S=WCl <sub>4</sub>
2 (linear)	$[(\eta^5\text{-C}_5\text{H}_5)(\text{CO})_2\text{Cr}\equiv\text{S}\equiv\text{Cr}(\text{CO})_2(\eta^5\text{-C}_5\text{H}_5)]^{(a)}$
2 (bent)	S <sub>n</sub> , H <sub>2</sub> S, H <sub>2</sub> S <sub>n</sub> , Me <sub>2</sub> S <sub>n</sub> , S <sub>n</sub> X <sub>2</sub> (Cl, Br), SO <sub>2</sub> , P <sub>4</sub> S <sub>n</sub> (bridging S), Se(SCN) <sub>2</sub> and "covalent" thiocyanates
3 (planar, D <sub>3h</sub> )	SO <sub>3</sub> (g), $\{[(\eta^5\text{-C}_5\text{H}_5)(\text{CO})_2\text{Mn}]_2\text{SO}_2\}$ , $\{[(\eta^5\text{-C}_5\text{H}_5)(\text{CO})_2\text{Mn}]_2\text{SO}\}^{(b)}$
3 (T-shaped planar)	
3 (pyramidal)	SSF <sub>2</sub> , OSOCl <sub>2</sub> , S <sub>8</sub> O(1 S), SO <sub>3</sub> <sup>2-</sup> , S <sub>2</sub> O <sub>4</sub> <sup>2-</sup> , S <sub>2</sub> O <sub>5</sub> <sup>2-</sup> (1 S), Me <sub>3</sub> S <sup>+</sup> , SF <sub>3</sub> <sup>+</sup>
4 (tetrahedral)	SO <sub>3</sub> (s) [i.e. cyclic S <sub>3</sub> O <sub>9</sub> or fibrous (SO <sub>3</sub> ) <sub>∞</sub> ], SO <sub>2</sub> Cl <sub>2</sub> , SO <sub>4</sub> <sup>2-</sup> , S <sub>2</sub> O <sub>6</sub> <sup>2-</sup> (O <sub>3</sub> SSO <sub>3</sub> <sup>2-</sup> ), S <sub>2</sub> O <sub>7</sub> <sup>2-</sup> (O <sub>3</sub> SOSO <sub>3</sub> <sup>2-</sup> ), S <sub>3</sub> O <sub>10</sub> <sup>2-</sup> , S <sub>5</sub> O <sub>16</sub> <sup>2-</sup> , ZnS (blende, and M = Be, Cd, Hg), ZnS(wurtzite, and M = Cd, Mn)
4 (seesaw) (ψ-tbp)	SF <sub>4</sub>
4 (pyramidal)	$[(\mu_4\text{-S})(\text{OsL}_n)_4]$ pyramidal clusters, <sup>(d)</sup> $[(\mu_4\text{-S})_2\text{Ru}_8\text{L}_m]$ bioctahedral cluster <sup>(e)</sup> , $[(\mu_4\text{-S})_2\text{Nb}_4(\text{SPh})_{12}]^{4-}$ octahedral $\{\text{S}_2\text{Nb}_4\}$ cluster <sup>(f)</sup>
5 (square pyramidal) (ψ-octahedral)	SF <sub>5</sub> <sup>-</sup> , SOF <sub>4</sub> , NiS (millerite structure)
6 (octahedral)	SF <sub>6</sub> , S <sub>2</sub> F <sub>10</sub> , MS(NaCl-type, M = Mg, Ca, Sr, Ba, Mn, Pb, Ln, Th, U, Pu)
6 (trigonal prismatic)	MS(NiAs-type), (M = Ti, V, Fe, Co, Ni), Hf <sub>2</sub> S
7 (mono-capped trigonal prismatic)	Ta <sub>6</sub> S, <sup>(g)</sup> Ti <sub>2</sub> S <sup>(h)</sup>
8 (cubic)	M <sub>2</sub> S (antifluorite-type, M = Li, Na, K, Rb)
9 (mono-capped square antiprismatic)	$[\text{Rh}_{17}(\text{CO})_{32}(\text{S})_2]^{3-}$ (encapsulated S) <sup>(i)</sup>
10 (bicapped square antiprismatic)	$[\text{Rh}_{10}(\text{CO})_{10}(\mu\text{-CO})_{12}\text{S}]^{2-}$ (encapsulated S) <sup>(j)</sup>

(a)Ref. 35. (b)Ref. 36. (c)Ref. 37. (d)Ref. 38. (e)Ref. 39. (f)Ref. 40. (g)Ref. 41. (h)Ref. 42. (i)Ref. 43. (j)Ref. 44.

<sup>35</sup>T. J. GREENHOUGH, B. W. S. KOLTHAMMER, P. LEGZDINS and J. TROTTER, *Inorg. Chem.* **18**, 3543–8 (1979). See also L. Y. GOH and T. C. W. MAK, *J. Chem. Soc., Chem. Commun.*, 1474–5 (1986).

<sup>36</sup>L. P. LORENZ, J. MESSELHÄUSER, W. HILLER and K. HAUG, *Angew. Chem. Int. Edn. Engl.* **24**, 228–9 (1985).

<sup>37</sup>P. H. W. LAU and J. C. MARTIN, *J. Am. Chem. Soc.* **100**, 7077–9 (1978).

<sup>38</sup>R. D. ADAMS, *Polyhedron* **4**, 2003–25 (1985).

<sup>39</sup>R. D. ADAMS, J. E. BABIN and M. TASI, *Inorg. Chem.* **25**, 4460–1 (1986).

<sup>40</sup>J. L. SEELA, J. C. HUFFMAN and G. CHRISTOU, *J. Chem. Soc., Chem. Commun.*, 1258–60 (1987).

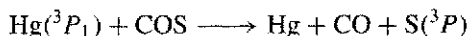
<sup>41</sup>H. F. FRANZEN and J. G. SMEGGL, *Acta Cryst.* **B26**, 125–9 (1970).

<sup>42</sup>J. P. OWENS, B. R. CONARD and H. F. FRANZEN, *Acta Cryst.* **23**, 77–82 (1967).

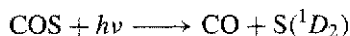
<sup>43</sup>J. L. VIDAL, R. A. FIATO, L. A. CROSBY and R. L. PRUEYTT, *Inorg. Chem.* **17**, 2574–82 (1978).

<sup>44</sup>G. CIANI, L. GARLASCHELLI, A. SIRONI and S. MARTINENGO, *J. Chem. Soc., Chem. Commun.*, 563–5 (1981).

methylenes, both singlet and triplet states are possible and these have different reactivities. The ground state is  $^3P_2$ , and the singlet state  $^1D_2$  lies  $110.52 \text{ kJ mol}^{-1}$  above this. Triplet state S atoms (with 2 unpaired electrons) can be generated by the Hg-photosensitized irradiation of COS:



Triplet S can also be generated by direct photolysis of  $\text{CS}_2$  ( $h\nu < 210 \text{ nm}$ ) or ethylene episulfide  $\overline{\text{CH}_2\text{CH}_2\text{S}}$  ( $h\nu 220\text{--}260 \text{ nm}$ ). Photolysis of  $\text{SPF}_3$  ( $h\nu 210\text{--}230 \text{ pm}$ ) generates singlet state S atoms (with no unpaired electrons) but the best syntheses of these is the direct primary photolysis of COS in the absence of Hg; this generates mainly singlet S (75%) with the rest being in the triplet state ( $^3P$ ):



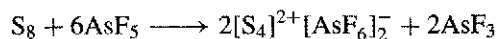
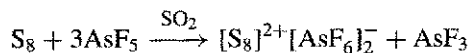
Generation of (excited state) singlet S in the presence of paraffins yields the corresponding mercaptan by a concerted single-step insertion:  $\text{RH} + \text{S}(^1D_2) \longrightarrow \text{RSH}$ . By contrast, paraffins are inert to triplet (ground state) S atoms. Singlet S undergoes analogous insertion reactions with  $\text{MeSiH}_3$ ,  $\text{SiMe}_4$  and  $\text{B}_2\text{H}_6$ . Olefins can undergo insertion of singlet S atoms on stereospecific addition of triplet S atoms; according to experimental conditions, the products are alkenyl mercaptans, vinylic mercaptans or episulfides. Analogous reactions with inorganic compounds appear to be a very promising field for future research. Generation of the reactive diatomic species  $\text{S}_2$  for synthetic purposes is also currently an active field.<sup>(45,46)</sup>

Sulfur compounds exhibit a rich and multifarious variety which derives not only from the numerous possible oxidation states of the element (from  $-2$  to  $+6$ ) but also from the range of bond types utilized (covalent, coordinate,

ionic and even metallic) and the multiplicity of coordination geometries adopted by the element. Oxidation states and their interrelationships as codified by oxidation state diagrams are dealt with more fully in the section on oxoacids of sulfur (p. 706) though the existence of several other series of compounds, notably the halides, also illustrates the element's versatility. The range of bond types, as reflected in the physical and chemical properties of the various compounds of the element, will become increasingly apparent throughout the rest of the chapter. The multiplicity of coordination geometries is amply demonstrated by the examples in Table 15.8. Most of these can be readily rationalized by the numerous variants of elementary bonding theory. See ref. 47 for a VSEPR treatment.

### Polyatomic sulfur cations

As long ago as 1804 C. F. Bucholz observed that sulfur dissolves in oleum to give clear, brightly coloured solutions which could be yellow, deep blue or red (or intermediate colours) depending on the strength of the oleum and the time of the reaction. These solutions are now known to contain  $\text{S}_n^{2+}$  cations, the structure of which has been elucidated during the past two decades mainly by elegant synthetic, Raman spectroscopic and crystallographic studies.<sup>(48–50)</sup> Selenium and tellurium behave similarly (p. 759). Sulfur can most conveniently be quantitatively oxidized using  $\text{SbF}_5$  or  $\text{AsF}_5$  in an inert solvent such as  $\text{SO}_2$ , e.g.:



<sup>47</sup> I. HARGITTAI, *The Structure of Volatile Sulfur Compounds*, D. Reidel Publ. Co., (Kluwer Academic Publ.), Dordrecht, 1985. 301 pp.

<sup>48</sup> R. J. GILLESPIE, *Chem. Soc. Rev.* **8**, 315–52 (1979).

<sup>49</sup> T. A. O'DONNELL, *Chem. Soc. Rev.* **16**, 1–43 (1987).

<sup>50</sup> N. BURFORD, J. PASSMORE and J. C. P. SANDERS, Chap. 2 in J. F. LIEBMAN and A. GREENBERG (eds.), *From Atoms to Polymers: Isoelectronic Analogies*, 1989, pp. 53–108.

<sup>45</sup> M. SCHMIDT and U. GÖRL, *Angew. Chem. Int. Edn. Engl.* **26** 887–8 (1987).

<sup>46</sup> T. L. GILCHRIST and J. E. WOOD, *J. Chem. Soc., Chem. Commun.*, 1460–1 (1992).

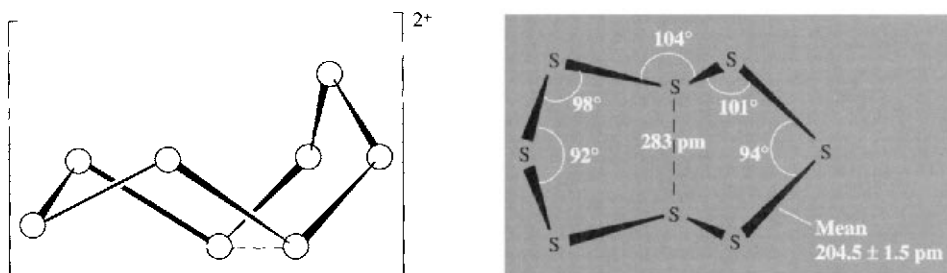


Figure 15.10 The structure and dimensions of the  $S_8^{2+}$  cation in  $[S_8]^{2+}[AsF_6]_2$ .

The bright-yellow solutions contain  $S_4^{2+}$ , a square-planar ring whose structure has been confirmed by an X-ray study on the unusual crystalline compound  $As_6F_{36}I_4S_{32}$ , i.e.  $[S_4]^{2+}[S_7I]_4[AsF_6]_6$  (p. 692). The S-S interatomic distance is 198 pm compared with 204 pm for a single-bonded species. Note also that  $S_4^{2+}$  is isoelectronic with the known heterocyclic compound  $S_2N_2$  (p. 725). The pale-yellow compound  $[S_4]^{2+}[SbF_6]_2$  has also been isolated.

The deep-blue solutions contain  $S_8^{2+}$ , and the X-ray structure of  $[S_8]^{2+}[AsF_6]_2$  reveals that the cation has an *exo-endo* cyclic structure with a long transannular bond as shown in Fig. 15.10 (see also p. 724). The bright-red solutions were originally thought to contain the  $S_{16}^{2+}$  cation and a compound thought to be  $S_{16}(AsF_6)_2$  was isolated; however, crystallographic study has shown<sup>(51)</sup> that the compound has the totally unexpected formulation  $[S_{19}]^{2+}[AsF_6]_2$  which could not have been distinguished from the earlier stoichiometry on the basis of the original analytical data. This astonishing cation consists of two 7-membered rings joined by a 5-atom chain. As shown in Fig. 15.11, one of the rings has a boat conformation whilst the other is disordered, existing as a 4:1 mixture of chair and boat conformations. S-S distances vary greatly from 187 to 239 pm and S-S-S angles vary from  $91.9^\circ$  to  $127.6^\circ$ . See also p. 692 for  $[S_7X]^+$  cations.

Solutions of sulfur in oleum also give rise to paramagnetic species, probably  $S_n^+$ , but the

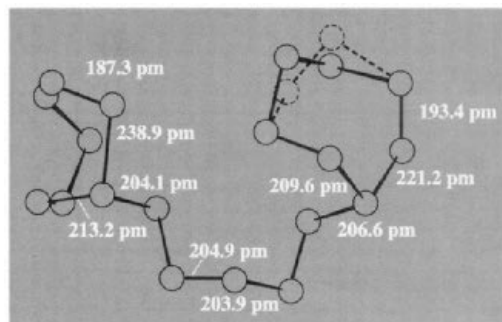


Figure 15.11 The structure and some of the dimensions of the disordered cation  $S_{19}^{2+}$  (see text).

nature of these has not yet been fully established. For polysulfur anions  $S_n^{2-}$ , see p. 681.

### Sulfur as a ligand

The S atom can act either as a terminal or a bridging ligand. The dianion  $S_2^{2-}$  is also an effective ligand, and chelating polysulfides  $-S_n-$  are well established. These various sulfur ligands will be briefly considered before dealing with the broad range of compounds in which S acts as the donor atom, e.g.  $H_2S$ ,  $R_2S$ , dithiocarbamates and related anions, 1,2-dithiolenes etc. Ligands in which S acts as a donor atom are usually classified as class-b ligands ("soft" Lewis bases), in contrast to oxygen donor-atom ligands which tend to be class-a or hard (p. 909). The larger size of the S atom and the consequent greater deformability of its electron cloud give a qualitative rationalization of this difference and the possible participation

<sup>51</sup> R. C. BURNS, R. J. GILLESPIE and J. F. SAWYER, *Inorg. Chem.* **19**, 1423-32 (1980).

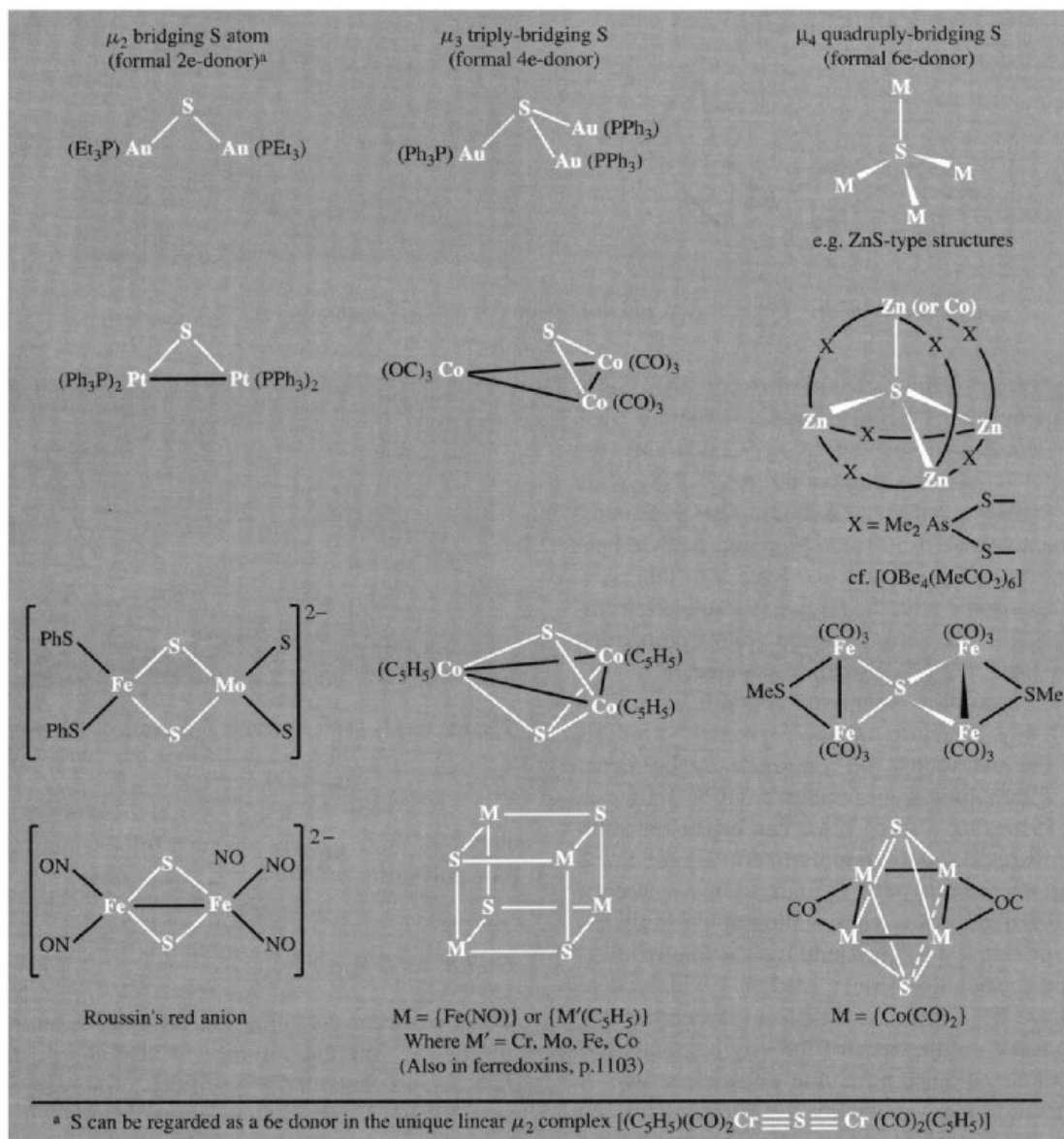


Figure 15.12 The S atom as a bridging ligand.

of  $d_{\pi}$  orbitals in bonding to sulfur has also been invoked (see comparison of N and P, p. 416).

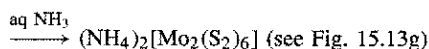
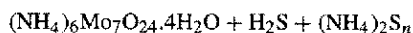
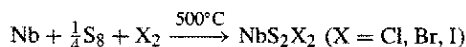
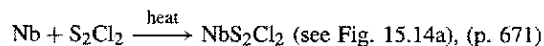
Some examples of the S atom as a bridging ligand are given in Fig. 15.12. In the  $\mu_2$  bridging mode S is usually regarded as a 2-electron donor, though in the linear bridge [(C<sub>5</sub>H<sub>5</sub>)(CO)<sub>2</sub>Cr]<sub>2</sub>S] it is probably best regarded

as a 6-electron donor.<sup>(35)</sup> In the  $\mu_3$  triply bridging mode S can be regarded as a 4-electron donor, using both its unpaired electrons and one lone-pair.<sup>(52)</sup> If the 3 bridged metal atoms

<sup>52</sup> H. VAHRENKAMP, *Angew. Chem. Int. Edn. Engl.* **14**, 322-9 (1975).

are different then a chiral tetrahedrane molecule results and this has permitted the recent (1980) resolution of the enantiomers of the first optically active metal cluster compound, the red complex  $[\{\text{Co}(\text{CO})_3\}\{\text{Fe}(\text{CO})_3\}\{\text{Mo}(\eta^5\text{-C}_5\text{H}_5)(\text{CO})_2\}\text{S}]$ .<sup>(53)</sup> The pseudo-cubane structure adopted by some of the  $\mu_3\text{-S}$  compounds is assuming added significance as a crucial structural unit in many biologically important systems, e.g. the  $\{(\text{RS})\text{FeS}\}_4$  units which cross-link the polypeptide chains in ferredoxins (p. 1103). In the  $\mu_4$ -mode 6-electrons are involved, if the bonding is considered to be predominantly covalent, though metal-sulfides are sometimes treated as compounds of  $\text{S}^{2-}$ . No molecular compounds are known in which S bridges 6 or 8 metal atoms though, again, these coordinations are prevalent in solid-state compounds, many of which have interatomic bonding which is far from being purely ionic.

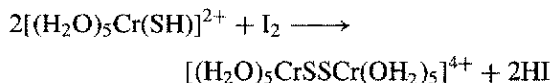
The disulfur ligand  $\text{S}_2$  (sometimes more helpfully considered as  $\text{S}_2^{2-}$ ) is attracting increasing attention since no other simple ligand is as versatile in the variety of its modes of coordination. Moreover, in one particular mode (see Type III, p. 669) it is particularly effective in stabilizing metal clusters. Many of the complexes of  $\text{S}_2$  were first obtained accidentally, and their seemingly bizarre stoichiometries only became intelligible after structural elucidation by X-ray crystallography. The complexes can be prepared by reacting metals or their compounds with: (a) a positive  $\text{S}_2$  group as in  $\text{S}_2\text{Cl}_2$ ,<sup>(54)</sup> (b) a neutral  $\text{S}_2$  group, usually derived from  $\text{S}_8$ ; (c) a negative  $\text{S}_2^{2-}$  group such as an alkaline polysulfide solution. Examples are:



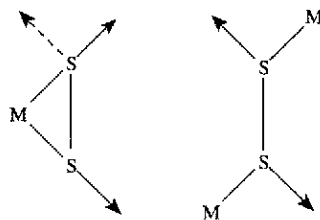
<sup>53</sup> F. RICHTER and H. VAHRENKAMP, *Angew. Chem. Int. Edn. Engl.* **19**, 65 (1980).

<sup>54</sup> M. J. ATHERTON and J. H. HOLLOWAY, *Adv. Inorg. Chem. Radiochem.* **22**, 171–98 (1979).

The S–S bond can also be formed by a direct coupling reaction, e.g.:



At least 8 modes of coordination are known (Table 15.9);<sup>(55)</sup> they are all based on either side-on  $\text{S}_2$  or bridging  $-\text{S}-\text{S}-$  with possible further ligation via one or two lone-pairs as shown schematically below:



Frequently, more than one type of coordination occurs in a given complex, e.g. Figs. 15.13b, c and g. Interestingly, there appear to be no known example of terminal “end-on” coordination,  $\text{M}-\text{S}-\text{S}$  (see dioxygen complexes, p. 615). Detailed descriptions of all the structures and their bonding are beyond the scope of this treatment but it will be noted from Table 15.9 that the S–S interatomic distances in disulfide complexes range from 201 to 209 pm. The following specific points of interest may also be mentioned. The orange-red anion  $[\text{Mo}_4(\text{NO})_4\text{S}_{13}]^{4-}$  (Fig. 15.13b) features two triangular arrays of Mo atoms joined by a common edge and with an angle of  $127.6^\circ$  between the two  $\text{Mo}_3$  planes; each plane has a  $\mu_3$ -bonded S atom above it ( $\text{Mo}-\text{S}$  250.1 pm) and there is a further unique  $\mu_4$ -bonded S atom which is 261.6 pm from each of the 4 Mo atoms. Four of the 5  $\text{S}_2^{2-}$  ligands are simultaneously bonded both end on ( $\text{Mo}-\text{S}$  246.5 pm) and side on ( $\text{Mo}-\text{S}$  249.2 pm) whilst the fifth is side-on only. The complex therefore has sulfur in five different bonding states. In the red complex  $[\text{Mn}_4(\text{CO})_{15}(\text{S}_2)_2]$  (Fig. 15.13c) the 2  $\text{S}_2^{2-}$  ligands are different (Types Ic and Id); the 4 Mn

<sup>55</sup> A. MULLER and W. JAEGERMANN, *Inorg. Chem.* **18**, 2631–3 (1979).

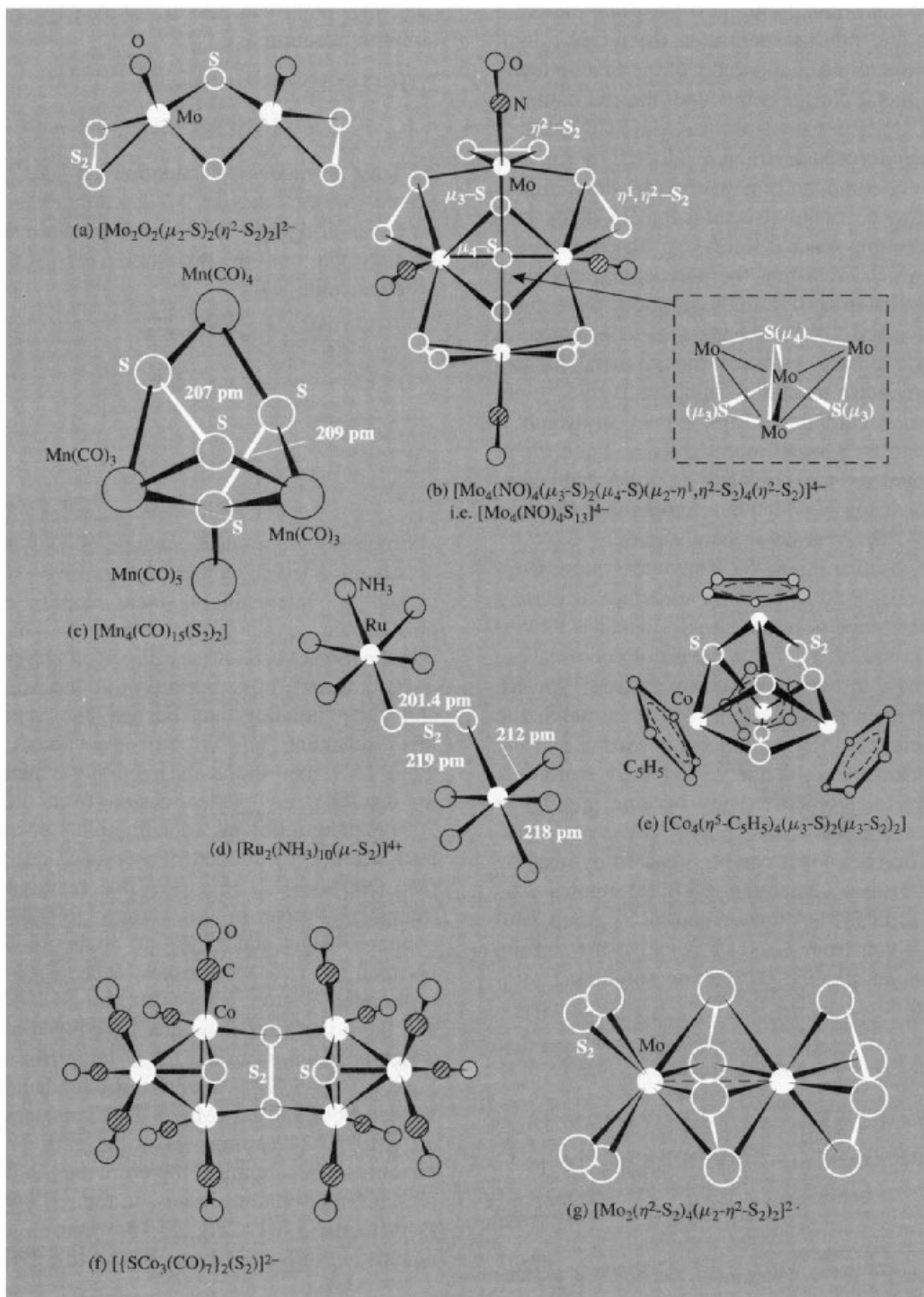
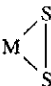
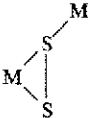
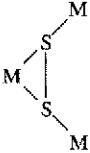
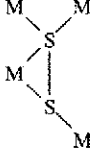
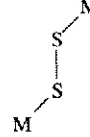
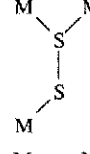
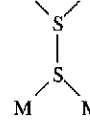
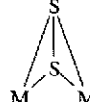


Figure 15.13 Structures of some disulfide complexes.

Table 15.9 Types of metal-disulfide complex

Type	Example	$d(S-S)/\text{pm}$	Structure
Ia 	$[\text{Mo}_2\text{O}_2\text{S}_2(\text{S}_2)_2]^{2-}$	208(1)	Figure 15.13a <sup>(56)</sup>
Ib 	$\{\text{Mo}_4(\text{NO})_4\text{S}_{13}\}^{4-}$	204.8(7)	Figure 15.13b <sup>(57)</sup>
Ic 	$[\text{Mn}_4(\text{CO})_{15}(\text{S}_2)_2]$	207	Figure 15.13c <sup>(58)</sup>
Id 	$[\text{Mn}_4(\text{CO})_{15}(\text{S}_2)_2]$	209	Figure 15.13c <sup>(58)</sup>
IIa 	$[\text{Ru}_2(\text{NH}_3)_{10}\text{S}_2]^{4+}$	201.4(1)	Figure 15.13d <sup>(59)</sup>
IIb 	$[\text{Co}_4(\eta^5\text{-C}_5\text{H}_5)_4(\mu_3\text{-S})_2(\mu_3\text{-S}_2)_2]$	201(3)	Figure 15.13e <sup>(60)</sup>
IIc 	$[\{\text{SCo}_3(\text{CO})_7\}_2\text{S}_2]$	204.2(14)	Figure 15.13f <sup>(61)</sup>
III 	$[\text{Mo}_2(\text{S}_2)_6]^{2-}$	204.3(5)	Figure 15.13g <sup>(62)</sup>

<sup>56</sup>W. CLEGG, N. MOHAN, A. MÜLLER, A. NEUMAN, W. RITTNER and G. M. SHELDRIK, *Inorg. Chem.* **19**, 2066-9 (1980).

<sup>57</sup>A. MÜLLER, W. ELTZNER and N. MOHAN, *Angew. Chem. Int. Edn. Engl.* **18**, 168-9 (1979).

<sup>58</sup>V. KÜLLMER, E. RÖTTINGER and H. VAHRENKAMP, *J. Chem. Soc., Chem. Commun.*, 782-3 (1977).

<sup>59</sup>R. C. ELDER and M. TRKULA, *Inorg. Chem.* **16**, 1048-51 (1977).

<sup>60</sup>V. A. UCHTMAN and L. F. DAHL, *J. Am. Chem. Soc.* **91**, 3756-63 (1969).

<sup>61</sup>D. L. STEVENSON, V. R. MAGNUSON and L. F. DAHL, *J. Am. Chem. Soc.* **89**, 3727-32 (1967).

<sup>62</sup>A. MÜLLER, W.-O. NOLTE and B. KREBS, *Angew. Chem. Int. Edn. Engl.* **17**, 279 (1978); A. MÜLLER, W.-O. NOLTE and B. KREBS, *Inorg. Chem.* **19**, 2835-6 (1980).

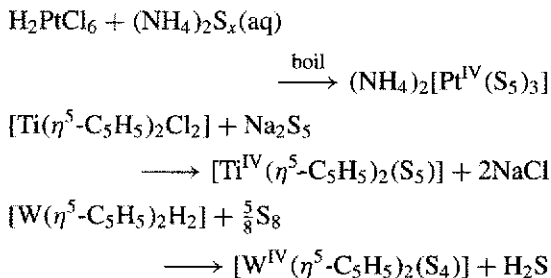


atoms are bonded, respectively, to 3, 3, 4 and 5 carbonyl ligands, but each achieves a distorted octahedral coordination by being bonded also to 3, 3, 2 and 1 S atoms respectively. There seems no reason to suppose that the diamagnetic bridged dinuclear anion  $[(\text{NC})_5\text{Co}^{\text{III}}\text{SSCo}^{\text{III}}(\text{CN})_5]^{6-}$  is not a formal Type IIa disulfido  $\text{S}_2^{2-}$  complex, but there is evidence<sup>(59)</sup> that the superficially analogous paramagnetic dinuclear ruthenium cation in Fig. 15.13d is, in fact, a mixed-valence supersulfido  $\text{S}_2^-$  complex:  $[(\text{H}_3\text{N})_5\text{Ru}^{\text{II}}\text{SSRu}^{\text{III}}(\text{NH}_3)_5]^{4+}$ . The bridged dinuclear cobalt anion undergoes a remarkable aerial oxidation in aqueous ethanol solutions at  $-15^\circ\text{C}$ ; one of the bridging S atoms only is oxidized and this results in the formation of a bridging thiosulfito group  $[(\text{NC})_5\text{CoSSO}_2\text{Co}(\text{CN})_5]^{6-}$  coordinated through the two S atoms to the two Co atoms.<sup>(63)</sup> Other recent examples of  $\text{S}_2$ -complexes include  $[\text{V}(\eta^5\text{-C}_5\text{Me}_5)_2(\eta^2\text{-S}_2)]$ ,<sup>(64)</sup>  $[\text{W}_2(\text{S})_2(\text{SH})(\mu\text{-}\eta^2\text{-S}_2)(\eta^2\text{-S}_2)_3]^-$ ,<sup>(65)</sup>  $[(\eta^5\text{-C}_5\text{Me}_5)_2\text{Fe}_2(\mu\text{-}\eta^2, \eta^2\text{-S}_2)]^{(66)}$  and  $[\text{Ru}_2\{\text{P}(\text{OMe})_3\}_2(\eta^5\text{-C}_5\text{H}_5)_2(\mu\text{-}\eta^1, \eta^1\text{-S}_2)_2]$ .<sup>(67)</sup>

Not all disulfide complexes are discrete molecular or ionic species and several solid-state compounds of  $\text{S}_2^{2-}$  are known in addition to the familiar pyrites and marcasite-type disulfides (p. 680). Examples are the chlorine-bridged polymeric  $\text{NbS}_2\text{Cl}_2$  mentioned on p. 667 (Fig. 15.14a) and the curious series of brown and red compounds formed by heating Mo or  $\text{MoS}_3$  with  $\text{S}_2\text{Cl}_2$ , e.g.<sup>(54)</sup>  $\text{MoS}_2\text{Cl}_2$ ,  $\text{MoS}_2\text{Cl}_3$  (Fig. 15.14b),  $\text{Mo}_2\text{S}_4\text{Cl}_5$  (Fig. 15.14c),  $\text{Mo}_2\text{S}_5\text{Cl}_3$  and  $\text{Mo}_3\text{S}_7\text{Cl}_4$ .

Complexes with chelating polysulfide ligands can be made either by reacting complex metal halides with solutions of polysulfides or by reacting hydrido complexes with elemental

sulfur, e.g.:



The red dianion  $[\text{PtS}_{15}]^{2-}$  was first made in 1903 but its structure as a chiral tris chelating pentasulfido complex (Fig. 15.15a) was not established until 1969.<sup>(68)</sup> It is a rare example of a "purely inorganic" (carbon-free) optically active species.<sup>(69)</sup> [Other examples are S. Heřmánek and J. Plešek's resolution of the main group element cluster compound  $i\text{-B}_{18}\text{H}_{22}$ ,<sup>(70)</sup> A. Werner's first-row transition-metal complex cation  $[\text{Co}\{(\mu\text{-OH})_2\text{Co}(\text{NH}_3)_4\}_3]^{6+}$ ,<sup>(71)</sup> and F. G. Mann's second-row complex anion  $\text{cis-}[\text{Rh}(\eta^2\text{-}(\text{NH})_2\text{-SO}_2)_2(\text{OH}_2)_2]^-$ .<sup>(72)</sup> The structure of the complex  $[\text{Ti}(\eta^5\text{-C}_5\text{H}_5)_2(\text{S}_5)]$  is in Fig. 15.15b; it has previously been mentioned in connection with the synthesis of *cyclo*-polysulfur allotropes (p. 657). The chair conformation of the 6-membered  $\text{TiS}_5$  ring undergoes chair-to-chair inversion above room temperature with an activation energy of about  $69\text{ kJ mol}^{-1}$ .<sup>(73)</sup> A similar ring inversion in  $[\text{Pt}(\text{S}_5)_3]^{2-}$  is even more facile and  $^{195}\text{Pt}$  n.m.r. studies lead to a value of  $50.5 \pm 1.3\text{ kJ mol}^{-1}$  for  $\Delta G^\ddagger$  at  $0^\circ\text{C}$ .<sup>(74)</sup> Other recent examples of chelating  $\text{S}_n^{2-}$  ligands occur in the dark red-brown dianion<sup>(75)</sup>  $[(\eta^2\text{-S}_5)\text{Fe}(\mu\text{-S})_2\text{Fe}(\eta^2\text{-S}_5)]^{2-}$  and in the intriguing black

<sup>63</sup> F. R. FRONCZEK, R. E. MARSH and W. P. SCHAEFER, *J. Am. Chem. Soc.* **104**, 3382–5 (1982).

<sup>64</sup> C. FLORIANO, S. GAMBARTTA, A. CHIESI-VILLA and C. GUASTINI, *J. Chem. Soc., Dalton Trans.*, 2099–103 (1987).

<sup>65</sup> F. SÉCHERESSE, J. M. MANOLI and C. POTVIN, *Inorg. Chem.* **25**, 3967–71 (1986).

<sup>66</sup> H. OGINO, H. TOBITA, S. INOMATA, and M. SHIMOI, *J. Chem. Soc., Chem. Commun.*, 586–7 (1988).

<sup>67</sup> P. M. TREICHEL, R. A. CRANE and K. J. HALLER, *Polyhedron* **9**, 1893–9 (1990).

<sup>68</sup> P. E. JONES and L. KATZ, *Acta Cryst.* **B25**, 745–52 (1969).

<sup>69</sup> R. D. GILLARD and F. L. WIMMER, *J. Chem. Soc., Chem. Commun.*, 936–7 (1978).

<sup>70</sup> S. HEŘMÁNEK and J. PLEŠEK, *Coll. Czech. Chem. Comm.* **35**, 2488–93 (1970).

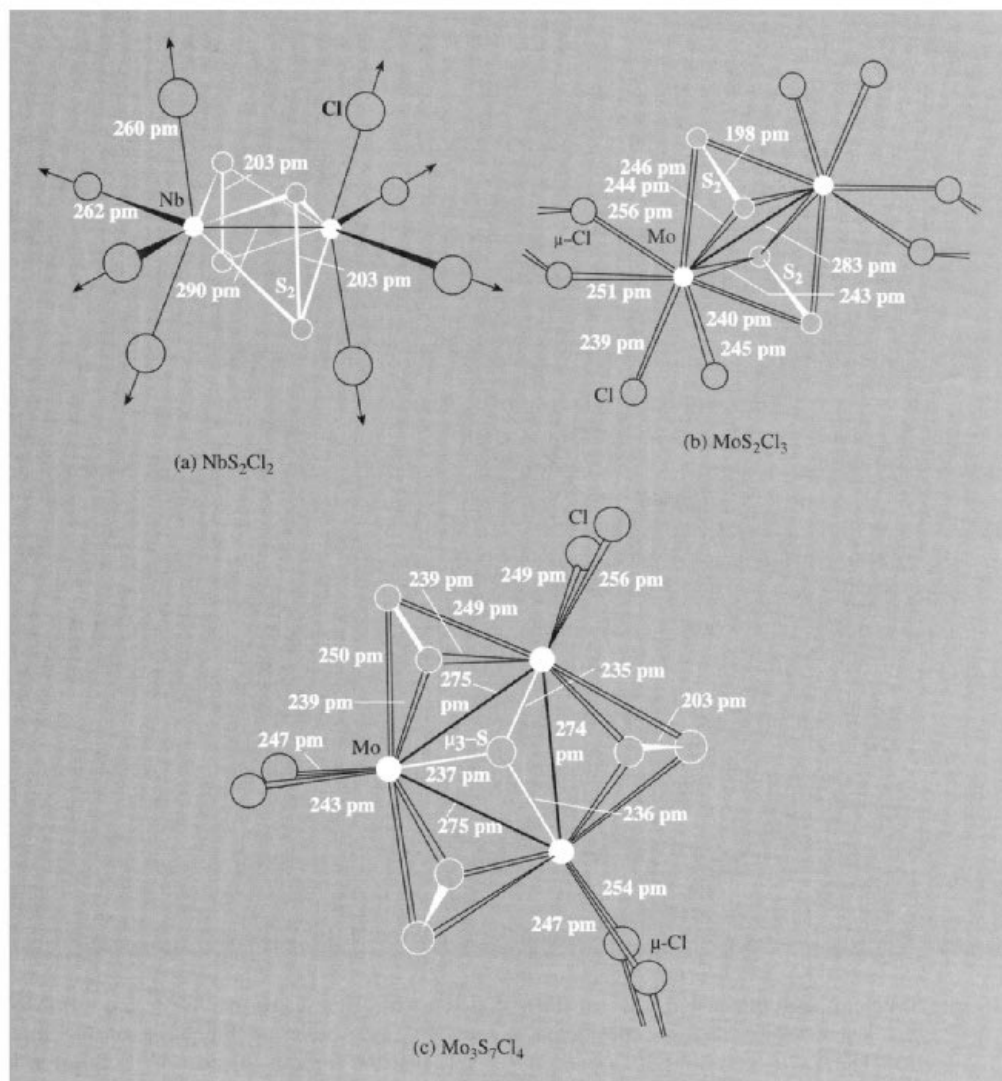
<sup>71</sup> A. WERNER, *Ber.* **47**, 3057–94 (1914).

<sup>72</sup> F. G. MANN, *J. Chem. Soc.* 412–19 (1933).

<sup>73</sup> E. W. ABEL, M. BOOTH and K. G. ORRELL, *J. Organometall. Chem.* **160**, 75–9 (1978).

<sup>74</sup> F. G. RIDDELL, R. D. GILLARD and F. L. WIMMER, *J. Chem. Soc., Chem. Commun.*, 332–3 (1982).

<sup>75</sup> D. COUCOUVANIS, D. SWENSON, P. STREMPLE and N. C. BAENZIGER, *J. Am. Chem. Soc.* **101**, 3392–4 (1979).



**Figure 15.14** Chlorine bridged polymeric structures of (a)  $\text{NbS}_2\text{Cl}_2$ , (b)  $\text{MoS}_2\text{Cl}_3$  and (c)  $\text{Mo}_3\text{S}_7\text{Cl}_4$ .

dianion  $[\text{Mo}_2\text{S}_{10}]^{2-}$  which features 4 different sorts of sulfur ligand and at least 6 different S-atom environments (Fig. 15.15c).<sup>(76)</sup> More complicated structures, including those featuring multidentate polymers or metal-sulfur clusters are continually being discovered in polysulfides whose apparently simple stoichiometry often

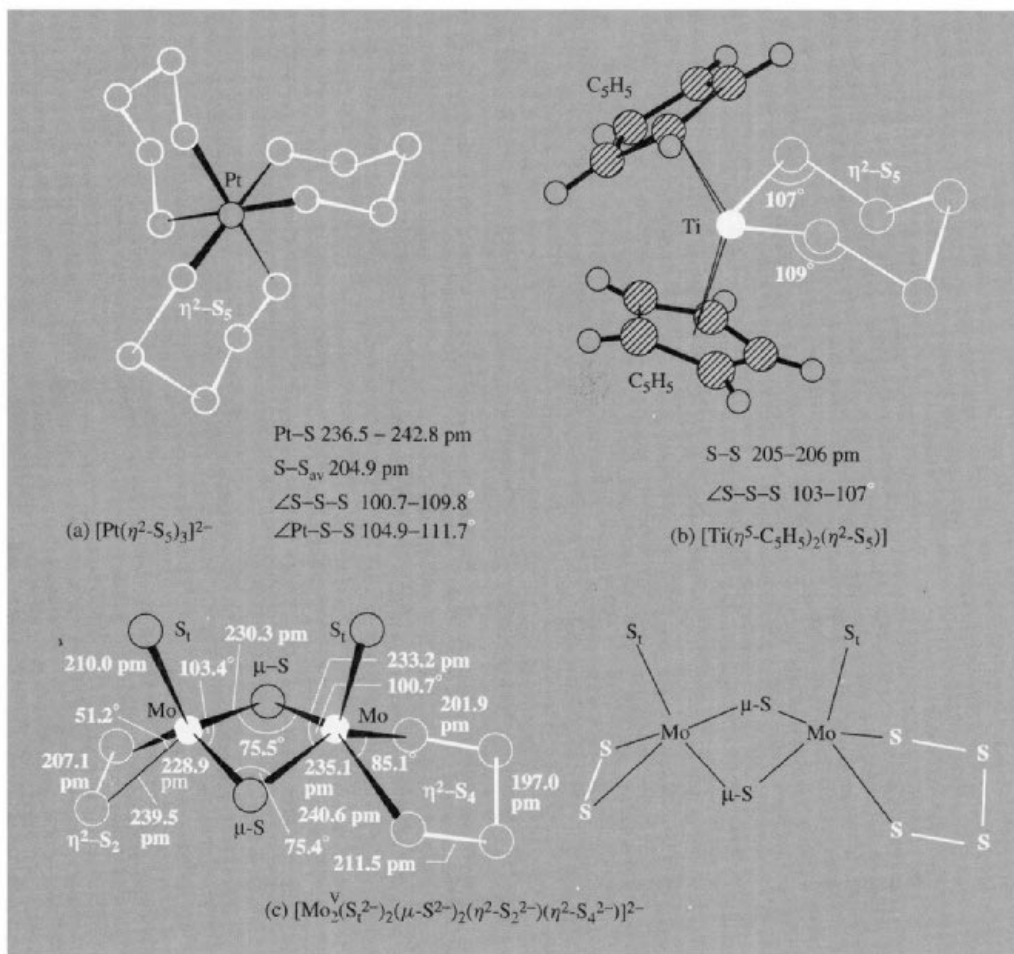
conceals an amazing structural complexity. Some recent examples are:  $[(\eta^5\text{-C}_5\text{Me}_5)_2\text{Th}(\eta^4\text{-S}_5)]$ ,<sup>(77)</sup>  $[\text{NMe}_4]^+[\text{Ag}(\text{S}_5)]_\infty$ ,<sup>(78)</sup>  $[\text{Cu}_4(\text{S}_5)_2(\text{py})_4]$ ,<sup>(79)</sup>

<sup>77</sup> D. A. WROBLESKI, D. T. CROMER, J. V. ORTIZ, T. B. RAUCHFUSS, R. R. RYAN and A. P. SATTELBERGER, *J. Am. Chem. Soc.* **108**, 174–5 (1986).

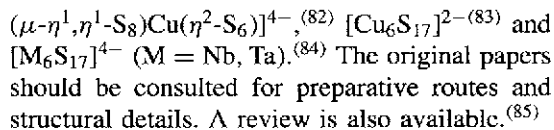
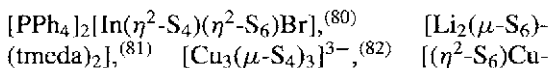
<sup>78</sup> R. M. H. BANDA, D. C. CRAIG, I. G. DANCE and M. L. SCUDDER, *Polyhedron* **8** 2379–83 (1989).

<sup>79</sup> E. RAMLI, T. B. RAUCHFUSS and C. L. STERN, *J. Am. Chem. Soc.* **112** 4043–4 (1990).

<sup>76</sup> W. CLEGG, G. CHRISTOU, C. D. GARNER and G. M. SHELDRICK, *Inorg. Chem.* **20**, 1562–6 (1981).



**Figure 15.15** Structure and dimensions of (a)  $[\text{Pt}(\eta^2\text{-S}_5)_3]^{2-}$ , (b)  $[\text{Ti}(\eta^5\text{-C}_5\text{H}_5)_2(\eta^2\text{-S}_5)]$  and (c)  $[\text{Mo}_2\text{S}_{10}]^{2-}$ : this last complex can be considered as an  $\text{Mo}^{\text{V}}$  derivative on the basis of the formulation  $[\text{Mo}_2^{\text{V}}(\text{S}_4^{2-})_2(\mu\text{-S}^{2-})_2(\eta^2\text{-S}_2^{2-})(\eta^2\text{-S}_4^{2-})]^{2-}$ . Note that the angles subtended by S atoms at Mo vary from 51.2° through 85.1° to 100.7° and 103.4°, the M-S distances from 211 pm through 229 and 235 pm to 241 pm, and the S-S distances from 197 to 211.5 pm with the  $\text{S}_2^{2-}$  group being 207 pm.



<sup>80</sup> S. DHINGRA and M. G. KANATZIDS, *Polyhedron* **10**, 1069–73 (1991). See also W. BUBENHEIM and U. MÜLLER, *Z. anorg. allg. Chem.* **620**, 1607–12 (1994) for  $[\text{In}(\eta^2\text{-S}_4)(\eta^2\text{-S}_6)\text{Cl}]^-$ .

<sup>81</sup> A. J. BANISTER (and 12 others), *J. Chem. Soc., Chem. Commun.*, 105–7 (1990).

<sup>82</sup> A. MÜLLER, F.-W. BAUMANN, H. BÖGGE, M. RÖMER, E. KRICKEMEYER and K. SCHMITZ, *Angew. Chem. Int. Edn. Engl.* **23**, 632–3 (1984).

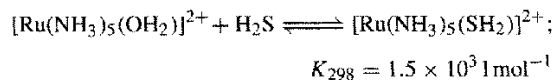
<sup>83</sup> A. MÜLLER, M. RÖMER, H. BÖGGE, E. KRICKEMEYER and D. BERGMANN, *J. Chem. Soc., Chem. Commun.*, 384–5 (1984).

<sup>84</sup> J. SOLA, Y. DO, J. M. BERG and R. H. HOLM, *J. Am. Chem. Soc.* **105**, 7784–6 (1983).

<sup>85</sup> M. DRAGANJAC and T. B. RAUCHFUSS, *Angew. Chem. Int. Edn. Engl.* **24** 742–57 (1985).

### Other ligands containing sulfur as donor atom

$\text{H}_2\text{S}$ , the simplest compound of sulfur, differs markedly from its homologue  $\text{H}_2\text{O}$  in complex-forming ability: whereas aquo complexes are extremely numerous and frequently very stable (p. 625),  $\text{H}_2\text{S}$  rarely forms simple adducts due to its ready oxidation to sulfur or its facile deprotonation to  $\text{SH}^-$  or  $\text{S}^{2-}$ .  $[\text{AlBr}_3(\text{SH}_2)]$  has long been known as a stable compound of tetrahedral  $\text{Al}^{(86)}$  but the few transition metal complexes having some degree of stability at room temperature are of more recent vintage: examples include  $[\text{Mn}(\eta^5\text{-C}_5\text{H}_5)(\text{CO})_2(\text{SH}_2)]$ ,  $[\text{W}(\text{CO})_5(\text{SH}_2)]$ , and the *triangulo* cluster complexes  $[\text{Ru}_3(\text{CO})_9(\text{SH}_2)]$  and  $[\text{Os}_3(\text{CO})_9(\text{SH}_2)]$ .<sup>(52,87)</sup> Action of  $\text{H}_2\text{S}$  on acidic aqueous solutions frequently precipitates the metal sulfide (cf. qualitative analysis separation schemes) but, in the presence of a reducing agent such as  $\text{Eu}^{\text{II}}$ ,  $\text{H}_2\text{S}$  can displace  $\text{H}_2\text{O}$  from the pale-yellow aquopentammine ruthenium(II) ion:



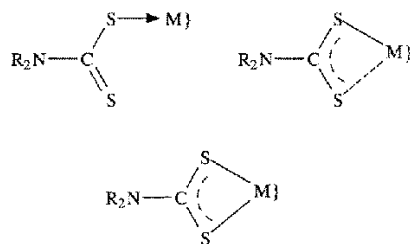
In the absence of  $\text{Eu}^{\text{II}}$ , oxidative deprotonation of the pale-yellow  $\text{H}_2\text{S}$  complex occurs to give the orange ruthenium(III) complex  $[\text{Ru}(\text{NH}_3)_5(\text{SH})]^{2+}$ . Other examples of complexes containing the  $\text{SH}^-$  ligand are  $[\text{Cr}(\text{OH}_2)_5(\text{SH})]^{2+}$ ,  $[\text{W}(\eta^5\text{-C}_5\text{H}_5)(\text{CO})_3(\text{SH})]$ ,  $[\text{Ni}(\eta^5\text{-C}_5\text{H}_5)(\text{PBU}_3)(\text{SH})]$ , *trans*- $[\text{PtH}(\text{PET}_3)_2(\text{SH})]$  and *trans*- $[\text{Pt}(\text{PET}_3)_2(\text{SH})_2]$ .<sup>(52,88,89)</sup>

The S-donor ligands  $\text{SO}$ ,  $\text{S}_2\text{O}_2$  and  $\text{SO}_2$  are mentioned in Section 15.2.5 and S-N ligands in Section 15.2.7. Thiocyanate ( $\text{SCN}^-$ ) is ambidentate, but towards heavier metals it

tends to be S-bonded rather than N-bonded. Bridging modes are also known (p. 324), including M-SCN-M and the rare S-only bridged  $\text{MS}(\text{CN})\text{M}$ .<sup>(90)</sup>

Organic thio ligands are well established, examples being the thiols  $\text{RSH}$  ( $\text{R} = \text{Et}$ ,  $\text{Pr}^n$ ,  $\text{Bu}'$ ,  $\text{Ph}$ ),<sup>(91)</sup> the thioethers  $\text{SMe}_2$ ,  $\text{SEt}_2$ , tetrahydrothiophene, etc., the chelating dithioethers, e.g.  $\text{MeS}(\text{CH}_2)_2\text{SMe}$ , and macro-cyclic ligands such as  $\{-(\text{CH}_2)_3\text{S}-\}_n$  with  $n = 3, 4$  etc.<sup>(92)</sup> Thiourea,  $(\text{H}_2\text{N})_2\text{C}=\text{S}$ , affords a further example. Factors affecting the stability of the resulting complexes have already been reviewed (p. 198). It is also notable that when  $\text{B}_{10}\text{H}_{14}$  reacts with solutions of thioethers in  $\text{OEt}_2$ , tetrahydrofuran, etc., it is the thio ligand rather than the oxygen-containing species which forms the stable *arachno*-bis adducts  $[\text{B}_{10}\text{H}_{12}(\text{SR}_2)_2]$  (p. 176).

Another large class of S-donor ligands comprises the dithiocarbamates  $\text{R}_2\text{NC}_2\text{S}_2^{2-}$  and related anions  $\text{YCS}_2^-$ , e.g. dithiocarbonylates  $\text{RCS}_2^-$ , xanthates  $\text{ROCS}_2^-$ , thioxanthates  $\text{RSCS}_2^-$ , dithiocarbonate  $\text{OCS}_2^{2-}$ , trithiocarbonate  $\text{SCS}_2^{2-}$  and dithiophosphinates  $\text{R}_2\text{PS}_2^-$  (see p. 509 for applications). Dithiocarbamates can function either as unidentate or bidentate (chelating) ligands:



<sup>90</sup> S. M. NELSON, F. S. ESHO and M. G. B. DREW, *J. Chem. Soc., Chem. Commun.*, 388-9 (1981).

<sup>91</sup> F. M. CONROY-LEWIS and S. J. SIMPSON, *J. Chem. Soc., Chem. Commun.*, 388-9 (1991) and references cited therein.

<sup>92</sup> S. CRAWLE, J. R. HARTMAN, D. J. WATKIN and S. R. COOPER, *J. Chem. Soc., Chem. Commun.*, 1083-4 (1986); C. M. THORNE, S. C. RAWLE, G. A. ADMANS and S. R. COOPER, *ibid.*, 306-7 (1987); S. C. RAWLE and S. R. COOPER, *ibid.*, 308-9 (1987); T. YOSHIDA, T. ADACHI, M. KAMINAKA and T. UEDA, *J. Am. Chem. Soc.* **110**, 4872-3 (1988). See also W. TREMEL, B. KREBS and G. HENKEL, *J. Chem. Soc., Chem. Commun.*, 1527-9 (1986).

<sup>86</sup> A. WEISS, R. PLASS, and AL. WEISS, *Z. anorg. allg. Chem.* **283**, 390-400 (1956).

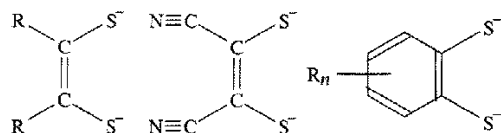
<sup>87</sup> C. G. KUEHN and H. TAUBE, *J. Am. Chem. Soc.* **98**, 689-702 (1976).

<sup>88</sup> T. RAMASAMI and A. G. SYKES, *Inorg. Chem.* **15**, 1010-14 (1976).

<sup>89</sup> I. M. BLACKLAWS, E. A. V. EBSWORTH, D. W. H. RANKIN and H. E. ROBERTSON, *J. Chem. Soc., Dalton Trans.*, 753-8 (1978).

In the chelating mode they frequently stabilize the metal centre in an unusually high apparent formal oxidation state, e.g.  $[\text{Fe}^{\text{IV}}(\text{S}_2\text{CNR}_2)_3]^+$  and  $[\text{Ni}^{\text{IV}}(\text{S}_2\text{CNR}_2)_3]^+$ . They also have a propensity for stabilizing novel stereochemical configurations, unusual mixed oxidation states (e.g. of Cu), intermediate spin states (e.g.  $\text{Fe}^{\text{III}}$ ,  $S = \frac{3}{2}$ ), and for forming a variety of tris chelated complexes of  $\text{Fe}^{\text{III}}$  which lie at the  ${}^2T_2 - {}^6A_1$  spin crossover (p. 1096).<sup>(93)</sup>

Dithiocarbamates and their analogues have 2 potential S-donor atoms joined to a single C atom and their complexes are sometimes called 1,1-dithiolato complexes. If the 2 S atoms are joined to adjacent C atoms then the equally numerous class of 1,2-dithiolato complexes results. Examples of chelating dithiolene ligands (drawn for convenience with localized valence bonds and ionic charges) are:



R = alkyl, aryl,  $\text{CF}_3$ , H

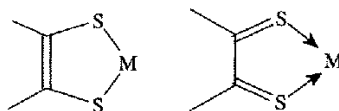
R = Me, F, Cl, H

Complexes of these ligands have been extensively studied during the past few decades not only because of the intrinsically interesting structural and bonding problems that they pose but also because of their varied industrial applications.<sup>(94-96)</sup> These include their use as highly specific analytical reagents, chromatographic supports, polarizers in sunglasses, mode-locking additives in neodymium lasers, semiconductors, fungicides, pesticides, vulcanization accelerators, high-temperature

wear-inhibiting additives in lubricants, polymerization and oxidation catalysts and even fingerprint developers in forensic investigations.

Complexes in which dithiolenes are the only ligands present can be classified according to six structural types as shown schematically in Fig. 15.16. For bis(dithiolato) complexes the planar structure (a) with  $D_{2h}$  local symmetry about the metal is the commonest mode but occasionally 5-coordinate dimers (b) are observed. The very rare metal-metal bonded 5-coordinate dimeric bis(dithiolato) structure (c) has been found for the palladium and platinum complexes  $[\{\text{M}(\text{S}_2\text{C}_2\text{H}_2)_2\}_2]$  with Pd-Pd 279 pm and Pt-Pt 275 pm. For tris(dithiolato) complexes two limiting geometries are possible: trigonal prismatic (Fig. 15.16d) and octahedral (Fig. 15.16f). The two geometries are related by a  $30^\circ$  twist of one triangular  $\text{S}_3$  face with respect to the other, and intermediate twists are also known (Fig. 15.16e). As a rough generalization, the less-common trigonal prismatic geometry (local  $D_{3h}$  symmetry) is adopted by "ligand-controlled" complexes which are often neutral or highly oxidized [e.g.  $\text{M}(\text{S}_2\text{C}_2\text{R}_2)_3$ , where M = V, Cr, Mo, W, Re], whereas the more usual octahedral ( $D_3$ ) geometry tends to be formed when the central metal dominates the stereochemistry as in the reduced anionic complexes. Thus reduction of the trigonal prismatic  $[\text{V}\{\text{S}_2\text{C}_2(\text{CN})_2\}_3]$  to the dianion  $[\text{V}\{\text{S}_2\text{C}_2(\text{CN})_2\}_3]^{2-}$  results in distortion to an intermediate geometry, whereas the iron analogue  $[\text{Fe}\{\text{S}_2\text{C}_2(\text{CN})_2\}_3]^{2-}$  has the chelated octahedral  $D_3$  structure. Intermediate geometries (Fig. 15.16e) have also been found for  $[\text{Mo}\{\text{S}_2\text{C}_2(\text{CN})_2\}_3]^{2-}$  and its W analogue.

There has been much discussion about the detailed bonding in 1,2-dithiolene complexes because of the alternative ways that the ring system can be described, e.g.:



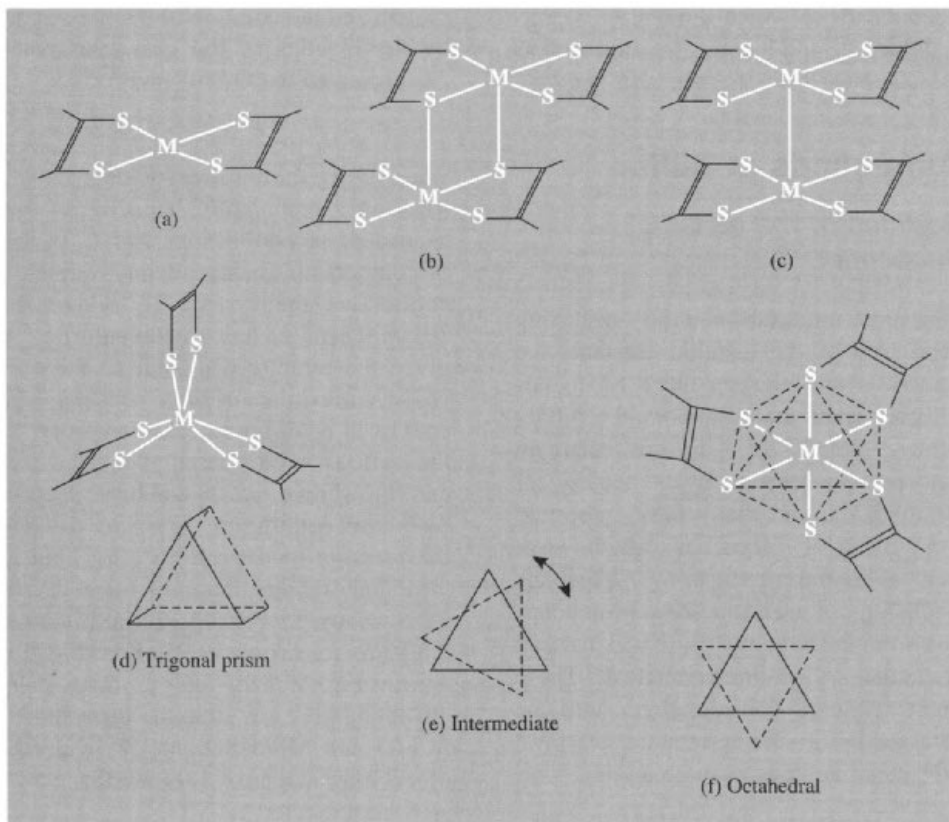
The formal oxidation state of the metal differs by 2 in these two limiting formulations (or

<sup>93</sup> R. L. MARTIN, in D. BANERJEA (ed.), *Coordination Chemistry - 20*, (International Conf. Calcutta, 1979) pp. 255-65, Pergamon Press, Oxford, 1980.

<sup>94</sup> R. EISENBERG, *Prog. Inorg. Chem.* **12**, 295-369 (1970).

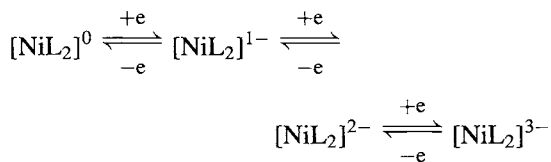
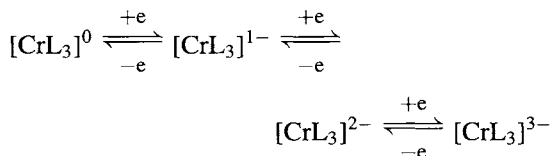
<sup>95</sup> R. P. BURNS and C. A. MCAULIFFE, *Adv. Inorg. Chem. Radiochem.* **22**, 303-48 (1979); R. P. BURNS, F. P. MCCULLOUGH and C. A. MCAULIFFE, *Adv. Inorg. Chem. Radiochem.* **23**, 211-80 (1980).

<sup>96</sup> A. M. BOND and R. L. MARTIN, *Coord. Chem. Revs.* **54**, 23-98 (1984).

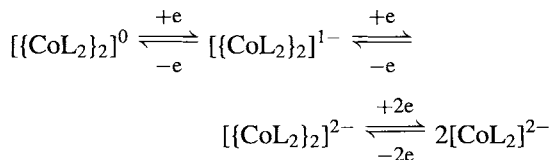


**Figure 15.16** Coordination geometries of bis- and tris-1,2-dithiolene complexes (see text).

by 6 in a tris complex). On this basis it is unclear whether the complex  $[\text{V}\{\text{S}_2\text{C}_2(\text{CN})_2\}_3]$  mentioned in the preceding paragraph should be formulated as  $\text{V}^{\text{VI}}(!)$  or  $\text{V}^0$ : it seems probable that an intermediate value would be more likely, but the example emphasizes the difficulty of assigning meaningful oxidation numbers to metal atoms in a redox series when the electronic configuration of the ligands themselves may also be undergoing change during reduction. Such reversible oxidation–reduction sequences are a characteristic feature of many 1,2-dithiolene complexes, e.g. for  $\text{L} = \{\text{S}_2\text{C}_2(\text{CN})_2\}$ :



and similarly for the Pd, Pt and other analogues.<sup>(97)</sup> Likewise for dimeric species with  $\text{L} = \{\text{S}_2\text{C}_2(\text{CF}_3)_2\}$ :



<sup>97</sup> W. E. GEIGER, T. E. MINES and F. E. SENFLEBER, *Inorg. Chem.* **14**, 2141–7 (1975); W. E. GEIGER, C. S. ALLEN, T. E. MINES and F. C. SENFLEBER, *Inorg. Chem.* **16**, 2003–8 (1977).

Mixed complexes in which a metal is coordinated by a dithiolene and by other ligands such as ( $\eta^5$ -C<sub>5</sub>H<sub>5</sub>), CO, NO, R<sub>3</sub>P, etc., are also known.

## 15.2 Compounds of Sulfur

### 15.2.1 Sulfides of the metallic elements<sup>(98,99)</sup>

Many of the most important naturally occurring minerals and ores of the metallic elements are sulfides (p. 648), and the recovery of metals from these ores is of major importance. Other metal sulfides, though they do not occur in nature, can be synthesized by a variety of preparative methods, and many have important physical or chemical properties which have led to their industrial production. Again, the solubility relations of metal sulfides in aqueous solution form the basis of the most widely used scheme of elementary qualitative analysis. These various more general considerations will be briefly discussed before the systematic structural chemistry of metal sulfides is summarized.

#### General considerations

When sulfide ores are roasted in air two possible reactions may occur:

- (a) conversion of the material to the oxide (as a preliminary to metal extraction, e.g. lead sulfide roasting);
- (b) formation of water-soluble sulfates which can then be used in hydrometallurgical processes.

The operating conditions (temperature, oxygen pressure, etc.) required to achieve each of these results depend on the thermodynamics of the

system and the duration of the roast is determined by the kinetics of the gas–solid reactions.<sup>(100)</sup> According to the Gibbs' phase rule:

$$F + P = C + 2$$

where  $F$  is the number of degrees of freedom (pressure, temperature, etc.),  $P$  is the number of phases in equilibrium and  $C$  is the number of components (independently variable chemical entities) in the system. It follows that, for a 3-component system (metal-sulfur-oxygen) at a given temperature and total pressure of the gas phase, a maximum of *three* condensed phases can coexist in equilibrium. The ranges of stability of the various solid phases at a fixed temperature can be shown on a stability diagram which plots the equilibrium pressure of SO<sub>2</sub> against the pressure of oxygen on a log–log graph. An idealized stability diagram for a divalent metal  $M$  is shown in Fig. 15.17a, and actual stability diagrams for copper at 950 K and lead at 1175 K are in Fig. 15.17b, and c. Note that, ideally, all boundaries are straight lines: those between  $M/MO$  and  $MS/MSO_4$  are vertical whereas the others have slopes of 1.0 ( $M/MS$ ), 1.5 ( $MS/MO$ ), and  $-0.5$  ( $MO/MSO_4$ ).<sup>†</sup>

The application of these generalizations to the extractive metallurgy of individual metals is illustrated at appropriate points in the text dealing with the chemistry of the various elements.

<sup>100</sup> C. B. ALCOCK, *Principles of Pyrometallurgy*, Chap. 2, pp. 15 ff., Academic Press, London, 1967.

<sup>†</sup> These simple relations can readily be deduced from the equilibria being represented. Thus at constant temperature:

$M/MO$  boundary:  $MO = M + \frac{1}{2}O_2(g)$ ;  $K = p^{1/2}(O_2)$ .  
Hence  $\log p(O_2) = 2 \log K = \text{constant}$  [i.e. independent of  $p(SO_2)$ ].

$MS/MSO_4$  boundary:  $MSO_4 = MS + 2O_2(g)$ ;  
 $K = p^2(O_2)$ . Hence  $\log p(O_2) = \frac{1}{2} \log K = \text{constant}$ .

$M/MS$  boundary:  $MS + O_2(g) = M + SO_2(g)$ ;  
 $K = p(SO_2)/p(O_2)$ . Hence  $\log p(SO_2) = \log K + \log p(O_2)$ , i.e. slope = 1.0.

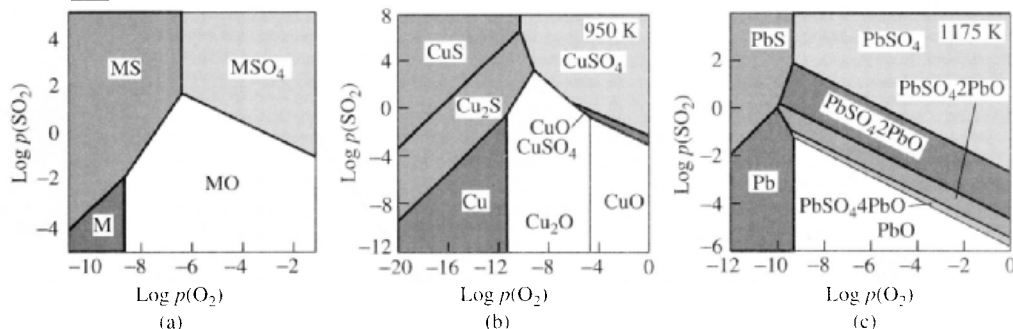
$MS/MO$  boundary:  $MS + \frac{3}{2}O_2(g) = MO + SO_2(g)$ ;  $K = p(SO_2)/p^{3/2}(O_2)$ . Hence  $\log p(SO_2) = \log K + \frac{3}{2} \log p(O_2)$ , i.e. slope = 1.5.

$MO/MSO_4$  boundary:  $MSO_4 = MO + SO_2(g) + \frac{1}{2}O_2(g)$ ;  
 $K = p(SO_2) \cdot p^{1/2}(O_2)$ . Hence  $\log p(SO_2) = \log K - \frac{1}{2} \log p(O_2)$ , i.e. slope =  $-0.5$ .

<sup>98</sup> F. JELLINEK, Sulfides, Chap. 19 in G. NICKLESS (ed.), *Inorganic Sulfur Chemistry*, pp. 669–747, Elsevier, Amsterdam, 1968. A comprehensive review with 631 references.

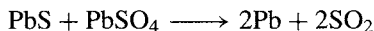
<sup>99</sup> D. J. VAUGHAN and J. R. CRAIG, *Mineral Chemistry of Metal Sulfides*, Cambridge University Press, Cambridge, 1978, 493 pp. A comprehensive account of the structure bonding and properties of mineral sulfides.



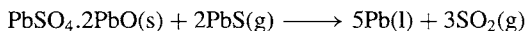


**Figure 15.17** Stability diagrams for the systems (a) metal (M)–sulfur–oxygen (idealized), (b) Cu–S–O and (c) Pb–S–O.

As noted above, the roasting of most metal sulfides yields either the oxide or sulfate. However, a few metals can be obtained directly by oxidation of their sulfides, and these all have the characteristic property that their oxides are much less stable than  $\text{SO}_2$ . Examples are Cu, Ag, Hg and the platinum metals. In addition, metallic Pb can be extracted by partial oxidation of galena to form a sulfate (the “Scotch hearth” or Newnham process, p. 370). The oversimplified reaction is:



However, as indicated in Fig. 15.17c, the system is complicated by the presence of several stable “basic sulfates”  $\text{PbSO}_4 \cdot n\text{PbO}$  ( $n = 1, 2, 4$ ), and these can react with gaseous PbS at lower metal-making temperatures, e.g.:



Metal sulfides can be prepared in the laboratory or on an industrial scale by a number of reactions; pure products are rarely obtained without considerable refinement and nonstoichiometric phases abound (p. 679). The more important preparative routes include:

- direct combination of the elements (e.g.  $\text{Fe} + \text{S} \longrightarrow \text{FeS}$ );
- reduction of a sulfate with carbon (e.g.  $\text{Na}_2\text{SO}_4 + 4\text{C} \longrightarrow \text{Na}_2\text{S} + 4\text{CO}$ );
- precipitation from aqueous solution by treatment with either acidified  $\text{H}_2\text{S}$  (e.g. the platinum metals; Cu, Ag, Au; Cd, Hg;

- Ge, Sn, Pb; As, Sb, Bi; Se, Te) or alkaline ( $\text{NH}_4$ )<sub>2</sub>S (e.g. Mn, Fe, Co, Ni, Zn; In, Tl);
- (d) saturation of an alkali hydroxide solution with  $\text{H}_2\text{S}$  to give MHS followed by reaction with a further equivalent of alkali (e.g.  $\text{KOH}(aq) + \text{H}_2\text{S} \longrightarrow \text{KHS} + \text{H}_2\text{O}$ ;  $\text{KHS} + \text{KOH} \longrightarrow \text{K}_2\text{S} + \text{H}_2\text{O}$ ).

This last method is particularly suitable for water-soluble sulfides, though frequently it is the hydrate that crystallizes, e.g.  $\text{Na}_2\text{S} \cdot 9\text{H}_2\text{O}$ ,  $\text{K}_2\text{S} \cdot 5\text{H}_2\text{O}$ . The hydrosulfides MHS can also be made by passing  $\text{H}_2\text{S}$  into solutions of metals in liquid  $\text{NH}_3$ . The colourless hygroscopic mixed metal sulfide  $\text{RbKS}$  was recently made by annealing a mixture of  $\text{K}_2\text{S}$  and  $\text{Rb}_2\text{S}$ .<sup>(100a)</sup>

Industrial applications of metal sulfides span the full time-scale from the earliest rise of the emerging chemical industry in the eighteenth century to the most recent developments of Li/S and Na/S power battery systems (see Panel). Reduction of  $\text{Na}_2\text{SO}_4$  by C was the first step in the now defunct Leblanc process (1791) for making  $\text{Na}_2\text{CO}_3$  (p. 71).  $\text{Na}_2\text{S}$  (or NaHS) is still used extensively in the leather industry for removal of hair from hides prior to tanning, for making organo-sulfur dyes, as a reducing agent for organic nitro compounds in the production of amines, and as a flotation agent for copper ores. It is readily oxidized by atmospheric  $\text{O}_2$  to give

<sup>100a</sup> H. SABROWSKY and P. VOGT, *Z. anorg. allg. Chem.*, **616**, 183–5 (1992).

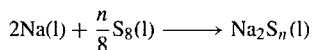


## Sodium-Sulfur Batteries

Alternatives to coal and hydrocarbon fuels as a source of power have been sought with increasing determination over the past three decades. One possibility is the Hydrogen Economy (p. 40). Another possibility, particularly for secondary, mobile sources of power, is the use of storage batteries. Indeed, electric vehicles were developed simultaneously with the first internal-combustion-engined vehicles, the first being made in 1888. In those days, over a century ago, electric vehicles were popular and sold well compared with the then noisy, inconvenient and rather unreliable petrol-engined vehicles. In 1899 an electric car held the world land-speed record at 105 km per hour. In the early years of this century, taxis in New York, Boston and Berlin were mainly electric; there were over 20000 electric vehicles in the USA and some 10000 cars and commercial vehicles in London. Even today (silent) battery-powered milk delivery vehicles are still operated in the UK. These use the traditional lead-sulfuric acid battery (p. 371), but this is extremely heavy and rather expensive.

The Na/S system has the potential to store 5-times as much energy (for the same weight) as the conventional lead battery and, in addition, shares with it the advantages of being silent, cheap to run, and essentially pollution-free: in general it is also reliable, has a long life and has extremely low maintenance costs. However, until recently it lacked the mileage range between successive chargings when compared with the highly developed petrol- or diesel-powered vehicles and it has a rather low performance (top speed and acceleration). A further disadvantage is the very long time taken to recharge the batteries (15–20 h) compared with the average time required to refill a petrol tank (1–2 min). Mixed power sources (petrol/electric battery) are a possible mode for development.

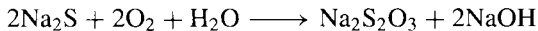
Conventional batteries consist of a liquid electrolyte separating two solid electrodes. In the Na/S battery this is inverted: a solid electrolyte separates two liquid electrodes: a ceramic tube made from the solid electrolyte sodium  $\beta$ -alumina (p. 249) separates an inner pool of molten sodium (mp 98°) from an outer bath of molten sulfur (mp 119°) and allows  $\text{Na}^+$  ions to pass through. The whole system is sealed and is encased in a stainless steel canister which also serves as the sulfur-electrode current collector. Within the battery, the current is passed by  $\text{Na}^+$  ions which pass through the solid electrolyte and react with the sulfur. The cell reaction can be written formally as



In the central compartment molten Na gives up electrons which pass through the external circuit and reduce the molten  $\text{S}_8$  to polysulfide ions  $\text{S}_n^{2-}$  (p. 681). The open circuit voltage is 2.08 V at 350°C. Since sulfur is an insulator the outer compartment is packed with porous carbon to provide efficient electrical conduction: the electrode volume is partially filled with sulfur when fully charged and is completely filled with sodium sulfide when fully discharged. To recharge, the polarity of the electrodes is changed and the passage of current forces the  $\text{Na}^+$  ions back into the central compartment where they are discharged as Na atoms.

Typical dimensions for the  $\beta$ -alumina electrolyte tube are 380 mm long, with an outer diameter of 28 mm, and a wall thickness of 1.5 mm. A typical battery for automotive power might contain 980 of such cells (20 modules each of 49 cells) and have an open-circuit voltage of 100 V. Capacity exceeds 50 kWh. The cells operate at an optimum temperature of 300–350°C (to ensure that the sodium polysulfides remain molten and that the  $\beta$ -alumina solid electrolyte has an adequate  $\text{Na}^+$  ion conductivity). This means that the cells must be thermally insulated to reduce wasteful loss of heat and to maintain the electrodes molten even when not in operation. Such a system is about one-fifth of the weight of an equivalent lead-acid traction battery and has a similar life (~1000 cycles).

thiosulfate:

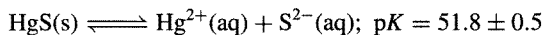


World production of  $\text{Na}_2\text{S}$  exceeds 150 000 tonnes pa and that of NaHS approaches 100 000 tpa. Barium sulfide (from  $\text{BaSO}_4 + \text{C}$ ) is the largest volume Ba compound manufactured but little of it is sold; almost all commercial Ba compounds are made by first making BaS and then converting it to the required compound.

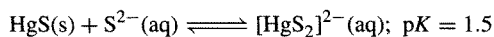
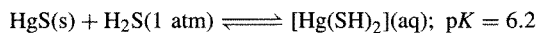
Metal sulfides vary enormously in their solubility in water. As expected, the (predominantly ionic) alkali metal sulfides and alkaline earth metal sulfides are quite soluble though there is appreciable hydrolysis which results in

strongly alkaline solutions ( $\text{M}_2\text{S} + \text{H}_2\text{O} \longrightarrow \text{MSH} + \text{MOH}$ ). Accordingly, solubilities depend sensitively not only on temperature but also on pH and partial pressure of  $\text{H}_2\text{S}$ . Thus, by varying the acidity, As can be separated from Pb, Pb from Zn, Zn from Ni, and Mn from Mg. In pure water the solubility of  $\text{Na}_2\text{S}$  is said to be 18.06 g per 100 g  $\text{H}_2\text{O}$  and for  $\text{Ba}_2\text{S}$  it is 7.28 g. In the case of some less-basic elements (e.g.  $\text{Al}_2\text{S}_3$ ,  $\text{Cr}_2\text{S}_3$ ) hydrolysis is complete and action of  $\text{H}_2\text{S}$  on solutions of the metal cation results in the precipitation of the hydroxide; likewise these sulfides (and  $\text{SiS}_2$ , etc.) react rapidly with water with evolution of  $\text{H}_2\text{S}$ .

By contrast with the water-soluble sulfides of Groups 1 and 2, the corresponding heavy metal sulfides of Groups 11 and 12 are amongst the least-soluble compounds known. Literature values are often wildly discordant, and care should be taken in interpreting the data. Thus, for black HgS the most acceptable value of the solubility product  $[\text{Hg}^{2+}][\text{S}^{2-}]$  is  $10^{-51.8} \text{ mol}^2 \text{ l}^{-2}$ , i.e.



However, this should not be taken to imply a concentration of only  $10^{-25.9} \text{ mol l}^{-1}$  for mercury in solution (i.e. less than  $10^{-2}$  of 1 atom of Hg per litre!) since complex formation can simultaneously occur to give species such as  $[\text{Hg}(\text{SH})_2]$  in weakly acid solutions and  $[\text{HgS}_2]^{2-}$  in alkaline solutions:



Hydrolysis also sometimes obtrudes.

### Structural chemistry of metal sulfides

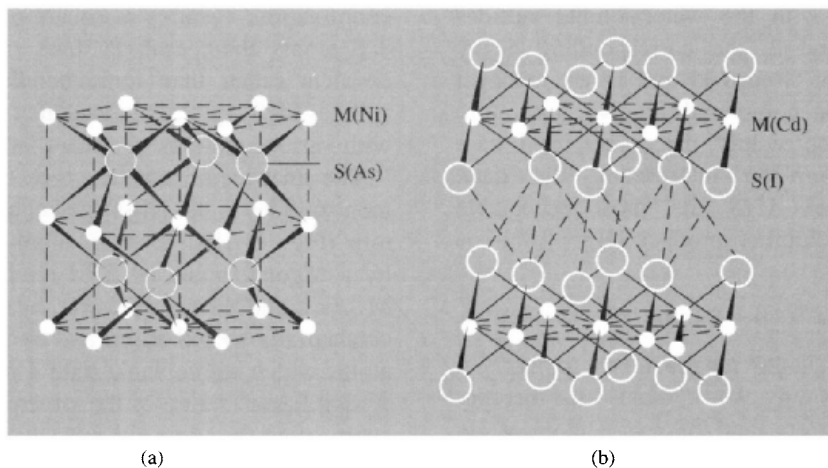
The predominantly ionic alkali metal sulfides  $\text{M}_2\text{S}$  (Li, Na, K, Rb, Cs) adopt the antifluorite structure (p. 118) in which each S atom is surrounded by a cube of 8 M and each M by a tetrahedron of S. The alkaline earth sulfides MS (Mg, Ca, Sr, Ba) adopt the NaCl-type 6:6 structure (p. 242) as do many other monosulfides of rather less basic metals ( $\text{M} = \text{Pb, Mn, La, Ce, Pr, Nd, Sm, Eu, Tb, Ho, Th, U, Pu}$ ). However, many metals in the later transition element groups show substantial trends to increasing covalency leading either to lower coordination numbers or to layer-lattice structures.<sup>(101)</sup> Thus MS (Be, Zn, Cd, Hg) adopt the 4:4 zinc blende structure (p. 1210) and ZnS, CdS and MnS also crystallize in the 4:4 wurtzite modification (p. 1210). In both of these structures both M and S are tetrahedrally coordinated, whereas PtS, which also has 4:4

coordination, features a square-planar array of 4 S atoms about each Pt, thus emphasizing its covalent rather than ionic bonding. Group 13 sulfides  $\text{M}_2\text{S}_3$  (p. 252) have defect ZnS structures with various patterns of vacant lattice sites.

The final major structure type found amongst monosulfides is the NiAs (nickel arsenide) structure (Fig. 15.18a). Each S atom is surrounded by a trigonal prism of 6 M atoms whilst each M has eightfold coordination, being surrounded octahedrally by 6 S atoms and by 2 additional M atoms which are coplanar with 4 of the S atoms. A significant feature of the structure is the close approach of the M atoms in chains along the (vertical) *c*-axis (e.g. 260 pm in FeS) and the structure can be regarded as transitional between the 6:6 NaCl structure and the more highly coordinated structures typical of metals. The NiAs structure is adopted by most first row transition-metal monosulfides MS ( $\text{M} = \text{Ti, V, Cr, Fe, Co, Ni}$ ) as well as by many selenides and tellurides of these elements.

The NiAs structure is closely related to the hexagonal layer-lattice  $\text{CdI}_2$  structure shown in Fig. 15.18b, this stoichiometry being achieved simply by leaving alternate M layers of the NiAs structure vacant. Disulfides  $\text{MS}_2$  adopting this structure include those of Ti, Zr, Hf, Ta, Pt and Sn; conversely,  $\text{Ti}_2\text{S}$  has the anti- $\text{CdI}_2$  structure. Progressive partial filling of the alternate metal layers leads to phases of intermediate composition as exemplified by the Cr/S system (Table 15.10). For some elements these intermediate phases have quite extensive ranges of composition, the limits depending on the temperature of the system. For example, at 1000°C there is a succession of non-stoichiometric titanium sulfides  $\text{TiS}_{0.97} - \text{TiS}_{1.06}$ ,  $\text{TiS}_{1.204} - \text{TiS}_{1.333}$ ,  $\text{TiS}_{1.377} - \text{TiS}_{1.594}$ ,  $\text{TiS}_{1.810} - \text{TiS}_{1.919}$ .<sup>(101)</sup> Many diselenides and ditellurides also adopt the  $\text{CdI}_2$  structure and in some there is an almost continuous nonstoichiometric variation in composition, e.g.  $\text{CoTe} \longrightarrow \text{CoTe}_2$ . A related 6:3 layer structure is the  $\text{CdCl}_2$ -type adopted by  $\text{TaS}_2$ , and the layer structures of  $\text{MoS}_2$  and  $\text{WS}_2$  are mentioned on p. 1018.

<sup>101</sup> N. N. GREENWOOD, *Ionic Crystals, Lattice Defects, and Nonstoichiometry*, Chap. 3, pp. 37-61; also pp. 153-5, Butterworths, London, 1968.



**Figure 15.18** Comparison of the nickel arsenide structure (a) adopted by many monosulfides  $MS$  with the cadmium iodide structure (b) adopted by some disulfides  $MS_2$ . The structures are related simply by removing alternate layers of  $M$  from  $MS$  to give  $MS_2$ .

**Table 15.10** Some sulfides of chromium (see text)

Nominal formula	Ratio Cr/S		Proportion of sites occupied in alternate layers	Random or ordered vacancies <sup>(a)</sup>
	calculated	observed		
$CrS^{(b)}$	1.000	$\approx 0.97$	1:1	None
$Cr_7S_8$	0.875	0.88–0.87	$1:\frac{3}{4}$	Random
$Cr_5S_6$	0.833	0.85	$1:\frac{2}{3}$	Ordered
$Cr_3S_4$	0.750	0.79–0.76	$1:\frac{1}{2}$	Ordered
$Cr_2S_3$	0.667	0.69–0.67	$1:\frac{1}{3}$	Ordered
$(CrS_2)$	0.500	Not observed	1:0	—

<sup>(a)</sup>Refers to the vacancies in the alternate metal layers.

<sup>(b)</sup> $CrS$  has a unique monoclinic structure intermediate between  $NiAs$  and  $PtS$  types.

Finally, many disulfides have a quite different structure motif, being composed of infinite three-dimensional networks of  $M$  and discrete  $S_2$  units. The predominate structural types are pyrites,  $FeS_2$  (also for  $M = Mn, Co, Ni, Ru, Os$ ), and marcasite (known only for  $FeS_2$  among the disulfides). Pyrites can be described as a distorted  $NaCl$ -type structure in which the rod-shaped  $S_2$  units ( $S-S$  217 pm) are centred on the  $Cl$  positions but are oriented so that they are inclined away from the cubic axes. The marcasite structure is a variant of the rutile structure ( $TiO_2$ ,

p. 961) in which the columns of edge-shared octahedra are rotated to give close approaches between pairs of  $S$  atoms in adjacent columns ( $S-S$  221 pm).

Many metal sulfides have important physical properties.<sup>(98,102)</sup> They range from insulators, through semiconductors to metallic conductors of electricity, and some are even superconductors,

<sup>102</sup>F. HULLIGER, *Struct. Bonding* (Berlin) **4**, 83–229 (1968). A comprehensive review with 532 references, 65 structural diagrams, and a 34-page appendix tabulating the known phases and their physical properties.

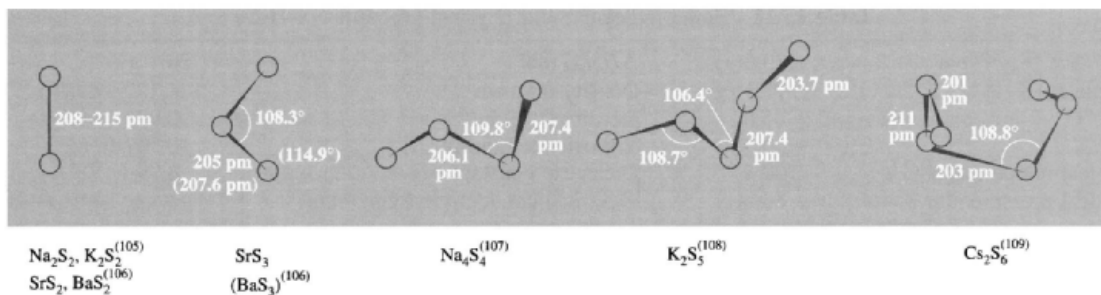


Figure 15.19 Structures of polysulfide anions  $S_n^{2-}$  in  $M_2S_n$  and  $BaS_n$ .

e.g.  $NbS_2$  (<6.2 K),  $TaS_2$  (<2.1 K),  $Rh_{17}S_{15}$  (<5.8 K),  $CuS$  (<1.62 K) and  $CuS_2$  (<1.56 K). Likewise they can be diamagnetic, paramagnetic, temperature-independent paramagnetic, ferromagnetic, antiferromagnetic or ferrimagnetic.

The structures of more complex ternary metal sulfides such as  $BaZrS_3$  (perovskite-type, p. 963),  $ZnAl_2S_4$  (spinel type, p. 247), and  $NaCrS_2$  (NaCl superstructure) introduce no new principles. Likewise, thiosalts, which may feature finite anions (e.g.  $Tl_3[VS_4]$ ), vertex-shared chains (e.g.  $Ba_2MnS_3$ ), edge-shared chains (e.g.  $KFeS_2$ ), double chains (e.g.  $Ba_2ZnS_3$ ), double layers (e.g.  $KCu_4S_3$ ) or three-dimensional frameworks (e.g.  $NH_4Cu_7S_4$ ).<sup>(103)</sup> Finite clusters also abound.<sup>(104)</sup>

### Anionic polysulfides

The pyrites and marcasite structures can be thought of as containing  $S_2^{2-}$  units though the variability of the interatomic distance and other properties suggest substantial deviation from a purely ionic description. Numerous higher polysulfides  $S_n^{2-}$  have been characterized, particularly for the more electropositive elements Na, K, Ba, etc. They are yellow at room temperature, turn dark red on being heated, and may be thought of as salts of the polysulfanes

(p. 683). Typical examples are  $M_2S_n$  ( $n = 2-5$  for Na, 2-6 for K, 6 for Cs),  $BaS_2$ ,  $BaS_3$ ,  $BaS_4$ , etc. The polysulfides, unlike the monosulfides, are low melting solids: published values for mps vary somewhat but representative values ( $^{\circ}C$ ) are:

$Na_2S$ 1180°	$Na_2S_2$ 484°	$Na_2S_4$ 294°	$Na_2S_5$ 255°	
$K_2S_3$ 292°	$K_2S_4$ ~145°	$K_2S_5$ 211°	$K_2S_6$ 196°	$BaS_3$ 554°

Structures are in Fig. 15.19. The  $S_3^{2-}$  ion is bent ( $C_{2v}$ ) and is isoelectronic with  $SCl_2$  (p. 689). The  $S_4^{2-}$  ion has twofold symmetry, essentially tetrahedral bond angles, and a dihedral angle of  $97.8^{\circ}$  (see p. 654). The  $S_5^{2-}$  ion also has approximately twofold symmetry (about the central S atom); it is a contorted but unbranched chain with bond angles close to tetrahedral and a small but significant difference between the terminal and internal S-S distances. The  $S_6^{2-}$  ion has alternating S-S distances, and bond angles in the range  $106.4-110.0^{\circ}$  (mean  $108.8^{\circ}$ ). Several of the references in Fig. 15.19 give preparative details: these can involve direct reaction of

<sup>105</sup> H. FOPPL, E. BUSMANN, and F.-K. FRORATH, *Z. anorg. allg. Chem.* **314**, 12-30 (1962).

<sup>106</sup> H. G. VON SCHNERING and N.-K. GOH, *Naturwissenschaften* **61**, 272 (1974).

<sup>107</sup> R. TEGMAN, *Acta Cryst.* **B29**, 1463-9 (1973).

<sup>108</sup> B. KELLY and P. WOODWARD, *J. Chem. Soc., Dalton Trans.*, 1314-6 (1976).

<sup>109</sup> S. C. ABRAHAMS and E. GRISON, *Acta Cryst.* **6**, 206-13 (1953).

<sup>103</sup> A. F. WELLS, *Structural Inorganic Chemistry*, 5th edn., Chap. 17 pp. 748-87, Oxford University Press, 1984.

<sup>104</sup> I. DANCE and K. FISHER, *Prog. Inorg. Chem.* **41**, 637-803 (1994). A comprehensive review with 503 references, 100 structural diagrams and 40 pages of tabulated material.

Table 15.11 Some molecular and physical properties of H<sub>2</sub>S

Distance (S–H)/pm	133.6(g)	$\Delta H_f^\circ/\text{kJ mol}^{-1}$	20.1(g)
Angle H–S–H	92.1°(g)	Density (s)/g cm <sup>-3</sup>	1.12 (–85.6°)
MP/°C	–85.6	Density (l)/g cm <sup>-3</sup>	0.993 (–85.6°)
BP/°C	–60.3	Viscosity/centipoise	0.547 (–82°)
Critical temperature/°C	100.4	Dielectric constant $\epsilon$	8.99 (–78°)
Critical pressure/atm	84	Electrical conductivity/ohm <sup>-1</sup> cm <sup>-1</sup>	$3.7 \times 10^{-11}$ (–78°)

stoichiometric amounts of the elements in sealed tubes or reaction of MSH with S in ethanol.<sup>(110)</sup>

It is interesting that, despite the unequivocal presence of the S<sub>3</sub><sup>2-</sup> ion in K<sub>2</sub>S<sub>3</sub>, BaS<sub>3</sub>, etc., a Raman spectroscopic study of molten “Na<sub>2</sub>S<sub>3</sub>” showed that the ion had disproportionated into S<sub>2</sub><sup>2-</sup> and S<sub>4</sub><sup>2-</sup>.<sup>(111)</sup>

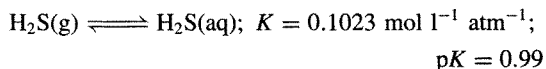
### 15.2.2 Hydrides of sulfur (sulfanes)

Hydrogen sulfide is the only thermodynamically stable sulfane; it occurs widely in nature as a result of volcanic or bacterial action and is, indeed, a prime source of elemental S (p. 647). It has been known since earliest times and its classical chemistry has been extensively studied since the seventeenth century.<sup>(112)</sup> H<sub>2</sub>S is a foul smelling, very poisonous gas familiar to all students of chemistry. Its smell is noticeable at 0.02 ppm but the gas tends to anaesthetize the olfactory senses and the intensity of the smell is therefore a dangerously unreliable guide to its concentration. H<sub>2</sub>S causes irritation at 5 ppm, headaches and nausea at 10 ppm and immediate paralysis and death at 100 ppm; it is therefore as toxic and as dangerous as HCN.

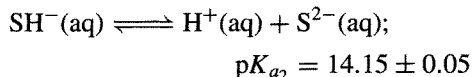
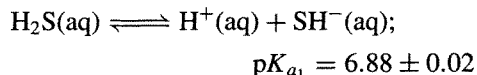
H<sub>2</sub>S is readily prepared in the laboratory by treating FeS with dilute HCl in a Kipp apparatus. Purer samples can be made by hydrolysing CaS, BaS or Al<sub>2</sub>S<sub>3</sub>, and the purest gas is prepared by direct reaction of the elements at 600°C.

Some physical properties are in Table 15.11:<sup>(113)</sup> comparison with the properties of water (p. 623) shows the absence of any appreciable H bonding in H<sub>2</sub>S.<sup>(114)</sup> Comparisons with H<sub>2</sub>Se, H<sub>2</sub>Te and H<sub>2</sub>Po are on p. 767.

H<sub>2</sub>S is readily soluble in both acidic and alkaline aqueous solutions. Pure water dissolves 4.65 volumes of the gas at 0° and 2.61 volumes at 20°; in other units a saturated solution is 0.1 M at atmospheric pressure and 25°, i.e.



In aqueous solution H<sub>2</sub>S is a weak acid (p. 49). At 20°:<sup>(115)</sup>



The chemistry of such solutions has been alluded to on p. 678. At low temperatures a hydrate H<sub>2</sub>S·5 $\frac{3}{4}$ H<sub>2</sub>O crystallizes. In acid solution H<sub>2</sub>S is also a mild reducing agent; e.g. even on standing in air solutions slowly precipitate sulfur. The gas burns with a bluish flame in air to give H<sub>2</sub>O and SO<sub>2</sub> (or H<sub>2</sub>O and S if the air supply is restricted). For adducts, see p. 673.

In very strongly acidic nonaqueous solutions (such as HF/SbF<sub>5</sub>) H<sub>2</sub>S acts as a base (proton acceptor) and the white crystalline

<sup>110</sup> G. WEDDIDEN, H. KLEINSCHMAGER and S. HOPPE, *J. Chem. Res. (S)*, 1978, 96; (*M*), 1978, 1101–12.

<sup>111</sup> G. J. JANZ *et al.*, *Inorg. Chem.* **15**, 1751–4, 1755–9, 1759–63 (1976).

<sup>112</sup> J. W. MELLOR, *A Comprehensive Treatise on Inorganic and Theoretical Chemistry*, Vol. 10, pp. 114–61, Longmans, London, 1930.

<sup>113</sup> F. FEHÉR, Liquid hydrogen sulfide, Chap. 4 in J. J. LAGOWSKI (ed.), *The Chemistry of Nonaqueous Solvents*, Vol. 3, pp. 219–40, Academic Press, New York, 1970.

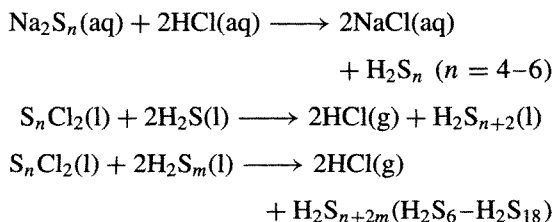
<sup>114</sup> A. N. FITCH and J. K. COCKROFT, *J. Chem. Soc., Chem. Commun.*, 515–6 (1990).

<sup>115</sup> M. WIDMER and G. SCHWARZENBACH, *Helv. Chim. Acta* **47**, 266–71 (1964).

solid  $[\text{SH}_3]^+[\text{SbF}_6]^-$  has been isolated from such solutions.<sup>(116)</sup> The compound, which is the first known example of a stable salt of  $\text{SH}_3^+$ , can be stored at room temperature in Teflon or Kel-F containers but attacks quartz. Vibrational spectroscopy confirms the pyramidal  $C_{3v}$  structure expected for a species isoelectronic with  $\text{PH}_3$  (p. 492). In the presence of an excess of  $\text{H}_2\text{S}$  at  $-80^\circ\text{C}$ , the trimercaptosulfonium salts  $[\text{S}(\text{SH})_3]^+\text{AsF}_6^-$  and  $[\text{S}(\text{SH})_3]^+\text{SbCl}_6^-$  can be prepared;<sup>(117)</sup> the cation is isoelectronic with  $\text{P}(\text{PH}_2)_3$  (p. 495) and is expected to have  $C_{3v}$  symmetry.

Polysulfanes,  $\text{H}_2\text{S}_n$ , with  $n = 2-8$  have been prepared and isolated pure, and many higher homologues have been obtained as mixtures with variable  $n$ . Our modern knowledge of these numerous compounds stems mainly from the elegant work of F. Fehér and his group in the 1950s. All polysulfanes have unbranched chains of  $n$  sulfur atoms thus reflecting the well-established propensity of this element towards catenation (p. 652). The polysulfanes are reactive liquids whose density  $d$ , viscosity  $\eta$ , and bp increase with increasing chain length.  $\text{H}_2\text{S}_2$ , the analogue of  $\text{H}_2\text{O}_2$ , is colourless but the others are yellow, the colour deepening with increasing chain length.

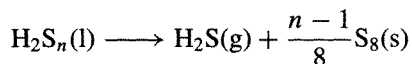
The polysulfanes were at one time made by fusing crude  $\text{Na}_2\text{S} \cdot 9\text{H}_2\text{O}$  with various amounts of sulfur and pouring the resulting polysulfide solution into an excess of dilute hydrochloric acid at  $-10^\circ\text{C}$ . The resulting crude yellow oil is a mixture mainly of  $\text{H}_2\text{S}_n$  ( $n = 4-7$ ). Polysulfanes can now also be readily prepared by a variety of other reactions, e.g.:



<sup>116</sup> K. O. CHRISTE, *Inorg. Chem.* **14**, 2230-3 (1975).

<sup>117</sup> R. MINKWITZ, R. KRAUSE, H. HÄRTNER and W. SAWODNY, *Z. anorg. allg. Chem.* **593**, 137-46 (1991).

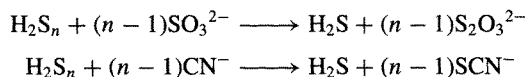
Purification is by low-pressure distillation. Some physical properties are in Table 15.12. Polysulfanes are readily oxidized and all are thermodynamically unstable with respect to disproportionation:



**Table 15.12** Some physical properties of polysulfanes<sup>(118)</sup>

Compound	$d_{20}/\text{g cm}^{-3}$	$P_{20}/\text{mmHg}$	BP/ $^\circ\text{C}$ (extrap)
$\text{H}_2\text{S}_2$	1.334	87.7	70
$\text{H}_2\text{S}_3$	1.491	1.4	170
$\text{H}_2\text{S}_4$	1.582	0.035	240
$\text{H}_2\text{S}_5$	1.644	0.0012	285
$\text{H}_2\text{S}_6$	1.688	—	—
$\text{H}_2\text{S}_7$	1.721	—	—
$\text{H}_2\text{S}_8$	1.747	—	—

This disproportionation is catalysed by alkali, and even traces dissolved from the surface of glass containers is sufficient to effect deposition of sulfur. They are also degraded by sulfite and by cyanide ions:



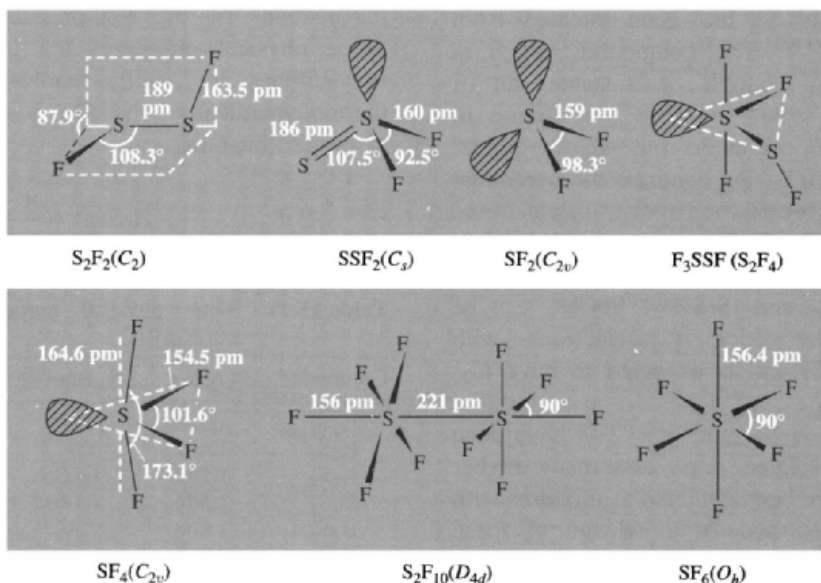
The former reaction, in particular, affords a convenient means of quantitative analysis by determination of the  $\text{H}_2\text{S}$  (precipitated as  $\text{CdS}$ ) and iodometric determination of the thiosulfate produced.

### 15.2.3 Halides of sulfur

#### Sulfur fluorides

The seven known sulfur fluorides are quite different from the other halides of sulfur in their stability, reactivity and to some extent even in their stoichiometries; it is therefore convenient to

<sup>118</sup> M. SCHMIDT and W. SIEBERT in *Comprehensive Inorganic Chemistry*, Vol. 2, Chap. 23, pp. 826-42, Pergamon Press, Oxford, 1973.



**Figure 15.20** Molecular structures of the sulfur fluorides.

consider them separately. Moreover, they have proved a rich field for both structural and theoretical studies since they form an unusually extensive and graded series of covalent molecular compounds in which S has the oxidation states 1, 2, 3, 4, 5 and 6, and in which it also exhibits all coordination numbers from 1 to 6 (if  $SF_5^-$  is also included). The compounds feature a rare example of structural isomerism amongst simple molecular inorganic compounds ( $FSSF$  and  $SSF_2$ ) and also a monomer–dimer pair ( $SF_2$  and  $F_3SSF$ ). The structures and physical properties will be described first, before discussing the preparative routes and chemical reactions.

*Structures and physical properties.* The molecular structure, point group symmetries, and dimensions of the sulfur fluorides are summarized in Fig. 15.20<sup>(119)</sup>  $S_2F_2$  resembles  $H_2O_2$ ,  $H_2S_2$ ,  $O_2F_2$  and  $S_2X_2$ , and detailed comparisons of bond distances, bond angles and dihedral angles are instructive. The isomer  $SSF_2$  (thiothionylfluoride) features 3-coordinate  $S^{IV}$  and 1-coordinate  $S^{II}$  and it is notable that the formally

double-bonded S–S distance is very close to that in the singly bonded isomer. The fugitive species  $SF_2$  has the expected bent configuration in the gas phase but is unique in readily undergoing dimerization by insertion of a second  $SF_2$  into an S–F bond. The structure of the resulting molecule  $F_3SSF$  is, in a sense, intermediate between those of  $S_2F_2$  and  $SF_4$ , being based on a trigonal bipyramid with the equatorial F atom replaced by an SF group. The fact that the  $^{19}F$  nmr spectrum at  $-100^\circ$  shows four distinct F resonances indicates that the 2 axial F atoms are non-equivalent, implying restricted rotation about the S–S bond.

The structure of  $SF_4$  is particularly significant. It is based on a trigonal bipyramid with one equatorial position occupied by the lone-pair; this distorts the structure by reducing the equatorial F–S–F bond angle from  $120^\circ$  to  $101.6^\circ$  and by repelling the axial  $F_{ax}$  atoms towards  $F_{eq}$ . There is also a significant difference between the (long) S– $F_{ax}$  and (short) S– $F_{eq}$  distances. Again, the low-temperature  $^{19}F$  nmr spectrum is precisely diagnostic of the  $C_{2v}$  structure, since the observed doublet of 1:2:1 triplets is consistent only with the two sets of 2 equivalent F atoms in this point group symmetry

<sup>119</sup> F. SEEL, *Adv. Inorg. Chem. Radiochem.* **16**, 297–333 (1974).

Table 15.13 Physical properties of some sulfur fluorides

	FSSF	S=SF <sub>2</sub>	SF <sub>4</sub>	SF <sub>6</sub>	S <sub>2</sub> F <sub>10</sub>
MP/°C	-133	-164.6	-121	-50.54	-52.7
BP/°C	+15	-10.6	-38	-63.8 (subl)	+30
Density(T°C)/g cm <sup>-3</sup>	—	—	1.919(-73°)	1.88(-50°)	2.08(0°)

(<sup>19</sup>F, like <sup>1</sup>H, has nuclear spin  $\frac{1}{2}$ ).<sup>(120)</sup> Thus, an axial lone-pair ( $C_{3v}$ ) would lead to a doublet and a quartet of integrated relative intensity 3:1, whereas all other conceivable symmetries ( $T_d$ ,  $C_{4v}$ ,  $D_{4h}$ ,  $D_{2d}$ ,  $D_{2h}$ ) would give a sharp singlet from the 4 equivalent F atoms. Above -98° the 30 MHz <sup>19</sup>F nmr spectrum of SF<sub>4</sub> gradually broadens and it coalesces at -47° into a single broad resonance which gradually sharpens again to a narrow singlet at higher temperatures; this is due to molecular fluxionality which permits intramolecular interchange of the axial and equatorial F atoms.

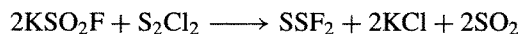
The structure of SF<sub>4</sub> can be rationalized on most of the simple bonding theories; the environment of S has 10 valency electrons and this leads to the observed structure in both valence-bond and electron-pair repulsion models. However, the rather high energy of the 3d orbitals on S make their full participation in bonding via sp<sup>3</sup>d<sub>2</sub> unlikely and, indeed, calculations<sup>(121)</sup> show that there may be as little as 12% d-orbital participation rather than the 50% implied by the scheme sp<sub>x</sub>p<sub>y</sub> + p<sub>z</sub>d<sub>2</sub>. Thus charge-transfer configurations or bonding via sp<sub>x</sub>p<sub>y</sub> + p<sub>z</sub> seem to be better descriptions, the p<sub>z</sub> orbital on S being involved in a 3-centre 4-electron bond with the 2 axial F atoms (cf. XeF<sub>2</sub>, p. 897).

The regular octahedral structure of SF<sub>6</sub> and the related structure of S<sub>2</sub>F<sub>10</sub> (Fig. 15.20) call for little comment except to note the staggered ( $D_{4d}$ ) arrangement of the two sets of F<sub>eq</sub> in S<sub>2</sub>F<sub>10</sub> and the unusually long S-S distance, both features presumably reflecting interatomic repulsion between the F atoms. SF<sub>6</sub> is also of

interest in establishing conclusively that S can be hexavalent. Its great stability (see below) contrasts with the non-existence of SH<sub>4</sub> and SH<sub>6</sub> despite the general similarity in S-F and S-H bond strengths; its existence probably reflects (a) the high electronegativity of F (p. 26), which facilitates the formation of either polar or 3-centre 4-electron bonds as discussed above for SF<sub>4</sub>, and (b) the lower bond energy of F<sub>2</sub> compared to H<sub>2</sub>, which for SH<sub>4</sub> and SH<sub>6</sub> favours dissociation into H<sub>2</sub>S + nH<sub>2</sub>.<sup>(122)</sup> For descriptions of the bonding which involve the use of 3d orbitals on sulfur, a net positive charge on the central atom would contract the d orbitals thereby making them energetically and spatially more favourable for overlap with the fluorine orbitals.

Some physical properties of the more stable sulfur fluorides are in Table 15.13. All are colourless gases or volatile liquids at room temperature. SF<sub>6</sub> sublimates at -63.8° (1 atm) and can only be melted under pressure (-50.8°). It is notable both for its extreme thermal and chemical stability (see below), and also for having a higher gas density than any other substance that boils below room temperature (5.107 times as dense as air).

*Synthesis and chemical reactions.* Disulfur difluoride, S<sub>2</sub>F<sub>2</sub>, can be prepared by the mild fluorination of sulfur with AgF in a rigorously dried apparatus at 125°. It is best handled in the gas phase at low pressures and readily isomerizes to thiothionylfluoride, SSF<sub>2</sub>, in the presence of alkali metal fluorides. SSF<sub>2</sub> can be made either by isomerizing S<sub>2</sub>F<sub>2</sub> or directly by the fluorination of S<sub>2</sub>Cl<sub>2</sub> using KF in SO<sub>2</sub>:

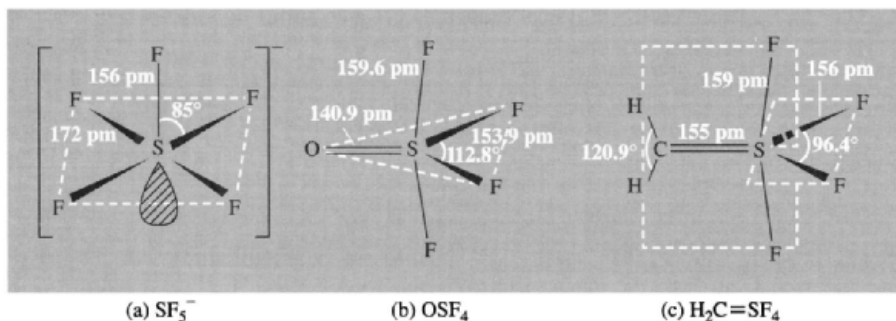


<sup>120</sup> F. A. COTTON, J. W. GEORGE and J. S. WAUGH, *J. Chem. Phys.* **28**, 994-5 (1958); E. MUETTERTIES and W. D. PHILLIPS, *J. Am. Chem. Soc.* **81**, 1084-8 (1959).

<sup>121</sup> P. J. HAY, *J. Am. Chem. Soc.* **99**, 1003-12 (1977).

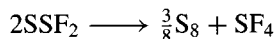
<sup>122</sup> G. M. SCHWENZER and H. F. SCHAEFFER, *J. Am. Chem. Soc.* **97**, 1393-7 (1975).



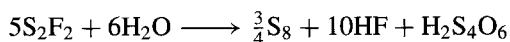


**Figure 15.21** Comparison of the structures of three species in which S has 12 valence electrons: (a) the  $\text{SF}_5^-$  ion in  $\text{RbSF}_5$ , as deduced from X-ray analysis,<sup>(123)</sup> (b)  $\text{OSF}_4$  as deduced from gas-phase electron diffraction<sup>(124)</sup> (note the wider angle  $\text{F}_{\text{eq}}\text{SF}_{\text{eq}}$  when compared with  $\text{SF}_4$  (Fig. 15.20) and the shorter distance  $\text{S}-\text{F}_{\text{ax}}$ ; the angle  $\text{F}_{\text{ax}}\text{SF}_{\text{ax}}$  is  $164.6^\circ$ ), and (c)  $\text{H}_2\text{CSF}_4$  (X-ray crystal structure at  $-160^\circ$ ).<sup>(125)</sup> The angle  $\text{F}_{\text{eq}}\text{SF}_{\text{eq}}$  is significantly smaller than in  $\text{SF}_4$  as is the angle  $\text{F}_{\text{ax}}\text{SF}_{\text{ax}}$  ( $170.4^\circ$ ); the methylene group is coplanar with the axial  $\text{SF}_2$  group as expected for  $p_\pi-d_\pi$   $\text{C}=\text{S}$  overlap and, unlike  $\text{SF}_4$ , the molecule is non-fluxional.

$\text{SSF}_2$  can be heated to  $250^\circ$  but is, in fact, thermodynamically unstable with respect to disproportionation, being immediately transformed to  $\text{SF}_4$  in the presence of acid catalysts such as  $\text{BF}_3$  or  $\text{HF}$ :



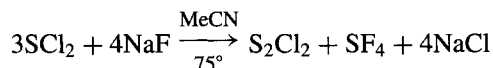
Both  $\text{S}_2\text{F}_2$  and  $\text{SSF}_2$  are rapidly hydrolysed by pure water to give  $\text{S}_8$ ,  $\text{HF}$  and a mixture of polythionic acids  $\text{H}_2\text{S}_n\text{O}_6$  ( $n$  4–6), e.g.:



Alkaline hydrolysis yields predominantly thiosulfate.  $\text{SSF}_2$  burns with a pale-blue flame when ignited, to yield  $\text{SO}_2$ ,  $\text{SOF}_2$  and  $\text{SO}_2\text{F}_2$ .

Sulfur difluoride,  $\text{SF}_2$ , is a surprisingly fugitive species in view of its stoichiometric similarity to the stable compounds  $\text{H}_2\text{S}$  and  $\text{SCl}_2$  (p. 689). It is best made by fluorinating gaseous  $\text{SCl}_2$  with activated  $\text{KF}$  (from  $\text{KSO}_2\text{F}$ ) or with  $\text{HgF}_2$  at  $150^\circ$ , followed by a tedious fractionation from the other sulfur fluorides ( $\text{FSSF}$ ,  $\text{SSF}_2$  and  $\text{SF}_4$ ) which form the predominant products. The chlorofluorides  $\text{ClSSF}$  and  $\text{ClSSF}_3$  are also formed. The compound can only be handled as a dilute gas under rigorously anhydrous conditions or at very low temperatures in a matrix of solid argon, and it rapidly dimerizes to give  $\text{F}_3\text{SSF}$ .

Sulfur tetrafluoride,  $\text{SF}_4$ , though extremely reactive (and valuable) as a selective fluorinating agent, is much more stable than the lower fluorides. It is formed, together with  $\text{SF}_6$ , when a cooled film of sulfur is reacted with  $\text{F}_2$ , but is best prepared by fluorinating  $\text{SCl}_2$  with  $\text{NaF}$  in warm acetonitrile solution:



$\text{SF}_4$  is unusual in apparently acting both as an electron-pair acceptor and an electron-pair donor (amphoteric Lewis acid-base). Thus pyridine forms a stable 1:1 adduct  $\text{C}_5\text{H}_5\text{NSF}_4$  which presumably has a pseudooctahedral (square-pyramidal) geometry. Likewise  $\text{CsF}$  (at  $125^\circ$ ) and  $\text{Me}_4\text{NF}$  (at  $-20^\circ$ ) form  $\text{CsSF}_5$  and  $[\text{NMe}_4]^+[\text{SF}_5]^-$  (Fig. 15.21a). By contrast,  $\text{SF}_4$  behaves as a donor to form 1:1 adducts with many Lewis acids; the stability decreases in the sequence  $\text{SbF}_5 > \text{AsF}_5 > \text{IrF}_5 > \text{BF}_3 > \text{PF}_5 > \text{AsF}_3$ . In view of the discussion on

<sup>123</sup> J. BITTNER, J. FUCHS and K. SEPELT, *Z. anorg. allg. Chem.* **551**, 182–90 (1988).

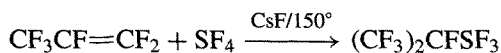
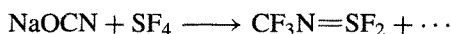
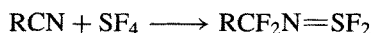
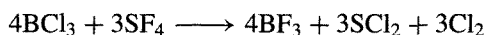
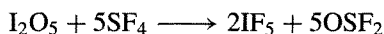
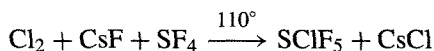
<sup>124</sup> L. HEDBERG and K. HEDBERG, *J. Phys. Chem.* **86**, 598–602 (1982).

<sup>125</sup> H. BOCK, J. E. BOGGS, G. KLEEMANN, D. LENTZ, H. OBERHAMMER, E. M. PETERS, K. SEPELT, A. SIMON and B. SOLOUKI, *Angew. Chem. Int. Edn. Engl.* **18**, 944–5 (1979).

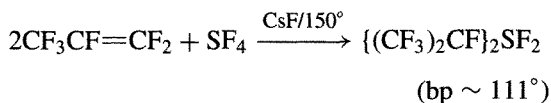
p. 198 it seems likely that SF<sub>4</sub> is acting here not as an S lone-pair donor but as a fluoride ion lone-pair donor and there is, indeed, infrared evidence to suggest that SF<sub>4</sub>.BF<sub>3</sub> is predominantly [SF<sub>3</sub>]<sup>+</sup>[BF<sub>4</sub>]<sup>-</sup>.

SF<sub>4</sub> rapidly decomposes in the presence of moisture, being instantly hydrolysed to HF and SO<sub>2</sub>. Despite this it has been increasingly used as a powerful and highly selective fluorinating agent for both inorganic and organic compounds. In particular it is useful for converting ketonic and aldehyde >C=O groups to >CF<sub>2</sub>, and carboxylic acid groups -COOH to -CF<sub>3</sub>. Similarly, ≡P=O groups are smoothly converted to ≡PF<sub>2</sub>, and >P(O)OH groups to >PF<sub>3</sub>. It also undergoes numerous oxidative addition reactions to give derivatives of S<sup>VI</sup>. The simplest of these are direct oxidation of SF<sub>4</sub> with F<sub>2</sub> or ClF (at 380°) to give SF<sub>6</sub> and SCIF<sub>5</sub> respectively. Analogous reactions with N<sub>2</sub>F<sub>4</sub>(*hν*) and F<sub>5</sub>SOOSF<sub>5</sub> yield SF<sub>5</sub>NF<sub>2</sub> and *cis*-SF<sub>4</sub>(OSF<sub>5</sub>)<sub>2</sub> respectively; likewise F<sub>5</sub>SOF (p. 688) yields F<sub>5</sub>SOSF<sub>5</sub>. Direct oxidation of SF<sub>4</sub> with O<sub>2</sub>, however, proceeds only slowly unless catalysed by NO<sub>2</sub>: the product is OSF<sub>4</sub>, which has a trigonal bipyramidal structure like SF<sub>4</sub> itself, but with the equatorial lone-pair replaced by the oxygen atom (Fig. 15.21b). A similar structure is adopted by the more recently prepared methylene compound H<sub>2</sub>C=SF<sub>4</sub> (Fig. 15.21c);<sup>(125)</sup> this is made by treating SF<sub>5</sub>-CH<sub>2</sub>Br with LiBu<sup>n</sup> at -110° and is more stable than the isoelectronic P or S ylides or metal carbene complexes, being stable in the gas phase up to 650° at low pressures.

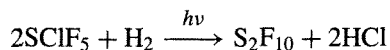
Some other reactions of SF<sub>4</sub> are:



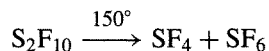
(bp 46°)



Disulfur decafluoride, S<sub>2</sub>F<sub>10</sub>, is obtained as a byproduct of the direct fluorination of sulfur to SF<sub>6</sub> but is somewhat tedious to separate and is more conveniently made by the photolytic reduction of SCIF<sub>5</sub> (prepared as above):



It is intermediate in reactivity between SF<sub>4</sub> and the very inert SF<sub>6</sub>. Unlike SF<sub>4</sub> it is not hydrolysed by water or even by dilute acids or alkalis and, unlike SF<sub>6</sub>, it is extremely toxic. It disproportionates readily at 150° probably by a free radical mechanism involving SF<sub>5</sub><sup>•</sup> (note the long, weak S-S bond; Fig. 15.20):



Similarly it reacts readily with Cl<sub>2</sub> and Br<sub>2</sub> to give SCIF<sub>5</sub> and SBrF<sub>5</sub>. It oxidizes KI (and I<sub>3</sub><sup>-</sup>) in acetone solution to give iodine (note SF<sub>4</sub> converts acetone to Me<sub>2</sub>CF<sub>2</sub>). S<sub>2</sub>F<sub>10</sub> reacts with SO<sub>2</sub> to give F<sub>5</sub>SSO<sub>2</sub>F and with NH<sub>3</sub> to give N≡SF<sub>3</sub>.

Sulfur hexafluoride is unique in its stability and chemical inertness: it is a colourless, odourless, tasteless, unreactive, non-flammable, non-toxic, insoluble gas prepared by burning sulfur in an atmosphere of fluorine. Because of its extraordinary stability and excellent dielectric properties it is extensively used as an insulating gas for high-voltage generators and switch gear: at a pressure of 2–3 bars it withstands 1.0–1.4 MV across electrodes 50 mm apart without breakdown, and at 10 bars it is used for high-power underground electrical transmission systems at 400 V and above. However, there is now some environmental concern at its use as an electrical transformer fluid and as an inert blanketing gas in magnesium metal casting, since even minute amounts may contribute to an atmospheric greenhouse effect (it is 6800 times as potent as CO<sub>2</sub>).

SF<sub>6</sub> can be heated to 500° without decomposition, and is unattacked by most metals, P, As, etc., even when heated. It is also unreactive towards



Other peroxy compounds:<sup>(130)</sup> SF<sub>5</sub>OOC(O)F,  
 SF<sub>5</sub>OSF<sub>4</sub>OOSF<sub>5</sub>, SF<sub>5</sub>OSF<sub>4</sub>OOSF<sub>4</sub>OSF<sub>5</sub>,  
 CF<sub>3</sub>OSF<sub>4</sub>OOSF<sub>5</sub>, CF<sub>3</sub>OSF<sub>4</sub>OOSF<sub>4</sub>OCF<sub>3</sub>,  
 (CF<sub>3</sub>SO<sub>2</sub>)<sub>2</sub>O<sub>2</sub>, HOSO<sub>2</sub>OOCF<sub>3</sub>,  
 CF<sub>3</sub>OOSO<sub>2</sub>OCF<sub>3</sub>.

Fluorosulfuric acid:<sup>(131)</sup> FSO<sub>2</sub>(OH), FSO<sub>3</sub><sup>-</sup>.

Of these the most extensively studied is fluorosulfuric acid, made by direct reaction of SO<sub>3</sub> and HF. Its importance derives from its use as a solvent system and from the fact that its mixtures with SbF<sub>5</sub> and SO<sub>3</sub> are amongst the strongest known acids (superacids, p. 570). Anhydrous HSO<sub>3</sub>F is a colourless, dense, mobile liquid which fumes in moist air: mp -89.0°, bp 162.7°; *d*<sub>25</sub> 1.726 g cm<sup>-3</sup>, *η*<sub>25</sub> 1.56 centipoise, *κ*<sub>25</sub> 1.085 × 10<sup>-4</sup> ohm<sup>-1</sup> cm<sup>-1</sup>.

Attention should also be directed to the growing number of perfluorocarbon-sulfur species which feature single, double or even triple C-S bonds, e.g.:

Single: (F<sub>5</sub>S)<sub>2</sub>CF<sub>2</sub>,<sup>(132)</sup> F<sub>4</sub>SCF<sub>2</sub>SF<sub>4</sub>CF<sub>2</sub>,<sup>(132)</sup>  
 [(F<sub>5</sub>S)C(CF<sub>3</sub>)<sub>2</sub>]<sup>-</sup>,<sup>(133)</sup> [(F<sub>5</sub>S)<sub>2</sub>C(CF<sub>3</sub>)]<sup>-</sup>,<sup>(133)</sup>  
 [F<sub>3</sub>SCF<sub>2</sub>S(F<sub>3</sub>)F]<sup>-</sup>;<sup>(134)</sup> see also footnote on  
 p. 690;

Double:

(F<sub>5</sub>S)(F<sub>3</sub>C)C=SF<sub>2</sub>,<sup>(135)</sup> (F<sub>3</sub>C)<sub>2</sub>C=SF<sub>2</sub>;<sup>(135)</sup>

Triple: (F<sub>3</sub>C)C≡SF<sub>3</sub>,<sup>(136-138)</sup> (F<sub>5</sub>S)C≡SF<sub>3</sub>.<sup>(139)</sup>

<sup>130</sup> R. A. DE MARCO and J. M. SHREEVE, *Adv. Inorg. Chem. Radiochem.* **16**, 109-76 (1974).

<sup>131</sup> A. W. JACHE, *Adv. Inorg. Chem. Radiochem.* **16**, 177-200 (1974).

<sup>132</sup> K. D. GUPTA, R. MEWS, A. WATERFELD, J. M. SHREEVE and H. OBERHAMMER, *Inorg. Chem.* **25**, 275-8 (1986).

<sup>133</sup> J. BITTNER, R. GERHARDT, K. MOOCK and K. SEPELT, *Z. anorg. allg. Chem.* **602**, 89-96 (1991).

<sup>134</sup> D. VIETS, W. HEILEMANN, A. WATERFELD, R. MEWS, S. BESSER, R. HERBST-IRMER, G. M. SHELDRIK and W.-D. STOHRER, *J. Chem. Soc., Chem. Commun.*, 1017-9 (1992).

<sup>135</sup> R. DAMERIUS, K. SEPELT and J. S. THRASHER, *Angew. Chem. Int. Edn. Engl.* **28**, 769-70 (1989).

<sup>136</sup> W. SAAK, G. HENKEL and S. POHL, *Angew. Chem. Int. Edn. Engl.* **23**, 150 (1984).

<sup>137</sup> B. PÖTTER, K. SEPELT, A. SIMON, E.-M. PETERS and B. HETTICH, *J. Am. Chem. Soc.* **107**, 980-5 (1985).

<sup>138</sup> D. A. DIXON and B. E. SMART, *J. Am. Chem. Soc.* **108**, 2688-91 (1986).

<sup>139</sup> R. GERHARDT, T. GRELBIG, J. BUSCHMANN, P. LUGER and K. SEPELT, *Angew. Chem. Int. Edn. Engl.* **27**, 1534-6 (1988).

Also notable are sulfur cyanide fluorides such as SF<sub>3</sub>CN,<sup>(140)</sup> SF<sub>2</sub>(CN)<sub>2</sub><sup>(140)</sup> and SF<sub>5</sub>CN<sup>(141,142)</sup> and the sulfinyl cyanide fluoride FS(O)CN.<sup>(140)</sup>

### Chlorides, bromides and iodides of sulfur

Sulfur is readily chlorinated by direct reaction with Cl<sub>2</sub> but the simplicity of the products obtained belies the complexity of the mechanisms involved. The reaction was first investigated by C. W. Scheele in 1774 and has been extensively studied since because of its economic importance (see below) and its intrinsic physicochemical interest. Direct chlorination of molten S followed by fractional distillation yields disulfur dichloride (S<sub>2</sub>Cl<sub>2</sub>) a toxic, golden-yellow liquid of revolting smell: mp -76°, bp 138°, *d*(20°) 1.677 g cm<sup>-3</sup>. The molecule has the expected C<sub>2</sub> structure (like S<sub>2</sub>F<sub>2</sub>, H<sub>2</sub>O<sub>2</sub>, etc.) with S-S 195 pm, S-Cl 206 pm, angle Cl-S-S 107.7°, and a dihedral angle of 85.2°.<sup>(143)</sup> Further chlorination of S<sub>2</sub>Cl<sub>2</sub>, preferably in the presence of a trace of catalyst such as FeCl<sub>3</sub>, yields the more-volatile, cherry-red liquid sulfur dichloride, SCl<sub>2</sub>: mp -122°, bp 59°, *d*(20°) 1.621 g cm<sup>-3</sup>. SCl<sub>2</sub> resembles S<sub>2</sub>Cl<sub>2</sub> in being foul-smelling and toxic, but is rather unstable when pure due to the decomposition equilibrium 2SCl<sub>2</sub> ⇌ S<sub>2</sub>Cl<sub>2</sub> + Cl<sub>2</sub>. However, it can be stabilized by the presence of as little as 0.01% PCl<sub>5</sub> and can be purified by distillation at atmospheric pressure in the presence of 0.1% PCl<sub>5</sub>.<sup>(144)</sup> The sulfur dichloride molecule is nonlinear (C<sub>2v</sub>) as expected, with S-Cl 201 pm and angle Cl-S-Cl 103°.

S<sub>2</sub>Cl<sub>2</sub> and SCl<sub>2</sub> both react readily with H<sub>2</sub>O to give a variety of products such as

<sup>140</sup> J. JACOBS and H. WILLNER, *Z. anorg. allg. Chem.* **619**, 1221-6 (1993).

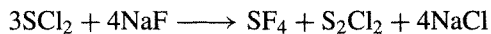
<sup>141</sup> O. LÖSKING and H. WILLNER, *Angew. Chem. Int. Edn. Engl.* **28**, 1255-6 (1989).

<sup>142</sup> J. S. THRASHER and K. V. MADAPPAT *Angew. Chem. Int. Edn. Engl.* **28**, 1256-8 (1989).

<sup>143</sup> C. J. MARSDEN, R. D. BROWN, and P. D. GODFREY, *J. Chem. Soc., Chem. Commun.*, 399-401 (1979).

<sup>144</sup> R. J. ROSSEN and F. R. WHITT, *J. Appl. Chem.* **10**, 229-37 (1960); see also the following paper (pp. 237-46) for large-scale distillation unit.

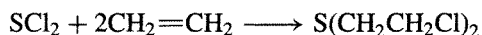
$\text{H}_2\text{S}$ ,  $\text{SO}_2$ ,  $\text{H}_2\text{SO}_3$ ,  $\text{H}_2\text{SO}_4$  and the polythionic acids  $\text{H}_2\text{S}_x\text{O}_6$ . Oxidation of  $\text{SCl}_2$  yields thionyl chloride ( $\text{OSCl}_2$ ) and sulfuryl chloride ( $\text{O}_2\text{SCl}_2$ ) (see Section 15.2.4). Reaction with  $\text{F}_2$  produces  $\text{SF}_4$  and  $\text{SF}_6$  (p. 686), whereas fluorination with  $\text{NaF}$  is accompanied by some disproportionation:



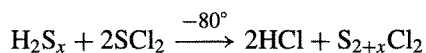
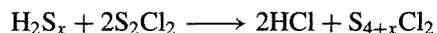
As indicated on p. 686, fluorination of  $\text{S}_2\text{Cl}_2$  with  $\text{KF}/\text{SO}_2$  occurs with concurrent isomerization to  $\text{SSF}_2$ . Both  $\text{S}_2\text{Cl}_2$  and  $\text{SCl}_2$  react with atomic N (p. 413) to give  $\text{NSCl}$  as the first step, and this can then react further with  $\text{S}_2\text{Cl}_2$  to give the ionic heterocyclic compound  $\text{S}_3\text{N}_2\text{Cl}^+\text{Cl}^-$  (p. 739). By contrast, reaction of  $\text{S}_2\text{Cl}_2$  with  $\text{NH}_4\text{Cl}$  at  $160^\circ$  (or with  $\text{NH}_3 + \text{Cl}_2$  in boiling  $\text{CCl}_4$ ) yields the cluster compound  $\text{S}_4\text{N}_4$  (p. 722). Treatment of  $\text{S}_2\text{Cl}_2$  with  $\text{Hg}(\text{SCN})_2$  yields colourless crystals of  $\text{S}_4(\text{CN})_4$ , mp  $-2^\circ$ , which are composed of unbranched chain molecules  $\text{NCSSSSCN}$  with essentially linear NCS groups ( $177.5^\circ$ ,  $178.4^\circ$ ) and the angles CSS  $98.6^\circ$  and SSS  $106.5^\circ$ ; interatomic distances are within the expected ranges, viz.  $\text{N}\equiv\text{C}$  113.4, C–S 169.6, outer S–S 206.8 and inner S–S 201.7 pm.<sup>(145)</sup>  $\text{SCl}_2$  acts as a ligand to Pd and Pt in the yellow 4-coordinate complex *trans*- $[\text{PdCl}_2(\text{SCl}_2)_2]$  and the red 6-coordinate complex *trans*- $[\text{PtCl}_4(\text{SCl}_2)_2]$ .<sup>(146)</sup> These are formed when either Pd or Pt metal is heated in a quartz ampoule with elemental S and  $\text{Cl}_2$  at  $200^\circ\text{C}$  for 4 days, and they decompose into  $\text{SCl}_2$  and  $\text{PdCl}_2$  or  $\text{PtCl}_4$ , respectively, on being heated.

$\text{S}_2\text{Cl}_2$  and  $\text{SCl}_2$  are important industrial chemicals. The main use for  $\text{S}_2\text{Cl}_2$  is in the vapour-phase vulcanization of certain rubbers, but other uses include its chlorinating action in the preparation of mono- and di-chlorohydrins, and the opening of some minerals in extractive metallurgy. Some idea of the scale of production can be gauged from the fact that  $\text{S}_2\text{Cl}_2$  is shipped in 50-tonne tank cars; smaller quantities are transported in drums containing 300 or 60 kg

of the liquid. Its less-stable homologue  $\text{SCl}_2$  is notable for its ready addition across olefinic double bonds: e.g., thiochlorination of ethene yields the notorious vesicant, mustard gas:



The compounds  $\text{SCl}_2$  and  $\text{S}_2\text{Cl}_2$  can be thought of as the first two members of an extended series of dichlorosulfanes  $\text{S}_n\text{Cl}_2$ . The lower electronegativity of Cl (compared with F) and the lower S–Cl bond energy (compared with S–F) enable the natural catenating propensity of S to have full reign and a series of dichlorosulfanes can be prepared in which S–S bonds in sulfur chains (and rings) can be broken and the resulting  $-\text{S}_n-$  oligomers stabilized by the formation of chain-terminating S–Cl bonds. The first eight members with  $n = 1 - 8$  have been isolated as pure compounds, and mixtures up to perhaps  $\text{S}_{100}\text{Cl}_2$  are known.<sup>†</sup> Specific compounds have been made by F. Fehér's group using the polysulfanes as starting materials (p. 683).<sup>(147)</sup>



The dichlorosulfanes are yellow to orange-yellow viscous liquids with an irritating odour. They are thermally and hydrolytically unstable.  $\text{S}_3\text{Cl}_2$  boils at  $31^\circ$  ( $10^{-4}$  mmHg) and has a density of  $1.744 \text{ g cm}^{-3}$  at  $20^\circ$ . Higher homologues have

<sup>†</sup> Several related series of compounds are also known in which Cl is replaced by a pseudohalogen such as  $-\text{CF}_3$  or  $-\text{C}_2\text{F}_5$ , e.g.  $\text{S}_n(\text{CF}_3)_2$  ( $n = 1-4$ ),  $\text{CF}_3\text{S}_n\text{C}_2\text{F}_5$  ( $n = 2-4$ ), and  $\text{S}_n(\text{C}_2\text{F}_5)_2$  ( $n = 2-4$ ). These can be prepared by the reaction of  $\text{CF}_3\text{I}$  and S vapour in a glow discharge followed by fractionation and glc separation; other routes include reaction of  $\text{CS}_2$  with  $\text{IF}_5$  at  $60-200^\circ$ , reaction of  $\text{CF}_3\text{I}$  with sulfur at  $310^\circ$ , and fluorination of  $\text{SCl}_2$  or related compounds with  $\text{NaF}$  or  $\text{KF}$  at  $150-250^\circ$ . (See, for example, T. Yasumura and R. J. Lagow, *Inorg. Chem.* **17**, 3108–10 (1978).)

<sup>147</sup> F. FEHÉR, pp. 370–9 in G. BRAUER (ed.), *Handbook of Preparative Inorganic Chemistry*, 2nd edn., Vol. 1, Academic Press, New York, 1963.

<sup>145</sup> R. STEUDEL, K. BERGEMANN and M. KUSTOS, *Z. anorg. allg. Chem.* **620**, 117–20 (1994).

<sup>146</sup> M. PAULUS and G. THIELE, *Z. anorg. allg. Chem.* **588**, 69–76 (1990).

even higher densities:

$n$ in $S_nCl_2$	1	2	3	4
Density(20°)/g cm <sup>-3</sup>	1.621	1.677	1.744	1.777
$n$ in $S_nCl_2$	5	6	7	8
Density(20°)/g cm <sup>-3</sup>	1.802	1.822	1.84	1.85

The higher chlorides of S (unlike the higher fluorides) are very unstable and poorly characterized. There is no evidence for molecular chloro analogues of SF<sub>4</sub>, S<sub>2</sub>F<sub>10</sub> and SF<sub>6</sub>, though SClF<sub>5</sub> is known (p. 687). Chlorination of SCl<sub>2</sub> by liquid Cl<sub>2</sub> at -78° yields a powdery off-white solid which begins to decompose when warmed above -30°. It analyses as SCl<sub>4</sub> and is generally formulated as SCl<sub>3</sub><sup>+</sup>Cl<sup>-</sup>, but little reliable structural work has been done on it. Consistent with this ionic formulation, reaction of SCl<sub>4</sub> with Lewis acids results in the formation of stable adducts; e.g. AlCl<sub>3</sub> yields the white solid SCl<sub>4</sub>.AlCl<sub>3</sub> which has been shown by vibrational spectroscopy on both the solid and the melt (125°) to be [SCl<sub>3</sub>]<sup>+</sup>[AlCl<sub>4</sub>]<sup>-</sup>.<sup>(148)</sup> The compound [SCl<sub>3</sub>]<sup>+</sup>[ICl<sub>4</sub>]<sup>-</sup> is also known (p. 693).<sup>(149)</sup> As expected from a species that is isoelectronic with PCl<sub>3</sub> the cation is pyramidal; dimensions are: S-Cl (average) 198.5 pm, angle Cl-S-Cl 101.3° (cf. PCl<sub>3</sub>: P-Cl 204.3 pm, angle Cl-P-Cl 100.1°). Other compounds containing [SCl<sub>3</sub>]<sup>+</sup> which have been characterized spectroscopically and by X-ray crystallography include those with [SbCl<sub>6</sub>]<sup>-</sup>, [UCl<sub>6</sub>]<sup>-</sup> and [AsF<sub>6</sub>]<sup>-</sup>.<sup>(150)</sup>

Sulfur bromides are but poorly characterized and there are few reliable data on them. SBr<sub>2</sub> probably does not exist at room temperature but has been claimed as a matrix-isolated product when a mixture of S<sub>2</sub>Cl<sub>2</sub>/SCl<sub>2</sub>:Br<sub>2</sub>:Ar in the ratio 1:1:150 is passed through an 80-W microwave discharge and the product condensed on a CsI

window at 9 K.<sup>(151)</sup> The dibromosulfanes S<sub>n</sub>Br<sub>2</sub> ( $n = 2-8$ ) are formed by the action of anhydrous HBr on the corresponding chlorides.<sup>(147)</sup> The best characterized compound (which can also be made directly from the elements at 100°C) is the garnet-red oily liquid S<sub>2</sub>Br<sub>2</sub> isostructural with S<sub>2</sub>Cl<sub>2</sub> (S-S 198 pm, S-Br 224 pm, angle Br-S-S 105°, dihedral angle 84 ± 11°). It has mp -46°, bp(0.18 mmHg) 54°, and  $d(20^\circ)$  2.629 g cm<sup>-3</sup>, but even at room temperature S<sub>2</sub>Br<sub>2</sub> tends to dissociate into its elements. Interestingly, the higher homologues have progressively lower densities (cf. S<sub>n</sub>Cl<sub>2</sub>). The unusual ionic compound [BrSSSBBr<sub>2</sub>]<sup>+</sup>[AsF<sub>6</sub>]<sup>-</sup> can be formed by reacting stoichiometric amounts of S, Br<sub>2</sub> and AsF<sub>5</sub> in liquid SO<sub>2</sub>.

$n$ in S <sub>n</sub> Br <sub>2</sub>	2	3	4	5	6	7	8
Density(20°)/g cm <sup>-3</sup>	2.629	2.52	2.47	2.41	2.36	2.33	2.30

Sulfur iodides are a topic of considerable current interest, although compounds containing S-I bonds were, in fact, unknown until fairly recently. The failure to prepare sulfur iodides by direct reaction of the elements probably reflects the comparative weakness of the S-I bond: an experimental value is not available but extrapolation from representative values for the bond energies of other S-X bonds leads to a value of ~170 kJ mol<sup>-1</sup>:

Bond	S-F	S-Cl	S-Br	S-I	S-S	I-I
Energy/ kJ mol <sup>-1</sup>	327	271	218	(~170)	225	150

The data indicate that formation of SI<sub>2</sub> from  $\frac{1}{8}S_8 + I_2$  and the formation of S<sub>2</sub>I<sub>2</sub> from  $\frac{1}{4}S_8 + I_2$  are both endothermic to the extent of ~35 kJ mol<sup>-1</sup>, implying that successful synthesis of these compounds must employ kinetically controlled routes to obviate decomposition back to the free elements.

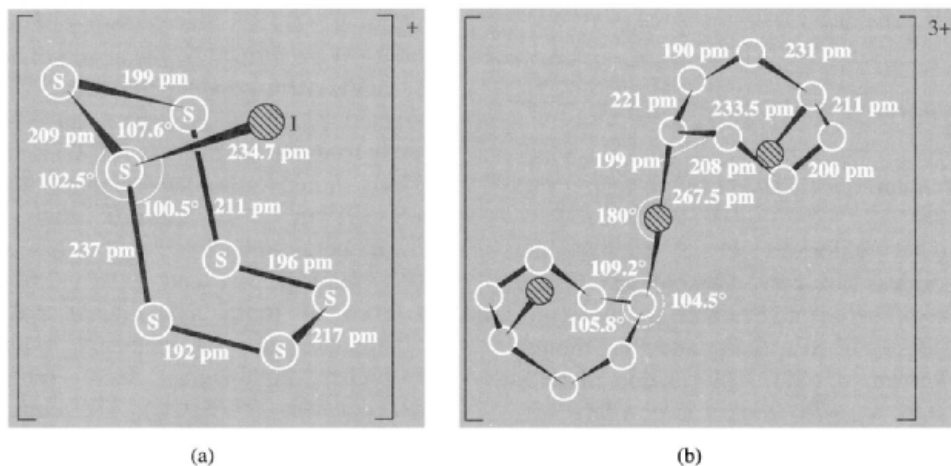
Pure S<sub>2</sub>I<sub>2</sub> was first isolated (as a dark reddish-brown solid) following the reaction of S<sub>2</sub>Cl<sub>2</sub> with

<sup>148</sup> G. MAMANTOV, R. MARASSI, F. W. POULSON, S. E. SPRINGER, J. P. WIAUX, R. HUGLEN and N. R. SMYLN, *J. Inorg. Nuclear Chem.* **41**, 260-1 (1979).

<sup>149</sup> A. J. EDWARDS, *J. Chem. Soc., Dalton Trans.*, 1723-5 (1978).

<sup>150</sup> B. H. CHRISTIAN, M. J. COLLINS, R. J. GILLESPIE and J. F. SAWYER, *Inorg. Chem.* **25**, 777-88 (1986), and references cited therein.

<sup>151</sup> M. FEUERHAN and G. VAHL, *Inorg. Nuclear Chem. Lett.* **16**, 5-8 (1980).

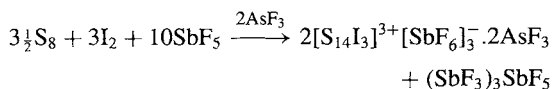


**Figure 15.22** (a) Structure of the iodocycloheptasulfur cation in  $[S_7I]^+[SbF_6]^-$ . The S–S–S angles in the  $S_7$  ring are in the range  $102.5$ – $108.4^\circ$  (mean  $105.6^\circ$ ).<sup>(154)</sup> (b) Structure of the centrosymmetric cation  $[(S_7I)_2I]^{3+}$  showing similar dimensions to those in  $[S_7I]^+$ .<sup>(156)</sup>

$HI/N_2$  in a freon solvent of  $-78^\circ$  in the presence of catalytic amounts of added  $I_2$ .<sup>(152)</sup> The darker brown solid  $OSI_2$  was formed similarly from  $OSCl_2$ .  $S_2I_2$  and  $OSI_2$  are both thermally unstable and decompose rapidly above about  $-30^\circ$  into S,  $I_2$  (and also  $SO_2$  in the case of  $OSI_2$ ).<sup>(152)</sup>  $S_2I_2$  was assigned  $C_2$  symmetry (like  $S_2F_2$ , p. 684) on the basis of its vibrational spectrum.<sup>(153)</sup>

The first X-ray crystal structure of a species containing an S–I bond was of the curious and unexpected cation  $[S_7I]^+$  which was found in the dark-orange compound  $[S_7I]^+[SbF_6]^-$  formed when iodine and sulfur react in  $SbF_5$  solution.<sup>(154)</sup> The structure of the cation is shown in Fig. 15.22a and features an  $S_7$  ring with alternating S–S distances and a pendant iodine atom; the conformation of the ring is the same as in  $S_7$ ,  $S_8$ , and  $S_8O$  (p. 696). The same cation was

found in  $[S_7I]_4^+[S_4]^{2+}[AsF_6]_6^{16-}$ <sup>(155)</sup> and a similar motif forms part of the iodo-bridged species  $[(S_7I)_2I]^{3+}$  (Fig. 15.22b);<sup>(156)</sup> this latter cation was formed during the reaction of  $S_8$  and  $I_2$  with  $SbF_5$  in the presence of  $AsF_3$  according to the reaction stoichiometry:



The very long S– $I_\mu$  bonds in the linear S–I–S bridge (267.5 pm) are notable and have been interpreted in terms of an S–I bond order of  $\frac{1}{2}$ . Even weaker  $S \cdots I$  interactions occur in the cation  $[S_2I_4]^{2+}$  which could, indeed, alternatively be regarded as an  $S_2^{2+}$  cation coordinated side-on by two  $I_2$  molecules (Fig. 15.23).<sup>(157)</sup> This

<sup>152</sup> D. K. PADMA, *Indian Journal of Chemistry* **12**, 417–8 (1974).

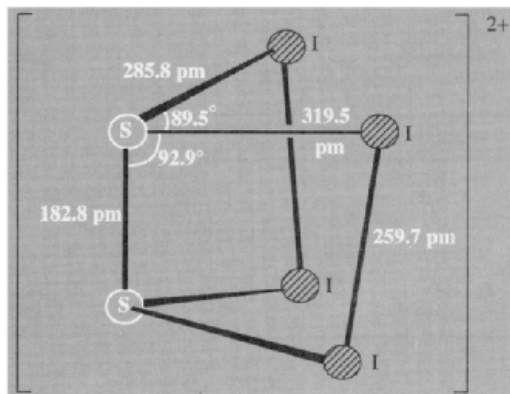
<sup>153</sup> V. G. VAHL and R. MINKWITZ, *Inorg. Nuclear Chem. Lett.* **13**, 213–5 (1977).

<sup>154</sup> J. PASSMORE, P. TAYLOR, T. K. WHIDDEN and P. S. WHITE, *J. Chem. Soc., Chem. Commun.*, 689 (1976). J. PASSMORE, G. SUTHERLAND, P. TAYLOR, T. K. WHIDDEN and P. S. WHITE, *Inorg. Chem.* **20**, 3839–45 (1981). The cation is also one of the products formed when an excess of S reacts with  $[I_3]^+[AsF_6]^-$  or  $[I_3]^+[As_2F_{11}]^-$  or  $AsF_5/I_2$ , or when  $[S_{16}]^{2+}[SbF_6]_2^-$  is iodinated with an excess of iodine.

<sup>155</sup> J. PASSMORE, G. SUTHERLAND and P. S. WHITE, *J. Chem. Soc., Chem. Commun.*, 330–1 (1980). (See also *Inorg. Chem.* **21**, 2717–23 (1982).)

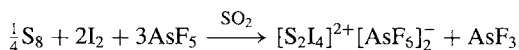
<sup>156</sup> J. PASSMORE, G. SUTHERLAND and P. S. WHITE, *J. Chem. Soc., Chem. Commun.*, 901–2 (1979). (See also *Inorg. Chem.* **21**, 2717–23 (1982).)

<sup>157</sup> J. PASSMORE, G. SUTHERLAND, T. WHIDDEN and P. S. WHITE, *J. Chem. Soc., Chem. Commun.*, 289–90 (1980). M. P. MURCHIE, J. P. JOHNSON, J. PASSMORE, G. W. SUTHERLAND, M. TAJIK, T. K. WHIDDEN, P. S. WHITE and F. GREIN, *Inorg. Chem.* **31**, 273–83 (1992). See also T. KLAPÖTKE and J. PASSMORE, *Accounts Chem. Research* **22**, 234–240 (1989).



**Figure 15.23** Structure of the  $[\text{S}_2\text{I}_4]^{2+}$  cation of  $C_2$  symmetry, showing the very short S–S distance and the rather short I–I distances; note also the S–I distances which are even longer than in the weak charge transfer complex  $[(\text{H}_2\text{N}_2\text{CS})_2\text{I}]^+$  (262.9 pm). The nonbonding  $\text{I}\cdots\text{I}$  distance is 426.7 pm.

curious right triangular prismatic conformation (notably at variance with that in the isoelectronic  $\text{P}_2\text{I}_4$  molecule) is associated with a very short S–S bond (bond order  $2\frac{1}{3}$ ) and rather short I–I distances (bond order  $1\frac{1}{3}$ ). The cation is formed in  $\text{AsF}_5/\text{SO}_2$  solution according to the equation:



Other species containing S–I bonds that have been characterized include the pseudopolyhalide anions  $[\text{I}(\text{SCN})_2]^-$  and  $[\text{I}_2(\text{SCN})]^-$ ,<sup>(158)</sup> and the dimethyliodosulfonium(IV) salts of  $[\text{Me}_2\text{SI}]^+$  with  $[\text{AsF}_6]^-$  and  $[\text{SbCl}_6]^-$  (which latter are thermally unstable above about  $-20^\circ$ ).<sup>(159)</sup>

We conclude this section with an amusing cautionary tale which illustrates the type of blunder that can still appear in the pages of a refereed journal (1975) when scientists (in this

case physicists) attempt to deduce the structure of a compound by spectroscopic techniques alone, without ever analysing the substance being investigated. The work<sup>(160)</sup> purported to establish the presence of a new molecule  $\text{Cl}_3\text{SI}$  in solid solution with an ionic complex  $[\text{SCl}_3]^+[\text{ICl}_2]^-$ , thus leading to an overall formula for the crystals of  $\text{S}_2\text{Cl}_8\text{I}_2$ . The mixed compound had apparently been made originally by M. Jaillard in 1860: he obtained it as beautiful transparent yellow-orange prismatic crystals by treating a mixture of sulfur and iodine with a stream of dry  $\text{Cl}_2$ . R. Weber obtained the same material in 1866 by passing  $\text{Cl}_2$  into a solution of  $\text{I}_2$  in  $\text{CS}_2$  but he reported a composition of  $\text{S}_2\text{Cl}_7\text{I}$  rather than Jaillard's  $\text{S}_2\text{Cl}_8\text{I}_2$ . The implausibility of forming a stable compound containing an S–I bond in this way, coupled with the perceptive recognition that the published Raman spectrum had bands that could be assigned to  $[\text{ICl}_4]^-$  rather than  $[\text{ICl}_2]^-$ , led P. N. Gates and A. Finch to reinvestigate the compound.<sup>(161)</sup> It transpired that the nineteenth-century workers had used  $\text{S}=16$  as the atomic weight of sulfur so the true chemical composition of the crystals was, in fact,  $\text{S}_2\text{Cl}_7\text{I}$ . The previous spectroscopic interpretation<sup>(160)</sup> was therefore totally incorrect and the compound was shown to be  $[\text{SCl}_3]^+[\text{ICl}_4]^-$ . This was later confirmed by a single-crystal X-ray diffraction study (p. 691).<sup>(149)</sup> In short, far from containing the new iodo-derivative  $\text{Cl}_3\text{SI}$ , the compound did not even contain an S–I bond.

### 15.2.4 Oxohalides of sulfur

Sulfur forms two main series of oxohalides, the thionyl dihalides  $\text{OS}^{\text{IV}}\text{X}_2$  and the sulfuryl dihalides  $\text{O}_2\text{S}^{\text{VI}}\text{X}_2$ . In addition, various other oxofluorides and peroxofluorides are known (p. 688). Thionyl fluorides and chlorides are colourless volatile liquids (Table 15.14);  $\text{OSBr}_2$  is rather less volatile and is orange-coloured.

<sup>158</sup> G. A. BOWMAKER and D. A. ROGERS, *J. Chem. Soc., Dalton Trans.*, 1146–51 (1981).

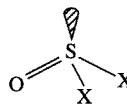
<sup>159</sup> R. MINKWITZ and H. PRENZEL, *Z. anorg. allg. Chem.* **548**, 91–102 (1987).

<sup>160</sup> Y. TAVARES-FORNERIS and R. FORNERIS, *J. Mol. Structure* **24**, 205–13 (1975).

<sup>161</sup> A. FINCH, P. N. GATES and T. H. PAGE, *Inorg. Chim. Acta* **25**, L49–L50 (1977).



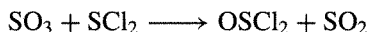
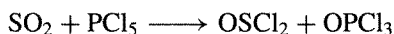
Table 15.14 Some properties of thionyl dihalides,



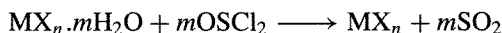
Property	OSF <sub>2</sub>	OSFCl	OSCl <sub>2</sub>	OSBr <sub>2</sub>
MP/°C	-110	-120	-101	-50
BP/°C	-44	12	76	140
<i>d</i> (O-S)/pm	141.2	—	145	145 (assumed)
<i>d</i> (S-X)/pm	158.5	—	207	227
angle O-S-X	106.8°	—	106°	108°
angle X-S-X	92.8°	—	114°(?)	96°

All have pyramidal molecules (*C<sub>s</sub>* point group for OSX<sub>2</sub>), and OSFCl is chiral though stereochemically labile. Dimensions are in Table 15.14; the short O-S distance is notable. The unstable compound OSI<sub>2</sub> was mentioned on p. 692.

The most important thionyl compound is OSCI<sub>2</sub> — it is readily prepared by chlorination of SO<sub>2</sub> with PCl<sub>5</sub> or, on an industrial scale, by oxygen-atom transfer from SO<sub>3</sub> to SCl<sub>2</sub>:



OSCl<sub>2</sub> reacts vigorously with water and is particularly valuable for drying or dehydrating readily hydrolysable inorganic halides:

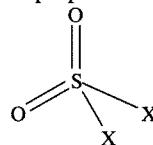


Examples are MgCl<sub>2</sub>·6H<sub>2</sub>O, AlCl<sub>3</sub>·6H<sub>2</sub>O, FeCl<sub>3</sub>·6H<sub>2</sub>O, etc. Thionyl chloride begins to decompose above its bp (76°) into S<sub>2</sub>Cl<sub>2</sub>, SO<sub>2</sub>, and Cl<sub>2</sub>; it is therefore much used as an oxidizing and chlorinating agent in organic chemistry. Fluorination with SbF<sub>3</sub>/SbF<sub>5</sub> gives OSF<sub>2</sub>; use of NaF/MeCN gives OSFCl or OSF<sub>2</sub> according to conditions. Thionyl chloride also finds some use as a nonaqueous ionizing solvent as does SO<sub>2</sub> (p. 700) and the formally related dimethylsulfoxide (dmsO), Me<sub>2</sub>SO (mp 18.6°, bp 189°, viscosity  $\eta_{25}$  1.996 centipoise, dielectric constant  $\epsilon_{25}$  46.7). OSF<sub>2</sub> is a useful low-temperature fluorinating agent in organic chemistry: it converts active C-H and P-H

groups into C-F and P-F, and replaces N-H with N-S(O)F.<sup>(162)</sup>

Sulfuryl halides, like their thionyl analogues, are also reactive, colourless, volatile liquids or gases (Table 15.15). The most important compound is O<sub>2</sub>SCL<sub>2</sub>, which is made on an industrial scale by direct chlorination of SO<sub>2</sub> in the presence of a catalyst such as activated charcoal (p. 274) or FeCl<sub>3</sub>. It is stable to 300° but begins to dissociate into SO<sub>2</sub> and Cl<sub>2</sub> above this: it is a useful reagent for introducing Cl or O<sub>2</sub>SCL into organic compounds. O<sub>2</sub>SCL<sub>2</sub> can be regarded as the acid chloride of H<sub>2</sub>SO<sub>4</sub> and, accordingly, slow hydrolysis (or ammonolysis) yields O<sub>2</sub>S(OH)<sub>2</sub> or O<sub>2</sub>S(NH<sub>2</sub>)<sub>2</sub>. Fluorination yields O<sub>2</sub>SF<sub>2</sub> (also prepared by SO<sub>2</sub> + F<sub>2</sub>) and comproportionation of this with O<sub>2</sub>SCL<sub>2</sub> and O<sub>2</sub>SBr<sub>2</sub> yield the corresponding O<sub>2</sub>SFX species.

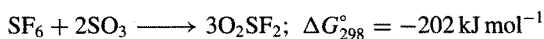
Table 15.15 Some properties of sulfuryl dihalides,



Property	O <sub>2</sub> SF <sub>2</sub>	O <sub>2</sub> SFCl	O <sub>2</sub> SCL <sub>2</sub>	O <sub>2</sub> SFBr
MP/°C	-120	-125	-54	-86
BP/°C	-55	7	69	41
<i>d</i> (O-S)/pm	140.5	—	143	—
<i>d</i> (S-X)/pm	153.0	—	199	—
angle O-S-O	124°	—	120°	—
angle X-S-X	96°	—	111°	—

<sup>162</sup> T. MAHMOOD and J. M. SHREEVE, *Inorg. Chem.* **24**, 1395-8 (1985).

All these compounds have (distorted) tetrahedral molecules, those of formula  $O_2SX_2$  having  $C_{2v}$  symmetry and the others  $C_s$ . Dimensions are in Table 15.15: the remarkably short O–S and S–F distances in  $O_2SF_2$  should be noted (cf. above). Indeed, the implied strength of bonding in this molecule is reflected by the fact that it can be made by reacting the normally extremely inert compound  $SF_6$  (p. 687) with the fluoro-acceptor  $SO_3$ :



A 20% conversion can be effected by heating the two compounds at  $250^\circ$  for 24 h.

### 15.2.5 Oxides of sulfur

At least thirteen proven oxides of sulfur are known to exist<sup>(163)</sup> though this profusion should not obscure the fact that  $SO_2$  and  $SO_3$  remain by far the most stable and unquestionably the most important economically. The six homocyclic polysulfur monoxides  $S_nO$  ( $5 < n < 10$ ) are made by oxidizing the appropriate *cyclo-S<sub>n</sub>* (p. 656) with trifluoroperoxoacetic acid,  $CF_3C(O)OOH$ , at  $-30^\circ$ . The dioxides  $S_7O_2$  and  $S_6O_2$  are also known. In addition there are the thermally unstable acyclic oxides  $S_2O$ ,  $S_2O_2$ ,  $SO$  and the fugitive species  $SOO$  and  $SO_4$ . Several other compounds were described in the older literature (pre-1950s) but these reports are now known to be in error. For example, the blue substance of composition “ $S_2O_3$ ” prepared from liquid  $SO_3$  and sulfur now appears to be a mixture of salts of the cations  $S_4^{2+}$  and  $S_8^{2+}$  (p. 664) with polysulfate anions. Likewise a “sulfur monoxide” prepared by P. W. Schenk in 1933 was shown by D. J. Meschi and R. J. Meyers in 1956 to be a mixture of  $S_2O$  and  $SO_2$ . The well-established lower oxides of S will be briefly reviewed before  $SO_2$  and  $SO_3$  are discussed in more detail.

#### Lower oxides<sup>(163)</sup>

Elegant work by R. Steudel and his group in Berlin has shown that, when *cyclo-S<sub>10</sub>*, *-S<sub>9</sub>*, and *-S<sub>8</sub>* are dissolved in  $CS_2$  and oxidized by freshly prepared  $CF_3C(O)O_2H$  at temperatures below  $-10^\circ$ , modest yields (10–20%) of the corresponding crystalline monoxides  $S_nO$  are obtained. Similar oxidation of *cyclo-S<sub>7</sub>*, and  $\alpha$ - and  $\beta$ - $S_6$  in  $CH_2Cl_2$  solution yields crystalline  $S_7O$ ,  $S_7O_2$ , and  $\alpha$ - and  $\beta$ - $S_6O$ . Crystals of  $S_6O_2$  and  $S_5O$  ( $d > -50^\circ$ ) have not yet been isolated but the compounds have been made in solution by the same technique.  $S_8O$  had previously been made (1972) by the reaction of  $OSCl_2$  and  $H_2S_7$  in  $CS_2$  at  $-40^\circ$ : it is one of the most stable compounds in the series and melts (with decomposition) at  $78^\circ$ . All the compounds are orange or dark yellow and decompose with liberation of  $SO_2$  and sulfur when warmed to room temperature or slightly above. Structures are in Fig. 15.24. It will be noted that  $S_7O$  is isoelectronic and isostructural with  $[S_7I]^+$  (p. 692). This invites the question as to whether  $S_7S$  can be prepared as a new structural isomer of *cyclo-S<sub>8</sub>*.

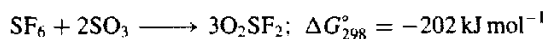
$S_8O$  reacts with  $SbCl_5$  in  $CS_2$  over a period of 9 days at  $-50^\circ$  to give a 71% yield of the unstable orange adduct  $S_8O.SbCl_5$ <sup>(164)</sup> its structure and dimensions are in Fig. 15.25a. It will be noted that the  $S_8O$  unit differs from molecular  $S_8O$  in having an equatorially bonded O atom and significantly different S–O and S–S interatomic distances. The X-ray crystal structure was determined at  $-100^\circ C$  as the adduct decomposes within 5 min at  $25^\circ$  to give  $OSCl_2$ ,  $SbCl_3$  and  $S_8$ . When a similar reaction was attempted with  $\beta$ - $S_6O$ , the novel dimer  $S_{12}O_2.2SbCl_5.3CS_2$  was obtained as orange crystals in 10% yield after 1 week at  $-50^\circ$ <sup>(165)</sup> (Fig. 15.25b). Formation of the centrosymmetric  $S_{12}O_2$  molecule, which is still unknown in the uncoordinated state, can be

<sup>164</sup> R. STEUDEL, T. SANDOW and J. STEIDEL, *J. Chem. Soc., Chem. Commun.*, 180–1 (1980).

<sup>165</sup> R. STEUDEL, J. STEIDEL and J. PICKARDT, *Angew. Chem. Int. Edn. Engl.* **19**, 325–6 (1980).

<sup>163</sup> *Gmelin Handbuch der Anorganischen Chemie*, 8th edn., Schwefel Oxide, Ergänzungsband 3, 1980, 344 pp.

All these compounds have (distorted) tetrahedral molecules, those of formula  $O_2SX_2$  having  $C_{2v}$  symmetry and the others  $C_s$ . Dimensions are in Table 15.15: the remarkably short O–S and S–F distances in  $O_2SF_2$  should be noted (cf. above). Indeed, the implied strength of bonding in this molecule is reflected by the fact that it can be made by reacting the normally extremely inert compound  $SF_6$  (p. 687) with the fluoro-acceptor  $SO_3$ :



A 20% conversion can be effected by heating the two compounds at  $250^\circ$  for 24 h.

### 15.2.5 Oxides of sulfur

At least thirteen proven oxides of sulfur are known to exist<sup>(163)</sup> though this profusion should not obscure the fact that  $SO_2$  and  $SO_3$  remain by far the most stable and unquestionably the most important economically. The six homocyclic polysulfur monoxides  $S_nO$  ( $5 < n < 10$ ) are made by oxidizing the appropriate *cyclo-S<sub>n</sub>* (p. 656) with trifluoroperoxoacetic acid,  $CF_3C(O)OOH$ , at  $-30^\circ$ . The dioxides  $S_7O_2$  and  $S_6O_2$  are also known. In addition there are the thermally unstable acyclic oxides  $S_2O$ ,  $S_2O_2$ ,  $SO$  and the fugitive species  $SOO$  and  $SO_4$ . Several other compounds were described in the older literature (pre-1950s) but these reports are now known to be in error. For example, the blue substance of composition “ $S_2O_3$ ” prepared from liquid  $SO_3$  and sulfur now appears to be a mixture of salts of the cations  $S_4^{2+}$  and  $S_8^{2+}$  (p. 664) with polysulfate anions. Likewise a “sulfur monoxide” prepared by P. W. Schenk in 1933 was shown by D. J. Meschi and R. J. Meyers in 1956 to be a mixture of  $S_2O$  and  $SO_2$ . The well-established lower oxides of S will be briefly reviewed before  $SO_2$  and  $SO_3$  are discussed in more detail.

#### Lower oxides<sup>(163)</sup>

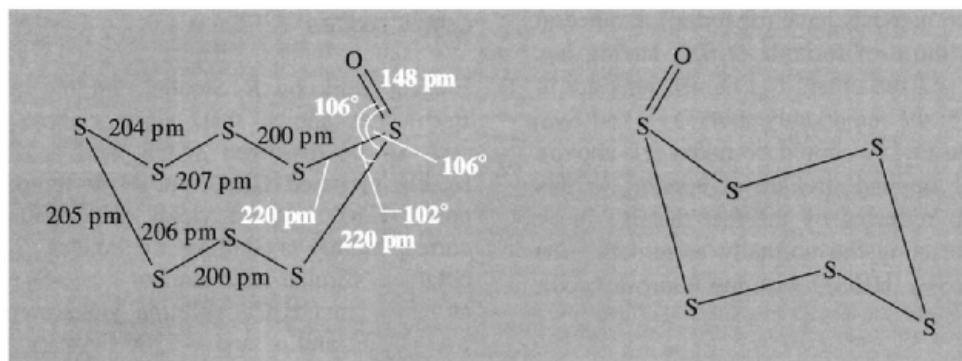
Elegant work by R. Steudel and his group in Berlin has shown that, when *cyclo-S<sub>10</sub>*, *-S<sub>9</sub>*, and *-S<sub>8</sub>* are dissolved in  $CS_2$  and oxidized by freshly prepared  $CF_3C(O)O_2H$  at temperatures below  $-10^\circ$ , modest yields (10–20%) of the corresponding crystalline monoxides  $S_nO$  are obtained. Similar oxidation of *cyclo-S<sub>7</sub>*, and  $\alpha$ - and  $\beta$ - $S_6$  in  $CH_2Cl_2$  solution yields crystalline  $S_7O$ ,  $S_7O_2$ , and  $\alpha$ - and  $\beta$ - $S_6O$ . Crystals of  $S_6O_2$  and  $S_5O$  ( $d > -50^\circ$ ) have not yet been isolated but the compounds have been made in solution by the same technique.  $S_8O$  had previously been made (1972) by the reaction of  $OSCl_2$  and  $H_2S_7$  in  $CS_2$  at  $-40^\circ$ : it is one of the most stable compounds in the series and melts (with decomposition) at  $78^\circ$ . All the compounds are orange or dark yellow and decompose with liberation of  $SO_2$  and sulfur when warmed to room temperature or slightly above. Structures are in Fig. 15.24. It will be noted that  $S_7O$  is isoelectronic and isostructural with  $[S_7I]^+$  (p. 692). This invites the question as to whether  $S_7S$  can be prepared as a new structural isomer of *cyclo-S<sub>8</sub>*.

$S_8O$  reacts with  $SbCl_5$  in  $CS_2$  over a period of 9 days at  $-50^\circ$  to give a 71% yield of the unstable orange adduct  $S_8O \cdot SbCl_5$ <sup>(164)</sup> its structure and dimensions are in Fig. 15.25a. It will be noted that the  $S_8O$  unit differs from molecular  $S_8O$  in having an equatorially bonded O atom and significantly different S–O and S–S interatomic distances. The X-ray crystal structure was determined at  $-100^\circ C$  as the adduct decomposes within 5 min at  $25^\circ$  to give  $OSCl_2$ ,  $SbCl_3$  and  $S_8$ . When a similar reaction was attempted with  $\beta$ - $S_6O$ , the novel dimer  $S_{12}O_2 \cdot 2SbCl_5 \cdot 3CS_2$  was obtained as orange crystals in 10% yield after 1 week at  $-50^\circ$ <sup>(165)</sup> (Fig. 15.25b). Formation of the centrosymmetric  $S_{12}O_2$  molecule, which is still unknown in the uncoordinated state, can be

<sup>164</sup> R. STEUDEL, T. SANDOW and J. STEIDEL, *J. Chem. Soc., Chem. Commun.*, 180–1 (1980).

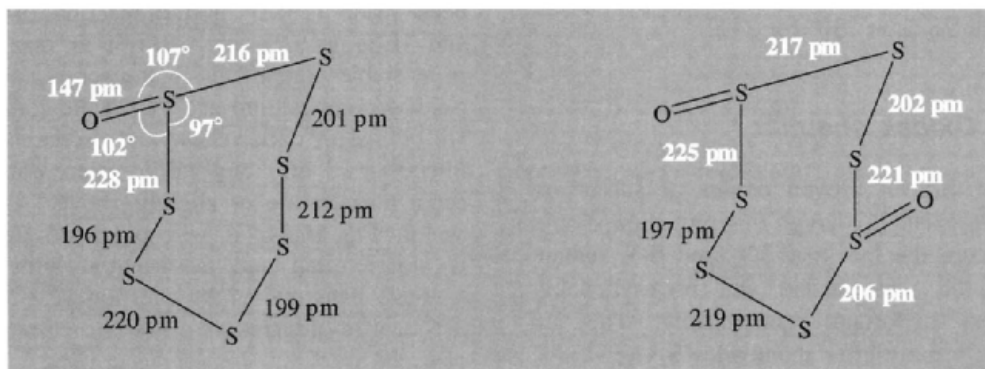
<sup>165</sup> R. STEUDEL, J. STEIDEL and J. PICKARDT, *Angew. Chem. Int. Edn. Engl.* **19**, 325–6 (1980).

<sup>163</sup> *Gmelin Handbuch der Anorganischen Chemie*, 8th edn., Schwefel Oxide, Ergänzungsband 3, 1980, 344 pp.



$S_8O$ : orange-yellow crystals,  
mp  $78^\circ$  (decomp)

$\alpha$ - $S_6O$ : orange-yellow crystals, mp  $39^\circ$  (d)  
 $\beta$ - $S_6O$ : dark orange, mp  $34^\circ$  (d)



$S_7O$ : orange crystals, mp  $55^\circ$  (d)

$S_7O_2$ : dark orange crystals,  
decomp  $>$  room temp

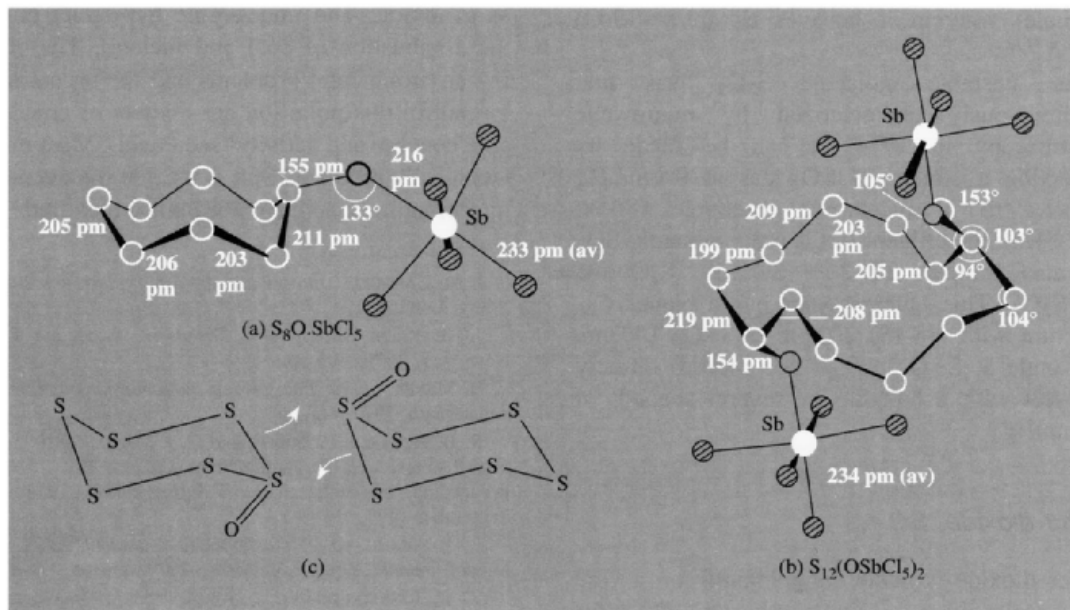
**Figure 15.24** Structures of  $S_8O$ ,  $S_7O$ ,  $S_7O_2$  and  $S_6O$ ; in each case the O atom adopts an axial conformation. For  $S_8O$  there is an alternation of S–S distances, the longest being adjacent to the exocyclic O atoms; S–S–S angles are in the range  $102$ – $108^\circ$  and dihedral angles (p. 654) vary from  $95^\circ$  to  $112^\circ$  (+ and –). For  $S_7O$  there is again an alternation in S–S distances; ring angles are in the range  $97$ – $106^\circ$  the smallest angle again being at the S atom carrying the pendant O. The structure of  $S_7O_2$  was deduced from its Raman spectrum, the interatomic distances ( $d/\text{pm}$ ) being computed from the relation  $\log(d/\text{pm}) = 2.881 - 0.213 \log(\nu/\text{cm}^{-1})$ . The two modifications  $\alpha$ - and  $\beta$ - $S_6O$  have the same Raman spectrum in solution.

explained in terms of a dipolar addition reaction (Fig. 15.25c). Its conformation differs drastically from the  $D_{3d}$  symmetry of the parent *cyclo*- $S_{12}$  (p. 658).

The fugitive species SO was first identified by its ultraviolet spectrum in 1929 but it is thermodynamically unstable and decomposes completely in the gas phase in less than 1 s. It is formed by reduction of  $SO_2$  with sulfur vapour in a glow discharge and its spectroscopic properties

have excited interest because of its relation to  $O_2$  ( $^3\Sigma^-$  ground state, p. 605). Molecular properties include internuclear distance 148.1 pm, dipole moment 1.55 D, equilibrium bond energy  $D_e$   $524 \text{ kJ mol}^{-1}$ . The use of transition-metal complexes to trap SO has received considerable attention.<sup>(166)</sup> It can bond in several modes including

<sup>166</sup> W. A. SCHENK, *Angew. Chem. Int. Edn. Engl.* **26**, 98–109 (1987).



**Figure 15.25** Molecular structure and dimensions of (a) the adduct  $S_8O \cdot SbCl_5$  at  $-100^\circ$ , and (b) the dimeric unit  $Sb_{12}O_2 \cdot 2SbCl_5$  in  $Sb_{12}O_2 \cdot 2SbCl_5 \cdot 3CS_2$  at  $-115^\circ C$ . (c) Possible dipolar addition of  $2S_8O$  to form  $S_{12}O_2$ .

4-centre-2 electron ( $4c-2e$ ) as in  $[Fe_3(CO)_9S(\mu_3-SO)]$ ,<sup>(167)</sup>  $2c-2e$  as in  $[IrCl(SO)(PR_3)_2]$ ,<sup>(168)</sup> and also  $3c-4e$  and  $3c-2e$  in several dinuclear transition-metal complexes.<sup>(169,170)</sup> A novel and unprecedented route to this last class of  $\mu-SO$  complexes involves the direct oxidative addition of  $OSCl_2$  to the  $Ni^0$  complex  $[Ni(cod)_2]$  in the presence of  $dppm$  ( $cod =$  cycloocta-1,5-diene,  $dppm = Ph_2PCH_2PPh_2$ ) to form the purple crystalline dinickel A-frame complex,  $[Ni_2(\mu-SO)(dppm)_2Cl_2]$ .<sup>(171)</sup> X-ray analysis reveals two slightly differing geometries, with  $SO$

144 and 145.9 pm, respectively (both shorter than in the free molecule, 148.1 pm), and with the  $SO$  ligand being tilted with respect to the  $Ni \cdots Ni$  vector.

$S_2O$  is also an unstable species but survives for several days in the gas phase at  $<1$  mmHg pressure. It is formed by decomposition of  $SO$  (above) and by numerous other reactions between S- and O-containing species but cannot be isolated as a pure compound. Typical recipes include: (a) passing a stream of  $OSCl_2$  at 0.1–0.5 mmHg over heated  $Ag_2S$  at  $160^\circ$ , (b) burning  $S_8$  in a stream of  $O_2$  at  $\sim 8$  mmHg pressure, and (c) passing  $SO_2$  at  $120^\circ$  and  $<1$  mmHg through a high-voltage discharge ( $\sim 5$  kV). Spectroscopic studies in the gas phase have shown it to be a nonlinear molecule (like  $O_3$  and  $SO_2$ ) with angle  $S-S-O$   $118^\circ$  and the interatomic distances  $S-S$  188,  $S-O$  146 pm.  $S_2O$  readily decomposes at room temperature to  $SO_2$  and sulfur. As with  $SO$ , the fugitive  $S_2O$  species can be trapped with transition-metal complexes (of Mn and Ir, for

<sup>167</sup> L. MARKÓ, B. MARKÓ-MONOSTORY, T. MADACH and H. VAHRENKAMP, *Angew. Chem. Int. Edn. Engl.* **19**, 226–7 (1980).

<sup>168</sup> W. A. SCHENK, J. LEISSNER and C. BURSCHKA, *Angew. Chem. Int. Edn. Engl.* **23**, 806–7 (1984).

<sup>169</sup> I.-P. LORENZ, J. MESSELHAUSER, W. HILLER and K. HAUG, *Angew. Chem. Int. Edn. Engl.* **3**, 24–5 (1985).

<sup>170</sup> G. BESENEI, C. L. LEE, J. GULINSKI, S. J. RETTIG, B. R. JAMES, D. A. NELSON and M. A. LILGA, *Inorg. Chem.* **26**, 3622–8 (1987).

<sup>171</sup> J. K. GONG, P. E. FANWICK and C. P. KUBIAK, *J. Chem. Soc., Chem. Commun.*, 1190–1 (1990).

example) wherein it behaves as an  $\eta^2$ -SS(O) ligand.<sup>(172)</sup>

The unstable molecule  $S_2O_2$  was first unambiguously characterized by microwave spectroscopy in 1974. It can be made by subjecting a stream of  $SO_2$  gas at 0.1 mmHg pressure to a microwave discharge (80 W, 2.45 GHz): the effluent gas is predominantly  $SO_2$  but also contains 20–30%  $SO$ , 5%  $S_2O$  and 5%  $S_2O_2$ . This latter species has a planar  $C_{2v}$  structure with  $r(S-S)$  202 pm,  $r(S-O)$  146 pm, and angle  $S-S-O$   $113^\circ$ ; it decomposes directly into  $SO$  with a half-life of several seconds at 0.1 mmHg.

### Sulfur dioxide, $SO_2$

Sulfur dioxide is made commercially on a very large scale either by the combustion of sulfur or  $H_2S$  or by roasting sulfide ores (particularly pyrite,  $FeS_2$ ) in air (p. 651). It is also produced

as a noxious and undesirable byproduct during the combustion of coal and fuel oil. The ensuing environmental problems and the urgent need to control this pollution are matters of considerable concern and activity (see Panel). Most of the technically produced  $SO_2$  is used in the manufacture of sulfuric acid (p. 708) but it also finds use

<sup>172</sup> G. A. UROVE and M. E. WELKER, *Organometallics* **7**, 1013–4 (1988).

<sup>173</sup> I. M. CAMPBELL, *Energy and the Atmosphere*, pp. 202–9, Wiley, London, 1977.

<sup>174</sup> J. HEICKLEN, *Atmospheric Chemistry*, Academic Press, New York, 1976, 406 pp.

<sup>175</sup> B. MEYER, *Sulfur, Energy, and the Environment*, Elsevier, Amsterdam, 1977, 448 pp.

<sup>176</sup> R. B. HUSAR, J. P. LODGE, and D. J. MOORE (eds.), *Sulfur in the Atmosphere*, Pergamon Press, Oxford, 1978, 816 pp. Proceedings of the International Symposium at Dubrovnik, September 1977.

<sup>177</sup> J. O. NRIAGU (ed.), *Sulfur in the Environment. Part 2. Ecological Impacts*, Wiley, Chichester, 1979, 494 pp.

<sup>178</sup> R. W. JOHNSON and G. E. GORDON (eds.), *The Chemistry of Acid Rain*, ACS Symposium **349**, 337 pp. (1987). See also M. Freemantle, *Chem. and Eng. News*, pp. 10–17, May 1, 1995.

<sup>179</sup> D. J. LITTLER (ed.), *Acid Rain*, CEBG Research, Special Issue No. 20, 64 pp. (1987), published by the Central Electricity Generating Board, Southampton SO4 4ZB. See also W. D. Halstead, *CEBG Research* **22**, 3–11 (1988).

## Atmospheric $SO_2$ and Environmental Pollution<sup>(173–179)</sup>

The pollution of air by smoke and sulfurous fumes is no new problem<sup>†</sup> but the quickening pace of industrial development during the nineteenth century, and the growing concern for both personal health and protection of the environment generally since the 1950s, has given added impetus to measures required to eliminate or at least minimize the hazard.

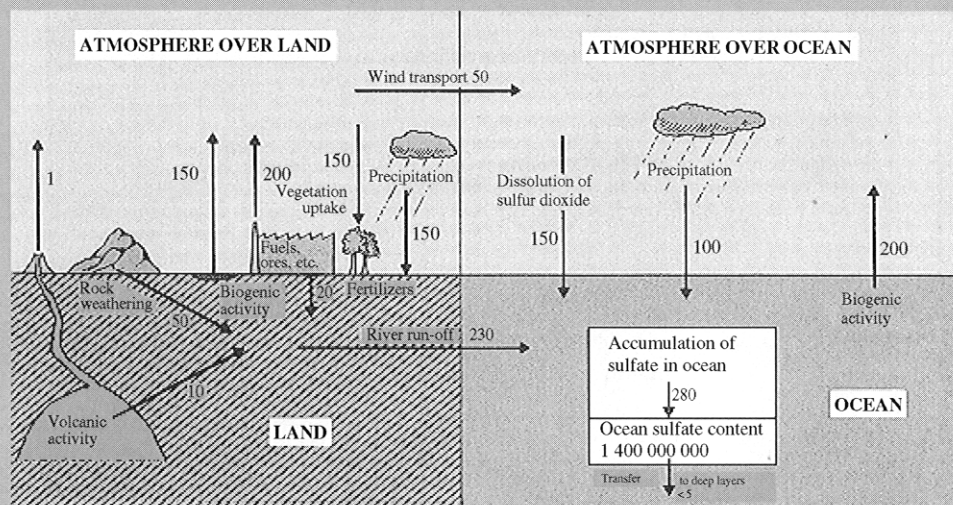
As indicated on p. 647, there are vast amounts of volatile sulfur compounds in the environment as a result of natural processes. Geothermal activity (especially volcanic) releases large amounts of  $SO_2$  together with smaller quantities of  $H_2S$ ,  $SO_3$ , elemental S and particulate sulfates. From a global viewpoint, however, this accounts for less than 1% of the naturally formed volatile S compounds (Fig. A). By far the most important source is the biological reduction of S compounds which occurs most readily in the presence of organic matter and under oxygen-deficient conditions. Much of this is released as  $H_2S$  but other compounds such as  $Me_2S$  are probably also implicated. The final natural source of atmospheric S compounds is sea-spray (sulfate is the second most abundant anion in sea-water being about one-seventh the concentration of chloride). Though much sulfur is transported as sulfate by wind-driven sea spray and by river run off, its environmental impact is not severe.

<sup>†</sup>One of the earliest tracts on the matter was John Evelyn's *Fumifugium, or the Inconvenience of the Aer and Smoake of London Dissipated* which he submitted (with little effect) to Charles II in 1661. Evelyn, a noted diarist and a founder Fellow of the Royal Society, outlined the problem as follows: "For when in all other places the Aer is most Serene and Pure, it is here [in London] Eclipsed with such a Cloud of Sulphure, as the Sun itself, which gives day to all the World besides, is hardly able to penetrate and impart it here; and the weary Traveller, at many Miles distance, sooner smells than sees the City to which he repairs. This is that pernicious Smoake which sullies all her Glory, superinducing a sooty Crust or Fur upon all that it lights, spoyling the moveables, tarnishing the Plate, Gildings, and Furniture, and corroding the very Iron-bars and hardest Stones with these piercing and acrimonious Spirits which accompany its Sulphure; and executing more in one year than exposed to the pure Aer of the Country it could effect in some hundreds."



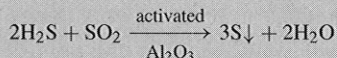
Much more serious is the effect of volatile S compounds (mainly  $\text{SO}_2$ ) released into the atmosphere as a result of man's domestic and industrial activities. This has been estimated to be some 200 million tonnes pa, and is comparable in amount to all the sulfur released by natural processes ( $\sim 310 \times 10^6$  tonnes pa). Unfortunately, by the very nature of its origin, this  $\text{SO}_2$  is released in the heart of densely populated areas and does great damage to the respiratory organs of man and animals, to buildings, and perhaps most seriously to plants, lake-waters and aquatic life as a result of "acid rain". Dispersal by means of high chimney stacks is inadequate since this merely transfers the problem to neighbouring regions. For example, only one-tenth of the serious  $\text{SO}_2/\text{H}_2\text{SO}_4$  pollution of lakes and streams in Sweden is as a result of atmospheric  $\text{SO}_2$  emissions in Sweden itself; one-tenth is due to emissions from the UK, and the remaining four-fifths is from industrial regions in northern Europe.

In Europe and the USA (and presumably elsewhere) the major source of  $\text{SO}_2$  pollution is in coal-based power generation; this, together with other coal consumption and coking operations accounts for some 60% of the emissions. A further 25% arises from oil-refinery operations, oil-fired power generation, and other oil consumption. Copper-smelting (together with much smaller amounts from zinc and lead ore processing) accounts for some 12% of the annual release of  $\text{SO}_2$ . The sulfuric acid manufacturing industry, which is the only one designed actually to make  $\text{SO}_2$  on a large scale, only contributes <2% to the total, probably because of the efficient design of the process.



**Figure A** The sulfur budget for the land-atmosphere-ocean system. Annual turnover rates are indicated in units of  $10^6$  tonnes (as estimated for 1977).<sup>(173)</sup>

Ultimately, pollution can only be avoided by complete removal of  $\text{SO}_2$  from the effluent gases, but this council of perfection is both technologically and economically unattainable. Many processes are available to reduce the  $\text{SO}_2$  concentration to very low figures, but the vast scale of power generation and domestic heating by coal and oil still results in substantial emission.  $\text{SO}_2$  can be removed by scrubbing with a slurry of "milk of lime",  $\text{Ca}(\text{OH})_2$ . Alternatively, partial reduction to  $\text{H}_2\text{S}$  using natural gas ( $\text{CH}_4$ ), naphtha or coal, followed by catalytic conversion to elemental sulfur by the Claus process can be used:



The detection of  $\text{SO}_2$  in the atmosphere has become a refined analytical procedure. Several techniques are available such as (a) absorption in aqueous  $\text{H}_2\text{O}_2$  and titration (or conductimetric determination) of the resulting  $\text{H}_2\text{SO}_4$  ( $\text{H}_2\text{O}_2 + \text{SO}_2 \longrightarrow \text{H}_2\text{SO}_4$ ); and (b) reaction with  $\text{Na}_2[\text{HgCl}_4]$  or  $\text{K}_2[\text{HgCl}_4]$ :



The resulting disulfite-mercurate is determined colorimetrically after addition of acidic pararosaniline and formaldehyde (P. W. West and G. C. Gaeke, 1956). Other methods are (c) flame-photometric monitoring of the gas stream using a reducing  $\text{H}_2$ /air flame and emission of  $\text{S}_2$  at 394 nm sensitive down to 1 part in  $10^9$  by volume and (d) pulsed fluorescent analyser using radiation in the region of 214 nm; this is specific for  $\text{SO}_2$  and response is linear over wide ranges down to 1 in  $10^9$ . Commercial instruments are available.

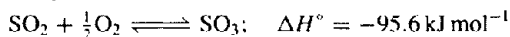
Table 15.16 Some molecular and physical properties of SO<sub>2</sub>

Property	Value	Property	Value
MP/°C	-75.5	Electrical conductivity $\kappa$ /ohm <sup>-1</sup> cm <sup>-1</sup>	<10 <sup>-8</sup>
BP/°C	-10.0	Dielectric constant $\epsilon$ (0°)	15.4
Critical temperature/°C	157.5	Dipole moment $\mu$ /D	1.62
Critical pressure/atm	77.7	Angle O-S-O	119°
Density(-10°)/g cm <sup>-3</sup>	1.46	Distance $r$ (S-O)/pm	143.1
Viscosity $\eta$ (0°)/centipoise	0.403	$\Delta H_f^\circ$ (g)/kJ mol <sup>-1</sup>	-296.9

as a bleach, disinfectant (Homer, p. 645), food preservative, refrigerant and nonaqueous solvent. Other chemical uses are in the preparation of sulfites and dithionites (p. 716) and, with Cl<sub>2</sub>, in the derivatization of hydrocarbons via sulfochlorination reactions. There is also much current interest in its properties as a multimode ligand (p. 701).

SO<sub>2</sub> is a colourless, toxic gas with a choking odour. Maximum permitted atmospheric concentration for humans is 5 ppm but many green plants suffer severe distress in concentrations as low as 1–2 ppm. SO<sub>2</sub> neither burns in air nor supports combustion. Some molecular and physical properties of the compound are in Table 15.16. Comparison of these properties with those of ozone (p. 607) is instructive. Note also that the S–O distance of 143.1 pm in SO<sub>2</sub> is less than that in unstable SO (148.1 pm) whereas the O–O distance of 127.8 pm in O<sub>3</sub> is greater than that in stable O<sub>2</sub> (120.7 pm). Furthermore the mean bond energy in SO<sub>2</sub> is 548 kJ mol<sup>-1</sup> which is greater than that for SO (524 kJ mol<sup>-1</sup>) whereas the mean bond energy in O<sub>3</sub> is 297 kJ mol<sup>-1</sup> which is less than the value for O<sub>2</sub> (490 kJ mol<sup>-1</sup>). This has been taken to imply an S–O bond order of at least 2 in SO<sub>2</sub>, compared with only 1.5 for O–O in O<sub>3</sub> (p. 607).

By far the most important chemical reaction of SO<sub>2</sub> is its further oxidation to SO<sub>3</sub> according to the equilibrium:



The equilibrium constant,  $K_p = p(\text{SO}_3)/[p(\text{SO}_2) \cdot p^{1/2}(\text{O}_2)]$ , decreases rapidly with increasing temperature; for example:  $\log K_p = 3.49$  at 800°C and  $-0.52$  at 1100°C. Thus for maximum oxidation during the manufacture of H<sub>2</sub>SO<sub>4</sub> it is necessary to work at lower temperatures and to increase the rate of reaction by use of catalysts.

Typical conditions would be to pass a mixture of SO<sub>2</sub> and air over Pt gauze or more commonly a V<sub>2</sub>O<sub>5</sub>/K<sub>2</sub>O contact catalyst supported on Kieselguhr or zeolite.

Gaseous SO<sub>2</sub> is readily soluble in water (3927 cm<sup>3</sup> SO<sub>2</sub> in 100 g H<sub>2</sub>O at 20°). Numerous species are present in this aqueous solution of "sulfurous acid" (p. 717). At 0° a cubic clathrate hydrate also forms with a composition ~SO<sub>2</sub>·6H<sub>2</sub>O; its dissociation pressure reaches 1 atm at 7.1°. The ideal composition would be SO<sub>2</sub>·5 $\frac{3}{4}$ H<sub>2</sub>O (p. 627).

In addition to the role of gaseous SO<sub>2</sub> in the manufacture of H<sub>2</sub>SO<sub>4</sub>, pure (liquid) SO<sub>2</sub> is manufactured on a large scale for the uses mentioned above. Typical production levels (in 1985) were 162 000 tonnes in USA and 65 000 tonnes in (West) Germany. About half of this is used in the manufacture of S-containing chemicals such as sulfites, hydrogen sulfites, thiosulfates, dithionites, salts of hydroxalkane-sulfinic acids and alkane sulfonates. It is also used in cellulose manufacture, in the chemical dressing of Mn-ores, in the removal of S-containing impurities from mineral oils, for food disinfection and preservation, and for treatment of water.

Liquid SO<sub>2</sub> has been much studied as a nonaqueous solvent.<sup>(180)</sup> Some of the early work (particularly on the physical properties of the solutions) is now known to be in error but

<sup>180</sup>T. C. WADDINGTON, Liquid sulfur dioxide, Chap. 6 in T. C. WADDINGTON (ed.), *Nonaqueous Solvent Systems*, pp. 253–84, Academic Press, London, 1965. W. KARCHER and H. HECHT, *Chemie in Flüssigem Schwefeldioxid*, Vol. 3, Part 2, of G. JANDER, H. SPAUNDAU and C. C. ADDISON, *Chemistry in Nonaqueous Ionizing Solvents*, pp. 79–193, Pergamon Press, Oxford, 1967. See also D. F. BUROW, Liquid sulfur dioxide, in J. J. LAGOWSKI (ed.), *Nonaqueous Solvents*, Vol. 3, pp. 138–85, Academic Press, New York, 1970.



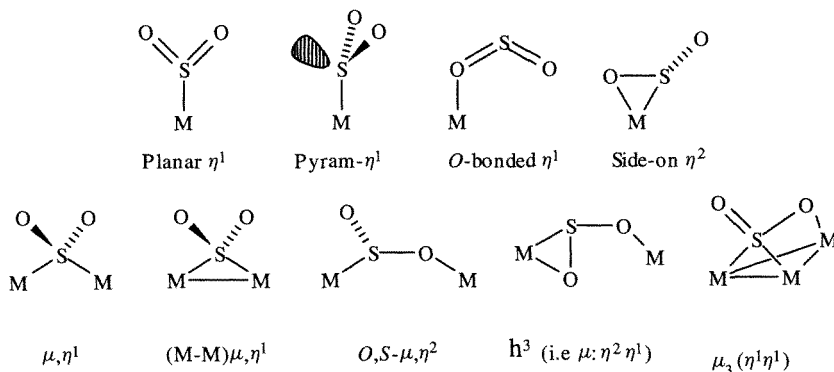
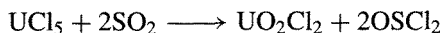
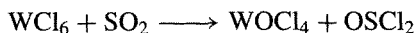
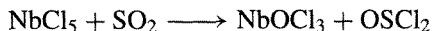


Figure 15.26 Various bonding modes of  $\text{SO}_2$  as a ligand.

the solvent is especially useful for carrying out a range of inorganic reactions. It is also an excellent solvent for proton nmr studies. In general, covalent compounds are very soluble: e.g.  $\text{Br}_2$ ,  $\text{ICl}$ ,  $\text{OSX}_2$ ,  $\text{BCl}_3$ ,  $\text{CS}_2$ ,  $\text{PCl}_3$ ,  $\text{OPCl}_3$  and  $\text{AsCl}_3$  are completely miscible, and most organic amines, ethers, esters, alcohols, mercaptans and acids are readily soluble. Many uni-univalent salts are moderately soluble, and those with ions such as the tetramethylammonium halides and the alkali metal iodides are freely so. The low dielectric constant of liquid  $\text{SO}_2$  leads to extensive ion-pair and ion-triplet formation but the solutions have limiting molar conductances in the range  $190\text{--}250 \text{ ohm}^{-1} \text{ cm}^2 \text{ mol}^{-1}$  at  $0^\circ$ . Solvate formation is exemplified by compounds such as  $\text{SnBr}_4 \cdot \text{SO}_2$  and  $2\text{TiCl}_4 \cdot \text{SO}_2$  (see below for  $\text{SO}_2$  as a ligand). Solvolysis reactions are also documented, e.g.:



Several other reaction types have also appeared in the literature but are sometimes purely formal schemes dating from the time when the solvent was (incorrectly) thought to undergo self-ionic dissociation into  $\text{SO}^{2+}$  and  $\text{SO}_3^{2-}$  or  $\text{SO}^{2+}$  and  $\text{S}_2\text{O}_5^{2-}$ . More recently it has been shown that, whereas neither  $\text{SO}_2$  nor  $\text{OSMe}_2$  (dmsO) react with first-row transition metals, the mixed solvent smoothly effects

dissolution of the metals with simultaneous oxidation of  $\text{S}^{\text{IV}}$  to  $\text{S}^{\text{VI}}$ , thereby enabling the production of crystalline solvated metal disulfates ( $\text{S}_2\text{O}_7^{2-}$ ) in high yield.<sup>(181)</sup> Examples are: colourless  $[\text{Ti}^{\text{IV}}(\text{OSMe}_2)_6][\text{S}_2\text{O}_7]_2$ , green  $[\text{V}^{\text{III}}(\text{OSMe}_2)_6][\text{S}_2\text{O}_7]_3$  and the salts  $[\text{M}^{\text{II}}(\text{OSMe}_2)_6][\text{S}_2\text{O}_7]$ , where  $\text{M} = \text{Mn}$  (yellow),  $\text{Fe}$  (pale green),  $\text{Co}$  (pale pink),  $\text{Ni}$  (green),  $\text{Cu}$  (pale blue),  $\text{Zn}$  (white) and  $\text{Cd}$  (white). This is by far the most convenient way to prepare pure disulfates. Dissolution of metals in  $\text{SO}_2$  mixed with other solvents such as dmf, dma, or hmpa also occurs, but in these cases there is no oxidation of the  $\text{S}^{\text{IV}}$ , and the product is usually the metal dithionite,  $\text{M}^{\text{II}}[\text{S}_2\text{O}_4]$ .

### Sulfur dioxide as a ligand

The coordination chemistry of  $\text{SO}_2$  has been extensively studied during the past two decades and at least 9 different bonding modes have been established.<sup>(166)</sup> These are illustrated schematically in Fig. 15.26 and typical examples are given in Table 15.17.<sup>(166,182)</sup> It is clear that nearly all the transition-metal complexes involve the metals in oxidation state zero or +1. Moreover,  $\text{SO}_2$  in the pyramidal  $\eta^1$ -clusters tends to be reversibly bound (being eliminated when

<sup>181</sup> W. D. HARRISON, J. B. GILL and D. C. GOODALL, *J. Chem. Soc., Dalton Trans.*, 847–50 (1979). See also *ibid.*, 2995–7 (1987); 728–9 (1988).

Table 15.17 Example of structurally characterized complexes containing SO<sub>2</sub>

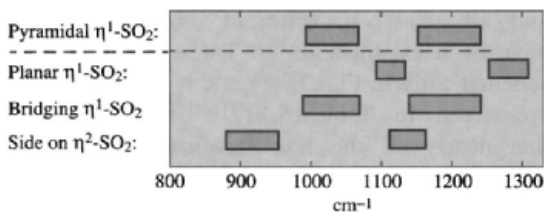
Planar $\eta^1$	Pyramidal $\eta^1$	O-bonded $\eta^1$	Side-on $\eta^2$
[Mn(C <sub>5</sub> H <sub>5</sub> )(CO) <sub>2</sub> (SO <sub>2</sub> )]	[RhCl(CO)(PPh <sub>3</sub> ) <sub>2</sub> (SO <sub>2</sub> )]	[SbF <sub>5</sub> (OSO)]	[Mo(CO) <sub>2</sub> (PMe <sub>3</sub> ) <sub>2</sub> ( $\eta^2$ -SO <sub>2</sub> )]
[RuCl(NH <sub>3</sub> ) <sub>4</sub> (SO <sub>2</sub> )]Cl	{[RhCl(PPh <sub>3</sub> ) <sub>2</sub> (SO <sub>2</sub> ) <sub>2</sub> ]}	{[Mg(OSO) <sub>2</sub> (AsF <sub>6</sub> ) <sub>2</sub> ] <sub>n</sub> }	[Mo(CO) <sub>2</sub> (bpy)( $\eta^2$ -SO <sub>2</sub> )]
[Os(CO)ClH(PCy <sub>3</sub> ) <sub>2</sub> (SO <sub>2</sub> )]	[IrCl(CO)(PPh <sub>3</sub> ) <sub>2</sub> (SO <sub>2</sub> )]	{[Ti( $\eta^6$ -C <sub>6</sub> H <sub>6</sub> )Cl <sub>4</sub> (OSO)] <sub>2</sub> }	[Mo( $\eta^2$ -S <sub>2</sub> CNEt <sub>2</sub> ) <sub>3</sub> ( $\eta^2$ -SO <sub>2</sub> )]
[Co(NO)(PPh <sub>3</sub> ) <sub>2</sub> (SO <sub>2</sub> )]	[Ir(SPh)(CO)- (PPh <sub>3</sub> ) <sub>2</sub> (SO <sub>2</sub> )]	[Mn(OPPh <sub>3</sub> ) <sub>4</sub> (OSO) <sub>2</sub> ] <sub>2</sub>	[RuCl( $\eta^2$ -S <sub>2</sub> CNEt <sub>2</sub> ) <sub>3</sub> ( $\eta^2$ -SO <sub>2</sub> )]
[Rh(C <sub>5</sub> H <sub>5</sub> )(C <sub>2</sub> H <sub>4</sub> )(SO <sub>2</sub> )]			[Rh(NO)( $\eta^2$ -S <sub>2</sub> CNEt <sub>2</sub> ) <sub>3</sub> - ( $\eta^2$ -SO <sub>2</sub> )]
[Ni(PPh <sub>3</sub> ) <sub>3</sub> (SO <sub>2</sub> )]	[Pt(PPh <sub>3</sub> ) <sub>3</sub> (SO <sub>2</sub> )]		
[Ni(PPh <sub>3</sub> ) <sub>2</sub> (SO <sub>2</sub> ) <sub>2</sub> ]	[Pt(PPh <sub>3</sub> ) <sub>2</sub> (SO <sub>2</sub> ) <sub>2</sub> ]		

Bridging $\eta^1$	M-M bridging $\eta^1$	Others
{[Fe(C <sub>5</sub> H <sub>5</sub> )(CO) <sub>2</sub> ] <sub>2</sub> ( $\mu$ -SO <sub>2</sub> )}	[Fe <sub>2</sub> (CO) <sub>8</sub> ( $\mu$ -SO <sub>2</sub> )]	<i>O,S</i> - $\mu$ - $\eta^2$ : [Rh <sub>2</sub> (PPh <sub>3</sub> ) <sub>4</sub> ( $\mu$ -Cl)- ( $\mu$ -OSO) <sub>2</sub> ] <sub>2</sub> (SO <sub>4</sub> )
{[Co( $\eta^5$ -C <sub>5</sub> H <sub>5</sub> )( $\mu$ -PR <sub>2</sub> ) <sub>2</sub> ] <sub>2</sub> ( $\mu$ SO <sub>2</sub> )}	[Fe <sub>2</sub> (C <sub>5</sub> H <sub>5</sub> ) <sub>2</sub> (CO) <sub>3</sub> ( $\mu$ -SO <sub>2</sub> )]	$\eta^3$ ( $\mu$ : $\eta^2$ $\eta^1$ ): {[Mo(CO) <sub>2</sub> (PPh <sub>3</sub> )- (py)( $\mu$ $\eta^3$ -SO <sub>2</sub> ) <sub>2</sub> ]. 2CH <sub>2</sub> Cl <sub>2</sub>
{[IrH(CO) <sub>2</sub> (PPh <sub>3</sub> ) <sub>2</sub> ] <sub>2</sub> ( $\mu$ -SO <sub>2</sub> )}	[Pd <sub>2</sub> Cl <sub>2</sub> (dpm) <sub>2</sub> ( $\mu$ -SO <sub>2</sub> )]	$\mu_3$ ( $\eta^1$ $\eta^1$ ): [Rh <sub>4</sub> ( $\mu$ -CO) <sub>4</sub> ( $\mu_3$ - SO <sub>2</sub> )[P(OPh) <sub>3</sub> ] <sub>4</sub> ]. $\frac{1}{2}$ C <sub>6</sub> H <sub>6</sub>
{[IrI(CO)(PPh <sub>3</sub> ) <sub>2</sub> ] <sub>2</sub> ( $\mu$ -SO <sub>2</sub> )}	[Pd <sub>3</sub> (CNBu <sup>t</sup> ) <sub>3</sub> ( $\mu$ -SO <sub>2</sub> ) <sub>2</sub> ]	[Pd <sub>5</sub> (PMe <sub>3</sub> ) <sub>5</sub> ( $\mu_2$ -SO <sub>2</sub> ) <sub>2</sub> - ( $\mu_3$ -SO <sub>2</sub> ) <sub>2</sub> ]
	[Pt <sub>3</sub> (PPh <sub>3</sub> ) <sub>3</sub> ( $\mu$ -SO <sub>2</sub> ) <sub>3</sub> ]	
	[Pt(PPh <sub>3</sub> ) <sub>3</sub> ( $\mu$ , $\eta^1$ -Ph)( $\mu$ - PPh <sub>2</sub> )( $\mu$ -SO <sub>2</sub> )]	

the complex is heated to <200° and recombining when the system is cooled to room temperature) whereas this tends not to be the case for the other bonding modes. Facile oxidation of the SO<sub>2</sub> by molecular O<sub>2</sub> to give coordinated sulfato complexes (SO<sub>4</sub><sup>2-</sup>) is also a characteristic of pyramidal  $\eta^1$ -SO<sub>2</sub> which is not shared by the other types.

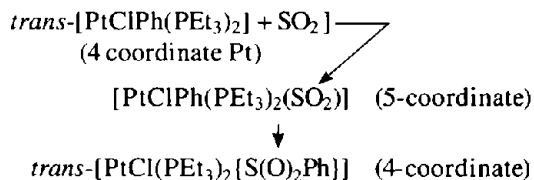
In the absence of X-ray crystallographic data vibrational spectroscopy can sometimes provide information concerning the mode of ligation, the position of the two  $\nu$ (SO) stretching modes in particular often providing a useful but not always reliable diagnostic.<sup>(182)</sup>



With such structural diversity it is perhaps not surprising that no certain method has been devised for theoretically predicting the mode of bonding to be expected in specific cases, although

plausible *post hoc* rationalization of the observed structure is sometimes possible.

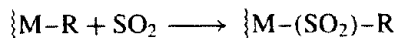
Sometimes coordination of SO<sub>2</sub> to an organometallic complex is followed by intramolecular insertion of SO<sub>2</sub> into the M-C  $\sigma$  bond, e.g.



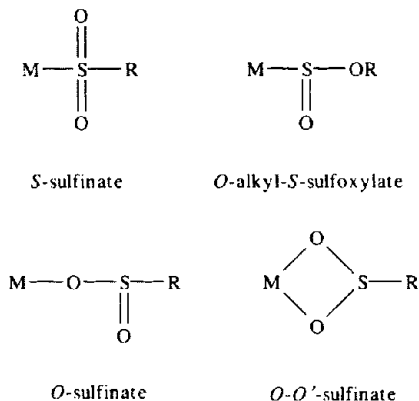
Intermolecular insertion of SO<sub>2</sub> can also occur (without prior formation of an isolable complex) and the general reaction can be represented by the equation:<sup>(183)</sup>

<sup>182</sup> G. J. KUBAS, *Inorg. Chem.* **18**, 182-8 (1979) and references therein. R. R. RYAN, G. J. KUBAS, D. C. MOODY and P. G. ELLER, *Structure and Bonding*, **46**, 47-100 (1981). More recent work can be found in the following references: J. SIELER *et al.* *Z. anorg. allg. Chem.* **549**, 171-6 (1987); E. WENSCHUH *et al.*, *Z. anorg. allg. Chem.* **600**, 55-60 (1991) and **603**, 21-4 (1991); E. SOLARI, C. FLORIANI and K. SCHENK, *J. Chem. Soc., Chem. Commun.*, 963-4 (1990); D. M. P. MINGOS *et al.* *J. Chem. Soc., Chem. Commun.*, 1048-9 (1988); *J. Chem. Soc., Dalton Trans.*, 1535-41 (1986); 1509-22 (1988); 261-8 (1992).

<sup>183</sup> A. WOJCIK, *Adv. Organomet. Chem.* **12**, 31-81 (1974).



where  $\{M$  represents a metal atom and its pendant ligands and R is an alkyl, aryl or related  $\sigma$ -bonded carbon group. The reaction is more flexible (though less important industrially) than the analogous carbonylation reaction of CO (p. 306) and can, in principle, lead to four different types of product:



Examples of all except possibly the second mode are known.

### Sulfur trioxide

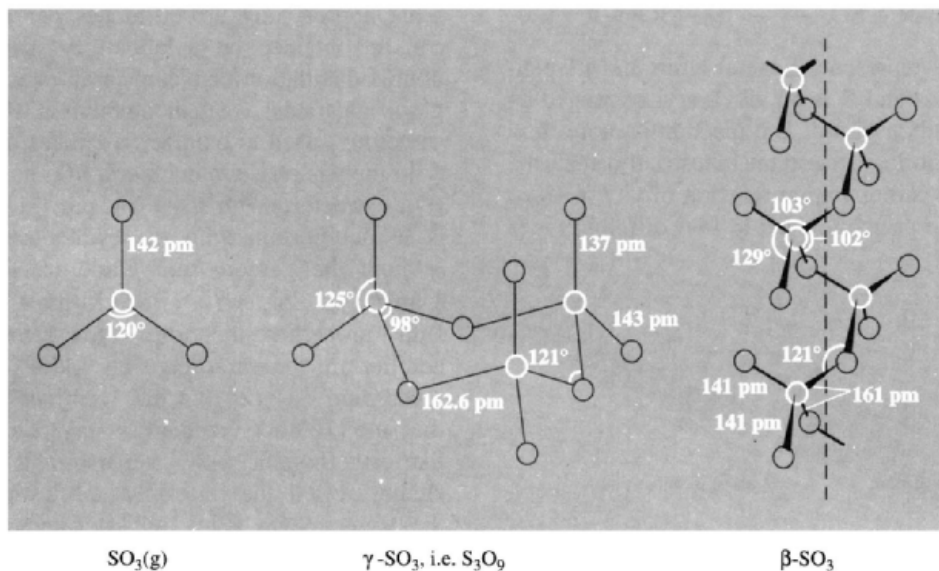
$SO_3$  is made on a huge scale by the catalytic oxidation of  $SO_2$  (p. 700): it is not usually isolated but is immediately converted to  $H_2SO_4$  (p. 708). It can also be obtained by the thermolysis of sulfates though rather high temperatures are required.  $SO_3$  is available commercially as a liquid: such samples contain small amounts (0.03–1.5%) of additives to inhibit polymerization. Typical additives are simple compounds of boron (e.g.  $B_2O_3$ ,  $B(OH)_3$ ,  $HBO_2$ ,  $BX_3$ ,  $MBF_4$ ,  $Na_2B_4O_7$ ), silica, siloxanes,  $SOCl_2$ , sulfonic acids, etc. The detailed mode of action of these additives remains obscure.  $SO_3$  is also readily available as fuming sulfuric acid (or oleum) which is a solution of 25–65%  $SO_3$  in  $H_2SO_4$  (p. 707). Because of its extremely aggressive reaction with most materials, pure anhydrous  $SO_3$  is difficult to handle although it is made in the USA (for example) on a

scale approaching 90 000 tonnes per annum. It can be obtained on a laboratory scale by the double distillation of oleum in an evacuated all-glass apparatus; a small amount of  $KMnO_4$  is sometimes used to oxidize any traces of  $SO_2$ .

In the gas phase, monomeric  $SO_3$  has a planar ( $D_{3h}$ ) structure with S–O 142 pm. This species is in equilibrium with the cyclic trimer  $S_3O_9$  in both the gaseous and liquid phases:  $K_p \approx 1 \text{ atm}^{-2}$  at  $25^\circ$ ,  $\Delta H^\circ \approx 125 \text{ kJ (mole } S_3O_9)^{-1}$ . Bulk properties therefore often refer to this equilibrium mixture, e.g. bp  $44.6^\circ\text{C}$ ,  $d(25^\circ)$   $1.903 \text{ g cm}^{-3}$ ,  $\eta(25^\circ)$  1.820 centipoise. Below the mp ( $16.86^\circ$ ), colourless crystals of ice-like orthorhombic  $\gamma$ - $SO_3$  separate and structural studies reveal that the only species present is the trimer  $S_3O_9$  (Fig. 15.27). Traces of water ( $10^{-3}$  mole%) lead to the rapid formation of glistening, white, needle-like crystals of  $\beta$ - $SO_3$  which is actually a mixture of fibrous, polymeric polysulfuric acids  $HO(SO_2O)_xH$ , where  $x$  is very large ( $\approx 10^3$ ). The helical chain structure of  $\beta$ - $SO_3$  is shown in Fig. 15.27 (cf. polyphosphates, p. 528). A third and still more stable form,  $\alpha$ - $SO_3$ , also requires traces of moisture or other polymerizing agent for its formation but involves some cross-linking between the chains to give a complex layer structure (mp  $62^\circ$ ). The standard enthalpies of formation ( $\Delta H_f^\circ/\text{kJ mol}^{-1}$ ) of the various forms of  $SO_3$  at  $25^\circ\text{C}$  are: gas  $-395.2$ , liquid  $-437.9$ ,  $\gamma$ -crystals  $-447.4$ ,  $\beta$ -crystals  $-449.6$ ,  $\alpha$ -solid  $-462.4$ .

$SO_3$  reacts vigorously and extremely exothermically with water to give  $H_2SO_4$ . Substoichiometric amounts yield oleums and mixtures of various polysulfuric acids (p. 712). Hydrogen halides give the corresponding halogenosulfuric acids  $HSO_3X$ .  $SO_3$  extracts the elements of  $H_2O$  from carbohydrates and other organic matter leaving a carbonaceous char. It acts as a strong Lewis acid towards a wide variety of inorganic and organic ligands to give adducts: e.g. oxides give  $SO_4^{2-}$ ,  $Ph_3P$  gives  $Ph_3P \cdot SO_3$  (with a rather long P–S bond, 217.6 pm)<sup>(184)</sup>

<sup>184</sup> R. L. BEDDOES and O. S. MILLS, *J. Chem. Research* (M) 2772–89 (1981); (S) 233 (1981); see also *J. Chem. Soc., Chem. Commun.*, 789–90 (1981).

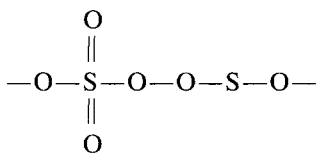


**Figure 15.27** Structure of the monomeric, trimeric and chain-polymeric forms of sulfur trioxide.

$\text{Ph}_3\text{AsO}$  gives  $\text{Ph}_3\text{AsO}\cdot\text{SO}_3$  etc. Frequently further reaction ensues: thus, under various conditions reaction with  $\text{NH}_3$  yields  $\text{H}_2\text{NSO}_3\text{H}$ ,  $\text{HN}(\text{SO}_3\text{H})_2$ ,  $\text{HN}(\text{SO}_3\text{NH}_4)_2$ ,  $\text{NH}_4\text{N}(\text{SO}_3\text{NH}_4)_2$ , etc.  $\text{SO}_3$  can also act as a ligand towards strong electron-pair acceptors such as  $\text{AsF}_3$ ,  $\text{SbF}_3$  and  $\text{SbCl}_3$ . It is reduced to  $\text{SO}_2$  by activated charcoal or by metal sulfides. The reaction with metal oxides (particularly  $\text{Fe}_3\text{O}_4$ ) to give sulfates is used industrially to rid stack-gases of unwanted byproduct  $\text{SO}_3$ .

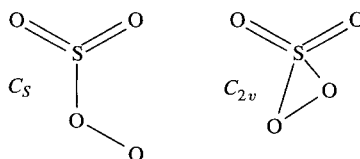
### Higher oxides

The reaction of gaseous  $\text{SO}_2$  or  $\text{SO}_3$  with  $\text{O}_2$  in a silent electric discharge gives colourless polymeric condensates of composition  $\text{SO}_{3+x}$  ( $0 < x < 1$ ). These materials are derived from  $\beta\text{-SO}_3$  by random substitution of oxo-bridges by peroxy-bridges:



Hydrolysis of the polymers yields  $\text{H}_2\text{SO}_4$  and  $\text{H}_2\text{SO}_5$  (p. 712), with  $\text{H}_2\text{O}_2$  and  $\text{O}_2$  as secondary products.

Monomeric neutral  $\text{SO}_4$  can be obtained by reaction of  $\text{SO}_3$  and atomic oxygen; photolysis of  $\text{SO}_3$ /ozone mixtures also yields monomeric  $\text{SO}_4$ , which can be isolated by inert-gas matrix techniques at low temperatures (15–78 K). Vibration spectroscopy indicates either an open peroxy  $C_s$  structure or a closed peroxy  $C_{2v}$  structure, the former being preferred by the most recent study, on the basis of agreement between observed and calculated frequencies and reasonable values for the force constants:<sup>(185)</sup>



The compound decomposes spontaneously below room temperature.

<sup>185</sup> P. LA BONVILLE, R. KUGEL, and J. R. FERRARO, *J. Chem. Phys.* **67**, 1477–81 (1977).

Table 15.18 Oxoacids of sulfur

Formula	Name	Ox. states	Schematic structure*	Salt
H <sub>2</sub> SO <sub>4</sub>	sulfuric	VI		sulfate, SO <sub>4</sub> <sup>2-</sup> H-sulfate, HOSO <sub>3</sub> <sup>-</sup>
H <sub>2</sub> S <sub>2</sub> O <sub>7</sub>	disulfuric	VI		disulfate, O <sub>3</sub> SOSO <sub>3</sub> <sup>2-</sup>
H <sub>2</sub> S <sub>2</sub> O <sub>3</sub>	thiosulfuric	IV, 0, (or VI, -II)		thiosulfate, SSO <sub>3</sub> <sup>2-</sup>
H <sub>2</sub> SO <sub>5</sub>	peroxomonosulfuric	VI		peroxomonosulfate, OOSO <sub>3</sub> <sup>2-</sup>
H <sub>2</sub> S <sub>2</sub> O <sub>8</sub>	peroxodisulfuric	VI		peroxodisulfate, O <sub>3</sub> SOOSO <sub>3</sub> <sup>2-</sup>
H <sub>2</sub> S <sub>2</sub> O <sub>6</sub>	dithionic*	V		dithionate, O <sub>3</sub> SSO <sub>3</sub> <sup>2-</sup>
H <sub>2</sub> S <sub>n+2</sub> O <sub>6</sub>	polythionic	V, 0		polythionate, O <sub>3</sub> S(S) <sub>n</sub> SO <sub>3</sub> <sup>2-</sup>
H <sub>2</sub> SO <sub>3</sub>	sulfurous*	IV		sulfite, SO <sub>3</sub> <sup>2-</sup> H-sulfite, HOSO <sub>2</sub> <sup>-</sup>
H <sub>2</sub> S <sub>2</sub> O <sub>5</sub>	disulfurous*	V, III		disulfite, O <sub>3</sub> SSO <sub>2</sub> <sup>2-</sup>
H <sub>2</sub> S <sub>2</sub> O <sub>4</sub>	dithionous*	III		dithionite, O <sub>2</sub> SSO <sub>2</sub> <sup>2-</sup>

\*Acids marked with an asterisk do not exist in the free state but are known as salts.

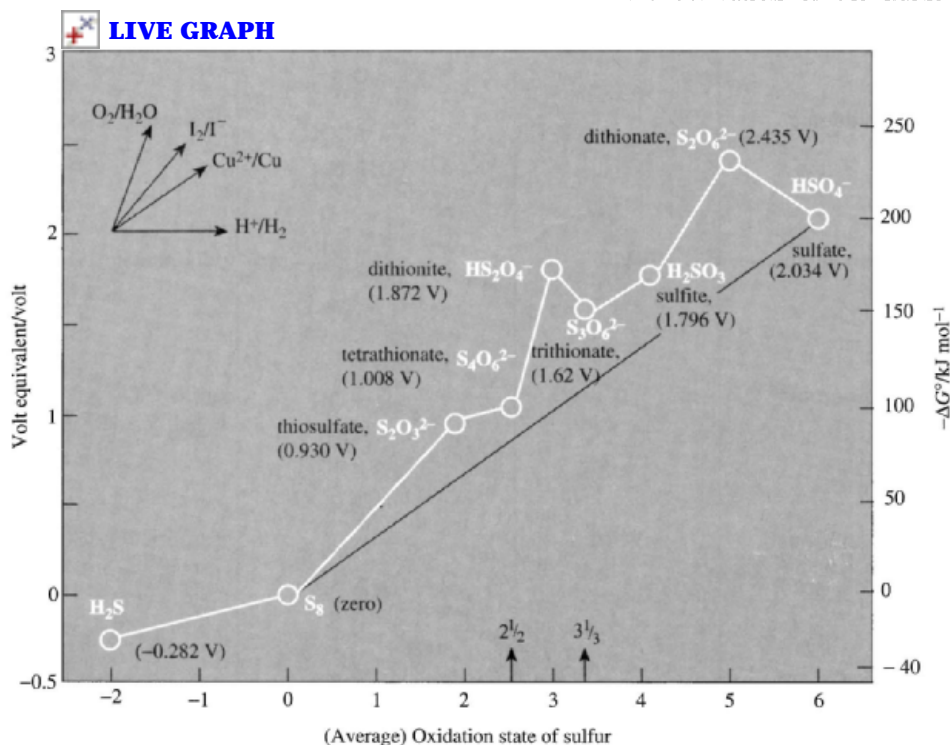
### 15.2.6 Oxoacids of sulfur

Sulfur, like nitrogen and phosphorus, forms many oxoacids though few of these can be isolated as the free acid and most are known either as aqueous solutions or as crystalline salts of the corresponding oxoacid anions. Sulfuric acid,  $\text{H}_2\text{SO}_4$ , is the most important of all industrial chemicals and is manufactured on an enormous scale, greater than for any other compound of any element (p. 407). Other compounds, such as thiosulfates, sulfites, disulfites and dithionites, are valuable reducing agents with a wide variety of applications. Nomenclature is somewhat confusing but is summarized in Table 15.18 which also gives an indication of the various oxidation states of S and a schematic representation of the structures. Previously claimed species such as "sulfoxylic acid" ( $\text{H}_2\text{SO}_2$ ), "thiosulfurous acid" ( $\text{H}_2\text{S}_2\text{O}_2$ ), and their salts are now thought not to exist.

**Table 15.19** Some standard reduction potentials of sulfur species ( $25^\circ$ , pH 0)

Couple	$E^\circ/V$
$2\text{H}_2\text{SO}_3 + \text{H}^+ + 2\text{e}^- \rightleftharpoons \text{HS}_2\text{O}_4^- + 2\text{H}_2\text{O}$	-0.082
$\text{S} + 2\text{H}^+ + 2\text{e}^- \rightleftharpoons \text{H}_2\text{S}$	+0.142
$\text{HSO}_4^- + 7\text{H}^+ + 6\text{e}^- \rightleftharpoons \text{S} + 4\text{H}_2\text{O}$	0.339
$\text{H}_2\text{SO}_3 + 4\text{H}^+ + 4\text{e}^- \rightleftharpoons \text{S} + 3\text{H}_2\text{O}$	0.449
$\text{S}_2\text{O}_3^{2-} + 6\text{H}^+ + 4\text{e}^- \rightleftharpoons 2\text{S} + 3\text{H}_2\text{O}$	0.465
$4\text{H}_2\text{SO}_3 + 4\text{H}^+ + 6\text{e}^- \rightleftharpoons \text{S}_4\text{O}_6^{2-} + 6\text{H}_2\text{O}$	0.509
$\text{S}_2\text{O}_6^{2-} + 4\text{H}^+ + 2\text{e}^- \rightleftharpoons 2\text{H}_2\text{SO}_3$	0.564
$\text{S}_2\text{O}_8^{2-} + 2\text{H}^+ + 2\text{e}^- \rightleftharpoons 2\text{HSO}_4^-$	2.123

Many of the sulfur oxoacids and their salts are connected by oxidation-reduction equilibria: some of the more important standard reduction potentials are summarized in Table 15.19 and displayed in graphic form as a volt-equivalent diagram (p. 435) in Fig. 15.28. By use of the couples in Table 15.19 data for many other oxidation-reduction equilibria can readily be calculated. (Indeed, it is an instructive exercise to check the derivation of the numerical data

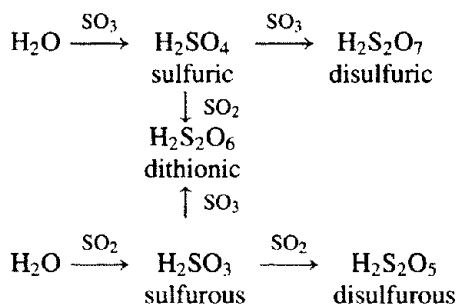


**Figure 15.28** Volt-equivalent diagram for sulfur-containing species in acid solution.

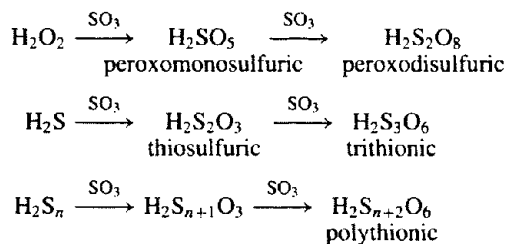
given in parentheses in Fig. 15.28 from the data given in Table 15.19 and to calculate the standard reduction potentials of other couples, e.g.  $\text{HSO}_4^-/\text{H}_2\text{S}$  0.289 V,  $\text{HSO}_4^-/\text{H}_2\text{SO}_3$  0.119 V,  $\text{H}_2\text{SO}_3/\text{S}_2\text{O}_3^{2-}$  0.433 V, etc.) Several important points emerge which are immediately apparent from inspection of Fig. 15.28. For example, it is clear that, in acid solutions, the gradient between  $\text{H}_2\text{S}$  and  $\text{S}_8$  is less than between  $\text{S}_8$  and any positive oxidation state, so that  $\text{H}_2\text{S}$  is thermodynamically able to reduce any oxoacid of sulfur to the element. Again, as all the intermediate oxoacids lie above the line joining  $\text{HSO}_4^-$  and  $\text{S}_8$ , it follows that all can ultimately disproportionate into sulfuric acid and the element. Similarly, any moderately powerful oxidizing agent should be capable of oxidizing the intermediate oxoacids to sulfuric acid (sometimes with concurrent precipitation of sulfur) though by suitable choice of conditions it is often possible to obtain kinetically stable intermediate oxidation states (e.g. the polythionates with the stable S-S linkages). It follows that all the oxoacids except  $\text{H}_2\text{SO}_4$  are moderately strong reducing agents (see below).

The formal interrelationship between the various oxoacids of sulfur can also be illustrated in a scheme<sup>(186)</sup> which places less emphasis on oxidation-reduction reactions but which is useful in suggesting possible alternative synthetic routes

to these oxoacids. Thus successive addition of  $\text{SO}_3$  or  $\text{SO}_2$  to  $\text{H}_2\text{O}$  can be represented by the scheme:



Likewise addition of  $\text{SO}_3$  to  $\text{H}_2\text{O}_2$ ,  $\text{H}_2\text{S}$  and  $\text{H}_2\text{S}_n$  generates the formulae of the other oxoacids as follows:



It should be emphasized that not all the processes in these schemes represent viable syntheses, and other routes are frequently preferred. The following sections give a fuller discussion of the individual oxoacids and their salts.

<sup>186</sup> M. SCHMIDT and W. SIEBERT. Oxyacids of sulfur, Section 2.4 in *Comprehensive Inorganic Chemistry*, Vol. 2, Chapter 23, pp. 868-98, Pergamon Press, Oxford, 1973.

<sup>187</sup> R. L. KUCZKOWSKI, R. D. SUENRAM and F. J. LOVAS, *J. Am. Chem. Soc.* **103**, 2561-6 (1981).

**Table 15.20** Some physical properties of anhydrous  $\text{H}_2\text{SO}_4$  and  $\text{D}_2\text{SO}_4$ <sup>(a)</sup>

Property	$\text{H}_2\text{SO}_4$	$\text{D}_2\text{SO}_4$
MP/°C	10.371	14.35
BP/°C	~300 (decomp)	—
Density(25°)/g cm <sup>-3</sup>	1.8267	1.8572
Viscosity(25°)/centipoise	24.55	24.88
Dielectric constant $\epsilon$	100	—
Specific conductivity $\kappa$ (25°)/ohm <sup>-1</sup> cm <sup>-1</sup>	$1.0439 \times 10^{-2}$	$0.2832 \times 10^{-2}$

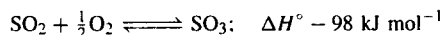
<sup>(a)</sup>In the gas phase  $\text{H}_2\text{SO}_4$  and  $\text{D}_2\text{SO}_4$  adopt the  $C_2$  conformation with r(O-H) 97 pm, r(S-OH) 157.4 pm, r(S-O) 142.2 pm; the various interatomic and dihedral angles were also determined and the molecular dipole moment calculated to be 2.73 D.<sup>(187)</sup>

## Industrial Manufacture of Sulfuric Acid

Sulfuric acid is the world's most important industrial chemical and is the cheapest bulk acid available in every country of the world. It was one of the first chemicals to be produced commercially in the USA (by John Harrison, Philadelphia, 1793); in Europe the history of its manufacture goes back even further — by at least two centuries.<sup>(188,189)</sup> Concentrated sulfuric acid ("oil of vitriol") was first made by the distillation of "green vitriol",  $\text{FeSO}_4 \cdot n\text{H}_2\text{O}$  and was needed in quantity to make  $\text{Na}_2\text{SO}_4$  from  $\text{NaCl}$  for use in the Leblanc Process (p. 71). This expensive method was replaced in the early eighteenth century by the burning of sulfur and Chile saltpetre ( $\text{NaNO}_3$ ) in the necks of large glass vessels containing a little water. The process was patented in 1749 by Joshua Ward (the Quack of Hogarth's *Harlot's Progress*) though it had been in use for several decades previously in Germany, France and England. The price plummeted 20-fold from £2 to 2 shillings per pound. It dropped by a further factor of 10 by 1830 following firstly John Roebuck's replacement (*ca.* 1755) of the fragile glass jars by lead-chambers of 200 ft<sup>3</sup> (5.7 m<sup>3</sup>) capacity, and, secondly, the discovery (by N. Clement and C. B. Désormes in 1793) that the amount of  $\text{NaNO}_3$  could be substantially reduced by admitting air for the combustion of sulfur. By 1860 James Muspratt (UK) was using lead chambers of 56 000 ft<sup>3</sup> capacity (1585 m<sup>3</sup>) and the process was continuous. The maximum concentration of acid that could be produced by this method was about 78% and until 1870 virtually the only source of oleum was the Nordhausen works (distillation of  $\text{FeSO}_4 \cdot n\text{H}_2\text{O}$ ). Today both processes have been almost entirely replaced by the modern contact process. This derives originally from Peregrine Philips' observation (patented in 1831) that  $\text{SO}_2$  can be oxidized to  $\text{SO}_3$  by air in the presence of a platinum catalyst.

The modern process uses a potassium-sulfate-promoted vanadium(V) oxide catalyst on a silica or kieselguhr support.<sup>(190)</sup> The  $\text{SO}_2$  is obtained either by burning pure sulfur or by roasting sulfide minerals (p. 651) notably iron pyrite, or ores of Cu, Ni and Zn during the production of these metals. On a worldwide basis about 65% of the  $\text{SO}_2$  comes from the burning of sulfur and some 35% by the roasting of sulfide ores but in some countries (e.g. the UK) over 95% comes from the former.

The oxidation of  $\text{SO}_2$  to  $\text{SO}_3$  is exothermic and reversible:



According to le Chatelier's principle the *yield* of  $\text{SO}_3$  will increase with increase in pressure, increase in excess  $\text{O}_2$  concentration, and removal of  $\text{SO}_3$  from the reaction zone; each of these factors will also increase the *rate* of conversion somewhat (by the law of mass action). Reaction rate will also increase substantially with increase in temperature but this will simultaneously decrease the yield of the exothermic forward reaction. Accordingly, a catalyst is required to accelerate the reaction without diminishing the yield. Optimum conditions involve an equimolar feed of  $\text{O}_2/\text{SO}_2$  (i.e. air/ $\text{SO}_2$ :5/1) and a 4-stage catalytic converter operating at the temperatures shown in the Figure.<sup>(123)</sup> (The  $\text{V}_2\text{O}_5$  catalyst is inactive below 400°C and breaks down above 620°C; it is dispersed as a thin film of molten salt on the catalyst support.) Such a converter may be 13 m high, 9 m in diameter, contain 80 tonnes of catalyst pellets and produce 500 tonnes per day of acid. The gas temperature rises during passage through the catalyst bed and is recooled by passage through external heat-exchanger loops between the first three stages. In the most modern "double-absorption" plants (IPA) the  $\text{SO}_3$  is removed at this stage before the residual  $\text{SO}_2/\text{O}_2$  is passed through a fourth catalyst bed for final conversion. The  $\text{SO}_3$  gas cannot be absorbed directly in water because it would first come into contact with the water-vapour above the absorber and so produce a stable mist of fine droplets of  $\text{H}_2\text{SO}_4$  which would then pass right through the absorber and out into the atmosphere. Instead, absorption is effected by 98%  $\text{H}_2\text{SO}_4$  in ceramic-packed towers and sufficient water is added to the circulating acid to maintain the required concentration. Commercial conc  $\text{H}_2\text{SO}_4$  is generally 96–98% to prevent undesirable solidification of the product. The main construction materials of the sulfur burner, catalytic converter, absorption towers and ducting are mild steel and stainless steel, and the major impurity in the acid is therefore  $\text{Fe}^{\text{II}}$  (10 ppm) together with traces of  $\text{SO}_2$  and  $\text{NO}_x$ .

Some idea of the accelerating demand for sulfuric acid can be gained from the following UK production figures:

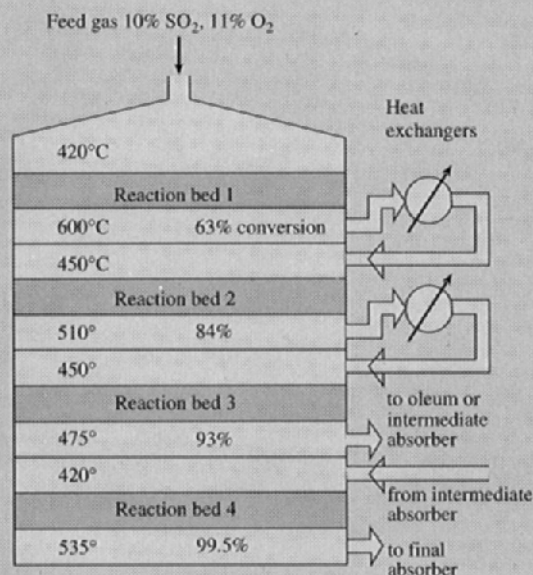
Year	1860	1870	1880	1890	1900	1917	1960	1980
10 <sup>3</sup> tonnes	260	560	900	870	1100	1400	2750	4750

<sup>188</sup>T. K. DERRY and T. I. WILLIAMS, *A Short History of Technology from the Earliest Times to AD 1900*, pp. 268, and 534–5, Oxford University Press, Oxford, 1960.

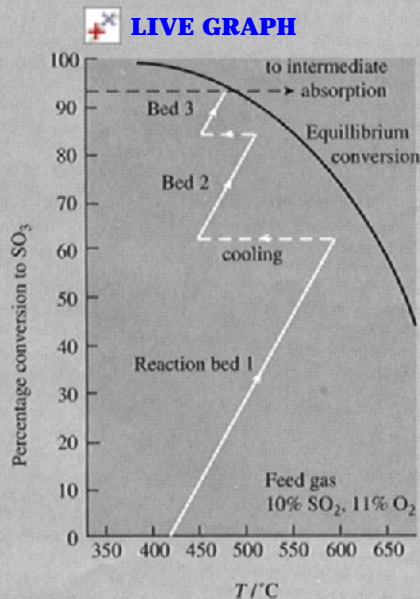
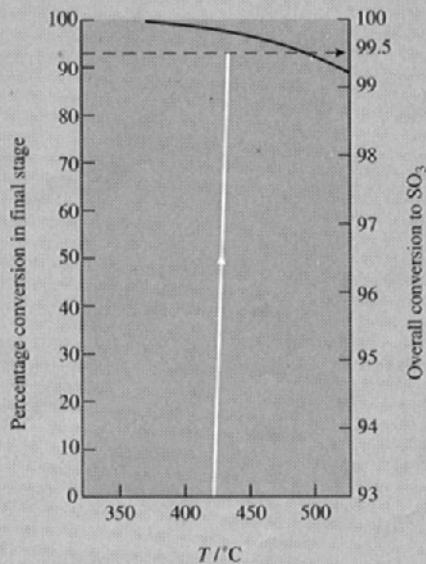
<sup>189</sup>L. F. HABER, *The Chemical Industry During the Nineteenth Century*, Oxford University Press, Oxford, 1958, 292 pp; L. F. HABER, *The Chemical Industry 1900–1930*, Oxford University Press, Oxford, 1971, 452 pp.

<sup>190</sup>A. PHILLIPS, in R. THOMPSON (ed.), *The Modern Inorganic Chemicals Industry*, pp. 183–200, The Chemical Society, London, 1977. See also W. BÜCHNER, R. SCHLIEBS, G. WINTER and K. H. BÜCHEL, *Industrial Inorganic Chemistry*, VCH Publishers, New York, pp. 108–20 (1989).





Schematic diagram of converter

Conversion versus temperature  
— first stage.Conversion versus temperature  
— final stage (reaction bed 4).

Double absorption (IPA) sulfuric acid plant.

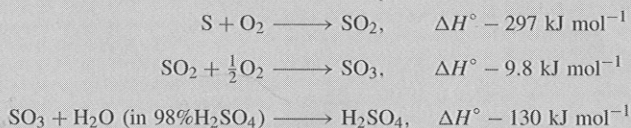
Figures for France, Germany and the USA were lower than these until the turn of the century, but then the USA began to outstrip the rest. At about the same time superphosphate manufacture overtook the Leblanc soda process as the main user of H<sub>2</sub>SO<sub>4</sub>. H<sub>2</sub>SO<sub>4</sub> production is now often taken as a reliable measure of a nation's industrial strength because it enters into so many industrial and manufacturing processes. Thus in 1900 production was equivalent to 4.05 million tonnes of 100% H<sub>2</sub>SO<sub>4</sub> distributed as follows (%):

UK	USA	Germany	France	Austria	Belgium	Russia	Japan
25.9	23.2	21.0	15.5	4.9	4.0	3.1	1.2

By 1976 world production was 113 million tonnes and the distribution changed to the following (%):

USA	USSR	Japan	Germany	France	Poland	UK	Canada	Spain	Italy	Others
25.6	17.7	5.4	4.1	3.5	3.2	2.9	2.8	2.5	2.4	29.9

This had increased to 145 million tonnes by 1986 (Europe 44%, USA/Canada 24%, Asia/Oceania 18%, Africa 9%, Latin America 5%). Such vast quantities require huge plants: these frequently have a capacity in excess of 2000 tonnes per day in the USA but are more commonly in the range 300–750 tonnes per day in Europe and smaller still in less industrialized countries. Even so, the energy flows are enormous as can be appreciated by scaling up the following reactions:



For example, the oxidation of S to SO<sub>3</sub> liberates nearly  $4 \times 10^9$  J per tonne of H<sub>2</sub>SO<sub>4</sub> of which ~3 GJ can be sold as energy in the form of steam and much of the rest used to pump materials around the plant, etc. A plant producing 750 tonnes per day of H<sub>2</sub>SO<sub>4</sub> produces ~25 MW of byproduct thermal energy, equivalent to ~7 MW of electricity if the steam is used to drive generators. Effective utilization of this energy is an important factor in minimizing the cost of sulfuric acid which remains a remarkably cheap commodity despite inflation (of the order of \$150 per tonne in 1994).

Environmental legislation in the USA requires that sulfur emitted from the stack (SO<sub>2</sub> and persistent H<sub>2</sub>SO<sub>4</sub> mist) must not exceed 0.3% of the sulfur burned (0.5% in the UK). Despite this, because of the vast scale of the industry, large quantities of unconverted SO<sub>2</sub> are vented to the atmosphere each year (say 0.3% of  $145 \times 10^6$  tonnes  $\times \frac{64}{98} = 284\,000$  tonnes SO<sub>2</sub> pa). It is a testament to the efficiency of the process that this represents a global impact of only some 780 tonnes SO<sub>2</sub> per day, which is minute compared with other sources of this pollution (p. 698).

The pattern of use of H<sub>2</sub>SO<sub>4</sub> varies from country to country and from decade to decade. Current US usage is dominated by fertilizer production (70%) followed by chemical manufacture, metallurgical uses, and petroleum refining (~5% each). In the UK the distribution of uses is more even: only 30% of the H<sub>2</sub>SO<sub>4</sub> manufactured is used in the fertilizer industry but 18% goes on paints, pigments and dyestuff intermediates, 16% on chemicals manufacture, 12% on soaps and detergents, 10% on natural and manmade fibres, and 2.5% on metallurgical applications.

## Sulfuric acid, H<sub>2</sub>SO<sub>4</sub>

Anhydrous sulfuric acid is a dense, viscous liquid which is readily miscible with water in all proportions: the reaction is extremely exothermic (~880 kJ mol<sup>-1</sup> at infinite dilution) and can result in explosive spattering of the mixture if the water is added to the acid; it is therefore important always to use the reverse order and add the acid to the water, slowly and with stirring. The large-scale preparation of sulfuric acid is a major industry in most countries and is described in the preceding Panel.

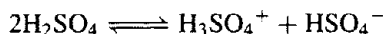
Some physical properties of anhydrous H<sub>2</sub>SO<sub>4</sub> (and D<sub>2</sub>SO<sub>4</sub>) are in Table 15.20 (p. 707).<sup>(191,192)</sup> In addition, several congruently melting hydrates,

H<sub>2</sub>SO<sub>4</sub>·*n*H<sub>2</sub>O, are known with *n* = 1, 2, 3, 4 (mps 8.5°, -39.5°, -36.4° and -28.3°, respectively). Other compounds in the H<sub>2</sub>O/SO<sub>3</sub> system are H<sub>2</sub>S<sub>2</sub>O<sub>7</sub> (mp 36°) and H<sub>2</sub>S<sub>4</sub>O<sub>13</sub> (mp 4°). Anhydrous H<sub>2</sub>SO<sub>4</sub> is a remarkable compound with an unusually high dielectric constant, and a very high electrical conductivity which results from the ionic self-dissociation (autoprotolysis) of the compound coupled with a proton-switch mechanism for the rapid

<sup>191</sup> R. J. GILLESPIE and E. A. ROBINSON, *Sulfuric acid*, Chap. 4 in T. C. WADDINGTON (ed.), *Nonaqueous Solvent Systems*, pp. 117–210, Academic Press, London, 1965. A definitive review with some 250 references.

<sup>192</sup> N. N. GREENWOOD and A. THOMPSON, *J. Chem. Soc.* 3474–84 (1959).

conduction of current through the viscous H-bonded liquid. For example, at 25° the single-ion conductances for  $\text{H}_3\text{SO}_4^+$  and  $\text{HSO}_4^-$  are 220 and 150 respectively, whereas those for  $\text{Na}^+$  and  $\text{K}^+$  which are viscosity-controlled are only 3–5. Anhydrous  $\text{H}_2\text{SO}_4$  thus has many features in common with anhydrous  $\text{H}_3\text{PO}_4$  (p. 518) but the equilibria are reached much more rapidly (almost instantaneously) in  $\text{H}_2\text{SO}_4$ :



$$K_{\text{ap}}(25^\circ) = [\text{H}_3\text{SO}_4^+][\text{HSO}_4^-] = 2.7 \times 10^{-4}$$

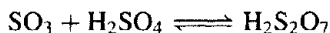
This value is compared with those for other acids and protonic liquids in Table 15.21.<sup>(191)</sup> the extent of autoprotolysis in  $\text{H}_2\text{SO}_4$  is greater than that in water by a factor of more than  $10^{10}$  and is exceeded only by anhydrous  $\text{H}_3\text{PO}_4$  and  $[\text{HBF}_3(\text{OH})]$  (p. 198). In addition to autoprotolysis,  $\text{H}_2\text{SO}_4$  undergoes ionic self-dehydration:



This arises from the primary dissociation of  $\text{H}_2\text{SO}_4$  into  $\text{H}_2\text{O}$  and  $\text{SO}_3$  which then react with further  $\text{H}_2\text{SO}_4$  as follows:



$$K_{\text{H}_2\text{O}}(25^\circ) = [\text{H}_3\text{O}^+][\text{HSO}_4^-]/[\text{H}_2\text{O}] \sim 1$$



$$K_{\text{H}_2\text{S}_2\text{O}_7}(25^\circ) = [\text{H}_3\text{SO}_4^+][\text{HS}_2\text{O}_7^-]/[\text{H}_2\text{S}_2\text{O}_7] \\ = 1.4 \times 10^{-2}$$

It is clear that “pure” anhydrous sulfuric acid, far from being a single substance in the bulk liquid phase, comprises a dynamic equilibrium involving at least seven well-defined species. The

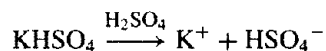
concentration of the self-dissociation products in  $\text{H}_2\text{SO}_4$  and  $\text{D}_2\text{SO}_4$  at 25° (expressed in millimoles of solute per kg solvent) are:

$\text{HSO}_4^-$	$\text{H}_3\text{SO}_4^+$	$\text{H}_3\text{O}^+$	$\text{HS}_2\text{O}_7^-$	$\text{H}_2\text{S}_2\text{O}_7$	$\text{H}_2\text{O}$	Total
15.0	11.3	8.0	4.4	3.6	0.1	42.4
$\text{DSO}_4^-$	$\text{D}_3\text{SO}_4^+$	$\text{D}_3\text{O}^+$	$\text{DS}_2\text{O}_7^-$	$\text{D}_2\text{S}_2\text{O}_7$	$\text{D}_2\text{O}$	Total
11.2	4.1	11.2	4.9	7.1	0.6	39.1

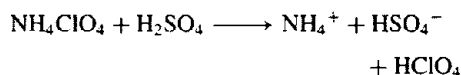
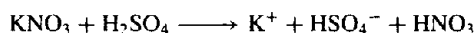
As the molecular weight of  $\text{H}_2\text{SO}_4$  is 98.078 it follows that 1 kg contains 10.196 mol; hence the predominant ions are present to the extent of about 1 millimole per mole of  $\text{H}_2\text{SO}_4$  and the total concentration of species in equilibrium with the parent acid is 4.16 millimole per mole. Many of the physical and chemical properties of anhydrous  $\text{H}_2\text{SO}_4$  as a nonaqueous solvent stem from these equilibria.

In the sulfuric acid solvent system, compounds that enhance the concentration of the solvo-cation  $\text{HSO}_4^-$  will behave as bases and those that give rise to  $\text{H}_3\text{SO}_4^+$  will behave as acids (p. 425). Basic solutions can be formed in several ways of which the following examples are typical:

- (a) Dissolution of metal hydrogen sulfates:



- (b) Solvolysis of salts of acids that are weaker than  $\text{H}_2\text{SO}_4$ :



- (c) Protonation of compounds with lone-pairs of electrons:

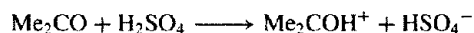
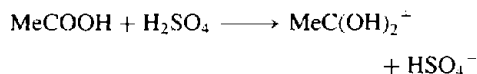
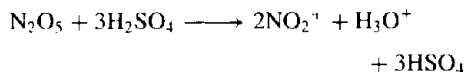
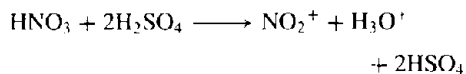


Table 15.21 Autoprotolysis constants at 25°

Compound	$-\log K_{\text{ap}}$	Compound	$-\log K_{\text{ap}}$	Compound	$-\log K_{\text{ap}}$
$\text{HBF}_3(\text{OH})$	$\sim -1$	$\text{HCO}_2\text{H}$	6.2	$\text{H}_2\text{O}_2$	12
$\text{H}_3\text{PO}_4$	$\sim 2$	$\text{HF}$	9.7	$\text{H}_2\text{O}$	14.0
$\text{H}_2\text{SO}_4$	3.6	$\text{MeCO}_2\text{H}$	12.6	$\text{D}_2\text{O}$	14.8
$\text{D}_2\text{SO}_4$	4.3	$\text{EtOH}$	18.9	$\text{NH}_3$	29.8



(d) Dehydration reactions:

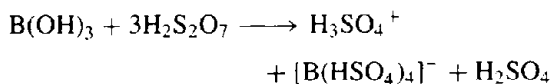


The reaction with  $\text{HNO}_3$  is quantitative, and the presence of large concentrations of the nitronium ion,  $\text{NO}_2^+$ , in solutions of  $\text{HNO}_3$ ,  $\text{MNO}_3$  and  $\text{N}_2\text{O}_5$  in  $\text{H}_2\text{SO}_4$  enable a detailed interpretation to be given of the nitration of aromatic hydrocarbons by these solutions.

Because of the high acidity of  $\text{H}_2\text{SO}_4$  itself, bases form the largest class of electrolytes and only few acids (proton donors) are known in this solvent system. As noted above,  $\text{H}_2\text{S}_2\text{O}_7$  acts as a proton donor to  $\text{H}_2\text{SO}_4$  and  $\text{HSO}_3\text{F}$  is also a weak acid:



One of the few strong acids is tetra(hydrogen sulfato)boric acid  $\text{B}(\text{HSO}_4)_4$ ; solutions of this can be obtained by dissolving boric acid in oleum:



Other strong acids are  $\text{H}_2\text{Sn}(\text{HSO}_4)_6$  and  $\text{H}_2\text{Pb}(\text{HSO}_4)_6$ .

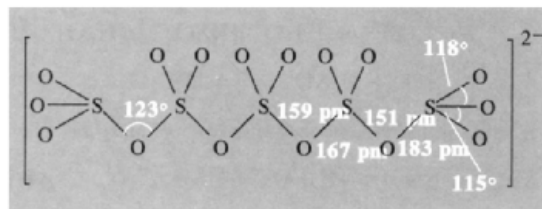
Sulfuric acid forms salts (sulfates and hydrogen sulfates) with many metals. These are frequently very stable and, indeed, they are the most important mineral compounds of several of the more electropositive elements. They have been discussed in detail under the appropriate elements. Sulfates can be prepared by:

- dissolution of metals in aqueous  $\text{H}_2\text{SO}_4$  (e.g. Fe);
- neutralization of aqueous  $\text{H}_2\text{SO}_4$  with metal oxides or hydroxides (e.g.  $\text{MOH}$ );
- decomposition of salts of volatile acids (e.g. carbonates) with aqueous  $\text{H}_2\text{SO}_4$ ;

- metathesis between a soluble sulfate and a soluble salt of the metal whose (insoluble) sulfate is required (e.g.  $\text{BaSO}_4$ );
- oxidation of metal sulfides or sulfites.

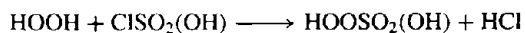
The sulfate ion is tetrahedral ( $\text{S}-\text{O}$  149 pm) and can act as a monodentate, bidentate (chelating) or bridging ligand. Examples are in Fig. 15.29. Vibrational spectroscopy is a useful diagnostic, as the progressive reduction in local symmetry of the  $\text{SO}_4$  group from  $T_d$  to  $C_{3v}$  and eventually  $C_{2v}$  increases the number of infrared active modes from 2 to 6 and 8 respectively, and the number of Raman active modes from 4 to 6 and 9.<sup>(193)</sup> (The effects of crystal symmetry and the overlapping of bands complicates the analysis but correct assignments are frequently still possible.)

Pairs of corner-shared  $\text{SO}_4$  tetrahedra are found in the disulfates,  $\text{S}_2\text{O}_7^{2-}$  ( $\text{S}-\text{O}_\mu-\text{S}$  124°,  $\text{S}-\text{O}_\mu$  164.5 pm,  $\text{S}-\text{O}_t$  144 pm); they are made by thermal dehydration of  $\text{MHSO}_4$ . Likewise the trisulfate ion  $\text{S}_3\text{O}_{10}^{2-}$  is known and also the pentasulfate ion,  $\text{S}_5\text{O}_{16}^{2-}$  whose structure indicates an alternation of  $\text{S}-\text{O}$  interatomic distances and very long  $\text{O}-\text{S}$  distances to the almost planar terminal  $\text{SO}_3$  groups:



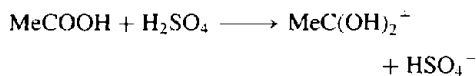
### Peroxosulfuric acids, $\text{H}_2\text{SO}_5$ and $\text{H}_2\text{S}_2\text{O}_8$

Anhydrous peroxomonosulfuric acid (Caro's acid) can be prepared by reacting chlorosulfuric acid with anhydrous  $\text{H}_2\text{O}_2$

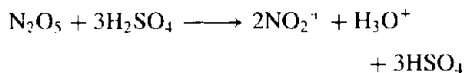
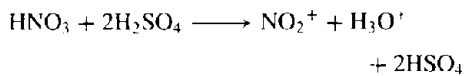


<sup>193</sup> K. NAKAMOTO, *Infrared Spectra of Inorganic and Coordination Compounds*, 2nd edn., Wiley, New York, 1970, 338 pp. (See also *J. Am. Chem. Soc.* **79**, 4904-8 (1957) for detailed correlation table.)





(d) Dehydration reactions:

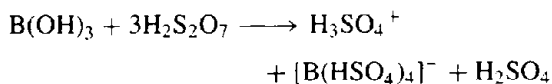


The reaction with  $\text{HNO}_3$  is quantitative, and the presence of large concentrations of the nitronium ion,  $\text{NO}_2^+$ , in solutions of  $\text{HNO}_3$ ,  $\text{MNO}_3$  and  $\text{N}_2\text{O}_5$  in  $\text{H}_2\text{SO}_4$  enable a detailed interpretation to be given of the nitration of aromatic hydrocarbons by these solutions.

Because of the high acidity of  $\text{H}_2\text{SO}_4$  itself, bases form the largest class of electrolytes and only few acids (proton donors) are known in this solvent system. As noted above,  $\text{H}_2\text{S}_2\text{O}_7$  acts as a proton donor to  $\text{H}_2\text{SO}_4$  and  $\text{HSO}_3\text{F}$  is also a weak acid:



One of the few strong acids is tetra(hydrogen sulfato)boric acid  $\text{B}(\text{HSO}_4)_4$ ; solutions of this can be obtained by dissolving boric acid in oleum:



Other strong acids are  $\text{H}_2\text{Sn}(\text{HSO}_4)_6$  and  $\text{H}_2\text{Pb}(\text{HSO}_4)_6$ .

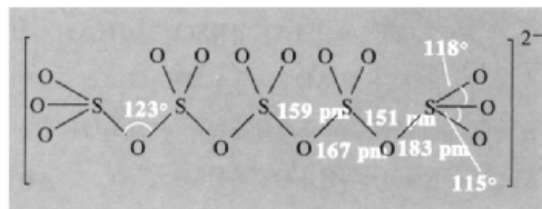
Sulfuric acid forms salts (sulfates and hydrogen sulfates) with many metals. These are frequently very stable and, indeed, they are the most important mineral compounds of several of the more electropositive elements. They have been discussed in detail under the appropriate elements. Sulfates can be prepared by:

- dissolution of metals in aqueous  $\text{H}_2\text{SO}_4$  (e.g. Fe);
- neutralization of aqueous  $\text{H}_2\text{SO}_4$  with metal oxides or hydroxides (e.g.  $\text{MOH}$ );
- decomposition of salts of volatile acids (e.g. carbonates) with aqueous  $\text{H}_2\text{SO}_4$ ;

- metathesis between a soluble sulfate and a soluble salt of the metal whose (insoluble) sulfate is required (e.g.  $\text{BaSO}_4$ );
- oxidation of metal sulfides or sulfites.

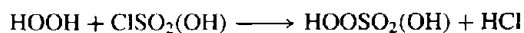
The sulfate ion is tetrahedral ( $\text{S}-\text{O}$  149 pm) and can act as a monodentate, bidentate (chelating) or bridging ligand. Examples are in Fig. 15.29. Vibrational spectroscopy is a useful diagnostic, as the progressive reduction in local symmetry of the  $\text{SO}_4$  group from  $T_d$  to  $C_{3v}$  and eventually  $C_{2v}$  increases the number of infrared active modes from 2 to 6 and 8 respectively, and the number of Raman active modes from 4 to 6 and 9.<sup>(193)</sup> (The effects of crystal symmetry and the overlapping of bands complicates the analysis but correct assignments are frequently still possible.)

Pairs of corner-shared  $\text{SO}_4$  tetrahedra are found in the disulfates,  $\text{S}_2\text{O}_7^{2-}$  ( $\text{S}-\text{O}_\mu-\text{S}$  124°,  $\text{S}-\text{O}_\mu$  164.5 pm,  $\text{S}-\text{O}_t$  144 pm); they are made by thermal dehydration of  $\text{MHSO}_4$ . Likewise the trisulfate ion  $\text{S}_3\text{O}_{10}^{2-}$  is known and also the pentasulfate ion,  $\text{S}_5\text{O}_{16}^{2-}$  whose structure indicates an alternation of  $\text{S}-\text{O}$  interatomic distances and very long  $\text{O}-\text{S}$  distances to the almost planar terminal  $\text{SO}_3$  groups:

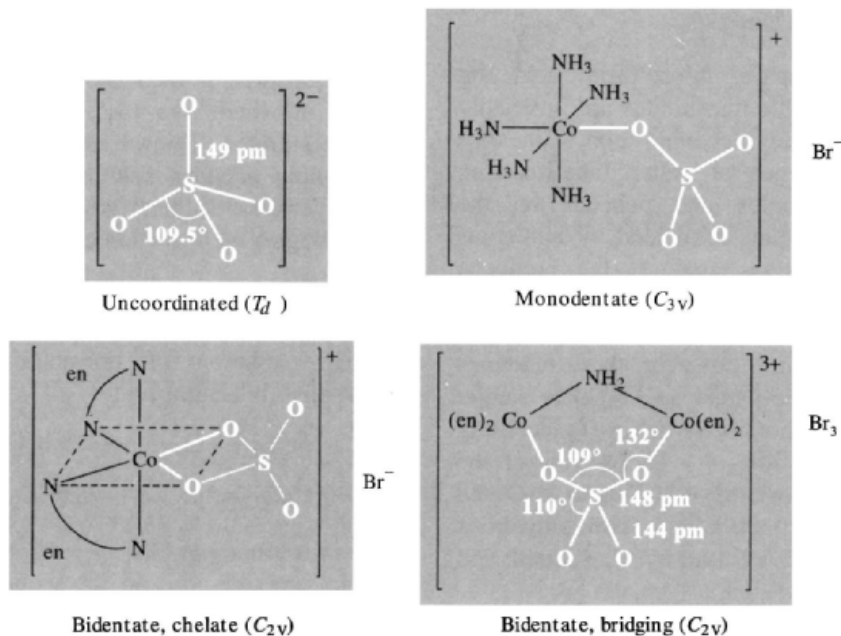


### Peroxosulfuric acids, $\text{H}_2\text{SO}_5$ and $\text{H}_2\text{S}_2\text{O}_8$

Anhydrous peroxomonosulfuric acid (Caro's acid) can be prepared by reacting chlorosulfuric acid with anhydrous  $\text{H}_2\text{O}_2$



<sup>193</sup> K. NAKAMOTO, *Infrared Spectra of Inorganic and Coordination Compounds*, 2nd edn., Wiley, New York, 1970, 338 pp. (See also *J. Am. Chem. Soc.* **79**, 4904-8 (1957) for detailed correlation table.)



**Figure 15.29** Examples of  $\text{SO}_4^{2-}$  as a ligand.

It is colourless, beautifully crystalline, and melts at  $45^\circ$ , but should be handled carefully because of the danger of explosions. It can also be made by the action of conc  $\text{H}_2\text{SO}_4$  on peroxydisulfates and is formed as a byproduct during the preparation of  $\text{H}_2\text{S}_2\text{O}_8$  by electrolysis of aqueous  $\text{H}_2\text{SO}_4$  (N. Caro, 1898). Its salts, which are preferably called trioxoperoxosulfates(2-) rather than peroxomonosulfates,<sup>(194)</sup> are unstable and the compound has few uses except those dependent on the formation of the  $\text{H}_2\text{O}_2$  during its decomposition. The structure of the anion  $[\text{HOOSO}_3]^-$ , which is the active principle of Caro's acid, has been determined by X-ray analysis of the hydrated salt  $\text{KHSO}_5 \cdot \text{H}_2\text{O}$ ; selected dimensions are O-O 140.0, S-O<sub>2</sub> 163.2, S-O<sub>1</sub> 143.5–144.4 pm, angle OOS  $109.4^\circ$ .<sup>(195)</sup>

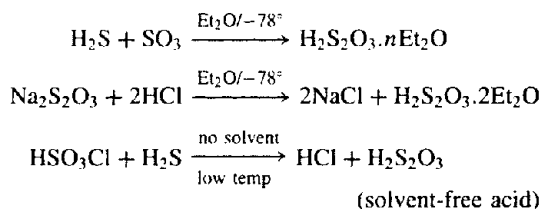
<sup>194</sup> G. J. LEIGH (ed.), *Nomenclature of Inorganic Chemistry* (The IUPAC 'Red Book'), Blackwell Scientific Publications, Oxford, 1990, pp. 268, 269.

<sup>195</sup> J. FLANAGAN, W. P. GRIFFITH and A. C. SKAPSKI, *J. Chem. Soc., Chem. Commun.*, 1574–5 (1984).

Peroxydisulfuric acid,  $\text{H}_2\text{S}_2\text{O}_8$ , is a colourless solid mp  $65^\circ$  (with decomposition). The acid is soluble in water in all proportions and its most important salts,  $(\text{NH}_4)_2\text{S}_2\text{O}_8$  and  $\text{K}_2\text{S}_2\text{O}_8$ , are also freely soluble. These salts are, in fact, easier to prepare than the acid and both are made on an industrial scale by anodic oxidation of the corresponding sulfates under carefully controlled conditions (high current density,  $T < 30^\circ$ , bright Pt electrodes, protected cathode). The structure of the peroxydisulfate ion [now preferably called hexaoxo- $\mu$ -peroxydisulfate(2-)]<sup>(194)</sup> is  $\text{O}_3\text{SOOSO}_3^{2-}$  with O-O 131 pm and S-O 150 pm. The compounds are used as oxidizing and bleaching agents. Thus, as can be seen from Table 15.19, the standard reduction potential  $\text{S}_2\text{O}_8^{2-}/\text{HSO}_4^-$  is 2.123 V, and  $E^\circ(\text{S}_2\text{O}_8^{2-}/\text{SO}_4^{2-})$  is similar (2.010 V); these are more positive than for any other aqueous couples except  $\text{H}_2\text{N}_2\text{O}_2$ ,  $2\text{H}^+/\text{N}_2$ ,  $2\text{H}_2\text{O}$  (2.85 V),  $\text{F}_2/2\text{F}^-$  (2.87 V) and  $\text{F}_2, 2\text{H}^+/2\text{HF}(\text{aq})$  (3.06) — see also  $\text{O}(\text{g})$ ,  $2\text{H}^+/\text{H}_2\text{O}$  (2.42 V),  $\text{OH}, \text{H}^+/\text{H}_2\text{O}$  (2.8 V).

### Thiosulfuric acid, H<sub>2</sub>S<sub>2</sub>O<sub>3</sub>

Attempts to prepare thiosulfuric acid by acidification of stable thiosulfates are invariably thwarted by the ready decomposition of the free acid in the presence of water. The reaction is extremely complex and depends on the conditions used, being dominated by numerous redox interconversions amongst the products: these can include sulfur (partly as *cyclo-S*<sub>6</sub>), SO<sub>2</sub>, H<sub>2</sub>S, H<sub>2</sub>S<sub>n</sub>, H<sub>2</sub>SO<sub>4</sub> and various polythionates. In the absence of water, however, these reactions are avoided and the parent acid is more stable: it decomposes quantitatively below 0° according to the reaction H<sub>2</sub>S<sub>2</sub>O<sub>3</sub> → H<sub>2</sub>S + SO<sub>3</sub> (cf. the analogous decomposition of H<sub>2</sub>SO<sub>4</sub> to H<sub>2</sub>O and SO<sub>3</sub> above its bp ~300°). Successful anhydrous syntheses have been devised by M. Schmidt and his group (1959–61), e.g.:

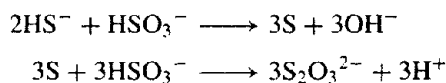


Combination of stoichiometric amounts of H<sub>2</sub>S and SO<sub>3</sub> at low temperature yields the white crystalline adduct H<sub>2</sub>S.SO<sub>3</sub> which is isomeric with thiosulfuric acid.

In contrast to the free acid, stable thiosulfate salts can readily be prepared by reaction of H<sub>2</sub>S on aqueous solutions of sulfites:

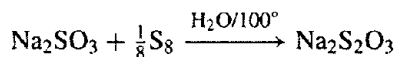


The reaction appears to proceed first by the formation of elemental sulfur which then equilibrates with more HSO<sub>3</sub><sup>-</sup> to form the product.<sup>(196)</sup>

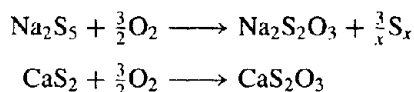


<sup>196</sup> G. W. HEUNISH, *Inorg. Chem.* **16**, 1411–13 (1979) and references therein.

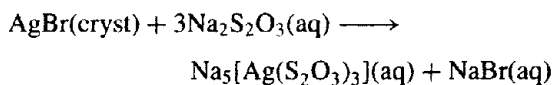
Consistent with this, experiments using HS<sup>-</sup> labelled with radioactive <sup>35</sup>S (p. 661) show that acid hydrolysis of the S<sub>2</sub>O<sub>3</sub><sup>2-</sup> produces elemental sulfur in which two-thirds of the <sup>35</sup>S activity is concentrated. Thiosulfates can also be made by boiling aqueous solutions of metal sulfites (or hydrogen sulfites) with elemental sulfur according to the stoichiometry



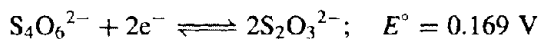
Aerial oxidation of polysulfides offers an alternative industrial route:



The thiosulfate ion closely resembles the SO<sub>4</sub><sup>2-</sup> ion in structure and can act as monodentate η<sup>1</sup>-S ligand, a monhapto bidentate bridging ligand (μ,η<sup>1</sup>-S), or a dihapto chelating η<sup>2</sup>-S,O ligand as illustrated in Fig. 15.30.<sup>(197)</sup> Hydrated sodium thiosulfate Na<sub>2</sub>S<sub>2</sub>O<sub>3</sub>·5H<sub>2</sub>O (“hypo”) forms large, colourless, transparent crystals, mp 48.5°; it is readily soluble in water and is used as a “fixer” in photography to dissolve unreacted AgBr from the emulsion by complexation:



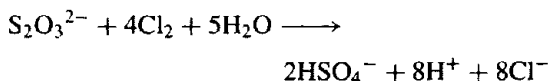
The thiosulfate ion is a moderately strong reducing agent as indicated by the couple



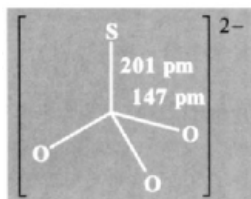
Thus the quantitative oxidation of S<sub>2</sub>O<sub>3</sub><sup>2-</sup> by I<sub>2</sub> to form tetrathionate and iodide is the basis for the iodometric titrations in volumetric analysis



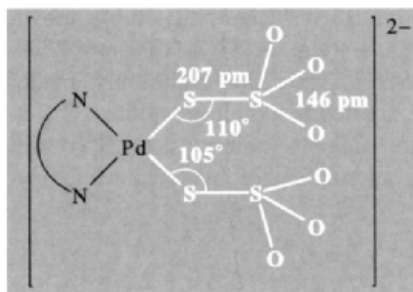
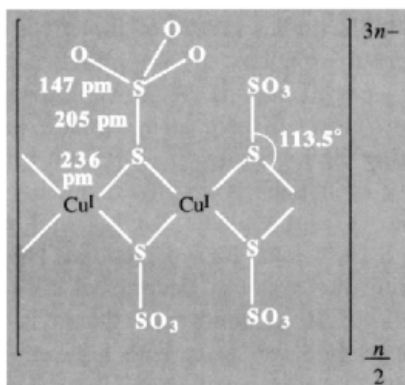
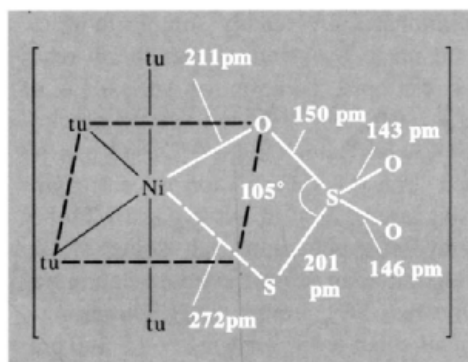
Stronger oxidizing agents take the reaction through to sulfate, e.g.:



<sup>197</sup> See p. 723 of ref. 103 for detailed references.



(a) Uncoordinated

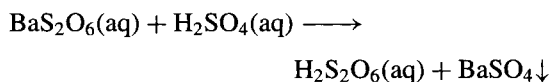
(b) Monodentate ( $\eta^1-S$ ): the  $S^{VI}$  atoms are not coplanar with the  $\{PdN_2S_2\}$  group(c) Monohapto bidentate bridging ( $\mu, \eta^1-S$ )(d) Dihapto bidentate chelating ( $\eta^2-S,O$ )

**Figure 15.30** Structure of the thiosulfate ion and its various modes of coordination: (a) uncoordinated  $S_2O_3^{2-}$ ; (b) monodentate ( $\eta^1-S$ ) in the anion of the orange complex  $[Pd^{II}(en)_2][Pd^{II}(en)(S_2O_3)_2]$ ; (c) monohapto bidentate bridging ( $\mu, \eta^1-S$ ) in the polymeric anion of the pale-violet mixed valence copper complex  $Na_4[Cu^I(NH_3)_4][Cu^I(S_2O_3)_2]_2$ ; and (d) dihapto chelating ( $\eta^2-S,O$ ) in the thiourea nickel complex  $[Ni(S_2O_3)(tu)_4] \cdot H_2O$ .

This reaction is the basis for the use of thiosulfates as “antichlorine” in the bleaching industry where they are used to destroy any excess of  $Cl_2$  in the fibres. Bromine, being intermediate between iodine and chlorine, can cause  $S_2O_3^{2-}$  to act either as a 1-electron or an 8-electron reducer according to conditions. For example, in an amusing and instructive experiment, if concentrated aqueous solutions of  $S_2O_3^{2-}$  and  $Br_2$  are titrated, and the titration is then repeated after having diluted both the  $S_2O_3^{2-}$  and  $Br_2$  solutions 100-fold, then the titre will be found to have increased by a factor of exactly 8.

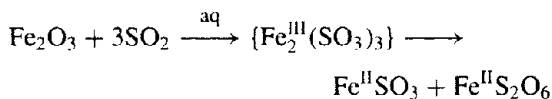
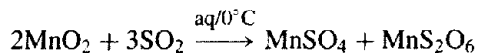
### Dithionic acid, $H_2S_2O_6$

In dithionic acid and dithionates,  $S_2O_6^{2-}$ , the oxidation state of the 2 S atoms has been reduced from VI to V by the formation of an S–S bond (Table 15.18, p. 705). The free acid has not been obtained pure, but quite concentrated aqueous solutions can be prepared by treatment of the barium salt with the stoichiometric amount of  $H_2SO_4$ :





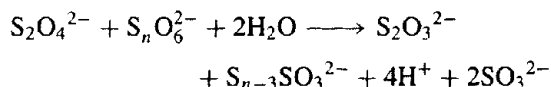
Crystalline dithionates are thermally stable above room temperature (e.g.  $\text{K}_2\text{S}_2\text{O}_6$  decomp  $258^\circ$  to  $\text{K}_2\text{SO}_4 + \text{SO}_2$ ). They are commonly made by oxidizing the corresponding sulfite. On a technical scale aqueous solutions of  $\text{SO}_2$  are oxidized by a suspension of hydrated  $\text{MnO}_2$  or  $\text{Fe}_2\text{O}_3$ :



All the dithionates are readily soluble in water and can be made by standard metathesis reactions. For example, addition of an excess of  $\text{Ba}^{\text{II}}$  ions to the  $\text{Mn}^{\text{II}}$  solution above precipitates  $\text{BaSO}_4$ , after which  $\text{BaS}_2\text{O}_6 \cdot 2\text{H}_2\text{O}$  can be crystallized. The  $[\text{O}_3\text{SSO}_3]^{2-}$  ion is centrosymmetric (staggered)  $D_{3d}$  in  $\text{Na}_2\text{S}_2\text{O}_6 \cdot 2\text{H}_2\text{O}$  but in the anhydrous potassium salt some of the  $\text{S}_2\text{O}_6^{2-}$  ions have an almost eclipsed configuration for the two  $\text{SO}_3$  groups ( $D_{3h}$ ). Dimensions are unremarkable: S-S 215 pm, S-O 143 pm, and angle S-S-O  $103^\circ$ . In a curious reaction between dibenzenechromium(0) and dry, oxygen-free  $\text{SO}_2$  in toluene, a red precipitate is formed which subsequently turns black. The unexpected product is  $[(\eta^6\text{-C}_6\text{H}_6)_2\text{Cr}]_2[\text{S}_4\text{O}_{10}]$ , which contains the dianion  $[\text{S}_4\text{O}_{10}]^{2-}$  formed by coordination of two  $\text{SO}_2$  molecules to a dithionate ion,  $[\text{O}_2\text{S} \rightarrow \text{OS}(\text{O})_2 - \text{S}(\text{O})_2\text{O} \leftarrow \text{SO}_2]^{2-}$  with S-S 221.8 pm, S-O 243.3 pm and angle S-O-S  $129.3^\circ$ .<sup>(198)</sup>

Dithionates are relatively stable towards oxidation in solution though strong oxidants such as the halogens, dichromate and permanganate oxidize them to sulfate. Powerful reductants (e.g.  $\text{Na}/\text{Hg}$ ) reduce dithionates to sulfites and dithionites ( $\text{S}_2\text{O}_4^{2-}$ ). In neutral and slightly acidic aqueous solutions dithionite itself decomposes by pH-dependent routes to thiosulfite ( $\text{S}_2\text{O}_3^{2-}$ ), sulfite ( $\text{SO}_3^{2-}$ ), sulfide ( $\text{S}^{2-}$ ), etc. These, and the products of the

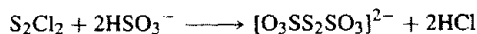
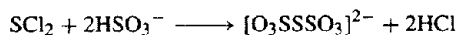
reactions of dithionites with polythionates ( $\text{S}_n\text{O}_6^{2-}$ ,  $n = 3-5$ ) have been studied by ion-pair chromatography:<sup>(199)</sup>



### Polythionic acids, $\text{H}_2\text{S}_n\text{O}_6$

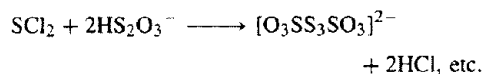
The numerous acids and salts in this group have a venerable history and the chemistry of systems in which they occur goes back to John Dalton's studies (1808) of the effect of  $\text{H}_2\text{S}$  on aqueous solutions of  $\text{SO}_2$ . Such solutions are now named after H. W. F. Wackenroder (1846) who subjected them to systematic study. Work during the following 60-80 y indicated the presence of numerous species including, in particular, the tetrathionate  $\text{S}_4\text{O}_6^{2-}$  and pentathionate  $\text{S}_5\text{O}_6^{2-}$  ions. New perceptions have emerged during the past few decades as a result of the work of H. Schmidt and others in Germany: just as  $\text{H}_2\text{S}$  can react with  $\text{SO}_3$  or  $\text{HSO}_3\text{Cl}$  to yield thiosulfuric acid,  $\text{H}_2\text{S}_2\text{O}_3$  (p. 714), so reaction with  $\text{H}_2\text{S}_2$  yields "disulfane monosulfonic acid",  $\text{HS}_2\text{SO}_3\text{H}$ ; likewise polysulfanes  $\text{H}_2\text{S}_n$  ( $n = 2-6$ ) yield  $\text{HS}_n\text{SO}_3\text{H}$ . Reaction at both ends of the polysulfane chain would yield "polysulfane disulfonic acids"  $\text{HO}_3\text{SS}_n\text{SO}_3\text{H}$  which are more commonly called polythionic acids ( $\text{H}_2\text{S}_{n+2}\text{O}_6$ ). Many synthetic routes are available, though mechanistic details are frequently obscure because of the numerous simultaneous and competing redox, catenation and disproportionation reactions that occur. Typical examples include:

- Interaction of  $\text{H}_2\text{S}$  and  $\text{SO}_2$  in Wackenroder's solution (see above).
- Reaction of chlorosulfanes with  $\text{HSO}_3^-$  or  $\text{HS}_2\text{O}_3^-$ , e.g.:



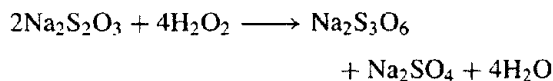
<sup>198</sup> C. ELSCHENBROICH, R. GONDRUM and W. MASSA, *Angew. Chem. Int. Edn. Engl.* **24**, 967-8 (1985).

<sup>199</sup> V. MUNCHOW and R. STEUDEL, *Z. anorg. allg. Chem.* **620**, 121-6 (1994).



- (c) Oxidation of thiosulfates with mild oxidants (p. 714) such as  $\text{I}_2$ ,  $\text{Cu}^{\text{II}}$ ,  $\text{S}_2\text{O}_8^{2-}$ ,  $\text{H}_2\text{O}_2$ .
- (d) Specific syntheses as noted below.

Sodium trithionate,  $\text{Na}_2\text{S}_3\text{O}_6$ , can be made by oxidizing sodium thiosulfate with cooled hydrogen peroxide solution



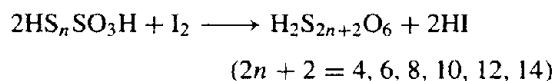
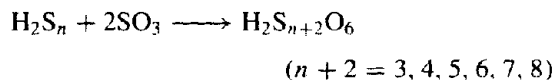
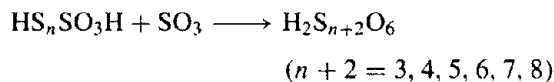
The potassium (but not the sodium) salt is obtained by the obscure reaction of  $\text{SO}_2$  on aqueous thiosulfate. Aqueous solutions of the acid  $\text{H}_2\text{S}_3\text{O}_6$  can then be obtained from  $\text{K}_2\text{S}_3\text{O}_6$  by treatment with tartaric acid or perchloric acid.

Sodium (and potassium) tetrathionate,  $\text{M}_2\text{S}_4\text{O}_6$ , can be made by oxidation of thiosulfate by  $\text{I}_2$  (p. 714) and the free acid liberated (in aqueous solution) by addition of the stoichiometric amount of tartaric acid.

Potassium pentathionate,  $\text{K}_2\text{S}_5\text{O}_6$ , can be made by adding potassium acetate to Wackenroder's solution and solutions of the free acid  $\text{H}_2\text{S}_5\text{O}_6$  can then be obtained by subsequent addition of tartaric acid.

Potassium hexathionate,  $\text{K}_2\text{S}_6\text{O}_6$ , is best synthesized by the action of  $\text{KNO}_2$  on  $\text{K}_2\text{S}_2\text{O}_3$  in conc  $\text{HCl}$  at low temperatures, though the ion is also a constituent of Wackenroder's solution.

Anhydrous polythionic acids can be made in ether solution by three general routes:



The structure of the trithionate ion (in  $\text{K}_2\text{S}_3\text{O}_6$ ) is shown in Fig. 15.31a and calls for little

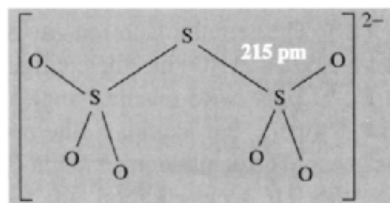
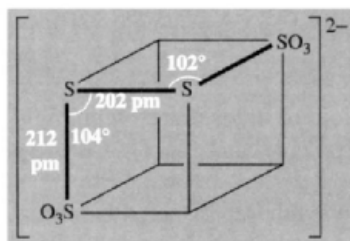
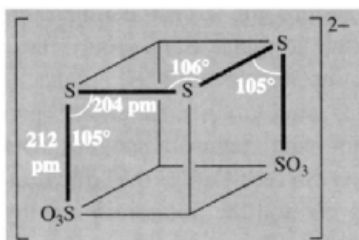
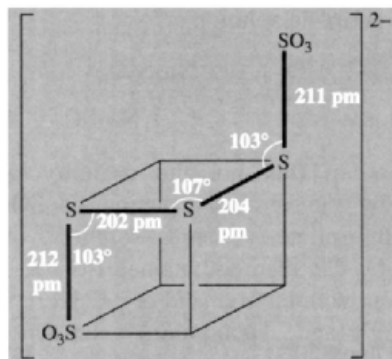
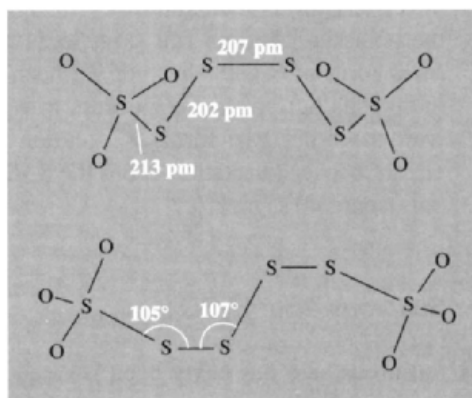
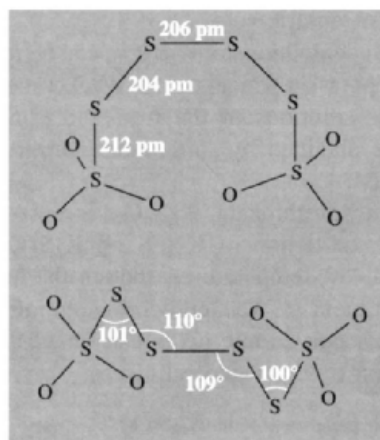
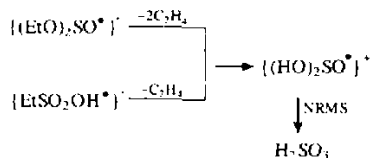
comment (cf. the disulfate ion  $\text{O}_3\text{SOSO}_3^{2-}$ , p. 712). The tetrathionate ion (in  $\text{BaS}_4\text{O}_6 \cdot 2\text{H}_2\text{O}$  and  $\text{Na}_2\text{S}_4\text{O}_6 \cdot 2\text{H}_2\text{O}$ ) has the configuration shown in Fig. 15.31b with dihedral angles close to  $90^\circ$  and a small, but definite, alternation in S–S distances. The pentathionate ion in  $\text{BaS}_5\text{O}_6 \cdot 2\text{H}_2\text{O}$  has the *cis* configuration in which the  $\text{S}_5$  unit can be regarded as part of an  $\text{S}_8$  ring (p. 655) from which 3 adjacent S atoms have been removed (Fig. 15.31c). By contrast, in the potassium salt  $\text{K}_2\text{S}_5\text{O}_6 \cdot 1\frac{1}{2}\text{H}_2\text{O}$  the pentathionate ion adopts the *trans* configuration in which the two terminal  $\text{SO}_3$  groups are on opposite sides of the central  $\text{S}_3$  plane (Fig. 15.31d). These structural differences persist in the seleno- and telluro-analogues  $\text{O}_3\text{SSeSSO}_3^{2-}$  and  $\text{O}_3\text{SSTeSSO}_3^{2-}$ , the dihydrated Ba salts being *cis* and the potassium hemihydrates being *trans*.<sup>(200)</sup> There are three possible rotameric forms of the hexathionate ion  $\text{S}_6\text{O}_6^{2-}$ : the extended *trans-trans* form analogous to spiral chains of fibrous sulfur (p. 660) occurs in the *trans*- $[\text{Co}^{\text{III}}(\text{en})_2\text{Cl}_2]^+$  salt (Fig. 15.31e), whereas the *cis-cis* form (analogous to *cyclo-S}\_8*) occurs in the potassium barium salt (Fig. 15.31f); the *cis-trans* form of  $\text{S}_6\text{O}_6^{2-}$  has not yet been observed in crystals but presumably occurs in equilibrium with the other two forms in solution since the energy barrier to rotation about the S–S bonds is only some  $40 \text{ kJ mol}^{-1}$ .

### Sulfurous acid, $\text{H}_2\text{SO}_3$

Sulfurous acid has never been isolated as a pure compound, although it has recently been detected in the gas phase by neutralization reionization mass spectrometry (NRMS) following the facile dissociative ionization (70 eV) of either diethyl sulfite or ethanesulfonic acid.<sup>(201)</sup>

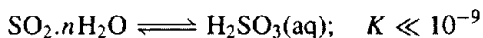
<sup>200</sup> O. FOSS, *IUPAC Additional Publication* (24th International Congress, Hamburg, 1973), Vol. 4, *Compounds of Non-Metals*, pp. 103–13. Butterworths, London, 1974, and references therein.

<sup>201</sup> D. SULZLE, M. VERHOEVEN, J. K. TERLOUW and H. SCHWARZ, *Angew. Chem. Int. Edn. Engl.* **27**, 1533–4 (1988).

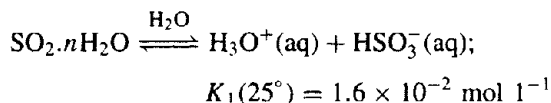
(a)  $S_3O_6^{2-}$ (b)  $S_4O_6^{2-}$ (c) *cis*- $S_5O_6^{2-}$ (d) *trans*- $S_5O_6^{2-}$ (e) *trans-trans*- $S_6O_6^{2-}$  (above: normal to the twofold axis; below: along this axis)(f) *cis-cis*- $S_6O_6^{2-}$  (above: normal to the twofold axis; below: along this axis)**Figure 15.31** Structures of some polythionate ions.<sup>(200)</sup>

The experimental finding was substantiated by high-level *ab initio* calculations. The unionized acid exists in only minute concentrations (if at all) in aqueous solutions of  $\text{SO}_2$ . However, its salts, the sulfites, are quite stable and many are known

in crystalline form; a second series of salts, the hydrogen sulfites  $\text{HSO}_3^-$ , are known in solution. Spectroscopic studies of aqueous solutions of  $\text{SO}_2$  suggest that the predominant species are various hydrates,  $\text{SO}_2 \cdot n\text{H}_2\text{O}$ ; depending on the concentration, temperature and pH, the ions present are  $\text{H}_3\text{O}^+$ ,  $\text{HSO}_3^-$  and  $\text{S}_2\text{O}_5^{2-}$  together with traces of  $\text{SO}_3^{2-}$ . The undissociated acid  $\text{OS}(\text{OH})_2$  has not been detected:



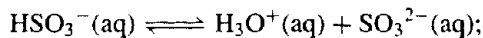
The first acid dissociation constant of "sulfurous acid" in aqueous solution is therefore defined as:



where

$$K_1 = \frac{[\text{H}_3\text{O}^+][\text{HSO}_3^-]}{[\text{total dissolved SO}_2] - [\text{HSO}_3^-] - [\text{SO}_3^{2-}]}$$

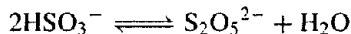
The second dissociation constant is given by the equation



$$K_2(25^\circ) = 1.0 \times 10^{-7} \text{ mol l}^{-1}$$

$$K_2 = \frac{[\text{H}_3\text{O}^+][\text{SO}_3^{2-}]}{[\text{HSO}_3^-]}$$

Most sulfites (except those of the alkali metals and ammonium) are rather insoluble; as indicated above such solutions contain the  $\text{HSO}_3^-$  ion predominantly, but attempts to isolate  $\text{M}^+\text{HSO}_3$  tend to produce disulfites (p. 720) by "dehydration":

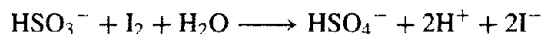


Only with large cations such as Rb, Cs and  $\text{NR}_4$  (R = Et, Bu<sup>n</sup>, *n*-pentyl) has it proved possible to isolate the solid sulfites  $\text{MHSO}_3$ .<sup>(202)</sup>

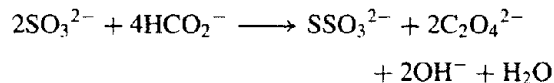
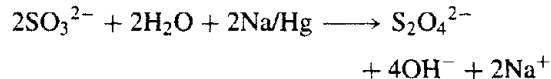
The sulfite ion  $\text{SO}_3^{2-}$  is pyramidal with  $C_{3v}$  symmetry: angle O-S-O 106°, S-O 151 pm. The hydrogen sulfite ion also appears to have  $C_{3v}$  symmetry both in the solid state and in solution, i.e. protonation occurs at S rather than

O to give  $\text{H-SO}_3^-$  rather than  $\text{HO-SO}_2^-$  ( $C_s$  symmetry). However, recent  $^{17}\text{O}$  nmr studies appear to provide evidence for the existence in solution of a dynamic equilibrium between the two isomers:  $\text{H-SO}_3^- \rightleftharpoons \text{HO-SO}_2^-$ .<sup>(203)</sup> The sulfite ion also coordinates through S in transition-metal complexes, e.g.  $[\text{Pd}(\text{NH}_3)_3(\eta^1\text{-SO}_3)]$ , *cis*- and *trans*- $[\text{Pt}(\text{NH}_3)_2(\eta^1\text{-SO}_3)_2]^{2-}$ . The structure of hydrogen-sulfito complex *trans*- $[\text{Ru}^{\text{II}}(\text{NH}_3)_4(\text{SO}_3\text{H})_2]$  is also S-bonded, implying a 1,2 proton shift to give  $\text{M}[\text{SO}_2(\text{OH})]$ .<sup>(204)</sup>

Sulfites and hydrogen sulfites are moderately strong reducing agents (p. 706) and, depending on conditions, are oxidized either to dithionate or sulfate. The reaction with iodine is quantitative and is used in volumetric analysis:



Conversely, sulfites can act as oxidants in the presence of strong reducing agents; e.g. sodium amalgam yields dithionite, and formates (in being oxidized to oxalates) yield thiosulfate:



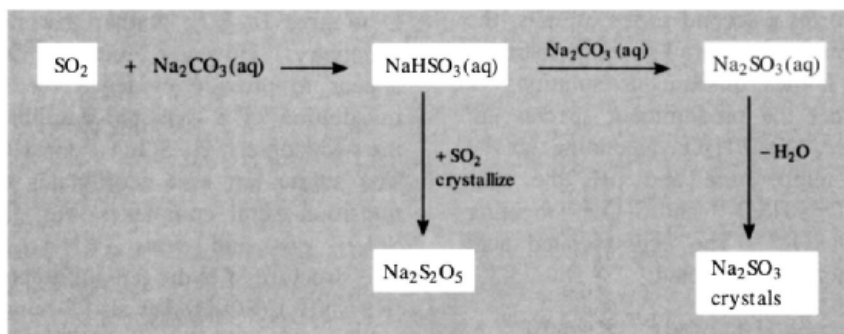
Thiosulfates also result from reduction of  $\text{SO}_3^{2-}$  or  $\text{HSO}_3^-$  with elemental sulfur (p. 714), whereas reduction with  $\text{H}_2\text{S}$  in Wackenroder's solution (pp. 716-7) yields polythionates. It is also notable that the sulfite ion is involved in the 6-electron sulfite reductase reaction:  $\text{SO}_3^{2-} + 6\text{H}^+ + 6\text{e}^- \longrightarrow \text{S}^{2-} + 3\text{H}_2\text{O}$ ;  $E^\circ = 0.380 \text{ V}$ . Indeed, there are only three such  $6\text{e}^-$  reductions known in the whole of biology, the other two being nitrite reductase ( $\text{NO}_2^- + 7\text{H}^+ + 6\text{e}^- \longrightarrow \text{NH}_3 + 2\text{H}_2\text{O}$ ) and nitrogenase ( $\text{N}_2 + 6\text{H}^+ + 6\text{e}^- \longrightarrow 2\text{NH}_3$ ).

On a technical scale, solutions of sodium hydrogen sulfite are prepared by passing  $\text{SO}_2$

<sup>203</sup> D. A. HORNER and R. E. CONNICK, *Inorg. Chem.* **25**, 2414-7 (1986).

<sup>204</sup> D. K. BREITINGER and R. BREITER, *Z. Naturforsch.* **45b**, 1651-6 (1990).

<sup>202</sup> R. MAYLOR, J. B. GILL and D. C. GOODALL, *J. Chem. Soc., Dalton Trans.*, 2001-3 (1972) and references therein.



into aqueous  $\text{Na}_2\text{CO}_3$ . As shown in the Scheme above, addition of a further equivalent of  $\text{Na}_2\text{CO}_3$  allows the normal sulfite to be crystallized, whereas addition of more  $\text{SO}_2$  yields the disulfite (see the next subsection below).

Crystallization of  $\text{Na}_2\text{SO}_3$  above  $37^\circ$  gives the anhydrous salt; below this temperature  $\text{Na}_2\text{SO}_3 \cdot 7\text{H}_2\text{O}$  is obtained. World production of the anhydrous salt exceeds 1 million tonnes pa; most is used in the paper pulp industry, but other applications are as an  $\text{O}_2$  scavenger in boiler-water treatment, and as a reducing agent in photography. Similarly,  $\text{K}_2\text{SO}_3 \cdot 2\text{H}_2\text{O}$  is obtained by passing  $\text{SO}_2$  into aqueous  $\text{KOH}$  until samples of the solution are neutral to phenolphthalein. For a compilation of critically evaluated solubility data, see ref. 205

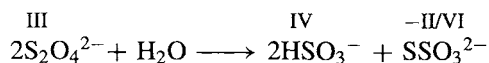
### Disulfurous acid, $\text{H}_2\text{S}_2\text{O}_5$

Like "sulfurous acid", disulfurous acid is unknown either in the free state or in solution. However, as indicated in the preceding section, its salts, are readily obtained from concentrated solutions of hydrogen sulfite:  $2\text{HSO}_3^- \rightleftharpoons \text{S}_2\text{O}_5^{2-} + \text{H}_2\text{O}$ . Unlike disulfates (p. 712), diphosphates (p. 522), etc., disulfites condense by forming an S-S bond. As indicated in Fig. 15.32a this S-S bond is rather long, but the S-O distances are unexceptional.

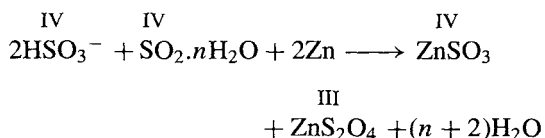
Acidification of solutions of disulfites regenerates  $\text{HSO}_3^-$  and  $\text{SO}_2$  again, and the solution chemistry of  $\text{S}_2\text{O}_5^{2-}$  is essentially that of the normal sulfites and hydrogen sulfites, despite the formal presence of  $\text{S}^{\text{V}}$  and  $\text{S}^{\text{III}}$  (rather than  $\text{S}^{\text{IV}}$ ) in the solid state.

### Dithionous acid, $\text{H}_2\text{S}_2\text{O}_4$

Dithionites,  $\text{S}_2\text{O}_4^{2-}$  are quite stable when anhydrous, but in the presence of water they disproportionate (slowly at  $\text{pH} \geq 7$ , rapidly in acid solution):

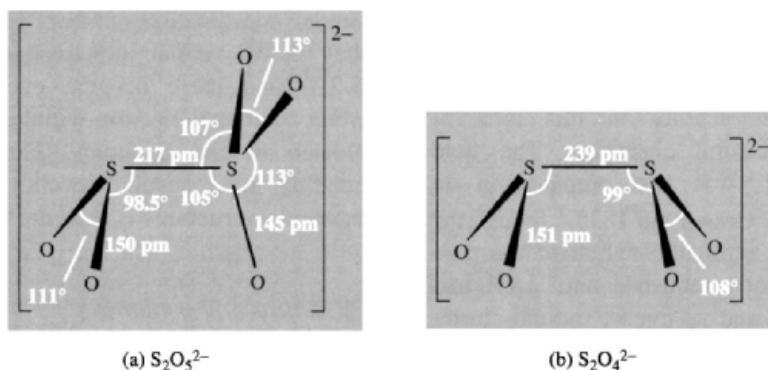


The parent acid has no independent existence and has not been detected in aqueous solution either. Sodium dithionite is widely used as an industrial reducing agent and can be prepared by reduction of sulfite using Zn dust, Na/Hg or electrolytically, e.g.:



The dihydrate  $\text{Na}_2\text{S}_2\text{O}_4 \cdot 2\text{H}_2\text{O}$  can be precipitated by "salting out" with  $\text{NaCl}$ . Air and oxygen must be excluded at all stages in the process to avoid reoxidation. The dithionite ion can also be produced *in situ* on an industrial scale by reaction

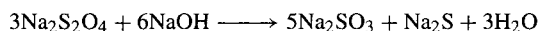
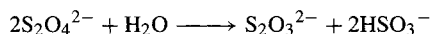
<sup>205</sup> M. R. MASSON, H. D. LUTZ and B. ENGELEN (eds.) *Sulfites, Selenites and Tellurites*, Pergamon Press, Oxford, 1986, 474 pp.



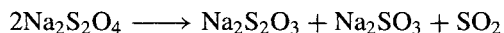
**Figure 15.32** Structure of (a) the disulfite ion  $\text{S}_2\text{O}_5^{2-}$  in  $(\text{NH}_4)_2\text{S}_2\text{O}_5$ , and (b) the dithionite ion  $\text{S}_2\text{O}_4^{2-}$  in  $\text{Na}_2\text{S}_2\text{O}_4 \cdot 2\text{H}_2\text{O}$ .

between  $\text{NaHSO}_3$  and  $\text{NaBH}_4$  (p. 167). Its main use is as a reducing agent in dyeing, bleaching of paper pulp, straw, clay, soaps, etc., and in chemical reductions (see below). Current worldwide demand is about 300 000 tonnes per annum.

The dithionite ion has a remarkable eclipsed structure of approximate  $C_{2v}$  symmetry (Fig. 15.32b). The extraordinarily long S–S distance (239 pm) and the almost parallel  $\text{SO}_2$  planes (dihedral angle  $30^\circ$ ) are other unusual features. Electron-spin-resonance studies have shown the presence of the  $\text{SO}_2^{\cdot -}$  radical ion in solution ( $\sim 300$  ppm), suggesting the establishment of a monomer-dimer equilibrium  $\text{S}_2\text{O}_4^{2-} \rightleftharpoons 2\text{SO}_2^{\cdot -}$ . Consistent with this, air-oxidation of alkaline dithionite solutions at  $30$ – $60^\circ$  are of order one-half with respect to  $[\text{S}_2\text{O}_4^{2-}]$ . Acid hydrolysis (second order with respect to  $[\text{S}_2\text{O}_4^{2-}]$ ) yields thiosulfate and hydrogen sulfite, whereas alkaline hydrolysis produces sulfite and sulfide:



Hydrated dithionites can be dehydrated by gentle warming, but the anhydrous salts themselves decompose on further heating. For example,  $\text{Na}_2\text{S}_2\text{O}_4$  decomposes rapidly at  $150^\circ$  and violently at  $190^\circ$ :



Dithionites are strong reducing agents and will reduce dissolved  $\text{O}_2$ ,  $\text{H}_2\text{O}_2$ ,  $\text{I}_2$ ,  $\text{IO}_3^-$  and  $\text{MnO}_4^-$ .

Likewise  $\text{Cr}^{\text{VI}}$  is reduced to  $\text{Cr}^{\text{III}}$  and  $\text{TiO}^{2+}$  to  $\text{Ti}^{\text{III}}$ . Heavy metal ions such as  $\text{Cu}^{\text{I}}$ ,  $\text{Ag}^{\text{I}}$ ,  $\text{Pb}^{\text{II}}$ ,  $\text{Sb}^{\text{III}}$  and  $\text{Bi}^{\text{III}}$  are reduced to the metal. Many of these reactions are useful in water-treatment and pollution control.

### 15.2.7 Sulfur–nitrogen compounds <sup>(206–210)</sup>

The study of S–N compounds is one of the most active areas of current inorganic research: many novel cyclic and acyclic compounds are being prepared which have unusual structures and which pose considerable problems in terms of simple bonding theory. The discovery in 1975 that the polymer  $(\text{SN})_x$  is a metal whose conductivity *increases* with decrease in

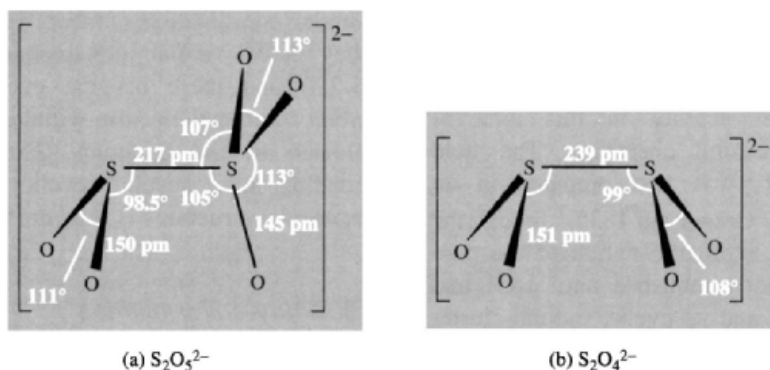
<sup>206</sup> M. BECKE-GOEHRING and E. FLUCK, Chap. 3 in C. B. COLBURN (ed.), *Developments in Inorganic Nitrogen Chemistry*, Vol. 1, pp. 150–240, Elsevier, Amsterdam, 1966.

<sup>207</sup> I. HAJDUC, *The Chemistry of Inorganic Ring Systems*, Part 2, (sulfur–nitrogen heterocycles), pp. 909–83, Wiley, London, 1970.

<sup>208</sup> H. G. HEAL, *The Inorganic Heterocyclic Chemistry of Sulfur, Nitrogen and Phosphorus*, Academic Press, London, 1981, 288 pp.

<sup>209</sup> H. W. ROESKY, *Adv. Inorg. Chem. Radiochem.* **22**, 239–301 (1979).

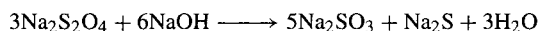
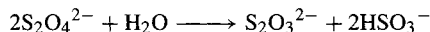
<sup>210</sup> *Gmelin Handbook of Inorganic Chemistry*, Sulfur–Nitrogen Compounds: Part 1, 288 pp (1977); Part 2, 333 pp (1985); Part 3, 325 pp (1987); Part 4, 272 pp (1987); Part 5, 276 pp (1990), Springer Verlag, Berlin.



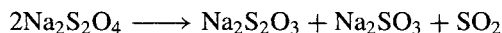
**Figure 15.32** Structure of (a) the disulfite ion  $\text{S}_2\text{O}_5^{2-}$  in  $(\text{NH}_4)_2\text{S}_2\text{O}_5$ , and (b) the dithionite ion  $\text{S}_2\text{O}_4^{2-}$  in  $\text{Na}_2\text{S}_2\text{O}_4 \cdot 2\text{H}_2\text{O}$ .

between  $\text{NaHSO}_3$  and  $\text{NaBH}_4$  (p. 167). Its main use is as a reducing agent in dyeing, bleaching of paper pulp, straw, clay, soaps, etc., and in chemical reductions (see below). Current worldwide demand is about 300 000 tonnes per annum.

The dithionite ion has a remarkable eclipsed structure of approximate  $C_{2v}$  symmetry (Fig. 15.32b). The extraordinarily long S–S distance (239 pm) and the almost parallel  $\text{SO}_2$  planes (dihedral angle  $30^\circ$ ) are other unusual features. Electron-spin-resonance studies have shown the presence of the  $\text{SO}_2^{\cdot -}$  radical ion in solution ( $\sim 300$  ppm), suggesting the establishment of a monomer-dimer equilibrium  $\text{S}_2\text{O}_4^{2-} \rightleftharpoons 2\text{SO}_2^{\cdot -}$ . Consistent with this, air-oxidation of alkaline dithionite solutions at  $30$ – $60^\circ$  are of order one-half with respect to  $[\text{S}_2\text{O}_4^{2-}]$ . Acid hydrolysis (second order with respect to  $[\text{S}_2\text{O}_4^{2-}]$ ) yields thiosulfate and hydrogen sulfite, whereas alkaline hydrolysis produces sulfite and sulfide:



Hydrated dithionites can be dehydrated by gentle warming, but the anhydrous salts themselves decompose on further heating. For example,  $\text{Na}_2\text{S}_2\text{O}_4$  decomposes rapidly at  $150^\circ$  and violently at  $190^\circ$ :



Dithionites are strong reducing agents and will reduce dissolved  $\text{O}_2$ ,  $\text{H}_2\text{O}_2$ ,  $\text{I}_2$ ,  $\text{IO}_3^-$  and  $\text{MnO}_4^-$ .

Likewise  $\text{Cr}^{\text{VI}}$  is reduced to  $\text{Cr}^{\text{III}}$  and  $\text{TiO}^{2+}$  to  $\text{Ti}^{\text{III}}$ . Heavy metal ions such as  $\text{Cu}^{\text{I}}$ ,  $\text{Ag}^{\text{I}}$ ,  $\text{Pb}^{\text{II}}$ ,  $\text{Sb}^{\text{III}}$  and  $\text{Bi}^{\text{III}}$  are reduced to the metal. Many of these reactions are useful in water-treatment and pollution control.

### 15.2.7 Sulfur–nitrogen compounds <sup>(206–210)</sup>

The study of S–N compounds is one of the most active areas of current inorganic research: many novel cyclic and acyclic compounds are being prepared which have unusual structures and which pose considerable problems in terms of simple bonding theory. The discovery in 1975 that the polymer  $(\text{SN})_x$  is a metal whose conductivity *increases* with decrease in

<sup>206</sup> M. BECKE-GOEHRING and E. FLUCK, Chap. 3 in C. B. COLBURN (ed.), *Developments in Inorganic Nitrogen Chemistry*, Vol. 1, pp. 150–240, Elsevier, Amsterdam, 1966.

<sup>207</sup> I. HAJDUC, *The Chemistry of Inorganic Ring Systems*, Part 2, (sulfur–nitrogen heterocycles), pp. 909–83, Wiley, London, 1970.

<sup>208</sup> H. G. HEAL, *The Inorganic Heterocyclic Chemistry of Sulfur, Nitrogen and Phosphorus*, Academic Press, London, 1981, 288 pp.

<sup>209</sup> H. W. ROESKY, *Adv. Inorg. Chem. Radiochem.* **22**, 239–301 (1979).

<sup>210</sup> *Gmelin Handbook of Inorganic Chemistry*, Sulfur–Nitrogen Compounds: Part 1, 288 pp (1977); Part 2, 333 pp (1985); Part 3, 325 pp (1987); Part 4, 272 pp (1987); Part 5, 276 pp (1990), Springer Verlag, Berlin.

temperature and which becomes superconducting below 0.33 K aroused tremendous additional interest and has stimulated still further the already substantial activity in this area of synthetic and structural chemistry. The field is not new.  $S_4N_4$  was first prepared in an impure form by W. Gregory in 1835,<sup>†</sup> though the stoichiometry and tetrameric nature of the pure compound were not established until 1851 and 1896 respectively, and its cyclic, pseudo-cluster structure was not revealed until 1944.<sup>(211)</sup> Other important compounds containing S–N bonds that date from the first half of the nineteenth century include sulfamic acid  $H[H_2NSO_3]$ , imidosulfonic acid  $HSO_3N=NH$ , sulfamide  $SO_2(NH_2)_2$ , nitrilotrisulfonic acid  $N(HSO_3)_3$ , hydroxy nitrilosulfonic acids  $HSO_3NH(OH)$  and  $(HSO_3)_2N(OH)$ , and their many derivatives (p. 743).

It will be convenient to describe first the binary sulfur nitrides  $S_xN_y$ , and then the related cationic and anionic species,  $S_xN_y^{n\pm}$ . The sulfur imides and other cyclic S–N compounds will then be discussed and this will be followed by sections on S–N–halogen and S–N–O compounds. Several compounds which feature isolated S←N, S–N, S=N and S≡N bonds have already been mentioned in the section on  $SF_4$ ; e.g.  $F_4S←NC_5H_5$ ,  $F_5S–NF_2$ ,  $F_2S=NCF_3$ , and  $F_3S≡N$  (p. 687). However, many SN compounds do not lend themselves to simple bond diagrams,<sup>(212)</sup> and formal oxidation states are often unhelpful or even misleading.

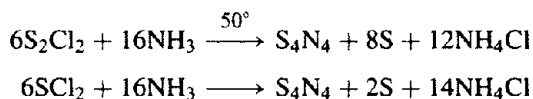
Nitrogen and sulfur are diagonally related in the periodic table and might therefore be expected to have similar electronic charge densities for

similar coordination numbers (p. 76). Likewise, they have similar electronegativities (N 3.0, S 2.5) and these become even more similar when additional electron-withdrawing groups are bonded to the S atoms. Extensive covalent bonding into acyclic, cyclic and polycyclic molecular structures is thus not unexpected.

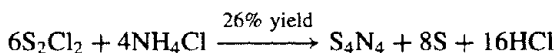
### (i) Binary sulfur nitrides

There is little structural similarity between the sulfur nitrides and the oxides of nitrogen (p. 443). The instability of NS when compared with the great stability of NO, and the paucity of thionitrosyl complexes have already been mentioned (p. 453), as has the difference between diatomic  $O_2$  and oligomeric or polymeric  $S_n$ . The compounds to be considered in this section are  $S_4N_4$ , *cyclo*- $S_2N_2$  and *catena*-(SN)<sub>x</sub> polymer, together with *cyclo*- $S_4N_2$ , *bicyclo*- $S_{11}N_2$ , and the higher homologues  $S_{15}N_2$ ,  $S_{16}N_2$ ,  $S_{17}N_2$  and  $S_{19}N_2$ . More recently, crystalline  $S_5N_6$  (the first binary sulfur nitride with more atoms of N than S) has been synthesized. The fugitive radicals  $SN^*$  and  $S_3N_3^*$  have also been characterized.

(a) *Tetrasulfur tetranitride*,  $S_4N_4$ . This is the most readily prepared sulfur nitride and is an important starting point for the preparation of many S–N compounds. It is obtained as orange-yellow, air-stable crystals<sup>†</sup> by passing  $NH_3$  gas into a warm solution of  $S_2Cl_2$  (or  $SCl_2$ ) in  $CCl_4$  or benzene; the overall stoichiometries of the mechanistically obscure reactions are:



Alternatively,  $NH_4Cl$  can be heated with  $S_2Cl_2$  at  $160^\circ$ :



<sup>†</sup> Crystalline  $S_4N_4$  is thermochromic, being pale yellow below about  $-30^\circ$ ; the colour deepens to orange at room temperature and to a deep red at  $100^\circ$  (cf. sulfur, p. 656).

<sup>†</sup> Disulfur dichloride was added to an aqueous solution of ammonia to give a yellow precipitate of sulfur contaminated with  $S_4N_4$ ; *J. Pharm. Chim.* **21**, 315 (1835).

<sup>211</sup> CHIA-SI LU and J. DONOHUE, *J. Am. Chem. Soc.* **66**, 818–27 (1944). D. CLARK, *J. Chem. Soc.* 1615–20 (1952).

<sup>212</sup> R. GLEITER, *Angew. Chem. Int. Edn. Engl.* **20**, 444–52 (1981); R. D. HARCOURT and H. M. HÜGEL, *J. Inorg. Nuclear Chem.* **43**, 239–52 (1981); A. A. BATTACHARYYA, A. BATTACHARYYA, R. R. ADKINS and A. G. TURNER, *J. Am. Chem. Soc.* **103**, 7458–65 (1981); R. C. HADDON, S. R. WASSERMAN, F. WUDL and G. R. J. WILLIAMS, *J. Am. Chem. Soc.* **102**, 6687–93 (1980).



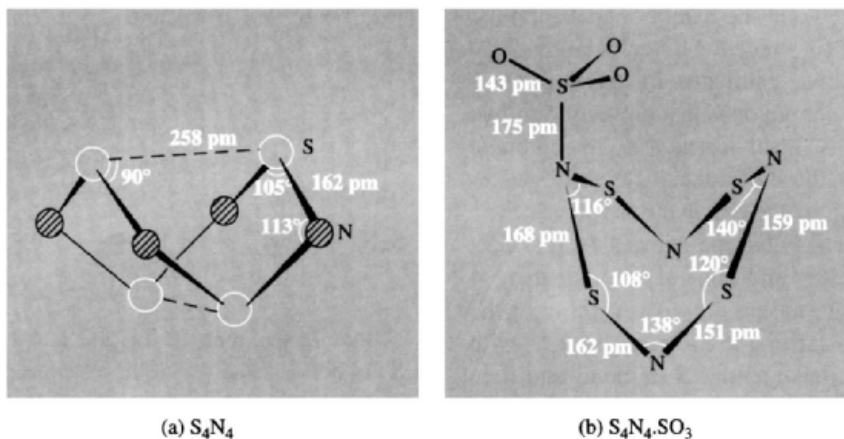
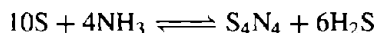


Figure 15.33 Structure of (a)  $S_4N_4$ , and (b)  $S_4N_4 \cdot SO_3$ .

The compound also results from the reversible equilibrium reaction of sulfur with anhydrous liquid ammonia:

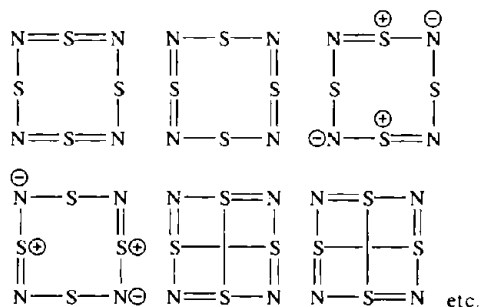


The  $H_2S$ , of course, reacts with further ammonia to form ammonium sulfides but the reaction can be made to proceed in the forward direction as written by addition of (soluble)  $AgI$  to precipitate  $AgS$  and form  $NH_4I$ .

$S_4N_4$  is kinetically stable in air but is endothermic with respect to its elements ( $\Delta H_f^\circ 460 \pm 8 \text{ kJ mol}^{-1}$ ) and may detonate when struck or when heated rapidly. This is due more to the stability of elementary sulfur and the great bond strength of  $N_2$  rather than to any inherent weakness in the S–N bonds. On careful heating  $S_4N_4$  melts at  $178.2^\circ$ . The structure (Fig. 15.33a) is an 8-membered heterocycle in the extreme cradle configuration; it has  $D_{2d}$  symmetry and resembles that of  $As_4S_4$  (p. 579) but with the sites of the Group 15 and Group 16 elements interchanged. The S–N distance of 162 pm is rather short when compared with the sum of the covalent radii (178 pm) and this, coupled with the equality of all the S–N bond distances in the molecule, has been attributed to some electron delocalization in the heterocycle. The trans-annular S···S distances (258 pm) are intermediate between bonding S–S (208 pm) and

nonbonding van der Waals (330 pm) distances; this suggests a weak but structurally significant bonding interaction between the pairs of S atoms. A study by gas-phase electron diffraction yields similar dimensions except that the trans-annular S···S distance is slightly longer (266.6 pm) probably because of the absence of constraining crystal packing forces.<sup>(213)</sup>

It is not possible to write down a single, satisfactory, classical bonding diagram for  $S_4N_4$  and, in valence-bond theory, numerous resonance hybrids must be considered of which the following are typical:



The extent to which each hybrid is incorporated into the full bonding description of the molecule will depend on the extent to which 3d orbitals

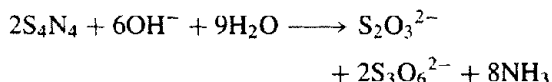
<sup>213</sup> A. J. DOWNS, T. L. JEFFERY and K. HAGEN, *Polyhedron* **8**, 2631–6 (1989).

on S are involved and the extent of trans-annular S-S bonding. More recent MO-calculations lead to semiquantitative estimates of these features and to electron charge densities on the individual atoms.<sup>(212)</sup> It is also instructive to compare the structure of the 44-(valence)electron species  $S_4N_4$  with those of the 46-electron species  $S_8^{2+}$  (p. 665) and the 48-electron species  $S_8$  (p. 655): successive formal addition of 2 and then 4 electron results in the progressive opening of the  $S_4N_4$  pseudocluster first to the *bicyclic*- $S_8^{2+}$  with a single weak trans-annular S-S bond and then to the open-crown structure of  $S_8$  with no trans-annular bonding at all.

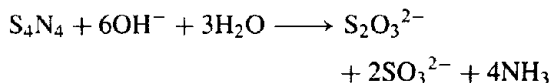
Interestingly, in the N-donor adducts  $S_4N_4 \cdot BF_3$  and  $S_4N_4 \cdot SbCl_5$  the  $S_4N_4$  ring adopts the alternative  $D_{2d}$  configuration of  $As_4S_4$ , with the 4 S atoms now coplanar instead of the 4 N atoms; the mean S-N distance increases slightly to 168 pm but the (nonbonding) trans-annular S...S distances are 380 pm. The same interchange occurs in  $S_4N_4 \cdot SO_3$  and Fig. 15.33b shows the substantial alternations in S-N distances and angles that are concurrently introduced into the ring. Likewise in the burgundy red salt  $[S_4N_4H]^+[BF_4]^-$ , formed by direct protonation of  $S_4N_4$  by  $HBF_4 \cdot Et_2O$  (S-N 157 pm, S-NH<sup>+</sup> 165 pm).<sup>(214)</sup> By contrast, in  $S_4N_4 \cdot CuCl$  the heterocycle acts as a bridging ligand between zigzag chains of  $(-Cu-Cl-)_\infty$ ; the  $S_4N_4$  retains the same conformation and almost the same dimensions as in the free molecule, with 2 of the 4 planar N atoms acting as a *cisoid* bridge and the 2 trans-annular S...S distances remaining short (259 and 263 pm).<sup>(215)</sup> It is not yet clear in detail what factors determine the ring conformation adopted (see also p. 656). Other complexes are mentioned below.

$S_4N_4$  is insoluble in and unreactive towards water but readily undergoes base hydrolysis with dilute NaOH solutions to give thiosulfate,

trithionate and ammonia:

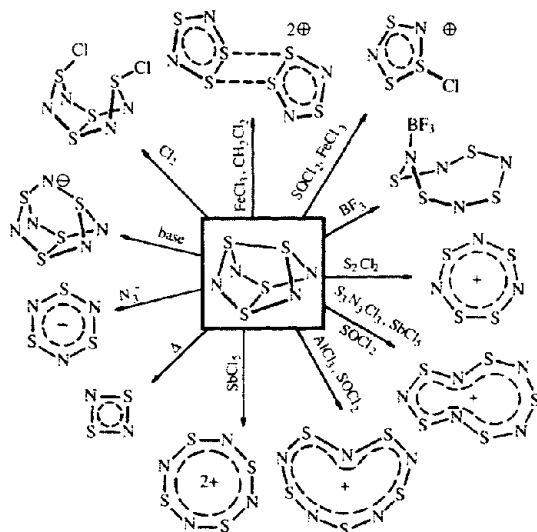


More concentrated alkali yields sulfite instead of trithionate:



Milder bases such as  $Et_2NH$  leave some of the S-N bonds intact to yield, for example,  $S(NEt_2)_2$ . The value of  $S_4N_4$  as a synthetic intermediate can be gauged from the representative reactions in the Scheme below<sup>(210)</sup> and in Table 15.22. It can be seen that these reactions embrace:

- conservation of the 8-membered heterocycle and attachment of substituents to S or N (or substitution of N by S);
- ring contraction to a 7-, 6-, 5- or 4-membered heterocycle with or without attachment of substituents;
- ring fragmentation into non-cyclic S-N groups (which sometimes then coordinate to metal centres);
- complete cleavage of all S-N bonds;
- formation of more complex heterocycles with 3 (or more) different heteroatoms.



<sup>214</sup> A. W. CORDES, C. G. MARCELLUS, M. C. NOBLE, R. T. OAKLEY and W. T. PENNINGTON, *J. Am. Chem. Soc.* **105**, 6008-12 (1983).

<sup>215</sup> U. THEWALT, *Angew. Chem. Int. Edn. Engl.* **15**, 765-6 (1976).

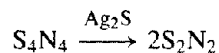
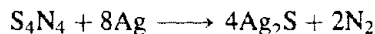
Table 15.22 Some further reactions of  $S_4N_4^{(206-210)}$ 

Reagents and conditions	Products	Ref. for structure, etc.
Vacuum thermolysis (Ag wool 300°)	$S_2N_2$ , (SN) <sub>x</sub>	pp. 726, 727
SnCl <sub>2</sub> (boiling C <sub>6</sub> H <sub>6</sub> + EtOH)	$S_4(NH)_4$	p. 735
NH <sub>3</sub>	$S_2N_2 \cdot NH_3$	
N <sub>2</sub> H <sub>4</sub> /SiO <sub>2</sub> (C <sub>6</sub> H <sub>6</sub> , 46°)	$S_{8-n}(NH)_n$ , n = 1–4	p. 735
S/CS <sub>2</sub> (heat in autoclave)	$S_4N_2$	
S <sub>2</sub> Cl <sub>2</sub>	$[S_4N_3]^+Cl^-$	
AgF <sub>2</sub> (cold CCl <sub>4</sub> )	$N_4(SF)_4$	
AgF <sub>2</sub> (hot CCl <sub>4</sub> )	NSF, NSF <sub>3</sub>	
Cl <sub>2</sub> (CCl <sub>4</sub> )	$N_3(SCl)_3$	
Br <sub>2</sub> (neat, heat in sealed tube)	$[S_4N_3]^+Br_3^-$	100% yield <sup>(216)</sup>
HX(CCl <sub>4</sub> ) X = F, Cl, Br	$[S_4N_3]^+X^-$	
HI	H <sub>2</sub> S, NH <sub>3</sub> , I <sub>2</sub>	
OSCl <sub>2</sub>	$S_3N_2O_2$	Fig. 15.34a
NiCl <sub>2</sub> /MeOH	$[Ni(S_2N_2H)_2]$ (also Co, Pd)	Fig. 15.34b
H <sub>2</sub> PtCl <sub>6</sub>	$[Pt(S_2N_2H)_2]$	Fig. 15.34b
PbI <sub>2</sub> /NH <sub>3</sub>	$[Pb(NSNS)(NH_3)]$	Fig. 15.34c

The molecular structures of the products are described as indicated at appropriate points in the text.  $S_3N_2O_2$  was at one time thought to be cyclic but X-ray diffraction analysis has revealed an open chain structure (Fig. 15.34a).<sup>(217)</sup> The structure of  $[Pt(S_2N_2H)_2]$  (Fig. 15.34b) is typical of several such compounds. When  $S_4N_4$  reacts with metal carbonyls in aprotic media, the products are the structurally similar  $[M(S_2N_2)_2]$  (M = Fe, Co, Ni). The pyramidal Pb<sup>II</sup> complex (Fig. 15.34c) is also notable, and features unequal S–N distances consistent with the bonding indicated. Still further reaction types are continually being discovered. For example, with the diphosphines  $Ph_2P(X)PPh_2$  (X = CH<sub>2</sub>CH<sub>2</sub> or NC<sub>4</sub>H<sub>8</sub>N),  $S_4N_4$  yields  $(N_3S_3)–NPPH_2(X)–PPh_2N–(S_3N_3)$ <sup>(218)</sup> whereas with platinum–metal complexes it forms adducts of the tridentate *S,S,N*-ligand *catena*- $S_4N_4^{2-}$ , e.g. *fac*- $[Ir(CO)Cl(\eta^3-S_4N_4)(PPh_3)]$ , Fig. 15.34d,<sup>(219)</sup>

*fac*- $[PtX_3(\eta^3-S_4N_4)]^-$  (X = Cl, Br, I)<sup>(220)</sup> and *mer*- $[PtCl_2(\eta^3-S_4N_4)(PMe_2Ph)]$ , (Fig 15.34e).<sup>(220)</sup>

(b) *Disulfur dinitrogen*,  $S_2N_2$ . When  $S_4N_4$  is carefully depolymerized by passing the heated vapour over Ag wool at 250–300° and 0.1–1.0 mmHg, the unstable cyclic dimer  $S_2N_2$  is obtained. The main purpose of the silver is to remove sulfur generated by the thermal decomposition of  $S_4N_4$ ; the  $Ag_2S$  so formed then catalyses the depolymerization of further  $S_4N_4$ :



In the absence of Ag/Ag<sub>2</sub>S the product is contaminated with  $S_4N_2$  (p. 728) formed by the reaction of the excess sulfur with either  $S_4N_4$  or  $S_2N_2$ . (See next subsection for discussion of possible mechanisms.)  $S_2N_2$  forms large colourless crystals which are insoluble in water but soluble in many organic solvents. The molecular structure is a square-planar ring ( $D_{2h}$ ) analogous to the isoelectronic cation

<sup>216</sup> G. WOLMERSHÄUSER and G. B. STREET, *Inorg. Chem.* **17**, 2685–6 (1978).

<sup>217</sup> J. WEISS, *Z. Naturforsch.* **16b**, 477 (1961); J. WEISS, *Fortsch. Chem. Forsch.* **5**, 635–62 (1966).

<sup>218</sup> C. J. THOMAS and M. N. S. RAO, *Z. anorg. allg. Chem.* **619**, 433–6 (1993), and references cited therein.

<sup>219</sup> F. EDELMANN, H. W. ROESKY, C. SPANG, M. NOLTEMEYER and G. M. SHELDRICK, *Angew. Chem. Int. Edn. Engl.* **25**, 931 (1986).

<sup>220</sup> V. C. GINN, P. F. KELLY, A. M. Z. SLAWIN, D. J. WILLIAMS and J. D. WOOLLINS, *Polyhedron* **12**, 1135–9 (1993). P. F. KELLY, R. N. SHEPPARD and J. D. WOOLLINS, *Polyhedron* **11**, 2605–9 (1992). See also P. F. KELLY and J. D. WOOLLINS, *Polyhedron* **8**, 2907–10 (1989).

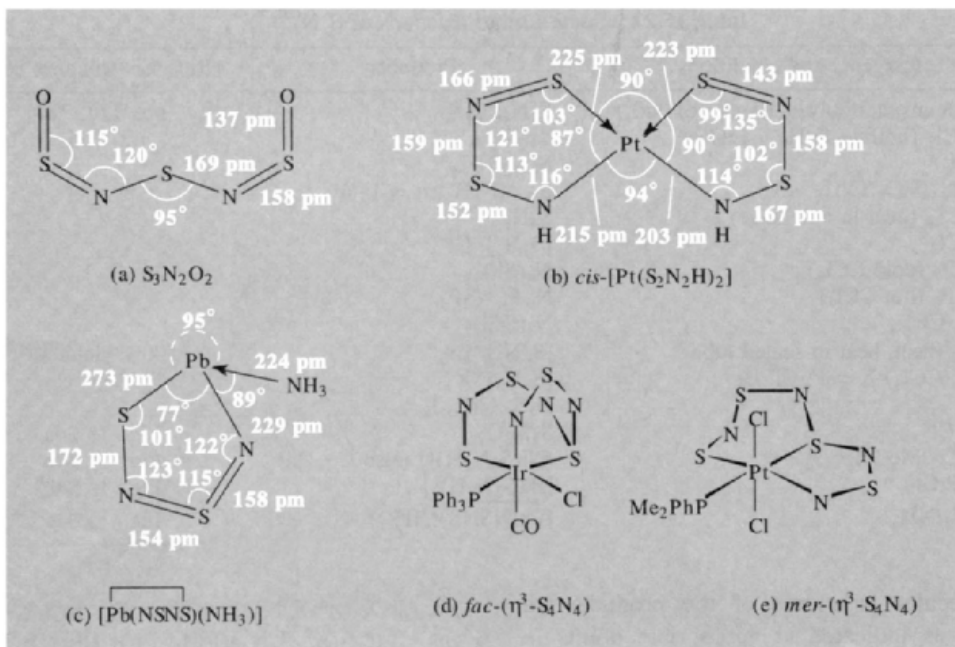


Figure 15.34 Structures of some SN compounds mentioned in Table 15.22 and the text.

$S_4^{2+}$  ( $D_{4h}$ , p. 665). Figure 15.35 shows the structure obtained by X-ray diffraction at  $-130^\circ$ <sup>(221)</sup> together with typical valence-bond representations.<sup>(212)</sup>

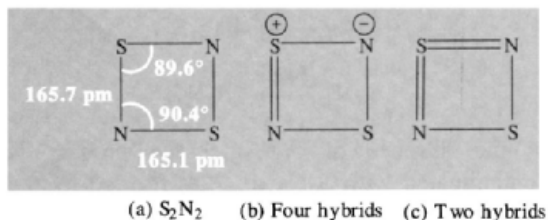


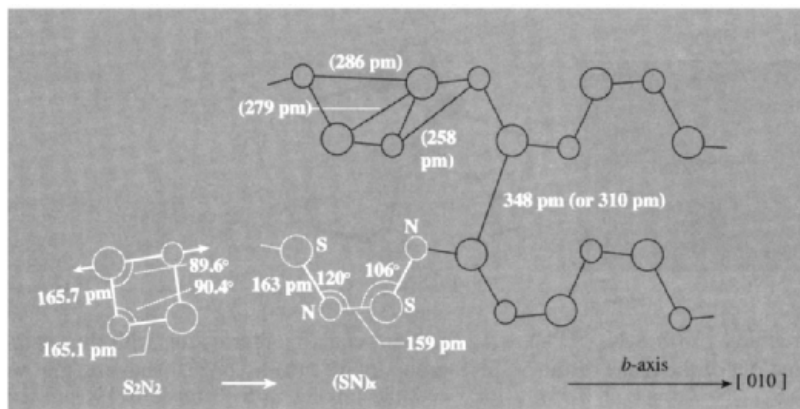
Figure 15.35 (a) Molecular structure and dimensions of  $S_2N_2$ ,<sup>(220)</sup> together with (b) minimal valence-bond representation and (c) additional valence-bond representation involving 3d S orbitals. (Note that the molecule has 6  $\pi$  electrons and 4 unshared electron-pairs superimposed on the square-planar  $\sigma$ -bonded structure.)

$S_2N_2$  decomposes explosively when struck or when warmed above  $30^\circ$ . Its chemistry

has therefore not been extensively studied. Reactions with  $NH_3$  and with aqueous alkali are similar to those of  $S_4N_4$ . It also forms adducts with Lewis bases, e.g.  $S_2N_2(SbCl_5)_2$ ; this latter is a yellow crystalline  $N$ -bonded complex which reacts with further  $S_2N_2$  to give the orange crystalline monoadduct  $S_2N_2 \cdot SbCl_5$ . The heterocycle remains planar and the S-N distances are almost the same as in the free  $S_2N_2$  molecule.

Undoubtedly the most exciting reaction of  $S_2N_2$  is its slow spontaneous polymerization in the solid state at room temperature to give crystalline  $(SN)_x$ . Crystals up to several millimetres in length can be grown. Not only is this an unusually facile topochemical reaction for a solid at low temperature but it results in an unprecedented metallic superconducting polymer, as discussed in the following subsection.

<sup>221</sup> A. G. MACDIARMID, C. M. MIKULSKI, P. J. RUSSO, M. S. SARAN, A. F. GARITO and A. J. HEEGER, *J. Chem. Soc., Chem. Commun.*, 476-7 (1975).



**Figure 15.36** Structure of fibrous  $(\text{SN})_x$  and its relation to  $\text{S}_2\text{N}_2$ .

(c) *Polythiazyl*,  $(\text{SN})_x$ .<sup>(222)</sup> Polymeric sulfur nitride, also known as polythiazyl, was first prepared by F. B. Burt in 1910 using a method that is still often used today — the solid-state polymerization of crystalline  $\text{S}_2\text{N}_2$  at room temperature (or preferably at  $0^\circ\text{C}$  over several days). Despite the bronze colour and metallic lustre of the polymer, over 50 y were to elapse before its metallic electrical conductivity, thermal conductivity and thermoelectric effect were investigated. By 1973 it had been established that  $(\text{SN})_x$  was indeed a metal down to liquid helium temperatures, and in 1975 the polymer was shown to be a superconductor below 0.26 K. (For higher-quality crystals the transition temperature rises to 0.33 K.) Values of the conductivity  $\sigma$  depend on the purity and crystallinity of the polymer and on the direction of measurement, being much greater along the fibres (*b*-axis) than across them. At room temperature typical values of  $\sigma_{\parallel}$  are  $1000\text{--}4000\text{ ohm}^{-1}\text{ cm}^{-1}$ , and this increases by as much as 1000-fold on cooling to 4.2 K. Typical values of the anisotropy ratio  $\sigma_{\parallel}/\sigma_{\perp}$  are  $\sim 50$  at room temperature and  $\sim 1000$  at 40 K.

The mechanism of formation of  $\text{S}_2\text{N}_2$  from  $\text{S}_4\text{N}_4$  and of the subsequent polymerization to  $(\text{SN})_x$  have been much studied and are very

sensitive to the exact conditions employed.<sup>(223)</sup> The use of the explosive intermediates  $\text{S}_4\text{N}_4$  and  $\text{S}_2\text{N}_2$  can be avoided by various alternative high-yield syntheses employing nonaqueous solvents. For example,  $(\text{SN})_x$  can be made in 65% yield by the reaction of  $\text{SiMe}_3(\text{N}_3)$  with  $\text{N}_3\text{S}_3\text{Cl}_3$ ,  $\text{N}_2\text{S}_3\text{Cl}_2$  or  $\text{N}_2\text{S}_3\text{Cl}$  (pp. 738, 739) in MeCN solution at  $-15^\circ\text{C}$  or by the reaction of  $\text{N}_3\text{S}_3\text{Cl}_3$  with an excess of  $\text{NaN}_3$ .<sup>(224)</sup> More recently still, the electrolytic reduction of  $\text{S}_5\text{N}_5^+\text{Cl}^-$  (p. 732) in liquid  $\text{SO}_2$  using a silver electrode has been used to deposit thin films of  $(\text{SN})_x$  on a variety of surfaces.<sup>(225)</sup>

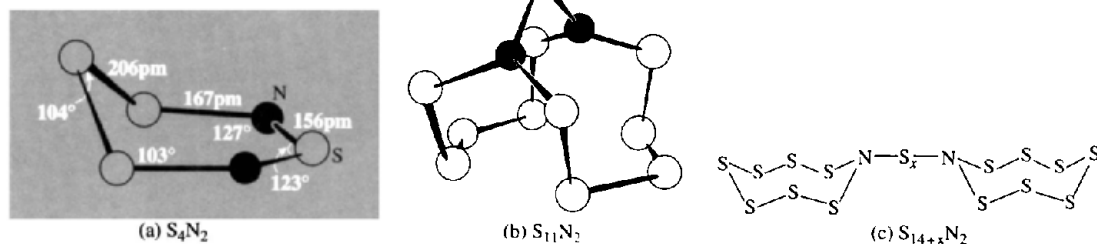
$(\text{SN})_x$  is much more stable than its precursor  $\text{S}_2\text{N}_2$ . When heated in air it decomposes explosively at about  $240^\circ\text{C}$  but it sublimes readily in vacuum at about  $135^\circ$ . The crystal structure reveals an almost planar chain polymer with the dimensions shown in Fig. 15.36. The S and N atoms deviate by about 17 pm from the mean plane. The structure should be compared

<sup>223</sup> H. BOCK, B. SOLOUKI and H. W. ROESKY, *Inorg. Chem.* **24**, 4425–7 (1985); E. BESENYEI, G. K. EIGENDORF and D. C. FROST, *Inorg. Chem.* **25**, 4404–8 (1986); M. J. ALMOND, A. J. DOWNS and T. L. JEFFERY, *Polyhedron* **7**, 629–34 (1988).

<sup>224</sup> F. A. KENNETT, G. K. MACLEAN, J. PASSMORE and M. N. S. RAO, *J. Chem. Soc., Dalton Trans.*, 851–7 (1982); A. J. BANISTER, Z. V. HAUPTMAN, J. PASSMORE, C.-M. WONG and P. S. WHITE, *J. Chem. Soc., Dalton Trans.*, 2371–9 (1986).

<sup>225</sup> A. J. BANISTER, Z. V. HAUPTMAN, J. M. RAWSON and S. T. WAIT, *J. Materials Chem.*, **6**, 1161–4 (1996).

<sup>222</sup> M. M. LABES, P. LOVE and L. F. NICHOLS, *Chem. Revs.* **79**, 1–15 (1979). A definitive review with 150 references.



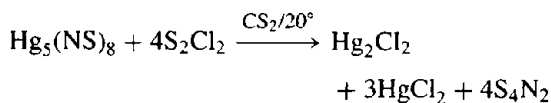
**Figure 15.37** Structures of (a)  $S_4N_2$ <sup>(226)</sup> showing the “half-chair” conformation with the central S of the  $S_3$  unit tilted out of the plane of the SNSNS group by  $55^\circ$ ; (b)  $S_{11}N_2$ <sup>(227)</sup> showing the two planar N atoms; (c)  $S_{14+x}N_2$  ( $x = 1, 2, 3, 5$ ) — for  $x = 2$  the linking S–S distance is 190 pm and S–N is 170 pm; for  $x = 3$  the linking S–S is 204 pm and S–N 171 pm<sup>(228)</sup>.

with that of helical  $S_\infty$  (p. 660), the (formal) replacement of alternate S atoms by N resulting both in a conformational change in the position of the atoms and an electronic change whereby 1 valence electron is removed for each SN unit in the chain. Polymerization is thought to occur by a one-point ring cleavage of each  $S_2N_2$  molecule followed by the formation of the *cis-trans*-polymer along the *a*-axis of the  $S_2N_2$  crystal which thereby transforms to the *b*-axis of the  $(SN)_x$  polymer.

There is intense current interest in these one-dimensional metals and several related partially halogenated derivatives have also been made, some of which have an even higher metallic conductivity, e.g. partial bromination of  $(SN)_x$  with  $Br_2$  vapour yields blue-black single crystals of  $(SNBr_{0.4})_x$  having a room-temperature conductivity of  $2 \times 10^4 \text{ ohm}^{-1} \text{ cm}^{-1}$  i.e. an order of magnitude greater than for the parent  $(SN)_x$  polymer. An even more facile preparation involves direct bromination of  $S_4N_4$  crystals ( $\sigma \sim 10^{-14} \text{ ohm}^{-1} \text{ cm}^{-1}$  at  $25^\circ$ ) with  $Br_2$  vapour at 180 mmHg over a period of hours; subsequent pumping at room temperature gives stoichiometries in the range  $(SNBr_{1.5})_x$  to  $(SNBr_{0.4})_x$  and further pumping at  $80^\circ\text{C}$  for 4 h reduces the halogen content to  $(SNBr_{0.25})_x$ . Similar highly conducting nonstoichiometric polymers can be obtained by treating  $S_4N_4$  with ICl, IBr and  $I_2$ , the increase in conductivity being more than 16 orders of magnitude.

(d) *Other binary sulfur nitrides.* Six further sulfur nitrides can be briefly mentioned:  $S_4N_2$ ,  $S_{11}N_2$  and  $(S_7N)_2S_x$  ( $x = 1, 2, 3, 5$ ); as can be seen from Fig. 15.37, these belong to three distinct structural classes. (For a fourth structure class, exemplified by  $S_5N_6$ , see p. 729.)

$S_4N_2$  is usually prepared by heating  $S_4N_4$  with a solution of sulfur in  $CS_2$  under pressure at  $100\text{--}120^\circ$ , though a more convenient laboratory preparation is now available by the reaction of activated Zn on  $N_3S_4Cl$ .<sup>(226)</sup> The compound also results from the thermolytic loss of  $N_2$  from  $S_4N_4$  which occurs when  $S_4N_4$  is heated under reflux in xylene for some hours. An alternative preparation (42% yield), which involves neither high pressure or high temperature, is the smooth reaction of solutions of  $Hg_5(NS)_8$  and  $S_2Cl_2$  in  $CS_2$ :



In all these reactions only the 1,3-diazaheterocycle (Fig. 15.37a) is obtained: the 1,1- and

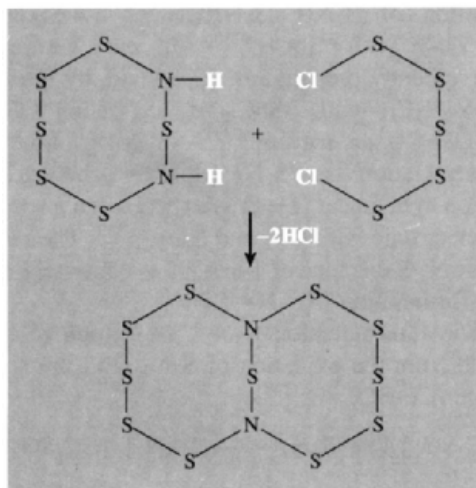
<sup>226</sup> R. W. H. SMALL, A. J. BANISTER and Z. V. HAUPTMAN, *J. Chem. Soc., Dalton Trans.*, 2188–91 (1981). T. CHIVERS, P. W. CODDING and R. T. OAKLEY, *J. Chem. Soc., Chem. Commun.*, 584–5 (1981). T. CHIVERS, P. W. CODDING, W. G. LAIDLAW, S. W. LIBLONG, R. T. OAKLEY and M. TRSIC, *J. Am. Chem. Soc.* **105**, 1186–92 (1983).

<sup>227</sup> H. GARCIA-FERNANDEZ, H. G. HEAL and G. TESTE DE SAGEY, *Compt. Rend.* **C275**, 323–6 (1972).

<sup>228</sup> H. GARCIA-FERNANDEZ, H. G. HEAL and G. TESTE DE SAGEY, *Compt. Rend.* **C282**, 241–3 (1976).

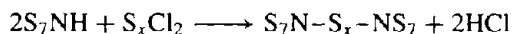
1,4-heterocycles and acyclic isomers are unknown (cf.  $N_2O_4$ , p. 455).  $S_4N_2$  forms opaque red-grey needles or transparent dark red prisms which melt at  $25^\circ$  to a dark-red liquid resembling  $Br_2$ . It decomposes explosively above  $100^\circ$ .  $S_4N_2$  appears to be a weaker ligand than either  $S_4N_4$  or  $S_2N_2$ : it does not react with  $BCl_3$  in  $CS_2$  solution, and  $SbCl_5$  gives a complex reaction mixture which contains  $S_4N_4 \cdot SbCl_5$  and  $[S_4N_3]^+ [SbCl_6]^-$  in addition to a poorly defined 1:1 adduct.

$S_{11}N_2$  is obtained as pale amber-coloured crystals by the double condensation of 1,3- $S_6(NH)_2$  with an equimolar amount of  $S_5Cl_2$  in the presence of pyridine:



Some polymer is also formed but this can be converted into the bicyclic  $S_{11}N_2$  by refluxing in  $CS_2$ . The X-ray crystal structure (Fig. 15.37b) shows that the 2 N atoms are planar.<sup>(227)</sup> This has been interpreted in terms of  $sp^2$  hybridization at N, with some delocalization of the  $p_\pi$  lone-pair of electrons into S-based orbitals, thus explaining the considerably diminished donor power of the molecule.  $S_{11}N_2$  is stable at room temperature but begins to decompose when heated above  $145^\circ$ .

The sulfur nitrides  $S_{15}N_2$  and  $S_{16}N_2$  are (formally) derived from *cyclo*- $S_8$  (or  $S_7NH$ ) and can be prepared by reacting  $S_7NH$  with  $SCl_2$  and  $S_2Cl_2$  respectively:



Both are yellow crystalline materials, stable at room temperature, and readily soluble in  $CS_2$  (Fig. 15.37c).<sup>(228)</sup> Compounds with  $x = 3$  and 5 can be prepared similarly.

Finally, in this subsection we mention the discovery of  $S_5N_6$  which is best prepared (73% yield) by the reaction of  $S_4N_5^-$  (p. 733) with  $Br_2$  in  $CH_2Cl_2$  at  $0^\circ C$  for several hours<sup>(229)</sup> Iodine reacts similarly but chlorine affords  $S_4N_5Cl$  (p. 731).  $S_5N_6$  forms orange crystals which are stable for prolonged periods at room temperature in an inert atmosphere, though they immediately blacken in air. It can be sublimed unchanged at  $45^\circ$  ( $10^{-2}$  mmHg) and decomposes above  $130^\circ$ . The structure (Fig. 15.38) features a molecular basket in which an  $-N=S-N-$  group bridges 2 S atoms of an  $S_4N_4$  cradle. Comparison with  $S_4N_4$  itself (p. 723) shows little change in the S–N distances in the cradle (161 pm) but the trans-annular S...S distances are markedly different: one is opened up from 258 pm to 394 pm (nonbonding) whereas the other contracts to 243 pm suggesting stronger trans-annular bonding between these 2 S atoms and the incipient formation of 2 fused 5-membered  $S_3N_2$  rings.

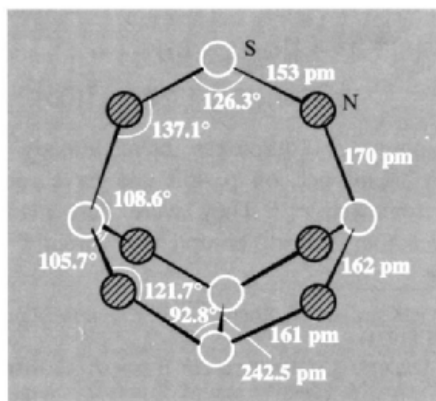


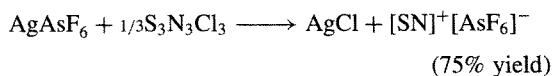
Figure 15.38 Structure of  $S_5N_6$ .

<sup>229</sup> T. CHIVERS and J. PROCTOR, *J. Chem. Soc., Chem. Commun.*, 642–3 (1978) and *Can. J. Chem.* **57**, 1286–93 (1979). See also W. S. SHELDRIK, M. N. S. RAO and H. W. ROESKY, *Inorg. Chem.* **19**, 538–43 (1980).

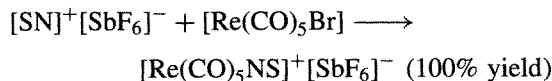
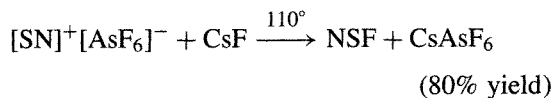
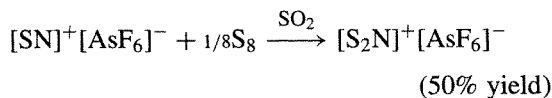
## (ii) Sulfur–nitrogen cations and anions

Numerous charged sulfur–nitrogen species have been synthesized in recent years, particularly those having an odd number of N atoms which would otherwise be paramagnetic. However, thio analogues of nitrites ( $\text{NO}_2^-$ , p. 461) and nitrates ( $\text{NO}_3^-$ , p. 465) are unknown.

The simplest stable sulfur–nitrogen species is the cation  $[\text{SN}]^+$  which was first prepared by the direct fluoride-ion transfer reaction between NSF and  $\text{AsF}_5$  or  $\text{SbF}_5$ .<sup>(230)</sup>  $[\text{NS}]^+[\text{AsF}_6]^-$  can also be prepared by reaction of an excess of  $\text{AsF}_5$  with  $\text{S}_3\text{N}_3\text{F}_3$  or by thermal decomposition of  $[\text{S}_3\text{N}_2\text{F}_2]^+[\text{AsF}_6]^-$ , but the simplest high-yield synthesis is by the reaction of  $\text{S}_3\text{N}_3\text{Cl}_3$  with an excess of  $\text{AgAsF}_6$  in liquid  $\text{SO}_2$ .<sup>(231)</sup>



The cation has considerable synthetic potential for a wide range of S/N compounds, e.g.<sup>(231,232)</sup>



Thionitrosyl complexes have already been briefly mentioned on p. 453 and have recently been reviewed.<sup>(233)</sup> They were first made<sup>(234)</sup> by reacting azido complexes directly with

<sup>230</sup> O. GLEMSER and W. KOCH, *Angew. Chem. Int. Edn. Engl.* **10**, 127 (1971).

<sup>231</sup> A. APBLET, A. J. BANISTER, D. BIRON, A. G. KENDRICK, J. PASSMORE, M. SCHRIEVER and M. STOJANAC, *Inorg. Chem.* **25**, 4451–2 (1986).

<sup>232</sup> G. HARTMANN and R. MEWS, *Angew. Chem. Int. Edn. Engl.* **24**, 202–3 (1985).

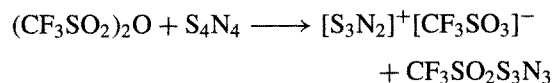
<sup>233</sup> J. D. WOOLLINS, Chap. 18 in R. STEUDEL (ed.), *The Chemistry of Inorganic Ring Systems*, Elsevier, Amsterdam, 1992, pp. 349–72.

<sup>234</sup> J. CHAIT and J. R. DILWORTH, *J. Chem. Soc., Chem. Commun.*, 508 (1974).

sulfur {e.g.  $[(\text{Et}_2\text{NCS})_3\text{Mo}\equiv\text{N}] + 1/8\text{S}_8 \longrightarrow [(\text{Et}_2\text{NCS})_3\text{Mo}(\text{NS})]$ }, but this reaction is not general. An alternative to direct metathesis with  $[\text{SN}]^+$  is dissociative oxidative addition {e.g.  $[\text{MCl}_2(\text{PPh}_3)_2] + 1/3(\text{S}_3\text{N}_3\text{Cl}_3) \longrightarrow [\text{MCl}_3(\text{NS})(\text{PPh}_3)_2]$ }. In the few complexes for which X-ray structural data are available the M–N–S group is essentially linear (170–177°) (see p. 453 and refs. 233, 235) but spectroscopic data on others suggest that bent and even  $\eta^1$ -bridging modes may be possible.

The dithionitronium cation  $[\text{S}_2\text{N}]^+$ , which is the sulfur analogue of the nitronium cation (p. 458), was first prepared as the crystalline salt  $[\text{S}_2\text{N}]^+[\text{SbCl}_6]^-$  by the complex oxidative reaction of  $\text{S}_7\text{NH}$ ,  $\text{S}_7\text{NBCl}_2$  or 1,4- $\text{S}_6(\text{NH})_2$  (p. 735) with  $\text{SbCl}_3$ .<sup>(236)</sup> It can be more conveniently prepared, in 30% yield, by reaction of  $\text{S}_3\text{N}_3\text{Cl}_3$  with  $3\text{SbCl}_5 + 3/8\text{S}_8$  using  $\text{OSCl}_2$  or  $\text{CH}_2\text{Cl}_2$  as solvent.<sup>(237)</sup> An X-ray structure determination on  $[\text{S}_2\text{N}]^+[\text{SbCl}_6]^-$  showed the cation to be linear ( $D_{\infty h}$ ) as expected for a species isoelectronic with  $\text{CS}_2$  and  $\text{NO}_2^+$ .<sup>(236)</sup> The rather short N–S distance of 146.4 pm is consistent with the formulation  $[\text{S}=\text{N}=\text{S}]^+$ .

The radical cation  $\text{S}_3\text{N}_2^+$  is formed in high yield from the oxidation of  $\text{S}_4\text{N}_4$  with the anhydride  $(\text{CF}_3\text{SO}_2)_2\text{O}$ .<sup>(238)</sup>



The product is a black-brown solid that is very sensitive to oxygen. The same cation can be obtained by oxidation of  $\text{S}_4\text{N}_4$  with  $\text{AsF}_5$  and is unusual in being the only sulfur–nitrogen (paramagnetic) radical that has been obtained as a stable crystalline salt. X-ray diffraction analysis shows the structure to be a planar 5-membered ring with approximate

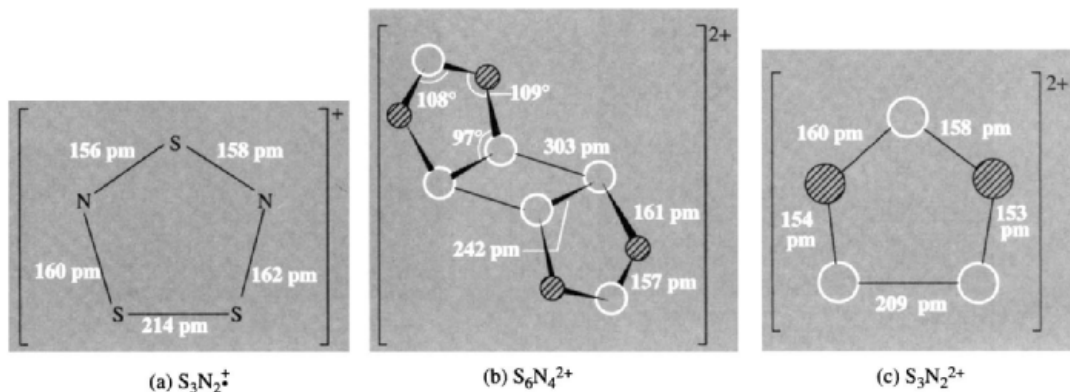
<sup>235</sup> J. BALDAS, J. BONNYMAN, M. F. MACKAY and G. A. WILLIAMS, *Aust. J. Chem.* **37**, 751–9 (1984).

<sup>236</sup> R. FAGGIANI, R. J. GILLESPIE, C. J. L. LOCK and J. D. TYRER, *Inorg. Chem.* **17**, 2975–8 (1978).

<sup>237</sup> A. J. BANISTER and A. G. KENDRICK, *J. Chem. Soc., Dalton Trans.*, 1565–7 (1987).

<sup>238</sup> R. J. GILLESPIE, J. P. KEMT and J. F. SAWYER, *Inorg. Chem.* **20**, 3784–99 (1981).

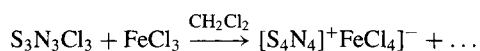
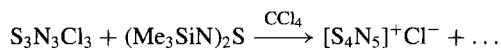
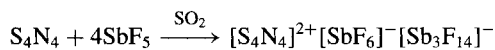
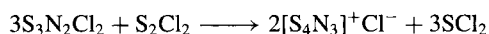
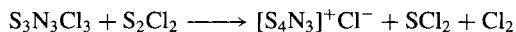




**Figure 15.39** Structures of (a) the planar radical cation  $S_3N_2^+$ , (b) its dimer  $S_6N_4^{2+}$  and (c) the corresponding planar diamagnetic dication  $S_3N_2^{2+}$ .

$C_{2v}$  symmetry (Fig. 15.39a). The corresponding diamagnetic dimer  $S_6N_4^{2+}$  was obtained in low yield by oxidation of  $S_3N_2Cl$  with  $ClSO_3H$ : its structure (Fig. 15.39b) consists of 2 symmetry-related planar  $S_3N_2^+$  units linked by 2 very long S–S bonds. Alternatively, the central  $S_4$  unit can be thought of as being bound by a 4-centre 6-electron bond. Even more remarkably, a diamagnetic  $6\pi$ -electron dication,  $[S_3N_2]^{2+}$ , which is less stable than its paramagnetic  $7\pi$ -electron analogue  $[S_3N_2]^+$ , has been prepared and characterized as the crystalline salt  $[S_3N_2]^{2+}[AsF_6]_2^-$ .<sup>(239)</sup> The planar conformation of the ring is retained, but the dimensions are significantly different (Fig. 15.39(c)) most notably in the shortening of the S–S and adjacent S–N bonds. The dictation is only stable in the crystalline phase; in  $SO_2$  solutions it reversibly dissociates into the paramagnetic species  $[SN]^+$  and  $[SNS]^+$ , the cycloaddition in the solid state apparently being driven by the high lattice energy of the 1:2 salt.

Cations containing 4 S atoms include  $S_4N_3^+$ ,  $S_4N_4^{2+}$  and  $S_4N_5^+$ , as well as the unique radical cation  $S_4N_4^+$ . The structures are in Fig. 15.40 and typical preparative routes are:<sup>(210, 240–241)</sup>



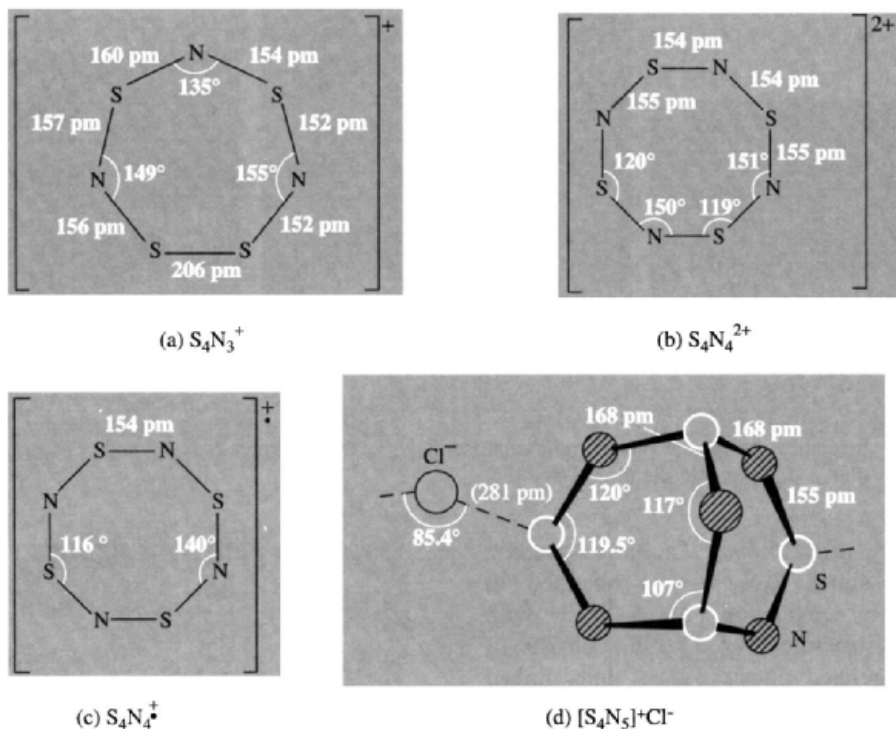
These compounds contain some fascinating and subtle structural and bonding problems. For example, the compound  $[S_4N_4]^{2+}[SbF_6]^- [Sb_3F_{14}]^-$  shows two structurally distinct cations, one with essentially equal S–N distances around the planar ring (Fig. 15.40b) and the other, also planar, but with alternating S–N distances of *ca.* 153 and 162 pm and with bond angles at S and N of  $127^\circ$  and  $143^\circ$ , respectively. By contrast, a non-planar boat-shaped structure was found for the dication in  $[S_4N_4]^{2+}[SbCl_6]_2^-$ .<sup>(240)</sup> The unusual radical cation  $[S_4N_4]^+$  occurs in the brown, moisture-sensitive compound  $[S_4N_4]^+[FeCl_4]^-$  and features a puckered 8-membered ring in which the four S atoms form an almost perfect square and all the S–N

<sup>240</sup> R. J. GILLESPIE, D. R. SLIM and J. D. TYRER, *J. Chem. Soc., Chem. Commun.*, 253–5 (1977). R. J. GILLESPIE, J. P. KENT, J. F. SAWYER, D. R. SLIM and J. D. TYRER, *Inorg. Chem.* **20**, 3799–812 (1981).

<sup>241</sup> T. CHIVERS, L. FIELDING, W. G. LAIDLAW and M. TRSIC, *Inorg. Chem.* **18**, 3379–87 (1979).

<sup>242</sup> U. MÜLLER, E. COMRADI, U. DEMANT and K. DEHNICKE, *Angew. Chem. Int. Edn. Engl.* **23**, 237–8 (1984).

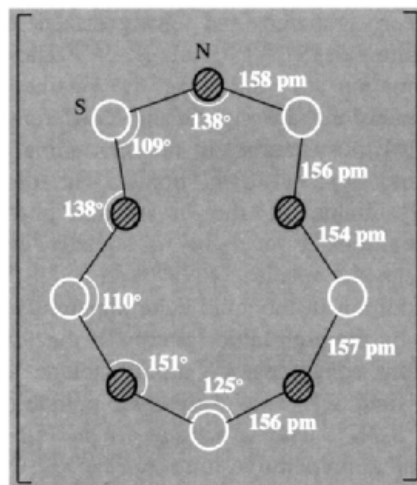
<sup>239</sup> W. V. F. BROOKS, T. S. CAMERON, F. GREIN, S. PARSONS, J. PASSMORE and M. J. SCHRIEVER, *J. Chem. Soc., Chem. Commun.*, 1079–81 (1991).



**Figure 15.40** Structure of (a) planar  $S_4N_3^+$ ; (b) planar  $S_4N_4^{2+}$  (see text); (c) puckered  $S_4N_4^+$ ; (d) a portion of the polymeric structure of  $[S_4N_5]^+Cl^-$  showing the trans-annular bridging N atom.

distances are essentially equal at 154 pm, but in which the four N atoms are located alternately 34, -59, 45 and -38 pm above and below the plane of the four S atoms. The original papers should be consulted for further details.

An interesting structural problem also emerges from the study of the final sulfur-nitrogen cation to be considered,  $S_5N_5^+$ . First made in 1972, this was originally thought to contain a planar, heart shaped 10-membered heterocycle on the basis of X-ray diffraction studies on  $[S_5N_5]^+[AlCl_4]^-$ ; however, it now seems likely that this is an artefact of disorder within the crystals and that the structure of the cation is as in Fig. 15.41<sup>(243)</sup> which is the



**Figure 15.41** Structure of  $S_5N_5^+$ .

<sup>243</sup> H. W. ROESKY, W. G. BÖWING, I. RAYMENT and H. M. M. SHEARER, *J. Chem. Soc., Chem. Commun.*, 735-6 (1975); A. J. BANISTER, J. A. DURRANT, I. RAYMENT and H. M. M. SHEARER, *J. Chem. Soc., Dalton Trans.*, 928-30

(1976). See also R. J. GILLESPIE, J. F. SAWYER, D. R. SLIM and J. D. TYRER, *Inorg. Chem.* **21**, 1296-302 (1982).

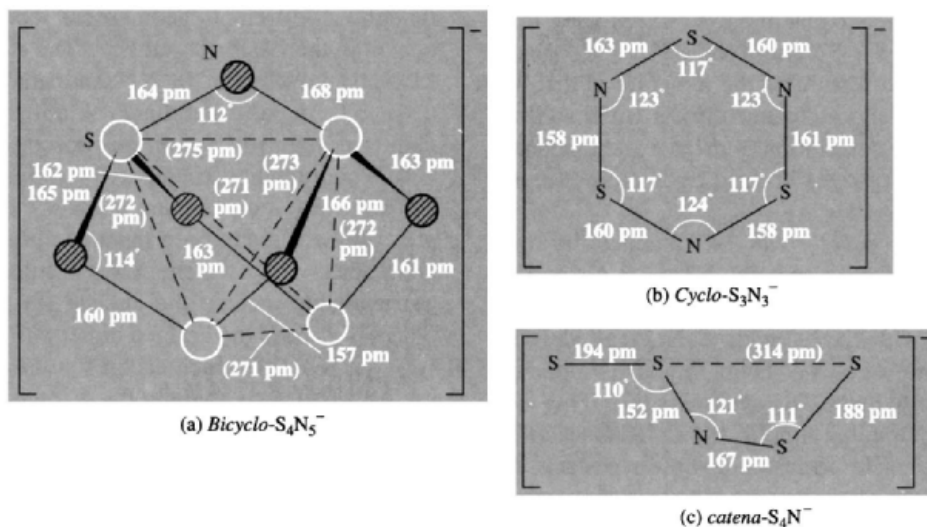
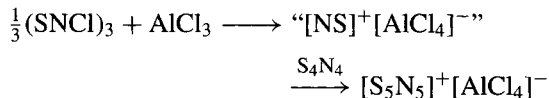


Figure 15.42 Structure of sulfur–nitrogen anions.

conformation observed in  $[\text{S}_5\text{N}_5]^+[\text{S}_3\text{N}_3\text{O}_4]^-$  and  $[\text{S}_5\text{N}_5]^+[\text{SnCl}_5(\text{POCl}_3)]^-$ . Salts such as the yellow  $[\text{S}_5\text{N}_5]^+[\text{AlCl}_4]^-$  and dark-orange  $[\text{S}_5\text{N}_5]^+[\text{FeCl}_4]^-$  can readily be prepared in high yield by adding  $\text{AlCl}_3$  (or  $\text{FeCl}_3$ ) to  $\text{S}_3\text{N}_3\text{Cl}_3$  in  $\text{SOCl}_2$  solution and then treating the adduct so formed with  $\text{S}_4\text{N}_4$ ; the overall stoichiometry can be represented as:



though the reaction is undoubtedly more complex and proceeds via the adduct  $(\text{SNCl})_3 \cdot 2\text{AlCl}_3$ .<sup>(244)</sup> Treatment of  $[\text{S}_5\text{N}_5]^+[\text{AlCl}_4]^-$  with thf yields pure  $[\text{S}_5\text{N}_5]\text{Cl}$  from which  $[\text{S}_5\text{N}_5]^+[\text{BF}_4]^-$  can readily be prepared.<sup>(245)</sup> The planar azulene-shaped cation also occurs in the crystalline adduct  $[\text{S}_5\text{N}_5]^+_4[\text{As}_8\text{Cl}_{28}]^{4-} \cdot 2\text{S}_4\text{N}_4$ .<sup>(246)</sup> Uncoordinated sulfur–nitrogen anions are less common than

S–N cations and all are of recent preparation:<sup>(247)</sup> *bicyclo-S<sub>4</sub>N<sub>5</sub><sup>-</sup>* (1976), *cyclo-S<sub>3</sub>N<sub>3</sub><sup>-</sup>* (1977) and *catena-S<sub>4</sub>N<sup>-</sup>* (1979), as well as the more fugitive species  $\text{S}_3\text{N}_3^-$  and  $\text{S}_7\text{N}_7^-$ . Structures are in Fig. 15.42.  $\text{S}_4\text{N}_5^-$  occurs as the product in a variety of reactions of  $\text{S}_4\text{N}_4$  with nucleophiles:<sup>(248)</sup> e.g. liquid  $\text{NH}_3$  or ethanolic solutions of  $\text{R}_2\text{NH}$ ,  $\text{MN}_3$  ( $\text{M} = \text{Li}, \text{Na}, \text{K}, \text{Rb}$ ),  $\text{KCN}$  or even  $\text{Na}_2\text{S}$ . The course of these reactions suggests the initial formation of  $\text{S}_3\text{N}_3^-$  which then reacts with further  $\text{S}_4\text{N}_4$  to give  $\text{S}_4\text{N}_5^-$ . The ammonium salt  $[\text{NH}_4]^+[\text{S}_4\text{N}_5]^-$  is a ubiquitous product of the reaction of ammonia with  $\text{S}_4\text{N}_4$ ,  $(\text{SNCl})_3$ ,  $\text{S}_2\text{Cl}_2$ ,  $\text{SCl}_2$  or  $\text{SCl}_4$ .<sup>(249)</sup> Yet another route is the methanolysis of  $(\text{Me}_3\text{SiN})_2\text{S}$ :



Subsequent metathesis with  $\text{Bu}_4\text{NOH}$  yielded yellow crystals suitable for X-ray structure analysis. The structure of  $[\text{S}_4\text{N}_5]^-$  (Fig. 15.42a)

<sup>244</sup> A. J. BANISTER and H. G. CLARKE, *J. Chem. Soc., Dalton Trans.*, 2661–3 (1972). See also A. J. BANISTER, A. J. FIELDER, R. G. HEY, and N. R. M. SMITH, *ibid.*, 1457–60.

<sup>245</sup> A. J. BANISTER, Z. V. HAUPTMAN, A. G. KENDRICK and R. W. H. SMALL, *J. Chem. Soc., Dalton Trans.*, 915–24 (1987).

<sup>246</sup> W. WILLING, U. MULLER, J. EICHER and K. DEHNICKE, *Z. anorg. allg. Chem.* **537**, 145–53 (1986).

<sup>247</sup> T. CHIVERS and R. T. OAKLEY *Topics in Current Chemistry*. Vol. 102, *Inorganic Ring Systems*, Springer Verlag, Berlin, 1982, pp. 117–47 (114 references).

<sup>248</sup> J. BOJES, T. CHIVERS, I. DRUMMOND and G. MACLEAN, *Inorg. Chem.* **17**, 3668–72 (1978).

<sup>249</sup> O. J. SCHERER and G. WOLMERSHÄUSER, *Chem. Ber.* **110**, 3241–4 (1977).

is closely related to that of  $S_4N_4$  (and  $S_4N_5^+$ ), one trans-annular  $S \cdots S$  being bridged by the fifth N atom.<sup>(250)</sup> One feature of the structure is that all the  $S \cdots S$  distances become almost equal so that an alternative description is of an  $S_4$  tetrahedron with 5 of the 6 edges bridged by N atoms, angle  $S-N-S$  112–114°.

The anion  $S_3N_3^-$  can be obtained by the action of azides (or metallic K) on  $S_4N_4$  or the reaction of KH on  $S_4(NH)_4$ .<sup>(251)</sup> Further reaction of  $S_3N_3^-$  with  $S_4N_4$  yields  $S_4N_5^-$  (as above). The structure of  $S_3N_3^-$  (Fig. 15.42b) is a planar ring of approximate  $D_{3h}$  symmetry.<sup>(251)</sup> This has interesting bonding implications. Thus each S in a heterocycle forms a  $\sigma$  bond to each of its neighbours (thereby using 2 electrons) and it also has an exocyclic lone-pair of electrons: this leaves 2 electrons to contribute to the  $\pi$  system of the heterocycle (which might or might not involve S 3d orbitals). Likewise, each N atom has 2 electrons in  $\sigma$  bonds, one exocyclic lone pair, and contributes one electron to the  $\pi$  system. Planar S–N heterocycles having 4–10 ring atoms are now known and all except the radical cation  $S_3N_2^+$  have  $(4n + 2)\pi$  electrons where  $n = 1, 2, \text{ or } 3$  as shown below:

Ring/size	4	5	6	7	8	10
Species	$S_2N_2$	$S_3N_2^+$	$S_3N_3^-$	$S_4N_3^+$	$S_4N_4^{2+}$	$S_5N_5^+$
Number of $\pi$ electrons	6	[7]	10	10	10	14

Thermal decomposition of  $[N(PPh_3)_2]^+ [S_4N_5]^-$  in MeCN yields sequentially the corresponding salts of  $S_3N_3^-$  and  $S_4N^-$  (50% yield). An X-ray crystallographic analysis of the dark-blue air-stable product  $[N(PPh_3)_2]^+ [S_4N]^-$  revealed the presence of the unique acyclic anion  $[SSNSS]^-$  whose structure is in Fig. 15.42c. The anion is planar with *cis-trans* configuration,

<sup>250</sup> W. FLUES, O. J. SCHERER, J. WEISS and G. WOLMERS-HÄUSER, *Angew. Chem. Int. Edn. Engl.* **15**, 379–80 (1976).

<sup>251</sup> J. BOJES, T. CHIVERS, W. G. LAIDLAW and M. TRSIC, *J. Am. Chem. Soc.* **101**, 4517–22 (1979), and references therein. See also R. JONES, P. F. KELLY, D. J. WILLIAMS and J. D. WOOLLINS, *Polyhedron* **6**, 1541–6 (1987); and P. N. JAGG, P. F. KELLY, H. S. RZEPA, D. J. WILLIAMS, J. D. WOOLLINS and W. WYLIE *J. Chem. Soc., Chem. Commun.*, 942–4 (1991).

though a different geometrical configuration occurs in the  $[AsPh_4]^+$  salt.<sup>(252)</sup> The existence of  $[S_4N]^-$  as well as of  $[S_7N]^-$  and small amounts of  $[S_3N]^-$  in sulfur-ammonia solutions has been demonstrated by  $^{14}N$  nmr spectroscopy.<sup>(253)</sup>

The coordination chemistry of sulfur–nitrogen anions is also a burgeoning field.<sup>(254)</sup> Some complexes have already been mentioned (pp. 725–6) and others for which X-ray structural data are available include the chelate  $[Pt(PPh_3)_2(\eta^2-SNSN)]$ <sup>(255)</sup> and the bridged dimer  $[{(Ph_3P)_2Pt}_2(\mu, \eta^2-S_2N_2)_2]$  in which each Pt atom is chelated by  $-SNSN-$  and then bridged to the other Pt atom by the coordinated N atom to form a central planar  $Pt_2N_2$  ring.<sup>(256)</sup> For coordinated  $[S_3N_2]^{2-}$  and  $[S_3N_4]^{2-}$  examples include the chelated titanocene derivatives  $[Ti(\eta^5-C_5H_5)_2(\eta^2-S_3N_2)]$  and  $[Ti(\eta^5-C_5H_5)_2(\eta^2-S_3N_4)]$  which feature the 6- and 8-membered ring systems  $\overline{TiSSNSN}$  and  $\overline{TiNSNSNSN}$ , respectively.<sup>(257)</sup> The chelating trianion  $[S_2N_3]^{3-}$  occurs in the 6-coordinate mixed ligand trisbidentate vanadium(V) complex  $[V(dtbc)(phen)(\eta^2-N_3S_2)]$  (*dtbc* = di-*t*-butylcatecholate,  $Bu_2C_6H_2O_2^{2-}$ ; *phen* = 1,10-phenanthroline)<sup>(258)</sup> and in the

<sup>252</sup> N. BUFORD, T. CHIVERS, A. W. CORDES, R. T. OAKLEY, W. T. PENNINGTON and P. N. SWEPSTON, *Inorg. Chem.* **20**, 4430–2 (1981). See also T. CHIVERS and C. LAU, *Inorg. Chem.* **21**, 453–5 (1982).

<sup>253</sup> T. CHIVERS, D. D. MCINTYRE, K. J. SCHMIDT and H. J. VOGEL, *J. Chem. Soc., Chem. Commun.*, 1341–2 (1990); see also T. CHIVERS and K. J. SCHMIDT, *ibid.* pp. 1342–3, for  $S_2N_2H]^-$ .

<sup>254</sup> P. F. KELLY and J. D. WOOLLINS, *Polyhedron* **5**, 607–32 (1986); T. CHIVERS and F. EDELMANN, *Polyhedron* **5**, 1661–99 (1986); H. W. ROESKY, in H. W. ROESKY (ed.), *Rings Clusters and Polymers of Main Group and Transition Elements*, Elsevier, Amsterdam, 1989, pp. 369–408; J. D. WOOLLINS, in R. STEUDEL (ed.), *The Chemistry of Inorganic Ring Systems*, Elsevier, Amsterdam, 1992, pp. 349–72.

<sup>255</sup> R. JONES, P. F. KELLY, D. J. WILLIAMS and J. D. WOOLLINS, *Polyhedron* **4**, 1947–50 (1985). See also P. A. BATES, M. B. HURSTHOUSE, P. F. KELLY and J. D. WOOLLINS, *J. Chem. Soc., Dalton Trans.*, 2367–70 (1986).

<sup>256</sup> R. JONES, P. F. KELLY, D. J. WILLIAMS and J. D. WOOLLINS, *J. Chem. Soc., Chem. Commun.*, 1325–6 (1985).

<sup>257</sup> C. G. MARCELLUS, R. T. OAKLEY, W. T. PENNINGTON and A. W. CORDES, *Organometallics* **5**, 1395–400 (1986).

<sup>258</sup> T. A. KABANOS, A. M. Z. SLAWIN, D. J. WILLIAMS and J. D. WOOLLINS, *J. Chem. Soc., Chem. Commun.*, 193–4

anionic complex  $[\text{WCl}_2\text{F}_2(\eta^2\text{-N}_3\text{S}_2)]^-$ .<sup>(259)</sup> Copper(I) and silver complexes of the  $[\text{S}_3\text{N}]^-$  ion are of older vintage, e.g.  $[\text{Cu}(\text{PPh}_3)_2(\eta^2\text{-SSNS})]$  and  $[\text{Cu}(\eta^2\text{-SSNS})_2]^-$ .<sup>(260)</sup>

(iii) Sulfur imides,  $\text{S}_{8-n}(\text{NH})_n$ <sup>(206)</sup>

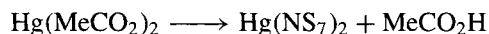
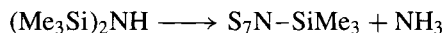
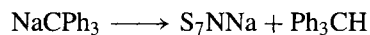
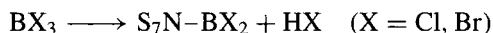
The NH group is “isoelectronic” with S and so can successively subrogate S in *cyclo*- $\text{S}_8$ . Thus we have already seen that reduction of  $\text{S}_4\text{N}_4$  with dithionite or with  $\text{SnCl}_2$  in boiling ethanol/benzene yields  $\text{S}_4(\text{NH})_4$ . Again, whereas reaction of  $\text{S}_2\text{Cl}_2$  or  $\text{SCl}_2$  with  $\text{NH}_3$  in non-polar solvents yields  $\text{S}_4\text{N}_4$ , heating these 2 reactants in

polar solvents such as dimethylformamide affords a range of sulfur imides. In a typical reaction 170 g  $\text{S}_2\text{Cl}_2$  and the corresponding amount of  $\text{NH}_3$  yielded:

$\text{S}_8$ (32 g)	$1,3\text{-S}_6(\text{NH})_2$ (0.98 g)	$1,3,5\text{-S}_5(\text{NH})_3$ (0.08 g)
$\text{S}_7\text{NH}$ (15.4 g)	$1,4\text{-S}_6(\text{NH})_2$ (2.3 g)	$1,3,6\text{-S}_5(\text{NH})_3$ (0.32 g)
	$1,5\text{-S}_6(\text{NH})_2$ (0.82 g)	

In no case have adjacent NH groups been observed.

$\text{S}_7\text{NH}$  is a stable pale-yellow compound, mp 113.5°; the structure is closely related to that of *cyclo*- $\text{S}_8$  as shown in Fig. 15.43a. The proton is acidic and undergoes many reactions of which the following are typical (see also p. 729):



(1990). See also P. F. KELLY, A. M. Z. SLAWIN, D. J. WILLIAMS and J. D. WOOLLINS *Polyhedron* **10**, 2337–40 (1991).

<sup>259</sup> H. BORGHOLTE, K. DEHNICKE, H. GOESMANN and D. FENSKE, *Z. anorg. allg. Chem.*, **586**, 159–65 (1990).

<sup>260</sup> J. BOJES, T. CHIVERS and P. W. CODDING, *J. Chem. Soc., Chem. Commun.*, 1171–3 (1981).

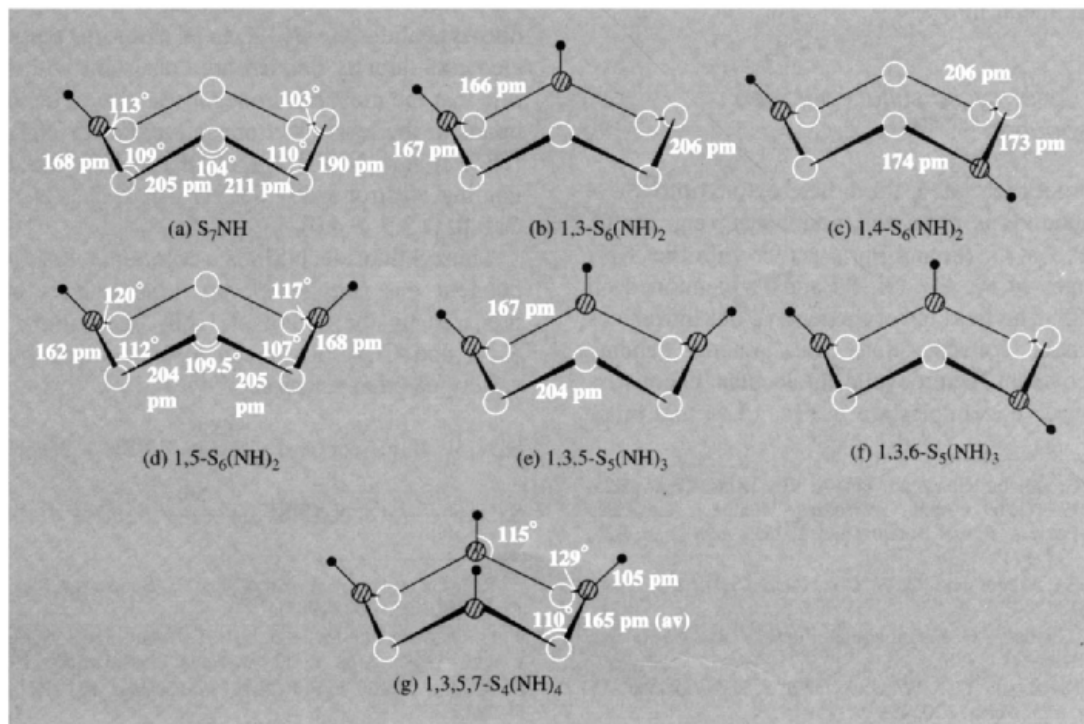


Figure 15.43 Structures of the various cyclo sulfur imides.

anionic complex  $[\text{WCl}_2\text{F}_2(\eta^2\text{-N}_3\text{S}_2)]^-$ .<sup>(259)</sup> Copper(I) and silver complexes of the  $[\text{S}_3\text{N}]^-$  ion are of older vintage, e.g.  $[\text{Cu}(\text{PPh}_3)_2(\eta^2\text{-SSNS})]$  and  $[\text{Cu}(\eta^2\text{-SSNS})_2]^-$ .<sup>(260)</sup>

(iii) Sulfur imides,  $\text{S}_{8-n}(\text{NH})_n$ <sup>(260)</sup>

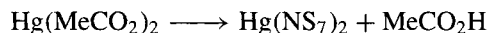
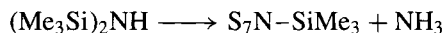
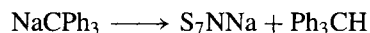
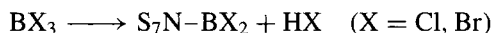
The NH group is “isoelectronic” with S and so can successively subrogate S in *cyclo-S*<sub>8</sub>. Thus we have already seen that reduction of  $\text{S}_4\text{N}_4$  with dithionite or with  $\text{SnCl}_2$  in boiling ethanol/benzene yields  $\text{S}_4(\text{NH})_4$ . Again, whereas reaction of  $\text{S}_2\text{Cl}_2$  or  $\text{SCl}_2$  with  $\text{NH}_3$  in non-polar solvents yields  $\text{S}_4\text{N}_4$ , heating these 2 reactants in

polar solvents such as dimethylformamide affords a range of sulfur imides. In a typical reaction 170 g  $\text{S}_2\text{Cl}_2$  and the corresponding amount of  $\text{NH}_3$  yielded:

$\text{S}_8$ (32 g)	$1,3\text{-S}_6(\text{NH})_2$ (0.98 g)	$1,3,5\text{-S}_5(\text{NH})_3$ (0.08 g)
$\text{S}_7\text{NH}$ (15.4 g)	$1,4\text{-S}_6(\text{NH})_2$ (2.3 g)	$1,3,6\text{-S}_5(\text{NH})_3$ (0.32 g)
	$1,5\text{-S}_6(\text{NH})_2$ (0.82 g)	

In no case have adjacent NH groups been observed.

$\text{S}_7\text{NH}$  is a stable pale-yellow compound, mp 113.5°; the structure is closely related to that of *cyclo-S*<sub>8</sub> as shown in Fig. 15.43a. The proton is acidic and undergoes many reactions of which the following are typical (see also p. 729):



(1990). See also P. F. KELLY, A. M. Z. SLAWIN, D. J. WILLIAMS and J. D. WOOLLINS *Polyhedron* **10**, 2337–40 (1991).

<sup>259</sup> H. BORGHOLTE, K. DEHNICKE, H. GOESMANN and D. FENSKE, *Z. anorg. allg. Chem.*, **586**, 159–65 (1990).

<sup>260</sup> J. BOJES, T. CHIVERS and P. W. CODDING, *J. Chem. Soc., Chem. Commun.*, 1171–3 (1981).

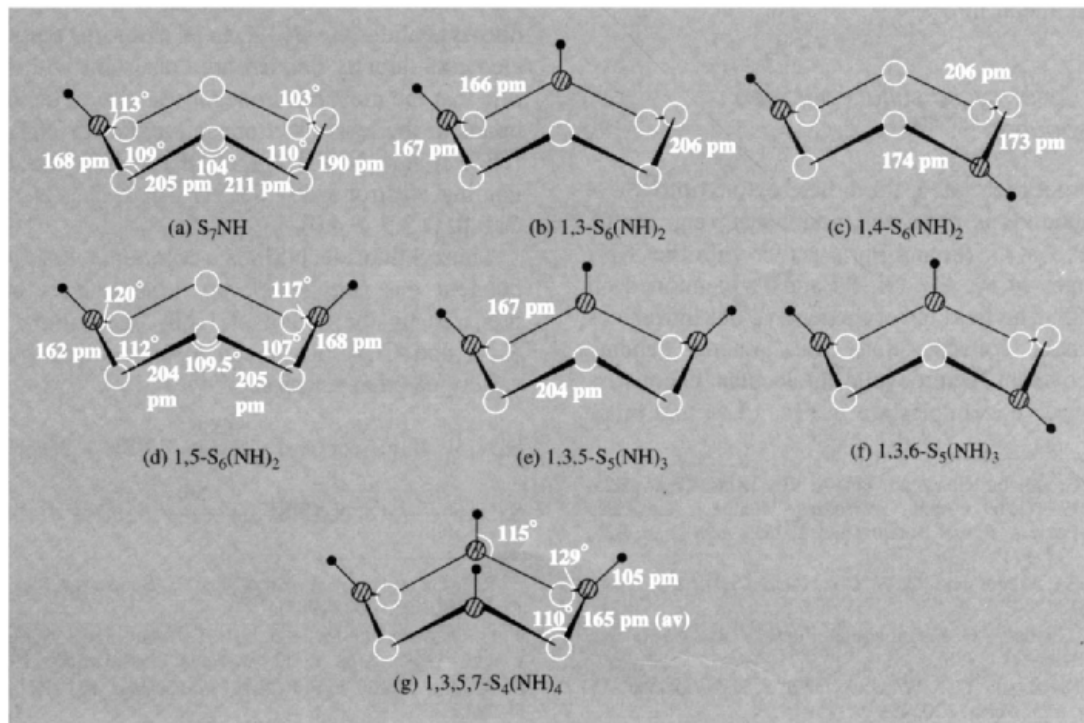


Figure 15.43 Structures of the various cyclo sulfur imides.

The 3 isomeric compounds  $S_6(NH)_2$  form stable colourless crystals and have the structures illustrated in Fig. 15.43b, c, and d.<sup>(208,261)</sup> The 1,3-, 1,4-, and 1,5-isomers melt at 130°, 133°, and 155° respectively. The 1,3,5- and 1,3,6-triimides melt with decomposition at 128° and 133° (Fig. 15.43e and f). The tetraimide,  $S_4(NH)_4$  (mp 145°) is structurally very similar (Fig. 15.43g):<sup>(262)</sup> the N atoms are each essentially trigonal planar and the heterocycle is somewhat flattened, the distance between the planes of the 4 N atoms and 4 S atoms being only 57 pm. The influence of extensive intermolecular H-bonding on the structure has been studied by electron deformation density techniques.<sup>(263)</sup>

Alkyl derivatives such as 1,4- $S_6(NR)_2$  and  $S_4(NR)_4$  can be synthesized by reacting  $S_2Cl_2$  with primary amines  $RNH_2$  in an inert solvent. Compounds such as 1,4- $S_2(NR)_4$  ( $R = -CO_2Et$ ) are now also well characterized.<sup>(264)</sup> The bis-adduct  $[Ag(S_4N_4H_4)_2]^+$  has been isolated as its perchlorate; this has a sandwich-like structure and is unique in being S-bonded rather than N-bonded to the metal ion.<sup>(265)</sup>

#### (iv) Other cyclic sulfur–nitrogen compounds<sup>(207,209)</sup>

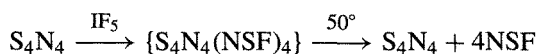
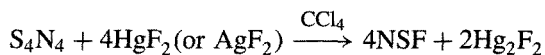
Incorporation of a third heteroatom into S–N compounds is now well established, e.g. for C, Si; P, As; O; Sn and Pb, together with the  $S_2N_2$  chelates of Fe, Co, Ni, Pd and Pt mentioned on p. 725. The field is very extensive but introduces no new concepts into the general scheme of covalent heterocyclic molecular chemistry. Illustrative examples are in Fig. 15.44 and fuller

details including X-ray structures for many of the compounds are in the references cited above. A selenium analogue of the dimer  $S_6N_4^{2+}$  (p. 731) has also been prepared and structurally characterized, viz.  $[SN_2Se_2Se_2N_2S]^{2+}$ .<sup>(266)</sup>

#### (v) Sulfur–nitrogen halogen compounds<sup>(267–9)</sup>

As with sulfur–halogen compounds (pp. 683–93) the stability of N–S–X compounds decreases with increase in atomic weight of the halogen. There are numerous fluoro and chloro derivatives but bromo and iodo derivatives are virtually unknown except for the nonstoichiometric  $(SNX_x)_\infty$  polymers (p. 728) and  $S(NX)_2$  (p. 740). Unlike the H atoms in the sulfur imides (p. 735) the halogen atoms are attached to S rather than N. Fluoro derivatives have been known since 1965 but some of the chloro compounds have been known for over a century. The simplest compounds are the nonlinear thiazyl halides  $N\equiv S-F$  and  $N\equiv S-Cl$ : these form a noteworthy contrast to the nonlinear nitrosyl halides  $O=N-X$ . In all cases, the pairs of elements directly bonded are consistent with the rule that the most electronegative atom of the trio bonds to the least electronegative, i.e.  $\{S(NH)\}_4$ ,  $\{N(SF)\}_{1,3,4}$ ,  $\{N(SCl)\}_{1,3}$ ,  $O(NF)$ ,  $O(NCl)$  (formal Pauling electronegativities: H 2.1, S 2.5, N 3.0, Cl 3.0, O 3.5, F 4.0).

Thiazyl fluoride, NSF, is a colourless, reactive, pungent gas (mp  $-89^\circ$ , bp  $+0.4^\circ$ ). It is best prepared by the action of  $HgF_2$  on a slurry of  $S_4N_4$  and  $CCl_4$  but it can also be made by a variety of other reactions:<sup>(267)</sup>



<sup>261</sup> J. C. VAN DE GRAMPPEL and A. VOS, *Acta Cryst.* **B25**, 611–17 (1969), and references therein. See also H. J. POSTMA, F. VAN BOLHUIS and A. VOS, *Acta Cryst.* **B27**, 2480–6 (1971).

<sup>262</sup> T. M. SABINE and G. W. COX, *Acta Cryst.* **28**, 574–7 (1967).

<sup>263</sup> D. GREGSON, G. KLEBE and H. FUESS, *J. Am. Chem. Soc.* **110**, 8488–93 (1988).

<sup>264</sup> J. NOVOSAD, D. J. WILLIAMS and J. D. WOOLLINS, *Z. anorg. allg. Chem.* **620**, 495–7 (1994).

<sup>265</sup> M. B. HURSTHOUSE, K. M. A. MALIK and S. N. NABI, *J. Chem. Soc., Dalton Trans.*, 355–9 (1980).

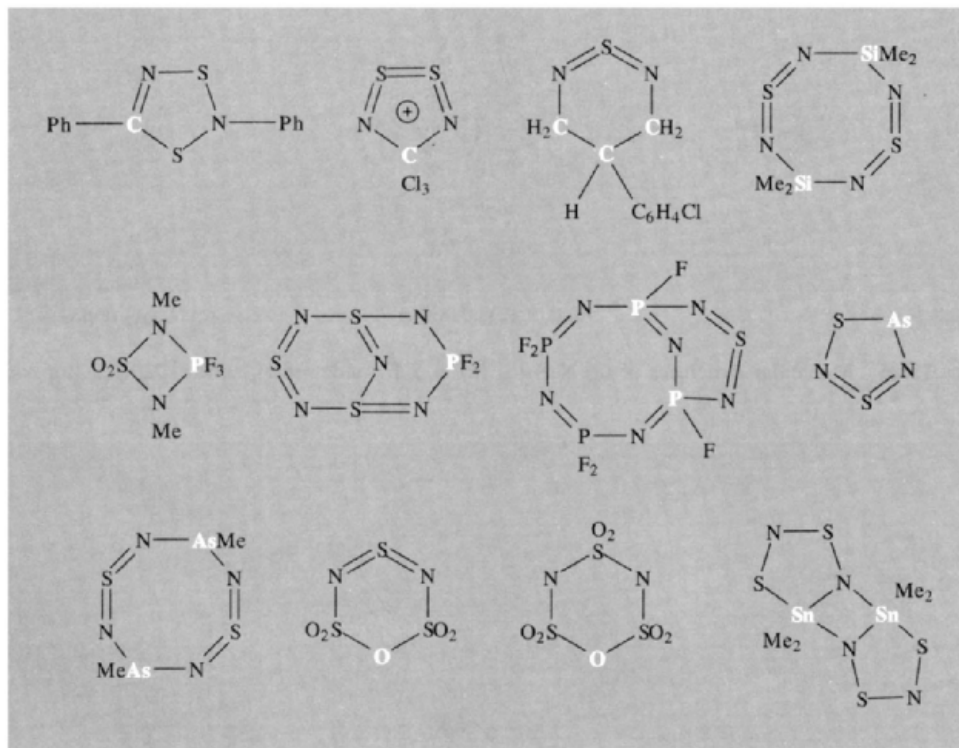
<sup>266</sup> R. J. GILLESPIE, J. P. KENT and J. F. SAWYER, *Inorg. Chem.* **20**, 4053–60 (1981).

<sup>267</sup> O. GLEMSER and M. FILD, in V. GUTMANN (ed.), *Halogen Chemistry*, Vol. 2, pp. 1–30, Academic Press, London, 1967.

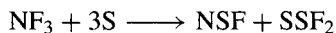
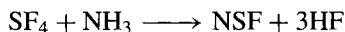
<sup>268</sup> R. MEWS, *Adv. Inorg. Chem. Radiochem.* **19**, 185–237 (1976).

<sup>269</sup> O. GLEMSER and R. MEWS, *Angew. Chem. Int. Edn. Engl.* **19**, 883–99 (1980).





**Figure 15.44** Some heterocyclic S–N compounds incorporating a third heteroelement.



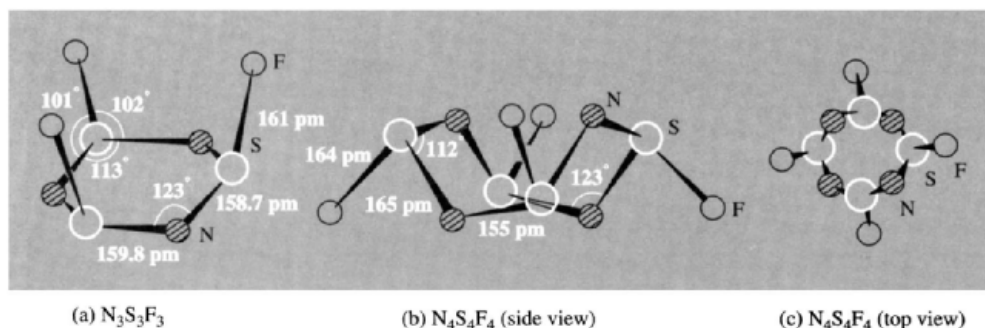
$\text{S}_4\text{N}_4$  can also be fluorinated to NSF (and other products) using  $\text{F}_2$  at  $-75^\circ$ ,  $\text{SeF}_4$  at  $-10^\circ$ , or  $\text{SF}_4$ . The molecular dimensions of NSF have been determined by microwave spectroscopy: N–S 145 pm, S–F 164 pm, angle at S  $116.5^\circ$ . The angle at S is very close to the angle at N in ONX ( $110$ – $117^\circ$ , p. 442). NSF can be stored at room temperature in copper or teflon vessels but it slowly decomposes in glass (more rapidly at  $200^\circ$ ) to form a mixture of  $\text{OSF}_2$ ,  $\text{SO}_2$ ,  $\text{SiF}_4$ ,  $\text{S}_4\text{N}_4$  and  $\text{N}_2$ . At room temperature and at pressures above 1 atm it trimerises to *cyclo*- $\text{N}_3\text{S}_3\text{F}_3$  (see below) but at lower pressures it affords  $\text{S}_4\text{N}_4$  admixed with yellow-green crystals of  $\text{S}_3\text{N}_2\text{F}_2$ ; this latter is of unknown structure but may well be the nonlinear acyclic species  $\text{FSN}=\text{S}=\text{NSF}$ .  $\text{N}_3\text{S}_3\text{F}_3$  is best made

by fluorinating *cyclo*- $\text{N}_3\text{S}_3\text{Cl}_3$  with  $\text{AgF}_2/\text{CCl}_4$ . The tetramer *cyclo*- $\text{N}_4\text{S}_4\text{F}_4$  is not obtained by polymerization of NSF monomer but can be readily made by fluorinating  $\text{S}_4\text{N}_4$  with a hot slurry of  $\text{AgF}_2/\text{CCl}_4$ . Some physical properties of these and other N–S–F compounds (p. 725) are compared in the following table:

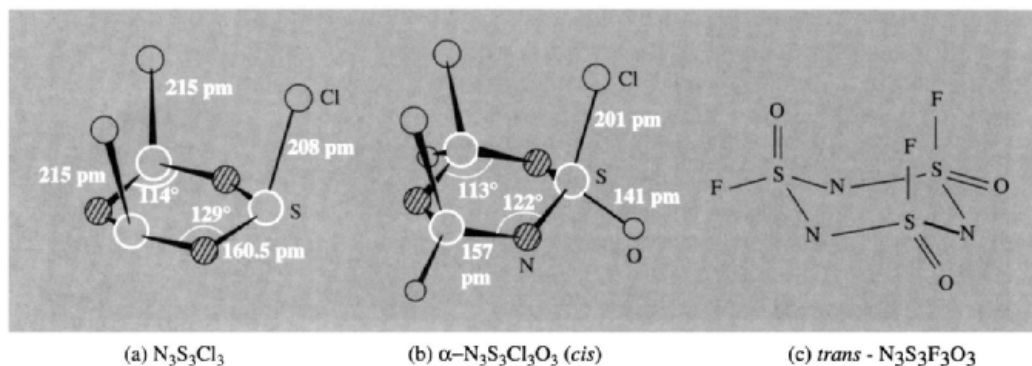
Compound	$\text{N}\equiv\text{S}-\text{F}$	$\text{S}_3\text{N}_2\text{F}_2$	$\text{N}_3\text{S}_3\text{F}_3$
MP/ $^\circ\text{C}$	-89	83	74.2
BP/ $^\circ\text{C}$	+0.4	-	92.5
Compound	$\text{N}_4\text{S}_4\text{F}_4$	$\text{N}\equiv\text{SF}_3$	$\text{FN}=\text{SF}_2$
MP/ $^\circ\text{C}$	153(d)	-72	-
BP/ $^\circ\text{C}$	-	27.1	-6.7

The structures of  $\text{N}_3\text{S}_3\text{F}_3$  and  $\text{N}_4\text{S}_4\text{F}_4$  are in Fig. 15.45. The former features a slightly puckered 6-membered ring (chair conformation) with essentially equal S–N distances around the ring and 3 eclipsed axial F atoms. By contrast,





**Figure 15.45** Molecular structures of (a)  $N_3S_3F_3$ , (b)  $N_4S_4F_4$  (side view), and (c)  $N_4S_4F_4$  (top view).



**Figure 15.46** Molecular structure of (a)  $N_3S_3Cl_3$ , (b)  $\alpha-N_3S_3Cl_3O_3$  (cis), and (c)  $trans-N_3S_3F_3O_3$ .

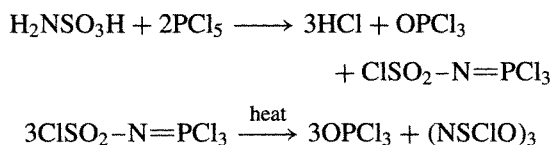
$N_4S_4F_4$  shows a pronounced alternation in S–N distances and only 2 of the F atoms are axial; it will also be noted that the conformation of the  $N_4S_4$  ring is very different to that in  $S_4N_4$  (p. 723) or  $S_4(NH)_4$  (p. 735). It is an interesting intellectual exercise to attempt to rationalize these striking structural differences.<sup>(270)</sup> The chemistry of these various NSF oligomers has not been extensively studied.  $N_3S_3F_3$  is stable in dry air but is hydrolysed by dilute aqueous NaOH to give  $NH_4F$  and sulfate.  $N_4S_4F_4$  is reported to form an N-bonded 1:1 adduct with  $BF_3$  whereas with  $AsF_5$  or  $SbF_5$  fluoride ion transfer occurs (accompanied by dethiazylation of the ring) to give  $[N_3S_3F_2]^+[MF_6]^-$  and  $[NS]^+[MF_6]^-$ .

In the chloro series, the compounds to be considered are  $N\equiv S-Cl$ ,  $cyclo-N_3S_3Cl_3$ ,  $cyclo-N_3S_3Cl_3O_3$ , and  $cyclo-N_4S_4Cl_2$ ; the ionic compounds  $[S_4N_3]^+Cl^-$  and  $[cyclo-N_2S_3Cl]^+Cl^-$  and  $[catena-N(SCl)_2]^+[BCl_4]^-$ ; together with various isomeric oxo- and fluoro-chloro derivatives. Thi-azyl chloride,  $NSCl$ , is best obtained by pyrolysis of the trimer in vacuum at  $100^\circ$ . It can also be made by the reaction of  $Cl_2$  on NSF (note that  $NSF + F_2 \longrightarrow NSF_3$ ) and by numerous other reactions.<sup>(267)</sup> It is a yellow-green gas that rapidly trimerizes at room temperature, and is isostructural with NSF.

By far the most common compound in the series is  $N_3S_3Cl_3$  (yellow needles, mp  $168^\circ$ ) which can be prepared by the direct action of  $Cl_2$  (or  $SOCl_2$ ) on  $S_4N_4$  in  $CCl_4$ , and which is also obtained in all reactions leading to  $NSCl$ . The structure (Fig. 15.46a) is very

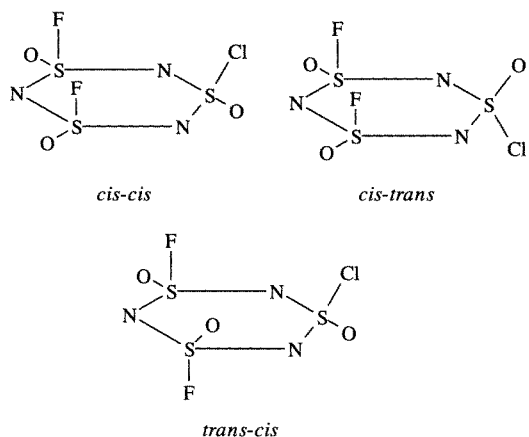
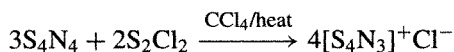
<sup>270</sup> S. M. OWEN and A. T. BROOKER, *A Guide to Modern Inorganic Chemistry*, Longman Scientific and Technical, Harlow 1991, pp. 120–1.

similar to that of  $N_3S_3F_3$  and comprises a slightly puckered ring with equal S–N distances of 160.5 pm and the N atoms only 18 pm above and below the plane of the 3 S atoms.  $N_3S_3Cl_3$  is sensitive to moisture and is oxidized by  $SO_3$  above  $100^\circ$  to  $N_3S_3Cl_3O_3$ ; at lower temperatures the adduct  $N_3S_3Cl_3 \cdot 6SO_3$  is formed and this dissociates at  $100^\circ$  to  $N_3S_3Cl_3 \cdot 3SO_3$ . A more efficient preparation of  $N_3S_3Cl_3O_3$  is by thermal decomposition of the product obtained by the reaction of amidosulfuric acid with  $PCl_5$ :



The compound is obtained in two isomeric forms from this reaction:  $\alpha$ , mp  $145^\circ$  and  $\beta$ , mp  $43^\circ$ . The structure of the  $\alpha$ -form is in Fig. 15.46b and is closely related to that of  $(NSCl)_3$  with uniform S–N distances around the ring. The  $\beta$ -form may have a different ring conformation but more probably involves *cis-trans* isomerism of the pendant Cl and O atoms. Fluorination of  $\alpha$ - $N_3S_3Cl_3O_3$  with KF in  $CCl_4$  yields the two isomeric fluorides *cis*- $N_3S_3F_3O_3$  (mp  $17.4^\circ$ ) and *trans*- $N_3S_3F_3O_3$  (mp  $-12.5^\circ$ ) (Fig. 15.46c). The structural assignment of the 2 isomers was made on the basis of  $^{19}F$  nmr. Fluorination with  $SbF_3$  under reduced pressure yields both the monofluoro and difluoro derivatives  $N_3S_3Cl_2FO_3$  and  $N_3S_3ClF_2O_3$ , each having 3 isomers which can be separated chromatographically and assigned by  $^{19}F$  nmr as indicated schematically in Fig. 15.47. Numerous other derivatives are known in which one or more halogen atom is replaced by  $-NH_2$ ,  $-N=SF_2$ ,  $-N=PCl_3$ ,  $-N=CHPh$ ,  $-OSiMe_3$ , etc.

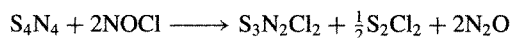
A different structure motif occurs in  $S_4N_3Cl$ . This very stable yellow compound features the  $S_4N_3^+$  cation (p. 732) and is obtained by many reactions, e.g.:



**Figure 15.47** Schematic representation of the three geometric isomers of  $N_3S_3ClF_2O_3$ . The three isomers of the monofluoro derivative are similar but with Cl and F interchanged.

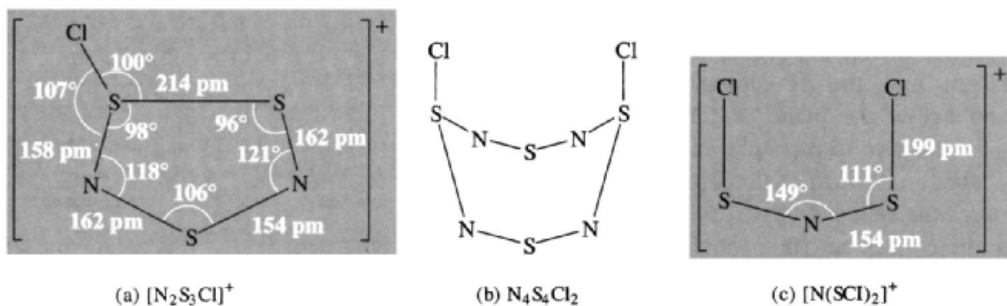
The chloride ion is readily replaced by other anions to give, for example, the orange-yellow  $[S_4N_3]Br$ , bronze-coloured  $[S_4N_3]SCN$ ,  $[S_4N_3]NO_3$ ,  $[S_4N_3]HSO_4$ , etc.

Chlorination of  $S_4N_4$  with  $NOCl$  or  $SOCl_2$  in a polar solvent yields  $S_3N_2Cl_2$ :



The crystal structure again reveals an ionic formulation,  $[N_2S_3Cl]^+Cl^-$ , this time with a slightly puckered 5-membered ring carrying a single pendant Cl atom as shown in Fig. 15.48a; the alternation of S–N distances and the rather small angles at the 2 directly linked S atoms are notable features. Reaction of  $[N_2S_3Cl]^+Cl^-$  with bis(trimethylsilyl)cyanamide,  $(Me_3Si)_2NCN$ , in MeCN yields dark red crystals of  $N_2S_3NCN$  (i.e.  $\overline{SNSNS=NCN}$ ) in which the essentially linear NCN group ( $176.4^\circ$ ) lies diagonally above the  $N_2S_3$ -ring with the angle  $S=N-C$  being  $119.0^\circ$ .<sup>(271)</sup> Yet a further chloride can be obtained by the partial chlorination of  $S_4N_4$  with  $Cl_2$  in  $CS_2$  solution below room temperature: one of the

<sup>271</sup> A. J. BANISTER, W. CLEGG, I. B. GORRELL, Z. V. HAUPTMAN and R. W. H. SMALL, *J. Chem. Soc., Chem. Commun.*, 1611–13 (1987).

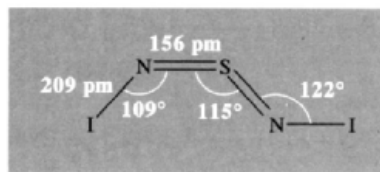


**Figure 15.48** Structure of (a) the cation in  $[\text{N}_2\text{S}_3\text{Cl}]^+\text{Cl}^-$ , (b)  $\text{N}_4\text{S}_4\text{Cl}_2$ , and (c)  $[\text{N}(\text{SCl})_2]^+$ .

trans-annular  $\text{S}\cdots\text{S}$  “bonds” is opened to give yellow crystals of  $\text{N}_4\text{S}_4\text{Cl}_2$  (Fig. 15.48b) and this derivatized heterocycle can be used to prepare several other compounds.<sup>(272)</sup>

Reaction of  $\text{NSF}_3$  with  $\text{BCl}_3$  yields the acyclic cation  $[\text{N}(\text{SCl})_2]^+$  as its  $\text{BCl}_4^-$  salt (Fig. 15.48c); the compound is very hygroscopic and readily decomposes to  $\text{BCl}_3$ ,  $\text{SCl}_2$ ,  $\text{S}_2\text{Cl}_2$ , and  $\text{N}_2$ .

The formation of highly conducting nonstoichiometric bromo and iodo derivatives of polythiazyl has already been mentioned (p. 728). It has been found that, whereas bromination of solid  $\text{S}_4\text{N}_4$  with gaseous  $\text{Br}_2$  yields conducting  $(\text{SNBr}_{0.4})_x$ , reaction with liquid bromine leads to the stable tribromide  $[\text{S}_4\text{N}_3]^+[\text{Br}_3]^-$ .<sup>(273)</sup> In contrast, the reaction of  $\text{S}_4\text{N}_4$  with  $\text{Br}_2$  in  $\text{CS}_2$  solution results in a (separable) mixture of  $[\text{S}_4\text{N}_3]^+[\text{Br}_3]^-$ ,  $[\text{S}_4\text{N}_3]^+\text{Br}^-$  and the novel ionic compound  $\text{CS}_3\text{N}_2\text{Br}_2$  which may be  $[\text{S}=\overset{\ominus}{\text{C}}-\text{S}=\text{N}=\text{S}=\overset{\oplus}{\text{N}}]^{2+}[\text{Br}^-]_2$  or  $[\text{S}=\overset{\ominus}{\text{C}}-\text{S}=\text{N}=\text{S}(\text{Br})=\overset{\oplus}{\text{N}}]^{2+}\text{Br}^-$ . The binary halides  $\text{SN}_2\text{Br}_2$  and  $\text{SN}_2\text{I}_2$  are also known. Thus  $\text{SF}_4$  reacts with  $(\text{Me}_3\text{Si})_2\text{NI}$  in  $\text{C}_2\text{F}_4\text{Cl}_2$  at  $0^\circ\text{C}$  to give  $\text{S}(\text{NI})_2$  as a shock-sensitive yellow crystalline powder composed of  $\text{I}-\text{N}=\text{S}=\text{N}-\text{I}$  molecules in *syn-anti* configuration.<sup>(274)</sup>



(vi) *Sulfur–nitrogen–oxygen compounds*<sup>(207)</sup>

This is a classic area of inorganic chemistry dating back to the middle of the last century and only a brief outline will be possible. It will be convenient first to treat the sulfur nitrogen oxides and then the amides, imides and nitrides of sulfuric acid. Hydrazides and hydroxylamides of sulfuric acid will also be considered. Some of these compounds have remarkable properties and some are implicated in the lead-chamber process for the manufacture of  $\text{H}_2\text{SO}_4$  (p. 708). The field is closely associated with the names of the great German chemists E. Frémy (~1845), A. Claus (~1870), F. Raschig (~1885–1925), W. Traube (~1890–1920), F. Ephraim (~1910), P. Baumgarten (~1925) and, in more recent years, M. Becke-Goehring (~1955) and F. Seel (~1955–65).

(a) *Sulfur–nitrogen oxides*. Trisulfur dinitrogen dioxide,  $\text{S}_3\text{N}_2\text{O}_2$ , is best made by treating  $\text{S}_4\text{N}_4$  with boiling  $\text{OSCl}_2$  under a stream of  $\text{SO}_2$ :



It is a yellow solid with an acyclic structure (Fig. 15.49a), cf  $\text{N}_2\text{O}_5$  (p. 458). Moist air converts  $\text{S}_3\text{N}_2\text{O}_2$  to  $\text{SO}_2$  and  $\text{S}_4\text{N}_4$  whereas  $\text{SO}_3$

<sup>272</sup> H. W. ROESKY, C. GRAF, M. N. S. RAO, B. KREBS and G. HENKEL, *Angew. Chem. Int. Edn. Engl.* **18**, 780–1 (1979), and references therein. H. W. ROESKY, M. N. S. RAO, C. GRAF, A. GIEREN and E. HADICKE, *Angew. Chem. Int. Edn. Engl.* **20**, 592–3 (1981).

<sup>273</sup> G. WOLMERSHÄUSER, G. B. STREET and R. D. SMITH,  $\text{CS}_3\text{N}_2\text{Br}_2$ , *Inorg. Chem.* **18**, 383–5 (1979).

<sup>274</sup> M. ROCK, P. BRAVIN and K. SEPPELT, *Z. anorg. allg. Chem.* **618**, 89–92 (1992).

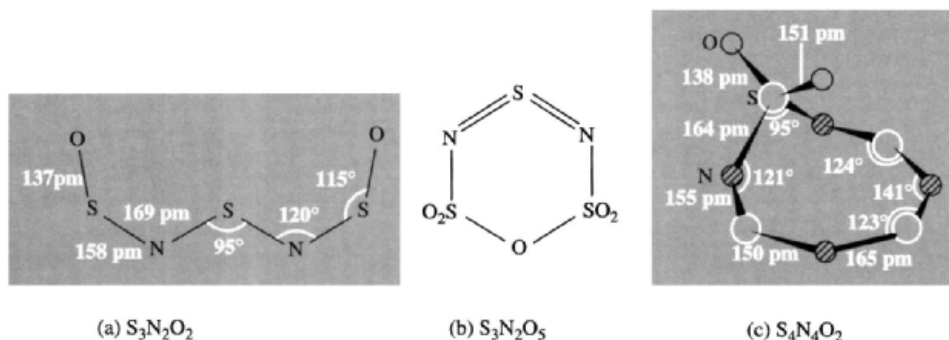
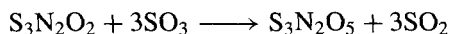
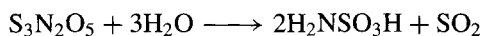


Figure 15.49 Structures of sulfur–nitrogen oxides.

oxidizes it smoothly to  $S_3N_2O_5$ :

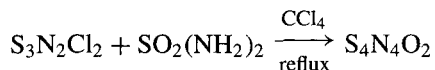


The pentoxide  $S_3N_2O_5$  can also be made directly from  $S_4N_4$  and  $SO_3$ . It forms colourless, strongly refracting crystals which readily hydrolyse to sulfamic acid:



It has a cyclic structure and may be regarded as a substituted diamide of disulfuric acid,  $H_2S_2O_7$  (Fig. 15.49b).

An alternative synthetic strategy for sulfur–nitrogen oxides is exemplified by the more recent reaction:<sup>(275)</sup>

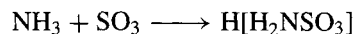
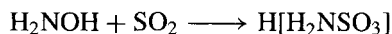


The product forms orange-yellow crystals, mp 166 (d), having a structure in which 1 S atom of an  $S_4N_4$  ring carries both O atoms. X-ray diffractometry shows substantial deviation from the parent  $S_4N_4$  structure, a notable feature being the coplanarity of the  $S_3N_2$  moiety furthest removed from the  $SO_2$  group (Fig. 15.49c). If  $S_4N_4O_2$  is allowed to react with 2 mols of  $SO_3$  in liquid  $SO_2$ , two further compounds are formed: the known  $S_3N_2O_5$  (Fig. 15.49b) and the novel greenish-black  $S_6N_5O_4$ , which is composed of separately stacked tricyclic radical cation dimers

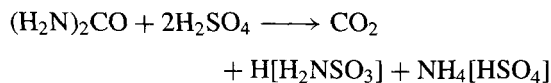
$[[S_3N_2]_2]^{2+}$  (Fig. 15.39b)) and the cyclic anion  $S_3N_3O_4^-$ , i.e.  $[O_2SNSNS(O)_2O]^-$ .<sup>(276)</sup> Numerous other *cyclic-* and *polycyclic-N/S/O* species have recently been prepared and structurally characterized.<sup>(277)</sup>

(b) *Amides of sulfuric acid.* Amidosulfuric acid (better known as sulfamic acid,  $H[H_2NSO_3]$ ), is a classical inorganic compound and an important industrial chemical. Formal replacement of both hydroxyl groups in sulfuric acid leads to sulfamide ( $(H_2N)_2SO_2$  (p. 742) which is also clearly related structurally to the sulfonyl halides  $X_2SO_2$  (p. 694).

Sulfamic acid can be made by many routes, including addition of hydroxylamine to  $SO_2$  and addition of  $NH_3$  to  $SO_3$ :



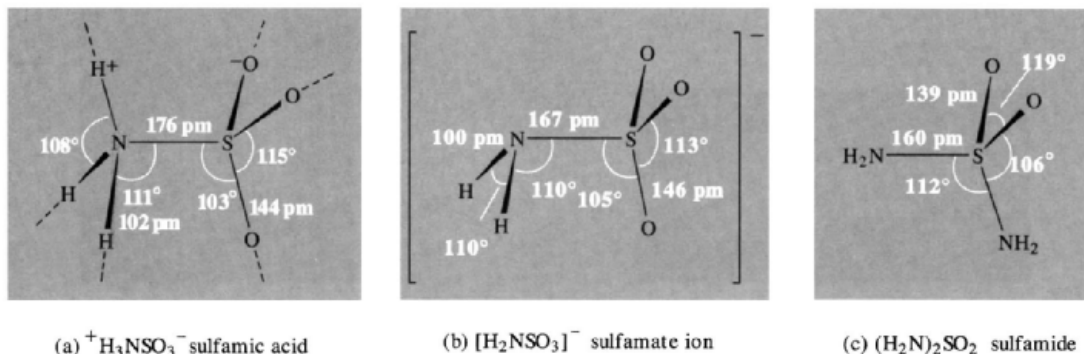
The industrial synthesis uses the strongly exothermic reaction between urea and anhydrous  $H_2SO_4$  (or dilute oleum):



<sup>276</sup> H. ROESKY, M. WITT, J. SCHIMKOWIAK, M. SCHMIDT, M. NOLTEMAYER and G. M. SHELDRIK, *Angew. Chem. Int. Edn. Engl.* **21**, 538–9 (1982).

<sup>277</sup> T. CHIVERS, R. T. OAKLEY, A. W. CORDES and W. T. PENNINGTON, *J. Chem. Soc., Chem. Commun.*, 1214–5 (1981). T. CHIVERS, A. W. CORDES, R. T. OAKLEY and W. T. PENNINGTON, *Inorg. Chem.* **22**, 2429–35 (1983). T. CHIVERS and M. HOJO, *Inorg. Chem.* **23**, 4088–93 (1984).

<sup>275</sup> H. W. ROESKY, W. SCHAPER, O. PETERSEN and T. MÜLLER, *Chem. Ber.* **110**, 2695–8 (1977).



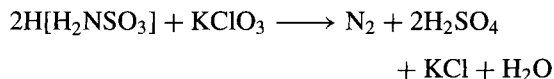
**Figure 15.50** The structures of (a) sulfamic acid, (b) the sulfamate ion, and (c) sulfamide.

Salts are obtained by direct neutralization of the acid with appropriate oxides, hydroxides, or carbonates. Sulfamic acid is a dry, non-volatile, non-hygroscopic, colourless, white, crystalline solid of considerable stability. It melts at  $205^\circ$ , begins to decompose at  $210^\circ$ , and at  $260^\circ$  rapidly gives a mixture of  $\text{SO}_2$ ,  $\text{SO}_3$ ,  $\text{N}_2$ ,  $\text{H}_2\text{O}$ , etc. It is a strong acid (dissociation constant  $1.01 \times 10^{-1}$  at  $25^\circ$  solubility  $\sim 25$  g per 100 g  $\text{H}_2\text{O}$ ) and, because of its physical form and stability, is a convenient standard for acidimetry. Over 50 000 tonnes are manufactured annually and its principal applications are in formulations for metal cleaners, scale removers, detergents and stabilizers for chlorine in aqueous solution.<sup>(278)</sup> Its salts are used in flame retardants, weed killers and for electroplating.

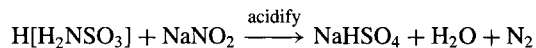
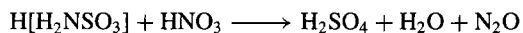
In the solid state sulfamic acid forms a strongly H-bonded network which is best described in terms of zwitterion units  ${}^+\text{H}_3\text{NSO}_3^-$  rather than the more obvious formulation as aminosulfuric acid,  $\text{H}_2\text{NSO}_2(\text{OH})$ . The zwitterion has the staggered configuration shown in Fig. 15.50a and the S–N distance is notably longer than in the sulfamate ion or sulfamide.

Dilute aqueous solutions of sulfamic acid are stable for many months at room temperature but at higher temperatures hydrolysis to  $\text{NH}_4[\text{HSO}_4]$  sets in. Alkali metal salts are stable in neutral and

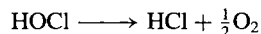
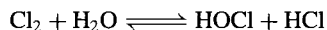
alkaline solutions even at the bp. Sulfamic acid is a monobasic acid in water (see Fig. 15.50b for structure of the sulfamate ion). In liquid ammonia solutions it is dibasic and, with Na for example, it forms  $\text{NaNH}_2\text{SO}_3\text{Na}$ . Sulfamic acid is oxidized to nitrogen and sulfate by  $\text{Cl}_2$ ,  $\text{Br}_2$  and  $\text{ClO}_3^-$ , e.g.:



Concentrated  $\text{HNO}_3$  yields pure  $\text{N}_2\text{O}$  whilst aqueous  $\text{HNO}_2$  reacts quantitatively to give  $\text{N}_2$ :



This last reaction finds use in volumetric analysis. The use of sulfamic acid to stabilize chlorinated water depends on the equilibrium formation of *N*-chlorosulfamic acid, which reduces loss of chlorine by evaporation, and slowly re-releases hypochlorous acid by the reverse hydrolysis:

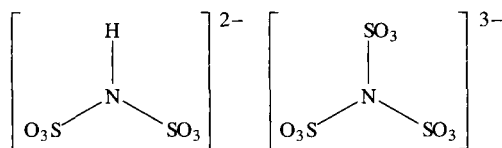
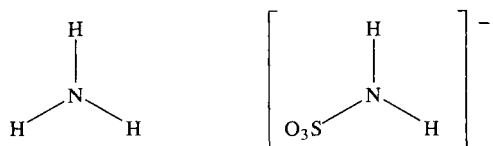


Sulfamide,  $(\text{H}_2\text{N})_2\text{SO}_2$ , can be made by ammonolysis of  $\text{SO}_3$  or  $\text{O}_2\text{SCL}_2$ . It is a colourless crystalline material, mp  $93^\circ$ , which begins to decompose above this temperature. It is soluble in water to give a neutral non-electrolytic solution but in boiling water it decomposes to ammonia and sulfuric acid. The structure (Fig. 15.50c)

<sup>278</sup> E. B. BELL, Sulfamic acid and sulfamates, *Kirk-Othmer Encyclopedia of Chemical Technology*, 3rd edn., Vol. 21, pp. 940–60, Wiley, New York, 1983.

can be compared with those of sulfuric acid,  $(\text{HO})_2\text{SO}_2$  (p. 710) and the sulfuryl halides  $\text{X}_2\text{SO}_2$  (p. 694).

(c) *Imido and nitrido derivatives of sulfuric acid.* In the preceding section the sulfamate ion and related species were regarded as being formed by replacement of an OH group in  $(\text{HO})\text{SO}_3^-$  or  $(\text{HO})_2\text{SO}_3$  by an  $\text{NH}_2$  group. They could equally well be regarded as sulfonates of ammonia in which each H atom is successively replaced by  $\text{SO}_3^-$  (or  $\text{SO}_3\text{H}$ ):

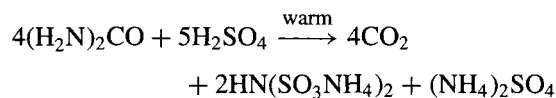


Imidodisulfate  
Imidodisulfonate

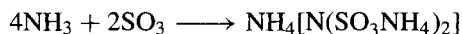
Nitridotrisulfate  
Nitriolotrisulfonate

Both sets of names are used in the literature. Free imidodisulfuric acid  $\text{HN}(\text{SO}_3\text{H})_2$  (which is isoelectronic with disulfuric acid  $\text{H}_2\text{S}_2\text{O}_7$ , p. 705) and free nitridotrisulfuric acid  $\text{N}(\text{SO}_3\text{H})_3$  are unstable, but their salts are well characterized and have been extensively studied.

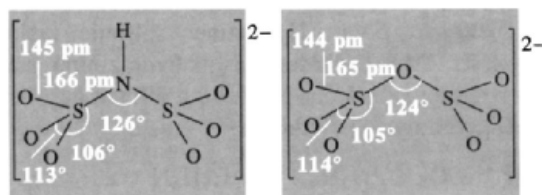
Imidodisulfuric acid derivatives can be prepared from urea by using less sulfuric acid than required for sulfamic acid (p. 741):



Addition of aqueous KOH liberates  $\text{NH}_3$  and affords crystalline  $\text{HN}(\text{SO}_3\text{K})_2$  on evaporation. All 3 H atoms in  $\text{HN}(\text{SO}_3\text{H})_2$  can be replaced by  $\text{NH}_4$  or  $\text{M}^I$ , e.g. the direct reaction of  $\text{NH}_3$  and  $\text{SO}_3$  yields the triammonium salt:

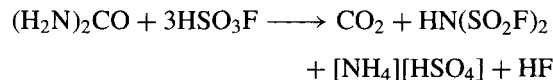


Imidodisulfates can also be obtained by hydrolysis of nitridotrisulfates (see below). Figure 15.51 compares the structure of the imidodisulfate and parent disulfate ions, as determined from the potassium salts. Comparison with the hydroxylamine derivative  $\text{K}[\text{HN}(\text{OH})\text{SO}_3]$  (below) is also instructive.

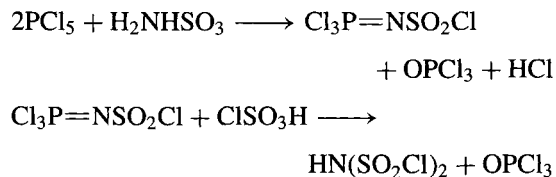


**Figure 15.51** Comparison of the structures of the imidodisulfate and disulfate ions in their potassium salts.

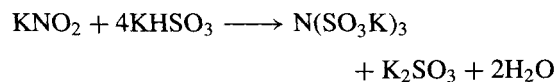
Fluoro and chloro derivatives of imidodisulfuric acid can be made by reacting  $\text{HSO}_3\text{F}$  or  $\text{HSO}_3\text{Cl}$  (rather than  $\text{H}_2\text{SO}_4$ ) with urea:



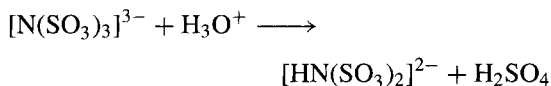
$\text{HN}(\text{SO}_2\text{F})_2$  melts at  $17^\circ$ , boils at  $170^\circ$  and can be further fluorinated with elemental  $\text{F}_2$  at room temperature to give  $\text{FN}(\text{SO}_2\text{F})_2$ , mp  $-79.9^\circ$ , bp  $60^\circ$ . The chloro derivative  $\text{HN}(\text{SO}_2\text{Cl})_2$  is a white crystalline compound, mp  $37^\circ$ : it is made in better yield from sulfamic acid by the following reaction sequence:



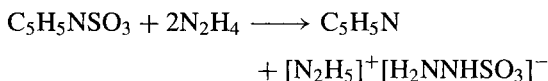
Salts of nitridotrisulfuric acid,  $\text{N}(\text{SO}_3\text{M}^I)_3$ , are readily obtained by the exothermic reaction of nitrites with sulfites or hydrogen sulfites in hot aqueous solution:



The dihydrate crystallizes as the solution cools. Such salts are stable in alkaline solution but hydrolyse in acid solution to imidodisulfate (and then more slowly to sulfamic acid):

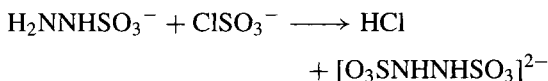


(d) *Hydrazine and hydroxylamine derivatives of sulfuric acid.* Hydrazine sulfonic acid,  $\text{H}_2\text{NNH.HSO}_3$  is obtained as its hydrazinium salt by reacting anhydrous  $\text{N}_2\text{H}_4$  with diluted gaseous  $\text{SO}_3$  or its pyridine adduct:



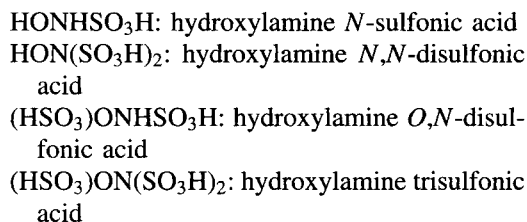
The free acid is monobasic,  $\text{pK}$  3.85; it is much more easily hydrolysed than sulfamic acid and has reducing properties comparable with those of hydrazine. Like sulfamic acid it exists as a zwitterion in the solid state:  $^+\text{H}_3\text{NNHSO}_3^-$ .

Symmetrical hydrazine disulfonic acid can be made by reacting a hydrazine sulfonate with a chlorosulfate:

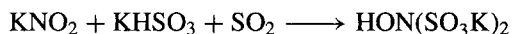


Oxidation of the dipotassium salt with  $\text{HOCl}$  yields the azodisulfonate  $\text{KO}_3\text{SN}=\text{NSO}_3\text{K}$ . Numerous other symmetrical and unsymmetrical hydrazine polysulfonate derivatives are known.

With hydroxylamine,  $\text{HONH}_2$ , 4 of the 5 possible sulfonate derivatives have been prepared as anions of the following acids:

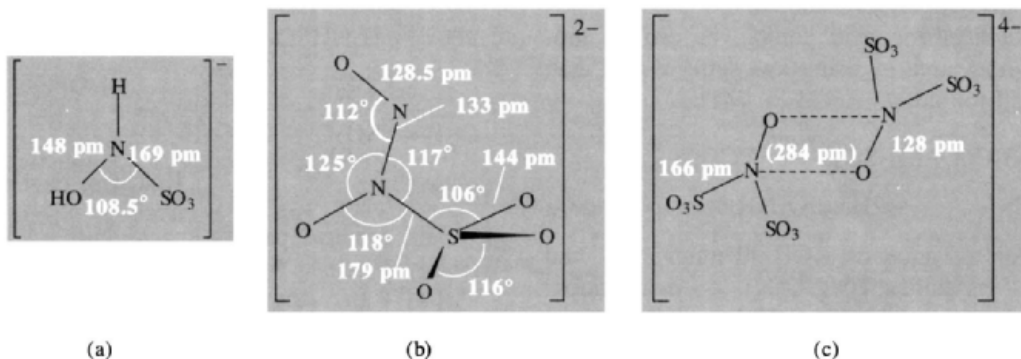


The first of these can be made by careful hydrolysis of the *N,N*-disulfonate which is itself made by the reaction of  $\text{SO}_2$  and a nitrite in cold alkaline solution:

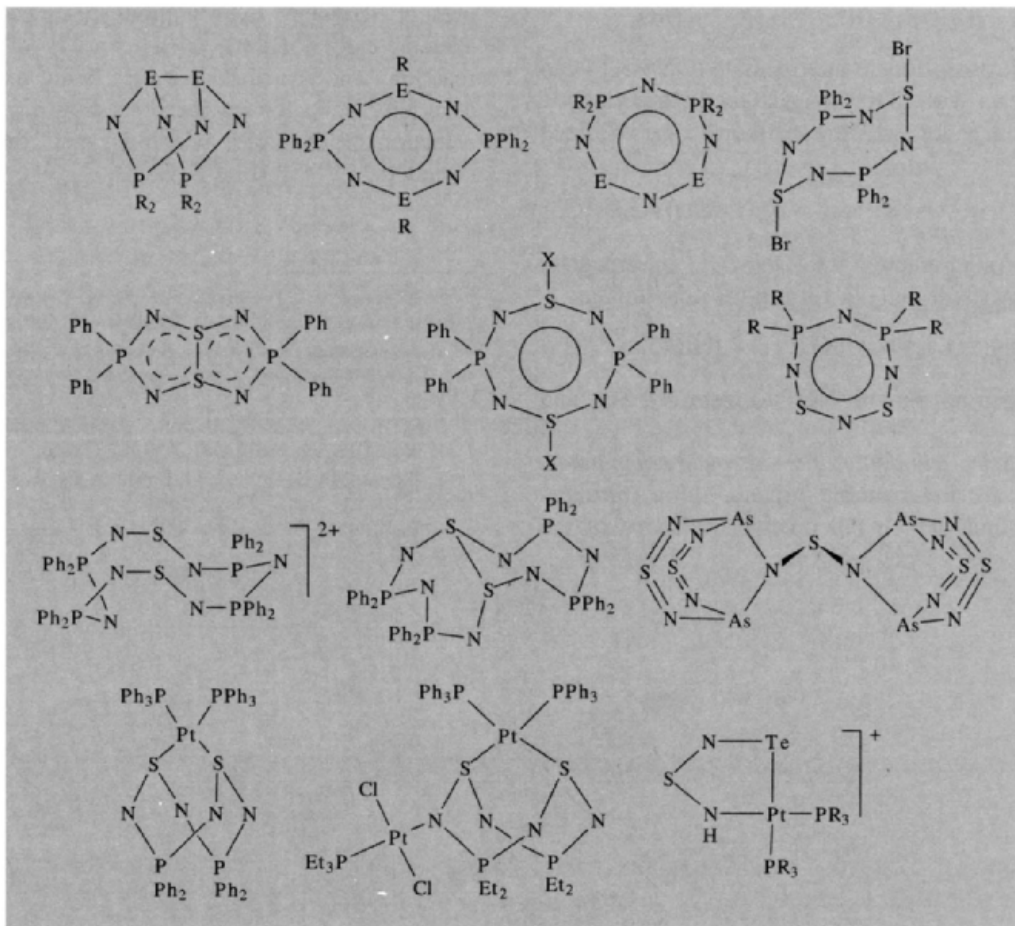


The potassium salt readily crystallizes from the cold solution thus preventing further reaction with the hydrogen sulfate to give nitridotrisulfate (p. 743). The structure of the hydroxylamine *N*-sulfonate ion is shown in Fig. 15.52a. The closely related *N*-nitrosohydroxylamine *N*-sulfonate ion (Fig. 15.52b) can be made directly by absorbing  $\text{NO}$  in alkaline  $\text{K}_2\text{SO}_3$  solution: the 6 atoms  $\text{ONN}(\text{O})\text{SO}$  all lie in one plane and the interatomic distances suggest an  $\text{S}-\text{N}$  single bond but considerable additional  $\pi$  bonding in the  $\text{N}-\text{N}$  bond.

Oxidation of hydroxylamine *N,N*-disulfonate with permanganate or  $\text{PbO}_2$  yields the intriguing

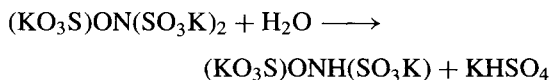


**Figure 15.52** Structures of various  $\text{S}-\text{N}$  oxoanions: (a) hydroxylamine-*N*-sulfonate, (b) *N*-nitrosohydroxylamine *N*-sulfonate and (c) the dimeric anion in Frémy's salt  $[\text{K}_2[\text{ON}(\text{SO}_3)_2]]_2$ .



nitrosodisulfonate  $K_2[ON(SO_3)_2]$ : this was first isolated by Frémy as a yellow solid which was subsequently shown to be dimeric and diamagnetic due to the formation of long  $N \cdots O$  bonds in the crystal (Fig. 15.52c). However, in aqueous solution the anion dissociates reversibly into the deep violet, paramagnetic monomer  $[ON(SO_3)_2]^{2-}$ .

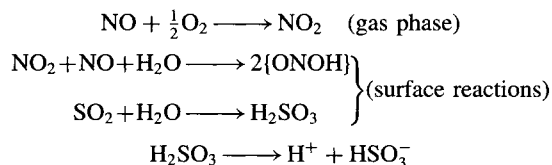
Hydroxylamine trisulfonates, e.g.  $(KO_3S)ON(SO_3K)_2$  are made by the reaction of  $K_2SO_3$  with potassium nitrosodisulfonate (Frémy's salt). Acidification of the product results in rapid hydrolysis to the *O,N*-disulfonate which can be isolated as the exclusive product:



Sulfonic acids containing nitrogen have long been implicated as essential intermediates in the synthesis of  $H_2SO_4$  by the lead-chamber process (p. 708) and, as shown by F. Seel and his group, the crucial stage is the oxidation of sulfite ions by the nitrosyl ion  $NO^+$ :



The  $NO^+$  ions are thought to be generated by the following sequence of reactions:



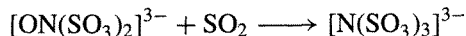




The nitrosulfonate intermediate  $[\text{ONSO}_3]^-$  can also react with  $\text{SO}_3^{2-}$  to give the hydroxylamine disulfonate ion which can likewise be oxidized by  $\text{NO}^+$ :



In a parallel reaction the  $[\text{ONSO}_3]^-$  intermediate can react with  $\text{SO}_2$  to form nitrilotrisulfonate:



This then reacts with  $\text{NO}^+$  to form  $\text{N}_2$ ,  $\text{SO}_3$  and  $\text{SO}_4^{2-}$ .

(e) *Selected other sulfur–nitrogen compounds.*

There are innumerable organo–sulfur–nitrogen compounds which fall outside the scope of the

present treatment. Even without the presence of skeletal carbon atoms, a rich variety of novel reactions and structural types is being explored as briefly indicated on the preceding page by a selection of examples which is itself far from complete.<sup>(279–282)</sup> (E = S, Se).

<sup>279</sup> N. BURFORD, T. CHIVERS, M. N. S. RAO and J. F. RICHARDSON, *Inorg. Chem.* **23**, 1946–52 (1984).

<sup>280</sup> M. HEBERHOLD, K. GULDAR, A. GIEREN, C. RUIZ-PEREZ and T. HÜBNER, *Angew. Chem. Int. Edn. Engl.* **26**, 82–3 (1987).

<sup>281</sup> P. F. KELLY, A. M. Z. SLAWIN, D. J. WILLIAMS and J. D. WOOLLINS, *Polyhedron* **9**, 2659–62 (1990).

<sup>282</sup> T. CHIVERS, D. D. DOXSEE, M. EDWARDS and R. W. HILTS, in R. STEUDEL (ed.), *The Chemistry of Inorganic Ring Systems*, Elsevier, Amsterdam, 1992, Chap. 15, pp. 271–94.

																1	2																																				
																H	He																																				
3	4																	5	6	7	8	9	10																														
Li	Be																	B	C	N	O	F	Ne																														
11	12																	13	14	15	16	17	18																														
Na	Mg																	Al	Si	P	S	Cl	Ar																														
19	20	21	22	23	24	25	26	27	28	29	30	31	32	33	34	35	36																																				
K	Ca	Sc	Ti	V	Cr	Mn	Fe	Co	Ni	Cu	Zn	Ga	Ge	As	Se	Br	Kr																																				
37	38	39	40	41	42	43	44	45	46	47	48	49	50	51	52	53	54	55	56																																		
Rb	Sr	Y	Zr	Nb	Mo	Tc	Ru	Rh	Pd	Ag	Cd	In	Sn	Sb	Te	I	Xe																																				
55	56	57	58	59	60	61	62	63	64	65	66	67	68	69	70	71	72	73	74	75	76	77	78	79	80	81	82	83	84	85	86																						
Cs	Ba	La	Hf	Ta	W	Re	Os	Ir	Pt	Au	Hg	Tl	Pb	Bi	Po	At	Rn																																				
87	88	89	90	91	92	93	94	95	96	97	98	99	100	101	102	103	104	105	106	107	108	109	110	111	112																												
Fr	Ra	Ac	Rf	Db	Sg	Bh	Hs	Mt	Cu	Cu	Cu	Cu	Cu	Cu	Cu	Cu	Cu																																				
																89	90	91	92	93	94	95	96	97	98	99	100	101	102	103																							
																Ce	Pr	Nd	Pm	Sm	Eu	Gd	Tb	Dy	Ho	Er	Tm	Yb	Lu																								
																91	92	93	94	95	96	97	98	99	100	101	102	103	104	105	106	107	108	109	110	111	112																
																Th	Pa	U	Np	Pu	Am	Cm	Bk	Cf	Es	Fm	Md	No	Lr																								

# 16

## Selenium, Tellurium and Polonium

### 16.1 The Elements<sup>(1-4)</sup>

#### 16.1.1 Introduction: history, abundance, distribution

Tellurium was the first of these three elements to be discovered. It was isolated by the Austrian chemist F. J. Müller von Reichenstein in 1782 a few years after the discovery of oxygen by J. Priestley and C. W. Scheele (p. 600), though the periodic group relationship between the elements was not apparent until nearly a century later (p. 20). Tellurium was first

observed in ores mined in the gold districts of Transylvania; Müller called it *metallum problematicum* or *aurum paradoxum* because it showed none of the properties of the expected antimony.<sup>(5)</sup> The name tellurium (Latin *tellus*, earth) is due to another Austrian chemist, M. H. Klaproth, the discoverer of zirconium and uranium.

Selenium was isolated some 35 y after tellurium and, since the new element resembled tellurium, it was named from the Greek *σελήνη*, *selene*, the moon. The discovery was made in 1817 by the Swedish chemist J. J. Berzelius (discoverer of Si, Ce and Th) and J. G. Gahn (discoverer of Mn);<sup>(5)</sup> they observed a reddish-brown deposit during the burning of sulfur obtained from Fahlun copper pyrites, and showed it to be volatile and readily reducible to the new element.

The discovery of polonium by Marie Curie in 1898 is a story that has been told many

<sup>1</sup> K. W. BAGNALL, Selenium, tellurium and polonium, Chap. 24 in *Comprehensive Inorganic Chemistry*, Vol. 2, pp. 935–1008, Pergamon Press, Oxford, 1973.

<sup>2</sup> R. A. ZINGARO and W. C. COOPER (eds.), *Selenium*, Van Nostrand, Reinhold, New York, 1974, 835 pp.

<sup>3</sup> W. C. COOPER (ed.), *Tellurium*, Van Nostrand, Reinhold, New York, 1971, 437 pp.

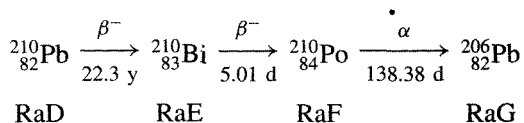
<sup>4</sup> N. B. MIKEEV, Polonium, *Chemiker Zeitung* **102**, 277–86 (1978). See also K. W. BAGNALL, *Radiochim. Acta.* **32**, 153–61 (1983). Polonium, *Gmelin Handbook of Inorganic and Organometallic Chemistry*, Suppl. Vol. 1, Springer-Verlag, Berlin, 1990, 425 pp.

<sup>5</sup> M. E. WEEKS, *Discovery of the Elements*, 6th edn., Journal of Chemical Education, Easton, Pa., 1956: pp. 303–37.

times.<sup>(6)</sup> The immense feat of processing huge quantities of uranium ore and of following the progress of separation by the newly discovered phenomenon of radioactivity (together with her parallel isolation of radium by similar techniques, p. 108), earned her the Nobel Prize for Chemistry in 1911. She had already shared the 1902 Nobel Prize for Physics with H. A. Becquerel and her husband P. Curie for their joint researches on radioactivity. Indeed, this was the first time, though by no means the last, that invisible quantities of a new element had been identified, separated, and investigated solely by means of its radioactivity. The element was named after Marie Curie's home country, Poland.

Selenium and tellurium are comparatively rare elements, being sixty-sixth and seventy-third respectively in order of crustal abundance; polonium, on account of its radioactive decay, is exceedingly unabundant. Selenium comprises some 0.05 ppm of the earth's crust and is therefore similar to Ag and Hg, which are each about 0.08 ppm, and Pd (0.015 ppm). Tellurium, at about 0.002 ppm can be compared with Au (0.004 ppm) and Ir (0.001 ppm). Both elements are occasionally found native, in association with sulfur, and many of their minerals occur together with the sulfides of chalcophilic metals (p. 648),<sup>(2,3)</sup> e.g. Cu, Ag, Au; Zn, Cd, Hg; Fe, Co, Ni; Pb, As, Bi. Sometimes the minerals are partly oxidized, e.g.  $MSeO_3 \cdot 2H_2O$  ( $M = Ni, Cu, Pb$ );  $PbTeO_3$ ,  $Fe_2(TeO_3)_3 \cdot 2H_2O$ ,  $FeTeO_4$ ,  $Hg_2TeO_4$ ,  $Bi_2TeO_4(OH)_4$ , etc. Selenolite,  $SeO_2$ , and tellurite,  $TeO_2$ , have also been found.

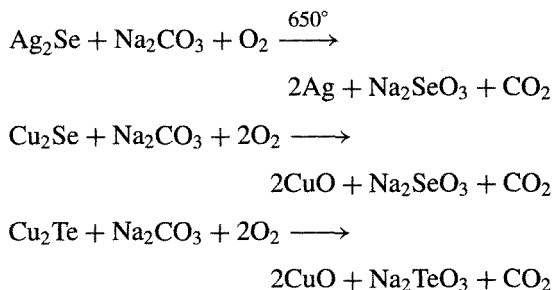
Polonium has no stable isotopes, all 27 isotopes being radioactive; of these only  $^{210}Po$  occurs naturally, as the penultimate member of the radium decay series:



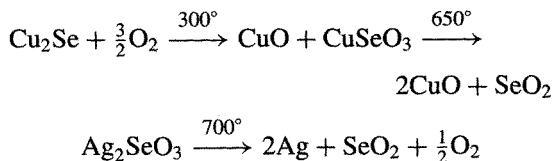
Because of the fugitive nature of  $^{210}Po$ , uranium ores contain only about 0.1 mg Po per tonne of ore (i.e.  $10^{-4}$  ppm). The overall abundance of Po in crustal rocks of the earth is thus of the order of  $3 \times 10^{-10}$  ppm.

### 16.1.2 Production and uses of the elements<sup>(2-4,7)</sup>

The main source of Se and Te is the anode slime deposited during the electrolytic refining of Cu (p. 1175); this mud also contains commercial quantities of Ag, Au and the platinum metals. Direct recovery from minerals is not usually economically viable because of their rarity. Selenium is also recovered from the sludge accumulating in sulfuric acid plants and from electrostatic precipitator dust collected during the processing of Cu and Pb. Detailed procedures for isolation and purification depend on the relative concentrations of Se, Te and other impurities, but a typical sequence involves oxidation by roasting in air with soda ash followed by leaching:



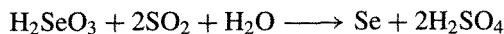
In the absence of soda ash,  $SeO_2$  can be volatilized directly from the roast:



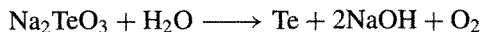
<sup>6</sup> Ref. 5, Chap. 29, pp. 803–43. See also E. FARBER, *Nobel Prize Winners in Chemistry 1901–1961*, Abelard-Schuman, London, Marie Skłodowska Curie, pp. 45–8. F. C. WOOD, Marie Curie, in E. FARBER (ed.), *Great Chemists*, pp. 1263–75. Interscience, New York, 1961.

<sup>7</sup> Kirk-Othmer *Encyclopedia of Chemical Technology*, 4th edn., 1997, Selenium and Selenium Compounds, Vol. 21, pp. 686–719, Tellurium and tellurium compounds, Vol. 22, pp. 659–79, 1983.

Separation of Se and Te can also be achieved by neutralizing the alkaline selenite and tellurite leach with  $\text{H}_2\text{SO}_4$ ; this precipitates the tellurium as a hydrous dioxide and leaves the more acidic selenous acid,  $\text{H}_2\text{SeO}_3$ , in solution from which 99.5% pure Se can be precipitated by  $\text{SO}_2$ :<sup>†</sup>



Tellurium is obtained by dissolving the dioxide in aqueous NaOH followed by electrolytic reduction:



The NaOH is regenerated and only make-up quantities are required. However, the detailed processes adopted industrially to produce Se and Te are much more complex and sophisticated than this outline implies.<sup>(2,3,7)</sup>

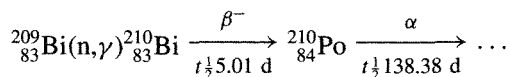
World production of refined Se in 1995 was ~2000 tonnes the largest producers being Japan (600 t), USA (360 t) and Canada (300 t). The pattern of use no doubt varies somewhat from country to country, but in the USA the largest single use of the element (35%) is as a decolorizer of glass (0.01–0.15 kg/tonne). Higher concentrations (1–2 kg/tonne) yield delicate pink glasses. The glorious selenium ruby glasses, which are the most brilliant reds known to glass-makers, are obtained by incorporating solid particles of cadmium sulfoselenide in the glass; the deepest ruby colour is obtained when Cd(S,Se) has about 10% CdS, but as the relative concentration of CdS increases the colour moderates to red (40% CdS), orange (75%) and yellow (100%). Cadmium sulfoselenides are also widely used as heat-resistant red pigments in plastics, paints, inks and enamels. Another very important application of elemental Se is in xerography, which has developed during the past four decades into the pre-eminent process for document copying, as witnessed by

<sup>†</sup> Very pure Se can be obtained by heating the crude material in  $\text{H}_2$  at  $650^\circ$  and then decomposing the  $\text{H}_2\text{Se}$  so formed by passing the gas through a silica tube at  $1000^\circ$ . Any  $\text{H}_2\text{S}$  present, being more stable than  $\text{H}_2\text{Se}$ , passes through the tube unchanged, whereas hydrides which are less stable than  $\text{H}_2\text{Se}$ , such as those of Te, P, As, Sb, are not formed in the initial reaction at  $650^\circ$ .

the ubiquitous presence of xerox machines in offices and libraries (see Panel). Related uses are as a photoconductor (selenium photoelectric cells) and as a rectifier in semiconductor devices (p. 258). Small amounts of ferroselenium are used to improve the casting, forging and machinability of stainless steels, and the dithiocarbamate  $[\text{Se}(\text{S}_2\text{CNET}_2)_4]$  finds some use in the processing of natural and synthetic rubbers. Selenium pharmaceuticals comprise a further small outlet. In addition to Se, Fe/Se, Cd(S,Se) and  $[\text{Se}(\text{S}_2\text{CNET}_2)_4]$  the main commercially available compounds of Se are  $\text{SeO}_2$ ,  $\text{Na}_2\text{SeO}_3$ ,  $\text{Na}_2\text{SeO}_4$ ,  $\text{H}_2\text{SeO}_4$  and  $\text{SeOCl}_2$  (q.v.).

Production of Te is on a much smaller scale: ca. 350 tonnes in 1978, dominated by USA, Canada and Japan. More than 70% of the Te is used in iron and steel production and in non-ferrous metals and alloys, and 25% for chemicals. A small amount of  $\text{TeO}_2$  is used in tinting glass, and Te compounds find some use as catalysts and as curing agents in the rubber industry. In addition to Te, Fe/Te and  $\text{TeO}_2$ , commercially important compounds include  $\text{Na}_2\text{TeO}_4$  and  $[\text{Te}(\text{S}_2\text{CNET}_2)_4]$ .

Polonium, because of its very low abundance and very short half-life, is not obtained from natural sources. Virtually all our knowledge of the physical and chemical properties of the element come from studies on  $^{210}\text{Po}$  which is best made by neutron irradiation of  $^{209}\text{Bi}$  in a nuclear reactor:

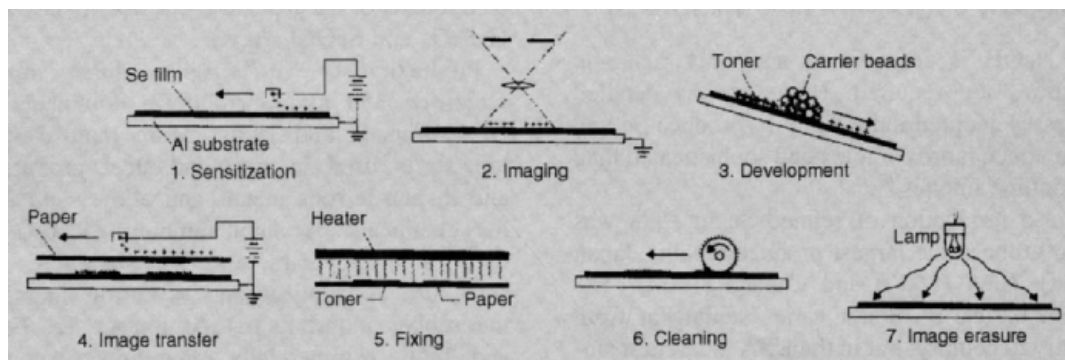


It will be recalled that  $^{209}\text{Bi}$  is 100% abundant and is the heaviest stable nuclide of any element (p. 550), but it is essential to use very high purity Bi to prevent unwanted nuclear side-reactions which would contaminate the product  $^{210}\text{Po}$ ; in particular Sc, Ag, As, Sb and Te must be <0.1 ppm and Fe <10 ppm. Polonium can be obtained directly in milligram amounts by fractional vacuum distillation from the metallic bismuth. Alternatively, it can be deposited spontaneously by electrochemical replacement onto the surface of a less electropositive metal

## Xerography

The invention of xerography by C. F. Carlson (USA) in the period 1934–42 was the culmination of a prolonged and concerted attack on the problem of devising a rapid, cheap and dry process for direct document copying without the need for the intermediate formation of a permanent photographic “negative”, or even the use of specially prepared photographic paper for the “print”. The discovery that vacuum-deposited amorphous or vitreous selenium was the almost ideal photoconductor for xerography was made in the Battelle Memorial Institute (Ohio, USA) in 1948. The dramatic success of these twin developments is witnessed by the vast number of xerox machines in daily use throughout the world today. However, early xerox equipment was not automatic. Models introduced in 1951 became popular for making offset masters, and rotary xerographic machines were introduced in 1959, but it was only after the introduction of the Xerox 914 copier in the early 1960s that electrophotography came of age. The word “xerography” derives from the Greek ξηρός, *xero* dry, γραφή, *graphy*, writing.

The sequential steps involved in commercial machines which employ reusable photoreceptors for generating xerox copies are shown in the figure<sup>(2)</sup> and further elucidated below.



1. *Sensitization of the photoreceptor.* The photoreceptor consists of a vacuum-deposited film of amorphous Se,  $\sim 50 \mu\text{m}$  thick, on an Al substrate; this is sensitized by electrostatic charging from a corona discharge using a field of  $\sim 10^5 \text{ V cm}^{-1}$ .

2. *Exposure and latent image formation.* The sensitized photoreceptor is exposed to a light and dark image pattern; in the light areas the surface potential of the photoconductor is reduced due to a photoconductive discharge. Since current can only flow perpendicular to the surface, this step produces an electrostatic-potential distribution which replicates the pattern of the image.

3. *Development of the image.* This is done using a mixture of black (or coloured) toner particles, typically  $10 \mu\text{m}$  in diameter, and spherical carrier beads ( $\sim 100 \mu\text{m}$  diameter). The toner particles become charged triboelectrically (i.e. by friction) and are preferentially attracted either by the surface fringe field at light–dark boundaries or (in systems with a developing electrode) by the absolute potential in the dark areas; they adhere to the photoreceptor, thus forming a visible image corresponding to the latent electrostatic image.

4. *Image transfer.* This is best done electrostatically by charging the print paper to attract the toner particles.

5. *Print fixing.* The powder image is made permanent by fusing or melting the toner particles into the surface of the paper, either by heat, by heat and pressure, or by solvent vapours.

6. *Cleaning.* Any toner still left on the photoreceptor after the transfer process is removed with a cloth web or brush, or by a combination of electrostatic and mechanical means.

7. *Image erasure.* The potential differences due to latent image formation are removed by flooding the photoreceptors with a sufficiently intense light source to drive the surface potential to some uniformly low value (typically  $\sim 100 \text{ V}$  corresponding to fields of  $\sim 10^4 \text{ V cm}^{-1}$ ); the photoreceptor is then ready for another print cycle.

The elegance, cheapness and convenience of xerography for document copying has led to rapid commercial development on a colossal scale throughout the world.

such as Ag. Solution techniques are unsuitable except on the trace scale (submicrogram amounts) because of the radiation damage caused by the intense radioactivity (p. 753). All

applications of Po depend on its radioactivity: it is an almost pure  $\alpha$ -emitter ( $E_\alpha$  5.30 MeV) and only 0.0011% of the activity is due to  $\gamma$ -rays ( $E_{\text{max}}$  0.803 MeV). Because of its short

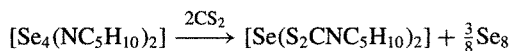
half-life (138.38 d) this entails a tremendous energy output of 141 W per gram of metal: in consequence, there is considerable self-heating of Po and its compounds. The element can therefore be used as a convenient light-weight heat source, or to generate spontaneous and reliable thermoelectric power for space satellites and lunar stations, since no moving parts are involved. Polonium also finds limited use as a neutron generator when combined with a light element of high  $\alpha, n$  cross-section such as beryllium:  ${}^9_4\text{Be}(\alpha, n){}^{12}_6\text{C}$ . The best yield (93 neutrons per  $10^6 \alpha$ -particles) is obtained with a BeO target.

### 16.1.3 Allotropy

At least eight structurally distinct forms of Se are known: the three red monoclinic polymorphs ( $\alpha$ ,  $\beta$  and  $\gamma$ ) consist of  $\text{Se}_8$  rings and differ only in the intermolecular packing of the rings in the crystals. Other ring sizes have recently been synthesized in the red allotropes *cyclo-Se*<sub>6</sub> and *cyclo-Se*<sub>7</sub>, and the heterocyclic analogues *cyclo-Se*<sub>5</sub>S and *cyclo-Se*<sub>5</sub>S<sub>2</sub>.<sup>(8)</sup> The grey, "metallic", hexagonal crystalline form features helical polymeric chains and these also occur, somewhat deformed, in amorphous red Se. Finally, vitreous black Se, the ordinary commercial form of the element, comprises an extremely complex and irregular structure of large polymeric rings having up to 1000 atoms per ring.

The  $\alpha$ - and  $\beta$ -forms of red crystalline  $\text{Se}_8$  are obtained respectively by the slow and rapid evaporation of  $\text{CS}_2$  or benzene solutions of black vitreous Se and more recently a third ( $\gamma$ ) form of red crystalline  $\text{Se}_8$  was obtained from the reaction

of dipiperidinotetraselane with solvent  $\text{CS}_2$ :<sup>(9)</sup>



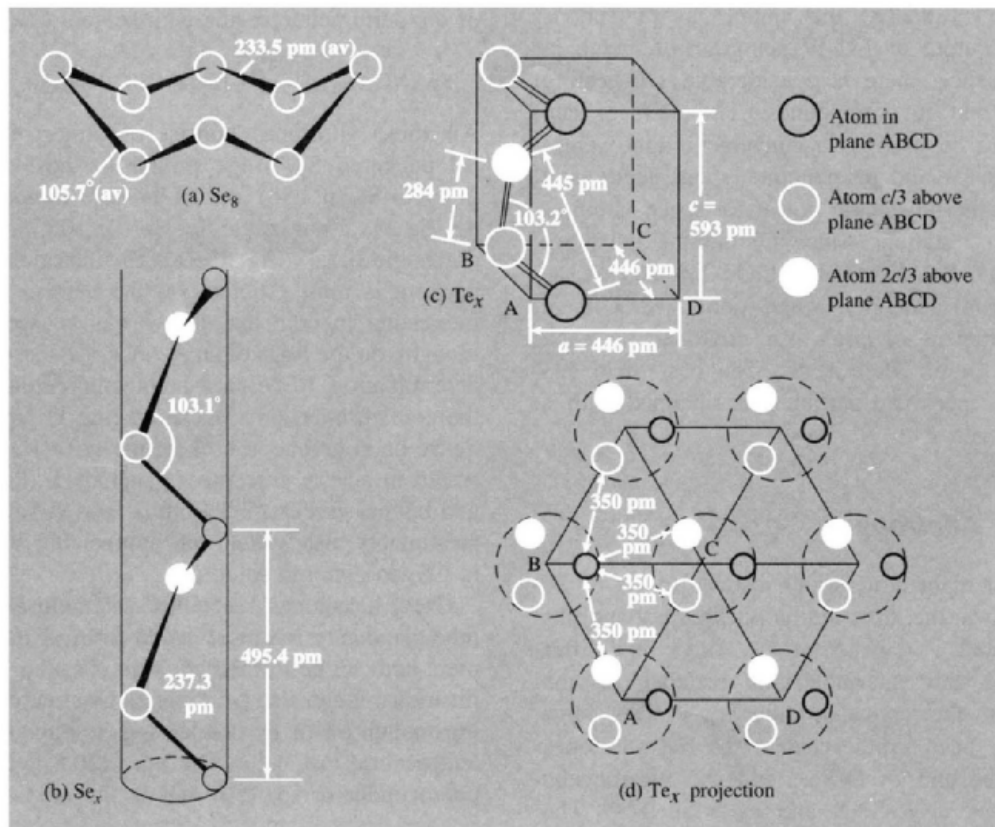
All three allotropes consist of almost identical puckered  $\text{Se}_8$  rings similar to those found in *cyclo-S*<sub>8</sub> (p. 658) and of average dimensions Se–Se 233.5 pm, angle Se–Se–Se 105.7°, dihedral angle 101.3° (Fig. 16.1a). The intermolecular packing is most efficient for the  $\alpha$ -form. [It is interesting to note that  $\beta$ - $\text{Se}_8$  was at one time thought, on the basis of an X-ray crystal structure determination, to be an 8-membered *chain* with the configuration of a puckered ring in which 1 Se–Se bond had been broken; the error was corrected in a very perceptive paper by L. Pauling and his co-workers.<sup>(10)</sup>] Both  $\alpha$ - and  $\beta$ - $\text{Se}_8$  (and presumably also  $\gamma$ - $\text{Se}_8$ ) are appreciably soluble in  $\text{CS}_2$  to give red solutions.

Grey, hexagonal, "metallic" selenium is thermodynamically the most stable form of the element and can be formed by warming other modifications; it can also be obtained by slowly cooling molten Se or by condensing Se vapour at a temperature just below the mp (220.5°). It is a photoconductor (p. 750) and is the only modification which conducts electricity. The structure (Fig. 16.1b) consists of unbranched helical chains with Se–Se 237.3 pm, angle Se–Se–Se 103.1°, and a repeat unit every 3 atoms (cf. fibrous sulfur, p. 660). The closest Se...Se distance between chains is 343.6 pm, which is very close to that in  $\text{Te}_x$  (350 pm) (see below). Grey  $\text{Se}_x$  is insoluble in  $\text{CS}_2$  and its density, 4.82 g cm<sup>-3</sup>, is the highest of any modification of the element. A related allotrope is red amorphous Se, formed by condensation of Se vapour onto a cold surface or by precipitation from aqueous solutions of selenous acid by treatment with  $\text{SO}_2$  (p. 755) or other reducing agents such as hydrazine hydrate. It is slightly soluble in  $\text{CS}_2$ , and has a deformed chain structure but does not conduct electricity. The heat of transformation to the stable hexagonal

<sup>8</sup> R. STEUDEL and E.-M. STRAUSS, in H. J. EMELÉUS and A. G. SHARPE, *Adv. Inorg. Chem. Radiochem.* **28**, 135–66 (1984). R. STEUDEL, M. PAPAVALSILIOU, E.-M. STRAUSS and R. LAITINEN, *Angew. Chem. Int. Edn. Engl.* **25**, 99–101 (1986) and references cited therein. See also R. STEUDEL and M. PAPAVALSILIOU, *Polyhedron* **7**, 581–3 (1988), R. STEUDEL, M. PRIDÖHL, H. HARTL and I. BRÜGAM, *Z. anorg. allg. Chem.* **619**, 1589–96 (1993).

<sup>9</sup> O. FOSS and V. JANICKIS, *J. Chem. Soc., Chem. Commun.*, 834–5 (1977).

<sup>10</sup> R. E. MARSH, L. PAULING and J. D. MCCULLOUGH, *Acta Cryst.* **6**, 71–5 (1953).



**Figure 16.1** Structures of various allotropes of selenium and the structure of crystalline tellurium: (a) the  $\text{Se}_8$  unit in  $\alpha$ -  $\beta$ - and  $\gamma$ -red selenium; (b) the helical Se chain along the  $c$ -axis in hexagonal grey selenium; (c) the similar helical chain in crystalline tellurium shown in perspective; and (d) projection of the tellurium structure on a plane perpendicular to the  $c$ -axis.

grey form has been variously quoted but is in the region of 5–10 kJ per mole of Se atoms.

Vitreous, black Se is the ordinary commercial form of the element, obtained by rapid cooling of molten Se; it is a brittle, opaque, bluish-black lustrous solid which is somewhat soluble in  $\text{CS}_2$ . It does not melt sharply but softens at about  $50^\circ$  and rapidly transforms to hexagonal grey Se when heated to  $180^\circ$  (or at lower temperatures when catalysed by halogens, amines, etc.). There has been much discussion about the structure but it seems to comprise rings of varying size up to quite high molecular weights. Presumably these rings cleave and polymerize into helical chains under the influence of thermal soaking or

catalysts. The great interest in the various allotropes of selenium and their stabilization or interconversion, stems from its use in photocells, rectifiers, and xerography (p. 750).<sup>(2)</sup>

Tellurium has only one crystalline form and this is composed of a network of spiral chains similar to those in hexagonal Se (Fig. 16.1c and d). Although the intra-chain Te–Te distance of 284 pm and the  $c$  dimension of the crystal (593 pm) are both substantially greater than for  $\text{Se}_x$  (as expected), nevertheless the closest interatomic distance between chains is almost identical for the 2 elements (Te...Te 350 pm). Accordingly the elements form a continuous range of solid solutions in which there is a random

Table 16.1 Production and properties of long-lived Po isotopes

Isotope	Production	$t_{\frac{1}{2}}$	$E_{\gamma}/\text{MeV}$	$A_r$ (relative atomic mass)
$^{208}\text{Po}$	$^{209}\text{Bi}(\text{d},3\text{n})$ or $(\text{p},2\text{n})$	2.898 y	5.11	207.9812
$^{209}\text{Po}$	$^{209}\text{Bi}(\text{d},2\text{n})$ or $(\text{p},\text{n})$	102 y	4.88	208.9824
$^{210}\text{Po}$	$^{209}\text{Bi}(\text{n},\gamma)$	138.376 d	5.305	209.9828

alternation of Se and Te atoms in the helical chains.<sup>(11)</sup> The homogeneous alloys  $\text{Se}_x\text{Te}_{1-x}$  can also, most remarkably, be prepared directly by hydrazine reduction of glycol solutions of  $x\text{SeO}_2$  and  $(1-x)\text{TeO}_2$  or other compounds of  $\text{Se}^{\text{IV}}$  and  $\text{Te}^{\text{IV}}$  such as dialkylselenites and tetraalkoxytelluranes); the lattice parameters and mp of the alloys vary steadily between those of the two end members Se and Te.<sup>(12)</sup> The rapid diminution in allotropic complexity from sulfur through selenium to tellurium is notable.

Polonium is unique in being the only element known to crystallize in the simple cubic form (6 nearest neighbours at 335 pm). This  $\alpha$ -form distorts at about  $36^\circ$  to a simple rhombohedral modification in which each Po also has 6 nearest neighbours at 335 pm. The precise temperature of the phase change is difficult to determine because of the self-heating of crystalline Po (p. 751) and it appears that both modifications can coexist from about  $18^\circ$  to  $54^\circ$ . Both are silvery-white metallic crystals with substantially higher electrical conductivity than Te.

### 16.1.4 Atomic and physical properties

Selenium, Te and Po are the three heaviest members of Group 16 and, like their congeners O and S, have two p electrons less than the next following noble gases. Selenium is normally said to have 6 stable isotopes though the heaviest of these ( $^{82}\text{Se}$ , 8.73% abundant) is actually an extremely long-lived  $\beta^-$  emitter,

$t_{\frac{1}{2}} 1.4 \times 10^{20}$  y. The most abundant isotope is  $^{80}\text{Se}$  (49.61%), and all have zero nuclear spin except the 7.63% abundant  $^{77}\text{Se}$  ( $I = \frac{1}{2}$ ), which is finding increasing use in nmr experiments.<sup>(13)</sup> Because of the plethora of isotopes the atomic weight is only known to about 1 part in 2600 (p. 16). Tellurium, with 8 naturally occurring stable isotopes, likewise suffers some imprecision in its atomic weight (1 part in 4300). The most abundant isotopes are  $^{130}\text{Te}$  (33.87%) and  $^{128}\text{Te}$  (31.70%), and again all have zero nuclear spin except the nmr active isotopes  $^{123}\text{Te}$  (0.905%) and  $^{125}\text{Te}$  (7.12%), which have spin  $\frac{1}{2}$ .<sup>(13)</sup>  $^{125}\text{Te}$  also has a low-lying nuclear isomer  $^{125\text{m}}\text{Te}$  which decays by pure  $\gamma$  emission ( $E_{\gamma}$  35.48 keV,  $t_{\frac{1}{2}}$  58 d) — this has found much use in Mössbauer spectroscopy.<sup>(14)</sup> Polonium, as we have seen (p. 748), has no stable isotopes. The 3 longest lived, together with their modes of production and other properties, are as shown in Table 16.1.

Several atomic and physical properties of the elements are given in Table 16.2. The trends to larger size, lower ionization energy and lower electronegativity are as expected. The trend to metallic conductivity is also noteworthy; indeed, Po resembles its horizontal neighbours Bi, Pb and Tl not only in this but in its moderately high density and notably low mp and bp.

<sup>13</sup> C. RODGER, N. SHEPPARD, H. C. E. MCFARLANE, and W. MCFARLANE, in R. K. HARRIS and B. R. MANN (eds.), *NMR and the Periodic Table*, pp. 402–19. Academic Press, London, 1978. H. C. E. MCFARLANE and W. MCFARLANE, in J. MASON (ed.) *Multinuclear NMR* pp. 417–35, Plenum Press, New York, 1987.

<sup>14</sup> N. N. GREENWOOD and T. C. GIBB, *Mössbauer Spectroscopy*, pp. 452–62, Chapman & Hall, London, 1971. F. J. BERRY, Chap. 8 in G. J. LONG (ed.) *Mössbauer Spectroscopy Applied to Inorganic Chemistry*, Vol. 2, Plenum Press, New York 1987, pp. 343–90.

<sup>11</sup> A. A. KUDRYAVTSEV, *The Chemistry and Technology of Selenium and Tellurium*, Collet's Publishers, London, 1974, 278 pp.

<sup>12</sup> T. W. SMITH, S. D. SMITH and S. S. BADESHA, *J. Am. Chem. Soc.* **106**, 7247–8 (1984).



Table 16.2 Some atomic and physical properties of selenium, tellurium and polonium

Property	Se	Te	Po
Atomic number	34	52	84
Number of stable isotopes	6	8	0
Electronic structure	[Ar]3d <sup>10</sup> 4s <sup>2</sup> 4p <sup>4</sup>	[Kr]4d <sup>10</sup> 5s <sup>2</sup> 5p <sup>4</sup>	[Xe]4f <sup>14</sup> 5d <sup>10</sup> 6s <sup>2</sup> 6p <sup>4</sup>
Atomic weight	78.96(± 0.03)	127.60(± 0.03)	(210)
Atomic radius (12-coordinate)/pm <sup>(a)</sup>	140 <sup>(a)</sup>	160 <sup>(a)</sup>	164 <sup>(a)</sup>
Ionic radius/pm (M <sup>2-</sup> )	198	221	(230?)
(M <sup>4+</sup> )	50	97	94
(M <sup>6+</sup> )	42	56	67
Ionization energy/kJ mol <sup>-1</sup>	940.7	869.0	813.0
Pauling electronegativity	2.4	2.1	2.0
Density(25°)/g cm <sup>-3</sup>	Hexag 4.189 α-monoclinic 4.389 Vitreous 4.285	6.25	α9.142 β9.352
MP/°C	217	452	246–254
BP/°C	685	990	962
Δ <i>H</i> <sub>atomization</sub> /kJ mol <sup>-1</sup>	206.7	192	—
Electrical resistivity(25°)/ohm cm	10 <sup>10(b)</sup>	1	α4.2 × 10 <sup>-5</sup> β4.4 × 10 <sup>-5</sup>
Band energy gap <i>E</i> <sub>g</sub> /kJ mol <sup>-1</sup>	178	32.2	0

<sup>(a)</sup>The 2-coordinate covalent radius is 119 pm for elemental Se and 142 pm for Te; the 6-coordinate metallic radius of Po is 168 pm.

<sup>(b)</sup>Depends markedly on purity, temperature and photon flux; resistivity of liquid Se at 400° is 1.3 × 10<sup>5</sup> ohm cm.

### 16.1.5 Chemical reactivity and trends

The elements in Group 16 share with the preceding main-group elements the tendency towards increasing metallic character as the atomic weight increases within the group. Thus O and S are insulators, Se and Te are semiconductors and Po is a metal. Parallel with this trend is the gradual emergence of cationic (basic) properties with Te, and these are even more pronounced with Po. For example, Se is not appreciably attacked by dilute HCl whereas Te dissolves to some extent in the presence of air; Po dissolves readily to yield pink solutions of Po<sup>II</sup> which are then rapidly oxidized further to yellow Po<sup>IV</sup> by the products of radiolytic decomposition of the solvent. Likewise, the structure and bonding of the halides of these elements depends markedly on both the electronegativity of the halogen and on the oxidation state of the central element, thereby paralleling the “ionic-covalent” transition which has already been discussed for the halides of P (p. 499), As and Sb (p. 558), and S (p. 691).

Selenium, Te and Po combine directly with most elements, though less readily than do O and S. The most stable compounds are (a) the selenides, tellurides and polonides (M<sup>2-</sup>) formed with the strongly positive elements of Groups 1, 2 and the lanthanides, and (b) the compounds with the electronegative elements O, F and Cl in which the oxidation states are +2, +4 and +6. The compounds tend to be less stable than the corresponding compounds of S (or O), and there are few analogues of the extensive range of sulfur–nitrogen compounds (p. 721). A similar trend (also noted in the preceding groups) is the decreasing thermal stability of the hydrides: H<sub>2</sub>O > H<sub>2</sub>S > H<sub>2</sub>Se > H<sub>2</sub>Te > H<sub>2</sub>Po. Selenium and tellurium share to a limited extent sulfur’s great propensity for catenation (see allotropy of the elements, polysulfanes, halides, etc.).

As found in preceding groups, there is a diminution in the stability of multiple bonds (e.g. to C, N, O) and a corresponding decrease in their occurrence as the atomic number of the group element increases. Thus O=C=O and (to a lesser extent) S=C=S are stable, whereas

Se=C=Se polymerizes readily, Se=C=Te is unstable and Te=C=Te is unknown. Again,

SO<sub>2</sub> is a (nonlinear) gaseous molecule,  $\text{O}=\text{S}=\text{O}$ ,

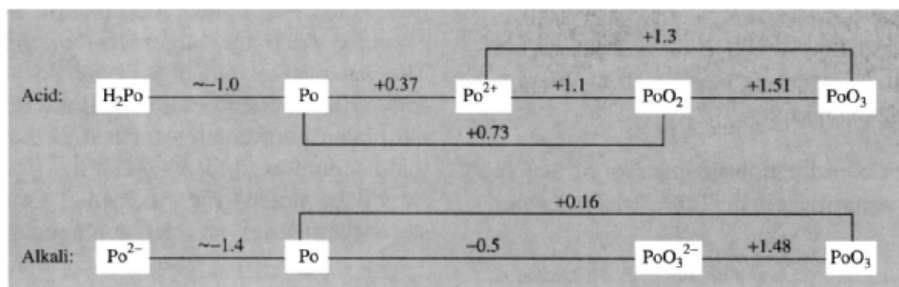
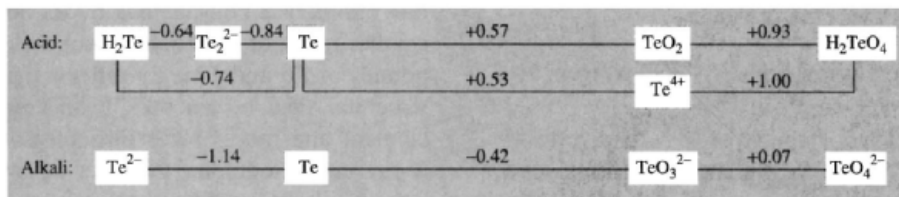
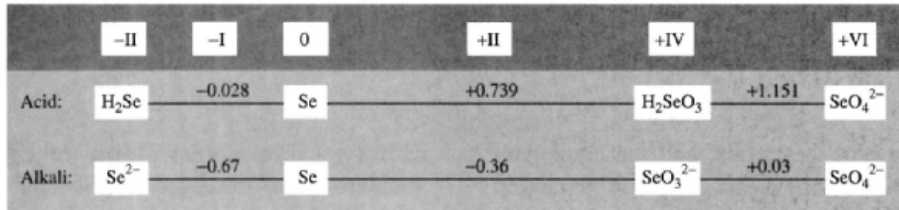
whereas SeO<sub>2</sub> is a chain polymer  $-\text{O}-\text{Se}(\text{=O})-$  (p. 779) and TeO<sub>2</sub> features 4-coordinate pseudo-trigonal-bipyramidal units  $\{\text{TeO}_4\}$  which are singly-bonded into extended layer or 3D structures (p. 779); in PoO<sub>2</sub> the coordination number increases still further to 8 and the compound adopts the typical "ionic" fluorite structure (p. 118). It can be seen that double bonds are less readily formed between 2 elements the greater the electronegativity difference between them and the smaller the sum of their individual electronegativities; this is paralleled by a diminution in double-bond formation with increasing size of the more electropositive element and the consequent decrease in bond energy.

The redox properties of the elements also show interesting trends. In common with several

elements immediately following the first (3d) transition series (especially Ge, As, Se, Br) selenium shows a marked resistance to oxidation up to its group valency, i.e. Se<sup>VI</sup>. For example, whereas HNO<sub>3</sub> readily oxidizes S to H<sub>2</sub>SO<sub>4</sub>, selenium gives H<sub>2</sub>SeO<sub>3</sub>. Again dehydration of H<sub>2</sub>SO<sub>4</sub> with P<sub>2</sub>O<sub>5</sub> yields SO<sub>3</sub> whereas H<sub>2</sub>SeO<sub>4</sub> gives SeO<sub>2</sub> +  $\frac{1}{2}$ O<sub>2</sub>. Likewise S forms a wide range of sulfones, R<sub>2</sub>SO<sub>2</sub>, but very few selenones are known; thus, Ph<sub>2</sub>SeO is not oxidized either by HNO<sub>3</sub> or by acidified K<sub>2</sub>Cr<sub>2</sub>O<sub>7</sub>, and alkaline KMnO<sub>4</sub> is required to produce Ph<sub>2</sub>SeO<sub>2</sub> (mp 155°). As noted in the isolation of the element (p. 749), SO<sub>2</sub> precipitates Se from acidified solutions of Se<sup>IV</sup>.

The standard reduction potentials of the elements in acid and alkaline solutions are summarized in the schemes below.<sup>(15)</sup> It is

<sup>15</sup> A. J. BARD, R. PARSONS and J. JORDAN, (eds.) *Standard Potentials in Aqueous Solution*, (IUPAC) Marcel Dekker, New York, 1985, 834 pp.



Standard reduction potentials of Se, Te and Po.<sup>(15)</sup>

Table 16.3 Coordination geometries of selenium, tellurium and polonium

Coordination number	Se	Te	Po
1	COSe, CSe <sub>2</sub> , NCSe <sup>-</sup> , MoSe <sub>4</sub> <sup>2-</sup> , WSe <sub>4</sub> <sup>2-</sup>	COTe, CSTe Te <sub>3</sub> <sup>2-</sup>	
2 (bent)	Se <sub>x</sub> , H <sub>2</sub> Se, R <sub>2</sub> Se <i>cyclo</i> -Se <sub>4</sub> <sup>2+</sup>	Te <sub>x</sub> , H <sub>2</sub> Te, R <sub>2</sub> Te, TeBr <sub>2</sub> <i>cyclo</i> -Te <sub>4</sub> <sup>2+</sup>	
(linear)	[L <sub>n</sub> Cr≡Se≡CrL <sub>n</sub> ] <sup>(a)</sup>		
3 (trigonal planar)	[(L <sub>n</sub> Cr) <sub>3</sub> (μ <sub>3</sub> -Se)] <sup>-(a)</sup>	TeO <sub>3</sub> (g)	
(pyramidal)	(SeO <sub>2</sub> ) <sub>x</sub> , SeOX <sub>2</sub> , SeMe <sub>3</sub> <sup>+</sup>	TeO <sub>3</sub> <sup>2-</sup> , TeMe <sub>3</sub> <sup>+</sup>	
4 (planar)	—	[TeBr <sub>2</sub> {SC(NH <sub>2</sub> ) <sub>2</sub> }] <sub>2</sub>	
(tetrahedral)	SeO <sub>4</sub> <sup>2-</sup> , SeO <sub>2</sub> Cl <sub>2</sub>	—	CdPo (ZnS)
(pseudo-trigonal bipyramidal)	R <sub>2</sub> SeX <sub>2</sub>	TeO <sub>2</sub> , Me <sub>2</sub> TeCl <sub>2</sub>	
5 (square pyramidal)	[SeOCl <sub>2</sub> py <sub>2</sub> ]	TeF <sub>5</sub> <sup>-</sup> , [TeL <sub>4</sub> Me] <sup>+</sup>	
(pentagonal planar)	—	[Te(S <sub>2</sub> COEt) <sub>3</sub> ] <sup>-</sup> (Fig. 16.2a)	
6 (octahedral)	SeF <sub>6</sub> , SeBr <sub>6</sub> <sup>2-</sup>	Te(OH) <sub>6</sub> , TeBr <sub>6</sub> <sup>2-</sup>	PoI <sub>6</sub> <sup>2-</sup> , Po metal CaPo (NaCl) MgPo (NiAs)
(trigonal prismatic)	VSe, CrSe, MnSe (NiAs)	ScTe, VTe, MnTe, (NiAs)	
(pentagonal pyramidal)	—	[Me Te(I){S <sub>2</sub> CNEt <sub>2</sub> }] <sub>2</sub> (Fig. 16.2b)	
7 (pentagonal bipyramidal)	—	[PhTe{S <sub>2</sub> CNEt <sub>2</sub> }] <sub>2</sub> - {S <sub>2</sub> P(OEt) <sub>2</sub> }] (Fig. 16.2c)	
8 (cubic)	—	TeF <sub>8</sub> <sup>2-</sup> (?)	Na <sub>2</sub> Po, PoO <sub>2</sub> (CaF <sub>2</sub> )

<sup>(a)</sup>{CrL<sub>n</sub>} = {Cr(η<sup>5</sup>-C<sub>5</sub>H<sub>5</sub>)(CO)<sub>2</sub>}<sup>(16)</sup>

instructive to plot these data, and the equivalent values for sulfur, as volt-equivalents *vs* oxidation state (pp. 435–8), when the following trends (in acid solution) become obvious:

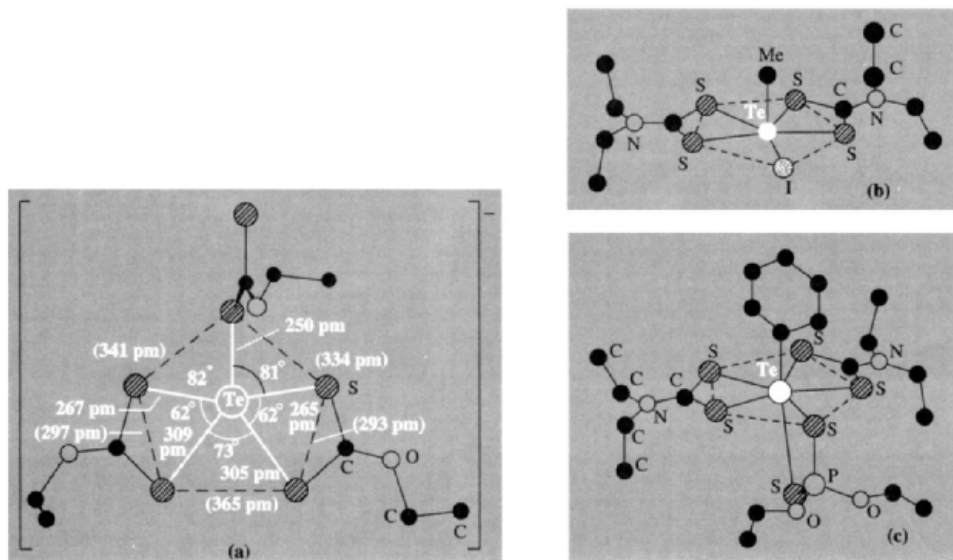
- (i) the decreasing stability of H<sub>2</sub>M from H<sub>2</sub>S to H<sub>2</sub>Po;
- (ii) the greater stability of M<sup>IV</sup> relative to M<sup>0</sup> and M<sup>VI</sup> for Se, Te and Po (but not for S, p. 706), as shown by the concavity of the graph;
- (iii) the anomalous position of Se in its higher oxidation states, as mentioned in the preceding paragraph.

The known coordination geometries of Se, Te and Po are summarized in Table 16.3 together

with typical examples. Most of the common geometries are observed for Se and Te, though twofold (linear) is rare and fivefold (trigonal bipyramidal) is conspicuous by its absence. The smaller range of established geometries for compounds of Po undoubtedly reflects the paucity of structural data occasioned by the rarity of this element and the extreme difficulty of obtaining X-ray crystallographic or other structural information. There appears, however, to be a clear preference for higher coordination numbers, as expected from the larger size of the Po atom. The various examples will be discussed more fully in subsequent sections but the rare pentagonal planar coordination formed in the ethyl xanthato complex [Te(η<sup>2</sup>-S<sub>2</sub>COEt)<sub>2</sub>(η<sup>1</sup>-S<sub>2</sub>COEt)]<sup>-</sup> should be noted (Fig. 16.2a);<sup>(17)</sup> Other unusual stereochemistries are the pentagonal pyramidal

<sup>16</sup> W. A. HERRMANN, J. ROHRMANN, E. HERDTWECK, H. BOCK and A. VELTMANN, *J. Am. Chem. Soc.* **108**, 3134–5 (1986).

<sup>17</sup> B. F. HOSKINS and C. D. PANNAN, *J. Chem. Soc., Chem. Commun.*, 408–9 (1975).



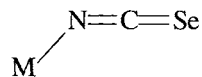
**Figure 16.2** Structure of (a) the anion  $[\text{Te}(\text{S}_2\text{COEt})_3]^-$ , the first authentic example of 5-coordinate pentagonal planar geometry,<sup>(17)</sup> (b)  $[\text{MeTe}(\text{I})\{\text{S}_2\text{CNET}_2\}_2]$ <sup>(18)</sup> and (c)  $[\text{PhTe}\{\text{S}_2\text{CNET}_2\}_2\{\text{S}_2\text{P}(\text{OEt})_2\}]^{(18)}$  (see text).

6-coordinate  $\text{Te}^{\text{IV}}$  in  $[\text{MeTe}(\text{I})\{\text{S}_2\text{CNET}_2\}_2]$ <sup>(18)</sup> and pentagonal bipyramidal 7-coordinate  $\text{Te}^{\text{IV}}$  in  $[\text{PhTe}\{\text{S}_2\text{CNET}_2\}_2\{\text{S}_2\text{P}(\text{OEt})_2\}]$ <sup>(18)</sup>; in both cases the crystallographic data suggest the presence of a stereochemically active lone pair of electrons which distorts the regular geometry of the coordination sphere. This structure is consistent with a pentagonal bipyramidal set of orbitals on  $\text{Te}^{\text{II}}$ , 2 of which are occupied by stereochemically active lone-pairs directed above and below the  $\text{TeS}_5$  plane. By contrast, the single lone-pairs in  $\text{Se}^{\text{IV}}\text{X}_6^{2-}$ ,  $\text{Te}^{\text{IV}}\text{X}_6^{2-}$  and  $\text{Po}^{\text{IV}}\text{I}_6^{2-}$  are sterically inactive and the 14-(valence)electron anions are accurately octahedral (see p. 776), as in molecular  $\text{Se}^{\text{VI}}\text{F}_6$ , which has only 12 valence electrons.

Other less-symmetrical coordination geometries for Se and Te occur in the  $\mu$ - $\text{Se}_2$  and  $\mu$ - $\text{Te}_2$  complexes and the polyatomic cluster cations  $\text{Se}_{10}^{2+}$  and  $\text{Te}_6^{4+}$ , as mentioned below.

The coordination chemistry of complexes in which Se is the donor atom has been

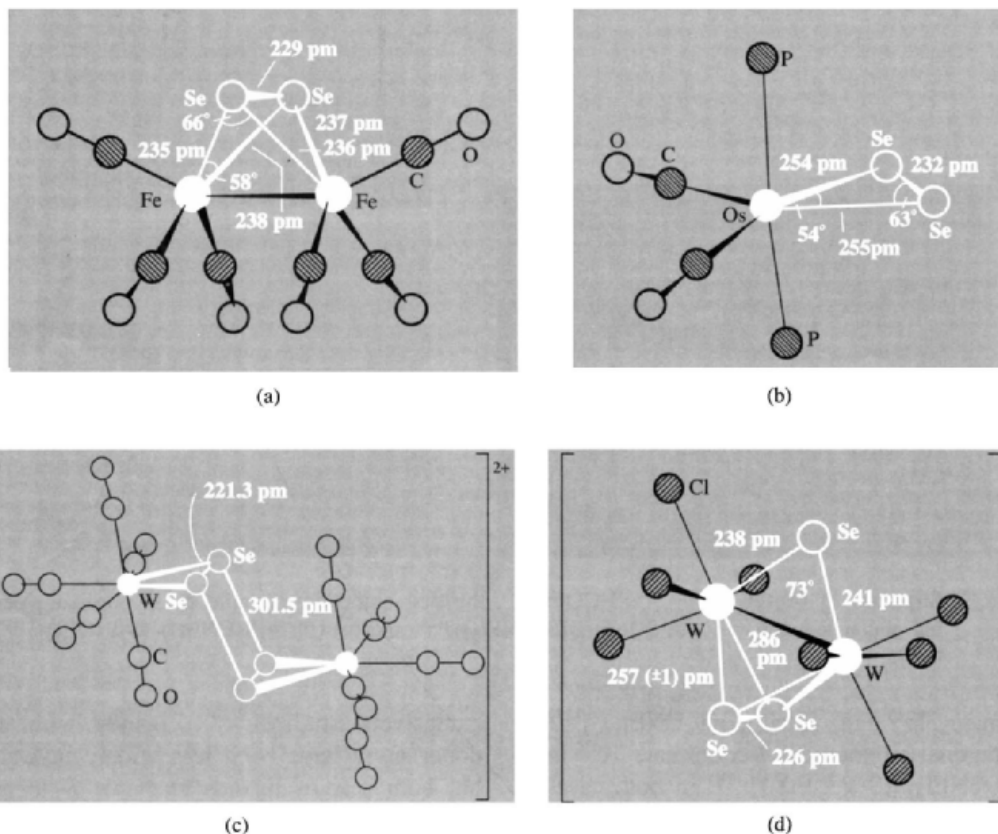
extensively studied.<sup>(2,19)</sup> Ligands with Te as donor atom have been less widely investigated but both sets of ligands resemble *S*-donor ligands (p. 673) rather than *O*-donor ligands in favouring b-class acceptors such as  $\text{Pd}^{\text{II}}$ ,  $\text{Pt}^{\text{II}}$  and  $\text{Hg}^{\text{II}}$ . The linear selenocyanate ion  $\text{SeCN}^-$ , like the thiocyanate ion (p. 324) is ambidentate, bonding via Se to heavy metals and via N (isoselenocyanate) to first-row transition metals, e.g.  $[\text{Ag}^{\text{I}}(\text{SeCN})_3]^{2-}$ ,  $[\text{Cd}^{\text{II}}(\text{SeCN})_4]^{2-}$ ,  $[\text{Pb}^{\text{II}}(\text{SeCN})_6]^{4-}$ , but  $[\text{Cr}^{\text{III}}(\text{NCSe})_6]^{3-}$  and  $[\text{Ni}(\text{NCSe})_4]^{2-}$ . The isoselenocyanate ligand often features nonlinear coordination



but in the presence of bulky ligands it tends to become linear  $\text{M}-\overset{\oplus}{\text{N}}\equiv\text{C}-\text{Se}^-$ . A bidentate bridging mode is also well established, e.g.  $\{\text{Cd}-\text{Se}-\text{C}-\text{N}-\text{Cd}\}$  and  $\{\text{Ag}-\text{Se}-\text{C}-\text{N}-\text{Cr}\}$ . Monodentate organoselenium ligands include

<sup>18</sup> D. DAKTERNIEKS, R. D. GIACOMO, R. W. GABLE and B. F. HOSKINS, *J. Am. Chem. Soc.* **110**, 6762–8 (1988). Later papers are reviewed in S. HUSEBYE and S. V. LINDEMAN, *Main Group Chemistry News*, 3(4), 8–16 (1996).

<sup>19</sup> S. E. LIVINGSTONE, *Q. Rev.* **19**, 386–425 (1965).



**Figure 16.3** Structures of some  $\eta^2$ -Se<sub>2</sub> complexes. (a) red [Fe<sub>2</sub>(CO)<sub>6</sub>( $\mu$ , $\eta^2$ -Se<sub>2</sub>)],<sup>(20)</sup> (b) reddish-purple [Os(CO)<sub>2</sub>(PPh<sub>3</sub>)<sub>2</sub>( $\eta^2$ -Se<sub>2</sub>)],<sup>(22)</sup> (c) the purple-black dication [W<sub>2</sub>(CO)<sub>8</sub>( $\mu$ : $\eta^2$ : $\eta^2$ -Se<sub>4</sub>)]<sup>2+</sup> and (d) brown [W<sub>2</sub>Cl<sub>8</sub>( $\mu$ -Se)( $\mu$ -Se<sub>2</sub>)]<sup>2-</sup><sup>(24)</sup>

R<sub>2</sub>Se, Ar<sub>2</sub>Se, R<sub>3</sub>P=Se and selenourea (H<sub>2</sub>N)<sub>2</sub>C=Se, all of which bond well to heavy metal acceptors. Tellurium appears to be analogous:<sup>(3)</sup> e.g. Me<sub>2</sub>Te.HgX<sub>2</sub>, C<sub>4</sub>H<sub>8</sub>Te.HgCl<sub>2</sub>, Ph<sub>2</sub>Te.HgX<sub>2</sub>, etc.

The structure of complexes containing the  $\eta^2$ -Se<sub>2</sub> ligand have recently been determined and, where appropriate, compared with analogous  $\eta^2$ -S<sub>2</sub>,  $\eta^2$ -P<sub>2</sub> and  $\eta^2$ -As<sub>2</sub> complexes (p. 587). Examples are in Fig. 16.3 and the original papers should be consulted for further details.<sup>(20-25)</sup> Complexes

which feature side-on  $\eta^2$ -Te<sub>2</sub> such as [Ni(ppp)( $\eta^2$ -Te<sub>2</sub>)] (ppp = Ph<sub>2</sub>PC<sub>2</sub>H<sub>4</sub>P(Ph)C<sub>2</sub>H<sub>4</sub>PPh<sub>2</sub>), analogous to the  $\eta^2$ -Se<sub>2</sub> complex in Fig. 16.3b are also

<sup>21</sup> D. J. JONES, T. MAKANI and J. ROZIÈRE, *J. Chem. Soc., Chem. Commun.*, 1275-80 (1986).

<sup>22</sup> D. H. FARRAR, K. R. GRUNDY, N. C. PAYNE, W. R. ROOPER and A. WALKER, *J. Am. Chem. Soc.* **101**, 6577-82 (1979).

<sup>23</sup> M. J. COLLINS, R. J. GILLESPIE, J. W. KOLIS and J. F. SAWYER, *Inorg. Chem.* **25**, 2057-61 (1986).

<sup>24</sup> M. G. B. DREW, G. W. A. FOWLES, E. M. PAGE and D. A. RICE, *J. Am. Chem. Soc.* **101**, 5827-8 (1979). The dark green rhodium complex [Rh( $\eta^5$ -C<sub>5</sub>Me<sub>5</sub>)<sub>2</sub>( $\mu$ -Se)( $\mu$ -Se<sub>2</sub>)] and the violet-brown osmium analogue [Os<sub>2</sub>( $\eta^5$ -C<sub>5</sub>Me<sub>5</sub>)<sub>2</sub>( $\mu$ -Se)( $\mu$ -Se<sub>2</sub>)] have a similar structure.<sup>(25)</sup>

<sup>25</sup> H. BRUNNER, W. MEIJER, B. NUBER, J. WACHTER and M. L. ZIEGLER, *Angew. Chem. Int. Edn. Engl.* **25** 907-8 (1986).

<sup>20</sup> C. F. CAMPANA, F. Y.-K. LO, and L. F. DAHL, *Inorg. Chem.* **18**, 3060-4 (1979); see also pp. 3047 and 3054. The mixed-metal cationic complex [FeW(CO)<sub>8</sub>( $\mu$ , $\eta^2$ -Se<sub>2</sub>)]<sup>2+</sup> has a similar structure.<sup>(21)</sup>

known,<sup>(26)</sup> as well as those which feature the  $\mu:\eta^2,\eta^2$  bridging mode:<sup>(27)</sup>



The tridentate triangulo ligand  $\eta^3\text{-cyclo-Te}_3$  has been characterized in the cationic complex  $[\text{W}(\text{CO})_4(\eta^3\text{-Te}_3)]^{2+}$ <sup>(28)</sup> [cf.  $\eta^3\text{-P}_3$  (p. 487),  $\eta^3\text{-As}_3$  (p. 588), etc.], and  $\mu_3\text{-}$  and  $\mu_4\text{-}$ bridging Te atoms have been found in the heptanuclear trimetallic cluster  $[\{\text{Fe}_2(\text{CO})_6\}(\mu_4\text{-Te})(\mu_3\text{-Te})\{\text{Re}_3(\text{CO})_{11}\}]$ <sup>(29)</sup> The core geometry of this latter cluster can be described as a  $\{\text{Fe}_2\text{Te}_2\}$  ‘butterfly’ with wing-tip Te atoms bridging a bent  $\text{Ru}_3$  unit.

The compounds of Se, Te and Po should all be treated as potentially toxic. Volatile compounds such as  $\text{H}_2\text{Se}$ ,  $\text{H}_2\text{Te}$  and organo derivatives are particularly dangerous and maximum permissible limits for air-borne concentrations are  $0.1 \text{ mg m}^{-3}$  (cf.  $10 \text{ mg m}^{-3}$  for HCN). The elements are taken up by the kidneys, spleen and liver, and even in minute concentrations cause headache, nausea and irritation of mucous membrane.

Organoselenium compounds in particular, once ingested, are slowly released over prolonged periods and result in foul-smelling breath and perspiration. The element is also highly toxic towards grazing sheep, cattle and other animals, and, at concentrations above about 5 ppm, causes severe disorders. Despite this, Se was found (in 1957) to play an essential dietary role in animals and also in humans — it is required in the formation of the enzyme glutathione peroxidase which is involved in fat metabolism. It has also been found that the incidence of kwashiorkor (severe protein malnutrition) in children is associated with inadequate uptake of Se, and it may well be involved in protection

against certain cancers. The average dietary intake of Se in the USA is said to be  $\sim 150 \mu\text{g}$  daily, usually in meat and sea food. Considerable caution should be taken in handling compounds of Se and Te, but the hazards should also be kept in perspective — no human fatalities directly attributable to either Se or Te poisoning have ever been recorded. The biochemistry and dietary aspects of Se have been reviewed.<sup>(30)</sup>

Polonium is extremely toxic at all concentrations and is never beneficial. Severe radiation damage of vital organs follows ingestion of even the minutest concentrations and, for the most commonly used isotope,  $^{210}\text{Po}$ , the maximum permissible body burden is  $0.03 \mu\text{Ci}$ , i.e.  $1100 \text{ Bq}$  ( $\equiv 1100 \text{ s}^{-1}$ ), equivalent to  $\sim 7 \times 10^{-12} \text{ g}$  of the element. Concentrations of airborne Po compounds must be kept below  $4 \times 10^{-11} \text{ mg m}^{-3}$ .

### 16.1.6 Polyatomic cations, $M_x^{n+}$

The brightly coloured solutions obtained when sulfur is dissolved in oleums (p. 664) are paralleled by similar behaviour of Se and Te. Indeed, the bright-red solutions of Te in  $\text{H}_2\text{SO}_4$  were noted by M. H. Klaproth in 1798 and the coloured solutions of Se in the same solvent were reported by G. Magnus in 1827. Systematic studies in a range of nonaqueous solvents have since shown that the polycations of Se and Te are less electropositive than their S analogues and can be prepared in a variety of strong acids such as  $\text{H}_2\text{SO}_4$ ,  $\text{H}_2\text{S}_2\text{O}_7$ ,  $\text{HSO}_3\text{F}$ ,  $\text{SO}_2/\text{AsF}_5$ ,  $\text{SO}_2/\text{SbF}_5$  and molten  $\text{AlCl}_3$ .<sup>(31,32)</sup> Typical reactions for Se are:

<sup>30</sup> R. J. SHAMBERGER, *Biochemistry of Selenium*, Plenum Press, New York, 1983, 334 pp. C. REILLY, *Selenium in Food and Health*, Blackie, London, 1996, 338 pp.

<sup>31</sup> R. J. GILLESPIE and J. PASSMORE, *Adv. Inorg. Chem. Radiochem.* **17**, 49–87 (1975). M. J. TAYLOR, *Metal–Metal Bonded States in Main Group Elements*, Academic Press, London, 1975, 211 pp. J. D. CORBETT, *Prog. Inorg. Chem.* **21**, 121–58 (1976). T. A. O'DONNELL, *Chem. Soc. Rev.* **16**, 1–43 (1987).

<sup>32</sup> N. BURFORD, J. PASSMORE and J. C. P. SANDERS, Chap. 2, Preparation, Structure and Energetics of the Homopolyatomic Cations of Groups 16 and 17, in J. F. LIEBMAN and A. GREENBURG (eds.), *From Atoms to Polymers: Isoelectronic Analogies*, VCH Publ., Florida, 1989, pp. 53–108. J. PASSMORE, Chap. 19 Homopolyatomic Selenium Cations

<sup>26</sup> M. DI VAIRA, M. PERUZZINI and P. STOPPIONI, *Angew. Chem. Int. Edn. Engl.* **26**, 916–7 (1987).

<sup>27</sup> M. DI VAIRA, M. PERUZZINI and P. STOPPIONI, *J. Chem. Soc., Chem. Commun.*, 374–5 (1986).

<sup>28</sup> R. FAGGIANI, R. J. GILLESPIE, C. CAMPANA and J. W. KOLIS, *J. Chem. Soc., Chem. Commun.*, 485–6 (1987).

<sup>29</sup> P. MATHUR, I. J. MAVUNKAL and A. L. RHEINGOLD, *J. Chem. Soc., Chem. Commun.*, 382–4 (1989).

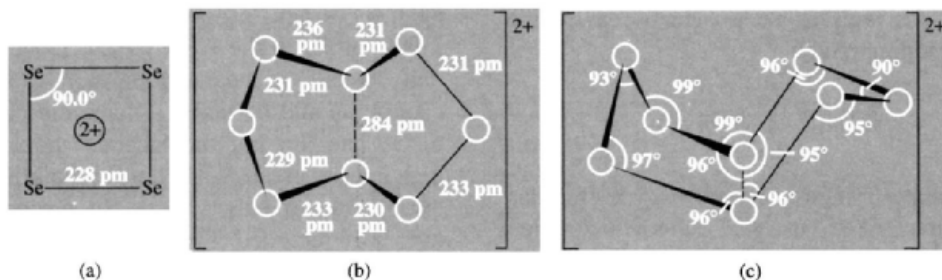


Figure 16.4 (a) Structure of  $[\text{Se}_4]^{2+}$ ; (b) and (c) views of  $[\text{Se}_8]^{2+}$ .

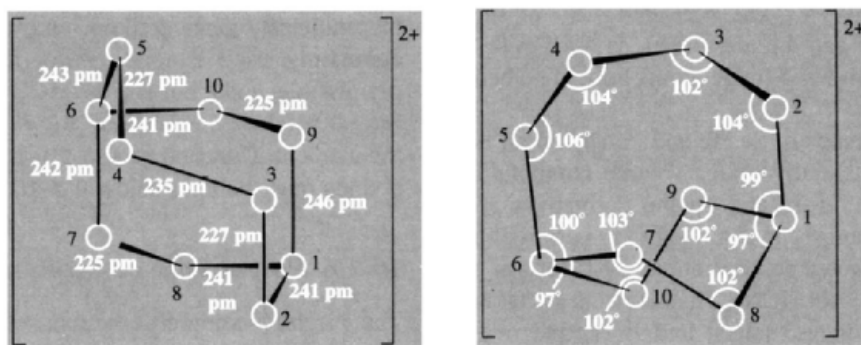
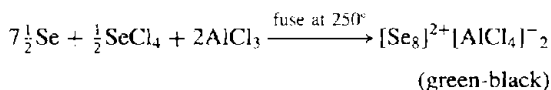
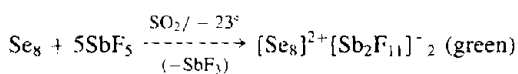
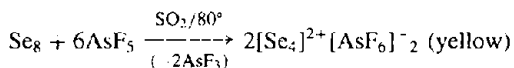
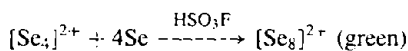
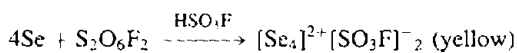


Figure 16.5 Structure of the  $[\text{Se}_{10}]^{2+}$  cation in  $\text{Se}_{10}(\text{SbF}_6)_2$  along the *b*- and *c*-axes of the crystal; angles  $\text{Se}(2)\text{-Se}(1)\text{-Se}(9)$  and  $\text{Se}(5)\text{-Se}(6)\text{-Se}(10)$  are each  $101.7^\circ$ .



X-ray crystal structure studies on  $[\text{Se}_4]^{2+}$ - $[\text{HS}_2\text{O}_7]^-$  show that the cation is square planar (like  $\text{S}_4^{2+}$ , p. 665) as in Fig. 16.4a. The Se-Se distance of 228 pm is significantly less than the value of 234 pm in  $\text{Se}_8$  and 237 pm in

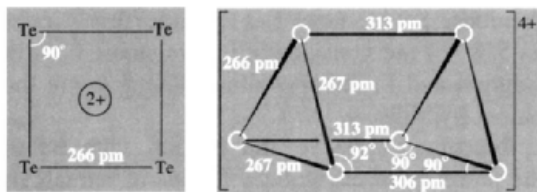
$\text{Se}_\infty$ , consistent with some multiple bonding. The structure of  $[\text{Se}_8]^{2+}$  in the salt  $[\text{Se}_8]^{2+}[\text{AlCl}_4]^-$  is in Fig. 16.4b and c: it comprises a bicyclo  $C_3$  structure with the *endo-exo* configuration with a long trans-annular link of 284 pm. Other Se-Se distances are very similar to those in  $\text{Se}_8$  itself, but the Se-Se-Se angles are significantly smaller in the cation, being  $\sim 96^\circ$  rather than  $106^\circ$ . More recently<sup>(33)</sup> the deep-red crystalline compound  $\text{Se}_{10}(\text{SbF}_6)_2$  has been isolated from the reaction of  $\text{SbF}_5$  with an excess of Se in  $\text{SO}_2$  under pressure at  $\sim 50^\circ$ . Two views of the bicyclic cation are shown in Fig. 16.5; it features a 6-membered boat-shaped ring linked across the middle of a zigzag chain of 4 further Se atoms. The Se-Se distances vary from 225 to 240 pm and Se-Se-Se angles range from

and Related Halo-polyselenium Cations, in R. Steudel (ed.), *The Chemistry of Inorganic Ring Systems*, Elsevier, Amsterdam, 1992, pp. 373-407.

<sup>33</sup>R. C. BURNS, W.-L. CHAN, R. J. GILLESPIE, W.-C. LUK, J. F. SAWYER and D. R. SLIM, *Inorg. Chem.* **19**, 1432-9 (1980).

97° to 106°, with 6 angles at the bridgehead atoms Se(1) and Se(6) being significantly smaller than the other 8 in the linking chains. The low-temperature disproportionation of  $Se_{10}^{2+}$  into  $Se_8^{2+}$  and a second species, probably  $Se_{17}^{2+}$ , i.e.  $\{Se_8-Sc-Se_8\}^{2+}$ , has been studied by  $^{77}Se$  nmr spectroscopy.<sup>(34)</sup> Heteronuclear species such as  $\{S_xSe_{4-x}\}^{2+}$  have also been identified by nmr techniques and characterized by X-ray structure analysis.<sup>(35)</sup> Analogous Se/Te heteronuclear cations are described below.

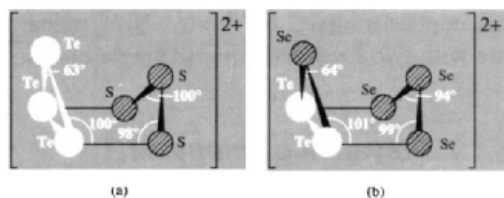
Polyatomic tellurium cations can be prepared by similar routes. The bright-red species  $Te_4^{2+}$ , like  $S_4^{2+}$  and  $Se_4^{2+}$ , is square planar with the Te-Te distance (266 pm) somewhat less than in the element (284 pm) (Fig. 16.6a). Oxidation of Te with  $AsF_5$  in  $AsF_3$  as solvent yields the brown crystalline compound  $Te_6(AsF_6)_4 \cdot 2AsF_3$ ; X-ray studies reveal the presence of  $[Te_6]^{4+}$  which is the first example of a simple trigonal prismatic cluster cation (Fig. 16.6b). The Te-Te distances between the triangular faces (313 pm) are substantially larger than those within the triangle (267 pm).<sup>(36)</sup> No Te analogue of  $S_8^{2+}$  and  $Se_8^{2+}$  had been identified until 1997 when the reaction of  $ReCl_4$  with Te and  $TeCl_4$  at 230° yielded silvery crystals of  $[Te_8]^{2+}[ReCl_6]^{2-}$  with Te-Te 272 pm (av), the shortest Te...Te distance being 315 pm.<sup>(36a)</sup> Previously (1990), oxidation



**Figure 16.6** Structure of the cations  $[Te_4]^{2+}$  and  $[Te_6]^{4+}$ .

of Te with  $WCl_6$  had yielded  $[Te_8][WCl_6]_2$  in which the  $Te_8^{2+}$  dication was found to have a more pronounced bicyclic structure of  $C_2$  symmetry with Te-Te 275.2 pm and the central transannular link being 299.3 pm.<sup>(36a)</sup>

Mixed Se/Te polatomic cations are also known. For example, when Se and Te are dissolved in 65% oleum at room temperature the resulting orange-brown solutions were shown by  $^{125}Te$  and  $^{123}Te$  nmr spectroscopy to contain the four species  $[Te_nSe_{4-n}]^{2+}$  ( $n = 1-4$ ) and the species  $[Se_4]^{2+}$  was also presumably present.<sup>(37)</sup> Likewise  $^{77}Se$  and  $^{125}Te$  multinuclear magnetic resonance studies on solutions obtained by oxidizing equimolar mixtures of Se and Te with  $AsF_5$  in  $SO_2$  reveal not only  $[Se_4]^{2+}$ ,  $[Te_4]^{2+}$  and  $[Te_6]^{4+}$  but also  $[TeSe_3]^{2+}$ , *cis*- and *trans*- $[Te_2Se_2]^{2+}$ ,  $[Te_3Se]^{2+}$ ,  $[Te_2Se_4]^{2+}$  and  $[Te_3Se_3]^{2+}$ .<sup>(38)</sup> The molecular structures of the sulfur analogue  $[Te_3S_3]^{2+}$  and of  $[Te_2Se_4]^{2+}$  have also been determined by X-ray diffractometry and found to have a boat-shaped 6-membered heterocyclic structure with a cross-ring bond as shown in Fig. 16.7. As expected, these  $M_6^{2+}$  species are more open than the corresponding  $Te_6^{4+}$  cluster because of the presence of 2 extra valency-shell electrons (p. 724). Other mixed species that have been characterized include  $[Te_2Se_6]^{2+}$  (cube, with diagonally placed Te)<sup>(39)</sup>



**Figure 16.7** Structures of the heteroatomic cluster cations (a)  $[Te_3S_3]^{2+}$  and (b)  $[Te_2Se_4]^{2-}$ .

<sup>34</sup> R. C. BURNS, M. J. COLLINS, R. J. GILLESPIE and G. J. SCHROBILGEN, *Inorg. Chem.* **25**, 4465-9 (1986); but see *Z. anorg. allg. Chem.* **623**, 780-4 (1977).

<sup>35</sup> M. J. COLLINS, R. J. GILLESPIE, J. F. SAWYER and G. J. SCHROBILGEN, *Inorg. Chem.* **25**, 2053-7 (1986).

<sup>36</sup> R. C. BURNS, R. J. GILLESPIE, W.-C. LUK and D. R. SLIM, *Inorg. Chem.* **18**, 3086-94 (1979).

<sup>36a</sup> J. BECK and K. MÜLLER-BUSCHBAUM, *Z. anorg. allg. Chem.* **623**, 409-13 (1997) and references therein.

<sup>37</sup> C. R. LASSIGNE and E. J. WELLS, *J. Chem. Soc., Chem. Commun.*, 956-7 (1978).

<sup>38</sup> G. J. SCHROBILGEN, R. C. BURNS and P. GRANGER, *J. Chem. Soc., Chem. Commun.*, 957-60 (1978). P. BOLDRINI, I. D. BROWN, M. J. COLLINS, R. J. GILLESPIE, E. MAHRAJH, D. R. SLIM and J. F. SAWYER, *Inorg. Chem.* **24**, 4302-7 (1985).

<sup>39</sup> M. J. COLLINS and R. J. GILLESPIE, *Inorg. Chem.* **23**, 1975-8 (1984).



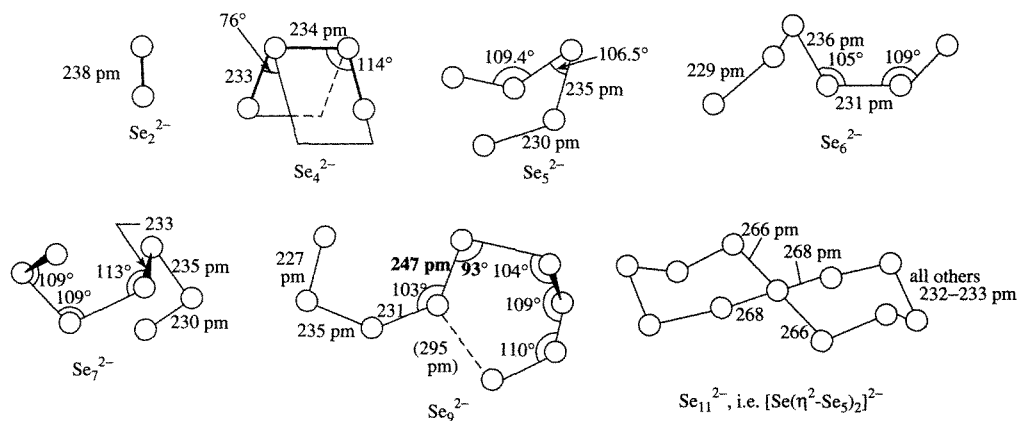


Figure 16.8 Structures of some dianions  $\text{Se}_x^{2-}$  (see text).

and  $[\text{Te}_4\text{S}_4]^{2+}$  (electron-rich  $\text{S}_4\text{N}_4$  cluster but with coplanar S atoms as in  $\text{As}_4\text{S}_4$ ).<sup>(40)</sup>

The mixed anionic species  $[\text{Te}_2\text{Te}_2]^{2-}$  (20 valence electrons) is butterfly-shaped with  $\text{Te}_2$  at the “hinge” and  $2\text{Te}$  at the “wing tips”,<sup>(41)</sup> in contrast to the 22 valence-electron cationic species  $\text{Te}_4^{2+}$  and  $\text{Se}_4^{2+}$  which are square planar. The remarkable cationic cluster species  $[(\text{NbI}_2)_3\text{O}(\text{Te}_4)(\text{Te}_2)_2]^{+}$  should also be noted: this was formed serendipitously in low yield as the monoiodide during the high-temperature reaction between  $\text{NbOI}_3$ , Te and  $\text{I}_2$  and features the bridging groups  $(\mu, \eta^2\text{-Te}_4)^{2+}$  and two  $(\mu, \eta^2\text{-Te}_2)$  in addition to  $(\mu_3\text{-O})^{2-}$  and six terminal  $\text{I}^-$ . This implies a mixed  $\text{Nb}^{\text{III}}$   $\text{Nb}^{\text{IV}}$   $\text{Nb}^{\text{IV}}$  oxidation state with two localized Nb–Nb single bonds.<sup>(42)</sup>

### 16.1.7 Polyatomic anions, $\text{M}_x^{2-}$

The synthesis, structural characterization and coordination chemistry of polyselenides,  $\text{Se}_x^{2-}$ , and polytellurides,  $\text{Te}_x^{2-}$ , is a burgeoning field which has sprung into prominence during the past decade. The seminal studies by E. Zintl and his

group during the 1930s showed that such species could be prepared by reduction of the elements with alkali metals in liquid ammonia, but it was the advent of  $^{77}\text{Se}$  and  $^{125}\text{Te}$  nmr techniques, and the use of crown and crypt complexes (p. 96) to prepare crystalline derivatives for X-ray structural analysis which provided the firm bases for further advances. The rich reaction chemistry and coordination properties soon followed. Comparisons with polysulfides and polysulfanes (pp. 681–3) are instructive. Thus, little is known about  $\text{H}_2\text{Se}_2$  and  $\text{H}_2\text{Te}_2$ , and nothing at all about the higher homologues  $\text{H}_2\text{Se}_x$  and  $\text{H}_2\text{Te}_x$ ; however, compounds containing the dianions  $\text{Se}_x^{2-}$  ( $x = 2\text{--}11$ ) and  $\text{Te}_x^{2-}$  ( $x = 2\text{--}5, 8\dots$ ) are considerably more stable both in solution and in the crystalline state than are the parent hydrides.

Reaction of  $\text{Na}_2\text{Se}$  and  $\text{Na}_2\text{Se}_2$  with Se in the presence of ethanolic solutions of tetraalkylammonium halides and catalytic amounts of  $\text{I}_2$  yields dark green or black crystalline polyselenides ( $x = 3, 5\text{--}9$ ) depending on the conditions used and the particular cation selected.<sup>(43)</sup> Tetraphenylphosphonium salts and crown ether complexes of alkali or alkaline earth cations in dimethylformamide solution can also be used.<sup>(44)</sup>

<sup>40</sup> R. FAGGIANI, R. J. GILLESPIE and J. E. VEKRIS, *J. Chem. Soc., Chem. Commun.*, 902–4 (1988).

<sup>41</sup> R. C. BURNS and J. D. CORBETT, *J. Am. Chem. Soc.* **103**, 2627–32 (1981).

<sup>42</sup> W. TREMEL, *J. Chem. Soc., Chem. Commun.*, 126–8 (1992).

<sup>43</sup> F. WELLER, J. ADEL and K. DEHNICKE, *Z. anorg. allg. Chem.* **548**, 125–32 (1987).

<sup>44</sup> D. FENSKE, C. KRAUS and K. DEHNICKE, *Z. anorg. allg. Chem.* **607**, 109–12 (1992). V. MÜLLER, A. AHLE,

Typical structures and dimensions of the resulting polyselenide dianions are shown in Fig. 16.8, though it should be emphasized that torsion angles, interatomic angles and even to some extent interatomic distances may depend on the counteraction chosen. Detailed references have been tabulated.<sup>(45)</sup> The triselenide ion,  $Se_3^{2-}$  has been identified as a moderately stable species in solution and in the solid state, but its X-ray structure has not been reported; it is presumably angular like  $S_3^{2-}$  and  $Te_3^{2-}$ . The evolution of the chains up to  $Se_7^{2-}$  is clear. The structure of  $Se_8^{2-}$  has also been determined in  $[Na(\text{crown})]_2[Se_8]^{2-}(Se_6, Se_7)$  which features a curious packing of the cation and the anion with an equimolar amount of neutral *cyclo- $Se_n$*  comprising variable amounts of  $Se_6$  and  $Se_7$ .<sup>(46)</sup> The structure of *catena- $Se_9^{2-}$*  has a relatively long central Se–Se bond (247 pm) which forms, at one end, a sharp angle of  $93^\circ$  to the adjacent Se atom; the Se at other end of the bond is approached rather closely by one of the terminal Se atoms (295 pm) to form an incipient 6-membered ring. The process continues in  $Se_{11}^{2-}$  which has a centrosymmetric spiro-bicyclic structure involving a central square-planar Se atom common to the two chair-conformation rings. The central bonds are again rather long (266–268 pm) and the structure may be described as a central  $Se^{2+}$  chelated by two  $\eta^2-Se_5^{2-}$  ligands (see below). The structure also has similarities with the anion in  $Cs^+_4[Se_{16}]^{4-}$ ,<sup>(47)</sup> which has a central planar formal  $Se^{2+}$  coordinated by one chelating  $\eta^2-Se_5^{2-}$  ligand (Se–Se 243 pm) and by two monohapto  $\eta^1-Se_5^{2-}$  ligands (Se–Se 299 pm), i.e.  $[Se(\eta^2-Se_5)(\eta^1-Se_5)_2]^{2-}$ .

Several of the *catena- $Se_x^{2-}$*  anions have proved to be effective chelating ligands to both main-group and transition metals. Synthesis of the

complexes is usually via direct reaction with the preformed anion or by synthesis of the anion in the presence of the appropriate metal centre. Examples are  $[Sn(\eta^2-Se_4)_3]^{2-}$ ,<sup>(48)</sup>  $[M(\eta^2-Se_4)_2]^{2-}$  ( $M = Zn, Cd, Hg, Ni, Pb^{II}$ ),<sup>(49)</sup>  $[Mo^{IV}(\eta^5-C_5H_5)(\eta^2-Se_4)_2]^{-}$ <sup>(50)</sup> and  $[M_3(Se_4)_6]^{3-}$ , i.e.  $\{[M(Se_4)_3]M\{(Se_4)_3M\}\}^{3-}$  ( $M = Cr$ ,<sup>(51)</sup>  $Co$ <sup>(52)</sup>), in which the two terminal  $M^{III}$  atoms have approximately *tris-tetraselenide* chelate coordination whilst the central  $M^{III}$  atom (also approximately octahedral) has  $(\mu-Se)_6$  coordination, achieved by sharing one ‘terminal’ Se atom from each of the six  $Se_4$  groups. The complex  $[Ti(\eta^5-C_5H_5)_2(\eta^2-Se_5)]$  reacts with  $SCl_2$ ,  $S_2Cl_2$  and  $SeCl_2$  to form, respectively,  $Se_5S$ ,  $Se_5S_2$  and  $Se_7$ .<sup>(53)</sup> Heterocyclic chelating ligands are also known, e.g. in  $[PtCl(PMe_2Ph)(\eta^2-Se_3N)]$ .<sup>(54)</sup> Note also the extraordinary 1900 pm long hexameric anion,  $[Ga_6Se_{14}]^{10-}$ , which is composed of a linear array of edge-sharing  $\{GaSe_4\}$  units, i.e.  $[Se_2\{Ga(\mu-Se)_2\}_5GaSe_2]^{10-}$ .<sup>(55)</sup>

Polytellurides,  $Te_x^{2-}$ , are less straightforward and often form complex units coordinated to metal centres.<sup>(56)</sup> The isolated ions  $Te_2^{2-}$  and

<sup>48</sup> S.-P. HUANG, S. DHINGRA and M. G. KANATZIDIS, *Polyhedron* **9**, 1389–95 (1990).

<sup>49</sup> R. M. H. BANDA, J. CUSICK, M. L. SCUDDER, D. C. CRAIG and I. G. DANCE, *Polyhedron* **8**, 1995–8 (1989). S. MAGULL, K. DEHNICKE and D. FENSKE, *Z. anorg. allg. Chem.* **608**, 17–22 (1992).

<sup>50</sup> R. M. H. BANDA, J. CUSICK, M. L. SCUDDER, D. C. CRAIG and I. G. DANCE, *Polyhedron* **8**, 1999–2001 (1989). See also J. CUSICK, M. L. SCUDDER, D. C. CRAIG and I. G. DANCE, *Polyhedron* **8**, 1139–41 (1989) for the more complex structures of tetranuclear Cu and Ag polyselenides.

<sup>51</sup> W. A. FLOMER, S. C. O’NEAL, W. T. PENNINGTON, D. JETER, A. W. CORDES and J. W. KOLIS, *Angew. Chem. Int. Edn. Engl.* **27**, 1702–3 (1988).

<sup>52</sup> J. CUSICK, M. L. SCUDDER, D. C. CRAIG and I. G. DANCE, *Aust. J. Chem.* **43**, 209–11 (1990).

<sup>53</sup> R. STEUDEL, M. PAPAVALIIOU, E.-M. STRAUSS and R. LAITINEN, *Angew. Chem. Int. Edn. Engl.* **25**, 99–101 (1986).

<sup>54</sup> P. F. KELLY, A. M. Z. SLAWIN, D. J. WILLIAMS and J. D. WOOLLINS, *J. Chem. Soc., Chem. Commun.*, 408–9 (1989).

<sup>55</sup> E. NIECKE, K. SCHWICHTENHÖVEL, H. G. SCHÄFER and B. KREBS, *Angew. Chem. Int. Edn. Engl.* **20**, 962–3 (1981).

<sup>56</sup> P. BÖTTCHER, *Angew. Chem. Int. Edn. Engl.* **27**, 759–72 (1988).

G. FRENZEN, B. NEUMÜLLER and K. DEHNICKE, *Z. anorg. allg. Chem.* **619**, 1247–56 (1993). V. MÜLLER, C. GREBE, U. MÜLLER and K. DEHNICKE, *Z. anorg. allg. Chem.* **619**, 416–20 (1993).

<sup>45</sup> J. CUSICK and I. DANCE, *Polyhedron* **10**, 2629–40 (1991).

<sup>46</sup> R. STAFFEL, U. MÜLLER, A. AHLE and K. DEHNICKE, *Z. Naturforsch.* **46b**, 1287–92 (1992).

<sup>47</sup> W. S. SHELDRIK and H. G. BRAUNBECK, *Z. Naturforsch.*, **44b** 1397–401 (1989).

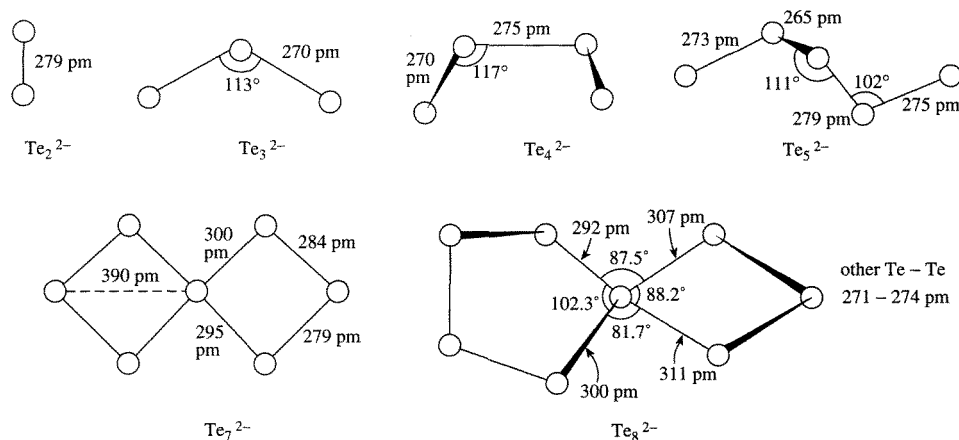


Figure 16.9 Structures of some dianions  $\text{Te}_x^{2-}$  (see text).

$\text{Te}_3^{2-}$  are found in  $\text{K}_2\text{Te}_2$ ,  $\text{Rb}_2\text{Te}_2$ <sup>(57)</sup> and  $[\text{K}(\text{crypt})]_2\text{Te}_3$ <sup>(58)</sup> — see Fig. 16.9. Likewise,  $\text{Te}_4^{2-}$  has been characterized in salts of crown ether complexes of Ca, Sr and Ba, and  $\text{Te}_5^{2-}$  as its salt with  $[\text{Ph}_3\text{PNPPH}_3]^+$ <sup>(59)</sup> (Fig. 16.9). The bicyclic polytellurides  $\text{Te}_7^{2-}$ <sup>(60)</sup> and  $\text{Te}_8^{2-}$ <sup>(61)</sup> are also known (Fig. 16.9). However, simple stoichiometry often conceals structural complexity as in the many alkali metal tellurides  $\text{MTe}_x$  ( $x = 1, 1.5, 2.5, 3, 4$ ).<sup>(56,62)</sup>

There is also a bewildering variety of structural motifs in polytelluride–ligand complexes as the brief selection in Fig. 16.10 indicates; the original papers should be consulted for preparative routes and other details. Thus, dissolution of the alloy  $\text{K}_2\text{Hg}_2\text{Te}_3$  in ethylenediamine, followed by treatment with a methanolic solution of  $[\text{NBu}_4^+]\text{Br}^-$ , yields the dark brown

compound  $[\text{NBu}_4^+]_4[\text{Hg}_4\text{Te}_{12}]^{6-}$ <sup>(63)</sup> this features the remarkable anion  $[\text{Hg}_4\text{Te}_{12}]^{4-}$  in which the four Hg atoms, which are coplanar, are coordinated in distorted tetrahedral fashion to an array of two  $\text{Te}^{2-}$ , two  $\text{Te}_2^{2-}$  and two  $\text{Te}_3^{2-}$  ligands (Fig. 16.10). By contrast, use of  $[\text{PPh}_4]^+$  as the counter-cation yields the unbranched, approximately planar, polymeric anion  $[\{\text{Hg}_2\text{Te}_5\}^{2-}]_\infty$  (Fig. 16.10) which contains  $\{\text{Hg}_2\text{Te}_3\}$  heterocycles joined by bridging  $\text{Te}_2^{2-}$  units.<sup>(63)</sup>  $\text{Cu}^{\text{I}}$  and  $\text{Ag}^{\text{I}}$  form discrete polytelluride complexes in  $[\text{PPh}_4]_2[\text{M}_2\text{Te}_{12}]$ <sup>(64)</sup> (Fig. 16.10) containing two chelating and one bridging  $\text{Te}_4^{2-}$  groups. A similar chelating mode occurs in  $[\text{Pd}(\eta^2\text{-Te}_4)_2]^{2-}$ .<sup>(65)</sup> Discrete  $[\text{HgTe}_7]^{2-}$  ions occur in the  $[\text{K}(\text{crown})_2]^+$  salt whereas the corresponding Zn derivative has a polymeric structure<sup>(66)</sup> (Fig. 16.10). The soluble cluster anion  $\text{NbTe}_{10}^{3-}$  is also notable; its structure has been determined in the black, crystalline tetraphenylphosphonium salt.<sup>(67)</sup> Cubane-like clusters occur

<sup>57</sup> P. BÖTTCHER, J. GETZSCHMANN and R. KELLER, *Z. anorg. allg. Chem.* **619**, 476–88 (1993).

<sup>58</sup> A. CÍŠAR and J. D. CORBETT, *Inorg. Chem.* **16**, 632–5 (1977).

<sup>59</sup> D. FENSKE, G. BAUM, H. WOLKERS, B. SCHREINER, F. WELLER and K. DEHNICKE, *Z. anorg. allg. Chem.* **619**, 489–99 (1993).

<sup>60</sup> B. HARBRECHT and A. SELMER, *Z. anorg. allg. Chem.* **620**, 1861–6 (1994).

<sup>61</sup> B. SCHREINER, K. DEHNICKE, K. MACZEK and D. FENSKE, *Z. anorg. allg. Chem.* **619**, 1414–8 (1993).

<sup>62</sup> J. BERNSTEIN and R. HOFFMANN, *Inorg. Chem.* **24**, 4100–8 (1985).

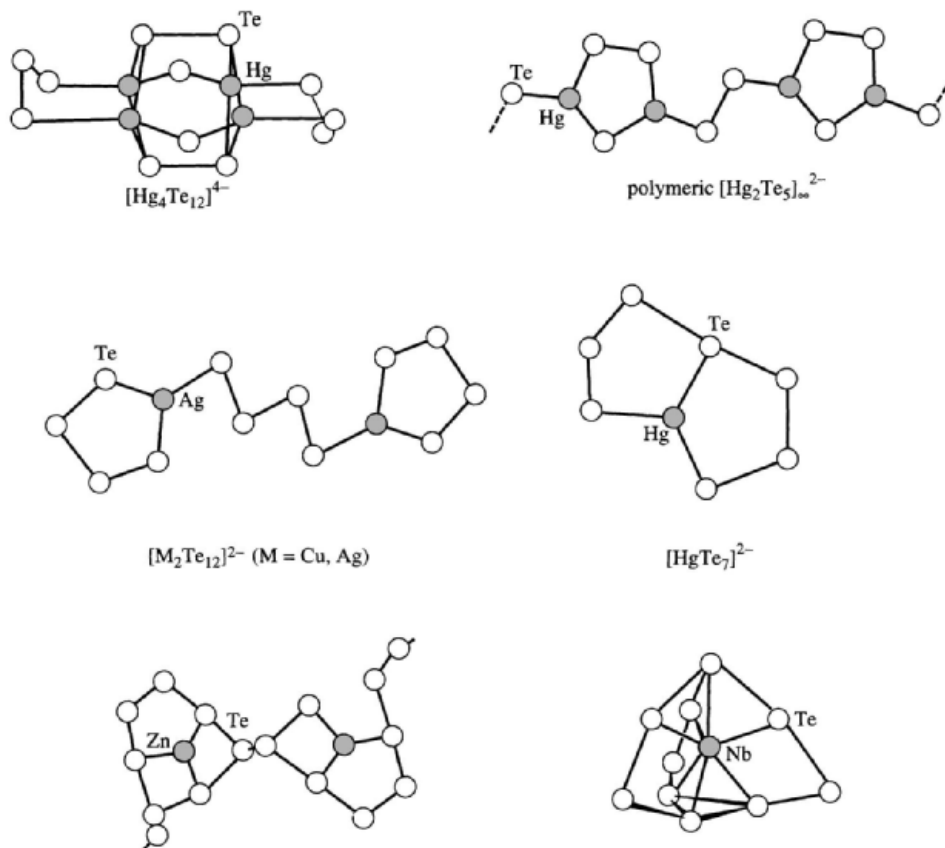
<sup>63</sup> R. C. HAUSHALTER, *Angew. Chem. Int. Edn. Engl.* **24**, 433–5 (1985).

<sup>64</sup> D. FENSKE, B. SCHREINER and K. DEHNICKE, *Z. anorg. allg. Chem.* **619**, 253–60 (1993).

<sup>65</sup> R. D. ADAMS, T. A. WOLFE, B. W. EICHHORN and R. C. HAUSHALTER, *Polyhedron* **8**, 701–3 (1989).

<sup>66</sup> U. MÜLLER, C. GREBE, B. NEUMÜLLER, B. SCHREINER and K. DEHNICKE, *Z. anorg. allg. Chem.* **619**, 500–6 (1993).

<sup>67</sup> W. A. FLOMER and J. W. KOLIS, *J. Am. Chem. Soc.* **110**, 3682–3 (1988).



**Figure 16.10** Structures of some metal-polytelluride complexes.

in  $[\text{NEt}_4]_3[\text{Fe}_4(\mu_3\text{-Te})_4(\text{TePh})_4] \cdot 2\text{MeCN}$ <sup>(68)</sup> and, perhaps surprisingly, in  $\text{NaTe}_3$  which has cubane-like interlinked clusters of  $\text{Te}_{12}^{6-}$ .<sup>(69)</sup> The trinuclear anion  $[\text{Cr}_3\text{Te}_{24}]^{3-}$  has the same structure as its Se analogue (p. 763).<sup>(51)</sup> Mention could also be made of the planar ion  $[\text{TeS}_3]^{2-}$  and the spiro-bicyclic  $[\text{Te}(\eta^2\text{-S}_5)_2]^{2-}$  in which the Te atom is also planar<sup>(70)</sup> (cf.  $\text{Se}_{11}^{2-}$  in Fig. 16.8).

<sup>68</sup> W. SIMON, A. WILK, B. KREBS and G. HENKEL, *Angew. Chem. Int. Edn. Engl.* **26**, 1009–10 (1987).

<sup>69</sup> P. BÖTTCHER and R. KELLER, *Z. anorg. allg. Chem.* **542**, 144–52 (1986).

<sup>70</sup> W. BUBENHEIM, G. FRENZEN and U. MÜLLER, *Z. anorg. allg. Chem.* **620** 1046–50 (1994).

## 16.2 Compounds of selenium, tellurium and polonium

### 16.2.1 Selenides, tellurides and polonides

All three elements combine readily with most metals and many non-metals to form binary chalcogenides. Indeed, selenides and tellurides are the most common mineral forms of these elements (p. 748). Nonstoichiometry abounds, particularly for compounds with the transition elements (where electronegativity differences are minimal and variable valency is favoured), and many of the chalcogenides can be considered

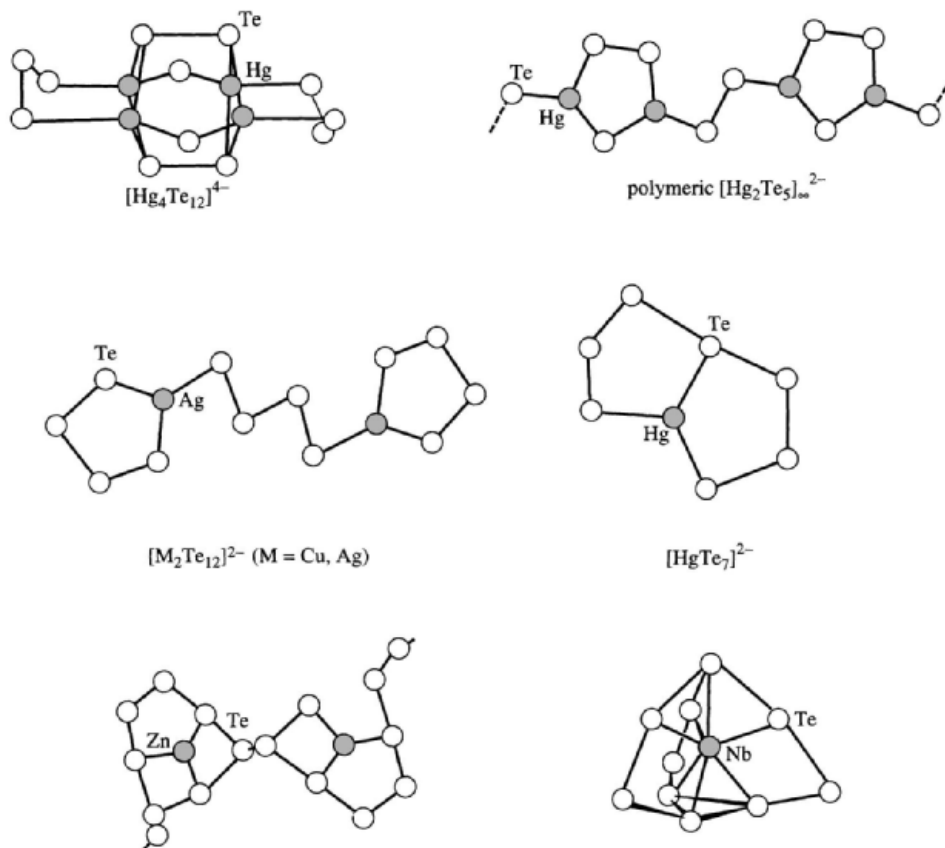


Figure 16.10 Structures of some metal-polytelluride complexes.

in  $[\text{NEt}_4]_3[\text{Fe}_4(\mu_3\text{-Te})_4(\text{TePh})_4] \cdot 2\text{MeCN}$ <sup>(68)</sup> and, perhaps surprisingly, in  $\text{NaTe}_3$  which has cubane-like interlinked clusters of  $\text{Te}_{12}^{6-}$ .<sup>(69)</sup> The trinuclear anion  $[\text{Cr}_3\text{Te}_{24}]^{3-}$  has the same structure as its Se analogue (p. 763).<sup>(51)</sup> Mention could also be made of the planar ion  $[\text{TeS}_3]^{2-}$  and the spiro-bicyclic  $[\text{Te}(\eta^2\text{-S}_5)_2]^{2-}$  in which the Te atom is also planar<sup>(70)</sup> (cf.  $\text{Se}_{11}^{2-}$  in Fig. 16.8).

<sup>68</sup> W. SIMON, A. WILK, B. KREBS and G. HENKEL, *Angew. Chem. Int. Edn. Engl.* **26**, 1009–10 (1987).

<sup>69</sup> P. BÖTTCHER and R. KELLER, *Z. anorg. allg. Chem.* **542**, 144–52 (1986).

<sup>70</sup> W. BUBENHEIM, G. FRENZEN and U. MÜLLER, *Z. anorg. allg. Chem.* **620** 1046–50 (1994).

## 16.2 Compounds of selenium, tellurium and polonium

### 16.2.1 Selenides, tellurides and polonides

All three elements combine readily with most metals and many non-metals to form binary chalcogenides. Indeed, selenides and tellurides are the most common mineral forms of these elements (p. 748). Nonstoichiometry abounds, particularly for compounds with the transition elements (where electronegativity differences are minimal and variable valency is favoured), and many of the chalcogenides can be considered

as metallic alloys. Many such compounds have important technological potentialities for solid-state optical, electrical and thermoelectric devices and have been extensively studied. For the more electropositive elements (e.g. Groups 1 and 2), the chalcogenides can be considered as "salts" of the acids,  $\text{H}_2\text{Se}$ ,  $\text{H}_2\text{Te}$ , and  $\text{H}_2\text{Po}$  (see next subsection).

The alkali metal selenides and tellurides can be prepared by direct reaction of the elements at moderate temperatures in the absence of air, or more conveniently in liquid ammonia solution. They are colourless, water soluble, and readily oxidized by air to the element. The structures adopted are not unexpected from general crystallochemical principles. Thus  $\text{Li}_2\text{Se}$ ,  $\text{Na}_2\text{Se}$  and  $\text{K}_2\text{Se}$  have the antifluorite structure (p. 118);  $\text{MgSe}$ ,  $\text{CaSe}$ ,  $\text{SrSe}$ ,  $\text{BaSe}$ ,  $\text{ScSe}$ ,  $\text{YSe}$ ,  $\text{LuSe}$ , etc., have the rock-salt structure (p. 242);  $\text{BeSe}$ ,  $\text{ZnSe}$  and  $\text{HgSe}$  have the zinc-blende structure (p. 1210); and  $\text{CdSe}$  has the wurtzite structure (p. 1210). The corresponding tellurides are similar, though there is not a complete 1:1 correspondence. Polonides can also be prepared by direct reaction and are amongst the stablest compounds of this element:  $\text{Na}_2\text{Po}$  has the antifluorite structure; the NaCl structure is adopted by the polonides of Ca, Ba, Hg, Pb and the lanthanide elements;  $\text{BePo}$  and  $\text{CdPo}$  have the ZnS structure and  $\text{MgPo}$  the nickel arsenide structure (p. 556). Decomposition temperatures of these polonides are about  $600 \pm 50^\circ\text{C}$  except for the less-stable  $\text{HgPo}$  (decomp  $300^\circ$ ) and the extremely stable lanthanide derivatives which do not decompose even at  $1000^\circ$  (e.g.  $\text{PrPo}$  mp  $1253^\circ$ ,  $\text{TmPo}$  mp  $2200^\circ\text{C}$ ).

Transition-element chalcogenides are also best prepared by direct reaction of the elements at  $400\text{--}1000^\circ\text{C}$  in the absence of air. They tend to be metallic nonstoichiometric alloys though intermetallic compounds also occur, e.g.  $\text{Ti}_{\sim 2}\text{Se}$ ,  $\text{Ti}_{\sim 3}\text{Se}$ ,  $\text{TiSe}_{0.95}$ ,  $\text{TiSe}_{1.05}$ ,  $\text{Ti}_{0.9}\text{Se}$ ,  $\text{Ti}_3\text{Se}_4$ ,  $\text{Ti}_{0.7}\text{Se}$ ,  $\text{Ti}_5\text{Se}_8$ ,  $\text{TiSe}_2$ ,  $\text{TiSe}_3$ , etc.<sup>(71,72)</sup>

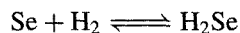
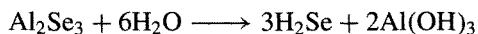
Fuller details of these many compounds are in the references cited.

Most selenides and tellurides are decomposed by water or dilute acid to form  $\text{H}_2\text{Se}$  or  $\text{H}_2\text{Te}$  but the yields, particularly of the latter, are poor.

Polychalcogenides are less stable than polysulfides (p. 681). Reaction of alkali metals with Se in liquid ammonia affords  $\text{M}_2\text{Se}_2$ ,  $\text{M}_2\text{Se}_3$  and  $\text{M}_2\text{Se}_4$ , and analogous polytellurides have also been reported (see preceding section). However many of these compounds are rather unstable thermally and tend to be oxidized in air.

### 16.2.2 Hydrides

$\text{H}_2\text{Se}$  (like  $\text{H}_2\text{O}$  and  $\text{H}_2\text{S}$ ) can be made by direct combination of the elements (above  $350^\circ$ ), but  $\text{H}_2\text{Te}$  and  $\text{H}_2\text{Po}$  cannot be made in this way because of their thermal instability.  $\text{H}_2\text{Se}$  is a colourless, offensive-smelling poisonous gas which can be made by hydrolysis of  $\text{Al}_2\text{Se}_3$ , the action of dilute mineral acids on  $\text{FeSe}$  or the surface-catalysed reaction of gaseous Se and  $\text{H}_2$ :



In this last reaction, conversion at first rises with increase in temperature and then falls because of increasing thermolysis of the product: conversion exceeds  $\sim 40\%$  between  $350\text{--}650^\circ$  and is optimum (64%) at  $520^\circ$ .

$\text{H}_2\text{Te}$  is also a colourless, foul-smelling toxic gas which is best made by electrolysis of 15–50% aqueous  $\text{H}_2\text{SO}_4$  at a Te cathode at  $-20^\circ$ , 4.5 A and 75–110 V. It can also be made by hydrolysis of  $\text{Al}_2\text{Te}_3$ , the action of hydrochloric acid on the tellurides of Mg, Zn or Al, or by reduction of  $\text{Na}_2\text{TeO}_3$  with  $\text{TiCl}_3$  in a buffered solution. The compound is unstable above  $0^\circ$  and decomposes in moist air and on exposure to light.  $\text{H}_2\text{Po}$  is even less stable and has only been made in trace amounts ( $\sim 10^{-10}$  g scale) by reduction of Po using Mg foil/dilute HCl and the reaction followed by radioactive tracer techniques.

<sup>71</sup> D. M. CHIZHIKOV and V. P. SHCHASTLIVYI, *Selenium and Selenides*, Collet's, London, 1968, 403 pp.

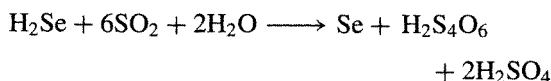
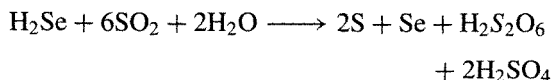
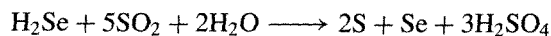
<sup>72</sup> F. HULLIGER, *Struct. Bonding (Berlin)*, **4**, 83–229 (1968).

Table 16.4 Some physical properties of H<sub>2</sub>O, H<sub>2</sub>S, H<sub>2</sub>Se, H<sub>2</sub>Te and H<sub>2</sub>Po

Property	H <sub>2</sub> O	H <sub>2</sub> S	H <sub>2</sub> Se	H <sub>2</sub> Te	H <sub>2</sub> Po
MP/°C	0.0	-85.6	-65.7	-51	-36(?)
BP/°C	100.0	-60.3	-41.3	-4	+37(?)
$\Delta H_f^\circ/\text{kJ mol}^{-1}$	-285.9	+20.1	+73.0	+99.6	—
Bond length (M-H)/pm	95.7	133.6	146	169	—
Bond angle (H-M-H) (g)	104.5°	92.1°	91°	90°	—
Dissociation constant:					
HM <sup>-</sup> , $K_1$	$1.8 \times 10^{-16}$	$1.3 \times 10^{-7}$	$1.3 \times 10^{-4}$	$2.3 \times 10^{-3}$	—
M <sup>2-</sup> , $K_2$	—	$7.1 \times 10^{-15}$	$\sim 10^{-11}$	$1.6 \times 10^{-11}$	—

Physical properties of the three gases are compared with those of H<sub>2</sub>O and H<sub>2</sub>S in Table 16.4. The trends are obvious, as is the "anomalous" position of water (p. 623). The densities of liquid and solid H<sub>2</sub>Se are 2.12 and 2.45 g cm<sup>-3</sup>. H<sub>2</sub>Te condenses to a colourless liquid ( $d$  4.4 g cm<sup>-3</sup>) and then to lemon-yellow crystals. Both gases are soluble in water to about the same extent as H<sub>2</sub>S, yielding increasingly acidic solutions (cf. acetic acid  $K_1 \sim 2 \times 10^{-5}$ ). Such solutions precipitate the selenides and tellurides of many metals from aqueous solutions of their salts but, since both H<sub>2</sub>Se and H<sub>2</sub>Te are readily oxidized (e.g. by air), elementary Se and Te are often formed simultaneously.

H<sub>2</sub>Se and H<sub>2</sub>Te burn in air with a blue flame to give the dioxide (p. 779). Halogens and other oxidizing agents (e.g. HNO<sub>3</sub>, KMnO<sub>4</sub>) also rapidly react with aqueous solutions to precipitate the elements. Reaction of H<sub>2</sub>Se with aqueous SO<sub>2</sub> is complex, the products formed depending critically on conditions (cf. Wackenroder's solution, p. 716): addition of the selenide to aqueous SO<sub>2</sub> yields a 2:1 mixture of S and Se together with oxoacids of sulfur, whereas addition of SO<sub>2</sub> to aqueous H<sub>2</sub>Se yields mainly Se:



H<sub>2</sub>Te undergoes oxidative addition to certain organometallic compounds, e.g. [Re( $\eta^5$ -C<sub>5</sub>Me<sub>5</sub>)-

(CO)<sub>2</sub>(thf)] reacts in thf solution at 25°C to give [HRe( $\eta^5$ -C<sub>5</sub>Me<sub>5</sub>)(CO)<sub>2</sub>(TeH)] and related dinuclear complexes.<sup>(73)</sup> The Te analogue of the hydroxide ion, TeH<sup>-</sup>, has been reported from time to time but has only recently been properly characterized crystallographically, in [PPh<sub>4</sub>]<sup>+</sup>[TeH]<sup>-</sup><sup>(74)</sup>

### 16.2.3 Halides

As with sulfur, there is a definite pattern to the stoichiometries of the known halides of the heavier chalcogens. Selenium forms no binary iodides whereas the more electropositive Te and Po do. Numerous chlorides and bromides are known for all 3 elements, particularly in oxidation states +1, +2 and +4. In the highest oxidation state, +6, only the fluorides MF<sub>6</sub> are known for the 3 elements; in addition SeF<sub>4</sub> and TeF<sub>4</sub> have been characterized but no fluorides of lower oxidation states except the fugitive FSeSeF, Se=SeF<sub>2</sub> and SeF<sub>2</sub> which can be trapped out at low temperature.<sup>(75,76)</sup> The compound previously thought to be Te<sub>2</sub>F<sub>10</sub> is now known to be O(TeF<sub>5</sub>)<sub>2</sub><sup>(76,77)</sup> (p. 778). Finally, Te forms a range of curious lower halides which

<sup>73</sup> W. A. HERRMANN, C. HECHT, E. HERDTWECK and H.-J. KNEUPER, *Angew. Chem. Int. Edn. Engl.* **26**, 132-4 (1987).

<sup>74</sup> J. C. HUFFMAN and R. C. HAUSHALTER, *Polyhedron* **8**, 531-2 (1989).

<sup>75</sup> B. COHEN and R. D. PEACOCK, *Adv. Fluorine Chem.* **6**, 343-85 (1970).

<sup>76</sup> E. ENGELBRECHT and F. SLADKY, *Adv. Inorg. Chem. Radiochem.* **24**, 189-223 (1981). This review also includes oxofluorides of Se and Te, and related anions.

<sup>77</sup> P. M. WATKINS, *J. Chem. Educ.*, **51**, 520-1 (1974).

are structurally related to the  $\text{Te}_x$  chains in elementary tellurium.

The known compounds are summarized in Table 16.5 which also lists their colour, mp, bp and decomposition temperature where these have been reported. It will be convenient to discuss the preparation, structure and chemical properties of these various compounds approximately in

ascending order of formal oxidation state. For comparable information on the halides of S, see pp. 683–93.

### Lower halides

The phase relations in the tellurium-halogen systems have only recently been elucidated

**Table 16.5** Halides of selenium, tellurium and polonium

Oxidation state	Fluorides	Chlorides	Bromides	Iodides
< 1		$\text{Te}_2\text{Cl}$ $\text{Te}_3\text{Cl}_2$ silver grey mp 238° (peritectic)	$\text{Te}_2\text{Br}$ grey needles mp 224 (peritectic)	$\text{Te}_2\text{I}$ silver grey [ $\text{Te}_2$ ] <sub>2</sub> (I <sub>2</sub> ) <sub>x</sub> ( $X \leq i$ ) metallic black
+1	(FSeSeF) and (Se=SeF <sub>2</sub> ) trapped at low temperature	$\text{Se}_2\text{Cl}_2$ yellow-brown liquid mp -85°, bp 130° (d)	( $\beta$ -) $\text{Se}_2\text{Br}_2$ blood-red liquid bp 225° (d) ( $\alpha$ -SeBr, mp +5°)	$\alpha$ - $\text{Te}_4\text{I}_4$ black mp 185°(peritectic) $\beta$ -TeI black
+2	(SeF <sub>2</sub> ) trapped at low temperature	(SeCl <sub>2</sub> ) d in vapour ("TeCl <sub>2</sub> ") black eutectic PoCl <sub>2</sub> dark ruby red mp 355°, subl 130°	(SeBr <sub>2</sub> ) d in vapour ("TeBr <sub>2</sub> ") brown d (see text) PoBr <sub>2</sub> purple-brown mp 270° (d)	(PoI <sub>2</sub> ) impure (from decomp of PoI <sub>4</sub> at 200°)
+4	SeF <sub>4</sub> colourless liquid mp -10°, bp 101°  TeF <sub>4</sub> colourless mp 129° d > 194°  PoF <sub>4</sub> (?) solid from decomp of PoF <sub>6</sub>	Se <sub>4</sub> Cl <sub>16</sub> colourless mp 305°, subl 196°  Te <sub>4</sub> Cl <sub>16</sub> pale-yellow solid. maroon liquid mp 223°, bp 390°  PoCl <sub>4</sub> yellow d > 200° to PoCl <sub>2</sub> mp 300°, bp ~ 390° extrapolated	$\alpha$ -Se <sub>4</sub> Br <sub>16</sub> orange-red mp 123° (also $\beta$ -Se <sub>4</sub> Br <sub>16</sub> )  Te <sub>4</sub> Br <sub>16</sub> yellow mp 388° (under Br <sub>2</sub> ) bp 414° (under Br <sub>2</sub> )  PoBr <sub>4</sub> bright red mp 330°, bp 360°/200 mmHg	Te <sub>4</sub> I <sub>16</sub> black mp 280°, d 100°  PoI <sub>4</sub> black d > 200°
+6	SeF <sub>6</sub> colourless gas mp -35° (2 atm), subl -47°  TeF <sub>6</sub> colourless gas mp -38°, subl -39°		<i>Mixed halides</i> TeBr <sub>2</sub> Cl <sub>2</sub> yellow solid, ruby-red liquid mp 292°, bp 415° TeBr <sub>2</sub> I <sub>2</sub> garnet-red crystals mp 325°, d 420° PoBr <sub>2</sub> Cl <sub>2</sub> salmon pink (PoCl <sub>2</sub> + Br <sub>2</sub> vap)	



and the results show a series of subhalides with various structural motifs based on the helical-chain structure of Te itself.<sup>(78)</sup> These are summarized in Fig. 16.11. Thus, reaction of Te and Cl<sub>2</sub> under carefully controlled conditions in a sealed tube<sup>(79)</sup> results in Te<sub>3</sub>Cl<sub>2</sub> (Fig. 16.11b) in which every third Te atom in the chain is oxidized by addition of 2 Cl atoms, thereby forming a series of 4-coordinate pseudo-trigonal-bipyramidal groups with axial Cl atoms linked by pairs of unmodified Te atoms –Te–Te–TeCl<sub>2</sub>–Te–Te–TeCl<sub>2</sub>–.<sup>(80)</sup> Te<sub>2</sub>Br and Te<sub>2</sub>I consist of zigzag chains of Te in planar arrangement (Fig. 16.11c); along the chain is an alternation of trigonal pyramidal (pseudo-tetrahedral) and square-planar (pseudo-octahedral) Te atoms. These chains are joined in pairs by cross-linking at the trigonal pyramidal Te atoms, thereby forming a ribbon of fused 6-membered Te rings in the boat configuration.<sup>(80)</sup> A similar motif occurs in β-TeI (Fig. 16.11d) which is formed by rapidly cooling partially melted α-TeI (see below) from 190°: in this case the third bond from the trigonal pyramidal Te atoms carries an I atom instead of being cross-linked to a similar chain.<sup>(81)</sup> The second, more stable modification, α-TeI, features tetrameric molecules Te<sub>4</sub>I<sub>4</sub> which are themselves very loosely associated into chains by Te–I...Te links (Fig. 16.11e); the non-planar Te<sub>4</sub> ring comprises two non-adjacent 3-coordinate trigonal pyramidal Te atoms bridged on one side by a single 2-coordinate Te atom and on the other by a 4-coordinate planar >TeI<sub>2</sub> group. An unrelated structure motif is found in the

unusual intercalation compound, [(Te<sub>2</sub>)<sub>2</sub>(I<sub>2</sub>)<sub>x</sub>] (x = 0.42–1.0),<sup>(82)</sup> which is obtained as shiny, metallic-black air-stable crystals by hydrothermal reaction of 67% HI (aq.) on a 1:1 mixture of Te and GeTe at ca. 170° followed by slow cooling (18 h). The structure comprises planar double layers of Te<sub>2</sub> units intercalated by I<sub>2</sub> up to the limiting formula [(Te<sub>2</sub>)<sub>2</sub>I<sub>2</sub>]. The Te atoms within the double layers exhibit distorted tetragonal pyramidal coordination with one short and four longer Te–Te distances (271.3 and 332.3 pm, respectively; cf. distances in Fig. 16.11). The I–I distance within the I<sub>2</sub> molecules is 286.6 pm (cf. 271.5 pm in solid iodine, p. 803). The semiconductivity and nonlinear optical properties of these various tellurium subhalides have been much studied for possible electronic applications.

The only other “monohalides” of these chalcogens are the highly coloured heavy liquids Se<sub>2</sub>Cl<sub>2</sub> (d<sub>25</sub> 2.774 g cm<sup>-3</sup>) and Se<sub>2</sub>Br<sub>2</sub> (d<sub>15</sub> 3.604 g cm<sup>-3</sup>). Both can be made by reaction of the stoichiometric amounts of the elements or better, by adding the halogen to a suspension of powdered Se in CS<sub>2</sub>. Reduction of SeX<sub>4</sub> with 3Se in a sealed tube at 120° is also effective. Se<sub>2</sub>Br<sub>2</sub> has a structure similar to that of S<sub>2</sub>Cl<sub>2</sub> and S<sub>2</sub>F<sub>2</sub> (pp. 689, 684) with a dihedral angle of 94°, angle Br–Se–Se 104° and a rather short Se–Se bond (224 pm, cf. 233.5 pm in monoclinic Se<sub>8</sub> and 237.3 pm in hexagonal Se<sub>∞</sub>).<sup>(83)</sup> The structure of Se<sub>2</sub>Cl<sub>2</sub> has not been determined but is probably similar. Se<sub>2</sub>Br<sub>2</sub> is, in fact, the metastable molecular form (also known as β-SeBr); the structure of the more stable α-SeBr is as yet unknown.

Several mixed species have been identified in nonaqueous solutions by <sup>77</sup>Se nmr spectroscopy. These include BrSeSeCl, Se<sub>3</sub>X<sub>2</sub> and Se<sub>4</sub>X<sub>2</sub>,<sup>(84)</sup> and ClSeSeCl, BrSeSeCl, ClSeSBr and

<sup>78</sup> R. KNIEP and A. RABENAU, *Topics in Current Chemistry* **111**, 145–92 (1983).

<sup>79</sup> A. RABENAU and H. RAU, *Z. anorg. allg. Chem.* **395**, 273–9 (1973).

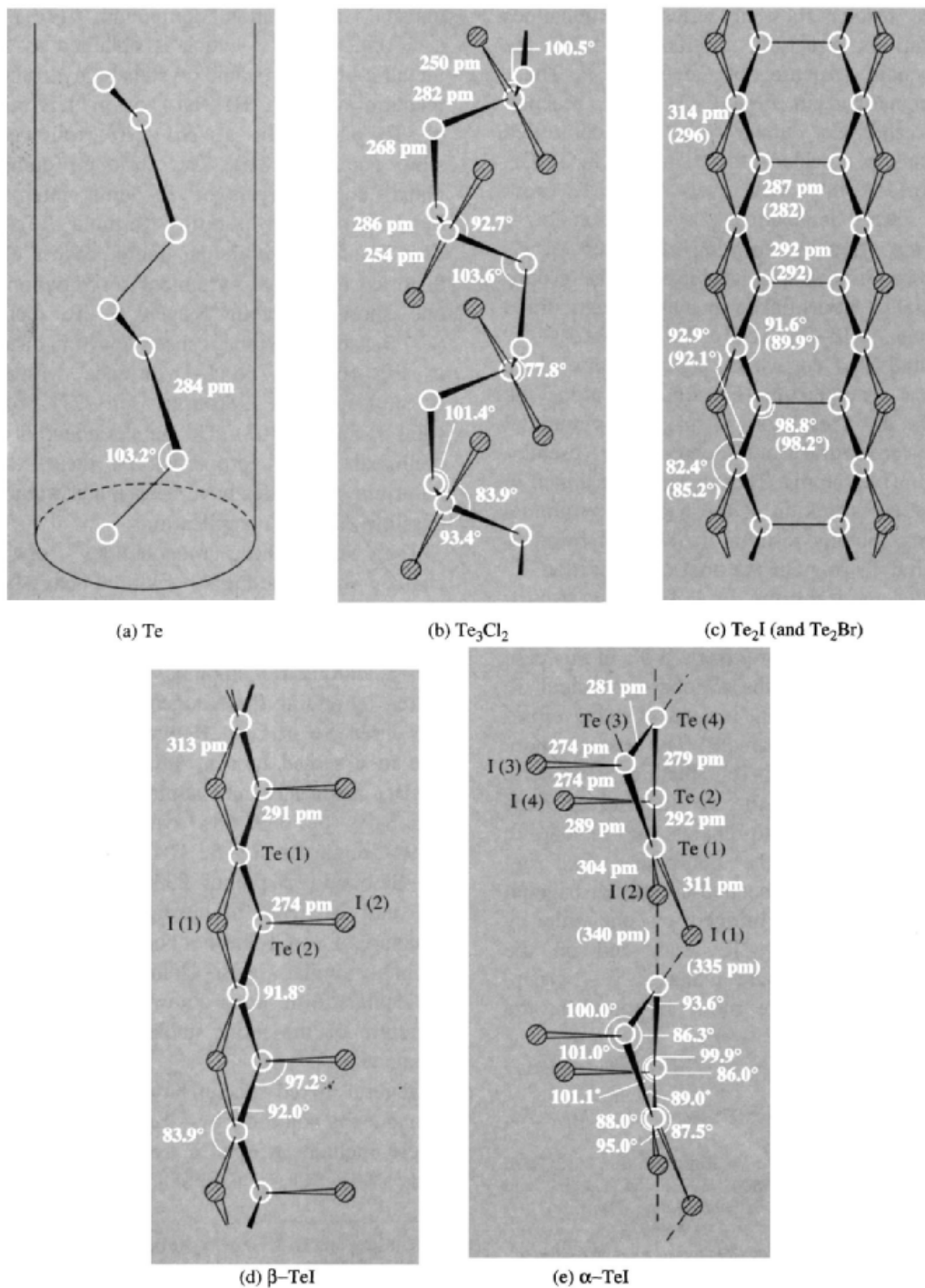
<sup>80</sup> R. KNIEP, D. MOOTZ and A. RABENAU, *Angew. Chem. Int. Edn. Engl.* **12**, 499–500 (1973). M. TAKEDA and N. N. GREENWOOD, *J. Chem. Soc., Dalton Trans.*, 631–6 (1976).

<sup>81</sup> R. KNIEP, D. MOOTZ and A. RABENAU, *Angew. Chem. Int. Edn. Engl.* **13**, 403–4 (1973). More complex chain and ribbon structures are observed for the ternary compounds α-AsSeI, β-AsSeI, α-AsTeI and β-AsTeI, all of which are isolectronic with Se<sub>∞</sub> and Te<sub>∞</sub> (R. KNIEP and H. D. RESKI, *Angew. Chem. Int. Edn. Engl.* **20**, 212–4 (1981)).

<sup>82</sup> R. KNIEP and H.-J. BEISTER, *Angew. Chem. Int. Edn. Engl.* **24**, 393–4 (1985).

<sup>83</sup> D. KATRYNIOK and R. KNIEP, *Angew. Chem. Int. Edn. Engl.* **19**, 645 (1980).

<sup>84</sup> M. LAMOUREUX and J. MILNE, *Polyhedron* **9**, 589–95 (1990).



**Figure 16.11** Structural relations between tellurium and its subhalides: (a) tellurium, (b)  $\text{Te}_3\text{Cl}_2$ , (c)  $\text{Te}_2\text{Br}$  and  $\text{Te}_2\text{I}$ , (d)  $\beta\text{-TeI}$ , and (e)  $\alpha\text{-TeI}$ .

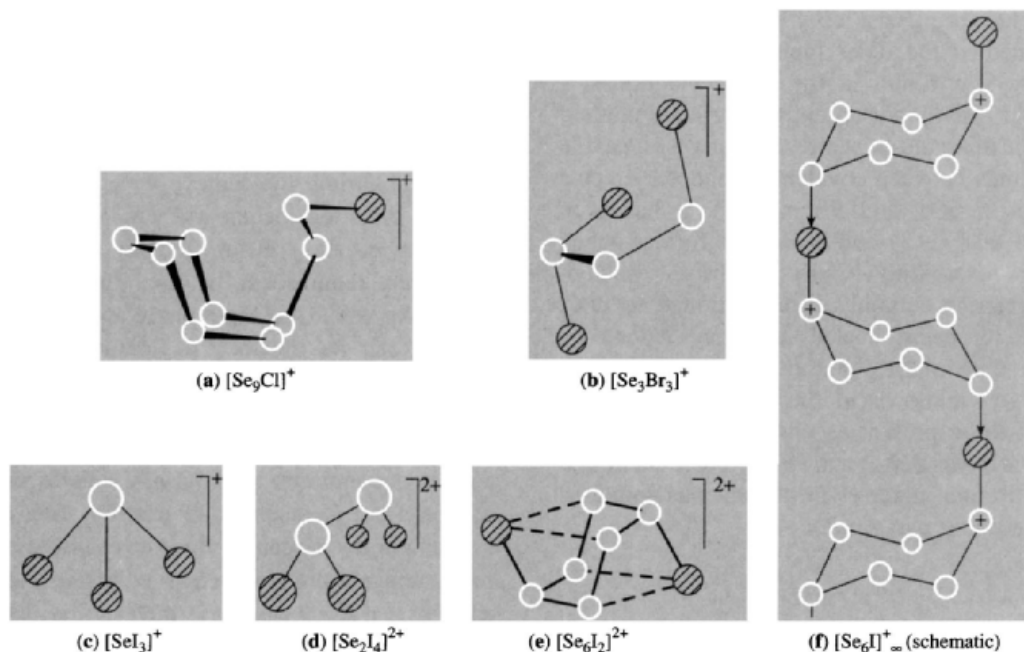


Figure 16.12 Structures of some selenium subhalide cations.

$\text{BrSeSBr}$ .<sup>(85)</sup>  $\text{ClSeSCl}$ , formed by mixing solutions of  $\text{S}_2\text{Cl}_2$  and  $\text{Se}_2\text{Cl}_2$ , has been reacted with titanocene pentasulfide (p. 672) to give mainly  $\text{S}_7$ ,  $\text{SeS}_6$  and  $1,2\text{-Se}_2\text{S}_5$ , plus smaller amounts of 6-, 8-, 9- and 12-membered Se/S ring molecules.<sup>(86)</sup> The related reaction with  $\text{SeBr}_2$  ( $\text{SeBr}_4 + \text{Se}$ ) in MeCN yields similar Se/S heterocycles.<sup>(87)</sup>

It is also convenient to mention here several cationic subhalide species that have recently been synthesized. Reaction of Se with  $[\text{NO}][\text{SbCl}_6]$  in liquid  $\text{SO}_2$  yields lustrous dark red crystals of  $[\text{Se}_9\text{Cl}]^+[\text{SbCl}_6]^-$  which is the first example of a 7-membered Se ring,  $[\text{cyclo-}\text{Se}_7\text{-SeSeCl}]^+$  (Fig. 16.12a).<sup>(88)</sup> Again, reaction of stoichiometric amounts of Se (or S),  $\text{Br}_2$

and  $\text{AsF}_5$  in liquid  $\text{SO}_2$  yields dark red crystals or  $[\text{Br}_2\text{Se-SeSeBr}]^+[\text{AsF}_6]^-$  (Fig. 16.12b)<sup>(89)</sup> or its S analogue. The first known binary Se/I species (albeit cationic rather than neutral) have been prepared<sup>(90)</sup> by reaction of  $\text{Se}_4^{2+}$  and  $\text{I}_2$  in  $\text{SO}_2$ : The species  $\text{SeI}_3^+$ ,  $\text{Se}_2\text{I}_4^{2+}$ ,  $\text{Se}_6\text{I}_2^{2+}$  were identified by  $^{77}\text{Se}$  nmr spectroscopy and subsequently assigned the definitive structures shown in Fig. 16.12c,d,e after X-ray diffraction analysis.<sup>(91)</sup> The polymeric cation  $[\text{Se}_6\text{I}]_\infty^+$  is also shown, (f).

Paradoxically, the most firmly established dihalides of the heavier chalcogens are the dark ruby-red  $\text{PoCl}_2$  and the purple-brown  $\text{PoBr}_2$  (Table 16.5). Both are formed by direct reaction of the elements or more conveniently by reducing  $\text{PoCl}_4$  with  $\text{SO}_2$  and  $\text{PoBr}_4$  with  $\text{H}_2\text{S}$  at  $25^\circ$ .

<sup>85</sup> J. MILNE, *J. Chem. Soc., Chem. Commun.*, 1048–9 (1991).

<sup>86</sup> R. STEUDEL, B. PLINKE, D. JENSEN and F. BAUMGART, *Polyhedron*, **10**, 1037–48 (1991).

<sup>87</sup> R. STEUDEL, D. JENSEN and F. BAUMGART, *Polyhedron* **9**, 1199–208 (1990).

<sup>88</sup> R. FAGGIANI, R. J. GILLESPIE, J. W. KOLIS and K. C. MALHOTRA, *J. Chem. Soc., Chem. Commun.*, 591–2 (1987).

<sup>89</sup> J. PASSMORE, M. TAJIK and P. S. WHITE, *J. Chem. Soc., Chem. Commun.*, 175–7 (1988).

<sup>90</sup> M. M. CARNELL, F. GREIN, M. MURCHIE, J. PASSMORE and C.-M. WONG, *J. Chem. Soc., Chem. Commun.*, 225–7 (1986).

<sup>91</sup> T. KLAPÖTKE and J. PASSMORE *Acc Chem. Res.* **22**, 234–40 (1989).

Doubt has been cast on "TeCl<sub>2</sub>" and "TeBr<sub>2</sub>" mentioned in the older literature since no sign of these was found in the phase diagrams.<sup>(79)</sup> However, this is not an entirely reliable method of establishing the existence of relatively unstable compounds between covalently bonded elements (cf. P/S, p. 506, and S/I, p. 691). It has been claimed that TeCl<sub>2</sub> and TeBr<sub>2</sub> are formed when fused Te reacts with CCl<sub>2</sub>F<sub>2</sub> or CBrF<sub>3</sub>,<sup>(92)</sup> though these materials certainly disproportionate to TeX<sub>4</sub> and Te on being heated and may indeed be eutectic-type phases in the system. SeCl<sub>2</sub> and SeBr<sub>2</sub> are unknown in the solid state but are thought to be present as unstable species in the vapour above SeX<sub>4</sub> and have been identified in equilibrium mixtures in nonaqueous solutions (see preceding paragraph).

### Tetrahalides

All 12 tetrahalides of Se, Te and Po are known except, perhaps, for SeI<sub>4</sub>. As with PX<sub>5</sub> (p. 498) and SX<sub>4</sub> (p. 691) these span the "covalent-ionic" border and numerous structural types are known; the stereochemical influence of the lone-pair of electrons (p. 377) is also prominent. SeF<sub>4</sub> is a colourless reactive liquid which fumes in air and crystallizes to a white hygroscopic solid (Table 16.5). It can be made by the controlled fluorination of Se (using F<sub>2</sub> at 0°, or AgF) or by reaction of SF<sub>4</sub> with SeO<sub>2</sub> above 100°. SeF<sub>4</sub> can be handled in scrupulously dried borosilicate glassware and is a useful fluorinating agent. Its structure in the gas phase, like that of SF<sub>4</sub> (p. 684), is pseudo-trigonal-bipyramidal with C<sub>2v</sub> symmetry; the dimensions shown in Fig. 16.13a were obtained by microwave spectroscopy. The same structure persists in solution but, with increasing concentration there is an increasing tendency to association *via* intermolecular F-bridges. The structure in the crystalline phase also has Se bonded to 4F atoms in a distorted pseudo-trigonal bipyramidal configuration as shown in

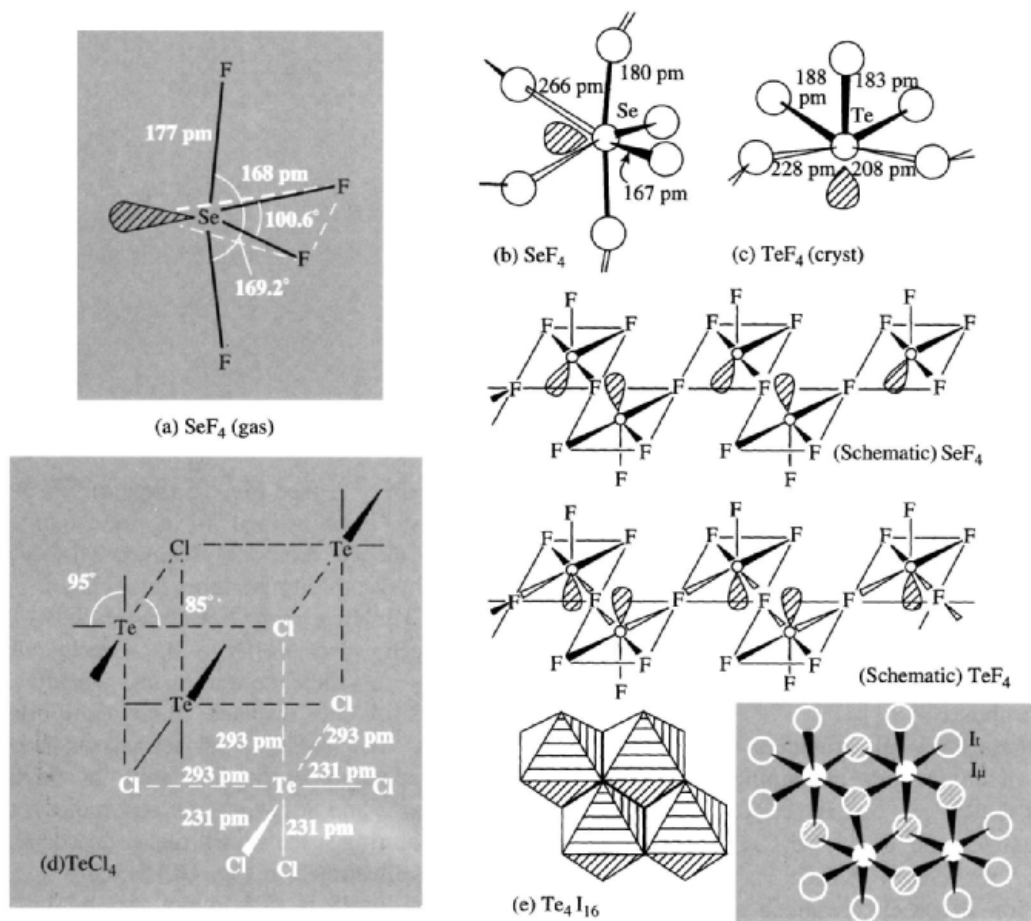
Fig. 16.13b (Se–F<sub>ax</sub> 180 pm, Se–F<sub>eq</sub> 167 pm, with axial and equatorial angles subtended at Se of 169.3° and 96.9°, respectively).<sup>(93)</sup> However, these pseudo-tbp molecules are arranged in layers by weaker intermolecular interactions to neighbouring molecules so as to form an overall distorted octahedral environment with two further Se···F at 266 pm (Fig. 16.13b) somewhat reminiscent of the structure found earlier for TeF<sub>4</sub> (see Fig. 16.13c and below).

TeF<sub>4</sub> can be obtained as colourless, hygroscopic, sublimable crystals by controlled fluorination of Te or TeX<sub>2</sub> with F<sub>2</sub>/N<sub>2</sub> at 0°, or more conveniently by reaction of SeF<sub>4</sub> with TeO<sub>2</sub> at 80°. It decomposes above 190° with formation of TeF<sub>6</sub> and is much more reactive than SeF<sub>4</sub>. For example, it readily fluorinates SiO<sub>2</sub> above room temperature and reacts with Cu, Ag, Au and Ni at 185° to give the metal tellurides and fluorides. Adducts with BF<sub>3</sub>, AsF<sub>5</sub> and SbF<sub>5</sub> are known (see also p. 776). Although probably monomeric in the gas phase, crystalline TeF<sub>4</sub> comprises chains of *cis*-linked square-pyramidal TeF<sub>5</sub> groups (Fig. 16.13c) similar to those in the isoelectronic (SbF<sub>4</sub><sup>–</sup>)<sub>n</sub> ions (p. 565). The lone-pair is alternately above and below the mean basal plane and each Te atom is displaced some 30 pm in the same direction. However, the local Te environment is somewhat less symmetrical than implied by this idealized description, and the Te–F distances span the range 183–228 pm.<sup>(93)</sup>

The other tetrahalides can all readily be made by direct reactions of the elements. Crystalline SeCl<sub>4</sub>, TeCl<sub>4</sub> and β-SeBr<sub>4</sub> are isotypic and the structural unit is a cubane-like tetramer of the same general type as [Me<sub>3</sub>Pt(μ<sub>3</sub>-Cl)]<sub>4</sub> (p. 1168). This is illustrated schematically for TeCl<sub>4</sub> in Fig. 16.13d: each Te is displaced outwards along a threefold axis and thus has a distorted octahedral environment. This can be visualized as resulting from repulsions due to the Te lone-pairs directed towards the cube centre and, in the limit, would result in the separation into

<sup>92</sup> E. E. AYNSLEY, *J. Chem. Soc.* 3016–9 (1953).  
E. E. AYNSLEY and R. H. WATSON, *J. Chem. Soc.* 2603–6 (1955).

<sup>93</sup> R. KNIEP, L. KORTE, R. KRYSCHI and W. POLL, *Angew. Chem. Int. Edn. Engl.* 23, 388–9 (1984).

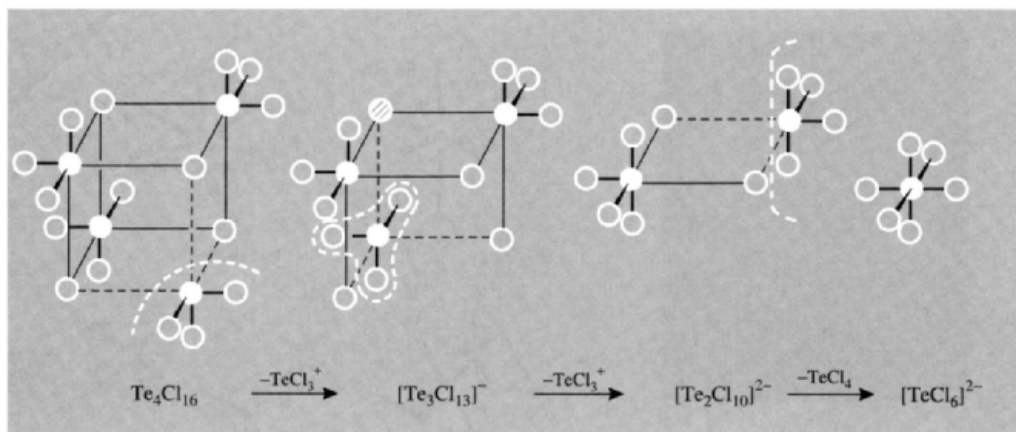


**Figure 16.13** Structures of some tetrahalides of Se and Te: (a)  $\text{SeF}_4$  (gas), (b) crystalline  $\text{SeF}_4$ , and schematic representation of the association of the pseudo-*tpb* molecules (see text), (c) coordination environment of Te in crystalline  $\text{TeF}_4$  and schematic representation of the polymerized square pyramidal units, (d) the tetrameric unit in crystalline  $(\text{TeCl}_4)_4$ , and (e) two representations of the tetrameric molecules in  $\text{Te}_4\text{I}_{16}$  showing the shared edges of the  $\{\text{Te}_6\}$  octahedral subunits.

$\text{TeCl}_3^+$  and  $\text{Cl}^-$  ions. Accordingly, the 3 tetrahalides are good electrical conductors in the fused state, and salts of  $\text{SeX}_3^+$  and  $\text{TeCl}_3^+$  can be isolated in the presence of strong halide ion acceptors, e.g.  $[\text{SeCl}_3]^+[\text{GaCl}_4]^-$ ,  $[\text{SeBr}_3]^+[\text{AlBr}_4]^-$ ,  $[\text{TeCl}_3]^+[\text{AlCl}_4]^-$ . In solution, however, the structure depends on the donor properties of the solvent:<sup>(94)</sup> in donor solvents such as MeCN,  $\text{Me}_2\text{CO}$  and EtOH the electrical conductivity

and vibrational spectra indicate the structure  $[\text{L}_2\text{TeCl}_3]^+\text{Cl}^-$ , where L is a molecule of solvent, whereas in benzene and toluene the compound dissolves as a non-conducting molecular oligomer which is tetrameric at a concentration of 0.1 molar but which is in equilibrium with smaller oligomeric units at lower concentrations. Removal of one  $\text{TeCl}_3^+$  unit from the cubane-like structure of  $\text{Te}_4\text{Cl}_{16}$  leaves the trinuclear anion  $\text{Te}_3\text{Cl}_{13}^-$  which can be isolated from benzene solutions as the salt of the large counter-cation  $\text{Ph}_3\text{C}^+$ ; the anion has the expected  $C_{3v}$  structure

<sup>94</sup> N. N. GREENWOOD, B. P. STRAUGHAN and A. E. WILSON, *J. Chem. Soc. (A)* 2209–12 (1968).



comprising three edge-shared octahedra with a central triply bridging Cl atom.<sup>(95)</sup> Removal of a further  $\text{TeCl}_3^+$  unit yields the edge-shared bi-octahedral dianion  $\text{Te}_2\text{Cl}_{10}^{2-}$  which was isolated as the crystalline salt  $[\text{AsPh}_4]_2^+ [\text{Te}_2\text{Cl}_{10}]^{2-}$ . Notional removal of a final  $\{\text{TeCl}_4\}$  unit leaves the octahedral anion  $\text{TeCl}_6^{2-}$  (p. 776) as in the scheme above.

Numerous crystal structures have been published of compounds containing the pyramidal cations  $\text{Se}^{\text{IV}}\text{Cl}_3^+$ ,  $\text{Se}^{\text{IV}}\text{Br}_3^+$ ,  $\text{Te}^{\text{IV}}\text{Cl}_3^+$ , etc.<sup>(96)</sup> and the anions  $\text{Se}^{\text{II}}\text{Cl}_4^{2-}$ ,  $\text{Se}^{\text{II}}\text{Cl}_6^{2-}$ ,<sup>(97)</sup>  $\text{Se}_3\text{Cl}_{13}^-$ ,  $\text{Se}_3\text{Br}_{13}^-$ ,<sup>(98)</sup>  $\text{SeCl}_5^-$ ,  $\text{TeCl}_5^-$ ,  $\text{TeCl}_6^{2-}$ , etc.<sup>(99)</sup> The anion structures are much as expected with the  $\text{Se}^{\text{II}}$  species featuring square planar (pseudo-octahedral) units, and the trinuclear  $\text{Se}^{\text{IV}}$  anions as in the tellurium analogue above. See also p. 776. There are, in addition, a fascinating series of bromoselenate(II) dianions based on fused planar  $\{\text{SeBr}_4\}$  units, e.g.  $\text{Se}_3\text{Br}_8^{2-}$ ,  $\text{Se}_4\text{Br}_{14}^{2-}$ ,

and  $\text{Se}_5\text{Br}_{12}^{2-}$ , (see Fig. 16.14a,b,c)<sup>(100)</sup>. Access has also been gained to a series of novel mixed-valence bromopolyselenate (II,IV) dianions by exploiting the dissociation equilibria  $\frac{1}{4}\text{Se}_4\text{Br}_{16} \rightleftharpoons \text{SeBr}_4 \rightleftharpoons \text{SeBr}_2 + \text{Br}_2$  and  $2\text{SeBr}_2 \rightleftharpoons \text{Se}_2\text{Br}_2 + \text{Br}_2$ . Careful addition of  $\text{Br}_2$  to such solutions in weakly polar organic solvents displaces these equilibria and permits the isolation of tetraalkylammonium or tetraphenylphosphonium salts of  $\text{Se}_2\text{Br}_8^{2-}$ ,  $\text{Se}_3\text{Br}_{10}^{2-}$ , and  $\text{Se}_4\text{Br}_{12}^{2-}$ , as dark red crystalline salts featuring fused square planar and octahedral units as illustrated in Fig. 16.15a,b,c.<sup>(101)</sup>

$\text{SeBr}_4$  itself is dimorphic: the  $\alpha$ -form, like  $\beta$ - $\text{SeBr}_4$  mentioned on p. 772, has a cubane-like tetrameric unit ( $\text{Se}-\text{Br}_\mu$  237 pm,  $\text{Se}-\text{Br}_\mu$  297 pm) but the two forms differ in the spacial arrangement of the tetramers.<sup>(102)</sup>  $\text{TeI}_4$  has yet another structure which involves a tetrameric arrangement of edge-shared  $\{\text{TeI}_6\}$  octahedra not previously encountered in binary inorganic compounds (Fig. 16.13e).<sup>(103)</sup> The molecule is close to idealized  $C_{2h}$  symmetry with each terminal octahedron sharing 2 edges with the 2 neighbouring central octahedra

<sup>95</sup> B. KREBS and V. PAULAT, *Z. Naturforsch.* **34b**, 900–5 (1979), and references therein.

<sup>96</sup> B. H. CHRISTIAN, M. J. COLLINS, R. J. GILLESPIE and J. F. SAWYER, *Inorg. Chem.* **25**, 777–88 (1986). B. NEUMÜLLER, C. LAU and K. DEHNICKE, *Z. anorg. allg. Chem.* **622**, 1847–53 (1996).

<sup>97</sup> B. KREBS, E. LÜHRS, R. WILLMER and F.-P. AHLERS, *Z. anorg. allg. Chem.* **592**, 17–34 (1991). See also H. FOLKERTS, K. DEHNICKE, J. MAGULL, H. GOESMANN and D. FENSKE, *Z. anorg. allg. Chem.* **620**, 1301–6 (1994).

<sup>98</sup> F.-P. AHLERS, E. LÜHRS and B. KREBS, *Z. anorg. allg. Chem.* **594**, 7–22 (1991).

<sup>99</sup> B. BORGSEN, F. WELLER and K. DEHNICKE, *Z. anorg. allg. Chem.* **596**, 55–61 (1991), and 2nd part of ref. 96.

<sup>100</sup> B. KREBS, F.-P. AHLERS and E. LÜHRS, *Z. anorg. allg. Chem.* **597**, 115–32 (1991).

<sup>101</sup> B. KREBS, E. LÜHRS and F.-P. AHLERS, *Angew. Chem. Int. Edn. Engl.* **28**, 187–9 (1989).

<sup>102</sup> P. BORN, R. KNIEP and D. MOOTZ, *Z. anorg. allg. Chem.* **451**, 12–24 (1979).

<sup>103</sup> V. PAULAT and B. KREBS, *Angew. Chem. Int. Edn. Engl.* **15**, 39–40 (1976).

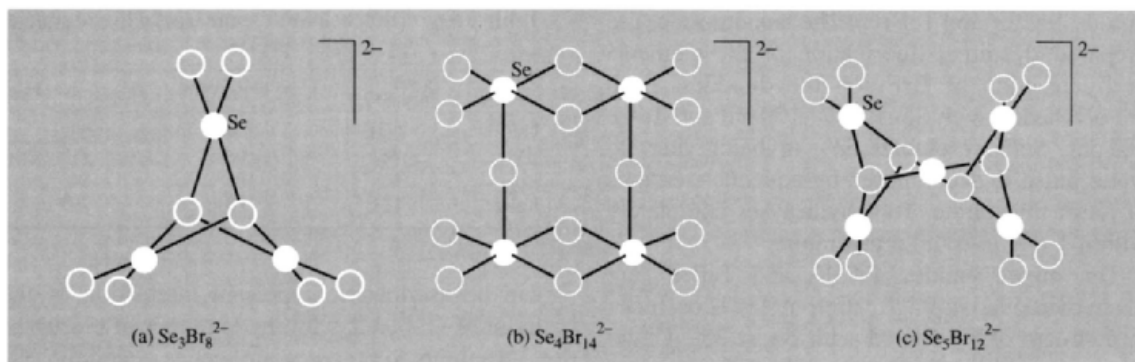


Figure 16.14 Structures of some bromoselenate(II) anions.

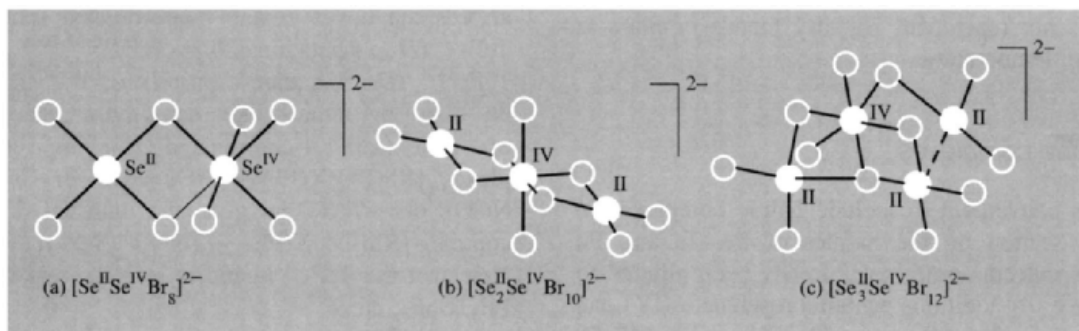
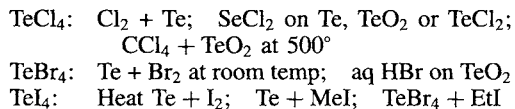


Figure 16.15 Structures of some mixed-valence bromopolyselenate(II,IV) anions.

and each central octahedron sharing 3 edges with its 3 neighbours (Te–I<sub>r</sub> 277 pm, Te–I<sub>μ<sub>2</sub></sub> 311 pm, Te–I<sub>μ<sub>3</sub></sub> 323 pm). There is no significant intermolecular I··I bonding. Comparison of the structures and bond data for the homologous series TeF<sub>4</sub>, TeCl<sub>4</sub>(TeBr<sub>4</sub>), TeI<sub>4</sub> reveals an increasing delocalization of the Te<sup>IV</sup> lone-pair. This effect is also observed in the compounds of other *ns*<sup>2</sup> elements (e.g. Sn<sup>II</sup>, Pb<sup>II</sup>, As<sup>III</sup>, Sb<sup>III</sup>, Bi<sup>III</sup>, I<sup>V</sup>; see pp. 380, 383, 568) and correlates with the gradation of electronegativities and the polarizing power of the halogens.

The detailed structures of PoX<sub>4</sub> are unknown. Some properties are in Table 16.5. PoF<sub>4</sub> is not well characterized. PoCl<sub>4</sub> forms bright-yellow monoclinic crystals which can be melted under an atmosphere of chlorine, and PoBr<sub>4</sub> has a fcc lattice with *a*<sub>0</sub> = 560 pm. These compounds and PoI<sub>4</sub> can be made by direct combination of the

elements or indirectly, e.g. by the chlorination of PoO<sub>2</sub> with HCl, PCl<sub>5</sub> or SOCl<sub>2</sub>, or by the reaction of PoO<sub>2</sub> with HI and 200°. Similar methods are used to prepare the tetrahalides of Se and Te, e.g.:



The two mixed tellurium(IV) halides listed in Table 16.5 were prepared by the action of liquid Br<sub>2</sub> on TeCl<sub>2</sub> to give the yellow solid TeBr<sub>2</sub>Cl<sub>2</sub>, and by the action of I<sub>2</sub> on TeBr<sub>2</sub> in ether solution to give the red crystalline TeBr<sub>2</sub>I<sub>2</sub>; their structures are as yet unknown.

### Hexahalides

The only hexahalides known are the colourless gaseous fluorides SeF<sub>6</sub> and TeF<sub>6</sub> and the volatile

liquids  $\text{TeClF}_5$  and  $\text{TeBrF}_5$ . The hexafluorides are prepared by direct fluorination of the elements or by reaction of  $\text{BrF}_3$  on the dioxides. Both are octahedral with  $\text{Se-F}$  167–170 pm and  $\text{Te-F}$  184 pm.  $\text{SeF}_6$  resembles  $\text{SF}_6$  in being inert to water but it is decomposed by aqueous solutions of KI or thiosulfate.  $\text{TeF}_6$  hydrolyses completely within 1 day at room temperature.

The mixed halides  $\text{TeClF}_5$  and  $\text{TeBrF}_5$  are made by oxidative fluorination of  $\text{TeCl}_4$  or  $\text{TeBr}_4$  in a stream of  $\text{F}_2$  diluted with  $\text{N}_2$  at  $25^\circ$ . Under similar conditions  $\text{TeI}_4$  gave only  $\text{TeF}_6$  and  $\text{IF}_5$ .  $\text{TeClF}_5$  can also be made by the action of  $\text{ClF}$  on  $\text{TeF}_4$ ,  $\text{TeCl}_4$  or  $\text{TeO}_2$  below room temperature; it is a colourless liquid, mp  $-28^\circ$ , bp  $13.5^\circ$ , which does not react with Hg, dry metals or glass at room temperature.

### Halide complexes

It is convenient to include halide complexes in this section on the halides of Se, Te and Po and, indeed, some have already been alluded to above. In addition, pentafluoroselenates(IV) can be obtained as rather unstable white solids  $\text{MSeF}_5$  by dissolving alkali metal fluorides or TlF in  $\text{SeF}_4$ . The crystal structure of  $\text{Me}_4\text{NSeF}_5$  features square-pyramidal  $\text{SeF}_5^-$  ions,<sup>(104)</sup> with  $\text{Se-F}_{\text{apex}}$  171 pm  $\text{Se-F}_{\text{base}}$  185 pm and the angle  $\text{F}_a\text{-Se-F}_b$   $84^\circ$ , implying that the Se atom and its lone pair of electrons lies some 20 pm below the basal plane (cf. Fig. 16.13b). The tellurium analogues are best prepared by dissolving MF and  $\text{TeO}_2$  in aqueous HF or  $\text{SeF}_4$ ; they are white crystalline solids. The  $\text{TeF}_5^-$  ion (like  $\text{SeF}_5^-$ ) has a distorted square-based pyramidal structure ( $C_{4v}$ ) in which the Te atom (and pendant lone-pair of electrons) is about 30 pm below the basal plane with  $\text{Te-F}_{\text{apex}}$  184 pm,  $\text{Te-F}_{\text{base}}$  196 pm and the angle  $\text{F}_a\text{-Te-F}_b$   $81^\circ$ <sup>(104)</sup> (cf.  $\text{TeF}_4$ , Fig. 16.13c). The resemblance to other isoelectronic  $\text{MF}_5^{n\pm}$  species is illustrated in Table 16.6; in each case, the fact that the distance  $\text{M-F}_{\text{base}}$  is greater than  $\text{M-F}_{\text{apex}}$  and that the angle  $\text{F}_{\text{apex}}\text{-M-F}_{\text{base}}$  is less than  $90^\circ$

**Table 16.6** Dimensions of some isoelectronic square-pyramidal species

Species	$\text{M-F}_{\text{apex}}/\text{pm}$	$\text{M-F}_{\text{base}}/\text{pm}$	$\angle\text{F}_{\text{apex}}\text{-M-F}_{\text{base}}$
$\text{SbF}_5^{2-}$	200	204	$83^\circ$
$\text{TeF}_5^-$	184	196	$81^\circ$
$\text{BrF}_5$	168	181	$84^\circ$
$\text{XeF}_5^+$	181	188	$79^\circ$

can be ascribed to repulsive interaction of the basal  $\text{M-F}$  bonds with the lone-pair of electrons.

Attempts to prepare compounds containing the  $\text{TeF}_6^{2-}$  ion have not been successful though numerous routes have been tried. However, reaction of  $\text{Me}_4\text{NF}$  with  $\text{TeF}_6$  in anhydrous MeCN affords the novel 7- and 8-coordinated species  $\text{TeF}_7^-$  ( $D_{5h}$ , pentagonal bipyramid)<sup>(105,106)</sup> and  $\text{TeF}_8^{2-}$  ( $D_{4d}$ , square antiprism),<sup>(105)</sup> There is also a remarkable heterolytic reaction of  $\text{TeF}_4$  with 4-coordinated rhodium complexes  $[\text{Rh}(\text{CO})\text{X}(\text{PEt}_3)_2]$ , ( $\text{X} = \text{Cl}, \text{Br}, \text{NCS}, \text{NCO}$ ) at  $-78^\circ\text{C}$  to give the unusual ionic complex  $[\text{Rh}(\text{CO})\text{X}(\text{PEt}_3)_2(\text{TeF}_3)]^+(\text{TeF}_5)^-$ .<sup>(107)</sup> Note that the  $\text{TeF}_3^+$  ligand is isoelectronic with  $\text{PF}_3$ ,  $\text{SbF}_3$ , etc.

By contrast to the absence of  $\text{TeF}_6^{2-}$ , compounds of the complex anions  $\text{SeX}_6^{2-}$  and  $\text{TeX}_6^{2-}$  ( $\text{X} = \text{Cl}, \text{Br}, \text{I}$ ) are readily prepared in crystalline form by direct reaction (e.g.  $\text{TeX}_4 + 2\text{MX}$ ) or by precipitating the complex from a solution of  $\text{SeO}_2$  or  $\text{TeO}_2$  in aqueous HX. Their most notable feature is a regular octahedral structure despite the fact that they are formally 14-electron species; it appears that with large monatomic ligands of moderate electronegativity the stereochemistry is dominated by inter-ligand repulsions and the lone-pair then either resides in an  $ns^2$  orbital for isolated ions or is delocalized in a low-energy solid-state band.<sup>(108)</sup> Similar results

<sup>105</sup> K. O. CHRISTE, J. P. C. SANDERS, G. J. SCHROBILGEN and W. W. WILSON, *J. Chem. Soc., Chem. Commun.*, 837–40 (1991) and references cited therein.

<sup>106</sup> A. R. MAHJOUB and K. SEPPELT, *J. Chem. Soc., Chem. Commun.*, 840–1 (1991).

<sup>107</sup> E. A. V. EBSWORTH, J. H. HOLLOWAY and P. G. WATSON, *J. Chem. Soc., Chem. Commun.*, 1443–4 (1991).

<sup>108</sup> For experimental results and theoretical discussion see I. D. BROWN, *Can. J. Chem.* **42**, 2758–67 (1964);

<sup>104</sup> A. R. MAHJOUB, D. LEOPOLD and K. SEPPELT, *Z. anorg. allg. Chem.* **618**, 83–8 (1992).



Table 16.7 Some physical properties of selenium oxohalides

Property	SeOF <sub>2</sub>	SeOCl <sub>2</sub>	SeOBr <sub>2</sub>	SeO <sub>2</sub> F <sub>2</sub>	(SeOF <sub>4</sub> ) <sub>2</sub>	F <sub>5</sub> SeOF	F <sub>5</sub> SeOOSF <sub>5</sub>
MP/°C	15	10.9	41.6	-99.5	-12	-54	-62.8
BP/°C	125	177.2	~220 (d)	-8.4	65	-29	76.3
Density/g cm <sup>-3</sup> (T°C)	2.80 (21.5°)	2.445 (16°)	3.38 (50°)	—	—	—	—

were noted for octahedral Sn<sup>II</sup> (p. 380) and Sb<sup>III</sup> (p. 568).

### 16.2.4 Oxohalides and pseudohalides<sup>(1)</sup>

Numerous oxohalides of Se<sup>IV</sup> and Se<sup>VI</sup> are known, SeOF<sub>2</sub> and SeOCl<sub>2</sub> are colourless, fuming, volatile liquids, whereas SeOBr<sub>2</sub> is a rather less-stable orange solid which decomposes in air above 50° (Table 16.7). The compounds can be conveniently made by reacting SeO<sub>2</sub> with the appropriate tetrahalide and their molecular structure is probably pyramidal (like SOX<sub>2</sub>, p. 694). SeOF<sub>2</sub> is an aggressive reagent which attacks glass, reacts violently with red phosphorus and with powdered SiO<sub>2</sub> and slowly with Si. In the solid state, X-ray studies have revealed that the pyramidal SeOF<sub>2</sub> units are linked by O and F bridges into layers thereby building a distorted octahedral environment around each Se with 3 close contacts (to O and 2F) and 3 (longer) bridging contacts grouped around the lone-pair to neighbouring units.<sup>(109)</sup> This contrasts with the discrete

D. S. URCH, *J. Chem. Soc.* 5775-81 (1964); N. N. GREENWOOD and B. P. STRAUGHAN, *J. Chem. Soc. (A)* 962-4 (1966); T. C. GIBB, R. GREATREX, N. N. GREENWOOD and A. C. SARMA, *J. Chem. Soc. (A)* 212-17 (1970). J. D. DONALDSON, S. D. ROSS, J. SILVER and P. WATKISS, *J. Chem. Soc., Dalton Trans.*, 1980-3 (1975), and references therein. There is, however, some very recent X-ray crystallographic evidence that the anion in [Bu<sup>t</sup>NH<sub>3</sub>]<sub>2</sub><sup>+</sup>[TeBr<sub>6</sub>]<sub>2</sub><sup>-</sup> is trigonally distorted, with 3 long bonds of 276 pm (av.) and 3 shorter bonds of 261 pm, although the corresponding TeCl<sub>6</sub><sup>2-</sup> salt had regular octahedral O<sub>h</sub> symmetry: see L.-J. BAKER, C. E. F. RICKARD and M. J. TAYLOR, *Polyhedron* **14**, 401-5 (1995).

<sup>109</sup> J. C. DEWAN and A. J. EDWARDS, *J. Chem. Soc., Dalton Trans.*, 2433-5 (1976).

molecular structure of SOF<sub>2</sub> and affords yet another example of the influence of preferred coordination number on the structure and physical properties of isovalent compounds, e.g. molecular BF<sub>3</sub> and 6-coordinate AlF<sub>3</sub>, molecular GeF<sub>4</sub> and the 6-coordinate layer lattice of SnF<sub>4</sub> and, to a less extent, molecular AsF<sub>3</sub> and F-bridged SbF<sub>3</sub>. (See also the Group 14 dioxides, etc.)

SeOCl<sub>2</sub> (Table 16.7) is a useful solvent: it has a high dielectric constant (46.2 at 20°), a high dipole moment (2.62 D in benzene) and an appreciable electrical conductivity (2 × 10<sup>-5</sup> ohm<sup>-1</sup> cm<sup>-1</sup> at 25°). This last has been ascribed to self-ionic dissociation resulting from chloride-ion transfer: 2SeOCl<sub>2</sub> ⇌ SeOCl<sup>+</sup> + SeOCl<sub>3</sub><sup>-</sup>.

Oxohalides of Se<sup>VI</sup> are known only for fluorine (Table 16.7). SeO<sub>2</sub>F<sub>2</sub> is a readily hydrolysable colourless gas which can be made by fluorinating SeO<sub>3</sub> with SeF<sub>4</sub> (or KBF<sub>4</sub> at 70°) or by reacting BaSeO<sub>4</sub> with HSO<sub>3</sub>F under reflux at 50°. Its vibrational spectra imply a tetrahedral structure with C<sub>2v</sub> symmetry as expected. By contrast, SeOF<sub>4</sub> is a dimer [F<sub>4</sub>Se(μ-O)<sub>2</sub>SeF<sub>4</sub>] in which each Se achieves octahedral coordination via the 2 bridging O atoms: the planar central Se<sub>2</sub>O<sub>2</sub> ring has Se-O 178 pm and angle Se-O-Se 97.5°, and Se-F<sub>eq</sub> and Se-F<sub>ax</sub> are 167 and 170 pm respectively.<sup>(110)</sup>

Two further oxofluorides of Se<sup>VI</sup> can be prepared by reaction of SeO<sub>2</sub> with a mixture of F<sub>2</sub>/N<sub>2</sub>: at 80° the main product is the "hypofluorite" F<sub>5</sub>SeOF whereas at 120° the peroxide F<sub>5</sub>SeOOSeF<sub>5</sub> predominates. The compounds (Table 16.7) can be purified by

<sup>110</sup> H. OBERHAMMER and K. SEPPALT, *Inorg. Chem.* **18**, 2226-9 (1979).

Table 16.7 Some physical properties of selenium oxohalides

Property	SeOF <sub>2</sub>	SeOCl <sub>2</sub>	SeOBr <sub>2</sub>	SeO <sub>2</sub> F <sub>2</sub>	(SeOF <sub>4</sub> ) <sub>2</sub>	F <sub>5</sub> SeOF	F <sub>5</sub> SeOOSF <sub>5</sub>
MP/°C	15	10.9	41.6	-99.5	-12	-54	-62.8
BP/°C	125	177.2	~220 (d)	-8.4	65	-29	76.3
Density/g cm <sup>-3</sup> (T°C)	2.80 (21.5°)	2.445 (16°)	3.38 (50°)	—	—	—	—

were noted for octahedral Sn<sup>II</sup> (p. 380) and Sb<sup>III</sup> (p. 568).

### 16.2.4 Oxohalides and pseudohalides<sup>(1)</sup>

Numerous oxohalides of Se<sup>IV</sup> and Se<sup>VI</sup> are known, SeOF<sub>2</sub> and SeOCl<sub>2</sub> are colourless, fuming, volatile liquids, whereas SeOBr<sub>2</sub> is a rather less-stable orange solid which decomposes in air above 50° (Table 16.7). The compounds can be conveniently made by reacting SeO<sub>2</sub> with the appropriate tetrahalide and their molecular structure is probably pyramidal (like SOX<sub>2</sub>, p. 694). SeOF<sub>2</sub> is an aggressive reagent which attacks glass, reacts violently with red phosphorus and with powdered SiO<sub>2</sub> and slowly with Si. In the solid state, X-ray studies have revealed that the pyramidal SeOF<sub>2</sub> units are linked by O and F bridges into layers thereby building a distorted octahedral environment around each Se with 3 close contacts (to O and 2F) and 3 (longer) bridging contacts grouped around the lone-pair to neighbouring units.<sup>(109)</sup> This contrasts with the discrete

molecular structure of SOF<sub>2</sub> and affords yet another example of the influence of preferred coordination number on the structure and physical properties of isovalent compounds, e.g. molecular BF<sub>3</sub> and 6-coordinate AlF<sub>3</sub>, molecular GeF<sub>4</sub> and the 6-coordinate layer lattice of SnF<sub>4</sub> and, to a less extent, molecular AsF<sub>3</sub> and F-bridged SbF<sub>3</sub>. (See also the Group 14 dioxides, etc.)

SeOCl<sub>2</sub> (Table 16.7) is a useful solvent: it has a high dielectric constant (46.2 at 20°), a high dipole moment (2.62 D in benzene) and an appreciable electrical conductivity (2 × 10<sup>-5</sup> ohm<sup>-1</sup> cm<sup>-1</sup> at 25°). This last has been ascribed to self-ionic dissociation resulting from chloride-ion transfer: 2SeOCl<sub>2</sub> ⇌ SeOCl<sup>+</sup> + SeOCl<sub>3</sub><sup>-</sup>.

Oxohalides of Se<sup>VI</sup> are known only for fluorine (Table 16.7). SeO<sub>2</sub>F<sub>2</sub> is a readily hydrolysable colourless gas which can be made by fluorinating SeO<sub>3</sub> with SeF<sub>4</sub> (or KBF<sub>4</sub> at 70°) or by reacting BaSeO<sub>4</sub> with HSO<sub>3</sub>F under reflux at 50°. Its vibrational spectra imply a tetrahedral structure with C<sub>2v</sub> symmetry as expected. By contrast, SeOF<sub>4</sub> is a dimer [F<sub>4</sub>Se(μ-O)<sub>2</sub>SeF<sub>4</sub>] in which each Se achieves octahedral coordination via the 2 bridging O atoms: the planar central Se<sub>2</sub>O<sub>2</sub> ring has Se-O 178 pm and angle Se-O-Se 97.5°, and Se-F<sub>eq</sub> and Se-F<sub>ax</sub> are 167 and 170 pm respectively.<sup>(110)</sup>

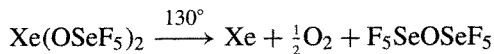
Two further oxofluorides of Se<sup>VI</sup> can be prepared by reaction of SeO<sub>2</sub> with a mixture of F<sub>2</sub>/N<sub>2</sub>: at 80° the main product is the "hypofluorite" F<sub>5</sub>SeOF whereas at 120° the peroxide F<sub>5</sub>SeOOSeF<sub>5</sub> predominates. The compounds (Table 16.7) can be purified by

D. S. URCH, *J. Chem. Soc.* 5775-81 (1964); N. N. GREENWOOD and B. P. STRAUGHAN, *J. Chem. Soc. (A)* 962-4 (1966); T. C. GIBB, R. GREATREX, N. N. GREENWOOD and A. C. SARMA, *J. Chem. Soc. (A)* 212-17 (1970). J. D. DONALDSON, S. D. ROSS, J. SILVER and P. WATKISS, *J. Chem. Soc., Dalton Trans.*, 1980-3 (1975), and references therein. There is, however, some very recent X-ray crystallographic evidence that the anion in [Bu<sup>t</sup>NH<sub>3</sub>]<sub>2</sub><sup>+</sup>[TeBr<sub>6</sub>]<sub>2</sub><sup>-</sup> is trigonally distorted, with 3 long bonds of 276 pm (av.) and 3 shorter bonds of 261 pm, although the corresponding TeCl<sub>6</sub><sup>2-</sup> salt had regular octahedral O<sub>h</sub> symmetry: see L.-J. BAKER, C. E. F. RICKARD and M. J. TAYLOR, *Polyhedron* **14**, 401-5 (1995).

<sup>109</sup> J. C. DEWAN and A. J. EDWARDS, *J. Chem. Soc., Dalton Trans.*, 2433-5 (1976).

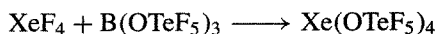
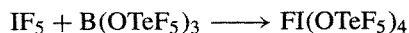
<sup>110</sup> H. OBERHAMMER and K. SEPPALT, *Inorg. Chem.* **18**, 2226-9 (1979).

fractional sublimation and are reactive, volatile, colourless solids. The analogous sulfur compounds were discussed on p. 688. The colourless liquid  $F_5SeOSeF_5$  (mp  $-85^\circ$ , bp  $53^\circ$ ) is made by a somewhat more esoteric route as follows:<sup>(111)</sup>



The corresponding tellurium analogue,  $F_5TeTeOF_5$ , is made by fluorinating  $TeO_2$  in a copper vessel at  $60^\circ$  using a stream of  $F_2/N_2$  (1:10); it is a colourless, mobile, unreactive liquid, mp  $-36.6^\circ$  bp  $59.8^\circ$ .<sup>(76,77)</sup> The Se–O–Se angle in  $F_5SeOSeF_5$  is  $142.4^\circ (\pm 1.9^\circ)$  as in the sulfur analogue, and the Te–O–Te angle is very similar ( $145.5 \pm 2.1^\circ$ ). The fluorination of Te in the presence of oxygen yields (in addition to  $Te_2F_{10}O$ , p. 767) the dense colourless liquids  $Te_3^{VI}O_2F_{14}$  and  $Te_6^{VI}O_5F_{26}$ . More purposeful synthetic routes have also been devised, leading to the isolation and structural characterization of the 6-coordinate  $Te^{VI}$  oxofluorides *cis*- and *trans*- $F_4Te(OTeF_5)_2$ , *cis*- and *trans*- $F_2Te(OTeF_5)_4$ ,  $FTe(OTeF_5)_5$  and even  $Te(OTeF_5)_6$ .<sup>(112)</sup> Similarly, thermolysis of  $B(OTeF_5)_3$  at  $600^\circ$  in a flow system yields the oxygen-bridged dimer  $Te_2O_2F_8$  analogous to  $Se_2O_2F_8$  above.  $Te_2O_2F_8$  is a colourless liquid with a garlic-like smell, mp  $28^\circ$ , bp  $77.5^\circ$ . The planar central  $Te_2O_2$  ring has Te–O 192 pm and angle Te–O–Te  $99.5^\circ$ , and again the equatorial Te–F distances (180 pm) are shorter than the axial ones (185 pm).<sup>(110)</sup>

The  $-OTeF_5$  group (like the  $-OSeF_5$  group) has a very high electronegativity as can be seen, for example, by the reactions of the ligand transfer reagent  $[B(OTeF_5)_3]$ :<sup>(113)</sup>



(see also p. 899)

Direct fluorination of  $B(OTeF_5)_3$  at  $115^\circ$  gives a 95% yield of the hypofluorite,  $F_5TeOF$ , as a colourless gas which condenses to a colourless liquid below  $0^\circ$  and finally to a glass at about  $-80^\circ$ ; the extrapolated bp is  $0.6^\circ$ .<sup>(114)</sup> The chlorine derivative,  $ClOTeF_5$ , the so-called teflic acid,  $HOTeF_5$ , and the teflate anion,  $F_5TeO^-$  (as caesium or tetraalkylammonium salts) are also useful synthons for a variety of metal derivatives, e.g.  $[Fe(OTeF_5)_3]$ ,<sup>(115)</sup>  $[Nb(OTeF_5)_6]^-$  and  $[Ta(OTeF_5)_6]^-$ .<sup>(116)</sup> Other examples are  $[Mn(CO)_5(OTeF_5)]$  and  $[Pt(\text{norbornadiene})(OTeF_5)_2]$ . The  $-OTeF_5$  group can also act as a bridging ligand, as in the dimeric  $Ag^I$  and  $Tl^I$  complexes,  $[\{(\eta^2\text{-tol})Ag\}_2(\mu\text{-}OTeF_5)_2]$ <sup>(117)</sup> and  $[\{(\eta^6\text{-mes})_2Tl\}_2(\mu\text{-}OTeF_5)_2]$ ,<sup>(118)</sup> which both feature a central planar  $M_2O_2$  core (tol = toluene,  $C_6H_5Me$ ; mes = mesitylene, 1,3,5- $C_6H_3Me_3$ ). The H-bonded anion  $[H(OTeF_5)_2]^-$  is also notable.<sup>(119)</sup>

Pseudohalides of Se in which the role of halogen is played by cyanide, thiocyanate or selenocyanate are known and, in the case of  $Se^{II}$  are much more stable with respect to disproportionation than are the halides themselves. Examples are  $Se(CN)_2$ ,  $Se_2(CN)_2$ ,  $Se(SeCN)_2$ ,  $Se(SCN)_2$ ,  $Se_2(SCN)_2$ . The selenocyanate ion  $SeCN^-$  is ambidentate like the thiocyanate ion, etc., p. 325), being capable of ligating to metal centres via either N or Se, as in the osmium(IV) complexes  $[OsCl_5(NCSe)]^{2-}$ ,  $[OsCl_5(SeCN)]^{2-}$ , and *trans*- $[OsCl_4(NCSe)(SeCN)]^{2-}$ .<sup>(120)</sup> Tellurium and polonium pseudohalogen analogues include  $Te(CN)_2$  and  $Po(CN)_4$  but have been much

<sup>114</sup> C. J. SCHACK and K. O. CHRISTE, *Inorg. Chem.* **23**, 2922 (1984).

<sup>115</sup> T. DREWS and K. SEPELT, *Z. anorg. allg. Chem.* **606**, 201–7 (1991).

<sup>116</sup> K. MOOCK and K. SEPELT, *Z. anorg. allg. Chem.* **561**, 132–8 (1988).

<sup>117</sup> S. H. STRAUSS, N. D. NOIROT and O. P. ANDERSON, *Inorg. Chem.* **24**, 4307–11 (1985).

<sup>118</sup> S. H. STRAUSS, N. D. NOIROT and O. P. ANDERSON, *Inorg. Chem.* **25**, 3851–3 (1986).

<sup>119</sup> S. H. STRAUSS, K. D. ABNEY and O. P. ANDERSON, *Inorg. Chem.* **25**, 2806–12 (1986).

<sup>120</sup> W. PREETZ and U. SELLERBERG, *Z. anorg. allg. Chem.* **589**, 158–66 (1988).

<sup>111</sup> H. OBERHAMMER and K. SEPELT, *Inorg. Chem.* **17**, 1435–9 (1978).

<sup>112</sup> D. LENTZ, H. PRITZKOW and K. SEPELT, *Inorg. Chem.* **17**, 1926–31 (1978).

<sup>113</sup> D. LENZ and K. SEPELT, *Angew. Chem. Int. Edn. Engl.* **17**, 355–6 and 356–61 (1978).

less studied than their Se counterparts. The long-sought tellurocyanate ion  $\text{TeCN}^-$  has finally been made, and isolated in crystalline form by the use of large counter-cations;<sup>(121)</sup> as expected, the anion is essentially linear (angle  $\text{Te}-\text{C}-\text{N}$   $175^\circ$ ), and the distances  $\text{Te}-\text{C}$  and  $\text{C}-\text{N}$  are 202 and 107 pm respectively.

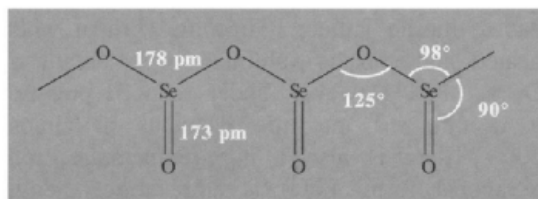
The selenohalides and tellurohalides of both main-group elements and transition metals have been compared with the corresponding thiohalides in two extensive reviews.<sup>(122)</sup> Other inorganic compounds of Se and Te, with bonds to N, P etc are described on pp. 783–6.

### 16.2.5 Oxides

The monoxides  $\text{SeO}$  and  $\text{TeO}$  have transient existence in flames but can not be isolated as stable solids.  $\text{PoO}$  has been obtained as a black, easily oxidized solid by the spontaneous radiolytic decomposition of the sulfoxide  $\text{PoSO}_3$ .

The dioxides of all 3 elements are well established and can be obtained by direct

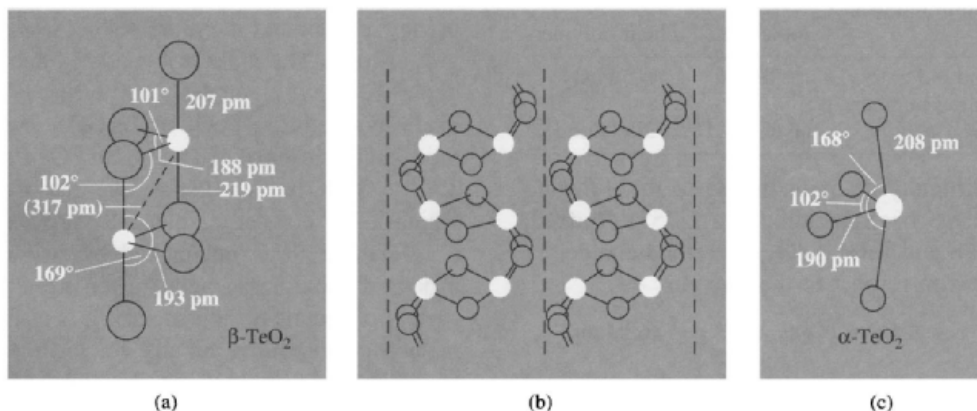
combination of the elements.  $\text{SeO}_2$  is a white solid which melts in a sealed tube to a yellow liquid at  $340^\circ$  (sublimes at  $315^\circ/760$  mmHg). It is very soluble in water to give selenous acid  $\text{H}_2\text{SeO}_3$  from which it can be recovered by dehydration. It is also very soluble (as a trimer) in  $\text{SeOCl}_2$  and in  $\text{H}_2\text{SO}_4$  in which it behaves as a weak base.  $\text{SeO}_2$  is thermodynamically less stable than either  $\text{SO}_2$  or  $\text{TeO}_2$  and is readily reduced to the elements by  $\text{NH}_3$ ,  $\text{N}_2\text{H}_4$  or aqueous  $\text{SO}_2$  (but not gaseous  $\text{SO}_2$ ). It also finds use as an oxidizing agent in organic chemistry. In the solid state  $\text{SeO}_2$  has a polymeric structure of corner-linked flattened  $\{\text{SeO}_3\}$  pyramids each carrying a pendant terminal O atom:



$\text{TeO}_2$  is dimorphic: the yellow, orthorhombic mineral tellurite ( $\beta\text{-TeO}_2$ ) has a layer structure in which pseudo-trigonal bipyramidal  $\{\text{TeO}_4\}$  groups form edge-sharing pairs (Fig. 16.16a) which then further aggregate into layers (Fig. 16.16b) by sharing the remaining vertices. By contrast, synthetic  $\alpha\text{-TeO}_2$  (“paratellurite”)

<sup>121</sup> A. S. FOUST, *J. Chem. Soc., Chem. Commun.*, 414–5 (1979).

<sup>122</sup> M. J. ATHERTON and J. H. HOLLOWAY, *Adv. Inorg. Chem. Radiochem.* **22**, 171–98 (1979). J. FENNER, A. RABENAU and G. TRAGESER, *Adv. Inorg. Chem. Radiochem.* **23**, 329–425 (1980).



**Figure 16.16** Structural units in crystalline  $\text{TeO}_2$ : (a) pair of edge-sharing pseudo-trigonal bipyramidal  $\{\text{TeO}_4\}$  groups in tellurite ( $\beta\text{-TeO}_2$ ) which aggregate into layers as shown in (b) by sharing the remaining vertices with neighbouring pairs, and (c) the  $\{\text{TeO}_4\}$  unit in paratellurite ( $\alpha\text{-TeO}_2$ ).

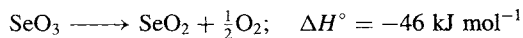
forms colourless tetragonal crystals in which very similar  $\{\text{TeO}_4\}$  units (Fig. 16.16c) share all vertices (angle  $\text{Te}-\text{O}-\text{Te}$   $140^\circ$ ) to form a rutile-like (p. 961) three-dimensional structure.  $\text{TeO}_2$  melts to a red liquid at  $733^\circ$  and is much less volatile than  $\text{SeO}_2$ . It can be prepared by the action of  $\text{O}_2$  on  $\text{Te}$ , by dehydrating  $\text{H}_2\text{TeO}_3$  or by thermal decomposition of the basic nitrate above  $400^\circ$ .  $\text{TeO}_2$  is not very soluble in water; it is amphoteric and shows a minimum in solubility (at  $\text{pH} \sim 4.0$ ). It is, however, very soluble in  $\text{SeOCl}_2$ .

$\text{PoO}_2$  is obtained by direct combination of the elements at  $250^\circ$  or by thermal decomposition of polonium(IV) hydroxide, nitrate, sulfate or selenate. The yellow (low-temperature) fcc form has a fluorite lattice; it becomes brown when heated and can be sublimed in a stream of  $\text{O}_2$  at  $885^\circ$ . However, under reduced pressure it decomposes into the elements at almost  $500^\circ$ . There is also a high-temperature, red, tetragonal form.  $\text{PoO}_2$  is amphoteric, though appreciably more basic than  $\text{TeO}_2$ : e.g. it forms the disulfate  $\text{Po}(\text{SO}_4)_2$  for which no  $\text{Te}$  analogue is known.

It is instructive to note the progressive trend to higher coordination numbers in the Group 16 dioxides, and the consequent influence on structure:

Compound	$\text{SO}_2$	$\text{SeO}_2$
Coordination number	2	3
Structure	molecule	chain polymers
Compound	$\text{TeO}_2$	$\text{PoO}_2$
Coordination number	4	8
Structure	layer or 3D	3D "fluorite"

The difficulty of oxidizing  $\text{Se}$  to the +6 state has already been mentioned (p. 755). Indeed, unlike  $\text{SO}_3$  and  $\text{TeO}_3$ ,  $\text{SeO}_3$  is thermodynamically unstable with respect to the dioxide:

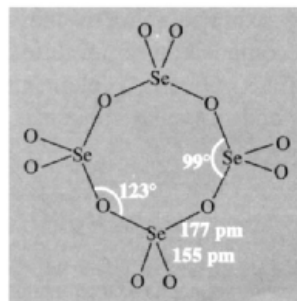


Some comparative figures for the standard heats of formation  $-\Delta H_f^\circ$  are in Table 16.8. Accordingly,  $\text{SeO}_3$  can not be made by direct oxidation of  $\text{Se}$  or  $\text{SeO}_2$  and is even hard to make by the dehydration of  $\text{H}_2\text{SeO}_4$  with  $\text{P}_2\text{O}_5$ ; a better

**Table 16.8**  $-\Delta H_f^\circ$  (298)/ $\text{kJ mol}^{-1}$  for  $\text{MO}_n$  from elements in standard states

$\text{SO}_2$	297	$\text{SeO}_2$	230	$\text{TeO}_2$	325
$\text{SO}_3$	432	$\text{SeO}_3$	184	$\text{TeO}_3$	348

route is to treat anhydrous  $\text{K}_2\text{SeO}_4$  with  $\text{SO}_3$  under reflux, followed by vacuum sublimation at  $120^\circ$ .  $\text{SeO}_3$  is a white, hygroscopic solid which melts at  $118^\circ$ , sublimes readily above  $100^\circ$  (40 mmHg) and decomposes above  $165^\circ$ . The crystal structure is built up from cyclic tetramers,  $\text{Se}_4\text{O}_{12}$ , which have a configuration very similar to that of  $(\text{PNCl}_2)_4$  (p. 538). In the vapour phase, however, there is some dissociation into the monomer. In the molten state  $\text{SeO}_3$  is probably polymeric like the isoelectronic polymetaphosphate ions (p. 528).



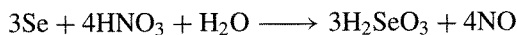
$\text{TeO}_3$  exists in two modifications. The yellow-orange  $\alpha$ -form and the more stable, less reactive, grey  $\beta$ -form. The  $\alpha$ - $\text{TeO}_3$  is made by dehydrating  $\text{Te}(\text{OH})_6$  (p. 782) at  $300$ – $360^\circ$ ; the  $\beta$ - $\text{TeO}_3$  is made by heating  $\alpha$ - $\text{TeO}_3$  or  $\text{Te}(\text{OH})_6$  in a sealed tube in the presence of  $\text{H}_2\text{SO}_4$  and  $\text{O}_2$  for 12 h at  $350^\circ$ .  $\alpha$ - $\text{TeO}_3$  has a structure like that of  $\text{FeF}_3$ , in which  $\text{TeO}_6$  octahedra share all vertices to give a 3D lattice. It is unattacked by water, but is a powerful oxidizing agent when heated with a variety of metals or non-metals. It is also soluble in hot concentrated alkalis to form tellurates (p. 782). The  $\beta$ -form is even less reactive but can be cleaved with fused  $\text{KOH}$ .

$\text{PoO}_3$  may have been detected on a tracer scale but has not been characterized with weighable amounts of the element.

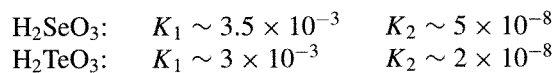
### 16.2.6 Hydroxides and oxoacids

The rich oxoacid chemistry of sulfur (pp. 705–21) is not paralleled by the heavier elements of the group. The redox relationships have already been summarized (p. 755). Apart from the dark-brown hydrated monoxide “Po(OH)<sub>2</sub>”, which precipitates when alkali is added to a freshly prepared solution of Po(II), only compounds in the +4 and +6 oxidation states are known.

Selenous acid, O=Se(OH)<sub>2</sub>, i.e. H<sub>2</sub>SeO<sub>3</sub>, and tellurous acid, H<sub>2</sub>TeO<sub>3</sub>, are white solids which can readily be dehydrated to the dioxide (e.g. in a stream of dry air). H<sub>2</sub>SeO<sub>3</sub> is best prepared by slow crystallization of an aqueous solution of SeO<sub>2</sub> or by oxidation of powdered Se with dilute nitric acid:



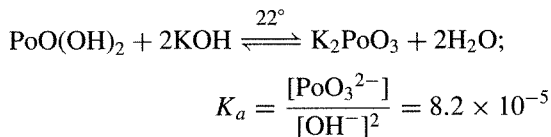
The less-stable H<sub>2</sub>TeO<sub>3</sub> is obtained by hydrolysis of a tetrahalide or acidification of a cooled aqueous solution of a telluride. Crystalline H<sub>2</sub>SeO<sub>3</sub> is built up of pyramidal SeO<sub>3</sub> groups (Se–O 174 pm) which are hydrogen-bonded to give an orthorhombic layer lattice. The detailed structure of H<sub>2</sub>TeO<sub>3</sub> is unknown. Both acids form acid salts MHSeO<sub>3</sub> and MHTeO<sub>3</sub> by reaction of the appropriate aqueous alkali. The neutral salts M<sub>2</sub>SeO<sub>3</sub> and M<sub>2</sub>TeO<sub>3</sub> can be obtained similarly or by heating the metal oxide with the appropriate dioxide. Dissociation constants have not been precisely determined but approximate values are:



Alkali diselenites M<sub>2</sub>Se<sub>2</sub>O<sub>5</sub> are also known and appear (on the basis of vibrational spectroscopy) to contain the ion [O<sub>2</sub>Se–O–SeO<sub>2</sub>]<sup>2-</sup>, with C<sub>2v</sub> symmetry and a nonlinear Se–O–Se bridge (cf. disulfite O<sub>3</sub>S–SO<sub>2</sub><sup>2-</sup>, p. 720). Selenous acid, in contrast to H<sub>2</sub>TeO<sub>3</sub>, can readily be oxidized to H<sub>2</sub>SeO<sub>4</sub> by ozone in strongly acid solution; it is reduced to elementary selenium by H<sub>2</sub>S, SO<sub>2</sub> or aqueous iodide solution.

Hydrated polonium dioxide, PoO(OH)<sub>2</sub>, is obtained as a pale-yellow flocculent precipitate by addition of dilute aqueous alkali to a solution

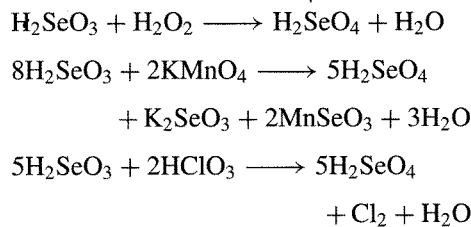
containing Po(IV). It is appreciably acidic, e.g.:



In the +6 oxidation state the oxoacids of Se and Te show little resemblance to each other. H<sub>2</sub>SeO<sub>4</sub> resembles H<sub>2</sub>SO<sub>4</sub> (p. 710) whereas orthotelluric acid Te(OH)<sub>6</sub> and polymetatelluric acid (H<sub>2</sub>TeO<sub>4</sub>)<sub>n</sub> are quite different.

Anhydrous H<sub>2</sub>SeO<sub>4</sub> is a viscous liquid which crystallizes to a white deliquescent solid (mp 62°). It loses water on being heated and combines readily with SeO<sub>3</sub> to give “pyroselenic acid”, H<sub>2</sub>Se<sub>2</sub>O<sub>7</sub> (mp 19°), and triselenic acid, H<sub>4</sub>Se<sub>3</sub>O<sub>11</sub> (mp 25°). It also resembles H<sub>2</sub>SO<sub>4</sub> in forming several hydrates: H<sub>2</sub>SeO<sub>4</sub>·H<sub>2</sub>O (mp 26°) and H<sub>2</sub>SeO<sub>4</sub>·4H<sub>2</sub>O (52°). Crystalline H<sub>2</sub>SeO<sub>4</sub> (*d* 2.961 g cm<sup>-3</sup>) comprises tetrahedral SeO<sub>4</sub> groups strongly H-bonded into layers through all 4 O atoms (Se–O 161 pm, O–H···O 261–268 pm). H<sub>2</sub>SeO<sub>4</sub> can be prepared by several routes:

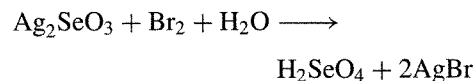
- (i) Oxidation of H<sub>2</sub>SeO<sub>3</sub> with H<sub>2</sub>O<sub>2</sub>, KMnO<sub>4</sub> or HClO<sub>3</sub>, which can be formally represented by the equations:



- (ii) Oxidation of Se with chlorine or bromine water, e.g.:

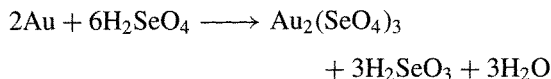


- (iii) Action of bromine water on a suspension of silver selenite:



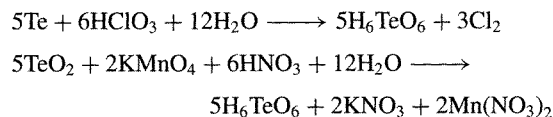
The acid dissociation constants of H<sub>2</sub>SeO<sub>4</sub> are close to those of H<sub>2</sub>SO<sub>4</sub>, e.g. K<sub>2</sub> (H<sub>2</sub>SeO<sub>4</sub>)

$1.2 \times 10^{-2}$ . Selenates resemble sulfates and both acids form a series of alums (p. 76). Selenic acid differs from  $\text{H}_2\text{SO}_4$ , however, in being a strong oxidizing agent: this is perhaps most dramatically shown by its ability to dissolve not only Ag (as does  $\text{H}_2\text{SO}_4$ ) but also Au, Pd (and even Pt in the presence of  $\text{Cl}^-$ ):

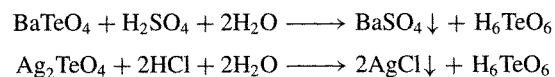


It oxidizes halide ions (except  $\text{F}^-$ ) to free halogen. Solutions of S, Se, Te and Po in  $\text{H}_2\text{SeO}_4$  are brightly coloured (cf. p. 664).

By contrast, the two main forms of telluric acid do not resemble  $\text{H}_2\text{SO}_4$  and  $\text{H}_2\text{SeO}_4$  and tellurates are not isomorphous with sulfates and selenates. Orthotelluric acid is a white solid, mp  $136^\circ$ , whose crystal structure is built up of regular octahedral molecules,  $\text{Te}(\text{OH})_6$ . This structure, which persists in solution (Raman spectrum), is also reflected in its chemistry; e.g. breaks occur in the neutralization curve at points corresponding to  $\text{NaH}_5\text{TeO}_6$ ,  $\text{Na}_2\text{H}_4\text{TeO}_6$ ,  $\text{Na}_4\text{H}_2\text{TeO}_6$  and  $\text{Na}_6\text{TeO}_6$ . Similar salts include  $\text{Ag}_6\text{TeO}_6$  and  $\text{Hg}_3\text{TeO}_6$ . Moreover diazomethane converts it to the hexamethyl ester  $\text{Te}(\text{OMe})_6$ . In this respect Te resembles its horizontal neighbours in the periodic table Sn, Sb and I which form the isoelectronic species  $[\text{Sn}(\text{OH})_6]^{2-}$ ,  $[\text{Sb}(\text{OH})_6]^-$  and  $\text{IO}(\text{OH})_5$ . Orthotelluric acid can be prepared by oxidation of powdered Te with chloric acid solution or oxidation of  $\text{TeO}_2$  with permanganate in nitric acid:

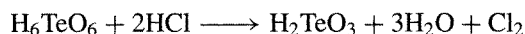
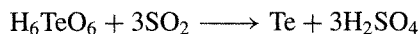


Alternatively, Te or  $\text{TeO}_2$  can be oxidized by  $\text{CrO}_3/\text{HNO}_3$  or by 30%  $\text{H}_2\text{O}_2$  under reflux. Acidification of a tellurate with an appropriate precipitating acid offers a further convenient route:



Crystallization from aqueous solutions below  $10^\circ$  gives the tetrahydrate  $\text{H}_6\text{TeO}_6 \cdot 4\text{H}_2\text{O}$ . The

anhydrous acid is stable in air at  $100^\circ$  but above  $120^\circ$  gradually loses water to give polymetateuric acid and allotelluric acid (see below). Unlike  $\text{H}_2\text{SO}_4$  and  $\text{H}_2\text{SeO}_4$ ,  $\text{H}_6\text{TeO}_6$  is a weak acid, approximate values of its successive dissociation constants being  $K_1 \sim 2 \times 10^{-8}$ ,  $K_2 \sim 10^{-11}$ ,  $K_3 \sim 3 \times 10^{-15}$ . It is a fairly strong oxidant, being reduced to the element by  $\text{SO}_2$  and to  $\text{H}_2\text{TeO}_3$  in hot HCl:



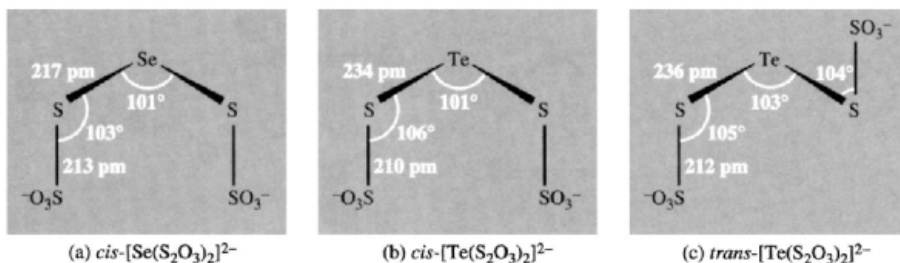
Polymetateuric acid  $(\text{H}_2\text{TeO}_4)_{\sim 10}$  is a white, amorphous hygroscopic powder formed by incomplete dehydration of  $\text{H}_6\text{TeO}_6$  in air at  $160^\circ$ . Alternatively, in aqueous solution the equilibrium  $n\text{H}_6\text{TeO}_6 \rightleftharpoons (\text{H}_2\text{TeO}_4)_n + 2n\text{H}_2\text{O}$  can be shifted to the right by increasing the temperature; rapid cooling then precipitates the sparingly soluble polymetateuric acid. The structure is unknown but appears to contain 6-coordinate Te. Allotelluric acid " $(\text{H}_2\text{TeO}_4)_3(\text{H}_2\text{O})_4$ " is an acid syrup obtained by heating  $\text{Te}(\text{OH})_6$  in a sealed tube at  $305^\circ$ : the compound has not been obtained pure but tends to revert to  $\text{H}_6\text{TeO}_6$  at room temperature or to  $(\text{H}_2\text{TeO}_4)_n$  when heated in air; indeed, it may well be a mixture of these two substances.

Tellurates are prepared by fusing a tellurite with a corresponding nitrate, by oxidizing a tellurite with chlorine, by or neutralizing telluric acid with a hydroxide.<sup>(123)</sup> An interesting variant is to heat intimate mixtures of  $\text{TeO}_3$  with metal oxides. For example, with  $\text{Rb}_2\text{O}$  at  $680^\circ$  for several weeks, colourless crystals having the unusual stoichiometry  $\text{Rb}_6\text{Te}_2^{\text{VI}}\text{O}_9$  were formed which contained both tetrahedral  $\text{TeO}_4^{2-}$  and trigonal bipyramidal  $\text{TeO}_5^{4-}$  groups, i.e.  $\text{Rb}_6[\text{TeO}_5][\text{TeO}_4]$ .<sup>(124)</sup>

Numerous peroxyacid or thioacid derivatives of Se and Te have been reported<sup>(1)</sup> but these add little to the discussion of the reaction chemistry or the structure types already

<sup>123</sup> Ref. 11, pp. 94–7.

<sup>124</sup> T. WISSER and R. HOPPE, *Z. anorg. allg. Chem.* **584**, 105–13 (1990).



**Figure 16.17** Structures and conformations of unbranched chain anions in (a)  $\text{Ba}[\text{Se}(\text{S}_2\text{O}_3)_2] \cdot 2\text{H}_2\text{O}$ , (b)  $\text{Ba}[\text{Te}(\text{S}_2\text{O}_3)_2] \cdot 2\text{H}_2\text{O}$ , and (c)  $(\text{NH}_4)_2[\text{Te}(\text{S}_2\text{O}_3)_2]$ .

described. Examples are peroxoselenous acid  $\text{HOSeO}(\text{OOH})$  (stable at  $-10^\circ$ ) and potassium peroxy-orthotellurate  $\text{K}_2\text{H}_4\text{TeO}_7$  which also loses oxygen at room temperature. Isomeric selenosulfates,  $\text{M}_2^1\text{SO}_3\text{Se}$ , and thioselenates,  $\text{M}_2^1\text{SeO}_3\text{S}$ , are known and can be made by the obvious routes of  $[\text{SO}_3^{2-}(\text{aq}) + \text{Se}]$  and  $[\text{SeO}_3^{2-}(\text{aq}) + \text{S}]$ . Likewise, colourless or yellow-green crystalline selenopolythionates  $\text{M}_2\text{Se}_x\text{S}_y\text{O}_6$  ( $x = 1, 2; y = 2, 4$ ) and orange-yellow telluropentathionates  $\text{M}_2^1\text{TeS}_4\text{O}_6$  are known. X-ray structure analysis reveals unbranched chains with various conformations as found for the polythionates themselves (p. 718).<sup>(125)</sup> Typical examples are in Fig. 16.17. It will be seen that these compounds contain Se and Te bonded to S rather than O and they therefore form a natural link with the Group 16 sulfides to be described in the next section.

### 16.2.7 Other inorganic compounds

The red compound  $\text{Se}_4\text{S}_4$ , obtained by fusing equimolar amounts of the elements, is a covalent molecular species which can be crystallized from benzene. Similar procedures yield  $\text{Se}_2\text{S}_6$ ,  $\text{SeS}_7$  and  $\text{TeS}_7$ , all of which are structurally related to  $\text{S}_8$  (p. 654; see also p. 763).

PoS forms as a black precipitate when  $\text{H}_2\text{S}$  is added to acidic solutions of polonium compounds. Its solubility product is  $\sim 5 \times 10^{-29}$ . The

action of aqueous ammonium sulfide on polonium(IV) hydroxide gives the same compound. It decomposes to the elements when heated to  $275^\circ$  under reduced pressure and is of unknown structure.

The chemistry of compounds containing Se–N and Te–N bonds has been very actively developed during the past decade and many new and unusual species are emerging.<sup>(126,127)</sup>  $\text{Se}_4\text{N}_4$  is an orange, shock sensitive crystalline compound which decomposes violently at  $160^\circ$ . It resembles its sulfur analogue (p. 722) in being thermochroic (yellow-orange at  $-195^\circ$ , red at  $+100^\circ$ ) and in having the same  $D_{2d}$  molecular structure.  $\text{Se}_4\text{N}_4$  can be made by reacting anhydrous  $\text{NH}_3$  with  $\text{SeBr}_4$  (or with  $\text{SeO}_2$  at  $70^\circ$  under pressure). A new red-brown crystalline modification,  $\beta\text{-Se}_4\text{N}_4$ , which has a very similar cluster structure but differs in the packing arrangement, has recently been prepared by reacting  $\text{SeO}_2$  with the phosphane imine,  $\text{Me}_3\text{SiNPMe}_3$ .<sup>(128)</sup> Tellurium nitride can be prepared similarly ( $\text{TeBr}_4 + \text{NH}_3$ ); it is a lemon-yellow, violently explosive compound with a formula that might be  $\text{Te}_3\text{N}_4$  rather than  $\text{Te}_4\text{N}_4$ ; its structure is unknown.

$\text{Se}_4\text{N}_4$  reacts with  $[\text{PtCl}_2(\text{PMe}_2\text{Ph})_2]$  in liquid ammonia (50 atm.) to give a quantitative yield of  $[\text{Pt}(\eta^2\text{-Se}_2\text{N}_2)(\text{PMe}_2\text{Ph})_2]$  which features a

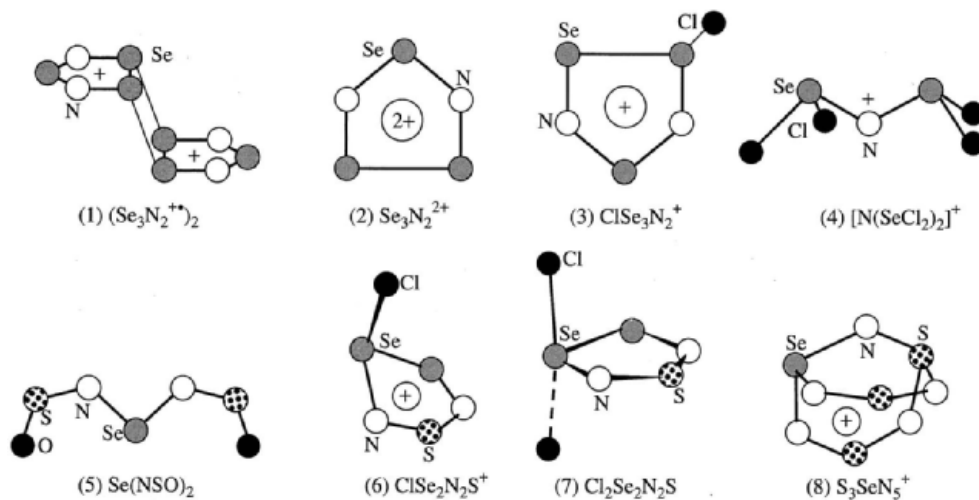
<sup>126</sup> M. BJÖRGVINSSON and H. W. ROESKY, *Polyhedron* **10**, 2353–70 (1991).

<sup>127</sup> P. F. KELLY, A. M. Z. SLAWIN, D. J. WILLIAMS and J. D. WOOLLINS, *Chem. Soc. Rev.* **21**, 245–52 (1992). T. M. KLAPÖTKE, in R. STEUDEL (ed.), *The Chemistry of Inorganic Ring Systems*, Elsevier, Amsterdam, 1992, pp. 409–27.

<sup>128</sup> H. FOLKERTS, B. NEUMÜLLER and K. DEHNICKE, *Z. anorg. allg. Chem.* **620**, 1011–15 (1994).

<sup>125</sup> A. F. WELLS, *Structural Inorganic Chemistry*, 5th edn., pp. 726–35, Oxford University Press, Oxford, 1984. See also *J. Chem. Soc., Dalton Trans.*, 1528–32 (1978) ( $\text{Pb}_2\text{Te}_3\text{O}_8$ ). *Inorg. Chem.* **19**, 1040–3, 1044–8, 1063–4 (1980) ( $\text{SeS}_3\text{O}_6^{2-}$ ,  $\text{Se}_2\text{S}_2\text{O}_6^{2-}$ ,  $\text{SeS}_2\text{O}_6^{2-}$ ).





5-membered  $\text{Pt}-\text{SeNSeN}$  heterocycle at the planar Pt centre.<sup>(129)</sup> A similar reaction with  $[\text{Pt}(\text{PPh}_3)_3]$  in  $\text{CH}_2\text{Cl}_2$  gives the analogous  $\text{PPh}_3$  complex plus the related dark-green dimer,  $[(\text{Ph}_3\text{P})\text{Pt}(\mu, \eta^2-\text{Se}_2\text{N}_2)_2\text{Pt}(\text{PPh}_3)]$ , in which the chelating ligand also bridges the two Pt atoms via the ipso-N atoms so as to form a central planar  $\text{Pt}_2\text{N}_2$  core which is also coplanar with the two planar 5-membered heterocycles.<sup>(130)</sup> Innumerable other Se/N species have been synthesized and characterized by X-ray diffraction analysis, e.g. the  $7\pi$ -electron radical cation  $\text{Se}_3\text{N}_2^{\cdot+}$  (1),<sup>(131)</sup> the  $6\pi$ -electron dication  $\text{Se}_3\text{N}_2^{2+}$  (2),<sup>(131)</sup>  $\text{ClSe}_3\text{N}_2$  (3),<sup>(132)</sup>  $[\text{N}(\text{SeCl}_2)_2]^+$  (4),<sup>(133)</sup>  $\text{Se}(\text{NSO})_2$  (5),<sup>(134)</sup>  $\text{ClSe}_3\text{N}_2\text{S}^+$  (6),<sup>(134)</sup>  $\text{Cl}_2\text{Se}_2\text{N}_2\text{S}$  (7),<sup>(134)</sup>  $[\text{S}_3\text{SeN}_5]^+$  (8),<sup>(134)</sup> etc. The original papers should be consulted for preparative procedures.

Metal complexes with Se/N ligands are also appearing in increasing numbers in the literature. Thus, *cyclo*- $\text{Se}_4\text{N}_2$  forms the red-brown donor-acceptor complexes  $[\text{SnCl}_4(\eta^1-\text{N}_2\text{Se}_4)_2]$  (9) and  $[\text{TiCl}_4(\eta^2-\text{N}_2\text{Se}_4)]$ ,<sup>(135)</sup> whereas reaction of  $[\text{Se}_2\text{SN}_2]_2\text{Cl}_2$  with *cis*- $[\text{PtCl}_2(\text{PMe}_2\text{Ph})_2]$  in liquid ammonia gives  $[\text{Pt}(\eta^2-\text{SeSN}_2)(\text{PMe}_2\text{Ph})_2]$  which in turn can be protonated with  $\text{HBF}_4$  to give  $[\text{Pt}(\eta^2-\text{SeSN}_2\text{H})(\text{PMe}_2\text{Ph})_2]^+$  (10).<sup>(136)</sup> The di-Se analogues with  $\eta^2-\text{Se}_2\text{N}_2^{2-}$  and  $\eta^2-\text{Se}_2\text{N}_2\text{H}^-$  have also been characterized.<sup>(137)</sup>

Heterocycles involving  $\text{P}^{\text{V}}$  include  $[1,5-(\text{Ph}_2\text{P})_2\text{N}_4(\text{SeMe})_2]$  (11), which has an 8-membered chair configuration with the two Se atoms displaced on either side of the  $\text{P}_2\text{N}_4$  plane, and the related  $[1,5-(\text{Ph}_2\text{P})_2\text{N}_4\text{Se}_2]$  (12).<sup>(138)</sup> The reaction of (12) with  $[\text{PtCl}_2(\text{PEt}_3)_2]$  gives the  $\eta^1$ -complexes (13), (14) which, in turn, can be oxidatively added to  $[\text{Pt}(\eta^2-\text{C}_2\text{H}_4)(\text{PPh}_3)_2]$  to give the  $\eta^2$ -Se,Se' complexes (15) and (16),<sup>(139)</sup>

<sup>129</sup> P. F. KELLY, J. D. WOOLLINS, *Polyhedron* **12**, 1129–33 (1993).

<sup>130</sup> P. F. KELLY, A. M. Z. SLAWIN, D. J. WILLIAMS and J. D. WOOLLINS, *Polyhedron* **9**, 1567–71 (1990).

<sup>131</sup> E. G. AWERE, J. PASSMORE, P. S. WHITE and T. M. KLAPÖTKE, *J. Chem. Soc., Chem. Commun.*, 1415–7 (1989).

<sup>132</sup> R. WOLLERT, B. NEUMÜLLER and K. DEHNICKE, *Z. anorg. allg. Chem.* **616**, 191–4 (1992).

<sup>133</sup> M. BRÖSCHAG, T. M. KLAPÖTKE, I. C. TORNIERTH-OETTING and P. S. WHITE, *J. Chem. Soc., Chem. Commun.*, 1390–1 (1992).

<sup>134</sup> A. HAAS, J. KASPROWSKI, K. ANGERMUND, P. BETZ, C. KRÜGER, Yi-H. TSAY and S. WERNER, *Chem. Ber.* **124**, 1895–906 (1991).

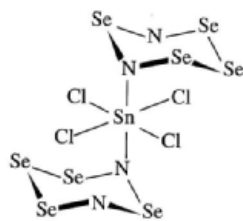
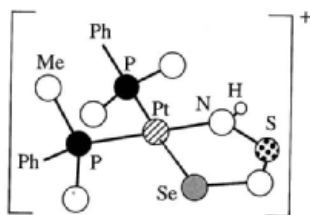
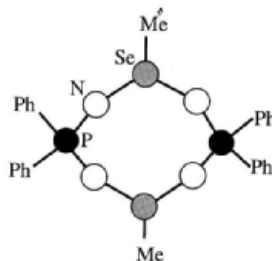
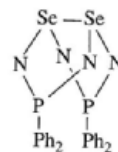
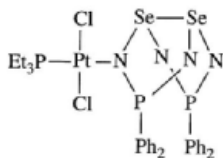
<sup>135</sup> S. VOGLER, M. SCHÄFER and K. DEHNICKE, *Z. anorg. allg. Chem.* **606**, 73–8 (1991).

<sup>136</sup> C. A. O'MAHONEY, I. P. PARKIN, D. J. WILLIAMS and J. D. WOOLLINS, *Polyhedron* **8**, 2215–7 (1989).

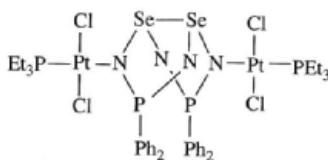
<sup>137</sup> P. F. KELLY, I. P. PARKIN, A. M. Z. SLAWIN, D. J. WILLIAMS and J. D. WOOLLINS, *Angew. Chem., Int. Edn. Engl.* **28**, 1047–9 (1989).

<sup>138</sup> T. CHIVERS, D. D. DOXSEE and J. F. FAIT, *J. Chem. Soc., Chem. Commun.*, 1703–5 (1989).

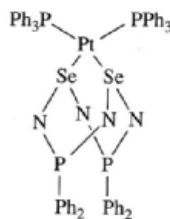
<sup>139</sup> T. CHIVERS, D. D. DOXSEE, R. W. HILTS, A. MEETSMA, M. PARVEZ and J. C. VAN DE GRAMPPEL, *J. Chem. Soc., Chem. Commun.*, 1330–2 (1992).

(9)  $[\text{SnCl}_4(\text{N}_2\text{Se}_4)_2]$ (10)  $[\text{Pt}(\text{SeSN}_2\text{H})(\text{PMe}_2\text{Ph})_2]^+$ (11)  $[(\text{PMe}_2\text{Ph})_2\text{Ni}_4(\text{SeMe})_2]$ (12)  $[(\text{Ph}_2\text{P})_2\text{N}_4\text{Se}_2]$ 

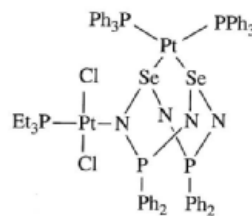
(13)



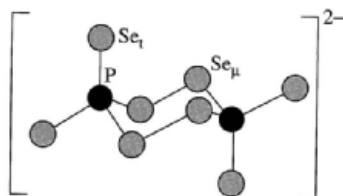
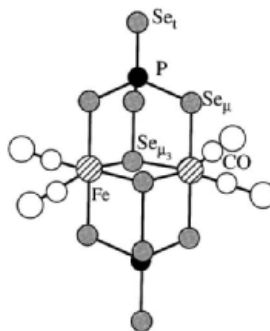
(14)



(15)



(16)

(17)  $\text{P}_2\text{Se}_8^{2-}$ (18)  $[\text{Fe}_2(\text{CO})_4(\text{PSe}_5)_2]$ 

Reaction of  $\text{P}_4\text{Se}_4$  with soluble polyselenides afforded the first isolated P/Se anion, the yellow  $\text{P}_2\text{Se}_8^{2-}$  (17) which further reacts with  $\text{Fe}(\text{CO})_5$  to generate the novel brown cluster anion  $[\text{Fe}_2(\text{CO})_4(\text{PSe}_5)_2]$  (18).<sup>(140)</sup> Numerous other examples are known; indeed, the whole field is still rapidly developing and many new types of compound are being synthesized and characterized each year.

Tellurium-chalcogen-nitrogen chemistry is also burgeoning. Typical examples include the red crystalline  $\text{Te}(\text{NSO})_2$ ,<sup>(141)</sup> isomorphous with

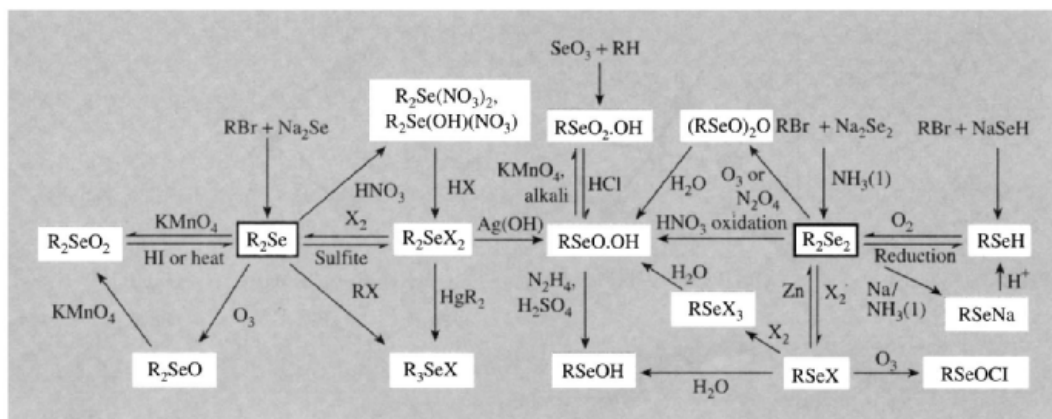
$\text{Se}(\text{NSO})_2$  (5), and the cationic heterocycle  $[\text{FTeNSNSeNSN}]^+[\text{TeF}_5]^-$ , which is formed, together with  $[\{\text{SeNSNSe}^*\}_2]^{2+}[\text{TeF}_5]^{2-}$ , when  $\text{Se}(\text{NSO})_2$  reacts with  $\text{TeF}_4$  in  $\text{CH}_2\text{Cl}_2$ .<sup>(142)</sup> The first stable tellurophosphorane complexes  $[\text{M}(\text{CO})_5(\text{Te}=\text{PBu}_3^t)]$  ( $\text{M} = \text{Cr}, \text{Mo}, \text{W}$ ) were prepared as dark-red crystals by photolysis of the hexacarbonyls in the presence of  $\text{Bu}_3^t\text{P}=\text{Te}$ , and the expected bent coordination at Te was confirmed by X-ray analysis (angle  $\text{W}-\text{Te}-\text{P}$   $120.1^\circ$ ).<sup>(143)</sup> By Contrast, reaction of  $\text{Et}_3\text{P}=\text{Te}$  with  $[\text{Mn}(\text{CH}_2\text{Ph})(\text{CO})_5]$  in refluxing toluene results in the insertion of Te into

<sup>140</sup> J. ZHAO, W. T. PENNINGTON and J. W. KOLIS, *J. Chem. Soc., Chem. Commun.*, 265–6 (1992).

<sup>141</sup> A. HAAS and R. POHL, *Chimia* **43**, 261–2 (1989). See also R. BOESE, F. DWORAK, A. HAAS and M. PRYKA, *Chem. Ber.* **128**, 477–80 (1995).

<sup>142</sup> A. HAAS and M. PRYKA, *Chem. Ber.* **128**, 11–22 (1995).

<sup>143</sup> N. KUHN, H. SCHUMANN and G. WOLMERSHÄUSER, *J. Chem. Soc., Chem. Commun.*, 1595–7 (1985).



Reaction scheme for the formation of organo-selenium compounds (X = halogen).

the Mn-CH<sub>2</sub> bond and the displacement of two CO ligands to yield the red crystalline solid [Mn(CO)<sub>3</sub>(PEt<sub>3</sub>)<sub>2</sub>(TeCH<sub>2</sub>Ph)], in which the three carbonyls are *mer* and the two tertiary phosphine ligands are *trans* to each other.<sup>(144)</sup>

The increasing basicity of the heavier members of Group 16 is reflected in the increasing incidence of oxoacid salts. Thus polonium forms Po(NO<sub>3</sub>)<sub>4</sub>·xN<sub>2</sub>O<sub>4</sub>, Po(SO<sub>4</sub>)<sub>2</sub>·xH<sub>2</sub>O, and a basic sulfate and selenate 2PoO<sub>2</sub>·SO<sub>3</sub> and 2PoO<sub>2</sub>·SeO<sub>3</sub>, all of which are white, and a hydrated yellow chromate Po(CrO<sub>4</sub>)<sub>2</sub>·xH<sub>2</sub>O. There is also fragmentary information on the precipitation of an insoluble polonium(IV) carbonate, iodate, phosphate and vanadate.<sup>(4)</sup> Tellurium(IV) forms a white basic nitrate 2TeO<sub>2</sub>·HNO<sub>3</sub> and a basic sulfate and selenate 2TeO<sub>2</sub>·XO<sub>3</sub>, and there are indications of a white, hygroscopic basic sulfate of selenium(IV), SeO<sub>2</sub>·SO<sub>3</sub> or SeOSO<sub>4</sub>. Most of these compounds have been prepared by evaporation of aqueous solutions of the oxide or hydrated oxide in the appropriate acid. There is no doubt that more imaginative nonaqueous synthetic routes could be devised, but the likely products seem rather uninteresting and the field has attracted little recent attention.

### 16.2.8 Organo-compounds<sup>(145-149)</sup>

Organoselenium and organotellurium chemistry is a large and expanding field which parallels but is distinct from organosulfur chemistry. The biochemistry of organoselenium compounds has also been much studied (p. 759). Organopolonium chemistry is almost entirely restricted to trace-level experiments because of the charring and decomposition of the compounds by the intense  $\alpha$  activity of polonium (pp. 749ff.).

The principal classes of organoselenium compound are summarized in the scheme above which indicates the central synthetic role of

<sup>145</sup> K. J. IRGOLIC and M. V. KUDCHADKER, The organic chemistry of selenium, Chap. 8 in ref. 2, pp. 408-545. H. E. GANTHER, Biochemistry of selenium, Chap. 9 in ref. 2, pp. 546-614. W. C. COOPER and J. R. GLOVER, The toxicology of selenium and its compounds, Chap. 11 in ref. 2, pp. 654-74.

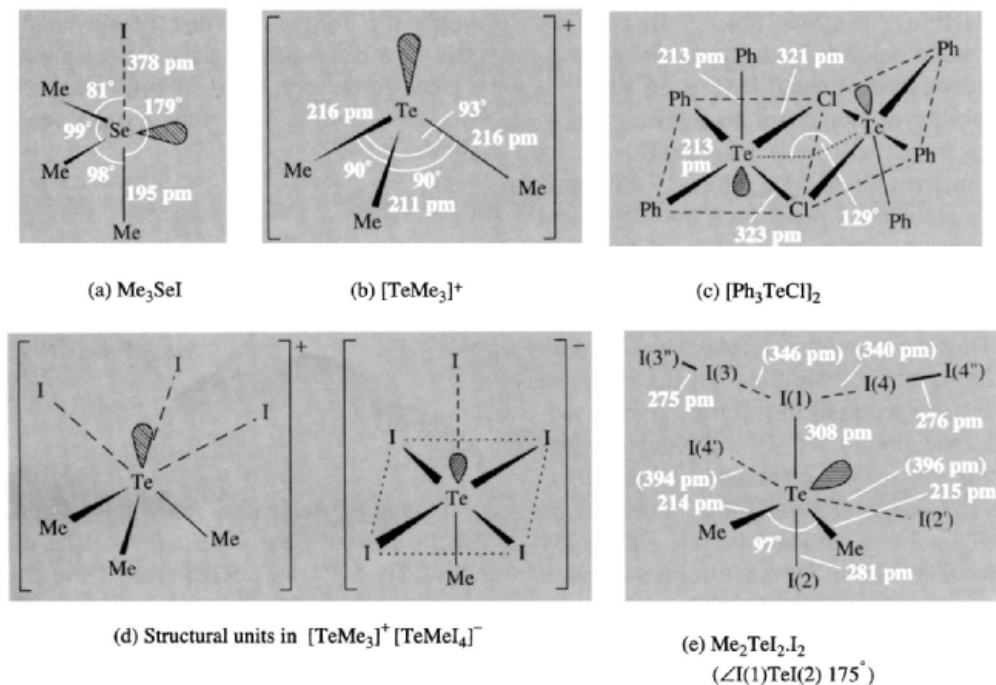
<sup>146</sup> R. A. ZINGARO and K. IRGOLIC, Organic compounds of tellurium, Chap 5 in ref. 3, pp. 184-280. W. C. COOPER, Toxicology of tellurium and its compounds, Chap. 7 in ref. 3, pp. 313-72.

<sup>147</sup> P. D. MAGNUS, Organic selenium and tellurium compounds, in D. BARTON and W. D. OLLIS (eds.), *Comprehensive Organic Chemistry*, Vol. 3, Chap. 12, pp. 491-538, Pergamon Press, Oxford, 1979.

<sup>148</sup> Specialist Periodical Reports of the Chemical Society (London), *Organic Compounds of Sulfur, Selenium and Tellurium*, Vols. 1-5 (1970-79).

<sup>149</sup> S. PATAI and Z. RAPPAPORT (eds.) *The Chemistry of Organic Selenium and Tellurium Compounds*, John Wiley (Interscience), Chichester, Vol. 1, 1986, 939 pp. Vol. 2 (S. PATAI, ed.), 1987, 864 pp.

<sup>144</sup> K. MCGREGOR, G. B. DEACON, R. S. DICKSON, G. D. FALLON, R. S. ROWE and B. O. WEST, *J. Chem. Soc., Chem. Commun.*, 1293-4 (1990).



**Figure 16.18** Some coordination environments of Se and Te in their organohalides.

the selenides  $\text{R}_2\text{Se}$  and diselenides  $\text{R}_2\text{Se}_2$ .<sup>(1)</sup> Detailed discussion of these and related tellurium compounds falls outside the scope of the present treatment. Other compounds such as the cyano derivatives (p. 778) and  $\text{CSe}_2$ ,  $\text{COSe}$ ,  $\text{COTe}$  and  $\text{CSTe}$  (p. 754) have already been briefly mentioned.

Tellurocarbonyl derivatives  $\text{R}^1\text{C}(=\text{Te})\text{OR}^2$  and telluroamides, e.g.  $\text{PhC}(=\text{Te})\text{NMe}_2$  (mp  $73^\circ$ ) have been prepared<sup>(150)</sup> and shown to be similar to, though more reactive than, the corresponding seleno derivatives.

Reaction of  $[\text{Se}_4]^{2+}[\text{AsF}_6]_2^-$  with  $\text{Ph}_2\text{Se}_2$  in liquid  $\text{SO}_2$  gives the bright orange compound  $[\text{Se}_6\text{Ph}_2]^{2+}[\text{AsF}_6]_2^- \cdot \text{SO}_2$  in which the  $\text{Se}_6$  ring adopts the boat conformation with pendent Ph groups in the 1- and 4-positions.<sup>(151)</sup> By contrast the reaction of  $\text{K}_2\text{CO}_3$  with red-Se in acetone in

the presence of  $[(\text{Ph}_3\text{P})_2\text{N}]\text{Cl}$  yields red crystals of  $[(\text{Ph}_3\text{P})_2\text{N}]^+[\text{Se}_5\text{C}(\text{Se})\text{C}(\text{O})\text{Me}]^-$ ; the anion, which adopts the chair conformation, is the first example of an  $\text{Se}_5\text{C}$  ring, and the C atom has exocyclic  $=\text{Se}$  and  $-\text{C}(\text{O})\text{Me}$  groups attached.<sup>(152)</sup>

Stoichiometry is frequently an inadequate guide to structure in organo-derivatives of Se and Te particularly when other elements (such as halogens) are also present. This arises from the incipient tendency of many of the compounds to undergo ionic dissociation or, conversely, to increase the coordination number of the central atom by dimerization or other oligomeric interactions. Thus  $\text{Me}_3\text{SeI}$  features pyramidal ions  $[\text{SeMe}_3]^+$  but these are each associated rather closely with 1 iodide which is colinear with 1  $\text{Me}-\text{Se}$  bond to give a distorted pseudotrigonal bipyramidal configuration (Fig. 16.18a).<sup>(125)</sup> A regular pyramidal cation can, however, be obtained by use of a large non-coordinating counteranion, as in

<sup>150</sup> K. A. LERSTRUP and L. HENRIKSEN, *J. Chem. Soc., Chem. Commun.*, 1102-3 (1979) and references therein.

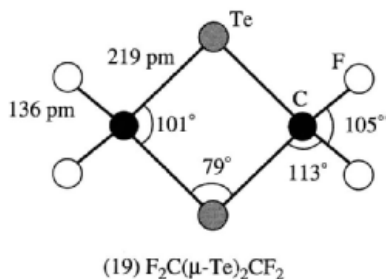
<sup>151</sup> R. FAGGIANI R. J. GILLESPIE and J. W. KOLIS *J. Chem. Soc., Chem. Commun.*, 592-3 (1987).

<sup>152</sup> T. CHIVERS, M. PARVEZ, M. PEACH and R. VOLLMERHAUS, *J. Chem. Soc., Chem. Commun.*, 1539-40 (1992).

[TeMe<sub>3</sub>]<sup>+</sup>[BPh<sub>4</sub>]<sup>-</sup> (Fig. 16.18b).<sup>(153)</sup> By contrast, Ph<sub>3</sub>TeCl is a chloride-bridged dimer with 5-coordinate square-pyramidal Te (Fig. 16.13c).<sup>(154)</sup> The possibility of isomerism also exists: e.g. 4-coordinate, monomeric molecular Me<sub>2</sub>TeI<sub>2</sub> and its ionic counterpart [TeMe<sub>3</sub>]<sup>+</sup>[TeMeI<sub>4</sub>]<sup>-</sup> in which interionic interactions make both the cation and the anion pseudo-6-coordinate (Fig. 16.18d).<sup>(125)</sup> Further complications obtrude when the halogen itself is capable of forming polyhalide units in the crystal. Thus reaction of molecular Me<sub>2</sub>TeI<sub>2</sub> with iodine readily affords Me<sub>2</sub>TeI<sub>4</sub> but the chemical behaviour and spectra of the product give no evidence for oxidation to Te(VI), and X-ray analysis indicates the formation of an adduct Me<sub>2</sub>TeI<sub>2</sub>·I<sub>2</sub> in which the axially disposed iodine atoms of the pseudo-trigonal-bipyramidal Me<sub>2</sub>TeI<sub>2</sub> are weakly bonded to molecules of iodine to form a network as shown in Fig. 16.18e<sup>(155)</sup> (cf. TlI<sub>3</sub>, p. 239).

Among the range of homoleptic organotellurium compounds that have recently been synthesized are the perfluoroalkyl derivatives Te(C<sub>n</sub>F<sub>2n+1</sub>)<sub>4</sub>, (n = 1–4).<sup>(156)</sup> Of these, the yellow oily liquid Te(CF<sub>3</sub>)<sub>4</sub> is the least stable, being both light- and temperature-sensitive. It reacts with fluorides to give the complex anion [Te(CF<sub>3</sub>)<sub>4</sub>F]<sup>-</sup> and with fluoride-ion acceptors to form the cation [Te(CF<sub>3</sub>)<sub>3</sub>]<sup>+</sup>. Te(CF<sub>3</sub>)<sub>4</sub> is made by reacting Te(CF<sub>3</sub>)<sub>2</sub>Cl<sub>2</sub> with Cd(CF<sub>3</sub>)<sub>2</sub> in MeCN. The higher members can be made directly from TeCl<sub>4</sub> and Cd(CF<sub>3</sub>)<sub>2</sub> are also viscous yellow liquids. The related TeMe<sub>4</sub> was first made in 1989 as a yellow pyrophoric liquid by treating TeCl<sub>4</sub> with LiMe in ether at -78°;<sup>(157)</sup> it can be oxidized by XeF<sub>2</sub> to the volatile white solid Me<sub>4</sub>TeF<sub>2</sub> which, when treated with ZnMe<sub>2</sub>, gave TeMe<sub>6</sub> as a white

solid.<sup>(158)</sup> TeMe<sub>6</sub>, the first peralkylated derivative of a hexavalent main-group element, can be heated for several hours at 140° without decomposition, and is thus much more stable than TeMe<sub>4</sub>.



Organopolytellurides (and polyselenides) are also known, e.g. ArTeTeAr (Ar = 2, 4, 6-Ph<sub>3</sub>C<sub>6</sub>H<sub>2</sub>-)<sup>(159)</sup> and RTeTeTeR (R = (Me<sub>3</sub>Si)<sub>3</sub>-C),<sup>(160)</sup> the stabilizing rôle of the bulky end groups is evident. [The related “isoelectronic” cation Bu<sub>3</sub>P<sup>+</sup>TeTeTePBu<sub>3</sub><sup>2+</sup> can also be noted;<sup>(161)</sup> it is prepared by oxidizing the tellurophosphorane Bu<sub>3</sub>P = Te (see p. 785) using ferricenium salts.] Related compounds are R<sub>2</sub>Se<sub>x</sub> (x = 2–7) and (RSe)<sub>2</sub>S<sub>y</sub> (y = 1–15).<sup>(162)</sup> Other compounds of note are the first “telluroketone”, Te = CF<sub>2</sub>,<sup>(163)</sup> a thermally unstable violet compound which readily dimerizes even below room temperature to the dark-red crystalline 1,3-ditellurethane (19). Cocondensation with its analogue, Se = CF<sub>2</sub> yields the corresponding volatile orange solid, 1-selena-3-tellurethane, F<sub>2</sub>C<sup>Te</sup>TeCF<sub>2</sub>Se.

<sup>158</sup> L. AHMED and J. A. MORRISON, *J. Am. Chem. Soc.* **112**, 7411–13 (1990).

<sup>159</sup> E. S. LANG, C. MAICHLE-MÖSSMER and J. STRÄHLE, *Z. anorg. allg. Chem.* **620**, 1678–85 (1994).

<sup>160</sup> F. SLADKY, B. BILDSTEIN, C. RIEKER, A. GIEREN, H. BETZ and T. HÜBNER, *J. Chem. Soc., Chem. Commun.*, 1800–1 (1985).

<sup>161</sup> N. KUHN, H. SCHUMANN and R. BOESE, *J. Chem. Soc., Chem. Commun.*, 1257–8 (1987).

<sup>162</sup> M. PRIDÖHL and R. STEUDEL, *Polyhedron* **12**, 2577–85 (1993).

<sup>163</sup> R. BOESE, A. HAAS and C. LIMBERG, *J. Chem. Soc., Chem. Commun.*, 1378–9 (1991) and *J. Chem. Soc., Dalton Trans.*, 2547–56 (1993).

<sup>153</sup> R. F. ZIOLO and J. M. TROUP, *Inorg. Chem.* **18**, 2271–4 (1979). See also, however, M. J. COLLINS, J. A. RIPMEESTER and J. F. SAWYER, *J. Am. Chem. Soc.* **110**, 8583–90 (1988).

<sup>154</sup> R. F. ZIOLO and M. EXTINE, *Inorg. Chem.* **19**, 2964–7 (1980).

<sup>155</sup> H. PRITZKOW, *Inorg. Chem.* **18**, 311–13 (1979).

<sup>156</sup> D. NAUMANN, H. BUTLER, J. FISCHER, J. HANKE, J. MOGIAS and B. WILKES, *Z. anorg. allg. Chem.* **608**, 69–72 (1992).

<sup>157</sup> R. W. GEDRIDGE, D. C. HARRIS, K. T. HIGA and R. A. NISSAN, *Organometallics* **8**, 2817–20 (1989).

# 17

## The Halogens: Fluorine, Chlorine, Bromine, Iodine and Astatine

### 17.1 The Elements

#### 17.1.1 Introduction

Compounds of the halogens have been known from earliest times and the elements have played a particularly important role during the past two hundred years in the development of both experimental and theoretical chemistry.<sup>(1)</sup> Some of this early history is summarized in Table 17.1. The name “halogen” was introduced by J. S. C. Schweigger in 1811 to describe the property of chlorine, at that time unique among the elements, of combining directly with metals to give salts (Greek  $\alpha\lambda\gamma\varsigma$ , sea salt, plus the root  $-\gamma\epsilon\nu$ , produce). The name has since been extended to cover all five members of Group 17 of the periodic table.

#### Fluorine

Fluorine derives its name from the early use of fluorspar ( $\text{CaF}_2$ ) as a flux (Latin *fluor*, flowing). The name was suggested to Sir Humphry Davy by A.-M. Ampère in 1812. The corrosive nature of hydrofluoric acid and the curious property that fluorspar has of emitting light when heated (“fluorescence”) were discovered in the seventeenth century. However, all attempts to isolate the element either by chemical reactions or by electrolysis were foiled by the extreme reactivity of free fluorine. Success was finally achieved on 26 June 1886 by H. Moissan who electrolysed a cooled solution of  $\text{KHF}_2$  in anhydrous liquid HF, using Pt/Ir electrodes sealed into a platinum U-tube sealed with fluorspar caps: the gas evolved immediately caused crystalline silicon to burst into flames, and Moissan reported the results to the Academy two days later in the following cautious words: “One can indeed make various hypotheses on the nature of the liberated gas; the simplest would be that *we are in the*

<sup>1</sup> M. E. WEEKS, *Discovery of the Elements*, 6th edn., Journal of Chemical Education, Easton, 1956, Chap. 27, ‘The halogen family’, pp. 729–77.

Table 17.1 Early history of the halogens and their compounds

3000 BC	Archaeological evidence for the use of rock-salt
~400 BC	Written records on salt (ascribed to Herodot)
~200 BC	Use of salt as part payment for services (salary)
~21 AD	Strabo described dyeworks for obtaining tyrian purple (dibromoindigo) in his <i>Geographica</i>
~100	Use of salt to purify noble metals
~900	Dilute hydrochloric acid prepared by Arabian alchemist Rhazes
~1200	Development of <i>aqua regia</i> (HCl/HNO <sub>3</sub> ) to dissolve gold — presumably Cl <sub>2</sub> was also formed
1529	Georgius Agricola described use of fluorspar as a flux
~1630	Chlorine recognized as a gas by Belgian physician J. B. van Helmont (see Scheele, 1774)
1648	Concentrated HCl prepared by J.L. Glauber (by heating hydrated ZnCl <sub>2</sub> and sand)
1670	H. Schwanhard (Nürnberg) found that CaF <sub>2</sub> + strong acid gave acid vapours (HF) that etched glass (used decoratively)
1678	J. S. Elsholtz described emission of bluish-white light when fluorspar was heated. Also described by J. G. Wallerius, 1750; the name “fluorescence” was coined in 1852 by G. G. Stokes
1768	First chemical study of fluorite undertaken by A. S. Marggraf
1771	Crude hydrofluoric acid prepared by C. W. Scheele
1772	Gaseous HCl prepared over mercury by J. Priestley
1774	C. W. Scheele prepared and studied gaseous chlorine (MnO <sub>2</sub> + HCl) but thought it was a compound
1785	Chemical bleaching (eau de Javel: aqueous KOH + Cl <sub>2</sub> ) introduced by C.-L. Berthollet
1787	N. Leblanc devised a technical process for obtaining NaOH from NaCl (beginnings of the chemical industry)
1798	Bleaching powder patented by C. Tennant (Cl <sub>2</sub> + slaked lime) following preparation of bleaching liquors from Cl <sub>2</sub> and lime solutions by T. Henry (1788)
1801	W. Cruickshank recommended use of Cl <sub>2</sub> as a disinfectant (widely used in hospitals by 1823; notably effective in the European cholera epidemic, 1831, and in the outbreak of puerperal fever, Vienna, 1845)
1802	Fluoride found in fossil ivory and teeth by D. P. Morichini (soon confirmed by J. J. Berzelius who found it also in bones)
1810	H. Davy announced proof of the elementary nature of chlorine to the Royal Society (15 November) and suggested the name “chlorine” (1811)
1811	B. Courtois isolated iodine by sublimation (H <sub>2</sub> SO <sub>4</sub> + seaweed ash)
1811	The term “halogen” introduced by J. S. C. Schweigger to denote the (then) unique property of the element chlorine to combine directly with metals to give salts
1812	A.-M. Ampère wrote to H. Davy (12 August) suggesting the name <i>le fluore</i> (fluorine) for the presumed new element in CaF <sub>2</sub> and HF (by analogy with <i>le chlore</i> , chlorine). Adopted by Davy in 1813
1814	Starch/iodine blue colour-reaction described by J.-J. Colin and H.-F. Gaultier de Claubry; developed by F. Stromeyer in the same year as an analytical test sensitive to 2–3 ppm iodine
1814	First interhalogen compound (ICl) prepared by J.L. Gay Lussac
1819	Potassium iodide introduced as a remedy for goitre by J.-F. Coindet (Switzerland), the efficacy of extracts from kelp having been known in China and Europe since the sixteenth century
1823	M. Faraday showed that “solid chlorine” was chlorine hydrate (Cl <sub>2</sub> ·~10H <sub>2</sub> O using present-day nomenclature). He also liquefied Cl <sub>2</sub> (5 March) by warming the hydrate in a sealed tube
1825	First iodine containing mineral (AgI) identified by A. M. del Rio (Mexico) and N.-L. Vauquelin (Paris)
1826	Bromine isolated by A.-J. Balard (aged 23 y)
1835	L. J. M. Daguerre’s photographic process (silver plate sensitized by exposure to iodine vapour)
~1840	Introduction of (light sensitive) AgBr into photography
1840	Iodine (as iodate) found in Chilean saltpetre by A. A. Hayes
1841	First mineral bromide (bromyrite, AgBr) discovered in Mexico by P. Berthier — later also found in Chile and France
1851	Diaphragm cell for the electrolytic generation of Cl <sub>2</sub> invented by C. Watt (London) but lack of electric generators delayed exploitation until 1886–90 (Matthes and Weber of Duisberg)
1857	Bromide therapy introduced by Lacoek as a sedative and anticonvulsant for treatment of epilepsy
1858	Discovery of Stassfurt salt deposits opened the way for bromine production (for photography and medicine) as a by-product of potash
1863	Alkali Act (UK) prohibited atmospheric pollution and enforced the condensation of by-product HCl from the Leblanc process
1886	H. Moissan isolated F <sub>2</sub> by electrolysis of KHF <sub>2</sub> /HF (26 June) after over 70 y of unsuccessful attempts by others (Nobel Prize for Chemistry 1906 — he died 2 months later)
1892–5	H. Y. Castner (US/UK) and C. Kellner (Vienna) independently developed commercial mercury-cathode cell for chlor-alkali production

Table 17.2 Halogens in the twentieth century

~1900	First manufacture of inorganic fluorides for aluminium industry
1902	J. C. Downs (of E. I. du Pont de Nemours, Delaware) patented the first practical molten-salt cell for $\text{Cl}_2$ and Na metal
1908	HCl shown to be present in gastric juices of animals by P. Sommerfeld
1909	P. Friedländer showed that Tyrian Purple from <i>Murex brandaris</i> was 6,6'-dibromoindigo (previously synthesized by F. Sachs in 1904)
1920	Bromine detected in blood and organs of humans and other animals and birds by A. Damiens
1928	T. Midgley, A. L. Henne and R. R. McNary synthesized Freon ( $\text{CCl}_2\text{F}_2$ ) as a non-flammable, non-toxic gas for refrigeration
1928	ClF made by O. Ruff <i>et al.</i> ( $\text{Cl}_2 + \text{F}_2$ at $250^\circ$ )
1930	IF <sub>7</sub> made by O. Ruff and R. Keim (IF <sub>5</sub> having been made in 1871 by G. Gore)
1930+	H. T. Dean <i>et al.</i> put the correlation between decreased incidence of dental caries and the presence of fluoride ions in drinking water on a quantitative basis
1931	First bulk shipment of commercial anhydrous HF (USA)
1938	R. J. Plunket discovered Teflon (polytetrafluoroethylene, PTFE)
1940	Astatine made via $^{209}\text{Bi}(\alpha,2n)$ by D. R. Corson, K. R. Mackenzie and E. Segré
1940–1	Industrial production of $\text{F}_2(\text{g})$ begun (in the UK and the USA for manufacture of $\text{UF}_6$ and in Germany for $\text{ClF}_3$ )
1950	Chemical shifts for $^{19}\text{F}$ and nmr signals for $^{35}\text{Cl}$ and $^{37}\text{Cl}$ first observed
1962	$\text{ClF}_3$ (the last halogen fluoride to be made) synthesized by W. Maya
1965	$\text{LaF}_3$ crystals developed by J. W. Ross and M. S. Frant as the first non-glass membrane electrode (for ion-selective determination of $\text{F}^-$ )
1965	Perchlorate ion established as a monodentate ligand (to Co) by X-ray crystallography, following earlier spectroscopic and conductimetric indications of coordination (1961)
1968	Perbromates first prepared by E. H. Appelman
1967	First example of $\mu(\eta^1, \eta^1)\text{-ClO}_4^-$ as a bidentate bridging ligand (to $\text{Ag}^+$ ); chelating $\eta^2\text{-ClO}_4^-$ identified in 1974
1971	HOF first isolated in weighable amounts (p. 856)
1986	First chemical synthesis of $\text{F}_2$ gas (p. 821)

presence of fluorine, but it would be possible, of course, that it might be a perfluoride of hydrogen or even a mixture of hydrofluoric acid and ozone. . . ." For this achievement, which had eluded some of the finest experimental chemists of the nineteenth century [including H. Davy (1813–14), G. Aimé (1833), M. Faraday (1834), C. J. and T. Knox (1836), P. Louyet (1846), E. Frémy (1854), H. Kammerer (1862) and G. Gore (1870)], and for his development of the electric furnace, Moissan was awarded the Nobel Prize for Chemistry in 1906.

Fluorine technology and the applications of fluorine-containing compounds have developed dramatically during the twentieth century.<sup>(2,3)</sup> Some highlights are included in Table 17.2 and will be discussed more fully in later sections.

Noteworthy events are the development of inert fluorinated oils, greases and polymers: Freon gases such as  $\text{CCl}_2\text{F}_2$  (1928) were specifically developed for refrigeration engineering; others were used as propellants in pressurized dispensers and aerosols; and the non-stick plastic polytetrafluoroethylene (PTFE or Teflon) was made in 1938. Inorganic fluorides, especially for the aluminium industry (p. 219) have been increasingly exploited from about 1900, and from 1940  $\text{UF}_6$  has been used in gaseous diffusion plants for the separation of uranium isotopes for nuclear reactor technology. The great oxidizing strength of  $\text{F}_2$  and many of its compounds with N and O have attracted the attention of rocket

compounds, pp. 267–466; Organic fluorine compounds, pp. 467–729.

<sup>3</sup> R. E. BANKS, D. W. A. SHARP and J. C. TATLOW (eds.), *Fluorine: the First Hundred years*, Elsevier, New York, 1987 399 pp.

<sup>2</sup> Kirk–Othmer *Encyclopedia of Chemical Technology*, 4th edn., Vol. 11, 1994: Fluorine pp. 241–67; In-organic fluorine

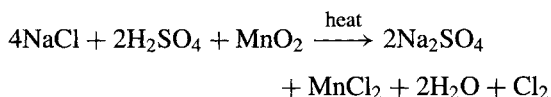


engineers and there have been growing large-scale industrial applications of anhydrous HF (p. 810).

The aggressive nature of HF fumes and solutions has been known since Schwanhard of Nürnberg used them for the decorative etching of glass. Hydrofluoric acid inflicts excruciatingly painful skin burns (p. 810) and any compound that might hydrolyse to form HF should be treated with great caution.<sup>(4)</sup> Maximum allowable concentration for continuous exposure to HF gas is 2–3 ppm (cf. HCN 10 ppm). The free element itself is even more toxic, maximum allowable concentration for a daily 8-h exposure being 0.1 ppm. Low concentrations of fluoride ion in drinking water have been known to provide excellent protection against dental caries since the classical work of H. T. Dean and his colleagues in the early 1930s; as there are no deleterious effects, even over many years, providing the total fluoride ion concentration is kept at or below 1 ppm, fluoridation has been a recommended and adopted procedure in several countries for many years (p. 810). However, at 2–3 ppm a brown mottling of teeth can occur and at 50 ppm harmful toxic effects are noted. Ingestion of 150 mg of NaF can cause nausea, vomiting, diarrhoea and acute abdominal pains though complete recovery is rapid following intravenous or intramuscular injection of calcium ions. The deliberate fluoridation of domestic water supplies has been a controversial, even polemical subject for several decades, though it is important to separate out the biological and toxicological aspects from the moral and philosophical aspects concerning the “right” of individuals to drink untreated water if they wish.<sup>(5–7)</sup>

## Chlorine

Chlorine was the first of the halogens to be isolated and common salt (NaCl) has been known from earliest times (see Table 17.1). Its efficacy in human diet was well recognized in classical antiquity and there are numerous references to its importance in the Bible. On occasion salt was used as part payment for the services of Roman generals and military tribunes (salary) and, indeed, it is an essential ingredient in mammalian diets (p. 68). The alchemical use of *aqua regia* (HCl/HNO<sub>3</sub>) to dissolve gold is also well documented from the thirteenth century onwards. Concentrated hydrochloric acid was prepared by J. L. Glauber in 1648 by heating hydrated ZnCl<sub>2</sub> and sand in a retort and the pure gas, free of water, was collected over mercury by J. Priestley in 1772. This was closely followed by the isolation of gaseous chlorine by C. W. Scheele in 1774: he obtained the gas by oxidizing nascent HCl with MnO<sub>2</sub> in a reaction which would now formally be written as:



However, Scheele believed he had prepared a *compound* (dephlogisticated marine acid air) and the misconception was compounded by C.-L. Berthollet who showed in 1785 that the action of chlorine on water releases oxygen: [Cl<sub>2</sub>(g) + H<sub>2</sub>O → 2HCl(soln) +  $\frac{1}{2}$ O<sub>2</sub>(g)]; he concluded that chlorine was a loose compound of HCl and oxygen and called it oxymuriatic acid.<sup>†</sup>

<sup>†</sup> *Muriatic acid* and *marine acid* were synonymous terms for what is now called hydrochloric acid, thus signifying its relation to the sodium chloride contained in brine (Latin *muria*) or sea water (Latin *mare*). Both names were strongly criticized by H. Davy in a scathing paper entitled “Some reflections on the nomenclature of oxymuriatic compounds” in *Phil. Trans. R. Soc.* for 1811: “To call a body which is not known to contain oxygen, and which cannot contain muriatic acid, oxymuriatic acid, is contrary to the principles of that nomenclature in which it is adopted; and an alteration of it seems necessary to assist the progress of the discussion, and to diffuse just ideas on the subject. If the great discoverer of this substance (i.e. Scheele) had signified it by any simple name it would have been proper to have referred to it; but

<sup>4</sup> A. J. FINKEL, Treatment of hydrogen fluoride injuries, *Adv. Fluorine Chem.* 7, 199–203 (1973).

<sup>5</sup> G. L. WALDBOTT (with A. W. BURGSTALLER and H. L. MCKINNEY, *Fluoridation: The Great Dilemma*, Colorado Press, Lawrence, Kansas, 1978, 423 pp.

<sup>6</sup> B. HILEMAN, Fluoridation of Water: A Special Report, *C & E News* August 1, 26–42 (1988). See also B. HILEMAN, *C & E News* February 25, 6–7 (1991).

<sup>7</sup> B. MARTIN, *Scientific Knowledge in Controversy: The Social Dynamics of the Fluoridation Debate*, State University of New York Press, Albany, N.Y. 1991, 256 pp.

The two decades from 1790 to 1810 were characterized by two major advances in chemical theory: Lavoisier's demolition of the phlogiston theory of combustion, and Davy's refutation of Lavoisier's contention that oxygen is a necessary constituent of all acids. Only when both these transformations had been achieved could the elementary nature of chlorine and the true composition of hydrochloric acid be appreciated, though some further time was to elapse (Dalton, Avogadro, Cannizaro) before gaseous chlorine was universally recognized to consist of diatomic molecules,  $\text{Cl}_2$ , rather than single atoms,  $\text{Cl}$ . The name, proposed by Davy in 1811, refers to the colour of the gas (Greek  $\chi\lambda\omega\rho\acute{o}\varsigma$ , *chloros*, yellowish or light green — cf. chlorophyll).

The bleaching power of  $\text{Cl}_2$  was discovered by Scheele in his early work (1774) and was put to technical use by Berthollet in 1785. This was a major advance on the previous time-consuming, labour-intensive, weather-dependent method of solar bleaching, and numerous patents followed (see Table 17.1). Indeed, the use of chlorine as a bleach remains one of its principal industrial applications (bleaching powder, elemental chlorine, hypochlorite solutions, chlorine dioxide, chloramines, etc.).<sup>(8)</sup> Another all-pervading use of chlorine, as a disinfectant and germicide, also dates from this period (1801), and the chlorination of domestic water supplies is now almost universal in developed countries. Again, as with fluoride, higher concentrations are toxic to humans: the gas is detectable by smell at 3 ppm, causes throat irritation at 15 ppm, coughing at 30 ppm, and rapid death at 1000 ppm. Prolonged exposure to concentrations above 1 ppm should be avoided.

Sodium chloride, by far the most abundant compound of chlorine, occurs in extensive evaporite deposits, saline lakes and brines, and in

the ocean (p. 795). It has played a dominant role in the chemical industry since its inception in the late eighteenth century (p. 71). The now defunct Leblanc process for obtaining  $\text{NaOH}$  from  $\text{NaCl}$  signalled the beginnings of large-scale chemical manufacture, and  $\text{NaCl}$  remains virtually the sole source of chlorine and hydrochloric acid for the vast present-day chlorine-chemicals industry.<sup>(8)</sup> This embraces not only the large-scale production and distribution of  $\text{Cl}_2$  and  $\text{HCl}$ , but also the manufacture of chlorinated methanes and ethanes, vinyl chloride, aluminium trichloride catalysts and the chlorides of  $\text{Mg}$ ,  $\text{Ti}$ ,  $\text{Zr}$ ,  $\text{Hf}$ , etc., for production of the metals. Details of many of these processes are to be found either in other chapters or in later sections of the present chapter. About 15 000 chlorinated compounds are currently used to varying degrees in commerce. Of these, the environmental and health hazards posed by certain polychlorinated hydrocarbons is now well established, though not all such compounds are dangerous: focused selective restrictions rather than a blanket banning of all organochlorine compounds is advocated.<sup>(9)</sup> The rôle of chlorofluorocarbons in the depletion of stratospheric ozone above the polar regions has already been mentioned (p. 608).

### Bromine

The magnificent purple pigment referred to in the Bible<sup>(10)</sup> and known to the Romans as Tyrian purple after the Phoenician port of Tyre (Lebanon), was shown by P. Friedländer in 1909 to be 6,6'-dibromoindigo. This precious dye was extracted in the early days from the small purple snail *Murex brandaris*, as many as 12 000 snails being required to prepare 1.5 g of dye. The element itself was isolated by A.-J. Balard in 1826 from the mother liquors remaining after the crystallization of sodium chloride and sulfate from the waters of the Montpellier salt marshes;

'dephlogisticated marine acid' is a term which can hardly be adopted in the present advanced area of the science. After consulting some of the most eminent chemical philosophers in the country, it has been judged most proper to suggest a name founded upon one of its most obvious and characteristic properties — its colour, and to call it *Chlorine*."

<sup>8</sup> J. S. SCONCE, *Chlorine: Its Manufacture, Properties and Uses*, Reinhold, New York, 1962, 901 pp.

<sup>9</sup> B. HILEMAN, *C & E News*, April 19, 11–20 (1993). See also B. HILEMAN, J. R. LONG and E. M. KIRSCHNER, *C & E News*, November 21, 12–26 (1994).

<sup>10</sup> Holy Bible, Ezekiel 27:7, 16.

the liquor is rich in  $\text{MgBr}_2$ , and the young Balard, then 23 y of age, noticed the deep yellow coloration that developed on addition of chlorine water. Extraction with ether and  $\text{KOH}$ , followed by treatment of the resulting  $\text{KBr}$  with  $\text{H}_2\text{SO}_4/\text{MnO}_2$ , yielded the element as a red liquid. Astonishingly rapid progress was possible in establishing the chemistry of bromine and in recognizing its elemental nature because of its similarity to chlorine and iodine (which had been isolated 15 y earlier). Indeed, J. von Liebig had missed discovering the element several years previously by misidentifying a sample of it as iodine monochloride.<sup>(1)</sup> Balard had proposed the name *muride*, but this was not accepted by the French Academy, and the element was named bromine (Greek  $\beta\rho\omega\mu\omicron\varsigma$ , stink) because of its unpleasant, penetrating odour. It is perhaps ironic that the name fluorine had already been pre-empted for the element in  $\text{CaF}_2$  and  $\text{HF}$  (p. 789) since bromine, as the only non-metallic element that is liquid at room temperature, would pre-eminently have deserved the name.

The first mineral found to contain bromine (bromyrite,  $\text{AgBr}$ ) was discovered in Mexico in 1841, and industrial production of bromides followed the discovery of the giant Stassfurt potash deposits in 1858. The major use at that time was in photography and medicine:  $\text{AgBr}$  had been introduced as the light-sensitive agent in photography about 1840, and the use of  $\text{KBr}$  as a sedative and anti-convulsant in the treatment of epilepsy was begun in 1857. Other major uses of bromine-containing compounds include their application as flame retardants and as phase-transfer catalysts. The scale of the present-day production of bromine and bromine chemicals will become clear in later sections of this chapter.<sup>(11)</sup>

### Iodine

The lustrous, purple-black metallic sheen of resublimed crystalline iodine was first observed

by the industrial chemist B. Courtois in 1811, and the name, proposed by J. L. Gay Lussac in 1813, reflects this most characteristic property (Greek  $\iota\omega\delta\eta\varsigma$ , violet-coloured). Courtois obtained the element by treating the ash of seaweed (which had been calcined to extract saltpetre and potash) with concentrated sulfuric acid. Extracts of the brown kelps and seaweeds *Fucus* and *Laminaria* had long been known to be effective for the treatment of goitre and it was not long before J. F. Coindet and others introduced pure  $\text{KI}$  as a remedy in 1819.<sup>(12)</sup> It is now known that the thyroid gland produces the growth-regulating hormone thyroxine, an iodinated amino acid:  $p\text{-(HO)-C}_6\text{H}_2(\text{I})_2\text{-O-C}_6\text{H}_2(\text{I})_2\text{-CH}_2\text{CH(NH}_2\text{)CO}_2\text{H}$ .

If the necessary iodine input is insufficient the thyroid gland enlarges in an attempt to garner more iodine: addition of 0.01%  $\text{NaI}$  to table salt (iodized salt) prevents this condition. Tincture of iodine is a useful antiseptic.

The first iodine-containing mineral ( $\text{AgI}$ ) was discovered in Mexico in 1825 but the discovery of iodate as an impurity in Chilean saltpetre in 1840 proved to be more significant industrially. The Chilean nitrate deposits provided the largest proportion of the world's iodine until overtaken in the late 1960s by Japanese production from natural brines (pp. 796, 799).

In addition to its uses in photography and medicine, iodine and its compounds have been much exploited in volumetric analysis (iodometry and iodimetry, p. 864). Organiodine compounds have also played a notable part in the development of synthetic organic chemistry, being the first compounds used in A. W. von Hofmann's alkylation of amines (1850), A. W. Williamson's synthesis of ethers (1851), A. Wurtz's coupling reactions (1855) and V. Grignard's reagents (1900).

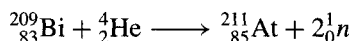
### Astatine

From its position in the periodic table, all isotopes of element 85 would be expected to

<sup>11</sup> D. PRICE, B. IDDON and B. J. WAKEFIELD, *Bromine Compounds: Chemistry and Applications*, Elsevier, Amsterdam 1988, 422 pp.

<sup>12</sup> E. BOOTH, *Chem. Ind. (Lond.)* 31 and 52-5 (1979).

be radioactive. Those isotopes that occur in the natural radioactive series all have half-lives of less than 1 min and thus occur in negligible amounts in nature (p. 796). Astatine (Greek *ἀστατος*, unstable) was first made and characterized by D. R. Corson, K. R. Mackenzie and E. Segré in 1940: they synthesized the isotope  $^{211}\text{At}$  ( $t_{1/2}$  7.21 h) by bombarding  $^{209}\text{Bi}$  with  $\alpha$ -particles in a large cyclotron:



In all, some 27 isotopes from  $^{194}\text{At}$  to  $^{220}\text{At}$  have now been prepared by various routes but all are short-lived. The only ones besides  $^{211}\text{At}$  having half-lives longer than 1 h are  $^{207}\text{At}$  (1.80 h),  $^{208}\text{At}$  (1.63 h),  $^{209}\text{At}$  (5.41 h), and  $^{210}\text{At}$  (8.1 h): this means that weighable amounts of astatine or its compounds cannot be isolated, and nothing is known of the bulk physical properties of the element. For example, the least-unstable isotope ( $^{210}\text{At}$ ) has a specific activity corresponding to 2 curies per  $\mu\text{g}$ , i.e.  $7 \times 10^{10}$  disintegrations per second per  $\mu\text{g}$ . The largest preparations of astatine to date have involved about 0.05  $\mu\text{g}$  and our knowledge of the chemistry of this element comes from extremely elegant tracer experiments, typically in the concentration range  $10^{-11}$ – $10^{-15}$  M. The most concentrated aqueous solutions of the element or its compounds ever investigated were only  $\sim 10^{-8}$  M.

### 17.1.2 Abundance and distribution

Because of their reactivity, the halogens do not occur in the free elemental state but they are both widespread and abundant in the form of their ions,  $X^-$ . Iodine also occurs as iodate (see below). In addition to large halide mineral deposits, particularly of NaCl and KCl, there are vast quantities of chloride and bromide in ocean waters and brines.

Fluorine is the thirteenth element in order of abundance in crustal rocks of the earth, occurring to the extent of 544 ppm (cf. twelfth Mn, 1060 ppm; fourteenth Ba, 390 ppm; fifteenth Sr, 384 ppm). The three most important minerals are

fluorite  $\text{CaF}_2$ , cryolite  $\text{Na}_3\text{AlF}_6$  and fluorapatite  $\text{Ca}_5(\text{PO}_4)_3\text{F}$ . Of these, however, only fluorite is extensively processed for recovery of fluorine and its compounds (p. 809). Cryolite is a rare mineral, the only commercial deposit being in Greenland, and most of the  $\text{Na}_3\text{AlF}_6$  needed for the huge aluminium industry (p. 219) is now synthetic. By far the largest amount of fluorine in the earth's crust is in the form of fluorapatite, but this contains only about 3.5% by weight of fluorine and the mineral is processed almost exclusively for its phosphate content. Despite this, about 7% of the domestic requirement for fluorine compounds in the USA was obtained from fluorosilicic acid recovered as a by-product of the huge phosphate industry (pp. 476, 520). Minor occurrences of fluorine are in the rare minerals topaz  $\text{Al}_2\text{SiO}_4(\text{OH},\text{F})_2$ , sellaite  $\text{MgF}_2$ , villiaumite  $\text{NaF}$  and bastnaesite  $(\text{Ce},\text{La})(\text{CO}_3)\text{F}$  (but see p. 1229). The insolubility of alkaline-earth and other fluorides precludes their occurrence at commercially useful concentrations in ocean water (1.2 ppm) and brines.

Chlorine is the twentieth most abundant element in crustal rocks where it occurs to the extent of 126 ppm (cf. nineteenth V, 136 ppm, and twenty-first Cr, 122 ppm). The vast evaporite deposits of NaCl and other chloride minerals have already been described (pp. 69, 73). Dwarfing these, however, are the inconceivably vast reserves in ocean waters (p. 69) where more than half the total average salinity of 3.4 wt% is due to chloride ions (1.9 wt%). Smaller quantities, though at higher concentrations, occur in certain inland seas and in subterranean brine wells, e.g. the Great Salt Lake, Utah (23% NaCl) and the Dead Sea, Israel (8.0% NaCl, 13.0%  $\text{MgCl}_2$ , 3.5%  $\text{CaCl}_2$ ).

Bromine is substantially less abundant in crustal rocks than either fluorine or chlorine; at 2.5 ppm it is forty-sixth in order of abundance being similar to Hf 2.8, Cs 2.6, U 2.3, Eu 2.1 and Sn 2.1 ppm. Like chlorine, the largest natural source of bromine is the oceans, which contain  $\sim 6.5 \times 10^{-3}\%$ , i.e. 65 ppm or 65 mg/l. The mass ratio Cl:Br is  $\sim 300:1$  in the oceans, corresponding to an atomic ratio

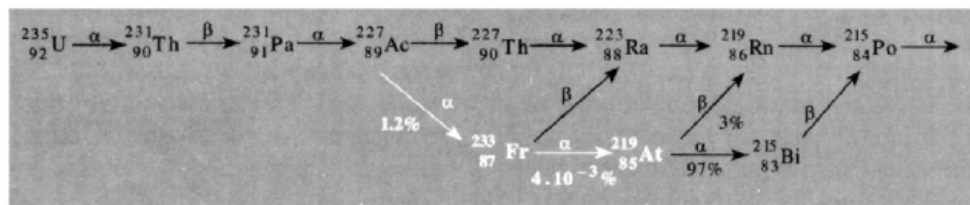
of  $\sim 660:1$ . Salt lakes and brine wells are also rich sources of bromine, and these are usually proportionately richer in bromine than are the oceans: the atom ratio Cl:Br spans the range  $\sim 200$ – $700$ . Typical bromide-ion concentrations in such waters are: Dead Sea 0.4% (4 g/l), Sakscoe Ozoro (Crimea) 0.28% and Searle's Lake (California) 0.085%.

Iodine is considerably less abundant than the lighter halogens both in the earth's crust and in the hydrosphere. It comprises 0.46 ppm of the crustal rocks and is sixtieth in order of abundance (cf. Tl 0.7, Tm 0.5, In 0.24, Sb 0.2). It occurs but rarely as iodide minerals, and commercial deposits are usually as iodates, e.g. lautarite,  $\text{Ca}(\text{IO}_3)_2$  and dietzeite,  $7\text{Ca}(\text{IO}_3)_2 \cdot 8\text{CaCrO}_4$ . Thus the caliche nitrate beds of Chile contain iodine in this form ( $\sim 0.02$ – $1$  wt% I). These mine workings soon replaced calcined seaweeds as the main source of iodine during the last century, but have recently been themselves overtaken by iodine recovered from brines. Brines associated with oil-well drillings in Louisiana and California were found to contain 30–40 ppm iodine in the 1920s, and independent subterranean brines were located at Midland, Michigan, in the 1960s, and in Oklahoma (1977), which is now the main US source. Natural brine wells in Japan (up to 100 ppm I) were discovered after the Second World War, and exploitation of these now ensures Japan first place among the world's iodine producers. The concentration of iodine in ocean waters is only 0.05 ppm, too low for commercial recovery, though brown seaweeds of the *Laminaria* family (and to a lesser extent *Fucus*) can concentrate this up to 0.45% of their dry weight (see above).

The fugitive radioactive element astatine can hardly be said to exist in nature though the punctillious would rightly point to its temporary participation in the natural radioactive series. Thus  $^{219}\text{At}$  ( $t_{1/2}$  54 s) occurs as a rare and inconspicuous branch ( $4 \times 10^{-3}\%$ ) of another minor branch (1.2%) of the  $^{235}\text{U}$  ( $4n + 3$ ) series (see scheme). Another branch ( $5 \times 10^{-4}\%$ ) at  $^{215}\text{Po}$  yields  $^{215}\text{At}$  by  $\beta$  emission before itself decaying by  $\alpha$  emission ( $t_{1/2} 1.0 \times 10^{-4}$  s); likewise  $^{218}\text{At}$  ( $t_{1/2} \sim 72$  s) is a descendant of the  $^{238}\text{U}$  ( $4n + 2$ ) series, and traces have been detected of  $^{217}\text{At}$  ( $t_{1/2}$  0.0323 s) and  $^{216}\text{At}$  ( $t_{1/2}$   $3.0 \times 10^{-4}$  s). Estimates suggest that the outermost kilometre of the earth's crust contains no more than 44 mg of astatine compared with 15 g of francium (p. 69) or the relatively abundant polonium (2500 tonnes) and actinium (7000 tonnes). Astatine can therefore be regarded as the rarest naturally occurring terrestrial element.

### 17.1.3 Production and uses of the elements

The only practicable large-scale method of preparing  $\text{F}_2$  gas is Moissan's original procedure based on the electrolysis of KF dissolved in anhydrous HF; (see however p. 821). Moissan used a mole ratio KF:HF of about 1:13, but this has a high vapour pressure of HF and had to be operated at  $-24^\circ$ . Electrolyte systems having mole ratios of 1:2 and 1:1 melt at  $\sim 72^\circ$  and  $\sim 240^\circ\text{C}$  respectively and have much lower vapour pressures of HF; accordingly



these compositions were subsequently favoured. Nowadays, medium-temperature cells (80–100°) are universally employed, being preferred over the high-temperature cells because (a) they have a lower pressure of HF gas above the cell, (b) there are fewer corrosion problems, (c) the anode has a longer life and (d) the composition of the electrolyte can vary within fairly wide limits without impairing the operating conditions or efficiency. The highly corrosive nature of the electrolyte, coupled with the aggressive oxidizing power of F<sub>2</sub>, pose considerable problems of handling, and these are exacerbated by the explosive reaction of F<sub>2</sub> with its co-product H<sub>2</sub>, so that accidental mixing of the gases must be prevented at all costs. Scrupulous absence of grease and other flammable contaminants must also be ensured since they can lead to spectacular fires which puncture the protective fluoride coating of the metal containers and cause the whole system to enflame. Another hazard in early generators was the formation of explosive graphite-fluorine compounds at the anode (p. 289). All these problems have now been overcome and F<sub>2</sub> can be routinely generated with safety both in the laboratory and on a large industrial scale.<sup>(2,13)</sup> A typical generator (Fig. 17.1) consists of a mild-steel pot (cathode) containing the electrolyte KF·2HF which is kept at 80–100°C either by a heating jacket when the cell is quiescent or by a cooling system when the cell is working. The anode consists of a central rod of compacted, ungraphitized carbon, and the product gases are kept separate by a skirt or diaphragm dipping below the electrolyte surface. The temperature is automatically controlled, as is the level of the electrolyte by controlled addition of make-up anhydrous HF. Laboratory generators usually operate at about 10–50 A whereas industrial production, employing banks of cells, may operate at 4000–6000 A and 8–12 V. An individual cell in such a bank might typically be 3.0 × 0.8 × 0.6 m and hold 1 tonne of electrolyte; it might have 12 anode

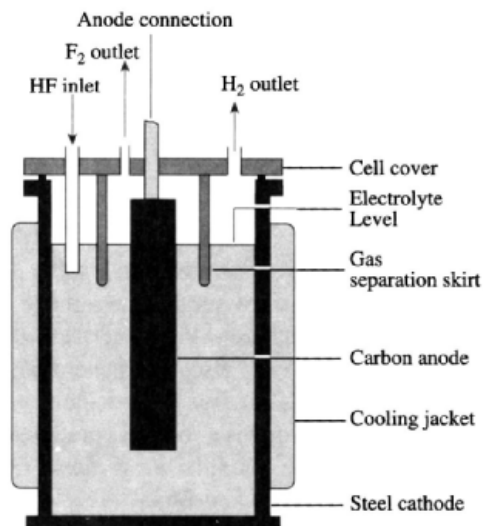


Figure 17.1 Schematic diagram of an electrolytic fluorine-generating cell.

assemblies each holding two anode blocks and produce 3–4 kg F<sub>2</sub> per hour. A large-scale plant can produce *ca.* 9 tonnes of liquefied F<sub>2</sub> per day. The total annual production in the USA and Canada exceeds 5000 tonnes, and similar though somewhat smaller amounts are produced in several European countries (UK, France, Germany, Italy, Russia). Production in Japan approaches 1000 tpa.

Cylinders of F<sub>2</sub> are now commercially available in various sizes from 230-g to 2.7-kg capacity; 1993 price ~\$110–260 per kg depending on cylinder size. The gas pressure is 2.86 MPa (~28 atm.) at 21°C. Liquid F<sub>2</sub> is shipped in tank trucks of 2.27 tonnes capacity, the container being itself cooled by a jacket of liquid N<sub>2</sub> which boils 8° below F<sub>2</sub>. Alternatively, it can be converted to ClF<sub>3</sub>, bp 11.7°C (p. 828), which is easier to handle and transport than F<sub>2</sub>. In fact, about 70–80% of the elemental F<sub>2</sub> produced is used captively for the manufacture of UF<sub>6</sub> for nuclear power generation (p. 1259). Another important use is in the production of SF<sub>6</sub> for dielectrics (p. 687). The captive use to manufacture the versatile fluorinating agents ClF<sub>3</sub>, BrF<sub>3</sub> and IF<sub>5</sub> is a third important outlet. Fluorination of W and Re to

<sup>13</sup> H. C. FIELDING and B. E. LEE, in R. THOMPSON (ed.), *The Modern Inorganic Chemicals Industry*, pp. 149–67, Chemical Society Special Publication No. 31, 1977.

their hexafluorides is also industrially important since these volatile compounds are used in chemical vapour deposition of W and Re films on intricately shaped components. Most other fluorinations of inorganic and organic compounds avoid the direct use of  $F_2$ . The former demand for liquid  $F_2$  as a rocket-fuel oxidizer has now ceased.

Chlorine is rarely generated on a laboratory scale since it is so readily available in cylinders of all sizes from 450 g (net) to 70 kg. When required it can also be generated by adding concentrated, air-free hydrochloric acid ( $d$  1.16 g cm<sup>-3</sup>) dropwise on to precipitated hydrated manganese dioxide in a flask fitted with a dropping funnel and outlet tube: the gas formation can be regulated by moderate heating and the  $Cl_2$  thus formed can be purified by passage through water (to remove HCl) and  $H_2SO_4$  (to remove  $H_2O$ ). The gas, whether generated in this way or obtained from a cylinder, can be further purified if necessary by passage through successive tubes containing CaO and  $P_2O_5$ , followed by condensation in a bath cooled by solid  $CO_2$  and fractionation in a vacuum line.

Industrial production of  $Cl_2$  and chlorine chemicals is on a vast scale and comprises a major section of the heavy chemical industry.<sup>(8,9,14,15)</sup> Some aspects have already been discussed on p. 793, and further details are in the Panel.

Bromine is invariably made on an industrial scale by oxidation of bromide ion with  $Cl_2$ . The main sources of  $Br^-$  are Arkansas brines (4000–5000 ppm) which account for most of US production, various brines and bitterns in Europe, the Dead Sea (4000–6000 ppm), and ocean waters (65 ppm). Following the oxidation of  $Br^-$  the  $Br_2$  is removed from the solution either by passage of steam (“steaming out”) or air (“blowing out”), and then condensed and purified. Although apparently simple, these unit operations must deal with highly reactive and corrosive materials, and the industrial processes have been ingeniously developed and refined

<sup>14</sup> R. W. PURCELL, The chor-alkali industry, in ref. 13, pp. 106–33. A. CAMPBELL, Chlorine and chlorination, *ibid.*, pp. 134–48.

<sup>15</sup> *Kirk-Othmer Encyclopedia of Chemical Technology*, 4th edn., 1, 938–1025 (1991).

### Industrial Production and Uses of Chlorine

The large-scale production of  $Cl_2$  is invariably achieved by the electrolytic oxidation of the chloride ion. Natural brines or aqueous solutions of NaCl can be electrolysed in an asbestos diaphragm cell or a mercury cathode cell, though these latter are being phased out for environmental and other reasons (p. 1225). Electrolysis of molten NaCl is also carried out on a large scale: in this case the co-product is Na rather than NaOH. Electrolysis of by-product HCl is also used where this is cheaply available. World consumption of  $Cl_2$  in 1987 exceeded 35 million tonnes. Production is dominated by the USA, but large tonnages are produced in all industrial countries: USA 30%, Western Europe 29%, Eastern Europe 15%, Japan 8.5%, Asia/Pacific 6.8%.  $Cl_2$  was ranked eighth among the large-volume chemicals manufactured in the USA during 1996. Diaphragm cells predominated though there is a growing interest in membrane cells in which the anolyte and catholyte are separated by a porous Nafion membrane (Nafion is a copolymer of tetrafluoroethylene and a perfluorosulfonylethoxy ether and the membrane is reinforced with a Teflon mesh).<sup>(15)</sup> In addition to cylinders of varying capacity up to 70 kg, chlorine can be transported in drums (865 kg), tank wagons (road: 15 tonnes; rail 27–90 tonnes), or barges (600–1200 tonnes).

The three main categories of use for  $Cl_2$  are:

- Production of organic compounds by chlorination and/or oxychlorination using a fluidized bed of copper chloride catalyst (pre-eminent amongst these are vinyl chloride monomer and propylene oxide which in the USA alone are produced on a scale of 9.0 and 2.0 million tonnes respectively). Production of chlorinated organic compounds accounts for about 63% of the  $Cl_2$  produced.
- Bleaches (for paper, pulp and textiles) sanitation and disinfection of municipal water supplies and swimming pools, sewage treatment and control. These uses account for about 19% of the  $Cl_2$  produced.
- Production of inorganic compounds, notably HCl,  $Cl_2O$ , HOCl,  $NaClO_3$ , chlorinated isocyanurates,  $AlCl_3$ ,  $SiCl_4$ ,  $SnCl_4$ ,  $PCl_3$ ,  $PCl_5$ ,  $POCl_3$ ,  $AsCl_3$ ,  $SbCl_3$ ,  $SbCl_5$ ,  $BiCl_3$ ,  $S_2Cl_2$ ,  $SCl_2$ ,  $SOCl_2$ ,  $ClF_3$ ,  $ICl$ ,  $ICl_3$ ,  $TiCl_3$ ,  $TiCl_4$ ,  $MoCl_5$ ,  $FeCl_3$ ,  $ZnCl_2$ ,  $Hg_2Cl_2$ ,  $HgCl_2$ , etc. (see index for page references to production and uses). About 18% of  $Cl_2$  production is used to manufacture inorganic chemicals.

to give optimum yields at the lowest possible operating costs.<sup>(16,17)</sup>

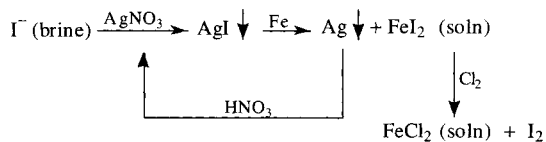
World production of Br<sub>2</sub> in 1990 was about 438 000 tonnes pa, i.e. about one-hundredth of the scale of the chlorine industry. The main producing countries are (tonnes): USA 177 000, Israel 135 000, Russia 60 000, UK 28 000, France 18 000 and Japan 15 000. The production capacity of Israel has recently increased almost threefold because of expanded facilities on the Dead Sea. Historically, bromine was shipped in individual 3-kg (net) bottles to minimize damage due to breakage, but during the 1960s bulk transport in monel metal drums (100-kg capacity) or lead-lined tanks (24 or 48 tonnes) was developed and these are now used for transport by road, rail and ship. The price of Br<sub>2</sub> in tank-car lots was \$975/kg in 1990.

The industrial usage of bromine has been dominated by the single compound ethylene dibromide which has been (with ethylene dichloride) a valuable gasoline (petrol) additive where it acts as a scavenger for lead from the anti-knock additive PbEt<sub>4</sub>. Environmental legislation has dramatically reduced the amount of leaded petrol produced and, accordingly, ethylene dibromide, which accounted for 90% of US bromine production in 1955, declined to 75% a decade later and now represents a mere 16% of the total bromine consumption in the USA (1990). Fortunately this decline has been matched by a steady increase in other applications and the industry worldwide has shown a modest growth. Most of these large-volume applications involve organic compounds, notably MeBr, which is one of the most effective nematocides known (i.e. kills worms) and is also used as a general pesticide (herbicide, fungicide and insecticide). Ethylene dibromide and dibromochloropropane are also used as pesticides. Bromine compounds are extensively used as fire retardants, especially for fibres, carpets, rugs and plastics; they are about 3–4 times as effective (weight for

weight) as chlorocompounds which gives them a substantial cost advantage.

Other uses of bromo-organics include high-density drilling fluids, dyestuffs and pharmaceuticals. Bromine is also used in water sanitation and to synthesize a wide range of inorganic compounds, e.g. AgBr for photography, HBr, alkali metal bromides, bromates, etc. (see later sections). An indication of the overall pattern of use (USA, 1990) is as follows: flame retardants 29%, ethylene dibromide 16%, agrochemicals 16% drilling fluids 11% inorganic bromides 5.5%, water treatment chemicals 5.5%, other 17%.

The commercial recovery of iodine on an industrial scale depends on the particular source of the element.<sup>(18)</sup> From natural brines, such as those at Midland (Michigan) or in Russia or Japan, chlorine oxidation followed by air blow-out as for bromine (above) is much used, the final purification being by resublimation. Alternatively the brine, after clarification, can be treated with just sufficient AgNO<sub>3</sub> to precipitate the AgI which is then treated with clean scrap iron or steel to form metallic Ag and a solution of FeI<sub>2</sub>; the Ag is redissolved in HNO<sub>3</sub> for recycling and the solution is treated with Cl<sub>2</sub> to liberate the I<sub>2</sub>:



The newest process to be developed oxidizes the brine with Cl<sub>2</sub> and then treats the solution with an ion-exchange resin: the iodine is adsorbed in the form of polyiodide which can be eluted with alkali followed by NaCl to regenerate the column. About 65% of the iodine consumed in the world comes from brines.

Recovery of iodine from Chilean saltpetre differs entirely from its recovery from brine since it is present as iodate. NaIO<sub>3</sub> is extracted from the caliche and is allowed to accumulate in the mother liquors from the crystallization of NaNO<sub>3</sub>

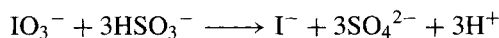
<sup>16</sup> R. B. McDONALD and W. R. MERRIMAN, pp. 168–82 of ref. 13.

<sup>17</sup> Ref. 2, Vol. 4 (1992), Bromine, pp. 536–60; Bromine compounds, pp. 560–89.

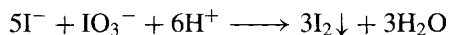
<sup>18</sup> Ref. 2, Vol. 14 (1995), Iodine and Iodine compounds, pp. 709–37.



until its concentration is about 6 g/l. Part is then drawn off and treated with the stoichiometric amount of sodium hydrogen sulfite required to reduce it to iodide:



The resulting acidic mixture is treated with just sufficient fresh mother liquor to liberate all the contained iodine:



The precipitated  $\text{I}_2$  is filtered off and the iodine-free filtrate returned to the nitrate-leaching cycle after neutralization of any excess acid with  $\text{Na}_2\text{CO}_3$ .

World production of  $\text{I}_2$  in 1992 approached 15 000 tonnes, the dominant producers being Japan 41%, Chile 40%, USA 10% and the former Soviet Union 9%. Crude iodine is packed in double polythene-lined fibre drums of 10–50-kg capacity. Resublimed iodine is transported in lined fibre drums (11.3 kg) or in bottles containing 0.11, 0.45 or 2.26 kg. The price of  $\text{I}_2$  has traditionally fluctuated wildly. Thus, because of acute over-supply in 1990 the price for  $\text{I}_2$  peaked at \$22/kg in 1988, falling to \$12/kg in 1990 and \$9.50/kg in 1992. Unlike  $\text{Cl}_2$  and  $\text{Br}_2$ , iodine has no predominant commercial outlet. About 50% is incorporated into a wide variety of organic compounds and about 15% each is accounted for as resublimed iodine, KI, and other inorganics. The end uses include catalysts for synthetic rubber manufacture, animal- and fowl-feed supplements,

stabilizers, dyestuffs, colourants and pigments for inks, pharmaceuticals, sanitary uses (tincture of iodine, etc.) and photographic chemicals for high-speed negatives. Uses of iodine compounds as smog inhibitors and cloud-seeding agents are small. In analytical chemistry  $\text{KHgI}_3$  forms the basis for Nessler's reagent for the detection of  $\text{NH}_3$ , and  $\text{Cu}_2\text{HgI}_4$  was used in Mayer's reagent for alkaloids. Iodides and iodates are standard reagents in quantitative volumetric analysis (p. 864).  $\text{Ag}_2\text{HgI}_4$  has the highest ionic electrical conductivity of any known solid at room temperature but this has not yet been exploited on a large scale in any solid-state device.

### 17.1.4 Atomic and physical properties

The halogens are volatile, diatomic elements whose colour increases steadily with increase in atomic number. Fluorine is a pale yellow gas which condenses to a canary yellow liquid, bp  $-188.1^\circ\text{C}$  (intermediate between  $\text{N}_2$ , bp  $-195.8^\circ$ , and  $\text{O}_2$ , bp  $-183.0^\circ\text{C}$ ). Chlorine is a greenish-yellow gas, bp  $-34.0^\circ$ , and bromine a dark-red mobile liquid, bp  $59.5^\circ$ : interestingly the colour of both elements diminishes with decrease in temperature and at  $-195^\circ$   $\text{Cl}_2$  is almost colourless and  $\text{Br}_2$  pale yellow. Iodine is a lustrous, black, crystalline solid, mp  $113.6^\circ$ , which sublimes readily and boils at  $185.2^\circ\text{C}$ .

Atomic properties are summarized in Table 17.3 and some physical properties are in Table 17.4.

**Table 17.3** Atomic properties of the halogens

Property	F	Cl	Br	I	At
Atomic number	9	17	35	53	85
Number of stable isotopes	1	2	2	1	0
Atomic weight	18.998 4032(9)	35.4527(9)	79.904(1)	126.90447(3)	(210)
Electronic configuration	$[\text{He}]2s^2 2p^5$	$[\text{Ne}]3s^2 3p^5$	$[\text{Ar}]3d^{10} 4s^2 4p^5$	$[\text{Kr}]4d^{10} 5s^2 5p^5$	$[\text{Xe}]4f^{14} 5d^{10} 6s^2 6p^5$
Ionization energy/ $\text{kJ mol}^{-1}$	1680.6	1255.7	1142.7	1008.7	[926]
Electron affinity/ $\text{kJ mol}^{-1}$	332.6	348.7	324.5	295.3	[270]
$\Delta H_{\text{dissoc}}/\text{kJ mol}(\text{X}_2)^{-1}$	158.8	242.58	192.77	151.10	—
Ionic radius, $\text{X}^-/\text{pm}$	133	184	196	220	—
van der Waals radius/pm	135	180	195	215	—
Distance X–X in $\text{X}_2/\text{pm}$	143	199	228	266	—

Table 17.4 Physical properties of the halogens

Property	F <sub>2</sub>	Cl <sub>2</sub>	Br <sub>2</sub>	I <sub>2</sub>
MP/°C	-219.6	-101.0	-7.25	113.6 <sup>(a)</sup>
BP/°C	-188.1	-34.0	59.5	185.2 <sup>(a)</sup>
<i>d</i> (liquid, T°C)/g cm <sup>-3</sup>	1.516(-188°)	1.655(-70°)	3.187 (0°)	3.960 <sup>(b)</sup> (120°)
$\Delta H_{\text{fusion}}/\text{kJ mol}(\text{X}_2)^{-1}$	0.51	6.41	10.57	15.52
$\Delta H_{\text{vap}}/\text{kJ mol}(\text{X}_2)^{-1}$	6.54	20.41	29.56	41.95
Temperature (°C) for 1% dissociation at 1 atm	765	975	775	575

<sup>(a)</sup>Solid iodine has a vapour pressure of 0.31 mmHg (41 Pa) at 25°C and 90.5 mmHg (12.07 kPa) at the mp (113.6°).

<sup>(b)</sup>Solid iodine has a density of 4.940 g cm<sup>-3</sup> at 20°C.

As befits their odd atomic numbers, the halogens have few naturally occurring isotopes (p. 3). Only one isotope each of F and I occurs in nature and the atomic weights of these elements are therefore known very accurately indeed (p. 17). Chlorine has two naturally occurring isotopes (<sup>35</sup>Cl 75.77%, <sup>37</sup>Cl 24.23%) as also does bromine (<sup>79</sup>Br 50.69%, <sup>81</sup>Br 49.31%). All isotopes of At are radioactive (p. 795). The ionization energies of the halogen atoms show the expected trend to lower values with increase in atomic number. The electronic configuration of each atom (*ns*<sup>2</sup>*np*<sup>5</sup>) is one p electron less than that of the next succeeding noble gas, and energy is evolved in the reaction X(g) + e<sup>-</sup> → X<sup>-</sup>(g). The electron affinity, which traditionally (though misleadingly) is given a positive sign despite the negative enthalpy change in the above reaction, is maximum for Cl, the value for F being intermediate between those for Cl and Br. Even more noticeable is the small enthalpy of dissociation for F<sub>2</sub> which is similar to that of I<sub>2</sub> and less than two-thirds of the value for Cl<sub>2</sub>.<sup>(19)</sup> In this connection it can be noted that N–N single bonds in hydrazines are weaker than the corresponding P–P bonds and that O–O single bonds in peroxides are weaker than the corresponding S–S bonds. This was explained (R. S. Mulliken and others, 1955) by postulating that partial p-d hybridization imparts some double-bond character

to the formal P–P, S–S and Cl–Cl single bonds thereby making them stronger than their first-row counterparts. However, following C. A. Coulson and others (1962), it seems unnecessary to invoke substantial d-orbital participation and the weakness of the F–F single bond is then ascribed to decreased overlap of bonding orbitals, appreciable internuclear repulsion and the relatively large electron–electron repulsions of the lone-pairs which are much closer together in F<sub>2</sub> than in Cl<sub>2</sub>.<sup>(20)</sup> The rapid diminution of bond-dissociation energies in the sequence N<sub>2</sub> ≫ O<sub>2</sub> ≫ F<sub>2</sub> is, of course, due to successive filling of the antibonding orbitals (p. 606), thus reducing the formal bond order from triple in N≡N to double and single in O=O and F–F respectively.

Radioactive isotopes of the halogens have found use in the study of isotope-exchange reactions and the mechanisms of various other reactions.<sup>(21,22)</sup> The properties of some of the most used isotopes are in Table 17.5. Many of these isotopes are available commercially. A fuller treatment with detailed references

<sup>20</sup> P. POLITZER, Anomalous properties of fluorine, *J. Am. Chem. Soc.* **91**, 6235–7 (1969); Some anomalous properties of oxygen and nitrogen, *Inorg. Chem.* **16**, 3350–1 (1977).

<sup>21</sup> M. F. A. DOVE and D. B. SOWERBY, in V. GUTMANN (ed.), *Halogen Chemistry*, Vol. 1, pp. 41–132, Academic Press, London, 1967.

<sup>22</sup> R. H. HERBER (ed.), *Inorganic Isotopic Syntheses*, W. H. Benjamin, New York, 1962; Radio-chlorine (B. J. MASTERS), pp. 215–26; Iodine-131 (M. KAHN), pp. 227–42. See also G. ANGELINI, M. SEPERANZA, C.-Y. SHIUE and A. P. WOLF, *J. Chem. Soc., Chem. Commun.*, 924–5 (1986) for radio fluorine (<sup>18</sup>F).

<sup>19</sup> J. BERKOWITZ and A. C. WAHL, *Adv. Fluorine Chem.* **7**, 147–74 (1973). A. A. WOOLF, *Adv. Inorg. Chem. Radiochem.* **24**, 1–55 (1981). J. J. TURNER, *MTP International Review of Science: Inorganic Chemistry Series 1*, Vol. 3, pp. 253–91, Butterworths, London, 1972.

Table 17.5 Some radioactive isotopes of the halogens

Isotope	Nuclear spin and parity	Half-life	Principal mode of decay ( $E/\text{MeV}$ )	Principal source
$^{18}\text{F}$	1+	109.77 min	$\beta^+$ (0.649)	$^{19}\text{F}(n,2n)$
$^{36}\text{Cl}$	2+	$3.01 \times 10^5$ y	$\beta^-$ (0.714)	$^{35}\text{Cl}(n,\gamma)$
$^{38}\text{Cl}$	2-	37.24 min	$\beta^-$ (4.81, 1.11, 2.77)	$^{37}\text{Cl}(n,\gamma)$
$^{80\text{m}}\text{Br}$	5-	4.42 h	$\gamma$ (internal trans) (0.086)	$^{79}\text{Br}(n,\gamma)$
$^{80}\text{Br}$	1+	17.68 min	$\beta^-$ (2.02, 1.35)	$^{80\text{m}}\text{Br}$ (IT)
$^{82}\text{Br}$	5-	35.30 h	$\beta^-$ (0.44)	$^{81}\text{Br}$ (n, $\gamma$ )
$^{125}\text{I}$	$\frac{5}{2}+$	60.2 d	Electron capture (0.035)	$^{123}\text{Sb}(\alpha,2n)$ , $^{124}\text{Te}(d,n)$ , or $^{125}\text{Xe}(\beta^-)$
$^{128}\text{I}$	1+	24.99 min	$\beta^-$ (2.12, 1.66)	$^{127}\text{I}(n,\gamma)$
$^{129}\text{I}$	$\frac{7}{2}+$	$1.57 \times 10^7$ y	$\beta^-$ (0.189)	U fission
$^{131}\text{I}$	$\frac{7}{2}+$	8.04 d	$\beta^-$ (0.806)	$^{130}\text{Te}(n,\gamma)$ , U or Pu fission

of the use of radioactive isotopes of the halogens, including exchange reactions, tracer studies of other reactions, studies of diffusion phenomena, radiochemical methods of analysis, physiological and biochemical applications, and uses in technology and industry is available.<sup>(23)</sup> Excited states of  $^{127}\text{I}$  and  $^{129}\text{I}$  have also been used extensively in Mössbauer spectroscopy.<sup>(24)</sup>

The nuclear spin of the stable isotopes of the halogens has been exploited in nmr spectroscopy. The use of  $^{19}\text{F}$  in particular, with its 100% abundance, convenient spin of  $\frac{1}{2}$  and excellent sensitivity, has resulted in a vast and continually expanding literature since  $^{19}\text{F}$  chemical shifts were first observed in 1950.<sup>(25)</sup> The resonances for  $^{35}\text{Cl}$  and  $^{37}\text{Cl}$  were also first observed in 1950.<sup>(26)</sup> Appropriate nuclear parameters are in Table 17.6. From this it is clear that the  $^{19}\text{F}$  resonance can be observed with high receptivity

at a frequency fairly close to that for  $^1\text{H}$ . Furthermore, since  $I < 1$  there is no nuclear quadrupole moment and hence no quadrupolar broadening of the resonance. The observed range of  $^{19}\text{F}$  chemical shifts is more than an order of magnitude greater than for  $^1\text{H}$  and spans more than 800 ppm of the resonance frequency.<sup>(27,28)</sup> The signal moves to higher frequency with increasing electronegativity and oxidation state of the attached atom thus following the usual trends. Results are regularly reviewed.<sup>(29)</sup> For other halogens, as seen from Table 17.6, the nuclear spin  $I$  is greater than  $\frac{1}{2}$  which means that the nuclear charge distribution is non-spherical; this results in a nuclear quadrupole moment, and resonance broadening due to quadrupolar relaxation severely restricts the use of the technique except for the halide ions  $\text{X}^-$  or for tetrahedral species such as  $\text{ClO}_4^-$  which have zero electric field gradient at the halogen nucleus. The receptivity is also much less

<sup>23</sup> A. J. DOWNS and C. J. ADAMS, in J. C. BAILAR, H. J. EMELÉUS, R. S. NYHOLM and A. F. TROTMAN-DICKENSON, *Comprehensive Inorganic Chemistry*, Vol. 2, pp. 1148-61 (Isotopes), Pergamon Press, Oxford, 1973.

<sup>24</sup> N. N. GREENWOOD and T. C. GIBB, *Mössbauer Spectroscopy*, pp. 462-82, Chapman & Hall, London, 1971. R. V. PARISH in G. J. LONG (ed.), *Mössbauer Spectroscopy Applied to Inorganic Chemistry*, Vol. 2, Chap. 9, 391-428 (1987). Plenum Press, New York.

<sup>25</sup> W. C. DICKENSON, *Phys. Rev.* **77**, 736-7 (1950). H. S. GUTOWSKY and C. J. HOFFMAN, *Phys. Rev.* **80**, 110-11 (1950).

<sup>26</sup> W. G. PROCTOR and F. C. YU, *Phys. Rev.* **77**, 716-7 (1950).

<sup>27</sup> J. W. EMSLEY, J. FEENEY and L. H. SUTCLIFFE, *High Resolution Nuclear Magnetic Resonance Spectroscopy*, Vols. 1 and 2, Pergamon Press, Oxford, 1966, Chap. 11, Fluorine-19, pp. 871-968.

<sup>28</sup> C. J. JAMESON in J. MASON (ed.) *Multinuclear NMR*, Plenum Press, New York, 1987. Fluorine, pp. 437-46. See also J. H. CLARK, E. M. GOODMAN, D. K. SMITH, S. J. BROWN and J. M. MILLER, *J. Chem. Soc., Chem. Commun.*, 657-8 (1986).

<sup>29</sup> *Annual Reports on NMR Spectroscopy*, Vol. 1 (1968)-Vol. 10b (1980) (Fluorine).

Table 17.6 Nuclear magnetic resonance parameters for the halogen isotopes

Isotope	Nuclear spin quantum no. $I$	NMR frequency rel to $^1\text{H}(\text{SiMe}_4)$ = 100.000	Relative receptivity $D_p^{(a)}$	Nuclear quadrupole moment $Q/ (e \cdot 10^{-28} \text{ m}^2)$
$^1\text{H}$	1/2	100.000	1.000	0
$^{19}\text{F}$	1/2	94.094	0.8328	0
$^{35}\text{Cl}$	3/2	9.809	$3.55 \times 10^{-3}$	$-8.2 \times 10^{-2}$
$^{37}\text{Cl}$	3/2	8.165	$6.44 \times 10^{-4}$	$-6.5 \times 10^{-2}$
$(^{79}\text{Br})^{(b)}$	3/2	25.140	$3.97 \times 10^{-2}$	0.33
$^{81}\text{Br}$	3/2	27.100	$4.87 \times 10^{-2}$	0.27
$^{127}\text{I}$	5/2	20.146	$9.34 \times 10^{-2}$	-0.79

<sup>(a)</sup>Receptivity  $D$  is proportional to  $\gamma^3 N I(I+1)$  where  $\gamma$  is the magnetogyric ratio,  $N$  the natural abundance of the isotope, and  $I$  the nuclear spin quantum number;  $D_p$  is the receptivity relative to that of the proton taken as 1.000.

<sup>(b)</sup>Less-favourable isotope.

Table 17.7 Interatomic distances in crystalline halogens (pm)

X	X-X	X...X		Ratio $\frac{\text{X...X}}{\text{X-X}}$
		Within layer	Between layers	
F	149	324	284	(1.91)
Cl	198	332, 382	374	1.68
Br	227	331, 379	399	1.46
I	272	350, 397	427	1.29

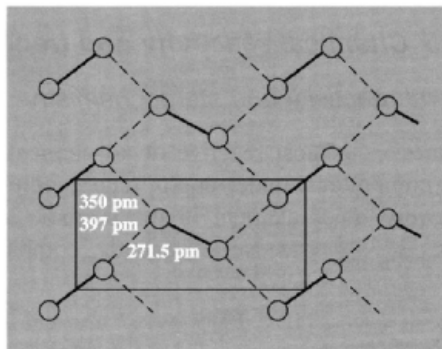
than for  $^1\text{H}$  or  $^{19}\text{F}$  which accordingly renders observation difficult. Despite these technical problems, much useful information has been obtained, especially in physicochemical and biological investigations.<sup>(30,31)</sup> The quadrupole moments of Cl, Br and I have also been exploited successfully in nuclear quadrupole resonance studies of halogen-containing compounds in the solid state.<sup>(32)</sup>

<sup>30</sup> B. LINDMAN and S. FORSEN, Chap. 13 in R. K. HARRIS and B. E. MANN (eds.), *NMR and the Periodic Table*, pp. 421-38, Academic Press, London, 1978. B. LINDMAN and S. FORSEN, Physicochemical and biological applications, Vol. 12 of P. DIEHL, E. FLUCK and R. KOSFELD (eds.), *NMR Basic Principles and Progress*, Springer-Verlag, Berlin, 1976, 365 pp.

<sup>31</sup> J. W. AKITT, in ref. 28, The quadrupolar halides Cl, Br and I, pp. 447-61.

<sup>32</sup> T. P. DAS and E. L. HAHN, *Nuclear Quadrupole Resonance Spectroscopy*, Academic Press, New York, 1958, 223 pp; E. A. C. LUCKEN, *Nuclear Quadrupole Coupling Constants*, Academic Press, London, 1969, 360 pp.

The molecular and bulk properties of the halogens, as distinct from their atomic and nuclear properties, were summarized in Table 17.4 and have to some extent already been briefly discussed. The high volatility and relatively low enthalpy of vaporization reflect the diatomic molecular structure of these elements. In the solid state the molecules align to give a layer lattice:  $\text{F}_2$  has two modifications (a low-temperature,  $\alpha$ -form and a higher-temperature,  $\beta$ -form) neither of which resembles the orthorhombic layer lattice of the isostructural  $\text{Cl}_2$ ,  $\text{Br}_2$  and  $\text{I}_2$ . The layer lattice is illustrated below for  $\text{I}_2$  the I-I distance of 271.5 pm is appreciably longer than in gaseous  $\text{I}_2$  (266.6 pm) and the closest interatomic approach between the molecules is 350 pm within the layer and 427 pm between layers (cf the van der Waals radius of 215 pm). These values are



compared with similar data for the other halogens in Table 17.7 from which two further features of interest emerge: (a) the intralayer intermolecular distances  $\text{Cl}\cdots\text{Cl}$  and  $\text{Br}\cdots\text{Br}$  are almost identical, and (b) the differences between intra- and inter-layer  $\text{X}\cdots\text{X}$  distances decreases with increase in atomic number. (Fluorine is not directly comparable because of its differing structure.)

As expected from their structures, the elements are poor conductors of electricity: solid  $\text{F}_2$  and  $\text{Cl}_2$  have negligible conductivity and  $\text{Br}_2$  has a value of  $\sim 5 \times 10^{-13} \text{ ohm}^{-1} \text{ cm}^{-1}$  just below the mp. Iodine single crystals at room temperature have a conductivity of  $5 \times 10^{-12} \text{ ohm}^{-1} \text{ cm}^{-1}$  perpendicular to the  $bc$  layer plane but this increases to  $1.7 \times 10^{-8} \text{ ohm}^{-1} \text{ cm}^{-1}$  within this plane; indeed, the element is a two-dimensional semiconductor with a band gap  $E_g \sim 1.3 \text{ eV}$  ( $125 \text{ kJ mol}^{-1}$ ). Even more remarkably, when crystals of iodine are compressed they become metallic, and at 350 kbar have a conductivity of  $\sim 10^4 \text{ ohm}^{-1} \text{ cm}^{-1}$ .<sup>(33)</sup> The metallic nature of the conductivity is confirmed by its negative temperature coefficient.

The ease of dissociation of the  $\text{X}_2$  molecules follows closely the values of the enthalpy of dissociation since the entropy change for the reaction is almost independent of X. Thus  $\text{F}_2$  at 1 atm pressure is 1% dissociated into atoms at  $765^\circ\text{C}$  but a temperature of  $975^\circ\text{C}$  is required to achieve the same degree of dissociation for  $\text{Cl}_2$ ; thereafter, the required temperature drops to  $775^\circ\text{C}$  for  $\text{Br}_2$  and  $575^\circ\text{C}$  for  $\text{I}_2$  (see also next section for atomic halogens).

### 17.1.5 Chemical reactivity and trends

#### General reactivity and stereochemistry

Fluorine is the most reactive of all elements. It forms compounds, under appropriate conditions, with every other element in the periodic table except He, Ar and Ne, frequently combining

directly and with such vigour that the reaction becomes explosive. Some elements such as  $\text{O}_2$  and  $\text{N}_2$  react less readily with fluorine (pp. 639, 438) and some bulk metals (e.g. Al, Fe, Ni, Cu) acquire a protective fluoride coating, though all metals react exothermically when powdered and/or heated. For example, powdered Fe (0.84 mm size, 20 mesh) is not attacked by liquid  $\text{F}_2$  whereas at 0.14 mm size (100 mesh) it ignites and burns violently. Perhaps the most striking example of the reactivity of  $\text{F}_2$  is the ease with which it reacts directly with Xe under mild conditions to produce crystalline xenon fluorides (p. 894). This great reactivity of  $\text{F}_2$  can be related to its small dissociation energy (p. 801) (which leads to low activation energies of reaction), and to the great strength of the bonds that fluorine forms with other elements. Both factors in turn can be related to the small size of the F atom and ensure that enthalpies of fluorination are much greater than those of other halogenations. Some typical average bond energies ( $\text{kJ mol}^{-1}$ ) illustrating these points are:

X	XX	HX	$\text{BX}_3$	$\text{AlX}_3$	$\text{CX}_4$
F	159	574	645	582	456
Cl	243	428	444	427	327
Br	193	363	368	360	272
I	151	294	272	285	239

The tendency for  $\text{F}_2$  to give  $\text{F}^-$  ions in solution is also much greater than for the other halogens as indicated by the steady decrease in oxidation potential ( $E^\circ$ ) for the reaction  $\text{X}_2(\text{soln}) + 2\text{e}^- \rightleftharpoons 2\text{X}^-(\text{aq})$ :

$\text{X}_2$	$\text{F}_2$	$\text{Cl}_2$	$\text{Br}_2$	$\text{I}_2$	$\text{At}_2$
$E^\circ/\text{V}$	2.866	1.395	1.087	0.615	$\sim 0.3$

The corresponding free energy changes can be calculated from the relation  $\Delta G = -nE^\circ F$  where  $n = 2$  and  $F = 96.485 \text{ kJ mol}^{-1}$ . Note that  $E^\circ(\text{F}_2/2\text{F}^-)$  is greater than the decomposition potential for water (p. 629). Note also the different sequence of values for  $E^\circ(\text{X}_2/2\text{X}^-)$  and for the electron affinities of  $\text{X}(\text{g})$  (p. 800). A similar "anomaly" was observed (p. 75) for  $E^\circ(\text{Li}^+/\text{Li})$  and the ionization energy of  $\text{Li}(\text{g})$ , and

<sup>33</sup> A. S. BALCHIN and H. G. DRICKAMER, *J. Chem. Phys.* **34**, 1948-9 (1961).

in both cases the reason is the same, namely the enhanced enthalpy of hydration of the smaller ions. Other redox properties of the halogens are compared on pp. 853–6.

It follows from the preceding paragraph that  $F_2$  is an extremely strong oxidizing element that can engender unusually high oxidation states in the elements with which it reacts, e.g.  $IF_7$ ,  $PtF_6$ ,  $PuF_6$ ,  $BiF_5$ ,  $TbF_4$ ,  $CmF_4$ ,  $KA_g^{III}F_4$  and  $AgF_2$ . Indeed, fluorine (like the other first-row elements Li, Be, B, C, N and O) is atypical of the elements in its group and for the same reasons. For all 7 elements deviations from extrapolated trends can be explained in terms of three factors:

- (1) their atoms are small;
- (2) their electrons are tightly held and not so readily ionized or distorted (polarized) as in later members of the group;
- (3) they have no low-lying d orbitals available for bonding.

Thus the ionization energy  $I_M$  is much greater for F than for the other halogens, thereby making formal positive oxidation states virtually impossible to attain. Accordingly, fluorine is exclusively univalent and its compounds are formed either by gain of 1 electron to give  $F^-$  ( $2s^2 2p^6$ ) or by sharing 1 electron in a covalent single bond. Note, however, that the presence of lone-pairs permits both the fluoride ion itself and also certain molecular fluorides to act as Lewis bases in which the coordination number of F is greater than 1, e.g. it is 2 for the bridging F atoms in  $As_2F_{11}^-$ ,  $Sb_3F_{16}^-$ ,  $Nb_4F_{20}$ ,  $(HF)_n$  and  $(BeF_2)_\infty$ . The coordination number of  $F^-$  can rise to 3 (planar) in compounds with the rutile structure (e.g.  $MgF_2$ ,  $MnF_2$ ,  $FeF_2$ ,  $CoF_2$ ,  $NiF_2$ ,  $ZnF_2$  and  $PdF_2$ ). Likewise, fourfold coordination (tetrahedral) is found in the zinc-blende-type structure of  $CuF$  and in the fluorite structure of  $CaF_2$ ,  $SrF_2$ ,  $BaF_2$ ,  $RaF_2$ ,  $CdF_2$ ,  $HgF_2$  and  $PbF_2$ . A coordination number of 6 occurs in the alkali metal fluorides  $MF$  (NaCl type). In many of these compounds  $F^-$  resembles  $O^{2-}$  stereochemically rather than the other halides, and the radii of the 2 ions are very similar ( $F^-$  133,  $O^{2-}$  140 pm, cf.  $Cl^-$  184,  $Br^-$  196 pm).

The heavier halogens, though markedly less reactive than fluorine, are still amongst the most reactive of the elements. Their reactivity diminishes in the sequence  $Cl_2 > Br_2 > I_2$ . For example,  $Cl_2$  reacts with CO, NO and  $SO_2$  to give  $COCl_2$ ,  $NOCl$  and  $SO_2Cl_2$ , whereas iodine does not react with these compounds. Again, in the direct halogenation of metals,  $Cl_2$  and  $Br_2$  sometimes produce a higher metal oxidation state than does  $I_2$ , e.g. Re yields  $ReCl_6$ ,  $ReBr_5$  and  $ReI_4$  respectively. Conversely, the decreasing ionization energies and increasing ease of oxidation of the elements results in the readier formation of iodine cations (p. 842) and compounds in which iodine has a higher stable oxidation state than the other halogens (e.g.  $IF_7$ ). The general reactivity of the individual halogens with other elements (both metals and non-metals) is treated under the particular element concerned. Reaction between the halogens themselves is discussed on p. 824. In general, reaction of  $X_2$  with compounds containing M–M, M–H or M–C bonds results in the formation of M–X bonds (M = metal or non-metal). Reaction with metal oxides sometimes requires the presence of C and the use of elevated temperatures.

The stereochemistry of the halogens in their various compounds is summarized in Table 17.8 and will be elucidated in more detail in subsequent sections.

Reactivity is enhanced in conditions which promote the generation of halogen atoms, though this does not imply that all reactions proceed via the intermediacy of X atoms. The reversible thermal dissociation of gaseous  $I_2 \rightleftharpoons 2I$  was first demonstrated by Victor Meyer in 1880 and has since been observed for the other halogens as well (p. 804). Atomic Cl and Br are more conveniently produced by electric discharge though, curiously, this particularly method is not successful for I. Microwave and radiofrequency discharges have also been used as well as optical dissociation by ultraviolet light. At room temperature and at pressures below 1 mmHg, up to 40% atomization can be achieved, the mean lives of the Cl and Br atoms in glass apparatus being of the order of a few milliseconds. The

Table 17.8 Stereochemistry of the halogens

CN	Geometry	F	Cl	Br	I
0	—	F <sup>•</sup> (g), F <sup>-</sup> (soln)	Cl <sup>•</sup> (g), Cl <sup>-</sup> (soln)	Br <sup>•</sup> (g), Br <sup>-</sup> (soln)	I <sup>•</sup> (g), I <sup>-</sup> (soln)
1	—	F <sub>2</sub> , ClF, BrF <sub>3</sub> , BF <sub>3</sub> , RF	Cl <sub>2</sub> , ICl, BCl <sub>3</sub> , RCl	Br <sub>2</sub> , IBr, BBr <sub>3</sub> , RBr	I <sub>2</sub> , IX, PI <sub>3</sub> , RI
2	Linear	Nb <sub>4</sub> F <sub>20</sub> NbF <sub>3</sub> (ReO <sub>3</sub> -type)	ClF <sub>2</sub> <sup>-</sup> YCl <sub>3</sub> (ReO <sub>3</sub> -type)	Br <sub>3</sub> <sup>-</sup> , (MeCN) <sub>2</sub> Br <sub>2</sub> CrBr <sub>3</sub> (ReO <sub>3</sub> -type)	I <sub>3</sub> <sup>-</sup> , ICl <sub>2</sub> <sup>-</sup> , BrICl <sup>-</sup> , Me <sub>3</sub> NI <sub>2</sub> BiI <sub>3</sub> (ReO <sub>3</sub> -type)
	Bent	(BeF <sub>2</sub> ) <sub>α</sub> , (HF) <sub>n</sub> , Sn <sub>4</sub> F <sub>8</sub>	ClO <sub>2</sub> , ClO <sub>2</sub> <sup>-</sup> , Al <sub>2</sub> Cl <sub>6</sub> , [Nb <sub>6</sub> Cl <sub>12</sub> ] <sup>2+</sup> , ClF <sub>2</sub> <sup>+</sup> BeCl <sub>2</sub> (polym), PdCl <sub>2</sub>	BrF <sub>2</sub> <sup>+</sup> , Al <sub>2</sub> Br <sub>6</sub>	IR <sub>2</sub> <sup>+</sup> , Al <sub>2</sub> I <sub>6</sub> , AuI(polymeric)
3	Trigonal pyramidal T-shaped		ClO <sub>3</sub> <sup>-</sup> , CdCl <sub>2</sub> , [Mo <sub>6</sub> Cl <sub>8</sub> ] <sup>4+</sup> ClF <sub>3</sub>	BrO <sub>3</sub> <sup>-</sup> , MgBr <sub>2</sub>  BrF <sub>3</sub>	HIO <sub>3</sub> , IO <sub>3</sub> <sup>-</sup> , CdI <sub>2</sub> RICl <sub>2</sub>
4	Planar Tetrahedral	MgF <sub>2</sub> (rutile) CaF <sub>2</sub> (fluorite) CuF (blende)	SrCl <sub>2</sub> (fluorite), ClO <sub>4</sub> <sup>-</sup> , FClO <sub>3</sub> , CuCl	BrO <sub>4</sub> <sup>-</sup> , FBrO <sub>3</sub> , CuBr BrF <sub>4</sub> <sup>-</sup>	IO <sub>4</sub> <sup>-</sup> CuI ICl <sub>4</sub> <sup>-</sup> , I <sub>2</sub> Cl <sub>6</sub>
	Square planar See-saw (C <sub>2v</sub> , or C <sub>s</sub> )		F <sub>3</sub> ClO, [F <sub>2</sub> ClO <sub>2</sub> ] <sup>-</sup>	F <sub>3</sub> BrO, [F <sub>2</sub> BrO <sub>2</sub> ] <sup>-</sup>	[F <sub>2</sub> IO <sub>2</sub> ] <sup>-</sup> , IF <sub>4</sub> <sup>+</sup>
5	Square pyramidal Trigonal bipyramidal		ClF <sub>5</sub> , [F <sub>4</sub> ClO] <sup>-</sup>  F <sub>3</sub> ClO <sub>2</sub>	BrF <sub>5</sub> , [F <sub>4</sub> BrO] <sup>-</sup>	IF <sub>5</sub> , [(F <sub>5</sub> TeO) <sub>4</sub> IO] <sup>-</sup> IO <sub>5</sub> <sup>3-</sup> (?)
6	Octahedral	NaF	NaCl	NaBr  BrF <sub>6</sub> <sup>-</sup>	IO <sub>6</sub> <sup>5-</sup> , F <sub>5</sub> IO, NaI, IF <sub>6</sub> <sup>+</sup> IF <sub>6</sub> <sup>-</sup> (?)
7	Distorted octahedral Pentagonal bipyramidal				IF <sub>7</sub>
	Hexagonal pyramidal		C <sub>6</sub> H <sub>6</sub> .Cl <sub>2</sub>	C <sub>6</sub> H <sub>6</sub> .Br <sub>2</sub>	
8	Cubic Square antiprismatic		CsCl, TlCl	CsBr, TlBr	CsI, TlI, Zr(IO <sub>3</sub> ) <sub>4</sub>

reason for the slow and relatively inefficient reversion to X<sub>2</sub> is the need for a 3-body collision in order to dissipate the energy of combination: X<sup>•</sup> + X<sup>•</sup> + M → X<sub>2</sub> + M<sup>\*</sup>. A fuller account of the production, detection and chemical reactions of atomic Cl, Br and I is on pages 1141–8 and 1165–72 of reference 23.

### Solutions and charge-transfer complexes<sup>(34)</sup>

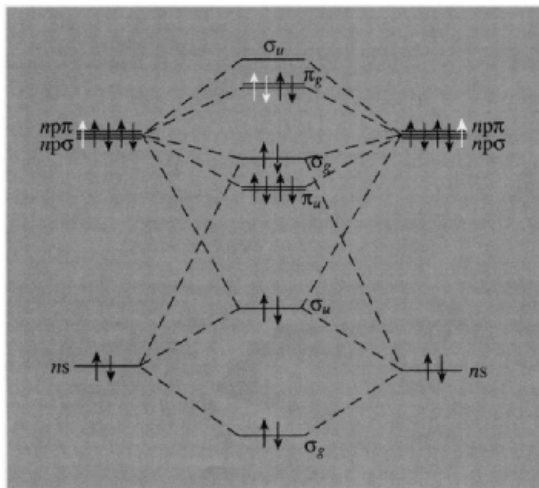
The halogens are soluble to varying extents in numerous solvents though their great reactivity

sometimes results in solvolysis or in halogenation of the solvent. Reactions with water are discussed on pp. 855ff. Iodine is only slightly soluble in water (0.340 g/kg at 25°, 4.48 g/kg at 100°). It is more soluble in aqueous iodide solutions due to the formation of polyiodides (p. 835) and these can achieve astonishing concentrations; e.g. the solution in equilibrium with solid iodine and KI<sub>7</sub>.H<sub>2</sub>O at 25° contains 67.8 wt% of iodine, 25.6% KI and 6.6% H<sub>2</sub>O. Iodine is also readily soluble in many organic solvents, typical values of its solubility at 25°C being (g/kg solvent): Et<sub>2</sub>O 337.3, EtOH 271.7, mesitylene 253.1, *p*-xylene 198.3, CS<sub>2</sub> 197.0, toluene 182.5, benzene 164.0, ethyl acetate 157, EtBr 146, EtCN 141,

<sup>34</sup> Ref. 23, pp. 1196–220.

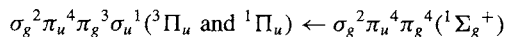
$C_2H_4Br_2$  115.1,  $Bu^iOH$  97,  $CHBr_3$  65.9,  $CHCl_3$  49.7, cyclohexane 27.9,  $CCl_4$  19.2, *n*-hexane 13.2, perfluoroheptane 0.12.

The most notable feature of such solutions is the dramatic dependence of their colour on the nature of the solvent chosen. Thus, solutions in aliphatic hydrocarbons or  $CCl_4$  are bright violet ( $\lambda_{max}$  520–540 nm), those in aromatic hydrocarbons are pink or reddish brown, and those in stronger donors such as alcohols, ethers or amines are deep brown ( $\lambda_{max}$  460–480 nm). This variation can be understood in terms of a weak donor–acceptor interaction leading to complex formation between the solvent (donor) and  $I_2$  (acceptor) which alters the optical transition energy. Thus, referring to the conventional molecular orbital energy diagram for  $I_2$  (or other  $X_2$ ) as shown in Fig. 17.2, the violet colour of  $I_2$  vapour can be seen to arise as a result of the excitation of an electron from the highest occupied MO (the antibonding  $\pi_g$  level) into the lowest unoccupied MO (the antibonding  $\sigma_u$  level). In non-coordinating solvents such as aliphatic hydrocarbons or their fluoro- or chloro-derivatives the transition energy (and hence the colour) remains essentially unmodified.



**Figure 17.2** Schematic molecular orbital energy diagram for diatomic halogen molecules. (For  $F_2$  the order of the upper  $\sigma_g$  and  $\pi_u$  bonding MOs is inverted.)

However, in electron-donor solvents, L, the vacant antibonding  $\sigma_u$  orbital of  $I_2$  acts as an electron acceptor thus weakening the I–I bond and altering the energy of the electronic transitions:



Consistent with this: (a) the solubility of iodine in the donor solvents tends to be greater than in the non-donor solvents (see list of solubilities), (b) brown solutions frequently turn violet on being heated, and brown again on cooling, due to the ready dissociation and reformation of the complex, and (c) addition of a small amount of a donor solvent to a violet solution turns the colour brown. Such donor solvents can be classified as (i) weak  $\pi$  donors (e.g. the aromatic hydrocarbons and alkenes), (ii) stronger  $\sigma$  donors such as nitrogen bases (amines, pyridines, nitriles), oxygen bases (alcohols, ethers, carbonyls), and organic sulfides and selenides.

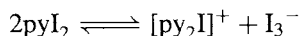
The most direct evidence for the formation of a complex  $L \rightarrow I_2$  in solution comes from the appearance of an intense new charge-transfer band in the near ultraviolet spectrum. Such a band occurs in the region 230–330 nm with a molar extinction coefficient  $\epsilon$  of the order of  $5 \times 10^3 - 5 \times 10^4 \text{ l mol}^{-1} \text{ cm}^{-1}$  and a half-width typically of  $4000 - 8000 \text{ cm}^{-1}$ . Detailed physico-chemical studies further establish that the formation constants of such complexes span the range  $10^{-1} - 10^4 \text{ l mol}^{-1}$  with enthalpies of formation  $5 - 50 \text{ kJ mol}^{-1}$ . Some typical examples are in Table 17.9. The donor strength of the various solvents (ligands) is rather independent of the particular halogen (or interhalogen) solute and follows the approximate sequence benzene < alkenes < polyalkylbenzenes  $\approx$  alkyl iodides  $\approx$  alcohols  $\approx$  ethers  $\approx$  ketones < organic sulfides < organic selenides < amines. Conversely, for a given solvent the relative acceptor strength of the halogens increases in the sequence  $Cl_2 < Br_2 < I_2 < IBr < ICl$ , i.e. they are class b or “soft” acceptors (p. 909). Further interactions may also occur in polar solvents leading to ionic dissociation which



Table 17.9 Some iodine complexes in solution

Donor solvent	Formation constant $K(20^\circ\text{C})/\text{l mol}^{-1}$	$-\Delta H_f/$ $\text{kJ mol}^{-1}$	Charge-transfer band		
			$\lambda_{\text{max}}/\text{nm}$	$\epsilon_{\text{max}}$	$\Delta\nu_{1/2}/\text{cm}^{-1}$
Benzene	0.15	5.9	292	16 000	5100
Ethanol	0.26	18.8	230	12 700	6800
Diethyl ether	0.97	18.0	249	5 700	6900
Diethyl sulfide	210	32.7	302	29 800	5400
Methylamine	530	29.7	245	21 200	6400
Dimethylamine	6 800	41.0	256	26 800	6450
Trimethylamine	12 100	50.6	266	31 300	8100
Pyridine	269	32.6	235	50 000	5200

renders the solutions electrically conducting, e.g.:



Numerous solid complexes have been crystallized from brown solutions of iodine and extensive X-ray structural data are available. Complexes of the type  $\text{L} \rightarrow \text{I} - \text{X}$  and  $\text{L} \rightarrow \text{I} - \text{X} \leftarrow \text{L}$

( $\text{L} = \text{Me}_3\text{N}$ , py, etc.;  $\text{X} = \text{I}$ , Br, Cl, CN) feature a linear configuration as expected from the involvement of the  $\sigma_u$  antibonding orbital of  $\text{IX}$  (Fig. 17.3a, b, c). When the ligand has two donor atoms (as in dioxan) or the donor atom has more than one lone-pair of electrons (as in acetone) the complexes can associate

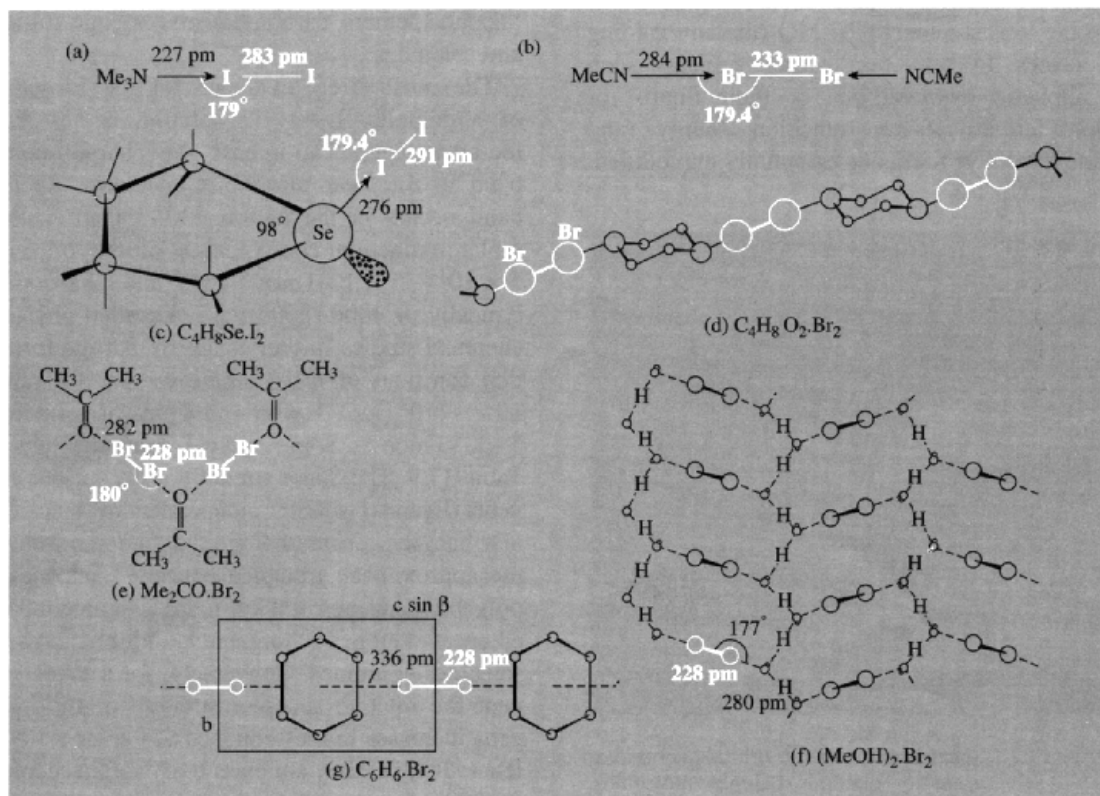


Figure 17.3 Structures of some molecular complexes of the halogens.

into infinite chains (Fig. 17.3d, e), whereas with methanol, the additional possibility of hydrogen bonding permits further association into layers (Fig. 17.3f). The structure of  $C_6H_6.Br_2$  is also included in Fig. 17.3(g). In all these examples, the lengthening of the X–X bond from that in the free halogen molecule is notable.

The intense blue colour of starch-iodine was mentioned on p. 790.

## 17.2 Compounds of Fluorine, Chlorine, Bromine and Iodine

### 17.2.1 Hydrogen halides, HX

It is common practice to refer to the molecular species HX and also the pure (anhydrous) compounds as hydrogen halides, and to call their aqueous solutions hydrohalic acids. Both the anhydrous compounds and their aqueous solutions will be considered in this section. HCl and hydrochloric acid are major industrial chemicals and there is also a substantial production of HF and hydrofluoric acid. HBr and hydrobromic acid are made on a much smaller scale and there seems to be little industrial demand for HI and hydriodic acid. It will be convenient to discuss first the preparation and industrial uses of the compounds and then to consider their molecular and bulk physical properties. The chemical reactivity of the anhydrous compounds and their acidic aqueous solutions will then be reviewed, and the section concludes with a discussion of the anhydrous compounds as nonaqueous solvents.

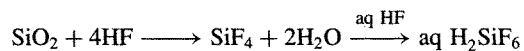
#### Preparation and uses

Anhydrous HF is almost invariably made by the action of conc  $H_2SO_4$  ( $\geq 95\%$ ) on “acid grade” fluorspar ( $\geq 98\%$   $CaF_2$ ):



As the reaction is endothermic heat must be supplied to obtain good yields in reasonable

time (e.g. 30–60 min at 200–250°C). Silica is a particularly undesirable impurity in the fluorspar since it consumes up to 6 moles of HF per mole of  $SiO_2$  by reacting to form  $SiF_4$  and then  $H_2SiF_6$ . A typical unit, producing up to 20 000 tonnes of HF pa, consists of an externally heated, horizontal steel kiln about 30 m long rotating at 1 revolution per minute. The product gas emerges at 100–150°C and, after appropriate treatment to remove solid, liquid and gaseous impurities, is condensed to give a 99% pure product which is then redistilled to give a final product of 99.9% purity. The technical requirements to enable the safe manufacture and handling of so corrosive a product are considerable.<sup>(2,13)</sup> In principle, HF could also be obtained from the wet-processing of fluorapatite to give phosphoric acid (p. 521) but the presence of  $SiO_2$  preferentially yields  $SiF_4$  and  $H_2SiF_6$  from which HF can only be recovered uneconomically.



Some of the  $H_2SiF_6$  so produced finds commercial outlets (p. 810), but it has been estimated that ~500 000 tonnes of  $H_2SiF_6$  is discarded annually by the US phosphoric acid industry, equivalent to ~1 million tonnes of fluorspar — enough to supply that nation’s entire requirements for HF. Production figures and major uses are in the Panel.

Hydrogen chloride is a major industrial chemical and is manufactured on a huge scale. It is also a familiar laboratory reagent both as a gas and as an aqueous acid. The industrial production and uses of HCl are summarized in the Panel on p. 811. One important method for synthesis on a large scale is the burning of  $H_2$  in  $Cl_2$ : no catalyst is needed but economic sources of the two elements are obviously required. Another major source of HCl is as a by-product of the chlorination of hydrocarbons (p. 798). The traditional “salt-cake” process of treating NaCl with conc  $H_2SO_4$  also remains an important industrial source of the acid. On a small laboratory scale, gaseous HCl can be made by treating concentrated aqueous hydrochloric acid

into infinite chains (Fig. 17.3d, e), whereas with methanol, the additional possibility of hydrogen bonding permits further association into layers (Fig. 17.3f). The structure of  $C_6H_6.Br_2$  is also included in Fig. 17.3(g). In all these examples, the lengthening of the X–X bond from that in the free halogen molecule is notable.

The intense blue colour of starch-iodine was mentioned on p. 790.

## 17.2 Compounds of Fluorine, Chlorine, Bromine and Iodine

### 17.2.1 Hydrogen halides, HX

It is common practice to refer to the molecular species HX and also the pure (anhydrous) compounds as hydrogen halides, and to call their aqueous solutions hydrohalic acids. Both the anhydrous compounds and their aqueous solutions will be considered in this section. HCl and hydrochloric acid are major industrial chemicals and there is also a substantial production of HF and hydrofluoric acid. HBr and hydrobromic acid are made on a much smaller scale and there seems to be little industrial demand for HI and hydriodic acid. It will be convenient to discuss first the preparation and industrial uses of the compounds and then to consider their molecular and bulk physical properties. The chemical reactivity of the anhydrous compounds and their acidic aqueous solutions will then be reviewed, and the section concludes with a discussion of the anhydrous compounds as nonaqueous solvents.

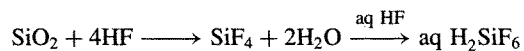
#### Preparation and uses

Anhydrous HF is almost invariably made by the action of conc  $H_2SO_4$  ( $\geq 95\%$ ) on “acid grade” fluorspar ( $\geq 98\%$   $CaF_2$ ):



As the reaction is endothermic heat must be supplied to obtain good yields in reasonable

time (e.g. 30–60 min at 200–250°C). Silica is a particularly undesirable impurity in the fluorspar since it consumes up to 6 moles of HF per mole of  $SiO_2$  by reacting to form  $SiF_4$  and then  $H_2SiF_6$ . A typical unit, producing up to 20 000 tonnes of HF pa, consists of an externally heated, horizontal steel kiln about 30 m long rotating at 1 revolution per minute. The product gas emerges at 100–150°C and, after appropriate treatment to remove solid, liquid and gaseous impurities, is condensed to give a 99% pure product which is then redistilled to give a final product of 99.9% purity. The technical requirements to enable the safe manufacture and handling of so corrosive a product are considerable.<sup>(2,13)</sup> In principle, HF could also be obtained from the wet-processing of fluorapatite to give phosphoric acid (p. 521) but the presence of  $SiO_2$  preferentially yields  $SiF_4$  and  $H_2SiF_6$  from which HF can only be recovered uneconomically.



Some of the  $H_2SiF_6$  so produced finds commercial outlets (p. 810), but it has been estimated that ~500 000 tonnes of  $H_2SiF_6$  is discarded annually by the US phosphoric acid industry, equivalent to ~1 million tonnes of fluorspar — enough to supply that nation’s entire requirements for HF. Production figures and major uses are in the Panel.

Hydrogen chloride is a major industrial chemical and is manufactured on a huge scale. It is also a familiar laboratory reagent both as a gas and as an aqueous acid. The industrial production and uses of HCl are summarized in the Panel on p. 811. One important method for synthesis on a large scale is the burning of  $H_2$  in  $Cl_2$ : no catalyst is needed but economic sources of the two elements are obviously required. Another major source of HCl is as a by-product of the chlorination of hydrocarbons (p. 798). The traditional “salt-cake” process of treating NaCl with conc  $H_2SO_4$  also remains an important industrial source of the acid. On a small laboratory scale, gaseous HCl can be made by treating concentrated aqueous hydrochloric acid

## Production and Uses of Hydrogen Fluoride

Anhydrous HF was first produced commercially in the USA in 1931 and in the UK from about 1942. By 1992 some eighteen countries were each producing at least 3000 tonnes pa with North America accounting for some 330 000 tonnes of the estimated annual world production of about 875 000 tonnes. A further 205 000 tonnes was used captively for production of  $\text{AlF}_3$ . Price in 1990 was about \$1.50/kg for the anhydrous acid and somewhat less for 70% acid. The primary suppliers ship HF in tank-cars of 20–91-tonne capacity and the product is also repackaged in steel cylinders holding 8.0–900 kg (2.7–635 kg in the UK). Lecture bottles contain 340 g HF. The 70% acid is shipped in tank-cars of 32–80-tonne capacity, tank trucks of 20-tonne capacity, and in polyethylene-lined drums holding 114 or 208 l.

The early need for HF was in the production of chlorofluorocarbons for refrigeration units and pressurizing gases. The large increase in aluminium production in 1935–40 brought an equivalent requirement for HF (for synthetic cryolite, p. 219) and these two uses still account for the bulk of HF produced in North America (comprising the single market of USA, Canada and Mexico), namely 53.0% and 24.3%, respectively. Other outlets are petroleum alkylation catalysts and steel pickling (3.8% each) and the nuclear industry (3.0%). The remaining 12.1% is distributed amongst traditional uses (such as glass etching and the frosting of light bulbs and television tubes, and the manufacture of fluoride salts), and newer applications such as rocket-propellant stabilizers, preparation of microelectronic circuits, laundry soaps and stain removers.

Probably about 50 000 tonnes of HF are used worldwide annually to make inorganic compounds other than  $\text{UF}_4/\text{UF}_6$  for the nuclear industry. Prominent amongst these products are:

$\text{NaF}$ : for water fluoridation, wood preservatives, the formulation of insecticides and fungicides, and use as a fluxing agent. It is also used to remove HF from gaseous  $\text{F}_2$  in the manufacture and purification of  $\text{F}_2$ .

$\text{SnF}_2$ : in toothpastes to prevent dental caries.

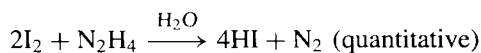
$\text{HBF}_4$  (aq) and metal fluoroborates: electroplating of metals, catalysts, fluxing in metal processing and surface treatment.

$\text{H}_2\text{SiF}_6$  and its salts: fluoridation of water, glass and ceramics manufacture, metal-ore treatment.

The highly corrosive nature of HF and aqueous hydrofluoric acid solutions have already been alluded to (pp. 792, 797) and great caution must be exercised in their handling. The salient feature of HF burns is the delayed onset of discomfort and the development of a characteristic white lesion that is excruciatingly painful. The progressive action of HF on skin is due to dehydration, low pH and the specific toxic effect of high concentrations of fluoride ions: these remove  $\text{Ca}^{2+}$  from tissues as insoluble  $\text{CaF}_2$  and thereby delay healing; in addition the immobilization of  $\text{Ca}^{2+}$  results in a relative excess of  $\text{K}^+$  within the tissue, so that nerve stimulation ensues. Treatment of HF burns involves copious sluicing with water for at least 15 min followed either by (a) immersion in (or application of wet packs of) cold  $\text{MgSO}_4$ , or (b) subcutaneous injection of a 10% solution of calcium gluconate (which gives rapid relief from pain), or (c) surgical excision of the burn lesion.<sup>(4)</sup> Medical attention is essential, even if the initial effects appear slight, because of the slow onset of the more serious symptoms.

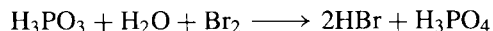
with conc  $\text{H}_2\text{SO}_4$ . Preparation of  $\text{DCl}$  is best effected by the action of  $\text{D}_2\text{O}$  on  $\text{PhCOCl}$  or a similar organic acid chloride;  $\text{PCl}_3$ ,  $\text{PCl}_5$ ,  $\text{SiCl}_4$ ,  $\text{AlCl}_3$ , etc., have also been used.

Similar routes are available for the production of  $\text{HBr}$  and  $\text{HI}$ . The catalysed combination of  $\text{H}_2$  and  $\text{Br}_2$  at elevated temperatures (200–400°C in the presence of  $\text{Pt}$ /asbestos, etc.) is the principal industrial route for  $\text{HBr}$ , and is also used, though on a relatively small scale, for the energetically less-favoured combination of  $\text{H}_2$  and  $\text{I}_2$  ( $\text{Pt}$  catalyst above 300°C). Commercially  $\text{HI}$  is more often prepared by the reaction of  $\text{I}_2$  with  $\text{H}_2\text{S}$  or hydrazine, e.g.:

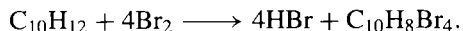


Reduction of the parent halogen with red phosphorus and water provides a convenient

laboratory preparation of both  $\text{HBr}$  and  $\text{HI}$ :



The rapid reaction of 1,2,3,4-tetrahydronaphthalene (tetralin) with  $\text{Br}_2$  at 20° affords an alternative small-scale preparation though only half the  $\text{Br}_2$  is converted, the other half being lost in brominating the tetralin:

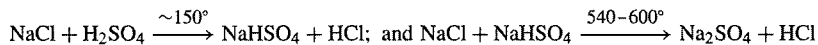


The action of conc  $\text{H}_2\text{SO}_4$  on metal bromides or iodides (analogous to the “salt-cake” process of  $\text{HCl}$ ) causes considerable oxidation of the product  $\text{HX}$  but conc  $\text{H}_3\text{PO}_4$  is satisfactory. Dehydration of the aqueous acids with  $\text{P}_2\text{O}_5$  is a viable alternative.  $\text{DBr}$  and  $\text{DI}$  are obtained by reaction of  $\text{D}_2\text{O}$  on  $\text{PBr}_3$  and  $\text{PI}_3$  respectively.

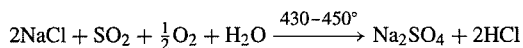
### Industrial Production and Uses of Hydrogen Chloride<sup>(35)</sup>

World production of HCl is of the order of 10 million tonnes pa, thus making it one of the largest volume chemicals to be manufactured. Four major processes account for the bulk of HCl produced, the choice of method invariably being dictated by the ready availability of the particular starting materials, the need for the co-products, or simply the availability of by-product HCl which can be recovered as part of an integrated process.

1. The classic salt-cake method was introduced with the Leblanc process towards the end of the eighteenth century and is still used to produce HCl where rock-salt mineral is cheaply available (as in the UK Cheshire deposits). The process is endothermic and takes place in two stages:



2. The Hargreaves process (late 19th C) is a variant of the salt-cake process in which NaCl is reacted with a gaseous mixture of SO<sub>2</sub>, air and H<sub>2</sub>O (i.e. "H<sub>2</sub>SO<sub>4</sub>") in a self-sustaining exothermic reaction:



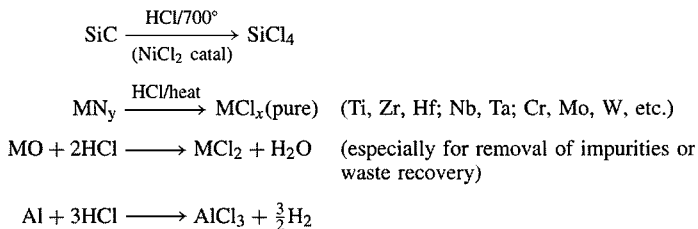
Again the economic operation of the process depends on abundant rock-salt or the need for the by-product Na<sub>2</sub>SO<sub>4</sub> for the paper and glass industries.

3. Direct synthesis of HCl by the burning of hydrogen in chlorine is the favoured process when high-purity HCl is required. The reaction is highly exothermic (~92 kJ/mol HCl) and requires specially designed burners and absorption systems.

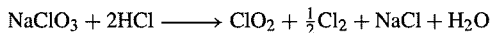
4. By-product HCl from the heavy organic-chemicals industry (p. 798) now accounts for over 90% of the HCl produced in the USA. Where such petrochemical industries are less extensive this source of HCl becomes correspondingly smaller. The crude HCl so produced may be contaminated with unreacted Cl<sub>2</sub>, organics, chloro-organics or entrained solids (catalyst supports, etc.), all of which must be removed.

Most of the byproduct HCl is used captively, primarily in oxyhydrochlorination processes for making vinyl chloride and chlorinated solvents or for Mg processing (p. 110). The scale of the industry is enormous; for example, 5.2 million tonnes of HCl per annum in the US alone (1993). HCl gas for industrial use can be transmitted without difficult over moderate distances in mild-steel piping or in tank cars or trailers. It is also available in cylinders of varying size down to laboratory scale lecture bottles containing 225 g. Aqueous hydrochloric acid consumption (1993) was 1.57 Mt (100% basis). Price for anhydrous HCl is ~\$330/tonne and for 31.4% aqueous acid ~\$73/tonne (1993) depending on plant location and amount required.

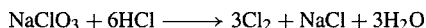
Industrial use of HCl gas for the manufacture of inorganic chemicals includes the preparation of anhydrous NH<sub>4</sub>Cl by direct reaction with NH<sub>3</sub> and the synthesis of anhydrous metal chlorides by reaction with appropriate carbides, nitrides, oxides or even the free metals themselves, e.g.:



HCl is also used in the industrial synthesis of ClO<sub>2</sub> (p. 846):



The reaction is catalysed by various salts of Ti, Mn, Pd and Ag which promote the formation of ClO<sub>2</sub> rather than the competing reaction which otherwise occurs:



*Panel continues*

<sup>35</sup>Kirk-Othmer's *Encyclopedia of Chemical Technology*, 4th Edn., Vol. 13, pp. 894–925 (1995).

HCl is also used in the production of  $\text{Al}_2\text{O}_3$  (p. 242) and  $\text{TiO}_2$  (p. 959), the isolation of Mg from sea water (p. 110), and in many extractive metallurgical processes for isolating or refining metals, e.g. Ge, Sn, V, Mn, Ta, W and Ra.

Aqueous HCl is also produced on a vast scale (e.g. 1.57 Mt/yr in the USA, 1993). Most of this is made and consumed captively at the site of production, predominantly for brine acidification prior to electrolysis in  $\text{Cl}_2$ /alkali cells. The largest merchant market use is for pickling steel and other metals to remove adhering oxide scale, and for the desulfurization of petroleum. It is also used in pH control (effluent neutralization, etc.), the desliming of hides and chrome tanning, ore beneficiation, the coagulation of latex and the production of aniline from  $\text{PhNO}_2$  for dyestuffs intermediates. The manufacture of gelatine requires large quantities of hydrochloric acid to decompose the bones used as raw materials — high purity acid must be used since much of the gelatine is used in foodstuffs for human consumption. Another food-related application is the hydrolysis of starch to glucose under pressure: this process is catalysed by small concentrations of HCl and is extensively used to produce “maple syrup” from maize (corn) starch. At higher concentrations of HCl wood (lignin) can be converted to glucose.

Other uses of HCl are legion and range from the purification of fine silica for the ceramics industry, and the refining of oils, fats and waxes, to the manufacture of chloroprene rubbers, PVC plastics, industrial solvents and organic intermediates, the production of viscose rayon yarn and staple fibre, and the wet processing of textiles (where hydrochloric acid is used as a sour to neutralize residual alkali and remove metallic and other impurities).

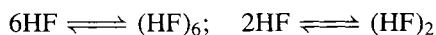
Anhydrous HBr is available in cylinders (6.8-kg and 68-kg capacity) under its own vapour pressure (24 atm at 25°C) and in lecture bottles (450-g capacity). Its main industrial use is in the manufacture of inorganic bromides and the synthesis of alkyl bromides either from alcohols or by direct addition to alkenes. HBr also catalyses numerous organic reactions. Aqueous HBr (48% and 62%) is available as a corrosive pale-yellow liquid in drums or in large tank trailers (15 000 l and 38 000 l).

There seem to be no large-scale uses for HI outside the laboratory, where it is used in various iodination reactions (lecture bottles containing 400 g HI are available). Commercial solutions contain 40–55 wt% of HI (cf. azeotrope at 56.9% HI, p. 815) and these solutions are thermodynamically much more stable than pure HI as indicated by the large negative free energy of solution.

### *Physical properties of the hydrogen halides*

HF is a colourless volatile liquid and an oligomeric H-bonded gas  $(\text{HF})_x$ , whereas the heavier HX are colourless diatomic gases at room temperature. Some molecular and bulk physical properties are summarized in Table 17.10. The influence of H bonding on the (low) vapour pressure, (long) liquid range and (high) dielectric constant of HF have already been discussed

(pp. 53–5). Note also that the viscosity of liquid HF is lower than that of water (or indeed of the other HX) and this has been taken to imply the absence of a three-dimensional network of H bonds such as occurs in  $\text{H}_2\text{O}$ ,  $\text{H}_2\text{SO}_4$ ,  $\text{H}_3\text{PO}_4$ , etc. However, it should be remembered that the viscosity of HF is quoted for 0°C, i.e. some 80° above its mp and only 20° below its bp; a more relevant comparison might be its value of 0.772 centipoise at –62.5° (i.e. 19° above its mp) compared with a value of 1.00 centipoise for water at 20°. Hydrogen bonding is also responsible for the association of HF molecules in the vapour phase: the vapour density of the gas over liquid HF reaches a maximum value of ~86 at –34°. At atmospheric pressure the value drops from 58 at 25° to 20.6 at 80° (the limiting vapour density of monomeric HF is  $\frac{20.0063}{2.0159} = 9.924$ ). These results, together with infrared and electron diffraction studies, indicate that gaseous HF comprises an equilibrium mixture of monomers and cyclic hexamers, though chain dimers may also occur under some conditions of temperature and pressure:



The crystal structure of HF shows it to consist of planar zigzag chain polymers with an F–H...F distance of 249 pm and an angle at F of 120.1°.

The other HX are not associated in the gaseous or liquid phases but the low-temperature forms of crystalline HCl and HBr both feature weakly

Table 17.10 Physical properties of the hydrogen halides

Property	HF	HCl	HBr	HI
MP/°C	-83.5	-114.2	-88.6	-51.0
BP/°C	19.5 <sup>(a)</sup>	-85.1	-67.1	-35.1
Liquid range (1 atm)/°C	103.0	29.1	21.5	15.9
Density(T°C)/g cm <sup>-3</sup>	1.002(0°) <sup>(b)</sup>	1.187(-114°)	2.603(-84°)	2.85(-47°)
Viscosity(T°C)/centipoise	0.256(0°)	0.51(-95°)	0.83(-67°)	1.35(-35.4°)
Dielectric constant, $\epsilon$	83.6(0°) <sup>(c)</sup>	9.28(-95°)	7.0(-85°)	3.39(-50°)
Electrical conductivity (T°C)/ohm <sup>-1</sup> cm <sup>-1</sup>	$\sim 10^{-6}$ (0°)	$\sim 10^{-9}$ (-85°)	$\sim 10^{-9}$ (-85°)	$\sim 10^{-10}$ (-50°)
$\Delta H_f^\circ(298^\circ)/\text{kJ mol}^{-1}$	-271.12	-92.31	-36.40	26.48
$\Delta G_f^\circ(298^\circ)/\text{kJ mol}^{-1}$	-273.22	-95.30	-53.45	1.72
$S^\circ(298^\circ)/\text{J mol}^{-1}\text{K}^{-1}$	173.67	186.80	198.59	206.48
$\Delta H_{\text{dissoc}}(\text{H-X})/\text{kJ mol}^{-1}$	573.98	431.62	362.50	294.58
$r_e(\text{H-X})/\text{pm}$	91.7	127.4	141.4	160.9
Vibrational frequency $\omega_e/\text{cm}^{-1}$	4138.33	2990.94(H <sup>35</sup> Cl) 2988.48(H <sup>37</sup> Cl)	2649.65	2309.53
Dipole moment $\mu/D$	1.86	1.11	0.788	0.382

<sup>(a)</sup>Vapour pressure of HF 363.8 mmHg (48.50 kPa) at 0°.

<sup>(b)</sup>Density of liquid HF 1.23 g cm<sup>-3</sup> near melting point. <sup>(c)</sup>Dielectric constant  $\epsilon$ (HF) 175 at -73°C.

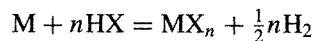
H-bonded zigzag chains similar to those in solid HF. At higher temperatures substantial disorder sets in.

The standard heats of formation  $\Delta H_f^\circ$  of gaseous HX diminish rapidly with increase in molecular weight and HI is endothermic. The very small (and positive) value for the standard free energy of formation  $\Delta G_f^\circ$  of HI indicates that (under equilibrium conditions) this species is substantially dissociated at room temperature and pressure. However, dissociation is slow in the absence of a catalyst. The bond dissociation energies of HX show a similar trend from the very large value of 574 kJ mol<sup>-1</sup> for HF to little more than half this (295 kJ mol<sup>-1</sup>) for HI.

### Chemical reactivity of the hydrogen halides

Anhydrous HX are versatile and vigorous reagents for the halogenation of metals, non-metals, hydrides, oxides and many other classes of compound, though reactions that are thermodynamically permissible do not always occur in the absence of catalysts, thermal initiation or photolytic encouragement, because

of kinetic factors. For example,<sup>(36)</sup> reaction of HX(g) with elements (M) can thermodynamically proceed according to the equation



providing that  $\Delta G$  for the reaction [i.e.  $\Delta G_f^\circ(\text{MX}_n) - n\Delta G_f^\circ(\text{HX}, \text{g})$ ] is negative. From the data in Table 17.10 this means that M could be oxidized to the  $n$ -valent halide  $\text{MX}_n$  if:

for the fluoride  $\Delta G_f^\circ(\text{MF}_n)$  is  $< -274n$  kJ mol<sup>-1</sup>

for the chloride  $\Delta G_f^\circ(\text{MCl}_n)$  is  $< -96n$  kJ mol<sup>-1</sup>

for the bromide  $\Delta G_f^\circ(\text{MBr}_n)$  is  $< -54n$  kJ mol<sup>-1</sup>

for the iodide  $\Delta G_f^\circ(\text{MI}_n)$  is  $< \sim 0$  kJ mol<sup>-1</sup>

Using tables of free energies of formation it is clear that most metals will react with most HX. Moreover, in many cases, e.g. with the alkali metals, alkaline earth metals, Zn, Al and the lanthanide elements, such reactions are extremely exothermic. It is also clear that Ag should react with HCl, HBr and HI but not with HF, and

<sup>36</sup> T. C. WADDINGTON, in V. GUTMANN (ed.), *Main Group Elements: Group VII and Noble Gases*, MTP International Review of Science: Inorganic Chemistry Series 1, Vol. 3, pp. 85-125, Butterworths, London, 1972.



Cu should form  $\text{CuF}_2$  with HF but not  $\text{CuX}_2$  with the other HX. Iron should give  $\text{FeCl}_3$  but in practice the reaction only proceeds to  $\text{FeCl}_2$ .  $\text{TiX}_4$  can be made, but only at high temperatures. Reactions of Si to form  $\text{SiX}_4$  are very favourable for  $\text{X} = \text{F}, \text{Cl}, \text{Br}$ , but only HF reacts at room temperature. With As, reaction with HF to give  $\text{AsF}_3$  is thermodynamically favourable but reactions with the other HX are not. Similar, though more complicated, schemes can be worked out for the reactions of HX with oxides, other halides, hydrides, etc.

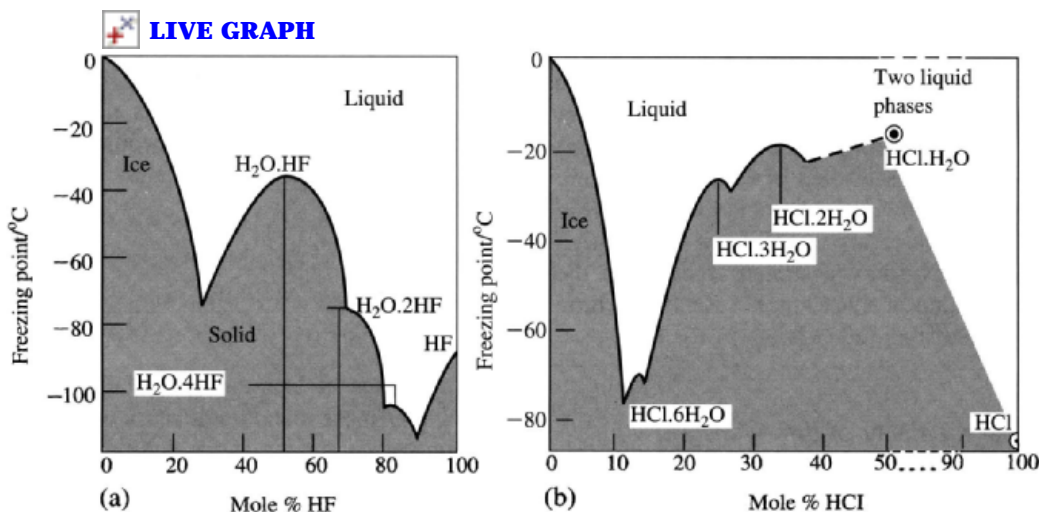
HF is miscible with water in all proportions and the phase diagram (Fig. 17.4a) shows the presence of three compounds:  $\text{H}_2\text{O} \cdot \text{HF}$  (mp  $-35.5^\circ$ ),  $\text{H}_2\text{O} \cdot 2\text{HF}$  (mp  $-75.5^\circ$ ) and  $\text{H}_2\text{O} \cdot 4\text{HF}$  (mp  $-100.4^\circ$ , i.e.  $17^\circ$  below the mp of pure HF). Recent X-ray studies have confirmed earlier conjectures that these compounds are best formulated as H-bonded oxonium salts  $[\text{H}_3\text{O}]\text{F}$ ,  $[\text{H}_3\text{O}][\text{HF}_2]^-$ , and  $[\text{H}_3\text{O}][\text{H}_3\text{F}_4]^-$  with three very strong H bonds per oxonium ion and average  $\text{O} \cdots \text{F}$  distances of 246.7, 250.2

and 253.6 pm respectively.<sup>(37)</sup> More recently, the low-temperature crystal structure of  $\text{Me}_4\text{NF} \cdot 5\text{HF}$  (decomp.  $-76^\circ\text{C}$ ) has revealed the presence of  $\text{H}_5\text{F}_6^-$ , i.e.  $[(\text{FH})_2\text{FHF}(\text{HF})_2]^-$ , with four terminal  $\text{F}-\text{H} \cdots \text{F}$  of 248.4 pm and a very strong central  $\text{F}-\text{H} \cdots \text{F}$  of 226.6 pm.  $\text{Me}_4\text{NF} \cdot 7\text{HF}$  was also identified (decomp.  $-110^\circ\text{C}$ ).<sup>(38)</sup> Another significant crystal structure, that of tris(ethylenediamine)zinc(II) fluoride dihydrate reveals the strongly H-bonded difluoride cluster  $[\text{F}_2(\text{H}_2\text{O})_2]^{2-}$  which adopts a diamond-shaped cyclic structure  $\text{F} \cdots \text{HOH} \cdots \text{F} \cdots \text{HOH} \cdots$  with  $\text{O}-\text{H} \cdots \text{F}$  distances of 258.6 and 267.9 pm and non-bonded distances across the lozenge of  $\text{O} \cdots \text{O}$  335 pm and  $\text{F} \cdots \text{F}$  406 pm.<sup>(39)</sup> Such H bonds are very relevant to the otherwise surprising observation that, unlike

<sup>37</sup> D. MOOTZ, *Angew. Chem. Int. Edn. Engl.* **20**, 791 (1981). See also J. EMSLEY and D. A. JOHNSON, *Polyhedron* **5**, 1109–10 (1986).

<sup>38</sup> D. MOOTZ and D. BOENIGK, *Z. anorg. allg. Chem.* **544**, 159–66 (1987).

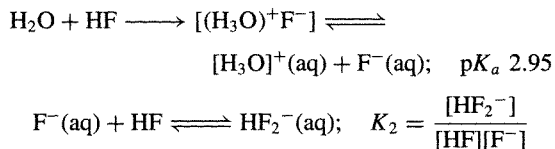
<sup>39</sup> J. EMSLEY, M. ARIF, P. A. BATES and M. B. HURSTHOUSE, *J. Chem. Soc., Chem. Commun.*, 738–9 (1989).



**Figure 17.4** The phase diagrams of the systems (a) HF/H<sub>2</sub>O and (b) HCl/H<sub>2</sub>O. Note that for hydrofluoric acid all the solvates contain  $\geq 1\text{HF}$  per H<sub>2</sub>O, whereas for hydrochloric acid they contain  $\leq 1\text{HCl}$  per H<sub>2</sub>O. This is because the H bonds  $\text{F}-\text{H} \cdots \text{F}$  and  $\text{F}-\text{H} \cdots \text{O}$  are *stronger* than  $\text{O}-\text{H} \cdots \text{O}$ , whereas  $\text{Cl}-\text{H} \cdots \text{Cl}$  and  $\text{Cl}-\text{H} \cdots \text{O}$  are *weaker* than  $\text{O}-\text{H} \cdots \text{O}$ . Accordingly the solvates in the former system have the crystal structures  $[\text{H}_3\text{O}]^+\text{F}^-$ ,  $[\text{H}_3\text{O}]^+[\text{HF}_2]^-$  and  $[\text{H}_3\text{O}]^+[\text{H}_3\text{F}_4]^-$ , whereas the latter are  $[\text{H}_3\text{O}]^+\text{Cl}^-$ ,  $[\text{H}_5\text{O}_2]^+\text{Cl}^-$  and  $[\text{H}_3\text{O}_2]^+\text{Cl}^-$ . H<sub>2</sub>O. The structures of HCl.6H<sub>2</sub>O and the metastable HCl.4H<sub>2</sub>O are not known.

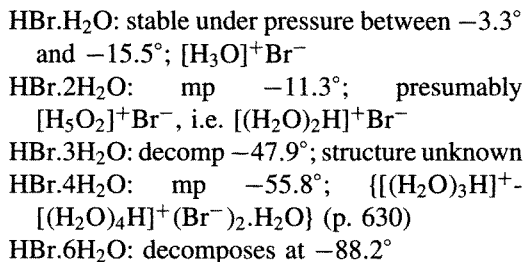


the other aqueous hydrohalic acids which are extremely strong, hydrofluoric acid is a very weak acid in aqueous solution. Indeed, the behaviour of such solutions is remarkable in showing a dissociation constant (as calculated from electrical conductivity measurements) that *diminishes* continuously on dilution. Detailed studies reveal the presence of two predominant equilibria:<sup>(40)</sup>



The dissociation constant for the first process is only  $1.1 \times 10^{-3} \text{ l mol}^{-1}$  at 25°C; this corresponds to  $pK_a$  2.95 and indicates a rather small free hydrogen-ion concentration (cf.  $\text{ClCH}_2\text{CO}_2\text{H}$ ,  $pK_a$  2.85) as a result of the strongly H-bonded, undissociated ion-pair  $[(\text{H}_3\text{O})^+\text{F}^-]$ . By contrast,  $K_2 = 2.6 \times 10^{-1} \text{ l mol}^{-1}$  ( $pK_2$  0.58), indicating that an appreciable number of the fluoride ions in the solution are coordinated by HF to give  $\text{HF}_2^-$  rather than by  $\text{H}_2\text{O}$  despite the very much higher concentration of  $\text{H}_2\text{O}$  molecules.

Numerous hydrates also occur in the  $\text{HCl}/\text{H}_2\text{O}$  system (Fig. 17.4b), e.g.  $\text{HCl} \cdot \text{H}_2\text{O}$  (mp  $-15.4^\circ$ ),  $\text{HCl} \cdot 2\text{H}_2\text{O}$  (mp  $-17.7^\circ$ ),  $\text{HCl} \cdot 3\text{H}_2\text{O}$  (mp  $-24.9^\circ$ ),  $\text{HCl} \cdot 4\text{H}_2\text{O}$  and  $\text{HCl} \cdot 6\text{H}_2\text{O}$  (mp  $-70^\circ$ ). The system differs from  $\text{HF}/\text{H}_2\text{O}$  not only in the stoichiometry of the hydrates but also in separating into two liquid phases at HCl concentrations higher than 1:1. The weakness of the  $\text{O}-\text{H} \cdots \text{Cl}$  hydrogen bond also ensures that there is very little impediment to complete ionic dissociation, and aqueous solutions of HCl (and also of HBr and HI) are strong acids; approximate values of  $pK_a$  are HCl  $-7$ , HBr  $-9$ , HI  $-10$ . The systems  $\text{HBr}/\text{H}_2\text{O}$  and  $\text{HI}/\text{H}_2\text{O}$  also show a miscibility gap at high concentrations of HX and also numerous hydrates which feature hydrated oxonium ions:

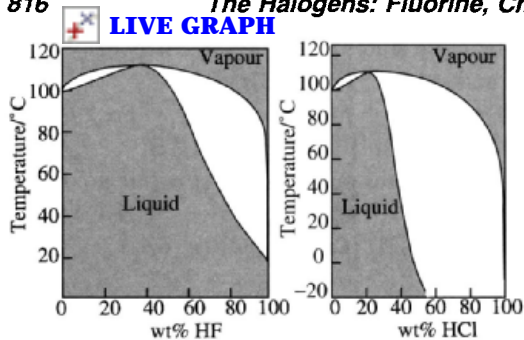


The compound  $\text{HI} \cdot \text{H}_2\text{O}$  does not appear as a stable hydrate in the phase diagram, but the vibrational spectra of frozen solutions of this composition indicate the formulation  $[\text{H}_3\text{O}]^+\text{I}^-$ . Higher hydrates appear at  $\text{HI} \cdot 2\text{H}_2\text{O}$  (mp  $\sim -43^\circ$ ),  $\text{HI} \cdot 3\text{H}_2\text{O}$  (mp  $\sim -48^\circ$ ), and  $\text{HI} \cdot 4\text{H}_2\text{O}$  (mp  $-36.5^\circ$ ).

Just as the solid/liquid phase equilibria in the systems  $\text{HX}/\text{H}_2\text{O}$  show several points of interest, so too do the liquid/gas phase equilibria. When dilute aqueous solutions of HX are heated to boiling the concentration of HX in the vapour is less than that in the liquid phase, so that the liquid becomes progressively more concentrated and the bp progressively rises until a point is reached at which the liquid has the same composition as the gas phase so that it boils without change in composition and at constant temperature. This mixture is called an azeotrope (Greek  $\alpha\acute{\iota}$ , without;  $\zeta\epsilon\acute{\iota}\eta$ , *zein*, to boil;  $\tau\rho\omicron\pi\acute{\eta}$ , *trope*, change). The phenomenon is illustrated for HF and HCl in Fig. 17.5. Conversely, when more concentrated aqueous solutions are boiled, the concentration of HX in the vapour is greater than that in the liquid phase which thereby becomes progressively diluted by distillation until the azeotropic mixture is again reached, whereupon distillation continues without change of composition and at constant temperature. The bps and azeotropic compositions at atmospheric pressure are listed below, together with the densities of the azeotropic acids at 25°C:

Azeotrope	HF	HCl	HBr	HI
BP (1 atm)/°C	112	108.58	124.3	126.7
g(HX)/100 g soln	38	20.22	47.63	56.7
Density(25°)/g cm <sup>-3</sup>	1.138	1.096	1.482	1.708

<sup>40</sup>L. G. SILLÉN and A. E. MARTELL, *Stability Constants of Metal-Ion Complexes*, Special Publication No. 17, pp. 256-7, The Chemical Society, London, 1964; *Supplement No. 1* (Special Publication No. 17), pp. 152-3 (1971). See also P. McTIGUE, T. A. O'DONNELL and B. VERITT, *Aust. J. Chem.* **38**, 1797-807 (1985).



**Figure 17.5** Liquid/gas phase equilibria for the systems HF/H<sub>2</sub>O and HCl/H<sub>2</sub>O showing the formation of maximum boiling azeotropes as described in the text.

Of course, the bp and composition of the azeotrope both vary with pressure, as illustrated below for the case of hydrochloric acid (1 mmHg = 0.1333 kPa):

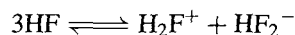
<i>P</i> /mmHg	50	250	500	700
BP/°C	48.72	81.21	97.58	106.42
g(HX)/100 g soln	23.42	21.88	20.92	20.36
Density(25°)/g cm <sup>-3</sup>	1.112	1.104	1.099	1.097
<i>P</i> /mmHg	<b>760</b>	800	1000	1200
BP/°C	<b>108.58</b>	110.01	116.19	122.98
g(HX)/100 g soln	<b>20.222</b>	20.16	19.73	19.36
Density(25°)/g cm <sup>-3</sup>	<b>1.0959</b>	1.095 <sub>5</sub>	1.093	1.091 <sub>5</sub>

The occurrence of such azeotropes clearly restricts the degree to which aqueous solutions of HX can be concentrated by evaporation. However, they do afford a ready means of obtaining solutions of precisely known concentration: in the case of hydrochloric acid, its azeotrope is particularly stable over long periods of time and has found much use in analytical chemistry.

### The hydrogen halides as nonaqueous solvents

The great synthetic value of liquid NH<sub>3</sub> as a nonaqueous solvent (p. 424) has encouraged the extensive study of the other neighbour of H<sub>2</sub>O in the periodic table, namely, HF.<sup>(36,41–44)</sup> Early studies were hampered by the aggressive nature of anhydrous HF towards glass and quartz,

but the pure acid can now be safely handled without contamination using fluorinated plastics such as polytetrafluoroethylene. The self-ionic dissociation of the solvent, as evidenced by the residual electrical conductivity of highly purified HF, can be represented as  $\text{HF} \rightleftharpoons \text{H}^+ + \text{F}^-$ ; however, since both ions will be solvated it is more usual to represent the equilibrium as



The fluoride ion has an anomalously high conductance,  $\lambda_{\infty}$ , as shown by the following values obtained at 0°:

Ion	Na <sup>+</sup>	K <sup>+</sup>	H <sub>2</sub> F <sup>+</sup>	BF <sub>4</sub> <sup>-</sup>	SbF <sub>6</sub> <sup>-</sup>	HF <sub>2</sub> <sup>-</sup>
$\lambda_{\infty}$ /ohm <sup>-1</sup> cm <sup>2</sup> mol <sup>-1</sup>	117	117	<b>79</b>	183	196	<b>273</b>

As the specific conductivity of pure HF is  $\sim 10^{-6}$  ohm<sup>-1</sup> cm<sup>2</sup> at 0°, these values imply concentrations of  $\text{H}_2\text{F}^+ = \text{HF}_2^- \simeq 2.9 \times 10^{-6}$  mol l<sup>-1</sup> and an ionic product for the liquid of  $\sim 8 \times 10^{-12}$  mol<sup>2</sup> l<sup>-2</sup> (cf. values of  $\sim 10^{-33}$  for NH<sub>3</sub> and  $\sim 10^{-14}$  for H<sub>2</sub>O).

The high dielectric constant, low viscosity and long liquid range of HF make it an excellent solvent for a wide variety of compounds. Whilst most inorganic fluorides give fluoride ions when dissolved (see next paragraph), a few solutes dissolve without ionization, e.g. XeF<sub>2</sub>, SO<sub>2</sub>, HSO<sub>3</sub>F, SF<sub>6</sub> and MF<sub>6</sub> (M = Mo, W, U, Re and Os). It is also probable that VF<sub>5</sub> and ReF<sub>7</sub> dissolve without ionizing. Perhaps more surprisingly liquid HF is now extensively used in biochemical research: carbohydrates, amino acids and proteins dissolve readily, frequently with only minor chemical consequences. In particular, complex organic compounds that are potentially

<sup>41</sup> H. H. HYMAN and J. J. KATZ, Chap. 2 in T. C. WADDINGTON (ed.), *Nonaqueous Solvent Systems*, pp. 47–81, Academic Press, London, 1965.

<sup>42</sup> M. KILPATRICK and J. G. JONES, Chap. 2 in J. J. LAGOWSKI (ed.), *The Chemistry of Nonaqueous Solvents*, pp. 43–99, Vol. 2, Academic Press, New York, 1967.

<sup>43</sup> T. A. O'DONNELL, Chap. 25 in *Comprehensive Inorganic Chemistry*, Vol. 2, pp. 1009–106, Pergamon Press, Oxford, 1973.

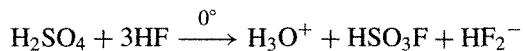
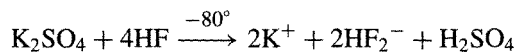
<sup>44</sup> R. J. GILLESPIE and J. LIANG, *J. Am. Chem. Soc.* **110**, 6053–7 (1988).

capable of eliminating the elements of water (e.g. cellulose, sugar esters, etc.) often dissolve without dehydration. Likewise globular proteins and many fibrous proteins that are insoluble in water, such as silk fibroin. These solutions are remarkably stable: e.g. the hormones insulin and ACTH were recovered after 2 h in HF at 0° with their biological activity substantially intact.

Many of the ionic fluorides of  $M^I$ ,  $M^{II}$  and  $M^{III}$  dissolve to give highly conducting solutions due to ready dissociation. Some typical values of the solubility of fluorides in HF are in Table 17.11: the data show the expected trend towards greater solubility with increase in ionic radius within the alkali metals and alkaline earth metals, and the expected decrease in solubility with increase in ionic charge so that  $MF > MF_2 > MF_3$ . This is dramatically illustrated by  $AgF$  which is 155 times more soluble than  $AgF_2$  and  $TiF$  which is over 7000 times more soluble than  $TiF_3$ .

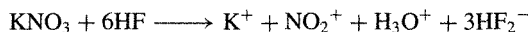
With inorganic solutes other than fluorides, solvolysis usually occurs. Thus chlorides, bromides and iodides give the corresponding fluorides with evolution of HX, and fluorides are also formed from oxides, hydroxides, carbonates and sulfites. Indeed, this is an excellent synthetic route for the preparation of anhydrous metal fluorides and has been used with good effect for  $TiF_4$ ,  $ZrF_4$ ,  $UF_4$ ,  $SnF_4$ ,  $VOF_3$ ,  $VF_3$ ,  $NbF_5$ ,  $TaF_5$ ,  $SbF_5$ ,  $MoO_2F_2$ , etc. (Note, however, that  $AgCl$ ,  $PdCl_2$ ,  $PtCl_4$ ,  $Au_2Cl_6$  and  $ICl$  are apparently exceptions.<sup>42</sup>) Less-extensive solvolysis occurs with sulfates, phosphates and certain other oxoanions. For example, a careful cryoscopic study of

solutions of  $K_2SO_4$  in HF (at  $\sim -84^\circ C$ ) gave a value of  $\nu = 5$  for the number of solute species in solution, but this increased to about 6 when determined by vapour-pressure depressions at 0°. These observations can be rationalized if unionized  $H_2SO_4$  is formed at the lower temperature and if solvolysis of this species to unionized  $HSO_3F$  sets in at the higher temperatures:



Consistent with this, the  $^{19}F$  nmr spectra of solutions at 0° showed the presence of  $HSO_3F$ , and separate cryoscopic experiments with pure  $H_2SO_4$  as the sole solute gave a value of  $\nu$  close to unity.

Solvolysis of phosphoric acids in the system HF/ $P_2O_5$ / $H_2O$  gave successively  $H_2PO_3F$ ,  $HPO_2F_2$  and  $H_3O^+PF_6^-$ , as shown by  $^{19}F$  and  $^{31}P$  nmr spectroscopy. Raman studies show that  $KNO_3$  solvolyses according to the reaction



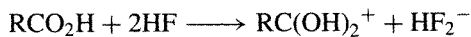
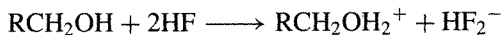
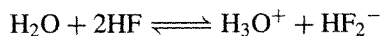
Permanganates and chromates are solvolysed by HF to oxide fluorides such as  $MnO_3F$  and  $CrO_2F_2$ .

Acid-base reactions in anhydrous HF are well documented. Within the Brønsted formalism, few if any acids would be expected to be sufficiently strong proton donors to be able to protonate the very strong proton-donor HF (p. 51), and this is borne out by observation. Conversely, HF can protonate many Brønsted bases, notably water,

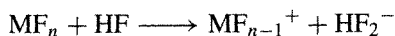
**Table 17.11** Solubility of some metal fluorides in anhydrous HF (in g/100 g HF and at 12°C unless otherwise stated)

LiF 10.3	NaF(11°) 30.1	NH <sub>4</sub> F(17°) 32.6	KF(8°) 36.5	RbF(20°) 110	CsF(10°) 199	<b>AgF</b> <b>83.2</b>	<b>TiF</b> <b>580</b>
Hg <sub>2</sub> F <sub>2</sub> 0.87	BeF <sub>2</sub> (11°) 0.015	MgF <sub>2</sub> 0.025	CaF <sub>2</sub> 0.817	SrF <sub>2</sub> 14.83	BaF <sub>2</sub> 5.60	<b>AgF<sub>2</sub></b> <b>0.54</b>	CaF <sub>2</sub> 0.010
HgF <sub>2</sub> 0.54	CdF <sub>2</sub> (14°) 0.201	ZnF <sub>2</sub> (14°) 0.024	CrF <sub>2</sub> (14°) 0.036	FeF <sub>2</sub> 0.006	NiF <sub>2</sub> 0.037	PbF <sub>2</sub> 2.62	
AlF <sub>3</sub> 0.002	CeF <sub>3</sub> 0.043	<b>TiF<sub>3</sub></b> <b>0.081</b>	MnF <sub>3</sub> 0.164	FeF <sub>3</sub> 0.008	CoF <sub>3</sub> 0.257	SbF <sub>3</sub> 0.536	BrF <sub>3</sub> 0.010

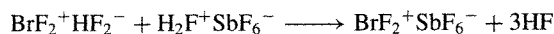
alcohols, carboxylic acids and other organic compounds having one or more lone-pairs on O, N, etc.:



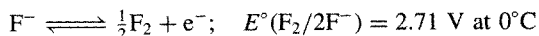
Alternatively, within the Lewis formalism, acids are fluoride-ion acceptors. The prime examples are  $\text{AsF}_5$  and  $\text{SbF}_5$  (which give  $\text{MF}_6^-$ ) and to a lesser extent  $\text{BF}_3$  which yields  $\text{BF}_4^-$ . A greater diversity is found amongst Lewis bases (fluoride-ion donors), typical examples being  $\text{XeF}_6$ ,  $\text{SF}_4$ ,  $\text{ClF}_3$  and  $\text{BrF}_3$ :



Such solutions can frequently be "neutralized" by titration with an appropriate Lewis acid, e.g.:



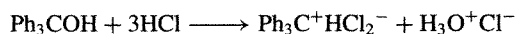
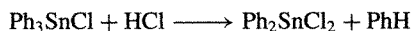
Oxidation-reduction reactions in HF form a particularly important group of reactions with considerable industrial application. The standard electrode potentials  $E^\circ(\text{M}^{n+}/\text{M})$  in HF follow the same sequence as for  $\text{H}_2\text{O}$  though individual values in the two series may differ by up to  $\pm 0.2$  V. Early examples showed that  $\text{CrF}_2$  and  $\text{UF}_4$  reduced HF to  $\text{H}_2$  whereas  $\text{VCl}_2$  gave  $\text{VF}_3$ ,  $2\text{HCl}$  and  $\text{H}_2$ . Of more significance is the very high potential needed for the anodic oxidation of  $\text{F}^-$  in HF:



This enables a wide variety of inorganic and organic fluorinations to be effected by the electrochemical insertion of fluorine. For example, the production of  $\text{NFH}_2$ ,  $\text{NF}_2\text{H}$  and  $\text{NF}_3$  by electrolysis of  $\text{NH}_4\text{F}$  in liquid HF represents the only convenient route to these compounds. Again,  $\text{CF}_3\text{CO}_2\text{H}$  is most readily obtained by electrolysis of  $\text{CH}_3\text{CO}_2\text{H}$  in HF. Other examples of anodic oxidations in HF are as follows:

Reactant	Products	Reactant	Products
$\text{NH}_4\text{F}$	$\text{NF}_3, \text{NF}_2\text{H}, \text{NMe}_3$ $\text{NFH}_2$		$(\text{CF}_3)_3\text{N}$
$\text{H}_2\text{O}$	$\text{OF}_2$	$(\text{MeCO})_2\text{O}$	$\text{CF}_3\text{COF}$
$\text{SCl}_2, \text{SF}_4$	$\text{SF}_6$	$\text{SMe}_2, \text{CS}_2$	$\text{CF}_3\text{SF}_5, (\text{CF}_3)_2\text{SF}_4$
$\text{NaClO}_4$	$\text{ClO}_3\text{F}$	$\text{MeCN}$	$\text{CF}_3\text{CN}, \text{C}_2\text{F}_5\text{NF}_2$

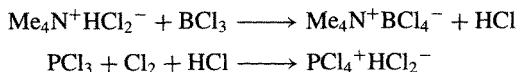
The other hydrogen halides are less tractable as solvents, as might be expected from their physical properties (p. 813), especially their low bps, short liquid ranges, low dielectric constants and negligible self-dissociation into ions. Nevertheless, they have received some attention, both for comparison with HF and as preparative media with their own special advantages.<sup>(36,45,46)</sup> In particular, because of their low bp and consequent ease of removal, the liquid HX solvent systems have provided convenient routes to  $\text{BX}_4^-$ ,  $\text{BF}_3\text{Cl}^-$ ,  $\text{B}_2\text{Cl}_6^{2-}$ ,  $\text{NO}_2\text{Cl}$ ,  $\text{Al}_2\text{Cl}_7^-$ ,  $\text{R}_2\text{SCI}^+$ ,  $\text{RSCl}_2^+$ ,  $\text{PCl}_3\text{Br}^+$ ,  $\text{Ni}_2\text{Cl}_4(\text{CO})_3$  (from nickel tetracarbonyl and  $\text{Cl}_2$ ) and  $\text{Ni}(\text{NO})_2\text{Cl}_2$  (from nickel tetracarbonyl and  $\text{NOCl}$ ). Solubilities in liquid HX are generally much smaller than in HF and tend to be restricted to molecular compounds (e.g.  $\text{NOCl}$ ,  $\text{PhOH}$ , etc.) or salts with small lattice energies, e.g. the tetraalkylammonium halides. Concentrations rarely attain  $0.5 \text{ mol l}^{-1}$  (i.e.  $0.05 \text{ mol}/100 \text{ g HF}$ ). Ready protonation of compounds containing lone-pairs or  $\pi$  bonds is observed, e.g. amines, phosphines, ethers, sulfides, aromatic olefins, and compounds containing  $-\text{C}\equiv\text{N}$ ,  $-\text{N}=\text{N}-$ ,  $>\text{C}=\text{O}$ ,  $>\text{P}=\text{O}$  etc. Of particular interest is the protonation of phosphine in the presence of  $\text{BX}_3$  to give  $\text{PH}_4^+\text{BCl}_4^-$ ,  $\text{PH}_4^+\text{BF}_3\text{Cl}^-$ , and  $\text{PH}_4^+\text{BBr}_4^-$ .  $\text{Fe}(\text{CO})_5$  affords  $[\text{Fe}(\text{CO})_5\text{H}]^+$  and  $[\text{Fe}(\eta^5\text{-C}_5\text{H}_5)(\text{CO})_2]_2$  yields  $[\text{Fe}(\eta^5\text{-C}_5\text{H}_5)(\text{CO})_2]_2\text{H}^+$ . Solvolysis is also well established:



<sup>45</sup> M. E. PEACH and T. C. WADDINGTON, Chap. 3 in T. C. WADDINGTON (ed.), *Nonaqueous Solvent Systems*, pp. 83–115, Academic Press, London, 1965.

<sup>46</sup> F. KLANBERG, Chap. 1 in J. J. LAGOWSKI (ed.), *The Chemistry of Nonaqueous Solvents*, Vol. 2, pp. 1–41, Academic Press, New York, 1967.

Likewise ligand replacement reactions and oxidations, e.g.:



The preparation and structural characterization of the ions  $\text{HX}_2^-$  has been an important feature of such work.<sup>(36)</sup> As expected, these H-bonded ions are much less stable than  $\text{HF}_2^-$  though crystalline salts of all three anions and of the mixed anions  $\text{HXY}^-$  (except  $\text{HBrI}^-$ ) have been isolated by use of large counter cations, typically  $\text{Cs}^+$  and  $\text{NR}_4^+$  ( $\text{R} = \text{Me}, \text{Et}, \text{Bu}^n$ ) — see pp. 1313–21, of ref. 23 for further details. Neutron and X-ray diffraction studies suggest that  $[\text{Cl}\cdots\text{H}\cdots\text{Cl}]^-$  can be either centrosymmetric or non-centrosymmetric depending on the crystalline environment. An example of the latter mode involves interatomic distances of 145 and 178 pm respectively and a bond angle of  $\sim 168^\circ$  ( $\text{Cl}\cdots\text{Cl}$  321.2 pm).<sup>(47)</sup>

## 17.2.2 Halides of the elements

The binary halides of the elements span a wide range of stoichiometries, structure types and properties which defy any but the most grossly oversimplified attempt at a unified classification. Indeed, interest in the halides as a class of compound derives in no small measure from this very diversity and from the fact that, being so numerous, there are many examples of well-developed and well-graded trends between the limiting cases. Thus the fluorides alone include  $\text{OF}_2$ , one of the most volatile molecular compounds known (bp  $-145^\circ$ ), and  $\text{CaF}_2$ , which is one of the least-volatile “ionic” compounds (bp  $2513^\circ\text{C}$ ). Between these extremes of discrete molecules on the one hand, and 3D lattices on the other, is a continuous sequence of oligomers, polymers and extended layer lattices which may be either predominantly covalent [e.g.  $\text{ClF}$ ,  $(\text{MoF}_5)_4$ ,

$(\text{CF}_2)_\infty$ ,  $(\text{CF})_\infty$ , p. 289] or substantially ionic [e.g.  $\text{Na}^+\text{F}^-(\text{g})$ ,  $(\text{SnF}_2)_4$ ,  $(\text{BeF}_2)_\infty$  (quartz type),  $\text{SnF}_4$ ,  $\text{NaF}$  (cryst)], or intermediate in bond type with secondary interactions also complicating the picture. The problems of classifying binary compounds according to presumed bond types or limiting structural characteristics have already been alluded to for the hydrides (p. 64), borides (p. 145), oxides, sulfides, etc. Such diversity and gradations are further compounded by the existence of four different halogens (F, Cl, Br, I) and by the possibility of numerous oxidation states of the element being considered, e.g.  $\text{CrF}_2$ ,  $\text{Cr}_2\text{F}_5$ ,  $\text{CrF}_3$ ,  $\text{CrF}_4$ ,  $\text{CrF}_5$  and  $\text{CrF}_6$ , or  $\text{S}_2\text{F}_2$ ,  $\text{SF}_2$ ,  $\text{SF}_4$ ,  $\text{S}_2\text{F}_{10}$  and  $\text{SF}_6$ .

A detailed discussion of individual halides is given under the chemistry of each particular element. This section deals with more general aspects of the halides as a class of compound and will consider, in turn, general preparative routes, structure and bonding. For reasons outlined on p. 805, fluorides tend to differ from the other halides either in their method of synthesis, their structure or their bond-type. For example, the fluoride ion is the smallest and least polarizable of all anions and fluorides frequently adopt 3D “ionic” structures typical of oxides. By contrast, chlorides, bromides and iodides are larger and more polarizable and frequently adopt mutually similar layer-lattices or chain structures (cf. sulfides). Numerous examples of this dichotomy can be found in other chapters and in several general references.<sup>(48–52)</sup> Because of this it is convenient to discuss fluorides as a group first, and then the other halides.

<sup>48</sup> V. GUTMANN (ed.), *Halogen Chemistry*, Academic Press, London, 1967; Vol. 1, 473 pp.; Vol. 2, 481 pp.; Vol. 3, 471 pp.

<sup>49</sup> R. COLTON and J. H. CANTERFORD, *Halides of the First Row Transition Elements*, Wiley, London, 1969, 579 pp.; *Halides of the Second and Third Row Transition Elements*, Wiley, London, 1968, 409 pp.

<sup>50</sup> Ref. 43, pp. 1062–1106; ref. 23, pp. 1232–80.

<sup>51</sup> A. F. WELLS, *Structural Inorganic Chemistry*, 5th edn. pp. 407–44, Oxford University Press, Oxford, 1984.

<sup>52</sup> B. MÜLLER, *Angew. Chem. Int. Edn. Engl.* **26**, 1081–97 (1987).

<sup>47</sup> W. KUCHEN, D. MOOTZ, H. SOMBERG, H. WUNDERLICH and H.-G. WUSSOW, *Angew. Chem. Int. Edn. Engl.* **17**, 869–70 (1978).

## Fluorides

Binary fluorides are known with stoichiometries that span the range from  $C_4F$  to  $IF_7$  (or even, possibly,  $XeF_8$ ). Methods of synthesis turn on the properties of the desired products.<sup>(50,53–57)</sup>

If hydrolysis poses no problem, fluorides can be prepared by halide metathesis in aqueous solution or by the reactions of aqueous hydrofluoric acid with an appropriate oxide, hydroxide, carbonate, or the metal itself. The following non-hydrated fluorides precipitate as easily filterable solids:  $LiF$ ,  $NaF$ ,  $NH_4F$ ;  $MgF_2$ ,  $CaF_2$ ,  $SrF_2$ ,  $BaF_2$ ;  $SnF_2$ ,  $PbF_2$ ;  $SbF_3$ . Gaseous  $SiF_4$  and  $GeF_4$  can also be prepared from aqueous HF. Furthermore, the following fluorides separate as hydrates that can readily be dehydrated thermally, though an atmosphere of HF is required to suppress hydrolysis except in the case of the univalent metal fluorides:

$KF \cdot 2H_2O$	$CuF_2 \cdot 4H_2O$	$AlF_3 \cdot H_2O$
$RbF \cdot 3H_2O$	$ZnF_2 \cdot 4H_2O$	$GaF_3 \cdot 3H_2O$
$CsF \cdot 1\frac{1}{2}H_2O$	$CdF_2 \cdot 4H_2O$	$InF_3 \cdot 3H_2O$
$TiF \cdot 2HF \cdot \frac{1}{2}H_2O$	$HgF_2 \cdot 2H_2O$	$LnF_3 \cdot xH_2O$
$AgF \cdot 4H_2O$	$MF_2 \cdot 6H_2O$	(Ln = lanthanide metal)
	(M = Fe, Co, Ni)	

By contrast  $BeF_2 \cdot xH_2O$ ,  $TiF_4 \cdot 2H_2O$  and  $ThF_4 \cdot 4H_2O$  cannot be dehydrated without hydrolysis.

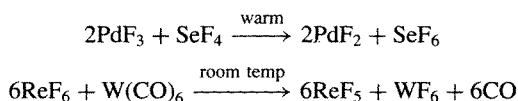
When hydrolysis is a problem then the action anhydrous HF on the metal (or chloride) may prove successful (e.g. the difluorides of Zn, Cd, Ge, Sn, Mn, Fe, Co, Ni; the trifluorides of Ga, In, Ti and the lanthanides; the tetrafluorides of

Ti, Zr, Hf, Th, U; and the pentafluorides of Nb and Ta). However, many higher fluorides require the use of a more aggressive fluorinating agent or even  $F_2$  itself. Typical of the fluorides prepared by oxidative fluorination with  $F_2$  are:

difluorides:	Ag, Xe
trifluorides:	Cl, Br, Mn, Co
tetrafluorides:	Sn, Pb, Kr, Xe, Mo, Mn, Ce, Am, Cm
pentafluorides:	As, Sb, Bi, Br, I, V, Nb, Ta, Mo
hexafluorides:	S, Se, Te, Xe, Mo, W, Tc, Ru, Os, Rh, Ir, Pt, U, Np, Pu
heptafluorides:	I, Re
octafluorides:	Xe(?)

Wherever possible the use of elementary  $F_2$  is avoided because of its cost and the difficulty of handling it; instead one of a graded series of halogen fluorides can often be used, the fluorinating power steadily diminishing in the sequence:  $ClF_3 > BrF_5 > IF_7 > ClF > BrF_3 > IF_5$ . Other “hard” oxidizing fluorinating agents are  $AgF_2$ ,  $CoF_3$ ,  $MnF_3$ ,  $PbF_4$ ,  $CeF_4$ ,  $BiF_5$  and  $UF_6$ . When selective fluorination of certain groups in organic compounds is required, then “moderate” fluorinating agents are employed, e.g.  $HgF_2$ ,  $SbF_5$ ,  $SbF_3/SbCl_5$ ,  $AsF_3$ ,  $CaF_2$  or  $KSO_2F$ . Such nucleophilic reagents may replace other halogens in halohydrocarbons by F but rarely substitute F for H. An electrophilic variant is  $ClO_3F$ . Most recently  $XeF_2$ , which is available commercially, has been used to effect fluorinations via radical cations: it can oxidatively fluorinate CC double bonds and can replace either aliphatic or aromatic H atoms with F. Even gentler are the “soft” fluorinating agents which do not cause fragmentation of functional groups, do not saturate double bonds, and do not oxidize metals to their highest oxidation states; typical of such mild fluorinating agents are the monofluorides of H, Li, Na, K, Rb, Cs, Ag and Tl and compounds such as  $SF_4$ ,  $SeF_4$ ,  $COF_2$ ,  $SiF_4$  and  $Na_2SiF_6$ .

The fluorination reactions considered so far can be categorized as metathesis, oxidation or substitution. Occasionally reductive fluorination is the preferred route to a lower fluoride. Examples are:



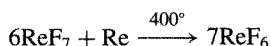
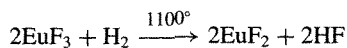
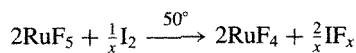
<sup>53</sup> E. L. MUETTERTIES and C. W. TULLOCK, Chap. 7 in W. L. JOLLY (ed.), *Preparative Inorganic Reactions*, Vol. 2, pp. 237–99 (1965). R. J. LAGOW and L. J. MARGRAVE, *Prog. Inorg. Chem.* **26**, 161–210 (1979). M. R. C. GERSTENBERGER and A. HAAS, *Angew. Chem. Int. Edn. Engl.* **20**, 647–67 (1981).

<sup>54</sup> J. PORTIER, *Angew. Chem. Int. Edn. Engl.* **15**, 475–86 (1976).

<sup>55</sup> R. D. PEACOCK, *Adv. Fluorine Chem.* **7**, 113–45 (1973).

<sup>56</sup> B. ZEMVA, K. LUTAR, A. JESIH, W. J. CASTEEL and N. BARTLETT, *J. Chem. Soc., Chem. Commun.*, 346–7 (1989).

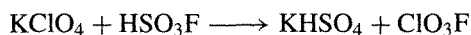
<sup>57</sup> G. A. OLAH, G. K. S. PRAKASH and R. D. CHAMBERS (eds.), *Synthetic Fluorine Chemistry*, Wiley, Chichester, 1992, 416 pp.



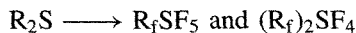
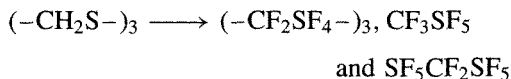
Further examples of this last type of reductive fluorination in which the element itself is used to reduce its higher fluoride are:

Product	ClF	CrF <sub>2</sub>	GeF <sub>2</sub>
Reactants	Cl <sub>2</sub> /ClF <sub>3</sub>	Cr/CrF <sub>3</sub>	Ge/GeF <sub>4</sub>
T/°C	350	1000	300
Product	MoF <sub>3</sub>	UF <sub>3</sub>	IrF <sub>4</sub>
Reactants	Mo/MoF <sub>5</sub>	U/UF <sub>4</sub>	Ir/IrF <sub>6</sub>
T/°C	400	1050	170
			Te/TeF <sub>6</sub>
			180

The final route to fluorine compounds is electrofluorination (anodic fluorination) usually in anhydrous or aqueous HF. The preparation of NF<sub>x</sub>H<sub>3-x</sub> (x = 1, 2, 3) has already been described (p. 818). Likewise a reliable route to OF<sub>2</sub> is the electrolysis of 80% HF in the presence of dissolved MF (p. 638). Perchloryl fluoride has been made by electrolysis of NaClO<sub>4</sub> in HF but a simpler route (p. 879) is the direct reaction of a perchlorate with fluorosulfuric acid:



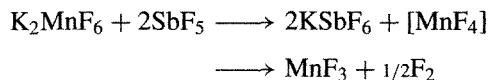
Electrolysis of organic sulfides in HF affords a variety of fluorocarbon derivatives:



where R<sub>f</sub> is a perfluoroalkyl group.

The application of the foregoing routes has led to the preparation and characterization of fluorides of virtually every element in the periodic table except the three lightest noble gases, He, Ne and Ar. The structures, bonding, reactivity, and industrial applications of these compounds will be found in the treatment of the individual elements and it is an instructive exercise to gather this information together in the form of comparative tables.<sup>(2,50,53-62)</sup>

One important postscript can be added — the achievement by K. O. Christe in 1986 of synthesizing fluorine itself by chemical means alone, a goal that had eluded chemists for at least 173 years.<sup>(63)</sup> In this context, the term *chemical synthesis* excludes techniques such as electrolysis, photolysis, discharge, etc., or the use of F<sub>2</sub> in the synthesis of any of the starting materials. It is well known that high oxidation states can often be stabilized by complex-ion formation. Christe's ingenious strategy was to treat just such a complex fluoride with a strong fluoride-ion acceptor, thus liberating the unstable metal fluoride which then spontaneously decomposed to a lower oxidation state with the liberation of F<sub>2</sub>. He chose to use K<sub>2</sub>MnF<sub>6</sub> and SbF<sub>5</sub>, both of which can be readily prepared from HF solutions without the use of F<sub>2</sub> itself:



The reaction was carried out in a passivated Teflon-stainless steel reactor at 150°C for 1 hour, and the yield was >40%. Fluorine pressures of more than 1 atm were generated in this way.

### Chlorides, bromides and iodides

A similar set of preparative routes is available as were outlined above for the fluorides, though the range of applicability of each method and the products obtained sometimes vary from halogen to halogen. When hydrolysis is not a problem

<sup>58</sup> A. J. EDWARDS, *Adv. Inorg. Chem. Radiochem.* **27**, 83-112 (1983).

<sup>59</sup> P. HAGENMÜLLER (ed.), *Inorganic Solid Fluorides*, Academic Press, N.Y., 1985, 628 pp.

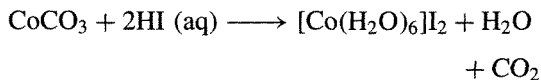
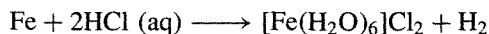
<sup>60</sup> J. F. LIEBMAN, A. GREENBERG and W. R. DOLBIER (eds.), *Fluorine-containing Molecules: Structure, Reactivity, Synthesis and Applications*, VCH Publishers, N.Y. 1988, 350 pp.

<sup>61</sup> A. E. COMYNS (ed.), *Fluoride Glasses*, Wiley, Chichester, 1989, 219 pp.

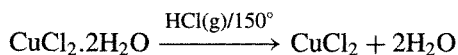
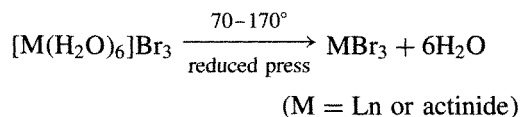
<sup>62</sup> J. S. THRASHER and S. H. STRAUSS (eds.) *Inorganic Fluorine Chemistry Towards the 21st Century*, ACS Symposium Series **555**, 1994, 437 pp.

<sup>63</sup> K. O. CHRISTE, *Inorg. Chem.* **25**, 3721-2 (1986). See also *C & E News*, March 2, pp. 4-5 (1987) for discussion of the implications.

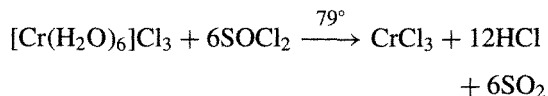
or when hydrated halides are sought, then wet methods are available, e.g. dissolution of a metal or its oxide, hydroxide or carbonate in aqueous hydrohalic acid followed by evaporative crystallization:



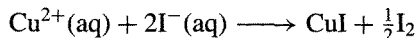
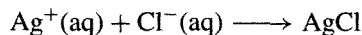
Dehydration can sometimes be effected by controlled removal of water using a judicious combination of gentle warming and either reduced pressure or the presence of anhydrous HX:



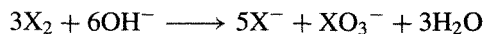
Hydrated chlorides that are susceptible to hydrolysis above room temperature can often be dehydrated by treating them with  $\text{SOCl}_2$  under reflux:



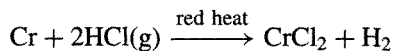
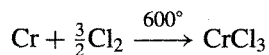
Alternative wet routes to hydrolytically stable halides are metathetical precipitation and reductive precipitation reactions, e.g.:



More complex is the hydrolytic disproportionation of the molecular halogens themselves in aqueous alkali which is a commercial route to several alkali-metal halides:

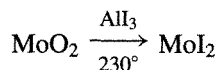
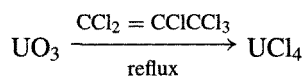
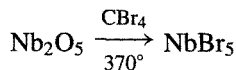
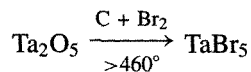
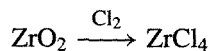


When the desired halide is hydrolytically unstable then dry methods must be used, often at elevated temperatures. Pre-eminent amongst these methods is the oxidative halogenation of metals (or non-metals) with  $\text{X}_2$  or HX; when more than one oxidation state is available  $\text{X}_2$  sometimes gives the higher and HX the lower, e.g.:

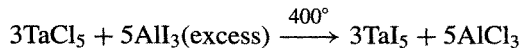
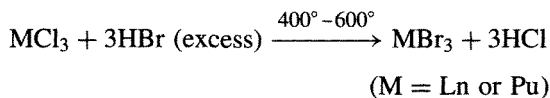
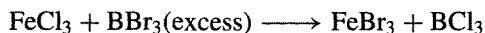


Similarly,  $\text{Cl}_2$  sometimes yields a higher and  $\text{Br}_2$  a lower oxidation state, e.g.  $\text{MoCl}_5$  and  $\text{MoBr}_3$ .

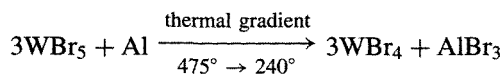
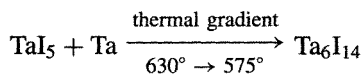
Other routes include the high-temperature halogenation of metal oxides, sometimes in the presence of carbon, to assist removal of oxygen; the source of halogen can be  $\text{X}_2$ , a volatile metal halide  $\text{CX}_4$  or another organic halide. A few examples of the many reactions that have been used industrially or for laboratory scale preparations are:



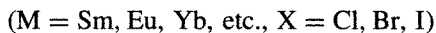
The last two of these reactions also feature a reduction in oxidation state. A closely related route is halogen exchange usually in the presence of an excess of the "halogenating reagent", e.g.:



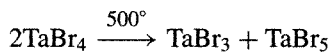
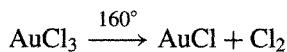
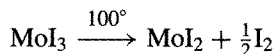
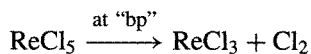
Reductive halogenation can be achieved by reducing a higher halide with the parent metal, another metal or hydrogen:







Alternatively, thermal decomposition or disproportionation can yield the lower halide:



Many significant trends are apparent in the structures of the halides and in their physical and chemical properties. The nature of the element concerned, its position in the periodic table, the particular oxidation state, and, of course, the particular halogen involved, all play a role. The majority of pre-transition metals (Groups 1, 2) together with Group 3, the lanthanides and the actinides in the +2 and +3 oxidation states form halides that are predominantly ionic in character, whereas the non-metals and metals in higher oxidation states ( $\geq +3$ ) tend to form covalent molecular halides. The "ionic-covalent transition" in the halides of Group 15 (P, As, Sb, Bi) and 16 (S, Se, Te, Po) has already been discussed at length (pp. 498, 558, 772) as has the tendency of the refractory transition metals to form cluster halides (pp. 991, 1021, etc.). The problems associated with the ionic bond model and its range of validity were considered in Chapter 4 (p. 79). Presumed bond types tend to show gradual rather than abrupt changes within series in which the central element, the oxidation state or the halogen are systematically varied. For example, in a sequence of chlorides of isoelectronic metals such as KCl, CaCl<sub>2</sub>, ScCl<sub>3</sub> and TiCl<sub>4</sub> the first member is predominantly ionic with a 3D lattice of octahedrally coordinated potassium ions; CaCl<sub>2</sub> has a framework structure (distorted rutile) in which Ca is surrounded by a distorted octahedron of 6Cl; ScCl<sub>3</sub> has a layer structure and TiCl<sub>4</sub> is a covalent molecular liquid.

The sudden discontinuity in physical properties at TiCl<sub>4</sub> is more a function of stoichiometry and coordination number than a sign of any discontinuous or catastrophic change in bond type. Numerous other examples can be found amongst the transition metal halides and the halides of the post-transition elements. In general, the greater the difference in electronegativity between the element and the halogen the greater will be the tendency to charge separation and the more satisfactory will be the ionic bond model. With increasing formal charge on the central atom or with decreasing electronegativity difference the more satisfactory will be the various covalent bond models. The complexities of the situation can be illustrated by reference to the bp (and mp) of the halides: for the more ionic halides these generally follow the sequence  $\text{MF}_n > \text{MCl}_n > \text{MBr}_n > \text{MI}_n$ , being dominated by coulombic interactions which are greatest for the small F<sup>-</sup> and least for the large I<sup>-</sup>, whereas for molecular halides the sequence is usually the reverse, viz.  $\text{MI}_n > \text{MBr}_n > \text{MCl}_n > \text{MF}_n$  being dictated rather by polarizability and London dispersion forces which are greatest for I and least for F. As expected, intermediate halides are less regular as the first sequence yields to the reverse, and no general pattern can be discerned. Physical techniques such as <sup>35,37</sup>Cl nmr spectroscopy and nuclear quadrupole resonance spectroscopy are being increasingly used to probe such trends.<sup>(64)</sup>

Similar observations hold for solubility. Predominantly ionic halides tend to dissolve in polar, coordinating solvents of high dielectric constant, the precise solubility being dictated by the balance between lattice energies and solvation energies of the ions, on the one hand, and on entropy changes involved in dissolution of the crystal lattice, solvation of the ions and modification of the solvent structure, on the other:  $[\Delta G(\text{cryst} \rightarrow \text{saturated soln}) = 0 = \Delta H - T\Delta S]$ . For a given cation (e.g. K<sup>+</sup>, Ca<sup>2+</sup>) solubility in water typically follows the sequence

<sup>64</sup> T. L. WEEDING and W. S. VEEMAN, *J. Chem. Soc., Chem. Commun.*, 946-8 (1989).

$MF_n < MCl_n < MBr_n < MI_n$ . By contrast for less-ionic halides with significant non-coulombic lattice forces (e.g. Ag) solubility in water follows the reverse sequence  $MI_n < MBr_n < MCl_n < MF_n$ . For molecular halides solubility is determined principally by weak intermolecular van der Waals' and dipolar forces, and dissolution is commonly favoured by less-polar solvents such as benzene,  $CCl_4$  or  $CS_2$ .

Trends in chemical reactivity are also apparent, e.g. ease of hydrolysis tends to increase from the non-hydrolysing predominantly ionic halides, through the intermediate halides to the readily hydrolysable molecular halides. Reactivity depends both on the relative energies of  $M-X$  and  $M-O$  bonds and also, frequently, on kinetic factors which may hinder or even prevent the occurrence of thermodynamically favourable reactions. Further trends become apparent within the various groups of halides and are discussed at appropriate points throughout the text.

### 17.2.3 Interhalogen compounds<sup>(65-67)</sup>

The halogens combine exothermically with each other to form interhalogen compounds of four stoichiometries:  $XY$ ,  $XY_3$ ,  $XY_5$  and  $XY_7$  where X is the heavier halogen. A few ternary compounds are also known, e.g.  $IFCl_2$  and  $IF_2Cl$ . For the hexatomic series, only the fluorides are known ( $ClF_5$ ,  $BrF_5$ ,  $IF_5$ ), and  $IF_7$  is the sole example of the octatomic series. All the interhalogen compounds are diamagnetic and contain an even number of halogen atoms. Similarly, the closely related polyhalide anions  $XY_{2n}^-$  and polyhalonium cations  $XY_{2n}^+$  ( $n = 1, 2, 3$ ) each have an odd

number of halogen atoms: these ions will be considered in subsequent sections (pp. 835, 839).

Related to the interhalogens chemically, are compounds formed between a halogen atom and a pseudohalogen group such as CN, SCN,  $N_3$ . Examples are the linear molecules  $ClCN$ ,  $BrCN$ ,  $ICN$  and the corresponding compounds  $XSCN$  and  $XN_3$ . Some of these compounds have already been discussed (p. 319) and need not be considered further. A microwave study<sup>(68)</sup> shows that chlorine thiocyanate is  $CISCN$  (angle  $Cl-S-C$   $99.8^\circ$ ) rather than  $CINCS$ , in contrast to the cyanate which is  $CINCO$ . The corresponding fluoro compound,  $FNCO$ , can be synthesized by several low-temperature routes but is not stable at room temperature and rapidly dimerizes to  $F_2NC(O)NCO$ .<sup>(69)</sup> The chemistry of iodine azide has been reviewed<sup>(70)</sup> — it is obtained as volatile, golden yellow, shock-sensitive needles by reaction of  $I_2$  with  $AgN_3$  in non-oxygen-containing solvents such as  $CH_2Cl_2$ ,  $CCl_4$  or benzene: the structure in the gas phase (as with  $FN_3$ ,  $ClN_3$  and  $BrN_3$  also) comprises a linear  $N_3$  group joined at an obtuse angle to the pendant X atom, thereby giving a molecule of  $C_s$  symmetry.

### Diatomic interhalogens, $XY$

All six possible diatomic compounds between F, Cl, Br and I are known. Indeed,  $ICl$  was first made (independently) by J. L. Gay Lussac and H. Davy in 1813–4 soon after the isolation of the parent halogens themselves, and its existence led J. von Liebig to miss the discovery of the new element bromine, which has similar properties (p. 794). The compounds vary considerably in thermal stability:  $ClF$  is extremely robust;  $ICl$  and  $IBr$  are moderately stable and can be obtained in very pure crystalline form at room temperature;  $BrCl$  readily dissociates reversibly into its

<sup>65</sup> Ref. 23, pp. 1476–1563, see also D. M. MARTIN, R. ROUSSON and J. M. WEULERSSE, in J. J. LAGOWSKI (ed.), *The Chemistry of Nonaqueous Solvents*, Chap. 3, pp. 157–95, Academic Press, New York, 1978.

<sup>66</sup> A. I. POPOV, Chap. 2, in V. GUTMANN (ed.), *MTP International Review of Science: Inorganic Chemistry Series* 1, Vol. 3, pp. 53–84, Butterworths, London, 1972.

<sup>67</sup> K. O. CHRISTE, *IUPAC Additional Publication 24th Int. Congr. Pure Appl. Chem.*, Hamburg, 1973, Vol. 4. *Compounds of Non-Metals*, pp. 115–41, Butterworths, London, 1974.

<sup>68</sup> R. J. RICHARDS, R. W. DAVIS and M. C. L. GERRY, *J. Chem. Soc., Chem. Commun.*, 915–6 (1980).

<sup>69</sup> K. GHOLIVAND and H. WILLNER, *Z. anorg. allg. Chem.* **550**, 27–34 (1987).

<sup>70</sup> K. DEHNICKE, *Angew. Chem. Int. Edn. Engl.* **18**, 507–14 (1979).

$MF_n < MCl_n < MBr_n < MI_n$ . By contrast for less-ionic halides with significant non-coulombic lattice forces (e.g. Ag) solubility in water follows the reverse sequence  $MI_n < MBr_n < MCl_n < MF_n$ . For molecular halides solubility is determined principally by weak intermolecular van der Waals' and dipolar forces, and dissolution is commonly favoured by less-polar solvents such as benzene,  $CCl_4$  or  $CS_2$ .

Trends in chemical reactivity are also apparent, e.g. ease of hydrolysis tends to increase from the non-hydrolysing predominantly ionic halides, through the intermediate halides to the readily hydrolysable molecular halides. Reactivity depends both on the relative energies of  $M-X$  and  $M-O$  bonds and also, frequently, on kinetic factors which may hinder or even prevent the occurrence of thermodynamically favourable reactions. Further trends become apparent within the various groups of halides and are discussed at appropriate points throughout the text.

### 17.2.3 Interhalogen compounds<sup>(65-67)</sup>

The halogens combine exothermically with each other to form interhalogen compounds of four stoichiometries:  $XY$ ,  $XY_3$ ,  $XY_5$  and  $XY_7$  where X is the heavier halogen. A few ternary compounds are also known, e.g.  $IFCl_2$  and  $IF_2Cl$ . For the hexatomic series, only the fluorides are known ( $ClF_5$ ,  $BrF_5$ ,  $IF_5$ ), and  $IF_7$  is the sole example of the octatomic series. All the interhalogen compounds are diamagnetic and contain an even number of halogen atoms. Similarly, the closely related polyhalide anions  $XY_{2n}^-$  and polyhalonium cations  $XY_{2n}^+$  ( $n = 1, 2, 3$ ) each have an odd

number of halogen atoms: these ions will be considered in subsequent sections (pp. 835, 839).

Related to the interhalogens chemically, are compounds formed between a halogen atom and a pseudohalogen group such as CN, SCN,  $N_3$ . Examples are the linear molecules  $ClCN$ ,  $BrCN$ ,  $ICN$  and the corresponding compounds  $XSCN$  and  $XN_3$ . Some of these compounds have already been discussed (p. 319) and need not be considered further. A microwave study<sup>(68)</sup> shows that chlorine thiocyanate is  $CISCN$  (angle  $Cl-S-C$   $99.8^\circ$ ) rather than  $CINCS$ , in contrast to the cyanate which is  $CINCO$ . The corresponding fluoro compound,  $FNCO$ , can be synthesized by several low-temperature routes but is not stable at room temperature and rapidly dimerizes to  $F_2NC(O)NCO$ .<sup>(69)</sup> The chemistry of iodine azide has been reviewed<sup>(70)</sup> — it is obtained as volatile, golden yellow, shock-sensitive needles by reaction of  $I_2$  with  $AgN_3$  in non-oxygen-containing solvents such as  $CH_2Cl_2$ ,  $CCl_4$  or benzene: the structure in the gas phase (as with  $FN_3$ ,  $ClN_3$  and  $BrN_3$  also) comprises a linear  $N_3$  group joined at an obtuse angle to the pendant X atom, thereby giving a molecule of  $C_s$  symmetry.

### Diatomic interhalogens, $XY$

All six possible diatomic compounds between F, Cl, Br and I are known. Indeed,  $ICl$  was first made (independently) by J. L. Gay Lussac and H. Davy in 1813–4 soon after the isolation of the parent halogens themselves, and its existence led J. von Liebig to miss the discovery of the new element bromine, which has similar properties (p. 794). The compounds vary considerably in thermal stability:  $ClF$  is extremely robust;  $ICl$  and  $IBr$  are moderately stable and can be obtained in very pure crystalline form at room temperature;  $BrCl$  readily dissociates reversibly into its

<sup>65</sup> Ref. 23, pp. 1476–1563, see also D. M. MARTIN, R. ROUSSON and J. M. WEULERSSE, in J. J. LAGOWSKI (ed.), *The Chemistry of Nonaqueous Solvents*, Chap. 3, pp. 157–95, Academic Press, New York, 1978.

<sup>66</sup> A. I. POPOV, Chap. 2, in V. GUTMANN (ed.), *MTP International Review of Science: Inorganic Chemistry Series* 1, Vol. 3, pp. 53–84, Butterworths, London, 1972.

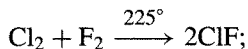
<sup>67</sup> K. O. CHRISTE, *IUPAC Additional Publication 24th Int. Congr. Pure Appl. Chem.*, Hamburg, 1973, Vol. 4. *Compounds of Non-Metals*, pp. 115–41, Butterworths, London, 1974.

<sup>68</sup> R. J. RICHARDS, R. W. DAVIS and M. C. L. GERRY, *J. Chem. Soc., Chem. Commun.*, 915–6 (1980).

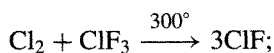
<sup>69</sup> K. GHOLIVAND and H. WILLNER, *Z. anorg. allg. Chem.* **550**, 27–34 (1987).

<sup>70</sup> K. DEHNICKE, *Angew. Chem. Int. Edn. Engl.* **18**, 507–14 (1979).

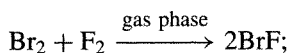
elements; BrF and IF disproportionate rapidly and irreversibly to a higher fluoride and Br<sub>2</sub> (or I<sub>2</sub>). Thus, although all six compounds can be formed by direct, controlled reaction of the appropriate elements, not all can be obtained in pure form by this route. Typical preparative routes (with comments) are as follows:



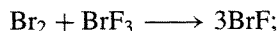
must be purified from ClF<sub>3</sub> and reactants



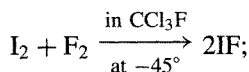
must be purified from excess ClF<sub>3</sub>



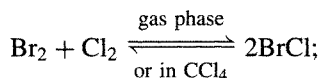
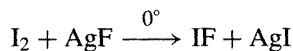
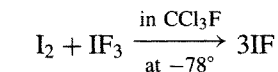
disproportionates to Br<sub>2</sub> + BrF<sub>3</sub> (and BrF<sub>5</sub>)  
at room temp



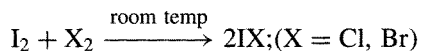
BrF favoured at high temp



disproportionates rapidly to I<sub>2</sub> + IF<sub>5</sub>  
at room temp



compound cannot be isolated free from  
Br<sub>2</sub> and Cl<sub>2</sub>



purify by fractional crystallization of  
the molten compound

In general the compounds have properties intermediate between those of the parent halogens, though a combination of aggressive chemical reactivity and/or thermal instability militates against the determination of physical properties such as mp, bp, etc., in some instances. However, even for such highly dissociated species as BrCl, precise molecular (as distinct from bulk) properties can be determined by spectroscopic techniques. Table 17.12 summarizes some of the more important physical properties of the

**Table 17.12** Physical properties of interhalogen compounds XY

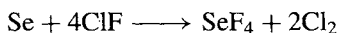
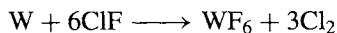
Property	ClF	BrF	IF	BrCl	ICl	IBr
Form at room temperature	Colourless gas	Pale brown (Br <sub>2</sub> )	Unstable	Red brown gas	Ruby red crystals	Black crystals
MP/°C	-155.6	ca. -33 Disprop <sup>(a)</sup>	— Disprop <sup>(a)</sup>	ca. -66 Dissoc <sup>(a)</sup>	27.2(α) 13.9(β)	41 Some dissoc
BP/°C	-100.1	ca. 20	—	ca. 5	97-100 <sup>(b)</sup>	~116 <sup>(b)</sup>
ΔH <sub>f</sub> <sup>o</sup> (298 K)/kJ mol <sup>-1</sup>	-56.5	-58.6	-95.4	+14.6	-35.3(α)	-10.5 (cryst)
ΔG <sub>f</sub> <sup>o</sup> (298 K)/kJ mol <sup>-1</sup>	-57.7	-73.6	-117.6	-1.0	-13.95(α)	+3.7(gas)
Dissociation energy/ kJ mol <sup>-1</sup>	252.5	248.6	~277	215.1	207.7	175.4
d(liq. T°C)/g cm <sup>-3</sup>	1.62(-100°)	—	—	—	3.095(30°)	3.762(42°)
r(X-Y)/pm	162.81	175.6	190.9	213.8	232.07	248.5
Dipole moment/D	0.881	1.29	—	0.57	0.65	1.21
κ(liq. T°C)/ ohm <sup>-1</sup> cm <sup>-1</sup>	1.9 × 10 <sup>-7</sup> (-128°)	—	—	—	5.50 × 10 <sup>-3</sup>	3.4 × 10 <sup>-4</sup>

<sup>(a)</sup>Substantial disproportionation or dissociation prevents meaningful determination of mp and bp; the figures merely indicate the approximate temperature range over which the (impure) compound is liquid at atmospheric pressure.

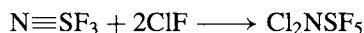
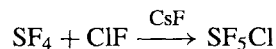
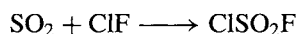
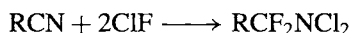
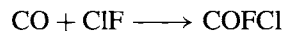
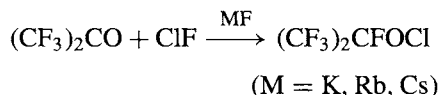
<sup>(b)</sup>Fused ICl and IBr both dissociate into the free halogens to some extent: ICl 0.4% at 25° (supercooled) and 1.1% at 100°C; IBr 8.8% at 25° (supercooled) and 13.4% at 100°C.

diatomic interhalogens. The most volatile compound, ClF, is a colourless gas which condenses to a very pale yellow liquid below  $-100^\circ$ . The least volatile is IBr; it forms black crystals in which the IBr molecules pack in a herringbone pattern similar to that in  $I_2$  (p. 803) and in which the internuclear distance  $r(\text{I}-\text{Br})$  is 252 pm. i.e. slightly longer than in the gas phase (248.5 pm). ICl is unusual in forming two crystalline modifications: the stable ( $\alpha$ ) form crystallizes as large, transparent ruby-red needles from the melt and features zigzag chains of molecules (Fig. 17.6) with two different ICl units and appreciable interchain intermolecular bonding. The packing is somewhat different in the yellow, metastable ( $\beta$ ) form (Fig. 17.6) which can be obtained as brownish-red crystals from strongly supercooled melts.

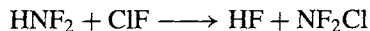
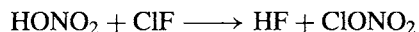
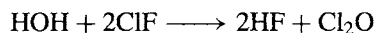
The chemical reactions of XY can be conveniently classified as (a) halogenation reactions, (b) donor-acceptor interactions and (c) use as solvent systems. Reactions frequently parallel those of the parent halogens but with subtle and revealing differences. ClF is an effective fluorinating agent (p. 820) and will react with many metals and non-metals either at room temperature or above, converting them to fluorides and liberating chlorine, e.g.:



It can also act as a chlorofluorinating agent by addition across a multiple bond and/or by oxidation, e.g.:



Reaction with OH groups or NH groups results in the exothermic elimination of HF and the (often violent) chlorination of the substrate, e.g.:



Lewis acid (fluoride-ion acceptor) behaviour is exemplified by reactions with NOF and MF to give  $[\text{NO}]^+[\text{ClF}_2]^-$  and  $\text{M}^+[\text{ClF}_2]^-$  respectively (M = alkali metal or  $\text{NH}_4$ ). Lewis base (fluoride ion donor) activity includes reactions with  $\text{BF}_3$  and  $\text{AsF}_5$ :

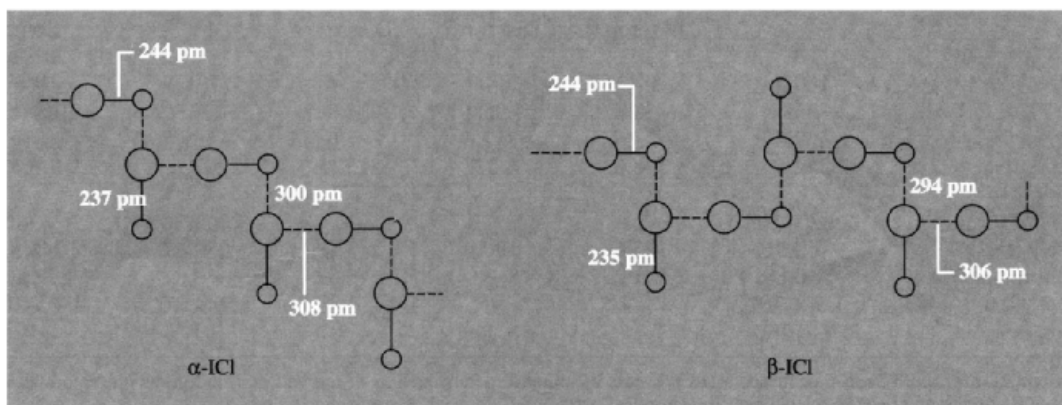
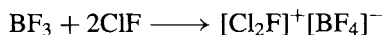
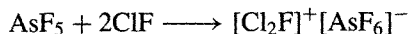


Figure 17.6 Structures of  $\alpha$ - and  $\beta$ -forms of crystalline ICl.

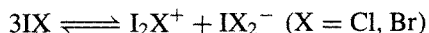


The linear polyhalide anion  $[\text{F}-\text{Cl}-\text{F}]^-$  and the angular polyhalonium cation  $[\text{F} \begin{array}{c} \text{Cl} \\ \diagup \quad \diagdown \\ \text{Cl} \end{array}]^+$  are members of a more extensive set of ions to be treated on pp. 835ff. ClF is commercially available in steel lecture bottles of 500-g capacity but must be handled with extreme circumspection in scrupulously dried and degreased apparatus constructed in steel, copper, Monel metal or nickel; fluorocarbon polymers such as Teflon can also be used, but not at elevated temperatures.

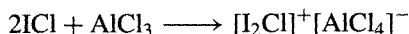
The reactivity of ICl and IBr, though milder than that of ClF is nevertheless still extremely vigorous and the compounds react with most metals including Pt and Au, but not with B, C, Cd, Pb, Zr, Nb, Mo or W. With ICl, phosphorus yields  $\text{PCl}_5$  and V conveniently yields  $\text{VCl}_3$  (rather than  $\text{VCl}_4$ ). Reaction with organic substrates depends subtly on the conditions chosen. For example, phenol and salicylic acid are chlorinated by ICl *vapour*, since homolytic dissociation of the ICl molecule leads to chlorination by  $\text{Cl}_2$  rather than iodination by the less-reactive  $\text{I}_2$ . By contrast, in  $\text{CCl}_4$  solution (low dielectric constant) iodination predominates, accompanied to a small extent by chlorination: this implies heterolytic fission and rapid electrophilic iodination by  $\text{I}^+$  plus some residual chlorination by  $\text{Cl}_2$  (or ICl). In a solvent of high dielectric constant, e.g.  $\text{PhNO}_2$ , iodination occurs exclusively.<sup>(71)</sup> Likewise BrF, in the presence of EtOH, rapidly and essentially quantitatively monobrominates aromatics such as PhX: when X = Me, Bu', OMe or Br, substitution is mainly or exclusively *para*, whereas with deactivating substituents (X =  $-\text{CO}_2\text{Et}$ ,  $-\text{CHO}$ ,  $-\text{NO}_2$ ) exclusively *meta*-bromination occurs.<sup>(72)</sup> A similar interpretation explains why IBr almost invariably brominates rather than iodates aromatic compounds due to its appreciable dissociation into  $\text{Br}_2$  and  $\text{I}_2$  in

solution and the much greater rate of reaction of bromination by  $\text{Br}_2$  compared with iodination by iodine.

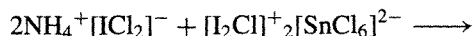
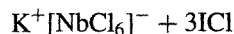
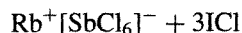
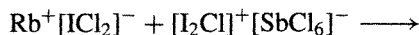
Both ICl and IBr are partly dissociated into ions in the fused state, and this gives rise to an appreciable electrical conductivity (Table 17.12). The ions formed by this heterolytic dissociation of IX are undoubtedly solvated in the melt and the equilibria can be formally represented as



The compounds can therefore be used as nonaqueous ionizing solvent systems (p. 424). For example the conductivity of ICl is greatly enhanced by addition of alkali metal halides or aluminium halides which may be considered as halide-ion donors and acceptors respectively:



Similarly pyridine gives  $[\text{pyI}]^+ [\text{ICl}_2]^-$  and  $\text{SbCl}_5$  forms a 2:1 adduct which can be reasonably formulated as  $[\text{I}_2\text{Cl}]^+ [\text{SbCl}_6]^-$ . By contrast, the 1:1 adduct with  $\text{PCl}_5$  has been shown by X-ray studies to be  $[\text{PCl}_4]^+ [\text{ICl}_2]^-$ . Solvoacid-solvobase reactions have been monitored by conductimetric titration; e.g. titration of solutions of RbCl and  $\text{SbCl}_5$  in ICl (or of KCl and  $\text{NbCl}_5$ ) shows a break at 1:1 molar proportions, whereas titration of  $\text{NH}_4\text{Cl}$  with  $\text{SnCl}_4$  shows a break at the 2:1 mole ratio:



The preparative utility of such reactions is, however, rather limited, and neither ICl or IBr has been much used except to form various mixed polyhalide species. Compounds must frequently

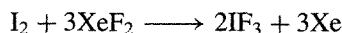
<sup>71</sup> F. W. BENNETT and A. G. SHARPE, *J. Chem. Soc.* 1383-4 (1950).

<sup>72</sup> S. ROZEN and M. BRAND, *J. Chem. Soc., Chem. Commun.*, 752-3 (1987).

be isolated by extraction rather than by precipitation, and solvolysis is a further complicating factor.

### Tetra-atomic interhalogens, $XY_3$

The compounds to be considered are  $ClF_3$ ,  $BrF_3$ ,  $IF_3$  and  $ICl_3$  ( $I_2Cl_6$ ). All can be prepared by direct reaction of the elements, but conditions must be chosen so as to avoid formation of mixtures of interhalogens of different stoichiometries.  $ClF_3$  is best formed by direct fluorination of  $Cl_2$  or  $ClF$  in the gas phase at 200–300° in Cu, Ni or Monel metal apparatus.  $BrF_3$  is formed similarly at or near room temperature and can be purified by distillation to give a pale straw-coloured liquid. With  $IF_3$ , which is only stable below –30° the problem is to avoid the more facile formation of  $IF_5$ ; this can be achieved either by the action of  $F_2$  on  $I_2$  suspended in  $CCl_3F$  at –45° or more elegantly by the low-temperature fluorination of  $I_2$  with  $XeF_2$ :



$I_2Cl_6$  is readily made as a bright-yellow solid by reaction of  $I_2$  with an excess of liquid chlorine at –80° followed by the low-temperature evaporation of the  $Cl_2$ ; care must be taken with this latter operation, however, because of the very ready dissociation of  $I_2Cl_6$  into  $ICl$  and  $Cl_2$ .

Physical properties are summarized in Table 17.13. Little is known of the unstable

$IF_3$  but  $ClF_3$  and  $BrF_3$  are well-characterized volatile molecular liquids. Both have an unusual T-shaped structure of  $C_{2v}$  symmetry, consistent with the presence of 10 electrons in the valency shell of the central atom (Fig. 17.7a,b). A notable feature of both structures is the slight deviation from colinearity of the apical F–X–F bonds, the angle being 175.0° for  $ClF_3$  and 172.4° for  $BrF_3$ ; this reflects the greater electrostatic repulsion of the nonbonding pair of electrons in the equatorial plane of the molecule. For each molecule the X–F<sub>apical</sub> distance is some 5–6% greater than the X–F<sub>equatorial</sub> distance but the mean X–F distance is very similar to that in the corresponding monofluoride. The structure of crystalline  $ICl_3$  is quite different, being built up of planar  $I_2Cl_6$  molecules separated by normal van der Waals' distances between the Cl atoms (Fig. 17.7c). The terminal I–Cl distances are similar to those in  $ICl$  but the bridging I–Cl distances are appreciably longer.

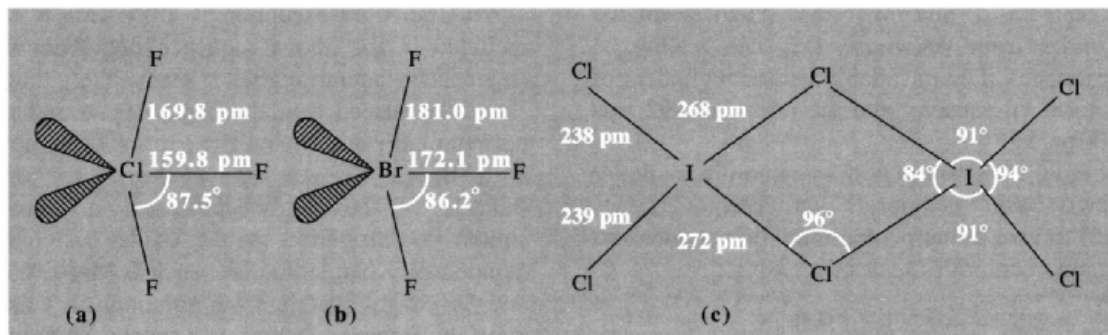
$ClF_3$  is one of the most reactive chemical compounds known<sup>(73)</sup> and reacts violently with many substances generally thought of as inert. Thus it spontaneously ignites asbestos, wood, and other building materials and was used in incendiary bomb attacks on UK cities during the Second World War. It reacts explosively with water and with most organic substances, though

<sup>73</sup> L. STEIN, in V. GUTMANN (ed.), *Halogen Chemistry*, Vol. 1, pp. 133–224, Academic Press, London, 1967.

**Table 17.13** Physical properties of interhalogen compounds  $XY_3$

Property	$ClF_3$	$BrF_3$	$IF_3$	$I_2Cl_6$
Form at room temperature	Colourless gas/liquid	Straw-coloured liquid	Yellow solid (decomp above –28°)	Bright yellow solid
MP/°C	–76.3	8.8	—	101 (16 atm)
BP/°C	11.8	125.8	—	—
$\Delta H_f^\circ(298\text{ K})/\text{kJ mol}^{-1}$	–164 (g)	–301 (l)	ca. –485 (g) calc	–89.3 (s)
$\Delta G_f^\circ(298\text{ K})/\text{kJ mol}^{-1}$	–124 (g)	–241 (l)	ca. –460 (g) calc	–21.5 (s)
Mean X–Y bond energy of $XY_3/\text{kJ mol}^{-1}$	174	202	ca. 275 (calc)	—
Density( $T^\circ\text{C}$ )/ $\text{g cm}^{-3}$	1.885 (0°)	2.803 (25°)	—	3.111 (15°)
Dipole moment/D	0.557	1.19	—	—
Dielectric constant $\epsilon(T^\circ)$	4.75 (0°)	—	—	—
$\kappa(\text{liq}, T^\circ\text{C})/\text{ohm}^{-1}\text{cm}^{-1}$	$6.5 \times 10^{-9}(0^\circ)$	$8.0 \times 10^{-3}(25^\circ)$	—	$8.6 \times 10^{-3}(102^\circ)$

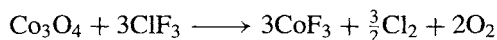
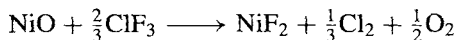
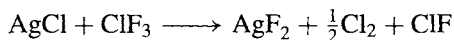




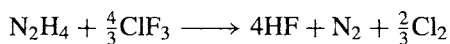
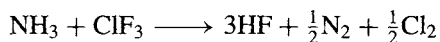
**Figure 17.7** Molecular structures of (a)  $\text{ClF}_3$  and (b)  $\text{BrF}_3$  as determined by microwave spectroscopy. An X-ray study of crystalline  $\text{ClF}_3$  gave slightly longer distances (171.6 and 162.1 pm) and a slightly smaller angle ( $87.0^\circ$ ). (c) Structure of  $\text{I}_2\text{Cl}_6$  showing planar molecules of approximate  $D_{2h}$  symmetry.

reaction can sometimes be moderated by dilution of  $\text{ClF}_3$  with an inert gas, by dissolution of the organic compound in an inert fluorocarbon solvent or by the use of low temperatures. Spontaneous ignition occurs with  $\text{H}_2$ , K, P, As, Sb, S, Se, Te, and powdered Mo, W, Rh, Ir and Fe. Likewise,  $\text{Br}_2$  and  $\text{I}_2$  enflame and produce higher fluorides. Some metals (e.g. Na, Mg, Al, Zn, Sn, Ag) react at room temperature until a fluoride coating is established; when heated they continue to react vigorously. Palladium, Pt and Au are also attacked at elevated temperatures and even Xe and Rn are fluorinated. Mild steel can be used as a container at room temperature and Cu is only slightly attacked below  $300^\circ$  but the most resistant are Ni and Monel metal. Very pure  $\text{ClF}_3$  has no effect on Pyrex or quartz but traces of HF, which are normally present, cause slow etching.

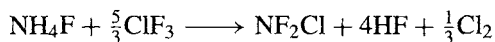
$\text{ClF}_3$  converts most chlorides to fluorides and reacts even with refractory oxides such as  $\text{MgO}$ ,  $\text{CaO}$ ,  $\text{Al}_2\text{O}_3$ ,  $\text{MnO}_2$ ,  $\text{Ta}_2\text{O}_5$  and  $\text{MoO}_3$  to form higher fluorides, e.g.:



With suitable dilution to moderate the otherwise violent reactions.  $\text{NH}_3$  gas and  $\text{N}_2\text{H}_4$  yield HF and the elements:

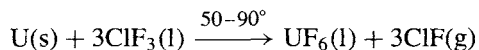


At one time this latter reaction was used in experimental rocket motors, the  $\text{ClF}_3$  oxidizer reacting spontaneously with the fuel ( $\text{N}_2\text{H}_4$  or  $\text{Me}_2\text{N}_2\text{H}_2$ ). At low temperatures  $\text{NH}_4\text{F}$  and  $\text{NH}_4\text{HF}_2$  react with liquid  $\text{ClF}_3$  when allowed to warm from  $-196$  to  $-5^\circ$  but the reaction is hazardous and may explode above  $-5^\circ$ :



The same products are obtained more safely by reacting gaseous  $\text{ClF}_3$  with a suspension of  $\text{NH}_4\text{F}$  or  $\text{NH}_4\text{HF}_2$  in a fluorocarbon oil.

$\text{ClF}_3$  is manufactured on a moderately large scale, considering its extraordinarily aggressive properties which necessitate major precautions during handling and transport. Production plant in Germany had a capacity of  $\sim 5$  tonnes/day in 1940 ( $\sim 1500$  tonnes pa). It is now used in the USA, the UK, France and Russia primarily for nuclear fuel processing.  $\text{ClF}_3$  is used to produce  $\text{UF}_6(\text{g})$ :

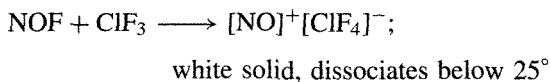
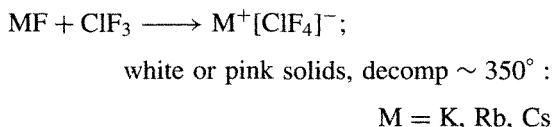
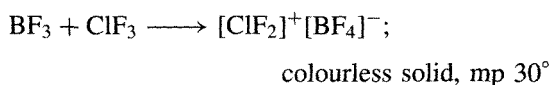
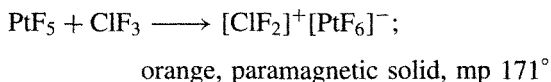
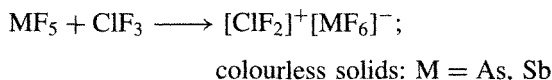


It is also invaluable in separating U from Pu and other fission products during nuclear fuel reprocessing, since Pu reacts only to give the (involatile)  $\text{PuF}_4$  and most fission products



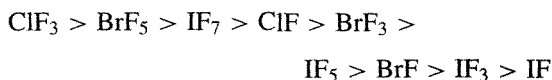
(except Te, I and Mo) also yield involatile fluorides from which the UF<sub>6</sub> can readily be separated. ClF<sub>3</sub> is available in steel cylinders of up to 82 kg capacity and the price in 1992 was \$100 per kg.

Liquid ClF<sub>3</sub> can act both as a fluoride ion donor (Lewis base) or fluoride ion acceptor (Lewis acid) to give difluorochloronium compounds and tetrafluorochlorides respectively, e.g.:



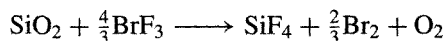
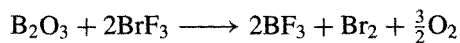
Despite these reaction products there is little evidence for an ionic self-dissociation equilibrium in liquid ClF<sub>3</sub> such as may be formally represented by  $2\text{ClF}_3 \rightleftharpoons \text{ClF}_2^+ + \text{ClF}_4^-$ , and the electrical conductivity of the pure liquid (p. 828) is only of the order of  $10^{-9} \text{ ohm}^{-1} \text{ cm}^{-1}$ . The structures of these ions are discussed more fully in subsequent sections.

Bromine trifluoride, though it reacts explosively with water and hydrocarbon tap greases, is somewhat less violent and vigorous a fluorinating agent than is ClF<sub>3</sub>. The sequence of reactivity usually quoted for the halogen fluorides is:

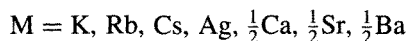
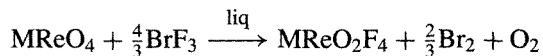


It can be seen that, for a given stoichiometry of XF<sub>n</sub>, the sequence follows the order Cl > Br > I and for a given halogen the reactivity of XF<sub>n</sub> diminishes with decrease in n, i.e. XF<sub>5</sub> > XF<sub>3</sub> >

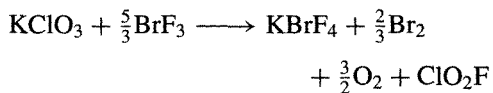
XF. (A possible exception is ClF<sub>5</sub>; this is not included in the above sequence but, from the fragmentary data available, it seems likely that it should be placed near the beginning — perhaps between ClF<sub>3</sub> and BrF<sub>5</sub>.) BrF<sub>3</sub> reacts vigorously with B, C, Si, As, Sb, I and S to form fluorides. It has also been used to prepare simple fluorides from metals, oxides and other compounds: volatile fluorides such as MoF<sub>6</sub>, WF<sub>6</sub> and UF<sub>6</sub> distil readily from solutions in which they are formed whereas less-volatile fluorides such as AuF<sub>3</sub>, PdF<sub>3</sub>, RhF<sub>4</sub>, PtF<sub>4</sub> and BiF<sub>5</sub> are obtained as residues on removal of BrF<sub>3</sub> under reduced pressure. Reaction with oxides often evolves O<sub>2</sub> quantitatively (e.g. B<sub>2</sub>O<sub>3</sub>, Tl<sub>2</sub>O<sub>3</sub>, SiO<sub>2</sub>, GeO<sub>2</sub>, As<sub>2</sub>O<sub>3</sub>, Sb<sub>2</sub>O<sub>3</sub>, SeO<sub>3</sub>, I<sub>2</sub>O<sub>5</sub>, CuO, TiO<sub>2</sub>, UO<sub>3</sub>):

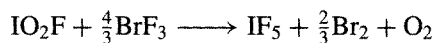
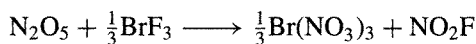


The reaction can be used as a method of analysis and also as a procedure for determining small amounts of O (or N) in metals and alloys of Li, Ti, U, etc. In cases when BrF<sub>3</sub> itself only partially fluorinates the refractory oxides, the related reagents KBrF<sub>4</sub> and BrF<sub>2</sub>SbF<sub>6</sub> have been found to be effective (e.g. for MgO, CaO, Al<sub>2</sub>O<sub>3</sub>, MnO<sub>2</sub>, Fe<sub>2</sub>O<sub>3</sub>, NiO, CeO<sub>2</sub>, Nd<sub>2</sub>O<sub>3</sub>, ZrO<sub>2</sub>, ThO<sub>2</sub>). Oxygen in carbonates and phosphates can also be determined by reaction with BrF<sub>3</sub>. Sometimes partial fluorination yields new compounds, e.g. perrhenates afford tetrafluoroperrhenates:



Likewise, K<sub>2</sub>Cr<sub>2</sub>O<sub>7</sub> and Ag<sub>2</sub>Cr<sub>2</sub>O<sub>7</sub> yield the corresponding MCrOF<sub>4</sub> (i.e. reduction from Cr<sup>VI</sup> to Cr<sup>V</sup>). Other similar reactions, which nevertheless differ slightly in their overall stoichiometry, are:



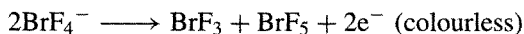
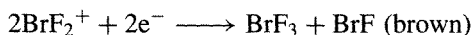


As with  $\text{ClF}_3$ ,  $\text{BrF}_3$  is used to fluorinate U to  $\text{UF}_6$  in the processing and reprocessing of nuclear fuel. It is manufactured commercially on a multitonne scale and is available as a liquid in steel cylinders of varying size up to 91 kg capacity. The US price in 1992 was  $\sim$ \\$80 per kg.

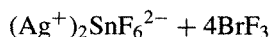
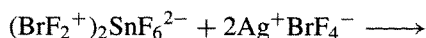
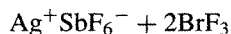
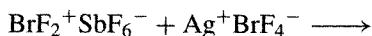
In addition to its use as a straight fluorinating agent,  $\text{BrF}_3$  has been extensively investigated and exploited as a preparative nonaqueous ionizing solvent. The appreciable electrical conductivity of the pure liquid (p. 828) can be interpreted in terms of the dissociative equilibrium



Electrolysis gives a brown coloration at the cathode but no visible change at the anode:

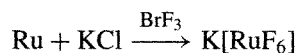
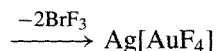


The specific conductivity decreases from  $8.1 \times 10^{-3} \text{ ohm}^{-1} \text{ cm}^{-1}$  at  $10^\circ$  to  $7.1 \times 10^{-3} \text{ ohm}^{-1} \text{ cm}^{-1}$  at  $55^\circ$  and this unusual behaviour has been attributed to the thermal instability of the  $\text{BrF}_2^+$  and  $\text{BrF}_4^-$  ions at higher temperatures. Consistent with the above scheme  $\text{KF}$ ,  $\text{BaF}_2$  and numerous other fluorides (such as  $\text{NaF}$ ,  $\text{RbF}$ ,  $\text{AgF}$ ,  $\text{NOF}$ ) dissolve in  $\text{BrF}_3$  with enhancement of the electrical conductivity due to the formation of the solvobases  $\text{KBrF}_4$ ,  $\text{Ba}(\text{BrF}_4)_2$ , etc. Likewise,  $\text{Sb}$  and  $\text{Sn}$  give solutions of the solvoacids  $\text{BrF}_2\text{SbF}_6$  and  $(\text{BrF}_2)_2\text{SnF}_6$ . Conductimetric titrations between these various species can be carried out, the end point being indicated by a sharp minimum in the conductivity:



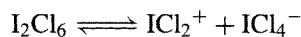
Other solvoacids that have been isolated include the  $\text{BrF}_2^+$  compounds of  $\text{AuF}_4^-$ ,  $\text{BiF}_6^-$ ,  $\text{NbF}_6^-$ ,

$\text{TaF}_6^-$ ,  $\text{RuF}_6^-$  and  $\text{PdF}_6^{2-}$  and reactions of  $\text{BrF}_3$  solutions have led to the isolation of large numbers of such anhydrous complex fluorides with a variety of cations.<sup>(73)</sup> Solvolysis sometimes complicates the isolation of a complex by evaporation of  $\text{BrF}_3$  and solvates are also known, e.g.  $\text{K}_2\text{TiF}_6 \cdot \text{BrF}_3$  and  $\text{K}_2\text{PtF}_6 \cdot \text{BrF}_3$ . It is frequently unnecessary to isolate the presumed reaction intermediates and the required complex can be obtained by the action of  $\text{BrF}_3$  on an appropriate mixture of starting materials:

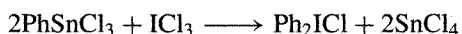


In these reactions  $\text{BrF}_3$  serves both as a fluorinating agent and as a nonaqueous solvent reaction medium.

Molten  $\text{I}_2\text{Cl}_6$  has been much less studied as an ionizing solvent because of the high dissociation pressure of  $\text{Cl}_2$  above the melt. The appreciable electrical conductivity may well indicate an ionic self-dissociation equilibrium such as

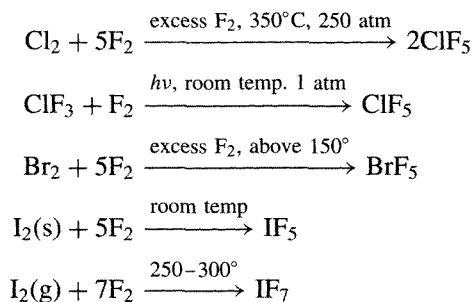


Such ions are known from various crystal-structure determinations, e.g.  $\text{K}[\text{ICl}_2] \cdot \text{H}_2\text{O}$ ,  $[\text{ICl}_2][\text{AlCl}_4]$  and  $[\text{ICl}_2][\text{SbCl}_6]$  (p. 839).  $\text{I}_2\text{Cl}_6$  is a vigorous chlorinating agent, no doubt due at least in part to its ready dissociation into  $\text{ICl}$  and  $\text{Cl}_2$ . Aromatic compounds, including thiophen,  $\text{C}_4\text{H}_4\text{S}$ , give chlorosubstituted products with very little if any iodination. By contrast, reaction of  $\text{I}_2\text{Cl}_6$  with aryl-tin or aryl-mercury compounds yield the corresponding diaryliodonium derivatives, e.g.:

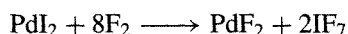
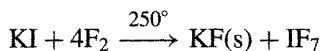
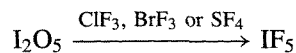
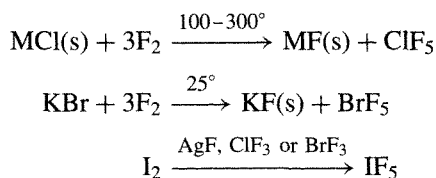


Hexa-atomic and octa-atomic interhalogens,  $\text{XF}_5$  and  $\text{IF}_7$

The three fluorides  $\text{ClF}_5$ ,  $\text{BrF}_5$  and  $\text{IF}_5$  are the only known hexa-atomic interhalogens, and  $\text{IF}_7$  is the sole representative of the octa-atomic class. The first to be made (1871) was  $\text{IF}_5$  which is the most readily formed of the iodine fluorides, whereas the more vigorous conditions required for the others delayed the synthesis of  $\text{BrF}_5$  and  $\text{IF}_7$  until 1930/1 and  $\text{ClF}_5$  until 1962. The preferred method of preparing all four compounds on a large scale is by direct fluorination of the element or a lower fluoride:



Small-scale preparations can conveniently be effected as follows:



This last reaction is preferred for  $\text{IF}_7$  because of the difficulty of drying  $\text{I}_2$ . ( $\text{IF}_7$  reacts with  $\text{SiO}_2$ ,  $\text{I}_2\text{O}_5$  or traces of water to give  $\text{OIF}_5$  from which it can be separated only with difficulty.)

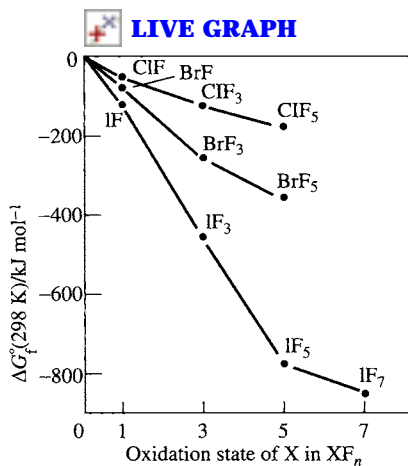
$\text{ClF}_5$ ,  $\text{BrF}_5$  and  $\text{IF}_7$  are extremely vigorous fluorinating reagents, being excelled in this only by  $\text{ClF}_3$ .  $\text{IF}_5$  is (relatively) a much milder fluorinating agent and can be handled in glass apparatus: it is manufactured in the USA on a scale of several hundred tonnes pa. It is available as a liquid in steel cylinders up to 1350 kg capacity (i.e.  $1\frac{1}{3}$  tonnes) and the price in 1992 was *ca.* \$50 per kg. All four compounds are colourless, volatile molecular liquids or gases at room temperature and their physical properties are given in Table 17.14. It will be seen that the liquid range of  $\text{IF}_5$  resembles that of  $\text{BrF}_3$  and that  $\text{BrF}_5$  is similar to  $\text{ClF}_3$ . The free energies of formation of these and the other halogen fluorides in the gas phase are compared in Fig. 17.8. The trends are obvious; it is also clear from the convexity (or concavity) of the lines that  $\text{BrF}$  and  $\text{IF}$  might be expected to disproportionate into the trifluoride and the parent halogen, whereas  $\text{ClF}_3$ ,  $\text{BrF}_3$  and  $\text{IF}_5$  are thermodynamically the most stable fluorides of Cl, Br and I respectively. Plots of average bond energies are in Fig. 17.9: for a

Table 17.14 Physical properties of the higher halogen fluorides

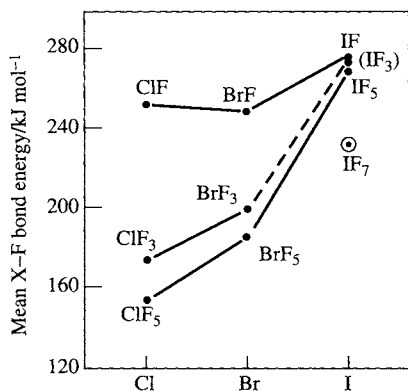
Property	$\text{ClF}_5$	$\text{BrF}_5$	$\text{IF}_5$	$\text{IF}_7$
MP/ $^\circ\text{C}$	-103	-60.5	9.4	6.5 (triple point)
BP/ $^\circ\text{C}$	-13.1	41.3	104.5	4.8 (subl 1 atm)
$\Delta H_f^\circ(\text{gas}, 298 \text{ K})/\text{kJ mol}^{-1}$	-255	429 <sup>(a)</sup>	-843 <sup>(b)</sup>	-962
$\Delta G_f^\circ(\text{gas}, 298 \text{ K})/\text{kJ mol}^{-1}$	-165	-351 <sup>(a)</sup>	-775 <sup>(b)</sup>	-842
Mean X-F bond energy/ kJ mol <sup>-1</sup>	154	187	269	232
$d_{\text{liq}}(T^\circ\text{C})/\text{g cm}^{-3}$	2.105 (-80°)	2.4716 (25°)	3.207 (25°)	2.669 (25°)
Dipole moment/D	—	1.51	2.18	0
Dielectric constant $\epsilon(T^\circ\text{C})$	4.28 (-80°)	7.91 (25°)	36.14 (25°)	1.75 (25°)
$\kappa(\text{liq at } T^\circ\text{C})/\text{ohm}^{-1} \text{ cm}^{-1}$	$3.7 \times 10^{-8}$ (-80°)	$9.9 \times 10^{-8}$ (25°)	$5.4 \times 10^{-6}$ (25°)	$<10^{-9}$ (25°)

<sup>(a)</sup>For liquid  $\text{BrF}_5$ :  $\Delta H_f^\circ(298 \text{ K}) -458.6 \text{ kJ mol}^{-1}$ ,  $\Delta G_f^\circ(298 \text{ K}) -351.9 \text{ kJ mol}^{-1}$ .

<sup>(b)</sup>For liquid  $\text{IF}_5$ :  $\Delta H_f^\circ(298 \text{ K}) -885 \text{ kJ mol}^{-1}$ ,  $\Delta G_f^\circ(298 \text{ K}) -784 \text{ kJ mol}^{-1}$ .



**Figure 17.8** Free energies of formation of gaseous halogen fluorides at 298 K.

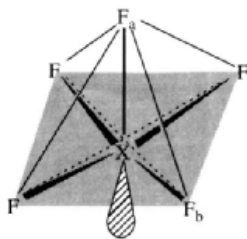


**Figure 17.9** Mean bond energies of halogen fluorides.

given value of  $n$  in  $\text{XF}_n$  the sequence of energies is  $\text{ClF}_n < \text{BrF}_n < \text{IF}_n$ , reflecting the increasing

difference in electronegativity between X and F.  $\text{ClF}$  is an exception. As expected, for a given halogen, the mean bond energy decreases as  $n$  increases in  $\text{XF}_n$ , the effect being most marked for Cl and least for I. Note that high bond energy (as in  $\text{BrF}$  and  $\text{IF}$ ) does not necessarily confer stability on a compound (why?).

The molecular structure of  $\text{XF}_5$  has been shown to be square pyramidal ( $C_{4v}$ ) with the central atom slightly below the plane of the four basal F atoms (Fig. 17.10). The structure is essentially the same in the gaseous, liquid and crystalline phases and has been established by some (or all) of the following techniques: electron diffraction, microwave spectroscopy, infrared and Raman spectroscopy,  $^{19}\text{F}$  nmr spectroscopy and X-ray diffraction analysis. This structure immediately explains the existence of a small permanent dipole moment, which would be absent if the structure were trigonal bipyramidal ( $C_{3v}$ ), and is consistent with the presence of 12 valence-shell electrons on the central atom X. Electrostatic effects account for the slight displacement of the four  $\text{F}_b$  away from the lone-pair of electrons and also the fact that  $\text{X}-\text{F}_b > \text{X}-\text{F}_a$ . The  $^{19}\text{F}$  nmr spectra of both  $\text{BrF}_5$  and  $\text{IF}_5$  consist of a highfield doublet (integrated relative area 4) and a 1:4:6:4:1 quintet of integrated area 1: these multiplets can immediately be assigned on the basis of  $^{19}\text{F}-^{19}\text{F}$  coupling and relative area to the 4 basal and the unique apical F atom respectively. The molecules are fluxional at higher temperatures: e.g. spin-spin coupling disappears in  $\text{IF}_5$  at  $115^\circ$  and further heating leads to broadening and coalescence of the two signals, but a sharp singlet could not be attained at still



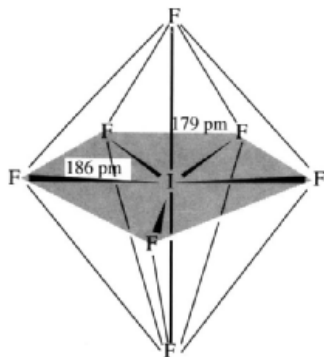
	$\text{ClF}_5$	$\text{BrF}_5$		$\text{IF}_5$	
	(gas)	(gas)	(cryst)	(gas)	(cryst)
$\text{X}-\text{F}_b/\text{pm}$	~172	177.4	178	186.9	189
$\text{X}-\text{F}_a/\text{pm}$	~162	168.9	168	184.4	186
$\angle \text{F}_a-\text{X}-\text{F}_b$	~ $90^\circ$ (assumed)	$84.8^\circ$	$84.5^\circ$	$81.9^\circ$	$80.9^\circ$

**Figure 17.10** Structure of  $\text{XF}_5$  (X = Cl, Br, I) showing X slightly below the basal plane of the four  $\text{F}_b$ .

higher temperatures because of accelerated attack of  $\text{IF}_5$  on the quartz tube.

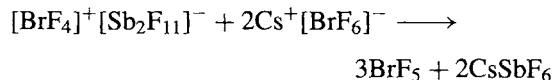
The structure of  $\text{IF}_7$  is generally taken to be pentagonal bipyramidal ( $D_{5h}$  symmetry) as originally suggested on the basis of infrared and Raman spectra (Fig. 17.11). Electron diffraction data have been interpreted in terms of slightly differing axial and equatorial distances and a slight deformation from  $D_{5h}$  symmetry due to a  $7.5^\circ$  puckering displacement and a  $4.5^\circ$  axial bending displacement. An assessment of the diffraction data permits the Delphic pronouncement<sup>(74)</sup> that, on the evidence available, it is not possible to demonstrate that the molecular symmetry is different from  $D_{5h}$ .

The very great chemical reactivity of  $\text{ClF}_5$  is well established but few specific stoichiometric reactions have been reported. Water reacts vigorously to liberate HF and form  $\text{FClO}_2$  ( $\text{ClF}_5 + 2\text{H}_2\text{O} \longrightarrow \text{FClO}_2 + 4\text{HF}$ ).  $\text{AsF}_5$  and  $\text{SbF}_5$  form 1:1 adducts which may well be ionic:  $[\text{ClF}_4]^+[\text{MF}_6]^-$ . A similar reaction with  $\text{BrF}_5$  yields a 1:2 adduct which has been shown by X-ray crystallography to be  $[\text{BrF}_4]^+[\text{Sb}_2\text{F}_{11}]^-$  (p. 841). Fluoride ion transfer probably also occurs with  $\text{SO}_3$  to give  $[\text{BrF}_4]^+[\text{SO}_3\text{F}]^-$ , but adducts with  $\text{BF}_3$ ,  $\text{PF}_5$  or  $\text{TiF}_4$  could not be formed. Conversely,  $\text{BrF}_5$  can act as a fluoride ion acceptor (from  $\text{CsF}$ ) to give  $\text{CsBrF}_6$  as a white, crystalline solid stable

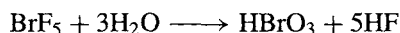


**Figure 17.11** Approximate structure of  $\text{IF}_7$  (see text).

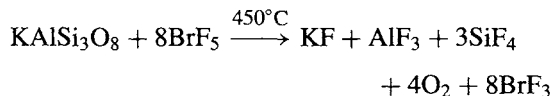
to about  $300^\circ$ , and this solvobase can be titrated with the solvoacid  $[\text{BrF}_4]^+[\text{Sb}_2\text{F}_{11}]^-$  according to the following stoichiometry:



$\text{BrF}_5$  reacts explosively with water but when moderated by dilution with MeCN gives bromic and hydrofluoric acids:



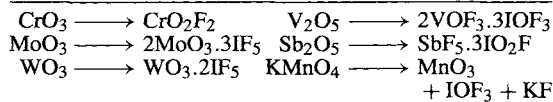
The vigorous fluorinating activity of  $\text{BrF}_5$  is demonstrated by its reaction with silicates, e.g.:



The chemical reactions of  $\text{IF}_5$  have been more extensively and systematically studied because the compound can be handled in glass apparatus and is much less vigorous a reagent than the other pentafluorides. The (very low) electrical conductivity of the pure liquid has been ascribed to slight ionic dissociation according to the equilibrium



Consistent with this, dissolution of  $\text{KF}$  increases the conductivity and  $\text{KIF}_6$  can be isolated on removal of the solvent. Likewise  $\text{NOF}$  affords  $[\text{NO}]^+[\text{IF}_6]^-$ . Antimony compounds yield  $\text{ISbF}_{10}$ , i.e.  $[\text{IF}_4]^+[\text{SbF}_6]^-$ , which can be titrated with  $\text{KSbF}_6$ . However, the milder fluorinating power of  $\text{IF}_5$  frequently enables partially fluorinated adducts to be isolated and in some of these the iodine is partly oxygenated. Complete structural identification of the products has not yet been established in all cases but typical stoichiometries are as follows:



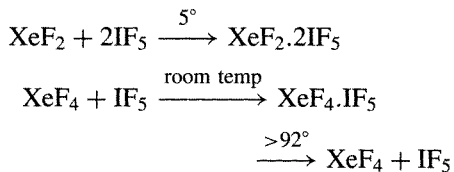
Potassium perhenate reacts similarly to  $\text{KMnO}_4$  to give  $\text{ReO}_3\text{F}$ . Similarly, the mild fluorinating

<sup>74</sup> J. D. DONOHUE, *Acta Cryst.* **18**, 1018–21 (1965).

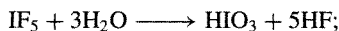
action of  $\text{IF}_5$  enables substituted iodine fluorides to be synthesized, e.g.:



$\text{IF}_5$  is unusual as an interhalogen in forming adducts with both  $\text{XeF}_2$  and  $\text{XeF}_4$ :



It should be emphasized that the reactivity of  $\text{IF}_5$  is mild only in comparison with the other halogen fluorides (p. 830). Reaction with water is extremely vigorous but the iodine is not reduced and oxygen is not evolved:



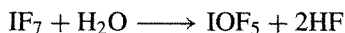
$$\Delta H = -92.3 \text{ kJ mol}^{-1}$$



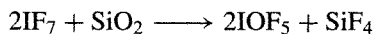
$$\Delta H = -497.5 \text{ kJ mol}^{-1}$$

Boron enflames in contact with  $\text{IF}_5$ ; so do P, As and Sb. Molybdenum and W enflame when heated and the alkali metals react violently. KH and  $\text{CaC}_2$  become incandescent in hot  $\text{IF}_5$ . However, reaction is more sedate with many other metals and non-metals, and compounds such as  $\text{CaCO}_3$  and  $\text{Ca}_3(\text{PO}_4)_2$  appear not to react with the liquid.

$\text{IF}_7$  is a stronger fluorinating agent than  $\text{IF}_5$  and reacts with most elements either in the cold or on warming. CO enflames in  $\text{IF}_7$  vapour but NO reacts smoothly and  $\text{SO}_2$  only when warmed.  $\text{IF}_7$  vapour hydrolyses without violence to  $\text{HIO}_4$  and HF; with small amounts of water at room temperature the oxyfluoride can be isolated:



The same compound is formed by action of  $\text{IF}_7$  on silica (at  $100^\circ$ ) and Pyrex glass:



$\text{IF}_7$  acts as a fluoride ion donor towards  $\text{AsF}_5$  and  $\text{SbF}_5$  and the compounds  $[\text{IF}_6]^+[\text{MF}_6]^-$  have

been isolated. Few complexes with alkali metal fluorides have been isolated but  $\text{CsF}$  and  $\text{NOF}$  form adducts which have been characterized by X-ray powder data, and formulated on the basis of Raman spectroscopy as  $\text{Cs}^+[\text{IF}_8]^-$  and  $[\text{NO}]^+[\text{IF}_8]^-$ .<sup>(75)</sup>

### 17.2.4 Polyhalide anions

Polyhalides anions of general formula  $\text{XY}_{2n}^-$  ( $n = 1, 2, 3, 4$ ) have been mentioned several times in the preceding section. They can be made by addition of a halide ion to an interhalogen compound, or by reactions which result in halide-ion transfer between molecular species. Ternary polyhalide anions  $\text{X}_m\text{Y}_n\text{Z}_p^-$  ( $m + n + p$  odd) are also known as are numerous polyiodides  $\text{I}_n^-$ . Stability is often enhanced by use of a large counter-cation, e.g.  $\text{Rb}^+$ ,  $\text{Cs}^+$ ,  $\text{NR}_4^+$ ,  $\text{PCl}_4^+$ , etc.; likewise, for a given cation, thermal stability is enhanced the more symmetrical the polyhalide ion and the larger the central atom (i.e. stability decreases in the sequence  $\text{I}_3^- > \text{IBr}_2^- > \text{ICl}_2^- > \text{I}_2\text{Br}^- > \text{Br}_3^- > \text{BrCl}_2^- > \text{Br}_2\text{Cl}^-$ ). The structures of many of these polyhalide anions have been established by X-ray diffraction analysis or inferred from vibrational spectroscopic data and in all cases the gross stereochemistry is consistent with the expectations of simple bond theories (p. 897); however, subtle deviations from the highest expected symmetry sometimes occur, probably due to crystal-packing forces and residual interactions between the various ions in the condensed phase.

Typical examples of linear (or nearly linear) triatomic polyhalides are in Table 17.15;<sup>(67,76)</sup> the structures are characterized by considerable variability of interatomic distances and these distances are individually always substantially greater than for the corresponding diatomic interhalogen (p. 825). Note also that for

<sup>75</sup> C. J. ADAMS, *Inorg. Nuclear Chem. Letters* **10**, 831–5 (1974).

<sup>76</sup> Ref. 23, pp. 1534–63 (Polyhalide anions) and references therein.

Table 17.15 Triatomic polyhalides [X-Y-Z]<sup>-</sup>

Polyhalide	Cations	Structure	Dimensions x/pm, y/pm	Angle
ClF <sub>2</sub> <sup>-</sup>	NO <sup>+</sup>	[F <sup>Δ</sup> Cl <sup>Δ</sup> F] <sup>-</sup>	x = y	~180°
	Rb <sup>+</sup> , Cs <sup>+</sup>	[F-Cl-F] <sup>-</sup>	x ≠ y	
Cl <sub>3</sub> <sup>-</sup>	NEt <sub>4</sub> <sup>+</sup> , NPr <sub>4</sub> <sup>+</sup> , NBu <sub>4</sub> <sup>+</sup>	[Cl-Cl-Cl] <sup>-</sup>	x = y	~180°
BrF <sub>2</sub> <sup>-</sup>	Cs <sup>+</sup>	[F-Br-F] <sup>-</sup>		
BrCl <sub>2</sub> <sup>-</sup>	Cs <sup>+</sup> , NR <sub>4</sub> <sup>+</sup> (R = Me, Et, Pr <sup>n</sup> , Bu <sup>n</sup> )	[Cl-Br-Cl] <sup>-</sup>	x = y	~180°
Br <sub>2</sub> Cl <sup>-</sup>		[Br-Br-Cl] <sup>-</sup>	x ≠ y	
Br <sub>3</sub> <sup>-</sup>	Me <sub>3</sub> NH <sup>+</sup> ( <sup>a</sup> )	[Br-Br-Br] <sup>-</sup>	x = y = 254	171°
	Cs <sup>+</sup> (and PBr <sub>4</sub> <sup>+</sup> )	[Br-Br-Br] <sup>-</sup>	244(239) 270(291)	177.5° (177.3°)
IF <sub>2</sub> <sup>-</sup>	NEt <sub>4</sub> <sup>+</sup>	[F-I-F] <sup>-</sup>		
IBrF <sup>-</sup>		[F-I-Br] <sup>-</sup>		
IBrCl <sup>-</sup>	NH <sub>4</sub> <sup>+</sup>	[Cl-I-Br] <sup>-</sup>	291 251	179°
ICl <sub>2</sub> <sup>-</sup>	NMe <sub>4</sub> <sup>+</sup> (and PCl <sub>4</sub> <sup>+</sup> )	[Cl-I-Cl] <sup>-</sup>	x = y = 255	180°
	piperazinium <sup>(b)</sup>	[Cl-I-Cl] <sup>-</sup>	247 269	180°
	triethylenediammonium <sup>(c)</sup>	[Cl-I-Cl] <sup>-</sup>	254(253) 267(263)	180° (180°)
IBr <sub>2</sub> <sup>-</sup>	Cs <sup>+</sup>	[Br-I-Br] <sup>-</sup>	262 278	178°
I <sub>2</sub> Cl <sup>-</sup>		[Cl-I-I] <sup>-</sup>		
I <sub>2</sub> Br <sup>-</sup>	Cs <sup>+</sup>	[Br-I-I] <sup>-</sup>	291 278	178°
I <sub>3</sub> <sup>-</sup>	AsPh <sub>4</sub> <sup>+</sup>	[I-I-I] <sup>-</sup>	x = y = 290	176°
	[PhCONH <sub>2</sub> ] <sub>2</sub> H <sup>+</sup>	[I-I-I] <sup>-</sup>	291 295	177°
	NEt <sub>4</sub> <sup>+</sup> (form I)	[I-I-I] <sup>-</sup>	293 294	180°
	(form II)		291 (& 289), 296 (& 298)	180° (& 178°)
	Cs <sup>+</sup> (and NH <sub>4</sub> <sup>+</sup> )	[I-I...I] <sup>-</sup>	283(282) 303(310)	176° (177°)

(<sup>a</sup>)In the compound [Me<sub>3</sub>NH]<sup>+</sup><sub>2</sub>Br<sup>-</sup>Br<sub>3</sub><sup>-</sup>; same dimensions for Br<sub>3</sub><sup>-</sup> in PhN<sub>2</sub>Br<sub>3</sub> and in [C<sub>6</sub>H<sub>7</sub>NH]<sub>2</sub>[SbBr<sub>6</sub>][Br<sub>3</sub>]. Other known values summarized in ref. 77

(<sup>b</sup>)piperazinium, [H<sub>2</sub>NC<sub>4</sub>H<sub>8</sub>NH<sub>2</sub>]<sup>2+</sup>.

(<sup>c</sup>)triethylenediammonium, [HN(C<sub>2</sub>H<sub>4</sub>)<sub>3</sub>NH]<sup>2+</sup>: compound contains 2 non-equivalent ICl<sub>2</sub><sup>-</sup> ions.

[Cl-I-Br]<sup>-</sup> the I-Cl distance is greater than the I-Br distance, and in [Br-I-I]<sup>-</sup> I-Br is greater than I-I. On dissociation, the polyhalide yields the solid monohalide corresponding to the smaller of the halogens present, e.g. CsICl<sub>2</sub> gives CsCl and ICl rather than CsI + Cl<sub>2</sub>. Likewise for CsIBrCl the favoured products are CsCl(s) + IBr(g) rather than CsBr(s) + ICl(g) or CsI(s) + BrCl(g). Thermochemical cycles have been developed to interpret these results.<sup>(76)</sup>

Penta-atomic polyhalide anions [XY<sub>4</sub>]<sup>-</sup> favour the square-planar geometry (*D*<sub>4h</sub>) as expected for species with 12 valence-shell electrons on the central atom. Examples are the Rb<sup>+</sup> and Cs<sup>+</sup> salts of [ClF<sub>4</sub>]<sup>-1</sup>, and KBrF<sub>4</sub> (in which Br-F is 189 pm and adjacent angles F-Br-F are 90° (±2°)). The symmetry of the anion is slightly

lowered in CsIF<sub>4</sub>(C<sub>2v</sub>) and also in KICl<sub>4</sub>.H<sub>2</sub>O (in which I-Cl is 242, 247, 253, and 260 pm and the adjacent angles Cl-I-Cl are 90.6°, 90.7°, 89.2° and 89.5°. Other penta-atomic polyhalide anions for which the structure has not yet been determined are [ICl<sub>3</sub>F]<sup>-</sup>, [IBrCl<sub>3</sub>]<sup>-</sup>, [I<sub>2</sub>Cl<sub>3</sub>]<sup>-</sup>, [I<sub>2</sub>BrCl<sub>2</sub>]<sup>-</sup>, [I<sub>2</sub>Br<sub>2</sub>Cl]<sup>-</sup>, [I<sub>2</sub>Br<sub>3</sub>]<sup>-</sup>, [I<sub>4</sub>Br]<sup>-</sup> and [I<sub>4</sub>Cl]<sup>-</sup>. Some of these may be "square planar" but the polyiodo species might well be more closely related to I<sub>5</sub><sup>-</sup>: the tetramethylammonium salt of this anion features a planar V-shaped array in which two I<sub>2</sub> units are bonded to a single iodide ion, i.e. [I(I<sub>2</sub>)<sub>2</sub>]<sup>-</sup> as in Fig. 17.12. The V-shaped ions are arranged in a planar array which bear an interesting relation to a (hypothetical) array of planar IX<sub>4</sub><sup>-</sup> ions.

Hepta-atomic polyhalide anions are exemplified by BrF<sub>6</sub><sup>-</sup> (K<sup>+</sup>, Rb<sup>+</sup> and Cs<sup>+</sup> salts) and IF<sub>6</sub><sup>-</sup> (K<sup>+</sup>, Cs<sup>+</sup>, NMe<sub>4</sub><sup>+</sup> and NEt<sub>4</sub><sup>+</sup> salts). The

<sup>77</sup>F. A. COTTON, G. E. LEWIS and W. SCHWOTZER, *Inorg. Chem.* **25**, 3528-9 (1986).

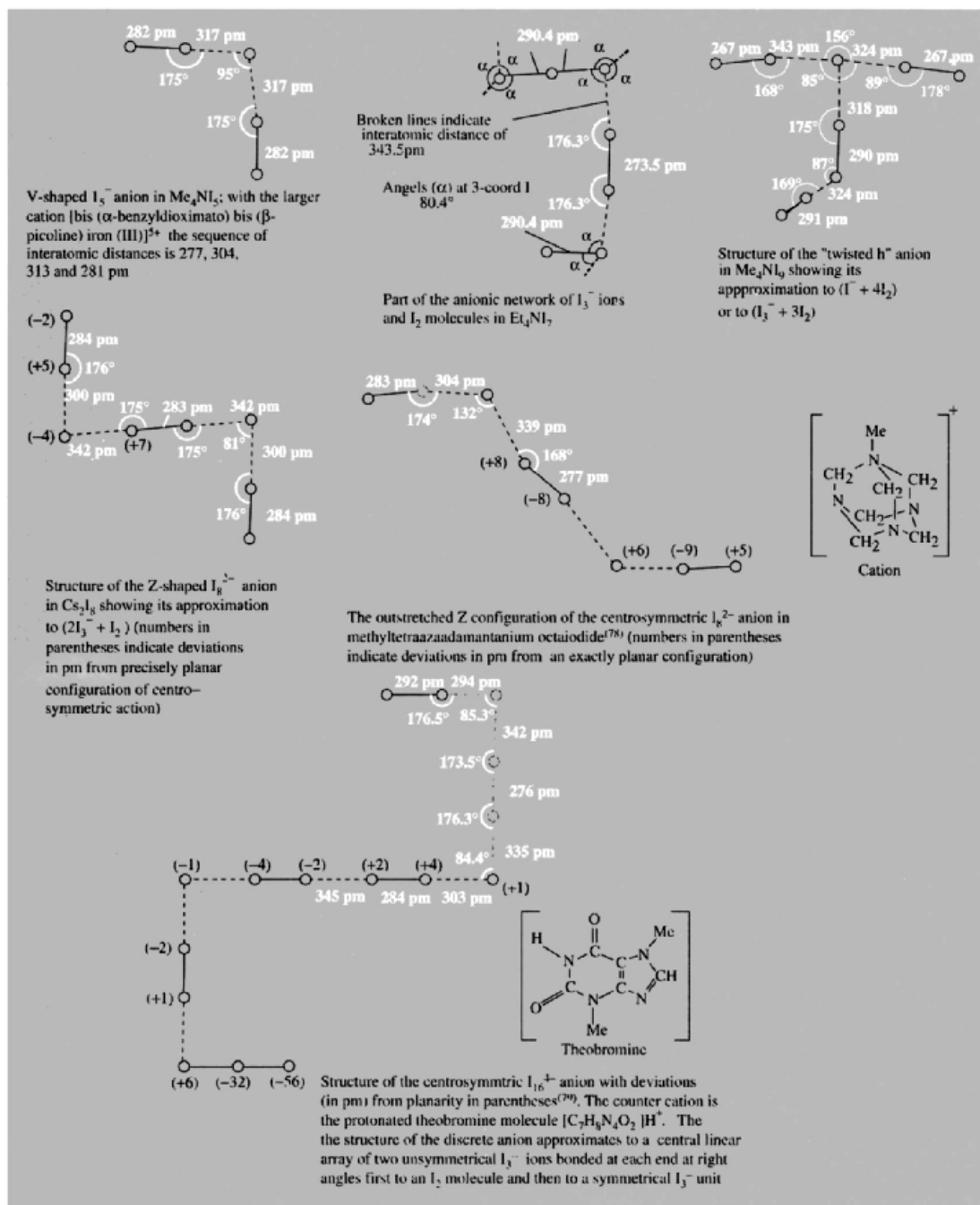


Figure 17.12 Structure of some polyiodides.

<sup>78</sup> P. K. HON, T. C. M. MAK and J. TROTTER, *Inorg. Chem.* **18**, 2916–7 (1979) and references therein.

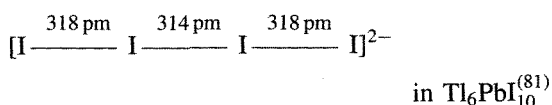
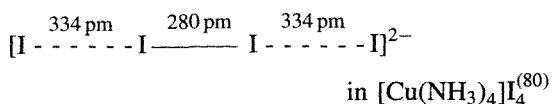
<sup>79</sup> F. H. HERSTEIN and M. KAPON, *J. Chem. Soc., Chem. Commun.*, 677–8 (1975).



anions have 14 valence-shell electrons on the central atom and spectroscopic studies indicate non-octahedral geometry ( $D_{3d}$  for  $\text{BrF}_6^-$ ). Other possible examples are  $\text{Br}_6\text{Cl}^-$  and  $\text{I}_6\text{Br}^-$  but these have not been shown to contain discrete hepta-atomic species and may be extended anionic networks such as that found in  $\text{Et}_4\text{NI}_7$  (Fig. 17.12).

$\text{IF}_7$  has been shown to act as a weak Lewis acid towards  $\text{CsF}$  and  $\text{NOF}$ , and the compounds  $\text{CsIF}_8$  and  $\text{NOIF}_8$  have been characterized by X-ray powder patterns and by Raman spectroscopy; they are believed to contain the  $\text{IF}_8^-$  anion.<sup>(75)</sup> A rather different structure motif occurs in the polyiodide  $\text{Me}_4\text{NI}_9$ ; this consists of discrete units with a "twisted h" configuration (Fig. 17.12). Interatomic distances within these units vary from 267 to 343 pm implying varying strengths of bonding, and the anions can be thought of as being built up either from  $\text{I}^- + 4\text{I}_2$  or from a central unsymmetrical  $\text{I}_3^-$  and  $3\text{I}_2$ . (The rather arbitrary recognition of discrete  $\text{I}_9^-$  anions is emphasized by the fact that the closest interionic  $\text{I} \cdots \text{I}$  contact is 349 pm which is only slightly greater than the 343 pm separating one  $\text{I}_2$  from the remaining  $\text{I}_7^-$  in the structure.)

The propensity for iodine to catenate is well illustrated by the numerous polyiodides which crystallize from solutions containing iodide ions and iodine. The symmetrical and unsymmetrical  $\text{I}_3^-$  ions (Table 17.15) have already been mentioned as have the  $\text{I}_5^-$  and  $\text{I}_9^-$  anions and the extended networks of stoichiometry  $\text{I}_7^-$  (Fig. 17.12). The stoichiometry of the crystals and the detailed geometry of the polyhalides depend sensitively on the relative concentrations of the components and the nature of the cation. For example, the linear  $\text{I}_4^{2-}$  ion may have the following dimensions:



(Note, however, that the overall length of the two  $\text{I}_4^{2-}$  ions is virtually identical.) Again, the  $\text{I}_8^{2-}$  anion is found with an acute-angled planar  $Z$  configuration in its  $\text{Cs}^+$  salt but with an outstretched configuration in the black methyltetraazaadamantanium salt (Fig. 17.12). The largest discrete polyiodide ion so far encountered is the planar centro-symmetric  $\text{I}_{16}^{4-}$  anion; this was shown by X-ray diffractometry<sup>(79)</sup> to be present in the dark-blue needle-shaped crystals of (theobromine) $_2 \cdot \text{H}_2\text{I}_8$  which had first been prepared over a century earlier by S. M. Jorgensen in 1869.

The bonding in these various polyiodides as in the other polyhalides and neutral interhalogens has been the subject of much speculation, computation and altercation. The detailed nature of the bonds probably depends on whether F is one of the terminal atoms or whether only the heavier halogens are involved. There is now less tendency than formerly to invoke much d-orbital participation (because of the large promotion energies required) and Mössbauer spectroscopic studies in iodine-containing species<sup>(82)</sup> also suggest rather scant s-orbital participation. The bonding appears predominantly to involve p orbitals only, and multicentred (partially delocalized) bonds such as are invoked in discussions of the isoelectronic xenon halides (p. 897) are currently favoured. However, no bonding model yet comes close to reproducing the range of interatomic distances and angles observed in the crystalline polyhalides.<sup>(76)</sup> There has also been much interest in the bis(ethylenedithio)tetrathiafulvalene layer-like compounds with polyhalide anions. For example,  $[(\text{BEDT}-\text{TTF})(\text{ICl}_2)]$  is a one-dimensional metal down to  $\sim 22 \text{ K}$  at which temperature it transforms to an insulator. The  $[\text{BrICl}]^-$  salt is similar, whereas with the larger

<sup>80</sup> E. DUBLER and L. LINOWSKY, *Helv. Chim. Acta* **58**, 2604-9 (1978).

<sup>81</sup> A. RABENAU, H. SCHULZ and W. STOEGER, *Naturwissenschaften* **63**, 245 (1976).

<sup>82</sup> N. N. GREENWOOD and T. C. GIBB, *Mössbauer Spectroscopy*, pp. 462-82, Chapman & Hall, London, 1971.

anions  $IBr_2^-$  and  $I_3^-$  the salts become ambient pressure superconductors.<sup>(83)</sup>

### 17.2.5 Polyhalonium cations $XY_{2n}^+$

Numerous polyhalonium cations have already been mentioned in Section 17.2.3 during the discussion of the self-ionization of interhalogen compounds and their ability to act as halide-ion donors. The known species are summarized in Table 17.16.<sup>(84,85)</sup> Preparations are usually by addition of the appropriate interhalogen and halide-ion acceptor, or by straightforward modification of this general procedure in which the interhalogen or halogen is also used as an oxidant. For example Au dissolves in  $BrF_3$  to give  $[BrF_2][AuF_4]$ ,  $BrF_3$  fluorinates and oxidizes  $PdCl_2$  and  $PdBr_2$  to  $[BrF_2][PdF_4]$ ;  $ClF_3$  converts

$AsCl_3$  to  $[ClF_2][AsF_6]$ ; stoichiometric amounts of  $I_2$ ,  $Cl_2$  and  $2SbCl_5$  yield  $[ICl_2][SbCl_6]$ . The fluorocations tend to be colourless or pale yellow but the colour deepens with increasing atomic weight so that compounds of  $ICl_2^+$  are wine-red or bright orange whilst  $I_2Cl^+$  compounds are dark brown or purplish black.

Structures are as expected from simple valency theory and the isoelectronic principle (20 valency electrons). Thus the triatomic species are bent, rather than linear, as illustrated in Fig. 17.13 for  $ClF_2^+$ ,  $BrF_2^+$  and  $ICl_2^+$ ; there is frequently some residual interionic interaction due to close approach of the cation and anion and this sometimes complicates the interpretation of vibrational spectroscopic data. In the case of  $[ICl_2][SbF_6]$  (Fig. 17.13c) the very short  $I \cdots F$  distance implies one of the strongest secondary interactions known between these two elements and the  $Sb-F \cdots I$  angle deviates appreciably from linearity.<sup>(86)</sup> The ion  $[Cl_2F]^+$  was originally thought to have the symmetrical

<sup>83</sup> T. J. EMGE and 12 others, *J. Am. Chem. Soc.* **108**, 695–702 (1986).

<sup>84</sup> J. SHAMIR, *Struct. Bonding* **37**, 141–210 (1979).

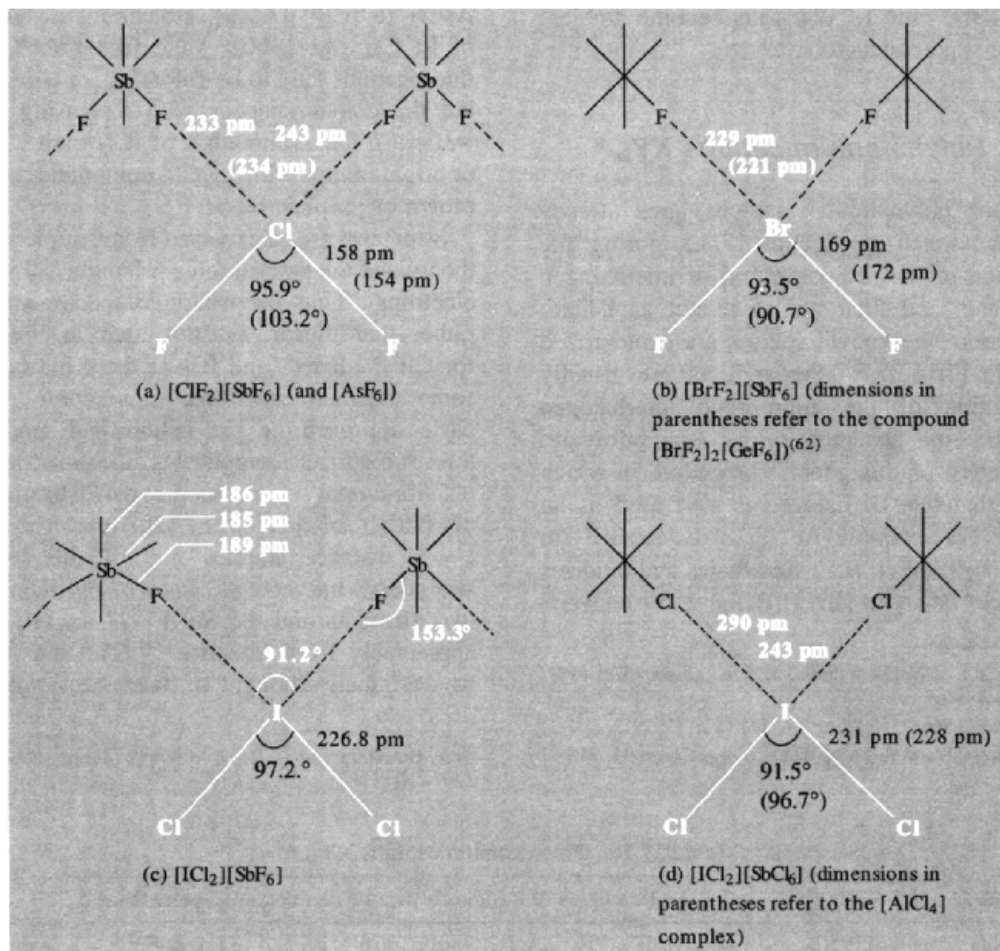
<sup>85</sup> T. BIRCHALL and R. D. MEYERS, *Inorg. Chem.* **21**, 213–7 (1982).

<sup>86</sup> T. BIRCHALL and R. D. MEYERS, *Inorg. Chem.* **20**, 2207–10 (1981).

**Table 17.16** Polyhalonium cations,  $XY_{2n}^+$

Cation	(Date) <sup>(a)</sup>	Examples of co-anions (mp of compound in parentheses)
$ClF_2^+$	(1950)	$BF_4^-$ (30°), $PF_6^-$ , $AsF_6^-$ , $SbF_6^-$ (78°), $PtF_6^-$ (171°), $SnF_6^{2-}$
$Cl_2F^+$	(1969)	$BF_4^-$ , $AsF_6^-$
$BrF_2^+$	(1949)	$PdF_4^-$ , $AuF_4^-$ , $AsF_6^-$ , $SbF_6^-$ (130°), $Sb_2F_{11}^-$ (33.5°), $BiF_6^-$ , $NbF_6^-$ , $TaF_6^-$ , $GeF_6^{2-}$ (subl 20°), $SnF_6^{2-}$ , $PtF_6^{2-}$ (136°), $SO_3F^-$
$IF_2^+$	(1968)	$BF_4^-$ , $AsF_6^-$ (d – 22°), $SbF_6^-$ (d 45°)
$ICl_2^+$	(1959)	$AlCl_4^-$ (105°), $SbCl_6^-$ (83.5°), $Sb_2F_{11}^-$ (62°), $SO_3F^-$ (42°), $SO_3Cl^-$ (8°)
$I_2Cl^+$	(1972)	$AlCl_4^-$ (53°), $SbCl_6^-$ (70°), $TaCl_6^-$ (102°), $SO_3F^-$ (40°)
$IBr_2^+$	(1971)	$Sb_2F_{11}^-$ (65°), $SO_3F^-$ (97°), $SO_3CF_3^-$ (75°)
$I_2Br^+$	(1974)	$SO_3F^-$ (70°)
$IBrCl^+$	(1973)	$SbCl_6^-$ , $SO_3F^-$ (65°)
$ClF_4^+$	(1967)	$AsF_6^-$ , $SbF_6^-$ (88°), $Sb_2F_{11}^-$ (64°), $PtF_6^-$
$BrF_4^+$	(1957)	$AsF_6^-$ , $Sb_2F_{11}^-$ (60°), $SnF_6^{2-}$
$IF_4^+$	(1950)	$SbF_6^-$ (103°), $Sb_2F_{11}^-$ , $PtF_6^-$ , $SO_3F^-$ , $SnF_6^{2-}$
$I_3Cl_2^+$	(1982)	$SbCl_6^-$ (47°)
$ClF_6^+$	(1972)	$PtF_6^-$ (d140°)
$BrF_6^+$	(1973)	$AsF_6^-$ , $Sb_2F_{11}^-$
$IF_6^+$	(1958)	$BF_4^-$ , $AsF_6^-$ (subl 120°), $SbF_6^-$ (175°), $Sb_2F_{11}^-$ , $[(SbF_5)_3F]^-$ (94°), $AuF_6^-$

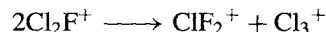
<sup>(a)</sup>The date given refers to the first isolation of a compound containing the cation, or the characterization of the cation in solution.



**Figure 17.13** Chain structures of compounds containing the triatomic cations  $\text{XY}_2^+$ : (a)  $[\text{ClF}_2][\text{SbF}_6]$  (with dimensions for  $[\text{ClF}_2][\text{AsF}_6]$  in parentheses); (b)  $[\text{BrF}_2][\text{SbF}_6]$ ; (c)  $[\text{ICl}_2][\text{SbF}_6]$  indicating slightly bent  $\text{Sb}-\text{F}\cdots\text{I}$  configuration and very short  $\text{I}\cdots\text{F}$  distance; and (d)  $[\text{ICl}_2][\text{SbCl}_6]$  (with dimensions for the  $[\text{AlCl}_4]^-$  salt in parentheses).

bent  $C_{2v}$  structure  $[\text{Cl}-\text{F}-\text{Cl}]^+$  but later Raman spectroscopic studies were interpreted on the basis of the unsymmetrical bent structure  $[\text{Cl}-\text{Cl}-\text{F}]^+$ . Calculations<sup>(87)</sup> suggest that the symmetrical  $C_{2v}$  structure is indeed the more stable form at least for the isolated cation and the question must be regarded as still open:

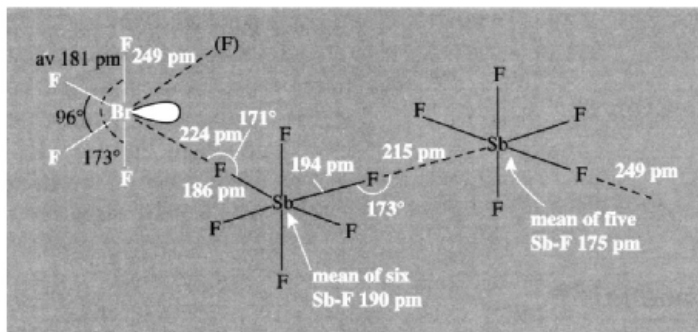
it may well be that the configuration adopted is determined by residual interactions in the solid state or in solution. In fact the ion is rather unstable in solution and disproportionates completely in  $\text{SbF}_5/\text{HF}$  even at  $-76^\circ$ :



The pentaatomic cations  $\text{ClF}_4^+$ ,  $\text{BrF}_4^+$  and  $\text{IF}_4^+$  are precisely isoelectronic with  $\text{SF}_4$ ,  $\text{SeF}_4$  and  $\text{TeF}_4$  and adopt the same T-shaped ( $C_{2v}$ ) configuration. This is illustrated in Fig. 17.14

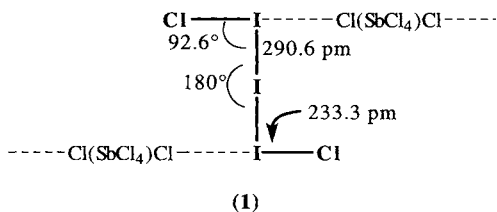
<sup>87</sup> B. D. JOSHI and K. MOROKUMA, *J. Am. Chem. Soc.* **101**, 1714-7 (1979), and references therein.

<sup>88</sup> A. J. EDWARDS and K. G. CHRISTE, *J. Chem. Soc., Dalton Trans.*, 175-7 (1976)



**Figure 17.14** Structure of  $[\text{BrF}_4][\text{Sb}_2\text{F}_{11}]$  (see text).

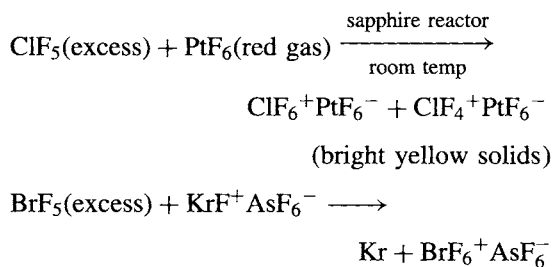
for the case of  $[\text{BrF}_4][\text{Sb}_2\text{F}_{11}]$ : again there are strong subsidiary interactions, the coordination about Br being pseudooctahedral with four short Br-F distances and two longer Br...F distances which are no doubt influenced by the presence of the stereochemically active nonbonding pair of electrons on the Br atom. In addition, the mean Sb-F distance in the central  $\text{SbF}_6$  unit is substantially longer than the mean of the five "terminal" Sb-F distances in the second unit and the structure can be described approximately as  $[\text{BrF}_4^+ \cdots \text{SbF}_6^- \cdots \text{SbF}_5]$ . The structure of the final pentaatomic cation,  $\text{I}_3\text{Cl}_2^+$  (1), is different and resembles that of  $\text{I}_5^+$  (p. 844) in being a planar centrosymmetric species with  $C_{2h}$  symmetry:<sup>(85)</sup>



It will be noted that the central I-I distance is close to that in  $\text{I}_5^+$  and that the terminal I-Cl distance is very similar to that in  $\beta\text{-ICl}$  (p. 826). There are also strong secondary interactions so as to form infinite zig-zag chains via *trans*-Cl atoms of the octahedral  $\text{SbCl}_6^-$  anions ( $\text{I} \cdots \text{Cl}$  294.1 pm, angle  $\text{Cl}-\text{I} \cdots \text{I}$  177.6°).

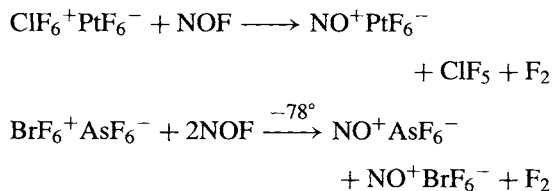
Of the heptaatomic cations,  $\text{IF}_6^+$  has been known for some time since it can be made

by fluoride-ion transfer from  $\text{IF}_7$ . Because  $\text{ClF}_7$  and  $\text{BrF}_7$  do not exist, alternative preparative procedures must be devised and compounds of  $\text{ClF}_6^+$  and  $\text{BrF}_6^+$  are of more recent vintage (Table 17.16). The cations have been made by oxidation of the pentafluorides with extremely strong oxidizers such as  $\text{PtF}_6$ ,  $\text{KrF}^+$ , or  $\text{KrF}_3^+$ , e.g.:<sup>(84)</sup>

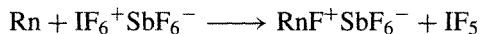
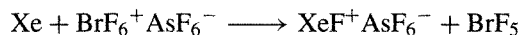
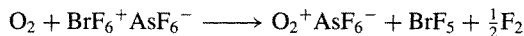


Vibrational spectra and  $^{19}\text{F}$  nmr studies on all three cations  $\text{XF}_6^+$  and the  $^{129}\text{I}$  Mössbauer spectrum of  $[\text{IF}_6][\text{AsF}_6]$  establish octahedral ( $O_h$ ) symmetry as expected for species isoelectronic with  $\text{SF}_6$ ,  $\text{SeF}_6$  and  $\text{TeF}_6$  respectively.

Attempts to prepare  $\text{ClF}_7$  and  $\text{BrF}_7$  by reacting the appropriate cation with  $\text{NOF}$  failed; instead the following reactions occurred:



As expected, the cations are extremely powerful oxidants, e.g.:



### 17.2.6 Halogen cations<sup>(84,89)</sup>

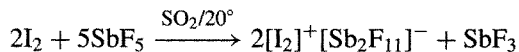
It has been known for many years that iodine dissolves in strongly oxidizing solvents such as oleum to give bright blue paramagnetic solutions, but only in 1966 was this behaviour unambiguously shown to be due to the formation of the diiodine cation  $\text{I}_2^+$ . (The production of similar brightly coloured solutions of S, Se and Te has already been discussed on pp. 664, 759.) The ionization energies of  $\text{Br}_2$  and  $\text{Cl}_2$ , whilst greater than that for  $\text{I}_2$  (Table 17.17), are nevertheless smaller than for  $\text{O}_2$ , which can likewise be oxidized to  $\text{O}_2^+$  (p. 616). Accordingly, compounds of the bright-red cationic species  $\text{Br}_2^+$  are now well established, but  $\text{Cl}_2^+$  is known only from its electronic band spectrum obtained in a low-pressure discharge tube. Some properties of the three diatomic cations  $\text{X}_2^+$  are compared with those of the parent halogen molecules  $\text{X}_2$  in Table 17.17; as expected, ionization reduces the interatomic distance and increases the vibration frequency ( $\nu \text{ cm}^{-1}$ ) and

**Table 17.17** Comparison of diatomic halogens  $\text{X}_2$  and their cations  $\text{X}_2^+$

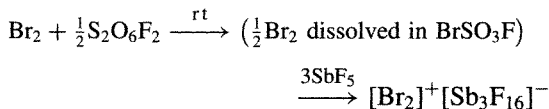
Species	$I/\text{kJ mol}^{-1}$	$r/\text{pm}$	$\nu/\text{cm}^{-1}$	$k/\text{N m}^{-1(a)}$	$\lambda_{\text{max}}/\text{nm}$
$\text{Cl}_2$	1110	199	554	316	330
$\text{Cl}_2^+$	—	189	645	429	—
$\text{Br}_2$	1014	228	319	238	410
$\text{Br}_2^+$	—	213	360	305	510
$\text{I}_2$	900	267	215	170	520
$\text{I}_2^+$	—	256	238	212	640

<sup>(a)</sup>Force constant  $k$  in newton/metre: 1 millidyne/Å = 100 N m<sup>-1</sup>.

force constant ( $k \text{ N m}^{-1}$ ). The principal synthetic routes to crystalline compounds of  $\text{Br}_2^+$  and  $\text{I}_2^+$  have been either (a) the comproportionation of  $\text{BrF}_3$ ,  $\text{BrF}_5$  or  $\text{IF}_5$  with the stoichiometric amount of halogen in the presence of  $\text{SbF}_5$ , or (b) the direct oxidation of the halogen by an excess of  $\text{SbF}_5$  or by  $\text{SbF}_5$  dissolved in  $\text{SO}_2$ , e.g.:

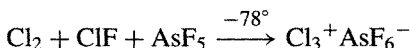


More recently<sup>(90)</sup> a simpler route has been devised which involves oxidation of  $\text{Br}_2$  or  $\text{I}_2$  with the peroxide  $\text{S}_2\text{O}_6\text{F}_2$  (p. 640) followed by solvolysis using an excess of  $\text{SbF}_5$ , e.g.:



The bright-red crystals of  $[\text{Br}_2]^+[\text{Sb}_3\text{F}_{16}]^-$  melt at 85.5°C to a cherry-red liquid. Dark-blue crystals of  $[\text{I}_2]^+[\text{Sb}_2\text{F}_{11}]^-$  melt sharply at 127°C and the corresponding blue solid  $[\text{I}_2]^+[\text{Ta}_2\text{F}_{11}]^-$  melts at 120°C. When solutions of  $\text{I}_2^+$  in  $\text{HSO}_3\text{F}$  are cooled below -60°C there is a dramatic colour change from deep blue to red as the cation dimerizes:  $2\text{I}_2^+ \rightleftharpoons \text{I}_4^{2+}$ . There is a simultaneous drop in the paramagnetic susceptibility of the solution and in its electrical conductivity. The changes are rapid and reversible, the blue colour appearing again on warming.

During the past 20 y numerous other highly coloured halogen cations have been characterized by Raman spectroscopy, X-ray crystallography, and other techniques, as summarized in Table 17.18. Typical preparative routes involve direct oxidation of the halogen (a) in the absence of solvent, (b) in a solvent which is itself the oxidant (e.g.  $\text{AsF}_5$ ) or (c) in a non-reactive solvent (e.g.  $\text{SO}_2$ ). Some examples are listed below:



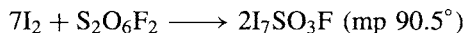
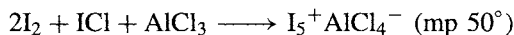
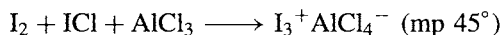
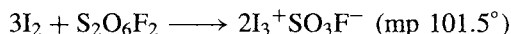
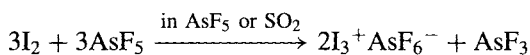
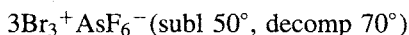
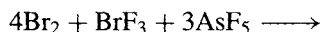
<sup>89</sup> R. J. GILLESPIE and J. PASSMORE *Adv. Inorg. Chem. Radiochem.* **17**, 49–87 (1975).

<sup>90</sup> W. W. WILSON, R. C. THOMPSON and F. AUBKE, *Inorg. Chem.* **19**, 1489–93 (1980).

**Table 17.18** Summary of known halogen cations

(Cl <sub>2</sub> <sup>+</sup> )	Br <sub>2</sub> <sup>+</sup> cherry red	I <sub>3</sub> <sup>+</sup> bright blue
Cl <sub>3</sub> <sup>+</sup> yellow	Br <sub>3</sub> <sup>+</sup> brown	I <sub>3</sub> <sup>+</sup> dark brown/black
	—	I <sub>4</sub> <sup>2+</sup> red-brown
	Br <sub>5</sub> <sup>+</sup> dark brown	I <sub>5</sub> <sup>+</sup> green/black <sup>(a)</sup>
	—	(I <sub>7</sub> <sup>+</sup> ) black

<sup>(a)</sup>[I<sub>5</sub>][AlCl<sub>4</sub>] is described as greenish-black needles, dark brown-red in thin sections.



Other compounds that have been prepared<sup>(91)</sup> include the dark-brown gold(III) complexes

<sup>(91)</sup> K. C. LEE and F. AUBKE, *Inorg. Chem.* **19**, 119–22 (1980).

Br<sub>3</sub>[Au(SO<sub>3</sub>F)<sub>4</sub>] (decomp ~150°C) and Br<sub>5</sub>[Au(SO<sub>3</sub>F)<sub>4</sub>] (mp 65°).

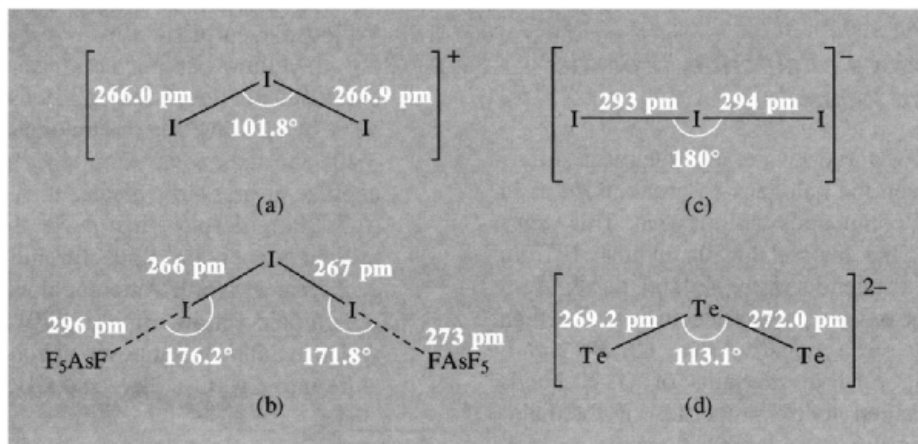
The triatomic cations X<sub>3</sub><sup>+</sup> are nonlinear and thus isostructural with other 20-electron species such as XY<sub>2</sub><sup>+</sup> (p. 839) and SCl<sub>2</sub> (p. 689). The contrast in bond lengths and angles between I<sub>3</sub><sup>+</sup> (Fig. 17.15)<sup>(92)</sup> and the linear 22-electron anion I<sub>3</sub><sup>-</sup> (p. 836) is notable, as is its similarity with the isoelectronic Te<sub>3</sub><sup>2-</sup> anion (p. 764). Likewise, Br<sub>3</sub>AsF<sub>6</sub> is isomorphous with I<sub>3</sub>AsF<sub>6</sub> and the non-linear cation has Br–Br 227.0 pm and an angle of 102.5°<sup>(93)</sup> (cf. Br<sub>3</sub><sup>-</sup>, Table 17.15). The structures of the penta-atomic cations Br<sub>5</sub><sup>+</sup> (2)<sup>(94)</sup> and I<sub>5</sub><sup>+</sup> (3)<sup>(95)</sup> have been determined by X-ray analysis of their AsF<sub>6</sub><sup>-</sup> salts and shown to have centrosymmetric C<sub>2h</sub> symmetry like the

<sup>(92)</sup> J. PASSMORE, G. SUTHERLAND and P. S. WHITE, *Inorg. Chem.* **20**, 2169–71 (1981).

<sup>(93)</sup> K. O. CHRISTE, R. BAU and D. ZHAO, *Z. anorg. allg. Chem.* **593**, 46–60 (1991).

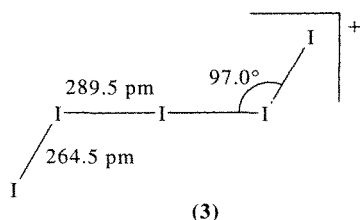
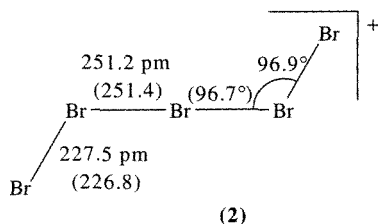
<sup>(94)</sup> H. HARTL, J. NOWICKI and R. MINKWITZ, *Angew. Chem. Int. Edn. Engl.* **30**, 328–9 (1991). See also K. O. CHRISTE, D. A. DIXON and R. MINKWITZ, *Z. anorg. allg. Chem.* **612**, 51–5 (1992).

<sup>(95)</sup> A. APBLET, F. GREIN, J. P. JOHNSON, J. PASSMORE and P. S. WHITE, *Inorg. Chem.* **25**, 422–6 (1986).



**Figure 17.15** The structure of (a) the nonlinear I<sub>3</sub><sup>+</sup> cation in I<sub>3</sub>AsF<sub>6</sub> and (b) the weaker cation–anion interactions along the chain (cf. Fig. 17.13). For comparison, the dimensions of (c) the linear 22-electron cation I<sub>3</sub><sup>-</sup> and (d) the nonlinear 20-electron cation Te<sub>3</sub><sup>2-</sup> are given. The data for this latter species refer to the compound [K(crypt)]<sub>2</sub>Te<sub>3</sub>.en; in K<sub>2</sub>Te<sub>3</sub> itself, where there are stronger cation–anion interactions, the dimensions are *r* = 280 pm and angle = 104.4°.

analogous cation  $I_3Cl_2^+$  (1) (p. 841). The figures in parenthesis in (2) refer to the  $SbF_6^-$  salt.



The black compound  $I_7SO_3F$  (mp  $90.5^\circ$ ) was established<sup>(96)</sup> as a local mp maximum in the phase diagram of the system  $I_2/S_2O_6F_2$ , together with the known compounds  $I_3SO_3F$  (mp  $101.5^\circ$ ),  $ISO_3F$  (mp  $50.2^\circ$ ), and  $I(SO_3F)_3$  (mp  $33.7^\circ$ ), but its structure has not been determined and there is at present no evidence for the presence of the discrete heptaatomic cation  $I_7^+$  in the crystals.

### 17.2.7 Oxides of chlorine, bromine and iodine

Perhaps nowhere else are the chemical differences between the halogens so pronounced as in their binary compounds with oxygen. This stems partly from the factors that distinguish F from its heavier congeners (p. 804) and partly from the fact that oxygen is less electronegative than F but more electronegative than Cl, Br and I. The varying relative strengths of O–X bonds and the detailed redox properties of the halogens also ensure considerable diversity in stoichiometry, structure, thermal stability and chemical reactivity of the various species. The binary

compounds between O and F have already been described (p. 638). About 25 further binary halogen oxide species are known, which vary from shock-sensitive liquids and short-lived free radicals to rather stable solids. It will be convenient to treat the 3 halogens separately though intercomparison of corresponding species is instructive and the chemistry is also, at times, related to that of the oxoacids (p. 853) and the halogen oxide fluorides (p. 875).

#### Oxides of chlorine<sup>(97,98)</sup>

Despite their instability (or perhaps because of it) the oxides of chlorine have been much studied and some (such as  $Cl_2O$  and particularly  $ClO_2$ ) find extensive industrial use. They have also assumed considerable importance in studies of the upper atmosphere because of the vulnerability of ozone in the stratosphere to destruction by the photolysis products of chlorofluorocarbons (p. 848). The compounds to be discussed are:

$Cl_2O$ : a brownish-yellow gas at room temperature (or red-brown liquid and solid at lower temperatures) discovered in 1834; it explodes when heated or sparked.

$Cl_2O_3$ : a dark-brown solid (1967) which explodes even below  $0^\circ$ .

$ClO_2$ : a yellow paramagnetic gas (deep-red paramagnetic liquid and solid) discovered in 1811 by H. Davy; the liquid explodes above  $-40^\circ$  and the gas at room temperature may explode at pressures greater than 50 mmHg (6.7 kPa); despite this more than half a million tonnes are made for industrial use each year in North America alone.

$Cl_2O_4$ : a pale-yellow liquid (1970),  $ClOClO_3$ , which readily decomposes at room temperature into  $Cl_2$ ,  $O_2$ ,  $ClO_2$  and  $Cl_2O_6$ .

<sup>97</sup> Ref. 23, pp. 1361–86. The oxides of the halogens.

<sup>98</sup> J. A. WOJCIWICZ, Dichlorine monoxide, hypochlorous acid and hypochlorites. *Kirk-Othmer Encyclopedia of Chemical Technology*, 4th edn., Wiley, New York, 1993, Vol. 5, pp. 932–68. J. J. KACZUR and D. W. CAWLFIELD, Chlorine dioxide, chlorous acid and chlorites, *ibid.*, pp. 968–91.

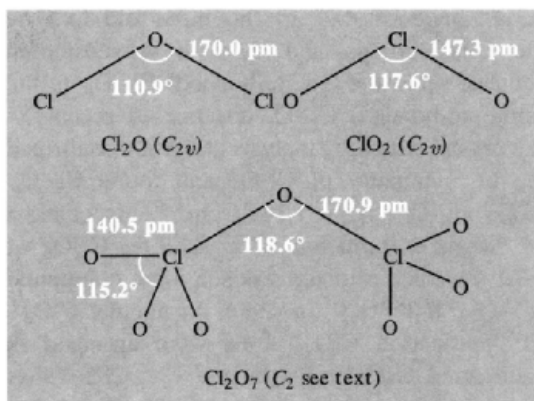
<sup>96</sup> C. CHUNG and G. H. CADY, *Inorg. Chem.* **11**, 2528–31 (1972).

$\text{Cl}_2\text{O}_6$ : a dark-red liquid (1843) which is in equilibrium with its monomer  $\text{ClO}_3$  in the gas phase; it decomposes to  $\text{ClO}_2$  and  $\text{O}_2$ .

$\text{Cl}_2\text{O}_7$ : a colourless oily liquid (1900) which can be distilled under reduced pressure.

In addition, there are the short-lived radical  $\text{ClO}$ , the chlorine peroxide radical  $\text{ClOO}$  (cf.  $\text{OCIO}$  above), and the tetroxide radical  $\text{ClO}_4$  (p. 850).

Some physical and molecular properties are summarized in Table 17.19. All the compounds are endothermic, having large positive enthalpies and free energies of formation. Structural data are in Fig. 17.16.  $\text{Cl}_2\text{O}$  has  $C_{2v}$  symmetry, as expected for a molecule with 20 valency-shell electrons; the dimensions indicate normal single bonds, and the bond angle can be compared with those for similar molecules such as  $\text{OF}_2$ ,  $\text{H}_2\text{O}$ ,  $\text{SCl}_2$ , etc. Chlorine dioxide,  $\text{ClO}_2$ , also has  $C_{2v}$  symmetry but there are only 19 valency-shell electrons and this is reflected in the considerable shortening of the  $\text{Cl}-\text{O}$  bonds and the increase in the bond angle, which is only  $1.7^\circ$  less than in the 18-electron species  $\text{SO}_2$  (p. 700).  $\text{ClO}_2$  is an interesting example of an odd-electron molecule which is stable towards dimerization (cf.  $\text{NO}$ , p. 445); calculations suggest that the odd electron is delocalized throughout the molecule and this probably explains the reluctance to dimerize. Indeed, there is no evidence of dimerization even



**Figure 17.16** Molecular structure and dimensions of gaseous molecules of chlorine oxides as determined by microwave spectroscopy ( $\text{Cl}_2\text{O}$  and  $\text{ClO}_2$ ) or electron diffraction ( $\text{Cl}_2\text{O}_7$ ).

in the liquid or solid phases, or in solution. This contrasts with the precisely isoelectronic thionite ion  $\text{SO}_2^-$  which exists as dithionite,  $\text{S}_2\text{O}_4^{2-}$ , albeit with a rather long  $\text{S}-\text{S}$  bond (p. 721). The trioxide  $\text{ClO}_3$  is also predominantly dimeric in the condensed phase (see below) as probably is  $\text{BrO}_2$  (p. 850).

The gaseous molecule of  $\text{Cl}_2\text{O}_7$  has  $C_2$  symmetry (Fig. 17.16) the  $\text{ClO}_3$  groups being twisted  $15^\circ$  from the staggered ( $C_{2v}$ ) configuration; the  $\text{Cl}-\text{O}_\mu$  bonds are also inclined

**Table 17.19** Physical and molecular properties of the oxides of chlorine

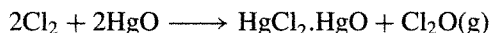
Property	$\text{Cl}_2\text{O}$	$\text{ClO}_2$	$\text{ClOClO}_3$	$\text{Cl}_2\text{O}_6(\text{l})$ ( $\rightleftharpoons 2\text{ClO}_3(\text{g})$ )	$\text{Cl}_2\text{O}_7$
Colour and form at room temperature	Yellow-brown gas	Yellow-green gas	Pale yellow liquid	Dark red liquid	Colourless liquid
Oxidation states of Cl	+1	+4	+1, +7	+6	+7
MP/ $^\circ\text{C}$	-120.6	-59	-117	3.5	-91.5
BP/ $^\circ\text{C}$	2.0	11	44.5 (extrap)	203 (extrap)	81
$d(\text{liq}, 0^\circ\text{C})/\text{g cm}^{-3}$	—	1.64	1.806	—	2.02
$\Delta H_f^\circ(\text{gas}, 25^\circ\text{C})/\text{kJ mol}^{-1}$	80.3	102.6	~180	(155)	272
$\Delta G_f^\circ(\text{gas}, 25^\circ\text{C})/\text{kJ mol}^{-1}$	97.9	120.6	—	—	—
$S^\circ(\text{gas}, 25^\circ\text{C})/\text{J K}^{-1} \text{mol}^{-1}$	265.9	256.7	327.2	—	—
Dipole moment $\mu/\text{D}^{(a)}$	$0.78 \pm 0.08$	$1.78 \pm 0.01$	—	—	$0.72 \pm 0.02$

<sup>(a)</sup> 1 D  $\equiv 3.3356 \times 10^{-30}$  C m.

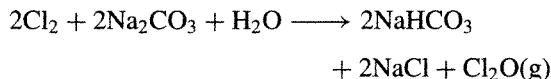


at an angle of  $4.7^\circ$  to the three-fold axis of the  $\text{ClO}_3$  groups and there is a substantial decrease from the (single-bonded)  $\text{Cl}-\text{O}_\mu$  to the (multiple-bonded)  $\text{Cl}-\text{O}_t$  distance. A recent X-ray crystal structure analysis at  $-160^\circ$  confirmed the  $C_2$  symmetry of  $\text{Cl}_2\text{O}_7$  and found  $\text{Cl}-\text{O}_\mu$  172.3 pm,  $\text{Cl}-\text{O}_t$  (av.) 141.6 pm.<sup>(99)</sup> By contrast an X-ray examination of crystalline  $\text{Cl}_2\text{O}_6$  at  $-70^\circ$  revealed a mixed-valence ionic compound  $[\text{Cl}^{\text{V}}\text{O}_2]^+[\text{Cl}^{\text{VII}}\text{O}_4]^-$  in which the angular  $\text{ClO}_2^+$  and tetrahedral  $\text{ClO}_4^-$  ions were arranged in a distorted CsCl-type structure.<sup>(100)</sup>  $\text{ClO}_2^+$  has  $\text{Cl}-\text{O}$  140.8 pm, angle  $\text{OClO}$   $118.9^\circ$ ;  $\text{ClO}_4^-$  has  $\text{Cl}-\text{O}$  (av) 144.3 pm. The structures of the other oxides of chlorine have not been rigorously established.

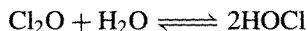
We next consider the synthesis and chemical reactions of the oxides of chlorine. Because the compounds are strongly endothermic and have large positive free energies of formation it is not possible to prepare them by direct reaction of  $\text{Cl}_2$  and  $\text{O}_2$ . Dichlorine monoxide,  $\text{Cl}_2\text{O}$ , is best obtained by treating freshly prepared yellow  $\text{HgO}$  and  $\text{Cl}_2$  gas (diluted with dry air or by dissolution in  $\text{CCl}_4$ ):



The reaction is convenient for both laboratory scale and industrial preparations. Another large-scale process is the reaction of  $\text{Cl}_2$  gas on moist  $\text{Na}_2\text{CO}_3$  in a tower or rotary tube reactor:



$\text{Cl}_2\text{O}$  is very soluble in water, a saturated solution at  $-9.4^\circ\text{C}$  containing 143.6 g  $\text{Cl}_2\text{O}$  per 100 g  $\text{H}_2\text{O}$ ; in fact the gas is the anhydride of hypochlorous acid, with which it is in equilibrium in aqueous solutions:

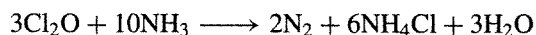


<sup>99</sup> A. SIMON and H. BORRMANN, *Angew. Chem. Int. Edn. Engl.* **27**, 1339–41 (1988).

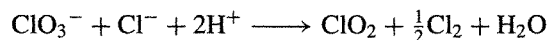
<sup>100</sup> K. M. TOBIAS and M. JANSEN, *Z. anorg. allg. Chem.* **550**, 16–26 (1987).

Much of the  $\text{Cl}_2\text{O}$  manufactured industrially is used to make hypochlorites, particularly  $\text{Ca}(\text{OCl})_2$ , and it is an effective bleach for wood-pulp and textiles.  $\text{Cl}_2\text{O}$  is also used to prepare chloroisocyanurates (p. 324) and chlorinated solvents (via mixed chain reactions in which  $\text{Cl}$  and  $\text{OCl}$  are the chain-propagating species).<sup>(101)</sup> Its reactions with inorganic reagents are summarized in the scheme opposite.

Gaseous mixtures of  $\text{Cl}_2\text{O}$  and  $\text{NH}_3$  explode violently: the overall stoichiometry of the reaction can be represented as

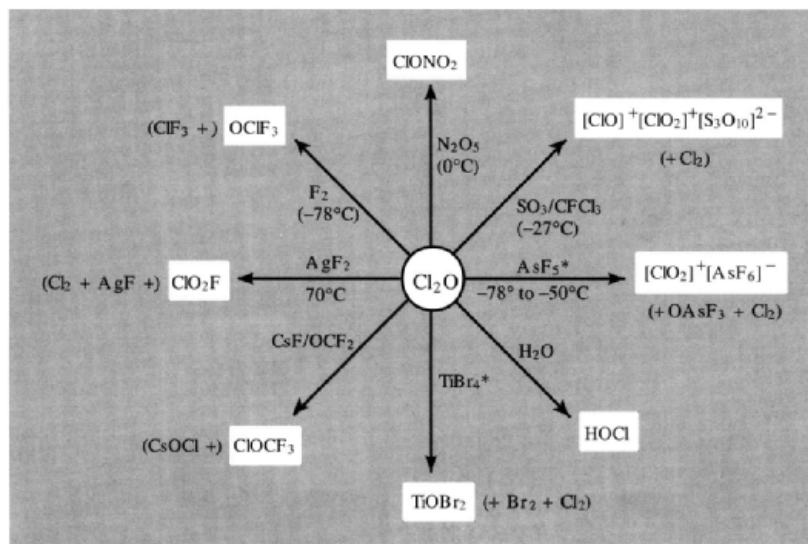


Chlorine dioxide,  $\text{ClO}_2$ , was the first oxide of chlorine to be discovered and is now manufactured on a massive scale for the bleaching of wood-pulp and for water treatment;<sup>(98,102)</sup> however, because of its explosive character as a liquid or concentrated gas, it must be made at low concentrations where it is to be used. For this reason, production statistics can only be estimated, but it is known that its use in the US wood-pulp and paper industry increased tenfold from 7800 tonnes in 1955 to 78 800 tonnes in 1970; thereafter captive production for this purpose increased less rapidly but the total US production of this gas for all purposes reached 361 000 tonnes in 1990. Production in Canada paralleled this growth and was 200 000 tonnes in 1990. Prices in 1992 were in the range \$1100–1800/tonne. Usually  $\text{ClO}_2$  is prepared by reducing  $\text{NaClO}_3$  with  $\text{NaCl}$ ,  $\text{HCl}$ ,  $\text{SO}_2$  or  $\text{MeOH}$  in strongly acid solution; other reducing agents that have been used on a laboratory scale include oxalic acid,  $\text{N}_2\text{O}$ ,  $\text{EtOH}$  and sugar. With  $\text{Cl}^-$  as reducing agent the formal reaction can be written:



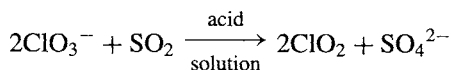
<sup>101</sup> J. J. RENARD and H. I. BOLKER, *Chem. Revs.* **76**, 487–505 (1976).

<sup>102</sup> W. J. MASSCHELEIN, *Chlorine Dioxide: Chemistry and Environmental Impact of Oxychlorine Compounds*, Ann Arbor Science Publishers, Ann Arbor, 1979, 190 pp. J. KATZ (ed.), *Ozone and Chlorine Dioxide Technology for Disinfection of Drinking Water*, Noyes Data Corp., Park Ridge, New Jersey, 1980, 659 pp.

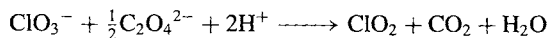


Scheme Some reactions of dichlorine monoxide. \*[In addition  $\text{AsCl}_3 \rightarrow \text{AsO}_2\text{Cl}$ ;  $\text{SbCl}_5 \rightarrow \text{SbO}_2\text{Cl}$ ;  $\text{VOCl}_3 \rightarrow \text{VO}_2\text{Cl}$ ;  $\text{TiCl}_4 \rightarrow \text{TiOCl}_2$ .] <sup>(101)</sup>

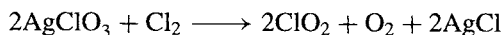
Contamination of the product with  $\text{Cl}_2$  gas is not always undesirable but can be avoided by using  $\text{SO}_2$ :



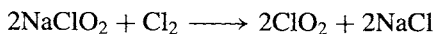
On a laboratory scale reduction of  $\text{KClO}_3$  with moist oxalic acid generates the gas suitably diluted with oxides of carbon:



Samples of pure  $\text{ClO}_2$  for measurement of physical properties can be obtained by chlorine reduction of silver chlorate at  $90^\circ\text{C}$ :

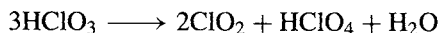


Chlorine oxidation of sodium chlorite has also been used on both an industrial scale (by mixing concentrated aqueous solutions) or on a laboratory scale (by passing  $\text{Cl}_2$ /air through a column packed with the solid chlorite):



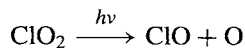
The production of  $\text{ClO}_2$  obviously hinges on the redox properties of oxochlorine species (p. 853)

and, indeed, the gas was originally obtained simply by the (extremely hazardous) disproportionation of chloric acid liberated by the action of concentrated sulfuric acid on a solid chlorate:

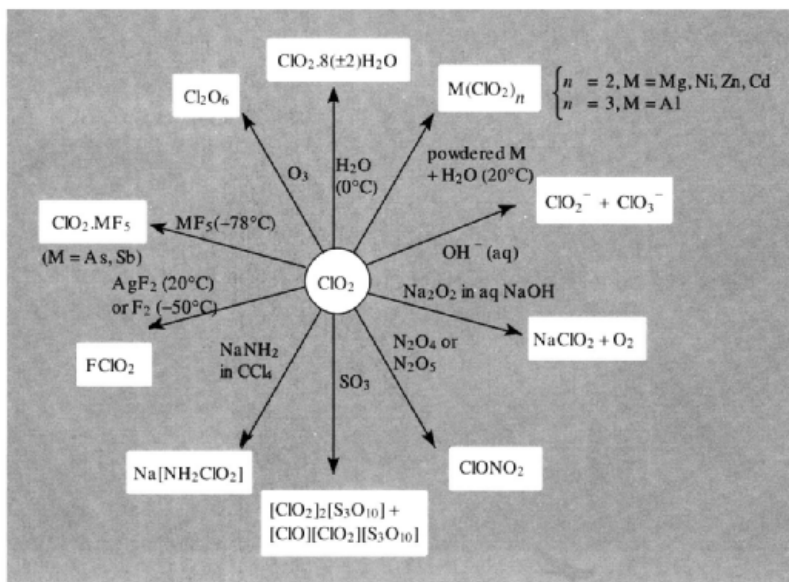


$\text{ClO}_2$  is a strong oxidizing agent towards both organic and inorganic materials and it reacts readily with S, P,  $\text{PX}_3$  and  $\text{KBH}_4$ . Some further reactions are in the scheme overleaf: <sup>(97)</sup>

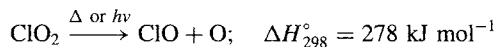
$\text{ClO}_2$  dissolves exothermically in water and the dark-green solutions, containing up to 8 g/l, decompose only very slowly in the dark. At low temperatures crystalline clathrate hydrates,  $\text{ClO}_2 \cdot n\text{H}_2\text{O}$ , separate ( $n \approx 6-10$ ). Illumination of neutral aqueous solutions initiates rapid photodecomposition to a mixture of chloric and hydrochloric acids:



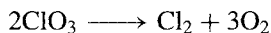
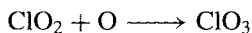
By contrast, alkaline solutions hydrolyse vigorously to a mixture of chlorite and chlorate (see scheme overleaf).



The photochemical and thermal decomposition of  $\text{ClO}_2$  both begin by homolytic scission of a Cl–O bond:



Subsequent reactions depend on conditions. Ultraviolet photolysis of isolated molecules in an inert matrix yields the radicals  $\text{ClO}$  and  $\text{ClOO}$ . At room temperature, photolysis of dry gaseous  $\text{ClO}_2$  yields  $\text{Cl}_2$ ,  $\text{O}_2$ , and some  $\text{ClO}_3$  which either dimerizes or is further photolysed to  $\text{Cl}_2$  and  $\text{O}_2$ :

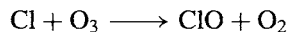


By contrast, photolysis of solid  $\text{ClO}_2$  at  $-78^\circ\text{C}$  produces some  $\text{Cl}_2\text{O}_3$  as well as  $\text{Cl}_2\text{O}_6$ :



The  $\text{ClO}$  radical in particular is implicated in environmentally sensitive reactions which lead to depletion of ozone and oxygen atoms in the

stratosphere.<sup>(103)</sup> Thus (as was first pointed out by M. J. Molina and F. S. Rowland in 1974<sup>(104)</sup>) chlorofluorocarbons such as  $\text{CFCl}_3$  and  $\text{CF}_2\text{Cl}_2$ , which have been increasingly used as aerosol spray propellants, refrigerants, solvents and plastic foaming agents (p. 304), have penetrated the stratosphere (10–50 km above the earth's surface) where they are photolysed or react with electronically excited  $\text{O}(^1D)$  atoms to yield Cl atoms and chlorine oxides; this leads to the continuous removal of  $\text{O}_3$  and O atoms via such reactions as:



i.e.  $\text{O} + \text{O}_3 \longrightarrow 2\text{O}_2$  plus regeneration of Cl

Depletion of  $\text{O}_3$  results in an increased penetration of ultraviolet light with wavelengths in the range 290–320 nm which may in time effect changes in climate and perhaps lead also to an increased incidence of skin cancer in

<sup>103</sup> R. J. DONOVAN, *Educ. in Chem.* **15**, 110–13 (1978).  
B. A. THRUSH, *Endeavour (New Series)* **1**, 3–6 (1977), and references therein.

<sup>104</sup> M. J. MOLINA and F. S. ROWLAND, *Nature* **249**, 810–12 (1974).

humans. Because of these concerns, the alarming increase in global sales of chlorofluorocarbons, which grew 15-fold between 1948 and 1973, has since been drastically reduced as shown by the following illustrative figures for CFC-11 and CFC-12 (tonnes):

	1948	1973	1983
CFCl <sub>3</sub> (CFC-11)	2 270	302 000	93 000
CF <sub>2</sub> Cl <sub>2</sub> (CFC-12)	2 220	383 000	120 000

The decrease is continuing due to global adherence to the provisions of the Montreal (1989) and London (1990) Protocols, and it is hoped that the most deleterious CFCs will eventually be phased out completely. As a result of their work, Rowland and Molina were awarded the Nobel Prize for Chemistry for 1995 (together with P. Crutzen, who showed how NO and NO<sub>2</sub> could similarly act as catalysts for the depletion of stratospheric ozone). Several excellent accounts giving more details of the chemistry and meteorology involved are available.<sup>(105–108)</sup>

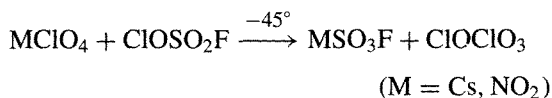
The great importance of the short-lived ClO radical has stimulated numerous investigations of its synthesis and molecular properties. Several routes are now available to this species (some of which have already been indicated above):

- thermal decomposition of ClO<sub>2</sub> or ClO<sub>3</sub>;
- decomposition of FClO<sub>3</sub> in an electric discharge;
- passage of a microwave or radio-frequency discharge through mixtures of Cl<sub>2</sub> and O<sub>2</sub>;
- reactions of Cl atoms with ClO or O<sub>3</sub> at 300 K;

- gas-phase photolysis of Cl<sub>2</sub>O, ClO<sub>2</sub> or mixtures of Cl<sub>2</sub> and O<sub>2</sub>.

It is an endothermic species with  $\Delta H_f^\circ(298\text{ K})$  101.8 kJ mol<sup>-1</sup>,  $\Delta G_f^\circ(298\text{ K})$  98.1 kJ mol<sup>-1</sup>,  $S^\circ(298\text{ K})$  226.5 J K<sup>-1</sup> mol<sup>-1</sup>. The interatomic distance Cl–O is 156.9 pm, its dipole moment is 1.24 D, and the bond dissociation energy  $D_0$  is 264.9 kJ mol<sup>-1</sup> (cf. BrO p. 851, IO p. 853).

Chlorine perchlorate ClOClO<sub>3</sub> is made by the following low-temperature reaction:



Little is known of its structure and properties; it is even less stable than ClO<sub>2</sub> and decomposes at room temperature to Cl<sub>2</sub>, O<sub>2</sub> and Cl<sub>2</sub>O<sub>6</sub>.

Dichlorine hexoxide, Cl<sub>2</sub>O<sub>6</sub>, is best made by ozonolysis of ClO<sub>2</sub>:



The dark-red liquid freezes to a solid which is yellow at –180°C. The structure in the liquid phase is not known but two possibilities have been considered. The Cl–Cl linked structure is superficially attractive as the product of dimerization of the paramagnetic gaseous species ClO<sub>3</sub>, but magnetic susceptibility studies of the equilibrium  $\text{Cl}_2\text{O}_6 \rightleftharpoons 2\text{ClO}_3$  in the liquid phase were flawed by the subsequent finding that there was no esr signal from ClO<sub>3</sub> and that ClO<sub>2</sub> (as an impurity) was the sole paramagnetic species present. Accordingly, the much-quoted value of 7.24 kJ mol<sup>-1</sup> for the derived heat of dimerization is without foundation. The alternative oxygen-bridged dimer, though requiring more electronic and geometric rearrangement of the presumed pyramidal \*ClO<sub>3</sub> monomers, is rather closer to the ionic structure [ClO<sub>2</sub>]<sup>+</sup>[ClO<sub>4</sub>]<sup>-</sup> which has been established by X-ray analysis (p. 846) of the solid. Cl<sub>2</sub>O<sub>6</sub> does, in fact, frequently behave as chloryl perchlorate in its reactions though experience with N<sub>2</sub>O<sub>4</sub> as “nitrosyl nitrate” (p. 455) engenders caution in attempting to deduce a geometrical structure from chemical reactions (cf. however, diborane, p. 165).

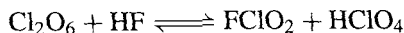
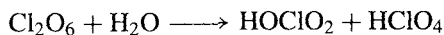
<sup>105</sup> F. S. ROWLAND and M. J. MOLINA, *Chem. & Eng. News*, August 15, 8–13 (1994).

<sup>106</sup> M. J. MOLINA and L. T. MOLINA, Chap. 2 in D. A. DUNNETTE and R. J. O'BRIEN (eds.), *The Science of Global Change: The Impact of Human Activities on the Environment*, ACS Symposium Series **483**, 24–35 (1992).

<sup>107</sup> R. P. WAYNE, *Chemistry of Atmospheres*, (2nd. edn.), Oxford University Press, Oxford, 1991, 456 pp.

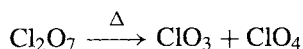
<sup>108</sup> P. S. ZURER, *Chem. & Eng. News*, May 24, 8–18 (1993). See also P. S. ZURER, *Chem. & Eng. News*, Jan. 2, 30–2 (1989) and Mar. 6, 29–31 (1989).

Hydrolysis of  $\text{Cl}_2\text{O}_6$  gives a mixture of chloric and perchloric acids, whereas anhydrous HF sets up an equilibrium:



Nitrogen oxides and their derivatives displace  $\text{ClO}_2$  to form nitrosyl and nitryl perchlorates. These and other reactions are summarized in the scheme below.

Dichlorine heptoxide,  $\text{Cl}_2\text{O}_7$ , is the anhydride of perchloric acid (p. 865) and is conveniently obtained by careful dehydration of  $\text{HClO}_4$  with  $\text{H}_3\text{PO}_4$  at  $-10^\circ\text{C}$  followed by cautious low-pressure distillation at  $-35^\circ\text{C}$  and 1 mmHg. The compound is a shock-sensitive oily liquid with physical properties and structure as already described (p. 845).  $\text{Cl}_2\text{O}_7$  is less reactive than the lower oxides of chlorine and does not ignite organic materials at room temperature. Dissolution in water or aqueous alkalis regenerates perchloric acid and perchlorates respectively. Thermal decomposition (which can be explosive) is initiated by rupture of a  $\text{Cl}-\text{O}_\mu$  bond, the activation energy being  $\sim 135 \text{ kJ mol}^{-1}$ :



### Oxides of bromine

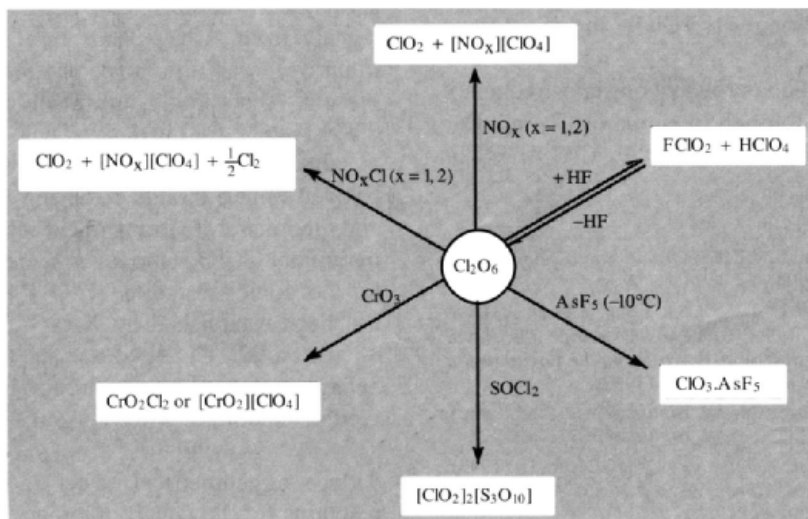
The oxides of Br are less numerous, far less studied, and much less well characterized than the ten oxide species of chlorine discussed in the preceding section. The reasonably well established compounds are listed below.

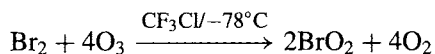
$\text{Br}_2\text{O}$ : a dark-brown solid moderately stable at  $-60^\circ$  (mp  $-17.5^\circ$  with decomposition), prepared by reaction of  $\text{Br}_2$  vapour on  $\text{HgO}$  (cf.  $\text{Cl}_2\text{O}$  p. 846) or better, by low-temperature vacuum decomposition of  $\text{BrO}_2$ . The molecule has  $C_{2v}$  symmetry in both the solid and vapour phase with  $\text{Br}-\text{O}$   $185 \pm 1$  pm and angle  $\text{BrOBr}$   $112 \pm 2^\circ$  as determined by EXAFS (extended X-ray absorption fine structure).<sup>(109)</sup> It oxidizes  $\text{I}_2$  to  $\text{I}_2\text{O}_5$ , benzene to 1,4-quinone, and yields  $\text{OBr}^-$  in alkaline solution.

“ $\text{BrO}_2$ ”: a pale yellow crystalline solid formed quantitatively by low-temperature ozonolysis of  $\text{Br}_2$ :<sup>†</sup>

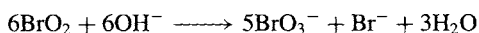
<sup>109</sup> W. LEVASON, J. S. OGDEN, M. D. SPICER and N. A. YOUNG, *J. Am. Chem. Soc.* **112**, 1019–22 (1990).

<sup>†</sup> Ozonolysis of  $\text{Br}_2$  at  $0^\circ\text{C}$  yields white, poorly characterized solids which, depending on the conditions used, have compositions close to  $\text{Br}_2\text{O}_5$ ,  $\text{Br}_3\text{O}_8$ , and  $\text{BrO}_3$ ; no structural data are available.





The structure has recently been shown by EXAFS to be bromine perbromate  $\text{BrOBrO}_3$  with  $\text{Br}^{\text{I}}-\text{O}$  186.2 pm,  $\text{Br}^{\text{VII}}-\text{O}$  160.5 pm and angle  $\text{BrOBr}$   $110 \pm 3^\circ$ ;<sup>(110)</sup> (cf.  $\text{ClOClO}_3$  and  $\text{BrOClO}_3$ ).  $\text{BrOBrO}_3$  is thermally unstable above  $-40^\circ\text{C}$  and decomposes violently to the elements at  $0^\circ\text{C}$ ; slower warming yields  $\text{BrO}_2$  (see above). Alkaline hydrolysis leads to disproportionation:



Reaction with  $\text{F}_2$  yields  $\text{FBrO}_2$  and with  $\text{N}_2\text{O}_4$  yields  $[\text{NO}_2]^+[\text{Br}(\text{NO}_3)_2]^-$ .

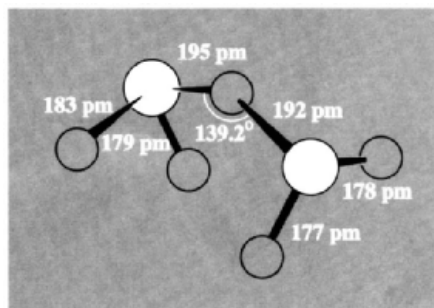
$\text{Br}_2\text{O}_3$ : an orange crystalline solid very recently isolated at  $-90^\circ$  from  $\text{CH}_2\text{Cl}_2$  solution after ozonization of  $\text{Br}_2$  in  $\text{CFCl}_3$ . It decomposes above  $-40^\circ$ , detonates if warmed rapidly to  $0^\circ$ , and was shown by X-ray analysis to be *syn*- $\text{BrOBrO}_2$  with  $\text{Br}^{\text{I}}-\text{O}$  184.5 pm,  $\text{Br}^{\text{V}}-\text{O}$  161.3 pm and angle  $\text{BrOBr}$   $111.6^\circ$ .<sup>(111)</sup> It is thus, formally, the anhydride of hypobromous and bromic acids.

In addition to these compounds the unstable monomeric radicals  $\text{BrO}$ ,  $\text{BrO}_2$  and  $\text{BrO}_3$  have been made by  $\gamma$ -radiolysis or flash photolysis of the anions  $\text{OBr}^-$ ,  $\text{BrO}_2^-$  and  $\text{BrO}_3^-$ . For  $\text{BrO}$  the interatomic distance is 172.1 pm, the dipole moment 1.55 D, and the thermodynamic properties  $\Delta H_f^\circ(298\text{ K})$  125.8  $\text{kJ mol}^{-1}$ ,  $\Delta G_f^\circ(298\text{ K})$  108.2  $\text{kJ mol}^{-1}$  and  $S^\circ(298\text{ K})$  237.4  $\text{J K}^{-1} \text{mol}^{-1}$ . Most recently<sup>(112)</sup> it has been shown that flash pyrolysis at  $800\text{--}1000^\circ\text{C}$  of a mixture containing  $\text{Br}_2/\text{O}_2/\text{Ar}$  yields bromine superoxide,  $[\text{BrOO}]^*$ , which can be trapped at 12 K and shown by ir- and uv-spectroscopy to be non-linear. Irradiation of

this species at 254 nm results in isomerization to bromine dioxide,  $[\text{OBrO}]^*$ , which is also non-linear (angle  $\sim 110^\circ$ ) and which can be reconverted to the superoxide by irradiating the matrix at wavelengths greater than 360 nm.

### Oxides of iodine

Iodine forms the most stable oxides of the halogens and  $\text{I}_2\text{O}_5$  was made (independently) by J. L. Gay Lussac and H. Davy in 1813. However, despite this venerable history the structure of the compound was not determined unambiguously until 1970. It is most conveniently prepared by dehydrating iodic acid (p. 863) at  $200^\circ\text{C}$  in a stream of dry air but it also results from the direct oxidation of  $\text{I}_2$  with oxygen in a glow discharge. The structure (Fig. 17.17) features molecular units of  $\text{O}_2\text{IOIO}_2$  formed by joining two pyramidal  $\text{IO}_3$  groups at a common oxygen. The bridging I–O distances correspond to single bonds, whereas the terminal I–O distances are substantially shorter.<sup>(113)</sup> There are also appreciable intermolecular interactions which join the molecular units into cross-linked chains; this gives each iodine pseudo-fivefold coordination, the sixth position of the distorted



**Figure 17.17** The structure of  $\text{I}_2\text{O}_5$  showing the dimensions and conformation of a single molecular unit. Note that the molecule has no mirror plane of symmetry so is not  $C_{2v}$ .

<sup>110</sup> T. R. GILSON, W. LEVASON, J. S. OGDEN, M. D. SPICER and N. A. YOUNG, *J. Am. Chem. Soc.* **114**, 5469–70 (1992).

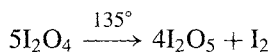
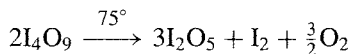
<sup>111</sup> R. KUSCHEL and K. SEPELT, *Angew. Chem. Int. Edn. Engl.* **32**, 1632–3 (1993).

<sup>112</sup> G. MAIER and A. BOTHUR, *Z. anorg. allg. Chem.* **621**, 743–6 (1995).

<sup>113</sup> K. SELTE and A. KJEKSHUS, *Acta Chem. Scand.* **24**, 1912–24 (1970).

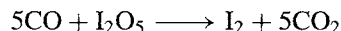
octahedron presumably being occupied by the lone-pair of electrons on the iodine atom.

$I_2O_5$  forms white, hygroscopic, thermodynamically stable crystals:  $\Delta H_f^\circ -158.1 \text{ kJ mol}^{-1}$ ,  $d$   $4.980 \text{ g cm}^{-3}$ . The compound is very soluble in water, reforming the parent acid  $HIO_3$ . So great is the affinity for water that commercial " $I_2O_5$ " consists almost entirely of  $HI_3O_8$ , i.e.  $I_2O_5 \cdot HIO_3$ . The interrelations between these compounds and the rather less stable oxides  $I_4O_9$  and  $I_2O_4$  are shown in the scheme below.  $I_4O_9$  is a hygroscopic yellow powder which decomposes to  $I_2O_5$  when heated above  $75^\circ$ ;  $I_2O_4$  forms diamagnetic lemon-yellow crystals ( $d$   $4.2 \text{ g cm}^{-3}$ ) which start to decompose above  $85^\circ$  and which rapidly yield  $I_2O_5$  at  $135^\circ$ :



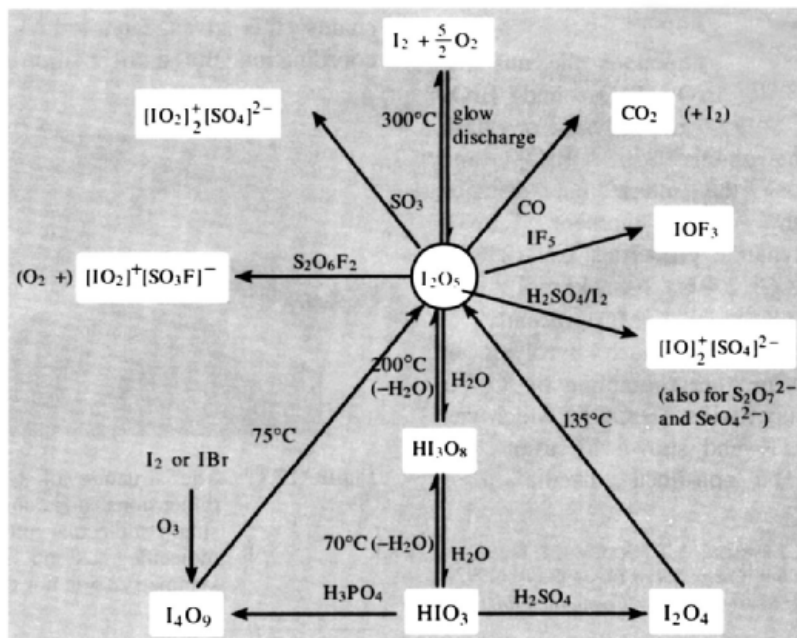
The structure of these oxides are unknown but  $I_4O_9$  has been formulated as  $I^{III}(I^V O_3)_3$  and  $I_2O_4$  as  $[IO]^{+}[IO_3]^{-}$ .

$I_2O_5$  is notable in being one of the few chemicals that will oxidize CO rapidly and completely at room temperature:



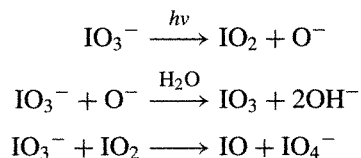
The reaction forms the basis of a useful analytical method for determining the concentration of CO in the atmosphere or in other gaseous mixtures.  $I_2O_5$  also oxidizes NO,  $C_2H_4$  and  $H_2S$ .  $SO_3$  and  $S_2O_6F_2$  yield iodyl salts,  $[IO_2]^{+}$ , whereas concentrated  $H_2SO_4$  and related acids reduce  $I_2O_5$  to iodosyl derivatives,  $[IO]^{+}$ . Fluorination of  $I_2O_5$  with  $F_2$ ,  $BrF_3$ ,  $SF_4$  or  $FCIO_2$  yields  $IF_5$  which itself reacts with the oxide to give  $OIF_3$ . It is also convenient to note here other related compounds which have recently been characterized:  $I(OTeF_5)_3$ ,  $O=I(OTeF_5)_3$ ,  $I(OTeF_5)_5$ ,  $[I(OTeF_5)_4]^{-}$  and  $[O=I(OTeF_5)_4]^{-}$ ; <sup>(114)</sup> all have the expected structures (cf. pp. 688, 777, 899, 904).

<sup>114</sup> L. TUROWSKY and K. SEPELT, *Z. anorg. allg. Chem.* **602**, 79–87 (1991), and references cited therein.



SCHEME: Preparation of reactions of iodine oxides.

In addition to the stable  $I_2O_5$  and moderately stable  $I_4O_9$  and  $I_2O_4$ , several short-lived radicals have been detected and characterized during  $\gamma$ -radiolysis and flash photolysis of iodates in aqueous alkali:



The endothermic radical IO has also been studied in the gas phase: the interatomic distance is 186.7 pm and the bond dissociation energy  $\sim 175 \pm 20 \text{ kJ mol}^{-1}$ . It thus appears that, although the higher oxides of iodine are much more stable than any oxide of Cl or Br, nevertheless, IO is much less stable than ClO (p. 849) or BrO (p. 851). Its enthalpy of formation and other thermodynamic properties are:  $\Delta H_f^\circ(298 \text{ K}) 175.1 \text{ kJ mol}^{-1}$ ,  $\Delta G_f^\circ(298 \text{ K}) 149.8 \text{ kJ mol}^{-1}$ ,  $S^\circ(298 \text{ K}) 245.5 \text{ J K}^{-1} \text{ mol}^{-1}$ .

### 17.2.8 Oxoacids and oxoacid salts

#### General considerations<sup>(115)</sup>

The preparative chemistry and technical applications of the halogen oxoacids and their salts have been actively pursued and developed for over two centuries (p. 790) and can now be very satisfactorily systematized in terms of general

thermodynamic principles. The thermodynamic data are codified in the form of reduction potentials and equilibrium constants and these, coupled with the relative rates of competing reactions, allow a vast range of aqueous solution chemistry of the halogens to be interrelated. Thus, although all the halogens are to some extent soluble in water, extensive disproportionation reactions and/or mutual redox reactions with the solvent can occur to an extent that depends crucially on conditions such as pH and concentration (which influence the thermodynamic variables) and the presence of catalysts or light quanta (which can overcome kinetic activation barriers). Fluorine is again exceptional and, because of its very high standard reduction potential,  $E^\circ(\frac{1}{2}F_2/F^-) + 2.866 \text{ V}$ , reacts very strongly with water at all values of pH (p. 629). Its inability to achieve formal oxidation states higher than +1 also limits the available oxoacids to hypofluorous acid HOF (p. 856). Numerous other oxoacids are known for the heavier halogens (Table 17.20) though most cannot be isolated pure and are stable only in aqueous solution or in the form of their salts. Anhydrous perchloric acid ( $HClO_4$ ), iodic acid ( $HIO_3$ ), paraperiodic acid ( $H_5IO_6$ ) and metaperiodic acid ( $HIO_4$ ) have been isolated as pure compounds.

The standard reduction potentials for Cl, Br and I species in acid and in alkaline aqueous solutions are summarized in Fig. 17.18. The couples  $\frac{1}{2}X_2/X^-$  are independent of pH and, together with the value for  $F_2$ , indicate a steadily decreasing oxidizing power of the halogens in the sequence  $F_2(+2.866 \text{ V}) > Cl_2(+1.358 \text{ V}) > Br_2(+1.066 \text{ V}) > I_2(+0.536 \text{ V})$ . Remembering

<sup>115</sup> Ref. 23, Chemical properties of the halogens — redox properties: aqueous solutions, pp. 1188–95; Oxoacids and oxoacid salts of the halogens, pp. 1396–1465.

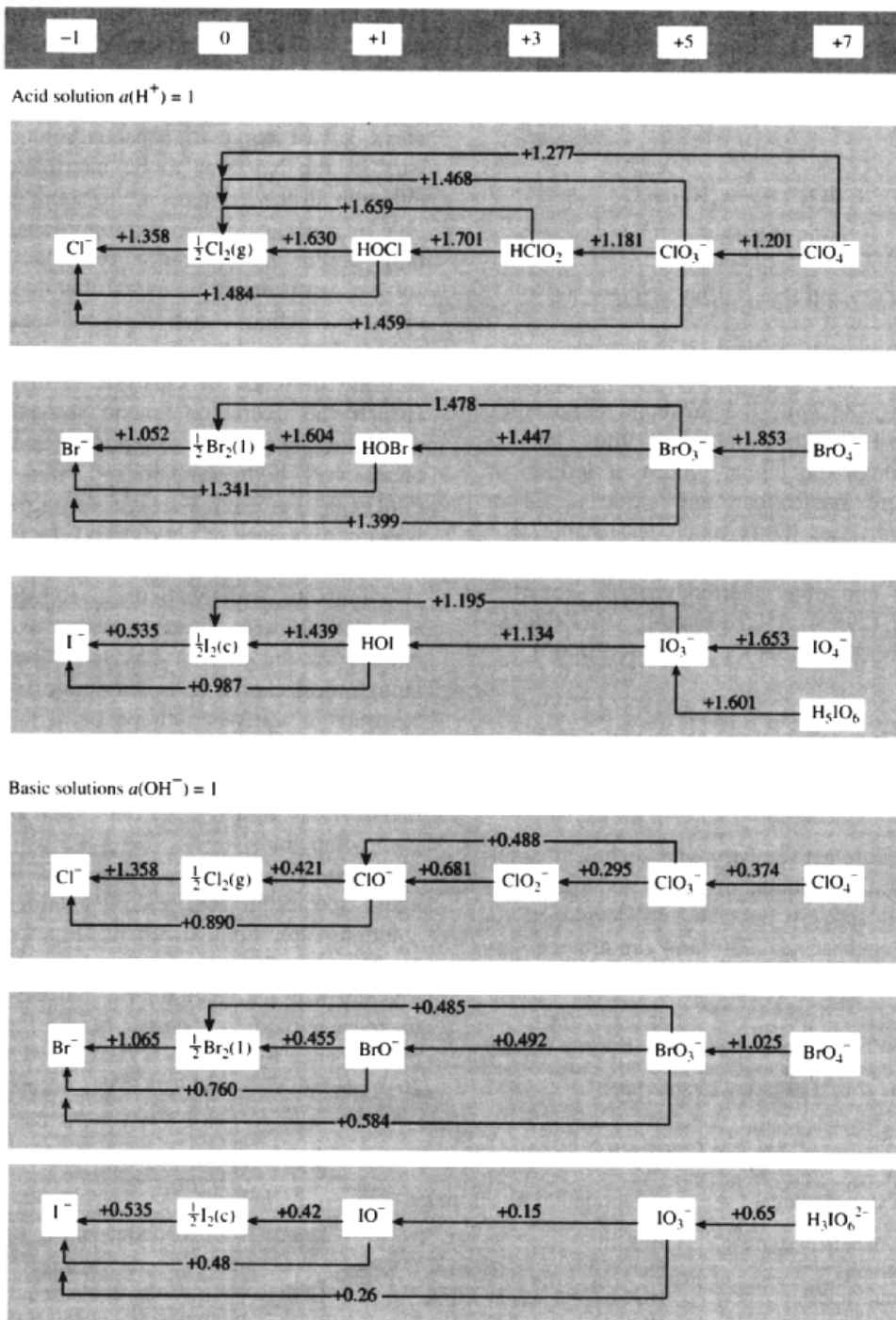
**Table 17.20** Oxoacids of the halogens

Generic name	Chlorine	Bromine	Iodine	Salts
Hypohalous acids <sup>(b)</sup>	HOCl <sup>(a)</sup>	HOBr <sup>(a)</sup>	HOI <sup>(a)</sup>	Hypohalites
Halous acids	HOClO <sup>(a)</sup>	(HOBrO?) <sup>(a)</sup>	—	Halites
Halic acids	HOClO <sub>2</sub> <sup>(a)</sup>	HOBrO <sub>2</sub> <sup>(a)</sup>	HOIO <sub>2</sub>	Halates
Perhalic acids	HOClO <sub>3</sub>	HOBrO <sub>3</sub> <sup>(a)</sup>	HOIO <sub>3</sub> , (HO) <sub>5</sub> IO, H <sub>4</sub> I <sub>2</sub> O <sub>7</sub>	Perhalates

<sup>(a)</sup>Stable only in aqueous solution.

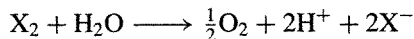
<sup>(b)</sup>HOF also known (p. 856).





**Figure 17.18** Standard reduction potentials for Cl, Br and I species in acid and alkaline solutions. For At see p. 886.

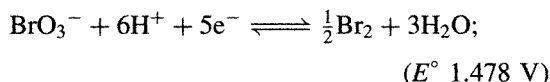
that  $E^\circ(\frac{1}{2}\text{O}_2/\text{H}_2\text{O}) = 1.229\text{ V}$  these values indicate that the potentials for the reaction.



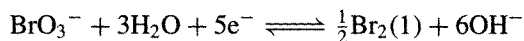
decrease in the sequence  $\text{F}_2(+1.637\text{ V}) > \text{Cl}_2(+0.129\text{ V}) > \text{Br}_2(-0.163\text{ V}) > \text{I}_2(-0.693\text{ V})$ . As already mentioned, this implies that  $\text{F}_2$  will oxidize water to  $\text{O}_2$  and the same should happen with chlorine in the absence of sluggish kinetic factors. In fact, were it not for the further fortunate circumstance of an appreciably higher overvoltage for oxygen, chlorine would not be evolved during the electrolysis of aqueous chloride solutions at low current densities: the phenomenon is clearly of great technical importance for the industrial preparation of chlorine by electrolysis of brines (p. 798).

For all other couples in Fig. 17.18 (i.e. for all couples involving oxygenated species) an increase in pH causes a dramatic reduction in  $E^\circ$  as expected (p. 435). For example, in acid solution the couple  $\text{BrO}_3^-/\frac{1}{2}\text{Br}_2(\text{l})$  refers to the

equilibrium reaction



The equilibrium constant clearly depends on the sixth power of the hydrogen-ion concentration and, when this is reduced (say to  $10^{-14}$  in 1 M alkali), the potential is likewise diminished by an amount  $\sim(RT/nF)\log_{10}[\text{H}^+]^6$ , i.e. by *ca.*  $(0.0592/5) \times 14 \times 6 \simeq 0.99\text{ V}$ . In agreement with this (Fig. 17.18) the potential at pH 14 is 0.485 V (calc  $\sim 0.49\text{ V}$ ) for the reaction



The data in Fig. 17.18 are presented in graphical form in Fig. 17.19 which shows the volt-equivalent diagrams (p. 436) for acid and alkaline solutions. It is clear from these that  $\text{Cl}_2$  and  $\text{Br}_2$  are much more stable towards disproportionation in acid solution (concave angle at  $\text{X}_2$ ) than in alkaline solutions (convex angle of

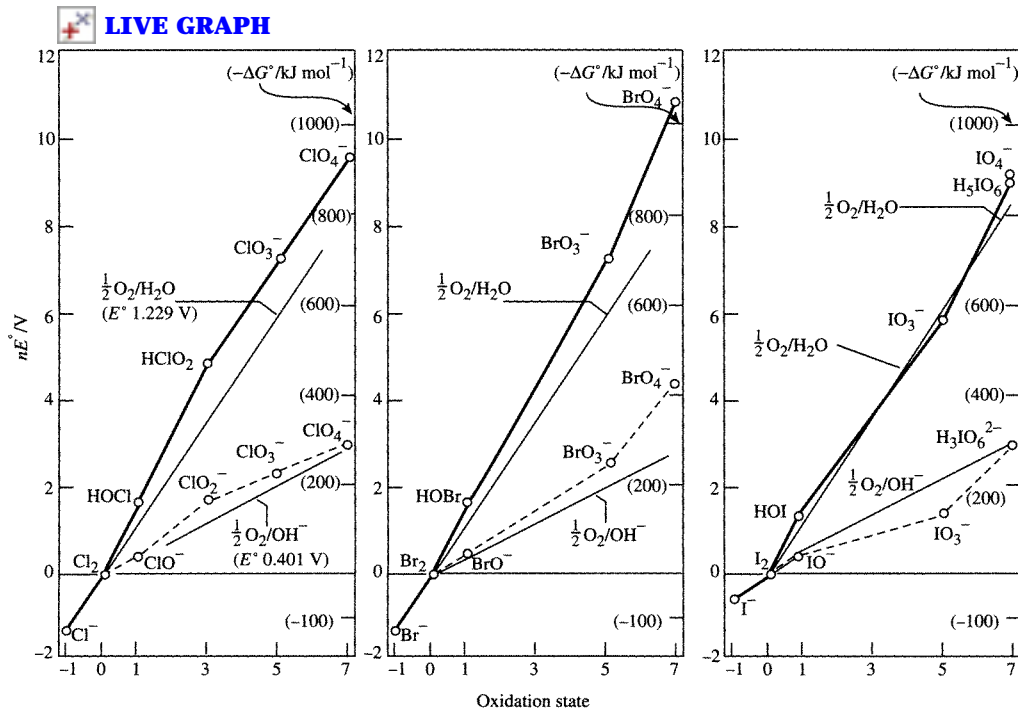
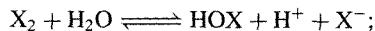


Figure 17.19 Volt-equivalent diagrams for Cl, Br and I.

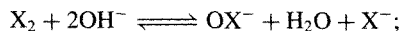
equilibrium constants:

acid solution :



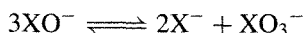
$$K_{ac} = \frac{[HOX][H^+][X^-]}{[X_2]}$$

alkaline solution :

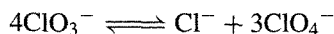


$$K_{alk} = \frac{[OX^-][X^-]}{[X_2][OH^-]^2}$$

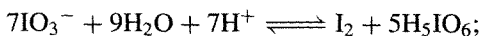
For  $Cl_2$ ,  $Br_2$  and  $I_2$ ,  $K_{ac}$  is  $4.2 \times 10^{-4}$ ,  $7.2 \times 10^{-9}$  and  $2.0 \times 10^{-13} \text{ mol}^2 \text{ l}^{-2}$  respectively, thereby favouring the free halogens, whereas  $K_{alk}$  is  $7.5 \times 10^{15}$ ,  $2 \times 10^8$  and  $30 \text{ mol}^{-1} \text{ l}$  respectively, indicating a tendency to disproportionation which is overwhelming for  $Cl_2$  but progressively less pronounced for  $Br_2$  and  $I_2$ . In actuality the situation is somewhat more complicated because of the tendency of the hypohalite ions themselves to disproportionate further to produce the corresponding halite ions:



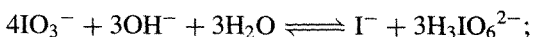
The equilibrium constant for this reaction is very favourable in each case:  $10^{27}$  for  $ClO^-$ ,  $10^{15}$  for  $BrO^-$ , and  $10^{20}$  for  $IO^-$ . However, particularly in the case of  $ClO^-$ , the rate of disproportionation is slow at room temperature and only becomes appreciable above  $70^\circ$ . Similarly, the disproportionation



has an equilibrium constant of  $10^{20}$  but the reaction is very slow even at  $100^\circ$ . By contrast, as indicated by the concavity of the volt-equivalent curve at  $BrO_3^-$  and  $IO_3^-$  (Fig. 17.19), the bromate and iodate ions are stable with respect to disproportionation (in both acid and alkaline solutions), e.g.:

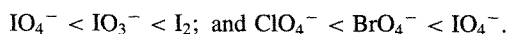
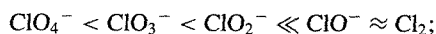


$$K = 10^{-85} \text{ mol}^{-8} \text{ l}^8$$



$$K = 10^{-44} \text{ mol}^{-3} \text{ l}^3$$

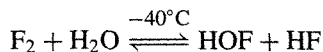
More detailed consideration of these various equilibria and other redox reactions of the halogen oxoacids will be found under the separate headings below. As expected, the rates of redox reactions of the halogen oxyanions will depend, sometimes crucially, on the precise conditions used. However, as a very broad generalization, they tend to become progressively faster as the oxidation state of the halogen decreases, i.e.:



The strengths of the monobasic acids increase rapidly with increase in oxidation state of the halogen in accordance with Pauling's rules (p. 50). For example, approximate values of  $pK_a$  are:  $HOCl$  7.52,  $HOClO$  1.94,  $HOClO_2$  - 3,  $HOClO_3$  - 10. The  $pK_a$  values of related acids increase in the sequence  $Cl < Br < I$ .

#### Hypohalous acids, HOX, and hypohalites, $XO^-$ (98,115)

Hypofluorous acid is the most recent of the halogen oxoacids to be prepared.<sup>(116)</sup> Traces were obtained in 1968 by photolysis of a mixture of  $F_2$  and  $H_2O$  in a matrix of solid  $N_2$  at 14–20 K but weighable amounts of the compound were first obtained by M. H. Studier and E. H. Appelman in 1971 by the fluorination of ice:



The isolation of HOF depends on removing it rapidly from the reaction zone so that it is prevented from reacting further with HF,  $F_2$  or  $H_2O$  (see below). The method used was to recirculate  $F_2$  at  $\sim 100 \text{ mmHg}$  through a Kel-F U-tube filled with moistened Räschi rings cut from Teflon "spaghetti" tubing (Kel-F is polymerized chlorotrifluoroethene; Teflon is polymerized tetrafluoroethene). The U-tube was held at about  $-40^\circ C$  and the effluent was passed through U-tubes cooled to  $-50^\circ$  and  $-79^\circ$  to

<sup>116</sup> E. H. APPELMAN, *Acc. Chem. Res.* 6, 113–7 (1973).

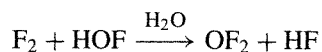
remove water and HF, and, finally, through a U-tube at  $-183^\circ$  to trap the HOF. The use of the  $-50^\circ$  trap was found to be critical because without it all of the HOF was caught in the  $-79^\circ$  with the  $\text{H}_2\text{O}$ , from which it could not be isolated because of subsequent reaction.

HOF is a white solid which melts at  $-117^\circ$  to a pale-yellow liquid. Its bp (extrap) is somewhat below room temperature and its volatility is thus comparable to that of HF with which it is always slightly contaminated. Spectroscopic data establish a nonlinear structure with H–O 96.4 pm, O–F 144.2 pm, and bond angle H–O–F  $97.2^\circ$ : this is the smallest known bond angle at an unrestricted O atom (cf. H–O–H  $104.7^\circ$ , F–O–F  $103.2^\circ$ ). It has been suggested that this arises in part from electrostatic attraction of the 2 terminal atoms, since nmr data lead to a charge of  $\sim +0.5e$  on H and  $\sim -0.5e$  on F. The negative charge on F is intermediate between those estimated for F in HF and  $\text{OF}_2$  and this emphasizes the strictly formal nature of the +1 oxidation state for F in HOF. Subsequently, the crystal structure of HOF was determined at  $-160^\circ$  in an experimental *tour de force*.<sup>(117)</sup> The dimensions were similar to those found for the gaseous molecule except for the expected artefact of a slightly shorter H–O distance due to the X-ray method (H–O 0.78 pm, O–F 144.2 pm, angle HOF  $101^\circ$ ). The molecules are arranged in chains along a screw axis parallel to the *b* axis of the crystal as a result of almost linear O–H $\cdots$ O bonds (angle  $163^\circ$ , O $\cdots$ O 289.5 pm).

The most prominent chemical property of HOF is its instability. It decomposes spontaneously (sometimes explosively) to HF and  $\text{O}_2$  with a half-life of *ca.* 30 min in a Teflon apparatus at room temperature and 100 mmHg. It reacts rapidly with water to produce HF,  $\text{H}_2\text{O}_2$  and  $\text{O}_2$ ; in dilute aqueous acid  $\text{H}_2\text{O}_2$  is the predominant product whereas in alkaline solution  $\text{O}_2$  is the principal O-containing product. The kinetics of these processes have been studied and, by use of  $^{18}\text{O}$ -enriched  $\text{H}_2\text{O}_2$ , it has

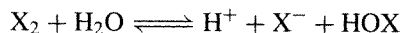
been shown, uniquely, that the  $\text{O}_2$  formed in the reaction,  $[\text{HOF} + \text{H}_2\text{O}_2 \rightarrow \text{O}_2 + \text{HF} + \text{H}_2\text{O}]$ , contains a substantial amount of oxygen from the HOF.<sup>(118)</sup>

HOF reacts with HF to reverse the equilibrium used in its preparation. It does not dehydrate to its formal anhydride  $\text{OF}_2$  but in the presence of  $\text{H}_2\text{O}$  it reacts with  $\text{F}_2$  to form this species.

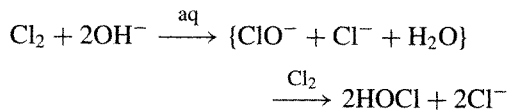


This reaction does not occur in the gas phase, however, in the absence of  $\text{H}_2\text{O}$ .

By contrast with the elusive though isolable HOF, the history of HOCl goes back over two centuries to the earliest experiments of C. W. Scheele with  $\text{Cl}_2$  in 1774 (p. 792), and the bleaching and sterilizing action of hypochlorites have long been used both industrially and domestically. HOCl, HOBr and HOI are all highly reactive, relatively unstable compounds that are known primarily in aqueous solutions. The most convenient preparation of such solutions is by perturbing the hydrolytic disproportionation equilibrium (p. 856):



by addition of  $\text{HgO}$  or  $\text{Ag}_2\text{O}$  so as to remove the halide ions. On an industrial scale, aqueous solutions of HOCl (containing  $\text{Cl}^-$ ) are readily prepared by reacting  $\text{Cl}_2$  with aqueous alkali. With strong bases  $\{\text{NaOH}, \text{Ca}(\text{OH})_2\}$  the reaction proceeds via the intermediate formation of hypochlorite, but this intermediate product is not formed with weaker bases such as  $\text{NaHCO}_3$  or  $\text{CaCO}_3$ :

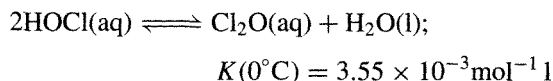


Chloride-free solutions (up to 5 M concentration) can be made by treating  $\text{Cl}_2\text{O}$  with water at  $0^\circ$  or industrially by passing  $\text{Cl}_2\text{O}$  gas into water. In fact, concentrated solutions of HOCl also contain appreciable amounts of  $\text{Cl}_2\text{O}$  which can form a

<sup>117</sup> W. POLL, G. PAWELKE, D. MOOTZ and E. H. APPELMAN, *Angew. Chem. Int. Edn. Engl.* **27**, 392–3 (1988).

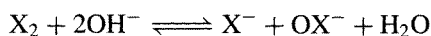
<sup>118</sup> E. H. APPELMAN and R. C. THOMPSON, *J. Am. Chem. Soc.*, **106**, 4167–72 (1984).

separate layer and which is probably the source of the yellow colour of such solutions:

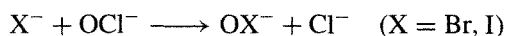


Organic solutions can be obtained in high yield by extracting HOCl from  $\text{Cl}^-$ -containing aqueous solutions into polar solvents such as ketones, nitriles or esters. Electrodialysis using semipermeable membranes affords an alternative route.

Solutions of the corresponding hypohalites can be made by the rapid disproportionation of the individual halogens in cold alkaline solutions (p. 856):



Such solutions are necessarily contaminated with halide ions and with the products of any subsequent decomposition of the hypohalite anions themselves. Alternative routes are the electrochemical oxidation of halides in cold dilute solutions or the chemical oxidation of bromides and iodides:

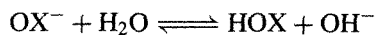


Hypochlorites can also be made by careful neutralization of aqueous solutions of hypochlorous acid or  $\text{Cl}_2\text{O}$ .

The most stable solid hypochlorites are those of Li, Ca, Sr and Ba (see below).  $\text{NaOCl}$  has only poor stability and cannot be isolated pure;  $\text{KOCl}$  is known only in solution, Mg yields a basic hypochlorite and impure Ag and Zn hypochlorites have been reported. Hydrated salts are also known. Solid, yellow, hydrated hypobromites  $\text{NaOBr} \cdot x\text{H}_2\text{O}$  ( $x = 5, 7$ ) and  $\text{KOBBr} \cdot 3\text{H}_2\text{O}$  can be crystallized from solutions obtained by adding  $\text{Br}_2$  to cold conc solutions of MOH but the compounds decompose above  $0^\circ\text{C}$ . No solid metal hypoiodites have yet been isolated.

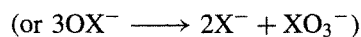
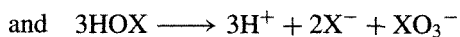
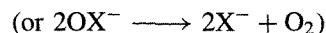
HOCl is more stable than HOBr and HOI and its microwave spectrum in the gas phase confirms the expected nonlinear geometry with H–O 97 pm, O–Cl 169.3 pm, and angle H–O–Cl  $103 \pm 3^\circ$  (cf. HOF, p. 857). All three

hypohalous acids are weak and solutions of their salts are therefore alkaline since the equilibrium



lies well to the right. Except at high pH, hypohalite solutions contain significant amounts of the undissociated acid. Approximate values for the acid dissociation constants  $K_a$  at room temperature are HOCl  $2.9 \times 10^{-8}$ , HOBr  $5 \times 10^{-9}$ , HOI  $\sim 10^{-11}$ ; these values are close to those of many  $\alpha$ -aminoacids and may also be compared with carbonic acid  $K_a$   $4.3 \times 10^{-7}$ , which is some 10 times stronger than HOCl, and phenol, which has  $K_a$   $1.3 \times 10^{-10}$ .

The manner and rate of decomposition of hypohalous acids (and hypohalite ions) in solution are much influenced by the concentration, pH and temperature of the solutions, by the presence or absence of salts which can act as catalysts, promoters or activators, and by light quanta. The main competing modes of decomposition are:



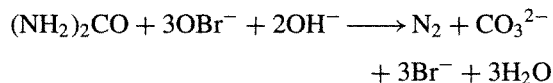
The acids decompose more readily than the anions so hypohalites are stabilized in basic solutions. The stability of the anions diminishes in the sequence  $\text{ClO}^- > \text{BrO}^- > \text{IO}^-$ .

Hypochlorites are amongst the strongest of the more common oxidizing agents and they react with inorganic species, usually by the net transfer of an O atom. Kinetic studies suggest that the oxidizing agent can be either HOCl or  $\text{OCl}^-$  in a given reaction, but rarely both simultaneously. Some typical examples are in Table 17.21. Hypochlorites react with ammonia and organic amino compounds to form chloramines. The characteristic "chlorine" odour of water that has been sterilized with hypochlorite is, in fact, due to chloramines produced from attack on bacteria. By contrast, hypobromites

**Table 17.21** Oxidation of inorganic substrates with HOCl or OCl<sup>-</sup>

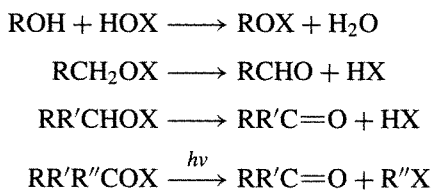
HOCl		OCl <sup>-</sup>	
Substrate	Products	Substrate	Products
HCO <sub>2</sub> <sup>-</sup>	CO <sub>3</sub> <sup>2-</sup>	ClO <sup>-</sup>	ClO <sub>2</sub> <sup>-</sup>
HC <sub>2</sub> O <sub>4</sub> <sup>-</sup>	CO <sub>2</sub>	ClO <sub>2</sub> <sup>-</sup>	ClO <sub>3</sub> <sup>-</sup>
OCN <sup>-</sup>	CO <sub>3</sub> <sup>2-</sup> , N <sub>2</sub> , NO <sub>3</sub> <sup>-</sup>	CN <sup>-</sup>	OCN <sup>-</sup>
NH <sub>3</sub>	NCl <sub>3</sub>	NH <sub>3</sub>	NH <sub>2</sub> Cl
NO <sub>2</sub> <sup>-</sup>	NO <sub>3</sub> <sup>-</sup>	SO <sub>3</sub> <sup>2-</sup>	SO <sub>4</sub> <sup>2-</sup>
H <sub>2</sub> O <sub>2</sub>	O <sub>2</sub>	IO <sub>3</sub> <sup>-</sup>	IO <sub>4</sub> <sup>-</sup>
S	SO <sub>4</sub> <sup>2-</sup>	Mn <sup>2+</sup>	MnO <sub>4</sub> <sup>-</sup>
Br <sup>-</sup>	Br <sub>2</sub> (acid)	Br <sup>-</sup>	OBr <sup>-</sup> , BrO <sub>3</sub> <sup>-</sup> (alkaline)
I <sup>-</sup>	I <sub>2</sub> (acid)	I <sup>-</sup>	OI <sup>-</sup> , IO <sub>3</sub> <sup>-</sup> (alkaline)

oxidize amines quantitatively to N<sub>2</sub>, a reaction that is exploited in the analysis of urea:



Other uses of hypohalous acids and hypohalites are described in the Panel.

This section concludes with a reminder that, in addition to the hypohalous acids HOX and metal hypohalites M(OX)<sub>n</sub>, various covalent (molecular) hypohalites are known. Hypochlorites are summarized in Table 17.22. All are volatile liquids or gases at room temperature and are discussed elsewhere (see Index). Organic hypohalites are unstable and rapidly expel HX or RX to form the corresponding aldehyde or ketone:



*Halous acids, HOXO, and halites,*  
XO<sub>2</sub><sup>-</sup> (98,115,119,120)

Chlorous acid is the least stable of the oxoacids of chlorine; it cannot be isolated but is known in dilute aqueous solution. HOBrO and HOIO are even less stable, and, if they exist at all, have only a fleeting presence in aqueous solutions. Several chlorites have been isolated and NaClO<sub>2</sub> is sufficiently stable to be manufactured as an article of commerce on the kilotonne pa scale. Little reliable information is available on bromites and still less is established for iodites which are essentially non-existent.

HClO<sub>2</sub> is formed (together with HClO<sub>3</sub>) during the decomposition of aqueous solutions of ClO<sub>2</sub> (p. 847) but the best laboratory preparation is to treat an aqueous suspension of Ba(ClO<sub>2</sub>)<sub>2</sub> with

<sup>119</sup> G. GORDON, R. G. KIEFFER and D. H. ROSENBLATT, *Progr. Inorg. Chem.* **15**, 201–86 (1972). The first half of this review deals with the aqueous solution chemistry of chlorous acid and chlorites.

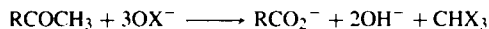
<sup>120</sup> F. SOLYMOSI, *Structure and Stability of Salts of the Halogen Oxyacids in the Solid Phase*, Wiley, UK, 1978, 468 pp.

**Table 17.22** Physical properties of some molecular hypochlorites

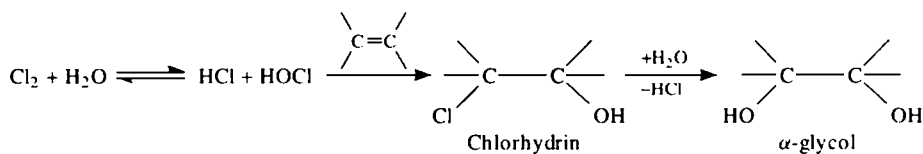
Compound	MP/°C	BP/°C	Compound	MP/°C	BP/°C
ClONO <sub>2</sub>	-107	18	ClOSeF <sub>5</sub>	-115	31.5
ClOClO <sub>3</sub>	-117	44.5	ClOTeF <sub>5</sub>	-121	38.5
ClOSO <sub>2</sub> F	-84.3	45.1	ClOOSF <sub>5</sub>	-130	26.4
ClOSF <sub>5</sub>	—	8.9	ClOOCF <sub>3</sub>	-132	-22

### Some Uses of Hypohalous Acids and Hypohalites

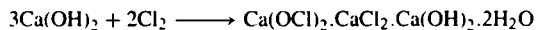
In addition to the applications indicated on p. 858, hypohalous acids are useful halogenating agents for both aromatic and aliphatic compounds. HOBr and HOI are usually generated *in situ*. The ease of aromatic halogenation increases in the sequence  $\text{OCl}^- < \text{OBr}^- < \text{OI}^-$  and is facilitated by salts of Pb or Ag. Another well-known reaction of hypohalites is their cleavage of methyl ketones to form carboxylates and haloform:



This is the basis of the iodoform test for the  $\text{CH}_3\text{CO}$  group. In addition to these reactions there is considerable industrial use for HOCl and hypochlorites in the manufacture of hydrazine (p. 427), chlorhydrins and  $\alpha$ -glycols:



By far the largest tonnage of hypochlorites is used for bleaching and sterilizing. "Liquid bleach" is an alkaline solution of NaOCl (pH  $\geq 11$ ); domestic bleaches have about 5% "available chlorine" content<sup>†</sup> whereas small-scale commercial installations such as laundries use  $\sim 12\%$  concentration. Chlorinated trisodium phosphate, which is a crystalline efflorescent product of approximate empirical composition  $(\text{Na}_3\text{PO}_4 \cdot 11\text{H}_2\text{O})_4 \cdot \text{NaOCl}$ , has 3.5–4.5% available Cl and is used in automatic dishwasher detergents, scouring powders, and acid metal cleaners for dairy equipment. Paper and pulp bleaching is effected by "bleach liquor", a solution of  $\text{Ca}(\text{OCl})_2$  and  $\text{CaCl}_2$ , yielding  $\sim 85 \text{ g l}^{-1}$  of "available chlorine". Powdered calcium hypochlorite,  $\text{Ca}(\text{OCl})_2 \cdot 2\text{H}_2\text{O}$  (70% available Cl), is used for swimming-pool sanitation whereas "bleaching powder",  $\text{Ca}(\text{OCl})_2 \cdot \text{CaCl}_2 \cdot \text{Ca}(\text{OH})_2 \cdot 2\text{H}_2\text{O}$  (obtained by the action of  $\text{Cl}_2$  gas on slaked lime) contains 35% available Cl and is used for general bleaching and sanitation:



The speciality chemical LiOCl (40% "Cl") is used when calcium is contra-indicated, such as in the sanitation of hard water and in some dairy applications. Some idea of the scale of these applications can be gained from the following production figures which relate to the USA:<sup>(98)</sup>

LiOCl  $\sim 2500$  tonnes pa. Price (1993)  $\sim \$ 2.80/\text{kg}$ .

NaOCl  $\sim 250000$  tpa (on a dry basis) used mainly for household liquid bleach, laundries, disinfection of swimming pools, municipal water supplies and sewage, and the industrial manufacture of  $\text{N}_2\text{H}_4$  and organic chemicals.

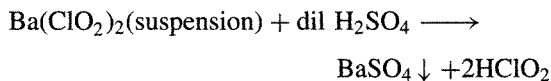
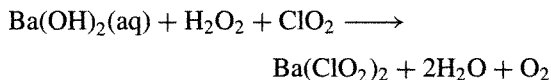
NaOCl  $(\text{Na}_3\text{PO}_4 \cdot 11\text{H}_2\text{O})_4$  was commercialized in 1930 and demand rose to 81000 tonnes in 1973. Use has dropped sharply since about 1980 (37000 tonnes in 1988, price  $\$ 0.70/\text{kg}$ ).

$\text{Ca}(\text{OCl})_2 \sim 85000$  tpa plus production facilities in numerous other countries (e.g. the USSR, Japan, South Africa and Canada).

Bleaching power is now much less used than formerly in highly industrialized countries but is still manufactured on a large scale in less-developed regions. In the USA its production peaked at 133000 tonnes in 1923 but had fallen to 23600 tonnes by 1955 and has not been reported since, though  $\sim 1160$  tonnes per annum were imported during the 1980s.

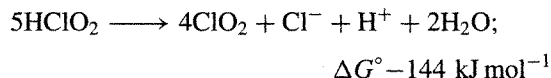
<sup>†</sup>"Available chlorine" content is defined as the weight of  $\text{Cl}_2$  which liberates the same amount of  $\text{I}_2$  from HI as does a given weight of the compound; it is often expressed as a percentage. For example, from the two (possibly hypothetical) stoichiometric equations  $\text{Cl}_2 + 2\text{HI} \rightarrow \text{I}_2 + 2\text{HCl}$  and  $\text{LiOCl} + 2\text{HI} \rightarrow \text{I}_2 + \text{LiCl} + \text{H}_2\text{O}$  it can be seen that 1 mol of  $\text{I}_2$  is liberated by 70.92 g  $\text{Cl}_2$  or by 58.4 g LiOCl. Whence the "available chlorine" content of pure LiOCl is  $(70.92/58.4) \times 100 = 121\%$ . The commercial product is usually diluted by sulfates to about one-third of this strength (see below).

dilute sulfuric acid:

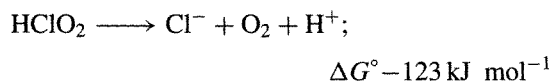
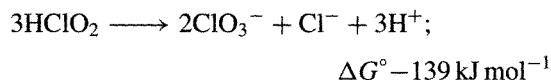


Evidence for the undissociated acid comes from spectroscopic data but the solutions cannot be concentrated without decomposition.  $\text{HClO}_2$  is a moderately strong acid  $K_a(25^\circ\text{C}) 1.1 \times 10^{-2}$  (cf  $\text{H}_2\text{SeO}_4 K_a 1.2 \times 10^{-2}$ ,  $\text{H}_4\text{P}_2\text{O}_7 K_a 2.6 \times 10^{-2}$ ).

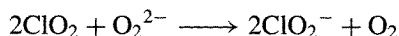
The decomposition of chlorous acid depends sensitively on its concentration, pH and the presence of catalytically active ions such as  $\text{Cl}^-$  which is itself produced during the decomposition. The main mode of decomposition (particularly if  $\text{Cl}^-$  is present) is to form  $\text{ClO}_2$ :



Competing modes produce  $\text{ClO}_3^-$  or evolve  $\text{O}_2$ :



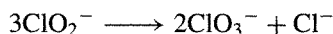
Metal chlorites are normally made by reduction of aqueous solutions of  $\text{ClO}_2$  in the presence of the metal hydroxide or carbonate. As with the preparation of  $\text{Ba(ClO}_2)_2$  above, the reducing agent is usually a peroxide since this adds no contaminant to the resulting chlorite solution:



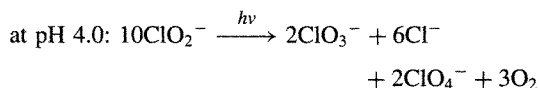
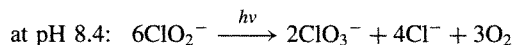
The  $\text{ClO}_2^-$  ion is nonlinear, as expected, and X-ray studies of  $\text{NH}_4\text{ClO}_2$  (at  $-35^\circ$ ) and of  $\text{AgClO}_2$  lead to the dimensions  $\text{Cl}-\text{O}$  156 pm, angle  $\text{O}-\text{Cl}-\text{O}$   $111^\circ$ . The chlorites of the alkali metals and alkaline earth metals are colourless or pale yellow. Heavy metal chlorites tend to explode or detonate when heated or struck (e.g. those of  $\text{Ag}^+$ ,  $\text{Hg}^+$ ,  $\text{Tl}^+$ ,  $\text{Pb}^{2+}$  and also those of  $\text{Cu}^{2+}$  and  $\text{NH}_4^+$ ). Sodium chlorite is the only one to

have sufficient stability and to be sufficiently inexpensive to be a major article of commerce (see below).

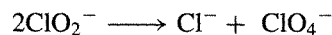
Anhydrous  $\text{NaClO}_2$  crystallizes from aqueous solutions above  $37.4^\circ$  but below this temperature the trihydrate is obtained. The commercial product contains about 80%  $\text{NaClO}_2$ . The anhydrous salt forms colourless deliquescent crystals which decompose when heated to  $175-200^\circ$ : the reaction is predominantly a disproportionation to  $\text{ClO}_3^-$  and  $\text{Cl}^-$  but about 5% of molecular  $\text{O}_2$  is also released (based on the  $\text{ClO}_2^-$  consumed). Neutral and alkaline aqueous solutions of  $\text{NaClO}_2$  are stable at room temperature (despite their thermodynamic instability towards disproportionation as evidenced by the reduction potentials on p. 854). This is a kinetic activation-energy effect and, when the solutions are heated near to boiling, slow disproportionation occurs:



Photochemical decomposition is rapid and the products obtained depend on the pH of the solution;



The stoichiometry in acid solution implies that, in addition to the more usual disproportionation into  $\text{ClO}_3^-$  and  $\text{Cl}^-$ , the following disproportionation also occurs:



The mechanisms of these various reactions have been the object of many studies.<sup>(98,115,119)</sup>

The main commercial applications of  $\text{NaClO}_2$  are in the bleaching and stripping of textiles, and as a source of  $\text{ClO}_2$  where required volumes are comparatively small. It is also used as an oxidant for removal of nitrogen oxide pollutants from industrial off-gases. The specific oxidizing properties of  $\text{NaClO}_2$  towards certain malodorous or toxic compounds such as unsaturated aldehydes, mercaptans, thioethers,

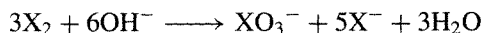


H<sub>2</sub>S and HCN have likewise led to its use for scrubbing the off-gases of processes where these noxious pollutants are formed. Production statistics are rather sparse but the main production plants are in Europe, which produced some 11 000 tonnes pa in 1990 and the USA, where production is expected to exceed 10 000 tpa in 1995. Other major producers are in Japan (~5000 tpa) and Canada (2700 tpa in 1990). The 1991 price for technical grade NaClO<sub>2</sub> in the USA was \$2.65/kg.

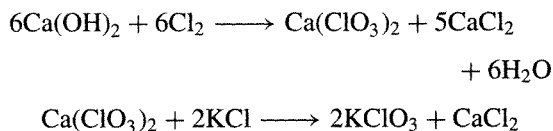
Crystalline barium bromite Ba(BrO<sub>2</sub>)<sub>2</sub>.H<sub>2</sub>O was first isolated in 1959; it can be made by treating the hypobromite with Br<sub>2</sub> at pH 11.2 and 0°C, followed by slow evaporation. Sr(BrO<sub>2</sub>)<sub>2</sub>.2H<sub>2</sub>O was obtained similarly.

### *Halic acids, HOXO<sub>2</sub>, and halates, XO<sub>3</sub><sup>-</sup>* (121,122)

Disproportionation of X<sub>2</sub> in hot alkaline solution has long been used to synthesize chlorates and bromates (see oxidation state diagrams, p. 855):

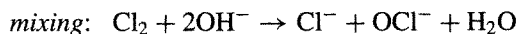
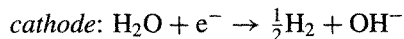
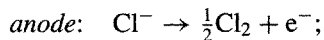


For example, J. von Liebig developed the technical preparation of KClO<sub>3</sub> by passing Cl<sub>2</sub> into a warm suspension of Ca(OH)<sub>2</sub> and then adding KCl to enable the less-soluble chlorate to crystallize on cooling:



However, only one-sixth of the halogen present is oxidized and alternative routes are more generally preferred for large-scale manufacture. Thus, the most important halate, NaClO<sub>3</sub>, is manufactured

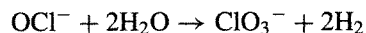
on a huge scale<sup>†</sup> by the electrolysis of brine in a diaphragmless cell which promotes efficient mixing. Under these conditions, the Cl<sub>2</sub> produced by anodic oxidation of Cl<sup>-</sup> reacts with cathodic OH<sup>-</sup> to give hypochlorite which then either disproportionates or is itself further anodically oxidized to ClO<sub>3</sub><sup>-</sup>:



*further disproportionation:*



*further anodic oxidation:*



Modern cells employ arrays of anodes (TiO<sub>2</sub> coated with a noble metal) and cathodes (mild steel) spaced 3 mm apart and carrying current at 2700 A m<sup>-2</sup> into brine (80–100 g l<sup>-1</sup>) at 60–80°C. Under these conditions current efficiency can reach 93% and 1 tonne of NaClO<sub>3</sub> can be obtained from 565 kg NaCl and 4535 kWh of electricity. The off-gas H<sub>2</sub> is also collected.

Bromates and iodates are prepared on a much smaller scale, usually by chemical oxidation. For example, Br<sup>-</sup> is oxidized to BrO<sub>3</sub><sup>-</sup> by aqueous hypochlorite (conveniently effected by passing

<sup>†</sup> World production of NaClO<sub>3</sub> (1989–91) exceeds 2 billion tonnes pa, Canada alone producing some 872 000 tpa, USA 630 000 tpa and Europe 421 000 tpa. Consumption in the USA exceeds production by some 50%, the rest being imported. The 1991 price (~\$480/tonne) was similar in both North America and Europe where, interestingly, the main consumers are Finland (156 800 tpa) and Sweden (109 700 tpa). The overwhelming use of NaClO<sub>3</sub> (95% in the USA) is in the manufacture of ClO<sub>2</sub>, mainly for bleaching paper pulp (p. 846). Other uses are to make perchlorates and other chlorates (3%), in uranium production (1% but declining sharply) and for agricultural uses (0.7%) such as herbicides, cotton defoliant and soya-bean desiccants. The use of NaClO<sub>3</sub> in pyrotechnic formulations is hampered by its hygroscopicity. KClO<sub>3</sub> does not suffer this disadvantage and is unexcelled as an oxidizer in fireworks and flares, the colours being obtained by admixture with salts of Sr (red), Ba (green), Cu (blue), etc. In addition KClO<sub>3</sub> is a crucial component in the head of "safety matches" (KClO<sub>3</sub>, S, Sb<sub>2</sub>S<sub>3</sub>, powdered glass and dextrin paste). Its price is very similar to that of NaClO<sub>3</sub>.

<sup>121</sup> Ref. 23, pp. 1418–35, Halic acids and halates.

<sup>122</sup> S. K. MENDIRATTA and B. L. DUNCAN, Chloric acid and chlorates, *Kirk-Othmer Encyclopedia of Chemical Technology*, 4th edn., Vol. 5, pp. 998–1016, Wiley, New York, 1993.

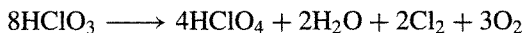
Cl<sub>2</sub> into alkaline solutions of Br<sup>-</sup>). Iodates can be prepared either by direct high-pressure oxidation of alkali metal iodides with oxygen at 600° or by oxidation of I<sub>2</sub> with chlorates:



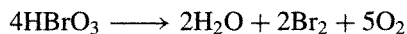
Salts of other metals are obtained by metathesis, and aqueous solutions of the corresponding acids are obtained by controlled addition of sulfuric acid to the barium salts:



Chloric acid, HClO<sub>3</sub>, is fairly stable in cold water up to about 30% concentration but, on being warmed, such solutions evolve Cl<sub>2</sub> and ClO<sub>2</sub>. Evaporation under reduced pressure can increase the concentration up to about 40% (~HClO<sub>3</sub>·7H<sub>2</sub>O) but thereafter it is accompanied by decomposition to HClO<sub>4</sub> and the evolution of Cl<sub>2</sub>, O<sub>2</sub> and ClO<sub>2</sub>:



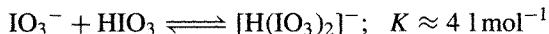
Likewise, aqueous HBrO<sub>3</sub> can be concentrated under reduced pressure to about 50% concentration (~HBrO<sub>3</sub>·7H<sub>2</sub>O) before decomposition obtrudes:



Both chloric and bromic acids are strong acids in aqueous solution ( $\text{p}K_a \lesssim 0$ ) whereas iodic acid is slightly weaker, with  $\text{p}K_a$  0.804, i.e.  $K_a$  0.157.

Iodic acid is more conveniently synthesized by oxidation of an aqueous suspension of I<sub>2</sub> either electrolytically or with fuming HNO<sub>3</sub>. Crystallization from acid solution yields colourless, orthorhombic crystals of α-HIO<sub>3</sub> which feature H-bonded pyramidal molecules of HOIO<sub>2</sub>:  $r(\text{I}-\text{O})$  181 pm,  $r(\text{I}-\text{OH})$  189 pm, angle O-I-O 101.4°, angle O-I-(OH) 97°. When heated to ~100°C iodic acid partly dehydrates to HI<sub>3</sub>O<sub>8</sub> (p. 852); this comprises an H-bonded array of composition HOIO<sub>2</sub>·I<sub>2</sub>O<sub>5</sub> in which the HIO<sub>3</sub> has almost identical dimensions to those in α-HIO<sub>3</sub>. Further heating to 200° results in complete dehydration to I<sub>2</sub>O<sub>5</sub>. In concentrated aqueous solutions

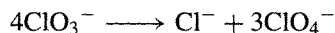
of HIO<sub>3</sub>, the iodate ions formed by deprotonation react with undissociated acid according to the equilibrium



Accordingly, crystallization of iodates from solutions containing an excess of HIO<sub>3</sub> sometimes results in the formation of hydrogen biiodates, M<sup>I</sup>H(IO<sub>3</sub>)<sub>2</sub>, or even dihydrogen triiodates, M<sup>I</sup>H<sub>2</sub>(IO<sub>3</sub>)<sub>3</sub>.

Chlorates and bromates feature the expected pyramidal ions XO<sub>3</sub><sup>-</sup> with angles close to the tetrahedral (106–107°). With iodates the interatomic angles at iodine are rather less (97–105°) and there are three short I–O distances (177–190 pm) and three somewhat longer distances (251–300 pm) leading to distorted perovskite structures (p. 963) with pseudo-sixfold coordination of iodine and piezoelectric properties (p. 58). In Sr(IO<sub>3</sub>)<sub>2</sub>·H<sub>2</sub>O the coordination number of iodine rises to 7 and this increases still further to 8 (square antiprism) in Ce(IO<sub>3</sub>)<sub>4</sub> and Zr(IO<sub>3</sub>)<sub>4</sub>.

The modes of thermal decomposition of the halates and their complex oxidation-reduction chemistry reflect the interplay of both thermodynamic and kinetic factors. On the one hand, thermodynamically feasible reactions may be sluggish, whilst, on the other, traces of catalyst may radically alter the course of the reaction. In general, for a given cation, thermal stability decreases in the sequence iodate > chlorate > bromate, but the mode and ease of decomposition can be substantially modified. For example, alkali metal chlorates decompose by disproportionation when fused:

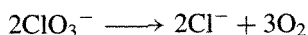


e.g. LiClO<sub>3</sub>, mp 125° (d 270°); NaClO<sub>3</sub>, mp 248° (d 265°); KClO<sub>3</sub>, mp 368° (d 400°).<sup>†</sup> However, in

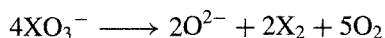
<sup>†</sup> Note, however, that thermal decomposition of NH<sub>4</sub>ClO<sub>3</sub> begins at 50°C and the compound explodes on further heating; this much lower decomposition temperature may result from prior proton transfer to give the less-stable acid: [NH<sub>4</sub>ClO<sub>3</sub> → NH<sub>3</sub> + HClO<sub>3</sub>].

A similar thermal instability afflicts NH<sub>4</sub>BrO<sub>3</sub> (d -5°) and NH<sub>4</sub>IO<sub>3</sub> (d ~ 100°).

the presence of a transition-metal catalyst such as  $\text{MnO}_2$  decomposition of  $\text{KClO}_3$  to  $\text{KCl}$  and oxygen begins at about  $70^\circ$  and is vigorous at  $100^\circ$



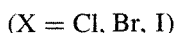
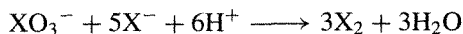
This is, indeed, a classic laboratory method for preparing small amounts of oxygen (p. 603). For bromates and iodates, disproportionation to halide and perchalate is not thermodynamically feasible and decomposition occurs either with formation of halide and liberation of  $\text{O}_2$  (as in the catalysed decomposition of  $\text{ClO}_3^-$  just considered), or by formation of the oxide:



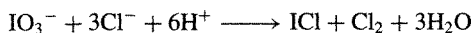
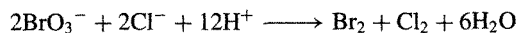
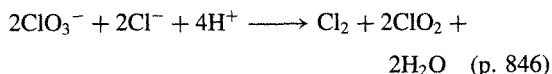
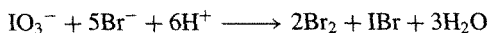
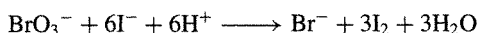
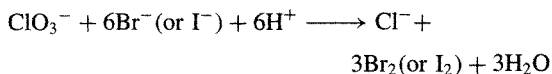
For all three halates (in the absence of disproportionation) the preferred mode of decomposition depends, again, on both thermodynamic and kinetic considerations. Oxide formation tends to be favoured by the presence of a strongly polarizing cation (e.g. magnesium, transition-metal and lanthanide halates), whereas halide formation is observed for alkali-metal, alkaline-earth and silver halates.

The oxidizing power of the halate ions in aqueous solution, as measured by their standard reduction potentials (p. 854), decreases in the sequence bromate  $\gtrsim$  chlorate  $>$  iodate but the rates of reaction follow the sequence iodate  $>$  bromate  $>$  chlorate. In addition, both the thermodynamic oxidizing power and the rate of reaction depend markedly on the hydrogen-ion concentration of the solution, being substantially greater in acid than in alkaline conditions (p. 855).

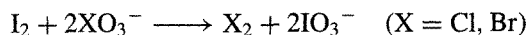
An important series of reactions, which illustrates the diversity of behaviour to be expected, is the comproportionation of halates and halides. Bromides are oxidized quantitatively to bromine and iodides to iodine, this latter reaction being much used in volumetric analysis:



Numerous variants are possible, e.g.:

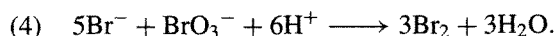
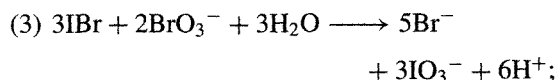
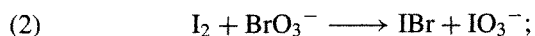


The greater thermodynamic stability of iodates enables iodine to displace  $\text{Cl}_2$  and  $\text{Br}_2$  from their halates:

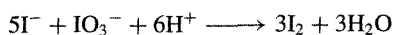


With bromate at pH 1.5–2.5 the reaction occurs in four stages:

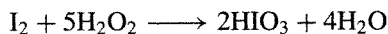
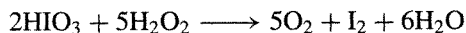
(1) an induction period in which a catalyst (probably  $\text{HOBr}$ ) is produced;



The dependence of reaction rates on pH and on the relative and absolute concentrations of reacting species, coupled with the possibility of autocatalysis and induction periods, has led to the discovery of some spectacular kinetic effects such as H. Landolt's "chemical clock" (1885): an acidified solution of  $\text{Na}_2\text{SO}_3$  is reacted with an excess of iodic acid solution in the presence of starch indicator — the induction period before the appearance of the deep-blue starch-iodine colour can be increased systematically from seconds to minutes by appropriate dilution of the solutions before mixing. With an excess of sulfite, free iodine may appear and then disappear as a single pulse due to the following sequence of reactions:



A true periodic reaction was discovered by W. C. Bray in 1921 and involves the reduction of iodic acid to  $I_2$  by  $H_2O_2$  followed by the reoxidation of  $I_2$  to  $HIO_3$ :



The net reaction is the disproportionation of  $H_2O_2$  to  $H_2O + \frac{1}{2}O_2$  and the starch indicator oscillates between deep blue and colourless as the iodine concentration pulsates.

Even more intriguing is the Belousov–Zhabotinskii class of oscillating reactions some of which can continue for hours. Such a reaction was first observed in 1959 by B. P. Belousov who noticed that, in stirred sulfuric acid solutions containing initially  $KBrO_3$ , cerium(IV) sulfate and malonic acid,  $CH_2(CO_2H)_2$ , the concentrations of  $Br^-$  and  $Ce^{4+}$  underwent repeated oscillations of major proportions (e.g. tenfold changes on a time-scale which was constant but which could be varied from a few seconds to a few minutes depending on concentrations and temperature). These observations were extended by A. M. Zhabotinskii in 1964 to the bromate oxidation of several other organic substrates containing a reactive methylene group catalysed either by  $Ce^{IV}/Ce^{III}$  or  $Mn^{III}/Mn^{II}$ . Not surprisingly these reactions have attracted considerable attention, but detailed studies of their mechanisms are beyond the scope of this chapter.<sup>(123–125)</sup>

The various reactions of bromates and iodates are summarized in the schemes on p. 866.<sup>(121)</sup>

The oxidation of halates to perhalates is considered further in the next section.

### Perhalic acid and perhalates

Because of their differing structures, chemical reactions and applications, perchloric acid and

the perchlorates are best considered separately from the various periodic acids and their salts; the curious history of perbromates also argues for their individual treatment.

### Perchloric acid and perchlorates<sup>(126–128)</sup>

The most stable compounds of chlorine are those in which the element is in either its lowest oxidation state (–I) or its highest (VII): accordingly perchlorates are the most stable oxo-compounds of chlorine (see oxidation-state diagram, (p. 855) and most are extremely stable both as solids and as solutions at room temperature. When heated they tend to decompose by loss of  $O_2$  (e.g.  $KClO_4$  above  $400^\circ$ ). Aqueous solutions of perchloric acid and perchlorates are not notable oxidizing agents at room temperature but when heated they become vigorous, even violent, oxidants. Considerable CAUTION should therefore be exercised when handling these materials, and it is crucial to avoid the presence of readily oxidizable organic (or inorganic) matter since this can initiate reactions of explosive intensity.

On an industrial scale, perchlorates are now invariably produced by the electrolytic oxidation of  $NaClO_3$  (see Panel, p. 867). Alternative routes have historical importance but are now only rarely used, even for small-scale laboratory syntheses.

Perchloric acid is best made by treating anhydrous  $NaClO_4$  or  $Ba(ClO_4)_2$  with concentrated HCl, filtering off the precipitated chloride and concentrating the filtrate by distillation. The azeotrope (p. 815) boils at  $203^\circ C$  and contains 71.6%  $HClO_4$  (i.e.  $HClO_4 \cdot 2H_2O$ ). The anhydrous acid is obtained by low-pressure distillation of the azeotrope ( $p < 1 \text{ mmHg} = 0.13 \text{ kPa}$ ) in an all-glass apparatus in the presence of fuming sulfuric acid. Commercially available perchloric acid is usually 60–62% ( $\sim 3.5H_2O$ ) or 70–72%

<sup>123</sup> R. J. FIELD, E. KÖRÖS and R. M. NOYES, *J. Am. Chem. Soc.* **94**, 8649–64 (1972).

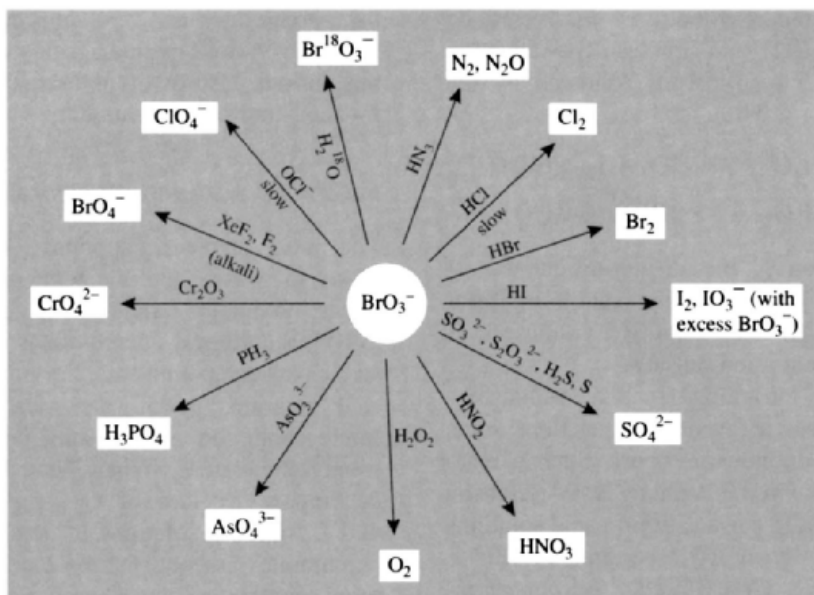
<sup>124</sup> R. M. NOYES, *J. Phys. Chem.* **94**, 4404–12 (1990).

<sup>125</sup> S. K. SCOTT, *Oscillations, Waves and Chaos in Chemical Kinetics*, Oxford Univ. Press, Oxford, 1994, 96 pp.

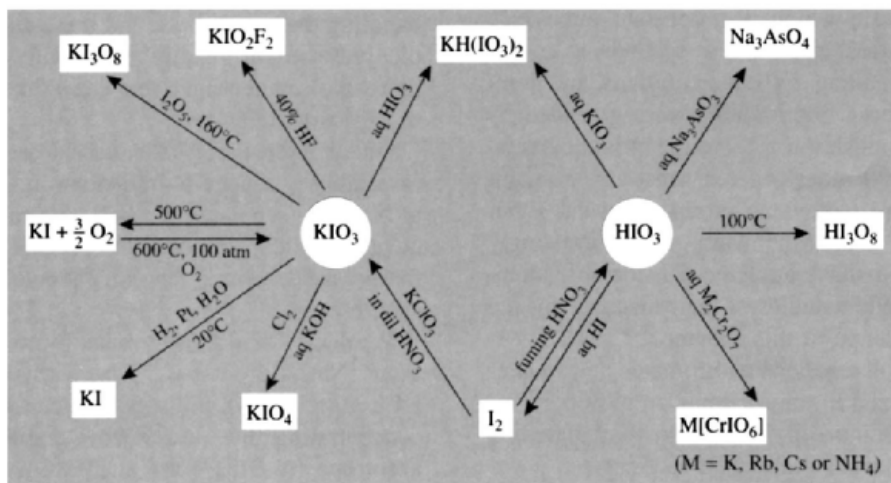
<sup>126</sup> Ref. 23, pp. 1435–60, Perhalic acids and perhalates.

<sup>127</sup> F. SOLYMOSI, *Structure and Stability of Salts of Halogen Oxyacids in the Solid Phase*, Wiley, New York, 1978, 468 pp.

<sup>128</sup> A. A. SCHILT, *Perchloric Acid and Perchlorates*, Northern Illinois University Press, 1979, 189 pp.



Some reactions of aqueous bromates.



Some reactions of iodates.

( $\sim 2\text{H}_2\text{O}$ ); more concentrated solutions are hygroscopic and are also unstable towards loss of  $\text{Cl}_2\text{O}_7$  or violent decomposition by accidental impurities.

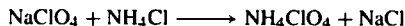
Pure  $\text{HClO}_4$  is a colourless mobile, shock-sensitive, liquid:  $d(25^\circ)$   $1.761\text{ g cm}^{-3}$ . At least 6 hydrates are known (Table 17.23). The structure of  $\text{HClO}_4$ , as determined by electron diffraction in the gas phase, is as shown in Fig. 17.20. This

molecular structure persists in the liquid phase, with some H bonding, and also in the crystalline phase, where an X-ray study at  $-160^\circ$  found three Cl–O distances of 142 pm and one of 161 pm<sup>(99)</sup> (very close to the dimensions of the extremely stable “isoelectronic” molecule,  $\text{FCIO}_3$  (140.4 and 161.9 pm, p. 879)). The (low) electrical conductivity and other physical properties of anhydrous  $\text{HClO}_4$  have been interpreted on the

### Production and Uses of Perchlorates

$\text{NaClO}_4$  is made by the electrolytic oxidation of aqueous  $\text{NaClO}_3$  using smooth Pt or  $\text{PbO}_2$  anodes and a steel cathode which also acts as the container. All other perchlorates, including  $\text{HClO}_4$ , are made either directly or indirectly from this  $\text{NaClO}_4$ . In a typical cell  $\text{NaClO}_3$  (600 g/l pH 6.5) is oxidized at 30–50°C with 90% current efficiency at 5000 A and 6.0 V with an anode current density of 3100  $\text{A m}^{-2}$  and an electrode separation of ~5 mm. The process can be either batch or continuous and energy consumption is ~2.5 kWh/kg. A small concentration of  $\text{Na}_2\text{Cr}_2\text{O}_7$  (1–5 g/l) is found to be extremely beneficial in inhibiting cathodic reduction of  $\text{ClO}_4^-$ .

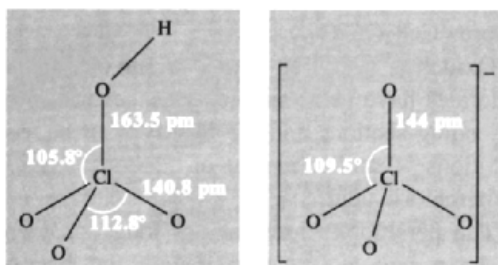
World production of perchlorates was less than 1800 tonnes pa until 1940 when wartime missile and rocket requirements boosted this tenfold. World production capacity peaked at around 40 000 tpa in 1963 but is now still above 30 000 tpa. More than half of this is converted to  $\text{NH}_4\text{ClO}_4$  for use as a propellant:



US production was severely disrupted by a series of devastating explosions in May 1988 which killed 2 people and injured several hundred.<sup>(129)</sup> Ultrapure  $\text{NH}_4\text{ClO}_4$  for physical measurements and research purposes can be made by direct neutralization of aqueous solutions of  $\text{NH}_3$  and  $\text{HClO}_4$ . One of the main current uses of  $\text{NH}_4\text{ClO}_4$  is in the Space Shuttle Programme: the two booster rockets use a solid propellant containing 70% by weight of  $\text{NH}_4\text{ClO}_4$ , this being the oxidizer for the “fuel” (powdered Al metal) which comprises most of the rest of the weight. Each shuttle launch requires about 770 tonnes of  $\text{NH}_4\text{ClO}_4$ .

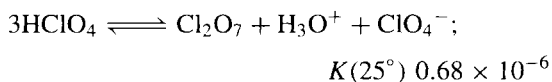
The annual consumption of 70%  $\text{HClO}_4$  is about 450 tonnes mainly for making other perchlorates. Most of the  $\text{NaClO}_4$  produced is used captively to make  $\text{NH}_4\text{ClO}_4$  and  $\text{HClO}_4$ , but about 725 tpa is used for explosives, particularly in slurry blasting formulations.

The two other perchlorates manufactured on a fairly large scale industrially are  $\text{Mg}(\text{ClO}_4)_2$  and  $\text{KClO}_4$ . The former is used as the electrolyte in “dry cells” (batteries), whereas  $\text{KClO}_4$  is a major constituent in pyrotechnic devices such as fireworks, flares, etc. Thus the white flash and thundering boom in fireworks displays are achieved by incorporating a compartment containing  $\text{KClO}_4/\text{S}/\text{Al}$ , whereas the flash powder commonly used in rock concerts and theatricals comprises  $\text{KClO}_4/\text{Mg}$ . Vivid blues, perhaps the most difficult pyrotechnic colour to achieve, are best obtained from the low temperature (< 1200° C) flame emission of  $\text{CuCl}$  in the 420–460 nm region: because of the instability of copper chlorate and perchlorate this colour is generated by ignition of a mixture containing 38%  $\text{KClO}_3$ , 29%  $\text{NH}_4\text{ClO}_3$ , and 14%  $\text{CuCO}_3$  bound with red gum (14%) and dextrin (5%).



**Figure 17.20** Structure of the gaseous molecule  $\text{HClO}_4$  and of the  $\text{ClO}_4^-$  anion.

basis of slight dissociation according to the overall equilibrium:



<sup>129</sup> R. J. SELTZER, *Chem. & Eng. News*, August 8, 7–15 (1988).

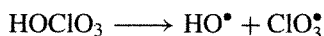
(cf.  $\text{H}_2\text{SO}_4$ , p. 711;  $\text{H}_3\text{PO}_4$ , p. 518, etc.). The monohydrate forms an H-bonded crystalline lattice  $[\text{H}_3\text{O}]^+[\text{ClO}_4]^-$  that undergoes a phase transition with rotational disorder above  $-30^\circ$ ; it melts to a viscous, highly ionized liquid at  $49.9^\circ$ . The other hydrates also feature hydroxonium ions  $[(\text{H}_2\text{O})_n\text{H}]^+$  as described more fully on p. 630. It is particularly notable that hydration does not increase the coordination number of Cl and in this perchloric acid differs markedly from periodic acid (p. 872). This parallels the difference between sulfuric and telluric acids in the preceding group (p. 782).

Anhydrous  $\text{HClO}_4$  is an extremely powerful oxidizing agent. It reacts explosively with most organic materials, ignites HI and  $\text{SOCl}_2$  and rapidly oxidizes Ag and Au. Thermal decomposition in the gas phase yields a mixture of HCl,  $\text{Cl}_2$ ,  $\text{Cl}_2\text{O}$ ,  $\text{ClO}_2$  and  $\text{O}_2$  depending on the conditions. Above  $310^\circ$  the decomposition is first

Table 17.23 Perchloric acid and its hydrates

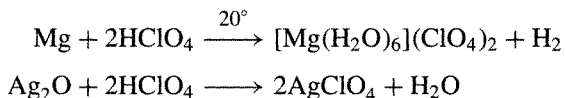
$n$ in $\text{HClO}_4 \cdot n\text{H}_2\text{O}$	Structure	MP/°C	BP/°C	$\Delta H_f^\circ/\text{kJ mol}^{-1}$
0	$\text{HOClO}_3$	-112	110 (expl)	-40.6 (liq)
0.25	$(\text{HClO}_4)_4 \cdot \text{H}_2\text{O}$	d-73.1	—	—
1	$[\text{H}_3\text{O}]^+[\text{ClO}_4]^-$	49.9	decomp	-382.2 (cryst)
2	$[\text{H}_5\text{O}_2]^+[\text{ClO}_4]^-$	-20.7	203	-688 (liq)
2.5	—	-33.1	—	—
3	$[\text{H}_7\text{O}_3]^+[\text{ClO}_4]^-$	-40.2	—	—
3.5	—	-45.9	—	—

order and homogeneous, the rate-determining step being homolytic fission of the Cl–OH bond:



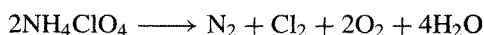
The hydroxyl radical rapidly abstracts an H atom from a second molecule of  $\text{HClO}_4$  to give  $\text{H}_2\text{O}$  plus  $\text{ClO}_4^\bullet$  and the 2 radicals  $\text{ClO}_3^\bullet$  and  $\text{ClO}_4^\bullet$  then decompose to the elements via the intermediate oxides. Above  $450^\circ$  the  $\text{Cl}_2$  produced reacts with  $\text{H}_2\text{O}$  to give  $2\text{HCl}$  plus  $\frac{1}{2}\text{O}_2$  whilst in the low-temperature range ( $150\text{--}310^\circ$ ) the decomposition is heterogeneous and second order in  $\text{HClO}_4$ .

Aqueous perchloric acid solutions exhibit very little oxidizing power at room temperature, presumably because of kinetic activation barriers, though some strongly reducing species slowly react, e.g.  $\text{Sn}^{\text{II}}$ ,  $\text{Ti}^{\text{III}}$ ,  $\text{V}^{\text{II}}$  and  $\text{V}^{\text{III}}$ , and dithionite. Others do not, e.g.  $\text{H}_2\text{S}$ ,  $\text{SO}_2$ ,  $\text{HNO}_2$ ,  $\text{HI}$  and, surprisingly,  $\text{Cr}^{\text{II}}$  and  $\text{Eu}^{\text{II}}$ . Electropositive metals dissolve with liberation of  $\text{H}_2$  and oxides of less basic metals also yield perchlorates. e.g. with 72% acid:



$\text{NO}$  and  $\text{NO}_2$  react to give  $\text{NO}^+\text{ClO}_4^-$  and  $\text{F}_2$  yields  $\text{FOClO}_3$  (p. 639).  $\text{P}_2\text{O}_5$  dehydrates the acid to  $\text{Cl}_2\text{O}_7$  (p. 850).

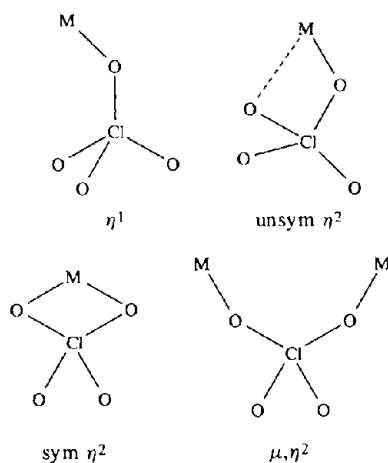
Perchlorates are known for most metals in the periodic table.<sup>(128)</sup> The alkali-metal perchlorates are thermally stable to several hundred degrees above room temperature but  $\text{NH}_4\text{ClO}_4$  deflagrates with a yellow flame when heated to  $200^\circ$ :



$\text{NH}_4\text{ClO}_4$  has a solubility in water of 20.2 g per 100 g solution at  $25^\circ$  and 135 g per 100 g liquid  $\text{NH}_3$  at the same temperature. Aqueous solubilities decrease in the sequence  $\text{Na} > \text{Li} > \text{NH}_4 > \text{K} > \text{Rb} > \text{Cs}$ ; indeed, the low solubility of the last 3 perchlorates in this series has been used for separatory purposes and even for gravimetric analysis (e.g.  $\text{KClO}_4$  1.99 g per 100 g  $\text{H}_2\text{O}$  at  $20^\circ$ ). Many of these perchlorates and those of  $\text{M}^{\text{II}}$  can also be obtained as hydrates.  $\text{AgClO}_4$  has the astonishing solubility of 557 g per 100 g  $\text{H}_2\text{O}$  at  $25^\circ$  and even in toluene its solubility is 101 g per 100 g  $\text{PhMe}$  at  $25^\circ$ . This has great advantages in the metathetic preparation of other perchlorates, particularly organic perchlorates, e.g.  $\text{RI}$  yields  $\text{ROClO}_3$ ,  $\text{Ph}_3\text{CCl}$  yields  $\text{Ph}_3\text{C}^+\text{ClO}_4^-$ , and  $\text{CCl}_4$  affords  $\text{CCl}_3\text{OCIO}_3$ .

Oxidation-reduction reactions involving perchlorates have been mentioned in several of the preceding sections and the reactivity of aqueous solutions is similar to that of aqueous solutions of perchloric acid.

The perchlorate ion was for long considered to be a non-coordinating ligand and has frequently been used to prepare “inert” ionic solutions of constant ionic strength for physicochemical measurements. Though it is true that  $\text{ClO}_4^-$  is a weaker ligand than  $\text{H}_2\text{O}$  it is not entirely toothless and, as shown schematically in Fig. 17.21, examples are known in which the perchlorate acts as a monodentate ( $\eta^1$ ), bidentate chelating ( $\eta^2$ ) and bidentate bridging ( $\mu, \eta^2$ ) ligand. The first unambiguous structural evidence for coordinated  $\text{ClO}_4^-$  was obtained in 1965 for the 5 coordinate cobalt(II)



**Figure 17.21** Coordination modes of  $\text{ClO}_4^-$  as determined by X-ray crystallography.

complex  $[\text{Co}(\text{OAsMePh}_2)_4(\eta^1\text{-OCIO}_3)_2]^{(130)}$  and this was quickly followed by a second example, the red 6-coordinate *trans* complex  $[\text{Co}(\eta^2\text{-MeSCH}_2\text{CH}_2\text{SMe})_2(\eta^1\text{-OCIO}_3)_2]^{(131)}$ . The two structures are shown in Fig. 17.22. The perchlorate ion has now been established as a monodentate ligand towards an s-block element (Ba),<sup>(132)</sup>

<sup>130</sup> P. PAULING, G. B. ROBERTSON and G. A. RODLEY, *Nature* **207**, 73–74 (1965).

<sup>131</sup> F. A. COTTON and D. L. WEAVER, *J. Am. Chem. Soc.* **87**, 4189–90 (1965).

<sup>132</sup> D. L. HUGHES, C. L. MORTIMER and M. R. TRUTER, *Acta Cryst.* **B34**, 800–7 (1978). *Inorg. Chim. Acta* **29**, 43–55 (1978).

a p-block element ( $\text{Sn}^{\text{II}}$  and  $\text{Sn}^{\text{IV}}$ ),<sup>(133)</sup> and an f-block element ( $\text{Sm}^{\text{III}}$ )<sup>(134)</sup> as well as to the d-block elements  $\text{Co}^{\text{II}}$ ,  $\text{Ni}^{\text{II}}$ ,  $\text{Cu}^{\text{II}}$  and  $\text{Ag}^{\text{I}}$ .<sup>(131,135)</sup> It is also known to function as a bidentate ligand towards Na,<sup>(136)</sup> Ba,<sup>(132)</sup>  $\text{Sn}^{\text{IV}}$ ,<sup>(133)</sup>  $\text{Sm}^{\text{III}}$ ,<sup>(134)</sup>  $\text{Ti}^{\text{IV}}$  in  $[\text{Ti}(\eta^2\text{-ClO}_4)_4]^{(137)}$  and  $\text{Ni}^{\text{II}}$  in  $[\text{Ni}(\eta^2\text{-ClO}_4)_2\text{L}_2]^+$  where L is a chiral bidentate organic ligand.<sup>(138)</sup> Sometimes both  $\eta^1$  and  $\eta^2$  modes occur in the same compound. The bidentate bridging mode occurs in the silver complex  $[\text{Ag}\{\mu, \eta^2\text{-OCl}(\text{O})_2\text{O}\}\text{-}(m\text{-xylene})_2]^{(139)}$ . The structure of appropriate segments of some of these compounds are in Fig. 17.23. The distinction between coordinated and non-coordinated (“ionic”) perchlorate is sometimes hard to make and there is an almost continuous

<sup>133</sup> R. C. ELDER, M. J. HEEG and E. DEUTSCH, *Inorg. Chem.* **17**, 427–31 (1978). C. BELIN, M. CHAABOUNI, J.-L. PASCAL, J. POTIER and J. ROZIERE, *J. Chem. Soc., Chem. Commun.*, 105–6 (1980).

<sup>134</sup> M. CIAMPOLINI, N. NARDI, R. CINI, S. MANGANI and P. ORIOLI, *J. Chem. Soc., Dalton Trans.*, 1983–6 (1979).

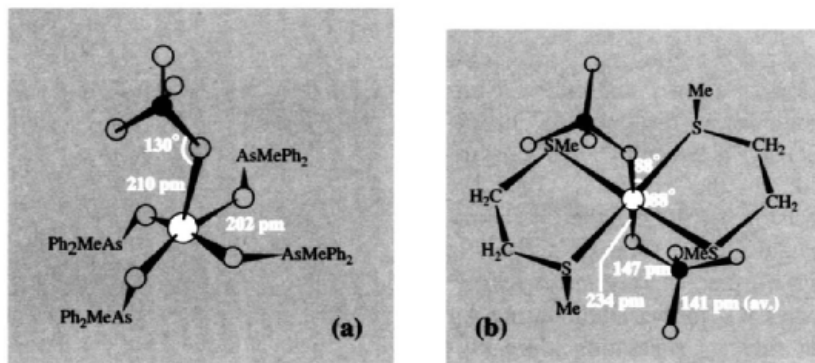
<sup>135</sup> F. MADAULE-AUBRY and G. M. BROWN, *Acta Cryst.* **B24**, 745–53 (1968). F. BIGOLI, M. A. PELLINGHELLI and A. TIRIPICCHIO, *Cryst. Struct. Comm.* **4**, 123–6 (1976). E. A. HALL GRIFFITH and E. L. AMMA, *J. Am. Chem. Soc.* **93**, 3167–72 (1971).

<sup>136</sup> H. MILBURN, M. R. TRUTER and B. L. VICKERY, *J. Chem. Soc., Dalton Trans.*, 841–6 (1974).

<sup>137</sup> M. FOURATI, M. CHAABOUNI, C. H. BELIN, M. CHARBONNEL, J.-L. PASCAL and J. POTIER, *Inorg. Chem.* **25**, 1386–90 (1986).

<sup>138</sup> D. A. HOUSE, P. J. STEEL and A. A. WATSON, *J. Chem. Soc., Chem. Commun.*, 1575–6 (1987).

<sup>139</sup> I. F. TAYLOR, E. A. HALL and E. L. AMMA, *J. Am. Chem. Soc.* **91**, 5745–9 (1969).



**Figure 17.22** The structures of monodentate perchlorate complexes (see text).



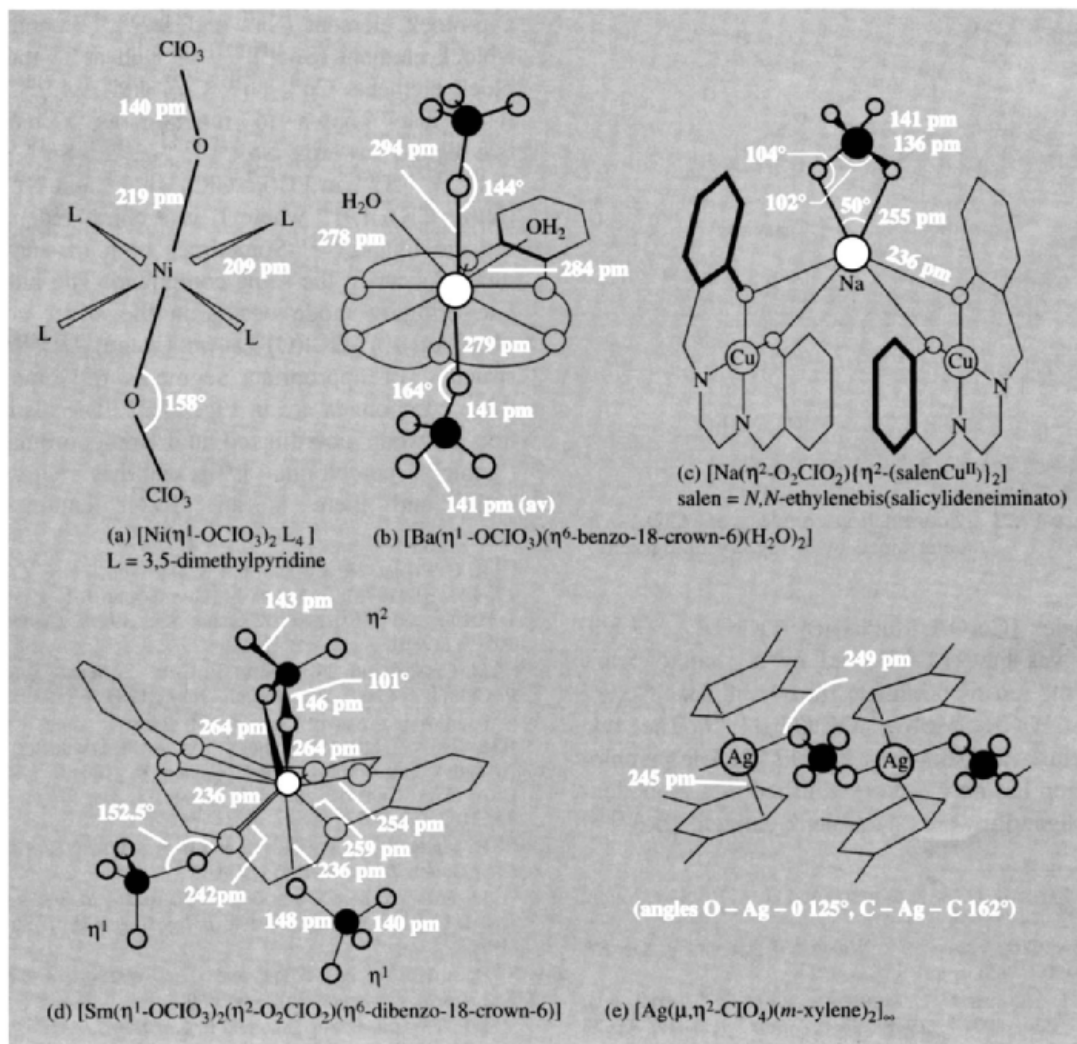
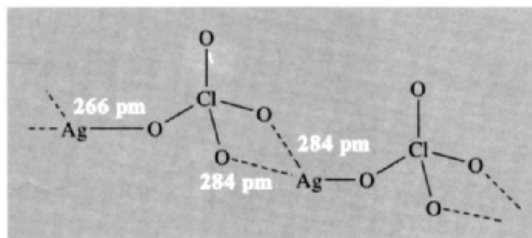


Figure 17.23 Examples of monodentate, chelating and bridging perchlorate ligands.

gradation between the two extremes. Similarly it is sometimes difficult to distinguish unambiguously between  $\eta^1$  and unsymmetrical  $\eta^2$  and, in the colourless complex  $[\text{Ag}(\text{cyclohexylbenzene})_2(\text{ClO}_4)]$ , the  $\eta^1$  bonding between Ag and  $\text{OCIO}_3$  (Ag–O 266 pm) is accompanied by a further weak symmetrical  $\eta^2$  bonding from each  $\text{ClO}_4$  to the neighbouring Ag (2Ag–O 284 pm) thereby generating a weakly-bridged chain-like structure involving pseudo- $\eta^3$  coordination of the perchlorate group.<sup>(135)</sup>



Because of its generally rather weak coordinating ability quite small changes can determine whether

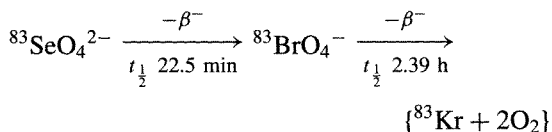
or not a perchlorate group coordinates and if so, in which mode. For example, the barium crown-ether dihydrate complex illustrated in Fig. 17.23 features 10-coordinate Ba with 6 oxygen atoms from the crown ring (Ba–O 280–285 pm), two H<sub>2</sub>O molecules (Ba–O 278 and 284 pm), and one of the perchlorates (Ba–O 294 pm) all on one side of the ring, and the other perchlorate (Ba–O 279 pm) below it. By contrast, the analogous strontium complex is a trihydrate with 9-coordinate Sr (six Sr–O from the crown ring at 266–272 pm, plus two H<sub>2</sub>O at 257, 259 pm, on one side of the ring, and one H<sub>2</sub>O on the other side at 255 pm); the ClO<sub>4</sub><sup>−</sup> ions are uncoordinated though they are H-bonded to the water molecules.

An even more dramatic change occurs with nickel(II) perchlorate complexes. Thus, the complex with 4 molecules of 3,5-dimethylpyridine (Fig. 17.23a) is blue, paramagnetic, and 6-coordinate with *trans*-(η<sup>1</sup>-OCIO<sub>3</sub>) ligands, whereas the corresponding complex with 3,4-dimethylpyridine is yellow and diamagnetic with square-planar Ni<sup>II</sup> and uncoordinated ClO<sub>4</sub><sup>−</sup> ions.<sup>(135,140)</sup> There is no steric feature of the structure which prevents the four 3,4-ligands from adopting the propeller-like configuration of the four 3,5-ligands thereby enabling Ni to accept two η<sup>1</sup>-OCIO<sub>3</sub>, or vice versa, and one must conclude that subtle differences in secondary valency forces and energies of packing are sufficient to dictate whether the complex that crystallizes is blue, paramagnetic and octahedral, or yellow, diamagnetic and square planar.

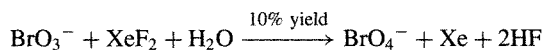
### Perbromic acid and perbromates

The quest for perbromic acid and perbromates and the various reasons adduced for their apparent non-existence make fascinating and salutary reading.<sup>(116)</sup> The esoteric radiochemical synthesis of BrO<sub>4</sub><sup>−</sup> in 1968 using the β-decay of radioactive <sup>83</sup>Se, whilst not providing a viable route to macroscopic quantities of perbromate,

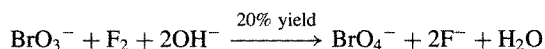
proved that this previously elusive species could exist:



This stimulated the search for a chemical synthesis. Electrolytic oxidation of aqueous LiBrO<sub>3</sub> produced a 1% yield of perbromate, but the first isolation of a solid perbromate salt (RbBrO<sub>4</sub>) was achieved by oxidation of BrO<sub>3</sub><sup>−</sup> with aqueous XeF<sub>2</sub>.<sup>(141)</sup>



The best synthesis is now by oxidation of alkaline solutions of BrO<sub>3</sub><sup>−</sup> using F<sub>2</sub> gas under rather specific conditions:<sup>(142)</sup>



In practice, F<sub>2</sub> is bubbled in until the solution is neutral, at which point excess bromate and fluoride are precipitated as AgBrO<sub>3</sub> and CaF<sub>2</sub>; the solution is then passed through a cation exchange column to yield a dilute solution of HBrO<sub>4</sub>. Several hundred grams at a time can be made by this route. The acid can be concentrated up to 6 M (55%) without decomposition and such solutions are stable for prolonged periods even at 100°. More concentrated solutions of HBrO<sub>4</sub> can be obtained but they are unstable; a white solid, possibly HBrO<sub>4</sub>·2H<sub>2</sub>O, can be crystallized.

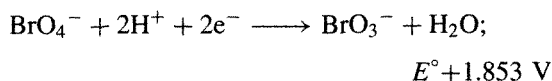
Pure KBrO<sub>4</sub> is isomorphous with KClO<sub>4</sub> and contains tetrahedral BrO<sub>4</sub><sup>−</sup> anions (Br–O 161 pm, cf. Cl–O 144 pm in ClO<sub>4</sub><sup>−</sup> and I–O 179 pm in IO<sub>4</sub><sup>−</sup>). Oxygen-18 exchange between 0.14 M KBrO<sub>4</sub> and H<sub>2</sub>O proceeds to less than 7% completion during 19 days at 94° in either acid or basic solutions and there is no sign of any increase in coordination number of Br; in this BrO<sub>4</sub><sup>−</sup> resembles ClO<sub>4</sub><sup>−</sup> rather than IO<sub>4</sub><sup>−</sup>. KBrO<sub>4</sub> is stable to 275–280° at which

<sup>140</sup> F. MADAULE-AUBRY, W. R. BUSING and G. M. BROWN, *Acta Cryst.* **B24**, 754–60 (1968).

<sup>141</sup> E. H. APPELMAN, *J. Am. Chem. Soc.* **90**, 1900–1 (1968); *Inorg. Chem.* **8**, 223–7 (1969).

<sup>142</sup> E. H. APPELMAN, *Inorg. Synth.* **13**, 1–9 (1972).

temperature it begins to dissociate into  $\text{KBrO}_3$  and  $\text{O}_2$ . Even  $\text{NH}_4\text{BrO}_4$  is stable to  $170^\circ$ . Dilute solutions of  $\text{BrO}_4^-$  show little oxidizing power at  $25^\circ$ ; they slowly oxidize  $\text{I}^-$  and  $\text{Br}^-$  but not  $\text{Cl}^-$ . More concentrated  $\text{HBrO}_4$  (3 M) readily oxidizes stainless steel and 12 M acid rapidly oxidizes  $\text{Cl}^-$ . The general inertness of  $\text{BrO}_4^-$  at room temperature stands in sharp contrast to its high thermodynamic oxidizing power, which is greater than that of any other oxohalogen ion that persists in aqueous solution. The oxidation potential is



(cf. 1.201 V for  $\text{ClO}_4^-$  and 1.653 for  $\text{IO}_4^-$ ). Accordingly, only the strongest oxidants would be expected to convert bromates to perbromates. As seen above,  $\text{F}_2/\text{H}_2\text{O}$  ( $E^\circ \sim 2.87 \text{ V}$ ) and  $\text{XeF}_2/\text{H}_2\text{O}$  ( $E^\circ \sim 2.64 \text{ V}$ ) are effective, but ozone ( $E^\circ 2.07 \text{ V}$ ) and  $\text{S}_2\text{O}_8^{2-}$  ( $E^\circ 2.01 \text{ V}$ ) are not, presumably for kinetic reasons. Thermochemical measurements<sup>(143)</sup> further show that  $\text{KBrO}_4$  is thermodynamically stable with respect to its elements, but less so than the corresponding  $\text{KClO}_4$  and  $\text{KIO}_4$ : this is not due to any significant difference in entropy effects or lattice energies and implies that the  $\text{Br}-\text{O}$  bond in  $\text{BrO}_4^-$  is substantially weaker than the  $\text{X}-\text{O}$  bond in the other perhalates. Some comparative data (298.15 K) are:

	$\text{KClO}_4$	$\text{KBrO}_4$	$\text{KIO}_4$
$\Delta H_f^\circ/\text{kJ mol}^{-1}$	-431.9	-287.6	-460.6
$\Delta G_f^\circ/\text{kJ mol}^{-1}$	-302.1	-174.1	-349.3

No entirely satisfactory explanation of these observations has been devised, though they are paralleled by the similar reluctance of other elements following the completion of the 3d subshell to achieve their highest oxidation states — see particularly Se (p. 755) and As (p. 552) immediately preceding Br in the periodic table. The detailed kinetics of several oxidation reactions involving aqueous solutions of  $\text{BrO}_4^-$

have been studied.<sup>(144)</sup> In general, the reactivity of perbromates lies between that of the chlorates and perchlorates which means that, after the perchlorates, perbromates are the least reactive of the known oxohalogen compounds. It has even been suggested<sup>(116)</sup> that earlier investigators may actually have made perbromates, but not realized this because they were expecting a highly reactive product rather than an inert one.

### Periodic acids and periodates<sup>(126)</sup>

At least four series of periodates are known, interconnected in aqueous solutions by a complex series of equilibria involving deprotonation, dehydration and aggregation of the parent acid  $\text{H}_5\text{IO}_6$  — cf. telluric acids (p. 782) and antimoninic acids (p. 577) in the immediately preceding groups. Nomenclature is summarized in Table 17.24, though not all of the fully protonated acids have been isolated in the free state. The structural relationship between these acids, obtained mainly from X-ray studies on their salts, are shown in Fig. 17.24.  $\text{H}_5\text{IO}_6$  itself (mp  $128.5^\circ$  decomp) consists of molecules of  $(\text{HO})_5\text{IO}$  linked into a three-dimensional array by  $\text{O}-\text{H}\cdots\text{O}$  bonds (10 for each molecule, 260–278 pm).

Periodates can be made by oxidation of  $\text{I}^-$ ,  $\text{I}_2$  or  $\text{IO}_3^-$  in aqueous solution. Industrial processes involve oxidation of alkaline  $\text{NaIO}_3$  either electrochemically (using a  $\text{PbO}_2$  anode) or with  $\text{Cl}_2$ :



Table 17.24 Nomenclature of periodic acids

Formula	Name	Alternative	Formal relation to $\text{H}_5\text{IO}_6$
$\text{H}_5\text{IO}_6$	Orthoperiodic	Paraperiodic	Parent
$\text{HIO}_4$	Periodic	Metaperiodic	$\text{H}_5\text{IO}_6 - 2\text{H}_2\text{O}$
" $\text{H}_3\text{IO}_5$ "	Mesoperiodic	Diperiodic	$\begin{cases} 2\text{H}_5\text{IO}_6 - 2\text{H}_2\text{O} \\ 2\text{H}_3\text{IO}_6 - 3\text{H}_2\text{O} \end{cases}$
$\text{H}_7\text{I}_3\text{O}_{14}$	Triperiodic		$3\text{H}_5\text{IO}_6 - 4\text{H}_2\text{O}$

<sup>143</sup> F. SCHREINER, D. W. OSBORNE, A. V. POCIUS and E. H. APPELMAN, *Inorg. Chem.* **9**, 2320–4 (1970).

<sup>144</sup> E. H. APPELMAN, U. K. KLÄNING and R. C. THOMPSON, *J. Am. Chem. Soc.* **101**, 929–34 (1979).

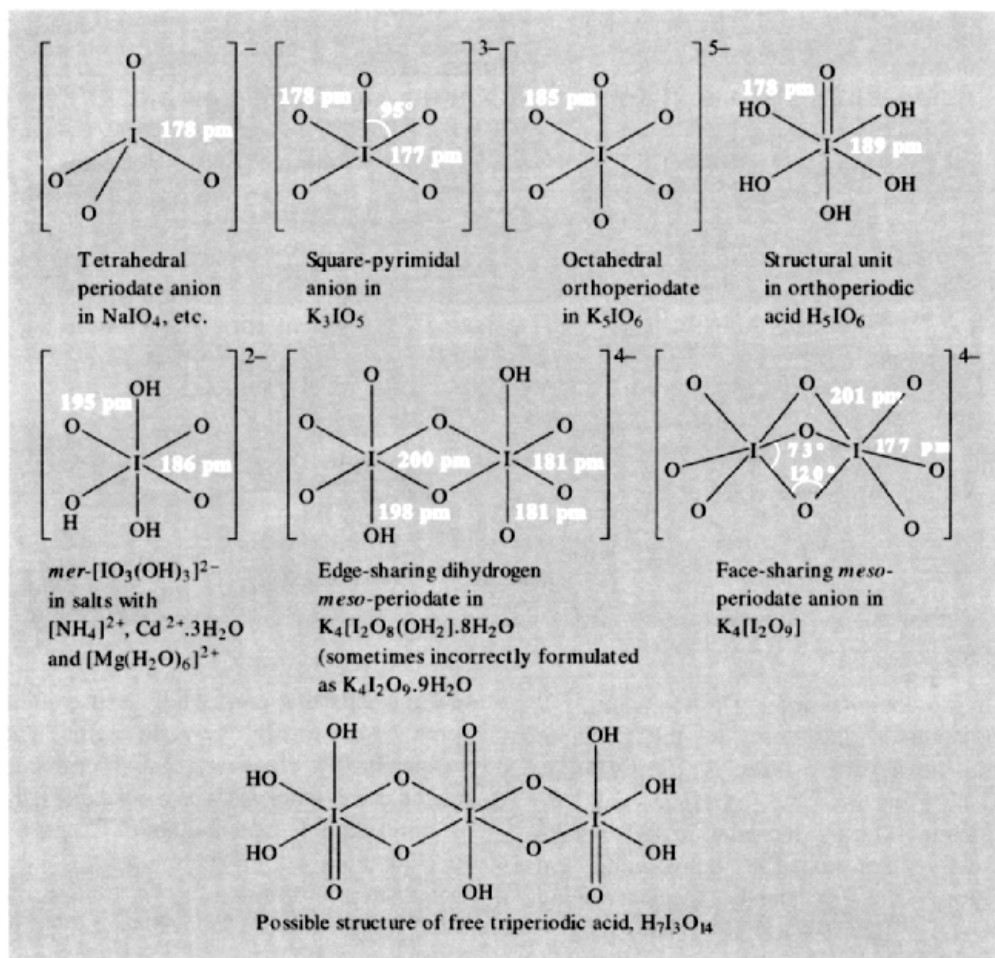
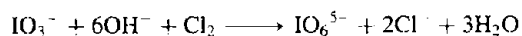
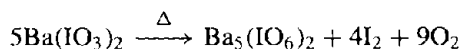


Figure 17.24 Structures of periodic acids and periodate anions.

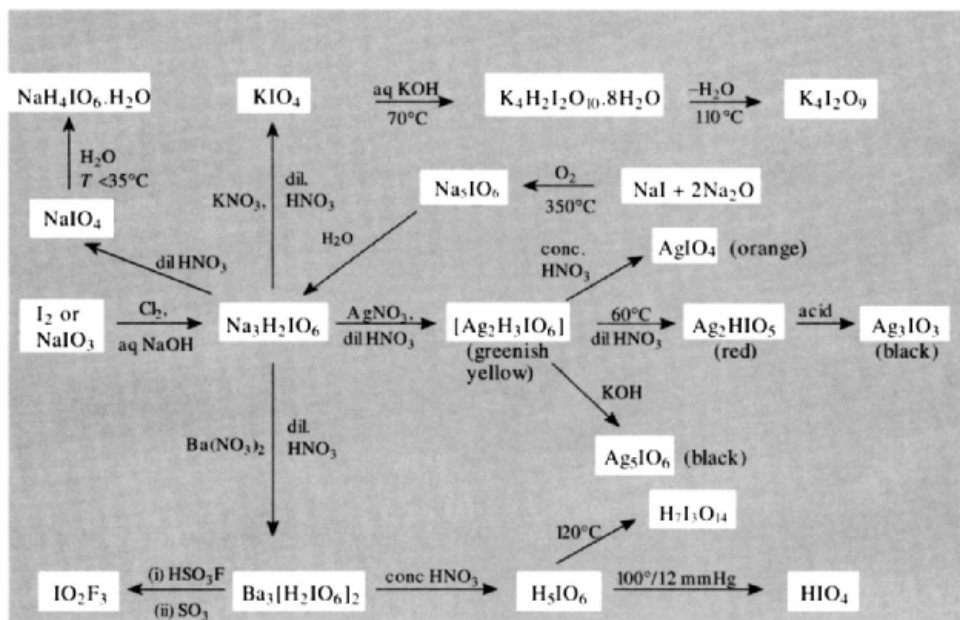


The product is the dihydrogen orthoperiodate  $\text{Na}_3\text{H}_2\text{IO}_6$ , which is a convenient starting point for many further preparations (see Scheme on next page). Paraperiodates of the alkaline earth metals can be made by the thermal disproportionation of the corresponding iodates, e.g.:



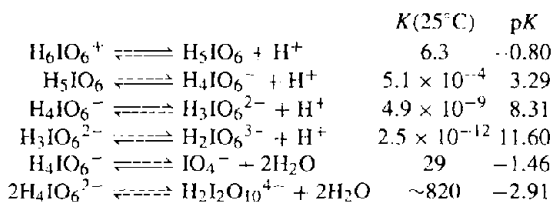
Aqueous solutions of periodic acid are best made by treating this barium salt with concentrated nitric acid. White crystals of

$\text{H}_5\text{IO}_6$  can be obtained from these solutions. Dehydration of  $\text{H}_5\text{IO}_6$  at  $120^\circ$  yields  $\text{H}_7\text{I}_3\text{O}_{14}$ , whereas heating to  $100^\circ$  under reduced pressure affords  $\text{HIO}_4$ . Attempts to dehydrate further do not yield the non-existent  $\text{I}_2\text{O}_7$  (p. 852); oxygen is progressively evolved to form the mixed oxide  $\text{I}_2\text{O}_5 \cdot \text{I}_2\text{O}_7$  and finally  $\text{I}_2\text{O}_5$ . Protonation of orthoperiodic acid with concentrated  $\text{HClO}_4$  yields the cation  $[\text{I}(\text{OH})_6]^+$ . Similarly, dissolution of crystalline  $\text{H}_5\text{IO}_6$  in 95%  $\text{H}_2\text{SO}_4$  (or  $\text{H}_2\text{SeO}_4$ ) at  $120^\circ$  yields colourless crystals of  $[\text{I}(\text{OH})_6][\text{HSO}_4]$  on slow cooling to room temperature and prolonged digestion of these with trichloroacetic acid extracts  $\text{H}_2\text{SO}_4$  to give the



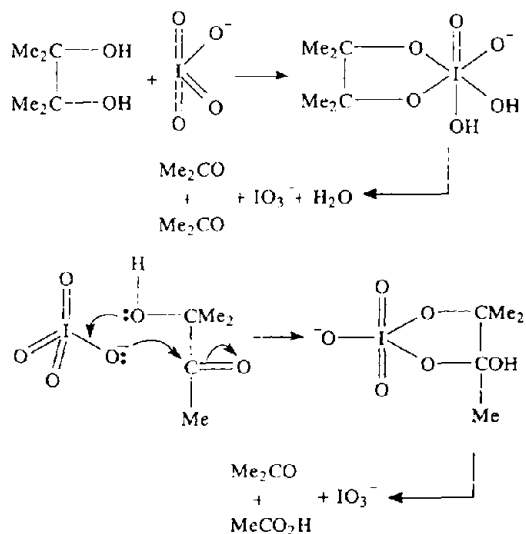
white, hygroscopic powder  $[\text{I}(\text{OH})_6]_2\text{SO}_4$ .<sup>(145)</sup> These compounds thus complete the series of octahedral hexahydroxo species  $[\text{Sn}(\text{OH})_6]^{2-}$ ,  $[\text{Sb}(\text{OH})_6]^-$ ,  $[\text{Te}(\text{OH})_6]$  and  $[\text{I}(\text{OH})_6]^+$ .

In aqueous solution increase in pH results in progressive deprotonation, dehydration and dimerization, the principal species being  $[(\text{HO})_4\text{IO}_2]^-$ ,  $[(\text{HO})_3\text{IO}_3]^{2-}$ ,  $[(\text{HO})_2\text{IO}_4]^{3-}$ ,  $[\text{IO}_4]^-$  and  $[(\text{HO})_2\text{I}_2\text{O}_8]^{4-}$ . The various equilibrium constants are:



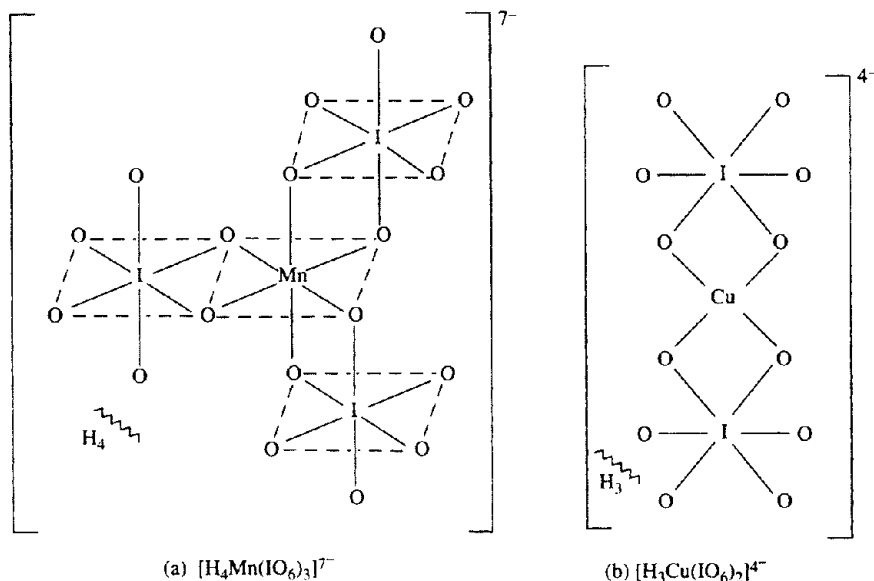
Periodates are both thermodynamically potent and kinetically facile oxidants. The oxidation potential is greatest in acid solution (p. 855) and can be progressively diminished by increasing the pH of the solution. In acid solution it is one of the

few reagents that can rapidly and quantitatively convert  $\text{Mn}^{\text{II}}$  to  $\text{Mn}^{\text{VII}}\text{O}_4^-$ . In organic chemistry it specifically cleaves 1,2-diols (glycols) and related compounds such as  $\alpha$ -diketones,  $\alpha$ -ketols,  $\alpha$ -aminoalcohols, and  $\alpha$ -diamines, e.g.:



In rigid systems only *cis*-difunctional groups are oxidized, the specificity arising from the

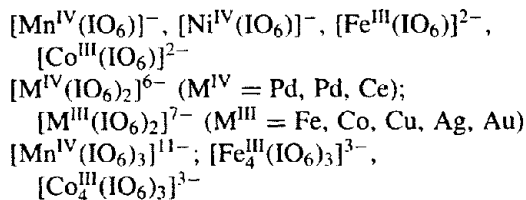
<sup>145</sup> H. SIEBERT and U. WOERNER, *Z. anorg. allgem. Chem.* **398**, 193-7 (1973).



**Figure 17.25** Structure of anions in  $\text{Na}_7[\text{H}_4\text{Mn}(\text{IO}_6)_3] \cdot 17\text{H}_2\text{O}$  and  $\text{Na}_3\text{K}[\text{H}_3\text{Cu}(\text{IO}_6)_2] \cdot 14\text{H}_2\text{O}$ .

formation of the cyclic intermediate. Such reactions have been widely used in carbohydrate and nucleic acid chemistry.

Periodates form numerous complexes with transition metals in which the octahedral  $\text{IO}_6^{5-}$  unit acts as a bidentate chelate. Examples are:



The stabilization of  $\text{Ni}^{\text{IV}}$ ,  $\text{Cu}^{\text{III}}$  and  $\text{Ag}^{\text{III}}$  is notable and many of the complexes have very high formation constants, e.g.  $[\text{Cu}(\text{IO}_6)_2]^{7-} \sim 10^{10}$ ,  $[\text{Co}(\text{IO}_6)_2]^{7-} \sim 10^{18}$ . The high formal charge on the anion is frequently reduced by protonation of the  $\{\text{I}(\mu\text{-O})_2\text{O}_4\}$  moiety, as in orthoperiodic acid itself. For example  $\text{H}_{11}[\text{Mn}(\text{IO}_6)_3]$  is a heptabasic acid with  $\text{p}K_1$  and  $\text{p}K_2 < 0$ ,  $\text{p}K_3$  2.75,  $\text{p}K_4$  4.35,  $\text{p}K_5$  5.45,  $\text{p}K_6$  9.55, and  $\text{p}K_7$  10.45. The crystal structure of  $\text{Na}_7[\text{H}_4\text{Mn}(\text{IO}_6)_3] \cdot 17\text{H}_2\text{O}$  features a 6-coordinate paramagnetic  $\text{Mn}^{\text{IV}}$  anion (Fig. 17.25a) whereas

the diamagnetic compound  $\text{Na}_3\text{K}[\text{H}_3\text{Cu}(\text{IO}_6)_2] \cdot 14\text{H}_2\text{O}$  has square-planar  $\text{Cu}^{\text{III}}$  (Fig. 17.25b).

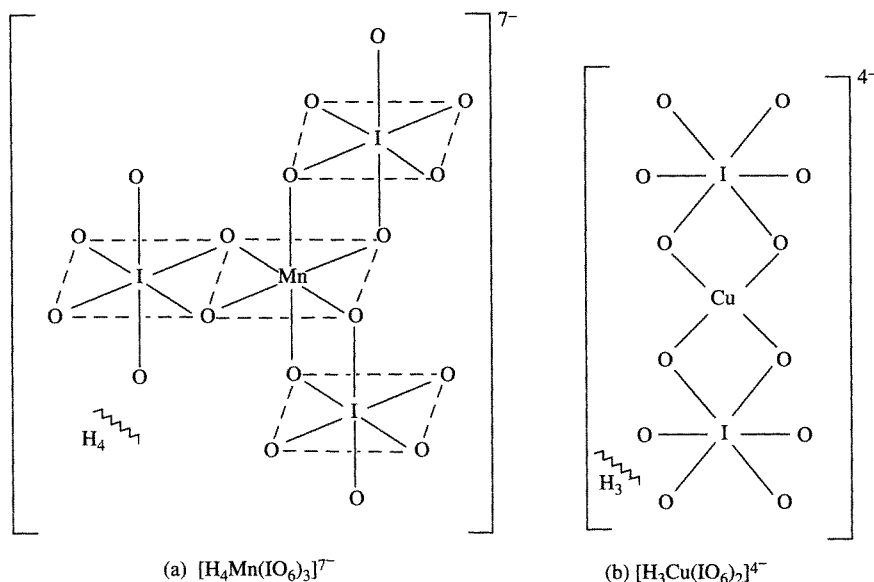
### 17.2.9 Halogen oxide fluorides and related compounds<sup>(146)</sup>

This section considers compounds in which X (Cl, Br or I) is bonded to both O and F, i.e.  $\text{F}_n\text{XO}_m$ . Oxofluorides  $-\text{OF}$  and peroxyfluorides  $-\text{OOF}$  have already been discussed (p. 638) and halogen derivatives of oxoacids, containing  $-\text{OX}$  bonds are treated in the following section (p. 883).

#### Chlorine oxide fluorides<sup>(147)</sup>

Of the 6 possible oxide fluorides of Cl, 5 have been characterized: they range in stability from the thermally unstable  $\text{FCl}^{\text{III}}\text{O}$  to the chemically rather inert perchloryl fluoride  $\text{FCl}^{\text{VII}}\text{O}_3$ . The others are  $\text{FCl}^{\text{V}}\text{O}_2$ ,  $\text{F}_3\text{Cl}^{\text{V}}\text{O}$  and  $\text{F}_3\text{Cl}^{\text{VII}}\text{O}_2$ .

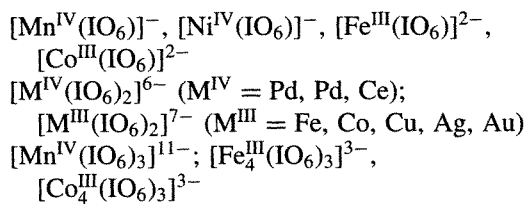
<sup>146</sup> Ref. 23, pp. 1386–96, The oxyfluorides of the halogens.  
<sup>147</sup> K. O. CHRISTE and C. J. SCHACK, *Adv. Inorg. Chem. Radiochem.* **18**, 319–98 (1976).



**Figure 17.25** Structure of anions in  $\text{Na}_7[\text{H}_4\text{Mn}(\text{IO}_6)_3] \cdot 17\text{H}_2\text{O}$  and  $\text{Na}_3\text{K}[\text{H}_3\text{Cu}(\text{IO}_6)_2] \cdot 14\text{H}_2\text{O}$ .

formation of the cyclic intermediate. Such reactions have been widely used in carbohydrate and nucleic acid chemistry.

Periodates form numerous complexes with transition metals in which the octahedral  $\text{IO}_6^{5-}$  unit acts as a bidentate chelate. Examples are:



The stabilization of  $\text{Ni}^{\text{IV}}$ ,  $\text{Cu}^{\text{III}}$  and  $\text{Ag}^{\text{III}}$  is notable and many of the complexes have very high formation constants, e.g.  $[\text{Cu}(\text{IO}_6)_2]^{7-} \sim 10^{10}$ ,  $[\text{Co}(\text{IO}_6)_2]^{7-} \sim 10^{18}$ . The high formal charge on the anion is frequently reduced by protonation of the  $\{\text{I}(\mu\text{-O})_2\text{O}_4\}$  moiety, as in orthoperiodic acid itself. For example  $\text{H}_{11}[\text{Mn}(\text{IO}_6)_3]$  is a heptabasic acid with  $\text{p}K_1$  and  $\text{p}K_2 < 0$ ,  $\text{p}K_3$  2.75,  $\text{p}K_4$  4.35,  $\text{p}K_5$  5.45,  $\text{p}K_6$  9.55, and  $\text{p}K_7$  10.45. The crystal structure of  $\text{Na}_7[\text{H}_4\text{Mn}(\text{IO}_6)_3] \cdot 17\text{H}_2\text{O}$  features a 6-coordinate paramagnetic  $\text{Mn}^{\text{IV}}$  anion (Fig. 17.25a) whereas

the diamagnetic compound  $\text{Na}_3\text{K}[\text{H}_3\text{Cu}(\text{IO}_6)_2] \cdot 14\text{H}_2\text{O}$  has square-planar  $\text{Cu}^{\text{III}}$  (Fig. 17.25b).

### 17.2.9 Halogen oxide fluorides and related compounds<sup>(146)</sup>

This section considers compounds in which X (Cl, Br or I) is bonded to both O and F, i.e.  $\text{F}_n\text{XO}_m$ . Oxofluorides  $-\text{OF}$  and peroxyfluorides  $-\text{OOF}$  have already been discussed (p. 638) and halogen derivatives of oxoacids, containing  $-\text{OX}$  bonds are treated in the following section (p. 883).

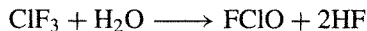
#### Chlorine oxide fluorides<sup>(147)</sup>

Of the 6 possible oxide fluorides of Cl, 5 have been characterized: they range in stability from the thermally unstable  $\text{FCl}^{\text{III}}\text{O}$  to the chemically rather inert perchloryl fluoride  $\text{FCl}^{\text{VII}}\text{O}_3$ . The others are  $\text{FCl}^{\text{V}}\text{O}_2$ ,  $\text{F}_3\text{Cl}^{\text{V}}\text{O}$  and  $\text{F}_3\text{Cl}^{\text{VI}}\text{O}_2$ .

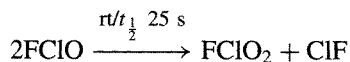
<sup>146</sup> Ref. 23, pp. 1386–96, The oxyfluorides of the halogens.  
<sup>147</sup> K. O. CHRISTE and C. J. SCHACK, *Adv. Inorg. Chem. Radiochem.* **18**, 319–98 (1976).

The remaining compound  $F_5Cl^{VII}O$  has been claimed but the report could not be confirmed. Fewer bromine oxide fluorides are known, only  $FBrO_2$ ,  $F_3BrO$  and possibly  $FBrO_3$  being characterized. The compounds of iodine include the  $I^V$  derivatives  $FIO_2$  and  $F_3IO$  and the  $I^{VII}$  derivatives  $FIO_3$ ,  $F_3IO_2$  and  $F_5IO$ . All the halogen oxide fluorides resemble the halogen fluorides (p. 824), to which they are closely related both structurally and chemically. Thus they tend to be very reactive oxidizing and fluorinating agents and several can act as Lewis acids or bases (or both) by gain or loss of fluoride ions, respectively.

The structures of the chlorine oxide fluorides are summarized in Fig. 17.26, together with those of related cationic and anionic species formed from the neutral molecules by gain or loss of  $F^-$ . The first conclusive evidence for free  $FCIO$  in the gas phase came in 1972 during a study of the hydrolysis of  $ClF_3$  with substoichiometric amounts of  $H_2O$  in a flow reactor:

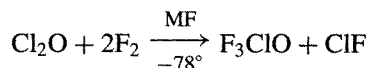


The compound is thermally unstable, and decomposes with a half-life of about 25 s at room temperature:

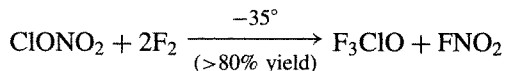


The compound can also be made by photolysis of a mixture of  $ClF$  and  $O_3$  in Ar at 4–15 K; evidence for the expected nonlinear by structure comes from vibration spectroscopy (Fig. 17.26a).

$F_3ClO$  was discovered in 1965 but not published until 1972 because of US security classification. It has low kinetic stability and is an extremely powerful fluorinating and oxidizing agent. It can be made in yields of up to 80% by fluorination of  $Cl_2O$  in the presence of metal fluorides, e.g. NaF:



However, the unpredictably explosive nature of  $Cl_2O$  in the liquid state renders this process somewhat hazardous and the best large-scale preparation is the low-temperature fluorination of  $ClONO_2$  (p. 884):



$F_3ClO$  is a colourless gas or liquid: mp  $-43^\circ$ , bp  $28^\circ$   $d(1, 20^\circ)$   $1.865 \text{ g cm}^{-3}$ . The compound

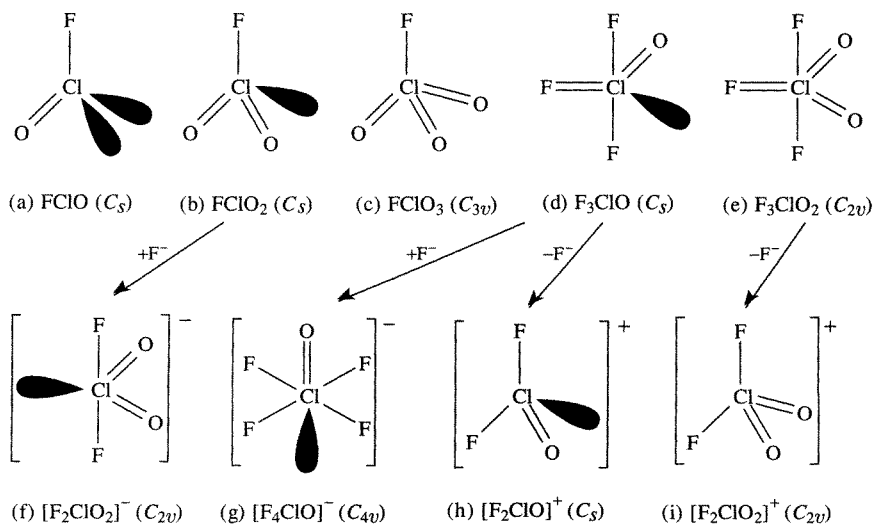
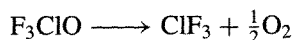


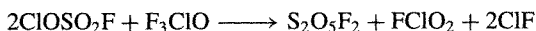
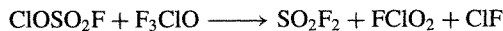
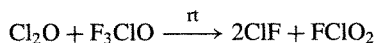
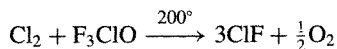
Figure 17.26 Structures of chlorine oxide fluorides and related cations and anions.



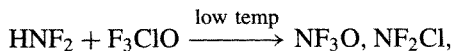
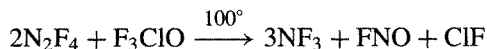
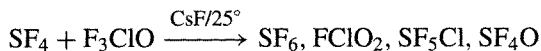
is stable at room temperature:  $\Delta H_f^\circ(\text{g}) = -148 \text{ kJ mol}^{-1}$ ,  $\Delta H_f^\circ(\text{l}) = -179 \text{ kJ mol}^{-1}$ . Its  $C_s$  structure (Fig. 17.26d) has been established by gas electron diffraction which also led to the dimensions  $\text{Cl}=\text{O}$  140.5 pm,  $\text{Cl}-\text{F}_{\text{eq}}$  160.3 pm,  $\text{Cl}-\text{F}_{\text{ax}}$  171.3 pm, and angle  $\text{F}_{\text{ax}}-\text{Cl}-\text{F}_{\text{ax}}$   $171^\circ$ ; other angles are  $\text{F}_{\text{ax}}-\text{Cl}-\text{F}_{\text{eq}}$   $88^\circ$ ,  $\text{F}_{\text{ax}}-\text{Cl}-\text{O}$   $95^\circ$  and  $\text{F}_{\text{eq}}-\text{Cl}-\text{O}$   $109^\circ$ .<sup>(148)</sup>  $\text{F}_3\text{ClO}$  can be handled in well-passivated metal, Teflon or Kel-F but reacts rapidly with glass or quartz. Its thermal stability is intermediate between those of  $\text{ClF}_3$  and  $\text{ClF}_5$  (p. 832) and it decomposes above  $300^\circ\text{C}$  according to



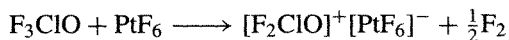
$\text{F}_3\text{ClO}$  tends to react slowly at room temperature but rapidly on heating or under ultraviolet irradiation. Typical of its fluorinating reactions are:



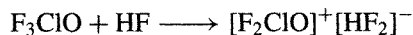
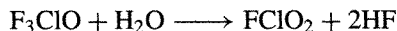
Combined fluorinating and oxygenating capacity is exemplified by the following (some of the reactions being complicated by further reaction of the products with  $\text{F}_3\text{ClO}$ ):



It reacts as a reducing agent towards the extremely strong oxidant  $\text{PtF}_6$ :

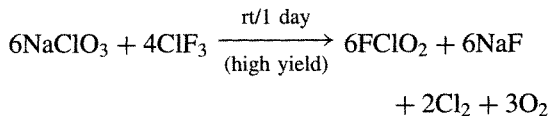


Hydrolysis with small amounts of water yields HF but this can react further by fluoride ion abstraction:

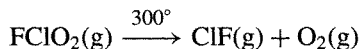


This last reaction is typical of many in which  $\text{F}_3\text{ClO}$  can act as a Lewis base by fluoride ion donation to acceptors such as  $\text{MF}_5$  ( $\text{M} = \text{P}, \text{As}, \text{Sb}, \text{Bi}, \text{V}, \text{Nb}, \text{Ta}, \text{Pt}, \text{U}$ ),  $\text{MoF}_4\text{O}$ ,  $\text{SiF}_4$ ,  $\text{BF}_3$ , etc. These products are all white, stable, crystalline solids (except the canary yellow  $\text{PtF}_6^-$ ) and contain the  $[\text{F}_2\text{ClO}]^+$  cation (see Fig. 17.26h) which is isostructural with the isoelectronic  $\text{F}_2\text{SO}$ . Chlorine trifluoride oxide can also act as a Lewis acid (fluoride ion acceptor) and is therefore to be considered as amphoteric (p. 225). For example  $\text{KF}$ ,  $\text{RbF}$  and  $\text{CsF}$  yield  $\text{M}^+[\text{F}_4\text{ClO}]^-$  as white solids whose stabilities increase with increasing size of  $\text{M}^+$ . Vibration spectroscopy establishes the  $C_{4v}$  structure of the anion (Fig. 17.29g).

The other  $\text{Cl}^{\text{V}}$  oxide fluoride  $\text{FClO}_2$  (1942) can be made by the low-temperature fluorination of  $\text{ClO}_2$  but is best prepared by the reaction:



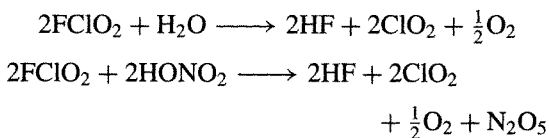
The  $C_s$  structure and dimensions (Fig. 17.26b) were established by microwave spectroscopy which also yielded a value for the molecular dipole moment  $\mu$  1.72 D. Other physical properties of this colourless gas are mp  $-115^\circ$  (or  $-123^\circ$ ), bp  $\sim -6^\circ$ ,  $\Delta H_f^\circ(\text{g}, 298 \text{ K}) -34 \pm 10 \text{ kJ mol}^{-1}$  [or  $-273 \text{ kJ mol}^{-1}$  when corrected for  $\Delta H_f^\circ(\text{HF}, \text{g})!$ ].  $\text{FClO}_2$  is thermally stable at room temperature in dry passivated metal containers and quartz. Thermal decomposition of the gas (first-order kinetics) only becomes measurable above  $300^\circ$  in quartz and above  $200^\circ$  in Monel metal:



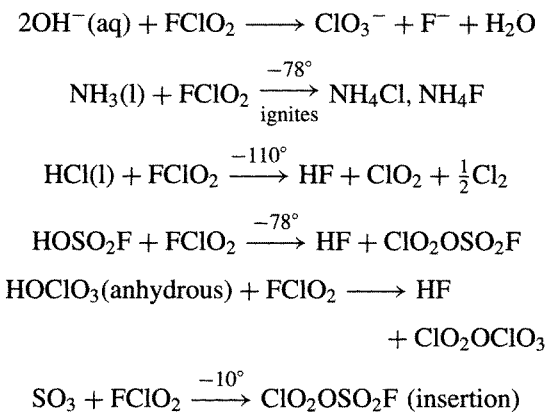
It is far more chemically reactive than  $\text{FClO}_3$  (p. 879) despite the lower oxidation state of Cl.

<sup>148</sup> H. OBERHAMMER and K. O. CHRISTIE, *Inorg. Chem.* **21**, 273-5 (1982).

Hydrolysis is slow at room temperature and the corresponding reaction with anhydrous  $\text{HNO}_3$  results in dehydration to the parent  $\text{N}_2\text{O}_5$ :

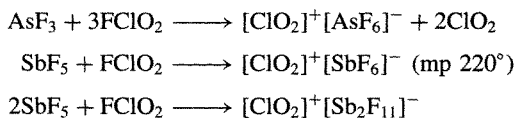


Other reactions with protonic reagents are:



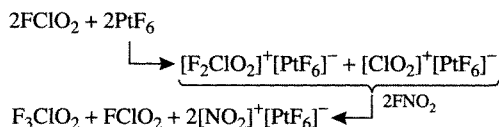
$\text{FCIO}_2$  explodes with the strong reducing agent  $\text{SO}_2$  even at  $-40^\circ$  and  $\text{HBr}$  likewise explodes at  $-110^\circ$ .

Chlorine dioxide fluoride is a good fluorinating agent and a moderately strong oxidant:  $\text{SF}_4$  is oxidized to  $\text{SF}_6$ ,  $\text{SF}_4\text{O}$  and  $\text{SF}_2\text{O}_2$  above  $50^\circ$ , whereas  $\text{N}_2\text{F}_4$  yields  $\text{NF}_3$ ,  $\text{FNO}_2$  and  $\text{FNO}$  at  $30^\circ$ .  $\text{UF}_4$  is oxidized to  $\text{UF}_5$  at room temperature and to  $\text{UF}_6$  at  $100^\circ$ . Chlorides (and some oxides) are fluorinated and the products can react further to form fluoro complexes. Thus, whereas  $\text{AlCl}_3$  yields  $\text{AlF}_3$ ,  $\text{B}_2\text{O}_3$  affords  $[\text{ClO}_2]^+[\text{BF}_4]^-$ , and the Lewis acid chlorides  $\text{SbCl}_5$ ,  $\text{SnCl}_4$  and  $\text{TiCl}_4$  yield  $[\text{ClO}_2]^+[\text{SbF}_6]^-$ ,  $[\text{ClO}_2]^{+}_2[\text{SnF}_6]^{2-}$  and  $[\text{ClO}_2]^{+}_2[\text{TiF}_6]^{2-}$ . Such complexes, and many others can, of course, be prepared directly from the corresponding fluorides either with or without concurrent oxidation, e.g.:

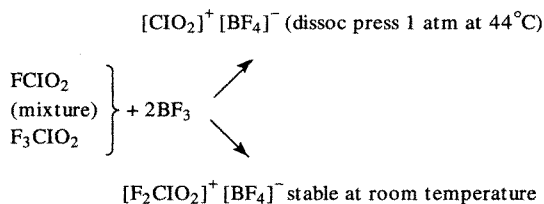


An X-ray study on this last compound showed the chloryl cation to have the expected nonlinear structure, with angle  $\text{OCIO } 122^\circ$  and  $\text{Cl-O } 131 \text{ pm}$ .  $\text{FCIO}_2$  can also act as a fluoride ion acceptor, though not so readily as  $\text{F}_3\text{ClO}$  above. For example  $\text{CsF}$  reacts at room temperature to give the white solid  $\text{Cs}[\text{F}_2\text{ClO}_2]$ ; this is stable at room temperature but dissociates reversibly into its components above  $100^\circ$ . The  $\text{C}_{2v}$  structure of  $[\text{F}_2\text{ClO}_2]^-$  (Fig. 17.26f) is deduced from its vibration spectrum.

The two remaining  $\text{Cl}^{\text{VII}}$  oxide fluorides are  $\text{F}_3\text{ClO}_2$  and  $\text{FCIO}_3$ . At one time  $\text{F}_3\text{ClO}_2$  was thought to exist in isomeric forms but the so-called violet form, previously thought to be the peroxo compound  $\text{F}_2\text{ClOOF}$  has now been discounted.<sup>(147)</sup> The well-defined compound  $\text{F}_3\text{ClO}_2$  was first made in 1972 as an extremely reactive colourless gas: mp  $-81.2^\circ$ , bp  $-21.6^\circ$ . It is a very strong oxidant and fluorinating agent and, because of its corrosive action, must be handled in Teflon or sapphire apparatus. It thus resembles the higher chlorine fluorides. The synthesis of  $\text{F}_3\text{ClO}_2$  is complicated and depends on an ingenious sequence of fluorine-transfer reactions as outlined below:

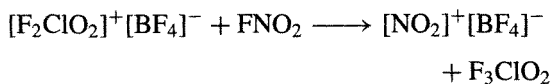


Fractional condensation at  $-112^\circ$  removes most of the  $\text{FCIO}_2$ , which is slightly less volatile than  $\text{F}_3\text{ClO}_2$ . The remaining  $\text{FCIO}_2$  is removed by complexing with  $\text{BF}_3$  and then relying on the greater stability of the  $\text{F}_3\text{ClO}_2$  complex:



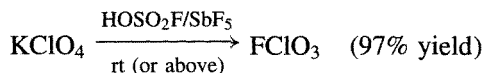
Pumping at  $20^\circ$  removes  $[\text{ClO}_2]^+[\text{BF}_4]^-$  as its component gases, leaving  $[\text{F}_2\text{ClO}_2]^+[\text{BF}_4]^-$  which, on treatment with  $\text{FNO}_2$ , releases the

desired product:



The whole sequence of reactions represents a *tour de force* in the elegant manipulation of extremely reactive compounds.  $\text{F}_3\text{ClO}_2$  is a violent oxidizing reagent but forms stable adducts by fluoride ion transfer to Lewis acids such as  $\text{BF}_3$ ,  $\text{AsF}_5$  and  $\text{PtF}_6$ . The structures of  $\text{F}_3\text{ClO}_2$  and  $[\text{F}_2\text{ClO}_2]^+$  have  $C_{2v}$  symmetry as expected (Fig. 17.26e and i).

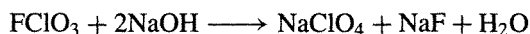
In dramatic contrast to  $\text{F}_3\text{ClO}_2$ , perchloryl fluoride ( $\text{FClO}_3$ ) is notably inert, particularly at room temperature. This colourless tetrahedral molecular gas (Fig. 17.26c) was first synthesized in 1951 by fluorination of  $\text{KClO}_3$  at  $-40^\circ$  and it can also be made (in 50% yield) by the action of  $\text{F}_2$  on an aqueous solution of  $\text{NaClO}_3$ . Electrolysis of  $\text{NaClO}_4$  in anhydrous  $\text{HF}$  has also been used but the most convenient route for industrial scale manufacture is the fluorination of a perchlorate with  $\text{SbF}_5$ ,  $\text{SbF}_5/\text{HF}$ ,  $\text{HOSO}_2\text{F}$  or perhaps best of all  $\text{HOSO}_2\text{F}/\text{SbF}_5$ :



Because of its remarkably low reactivity at room temperature and its very high specific impulse, the gas has been much studied as a rocket propellant oxidizer (e.g. it compares favourably with  $\text{N}_2\text{O}_4$  and with  $\text{ClF}_3$  as an oxidizer for fuels such as  $\text{N}_2\text{H}_4$ ,  $\text{Me}_2\text{NNH}_2$  and  $\text{LiH}$ ).  $\text{FClO}_3$  has mp  $-147.8^\circ$ , bp  $-46.7^\circ$ ,  $d(1, -73^\circ\text{C})$   $1.782 \text{ g cm}^{-3}$ , viscosity  $\eta(-73^\circ)$  0.55 centipoise. The extremely low dipole moment ( $\mu = 0.023 \text{ D}$ ) is particularly noteworthy.  $\text{FClO}_3$  has high kinetic stability despite its modest thermodynamic instability:  $\Delta H_f^\circ(\text{g}, 298 \text{ K}) -23.8 \text{ kJ mol}^{-1}$ ,  $\Delta G_f^\circ(\text{g}, 298 \text{ K}) +48.1 \text{ kJ mol}^{-1}$ .  $\text{FClO}_3$  offers the highest known resistance to dielectric breakdown for any gas (30% greater than for  $\text{SF}_6$ , p. 687) and has been used as an insulator in high-voltage systems.

Perchloryl fluoride is thermally stable up to about  $400^\circ$ . Above  $465^\circ$  it undergoes decomposition with first-order kinetics and an

activation energy of  $244 \text{ kJ mol}^{-1}$ . Hydrolysis is slow even at  $250\text{--}300^\circ$  and quantitative reaction is only achieved with concentrated aqueous hydroxide in a sealed tube under high pressure at  $300^\circ\text{C}$ :



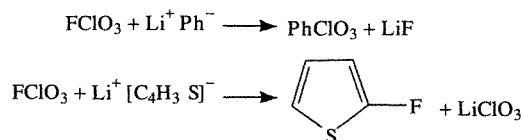
However, alcoholic  $\text{KOH}$  effects a similar quantitative reaction at  $25^\circ\text{C}$ . Reaction with liquid  $\text{NH}_3$  is also smooth particularly in the presence of a strong nucleophile such as  $\text{NaNH}_2$ :



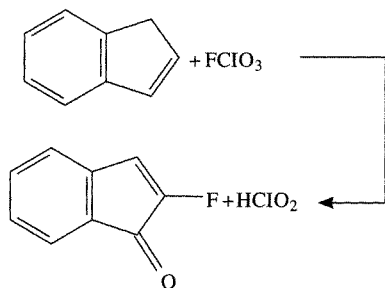
Metallic Na and K react only above  $300^\circ$ .

$\text{FClO}_3$  shows no tendency to form adducts with either Lewis acids or bases. This is in sharp contrast to most of the other oxide fluorides of chlorine discussed above and has been related to the preferred tetrahedral ( $C_{3v}$ ) geometry as compared with the planar ( $D_{3h}$ ) and trigonal bipyramidal ( $D_{3h}$ ) geometries expected for  $[\text{ClO}_3]^+$  and  $[\text{F}_2\text{ClO}_3]^-$  respectively. Conversely the pseudo-trigonal bipyramidal  $C_s$  structure  $\text{F}_3\text{ClO}$  gains stability when converted to the pseudo-tetrahedral  $[\text{F}_2\text{ClO}]^+$  or pseudo-octahedral  $[\text{F}_4\text{ClO}]^-$  (see Fig. 17.26).

In reactions with organic compounds  $\text{FClO}_3$  acts either as an oxidant or as a 1- or 2-centre electrophile which can therefore be used to introduce either F, a  $-\text{ClO}_3$  group, or both F and O into the molecule. As  $\text{FClO}_3$  is highly susceptible to nucleophilic attack at Cl it reacts readily with organic anions:



Compounds having a cyclic double bond conjugated to an aromatic ring (e.g. indene) undergo oxofluorination, with  $\text{FClO}_3$  acting as a 2-centre electrophile:



$\text{FClO}_3$  also acts as a mild fluorinating agent for compounds possessing a reactive methylene group, e.g.:



It is particularly useful for selective fluorination of steroids.

### Bromine oxide fluorides<sup>(149)</sup>

These compounds are less numerous and rather less studied than their chlorine analogues; indeed, until fairly recently only  $\text{FBrO}_2$  was well characterized. The known species are:

Oxidation state of Br	Cations	Neutral species	Anions
V	$[\text{BrO}_2]^+$ $[\text{F}_2\text{BrO}]^+$	<b><math>\text{FBrO}_2</math></b> (1955) <b><math>\text{F}_3\text{BrO}</math></b> (1976)	$[\text{F}_2\text{BrO}_2]^-$ $[\text{F}_4\text{BrO}]^-$
VII		<b><math>\text{FBrO}_3</math></b> (1969)	

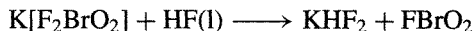
Despite several attempts at synthesis, there is little or no evidence for the existence of  $\text{FBrO}$ ,  $\text{F}_3\text{BrO}_2$  or  $\text{F}_5\text{BrO}$ . The bromine oxide fluorides are somewhat less thermally stable than their chlorine analogues and somewhat more reactive chemically. The structures are as already described for the chlorine oxide fluorides (Fig. 17.26).

Bromyl fluoride,  $\text{FBrO}_2$ , is a colourless liquid, mp  $-9^\circ$ , which attacks glass at room temperature and which undergoes rapid decomposition

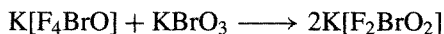
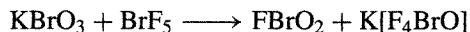
above  $55^\circ$ :



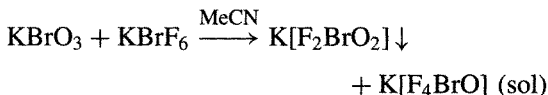
It is best prepared by fluorine transfer reactions such as



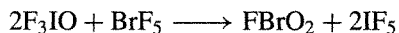
The  $\text{K}[\text{F}_2\text{BrO}_2]$  can be prepared by fluorination of  $\text{KBrO}_3$  with  $\text{BrF}_5$  in the presence of a trace of HF:



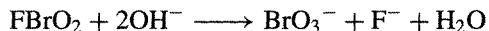
However, the most convenient method of preparation of  $\text{K}[\text{F}_2\text{BrO}_2]$  is by reaction of  $\text{KBrO}_3$  with  $\text{KBrF}_6$  in MeCN:



Bromyl fluoride is also produced by fluorine-oxygen exchange between  $\text{BrF}_5$  and oxoiodine compounds (p. 881), e.g.:

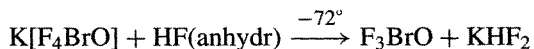
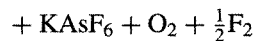


As with  $\text{FClO}_2$  and  $\text{FIO}_2$ , hydrolysis regenerates the halate ion, the reaction with  $\text{FBrO}_2$  being of explosive violence. Hydrolysis in basic solution at  $0^\circ$  can be represented as



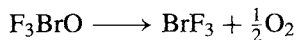
Organic substances react vigorously, often enflaming. Co-condensation of  $\text{FBrO}_2$  with the Lewis acid  $\text{AsF}_5$  produced  $[\text{BrO}_2]^+[\text{AsF}_6]^-$ . Vibrational spectra establish the expected non-linear structure of the cation (3 bands active in both Raman and infrared).  $\text{FBrO}_2$  can also react as a fluoride ion acceptor (from KF).

Bromine oxide trifluoride,  $\text{F}_3\text{BrO}$ , is made by reaction of  $\text{K}[\text{F}_4\text{BrO}]$  with a weak Lewis acid:

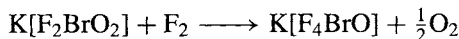


<sup>149</sup> R. J. GILLESPIE and P. H. SPEKKENS, *Israel J. Chem.* **17**, 11-19 (1978). R. BOUGON, T. B. HUY, P. CHARPIN, R. J. GILLESPIE and P. H. SPEKKENS, *J. Chem. Soc., Dalton Trans.*, 6-12 (1979).

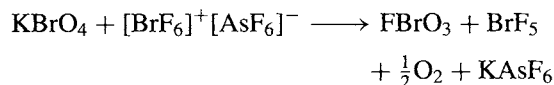
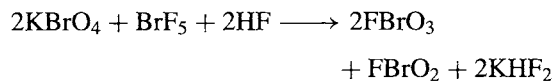
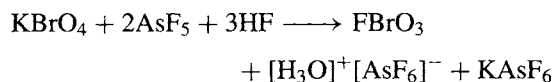
The product is a white solid which melts to a clear liquid at about  $-5^\circ$ ; it is only marginally stable at room temperature and slowly decomposes with loss of oxygen:



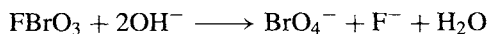
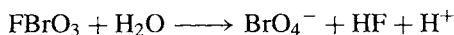
The molecular symmetry is  $C_s$  (like  $\text{F}_3\text{ClO}$ ; Fig. 17.26d) and there is some evidence for weak intermolecular association via  $\text{F}_{\text{ax}}-\text{Br}\cdots\text{F}_{\text{ax}}$  bonding. Fluoride ion transfer reactions have been established and yield compounds such as  $[\text{F}_2\text{BrO}]^+[\text{AsF}_6]^-$ ,  $[\text{F}_2\text{BrO}]^+[\text{BF}_4]^-$  and  $\text{K}[\text{F}_4\text{BrO}]$ , though this last compound is more conveniently made independently, e.g. by the reaction of  $\text{KBrO}_3$  with  $\text{KBrF}_6$  mentioned above, or by direct fluorination of  $\text{K}[\text{F}_2\text{BrO}_2]$ :



Perbromyl fluoride,  $\text{FBrO}_3$ , is made by fluorinating the corresponding perbromate ion with  $\text{AsF}_5$ ,  $\text{SbF}_5$ ,  $\text{BrF}_5$  or  $[\text{BrF}_6]^+[\text{AsF}_6]^-$  in HF solutions. The reactions are smooth and quantitative at room temperature:



Perbromyl fluoride is a reactive gas which condenses to a colourless liquid (bp  $2.4^\circ$ ) and then solidifies to a white solid (mp ca.  $-110^\circ$ ). It has the expected  $C_{3v}$  symmetry Fig. 17.27 and decomposes slowly at room temperature; it is more reactive than  $\text{FClO}_3$  and, unlike that compound, it reacts rapidly with water, aqueous base and even glass:



Fluoride ion transfer reactions have not been established for  $\text{FBrO}_3$  and may be unlikely, (see p. 879).

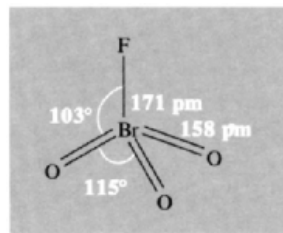
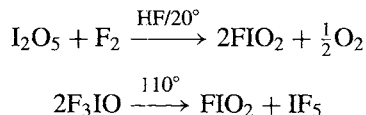


Figure 17.27 Structure of  $\text{FBrO}_3$  as determined by gas-phase electron diffraction.

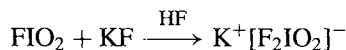
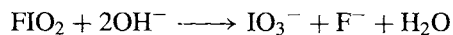
### Iodine oxide fluorides

The compounds to be considered are the  $\text{I}^{\text{V}}$  derivatives  $\text{FIO}_2$  and  $\text{F}_3\text{IO}$  and the  $\text{I}^{\text{VII}}$  derivatives  $\text{FIO}_3$ ,  $\text{F}_3\text{IO}_2$  and  $\text{F}_5\text{IO}$ . Note that, unlike Cl, no  $\text{I}^{\text{III}}$  compound  $\text{FIO}$  has been reported and that, conversely,  $\text{F}_5\text{IO}$  (but not  $\text{F}_5\text{ClO}$ ) has been characterized.

$\text{FIO}_2$  has been prepared both by direct fluorination of  $\text{I}_2\text{O}_5$  in anhydrous HF at room temperature and by thermal dismutation of  $\text{F}_3\text{IO}$ :

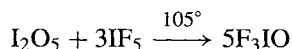


Unlike gaseous molecular  $\text{FClO}_2$ , it is a colourless polymeric solid which decomposes without melting when heated above  $200^\circ$ . Like the other halyl fluorides it readily undergoes alkaline hydrolysis and also forms a complex with  $\text{F}^-$ :



An X-ray study of this latter complex reveals a  $C_{2v}$  anion as in the chlorine analogue (Fig. 17.28a). This is closely related to the  $C_s$  structure of the neutral molecule  $\text{F}_3\text{IO}$  (Fig. 17.28b).

$\text{F}_3\text{IO}$  is prepared as colourless crystals by dissolving  $\text{I}_2\text{O}_5$  in boiling  $\text{IF}_5$  and then cooling the mixture:



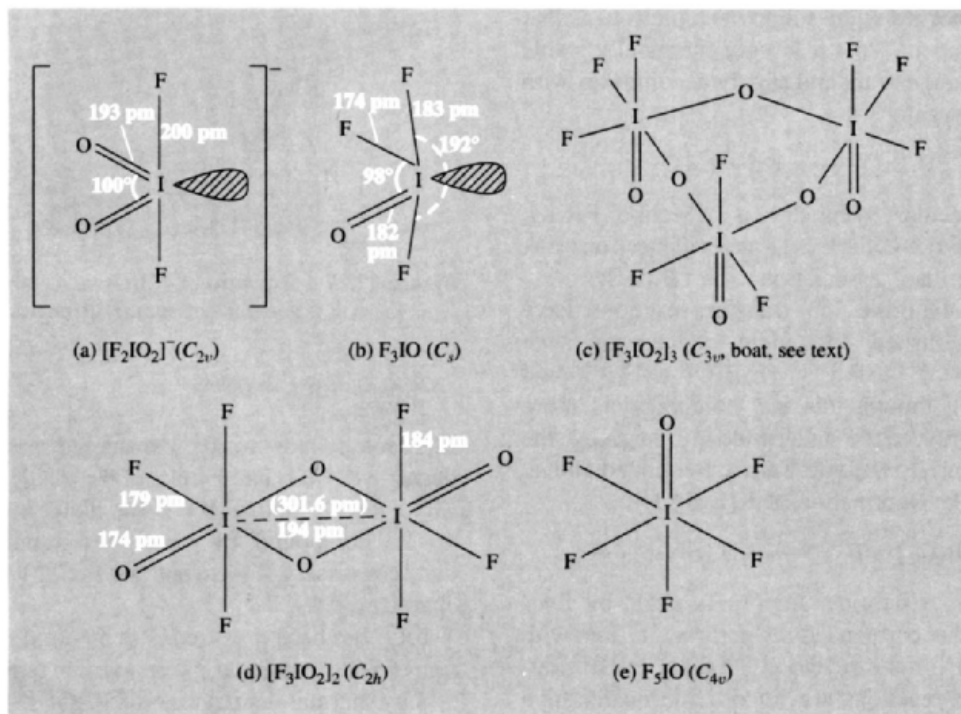
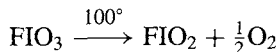


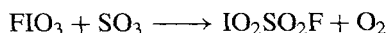
Figure 17.28 Structures of iodine oxide fluorides.

Above  $110^\circ$  it dismutates into  $FIO_2$  and  $IF_5$  as mentioned above.

Of the  $I^{VII}$  oxide fluorides  $FIO_3$  has been prepared by the action of  $F_2$ /liquid HF on  $HIO_4$ . It is a white, crystalline solid, stable in glass but decomposing with loss of oxygen on being heated:



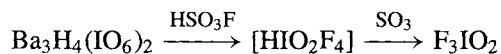
Unlike its analogue  $FClO_3$  it forms adducts with  $BF_3$  and  $AsF_5$ , possibly by  $F^-$  donation to give  $[IO_3]^+[BF_4]^-$  and  $[IO_3]^+[AsF_6]^-$ , though the structures have not yet been determined. Alternatively, the coordination number of the central I atom might be increased.  $SO_3$  reduces  $FIO_3$  to iodyl fluorosulfate:



Like  $FClO_3$  it reacts with  $NH_3$  but the products have not been fully characterized.

$F_3IO_2$ , first made in 1969, has posed an interesting structural problem. The yellow solid, mp

$41^\circ$ , can be prepared by partial fluorination of a periodate with fluorosulfuric acid:



Unlike monomeric  $F_3ClO_2$  (p. 878) the structure is oligomeric not only in the solid state but also in the gaseous and solution phases. This arises from the familiar tendency of iodine to increase its coordination number to 6. Fluorine-19 nmr and Raman spectroscopy of  $F_3IO_2$  dissolved in  $BrF_3$  at  $-48^\circ$  have been interpreted in terms of a *cis*-oxygen-bridged trimer with axial terminal O atoms and a  $C_{3v}$  boat conformation (Fig. 17.28c).<sup>(150)</sup> On warming the solution to  $50^\circ$  there is a fast interconversion between this and the  $C_s$  chair conformer. The vibration spectrum of the gas phase at room temperature has been interpreted in terms of a centrosymmetric dimer

<sup>150</sup>R. J. GILLESPIE and J. P. KRASZNAI, *Inorg. Chem.* **15**, 1251-6 (1976).

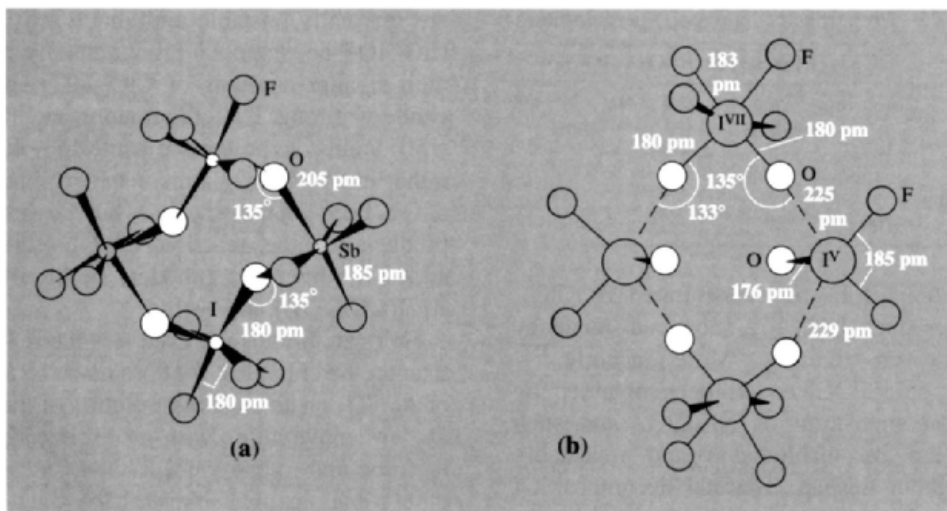


Figure 17.29 Structures of dimeric adducts of  $F_3IO_2$ .

(Fig. 17.28d). There is significant dissociation into monomers at  $100^\circ$  and this is almost complete at  $185^\circ$ . The centrosymmetric dimer has also been found in an X-ray study of the crystalline solid at  $-80^\circ$  (Fig. 17.28d).<sup>(151)</sup> Complexes of  $F_3IO_2$  with  $AsF_5$ ,  $SbF_5$ ,  $NbF_5$  and  $TaF_5$  have been studied:<sup>(152)</sup> they are oxygen-bridged polymers with alternating  $\{F_4IO_2\}$  and  $\{O_2MF_4\}$  groups. For example, the crystal structure of the complex with  $SbF_5$  shows it to be dimeric (Fig. 17.29a).<sup>(153)</sup> A similar structure motif is found in the adduct  $F_3IO.F_3IO_2$  which features alternating 5- and 6-coordinate I atoms (Fig. 17.29b),<sup>(154)</sup> the structure can be regarded as a cyclic dimer of the ion pair  $[F_2IO]^+[F_4IO_2]^-$ . See also p. 885 for the mixed valence oxo-iodine polymeric cation in  $[(IO_2)_3]^+HSO_4^-$ .

Finally in this section we mention iodine oxide pentafluoride,  $F_5IO$ , obtained as a colourless liquid, mp  $45^\circ$ , when  $IF_7$  is allowed to react with water, silica, glass or  $I_2O_5$ . As implied

by its preparation from water,  $F_5IO$  is not readily hydrolysed. Vibrational spectroscopy and  $^{19}F$  nmr studies point to the 6-coordinate  $C_{4v}$  geometry in Fig. 17.28e (i.e.  $IV^{II}$ ) rather than the alternative 5-coordinate structure  $F_4IV^V OF$ . Microwave spectroscopy yields a value of 1.08 D for the molecular dipole moment.

### 17.2.10 Halogen derivatives of oxoacids

Numerous compounds are known in which the H atom of an oxoacid has been replaced by a halogen atom. Examples are:

halogen(I) perchlorates	$XOCIO_3$ (X=F, Cl, Br, ?I)
halogen(I) fluorosulfates	$XOSO_2F$ (X=F, Cl, Br, I)
halogen(I) nitrates	$XONO_2$ (X=F, Cl, Br, I)

In addition, halogen(III) derivatives such as  $Br(ONO_2)_3$ ,  $I(ONO_2)_3$ ,  $Br(OSO_2F)_3$  and  $I(OSO_2F)_3$  are known, as well as complexes  $M^I-[X^I(ONO_2)_2]$ ,  $M^I-[I^{III}(ONO_2)_4]$ ,  $M^I-[X^{III}(OSO_2F)_4]$  (X=Br, I). In general, thermal stability decreases with increase in atomic number of the halogen.

The properties of halogen(I) perchlorates are in Table 17.25.  $FOClO_3$  was originally prepared

<sup>151</sup> L. E. SMART, *J. Chem. Soc., Chem. Commun.*, 519–20 (1977).

<sup>152</sup> R. J. GILLESPIE and J. P. KRASZNAI, *Inorg. Chem.* **16**, 1384–92 (1977).

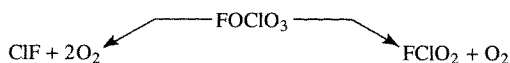
<sup>153</sup> A. J. EDWARDS and A. A. K. HANA, *J. Chem. Soc., Dalton Trans.*, 1734–6 (1980).

<sup>154</sup> R. J. GILLESPIE, J. P. KRASZNAI and D. R. SLIM, *J. Chem. Soc., Dalton Trans.*, 481–3 (1980).

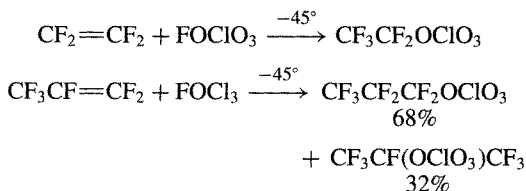
Table 17.25 Properties of halogen(I) perchlorates

Property	FOClO <sub>3</sub>	ClOClO <sub>3</sub>	BrOClO <sub>3</sub>	IOClO <sub>3</sub>
Colour	Colourless	Pale yellow	Red	Not obtained pure
MP/°C	-167.3	-117	< -78	
BP/°C	-15.9	44.5	—	
Decomp temp /°C	~100	20	-20	

by the action of F<sub>2</sub> on concentrated HOClO<sub>3</sub>, but the product had a pronounced tendency to explode on freezing. More recently,<sup>(155)</sup> extremely pure FOClO<sub>3</sub> has been obtained by thermal decomposition of NF<sub>4</sub>ClO<sub>4</sub> and such samples can be manipulated and repeatedly frozen without mishap. Thermal decomposition occurs via two routes:

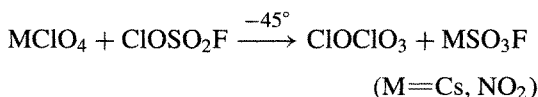


It readily oxidizes iodide ions:  $\text{FOClO}_3 + 2\text{I}^- \longrightarrow \text{ClO}_4^- + \text{F}^- + \text{I}_2$ . FOClO<sub>3</sub> also adds to C=C double bonds in fluorocarbons to give perfluoroalkyl perchlorates:



The formation of isomers in this last reaction implies a low bond polarity of FO- in FOClO<sub>3</sub>.

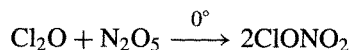
Chlorine perchlorate, ClOClO<sub>3</sub>, is made by low-temperature metathesis:



The bromine analogue can be made similarly using BrOSO<sub>2</sub>F at -20° or by direct bromination of ClOClO<sub>3</sub> with Br<sub>2</sub> at -45°. Both compounds

are thermally unstable and shock sensitive; e.g. ClOClO<sub>3</sub> decomposes predominantly to Cl<sub>2</sub>O<sub>6</sub> with smaller amounts of ClO<sub>2</sub>, Cl<sub>2</sub> and O<sub>2</sub> on gentle warming. Direct iodination of ClOClO<sub>3</sub> at -50° yields the polymeric white solid I(OClO<sub>3</sub>)<sub>3</sub> rather than IOClO<sub>3</sub>; this latter compound has never been obtained pure but is among the products of the reaction of I<sub>2</sub> with AgClO<sub>4</sub> at -85°, the other products being I(OClO<sub>3</sub>)<sub>3</sub>, Ag[I(OClO<sub>3</sub>)<sub>2</sub>] and AgI.

Halogen nitrates are even less thermally stable than the perchlorates: they are made by the action of AgNO<sub>3</sub> on an alcoholic solution of the halogen at low temperature. With an excess of AgNO<sub>3</sub>, bromine and iodine yield X(ONO<sub>2</sub>)<sub>3</sub>. Numerous other routes are available; e.g., the reaction of ClF on HONO<sub>2</sub> gives a 90% yield of ClONO<sub>2</sub> and the best preparation of this compound is probably the reaction



Some physical properties are in Table 17.26. Both FONO<sub>2</sub> and ClONO<sub>2</sub> feature planar NO<sub>3</sub> groups with the halogen atom out of the plane. ClONO<sub>2</sub> has been used to convert metal chlorides to anhydrous metal nitrates, e.g. Ti(NO<sub>3</sub>)<sub>4</sub>. Likewise ICl<sub>3</sub> at -30° yields I(ONO<sub>2</sub>)<sub>3</sub>. ClONO<sub>2</sub> and IONO<sub>2</sub> add across C=C double bonds, e.g.:

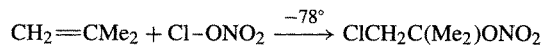


Table 17.26 Some properties of halogen(I) nitrates

Property	FONO <sub>2</sub>	ClONO <sub>2</sub>	BrONO <sub>2</sub>	IONO <sub>2</sub>
Colour	Colourless	Colourless	Yellow	Yellow
MP/°C	-175	-107	-42	—
BP/°C	-45.9	18	—	—
Decomp temp/°C	Ambient	Ambient	<0	<0
ΔH <sub>f</sub> <sup>o</sup> (g, 298 K)/ kJ mol <sup>-1</sup>	+10.5	+29.2	—	—
ΔG <sub>f</sub> <sup>o</sup> (g, 298 K)/ kJ mol <sup>-1</sup>	+73.5	+92.4	—	—

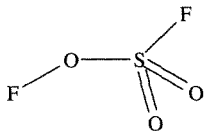
Several other reactions have been studied but the overall picture is one of thermal instability,

<sup>155</sup> C. J. SCHACK and K. O. CHRISTE, *Inorg. Chem.* **18**, 2619–20 (1979). For vibrational spectra, thermodynamic properties and confirmation of C<sub>s</sub> structure see K. O. CHRISTE and E. C. CURTIS, *Inorg. Chem.* **21**, 2938–45 (1982).

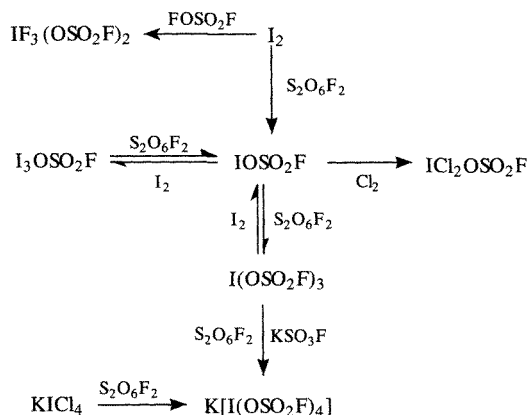


hazardous explosions, and vigorous chemical reactivity leading to complex mixtures of products.

The halogen fluorosulfates are amongst the most stable of the oxoacid derivatives of the halogens. FOSO<sub>2</sub>F is made by direct addition of F<sub>2</sub> to SO<sub>3</sub> and the others are made by direct combination of the halogen with an equimolar quantity of peroxodisulfuryl difluoride, S<sub>2</sub>O<sub>6</sub>F<sub>2</sub> (p. 640). With an excess of S<sub>2</sub>O<sub>6</sub>F<sub>2</sub>, bromine and iodine yield X(OSO<sub>2</sub>F)<sub>3</sub>. An alternative route to ClOSO<sub>2</sub>F is the direct addition of ClF to SO<sub>3</sub>, whilst BrOSO<sub>2</sub>F and IOSO<sub>2</sub>F can be made by thermal decomposition of the corresponding X(OSO<sub>2</sub>F)<sub>3</sub>. The halogen fluorosulfates are thermally unstable, moisture sensitive, highly reactive compounds. Some physical properties are summarized in Table 17.27. The vibrational spectra of FOSO<sub>2</sub> and ClOSO<sub>2</sub>F are consistent with C<sub>s</sub> molecular symmetry as in HOSO<sub>2</sub>F:



Much of the chemistry of the halogen fluorosulfates resembles that of the interhalogens (p. 824) and in many respects the fluorosulfate group can be regarded as a pseudohalogen (p. 319). There is some evidence of ionic self-dissociation and reactions can be classified as exchange, addition, displacement and complexation. This is illustrated for the iodine fluorosulfates in the following scheme:<sup>(156)</sup>



BrOSO<sub>2</sub>F has also been used to prepare new *N*-bromo sulfonyl imides such as (CF<sub>3</sub>SO<sub>2</sub>)<sub>2</sub>NBr.<sup>(157)</sup> Other novel compounds include [I(OSO<sub>2</sub>F)<sub>2</sub>]<sup>+</sup>I<sup>-</sup><sup>(158)</sup> and the mixed valent iodine (III,V) polyanion in [(IO<sub>2</sub>)<sub>3</sub>]<sup>+</sup>HSO<sub>4</sub><sup>-</sup>.<sup>(159)</sup>

## 17.3 The Chemistry of Astatine<sup>(160,161)</sup>

All isotopes of element 85, astatine, are intensely radioactive with very short half-lives (p. 795). As a consequence weighable amounts of the element or its compounds cannot be prepared and no bulk properties are known. The chemistry of the element must, of necessity, be studied by tracer techniques on extremely dilute solutions, and this introduces the risk of experimental errors and the consequent possibility of erroneous

**Table 17.27** Some physical properties of halogen fluorosulfates<sup>(a)</sup>

Property	FOSO <sub>2</sub> F	ClOSO <sub>2</sub> F	BrOSO <sub>2</sub> F	IOSO <sub>2</sub> F
Colour	Colourless	Yellow	Red-brown	Black
State at room temp	Gas	Liquid	Liquid	Solid
MP/°C	-158.5	-84.3	-31.5	51.5
BP/°C	-31.3	45.1	117.3	—

<sup>(a)</sup>Br(OSO<sub>2</sub>F)<sub>3</sub> is a pale yellow solid, mp 59°; I(OSO<sub>2</sub>F)<sub>3</sub> is a pale yellow solid, mp 32°.

<sup>157</sup> S. SINGH and D. D. DESMARTEAU, *Inorg. Chem.* **25**, 4596-7 (1986).

<sup>158</sup> M. J. COLLINS, G. DÉNÈS and R. J. GILLESPIE, *J. Chem. Soc., Chem. Commun.*, 1296-7 (1984).

<sup>159</sup> A. REHR and M. JANSEN, *Z. anorg. allg. Chem.* **608**, 159-65 (1992).

<sup>160</sup> E. H. APPELMAN, Astatine, Chap. 6 in *MTP International Review of Science, Inorganic Chemistry*, Series 1. Vol. 3, *Main Group Elements Group VII and Noble Gases*, pp. 181-98, Butterworths, London, 1972; see also ref. 23, pp. 1573-94, Astatine.

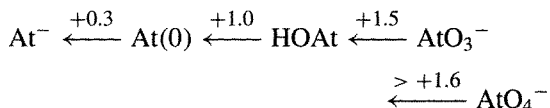
<sup>161</sup> T. J. RUTH, M. DOMBSKY, J. M. D'AURIA and T. E. WARD, *Radiochemistry of Astatine*, US Dept. of Energy, Nuclear Science Series NAS-NS-3064 (DE 880 15386), Washington, DC, 1988, 80 pp.

<sup>156</sup> Ref. 23, pp. 1466-75, Halogen derivatives of oxyacids.

conclusions. Nevertheless, a picture of the element is emerging, as outlined below. The synthesis of the element (p. 795), its natural occurrence in rare branches of the  $^{235}\text{U}$  decay series (p. 796), and its atomic properties (p. 800) have already been mentioned.

The chemistry of At is most conveniently studied using  $^{211}\text{At}$  ( $t_{1/2}$  7.21 h). This isotope is prepared by  $\alpha$ -particle bombardment of  $^{209}\text{Bi}$  using acceleration energies in the range 26–29 MeV. Higher energies result in the concurrent formation of  $^{210}\text{At}$  and  $^{209}\text{At}$  which complicate the subsequent radiochemical assays. The Bi is irradiated either as the metal or its oxide and the target must be cooled to avoid volatilization of the At produced. Astatine is then removed by heating the target to 300–600° (i.e. above the mp of Bi, 217°) in a stream of  $\text{N}_2$  and depositing the sublimed element on a glass cold finger or cooled Pt disc. Aqueous solutions of the element can be prepared by washing the cold finger or disc with dilute  $\text{HNO}_3$  or  $\text{HCl}$ . Alternatively, the irradiated target can be dissolved in perchloric acid containing a little iodine as carrier for the astatine; the Bi is precipitated as phosphate and the aqueous solution of AtI used as it is or the activity can be extracted into  $\text{CCl}_4$  or  $\text{CHCl}_3$ .

Five oxidation states of At have been definitely established (–I, 0, +I, V, VII) and one other (III) has been postulated. The standard oxidation potentials connecting these states in 0.1 M acid solution are  $E^\circ/V$ ):



These values should be compared with those for the other halogens (in 1 M acid) (p. 854). Noteworthy features are that At is the only halogen with an oxidation state between 0 and V that is thermodynamically stable towards disproportionation, and that the smooth trends in the values of  $E^\circ(\frac{1}{2}\text{X}_2/\text{X}^-)$  and  $E^\circ(\text{HOX}/\frac{1}{2}\text{X}_2)$  continue to At.

The astatide ion  $\text{At}^-$  (which coprecipitates with  $\text{AgI}$ ,  $\text{TlI}$ ,  $\text{PtI}_2$  or  $\text{PdI}_2$ ) can be obtained from  $\text{At}(0)$  or  $\text{AtI}$  using moderately powerful reducing agents, e.g.  $\text{Zn}/\text{H}^+$ ,  $\text{SO}_2$ ,  $\text{SO}_3^{2-}/\text{OH}^-$ ,  $[\text{Fe}(\text{CN})_6]^{4-}$  or  $\text{As}^{\text{III}}$ . Reoxidation to  $\text{At}(0)$  can be effected by the weak oxidants  $[\text{Fe}(\text{CN})_6]^{3-}$ ,  $\text{As}^{\text{V}}$  or dilute  $\text{HNO}_3$ . Oxidants of intermediate power (e.g.  $\text{Cl}_2$ ,  $\text{Br}_2$ ,  $\text{Fe}^{3+}$ ,  $\text{Cr}_2\text{O}_7^{2-}$ ,  $\text{VO}^{2+}$ ) convert astatine to an intermediate oxidation state which is most probably  $\text{AtO}^-$  or  $\text{At}^+$  and which does not extract into  $\text{CCl}_4$ . Powerful oxidants ( $\text{Ce}^{\text{IV}}$ ,  $\text{NaBiO}_3$ ,  $\text{S}_2\text{O}_8^{2-}$ ,  $\text{IO}_4^-$ ) convert  $\text{At}(0)$  directly to  $\text{AtO}_3^-$  (carried by  $\text{AgIO}_3$ ,  $\text{Ba}(\text{IO}_3)_2$ , etc., and not extractable into  $\text{CCl}_4$ ). The perastatate ion,  $\text{AtO}_4^-$ , was first conclusively prepared by V. A. Khalkin's group in the USSR in 1970 using solid  $\text{XeF}_2$  in hot  $\text{NaOH}$  solution at  $\text{pH} \sim 10$ . It is unstable in acid solutions, being completely decomposed to  $\text{AtO}_3^-$  within 5–10 minutes at  $\text{pH} 1$  and  $90^\circ\text{C}$ , for example.

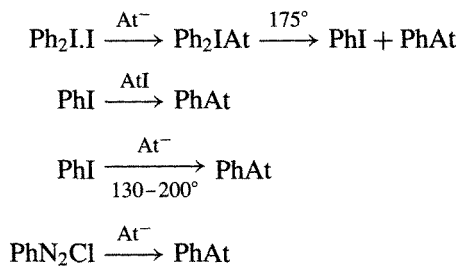
$\text{At}(0)$  reacts with halogens  $\text{X}_2$  to produce interhalogen species  $\text{AtX}$ , which can be extracted into  $\text{CCl}_4$ , whereas halide ions  $\text{X}^-$  yield polyhalide ions  $\text{AtX}_2^-$  which are not extracted by  $\text{CCl}_4$  but can be extracted into  $\text{Pr}_2\text{O}$ . The equilibrium formation constants of the various trihalide ions are intercompared in Table 17.28.

A rudimentary chemistry of organic derivatives of astatine is emerging, but the problems of radiation damage, product separation and tracer

**Table 17.28** Formation constants for trihalide ions at  $25^\circ\text{C}$

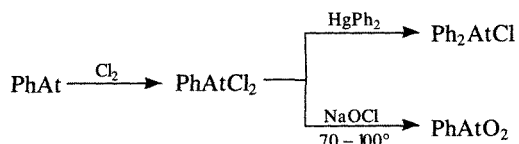
Reaction	$K/\text{l mol}^{-1}$	Reaction	$K/\text{l mol}^{-1}$
$\text{Cl}_2 + \text{Cl}^- \rightleftharpoons \text{Cl}_3^-$	0.12	$\text{AtI} + \text{Br}^- \rightleftharpoons \text{AtIBr}^-$	120
$\text{Br}_2 + \text{Cl}^- \rightleftharpoons \text{Br}_2\text{Cl}^-$	1.4	$\text{ICl} + \text{Cl}^- \rightleftharpoons \text{ICl}_2^-$	170
$\text{I}_2 + \text{Cl}^- \rightleftharpoons \text{I}_2\text{Cl}^-$	3	$\text{AtBr} + \text{Br}^- \rightleftharpoons \text{AtBr}_2^-$	320
$\text{AtI} + \text{Cl}^- \rightleftharpoons \text{AtICl}^-$	9	$\text{IBr} + \text{Br}^- \rightleftharpoons \text{IBr}_2^-$	440
$\text{Br}_2 + \text{Br}^- \rightleftharpoons \text{Br}_3^-$	17	$\text{I}_2 + \text{I}^- \rightleftharpoons \text{I}_3^-$	800
$\text{IBr} + \text{Cl}^- \rightleftharpoons \text{IBrCl}^-$	43	$\text{AtI} + \text{I}^- \rightleftharpoons \text{AtI}_2^-$	2000

identification, already severe for inorganic compounds of astatine, are even worse with organic derivatives. Two reviews are available.<sup>(162,163)</sup> Various compounds of the type RAt, RAtCl<sub>2</sub>, R<sub>2</sub>AtCl and RAtO<sub>2</sub> (R = phenyl or *p*-tolyl) have been synthesized using astatine-labelled iodine reagents, e.g.:



<sup>162</sup> K. BEREI and L. VASAROS, The Organic Chemistry of Astatine, in S. PATAI and Z. RAPPAPORT (eds.), *The Chemistry of Organic Functional Groups*, Wiley, New York, 1983.

<sup>163</sup> H. H. COENEN, S. M. MOERLEIN and G. STÖCKLIN, *Radiochem. Acta* **34**, 47-68 (1983).



In addition, demercuration reactions have resulted in a wide variety of rather complex compounds including aromatic aminoacids, steroids, imidazols, etc. in good yields (at the tracer level). The driving force in these studies has been the hope of incorporating <sup>211</sup>At into biologically active compounds for therapeutic use.

Astatine has been shown to be superior to radio-iodine for the destruction of abnormal thyroid tissue (p. 794) because of the localized action of the emitted  $\alpha$ -particles which dissipate 5.9 MeV within a range of 70  $\mu\text{m}$  of tissue, whereas the much less energetic  $\beta$ -rays of radio-iodine have a maximum range of *ca.* 2000  $\mu\text{m}$ . However, its general inaccessibility and high cost render its extensive application unlikely.

		H He																		B C N O F Ne											
3	4																	13	14	15	16	17	18								
Li	Be																	Al	Si	P	S	Cl	Ar								
11	12																	19	20	21	22	23	24								
Na	Mg																	K	Ca	Sc	Ti	V	Cr								
19	20	21	22	23	24	25	26	27	28	29	30	31	32	33	34	35	36														
K	Ca	Sc	Ti	V	Cr	Mn	Fe	Co	Ni	Cu	Zn	Ga	Ge	As	Se	Br	Kr														
37	38	39	40	41	42	43	44	45	46	47	48	49	50	51	52	53	54														
Rb	Sr	Y	Zr	Nb	Mo	Tc	Ru	Rh	Pd	Ag	Cd	In	Sn	Sb	Te	I	Xe														
55	56	57	58	59	60	61	62	63	64	65	66	67	68	69	70	71	72														
Cs	Ba	La	Hf	Ta	W	Re	Os	Ir	Pt	Au	Hg	Tl	Pb	Bi	Po	At	Rn														
87	88	89	90	91	92	93	94	95	96	97	98	99	100	101	102	103	104														
Fr	Ra	Ac	Rf	Db	Sg	Bh	Hs	Mt	Uun	Uun	Uub																				
																		58 59 60 61 62 63 64 65 66 67 68 69 70 71 72													
																		Ce	Pr	Nd	Pm	Sm	Eu	Gd	Tb	Dy	Ho	Er	Tm	Yb	Lu
																		88 89 90 91 92 93 94 95 96 97 98 99 100 101 102 103 104													
																		Th	Pa	U	Np	Pu	Am	Cm	Bk	Cf	Es	Fm	Md	No	Lr

# 18

## The Noble Gases: Helium, Neon, Argon, Krypton, Xenon and Radon

### 18.1 Introduction

In 1785 H. Cavendish in his classic work on the composition of air (p. 406) noted that, after repeatedly sparking a sample of air with an excess of O<sub>2</sub>, there was a small residue of gas which he was unable to remove by chemical means and which he estimated with astonishing accuracy to be “not more than  $\frac{1}{120}$ th part of the whole”. He could not further characterize this component of air, and its identification as argon had to wait for more than a century. But first came the discovery of helium, which is unique in being the only element discovered extraterrestrially before being found on earth. During the solar eclipse of 18 August 1868, a new yellow line was observed close to the sodium D lines in the spectrum of the sun’s chromosphere. This led J. N. Lockyer (founder in 1869 of the journal *Nature*) and E. Frankland to suggest the existence of a new element which, appropriately, they named helium (Greek  $\eta\lambda\iota\omicron\varsigma$ , the sun). The same line was observed by L. Palmieri in 1881

in the spectrum of volcanic gas from Mount Vesuvius, and the terrestrial existence of helium was finally confirmed by W. Ramsay<sup>(1)</sup> in the course of his intensive study of atmospheric gases which led to the recognition of a new group in the periodic table. This work was initiated by the physicist, Lord Rayleigh, and was recognized in 1904 by the award of the Nobel Prizes for Chemistry and Physics to Ramsay and Rayleigh respectively.

In order to test Prout’s hypothesis (that the atomic weights of all elements are multiples of that of hydrogen) Rayleigh made accurate measurements of the densities of common gases and found, to his surprise, that the density of nitrogen obtained from air by the removal of O<sub>2</sub>, CO<sub>2</sub> and H<sub>2</sub>O was consistently about 0.5% higher than that of nitrogen obtained chemically from ammonia. Ramsay then treated “atmospheric nitrogen” with heated magnesium ( $3\text{Mg} + \text{N}_2 \longrightarrow \text{Mg}_3\text{N}_2$ ), and was left with a small amount of a much

<sup>1</sup> M. W. TRAVERS, *Life of Sir William Ramsay*, E. Arnold, London, 1956.

denser, monatomic gas<sup>†</sup> which, in a joint paper [*Proc. R. Soc.* **57**, 265 (1895)], was identified as a new element which was named *argon* (Greek ἀργόν, idle or lazy) because of its inert nature. Unfortunately there was no space for a new and unreactive, gaseous, element in the periodic table (p. 20), which led to Ramsay's audacious suggestion that a whole new group might be accommodated. By 1898 Ramsay and M. W. Travers had isolated three further new elements by the low-temperature distillation of liquid air (which had only recently become available) and characterized them by spectroscopic analysis: krypton (Greek κρυπτόν, hidden, concealed), neon (Greek νέον, new) and xenon (Greek ξένον, strange).

In 1895 Ramsay also identified helium as the gas previously found occluded in uranium minerals and mistakenly reported as nitrogen. Five years later he and Travers isolated helium from samples of atmospheric neon.

Element 86, the final member of the group, is a short-lived, radioactive element, formerly known as radium-emanation or niton or, depending on which radioactive series it originates in (i.e. which isotope) as radon, thoron, or actinon. It was first isolated and studied in 1902 by E. Rutherford and F. Soddy and is now universally known as radon (from radium and the termination -on adopted for the noble gases; Latin *radius*, ray).

Once the existence of the new group had been established it was apparent that it not only fitted into the periodic table but actually improved it by providing a bridge between the strongly electronegative halogens and strongly electropositive alkali metals. The elements became known as "inert gases" comprising Group 0, though A. von Antropoff suggested that a maximum valency of eight might be attainable and designated them as Group VIIIB. They have also been described as

the "rare gases" but, since the lighter members are by no means rare and the heavier ones are not entirely inert, "noble" gases seems a more appropriate name and has come into general use during the past three decades as has their designation as Group 18 of the periodic table.

The apparent inertness of the noble gases gave them a key position in the electronic theories of valency as developed by G. N. Lewis (1916) and W. Kossel (1916) and the attainment of a "stable octet" was regarded as a prime criterion for bond formation between atoms (p. 21). Their monatomic, non-polar nature makes them the most nearly "perfect" gases known, and has led to continuous interest in their physical properties.

## 18.2 The Elements

### 18.2.1 Distribution, production and uses<sup>(2,3)</sup>

Helium is the second most abundant element in the universe (76% H, 23% He) as a result of its synthesis from hydrogen (p. 9) but, being too light to be retained by the earth's gravitational field, all primordial helium has been lost and terrestrial helium, like argon, is the result of radioactive decay (<sup>4</sup>He from  $\alpha$ -decay of heavier elements, <sup>40</sup>Ar from electron capture by <sup>40</sup>K (p. 18).

The noble gases make up about 1% of the earth's atmosphere in which their major component is Ar. Smaller concentrations are occluded in igneous rocks, but the atmosphere is the principal commercial source of Ne, Ar, Kr and Xe, which are obtained as by-products of the liquefaction and separation of air (p. 604). Some Ar is also obtained from synthetic ammonia plants in which it accumulates after entering as impurity in the N<sub>2</sub> and H<sub>2</sub> feeds. World production of

<sup>†</sup> The molecular weight (mean relative molecular mass) was obtained by determination of density but, in order to determine that the gas was monatomic and its atomic and molecular weights identical, it was necessary to measure the velocity of sound in the gas and to derive from this the ratio of its specific heats: kinetic theory predicts that  $C_p/C_v = 1.67$  for a monatomic and 1.40 for a diatomic gas.

<sup>2</sup> Helium group gases, in *Kirk-Othmer Encyclopedia of Chemical Technology*, 4th edn, Vol. 13, pp. 1-53. Wiley-Interscience, New York, 1995.

<sup>3</sup> W. J. GRANT and S. L. REDFEARN, *Industrial gases*, in R. THOMPSON (ed.), *The Modern Inorganic Chemicals Industry*, pp. 273-301. The Chemical Society, London, 1977.

Ar in 1975 was 700 000 tonnes for use mainly as an inert atmosphere in high-temperature metallurgical processes and, in smaller amounts, for filling incandescent lamps. By 1993, production had increased considerably and 716 000 tonnes ( $427 \times 10^6 \text{ m}^3$ ) were produced in the USA alone. The price was  $\$0.76/\text{m}^3$  for bulk supplies and  $\$2.6\text{--}8.5/\text{m}^3$  for laboratory quantities, depending on purity. Along with Ne, Kr and Xe, which are produced on a much smaller scale, Ar is also used in discharge tubes — the so-called neon lights for advertisements — (the colour produced depending on the particular mixture of gases used). They are also used in fluorescent tubes, though here the colour produced depends not on the gas but on the phosphor which is coated on the inside walls of the tube. Lasers are another important application, though the actual amount of gas required for this use is minute compared with the other uses.

Although the concentration of He in the atmosphere is five times that of Kr and sixty times that of Xe (see Table 18.1), its recovery from this source is uneconomical compared to that from natural gas if more than 0.4% He is present. This concentration is attained in a number of gases in the USA (concentrations as high as 7% are known) and in eastern Europe (mainly Poland). Some  $99 \times 10^6 \text{ m}^3$  (16 800 tonnes) of He was produced in the USA in 1993, the bulk price being  $\$1.77/\text{m}^3$  ( $\$2.30/\text{m}^3$  for liquid He). Laboratory quantities were in the range  $\$5.00\text{--}45.00/\text{m}^3$  depending on purity. The former use of He as a non-flammable gas (it has a lifting power of approximately 1 kg per  $\text{m}^3$ ) in airships is no longer important, though it is still employed in meteorological balloons. The primary domestic use of He (30%) is as a cryogenic fluid for temperatures at or below 4.2 K; as much as two-thirds of this is for magnetic resonance imaging and other nmr instruments. Other major uses are in arc welding (21%), pressurizing and purging (11%). The choice between Ar and He for these purposes is determined by cost and, except in the USA, this generally favours Ar. Smaller, but important, uses for He are:

- (a) as a substitute for  $\text{N}_2$  in synthetic breathing gas for deep-sea diving (its low solubility

in blood minimizes the degassing which occurs with  $\text{N}_2$  when divers are depressurized and which produces the sometimes fatal “bends”);

- (b) as a leak detector;  
 (c) as a coolant in HTR nuclear reactors (p. 1258);  
 (d) as a flow-gas in gas-liquid chromatography;  
 (e) for deaeration of solutions and as a general inert diluent or inert atmosphere.

The price per  $\text{m}^3$  of the other noble gases is considerably higher (Ne  $\$70$ , Kr  $\$350$  and Xe  $\$3500$ , and this tends to restrict their usage to specialist applications only. Radon has been used in the treatment of cancer and as a radioactive source in testing metal castings but, because of its short half-life (3.824 days) it has been superseded by more convenient materials. Such small quantities as are required are obtained as a decay product of  $^{226}\text{Ra}$  (1 g of which yields  $0.64 \text{ cm}^3$  in 30 days).

### 18.2.2 Atomic and physical properties of the elements<sup>(2-4)</sup>

Some of the important properties of the elements are given in Table 18.1. The imprecision of the atomic weights of Kr and Xe reflects the natural occurrence of several isotopes of these elements. For He, however, and to a lesser extent Ar, a single isotope predominates ( $^4\text{He}$ , 99.999 863%;  $^{40}\text{Ar}$ , 99.600%) and much greater precision is possible. The natural preponderance of  $^{40}\text{Ar}$  is indeed responsible for the well-known inversion of atomic weight order of Ar and K in the periodic table, and the position of Ar in front of K was only finally accepted when it was shown that the atomic weight of He placed it in front of Li. The second isotope of helium,  $^3\text{He}$ , has only been available in significant amounts since

<sup>4</sup> A. H. COCKETT and K. C. SMITH, Chap. 5 in *Comprehensive Inorganic Chemistry*, Vol. 1, pp. 139–211, Pergamon Press, Oxford, 1973. G. A. COOK (ed.), *Argon, Helium and the Rare Gases*, 2 vols, Interscience, New York, 1961, 818 pp.

Table 18.1 Some properties of the noble gases

Property	He	Ne	Ar	Kr	Xe	Rn
Atomic number	2	10	18	36	54	86
Number of naturally occurring isotopes	2	3 <sup>(a)</sup>	3	6	9	(1)
Atomic weight	4.002 602(2)	20.179 7(6)	39.948(1)	83.80(1)	131.29(2)	(222) <sup>(b)</sup>
Abundance in dry air/ppm by vol	5.24	18.21	9340	1.14	0.087	Variable traces <sup>(c)</sup>
Abundance in igneous rocks/ppm by wt	$3 \times 10^{-3}$	$7 \times 10^{-5}$	$4 \times 10^{-2}$	—	—	$1.7 \times 10^{-10}$
Outer shell electronic configuration	1s <sup>2</sup>	2s <sup>2</sup> 2p <sup>6</sup>	3s <sup>2</sup> 3p <sup>6</sup>	4s <sup>2</sup> 4p <sup>6</sup>	5s <sup>2</sup> 5p <sup>6</sup>	6s <sup>2</sup> 6p <sup>6</sup>
First ionization energy/kJ mol <sup>-1</sup>	2372	2080	1520	1351	1170	1037
BP/K	4.215	27.09	87.28	119.80	165.03	211
°C	-268.93	-246.06	-185.86	-153.35	-108.13	-62
MP/K	— <sup>(d)</sup>	24.56	83.80	115.76	161.37	202
°C	—	-248.61	-189.37	-157.20	-111.80	-71
$\Delta H_{\text{vap}}$ /kJ mol <sup>-1</sup>	0.08	1.74	6.52	9.05	12.65	18.1
Density at STP/mg cm <sup>-3</sup>	0.178 50	0.899 94	1.7838	3.7493	5.8971	9.73
Thermal conductivity at 0°C/J s <sup>-1</sup> m <sup>-1</sup> K <sup>-1</sup>	0.1418	0.0461	0.0169	0.008 74	0.005 06	
Solubility in water at 20°C/cm <sup>3</sup> kg <sup>-1</sup>	8.61	10.5	33.6	59.4	108.1	230

<sup>(a)</sup>In the pioneering work of J. J. Thomson and F. W. Aston on mass-spectrometry, neon was the first non-radioactive element shown to exist in different isotopic forms.

<sup>(b)</sup>The relative atomic mass of this nuclide is 222.0176.

<sup>(c)</sup>Mean value  $\sim 6 \times 10^{-14}$ .

<sup>(d)</sup>Helium is the only liquid which cannot be frozen by the reduction of temperature alone. Pressure must also be applied. It is also the only substance lacking a "triple point", i.e. a combination of temperature and pressure at which solid, liquid and gas coexist in equilibrium.

the 1950s when it began to accumulate as a  $\beta$ -decay product of tritium stored for thermonuclear weapons.

All the elements have stable electronic configurations (1s<sup>2</sup> or  $ns^2np^6$ ) and, under normal circumstances are colourless, odourless and tasteless monatomic gases. The non-polar, spherical nature of the atoms which this implies, leads to physical properties which vary regularly with atomic number. The only interatomic interactions are weak van der Waals forces. These increase in magnitude as the polarizabilities of the atoms increase and the ionization energies decrease, the effect of both factors therefore being to increase the interactions as the sizes of the atoms increase. This is shown most directly by the enthalpy of vaporization, which is a measure of the energy required to overcome the

interactions, and increases from He to Rn by a factor of over 200. However,  $\Delta H_{\text{vap}}$  is in all cases small and bps are correspondingly low, that of He being the lowest of any substance.

The stability of the electronic configuration is indicated by the fact that each element has the highest ionization energy in its period, though the value decreases down the group as a result of increasing size of the atoms. For the heavier elements is it actually smaller than for first-row elements such as O and F with consequences for the chemical reactivities of the noble gases which will be considered in the next section. Nuclear properties, particularly for xenon, have been exploited for nmr spectroscopy<sup>(5)</sup> and Mössbauer

<sup>5</sup>C. J. JAMESON in J. MASON (ed.), *Multinuclear NMR*, Plenum Press, New York, 1987, pp. 463–77.

spectroscopy<sup>(6)</sup> (p. 896). The environmental health hazard posed by the natural generation of radioactive radon gas should also be noted.<sup>(7)</sup>

As the first member of this unusual group He has, of course, a number of unique properties. Among these is the astonishing transition from so-called HeI to HeII which occurs around 2.2 K (the  $\lambda$ -point temperature) when liquid He ( $^4\text{He}$  to be precise, since  $^3\text{He}$  does not behave in this way until 1–3 millikelvin) is cooled by continuous pumping. The transition is clearly seen as the sudden cessation of turbulent boiling, even though evaporation continues. HeI is a normal liquid but at the transition the specific heat increases abruptly by a factor of 10, the thermal conductivity by the order of  $10^6$ , and the viscosity, as measured by its flow through a fine capillary, becomes effectively zero (hence its description as a “superfluid”). HeII also has the curious ability to cover, with a film a few hundred atoms thick, all solid surfaces which are connected to it and are below the  $\lambda$  point. This can be spectacularly demonstrated by dipping the bottom of a suitable container into a bath of HeII. Once the vessel has cooled, liquid He flows, apparently without friction, up and over the edge of the container until the levels inside and outside are equal. These phenomena are evidently the result of quantum effects on a macroscopic scale, and HeII is believed to consist of two components: a true superfluid with zero viscosity and entropy, together with a normal fluid, the fraction of the former increasing to 1 at absolute zero. No completely satisfactory explanation of these phenomena is yet available.

Finally, a property of practical importance which may be noted is the ability of noble gases, especially He, to diffuse through many materials commonly used in laboratories. Rubber and PVC

are cases in point, and He will even diffuse through most glasses so that glass Dewar vessels cannot be used in cryoscopic work involving liquid He.

## 18.3 Chemistry of the Noble Gases<sup>(8–12)</sup>

The discovery of the noble gases was a direct result of their unreactive nature, and early unsuccessful attempts to induce chemical reactions reinforced the belief in their inertness. Nevertheless, attempts were made to make the heavier gases react, and in 1933 Linus Pauling, from a consideration of ionic radii, suggested that  $\text{KrF}_6$  and  $\text{XeF}_6$  should be preparable. D. M. Yost and A. L. Kaye attempted to prepare the latter by passing an electric discharge through a mixture of Xe and  $\text{F}_2$  but failed<sup>†</sup> and, until “ $\text{XePtF}_6$ ” was prepared in 1962, the only compounds of the noble gases which could be prepared were clathrates.

While investigating the chemistry of  $\text{PtF}_6$ , N. Bartlett noticed that its accidental exposure to air produced a change in colour, and with D. H. Lohmann he later showed this to be  $\text{O}_2^{+}[\text{PtF}_6]^{-}$ .<sup>(13)</sup> Recognizing that  $\text{PtF}_6$  must therefore be an oxidizing agent of unprecedented power, he noted that Rn and Xe should similarly be oxidizable by this reagent since the first ionization energy of Rn is less than, and that of

<sup>8</sup> N. BARTLETT and F. E. SLADKY, Chap. 6, in *Comprehensive Inorganic Chemistry*, Vol. 1, pp. 213–330, Pergamon Press, Oxford, 1973.

<sup>9</sup> D. T. HAWKINS, W. E. FALCONER and N. BARTLETT, *Noble Gas Compounds, A Bibliography 1962–1976*. Plenum Press, New York, 1978.

<sup>10</sup> J. H. HOLLOWAY, *Noble-gas Chemistry*, Methuen, London, 1968, 213 pp. See also *Chem. in Britain*, July 1987, pp. 658–64.

<sup>11</sup> K. SEPPELT and D. LENTZ, *Progr. Inorg. Chem.* **29**, 167–202 (1982).

<sup>12</sup> pp. 38–53 of ref. 2.

<sup>13</sup> N. BARTLETT and D. H. LOHMANN, *Proc. Chem. Soc.* 1962, 115–6.

<sup>†</sup> By what must have seemed to these workers a cruel irony, essentially the same method, but using sunlight instead of a discharge, when tried 30 years later produced  $\text{XeF}_2$ .

<sup>6</sup> N. N. GREENWOOD and T. C. GIBB, *Mössbauer Spectroscopy*, Chapman and Hall, London 1971, <sup>83</sup>Kr pp. 437–41; <sup>129</sup>Xe, <sup>131</sup>Xe pp. 482–6.

<sup>7</sup> P. K. HOPKE (ed.), *Radon and its Decay Products: Occurrence, Properties and Health Effects* ACS Symposium Series No. 331, 1986, 586 pp. D. J. HANSON, *Chem. & Eng. News*, Feb. 6, 1989, pp. 7–13. A. F. GARDNER, R. S. GILLET and P. S. PHILLIPS, *Chem. in Britain*, April 1992, pp. 344–8.



Xe is comparable to, that of molecular oxygen ( $1175 \text{ kJ mol}^{-1}$  for  $\text{O}_2 \rightarrow \text{O}_2^+ + \text{e}^-$ ). He quickly proceeded to show that deep-red  $\text{PtF}_6$  vapour spontaneously oxidized Xe to produce an orange-yellow solid and announced this in a brief note.<sup>(14)</sup> Within a few months  $\text{XeF}_4$  and  $\text{XeF}_2$  had been synthesized in other laboratories.<sup>(15,16)</sup> Noble-gas chemistry had begun.

Isolable compounds are obtained only with the heavier noble gases Kr and Xe; radon also reacts with  $\text{F}_2$  but isolation and characterization of products is hampered by its intense radioactivity which is not only hazardous but also decomposes the reagents involved. The compounds usually involve bonds to F or O, in most cases exclusively so. However, a growing number of compounds involving bonds to Cl, N and even C are becoming known (p. 901). Chemical combinations involving the lighter noble gases have been observed but are very unstable, and frequently occur only as transient species (p. 903).

### 18.3.1 Clathrates

Probably the most familiar of all clathrates are those formed by Ar, Kr and Xe with quinol,  $1,4\text{-C}_6\text{H}_4(\text{OH})_2$ , and with water. The former are obtained by crystallizing quinol from aqueous or other convenient solution in the presence of the noble gas at a pressure of 10–40 atm. The quinol crystallizes in the less-common  $\beta$ -form, the lattice of which is held together by hydrogen bonds in such a way as to produce cavities in the ratio 1 cavity: 3 molecules of quinol. Molecules of gas (G) are physically trapped in these cavities, there being only weak van der Waals interactions between

“guest” and “host” molecules. The clathrates are therefore nonstoichiometric but have an “ideal” or “limiting” composition of  $[\text{G}\{\text{C}_6\text{H}_4(\text{OH})_2\}_3]$ . Once formed they have considerable stability but the gas is released on dissolution or melting. Similar clathrates are obtained with numerous other gases of comparable size, such as  $\text{O}_2$ ,  $\text{N}_2$ , CO and  $\text{SO}_2$  (the first clathrate to be fully characterized, by H. M. Powell in 1947) but not He or Ne, which are too small or insufficiently polarizable to be retained.

Noble gas hydrates are formed similarly when water is frozen under a high pressure of gas (p. 626). They have the ideal composition,  $[\text{G}_8(\text{H}_2\text{O})_{46}]$ , and again are formed by Ar, Kr and Xe but not by He or Ne. A comparable phenomenon occurs when synthetic zeolites (molecular sieves) are cooled under a high pressure of gas, and Ar and Kr have been encapsulated in this way (p. 358). Samples containing up to 20% by weight of Ar have been obtained.

Clathrates provide a means of storing noble gases and of handling the various radioactive isotopes of Kr and Xe which are produced in nuclear reactors.

### 18.3.2 Compounds of xenon

The chemistry of Xe is much the most extensive in this group and the known oxidation states of Xe range from +2 to +8. Details of some of the more important compounds are given in Table 18.2. There is clearly a rich variety of stereochemistries, though the description of these depends on whether only nearest-neighbour atoms are considered or whether the supposed disposition of lone-pairs of electrons is also included. Weaker secondary interactions in crystalline compounds also tend to increase the number of atoms surrounding a central Xe atom. For example,  $[\text{XeF}_5]^+[\text{AsF}_6]^-$  has 5 F at 179–182 pm and three further F at 265–281 pm, whereas  $[\text{XeF}_5]^+[\text{RuF}_6]^-$  has 5 F at 179–184 pm and four further F at 255–292 pm. If only the most closely bonded atoms are counted, then Xe is known with all coordination numbers from 0 to 8 as shown schematically in Table 18.3.

<sup>14</sup> N. BARTLETT, *Proc. Chem. Soc.* 1962, 218.

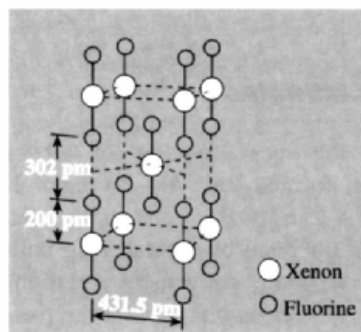
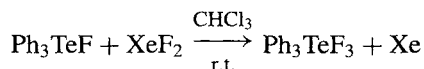
<sup>15</sup> H. H. CLAASSEN, H. SELIG and J. G. MALM, *J. Am. Chem. Soc.* **84**, 3593 (1962). See also P. LAZLO and G. J. SCHROBILGEN, *Angew. Chem. Int. Edn. Engl.* **28**, 636 (1989) for further detailed chronology of the first synthesis of  $\text{XeF}_4$ .

<sup>16</sup> R. HOPPE, W. DÄHNE, H. MATTAUCH and K. H. RÖDDER, *Angew. Chem.* **74**, 903 (1962). See also note on priorities by W. KLEMM, *Nachr. Chem. Tech. Lab.* **30**, 963 (1982).

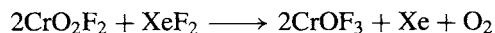
Table 18.2 Some compounds of xenon with fluorine and oxygen

Oxidation State	Compound	MP/°C	Stereochemistry of Xe	
			Actual	Pseudo, i.e. with electron lone-pairs (in parentheses) included
+2	XeF <sub>2</sub>	129	<i>D</i> <sub>∞h</sub> , linear	Trigonal bipyramidal (3)
+4	XeF <sub>4</sub>	117.1	<i>D</i> <sub>4h</sub> , square planar	Octahedral (2)
+6	XeF <sub>6</sub>	49.5	Distorted octahedral (fluxional)	Pentagonal bipyramidal or capped octahedral (1)
	[XeF <sub>5</sub> ] <sup>+</sup> [AsF <sub>6</sub> ] <sup>-</sup>	130.5	<i>C</i> <sub>4v</sub> , square pyramidal	Octahedral (1)
	CsXeF <sub>7</sub>	dec > 40		
	[NO] <sup>+</sup> <sub>2</sub> [XeF <sub>8</sub> ] <sup>2-</sup>		<i>D</i> <sub>4d</sub> , square antiprismatic	(Lone-pair inactive)
	XeOF <sub>4</sub>	(-46)	<i>C</i> <sub>4v</sub> , square pyramidal	Octahedral (1)
	XeO <sub>2</sub> F <sub>2</sub>	30.8	<i>C</i> <sub>2v</sub> , "see-saw"	Trigonal bipyramidal (1)
	CsXeOF <sub>5</sub>		Distorted octahedral	Capped octahedral (1)
	KXeO <sub>3</sub> F		Square pyramidal (chain)	Octahedral (1)
+8	XeO <sub>3</sub>	explodes	<i>C</i> <sub>3v</sub> , pyramidal	Tetrahedral (1)
	XeO <sub>4</sub>	-35.9	<i>T</i> <sub>d</sub> , tetrahedral	(No lone-pairs on Xe)
	XeO <sub>3</sub> F <sub>2</sub>	-54.1	<i>D</i> <sub>3h</sub> , trigonal bipyramidal	Trigonal bipyramidal
	Ba <sub>2</sub> XeO <sub>6</sub>	dec > 300	<i>O</i> <sub>h</sub> , octahedral	(No lone-pairs on Xe)

The three fluorides of Xe can be obtained by direct reaction but conditions need to be carefully controlled if these are to be produced individually in pure form. XeF<sub>2</sub> can be prepared by heating F<sub>2</sub> with an excess of Xe to 400°C in a sealed nickel vessel or by irradiating mixtures of Xe and F<sub>2</sub> with sunlight. The product is a white, crystalline solid consisting of parallel linear XeF<sub>2</sub> units (Fig. 18.1). It is sublimable and its infrared and Raman spectra show that the linear molecular structure is retained in the vapour. XeF<sub>2</sub> is a versatile mild fluorinating agent and will, for instance, difluorinate olefins (alkenes). Oxidative fluorination of MeI yields MeIF<sub>2</sub>, and similar reactions yield Me<sub>2</sub>EF<sub>2</sub> (E = S, Se, Te) and Me<sub>3</sub>EF<sub>2</sub> (E = P, As, Sb).<sup>(17)</sup> A related reaction was used to prepare the organotellurium(VI) compound *mer*-Ph<sub>3</sub>TeF<sub>3</sub>.<sup>(18)</sup>

Figure 18.1 The unit cell of crystalline XeF<sub>2</sub>.

Reductive fluorination is exemplified by the high-yield synthesis of crystalline CrOF<sub>3</sub> at 275°C:<sup>(19)</sup>



XeF<sub>2</sub> sequentially fluorinates Ir<sub>4</sub>(CO)<sub>12</sub> dissolved in anhydrous HF yielding, initially, the novel neutral complexes *mer*- and *fac*-[Ir(CO)<sub>3</sub>F<sub>3</sub>].<sup>(20)</sup>

<sup>17</sup> A. M. FORSTER and A. J. DOWNS, *Polyhedron* **4**, 1625-35 (1985).

<sup>18</sup> A. S. SECCO, K. ALAM, B. J. BLACKBURN and A. F. JANZEN, *Inorg. Chem.* **25** 2125-9 (1986).

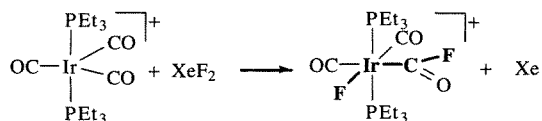
<sup>19</sup> M. MCHUGHES, R. D. WILLETT, H. B. DAVIS and G. L. GARD, *Inorg. Chem.* **25**, 426-7 (1986).

<sup>20</sup> S. A. BREWER, J. H. HOLLOWAY, E. G. HOPE and P. G. WATSON, *J. Chem. Soc., Chem. Commun.*, 1577-8 (1992).

Table 18.3 Stereochemistry of xenon

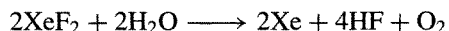
CN	Stereochemistry	Examples	Structure
0	—	Xe(g)	Xe
1	—	[XeF] <sup>+</sup> , [XeOTeF <sub>5</sub> ] <sup>-</sup>	Xe—
2	Linear	XeF <sub>2</sub> , [FXeFXeF] <sup>+</sup> , FXeOSO <sub>2</sub> F	—Xe—
3	Pyramidal	XeO <sub>3</sub>	
	T-shaped	[XeF <sub>3</sub> ] <sup>+</sup> , XeOF <sub>2</sub>	—Xe— 
4	Tetrahedral	XeO <sub>4</sub>	
	Square	XeF <sub>4</sub>	—Xe—     
	C <sub>2v</sub> , “see-saw”	XeO <sub>2</sub> F <sub>2</sub>	—Xe— / \
5	Trigonal bipyramidal	XeO <sub>3</sub> F <sub>2</sub>	
	Square pyramidal	XeOF <sub>4</sub> , [XeF <sub>5</sub> ] <sup>+</sup>	
6	Octahedral Distorted octahedral	[XeO <sub>6</sub> ] <sup>4-</sup> XeF <sub>6</sub> (g), [XeOF <sub>5</sub> ] <sup>-</sup>	
7	(?)	CsXeF <sub>7</sub>	
8	Square antiprismatic	[XeF <sub>8</sub> ] <sup>2-</sup>	

By contrast, reaction of XeF<sub>2</sub> with the iridium carbonyl complex cation [Ir(CO)<sub>3</sub>(PEt<sub>3</sub>)<sub>2</sub>]<sup>+</sup> in CH<sub>2</sub>Cl<sub>2</sub> results in addition across one of the Ir–CO bonds to give the first example of a metal fluoroacyl complex:<sup>(21)</sup>



The product was isolated as white, air-sensitive crystals of the BF<sub>4</sub><sup>-</sup> and PF<sub>6</sub><sup>-</sup> salts.

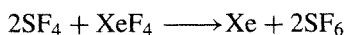
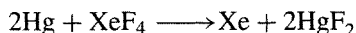
XeF<sub>2</sub> dissolves in water to the extent of 25 g dm<sup>-3</sup> at 0°C, the solution being fairly stable (half-life ~7 h at 0°C) unless base is present, in which case almost instantaneous decomposition takes place:



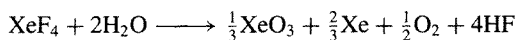
The aqueous solutions are powerful oxidizing agents, converting 2Cl<sup>-</sup> to Cl<sub>2</sub>, Ce<sup>III</sup> to Ce<sup>IV</sup>, Cr<sup>III</sup> to Cr<sup>VI</sup>, Ag<sup>I</sup> to Ag<sup>II</sup>, and even BrO<sub>3</sub><sup>-</sup> to BrO<sub>4</sub><sup>-</sup> (p. 871).

<sup>21</sup> A. J. BLAKE, R. W. COCKMAN, E. A. V. EBSWORTH and J. H. HOLLOWAY, *J. Chem. Soc., Chem. Commun.*, 529–30 (1988).

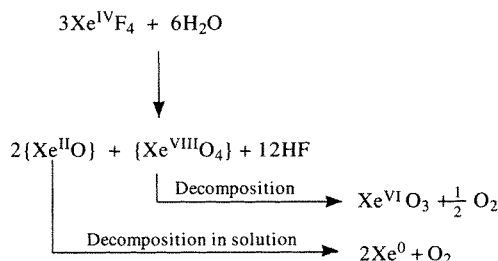
XeF<sub>4</sub> is best prepared by heating a 1:5 volume mixture of Xe and F<sub>2</sub> to 400°C under 6 atm pressure in a nickel vessel. It also is a white, crystalline, easily sublimed solid; the molecular shape is square planar (Xe–F 195.2 pm) and is essentially the same in both the solid and gaseous phases. Its properties are similar to those of XeF<sub>2</sub> except that it is a rather stronger fluorinating agent, as shown by the reactions:



It is also hydrolysed instantly by water, yielding a variety of products which include XeO<sub>3</sub>:



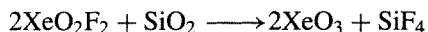
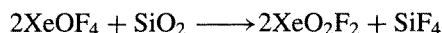
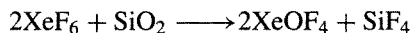
This reaction is indeed a major hazard in Xe/F chemistry, since XeO<sub>3</sub> is highly explosive, and the complete exclusion of moisture is therefore essential (see p. 165 of ref. 10). Interestingly, the maximum yield of XeO<sub>3</sub> is 33% rather than the 50% that would be expected from a simple disproportionation of 2Xe<sup>IV</sup> → Xe<sup>VI</sup> + Xe<sup>II</sup>, and the following reaction sequence has been suggested to explain this:



The stoichiometry of the reaction also depends sensitively on the precise conditions of hydrolysis.<sup>(22)</sup>

XeF<sub>6</sub> is produced by the prolonged heating of 1:20 volume mixtures of Xe and F<sub>2</sub> at 250–300°C under 50–60 atm pressure in a nickel vessel. It is a crystalline solid, even more volatile than XeF<sub>2</sub>

and XeF<sub>4</sub>, and although colourless in the solid it is yellow in the liquid and gaseous phases. It is also more reactive than the other fluorides, being both a stronger oxidizing and a stronger fluorinating agent. Hydrolysis occurs with great vigour and the compound cannot be handled in glass or quartz apparatus because of a stepwise reaction which finally produces the dangerous XeO<sub>3</sub>:



The structure of XeF<sub>6</sub> was the source of some controversy for more than a decade after its discovery in 1963. This was partly a result of the obvious problems associated with a substance which attacks most of the materials used to construct apparatus for structural determinations. It is now clear that in the gaseous phase this seemingly simple molecule is not a regular octahedron; it appears to be a non-rigid, distorted octahedron although, in spite of numerous theoretical studies, the precise nature of the distortion is uncertain (see, for instance, p. 299 of ref. 8). In the crystalline state at least four different forms of XeF<sub>6</sub> are known comprising square-pyramidal XeF<sub>5</sub><sup>+</sup> ions bridged by F<sup>−</sup> ions. Three of these forms are tetramers, [(XeF<sub>5</sub><sup>+</sup>)F<sup>−</sup>]<sub>4</sub>, while in the fourth and best-characterized cubic form,<sup>(23)</sup> the unit cell comprises 24 tetramers and 8 hexamers, [(XeF<sub>5</sub><sup>+</sup>)F<sup>−</sup>]<sub>6</sub> (Fig. 18.2).

The nature of the bonding in these xenon fluorides is discussed in the Panel opposite.

Apart from XeF, which is the light-emitting species in certain Xe/F<sub>2</sub> lasers, there is no evidence for the existence of any odd-valent fluorides. Reports of XeF<sub>8</sub> have not been confirmed. Of the other halides, XeCl<sub>2</sub>, XeBr<sub>2</sub> and XeCl<sub>4</sub> have been detected by Mössbauer spectroscopy as products of the β-decay of their <sup>129</sup>I

<sup>22</sup> J. L. HUSTON, *Inorg. Chem.* **21**, 685–8 (1982).

<sup>23</sup> R. D. BURBANK and G. R. JONES, *J. Am. Chem. Soc.* **96**, 43–8 (1974).

### Bonding in Noble Gas Compounds

As it was widely believed, prior to 1962, that the noble gases were chemically inert because of the stability, if not inviolability, of their electronic configurations, the discovery that compounds could in fact be prepared, immediately necessitated a description of the bonding involved. A variety of approaches has been suggested,<sup>(24)</sup> none of which is universally applicable. The simplest molecular-orbital description is that of the 3-centre, 4-electron  $\sigma$  bond in  $\text{XeF}_2$ , which involves only valence shell p orbitals and eschews the use of higher energy d orbitals. The orbitals involved are the colinear set comprising the  $5p_x$  orbital of Xe, which contains 2 electrons, and the  $2p_x$  orbitals from each of the F atoms, each containing 1 electron. The possible combinations of these orbitals are shown in Fig. A and yield 1 bonding, 1 nonbonding, and 1 antibonding orbital. A single bonding pair of electrons is responsible for binding all 3 atoms, and the occupation of the nonbonding orbital, situated largely on the F atoms, implies significant ionic character. The scheme should be compared with the 3-centre, 2-electron bonding proposed for boron hydrides (p. 158).

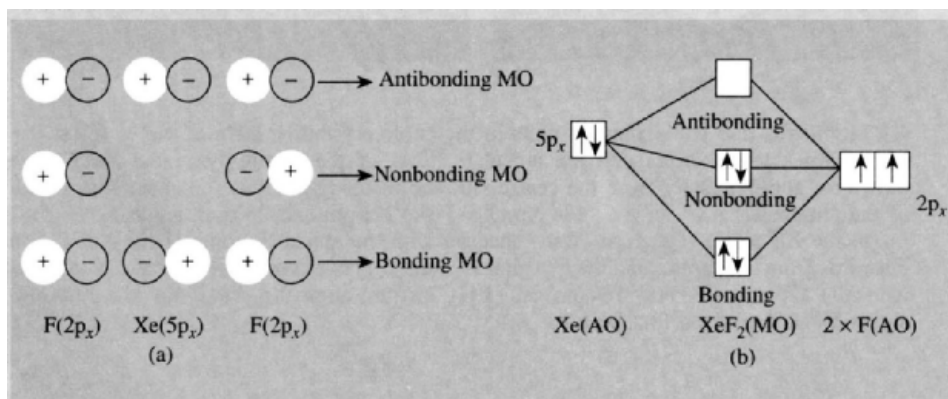


Fig. A. Molecular-orbital representation of the 3-centre F-Xe-F bond. (a) The possible combinations of colinear  $p_x$  atomic orbitals, and (b) the energies of the resulting MOs (schematic).

A similar treatment, involving two 3-centre bonds accounts satisfactorily for the planar structure of  $\text{XeF}_4$  but fails when applied to  $\text{XeF}_6$  since three 3-centre bonds would produce a regular octahedron instead of the distorted structure actually found. An improvement is possible if involvement of the Xe 5d orbitals is invoked,<sup>(25)</sup> since this produces a triplet level which would be subject to a Jahn-Teller distortion (p. 1021). However, the approach which has most consistently rationalized the stereochemistries of noble-gas compounds (as distinct from their bonding) is the electron-pair repulsion theory of Gillespie and Nyholm.<sup>(26)</sup> This assumes that stereochemistry is determined by the repulsions between valence-shell electron-pairs, both nonbonding and bonding, and that the former exert the stronger effect. Thus, in  $\text{XeF}_2$  the Xe is surrounded by 10 electrons (8 from Xe and 1 from each F) distributed in 5 pairs; 2 bonding and 3 nonbonding. The 5 pairs are directed to the corners of a trigonal bipyramid and, because of their greater mutual repulsions, the 3 nonbonding pairs are situated in the equatorial plane at  $120^\circ$  to each other, leaving the 2 bonding pairs perpendicular to the plane and so producing a linear F-Xe-F molecule.

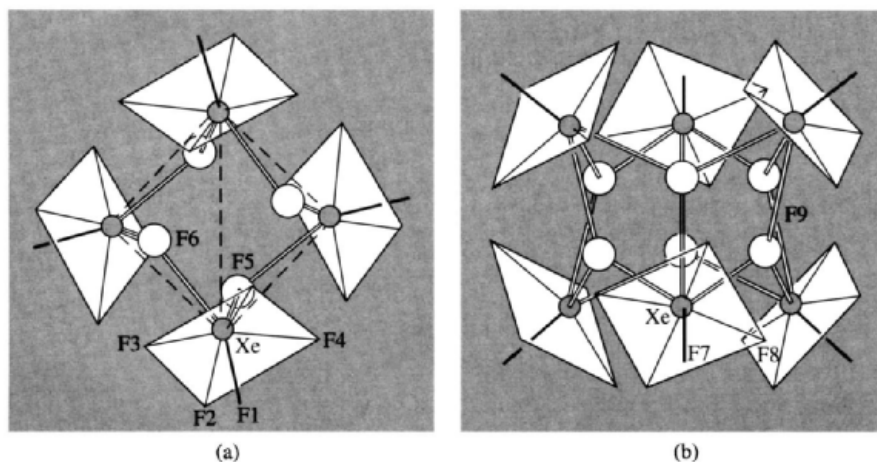
In the same way  $\text{XeF}_4$ , with 6 electron-pairs, is considered as pseudo-octahedral with its 2 nonbonding pairs trans to each other, leaving the 4 F atoms in a plane around the Xe. More distinctively, the 7 electron-pairs of  $\text{XeF}_6$  suggest the possibility of a non-regular octahedral geometry and imply a distorted structure based on either a monocapped octahedral or a pentagonal pyramidal arrangement of electron-pairs, with the Xe-F bonds bending away from the projecting nonbonding pair.

It is an instructive exercise to devise similar rationalizations for the xenon oxides and oxofluorides listed in Table 18.3.

<sup>24</sup> C. A. COULSON, *J. Chem. Soc.* 1442-54 (1964). J. G. MALM, H. SELIG, J. JORTNER and S. A. RICE, *Chem. Revs.* **65**, 199-236 (1965)

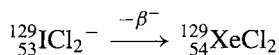
<sup>25</sup> G. L. GOODMAN, *J. Chem. Phys.* **56**, 5038-41 (1972).

<sup>26</sup> R. J. GILLESPIE, *Molecular Geometry*, van Nostrand Reinhold, London, 1972, 228 pp.



**Figure 18.2** (a) Tetrameric, and (b) hexameric units in the cubic crystalline form of  $\text{XeF}_6$ . In (a) the Xe atoms ( $\odot$ ) form a tetrahedron, with the apical F atoms of the square-pyramidal  $\text{XeF}_5^+$  ions pointing outwards, approximately from the centre, and the bridging  $\text{F}^-$  ions ( $\circ$ ) near four of the six edges of the tetrahedron: Xe–F(1–5) 184 pm, Xe–F(6), 223 pm and 260 pm, angle Xe–F(6)–Xe 120.7°. In (b) the Xe atoms ( $\odot$ ) form an octahedron with the apical F atoms of the  $\text{XeF}_5^+$  ions pointing outwards from the centre, and the bridging  $\text{F}^-$  ions ( $\circ$ ) over six of the eight faces of the octahedron: Xe–F(7) 175 pm, Xe–F(8) 188 pm, Xe–F(9) 256 pm, angle Xe–F(9)–Xe 118.8°.  $\text{XeF}_5^+$  ions are shown in skeletal form for clarity.

analogues, for instance:



$\text{XeCl}_2$  has also been trapped in a matrix of solid Xe after  $\text{Xe}/\text{Cl}_2$  mixtures had been passed through a microwave discharge, but these halides are too unstable to be chemically characterized.

It is from the binary fluorides that other compounds of xenon are invariably prepared, by reactions which fall mostly into four classes:

- with  $\text{F}^-$  acceptors, yielding fluorocations of xenon;
- with  $\text{F}^-$  donors, yielding fluoroanions of xenon;
- F/H metathesis between  $\text{XeF}_2$  and an anhydrous acid;
- hydrolysis, yielding oxofluorides, oxides and xenates.

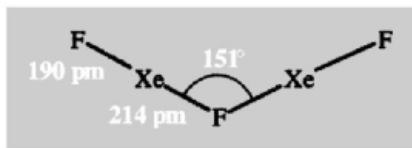
(a) *Reactions with  $\text{F}^-$  acceptors.*  $\text{XeF}_2$  has a more extensive  $\text{F}^-$  donor chemistry than has  $\text{XeF}_4$ ; it reacts with the pentafluorides of P,

As, Sb, I, as well as with metal pentafluorides, to form salts of the types  $[\text{XeF}]^+[\text{MF}_6]^-$ ,  $[\text{XeF}]^+[\text{M}_2\text{F}_{11}]^-$  and  $[\text{Xe}_2\text{F}_3]^+[\text{MF}_6]^-$ . The  $[\text{XeF}]^+$  ions are apparently always weakly attached to the counter-anion forming linear  $\text{F}-\text{Xe}\cdots\text{F}-\text{M}$  units with one short and one long Xe–F bond, while the  $[\text{Xe}_2\text{F}_3]^+$  ions are V-shaped (see p. 899; cf. isoelectronic  $\text{I}_5^-$  with central angle 95°, p. 837). With  $\text{SbF}_5$  the bright-green paramagnetic  $\text{Xe}_2^+$  cation has been identified as a further product.<sup>(27)</sup>  $\text{MOF}_4$  ( $\text{M} = \text{W}, \text{Mo}$ ) are also weak  $\text{F}^-$  acceptors and form  $[\text{XeF}]^+[\text{MOF}_5]^-$ , which again contain linear  $\text{F}-\text{Xe}\cdots\text{F}-\text{M}$  units.<sup>(28)</sup> The  $\text{XeF}^+$  cation is an excellent Lewis acid and this property has been used to prepare a range of compounds featuring Xe–N bonds<sup>(29)</sup> (see also p. 902).

<sup>27</sup> L. STEIN and W. H. HENDERSON, *J. Am. Chem. Soc.* **102**, 2856–7 (1980).

<sup>28</sup> J. H. HOLLOWAY and G. J. SCHROBILGEN, *Inorg. Chem.* **19**, 2632–40 (1980).

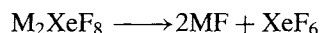
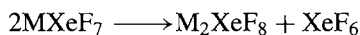
<sup>29</sup> G. J. SCHROBILGEN, Chap. 1 in G. A. OLAH, R. D. CHAMBERS and G. K. S. PRAKASH (eds.), *Synthetic Fluorine Chemistry*, John Wiley, New York, 1992, pp. 1–30.



Although the orange-yellow solid prepared by Bartlett (p. 892) was originally formulated as  $\text{Xe}^+[\text{PtF}_6]^-$ , it was subsequently found to have the variable composition  $\text{Xe}(\text{PtF}_6)_x$ ,  $x$  lying between 1 and 2. The material has still not been fully characterized but probably contains both  $[\text{XeF}]^+[\text{PtF}_6]^-$  and  $[\text{XeF}]^+[\text{Pt}_2\text{F}_{11}]^-$ .

$\text{XeF}_4$  forms comparable complexes only with the strongest  $\text{F}^-$  acceptors such as  $\text{SbF}_5$  and  $\text{BiF}_5$ , but  $\text{XeF}_6$  combines with a variety of pentafluorides to yield 1:1 adducts. In view of the structure of  $\text{XeF}_6$  (see Fig. 18.2) it is not surprising that these adducts contain  $\text{XeF}_5^+$  cations, as for instance in  $[\text{XeF}_5]^+[\text{AsF}_6]^-$  and  $[\text{XeF}_5]^+[\text{PtF}_6]^-$ . In a similar manner, reactions with  $\text{FeF}_3$  and  $\text{CoF}_3$  yield  $[\text{XeF}_5][\text{MF}_4]$  in which layers of corner-sharing  $\text{FeF}_6$  octahedra are separated by  $[\text{XeF}_5]^+$  ions.<sup>(30)</sup>

(b) *Reactions with  $\text{F}^-$  donors.*  $\text{F}^-$  acceptor behaviour of xenon fluorides is evidently confined to  $\text{XeF}_6$  which reacts with alkali metal fluorides to form  $\text{MXeF}_7$  ( $\text{M} = \text{Rb}, \text{Cs}$ ) and  $\text{M}_2\text{XeF}_8$  ( $\text{M} = \text{Na}, \text{K}, \text{Rb}, \text{Cs}$ ). These compounds lose  $\text{XeF}_6$  when heated:

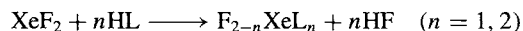


Their thermal stability increases with molecular weight. Thus the Cs and Rb octafluoro complexes only decompose above  $400^\circ\text{C}$ , whereas the Na complex decomposes below  $100^\circ\text{C}$ . NaF can therefore conveniently be used to separate  $\text{XeF}_6$  from  $\text{XeF}_2$  and  $\text{XeF}_4$ , with which it does not react, the purified  $\text{XeF}_6$  being regenerated on heating.

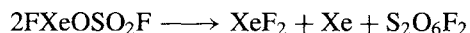
A similar product,  $[\text{NO}]^+_2[\text{XeF}_8]^{2-}$ , is formed with NOF and its anion has been shown by X-ray

crystallography to be a slightly distorted square antiprism<sup>(31)</sup> (probably due to weak  $\text{F}\cdots\text{NO}^+$  interactions). The absence of any clearly defined ninth coordination position for the lone-pair of valence electrons which is present, implies that this must be stereochemically inactive.

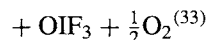
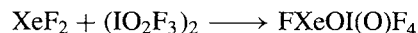
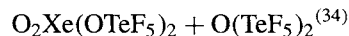
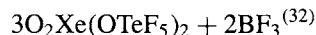
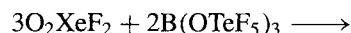
(c) *F/H metathesis between  $\text{XeF}_2$  and an anhydrous acid:*



where  $\text{L} = \text{OTeF}_5, \text{OSeF}_5, \text{OSO}_2\text{F}, \text{OCIO}_3, \text{ONO}_2, \text{OC}(\text{O})\text{Me}, \text{OC}(\text{O})\text{CF}_3, \text{OSO}_2\text{Me}$  and  $\text{OSO}_2\text{CF}_3$  (see also p. 902 for an analogous reaction with  $\text{HN}(\text{OSO}_2\text{F})_2$ ). The compounds are colourless or pale yellow and many are thermodynamically unstable. The perchlorate (mp  $16.5^\circ$ ) is dangerously explosive. The fluoro-sulfate (mp  $36.6^\circ$ ) can be stored for many weeks at  $0^\circ$  but decomposes with a half-life of a few days at  $20^\circ$ .



The molecular structure of  $\text{FXeOSO}_2\text{F}$  is in Fig. 18.3a. Many other such compounds have been made by similar routes e.g.  $\text{O}_2\text{Xe}(\text{F})(\text{OTeF}_5)$ ,  $\text{O}_2\text{Xe}(\text{OTeF}_5)_2$ ,  $\text{OXeF}_{4-n}(\text{OTeF}_5)_n$  ( $n = 1-4$ ) and  $\text{XeF}_{4-n}(\text{OTeF}_5)_n$  ( $n = 1-4$ );<sup>(32)</sup>  $\text{FXeOI}(\text{O})\text{F}_4$  and  $\text{Xe}\{\text{OI}(\text{O})\text{F}_4\}_2$ ;<sup>(33)</sup>  $\text{FXeOP}(\text{O})\text{F}_2$  and  $\text{Xe}\{\text{OP}(\text{O})\text{F}_2\}_2$  etc. Typical reactions are:



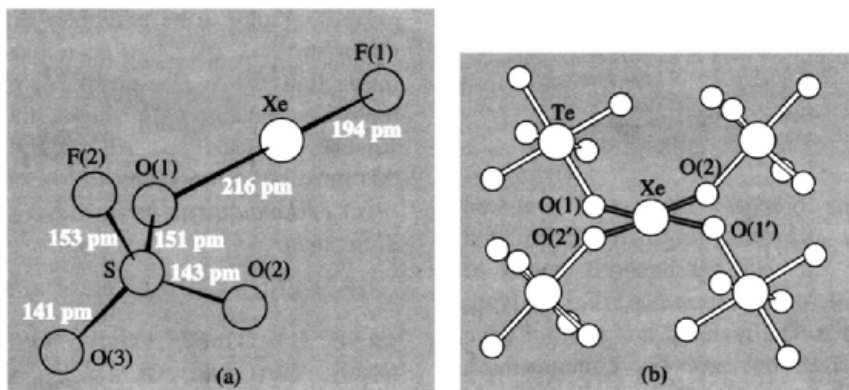
<sup>31</sup> S. W. PETERSON, J. H. HOLLOWAY, B. A. COYLE and J. M. WILLIAMS, *Science*, **173**, 1238-9 (1971).

<sup>32</sup> G. A. SCHUMACHER and G. J. SCHROBILGEN, *Inorg. Chem.* **23**, 2923-9 (1984).

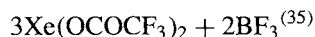
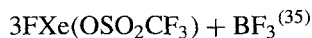
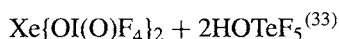
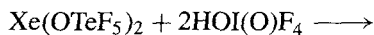
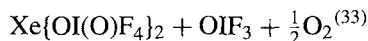
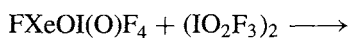
<sup>33</sup> R. G. STYRET and G. J. SCHROBILGEN, *J. Chem. Soc., Chem. Commun.*, 1529-30 (1985).

<sup>34</sup> L. TUROWSKY and K. SEPPERT, *Z. anorg. allg. Chem.* **609**, 153-6 (1992).

<sup>30</sup> J. SLIVNIK, B. ZEMVA, M. BOHINC, D. HANZEL, J. GRANNEC and P. HAGENMULLER, *J. Inorg. Nucl. Chem.* **38**, 997-1000 (1976).



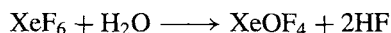
**Figure 18.3** (a) The molecular structure of  $\text{FXeOSO}_2\text{F}$ . Precision of bond lengths is *ca.* 1 pm (uncorrected for thermal motion). The angle  $\text{F}(1)\text{-Xe-O}(1)$  is  $177.5 \pm 0.4^\circ$  and angle  $\text{Xe-O}(1)\text{-S}$  is  $123.4 \pm 0.6^\circ$ . (b) The molecular structure of  $\text{Xe}(\text{OTeF}_5)_4$  (see text)



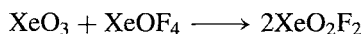
The molecular structure of yellow crystalline  $\text{Xe}(\text{OTeF}_5)_4$  has been determined by X-ray analysis (see Fig. 18.3b);<sup>(34)</sup> the Xe atom is surrounded by a square-planar array of four O atoms, with the adjacent  $\text{TeF}_5$  groups pointing, curiously, pair-wise up and down from this plane ( $\text{Xe-O}$  203.9(5) and 202.6(5) pm,  $\text{Te-O}$  188.5 pm).

(d) *Hydrolysis and related reactions.* Two  $\text{Xe}^{\text{VI}}$  oxofluorides,  $\text{XeOF}_4$  and  $\text{XeO}_2\text{F}_2$ , have been characterized, and the  $\text{Xe}^{\text{VIII}}$  derivative  $\text{XeO}_3\text{F}_2$  (mp.  $-54.1^\circ\text{C}$ )<sup>(22)</sup> is also known (see below).  $\text{XeOF}_4$  is a colourless volatile liquid with a square-pyramidal molecular structure, the O atom being at the apex. It can be prepared by the

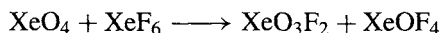
controlled hydrolysis of  $\text{XeF}_6$ :



Its most pronounced chemical characteristic is its propensity to hydrolyse further to  $\text{XeO}_2\text{F}_2$  and then  $\text{XeO}_3$  (p. 901). This reaction is difficult to control, and the low-melting, colourless solid,  $\text{XeO}_2\text{F}_2$ , is more reliably obtained by the reaction:



An analogous reaction with  $\text{XeO}_4$  (see p. 901) is:



Indeed, many of the reactions of the xenon oxides, fluorides and oxofluorides can be systematized in terms of generalized acid-base theory in which any acid (here defined as an oxide acceptor) can react with any base (oxide donor) lying beneath it in the sequence of descending acidity:  $\text{XeF}_6 > \text{XeO}_2\text{F}_4 > \text{XeO}_3\text{F}_2 > \text{XeO}_4 > \text{XeOF}_4 > \text{XeF}_4 > \text{XeO}_2\text{F}_2 > \text{XeO}_3 \approx \text{XeF}_2$ .<sup>(22)</sup>

In addition, oxofluoro anions may be produced by treating hydrolysis products with  $\text{F}^-$ . Thus aqueous  $\text{XeO}_3$  and  $\text{MF}$  ( $\text{M} = \text{K}, \text{Cs}$ ) yield the stable white solids  $\text{M}[\text{XeO}_3\text{F}]$  in which the anion consists of chains of pseudo-octahedral Xe atoms (the lone-pair of valence electrons occupying one of the six positions) linked by angular F bridges.

<sup>35</sup> B. CREMER-LOBER, H. BUTLER, D. NAUMANN and W. TYRRA, *Z. anorg. allg. Chem.* **607**, 34–40 (1992).



Again, the reaction of  $\text{XeOF}_4$  and dry  $\text{CsF}$  has been shown to yield the labile  $\text{Cs}[(\text{XeOF}_4)_3\text{F}]$  in which the anion consists of three equivalent  $\text{XeOF}_4$  groups attached to a central  $\text{F}^-$  ion.<sup>(36)</sup> The ready loss of  $2\text{XeOF}_4$  produces the more stable  $\text{CsXeOF}_5$ , the anion of which has a distorted octahedral geometry, the lone-pair of electrons again being stereochemically active and apparently occupying an octahedral face.

Complete hydrolysis of  $\text{XeF}_6$  is the route to  $\text{XeO}_3$ . The most effective control of this potentially violent reaction is achieved by using a current of dry  $\text{N}_2$  to sweep  $\text{XeF}_6$  vapour into water:<sup>(37)</sup>

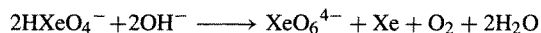


The HF may then be removed by adding  $\text{MgO}$  to precipitate  $\text{MgF}_2$  and the colourless deliquescent solid  $\text{XeO}_3$  obtained by evaporation. The aqueous solution known as "xenic acid" is quite stable if all oxidizable material is excluded, but the solid is a most dangerous explosive (reported to be comparable to TNT) which is easily detonated. The X-ray analysis, made even more difficult by the tendency of the crystals to disintegrate in an X-ray beam, shows the solid to consist of trigonal pyramidal  $\text{XeO}_3$  units, with the xenon atom at the apex<sup>(38)</sup> (cf. the isoelectronic iodate ion  $\text{IO}_3^-$ ; p. 863).

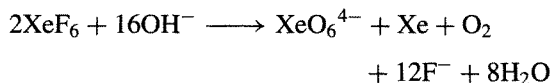
In aqueous solution  $\text{XeO}_3$  is an extremely strong oxidizing agent (for  $\text{XeO}_3 + 6\text{H}^+ + 6\text{e}^- \rightleftharpoons \text{Xe} + 3\text{H}_2\text{O}$ ;  $E^\circ = 2.10$  V), but may be kinetically slow; the oxidation of  $\text{Mn}^{\text{II}}$  takes hours to produce  $\text{MnO}_2$  and days before  $\text{MnO}_4^-$  is obtained. Treatment of aqueous  $\text{XeO}_3$  with alkali produces xenate ions:



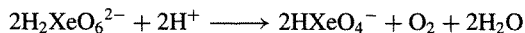
However, although some salts have been isolated, alkaline solutions are not stable and immediately, if slowly, begin to disproportionate into  $\text{Xe}^{\text{VIII}}$  (perxenates) and Xe gas by routes such as:



Similar results are obtained by the alkaline hydrolysis of  $\text{XeF}_6$ :



The most efficient production of perxenate is the treatment of  $\text{XeO}_3$  in aqueous  $\text{NaOH}$  with ozone, when  $\text{Na}_4\text{XeO}_6 \cdot 2\frac{1}{5}\text{H}_2\text{O}$  precipitates almost quantitatively. The crystal structures of  $\text{Na}_4\text{XeO}_6 \cdot 6\text{H}_2\text{O}$  and  $\text{Na}_4\text{XeO}_6 \cdot 8\text{H}_2\text{O}$  show them to contain octahedral  $\text{XeO}_6^{4-}$  units with  $\text{Xe}-\text{O}$  184 pm and 186.4 pm respectively. Perxenates of other alkali metals ( $\text{Li}^+$ ,  $\text{K}^+$ ) and of several divalent and trivalent cations (e.g.  $\text{Ba}^{2+}$ ,  $\text{Am}^{3+}$ ) have also been prepared. They are colourless solids, thermally stable to over  $200^\circ\text{C}$ , and contain octahedral  $\text{XeO}_6^{4-}$  ions. They are powerful oxidizing agents, the reduction of  $\text{Xe}^{\text{VIII}}$  to  $\text{Xe}^{\text{VI}}$  in aqueous acid solution being very rapid. The oxidation of  $\text{Mn}^{\text{II}}$  to  $\text{MnO}_4^-$  by perxenates, unlike that by  $\text{XeO}_3$ , is thus immediate and is accompanied by evolution of  $\text{O}_2$ :



The addition of solid  $\text{Ba}_2\text{XeO}_6$  to cold conc  $\text{H}_2\text{SO}_4$  produces the second known oxide of xenon,  $\text{XeO}_4$ . This is an explosively unstable gas which may be condensed in a liquid nitrogen trap. The solid tends to detonate when melted but small sublimed crystals have been shown to melt sharply at  $-35.9^\circ\text{C}$ .<sup>(22)</sup>  $\text{XeO}_4$  has only been incompletely studied, but electron diffraction and infrared evidence show the molecule to be tetrahedral.

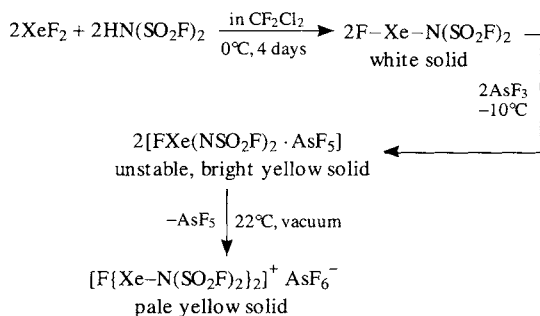
Whilst the great bulk of noble-gas chemistry concerns  $\text{Xe}-\text{F}$  or  $\text{Xe}-\text{O}$  bonds, attempts to bond Xe to certain other atoms have also been successful. Compounds containing  $\text{Xe}-\text{N}$  bonds have been produced by the replacement of F

<sup>36</sup> G. J. SCHROBILGEN, D. MARTIN-ROVET, P. CHARPIN and M. LANCE, *J. Chem. Soc., Chem. Commun.*, 894-7 (1980). J. H. HOLLOWAY, V. KAUČIČ, D. MARTIN-ROVET, D. R. RUSSELL, G. J. SCHROBILGEN and H. SELIG, *Inorg. Chem.* **24**, 678-83 (1985).

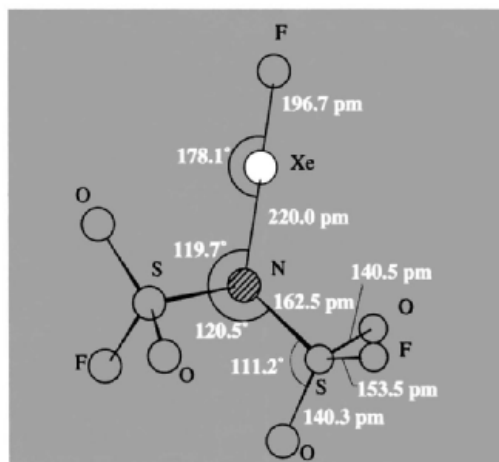
<sup>37</sup> B. JASELSKIS, T. M. SPITTLER and J. L. HUSTON, *J. Am. Chem. Soc.* **88**, 2149-50 (1966).

<sup>38</sup> D. H. TEMPLETON, A. ZALKIN, J. D. FORRESTER and S. M. WILLIAMSON, *J. Am. Chem. Soc.* **85**, 817 (1963).

atoms by  $-\text{N}(\text{SO}_2\text{F})_2$  groups.<sup>(39)</sup> The relevant reactions may be represented as:



The first (white) product has been characterized by X-ray diffraction at  $-55^\circ$  and features a linear F-Xe-N group and a planar N atom (Fig. 18.4).<sup>(40)</sup> On the basis of Raman and  $^{19}\text{F}$  nmr data, the cation of the final (pale yellow) product is believed to be essentially like the V-shaped  $[\text{Xe}_2\text{F}_3]^+$  cation but with the 2 terminal F atoms replaced by

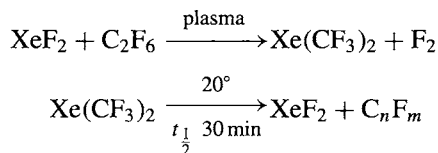


**Figure 18.4** The structure of  $\text{FXeN}(\text{SO}_2\text{F})_2$  ( $C_2$  symmetry) showing essentially linear Xe and planar N. Other bond angles are  $\text{OSO } 122.6^\circ$ ,  $\text{OSF } 106.3^\circ$ ,  $\text{NSO } 107.2^\circ$  and  $111.2^\circ$ ,  $\text{NSF } 101.2^\circ$ .

<sup>39</sup> D. D. DESMARTEAU, *J. Am. Chem. Soc.* **100**, 6270-1 (1978). D. D. DESMARTEAU, R. D. LEBLOND, S. F. HOSSAIN and D. NOTHE, *J. Am. Chem. Soc.* **103**, 7734-9 (1981).

$-\text{N}(\text{SO}_2\text{F})_2$  groups.<sup>(40)</sup> The related compound  $[\text{Xe}\{\text{N}(\text{SO}_2\text{F})_2\}_2]$  was the first to feature an Xe atom bonded to two N atoms.<sup>(41)</sup> The cations  $[\text{XeN}(\text{SO}_2\text{F})_2]^+$  and  $[\text{F}\{\text{XeN}(\text{SO}_2\text{F})_2\}_2]^+$  have also been characterized and the X-ray structure of  $[\text{XeN}(\text{SO}_2\text{F})_2]^+[\text{Sb}_3\text{F}_{16}]^-$  determined.<sup>(42)</sup> An important new synthetic strategy was introduced by G. J. Schrobilgen who exploited the Lewis acid (electron-pair acceptor) properties of the  $\text{XeF}^+$  cation to prepare a wide range of stable nitrile adducts featuring Xe-N bonds, e.g.  $[\text{RC}\equiv\text{NXeF}]^+\text{AsF}_6^-$  ( $\text{R} = \text{H, Me, CH}_2\text{F, Et, C}_2\text{F}_5, \text{C}_3\text{F}_7, \text{C}_6\text{F}_5$ ).<sup>(43)</sup> Similarly, perfluoropyridine ligands have been used to prepare  $[\text{4-RC}_5\text{F}_4\text{NXeF}]^+$  cations ( $\text{R} = \text{F, CF}_3$ ) in HF or  $\text{BrF}_5$  solutions at temperatures below  $-30^\circ\text{C}$ .<sup>(44)</sup> Other cationic species involving Xe-N bonds include  $[\text{F}_3\text{S}\equiv\text{NXeF}]^+$ ,  $[\text{F}_4\text{S}=\text{NXe}]^+$ ,  $[\text{F}_5\text{SN}(\text{H})\text{Xe}]^+$ ,  $[\text{F}_5\text{TeN}(\text{H})\text{Xe}]^+$ ,  $[\text{p-C}_3\text{F}_3\text{N}_2\text{NXeF}]^+$ ,  $[\text{MeC}\equiv\text{NXeOTeF}_5]^+$ ,  $[\text{C}_5\text{F}_5\text{-NXeOTeF}_5]^+$  and  $[\text{F}_3\text{S}\equiv\text{NXeOSeF}_5]^+$ . Over three dozen such compounds are now known and The field has been recently reviewed.<sup>(29)</sup>

Fewer compounds with Xe-C bonds have been characterized. The first to be claimed was synthesized by the plasma reaction of  $\text{XeF}_2$  with  $\text{CF}_3^\bullet$  radicals; the volatile waxy white solid produced,  $\text{Xe}(\text{CF}_3)_2$ , decomposed at room temperature with a half-life of about 30 min.<sup>(45)</sup>



<sup>40</sup> J. F. SAWYER, G. J. SCHROBILGEN and S. J. SUTHERLAND, *J. Chem. Soc., Chem. Commun.*, 210-11 (1982).

<sup>41</sup> G. A. SCHUMACHER and G. J. SCHROBILGEN, *Inorg. Chem.* **22**, 2178-83 (1983).

<sup>42</sup> R. FAGGIANI, D. K. KENNEPOHL, C. J. L. LOCK and G. J. SCHROBILGEN, *Inorg. Chem.* **25**, 563-71 (1986).

<sup>43</sup> A. A. A. EMARA and G. J. SCHROBILGEN, *J. Chem. Soc., Chem. Commun.*, 1644-6 (1987).

<sup>44</sup> A. A. A. EMARA and G. J. SCHROBILGEN, *J. Chem. Soc., Chem. Commun.*, 257-9 (1988).

<sup>45</sup> L. J. TURBINI, R. E. AIKMAN and R. J. LAGOW, *J. Am. Chem. Soc.* **101**, 5833-4 (1979).

However, the first compound to have a stable Xe–C bond was reported independently by two groups in 1989:<sup>(46)</sup> reaction of XeF<sub>2</sub> with an excess of B(C<sub>6</sub>F<sub>5</sub>)<sub>3</sub> in MeCN or CH<sub>2</sub>Cl<sub>2</sub> yielded [XeC<sub>6</sub>F<sub>5</sub>]<sup>+</sup>[B(C<sub>6</sub>F<sub>5</sub>)<sub>3</sub>F]<sup>−</sup> which was characterized by its chemical reactions and by <sup>129</sup>Xe and <sup>19</sup>F nmr spectroscopy. The compound can be isolated as a colourless solid. Several other similar compounds have since been synthesized at temperatures below −40°C, e.g. [XeC<sub>6</sub>H<sub>4</sub>R]<sup>+</sup>[B(C<sub>6</sub>H<sub>4</sub>R)<sub>n</sub>F<sub>4−n</sub>]<sup>−</sup> (R = *m*-F, *p*-F, *m*-CF<sub>3</sub>, *p*-CF<sub>3</sub>), (*n* = 0, 1, 2).<sup>(47)</sup> An X-ray structure analysis of the adduct, [MeC≡N→Xe–C<sub>6</sub>F<sub>5</sub>]<sup>+</sup>[(C<sub>6</sub>F<sub>5</sub>)<sub>2</sub>BF<sub>2</sub>]<sup>−</sup> at −123°C established the Xe–C distance as 209.2(8) pm and the coordinate link N→Xe as 268.1(8) pm (substantially longer than the Xe–N distance in Fig. 18.4; the angle C–Xe–N is 174.5(3)°).<sup>(48)</sup> The alkynyl xenonium compound [Bu'C≡C–Xe]<sup>+</sup>BF<sub>4</sub><sup>−</sup> has also been characterized.<sup>(49)</sup>

The most recent extension of xenon chemistry is the formation of a compound containing a Xe–Xe bond.<sup>(49a)</sup> Thus, when the yellow compound XeF<sup>+</sup>Sb<sub>2</sub>F<sub>11</sub><sup>−</sup> was reacted with Xe in “magic acid” (HF/SbF<sub>5</sub>), dark-green crystals of Xe<sub>2</sub><sup>+</sup>Sb<sub>4</sub>F<sub>21</sub><sup>−</sup> were formed at −30°C. An X-ray structure analysis at −143°C revealed that the Xe–Xe<sup>+</sup> bond length was 308.7(1) pm, making it the longest element–element bond yet known [cf. 304.1(1) pm for Re–Re in Re<sub>2</sub>(CO)<sub>10</sub>].

### 18.3.3 Compounds of other noble gases

No stable compounds of He, Ne or Ar are known. Radon apparently forms a difluoride and some

complexes such as [RnF]<sup>+</sup>X<sup>−</sup> (X<sup>−</sup> = SbF<sub>6</sub><sup>−</sup>, TaF<sub>6</sub><sup>−</sup>, BiF<sub>6</sub><sup>−</sup>), but the evidence is based solely on radiochemical tracer techniques since Rn has no stable isotopes.<sup>(50)</sup> The remaining noble gas, Kr, has an emerging chemistry though this is less extensive than that of Xe.

Apart from the violet free radical KrF, which has been generated in minute amounts by  $\gamma$ -radiation of KrF<sub>2</sub> and exists only below −153°C, the chemistry of Kr was for some time confined to the difluoride and its derivatives. An early claim for KrF<sub>4</sub> remains unsubstantiated. The volatile, colourless solid, KrF<sub>2</sub>, is produced when mixtures of Kr and F<sub>2</sub> are cooled to temperatures near −196°C and then subjected to electric discharge, or irradiated with high-energy electrons or X-rays. It is a thermally (and thermodynamically) unstable compound which slowly decomposes even at room temperature. It has the same linear molecular structure as XeF<sub>2</sub> (Kr–F 188.9 pm) but, consistent with its lower stability, is a stronger fluorinating agent and is rapidly decomposed by water without requiring the addition of a base. KrF<sub>2</sub> has been used as a specialist reagent to prepare high oxidation state fluorides. Reaction with Ag or AgF in HF gave the new fluoride AgF<sub>3</sub>;<sup>(51)</sup> high-purity MnF<sub>4</sub> was prepared from MnF<sub>2</sub>/HF via the adducts 2KrF<sub>2</sub>.MnF<sub>4</sub> and KrF<sub>2</sub>.MnF<sub>4</sub>;<sup>(52)</sup> the square-pyramidal CrF<sub>4</sub>O (mp. 55°C) was obtained by an improved route from CrO<sub>2</sub>F<sub>2</sub>/HF.<sup>(53)</sup> KrF<sub>2</sub> also affords an unusual and extremely useful room-temperature route to NpF<sub>6</sub> and PuF<sub>6</sub>, thus avoiding the necessity of using F<sub>2</sub> at high temperatures, the compound O<sub>2</sub>F<sub>2</sub> being the only other reagent known to do this.<sup>(54)</sup>

Complexes of KrF<sub>2</sub> are analogous to those of XeF<sub>2</sub> and are confined to cationic species

<sup>46</sup> D. NAUMANN and W. TYRRA, *J. Chem. Soc., Chem. Commun.*, 47–50 (1989). H. J. FROHN and S. JAKOBS, *J. Chem. Soc., Chem. Commun.*, 625–7 (1989).

<sup>47</sup> H. J. FROHN and C. ROSSBACH, *Z. anorg. allg. Chem.* **619**, 1672–8 (1993).

<sup>48</sup> H. J. FROHN, S. JACOBS and G. HENKEL, *Angew. Chem. Int. Edn. Engl.* **28**, 1506–7 (1989).

<sup>49</sup> V. V. ZHDANKIN, P. J. STANG and N. S. ZEFIROV, *J. Chem. Soc., Chem. Commun.*, 578–9 (1992).

<sup>49a</sup> T. DREWS and K. SEPPELT, *Angew. Chem. Int. Edn. Engl.* **36**, 273–4 (1997), and references cited therein.

<sup>50</sup> L. STEIN, *Inorg. Chem.* **23**, 3670–1 (1984).

<sup>51</sup> R. BOUGON, T. B. HUY, M. LANCE and H. ABAZLI, *Inorg. Chem.* **23**, 3667–8 (1984).

<sup>52</sup> K. LUTAR, A. JESIH and B. ŽEMVA, *Polyhedron* **7**, 1217–9 (1988).

<sup>53</sup> K. O. CHRISTE, W. W. WILSON and R. A. BOUGON, *Inorg. Chem.* **25**, 2163–9 (1986).

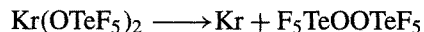
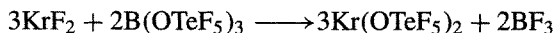
<sup>54</sup> L. B. ASPREY, P. G. ELLER and S. A. KINKEAD, *Inorg. Chem.* **25**, 670–2 (1986).

which can be generated by reaction with  $F^-$  acceptors. Thus, such compounds as  $[KrF]^+[MF_6]^-$ ,  $[Kr_2F_3]^+[MF_6]^+$  ( $M = As, Sb$ ) are known, and also  $[KrF]^+[MoOF_5]^-$  and  $[KrF]^+[WOF_5]^-$  which have been prepared and characterized by  $^{19}F$  nmr and Raman spectroscopy.<sup>55</sup> In addition, adducts of  $KrF^+$  with nitrile donors have been synthesized, analogous to those of  $XeF^+$  described in the preceding section, e.g.  $[RC\equiv NKrF]^+$  ( $R = Me, CF_3, C_2F_5, n-C_3F_5$ ).<sup>(29,56)</sup>

<sup>55</sup> J. H. HOLLOWAY and G. J. SCHROBILGEN, *Inorg. Chem.* **20**, 3363–8 (1981).

<sup>56</sup> G. J. SCHROBILGEN, *J. Chem. Soc., Chem. Commun.*, 863–5 and 1506–8 (1988).

The formation of the first compound having Kr–O bonds has been documented by using  $^{19}F$  and  $^{17}O$  nmr spectroscopy of  $^{17}O$ -enriched samples to follow the synthesis and decomposition of the thermally unstable compound,  $[Kr(OTeF_5)_2]$ , according to the reactions:<sup>(57)</sup>



<sup>57</sup> J. C. P. SAUNDERS and G. J. SCHROBILGEN, *J. Chem. Soc., Chem. Commun.*, 1576–8 (1989).

																1	2																										
		3	4																	5	6	7	8	9	10																		
		Li	Be																	B	C	N	O	F	Ne																		
		11	12																	13	14	15	16	17	18																		
		Na	Mg																	Al	Si	P	S	Cl	Ar																		
		19	20	21	22	23	24	25	26	27	28	29	30	31	32	33	34	35	36																								
		K	Ca	Sc	Ti	V	Cr	Mn	Fe	Cu	Ni	Cd	Zn	Ga	Ge	As	Se	Br	Kr																								
		37	38	39	40	41	42	43	44	45	46	47	48	49	50	51	52	53	54																								
		Rb	Sr	Y	Zr	Nb	Mo	Tc	Ru	Rh	Pd	Ag	Cd	In	Sn	Sb	Te	I	Xe																								
		55	56	57	58	59	60	61	62	63	64	65	66	67	68	69	70	71	72	73	74	75	76	77	78	79	80	81	82	83	84	85	86	87	88	89	90						
		Cs	Ba	La	Hf	Ta	W	Re	Os	Ir	Pt	Au	Hg	Tl	Pb	Bi	Po	At	Rn																								
		87	88	89	90	91	92	93	94	95	96	97	98	99	100	101	102	103	104	105	106	107	108	109	110	111	112	113	114	115	116	117	118	119	120								
		Fr	Ra	Ac	Rf	Db	Sg	Bh	Hs	Mt	Uun	Uuu	Uub																														
																105	106	107	108	109	110	111	112	113	114	115	116	117	118	119	120												
																Ce	Pr	Nd	Pm	Sm	Eu	Gd	Tb	Dy	Ho	Er	Tm	Yb	Lu														
																105	106	107	108	109	110	111	112	113	114	115	116	117	118	119	120												
																Th	Pa	U	Np	Pu	Am	Cm	Bk	Cf	Es	Fm	Md	No	Lr														

# 19

## Coordination and Organometallic Compounds

### 19.1 Introduction

The three series of elements arising from the filling of the 3d, 4d and 5d shells, and situated in the periodic table following the alkaline earth metals, are commonly described as “transition elements”, though this term is sometimes also extended to include the lanthanide and actinide (or inner transition) elements. They exhibit a number of characteristic properties which together distinguish them from other groups of elements:

- (i) They are all metals and as such are lustrous and deformable and have high electrical and thermal conductivities. In addition, their melting and boiling points tend to be high and they are generally hard and strong.
- (ii) Most of them display numerous oxidation states which vary by steps of 1 rather than 2 as is usually the case with those

main-group elements which exhibit more than one oxidation state.

- (iii) They have an unparalleled propensity for forming coordination compounds with Lewis bases.

(i) and (ii) will be dealt with more fully in later chapters but it is the purpose of the present chapter to expand the theme of (iii).

A coordination compound, or complex, is formed when a Lewis base (ligand)<sup>(1)</sup> is attached to a Lewis acid (acceptor) by means of a “lone-pair” of electrons. Where the ligand is composed of a number of atoms, the one which is directly attached to the acceptor is called the “donor atom”. This type of bonding has already been discussed (p. 198) and is exemplified by the addition compounds formed by the trihalides of the elements of Group 13 (p. 237); it is also the basis of much of the chemistry of the

<sup>1</sup> W. H. BROCK, K. A. JENSEN, C. K. JØRGENSEN and G. B. KAUFFMAN, *Ambix* 27, 171–83 (1981).

transition elements. The precise nature of the bond between a transition metal ion and a ligand varies enormously and the term “donor atom” is often used in situations where its literal meaning should not be assumed. Although inevitably the line of demarcation is rather ill-defined, it is conventional to distinguish two extremes. On the one hand, are those cases in which the bond may be considered profitably as a single  $\sigma$  bond, or even a purely electrostatic interaction, and in which the metal has an oxidation state of +2 or higher. On the other hand, are those cases where the bonding is multiple, the ligand acting simultaneously as both a  $\sigma$  donor and a  $\pi$  acceptor (p. 922) and in which the metal usually has a formal oxidation state of +1 or less, though the significance of such values is often unclear. Compounds of the former type are commonly described as “classical” or “Werner” complexes since it was through the investigation of such materials that A. Werner in the period 1893–1913 laid the foundations of coordination chemistry<sup>(2)</sup> (see also p. 912). Compounds of the latter type are exemplified by the carbonyls and other organometallic compounds.

## 19.2 Types of Ligand

Ligands are most conveniently classified according to the number of potential donor atoms which they contain and are known as uni-, bi-, ter-, quadri-, quinqi- and sexi-dentate accordingly as the number is 1, 2, 3, 4, 5 or 6. Unidentate ligands may be simple monatomic ions such as halide ions, or polyatomic ions or molecules which contain a donor atom from Groups 16, 15 or even 14 (e.g.  $\text{CN}^-$ ). Bidentate ligands are frequently chelating ligands (from Greek  $\chi\eta\lambda\eta$ , crab’s claw) and, with the metal ion, produce chelate rings<sup>(3)</sup>

<sup>2</sup> G. B. KAUFFMAN, *Alfred Werner Founder of Coordination Theory*, Springer, Berlin, 1966, 127 pp. G. B. Kauffman (ed.) *Coordination Chemistry: A Century of Progress*, ACS Symposium Series 565, Washington DC, 1994, 464 pp.

<sup>3</sup> C. F. BELL, *Principles and Applications of Metal Chelation*, Oxford University Press, Oxford, 1977, 147 pp.

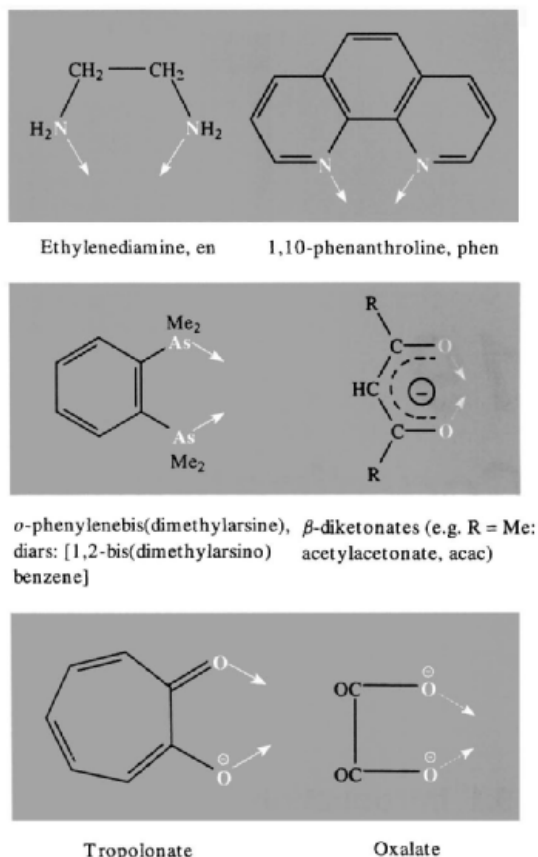
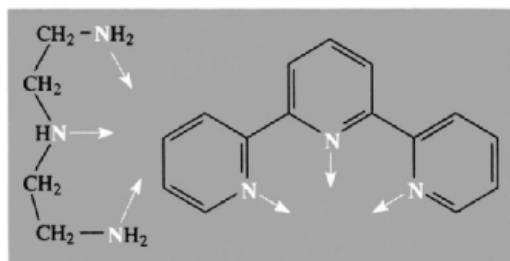


Figure 19.1 Some bidentate ligands.

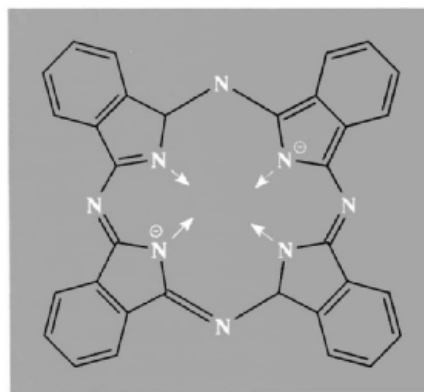
which in the case of the most commonly occurring bidentate ligands are 5- or 6-membered, e.g.: see Fig. 19.1. Terdentate ligands produce 2 ring systems when coordinated to a single metal ion and in consequence may impose structural limitations on the complex, particularly where rigidity is introduced by the incorporation of conjugated double bonds within the rings. Thus diethylenetriamine, dien (1), being flexible is stereochemically relatively undemanding, whereas terpyridine, terpy (2), can only coordinate when the 3 donor nitrogen atoms and the metal ion are in the same plane.

Quadridentate ligands produce 3, and in some cases 4, rings on coordination, and so even greater restrictions on the stereochemistry of the complex may be imposed by an

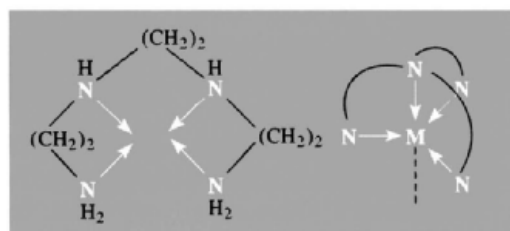


(1)

(2)



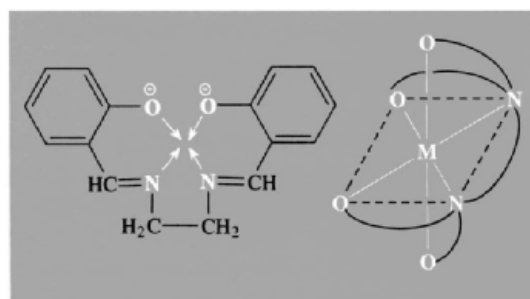
(5)



(3)

(4)

appropriate choice of ligand. The open-chain ligand triethylenetetramine, trien (3), is, like dien, flexible and undemanding, whereas triethylaminetriamine, tren, i.e.  $N(CH_2CH_2NH_2)_3$ , is one of the so-called “tripod” ligands which are quite unable to give planar coordination but instead favour trigonal bipyramidal structures (4). By contrast, the highly conjugated phthalocyanine<sup>(4)</sup> (5), which is an example of the class of macrocyclic ligands of which the crown ethers have already been mentioned (p. 96), forces the complex to adopt a virtually planar structure and has proved to be a valuable model for the naturally occurring porphyrins which, for instance, are involved in haem (p. 1100),  $B_{12}$  (p. 1138) and the chlorophylls (p. 125). Another well-known ligand, which has been used to synthesize oxygen-carrying molecules, is bis(salicylaldehyde)ethylenediimine, salen (6). Quinquidentate and sexidentate ligands are most familiarly exemplified by the anions derived from ethylenediaminetetraacetic acid,  $edtaH_4$  i.e.  $(HO_2CCH_2)_2N(CH_2)_2N(CH_2CO_2H)_2$ , which is



(6)

(7)

used with remarkable versatility in the volumetric analysis of metal ions. As the fully ionized anion,  $edta^{4-}$ , it has 4 oxygen and 2 nitrogen donor atoms and has the flexibility to wrap itself around a variety of metal ions to produce a pseudo-octahedral complex involving five 5-membered rings as in (7).

In the incompletely ionized form,  $edtaH^{3-}$ , one of the oxygen atoms is no longer able to coordinate to the metal and the anion is quinquidentate.

Ambidentate ligands possess more than 1 donor atom and can coordinate through either one or the other. This leads to the possibility of “linkage” isomerism (p. 920). The commonest examples are the ions  $NO_2^-$  (p. 463) and  $SCN^-$  (p. 325). Such ligands can also coordinate via both donor sites simultaneously, thereby acting as bridging ligands.

In the case of organometallic compounds the most satisfactory way of classifying the ligands

<sup>4</sup> C. C. LEZNOFF and A. B. P. LEVER (eds.), *Phthalocyanines, Properties and Applications*, V.C.H., Weinheim, 1990, 336 pp.

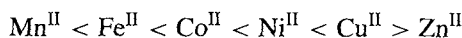




		1		2																																																																					
		H		He																																																																					
3	4											5	6	7	8	9	10																																																								
Li	Be											B	C	N	O	F	Ne																																																								
11	12											13	14	15	16	17	18																																																								
Na	Mg											Al	Si	P	S	Cl	Ar																																																								
19	20	21	22	23	24	25	26	27	28	29	30	31	32	33	34	35	36																																																								
K	Ca	Sc	Ti	V	Cr	Mn	Fe	Co	Ni	Cu	Zn	Ga	Ge	As	Se	Br	Kr																																																								
37	38	39	40	41	42	43	44	45	46	47	48	49	50	51	52	53	54																																																								
Rb	Sr	Y	Zr	Nb	Mo	Tc	Ru	Rh	Pd	Ag	Cd	In	Sn	Sb	Te	I	Xe																																																								
55	56	57	72	73	74	75	76	77	78	79	80	81	82	83	84	85	86																																																								
Cs	Ba	La	Hf	Ta	W	Re	Os	Ir	Pt	Au	Hg	Tl	Pb	Bi	Po	At	Rn																																																								
87	88	89																																																																							
Fr	Ra	Ac																																																																							
<table border="1" style="width: 100%; text-align: center;"> <tr> <td>58</td><td>59</td><td>60</td><td>61</td><td>62</td><td>63</td><td>64</td><td>65</td><td>66</td><td>67</td><td>68</td><td>69</td><td>70</td><td>71</td> </tr> <tr> <td>Ce</td><td>Pr</td><td>Nd</td><td>Pm</td><td>Sm</td><td>Eu</td><td>Gd</td><td>Tb</td><td>Dy</td><td>Ho</td><td>Er</td><td>Tm</td><td>Yb</td><td>Lu</td> </tr> <tr> <td>90</td><td>91</td><td>92</td><td>93</td><td>94</td><td>95</td><td>96</td><td>97</td><td>98</td><td>99</td><td>100</td><td>101</td><td>102</td><td>103</td> </tr> <tr> <td>Th</td><td>Pa</td><td>U</td><td>Np</td><td>Pu</td><td>Am</td><td>Cm</td><td>Bk</td><td>Cf</td><td>Es</td><td>Fm</td><td>Md</td><td>No</td><td>Lr</td> </tr> </table>																		58	59	60	61	62	63	64	65	66	67	68	69	70	71	Ce	Pr	Nd	Pm	Sm	Eu	Gd	Tb	Dy	Ho	Er	Tm	Yb	Lu	90	91	92	93	94	95	96	97	98	99	100	101	102	103	Th	Pa	U	Np	Pu	Am	Cm	Bk	Cf	Es	Fm	Md	No	Lr
58	59	60	61	62	63	64	65	66	67	68	69	70	71																																																												
Ce	Pr	Nd	Pm	Sm	Eu	Gd	Tb	Dy	Ho	Er	Tm	Yb	Lu																																																												
90	91	92	93	94	95	96	97	98	99	100	101	102	103																																																												
Th	Pa	U	Np	Pu	Am	Cm	Bk	Cf	Es	Fm	Md	No	Lr																																																												
Class a			Class b			Borderline																																																																			

Figure 19.2 Classification of acceptor atoms in their common oxidation states.

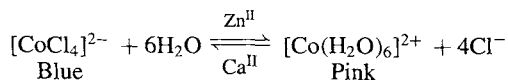
particular ligand involved, usually vary in the Irving–Williams<sup>(6)</sup> order (1953):



which is the reverse of the order for the cation radii (p. 1295). These observations are consistent with the view that, at least for metals in oxidation states +2 and +3, the coordinate bond is largely electrostatic. This was a major factor in the acceptance of crystal field theory (see pp. 921–3).

(ii) *The relationship between metal and donor atom.*<sup>(6a)</sup> Some metal ions (known as class-a acceptors or alternatively as “hard” acids) form their most stable complexes with ligands containing N, O or F donor atoms. Others (known as class-b acceptors or alternatively as “soft” acids) form their most stable complexes with ligands whose donor atoms are the heavier elements of the N, O or F groups. The metals of

Groups 1 and 2 along with the inner transition elements and the early members of the transition series (Groups 3 → 6) fall into class-a. The transition elements Rh, Pd, Ag and Ir, Pt, Au, Hg comprise class-b, while the remaining transition elements may be regarded as borderline (Fig. 19.2). The difference between the class-a elements of Group 2 and the borderline class-b elements of Group 12 is elegantly and colourfully illustrated by the equilibrium



If  $\text{Ca}^{\text{II}}$  is added it pushes the equilibrium to the left by bonding preferentially to  $\text{H}_2\text{O}$ , whereas  $\text{Zn}^{\text{II}}$ , with its partial b character (p. 1206), prefers the heavier  $\text{Cl}^-$  and so pushes the equilibrium to the right.

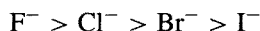
It seems that, as suggested by Ahrland *et al.*<sup>(7)</sup> in 1958, this distinction can be explained at least partly on the basis that class-a acceptors are the

<sup>6</sup> H. M. N. H. IRVING and R. J. P. WILLIAMS, *J. Chem. Soc.* 1953, 3192–210.

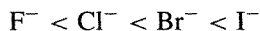
<sup>6a</sup> R. G. PEARSON, *Coord. Chem. Revs.* **100**, 403–25 (1990).

<sup>7</sup> S. AHRLAND, J. CHATT and N. R. DAVIES, *Q. Revs.* **12**, 265–76 (1958).

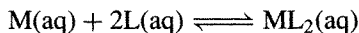
more electropositive elements which tend to form their most stable complexes with ligands favouring electrostatic bonding, so that, for instance, the stabilities of their complexes with halide ions should decrease in the order



Class-b acceptors on the other hand are less electropositive, have relatively full d orbitals, and form their most stable complexes with ligands which, in addition to possessing lone-pairs of electrons, have empty  $\pi$  orbitals available to accommodate some charge from the d orbitals of the metal. The order of stability will now be the reverse of that for class-a acceptors, the increasing accessibility of empty d orbitals in the heavier halide ions for instance, favouring an increase in stability of the complexes in the sequence

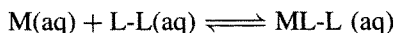


(iii) *The type of ligand.* In comparing the stabilities of complexes formed by different ligands, one of the most important factors is the possible formation of chelate rings. If L is a unidentate ligand and L-L a bidentate ligand, the simplest illustration of this point is provided by comparing the two reactions:



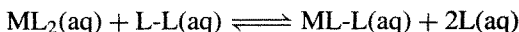
$$\text{for which } \beta_L = \frac{[ML_2]}{[M][L]^2}$$

and



$$\text{for which } \beta_{L-L} = \frac{[ML-L]}{[M][L-L]}$$

or alternatively by considering the replacement reaction obtained by combining them:



$$\text{for which } K = \frac{[ML-L][L]^2}{[ML_2][L-L]} = \frac{\beta_{L-L}}{\beta_L}$$

Experimental evidence shows overwhelmingly that, providing the donor atoms of L and L-L are the same element and that the chelate ring

formed by the coordination of L-L does not involve undue strain, L-L will replace L and the equilibrium of the replacement reaction will be to the right. This stabilization due to chelation is known as the *chelate effect*<sup>(8)</sup> and is of great importance in biological systems as well as in analytical chemistry.

The effect is frequently expressed as  $\beta_{L-L} > \beta_L$  or  $K > 1$  and, when values of  $\Delta H^\circ$  are available,  $\Delta G^\circ$  and  $\Delta S^\circ$  are calculated from the thermodynamic relationships

$$\Delta G^\circ = -RT \ln \beta \text{ and } \Delta G^\circ = \Delta H^\circ - T\Delta S^\circ$$

On the basis of the values of  $\Delta S^\circ$  derived in this way it appears that the chelate effect is usually due to more favourable entropy changes associated with ring formation. However, the objection can be made that  $\beta_L$  and  $\beta_{L-L}$  as just defined have different dimensions and so are not directly comparable. It has been suggested that to surmount this objection concentrations should be expressed in the dimensionless unit "mole fraction" instead of the more usual  $\text{mol dm}^{-3}$ . Since the concentration of pure water at 25°C is approximately  $55.5 \text{ mol dm}^{-3}$ , the value of concentration expressed in mole fractions =  $\text{conc in mol dm}^{-3}/55.5$ . Thus, while  $\beta_L$  is thereby increased by the factor  $(55.5)^2$ ,  $\beta_{L-L}$  is increased by the factor  $(55.5)$  so that the derived values of  $\Delta G^\circ$  and  $\Delta S^\circ$  will be quite different. The effect of this change in units is shown in Table 19.1 for the  $\text{Cd}^{II}$  complexes of L = methylamine and L-L = ethylenediamine. It appears that the entropy advantage of the chelate, and with it the chelate effect itself, virtually disappears when mole fractions replace  $\text{mol dm}^{-3}$ .

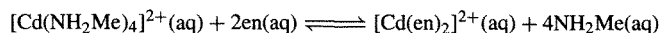
The resolution of this paradox lies in the assumptions about standard (reference), states which are unavoidably involved in the above definitions of  $\beta_L$  and  $\beta_{L-L}$ . In order to ensure that  $\beta_L$  and  $\beta_{L-L}$  are dimensionless (as they have to be if their logarithms are to be used) when concentrations are expressed in units which have dimensions, it is necessary to use the ratios of the actual concentrations to the concentrations of

<sup>8</sup> D. C. MUNRO, *Chem. Br.* **13**, 100-5 (1977).

**Table 19.1** Stability constants and thermodynamic functions for some complexes of Cd<sup>II</sup> at 25°C

Complex	log $\beta$	$\Delta H^\circ$ (kJ mol <sup>-1</sup> )	$\Delta G^\circ$ (kJ mol <sup>-1</sup> )	$T\Delta S^\circ$ (kJ mol <sup>-1</sup> )
(a) [Cd(NH <sub>2</sub> Me) <sub>4</sub> ] <sup>2+</sup>	6.55 <i>13.53</i>	-57.32	-37.41 <i>-72.20</i>	-19.91 <i>+19.98</i>
(b) [Cd(en) <sub>2</sub> ] <sup>2+</sup>	10.62 <i>14.11</i>	-56.48	-60.67 <i>-80.51</i>	+4.19 <i>+24.04</i>
Difference (b)-(a)	4.07 <i>0.58</i>	+0.84	-23.26 <i>-3.31</i>	+24.1 <i>+4.06</i>

Values in roman type are based on concentrations expressed in mol dm<sup>-3</sup>. Values in *italics* are based on concentrations expressed in mole fractions. The difference (b)-(a) refers to the replacement reaction



some standard state. Accordingly, the expression for any  $\beta$  should incorporate an additional factor composed of standard state concentrations, and the expression  $\Delta G^\circ = -RT \ln \beta$  should have an additional term involving the logarithm of this factor. Not to include this factor and this term inevitably implies the choice of standard states of concentration = 1 in whatever units are being used. Only in this way can the factor associated with  $\beta$  be 1 and its logarithm zero. It should be stressed, however, that irrespective of these definitional niceties, it remains true as stated above that chelating ligands which form unstrained complexes always tend to displace their monodentate counterparts under normally attainable experimental conditions.

Probably the most satisfactory model with which to explain the chelate effect is that proposed by G. Schwarzenbach<sup>(9)</sup> If L and L-L are present in similar concentrations and are competing for two coordination sites on the metal, the probability of either of them coordinating to the first site may be taken as equal. However, once one end of L-L has become attached it is much more likely that the second site will be won by its other end than by L, simply because its other end must be held close to the second site and its effective concentration where it matters is therefore much

higher than the concentration of L. Because  $\Delta G^\circ$  refers to the transfer of the separate reactants at concentrations = 1 to the products, also at concentrations = 1, it is clear from this model that the advantage of L-L over L, as denoted by  $\Delta G^\circ$  or  $\beta$ , will be greatest when the units of concentration are such that a value of 1 corresponds to a dilute solution. Conversely, where a value of 1 corresponds to an exceedingly high concentration, the advantage will be much less and may even disappear. In normal practice even a concentration of 1 mol dm<sup>-3</sup> is regarded as high, and a concentration of 1 mole fraction is so high as to be of only hypothetical significance, so it need cause no surprise that the choice of the latter unit should lead to rather bizarre results.

The chelate effect is usually most pronounced for 5- and 6-membered rings. Smaller rings generally involve excessive strain while increasingly large rings offer a rapidly decreasing advantage for coordination to the second site. Naturally the more rings there are in a complex the greater the total increase in stability. If a multidentate ligand is also cyclic, and there are no unfavourable steric effects, a further increase in the stability of its complexes accrues. Favourable entropy changes can again be invoked to explain this *macrocyclic effect*. Since a macrocyclic ligand has very little rotational entropy even before coordination, the net increase in entropy when it does coordinate is expected to be even greater than in the case of a comparable non-cyclic ligand.

<sup>9</sup>G. SCHWARZENBACH. *Helv. Chim. Acta* **35**, 2344-59 (1952).

## 19.4 The Various Coordination Numbers<sup>(10)</sup>

In 1893 at the age of 26, Alfred Werner<sup>†</sup> produced his classic coordination theory.<sup>(2,11)</sup> It is said that, after a dream which crystallized his ideas, he set down his views and by midday had written the paper which was the starting point for work which culminated in the award of the Nobel Prize for Chemistry in 1913. The main thesis of his argument was that metals possess two types of valency: (i) the primary, or ionizable, valency which must be satisfied by negative ions and is what is now referred to as the "oxidation state"; and (ii) the secondary valency which has fixed directions with respect to the central metal and can be satisfied by either negative ions or neutral molecules. This is the basis for the various stereochemistries found amongst coordination compounds. Without the armoury of physical methods available to the modern chemist, in particular X-ray crystallography, the early workers were obliged to rely on purely chemical methods to identify the more important of these stereochemistries. They did this during the next 20 y or so, mainly by preparing vast numbers of complexes of various metals of such stoichiometry that the number of isomers which could be produced would distinguish between alternative stereochemistries.

The term "secondary valency" has been superseded by the term "coordination number". This may be defined as the number of donor atoms associated with the central metal atom or ion. For many years a distinction was made between coordination number in this sense and in

the crystallographic sense, where it is the number of nearest-neighbour ions of opposite charge in an ionic crystal. Though the former definition applies to species which can exist independently in the solid or in solution, while the latter applies to extended lattice systems, the distinction is rather artificial, particularly in view of the fact that crystal field theory (one of the theories of bonding most commonly applied to coordination compounds) assumes that the coordinate bond is entirely ionic! Indeed, the concept can be extended to all molecules.  $\text{TiCl}_4$ , for instance, can be regarded as a complex of  $\text{Ti}^{4+}$  with 4  $\text{Cl}^-$  ions in which one lone-pair of electrons on each of the latter is completely shared with the  $\text{Ti}^{4+}$  to give essentially covalent bonds.

The most commonly occurring coordination numbers for transition elements are 4 and 6, but all values from 2 to 9 are known and a few examples of even higher ones have been established. The more important factors determining the most favourable coordination number for a particular metal and ligand are summarized below. However it is important to realize that, with so many factors involved, it is not difficult to provide facile explanations of varying degrees of plausibility for most experimental observations, and it is therefore prudent to treat such explanations with caution.

(i) If electrostatic forces are dominant the attractions between the metal and the ligands should exceed the destabilizing repulsions between the ligands. The attractions are proportional to the product of the charges on the metal and the ligand whereas the repulsions are proportional to the square of the ligand charge. High cation charge and low ligand charge should consequently favour high coordination numbers, e.g. halide ions usually favour higher coordination numbers than does  $\text{O}^{2-}$ .

(ii) There must be an upper limit to the number of molecules (atoms) of a particular ligand which can physically be fitted around a particular cation. For monatomic ligands this limit will be dependent on the radius ratio of cation and anion, just as is the case with extended crystal lattices.

(iii) Where covalency is important the distribution of charge is equalized by the transference

<sup>10</sup> G. WILKINSON, R. D. GILLARD and J. A. MCCLEVERTY (eds.), *Comprehensive Coordination Chemistry*, Pergamon Press, Oxford, Vol. 1, 1987, 613 pp. D. L. KEPERT, *Inorganic Stereochemistry*, Springer-Verlag, Berlin, 1982, 227 pp. J. A. DAVIES, C. M. HOCKENSMITH, V. YU. KUKUSHKIN and YU. N. KUKUSHKIN, *Synthetic Coordination Chemistry: Principles and Practise*, World Scientific Publ., Singapore, 1996, 452 pp.

<sup>11</sup> G. B. KAUFFMAN, *Inorganic Coordination Compounds*, Wiley, New York, 1981, 205 pp.

<sup>†</sup> Born in Mulhouse, Alsace, in 1866, he was French by birth, German in upbringing, and, working in Zürich, he became a Swiss citizen in 1894.

of charge in the form of lone-pairs of electrons from ligands to cation. The more polarizable the ligand the lower the coordination number required to satisfy the particular cation though, if back-donation of charge from cation to ligand via suitable  $\pi$  orbitals is possible, then more ligands can be accommodated. Thus the species most readily formed with  $\text{Fe}^{\text{III}}$  in aqueous solutions are  $[\text{FeF}_5(\text{H}_2\text{O})]^{2-}$  for the non-polarizable  $\text{F}^-$ ,  $[\text{FeCl}_4]^-$  for the more polarizable  $\text{Cl}^-$ , but  $[\text{Fe}(\text{CN})_6]^{3-}$  for  $\text{CN}^-$  which, though it is even more polarizable, also possesses empty antibonding  $\pi$  orbitals suitable for back-donation.

(iv) The availability of empty metal orbitals of suitable symmetries and energies to accommodate electron-pairs from the ligands must also be important in covalent compounds. This is probably one of the main reasons why the lowest coordination numbers (2 and 3) are to be found in the Ag, Au, Hg region of the periodic table where the d shell has been filled. However, it would be unwise to draw the converse conclusion that the highest coordinations are found amongst the early members of the transition and inner-transition series because of the availability of empty d or f orbitals. It seems more likely that these high coordination numbers are achieved by electrostatic attractions between highly charged but rather large cations and a large number of relatively non-polarizable ligands.

Representative examples of the stereochemistries associated with each of the various coordination numbers will now be discussed.

### Coordination number 2

Examples of this coordination number are virtually confined to linear  $D_{\infty h}$  complexes of  $\text{Cu}^{\text{I}}$ ,  $\text{Ag}^{\text{I}}$ ,  $\text{Au}^{\text{I}}$ , and  $\text{Hg}^{\text{II}}$  of which a well-known instance is the ammine formed when ammonia is added to an aqueous solution of  $\text{Ag}^+$ :  $[\text{H}_3\text{N}-\text{Ag}-\text{NH}_3]^+$

### Coordination number 3<sup>(12)</sup>

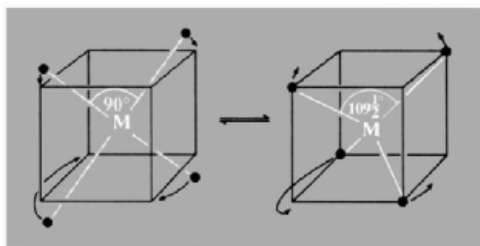
This is rather rare and even in  $[\text{HgI}_3]^-$ , the example usually cited, the coordination number is

dependent on the counter cation. In  $[\text{SMe}_3][\text{HgI}_3]$  the  $\text{Hg}^{\text{II}}$  lies at the centre of an almost equilateral triangle of iodide ions ( $D_{3h}$ ) whereas in  $[\text{NMe}_4][\text{HgI}_3]$  the anion apparently polymerizes into loosely linked chains of 4-coordinate  $\text{Hg}^{\text{II}}$ . Other examples feature bulky ligands, e.g. the trigonal planar complexes  $[\text{Fe}\{\text{N}(\text{SiMe}_3)_2\}_3]$ ,  $[\text{Cu}\{\{\text{SC}(\text{NH}_2)_2\}_3\}\text{Cl}]$  and  $[\text{Cu}(\text{SPPPh}_3)_3]\text{ClO}_4$ .

### Coordination number 4

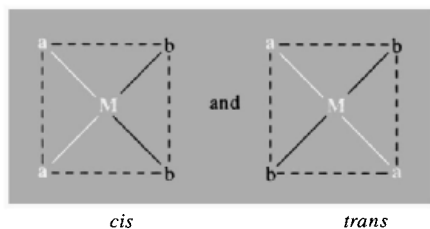
This is very common and usually gives rise to stereochemistries which may be regarded essentially as either tetrahedral  $T_d$  or (square) planar  $D_{4h}$ . Where a complex may be thought to have been formed from a central cation with a spherically symmetrical electron configuration, the ligands will lie as far from each other as possible, that is they will be tetrahedrally disposed around the cation. This has already been seen in complex anions such as  $\text{BF}_4^-$  and is also common amongst complexes of transition metals in their group oxidation states and of  $d^5$  and  $d^{10}$  ions.  $[\text{MnO}_4]^-$ ,  $[\text{Ni}(\text{CO})_4]$  and  $[\text{Cu}(\text{py})_4]^+$ , respectively, exemplify these types. Central cations with other d configurations, in particular  $d^8$ , may give rise to a square-planar stereochemistry and the complexes of  $\text{Pd}^{\text{II}}$  and  $\text{Pt}^{\text{II}}$  are predominantly of this type. Then again, the difference in energy between tetrahedral and square-planar forms may be only slight, in which case both forms may be known or, indeed, interconversions may be possible as happens with a number of  $\text{Ni}^{\text{II}}$  complexes (p. 1159). In the  $\text{M}_2\text{CuX}_4$  series of complexes of  $\text{Cu}^{\text{II}}$ , variation of  $\text{M}^{\text{I}}$  and X gives complex anions with stereochemistries ranging from square planar, e.g.  $(\text{NH}_4)_2[\text{CuCl}_4]$ , to almost tetrahedral, e.g.  $\text{Cs}_2[\text{CuBr}_4]$ . Figure 19.3 shows that the change from square planar to tetrahedral requires a  $90^\circ$  rotation of one L,L pair and a  $19\frac{1}{2}^\circ$  change in the LML angles, and a continuous range of distortions from one extreme to the other would appear to be feasible.

<sup>12</sup> P. G. ELLER, D. C. BRADLEY, M. B. HURSTHOUSE and D. W. MEEK, *Coord. Chem. Revs.* **24**, 1-95 (1977).



**Figure 19.3** Schematic interconversion of square planar and tetrahedral geometries.

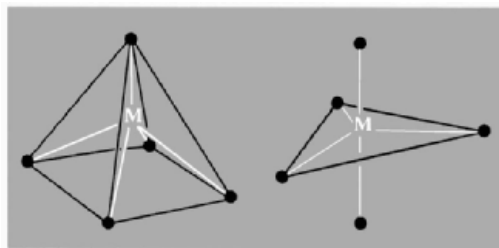
Four-coordinate complexes provide good examples of the early use of preparative methods for establishing stereochemistry. For complexes of the type  $[Ma_2b_2]$ , where a and b are unidentate ligands, a tetrahedral structure cannot produce isomerism whereas a planar structure leads to *cis* and *trans* isomers (see below). The preparation of 2 isomers of  $[PtCl_2(NH_3)_2]$ , for instance, was taken as good evidence for their planarity.<sup>†</sup>



### Coordination number 5

Five-coordinate complexes are far more common than was once supposed and are now known for all configurations from  $d^1$  to  $d^9$ . Two limiting stereochemistries may be distinguished (Fig. 19.4). One of the first authenticated examples of 5-coordination was  $[VO(acac)_2]$  which has the square-pyramidal  $C_{4v}$  structure with the  $=O$  occupying the unique apical site. However, many of the complexes with this coordination number have structures intermediate between the

<sup>†</sup> On the basis of this evidence alone it is logically possible that one isomer could be tetrahedral. Early coordination chemists, however, assumed that the directions of the "secondary valencies" were fixed, which would preclude this possibility. X-ray structural analysis shows that, in the case of  $Pt^{II}$  complexes, they were correct.



Square pyramidal

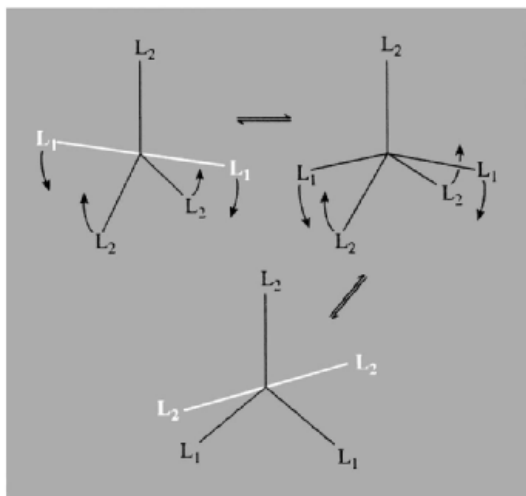
Trigonal bipyramidal

**Figure 19.4** Limiting stereochemistries for 5-coordination.

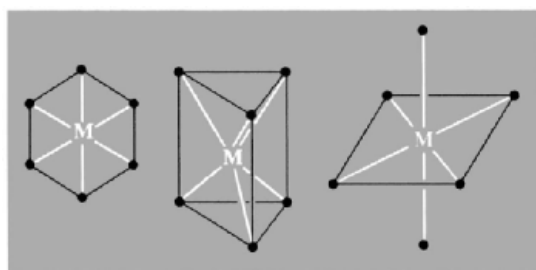
two extremes and it appears that the energy required for their interconversion is frequently rather small. Because of this stereochemical non-rigidity a number of 5-coordinate compounds behave in a manner described as "fluxional". That is, they exist in two or more configurations which are chemically equivalent and which interconvert at such a rate that some physical measurement (commonly nmr) is unable to distinguish the separate configurations and instead "sees" only their time-average. If  $ML_5$  has a trigonal bipyramidal  $D_{3h}$  structure then 2 ligands must be "axial" and 3 "equatorial", but interchange via a square-pyramidal intermediate is possible (Fig. 19.5). This mechanism has been suggested as the reason why the  $^{13}C$  nmr spectrum of trigonal bipyramidal  $Fe(CO)_5$  (p. 1104) fails to distinguish two different kinds of carbon nuclei. See also the discussion of  $PF_5$  on p. 499.

### Coordination number 6

This is the most common coordination number for complexes of transition elements. It can be seen by inspection that, for compounds of the type  $(Ma_4b_2)$ , the three symmetrical structures (Fig. 19.6) can give rise to 3, 3 and 2 isomers respectively. Exactly the same is true for compounds of the type  $[Ma_3b_3]$ . In order to determine the stereochemistry of 6-coordinate complexes very many examples of such compounds were prepared, particularly with  $M = Cr^{III}$  and  $Co^{III}$ , and in no case was more than 2 isomers found. This, of course, was only negative evidence for the octahedral structure, though the



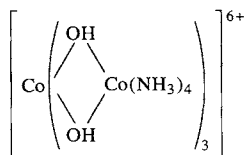
**Figure 19.5** The interconversion of trigonal bipyramidal configurations via a square-pyramidal intermediate. Notice that the  $L_1$  ligands, which in the left-hand tbp are axial, become equatorial in the right-hand tbp and simultaneously 2 of the  $L_2$  ligands change from equatorial to axial.



Planar      Trigonal prismatic      Octahedral

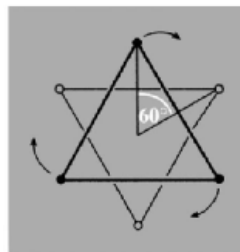
**Figure 19.6** Possible stereochemistries for 6-coordination.

sheer volume of it made it rather compelling. More positive evidence was provided by Werner, who in 1914 achieved the first resolution into optical isomers of an entirely inorganic compound, since

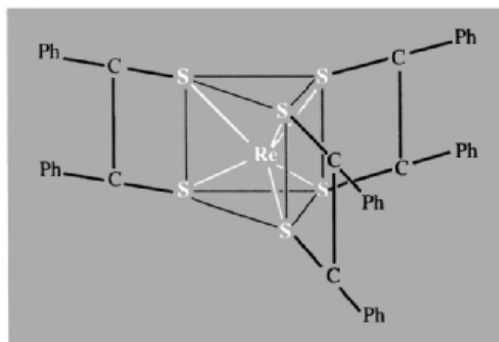


neither the planar nor trigonal prismatic structures can give rise to such optical isomers.

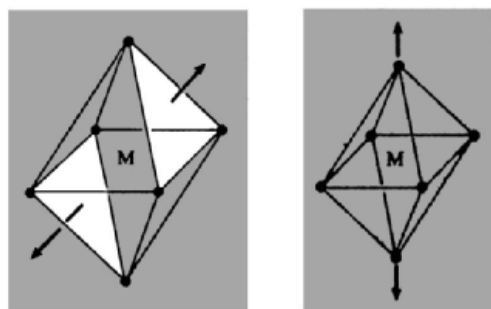
Nevertheless, it cannot be assumed that every 6-coordinate complex is octahedral. In 1923 the first example of trigonal prismatic coordination was reported for the infinite layer lattices of  $\text{MoS}_2$  and  $\text{WS}_2$ . A limited number of further examples are now known following the report in 1965 of the structure of  $[\text{Re}(\text{S}_2\text{C}_2\text{Ph}_2)_3]$  (Fig. 19.7). Intermediate structures also occur and can be defined by the “twist angle” which is the angle through which one face of an octahedron has been rotated with respect to the opposite face as “viewed along” a threefold axis of the octahedron. A twist angle of  $60^\circ$  suffices to convert an octahedron into a trigonal prism:



In fact the vast majority of 6-coordinate complexes are indeed octahedral or distorted octahedral. In addition to the twist distortion just considered distortions can be of two other types: trigonal and tetragonal distortions which mean compression or elongation along a threefold and a fourfold axis of the octahedron respectively (Fig. 19.8).



**Figure 19.7** Trigonal prismatic structure of  $[\text{Re}(\text{S}_2\text{C}_2\text{Ph}_2)_3]$ .



Trigonal elongation

Tetragonal elongation

**Figure 19.8** Distortions of octahedral geometry.

### Coordination number 7

There are three main stereochemistries for complexes of this coordination number: pentagonal bipyramidal  $D_{5h}$ , capped trigonal prismatic  $C_{2v}$  and capped octahedral  $C_{3v}$ , the last two being obtained by the addition of a seventh ligand either above one of the rectangular faces of a trigonal prism or above a triangular face of an octahedron respectively. These structures may conveniently be visualized as having the ligating atoms which form the coordination polyhedra on the surfaces of circumscribed spheres (Fig. 19.9).

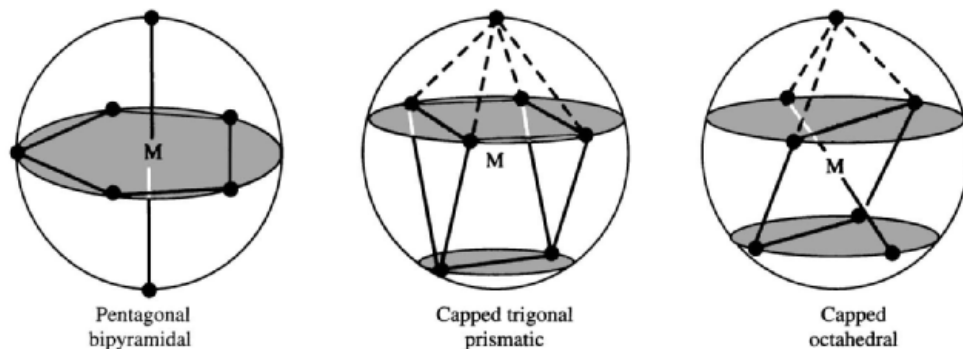
As with other high coordination numbers, there seems to be little difference in energy between these structures. Factors such as the number of counter ions and the stereochemical requirements of chelating ligands are probably decisive and *a priori* arguments are unreliable in predicting

the geometry of a particular complex.  $[\text{ZrF}_7]^{3-}$  and  $[\text{HfF}_7]^{3-}$  have the pentagonal bipyramidal structure, whereas the bivalent anions,  $[\text{NbF}_7]^{2-}$  and  $[\text{TaF}_7]^{2-}$  are capped trigonal prismatic. The capped octahedral structure is exemplified by  $[\text{NbOF}_6]^{3-}$ .

### Coordination number 8<sup>(13,14)</sup>

The most symmetrical structure possible is the cube  $O_h$  but, except in extended ionic lattices such as those of  $\text{CsCl}$  and  $\text{CaF}_2$ , it appears that inter-ligand repulsions are nearly always (but see p. 1275) reduced by distorting the cube, the two most important resultant structures being the square antiprism  $D_{4h}$  and the dodecahedron  $D_{2d}$  (Fig. 19.10).

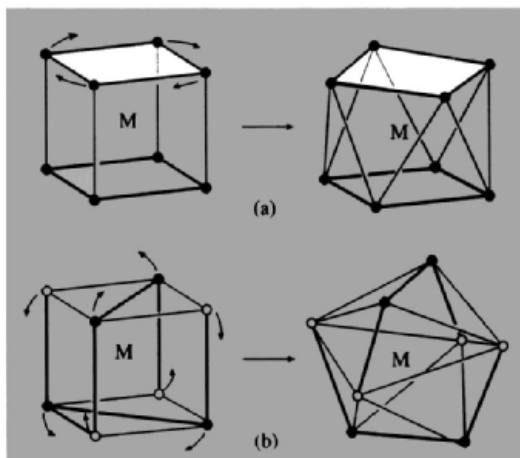
Again, these forms are energetically very similar; distortions from the idealized structures make it difficult to specify one or other, and the particular structure actually found must result from the interplay of many factors.  $[\text{TaF}_8]^{3-}$ ,  $[\text{ReF}_8]^{2-}$  and  $[\text{Zr}(\text{acac})_4]$  are square antiprismatic, whereas  $[\text{ZrF}_8]^{4-}$  and  $[\text{Mo}(\text{CN})_8]^{4-}$  are dodecahedral. The nitrates  $[\text{Co}(\text{NO}_3)_4]^{2-}$  and  $\text{Ti}(\text{NO}_3)_4$  may both be regarded as dodecahedral, the former with some distortion. Each nitrate ion is bidentate but the 2

Pentagonal  
bipyramidalCapped trigonal  
prismaticCapped  
octahedral**Figure 19.9** The three main stereochemistries for 7-coordination.

<sup>13</sup> I. G. SHTEREV, G. St. NIKOLOV, N. TRENDAFILOVA and R. KIROV, *Polyhedron*, **10**, 393–402 (1991).

<sup>14</sup> C. W. HAIGH, *Polyhedron*, **15**, 605–43 (1996).



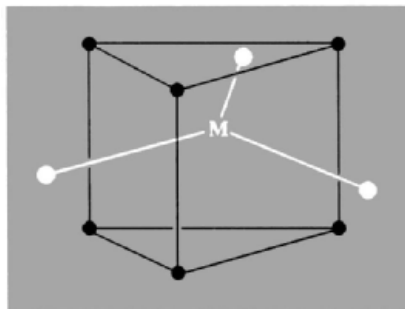


**Figure 19.10** (a) Conversion of cube to square antiprism by rotation of one face through  $45^\circ$  (b) Conversion of cube into dodecahedron.

oxygen atoms are necessarily close together so that the structure of the complexes is probably more easily visualized from the point of view of the 4 nitrogen atoms which form a flattened tetrahedron around the metal (p. 966).

### Coordination number 9

The stereochemistry of most 9-coordinate complexes approximates to the tri-capped trigonal prism  $D_{3h}$ , formed by placing additional ligands above the three rectangular faces of a trigonal prism:

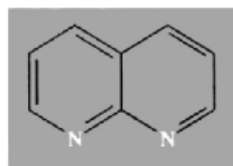


Amongst the known examples of this arrangement are a number of  $[M(\text{H}_2\text{O})_9]^{3+}$  hydrates of lanthanide salts and  $[\text{ReH}_9]^{2-}$ . The latter is

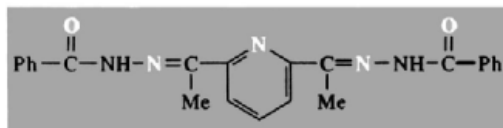
interesting in that it is presumably only the small size of the H ligand which allows such a high coordination number for rhenium. Very occasionally 9-coordination results in a capped square antiprismatic  $C_{4v}$  arrangement in which the ninth ligand lies above one of the square faces, e.g. the Cl-bridged  $[\{\text{LaCl}(\text{H}_2\text{O})_7\}_2]^{4+}$ .

### Coordination numbers above 9

Such high coordination numbers are not common and it is difficult to generalize about their structures since so few have been accurately determined. They are found mainly with ions of the early lanthanide and actinide elements and it is therefore tempting to assume that the availability of empty and accessible f orbitals is necessary for their formation. However, it appears that the bonding is predominantly ionic and that the really important point is that these are the elements which provide stable cations with charges high enough to attract a large number of anions and yet are large enough to ensure that the inter-ligand repulsions are not unacceptably high.  $\text{K}_4[\text{Th}(\text{O}_2\text{CCO}_2)_4(\text{H}_2\text{O})_2] \cdot 2\text{H}_2\text{O}$  (bicapped square antiprism  $D_{4d}$ ) and  $[\text{La}(\text{edta})(\text{H}_2\text{O})_4]$  afford examples of 10-coordination. Higher coordination numbers are reached only by chelating ligands such as  $\text{NO}_3^-$ ,  $\text{SO}_4^{2-}$ , and 1,8-naphthyridine (8) with donor atoms close together (i.e. ligands with only a small "bite").  $[\text{La}(\text{dapbaH})(\text{NO}_3)_3]$ , is a good example (see



(8)



(9)

also p. 1276): in it the 5 donor atoms of the dapbaH, i.e. 2,6-diacetylpyridinebis(benzoic acid hydrazone) (9), are situated in a plane, with the N atoms (but not the donor oxygens) of the 3 bidentate nitrates in a second plane at right angles to the first.  $\text{Ce}_2\text{Mg}_3(\text{NO}_3)_{12}\cdot 24\text{H}_2\text{O}$  contains 12-coordinate Ce in the complex ion  $[\text{Ce}(\text{NO}_3)_6]^{3-}$ . This has a distorted icosahedral stereochemistry, though it is more easily visualized as an octahedral arrangement of the nitrogen atoms around the  $\text{Ce}^{\text{III}}$ . Another example is  $[\text{Pr}(\text{naph})_6]^{3+}$  where naph is 1,8-naphthyridine (8).

Higher coordination numbers (up to 16) are known, particularly among organometallic compounds (pp. 940–3) and metal borohydrides (p. 168).

In addition to coordination compounds in which a central metal atom is surrounded by a polyhedral array of donor atoms, a large and rapidly increasing number of “cluster” compounds<sup>(15–18)</sup> is known in which a group of metal atoms is held together largely by M–M bonds. Where more than three metal atoms are involved, they themselves form polyhedral arrays which may be considered as conceptual intermediates between mononuclear classical complexes and the non-molecular lattice structures of binary and ternary compounds of transition metals. A distinction is sometimes made between “clusters” which owe their stability to M–M bonds, and “cages” which are held together by ligand bridges, but the distinction is not rigidly adhered to.

Cluster and cage structures are widespread in the chemistry of main group elements, being particularly extensive in the case of boron (Chap. 6). For transition elements the principal

areas of interest are the lower halides of elements towards the left of the d-block, and carbonyls of elements towards the right of the d-block, the latter being an especially active area. The possibility that metal clusters of high nuclearity might mimic the behaviour of metal surfaces (the “surface-cluster analogy”) has stimulated synthetic chemists to search for materials with high catalytic activity.<sup>(19)</sup> Such materials, particularly if soluble, should also provide better insight into the catalytic activity of metal surfaces. Unfortunately these objectives have so far proved largely elusive and in only a few cases can catalytic activity be attributed confidently to a cluster itself rather than to its fragmentation products.

These and other classes of cluster compounds will be dealt with more fully in later chapters devoted to the chemistry of the metals involved.

## 19.5 Isomerism<sup>(20)</sup>

Isomers are compounds with the same chemical composition but different structures, and the possibility of their occurrence in coordination compounds is manifest. Their importance in the early elucidation of the stereochemistries of complexes has already been referred to and, though the purposeful preparation of isomers is no longer common, the preparative chemist must still be aware of the diversity of the compounds which can be produced. The more important types of isomerism are listed below.

### Conformational isomerism

In principle this type of isomerism (also known as “polytopal” isomerism) is possible with any coordination number for which there is more than one known stereochemistry. However, to actually occur the isomers need to be of comparable stability, and to be separable there

<sup>15</sup> M. MOSKOVITS, *Metal Clusters*, Wiley, New York, 1986, 313 pp.

<sup>16</sup> I. G. DANCE, Chap. 5 in *Comprehensive Coordination Chemistry*, Vol. 1, pp. 135–78, Pergamon Press, Oxford, 1987.

<sup>17</sup> D. F. SHRIVER, H. D. KAESZ and R. D. ADAMS, *The Chemistry of Metal Cluster Complexes*, VCH, New York, 1990, 439 pp.

<sup>18</sup> D. M. P. MINGOS and D. I. WALES, *Introduction to Cluster Chemistry*, Prentice Hall, New York, 1990, 318 pp.

<sup>19</sup> B. C. GATES, L. GUCZI and H. KNÖZINGER (eds.) *Metal Clusters in Catalysis*, Vol. 29 of *Studies in Surface Science and Catalysis*, Elsevier, Amsterdam, 1986, 648 pp.

<sup>20</sup> J. MACB. HARROWFIELD, Chap. 6 in *Comprehensive Coordination Chemistry*, Vol. 1, pp. 179–212, Pergamon Press, Oxford, 1987.

must be a significant energy barrier preventing their interconversion. This behaviour is confined primarily to 4-coordinate nickel(II), an example being  $[\text{NiCl}_2\{\text{P}(\text{CH}_2\text{Ph})\text{Ph}_2\}_2]$  which is known in both planar and tetrahedral forms (p. 1160).

### Geometrical isomerism

This is of most importance in square-planar and octahedral compounds where ligands, or more specifically donor atoms, can occupy positions next to one another (*cis*) or opposite each other (*trans*) (Fig. 19.11).

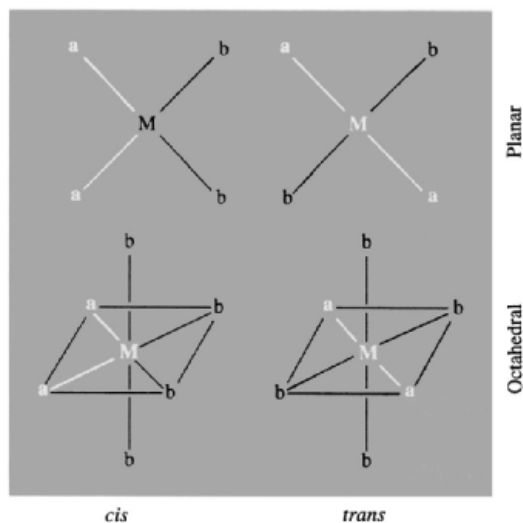


Figure 19.11 *Cis* and *trans* isomerism.

A similar type of isomerism occurs for  $[\text{Ma}_3\text{b}_3]$  octahedral complexes since each trio of donor atoms can occupy either adjacent positions at the corners of an octahedral face (*facial*) or positions around the meridian of the octahedron (*meridional*). (Fig. 19.12.) Geometrical isomers differ in a variety of physical properties, amongst which dipole moment and visible/ultraviolet spectra are often diagnostically important.

### Optical isomerism

Optical isomers, enantiomorphs or enantiomers, as they are also known, are pairs of molecules

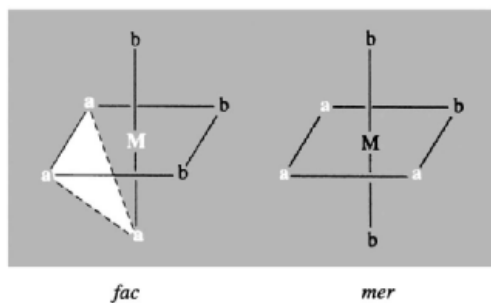


Figure 19.12 Facial and meridional isomers.

which are non-superimposable mirror images of each other. Such isomers have the property of chirality (from Greek  $\chi\epsilon\iota\rho$ , hand), i.e. handedness, and virtually the only physical or chemical difference between them is that they rotate the plane of polarized light, one of them to the left and the other to the right. They are consequently designated as laevo (*l* or  $-$ ) and dextro (*d* or  $+$ ) isomers.

A few cases of optical isomerism are known for planar and tetrahedral complexes involving unsymmetrical bidentate ligands, but by far the most numerous examples are afforded by octahedral compounds of chelating ligands, e.g.  $[\text{Cr}(\text{oxalate})_3]^{2-}$  and  $[\text{Co}(\text{edta})]^-$  (Fig. 19.13).

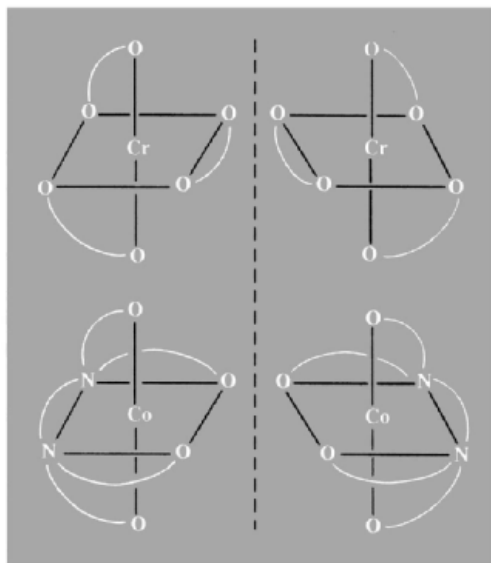
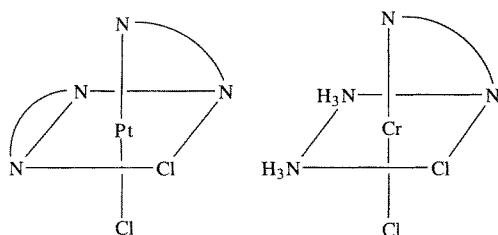


Figure 19.13 Non-superimposable mirror images.

Where unidentate ligands are present, the ability to effect the resolution of an octahedral complex (i.e. to separate 2 optical isomers) is proof that the 2 ligands are *cis* to each other. Resolution of  $[\text{PtCl}_2(\text{en})_2]^{2-}$  therefore shows it to be *cis* while of the 2 known geometrical isomers of  $[\text{CrCl}_2\text{en}(\text{NH}_3)_2]^+$  the one which can be resolved must have the *cis-cis* structure since the *trans* form would give a superimposable, and therefore identical, mirror image:



### Ionization isomerism

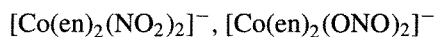
This type of isomerism occurs when isomers produce different ions in solution, and is possible in compounds which consists of a complex ion with a counter ion which is itself a potential ligand. The pairs:  $[\text{Co}(\text{NH}_3)_5(\text{NO}_3)]\text{SO}_4$ ,  $[\text{Co}(\text{NH}_3)_5(\text{SO}_4)]\text{NO}_3$  and  $[\text{PtCl}_2(\text{NH}_3)_4]\text{Br}_2$ ,  $[\text{PtBr}_2(\text{NH}_3)_4]\text{Cl}_2$ , and the series  $[\text{CoCl}(\text{en})_2(\text{NO}_2)]\text{SCN}$ ,  $[\text{CoCl}(\text{en})_2(\text{SCN})]\text{NO}_2$ ,  $[\text{Co}(\text{en})_2(\text{NO}_2)(\text{SCN})]\text{Cl}$  are examples of ionization isomers.

A subdivision of this type of isomerism, known as "hydrate isomerism", occurs when water may be inside or outside the coordination sphere. It is typified by  $\text{CrCl}_3 \cdot 6\text{H}_2\text{O}$  which exists in the three distinct forms  $[\text{Cr}(\text{H}_2\text{O})_6]\text{Cl}_3$  (violet),  $[\text{CrCl}(\text{H}_2\text{O})_5]\text{Cl}_2 \cdot \text{H}_2\text{O}$  (pale green), and  $[\text{CrCl}_2(\text{H}_2\text{O})_4]\text{Cl} \cdot 2\text{H}_2\text{O}$  (dark green). These are readily distinguished by the action of  $\text{AgNO}_3$  in aqueous solution which immediately precipitates 3, 2 and 1 chloride ions respectively.

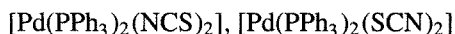
### Linkage isomerism

This is in principle possible in any compound containing an ambidentate ligand. However, that

such a ligand can *under different circumstances* coordinate through either of the 2 different donor atoms is by no means a guarantee that it will form isolable linkage isomers with the same cation. In fact, in only a very small proportion of the complexes of ambidentate ligands can linkage isomers actually be isolated, and these are confined largely to complexes of  $\text{NO}_2^-$  (p. 463) and, to a lesser extent,  $\text{SCN}^-$  (p. 325). Examples are:



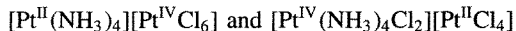
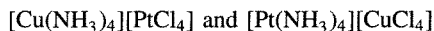
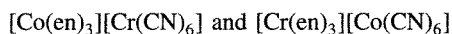
and



It should be noted that, by convention, the ambidentate ligand is always written with its donor atom first, i.e.  $\text{NO}_2$  for the nitro,  $\text{ONO}$  for the nitrito,  $\text{NCS}$  for the *N*-thiocyanato and  $\text{SCN}$  for the *S*-thiocyanato complex. Differences in infrared spectra arising from the differences in bonding are often used to distinguish between such isomers.

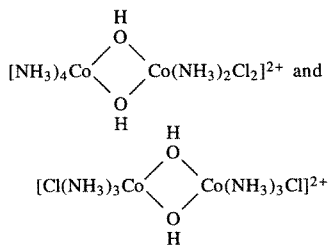
### Coordination isomerism

In compounds made up of both anionic and cationic complexes it is possible for the distribution of ligands between the ions to vary and so lead to isomers such as:



It can be seen that other intermediate isomers are feasible but in the above cases they have not been isolated. Substantial differences in both physical and chemical properties are to be expected between coordination isomers.

When the two coordinating centres are not in separate ions but are joined by bridging groups, the isomers are often distinguished as "coordination position isomers" as is the case for:



### Polymerization isomerism

Compounds whose molecular compositions are multiples of a simple stoichiometry are polymers, strictly, only if they are formed by repetition of the simplest unit. However, the name “polymerization isomerism” is applied rather loosely to cases where the same stoichiometry is retained but where the molecular arrangements are different. The stoichiometry  $\text{PtCl}_2(\text{NH}_3)_2$  applies to the 3 known compounds,  $[\text{Pt}(\text{NH}_3)_4][\text{PtCl}_4]$ ,  $[\text{Pt}(\text{NH}_3)_4][\text{PtCl}_3(\text{NH}_3)]_2$ , and  $[\text{PtCl}(\text{NH}_3)_3]_2[\text{PtCl}_4]$  (in addition to the *cis* and *trans* isomers of monomeric  $[\text{PtCl}_2(\text{NH}_3)_2]$ ). There are actually 7 known compounds with the stoichiometry  $\text{Co}(\text{NH}_3)_3(\text{NO}_2)_3$ . Again it is clear that considerable differences are to be expected in the chemical properties and in physical properties such as conductivity.

### Ligand isomerism

Should a ligand exist in different isomeric forms then of course the corresponding complexes will also be isomers, often described as “ligand isomers”. In  $[\text{CoCl}(\text{en})_2(\text{NH}_2\text{C}_6\text{H}_4\text{Me})]\text{Cl}_2$ , for instance, the toluidine may be of the *o*-, *m*- or *p*- form.

## 19.6 The Coordinate Bond<sup>(21)</sup>

(see also p. 198)

The concept of the coordinate bond as an interaction between a cation and an ion or

molecule possessing a lone-pair of electrons can be accepted before specifying the nature of that interaction. Indeed, it is now evident that in different complexes the bond can span the whole range from electrostatic to covalent character. This is why the various theories which have been accorded popular favour at different times have been acceptable and useful even though based on apparently incompatible assumptions. This dichotomy is reflected in the now obsolete adjectives “dative-covalent”, “semi-polar” and “co-ionic”, which have been used to describe the coordinate bond. The first of these descriptions arises from the idea advanced by N. V. Sidgwick in 1927, that the coordinate bond is a covalent bond formed by the donation of a lone-pair of electrons from the donor atom to the central metal. Since noble gases are extremely unreactive, and compounds in which atoms have attained the electronic configuration of a noble gas either by sharing or transferring electrons also tend to be stable, Sidgwick further suggested that, in complexes, the metal would tend to surround itself with sufficient ligands to ensure that the number of electrons around it (its “effective atomic number” or EAN) would be the same as that of the next noble gas. If this were true then a metal would have a unique coordination number for each oxidation state, which is certainly not always the case. However, the EAN rule is still of use in rationalizing the coordination numbers and structures of simple metal carbonyls.

In his *valence bond theory* (VB), L. Pauling extended the idea of electron-pair donation by considering the orbitals of the metal which would be needed to accommodate them, and the stereochemical consequences of their hybridization (1931–3). He was thereby able to account for much that was known in the 1930s about the stereochemistry and kinetic behaviour of complexes, and demonstrated the diagnostic value of measuring their magnetic properties. Unfortunately the theory offers no satisfactory explanation of spectroscopic properties and so was

<sup>21</sup> B. N. FIGGIS, Chap. 7 in *Comprehensive Coordination Chemistry*, Vol. 1, pp. 213–80, Pergamon Press, Oxford, 1987. S. F. A. KETTLE, *Physical Inorganic Chemistry*, A

*Coordination Chemistry Approach*, pp. 95–237, Spektrum, Oxford, 1996.

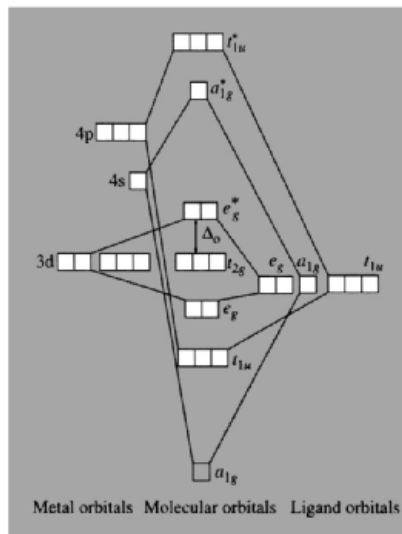
eventually superseded by *crystal field theory* (CF).

About the same time that VB theory was being developed, CF theory was also being used by H. Bethe, J. H. van Vleck and other physicists to account for the colours and magnetic properties of hydrated salts of transition metals (1933–6). It is based on what, to chemists, appeared to be the outrageous assumption that the coordinate bond is entirely electrostatic. Nevertheless, in the 1950s a number of theoretical chemists used it to interpret the electronic spectra of transition metal complexes. It has since been remarkably successful in explaining the properties of  $M^{II}$  and  $M^{III}$  ions of the first transition series, especially when modifications have been incorporated to include the possibility of some covalency. (The theory is then often described as *ligand field theory*, but there is no general agreement on this terminology.)

In order to take full account of both ionic and covalent character, recourse must be made to *molecular orbital theory* (MO) which, like the VB and CF theories, originated in the 1930s. It has gained increasing ground with the development of powerful high-speed computers and the ready accessibility of software programmes which enable either semi-empirical or complex *ab initio* calculations to be carried out reliably and rapidly. There is still a place, however, for the pictorial representation of localized two-centre or three-centre bonds in elementary descriptions of bonding.

The fundamental assumption of MO theory is that metal and ligand orbitals will overlap and combine, providing they are of the correct symmetries to do so and have similar energies. In one approximation the appropriate AOs of the metal and atomic or molecular orbitals of the ligand, are used to produce the MOs by the linear combination of atomic orbitals (LCAO) method. Since combination of metal and ligand orbitals of widely differing energies can be neglected, only valence orbitals are considered.

In the case of an octahedral complex  $ML_6$ , the metal has six  $\sigma$  orbitals, i.e. the  $e_g$  pair of the  $nd$  set, together with the  $(n+1)s$  and the three  $(n+1)p$ . The ligands each have one



**Figure 19.14** Molecular orbital diagram for an octahedral complex of a first series transition metal (only  $\sigma$  interactions are considered in this simplified diagram).

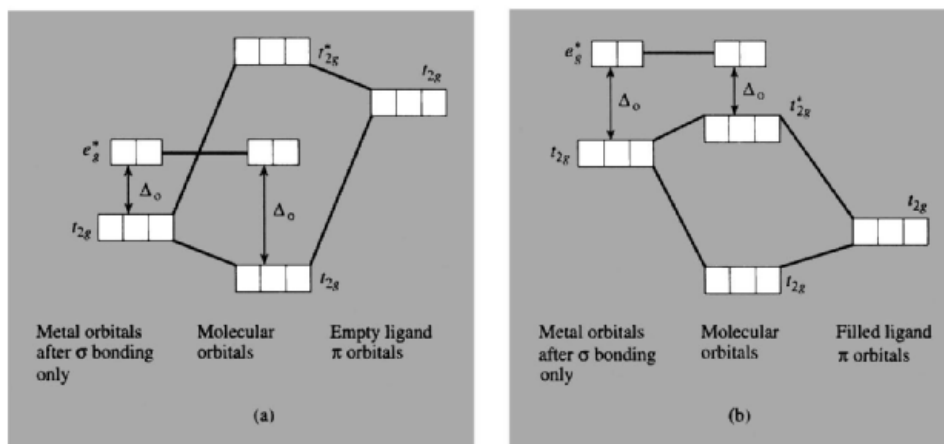
$\sigma$  orbital (containing the lone-pair of electrons) and these are combined to give orbitals with the correct symmetry to overlap with the metal  $\sigma$  orbitals (Fig. 19.14). The 6 electron pairs from the ligands are placed in the six lowest MOs, leaving the non-axial, and hence non- $\sigma$ -bonding, metal  $t_{2g}$  and the antibonding  $e_g^*$  orbitals to accommodate the electrons originally on the metal. This central portion of the figure is the same as the  $e_g/t_{2g}$  splitting defined in CF theory, with the difference that the  $e_g^*$  orbitals now have some ligand character which implies covalency. The lower in energy the ligand orbitals are with respect to the AOs of the metal the nearer is the bonding to the electrostatic extreme. Conversely, the nearer in energy the ligand orbitals are to the AOs of the metal the more nearly can the bonding be described as electron pair donation by the ligand as in VB theory. Indeed, the metal character of the bonding MOs is derived from just those metal orbitals used in VB theory to produce the  $d^2sp^3$  hybrids which accommodate the electron pairs donated by the ligands.

If the ligand possesses orbitals of  $\pi$  as well as  $\sigma$  symmetry the situation is drastically changed

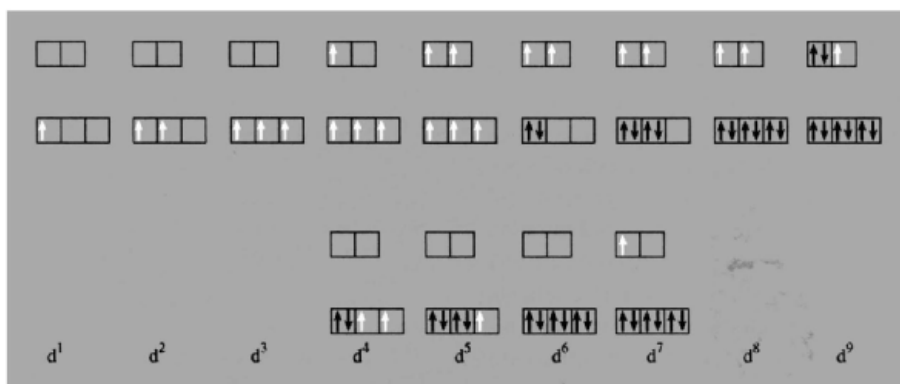
because of the overlap of these orbitals with the  $t_{2g}$  orbitals of the metal. Two situations may arise. Either the ligand  $\pi$  orbitals are empty and of higher energy than the metal  $t_{2g}$ , or they are filled and of lower energy than the metal  $t_{2g}$  orbitals (Fig. 19.15). The former in effect increases  $\Delta_o$ , the separation of the  $t_{2g}$  and  $e_g^*$  orbitals, and is the more important case, including ligands such as CO,  $\text{NO}^+$  and  $\text{CN}^-$ . This type of covalency, called  $\pi$  bonding or back bonding, provides a plausible explanation for the stability of such compounds as the metal carbonyls (pp. 926–9).

If  $\Delta_o$  is large enough then electrons which would otherwise remain unpaired in the  $e_g$

orbitals may instead be forced to pair in the lower  $t_{2g}$  orbitals. For metal ions with  $d^4$ ,  $d^5$ ,  $d^6$  and  $d^7$  configurations therefore two possibilities arise depending on the magnitude of  $\Delta_o$ . If  $\Delta_o$  is small (compared with electron–electron repulsion energies within one orbital) then the maximum possible number of electrons remain unpaired and the configurations are known as “spin-free” or “high-spin”. If  $\Delta_o$  is large then electrons are forced to pair in the lower  $t_{2g}$  set and the configurations are known as “spin-paired” or “low-spin”. This is summarized in Fig. 19.16.



**Figure 19.15** Possible effects of  $\pi$  bonding on  $\Delta_o$ : (a) when ligand  $\pi$  orbitals are empty, and (b) when ligand  $\pi$  orbitals are filled.



**Figure 19.16** The possible high-spin and low-spin configurations arising as a result of the imposition of an octahedral crystal field on a transition metal ion.

Similar MO treatments are possible for tetrahedral and square planar complexes but are increasingly complicated.

## 19.7 Organometallic Compounds

This section gives a brief overview of the vast and burgeoning field of organometallic chemistry. The term *organometallic* is somewhat vague since definitions of *organo* and *metallic* are themselves necessarily imprecise. We use the term to refer to compounds that involve at least one close M–C interaction: this includes metal complexes with ligands such as CO, CO<sub>2</sub>, CS<sub>2</sub> and CN<sup>−</sup> but excludes “ionic” compounds such as NaCN or Na acetate; it also excludes metal alkoxides M(OR)<sub>n</sub> and metal complexes with organic ligands such as C<sub>5</sub>H<sub>5</sub>N, PPh<sub>3</sub>, OEt<sub>2</sub>, SMe<sub>2</sub>, etc., where the donor atom is not carbon. A permissive view is often taken in the literature of what constitutes a “metal” and the elements B; Si, Ge; As, Sb; Se and Te are frequently included for convenience and to give added perspective. However, it is not helpful to include as metals all elements less electronegative than C since this includes I, S and P. Metal carbides (p. 297) and graphite intercalation compounds (p. 293) are also normally excluded. Further treatment of organometallic compounds will be found throughout the book under each individual element.

No area of chemistry produces more surprises and challenges and the whole field of organometallic chemistry continues to be one of great excitement and activity. A rich harvest of new and previously undreamed of structure types is reaped each year, the rewards of elegant and skilful synthetic programmes being supplemented by an unusual number of chance discoveries and totally unsuspected reactions. Synthetic chemists can take either a buccaneering or an intellectual approach (or both); structural chemists are able to press their various techniques to the limit in elucidating the products formed; theoretical chemists and reaction kineticists, though badly

outpaced in predictive work, provide an invaluable underlying rationale for various aspects of the continually evolving field and just occasionally run ahead of the experimentalists; industrial chemists can exploit and extend the results by developing numerous catalytic processes of immense importance. The field is not new, but was transformed in 1952 by the recognition of the “sandwich” structure of dicyclopentadienyliron (ferrocene).<sup>(22,23)</sup> Compendia and extended reviews<sup>(24–27)</sup> are available on various aspects, and continued progress is summarized in annual volumes.<sup>(28,29)</sup>

The various classes of ligands and attached groups that occur in organometallic compounds are summarized in Table 19.2, and these will be briefly discussed in the following paragraphs. Aspects which concern the general chemistry of carbon will be emphasized in order to give coherence and added significance to the more detailed treatment of the organometallic chemistry of individual elements given in other sections, e.g. Li (p. 102), Be (p. 127), Mg (p. 131), etc.

---

<sup>22</sup> G. WILKINSON, M. ROSENBLUM, M. C. WHITING and R. B. WOODWARD, *J. Am. Chem. Soc.* **74**, 2125–6 (1952). For some personal recollections on the events leading up to this paper, see G. WILKINSON, *J. Organometallic Chem.* **100**, 273–8 (1975).

<sup>23</sup> J. S. THAYER, *Adv. Organometallic Chem.* **13**, 1–49 (1975).

<sup>24</sup> G. WILKINSON, F. G. A. STONE and E. W. ABEL (eds.), *Comprehensive Organometallic Chemistry*, 9 Vols., Pergamon Press, Oxford, 1982, 9569 pp. E. W. ABEL, F. G. A. STONE and G. WILKINSON (eds.), *Comprehensive Organometallic Chemistry II*, 14 Vols, Pergamon Press, Oxford, 1995, approx. 8750 pp.

<sup>25</sup> F. A. COTTON and G. WILKINSON, *Advanced Inorganic Chemistry*, 5th edn., Wiley, New York, 1988, particularly Chaps. 22–29, pp. 1021–334.

<sup>26</sup> *Dictionary of Organometallic Compounds*, Chapman and Hall, London, Vols. 1–3, (1984), J. BUCKINGHAM (ed.); Supplement 1 (1985)–Supplement 5 (1989), Index (1990), J. F. MACINTYRE (ed).

<sup>27</sup> *The Chemistry of the Metal–Carbon Bond*, Wiley, Chichester, Vols. 1–3 (1985), F. R. HARTLEY and S. PATAI (eds.); Vol. 4 (1987), Vol. 5 (1989), F. R. HARTLEY (ed.).

<sup>28</sup> F. G. A. STONE and R. WEST (eds.), *Advances in Organometallic Chemistry*, Academic Press, New York, Vol. 1 (1964)–Vol. 40 (1996).

<sup>29</sup> *Organometallic Chemistry Reactions*, Wiley, Vol. 1, (1967)–Vol. 12 (1981).



Similar MO treatments are possible for tetrahedral and square planar complexes but are increasingly complicated.

## 19.7 Organometallic Compounds

This section gives a brief overview of the vast and burgeoning field of organometallic chemistry. The term *organometallic* is somewhat vague since definitions of *organo* and *metallic* are themselves necessarily imprecise. We use the term to refer to compounds that involve at least one close M–C interaction: this includes metal complexes with ligands such as CO, CO<sub>2</sub>, CS<sub>2</sub> and CN<sup>−</sup> but excludes “ionic” compounds such as NaCN or Na acetate; it also excludes metal alkoxides M(OR)<sub>n</sub> and metal complexes with organic ligands such as C<sub>5</sub>H<sub>5</sub>N, PPh<sub>3</sub>, OEt<sub>2</sub>, SMe<sub>2</sub>, etc., where the donor atom is not carbon. A permissive view is often taken in the literature of what constitutes a “metal” and the elements B; Si, Ge; As, Sb; Se and Te are frequently included for convenience and to give added perspective. However, it is not helpful to include as metals all elements less electronegative than C since this includes I, S and P. Metal carbides (p. 297) and graphite intercalation compounds (p. 293) are also normally excluded. Further treatment of organometallic compounds will be found throughout the book under each individual element.

No area of chemistry produces more surprises and challenges and the whole field of organometallic chemistry continues to be one of great excitement and activity. A rich harvest of new and previously undreamed of structure types is reaped each year, the rewards of elegant and skilful synthetic programmes being supplemented by an unusual number of chance discoveries and totally unsuspected reactions. Synthetic chemists can take either a buccaneering or an intellectual approach (or both); structural chemists are able to press their various techniques to the limit in elucidating the products formed; theoretical chemists and reaction kineticists, though badly

outpaced in predictive work, provide an invaluable underlying rationale for various aspects of the continually evolving field and just occasionally run ahead of the experimentalists; industrial chemists can exploit and extend the results by developing numerous catalytic processes of immense importance. The field is not new, but was transformed in 1952 by the recognition of the “sandwich” structure of dicyclopentadienyliron (ferrocene).<sup>(22,23)</sup> Compendia and extended reviews<sup>(24–27)</sup> are available on various aspects, and continued progress is summarized in annual volumes.<sup>(28,29)</sup>

The various classes of ligands and attached groups that occur in organometallic compounds are summarized in Table 19.2, and these will be briefly discussed in the following paragraphs. Aspects which concern the general chemistry of carbon will be emphasized in order to give coherence and added significance to the more detailed treatment of the organometallic chemistry of individual elements given in other sections, e.g. Li (p. 102), Be (p. 127), Mg (p. 131), etc.

---

<sup>22</sup> G. WILKINSON, M. ROSENBLUM, M. C. WHITING and R. B. WOODWARD, *J. Am. Chem. Soc.* **74**, 2125–6 (1952). For some personal recollections on the events leading up to this paper, see G. WILKINSON, *J. Organometallic Chem.* **100**, 273–8 (1975).

<sup>23</sup> J. S. THAYER, *Adv. Organometallic Chem.* **13**, 1–49 (1975).

<sup>24</sup> G. WILKINSON, F. G. A. STONE and E. W. ABEL (eds.), *Comprehensive Organometallic Chemistry*, 9 Vols., Pergamon Press, Oxford, 1982, 9569 pp. E. W. ABEL, F. G. A. STONE and G. WILKINSON (eds.), *Comprehensive Organometallic Chemistry II*, 14 Vols, Pergamon Press, Oxford, 1995, approx. 8750 pp.

<sup>25</sup> F. A. COTTON and G. WILKINSON, *Advanced Inorganic Chemistry*, 5th edn., Wiley, New York, 1988, particularly Chaps. 22–29, pp. 1021–334.

<sup>26</sup> *Dictionary of Organometallic Compounds*, Chapman and Hall, London, Vols. 1–3, (1984), J. BUCKINGHAM (ed.); Supplement 1 (1985)–Supplement 5 (1989), Index (1990), J. F. MACINTYRE (ed).

<sup>27</sup> *The Chemistry of the Metal–Carbon Bond*, Wiley, Chichester, Vols. 1–3 (1985), F. R. HARTLEY and S. PATAI (eds.); Vol. 4 (1987), Vol. 5 (1989), F. R. HARTLEY (ed.).

<sup>28</sup> F. G. A. STONE and R. WEST (eds.), *Advances in Organometallic Chemistry*, Academic Press, New York, Vol. 1 (1964)–Vol. 40 (1996).

<sup>29</sup> *Organometallic Chemistry Reactions*, Wiley, Vol. 1, (1967)–Vol. 12 (1981).

**Table 19.2** Classification of organometallic ligands according to the number of attached C atoms<sup>(a)</sup>

Number	Examples
$\eta^1$ , monohapto	Alkyl ( $-\text{R}$ ), aryl ( $-\text{Ar}$ ), perfluoro ( $-\text{R}_f$ ), acyl ( $-\text{CR}$ ), $\sigma$ -allyl ( $-\text{CH}_2\text{CH}=\text{CH}_2$ ), $\sigma$ -ethynyl ( $-\text{C}\equiv\text{CR}$ ), CO, CO <sub>2</sub> , CS <sub>2</sub> , CN <sup>-</sup> , isocyanide (RNC), <div style="text-align: center;"> <math>\begin{array}{c} \text{O} \\    \\ \text{C} \end{array}</math> </div> carbene ( $=\text{CR}_2$ , $=\text{C} \begin{array}{l} \text{OR}' \\ \text{R} \end{array}$ , $=\text{C} \begin{array}{l} \text{OR} \\ \text{NHAr} \end{array}$ , $=\text{C}_{\text{cyclo}}$ , etc.) carbyne ( $\equiv\text{CR}$ , $\equiv\text{CAr}$ ), carbido (C)
$\eta^2$ , dihapto	Alkene ( $\text{>C}=\text{C}<$ ), perfluoroalkene (e.g. C <sub>2</sub> F <sub>4</sub> ), alkyne ( $-\text{C}\equiv\text{C}-$ ), etc. [non-conjugated dienes are bis-dihapto]
$\eta^3$ , trihapto	$\pi$ -Allyl ( $\text{>C}-\text{C}-\text{C}<$ )
$\eta^4$ , tetrahapto	Conjugated diene (e.g. butadiene), cyclobutadiene derivatives
$\eta^5$ , pentahapto	Dieryl (e.g. cyclopentadienyl derivatives, cycloheptadienyl derivatives)
$\eta^6$ , hexahapto	Arene (e.g. benzene, substituted benzenes) cycloheptatriene, cycloocta-1,3,5-triene
$\eta^7$ , heptahapto	Tropylium (cycloheptatrienyl)
$\eta^8$ , octahapto	Cyclooctatetraene

<sup>(a)</sup>Many ligands can bond in more than one way: e.g. allyl can be  $\eta^1$  ( $\sigma$ -allyl) or  $\eta^3$  ( $\pi$ -allyl); cyclooctatetraene can be  $\eta^4$  (1,3-diene),  $\eta^4$  (chelating, 1,5-diene),  $\eta^6$  (1,3,5-triene),  $\eta^6$  (bis-1,2,3,-5,6,7- $\pi$ -allyl),  $\eta^8$  (1,3,5,7-tetraene), etc.

### 19.7.1 Monohapto ligands

Alkyl and aryl derivatives of many main-group metals have already been discussed in previous chapters, and compounds such as PbMe<sub>4</sub> and PbEt<sub>4</sub> are made on a huge scale, larger than all other organometallics put together (p. 371). The alkyl and aryl groups are usually regarded as 1-electron donors but it is important to remember that even a monohapto 1-electron donor can bond simultaneously to more than 1 metal atom, e.g. to 2 in Al<sub>2</sub>Me<sub>6</sub> (p. 259), 3 in Li<sub>4</sub>Bu<sub>4</sub>' (p. 105) and 4 in [Li<sub>4</sub>Me<sub>4</sub>]<sub>n</sub>. Similarly, an  $\eta^1$  ligand such as CO, which is often regarded as a 2-electron donor, can bond simultaneously to either 1, 2 or 3 metal atoms (p. 928). There is thus an important distinction to be drawn between (a) hapticity (the number of C atoms in the organic group that are closely associated with a metal atom), (b) metal connectivity (the number of M atoms simultaneously bonded to the organic group), and (c) the number of ligand electrons formally involved in bonding to the metal atom(s). The

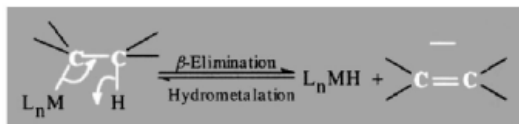
metal connectivity is also to be distinguished from the coordination number of the C atom, which also includes all other atoms or groups attached to it: e.g. the bridging C atoms in Al<sub>2</sub>Me<sub>6</sub> are monohapto with a metal connectivity of 2 and a coordination number of 5.

Although zinc alkyls were first described by E. Frankland in 1849 and the alkyls and aryls of most main group elements had been prepared and often extensively studied during the subsequent 100 y, very few such compounds were known for the transition metals even as recently as the late 1960s. The great burst of more recent activity stems from the independent suggestion<sup>(30,31)</sup> that M-C bonds involving transition elements are not inherently weak and that kinetically stable complexes can be made by a suitable choice of organic groups. In particular, the use of groups which have no  $\beta$ -hydrogen atom (e.g.  $-\text{CH}_2\text{Ph}$ ,

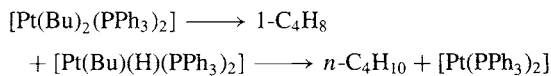
<sup>30</sup> M. R. COLLIER, M. F. LAPPERT and M. M. TRUELOCK, *J. Organometallic Chem.* **25**, C36-8 (1970).

<sup>31</sup> G. YAGUPSKY, W. MOWAT, A. SHORTLAND and G. WILKINSON, *J. Chem. Soc., Chem. Commun.*, 1369-71 (1970).

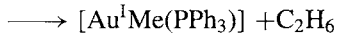
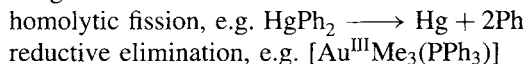
$-\text{CH}_2\text{CMe}_3$ , or  $-\text{CH}_2\text{SiMe}_3$ ) often leads to stable complexes since this prevents at least one facile decomposition route namely  $\beta$ -elimination.



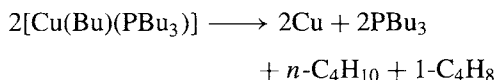
The reverse reaction (formation of metal alkyls by addition of alkenes to  $\text{M}-\text{H}$ ) is the basis of several important catalytic reactions such as alkene hydrogenation, hydroformylation, hydroboration, and isomerization. A good example of decomposition by  $\beta$ -elimination is the first-order intramolecular reaction:



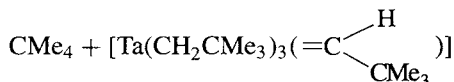
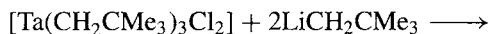
$\beta$ -Elimination reactions have been much studied but should not be over emphasized since other decomposition routes must also be considered. Amongst these are:



binuclear elimination (or formation of Bu radicals) e.g.



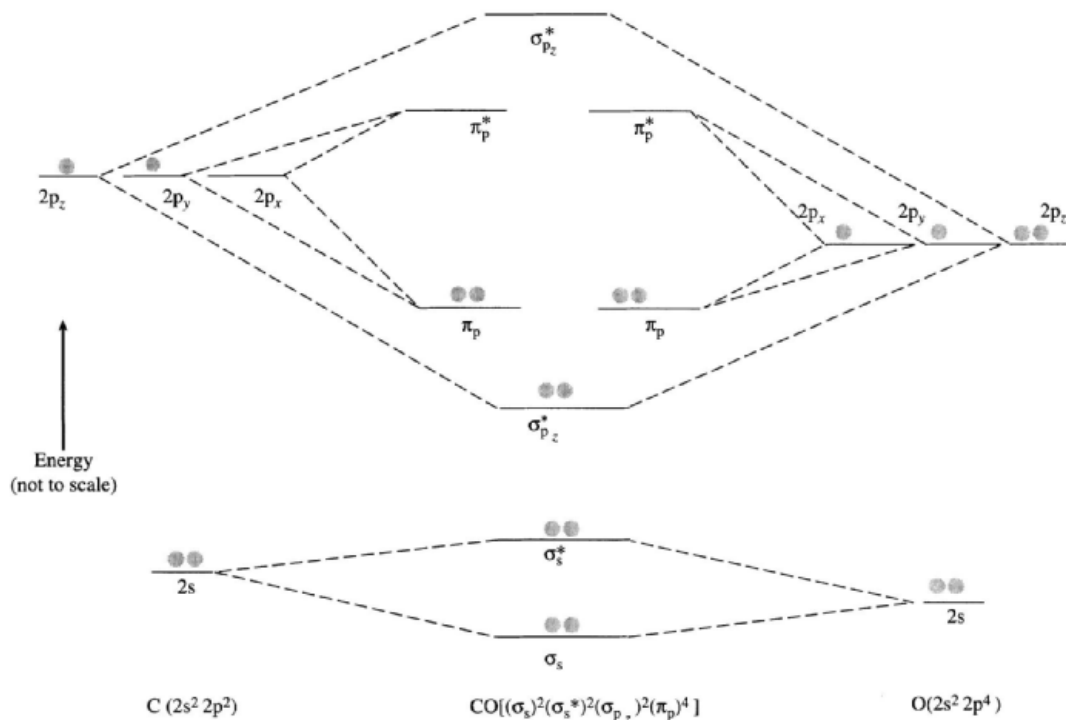
$\alpha$ -Elimination to give a carbene complex, e.g.



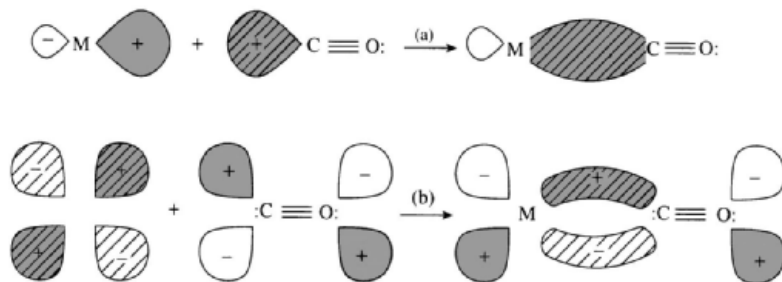
Stabilization of  $\eta^1$ -alkyl and -aryl derivatives of transition metals can be enhanced by the judicious inclusion of various other stabilizing ligands in the complex, even though such ligands are known not to be an essential prerequisite. Particularly efficacious are potential  $\pi$  acceptors (see below) such as  $\text{AsPh}_3$ ,  $\text{PPh}_3$ ,

$\text{CO}$  or  $\eta^5\text{-C}_5\text{H}_5$  in combination with the heavier transition metals since the firm occupation of coordination sites prevents their use for concerted decomposition routes. Steric protection may also be implicated. Similar arguments have been used to interpret the observed increase in stability of  $\eta^1$  complexes in the sequence alkyl < aryl < *o*-substituted aryl < ethynyl ( $-\text{C}\equiv\text{CH}$ ).

The next group of  $\eta^1$  ligands comprise the isoelectronic species,  $\text{CO}$ ,  $\text{CN}^-$  and  $\text{RNC}$ . They are closely related to other 14-electron (10 valence electron) ligands such as  $\text{N}_2$  and  $\text{NO}^+$  (and also to tertiary phosphines and arsines, and to organic sulfides, selenides, etc.), and it is merely the presence of C as the donor atom which classifies their complexes as organometallics. All have characteristic donor properties that distinguish them from simple electron-pair donors (Lewis bases, p. 198) and these have been successfully interpreted in terms of a synergic or mutually reinforcing interaction between  $\sigma$  donation from ligand to metal and  $\pi$  back donation from metal to ligand as elaborated below.  $\text{CO}$  is undoubtedly the most important and most widely studied of all organometallic ligands and it is the prototype for this group of so-called  $\pi$ -acceptor ligands. The currently accepted view of the bonding is represented diagrammatically in Figs. 19.17 and 19.18. Figure 19.17 shows a schematic molecular orbital energy level diagram for the heteronuclear diatomic molecule  $\text{CO}$ . The AOs lie deeper in O than in C because of the higher effective nuclear charge on O; consequently O contributes more to bonding MOs and C contributes more to the antibonding MOs. It can be seen that all the bonding MOs are filled and, in this description, the  $\text{CO}$  molecule can be said to have a triple bond  $:\text{C}\equiv\text{O}:$  with the lone-pair on carbon weakly available for donation to an acceptor. The top part (a) of Fig. 19.18 shows the formation of a  $\sigma$  bond by donation of the lone-pair into a suitably directed hybrid orbital on M, and the lower part (b) shows the accompanying back donation from a filled metal d orbital into the vacant antibonding  $\text{CO}$  orbital having  $\pi$  symmetry (one node) with respect to the bonding axis. This



**Figure 19.17** Schematic molecular energy level diagram for CO. The 1s orbitals have been omitted as they contribute nothing to the bonding. A more sophisticated treatment would allow some mixing of the 2s and  $2p_z$  orbitals in the bonding direction (z) as implied by the orbital diagram in Fig. 19.18.



**Figure 19.18** Schematic representation of the orbital overlaps leading to M–CO bonding: (a)  $\sigma$  overlap and donation from the lone-pair on C into a vacant (hybrid) metal orbital to form a  $\sigma$  M←C bond, and (b)  $\pi$  overlap and the donation from a filled  $d_{xz}$  or  $d_{yz}$  orbital on M into a vacant antibonding  $\pi_p^*$  orbital on CO to form a  $\pi$  M→C bond.

at once interprets why CO, which is a very weak  $\sigma$  donor to Lewis acids such as  $BF_3$  and  $AlCl_3$ , forms such strong complexes with transition elements, since the drift of  $\pi$ -electron density from M to C tends to make the

ligand more negative and so enhances its  $\sigma$ -donor power. The pre-existing negative charge on  $CN^-$  increases its  $\sigma$ -donor propensity but weakens its effectiveness as a  $\pi$  acceptor. It is thus possible to rationalize many chemical

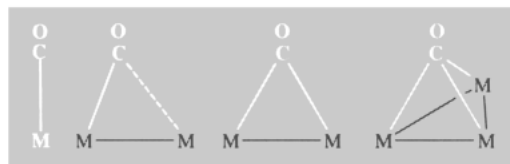
**Table 19.3** Known neutral binary metal carbonyls. Osmium also forms  $\text{Os}_5(\text{CO})_{16}$ ,  $\text{Os}_5(\text{CO})_{19}$ ,  $\text{Os}_6(\text{CO})_{18}$ ,  $\text{Os}_6(\text{CO})_{20}$ ,  $\text{Os}_7(\text{CO})_{21}$  and  $\text{Os}_8(\text{CO})_{23}$ . Carbonyls of elements in the shaded area are either very unstable or anionic or require additional ligands besides CO for stabilization

3	4	5	6	7	8	9	10	11	12
	Ti	$\text{V}(\text{CO})_6$	$\text{Cr}(\text{CO})_6$	$\text{Mn}_2(\text{CO})_{10}$	$\text{Fe}(\text{CO})_5$ $\text{Fe}_2(\text{CO})_9$ $\text{Fe}_3(\text{CO})_{12}$	$\text{Co}_2(\text{CO})_8$ $\text{Co}_4(\text{CO})_{12}$ $\text{Co}_6(\text{CO})_{16}$	$\text{Ni}(\text{CO})_4$	Cu	
	Zr	Nb	$\text{Mo}(\text{CO})_6$	$\text{Tc}_2(\text{CO})_{10}$ $\text{Tc}_3(\text{CO})_{12}$	$\text{Ru}(\text{CO})_5$ $\text{Ru}_2(\text{CO})_9$ $\text{Ru}_3(\text{CO})_{12}$	$\text{Rh}_2(\text{CO})_8$ $\text{Rh}_4(\text{CO})_{12}$ $\text{Rh}_6(\text{CO})_{16}$	Pd	Ag	
	Hf	Ta	$\text{W}(\text{CO})_6$	$\text{Re}_2(\text{CO})_{10}$	$\text{Os}(\text{CO})_5$ $\text{Os}_2(\text{CO})_9$ $\text{Os}_3(\text{CO})_{12}$	$\text{Ir}_2(\text{CO})_8$ $\text{Ir}_4(\text{CO})_{12}$ $\text{Ir}_6(\text{CO})_{16}$	Pt	Au	

observations by noting that effectiveness as a  $\sigma$  donor decreases in the sequence  $\text{CN}^- > \text{RNC} > \text{NO}^+ \sim \text{CO}$  whereas effectiveness as a  $\pi$  acceptor follows the reverse sequence  $\text{NO}^+ > \text{CO} \gg \text{RNC} > \text{CN}^-$ . By implication, back donation into antibonding CO orbitals weakens the CO bond and this is manifest in the slight increase in interatomic distance from 112.8 pm in free CO to  $\sim 115$  pm in many complexes. There is also a decrease in the C–O force constant, and the drop in the infrared stretching frequency from  $2143 \text{ cm}^{-1}$  in free CO to  $2125\text{--}1850 \text{ cm}^{-1}$  for terminal COs in neutral carbonyls has been interpreted in the same way.

The occurrence of stable neutral binary carbonyls is restricted to the central area of the d block (Table 19.3), where there are low-lying vacant metal orbitals to accept  $\sigma$ -donated lone-pairs and also filled d orbitals for  $\pi$  back donation. Outside this area carbonyls are either very unstable (e.g. Cu, Ag, p. 1199), or anionic, or require additional ligands besides CO for stabilization. As with boranes and carboranes (p. 181), CO can be replaced by isoelectronic equivalents such as  $2e^-$ ,  $\text{H}^-$ ,  $2\text{H}^+$  or L. Mean bond dissociation energies  $\bar{D}(\text{M}–\text{CO})/\text{kJ mol}^{-1}$  increase in the sequence  $\text{Cr}(\text{CO})_6$  109,  $\text{Mo}(\text{CO})_6$  151,  $\text{W}(\text{CO})_6$  176, and in the sequence  $\text{Mn}_2(\text{CO})_{10}$  100,  $\text{Fe}(\text{CO})_5$  121,  $\text{Co}_2(\text{CO})_8$  138,  $\text{Ni}(\text{CO})_4$  147.

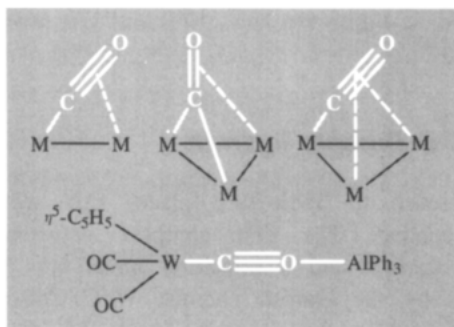
CO can act as a terminal ligand, as an unsymmetrical or symmetrical bridging ligand ( $\mu_2$ -CO) or as a triply bridging ligand ( $\mu_3$ -CO):



In all these cases CO is  $\eta^1$  but the connectivity to metal increases from 1 to 3. It is notable that in the  $\mu_2$ -bridging carbonyls the angle  $\text{M}–\text{C}(\text{O})–\text{M}$  is usually very acute ( $77\text{--}80^\circ$ ), whereas in organic carbonyls the  $\text{C}–\text{C}(\text{O})–\text{C}$  angle is typically  $120\text{--}124^\circ$ . This suggests a fundamentally differing bonding mode in the two cases and points to the likelihood of a 2-electron 3-centre bond (p. 158) for the bridging metal carbonyls. The hapticity can also rise, and structural determinations indicate that one or both of the  $\pi^*$  orbitals in CO contribute to  $\eta^2$  bonding to 1 or 2 M atoms.<sup>(32)</sup> A bis- $\eta^1$ -bridging mode has also been detected in an  $\text{AlPh}_3$  adduct,<sup>(33)</sup> reminiscent of the bridging mode in the isoelectronic  $\text{CN}^-$  ligand (p. 322):

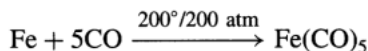
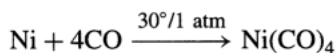
<sup>32</sup> C. P. HORWITZ and D. F. SHRIVER, *Adv. Organometallic Chem.* **23**, 219–305 (1984).

<sup>33</sup> J. M. BURLICH, M. E. LEONOWICZ, R. B. PETERSEN and R. E. HUGHES, *Inorg. Chem.* **18**, 1097–105 (1979).

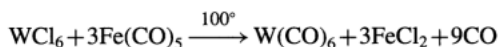
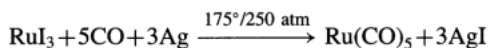
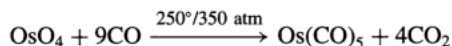


Numerous examples of metal carbonyls will be found in later chapters dealing with the chemistry of the individual transition metals. CO also has an unrivalled capacity for stabilizing metal clusters and for inserting into M–C bonds (p. 309). Synthetic routes include:

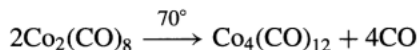
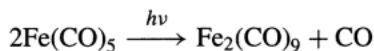
(a) direct reaction, e.g.:



(b) reductive carbonylation, e.g.:



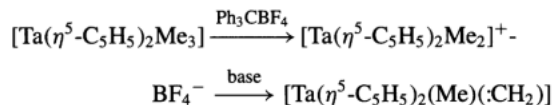
(c) photolysis or thermolysis, e.g.:



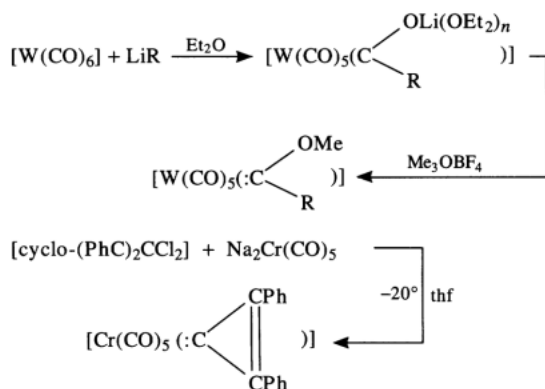
The remaining classes of monohapto organic ligands listed in Table 19.2 are carbene ( $=\text{CR}_2$ ), carbyne ( $\equiv\text{CR}$ ), and carbido (C). Stable carbene complexes were first reported in 1964 by E. O. Fischer and A. Maasböl.<sup>(34)</sup> Initially they

were of the type  $[\text{W}(\text{CO})_5(\text{C}(\text{OMe})_2\text{R})]$ , and it was

not until 1968 that the first homonuclear carbene complex was reported  $[\text{Cr}(\text{CO})_5(\text{C}(\text{CPh})_2)]$ ; isolation of a carbene containing the parent methylene group  $:\text{CH}_2$  was not achieved until 1975.<sup>(35)</sup>



Other preparative routes are:



The metal is in the formal oxidation state zero. As expected, the M–C bonds are somewhat shorter than M–R bonds to alkyls, but they are noticeably longer than M–CO bonds suggesting only limited double-bond character  $\text{M}=\text{C}$ , e.g.:

in $[\text{Ta}(\eta^5\text{-C}_5\text{H}_5)_2(\text{Me})(\text{CH}_2)]$	Ta–CH <sub>2</sub> 220.6 pm
	Ta–CH <sub>3</sub> 225 pm
in $[\text{W}(\text{CO})_5(\text{C}(\text{OMe})\text{Ph})]$	W–C(OMe)Ph 205 pm
	W–CO 189 pm
in $[\text{Cr}(\text{CO})_4(\text{C}(\text{OMe})\text{Me})(\text{PPh}_3)]$	Cr–C(OMe)Me 204 pm
	Cr–CO 186 pm

Carbene complexes are highly reactive species.<sup>(36)</sup>

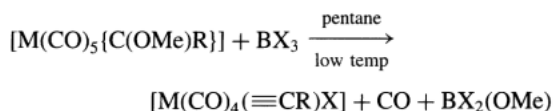
Carbyne complexes were first made in 1973 by the unexpected reaction of methoxycarbene

<sup>35</sup> R. R. SCHROCK, *J. Am. Chem. Soc.* **97**, 6577–8 (1975); L. J. GUGGENBERGER and R. R. SCHROCK, *ibid.* 6578–9.

<sup>36</sup> K. H. DÖTZ, H. FISCHER, P. HOFMANN, F. R. KREISSL, U. SCHUBERT and K. WEISS, *Transition Metal Carbene Complexes*, Verlag Chemie, Weinheim, 1983, 264 pp.

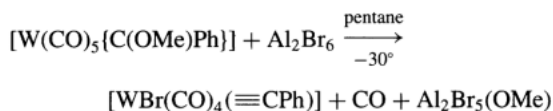
<sup>34</sup> E. O. FISCHER, *Adv. Organometallic Chem.* **14**, 1–32 (1976).

complexes with boron trihalides:



M = Cr, Mo, W; R = Me, Et, Ph; X = Cl, Br, I

Several other routes are now also available in which  $\text{BX}_3$  is replaced by  $\text{AlCl}_3$ ,  $\text{GaCl}_3$ ,  $\text{Al}_2\text{Br}_6$ ,  $\text{Ph}_3\text{PBr}_2$ , e.g.:



X-ray studies reveal the expected short M–CR distance, but the bond angle at the carbyne C atom is not always linear. Some structural data are annexed, see below. A compound which features all three types of  $\eta^1$  ligand, alkyl, alkylidene and alkylidyne, is the red, square-pyramidal tungsten(VI) complex  $[\text{W}(\equiv\text{CCMe}_3)(=\text{CHCMe}_3)(\text{CH}_2\text{CMe}_3)(\text{Me}_2\text{PCH}_2\text{CH}_2\text{PMe}_2)]$  in which the W–C distance is 226 pm to neopentyl, 194 pm to neopentylidene, and 176 pm to the apical neopentylidyne ligand; the corresponding

W–C–C angles are  $125^\circ$ ,  $150^\circ$  and  $175^\circ$  respectively.<sup>(37)</sup>

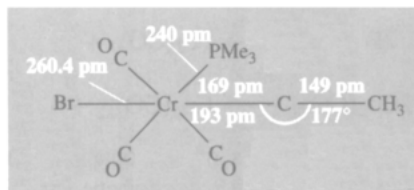
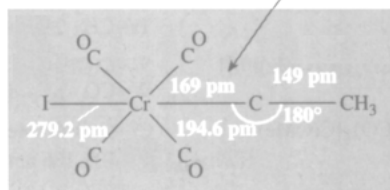
### 19.7.2 Dihapto ligands

Reference to Table 19.2 places this section in context. The first complex between a hydrocarbon and a transition metal was isolated by the Danish chemist W. C. Zeise in 1825 and in the following years he characterized the pale-yellow compound now formulated as  $\text{K}[\text{Pt}(\eta^2\text{-C}_2\text{H}_4)\text{Cl}_3]\cdot\text{H}_2\text{O}$ .<sup>†</sup> Zeise's salt, and a few closely related complexes such as the chloro-bridged binuclear compound  $[\text{Pt}_2(\eta^2\text{-C}_2\text{H}_4)(\mu_2\text{-Cl})_2\text{Cl}_2]$ , remained as chemical curiosities and a considerable theoretical embarrassment for over 100 y but are now seen as the archetypes of a large family of complexes based on the bonding of unsaturated organic

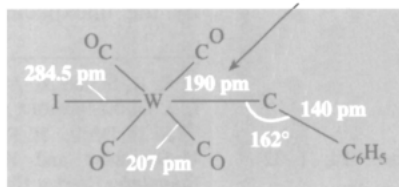
<sup>37</sup> M. R. CHURCHILL and W. J. YOUNGS, *Inorg. Chem.* **18**, 2454–8 (1979).

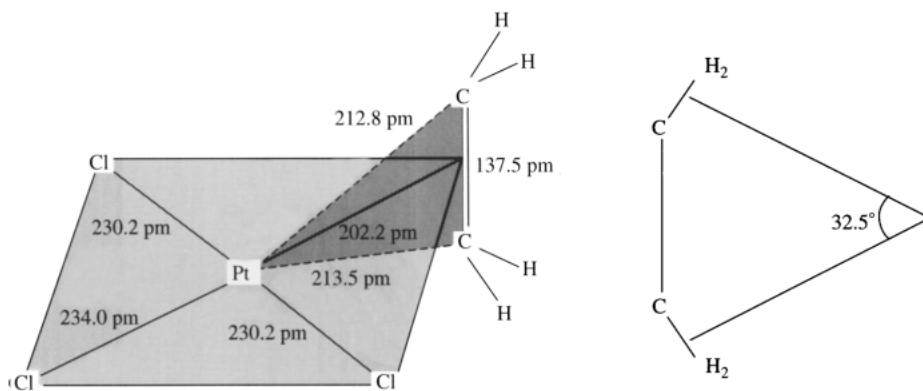
<sup>†</sup> The original reaction was obscure: Zeise heated a mixture of  $\text{PtCl}_2$  and  $\text{PtCl}_4$  in EtOH under reflux and then treated the resulting black solid with aqueous KCl and HCl to give ultimately the cream-yellow product. Subsequently the compound was isolated by direct reaction of  $\text{C}_2\text{H}_4$  with  $\text{K}_2[\text{PtCl}_4]$  in aqueous HCl.

This is the shortest known Cr–C distance cf. 217–222 pm in Cr–C single bonds and 191 pm in  $\text{Cr}(\text{CO})_6$



Cf. 227–232 pm for W–C single bond and 206 pm in  $\text{W}(\text{CO})_6$





**Figure 19.19** Structure of the anion of Zeise's salt,  $[\text{Pt}(\eta^2\text{-C}_2\text{H}_2)\text{Cl}_3]^-$ ; standard deviations are Pt–Cl 0.2 pm, Pt–C 0.3 pm, and C–C 0.4 pm.

molecules to transition metals. The structure of the anion of Zeise's salt has been extensively studied and neutron diffraction data<sup>(38)</sup> are in Fig. 19.19. Significant features are (a) the C=C bond is perpendicular to the PtCl<sub>3</sub> plane and is only 3.8 pm longer than in free C<sub>2</sub>H<sub>4</sub>, (b) the C<sub>2</sub>H<sub>4</sub> group is significantly distorted from planarity, each C being 16.4 pm from the plane of 4H, (c) the angle between the normals to the CH<sub>2</sub> planes is 32.5°, and (d) there is an unambiguous *trans*-effect (p. 1163), i.e. the Pt–Cl distance *trans* to C<sub>2</sub>H<sub>4</sub> is longer than the 2 *cis*-Pt–Cl distances by 3.8 pm (19 standard deviations).

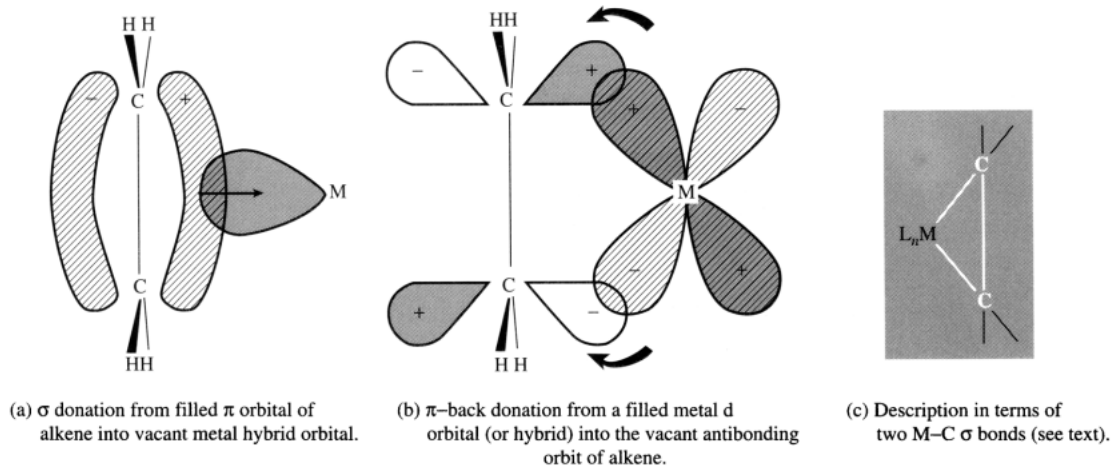
The key to our present understanding of the bonding in Zeise's salt and all other alkene complexes stems from the perceptive suggestion by M. J. S. Dewar in 1951 that the bonding involves electron donation from the  $\pi$  bond of the alkene into a vacant metal orbital of  $\sigma$  symmetry; this idea was modified and elaborated by J. Chatt and L. A. Duncanson in a seminal paper in 1953 and the Dewar–Chatt–Duncanson theory forms the basis for most subsequent discussion. The bonding is considered to arise from two interdependent components as illustrated schematically in Fig. 19.20 (a) and (b). In the first part,  $\sigma$  overlap between the filled  $\pi$  orbital of

ethene and a suitably directed vacant hybrid metal orbital forms the “electron-pair donor bond”. This is reinforced by the second component, (b), which derives from overlap of a filled metal d orbital with the vacant antibonding orbital of ethene; these orbitals have  $\pi$  symmetry with respect to the bonding axis and allow  $\text{M} \rightarrow \text{C}_2$   $\pi$  back bonding to assist the  $\sigma_{\text{C}_2 \rightarrow \text{M}}$  bond synergically as for CO (p. 927). The flexible interplay of these two components allows a wide variety of experimental observations to be rationalized: in particular the theory convincingly interprets the orientation of the alkene with respect to the metal and the observed lengthening of the C–C bond. However, the details of the distortion of the alkene from planarity are less easy to quantify on the model and evidence is accumulating which suggests that the extent of  $\pi$  back bonding may have been overemphasized for some systems in the past. At the other extreme back donation may become so dominant that C–C distances approach values to be expected for a single bond and the interaction would be described as oxidative addition to give a metallacyclopropane ring involving two 2-electron 2-centre M–C bonds (see Fig. 19.20(c)).

For example, tetracyanoethylene has a formal C=C double bond (133.9 pm) in the free ligand but in the complex  $[\text{Pt}[\text{C}_2(\text{CN})_4]\{\text{PPh}_3\}_2]$  the C–C distance (152 pm) is that of a single bond and the CN groups are bent away from the

<sup>38</sup> R. A. LOVE, T. F. KOETZLE, G. J. B. WILLIAMS, L. C. ANDREWS and R. BAU, *Inorg. Chem.* **14**, 2653–7 (1975).

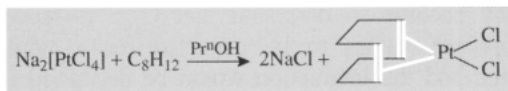




**Figure 19.20** Schematic representation of the two components, (a) and (b), of an  $\eta^2$ -alkene-metal bond.

Pt and 2P atoms; moreover, the 2P and 2C that are bonded to Pt are nearly coplanar, as expected for  $\text{Pt}^{\text{II}}$  but not as in (tetrahedral) 4-coordinate  $\text{Pt}^0$  complexes.  $[\text{Rh}(\text{C}_2\text{F}_4)\text{Cl}(\text{PPh}_3)_2]$  affords another example of the tendency to form a metallacyclopropane-type complex (C-C 141 pm) with pseudo-5-coordinate  $\text{Rh}^{\text{III}}$  rather than a pseudo-4-coordinate  $\eta^2$ -alkene complex of  $\text{Rh}^{\text{I}}$ . However, the two descriptions are not mutually exclusive and, in principle, there can be a continuous gradation between them.

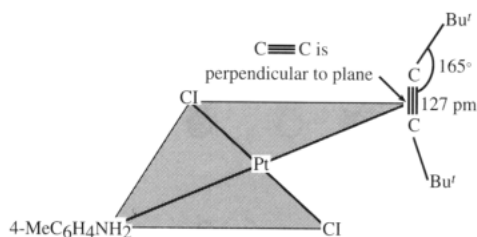
Compounds containing M- $\eta^2$ -alkene bonds are generally prepared by direct replacement of a less strongly bound ligand such as a halide ion (cf. Zeise's salt), a carbonyl, or another alkene. Chelating dialkene complexes can be made similarly, e.g. with *cis-cis*-cycloocta-1,5-diene (cod):



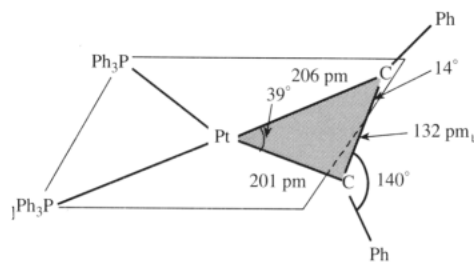
Numerous examples are given in later sections dealing with the chemistry of individual transition metals. Few, if any,  $\eta^2$ -alkene or -diene complexes have been reported for the first three transition-metal groups (why?), but all later groups are well represented, including  $\text{Cu}^{\text{I}}$ ,  $\text{Ag}^{\text{I}}$  and  $\text{Au}^{\text{I}}$ . Indeed, an industrial method for the

separation of alkenes uses the differing stabilities of their complexes with  $\text{CuCl}$ . For many metals it is found that increasing alkyl substitution of the alkene lowers the stability of the complex and that *trans*-substituted alkenes give less stable complexes than do *cis*-substituted alkenes. For  $\text{Rh}^{\text{I}}$  complexes F substitution of the alkene enhances the stability of the complex and Cl substitution lowers it.

Alkyne complexes have been less studied than alkene complexes but are similar. Preparative routes are the same and bonding descriptions are also analogous. In some cases, e.g. the pseudo-4-coordinate complex  $[\text{Pt}(\eta^2\text{-C}_2\text{Bu}'_2)\text{Cl}_2(4\text{-toluidine})]$  (Fig. 19.21) the  $\text{C}\equiv\text{C}$  bond remains short and the alkyne group is normal to the plane of coordination; in others, e.g. the pseudo-3-coordinate complex  $[\text{Pt}(\eta^2\text{-C}_2\text{Ph}_2)(\text{PPh}_3)_2]$  (Fig. 19.22), the alkyne group is almost in the plane ( $14^\circ$ ) and the attached substituents are bent back to an angle of  $140^\circ$  suggesting a formulation intermediate between 3-coordinate  $\text{Pt}^0$  and 4-coordinate  $\text{Pt}^{\text{II}}$ . One important difference between alkynes and alkenes is that the former have a triple bond which can be described in terms of a  $\sigma$  bond and two mutually perpendicular  $\pi$  bonds. The possibility thus arises that  $\eta^2$ -alkynes can function as bridging ligands and several such complexes have been characterized.

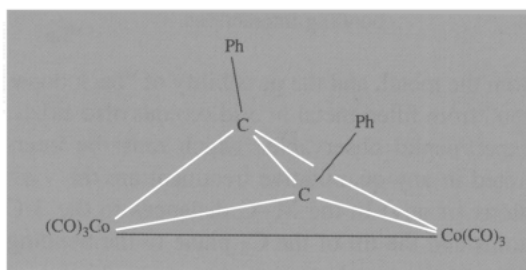


**Figure 19.21** Structure of  $[\text{Pt}(\eta^2\text{-C}_2\text{Bu}'_2)\text{Cl}_2(4\text{-toluidine})]$ .



**Figure 19.22** Structure of  $[\text{Pt}(\eta^2\text{-C}_2\text{Ph}_2)(\text{PPh}_3)_2]$ .

The classic example is  $[\text{Co}_2(\text{CO})_6(\text{C}_2\text{Ph}_2)]$  which is formed by direct displacement of the 2 bridging carbonyls in  $[\text{Co}_2(\text{CO})_8]$  to give the structure sketched below:



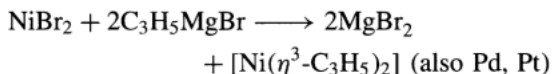
The C-C group lies above and at right angles to the Co-Co vector; the C-C distance is 146 pm (27 pm greater than in the free alkyne) and this has been taken to indicate extensive back donation from the 2 Co atoms. The Co-Co distance is 247 pm compared with 252 pm in  $\text{Co}_2(\text{CO})_8$ . A rather different situation is found in  $[\text{Ru}_4(\mu_4\text{-}\eta^1, \eta^2\text{-C}_2)(\mu\text{-PPh}_2)_2(\text{CO})_{12}]$ , where a  $\mu_4\text{-}\eta^1, \eta^2\text{-acetylide}$  dianion bridges two  $\{\text{Ru}_2(\mu\text{-PPh}_2)(\text{CO})_6\}$  units. Here, the steric demands of the other ligands make the C-C bridge almost coplanar with the two  $\eta^2$ -bonded

Ru atoms, and reduced  $\pi$ -bonding is indicated by a much shorter (127.5 pm) C-C distance.<sup>(38a)</sup>

### 19.7.3 Trihapto ligands

The possibility that the allyl group  $\text{CH}_2=\text{CH}-\text{CH}_2-$  can act as an  $\eta^3$  ligand was recognized independently by several groups in 1960 and since then the field has flourished, partly because of its importance in homogeneous catalysis and partly because of the novel steric possibilities and interconversions that can be studied by proton nmr spectroscopy. Many synthetic routes are available of which the following are representative.

(a) Allyl Grignard reagent:

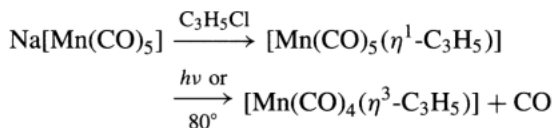


A mixture of *cis* and *trans* isomers is obtained:



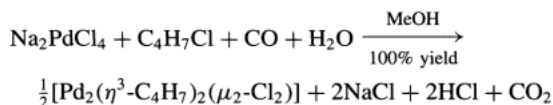
*Tris*-( $\eta^3$ -allyl) complexes  $[\text{M}(\text{C}_3\text{H}_5)_3]$  can be prepared similarly for V, Cr, Fe, Co, Rh, Ir, and *tetrakis* complexes  $[\text{M}(\eta^3\text{-C}_3\text{H}_5)_4]$  for Zr, Th, Mo and W.

(b) Conversion of  $\eta^1$ -allyl to  $\eta^3$ -allyl:



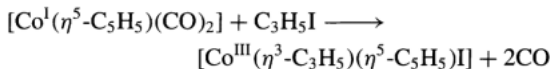
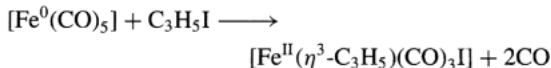
Similarly many other  $\eta^1$ -allyl carbonyl complexes convert to  $\eta^3$ -allyl complexes with loss of 1 CO.

(c) From allylic halides (e.g. 2-methylallyl chloride):

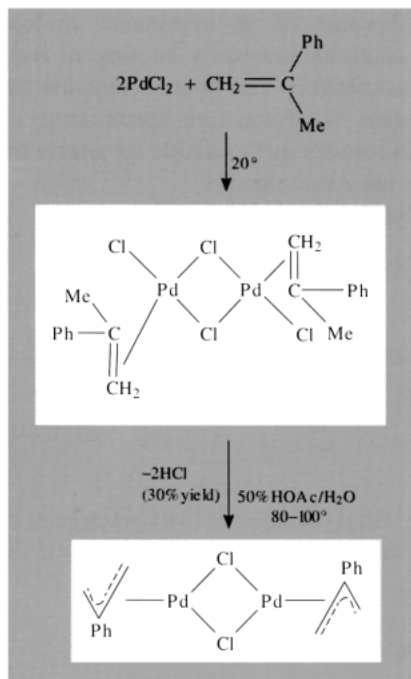


<sup>38a</sup> M. I. BRUCE, M. R. SNOW, E. R. T. TIEKINK and M. L. WILLIAMS, *J. Chem. Soc., Chem. Commun.*, 701-2 (1986).

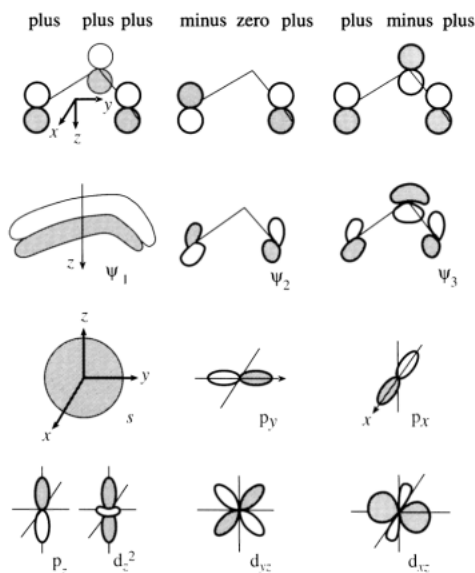
(d) Oxidative addition of allyl halides, e.g.:



(e) Elimination of HCl from an alkene metal halide complex, e.g.:



The bonding in  $\eta^3$ -allylic complexes can be described in terms of the qualitative MO theory illustrated in Fig. 19.23. The  $p_z$  orbitals on the 3 allylic C atoms can be combined to give the 3 orbitals shown in the upper part of Fig. 19.23; each retains  $\pi$  symmetry with respect to the  $C_3$  plane but has, in addition, 0, 1 or 2 nodes perpendicular to this plane. The metal orbitals of appropriate symmetry to form bonding MOs with these 3 combinations are shown in the lower part of Fig. 19.23. The extent to which these orbitals are, in fact, involved in bonding depends on their relative energies, their radial diffuseness and the actual extent of orbital overlap. Electrons to fill these bonding MOs can be thought of as coming both from the allylic  $\pi$ -electron cloud and

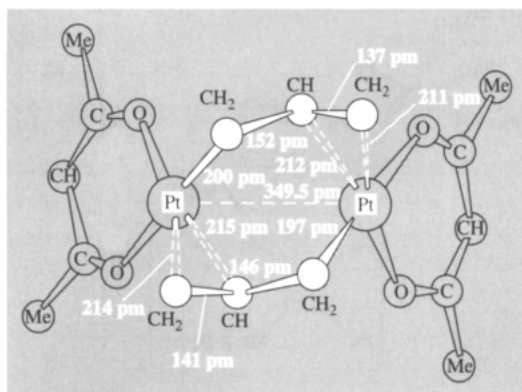


**Figure 19.23** Schematic illustration of possible combinations of orbitals in the  $\pi$ -allylic complexes. The bonding direction is taken to be the  $z$ -axis with the M atom below the  $C_3$  plane. Appropriate combinations of  $p_\pi$  orbitals on the 3 C are shown in the top half of the figure, and beneath them are the metal orbitals with which they are most likely to form bonding interactions.

from the metal, and the possibility of “back donation” from filled metal hybrid orbitals also exists. Experimental observables which must be interpreted in any quantitative treatment are the variations (if any) in the M–C distances to the 3 C atoms and the tilt of the  $C_3$  plane to the bonding plane of the metal atom.

In addition to acting as an  $\eta^1$  and an  $\eta^3$  ligand the allyl group can also act as a bridging ligand by  $\eta^1$  bonding to one metal atom and  $\eta^2$  bonding via the alkene function to a second metal atom. For example  $[\text{Pt}_2(\text{acac})_2(\eta^1, \eta^2\text{-C}_3\text{H}_5)_2]$  has the dimeric structure shown in Fig. 19.24. The compound was made from  $[\text{Pt}(\eta^3\text{-C}_3\text{H}_5)_2]$  by treatment first with HCl to give polymeric  $[\text{Pt}(\text{C}_3\text{H}_5)\text{Cl}]$  and then with thallium(I) acetylacetonate.

Many  $\eta^3$ -allyl complexes are fluxional (p. 914) at room temperature or slightly above,

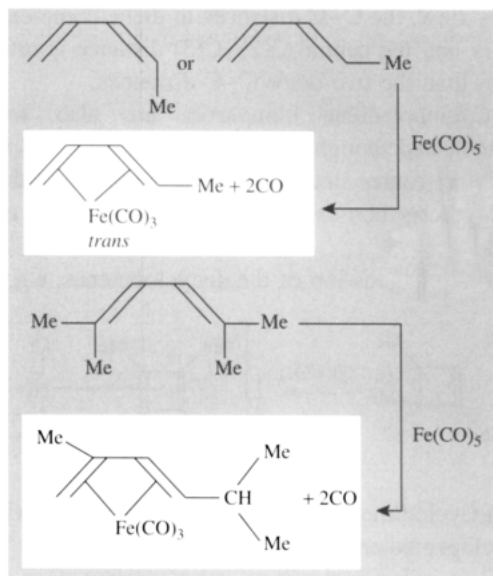


**Figure 19.24** Structure of  $[\text{Pt}_2(\text{acac})_2(\mu\text{-C}_3\text{H}_5)_2]$  showing the bridging allyl groups, each  $\eta^1$  bonded to 1 Pt and  $\eta^2$ -bonded to the other. Interatomic distances are in pm with standard deviations of  $\sim 5$  pm for Pt–C and  $\sim 7$  for C–C. The distance of Pt to the centre of the  $\eta^2$ -C<sub>2</sub> group is 201 pm, very close to the  $\eta^1$ -Pt–C distance of 199 pm.

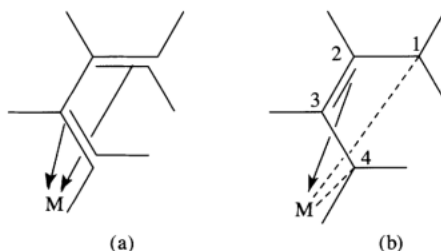
and this property has been extensively studied by  $^1\text{H}$  nmr spectroscopy. Exceedingly complex patterns can emerge. The simplest interchange that can occur is between those H atoms which are on the side nearer the metal (*syn*) and those which are on the side away from the metal (*anti*) probably via a short-lived  $\eta^1$ -allyl metal intermediate. The fluxional behaviour can be slowed down by lowering the temperature, and separate resonances from the various types of H atom are then observed. Fluxionality can also sometimes be quenched by incorporating the allylic group in a ring system which restricts its mobility.

### 19.7.4 Tetrahapto ligands

Conjugated dienes such as butadiene and its open-chain analogues can act as  $\eta^4$  ligands; the complexes are usually prepared from metal carbonyl complexes by direct replacement of 2CO by the diene. Isomerization or rearrangement of the diene may occur as indicated schematically below:



No new principles are involved in describing the bonding in these complexes and appropriate combinations of the  $4p_\pi$  orbitals on the diene system can be used to construct MOs with the metal-based orbitals for donation and back donation of electron density.<sup>(39)</sup> As with ethene, two limiting cases can be envisaged which can be represented schematically as in Fig. 19.25. Consistent with



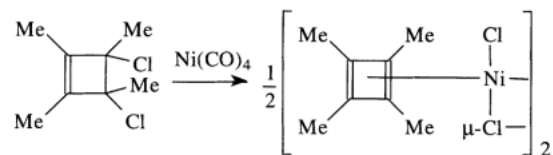
**Figure 19.25** Schematic representation of the two formal extremes of bonding in 1,3-diene complexes. In (a) the bonding is considered as two almost independent  $\eta^2$ -alkene–metal bonds, whereas in (b) there are  $\sigma$  bonds to C(1) and C(4) and an  $\eta^2$ -alkene–metal bond from C(2)–C(3).

<sup>39</sup> D. M. P. MINGOS, *J. Chem. Soc., Dalton Trans.*, 20–35 (1977).

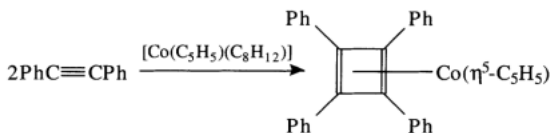
this view, the C–C distances in diene complexes vary and the central C(2)–C(3) distance is often less than the two outer C–C distances.

Cyclobutadiene complexes are also well established though they must be synthesized by indirect routes since the parent dienes are either unstable or non-existent. Four general routes are available:

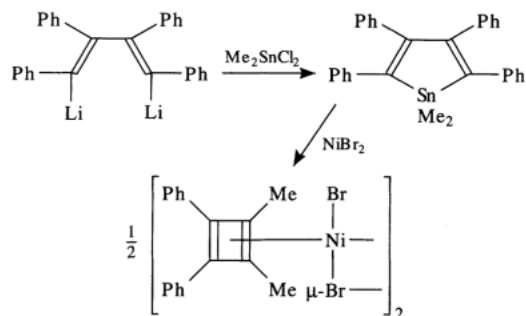
(a) Dehalogenation of dihalocyclobutenes, e.g.:



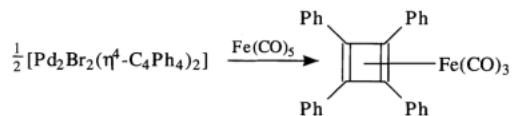
(b) Cyclodimerization of alkynes, e.g. with cyclopentadienyl-(cycloocta-1,5-diene)cobalt:



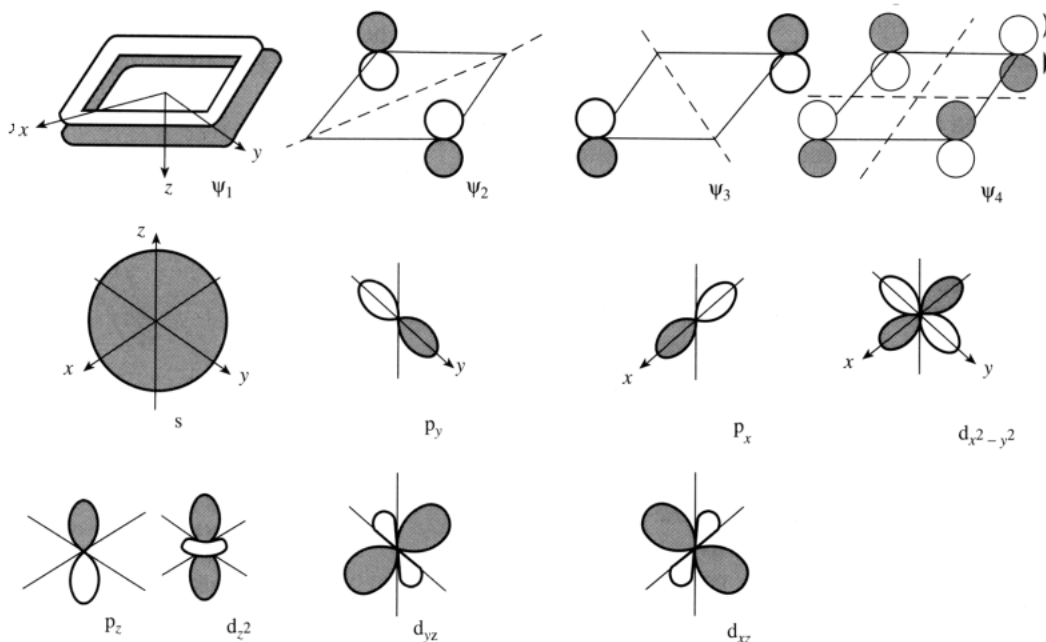
(c) From metallacyclopentadienes:



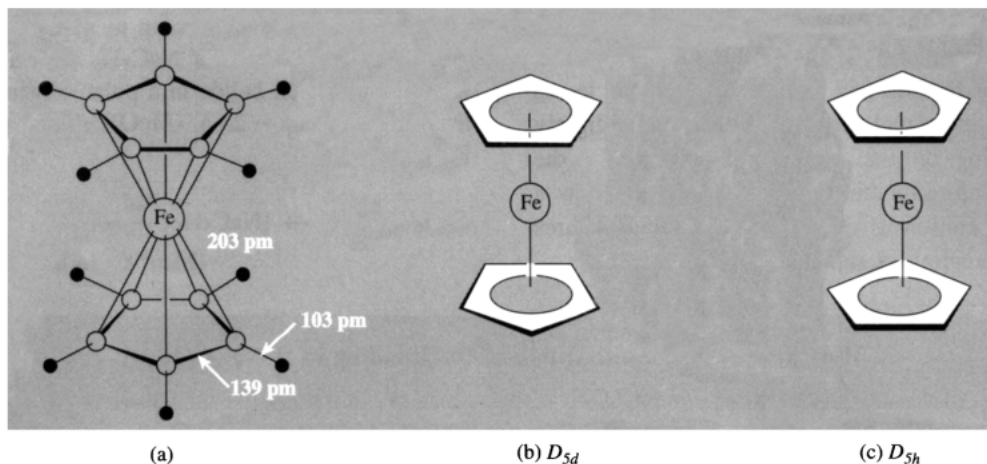
(d) Ligand exchange from other cyclobutadiene complexes, e.g.:



A schematic interpretation of the bonding in cyclobutadiene complexes can be given within the framework outlined in the preceding sections and this is illustrated in Fig. 19.26.



**Figure 19.26** Orbitals used in describing the bonding in metal- $\eta^2$ -cyclobutadiene complexes. The sign convention and axes are as in Fig. 19.23.



**Figure 19.27** Structure of ferrocene,  $[\text{Fe}(\eta^5\text{-C}_5\text{H}_5)_2]$ , and a conventional “shorthand” representation.

Cyclobutadiene complexes afford a classic example of the stabilization of a ligand by coordination to a metal and, indeed, were predicted theoretically on this basis by H. C. Longuet-Higgins and L. E. Orgel (1956) some 3 y before the first examples were synthesized. In the (hypothetical) free cyclobutadiene molecule 2 of the 4  $\pi$ -electrons would occupy  $\psi_1$  and there would be an unpaired electron in each of the 2 degenerate orbitals  $\psi_2$ ,  $\psi_3$ . Coordination to a metal provides further interactions and avoids this unstable configuration. See also the discussion on ferroborationes (p. 174).

### 19.7.5 Pentahapto ligands

The importance of bis(cyclopentadienyl)iron  $[\text{Fe}(\eta^5\text{-C}_5\text{H}_5)_2]$  in the development of organometallic chemistry has already been alluded to (p. 924). The compound, which forms orange crystals, mp  $174^\circ$ , has extraordinary thermal stability ( $>500^\circ$ ) and a remarkable structure which was unique when first established. It also has an extensive aromatic-type reaction chemistry which is reflected in its common name “ferrocene”. The molecular structure of ferrocene in the crystalline state features two parallel cyclopentadienyl rings: at one time these

rings were thought to be staggered ( $D_{5d}$ ) as in Fig. 19.27a and b since only this was compatible with the molecular inversion centre required by the crystallographic space group ( $C_{2h}^5$ ,  $Z = 2$ ). However, gas-phase electron diffraction data suggest that the equilibrium structure of ferrocene is eclipsed ( $D_{5h}$ ) as in Fig. 19.27c rather than staggered, with a rather low barrier to internal rotation of  $\sim 4 \text{ kJ mol}^{-1}$ . X-ray crystallographic<sup>(40)</sup> and neutron diffraction studies<sup>(41)</sup> confirm this general conclusion, the space-group symmetry requirement being met by a disordered arrangement of nearly eclipsed molecules (rotation angle between the rings  $\sim 9^\circ$  rather than  $0^\circ$  for precisely eclipsed or  $36^\circ$  for staggered conformation). Below 169 K the molecules become ordered, the rotation angle remaining  $\sim 9^\circ$ . The perpendicular distance between the rings is 325 pm (cf. graphite 335 pm) and the mean interatomic distances are Fe–C  $203 \pm 2$  pm and C–C  $139 \pm 6$  pm. The Ru and Os analogues  $[\text{M}(\eta^5\text{-C}_5\text{H}_5)_2]$  have similar molecular structures with eclipsed parallel  $\text{C}_5$  rings. A molecular-orbital description of the bonding can be developed along the lines indicated in

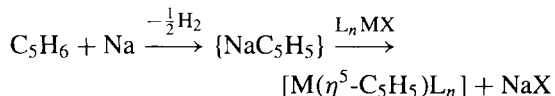
<sup>40</sup> P. SEILER and J. D. DUNITZ, *Acta Cryst.* **B35**, 1068–74 (1979).

<sup>41</sup> F. TAKUSAGAWA and T. F. KOETZLE, *Acta Cryst.* **B35**, 1074–81 (1979).



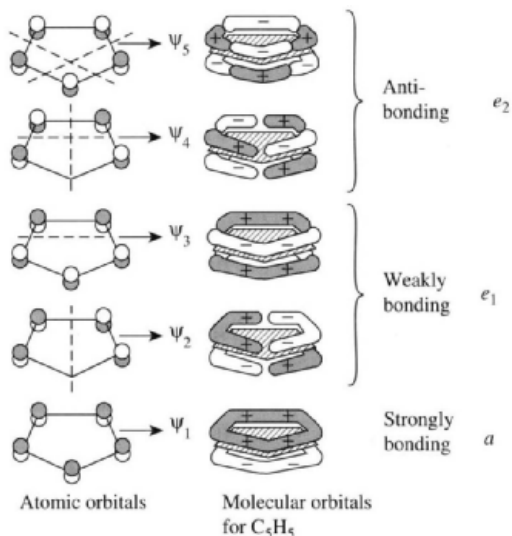
previous sections. Because of the importance of ferrocene, numerous calculations have been made of the detailed sequence of energy levels in the molecule; though these differ slightly depending on the assumptions made and the computational methods adopted, there is now a general consensus concerning the main features of the bonding as shown in the Panel.

A general preparative route to  $\eta^5\text{-C}_5\text{H}_5$  compounds is the reaction of  $\text{NaC}_5\text{H}_5$  with a metal halide or complex halide in a polar solvent such as thf,  $\text{Me}_2\text{O}$  (bp  $-23^\circ$ ),  $(\text{MeO})_2\text{C}_2\text{H}_4(\text{OMe})$ , or  $\text{HC}(\text{O})\text{NMe}_2$ :



### A Molecular Orbital Description of the Bonding in $[\text{Fe}(\eta^5\text{-C}_5\text{H}_5)_2]$

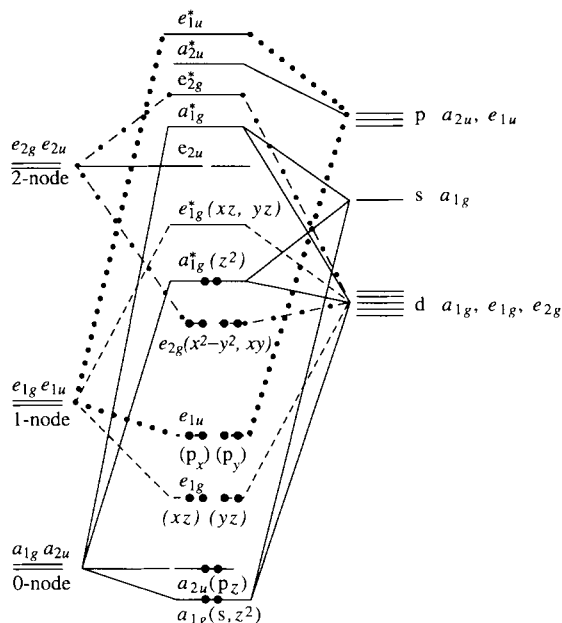
The 5  $p_\pi$  atomic orbitals on the planar  $\text{C}_5\text{H}_5$  group can be combined to give 5 group MOs as shown in Fig. A; one combination has the full symmetry of the ring ( $a_1$ ) and there are two doubly degenerate combinations ( $e_1$  and  $e_2$ ) having respectively 1 and 2 planar nodes at right angles to the plane of the ring. These 5 group MOs can themselves be combined in pairs with a similar set from the second  $\text{C}_5\text{H}_5$  group before combining with metal orbitals. Each of the combinations [(ligand orbitals) + (metal orbitals)] leads, in principle, to a bonding MO of the molecule, providing that the energy of the two component sets is not very different. There are an equal number of antibonding combinations with the sign [(ligand orbitals) - (metal orbital)].



**Figure A** The  $\pi$  molecular orbitals formed from the set of  $p_\pi$  orbitals of the  $\text{C}_5\text{H}_5$  ring.

Calculation of the detailed sequence of energy levels arising from these combinations poses severe computational problems but a schematic indication of the sequence (not to scale) is shown in Fig. B. Thus, starting from the foot of the figure, the  $a_{1g}$  bonding MO is mainly ligand-based with only a slight admixture of the Fe 4s and  $3d_{z^2}$  orbitals. Similarly, the  $a_{2g}$  level has little, if any, admixture of the even higher-lying Fe  $4p_z$  orbital with which it is formally able to combine. The  $e_{1g}$  MO arises from the bonding combination of the ligand  $e_{1g}$  orbitals with Fe  $3d_{xz}$  and  $3d_{yz}$  and this is the main contribution to the stability of the complex; the corresponding antibonding  $e_{1g}^*$  are unoccupied in the ground state but will be involved in optical transitions. The  $e_{1u}$  bonding MOs are again mainly ligand-based but with some contribution from Fe  $4p_x$  and  $4p_y$ , etc. It can be seen that there is room for just 18 electrons in bonding and nonbonding MOs and that the antibonding MOs are unoccupied. In terms of electron counting the 18 electrons can be thought of as originating from the Fe atom (8e) and the two  $\text{C}_5\text{H}_5$  groups ( $2 \times 5e$ ) or from an  $\text{Fe}^{\text{II}}$  ion (6e) and two  $\text{C}_5\text{H}_5^-$  groups ( $2 \times 6e$ ).

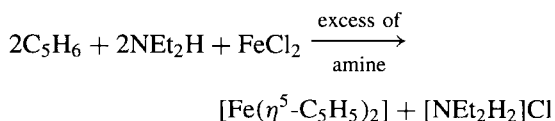
Panel continues



**Figure B** A qualitative molecular orbital diagram for ferrocene. The subscripts *g* and *u* refer to the parity of the orbitals: *g* (German *gerade*, even) indicates that the orbital (or orbital combination) is symmetric with respect to inversion, whereas the subscript *u* (*ungerade*, odd) indicates that it is antisymmetric with respect to inversion. Only orbitals with the same parity can combine.

The stability of  $[\text{Fe}(\eta^5\text{-C}_5\text{H}_5)_2]$  compared with the 19 electron system  $[\text{Co}(\eta^5\text{-C}_5\text{H}_5)_2]$  and the 20-electron system  $[\text{Ni}(\eta^5\text{-C}_5\text{H}_5)_2]$  is readily interpreted on this bonding scheme since these latter species have 1 and 2 easily oxidizable electrons in the antibonding  $e_{1u}^*$  orbitals. Similarly,  $[\text{Cr}(\eta^5\text{-C}_5\text{H}_5)_2]$  (16e) and  $[\text{V}(\eta^5\text{-C}_5\text{H}_5)_2]$  (15e) have unfilled bonding MOs and are highly reactive. However, attachment of additional groups or ligands destroys the  $D_{5d}$  (or  $D_{5h}$ ) symmetry of the simple metallocene and this modifies the orbital diagram. This also happens when ferrocene is protonated to give the 18-electron cation  $[\text{Fe}(\eta^5\text{-C}_5\text{H}_5)_2\text{H}]^+$  and when the (bent) isoelectronic neutral molecules  $[\text{Re}(\eta^5\text{-C}_5\text{H}_5)_2\text{H}]$  (p. 1067) and  $[\text{Mo}(\eta^5\text{-C}_5\text{H}_5)_2\text{H}_2]$  (p. 1038) are considered. An excellent discussion of the bonding in such “bent metallocenes” has been given.<sup>(42)</sup>

A very convenient though somewhat less general method is to use a strong nitrogen base to deprotonate the  $\text{C}_5\text{H}_6$ :



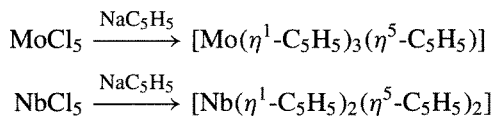
An enormous number of  $\eta^5\text{-C}_5\text{H}_5$  complexes is now known. Thus the isoelectronic yellow

$\text{Co}^{\text{I}}$  species  $[\text{Co}(\eta^5\text{-C}_5\text{H}_5)_2]^+$  is stable in aqueous solutions and its salts are thermally stable to  $\sim 400^\circ$ . The bright-green paramagnetic complex  $[\text{Ni}(\eta^5\text{-C}_5\text{H}_5)_2]$ , mp  $173^\circ$  (d), is fairly stable as a solid but is rapidly oxidized to  $[\text{Ni}(\eta^5\text{-C}_5\text{H}_5)_2]^+$ . In contrast, the scarlet, paramagnetic complex  $[\text{Cr}(\eta^5\text{-C}_5\text{H}_5)_2]$ , mp  $173^\circ$ , is very air sensitive; it dissolves in aqueous HCl to give  $\text{C}_5\text{H}_6$  and a blue cation which is probably  $[\text{Cr}(\eta^5\text{-C}_5\text{H}_5)\text{Cl}(\text{H}_2\text{O})_n]^+$ . Other stoichiometries are exemplified by  $[\text{Ti}(\eta^5\text{-C}_5\text{H}_5)_3]$  and  $[\text{M}(\eta^5\text{-C}_5\text{H}_5)_4]$ , where M is Zr, Hf, Th.

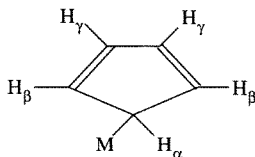
<sup>42</sup> J. W. LAUHER and R. HOFFMAN, *J. Am. Chem. Soc.* **98**, 1729–42 (1976), and references therein.



Innumerable derivatives have been synthesized in which one or more  $\eta^5\text{-C}_5\text{H}_5$  group is present in a mononuclear or polynuclear metal complex together with other ligands such as CO, NO, H or X. It should also be borne in mind that  $\text{C}_5\text{H}_5$  can act as an  $\eta^1$ -ligand by forming a  $\sigma$  M-C bond and mixed complexes are sometimes obtained, e.g.  $[\text{Be}(\eta^1\text{-C}_5\text{H}_5)(\eta^5\text{-C}_5\text{H}_5)]$  (see p. 130). Likewise:



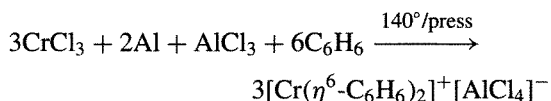
Such  $\eta^1\text{-C}_5\text{H}_5$  complexes are often found to be fluxional in solution at room temperature, the 5 H atoms giving rise to a single sharp  $^1\text{H}$  nmr resonance. At lower temperatures the spectrum usually broadens and finally resolves into the expected complex spectrum at temperatures which are sufficiently low to prevent interchange on the nmr time scale ( $\sim 10^{-3}$  s). Numerous experiments have been devised to elucidate the mechanism by which the H atoms become equivalent and, at least in some systems, it seems likely that a non-dissociative (unimolecular) 1,2-shift occurs.



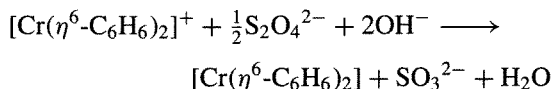
### 19.7.6 Hexahapto ligands

Arenes such as benzene and its derivatives can form complexes precisely analogous to ferrocene and related species. Though particularly exciting when first recognized as  $\eta^6$  complexes in 1955 these compounds introduce no new principles and need only be briefly considered here. Curiously, the first such compounds were made as long ago as 1919 when F. Hein reacted  $\text{CrCl}_3$  with  $\text{PhMgBr}$  to give compounds which he formulated as "polyphenylchromium" compounds  $[\text{CrPh}_n]^{0,+1}$  ( $n = 2, 3, \text{ or } 4$ ); their true nature

as  $\eta^6$ -arene complexes of benzene and diphenyl was not recognized until over 35 y later.<sup>(43)</sup> The best general method for making bis( $\eta^6$ -arene) metal complexes is due to E. O. Fischer and W. Hafner (1955) who devised it originally for dibenzenechromium — the isoelectronic analogue of ferrocene:  $\text{CrCl}_3$  was reduced with Al metal in the presence of  $\text{C}_6\text{H}_6$ , using  $\text{AlCl}_3$  as a catalyst:

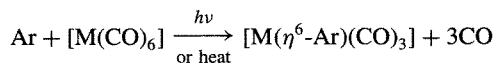


The yield is almost quantitative and the orange-yellow  $\text{Cr}^I$  cation can be reduced to the neutral species with aqueous dithionite:

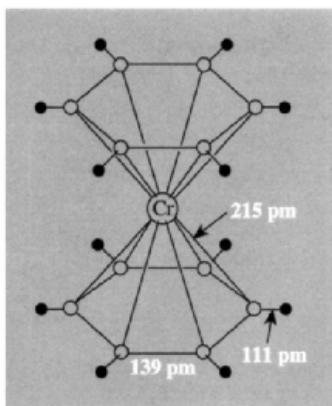


Dibenzenechromium(0) forms dark-brown crystals, mp  $284^\circ$ , and the molecular structure (Fig. 19.28) comprises plane parallel rings in eclipsed configuration above and below the Cr atom ( $D_{6h}$ ); the C-H bonds are tilted slightly towards the metal and, most significantly, the C-C distances show no alternation around the rings. A bonding scheme can be constructed as for ferrocene (p. 938) using the six  $p_z$  orbitals on each benzene ring.

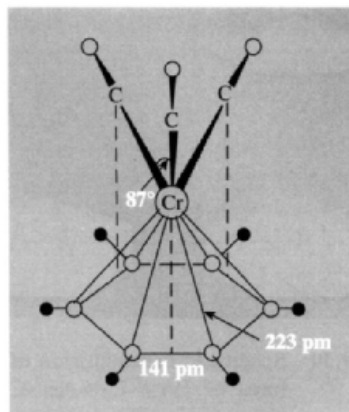
Bis ( $\eta^6$ -arene) metal complexes have been made for many transition metals by the Al/ $\text{AlCl}_3$  reduction method and cationic species  $[\text{M}(\eta^6\text{-Ar})_2]^{n+}$  are also well established for  $n = 1, 2, \text{ and } 3$ . Numerous arenes besides benzene have been used, the next most common being 1,3,5- $\text{Me}_3\text{C}_6\text{H}_3$  (mesitylene) and  $\text{C}_6\text{Me}_6$ . Reaction of arenes with metal carbonyls in high-boiling solvents or under the influence of ultraviolet light results in the displacement of 3CO and the formation of arene-metal carbonyls:



<sup>43</sup> H. ZEISS, P. J. WHEATLEY and H. J. S. WINKLER, *Benzene-Metal Complexes*, Ronald Press, New York, 1966, 101 pp.



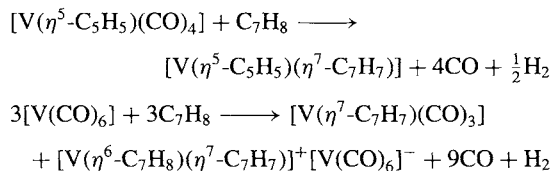
**Figure 19.28** The eclipsed ( $D_{6h}$ ) structure of  $[\text{Cr}(\eta^6\text{-C}_6\text{H}_6)_2]$  as revealed by X-ray diffraction, showing the two parallel rings 323 pm apart. Neutron diffraction shows the H atoms are tilted slightly towards the Cr, and electron diffraction on the gaseous compound shows that the eclipsed configuration is retained without rotation.



**Figure 19.29** The structure of  $[\text{Cr}(\eta^6\text{-C}_6\text{H}_6)(\text{CO})_3]$  showing the three CO groups in staggered configuration with respect to the benzene ring: the Cr–O distance is 295 pm and the plane of the 3 O atoms is parallel to the plane of the ring.

For Cr, Mo and W the benzenetricarbonyl complexes are yellow solids melting at  $162^\circ$ ,  $125^\circ$ , and  $140^\circ$ , respectively. The structure of  $[\text{Cr}(\eta^6\text{-C}_6\text{H}_6)(\text{CO})_3]$  is in Fig. 19.29. In general,  $\eta^6$ -arene complexes are more reactive than their  $\eta^5\text{-C}_5\text{H}_5$  analogues and are thermally less stable.

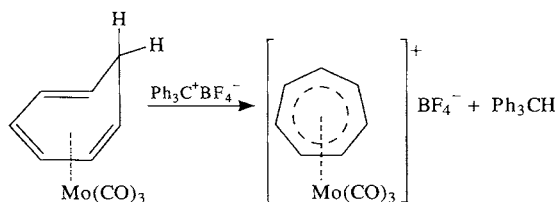
In some cases the loss of hydrogen may occur spontaneously, e.g.:

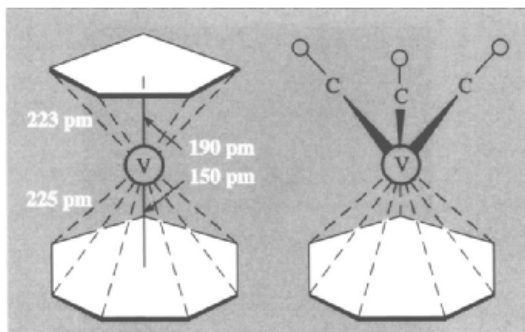


The purple paramagnetic complex  $[\text{V}(\eta^5\text{-C}_5\text{H}_5)(\eta^7\text{-C}_7\text{H}_7)]$  and the dark-brown diamagnetic complex  $[\text{V}(\eta^7\text{-C}_7\text{H}_7)(\text{CO})_3]$  both feature symmetrical planar  $\text{C}_7$  rings as illustrated in Fig. 19.30. The bonding appears to be similar to that in  $\eta^5\text{-C}_5\text{H}_5$  and  $\eta^6\text{-C}_6\text{H}_6$  complexes but, as expected from the large number of bonding electrons formally provided by the ligand, its complexes are restricted to elements in the early part of the transition series, e.g. V, Cr, Mo,  $\text{Mn}^{\text{I}}$ . For  $[\text{V}(\eta^5\text{-C}_5\text{H}_5)(\eta^7\text{-C}_7\text{H}_7)]$  the rings are “eclipsed” as shown, and a notable feature of the structure is the substantially closer approach of the  $\text{C}_7\text{H}_7$  ring to the V atom, suggesting that equality of V–C distances to the 2 rings is the controlling factor; consistent with this V–C(7 ring) is 225 pm and V–C(5 ring) is 223 pm. In addition to acting as an

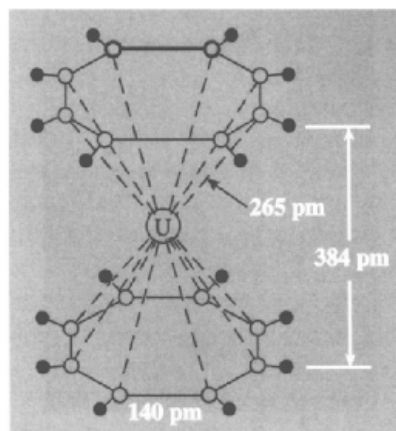
### 19.7.7 Heptahapto and octahapto ligands

Treatment of cycloheptatriene complexes of the type  $[\text{M}(\eta^6\text{-C}_7\text{H}_8)(\text{CO})_3]$  ( $\text{M} = \text{Cr}, \text{Mo}, \text{W}$ ) with  $\text{Ph}_3\text{C}^+\text{BF}_4^-$  results in hydride abstraction to give orange-coloured  $\eta^7$ -cycloheptatrienyl (or tropylium) complexes:





**Figure 19.30** Schematic representation of the structures of  $[\text{V}(\eta^5\text{-C}_5\text{H}_5)(\eta^7\text{-C}_7\text{H}_7)]$  and  $[\text{V}(\eta^7\text{-C}_7\text{H}_7)(\text{CO})_3]$  (see text).

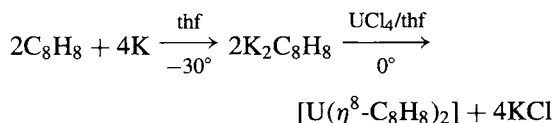


**Figure 19.31** The structure of  $[\text{U}(\eta^8\text{-C}_8\text{H}_8)_2]$  showing  $D_{8h}$  symmetry.

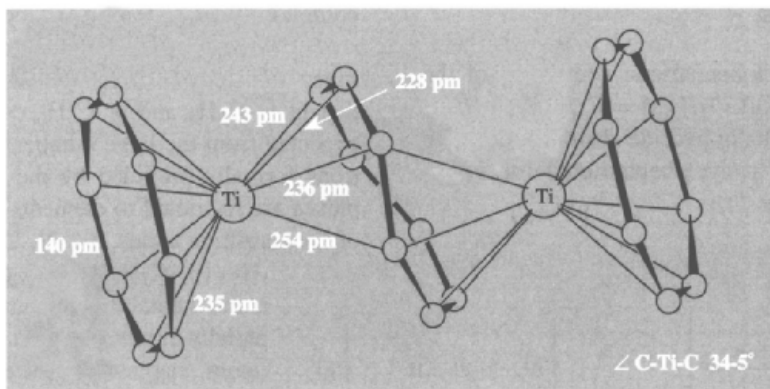
$\eta^7$  ligand, cycloheptatrienyl can also bond in the  $\eta^5, \eta^3$ , and even  $\eta^1$  mode (see ref. 44 on p. 943).

Octahapto ligands are rare but cyclooctatetraene fulfils this role in some of its complexes — the metal must clearly have an adequate number of unfilled orbitals and be large enough to bond effectively with such a large ring. Th, Pa, U, Np and Pu satisfy these criteria and the complexes  $[\text{M}(\eta^8\text{-C}_8\text{H}_8)_2]$  have been shown by X-ray crystallography to have eclipsed parallel planar rings (Fig. 19.31). The deep-green U complex can be made by reducing  $\text{C}_8\text{H}_8$  with K in dry thf and then reacting the intense yellow

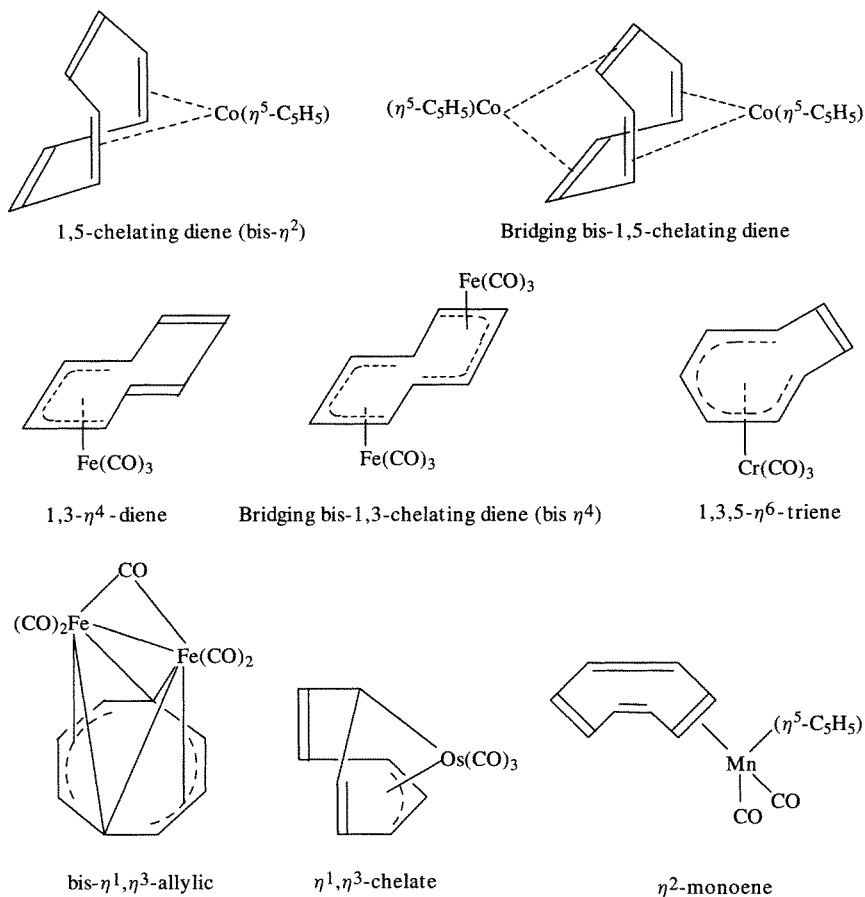
solution of  $\text{K}_2\text{C}_8\text{H}_8$  with  $\text{UCl}_4$ :



The compound inflames in air but is stable in aqueous acid or alkali solutions. The colourless complex  $[\text{Th}(\eta^8\text{-C}_8\text{H}_8)_2]$ , yellow complexes  $[\text{Pa}(\eta^8\text{-C}_8\text{H}_8)_2]$  and  $[\text{Np}(\eta^8\text{-C}_8\text{H}_8)_2]$  and the cherry red compound  $[\text{Pu}(\eta^8\text{-C}_8\text{H}_8)_2]$  are prepared similarly. One of the very few



**Figure 19.32** Structure of  $[\text{Ti}_2(\text{C}_8\text{H}_8)_3]$  showing it to be  $[(\text{Ti}(\eta^8\text{-C}_8\text{H}_8))_2\mu\text{-}(\eta^4, \eta^4\text{-C}_8\text{H}_8)]$ . Ti-C to outer 16C = 235 pm. H atoms are omitted for clarity.



**Figure 19.33** Some further coordinating modes of  $C_8H_8$ .

examples of  $\eta^8$  bonding to a d-block element is in the curious complex  $Ti_2(C_8H_8)_3$ . As shown in Fig. 19.32, two of the ligands are planar  $\eta^8$  donors whereas the central puckered ring bridges the 2 Ti atoms in a bis- $\eta^4$ -mode. It is made by treating  $Ti(OBu^t)_4$  with  $C_8H_8$  in the presence of  $AlEt_3$ .

In addition to acting as an  $\eta^8$  ligand,  $C_8H_8$  can coordinate in other modes,<sup>(44)</sup> some of which are illustrated in Fig. 19.33. Many of these complexes show fluxional behaviour<sup>(45)</sup> in solution (p. 935) and the distinction between the various types of bonding is not as clear-cut as implied by the limiting structures in Fig. 19.33.

<sup>44</sup>G. DEGANELLO, *Transition Metal Complexes of Cyclic Polyolefins*. Academic Press, London, 1980, 476 pp.

<sup>45</sup>D. M. HEINEKEY and W. A. G. GRAHAM, *J. Am. Chem. Soc.* **101**, 6115–6 (1979).

																1	2																				
																H	He																				
3	4															5	6	7	8	9	10																
Li	Be															B	C	N	O	F	Ne																
11	12															13	14	15	16	17	18																
Na	Mg															Al	Si	P	S	Cl	Ar																
19	20	21	22	23	24	25	26	27	28	29	30	31	32	33	34	35	36																				
K	Ca	Sc	Ti	V	Cr	Mn	Fe	Co	Ni	Cu	Zn	Ga	Ge	As	Se	Br	Kr																				
37	38	39	40	41	42	43	44	45	46	47	48	49	50	51	52	53	54																				
Rb	Sr	Y	Zr	Nb	Mo	Tc	Ru	Rh	Pd	Ag	Cd	In	Sn	Sb	Te	I	Xe																				
55	56	57	58	59	60	61	62	63	64	65	66	67	68	69	70	71	72																				
Cs	Ba	La	Hf	Ta	W	Re	Os	Ir	Pt	Au	Hg	Tl	Pb	Bi	Po	At	Rn																				
87	88	89	90	91	92	93	94	95	96	97	98	99	100	101	102	103	104																				
Fr	Ra	Ac	Th	Pa	U	Np	Pu	Am	Cm	Bk	Cf	Es	Fm	Md	No	Lr																					
																		105	106	107	108	109	110	111	112												
																		Ce	Pr	Nd	Pm	Sm	Eu	Gd	Tb	Dy	Ho	Er	Tm	Yb	Lu						
																		Th	Pa	U	Np	Pu	Am	Cm	Bk	Cf	Es	Fm	Md	No	Lr						

# 20

## Scandium, Yttrium, Lanthanum and Actinium

### 20.1 Introduction

In 1794 the Finnish chemist J. Gadolin, while examining a mineral that had recently been discovered in a quarry at Ytterby, near Stockholm, isolated what he thought was a new oxide (or “earth”) which A. G. Ekeberg in 1797 named yttria. In fact it was a mixture of a number of metal oxides from which yttrium oxide was separated by C. G. Mosander in 1843. This is actually part of the fascinating story of the “rare earths” to which we shall return in Chapter 30. The first sample of yttrium metal, albeit very impure, was obtained by F. Wöhler in 1828 by the reduction of the trichloride by potassium.

Four years before isolating yttria, Mosander extracted lanthanum oxide as an impurity from cerium nitrate (hence the name from Greek *λανθάνειν*, to hide), but it was not until 1923 that metallic lanthanum in a relatively pure form was obtained, by electrolysis of fused halides.

Scandium, the first member of the group, is also present in the Swedish ores from which

yttrium and lanthanum had been extracted, but in only very small amounts and, probably for this reason, its discovery was delayed until 1879 when L. F. Nilsen isolated a new oxide and named it scandia. A few years later and with larger amounts at his disposal, P. T. Cleve prepared a large number of salts from this oxide and was able to show that it was the oxide of a new element whose properties tallied very closely indeed with those predicted by D. I. Mendeleev for ekaboron, an element missing from his classification (p. 29). It was only in 1937 that the metal itself was prepared by the electrolysis of molten chlorides of potassium, lithium and scandium, and only in 1960 that the first pound of 99% pure metal was produced.

The final member of the group, actinium, was identified in uranium minerals by A. Debierne in 1899, the year after P. and M. Curie had discovered polonium and radium in the same minerals. However, the naturally occurring isotope,  $^{227}\text{Ac}$ , is a  $\beta^-$  emitter with a half-life of 21.77 y and the intense  $\gamma$  activity of its decay products makes it difficult to study.

## 20.2 The Elements<sup>(1,2,3)</sup>

### 20.2.1 Terrestrial abundance and distribution

With the exception of actinium, which is found naturally only in traces in uranium ores, these elements are by no means rare though they were once thought to be so: Sc 25, Y 31, La 35 ppm of the earth's crustal rocks, (cf. Co 29 ppm). This was, no doubt, at least partly because of the considerable difficulty experienced in separating them from other constituent rare earths. As might be expected for class-a metals, in most of their minerals they are associated with oxoanions such as phosphate, silicate and to a lesser extent carbonate.

Scandium is very widely but thinly distributed and its only rich mineral is the rare thortveitite,  $\text{Sc}_2\text{Si}_2\text{O}_7$  (p. 348), found in Norway, but since scandium has only small-scale commercial use, and can be obtained as a byproduct in the extraction of other materials, this is not a critical problem. Yttrium and lanthanum are invariably associated with lanthanide elements, the former (Y) with the heavier or "Yttrium group" lanthanides in minerals such as xenotime,  $\text{M}^{\text{III}}\text{PO}_4$  and gadolinite,  $\text{M}_2^{\text{III}}\text{M}_3^{\text{II}}\text{Si}_2\text{O}_{10}$  ( $\text{M}^{\text{II}} = \text{Fe, Be}$ ), and the latter (La) with the lighter or "cerium group" lanthanides in minerals such as monazite,  $\text{M}^{\text{III}}\text{PO}_4$  and bastnaesite,  $\text{M}^{\text{III}}\text{CO}_3\text{F}$ . This association of similar metals is a reflection of their ionic radii. While  $\text{La}^{\text{III}}$  is similar in size to the early lanthanides which immediately follow it in the periodic table,  $\text{Y}^{\text{III}}$ , because of the steady fall in ionic radius along the lanthanide series (p. 1234), is more akin to the later lanthanides.

<sup>1</sup> R. C. VICKERY, Scandium, yttrium and lanthanum, Chap. 31 in *Comprehensive Inorganic Chemistry*, Vol. 3, pp. 329–53, Pergamon Press, Oxford, 1973, and references therein. C. T. HOROVITZ (ed.), *Scandium: Its Occurrence, Chemistry, Physics, Metallurgy, Biology and Technology*, Academic Press, London, 1975, 598 pp.

<sup>2</sup> S. COTTON, *Lanthanides and Actinides*, Macmillan, Basingstoke, 1991, 192 pp.

<sup>3</sup> K. A. GSCHNEIDER and L. EYRING (eds) *Handbook of the Physics and Chemistry of Rare Earths*, Vols 1–21, 1978–1995, Elsevier, Amsterdam.

### 20.2.2 Preparation and uses of the metals

Some scandium is obtained from thortveitite, which contains 35–40%  $\text{Sc}_2\text{O}_3$ , but most is obtained as a byproduct in the processing of uranium ores which contain only about 0.02%  $\text{Sc}_2\text{O}_3$ , and in the production of tungsten. Its applications, for instance in laser crystals and coatings, are highly specialized and the amount consumed is low, though increasing.

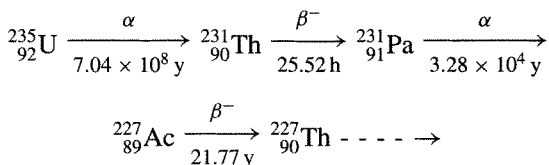
Yttrium and lanthanum are both obtained from lanthanide minerals and the method of extraction depends on the particular mineral involved. Digestions with hydrochloric acid, sulfuric acid, or caustic soda are all used to extract the mixture of metal salts. Prior to the Second World War the separation of these mixtures was effected by fractional crystallizations, sometimes numbered in their thousands. However, during the period 1940–45 the main interest in separating these elements was in order to purify and characterize them more fully. The realization that they are also major constituents of the products of nuclear fission effected a dramatic sharpening of interest in the USA. As a result, ion-exchange techniques were developed and, together with selective complexation and solvent extraction, these have now completely supplanted the older methods of separation (p. 1228). In cases where the free metals are required, reduction of the trifluorides with metallic calcium can be used.

Yttrium has important roles in the field of electronics, providing the basis of the phosphors used to produce the red colour on television screens and, in the form of garnets such as  $\text{Y}_3\text{Fe}_5\text{O}_{12}$ , being employed as microwave filters in radar. Because of its low neutron absorption cross-section, yttrium has potential as a moderator in nuclear reactors though this use has yet to be developed. It was, however, the announcement in 1986/87 of the *high temperature superconductors*,  $\text{La}_{2-x}\text{Sr}_x\text{CuO}_4$  and  $\text{YBa}_2\text{Cu}_3\text{O}_{7-x}$  which produced the highest, though as yet unfulfilled, hopes of commercial exploitation. The latter compound has a critical temperature,  $T_c \sim 95 \text{ K}$ , below which it is

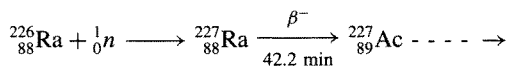
superconducting. This temperature, crucially, can be attained using liquid nitrogen rather than liquid helium as refrigerant and a continuing spate of publications on these and related materials has been generated (p. 1182).

Lanthanum has also found modest uses. Its oxide is an additive in high-quality optical glasses to which it imparts a high refractive index (sparkle) and has been suggested for a variety of catalytic uses. "Mischmetal", an unseparated mixture of lanthanide metals containing about 25% La, is used in making lighter flints, and more importantly in the production of alloy steels. (p. 1232).

Actinium occurs naturally as a decay product of  $^{235}\text{U}$ :



but the half-lives are such that one tonne of the naturally occurring uranium ore contains on average only about 0.2 mg of Ac. An alternative source is the neutron irradiation of  $^{226}\text{Ra}$  in a nuclear reactor:



In either case, ion-exchange or solvent extraction techniques are needed to separate the element and, at best, it can be produced in no more than milligram quantities. Large-scale use is therefore impossible even if desired.

### 20.2.3 Properties of the elements

A number of the properties of Group 3 elements are summarized in Table 20.1. Each of the elements has an odd atomic number and so has few stable isotopes. All are rather soft, silvery-white metals, and they display the gradation in properties that might be expected for elements immediately following the strongly electropositive alkaline-earth metals and preceding the transition elements proper. Each is less electropositive than its predecessor in Group 2 but more electropositive than its successors in transition series, while the increasingly electropositive character of the heavier elements of the group is in keeping with the increase in size. The inverse trends in electronegativity are illustrated in Fig. 20.1.

As is the case for boron and aluminium (in Group 13), the underlying electron cores are those of the preceding noble gases and indeed, as was pointed out in Chapter 7, a much more

**Table 20.1** Some properties of Group 3 elements

Property	Sc	Y	La	Ac
Atomic number	21	39	57	89
Number of naturally occurring isotopes	1	1	2	(2)
Atomic weight	44.955910(8)	88.90585(2)	138.9055(2)	227.0277 <sup>(a)</sup>
Electronic configuration	[Ar]3d <sup>1</sup> 4s <sup>2</sup>	[Kr]4d <sup>1</sup> 5s <sup>2</sup>	[Xe]5d <sup>1</sup> 6s <sup>2</sup>	[Rn]6d <sup>1</sup> 7s <sup>2</sup>
Electronegativity	1.3	1.2	1.1	1.1
Metal radius (12-coordinate)/pm	162	180	187	—
Ionic radius (6-coordinate)/pm	74.5	90.0	103.2	112
$E^\circ(\text{M}^{3+} + 3e^- = \text{M(s)})/\text{V}$	-2.03	-2.37	-2.37	-2.6
MP/°C	1539	1530	920	817
BP/°C	2748	3264	3420	2470
$\Delta H_{\text{fus}}/\text{kJ mol}^{-1}$	15.77	11.5	8.5	(10.5)
$\Delta H_{\text{vap}}/\text{kJ mol}^{-1}$	332.71	367	402	(293)
$\Delta H_{\text{f}}(\text{monatomic gas})/\text{kJ mol}^{-1}$	376 (±20)	425 (±8)	423 (±6)	—
Density (20°C)/g cm <sup>-3</sup>	3.0	4.5	6.17	—
Electrical resistivity (20°C)/μohm cm	50-61	57-70	57-80	—

<sup>(a)</sup>This value is for the radioisotope with the longest half-life ( $^{227}\text{Ac}$ ).



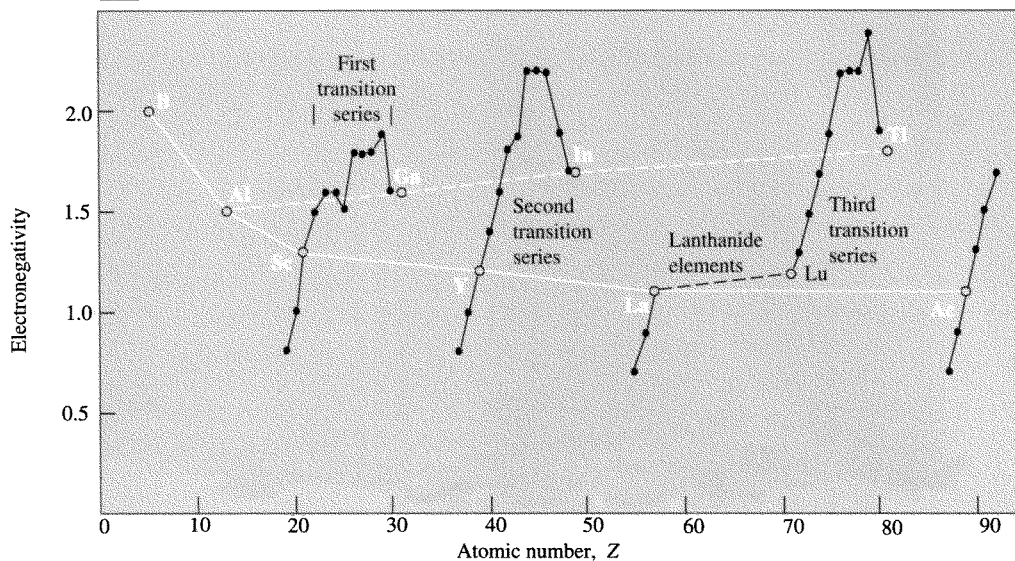


Figure 20.1 Electronegativity of the elements in Groups 3 and 13.

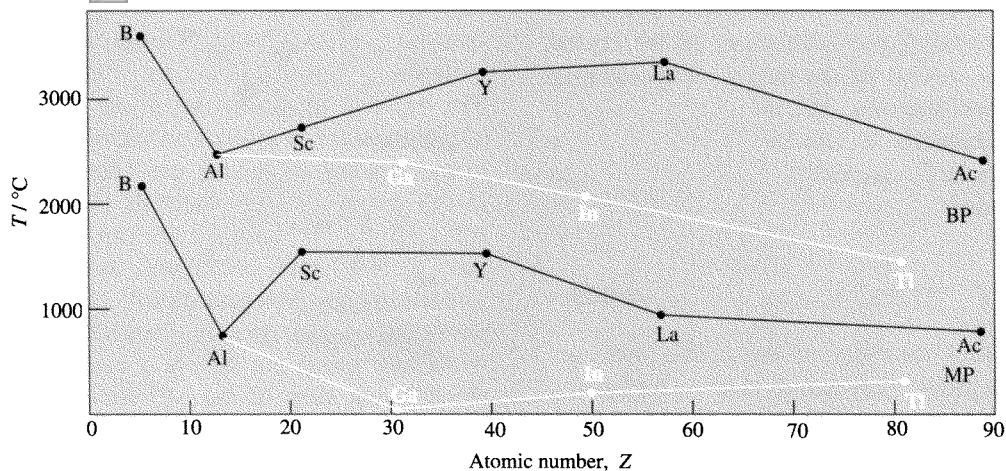


Figure 20.2 Mps and bps of the elements in Groups 3 and 13.

regular variation in atomic properties occurs in passing from B and Al to Group 3 than to heavier congeners in Group 13 (p. 223). However, the presence of a d electron on each of the atoms of this group (in contrast to the p electron in the atoms of B, Al and the other elements in Group 13) has consequences which can be seen in some of the bulk properties of the metals. For instance, the mps and bps (Fig. 20.2), along with

the enthalpies associated with these transitions, all show discontinuous increases in passing from Al to Sc rather than to Ga, indicating that the d electron has a more cohesive effect than the p electron. It appears that this is due to d electrons forming more localized bonds within the metals. Thus, although Sc, Y and La have typically metallic (hcp) structures (with other metallic modifications at higher temperatures),



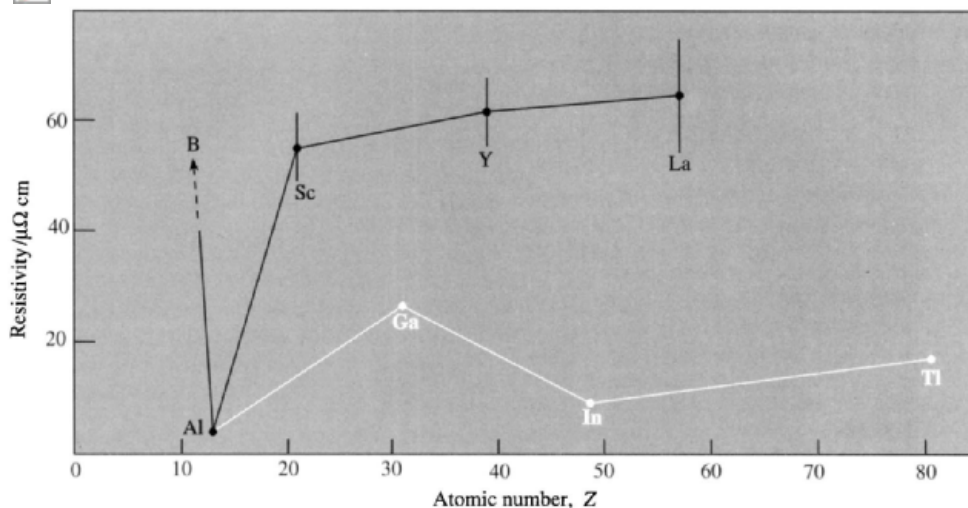


Figure 20.3 Resistivities of the elements in Groups 3 and 13.

their electrical resistivities are much higher than that of Al (Fig. 20.3). Admittedly, resistivity is a function of thermal vibrations of the crystal lattice as well as of the degree of localization of valence electrons, but even so the marked changes between Al and Sc seem to indicate a marked reduction in the mobility of the d electron of the latter.

#### 20.2.4 Chemical reactivity and trends

The general reactivity of the metals increases down the group. They tarnish in air — La rapidly, but Y much more slowly because of the formation of a protective oxide coating — and all burn easily to give the oxides  $M_2O_3$ . They react with halogens at room temperature and with most non-metals on warming. They reduce water with evolution of hydrogen, particularly if finely divided or heated, and all dissolve in dilute acid. Strong acids produce soluble salts whereas weak acids such as HF,  $H_3PO_4$  and  $H_2C_2O_4$  produce sparingly soluble or insoluble salts.

In the main, the chemistry of these elements concerns the formation of a predominantly ionic +3 oxidation state arising from the loss of all 3 valence electrons and giving a well-defined

cationic aqueous chemistry. Because of this, although each member of this group is the first member of a transition series, its chemistry is largely atypical of the transition elements. The variable oxidation states and the marked ability to form coordination compounds with a wide variety of ligands are barely hinted at in this group although materials containing the metals in low oxidation states can be prepared (see p. 949) and a limited organometallic (predominantly cyclopentadienyl) chemistry has developed. Differences in chemical behaviour within the group are largely a consequence of the differing sizes of the  $M^{III}$  ions. Scandium, the lightest of these elements, with the smallest ionic radius, is the least basic and the strongest complexing agent, with properties not unlike those of aluminium. Its aqueous solutions are appreciably hydrolysed and its oxide has some acidic properties. On the other hand, lanthanum and actinium (in so far as its properties have been examined) show basic properties approaching those of calcium.

Most structural studies have relied exclusively on the use of X-ray techniques but these elements have nuclei,  $^{45}\text{Sc}$ ,  $^{89}\text{Y}$  and  $^{139}\text{La}$  with abundances in excess of 99.9% and  $I = \frac{7}{2}, \frac{1}{2}, \frac{7}{2}$  respectively. The application of nmr studies is therefore

becoming increasingly important,<sup>(4)</sup> mainly on solutions but also for solid-state work.<sup>(5)</sup>

## 20.3 Compounds of Scandium, Yttrium, Lanthanum and Actinium

### 20.3.1 Simple compounds<sup>(6)</sup>

The oxides,  $M_2O_3$ , are white solids which can be prepared directly from the elements. In  $Sc_2O_3$  and  $Y_2O_3$  the metals are 6-coordinate but the larger  $La^{III}$  ion adopts this structure only at elevated temperatures, a 7-coordinate structure being normally more stable. When water is added to  $La_2O_3$  it "slakes" like lime with evolution of much heat and a hissing sound. The hydroxides,  $M(OH)_3$ , (or in the case of scandium possibly the hydrated oxide) are obtained as gelatinous precipitates from aqueous solutions of the metal salts by addition of alkali hydroxide. In the case of scandium only, this precipitate can be dissolved in an excess of conc NaOH to give anionic species such as  $[Sc(OH)_6]^{3-}$ . Yttrium and lanthanum hydroxides possess only basic properties, and the latter especially will absorb atmospheric  $CO_2$  to form basic carbonates.

Dissolution of the oxide or hydroxide in the appropriate acid provides the most convenient method for producing the salts of the colourless, diamagnetic  $M^{III}$  ions. Such solutions, especially those of  $Sc^{III}$ , are significantly hydrolysed with the formation of polymeric hydroxy species.

With the exception of the fluorides, the halides are all very water-soluble and deliquescent. Precipitation of the insoluble fluorides can be used as a qualitative test for these elements. The distinctive ability of  $Sc^{III}$  to form complexes is illustrated by the fact that an excess of  $F^-$  causes the first-precipitated  $ScF_3$  to redissolve as

$[ScF_6]^{3-}$ ; indeed,  $M_3[ScF_6]$ ,  $M = NH_4, Na, K$ , were isolated as long ago as 1914. The anhydrous halides are best prepared by direct reaction of the elements rather than by heating the hydrates which causes hydrolysis. Heating the hydrated chlorides, for instance, gives  $Sc_2O_3$ ,  $YOCl$  and  $LaOCl$  respectively, though to produce  $AcOCl$  it is necessary to use superheated steam. The anhydrous halides illustrate nicely the effects of ionic size on the coordination number of the metal<sup>(2)</sup>. In all four of its halides scandium is 6-coordinate. So too is yttrium except in its fluoride where it has eight near neighbours and one slightly further away (8 + 1). The larger lanthanum however has 9 + 2 coordination in its fluoride, but is 9-coordinate in its chloride and bromide and 8-coordinate in its iodide.

Sulfates and nitrates are known and in all cases they decompose to the oxides on heating. Double sulfates of the type  $M_2^{III}(SO_4)_3 \cdot 3Na_2SO_4 \cdot 12H_2O$  can be prepared, and La (unlike Sc and Y) forms a double nitrate,  $La(NO_3)_3 \cdot 2NH_4NO_3 \cdot 4H_2O$ , which is of the type once used extensively in fractional crystallization procedures for separating individual lanthanides.

Reaction of the metals with hydrogen produces highly conducting materials with the composition  $MH_2$ , similar to the metallic nonstoichiometric hydrides of the subsequent transition elements (pp. 66–7). Except in the case of  $ScH_2$ , further  $H_2$  can then be absorbed causing a diminution of electrical conductivity until materials similar to the ionic hydrides of the alkaline-earth metals, and with the limiting composition  $MH_3$ , are produced. The dihydrides, though ostensibly containing the divalent metals, are probably best considered as pseudo-ionic compounds of  $M^{3+}$  and  $2H^-$  with the extra electron in a conduction band. However, the question of the type of bonding is still controversial, as was explained more fully in Chapter 3 (p. 66).

Another example of a "divalent" metal of this group, but which in fact is probably entirely analogous to the dihydrides, is  $LaI_2$ . However, the most extensive set of examples of these metals in low formal oxidation states is provided by the binary and ternary halides produced by

<sup>4</sup> J. MASON, *Polyhedron* **8**, 1657–68 (1989).

<sup>5</sup> A. R. THOMPSON and E. OLDFIELD, *J. Chem. Soc., Chem. Commun.*, 27–9 (1987).

<sup>6</sup> G. MEYER and L. R. MORSS (eds.), *Synthesis of Lanthanide and Actinide Compounds*, Kluwer Acad. Publ., Dordrecht, 1991, 367 pp.

prolonged heating of the reactants in sealed tantalum or niobium vessels to temperatures sometimes in excess of 1000°C. Starting with  $\text{ScX}_3$  and Sc metal along with the appropriate alkali metal halide, several compounds of the series  $\text{M}^I\text{ScX}_3$  have been obtained containing octahedrally coordinated  $\text{Sc}^{II}$  in linear  $[\text{ScX}_3^-]$  chains<sup>(7)</sup>.  $\text{ScCl}_3 + \text{Sc}$  yield no less than five reduced phases, dark-coloured and sensitive to oxygen and moisture<sup>(8)</sup>:

$\text{Sc}_7\text{Cl}_{12}$  consists of discrete  $[\text{Sc}_6\text{Cl}_{12}]^{3-}$  clusters, similar to the  $\text{M}_6\text{Cl}_{12}$  clusters of Nb and Ta (p. 991), along with separate  $\text{Sc}^{3+}$  ions;

$\text{Sc}_5\text{Cl}_8$  is best regarded as  $(\text{ScCl}_2^+)_n - (\text{Sc}_4\text{Cl}_6^-)_n$  in which edge-sharing  $\text{ScCl}_6$  octahedra and edge-sharing  $\text{Sc}_6$  octahedra lie in parallel chains;

$\text{Sc}_2\text{Cl}_3$  and its Br analogue are of unknown structure, as are reported  $\text{La}_2\text{X}_3$  phases, though  $\text{Y}_2\text{Cl}_3$  and  $\text{Y}_2\text{Br}_3$  have been shown to consist of parallel chains of  $\text{Y}_6$  octahedra, the chains being linked by Cl atoms;

$\text{Sc}_7\text{Cl}_{10}$  is composed of a double chain of  $\text{Sc}_6$  octahedra sharing edges, and a parallel chain of  $\text{ScCl}_6$  octahedra<sup>(9)</sup>;

$\text{ScCl}$ , made up of close-packed layers of Sc and Cl atoms in the sequence Cl-Sc-Sc-Cl has, like analogous Y and La materials with Cl and Br, since been shown to have been stabilised by interstitial H impurity.<sup>(10)</sup>

The ability of B, C and N as well as H to stabilize many of these reduced phases is at once a major preparative problem<sup>(11)</sup> and also a source of an

expanding area of cluster chemistry of which  $\text{Sc}_7\text{X}_{12}\text{Z}$  ( $\text{Z} = \text{C}$ ;  $\text{X} = \text{Br}$ ,  $\text{I}$ .  $\text{Z} = \text{B}$ ;  $\text{X} = \text{I}$ ), best regarded as  $\text{Sc}(\text{Sc}_6\text{X}_{12}\text{Z})$ , are examples.<sup>(12)</sup>

### 20.3.2 Complexes<sup>(13,14)</sup>

Compared to later elements in their respective transition series, scandium, yttrium and lanthanum have rather poorly developed coordination chemistries and form weaker coordinate bonds, lanthanum generally being even less inclined to form strong coordinate bonds than scandium. This is reflected in the stability constants of a number of relevant 1:1 metal-edta complexes:

Metal ion	$\text{Sc}^{III}$	$\text{Y}^{III}$	$\text{La}^{III}$	$\text{Fe}^{III}$	$\text{Co}^{III}$
$\log_{10} K_1$	23.1	18.1	15.5	25.5	36.0

This may seem somewhat surprising in view of the charge of +3 ions, but this is coupled with appreciably larger ionic radii and also with greater electropositive character which inhibits covalent contribution to their bonding. Lanthanum of course exhibits these characteristics more clearly than Sc, and, while La and Y closely resemble the lanthanide elements, Sc has more similarity with Al. Even Sc however is a class-a acceptor, complexing most readily with O-donor ligands particularly if chelating. Complexes with N-donor and halide ligands are less well-characterized and those with S-donors are largely confined to the Y and La complexes with dithiocarbamates and dithiophosphinates,  $[\text{M}(\text{S}_2\text{CNET}_2)_3]$  and  $[\text{M}(\text{S}_2\text{P}(\text{C}_6\text{H}_{11})_2)_3]$ .

The complex anion  $[\text{ScF}_6]^{3-}$  has already been mentioned and, while there is a fairly extensive series of halo complexes with a

<sup>7</sup> A. LACHGAR, D. S. DUDIS, P. K. DORHOUT and J. D. CORBETT, *Inorg. Chem.* **30**, 3321-6 (1991).

<sup>8</sup> J. D. CORBETT, *Acc. Chem. Res.* **14**, 239-46 (1981).

<sup>9</sup> F. J. DI SALVO, J. V. WASZCZAK, W. M. WALSH, Jr., L. W. RUPP and J. D. CORBETT, *Inorg. Chem.* **24**, 4624-5 (1985).

<sup>10</sup> See p. 176 of A. SIMON, *Angew. Chem. Int. Edn. Engl.*, **27**, 159-83 (1988). Hj. MATTAUSCH, R. EGER, J. D. CORBETT and A. SIMON, *Z. anorg. allg. Chem.* **616**, 157-61 (1992).

<sup>11</sup> J. D. CORBETT in *Synthesis of Lanthanide and Actinide Compounds*, pp. 159-73, Kluwer Acad. Publ., Dordrecht, (1991).

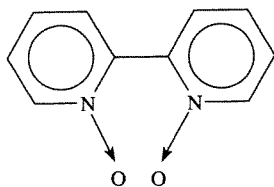
<sup>12</sup> D. S. DUDIS, J. D. CORBETT and S-J. HWU, *Inorg. Chem.* **25**, 3434-8 (1986).

<sup>13</sup> G. A. MELSON and R. W. STOTZ, *Coord. Chem. Revs.* **7**, 133-60 (1971).

<sup>14</sup> F. A. HART, Scandium, Yttrium and the Lanthanides, in *Comprehensive Coordination Chemistry*, Vol. 3, pp. 1059-127, Pergamon Press, Oxford, 1987.

variety of stereochemistries, they must normally be prepared<sup>(15)</sup> by dry methods to avoid hydrolysis, and iodo complexes are invariably unstable. Other complexes such as  $[\text{Sc}(\text{dmsO})_6]^{3+}$  (where dmsO is dimethylsulfoxide,  $\text{Me}_2\text{SO}$ ),  $[\text{Sc}(\text{bipy})_3]^{3+}$ ,  $[\text{Sc}(\text{bipy})_2(\text{NCS})_2]^+$  and  $[\text{Sc}(\text{bipy})_2\text{Cl}_2]^+$  exhibit scandium's usual coordination number of 6. Data for corresponding Y and La compounds are limited but in  $[\text{Y}(\text{OH})(\text{H}_2\text{O})_2(\text{phen})_2]\text{Cl}_4 \cdot 2(\text{phen}) \cdot \text{MeOH}$  the yttrium is 8-coordinate with square antiprismatic geometry,<sup>(16)</sup> and in  $[\text{La}(\text{NO}_3)_3(\text{bipy})_2]$  the lanthanum is 10-coordinate. This is illustrative of the general trend in moving down the group that coordination numbers greater than 6 become the rule rather than the exception. It seems likely that in aqueous solutions, in the absence of other preferred ligands,  $\text{Y}^{\text{III}}$  is directly coordinated to 8 water molecules and  $\text{La}^{\text{III}}$  to 9 and in  $\text{M}(\text{OH})_3$ , ( $\text{M} = \text{Y}, \text{La}$ ) the metal ion is 9-coordinate with a stereochemistry approximating to tri-capped trigonal prismatic.

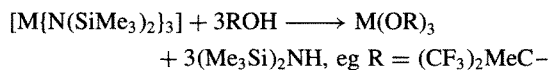
A coordination number of 8 is probably the most characteristic of La and possibly even of Y, with the square antiprism and the dodecahedron being the preferred stereochemistries. The acac complexes referred to below are good examples of the former type, while  $\text{Cs}[\text{Y}(\text{CF}_3\text{COCHCOCF}_3)_4]$  typifies the latter. On the basis of ligand-ligand repulsions the cubic arrangement is expected to be much less favoured in discrete complexes, but, nonetheless, the complex  $[\text{La}(\text{bipyO}_2)_4]\text{ClO}_4$ , in which  $\text{bipyO}_2$  is 2,2'-bipyridine dioxide, has been shown to be very nearly cubic.



The gradation of properties within this group is also illustrated by the oxalates and  $\beta$ -diketonates

which are formed. On addition of alkali-metal oxalate to aqueous solutions of  $\text{M}^{\text{III}}$ , oxalate precipitates form but their solubilities in an excess of the alkali-metal oxalate decrease very markedly down the group. Scandium oxalate dissolves readily with evidence of such anionic species as  $[\text{Sc}(\text{C}_2\text{O}_4)_2]^-$ . Yttrium oxalate also dissolves to some extent but lanthanum oxalate dissolves only slightly. All three elements form acetylacetonates: that of scandium is usually anhydrous,  $[\text{Sc}(\text{acac})_3]$ , and presumably pseudo-octahedral:  $[\text{Y}(\text{acac})_3(\text{H}_2\text{O})]$  is 7-coordinate with a capped trigonal prismatic structure (p. 916);  $[\text{Y}(\text{acac})_3(\text{H}_2\text{O})_2] \cdot \text{H}_2\text{O}$  and  $[\text{La}(\text{acac})_3(\text{H}_2\text{O})_2]$  are 8-coordinate with distorted square-antiprismatic structures (p. 917); the scandium compound can be sublimed without decomposition whereas the yttrium and lanthanum compounds decompose at about  $500^\circ\text{C}$  and dehydration without decomposition or polymerization is difficult.

The alkoxides and aryloxides, particularly of yttrium have excited recent interest.<sup>(17)</sup> This is because of their potential use in the production of electronic and ceramic materials,<sup>(18)</sup> in particular high temperature superconductors, by the deposition of pure oxides (metallo-organic chemical vapour deposition, MOCVD). They are moisture sensitive but mostly polymeric and involatile and so attempts have been made to inhibit polymerization and produce the required volatility by using bulky alkoxide ligands.  $\text{M}(\text{OR})_3$ ,  $\text{R} = 2,6$ -di-*tert*-butyl-4-methylphenoxide, are indeed 3-coordinate (pyramidal) monomers but still not sufficiently volatile. More success has been achieved with fluorinated alkoxides, prepared by reacting the parent alcohols with the metal tris-(bis-trimethylsilylamides):



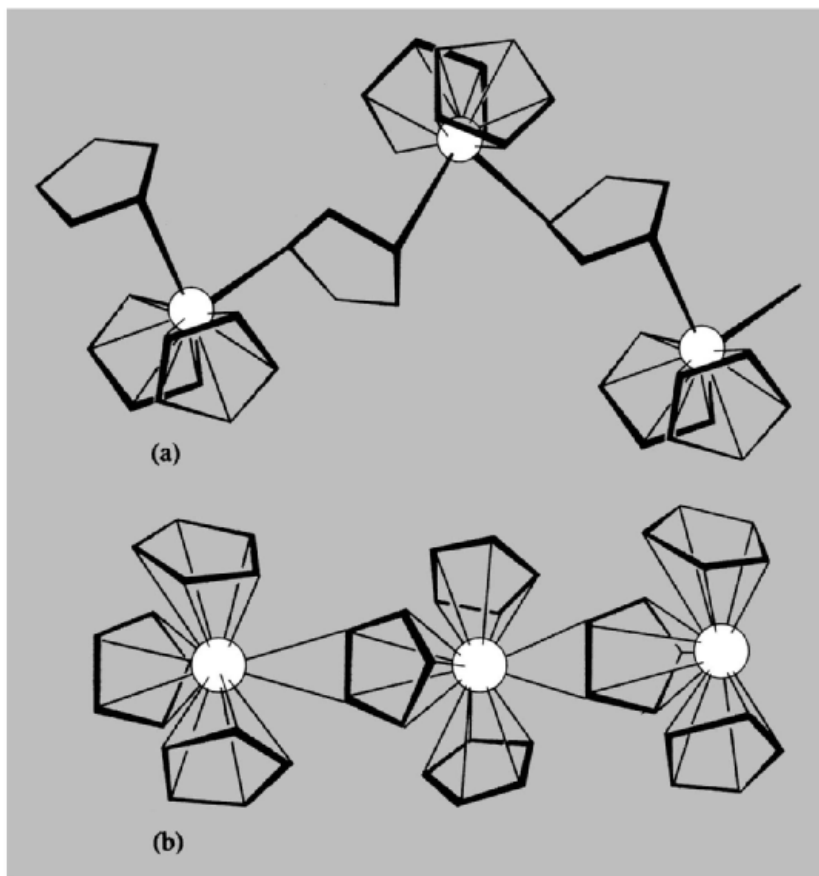
The Y and La compounds, though polymeric, are surprisingly volatile but, using

<sup>15</sup> G. MEYER, p. 145–58 in ref. 6.

<sup>16</sup> M. D. GRILLONE, F. BENETOLLO and G. BOMBIERI *Polyhedron* **10**, 2171–7 (1991).

<sup>17</sup> R. C. MEHROTRA, A. SINGH and U. M. TRIPATHI, *Chem. Revs.* **91**, 1287–303 (1991).

<sup>18</sup> D. C. BRADLEY, *Chem. Revs.* **89**, 1317–22 (1989).



**Figure 20.4** (a) The structure of  $[\text{Sc}(\text{C}_5\text{H}_5)_3]$ . (b) The structure of  $[\text{La}(\text{C}_5\text{H}_5)_3]$ . Note that the “total connectivity” of the ligands around each Sc atom is 12 as compared to 17 for the larger La.

thf as solvent, volatile octahedral monomers  $[\text{M}(\text{OR})_3(\text{thf})_3]$ ,  $\text{M} = \text{Y}, \text{La}$ , are obtained.<sup>(19)</sup> With 2,6-diphenylphenolate ligands the coordination number 5 is stabilized in the distorted trigonal-bipyramidal  $[\text{La}(\text{Odpp})_3(\text{thf})_2](\text{thf})$ .<sup>(20)</sup>

EDTA complexes of La and the lanthanides are known.  $\text{K}[\text{La}(\text{edta})(\text{H}_2\text{O})_3] \cdot 5\text{H}_2\text{O}$  is a 9-coordinate complex but steric constraints imposed by the edta produce deviations from a tricapped trigonal prismatic structure.  $[\text{La}(\text{edtaH})$

$(\text{H}_2\text{O})_4] \cdot 3\text{H}_2\text{O}$  is 10-coordinate and its structure is probably best regarded as being based on the same structure but with an extra water “squeezed” between the three coordinated water molecules.

The highest coordination numbers of all are attained with the aid of chelating ligands, such as  $\text{SO}_4^{2-}$  and  $\text{NO}_3^-$ , with very small “bites” (p. 917). In  $\text{La}_2(\text{SO}_4)_3 \cdot 9\text{H}_2\text{O}$  there are actually two types of  $\text{La}^{\text{III}}$ , one being coordinated to 12 oxygens in  $\text{SO}_4^{2-}$  ions while the other is coordinated to 6 water molecules and 3 oxygens in  $\text{SO}_4^{2-}$  ions. In  $[\text{Y}(\text{NO}_3)_5]^{2-}$  the  $\text{Y}^{\text{III}}$  is 10-coordinate and in  $[\text{Sc}(\text{NO}_3)_5]^{2-}$ , even though one of the nitrate ions is only unidentate (p. 469), the coordination number of 9 is extraordinarily high for scandium.

<sup>19</sup> D. C. BRADLEY, H. CHUDZYNSKA, M. E. HAMMOND, M. B. HURSTHOLISE, M. MOTEVALLI and W. RUOWEN, *Polyhedron* **11**, 375–9 (1992).

<sup>20</sup> G. B. DEACON, B. M. GATEHOUSE, Q. SHEN, G. N. WARD and E. R. T. TIEKINK, *Polyhedron* **12**, 1289–94 (1993).

The low symmetries of many of the above highly coordinated species, which appear to be determined largely by the stereochemical requirements of the ligands, together with the fact that these high coordination numbers are attained almost exclusively with oxygen-donor ligands, are consistent with the belief that the bonding is essentially of an electrostatic rather than a directional covalent character.

### 20.3.3 Organometallic compounds<sup>(2,21,22)</sup>

In view of the electronic structures of the elements of this group, little interaction with  $\pi$ -acceptor ligands is to be expected, though cocondensation of metal vapours with an excess of the bulky ligand, 1,3,5-tri-*tert*-butylbenzene at 77 K yields the unstable sandwich compounds  $[M(\eta^6\text{-Bu}_3\text{C}_6\text{H}_3)_2]$ ,  $M = \text{Sc, Y}$  which are the first examples of these metals in oxidation state zero.<sup>(23)</sup> The organometallic chemistry of this group, as of the lanthanides, is instead dominated by compounds involving cyclopentadiene and its methyl-substituted derivatives.<sup>(23)</sup> Though many

are thermally stable, they are invariably sensitive to moisture and oxygen. The first to be prepared were the ionic cyclopentadienides,  $M(\text{C}_5\text{H}_5)_3$ , formed by the reactions of anhydrous  $\text{MCl}_3$  with  $\text{NaC}_5\text{H}_5$  in tetrahydrofuran and purified by vacuum sublimation at 200–250°C. The solids are polymeric,  $[\text{Sc}(\text{C}_5\text{H}_5)_3]$  being made up of zig-zag chains of  $\{\text{Sc}(\eta^5\text{-C}_5\text{H}_5)_2\}$  groups joined by  $\eta^1:\eta^1\text{-C}_5\text{H}_5$  bridges,<sup>(24)</sup> (Fig. 20.4a), whereas in the lanthanum analogue the zig-zag chains of  $\{\text{La}(\eta^5\text{-C}_5\text{H}_5)_2\}$  groups are joined by  $\eta^5:\eta^2\text{-C}_5\text{H}_5$  bridges<sup>(25)</sup> (Fig. 20.4b). They are reactive compounds and form “tetrahedral” monomers,  $[\text{M}(\text{C}_5\text{H}_5)_3\text{L}]$  with neutral ligands such as ammonia and phosphines.

The  $\text{M}(\text{C}_5\text{H}_5)_2\text{Cl}$  compounds, which are actually Cl-bridged dimers,  $[(\text{C}_5\text{H}_5)\text{M}(\mu\text{-Cl})_2\text{M}(\text{C}_5\text{H}_5)]$ , provide an extensive substitution chemistry in which  $\mu\text{-Cl}$  can be replaced by a variety of ligands including H, CN,  $\text{NH}_2$ , MeO and alkyl groups.

Monomeric alkyl compounds of the form  $\text{MR}_3$  have also been obtained for Sc and Y, where the alkyl groups are of the types  $\text{Me}_3\text{SiCH}_2$  and  $\text{Me}_3\text{CCH}_2$  which are bulky and contain no  $\beta$  hydrogen atoms (p. 926).

<sup>21</sup> T. J. MARKS and R. D. ERNST, Chap 21 in *Comprehensive Organometallic Chemistry*, Vol. 3, pp. 173–270, Pergamon Press, Oxford, 1982.

<sup>22</sup> M. N. BOCHKAREV, L. N. ZAKHAROV and G. S. KALININA, *Organoderivatives of Rare Earth Elements*, Kluwer Academic Publishers, Dordrecht, 1995, 532 pp.

<sup>23</sup> F. G. N. CLOKE, K. KHAN and R. N. PERUTZ, *J. Chem. Soc., Chem. Commun.*, 1372–3 (1991).

<sup>24</sup> J. L. ATWOOD and K. D. SMITH, *J. Am. Chem. Soc.* **95**, 1488–91 (1973).

<sup>25</sup> S. H. EGGERS, J. KOPF and R. D. FISCHER, *Organometallics* **5**, 383–5 (1986).

																1	2																																						
																H	He																																						
3	4											5	6	7	8	9	10																																						
Li	Be											B	C	N	O	F	Ne																																						
11	12											13	14	15	16	17	18																																						
Na	Mg											Al	Si	P	S	Cl	Ar																																						
19	20	21	22	23	24	25	26	27	28	29	30	31	32	33	34	35	36																																						
K	Ca	Sc	Ti	V	Cr	Mn	Fe	Co	Ni	Cu	Zn	Ga	Ge	As	Se	Br	Kr																																						
37	38	39	40	41	42	43	44	45	46	47	48	49	50	51	52	53	54																																						
Rb	Sr	Y	Zr	Nb	Mo	Tc	Ru	Rh	Pd	Ag	Cd	In	Sn	Sb	Te	I	Xe																																						
55	56	57	58	59	60	61	62	63	64	65	66	67	68	69	70	71	72	73	74	75	76	77	78	79	80	81	82	83	84	85	86																								
Cs	Ba	La	Hf	Ta	W	Re	Os	Ir	Pt	Au	Hg	Tl	Pb	Bi	Po	At	Rn																																						
87	88	89	90	91	92	93	94	95	96	97	98	99	100	101	102	103	104																																						
Fr	Ra	Ac	Rf	Db	Sg	Bh	Hs	Mt	Uun	Uuu	Uub																																												
																		89	90	91	92	93	94	95	96	97	98	99	100	101	102	103	104	105	106	107	108	109	110	111	112	113	114	115	116	117	118	119	120						
																		Ce	Pr	Nd	Pm	Sm	Eu	Gd	Tb	Dy	Ho	Er	Tm	Yb	Lu																								
																		Th	Pa	U	Np	Pu	Am	Cm	Bk	Cf	Es	Fm	Md	No	Lr																								

# 21

## Titanium, Zirconium and Hafnium

### 21.1 Introduction

In 1791 William Gregor, a Cornish vicar and amateur chemist, examined sand from the local river Helford. Using a magnet he extracted a black material (now called ilmenite) from which he removed iron by treatment with hydrochloric acid. The residue, which dissolved only with difficulty in concentrated sulfuric acid, was the impure oxide of a new element, and Gregor proceeded to discover the reactions which were to form the basis of the production of virtually all  $\text{TiO}_2$  up to about 1960. Four years later the German chemist M. H. Klaproth independently discovered the same oxide (or “earth”), in a sample of ore now known to be rutile, and named the element titanium after the Titans who, in Greek mythology, were the children of Heaven and Earth condemned to live amongst the hidden fires of the earth. Klaproth had previously (1789) isolated the oxide of zirconium from a sample of zircon,  $\text{ZrSiO}_4$ . Various forms of zircon (Arabic *zargun*) have been known as gemstones since ancient times. Impure samples of the two metals were prepared by J. J. Berzelius (Sweden) in 1824 (Zr) and 1825 (Ti) but samples

of high purity were not obtained until much later. M. A. Hunter (USA) reduced  $\text{TiCl}_4$  with sodium in 1910 to obtain titanium, and A. E. van Arkel and J. H. de Boer (Netherlands) produced zirconium in 1925 by their iodide-decomposition process (see below).

The discovery of hafnium was one of chemistry’s more controversial episodes<sup>(1)</sup>. In 1911 G. Urbain, the French chemist and authority on “rare earths”, claimed to have isolated the element of atomic number 72 from a sample of rare-earth residues, and named it celtium. With hindsight, and more especially with an understanding of the consequences of H. G. J. Moseley’s and N. Bohr’s work on atomic structure, it now seems very unlikely that element 72 could have been found in the necessary concentrations along with rare earths. But this knowledge was lacking in the early part of the century and, indeed, in 1922 Urbain and A. Dauvillier claimed to have X-ray evidence to support the discovery. However, by that time Niels Bohr had developed his atomic theory and so was confident that element 72 would be a

<sup>1</sup> R. T. ALLSOP, *Educ. Chem.* **10**, 222–3 (1973).

member of Group 4 and was more likely to be found along with zirconium than with the rare earths. Working in Bohr's laboratory in Copenhagen in 1922/3, D. Coster (Netherlands) and G. von Hevesy (Hungary) used Moseley's method of X-ray spectroscopic analysis to show that element 72 was present in Norwegian zircon, and it was named hafnium (*Hafnia*, Latin name for Copenhagen). The separation of hafnium from zirconium was then effected by repeated recrystallizations of the complex fluorides and hafnium metal was obtained by reduction with sodium. For rutherfordium ( $Z = 104$ ) see pp. 1280–82.

## 21.2 The Elements<sup>(2)</sup>

### 21.2.1 Terrestrial abundance and distribution

Titanium, which comprises 0.63% (i.e. 6320 ppm) of the earth's crustal rocks, is a very abundant element (ninth of all elements, second of the transition elements), and, of the transition elements, only Fe, Ti and Mn are more abundant than zirconium (0.016%, 162 ppm). Even hafnium (2.8 ppm) is as common as Cs and Br.

That these elements have in the past been considered unfamiliar has been due largely to the difficulties involved in preparing the pure metals and also to their rather diffuse occurrence. Like their predecessors in Group 3, they are classified as type-a metals and are found as silicates and oxides in many siliceous materials. These are frequently resistant to weathering and so often accumulate in beach deposits which can be profitably exploited.

The two most important minerals of titanium are ilmenite ( $\text{FeTiO}_3$ ) and rutile ( $\text{TiO}_2$ ). The former is a black sandy material mined in Canada, the USA, Australia, Scandinavia and Malaysia, while the latter is mined principally in Australia. Zirconium's main minerals are zircon ( $\text{ZrSiO}_4$ )

and baddeleyite ( $\text{ZrO}_2$ ) mined mainly in Australia, the Republic of S. Africa, USA and the former USSR and invariably containing hafnium, most commonly in quantities around 2% of the zirconium content. Only in a few minerals, such as alvite,  $\text{MSiO}_4 \cdot x\text{H}_2\text{O}$  ( $M = \text{Hf, Th, Zr}$ ), does the hafnium content occasionally exceed that of zirconium. As a result of the lanthanide contraction (p. 1232) the ionic radii of Zr and Hf are virtually identical and their association in nature parallels their very close chemical similarity.

### 21.2.2 Preparation and uses of the metals<sup>(3)</sup>

Viable methods of producing the metals from oxide ores have to surmount two problems. In the first place, reduction with carbon is not possible because of the formation of intractable carbides (p. 299), and even reduction with Na, Ca or Mg is unlikely to remove all the oxygen. In addition, the metals are extremely reactive at high temperatures and, unless prepared in the absence of air, will certainly be contaminated with oxygen and nitrogen.

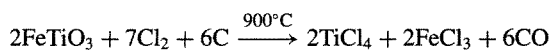
In 1932 Wilhelm Kroll of Luxembourg produced titanium by reducing  $\text{TiCl}_4$  with calcium and then later (1940) with magnesium and even sodium. The expense of this process was a severe deterrent to any commercial use of titanium. However, the metal has a very low density (~57% that of steel) combined with good mechanical strength and, in fact, when alloyed with small quantities of such metals as Al and Sn, has the highest strength:weight ratio of any of the engineering metals. Accordingly, about 1950, a demand developed for titanium for the manufacture of gas-turbine engines, and this demand has rapidly increased as production and fabrication problems have been overcome. Its major uses are still in the aircraft industry

<sup>2</sup> R. J. H. CLARK, Chap. 32, pp. 355–417, and D. C. BRADLEY and P. THORNTON, Chap. 33, pp. 419–90, in *Comprehensive Inorganic Chemistry*, Vol. 3, Pergamon Press, Oxford, 1973.

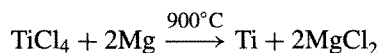
<sup>3</sup> Kirk–Othmer *Encyclopedia of Chemical Technology*, 4th edn. Interscience. New York. For Ti, See Vol. 24, 1997, pp. 186–349; for Zr, See Vol. 25, 1998, pp. 853–96; for Hf, See Vol. 12, 1994, pp. 861–81.



for the production of both engines and airframes, but it is also widely used in chemical processing and marine equipment. Current world production capacity is estimated to exceed 120 000 tonnes pa though actual production is less than this. The Kroll method still dominates the industry: in this ilmenite or rutile is heated with chlorine and carbon, e.g.:



The  $\text{TiCl}_4$  is fractionally distilled from  $\text{FeCl}_3$  and other impurities and then reduced with molten magnesium in a sealed furnace under Ar,



Molten  $\text{MgCl}_2$  is tapped off periodically and, after cooling, residual  $\text{MgCl}_2$  and any excess of magnesium are removed by leaching with water and dilute hydrochloric acid or by distillation, leaving titanium "sponge" which, after grinding and cleaning with aqua regia (1:3 mixture of concentrated nitric and hydrochloric acids), is melted under argon or vacuum and cast into ingots. The use of sodium instead of magnesium requires little change in the basic process but gives a more readily leached product. This yields titanium metal in a granular form which is fabricated by somewhat different techniques and has been preferred by some users.

Zirconium, too, is produced commercially by the Kroll process, but the van Arkel-de Boer process is also useful when it is especially important to remove all oxygen and nitrogen. In this latter method the crude zirconium is heated in an evacuated vessel with a little iodine, to a temperature of about  $200^\circ\text{C}$  when  $\text{ZrI}_4$  volatilizes. A tungsten or zirconium filament is simultaneously electrically heated to about  $1300^\circ\text{C}$ . This decomposes the  $\text{ZrI}_4$  and pure zirconium is deposited on the filament. As the deposit grows the current is steadily increased so as to maintain the temperatures. The method is applicable to many metals by judicious adjustment of the temperatures. Zirconium has a high corrosion resistance and in certain chemical plants is preferred to alternatives such as stainless

steel, titanium and tantalum. It is also used in a variety of alloy steels and, when added to niobium, forms a superconducting alloy which retains its superconductivity in strong magnetic fields. The small percentage of hafnium normally present in zirconium is of no detriment in these cases and may even improve its properties, but a further important use for zirconium is as a cladding for uranium dioxide fuel rods in water-cooled nuclear reactors. When alloyed with  $\sim 1.5\%$  tin, its corrosion resistance and mechanical properties, which are stable under irradiation, coupled with its extremely low absorption of "thermal" neutrons, make it an ideal material for this purpose. Unfortunately, hafnium is a powerful absorber of thermal neutrons (600 times more so than Zr) and its removal, though difficult, is therefore necessary. Solvent extraction methods, taking advantage of the different solubilities of, for instance, the two nitrates in tri-*n*-butyl phosphate or the thiocyanates in hexone (methyl isobutyl ketone) have been developed and reduce the hafnium content to less than 100 ppm. The neutron absorbing ability of hafnium is not always disadvantageous, however, since it is the reason for hafnium's use for reactor control rods in nuclear submarines. Hafnium is produced in the same ways as zirconium but on a much smaller scale. For rutherfordium see p. 1281.

### 21.2.3 Properties of the elements

Table 21.1 summarizes a number of properties of these elements. The difficulties in attaining high purity has led to frequent revision of the estimates of several of these properties. Each element has a number of naturally occurring isotopes and, in the case of zirconium and hafnium, the least abundant of these is radioactive, though with a very long half-life ( $^{96}_{40}\text{Zr}$ , 2.76%,  $3.6 \times 10^{17}$  y;  $^{174}_{72}\text{Hf}$ , 0.162%,  $2.0 \times 10^{15}$  y).

The elements are all lustrous, silvery metals with high mps and they have typically metallic hcp structures which transform to bcc at high temperatures ( $882^\circ$ ,  $870^\circ$  and  $1760^\circ\text{C}$  for Ti, Zr and Hf). They are better conductors of

Table 21.1 Some properties of Group 4 elements

Property	Ti	Zr	Hf
Atomic number	22	40	72
Number of naturally occurring isotopes	5	5	6
Atomic weight	47.867(1)	91.224(2)	178.49(2)
Electronic configuration	[Ar]3d <sup>2</sup> 4s <sup>2</sup>	[Kr]4d <sup>2</sup> 5s <sup>2</sup>	[Xe]4f <sup>14</sup> 5d <sup>2</sup> 6s <sup>2</sup>
Electronegativity	1.5	1.4	1.3
Metal radius/pm	147	160	159
Ionic radius (6-coordinate)/pm	M(IV) 60.5 M(III) 67.0 M(II) 86	72 — —	71 — —
MP/°C	1667	1857	2222 (or 2467)
BP/°C	3285	4200	4450
$\Delta H_{\text{fus}}/\text{kJ mol}^{-1}$	18.8	19.2	(25)
$\Delta H_{\text{vap}}/\text{kJ mol}^{-1}$	425 ( $\pm 11$ )	567	571 ( $\pm 25$ )
$\Delta H_{\text{f}}(\text{monatomic gas})/\text{kJ mol}^{-1}$	469 ( $\pm 4$ )	612 ( $\pm 11$ )	611 ( $\pm 17$ )
Density (25°C)/g cm <sup>-3</sup>	4.50	6.51	13.28
Electrical resistivity (20°C)/ $\mu\text{ohm cm}$	42.0	40.0	35.1

heat and electricity than their predecessors in Group 3 but are not to be regarded as “good” conductors in comparison with most other metals. The enthalpies of fusion, vaporization and atomization have also increased, indicating that the additional d electron has in each case contributed to stronger metal bonding. As was noticed in comparing groups 3 and 13, similarly for groups 4 and 14, the d electrons of the first group contribute more effectively to the metal–metal bonding in the bulk materials than do the p electrons of the heavier members of the latter group (Ge, Sn, Pb). Figure 21.1 illustrates the consequent discontinuous increases in mp, bp and enthalpy of atomization in passing from C

and Si to Ti, Zr and Hf, rather than to Ge, Sn and Pb.

The mechanical properties of these metals are markedly affected by traces of impurities such as O, N and C which have an embrittling effect on the metals, making them difficult to fabricate.

The effect of the lanthanide contraction on the metal and ionic radii of hafnium has already been mentioned. That these radii are virtually identical for zirconium and hafnium has the result that the ratio of their densities, like that of their atomic weights, is very close to Zr:Hf = 1:2.0. Indeed, the densities, the transition temperatures and the neutron-absorbing abilities are the only common properties of these two elements which differ

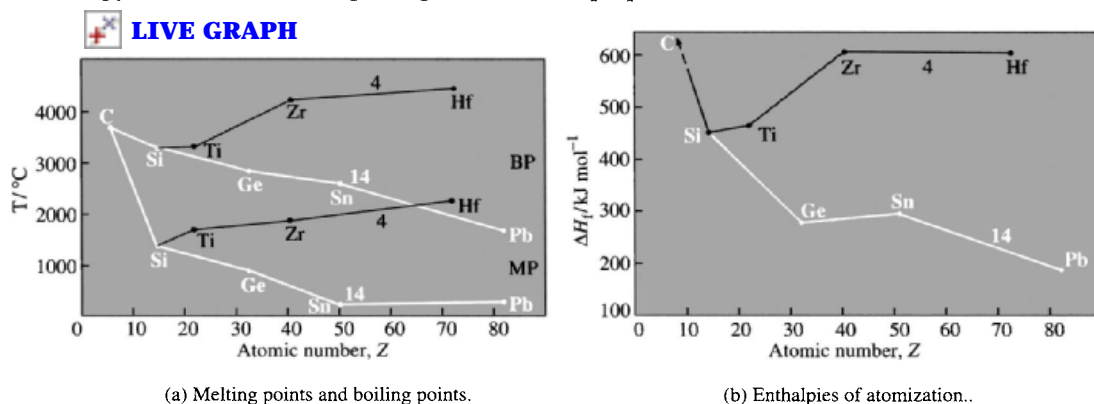


Figure 21.1 Trends in some properties of elements of Groups 4 and 14.

significantly. This close similarity of second and third members is noticeable in all subsequent groups of the transition elements but is never more pronounced than here.

### 21.2.4 Chemical reactivity and trends

The elements of this group are relatively electropositive but less so than those of Group 3. If heated to high temperatures they react directly with most non-metals, particularly oxygen, hydrogen (reversibly), and, in the case of titanium, nitrogen (Ti actually burns in  $N_2$ ). When finely divided the metals are pyrophoric and for this reason care is necessary when machining them to avoid the production of fine waste chips. In spite of this inherent reactivity, the most noticeable feature of these metals in the massive form at room temperature is their outstanding resistance to corrosion, which is due to the formation of a dense, adherent, self-healing oxide film. This is particularly striking in the case of zirconium. With the exception of hydrofluoric acid (which is the best solvent, probably because of the formation of soluble fluoro complexes) mineral acids have little effect unless hot. Even when hot, aqueous alkalis do not attack the metals. The presence of oxidizing agents such as nitric acid frequently reduces the reactivity of the metals by ensuring the retention of the protective oxide film.

The chemistry of hafnium has not received the same attention as that of titanium or zirconium, but it is clear that its behaviour follows that of zirconium very closely indeed with only minor differences in such properties as solubility and volatility being apparent in most of their compounds. The most important oxidation state in the chemistry of these elements is the group oxidation state of +4. This is too high to be ionic, but zirconium and hafnium, being larger, have oxides which are more basic than that of titanium and give rise to a more extensive and less-hydrolysed aqueous chemistry. In this oxidation state, particularly in the case of the dioxide and tetrachloride, titanium shows many similarities with tin which is of much the same size. A large

number of coordination compounds of the  $M^{IV}$  metals have been studied<sup>(4)</sup> and complexes such as  $[MF_6]^{2-}$  and those with *O*- or *N*- donor ligands are especially stable.

The  $M^{IV}$  ions, though much smaller than their triply charged predecessors in Group 3, are, nonetheless, sufficiently large, bearing in mind their high charge, to attain a coordination number of 8 or more, which is certainly higher than is usually found for most transition elements. Eight is not a common coordination number for the first member, titanium, but is very well known for zirconium and hafnium, and the spherical symmetry of the  $d^0$  configuration allows a variety of stereochemistries.

Lower oxidation states are rather sparsely represented for Zr and Hf. Even for Ti they are readily oxidized to +4 but they are undoubtedly well defined and, whatever arguments may be advanced against applying the description to Sc, there is no doubt that Ti is a "transition metal". In aqueous solution  $Ti^{III}$  can be prepared by reduction of  $Ti^{IV}$ , either with Zn and dilute acid or electrolytically, and it exists in dilute acids as the violet, octahedral  $[Ti(H_2O)_6]^{3+}$  ion (p. 970). Although this is subject to a certain amount of hydrolysis, normal salts such as halides and sulfates can be separated.  $Zr^{III}$  and  $Hf^{III}$  are known mainly as the trihalides or their derivatives and have no aqueous chemistry since they reduce water. Table 21.2 (p. 960) gives the oxidation states and stereochemistries found in the complexes of Ti, Zr and Hf along with illustrative examples. (See also pp. 1281–2.)

$M-C$   $\sigma$  bonds are not strong and, as might be expected for metals with so few *d* electrons, little help is available from synergic  $\pi$  bonding: for instance, of the simple carbonyls only  $Ti(CO)_6$  has been reported, and that only on the basis of spectroscopic evidence. However, as will be seen on p. 972, the discovery that titanium compounds can be used to

<sup>4</sup> C. H. McAULIFFE and D. S. BARRATT, Chap. 31, pp. 323–61, and R. J. FAY, Chap. 32, pp. 363–451, in *Comprehensive Coordination Chemistry*, Vol. 3, Pergamon Press, Oxford, 1987.

### Titanium Dioxide as a Pigment (See page 961)

Of all white pigments, TiO<sub>2</sub> is now the most widely used: the impressive growth in demand is shown in Table A:<sup>(5)</sup>

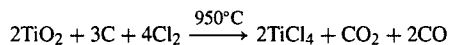
**Table A** Annual world production of TiO<sub>2</sub>

Year	1925	1937	1975	1993
TiO <sub>2</sub> /tonnes	5000	100 000	2 000 000	3 730 000

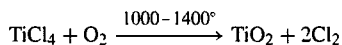
Its major use is in the manufacture of paint, and other important uses are as a surface coating on paper and as a filler in rubber and plastics.

The value of TiO<sub>2</sub> as a pigment is due to its exceptionally high refractive index in the visible region of the spectrum. Thus although large crystals are transparent, fine particles scatter light so strongly that they can be used to produce films of high opacity<sup>†</sup>. Table B gives the refractive indices of a number of relevant materials. In the manufacture of TiO<sub>2</sub> either the anatase or the rutile form is produced depending on modifications in the process employed. Because of its slightly higher refractive index, rutile has a somewhat greater opacity and most of the TiO<sub>2</sub> currently produced is of this form.

In addition to these optical properties, TiO<sub>2</sub> is chemically inert which is why it displaced "white lead", 2PbCO<sub>3</sub>.Pb(OH)<sub>2</sub>; in industrial atmospheres this formed PbS (black) during the production of or weathering of the paint and was also a toxic hazard. Unfortunately the naturally occurring forms of TiO<sub>2</sub> are invariably coloured, sometimes intensely, by impurities, and expensive processing is required to produce pigments of acceptable quality. The two main processes in use are the *sulfate process* and the *chloride process* (Fig. A, p. 960), which account for approximately 56% and 44% respectively of total world production. The principal reactions of the chloride process are:



and



It is most economical when high-grade ores are used, becoming less economical with poorer feed materials containing iron, because of the production of chloride wastes from which the chlorine cannot be recovered. By contrast the sulfate process cannot make use of rutile which does not dissolve in sulfuric acid, but is able to operate on lower grade ores. However, the capital cost of plant for the sulfate process is higher, and disposal of waste has proved environmentally more difficult, so that most new plant is designed for the chloride process.

The physical properties of the base pigments produced from both processes are further improved by slurring in water and selectively precipitating on the finely divided particles a surface coating of SiO<sub>2</sub>, Al<sub>2</sub>O<sub>3</sub>, or TiO<sub>2</sub> itself.

**Table B** Refractive indices of some pigments and other materials

Substance	Refractive index	Substance	Refractive index	Substance	Refractive index
NaCl	1.54	BaSO <sub>4</sub>	1.64–1.65	Diamond	2.42
CaCO <sub>3</sub>	1.53–1.68	ZnO	2.0	TiO <sub>2</sub> (anatase)	2.49–2.55
SiO <sub>2</sub>	1.54–1.56	ZnS	2.36–2.38	TiO <sub>2</sub> (rutile)	2.61–2.90

*Panel continues*

<sup>5</sup>R. S. DARBY and J. LEIGHTON, in *The Modern Inorganic Chemicals Industry*, pp. 354–74, Special Publication No. 31, (1977), The Chemical Society, London. *Metals and Minerals Ann. Rev.*, 75–6 (1992).

<sup>†</sup>The smaller the particle size, the lower the wavelength at which maximum scattering occurs. Thus, ultrafine (20–50 nm) TiO<sub>2</sub> is used as a UV filter in skin care and cosmetic products. (Sec V. P. S. JUDIN, *Chem. Br.* **29**, 503–5 (1993).)

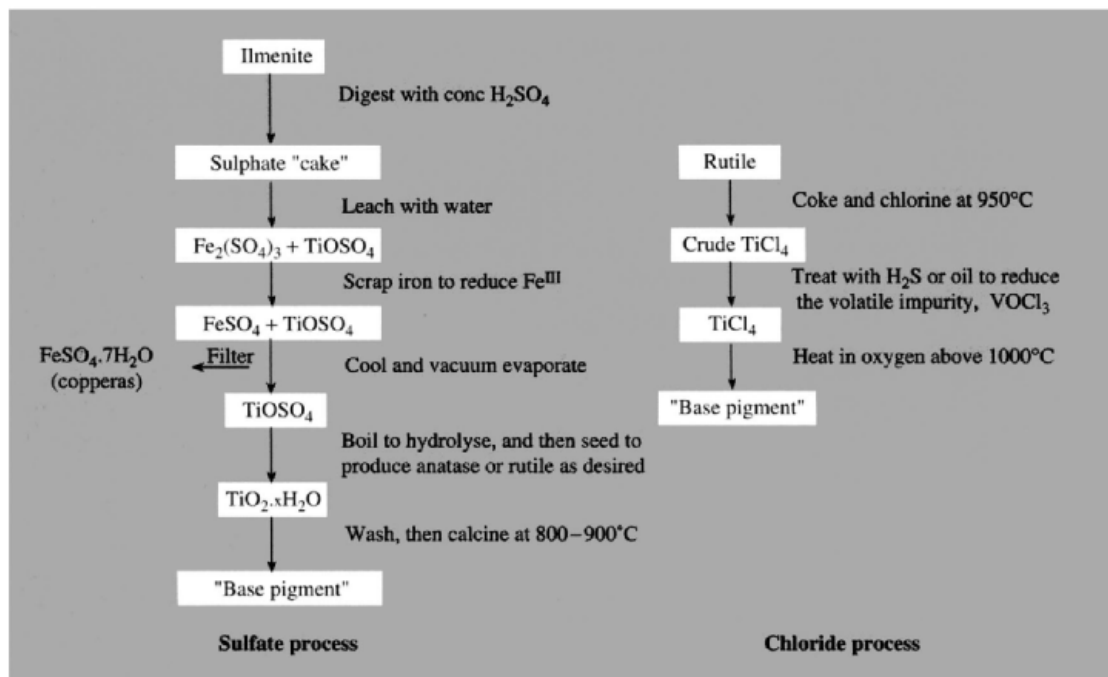
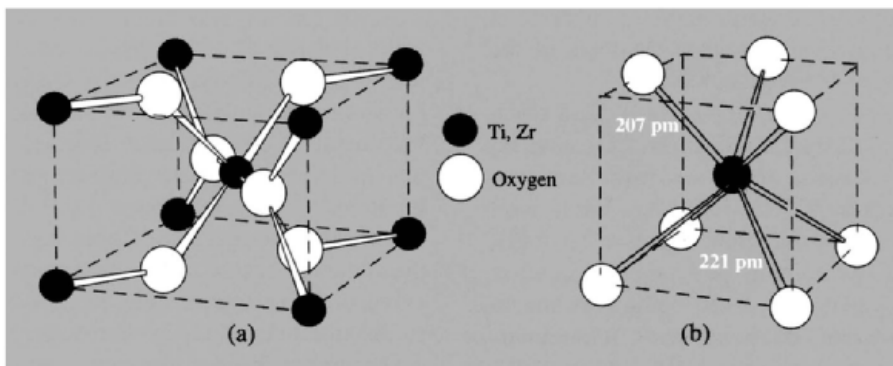


Figure A Flow diagrams for the manufacture of  $\text{TiO}_2$  pigments.

Table 21.2 Oxidation states and stereochemistries of titanium, zirconium and hafnium

Oxidation state	Coordination number	Stereochemistry	Ti	Zr/Hf
-1 ( $d^5$ )	6	Octahedral	$[\text{Ti}(\text{bipy})_3]^-$	$[\text{Zr}(\text{bipy})_3]^-$
0 ( $d^4$ )	6	Octahedral	$[\text{Ti}(\text{bipy})_3]$	$[\text{Zr}(\text{bipy})_3]$
2 ( $d^2$ )	6	Octahedral	$\text{TiCl}_2$	Layer structures and clusters
	12	—	$[\text{Ti}(\eta^5\text{-C}_5\text{H}_5)_2(\text{CO})_2]$	$[\text{M}(\eta^5\text{-C}_5\text{H}_5)_2(\text{CO})_2]$
3 ( $d^1$ )	3	Planar	$[\text{Ti}\{\text{N}(\text{SiMe}_3)_2\}_3]$	
	5	Trigonal bipyramidal	$[\text{TiBr}_3(\text{NMe}_3)_2]$	
	6	Octahedral	$[\text{Ti}(\text{urea})_6]^{3+}$	$\text{ZrX}_3$ (Cl, Br, I), $\text{HfI}_3$
4 ( $d^0$ )	4	Tetrahedral	$\text{TiCl}_4$	$\text{ZrCl}_4(\text{g})$ (solid is octahedral)
	5	Trigonal bipyramidal	$[\text{TiOCl}_2(\text{NMe}_3)_2]$	—
		Square pyramidal	$[\text{TiOCl}_4]^{2-}$	—
	6	Octahedral	$[\text{TiF}_6]^{2-}$	$[\text{ZrF}_6]^{2-}$ , $\text{ZrCl}_4(\text{s})$
	7	Pentagonal bipyramidal	$[\text{TiCl}(\text{S}_2\text{CNMe}_2)_3]$	$[\text{NH}_4]^+[\text{ZrF}_7]^{3-}$
		Capped trigonal prismatic	$[\text{TiF}_5(\text{O}_2)]^{3-}$	$[\text{Zr}_2\text{F}_{13}]^{5-}$
	8	Dodecahedral	$[\text{Ti}(\eta^2\text{-NO}_3)_4]$	$[\text{Zr}(\text{C}_2\text{O}_4)_4]^{4-}$
		Square antiprismatic	—	$[\text{Zr}(\text{acac})_4]$
	11	—	$[\text{Ti}(\eta^5\text{-C}_5\text{H}_5)(\text{S}_2\text{CNMe}_2)_3]$	$[\text{Zr}(\eta^5\text{-C}_5\text{H}_5)(\text{S}_2\text{CNMe}_2)_3]$
	12	—	—	$[\text{M}(\eta^3\text{-BH}_4)_4]$



**Figure 21.2** (a) The tetragonal unit cell of rutile, TiO<sub>2</sub>. (b) The coordination of Zr<sup>IV</sup> in baddeleyite ZrO<sub>2</sub>; the 3 O atoms in the upper plane are each coordinated by 3 Zr atoms in a plane, whereas the 4 lower O atoms are each tetrahedrally coordinated by 4 Zr atoms.

catalyse the polymerization of alkenes (olefins) turned organo-titanium chemistry into a topic of major commercial importance and has produced an extensive chemistry. The organometallic chemistry of Zr and Hf, though less developed than that of Ti, has grown rapidly in recent years.

## 21.3 Compounds of Titanium, Zirconium and Hafnium

The binary hydrides (p. 64), borides (p. 145), carbides (p. 299) and nitrides (p. 417) are hard, refractory, nonstoichiometric materials with metallic conductivities. They have already been discussed in relation to comparable compounds of other metals in earlier chapters.

### 21.3.1 Oxides and sulfides

The main oxides are the dioxides. In fact, TiO<sub>2</sub> is by far the most important compound formed by the elements of this group, its importance arising predominantly from its use as a white pigment (see Panel, p. 959). It exists at room temperature in three forms — rutile, anatase and brookite, each of which occurs naturally. Each contains 6-coordinate titanium but rutile is the most common form, both in nature and as produced commercially, and the others transform into it on heating. The rutile

structure is based on a slightly distorted hcp of oxygen atoms with half the octahedral interstices being occupied by titanium atoms. The octahedral coordination of the titanium atoms and trigonal planar coordination of the oxygen can be seen in Fig. 21.2. This is a structure commonly adopted by ionic dioxides and difluorides where the relative sizes of the ions are such as to favour 6-coordination (i.e. when the radius ratio of cation:anion lies in the range 0.73 to 0.41).<sup>(6)</sup> Anatase and brookite are both based on cubic rather than hexagonal close packing of oxygen atoms, but again the titanium atoms occupy half the octahedral interstices. TiO<sub>2</sub> melts at 1892 ± 30°C when heated in an atmosphere of O<sub>2</sub>; when heated in air the compound tends to lose oxygen and then melts at 1843 ± 15°C (TiO<sub>1.985</sub>).

Though it is unreactive, rutile can be reduced with difficulty to give numerous nonstoichiometric oxide phases, the more important of which are the Magnéli-type phases Ti<sub>n</sub>O<sub>2n-1</sub> (4 ≤ n ≤ 9), the lower oxides Ti<sub>3</sub>O<sub>5</sub> and Ti<sub>2</sub>O<sub>3</sub>, and the broad, nonstoichiometric phase TiO<sub>x</sub> (0.70 ≤ x ≤ 1.30). The Magnéli phases Ti<sub>n</sub>O<sub>2n-1</sub> are built up of slabs of rutile-type structure with a width of nTiO<sub>6</sub> octahedra and with adjacent slabs mutually related by a crystallographic shear which conserves oxygen atoms by an increased sharing

<sup>6</sup> A. F. WELLS, *Structural Inorganic Chemistry*, 5th edn., Chap. 7, pp. 312–19, Oxford University Press, Oxford, 1984.

between adjacent octahedra.  $\text{Ti}_4\text{O}_7$  is metallic at room temperature but the other members of the series tend to be semiconductors.

Of the lower oxides  $\text{Ti}_3\text{O}_5$  is a blue-black material prepared by the reduction  $\text{TiO}_2$  with  $\text{H}_2$  at  $900^\circ\text{C}$ ; it shows a transition from semiconductor to metal at  $175^\circ\text{C}$ .  $\text{Ti}_2\text{O}_3$  is a dark-violet material with the corundum structure (p. 243); it is prepared by reacting  $\text{TiO}_2$  and Ti metal at  $1600^\circ\text{C}$  and is generally inert, being resistant to most reagents except oxidizing acids. It has a narrow composition range ( $x = 1.49\text{--}1.51$  in  $\text{TiO}_x$ ) and undergoes a semiconductor-to-metal transition above  $\sim 200^\circ\text{C}$ .

$\text{TiO}$ , a bronze coloured, readily oxidized material, is again prepared by the reaction of  $\text{TiO}_2$  and Ti metal. It has a defect rock-salt structure which tolerates a high proportion of vacancies (Schottky defects) in both Ti and O sites and so is highly nonstoichiometric<sup>(7)</sup> with a composition range at  $1700^\circ\text{C}$  of  $\text{TiO}_{0.75}$  to  $\text{TiO}_{1.25}$ . This range diminishes somewhat at lower temperatures and, at equilibrium below about  $900^\circ\text{C}$ , various ordered phases separate with smaller ranges of composition-variation, e.g.  $\text{TiO}_{0.9}\text{--TiO}_{1.1}$  and  $\text{TiO}_{1.25}$  (i.e.  $\text{Ti}_4\text{O}_5$ ). In this latter compound the tetragonal unit cell can be thought of as being related to the NaCl-type structure: there are 10 Ti sites and 10 oxygen sites but 2 of the Ti sites are vacant in a regular or ordered way to generate the structure of  $\text{Ti}_4\text{O}_5$ . A high-temperature ( $>3000^\circ\text{C}$ ) form of  $\text{TiO}$  has been prepared with the unusual feature of  $\text{Ti}^{2+}$  in a trigonal prismatic array of oxygen atoms.<sup>(7a)</sup>

Finally, oxygen is soluble in metallic titanium up to a composition of  $\text{TiO}_{0.5}$  with the oxygen atoms occupying octahedral sites in the hcp metal lattice: distinct phases that have been crystallographically characterized are  $\text{Ti}_6\text{O}$ ,  $\text{Ti}_3\text{O}$  and  $\text{Ti}_2\text{O}$ . It seems likely that in all these reduced oxide phases there is extensive metal-metal bonding.

In the case of zirconium and hafnium there is little evidence of stable phases other than  $\text{MO}_2$ , and at room temperature  $\text{ZrO}_2$  (baddeleyite) and the isomorphous  $\text{HfO}_2$  have a structure in which the metal is 7-coordinate (Fig. 21.2(b)).  $\text{ZrO}_2$  has at least two more high-temperature modifications (tetragonal above  $1100^\circ\text{C}$  and cubic, fluorite-type, above  $2300^\circ\text{C}$ ) but it is notable that, presumably because of the greater size of Zr compared to Ti, neither of them has the 6-coordinate rutile structure.  $\text{ZrO}_2$  is unreactive, has a low coefficient of thermal expansion, and a very high melting point ( $2710 \pm 25^\circ\text{C}$ ) and is therefore a useful refractory material, being used in the manufacture of crucibles and furnace cores. However, the phase change at  $1100^\circ$  severely restricts the use of pure  $\text{ZrO}_2$  as a refractory because repeated thermal cycling through this temperature causes cracking and disintegration — the problem is avoided by using solid solutions of CaO or MgO in the  $\text{ZrO}_2$  since these retain the cubic fluorite structure throughout the temperature range.  $\text{ZrO}_2$  has also recently been produced in fibrous form suitable for weaving into fabrics, as already mentioned for  $\text{Al}_2\text{O}_3$  (p. 244), and its chemical inertness and refractivity — coupled with an apparent lack of toxicity — can be expected to lead to increasing applications as an insulator and for the filtration of corrosive liquids. Production of  $\text{ZrO}_2$  concentrates in 1991 was about 870 000 t, Australia being the most important source.

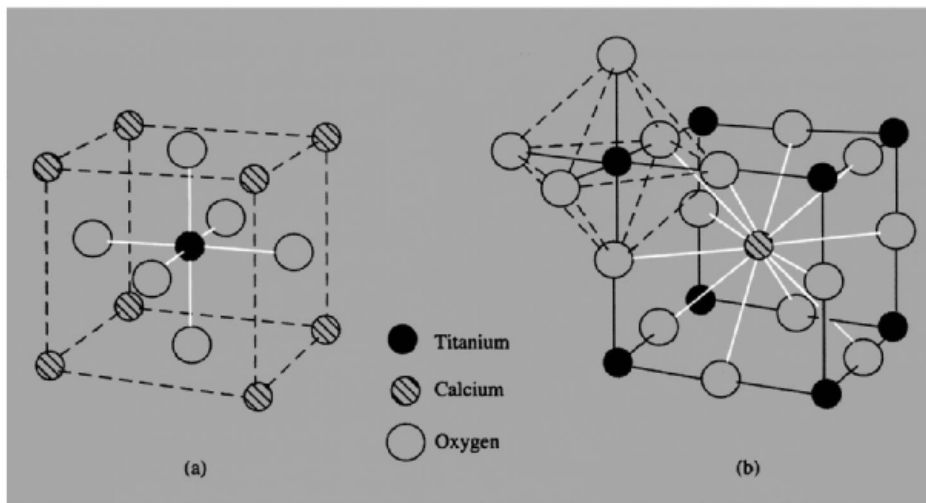
The sulfides have been less thoroughly examined than the oxides but it is clear that a number of stable phases can be produced and nonstoichiometry is again prevalent (p. 679). The most important are the disulfides, which are semiconductors with metallic lustre.  $\text{TiS}_2$  and  $\text{ZrS}_2$  have the  $\text{CdI}_2$  structure (p. 1211) in which the cations occupy the octahedral sites between alternate layers of hcp anions.

### 21.3.2 Mixed (or complex) oxides

Although the dioxides,  $\text{MO}_2$ , are notable for their inertness, particularly if they have been heated, fusion or firing at high temperatures (sometimes up to  $2500^\circ\text{C}$ ) with the stoichiometric

<sup>7</sup> D. J. M. BEVAN, Chap. 49, pp. 453–540 in *Comprehensive Inorganic Chemistry*, Vol. 3, Pergamon Press, Oxford, 1973.

<sup>7a</sup> S. MÖHR and H. MÜLLER-BUSCHBAUM, *Z. anorg. allg. Chem.* **620**, 1175–8 (1994).



**Figure 21.3** Two representations of the structure of perovskite,  $\text{CaTiO}_3$ , showing (a) the octahedral coordination of Ti, and (b) the twelve-fold coordination of Ca by oxygen. Note the relation of (b) to the cubic structure of  $\text{ReO}_3$  (p. 1047).

amounts of appropriate oxides produces a number of “titanates”, “zirconates”, and “hafnates”. The titanates are of two main types: the orthotitanates  $\text{M}_2^{\text{II}}\text{TiO}_4$  and the metatitanates  $\text{M}^{\text{II}}\text{TiO}_3$ . The names are misleading since the compounds almost never contain the discrete ions  $[\text{TiO}_4]^{4-}$  and  $[\text{TiO}_3]^{2-}$  analogous to phosphates or sulfites. Rather, the structures comprise three-dimensional networks of ions which are of particular interest and importance because two of the metatitanates are the archetypes of common mixed metal oxide structures.

When  $\text{M}^{\text{II}}$  is approximately the same size as  $\text{Ti}^{\text{IV}}$  (i.e.  $\text{M} = \text{Mg}, \text{Mn}, \text{Fe}, \text{Co}, \text{Ni}$ ) the structure is that of *ilmenite*,  $\text{FeTiO}_3$ , which consists of hcp oxygens with one-third of the octahedral interstices occupied by  $\text{M}^{\text{II}}$  and another third by  $\text{Ti}^{\text{IV}}$ . This is essentially the same structure as corundum ( $\text{Al}_2\text{O}_3$ , p. 243) except that in that case there is only one type of cation which occupies two-thirds of the octahedral sites.

If, however,  $\text{M}^{\text{II}}$  is significantly larger than  $\text{Ti}^{\text{IV}}$  (e.g.  $\text{M} = \text{Ca}, \text{Sr}, \text{Ba}$ ), then the preferred structure is that of *perovskite*,<sup>(8)</sup>  $\text{CaTiO}_3$ . This

can be envisaged as a ccp array of calcium and oxygen atoms, with the former regularly disposed, and the titanium atoms then occupying octahedral sites formed by oxygen atoms only and so being as remote as possible from the calciums (Fig. 21.3). The  $\text{Ba}^{\text{II}}$  ion is so large and expands the perovskite lattice to such an extent that the titanium is too small to fill the octahedral interstice which accommodates it. This leads to ferroelectric and piezoelectric behaviour as discussed in Chapter 3 (p. 57). In consequence,  $\text{BaTiO}_3$  has found important applications in the production of compact capacitors (because of its high permittivity) and as a ceramic transducer in devices such as microphones and gramophone pick-ups. For such purposes it compares favourably with Rochelle salt (sodium potassium tartrate,  $\text{NaKC}_4\text{H}_4\text{O}_6$ ) in terms of thermal stability, and with quartz in terms of the strength of the effect.

$\text{M}_2^{\text{II}}\text{TiO}_4$  ( $\text{M} = \text{Mg}, \text{Zn}, \text{Mn}, \text{Fe}, \text{Co}$ ) have the *spinel* structure ( $\text{MgAl}_2\text{O}_4$ , p. 248) which is the third important structure type adopted by many mixed metal oxides; in this the cations occupy both octahedral and tetrahedral sites in a ccp array of oxide ions.  $\text{Ba}_2\text{TiO}_4$ , although having the same stoichiometry, is unique amongst titanates in that

<sup>8</sup> A. RELLER and T. WILLIAMS, *Chem. Br.*, **25**, 1227–30 (1989).



it contains discrete  $[\text{TiO}_4]^{4-}$  ions which have a somewhat distorted tetrahedral structure.

High-temperature reduction of  $\text{Na}_2\text{TiO}_3$  with hydrogen produces nonstoichiometric materials,  $\text{Na}_x\text{TiO}_2$  ( $x = 0.20\text{--}0.25$ ), called titanium "bronzes" by analogy with the better-known tungsten bronzes (p. 1016). They have a blue-black, metallic appearance with high electrical conductivity and are chemically inert (even hydrofluoric acid does not attack them).

"Zirconates" and "hafnates" can be prepared by firing appropriate mixtures of oxides, carbonates or nitrates. None of them are known to contain discrete  $[\text{MO}_4]^{4-}$  or  $[\text{MO}_3]^{2-}$  ions. Compounds  $\text{M}^{\text{II}}\text{ZrO}_3$  usually have the perovskite structure whereas  $\text{M}^{\text{II}}\text{ZrO}_4$  frequently adopt the spinel structure.

### 21.3.3 Halides

The most important of these are the tetrahalides, all 12 of which are known. The titanium compounds (Table 21.3) show an interesting gradation in colour, the charge-transfer band moving steadily to lower energies (i.e. absorbing increasingly in the visible region of the spectrum) as the anion becomes more easily oxidized ( $\text{F}^-$  to  $\text{I}^-$ ) by the small, highly polarizing titanium cation. The larger  $\text{Zr}^{\text{IV}}$  and  $\text{Hf}^{\text{IV}}$ , however, do not have the same polarizing effect and their tetrahalides are all white solids; the fluorides are involatile but the other tetrahalides sublime readily at temperatures in the range  $320\text{--}430^\circ\text{C}$ .

**Table 21.3** Some physical properties of titanium tetrahalides

Compound	Colour	MP/ $^\circ\text{C}$	BP/ $^\circ\text{C}$
$\text{TiF}_4$	White	284	—
$\text{TiCl}_4$	Colourless	-24	136.5
$\text{TiBr}_4$	Orange	38	233.5
$\text{TiI}_4$	Dark brown	155	377

Though numerous preparative methods are possible besides the direct action of the halogen on the metal, convenient general procedures are as follows:

*tetrafluorides* by the action of anhydrous HF on the tetrachloride;

*tetrachlorides and tetrabromides* by passing the halogen over the heated dioxide in the presence of a reducing agent such as carbon (this reaction is central to the chloride process for manufacturing  $\text{TiO}_2$ , p. 959);

*tetraiodides* by the iodination of the dioxide with aluminium triiodide at a temperature of  $130\text{--}400^\circ$  depending on the metal ( $3\text{MO}_2 + 4\text{AlI}_3 \longrightarrow 3\text{MI}_4 + 2\text{Al}_2\text{O}_3$ ).

Not all the structures have been determined but in the vapour phase all the tetrahalides of titanium and probably all those of zirconium and hafnium have monomeric, tetrahedral structures. In the solid,  $\text{TiF}_4$  is a polymer consisting of corner-sharing  $\{\text{TiF}_6\}$  octahedra,<sup>(8a)</sup> but the other tetrahalides of titanium retain the tetrahedral configuration around the metal even in the solids. The larger zirconium exhibits higher coordination numbers. Thus solid  $\text{MF}_4$  contain 8-coordinate (square antiprismatic) metal atoms while the tetrachlorides and bromides are polymers consisting of zigzag chains of edge-sharing  $\{\text{MX}_6\}^{2-}$  octahedra.

All the tetrahalides, but especially the chlorides and bromides, behave as Lewis acids dissolving in polar solvents to give rise to series of addition compounds; they also form complex anions with halides. They are all hygroscopic and hydrolysis follows the same pattern as complex formation, with the chlorides and bromides being more vulnerable than the fluorides and iodides.  $\text{TiCl}_4$  fumes in and is completely hydrolysed by moist air ( $\text{TiCl}_4 + 2\text{H}_2\text{O} \longrightarrow \text{TiO}_2 + 4\text{HCl}$ ); a variety of intermediate hydrolysis products, such as the oxochlorides  $\text{MOCl}_2$ , can be formed with aqueous HCl of varying concentration. Even in conc HCl,  $\text{ZrCl}_4$  gives  $\text{ZrOCl}_2 \cdot 8\text{H}_2\text{O}$ . This contains the tetrameric cation  $[\text{Zr}_4(\text{OH})_8(\text{H}_2\text{O})_{16}]^{8+}$  in which the 4 zirconium atoms are connected in a ring by 4 pairs of  $\text{OH}^-$  bridges and each zirconium atom is dodecahedrally coordinated to 8 oxygen atoms. The fluorides are less susceptible

<sup>8a</sup>H. BIALOWONS, M. MÜLLER and B. G. MÜLLER, *Z. anorg. allg. Chem.* **621**, 1227-31 (1995).

to hydrolysis and, though aqueous HF produces the oxofluorides,  $\text{MOF}_2$ , the hydrates  $\text{TiF}_4 \cdot 2\text{H}_2\text{O}$ ,  $\text{MF}_4 \cdot \text{H}_2\text{O}$ , and  $\text{MF}_4 \cdot 3\text{H}_2\text{O}$  ( $\text{M} = \text{Zr}, \text{Hf}$ ) can be produced. Rather curiously the trihydrates of  $\text{ZrF}_4$  and  $\text{HfF}_4$  actually have different structures, though both contain 8-coordinated metal atoms. The zirconium compound is essentially dimeric  $[(\text{H}_2\text{O})_3\text{F}_3\text{Zr}(\mu\text{-F})_2\text{ZrF}_3(\text{H}_2\text{O})_3]$  with dodecahedral Zr, whereas the hafnium compound consists of infinite chains of octahedral  $[\text{>HfF}_2(\text{H}_2\text{O})_2(\mu\text{-F})_2]$  with the third water molecule held in the lattice.

Besides being important as an intermediate in one of the processes for making  $\text{TiO}_2$ ,  $\text{TiCl}_4$  is also used to produce Ziegler–Natta catalysts (p. 972) for the polymerization of ethylene (ethene) and is the starting point for the production of most of the commercially important organic titanium compounds (in most cases these are actually titanium alkoxides rather than true organometallic compounds). The iodides  $\text{MI}_4$  are all utilized in the van Arkel–de Boer process for producing pure metals (p. 956).

All the trihalides except  $\text{HfF}_3$  have been prepared,<sup>†</sup> the most general method being the high-temperature reduction of the tetrahalide with the metal, though a variety of other methods have been used especially for the titanium compounds. Since the tetrahalides are quite stable to reduction, lower halides are not easily prepared in a pure state, incomplete reactions and the presence of excess metal being common. Apart from  $\text{TiF}_3$ , which, as expected for a  $d^1$  ion, has a magnetic moment of 1.85 BM at room temperature, and only shows signs of magnetic interactions below about 60 K,<sup>(9)</sup> all compounds have low magnetic moments, indicative of appreciable M–M bonding. They are coloured, halogen-bridged polymers in which one third of the octahedral interstices of an hcp lattice of halide ions is occupied by metal atoms. In the cases of  $\alpha\text{-TiCl}_3$  and  $\alpha\text{-TiBr}_3$  this takes the form of the “ $\text{BiI}_3$ ” structure which is comprised of layers of edge-sharing

octahedra; the remainder adopt the “ $\beta\text{-TiCl}_3$ ” structure, comprised of chains of face-sharing octahedra.<sup>(10)</sup> In most, if not all, of the latter cases M–M bonds occur between pairs of metal atoms as a result of distortions leading, in the case of  $\text{ZrI}_3$  for instance,<sup>(11)</sup> to alternate Zr–Zr distances of 317.2 and 350.7 pm.  $\text{TiF}_3$  also differs in being stable in air unless heated whereas the others show reducing properties; indeed,  $\text{ZrX}_3$  and  $\text{HfX}_3$  reduce water and so have no aqueous chemistry, but aqueous solutions of  $\text{TiX}_3$  are stable if kept under an inert atmosphere. Hexahydrates  $\text{TiX}_3 \cdot 6\text{H}_2\text{O}$  are well known and the chloride is notable in that, like its chromium(III) analogue, it exhibits hydrate isomerism, existing as violet  $[\text{Ti}(\text{H}_2\text{O})_6]^{3+}\text{Cl}_3^-$  and green  $[\text{TiCl}_2(\text{H}_2\text{O})_4]^{+}\text{Cl}^- \cdot 2\text{H}_2\text{O}$ .

$\text{TiX}_2$  ( $\text{X} = \text{Cl}, \text{Br}, \text{I}$ ) have been prepared by reduction of  $\text{TiX}_4$  with Ti metal and are black solids with the  $\text{CdI}_2$  structure (p. 1211) but their low magnetic moments again indicate extensive M–M bonding. They are very strongly reducing and decompose water.  $\text{Ti}_7\text{X}_{16}$  ( $\text{X} = \text{Cl}, \text{Br}$ ) have also been prepared. They are black crystalline solids sensitive to hydrolysis and oxidation and can be regarded as being composed of octahedrally coordinated  $\text{Ti}^{\text{IV}}$  and  $\text{Ti}^{\text{II}}$  in the ratio of 1:6 (i.e.  $\text{TiCl}_4 \cdot 6\text{TiCl}_2$ ) with the bivalent metal ions arranged in triangular groups involving Ti–Ti bonds. Incorporation of KCl in the chloride reaction mix yields<sup>(12)</sup> the structurally related  $\text{KTi}_4\text{Cl}_{11}$  but the structural diversity of reduced Ti halides does not yet match that of Zr.

Products of the high temperature (typically 750–850°C) reduction of  $\text{ZrX}_4$  ( $\text{X} = \text{Cl}, \text{Br}, \text{I}$ ) with Zr metal in various proportions, have provided intriguing structural problems. Black phases initially thought to be  $\text{ZrX}_2$  and made up of  $\text{Zr}_6\text{X}_{12}$  clusters, isostructural with the well-known  $[\text{M}_6\text{X}_{12}]^{n+}$  clusters of Nb and Ta, (p. 992), were subsequently shown to contain

<sup>10</sup> See pp. 167 and 196 of U. MÜLLER, *Inorganic Structural Chemistry*, 2nd edn., Wiley, New York, (1992).

<sup>11</sup> A. LACHGAR, D.S. DUDIS and J.D. CORBETT, *Inorg. Chem.* **29**, 2242–6 (1990).

<sup>12</sup> J. ZHANG, R.Y. QI and J.D. CORBETT, *Inorg. Chem.* **30**, 4794–8 (1991).

<sup>†</sup>  $\text{ZrF}_3$  may also be doubted (see p. 150 of D. SMITH, *Inorganic Substances*, Cambridge Univ. Press, Cambridge, 1990).

<sup>9</sup> R. HOPPE and ST. BECKER, *Z. anorg. allg. Chem.* **568**, 126–35 (1989).

impurity atoms situated inside the  $Zr_6$  octahedra which they actually stabilize. The materials are correctly formulated as  $Zr_6X_{12}Z$  and, if alkali metal halides are incorporated in the reaction mix a whole series of phases based on the  $[Zr_6X_{12}Z]$  cluster unit is obtained, of which the chlorides and iodides have so far been most thoroughly studied. Z is most commonly H, Be, B, C or N (dark orange to red products), but may also be Cr, Mn, Fe or Co (green, blue or purple products). In all cases the same basic  $Zr_6X_{12}Z$  cluster unit is involved, though several structure types result from the differing ways in which these are connected.<sup>(13)</sup> In most cases it appears that stability is attained when 14 electrons are available for cluster bonding (i.e. total number of valence electrons from  $Zr_6$  and Z, adjusted for overall charge, less 12 required by  $X^{-12}$ ) where Z is a main-group element, but 18 electrons where Z is a transition element. It has been suggested that the presence of Z is essential for the stabilisation of these clusters, but  $Zr_6Cl_{12}(PMe_2Ph)_6$  appears to consist entirely of empty  $Zr_6Cl_{12}$  clusters with a phosphine attached externally to each Zr atom.<sup>(14)</sup>

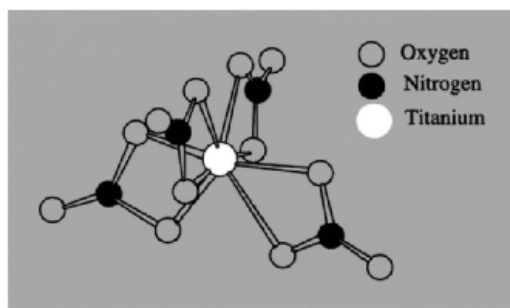
By contrast, ZrCl and ZrBr, also prepared by the high temperature reduction of  $ZrX_4$  with the metal, appear to be genuine binary halides. They are comprised of hcp double layers of metal atoms surrounded by layers of halide ions, leading to metallic conduction in the plane of the layers, and they are thermally more stable than the less reduced phases. ZrI has not been obtained, possibly because of the large size of the iodide ion, and, less surprisingly, attempts to prepare reduced fluorides have been unsuccessful.

### 21.3.4 Compounds with oxoanions

Because of the high ratio of ionic charge to radius, normal salts of  $Ti^{IV}$  cannot be

prepared from aqueous solutions, which only yield basic, hydrolysed species. Even with  $Zr^{IV}$  and  $Hf^{IV}$ , normal salts such as  $Zr(NO_3)_4 \cdot 5H_2O$  and  $Zr(SO_4)_2 \cdot 4H_2O$  can only be isolated if the solution is sufficiently acidic, whilst basic salts and anionic complexes are readily obtained. Several oxometal(IV) compounds (i.e. "titanyl", "zirconyl") have been isolated but do not contain discrete  $MO^{2+}$  ions, being polymeric in the solid state. Thus,  $TiOSO_4 \cdot H_2O$  contains chains of  $-Ti-O-Ti-O-$  with each Ti being approximately octahedrally coordinated to 2 bridging oxygen atoms, 1 water molecule and an oxygen atom from each of 3 sulfates;  $ZrO(NO_3)_2$  is also an oxygen-bridged chain, though hydroxy bridging, as in  $ZrOCl_2 \cdot 8H_2O$  mentioned above, is more common. By contrast, ion-exchange studies on aqueous solutions of  $Ti^{IV}$  in 2M  $HClO_4$  are consistent with the presence of monomeric doubly-charged cationic species rather than polymers, though it is not clear whether the predominant species is  $[TiO]^{2+}$  or  $[Ti(OH)_2]^{2+}$ .

The anhydrous nitrates can be prepared by the action of  $N_2O_5$  on  $MCl_4$ .  $Ti(NO_3)_4$  is a white sublimable and highly reactive compound (mp  $58^\circ C$ ) in which the bidentate nitrate ions are disposed tetrahedrally around the titanium which thereby attains a coordination number of 8 (Fig. 21.4). Infrared evidence suggests that  $Zr(NO_3)_4$  is isostructural but hafnium nitrate



**Figure 21.4** The molecular structure of  $Ti(NO_3)_4$ . Eight O atoms form a dodecahedron around the Ti and the 4 N atoms form a flattened tetrahedron.

<sup>13</sup> R. P. ZIEBARTH and J. D. CORBETT, *Acc. Chem. Res.* **22**, 256–62 (1989).

<sup>14</sup> F. A. COTTON, P. A. KIBALA and W. J. ROTH, *J. Am. Chem. Soc.* **110** 298–300 (1988).

## §21.3.5

sublimes under vacuum at 100°C as the adduct  $\text{Hf}(\text{NO}_3)_4 \cdot \text{N}_2\text{O}_5$ .

Zirconium phosphates ( $\alpha$ -form:  $\text{Zr}(\text{HPO}_4)_2 \cdot \text{H}_2\text{O}$ ,  $\beta$ -form:  $\text{Zr}(\text{HPO}_4)_2 \cdot 2\text{H}_2\text{O}$ ) have layered structures with cation-exchange properties due to the replaceable, acidic hydrogens. Intercalation of organic molecules causes swelling of the structures and increases their versatility as ion-exchangers.

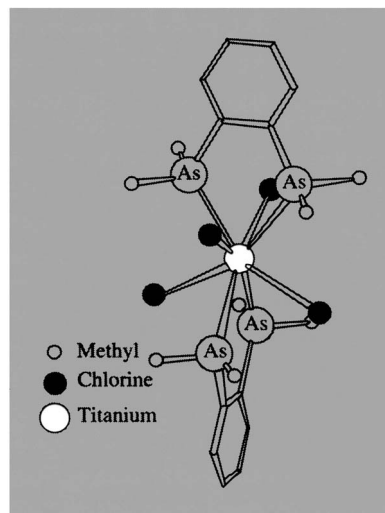
In oxidation states lower than +4, only  $\text{Ti}^{\text{III}}$  forms a sulfate and this gives rise to the alums,  $\text{MTi}(\text{SO}_4)_2 \cdot 12\text{H}_2\text{O}$  ( $M = \text{Rb}, \text{Cs}$ ), containing the octahedral hexaaquotitanium(III) ion.

### 21.3.5 Complexes<sup>(4,15)</sup>

#### Oxidation state IV ( $d^0$ )

A very large number of these complexes, particularly of titanium, have been prepared and, as is to be expected for the  $d^0$  configuration, they are invariably diamagnetic. Hydrolysis, resulting in polymeric species with  $-\text{OH}-$  or  $-\text{O}-$  bridges, is common especially with titanium and is still a preparative problem with zirconium and hafnium, though acidic solutions if sufficiently dilute ( $<10^{-4}$  M) probably contain the  $\text{Zr}^{4+}(\text{aq})$  ion<sup>(16)</sup>. A coordination number of 6 is the most usual for  $\text{Ti}^{\text{IV}}$  but 7- and even 8-coordination is possible. However, these high coordination numbers are much more characteristic of  $\text{Zr}^{\text{IV}}$  and  $\text{Hf}^{\text{IV}}$ , whose complexes are more labile (consistent with greater electrostatic character in the bonding). Furthermore, because changes in geometry entail smaller changes in energy for higher coordination numbers, these include a greater variety of stereochemistries.

The neutral and anionic adducts of the halides constitute a large proportion of the complexes of  $\text{Ti}^{\text{IV}}$ , and the alkoxides (also prepared from  $\text{TiCl}_4$ ) are of commercial importance (p. 968).



**Figure 21.5** Molecular structure of  $[\text{TiCl}_4(\text{diars})_2]$ . The dodecahedral coordination is produced by two interpenetrating tetrahedra (slightly distorted) of chlorine and arsenic atoms.

$\text{TiF}_4$  forms 6-coordinate adducts mainly with *O*- and *N*-donor ligands, and complexes of the type  $\text{TiF}_4\text{L}$  have all the appearances of fluorine-bridged polymers.  $\text{TiCl}_4$  and  $\text{TiBr}_4$  are especially prolific and are clearly “softer” acceptors than the fluoride. They form mainly yellow to red adducts of the types  $[\text{MX}_4\text{L}_2]$  and  $[\text{MX}_4(\text{L-L})]$  with ligands such as ethers, ketones,  $\text{OPCl}_3$ , amines, imines, nitriles, thiols and thioethers. Zirconium and hafnium analogues occur but are often less well characterized because of insolubility and also difficulty in preparing samples suitable for X-ray analysis. Phosphorus- and *As*-donor ligands also complex readily with the chlorides of all three metals, particularly as chelates, and are of interest in that they produce coordination numbers which, for titanium, are unusually high. Thus *o*-phenylenebis(dimethyldiarsine), diars, and its phosphorus analogue form not only the 6-coordinate  $[\text{MX}_4(\text{L-L})]$  but also the 8-coordinate  $[\text{MX}_4(\text{L-L})_2]$ .  $[\text{TiCl}_4(\text{diars})_2]$  (Fig. 21.5) was in fact one of the first examples of an 8-coordinate complex of a first-row transition element. The terdentate arsine,  $\text{MeC}(\text{CH}_2\text{AsMe}_2)_3$ , forms a 1:1

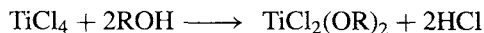
<sup>15</sup> N. SERPONE, M. A. JAMIESON and E. PELIZZETTI, *Coord. Chem. Revs.* **90**, 243–315 (1988); R. FAY *ibid.* **80**, 131–56 (1987).

<sup>16</sup> D. H. DEVIA and A. G. SYKES, *Inorg. Chem.* **20**, 910–13 (1981).

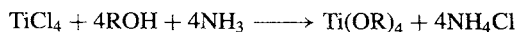
adduct with  $\text{TiCl}_4$  which is monomeric and so presumably 7-coordinate.  $[\text{TiCl}_4\text{L}]$  adducts are usually 6-coordinate dimers with double chloride bridges.

Octahedral, anionic complexes,  $[\text{MX}_6]^{2-}$ , show a marked increase in susceptibility to hydrolysis and consequent difficulty in preparation, in passing from the stable fluorides to the heavier halides, with the result that the hexaiodo complexes cannot be isolated. The fluorozirconates and fluorohafnates display considerable variety, complexes of the types  $[\text{MF}_7]^{3-}$ ,  $[\text{M}_2\text{F}_{14}]^{6-}$ , and  $[\text{MF}_8]^{4-}$  having been prepared, often by fusion of the appropriate fluorides. In  $\text{Na}_3\text{ZrF}_7$  the anion has the 7-coordinate pentagonal bipyramidal structure; in  $\text{Li}_6[\text{BeF}_4][\text{ZrF}_8]$  the zirconium anion is 8-coordinate, dodecahedral (distorted); in  $\text{Cu}_6[\text{ZrF}_8] \cdot 12\text{H}_2\text{O}$  it is 8-coordinate, square antiprismatic, and in  $\text{Cu}_3[\text{Zr}_2\text{F}_{14}] \cdot 18\text{H}_2\text{O}$  dimerization by the edge-sharing of two square antiprisms maintains 8-coordination. Stoichiometry does not, however, define coordination type, and this is very well illustrated by the ostensibly  $[\text{MF}_6]^{2-}$  complexes which may contain 6-, 7-, or 8-coordinate  $\text{Zr}^{\text{IV}}$  or  $\text{Hf}^{\text{IV}}$  depending on the counter anion. In  $\text{Rb}_2\text{MF}_6$ , M is indeed octahedrally coordinated, but in  $(\text{NH}_4)_2\text{MF}_6$  and  $\text{K}_2\text{MF}_6$  polymerization occurs to give respectively 7- and 8-coordinate species.

Alkoxides of all 3 metals are well characterized but it is those of titanium which are of particular importance. The solvolysis of  $\text{TiCl}_4$  with an alcohol yields a dialkoxide:



If dry ammonia is added to remove the HCl, then the tetraalkoxides can be produced:



These alkoxides are liquids or sublimable solids and, unless the steric effects of the alkyl chain prevent it, apparently attain octahedral coordination of the titanium by polymerization (Fig. 21.6). The lower alkoxides are especially sensitive to moisture, hydrolysing to the dioxide. Application of these "organic titanates" (as they are frequently described) can therefore give a

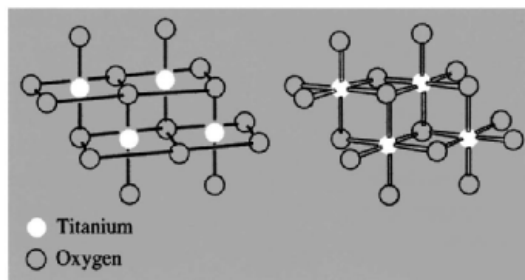


Figure 21.6 Two representations of the tetrameric structure of  $[\text{Ti}(\text{OEt})_4]_4$ .

thin, transparent, and adherent coating of  $\text{TiO}_2$  to a variety of materials merely by exposure to the atmosphere. In this way they are used to waterproof fabrics and also in heat-resistant paints. They are also used on glass and enamels which, after firing, retain a coating of  $\text{TiO}_2$  which confers a resistance to scratching and often enhances the appearance. However, the most important commercial application is in the production of "thixotropic" paints which do not "drip" or "run". For this the  $\text{Ti}(\text{OR})_4$  is chelated with ligands such as  $\beta$ -diketonates to give products of the type  $[\text{Ti}(\text{OR})_2(\text{L-L})_2]$  which are water soluble and more resistant to hydrolysis. In concentrations of 1% or less, they form gels with the cellulose ether colloids used to thicken latex paints and so produce the desired characteristics. Titanium tartrate complexes, probably dimeric species such as  $[\text{Ti}_2(\text{tartrate})_2(\text{OR})_4]$ , are also useful catalysts in asymmetric epoxidations of allylic alcohols.<sup>(17)</sup>

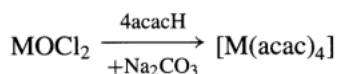
One of the most sensitive methods for estimating titanium (or, conversely, for estimating  $\text{H}_2\text{O}_2$ ) is to measure the intensity of the orange colour produced when  $\text{H}_2\text{O}_2$  is added to acidic solutions of titanium(IV). The colour is due<sup>(18)</sup> to the peroxo complex,  $[\text{Ti}(\text{O}_2)(\text{OH})(\text{H}_2\text{O})_x]^+$ , though alkaline solutions are needed before crystalline solids such as  $\text{M}_3^1[\text{Ti}(\text{O}_2)\text{F}_5]$  or  $\text{M}_2^1[\text{Ti}(\text{O}_2)(\text{SO}_4)_2]$

<sup>17</sup> R. A. JOHNSON and K. B. SHARPLESS, Chap. 3.2, pp. 389–436 in *Comprehensive Organic Synthesis*, Vol. 7, Pergamon Press, Oxford, 1991.

<sup>18</sup> E. M. NOUR and S. MORSY, *Inorg. Chim. Acta* **117**, 45–8 (1986).

can be isolated. The peroxy ligand is apparently bidentate, the 2 oxygen atoms being equidistant from the metal (see also p. 615).

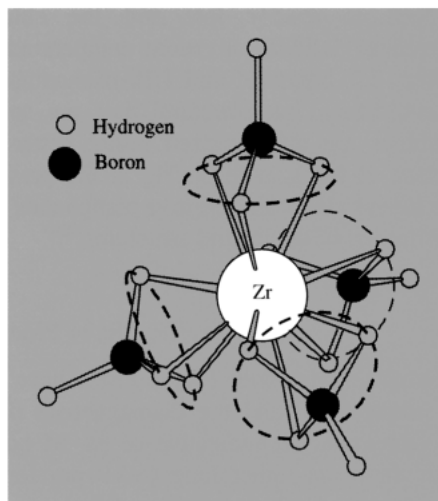
Not surprisingly, in view of their greater size, zirconium and hafnium show a greater preference than titanium for *O*-donor ligands as well as for high coordination numbers, and this is shown by the greater variety of  $\beta$ -diketonates, carboxylates and sulfato complexes which they form. Bis- $\beta$ -diketonates such as  $[\text{MCl}_2(\text{acac})_2]$  of all 3 metals are made by the reaction of  $\text{MCl}_4$  and the  $\beta$ -diketone in inert solvents such as benzene. They are octahedral with *cis*-chlorides. In addition, Zr and Hf form the monomeric, 7-coordinate  $[\text{MCl}(\text{acac})_3]$  complexes which have a distorted pentagonal bipyramidal stereochemistry. Also, providing alkali is present to remove the labile proton, Zr and Hf will yield the tetrakis complexes in aqueous solution:



These too are monomeric, and the 8-coordinate structure has a square-antiprismatic arrangement of oxygen atoms around M.

Monocarboxylates of the types  $[\text{Zr}(\text{carbox})_4]$ ,  $[\text{ZrO}(\text{carbox})_3(\text{H}_2\text{O})_x]$  and  $[\text{ZrO}(\text{OH})(\text{carbox})(\text{H}_2\text{O})_x]$  are well known, as are the corresponding dicarboxylates. It is interesting that the tetrakis(oxalates),  $\text{Na}_4[\text{M}(\text{C}_2\text{O}_4)_4] \cdot 3\text{H}_2\text{O}$ , adopt the dodecahedral stereochemistry in contrast to the square-antiprismatic stereochemistry of  $[\text{M}(\text{acac})_4]$ , possibly because the smaller "bite" of the oxalate ion compared to that of acac favours the dodecahedral form (p. 916). It may also be noted that, although optical and geometrical isomerism is conceivable for these stereochemistries, intramolecular rearrangement of the ligands is too rapid for sets of isomers of the above compounds (or, indeed, of any compound of  $\text{Zr}^{\text{IV}}$  or  $\text{Hf}^{\text{IV}}$ ) to have been isolated.

Intramolecular rearrangement evidently also occurs in the borohydride,  $[\text{Zr}(\text{BH}_4)_4]$  (p. 168). X-ray analysis of a single crystal at  $-160^\circ\text{C}$  (at which temperature thermal vibrations are sufficiently reduced to allow the positions of the hydrogen atoms to be determined) showed



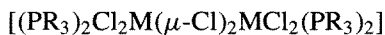
**Figure 21.7** Molecular structure  $[\text{Zr}(\text{BH}_4)_4]$  showing 4 trihapto  $\text{BH}_4$  groups.

it to have  $T_d$  symmetry (Fig. 21.7), with triple-hydrogen bridges, implying two types of hydrogen. Yet the proton nmr distinguishes only one type of proton, so that rapid intramolecular rearrangement is indicated. The structure of the hafnium compound has not been determined but its properties are so similar that its structure may be assumed to be the same. Both compounds are rather unstable, have virtually the same mp ( $\sim 29^\circ\text{C}$ ) and are the most volatile compounds yet known for zirconium and hafnium. The type of bonding involved is a matter of some uncertainty. The volatility is indicative of covalency, but how many electrons the borohydride groups should be regarded as donating to the metal is open to doubt.

### Oxidation state III ( $d^1$ )

The coordination chemistry of this oxidation state is virtually confined to that of titanium. Reduction of zirconium and hafnium from the quadrivalent to the trivalent state is not easy and cannot be attempted in water which is itself reduced by  $\text{Zr}^{\text{III}}$  and  $\text{Hf}^{\text{III}}$ . A few adducts of the trihalides of these two elements with *N*- or *P*- donor ligands have been prepared.  $\text{ZrBr}_3$  treated with liquid ammonia yields a hexaammine stable to room temperature

but  $\text{NH}_3$  is readily lost and the chloride only retains  $2.5\text{NH}_3$  at room temperature.<sup>(19)</sup> Pyridine, 2,2'-bipyridyl and 1,10-phenanthroline also coordinate, but structural data are sparse. Phosphines are characterized rather better and reduction of  $\text{MCl}_4$  with  $\text{Na/Hg}$  in the presence of the ligand yields air-sensitive compounds with edge-sharing, bi-octahedral structures:<sup>(20)</sup>



Analogous iodides with  $\text{PR}_3 = \text{PMe}_3$  have also been prepared,<sup>(21)</sup> and the diamagnetism of all these compounds is indicative of  $\text{M-M}$  bonds, though these are rather long ( $\sim 310$  pm for the chlorides and  $\sim 340$  pm for the iodides).

Titanium(III) is also prone to aerial oxidation. Most of the complexes of titanium(III) are octahedral and are produced by reacting  $\text{TiCl}_3$  with an excess of the ligand, giving rise to stoichiometries such as  $[\text{TiL}_6]\text{X}_3$ ,  $[\text{TiL}_4\text{X}_2]\text{X}$ ,  $[\text{TiL}_3\text{X}_3]$  and  $\text{M}_3^1[\text{TiX}_6]$  ( $\text{L} =$  neutral unidentate ligand,  $\text{X} =$  singly charged anion) (Table 21.4) together with corresponding complexes involving multidentate ligands.

The first of these types is most familiarly represented by the hexaquo ion which is present in acidic aqueous solutions and, in the solid state, in the alum  $\text{CsTi}(\text{SO}_4)_2 \cdot 12\text{H}_2\text{O}$ . In fact few other neutral ligands besides water form a  $[\text{TiL}_6]^{3+}$  complex. Urea is one of these few and  $[\text{Ti}(\text{OCN}_2\text{H}_4)_6]\text{I}_3$ , in which the urea ligands coordinate to the titanium via their oxygen atoms, is one of the compounds of titanium(III) most resistant to oxidation.

Hydrate isomerism of  $\text{TiCl}_3 \cdot 6\text{H}_2\text{O}$ , yielding  $[\text{TiCl}_2(\text{H}_2\text{O})_4]^+\text{Cl}^-$  as one of the isomers, has already been referred to (p. 965) and analogous complexes are formed by a variety of alcohols. Neutral complexes,  $[\text{TiL}_3\text{X}_3]$  have been characterized for a variety of ligands such

as tetrahydrofuran ( $\text{C}_4\text{H}_8\text{O}$ ), dioxan ( $\text{C}_4\text{H}_8\text{O}_2$ ), acetonitrile, pyridine and picoline, while anionic complexes  $[\text{TiX}_6]^{3-}$  ( $\text{X} = \text{F, Cl, Br, NCS}$ ) have been prepared by electrolytic reduction of melts or by other nonaqueous methods. An interesting binuclear complex,  $(\text{NMe}_4)[\text{Ti}(\text{H}_2\text{O})_4\text{F}_2][\text{TiF}_6] \cdot \text{H}_2\text{O}$  is obtained by reacting  $\text{TiCl}_3$  with  $\text{NMe}_4\text{F}$  in dimethylformamide. It contains *trans*- $[\text{Ti}^{\text{III}}(\text{H}_2\text{O})_4\text{F}_2]^+$  cations and  $[\text{Ti}^{\text{IV}}\text{F}_6]^{2-}$  anions.<sup>(22)</sup>

Interpretation of the electronic spectrum of  $\text{Ti}^{\text{III}}$  in aqueous solution was an early landmark in the development of Crystal Field Theory, the observed broad band being assigned to the  ${}^2E_g \leftarrow 2T_{2g}$  transition (promotion of an electron from a  $t_{2g}$  to an  $e_g$  orbital). However, the absorption band actually observed for this and for other octahedral complexes of  $\text{Ti}^{\text{III}}$  is never of the symmetrical shape expected for a single transition, but is rather an asymmetrical peak with a (usually) distinct shoulder on the low-energy side<sup>(4)</sup>. The whole absorption "envelope" is apparently made up of two superimposed bands whose positions are indicated in Table 21.4 and which are generally assumed to be a consequence of the Jahn-Teller effect (p. 1021) acting on the excited term. The value of  $10Dq$  is usually identified with the energy of the stronger of the two bands rather than an average, and the results in Table 21.4 indicate that this varies with the ligand in the order:



which agrees with the spectrochemical series established for other metals.

The  $t_{2g}^1$  ground configuration in a perfectly octahedral crystal field is expected to produce a magnetic moment of approx. 1.86 BM at room temperature, decreasing to zero at 0 K. Although observed magnetic moments of  $\text{Ti}^{\text{III}}$  compounds do indeed decrease with temperature, the effects of distortions (which split the ground  ${}^2T_{2g}$  term) and partial covalency of the metal-ligand bond (which delocalizes the single electron from the

<sup>19</sup> E. L. BOYLE, E. S. DODSWORTH, D. NICHOLLS and T. A. RYAN, *Inorg. Chim. Acta* **100**, 281-4 (1985).

<sup>20</sup> F. A. COTTON, P. A. KIBALA and W. A. WOJTCZAK, *Inorg. Chim. Acta* **177**, 1-3 (1990).

<sup>21</sup> F. A. COTTON, M. SHANG and W. A. WOJTCZAK, *Inorg. Chem.* **30**, 3670-5 (1991).

<sup>22</sup> L. KIRIAZIS and R. MATTES, *Z. anorg. allg. Chem.* **593**, 90-8 (1991).

**Table 21.4** Spectroscopic and magnetic properties of some complexes of titanium(III)

Complex	Colour	${}^2E_g \leftarrow {}^2T_{2g}/(\text{cm}^{-1})$	$\mu$ (room temperature)/ BM
$[\text{Cs}(\text{H}_2\text{O})_6][\text{Ti}(\text{H}_2\text{O})_6][\text{SO}_4]_2$	Red-purple	19 900, 18 000	1.79
$[\text{Ti}(\text{urea})_6]_3$	Blue	17 550, 16 000	1.77
$[\text{TiCl}_3(\text{NCMe})_3]$	Blue	17 100, 14 700	1.68
$[\text{TiCl}_3(\text{NC}_5\text{H}_5)_3]$	Green	16 600, Asym <sup>(a)</sup>	1.63
$[\text{TiCl}_3(\text{thf})_3]$	Blue-green	14 700, 13 500	1.70
$[\text{TiCl}_3(\text{dioxan})_3]$	Blue-green	15 150, 13 400	1.69
$[\text{NH}_4]_3[\text{TiF}_6]$	Purple	19 000, 15 100	1.78
$[\text{C}_5\text{H}_5\text{NH}]_3[\text{TiCl}_6]$	Orange	12 750, 10 800	1.78
$[\text{C}_5\text{H}_5\text{NH}]_3[\text{TiBr}_6]$	Orange	11 400, 9 650	1.81
$[\text{NBu}_4]_3[\text{Ti}(\text{NCS})_6]$	Dark violet	18 400, Asym <sup>(a)</sup>	1.81

<sup>(a)</sup>The band "envelope" is asymmetrical with insufficient resolution to identify the position of the weaker component.

metal) lead to lower values at room temperature (see Table 21.4) and less temperature dependence than would have been expected.<sup>(23)</sup>

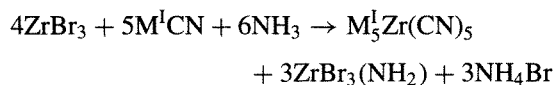
Amongst the few complexes of  $\text{Ti}^{\text{III}}$  which have been shown to be non-octahedral are  $[\text{TiBr}_3(\text{NMe}_2)_2]$  and  $[\text{Ti}\{\text{N}(\text{SiMe}_3)_2\}_3]$ . The former has a 5-coordinate, trigonal bipyramidal structure while the latter is one of a series of complexes of trivalent metals which have a 3-coordinate, planar structure. It appears that the silylamide ligands are simply too bulky for the  $\text{Ti}^{\text{III}}$  ion to accommodate more than three of them, and this consideration overrides any preference which the metal might have for a higher coordination number.

### Lower oxidation states

Apart from  $\text{TiO}$  and the lower halides already mentioned, the chemistry of these metals in oxidation states lower than 3 is not well established. Addition compounds of the type  $[\text{TiCl}_2\text{L}_2]$  can be formed with difficulty with ligands such as dimethylformamide and acetonitrile, but their magnetic properties suggest that they also are polymeric with appreciable metal-metal bonding. However, the electronic spectra of  $\text{Ti}^{\text{II}}$  in  $\text{TiCl}_2/\text{AlCl}_3$  melts and also of  $\text{Ti}^{\text{II}}$  incorporated in  $\text{NaCl}$  crystals (prepared by

the reaction of  $\text{CdCl}_2$  and titanium in molten  $\text{NaCl}$  and subsequent sublimation of  $\text{Cd}$  metal) have been shown to be as expected for a  $d^2$  ion in an octahedral field.

The versatility of cyanide and bipyridyl ligands has been used to stabilize low oxidation states. By using potassium in liquid ammonia,  $\text{K}_3\text{Ti}^{\text{III}}(\text{CN})_6$  is reduced to  $\text{K}_2\text{Ti}^{\text{II}}(\text{CN})_4$  and  $\text{TiBr}_3 + \text{KCN}$  to  $\text{K}_4\text{Ti}^0(\text{CN})_4$ . With  $\text{ZrBr}_3$  and  $\text{M}^{\text{I}}\text{CN}$  ( $\text{M}^{\text{I}} = \text{K}, \text{Rb}$ ) in liquid ammonia, ammonolysis occurs and zerovalent Zr is produced:



Reduction of  $\text{MCl}_4$  ( $\text{M} = \text{Ti}, \text{Zr}$ ) in tetrahydrofuran by lithium in the presence of bipyridyl yields a series of darkly coloured, very air-sensitive compounds of the types  $[\text{M}(\text{bipy})_3]$ ,  $\text{Li}[\text{M}(\text{bipy})_3]$  and  $\text{Li}_2[\text{M}(\text{bipy})_3]$  with varying amounts of solvent of crystallization, implying oxidation states of 0, -1 and -2. However, delocalization of charge in the  $\pi^*$  orbitals of the ligands facilitates reduction of the ligands and assigning oxidation states to the metals under these circumstances is a purely formal exercise. A more "realistic" claim to zero oxidation state in Zr and Hf compounds is provided by  $[\text{M}(\eta\text{-PhMe})_2(\text{PMe}_3)]$ . Metal vapour was produced from an "electron-gun furnace" and condensed with an excess of toluene and trimethylphosphine at  $-196^\circ\text{C}$ . On warming up, a dark-green solution was produced from which the pure solids were isolated.

<sup>23</sup> For a fuller account, see pp. 58-61 of R. L. CARLIN, *Magnetochemistry*, Springer-Verlag, Berlin (1986).



### Ziegler–Natta Catalysts<sup>(27)</sup>

The original ICI process for producing polythene involved the use of high temperatures and pressures but K. Ziegler discovered that, in the presence of a mixture of  $\text{TiCl}_4$  and  $\text{AlEt}_3$  in a hydrocarbon solvent, the polymerization will take place at room temperature and atmospheric pressure. G. Natta then showed that by suitable modification of the catalyst stereoregular polymers of almost any alkene (olefin),  $\text{CH}_2=\text{CHR}$ , can be produced. In general, these catalysts can be formed from an alkyl of Li, Be or Al together with a halide of one of the metals of Groups 4 to 6 in an oxidation state less than its maximum. As a result of their work, Ziegler and Natta were jointly awarded the 1963 Nobel Prize for Chemistry. Because of its commercially sensitive nature, much of the voluminous literature on this subject is in the form of patents, but a great deal of work has also been directed at ascertaining the mechanism of the catalyst. The initial reaction of  $\text{TiCl}_4$  and  $\text{AlEt}_3$  produces insoluble  $\text{TiCl}_3$  (alternatively, preformed  $\text{TiCl}_3$  can be used). The most plausible sequence of events on the surface of this catalyst is then as illustrated in Fig. A:

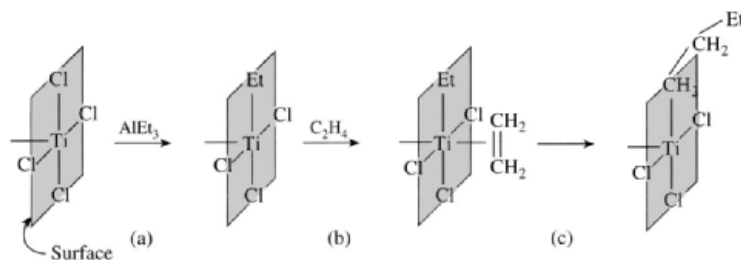


Figure A Possible mechanism of Ziegler–Natta catalyst.

- one of the chlorine atoms coordinated to a titanium atom is replaced by an ethyl group from  $\text{AlEt}_3$ ,
- then, because the titanium atom on the surface of the solid has a vacant coordination site, a molecule of ethylene (ethene) can attach itself;
- migration of the ethyl group to the ethylene by a well-known process known as “*cis*-insertion” occurs.

The result of this *cis*-insertion is that a vacant site is left behind, and this can be occupied by another ethylene molecule and steps (a) and (b) repeated indefinitely.

The efficacy of the catalyst seems to lie in the fact that in the case of propylene ( $\text{CH}_2=\text{CH}-\text{CH}_3$ ), for instance, the steric hindrance inherent in the surface coordination sites ensures that the polymer which is produced is stereoregular. Such a stereoregular polymer is stronger and has a higher mp than the non-regular (so-called “atactic”) polymer. Furthermore, while the titanium provides bonds sufficiently strong to be able to hold the olefin and the alkyl in the correct orientations for reaction, they are not so strong as to prevent the migration which is essential to the reaction. For an alternative suggestion for the mechanism of catalysis, see p. 261.

#### 21.3.6 Organometallic compounds<sup>(24,25)</sup>

Until the 1950s this was an unexplored area of chemistry, but then two events occurred:

<sup>24</sup> M. BOTTRILL, P. D. GAVENS, J. W. KELLAND and J. MCKEENING, Chap. 22, pp. 271–547, and D. J. CARDIN, M. F. LAPPERT, C. L. RASTON and P. I. RILEY, Chap. 23, pp. 549–646, in *Comprehensive Organometallic Chemistry*, Vol. 3, Pergamon Press, Oxford, 1982.

<sup>25</sup> D. J. CARDIN, M. F. LAPPERT and C. L. RASTON, *Chemistry of Organo-Zirconium and -Hafnium Compounds*, Ellis Horwood, Chichester, 1986, 451 pp. D. COZAK and M. MELNIK, *Coord. Chem. Rev.* **74**, 53–99 (1986).

ferrocene was discovered (pp. 937, 1109) and K. Ziegler<sup>(26)</sup> catalysed the polymerization of ethylene using an organo-titanium derivative. The first event initiated a systematic study of cyclopentadienyl compounds, and so led to the preparation of the most stable of the organometallic compounds of this group, while the second event provided a strong commercial incentive for the investigation of this field (see Panel).

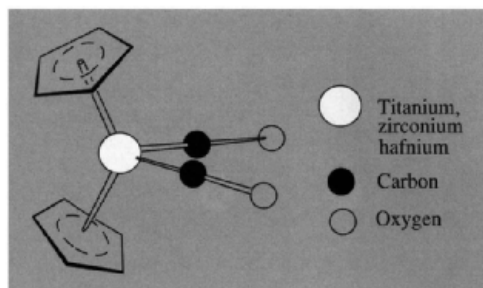
<sup>26</sup> K. ZIEGLER, E. HOLZKAMP, H. BREILAND and H. MARTIN, *Angew. Chem.* **67**, 541–7 (1955).

<sup>27</sup> See pp. 475–547 of ref. 24.

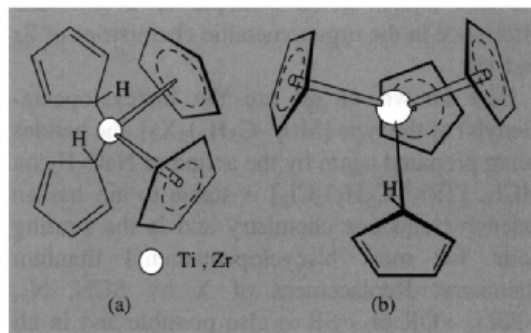
In sharp contrast to the Group 14 elements Ge, Sn and Pb, Group 4 metals form relatively few alkyl and aryl compounds and those which are known are very unstable to both air and water. Thermal stabilization is provided by ligands which lack  $\beta$ -hydrogens (p. 926) or are bulky. Thus  $\text{MET}_4$  are unknown;  $\text{MMe}_4$  can be prepared by the reactions of  $\text{LiMe}$  and  $\text{MCl}_4$  in ether at low temperatures, but the yellow titanium and the red zirconium compounds decompose to the metals at temperatures above  $-20$  and  $-15^\circ\text{C}$  respectively;  $\text{M}(\text{CH}_2\text{SiMe}_3)_4$  of all three metals are stable at room temperature. Another homoleptic alkyl is of interest because of its unusual structure. X-ray analysis has shown the anion of  $[\text{Li}(\text{tmed})]_2[\text{ZrMe}_6]$  to be the first  $\text{ML}_6$  complex to have a trigonal bipyramidal structure and nmr studies indicate that this is retained in solution.<sup>(28)</sup>

Perhaps because of inadequate or non-existent back-bonding (p. 923), the only neutral, binary carbonyl so far reported is  $\text{Ti}(\text{CO})_6$  which has been produced by condensation of titanium metal vapour with CO in a matrix of inert gases at 10–15 K, and identified spectroscopically. By contrast, if  $\text{MCl}_4$  ( $\text{M} = \text{Ti}, \text{Zr}$ ) in dimethoxyethane is reduced with potassium naphthalene in the presence of a crown ether (to complex the  $\text{K}^+$ ) under an atmosphere of CO,  $[\text{M}(\text{CO})_6]^{2-}$  salts are produced.<sup>(29)</sup> These not only involve the metals in the exceptionally low formal oxidation state of  $-2$  but are thermally stable up to 200 and  $130^\circ\text{C}$  respectively. However, the majority of their carbonyl compounds are stabilized by  $\pi$ -bonded ligands, usually cyclopentadienyl,<sup>(30)</sup> as in  $[\text{M}(\eta^5\text{-C}_5\text{H}_5)_2(\text{CO})_2]$  (Fig. 21.8).

Indeed, it is the cyclopentadienyls which provide the major part of the organometallic chemistry of this group and they are known for metal oxidation states of IV, III and II though III



**Figure 21.8** Molecular structure of  $[\text{M}(\eta^5\text{-C}_5\text{H}_5)_2(\text{CO})_2]$ . For  $\text{M} = \text{Ti}$  the  $\text{C}_5\text{H}_5$  rings are “eclipsed” as shown here, but for  $\text{M} = \text{Hf}$  they are “staggered”. Essentially the same structure is found in other  $[\text{M}(\eta^5\text{-C}_5\text{H}_5)_2\text{L}_2]$  molecules, but the conformation of the two  $\text{C}_5\text{H}_5$  rings varies in an apparently unsystematic manner.



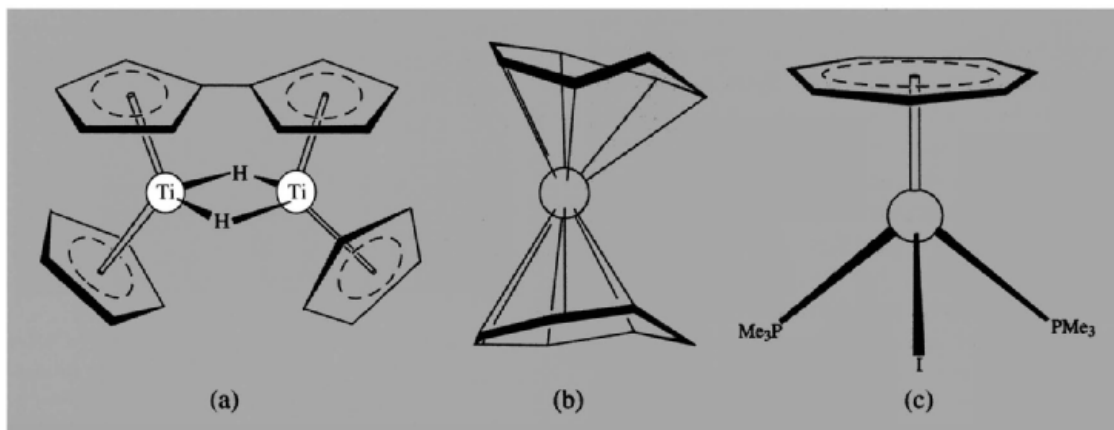
**Figure 21.9** (a) Molecular structure of (a)  $\text{Ti}(\text{C}_5\text{H}_5)_4$ . (b)  $\text{Zr}(\text{C}_5\text{H}_5)_4$ .

and II are rather sparsely represented for Zr and Hf. The compounds  $\text{M}(\text{C}_5\text{H}_5)_4$  are prepared from  $\text{MCl}_4$  and  $\text{NaC}_5\text{H}_5$  and the structure of the green-black titanium compound is shown in Fig. 21.9a. It is therefore formulated as  $[\text{Ti}(\eta^1\text{-C}_5\text{H}_5)_2(\eta^5\text{-C}_5\text{H}_5)_2]$  (p. 940). Rather surprisingly, the  $^1\text{H}$  nmr distinguishes only one type of proton at room temperature and it is evident that fluxional processes render all 20 protons indistinguishable. The yellow hafnium analogue is isostructural but the yellow-orange zirconium compound contains 1 monohapto- and 3 pentahapto-rings,  $[\text{Zr}(\eta^1\text{-C}_5\text{H}_5)(\eta^5\text{-C}_5\text{H}_5)_3]$  Fig. 21.9b. This formulation is unexpected since it entails a formally 20-electron

<sup>28</sup> P. M. MORSE and G. S. GIROLAMI, *J. Am. Chem. Soc.* **111**, 4114–6 (1989).

<sup>29</sup> K. M. CHI, S. R. FRERICHS, S. B. PHILSON and J. E. ELLIS, *Angew. Chem. Int. Edn. Engl.* **26**, 1190–1 (1987) and *J. Am. Chem. Soc.* **110**, 303–4 (1988).

<sup>30</sup> D. J. SIKORA, D. W. MACOMBER and M. D. RAUSCH, *Adv. Organometallic Chem.* **25**, 318–80 (1986).



**Figure 21.10** (a) “Dimeric”  $\text{Ti}(\text{C}_5\text{H}_5)_2$ , actually  $(\mu\text{-}(\eta^5\text{-}\eta^5\text{-fulvalene-(di-}(\mu\text{-hydrido)-bis}(\eta^5\text{-cyclopentadienyl)-titanium)$ , (b)  $\text{Zr}(\eta^6\text{-C}_7\text{H}_8)_2$  and (c)  $\text{Zr}(\eta^7\text{-C}_7\text{H}_7)(\text{PMe}_3)_2\text{I}$ .

configuration; the two compounds also provided the first authenticated example of a structural difference in the organometallic chemistries of Zr and Hf.

Best known of all are the bis(cyclopentadienyls) of the type  $[\text{M}(\eta^5\text{-C}_5\text{H}_5)_2\text{X}_2]$ , the halides being prepared again by the action of  $\text{NaC}_5\text{H}_5$  on  $\text{MCl}_4$ .  $[\text{Ti}(\eta^5\text{-C}_5\text{H}_5)_2\text{Cl}_2]$  is stable to air, has an extensive aqueous chemistry and is the starting point for most biscyclopentadienyl titanium chemistry. Replacement of X by SCN,  $\text{N}_3$ ,  $\text{-NR}_2$ ,  $\text{-OR}$  or  $\text{-SR}$  is also possible and in all cases the structures are distorted tetrahedral with both rings pentahapto (Fig. 21.8). Interesting derivatives of the type  $[(\text{C}_5\text{H}_5)_2\text{Ti}(\text{CH}_2)_4]$  have also been produced. Amongst the many other reactions of the dihalides, ring replacement to give compounds such as  $[\text{Ti}(\text{C}_5\text{H}_5)\text{X}_3]$  and reductions to  $[\text{Ti}(\text{C}_5\text{H}_5)_2\text{X}]$  and  $[\text{Ti}(\text{C}_5\text{H}_5)_2]$  may be noted. The last of these is of interest as a potential analogue of ferrocene. Several preparative routes have been suggested, and the usual product is a dark-green, pyrophoric, diamagnetic dimer, though a monomeric isomer may be produced in some cases as an intermediate. The structure of the dimer has been shown by X-ray crystallography<sup>(30a)</sup> to be that

in Fig. 21.10a, confirming earlier results based on  $^{13}\text{C}$  nmr. Attempts to prepare a zirconium analogue have yielded a variety of products, some dinuclear others polymeric but, as with titanium, no true mononuclear metallocene. A number of cyclopentadienyl and related compounds of titanium and zirconium have been found to absorb molecular nitrogen, which in some cases can be recovered in a reduced form (i.e. as ammonia or hydrazine) upon hydrolysis, and the first example of dinitrogen complexation by a non-cyclopentadienyl Ti system has recently been reported.<sup>(31)</sup> While this has obvious interest as a potential route to nitrogen fixation, a compound which can be regenerated and so act catalytically has so far proved elusive.

Although the chemistry of zirconium in its lower oxidation states is still relatively unexplored, it is developing. Examples which offer the possibility of further exploitation include the blue, paramagnetic zirconium(III) compound<sup>(32)</sup>  $[\text{L}_2\text{Zr}(\mu\text{-Cl})_2\text{ZrL}_2]$   $\{\text{L} = \text{C}_5\text{H}_3(\text{SiMe}_3)_2\text{-1,3}\}$ , and the “sandwich” and “half-sandwich” compounds derived from cycloheptatriene: red

<sup>31</sup> N. BEYDOUN, R. DUCHATEAU and S. GAMBAROTTA, *J. Chem. Soc., Chem. Commun.*, 244–6 (1992).

<sup>32</sup> P. B. HITCHCOCK, M. F. LAPPERT, G. A. LAWLESS, H. OLIVIER and E. J. RYAN, *J. Chem. Soc., Chem. Commun.*, 474–6 (1992).

<sup>30a</sup> S. I. TROYANOV, H. ANTROPIUSOVA and K. MACG, *J. Organometallic Chem.* **427**, 49–55 (1992).

$[\text{Zr}^0(\eta^6\text{-C}_7\text{H}_8)_2]^{(33)}$  and blue,  $[\text{Zr}^{\text{II}}(\eta^7\text{-C}_7\text{H}_7)\text{-(PMe}_3)_2\text{I}]^{(34)}$  (Fig. 21.10b and c).

Considerable attention is also being given to the anti-tumor activity of titanium compounds.

---

<sup>33</sup> M. L. H. GREEN and N. M. WALKER, *J. Chem. Soc., Chem. Commun.*, 850–2 (1989).

<sup>34</sup> *ibid.*, pp. 908–9.

Amongst these are bis(cyclopentadienyl) and bis( $\beta$ -diketonate) derivatives, some of which are undergoing clinical trials,<sup>(35)</sup> in the hope that they will provide more extensive application than cisplatin (pp. 1163–4).

---

<sup>35</sup> B. K. KEPPLER, C. FRIESEN, H. G. MORITZ, H. VONGERICHTEN and E. VOGEL, *Struct. and Bonding* **78**, 97–127 (1991).

																1	2																
																H	He																
3	4															5	6	7	8	9	10												
Li	Be															B	C	N	O	F	Ne												
11	12															13	14	15	16	17	18												
Na	Mg															Al	Si	P	S	Cl	Ar												
19	20	21	22	23	24	25	26	27	28	29	30	31	32	33	34	35	36																
K	Ca	Sc	Ti	V	Cr	Mn	Fe	Co	Ni	Cu	Zn	Ga	Ge	As	Se	Br	Kr																
37	38	39	40	41	42	43	44	45	46	47	48	49	50	51	52	53	54																
Rb	Sr	Y	Zr	Nb	Mo	Tc	Ru	Rh	Pd	Ag	Cd	In	Sn	Sb	Te	I	Xe																
55	56	57	58	59	60	61	62	63	64	65	66	67	68	69	70	71	72																
Cs	Ba	La	Hf	Ta	W	Re	Os	Ir	Pt	Au	Hg	Tl	Pb	Bi	Po	At	Rn																
87	88	89	90	91	92	93	94	95	96	97	98	99	100	101	102	103	104																
Fr	Ra	Ac	Rf	Db	Sg	Bh	Hs	Mt	Uuo	Uuq	Uub																						
105	106	107	108	109	110	111	112	113	114	115	116	117	118	119	120	121	122																
Th	Pa	U	Np	Pu	Am	Cm	Bk	Cf	Es	Fm	Md	No	Lr																				

# 22

## Vanadium, Niobium and Tantalum

### 22.1 Introduction

The discoveries of all three of these elements were made at the beginning of the nineteenth century and were marked by initial uncertainty and confusion due, in the case of the heavier pair of elements, to the overriding similarity of their chemistries. (See p. 1282 for element 105, dubnium.)

A. M. del Rio in 1801 claimed to have discovered the previously unknown element 23 in a sample of Mexican lead ore and, because of the red colour of the salts produced by acidification, he called it erythronium. Unfortunately he withdrew his claim when, 4 years later, it was (incorrectly) suggested by the Frenchman, H. V. Collett-Desotils, that the mineral was actually basic lead chromate. In 1830 the element was “rediscovered” by N. G. Sefström in some Swedish iron ore. Because of the richness and variety of colours found in its compounds he called it vanadium after Vanadis, the Scandinavian goddess of beauty. One year later F. Wöhler established the identity of vanadium and erythronium. The metal itself was isolated in a reasonably pure form in 1867 by H. E. Roscoe who reduced the chloride with hydrogen, and he was

also responsible for much of the early work on the element.

In the same year that del Rio found his erythronium, C. Hatchett examined a mineral which had been sent to England from Massachusetts and had lain in the British Museum since 1753. From it he isolated the oxide of a new element which he named columbium, and the mineral columbite, in honour of its country of origin. Meanwhile in Sweden A. G. Ekeberg was studying some Finnish minerals and in 1802 claimed to have identified a new element which he named tantalum because of the difficulty he had had in dissolving the mineral in acids.<sup>†</sup> It was subsequently thought that the two elements were one and the same, and this view persisted until at least 1844 when H. Rose examined a columbite sample and showed that two distinct elements were involved.

<sup>†</sup> The classical allusion refers to Tantalus, the mythical king of Phrygia, son of Zeus and a nymph, who was condemned for revealing the secrets of the gods to man: one of his punishments was being made to stand in Tartarus up to his chin in water, which constantly receded as he stooped to drink. As Ekeberg wrote (1802): “This metal I call *tantalum* . . . partly in allusion to its incapacity, when immersed in acid, to absorb any and be saturated.”

One was Ekeberg's tantalum and the other he called niobium (Niobe was the daughter of Tantalus). Despite the chronological precedence of the name columbium, IUPAC adopted niobium in 1950, though columbium is still sometimes used in US industry. Impure niobium metal was first isolated by C. W. Blomstrand in 1866 by the reduction of the chloride with hydrogen, but the first pure samples of metallic niobium and tantalum were not prepared until 1907 when W. von Bolton reduced the fluorometallates with sodium.

## 22.2 The Elements

### 22.2.1 Terrestrial abundance and distribution

The abundances of these elements decrease by approximately an order of magnitude from V to Nb and again from Nb to Ta. Vanadium has been estimated to comprise about 136 ppm (i.e. 0.0136%) of the earth's crustal rocks, which makes it the nineteenth element in order of abundance (between Zr, 162 ppm, and Cl, 126 ppm); it is the fifth most abundant transition metal after Fe, Ti, Mn and Zr. It is widely, though sparsely, distributed; thus although more than 60 different minerals of vanadium have been characterized, there are few concentrated deposits and most of it is obtained as a coproduct along with other materials. Its major commercial source is the titaniferous magnetites of South Africa, the former USSR and China. One of its important minerals is the polysulfide, patronite,  $VS_4$ , but, being a class-a metal, it is more generally associated with oxygen. For example, vanadinite approximates to lead chloride vanadate,  $PbCl_2 \cdot 3Pb_3(VO_4)_2$ , and carnotite to potassium uranyl vanadate,  $K(UO_2)(VO_4) \cdot 1.5H_2O$ . Vanadium is also found in some crude oils, in particular those from Venezuela and Canada, and can be recovered from the oil residues and from flue dusts after burning.

The crustal abundances of niobium and tantalum are 20 ppm and 1.7 ppm, comparable to N (19 ppm), Ga (19 ppm), and Li (18 ppm),

on the one hand, and to As (1.8 ppm) and Ge (1.5 ppm), on the other. Of course, in view of their chemical similarities. Nb and Ta usually occur together, and their most widespread mineral,  $(Fe,Mn)M_2O_6$  ( $M = Nb, Ta$ ), is known as columbite or tantalite, depending on which metal preponderates. Until the 1950s, this was the major source of both metals, with significant amounts obtained also as a byproduct of the extraction of tin in SE Asia and Nigeria. The discovery of a huge, high grade (2.5%  $Nb_2O_5$ ) deposit of pyrochlore,  $NaCaNb_2O_6F$ , in Brazil totally changed the pattern. Nb is now obtained chiefly from Brazil; Ta from Australia, Canada and SE Asia but its production is heavily dependent on demand for Sn.

### 22.2.2 Preparation and uses of the metals

Because it is usually produced along with other metals, the availability of vanadium and the economics of its production<sup>(1)</sup> are intimately connected with the particular coproduct involved.

The usual extraction procedure is to roast the crushed ore, or vanadium residue, with NaCl or  $Na_2CO_3$  at 850°C. This produces sodium vanadate,  $NaVO_3$ , which is leached out with water. Acidification with sulfuric acid to pH 2–3 precipitates "red cake", a polyvanadate which, on fusing at 700°C, gives a black, technical grade vanadium pentoxide. Reduction is then necessary to obtain the metal, but, since about 80% of vanadium produced is used as an additive to steel, it is usual to effect the reduction in an electric furnace in the presence of iron or iron ore to produce ferrovandium, which can then be used without further refinement. Carbon was formerly used as the reductant, but it is difficult to avoid the formation of an intractable carbide, and so it has been superseded by aluminium or, more commonly, ferrosilicon (p. 330) in which case lime is also added to remove the silica as a slag of calcium silicate. If pure vanadium metal is required it can

<sup>1</sup> C. K. GUPTA and N. KRISHNAMURTHY, *Extractive Metallurgy of Vanadium*, Elsevier, Amsterdam, 1992, 689 pp.

be obtained by reduction of  $VCl_5$  with  $H_2$  or Mg, by reduction of  $V_2O_5$  with Ca, or by electrolysis of partially refined vanadium in fused alkali metal chloride or bromide.

The benefit of vanadium as an additive in steel is that it forms  $V_4C_3$  with any carbon present, and this disperses to produce a fine-grained steel which has increased resistance to wear and is stronger at high temperatures. Such steels are widely used in the manufacture of springs and high-speed tools. In 1995, world consumption of vanadium metal, alloys and concentrates exceeded 33 000 tonnes of contained vanadium.

Production of niobium and tantalum is on a smaller scale and the processes involved are varied and complicated. Alkali fusion, or digestion of the ore with acids can be used to solubilize the metals, which can then be separated from each other. The process originally developed by M. C. Marignac in 1866 and in use for a century utilized the fact that in dil HF tantalum tends to form the sparingly soluble  $K_2TaF_7$ , whereas niobium forms the soluble  $K_3NbOF_5 \cdot 2H_2O$ . Nowadays it is more usual to employ a solvent extraction technique. For instance, tantalum can be extracted from dilute aqueous HF solutions by methyl isobutyl ketone, and increasing the acidity of the aqueous phase allows niobium to be extracted into a fresh batch of the organic phase. The metals can then be obtained, after conversion to the pentoxides, by reduction with Na or C, or by the electrolysis of fused fluorides. In 1995, world production of contained metal was in the region of 18 000 tonnes for Nb and 1000 tonnes for Ta.

Niobium finds use in the production of numerous stainless steels for use at high temperatures, and Nb/Zr wires are used in superconducting magnets. The extreme corrosion-resistance of tantalum at normal temperatures (due to the presence of an exceptionally tenacious film of oxide) leads to its application in the construction of chemical plant, especially where it can be used as a liner inside cheaper metals. Its complete inertness to body fluids makes it the ideal material for surgical use in bone repair and internal suturing.

It is widely used by the electronics industry in the manufacture of capacitors, where the oxide film is an efficient insulator, and as a filament or filament support. Indeed, it was for a while widely used to replace carbon as the filament in incandescent light bulbs but, by about 1911, was itself superseded by tungsten.

### 22.2.3 Atomic and physical properties of the elements

Some of the important properties of Group 5 elements are summarized in Table 22.1. Having odd atomic numbers, they have few naturally occurring isotopes; Nb only 1 and V and Ta 2 each, though the second ones are present only in very low abundance ( $^{50}V$  0.250%,  $^{180}Ta$  0.012%). As a consequence (p. 17) their atomic weights have been determined with considerable precision. On the other hand, because of difficulties in removing all impurities, reported values of their bulk properties have often required revision.

All three elements are shiny, silvery metals with typically metallic bcc structures. When very pure they are comparatively soft and ductile but impurities usually have a hardening and embrittling effect. When compared to the elements of Group 4 the expected trends are apparent. These elements are slightly less electropositive and are smaller than their predecessors, and the heavier pair Nb and Ta are virtually identical in size as a consequence of the lanthanide contraction. The extra d electron again appears to contribute to stronger metal-metal bonding in the bulk metals, leading in each case to a higher mp, bp and enthalpy of atomization. Indeed, these quantities reach their maximum values in this and the following group. In the first transition series, vanadium is the last element before some of the  $(n-1)d$  electrons begin to enter the inert electron-core of the atom and are therefore not available for bonding. As a result, not only is its mp the highest in the series but it is the last element whose compounds in the group oxidation state (i.e. involving all  $(n-1)d$  and  $ns$  electrons) are not strongly oxidizing. In the second and

Table 22.1 Some properties of Group 5 elements

Property	V	Nb	Ta
Atomic number	23	41	73
Number of naturally occurring isotopes	2	1	2
Atomic weight	50.9415(1)	92.90638(2)	180.9479(1)
Electronic configuration	[Ar]3d <sup>3</sup> 4s <sup>2</sup>	[Kr]4d <sup>3</sup> 5s <sup>2</sup>	[Xe]4f <sup>14</sup> 5d <sup>3</sup> 6s <sup>2</sup>
Electronegativity	1.6	1.6	1.5
Metal radius (12-coordinate)/pm	134	146	146
Ionic radius (6-coordinate)/pm	54	64	64
	IV	68	68
	III	72	72
	II	—	—
MP/°C	1915	2468	2980
BP/°C	3350	4758	5534
$\Delta H_{\text{fus}}/\text{kJ mol}^{-1}$	17.5	26.8	24.7
$\Delta H_{\text{vap}}/\text{kJ mol}^{-1}$	459.7	680.2	758.2
$\Delta H_{\text{f}}(\text{monoatomic gas})/\text{kJ mol}^{-1}$	510 ( $\pm 29$ )	724	782 ( $\pm 6$ )
Density (20°C)/g cm <sup>-3</sup>	6.11	8.57	16.65
Electrical resistivity (20°C)/ $\mu\text{ohm cm}$	~25	~12.5	(12.4)

third series the entry of  $(n - 1)d$  electrons into the electron core is delayed somewhat and it is molybdenum and tungsten in Group 6 whose mps are the highest.

### 22.2.4 Chemical reactivity and trends

The elements of Group 5 are in many ways similar to their predecessors in Group 4. They react with most non-metals, giving products which are frequently interstitial and nonstoichiometric, but they require high temperatures to do so. Their general resistance to corrosion is largely due to the formation of surface films of oxides which are particularly effective in the case of tantalum. Unless heated, tantalum is appreciably attacked only by oleum, hydrofluoric acid or, more particularly, a hydrofluoric/nitric acid mixture. Fused alkalis will also attack it. In addition to these reagents, vanadium and niobium are attacked by other hot concentrated mineral acids but are resistant to fused alkali.

The most obvious factor in comparing the chemistry of the three elements is again the very close similarity of the second and third members although, in this group, slight differences can be discerned as will be discussed shortly. The

stability of the lower oxidation states decreases as the group is descended. As a result, although each element shows formal oxidation states from +5 down to -3, the most stable one in the case of vanadium under normal conditions is the +4, and even the +3 and +2 oxidation states (which are admittedly strongly reducing) have well-characterized cationic aqueous chemistries; by contrast most of the chemistries of niobium and tantalum are confined to the group oxidation state +5. Of the halogens, only the strongly oxidizing fluorine produces a pentahalide of vanadium, and the other vanadium(V) compounds are based on the oxohalides and the pentoxide. The pentoxide also gives rise to the complicated but characteristic aqueous chemistry of the polymerized vanadates (isopolyvanadates) which anticipates the even more extensive chemistry of the polymolybdates and polytungstates; this is only incompletely mirrored by niobium and tantalum.

The +4 oxidation state, which for Nb and Ta is best represented by their halides, is most notable for the uniquely stable  $\text{VO}^{2+}$  (vanadyl) ion which retains its identity throughout a wide variety of reactions and forms many complexes. Indeed it is probably the most stable diatomic ion known. The  $\text{M}^{\text{IV}}$  ions have only slightly smaller radii



Table 22.2 Oxidation states and stereochemistries of compounds of vanadium, niobium and tantalum

Oxidation state	Coordination number	Stereochemistry	V	Nb/Ta
-3 (d <sup>8</sup> )	5	—	[V(CO) <sub>5</sub> ] <sup>3-</sup>	[M(CO) <sub>5</sub> ] <sup>3-</sup>
-1 (d <sup>6</sup> )	6	Octahedral	[V(CO) <sub>6</sub> ] <sup>-</sup>	[M(CO) <sub>6</sub> ] <sup>-</sup>
0 (d <sup>5</sup> )	6	Octahedral	[V(CO) <sub>6</sub> ]	—
1 (d <sup>4</sup> )	6	Octahedral	[V(bipy) <sub>3</sub> ] <sup>+</sup>	—
	7	Capped octahedral	—	[TaH(CO) <sub>2</sub> (diphos) <sub>2</sub> ]
2 (d <sup>3</sup> )	4	Square planar	—	NbO
	6	Octahedral	[V(CN) <sub>6</sub> ] <sup>4-</sup>	TaO(?)
		Trigonal prismatic	VS	NbS
3 (d <sup>2</sup> )	3	Planar	[V{N(SiMe <sub>3</sub> ) <sub>2</sub> }] <sub>3</sub>	—
	4	Tetrahedral	[VCl <sub>4</sub> ] <sup>-</sup>	—
	5	Trigonal bipyramidal	[VCl <sub>3</sub> (NMe <sub>3</sub> ) <sub>2</sub> ]	—
	6	Octahedral	[V(C <sub>2</sub> O <sub>4</sub> ) <sub>3</sub> ] <sup>3-</sup>	[Nb <sub>2</sub> Cl <sub>9</sub> ] <sup>3-</sup>
		Trigonal prismatic	—	LiNbO <sub>2</sub>
	7	Complex	—	[Ta(CO)Cl <sub>3</sub> (PMe <sub>2</sub> Ph) <sub>3</sub> ].EtOH
	8	Dodecahedral	—	[Nb(CN) <sub>8</sub> ] <sup>5-</sup>
4 (d <sup>1</sup> )	4	Tetrahedral	VCl <sub>4</sub>	[Nb(NEt <sub>2</sub> ) <sub>4</sub> ] (not Ta)
	5	Trigonal bipyramidal	[VOCl <sub>2</sub> (NMe <sub>3</sub> ) <sub>2</sub> ]	—
		Square pyramidal	[VO(acac) <sub>2</sub> ]	—
	6	Octahedral	[VCl <sub>4</sub> (bipy)]	[MCl <sub>6</sub> ] <sup>2-</sup>
	7	Pentagonal bipyramidal	—	[NbF <sub>7</sub> ] <sup>3-</sup>
	8	Dodecahedral	[VCl <sub>4</sub> (diars) <sub>2</sub> ]	[NbCl <sub>4</sub> (diars) <sub>2</sub> ] (not Ta)
		Square antiprismatic	[V(S <sub>2</sub> CMe) <sub>4</sub> ] <sup>(a)</sup>	[Nb(β-diketonate) <sub>4</sub> ]
5 (d <sup>0</sup> )	4	Tetrahedral	VOCl <sub>3</sub>	ScNbO <sub>4</sub>
	5	Trigonal bipyramidal	VCl <sub>5</sub> (g)	MF <sub>5</sub> (g)
		Square pyramidal	[VOF <sub>4</sub> ] <sup>-</sup>	[M(NMe <sub>2</sub> ) <sub>5</sub> ]
	6	Octahedral	[VF <sub>6</sub> ] <sup>-</sup>	[MF <sub>6</sub> ] <sup>-</sup>
		Trigonal prismatic	—	[M(S <sub>2</sub> C <sub>6</sub> H <sub>4</sub> ) <sub>3</sub> ] <sup>-</sup>
	7	Pentagonal bipyramidal	[VO(S <sub>2</sub> CNEt <sub>2</sub> ) <sub>3</sub> ]	[TaS(S <sub>2</sub> CNEt <sub>2</sub> ) <sub>3</sub> ]
		Capped trigonal prismatic	—	[MF <sub>7</sub> ] <sup>2-</sup>
	8	Dodecahedral	[V(O <sub>2</sub> ) <sub>4</sub> ] <sup>3-</sup>	[M(O <sub>2</sub> ) <sub>4</sub> ] <sup>3-</sup>
		Square antiprismatic	—	[Ta(S <sub>2</sub> CNMe <sub>2</sub> ) <sub>4</sub> ] <sup>+</sup>
				[MF <sub>8</sub> ] <sup>3-</sup>

<sup>(a)</sup>Tetrakis(dithioacetato)vanadium(IV) was originally classified as dodecahedral. Re-examination has shown that its unit cell in fact contains two independent metal sites. One is indeed dodecahedral but the other is square antiprismatic; C. W. HAIGH, *Polyhedron* **14**, 2871–8 (1995).

than those of Group 4, and, again, coordination numbers as high as 8 are found. In the +5 state, however, only Nb and Ta are sufficiently large to achieve this coordination number with ligands other than bidentate ones with very small “bites”, such as the peroxy group. Table 22.2 illustrates the various oxidation states and stereochemistries of compounds of V, Nb and Ta.

Niobium and tantalum provide no counterpart to the cationic chemistry of vanadium in the +3 and +2 oxidation states. Instead, they form a series of “cluster” compounds based

on octahedral M<sub>6</sub>X<sub>12</sub> units. The occurrence of such compounds is largely a consequence of the strength of metal–metal bonding in this part of the periodic table (as reflected in high enthalpies of atomization), and similar cluster compounds are found also for molybdenum and tungsten.

Compounds containing M–C σ-bonds are frequently unstable and do not give rise to an extensive chemistry (p. 999). Vanadium forms a neutral (paramagnetic) hexacarbonyl which, though not very stable, contrasts with that of titanium in that it can at least be prepared in

quantity. All three elements give a number of  $\eta^5$ -cyclopentadienyl derivatives.

## 22.3 Compounds of Vanadium, Niobium and Tantalum<sup>(2,3)</sup>

The binary hydrides (p. 67), borides (p. 148), carbides (p. 299), and nitrides (p. 418) of these metals have already been discussed and will not be described further except to note that, as with the analogous compounds of Group 4, they are hard, refractory and nonstoichiometric materials with high conductivities. The intriguing cryo-compound  $[V(N_2)_6]$  has been isolated by cocondensing V atoms and  $N_2$  molecules at 20–25 K; it has an infrared absorption at  $2100\text{ cm}^{-1}$  and its d–d and charge-transfer spectra are strikingly similar to those of the isoelectronic 17-electron species  $[V(CO)_6]$ .

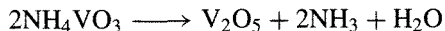
### 22.3.1 Oxides

Table 22.3 gives the principal oxides formed by the elements of this group. Besides the 4 oxides of vanadium shown, a number of other phases of intermediate composition have been identified and the lower oxides in particular have wide ranges of homogeneity.  $V_2O_5$  is orange yellow when pure (due to charge transfer) and is the final product when the metal is heated in an excess of oxygen, but contamination with lower oxides is then common and a better method is to heat

**Table 22.3** Oxides of Group 5 metals

Oxidation state:	+5	+4	+3	+2
V	$V_2O_5$	$VO_2$	$V_2O_3$	VO
Nb	$Nb_2O_5$	$NbO_2$	—	NbO
Ta	$Ta_2O_5$	$TaO_2$	—	(TaO)

ammonium “metavanadate”:



On the basis of simple radius ratio arguments, vanadium(V) is expected to be rather large for tetrahedral coordination to oxygen, but rather small for octahedral coordination. It is perhaps not surprising therefore that, though the structure of  $V_2O_5$  is somewhat complicated, it consists essentially of distorted trigonal bipyramids of  $VO_5$  sharing edges to form zigzag double chains. Another, metastable, form has been prepared which differs from the normal one in the relative dispositions of adjacent parallel chains.<sup>(4)</sup>  $V_2O_5$  is homogeneous over only a small range of compositions but loses oxygen reversibly on heating, which is probably why it is such a versatile catalyst. For instance, it catalyses the oxidation of numerous organic compounds by air or hydrogen peroxide, and the reduction of olefins (alkenes) and of aromatic hydrocarbons by hydrogen, but most importantly it catalyses the oxidation of  $SO_2$  to  $SO_3$  in the contact process for the manufacture of sulfuric acid (p. 708). For this purpose it replaced metallic platinum which, besides being far more expensive, was also prone to “poisoning” by impurities such as arsenic.  $V_2O_5$  is amphoteric. It is slightly soluble in water, giving a pale yellow, acidic solution. It dissolves in acids producing salts of the pale-yellow dioxovanadium(V) ion,  $[VO_2]^+$ , and in alkalis producing colourless solutions which, at high pH, contain the orthovanadate ion,  $VO_4^{3-}$ . At intermediate pHs a series of hydrolysis-polymerization reactions occur yielding the isopolyvanadates to be discussed in the next section. It is also a mild oxidizing agent and in aqueous solution is reduced by, for instance, hydrohalic acids to vanadium(IV). In the solid, mild reduction with CO,  $SO_2$ , or fusion with oxalic acid gives the deep-blue  $VO_2$ .

At room temperature  $VO_2$  has a rutile-like structure (p. 961) distorted by the presence of pairs of vanadium atoms bonded together. Above  $70^\circ\text{C}$ , however, an undistorted rutile

<sup>2</sup> D. L. KEPERT, *The Early Transition Metals*, Chap. 3, V, Nb, Ta, pp. 142–254, Academic Press, London, 1972.

<sup>3</sup> R. J. H. CLARK, Chap. 34, pp. 491–551, and D. BROWN, Chap. 35, pp. 553–622, in *Comprehensive Inorganic Chemistry*, Vol. 3, Pergamon Press, Oxford, 1973.

<sup>4</sup> J. M. COCCIANTELLI, P. GRAVEREAU, M. POUCHARD and P. HAGENMULLER, *J. Solid State Chem.*, **93**, 497–502 (1991).

structure is adopted as the atoms in each pair separate, breaking the localized V–V bonds and releasing the bonding electrons, so causing a sharp increase in electrical conductivity and magnetic susceptibility. It is again amphoteric, dissolving in non-oxidizing acids to give salts of the blue oxovanadium(IV) (vanadyl) ion  $[\text{VO}]^{2+}$ , and in alkali to give the yellow to brown vanadate(IV) (hypovanadate) ion  $[\text{V}_4\text{O}_9]^{2-}$ , or at high pH  $[\text{VO}_4]^{4-}$ . Like the vanadium(V) system, a number of polyanions are produced at intermediate pH. Between  $\text{V}_2\text{O}_5$  and  $\text{VO}_2$  is a succession of phases  $\text{V}_n\text{O}_{2n+1}$  of which  $\text{V}_3\text{O}_7$ ,  $\text{V}_4\text{O}_9$  and  $\text{V}_6\text{O}_{13}$  have been characterized.

Further reduction with  $\text{H}_2$ , C or CO produces a series of discrete chemical-shear phases (Magnéli phases) of general formula  $\text{V}_n\text{O}_{2n-1}$  based on a rutile structure with periodic defects (p. 961), before the black, refractory sesquioxide  $\text{V}_2\text{O}_3$  is reached. Examples are  $\text{V}_4\text{O}_7$ ,  $\text{V}_5\text{O}_9$ ,  $\text{V}_6\text{O}_{11}$ ,  $\text{V}_7\text{O}_{13}$  and  $\text{V}_8\text{O}_{15}$ . The oxides VO,  $\text{V}_2\text{O}_3$  and  $\text{V}_3\text{O}_5$  also conform to the general formula  $\text{V}_n\text{O}_{2n-1}$ , but this is a purely formal relation and their structures are not related by chemical-shear to those of the Magnéli phases.

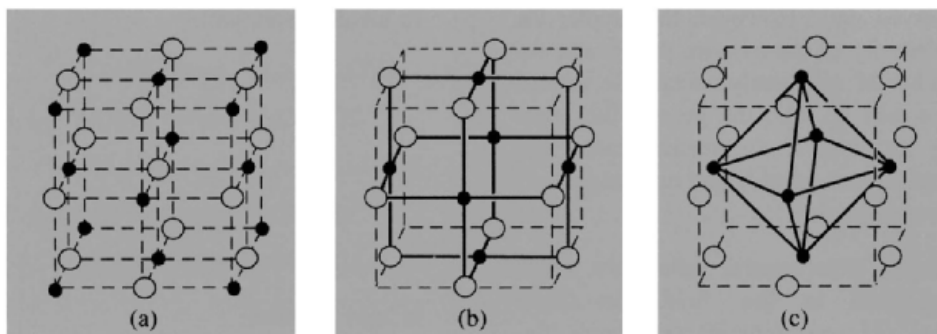
$\text{V}_2\text{O}_3$  has a corundum structure (p. 243) and is notable for the transition occurring as it is cooled below about 170 K when its electrical conductivity changes from metallic to insulating in character. Chemically it is entirely basic, dissolving in aqueous acids to give blue or green vanadium(III) solutions which are strongly reducing. On still further reducing the oxide system, the corundum structure is retained down to compositions as low as  $\text{VO}_{1.35}$ , after which the grey metallic monoxide VO, with a defect rock-salt structure, is formed. This too is markedly nonstoichiometric with a composition range from  $\text{VO}_{0.8}$  to  $\text{VO}_{1.3}$ . In all, therefore, at least 13 distinct oxide phases of vanadium have been identified between  $\text{VO}_{\sim 1}$  and  $\text{V}_2\text{O}_5$ .

Niobium and tantalum also form various oxide phases but they are not so extensive or well characterized as those of vanadium. Their pentoxides are relatively much more stable and difficult to reduce. As they are attacked by conc HF and will dissolve in fused alkali, they may perhaps

be described as amphoteric, but inertness is the more obvious characteristic. Their structures are extremely complicated and  $\text{Nb}_2\text{O}_5$  in particular displays extensive polymorphism. It is interesting to note that the polymorphs of  $\text{Nb}_2\text{O}_5$  and  $\text{Ta}_2\text{O}_5$  are by no means all analogous.

High temperature reduction of  $\text{Nb}_2\text{O}_5$  with hydrogen gives the bluish-black dioxide  $\text{NbO}_2$  which has a distorted rutile structure. As in  $\text{VO}_2$  the distortion is caused by pairs of metal atoms evidently bonded together, but the distortion is in a different direction. Between  $\text{Nb}_2\text{O}_5$  and  $\text{NbO}_2$  there is a homologous series of structurally related phases of general formula  $\text{Nb}_{3n+1}\text{O}_{8n-2}$  with  $n = 5, 6, 7, 8$  (i.e.  $\text{Nb}_8\text{O}_{19}$ ,  $\text{Nb}_{19}\text{O}_{46}$ ,  $\text{Nb}_{11}\text{O}_{27}$  and  $\text{Nb}_{25}\text{O}_{62}$ ). In addition, oxides of formula  $\text{Nb}_{12}\text{O}_{29}$  and  $\text{Nb}_{47}\text{O}_{116}$  have been reported: the numerical relationship to  $\text{Nb}_2\text{O}_5$  is clear since  $\text{Nb}_{12}\text{O}_{29}$  is  $(12\text{Nb}_2\text{O}_5 - 2\text{O})$  and  $2\text{Nb}_{47}\text{O}_{116}$  (or  $\text{Nb}_{94}\text{O}_{232}$ ) is  $(47\text{Nb}_2\text{O}_5 - 3\text{O})$ . Further reduction produces the grey monoxide NbO which has a cubic structure and metallic conductivity but differs markedly from its vanadium analogue in that its composition range is only  $\text{NbO}_{0.982}$  to  $\text{NbO}_{1.008}$ . The structure is a unique variant of the rock-salt NaCl structure (p. 242) in which there are vacancies (Nb) at the eight corners of the unit cell and an O vacancy at its centre (Fig. 22.1). The structure could therefore be described as a vacancy-defect NaCl structure  $\text{Nb}_{0.75}\square_{0.25}\text{O}_{0.75}\square_{0.25}$ , but as all the vacancies are ordered it is better to consider it as a new structure type in which both Nb and O form 4 coplanar bonds. The central feature is a 3D framework of  $\text{Nb}_6$  octahedral clusters (Nb–Nb 298 pm, cf. Nb–Nb 285 pm in Nb metal) and this accounts for the metallic conductivity of the compound. The structure is reminiscent of the structure-motif of the lower halides of Nb and Ta (p. 992) and the retention of the  $\text{Nb}_6$  clusters rather than the adoption of the ionic NaCl-type structure can similarly be related to the high heats of sublimation of Nb and neighbouring metals. (For a fuller discussion of the bonding, see ref. 5.)

<sup>5</sup> J. K. BURDETT and T. HUGHBANKS, *J. Am. Chem. Soc.* **106**, 3101–13 (1984).



**Figure 22.1** (a) NaCl (MgO) showing all sites occupied by M(●) and O(○). (b) NbO showing planar coordination of Nb (and O) and vacancies at the cube corners (Nb) and centre (O). (c) NbO as in (b), but emphasizing the octahedral Nb<sub>6</sub> cluster (joined by corner sharing to neighbouring unit cells).

The heavier metal tantalum is distinctly less inclined than niobium to form oxides in lower oxidation states. The rutile phase TaO<sub>2</sub> is known but has not been studied, and a cubic rock-salt-type phase TaO with a narrow homogeneity range has also been reported but not yet fully characterized. Ta<sub>2</sub>O<sub>5</sub> has two well-established polymorphs which have a reversible transition temperature at 1355°C but the detailed structure of these phases is too complex to be discussed here.

### 22.3.2 Polymetallates<sup>(6-8b)</sup>

The amphoteric nature of V<sub>2</sub>O<sub>5</sub> has already been noted. In fact, if the colourless solution produced by dissolving V<sub>2</sub>O<sub>5</sub> in strong aqueous alkali such as NaOH is gradually acidified, it first deepens in colour, becoming orange to red as the neutral point is passed; it then darkens further and, around pH 2, a brown precipitate of hydrated V<sub>2</sub>O<sub>5</sub> separates and redissolves at

still lower pHs to give a pale-yellow solution. As a result of spectrophotometric studies there is general agreement that the predominant species in the initial colourless solution is the tetrahedral VO<sub>4</sub><sup>3-</sup> ion and, in the final pale-yellow solution, the angular VO<sub>2</sub><sup>+</sup> ion. In the intervening orange to red solutions a complicated series of hydrolysis-polymerization reactions occur, which have direct counterparts in the chemistries of Mo and W and to a lesser extent Nb, Ta and Cr. The polymerized species involved are collectively known as isopolymetallates or isopolyanions. The determination of the equilibria involved in their formation, as well as their stoichiometries and structures, has been a confused and disputed area, some aspects of which are by no means settled even now. That this is so is perfectly understandable because:

- (i) Some of the equilibria are reached only slowly (possibly months in some cases) and it is likely that much of the reported work has been done under non-equilibrium conditions.
- (ii) Often in early work, solid species were crystallized from solution and their stoichiometries, quite unjustifiably as it turns out, were used to infer the stoichiometries of species in solution.
- (iii) When a series of experimental measurements has been made it is usual to see what combination of plausible ionic species will best account for the

<sup>6</sup> M. T. POPE, Iso- and Hetero-polyanions, Chap. 38 in *Comprehensive Coordination Chemistry*, Vol. 3, pp. 1028–58, Pergamon Press, Oxford, 1987.

<sup>7</sup> M. T. POPE, *Heteropoly and Isopoly Oxometalates*, Springer Verlag, Berlin, 1983, 180 pp.

<sup>8</sup> M. T. POPE and A. MÜLLER, *Angew. Chem. Int. Edn. Engl.* **30**, 34–48 (1991).

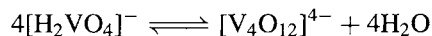
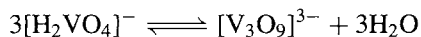
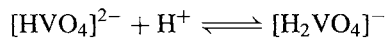
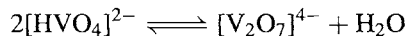
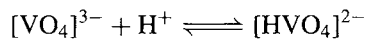
<sup>8a</sup> G. M. MAKSIMOV, *Russ. Chem. Rev. (Engl. Transl.)* **64**, 445–61 (1995).

<sup>8b</sup> M. I. KHAN and J. ZUBIETA, *Prog. Inorg. Chem.* **43**, 1–149 (1995).

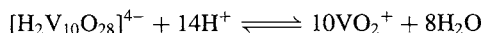
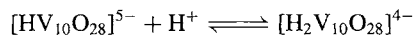
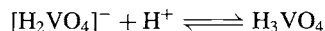
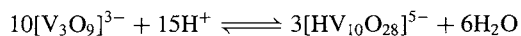
observed data. However, the greater the complexity of the system, the greater the number of apparently acceptable models there will be, and the greater the accuracy required if the measurements are to distinguish reliably and unambiguously between them.

Of the many experimental techniques which have been used in this field, the more important are: pH measurements, cryoscopy, ion-exchange and ultraviolet/visible spectroscopy for studying the stoichiometry of the equilibria, and infrared/Raman and nmr spectroscopy for studying the structures of the ions in solution, where oxygen-17 and metal atom nmr spectroscopy are playing an increasingly important role. Probably the best summary of our current understanding of the vanadate system is given by Fig. 22.2. This shows how the existence of the various vanadate species depends on the pH and on the total concentration of vanadium.<sup>(7)</sup> Their occurrence can be accounted for by protonation and condensation equilibria such as the following:

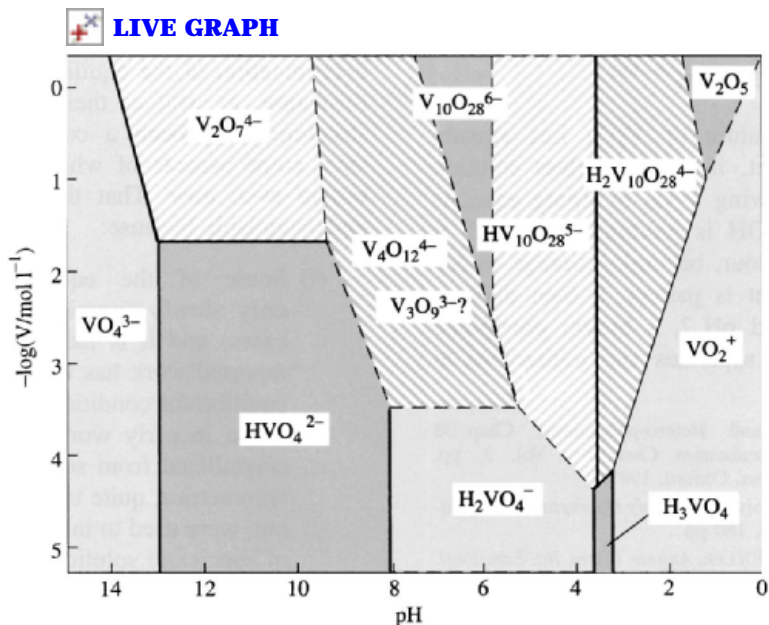
In alkaline solution:



In acid solution:



In these equilibria the site of protonation in the species  $[\text{HVO}_4]^{2-}$ ,  $[\text{H}_2\text{VO}_4]^{-}$  etc., is an oxygen atom (not vanadium); a more precise representation would therefore be  $[\text{VO}_3(\text{OH})]^{2-}$ ,  $[\text{VO}_2(\text{OH})_2]^{-}$  etc. However, the customary formulation is retained for convenience (cf.  $\text{HNO}_3$ ,  $\text{HSO}_4^{-}$ ,  $\text{H}_2\text{SO}_4$ , etc.).



**Figure 22.2** Occurrence of various vanadate and polyvanadate species as a function of pH and total concentration of vanadium.

It is evident from Fig. 22.2 that only in very dilute solutions are monomeric vanadium ions found and any increase in concentrations, particularly if the solution is acidic, leads to polymerization.  $^{51}\text{V}$  nmr work indicates that, starting from the alkaline side, the various ionic species are all based on 4-coordinate vanadium(V) in the form of linked  $\text{VO}_4$  tetrahedra until the decavanadates appear. These evidently involve a higher coordination number, but whether or not it is the same in solution as in the solids which can be separated is uncertain. However, it is interesting to note that similarities between the vanadate and chromate systems cease with the appearance of the decavanadates which have no counterpart in chromate chemistry. The smaller chromium(VI) is apparently limited to tetrahedral coordination with oxygen, whereas vanadium(V) is not.

More information is of course available on the structures of the various crystalline vanadates which can be separated from solution. Traditionally, the colourless salts obtained from alkaline solution were called ortho-, pyro-, or metavanadates by analogy with the phosphates of corresponding stoichiometry. "Ortho"-vanadates,  $\text{M}_3\text{VO}_4(\text{aq})$ , apparently contain discrete, tetrahedral,  $\text{VO}_4^{3-}$  ions; "pyro"-vanadates,  $\text{M}_4\text{V}_2\text{O}_7(\text{aq})$ , contain dinuclear  $[\text{V}_2\text{O}_7]^{4-}$  ions consisting of 2  $\text{VO}_4$  tetrahedra sharing a corner; the structures of "meta"-vanadates depend on the state of hydration (Fig. 22.3) but in no cases do they involve discrete  $\text{VO}_3^-$  ions. Anhydrous metavanadates such as  $\text{NH}_4\text{VO}_3$  contain infinite chains of corner-linked  $\text{VO}_4$  tetrahedra, while hydrated metavanadates, such as  $\text{KVO}_3 \cdot \text{H}_2\text{O}$ , contain infinite chains of approximately trigonal bipyramidal  $\text{VO}_5$  units, not unlike those in  $\text{V}_2\text{O}_5$ . From the bright orange, acidic solutions, orange, crystalline decavanadates such as  $\text{Na}_6\text{V}_{10}\text{O}_{28} \cdot 18\text{H}_2\text{O}$  are obtained: the anion  $[\text{V}_{10}\text{O}_{28}]^{6-}$  is made up of 10  $\text{VO}_6$  octahedra, two representations of which are shown in Fig. 22.3.  $^{51}\text{V}$  and  $^{17}\text{O}$  nmr evidence shows that this is present in solution, and it can be isolated with a variety of counter cations — indeed it occurs naturally in at least three minerals. Other compounds such as  $(\text{PyH})_4[\text{V}_{10}\text{O}_{28}\text{H}_2]$

can also be crystallized<sup>(9)</sup> in which outer oxygen atoms of the polyanion are protonated<sup>†</sup>, while refluxing the tetra-*n*-butyl ammonium salt of the decavanadate in acetonitrile has been shown<sup>(10)</sup> to yield the dark-red inclusion compound  $[(n\text{-C}_4\text{H}_9\text{N})_4[\text{MeCN}(\text{V}_{12}\text{O}_{32})]^{4-}]$  in which the MeCN molecule sits inside the now basket-shaped polyanion.

Because of potential applications in catalysis and in providing convenient models for biological systems (for example, the chemical similarities of  $\text{VO}^{n+}$  and  $\text{Fe}^{n+}$  may be harnessed to study iron storage and transport proteins), a more diverse chemistry has so far been developed for reduced polyvanadates exhibiting a whole range of  $\text{V}^{\text{V}}$  to  $\text{V}^{\text{IV}}$  ratios. At the reduced extreme of this range, prolonged heating (4 days at  $200^\circ\text{C}$ ) of  $\text{NH}_4\text{VO}_3$  and  $\text{EtC}(\text{CH}_2\text{OH})_3$  produces black crystals of the  $\text{V}^{\text{IV}}$  compound<sup>(11)</sup>  $(\text{NH}_4)_4[\text{V}_{10}\text{O}_{16}(\text{EtC}(\text{CH}_2\text{O})_3)_4] \cdot 4\text{H}_2\text{O}$ , in the anion of which, twelve of the oxygen atoms in the  $\text{V}_{10}\text{O}_{28}$  cluster are provided by bridging alkoxy groups. The same research workers have also used this hydrothermal technique to prepare another decavanadate(IV) material which contains chiral, interpenetrating double helices of vanadium phosphate units.<sup>(12)</sup> Still higher nuclearity is found in the dark brown  $\text{M}'_{12}[\text{V}_{18}\text{O}_{42}] \cdot n\text{H}_2\text{O}$  crystallized from alkaline solutions of  $\text{VO}_2$ . The anion consists this time of  $\text{VO}_5$  square pyramids, the bases of which by corner- and edge-sharing form an almost spherical cavity of diameter  $\sim 450$  pm (Fig. 22.3f). It has the extraordinary ability to encapsulate *negatively* charged ions, as in

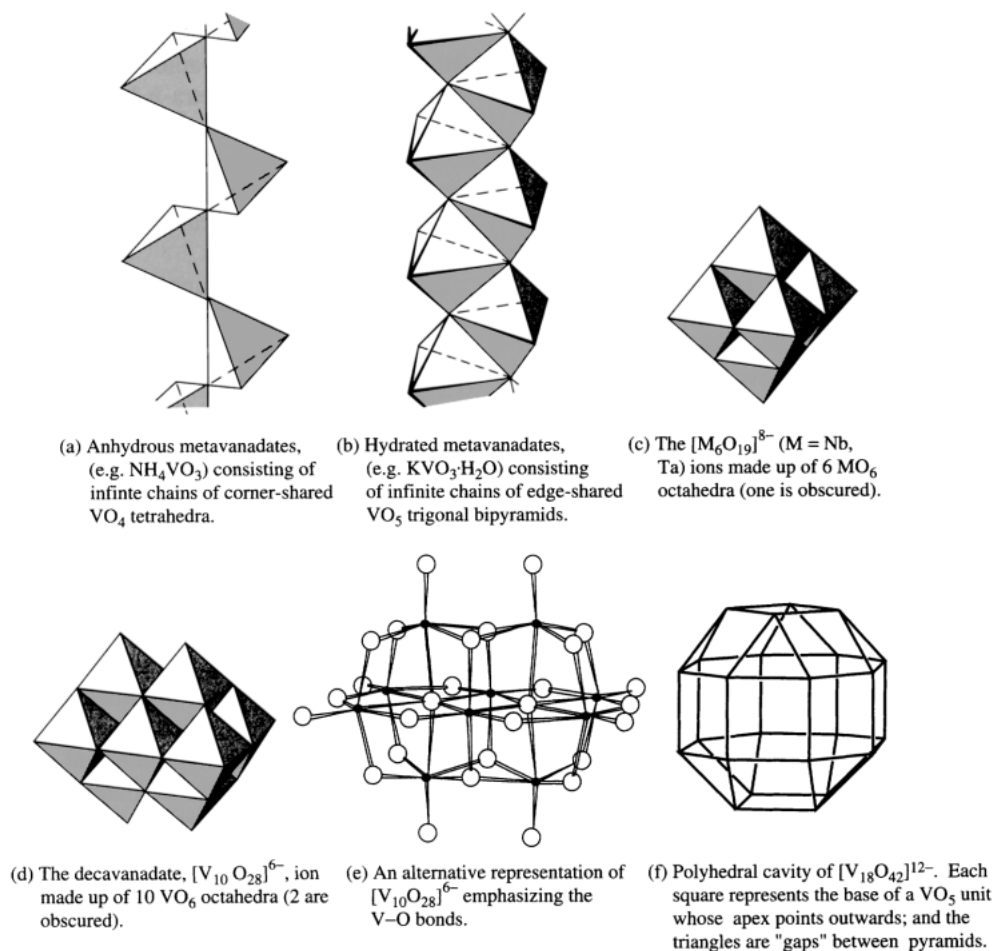
<sup>†</sup> Although protonation usually occurs on outer oxygen atoms (Fig. 22.3e), an exception is provided by  $[\text{NH}_3(\text{C}_6\text{H}_{13})][\text{V}_{10}\text{O}_{28}\text{H}_2]$  in which the protons have been located on triply linked, inner oxygen atoms. See P. ROMAN, A. ARANZABE, A. LUQUE, J. M. G.-ZORILLA and M. M.-RIPOLL, *J. Chem. Soc., Dalton Trans.*, 2225–31 (1995).

<sup>9</sup> J. M. ARRIETA, *Polyhedron* **11**, 3045–68 (1992).

<sup>10</sup> V. W. DAY, W. G. KLEMPERER and O. M. YAGHI, *J. Am. Chem. Soc.* **111**, 5959–61 (1989).

<sup>11</sup> M. I. KHAN, Q. CHEN and J. ZUBIETA, *J. Chem. Soc., Chem. Commun.*, 305–6 (1992).

<sup>12</sup> V. SOGHOMONIAN, Q. CHEN, R. C. HAUSHALTER, J. ZUBIETA and C. J. CONNOR, *Science* **259**, 1596–9 (1993).



**Figure 22.3** The structures of some isopoly-anions in the solid state using, where relevant, the conventional representation in which each polyhedron contains a metal atom and each vertex of a polyhedron represents an oxygen atom.

the compounds,<sup>(13)</sup>  $\text{M}_9[\text{H}_4\text{V}_{18}\text{O}_{42}\text{X}].n\text{H}_2\text{O}$  ( $\text{M} = \text{Cs}, n = 12, \text{X} = \text{Br}, \text{I}; \text{M} = \text{K}, n = 16, \text{X} = \text{Cl}$ ). Amongst the mixed,  $\text{V}^{\text{V}}, \text{V}^{\text{IV}}$  polyvanadates nuclearities up to 34 have been attained,<sup>(14)</sup> as in  $\text{K}_{10}[\text{V}_{34}\text{O}_{82}].20\text{H}_2\text{O}$ . In these materials the coordination of the metal can be octahedral ( $\text{V}^{\text{V}}, \text{V}^{\text{IV}}$ ), square pyramidal ( $\text{V}^{\text{V}}, \text{V}^{\text{IV}}$ ), trigonal bipyramidal ( $\text{V}^{\text{V}}$ ) and tetrahedral ( $\text{V}^{\text{V}}$ ), and the

magnetic moment per  $\text{V}^{\text{IV}}$  atom decreases as the proportion of  $\text{V}^{\text{IV}}$  atoms increases (indicating increasing M–M interaction). To rationalize this rich variety of structures it has been suggested<sup>(15)</sup> that they may be conceptually derived from that of  $\text{V}_2\text{O}_5$ .

Heteropolyanions, in which an atom of a different element is incorporated, usually at the centre of a cage-like structure, are most abundant in Group 6 (p. 1013) but increasing numbers are to

<sup>13</sup> A. MÜLLER, M. PENK, R. ROHLFING, E. KRICKEMEYER and J. DÖRING, *Angew. Chem. Int. Edn. Engl.* **29**, 926–7 (1990).

<sup>14</sup> A. MÜLLER, R. ROHLFING, J. DÖRING and M. PENK, *Angew. Chem. Int. Edn. Engl.* **30**, 588–60 (1991).

<sup>15</sup> W. KLEMPERER, T. A. MARQUART and O. M. YAGHI, *Angew. Chem. Int. Edn. Engl.* **31**, 49–51 (1992).

be found in this group also. For vanadium(V) the  $[XV_{14}O_{42}]^{9-}$  ions ( $X = P, As$ ) are composed of an X atom tetrahedrally coordinated to four oxygen atoms at the centre of a "Keggin" anion (p. 1014) which is capped by two VO groups.<sup>(16)</sup> Reduced species, because of their lower overall anionic charge, allow the formation of clusters of higher nuclearity and several of these have been reported.<sup>(8)</sup>

Fusion of  $Nb_2O_5$  and  $Ta_2O_5$  with an excess of alkali hydroxides or carbonates, followed by dissolution in water, produces solutions of isopolyanions but not in the variety produced with vanadium. It appears that, down to pH 11,  $[M_6O_{19}]^{8-}$  ions are present; in the case of niobium protonation occurs at lower pH to give  $[HNb_6O_{19}]^{7-}$ . The presence of discrete  $MO_4^{3-}$  ions in strongly alkaline solutions is uncertain. Below pH  $\sim 7$  for Nb and pH  $\sim 10$  for Ta, precipitation of the hydrous oxides occurs. Salts such as  $K_8M_6O_{19} \cdot 16H_2O$  can be crystallized from the alkaline solutions and contain  $[M_6O_{19}]^{8-}$  ions which are made up of octahedral groupings of 6  $MO_6$  octahedra (Fig. 22.3). A decaniobate, exactly analogous to the decavanadate, has also been isolated and it is possible that such species exist also in solution at low pH.

Most niobates and tantalates, however, are insoluble and may be regarded as mixed oxides in which the Nb or Ta is octahedrally coordinated and with no discrete anion present. Thus  $KMO_3$ , known inaccurately (since they have no discrete  $MO_3^-$  anions) as metaniobates and metatantalates, have the perovskite (p. 963) structure. Several of these perovskites have been characterized and some have ferroelectric and piezoelectric properties (p. 57). Because of these properties,  $LiNbO_3$  and  $LiTaO_3$  have been found to be attractive alternatives to quartz as "frequency filters" in communications devices.

A number of nonstoichiometric "bronzes" are also known<sup>(17)</sup> which, like the titanium bronzes

already mentioned (p. 964) and the better known tungsten bronzes (p. 1016), are characterized by very high electrical conductivities and characteristic colours. For instance,  $Sr_xNbO_3$  ( $x = 0.7-0.95$ ) varies in colour from deep blue to red as the Sr content increases. Fusion of mixtures of appropriate oxides of niobium and alkali metals produces black powders (shiny, golden *single* crystals) of  $NaNb_{10}O_{18}$  (metallic conductance)<sup>(18)</sup> and  $KNb_8O_{14}$  (semiconductor),<sup>(19)</sup> both of which are made up of  $Nb^V O_6$  octahedra and  $Nb_6O_{12}$  clusters analogous to the  $M_6X_{12}$  halide cluster (p. 992).  $Li_xNbO_2$  ( $x \sim 0.5$ ) has been shown<sup>(20)</sup> to be a superconductor below 5 K, and is notable as the first superconductor involving an early transition metal oxide which has a layered rather than a 3D structure. It is, indeed, the search for better superconductors and battery electrode materials which is responsible for the upsurge in interest in early transition metal oxides, and further expansion of this area of chemistry is to be expected.

### 22.3.3 Sulfides, selenides and tellurides

All three metals form a wide variety of binary chalcogenides which frequently differ both in stoichiometry and in structure from the oxides. Many have complex structures which are not easily described, and detailed discussion is therefore inappropriate. The various sulfide phases are listed in Table 22.4: phases approximating to the stoichiometry  $MS$  have the NiAs-type structure (p. 556) whereas  $MS_2$  have layer lattices related to  $MoS_2$  (p. 1018),  $CdI_2$ , or  $CdCl_2$  (p. 1212). Sometimes complex layer-sequences occur in which the 6-coordinate metal atom is alternatively octahedral and trigonal prismatic. Most of the phases exhibit

<sup>16</sup> G.-Q. HUANG, S.-W. ZHANG, Y.-G. WEI and M.-C. SHAO, *Polyhedron* **12**, 1483-5 (1993).

<sup>17</sup> P. HAGENMULLER, Chap. 50 in *Comprehensive Inorganic Chemistry*, Vol. 4, pp. 541-605, Pergamon Press, Oxford, 1973.

<sup>18</sup> J. KÖHLER and A. SIMON, *Z. anorg. allg. Chem.* **572**, 7-17 (1989).

<sup>19</sup> J. KÖHLER, R. TISCHTAN and A. SIMON, *J. Chem. Soc., Dalton Trans.*, 829-32 (1991).

<sup>20</sup> M. GESELBRACHT, T. J. RICHARDSON and A. M. STACY, *Nature* **345**, 324-6 (1990).



Table 22.4 Sulfides of vanadium, niobium and tantalum

V <sub>3</sub> S	Nb <sub>21</sub> S <sub>8</sub>	Ta <sub>6</sub> S	V <sub>2</sub> S <sub>3</sub>	—	—
—	—	Ta <sub>2</sub> S	V <sub>5</sub> S <sub>8</sub>	Nb <sub>1+x</sub> S <sub>2</sub>	Ta <sub>1+x</sub> S <sub>2</sub>
V <sub>5</sub> S <sub>4</sub>	—	—	—	NbS <sub>2</sub>	TaS <sub>2</sub>
VS	NbS <sub>1-x</sub>	TaS	—	NbS <sub>3</sub>	TaS <sub>3</sub>
V <sub>7</sub> S <sub>8</sub>	—	—	VS <sub>4</sub>	—	—
V <sub>3</sub> S <sub>4</sub>	Nb <sub>3</sub> S <sub>4</sub>	—			

Table 22.5 Selenides and tellurides of vanadium, niobium and tantalum

V <sub>2</sub> Se	—	—	—	—	—
V <sub>5</sub> Se <sub>4</sub>	Nb <sub>5</sub> Se <sub>4</sub>	—	V <sub>5</sub> Te <sub>4</sub>	Nb <sub>5</sub> Te <sub>4</sub>	—
VSe	NbSe	—	VTe <sub>1+x</sub>	—	TaTe
V <sub>7</sub> Se <sub>8</sub>	—	—	—	—	—
V <sub>3</sub> Se <sub>4</sub>	Nb <sub>3</sub> Se <sub>4</sub>	—	V <sub>3</sub> Te <sub>4</sub>	Nb <sub>3</sub> Te <sub>4</sub>	—
(V <sub>2</sub> Se <sub>3</sub> )	Nb <sub>2</sub> Se <sub>3</sub>	Ta <sub>2</sub> Se <sub>3</sub>	V <sub>2</sub> Te <sub>3</sub>	—	—
V <sub>5</sub> Se <sub>8</sub>	—	—	V <sub>5</sub> Te <sub>8</sub>	—	—
—	Nb <sub>1+x</sub> Se <sub>2</sub>	Ta <sub>1+x</sub> Se <sub>2</sub>	V <sub>1+x</sub> Te <sub>2</sub>	Nb <sub>1+x</sub> Te <sub>2</sub>	Ta <sub>1-x</sub> Te <sub>2</sub>
VSe <sub>2</sub>	NbSe <sub>2</sub>	TaSe <sub>2</sub>	VTe <sub>2</sub>	NbTe <sub>2</sub>	TaTe <sub>2</sub>
—	—	TaSe <sub>3</sub>	—	—	—
—	NbSe <sub>4</sub>	—	—	NbTe <sub>4</sub>	TaTe <sub>4</sub>

metallic conductivity and magnetic properties range from diamagnetic (e.g. VS<sub>4</sub>), through paramagnetic (VS, V<sub>2</sub>S<sub>3</sub>), to antiferromagnetic (V<sub>7</sub>S<sub>8</sub>). Selenides and tellurides show a similar profusion of stoichiometries and structural types (Table 22.5).

In addition to these binary chalcogenides, many of which exist over wide ranges of composition because of the structural relation between the NiAs and CdI<sub>2</sub> structure types (p. 556), several ternary phases have been studied. Some, like BaVS<sub>3</sub> and BaTaS<sub>3</sub> have three-dimensional structures in which the Ba and V(Ta) are coordinated by 12 and 6 S atoms respectively. Other compounds such as the easily hydrolysed (NH<sub>4</sub>)<sub>3</sub>VS<sub>4</sub>, which has been known for over a century, and M<sub>3</sub><sup>I</sup>VS<sub>4</sub> (M = Na, K, Tl) prepared by heating stoichiometric amounts of the elements under vacuum<sup>(21)</sup> contain the discrete, tetrahedral [VS<sub>4</sub>]<sup>3-</sup> anion. The cluster chemistry of the thiometallates of this group, however, is not comparable to that of the oxometallates. It is very limited and whereas, for instance, (Et<sub>4</sub>N)<sub>4</sub>[M<sub>6</sub>S<sub>17</sub>].3CH<sub>3</sub>CN (M = Nb,

Ta) contains a discrete [M<sub>6</sub>S<sub>17</sub>]<sup>4-</sup> anion,<sup>(22)</sup> the stoichiometrically analogous M<sub>4</sub><sup>I</sup>Nb<sub>6</sub>O<sub>17</sub>·0.3H<sub>2</sub>O has an extended structure.

### 22.3.4 Halides and oxohalides

The known halides of vanadium, niobium and tantalum, are listed in Table 22.6. These are illustrative of the trends within this group which have already been alluded to. Vanadium(V) is only represented at present by the fluoride, and even vanadium(IV) does not form the iodide, though all the halides of vanadium(III) and vanadium(II) are known. Niobium and tantalum, on the other hand, form all the halides in the high oxidation state, and are in fact unique (apart only from protactinium) in forming pentafluorides. However in the +4 state, tantalum fails to form a fluoride and neither metal produces a trifluoride. In still lower oxidation states, niobium and tantalum give a number of (frequently nonstoichiometric) cluster compounds which can be considered to involve fragments of the metal lattice.

<sup>21</sup> A. T. HARRISON and O. W. HAWORTH, *J. Chem. Soc., Dalton Trans.*, 1405–9 (1986).

<sup>22</sup> J. SOLA, Y. DO, J. M. BERG and R. H. HOLM, *Inorg. Chem.* **24**, 1706–13 (1985).

Table 22.4 Sulfides of vanadium, niobium and tantalum

V <sub>3</sub> S	Nb <sub>21</sub> S <sub>8</sub>	Ta <sub>6</sub> S	V <sub>2</sub> S <sub>3</sub>	—	—
—	—	Ta <sub>2</sub> S	V <sub>5</sub> S <sub>8</sub>	Nb <sub>1+x</sub> S <sub>2</sub>	Ta <sub>1+x</sub> S <sub>2</sub>
V <sub>5</sub> S <sub>4</sub>	—	—	—	NbS <sub>2</sub>	TaS <sub>2</sub>
VS	NbS <sub>1-x</sub>	TaS	—	NbS <sub>3</sub>	TaS <sub>3</sub>
V <sub>7</sub> S <sub>8</sub>	—	—	VS <sub>4</sub>	—	—
V <sub>3</sub> S <sub>4</sub>	Nb <sub>3</sub> S <sub>4</sub>	—			

Table 22.5 Selenides and tellurides of vanadium, niobium and tantalum

V <sub>2</sub> Se	—	—	—	—	—
V <sub>5</sub> Se <sub>4</sub>	Nb <sub>5</sub> Se <sub>4</sub>	—	V <sub>5</sub> Te <sub>4</sub>	Nb <sub>5</sub> Te <sub>4</sub>	—
VSe	NbSe	—	VTe <sub>1+x</sub>	—	TaTe
V <sub>7</sub> Se <sub>8</sub>	—	—	—	—	—
V <sub>3</sub> Se <sub>4</sub>	Nb <sub>3</sub> Se <sub>4</sub>	—	V <sub>3</sub> Te <sub>4</sub>	Nb <sub>3</sub> Te <sub>4</sub>	—
(V <sub>2</sub> Se <sub>3</sub> )	Nb <sub>2</sub> Se <sub>3</sub>	Ta <sub>2</sub> Se <sub>3</sub>	V <sub>2</sub> Te <sub>3</sub>	—	—
V <sub>5</sub> Se <sub>8</sub>	—	—	V <sub>5</sub> Te <sub>8</sub>	—	—
—	Nb <sub>1+x</sub> Se <sub>2</sub>	Ta <sub>1+x</sub> Se <sub>2</sub>	V <sub>1+x</sub> Te <sub>2</sub>	Nb <sub>1+x</sub> Te <sub>2</sub>	Ta <sub>1-x</sub> Te <sub>2</sub>
VSe <sub>2</sub>	NbSe <sub>2</sub>	TaSe <sub>2</sub>	VTe <sub>2</sub>	NbTe <sub>2</sub>	TaTe <sub>2</sub>
—	—	TaSe <sub>3</sub>	—	—	—
—	NbSe <sub>4</sub>	—	—	NbTe <sub>4</sub>	TaTe <sub>4</sub>

metallic conductivity and magnetic properties range from diamagnetic (e.g. VS<sub>4</sub>), through paramagnetic (VS, V<sub>2</sub>S<sub>3</sub>), to antiferromagnetic (V<sub>7</sub>S<sub>8</sub>). Selenides and tellurides show a similar profusion of stoichiometries and structural types (Table 22.5).

In addition to these binary chalcogenides, many of which exist over wide ranges of composition because of the structural relation between the NiAs and CdI<sub>2</sub> structure types (p. 556), several ternary phases have been studied. Some, like BaVS<sub>3</sub> and BaTaS<sub>3</sub> have three-dimensional structures in which the Ba and V(Ta) are coordinated by 12 and 6 S atoms respectively. Other compounds such as the easily hydrolysed (NH<sub>4</sub>)<sub>3</sub>VS<sub>4</sub>, which has been known for over a century, and M<sub>3</sub><sup>I</sup>VS<sub>4</sub> (M = Na, K, Tl) prepared by heating stoichiometric amounts of the elements under vacuum<sup>(21)</sup> contain the discrete, tetrahedral [VS<sub>4</sub>]<sup>3-</sup> anion. The cluster chemistry of the thiometallates of this group, however, is not comparable to that of the oxometallates. It is very limited and whereas, for instance, (Et<sub>4</sub>N)<sub>4</sub>[M<sub>6</sub>S<sub>17</sub>].3CH<sub>3</sub>CN (M = Nb,

Ta) contains a discrete [M<sub>6</sub>S<sub>17</sub>]<sup>4-</sup> anion,<sup>(22)</sup> the stoichiometrically analogous M<sub>4</sub><sup>I</sup>Nb<sub>6</sub>O<sub>17</sub>·0.3H<sub>2</sub>O has an extended structure.

### 22.3.4 Halides and oxohalides

The known halides of vanadium, niobium and tantalum, are listed in Table 22.6. These are illustrative of the trends within this group which have already been alluded to. Vanadium(V) is only represented at present by the fluoride, and even vanadium(IV) does not form the iodide, though all the halides of vanadium(III) and vanadium(II) are known. Niobium and tantalum, on the other hand, form all the halides in the high oxidation state, and are in fact unique (apart only from protactinium) in forming pentafluorides. However in the +4 state, tantalum fails to form a fluoride and neither metal produces a trifluoride. In still lower oxidation states, niobium and tantalum give a number of (frequently nonstoichiometric) cluster compounds which can be considered to involve fragments of the metal lattice.

<sup>21</sup> A. T. HARRISON and O. W. HAWORTH, *J. Chem. Soc., Dalton Trans.*, 1405–9 (1986).

<sup>22</sup> J. SOLA, Y. DO, J. M. BERG and R. H. HOLM, *Inorg. Chem.* **24**, 1706–13 (1985).

Table 22.6 Halides of vanadium, niobium and tantalum<sup>(a)</sup> (mp, bp/°C)

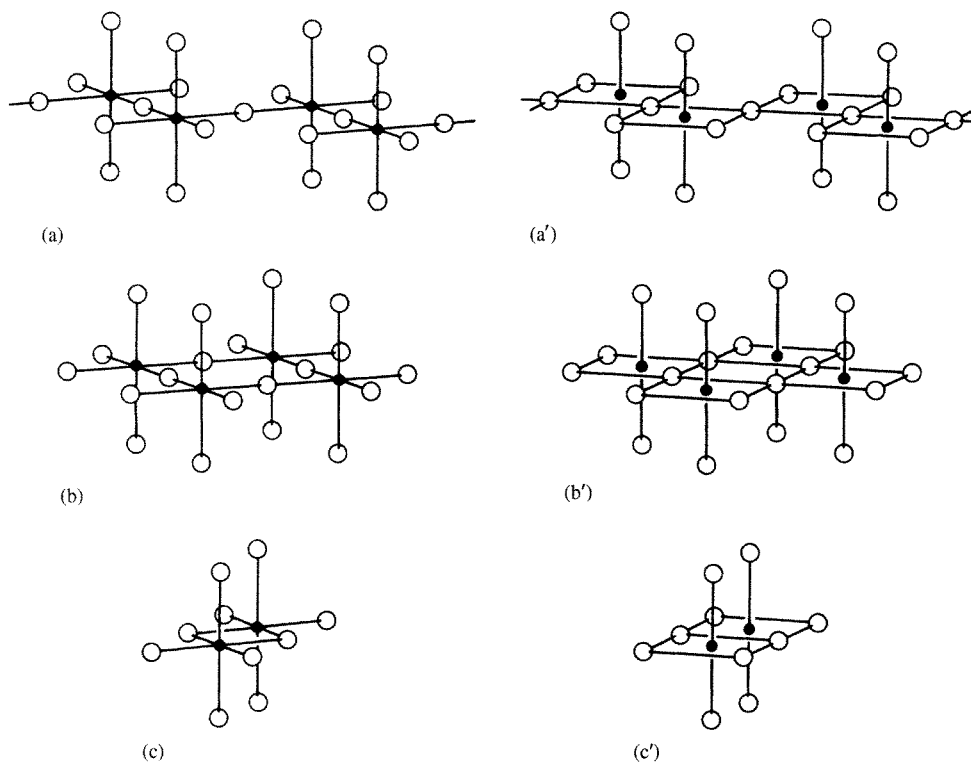
Oxidation state	Fluorides	Chlorides	Bromides	Iodides
+5	VF <sub>5</sub> colourless mp 19.5°, bp 48.3°	—	—	—
	NbF <sub>5</sub> white mp 79°, bp 234°	NbCl <sub>5</sub> yellow mp 203°, bp 247°	NbBr <sub>5</sub> orange mp 254°, bp 360°	NbI <sub>5</sub> brass coloured
	TaF <sub>5</sub> white mp 97°, bp 229°	TaCl <sub>5</sub> white mp 210°, bp 233°	TaBr <sub>5</sub> pale yellow mp 280°, bp 345°	TaI <sub>5</sub> black mp 496°, bp 543°
+4	VF <sub>4</sub> lime green (subl > 150°)	VCl <sub>4</sub> red-brown mp -26°, bp 148°	VBr <sub>4</sub> magenta (d - 23°)	—
	NbF <sub>4</sub> black (d > 350°)	NbCl <sub>4</sub> violet-black	NbBr <sub>4</sub> dark brown	NbI <sub>4</sub> dark grey mp 503°
+3	—	TaCl <sub>4</sub> black	TaBr <sub>4</sub> dark blue	TaI <sub>4</sub>
	VF <sub>3</sub> yellow-green mp 800°	VCl <sub>3</sub> red-violet	VBr <sub>3</sub> grey-brown	VI <sub>3</sub> brown-black
	NbF <sub>3</sub> (?) blue	NbCl <sub>3</sub> black	NbBr <sub>3</sub> dark brown	NbI <sub>3</sub>
+2	TaF <sub>3</sub> (?) blue	TaCl <sub>3</sub> black	TaBr <sub>3</sub>	—
	VF <sub>2</sub> blue	VCl <sub>2</sub> pale green (subl 910°)	VBr <sub>2</sub> orange-brown (subl 800°)	VI <sub>2</sub> red-violet

<sup>(a)</sup>Niobium and Ta also form a number of polynuclear halides in which the metal has non-integral oxidation states (see text).

VF<sub>5</sub> and all pentahalides of Nb and Ta can be prepared conveniently by direct action of the appropriate halogen on the heated metal. They are all relatively volatile, hydrolysable solids (indicative of the covalency to be anticipated in such a high oxidation state) in which the metals attain octahedral coordination by means of halide bridges (Fig. 22.4). VF<sub>5</sub> is an infinite chain polymer, whereas NbF<sub>5</sub> and TaF<sub>5</sub> are tetramers, and the chlorides and bromides are dimers. The colours vary from white fluorides, yellow chlorides, and orange bromides, to brown iodides. The decreasing energy of the charge-transfer bands responsible for these colours is a reflection of the increasing polarizability of the anions from F<sup>-</sup> to I<sup>-</sup>, and for each anion usually the least readily reduced Ta produces the palest colour. All the pentahalides can be

sublimed in an atmosphere of the appropriate halogen and they are then monomeric, probably trigonal bipyramidal. Potentially they are all Lewis acids but their ability to form adducts (LMX<sub>5</sub>) diminishes and the iodides rarely do so.

The tetrahalides can be prepared by direct action of the elements. However, whereas VF<sub>4</sub> tends to disproportionate into VF<sub>5</sub> + VF<sub>3</sub> and must be sublimed from them, VCl<sub>4</sub> and VBr<sub>4</sub> tend to dissociate into VX<sub>3</sub> +  $\frac{1}{2}$ X<sub>2</sub> and so require the presence of an excess of halogen. Even so, VBr<sub>4</sub> has only been isolated by quenching the mixed vapours at -78°C. VF<sub>4</sub> is a bright-green hygroscopic solid, probably consisting of fluorine-bridged VF<sub>6</sub> octahedra. VCl<sub>4</sub> is a red-brown oil, rapidly hydrolysed by water to give solutions of oxovanadium(IV) chloride, and magnetic and spectroscopic evidence indicate that

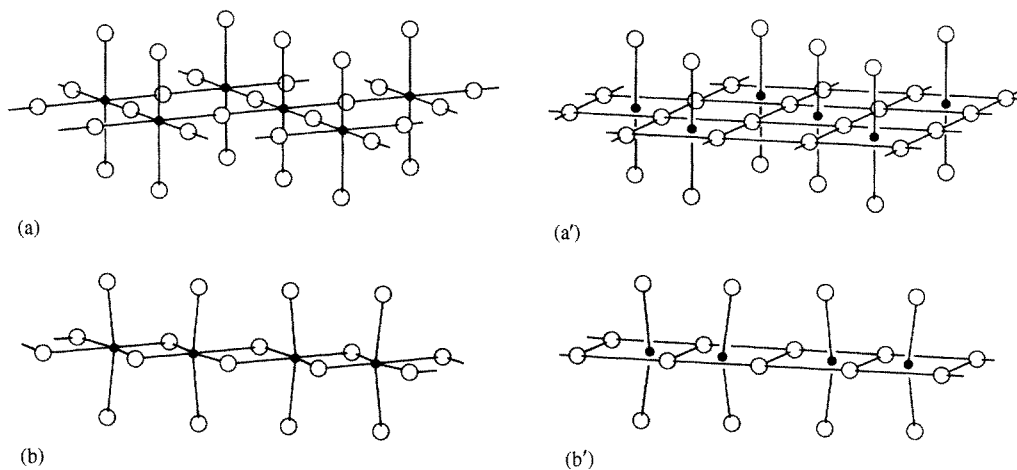


**Figure 22.4** Alternative representations of: (a) infinite chains of vanadium atoms in  $\text{VF}_5$ , (b) tetrameric structures of  $\text{NbF}_5$  and  $\text{TaF}_5$ , and (c) dimeric structure of  $\text{MX}_5$  ( $\text{M} = \text{Nb}, \text{Ta}$ ;  $\text{X} = \text{Cl}, \text{Br}$ ).

it consists of unassociated tetrahedral molecules. As far as its properties are known, the magenta-coloured  $\text{VBr}_4$  is similar.

The Nb and Ta tetrahalides (except  $\text{TaF}_4$  which is unknown, and  $\text{NbI}_4$  which is prepared by thermal decomposition of  $\text{NbI}_5$ ) are generally prepared by reduction of the corresponding pentahalide and are all readily hydrolysed.  $\text{NbF}_4$  is a black involatile solid and its low magnetic moment suggests extensive metal-metal interaction, presumably via the intervening  $\text{F}^-$  ions since it consists of infinite sheets of  $\text{NbF}_6$  octahedra (Fig. 22.5a). The chlorides, bromides and iodides are brown to black solids with a chain structure (Fig. 22.5b) in which pairs of metal atoms are displaced towards each other, so facilitating the interaction which leads to their diamagnetism.

The vanadium trihalides are all crystalline, polymeric solids in which the vanadium is 6-coordinate.  $\text{VF}_3$  is prepared by the action of HF on heated  $\text{VCl}_3$  and this, along with  $\text{VBr}_3$  and  $\text{VI}_3$ , can be prepared by direct action of the elements under appropriate conditions. They are coloured and have magnetic moments slightly lower than the spin-only value of 2.83 BM corresponding to 2 unpaired electrons. Apart from the trifluoride, which is not very readily oxidized nor very soluble in water, they are easily oxidized by air and are very hygroscopic, forming aqueous solutions of  $[\text{V}(\text{H}_2\text{O})_6]^{3+}$ . As with the other lower halides of Nb and Ta, the trihalides are obtained by reduction or thermal decomposition of their pentahalides. Despite claims for the existence of  $\text{NbF}_3$  and  $\text{TaF}_3$  it is probable that these blue materials are

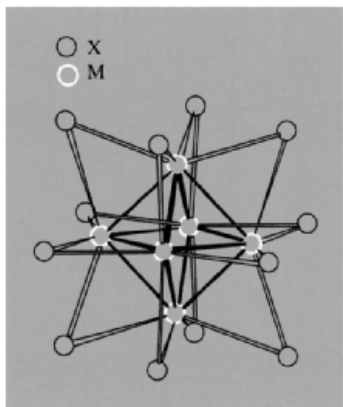


**Figure 22.5** Alternative representations of: (a) the sheet structure of  $\text{NbF}_4$  and (b) the chain structure of  $\text{MX}_4$  ( $M = \text{Nb, Ta}$ ;  $X = \text{Cl, Br, I}$ ) showing the displacement of the metal atoms which leads to diamagnetism.

actually oxide fluorides but, because  $\text{O}^{2-}$  and  $\text{F}^-$  are isoelectronic and very similar in size, they are difficult to distinguish by X-ray methods. The remaining 5 known trihalides of this pair of metals are dark coloured, rather unreactive materials. The  $\text{Nb}-\text{Cl}$  system has been the most thoroughly studied but the others appear to be entirely analogous. They are nonstoichiometric and the composition “ $\text{MX}_3$ ” is best considered as a single unexceptional point within a broad homogeneous phase based on hcp halide ions. At one extreme is  $\text{M}_3\text{X}_8$  (i.e.  $\text{MX}_{2.67}$ ) in which one-quarter of the octahedral sites are empty and the others occupied by triangular groups of metal atoms. Of the 15 valence electrons provided by the 3 metal atoms, 8 are lost by ionization and transfer to the 8 Cl atoms and, of the remaining 7 available for metal–metal bonding, 6 are considered to be in bonding orbitals and 1 in a nonbonding orbital. This accounts for the magnetic moment of 1.86 BM for each trinuclear cluster in  $\text{Nb}_3\text{Cl}_8$ . Metal deficiency then produces stoichiometries to somewhat beyond  $\text{MX}_3$  (i.e.  $\text{M}_{2.67-x}\text{X}_8$ ) after which the  $\text{MX}_4$  phase separates, containing pairs of interacting metal atoms, as already mentioned (i.e.  $\text{M}_2\text{X}_8$ ).

In the still lower oxidation state, +2, the halides of vanadium on the one hand, and niobium and tantalum, on the other, diverge still further. The dihalides of V are prepared by reduction of the corresponding trihalides and have simple structures based on the close-packing of halide ions: the rutile structure (p. 961) for  $\text{VF}_2$ , and the  $\text{CdI}_2$  structure (p. 1212) for the others. They are strongly reducing and hygroscopic, dissolving in water to give lavender-coloured solutions of  $[\text{V}(\text{H}_2\text{O})_6]^{2+}$ . By contrast, high-temperature reductions of  $\text{NbX}_5$  or  $\text{TaX}_5$  with the metals (or Na or Al) yield a series of phases based on  $[\text{M}_6\text{X}_{12}]^{n+}$  units consisting of octahedral clusters of metal atoms with the halogen atoms situated above each edge of the octahedra (Fig. 22.6). These may be surrounded by:

- Four similar units, with each of which a halogen atom is shared, producing a sheet structure with the composition  $[\text{M}_6\text{X}_{12}]\text{X}_{4/2} = \text{M}_6\text{X}_{14}$  (i.e.  $\text{MX}_{2.3}$ ). These compounds are diamagnetic as a result of the metal–metal bonding.
- Six similar units, with each of which a halogen atom is shared, producing a



**Figure 22.6**  $[M_6X_{12}]^{n+}$  cluster with X bridges over each edge of the octahedron of metal ions.

three-dimensional array with the composition  $[M_6X_{12}]X_{6/2} = M_6X_{15}$  (i.e.  $MX_{2.5}$ ). These have magnetic moments corresponding to 1 unpaired electron per hexamer and so indicate the same metal–metal bonding within the cluster as in (a).

By incorporation of alkali metal halides in the reaction mix, materials of composition  $M_4^- [M_6X_{18}]$  can be produced in which each  $M_6X_{12}$  unit has a further six X atoms attached to its apices, so forming discrete clusters.

Many of these cluster compounds are water-soluble and yield solutions in which the clusters are retained throughout chemical reactions. These reactions include attachment of a variety of ligands at the apical (or “terminal”) sites as well as reversible oxidations of the clusters. Thus, it has been possible<sup>(23)</sup> to isolate  $Rb_4[Nb_6Br_{12}(N_3)_6] \cdot 2H_2O$  from aqueous methanolic solutions, and from aqueous alcoholic solutions of  $[M_6X_{12}]X_2 \cdot 8H_2O$  ( $M = Nb, Ta; X = Cl, Br$ )<sup>(23a)</sup> the insoluble, diamagnetic compounds  $[M_6X_{12}(ROH)_6]X_2$ . In these compounds all the terminal coordination sites are occupied by azide groups and aliphatic alcohols respectively. In addition  $[M_6X_{12}]^{2+}$  (diamagnetic) can also be

oxidized to  $[M_6X_{12}]^{3+}$  (1 unpaired electron) and then to  $[M_6X_{12}]^{4+}$  (diamagnetic), and compounds such as  $M_6X_{14}$ ,  $M_6X_{15}$  and  $M_6X_{16}$ , usually with 7 or 8 molecules of  $H_2O$ , can be crystallized. Although terminal ligands are generally more labile than the bridging halogen atoms, isomers of the green  $[Ta_6Cl_{12}(\mu-Cl)_2(PR_3)_4]$  in which the terminal chlorines are either *cis* or *trans* have been isolated by column chromatography. The isomerism was then retained<sup>(24)</sup> when the individual isomers were oxidized by  $NOBF_4$  or  $AgBF_4$  to the orange to brown  $BF_4^-$  salts of  $[Ta_6Cl_{12}(\mu-Cl)_2(PR_3)_4]^{n+}$  ( $n = 1, 2$ ).

The  $[M_6X_8]$  cluster unit in which halogen atoms are situated above each *face* of the  $M_6$  octahedron is far less common here than in Group 6 (p. 1022) but does occur in the unusual compound,  $Nb_6I_{11}$ . This consists of a 3D array of six  $[Nb_6I_8]$  units joined by shared iodines:  $[Nb_6I_8]I_{6/2} = Nb_6I_{11}$ . It absorbs hydrogen and, in 1967, provided the first example of a metal atom cluster with an encapsulated H atom at its centre.<sup>(25)</sup> Both  $Nb_6I_{11}$  and  $HNb_6I_{11}$  exhibit a “spin-crossover”: 1 to 3 unpaired electrons at 274 K for the former, and diamagnetic to 2 unpaired electrons at 324 K for the latter.<sup>(26)</sup>

The cluster compounds of this group may be regarded as intermediate between the  $[M_6X_8]^{n+}$  type of Group 6 (p. 1022) which generally possess sufficient electrons (24) to allow M–M single bonds on each edge of the octahedron, and the comparatively electron-poor clusters of Groups 3 and 4 (p. 950 and 965) which generally require the presence of an interstitial atom to stabilize them.<sup>(27)</sup>

The known oxohalides are listed in Table 22.7. They are generally prepared from the oxides but are not particularly well known and, as can be seen, are limited almost entirely to the oxidation states of +4 and +5. Those in the

<sup>24</sup> H. IMOTO, S. HAYAKAWA, N. MORITA and T. SAITO, *Inorg. Chem.* **29**, 2007–14 (1990).

<sup>25</sup> A. SIMON, F. STOLLMAIER, D. GREGSON and H. FUESS, *J. Chem. Soc., Dalton Trans.*, 431–4 (1987).

<sup>26</sup> H. IMOTO and A. SIMON, *Inorg. Chem.* **21**, 308–19 (1982).

<sup>27</sup> A. SIMON, *Angew. Chem. Int. Edn. Engl.* **27**, 159–83 (1988).

<sup>23</sup> H.-J. MEYER, *Z. anorg. allg. Chem.* **621**, 921–4 (1995).

<sup>23a</sup> A. KASHTA, N. BRNICEVIC and R. E. MCCARLEY, *Polyhedron* **10**, 2031–6 (1991).

Table 22.7 Oxohalides of vanadium, niobium and tantalum<sup>(28)</sup>

Oxidation state	Fluorides		Chlorides		Bromides		Iodides	
+5	VOF <sub>3</sub> yellow mp 300° bp 480°	VO <sub>2</sub> F brown	VOCl <sub>3</sub> yellow mp -77° bp 127°	VO <sub>2</sub> Cl orange	VOBr <sub>3</sub> deep red (d 180°)			—
	TaOF <sub>3</sub>	NbO <sub>2</sub> F white TaO <sub>2</sub> F	NbOCl <sub>3</sub> white TaOCl <sub>3</sub> white	NbO <sub>2</sub> Cl white TaO <sub>2</sub> Cl white	NbOBr <sub>3</sub> yellow-brown TaOBr <sub>3</sub> pale yellow	NbO <sub>2</sub> Br brown TaO <sub>2</sub> Br orange-gold	NbOI <sub>3</sub> black TaOI <sub>3</sub>	NbO <sub>2</sub> I red TaO <sub>2</sub> I
+4	VOF <sub>2</sub> yellow		VOCl <sub>2</sub> green		VOBr <sub>2</sub> yellow-brown (d 180°)			
			NbOCl <sub>2</sub> black TaOCl <sub>2</sub>		NbOBr <sub>2</sub>  TaOBr <sub>2</sub> black		NbOI <sub>2</sub> black TaOI <sub>2</sub> black	
+3	—		VOCl yellow-brown bp 127°		VOBr violet (d 480°)			

former oxidation state are relatively stable but those in the latter are notably hygroscopic and hydrolyse vigorously to the hydrous pentoxides. The Nb(V) and Ta(V) compounds are rather volatile, though less so than the pentahalides. NbOCl<sub>3</sub> is the best known, mainly because of its propensity for occurring as an unwanted impurity in the preparation of VCl<sub>5</sub> if O<sub>2</sub> is not rigorously excluded or, more specially, if V<sub>2</sub>O<sub>5</sub> is used.

### 22.3.5 Compounds with oxoanions

The group oxidation state of +5 is too high to allow the formation of simple ionic salts even for Nb and Ta, and in lower oxidation states the higher sublimation energies of these heavier metals, coupled with their ease of oxidation, again militates against the formation of simple salts of the oxoacids. As a consequence the only simple oxoanion salts are the sulfates of vanadium in the oxidation states +3 and +2. These can be crystallized from aqueous solutions as hydrates and are both strongly

reducing. They give rise to blue-violet alums, MV(SO<sub>4</sub>)<sub>2</sub>·12H<sub>2</sub>O, the ammonium alum being air-stable when dry, and to the reddish-violet Tutton's salts, M<sub>2</sub>V(SO<sub>4</sub>)<sub>2</sub>·6H<sub>2</sub>O, the ammonium analogue of which is again relatively more stable to oxidation.

In the higher oxidation states partially hydrolysed species dominate the aqueous chemistry, the most important being the oxovanadium(IV), or vanadyl, ion VO<sup>2+</sup>. This gives the sulfate VOSO<sub>4</sub>·5H<sub>2</sub>O, containing monodentate sulfate and octahedrally coordinated vanadium, and the polymeric VOSO<sub>4</sub>. Oxovanadium(V) species are not well characterized, outside the oxohalides VOX<sub>3</sub>, but in strongly acid solutions VO<sub>2</sub><sup>+</sup> is formed and reportedly gives the nitrate VO<sub>2</sub>(NO<sub>3</sub>). The VO<sub>2</sub><sup>+</sup> ion is also found in anionic complexes such as [VO<sub>2</sub>(oxalate)<sub>2</sub>]<sup>3-</sup> and in all cases the oxygens are mutually *cis* as they are in the isoelectronic MoO<sub>2</sub><sup>2+</sup> (p. 1024). Niobium and tantalum produce a variety of complicated and ill-defined, but probably polymeric, species which include the nitrates, MO(NO<sub>3</sub>)<sub>3</sub>, sulfates such as Nb<sub>2</sub>O(SO<sub>4</sub>), and double sulfates such as (NH<sub>4</sub>)<sub>6</sub>Nb<sub>2</sub>O(SO<sub>4</sub>)<sub>7</sub>, all of which are extremely readily hydrolysed.

<sup>28</sup> H. SCHÄFER, R. GERKEN and L. ZYLKA, *Z. anorg. allg. Chem.* **534**, 209–15 (1986).

### 22.3.6 Complexes<sup>(29,30)</sup>

#### Oxidation state V (d<sup>0</sup>)

Vanadium (V) has a great affinity for *O*-donors: the extensive chemistry of the polyoxometallates has already been discussed and complexes not involving oxygen, such as the white diamagnetic hexafluorovanadates, MVF<sub>6</sub>, are extremely susceptible to hydrolysis. If H<sub>2</sub>O<sub>2</sub> is added to aqueous solutions of [VO<sub>4</sub>]<sup>3-</sup> a series of substituted products is obtained depending on pH. Using Raman and <sup>51</sup>V nmr spectroscopy to compare the solutions with compounds of known compositions and structures, suggests<sup>(31)</sup> that the red-brown acidic solutions contain [VO(O<sub>2</sub>)(H<sub>2</sub>O)<sub>4</sub>]<sup>+</sup> and that in progressively more alkaline solutions, [VO(O<sub>2</sub>)<sub>2</sub>(H<sub>2</sub>O)]<sup>-</sup>, [VO<sub>2</sub>(O<sub>2</sub>)<sub>2</sub>(H<sub>2</sub>O)]<sup>3-</sup>, [VO(O<sub>2</sub>)<sub>3</sub>]<sup>3-</sup> and [V(O<sub>2</sub>)<sub>4</sub>]<sup>3-</sup> are among the species produced until, from strongly alkaline solutions, blue-violet crystals of M<sub>3</sub>[V(O<sub>2</sub>)<sub>4</sub>].*n*H<sub>2</sub>O (M<sup>I</sup> = Li, Na, K, NH<sub>4</sub>) are deposited. Like the corresponding Cr ion (p. 637), [V(O<sub>2</sub>)<sub>4</sub>]<sup>3-</sup> is 8-coordinate and dodecahedral, but such a high coordination number is not common for vanadium. Niobium and tantalum produce similar peroxy-compounds, e.g. pale yellow K<sub>3</sub>[Nb(O<sub>2</sub>)<sub>4</sub>] and white K<sub>3</sub>[Ta(O<sub>2</sub>)<sub>4</sub>].

However, most complexes of Nb<sup>V</sup> and Ta<sup>V</sup> are derived from the pentahalides. NbF<sub>5</sub> and TaF<sub>5</sub> dissolve in aqueous solutions of HF to give [MOF<sub>5</sub>]<sup>2-</sup> and, if the concentration of HF is increased, [MF<sub>6</sub>]<sup>-</sup>. This is normally the highest coordination number attained in solution though some [NbF<sub>7</sub>]<sup>2-</sup> may form, and [TaF<sub>7</sub>]<sup>2-</sup> definitely does form, in very high concentrations of HF. However, by suitably regulating the concentration of metal, fluoride ion and HF, octahedral

[MF<sub>6</sub>]<sup>-</sup>, capped trigonal prismatic [MF<sub>7</sub>]<sup>2-</sup>, and even square-antiprismatic [MF<sub>8</sub>]<sup>3-</sup> salts can all be isolated. By contrast with the fluorides, aqueous solutions of MCl<sub>5</sub> and MBr<sub>5</sub> (M = Nb, Ta) yield only oxochloro- and oxobromo-complexes, though the application of non-aqueous procedures allows their use as starting materials.

Niobium(V) is generally considered to be a class-a metal, but the SCN<sup>-</sup> ligand yields a series of both *N*-bonded thiocyanato and *S*-bonded isothiocyanato complexes, e.g. [Nb(NCS)<sub>*n*</sub>(SCN)<sub>6-*n*</sub>]<sup>-</sup> (*n* = 0, 2, 4, 5, 6). Furthermore, dithiocarbamates, dodecahedral [M(S<sub>2</sub>CNR<sub>2</sub>)<sub>4</sub>]<sup>+</sup>, and dithiolates,<sup>(32)</sup> [M(SCH<sub>2</sub>CH<sub>2</sub>S)<sub>3</sub>]<sup>-</sup> with stereochemistry midway between octahedral and trigonal-prismatic, are known for both Nb and Ta. The pentahalides of these two metals act as Lewis acids and form complexes of the type MX<sub>5</sub>L with *O*, *S*, *N*, *P*, and *As* donor ligands.

#### Oxidation state IV (d<sup>1</sup>)

The tetrahalides are Lewis acids and produce a number of adducts with a variety of donor atoms, the most common coordination number being 6. [VF<sub>4</sub>L] (L = NH<sub>3</sub>, py) are insoluble in common organic solvents, have magnetic moments of about 1.8 BM, and are thought to be fluorine-bridged polymers. [VCl<sub>4</sub>2L] (L = py, MeCN, aldehydes, etc.) and VCl<sub>4</sub>(L-L) (L-L = bipy, phen, diars) are brown paramagnetic, readily hydrolysed compounds assumed to be 6-coordinate monomers. Similar compounds of Nb and Ta are also paramagnetic and the metal-metal bonding which led to the diamagnetism of the parent tetrahalides is presumed to have been broken to give adducts which again are 6-coordinate monomers. Hexahalo-complexes [MX<sub>6</sub>]<sup>2-</sup> (M = V, X = F, Cl; M = Nb, Ta, X = Cl, Br) are known, the vanadium compounds being especially sensitive to moisture though stable to air.

<sup>29</sup> L. V. BOAS and L. C. PESSOA, Vanadium, Chap. 33, pp. 453-583, and L. G. HUBERT-PFALZGRAF, M. POSTEL and J. G. RIESS, Niobium and Tantalum, Chap. 34, pp. 585-697 in *Comprehensive Coordination Chemistry*, Vol. 3, Pergamon Press, Oxford, 1987.

<sup>30</sup> R. W. BERG, *Coord. Chem. Revs.* **113**, 1-130 (1992).

<sup>31</sup> N. J. CAMPBELL, A. C. DENGEL and W. P. GRIFFITH, *Polyhedron* **8**, 1379-86 (1989). See also A. BUTLER, M. J. CLAGUE and G. E. MEISTER, *Chem. Revs.* **94**, 625-38 (1994).

<sup>32</sup> K. TATSUMI, Y. SEKIGUCHI, A. NAKAMURA, R. E. CRAMER and J. J. RUPP, *Angew. Chem. Int. Edn. Engl.* **25**, 86-7 (1986).



Higher coordination numbers are also found. Vanadium and Nb produce the dodecahedral  $[\text{MCl}_4(\text{diars})_2]$  just like the Group 4 metals. This is probably the most common stereochemistry for this coordination number but others are possible; differences in energy are slight and this facilitates non-rigidity. For example the yellow-coloured solid  $\text{K}_4[\text{Nb}(\text{CN})_8] \cdot 2\text{H}_2\text{O}$  contains dodecahedral niobium(IV) (like its molybdenum isomorph), whereas esr and infrared data suggest that, in solution, the anion has the square-antiprismatic configuration. Likewise, the deep-red niobium(III) complex  $\text{K}_5[\text{Nb}(\text{CN})_8]$  adopts a dodecahedral ( $D_{2d}$ ) configuration for the anion in the crystal whereas the single  $^{13}\text{C}$  nmr signal in aqueous solution implies either a square-pyramidal ( $D_{4d}$ ) or fluxional ( $D_{2d}$ ) structure.

The major contrast with the Group 4 metals is the stability of  $\text{VO}^{2+}$  complexes which are the most important and the most widely studied of the vanadium(IV) complexes, and are the usual products of the hydrolysis of other vanadium(IV) complexes.  $\text{VO}^{2+}$  behaves as a class-a cation, forming stable compounds with *F* (especially), *Cl*, *O*, and *N* donor ligands. These “vanadyl” complexes are generally blue to green and can be cationic, neutral or anionic. They are very frequently 5-coordinate in which case the stereochemistry is almost invariably square pyramidal.  $[\text{VO}(\text{acac})_2]$  (Fig. 22.7) is the archetypal example of this geometry in coordination compounds. In this and in similar compounds the  $\text{V}=\text{O}$  bond length is  $\sim 157\text{--}168$  pm which is about 50 pm shorter than the 4 equatorial  $\text{V}\text{--}\text{O}$  bonds. This, as well as spectroscopic evidence, is consistent with the

formulation of the bond as double. A sixth ligand may be weakly bonded *trans* to the  $\text{V}=\text{O}$  to produce a distorted octahedral structure; the concomitant reduction in the stretching frequency of the  $\text{V}=\text{O}$  bond generally within the range,  $985 \pm 50 \text{ cm}^{-1}$  has been interpreted in terms of electron donation from this sixth ligand, thereby making the vanadium atom less able to accept charge from the oxygen and so reducing the bond order. Tetradentate Schiff bases, produced for instance by the condensation of salicylaldehyde with primary diamines, in most cases give entirely analogous compounds, but some are yellow and may be polymeric with the vanadium attaining 6-coordination by “stacking” so that the sixth position of each vanadium is occupied by the oxygen from the  $\text{V}=\text{O}$  beneath. The black  $[\text{V}(\text{salen})_4(\mu\text{-O})_3](\text{BF}_4)_2$  [ $\text{H}_2\text{salen} = N,N'$ -ethylenebis(salicylideneimine), p. 907] has recently been shown to be tetrameric with a linear  $\text{V}\text{--}\text{O}\text{--}\text{V}\text{--}\text{O}\text{--}\text{V}\text{--}\text{O}\text{--}\text{V}$  chain.<sup>(33)</sup>

In spite of the evident proclivity of  $\text{VO}^{2+}$  to form square pyramidal or distorted octahedral complexes, it must not be assumed that 5-coordination inevitably results in the former shape.  $[\text{VOCl}_2(\text{NMe}_3)_2]$  is in fact trigonal bipyramidal (Fig. 22.8), no doubt because of a dominant steric effect of the bulky trimethylamine ligands rather than any electronic effect. Most oxovanadium(IV) complexes are magnetically simple, having virtually “spin-only” moments of 1.73 BM corresponding to 1 unpaired electron, but their electronic spectra are less easily understood. This is primarily due to the presence of a strong  $\pi$  contribution to the bond between the vanadium and the oxygen which makes it difficult to assign an unequivocal sequence to the molecular orbitals involved.<sup>(34)</sup>

Some square pyramidal derivatives of thiovanadyl,  $(\text{V}=\text{S})^{2+}$ , have also been prepared from the corresponding vanadyl complexes: deep magenta  $[\text{VS}(\text{salen})]$  and  $[\text{VS}(\text{acen})]$  [ $\text{H}_2\text{acen} = N,N'$ -ethylenebis(acetylacetyloneimine)] by

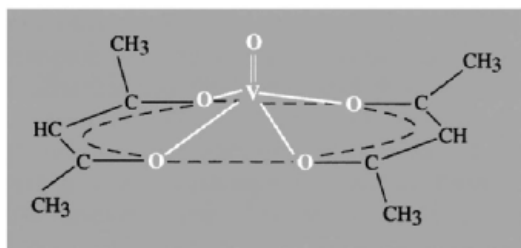
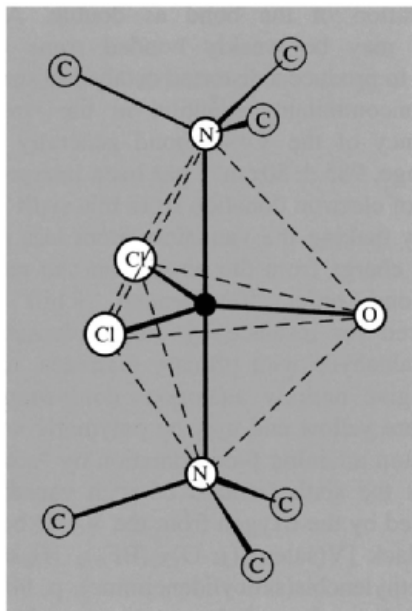


Figure 22.7 The square-pyramidal structure of  $[\text{VO}(\text{acac})_2]$ .

<sup>33</sup> A. HILLS, D. L. HUGHES, G. J. LEIGH and J. R. SANDERS *J. Chem. Soc., Chem. Commun.*, 827–9 (1991).

<sup>34</sup> A. B. P. LEVER, *Inorganic Electronic Spectra*, 2nd edn., pp. 384–91, Elsevier Amsterdam, 1984.



**Figure 22.8** The trigonal bipyramidal structure of  $[\text{VOCl}_2(\text{NMe}_3)_2]$ .

the action of  $\text{B}_2\text{S}_3$  in  $\text{CH}_2\text{Cl}_2$ ; brown  $[\text{VS}(\text{SCH}_2\text{-CH}_2\text{S})_2]^{2-}$  by the action of  $(\text{Me}_3\text{Si})_2\text{S}$  in  $\text{MeCN}$ .<sup>(35)</sup> The exclusion of air and moisture throughout these preparations is essential in order to avoid reversion to vandyl complexes.

### Oxidation state III ( $d^2$ )

Until comparatively recently only vanadium had a significant  $\text{M}^{\text{III}}$  coordination chemistry and even so the majority of its compounds are easily oxidized and must be prepared with air rigorously excluded. The usual methods are to use  $\text{VCl}_3$  as the starting material, or to reduce solutions of vanadium(V) or (IV) electrolytically. However, the reduction of pentahalides of Nb and Ta by Na amalgam or Mg, has facilitated the expansion of  $\text{Nb}^{\text{III}}$  and  $\text{Ta}^{\text{III}}$  chemistry particularly with *S*- and *P*-donor ligands.

The chemistry of vanadium(III) closely parallels that of titanium(III) and it likewise favours octahedral coordination. The interpretation of the electronic spectra of its complexes, as the prime examples of  $d^2$  ions in an octahedral field, provided the stimulus for early preparative work in this area. In general, the spectra are characterized by two bands in the visible region with a further much more intense absorption in the ultraviolet. The two former bands are believed to arise from *d-d* transitions and others from charge-transfer. Since the  $d^2$  configuration in a cubic field is expected to give rise to three spin-allowed transitions it is assumed that the most energetic of these is obscured by the charge-transfer band. Table 22.8 gives data for some octahedral vanadium(III) complexes (see also ref. 34, pp. 400–6). It turns out, on examination of data such as these, that a coherent interpretation of the spectra is only possible if the bands are assigned (Fig. 22.9) as:

$$\nu_1 = {}^3T_{2g}(F) \leftarrow {}^3T_{1g}(F)$$

$$\nu_2 = {}^3T_{1g}(P) \leftarrow {}^3T_{1g}(F)$$

and the third, obscured one, therefore as:

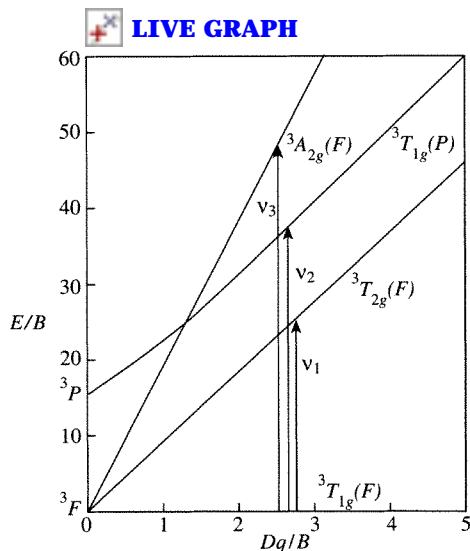
$$\nu_3 = {}^3A_{2g}(F) \leftarrow {}^3T_{1g}(F)$$

*B* is the Racah “interelectronic repulsion parameter”. It is included in Fig. 22.9 in order to retain generality and obviate the necessity of drawing separate diagrams for each  $d^2$  metal ion. The expansion of *d*-electron charge on complexation reduces its value as compared to the value for the free-ion ( $860\text{ cm}^{-1}$ ). In general the electronic spectra of these 6-coordinate complexes are accounted for moderately well on the assumption of basically octahedral crystal fields, but the inclusion of trigonal distortions gives more satisfactory results. The magnetic moments of  $d^2$  ions in perfectly octahedral fields are expected to involve “orbital contribution” which varies with temperature. In practice the moments at room temperature rarely exceed the spin-only value and their variation with temperature is less than anticipated for a *T* ground term. This also is in accord with the presence of some distortion which splits the

<sup>35</sup> G. CHRISTOU, D. HEINRICH, J. K. MONEY, J. R. RAMBO, J. C. HUFFMAN and K. FOLTING *Polyhedron*, **8**, 1723–7 (1989).

Table 22.8 Typical octahedral complexes of vanadium(III)

Complex	Colour	$\nu_1/\text{cm}^{-1}$	$\nu_2/\text{cm}^{-1}$	$10Dq/\text{cm}^{-1}$	$B/\text{cm}^{-1}$	$\mu/\text{BM}$ (room temperature)
$[\text{NH}_4][\text{V}(\text{H}_2\text{O}_6)[\text{SO}_4]_2 \cdot 6\text{H}_2\text{O}$	Blue-violet	17 800	25 700	19 200	620	2.80
$[\text{VCl}_3(\text{MeCN})_3]$	Green	14 400	21 400	15 500	540	2.79
$[\text{VCl}_3(\text{thf})_3]$	Orange	13 300	19 900	14 000	553	2.80
$\text{K}_3[\text{VF}_6]$	Green	14 800	23 250	16 100	649	2.79
$[\text{pyH}]_3[\text{VCl}_6]$	Purple-pink	16 650	18 350	12 650	513	2.71

Figure 22.9 Energy Level diagram for a  $d^2$  ion in an octahedral crystal field.

${}^3T_{2g}$  ground term and so reduces the temperature dependence of the magnetic moment.

Cationic complexes of the type  $[\text{VL}_6]^{3+}$  of which  $[\text{V}(\text{H}_2\text{O}_6)]^{3+}$  is the best-known example are actually rather rare, the action of  $\text{NH}_3$  on  $\text{VX}_3$  for instance, causing ammonolysis of the  $\text{V}-\text{X}$  bond to produce  $\text{VX}_2(\text{NH}_2)_n\text{NH}_3$ . Anionic  $[\text{VX}_6]^{3-}$ ,  $[\text{VX}_5\text{L}]^{2-}$ ,  $[\text{VX}_4\text{L}_2]^-$  and neutral  $[\text{VCl}_3\text{L}_3]$  are more common. Dithiolates  $[\text{V}_2(\text{SCH}_2\text{CH}_2\text{S})_4]^{2-}$  with four sulfur atoms bridging the two vanadium atoms are also known (Fig. 22.10a), their diamagnetism and short  $\text{V}-\text{V}$  distances (260 pm) indicating  $\text{M}-\text{M}$  bonding.

In spite of the preponderance of 6-coordinate complexes, other coordination numbers are known: the ions  $[\text{VCl}_4]^-$  and  $[\text{VBr}_4]^-$  are tetrahedral and are notable in that 4-coordination

with ligands other than  $O$ -donors is common only later in the transition series. Their spectra exhibit two bands in the regions of  $9000\text{ cm}^{-1}$  and  $15000\text{ cm}^{-1}$  which are assigned to  ${}^3T_1(F) \leftarrow {}^3A_2$  and  ${}^3T_1(P) \leftarrow {}^3A_2$  transitions respectively, corresponding quite reasonably to values of  $\Delta_t$  of about  $5000$  to  $5500\text{ cm}^{-1}$ . Their magnetic moments too are about 2.7 BM and independent of temperature, as expected.

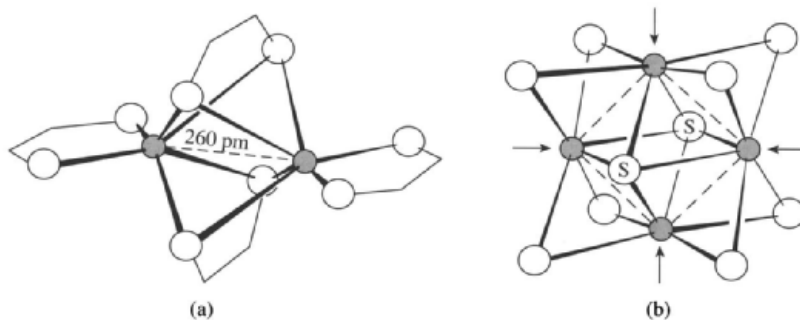
Neutral complexes of the type  $[\text{VX}_3(\text{NMe}_3)_2]$  ( $\text{X} = \text{Cl}, \text{Br}$ ) are trigonal bipyramidal with the trimethylamines occupying the axial positions. By contrast  $[\text{V}\{\text{N}(\text{SiMe}_3)_2\}_3]$  has a 3-coordinate, planar structure, presumably because the bis(trimethylsilyl)amido ligands are too big for the  $\text{V}^{\text{III}}$  to accommodate more. The 7-coordinate  $\text{K}_4[\text{V}(\text{CN})_7] \cdot 2\text{H}_2\text{O}$  has a pentagonal bipyramidal structure and is a rare example of a 7-coordinated transition metal complex which persists in solution and in which the ligand is not  $\text{F}^-$ .

A few trinuclear oxo-centred carboxylates  $[\text{V}_3\text{O}(\text{RCOO})_6\text{L}_3]^+$  of a type more common for later transition metals (see Fig. 23.9, p. 1030) have been obtained,<sup>(36)</sup> as well as  $[\text{Nb}_3\text{O}_2(\text{MeCOO})_6(\text{thf})_3]^+$  whose structure differs essentially only in that there are **two** bridging  $O$  atoms above and below the  $\text{Nb}_3$  plane.<sup>(37)</sup>

With  $S$ - and  $P$ - donor ligands such as  $\text{SMe}_2$  and  $\text{PMe}_3$ ,  $\text{M}_2\text{Cl}_6\text{L}_4$  ( $\text{M} = \text{Nb}, \text{Ta}$ ) consisting of a pair of edge-sharing octahedra are formed. For Nb, but interestingly not for

<sup>36</sup> F. A. COTTON, M. W. EXTINE, L. R. FALVELLO, D. B. LEWIS, G. E. LEWIS, C. A. MURILLO, W. SCHWOTZER, M. TOMAS and J. M. TROUP, *Inorg. Chem.* **25**, 3505–12 (1986).

<sup>37</sup> F. A. COTTON, M. P. DIEBOLD, R. LLUSAR and W. J. ROTH, *J. Chem. Soc., Chem. Commun.*, 1276–8 (1986).



**Figure 22.10** (a) dithiolates  $[\text{V}_2(\text{SCH}_2\text{CH}_2\text{S})_4]^{2-}$ . (b)  $[\text{Nb}_4\text{S}_2(\text{SPh})_{12}]^{4-}$  and  $[\text{Nb}_4\text{S}_2(\text{SPh})_8(\text{PMe}_2\text{R})_4]$  in which the four arrowed coordination sites are occupied by  $\text{SPh}^-$  and  $\text{PMe}_2\text{R}$  respectively. Unlabelled S atoms in (b) all have an attached Ph which is not shown. Nb–Nb(av)  $\sim 282$  pm.

Ta, tetranuclear, orange coloured derivatives  $\text{Li}_4[\text{Nb}_4\text{S}_2(\text{SPh})_{12}]^{38}$  and  $[\text{Nb}_4\text{S}_2(\text{SPh})_8(\text{PMe}_2\text{R})_4]$  (R = Me, Ph)<sup>39</sup> have been shown to have a common and rather stable central unit of four Nb atoms in a square plane with two  $\mu_4$ -S atoms above and below it (Fig. 22.10b). The diamagnetism and average Nb–Nb separations of approx 282 pm are consistent with single bonds between adjacent Nb atoms.

### Oxidation state II ( $d^3$ )

The coordination chemistry of this oxidation state is not well-developed. Vanadium(II) complexes are usually prepared by electrolytic or zinc reduction of acidic solutions of vanadium in one of its higher oxidation states. The resulting blue-purple solutions are strongly reducing, and reduction of the water is, in general, only prevented by the presence of acid. Several salts and double sulfates which contain the  $[\text{V}(\text{H}_2\text{O})_6]^{2+}$  ion are known and there are adducts of  $\text{VCl}_2$  of the type  $[\text{VCl}_2\text{L}_4]$ , where L is one of a number of *O*- or *N*-donor ligands. The spectroscopic and magnetic properties of these compounds are typical of a  $d^3$  ion and their interpretation follows closely that for the chromium(III) ion (p. 1028). Also

typical of a  $d^3$  ion is the fact that vanadium(II) is kinetically inert and undergoes substitution reactions only slowly.

Other complexes of the type  $[\text{VCl}_2\text{L}_2]$  are distinguished by their colour (green) and magnetic moment ( $\sim 3.2$  BM), well below the spin-only value for 3 unpaired electrons, and some at least are halogen-bridged oligomers. Carboxylate derivatives such as the trinuclear  $[\text{V}_3(\text{RCOO})_6(\text{Me}_2\text{NCHCHNMe}_2)_2]$  have recently been prepared<sup>40</sup> as has the binuclear  $[\text{V}_2(\text{RNCHNR})_4]$  (R = *p*- $\text{MeC}_6\text{H}_4$ ).<sup>41</sup> The former contains an almost linear chain of V atoms held together by carboxylate bridges and, in the latter, the pair of V atoms bridged by the four ligands, are so close (197.8 pm) that a  $\text{V}\equiv\text{V}$  bond is indicated (for single- and double-bonded V–V species, separations of approx. 260 and 220 pm, respectively, are common).

Organometallic compounds apart, oxidation states below +2 are best represented by complexes with tris-bidentate nitrogen-donor ligands such as 2,2'-bipyridyl. Reduction by  $\text{LiAlH}_4$  in thf yields tris(bipyridyl) complexes in which the formal oxidation state of vanadium is +2 to –1. Magnetic moments are compatible with low-spin configurations of the metal but,

<sup>38</sup> J. L. SEELA, J. C. HUFFMAN and G. CHRISTOU, *J. Chem. Soc., Chem. Commun.*, 1258–60 (1987).

<sup>39</sup> E. B. KIBALA, F. A. COTTON and P. A. KIBALA, *Polyhedron* **9**, 1689–94 (1990).

<sup>40</sup> J. J. H. EDEMA, S. GAMBAROTTO, S. HAO and C. BEN-SIMON, *Inorg. Chem.* **30**, 2584–6 (1991).

<sup>41</sup> F. A. COTTON, L. M. DANIELS and C. A. MURILLO, *Angew. Chem. Int. Edn. Engl.* **31**, 737–8 (1992).

as with the analogous compounds of titanium, it may well be that they would be better regarded as complexes with reduced, i.e. anionic, ligands.

### 22.3.7 The biochemistry of vanadium<sup>(41a)</sup>

Certain vertebrates have an astonishing ability to accumulate vanadium in their blood. For example, the ascidian seaworm *Phallusia mammilata* has a blood concentration of V up to 1900 ppm, which represents more than a millionfold concentration with respect to the sea-water in which it lives. The related organism *Ascidia nigra* has an even more spectacular accumulation with concentrations up to 1.45% V (i.e. 14 500 ppm) in its blood cells, which also contain considerable concentrations of sulfuric acid (pH ~ 0). One possibility that has been mooted is that the ascidia accumulates vanadate and polyvanadate ions in mistake for phosphate and polyphosphates (p. 528).

Indeed, the observation that vanadate is a potent inhibitor of phosphate-recognizing enzyme systems was a great stimulus to work in this area, but it now seems likely that its action is more complicated than simple mimicry of phosphates.<sup>(42)</sup> This is germane to obtaining an understanding of the antitumor activity of  $[V(\eta^5-C_5H_5)_2Cl_2]$ .

A number of nitrogen-fixing bacteria contain vanadium and it has been shown that in one of these, *Azotobacter*, there are three distinct nitrogenase systems based in turn on Mo, V and Fe, each of which has an underlying functional and structural similarity.<sup>(43)</sup> This discovery has prompted a search for models and the brown  $V^{-1}$  compound  $[Na(thf)]^+[V(N_2)_2(dppe)_2]$  (dppe =  $Ph_2PCH_2CH_2PPh_2$ ) has recently been prepared by reduction of  $VCl_3$  by sodium naphthalenide

in the presence of dppe.<sup>(44)</sup> Acidification achieves partial nitrogen fixation since one of the four N atoms is converted to  $NH_3$ .

### 22.3.8 Organometallic compounds<sup>(45)</sup>

The organometallic chemistry of this group developed rather slowly but there has been a surge of interest, especially in Nb and Ta, in the last decade or so. The chemistry of  $\sigma$  alkyls or aryls is less well developed than for many other elements but  $[V^{III}\{CH(SiMe_3)_2\}_3]$ ,  $[V^{IV}(CH_2SiMe_3)_4]$ , and  $[V^VO(CH_2SiMe_3)_3]$  have been isolated. In these compounds the possibility of decomposition by alkene elimination or other routes is circumvented by the absence of  $\beta$  hydrogen atoms (p. 926) and the bulkiness of the trimethylsilylmethyl groups. Complexes such as  $[MMe_5(dmpe)]$  ( $M = Nb, Ta$ ;  $dmpe = Me_2PCH_2CH_2PMe_2$ ) decompose spontaneously above room temperature and, although free  $TaMe_5$  has been isolated, it can explode spontaneously at room temperature even in the absence of air. Despite this instability, the Ta–Me bond itself is rather strong: thermochemical studies have shown that the mean bond dissociation energy  $D(Ta-Me)$  in  $TaMe_5$  is  $261 \pm 6 \text{ kJ mol}^{-1}$ , which is substantially greater than, for example, the mean dissociation energy  $D(W-CO)$  of  $178 \pm 3 \text{ kJ mol}^{-1}$  in the kinetically much more stable  $W(CO)_6$ . Expanding the coordination sphere of the metal by the addition of other ligands such as  $C_5H_5^-$ , halides and phosphines often increases the thermal stability.

Reduction of  $MCl_5$  or  $MCl_3$  under an atmosphere of CO yields salts of the  $[M(CO_6)]^-$  ions ( $M = V, Nb, Ta$ )<sup>(46)</sup> which have the noble gas electron configuration. Using Na as reductant

<sup>44</sup> D. REHDER, C. WOITHA, W. PRIEBSCHE and M. GAILUS *J. Chem. Soc., Chem. Commun.*, 364–5 (1992).

<sup>45</sup> M. G. CONNELLY, Vanadium, Chap. 24, pp. 648–704, and J. A. LABINGER, Niobium and Tantalum, Chap. 25, pp. 706–82 in *Comprehensive Organometallic Chemistry*, Vol. 3, Pergamon Press, Oxford, 1982.

<sup>46</sup> S. C. SRIVASTAVA and A. K. SHRIMAL, *Polyhedron* **7**, 1639–65 (1988).

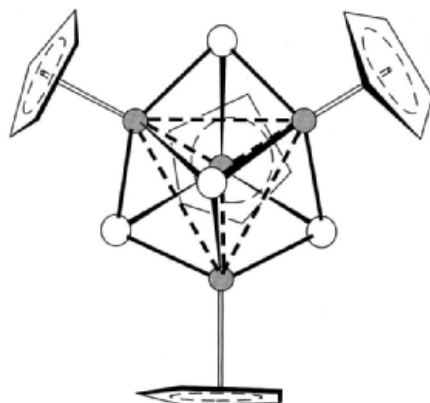
<sup>41a</sup> H. SIGEL and A. SIGEL (eds.), *Metal Ions in Biological Systems*, Vol. 31, Marcel Dekker, New York, 1995, 779 pp.

<sup>42</sup> A. BUTLER and C. J. CARRANO, *Coord. Chem. Revs.* **109**, 61–105 (1991).

<sup>43</sup> R. R. EADY, *Adv. Inorg. Chem.* **36**, 77–102 (1991).

with pyridine or diglyme as solvent requires high temperatures and pressures, but the application of high-energy ultrasound or the use of Mg/Zn as reductant allows less forcing conditions. In the case of the V salt, but not those of Nb and Ta, acidification and extraction with petroleum ether yields volatile, blue-green, pyrophoric crystals of  $V(CO)_6$ . Unlike other formally odd-electron transition metal carbonyls, this does not attain the noble gas configuration by dimerization and the formation of a M–M bond. It is in fact monomeric and isomorphous with Group 6 octahedral hexacarbonyls (p. 1037); it undergoes substitution reactions typical of metal carbonyls, but is unique amongst simple carbonyls in being paramagnetic with a moment at room temperature of 1.81 BM. Further reduction of  $[Na(diglyme)_2][M(CO)_6]$  with Na metal in liquid  $NH_3$  yields the super-reduced 18-electron species  $[M(CO)_5]^{3-}$  which contain M in their lowest known formal oxidation state ( $-3$ ).<sup>(47)</sup> Although sensitivity is somewhat dependent on the counter-cation involved, several of the salts of these ions are hazardously shock and temperature sensitive. Direct synthesis of  $V(CO)_6$ ,  $V_2(CO)_{12}$  and  $M(CO)_n$  ( $M = V, n = 1-5$ ;  $M = Ta, n = 1-6$ ) by condensation of vanadium vapour with CO in a matrix of noble gases is possible. The same technique has also been used to prepare the hexakis(dinitrogen) compound,  $[V(N_2)_6]$  (p. 981) which is isoelectronic and probably isostructural with the hexacarbonyl.

With the cyclopentadienyl ligand, vanadium forms the simple “sandwich” compound, “vanadocene”.  $[V(\eta^5-C_5H_5)_2]$  which is dark violet, paramagnetic (3 unpaired electrons) and extremely air-sensitive. Oxidative addition reactions are possible and provide compounds such as  $[V(\eta^5-C_5H_5)_2Cl_n]$  ( $n = 1, 2, 3$ ) and  $[V(\eta^5-C_5H_5)_2R_2]$ , while its reaction with dithioacetic acid produces the dark-brown tetramer  $[V_4(\eta^5-C_5H_5)_4(\mu_3-S_4)]$ , Fig. 22.11.<sup>(48)</sup> With four  $V^{III}$  atoms, eight electrons are available for six V–V bonds and the implied bond order of 2/3

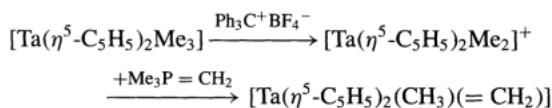


**Figure 22.11**  $[V_4(\eta^5-C_5H_5)_4(\mu_3-S_4)]$  the centre of which is a tetrahedron of V atoms face-capped by S atoms.

is consistent with the observed average V–V separation of 287.6 pm and magnetic moment of 2.65 BM at room temperature.

Niobium and tantalum do not form simple, thermally stable sandwich compounds. Niobocene is actually a dimer and a hydride (Fig. 22.12a). They do however form  $[M(\eta^5-C_5H_5)_4]$  (p. 940) in which two rings are  $\eta^5$ - and two  $\eta^1$ -bonded, and there are many bis(cyclopentadienyl) compounds of the types  $[M(\eta^5-C_5H_5)_2X_2]$  and  $[M(\eta^5-C_5H_5)_2R_2]$  in which, if the  $C_5H_5$  is taken as a single ligand, the coordination geometry is pseudo-tetrahedral.  $[M(\eta^5-C_5H_5)_2X_3]$  and  $[M(\eta^5-C_5H_5)_2R_3]$  are also known.

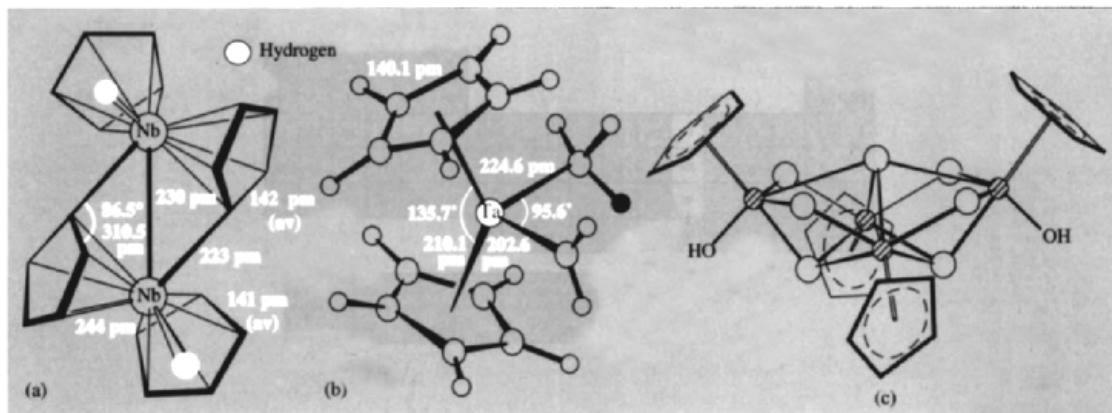
An important compound is the mixed methyl-methylene derivative of bis(cyclopentadienyl)tantalum(V) prepared by the following sequence of high-yield reactions:



The structure of the pale buff-coloured product is shown in Fig. 22.12b and this allows a direct comparison between the three Ta–C distances: Ta=CH<sub>2</sub> 203 pm, Ta–CH<sub>3</sub> 225 pm, and Ta–C(C<sub>5</sub>H<sub>5</sub>) 216 pm. It will also be noted that the two cyclopentadienyl rings are eclipsed and that the CH<sub>2</sub> group orients perpendicular to the C–Ta–C plane.

<sup>47</sup> J. E. ELLIS, *Adv. Organometallic Chem.* **31**, 1–52 (1990).

<sup>48</sup> S. A. DURAJ, M. T. ANDRAS and B. RIHTER, *Polyhedron* **8**, 2763–7 (1989).



**Figure 22.12** (a) The structure of dimeric  $[\text{Nb}(\eta^5\text{-C}_5\text{H}_5)\text{H}-\mu\text{-(}\eta^5,\eta^1\text{-C}_5\text{H}_4\text{)}]_2$ . The observed diamagnetism of this compound is consistent with the Nb–Nb bond shown. Each of the two bridging rings is  $\eta^5$ -bonded to one Nb and  $\eta^1$ -bonded to the other. (b) The structure of  $[\text{Ta}(\eta^5\text{-C}_5\text{H}_5)_2(\text{CH}_3)(=\text{CH}_2)]$ . (c) The structure of  $[\text{Ta}_4(\eta^5\text{-C}_5\text{Me}_5)_4(\mu_2\text{-O})_4(\mu_3\text{-O})_2(\mu_4\text{-O})(\text{OH})_2]$ .

Cationic cyclopentadienyl complexes are not common in this group, but recent examples whose structures have been determined include  $[\text{Nb}^{\text{V}}(\eta^5\text{-C}_5\text{H}_5)_2\text{Cl}_2]\text{BF}_4$ <sup>(49)</sup> and  $[\text{Nb}(\eta^5\text{-C}_5\text{H}_5)_2\text{L}_2](\text{BF}_4)_2$  (L = CNMe and NCMe),<sup>(50)</sup> which have pseudo-tetrahedral symmetry. Mono(cyclopentadienyl), or “half-sandwich” poly-oxo complexes are of interest as hydrocarbon-soluble models for oxide catalysts. The action of water on  $[\text{Ta}(\eta^5\text{-C}_5\text{Me}_5)(\text{PMe}_3)_2]$  yields the colourless  $[\text{Ta}_4(\eta^5\text{-C}_5\text{Me}_5)_4\text{O}_7(\text{OH})_2]$  which has a tetranuclear “butterfly” core (Fig. 22.12c).<sup>(51)</sup>

<sup>49</sup>K. H. THIELE, W. KUBAK, J. SIELER, H. BORRMANN and A. SIMON, *Z. anorg. allgem. Chem.* **587**, 80–90 (1990).

<sup>50</sup>M. A. A. De C. T. CARRONDO, J. MORAIS, C. C. ROMAO and M. J. ROMAO, *Polyhedron* **12**, 765–70 (1993).

<sup>51</sup>V. C. GIBSON, T. P. KEE and W. CLEGG, *J. Chem. Soc., Chem. Commun.*, 29–30 (1990).

The chemistry of these metals with ring systems other than cyclopentadienyl has been little developed but, since larger rings afford more bonding electrons it would seem that the relatively electron-poor, early transition elements (see p. 941) should provide a field of study ripe for expansion. Reduction of  $\text{NbCl}_4$  by Na/Hg in thf in the presence of cycloheptatriene and  $\text{PMe}_3$  provides a convenient route and several  $\text{C}_7$ -ring compounds have been prepared<sup>(52)</sup> including the blue-green, 17-electron complex  $[\text{Nb}^{\text{II}}(\eta^7\text{-C}_7\text{H}_7)(\text{PMe}_3)_2\text{I}]$  which is isomorphous with the previously described Zr analogue (Fig. 21.10c).

<sup>52</sup>M. L. H. GREEN, P. MOUNTFORD, P. SCOTT and V. S. B. MTETWA, *Polyhedron* **10**, 389–92 (1991), and *J. Chem. Soc., Chem. Commun.*, 314–5 (1992).

																1		2																							
																H		He																							
3												4		5		6		7		8		9		10																	
Li												Be		B		C		N		O		F		Ne																	
11												12		13		14		15		16		17		18																	
Na												Mg		Al		Si		P		S		Cl		Ar																	
19												20		21		22		23		24		25		26		27		28		29		30									
K		Ca		Sc		Ti		V		Cr		Mn		Fe		Co		Ni		Cu		Zn		Ga		Ge		As		Se		Br		Kr							
37		38		39		40		41		42		43		44		45		46		47		48		49		50		51		52		53		54							
Rb		Sr		Y		Zr		Nb		Mo		Tc		Ru		Rh		Pd		Ag		Cd		In		Sn		Sb		Te		I		Xe							
55		56		57		58		59		60		61		62		63		64		65		66		67		68		69		70		71		72		73					
Cs		Ba		La		Ce		Pr		Nd		Pm		Sm		Eu		Gd		Tb		Dy		Ho		Er		Tm		Yb		Lu									
87		88		89		90		91		92		93		94		95		96		97		98		99		100		101		102		103		104		105					
Fr		Ra		Ac		Rf		Db		Sg		Bh		Hs		Mt		Uun		Uuu		Uub																			
																106		107		108		109		110		111		112		113		114		115		116		117		118	
																Lv		Ts		Og		Nh		Fl		Mc		Lr													

# 23

## Chromium, Molybdenum and Tungsten

### 23.1 Introduction

The discoveries of these elements span a period of about 20 y at the end of the eighteenth century. In 1778 the famous Swedish chemist C. W. Scheele produced from the mineral molybdenite ( $\text{MoS}_2$ ) the oxide of a new element, thereby distinguishing the mineral from graphite with which it had hitherto been thought to be identical. Molybdenum metal was isolated 3 or 4 y later by P. J. Hjelm by heating the oxide with charcoal. The name is derived from the Greek word for lead ( $\mu\acute{o}\lambda\upsilon\beta\delta\omicron\varsigma$ , *molybdos*), owing to the ancient confusion between any soft black minerals which could be used for writing (this is further illustrated by the use of the names “plumbago” and “black lead” for graphite).

In 1781 Scheele, and also T. Bergman, isolated another new oxide, this time from the mineral now known as scheelite ( $\text{CaWO}_4$ ) but then called “tungsten” (Swedish *tung sten*, heavy stone). Two years later the Spanish brothers J. J.

and F. d’Elhuyar showed that the same oxide was a constituent of the mineral wolframite and reduced it to the metal by heating with charcoal. The name “wolfram”, from which the symbol of the element is derived, is still widely used in the German literature and is recommended by IUPAC, but the allowed alternative “tungsten” is used in the English-speaking world.

Finally, in 1797, the Frenchman L. N. Vauquelin discovered the oxide of a new element in a Siberian mineral, now known as crocoite ( $\text{PbCrO}_4$ ), and in the following year isolated the metal itself by charcoal reduction. This was subsequently named chromium (Greek  $\chi\rho\omega\mu\iota\alpha$ , *chroma*, colour) because of the variety of colours found in its compounds. Since their discoveries the metals and their compounds have become vitally important in many industries and, as one of the biologically active transition elements, molybdenum has been the subject of a great deal of attention in recent years, especially in the field of nitrogen fixation (p. 1035).



## 23.2 The Elements

### 23.2.1 Terrestrial abundance and distribution

Chromium, 122 ppm of the earth's crustal rocks, is comparable in abundance with vanadium (136 ppm) and chlorine (126 ppm), but molybdenum and tungsten (both ~1.2 ppm) are much rarer (cf. Ho 1.4 ppm, Tb 1.2 ppm), and the concentration in their ores is low. The only ore of chromium of any commercial importance is chromite,  $\text{FeCr}_2\text{O}_4$ , which is produced principally in southern Africa (where 96% of the known reserves are located), the former Soviet Union and the Philippines. Other less plentiful sources are crocoite,  $\text{PbCrO}_4$ , and chrome ochre,  $\text{Cr}_2\text{O}_3$ , while the gemstones emerald and ruby owe their colours to traces of chromium (pp. 107, 242).

The most important ore of molybdenum is the sulphide molybdenite,  $\text{MoS}_2$ , of which the largest known deposit is in Colorado, USA, but it is also found in Canada and Chile. Less important ores are wulfenite,  $\text{PbMoO}_4$ , and powellite,  $\text{Ca}(\text{Mo},\text{W})\text{O}_4$ .

Tungsten occurs in the form of the tungstates scheelite,  $\text{CaWO}_4$ , and wolframite,  $(\text{Fe},\text{Mn})\text{WO}_4$ , which are found in China (thought to have perhaps 75% of the world's reserves), the former Soviet Union, Korea, Austria and Portugal.

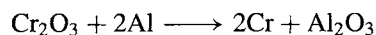
### 23.2.2 Preparation and uses of the metals

Chromium is produced in two forms:<sup>(1)</sup>

- (a) Ferrochrome by the reduction of chromite with coke in an electric arc furnace. A low-carbon ferrochrome can be produced by using ferrosilicon (p. 330) instead of coke as the reductant. This iron/chromium alloy is used directly as an additive

to produce chromium-steels which are "stainless" and hard.

- (b) Chromium metal by the reduction of  $\text{Cr}_2\text{O}_3$ . This is obtained by aerial oxidation of chromite in molten alkali to give sodium chromate,  $\text{Na}_2\text{CrO}_4$ , which is leached out with water, precipitated and then reduced to the Cr(III) oxide by carbon. The oxide can be reduced by aluminium (aluminothermic process) or silicon:



The main use of the chromium metal so produced is in the production of non-ferrous alloys, the use of pure chromium being limited because of its low ductility at ordinary temperatures. Alternatively, the  $\text{Cr}_2\text{O}_3$  can be dissolved in sulphuric acid to give the electrolyte used to produce the ubiquitous chromium-plating which is at once both protective and decorative.

The sodium chromate produced in the isolation of chromium is itself the basis for the manufacture of all industrially important chromium chemicals. World production of chromite ores approached 12 million tonnes in 1995.

Molybdenum is obtained as a primary product but mainly as a byproduct in the production of copper. In either case  $\text{MoS}_2$  is separated by flotation and then roasted to  $\text{MoO}_3$ . In the manufacture of stainless steel and high-speed tools, which account for about 85% of molybdenum consumption, the  $\text{MoO}_3$  may be used directly or after conversion to ferromolybdenum by the aluminothermic process. Otherwise, further purification is possible by dissolution in aqueous ammonia and crystallization of ammonium molybdate (sometimes as the dimolybdate,  $[\text{NH}_4]_2[\text{Mo}_2\text{O}_7]$ , sometimes as the paramolybdate,  $[\text{NH}_4]_6[\text{Mo}_7\text{O}_{24}] \cdot 4\text{H}_2\text{O}$ , depending on conditions), which is the starting material for the manufacture of molybdenum chemicals. Pure molybdenum, which finds important applications as a catalyst in a variety of petrochemical processes and as an electrode material, can be

<sup>1</sup> Kirk-Othmer, *Encyclopedia of Chemical Technology*, 4th edn., Vol. 6, pp. 228-63, Interscience, New York, 1993.

obtained by hydrogen reduction of ammonium molybdate. In 1995 world production of molybdenum ores was equivalent to 130 000 tonnes of contained Mo.

The isolation of tungsten is effected by the formation of "tungstic acid" (hydrous  $\text{WO}_3$ ), but the chemical route chosen depends on the ore being used. After pulverization and concentration of the ore:

- (a) Wolframite is converted to soluble alkali tungstate either by fusing with NaOH and leaching the cooled product with water, or by protracted boiling with aqueous alkali. Acidification with hydrochloric acid then precipitates the tungstic acid.
- (b) Scheelite is converted to insoluble tungstic acid by direct treatment with hydrochloric acid and separated from the soluble salts of other metals.

Tungstic acid is then roasted to  $\text{WO}_3$  which is reduced to the metal by heating with hydrogen at  $850^\circ\text{C}$ . Half of the tungsten produced is used as the carbide, WC, which is extremely hard and wear-resistant and so ideal as a tool-tip. Other

major uses are in the production of numerous heat-resistant alloys, but the most important use of the *pure* metal is still as a filament in electric light bulbs, in which role it has never been bettered since it was first used in 1908. In 1995, world production of tungsten ores contained 31 000 tonnes of tungsten.

Both molybdenum and tungsten are obtained initially in the form of powders and, since fusion is impracticable because of their high mps, they are converted to the massive state by compression and sintering under  $\text{H}_2$  at high temperatures.

### 23.2.3 Properties of the elements

As can be seen from Table 23.1, which summarizes some of the important properties of Group 6, each of these elements has several naturally occurring isotopes which imposes limits on the precision with which their atomic weights have been determined, especially for Mo and W.

The elements all have typically metallic bcc structures and in the massive state are lustrous, silvery, and (when pure) fairly soft. However, the most obvious characteristic at least of

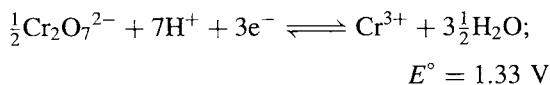
**Table 23.1** Some properties of Group 6 elements

Property	Cr	Mo	W
Atomic number	24	42	74
Number of naturally occurring isotopes	4	7	5
Atomic weight	51.9961(6)	95.94(1)	183.84(1)
Electronic configuration	$[\text{Ar}]3d^54s^1$	$[\text{Kr}]4d^55s^1$	$[\text{Xe}]4f^{14}5d^46s^2$
Electronegativity	1.6	1.8	1.7
Metal radius (12-coordinate)/pm	128	139	139
Ionic radius (6-coordinate)/pm	VI V IV III II <sup>(a)</sup>	44 49 55 61.5	59 61 65 69
	73 (ls), 80 (hs)	—	—
MP/ $^\circ\text{C}$	1900	1620	3422
BP/ $^\circ\text{C}$	2690	4650	(5500)
$\Delta H_{\text{fus}}/\text{kJ mol}^{-1}$	21( $\pm$ 2)	28( $\pm$ 3)	(35)
$\Delta H_{\text{vap}}/\text{kJ mol}^{-1}$	342( $\pm$ 6)	590( $\pm$ 21)	824( $\pm$ 21)
$\Delta H_{\text{f}}$ (monatomic gas)/ $\text{kJ mol}^{-1}$	397( $\pm$ 3)	664( $\pm$ 13)	849( $\pm$ 13)
Density ( $20^\circ\text{C}$ )/ $\text{g cm}^{-3}$	7.14	10.28	19.3
Electrical resistivity ( $20^\circ\text{C}$ )/ $\mu\text{ohm cm}$	13	$\sim$ 5	$\sim$ 5

<sup>(a)</sup>Radius depends on whether Cr(II) is low-spin (ls) or high-spin (hs).

molybdenum and tungsten, is their refractive nature, and tungsten has the highest mp of all metals — indeed, of all elements except carbon. For this reason, metallic Mo and W are fabricated by the techniques of powder metallurgy and, in consequence, many of their bulk physical properties depend critically on the nature of their mechanical history.

As in the preceding transition-metal groups, the refractory behaviour and the relative stabilities of the different oxidation states can be explained by the role of the  $(n - 1)d$  electrons. Compared to vanadium, chromium has a lower mp, bp and enthalpy of atomization which implies that the 3d electrons are now just beginning to enter the inert electron core of the atom, and so are less readily delocalized by the formation of metal bonds. This is reflected too in the fact that the most stable oxidation state has dropped to +3, while chromium(VI) is strongly oxidizing:



For the heavier congeners, tungsten in the group oxidation state is much more stable to reduction, and it is apparently the last element in the third transition series in which all the 5d electrons participate in metal bonding.

### 23.2.4 Chemical reactivity and trends

At ambient temperatures all three elements resist atmospheric attack, which is why chromium is so widely used to protect other more reactive metals. They become more susceptible to attack at high temperatures, when they react with many non-metals giving frequently interstitial and non-stoichiometric products. Chromium reacts more readily with acids than does either molybdenum or tungsten though its reactivity depends on its purity and it can easily be rendered passive. Thus, it dissolves readily in dil HCl but, if very pure, will often resist dil  $\text{H}_2\text{SO}_4$ ; again,  $\text{HNO}_3$ , whether

dilute or concentrated, and aqua regia will render it passive for reasons which are by no means clear. In the presence of oxidizing agents such as  $\text{KNO}_3$  or  $\text{KClO}_3$ , alkali melts rapidly attack the metals producing  $\text{MO}_4^{2-}$ .

Once again the two heavier elements are closely similar to each other and show marked differences from the lightest element. This is reflected particularly in the relative stabilities of the oxidation states, all of which are known from +6 down to -2.

The stability of the group oxidation state +6 was referred to above and it may be further noted that, while chromium(VI) tends to form poly oxoanions, the diversity of these is but a pale shadow of that of the polymolybdates and polytungstates (p. 1009). Oxidation states +5 and +4 are represented by chromium largely as unstable intermediates, and +3 is much its most stable oxidation state, the symmetrical  $t_{2g}^3$  configuration leading to a coordination chemistry, the fecundity of which is exceeded only by that of cobalt(III). Chromium(II) is strongly reducing ( $\text{Cr}^{3+}/\text{Cr}^{2+}$ ,  $E^\circ - 0.41 \text{ V}$ ) but it still has an extensive cationic chemistry. By contrast, the chemistry of molybdenum and tungsten in oxidation states +5 to +2 is dominated by clusters and multiple-bonded species which, particularly in the case of molybdenum, has produced an effusion of publications in recent years. This is due not only to the intrinsically interesting chemistry involved but also because of molybdenum's role in biological processes and, catalytically, in the hydrodesulfurization (HDS) process for removing S-compounds from petroleum feedstocks. In the still lower oxidation states, found in compounds with  $\pi$ -acceptor ligands, the metals are quite similar.

Table 23.2 lists the oxidation states of the elements along with representative examples of their compounds. Coordination numbers as high as 12 can be attained, but those over 7 in the case of Cr and 9 in the cases of Mo and W involve the presence of the peroxo ligand or  $\pi$ -bonded aromatic rings systems such as  $\eta^5\text{-C}_5\text{H}_5^-$  or  $\eta^6\text{-C}_6\text{H}_6$ .

**Table 23.2** Oxidation states and stereochemistries of compounds of chromium, molybdenum and tungsten

Oxidation state	Coordination number	Stereochemistry	Cr	Mo/W
-4	4	Tetrahedral	[Cr(CO) <sub>4</sub> ] <sup>4-</sup>	[M(CO) <sub>4</sub> ] <sup>4-</sup>
-2 (d <sup>8</sup> )	5	Trigonal bipyramidal(?)	[Cr(CO) <sub>5</sub> ] <sup>2-</sup>	[M(CO) <sub>5</sub> ] <sup>2-</sup>
-1 (d <sup>7</sup> )	6	Octahedral	[Cr <sub>2</sub> (CO) <sub>10</sub> ] <sup>2-</sup>	[M <sub>2</sub> (CO) <sub>10</sub> ] <sup>2-</sup>
0 (d <sup>6</sup> )	6	Octahedral	[Cr(bipy) <sub>3</sub> ]	[M(CO) <sub>6</sub> ]
1 (d <sup>5</sup> )	9	—	[Cr(η <sup>6</sup> -C <sub>6</sub> H <sub>6</sub> )(CO) <sub>3</sub> ]	—
	12	—	[Cr(η <sup>6</sup> -C <sub>6</sub> H <sub>6</sub> ) <sub>2</sub> ]	—
	6	Octahedral	[Cr(CNR) <sub>6</sub> ] <sup>+</sup>	[MoCl(N <sub>2</sub> )(diphos) <sub>2</sub> ]
	8	—	—	[Mo(η <sup>5</sup> -C <sub>5</sub> H <sub>5</sub> )(CO) <sub>3</sub> ]
2 (d <sup>4</sup> )	11	—	—	[Mo(η <sup>5</sup> -C <sub>5</sub> H <sub>5</sub> )(η <sup>6</sup> -C <sub>6</sub> H <sub>6</sub> )]
	12	—	—	[Mo(η <sup>6</sup> -C <sub>6</sub> H <sub>6</sub> ) <sub>2</sub> ] <sup>+</sup>
	4	Tetrahedral	[CrI <sub>2</sub> (OPPh <sub>3</sub> ) <sub>2</sub> ]	—
	4	Square Planar	{Cr(acac) <sub>2</sub> }	—
	5	Trigonal bipyramidal	[CrBr{N(C <sub>2</sub> H <sub>4</sub> NMe <sub>2</sub> ) <sub>3</sub> }] <sup>+</sup>	—
		Square pyramidal	—	[Mo <sub>2</sub> Cl <sub>8</sub> ] <sup>4-</sup> , [W <sub>2</sub> Me <sub>8</sub> ] <sup>4-</sup>
	6	Octahedral	[Cr(en <sub>3</sub> ) <sub>2</sub> ] <sup>2+</sup>	[M(diars) <sub>2</sub> I <sub>2</sub> ]
	7	Capped trigonal prismatic	[Cr(CO) <sub>2</sub> (diars) <sub>2</sub> X] <sup>+</sup>	[Mo(CNR) <sub>7</sub> ] <sup>2+</sup> †
		Pentagonal bipyramidal	—	[MoH(η <sup>2</sup> -O <sub>2</sub> CCF <sub>3</sub> ){P(OMe) <sub>3</sub> }] <sub>4</sub>
	8	—	[Cr(η <sup>5</sup> -C <sub>5</sub> H <sub>5</sub> )Cl(NO) <sub>2</sub> ]	—
3 (d <sup>3</sup> )	9	—	—	[W(η <sup>5</sup> -C <sub>5</sub> H <sub>5</sub> )(CO) <sub>3</sub> Cl], M <sub>6</sub> Cl <sub>12</sub> clusters
	10	—	[Cr(η <sup>5</sup> -C <sub>5</sub> H <sub>5</sub> ) <sub>2</sub> ]	—
	3	Planar	[Cr(NPr <sub>2</sub> ) <sub>3</sub> ]	—
	4	Tetrahedral	[CrCl <sub>4</sub> ] <sup>-</sup>	[(RO) <sub>3</sub> Mo≡Mo(OR) <sub>3</sub> ], [(R <sub>2</sub> N) <sub>3</sub> W≡W(NR <sub>2</sub> ) <sub>3</sub> ]
	5	Trigonal bipyramidal	[CrCl <sub>3</sub> (NMe <sub>3</sub> ) <sub>2</sub> ]	—
	6	Octahedral	[Cr(NH <sub>3</sub> ) <sub>6</sub> ] <sup>3+</sup>	[M <sub>2</sub> Cl <sub>9</sub> ] <sup>3-</sup>
	7	?	—	[WBr <sub>2</sub> (CO) <sub>3</sub> (diars)] <sup>+</sup>
8 or 12	8	Dodecahedral(?)	—	[Mo(CN) <sub>7</sub> (H <sub>2</sub> O)] <sup>4-</sup>
	8 or 12	—	—	[Mo(η <sup>1</sup> -C <sub>5</sub> H <sub>5</sub> )(η <sup>1</sup> -C <sub>5</sub> H <sub>5</sub> ) <sub>2</sub> (NO)], x = 3 or 5
4 (d <sup>2</sup> )	4	Tetrahedral	[Cr(OBu <sup>t</sup> ) <sub>4</sub> ]	[Mo(NMe <sub>2</sub> ) <sub>4</sub> ]
	6	Octahedral	[CrF <sub>6</sub> ] <sup>2-</sup>	[MCl <sub>6</sub> ] <sup>2-</sup>
		Trigonal prismatic	—	MS <sub>2</sub>
	8	Dodecahedral	[CrH <sub>4</sub> (dmpe) <sub>2</sub> ] <sup>(a)</sup>	[M(CN) <sub>8</sub> ] <sup>4-</sup>
		Square antiprismatic(?)	—	Mo(S <sub>2</sub> CNMe <sub>2</sub> ) <sub>4</sub> , [M(picolate)] <sub>4</sub>
5 (d <sup>1</sup> )	12	—	—	[M(η <sup>5</sup> -C <sub>5</sub> H <sub>5</sub> ) <sub>2</sub> X <sub>2</sub> ]
	4	Tetrahedral	[CrO <sub>4</sub> ] <sup>3-</sup>	—
	5	Square pyramidal	[CrOCl <sub>4</sub> ] <sup>-</sup>	—
		Trigonal bipyramidal	CrF <sub>5</sub> (g)	MoCl <sub>5</sub> (g)
	6	Octahedral	[CrOCl <sub>5</sub> ] <sup>2-</sup>	[MF <sub>6</sub> ] <sup>-</sup>
	8	Dodecahedral	[Cr(O <sub>2</sub> ) <sub>4</sub> ] <sup>3-</sup>	[M(CN) <sub>8</sub> ] <sup>3-</sup>
6 (d <sup>0</sup> )	13	—	—	[W(η <sup>5</sup> -C <sub>5</sub> H <sub>5</sub> ) <sub>2</sub> H <sub>3</sub> ]
	4	Tetrahedral	[CrO <sub>4</sub> ] <sup>2-</sup>	[MO <sub>4</sub> ] <sup>2-</sup>
	5	?	—	[MOX <sub>4</sub> ]
		Square pyramidal	—	[W(≡CCMe <sub>3</sub> )(=CHCMe <sub>3</sub> )- (CH <sub>2</sub> CMe <sub>3</sub> ){(PMe <sub>2</sub> CH <sub>2</sub> ) <sub>2</sub> }]
	6	Octahedral	CrF <sub>6</sub>	{MO <sub>6</sub> } in polymetallates
		Trigonal prismatic	—	[M(S <sub>2</sub> C <sub>2</sub> H <sub>2</sub> ) <sub>3</sub> ]
	7	Pentagonal bipyramidal	—	[WOCl <sub>4</sub> (diars)]
	8	?	—	[MF <sub>8</sub> ] <sup>2-</sup>
	9	Tricapped trigonal prismatic (C <sub>2v</sub> )	—	[WH <sub>6</sub> (PPhPr <sub>2</sub> ) <sub>3</sub> ]

† The structure of these complexes is not regular and has been described as “4:3 (C<sub>s</sub>) piano stool”, which is obtained by slight distortion of a capped trigonal prism (C<sub>2v</sub>).

<sup>(a)</sup> dmpe, 1,2-bis(dimethylphosphino)ethane, Me<sub>2</sub>PCH<sub>2</sub>CH<sub>2</sub>PMe<sub>2</sub>.

Table 23.3 Oxides of Group 6

Oxidation state:	+6	Intermediate	+4	+3
Cr	CrO <sub>3</sub>	Cr <sub>3</sub> O <sub>8</sub> , Cr <sub>2</sub> O <sub>5</sub> , Cr <sub>5</sub> O <sub>12</sub> , etc.	CrO <sub>2</sub>	Cr <sub>2</sub> O <sub>3</sub>
Mo	MoO <sub>3</sub>	Mo <sub>9</sub> O <sub>26</sub> , Mo <sub>8</sub> O <sub>23</sub> , Mo <sub>5</sub> O <sub>14</sub> , Mo <sub>17</sub> O <sub>47</sub> , Mo <sub>4</sub> O <sub>11</sub>	MoO <sub>2</sub>	—
W	WO <sub>3</sub>	W <sub>49</sub> O <sub>119</sub> , W <sub>50</sub> O <sub>148</sub> , W <sub>20</sub> O <sub>58</sub> , W <sub>18</sub> O <sub>49</sub>	WO <sub>2</sub>	—

## 23.3 Compounds of Chromium, Molybdenum and Tungsten<sup>(2,3,3a)</sup>

The binary borides (p. 145), carbides (p. 299), and nitrides (p. 418) have already been discussed. Suffice it to note here that the chromium atom is too small to allow the ready insertion of carbon into its lattice, and its carbide is consequently more reactive than those of its predecessors. As for the hydrides, only CrH is known which is consistent with the general trend in this part of the periodic table that hydrides become less stable across the d block and down each group.

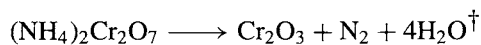
### 23.3.1 Oxides<sup>(2,4)</sup>

The principal oxides formed by the elements of this group are given in Table 23.3 above.

CrO<sub>3</sub>, as is to be expected with such a small cation, is a strongly acidic and rather covalent oxide with a mp of only 197°C. Its deep-red crystals are made up of chains of corner-shared CrO<sub>4</sub> tetrahedra. It is commonly called "chromic acid" and is generally prepared by the addition of conc H<sub>2</sub>SO<sub>4</sub> to a saturated aqueous solution of a dichromate. Its strong oxidizing properties are widely used in organic chemistry. CrO<sub>3</sub> melts with some decomposition and, if heated above

220–250°, it loses oxygen to give a succession of lower oxides until the green Cr<sub>2</sub>O<sub>3</sub> is formed.

Like the analogous oxides of Ti, V and Fe, Cr<sub>2</sub>O<sub>3</sub> has the corundum structure (p. 243), and it finds wide applications as a green pigment. It is a semiconductor and is antiferromagnetic below 35°C. Cr<sub>2</sub>O<sub>3</sub> is the most stable oxide of chromium and is the final product of combustion of the metal, though it is more conveniently obtained by heating ammonium dichromate:



When produced by such dry methods it is frequently unreactive but, if precipitated as the hydrous oxide (or "hydroxide") from aqueous chromium(III) solutions it is amphoteric. It dissolves readily in aqueous acids to give an extensive cationic chemistry based on the [Cr(H<sub>2</sub>O)<sub>6</sub>]<sup>3+</sup> ion, and in alkalis to produce complicated, extensively hydrolysed chromate(III) species ("chromites").

The third major oxide of chromium is the brown-black, CrO<sub>2</sub>, which is an intermediate product in the decomposition of CrO<sub>3</sub> to Cr<sub>2</sub>O<sub>3</sub> and has a rutile structure (p. 961). It has metallic conductivity and its ferromagnetic properties lead to its commercial importance in the manufacture of magnetic recording tapes which are claimed to give better resolution and high-frequency response than those made from iron oxide. Other more or less stable phases with compositions between CrO<sub>2</sub> and CrO<sub>3</sub> have been identified but are of little importance.

The trioxides of molybdenum and tungsten differ from CrO<sub>3</sub> in that, though they are acidic and dissolve in aqueous alkali to give salts of

<sup>2</sup> E. R. BRAITHWAITE and J. HABER (eds.), *Molybdenum: An Outline of its Chemistry and Uses*, Elsevier, Amsterdam 1994, 662 pp.

<sup>3</sup> C. L. ROLLINSON, Chap. 36 in *Comprehensive Inorganic Chemistry*, Vol. 3, pp. 623–769, Pergamon Press, Oxford, 1973.

<sup>3a</sup> *Encyclopedia of Inorganic Chemistry*, Wiley, Chichester, 1994: for Cr see Vol. 2, pp. 666–78; for Mo see Vol. 5, pp. 2304–30; for W see Vol. 6, pp. 4240–68.

<sup>4</sup> M. T. POPE, Molybdenum oxygen chemistry, *Prog. Inorg. Chem.* **39**, 181–257 (1991); pp. 181–94 deals with oxides.

<sup>†</sup> In 1986 the initial drying of the dichromate in a rotary vacuum drier, resulted in a serious explosion in Ohio. The cause was not obvious but the presence of an organic contaminant must be a possibility.

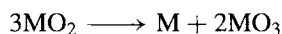
the  $\text{MO}_4^{2-}$  ions, they are insoluble in water and have no appreciable oxidizing properties, being the final products of the combustion of the metals.  $\text{MoO}_3$  and  $\text{WO}_3$  have mps of 795 and  $1473^\circ\text{C}$  respectively (i.e. much higher than for  $\text{CrO}_3$ ) and their crystal structures are different. The white  $\text{MoO}_3$  has an unusual layer structure composed of distorted  $\text{MoO}_6$  octahedra while the yellow  $\text{WO}_3$  (like  $\text{ReO}_3$  see p. 1047) consists of a three-dimensional array of corner-linked  $\text{WO}_6$  octahedra. In fact,  $\text{WO}_3$  is known in at least seven polymorphic forms and is unique in being the only oxide of any element that can undergo numerous facile crystallographic transitions near room temperature. Thus the monoclinic  $\text{ReO}_3$ -type phase (which is slightly distorted from cubic by  $W-W$  interactions) transforms to a ferroelectric monoclinic phase when cooled to  $-43^\circ\text{C}$ , and transforms to another monoclinic variety above  $+20^\circ\text{C}$ ; there are further transitions to an orthorhombic phase at  $325^\circ$  and to a succession of tetragonal phases at  $725^\circ$ ,  $900^\circ$  and  $1225^\circ$ .

If either  $\text{MoO}_3$  or  $\text{WO}_3$  is heated *in vacuo* or is heated with the powdered metal, reduction occurs until eventually  $\text{MO}_2$  with a distorted rutile structure (p. 961) is formed. In between these extremes, however, lie a variety of intensely coloured (usually violet or blue) phases whose structural complexity has excited great interest over many years.<sup>(5)</sup> Following the pioneer work of the Swedish chemist A. Magnéli in the late 1940s these materials, which were originally thought to consist of a comparatively small number of rather grossly nonstoichiometric phases, are now known to be composed of a much larger number of distinct and accurately stoichiometric phases with formulae such as  $\text{Mo}_4\text{O}_{11}$ ,  $\text{Mo}_{17}\text{O}_{47}$ ,  $\text{Mo}_8\text{O}_{23}$ ,  $\text{W}_{18}\text{O}_{49}$  and  $\text{W}_{20}\text{O}_{58}$ . As oxygen is progressively eliminated, a whole series of  $\text{M}_n\text{O}_{3n-1}$  stoichiometries is feasible between the  $\text{MO}_3$  structure containing *corner-shared*  $\text{MO}_6$  octahedra and the rutile structure consisting of

edge-shared  $\text{MO}_6$  octahedra. These are produced as slabs of corner-shared octahedra move so as to share edges with the octahedra of identical adjacent slabs. This is the phenomenon of crystallographic shear and occurs in an ordered fashion throughout the solid.<sup>(6)</sup> The situation is further complicated by the formation of structures involving (a) 7-coordinate, and (b) 4-coordinate, alongside the more prevalent 6-coordinate, metal atoms. The reasons for the formation of these intermediate phases is by no means fully understood but, although their "nonstoichiometric"  $\text{M}:\text{O}$  ratios imply mixed valence compounds, their largely metallic conductivities suggest that the electrons released as oxygen is removed are in fact delocalized within a conduction band permeating the whole lattice.

Reduction of a solution of a molybdate(VI), or of a suspension of  $\text{MoO}_3$ , in water or acid by a variety of reagents including  $\text{Sn}^{\text{II}}$ ,  $\text{SO}_2$ ,  $\text{N}_2\text{H}_4$ ,  $\text{Cu}/\text{acid}$  or  $\text{Sn}/\text{acid}$ , leads to the production of intense blue, sometimes transient, and probably colloidal products, referred to rather imprecisely as *molybdenum blues*. They appear to be oxide/hydroxide species of mixed valence, forming a series between the extremes of  $\text{Mo}^{\text{VI}}\text{O}_3$  and  $\text{Mo}^{\text{V}}\text{O}(\text{OH})_3$ , but a precise explanation of their colour is lacking. Their formation can be used as a sensitive test for the presence of reducing agents. The behaviour of tungsten is entirely analogous to that of molybdenum and, as will be seen presently, the reduction of heteropolyanions of these metals produces similar coloured products which may be distinguished from the above "blues" as "heteropoly blues" (though this is not always done).

The dioxides of molybdenum (violet) and tungsten (brown) are the final oxide phases produced by reduction of the trioxides with hydrogen; they have rutile structures sufficiently distorted to allow the formation of  $\text{M}-\text{M}$  bonds and concomitant metallic conductivity and diamagnetism. Strong heating causes disproportionation:



<sup>5</sup> D. J. M. BEVAN, Chap. 49 in *Comprehensive Inorganic Chemistry*, Vol. 4, pp. 491-7, Pergamon Press, Oxford, 1973.

<sup>6</sup> See p. 148 of ref. 2.

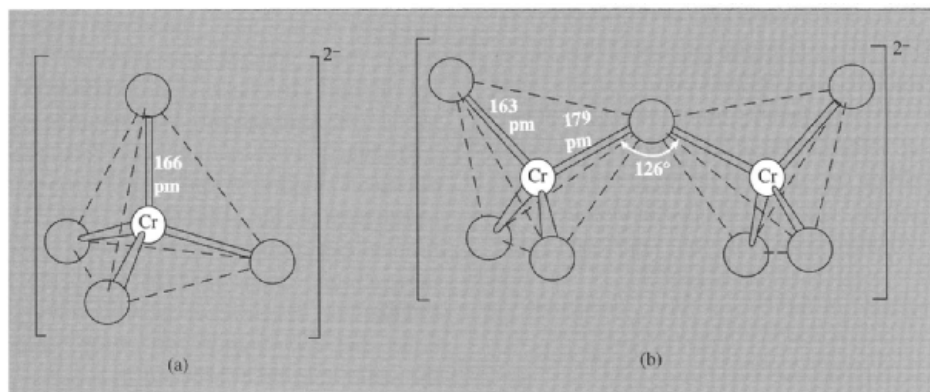
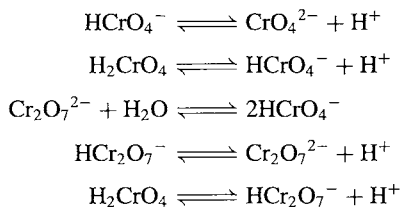


Figure 23.1 (a)  $\text{CrO}_4^{2-}$  ion, and (b)  $\text{Cr}_2\text{O}_7^{2-}$  ion.

No other oxide phases below  $\text{MO}_2$  have been established but a yellow “hydroxide”, precipitated by alkali from aqueous solutions of chromium(II), spontaneously evolves  $\text{H}_2$  and forms a chromium(III) species of uncertain composition. The sulfides, selenides and tellurides of this triad are considered on p. 1017.

### 23.3.2 Isopolymetallates (4.7.8.9.9a)

Acidification of aqueous solutions of the yellow, tetrahedral chromate ion,  $\text{CrO}_4^{2-}$ , initiates a series of labile equilibria involving the formation of the orange-red dichromate ion,  $\text{Cr}_2\text{O}_7^{2-}$ :



However, estimates of equilibrium constants (see for instance, *Comprehensive Coordination*

*Chemistry*, Vol. 3, p. 699) have been questioned and it appears that the concentration of  $\text{HCrO}_4^-$  is much lower than was previously supposed, the ion being undetectable by Raman and uv-visible spectroscopic techniques.<sup>(9b)</sup> Because of the lability of these equilibria the addition of the cations  $\text{Ag}^I$ ,  $\text{Ba}^{II}$  or  $\text{Pb}^{II}$  to aqueous dichromate solutions causes their immediate precipitation as insoluble chromates rather than their more soluble dichromates. Polymerization beyond the dichromate ion is apparently limited to the formation of tri- and tetra-chromates ( $\text{Cr}_3\text{O}_{10}^{2-}$  and  $\text{Cr}_4\text{O}_{13}^{2-}$ ), which can be crystallized as alkali-metal salts from very strongly acid solutions. These anions, as well as the dichromate ion, are formed by the corner sharing of  $\text{CrO}_4$  tetrahedra, giving Cr–O–Cr angles very roughly in the region of  $120^\circ$  (Fig. 23.1). The simplicity of this anionic polymerization of chromium, as compared to that shown by the elements of the preceding groups and the heavier elements of the present triad, is probably due to the small size of  $\text{Cr}^{VI}$ . This evidently limits it to tetrahedral rather than octahedral coordination with oxygen, whilst simultaneously favouring Cr–O double bonds and so inhibiting the sharing of attached oxygens.

Sodium dichromate,  $\text{Na}_2\text{Cr}_2\text{O}_7 \cdot 2\text{H}_2\text{O}$ , produced from the chromate is commercially much

<sup>7</sup> M. T. POPE, *Heteropoly and Isopoly Oxometalates*, Springer Verlag, Berlin, 1983, 180 pp. Also Chap. 38 in *Comprehensive Coordination Chemistry*, Vol. 3, pp. 1028–58, Pergamon Press, Oxford, 1987.

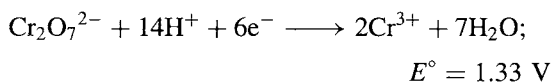
<sup>8</sup> Polyoxometalate Symposium Report (Engl.), *Comptes Rendus Acad. Sci. IIC*, **1**, 297–403 (1998).

<sup>9</sup> M. T. POPE and A. MÜLLER, *Angew. Chem. Int. Edn. Engl.* **30**, 34–48 (1991).

<sup>9a</sup> M. I. KHAN and J. ZUBIETA, *Prog. Inorg. Chem.* **43**, 1–149 (1995).

<sup>9b</sup> V. G. POULOPOULOU, E. VRACHNOU, S. KOINIS and D. KATAKIS, *Polyhedron* **16**, 521–4 (1997).

the most important compound of chromium. It yields a wide variety of pigments used in the manufacture of paints, inks, rubber and ceramics, and from it are formed a host of other chromates used as corrosion inhibitors and fungicides, etc. It is also the oxidant in many organic chemical processes; likewise, acidified dichromate solutions are used as strong oxidants in volumetric analysis:



For this purpose the potassium salt  $\text{K}_2\text{Cr}_2\text{O}_7$  is preferred since it lacks the hygroscopic character of the sodium salt and may therefore be used as a primary standard.

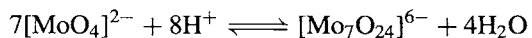
The polymerization of acidified solutions of molybdenum(VI) or tungsten(VI) yields the most complicated of all the polyanion systems and, in spite of the fact that the tungsten system has been the most intensively studied, it is still probably the least well understood. This arises from the problem inevitably associated with studies of such equilibria, and which were noted (p. 983) in the discussion of the Group 5 isopolyanions. It must also be admitted that, whilst the observed structures of individual polyanions are reasonable, it is often difficult to explain why, under given circumstances, a particular degree of aggregation or a particular structure is preferred over other possibilities.

When the trioxides of molybdenum and tungsten are dissolved in aqueous alkali, the resulting solutions contain tetrahedral  $\text{MO}_4^{2-}$  ions and simple, or "normal", molybdates and tungstates such as  $\text{Na}_2\text{MoO}_4$  can be crystallized from them. If these solutions are made strongly acid, precipitates of yellow "molybdic acid",  $\text{MoO}_3 \cdot 2\text{H}_2\text{O}$ , or white "tungstic acid",  $\text{WO}_3 \cdot 2\text{H}_2\text{O}$  are obtained which convert to the monohydrates if warmed. At pHs between these two extremes, however, polymerization occurs and salts can be crystallized,<sup>(10)</sup> the anions of which are almost invariably made up of  $\text{MO}_6$  octahedra. A plethora of

physical techniques<sup>(7)</sup> has been used to characterize these species and unravel the complexity of their structures. Examination of the alkali metal (or ammonium) and alkaline earth salts, particularly by X-ray analysis, forms the basis of classical studies of the isopoly-molybdates and -tungstates in the solid state. Modern nmr techniques (especially pulsed Fourier transform) have increasingly been used to study the solutions themselves. Even so it is only with great difficulty that the structure of an ion, determined in the solid, can be confirmed in solution.

Important differences distinguish the molybdenum and tungsten systems. In aqueous solution, equilibration of the molybdenum species is complete within a matter of minutes whereas for tungsten this may take several weeks; it also transpires that whereas the basic unit of most isopolymolybdates is an  $\text{MO}_6$  octahedron with a pair of *cis*-terminal oxygens, that of the isopolytungstates is more commonly an  $\text{MO}_6$  octahedron with only one terminal oxygen. The two must therefore be considered separately.

Undoubtedly the first major polyanion formed when the pH of an aqueous molybdate solution is reduced below about 6 is the heptamolybdate  $[\text{Mo}_7\text{O}_{24}]^{6-}$ , traditionally known as the paramolybdate:



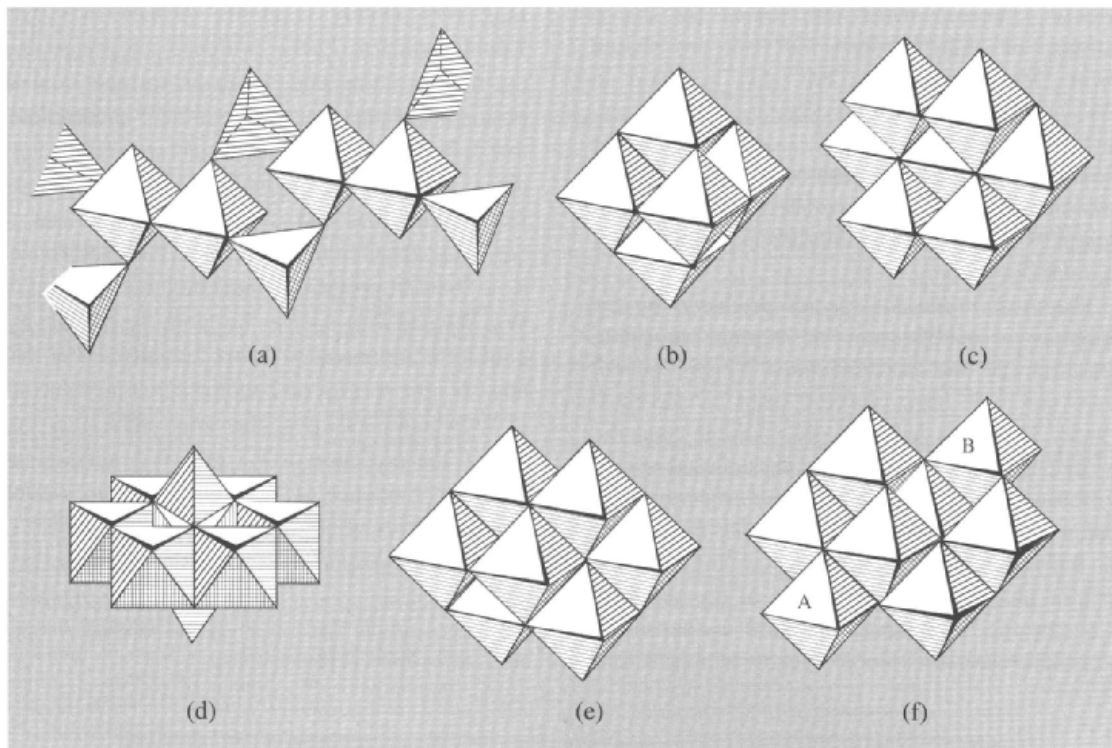
This may be crystallized from aqueous solution and, by the addition of diethylenetriamine,  $(\text{H}_3\text{dien})_2[\text{Mo}_7\text{O}_{24}] \cdot 4\text{H}_2\text{O}$  has been obtained<sup>(11)</sup> as two distinct polymorphs. Both contain discrete  $[\text{Mo}_7\text{O}_{24}]^{6-}$  ions but differ in the way these are packed in the crystals.

Anions with 8, and probably 16–18, Mo atoms also appear to be formed, before increasing acidity suffices to precipitate the hydrous oxide. It is clear from the above equation that the condensation of  $\text{MoO}_4$  polyhedra to produce these large polyanions requires large quantities of strong acid as the supernumerary oxygen atoms are removed in the form of water molecules. Careful

<sup>10</sup> *Inorganic Syntheses*, 27, Chap. 3 pp. 71–135 (1990), gives several detailed preparations.

<sup>11</sup> P. ROMAN, A. LUQUE, A. ARANZABE and J. M. GUTIERREZ-ZORRILLA, *Polyhedron* 11, 2027–38 (1992).





**Figure 23.2** Idealized structures of isopolymolybdate ions. (a) Polymeric  $[\text{Mo}_2\text{O}_7]^{2-}$ , chain as found in the  $\text{NH}_4^+$  salt. The  $[\text{NBu}_4]^+$  salt contains discrete  $[\text{Mo}_2\text{O}_7]^{2-}$  ions, comparable to  $[\text{Cr}_2\text{O}_7]^{2-}$  (p. 1009) but with an  $\text{M}-\text{O}-\text{M}$  angle of  $154^\circ$  compared to  $126^\circ$ . (b)  $[\text{Mo}_6\text{O}_{19}]^{2-}$  (the sixth octahedron is obscured). (c) Paramolybdate,  $[\text{Mo}_7\text{O}_{24}]^{6-}$ ; this is the Anderson structure and can be viewed as an  $\text{M}_{10}\text{O}_{28}$  structure (Fig. 22.3, p. 986) with a line of three octahedra removed. (d)  $\alpha$ - $[\text{Mo}_8\text{O}_{26}]^{4-}$ ; a ring of six octahedra capped by two tetrahedra. (e)  $\beta$ - $[\text{Mo}_8\text{O}_{26}]^{4-}$  (one octahedron is obscured). (f)  $\gamma$ - $[\text{Mo}_8\text{O}_{26}]^{4-}$ . One of the three terminal coordination positions in each octahedron A and B is unoccupied. Filling them with suitable ligands stabilizes this otherwise labile ion.

adjustment of acidity, concentration and temperature, often coupled with slow crystallization, can produce solids containing many other ions which are apparently not present in solution. Mixtures abound, but amongst the distinct species which have been characterized are: the dimolybdate,  $[\text{Mo}_2\text{O}_7]^{2-}$ ; the hexamolybdate,  $[\text{Mo}_6\text{O}_{19}]^{2-}$ ; and the octamolybdate,  $[\text{Mo}_8\text{O}_{26}]^{4-}$ , for which there are  $\alpha$ - and  $\beta$ -isomers. The latter is the one usually obtained from aqueous solutions, but large counter ions or non-aqueous solvents have been used to prepare the former. A third ( $\gamma$ ), coordinatively unsaturated form containing two 5-coordinate Mo atoms has been

suggested as an intermediate in the  $\alpha \rightleftharpoons \beta$  equilibrium, and has been isolated<sup>(12)</sup> as the salt  $[\text{Me}_3\text{N}(\text{CH}_2)_6\text{NMe}_3]_2[\text{Mo}_8\text{O}_{26}]\cdot 2\text{H}_2\text{O}$ . Stabilization of the  $\gamma$ -configuration is also possible by completing the octahedral coordination spheres of the 5-coordinate Mo atoms with suitable ligands such as pyridine or pyrazole.<sup>(13)</sup> Figure 23.2 depicts the structures of these ions and it can be seen that the basic units are

<sup>12</sup> M. L. NIVEN, J. J. CRUYWAGEN and J. B. B. HEYNS, *J. Chem. Soc., Dalton Trans.*, 2007–11 (1991).

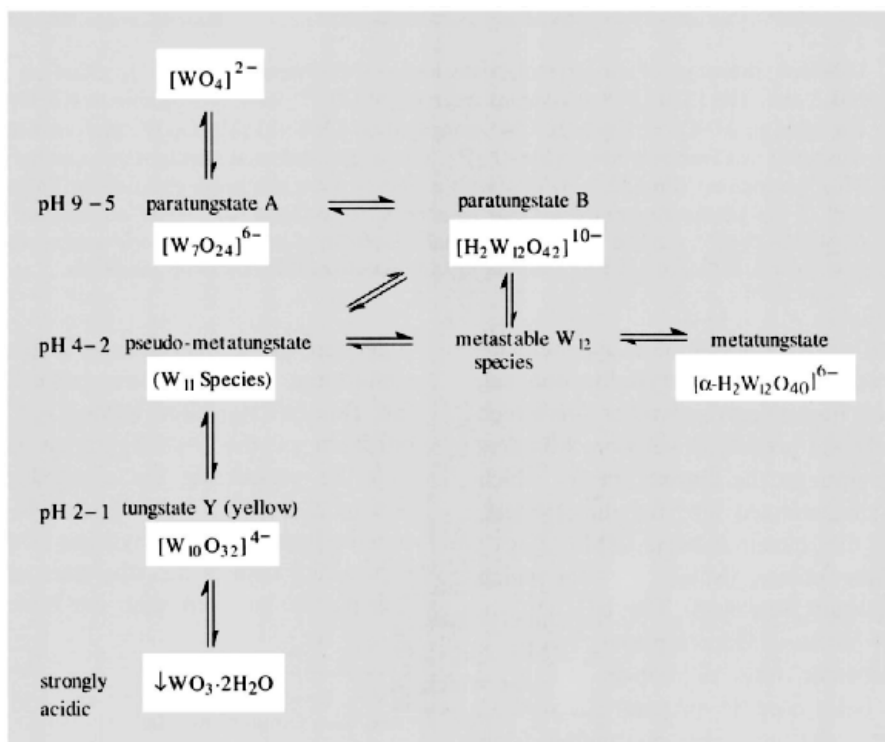
<sup>13</sup> P. GILI, P. MARTIN-ZARZA, G. MARTIN-REYES, J. M. ARRITA and G. MADARIAGA, *Polyhedron* **11**, 115–21 (1992).

MoO<sub>6</sub> octahedra which are joined by shared corners or shared edges, but not by shared faces. MoO<sub>4</sub> tetrahedra are also involved in [Mo<sub>2</sub>O<sub>7</sub><sup>2-</sup>]<sub>n</sub> and in a few other ions. The structure of [Mo<sub>36</sub>O<sub>112</sub>(H<sub>2</sub>O)<sub>16</sub>]<sup>8-</sup>, one of the larger isopolyanions (but see Panel on p. 1015) consists predominantly of MoO<sub>6</sub> octahedra but includes, uniquely in the isopolymolybdates, MoO<sub>7</sub> pentagonal bipyramids.

The most important species produced by the progressive acidification of normal tungstate solutions are the paratungstates which, indeed, were the only ones reported prior to the mid-1940s. They are generally less soluble than the normal tungstates and can be crystallized over a period of several days. Further acidification produces metatungstates which are rather more soluble but will crystallize either on standing for some months or on prolonged heating of the solution. It seems that comparatively rapid condensation produces relatively soluble species which, if left,

will very slowly condense further into less-soluble species. Early evidence suggested that the first paratungstate, A, to be formed in solution is a hexamer but evidence later accumulated that a heptamer is produced, just as with molybdates. For instance, potentiometric data obtained from dilute (0.1 and 0.001 molar) solutions of Na<sub>2</sub>WO<sub>4</sub>·2H<sub>2</sub>O in the range pH 7.8–5 and treated by a “best-fit program”, indicated the presence of W<sub>6</sub>, W<sub>7</sub> and W<sub>12</sub> species but with the W<sub>6</sub> always a minor component.<sup>(14)</sup> More recently, <sup>183</sup>W, <sup>17</sup>O and <sup>1</sup>H nmr spectra of 2 molar aqueous solutions of WO<sub>3</sub> and LiOH over the range pH 8–1.5 confirmed the presence of W<sub>7</sub> and W<sub>12</sub> species but found no evidence of W<sub>6</sub>; they revealed a complicated series of equilibria in which a variety of protonations played a crucial role, and involving

<sup>14</sup> J. J. CRUYWAGEN and I. F. J. van der MERWE, *J. Chem. Soc., Dalton Trans.*, 1701–5 (1987).

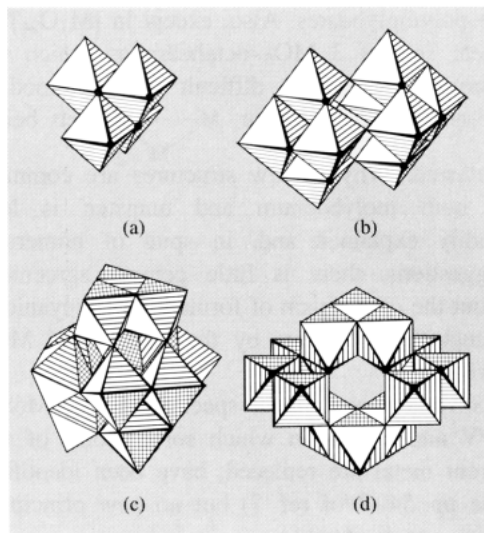


Reaction scheme for the condensation of tungstate ions in aqueous solution.

a  $W_{11}$  species of uncertain composition.<sup>(15)</sup> The much simplified reaction scheme at the foot of the previous page outlines the situation but it must be noted that concentration, temperature, rate of acidification and counter cation will all affect the details of a particular system.

Amongst the crystalline products obtained from aqueous solution are,  $(NH_4)_{10}[H_2W_{12}O_{42}] \cdot 10H_2O$ ,  $Na_6[H_2W_{12}O_{40}] \cdot 29H_2O$ ,  $K_4[W_{10}O_{32}] \cdot 4H_2O$  and  $Na_6[W_7O_{24}] \cdot 14H_2O$ . The compound  $Na_5[H_3W_6O_{22}] \cdot 18H_2O$  has recently been precipitated by acetone from a non-equilibrated aqueous solution<sup>(15a)</sup> and the structure of the anion may be considered to be derived from that of  $[W_7O_{24}]^{6-}$  (which is like that of its Mo analogue, Fig. 23.2c) by removal of an outer octahedron from the middle row of three. Another hexatungstate,  $[W_6O_{19}]^{2-}$  isostructural with its Mo analogue, can be obtained from methanolic solutions.  $Li_{14}(WO_4)_3(W_4O_{16}) \cdot 4H_2O$  has also been crystallized from aqueous solution and shown to contain the discrete ion,  $[W_4O_{16}]^{8-}$  though there is no direct evidence that this is present in solution. The structures<sup>†</sup> of these anions are described in Fig. 23.3.

Many attempts have been made to rationalize the structures and mechanisms of formation of polymetallates. Lipscomb observed that no individual  $MO_6$  octahedral unit ever has more than two unshared, i.e. terminal oxygens (exceptions appear to be stable only in the solid state) and this has been explained on the basis of  $\pi$ -bonding between the metal and terminal oxygen atoms: more than two of these



**Figure 23.3** Idealized structures of isopolytungstate ions. (a)  $[W_4O_{16}]^{8-}$  (b)  $[W_{10}O_{32}]^{4-}$ , composed of two identical  $W_5O_{16}$  groups. (c) The metatungstate ion,  $[H_2W_{12}O_{40}]^{6-}$  (d) The paratungstate B ion,  $[H_2W_{12}O_{42}]^{10-}$ . As in the metatungstate, the protons appear to reside in the cavity of the ion but, unlike those of the metatungstate, exchange rapidly with protons from solvent water.

<sup>15</sup> J. J. HASTINGS and O. W. HOWARTH, *J. Chem. Soc., Dalton Trans.*, 209–15 (1992).

<sup>15a</sup> H. HARTL, R. PALM and J. FUCHS, *Angew. Chem. Int. Edn. Engl.* **32**, 1492–4 (1993).

<sup>†</sup> It is instructive to recall a particular problem facing early workers in establishing these structures by X-ray diffraction. Large scattering by the heavy tungsten atoms made it extremely difficult to locate the positions of the lighter oxygen atoms and this sometimes led to ambiguity in the assignment of precise structures (relative scattering  $O/W = (8/74)^2 = 1/86$ , cf.  $H/C = (1/6)^2 = 1/36$ ). This is no longer a problem because of the greater precision of modern techniques of X-ray data acquisition and processing, but good-quality crystals are still necessary and these may be very difficult to produce.

would so weaken and lengthen the *trans*-bonds holding the metal to the polyanion that it would become detached. Electrostatic repulsions between neighbouring metal ions will reinforce the distorting effect of  $M-O \pi$ -bonding, causing the metal ions to move off-centre in the  $MO_6$  octahedra which are connected to each other. The effect increases as the mode of attachment changes from corner-sharing to edge-sharing. Thus, while the avoidance of unfavourably high, overall anionic charge favours edge-sharing as opposed to corner-sharing (thereby reducing the number of  $O^{2-}$  ions), the off-centre distortions become increasingly difficult to accommodate as the size of the polyanion increases. Ultimately edge-sharing is no longer possible, and this stage is reached by  $W^{VI}$  before it occurs with the smaller  $Mo^{VI}$ . Inspection of Figs. 23.2 and 23.3 shows the greater incidence of corner-sharing in the higher polytungstates than in

the polymolybdates. Also, except in  $[M_7O_{24}]^{6-}$ , linear sets of 3  $MO_6$  octahedra on which the distortions are most difficult to accommodate are not found, triangular  $M \cdots M$  sets being



preferred. Why so few structures are common to both molybdenum and tungsten is less readily explained and, in spite of numerous suggestions, there is little general agreement about the mechanism of formation of polyanions except that it occurs by the addition of  $MO_4$  tetrahedra.

Several mixed metal species, Mo/W, Mo/V, W/V and W/Nb, in which some atoms of the parent metal are replaced, have been identified (see pp. 54–7 of ref. 7) but no new principles are as yet discernible.

### 23.3.3 Heteropolymetallates<sup>(7,8,9)</sup>

In 1826 J. J. Berzelius found that acidification of solutions containing both molybdate and phosphate produced a yellow crystalline precipitate. This was the first example of a heteropolyanion and it actually contains the phosphomolybdate ion,  $[PMo_{12}O_{40}]^{3-}$ , which can be used in the quantitative estimation of phosphate. Since its discovery a host of other heteropolyanions have been prepared, mostly with molybdenum and tungsten but with more than 50 different heteroatoms, which include many non-metals and most transition metals — often in more than one oxidation state. Unless the heteroatom contributes to the colour, the heteropoly-molybdates and -tungstates are generally of varying shades of yellow. The free acids and the salts of small cations are extremely soluble in water but the salts of large cations such as  $Cs^I$ ,  $Ba^{II}$  and  $Pb^{II}$  are usually insoluble. The solid salts are noticeably more stable thermally than are the salts of isopolyanions. Heteropoly compounds have been applied extensively as catalysts in the petrochemicals industry, as precipitants for numerous dyes with which they form “lakes” and, in the case of the Mo compounds, as flame retardants.

In these ions the heteroatoms are situated inside “cavities” or “baskets” formed by  $MO_6$  octahedra of the parent M atoms and are bonded to oxygen atoms of the adjacent  $MO_6$  octahedra. The stereochemistry of the heteroatom is determined by the shape of the cavity which in turn depends on the ratio of the number of heteroatoms to parent atoms. Three major and a number of minor classes are found.

*1:12, tetrahedral.* These are found for both Mo and W but the latter are far more numerous and stable than the former. They occur with small heteroatoms such as  $P^V$ ,  $As^V$ ,  $Si^{IV}$  and  $Ge^{IV}$  which yield tetrahedral oxoanions, and they are the most readily obtained and best known of the heteropolyanions. Keggin<sup>(16)</sup> first determined the structure of the phosphotungstate, which was known to be isomorphous with the metatungstate, and his name is given to this structure type (Fig. 23.3c). The hetero-atom, or in the case of metatungstate a pair of protons, is situated in the tetrahedral inner cavity of the parent ion (Panel opposite). For the tungstates,  $Fe^{III}$ ,  $Co^{II}$  and  $Zn^{II}$  derivatives are known, the second of which is of interest: it is readily formed, since tetrahedrally coordinated  $Co^{II}$  is not unusual, but oxidation yields  $[Co^{III}W_{12}O_{40}]^{5-}$  in which the very unusual, high-spin, tetrahedral  $Co^{III}$  is trapped. Nor is tetrahedral coordination common for  $Cu^{II}$  but it is found in a recently reported<sup>(17)</sup> polyanion of this class containing both  $Cu^{II}$  and 2H as heteroatoms (giving an overall stoichiometry of  $\{Cu_{0.4}(H_2)_{0.6}\}$  for the hetero “atom”). The structure of these compounds is now known as the  $\alpha$ -Keggin structure since an isomeric  $\beta$ -Keggin structure has been identified for the heteropolyanions, “ $XMo_{12}$ ” ( $X = Si, Ge, P, As$ ) and “ $XW_{12}$ ” ( $X = Si, Ge$ ). Also  $\beta$ - $[H_2W_{12}O_{40}]^{6-}$  has been implicated in the isopolytungstate equilibria.<sup>(15)</sup> “Lacunary” ions, or their derivatives, are obtained by the nominal loss of one or more  $MO_6$  octahedra (actually the stoichiometric loss of that number of MO

<sup>16</sup> J. F. KEGGIN, *Proc. R. Soc. A*, **144**, 75–100 (1934)

<sup>17</sup> H.-J. LUNK, S. GIESE, J. FUCHS and R. STÖSSER, *Z. anorg. allg. Chem.* **619**, 961–8 (1993).

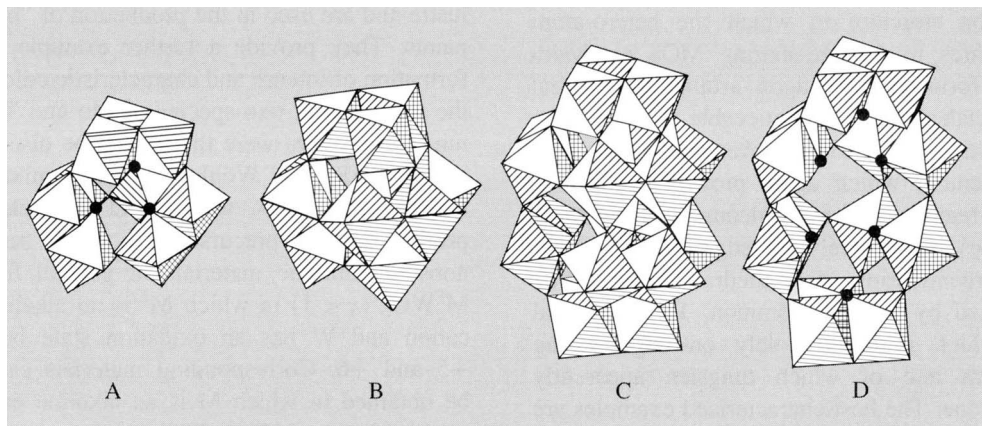
## Large Polymetallates

With the objective of producing model systems to mimic the metal oxide surfaces of catalysts, a great deal of effort has been devoted to the preparation of large polymetallate structures.

The  $\alpha$ -Keggin structure of  $[\text{PW}_{12}\text{O}_{40}]^{3-}$  and the metatungstate,  $[\text{H}_2\text{W}_{12}\text{O}_{40}]^{6-}$  can be seen (Fig 23.3) to be composed of four identical "tritungstate" or  $\text{W}_3$  groups. Each of these is made up of three edge-sharing  $\text{WO}_6$  octahedra, and the four groups are linked to each other by corner-sharing so as to enclose the heteroatom. This is more clearly seen in A where one of the  $\text{W}_3$  groups has been omitted and the oxygens which are nearest neighbours to the heteroatom are marked by dots. The  $\beta$ -Keggin structure, B, is derived from the  $\alpha$ -form by rotation of one  $\text{W}_3$  group (in this case the top one) through  $60^\circ$ . In principle, similar rotation of the other three  $\text{W}_3$  groups would yield  $\gamma$ ,  $\delta$  and  $\epsilon$  isomers.

The Dawson structure, C, can be visualized as being formed by removing the three basal octahedra from each of two  $\alpha$ -Keggin ions which are then fused together. By omitting the four octahedra at the front, the oxygens associated with the 2 heteroatoms can be seen more clearly (D).

Still larger heteropolyanions are possible by using  $\text{As}^{\text{III}}$  as the heteroatom. The lone-pair of electrons of this atom makes it too large to fit inside the Keggin ion, and the lacunary  $[\text{AsW}_9\text{O}_{33}]^{9-}$  is formed instead. By judicious use of this as a "building block,"  $[\text{As}_4\text{W}_{40}\text{O}_{140}]^{28-}$  has been prepared. Similar use of  $[\text{P}_2\text{W}_{12}\text{O}_{48}]^{12-}$ , produced by degrading the Dawson structure by raising the pH, has yielded<sup>(18)</sup>  $[\text{P}_4\text{W}_{48}\text{O}_{184}]^{40-}$ .



The largest polymetallates so far reported, however, are the mixed valence ( $\text{Mo}^{\text{VI}}$ ,  $\text{Mo}^{\text{V}}$ ) nitrosyls obtained by the more straightforward, if less systematic, method of heating acidified aqueous solutions of  $\text{MoO}_4^-$  and  $\text{NH}_2\text{OH}$  with  $\text{VO}_3^-$ . Depending on concentration and whether the solutions are refluxed or heated without stirring, a variety of products has been obtained<sup>(19)</sup> including the mixed metal  $[\text{Mo}_{57}\text{V}_6\text{O}_{183}(\text{NO})_6(\text{H}_2\text{O})_{18}]^{16-}$  and the spectacular  $[\text{Mo}_{154}\text{O}_{420}(\text{NO})_{14}(\text{H}_2\text{O})_{70}]^{n-}$  ( $n = 25 \pm 5$ ). Both are dark blue and are composed of edge- and corner-sharing  $\text{MoO}_6$  octahedra and  $\{\text{Mo}(\text{NO})\text{O}_6\}$  pentagonal bipyramids, along with  $\text{V}^{\text{IV}}\text{O}_6$  octahedra in the case of the former. The latter has the overall shape of a car (automobile) tyre and, in spite of its large molar mass, its large surface area, bristling with  $\text{H}_2\text{O}$  and  $\text{OH}$  ligands, renders it readily soluble in water from which it can be recrystallized without decomposition in the absence of air.

units). The hetero atom is then held in an open "basket" rather than being totally enclosed. The

most numerous of such ions<sup>(9)</sup> are the Keggin derivatives,  $[\text{XM}_{11}\text{O}_{39}]^{n-}$  ( $\text{M} = \text{Mo}, \text{W}$ ;  $\text{X} = \text{P}$ ,

<sup>18</sup> Y. JEANNIN, G. HERVE and A. PROUST, *Inorg. Chim. Acta* **198**–**200**, 319–36 (1992).

<sup>19</sup> S.-W. ZHANG, G.-Q. HUANG, M.-C. SHAO and Y.-Q. TANG, *J. Chem. Soc., Chem. Commun.*, 37–8

(1993). A. MÜLLER, E. KRICKEMEYER, J. MEYER, H. BOGGE, F. PETERS, W. PLASS, E. DIEMANN, S. DILLINGER, F. NONNENBRUCH, M. RANDEATH and C. MENKE, *Angew. Chem. Int. Edn. Engl.* **34**, 2122–4 (1995).

As, Si, etc.) which are able to act as ligands to a variety of transition metal cations as well as to organometallic groups such as SnR, AsR and Ti ( $\eta^5$ -C<sub>5</sub>H<sub>5</sub>).

2:18, *tetrahedral*. If acidic solutions of the 1:12 anions  $[X^V M_{12} O_{40}]^{3-}$  (X = P, As; M = Mo, W) are allowed to stand, the 2:18  $[X_2 M_{18} O_{62}]^{6-}$  ions are gradually produced and can be isolated as their ammonium or potassium salts. The ion is best considered to be formed from two lacunary, 1:9 ions fused together and is generally known as the Dawson structure.

1:6, *octahedral*. These are formed with larger heteroatoms such as Te<sup>VI</sup>, I<sup>VII</sup>, Co<sup>III</sup> and Al<sup>III</sup> and are usually obtained from slightly acidic (pH 4–5) aqueous solutions. They adopt the Anderson structure in which the hetero-atom coordinates to 6 edge-sharing MO<sub>6</sub> octahedra in the form of a hexagon around the central XO<sub>6</sub> octahedron. It is noticeable that tungsten forms this type of ion less frequently than does molybdenum, which again probably reflects a greater readiness of molybdenum to form large structures based solely on edge-sharing, rather than corner-sharing, of octahedra. This is further reinforced by the less common, 1:9 octahedral type which is based solely on edge-sharing octahedra and of which tungsten apparently forms none. The best characterized examples are  $[Mn^{IV} Mo_9 O_{32}]^{6-}$  and  $[Ni^{IV} Mo_9 O_{32}]^{6-}$ , prepared by the oxidation of X<sup>II</sup> molybdate solutions with peroxodisulfate, the kinetics of which have been investigated.<sup>(20)</sup>

Mild and reversible reduction of 1:12 and 2:18 heteropoly-molybdates and -tungstates produces characteristic and very intense blue colours (“heteropoly blues”) which find application in the quantitative determinations of Si, Ge, P and As, and commercially as dyes and pigments. The reductions are most commonly of 2 electron equivalents but may be of 1 and up to 6 electron equivalents. Many of the reduced anions can be isolated as solid salts in which the unreduced structure remains essentially unchanged and

the heteroatom is not normally involved; i.e. even Fe<sup>III</sup>W<sub>12</sub> is reduced to Fe<sup>III</sup>W<sup>V</sup>W<sub>11</sub><sup>VI</sup> not to Fe<sup>II</sup>W<sub>12</sub>, although Co<sup>III</sup>W<sub>12</sub> is reduced to Co<sup>II</sup>W<sub>12</sub>. 1- or 2-electron reductions evidently occur on individual M atoms, producing a proportion of M<sup>V</sup> ions. Transfer of electrons from M<sup>V</sup> to M<sup>VI</sup> ions is then responsible for the intense “charge-transfer” absorption. In the highly reduced species, limited delocalization is probable.

### 23.3.4 Tungsten and molybdenum bronzes

These materials owe their name to their metallic lustre and are used in the production of “bronze” paints. They provide a further example of the formation of intense and characteristic colours by the reduction of oxo-species of Mo and W. The tungsten bronzes were the first to be discovered when, in 1823, F. Wöhler reduced a mixture of Na<sub>2</sub>WO<sub>4</sub> and WO<sub>3</sub> with H<sub>2</sub> at red heat. The product was the precursor of a whole series of nonstoichiometric materials of general formula M<sup>I</sup><sub>x</sub>WO<sub>3</sub> (x < 1) in which M<sup>I</sup> is an alkali metal cation and W has an oxidation state between +5 and +6. Corresponding materials can also be obtained in which M is an alkaline earth or lanthanide metal. The alkali-metal molybdenum bronzes<sup>(21)</sup> are analogous to, but less well-known than, those of tungsten, being less stable and requiring high pressure for their formation; they were not produced until the 1960s. The lower stability of the molybdenum bronzes may be a consequence of the greater tendency of Mo<sup>V</sup> to disproportionate as compared to W<sup>V</sup>.

Tungsten bronzes can be prepared by a variety of reductive techniques but probably the most general method consists of heating the normal tungstate with tungsten metal. They are extremely inert chemically, being resistant both to alkalis and to acids, even when hot and concentrated. Their colours depend in the proportion of M and W present. In the case of sodium

<sup>20</sup> S. J. DUNNE, R. C. BURNS and G. A. LAWRENCE, *Aust. J. Chem.* **45**, 1943–52 (1992).

<sup>21</sup> M. GREENBLATT, *Chem. Revs.* **88**, 31–53 (1988).



tungsten bronze the colour varies from golden yellow, when  $x \sim 0.9$ , through shades of orange and red to bluish-black when  $x \sim 0.3$ . Within this range of  $x$ -values the structure consists of corner-shared  $\text{WO}_6$  octahedra<sup>†</sup> as in  $\text{WO}_3$  (p. 1008), with  $\text{Na}^+$  ions in the interstices — in other words an M-deficient perovskite lattice (p. 963). The observed electrical conductivities are metallic in magnitude and decrease linearly with increase in temperature, suggesting the existence of a conduction band of delocalized electrons. Measurements of the Hall effect (used to measure free electron concentrations) indicate that the concentration of free electrons equals the concentration of sodium atoms, implying that the conduction electrons arise from the complete ionization of sodium atoms. Several mechanisms have been suggested for the formation of this conduction band but it seems most likely that the  $t_{2g}$  orbitals of the tungsten overlap, not directly (since adjacent W atoms are generally more than 500 pm apart) but via oxygen  $p\pi$  orbitals, so forming a partly filled  $\pi^*$  band permeating the whole  $\text{WO}_3$  framework. If the value of  $x$  is reduced below about 0.3 the resulting electrical properties are semiconducting rather than metallic. This change coincides with structural distortions which probably disrupt the mechanism by which the conduction band is formed and instead cause localization of electrons in  $t_{2g}$  orbitals of specific tungsten atoms.

### 23.3.5 Sulfides<sup>(2)</sup>, selenides and tellurides

The sulfides of this triad, though showing some similarities in stoichiometry to the principal

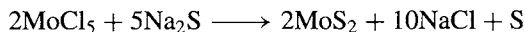
<sup>†</sup> This corner-sharing in tungsten bronzes is to be compared with a mixture of corner and edge-sharing in molybdenum bronzes which presumably occurs, as in the case of the polymetallates, because the increased electrostatic repulsion entailed in edge-sharing is less disruptive when the smaller Mo is involved. The prevalence of edge-sharing is still more marked in the vanadium and titanium bronzes (pp. 987, 964) where the smaller charges on the metal ions produce correspondingly smaller repulsions.

oxides (p. 1007), tend to be more stable in the lower oxidation states of the metals. Thus Cr forms no trisulfide and it is the di- rather than the tri-sulfides of Mo and W which are the more stable. However, tungsten (unlike Cr and Mo) does not form  $\text{M}_2\text{S}_3$ . Many of the compounds are nonstoichiometric, most are metallic (or at least semiconducting), and they exhibit a wide variety of magnetic behaviour encompassing diamagnetic, paramagnetic, antiferro-, ferri- and ferro-magnetic.

$\text{Cr}_2\text{S}_3$  is formed by heating powdered Cr with sulfur, or by the action of  $\text{H}_2\text{S}(\text{g})$  on  $\text{Cr}_2\text{O}_3$ ,  $\text{CrCl}_3$  or Cr. It decomposes to CrS on being heated, via a number of intermediate phases which approximate in composition to  $\text{Cr}_3\text{S}_4$ ,  $\text{Cr}_5\text{S}_6$  and  $\text{Cr}_7\text{S}_8$ . The structural relationship between these various phases can most readily be understood by reference to the NiAs– $\text{CdI}_2$  structure motif. Removal of all the M atoms from alternate layers of the NiAs structure (p. 555) yields the  $\text{CdI}_2$  layer lattice (p. 1212). Between these two extremes, removal of a proportion of M atoms results in the above phases as follows: if one quarter of the Cr atoms are removed from alternate layers  $\text{Cr}_7\text{S}_8$  results; if one third,  $\text{Cr}_5\text{S}_6$  results; if two thirds,  $\text{Cr}_4\text{S}_6$  (ie  $\text{Cr}_2\text{S}_3$ ) results and if half,  $\text{Cr}_3\text{S}_4$  results. Of these various phases  $\text{Cr}_2\text{S}_3$  and CrS are semiconductors, whereas  $\text{Cr}_7\text{S}_8$ ,  $\text{Cr}_5\text{S}_6$  and  $\text{Cr}_3\text{S}_4$  are metallic, and all exhibit magnetic ordering. The corresponding selenides  $\text{CrSe}$ ,  $\text{Cr}_7\text{Se}_8$ ,  $\text{Cr}_3\text{Se}_4$ ,  $\text{Cr}_2\text{Se}_3$ ,  $\text{Cr}_5\text{Se}_6$  and  $\text{Cr}_7\text{Se}_{12}$  are broadly similar, as are the tellurides  $\text{CrTe}$ ,  $\text{Cr}_7\text{Te}_8$ ,  $\text{Cr}_5\text{Te}_6$ ,  $\text{Cr}_3\text{Te}_4$ ,  $\text{Cr}_2\text{Te}_3$ ,  $\text{Cr}_5\text{Te}_8$  and  $\text{CrTe}_{\sim 2}$ .

Of the many molybdenum sulfides which have been reported, only  $\text{MoS}$ ,  $\text{MoS}_2$  and  $\text{Mo}_2\text{S}_3$  are well established. A hydrated form of the trisulfide of somewhat variable composition is precipitated from aqueous molybdate solutions by  $\text{H}_2\text{S}$  in classical analytical separations of molybdenum, but it is best prepared by thermal decomposition of the thiomolybdate,  $(\text{NH}_4)_2\text{MoS}_4$ .  $\text{MoS}$  is formed by heating the calculated amounts of Mo and S in an evacuated tube. The black  $\text{MoS}_2$ , however, is the most stable sulfide and, besides being the principal ore of Mo,

is much the most important Mo compound commercially. In 1923 its structure was shown by R. G. Dickinson and L. Pauling (in the latter's first research paper) to consist of layers of MoS<sub>2</sub> in which the molybdenum atoms are each coordinated to 6 sulfides, but forming a trigonal prism rather than the more usual octahedron. This layer structure promotes easy cleavage and graphite-like lubricating properties, which have led to its widespread use as a lubricant both dry and in suspensions in oils and greases. It also has applications as a catalyst in many hydrogenation reactions and, even when the original catalyst takes the form of an oxide, it is likely that impurities (which often "poison" other catalysts) quickly produce a sulfide catalytic system. High-purity MoS<sub>2</sub> is normally prepared by heating the elements at 1000°C for several days. The reaction of anhydrous MoCl<sub>5</sub> and Na<sub>2</sub>S offers a promising alternative.<sup>(22)</sup>



It is so exothermic as to burst into flame on mixing, and is complete within seconds.

WS<sub>3</sub> and WS<sub>2</sub> are similar to their molybdenum analogues and all 4 compounds are diamagnetic semiconductors.

Selenides and tellurides are, again, broadly similar to the sulfides in structure and properties.

The oxygen atoms of MO<sub>4</sub><sup>2-</sup> can be replaced successively by sulfur, and all four thiometallates, MO<sub>3</sub>S<sup>2-</sup>, MO<sub>2</sub>S<sub>2</sub><sup>2-</sup>, MOS<sub>3</sub><sup>2-</sup> and MS<sub>4</sub><sup>2-</sup> have been prepared; the thiomolybdates a century ago. They are useful reagents for the preparation of metal-sulfur clusters, and act as ligands, usually chelating but also as bridging groups.<sup>(23)</sup>

MSe<sub>4</sub><sup>2-</sup> have also been known for a considerable time but are less familiar. They may

be prepared conveniently by treating K<sub>2</sub>Se<sub>3</sub> with M(CO)<sub>6</sub> in dmf.<sup>(24)</sup>

Remarkable physical properties are found in a series of ternary molybdenum chalcogenides, M<sub>x</sub>Mo<sub>6</sub>X<sub>8</sub>, known as Chevrel phases.<sup>(25)</sup> The first of these was PbMo<sub>6</sub>S<sub>8</sub> but over 40 metals have been incorporated in the series, and both Se and Te analogues occur. These phases are black crystalline materials, prepared from the elements at temperatures of 1000–1100°C, and the [Mo<sub>6</sub>X<sub>8</sub>] cluster, composed of an octahedron of Mo atoms face-capped by X atoms, is the basic structural unit (cf Mo, W dihalides, p. 1022). The clusters are linked because the otherwise free apical coordination site of each Mo is occupied by an X atom of an adjacent cluster, while the M<sub>x</sub> atoms are intercalated in the channels between the clusters. That these bridges are strong, is evident from the observed intercluster Mo–Mo distances of only 310–360 pm compared to approx. 270 pm for Mo atoms within a cluster — which are not bridged. With *x* = 0, the metastable Mo<sub>6</sub>X<sub>8</sub> (obtained by "deintercalation" of M<sub>x</sub>Mo<sub>6</sub>X<sub>8</sub> with HCl, rather than by direct synthesis) has only 20 electrons per cluster (6 × 6 metal valence electrons less 2 × 8 used in bonding to X<sub>8</sub>). This is 4 short of the 24 required for Mo–Mo single bonds along each of the edges of the cluster, and may be the cause of the observed trigonal distortion. Intercalation of M<sub>x</sub> atoms provides up to 4 electrons which make good this deficit thereby strengthening and shortening the Mo–Mo bonds and reducing the distortion.<sup>†</sup> PbMo<sub>6</sub>S<sub>8</sub> has 22 electrons per cluster. The electron "holes" facilitate conduction, and below 14 K it is a superconductor. This, and several other Chevrel phases retain their superconductivity in the presence of exceptionally strong magnetic fields, and attempts to produce technically acceptable superconductors by extruding filaments in a copper matrix have been

<sup>24</sup> S. C. O'NEAL and J. W. COLIS, *J. Am. Chem. Soc.* **110**, 1971–3 (1988).

<sup>25</sup> R. CHEVREL, M. HIRRIEN and M. SERGENT, *Polyhedron* **5**, 87–94 (1986).

<sup>†</sup> An alternative interpretation, supported by evidence from relevant molecular compounds is that the distortions are the result of intercluster M–X interactions (see p. 1031)

<sup>22</sup> P. R. BONNEAU, R. F. JARVIS and R. B. KANER, *Nature* **349**, 510–2 (1991).

<sup>23</sup> M. A. GREANEY and E. I. STIEFEL, *J. Chem. Soc., Chem Commun.*, 1679–80 (1992).



promising. Apparently, no tungsten analogues are yet known.

### 23.3.6 Halides and oxohalides<sup>(2,3)</sup>

The known halides of chromium, molybdenum and tungsten are listed in Table 23.4. The observed trends are as expected. The group

oxidation state of +6 is attained by chromium only with the strongly oxidizing fluorine, and even tungsten is unable to form a hexaiodide. Precisely the same is true in the +5 oxidation state, and in the +4 oxidation state the iodides have a doubtful or unstable existence. In the lower oxidation states all the chromium halides are known, but molybdenum has not yet been induced to form a difluoride nor tungsten a di- or

**Table 23.4** Halides of Group 6 (mp/°C)

Oxidation state	Fluorides	Chlorides	Bromides	Iodides
+6	CrF <sub>6</sub> yellow ( <i>d</i> > -100°)			
	MoF <sub>6</sub> colourless (17.4°) bp 34°	(MoCl <sub>6</sub> ) black		
	WF <sub>6</sub> colourless (1.9°) bp 17.1°	WCl <sub>6</sub> dark blue (275°) bp 346°	WBr <sub>6</sub> dark blue (309°)	
+5	CrF <sub>5</sub> red (34°) bp 117°			
	MoF <sub>5</sub> yellow (67°) bp 213°	MoCl <sub>5</sub> black (194°) bp 268°		
	WF <sub>5</sub> yellow	WCl <sub>5</sub> dark green (242°) bp 286°	WBr <sub>5</sub> black	
+4	CrF <sub>4</sub> violet-amethyst <sup>(a)</sup>	CrCl <sub>4</sub> ( <i>d</i> > 600°, gas phase)	CrBr <sub>4</sub> ?	CrI <sub>4</sub>
	MoF <sub>4</sub> pale green	MoCl <sub>4</sub> black	MoBr <sub>4</sub> black	MoI <sub>4</sub> ?
	WF <sub>4</sub> red-brown	WCl <sub>4</sub> black	WBr <sub>4</sub> black	WI <sub>4</sub> ?
+3	CrF <sub>3</sub> green (1404°)	CrCl <sub>3</sub> red-violet (1150°)	CrBr <sub>3</sub> very dark green (1130°)	CrI <sub>3</sub> very dark green
	MoF <sub>3</sub> brown (>600°)	MoCl <sub>3</sub> very dark red (1027°)	MoBr <sub>3</sub> green (977°)	MoI <sub>3</sub> black (927°)
		WCl <sub>3</sub> red	WBr <sub>3</sub> black ( <i>d</i> > 80°)	WI <sub>3</sub>
+2	CrF <sub>2</sub> green (894°)	CrCl <sub>2</sub> white (820°)	CrBr <sub>2</sub> white (842°)	CrI <sub>2</sub> red-brown (868°)
		MoCl <sub>2</sub> yellow ( <i>d</i> > 530°)	MoBr <sub>2</sub> yellow-red ( <i>d</i> > 900°)	MoI <sub>2</sub>
		WCl <sub>2</sub> yellow	WBr <sub>2</sub> yellow	WI <sub>2</sub> brown

<sup>(a)</sup>It is probable that previously reported green samples were largely CrF<sub>3</sub>; O. KRAMER and B. G. MÜLLER, *Z. anorg. allg. Chem.* **621**, 1969-72 (1995).

tri-fluoride. Similarly, in the oxohalides (which are largely confined to the +6 and +5 oxidation states, see p. 1023) tungsten alone forms an oxiodide, while only chromium (as yet) forms an oxofluoride in the lower of these oxidation states.

All the known hexahalides can be prepared by the direct action of the halogen on the metal and all are readily hydrolysed. The yellow  $\text{CrF}_6$ , however, requires a temperature of  $400^\circ\text{C}$  and a pressure of 200–300 atms for its formation, and reduction of the pressure causes it to dissociate into  $\text{CrF}_5$  and  $\text{F}_2$  even at temperatures as low as  $-100^\circ\text{C}$ . The monomeric and octahedral hexafluorides  $\text{MoF}_6$  and  $\text{WF}_6$  are colourless liquids and the former is strongly oxidizing. Only tungsten is known with certainty to produce other hexahalides and these are the dark-blue solids  $\text{WCl}_6$  and  $\text{WBr}_6$ , the latter in particular being susceptible to reduction.

Of the pentahalides, chromium again forms only the fluoride which is a strongly oxidizing, bright red, volatile solid prepared from the elements using less severe conditions than for  $\text{CrF}_6$ .  $\text{MoF}_5$  and  $\text{WF}_5$  can be prepared by reduction of the hexahalides with the metal but the latter disproportionates into  $\text{WF}_6$  and  $\text{WF}_4$  if heated above about  $80^\circ\text{C}$ . They are yellow volatile solids, isostructural with the tetrameric  $(\text{NbF}_5)_4$  and  $(\text{TaF}_5)_4$  (Fig. 22.4b, p. 990). Similarity with Group 5 is again evident in the pentachlorides of Mo and W,  $\text{MoCl}_5$  being the most extensively studied of the pentahalides. These, respectively, black and dark-green solids are obtained by direct reaction of the elements under carefully controlled conditions and have the same dimeric structure as their Nb and Ta analogues (Fig. 22.4c, p. 990).  $\text{WBr}_5$  can be prepared similarly but is not yet well characterized.

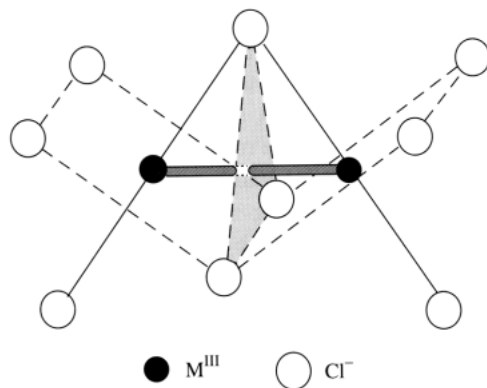
The tetrahalides are scarcely more numerous or familiar than the hexa- and penta-halides, the 3 tetraiodides together with  $\text{CrBr}_4$  and  $\text{CrCl}_4$  being either of uncertain existence or occurring only at high temperatures in the gaseous phase. The most stable representatives are the fluorides:  $\text{CrF}_4$  is an unreactive solid;  $\text{MoF}_4$  is an involatile green solid; and  $\text{WF}_4$  begins

to decompose only when heated above  $800^\circ$ .  $\text{MoCl}_4$  exists in two crystalline modifications:  $\alpha\text{-MoCl}_4$  is probably made up of linear chains of edge-shared octahedra, whereas  $\beta\text{-MoCl}_4$  has a unique structure composed of hexameric cyclic molecules  $(\text{MoCl}_4)_6$  generated by edge-shared  $\{\text{MoCl}_6\}$  octahedra with  $\text{Mo}-\text{Cl}_l$  220 pm,  $\text{Mo}-\text{Cl}_\mu$  243 and 251 pm and  $\text{Mo}\cdots\text{Mo}$  367 pm. General preparative methods include controlled reaction of the elements, reduction of higher halides, and halogenation of lower halides. The tetrahalides of Mo and W are readily oxidized and hydrolysed and produce some adducts of the form  $\text{MX}_4\text{L}_2$ .

The trihalides show major differences between the 3 metals. All 4 of the chromium trihalides are known, this being much the most stable oxidation state for chromium; they can be prepared by reacting the halogen and the metal, though  $\text{CrF}_3$  is better obtained from HF and  $\text{CrCl}_3$  at  $500^\circ\text{C}$ . The fluoride is green, the chloride red-violet, and the bromide and iodide dark green to black. In all cases layer structures lead to octahedral coordination of the metal.  $\text{CrCl}_3$  consists of a ccp lattice of chloride ions with  $\text{Cr}^{\text{III}}$  ions occupying two-thirds of the octahedral sites of alternate layers. The other alternate layers of octahedral sites are empty and, without the cohesive effect of the cations, easy cleavage in these planes is possible and this accounts for the flaky appearance. Stable, hydrated forms of  $\text{CrX}_3$  can also be readily obtained from aqueous solutions, and  $\text{CrCl}_3 \cdot 6\text{H}_2\text{O}$  provides a well-known example of hydrate isomerism, mentioned on p. 920. In view of this clear ability of  $\text{Cr}^{\text{III}}$  to aquate it may seem surprising that anhydrous  $\text{CrCl}_3$  is quite insoluble in pure water (though it dissolves rapidly on the addition of even a trace of a reducing agent). It appears that the reducing agent produces at least some  $\text{Cr}^{\text{II}}$  ions. Solubilization then follows as a result of electron transfer from  $[\text{Cr}(\text{aq})]^{2+}$  in solution via a chloride bridge to  $\text{Cr}^{\text{III}}$  in the solid, which leaves  $[\text{Cr}(\text{aq})]^{3+}$  in solution and  $\text{Cr}^{\text{II}}$  in the solid. The latter is kinetically far more labile than  $\text{Cr}^{\text{III}}$  and can readily leave the solid and aquate, so starting the cycle again and rapidly dissolving the solid.

The Mo trihalides are obtained by reducing a higher halide with the metal (except for the triiodide which, being the highest stable iodide, is best prepared directly). They are insoluble in water and generally inert.  $\text{MoCl}_3$  is structurally similar to  $\text{CrCl}_3$  but is distorted so that pairs of Mo atoms lie only 276 pm apart which, in view of the low and temperature-dependent magnetic moment, is evidently close enough to permit appreciable Mo–Mo interaction. Electrolytic reduction of a solution of  $\text{MoO}_3$  in aqueous HCl changes the colour to green, then brown, and finally red, when complexes of the octahedral  $[\text{MoCl}_6]^{3-}$ ,  $[\text{MoCl}_5(\text{H}_2\text{O})]^{2-}$  and  $[\text{Mo}_2\text{Cl}_9]^{3-}$  can be isolated using suitable cations. The diversity of the coordination chemistry of molybdenum(III) is, however, in no way comparable to that of chromium(III).

By contrast, the tungsten trihalides (the trifluoride is not known) are “cluster” compounds similar to those of Nb and Ta. The trichloride and tribromide are prepared by halogenation of the dihalides. The structure of the former is based on the  $[\text{M}_6\text{X}_{12}]^{n+}$  cluster (Fig. 22.6) with a further 6 Cl atoms situated above the apical W atoms.  $\text{WBr}_3$ , on the other hand, has a structure based on the  $[\text{M}_6\text{X}_8]^{n+}$  cluster (see Fig. 23.5), but as it is formed by only a 2-electron oxidation of  $[\text{W}_6\text{Br}_8]^{4+}$  it does not contain tungsten(III) and is best formulated as  $[\text{W}_6\text{Br}_8]^{6+}(\text{Br}_4^{2-})(\text{Br}^-)_2$ , where  $(\text{Br}_4^{2-})$  represents a bridging polybromide group. Electrolytic reduction of  $\text{WO}_3$  in aqueous HCl fails to produce the mononuclear complexes obtained with molybdenum, but forms the green  $[\text{W}_2\text{Cl}_9]^{3-}$  ion. This and its Cr and Mo analogues provide an interesting reflection of the increasing strength of M–M bonding in the order  $\text{Cr}^{\text{III}} < \text{Mo}^{\text{III}} < \text{W}^{\text{III}}$ . The structure consists of 2  $\text{MCl}_6$  octahedra sharing a common face (Fig. 23.4) which allows the possibility of direct M–M bonding. In the Cr ion the Cr atoms are 312 pm apart, being actually displaced in their  $\text{CrO}_6$  octahedra away from each other. The magnetic moment of  $[\text{Cr}_2\text{Cl}_9]^{3-}$  is normal for a metal ion with 3 unpaired electrons and indicates the absence of Cr–Cr bonding. In  $[\text{Mo}_2\text{Cl}_9]^{3-}$  the Mo atoms are 267 pm apart and the magnetic



**Figure 23.4** Structure of  $[\text{M}_2\text{Cl}_9]^{3-}$  showing the M–M bond through the shared face of two inclined  $\text{MCl}_6$  octahedra. See also Fig. 7.9, p. 240, for an alternative representation of the confacial bioctahedral structure.

moment is low and temperature dependent, indicating appreciable Mo–Mo bonding. Finally,  $[\text{W}_2\text{Cl}_9]^{3-}$  is diamagnetic: the metal atoms are displaced towards each other, being only 242 pm apart (compared to 274 pm in the metal itself), consistent with a W–W triple bond (p. 1030).

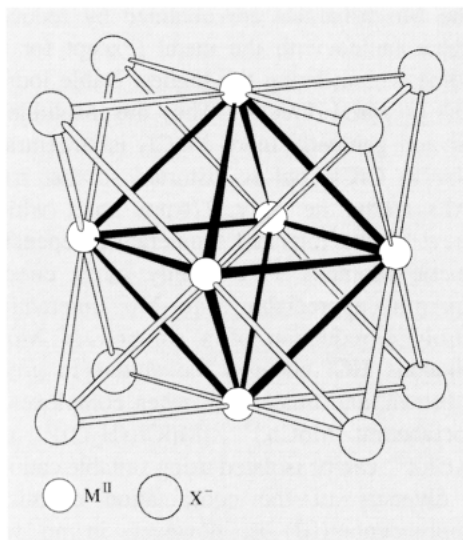
Anhydrous chromium dihalides are conveniently prepared by reduction of the trihalides with  $\text{H}_2$  at 300–500°C, or by the action of HX (or  $\text{I}_2$  for the diiodide) on the metal at temperatures of the order of 1000°C. They are all deliquescent and the hydrates can be obtained by reduction of the trihalides using pure chromium metal and aqueous HX. All have distorted octahedral structures as anticipated for a metal ion with the  $d^4$  configuration which is particularly susceptible to Jahn–Teller distortion<sup>†</sup>. This is typified by  $\text{CrF}_2$ , which adopts a distorted rutile structure in which

<sup>†</sup> A theorem proposed by H. A. Jahn and E. Teller (1937) states that a molecule in a degenerate electronic state will be unstable and will undergo a geometrical distortion that lowers its symmetry and splits the degenerate state. *Jahn–Teller* distortions are particularly important and well-documented for octahedrally coordinated metal ions whose  $e_g$  (i.e. axial) orbitals are unequally occupied:  $t_{2g}^3 e_g^1$  (high-spin  $\text{Cr}^{\text{II}}$  and  $\text{Mn}^{\text{III}}$ ),  $t_{2g}^6 e_g^1$  (low-spin  $\text{Co}^{\text{II}}$  and  $\text{Ni}^{\text{III}}$ ) and  $t_{2g}^6 e_g^3$  ( $\text{Cu}^{\text{II}}$ ). They are generally manifested by an elongation of the bonds on one axis, and may be ascribed to the  $d_{z^2}$  orbital containing 1

4 fluoride ions are 200 pm from the chromium atom while the remaining 2 are 243 pm away. The strongly reducing properties of chromium(II) halides contrast, at first sight surprisingly, with the redox stability of the molybdenum(II) halides. Even the tungsten(II) halides, which admittedly are also strong reducing agents (being oxidized to their trihalides), may by their very existence be thought to depart from the expected trend.

Of the various preparative methods available for the dihalides of Mo and W, thermal decomposition or reduction of higher halides is the most general. The reason for their enhanced stability lies in the prevalence of metal-atom clusters, stabilized by M-M bonding. All 6 of these dihalides (Mo and W do not form difluorides) are isomorphous,<sup>(26)</sup> with a structure based on the  $[M_6X_8]^{4+}$  unit briefly mentioned above for  $WBr_3$  (see also Chevrel phases p. 1018). It can be seen (Fig. 23.5) that in this cluster each metal atom has a free coordination position. In the dihalides themselves, these positions are occupied by  $6X^-$  ions, 4 of them bridging to other  $[M_6X_8]^{4+}$  units, giving the composition  $[M_6X_8]X_2X_{4/2} = MX_2$ . Although precise details of the bonding scheme are not settled it is clear that in each cluster the 6 metals contribute  $6 \times 6 = 36$  valence electrons of which 4 are transferred to the counter anions, so producing the net charge, and 8 are used in bonding to the 8 chlorines of the cluster. Twenty-four electrons remain which can provide M-M bonds along each of the 12 edges of the octahedron of metal atoms accounting for the observed diamagnetism. Unlike the  $M_6$  clusters of the "electron-poor" elements of groups 3, 4 and 5 (pp. 950, 965 and 992) the incorporation of interstitial atoms offers no additional stability and is not observed.

The six outer halide ions are readily replaced, leaving the  $[M_6X_8]^{4+}$  core intact throughout a



**Figure 23.5**  $[M_6X_8]^{4+}$  clusters with X bridges over each face of the octahedron of metal ions.

variety of substitution reactions. The eight core halogens are far less labile, but prolonged heating (16 h at 500°C) of  $[Mo_6Cl_8Br_4]^{2-}$  for instance, has been shown<sup>(27)</sup> by  $^{19}F$  nmr spectroscopy to yield a mixture containing all 22 possible isomers of the  $[Mo_6Br_nCl_{8-n}]^{4+}$  cluster. Oxidation of  $WBr_2$  with  $Br_2$  yields brownish-black crystals of the molecular cluster compound  $W_6Br_{14}$  in which a non-bridging Br completes the coordination sphere of each metal atom in the  $\{W_6Br_8\}$  core.<sup>(27a)</sup>

The oxohalides of all three elements (Table 23.5) are very susceptible to hydrolysis and their oxidizing properties decrease in the order  $Cr > Mo > W$ . They are yellow to red liquids or volatile solids; probably the best known is the deep-red liquid, chromyl chloride,  $CrO_2Cl_2$ . It is most commonly encountered as the distillate in qualitative tests for chromium or chloride and can be obtained by heating a dichromate and chloride in conc  $H_2SO_4$ ; it is an extremely aggressive oxidizing agent. The Mo and W oxohalides

electron more than the  $d_{x^2-y^2}$ , so preventing ligands on the z-axis approaching as close as those on the x and y

<sup>26</sup> An amorphous form of  $MoCl_2$  is also known, whose spectroscopic properties suggest the presence of tetranuclear units; see W. W. BEERS and R. E. MCCARLEY, *Inorg. Chem.* **24**, 472-5 (1985).

<sup>27</sup> P. BRÜCKNER, G. PETERS and W. PREETZ, *Z. anorg. allg. Chem.* **619**, 551-8 (1993).

<sup>27a</sup> J. SASSMANSHAUSEN and H.-G. VON SCHNERING, *Z. anorg. allg. Chem.* **620**, 1312-20 (1994).

Table 23.5 Oxohalides of Group 6 (mp/°C)

Oxidation state	Fluorides		Chlorides		Bromides		Iodides
+6	CrOF <sub>4</sub> red (55°)	CrO <sub>2</sub> F <sub>2</sub> violet (32°)		CrO <sub>2</sub> Cl <sub>2</sub> red (-96.5°) bp 117°		CrO <sub>2</sub> Br <sub>2</sub> red (d < rt)	
	MoOF <sub>4</sub> white (97°) bp 186°	MoO <sub>2</sub> F <sub>2</sub> white (subl 270°)	MoOCl <sub>4</sub> green (101°) bp 159°	MoO <sub>2</sub> Cl <sub>2</sub> pale yellow (175°) bp 250°		MoO <sub>2</sub> Br <sub>2</sub> purple-brown	
	WOF <sub>4</sub> white (101°) bp 186°	WO <sub>2</sub> F <sub>2</sub> white	WOCl <sub>4</sub> red (209°) bp 224°	WO <sub>2</sub> Cl <sub>2</sub> pale yellow (265°)	WOBBr <sub>4</sub> dark brown (277°) or black (321°)	WO <sub>2</sub> Br <sub>2</sub> red	WO <sub>2</sub> I <sub>2</sub> green
+5	CrOF <sub>3</sub>		CrOCl <sub>3</sub> dark red				
	MoOF <sub>3</sub> green, also dark blue		MoOCl <sub>3</sub> black (d > 200°)	MoO <sub>2</sub> Cl	MoOBr <sub>3</sub> black (subl 270° vac)		
+3			WOCl <sub>3</sub> olive green		WOBBr <sub>3</sub> dark brown		WO <sub>2</sub> I
			CrOCl green		CrOBr		

Cr<sup>IV</sup>OCl<sub>2</sub> has been observed in the gaseous phase by means of mass spectrometry.<sup>(29)</sup>

are prepared by a variety of oxygenation and halogenation reactions which frequently produce mixtures, and many specific preparations have therefore been devised.<sup>(28)</sup> They are possibly best known as impurities in preparations of the halides from which air or moisture have been inadequately excluded, and their formation is indicative of the readiness with which metal-oxygen bonds are formed by these elements in high oxidation states.

### 23.3.7 Complexes of chromium, molybdenum and tungsten<sup>(3,30,31)</sup>

#### Oxidation state VI (d<sup>0</sup>)

No halogeno complexes of the type [MX<sub>6+x</sub>]<sup>x-</sup> are known and, although homoleptic imido

complexes, Li<sub>2</sub>[M(NBu<sup>t</sup>)<sub>4</sub>] (M = Cr, Mo, W), containing tetrahedrally coordinated M<sup>VI</sup> have been prepared,<sup>(32)</sup> the coordination chemistry of this oxidation state is centred mainly on oxo and peroxo complexes. The former class includes chromyl alkoxides<sup>(33)</sup> and adducts of tungsten oxohalides such as [WOX<sub>5</sub>]<sup>-</sup> and [WO<sub>2</sub>X<sub>4</sub>]<sup>2-</sup> (X = F, Cl), but most are octahedral chelates of

<sup>29</sup> V. PLIES, *Z. anorg. allg. Chem.* **602**, 97-104 (1991).

<sup>30</sup> L. F. LARKWORTHY, K. B. NOLAN and P. O'BRIEN, *Chromium*, Chap. 35, pp. 699-969, A. G. SYKES, G. J. HUNT, R. L. RICHARDS, C. D. GARNER, J. M. CHARNOCK and E. I. STIEFEL, *Molybdenum*, Chap. 36, pp. 1229-444, and Z. DORI, *Tungsten*, Chap. 37, pp. 973-1022, in *Comprehensive Coordination Chemistry*, Vol. 3, Pergamon Press, Oxford, 1987. For Chromium see also D. A. HOUSE, *Adv. Inorg. Chem.* **44**, 341-73 (1997).

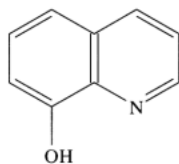
<sup>31</sup> R. COLTON, *Coord. Chem. Revs.* **90**, 1-109 (1988).

<sup>32</sup> A. A. DANOPOULOS and G. WILKINSON, *Polyhedron* **9**, 1009-10 (1990).

<sup>33</sup> S. L. CHADHA, V. SHARMA and A. SHARMA, *J. Chem. Soc., Dalton Trans.*, 1253-5 (1987).

<sup>28</sup> Ref. 2, pp. 275-81.

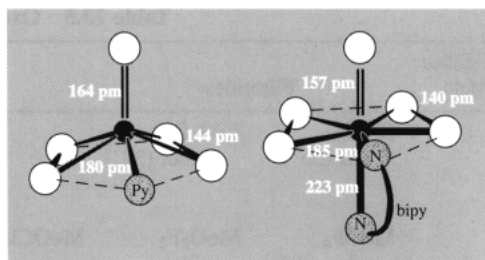
the types  $[\text{MO}_2\text{X}_2(\text{L-L})]^{(34)}$  and  $[\text{MO}_2(\text{L-L}^-)_2]$  ( $\text{M} = \text{Mo}, \text{W}$ ). In the  $\text{MO}_2^{2+}$  group of these compounds the oxygen atoms are mutually *cis*, thereby maximizing the  $\text{O}(p_\pi) \rightarrow \text{M}(d_\pi)$  bonding, and the group is reminiscent of the uranyl  $\text{UO}_2^{2+}$  ion (p. 1273), though its chemistry is by no means as extensive and the latter is a linear ion. The best-known example of this type of compound is  $[\text{MoO}_2(\text{oxinate})_2]$  used for the gravimetric determination of molybdenum; oxine is 8-hydroxyquinoline, i.e.



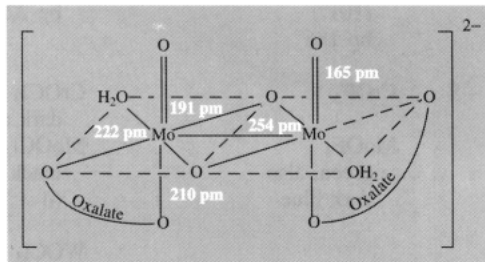
The peroxy-complexes provide further examples of the ability of oxygen to coordinate to the metals in their high oxidation states. The production of blue solutions when acidified dichromates are treated with  $\text{H}_2\text{O}_2$  is a qualitative test for chromium.<sup>†</sup> The colour arises from the unstable  $\text{CrO}_5$  which can, however, be stabilized by extraction into ether, and blue solid adducts such as  $[\text{CrO}_5(\text{py})]$  can be isolated. This is more correctly formulated as  $[\text{CrO}(\text{O}_2)_2\text{py}]$  and has an approximately pentagonal pyramidal structure (Fig. 23.6a). Bidentate ligands, such as phenanthroline and bipyridyl produce pentagonal bipyramidal complexes in which the second N-donor atom is loosely bonded *trans* to the  $=\text{O}$  (Fig. 23.6b). This 7-coordinate structure is favoured in numerous peroxy-complexes of Mo and W, and the dark-red peroxy anion  $[\text{Mo}(\text{O}_2)_4]^{2-}$  is 8-coordinate, with Mo–O 197 pm and O–O 155 pm.

### Oxidation state V ( $d^1$ )

This is an unstable state for chromium and, apart from the fluoride and oxohalides already



**Figure 23.6** Molecular structures of (a)  $[\text{CrO}(\text{O}_2)_2\text{py}]$  and (b)  $[\text{CrO}(\text{O}_2)_2(\text{bipy})]$ .



**Figure 23.7** The dimeric, oxygen bridged,  $[\text{Mo}_2\text{O}_4(\text{C}_2\text{O}_4)_2(\text{H}_2\text{O})_2]^{2-}$  showing the close approach of the 2 Mo atoms and unusually large range of Mo–O distances from 165 to 222 pm.

mentioned, it is represented primarily by the blue to black chromates of the alkali and alkaline earth metals and the red-brown tetraperoxo-chromate(V). The former contain the tetrahedral  $[\text{CrO}_4]^{3-}$  ion and hydrolyse with disproportionation to Cr(III) and Cr(VI). The latter can be isolated as rather more stable salts from alkaline solutions of dichromate treated with  $\text{H}_2\text{O}_2$ . These red salts contain the paramagnetic 8-coordinate, dodecahedral,  $[\text{Cr}(\text{O}_2)_4]^{3-}$  ion, which is isomorphous with the corresponding complex ions of the Group 5 metals (p. 994). The  $\eta^2$ - $\text{O}_2$  groups are unsymmetrically coordinated, with Cr–O 185 and 195 pm and the O–O distance 141 pm.

The heavier elements have a much more extensive +5 chemistry including, in the case of molybdenum, a number of compounds of considerable biological interest which will be discussed separately (p. 1035). A variety of reactions involving fusion and nonaqueous

<sup>34</sup> K. DREISCH, C. ANDERSSON and C. STÄLHANDSKE, *Polyhedron* **11**, 2143–50 (1992).

<sup>†</sup> The acidity is important. In alkaline solution  $[\text{Cr}^{\text{V}}(\text{O}_2)_4]^{3-}$  is produced, but from neutral solutions explosive violet salts, probably containing  $[\text{Cr}^{\text{VI}}\text{O}(\text{O}_2)_2\text{OH}]^-$ , are produced.

solvents has been used to produce octahedral hexahalogeno complexes. These are very susceptible to hydrolysis, and the affinity of Mo<sup>V</sup> for oxygen is further demonstrated by the propensity of MoCl<sub>5</sub> to produce green oxomolybdenum(V) compounds by oxygen-abstraction from appropriate oxygen-containing materials. This leads to a number of well-characterized complexes of the type [MoOCl<sub>3</sub>L] and [MoOCl<sub>3</sub>L<sub>2</sub>]. Oxomolybdenum(V) compounds are also obtained from aqueous solution and include monomeric species such as [MoOX<sub>5</sub>]<sup>2-</sup> (X = Cl, Br, NCS) and dimeric, oxygen-bridged complexes such as [Mo<sub>2</sub>O<sub>4</sub>(C<sub>2</sub>O<sub>4</sub>)<sub>2</sub>(H<sub>2</sub>O)<sub>2</sub>]<sup>2-</sup> (Fig. 23.7) which may be considered to be derived from the orange-yellow aquo ion [Mo<sub>2</sub>O<sub>4</sub>(H<sub>2</sub>O)<sub>6</sub>]<sup>2+</sup>. Whereas the monomeric compounds are paramagnetic with magnetic moments corresponding to 1 unpaired electron, the binuclear compounds are diamagnetic, or only slightly paramagnetic, suggesting appreciable metal-metal interaction occurring either directly or via the bridging oxygens.

Also of interest are the octacyano complexes, [M(CN)<sub>8</sub>]<sup>3-</sup> (M = Mo, W), which are commonly prepared by oxidation of the M<sup>IV</sup> analogues (using MnO<sub>4</sub><sup>-</sup> or Ce<sup>IV</sup>) and whose structures apparently vary, according to the environment and counter cation, between the energetically similar square-antiprismatic and dodecahedral forms.<sup>(35)</sup>

### Oxidation state IV (d<sup>2</sup>)

As for the previous oxidation state, the chemistries of Mo<sup>IV</sup> and W<sup>IV</sup> are much more extensive than that of Cr<sup>IV</sup> which is largely confined to peroxo- and fluoro- complexes. [Cr(O<sub>2</sub>)<sub>2</sub>(NH<sub>3</sub>)<sub>3</sub>], which has a dark red-brown metallic lustre, may be obtained either by treating [Cr(O<sub>2</sub>)<sub>4</sub>]<sup>3-</sup> with warm aqueous ammonia or by the action of H<sub>2</sub>O<sub>2</sub> on ammoniacal solutions of (NH<sub>4</sub>)<sub>2</sub>CrO<sub>4</sub>. It has a pentagonal bipyramidal structure in which the peroxo- groups occupy

four of the planar positions, and the NH<sub>3</sub> molecules are replaceable by other ligands. The very hydrolysable salts of [CrF<sub>6</sub>]<sup>2-</sup> are obtained by direct fluorination of anhydrous CrCl<sub>3</sub> and an alkali metal chloride.

More or less hydrolysable hexahalogeno salts of [MX<sub>6</sub>]<sup>2-</sup> (M = Mo, X = F, Cl, Br; M = W, X = Cl, Br) are also known and the yellow octacyano compounds have provided structural interest ever since the classical work of J. I. Hoard in 1939 established K<sub>4</sub>[Mo(CN)<sub>8</sub>].2H<sub>2</sub>O as the first example of an 8-coordinate complex. This and its W analogue have dodecahedral (*D*<sub>2d</sub>) structures and their diamagnetism arises from the splitting of their d-orbitals which stabilizes one (probably the d<sub>xy</sub>) to such an extent that the two d electrons pair in it. The energy barrier between dodecahedral and square antiprismatic (*D*<sub>4d</sub>) structures is, however, small and the latter is obtained if the K<sup>+</sup> counter cations are replaced by Cd<sup>2+</sup>.<sup>95</sup> Mo and <sup>14</sup>N nmr studies show<sup>(35a)</sup> that the ion is dodecahedral in aqueous solution and that the equivalence of the eight CN groups (indicating the more symmetrical *D*<sub>4d</sub> form), implied by earlier <sup>13</sup>C work, arises from rapid tumbling of the ion rather than fluxional rearrangement. Photolysis of the otherwise stable [M(CN)<sub>8</sub>]<sup>4-</sup> solutions causes loss of four CN<sup>-</sup> ions to give octahedral oxo compounds such as K<sub>4</sub>[MO<sub>2</sub>(CN)<sub>4</sub>].6H<sub>2</sub>O (M = Mo, W).

Other mononuclear complexes include the tetrahedral [Mo(NMe<sub>2</sub>)<sub>4</sub>] and the octahedral Li<sub>2</sub>[Mo(NMe<sub>2</sub>)<sub>6</sub>].2thf<sup>(36)</sup> but recent interest in the chemistry of the M<sup>IV</sup> ion has centred on the trinuclear oxo and thio complexes of Mo and W, particularly the former. They are of three main types. The first may be conceptually based on the [M<sub>3</sub>O<sub>13</sub>] unit found in the aquo ions [M<sub>3</sub>O<sub>4</sub>(H<sub>2</sub>O)<sub>9</sub>]<sup>4+</sup> (M = Mo,<sup>(37)</sup> W). It contains a

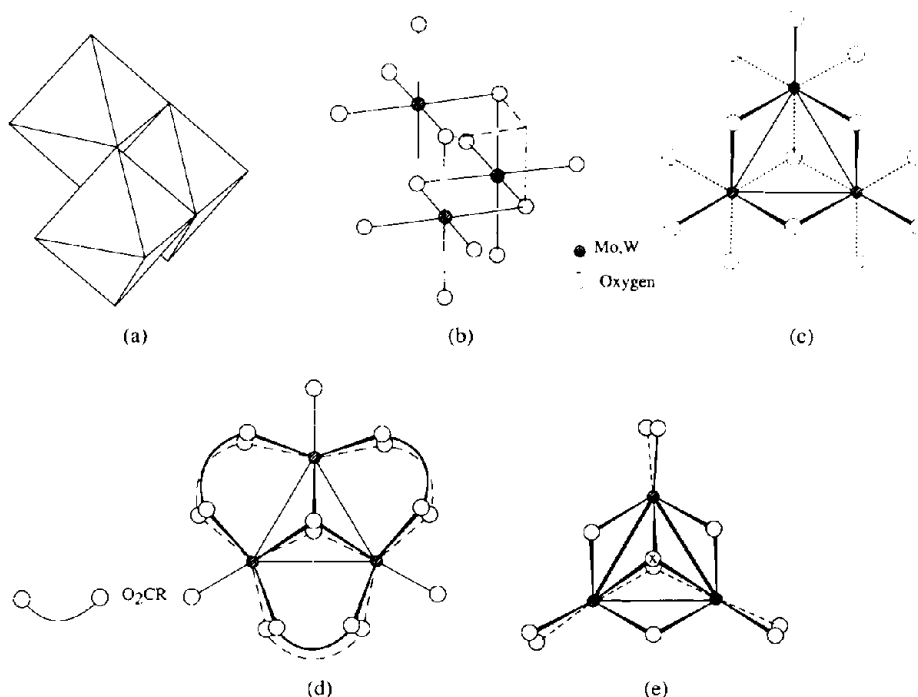
<sup>35a</sup> R. T. C. BROWNLEE, B. P. SHEHAN and A. G. WEDD, *Inorg. Chem.* **26**, 2022-4 (1987).

<sup>36</sup> M. H. CHISHOLM, C. E. HAMMOND and J. C. HUFFMAN, *Polyhedron* **7**, 399-400 (1988).

<sup>37</sup> Preparations of the various aquo ions of Mo in oxidation states II to V are given in D. T. RICHENS and A. G. SYKES, *Inorg. Synth.* **23**, 130-40 (1985).

<sup>35</sup> J. G. LEIPOLDT, S. S. BASSON and A. ROODT, *Adv. Inorg. Chem.* **40**, 241-322 (1994).





**Figure 23.8** Trinuclear, M–M bonded species of  $\text{Mo}^{\text{IV}}$  and  $\text{W}^{\text{IV}}$ . (a) (b) and (c) are alternative representations of the  $\text{M}_3\text{O}_{13}$  unit: (a) emphasizes its relationship to the edge-sharing octahedra of the  $\text{M}_3$  group in polymetallate ions; (b) shows the  $(\mu_3\text{-O})$   $(\mu_2\text{-O})_3$  bridges and M–M bonds of its  $\text{M}_3\text{O}_4$  “incomplete cubane” core; and (c) emphasizes its triangular centre by viewing from the unoccupied corner of the cuboid. (d) and (e) offer the same perspective as (c) but of  $[\text{M}_3\text{O}_2(\text{O}_2\text{CR})_6(\text{H}_2\text{O})_3]^{2+}$  and  $[\text{M}_3(\mu_3\text{-X})(\mu_3\text{-OR})(\text{OR})_9]$  structures respectively.

triangle of M–M bonded metals capped by a single oxygen on one side and on the other side three oxygens bridge each pair of metal atoms. It may be viewed either as a reduced form of the  $\text{M}_3$  group found in polymetallate ions, or as an “incomplete cubane-type” of complex<sup>(38)</sup> (Fig. 23.8). Some, or all, of the nine water molecules of the aquo ion are replaceable by a variety of ligands including oxalate, edta and  $\text{NCS}^-$ , and thio derivatives<sup>(38a)</sup> containing  $\text{M}_3\text{O}_3\text{S}$ ,  $\text{M}_3\text{O}_2\text{S}_2$ ,  $\text{M}_3\text{OS}_3$  and  $\text{M}_3\text{S}_4$  cores have been prepared. In the mixed O/S species, S appears always to occupy the  $\mu_3$ -position. M–M bond lengths are about 250 pm for  $\text{M}_3\text{O}_4$  species increasing to 270–280 pm for  $\text{M}_3\text{S}_4$ , there

being very little difference between Mo and W compounds. Preparative routes vary but usually involve reduction from  $\text{M}^{\text{VI}}$  or  $\text{M}^{\text{V}}$ , often by the use of  $\text{NaBH}_4$ . Se and Te analogues of the Mo compounds are also known and an Se analogue for W has recently been reported.<sup>(39)</sup>

The second type of trinuclear compounds containing  $[\text{M}_3\text{O}_2(\text{O}_2\text{CR})_6(\text{H}_2\text{O})_3]^{2+}$  and obtained by the reaction of  $\text{M}(\text{CO})_6$  ( $\text{M} = \text{Mo}, \text{W}$ ) with carboxylic acids, features a similar triangle of M–M bonded metal atoms but this time capped on *both* sides by  $\mu_3\text{-O}$  atoms (Fig. 23.8d). Complexes in which either one or both of these capping atoms are replaced by  $\mu_3\text{-CR}$ , alkylidene,

<sup>39</sup> V. P. FEDIN, M. N. SOKOLOV, A. V. VIROVETS, N. V. POD-BEREZSKAY and V. Y. FEDEROV, *Polyhedron* **11**, 2973–4 (1992).

<sup>38</sup> T. SHIBAHARA, *Adv. Inorg. Chem.* **37**, 143–73 (1991).

<sup>38a</sup> T. SAITO, *Adv. Inorg. Chem.* **44**, 45–92 (1997).

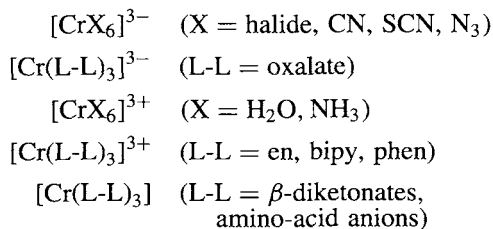


groups are also obtainable and all these biccapped species are notable for their kinetic inertness. The third trinuclear type is that of the alkoxides  $[M_3(\mu_3-X)(\mu_3-OR)(OR)_9]$  ( $M = Mo, W; X = O, NH$ )<sup>(40)</sup> which again are biccapped but with only single bridges spanning the M–M bonds (Fig. 23.8e).

### Oxidation state III ( $d^3$ )

This is by far the most stable and best-known oxidation state for chromium and is characterized by thousands of compounds, most of them prepared from aqueous solutions. By contrast, unless stabilized by M–M bonding, molybdenum(III) compounds are sparse and hardly any are known for tungsten(III). Thus Mo, but not W, has an aquo ion  $[Mo(H_2O)_6]^{3+}$ , which gives rise to complexes  $[MoX_6]^{3-}$  ( $X = F, Cl, Br, NCS$ ). Direct action of acetylacetonate on the hexachloromolybdate(III) ion produces the sublimable  $[Mo(acac)_3]$  which, however, unlike its chromium analogue, is oxidized by air to  $Mo^V$  products. A black  $Mo^{III}$  cyanide,  $K_4Mo(CN)_7 \cdot 2H_2O$ , has been precipitated from aqueous solution by the addition of ethanol. Its magnetic moment ( $\sim 1.75$  BM) is consistent with 7-coordinate  $Mo^{III}$  in which the loss of degeneracy of the  $t_{2g}$  orbitals has caused pairing of 2 of the three d electrons.

Chromium(III) forms stable salts with all the common anions and it complexes with virtually any species capable of donating an electron-pair. These complexes may be anionic, cationic, or neutral and, with hardly any exceptions, are hexacoordinate and octahedral, e.g.:



There is also a multitude of complexes with 2 or more different ligands, such as the pentaammines  $[Cr(NH_3)_5X]^{n+}$  which have been extensively used in kinetic studies. These various complexes are notable for their kinetic inertness, which is compatible with the half-filled  $t_{2g}$  level arising from an octahedral  $d^3$  configuration and is the reason why many thermodynamically unstable complexes can be isolated. Ligand substitution and rearrangement reactions are slow (half-times are of the order of hours), with the result that the preparation of different, solid, isomeric forms of a compound was the classical means of establishing stereochemistry and the reason why early coordination chemists devoted so much attention to  $Cr^{III}$  complexes. For precisely the same reason, however, the preparation of these complexes is not always straightforward. Salts such as the hydrated sulfate and halides, which might seem obvious starting materials, themselves contain coordinated water or anions and these are not always easily displaced. Simple addition of the appropriate ligand to an aqueous solution of a  $Cr^{III}$  salt is therefore not a usual preparative method, though in the presence of charcoal it is feasible in the case, for instance, of  $[Cr(en)_3]^{3+}$ . Some alternative routes, which avoid these pre-formed inert complexes, are:

- (i) *Anhydrous methods*: ammine and amine complexes can be prepared by the reaction of  $CrX_3$  with  $NH_3$  or amine, and salts of  $[CrX_6]^{3-}$  anions are best obtained by fusion of  $CrX_3$  with the alkali metal salt.
- (ii) *Oxidation of Cr(II)*: ammine and amine complexes can also be prepared by the aerial oxidation of mixtures of aqueous  $[Cr(H_2O)_6]^{2+}$  (which is kinetically labile) and the appropriate ligands.
- (iii) *Reduction of Cr(VI)*:  $CrO_3$  and dichromates are commonly used to prepare such complexes as  $K_3[Cr(C_2O_4)_3]$  and  $NH_4[Cr(NH_3)_2(NCS)_4] \cdot H_2O$  (Reinecke's salt).

<sup>40</sup> M. H. CHISHOLM, D. L. CLARK, M. J. HAMPDEN-SMITH and D. H. HOFFMAN, *Angew. Chem. Int. Edn. Engl.* **28**, 432–44 (1989).

The violet hexaquo ion,  $[Cr(H_2O)_6]^{3+}$ , occurs in the chrome alums,  $Cr_2(SO_4)_3 \cdot M_2SO_4 \cdot 24H_2O$

Table 23.6 Spectroscopic data for typical octahedral complexes of chromium(III)

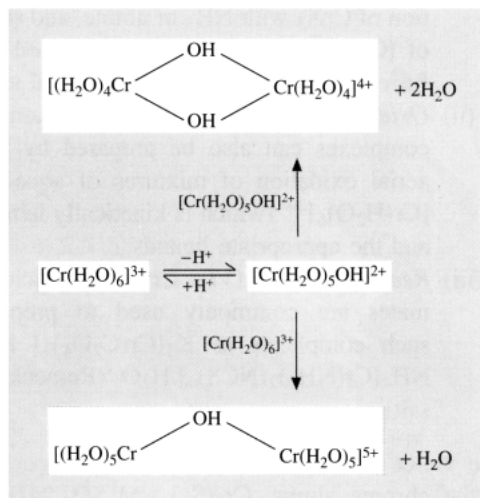
Complex	Colour	$\nu_1/\text{cm}^{-1}$	$\nu_2/\text{cm}^{-1}$	$\nu_3/\text{cm}^{-1}$	$10Dq/\text{cm}^{-1}$	$B/\text{cm}^{-1}$	$\mu_{\pi}/\text{BM}^{(a)}$
$\text{K}[\text{Cr}(\text{H}_2\text{O})_6][\text{SO}_4]_2 \cdot 6\text{H}_2\text{O}$	Violet	17 400	24 500	37 800	17 400	725	3.84
$\text{K}_3[\text{Cr}(\text{C}_2\text{O}_4)_3] \cdot 3\text{H}_2\text{O}$	Reddish-violet	17 500	23 900		17 500	620	3.84
$\text{K}_3[\text{Cr}(\text{NCS})_6] \cdot 4\text{H}_2\text{O}$	Purple	17 800	23 800		17 800	570	3.77
$[\text{Cr}(\text{NH}_3)_6]\text{Br}_3$	Yellow	21 550	28 500		21 550	650	3.77
$[\text{Cr}(\text{en})_3]\text{I}_3 \cdot \text{H}_2\text{O}$	Yellow	21 600	28 500		21 600	650	3.84
$\text{K}_3[\text{Cr}(\text{CN})_6]$	Yellow	26 700	32 200		26 700	530	3.87

<sup>(a)</sup>Room temperature value of  $\mu_e$ .

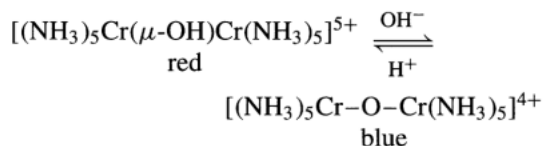
(e.g.  $[\text{K}(\text{H}_2\text{O})_6][\text{Cr}(\text{H}_2\text{O})_6][\text{SO}_4]_2$ ), but in hydrated salts and aqueous solutions, green species, produced by the replacement of some of the water molecules by other ligands, are more usual. So, the common form of the hydrated chloride is the dark-green *trans*- $[\text{CrCl}_2(\text{H}_2\text{O})_4]\text{Cl} \cdot 2\text{H}_2\text{O}$ , and other isomers are known (see p. 920).

Chromium(III) is the archetypal  $d^3$  ion and the electronic spectra and magnetic properties of its complexes have therefore been exhaustively studied<sup>(41)</sup> (see Panel). Data for a representative sample of complexes are given in Table 23.6.

One of the most obvious characteristics of  $\text{Cr}^{\text{III}}$  is its tendency to hydrolyse and form polynuclear complexes containing  $\text{OH}^-$  bridges. This is thought to occur by the loss of a proton from coordinated water, followed by coordination of the  $\text{OH}^-$  so formed to a second cation:



The ease with which the proton is removed can be judged by the fact that the hexaquo ion ( $\text{p}K_a \sim 4$ ) is almost as strong an acid as formic acid. Further deprotonation and polymerization can occur and, as the pH is raised, the final product is hydrated chromium(III) oxide or “chromic hydroxide”. Formation of this is the reason why amine complexes are not prepared by simple addition of the amine base to an aqueous solution of  $\text{Cr}^{\text{III}}$ . By methods which commonly start with  $\text{Cr}^{\text{II}}$ , binuclear compounds such as  $[(\text{en})_2\text{Cr}(\mu_2\text{-OH})_2\text{Cr}(\text{en})_2]$  and  $[(\text{NH}_3)_5\text{Cr}(\mu\text{-OH})\text{Cr}(\text{NH}_3)_5]\text{X}_5$  are obtained. These have temperature-dependent magnetic moments, somewhat lower than those usual for octahedral  $\text{Cr}^{\text{III}}$  and indicative of weak antiferromagnetic interaction via the bent  $\text{Cr}\text{-O}(\text{H})\text{-Cr}$  bridges. Stronger antiferromagnetic interaction (magnetic moment per metal atom at room temperature  $\sim 1.3 \text{ BM}$  falling to zero below 100 K) is found in the oxo-bridged derivative of the latter compound:

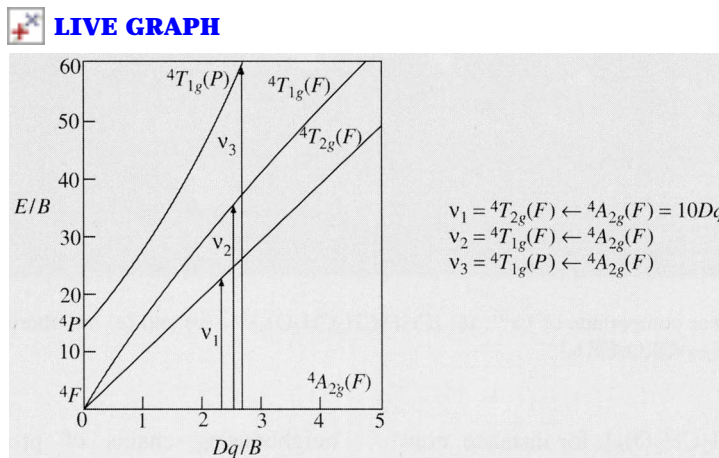


The linear  $\text{Cr}\text{-O}\text{-Cr}$  bridge evidently permits pairing of the d electrons of the 2 metal atoms via  $d_{\pi}\text{-p}_{\pi}$  bonds, much more readily than the bent  $\text{Cr}\text{-OH}\text{-Cr}$  bridge. Blue  $[\text{LCr}(\mu_2\text{-O})(\mu_2\text{-O}_2\text{CMe})_2\text{CrL}]$  ( $\text{L} = 1,4,7\text{-trimethyl-1,4,7-triazacyclononane}$ ), produced similarly by

<sup>41</sup> A. B. P. LEVER *Inorganic Electronic Spectroscopy*, (2nd edn.), pp. 417–28, Elsevier, Amsterdam, 1984.

### Electronic Spectra and Magnetic Properties of Chromium(III)

In an octahedral field the free-ion ground  ${}^4F$  term of a  $d^3$  ion is split into an  $A$  and two  $T$  terms which, along with the excited  ${}^4T(P)$  term (Fig. A), give rise to the possibility of three spin-allowed d-d transitions of which the one of lowest energy is a direct measure of the crystal field splitting,  $\Delta$  or  $10Dq$ :



**Figure A** Energy Level diagram for a  $d^3$  ion in an octahedral crystal field.

Assignment of the observed bands to these transitions, provides an estimate of  $B$ , the Racah "interelectron repulsion parameter." Its value (Table 23.6) is invariably below that of the free-ion ( $1030\text{ cm}^{-1}$ ) because the expansion of d-electron charge on complexation reduces the interelectronic repulsions.

The magnetic moment arising from the ground  ${}^4A$  term is expected to be close to the spin-only value of  $3.87\text{ BM}$  and independent of temperature. In practice, providing the compounds are mononuclear, these expectations are realized remarkably well apart from the fact that, as was noted for octahedral complexes of vanadium(III), the third high-energy band in the spectrum is usually wholly or partially obscured by more intense charge-transfer absorption.

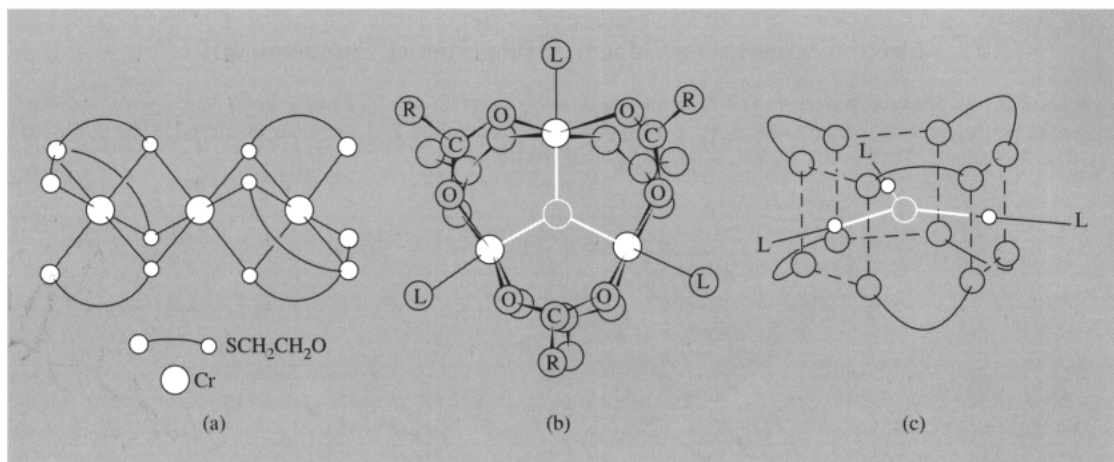
In addition to the terms so far mentioned there are a number of spin doublets and, in the  $\text{Cr}^{3+}$  ions of ruby ( $\alpha\text{-Al}_2\text{O}_3$ , corundum, in which a small proportion of  $\text{Al}^{3+}$  ions have been replaced by  $\text{Cr}^{3+}$ ), two of these ( ${}^2E_g$  and  ${}^2T_{1g}$ ) lie just below the  ${}^4T_{2g}$ . Ions excited to the  ${}^4T_{2g}$  may decay back to the ground level with *spontaneous emission* of radiation but some will decay instead to the doublets, the small energy difference being converted to lattice vibrations. The rate of decay by spontaneous emission from the doublets to the ground level is however slow, being spin-forbidden, but can be induced by interaction with photons of the same energy as those to be emitted (i.e. *stimulated emission*). This situation is exploited in the ruby laser,<sup>(42)</sup> in which a rod of ruby is irradiated by intense light of appropriate frequency to continually excite and re-excite the  $\text{Cr}^{3+}$  ions to the  ${}^4T_{2g}$  term. This *optical pumping* has the effect of steadily building up the population of the doublets. At suitable intervals the photons from the small proportion of ions which do spontaneously decay from the doublets are reflected by mirrors back through the rod where they interact with the excited ions, triggering their decay. This produces a burst of extremely intense radiation which is monochromatic, coherent and virtually non-divergent.

deprotonation of a pink, OH-bridged species but, crucially, with a  $120^\circ$  Cr-O-Cr bridge, shows only weak antiferromagnetic interaction.<sup>(43)</sup>

Examples of O atoms providing  $\pi$  pathways for antiferromagnetic interaction are also to be found among trinuclear compounds of  $\text{Cr}^{\text{III}}$ .

<sup>42</sup> J. A. DUFFY, *Bonding, Energy Levels and Bands*, pp. 72-7, Longman, Harlow, 1990.

<sup>43</sup> L. L. MARTIN, K. WIEGHARDT, G. BLONDIN, J.-J. GIRERD, B. NUBER and J. WEISS, *J. Chem. Soc., Chem. Commun.*, 1767-9 (1990).



**Figure 23.9** Trinuclear compounds of Cr<sup>III</sup>: (a)  $[\text{Cr}_3(\text{SCH}_2\text{CH}_2\text{O})_6]^{3-}$ . (b) and (c) are alternative representations of  $[\text{Cr}_3(\mu_3\text{-O})(\text{O}_2\text{CR})_6]^+$ .

( $\text{PPh}_4$ )<sub>2</sub>Na[Cr<sub>3</sub>(SCH<sub>2</sub>CH<sub>2</sub>O)<sub>6</sub>], for instance, consists of three face-sharing octahedra in which the Cr<sup>III</sup> atoms are linearly aligned and the O-, S-donor ligands are arranged so that all bridging atoms are oxygens<sup>(44)</sup> (Fig. 23.9a). A whole series of “basic” carboxylates of the general type  $[\text{Cr}_3\text{O}(\text{RCOO})_6\text{L}_3]^+$  show weak interactions and have the structure (Fig. 23.9b,c) common to carboxylates of other M<sup>III</sup> atoms and containing a central μ<sub>3</sub>-O.<sup>(45)</sup>

Hydrolysed, polynuclear Cr<sup>III</sup> complexes are of considerable commercial importance in the dyeing and tanning industries. In the former the role is that of a mordant to the dye. In leather production it is necessary to treat animal hides to prevent putrefaction and to render them supple when dry. Traditionally, tannin was used, hence the name of the process, but this was superseded towards the end of the nineteenth century by solutions of chromium(III) sulfate. After soaking in sulfuric acid the hides are impregnated with the Cr<sup>III</sup> solution. This is subsequently made alkaline, when the polynuclear complexes form and bridge

neighbouring chains of proteins, presumably by coordinating to the carboxyl groups of the proteins.

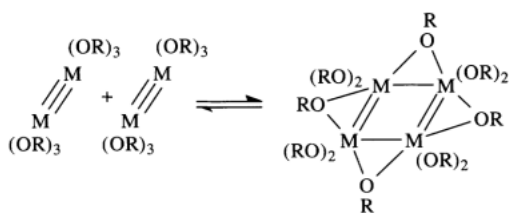
The bulk of the chemistry of Mo<sup>III</sup> and W<sup>III</sup> is associated with M≡M bonded species<sup>(46)</sup> which have been extensively studied for over a decade. M<sub>2</sub>X<sub>6</sub> compounds are commonly found with X = NR<sub>2</sub>, OR, CH<sub>2</sub>SiMe<sub>3</sub>, SAr and more recently SeAr,<sup>(47)</sup> and are generally both oxygen- and moisture-sensitive. The usual preparative route is by reacting metal halides with LiNR<sub>2</sub> followed by ligand substitution of the M<sub>2</sub>(NR<sub>2</sub>)<sub>6</sub> so obtained, and the products are of the type X<sub>3</sub>M≡MX<sub>3</sub> in which the two MX<sub>3</sub> halves are staggered with respect to each other. The σ<sup>2</sup>π<sup>4</sup> triple bond is readily understood from the MO diagram of Fig. 23.12 (p. 1033), given that the two d<sup>3</sup> metal ions contribute six electrons for M–M bonding. Neutral ligands can sometimes be added, to yield LX<sub>3</sub>M≡MX<sub>3</sub>L, and a series of tetranuclear products has been obtained by dimerization of M<sub>2</sub>(OR)<sub>6</sub>

<sup>44</sup> J. R. NICHOLSON, G. CHRISTOU, R.-J. WANG, J. C. HUFFMAN, H.-R. CHANG and D. N. HENDRICKSON, *Polyhedron* **19**, 2255–63 (1991).

<sup>45</sup> R. D. CANNON and R. P. WHITE, *Prog. Inorg. Chem.* **36**, 195–298 (1988).

<sup>46</sup> F. A. COTTON and R. A. WALTON, *Multiple Bonds between Atoms*, 2nd edn., Oxford Univ. Press, Oxford, 1993, 787 pp.

<sup>47</sup> M. H. CHISHOLM, J. C. HUFFMAN, I. P. PARKIN and W. E. STREIB, *Polyhedron* **9**, 2941–52 (1990).



The precise shape of the  $M_4$  core can be varied by partial substitution of OR with halide, and ranges from square to “butterfly” but apparently never tetrahedral<sup>(48)</sup>

Another type of triply bonded species is represented by the purple and unusually air-stable,  $Cs_2[Mo_2(HPO_4)_4(H_2O)_2]$ , prepared by the reaction of  $K_4MoCl_8 \cdot 2H_2O$  and  $CsCl$  in aqueous  $H_3PO_4$ . Here the cation has the dinuclear structure more commonly found in the divalent carboxylates (see below) and the  $M \equiv M$  bond is supported by phosphate bridges.

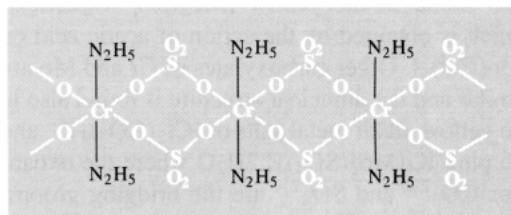
Although having formal oxidation states of  $2\frac{2}{3}$  per metal, it is opportune to mention here important molecular analogues of the Chevrel phases.<sup>(49)</sup>  $M_6S_8(PEt_3)_6$ , ( $M = Mo, W$ ) have the same octahedral  $[M_6S_8]$  core found in Chevrel phases (with the addition of terminal phosphines on each metal) but without the trigonal elongation found in the latter (p. 1018). That both are 20-electron clusters is compelling evidence that the distortion arises from intercluster interactions, which are absent in the molecular compounds, rather than because the number of cluster electrons is insufficient to form  $M-M$  bonds along all twelve edges of the octahedron.

### Oxidation state II ( $d^4$ )

For chromium, this oxidation state is characterized by the aqueous chemistry of the strongly reducing  $Cr^{II}$  cation, and a noticeable tendency to form dinuclear compounds with multiple metal–metal bonds. This tendency is even more

marked in the case of molybdenum but, perhaps surprisingly, is much less so in the case of tungsten,<sup>†</sup> though single  $M-M$  bonds are present in the  $[M_6X_8]^{4+}$  clusters of the dihalides of both Mo and W (p. 1022).

With the exception of the nitrate, which has not been prepared because of internal oxidation–reduction, the simple hydrated, sky-blue, salts of chromium(II) are best obtained by the reaction of the appropriate dilute acid with pure chromium metal, air being rigorously excluded. A variety of complexes is formed, especially with  $N$ -donor chelating ligands which commonly produce stoichiometries such as  $[Cr(L-L)_3]^{2+}$  and  $[Cr(L-L)_2X_2]$ . They (and other complexes of  $Cr^{II}$ ) are generally extremely sensitive to atmospheric oxidation if moist, but are considerably more stable when dry, probably the most air-stable of all being the pale-blue hydrazinium sulfate,  $(N_2H_5^+)_2Cr^{II}(SO_4)_2$ . In the solid state this consists of linear chains of  $Cr^{II}$  ions, bridged by  $SO_4^{2-}$  ions:



The majority of  $Cr^{II}$  complexes are octahedral and can be either high-spin ( $t_{2g}^3 e_g^1$ ) or low-spin ( $t_{2g}^4$ ). The former are characterized by magnetic moments close to 4.90 BM and visible/ultraviolet spectra consisting typically of a broad band in the region of  $16\,000\text{ cm}^{-1}$  with another band around  $10\,000\text{ cm}^{-1}$ . Since a  $d^4$  ion in a perfectly octahedral field can give rise to only one  $d-d$  transition it is clear that some lowering of symmetry has occurred. Indeed, this is expected as a consequence of the Jahn–Teller effect, even when the metal is surrounded by 6 equivalent donor atoms. The splitting of the free-ion  $^5D$

<sup>48</sup> M. H. CHISHOLM, C. E. HAMMOND, J. C. HUFFMAN and J. D. MARTIN, *Polyhedron* **9**, 1829–41 (1990).

<sup>49</sup> T. SAITO, N. YAMAMOTO, T. NAGASE, T. TSUBOI, K. KOBAYASHI, T. YAMAGATA, H. IMOTO and K. UNOURA, *Inorg. Chem.* **29**, 764–70 (1990).

<sup>†</sup> A major reason for their comparative paucity is that the dinuclear acetate, which in the case of Mo is the most common starting material in the preparation of quadruply bonded dimeric complexes, is unknown for W.

term is shown in Fig. 23.10 and the two observed bands are assigned to superimposed  ${}^5B_{2g} \leftarrow {}^5B_{1g}$  and  ${}^5E_g \leftarrow {}^5B_{1g}$  transitions and to the  ${}^5A_{1g} \leftarrow {}^5B_{1g}$  transition respectively. The low-spin, intensely coloured compounds such as  $K_4[Cr(CN)_6] \cdot 3H_2O$  and  $[Cr(L-L)_3]X_2 \cdot nH_2O$  ( $L-L = \text{bipy, phen; } X = \text{Cl, Br, I}$ ) have magnetic moments in the range 2.74–3.40 BM and electronic spectra showing clear evidence of extensive  $\pi$  bonding, as is to be expected with such ligands.

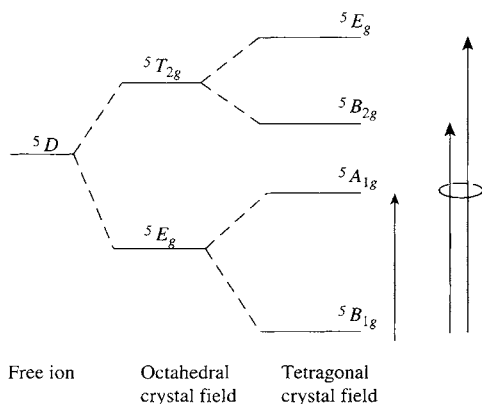
Although distorted octahedral geometry is certainly the most usual,  $Cr^{II}$  has a varied stereochemistry, as indicated in Table 23.2 (p. 1006).

One of the best known of  $Cr^{II}$  compounds, and one which has often been used as the starting material in preparations of other  $Cr^{II}$  compounds, is the acetate, itself obtained by addition of sodium acetate to an aqueous solution of a  $Cr^{II}$  salt. The red colour of the hydrated acetate is in sharp distinction to the blue of the simple salts — a contrast reflected in its dinuclear, bridged structure (Fig. 23.11a). This structure is also found in the yellow  $[Mo_2(\mu, \eta^2-O_2CMe)_4]$  which is obtained by the action of acetic acid on  $[Mo(CO)_6]$ . Other carboxylates of Cr and Mo are similar and the dinuclear structure is found also in the yellow alkali metal salts of  $[Cr_2(CO_3)_4]^{4-}$  and the pink  $K_4[Mo_2(SO_4)_4] \cdot 2H_2O$  where the oxoanions  $CO_3^{2-}$  and  $SO_4^{2-}$  are the bridging groups. Although an exact structure determination is lacking it is likely that the violet dihydrate,

obtained by partial dehydration of the blue “double sulphate”  $Cs_2SO_4 \cdot CrSO_4 \cdot 6H_2O$ , is of the same type in which case the formulation  $Cs_4[Cr_2(\mu, \eta^2-SO_4)_4(H_2O)_2] \cdot 2H_2O$  would be appropriate.  $[NBU_4]_2[Cr(NCS)_4]$  exists in two forms in which the usual correlation between structure and colour of  $Cr^{II}$  salts is reversed.<sup>(49a)</sup> The red form contains the mononuclear, planar  $[Cr(NCS)_4]^{2-}$  ion whereas the blue form contains the dinuclear  $[(NCS)_3Cr(\mu-NCS)_2Cr(NCS)_3]^{4-}$  ion featuring bridging thiocyanates (p. 324).

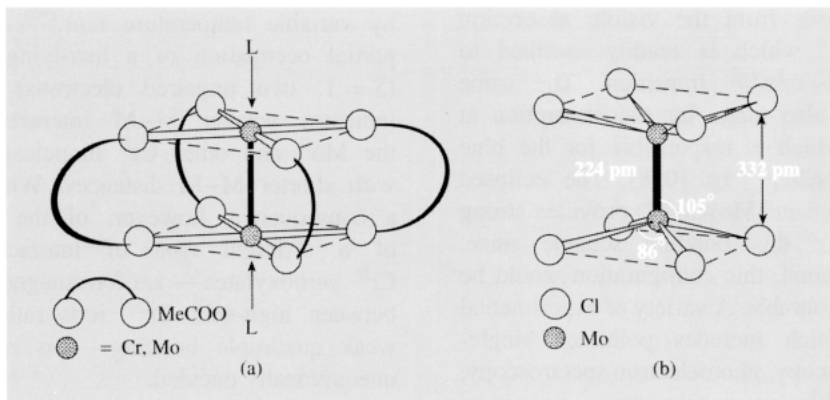
The reaction of conc HCl and molybdenum acetate at 0°C produces the diamagnetic red anion  $[Mo_2Cl_8]^{4-}$  (Fig. 23.11b) in which the 2  $MoCl_4$  are in the “eclipsed” orientation relative to each other and are held together solely by the Mo–Mo bond. At somewhat higher temperatures (~50°C) the above reactants also produce the  $[Mo_2Cl_8H]^{3-}$  ion which has the  $[M_2^{III}Cl_7]^{3-}$  structure (Fig. 23.4) but with one of the bridging Cl atoms replaced by a H atom.

An abundance of dinuclear compounds with a wide range of bridging groups involving not only the O–C–O unit of the carboxylates but also N–C–O, N–C–N, N–N–N and C–C–O, or like  $[Mo_2Cl_8]^{4-}$  with no bridging groups at all, are now known for  $Cr^{II}$  and  $Mo^{II}$ , particularly the latter.  $W^{II}$  also forms a comparatively small number and analogues of the isoelectronic  $Re^{III}$  and  $Tc^{III}$  are well-known (p. 1058–9). The  $Cr^{II}$  compounds apart, all these compounds whether bridged or not are diamagnetic, have very short M–M distances and clearly involve M–M bonds the precise nature of which has excited considerable attention<sup>(46)</sup>. The best simple description of the  $d^4$  systems is that shown in Fig. 23.12. The  $d_{x^2-y^2}$  orbital is assumed to have been used in  $\sigma$  bonding to the ligands and the four d electrons on each metal atom are then used to form a M–M quadruple bond ( $\sigma + 2\pi + \delta$ ) as originally proposed by B. N. Figgis and R. L. Martin for the bonding in dinuclear chromium(II) acetate (*J. Chem. Soc.* 3837–46 (1956)). The characteristic

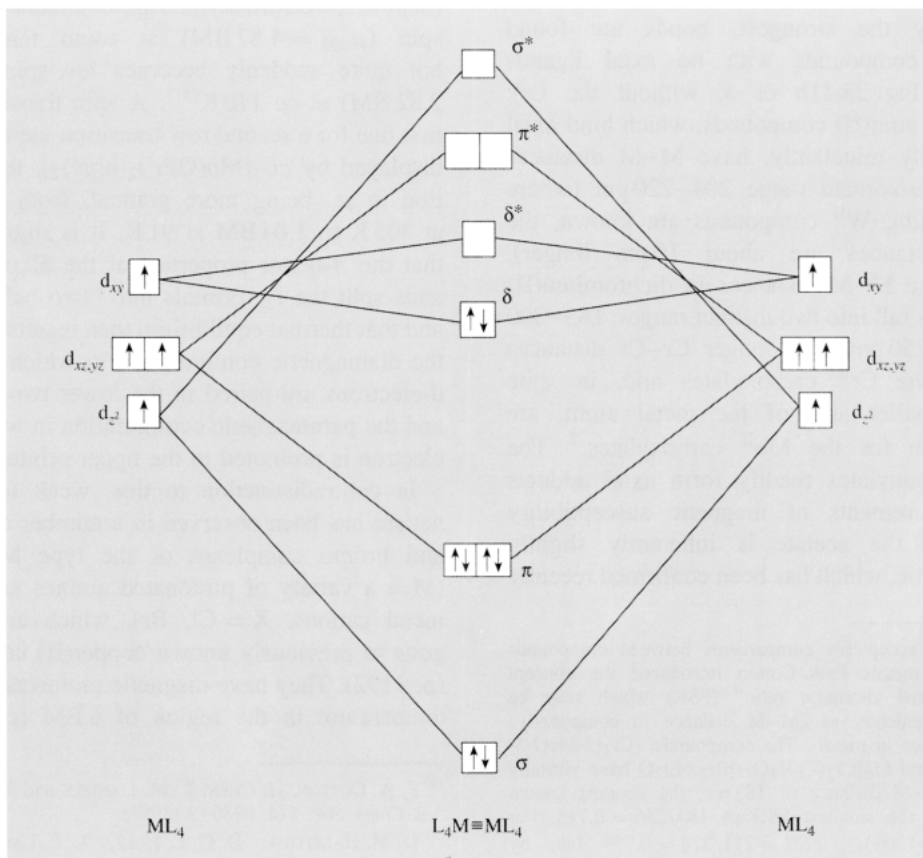


**Figure 23.10** Crystal field splitting of the  ${}^5D$  term of a  $d^4$  ion.

<sup>49a</sup> L. F. LARKWORTHY, G. A. LEONARD, D. C. POVEY, S. S. TANDON, B. J. TUCKER and G. W. SMITH, *J. Chem. Soc., Dalton Trans.*, 1425–8 (1994).



**Figure 23.11** (a)  $[M_2(\mu, \eta^2\text{-O}_2\text{CMe})_4]$ ,  $M = \text{Cr, Mo}$ . In the case of Cr, but not Mo, the hydrate and other adducts can be formed by attachment of  $\text{H}_2\text{O}$  (or in general, L) molecules as arrowed. (b)  $[\text{Mo}_2\text{Cl}_8]^{4-}$ .



**Figure 23.12** Simplified MO diagram showing the formation of an M–M quadruple bond in  $M_2L_8$  systems of  $d^4$  metal ions giving a ground configuration of  $\sigma^2\pi^4\delta^2$  (the  $d_{x^2-y^2}$ , along with  $p_x$ ,  $p_y$  and  $s$  orbitals of the metal ions are assumed to be used in the formation of M–L  $\sigma$  bonds).



red colour arises from the visible absorption at  $19\,000\text{ cm}^{-1}$  which is readily ascribed to the  $\sigma^2\pi^4\delta\delta^* \leftarrow \sigma^2\pi^4\delta^2$  transition. The same assignment is also made for the absorption at  $14\,300\text{ cm}^{-1}$  which is responsible for the blue colour of  $[\text{Re}_2\text{Cl}_8]^{2-}$  (p. 1058). The eclipsed orientation noted in  $[\text{Mo}_2\text{Cl}_8]^{4-}$  provides strong confirmation of this bonding scheme since, without the  $\delta$  bond, this configuration would be sterically unfavourable. A variety of experimental techniques, which includes polarized single-crystal spectroscopy, photoelectron spectroscopy, and X-ray emission spectroscopy, has been used to further substantiate this view of the bonding. Accurately determined M–M distances provide the most readily available indication of bond strength. The shortest, and therefore presumably the strongest, bonds are found in those compounds with no axial ligands (i.e. like Fig. 23.11b or a, without the Ls). Dimolybdenum(II) compounds, which bind axial ligands only reluctantly, have M–M distances in the approximate range 204–220 pm (where corresponding W<sup>II</sup> compounds are known, the W–W distances are about 10 pm longer), whereas the M–M distances in dichromium(II) compounds fall into two distinct ranges: 183–200 and 220–250 pm. The longer Cr–Cr distances refer to the Cr<sup>II</sup> carboxylates and, in spite of the smaller size of the metal atom, are longer than for the Mo<sup>II</sup> carboxylates.<sup>†</sup> The Cr(II) carboxylates readily form axial adducts and measurements of magnetic susceptibility show that the acetate is inherently slightly paramagnetic, which has been confirmed recently

<sup>†</sup> To effect acceptable comparisons between compounds of different metals F. A. Cotton introduced the concept of the “formal shortness ratio” (FSR) which may be defined conveniently as (M–M distance in compound) : (M–M distance in metal). The compounds,  $[\text{Cr}_2(2\text{-MeO-5-MeC}_6\text{H}_3)_4]$  and  $\text{Li}_6[\text{Cr}_2(\text{C}_6\text{H}_4\text{O})_4]\text{Br}_2 \cdot 6\text{Et}_2\text{O}$  have virtually the same M–M distance of 183 pm, the shortest known and yielding the smallest FSR of  $183/256 = 0.715$ . For  $[\text{Mo}_2(\mu, \eta^2\text{-O}_2\text{CMe})_4]$ ,  $\text{FSR} = 211/278 = 0.759$  but, by contrast, for  $[\text{Cr}_2(\mu, \eta^2\text{-O}_2\text{CMe})_4] \cdot 2\text{H}_2\text{O}$   $\text{FSR} = 236/256 = 0.922$ . For comparison, the strongest homonuclear bonds for which bond energies are accurately known are  $\text{N}\equiv\text{N}$  and  $\text{C}\equiv\text{C}$  and their FSRs are  $110/140 = 0.786$  and  $120.6/154 = 0.783$  respectively.

by variable temperature nmr.<sup>(50)</sup> This implies partial occupation of a low-lying spin triplet ( $S = 1$ , two unpaired electrons) and clearly indicates weaker M–M interaction than in the Mo<sup>II</sup> and other Cr<sup>II</sup> dinuclear compounds with shorter M–M distances. Whether this is a consequence, however, of the involvement of a different *type* of interaction in the Cr<sup>II</sup> carboxylates — antiferromagnetic coupling between high-spin Cr<sup>2+</sup> ions rather than just weak quadruple bonding — has not yet been unequivocally decided.

Interesting spin transitions are also observed: Although the reddish-purple  $[\text{CrI}_2(\text{dmpe})_2]$ , (dmpe = 1,2-bis(dimethylphosphino)ethane) is low-spin, the purple-brown  $[\text{CrI}_2(\text{depe})_2]$ , (depe = 1,2-bis(diethylphosphino)ethane) is high-spin ( $\mu_{295} = 4.87\text{ BM}$ ) at room temperature but quite suddenly becomes low-spin ( $\mu_{90} = 2.82\text{ BM}$ ) at *ca* 170 K<sup>(51)</sup>. A spin transition, the first one for a second row transition metal, is also displayed by *cis*- $[\text{Mo}(\text{OPr}^i)_2(\text{bipy})_2]$ , the reduction in  $\mu_e$  being more gradual, from 1.96 BM at 305 K to 1.04 BM at 91 K. It is suggested<sup>(52)</sup> that the  $\pi$ -donor properties of the alkoxide ligands split the  $t_{2g}$  orbitals into “two below one” and that thermal equilibrium then results between the diamagnetic configuration in which the four d-electrons are paired in the lower two orbitals, and the paramagnetic configuration in which one electron is promoted to the upper orbital.

In contradistinction to this, weak ferromagnetism has been observed in a number of chloro and bromo complexes of the type  $\text{M}_2[\text{CrX}_4]$  (M = a variety of protonated amines and alkali metal cations, X = Cl, Br), which are analogous to previously known copper(II) complexes (p. 1192). They have magnetic moments at room temperature in the region of 6 BM (compared

<sup>50</sup> F. A. COTTON, H. CHEN, L. M. DANIELS and X. FENG, *J. Am. Chem. Soc.* **114**, 8980–3 (1992).

<sup>51</sup> D. M. HALEPOTO, D. G. L. HOLT, L. F. LARKWORTHY, G. J. LEIGH, D. C. POVEY and G. W. SMITH *J. Chem. Soc., Chem. Commun.*, 1322–3 (1989), *Polyhedron* **8**, 1821–2 (1989).

<sup>52</sup> M. H. CHISHOLM, E. M. KOBER, D. J. IRONMONGER and P. THORTON, *Polyhedron* **4**, 1869–74 (1985).



to 4.9 BM expected for magnetically dilute  $\text{Cr}^{\text{II}}$  and these increase markedly as the temperature is lowered, the ferromagnetic interactions evidently being transmitted via Cr–Cl–Cr bridges. The electronic spectra consist of the usual absorptions expected for tetragonally distorted octahedral complexes of  $\text{Cr}^{\text{II}}$  but with two sharp and intense bands characteristically superimposed at higher energies (around 15 500 and 18 500  $\text{cm}^{-1}$ ). These are ascribed to spin-forbidden transitions intensified by the magnetic exchange.

Complexes in which the metal exhibits still lower oxidation states (such as I, 0, –I, –II) occur amongst the organometallic compounds (pp. 1006 and 1037).

### 23.3.8 Biological activity and nitrogen fixation

It appears that chromium(III) is an essential trace element<sup>(52a)</sup> in mammalian metabolism and, together with insulin, is responsible for the clearance of glucose from the blood-stream. Tungsten too has been found to have a role in some enzymes converting  $\text{CO}_2$  into formic acid but, from the point of view of biological activity, the focus of interest in this group is unquestionably on molybdenum.

In animal metabolism, oxomolybdoenzymes catalyse a number of oxidation processes. These oxidases contain  $\text{Mo}^{\text{VI}}$  coordinated to terminal O and S atoms, and their action appears to involve loss of an O or S atom along with reduction to  $\text{Mo}^{\text{V}}$  or  $\text{Mo}^{\text{IV}}$ . It is, however, the role of molybdenum in nitrogen fixation which has received most attention.

It is estimated that each year approximately 150 million tonnes of nitrogen are fixed biologically compared to 120 million tonnes fixed industrially by the Haber process (p. 421). In both cases  $\text{N}_2$  is converted to  $\text{NH}_3$ , requiring the rupture of the  $\text{N}\equiv\text{N}$  triple bond which has the highest dissociation energy (945.41  $\text{kJ mol}^{-1}$ )

of any homonuclear diatomic molecule. This is an inescapable toll exacted by  $\text{N}_2$  no matter how the fixation is achieved. In the Haber process it is paid by using high temperatures and pressures. Nature pays it by consuming 1 kg of glucose for every 14 g of  $\text{N}_2$  fixed, but does so *under ambient conditions*. It is this last fact which provides the economic spur to achieve an understanding of the mechanism of the natural process.

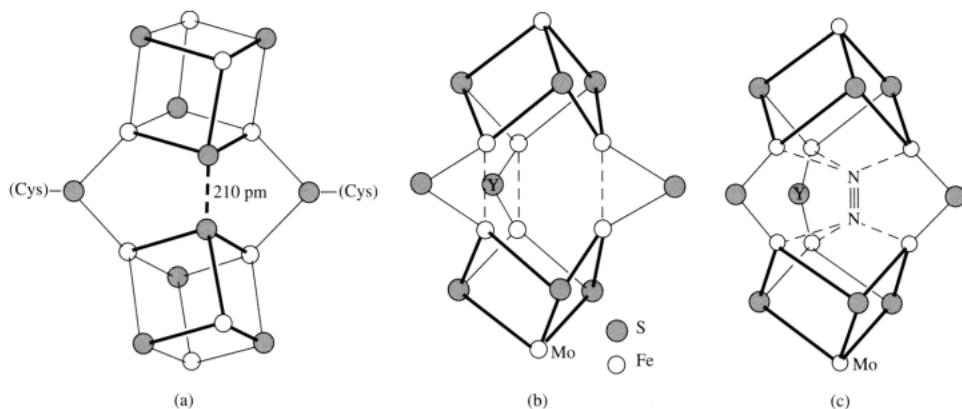
Nitrogen fixation takes place in a wide variety of bacteria, the best known of which is *rhizobium* which is found in nodules on the roots of leguminous plants such as peas, beans, soya and clover. The essential constituents of this and all other nitrogen-fixing bacteria are:

- (i) adenosine triphosphate (ATP) which is a highly active energy transfer agent (p. 528), operating by means of its hydrolysis which requires the presence of  $\text{Mg}^{2+}$ ;
- (ii) ferredoxin,  $\text{Fe}_4\text{S}_4(\text{SR})_4$  (p. 1102), which is an efficient electron-transfer agent that can be replaced in artificial systems by reducing agents such as dithionite,  $[\text{S}_2\text{O}_4]^{2-}$ ;
- (iii) a metallo-enzyme.

These metallo-enzymes are “nitrogenases” which have been isolated in an active form from several different bacteria and in a pure form from a number of these. The presence of Mo is not essential in all cases<sup>(53)</sup> (a vanadium nitrogenase is known — see p. 999) but is evidently a necessary component of most nitrogenases even though its precise function is unclear. These molybdenum nitrogenases consist of two distinct proteins. One, containing Fe but no Mo and therefore known as “Fe protein”, is yellow and extremely air-sensitive. Its molecular weight is about 60 000 and its structure involves an  $\text{Fe}_4\text{S}_4$ , ferredoxin-like cluster. The other protein contains both Mo and Fe and is known as “MoFe protein.” It is brown, air-sensitive, has a molecular weight in the approximate range 220 000 to 240 000, and

<sup>52a</sup> S. A. KATZ and H. SALEM, *The Biological and Environmental Chemistry of Chromium*, VCH, Weinheim, 1994, 214pp.

<sup>53</sup> R. R. EADY, *Adv. Inorg. Chem.* **36**, 77–102 (1991).



**Figure 23.13** Metal centres in the FeMo protein of nitrogenase. (a) P-cluster pair. Each of the four outer Fe atoms is further coordinated to the S of a cysteine group. (b) FeMo cofactor. (Y is probably S, O or N.) Fe–Fe bridge distances are in the range 240–260 pm, suggesting weak Fe–Fe interactions. The Mo achieves 6-coordination by further bonds to N (of histidine) and two O atoms (of a chelating homocitrate), while the Fe at the opposite end of the cofactor is tetrahedrally coordinated by attachment of a cysteine. (c) Possible intermediate in the interaction of  $N_2$  with FeMo cofactor.

contains the actual site of the  $N_2$  reduction.<sup>†</sup> Most of the isolated forms of MoFe protein contain 2 atoms of Mo and about 30 atoms each of Fe and S. These atoms are arranged in 6 metal centres: 4 so-called P-clusters each made up of  $Fe_4S_4$  units, and 2 Fe–Mo cofactors (FeMoco) in which the Mo is thought to be present as  $Mo^{IV}$ . Unfortunately, investigation of the structures of these proteins is hampered by the extreme sensitivity of nitrogenase to oxygen and the inherent difficulty of obtaining pure crystalline derivatives from biological materials. (Bacteria evidently protect nitrogenase from oxygen by a process of respiration,  $O_2 \rightarrow CO_2$ , but if too much oxygen is present the system cannot cope and nitrogen fixation ceases.) The recent determination of the structure of the nitrogenase from *Azotobacter vinelandii*<sup>(54)</sup> is therefore a remarkable achievement of X-ray crystallography, building upon results previously obtained from esr, Mössbauer spectroscopy and X-ray absorption spectroscopy (analysis of the

“extended X-ray absorption fine structure” or EXAFS).<sup>(55)</sup>

It turns out that each of the two FeMo cofactors consists of an  $Fe_4S_3$  and an  $Fe_3MoS_3$  incomplete cubane cluster. These are linked by two S bridges and a third bridging atom (Y), not identified with certainty, but possibly a well-ordered O or N or, alternatively, a less well-ordered S. Three atoms in each cluster are close enough to form interacting pairs across the bridge (Fig 23.13a). The P-clusters form two pairs, each pair consisting of two  $Fe_4S_4$  cubane clusters linked by two cysteine thiol bridges and a disulfide bond (Fig. 23.13b). Cleavage and re-formation of this disulfide bridge *could* provide the mechanism for a  $2e^-$  redox process. Mössbauer studies suggest that, in their most reduced form, the iron atoms of the P-clusters are in the 2+ oxidation state, unprecedented in biological  $Fe_4S_4$  systems. The reduction of  $N_2$  apparently involves the following steps:

- (i) reduction by ferredoxin of the Fe protein’s  $Fe_4S_4$  cluster, which is situated in an exposed position at the surface of the protein;

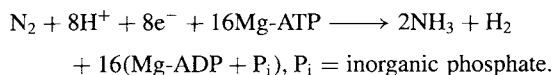
<sup>†</sup> Isolated nitrogenases will also reduce other species such as  $CN^-$  and  $N_3^-$  containing a triple bond, as well as reducing acetylenes to olefins.

<sup>54</sup> D. C. REES, M. K. CHAN and J. KIM, *Adv. Inorg. Chem.* **40**, 89–119 (1993).

<sup>55</sup> C. D. GARNER, *Adv. Inorg. Chem.* **36**, 303–39 (1991).

- (ii) one-electron transfer from the Fe protein to a P-cluster pair of the FeMo protein, by a process involving the hydrolysis of ATP;
- (iii) two-electron transfer, within the FeMo protein, from a P-cluster pair (whose environment is essentially hydrophobic) to an FeMo cofactor (whose environment is essentially hydrophilic);
- (iv) electron and proton transfer to N<sub>2</sub> which is almost certainly attached to the FeMo cofactor.

The overall reaction can be represented as:



Aspects of the process still requiring clarification include details of the electron flow between redox centres; the pathways for entry and exit of N<sub>2</sub>, NH<sub>3</sub> and H<sub>2</sub> (presumably structural rearrangements are needed); the role of Mg-ATP; and the nature of the interaction between N<sub>2</sub> and the FeMo cofactor which is central to the whole process. Persuasive arguments had been advanced for an intermediate involving 2 Mo atoms bridged by N<sub>2</sub><sup>(56)</sup>, yet in the determined structure the Mo atoms are too far apart to form a binuclear intermediate of this kind. On the other hand it has been plausibly suggested<sup>(55)</sup> that a reduced form of the FeMo cofactor might be sufficiently open at its centre to allow the insertion of N<sub>2</sub> so forming a bridged intermediate in which Fe-N interactions replace weak Fe-Fe bonds (Fig. 23.13c). The concomitant weakening of the N≡N bond would facilitate subsequent reduction of the N<sub>2</sub> bridge.

Further developments in this field may be confidently expected.

### 23.3.9 Organometallic compounds<sup>(57,58)</sup>

In this group a not-insignificant number of M-C σ-bonded compounds are known but are very unstable (MMe<sub>6</sub> is known only for W and this

explodes in air and can detonate in a vacuum) unless stabilized either by ligands lacking β-hydrogen atoms (p. 925) or by dimerizing and forming M-M bonds. Thus trimethylsilylmethyl (-CH<sub>2</sub>SiMe<sub>3</sub>) yields [Cr(tms)<sub>4</sub>] and the dimers [(tms)<sub>3</sub>M≡M(tms)<sub>3</sub>], (M = Mo, W). As with the preceding group, however, the bulk of organometallic chemistry is concerned with the metals in low oxidation states stabilized by π bonding ligands such as CO, cyclopentadienyl and, in this group, η<sup>6</sup>-arenes. Cyanides have been discussed on pp. 1025-32.

Stable, colourless, crystalline hexacarbonyls, M(CO)<sub>6</sub>, are prepared by reductive carbonylation of compounds (often halides) in higher oxidation states and are octahedral and diamagnetic as anticipated from the 18-electron rule (p. 1134). Replacement of the carbonyl groups by either π-donor or σ-donor ligands is possible, giving a host of materials of the form [M(CO)<sub>6-x</sub>L<sub>x</sub>] or [M(CO)<sub>6-2x</sub>(L-L)<sub>x</sub>] (e.g. L = NO, NH<sub>3</sub>, CN, PF<sub>3</sub>; L-L = bipy, butadiene). [M(CO)<sub>5</sub>X]<sup>-</sup> ions (X = halogen, CN or SCN) are formed in this way. The low-temperature reaction (-78°) of the halogens with [Mo(CO)<sub>6</sub>] or [W(CO)<sub>6</sub>] (but not with [Cr(CO)<sub>6</sub>]) produces the M<sup>II</sup> carbonyl halides, [M(CO)<sub>4</sub>X<sub>2</sub>] from which many adducts, [M(CO)<sub>3</sub>L<sub>2</sub>X<sub>2</sub>], are obtained. Although not all of these have been fully characterized, those that have are 7-coordinated and mostly capped octahedral. Reduction of the hexacarbonyls with a borohydride in liquid ammonia forms dimeric [M<sub>2</sub>(CO)<sub>10</sub>]<sup>2-</sup> which are isostructural with the isoelectronic [Mn<sub>2</sub>(CO)<sub>10</sub>] (p. 1062). Hydrolysis of these dimers produces the yellow hydrides [(CO)<sub>5</sub>M-H-M(CO)<sub>5</sub>] which maintain the 18 valence electron configuration by means of a 3-centre, 2-electron M-H-M bond. Neutron diffraction studies show these bridges to be non-linear as expected, the actual degree of bending probably being influenced by crystal-packing forces arising from different counter-cations. A

<sup>57</sup> S. W. KIRTLLEY, R. DAVIS and L. A. P. KANE-MAGUIRE, Chap. 26, pp. 783-1077, Chap. 27, pp. 1079-253 and Chap. 28, pp. 1255-384 in *Comprehensive Organometallic Chemistry*, Vol. 3, Pergamon Press, Oxford, 1982.

<sup>58</sup> pp. 277-402 of ref. 2.

<sup>56</sup> A. E. SHILOV, *Pure Appl. Chem.* **64**, 1409-20 (1992).

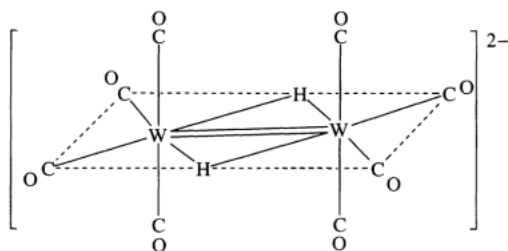
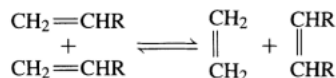


Figure 23.14 Structure of  $[\text{H}_2\text{W}_2(\text{CO})_8]^{2-}$ .

related compound,  $[\text{NEt}_4]_2^+[\text{H}_2\text{W}_2(\text{CO})_8]^{2-}$  is of interest because it has 2 hydrogen bridges and a W–W distance indicative of a W–W double bond (301.6 pm compared to about 320 pm for a W–W single bond) (Fig. 23.14). The compound also illustrates the improved refinement now possible with modern X-ray methods (p. 1013) and it was, in fact, the first case of the successful location of hydrogens bridging third-row transition metals. Reduction of the hexacarbonyls using Na metal in liquid  $\text{NH}_3$  yields the super-reduced, 18-electron species  $[\text{M}(\text{CO})_4]^{4-}$ .

$\text{M}(\text{CO})_6$  and other Mo and W compounds catalyse alkene metathesis<sup>†</sup> by the formation of

<sup>†</sup> This general reaction involves the cleavage of two C=C bonds and the formation of two new ones:



active alkylidene (p. 930) intermediates. This has stimulated the study of Mo and W alkylidenes (also alkylidyne which are similarly active in alkyne metathesis)<sup>(58)</sup>

Metallocenes,  $[\text{M}^{\text{II}}(\eta^5\text{-C}_5\text{H}_5)_2]$ , analogous to ferrocene would have only 16 valence electrons and could therefore be considered “electron deficient”. Chromocene can be formed by the action of sodium cyclopentadienide on  $[\text{Cr}(\text{CO})_6]$ . It is isomorphous with ferrocene but paramagnetic and much more reactive. Monomeric molybdocene and tungstocene polymerize above 10 K to red-brown polymeric solids,  $[\text{M}^{\text{II}}(\text{C}_5\text{H}_5)_2]_n$ . They are obtained by photolytic decomposition of yellow,  $[\text{M}^{\text{II}}(\eta^5\text{-C}_5\text{H}_5)_2\text{H}_2]$  which are “bent” molecules (Fig 23.15a), themselves prepared by the action of  $\text{NaBH}_4$  on  $\text{MCl}_5$  and  $\text{NaC}_5\text{H}_5$  in thf. With Mo and W hexacarbonyls, conditions similar to those used to prepare chromocene produce only  $[(\eta^5\text{-C}_5\text{H}_5)\text{M}^{\text{I}}(\text{CO})_3]_2$ , (Fig. 23.15b) in which dimerization achieves the 18-valence-electron configuration by means of an M–M bond. The chromium analogue of these dimers has one of the longest M–M bonds found in dinuclear transition metal compounds (328.1 pm). Its reactivity allows ready insertion of a variety of groups which includes S and Se yielding

and can be used to convert propylene into ethylene for subsequent polymerization or oligomerization.

<sup>58</sup> See for instance: J. KRESS and J. A. OSBORN, *Angew. Chem. Int. Edn. Engl.* **31**, 1585–7 (1992); A. MAYR and C. M. BASTOS, *Prog. Inorg. Chem.* **40**, 1–98 (1992).

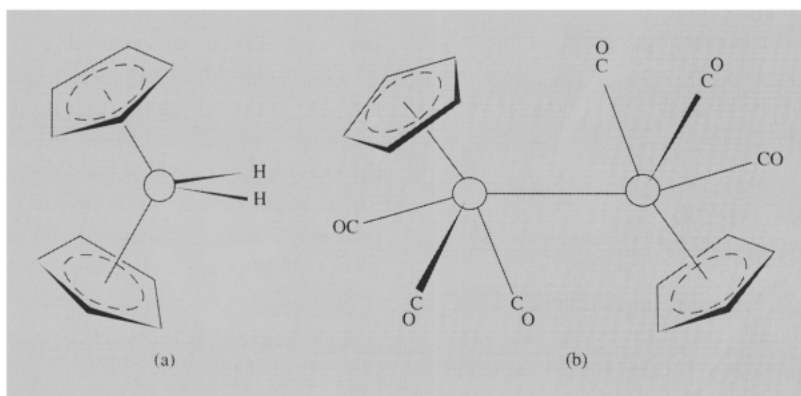


Figure 23.15 (a) The “bent” molecules  $[\text{M}^{\text{II}}(\eta^5\text{-C}_5\text{H}_5)_2\text{H}_2]$  (b)  $[\text{M}^{\text{I}}(\eta^5\text{-C}_5\text{H}_5)(\text{CO})_3]_2$  (M = Mo, W).

products such as  $[\text{Cr}_2(\eta^5\text{-C}_5\text{H}_5)_2(\text{CO})_4\text{E}_2]$ , while cleavage of the bond with  $\text{Ph}_2\text{E}_2$  gives  $[\text{Cr}(\eta^5\text{-C}_5\text{H}_5)(\text{CO})_3(\text{EPh})]$  ( $\text{E} = \text{S}, \text{Se}$ )<sup>(59)</sup>. Of the many other cyclopentadienyl derivatives the Mo and W halides  $[\text{M}(\eta^5\text{-C}_5\text{H}_5)_2\text{X}_2]$  and dimeric  $[\text{M}_2(\eta^5\text{-C}_5\text{H}_5)_2\text{X}_4]$ , which are useful precursors in other syntheses<sup>(60)</sup> may be mentioned.

Of greater stability than the monomeric metallocenes in this group are the dibenzene sandwich compounds which are isoelectronic with ferrocene and of which the dark brown  $[\text{Cr}(\eta^6\text{-C}_6\text{H}_6)_2]$  was the first to be prepared (p. 940) and remains the best known. The green  $[\text{Mo}(\eta^6\text{-C}_6\text{H}_6)_2]$  and yellow-green  $[\text{W}(\eta^6\text{-C}_6\text{H}_6)_2]$  are also well characterized and all contain the metal in the formal oxidation state of zero. As the 12 C atoms in  $[\text{M}(\eta^6\text{-C}_6\text{H}_6)_2]$  are equidistant from the central metal atom, the coordination number of M is 12, though, of course, only 6 bonding molecular orbitals are primarily involved in linking the

two ligand molecules to M. The compounds are more susceptible to oxidation than is the isoelectronic ferrocene and all are converted to paramagnetic salts of  $[\text{M}^I(\eta^6\text{-C}_6\text{H}_6)_2]^+$ : the ease with which this process takes place increases in the order  $\text{Cr} < \text{Mo} < \text{W}$ . Since CO groups are evidently better  $\pi$ -acceptors than  $\text{C}_6\text{H}_6$ , replacement of one of the benzene ligands in  $[\text{M}(\text{C}_6\text{H}_6)_2]$  by three carbonyls giving, for instance,  $[\text{Cr}(\eta^6\text{-C}_6\text{H}_6)(\text{CO})_3]$ , appreciably improves the resistance to oxidation because the electron density on the metal is lowered.  $[\text{W}(\eta^6\text{-C}_6\text{H}_6)_2]$  is reversibly protonated by dilute acids to give  $[\text{W}(\eta^6\text{-C}_6\text{H}_6)_2\text{H}]^+$ .

As in the previous group, a potentially productive route into C<sub>7</sub>-ring chemistry is provided by the reduction of a metal halide with Na/Hg in thf in the presence of cycloheptatriene. With  $\text{MoCl}_5$ ,  $[\text{Mo}(\eta^7\text{-C}_7\text{H}_7)(\eta^7\text{-C}_7\text{H}_9)]$  is produced and a variety of derivatives have already been obtained.<sup>(61)</sup>

<sup>59</sup>L. Y. GOH, Y. Y. LIM, M. S. TAY, T. C. W. MAK and Z. Y. ZHOU, *J. Chem. Soc., Dalton Trans.*, 1239–42 (1992).

<sup>60</sup>M. L. H. GREEN and P. MOUNTFORD, *Chem. Soc. Revs.* **21**, 29–38 (1992).

<sup>61</sup>M. L. H. GREEN, D. K. P. NG and R. C. TOVEY, *J. Chem. Soc., Chem. Commun.*, 918–9 (1992).

																1	2																		
																H	He																		
3	4															5	6	7	8	9	10														
Li	Be															B	C	N	O	F	Ne														
11	12															13	14	15	16	17	18														
Na	Mg															Al	Si	P	S	Cl	Ar														
19	20	21	22	23	24	25	26	27	28	29	30	31	32	33	34	35	36																		
K	Ca	Sc	Ti	V	Cr	Mn	Fe	Cu	Ni	Cu	Zn	Ga	Ge	As	Se	Br	Kr																		
37	38	39	40	41	42	43	44	45	46	47	48	49	50	51	52	53	54																		
Rb	Sr	Y	Zr	Nb	Mo	Tc	Ru	Rh	Pd	Ag	Cd	In	Sn	Sb	Te	I	Xe																		
55	56	57	58	59	60	61	62	63	64	65	66	67	68	69	70	71	72																		
Cs	Ba	La	Hf	Ta	W	Re	Os	Ir	Pt	Au	Hg	Tl	Pb	Bi	Po	At	Rn																		
87	88	89	90	91	92	93	94	95	96	97	98	99	100	101	102	103	104																		
Fr	Ra	Ac	Rf	Db	Sg	Bh	Hs	Mt	Uun	Uuu	Uub																								
																		89	90	91	92	93	94	95	96	97	98	99	100	101	102	103	104	105	
																		Ce	Pr	Nd	Pm	Sm	Eu	Gd	Tb	Dy	Ho	Er	Tm	Yb	Lu				
																		91	92	93	94	95	96	97	98	99	100	101	102	103	104	105			
																		Th	Pa	U	Np	Pu	Am	Cm	Bk	Cf	Es	Fm	Md	No	Lr				

# 24

## Manganese, Technetium and Rhenium

### 24.1 Introduction

In terms of history, abundance and availability, it is difficult to imagine a greater contrast than exists in this group between manganese and its congeners, technetium and rhenium. Millions of tonnes of manganese are used annually, and its most common mineral, pyrolusite, has been used in glassmaking since the time of the Pharaohs. On the other hand, technetium and rhenium are exceedingly rare and were only discovered comparatively recently, the former being the first new element to have been produced artificially and the latter being the last naturally occurring element to be discovered.

Metallic manganese was first isolated in 1774 when C. W. Scheele recognized that pyrolusite contained a new element, and his fellow Swede, J. G. Gahn, heated the  $\text{MnO}_2$  with a mixture of charcoal and oil. The purity of this sample of the metal was low, and high-purity (99.9%) manganese was only produced in the 1930s when electrolysis of  $\text{Mn}^{\text{II}}$  solutions was used.

In Mendeleev's table, this group was completed by the then undiscovered eka-manganese ( $Z = 43$ ) and dvi-manganese ( $Z = 75$ ). Confirmation of the existence of these missing elements was not obtained until H. G. J. Moseley had introduced the method of X-ray spectroscopic analysis. Then in 1925 W. Noddack, I. Tacke (later Frau Noddack) and O. Berg discovered element 75 in a sample of gadolinite (a basic silicate of beryllium, iron and lanthanides) and named it rhenium after the river Rhine. The element was also discovered, independently by F. H. Loring and J. F. G. Druce, in manganese compounds, but is now most usually recovered from the flue dusts produced in the roasting of  $\text{CuMo}$  ores.

The Noddacks also claimed to have detected element 43 and named it masurium after Masuren in Prussia. This claim proved to be incorrect, however, and the element was actually detected in 1937 in Italy by C. Perrier and E. Segré in a sample of molybdenum which had been bombarded with deuterons in the cyclotron of E. O. Lawrence in California. It was present in the form of the  $\beta^-$  emitters  $^{95\text{m}}\text{Tc}$  and  $^{97\text{m}}\text{Tc}$

with half-lives of 61 and 90 days respectively. The name technetium (from Greek τεχνικός, artificial) is clearly appropriate even though minute traces of the more stable  $^{99}\text{Tc}$  (half-life =  $2.11 \times 10^5$  y) do occur naturally as a result of spontaneous fission of uranium.

## 24.2 The Elements

### 24.2.1 Terrestrial abundance and distribution

The natural abundance of technetium is, as just indicated, negligibly small. The concentration of rhenium in the earth's crust is extremely low (of the order of  $7 \times 10^{-8}\%$ , i.e. 0.0007 ppm) and it is also very diffuse. Being chemically akin to molybdenum it is in molybdenites that its highest concentrations (0.2%) are found. By contrast, manganese (0.106%, i.e. 1060 ppm of the earth's crustal rocks) is the twelfth most abundant element and the third most abundant transition element (exceeded only by iron and titanium). It is found in over 300 different and widely distributed minerals of which about twelve are commercially important. As a class-a metal it occurs in primary deposits as the silicate. Of more commercial importance are the secondary deposits of oxides and carbonates such as pyrolusite ( $\text{MnO}_2$ ), which is the most common, hausmannite ( $\text{Mn}_3\text{O}_4$ ), and rhodochrosite ( $\text{MnCO}_3$ ). These have been formed by weathering of the primary silicate deposits and are found in the former USSR, Gabon, South Africa, Brazil, Australia, India and China.

A further consequence of this weathering is that colloidal particles of the oxides of manganese, iron and other metals are continuously being washed into the sea where they agglomerate and are eventually compacted into the "manganese nodules" (so called because Mn is the chief constituent), first noted during the voyage of HMS *Challenger* (1872–6). Following a search in the Pacific organized by the University of California during the International Geophysical Year (1957), the magnitude and potential value of manganese nodules became

apparent. More than  $10^{12}$  tonnes are estimated to cover vast areas of the ocean beds and a further  $10^7$  tonnes are deposited annually. The composition varies but the dried nodules generally contain between 15 and 30% of Mn. This is less than the 35% normally regarded as the lower limit required for present-day commercial exploitation but, since the Mn is accompanied not only by Fe but more importantly by smaller amounts of Ni, Cu and Co, the combined recovery of Ni, Cu and Co, with Mn effectively as a byproduct could well be economical if performed on a sufficient scale. The technical, legal, and political problems involved are enormous, but perhaps even more importantly, overcapacity in conventional means of production has so far inhibited the exploitation of these reserves.

### 24.2.2 Preparation and uses of the metals

Over ninety per cent of all the manganese ores produced are used in steel manufacture, mostly in the form of ferromanganese.<sup>(1)</sup> This contains about 80% Mn and is made by reducing appropriate amounts of  $\text{MnO}_2$  and  $\text{Fe}_2\text{O}_3$  with coke in a blast furnace or, if cheap electricity is available, in an electric-arc furnace. Dolomite or limestone is also added to remove silica as a slag. Where the Mn content is lower (because of the particular ores used) the product is known as silicomanganese (65–70% Mn, 15–20% Si) or spiegeleisen (5–20% Mn). Where pure manganese metal is required it is prepared by the electrolysis of aqueous manganase(II) sulfate. Ore with an Mn content of over 8 million tonnes was produced in 1995, the most important sources being the former Soviet Union, the Republic of South Africa, Gabon and Australia.

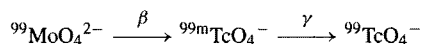
All steels contain some Mn, and its addition in 1856 by R. Mushet ensured the success of the Bessemer process. It serves two main purposes. As a "scavenger" it combines with sulfur to form

<sup>1</sup> Kirk-Othmer Encyclopedia of Chemical Technology, 4th edn., Vol. 15, pp. 963–91, Interscience, New York, 1995.

## Technetium in Diagnostic Nuclear Medicine<sup>(2)</sup>

<sup>99m</sup>Tc is one of the most widely used isotopes in nuclear medicine. It is injected into the patient in the form of a saline solution of a compound, chosen because it will be absorbed by the organ under investigation, which can then be "imaged" by an X-ray camera or scanner. Its properties are ideal for this purpose: it decays into <sup>99</sup>Tc by internal transition and  $\gamma$ -emission of sufficient energy to allow the use of physiologically insignificant quantities (nmol or even pmol — a permissible dose of 1 mCi corresponds to 1.92 pmol of <sup>99m</sup>Tc) and a half-life (6.01 h) short enough to preclude radiological damage due to prolonged exposure. It is obtained from <sup>99</sup>Mo ( $t_{1/2} = 65.94$  h), which in turn is obtained from the fission products of natural or reactor uranium, or else by neutron irradiation of <sup>98</sup>Mo.

Although details vary considerably, the <sup>99</sup>Mo is typically incorporated in a "generator" in the form of  $\text{MoO}_4^{2-}$  absorbed on a substrate such as alumina where it decays according to the scheme:



These generators can be made available virtually anywhere and, when required,  $\text{TcO}_4^-$  is eluted from the substrate and reduced ( $\text{Sn}^{\text{II}}$  is a common, but not the sole, reductant) in the presence of an appropriate ligand, ready for immediate use. A wide range of *N*-, *P*- and *S*-donor ligands has been used to prepare complexes of Tc, mainly in oxidation states III, IV and V, which are absorbed preferentially by different organs. Though the circumstances of clinical usage mean that the precise formulation of the compound actually administered is frequently uncertain,<sup>†</sup> the imaging of brain, heart, lung, bone and tumours etc. is possible. It is the search for compounds of increased specificity which has stimulated most of the recent work on the coordination chemistry of Tc.

<sup>†</sup> Interconversion between different oxidation states occurs easily for Tc (see Section 24.2.4.), and its control often requires careful adjustment of pH and the relative excess of reductant used.

MnS which passes into the slag and prevents the formation of FeS which would induce brittleness, and it also combines with oxygen to form MnO, so preventing the formation of bubbles and pinholes in the cold steel. Secondly, the presence of Mn as an alloying metal increases the hardness of the steel. The hard, non-magnetic Hadfield steel containing about 13% Mn and 1.25% C, is the best known, and is used when resistance to severe mechanical shock and wear is required, e.g. for excavators, dredgers, rail crossings, etc.

Important, but less extensive, uses are found in the production of non-ferrous alloys. It is a scavenger in several Al and Cu alloys, while "manganin" is a well-known alloy (84% Cu, 12% Mn, 4% Ni) which is used in electrical instruments because the temperature coefficient of its resistivity is almost zero. A variety of other major uses have been found for Mn in the form of

its compounds and these will be dealt with later under the appropriate headings.

Technetium is obtained from nuclear power stations where it makes up about 6% of uranium fission products and is recovered from these after storage for several years to allow the highly radioactive, short-lived fission products to decay. The original process used the precipitation of  $[\text{AsPh}_4]^+[\text{ClO}_4]^-$  to carry with it  $[\text{AsPh}_4]^+[\text{TcO}_4]^-$  and so separate the Tc from other fission products, but solvent extraction and ion-exchange techniques are now used. The metal itself can be obtained by the high-temperature reduction of either  $\text{NH}_4\text{TcO}_4$  or  $\text{Tc}_2\text{S}_7$  with hydrogen. <sup>99</sup>Tc is the isotope available in kg quantities and the one used for virtually all chemical studies. Because of its long half-life it is not a major radiation hazard and, with standard manipulative techniques, can be safely handled in mg quantities. However, the main interest in Tc is its role in nuclear medicine, and here it is the metastable  $\gamma$ -emitting isotope <sup>99m</sup>Tc which is used (see Panel).

<sup>2</sup> S. JURISSON, D. BERNING, W. JIA and D. MA, *Chem. Revs.*, **93**, 1137–56 (1993). K. SCHWOCHALL, *Angew. Chem. Int. Edn. Engl.* **33**, 2258–67 (1994).



In the roasting of molybdenum sulfide ores, any rhenium which might be present is oxidized to volatile  $\text{Re}_2\text{O}_7$  which collects in the flue dusts and is the usual source of the metal via conversion to  $(\text{NH}_4)\text{ReO}_4$  and reduction by  $\text{H}_2$  at elevated temperatures. Being highly refractory and corrosion-resistant, rhenium metal would no doubt find widespread use were it not for its scarcity and consequent high cost. As it is, uses are essentially small scale. These include bimetallic Pt/Re catalysts for the production of lead-free, high octane petroleum products, high temperature superalloys for jet engine components, mass spectrometer filaments, furnace heating elements and thermocouples. World production is about 35 tonnes annually.

### 24.2.3 Properties of the elements

Some of the important properties of Group 7 elements are summarized in Table 24.1. Technetium is an artificial element, so its atomic weight depends on which isotope has been produced. The atomic weights of Mn and Re, however, are known with considerable accuracy. In the case of

the former this is because it has only 1 naturally occurring isotope and, in the case of the latter, because it has only 2 and the relative proportions of these in terrestrial samples are essentially constant ( $^{185}\text{Re}$  37.40%,  $^{187}\text{Re}$  62.60%).

In the solid state all three elements have typically metallic structures. Technetium and Re are isostructural with hcp lattices, but there are 4 allotropes of Mn of which the  $\alpha$ -form is the one stable at room temperature. This has a bcc structure in which, for reasons which are not clear, there are 4 distinct types of Mn atom. It is hard and brittle, and noticeably less refractory than its predecessors in the first transition series.

In continuance of the trends already noticed, the most stable oxidation state of manganese is +2, and in the group oxidation state of +7 it is even more strongly oxidizing than Cr(VI). Evidently the 3d electrons are more tightly held by the Mn atomic nucleus and this reduced delocalization produces weaker metallic bonding than in Cr. The same trends are also starting in the second and third series with Tc and Re, but are less marked, and Re in particular is very refractory, having a mp which is second only to that of tungsten amongst transition elements.

Table 24.1 Some properties of Group 7 elements

Property	Mn	Tc	Re
Atomic number	25	43	75
Number of naturally occurring isotopes	1	—	2
Atomic weight	54.938049(9)	98.9063 <sup>(a)</sup>	186.207(1)
Electronic configuration	[Ar]3d <sup>5</sup> 4s <sup>2</sup>	[Kr]4d <sup>6</sup> 5s <sup>1</sup>	[Xe]4f <sup>14</sup> 5d <sup>5</sup> 6s <sup>2</sup>
Electronegativity	1.5	1.9	1.9
Metal radius (12-coordinate)/pm	127	136	137
Ionic radius/pm	46	56	53
(4-coordinate if marked*; otherwise 6-coordinate)	25.5*	—	55
	V	60	58
	IV	64.5	63
	III	—	—
	II	—	—
MP/°C	1244	2200	3180
BP/°C	2060	4567	(5650)
$\Delta H_{\text{fus}}/\text{kJ mol}^{-1}$	(13.4)	23.8	34(±4)
$\Delta H_{\text{vap}}/\text{kJ mol}^{-1}$	221(±8)	585	704
$\Delta H_{\text{f}}$ (monatomic gas)/kJ mol <sup>-1</sup>	281(±6)	—	779(±8)
Density (25°C)/g cm <sup>-3</sup>	7.43	11.5	21.0
Electrical resistivity (20°C)/μohm cm	185.0	—	19.3

<sup>(a)</sup>This refers to  $^{99}\text{Tc}$  ( $t_{1/2} 2.11 \times 10^5$  y). For  $^{97}\text{Tc}$  ( $t_{1/2} 2.6 \times 10^6$  y) and  $^{98}\text{Tc}$  ( $t_{1/2} 4.2 \times 10^6$  y) the values are 96.9064 and 97.9072 respectively.

### 24.2.4 Chemical reactivity and trends

Manganese is more electropositive than any of its neighbours in the periodic table and the metal is more reactive, especially when somewhat impure. In the massive state it is superficially oxidized on exposure to air but will burn if finely divided. It liberates hydrogen from water and dissolves readily in dilute aqueous acids to form manganese(II) salts. With non-metals it is not very reactive at ambient temperatures but frequently reacts vigorously when heated. Thus it burns in oxygen, nitrogen, chlorine and fluorine giving  $\text{Mn}_3\text{O}_4$ ,  $\text{Mn}_3\text{N}_2$ ,  $\text{MnCl}_2$  and  $\text{MnF}_2 + \text{MnF}_3$  respectively, and it combines directly with B, C, Si, P, As and S.

Technetium and rhenium metals are less reactive than manganese and, as is to be expected for the two heavier elements, they are closely similar to each other. In the massive form they resist oxidation and are only tarnished slowly in moist air. However, they are normally produced as sponges or powders in which case they are more reactive. Heated in oxygen they burn to give volatile heptaoxides ( $\text{M}_2\text{O}_7$ ), and with fluorine they give  $\text{TcF}_5 + \text{TcF}_6$  and  $\text{ReF}_6 + \text{ReF}_7$  respectively.  $\text{MS}_2$  can also be produced by direct action. Although insoluble in hydrofluoric and hydrochloric acids, the metals dissolve readily in oxidizing acids such as  $\text{HNO}_3$  and conc  $\text{H}_2\text{SO}_4$  and also in bromine water, when "pertechnetic" and "perrhenic" acids ( $\text{HMO}_4$ ) are formed.

Because of the differing focus of interest in these elements their chemistries have not developed in parallel and the data on which strict comparisons might be based are not always available. Nevertheless many of the similarities and contrasts expected in the chemistry of transition elements are evident in this triad. The relative stabilities of different oxidation states in aqueous, acidic solutions are summarized in Table 24.2 and Fig. 24.1.

The most obvious features of Fig. 24.1 are the relative positions of the +2 oxidation states. For manganese this state, represented by the high-spin  $\text{Mn}^{\text{II}}$  cation, is much the most stable. This may be taken as an indication of the stability of the symmetrical  $d^5$  electron configuration.

Table 24.2  $E^\circ$  for some manganese, technetium and rhenium couples in acid solution at 25°C

Couple	$E^\circ/\text{V}$
$\text{Mn}^{2+}(\text{aq}) + 2\text{e}^- \rightleftharpoons \text{Mn}(\text{s})$	-1.185
$\text{Mn}^{3+}(\text{aq}) + 3\text{e}^- \rightleftharpoons \text{Mn}(\text{s})$	-0.283
$\text{MnO}_2 + 4\text{H}^+ + 4\text{e}^- \rightleftharpoons \text{Mn}(\text{s}) + 2\text{H}_2\text{O}$	0.024
$\text{MnO}_4^{2-} + 8\text{H}^+ + 4\text{e}^- \rightleftharpoons \text{Mn}^{2+}(\text{aq}) + 4\text{H}_2\text{O}$	1.742
$\text{MnO}_4^- + 8\text{H}^+ + 5\text{e}^- \rightleftharpoons \text{Mn}^{2+}(\text{aq}) + 4\text{H}_2\text{O}$	1.507
$\text{Tc}^{2+}(\text{aq}) + 2\text{e}^- \rightleftharpoons \text{Tc}(\text{s})$	0.400
$\text{TcO}_2 + 4\text{H}^+ + 4\text{e}^- \rightleftharpoons \text{Tc}(\text{s}) + 2\text{H}_2\text{O}$	0.272
$\text{TcO}_3 + 2\text{H}^+ + 2\text{e}^- \rightleftharpoons \text{TcO}_2 + \text{H}_2\text{O}$	0.757
$\text{TcO}_4^- + 8\text{H}^+ + 5\text{e}^- \rightleftharpoons \text{Tc}^{2+}(\text{aq}) + 4\text{H}_2\text{O}$	0.500
$\text{Re}^{3+}(\text{aq}) + 3\text{e}^- \rightleftharpoons \text{Re}(\text{s})$	0.300
$\text{ReO}_2 + 4\text{H}^+ + 4\text{e}^- \rightleftharpoons \text{Re}(\text{s}) + 2\text{H}_2\text{O}$	0.251
$\text{ReO}_3 + 6\text{H}^+ + 3\text{e}^- \rightleftharpoons \text{Re}^{3+}(\text{aq}) + 3\text{H}_2\text{O}$	0.318
$\text{ReO}_4^{2-} + 8\text{H}^+ + 3\text{e}^- \rightleftharpoons \text{Re}^{3+}(\text{aq}) + 4\text{H}_2\text{O}$	0.795
$\text{ReO}_4^- + 8\text{H}^+ + 4\text{e}^- \rightleftharpoons \text{Re}^{3+}(\text{aq}) + 4\text{H}_2\text{O}$	0.422

However, like the mp, bp and enthalpy of atomization, it also reflects the weaker cohesive forces in the metallic lattice since for Tc and Re, which have much stronger metallic bonding, the +2 state is of little importance and the occurrence of cluster compounds with M–M bonds is a dominant feature of rhenium(III) chemistry. The almost uniform slope of the plot for Tc presages the facile interconversion between oxidation states, observed for this element.

Another marked contrast is evident in the +7 oxidation state where the manganate(VII) (permanganate) ion is an extremely strong oxidizing agent but  $(\text{TcO}_4)^-$  and  $(\text{ReO}_4)^-$  show only mild oxidizing properties. Indeed, the greater stability of Tc and Re compared to Mn in any oxidation state higher than +2 is apparent, as will be seen more fully in the following account of individual compounds.

Table 24.3 lists representative examples of the compounds of these elements in their various oxidation states. The wide range of the oxidation states is particularly noteworthy. It arises from the fact that, in moving across the transition series, the number of d electrons has increased and, in this mid-region, the d orbitals have not yet sunk energetically into the inert electron core. The number of d electrons available for bonding is consequently maximized, and not

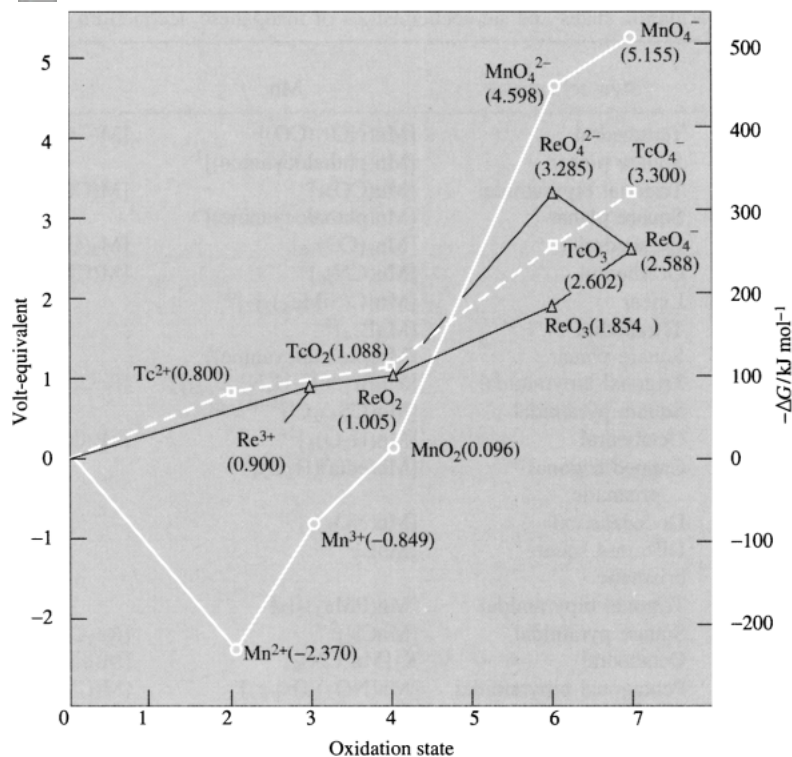


Figure 24.1 Plot of volt-equivalent versus oxidation state for Mn, Tc and Re.

only are high oxidation states possible, but back donation of electrons from metal to ligand is also facilitated with resulting stabilization of low oxidation states.

A further point of interest is the noticeably greater tendency of rhenium, as compared to either manganese or technetium, to form compounds with high coordination numbers.

## 24.3 Compounds of Manganese, Technetium and Rhenium<sup>(3)</sup>

Binary borides (p. 145), carbides (p. 297), and nitrides (p. 417) have already been mentioned.

<sup>3</sup> R. D. W. KEMMITT, Chap. 37, pp. 771–876; R. D. PEACOCK Chap. 38, pp. 877–903 and Chap. 39, pp. 905–78, in *Comprehensive Inorganic Chemistry*, Vol. 3, Pergamon Press, Oxford, 1973. (See also nine reviews devoted to the chemistry of Tc and Re in *Topics in Current Chemistry* **176**, 1996, 291 pp.)

Manganese, like chromium (and also the succeeding elements in the first transition series), is too small to accommodate interstitial carbon without significant distortion of the metal lattice. As a consequence it forms a number of often readily hydrolysed carbides with rather complicated structures.

Hydrido complexes are well-known but simple binary hydrides are not, which is in keeping with the position of these metals in the “hydrogen gap” portion of the periodic table (p. 67).

### 24.3.1 Oxides and chalcogenides

All three metals form heptoxides (Table 24.4) but, whereas  $\text{Tc}_2\text{O}_7$  and  $\text{Re}_2\text{O}_7$  are the final products formed when the metals are burned in an excess of oxygen,  $\text{Mn}_2\text{O}_7$  requires prior oxidation of the manganese to the +7 state. It separates as a reddish-brown explosive oil from the green

Table 24.3 Oxidation states and stereochemistries of manganese, technetium and rhenium

Oxidation state	Coordination number	Stereochemistry	Mn	Tc/Re
-3 (d <sup>10</sup> )	4	Tetrahedral	[Mn(NO) <sub>3</sub> (CO)]	[M(CO) <sub>4</sub> ] <sup>3-</sup>
-2 (d <sup>9</sup> )	4	Square planar	[Mn(phthalocyanine)] <sup>2-</sup>	—
-1 (d <sup>8</sup> )	5	Trigonal bipyramidal	[Mn(CO) <sub>5</sub> ] <sup>-</sup>	[M(CO) <sub>5</sub> ] <sup>-</sup>
	4	Square planar	[Mn(phthalocyanine)] <sup>-</sup>	—
0 (d <sup>7</sup> )	6	Octahedral	[Mn <sub>2</sub> (CO) <sub>10</sub> ]	[M <sub>2</sub> (CO) <sub>10</sub> ]
1 (d <sup>6</sup> )	6	Octahedral	[Mn(CN) <sub>6</sub> ] <sup>5-</sup>	[M(CN) <sub>6</sub> ] <sup>5-</sup>
2 (d <sup>5</sup> )	2	Linear	[Mn{C(SiMe <sub>3</sub> ) <sub>3</sub> ] <sub>2</sub> ] <sup>(a)</sup>	—
	4	Tetrahedral	[MnBr <sub>4</sub> ] <sup>2-</sup>	—
	5	Square planar	[Mn(phthalocyanine)]	—
	5	Trigonal bipyramidal	[MnBr{N(C <sub>2</sub> H <sub>4</sub> NMe <sub>2</sub> ) <sub>3</sub> }] <sup>+</sup>	[ReCl(dppe) <sub>2</sub> ] <sup>+</sup>
		Square pyramidal	[Mn(CS <sub>4</sub> ) <sub>2</sub> Cl] <sup>3-(b)</sup>	—
	6	Octahedral	[Mn(H <sub>2</sub> O) <sub>6</sub> ] <sup>2+</sup>	[M(diars) <sub>2</sub> Cl <sub>2</sub> ]
	7	Capped trigonal prismatic	[Mn(edta)(H <sub>2</sub> O)] <sup>2-</sup>	—
	8	Dodecahedral	[Mn(NO <sub>3</sub> ) <sub>4</sub> ] <sup>2-</sup>	—
		Distorted square prismatic	[MnL] <sup>2+(c)</sup>	—
	5	Trigonal bipyramidal	[Mn(PMe <sub>3</sub> ) <sub>2</sub> I <sub>3</sub> ]	—
3(d <sup>4</sup> )	6	Square pyramidal	[MnCl <sub>5</sub> ] <sup>2-</sup>	[Re <sub>2</sub> Cl <sub>8</sub> ] <sup>2-</sup>
	6	Octahedral	K <sub>3</sub> [Mn(CN) <sub>6</sub> ]	[M(diars) <sub>2</sub> Cl <sub>2</sub> ] <sup>+</sup>
	7	Pentagonal bipyramidal	[Mn(NO <sub>3</sub> ) <sub>3</sub> (bipy)]	[M(CN) <sub>7</sub> ] <sup>4-</sup>
	11	See Fig. 24.11a	—	[Re(η <sup>5</sup> -C <sub>5</sub> H <sub>5</sub> ) <sub>2</sub> H]
4 (d <sup>3</sup> )	5	—	—	[(Me <sub>3</sub> SiCH <sub>2</sub> ) <sub>4</sub> Re(N <sub>2</sub> )- Re(CH <sub>2</sub> SiMe <sub>3</sub> ) <sub>4</sub> ]
	6	Octahedral	[MnF <sub>6</sub> ] <sup>2-</sup>	[Ml <sub>6</sub> ] <sup>2-</sup>
5 (d <sup>2</sup> )	4	Tetrahedral	[MnO <sub>4</sub> ] <sup>3-</sup>	—
	5	Trigonal bipyramidal (?)	—	ReF <sub>5</sub>
		Square pyramidal	—	[MOCl <sub>4</sub> ] <sup>-</sup>
	6	Octahedral	—	[Tc(NCS) <sub>6</sub> ] <sup>-</sup> , [ReNCl <sub>2</sub> (PEt <sub>2</sub> Ph) <sub>3</sub> ]
6 (d <sup>1</sup> )	8	Dodecahedral	—	[M(diars) <sub>2</sub> Cl <sub>4</sub> ] <sup>+</sup>
	4	Tetrahedral	[MnO <sub>4</sub> ] <sup>2-</sup>	[ReO <sub>4</sub> ] <sup>2-</sup>
	5	Square pyramidal	—	ReOCl <sub>4</sub>
	6	Trigonal prismatic	—	[Re(S <sub>2</sub> C <sub>2</sub> Ph <sub>2</sub> ) <sub>3</sub> ] (see p. 1055)
	6	Octahedral	—	ReF <sub>6</sub>
	8	Dodecahedral	—	[ReMe <sub>8</sub> ] <sup>2-</sup>
		Square antiprismatic	—	[ReF <sub>8</sub> ] <sup>2-</sup>
	4	Tetrahedral	[MnO <sub>4</sub> ] <sup>-</sup>	[MO <sub>4</sub> ] <sup>-</sup>
7 (d <sup>0</sup> )	5	Trigonal bipyramidal	—	[ReO <sub>2</sub> Me <sub>3</sub> ]
	6	Octahedral	—	[ReO <sub>3</sub> Cl <sub>3</sub> ] <sup>2-</sup>
	7	Pentagonal bipyramidal	—	ReF <sub>7</sub>
	9	Tricapped trigonal prismatic	—	[ReH <sub>9</sub> ] <sup>2-</sup>

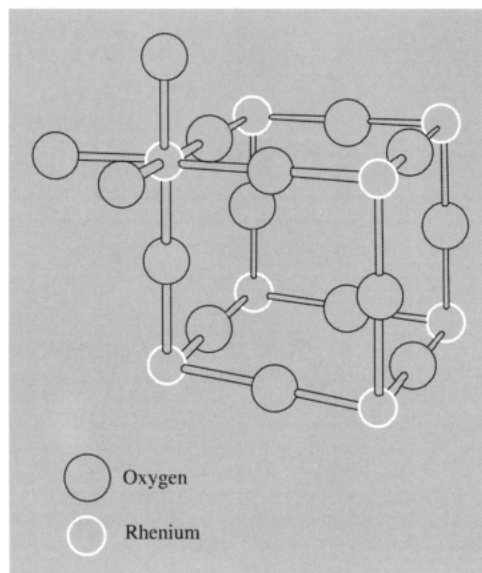
(a) N. H. BUTTRUS, C. EABORN, P. B. HITCHCOCK, J. D. SMITH and A. C. SULLIVAN *J. Chem. Soc., Chem. Commun.* 1380-1 (1985).(b) S.-B. YU and R. H. HOLM, *Polyhedron* **12**, 263-6 (1993).(c) L = 1,4,7,10-tetrakis(pyrazol-1-ylmethyl)-1,4,7,10-tetraazacyclododecane. See M. DI VAIRA, F. MANI and P. STOPPIONI, *J. Chem. Soc., Dalton Trans.*, 1127-30 (1992).

Table 24.4 Oxides of Group 7

Ox. state	+7	+6	+5	+4	+3	+2
Mn	Mn <sub>2</sub> O <sub>7</sub>			MnO <sub>2</sub>	Mn <sub>2</sub> O <sub>3</sub> Mn <sub>3</sub> O <sub>4</sub>	MnO
Tc	Tc <sub>2</sub> O <sub>7</sub>	TcO <sub>3</sub> (?)		TcO <sub>2</sub>		
Re	Re <sub>2</sub> O <sub>7</sub>	ReO <sub>3</sub>	Re <sub>2</sub> O <sub>5</sub>	ReO <sub>2</sub>		

solutions produced by the action of conc H<sub>2</sub>SO<sub>4</sub> on a manganate(VII) salt. On standing, it slowly loses oxygen to form MnO<sub>2</sub> but detonates around 95°C and will explosively oxidize most organic materials. The molecule is composed of 2 corner-sharing MnO<sub>4</sub> tetrahedra with a bent Mn–O–Mn bridge. The liquid solidifies at 5.9°C to give red crystals in which the dimeric units persist with an Mn–O–Mn angle<sup>(4)</sup> of 120.7°. The other 2 heptoxides are yellow solids whose volatility provides a useful means of purifying the elements and, as has been pointed out, is a crucial factor in the commercial production of rhenium (Tc<sub>2</sub>O<sub>7</sub>: mp 119.5°, bp 310.6°; Re<sub>2</sub>O<sub>7</sub>: mp 300.3°, bp 360.3°). In the vapour phase both consist of corner-sharing MO<sub>4</sub> tetrahedra but, whereas this structure is retained in the solid phase by Tc<sub>2</sub>O<sub>7</sub> (linear Tc–O–Tc), solid Re<sub>2</sub>O<sub>7</sub> has an unusual structure consisting of polymeric double layers of corner-sharing ReO<sub>4</sub> tetrahedra alternating with ReO<sub>6</sub> octahedra. The same basic unit, though this time discrete, is found in the dihydrate which is therefore best formulated as [O<sub>3</sub>Re–O–ReO<sub>3</sub>(H<sub>2</sub>O)<sub>2</sub>] and is obtained by careful evaporation of an aqueous solution of the heptoxide. The structure breaks down, however, if the solution is kept for a period of months. Crystals of perrhenic acid monohydrate, HReO<sub>4</sub>·H<sub>2</sub>O, are deposited and consist of fairly regular ReO<sub>4</sub><sup>−</sup> tetrahedra and H<sub>3</sub>O<sup>+</sup> ions linked by hydrogen bridges.<sup>(5)</sup>

Only rhenium forms a stable trioxide. It is a red solid with a metallic lustre and is obtained by the reduction of Re<sub>2</sub>O<sub>7</sub> with CO. ReO<sub>3</sub> has a structure in which each Re is



**Figure 24.2** The structure of ReO<sub>3</sub>. Note the similarity to perovskite (p. 963) which can be understood as follows: if the Re atom, which is shown here with its full complement of 6 surrounding O atoms, is imagined to be the small cation at the centre of Fig. 21.3(a), then the perovskite structure is obtained by placing the large cations (Ca<sup>II</sup>) into the centre of the cube drawn above and in the 7 other equivalent positions around the Re.

octahedrally surrounded by oxygens (Fig. 24.2). It has an extremely low electrical resistivity which decreases with decrease in temperature like a true metal:  $\rho_{300\text{K}} 10 \mu\text{ohm cm}$ ,  $\rho_{100\text{K}} 0.6 \mu\text{ohm cm}$ . It is clear that the single valency electron on each Re atom is delocalized in a conduction band of the crystal. ReO<sub>3</sub> is unreactive towards water and aqueous acids and alkalis, but when boiled with conc alkali it disproportionates into ReO<sub>4</sub><sup>−</sup> and ReO<sub>2</sub>. A blue pentoxide Re<sub>2</sub>O<sub>5</sub> has been reported but is also prone to disproportionation into +7 and +4 species.

The +4 oxidation state is the only one in which all three elements form stable oxides, but only in the case of technetium is this the most stable oxide. TcO<sub>2</sub> is the final product when any Tc/O

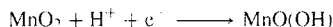
<sup>4</sup> R. DRONSKOWSKI, B. KREBS, A. SIMON, G. MILLER and B. HETTICH, *Z. anorg. allg. Chem.* **558**, 7–20 (1988).

<sup>5</sup> G. WLTSCHEK, I. SVOBODA and H. FUESS, *Z. anorg. allg. Chem.* **619**, 1679–81 (1993).

### Applications of Manganese Dioxide<sup>(6)</sup>

Although the primary use of manganese is in the production of steel it also finds widespread and important uses in non-metallurgical industries. These frequently use the manganese as MnO<sub>2</sub> but even where this is not the case the dioxide is invariably the starting material.

The largest non-metallurgical use of MnO<sub>2</sub> is in the manufacture of dry-cell batteries (p. 1204) which accounts for about half a million tonnes of ore annually. The most common dry batteries are of the carbon-zinc Leclanché type in which carbon is the positive pole. MnO<sub>2</sub> is incorporated as a depolarizer to prevent the undesirable liberation of hydrogen gas on to the carbon, probably by the reaction



Only the highest quality MnO<sub>2</sub> ore can be used directly for this purpose, and "synthetic dioxide", usually produced electrolytically by anodic oxidation of manganese(II) sulfate, is increasingly employed.

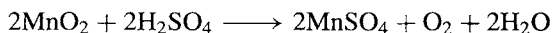
The brick industry is another major user of MnO<sub>2</sub> since it can provide a range of red to brown or grey tints. In the manufacture of glass its use as a decolourizer (hence "glassmaker's soap") is its most ancient application. Glass always contains iron at least in trace amounts, and this imparts a greenish colour; the addition of MnO<sub>2</sub> to the molten glass produces red-brown Mn<sup>III</sup> which equalizes the absorption across the visible spectrum so giving a "colourless", i.e. grey glass. In recent times selenium compounds have replaced MnO<sub>2</sub> for this application, but in larger proportions the latter is still used to make pink to purple glass.

The oxidizing properties of MnO<sub>2</sub> are utilized in the oxidation of aniline for the preparation of hydroquinone which is important as a photographic developer and also in the production of dyes and paints.

In the electronics industry the advantages of higher electrical resistivity and lower cost of ceramic ferrites (M<sup>II</sup>Fe<sub>2</sub>O<sub>4</sub>) (p. 1081) over metallic magnets have been recognized since the 1950s and the "soft" ferrites (M<sup>II</sup> = Mn, Zn) are the most common of these. They are used on the sweep transformer and deflection yoke of a television set and, of course, MnO<sub>2</sub>, either natural or synthetic, is required in their production.

system is heated to high temperatures, but ReO<sub>2</sub> disproportionates at 900°C into Re<sub>2</sub>O<sub>7</sub> and the metal. Hydrated TcO<sub>2</sub> and ReO<sub>2</sub> may be conveniently prepared by reduction of aqueous solutions of MO<sub>4</sub><sup>-</sup> with zinc and hydrochloric acid and are easily dehydrated. TcO<sub>2</sub> is dark brown and ReO<sub>2</sub> is blue-black: both solids have distorted rutile structures like MoO<sub>2</sub> (p. 1008).

It is MnO<sub>2</sub>, however, which is by far the most important oxide in this group, though it is not the most stable oxide of manganese, decomposing to Mn<sub>2</sub>O<sub>3</sub> above about 530°C and being a useful oxidizing agent. Hot concentrated sulfuric and hydrochloric acids reduce it to manganese(II):



the latter reaction being formerly the basis of the manufacture of chlorine. It is, however, extremely insoluble and, as a consequence, often unreactive. As pyrolusite it is the most plentiful ore of

manganese and it finds many industrial uses (see Panel).

The structural history of MnO<sub>2</sub> is complex and confused due largely to the prevalence of nonstoichiometry and the fact that in its hydrated forms it behaves as a cation-exchanger. Many of the various polymorphs which have been reported are probably therefore simply impure forms. The only stoichiometric form is the so-called β-MnO<sub>2</sub>, which is that of pyrolusite and possesses the rutile structure (p. 961), but even here a range of composition from MnO<sub>1.93</sub> to MnO<sub>2.0</sub> is possible. β-MnO<sub>2</sub> can be prepared by careful decomposition of manganese(II) nitrate but, when precipitated from aqueous solutions, for instance by reduction of alkaline MnO<sub>4</sub><sup>-</sup>, the hydrated MnO<sub>2</sub> has a more open structure which exhibits cation-exchange properties and cannot be fully dehydrated without some loss of oxygen.

Apart from the black Re<sub>2</sub>O<sub>3</sub>·2H<sub>2</sub>O (which is readily oxidized to the dioxide and is prepared by boiling ReCl<sub>3</sub> in air-free water) oxides of oxidation states below +4 are known only for manganese. Mn<sub>3</sub>O<sub>4</sub> is formed when any

<sup>6</sup> *Ulmann's Encyclopedia of Industrial Chemistry*, Vol. A16, pp. 123-43, VCH, Weinheim, 1990.

oxide of manganese is heated to about 1000°C in air and is the black mineral, hausmannite. It has the spinel structure (p. 247) and as such is appropriately formulated as  $\text{Mn}^{\text{II}}\text{Mn}^{\text{III}}\text{O}_4$ , with  $\text{Mn}^{\text{II}}$  and  $\text{Mn}^{\text{III}}$  occupying tetrahedral and octahedral sites respectively within a ccp lattice of oxide ions; there is, however, a tetragonal distortion due to a Jahn–Teller effect (p. 1021) on  $\text{Mn}^{\text{III}}$ . A related structure, but with fewer cation sites occupied, is found in the black  $\gamma$ - $\text{Mn}_2\text{O}_3$  which can be prepared by aerial oxidation and subsequent dehydration of the hydroxide precipitated from aqueous  $\text{Mn}^{\text{II}}$  solutions. If  $\text{MnO}_2$  is heated less strongly (say <800°C) than is required to produce  $\text{Mn}_3\text{O}_4$ , then the more stable  $\alpha$ -form of  $\text{Mn}_2\text{O}_3$  results which has a structure involving 6-coordinate Mn but with 2 Mn–O bonds longer than the other 4. This is no doubt a further manifestation of the Jahn–Teller effect expected for the high-spin  $d^4$   $\text{Mn}^{\text{III}}$  ion and is presumably the reason why  $\text{Mn}_2\text{O}_3$ , alone among the oxides of transition metal  $\text{M}^{\text{III}}$  ions, does not have the corundum (p. 242) structure.

Reduction with hydrogen of any oxide of manganese produces the lowest oxide, the grey to green MnO. This is an entirely basic oxide, dissolving in acids and giving rise to the aqueous  $\text{Mn}^{\text{II}}$  cationic chemistry. It has a rock-salt structure and is subject to nonstoichiometric variation ( $\text{MnO}_{1.00}$  to  $\text{MnO}_{1.045}$ ), but its main interest is that it is a classic example of an antiferromagnetic compound. If the temperature is reduced below about 118 K (its Néel point), a rapid fall in magnetic moment takes place as the electron spins on adjacent Mn atoms pair-up. This is believed to take place by the process of “superexchange” by which the interaction is transferred through intervening, non-magnetic, oxide ions. ( $\text{MnO}_2$  is also antiferromagnetic below 92 K whereas the alignment in  $\text{Mn}_3\text{O}_4$  results in ferrimagnetism below 43 K.)

The sulfides are fewer and less familiar than the oxides but, as is to be expected, favour lower oxidation states of the metals. Thus manganese forms  $\text{MnS}_2$  which has the pyrite structure (p. 680) with discrete  $\text{Mn}^{\text{II}}$  and  $\text{S}_2^{-\text{II}}$  ions and is converted on heating to MnS and

sulfur. This green MnS is the most stable manganese sulfide and, like MnO, has a rock-salt structure and is strongly antiferromagnetic ( $T_N - 121^\circ\text{C}$ ). Less-stable red forms are also known and the pale-pink precipitate produced when  $\text{H}_2\text{S}$  is bubbled through aqueous  $\text{Mn}^{\text{II}}$  solutions is a hydrated form which passes very slowly into the green variety. The corresponding selenides are very similar:  $\text{Mn}^{\text{II}}\text{Se}_2$  (pyrite-type), and  $\text{MnSe}$  (NaCl-type), antiferromagnetic with  $T_N - 100^\circ\text{C}$ .

Technetium and rhenium favour higher oxidation states in their binary chalcogenides. Both form black diamagnetic heptasulfides,  $\text{M}_2\text{S}_7$ , which are isomorphous and which decompose to  $\text{M}^{\text{IV}}\text{S}_2$  and sulfur on being heated. These disulfides, unlike the pyrite-type  $\text{Mn}^{\text{II}}\text{S}_2$ , contain monatomic  $\text{S}^{-\text{II}}$  units. The diselenides are similar.  $\text{TcS}_2$ ,  $\text{TcSe}_2$  and  $\text{ReS}_2$  feature trigonal prismatic coordination of  $\text{M}^{\text{IV}}$  by S (or Se) in a layer-lattice structure which is isomorphous with a rhombohedral polymorph of  $\text{MoS}_2$ .  $\text{ReSe}_2$  also has a layer structure but the  $\text{Re}^{\text{IV}}$  atoms are octahedrally coordinated.

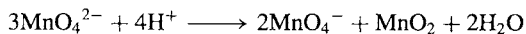
Lower formal oxidation states are stabilized, however, by M–M bonding in ternary chalcogenides such as  $\text{M}_4^{\text{I}}\text{M}_6\text{Q}_{12}$ ,  $\text{M}_4^{\text{I}}\text{M}_6\text{Q}_{13}$  ( $\text{M}^{\text{I}}$  = alkali metal;  $\text{M} = \text{Re}, \text{Tc}$ ;  $\text{Q} = \text{S}, \text{Se}$ ) and the recently reported<sup>(7)</sup>  $\text{M}_{10}^{\text{I}}\text{M}_6\text{S}_{14}$ . Their structures are all based on the face-capped, octahedral  $\text{M}_6\text{X}_8$  cluster unit found in Chevrel phases (p. 1018) and in the dihalides of Mo and W (p. 1022).

### 24.3.2 Oxoanions

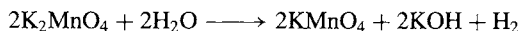
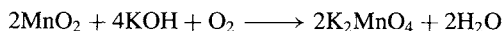
The lower oxides of manganese are basic and react with aqueous acids to give salts of  $\text{Mn}^{\text{II}}$  and  $\text{Mn}^{\text{III}}$  cations. The higher oxides, on the other hand, are acidic and react with alkalis to yield oxoanion salts, but the polymerization which was such a feature of the chemistry of the preceding group is absent here.

<sup>7</sup> W. BRONGER, M. KANERT, M. LOVENICH and D. SCHMITZ, *Z. anorg. allg. Chem.* **619**, 2015–20 (1993).

Fusion of  $\text{MnO}_2$  with an alkali metal hydroxide and an oxidizing agent such as  $\text{KNO}_3$  produces very dark-green manganate(VI) salts (manganates) which are stable in strongly alkaline solution but which disproportionate readily in neutral or acid solution (see Fig. 24.1):

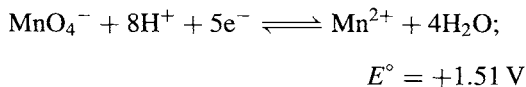


The deep-purple manganate(VII) salts (permanganates) may be prepared in aqueous solution by oxidation of manganese(II) salts with very strong oxidizing agents such as  $\text{PbO}_2$  or  $\text{NaBiO}_3$ . They are manufactured commercially by alkaline oxidative fusion of  $\text{MnO}_2$  followed by the electrolytic oxidation of manganate(VI):

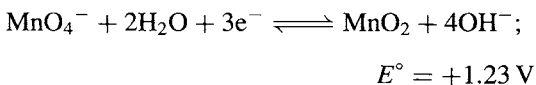


The most important manganate(VII) is  $\text{KMnO}_4$  of which several tens of thousands of tonnes are produced annually. It is a well-known oxidizing agent, used analytically:

in acid solution:



in alkaline solution:



It is also important as an oxidizing agent in the industrial production of saccharin and benzoic acid, and medically as a disinfectant. It is increasingly being used also for purifying water, since it has the dual advantage over chlorine that it does not affect the taste, and the  $\text{MnO}_2$  produced acts as a coagulant for colloidal impurities.

Reduction of  $\text{KMnO}_4$  with aqueous  $\text{Na}_2\text{SO}_3$  produces the bright-blue tetraoxomanganate(V) (hypomanganate),  $\text{MnO}_4^{3-}$ , which has also been postulated as a reaction intermediate in some organic oxidations; it is not stable, being prone to disproportionation.

All  $[\text{MnO}_4]^{n-}$  ions are tetrahedral with  $\text{Mn}-\text{O}$  162.9 pm in  $\text{MnO}_4^-$  and 165.9 pm in  $\text{MnO}_4^{2-}$ .  $\text{K}_2\text{MnO}_4$  is isomorphous with  $\text{K}_2\text{SO}_4$  and  $\text{K}_2\text{CrO}_4$ . By contrast, the only tetrahedral oxoanions of Tc and Re are the tetraoxotechnetate(VII) (pertechnetate) and tetraoxorhenate(VII) (perrhenate) ions.  $\text{HTcO}_4$  and  $\text{HReO}_4$  are strong acids like  $\text{HMnO}_4$  and are formed when the heptoxides are dissolved in water. From such solutions dark-red crystals with the composition  $\text{HTcO}_4$  in the case of technetium and, in the case of rhenium, yellowish crystals of  $\text{Re}_2\text{O}_7 \cdot 2\text{H}_2\text{O}$  or  $\text{HReO}_4 \cdot \text{H}_2\text{O}$  (p. 1047) can be obtained.

$[\text{TcO}_4]^-$  and  $[\text{ReO}_4]^-$  provide the starting point for virtually all the Tc and Re chemistry. They are produced whenever compounds of Tc and Re are treated with oxidizing agents such as nitric acid or hydrogen peroxide and, although reduced in aqueous solution by, for instance,  $\text{Sn}^{\text{II}}$ ,  $\text{Fe}^{\text{II}}$ ,  $\text{Ti}^{\text{III}}$  and  $\text{I}^-$ , they are much weaker oxidizing agents than  $[\text{MnO}_4]^-$ . In further contrast to  $[\text{MnO}_4]^-$  they are also stable in alkaline solution and are colourless whereas  $[\text{MnO}_4]^-$  is an intense purple. In fact, the absorption spectra of the 3  $[\text{MO}_4]^{-1}$  ions are very similar, arising in each case from charge transfer transitions between  $\text{O}^{2-}$  and  $\text{M}^{\text{VII}}$ , but the energies of these transitions reflect the relative oxidizing properties of  $\text{M}^{\text{VII}}$ . Thus the intense colour of  $[\text{MnO}_4]^-$  arises because the absorption occurs in the visible region, whereas for  $[\text{ReO}_4]^-$  it has shifted to the more energetic ultraviolet, and the ion is therefore colourless.  $[\text{TcO}_4]^-$  is also normally colourless but the absorption starts on the very edge of the visible region and it may be that the red colour of crystalline  $\text{HTcO}_4$ , and other transient red colours which have been reported in some of its reactions, are due to slight distortions of the ion from tetrahedral symmetry causing the absorption to move sufficiently for it to "tail" into the blue end of the visible, thereby imparting a red coloration.  $[\text{MO}_4]^-$  ions might be expected to act as Lewis bases (cf  $\text{ClO}_4^-$  p. 868) and, indeed, several mono- and bis-  $[\text{ReO}_4]^-$  complexes with  $\text{Co}^{\text{II}}$ ,  $\text{Ni}^{\text{II}}$  and  $\text{Cu}^{\text{II}}$  have been



Table 24.5 Halides of Group 7

Oxidation state	Fluorides	Chlorides	Bromides	Iodides
+7	ReF <sub>7</sub> yellow mp 48.3°, bp 73.7°			
+6	TcF <sub>6</sub> yellow mp 37.4°, bp 55.3° ReF <sub>6</sub> yellow mp 18.5°, bp 33.7°	TcCl <sub>6</sub> green mp 25° ReCl <sub>6</sub> red-green mp 29° (dichroic)		
+5	TcF <sub>5</sub> yellow mp 50°, bp (d) ReF <sub>5</sub> yellow-green mp 48°, bp(extrap) 221°	— ReCl <sub>5</sub> brown-black mp 220°	ReBr <sub>5</sub> dark brown (d 110°)	
+4	MnF <sub>4</sub> blue (d above rt) — ReF <sub>4</sub> blue (subl >300°)	— TcCl <sub>4</sub> red (subl >300°) ReCl <sub>4</sub> purple-black (d 300°)	— (?TcBr <sub>4</sub> ) (red-brown) ReBr <sub>4</sub> dark red	ReI <sub>4</sub> black (d above rt)
+3	MnF <sub>3</sub> red-purple —	— [ReCl <sub>3</sub> ] <sub>3</sub> dark red (subl 500°) (d)	— [ReBr <sub>3</sub> ] <sub>3</sub> red-brown	— [ReI <sub>3</sub> ] <sub>3</sub> lustrous black (d on warming)
+2	MnF <sub>2</sub> pale pink mp 920°	MnCl <sub>2</sub> pink mp 652°, bp ~1200°	MnBr <sub>2</sub> rose mp 695°	MnI <sub>2</sub> pink mp 613°

characterized, and both unidentate and bridging modes identified.<sup>(8)</sup>

Fusion of rhenates(VII) with a basic oxide yields so-called ortho- and meso-perrhenates (M<sub>5</sub>ReO<sub>6</sub> and M<sub>3</sub>ReO<sub>5</sub>, M = Na,  $\frac{1}{2}$ Ca, etc.) while addition of rhenium metal to the fusion (and exclusion of oxygen) produces rhenate(VI) (e.g. Ca<sub>3</sub>ReO<sub>6</sub>). There is evidence suggesting the existence of [ReO<sub>6</sub>]<sup>5-</sup> and [ReO<sub>6</sub>]<sup>6-</sup> but it may be better to regard all these compounds as mixed oxides. In any case, it is clear that the coordination sphere of the metal has

expanded compared to that of the smaller Mn in the tetrahedral [MnO<sub>4</sub>]<sup>n-</sup> ions. Comparable technetium compounds have also been prepared.

### 24.3.3 Halides and oxohalides

The known halides and oxohalides of this group are listed in Tables 24.5 and 24.6 respectively.

The highest halide of each metal is of course a fluoride: ReF<sub>7</sub> (the only thermally stable heptahalide of a transition metal), TcF<sub>6</sub>, and MnF<sub>4</sub>. This again indicates the diminished ability of manganese to attain high oxidation states when compared not only to Tc and Re but also to

<sup>8</sup> M. C. CHAKRAVORTY, *Coord. Chem. Revs.* **106**, 205–25 (1990).

Table 24.6 Oxohalides of Group 7

Oxidation state		Fluorides		Chlorides	Bromides
+7	—	—	MnO <sub>3</sub> F dark green mp -78°, bp(extrap) 60°	MnO <sub>3</sub> Cl vol green liq	—
	—	—	TcO <sub>3</sub> F yellow mp 18.3°, bp ~100°	TcO <sub>3</sub> Cl colourless	—
+6	ReOF <sub>5</sub> cream mp 43.8°, bp 73.0°	ReO <sub>2</sub> F <sub>2</sub> yellow mp 90°, bp 185°	ReO <sub>3</sub> F yellow mp 147°, bp 164°	ReO <sub>3</sub> Cl colourless mp 4.5°, bp 130°	ReO <sub>3</sub> Br colourless mp 39.5°
	—	—	—	MnO <sub>2</sub> Cl <sub>2</sub> vol brown liq	—
+5	TcOF <sub>4</sub> blue mp 134° bp(extrap) 165°	—	—	TcOCl <sub>4</sub> blue	—
	ReOF <sub>4</sub> blue mp 108°, bp 171°	—	—	ReOCl <sub>4</sub> brown mp 30°, bp(extrap) 228°	ReOBr <sub>4</sub> blue
	—	—	—	MnOCl <sub>3</sub> vol liq	—
+5	—	—	—	TcOCl <sub>3</sub>	TcOBr <sub>3</sub> black
	ReOF <sub>3</sub> black	—	—	—	—

chromium, which forms CrF<sub>5</sub> and CrF<sub>6</sub>. The most interesting of the lower halides are the rhenium trihalides which exist as trimeric clusters which persist throughout much of the chemistry of Re<sup>III</sup>.

Apart from ReF<sub>5</sub>, which is produced when ReF<sub>6</sub> is reduced by tungsten wire at 600°C, all the known penta-, hexa- and hepta- halides of Re and Tc can be prepared directly from the elements by suitably adjusting the temperature and pressure, although various specific methods have been suggested. They are volatile solids varying in colour from pale yellow (ReF<sub>7</sub>) to dark brown (ReBr<sub>5</sub>), and are readily hydrolysed by water with accompanying disproportionation into the comparatively more stable [MO<sub>4</sub>]<sup>-</sup> and MO<sub>2</sub>, e.g.:



Because of the tendency to produce mixtures of the halides, and the facile formation of oxohalides if air and moisture are not rigorously excluded (or even, in some cases, also by attacking glass), not all of these halides have been characterized as well as might be desired. There is spectroscopic evidence that ReF<sub>7</sub> has a pentagonal bipyramidal structure, and ReX<sub>6</sub> are probably octahedral. ReCl<sub>5</sub> is actually a dimer, Cl<sub>4</sub>Re(μ-Cl)<sub>2</sub>ReCl<sub>4</sub>, in which the rhenium is octahedrally coordinated.

The tetrahalides are made by a variety of methods. MnF<sub>4</sub>, being the highest halide formed by Mn, can be prepared directly from the elements, as can TcCl<sub>4</sub>, which is the only thermally stable chloride of Tc. TcCl<sub>4</sub> is a red sublimable solid consisting of infinite chains of edge-sharing TcCl<sub>6</sub> octahedra. By contrast the

black  $\text{ReCl}_4$ , which is prepared by heating  $\text{ReCl}_3$  and  $\text{ReCl}_5$  in a sealed tube at  $300^\circ\text{C}$ , is made up of pairs of  $\text{ReCl}_6$  octahedra which share faces (as in  $[\text{W}_2\text{Cl}_9]^{3-}$ , p. 1021), these dimeric units then being linked in chains by corner-sharing. The closeness of the Re atoms in each pair (273 pm) is indicative of a metal–metal bond though not so pronounced as the more extensive metal–metal bonding found in  $\text{Re}^{\text{III}}$  chemistry.

$\text{MnF}_3$  is a red-purple, reactive, but thermally stable solid; it is prepared by fluorinating any of the  $\text{Mn}^{\text{II}}$  halides and its crystal lattice consists of  $\text{MnF}_6$  octahedra which are distorted, presumably because of the Jahn–Teller effect expected for  $d^4$  ions. The  $\text{Re}^{\text{III}}$  halides are obtained by thermal decomposition of  $\text{ReCl}_5$ ,  $\text{ReBr}_5$  and  $\text{ReI}_4$ . The dark-red chloride is composed of triangular clusters of chloride-bridged Re atoms with 1 of the 2 out-of-plane Cl on each Re bridging to adjacent trimeric clusters (Fig. 24.3). After allowing for the Re–Cl bonds, each  $\text{Re}^{\text{III}}$  has a  $d^4$  configuration and the observed diamagnetism can be accounted for by assuming that these four d electrons on each Re are used in forming

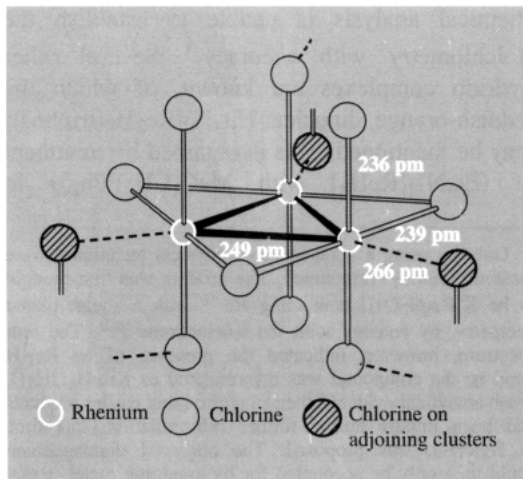
double bonds ( $\sigma + \pi$ ) to its 2 Re neighbours. The Re–Re distance of 249 pm is consistent with this (cf. 275 pm in Re metal).  $\text{Re}_3\text{Cl}_9$  can be sublimed under vacuum but the green colour of the vapour probably indicates breakdown of the cluster in the vapour phase. The compound dissolves in water to give a red solution which slowly hydrolyses to hydrated  $\text{Re}_2\text{O}_3$ , and in conc hydrochloric acid it gives a red solution which is stable to oxidation and from which can be precipitated hydrates of  $\text{Re}_3\text{Cl}_9$  and a number of complex chlorides in which the trimeric clusters persist.<sup>(9)</sup>

$\text{Re}_3\text{Br}_9$  is similar to  $\text{Re}_3\text{Cl}_9$  but the iodide, which is a black solid and is similarly trinuclear, differs in that it is thermally less stable and only 2 Re atoms in each cluster are linked to adjacent clusters, thereby forming infinite chains of trimeric units rather than planar networks.

Except for the possible existence of  $\text{ReI}_2$ , the only simple dihalides of this group that are known (so far) are those of manganese. They are pale-pink salts obtained by simply dissolving the metal or carbonate in aqueous HX.  $\text{MnF}_2$  is insoluble in water and forms no hydrate, but the others form a variety of very water-soluble hydrates of which the tetrahydrates are the most common.

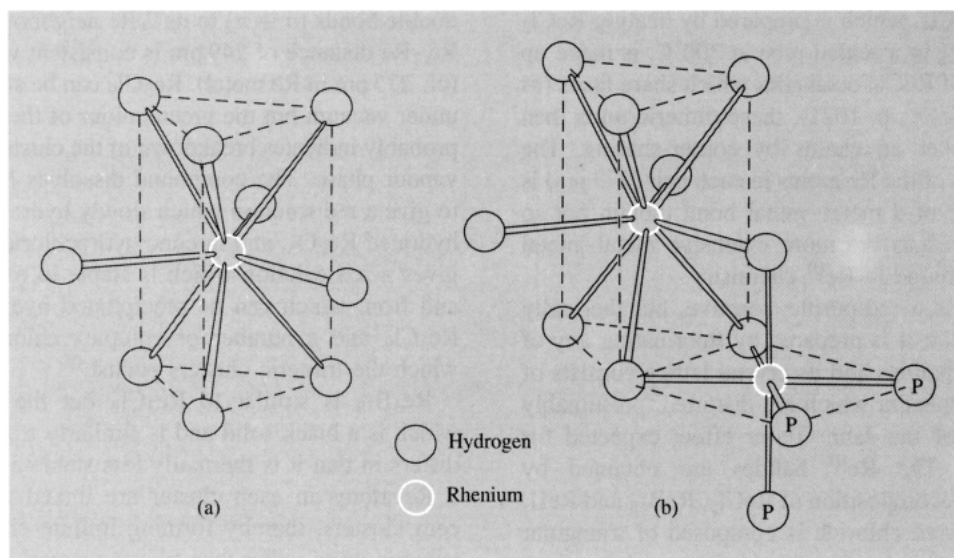
The oxohalides of manganese are green liquids (except  $\text{MnO}_2\text{Cl}_2$  which is brown); they are notable for their explosive instability.  $\text{MnO}_3\text{F}$  can be prepared by treating  $\text{KMnO}_4$  with fluorosulfuric acid,  $\text{HSO}_3\text{F}$ , whereas reaction of  $\text{Mn}_2\text{O}_7$  with chlorosulfuric acid yields  $\text{MnO}_3\text{Cl} + \text{MnO}_2\text{Cl}_2 + \text{MnOCl}_3$ .

The oxohalides of technetium and rhenium are more numerous than those of manganese and are not so unstable, although all of them readily hydrolyse (with dis-proportionation to  $[\text{MO}_4]^-$  and  $\text{MO}_2$  in the case of oxidation states +5 and +6). In this respect they may be regarded as being intermediate between the halides and the oxides which, in the higher oxidation states, are the more stable. Treatment of the oxides with the halogens, or the halides with oxygen are common preparative methods. The structures are not all



**Figure 24.3** Idealized structure of  $\text{Re}_3\text{Cl}_9$ ; in crystalline  $\text{ReCl}_3$  the trimeric units are linked into planar hexagonal networks. The coordination sites occupied by Cl from adjoining clusters can readily be occupied by a variety of other ligands instead.

<sup>9</sup> M. IRMLER and G. MEYER, *Z. anorg. allg. Chem.* **581**, 104–10 (1990); B. JUNG, G. MEYER and E. HERDTWECK, *ibid.* **604**, 27–33 (1991).



**Figure 24.4** (a) The tricapped trigonal prismatic structure of the  $[\text{ReH}_9]^{2-}$  anion. (b)  $[\text{Re}_2(\mu\text{-H})_3\text{H}_6\text{MeC}(\text{CH}_2\text{-PPh}_2)_3]^-$ . For clarity, only the P atoms of the triphos ligand are shown.

known with certainty, but  $\text{ReOCl}_4$  may be noted as an example of a square-pyramidal structure.

### 24.3.4 Complexes of manganese, technetium and rhenium<sup>(3,10,11)</sup>

#### Oxidation state VII ( $d^0$ )

The coordination chemistry of this oxidation state is confined mainly to a few readily hydrolysed oxohalide complexes of Re such as  $\text{KReO}_2\text{F}_4$ . Exceptions to this limitation are provided by the isomorphous hydrides  $\text{K}_2\text{MH}_9$  of Tc and Re which formally involve  $\text{M}^{\text{VII}}$  and  $\text{H}^-$ . The rhenium analogue was the first to be prepared as the colourless, diamagnetic product of the reduction of  $\text{KReO}_4$  by potassium in aqueous diaminoethane (ethylenediamine). The

elucidation of its structure (Fig. 24.4a) illustrates vividly the problems associated with identifying a novel compound when its isolation in a pure form is difficult and when conventional chemical analysis is unable to establish the stoichiometry with accuracy.<sup>†</sup> Several other hydrido complexes are known, of which the reddish-orange, dinuclear  $(\text{Et}_4\text{N})[\text{Re}_2\text{H}_9(\text{triphos})]$  may be mentioned. This is obtained by treatment of  $(\text{Et}_4\text{N})_2[\text{ReH}_9]$  with  $\text{MeC}(\text{CH}_2\text{PPh}_2)_3$  in

<sup>†</sup> Only by using a wide range of physical techniques were these difficulties surmounted. The product was first thought to be  $\text{K}[\text{Re}(\text{H}_2\text{O})_4]$  containing  $\text{Re}^{-1}$  with a square-planar geometry, by analogy with the isoelectronic  $\text{Pt}^{\text{II}}$ . The nmr spectrum, however, indicated the presence of an  $\text{Re-H}$  bond so the compound was reformulated as  $\text{KReH}_4 \cdot 2\text{H}_2\text{O}$ . Fresh analytical evidence then suggested that earlier products had been impure and a further reformulation, this time as  $\text{K}_2\text{ReH}_8$ , was proposed. The observed diamagnetism could then only be accounted for by assuming metal-metal bonding between the implied  $d^1$  rhenium(VI) atoms, but X-ray analysis showing the Re atoms to be 550 pm apart, precluded this possibility. The problem was finally resolved when a neutron diffraction study established the formula as  $\text{K}_2\text{ReH}_9$  and the structure is tricapped trigonal prismatic. The nmr spectrum actually shows only one proton signal in spite of the existence of distinct capping and prismatic protons, and this is thought to be due to rapid exchange between the sites.

<sup>10</sup> B. CHISWELL, E. D. MCKENZIE and L. F. LINDOY, *Manganese*, Chap. 41, pp. 1–122; K. A. CONNER and R. A. WALTON, *Rhenium*, Chap. 43, pp. 125–213 in *Comprehensive Coordination Chemistry*, Vol. 4, Pergamon Press, Oxford, 1987.

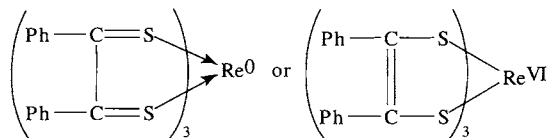
<sup>11</sup> J. BALDAS, *Adv. Inorg. Chem.* **41**, 2–123 (1994) and F. TISATO, F. REFOSCO and G. BANDOLI, *Coord. Chem. Revs.* **135/136**, 325–97 (1994) are devoted to technetium.

MeCN. The structure of the anion (Fig 24.4b) can be envisaged as a tridentate  $[\text{ReH}_9]^{2-}$  ligand coordinated to  $\text{Re}(\text{triphos})^+$ , and, since the metal atoms are only 259.4 pm apart, is said to involve an  $\text{Re}\equiv\text{Re}$  triple bond<sup>(12)</sup> (in which case the  $[\text{ReH}_9]^{2-}$  should be regarded as tetradentate and its Re atom as 10-coordinated).

### Oxidation state VI ( $d^1$ )

Again, fluoro and oxo complexes of rhenium predominate. The reaction of KF and  $\text{ReF}_6$  in an inert PTFE vessel yields pink  $\text{K}_2[\text{ReF}_8]$ , the anion of which has a square-prismatic structure; hydrolysis converts it to  $\text{K}[\text{ReOF}_5]$ .

An interesting compound which is usually included in discussions of  $\text{Re}^{\text{VI}}$  chemistry is the green crystalline dithiolate,  $[\text{Re}(\text{S}_2\text{C}_2\text{Ph}_2)_3]$ . This was the first authenticated example of a trigonal prismatic complex (Fig. 19.6, p. 915) but besides its structural interest it has, along with other complexes of such ligands, posed problems regarding the oxidation state of the metal. The ligand may be thought to coordinate in either of two extreme ways (or some intermediate state between them):



The difference between the two extremes is essentially that, in the former, the Re retains its valence electrons in its d orbitals whereas in the latter it loses 6 of them to delocalized ligand orbitals. In either case paramagnetism is anticipated since rhenium has an odd number of valence electrons. The magnetic moment of 1.79 BM corresponding to 1 unpaired electron, and esr evidence showing that this electron is situated predominantly on the ligands, indicates that an intermediate oxidation state is involved

<sup>12</sup> S. C. ABRAHAMS, A. P. GINSBERG, T. F. KOETZLE, P. MARSH and C. R. SPRINKLE, *Inorg. Chem.* **25**, 2500–10 (1986).

but does not specify which one. Because of this uncertainty, dithiolate ligands, and others like them, have been expressively termed “non-innocent” ligands by C. K. Jørgensen.<sup>(13)</sup>

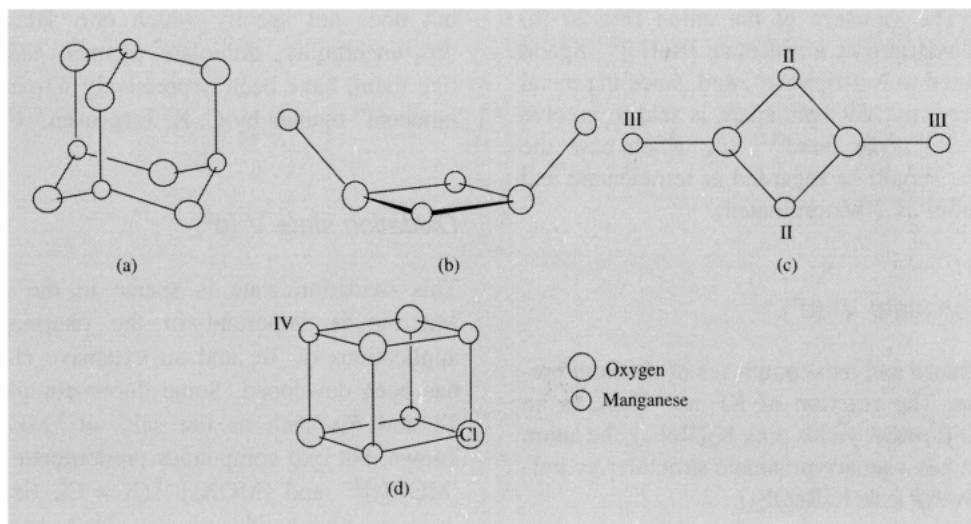
### Oxidation state V ( $d^2$ )

This oxidation state is sparse in the case of Mn but is important in the pharmaceutical applications of Tc, and an extensive chemistry has been developed. Some fluoro complexes of Tc and Re such as the salts of  $[\text{MF}_6]^-$  are known, but oxo compounds predominate and, in  $[\text{MOC}_5]^{2-}$  and  $[\text{MOX}_4]^-$  ( $\text{X} = \text{Cl}, \text{Br}, \text{I}$ ) for instance, other halides are also able to coordinate.  $[\text{MOX}_4]^-$  is square pyramidal with apical  $\text{M}=\text{O}$  and the  $\text{MO}^{3+}$  moiety is reminiscent of  $\text{VO}^{2+}$ , being found in other compounds (particularly those containing phosphines) and labilizing whatever ligand is *trans* to it. The ir stretching frequency of the  $\text{M}=\text{O}$  bond is conveniently used for its detection, lying in the range  $890\text{--}1020\text{ cm}^{-1}$  for  $\text{Tc}=\text{O}$  and generally about  $20\text{ cm}^{-1}$  lower for  $\text{Re}=\text{O}$ . The  $\text{M}\equiv\text{N}$  group also stabilizes the oxidation state, probably because the  $\pi$  bonds are able to reduce the charge on the  $\text{M}^{\text{V}}$ ; it is found in compounds such as  $[\text{MNX}_2(\text{PR}_3)_3]$  and  $[\text{MNX}_2(\text{PR}_3)_2]$  ( $\text{X} = \text{Cl}, \text{Br}, \text{I}$ ) produced when  $[\text{MO}_4]^-$  is reduced by hydrazine in the presence of appropriate ligands, of which phosphines are especially useful.<sup>(14)</sup> The ir stretching frequency is again of diagnostic value being found in the approximate range of  $1050\text{--}1100\text{ cm}^{-1}$  for  $\text{Tc}\equiv\text{N}$  and  $20\text{ cm}^{-1}$  or so lower for  $\text{Re}\equiv\text{N}$ . Eight-coordinate and probably dodecahedral  $[\text{ReCl}_4(\text{diars})_2]\text{ClO}_4$  has been prepared and the Tc analogue is notable as the first example of 8-coordinate technetium.

<sup>13</sup> C. K. JØRGENSEN, *Oxidation Numbers and Oxidation States*, Springer-Verlag, Berlin, 1969, 291 pp.

<sup>14</sup> For other  $\text{Tc}\equiv\text{N}$  compounds see for instance: G. A. WILLIAMS and J. BALDAS, *Aust. J. Chem.* **42**, 875–84 (1989); C. M. ARCHER, J. R. DILWORTH, J. D. KELLY and M. MCPARTLIN, *Polyhedron* **8**, 1879–81 (1989).





**Figure 24.5** Cores of some  $Mn_4$  complexes. (a) Adamantane  $\{Mn_4^{IV}O_6\}$  in  $[Mn_4O_6(tacn)_4]^{4+}$ . (b) Butterfly  $\{Mn_2^{III}O_2\}$  in  $[Mn_4O_2(MeCOO)_7(bipy)_2]^+$ . (c) Planar  $\{Mn_2^{II}Mn_2^{III}O_2\}$  in  $[Mn_4O_2(MeCOO)_6(bipy)_2]$ . (d) Cubane  $\{Mn_3^{III}Mn^{IV}O_3Cl\}$  in  $[Mn_4O_3Cl_4(MeCOO)_3py_3]$ .

### Oxidation state IV ( $d^3$ )

This is apparently the highest oxidation state in which manganese is able to form complexes. Monomeric complexes are sparse, though  $K_2[MnX_6]$ , where  $X = F, Cl, IO_3$  and  $CN$  are known, but di- and poly-meric compounds are more numerous and have received attention as models for the water-oxidizing enzyme, *Photosystem II*,<sup>(15)</sup> important in plant photosynthesis. An  $Mn(\mu-O)_2Mn$  core is thought to be involved and the redox behaviour of compounds such as  $[(L-L)_2Mn(\mu-O)_2Mn(L-L)_2]^{n+}$  ( $L-L = 1,10$ -phenanthroline,  $2,2'$ -bipyridyl;  $n = 2, 3, 4$ , implying  $Mn^{III}-Mn^{III}$ ,  $Mn^{III}-Mn^{IV}$  and  $Mn^{IV}-Mn^{IV}$  pairings) has been studied.<sup>(16)</sup> Schiff bases and carboxylate ligands have also been used and complexes with OH bridges and also triply bridged complexes have been

produced. Fully oxidized  $Mn^{IV}-Mn^{IV}$  species are often observed only electrochemically and not completely characterized. An exception is the  $Mn^{IV}$  tetramer,  $[Mn_4O_6(tacn)_4]^{4+}$  prepared by aerial oxidation of  $Mn^{2+}$  in the presence of 1,4,7-triazacyclononane. The core of this has the adamantane structure, each Mn being facially coordinated to one tacn and three  $\mu_2$ -oxygens (Fig. 24.5a).

Relatively few compounds of  $Tc^{IV}$  have radiopharmaceutical use, and its chemistry in this oxidation state has therefore been comparatively neglected. For both the heavier elements the preference for oxo compounds is diminishing while the tendency to form  $M-M$  multiple bonds has not yet acquired the importance to be found in more reduced states. The most important compounds are the salts of  $[MX_6]^{2-}$  [ $M = Tc, Re; X = F, Cl, Br, I$ ]. The fluoro complexes are obtained by the reaction of HF on one of the other halogeno complexes and these in turn are obtained by reducing  $[MO_4]^-$  (commonly by using  $I^-$ ) in aqueous HX. The corresponding Tc and Re complexes are closely similar, but an interesting difference between  $Tc^{IV}$  and  $Re^{IV}$  is found in their behaviour with  $CN^-$ . The reaction

<sup>15</sup> V. K. YACHANDRA, K. SAUER and M. P. KLEIN, *Chem. Revs.* **96**, 2927–50 (1996); R. MANCHANDA, G. W. BRUDVIG, and R. H. CRABTREE, *Coord. Chem. Revs.* **144**, 1–38 (1995).

<sup>16</sup> G. W. BRUDVIG and R. H. CRABTREE, *Prog. Inorg. Chem.* **37**, 99–142 (1989); J. B. VINCENT and G. CHRISTOU, *Adv. Inorg. Chem.* **33**, 197–258 (1989); K. WIEGHARDT, *Angew. Chem. Int. Edn. Engl.* **28**, 1153–72 (1989).

of KCN and  $K_2ReI_6$  in methanol yields a mixture of  $K_4[Re^{III}(CN)_7] \cdot 2H_2O$  and  $K_3[Re^{VO}_2(CN)_4]$  whereas the analogous reaction of KCN and  $K_2TcI_6$  produces a reddish-brown, paramagnetic precipitate, thought to be  $K_2[Tc(CN)_6]$ .

### Oxidation state III ( $d^4$ )

Nearly all manganese(III) complexes are octahedral and high-spin with magnetic moments close to the spin-only value of 4.90 BM expected for 4 unpaired electrons. The  $d^4$  configuration is also expected to be subject to Jahn–Teller distortions (p. 1021). For reasons which are not obvious, the  $[Mn(H_2O)_6]^{3+}$  ion in the alum  $CsMn(SO_4)_2 \cdot 12H_2O$  does not display the appreciable distortion from octahedral symmetry (elongation of two *trans* bonds) found, for instance, in solid  $MnF_3$ , the octahedral  $Mn^{III}$  sites of  $Mn_3O_4$ ,  $[Mn(acac)_3]$  and in tris(tropolonato)manganese(III). Manganese(III) is strongly oxidizing in aqueous solution with a marked tendency to disproportionate into  $Mn^{IV}$  (i.e.  $MnO_2$ ) and  $Mn^{II}$  (see Fig. 24.1). It is, however, stabilized by *O*-donor ligands, as evidenced by the way in which the virtually white  $Mn(OH)_2$  rapidly darkens in air as it oxidizes to hydrous  $Mn_2O_3$  or  $MnO(OH)$ , and by the preparation of  $[Mn(acac)_3]$  via the aerial oxidation of aqueous  $Mn^{II}$  in the presence of acetylacetonate.  $K_3[Mn(C_2O_4)_3] \cdot 3H_2O$  is also known, while the complexing oxoanions, phosphate and sulfate, have a stabilizing effect on aqueous solutions. The main preparative routes to  $Mn^{III}$  are by reduction of  $KMnO_4$  or oxidation of  $Mn^{II}$ . The latter may be effected electrolytically but a common method is by way of the red-brown acetate. This is similar to the “basic” acetate of chromium(III) and so involves the  $[Mn_3O(MeCOO)_6]^+$  unit (see Fig. 23.9, p. 1030). The hydrate is prepared by oxidation of manganese(II) acetate with  $KMnO_4$  in glacial acetic acid, and the anhydrous salt by the action of acetic hydride on hydrated manganese(II) nitrate.

The field of oxo-bridged polynuclear complexes of manganese, much of it involving mixed

oxidation states and facile redox behaviour, is expanding rapidly<sup>(16)</sup>. Oxidation of an ethanolic solution of  $Mn^{II}$  acetate by  $(Bu_4N)MnO_4$  in the presence of acetic acid and pyridine can yield either the  $Mn^{III}$  compound,  $[Mn_3O(MeCOO)_6py_3]^+$  or the  $Mn^{II}Mn^{III}$  compound,  $[Mn_3O(MeCOO)_6py_3]$ . Addition of bipyridyl to solutions of these in MeCN gives the tetranuclear,  $[Mn_4O_2(MeCOO)_7(bipy)_2]^+$  and  $[Mn_4O_2(MeCOO)_6(bipy)_2]$  respectively. The structures of the cores of these and other  $Mn_4$  complexes<sup>(17)</sup> are given in Fig. 24.5.

Still higher nuclearities, up to 12 in  $[Mn_{12}O_{12}(RCOO)_{16}(H_2O)_4]$  ( $R = Me, Ph$ ), have been reported.<sup>(18)</sup> The cores of these two compounds, which are of interest as potential building blocks in the preparation of molecular ferromagnets, consist of a central  $[Mn_4^V(\mu-O)_4]$  cubane linked by *O*-bridges to eight Mn atoms.

The most important low-spin octahedral complex of  $Mn^{III}$  is the dark-red cyano complex,  $[Mn(CN)_6]^{3-}$ , which is produced when air is bubbled through an aqueous solution of  $Mn^{II}$  and  $CN^-$ .  $[MnX_5]^{2-}$  ( $X = F, Cl$ ) are also known; the chloro ion, at least when combined with the cation  $[bipyH_2]^{2+}$ , is notable as an example of a square pyramidal manganese complex.

Technetium(III) complexes are accessible especially if stabilized by back-bonding ligands, and are most commonly 6-coordinate.  $[TcCl_2(diars)_2]ClO_4$ , prepared by the reaction of *o*-phenylenebisdimethylarsine and HCl with  $HTcO_4$  in aqueous alcohol, is probably the best known. The rhenium(III) analogue is isomorphous but requires the help of a reducing agent such as  $H_3PO_2$  to effect the reduction from  $[ReO_4]^-$ . Other examples are  $[Tc(NCS)_6]^{3-}$  and  $[Tc(thiourea)_6]^{3+}$ . However, 7-coordinate compounds such as  $[M(CN)_7]^{4-}$  are also known and, more recently, it has been reported<sup>(19)</sup> that the

<sup>17</sup> V. MCKEE, *Adv. Inorg. Chem.* **40**, 323–410 (1994).

<sup>18</sup> P. D. W. BOYD, Q. LI, J. B. VINCENT, K. FOLTING, H.-R. CHANG, W. E. STREIB, J. C. HUFFMAN, G. CHRISTOU and D. N. HENDRICKSON, *J. Am. Chem. Soc.* **110**, 8537–9 (1988).

<sup>19</sup> C. M. ARCHER, J. R. DILWORTH, P. JOBANPUTRA, R. M. THOMPSON, M. MCPARTLIN, P. C. POVEY, G. W. SMITH and J. D. KELLY, *Polyhedron* **9**, 1497–1502 (1990).

reaction of  $[\text{MOC}l_4]^-$  with excess arylhydrazine and  $\text{PPh}_3$  in ethanol gives 5-coordinate, diamagnetic,  $[\text{MCl}(\text{N}_2\text{Ar})_2(\text{PPh}_3)_2]$ .

In general  $\text{Re}^{\text{III}}$  is readily oxidized to  $\text{Re}^{\text{IV}}$  or  $\text{Re}^{\text{VII}}$  unless it is stabilized by metal-metal bonding<sup>(20)</sup> as in the case of the trihalides already discussed. Rhenium(III) complexes with  $\text{Cl}^-$  and  $\text{Br}^-$  have been characterized and are of two types,  $[\text{Re}_3\text{X}_{12}]^{3-}$  and  $[\text{Re}_2\text{X}_8]^{2-}$ , both of which involve multiple Re-Re bonds. If  $\text{Re}_3\text{Cl}_9$  or  $\text{Re}_3\text{Br}_9$  are dissolved in conc HCl or conc HBr respectively, stable, red, diamagnetic salts may be precipitated by adding a suitable monovalent cation. Their stoichiometry is  $\text{M}^1\text{ReX}_4$  and they were formerly thought to be unique examples of low-spin, tetrahedral complexes. X-ray analysis, however, showed that the anions are trimeric with the same structure as the halides (Fig. 24.3) and likewise incorporating Re=Re double bonds. Their chemistry reflects their structure since 3 halide ions per trimeric unit can be replaced by ligands such as MeCN,  $\text{Me}_2\text{SO}$ ,  $\text{Ph}_3\text{PO}$  and  $\text{PEt}_2\text{Ph}$  yielding neutral complexes  $[\text{Re}_3\text{X}_9\text{L}_3]$ .

The blue diamagnetic complexes  $[\text{Re}_2\text{X}_8]^{2-}$  are produced when  $[\text{ReO}_4]^-$  in aqueous HCl or HBr is reduced by  $\text{H}_3\text{PO}_2$  and they can then be precipitated by the addition of a suitable cation. A more efficient method, which also yields a product soluble in polar organic solvents, is the reaction of  $(\text{NBu}_4)\text{ReO}_4$  with refluxing benzoyl chloride followed by the addition of a solution of  $(\text{NBu}_4)\text{Cl}$  in ethanol saturated with HCl. Salts of  $[\text{Re}_2\text{X}_8]^{2-}$  are the starting points for almost all dirhenium(III) compounds and the ion provided one of the first examples of a quadruple bond in a stable compound (see pp. 1032, 1034). The structure of  $[\text{Re}_2\text{Cl}_8]^{2-}$  is shown in Fig. 24.6 and, as in  $[\text{Mo}_2\text{Cl}_8]^{4-}$  (Fig. 23.11, p. 1033), the chlorine atoms are eclipsed. In both ions the metal has a  $d^4$  configuration which is to be expected if a  $\delta$ -bond is present.  $[\text{Re}_2\text{Cl}_8]^{2-}$  can be reduced polarographically to unstable  $[\text{Re}_2\text{Cl}_8]^{3-}$  and  $[\text{Re}_2\text{Cl}_8]^{4-}$ , and also undergoes a variety of substitution reactions (Fig. 24.6b,c,d).

One Cl on each Re may be replaced by phosphines, while  $\text{MeSCH}_2\text{CH}_2\text{SMe}$  (dth) takes up 4 coordination positions on 1 Re to give  $[\text{Re}_2\text{Cl}_5(\text{dth})_2]$ . In this case the average oxidation state of the rhenium has been reduced to +2.5. The reduction in bond order from 4 to 3.5, which the addition of a  $\delta^*$  electron implies, causes some lengthening of the Re-Re distance and the configuration is staggered. Carboxylates are able to bridge the metal atoms forming complexes of the type  $[\text{Re}_2\text{Cl}_2(\text{O}_2\text{CR})_4]$  which are clearly analogous to the dimeric carboxylates found in the previous group.

In the octachloro technetium system, by contrast, the paramagnetic  $[\text{Tc}_2\text{Cl}_8]^{3-}$  is the most readily obtained species. The Tc has a formal oxidation state of +2.5 with a  $d(\text{Tc-Tc})$  210.5 pm and the configuration is eclipsed. The pale green  $[\text{NBu}_4]_2^+[\text{Tc}_2^{\text{III}}\text{Cl}_8]^{2-}$  can be isolated from the products of reduction of  $[\text{TcCl}_6]^{2-}$  with  $\text{Zn}/\text{HCl}(\text{aq})$ . The compound is strictly isomorphous with  $[\text{NBu}_4]_2^+[\text{Re}_2\text{Cl}_8]^{2-}$  and has  $(\text{Tc-Tc})$  214.7 pm. The reason for the increase in Tc-Tc distance on removal of the  $\delta^*$  electron, and the consequent increase in the presumed bond order from 3.5 to 4, is not clear, but has been ascribed to a decrease in the strength of  $\sigma$  and  $\pi$  bonding caused by orbital contraction occurring as the charge on the metal core (and hence the bond order) increases.<sup>(21)</sup>

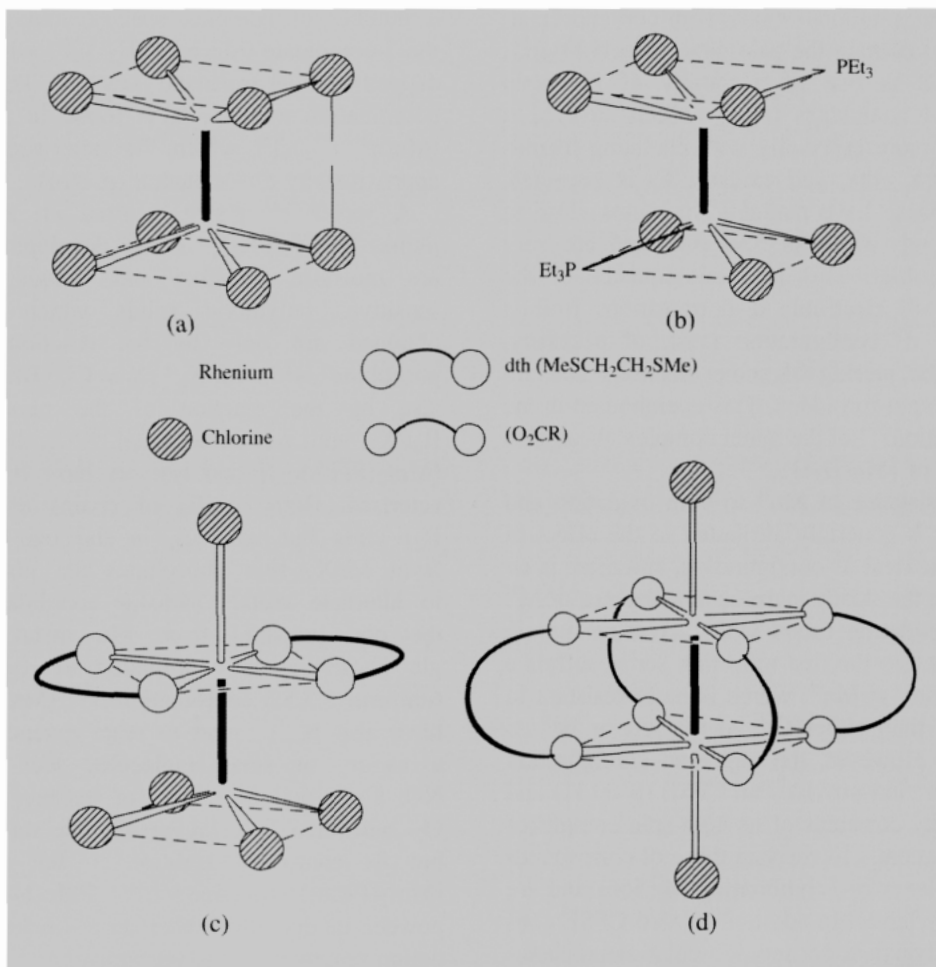
### Oxidation state II ( $d^5$ )

The chemistry of technetium(II) and rhenium(II) is meagre and mainly confined to arsine and phosphine complexes. The best known of these are  $[\text{MCl}_2(\text{diars})_2]$ , obtained by reduction with hypophosphite and  $\text{Sn}^{\text{II}}$  respectively from the corresponding  $\text{Tc}^{\text{III}}$  and  $\text{Re}^{\text{III}}$  complexes, and in which the low oxidation state is presumably stabilized by  $\pi$  donation to the ligands. This oxidation state, however, is really best typified by manganese for which it is the most thoroughly studied and, in aqueous solution, by far the most

<sup>20</sup> F. A. COTTON and R. A. WALTON, *Multiple Bonds between Atoms*, 2nd edn., Oxford University Press, Oxford, 1993, 787 pp.

<sup>21</sup> p. 123 of ref. 20.

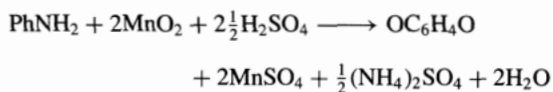




**Figure 24.6** Some complexes of Re with multiple Re-Re bonds: (a)  $[\text{Re}_2\text{Cl}_8]^{2-}$ . (b)  $[\text{Re}_2\text{Cl}_6(\text{PEt}_3)_2]$ . (c)  $[\text{Re}_2\text{Cl}_5(\text{dth})_2]$ . (d)  $[\text{Re}_2(\text{O}_2\text{CR})_4\text{Cl}_2]$ .

stable; accordingly it provides the most extensive cationic chemistry in this group.

Salts of manganese(II) are formed with all the common anions and most are water-soluble hydrates. The most important of these commercially and hence the most widely produced is the sulfate, which forms several hydrates of which  $\text{MnSO}_4 \cdot 5\text{H}_2\text{O}$  is the one commonly formed. It is manufactured either by treating pyrolusite with sulfuric acid and a reducing agent, or as a byproduct in the production of hydroquinone ( $\text{MnO}_2$  is used in the conversion of aniline to quinone):



It is the starting material for the preparation of nearly all manganese chemicals and is used in fertilizers in areas of the world where there is a deficiency of Mn in the soil, since Mn is an essential trace element in plant growth. The anhydrous salt has a surprising thermal stability; it remains unchanged even at red heat, whereas the sulfates of  $\text{Fe}^{\text{II}}$ ,  $\text{Co}^{\text{II}}$  and  $\text{Ni}^{\text{II}}$  all decompose under these conditions.

Aqueous solutions of salts with non-coordinating anions contain the pale-pink,  $[\text{Mn}(\text{H}_2\text{O})_6]^{2+}$ , ion which is one of a variety of high-spin octahedral complexes ( $t_{2g}^3 e_g^2$ ) which have been prepared more especially with chelating ligands such as en, edta, and oxalate. As is expected, most of these have magnetic moments close to the spin-only value of 5.92 BM, and are very pale in colour. This is a consequence of the fact that all electronic d-d transitions from a high-spin  $d^5$  configuration must, of necessity, involve the pairing of some electrons and are therefore spin-forbidden. This is embodied in the interpretation<sup>(22)</sup> of the rather complex absorption spectrum of  $[\text{Mn}(\text{H}_2\text{O})_6]^{2+}$ .

The resistance of  $\text{Mn}^{\text{II}}$  to both oxidation and reduction is generally attributed to the effect of the symmetrical  $d^5$  configuration, and there is no doubt that the steady increase in resistance of  $\text{M}^{\text{II}}$  ions to oxidation found with increasing atomic number across the first transition series suffers a discontinuity at  $\text{Mn}^{\text{II}}$ , which is more resistant to oxidation than either  $\text{Cr}^{\text{II}}$  to the left or  $\text{Fe}^{\text{II}}$  to the right. However, the high-spin configuration of the  $\text{Mn}^{\text{II}}$  ion provides no CFSE (p. 1131) and the stability constants of its high-spin complexes are consequently lower than those of corresponding complexes of neighbouring  $\text{M}^{\text{II}}$  ions and are kinetically labile. In addition, a zero CFSE confers no advantage on any particular stereochemistry which must be one of the reasons for the occurrence of a wider range of stereochemistries for  $\text{Mn}^{\text{II}}$  than is normally found for  $\text{M}^{\text{II}}$  ions.

Green-yellow salts of the tetrahedral  $[\text{MX}_4]^{2-}$  ( $X = \text{Cl}, \text{Br}, \text{I}$ ) ions can be obtained from ethanolic solutions and are well characterized. Furthermore, a whole series of adducts  $[\text{MnX}_2\text{L}_2]$  ( $X = \text{Cl}, \text{Br}, \text{I}$ ) are known where L is an  $N$ -,  $P$ - or  $As$ -donor ligand, and both octahedral and tetrahedral stereochemistries are found. Of interest because of the possible role of manganese porphyrins in photosynthesis is  $[\text{Mn}^{\text{II}}(\text{phthalocyanine})]$  which is square planar. The reaction of aqueous edta with  $\text{MnCO}_3$  yields

a number of complex species, amongst them the 7-coordinate  $[\text{Mn}(\text{edta})(\text{H}_2\text{O})]^{2-}$  which has a capped trigonal prismatic structure. The highest coordination number, 8, is found in the anion  $[\text{Mn}(\eta^2\text{-NO}_3)_4]^{2-}$  which, like other such ions, is approximately dodecahedral (p. 916).

A varied chemistry, centred on the phosphines  $[\text{MnX}_2(\text{PR}_3)]$ , is also developing. These are moisture sensitive and, frequently, air-sensitive, polymeric solids which can be obtained not only by the reaction of the phosphine with  $\text{MnX}_2$  ( $X = \text{Cl}, \text{Br}, \text{I}$ ), but also by the reaction of the phosphorane,  $\text{R}_3\text{PX}_2$ , with powdered metal.<sup>(23)</sup> In the case of  $[\text{MnI}_2(\text{PPhMe}_2)]$  two isomers have been characterised. Both consist of chains of  $[\text{Mn}(\mu\text{-I})_2]$  units but whereas, in the one prepared from  $\text{MnX}_2$  two phosphines are coordinated to alternate metals (4,6,4,6 coordination), in the one prepared from Mn metal, a single phosphine is coordinated to each metal (uniform 5,5,5,5 coordination).<sup>(23)</sup>  $[\text{MnX}_2(\text{PR}_3)]$  have also been found to react reversibly with a variety of small molecules such as CO, NO,  $\text{C}_2\text{H}_4$  and  $\text{SO}_2$  (see for instance ref. 24).  $\text{O}_2$  will also react reversibly in some cases but its controlled addition to the pale-pink  $[\text{MnI}_2(\text{PMe}_3)]$  (obtained from  $\text{PMe}_3\text{I}_2$  and Mn powder in dry ethyl ether as a 4,6,4,6 coordination polymer) yields successively<sup>(25)</sup> the dark-red dimer,  $[\text{Mn}^{\text{III}}(\text{PMe}_3)_2(\mu\text{-I})\text{Mn}^{\text{II}}(\text{PMe}_3)_2\text{I}_2]$  (involving approximately tetrahedral  $\text{Mn}^{\text{III}}$  and trigonal bipyramidal  $\text{Mn}^{\text{II}}$ ) and finally the dark-green, trigonal bipyramidal  $[\text{Mn}^{\text{III}}(\text{PMe}_3)_2\text{I}_3]$ .

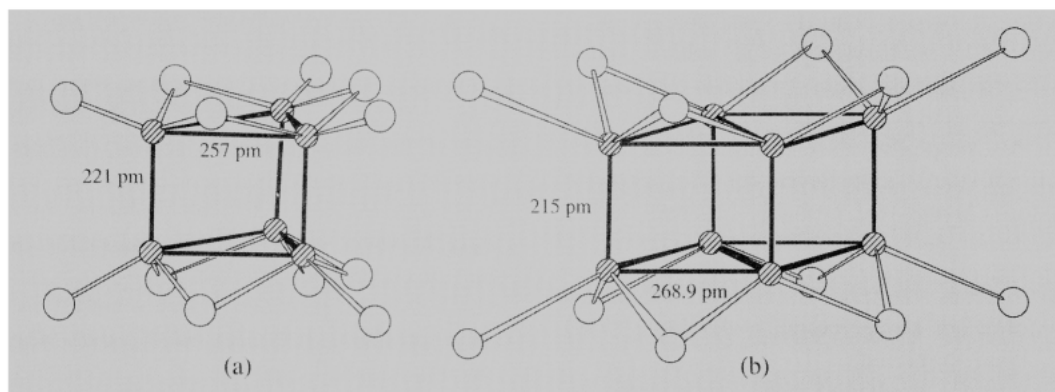
Spin-pairing in manganese(II) requires a good deal of energy and is achieved only by ligands such as  $\text{CN}^-$  and CNR which are high in the spectrochemical series. The low-spin complexes.  $[\text{Mn}(\text{CN})_6]^{4-}$  and  $[\text{Mn}(\text{CNR})_6]^{2+}$  are presumed

<sup>23</sup> S. M. GODFREY, D. G. KELLY, A. G. MACKIE, P. P. MACRORY, C. A. MCAULIFFE, R. G. PRITCHARD and S. M. WATSON, *J. Chem. Soc., Chem. Commun.* 1447-9 (1991).

<sup>24</sup> D. S. BARRATT, G. A. GOTT and C. A. MCAULIFFE, *J. Chem. Soc., Dalton Trans.*, 2065-70 (1988).

<sup>25</sup> C. A. MCAULIFFE, S. M. GODFREY, A. G. MACKIE, and R. G. PRITCHARD, *J. Chem. Soc., Chem. Commun.* 483-5 (1992).

<sup>22</sup> A. B. P. LEVER, *Inorganic Electronic Spectroscopy*, 2nd edn., pp. 448-52, Elsevier, Amsterdam, 1984.



**Figure 24.7** (a) Trigonal prismatic  $[\text{Tc}_6\text{Cl}_{12}]^{2-}$  (b)  $[\text{Tc}_8\text{Br}_{12}]^{n+}$ . The bond lengths shown are for  $n = 1$ , i.e.  $[\text{Tc}_8\text{Br}_{12}]\text{Br}\cdot 2\text{H}_2\text{O}$ . The very short bonds holding together the triangular faces in (a) and the rhombohedral faces in (b) are consistent with  $\text{Tc}\equiv\text{Tc}$  triple bonds.

to involve appreciable  $\pi$  bonding and this covalency brings with it a susceptibility to oxidation. Just as  $\text{Mn}^{\text{II}}$  hydroxide undergoes aerial oxidation to  $\text{Mn}^{\text{III}}$  so, in the presence of excess  $\text{CN}^-$ , aqueous solutions of the blue-violet  $[\text{Mn}(\text{CN})_6]^{4-}$  are oxidized by air to the dark red  $[\text{Mn}(\text{CN})_6]^{3-}$ .

### Lower oxidation states

Cyano complexes of the metals of this group in high oxidation states have already been referred to. The tolerance of  $\text{CN}^-$  to a range of metal oxidation states, arising, on the one hand, from its negative charge and, on the other, from its ability to act as a  $\pi$ -acceptor, is further demonstrated by the formation (albeit requiring reduction with potassium amalgam) of the  $\text{M}^{\text{I}}$  complexes,  $\text{K}_5[\text{M}(\text{CN})_6]$  ( $\text{M} = \text{Mn}, \text{Tc}, \text{Re}$ ). However, claims for the formation of cyano complexes with oxidation state zero are less reliable.

Reduction of  $[\text{MO}_4]^-$  in hydrohalic acid by  $\text{H}_2$  under pressure is an alternative method for preparing  $[\text{Re}_2\text{X}_8]^{2-}$ . In the case of technetium, however, further reduction occurs, yielding  $[\text{Tc}_2\text{X}_8]^{3-}$  along with higher nuclearity clusters in which the oxidation state of the metal is below 2.<sup>(26)</sup> Chloride species include  $[\text{Tc}_6\text{Cl}_{14}]^{3-}$  and  $[\text{Tc}_6\text{Cl}_{12}]^{2-}$

with the trigonal prismatic structure shown in Fig. 24.7a. Bromide species<sup>(27)</sup> additionally include hexanuclear octahedral species and the octanuclear prismatic,  $[\text{Tc}_8\text{X}_{12}]^{n+}$  ( $n = 0, 1$ ) (Fig. 24.7b). Other examples of complexes in which Mn, Tc and Re are in lower oxidation states are considered in section 24.3.6 on organometallic compounds.

### 24.3.5 The biochemistry of manganese<sup>(16,18)</sup>

Traces of manganese are found in many plants and bacteria, and a healthy human adult contains about 10–20 mg of Mn.

In many manganeseoproteins the manganese is in the II oxidation state and can often be replaced by magnesium(II) without loss of function. In other cases, where redox activity is involved, some naturally occurring forms containing either manganese or iron are known. The most important natural role of manganese, however, is in the oxidation of water in green plant photosynthesis (p. 125) where its presence in photosystemII (PSII) is essential. Here, absorbed radiation provides the energy for the oxidation

<sup>27</sup> V. I. SPITZIN, S. V. KRYUTCHKOV, M. S. GRIGORIEV and A. F. KUZINA, *Z. anorg. allg. Chem.* **563**, 136–52 (1988).

<sup>26</sup> pp. 559–63 of ref. 20.

of water, dioxygen being evolved and electrons transferred to photosystemI (PSI) where NADP is reduced. The oxidation proceeds by four 1-photon, 1-electron steps and it appears that it is the redox properties of a group of Mn atoms which provide stable stages for this stepwise oxidation. Manganese probably has two further functions:

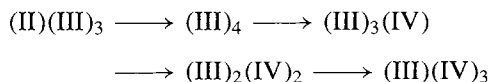
- (a) to act as a template holding two molecules of water close enough to facilitate O–O bond formation;
- (b) to make the bound water more acidic, so facilitating loss of H<sup>+</sup>

It is no doubt significant that the equilibrium constant for the reaction



is larger for Mn<sup>III</sup> than for any other trivalent, first row transition metal ion.

Although definitive crystallographic data are lacking it seems clear that the “water oxidizing centre” (WOC) or “oxygen evolving complex” (OEC) of PSII contains four Mn atoms and it is believed that these are arranged in one of the cluster forms shown in Fig. 24.5. Physical techniques which have been used to study these proteins include esr, uv-visible spectroscopy, magnetic measurements and EXAFS. Two Mn–Mn distances, 270 and 330 pm are indicated, with *O*-, *N*- and possible *Cl*-donor atoms, giving a core of fairly low symmetry. A plausible sequence of oxidation state changes for the four Mn atoms consistent with, but by no means defined by, the available data would be:



Efforts have been made to reproduce these characteristics in model systems, and molecules with the core structures already described have been prepared. Though none as yet has shown any photoredox activity the 270 pm distance has been shown to be consistent with ( $\mu$ -oxo)<sub>2</sub> bridges and 330 pm with  $\mu$ -oxo or  $\mu$ -oxo- $\mu$ -carboxylate bridges. Several mechanistic proposals have been made incorporating these features.

### 24.3.6 Organometallic compounds

Carbonyls, cyclopentadienyls and their derivatives occupy a central position in the chemistry of this as of preceding groups, the bonding involved and even their stoichiometries having in some cases posed difficult problems. Increasingly, however, interest has focused on the chemistry of compounds involving M–C  $\sigma$  bonds, of which rhenium provides as rich a variety as any transition metal. It is also notable that, whereas the organometallic chemistry of manganese is largely limited to oxidation states 0, I and II, that of rhenium extends to VII.<sup>(28,29)</sup>

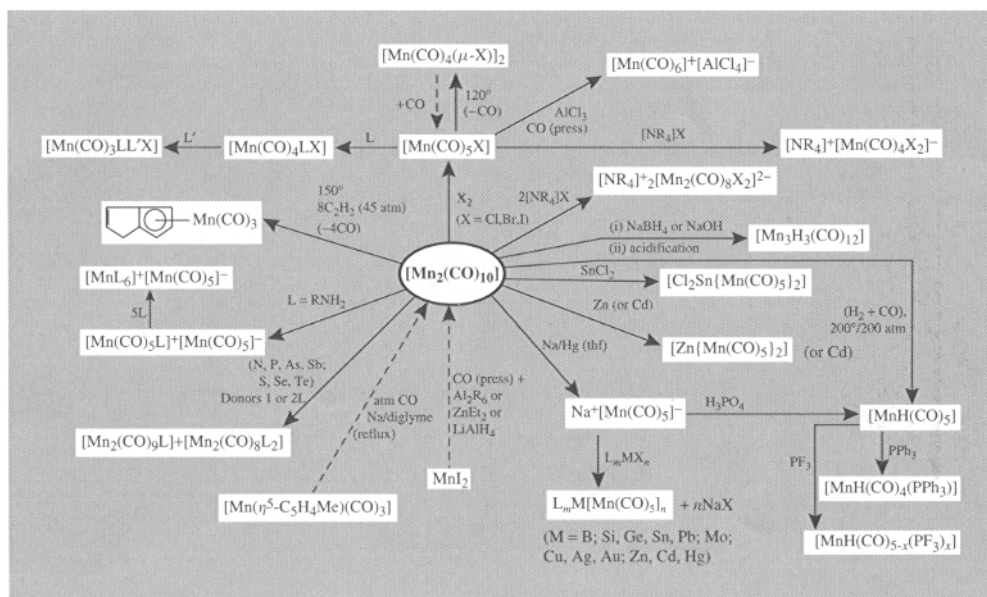
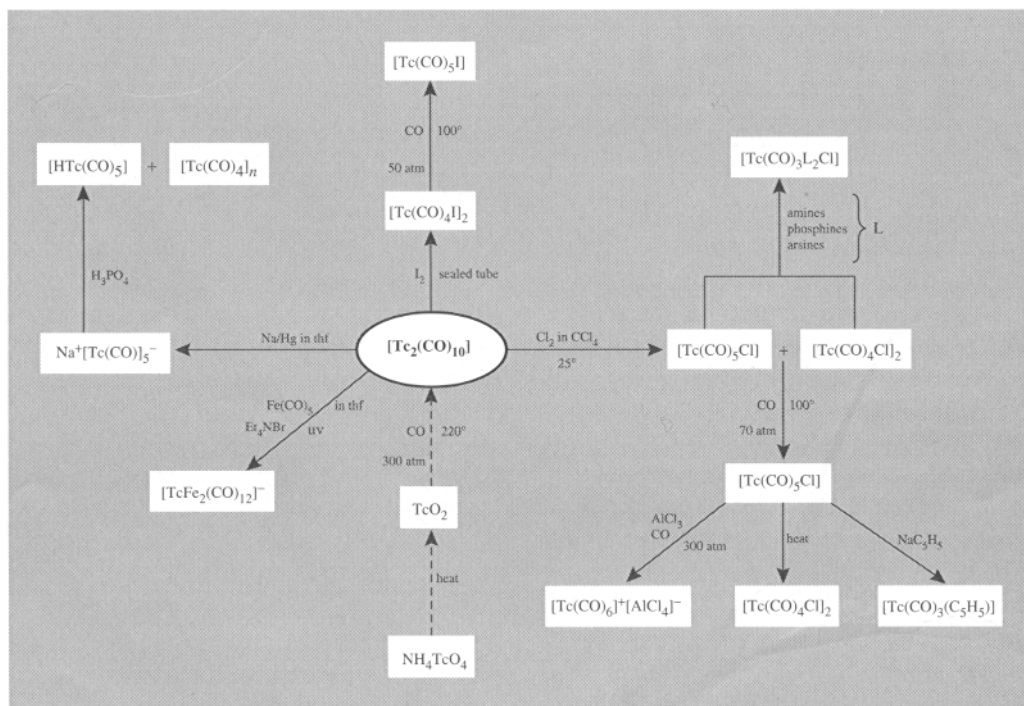
Only one well-characterized binary carbonyl is formed by each of the elements of this group. That of manganese is best prepared by reducing MnI<sub>2</sub> (e.g. with LiAlH<sub>4</sub>) in the presence of CO under pressure. Those of technetium and rhenium are made by heating their heptoxides with CO under pressure. They are sublimable, isomorphous, crystalline solids: golden-yellow for [Mn<sub>2</sub>(CO)<sub>10</sub>], mp 154°, and colourless for [Tc<sub>2</sub>(CO)<sub>10</sub>], mp 160° and [Re<sub>2</sub>(CO)<sub>10</sub>], mp 177°. Their stabilities in air show a regular gradation: manganese carbonyl is quite stable below 110°C, technetium carbonyl decomposes slowly and rhenium carbonyl may ignite spontaneously. The empirical stoichiometry M(CO)<sub>5</sub> would imply a paramagnetic molecule with 17 valence electrons, but the observed diamagnetism (for Mn and Re) suggests at least a dimeric structure. In fact, X-ray analysis reveals the structure shown in Fig. 24.8(a) in which two M(CO)<sub>5</sub> groups in staggered configuration are held together by an M–M bond, unsupported by bridging ligands (cf. S<sub>2</sub>F<sub>10</sub>, p. 684).

Very many derivatives of the carbonyls of Mn,<sup>(30)</sup> Tc and Re have been prepared since the parent carbonyls were first synthesized in 1949, 1961 and 1941 respectively:<sup>(3)</sup> among the more important are the carbonylate anions,

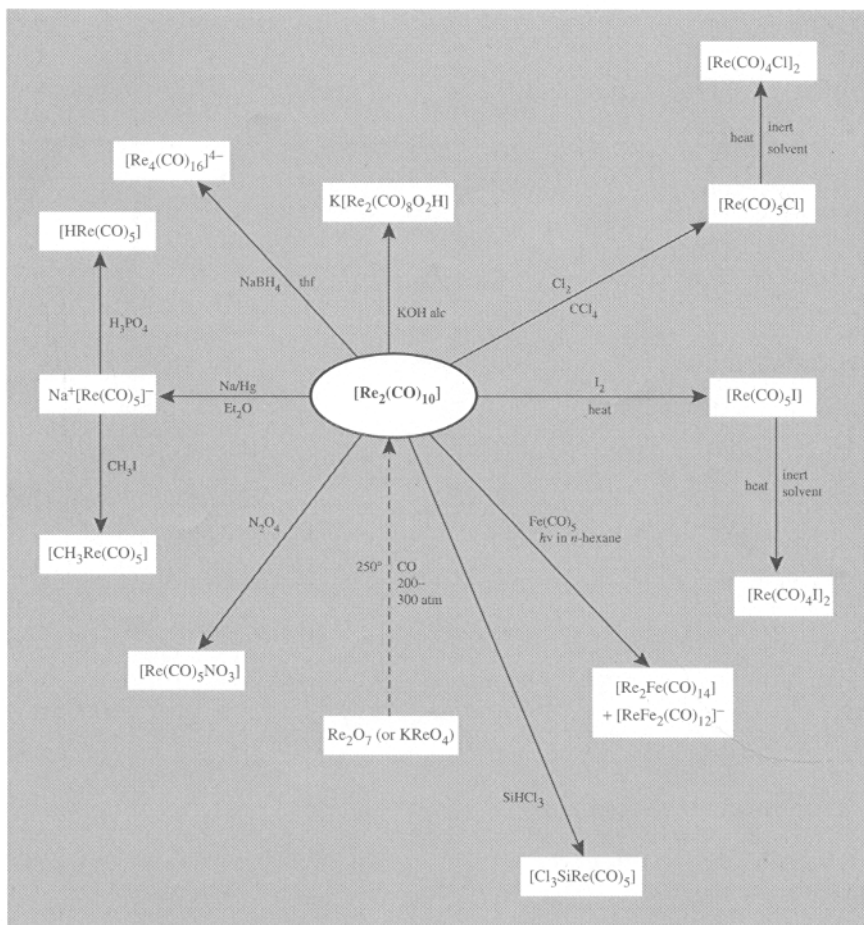
<sup>28</sup> C. P. CASEY, *Science* **259**, 1552–8 (1993).

<sup>29</sup> W. A. HERRMANN, *Angew. Chem. Int. Edn. Engl.* **27**, 1297–313 (1988).

<sup>30</sup> C. E. HOLLOWAY and M. MELNIK, *J. Organometallic Chem.* **396**, 129–246 (1990).

SCHEME A Some reactions of  $[\text{Mn}_2(\text{CO})_{10}]$  and its derivatives.<sup>(31)</sup>SCHEME B Some reactions of  $[\text{Tc}_2(\text{CO})_{10}]$  and its derivatives.<sup>(32)</sup><sup>31</sup>R. D. W. KEMMIT, pp. 839–51 in *Comprehensive Inorganic Chemistry*, Vol. 3, Pergamon Press, Oxford 1973.<sup>32</sup>R. D. PEACOCK, *ibid.*, p. 899 for Scheme B, p. 953 for Scheme C and p. 954 for Scheme D.



SCHEME C Some reactions of rhenium carbonyl.<sup>(32)</sup>

the carbonyl cations, and the carbonyl hydrides. Typical reactions are summarized in schemes A, B, C and D (this last on p. 1067).

Sodium amalgam reductions of  $M_2(CO)_{10}$  give  $Na^+[M(CO)_5]^-$  and, indeed, further reduction<sup>(33)</sup> leads to the “super reduced” species  $[M(CO)_4]^{3-}$  in which the metals exhibit their lowest known formal oxidation state of  $-3$ . On the other hand, treatment of  $[M(CO)_5Cl]$  with  $AlCl_3$  and CO under pressure produces  $[M(CO)_6]^+AlCl_4^-$  from which other salts of the cation can be obtained.

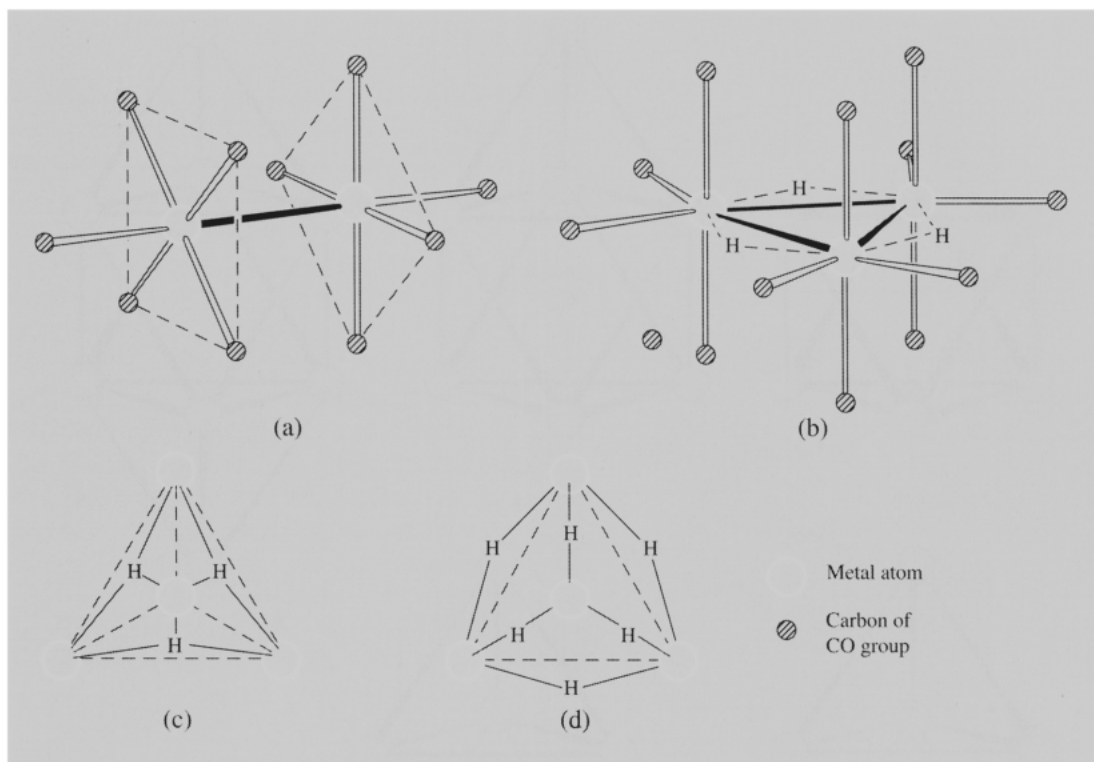
Acidification of  $[M(CO)_5]^-$  produces the octahedral and monomeric,  $[MH(CO)_5]$ , and a number of polymeric carbonyls have been

obtained by reduction of  $[M_2(CO)_{10}]$ , including interesting hydrogen-bridged complexes such as  $[H_3Mn_3(CO)_{12}]$  (the first transition metal cluster in which the H atoms were located),  $[H_4Re_4(CO)_{12}]$  and  $[H_6Re_4(CO)_{12}]^{2-}$  (Fig. 24.8). The tendency to form high nuclearity carbonyl clusters is, however, much less evident for Mn than for Re. The largest so far obtained for Mn is the heptanuclear,  $[Mn_7(\mu_3-OH)_8(CO)_8]^{34}$  but this is exceptional, there being very few others with nuclearities higher than four.<sup>(30)</sup>

By contrast, the stronger M–M bonds characteristic of Re, help to provide a wider

<sup>33</sup> J. E. ELLIS, *Adv. Organometallic Chem.* **31**, 52 (1990).

<sup>34</sup> M. D. CLERK and M. J. ZAWOROTKO, *J. Chem. Soc. Chem. Commun.* 1607–8 (1991).



**Figure 24.8** Some carbonyls and carbonyl hydrides of Group 7 metals. (a)  $[M_2(CO)_{10}]$ ,  $M = Mn, Tc, Re$  (Mn–Mn 293 pm, Tc–Tc 304 pm, Re–Re 302 pm). (b)  $[H_3Mn_3(CO)_{12}]$ . Mn–Mn 311 pm. (c)  $[H_4Re_4(CO)_{12}]$ , Re–Re 289.6–294.5 pm. (In this structure the 4 Re atoms lie at the corners of a tetrahedron, the faces of which are bridged by 4 H atoms; the molecule is viewed from above one Re which obscures the fourth H. For clarity the CO groups are not shown but 3 are attached to each Re so as to “eclipse” the edges of the tetrahedron.) (d)  $[H_6Re_4(CO)_{12}]^{2-}$ , Re–Re 314.2–317.2 pm. (As in (c) the 4 Re atoms lie at the corners of a tetrahedron and the CO groups have been omitted for clarity. The 3 CO groups attached to each Re are now “staggered” with respect to the edges of the tetrahedron, whilst the H atoms (6) are presumed to bridge these edges.)

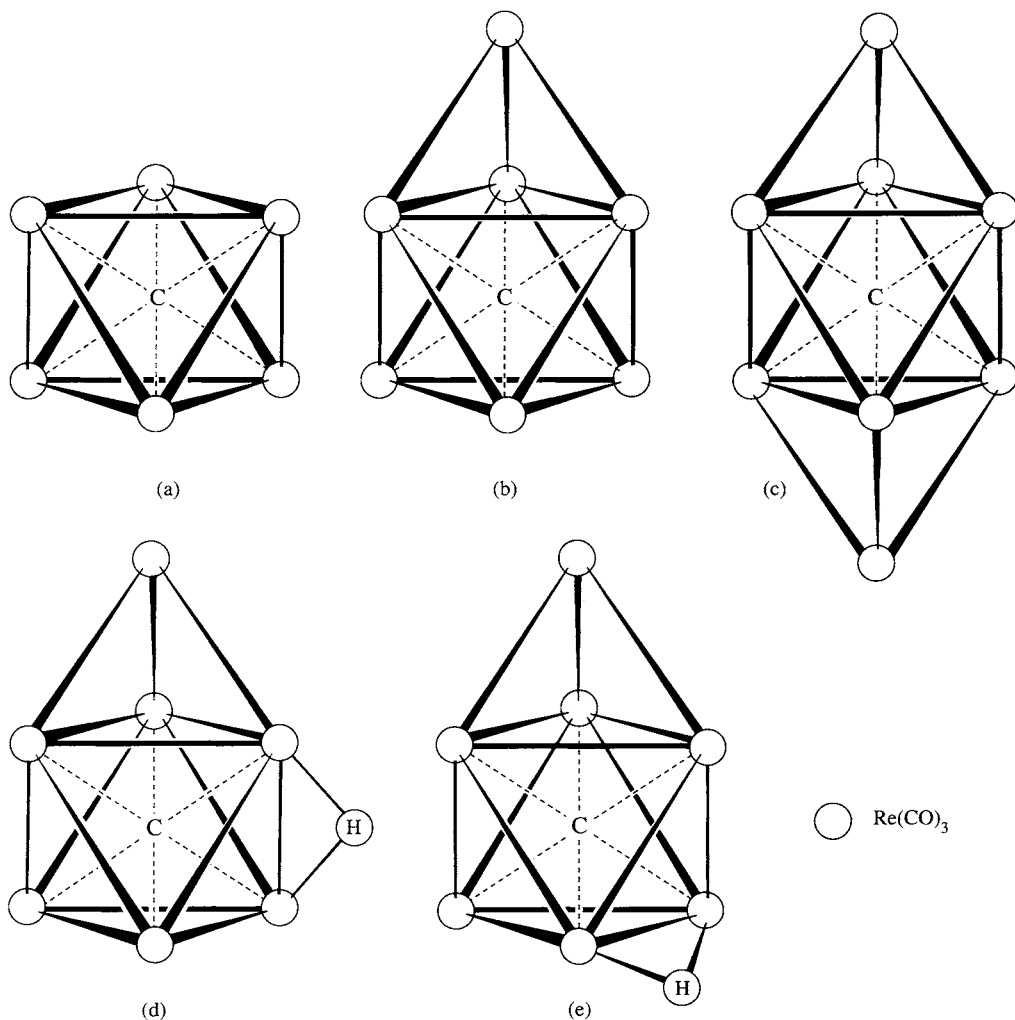
variety<sup>(35)</sup> of which the carbon-centred clusters  $[H_2Re_6C(CO)_{18}]^{2-}$ ,  $[Re_7C(CO)_{21}]^{3-}$  and  $[Re_8C(CO)_{24}]^{2-}$  (Fig. 24.9), obtained by the pyrolytic reduction of  $Re_2(CO)_{10}$  with varying proportions of Na in thf, may be mentioned. The H atoms in the first of these clusters, though not positively located, were thought to be face-capping (i.e.  $\mu_3$ ). On the other hand  $[Re_7HC(CO)_{21}]^{2-}$ , which is obtained by treating a salt of  $[Re_7C(CO)_{21}]^{3-}$  in acetone or thf with a strong acid such as  $HBF_4$  or  $H_2SO_4$ , exists in two isomeric forms and potential

energy computations suggest that both contain a  $\mu$ -H atom and differ in the cluster edge which this bridges<sup>(36)</sup> (Fig. 24.9d and e).

When  $MnCl_2$  in thf is treated with  $C_5H_5Na$ , amber-coloured crystals of manganocene,  $[Mn(C_5H_5)_2]$ , mp  $172^\circ$ , are produced. It is very sensitive to both air and water and is a most unusual compound. At room temperature it is polymeric with  $Mn(\eta^5-C_5H_5)$  units linked by bridging  $C_5H_5$  groups in a zig-zag arrangement.

<sup>35</sup> T. J. HENLY, *Coord. Chem. Revs.* **93**, 269–95 (1989).

<sup>36</sup> T. BERINGHELLI, G. D’ALFONSO, G. CIANI, A. SIRONI and H. MOLINARI, *J. Chem. Soc., Dalton Trans.*, 1281–7 (1988).



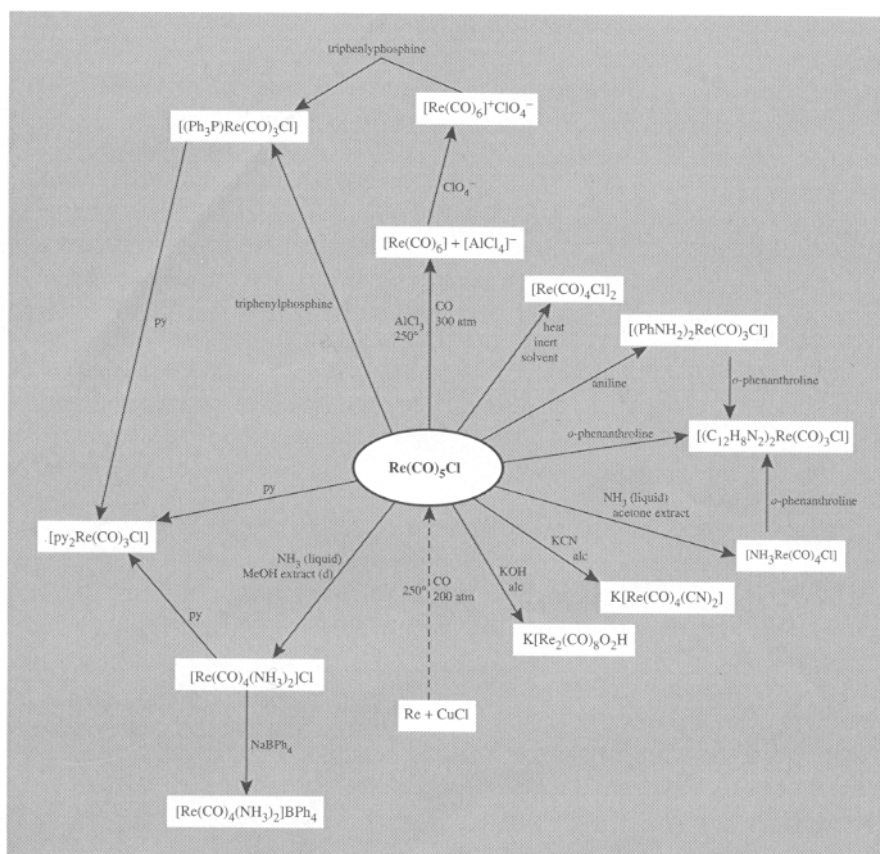
**Figure 24.9** Cluster carbonyls of rhenium containing an encapsulated carbon atom. (a) Octahedral  $[\text{H}_2\text{Re}_6\text{C}(\text{CO})_{18}]^{2-}$ . (b) Monocapped octahedral  $[\text{Re}_7\text{C}(\text{CO})_{21}]^{3-}$ . (c) *trans*-bicapped octahedral  $[\text{Re}_8\text{C}(\text{CO})_{24}]^{2-}$ . (d) and (e) isomers of  $[\text{Re}_7\text{HC}(\text{CO})_{21}]^{2-}$  differing in the position of their  $\mu\text{-H}$  atom.

At about  $159^\circ\text{C}$  it turns pink and adopts the “sandwich” structure, expected for  $[\text{M}(\text{C}_5\text{H}_5)_2]$  compounds, and this is retained in the gaseous phase and in hydrocarbon solutions. Using substituted cyclopentadienyls a variety of analogous sandwich compounds have been prepared<sup>(37)</sup> and their magnetic properties indicate that the

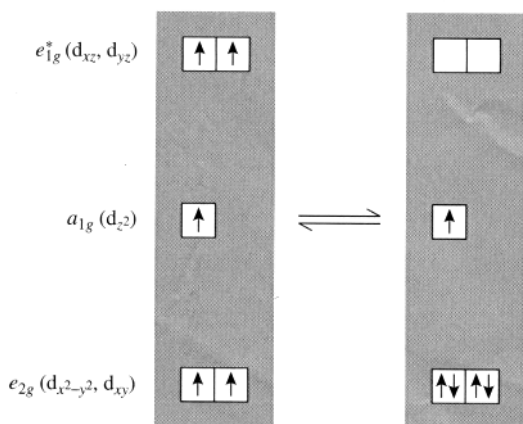
high-spin (5 unpaired electrons) and low-spin (1 unpaired electron) configurations are sufficiently close together to produce an equilibrium between the two in many cases (Fig. 24.10). The spin state depends on the nature and number of substituents in the  $\text{C}_5$  ring and also on solvent and temperature. Electron donating substituents, such as methyl, enhance the covalent character of the  $\text{Mn}-\text{C}$  bonding and favour the low-spin configuration. Thus  $[\text{Mn}(\eta^5\text{-C}_5\text{Me}_5)_2]$

<sup>37</sup> N. HEBENDANZ, F. H. KÖHLER, G. MÜLLER and J. REIDE, *J. Am. Chem. Soc.* **108**, 3281–9 (1986).





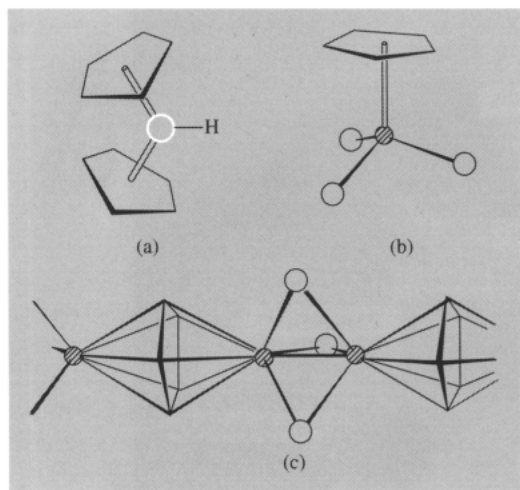
SCHEME D Some reactions of rhenium carbonyl chloride.



**Figure 24.10** Spin equilibrium in  $[\text{Mn}(\eta^5\text{-C}_5\text{H}_4\text{-Me})_2]$ : the orbitals shown here are the mainly metal-based orbitals in the centre of the MO diagram for metallocenes (see Fig. B, p. 939).

is exclusively low-spin,  $[\text{Mn}(\eta^5\text{-C}_5\text{H}_4\text{Me})_2]$  and other monoalkyl substituted ring systems exhibit spin-equilibria, while manganocene itself with a magnetic moment of 5.86 BM in hydrocarbon solvents at room temperature, is almost (but not entirely) high-spin.

Apart from the formation of  $[\text{Re}(\eta^5\text{-C}_5\text{H}_5)_2]$  on  $\text{N}_2$  matrices at 20 K, Tc and Re analogues of manganocene have not been prepared. Instead, when  $\text{TcCl}_4$  or  $\text{ReCl}_5$  are treated with  $\text{NaC}_5\text{H}_5$  in thf, the diamagnetic, yellow crystalline hydrides,  $[\text{M}(\eta^5\text{-C}_5\text{H}_5)_2\text{H}]$  are obtained (Fig. 24.11a). The protons on the cyclopentadienyl rings give rise to only one nmr signal, presumably because of rapid rotation of the rings about the metal-ring axis making the protons indistinguishable. As with Mn, however, methyl substitution has a stabilizing effect and purple  $[\text{Re}(\eta^5\text{-C}_5\text{Me}_5)_2]$



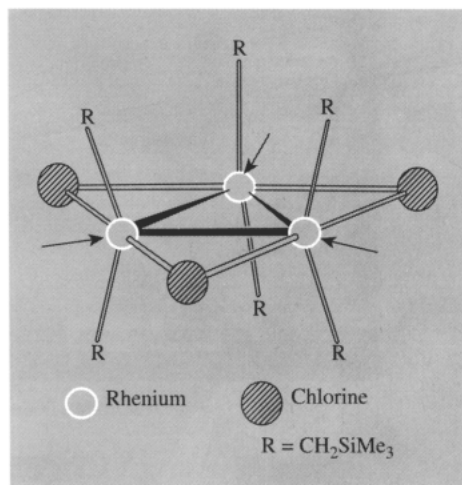
**Figure 24.11** (a)  $[M(\eta^5\text{-C}_5\text{H}_5)_2\text{H}]$  ( $M = \text{Tc, Re}$ ) (b)  $[\text{Re}(\eta^5\text{-C}_5\text{Me}_5)\text{O}_3]$  (The structure of  $[\text{Re}(\eta^5\text{-C}_5\text{Me}_5)\text{O}_3]$  is presumed to be identical but was not determined because of the lack of suitable single crystals<sup>(29)</sup>. (c) Section of the linear chain  $[\text{Tc}_2(\text{C}_5\text{Me}_5)\text{O}_3]_n$ .

is readily obtained by photolysis of a solution of  $[\text{Re}(\eta^5\text{-C}_5\text{Me}_5)_2\text{H}]$  in pentane. It is low-spin at low temperatures but has a minor contribution from the high-spin configuration at room temperature.<sup>(38)</sup>

Pentamethylcyclopentadienyl compounds also provide a convenient route into high-valent organorhenium chemistry.<sup>(29)</sup> Oxidation of  $[\text{Re}^I(\eta^5\text{-C}_5\text{Me}_5)(\text{CO})_3]$  by  $\text{H}_2\text{O}_2$  in a two-phase water–benzene system gives high yields of lemon yellow  $[\text{Re}(\eta^5\text{-C}_5\text{Me}_5)\text{O}_3]$  (Fig. 24.11b) which, being stable in air even up to  $140^\circ\text{C}$ , demonstrates the remarkable stabilizing effect of oxygen on Re in high oxidation states. The same procedure<sup>(39)</sup> in the case of technetium raises its oxidation state only to 3.5, forming yellow  $[\text{Tc}_2(\text{C}_5\text{Me}_5)\text{O}_3]_n$  (Fig. 24.11c) in which linear chains of Tc atoms are bridged alternately by  $(\mu\text{-C}_5\text{Me}_5)$  and  $(\mu\text{-O})_3$

with Tc–Tc distances respectively of 407.7(4) and the unusually short 186.7(4) pm.

Manganese(II) forms alkyls with a distinct tendency to polymerize. Thus the bright orange  $\text{Mn}(\text{CH}_2\text{SiMe}_3)_2$  is a polymer in which each Mn attains tetrahedral coordination, being doubly bridged to each adjacent metal by two  $\text{CH}_2\text{SiMe}_3$  groups (each Mn–C–Mn bridge is best regarded as a three-centre, two-electron bond). Red-brown  $\text{Mn}(\text{CH}_2\text{CMe}_3)_2$  is similarly bridged but, for no obvious reason, is only tetrameric, a terminal ligand being attached to each of the two outer Mn atoms which are therefore only 3-coordinate.



**Figure 24.12** Rhenium clusters:  $[\text{Re}_3\text{Cl}_3\text{R}_6]$ ; arrows indicate vacant coordination sites where further ligands can be attached.

The simplest of the  $\sigma$ -bonded Re–C compounds is the green, paramagnetic, crystalline, thermally unstable  $\text{ReMe}_6$ , which, after  $\text{WMe}_6$ , was only the second hexamethyl transition metal compound to be synthesized (1976). It reacts with  $\text{LiMe}$  to give the unstable, pyrophoric,  $\text{Li}_2[\text{ReMe}_8]$ , which has a square-antiprismatic structure, and incorporation of oxygen into the coordination sphere greatly increases the stability, witness  $\text{Re}^{\text{VI}}\text{OMe}_4$ , which is thermally stable up to  $200^\circ\text{C}$ , and  $\text{Re}^{\text{VII}}\text{O}_3\text{Me}$ , which is stable in air. The interaction of  $[\text{ReCl}_4(\text{thf})_2]$

<sup>38</sup> J. A. BANDY, F. G. N. CLOKE, G. COOPER, J. P. DAY, R. B. GIRLING, R. G. GRAHAM, J. C. GREEN, R. GRINTER and R. N. PERUTZ, *J. Am. Chem. Soc.* **110**, 5039–50 (1988).

<sup>39</sup> B. KANELAKOPOULOS, B. NUBER, K. RAPTIS and M. L. ZIEGLER, *Angew. Chem. Int. Edn. Engl.* **28**, 1055 (1989).

with (o-tolyl)MgBr in thf yields the dark red, paramagnetic tetraaryl,  $[\text{Re}(\text{2-MeC}_6\text{H}_4)_4]^{(40)}$ . This highly air-sensitive compound, if treated with  $\text{PMe}_2\text{R}$  ( $\text{R} = \text{Me, Ph}$ ), is converted into the thermally stable and rather inert benzyne,  $[\text{Re}(\eta^2\text{-C}_6\text{H}_3\text{Me})(\text{PMe}_2\text{R})_2(\text{2-MeC}_6\text{H}_4)_2]^{(41)}$ .

A whole series of alkyl cluster compounds  $\text{Re}_3\text{Cl}_3\text{R}_6$  has been prepared by reacting  $\text{Re}_3\text{Cl}_9$  with a large excess of  $\text{RMgCl}$  in

thf. The blue diamagnetic trimethylsilylmethyl complex (Fig. 24.12) is best known. A red isomer has been obtained in which the Cl bridges have exchanged positions with three of the terminal alkyls, and it is also possible to replace the Cl bridges by  $\text{CH}_3$  to produce,  $[\text{Re}_3(\mu\text{-CH}_3)_3(\text{CH}_2\text{SiMe}_3)_6]$ . Adducts,  $[\text{Re}_3\text{Cl}_3(\text{CH}_2\text{SiMe}_3)_6\text{L}_3]$  ( $\text{L} = \text{CO, H}_2\text{O}$ ) can be obtained, but phosphines tend to cause cleavage of the  $\text{Re}_3$  ring instead of forming adducts.

---

<sup>40</sup> P. SAVAGE, G. WILKINSON, M. MOTEVALLI and M. B. HURSTHOUSE, *J. Chem. Soc., Dalton Trans.*, 669–73 (1988).

---

<sup>41</sup> J. ARNOLD, G. WILKINSON, B. HUSSAIN and M. B. HURSTHOUSE *J. Chem. Soc., Chem. Commun.* 704–5 (1988).

		1		2													
		H		He													
3	4											5	6	7	8	9	10
Li	Be											B	C	N	O	F	Ne
11	12											13	14	15	16	17	18
Na	Mg											Al	Si	P	S	Cl	Ar
19	20	21	22	23	24	25	26	27	28	29	30	31	32	33	34	35	36
K	Ca	Sc	Ti	V	Cr	Mn	Fe	Co	Ni	Cu	Zn	Ga	Ge	As	Se	Br	Kr
37	38	39	40	41	42	43	44	45	46	47	48	49	50	51	52	53	54
Rb	Sr	Y	Zr	Nb	Mo	Tc	Ru	Rh	Pd	Ag	Cd	In	Sn	Sb	Te	I	Xe
55	56	57	58	59	60	61	62	63	64	65	66	67	68	69	70	71	72
Cs	Ba	La	Hf	Ta	W	Re	Os	Ir	Pt	Au	Hg	Tl	Pb	Bi	Po	At	Rn
87	88	89	90	91	92	93	94	95	96	97	98	99	100	101	102	103	104
Fr	Ra	Ac	Rf	Db	Sg	Bh	Hs	Mt	Uun	Uun	Uun	Uun	Uun	Uun	Uun	Uun	Uun
88	89	90	91	92	93	94	95	96	97	98	99	100	101	102	103	104	105
Ce	Pr	Nd	Pm	Sm	Eu	Gd	Tb	Dy	Ho	Er	Tm	Yb	Lu				
90	91	92	93	94	95	96	97	98	99	100	101	102	103	104	105	106	107
Th	Pa	U	Np	Pu	Am	Cm	Bk	Cf	Es	Fm	Md	No	Lr				

# 25

## Iron, Ruthenium and Osmium

### 25.1 Introduction

The nine elements, Fe, Ru, Os; Co, Rh, Ir; Ni, Pd and Pt, together formed Group VIII of Mendeleev's periodic table. They will be treated here, like the other transition elements, in "vertical" triads, but because of the marked "horizontal" similarities it is not uncommon for Fe, Co and Ni to be distinguished from the other six elements (known collectively as the "platinum" metals) and the two sets of elements considered separately.

The triad Fe, Ru and Os is dominated, as indeed is the whole block of transition elements, by the immense importance of iron. This element has been known since prehistoric times and no other metal has played a more important role in man's material progress. Iron beads dating from around 4000 BC were no doubt of meteoric origin, and later samples, produced by reducing iron ore with charcoal, were not cast because adequate temperatures were not attainable without the use of some form of bellows. Instead, the spongy material produced by low-temperature reduction would have had to be shaped by prolonged hammering. It seems that iron was first smelted by the Hittites in Asia

Minor sometime in the third millennium BC, but the value of the process was so great that its secret was carefully guarded and it was only with the eventual fall of the Hittite empire around 1200 BC that the knowledge was dispersed and the "Iron Age" began.<sup>(1)</sup> In more recent times the introduction of coke as the reductant had far-reaching effects, and was one of the major factors in the initiation of the Industrial Revolution. The name "iron" is Anglo-Saxon in origin (*iren*, cf. German *Eisen*). The symbol Fe and words such as "ferrous" derive from the Latin *ferrum*, iron.

Biologically, iron plays crucial roles in the transport and storage of oxygen and also in electron transport, and it is safe to say that, with only a few possible exceptions in the bacterial world, there would be no life without iron. Again, within the last forty years or so, the already rich organometallic chemistry of iron has been enormously expanded, and work in the whole field given an added impetus by the discovery and characterization of ferrocene.<sup>(2)</sup>

<sup>1</sup> V. G. CHILDE, *What Happened in History*, pp. 182–5, Penguin Books, London, 1942.

<sup>2</sup> J. S. THAYER, *Adv. Organometallic Chem.* **13**, 1–49 (1975).

Ruthenium and osmium, though interesting and useful, are in no way comparable with iron and are relative newcomers. They were discovered independently in the residues left after crude platinum had been dissolved in aqua regia; ruthenium in 1844 from ores from the Urals by K. Klaus<sup>(2a)</sup> who named it after *Ruthenia*, the Latin name for Russia; and osmium in 1803 by S. Tennant who named it from the Greek word for odour (ὄσμη, *osme*) because of the characteristic and pungent smell of the volatile oxide, OsO<sub>4</sub>. (CAUTION: OsO<sub>4</sub> is very toxic.)

## 25.2 The Elements Iron, Ruthenium and Osmium

### 25.2.1 Terrestrial abundance and distribution

Ruthenium and osmium are generally found in the metallic state along with the other “platinum” metals and the “coinage” metals. The major source of the platinum metals are the nickel–copper sulfide ores found in South Africa and Sudbury (Canada), and in the river sands of the Urals in Russia. They are rare elements, ruthenium particularly so, their estimated abundances in the earth’s crustal rocks being but 0.0001 (Ru) and 0.005 (Os) ppm. However, as in Group 7, there is a marked contrast between the abundances of the two heavier elements and that of the first.

The nuclei of iron are especially stable, giving it a comparatively high cosmic abundance (Chap. 1, p. 11), and it is thought to be the main constituent of the earth’s core (which has a radius of approximately 3500 km, i.e. 2150 miles) as well as being the major component of “siderite” meteorites. About 0.5% of the lunar soil is now known to be metallic iron and, since on average this soil is 10 m deep, there must be  $\sim 10^{12}$  tonnes of iron on the moon’s surface. In the earth’s crustal rocks (6.2%, i.e. 62 000 ppm) it is the fourth most abundant element (after oxygen, silicon and aluminium) and the second most abundant metal. It is also widely distributed,

as oxides and carbonates, of which the chief ones are: haematite (Fe<sub>2</sub>O<sub>3</sub>), magnetite (Fe<sub>3</sub>O<sub>4</sub>), limonite ( $\sim 2\text{Fe}_2\text{O}_3 \cdot 3\text{H}_2\text{O}$ ) and siderite (FeCO<sub>3</sub>). Iron pyrite (FeS<sub>2</sub>) is also common but is not used as a source of iron because of the difficulty in eliminating the sulfur. The distribution of iron has been considerably influenced by weathering. Leaching from sulfide and silicate deposits occurs readily as FeSO<sub>4</sub> and Fe(HCO<sub>3</sub>)<sub>2</sub> respectively. In solution, these are quickly oxidized, and even mildly alkaline conditions cause the precipitation of iron(III) oxide. Because of their availability, production of iron ores can be confined to those of the highest grade in gigantic operations.

### 25.2.2 Preparation and uses of the elements

Pure iron, when needed, is produced on a relatively small scale by the reduction of the pure oxide or hydroxide with hydrogen, or by the carbonyl process in which iron is heated with carbon monoxide under pressure and the Fe(CO)<sub>5</sub> so formed decomposed at 250°C to give the powdered metal. However, it is not in the pure state but in the form of an enormous variety of steels that iron finds its most widespread uses, the world’s annual production being over 700 million tonnes.

The first stage in the conversion of iron ore to steel is the *blast furnace* (see Panel), which accounts for the largest tonnage of any metal produced by man. In it the iron ore is reduced by coke,<sup>†</sup> while limestone removes any sand or clay as a slag. The molten iron is run off to be cast into moulds of the required shape or into ingots (“pigs”) for further processing — hence the names “cast-iron” or “pig-iron”. This is an

<sup>†</sup> The actual reducing agent is, in the main, CO. Direct reduction of the ore using H<sub>2</sub>, CO or CO + H<sub>2</sub> gas (produced from natural gas or fossil fuels) now accounts for about 4% of the world’s total production of iron. With a much lower operating temperature than that of the blast furnace, reduction is confined to the ore, producing a “sponge” iron and leaving the gangue relatively unchanged. This offers a potential economy in fuel providing that the quantity and composition of the gangue do not adversely affect the subsequent conversion to steel — which is most commonly by the electric arc furnace.

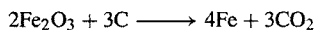
<sup>2a</sup> V. N. PITCHKOV, *Platinum Metals Rev.* **40**, 181–8 (1996).

### Iron<sup>(3,4)</sup> and Steel<sup>(5)</sup>

About 1773, in order to overcome a shortage of timber for the production of charcoal, Abraham Darby developed a process for producing carbon (coke) from coal and used this instead of charcoal in his blast furnace at Coalbrookdale in Shropshire. The impact was dramatic. It so cheapened and increased the scale of ironmaking that in the succeeding decades Shropshire iron was used to produce for the first time: iron cylinders for steam-engines, iron rails, iron boats and ships, iron aqueducts, and iron-framed buildings. The iron bridge erected nearby over the River Severn in 1779, gave its name to the small town which grew around it and still stands, a monument to the process which "opened up" the iron industry to the Industrial Revolution.

The blast furnace (Fig. A, opposite) remains the basis of ironmaking though the scale, if not the principle, has changed considerably since the eighteenth century: the largest modern blast furnaces have hearths 14 m in diameter and produce up to 10 000 tonnes of iron daily.

The furnace is charged with a mixture of the ore (usually haematite), coke and limestone, then a blast of hot air, or air with fuel oil, is blown in at the bottom. The coke burns and such intense heat is generated that temperatures approaching 2000°C are reached near the base of the furnace and perhaps 200°C at the top. The net result is that the ore is reduced to iron, and siliceous gangue forms a slag (mainly CaSiO<sub>3</sub>) with the limestone:



The molten iron, and the molten slag which floats on the iron, collect at the bottom of the furnace and are tapped off separately. As the charge moves down, the furnace is recharged at the top, making the process continuous. Of course the actual reactions taking place are far more numerous than this and only the more important ones are summarized in Fig. A. The details are exceedingly complex and still not fully understood. At least part of the reason for this complexity is the rapidity with which the blast passes through the furnace (~10 s) which does not allow the gas-solid reactions to reach equilibrium. The main reduction occurs near the top, as the hot rising gases meet the descending charge. Here too the limestone is converted to CaO. Reduction to the metal is completed at somewhat higher temperatures, after which fusion occurs and the iron takes up Si and P in addition to C. The deleterious uptake of S is considerably reduced if manganese is present, because of the formation of MnS which passes into the slag. For this the slag must be adequately fluid and to this end the ratio of base (CaO):acid (SiO<sub>2</sub>, Al<sub>2</sub>O<sub>3</sub>) is maintained by the addition, if necessary, of gravel (SiO<sub>2</sub>). The slag is subsequently used as a building material (breeze blocks, wall insulation) and in the manufacture of some types of cement.

Traditionally, pig-iron was converted to wrought-iron by the "puddling" process in which the molten iron was manually mixed with haematite and excess carbon and other impurities burnt out. Some wrought-iron was then converted to steel by essentially small-scale and expensive methods, such as the Cementation process (prolonged heating of wrought-iron bars with charcoal) and the crucible process (fusion of wrought-iron with the correct amount of charcoal). In the mid-nineteenth century, production was enormously increased by the introduction of the *Bessemer process* in which the carbon content of molten pig-iron in a "converter" was lowered by blasting compressed air through it. The converter was lined with silica or limestone in order to form a molten slag with the basic or acidic impurities present in the pig-iron. Air and appropriate linings were also employed in the *Open-hearth process* which allowed better control of the steel's composition, but both processes have now been supplanted by the *Basic oxygen* and *Electric arc* processes.

*Basic oxygen process (BOP)*. This process, of which there are several modifications, originated in Austria in 1952, and because of its greater speed has since become by far the most common means of producing steel. A jet of pure oxygen is blown through a retractable steel "lance" into, or over the surface of, the molten pig-iron which is contained in a basic-lined furnace. Impurities form a slag which is usually removed by tilting the converter.

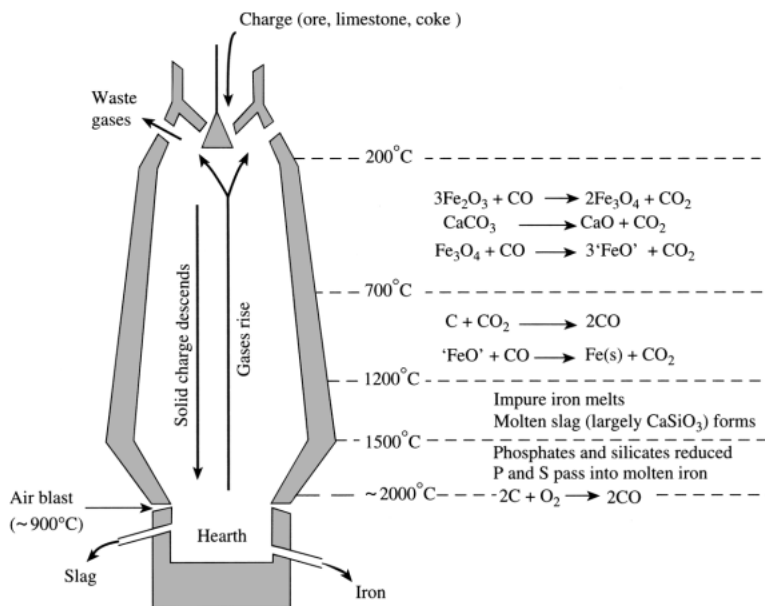
*Electric arc process*. Patented by Siemens in 1878, this uses an electric current through the metal (direct-arc), or an arc just above the metal (indirect-arc), as a means of heating. It is widely used in the manufacture of alloy- and other high-quality steels.

World production of iron ore in 1995 was 1020 million tonnes (Mt) (China 25%, Brazil 18%, former USSR 14%, Australia 12.9%, India and USA 6% each). In the same year world production of raw steel was 748 Mt (Western Europe 22.7%, N. America 16.2%, Japan 13.6%, China 12.4%, former USSR 10.6% and S. America 4.7%).

<sup>3</sup>Kirk-Othmer *Encyclopedia of Chemical Technology*, 4th edn., Vol. 14, pp. 829–72, Interscience, New York, 1995.

<sup>4</sup>Ullmann's *Encyclopedia of Industrial Chemistry*, 5th edn., Vol. A21, pp. 461–590, VCH, Weinheim, 1989.

<sup>5</sup>Ref. 4, Vol. A25, pp. 63–307, 1994.



**Figure A** Blast furnace (diagrammatic).

impure form of iron, containing about 4% of carbon along with variable amounts of Si, Mn, P and S. It is hard but notoriously brittle. To eradicate this disadvantage the non-metallic impurities must be removed. This can be done by oxidizing them with haematite in the now obsolete “puddling process”, producing the much purer “wrought-iron”, which is tough and malleable and ideal for mechanical working. Nowadays, however, the bulk of pig-iron is converted into steel containing 0.5–1.5% C but very little S or P. The oxidation in this case is most commonly effected in one of a number of related processes by pure oxygen (basic oxygen process, or BOP), but open-hearth and electric arc furnaces are also used, while the Bessemer Converter (see Panel) was of great historical importance. This “mild steel” is cheaper than wrought-iron and stronger and more workable than cast-iron; it also has the advantage over both that it can be hardened by heating to redness and then cooling rapidly (quenching) in water or mineral oil, and “tempered” by re-heating to 200–300°C and cooling more slowly. The hardness, resilience and ductility can be controlled by varying the temperature and the

rate of cooling as well as the precise composition of the steel (see below). Alloy steels, with their enormous variety of physical properties, are prepared by the addition of the appropriate alloying metal or metals.

All the platinum group metals are isolated from “platinum concentrates” which are commonly obtained either from “anode slimes” in the electrolytic refining of nickel and copper, or as “converter matte” from the smelting of sulfide ores.<sup>(6)</sup> The details of the procedure used differ from location to location and depend on the composition of the concentrate. Classical methods of separation, relying on selective precipitation, are still widely employed but solvent extraction and ion exchange techniques are increasingly being introduced to effect the primary separations (p. 1147).

Ru and Os are usually removed by distillation of their tetroxides immediately after the initial dissolution with hydrochloric acid and chlorine. Collection of the tetroxides in alcoholic NaOH and aqueous HCl respectively yields  $\text{OsO}_2(\text{NH}_3)_4\text{Cl}_2$  and  $(\text{NH}_4)_3\text{RuCl}_6$  from which the metals are

<sup>6</sup> Ref. 4, Vol. A21, pp. 86–105, 1992.

Table 25.1 Some properties of the elements iron, ruthenium and osmium

Property	Fe	Ru	Os
Atomic number	26	44	76
Number of naturally occurring isotopes	4	7	7
Atomic weight	55.845(2)	101.07(2)	190.23(3)
Electronic configuration	[Ar]3d <sup>6</sup> 4s <sup>2</sup>	[Kr]4d <sup>7</sup> 5s <sup>1</sup>	[Xe]4f <sup>14</sup> 5d <sup>6</sup> 6s <sup>2</sup>
Electronegativity	1.8	2.2	2.2
Metal radius (12-coordinate)/pm	126	134	135
Effective ionic radius/pm	VIII	36 <sup>(a)</sup>	39 <sup>(a)</sup>
(4-coordinate if marked <sup>(a)</sup> , VII otherwise 6-coordinate)	—	38 <sup>(a)</sup>	52.5
	VI	—	54.5
	V	56.5	57.5
	IV	62	63
	III	68	—
	II	—	—
MP/°C	1535	2282(±20)	3045(±30)
BP/°C	2750	extrap 4050(±100)	extrap 5025(±100)
$\Delta H_{\text{fus}}/\text{kJ mol}^{-1}$	13.8	~25.5	31.7
$\Delta H_{\text{vap}}/\text{kJ mol}^{-1}$	340(±13)	—	738
$\Delta H_{\text{f}}(\text{monatomic gas})/\text{kJ mol}^{-1}$	398(±17)	640	791(±13)
Density (20°C)/g cm <sup>-3</sup>	7.874	12.37	22.59
Electrical resistivity (20°C)/μohm cm	9.71	6.71	8.12

<sup>(a)</sup>Refers to coordination number 4. ls = low spin, hs = high spin.

obtained by ignition in H<sub>2</sub>. The metals are in the form of powder or sponge and are usually consolidated by powder-metallurgical techniques. Major uses of ruthenium are as a coating for titanium anodes in the electrolytic production of Cl<sub>2</sub> and, more recently, as a catalyst in the production of ammonia (p. 421). Osmium is used in dentistry as a hardening agent in gold alloys. However, Ru and Os, along with Ir, are regarded as the minor platinum metals, being obtained largely as byproducts in the production of Pt, Pd and Rh, and their annual world production is only of the order of tonnes. (Weights of Ru and Os, as of most precious metals, are generally quoted in troy ounces: 1 troy ounce = 1.097 avoirdupois ounce = 31.103 g.)

### 25.2.3 Properties of the elements

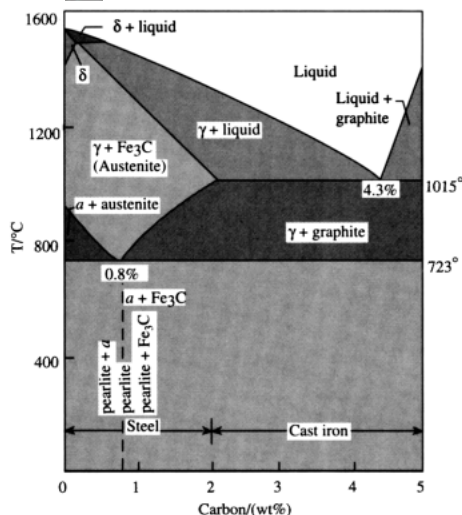
Table 25.1 summarizes some of the important properties of Fe, Ru and Os. The two heavier elements in particular have several naturally occurring isotopes, and difficulties in obtaining calibrated measurements of their

relative abundances limit the precision with which their atomic weights can be determined. Osmium is the densest of all elements, surpassing iridium by the tiniest of margins.<sup>(7)</sup>

All three elements are lustrous and silvery in colour. Iron when pure is fairly soft and readily worked, but ruthenium and osmium are less tractable in this respect. The structures of the solids are typically metallic, being hcp for the two heavier elements and bcc for iron at room temperature ( $\alpha$ -iron). However, the behaviour of iron is complicated by the existence of a fcc form ( $\gamma$ -iron) at higher temperatures (above 910°), reverting to bcc again ( $\delta$ -iron) at about 1390°, some 145° below its mp. Technologically, the carbon content is crucial, as can be seen from the Fe/C phase diagram (Fig. 25.1), which also throws light on the hardening and tempering

<sup>7</sup>Densities are calculated from crystallographic data and depend on a knowledge of the wavelength of the X-rays, Avogadro's constant and the atomic weight of the element. Using the best available data the densities of Os and Ir are calculated to be  $22.587 \pm 0.009$  and  $22.562 \pm 0.009$  g cm<sup>-3</sup> respectively at 20°C. J. W. ARBLASTER, *Platinum Metals Rev.* **33**, 14–16 (1989). *ibid.*, **39**, 164 (1995).





**Figure 25.1** The iron-carbon phase diagram for low concentrations of carbon.

processes already referred to. The lowering of the mp from  $1535^{\circ}$  to  $1015^{\circ}\text{C}$  when the C content reaches 4.3%, facilitates the fusion of iron in the blast furnace, and the lower solubility of  $\text{Fe}_3\text{C}$  (“cementite”) in  $\alpha$ -iron as compared to  $\delta$ - and  $\gamma$ -iron leads to the possibility of producing metastable forms by varying the rate of cooling of hot steels. At elevated temperatures a solid solution of  $\text{Fe}_3\text{C}$  in  $\gamma$ -iron, known as “austenite”, prevails. If 0.8% C is present, slow cooling below  $723^{\circ}\text{C}$  causes  $\text{Fe}_3\text{C}$  to separate forming alternate layers with the  $\alpha$ -iron. Because of its appearance when polished, this is known as “pearlite” and is rather soft and malleable. If, however, the cooling is rapid (quenching) the separation is suppressed and the extremely hard and brittle “martensite” is produced. Reheating to an intermediate temperature tempers the steel by modifying the proportions of hard and malleable forms. If the C content of the steel is below 0.8% then slow cooling gives a mixture of pearlite and  $\alpha$ -iron and, if higher than 0.8% a mixture of pearlite and  $\text{Fe}_3\text{C}$ . Varying the proportion of carbon in the steel thereby further extends the range of physical properties which can be attained by appropriate heat treatment.

The magnetic properties of iron are also dependent on purity and heat treatment. Up to  $768^{\circ}\text{C}$

(the Curie point) pure iron is ferromagnetic as a result of extensive magnetic interactions between unpaired electrons on adjacent atoms, which cause the electron spins to be aligned in the same direction, so producing exceedingly high magnetic susceptibilities and the characteristic ferromagnetic properties of “saturation” and “hysteresis”. The existence of unpaired electrons on the individual atoms, as opposed to being delocalized in bands permeating the lattice, can be rationalized at least partly by supposing that in the bcc lattice the metal  $d_{z^2}$  and  $d_{x^2-y^2}$  orbitals, which are not directed towards nearest neighbours, are therefore nonbonding and so can retain 2 unpaired electrons on the atom. On the other hand, electrons in the remaining three d orbitals participate in the formation of a conduction band of predominantly paired electrons. At temperatures above the Curie temperature, thermal energy overcomes the interaction between the electrons localized on individual atoms; their mutual alignment is broken, and normal paramagnetic behaviour ensues. This is sometimes referred to as  $\beta$ -iron ( $768\text{--}910^{\circ}$ ) though the crystal structure remains bcc as in ferromagnetic  $\alpha$ -iron. For the construction of permanent magnets, cobalt steels are particularly useful, whereas for the “soft” irons used in electric motors and transformer cores (where the magnetization undergoes rapid reversal) silicon steels are preferred.

The mps and bps and enthalpies of atomization indicate that the  $(n-1)d$  electrons are contributing to metal bonding less than in earlier groups although, possibly due to an enhanced tendency for metals with a  $d^5$  configuration to resist delocalization of their d electrons, Mn and to a lesser extent Tc occupy “anomalous” positions so that for Fe and Ru the values of these quantities are actually higher than for the elements immediately preceding them. In the third transition series Re appears to be “well-behaved” and the changes from  $\text{W} \rightarrow \text{Re} \rightarrow \text{Os}$  are consequently smooth.

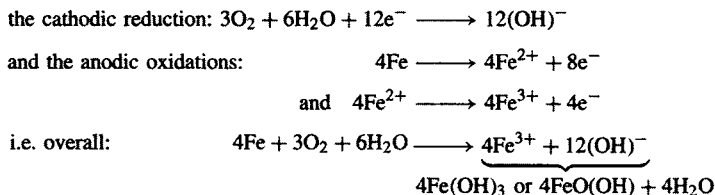
### 25.2.4 Chemical reactivity and trends

As expected, contrasts between the first element and the two heavier congeners are noticeable,

### Rusting of Iron<sup>(8)</sup>

The economic importance of rusting can scarcely be overestimated. Although precision is impossible, it is likely that the cost of corrosion is over 1% of the world's economy.

Rusting of iron consists of the formation of hydrated oxide,  $\text{Fe}(\text{OH})_3$  or  $\text{FeO}(\text{OH})$ , and is evidently an electrochemical process which requires the presence of water, oxygen and an electrolyte — in the absence of any one of these rusting does not occur to any significant extent. In air, a relative humidity of over 50% provides the necessary amount of water. The mechanism is complex<sup>(9)</sup> and will depend in detail on the prevailing conditions, but may be summarized as:



The presence of the electrolyte is required to provide a pathway for the current and, in urban areas, this is commonly iron(II) sulfate formed as a result of attack by atmospheric  $\text{SO}_2$  but, in seaside areas, airborne particles of salt are important. Because of its electrochemical nature, rusting may continue for long periods at a more or less constant rate, in contrast to the formation of an anhydrous oxide coating which under dry conditions slows down rapidly as the coating thickens.

The anodic oxidation of the iron is usually localized in surface pits and crevices which allow the formation of adherent rust over the remaining surface area. Eventually the lateral extension of the anodic area undermines the rust to produce loose flakes. Moreover, once an adherent film of rust has formed, simply painting over gives but poor protection. This is due to the presence of electrolytes such as iron(II) sulfate in the film so that painting merely seals in the ingredients for anodic oxidation. It then only requires the exposure of some other portion of the surface, where cathodic reduction can take place, for rusting beneath the paint to occur.

The protection of iron and steel against rusting takes many forms, including: simple covering with paint; coating with another metal such as zinc (galvanizing) or tin; treating with "inhibitors" such as chromate(VI) or (in the presence of air) phosphate or hydroxide, all of which produce a coherent protective film of  $\text{Fe}_2\text{O}_3$ . Another method uses sacrificial anodes, most usually Mg or Zn which, being higher than Fe in the electrochemical series, are attacked preferentially. In fact, the Zn coating on galvanized iron is actually a sacrificial anode.

both in the reactivity of the elements and in their chemistry. Iron is much the most reactive metal of the triad, being pyrophoric if finely divided and dissolving readily in dilute acids to give  $\text{Fe}^{\text{II}}$  salts; however, it is rendered passive by oxidizing acids such as concentrated nitric and chromic, due to the formation of an impervious oxide film which protects it from further reaction but which is immediately removed by acids such as hydrochloric. Ruthenium and osmium, on the other hand, are virtually unaffected by non-oxidizing acids, or even aqua regia. Iron also reacts fairly easily with most non-metals whereas ruthenium and osmium do so only with difficulty at high temperatures, except in the case of

oxidizing agents such as  $\text{F}_2$  and  $\text{Cl}_2$ . Indeed, it is with oxidizing agents generally that Ru and Os metals are most reactive. Thus Os is converted to  $\text{OsO}_4$  by conc nitric acid and both metals can be dissolved in molten alkali in the presence of air or, better still, in oxidizing flux such as  $\text{Na}_2\text{O}_2$  or  $\text{KClO}_3$  to give the ruthenates and osmates  $[\text{RuO}_4]^{2-}$  and  $[\text{OsO}_2(\text{OH})_4]^{2-}$  respectively. If the aqueous extracts from these fusions are treated with  $\text{Cl}_2$  and heated, the tetroxides distil off, providing convenient preparative starting materials as well as the means of recovering the elements.

Ruthenium and Os are stable to atmospheric attack though if Os is very finely divided it gives off the characteristic smell of  $\text{OsO}_4$ . By contrast, iron is subject to corrosion in the form of rusting which, because of its great economic importance, has received much attention (see Panel above).

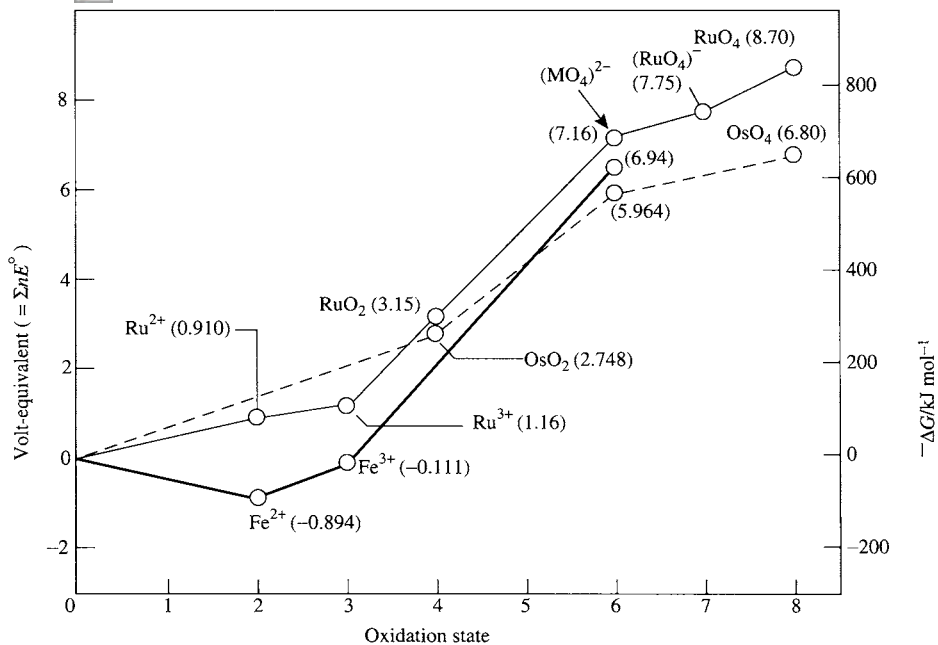
<sup>8</sup> U. R. EVANS, *An Introduction to Metallic Corrosion*, Arnold, London, 3rd edn, 1981, 320 pp.

<sup>9</sup> T. E. GRAEDEL and R. P. FRANKENTHAL, *J. Electrochem. Soc.* **137**, 2385–94 (1990).

**Table 25.2** Standard reduction potentials for iron, ruthenium and osmium in acidic aqueous solution<sup>(a)</sup>

Half reaction	$E^\circ/V$	Volt-equivalent
$\text{Fe}^{2+} + 2e^- \rightleftharpoons \text{Fe}$	-0.447	-0.894
$\text{Fe}^{3+} + 3e^- \rightleftharpoons \text{Fe}$	-0.037	-0.111
$(\text{FeO}_4)^{2-} + 8\text{H}^+ + 3e^- \rightleftharpoons \text{Fe}^{3+} + 4\text{H}_2\text{O}$	2.20	6.49
$\text{Ru}^{2+} + 2e^- \rightleftharpoons \text{Ru}$	0.455	0.910
$\text{Ru}^{3+} + e^- \rightleftharpoons \text{Ru}^{2+}$	0.249	1.159
$\text{RuO}_2 + 4\text{H}^+ + 2e^- \rightleftharpoons \text{Ru}^{2+} + 2\text{H}_2\text{O}$	1.120	3.150
$(\text{RuO}_4)^{2-} + 8\text{H}^+ + 4e^- \rightleftharpoons \text{Ru}^{2+} + 4\text{H}_2\text{O}$	1.563	7.162
$(\text{RuO}_4)^- + 8\text{H}^+ + 5e^- \rightleftharpoons \text{Ru}^{2+} + 4\text{H}_2\text{O}$	1.368	7.750
$\text{RuO}_4 + 4\text{H}^+ + 4e^- \rightleftharpoons \text{RuO}_2 + 2\text{H}_2\text{O}$	1.387	8.698
$\text{OsO}_2 + 4\text{H}^+ + 4e^- \rightleftharpoons \text{Os} + 2\text{H}_2\text{O}$	0.687	2.748
$(\text{OsO}_4)^{2-} + 8\text{H}^+ + 6e^- \rightleftharpoons \text{Os} + 4\text{H}_2\text{O}$	0.994	5.964
$\text{OsO}_4 + 8\text{H}^+ + 8e^- \rightleftharpoons \text{Os} + 4\text{H}_2\text{O}$	0.85	6.80

(a) See also Table A (p. 1093) and Table 25.8 (p. 1101).

 **LIVE GRAPH**
**Figure 25.2** Plot of volt-equivalent against oxidation state for Fe, Ru and Os in acidic aqueous solution.

In moving across the transition series, iron is the first element which fails to attain its group oxidation state (+8). The highest oxidation state known (so far) is +6 in  $[\text{FeO}_4]^{2-}$  and even this is extremely easily reduced. On the

other hand, ruthenium and osmium do attain the group oxidation state of +8, though they are the last elements to do so in the second and third transition series, and this is consequently the highest oxidation state for any element (see also

Xe<sup>VIII</sup>, p. 894). Ruthenium(VIII) is significantly less stable than Os<sup>VIII</sup> and it is clear that the second- and third-row elements, though similar, are by no means as alike as for earlier element-pairs in the transition series. The same gradation within the triad is well illustrated by the reactions of the metals with oxygen. All react on heating, but their products are, respectively, Fe<sub>2</sub>O<sub>3</sub> and Fe<sub>3</sub>O<sub>4</sub>, Ru<sup>IV</sup>O<sub>2</sub> and Os<sup>VIII</sup>O<sub>4</sub>. In general terms it can be said that the most common oxidation states

for the three elements are +2 and +3 for Fe, +3 for Ru, and +4 for Os. And, while Fe (and to a lesser extent Ru) has an extensive aqueous cationic chemistry in its lower oxidation states, Os has none. Table 25.2 and Fig. 25.2 summarize the relative stabilities of the various oxidation states in acidic aqueous solution.

A selection of representative examples of compounds of the three elements is given in Table 25.3. As in the preceding group there is

**Table 25.3** Oxidation states and stereochemistries of some compounds of iron, ruthenium and osmium

Oxidation state	Coordination number	Stereochemistry	Fe	Ru, Os
-2 (d <sup>10</sup> )	4	Tetrahedral	[Fe(CO) <sub>4</sub> ] <sup>2-</sup>	[M(CO) <sub>4</sub> ] <sup>2-</sup>
-1 (d <sup>9</sup> )	5	Trigonal bipyramidal	[Fe <sub>2</sub> (CO) <sub>8</sub> ] <sup>2-</sup>	
0 (d <sup>8</sup> )	5	Trigonal bipyramidal	[Fe(CO) <sub>5</sub> ]	[M(CO) <sub>5</sub> ](?)
	6	Octahedral (D <sub>3</sub> )	[Fe(bipy) <sub>3</sub> ]	
	7	Face-capped octahedral	[Fe <sub>2</sub> (CO) <sub>9</sub> ]	
1 (d <sup>7</sup> )	2	Linear	[FeO <sub>2</sub> ] <sup>3-</sup>	
	6	Octahedral	[Fe(NO)(H <sub>2</sub> O) <sub>5</sub> ] <sup>2+</sup>	[Os(NH <sub>3</sub> ) <sub>6</sub> ] <sup>+</sup>
	9	(See Fig. 25.15(a))	[(Fe(η <sup>5</sup> -C <sub>5</sub> H <sub>5</sub> )(CO)(μ-CO)) <sub>2</sub> ]	
2 (d <sup>6</sup> )	4	Tetrahedral	[FeCl <sub>4</sub> ] <sup>2-</sup>	[RuH{N(SiMe <sub>3</sub> ) <sub>2</sub> }(PPh <sub>3</sub> ) <sub>2</sub> ]
		Square planar	BaFeSi <sub>4</sub> O <sub>10</sub>	
	5	Trigonal bipyramidal	[FeBr{N(C <sub>2</sub> H <sub>4</sub> NMe <sub>2</sub> ) <sub>3</sub> }] <sup>+</sup>	
		Square pyramidal	[Fe(OAsMe <sub>3</sub> ) <sub>4</sub> (ClO <sub>4</sub> )] <sup>+</sup>	[RuCl <sub>2</sub> (PPh <sub>3</sub> ) <sub>3</sub> ]
	6	Octahedral	[Fe(H <sub>2</sub> O) <sub>6</sub> ] <sup>2+</sup>	[M(CN) <sub>6</sub> ] <sup>4-</sup>
	7	(p. 174)	[Fe(η <sup>4</sup> -B <sub>4</sub> H <sub>8</sub> )(CO) <sub>3</sub> ]	
	8	(See Fig. 25.15c)	[Fe(η <sup>1</sup> -C <sub>5</sub> H <sub>5</sub> )(η <sup>5</sup> -C <sub>5</sub> H <sub>5</sub> )(CO) <sub>2</sub> ]	
	10	Sandwich	[Fe(η <sup>5</sup> -C <sub>5</sub> H <sub>5</sub> ) <sub>2</sub> ]	[M(η <sup>5</sup> -C <sub>5</sub> H <sub>5</sub> ) <sub>2</sub> ]
3 (d <sup>5</sup> )	3	Planar	[Fe{N(SiMe <sub>3</sub> ) <sub>2</sub> ] <sub>3</sub> ]	
	4	Tetrahedral	[FeCl <sub>4</sub> ] <sup>-</sup>	
	5	Square pyramidal	[Fe(acac) <sub>2</sub> Cl]	
	6	Octahedral	[Fe(CN) <sub>6</sub> ] <sup>3-</sup>	[MCl <sub>6</sub> ] <sup>3-</sup>
	7	Pentagonal bipyramidal	[Fe(edta)(H <sub>2</sub> O)] <sup>-</sup>	
	8	Dodecahedral	[Fe(NO <sub>3</sub> ) <sub>4</sub> ] <sup>-</sup>	
4 (d <sup>4</sup> )	6	Octahedral	[Fe(diars) <sub>2</sub> Cl <sub>2</sub> ] <sup>2+</sup>	[MCl <sub>6</sub> ] <sup>2-</sup>
	4	Tetrahedral		OsCy <sub>4</sub>
5 (d <sup>3</sup> )	4	Tetrahedral	[FeO <sub>4</sub> ] <sup>3-</sup>	
	6	Octahedral		[MF <sub>6</sub> ] <sup>-</sup>
6 (d <sup>2</sup> )	4	Tetrahedral	[FeO <sub>4</sub> ] <sup>2-</sup>	[RuO <sub>4</sub> ] <sup>2-</sup>
	5	Square pyramidal		[OsNCl <sub>4</sub> ] <sup>-</sup>
		Trigonal bipyramidal		[RuO <sub>5</sub> ] <sup>4-(a)</sup>
	6	Octahedral		[OsO <sub>2</sub> (OH) <sub>4</sub> ] <sup>2-</sup>
7 (d <sup>1</sup> )	4	Tetrahedral		[MO <sub>4</sub> ] <sup>-</sup>
	6	Octahedral		[OsOF <sub>5</sub> ]
	7	Pentagonal bipyramidal		OsF <sub>7</sub>
8 (d <sup>0</sup> )	4	Tetrahedral		MO <sub>4</sub>
	6	Octahedral		[OsO <sub>4</sub> F <sub>2</sub> ] <sup>2-</sup>

<sup>(a)</sup>Both tetrahedral and trigonal bipyramidal Ru<sup>VI</sup> occur in the single compound, CsK<sub>5</sub>[RuO<sub>5</sub>][RuO<sub>4</sub>]; D. FISCHER and R. HOPPE, *Z. anorg. allg. Chem.* **617**, 37-44 (1992).

Table 25.4 Electronic spin-states of iron

Spin quantum number (S)	Ion	Electronic configuration	Typical compounds
0 (diamagnetic)	Low-spin Fe <sup>II</sup>	$t_{2g}^6$	K <sub>4</sub> [Fe(CN) <sub>6</sub> ].3H <sub>2</sub> O HbO <sub>2</sub> (oxygenated haemoglobin)
$\frac{1}{2}$ (1 unpaired e <sup>-</sup> )	Low-spin Fe <sup>III</sup>	$t_{2g}^5$	K <sub>3</sub> [Fe(CN) <sub>6</sub> ], HbCN
1 (2 unpaired e <sup>-</sup> )	Low-spin Fe <sup>I</sup>	$t_{2g}^6 e_g^1$	[Fe(diars)(CO) <sub>2</sub> I]
	Low-spin Fe <sup>IV</sup>	$t_{2g}^4 e_g^2$	[Fe(diars) <sub>2</sub> Cl <sub>2</sub> ](ClO <sub>4</sub> ) <sub>2</sub>
$\frac{3}{2}$ (3 unpaired e <sup>-</sup> )	Tetrahedral Fe <sup>VI</sup>	$e^3$	Ba[FeO <sub>4</sub> ]
	Distorted square pyramidal Fe <sup>III</sup>	$d_{x^2-y^2}^2 d_{yz}^1 d_{xz}^1 d_{z^2}^1$	[Fe(S <sub>2</sub> CNR <sub>2</sub> ) <sub>2</sub> Cl]
2 (4 unpaired e <sup>-</sup> )	High-spin Fe <sup>II</sup>	$t_{2g}^4 e_g^2$	[Fe(H <sub>2</sub> O) <sub>6</sub> ] <sup>2+</sup> , deoxyhaemoglobin
$\frac{5}{2}$ (5 unpaired e <sup>-</sup> )	High-spin Fe <sup>III</sup>	$t_{2g}^3 e_g^2$	[Fe(acac) <sub>3</sub> ], iron-transport proteins

a remarkably wide range of oxidation states, particularly for Ru and Os, and, although it is now evident that as the size of the atoms decreases across each period the tendency to form compounds with high coordination numbers is diminishing, Os has a greater tendency than Ru to adopt a coordination number of 6 in the higher oxidation states. Thus OsO<sub>4</sub> expands its coordination sphere far more readily than RuO<sub>4</sub> to form complexes such as [OsO<sub>4</sub>(OH)<sub>2</sub>]<sup>2-</sup>, and Os has no 4-coordinate analogue of [RuO<sub>4</sub>]<sup>2-</sup>.

Iron is notable for the range of electronic spin states to which it gives rise. The values of *S* which are found include every integral and half-integral value from 0 to  $\frac{5}{2}$  i.e. every value possible for a d-block element (Table 25.4).

## 25.3 Compounds of Iron<sup>(10)</sup>, Ruthenium<sup>(11)</sup> and Osmium

The borides (p. 145), carbides (pp. 297, 1074), and nitrides (p. 417) have been discussed previously. Binary hydrides are not formed but prolonged heating of powdered Mg and Fe under a high pressure of H<sub>2</sub> yields MgFeH<sub>6</sub> containing the octahedral hydrido anion, [FeH<sub>6</sub>]<sup>4-</sup> which satisfies the 18-electron rule.

### 25.3.1 Oxides and other chalcogenides

The principal oxides of the elements<sup>(12)</sup> of this group are given in Table 25.5.

Table 25.5 The oxides of iron, ruthenium and osmium

Oxidation state	+8	+4	+3	+2
Fe			Fe <sub>2</sub> O <sub>3</sub>	FeO
Ru		RuO <sub>4</sub>	RuO <sub>2</sub>	
Os		OsO <sub>4</sub>	OsO <sub>2</sub>	

Three oxides of iron may be distinguished, but are all subject to nonstoichiometry. The lowest is FeO which is obtained by heating iron in a low partial pressure of O<sub>2</sub> or as a fine, black pyrophoric powder by heating iron(II) oxalate *in vacuo*. Below about 575°C it is unstable towards disproportionation into Fe and Fe<sub>3</sub>O<sub>4</sub> but can be obtained as a metastable phase if cooled rapidly. It has a rock-salt structure but is always deficient in iron, with a homogeneity range of Fe<sub>0.84</sub>O to Fe<sub>0.95</sub>O. Treatment of any aqueous solution of Fe<sup>II</sup> with alkali produces a flocculent precipitate. If air is rigorously excluded this is the virtually white Fe(OH)<sub>2</sub> which is almost entirely basic in character, dissolving readily in non-oxidizing acids to give Fe<sup>II</sup> salts but

<sup>10</sup> *Chemistry of Iron* (J. SILVER, ed.), Blackie, London, 1993, 306 pp.

<sup>11</sup> E. A. SEDDON and K. R. SEDDON, *The Chemistry of Ruthenium*, Elsevier, Amsterdam, 1984, 1374 pp.

<sup>12</sup> U. SCHWERTMANN and R. M. CORNELL, *Iron Oxides in the Laboratory*, VCH, Weinheim, 1991, 137 pp.

showing only slight reactivity towards alkali. It gradually decomposes, however, to  $\text{Fe}_3\text{O}_4$  with evolution of hydrogen and in the presence of oxygen darkens rapidly and eventually forms the reddish-brown hydrated iron(III) oxide.  $\text{Fe}_3\text{O}_4$  is a mixed  $\text{Fe}^{\text{II}}/\text{Fe}^{\text{III}}$  oxide which can be obtained by partial oxidation of  $\text{FeO}$  or, more conveniently, by heating  $\text{Fe}_2\text{O}_3$  above about  $1400^\circ\text{C}$ . It has the inverse spinel structure. Spinel is of the form  $\text{M}^{\text{II}}\text{M}_2^{\text{III}}\text{O}_4$  and in the normal spinel (p. 247) the oxide ions form a ccp lattice with  $\text{M}^{\text{II}}$  ions occupying tetrahedral sites and  $\text{M}^{\text{III}}$  ions octahedral sites. In the inverse structure half the  $\text{M}^{\text{III}}$  ions occupy tetrahedral sites, with the  $\text{M}^{\text{II}}$  and the other half of the  $\text{M}^{\text{III}}$  occupying octahedral sites.<sup>†</sup>  $\text{Fe}_3\text{O}_4$  occurs naturally as the mineral magnetite or lodestone. It is a black, strongly ferromagnetic substance (or, more strictly, "ferromagnetic" — see p. 1081), insoluble in water and acids. Its electrical properties are not simple, but its rather high conductivity may be ascribed to electron transfer between  $\text{Fe}^{\text{II}}$  and  $\text{Fe}^{\text{III}}$ .

$\text{Fe}_2\text{O}_3$  is known in a variety of modifications of which the more important are the  $\alpha$ - and  $\gamma$ -forms. When aqueous solutions of iron(III) are treated with alkali, a gelatinous reddish-brown precipitate of hydrated oxide is produced (this is amorphous to X-rays and is not simple  $\text{Fe}(\text{OH})_3$ , but probably  $\text{FeO}(\text{OH})$ ); when heated to  $200^\circ\text{C}$ , this gives the red-brown  $\alpha$ - $\text{Fe}_2\text{O}_3$ . Like  $\text{V}_2\text{O}_3$  and  $\text{Cr}_2\text{O}_3$  this has the corundum structure (p. 243) in which the oxide ions are hcp and the metal ions occupy octahedral sites. It occurs naturally as the mineral haematite and, besides its overriding importance as a source of the metal (p. 1072), it is used (a) as a pigment, (b) in the preparation of rare earth/iron garnets and

other ferrites (p. 1081), and (c) as a polishing agent — jewellers' rouge. The second variety  $\gamma$ - $\text{Fe}_2\text{O}_3$  is metastable and is obtained by careful oxidation of  $\text{Fe}_3\text{O}_4$ , like which it is cubic and ferrimagnetic. If heated *in vacuo* it reverts to  $\text{Fe}_3\text{O}_4$  but heating in air converts it to  $\alpha$ - $\text{Fe}_2\text{O}_3$ . It is the most widely used magnetic material in the production of magnetic recording tapes.

The interconvertibility of  $\text{FeO}$ ,  $\text{Fe}_3\text{O}_4$  and  $\gamma$ - $\text{Fe}_2\text{O}_3$  arises because of their structural similarity. Unlike  $\alpha$ - $\text{Fe}_2\text{O}_3$ , which is based on a hcp lattice of oxygen atoms, these three compounds are all based on ccp lattices of oxygen atoms. In  $\text{FeO}$ ,  $\text{Fe}^{\text{II}}$  ions occupy the octahedral sites and nonstoichiometry arises by oxidation, when some  $\text{Fe}^{\text{II}}$  ions are replaced by two-thirds their number of  $\text{Fe}^{\text{III}}$  ions. Continued oxidation produces  $\text{Fe}_3\text{O}_4$  in which the  $\text{Fe}^{\text{II}}$  ions are in octahedral sites, but the  $\text{Fe}^{\text{III}}$  ions are distributed between both octahedral and tetrahedral sites. Eventually, oxidation leads to  $\gamma$ - $\text{Fe}_2\text{O}_3$  in which all the cations are  $\text{Fe}^{\text{III}}$  which are randomly distributed between octahedral and tetrahedral sites. The oxygen lattice remains intact throughout but contracts somewhat as the number of iron atoms which it accommodates diminishes.

Ruthenium and osmium have no oxides comparable to those of iron and, indeed, the lowest oxidation state in which they form oxides is +4.  $\text{RuO}_2$  is a blue to black solid, obtained by direct action of the elements at  $1000^\circ\text{C}$ , and has the rutile (p. 961) structure. The intense colour has been suggested as arising from the presence of small amounts of Ru in another oxidation state, possibly +3.  $\text{OsO}_2$  is a yellowish-brown solid, usually prepared by heating the metal at  $650^\circ\text{C}$  in NO. It, too, has the rutile structure.

The most interesting oxides of Ru and Os, however, are the volatile, yellow tetroxides,  $\text{RuO}_4$  (mp  $25^\circ\text{C}$ , bp  $130^\circ\text{C}$ <sup>(13)</sup>) and  $\text{OsO}_4$  (mp  $40^\circ\text{C}$ , bp  $130^\circ\text{C}$ ). They are tetrahedral molecules and the latter is perhaps the best-known compound of osmium. It is produced by aerial oxidation of the heated metal or by oxidizing other compounds of osmium with

<sup>†</sup> Although  $\text{Fe}_3\text{O}_4$  is an inverse spinel it will be recalled that  $\text{Mn}_3\text{O}_4$  (pp. 1048–9) is normal. This contrast can be explained on the basis of crystal field stabilization. Manganese(II) and  $\text{Fe}^{\text{III}}$  are both  $d^5$  ions and, when high-spin, have zero CFSE whether octahedral or tetrahedral. On the other hand,  $\text{Mn}^{\text{III}}$  is a  $d^4$  and  $\text{Fe}^{\text{II}}$  a  $d^6$  ion, both of which have greater CFSEs in the octahedral rather than the tetrahedral case. The preference of  $\text{Mn}^{\text{III}}$  for the octahedral sites therefore favours the spinel structure, whereas the preference of  $\text{Fe}^{\text{II}}$  for these octahedral sites favours the inverse structure.

<sup>13</sup> Y. KODA, *J. Chem. Soc., Chem. Commun.*, 1347–8 (1986).

nitric acid. It dissolves in aqueous alkali to give  $[\text{Os}^{\text{VIII}}\text{O}_4(\text{OH})_2]^{2-}$  and oxidizes conc (but not dil) hydrochloric acid to  $\text{Cl}_2$ , being itself reduced to  $\text{H}_2\text{OsCl}_6$ . It is used in organic chemistry to oxidize  $\text{C}=\text{C}$  bonds to *cis*-diols and is also employed as a biological stain. Unfortunately, it is extremely toxic and its volatility renders it particularly dangerous.  $\text{RuO}_4$  is, appreciably less stable and will oxidize dil as well as conc  $\text{HCl}$ , while in aqueous alkali it is reduced to  $[\text{Ru}^{\text{VI}}\text{O}_4]^{2-}$ . If heated above  $100^\circ\text{C}$  it decomposes explosively to  $\text{RuO}_2$  and is liable to do the same at room temperature if brought into contact with oxidizable organic solvents such as ethanol. Its preparation obviously requires stronger oxidizing agents than that of  $\text{OsO}_4$ ; nitric acid alone will not suffice and instead the action of  $\text{KMnO}_4$ ,  $\text{KIO}_4$  or  $\text{Cl}_2$  on acidified solutions of a convenient Ru compound is used.

The sulfides are fewer in number than the oxides and favour lower metal oxidation states. Iron forms 3 sulfides (p. 680).  $\text{FeS}$  is a grey, nonstoichiometric material, obtained by direct action of the elements or by treating aqueous  $\text{Fe}^{\text{II}}$  with alkali metal sulfide. It has a NiAs structure (p. 679) in which each metal atom is octahedrally surrounded by anions but is also quite close to 2 other metal atoms. It oxidizes readily in air and dissolves in aqueous acids with evolution of  $\text{H}_2\text{S}$ .  $\text{FeS}_2$  can be prepared by heating  $\text{Fe}_2\text{O}_3$  in  $\text{H}_2\text{S}$  but is most commonly encountered as the yellow mineral pyrites. This does not contain  $\text{Fe}^{\text{IV}}$  but is composed of  $\text{Fe}^{\text{II}}$  and  $\text{S}_2^{2-}$  ions in a distorted rock-salt arrangement, its diamagnetism indicating low-spin  $\text{Fe}^{\text{II}}(d^6)$ . It is very unreactive unless heated, when it gives  $\text{Fe}_2\text{O}_3 + \text{SO}_2$  in air, or  $\text{FeS} + \text{S}$  in a vacuum.  $\text{Fe}_2\text{S}_3$  is the unstable black precipitate resulting when aqueous  $\text{Fe}^{\text{III}}$  is treated with  $\text{S}^{2-}$ , and is rapidly oxidized in moist air to  $\text{Fe}_2\text{O}_3$  and  $\text{S}$ .

Ruthenium and osmium form only disulfides. These have the pyrite structure and are diamagnetic semiconductors; this implies that they contain  $\text{M}^{\text{II}}$ .  $\text{RuSe}_2$ ,  $\text{RuTe}_2$ ,  $\text{OsSe}_2$  and  $\text{OsTe}_2$  are very similar. All 6 dichalcogenides are obtained directly from the elements.

### 25.3.2 Mixed metal oxides and oxoanions<sup>(14)</sup>

The “ferrites” and “garnets” of iron are mixed metal oxides of considerable technological importance. They are obtained by heating  $\text{Fe}_2\text{O}_3$  with the carbonate of the appropriate metal. The ferrites have the general form  $\text{M}^{\text{II}}\text{Fe}_2^{\text{III}}\text{O}_4$ . Some adopt the *normal* spinel structure and others the *inverse* spinel structure (p. 248) as just described for  $\text{Fe}_3\text{O}_4$  (which can itself be regarded as the ferrite  $\text{Fe}^{\text{II}}\text{Fe}_2^{\text{III}}\text{O}_4$ ). In inverse spinels the unpaired electrons of all the cations in octahedral sites ( $\text{M}^{\text{II}}$  and half the  $\text{M}^{\text{III}}$ ) are magnetically coupled parallel to give a ferromagnetic sublattice, while the unpaired electrons of all the cations in tetrahedral sites (the remaining  $\text{M}^{\text{III}}$ ) are similarly but independently coupled parallel to give a second ferromagnetic sublattice. The spins of one sublattice, however, are antiparallel to those of the other. If the cations in the octahedral sites have the same total number of unpaired electrons as those in the tetrahedral sites, then the effects of 2 ferromagnetic sublattices are mutually compensating and “antiferromagnetism” results; but where the sublattices are not balanced then a type of ferromagnetism known as ferrimagnetism results, the explanation of which was first given by L. Néel in 1948 (Nobel Prize for Physics, 1970). Important applications of inverse spinel ferrites are as cores in high-frequency transformers (where they have the advantage over metals of being free from eddy-current losses), and in computer memory systems.

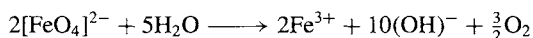
So-called “hexagonal ferrites” such as  $\text{BaFe}_{12}\text{O}_{19}$  are ferrimagnetic and are used to construct permanent magnets. A third type of ferrimagnetic mixed oxides are the garnets,  $\text{M}_3^{\text{III}}\text{Fe}_5\text{O}_{12}$ , of which the best known is yttrium iron garnet (YIG) used as a microwave filter in radar.

Mixed oxides of  $\text{Fe}^{\text{IV}}$  such as  $\text{M}_4^{\text{I}}\text{FeO}_4$  and  $\text{M}_2^{\text{II}}\text{FeO}_4$  can be prepared by heating  $\text{Fe}_2\text{O}_3$  with the appropriate oxide or hydroxide in

<sup>14</sup> A. F. WELLS, *Structural Inorganic Chemistry*, 5th edn., Complex oxides, pp. 575–625, Oxford University Press, Oxford, 1984.



oxygen. These do not contain discrete  $[\text{FeO}_4]^{4-}$  anions and, as was seen above, mixed oxides of  $\text{Fe}^{\text{III}}$  are generally based on close-packed oxide lattices with no iron-containing anions. However, oxoanions of iron are known and are usually based on the  $\text{FeO}_4$  tetrahedron.<sup>†</sup> Thus for iron(III),  $\text{Na}_5\text{FeO}_4$ ,  $\text{K}_6[\text{Fe}_2\text{O}_6]$  (2 edge-sharing tetrahedra), and  $\text{Na}_{14}[\text{Fe}_6\text{O}_{16}]$  (rings of 6 corner-sharing tetrahedra), have been prepared and more recently, for iron(V),  $\text{K}_3[\text{FeO}_4]$ .<sup>(15)</sup> But the best-known oxoanion of iron is the ferrate(VI) prepared by oxidizing a suspension of hydrous  $\text{Fe}_2\text{O}_3$  in conc alkali with chlorine, or by the anodic oxidation of iron in conc alkali. The tetrahedral  $[\text{FeO}_4]^{2-}$  ion is red-purple and is an extremely strong oxidizing agent. It oxidizes  $\text{NH}_3$  to  $\text{N}_2$  even at room temperature and, although it can be kept for a period of hours in alkaline solution, in acid or neutral solutions it rapidly oxidizes the water, so liberating oxygen:



The distinction between the first member of the group and the two heavier members, which was seen to be so sharp in the early groups of transition metals, is much less obvious here. The only unsubstituted, discrete oxoanions of the heavier pair of metals are the tetrahedral  $[\text{Ru}^{\text{VII}}\text{O}_4]^-$  and  $[\text{Ru}^{\text{VI}}\text{O}_4]^{2-}$ . This behaviour is akin to that of iron or, even more, to that of manganese, whereas in the osmium analogues the metal always increases its coordination number by the attachment of extra  $\text{OH}^-$  ions. If  $\text{RuO}_4$  is dissolved in cold dilute  $\text{KOH}$ , or aqueous  $\text{K}_2\text{RuO}_4$  is oxidized by chlorine, virtually black crystals of  $\text{K}[\text{Ru}^{\text{VII}}\text{O}_4]$  ("perruthenate") are deposited. These are unstable unless dried and are reduced by water, especially if alkaline, to the orange

$[\text{Ru}^{\text{VI}}\text{O}_4]^{2-}$  ("ruthenate") by a mechanism which is thought to involve octahedral intermediates of the type  $[\text{RuO}_4(\text{OH})_2]^{3-}$  and  $[\text{RuO}_4(\text{OH})_2]^{2-}$ .  $\text{K}_2[\text{RuO}_4]$  is obtained by fusing  $\text{Ru}$  metal with  $\text{KOH}$  and  $\text{KNO}_3$ .

By contrast, dissolution of  $\text{OsO}_4$  in cold aqueous  $\text{KOH}$  produces deep-red crystals of  $\text{K}_2[\text{Os}^{\text{VIII}}\text{O}_4(\text{OH})_2]$  ("perosmate"), which is easily reduced to the purple "osmate",  $\text{K}_2[\text{Os}^{\text{VI}}\text{O}_2(\text{OH})_4]$ . The anions in both cases are octahedral with, respectively, *trans*  $\text{OH}$  and *trans*  $\text{O}$  groups.

By heating the metal with appropriate oxides or carbonates of alkali or alkaline earth metals, a number of mixed oxides of  $\text{Ru}$  and  $\text{Os}$  have been made. They include  $\text{Na}_5\text{Os}^{\text{VII}}\text{O}_6$ ,  $\text{Li}_6\text{Os}^{\text{VI}}\text{O}_6$  and the "ruthenites",  $\text{M}^{\text{II}}\text{Ru}^{\text{IV}}\text{O}_3$ , in all of which the metal is situated in octahedral sites of an oxide lattice.  $\text{Ru}^{\text{V}}$  (octahedral) has now also been established by  $^{99}\text{Ru}$  Mössbauer spectroscopy as a common stable oxidation state in mixed oxides such as  $\text{Na}_3\text{Ru}^{\text{V}}\text{O}_4$ ,  $\text{Na}_4\text{Ru}^{\text{V}}\text{O}_7$ , and the ordered perovskite-type phases  $\text{M}_2^{\text{II}}\text{Ln}^{\text{III}}\text{Ru}^{\text{V}}\text{O}_6$ .

### 25.3.3 Halides and oxohalides

The known halides of this group are listed in Table 25.6. As in the preceding group the highest halide is a heptafluoride, but  $\text{OsF}_7$  (unlike  $\text{ReF}_7$ ) is thermally unstable. It was for many years thought that  $\text{OsF}_8$  existed but the yellow crystalline material to which the formula had been ascribed turned out to be  $\text{OsF}_6$ , the least unstable of the platinum metal hexafluorides. (In view of the propensity of higher fluorides to attack the vessels containing them, to disproportionate and to hydrolyse, it is not surprising that early reports on them sometimes proved to be erroneous.) The highest chloride is  $\text{OsCl}_5$  and, rather unexpectedly perhaps, neither ruthenium nor iron form a chloride in an oxidation state higher than +3. Iron in fact does not form even a fluoride in an oxidation state higher than this and its halides are confined to the +3 and +2 states.

$\text{OsF}_7$  has been obtained as a yellow solid by direct action of the elements at  $600^\circ\text{C}$

<sup>†</sup> An exception is  $\text{K}_3[\text{FeO}_2]$  which contains the linear  $[\text{O}-\text{Fe}^{\text{I}}-\text{O}]^{3-}$  anion (see p. 1166). It is surprisingly prepared as garnet-red crystals when a mixture of  $\text{K}_6[\text{CdO}_4]$  and  $\text{CdO}$  is subjected to prolonged heating at  $450^\circ\text{C}$  in a closed iron cylinder and reacts with the cylinder walls! F. BERNARD and R. HOPPE, *Z. anorg. allg. Chem.* **619**, 969–75 (1993).

<sup>15</sup> R. HOPPE and K. MADER *Z. anorg. allg. Chem.* **586**, 115–24 (1990).



Table 25.6 Halides of iron, ruthenium and osmium (mp/°C)

Oxidation state	Fluorides	Chlorides	Bromides	Iodides
+7	OsF <sub>7</sub> yellow			
+6	RuF <sub>6</sub> dark brown (54°) OsF <sub>6</sub> yellow (33°)			
+5	RuF <sub>5</sub> dark green (86.5°) OsF <sub>5</sub> blue (70°)	OsCl <sub>5</sub> black (d > 160°)		
+4	RuF <sub>4</sub> yellow OsF <sub>4</sub> yellow (230°)	OsCl <sub>4</sub> red (also black form)	OsBr <sub>4</sub> black (d 350°)	
+3	FeF <sub>3</sub> pale green (>1000°) RuF <sub>3</sub> dark brown (d > 650°)	FeCl <sub>3</sub> brown-black (306°) RuCl <sub>3</sub> black (α) dark brown (β) OsCl <sub>3</sub> dark grey (d 450°)	FeBr <sub>3</sub> red-brown (d > 200°) RuBr <sub>3</sub> dark brown (d > 400°)	FeI <sub>3</sub> black RuI <sub>3</sub> black
+2	FeF <sub>2</sub> white (>1000°)	FeCl <sub>2</sub> pale yellow (674°) RuCl <sub>2</sub> brown	FeBr <sub>2</sub> yellow-green (d 684°) RuBr <sub>2</sub> black	OsI <sub>3</sub> black FeI <sub>2</sub> grey RuI <sub>2</sub> blue OsI <sub>2</sub> black
+1				OsI metallic grey

and a pressure of 400 atm, but under less drastic conditions OsF<sub>6</sub> is produced, as is RuF<sub>6</sub>. This latter pair are low-melting, yellow and brown solids, respectively, hydrolysing violently with water and with a strong tendency to disproportionate into F<sub>2</sub> and lower halides. The pentafluorides are both polymeric, easily hydrolysed solids obtained by specific oxidations or reduction of other fluorides, and their structures involve [MF<sub>5</sub>]<sub>4</sub> units in which 4 corner-sharing MF<sub>6</sub> octahedra form a ring (Fig. 25.3).

The tetrafluorides are yellow solids, probably polymeric, and are obtained by reducing RuF<sub>5</sub> with I<sub>2</sub>, and OsF<sub>6</sub> with W(CO)<sub>6</sub>. The tetrachloride and tetrabromide of osmium require pressure as well as heat in their preparations from the

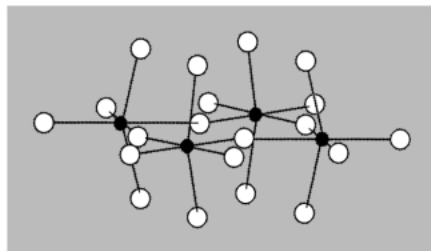
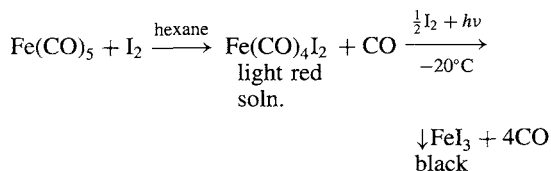


Figure 25.3 Tetrameric pentafluorides of Ru and Os, [M<sub>4</sub>F<sub>20</sub>]. Their structures are similar to, but more distorted than, those of the pentafluorides of Nb and Ta (see Fig. 22.4).

elements and are black solids, the bromide consisting of OsBr<sub>6</sub> octahedra connected by shared edges.

In the +3 and +2 oxidation states those halides of osmium which have been reported are poorly characterized, grey or black solids. The compound obtained by thermal decomposition of  $\text{OsBr}_4$  and previously thought to be  $\text{OsBr}_3$  has since been shown<sup>(16)</sup> to be  $\text{Os}_2\text{OBr}_6$ , the chloride analogue of which is also known. For ruthenium,  $\text{RuCl}_3$  is well known and, as the anhydrous compound, exists in two forms: heating Ru metal at  $330^\circ\text{C}$  in CO and  $\text{Cl}_2$  produces the dark-brown  $\beta$ -form which if heated above  $450^\circ\text{C}$  in  $\text{Cl}_2$  is converted to the black  $\alpha$ -form which is isomorphous with  $\text{CrCl}_3$  (p. 1020). Evaporation of a solution of  $\text{RuO}_4$  in hydrochloric acid in a stream of HCl gas produces red  $\text{RuCl}_3 \cdot 3\text{H}_2\text{O}$ ; aqueous solutions contain both  $[\text{Ru}(\text{H}_2\text{O})_6]^{3+}$  and chloro-substituted species and are easily hydrolysed and oxidized to  $\text{Ru}^{\text{IV}}$ . Where impurities due to such reactions are suspected, conversion back to  $\text{Ru}^{\text{III}}$  chloride can be effected by repeated evaporations to dryness with conc HCl. This gives a uniform though rather poorly characterized product that is widely used as the starting material in ruthenium chemistry.

All the anhydrous +3 and +2 halides of iron are readily obtained, except for iron(III) iodide, where the oxidizing properties of  $\text{Fe}^{\text{III}}$  and the reducing properties of  $\text{I}^-$  lead to thermodynamic instability. It has, however, been prepared<sup>(17)</sup> in mg quantities by the following reaction, with air and moisture rigorously excluded,



The other anhydrous  $\text{FeX}_3$  can be prepared by heating the elements (though in the case of  $\text{FeBr}_3$  the temperature must not rise above  $200^\circ\text{C}$  otherwise  $\text{FeBr}_2$  is formed). The fluoride, chloride and bromide are respectively white, dark

brown and reddish-brown. The crystalline solids contain  $\text{Fe}^{\text{III}}$  ions octahedrally surrounded by halide ions and decompose to  $\text{FeX}_2 + \frac{1}{2}\text{X}_2$  if heated strongly under vacuum.  $\text{FeCl}_3$  sublimes above  $300^\circ\text{C}$  and vapour pressure measurements show the vapour to contain dimeric  $\text{Fe}_2\text{Cl}_6$ , like  $\text{Al}_2\text{Cl}_6$  consisting of 2 edge-sharing tetrahedra. The trifluoride is sparingly soluble, and the chloride and bromide very soluble in water and they crystallize as white  $\text{FeF}_3 \cdot 4\text{H}_2\text{O}$  (converting above  $50^\circ\text{C}$  to the pink trihydrate),<sup>(18)</sup> yellow-brown  $\text{FeCl}_3 \cdot 6\text{H}_2\text{O}$  and dark-green  $\text{FeBr}_3 \cdot 6\text{H}_2\text{O}$ . The chloride is probably the most widely used etching material, being particularly important for etching copper in the production of electrical printed circuits. It is also used in water treatment as a coagulant (by producing a "ferric hydroxide" floc which removes organic matter and suspended solids) in cases where the  $\text{SO}_4^{2-}$  of the more widely used iron(III) sulfate is undesirable.

Of the anhydrous dihalides of iron the iodide is easily prepared from the elements but the others are best obtained by passing HX over heated iron. The white (or pale-green) difluoride has the rutile structure the pale-yellow dichloride the  $\text{CdCl}_2$  structure (based on ccp anions, p. 1212) and the yellow-green dibromide and grey diiodide the  $\text{CdI}_2$  structure (based on hcp anions, p. 1212), in all of which the metal occupies octahedral sites. All these iron dihalides dissolve in water and form crystalline hydrates which may alternatively be obtained by dissolving metallic iron in the aqueous acid.

Apart from the pale green  $\text{RuOF}_4$  and the oxochlorides already referred to, oxohalides are largely confined to the oxofluorides of osmium,<sup>(19)</sup>  $\text{OsO}_3\text{F}_2$ ,  $\text{OsO}_2\text{F}_3$ ,  $\text{OsOF}_5$ ,  $\text{OsOF}_4$  and the recently confirmed<sup>(20)</sup>  $\text{OsO}_2\text{F}_4$ , previously thought to be  $\text{OsOF}_6$ . The compounds of  $\text{Os}^{\text{VIII}}$  are orange and red solids and those of the lower oxidation states are yellow to green. Typical preparations involve

<sup>18</sup> D. G. KARRAKER and P. K. SMITH, *Inorg. Chem.* **31**, 1119–20 (1992).

<sup>19</sup> J. H. HOLLOWAY and D. LAYCOCK, *Adv. Inorg. Chem. Radiochem.* **28**, 73–99 (1984).

<sup>20</sup> K. O. CHRISTE and R. BOUGON, *J. Chem. Soc., Chem. Commun.*, 1056 (1992).

<sup>16</sup> H. SCHÄFER, *Z. anorg. allg. Chem.* **535**, 219–20 (1986).

<sup>17</sup> K. B. YOON and J. K. KOCHI, *Inorg. Chem.* **29**, 869–74 (1990).

the action of various fluorinating agents on OsO<sub>4</sub> but they are subject to disproportionation and not easily prepared in pure form.

### 25.3.4 Complexes<sup>(10,11,21,22,23)</sup>

#### Oxidation state VIII (d<sup>0</sup>)

Iron forms barely any complexes in oxidation states above +3, and in the +8, +7 and +6 states those of ruthenium are less numerous than those of osmium. Ru<sup>VIII</sup> complexes are confined to a few unstable (sometimes explosive) amine adducts of RuO<sub>4</sub>. The “perosmates” (p. 1082) are, of course, adducts of OsO<sub>4</sub>, but the most stable Os<sup>VIII</sup> complexes are the “osmiamates”, [OsO<sub>3</sub>N]<sup>-</sup> (p. 419). Pale-yellow crystals of K[OsO<sub>3</sub>N] are obtained when solutions of OsO<sub>4</sub> in aqueous KOH (i.e. the perosmate) are treated with ammonia: the compound has been known since 1847 and A. Werner formulated it correctly in 1901. The anion is isoelectronic with OsO<sub>4</sub> and has a distorted tetrahedral structure (C<sub>3v</sub>), while its infrared spectrum shows  $\nu_{\text{Os-N}} = 1023 \text{ cm}^{-1}$ , consistent with an Os≡N triple bond. Hydrochloric and hydrobromic acids reduce K[OsO<sub>3</sub>N] to red, K<sub>2</sub>[Os<sup>VI</sup>NX<sub>5</sub>].

#### Oxidation state VII (d<sup>1</sup>)

Fluorides and oxo compounds of Ru<sup>VII</sup> and Os<sup>VII</sup> have already been mentioned, and salts such as (R<sub>4</sub>N)[RuO<sub>4</sub>], (R = *n*-propyl, *n*-butyl) are useful reagents to oxidize a variety of organic materials without attacking double or allylic bonds.<sup>(24)</sup>

<sup>21</sup> P. N. HAWKER and M. V. TWIGG, *Iron(II) and Lower States*, Chap. 44.1, pp. 1179–288; S. M. NELSON, *Iron(III) and Higher States*, Chap. 44.2, pp. 217–76; M. SCHRÖDER and T. A. STEPHENSON, *Ruthenium*, Chap. 45, pp. 277–518; W. P. GRIFFITH, *Osmium*, Chap. 46, pp. 519–633 in *Comprehensive Coordination Chemistry*, Vol. 4, Pergamon Press, Oxford, 1987.

<sup>22</sup> C.-M. CHE and V. W.-W. YAM, High valent compounds of Ruthenium and Osmium, *Adv. Inorg. Chem.* **39**, 233–325 (1992).

<sup>23</sup> P. A. LAY and W. D. HARMAN, Recent advances in osmium chemistry, *Adv. Inorg. Chem.* **37**, 219–380 (1991).

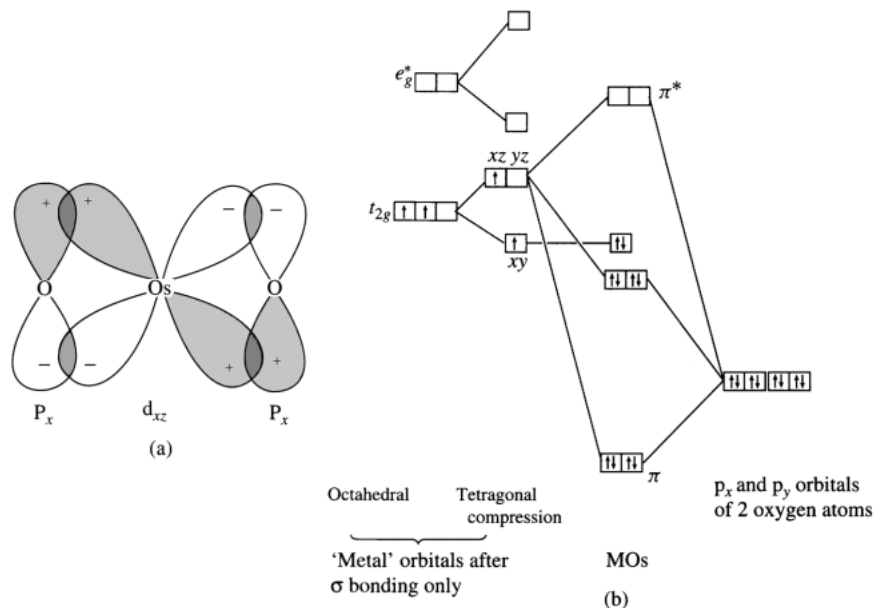
<sup>24</sup> W. P. GRIFFITH, *Platinum Metals Rev.* **33**, 181–5 (1989).

#### Oxidation state VI (d<sup>2</sup>)

The most important members of this class are the osmium nitrido, and the “osmyl” complexes. The reddish-purple K<sub>2</sub>[OsNCl<sub>5</sub>] mentioned above is the result of reducing the osmiamate. The anion has a distorted octahedral structure with a formal triple bond Os≡N (161 pm) and a pronounced “*trans*-influence” (pp. 1163–4), i.e. the Os–Cl distance *trans* to Os–N is much longer than the Os–Cl distances *cis* to Os–N (261 and 236 pm respectively). The anion [OsNCl<sub>5</sub>]<sup>2-</sup> also shows a “*trans*-effect” in that the Cl opposite the N is more labile than the others, leading, for instance, to the formation of [Os<sup>VI</sup>NCl<sub>4</sub>]<sup>-</sup>, which has a square-pyramidal structure with the N occupying the apical position.

The osmyl complexes, of which the osmate ion [Os<sup>VI</sup>O<sub>2</sub>(OH)<sub>4</sub>]<sup>2-</sup> may be regarded as the precursor, are a series of diamagnetic complexes containing the linear O=Os=O group together with 4 other, more remote, donor atoms which occupy the equatorial plane. That the Os–O bonds are double (i.e. 1σ and 1π) is evident from the bond lengths of 175 pm – very close to those of 172 pm in OsO<sub>4</sub>. The diamagnetism can then be explained using the MO approach outlined in Chapter 19, but modified to allow for the tetragonal compression along the axis of the osmyl group (taken to define the *z*-axis). On this model, the effect of 6 σ interactions produces the molecular orbitals shown in Fig. 19.14 (p. 922). The tetragonal compression then splits the essentially metallic *t*<sub>2g</sub> and *e*<sub>g</sub><sup>\*</sup> sets, as shown to the left of Fig. 25.4b. Two 3-centre π bonds are then formed, one by overlap of the metal d<sub>xz</sub> orbital with the p<sub>x</sub> orbitals of the 2 oxygen atoms (Fig. 25.4a), the second similarly by d<sub>yz</sub> and p<sub>y</sub> overlap. Each 3-centre interaction produces 1 bonding, 1 virtually nonbonding, and 1 antibonding MO, as shown. The metal d<sub>xy</sub> orbital remains unchanged and, in effect, the two d electrons of the Os are obliged to pair-up in it since other empty orbitals are inaccessible to them.

The {Os<sup>VI</sup>O<sub>2</sub>}<sup>2+</sup> group has a formal similarity to the more familiar uranyl ion [UO<sub>2</sub>]<sup>2+</sup> and is present in a variety of octahedral complexes



**Figure 25.4** Proposed  $\pi$  bonding in osmyl complexes: (a) 3-centre  $\pi$  bond formed by overlap of ligand  $p_x$  and metal  $d_{xz}$  orbitals (a similar bond is produced by  $p_y$  and  $d_{yz}$  overlap), and (b) MO diagram (see text).

in which the 4 equatorial sites are occupied by ligands such as  $\text{OH}^-$ , halides,  $\text{CN}^-$ ,  $(\text{C}_2\text{O}_4)^{2-}$ ,  $\text{NO}_2^-$ ,  $\text{NH}_3$  and phthalocyanine. These are obtained from  $\text{OsO}_4$  or potassium osmate.

A few analogous but less stable trans-dioxoruthenium(VI) compounds such as the bright yellow  $[\text{RuO}_2(\text{O}_2\text{CCH}_3)_2\text{py}_2]$  ( $\text{Ru}-\text{O} = 172.6 \text{ pm}$ ) are also known.<sup>(25)</sup>

### Oxidation state V ( $d^3$ )

This is not a very stable state for this group of metals in solution,  $[\text{MF}_6]^-$  and  $[\text{OsCl}_6]^-$  being amongst the few established examples. It is, however, well-characterized and stable in numerous solid-state oxide systems (p. 1082).

### Oxidation state IV ( $d^4$ )

Under normal circumstances this is the most stable oxidation state for osmium and the

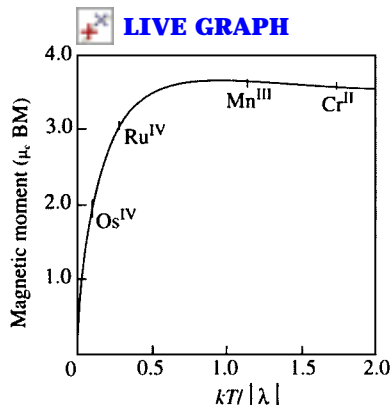
$[\text{OsX}_6]^{2-}$  complexes ( $\text{X} = \text{F}, \text{Cl}, \text{Br}, \text{I}$ ) are particularly well known.  $[\text{RuX}_6]^{2-}$  ( $\text{X} = \text{F}, \text{Cl}, \text{Br}$ ) are also familiar but can more readily be reduced to  $\text{Ru}^{\text{III}}$ . All these  $[\text{MX}_6]^{2-}$  ions are octahedral and low-spin, with 2 unpaired electrons. Their magnetic properties are interesting and highlight the limitations of using "spin-only" values of magnetic moments in assessing the number of unpaired electrons (see Panel).

The action of hydrochloric acid on  $\text{RuO}_4$  in the presence of  $\text{KCl}$  produces a deep-red crystalline material, of stoichiometry  $\text{K}_2[\text{RuCl}_5(\text{OH})]$ , but its diamagnetism precludes this simple formulation. The compound is in fact  $\text{K}_4[\text{Cl}_5\text{Ru}-\text{O}-\text{RuCl}_5]$  and is of interest as providing an early application of simple MO theory to a linear  $\text{M}-\text{O}-\text{M}$  system (not unlike the later treatment of the osmyl group). If the  $\text{Ru}-\text{O}-\text{Ru}$  axis is taken as the  $z$ -axis and each  $\text{Ru}^{\text{IV}}$  is regarded as being octahedrally coordinated, then the low-spin configuration of each  $\text{Ru}^{\text{IV}}$  ion is  $d_{xy}^2 d_{xz}^1 d_{yz}^1$ . The diamagnetism is accounted for on the basis of two 3-centre  $\pi$  bonds, one arising from overlap

<sup>25</sup> S. PERRIER, T. C. LAU and J. K. KOCHI, *Inorg. Chem.* **29**, 4190–5 (1990).

### Magnetic Properties of Low-spin, Octahedral $d^4$ Ions

That halide ligands should cause spin-pairing may in itself seem surprising, but this is not all. The regular, octahedral complexes of  $\text{Os}^{\text{IV}}$  have magnetic moments at room temperature in the region of 1.48 BM and these decrease rapidly as the temperature is reduced. Even the moments of similar complexes of  $\text{Ru}^{\text{IV}}$  (which at around 2.9 BM are close to the "spin-only moment" expected solely from the angular momentum of 2 unpaired electrons) fall sharply with temperature. In the first place, low-spin configurations are much more common for the second- and third-row than for first-row transition elements and this is due to (a) the higher nuclear charges of the heavier elements which exert stronger attractions on the ligands so that a given set of ligands produces a greater splitting of the metal d orbitals, and (b) the larger sizes of 4d and 5d orbitals compared to 3d orbitals, with the result that interelectronic repulsions, which tend to oppose spin-pairing, are lower in the former cases. These factors explain why the halide complexes of  $\text{Os}^{\text{IV}}$  and  $\text{Ru}^{\text{IV}}$  are low-spin but what of the temperature dependence and their magnetic behaviour? This arises from the effect of "spin-orbit coupling" which can be summarized in a plot of  $\mu_e$  versus  $kT/|\lambda|$  (Fig. A).  $\lambda$  is the spin-orbit coupling constant for a particular ion and is indicative of the strength of the coupling between the angular momentum vectors associated with  $S$  and  $L$ , and also of the magnitude of the splitting of the ground term of the ion ( ${}^3T_1$ , in the case of low-spin  $d^4$ ). When  $|\lambda|$  is of comparable magnitude to  $kT$ ,  $\mu_e \sim 3.6$  BM, which is the spin-only moment (2.83 BM) plus a contribution from the orbital angular momentum. Thus,  $\text{Cr}^{\text{II}}$  ( $\lambda = -115 \text{ cm}^{-1}$ ) and  $\text{Mn}^{\text{II}}$  ( $\lambda = -178 \text{ cm}^{-1}$ ) at room temperature ( $kT \sim 200 \text{ cm}^{-1}$ ), lie on the flat portion of the curve and so have magnetic moments of about 3.6 BM which only begin to fall at appreciably lower temperatures. On the other hand,  $\text{Ru}^{\text{IV}}$  ( $\lambda = -700 \text{ cm}^{-1}$ ) and  $\text{Os}^{\text{IV}}$  ( $\lambda \sim -2000 \text{ cm}^{-1}$ ) have moments which at room temperature are already on the steep portion of the curve and so are extremely dependent on temperature. In each case, as the temperature approaches 0 K so also  $\mu_e \rightarrow 0$ , corresponding to a coupling of  $L$  and  $S$  vectors in opposition and their associated magnetic moments therefore cancelling each other.



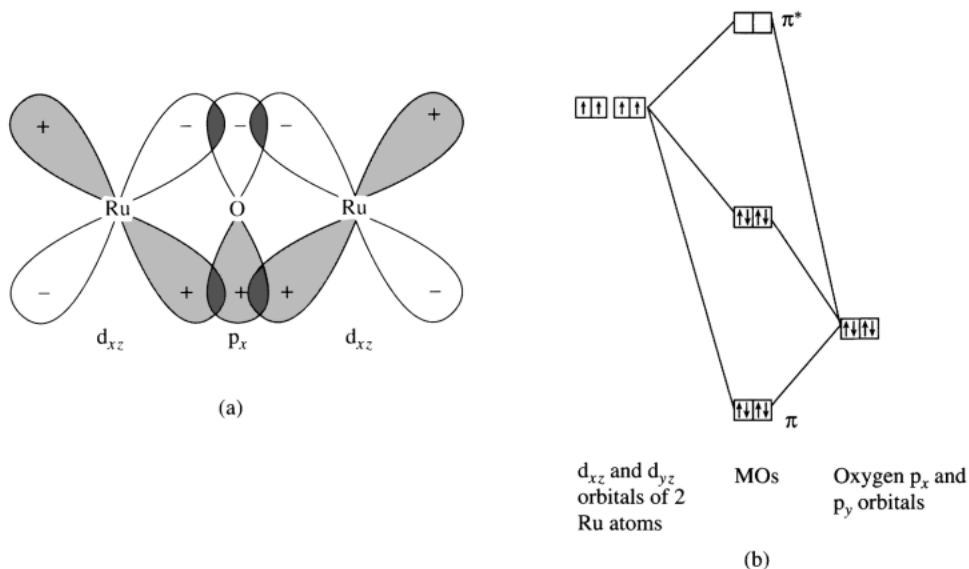
**Figure A** The variation with temperature and spin-orbit coupling constant, of the magnetic moments of octahedral, low-spin,  $d^4$  ions. (The values of  $\mu_e$  at 300 K are marked for individual ions).

All  $d^n$  configurations with  $T$  ground terms give rise to magnetic moments which are lower for second- and third-row than for first-row transition elements and are temperature dependent, but in no case so dramatically as for low-spin  $d^4$ .

of the oxygen  $p_x$  orbital and the two  $d_{xz}$  orbitals of the Ru ions, and the other similarly from  $p_y$  and  $d_{yz}$  overlap (Fig. 25.5). The bromo analogue apparently does not exist.<sup>(26)</sup>

Ruthenium(IV) produces few other complexes of interest but osmium(IV) yields several sulfite complexes (e.g.  $[\text{Os}(\text{SO}_3)_6]^{8-}$  and substituted derivatives) as well as a number of complexes, such as  $[\text{Os}(\text{bipy})\text{Cl}_4]$  and  $[\text{Os}(\text{diars})_2\text{X}_2]^{2+}$  ( $\text{X} = \text{Cl}, \text{Br}, \text{I}$ ), with mixed halide and Group 15 donor atoms. The iron analogues of the latter complexes (with  $\text{X} = \text{Cl}, \text{Br}$ ), are obtained by oxidation of

<sup>26</sup> D. APPLEBY, R. I. CRISP, P. B. HITCHCOCK, C. L. HUSSEY, T. A. RYAN, J. R. SANDERS, K. R. SEDDON, J. E. TURP and J. A. ZORA, *J. Chem. Soc., Chem. Commun.*, 483-5 (1986).



**Figure 25.5**  $\pi$  bonding in  $[\text{Ru}_2\text{OCl}_{10}]^{4-}$ : (a) 3-centre  $\pi$  bond formed by overlap of an oxygen  $p_x$  and ruthenium  $d_{xz}$  orbitals (another similar bond is produced by  $p_y$  and  $d_{yz}$  overlap), and (b) MO diagram.

$[\text{Fe}(\text{diars})_2\text{X}_2]^+$  with conc  $\text{HNO}_3$  and provide rare examples of complexes containing iron in an oxidation state higher than +3. The halide ions are *trans* to each other and a reduction in the magnetic moment at 293 K from a value of  $\sim 3.6$  BM (which might have been expected, since  $\lambda = -260 \text{ cm}^{-1}$  for  $\text{Fe}^{\text{IV}}$  — see Panel) to 2.98 BM is explained by a large tetragonal distortion.

### Oxidation state III ( $d^5$ )

Ruthenium(III) and osmium(III) complexes are all octahedral and low-spin with 1 unpaired electron. Iron(III) complexes, on the other hand, may be high or low spin, and even though an octahedral stereochemistry is the most common, a number of other geometries are also found. In other respects, however there is a gradation down the triad, with  $\text{Ru}^{\text{III}}$  occupying an intermediate position between  $\text{Fe}^{\text{III}}$  and  $\text{Os}^{\text{III}}$ . For iron the oxidation state +3 is one of its two most common and for it there is an extensive, simple, cationic chemistry (though the aquo

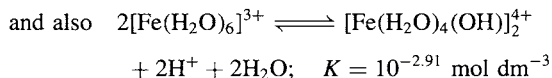
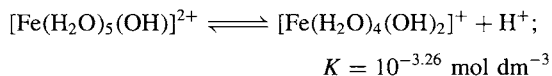
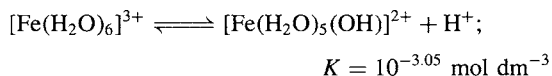
ion,  $[\text{Fe}(\text{H}_2\text{O})_6]^{3+}$ , is too readily hydrolysed to be really common). For ruthenium it is the best-known oxidation state and  $[\text{Ru}(\text{H}_2\text{O})_6]^{3+}$ , which can be obtained by oxidation of the divalent ion (p. 1095), has been characterized<sup>(27)</sup> in the toluene sulfonate,  $[\text{Ru}(\text{H}_2\text{O})_6](\text{tos})_3$  and the caesium alum (see below). For osmium, however,  $\text{Os}^{\text{III}}$  is a distinctly less-common oxidation state, being readily oxidized to  $\text{Os}^{\text{IV}}$  or even, in the presence of  $\pi$ -acceptor ligands such as  $\text{CN}^-$ , reduced to  $\text{Os}^{\text{II}}$ . There is no evidence of a simple aquo ion of osmium in this or indeed in any other oxidation state.

Except with anions such as iodide (but see p. 1084) which have reducing tendencies, iron(III) forms salts with all the common anions, and these may be crystallized in pale-pink or pale-violet hydrated forms. These presumably contain the  $[\text{Fe}(\text{H}_2\text{O})_6]^{3+}$  cation, and the iron alums certainly do. These alums have the composition  $\text{Fe}_2(\text{SO}_4)_3\text{M}_2^{\text{I}}\text{SO}_4 \cdot 24\text{H}_2\text{O}$  and can be formulated  $[\text{M}^{\text{I}}(\text{H}_2\text{O})_6][\text{Fe}^{\text{III}}(\text{H}_2\text{O})_6][\text{SO}_4]_2$ .

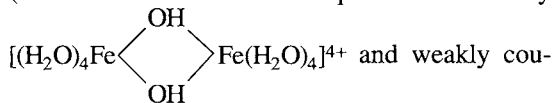
<sup>27</sup> F. JOENSEN and C. E. SCHAFFER, *Acta. Chem. Scand. Ser. A*, **38**, 819–20 (1984).

Like the analogous chrome alums they find use as mordants in dyeing processes. The sulfate is the cheapest salt of  $\text{Fe}^{\text{III}}$  and forms no less than 6 different hydrates (12, 10, 9, 7, 6 and 3 mols of  $\text{H}_2\text{O}$  of which  $9\text{H}_2\text{O}$  is the most common); it is widely used as a coagulant in the treatment not only of potable water but also of sewage and industrial effluents.

In the crystallization of these hydrated salts from aqueous solutions it is essential that a low pH (high level of acidity) is maintained, otherwise hydrolysis occurs and yellow impurities contaminate the products. Similarly, if the salts are redissolved in water, the solutions turn yellow/brown. The hydrolytic processes are complicated, and, in the presence of anions with appreciable coordinating tendencies, are further confused by displacement of water from the coordination sphere of the iron. However, in aqueous solutions of salts such as the perchlorate the following equilibria are important:



(The dimer in the third equation is actually



pled electron spins on the 2 metal ions reduce the magnetic moment per iron below the spin-only value for 5 unpaired electrons.)

It is evident therefore that  $\text{Fe}^{\text{III}}$  salts dissolved in water produce highly acidic solutions and the simple, pale-violet, hexaaquo ion only predominates if further acid is added to give pH  $\sim 0$ . At somewhat higher values of pH the solution becomes yellow due to the appearance of the above hydrolysed species and if the pH is raised above 2–3, further condensation occurs, colloidal gels begin to form, and eventually a

reddish-brown precipitate of hydrous iron(III) oxide is formed (see p. 1080).

The colours of these solutions are of interest. Iron(III) like manganese(II), has a  $d^5$  configuration and its absorption spectrum might therefore be expected to consist similarly of weak spin-forbidden bands. However, a crucial difference between the ions is that  $\text{Fe}^{\text{III}}$  carries an additional positive charge, and its correspondingly greater ability to polarize coordinated ligands produces intense, charge-transfer absorptions at much lower energies than those of  $\text{Mn}^{\text{II}}$  compounds. As a result, only the hexaaquo ion has the pale colouring associated with spin-forbidden bands in the visible region of the spectrum, while the various hydrolysed species have charge transfer bands, the edges of which tail from the ultraviolet into the visible region producing the yellow colour and obscuring weak d–d bands.<sup>(28)</sup> Even the hexaaquo ion's spectrum is dominated in the near ultraviolet by charge transfer, and a full analysis of the d–d spectrum of this and of other  $\text{Fe}^{\text{III}}$  complexes is consequently not possible.

Iron(III) forms a variety of cationic, neutral and anionic complexes, but an interesting feature of its coordination chemistry is a marked preference (not shown by  $\text{Cr}^{\text{III}}$  with which in many other respects it is similar) for *O*-donor as opposed to *N*-donor ligands. Ammines of  $\text{Fe}^{\text{III}}$  are unstable and dissociate in water; chelating ligands such as bipy and phen which induce spin-pairing produce more stable complexes, but even these are less stable than their  $\text{Fe}^{\text{II}}$  analogues. Thus, whereas deep-red aqueous solutions of  $[\text{Fe}(\text{phen})_3]^{2+}$  are indefinitely stable, the deep-blue solutions of  $[\text{Fe}(\text{phen})_3]^{3+}$  slowly turn khaki-coloured as polymeric hydroxo species form. By contrast, the intense colours produced when phenols or enols are treated with  $\text{Fe}^{\text{III}}$ , and which are used as characteristic tests for these organic materials, are due to the formation of Fe–O complexes. Again, the addition of phosphoric acid to yellow, aqueous solutions of  $\text{FeCl}_3$ , for instance, decolourizes them because

<sup>28</sup> A. B. P. LEVER, *Inorganic Electronic Spectroscopy*, 2nd edn., pp. 329–34 and 452–3, Elsevier, Amsterdam, 1984.

of the formation of phosphato complexes such as  $[\text{Fe}(\text{PO}_4)_3]^{6-}$  and  $[\text{Fe}(\text{HPO}_4)_3]^{3-}$ . The deep-red  $[\text{Fe}(\text{acac})_3]$  and the green  $[\text{Fe}(\text{C}_2\text{O}_4)_3]^{3-}$  are other examples of complexes with oxygen-bonded ligands although the latter, whilst very stable towards dissociation, is photosensitive due to oxidation of the oxalate ion by  $\text{Fe}^{\text{III}}$  and so decomposes to  $\text{Fe}(\text{C}_2\text{O}_4)$  and  $\text{CO}_2$ .

Complexes with mixed *O*- and *N*-donor ligands such as edta and Schiff bases are well known and  $[\text{Fe}(\text{edta})(\text{H}_2\text{O})]^-$  and  $[\text{Fe}(\text{salen})\text{Cl}]$  are examples of 7-coordinate (pentagonal bipyramidal) and 5-coordinate (square-pyramidal) stereochemistries respectively.

As in the case of  $\text{Cr}^{\text{III}}$ , oxo-bridged species with magnetic moments reduced below the spin-only value (5.9 BM in the case of high-spin  $\text{Fe}^{\text{III}}$ ) are known.  $[\text{Fe}(\text{salen})_2\text{O}]$ , for instance, has a moment of 1.9 BM at 298 K which falls to 0.6 BM at 80 K and the interaction between the electron spins on the 2 metal ions is transmitted across an Fe–O–Fe bridge, bent at an angle of  $140^\circ$ . Trinuclear, basic carboxylates,  $[\text{Fe}_3\text{O}(\text{O}_2\text{CR})_6\text{L}_3]^+$ , are, however, entirely analogous to their  $\text{Cr}^{\text{III}}$  counterparts (p. 1030).<sup>(29)</sup>

Halide complexes decrease markedly in stability from  $\text{F}^-$  to  $\text{I}^-$ . Fluoro complexes are quite stable and in aqueous solutions the predominant species is  $[\text{FeF}_5(\text{H}_2\text{O})]^{2-}$  while isolation of the solid and fusion with  $\text{KHF}_2$  yields  $[\text{FeF}_6]^{3-}$ . Chloro complexes are appreciably less stable, and tetrahedral rather than octahedral coordination is favoured.<sup>†</sup>  $[\text{FeCl}_4]^-$  can be isolated in yellow salts with large cations such as  $[\text{RN}_4]^+$  from ethanolic solutions or conc HCl.  $[\text{FeBr}_4]^-$  and  $[\text{FeI}_4]^-$  are also known but are readily reduced to  $\text{Fe}^{\text{II}}$  either by internal

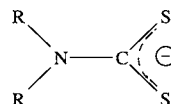
oxidation–reduction or by the action of excess ligand.<sup>(30)</sup>

The blood-red colour produced by mixing aqueous solutions of  $\text{Fe}^{\text{III}}$  and  $\text{SCN}^-$  (and which provides a well-known test for  $\text{Fe}^{\text{III}}$ ) is largely due to  $[\text{Fe}(\text{SCN})(\text{H}_2\text{O})_5]^{2+}$  but, in addition to this, the simple salt  $\text{Fe}(\text{SCN})_3$  and salts of complexes such as  $[\text{Fe}(\text{SCN})_4]^-$  and  $[\text{Fe}(\text{SCN})_6]^{3-}$  can also be isolated.

The high-spin  $d^5$  configuration of  $\text{Fe}^{\text{III}}$ , like that of  $\text{Mn}^{\text{II}}$ , confers no advantage by virtue of CFSE (p. 1131) on any particular stereochemistry. Some examples of its consequent ability to adopt stereochemistries other than octahedral have just been mentioned and further examples are given in Table 25.3 (p. 1078). These cover the range of coordination numbers from 3 to 8.

Further similarity with  $\text{Mn}^{\text{II}}$  may be seen in the fact that the vast majority of the compounds of  $\text{Fe}^{\text{III}}$  are high-spin. Only ligands such as bipy and phen (already mentioned) and  $\text{CN}^-$ , which are high in the spectrochemical series, can induce spin-pairing. The low-spin  $[\text{Fe}(\text{CN})_6]^{3-}$ , which is best known as its red, crystalline potassium salt, is usually prepared by oxidation of  $[\text{Fe}(\text{CN})_6]^{4-}$  with, for instance,  $\text{Cl}_2$ . It should be noted that in  $[\text{Fe}(\text{CN})_6]^{3-}$  the  $\text{CN}^-$  ligands are sufficiently labile to render it poisonous, in apparent contrast to  $[\text{Fe}(\text{CN})_6]^{4-}$ , which is kinetically more inert. Dilute acids produce  $[\text{Fe}(\text{CN})_5(\text{H}_2\text{O})]^{2-}$ , and other pentacyano complexes are known.

$\text{Fe}^{\text{III}}$  complexes in general have magnetic moments at room temperature which are close to 5.92 BM if they are high-spin and somewhat in excess of 2 BM (due to orbital contribution) if they are low-spin. A number of complexes, however, were prepared in 1931 by L. Cambi and found to have moments intermediate between these extremes. They are the iron(III)-*N,N*-dialkyldithiocarbamates,  $[\text{Fe}(\text{S}_2\text{CNR}_2)_3]$ , in which the ligands are:



<sup>30</sup> S. POHL, U. BIERBACH and W. SAAK, *Angew. Chem. Int. Edn. Engl.* **28**, 776–7 (1989).

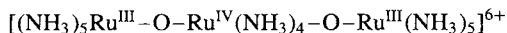
<sup>29</sup> R. D. CANNON and R. P. WHITE, *Prog. Inorg. Chem.* **36**, 195–298 (1988).

<sup>†</sup> In the compound, previously assumed to be  $(\text{pyH})_3[\text{Fe}_2\text{Cl}_9]$  with the anion composed of a pair of face-sharing octahedra, the iron is in fact coordinated tetrahedrally and the correct formulation is,  $[(\text{pyH})_3\text{Cl}][\text{FeCl}_4]_2$ , see R. SHAVIV, C. B. LOWE, J. A. ZORA, C. B. AAKERÖY, P. B. HITCHCOCK, K. R. SEDDON and R. L. CARLIN, *Inorg. Chim. Acta* **198–200**, 613–21 (1992).



so that the  $\text{Fe}^{\text{III}}$  is surrounded octahedrally by 6 sulfur atoms. They provide well documented examples of high-spin/low-spin crossover (i.e. spin equilibria) (see Panel p. 1096).

Ruthenium(III) forms extensive series of halide complexes, the aquo-chloro series being probably the best characterized of all its complexes. The  $\text{Ru}^{\text{III}}/\text{Cl}^-/\text{H}_2\text{O}$  system has received extensive study, especially by ion-exchange techniques. The ions  $[\text{RuCl}_n(\text{H}_2\text{O})_{6-n}]^{(n-3)-}$  from  $n = 6$  to  $n = 0$  have all been identified in solution and a number also isolated as solids.  $\text{K}_3[\text{RuF}_6]$  can be obtained from molten  $\text{RuCl}_3/\text{KHF}_2$ . Several bromo complexes have been reported amongst them the dimeric anion  $[\text{Ru}_2\text{Br}_9]^{3-}$  which, like its chloro analogue, is composed of a pair of face-sharing octahedra. There are, however, no iodo complexes and, whilst  $[\text{Os}(\text{CN})_6]^{3-}$  as well as the  $\text{Fe}^{\text{III}}$  analogue are known and some substituted cyano complexes of  $\text{Ru}^{\text{III}}$  have been prepared, the parent  $[\text{Ru}(\text{CN})_6]^{3-}$  has only recently been isolated as the brilliant yellow  $(\text{Bu}^n_4\text{N})^+$  salt by aerial oxidation of dmf solution of  $[\text{Ru}(\text{CN})_6]^{2+}$ .<sup>(31)</sup>  $\text{Ru}^{\text{III}}$  is much more amenable to coordination with *N*-donor ligands than is  $\text{Fe}^{\text{III}}$ , and forms ammines with from 3 to 6  $\text{NH}_3$  ligands (the extra ligands making up octahedral coordination are commonly  $\text{H}_2\text{O}$  or halides) as well as complexes with bipy and phen. Treatment of “ $\text{RuCl}_3$ ” with aqueous ammonia in air slowly yields an extremely intense red solution (ruthenium red) from which a diamagnetic solid can be isolated, apparently of the form:



Its diamagnetism can be explained on the basis of  $\pi$  overlap, producing polycentre molecular orbitals essentially the same as used for  $[\text{Ru}_2\text{OCl}_{10}]^{4-}$  (see Fig. 25.5). It is stable in either acid or alkali and its acid solution can be used as an extremely sensitive test for oxidizing agents since even such a mild reagent as iron(III) chloride oxidizes the red, 6+ cation to a yellow, paramagnetic, 7+ cation of the same constitution (a change which is detectable in solutions containing less than 1 ppm Ru).

Trinuclear basic acetates  $[\text{Ru}_3\text{O}(\text{O}_2\text{CMe})_6\text{L}_3]^+$  have also been prepared apparently with the same constitution as the analogous  $\text{Fe}^{\text{III}}$  and  $\text{Cr}^{\text{III}}$  compounds (p. 1030).

For osmium, halogeno complexes are less diverse but the reaction of acetic acid/acetic anhydride with  $[\text{OsCl}_6]^{2-}$  yields brown  $\text{Os}_2(\text{O}_2\text{CMe})_4\text{Cl}_2$  which, if treated as a suspension in anhydrous ethanol with gaseous  $\text{HX}$  ( $\text{X} = \text{Cl}, \text{Br}$ ), yields  $[\text{Os}_2\text{X}_8]^{2-}$ . These diamagnetic ions are notable for the presence of the  $\text{Os}\equiv\text{Os}$  triple bond unsupported by bridging ligands. The triply bridged  $[\text{Os}_2\text{Br}_9]^{3-}$  is also known.<sup>(32)</sup>

### Oxidation state II ( $d^6$ )

This is the second of the common oxidation states for iron and is familiar for ruthenium, particularly with Group 15-donor ligands ( $\text{Ru}^{\text{II}}$  probably forms more nitrosyl complexes than any other metal). Osmium(II) also produces a considerable number of complexes but is usually more strongly reducing than  $\text{Ru}^{\text{II}}$ .

Iron(II) forms salts with nearly all the common anions.<sup>†</sup> These are usually prepared in aqueous solution either from the metal or by reduction of the corresponding  $\text{Fe}^{\text{III}}$  salt. In the absence of other coordinating groups these solutions contain the pale-green  $[\text{Fe}(\text{H}_2\text{O})_6]^{2+}$  ion which is also present in solids such as  $\text{Fe}(\text{ClO}_4)_2 \cdot 6\text{H}_2\text{O}$ ,  $\text{FeSO}_4 \cdot 7\text{H}_2\text{O}$  and the well-known “Mohr’s salt”,  $(\text{NH}_4)_2\text{SO}_4 \cdot \text{FeSO}_4 \cdot 6\text{H}_2\text{O}$  introduced into volumetric analysis by K. F. Mohr in the 1850s.<sup>‡</sup>

<sup>31</sup> S. ELLER and R. D. FISCHER, *Inorg. Chem.*, **29**, 1289–90 (1990).

<sup>32</sup> G. A. HEATH and D. G. HUMPHREY, *J. Chem. Soc., Chem. Commun.*, 672–3 (1990).

<sup>†</sup> An exception is  $\text{NO}_2^-$  which instantly oxidizes  $\text{Fe}^{\text{II}}$  to  $\text{Fe}^{\text{III}}$  and liberates NO.  $\text{Fe}(\text{BrO}_3)_2$  and  $\text{Fe}(\text{IO}_3)_2$  also are unstable.

<sup>‡</sup> K. F. Mohr (1806–79) was Professor of Pharmacy at the University of Bonn. Among his many inventions were the specific gravity balance, the burette, the pinch clamp, the cork borer, and the use of the so-called Liebig condenser for refluxing. In addition to his introduction of iron(II) ammonium sulfate as a standard reducing agent he devised Mohr’s method for titrating halide solutions with silver ions

The hydrolysis (which in the case of Fe<sup>III</sup> produces acidic solutions) is virtually absent, and in aqueous solution the addition of CO<sub>3</sub><sup>2-</sup> does not result in the evolution of CO<sub>2</sub> but simply in the precipitation of white FeCO<sub>3</sub>. The moist precipitate oxidizes rapidly on exposure to air but in the presence of excess CO<sub>2</sub> the slightly soluble Fe(HCO<sub>3</sub>)<sub>2</sub> is formed. It is the presence of this in natural underground water systems, leading to the production of FeCO<sub>3</sub> on exposure to air, followed by oxidation to iron(III) oxide, which leads to the characteristic brown deposits found in many streams.

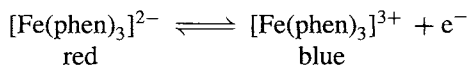
The possibility of oxidation to Fe<sup>III</sup> is a crucial theme in the chemistry of Fe<sup>II</sup> and most of its salts are unstable with respect to aerial oxidation, though double sulfates are much less so (e.g. Mohr's salt above). However, the susceptibility of Fe<sup>II</sup> to oxidation is dependent on the nature of the ligands attached to it and, in aqueous solution, on the pH. Thus the solid hydroxide and alkaline solutions are very readily oxidized whereas acid solutions are much more stable (see Panel opposite).

Iron(II) forms complexes with a variety of ligands. As is to be expected, in view of its smaller cationic charge, these are usually less stable than those of Fe<sup>III</sup> but the antipathy to *N*-donor ligands is less marked. Thus [Fe(NH<sub>3</sub>)<sub>6</sub>]<sup>2+</sup> is known whereas the Fe<sup>III</sup> analogue is not; also there are fewer Fe<sup>II</sup> complexes with *O*-donor ligands such as acac and oxalate, and they are less stable than those of Fe<sup>III</sup>. High-spin octahedral complexes of Fe<sup>II</sup> have a free-ion <sup>5</sup>*D* ground term, split by the crystal field into a ground <sup>5</sup>*T*<sub>2g</sub> and an excited <sup>5</sup>*E*<sub>g</sub> term. A magnetic moment of around 5.5 BM (i.e. 4.90 BM + orbital contribution) is expected for pure octahedral symmetry but, in practice, distortions produce values in the range 5.2–5.4 BM. Similarly, in the electronic spectrum, the expected single band due to the <sup>5</sup>*E*<sub>g</sub>(*t*<sub>2g</sub><sup>3</sup>*e*<sub>g</sub><sup>3</sup>) ← <sup>5</sup>*T*<sub>2g</sub>(*t*<sub>2g</sub><sup>4</sup>*e*<sub>g</sub><sup>2</sup>) transition is broadened

or split. Besides stereochemical distortions, spin-orbit coupling and a Jahn-Teller effect in the excited configuration (footnote p. 1021) help to broaden the band, the main part of which is usually found between 10 000 and 11 000 cm<sup>-1</sup>. The d-d spectra of low-spin Fe<sup>II</sup> (which is isoelectronic with Co<sup>III</sup>) are not so well documented, being generally obscured by charge-transfer absorption (p. 1128).

Most Fe<sup>II</sup> complexes are octahedral but several other stereochemistries are known (Table 25.3). [FeX<sub>4</sub>]<sup>2-</sup> (X = Cl, Br, I, NCS) are tetrahedral. A single absorption around 4000 cm<sup>-1</sup> due to the <sup>5</sup>*T*<sub>2</sub> ← <sup>5</sup>*E* transition is as expected, but magnetic moments of these and other apparently tetrahedral complexes are reported to lie in the range 5.0–5.4 BM, and the higher values are difficult to explain.

Low-spin, octahedral complexes are formed by ligands such as bipy, phen and CN<sup>-</sup>, and their stability is presumably enhanced by the symmetrical *t*<sub>2g</sub><sup>6</sup> configuration. [Fe(bipy)<sub>3</sub>]<sup>2+</sup> and [Fe(phen)<sub>3</sub>]<sup>2+</sup> are stable, intensely red complexes, the latter being employed as the redox indicator, "ferroin", due to the sharp colour change which occurs when strong oxidizing agents are added to it:



Mono- and bis-phenanthroline complexes can be prepared but these are both high-spin and, because of the increase in CFSE (p. 1131) accompanying spin pairing (<sup>2</sup>/<sub>5</sub>Δ<sub>0</sub> → <sup>12</sup>/<sub>5</sub>Δ<sub>0</sub>), addition of phenanthroline to aqueous Fe<sup>II</sup> leads almost entirely to the formation of the tris complex rather than mono or bis, even though the Fe<sup>II</sup> is initially in great excess. Pale-yellow K<sub>4</sub>[Fe(CN)<sub>6</sub>].3H<sub>2</sub>O can be crystallized from aqueous solutions of iron(II) sulfate and an excess of KCN: this is clearly more convenient than the traditional method of fusing nitrogeous animal residues (hides, horn, etc.) with iron and K<sub>2</sub>CO<sub>3</sub>. The hexacyanoferrate(II) anion (ferrocyanide) is kinetically inert and is said to be non-toxic, but HCN is liberated by the addition of dilute acids.

in the presence of chromate as indicator, and was instrumental in establishing titrimetric methods generally for quantitative analysis.

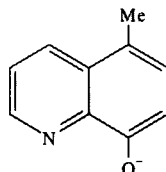
### The Fe<sup>III</sup>/Fe<sup>II</sup> Couples

A selection of the standard reduction potentials for some iron couples is given in Table A, from which the importance of the participating ligand can be judged (see also Table 25.8 for biologically important iron proteins). Thus Fe<sup>III</sup>, being more highly charged than Fe<sup>II</sup> is stabilized (relatively) by negatively charged ligands such as the anions of edta and derivatives of 8-hydroxyquinoline, whereas Fe<sup>II</sup> is favoured by neutral ligands which permit some charge delocalization in  $\pi$ -orbitals (e.g. bipy and phen).

**Table A**  $E^\circ$  at 25°C for some Fe<sup>III</sup>/Fe<sup>II</sup> couples in acid solution

Fe <sup>III</sup>	Fe <sup>II</sup>	$E^\circ/V$
[Fe(phen) <sub>3</sub> ] <sup>3+</sup> + e <sup>-</sup>	⇌ [Fe(phen) <sub>3</sub> ] <sup>2+</sup>	1.12
[Fe(bipy) <sub>3</sub> ] <sup>3+</sup> + e <sup>-</sup>	⇌ [Fe(bipy) <sub>3</sub> ] <sup>2+</sup>	0.96
[Fe(H <sub>2</sub> O) <sub>6</sub> ] <sup>3+</sup> + e <sup>-</sup>	⇌ [Fe(H <sub>2</sub> O) <sub>6</sub> ] <sup>2+</sup>	0.77
[Fe(CN) <sub>6</sub> ] <sup>3-</sup> + e <sup>-</sup>	⇌ [Fe(CN) <sub>6</sub> ] <sup>4-</sup>	0.36
[Fe(C <sub>2</sub> O <sub>4</sub> ) <sub>3</sub> ] <sup>3-</sup> + e <sup>-</sup>	⇌ [Fe(C <sub>2</sub> O <sub>4</sub> ) <sub>2</sub> ] <sup>2-</sup> + (C <sub>2</sub> O <sub>4</sub> ) <sup>2-</sup>	0.02
[Fe(edta)] <sup>-</sup> + e <sup>-</sup>	⇌ [Fe(edta)] <sup>2-</sup>	-0.12
[Fe(quin) <sub>3</sub> ] + e <sup>-</sup>	⇌ [Fe(quin) <sub>2</sub> ] + quin <sup>-(a)</sup>	-0.30

<sup>(a)</sup>quin<sup>-</sup> = 5-methyl-8-hydroxyquinolate.



The value of  $E^\circ$  for the couple involving the simple aquated ions, shows that Fe<sup>II</sup>(aq) is thermodynamically stable with respect to hydrogen; which is to say that Fe<sup>III</sup>(aq) is spontaneously reduced by hydrogen gas (see p. 435). However, under normal circumstances, it is not hydrogen but atmospheric oxygen which is important and, for the process  $\frac{1}{2}\text{O}_2 + 2\text{H}^+ + 2\text{e}^- \rightleftharpoons \text{H}_2\text{O}$ ,  $E^\circ = 1.229\text{ V}$ , i.e. oxygen gas is sufficiently strong an oxidizing agent to render [Fe(H<sub>2</sub>O)<sub>6</sub>]<sup>2+</sup> (and, indeed, all other Fe<sup>II</sup> species in Table A) unstable wrt atmospheric oxidation. In practice the oxidation in acidic solutions is slow and, if the pH is increased, the potential for the Fe<sup>III</sup>/Fe<sup>II</sup> couple remains fairly constant until the solution becomes alkaline and hydrous Fe<sub>2</sub>O<sub>3</sub> (considered here for convenience to be Fe(OH)<sub>3</sub>) is precipitated. But here the change is dramatic, as explained below.

The actual potential  $E$  of the couple is given by the Nernst equation,

$$E = E^\circ - \frac{RT}{nF} \ln \frac{[\text{Fe}^{\text{II}}]}{[\text{Fe}^{\text{III}}]}$$

where  $E = E^\circ$  when all activities are unity. However, once precipitation occurs, the activities of the iron species are far from unity; they are determined by the solubility products of the 2 hydroxides. These are:

$$[\text{Fe}^{\text{II}}][\text{OH}^-]^2 \sim 10^{-14} (\text{mol dm}^{-3})^3 \text{ and } [\text{Fe}^{\text{III}}][\text{OH}^-]^3 \sim 10^{-36} (\text{mol dm}^{-3})^4$$

Therefore when  $[\text{OH}^-] = 1 \text{ mol dm}^{-3}$ ,  $\frac{[\text{Fe}^{\text{II}}]}{[\text{Fe}^{\text{III}}]} \sim 10^{22}$

Hence  $E \sim 0.771 - 0.05916 \log_{10}(10^{22}) = 0.771 - 1.301 = -0.530\text{ V}$

Thus by making the solution alkaline the sign of  $E$  has been reversed and the susceptibility of Fe<sup>II</sup>(aq) to oxidation (i.e. its reducing power) enormously increased. This is why white, precipitated Fe(OH)<sub>2</sub> and FeCO<sub>3</sub> are rapidly darkened by aerial oxidation and why Fe<sup>II</sup> in alkaline solution will reduce nitrates to ammonia and copper(II) salts to metallic copper.

Addition of  $K_4[Fe^{II}(CN)_6]$  to aqueous  $Fe^{III}$  produces the intensely blue precipitate, Prussian blue.<sup>(32a)</sup> The X-ray powder pattern and Mössbauer spectrum of this are the same as those of Turnbull's blue which is produced by the converse addition of  $K_3[Fe^{III}(CN)_6]$  to aqueous  $Fe^{II}$ . By varying the conditions and proportions of the reactants, a whole range of these blue materials can be produced of varying composition with some, which are actually colloidal, described as soluble Prussian blue. They have found application as pigments in the manufacture of inks and paints since their discovery in 1704 and, in 1840, their formation on sensitized paper was utilized in the production of blueprints. It appears that all these materials have the same basic structure. This consists of a cubic lattice of low-spin  $Fe^{II}$  and high-spin  $Fe^{III}$  ions with cyanide ions lying linearly along the cube edges, and water molecules situated inside the cubes. The intense colour is due to charge-transfer from  $Fe^{II}$  to  $Fe^{III}$ . Unfortunately, detailed characterizations are bedevilled by difficulties in obtaining satisfactory single crystals and reproducible compositions. Good quality single crystals formulated as  $Fe_4[Fe(CN)_6]_3 \cdot xH_2O$  ( $x = 14-16$ ) can be produced by the slow diffusion of  $H_2O$  vapour into a solution of  $Fe^{III}$  and  $[Fe(CN)_6]^{4-}$  in conc HCl. This has the same basic lattice but with some of the  $Fe^{II}$  and  $CN^-$  sites occupied by water. Less delicate methods lead to the absorption of alkali metal ions (particularly  $K^+$ ) and to formulations such as  $M^I Fe^{II} Fe^{III}(CN)_6 \cdot xH_2O$ . The same structure motif is found in  $Fe^{III} Fe^{III}(CN)_6$  and in the virtually white, readily oxidizable  $K_2 Fe^{II} Fe^{II}(CN)_6$ , the former having no counter cations while the  $K^+$  ions of the latter fill all the lattice cubes. Having all their iron atoms in a uniform oxidation state, however, these two compounds lack the intense colour of the Prussian blues.

It is possible to replace 1  $CN^-$  in the hexacyanoferrate(II) ion with  $H_2O$ ,  $CO$ ,  $NO_2^-$ , and, most importantly, with  $NO^+$ . The "nitroprusside" ion  $[Fe(CN)_5NO]^{2-}$  can be produced by the

action of 30% nitric acid on either  $[Fe(CN)_6]^{4-}$  or  $[Fe(CN)_6]^{3-}$ . That it formally contains  $Fe^{II}$  and  $NO^+$  (rather than  $Fe^{III}$  and  $NO$ ) is evident from its diamagnetism, although Mössbauer studies indicate that there is appreciable  $\pi$  delocalization of charge from the  $t_{2g}$  orbitals of the  $Fe^{II}$  to the nitrosyl and cyanide groups. The red colour of  $[Fe(CN)_5(NOS)]^{4-}$ , formed by the addition of sulfide ion, is used in a common qualitative test for sulfur. Another qualitative test involving an iron nitrosyl is the "brown ring" test for  $NO_3^-$ , using iron(II) sulfate and conc  $H_2SO_4$  in which  $NO$  is produced. The brown colour, which appears to be due to charge-transfer, evidently arises from a cationic iron nitrosyl complex which has a magnetic moment  $\sim 3.9$  BM; it is therefore formulated as  $[Fe(NO)(H_2O)_5]^{2+}$  in which the iron can be considered formally to be in the +1 oxidation state.

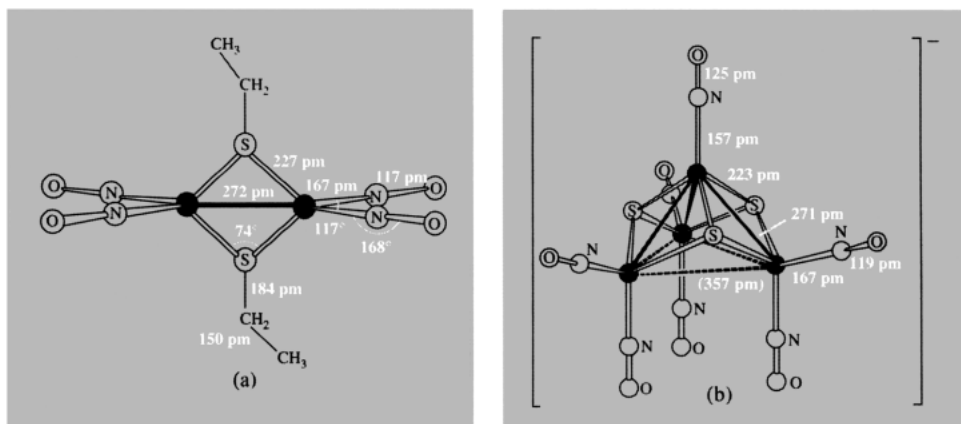
Roussin's "red" and "black" salts, formulated respectively as  $K_2[Fe_2(NO)_4S_2]$  and  $K[Fe_4(NO)_7S_3]$ , are obtained by the action of  $NO$  on  $Fe^{II}$  in the presence of  $S^{2-}$  and are structurally interesting. In both cases the iron atoms are pseudo-tetrahedrally coordinated (Fig. 25.6) and, though the assignment of formal oxidation states has only doubtful significance, their diamagnetism and the presence of rather short  $Fe-Fe$  distances are indicative of some direct metal-metal interaction. The  $[NEt_4]^+$  black salt in acetonitrile solution has been reversibly reduced electrochemically<sup>(33)</sup> to  $[Fe_4(NO)_7S_3]^{n-}$  ( $n = 1-4$ ), the  $n = 2$  and 3 compounds being isolated and shown to retain essentially the same structure, though somewhat expanded, as expected with the extra charge.

These, and related, iron nitrosyl compounds have excited considerable interest because of their biological activity.<sup>(34)</sup> Nitroprusside induces muscle relaxation and is therefore used to control high blood pressure. Roussin's black salt has antibacterial activity under conditions relevant to

<sup>33</sup> S. D'ADDARIO, F. DEMARTIN, L. GROSSI, M. C. IAPALUCCI, F. LASCHI, G. LONGONI and F. ZANELLO, *Inorg. Chem.* **32**, 1153-60 (1993).

<sup>34</sup> A. R. BUTLER, C. GLIDEWELL and S. M. GLIDEWELL, *Polyhedron*, **11**, 591-6 (1992).

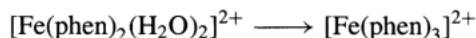
<sup>32a</sup> K. R. DUNBAR and R. A. HEINTZ, *Prog. Inorg. Chem.* **45**, 283-391 (1997).



**Figure 25.6** The structure of Roussin's salts: (a) the ethyl ester  $[\text{Fe}(\text{NO})_2\text{SET}]_2$  of the red salt showing pseudo-tetrahedral coordination of each iron ( $\text{Fe}-\text{Fe} = 272 \text{ pm}$ ), and (b) the anion of the black salt  $\text{Cs}[\text{Fe}_4(\text{NO})_7\text{S}_3] \cdot \text{H}_2\text{O}$  showing a pyramid of 4 Fe atoms with an S atom above each of its three non-horizontal faces ( $\text{Fe}_{\text{apex}}-\text{Fe}_{\text{base}} = 271 \text{ pm}$ ,  $\text{Fe}_{\text{base}} \cdots \text{Fe}_{\text{base}} 357 \text{ pm}$ ). (The anion may alternatively be viewed as an  $\text{Fe}_3\text{S}_3$  ring with the "chair" conformation.) Note that even the short Fe-Fe distances are appreciably greater than the Fe-Fe "single-bond" distance of  $\sim 250 \text{ pm}$ .

food-processing, while some of the red esters promote the activity of certain environmental carcinogens.

In addition to high-spin octahedral complexes with magnetic moments in excess of 5 BM, and diamagnetic, low-spin octahedral complexes,  $\text{Fe}^{\text{II}}$  affords further examples of high-spin/low-spin transitions within a given compound (see Panel, p. 1096). It has already been noted that a change from high-spin to low-spin accompanies the change,



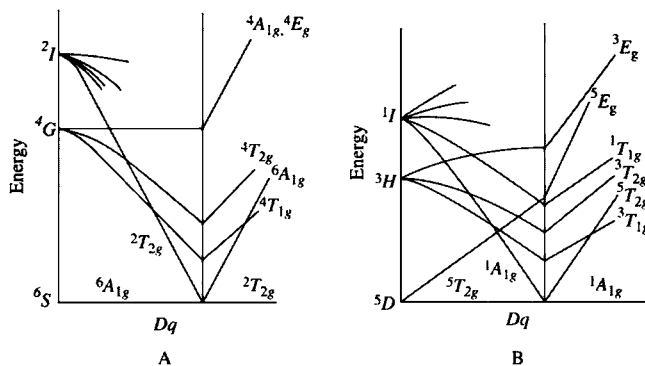
so it is no great surprise that spin transitions have been found in  $[\text{Fe}(\text{phen})_2\text{X}_2]$  ( $\text{X} = \text{NCS}$ ,  $\text{NCS}_e$ ) complexes and their bipy analogues. These evidently lie just to the high-field side of the crossover since at temperatures below  $-125^\circ\text{C}$  the compounds are almost diamagnetic (what paramagnetism there is probably due to impurity), while at some temperature between  $-125^\circ\text{C}$  and  $-75^\circ\text{C}$  depending on the compound, the moment quite suddenly rises to over 5 BM. Confirmation of the transition in these and other  $\text{Fe}^{\text{II}}$  complexes has been provided by electronic and Mössbauer spectroscopy.

Apart from compounds such as  $[\text{RuCl}_2(\text{PPh}_3)_3]$ , which is square pyramidal because the sixth coordinating position is stereochemically blocked,  $\text{Ru}^{\text{II}}$  compounds (and also  $\text{Os}^{\text{II}}$  compounds) are octahedral and diamagnetic.  $[\text{Ru}(\text{H}_2\text{O})_6]^{2+}$  can be prepared in aqueous solution by electrolytic reduction of  $[\text{RuCl}_5(\text{H}_2\text{O})]^{2-}$  using  $\text{Pt}/\text{H}_2$  and, though readily oxidized to  $\text{Ru}^{\text{III}}$  (p. 1088), has been isolated and characterized<sup>(27)</sup> in the pink  $[\text{Ru}(\text{H}_2\text{O})_6](\text{tos})_2$  and the sulfates  $\text{M}_2[\text{Ru}(\text{H}_2\text{O})_6](\text{SO}_4)_2$  ( $\text{M} = \text{Rb}$ ,  $\text{NH}_4$ ). The cyano complexes  $[\text{Ru}(\text{CN})_6]^{4-}$  and  $[\text{Ru}(\text{CN})_5\text{NO}]^{2-}$ , analogous to their iron counterparts, are also known but the most notable compounds of  $\text{Ru}^{\text{II}}$  are undoubtedly its complexes with Group 15 donor ligands, such as the amines and nitrosyls.

$[\text{Ru}(\text{NH}_3)_6]^{2+}$  and corresponding tris chelates with en, bipy and phen, etc., are obtained from "RuCl<sub>3</sub>" with Zn powder as a reducing agent. The hexammine is a strongly reducing substance and  $[\text{Ru}(\text{bipy})_3]^{2+}$ , although thermally very stable, is capable of photochemical excitation involving the promotion of an electron from a molecular orbital of essentially metal character to one of an essentially ligand character, after which its oxidation is possible. A number of similar

Spin Equilibria<sup>(35–38)</sup>

Because the d-orbitals of a metal in an octahedral complex split into  $t_{2g}$  and  $e_g^*$  sets (p. 922), each of the  $d^4$ – $d^7$  configurations can exist in either high-spin or low-spin configurations, depending on whether the energy ( $P$ ) required to force spin-pairing is greater or smaller than the orbital splitting ( $\Delta_0$  or  $10Dq$ ). This is illustrated in the energy level diagrams (Figs. A and B) for  $d^5$  and  $d^6$  ions where in each case at a critical value of  $\Delta_0$  (the crossover point), the ground terms of the high- and low-spin configurations ( ${}^6A_{1g}$  and  ${}^2T_{2g}$  respectively for  $d^5$ ,  ${}^5T_{2g}$  and  ${}^1A_{1g}$  for  $d^6$ ) are equal. Close to the crossover point both terms are thermally accessible and a Boltzmann distribution of molecules between the two states can be envisaged.



Energy level diagrams for, A  $d^5$  ions and B  $d^6$  ions.

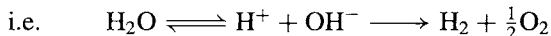
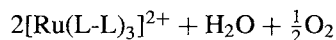
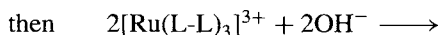
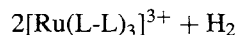
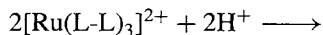
This simple explanation accounts quite well for a variety of dithiocarbamate complexes of iron(III) whose magnetic moments rise gradually from about 2.3 BM (corresponding to low-spin  $d^5$ ) at very low temperatures to > 4 BM (corresponding to roughly equal populations in the two states) above room temperature.

However, the emptying of the  $e_g^*$  orbitals in changing from high- to low-spin allows a shortening of metal-ligand distances with a corresponding increase in  $\Delta_0$ . Such a situation does not correspond to the crossover point since the two isomers occupy different positions on the  $\Delta_0$  axis. In solutions, conversion of one isomer to the other is usually facile and equilibrium readily established. In solids, on the other hand, molecules are coupled by lattice vibrations and the conversion is often accompanied by a change of phase. The iron(II) compound  $[\text{Fe}(\text{phen})_2(\text{NCS})_2]$  is a good example of this, the change in magnetic moment being far too abrupt to be accounted for by a simple Boltzmann distribution between thermally accessible spin states.

Spin equilibria have been investigated by bulk magnetic measurements, X-ray crystallography, vibrational, electronic, Mössbauer, esr and nmr spectroscopy and also at high pressures. Besides their obvious intrinsic interest, they have biological relevance because of the change in spin when haemoglobin is oxygenated (p. 1099). Geologically, the high-spin iron(II) in minerals such as olivine (p. 347) becomes low-spin under high pressure in the earth's mantle. Since some spin-transitions can be induced optically, there are also possible light storage applications.

complexes with substituted bipyridyl ligands luminesce in visible light,<sup>(39)</sup> and considerable effort is being devoted to preparing suitable derivatives which could be used to catalyze the

photolytic decomposition of water, with a view to the conversion of solar energy into hydrogen fuel.



<sup>35</sup> L. L. MARTIN, R. L. MARTIN and A. M. SARGESON, *Polyhedron* **13**, 1969–80 (1994).

<sup>36</sup> E. KÖNIG, *Structure and Bonding* **76**, 51–152 (1991).

<sup>37</sup> H. TOFLUND, *Coord. Chem. Revs.* **94**, 67–108 (1989).

<sup>38</sup> J. K. BEATTY, *Adv. Inorg. Chem.* **32**, 1–53 (1988).

<sup>39</sup> E. KRAUSZ and J. FERGUSON, *Prog. Inorg. Chem.* **37**, 293–390 (1989).

The pentaammine derivative,  $[\text{Ru}(\text{NH}_3)_5\text{N}_2]^{2+}$ , when prepared in 1965 by the reduction of aqueous  $\text{RuCl}_3$  with  $\text{N}_2\text{H}_4$ , was the first dinitrogen complex to be produced (p. 414). It contains the linear Ru–N–N group ( $\nu_{(\text{N}-\text{N})} = 2140 \text{ cm}^{-1}$ ). The dinuclear derivative  $[(\text{NH}_3)_5\text{Ru}-\text{N}-\text{N}-\text{Ru}(\text{NH}_3)_5]^{4+}$  with a linear Ru–N–N–Ru bridge ( $\nu_{(\text{N}-\text{N})} = 2100 \text{ cm}^{-1}$  compared to  $2331 \text{ cm}^{-1}$  for  $\text{N}_2$  itself) is also known (see pp. 414 and 1035 for a fuller discussion of the significance of  $\text{N}_2$  complexes).

The nitrosyl complex  $[\text{Ru}(\text{NH}_3)_5\text{NO}]^{3+}$ , which is obtained by the action of  $\text{HNO}_2$  on  $[\text{Ru}(\text{NH}_3)_6]^{2+}$ , is isoelectronic with  $[\text{Ru}(\text{NH}_3)_5\text{N}_2]^{2+}$  and is typical of a whole series of  $\text{Ru}^{\text{II}}$  nitrosyls.<sup>(11,21)</sup> They are prepared using reagents such as  $\text{HNO}_3$  and  $\text{NO}_2^-$  and are invariably mononitrosyls, the 1 NO apparently sufficing to satisfy the  $\pi$ -donor potential of  $\text{Ru}^{\text{II}}$ . The RuNO group is characterized by a short Ru–N distance in the range 171–176 pm, and a stretching mode  $\nu_{(\text{N}-\text{O})}$  in the range 1930–1845  $\text{cm}^{-1}$ , consistent with the formulation  $\text{Ru}^{\text{II}}=\overset{+}{\text{N}}=\text{O}$ . The other ligands making up the octahedral coordination include halides, O-donor anions, and neutral, mainly Group 15 donor ligands.

The stability of ruthenium nitrosyl complexes poses a practical problem in the processing of wastes from nuclear power stations.  $^{106}\text{Ru}$  is a major fission product of uranium and plutonium and is a  $\beta^-$  and  $\gamma$  emitter with a half-life of 1 year (374d). The processing of nuclear wastes depends largely on the solvent extraction of nitric acid media, using tri-*n*-butyl phosphate (TBP) as the solvent (p. 1261). In the main, the uranium and plutonium enter the organic phase while fission products such as Cs, Sr and lanthanides remain in the aqueous phase. Unfortunately, by this procedure Ru is less effectively removed from the U and Pu than any other contaminant. The reason for this problem is the coordination of TBP to stable ruthenium nitrosyl complexes which are formed under these conditions. This confers on the ruthenium an appreciable solubility in the organic phase, thereby necessitating several extraction cycles for its removal.

Osmium(II) forms no hexaquo complex and  $[\text{Os}(\text{NH}_3)_6]^{2+}$ , which may possibly be present in potassium/liquid  $\text{NH}_3$  solutions, is also unstable.  $[\text{Os}(\text{NH}_3)_5\text{N}_2]^{2+}$  and other dinitrogen complexes are known but only ligands with good  $\pi$ -acceptor properties, such as  $\text{CN}^-$ , bipy, phen, phosphines and arsines, really stabilize  $\text{Os}^{\text{II}}$ , and these form complexes similar to their  $\text{Ru}^{\text{II}}$  analogues.

### Mixed Valence Compounds of Ruthenium<sup>(40)</sup>

Ruthenium provides more examples of dinuclear compounds in which the metal is present in a mixture of oxidation states (or in a non-integral oxidation state) than any other element.

Heating  $\text{RuCl}_3 \cdot 3\text{H}_2\text{O}$  in acetic acid/acetic anhydride under reflux yields brown  $[\text{Ru}_2(\text{O}_2\text{CCH}_3)_4]\text{Cl}$  (cf Os p. 1091) in which the metals are linked by four acetate bridges in the manner of  $\text{Cr}^{\text{II}}$  and  $\text{Mo}^{\text{II}}$  carboxylates (p. 1033). In this and analogous carboxylates, Ru = Ru 224–230 pm with magnetic moments indicative of three unpaired electrons; this can be explained by the assumption that the  $\pi^*$  and  $\delta^*$  orbitals (see Fig. 23.14) are close enough in energy to afford the  $\pi^*\delta^*$  configuration.<sup>(41)</sup> Treatment of  $[\text{Ru}(\text{NH}_3)_6]^{2+}$  in conc. HCl produces the intensely coloured *ruthenium blue*,  $[(\text{NH}_3)_5\text{Ru}(\mu\text{-Cl})_3\text{Ru}(\text{NH}_3)_5]^{2+}$  (Ru–Ru 275.3 pm). In all these cases the metal atoms are indistinguishable and are assigned an oxidation state of 2.5.

The “Creutz–Taube” anion,  $[(\text{NH}_3)_5\text{Ru}\{\text{N}(\text{CH}=\text{CH})_2\text{N}\}\text{Ru}(\text{NH}_3)_5]^{5+}$  displays more obvious redox properties, yielding both 4+ and 6+ species, and much interest has focused on the extent to which the pyrazine bridge facilitates electron transfer. A variety of spectroscopic studies supports the view that low-energy electron tunnelling across the bridge delocalizes the charge, making the 5+ ion symmetrical. Other complexes, such as the anion  $[(\text{CN})_5\text{Ru}^{\text{II}}(\mu\text{-CN})\text{Ru}^{\text{III}}(\text{CN})_5]^-$ , are asymmetric

<sup>40</sup> R. J. CRUTCHLEY, *Adv. Inorg. Chem.* **41**, 273–325 (1994).

<sup>41</sup> F. A. COTTON and R. A. WALTON, pp. 399–430 *Multiple Bonds between Metal Atoms*, Clarendon Press, Oxford (1993).

Table 25.7 Naturally occurring iron proteins

Name	Donor atoms. Stereochemistry of Fe	Function	Source	Approximate Mol wt	No. of Fe atoms
<i>Haem proteins</i>					
Haemoglobin	$5 \times N$ Square pyramidal	O <sub>2</sub> transport	Animals	64 500	4
Myoglobin	$5 \times N$ Square pyramidal	O <sub>2</sub> storage	Animals	17 800	1
Cytochromes	$5 \times N + S$ Octahedral	Electron transfer	Bacteria, plants, animals	12 400	4
<i>NHIP (non-haem iron proteins)</i>					
Transferrin		Scavenging Fe	Animals	80 000	2
Ferritin		Storage of Fe	Animals	460 000	20% Fe
Ferredoxins	$4 \times S$ Distorted tetrahedral	Electron transfer	Bacteria, plants, animals	6000–12 000	2–8
Rubridoxins	$4 \times S$ Distorted tetrahedral	Electron transfer	Bacteria	6000	1
“MoFe protein”	$4 \times S$ Distorted tetrahedral	Nitrogen fixation (see p. 1035)	In nitrogenase	220 000–240 000	24–36
“Fe protein”					

and are thought to have potential use in laser technology.<sup>(42)</sup>

### Lower oxidation states

With rare exceptions, such as  $[\text{Fe}(\text{bipy})_3]^0$ , oxidation states lower than +2 are represented only by carbonyls, phosphines, and their derivatives. These will be considered together with other organometallic compounds in Section 25.3.6.

### 25.3.5 The biochemistry of iron<sup>(43–45)</sup>

Iron is the most important transition element involved in living systems, being vital to both

plants and animals. The stunted growth of the former is well known on soils which are either themselves deficient in iron, or in which high alkalinity renders the iron too insoluble to be accessible to the plants. Very efficient biological mechanisms exist to control the uptake and transport of iron and to ensure its presence in required concentrations. The adult human body contains about 4 g of iron (i.e. ~0.005% of body weight), of which about 3 g are in the form of haemoglobin, and this level is maintained by absorbing a mere 1 mg of iron per day — a remarkably economical utilization.

Proteins involving iron have two major functions:

- (a) oxygen transport and storage;
- (b) electron transfer.

Ancillary to the proteins performing these functions are others which transport and store the iron itself. All these proteins are conveniently categorized according to whether or not they contain haem, and the more important classes found in nature are listed in Table 25.7.

<sup>42</sup> W. M. LAIDLAW, R. G. DENNING, T. VERBIEST, E. CHAUHARD and A. PERSOONS, *Nature* **363**, 58–60 (1993).

<sup>43</sup> J. G. LEIGH, G. R. MOORE and M. T. WILSON, *Biological Iron*, Chap. 6, pp. 181–243; A. K. POWELL, *Models for Iron Biomolecules*, Chap. 7, pp. 244–74, in ref. 10.

<sup>44</sup> R. CRICHTON, *Inorganic Biochemistry of Iron Metabolism*, Ellis Horwood, Hemel Hempstead, 1991, 212 pp.

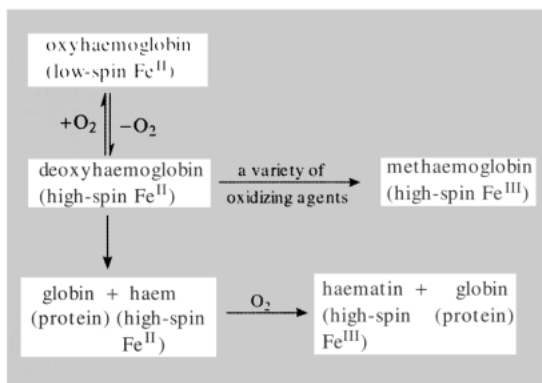
<sup>45</sup> W. KAIM and B. SCHWEDERSKI, *Bioinorganic Chemistry: Inorganic Elements in the Chemistry of Life*, Wiley, Chichester, 1994, 401 pp.



### Haemoglobin and myoglobin

Haemoglobin (see p. 126) is the oxygen-carrying protein in red blood-cells (erythrocytes) and is responsible for their colour. Its biological function is to carry  $O_2$  in arterial blood from the lungs to the muscles, where the oxygen is transferred to the immobile myoglobin, which stores it so that it is available as and when required for the generation of energy by the metabolic oxidation of glucose. At this point the haemoglobin picks up  $CO_2$ , which is a product of the oxidation of glucose, and transports it in venous blood back to the lungs.†

In haemoglobin which has no  $O_2$  attached (and is therefore known as deoxyhaemoglobin or reduced haemoglobin), the iron is present as high-spin  $Fe^{II}$  and the reversible attachment of  $O_2$  (giving oxyhaemoglobin) changes this to diamagnetic, low-spin  $Fe^{II}$  without affecting the metal's oxidation state. This is remarkable, the more so because, if the globin is removed by treatment with HCl/acetone, the isolated haem in water entirely loses its  $O_2$ -carrying ability, being instead oxidized by air to haematin in which the iron is high-spin  $Fe^{III}$ :



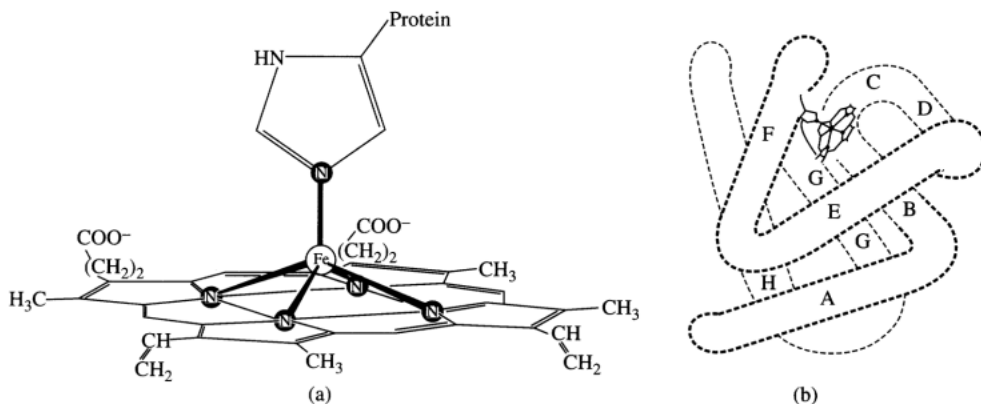
The key to the explanation lies in (a) the observation that in general the ionic radius of  $Fe^{II}$  (and also, for that matter, of  $Fe^{III}$ ) decreases by roughly 20% when the configuration changes

† Human arterial blood can absorb over 50 times more oxygen than can water, and venous blood can absorb 20 times more  $CO_2$  than water can.

from high- to low-spin (see Table 25.1), and (b) the structure of haemoglobin.

As a result of intensive study, enough is known about the structure of haemoglobin to allow the broad principles of its operation to be explained. It is made up of 4 subunits, each of which consists of a protein (globin), in the form of a folded helix or spiral, attached to 1 iron-containing group (haem). The proteins are of two types, one denoted as  $\alpha$  consists of 141 amino acids, the other denoted as  $\beta$  consists of 146 amino acids. The polar groups of each protein are on the outside of the structure leaving a hydrophobic interior. The haem group, which is held in a protein "pocket" is therefore in a hydrophobic environment. Within the haem group the iron is coordinated to 4 nitrogen atoms of the planar group known as protoporphyrin IX (PIX). In the case of deoxyhaemoglobin the  $Fe^{II}$ , being high-spin, is too large to fit easily inside the hole provided by the porphyrin ring and is situated 55 pm above the ring which, in turn, is slightly bent into a domed shape, the better to accommodate the  $Fe^{II}$ . The fifth coordination site, away from the ring, is occupied by an imidazole nitrogen of a *proximal* histidine of the globin (Fig. 25.7). The vacant sixth site, below the ring, is essentially vacant, "reserved" for the  $O_2$  but with another (*distal*) histidine restricting access. This is the so-called "tense" (deoxyT) form in which the 4 subunits of deoxyhaemoglobin are held together in an approximately tetrahedral arrangement by electrostatic  $-NH_3^+ \dots \bar{O}OC-$  "salt bridges."

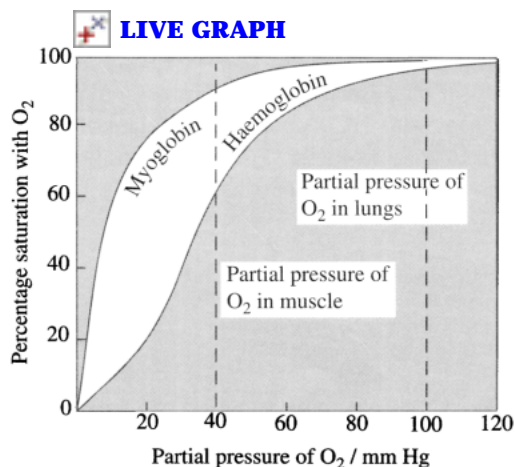
In order that  $O_2$  may bond to the haem, the *distal* histidine must swing away but, once the  $O_2$  is attached, it swings back to form a hydrogen bond with the  $O_2$ . The  $Fe^{II}$  becomes low-spin and the oxyT form, which is still domed, "relaxes" to the planar oxyR form as the now smaller  $Fe^{II}$  slips into the ring which becomes planar again. When this occurs to one of the 4 subunits of deoxyhaemoglobin the movement of the Fe, and of the histidines attached to it, is communicated through the protein chains to the other subunits. This produces a rotation and linear movement of one  $\alpha\beta$  pair w.r.t. the other which, crucially,



**Figure 25.7** Haemoglobin: (a) The haem group, composed of the planar PIX molecule and iron, and shown here attached to the globin via an imidazole-nitrogen which completes the square pyramidal coordination of the  $\text{Fe}^{\text{II}}$ , and (b) myoglobin showing, diagrammatically, the haem group in a “pocket” formed by the folded protein. The globin chain is actually in the form of 8 helical sections, labelled A to H, and the haem is situated between the E and F sections. The 4 subunits of haemoglobin are similar.

converts the other 3 subunits to the deoxyR form, greatly increasing their affinity for  $\text{O}_2$ . The effect of attaching one  $\text{O}_2$  to haemoglobin is therefore to greatly increase its affinity for more.

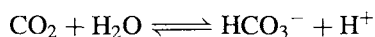
Conversely, as  $\text{O}_2$  is removed from oxyhaemoglobin the reverse conformational changes occur and successively decrease its affinity for oxygen. This is the phenomenon of *cooperativity*, and its physiological importance lies in the fact that it allows the efficient transfer of oxygen from oxyhaemoglobin to myoglobin. This is because myoglobin contains only 1 haem group and can be regarded crudely as a single haemoglobin subunit. It therefore cannot display a cooperative effect and at lower partial pressures of oxygen it has a greater affinity than haemoglobin for oxygen. This can be seen in Fig. 25.8 which shows that, while haemoglobin is virtually saturated with  $\text{O}_2$  in the lungs, when it experiences the lower partial pressures of oxygen in the muscle tissue its affinity for  $\text{O}_2$  has fallen off so much more rapidly than that of myoglobin that oxygen transfer ensues. Indeed, the actual situation is even more effective than this, because the affinity of haemoglobin for oxygen decreases when the pH is lowered (this is called the Bohr effect and arises in a complicated manner from the effect



**Figure 25.8** Oxygen dissociation curves for haemoglobin and myoglobin, showing how haemoglobin is able to absorb  $\text{O}_2$  efficiently in the lungs yet transfer it to myoglobin in muscle tissue.

of pH on the salt bridges holding the subunits together). Since the  $\text{CO}_2$  released in the muscle lowers the pH, it thereby facilitates the transfer of oxygen from the oxyhaemoglobin, and the greater the muscular activity the more the release of  $\text{CO}_2$  helps to meet the increased demand for oxygen. Excess  $\text{CO}_2$  is then removed from the tissue,

predominantly in the form of soluble  $\text{HCO}_3^-$  ions whose formation is facilitated by the protein chains of deoxyhaemoglobin which act as a buffer by picking up the accompanying protons.



The mode of bonding of the  $\text{O}_2$  to Fe is important. In oxyhaemoglobin the hydrogen bonding to the *distal* histidine tilts the  $\text{O}_2$  and produces an Fe–O–O angle of about  $120^\circ$ . This geometry (which hinders the formation of the Fe–O–Fe or Fe– $\text{O}_2$ –Fe bridge believed to be an intermediate in  $\text{Fe}^{\text{II}}$  to  $\text{Fe}^{\text{III}}$  oxidations) along with the hydrophobic environment which inhibits electron transfer, together prevent the oxidation of  $\text{Fe}^{\text{II}}$  which would destroy the haemoglobin.

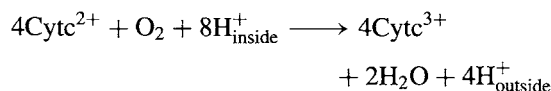
The poisoning effect of molecules such as CO and  $\text{PF}_3$  (p. 495) arises simply from their ability to bond reversibly to haem in the same manner as  $\text{O}_2$ , but much more strongly, so that oxygen transport is prevented. The cyanide ion  $\text{CN}^-$  can also displace  $\text{O}_2$  from oxyhaemoglobin but its very much greater toxicity at small concentrations stems not from this but from its interference with the action of cytochrome a.

### Cytochromes<sup>(46)</sup>

The haem unit was evidently a most effective evolutionary development since it is found not only in the oxygen-transporting substances but also in electron transporters such as the cytochromes which are scattered widely throughout nature. There are three main types of cytochromes, a, b and c, members of each type being distinguished by subscripts, and their role is as intermediates in the metabolic oxidation of glucose by molecular oxygen. The iron of the haem group is attached to an associated protein by an imidazole N just as in haemoglobin and myoglobin. In most a and b cytochromes the sixth coordination site of the iron is also occupied by an imidazole N but, in type c and some type b cytochromes, it is occupied by a tightly bound

S from a methionine residue rendering these cytochromes inert not only to oxygen but also to the poisons which affect oxygen carriers. Electron transfer is effected in a series of steps, in each of which the oxidation state of the iron which is normally in a low-spin configuration oscillates between +2 and +3. Since the cytochromes are involved in the order b,c,a, the reduction potential of each step is successively increased (Table 25.8), so forming a “redox gradient”. This allows energy from the glucose oxidation to be released gradually and to be stored in the form of adenosine triphosphate (ATP) (see also p. 528).

The link with the final electron acceptor,  $\text{O}_2$ , is the enzyme cytochrome c oxidase which spans the inner membrane of the mitochondrion. It consists of cytochromes a and  $\text{a}_3$  along with two, or possibly three, Cu atoms. The details of its action are not fully established but the overall reaction catalysed by the enzyme is:



indicating the transport not only of electrons but also of protons across the mitochondrial membrane. As the end member of the redox gradient it differs from the other members in bonding  $\text{O}_2$  directly and so being extremely susceptible to poisoning by  $\text{CN}^-$ .

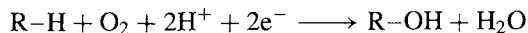
Another important group of cytochromes, found in plants, bacteria and animals is cytochrome P-450, so-called because of the absorption at 450 nm characteristic of their complexes with CO. Their function is to activate

**Table 25.8** Reduction potentials of some iron proteins

Iron protein	Oxidation states of Fe	$E^\circ/\text{V}$
Cytochrome $\text{a}_3$	$\text{Fe}^{\text{III}}/\text{Fe}^{\text{II}}$	0.4
Cytochrome b	$\text{Fe}^{\text{III}}/\text{Fe}^{\text{II}}$	0.02
Cytochrome c	$\text{Fe}^{\text{III}}/\text{Fe}^{\text{II}}$	0.26
Rubredoxin	$\text{Fe}^{\text{III}}/\text{Fe}^{\text{II}}$	–0.06
2-Fe plant ferredoxins	$\text{Fe}^{\text{III}}/\text{fractional}$	–0.40
4-Fe bacterial ferredoxins	Fractional/fractional	–0.37
8-Fe bacterial ferredoxins	Fractional/fractional	–0.42

<sup>46</sup> See p. 206–8 of ref. 45.

O<sub>2</sub> sufficiently to facilitate its cleavage and so catalyse the reaction,



thus making R-H water soluble and aiding its elimination. They have molecular weights in the region of 50 000 and O<sub>2</sub> bonds to the haem in a manner similar to that in haemoglobin but with cysteine instead of histidine in the *proximal* position. The S donor atom of the cysteine is helpful in stabilizing an Fe<sup>IV</sup>=O group the oxygen of which is then inserted into the R-H bond.

### *Iron-sulfur proteins*<sup>(47,48)</sup>

In spite of the obvious importance and diversity of haem proteins, comparable functions, especially that of electron transfer, are performed by non-haem iron proteins (NHIP).<sup>†</sup> These too are widely distributed (well over 100 are now known), different types being involved in nitrogen fixation (p. 1035) and photosynthesis as well as in the metabolic oxidation of sugars prior to the involvement of the cytochromes mentioned above. The NHIP responsible for electron transfer are the iron-sulfur proteins which are of relatively low molecular weight (6000–12 000) and contain 1, 2, 4 or 8 Fe atoms which, in all the structures which have been definitely established, are each coordinated to 4 S atoms in an approximately tetrahedral manner. As a consequence of the small ligand fields associated in the tetrahedral coordination, these all contain iron in the high-spin configuration. Nearly all NHIP are notable for reduction potentials in the unusually low range –0.05 to –0.49 V (Table 25.8), indicating their ability to act as reducing agents at the low-potential end of biochemical processes.

The simplest NHIP is rubredoxin, in which the single iron atom is coordinated (Fig. 25.9a) to 4 S atoms belonging to cysteine residues in the protein chain. It differs from the other Fe-S proteins in having no labile sulfur (i.e. inorganic sulfur which can be liberated as H<sub>2</sub>S by treatment with mineral acid; sulfur atoms of this type are not part of the protein, but form bridges between Fe atoms.)

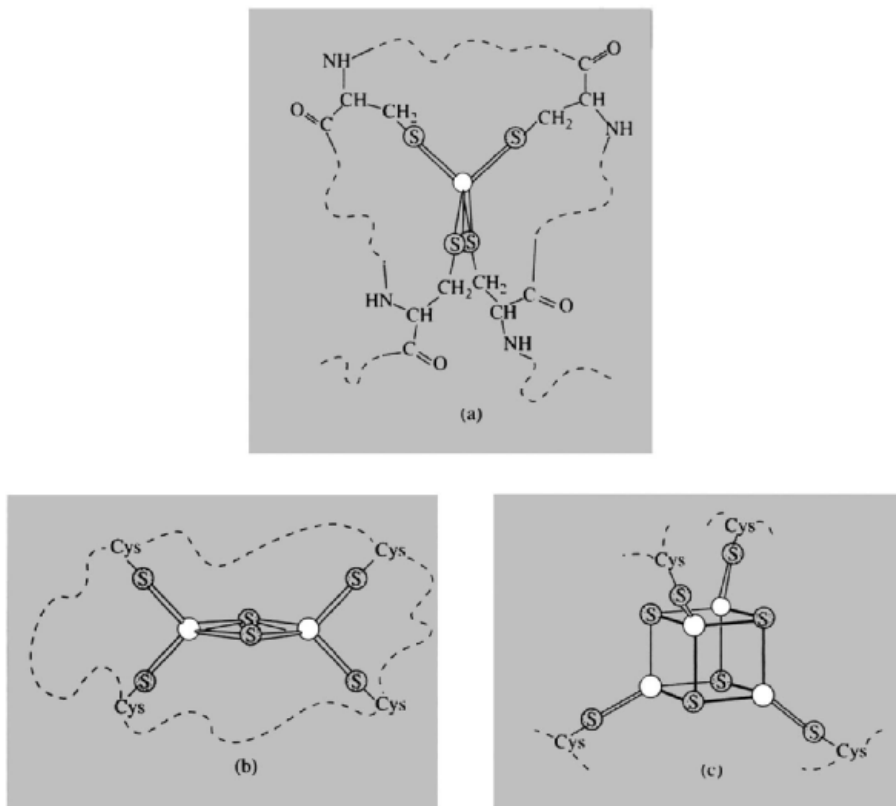
NHIP with more than one Fe are conveniently classified as [2Fe–2S], [3Fe–4S] and [4Fe–4S] types. The first of these, the so-called plant ferredoxins act as 1-electron transfer agents and contain 2 Fe atoms joined by S bridges with terminal cysteine groups (Fig. 25.9b). The 2 Fe atoms in the oxidized form are high-spin Fe(III) but very low magnetic moments are observed because of strong spin-spin interaction via the bridging atoms. The iron centres are not equivalent however, and esr evidence suggests that in the reduced form they exist as Fe(III) and Fe(II) rather than both having a fractional oxidation state of +2.5.

The existence of [3Fe–4S] ferredoxins has been established by Mössbauer spectroscopy only comparatively recently. The cluster consists essentially of the cubane [4Fe–4S] with one corner removed, the irons being high-spin Fe(III) in the oxidized form and Fe(II) + 2Fe(III) in the reduced. The most common and most stable of the ferredoxins, however, are the [4Fe–4S] type (Fig. 25.9c). In these clusters the 4 × Fe and 4 × S atoms form 2 interpenetrating tetrahedra which together make up a distorted cube in which each Fe atom is additionally coordinated to a cysteine sulfur to give it an approximately tetrahedral coordination sphere. The cluster, like the 2-Fe dimer, acts as a 1-electron transfer agent so that an 8-Fe protein, in which there are two [4Fe–4S] units with centres about 1200 pm apart can effect a 2-electron transfer. Why 4 Fe atoms are required to transfer 1 electron is not obvious. Synthetic analogues, prepared by reacting FeCl<sub>3</sub>, NaHS and an appropriate thiol (or still better FeCl<sub>3</sub>, elemental sulfur and the Li salt of a thiol), have properties similar to those of the natural proteins and have been used

<sup>47</sup> R. CAMMACK (ed.) *Adv. Inorg. Chem.* **38**, 1992, 487 pp. Whole volume devoted to Fe-S proteins.

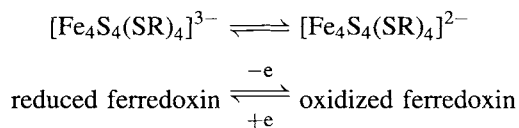
<sup>48</sup> I. BERTINI, S. CUIRLI and C. LUCHINAT, *Structure and Bonding*, **83**, 1–53 (1995).

<sup>†</sup> The oxygen-carrying function is performed in some invertebrates by haemerythrin which, in spite of its name, does not contain haem. It is a diiron-oxygen protein. See K. K. ANDERSON and A. GRÄLUND, *Adv. Inorg. Chem.* **43**, 359–408 (1995).



**Figure 25.9** Some non-haem iron proteins: (a) rubredoxin in which the single Fe is coordinated, almost tetrahedrally, to 4 cysteine-sulfurs, (b) plant ferredoxin,  $[\text{Fe}_2\text{S}_2(\text{S-Cys})_4]$ , (c)  $[\text{Fe}_4\text{S}_4(\text{S-Cys})_4]$  cube of bacterial ferredoxins. (This is in fact distorted, the  $\text{Fe}_4$  and  $\text{S}_4$  making up the two interpenetrating tetrahedra, of which the latter is larger than the former).

extensively in attempts to solve this problem.<sup>(43)</sup> The esr, electronic, and Mössbauer spectra, as well as the magnetic properties of the synthetic  $[\text{Fe}_4\text{S}_4(\text{SR})_4]^{3-}$  anions, are similar to those of the reduced ferredoxins, whose redox reaction is therefore mirrored by:



This indicates a change in the formal oxidation state of the iron from +2.25 to +2.5, and mixed  $\text{Fe}^{\text{III}}/\text{Fe}^{\text{II}}$  species have been postulated. However, it appears likely that these clusters are best regarded as electronically delocalized systems in which all the Fe atoms are equivalent.

4-Fe proteins are also known in which the diamagnetic, oxidized  $[\text{Fe}_4\text{S}_4(\text{SR})_4]^{2-}$  can be further oxidized at high potentials of about +0.35 V (hence “high potential iron sulfur proteins”, HIPIP) to paramagnetic ( $S = 1/2$ ),  $[\text{Fe}_4\text{S}_4(\text{SR})_4]^-$  species. Structural details and, indeed, biological function are still unclear.

Other non-haem proteins, distinct from the above iron-sulfur proteins are involved in the roles of iron transport and storage. Iron is absorbed as  $\text{Fe}^{\text{II}}$  in the human duodenum and passes into the blood as the  $\text{Fe}^{\text{III}}$  protein, transferrin.<sup>(49)</sup> The  $\text{Fe}^{\text{III}}$  is in a distorted octahedral environment consisting of  $1 \times \text{N}$ ,  $3 \times \text{O}$  and a chelating carbonate ion which

<sup>49</sup> E. N. BAKER, *Adv. Inorg. Chem.* **41**, 389–463 (1994)

apparently “locks” the iron into the binding site. This has a stability constant sufficiently high for the uncombined protein to strip  $\text{Fe}^{\text{III}}$  from such stable complexes as those with phosphate and citrate ions, and so it very efficiently scavenges iron from the blood plasma. The iron is then transported to the bone marrow where it is released from the transferrin (presumably after the temporary reduction of  $\text{Fe}^{\text{III}}$  to  $\text{Fe}^{\text{II}}$  since the latter's is a much less-stable complex), to be stored as ferritin, prior to its incorporation into haemoglobin. Ferritin is a water-soluble material consisting of a layer of protein encapsulating iron(III) hydroxyphosphate to give an overall iron content of about 20%.

### 25.3.6 Organometallic compounds<sup>(50)</sup>

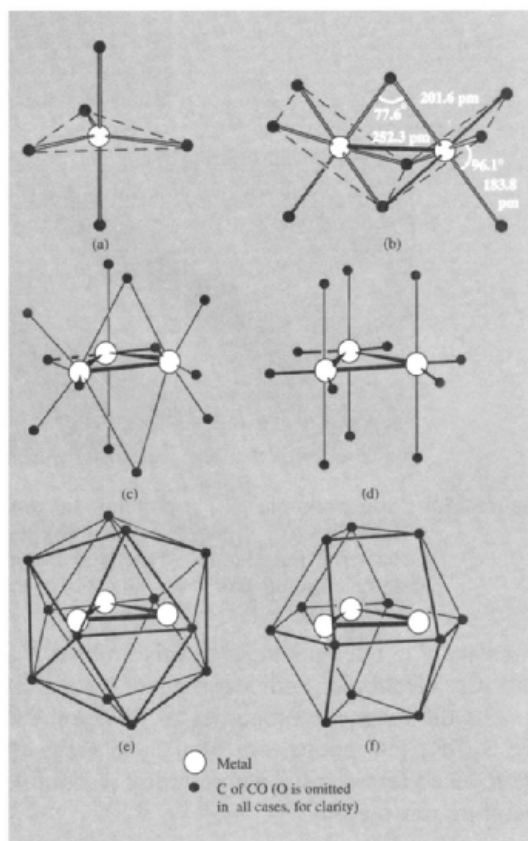
Within the field of organometallic chemistry, iron has long held a dominant position, and the last decade has seen explosive growth in the organic chemistry of ruthenium and osmium, particularly in the cluster chemistry<sup>(51)</sup> of osmium carbonyls. Carbonyls and metallocenes occupy dominant positions in this diverse field. Thus, although alkyls and aryls are known, they are only obtained with bulky groups which cannot undergo  $\beta$ -elimination (p. 925) or if the M–C  $\sigma$  bonds are stabilized by  $\pi$ -bonding ligands such as CO and P-donors.

#### Carbonyls (see p. 926)

Having the  $d^6s^2$  configuration, the elements of this triad are able to conform with the 18-electron rule by forming mononuclear carbonyls of the type  $\text{M}(\text{CO})_5$ . These are volatile liquids which can be prepared by the direct action of CO on the powdered metal ( $\text{Fe}^\dagger$  and Ru) or by the action of

CO on the tetroxide (Os), in each case at elevated temperatures and pressures.

$\text{Fe}(\text{CO})_5$  is a highly toxic substance discovered in 1891, the only previously known metal carbonyl being  $\text{Ni}(\text{CO})_4$ . Like its thermally unstable Ru and Os analogues, its structure is trigonal bipyramidal (Fig. 25.10a) but its  $^{13}\text{C}$  nmr spectrum indicates that all 5 carbon atoms are equivalent and this is explained by the molecules' fluxional behaviour (p. 914).



**Figure 25.10** Some carbonyls of Fe, Ru and Os: (a)  $\text{M}(\text{CO})_5$ ; M = Fe, Ru, Os. (b)  $\text{Fe}_2(\text{CO})_9$ ; Fe–Fe = 252.3 pm. (c)  $\text{Fe}_2(\text{CO})_{12}$ ; 1 Fe–Fe = 256 pm, 2 Fe–Fe = 268 pm. (d)  $\text{M}_3(\text{CO})_{12}$ ; M = Ru, Os, Ru–Ru = 285 pm, Os–Os = 288 pm. (e) and (f) are alternative representations of (c) and (d) emphasizing respectively the icosahedral and anti-cubeoctahedral arrangements of the CO ligands.

<sup>50</sup> P. L. PAUSON, Chap. 4 in *Chemistry of Iron*, pp. 73–170, Blackie, London, 1993.

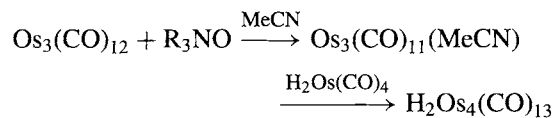
<sup>51</sup> A. J. AMOROSO, L. H. GADE, B. F. G. JOHNSON, J. LEWIS, P. R. RAITHY and W. T. WONG, *Angew. Chem. Int. Edn. Engl.* **30**, 107–9 (1991); B. H. S. THIMMAPPA, *Coord. Chem. Revs.* **143**, 1–35 (1995).

<sup>†</sup> The presence of  $\text{Fe}(\text{CO})_5$  in commercial cylinders of carbon monoxide at levels of 50 ppm has been reported (*Chem. in Brit.* **28**, 517 (1992)).

Exposure of  $\text{Fe}(\text{CO})_5$  in organic solvents to ultraviolet light produces volatile orange crystals of the enneacarbonyl,  $\text{Fe}_2(\text{CO})_9$ . Its structure consists of two face-sharing octahedra (Fig. 25.10b). An electron count shows that the dimer has a total of 34 valence electrons, i.e. 17 per iron atom. The observed diamagnetism is therefore explained by the presence of an Fe–Fe bond which is consistent with an interatomic separation virtually the same as in the metal itself. It is of interest that Ru and Os counterparts of  $\text{Fe}_2(\text{CO})_9$  are not only thermally less stable (the former especially so) but apparently are also structurally different, having an M–M bond supported by only 1 CO bridge. The carbonyls, which are produced along with the pentacarbonyls of Ru and Os and were initially thought to be enneacarbonyls, are in fact trimers,  $\text{M}_3(\text{CO})_{12}$ , which also differ structurally from  $\text{Fe}_3(\text{CO})_{12}$  (Fig. 25.10c to f). This dark-green solid, which is best obtained by oxidation of  $[\text{FeH}(\text{CO})_4]^-$  (see below), has a triangular structure in which two of the iron atoms are bridged by a pair of carbonyl groups, and can be regarded as being derived from  $\text{Fe}_2(\text{CO})_9$  by replacing a bridging CO with  $\text{Fe}(\text{CO})_4$ . The Ru and Os compounds (orange and yellow respectively), on the other hand, have a more symmetrical structure in which all the metal atoms are equivalent and are held together solely by M–M bonds. It has been suggested (Johnson's Ligand Polyhedral Model<sup>(52)</sup>) that the structure of the iron compound is determined not by the major bonding forces but by the interactions between the 12 CO ligands which in fact form an icosahedral array. This accommodates an  $\text{Fe}_3$  triangle with Fe–Fe distances similar to those in the metal, but not the larger  $\text{Ru}_3$  and  $\text{Os}_3$  triangles which force the ligands to adopt the less dense anticubeoctahedral form. As with the mononuclear carbonyl, the  $^{13}\text{C}$  nmr spectrum of the iron compound indicates C atom equivalence but this can be accounted for by oscillation of the  $\text{Fe}_3$  triangle without disruption of the icosahedral

array of CO ligands.<sup>(52)</sup> In solution, a non-bridged isomer is formed, different from the  $\text{Ru}_3$  and  $\text{Os}_3$  carbonyls and again probably retaining the icosahedral arrangement of ligands.

The chemistry of these carbonyls, especially those of Os, is extensive and displays an astonishing structural diversity which has been exploited particularly by the Cambridge group of J. Lewis.<sup>(53)</sup>  $\text{Os}_3(\text{CO})_{12}$  is the starting material for the preparation of other  $\text{Os}_3$  species and for clusters of higher nuclearity.<sup>(54)</sup> It is itself prepared by the reaction of  $\text{OsO}_4$  and CO under high pressure and is more stable than its Ru counterpart, which has a weaker M–M bond enthalpy ( $76 \text{ kJ mol}^{-1}$  compared to  $94 \text{ kJ mol}^{-1}$  in  $\text{Os}_8(\text{CO})_{12}$ ) and fragments rather easily. Thermolysis of  $\text{Os}_3(\text{CO})_{12}$  at  $200^\circ\text{C}$  yields mainly  $\text{Os}_6(\text{CO})_{18}$  along with smaller quantities of  $\text{Os}_5(\text{CO})_{16}$ ,  $\text{Os}_7(\text{CO})_{21}$  (Fig. 25.11) and  $\text{Os}_8(\text{CO})_{23}$ . By careful adjustment of conditions, thermal and photochemical methods can give good yields of selected products but more rational methods have also been developed. Nucleophilic attack, by amine oxides for instance, removes CO (as  $\text{CO}_2$ ) allowing a vacant site to be filled by a donor solvent such as MeCN. The products may themselves be pyrolysed or the solvent molecules replaced by metal nucleophiles such as  $\text{H}_2\text{Os}(\text{CO})_4$ :



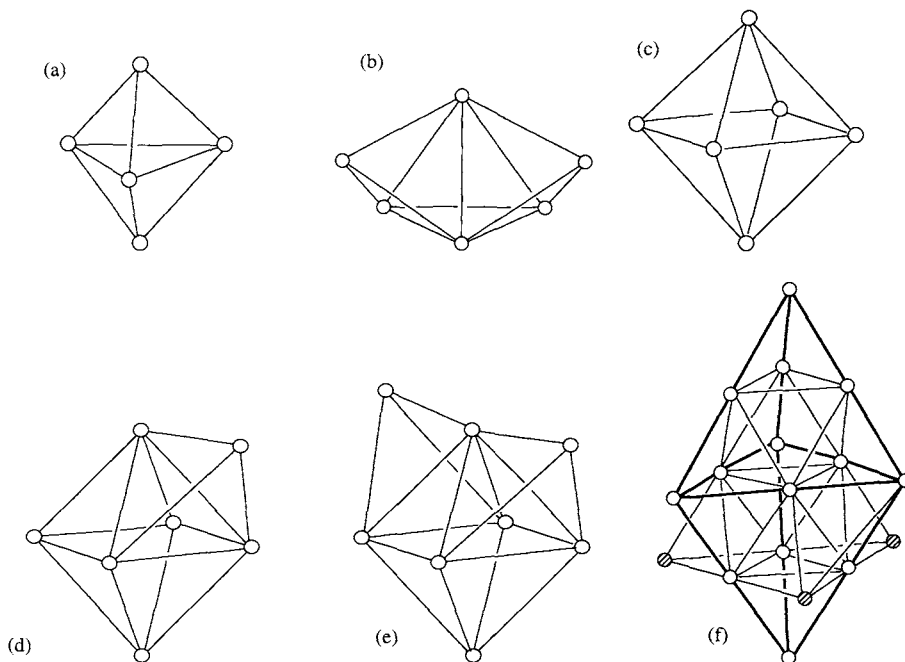
### Carbonyl hydrides and carbonylate anions

The treatment of iron carbonyls with aqueous or alcoholic alkali can, by varying the conditions, be used to produce a series of interconvertible carbonylate anions:  $[\text{HFe}(\text{CO})_4]^-$ ,  $[\text{Fe}(\text{CO})_4]^{2-}$ ,  $[\text{Fe}_2(\text{CO})_8]^{2-}$ ,  $[\text{HFe}_3(\text{CO})_{11}]^-$  and  $[\text{Fe}_4(\text{CO})_{13}]^{2-}$ . Of these the first has a distorted trigonal bipyramidal structure with axial H, the second

<sup>52</sup> B. F. G. JOHNSON and Y. V. ROBERTS, *Polyhedron* **12**, 977–90 (1993).

<sup>53</sup> J. LEWIS, *Chem. in Brit.* **24**(5), 795–800 (1988).

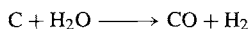
<sup>54</sup> A. J. DEEMING, *Adv. Organomet. Chem.* **26**, 1–96 (1986).



**Figure 25.11** Metal frameworks of some high-nuclearity binary carbonyl and carbonylate clusters of osmium: (a)  $\text{Os}_5(\text{CO})_{16}$  (trigonal bipyramid); (b)  $\text{Os}_6(\text{CO})_{18}$  (bicapped tetrahedron, or capped trigonal bipyramid); (c)  $[\text{Os}_6(\text{CO})_{18}]^{2-}$  (octahedron); (d)  $\text{Os}_7(\text{CO})_{21}$  (capped octahedron); (e)  $[\text{Os}_8(\text{CO})_{22}]^{2-}$  (bicapped octahedron); (f)  $[\text{Os}_{17}(\text{CO})_{36}]^{2-}$  (3 shaded atoms cap an  $\text{Os}_{14}$  trigonal bipyramid).

is isoelectronic and isostructural with  $\text{Ni}(\text{CO})_4$ , the third is isoelectronic with  $\text{Co}_2(\text{CO})_8$  and isostructural with the isomer containing no CO bridges, while the trimeric and tetrameric anions have the cluster structures shown in Fig. 25.12. The related ruthenium complexes  $[\text{HRu}_3(\text{CO})_{11}]^-$  and  $[\text{H}_3\text{Ru}_4(\text{CO})_{12}]^-$ , are of interest as possible catalysts for the “water-gas shift reaction”.<sup>†</sup>

<sup>†</sup> Water-gas is produced by the high-temperature reaction of water and C:



and is therefore a mixture of  $\text{H}_2\text{O}$ ,  $\text{CO}$  and  $\text{H}_2$ . By suitably adjusting the relative proportions of  $\text{CO}$  and  $\text{H}_2$ , “synthesis gas” is obtained which can be used for the synthesis of methanol and hydrocarbons (the Fischer–Tropsch process). It is this catalytically controlled adjustment:



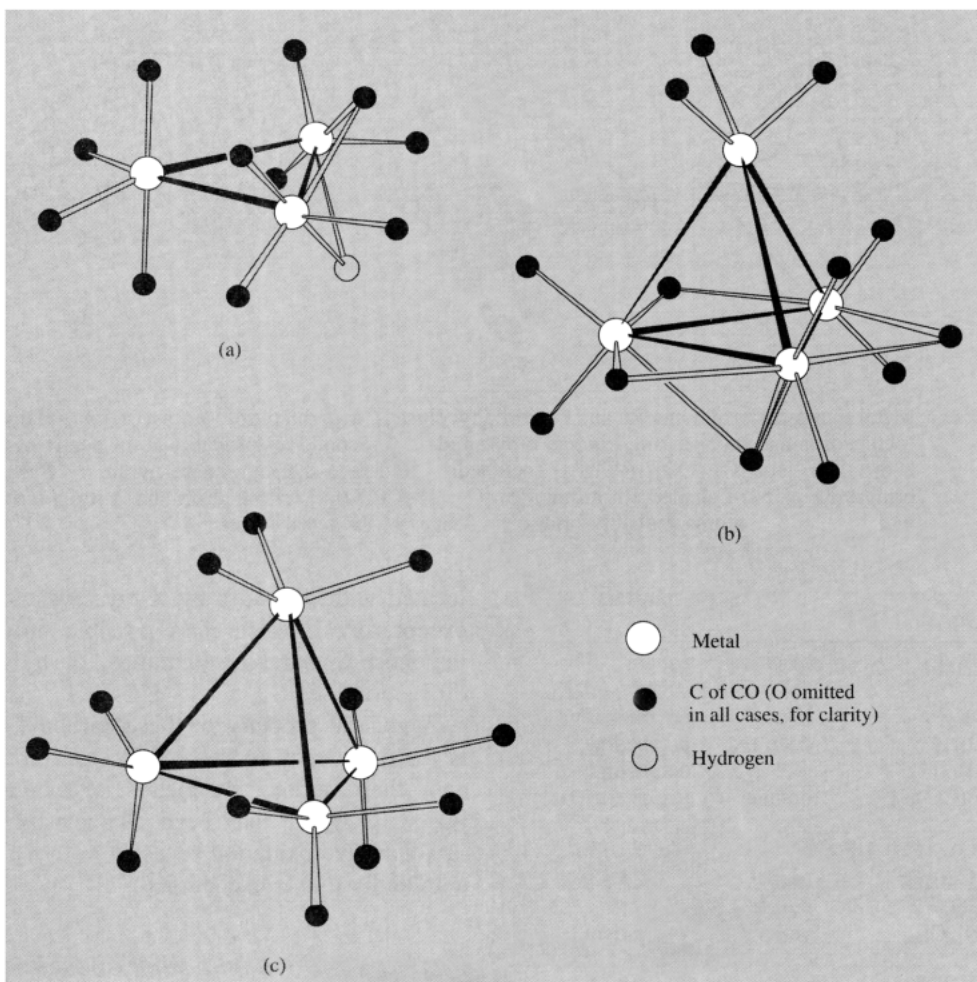
which is the water-gas shift reaction (WGSR) (see p. 421).

Reduction of the pH of solutions of carbonylate anions yields a variety of protonated species and, from acid solutions, carbonyl hydrides such as the unstable, gaseous  $\text{H}_2\text{Fe}(\text{CO})_4$  and the polymeric liquids  $\text{H}_2\text{Fe}_2(\text{CO})_8$  and  $\text{H}_2\text{Fe}_3(\text{CO})_{11}$  are liberated. The use of ligand-replacement reactions to yield hydrides of higher nuclearity has already been noted.

Thermolysis of binary carbonyls or of their partially substituted derivatives, either under vacuum or in solutions, has been used to produce carbonyls and carbonylate anions with an unparalleled range of structures (Fig. 25.11). The Ru chemistry, though less well developed, mostly parallels that of Os.<sup>(55)</sup> These compounds are interesting not only for their catalytic potential but also for the preparative and theoretical problems they pose. Almost all these

<sup>55</sup> See for instance L. MA, G. WILLIAMS and J. R. SHAPLEY, *Coord. Chem. Revs.* **128**, 261–84 (1993).



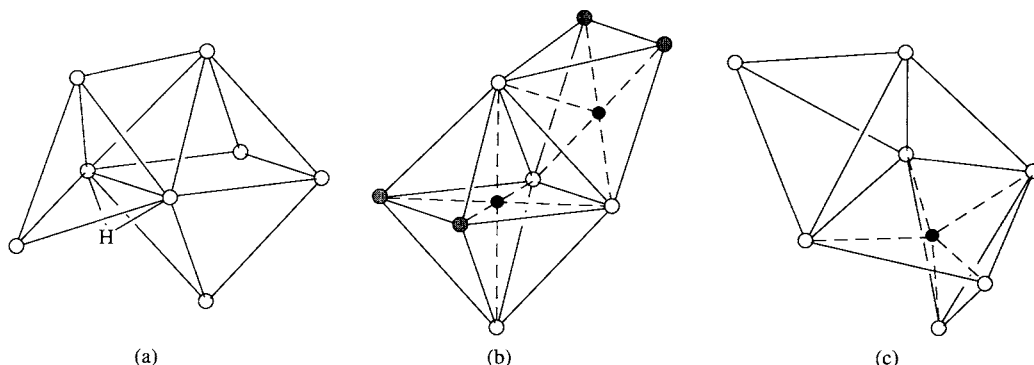


**Figure 25.12** Some small carbonylate anion clusters of Fe, Ru and Os: (a)  $[\text{HM}_3(\text{CO})_{11}]^-$ ;  $\text{M} = \text{Fe}, \text{Ru}$ . (b)  $[\text{Fe}_4(\text{CO})_{13}]^{2-}$ . (c)  $[\text{H}_3\text{Ru}_4(\text{CO})_{12}]^-$ . [The H atoms are not shown in (c) because this ion exists in two isomeric forms: (i) the 3 H atoms bridge the edges of a single face of the tetrahedron, and (ii) the 3 H atoms bridge three edges of the tetrahedron which do not form a face.]

polyhedral clusters are networks of triangular faces, are diamagnetic and have structures which can be rationalized by electron-counting arguments. However, in applying these rules it has to be noted that where an  $\text{M}(\text{CO})_3$  group “caps” a triangular face it has no effect on the skeletal electron count of the central polyhedron. Nor do such rules predict structures *precisely*. The  $[\text{H}_2\text{M}_6(\text{CO})_{18}]$ ,  $[\text{HM}_6(\text{CO})_{18}]^-$  and  $[\text{M}_6(\text{CO})_{18}]^{2-}$  clusters, for instance, while being stoichiometrically the same for  $\text{M} = \text{Ru}$  and  $\text{M} =$

Os, and having the same essentially octahedral skeletons, nevertheless differ appreciably in the disposition of the attached carbonyl groups. The incorporation of interstitial (encapsulated) atoms such as C, H, S, N, P and, more recently, B<sup>(56)</sup> is a widespread and frequently stabilizing feature of these clusters. Carbido clusters are the most common the C contributing 4 electrons

<sup>56</sup> C. E. HOUSECROFT, D. A. MATTHEWS, A. RHEINGOLD and X. SONG, *J. Chem. Soc., Chem. Commun.*, 842–3 (1992).



**Figure 25.13** Metal frameworks of some Ru and Os carbonyl clusters with interstitial atoms. (a)  $[\text{Ru}_8(\text{H})_2(\text{CO})_{21}]^{2-}$  (octahedron and face-sharing trigonal bipyramid); the second H is probably at the centre of the octahedron. (b)  $[\text{Ru}_8(\text{C})_2(\text{CO})_{17}(\text{PPh}_2)_2]$  (octahedron and face-sharing square pyramid);  $\text{PPh}_2$  ligands bridge the pairs of shaded Ru atoms. (c)  $[\text{Os}_7(\text{H})_2\text{C}(\text{CO})_{19}]$  (tetrahedron and 3 irregularly spaced metal atoms); H atoms probably bridge two edges of the tetrahedron.

**Table 25.9** Some metal carbonyl clusters with interstitial atoms

$[\text{Fe}_5\text{C}(\text{CO})_{15}]$	black	square pyramidal*
$[\text{Fe}_6\text{C}(\text{CO})_{16}]^{2-}$	black	octahedral
$[\text{Ru}_6\text{C}(\text{CO})_{17}]$	deep red	octahedral
$[\text{Ru}_6\text{H}(\text{CO})_{18}]^-$	red	octahedral
$[\text{Ru}_6(\text{H})_2\text{B}(\text{CO})_{18}]^-$	orange	trig. prism (H bridges) <sup>(55)</sup>
$[\text{Ru}_8\text{C}_2(\text{CO})_{17}(\text{PPh}_2)_2]$	black	Fig. 25.13b
$[\text{Ru}_8(\text{H})_2(\text{CO})_{21}]^{2-}$	black	Fig. 25.13a
$[\text{Ru}_{10}\text{C}_2(\text{CO})_{24}]^{2-}$	purple	bis oct.
$[\text{Os}_6\text{P}(\text{CO})_{18}\text{Cl}]$	yellow	trig. prism (Cl bridge)
$[\text{Os}_7\text{C}(\text{H})_2(\text{CO})_{19}]$	green	Fig. 25.13c
$[\text{Os}_8\text{C}(\text{CO})_{21}]$	purple	bicapped oct.
$[\text{Os}_9\text{H}(\text{CO})_{24}]$	brown	tricapped oct.
$[\text{Os}_{10}\text{C}(\text{CO})_{24}]^{2-}$	pink-red	tetracapped oct.

\*corresponding Ru and Os compounds are red and orange respectively.

to the formal electron count and originating possibly from the solvent or, more often, from cleavage of a CO ligand. This is especially true for Ru where the formation of carbido clusters is a general consequence of thermolysis. Some illustrative examples of these compounds are listed in Table 25.9.

The encapsulated atom usually occupies the centre of the polyhedron of metals (or its base in the case of square pyramids). Its position can be

located with precision by X-ray crystallography except for H, when it is possible only under the most favourable conditions, or by neutron diffraction.

A general property of these carbonyl clusters is their tendency to behave as electron "sinks", and their redox chemistry is extensive.<sup>(57)</sup>  $[\text{Os}_{10}\text{C}(\text{CO})_{24}]^{n-}$  has been characterized in no less than five oxidation states ( $n = 0-4$ ); though admittedly this is exceptional.

### Carbonyl halides and other substituted carbonyls

Numerous carbonyl halides, of which the best known are octahedral compounds of the type  $[\text{M}(\text{CO})_4\text{X}_2]$  are obtained by the action of halogen on  $\text{Fe}(\text{CO})_5$ , or CO on  $\text{MX}_3$  ( $\text{M} = \text{Ru}, \text{Os}$ ). Stepwise substitution of the remaining CO groups is possible by  $\text{X}^-$  or other ligands such as N, P and As donors.

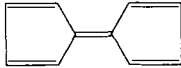
Direct substitution of the carbonyls themselves is of course possible. Besides Group 15 donor ligands, unsaturated hydrocarbons give especially interesting products. The iron carbonyl acetylenes provided early examples of the use of carbonyls in organic synthesis. From them a wide variety

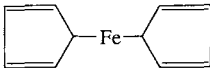
<sup>57</sup> S. R. DRAKE, *Polyhedron* 9, 455-74 (1990).

of cyclic compounds can be obtained as a result of condensation of coordinated acetylenes with themselves and/or CO. The complexes involving the acetylenes alone are usually unstable intermediates which are only separable when bulky substituents are incorporated on the acetylene. More usually, complexes of the condensed cyclic products are isolated. These ring systems include quinones, hydroquinones, cyclobutadienes and cyclopentadienones, the specific product depending on the particular iron carbonyl used and the precise conditions of the reaction.

### Ferrocene and other cyclopentadienyls

Bis(cyclopentadienyl)iron,  $[\text{Fe}(\eta^5\text{-C}_5\text{H}_5)_2]$ , or, to give it the more familiar name coined by M. C. Whiting, “ferrocene”, is the compound whose discovery in the early 1950s utterly transformed the study of organometallic chemistry.<sup>(2)</sup> Yet the two groups of organic chemists who independently made the discovery, did so accidentally. P. L. Pauson and T. J. Kealy (*Nature* **168**, 1039 (1951)) were attempting to synthesize ful-

valene, , by reacting the Grignard reagent cyclopentadienyl magnesium bromide with  $\text{FeCl}_3$ , but instead obtained orange crystals (mp  $173^\circ\text{C}$ ) containing  $\text{Fe}^{\text{II}}$  and analysing for  $\text{C}_{10}\text{H}_{10}\text{Fe}$ . In a paper submitted simultaneously (*J. Chem. Soc.* 632 (1952)), S. A. Miller, T. A. Tebboth and J. F. Tremaine reported passing cyclopentadiene and  $\text{N}_2$  over a reduced iron catalyst as part of a programme to prepare amines and they too obtained  $\text{C}_{10}\text{H}_{10}\text{Fe}$ .<sup>†</sup>

The initial structural formulation was , but the correct formulation, an unprecedented “sandwich” compound, was soon to follow. For this and for subsequent independent work in this field, G. Wilkinson and

E. O. Fischer shared the 1973 Nobel Prize for Chemistry.

The structure of ferrocene and an MO description of its bonding have already been given (p. 937). The rings are virtually eclipsed as they are in the analogous ruthenocene (light-yellow, mp  $199^\circ\text{C}$ ) and osmocene (white, mp  $229^\circ\text{C}$ ).

This is also the case in the decamethylmetallocenes of Ru and Os but not in the iron analogue which has a staggered conformation, presumably due to steric crowding around the smaller metal.

$[\text{M}(\eta^5\text{-C}_5\text{H}_5)_2]$  satisfy the 18-electron rule (p. 1134) and are stable to air and water but are readily oxidized. From ferrocene the blue-green, paramagnetic ferricinium ion,  $[\text{Fe}^{\text{III}}(\eta^5\text{-C}_5\text{H}_5)_2]^+$ , is produced whereas the Ru and Os monocations are unstable, oxidizing further to  $[\text{M}^{\text{IV}}(\eta\text{-C}_5\text{H}_5)_2]^{2+}$  or dimerizing to  $[(\eta^5\text{-C}_5\text{H}_5)_2\text{M}^{\text{III}}\text{-M}^{\text{III}}(\eta^5\text{-C}_5\text{H}_5)_2]^{2+}$ . The decamethylferricinium salt,  $[\text{Fe}(\eta^5\text{-C}_5\text{Me}_5)_2][\text{tcne}]$ , (tcne = tetracyanoethylene) is a dark green crystalline material consisting of linear chains of alternating anions and cations.<sup>(58)</sup> It has the astonishing property of being a 1D molecular ferromagnet (with a saturation magnetisation greater than that of metallic iron itself on a molar basis), although the mechanism by which this originates is not yet settled.

The most notable chemistry of the biscyclopentadienyls results from the aromaticity of the cyclopentadienyl rings. This is now far too extensively documented to be described in full but an outline of some of its manifestations is in Fig. 25.14. Ferrocene resists catalytic hydrogenation and does not undergo the typical reactions of conjugated dienes, such as the Diels–Alder reaction. Nor are direct nitration and halogenation possible because of oxidation to the ferricinium ion. However, Friedel–Crafts acylation as well as alkylation and metallation reactions, are readily effected. Indeed, electrophilic substitution of ferrocene occurs with such facility compared to, say, benzene ( $3 \times 10^6$  faster) that some explanation is called for. It has been suggested that,

<sup>†</sup> In retrospect it seems likely that ferrocene was actually first prepared as volatile yellow crystals in the 1930s by chemists at Union Carbide who passed dicyclopentadiene through a heated iron tube, but the significance was not then realized.

<sup>58</sup> J. S. MILLER and A. J. EPSTEIN, *Chem. Brit.* **30**(6), 477–80 (1994).

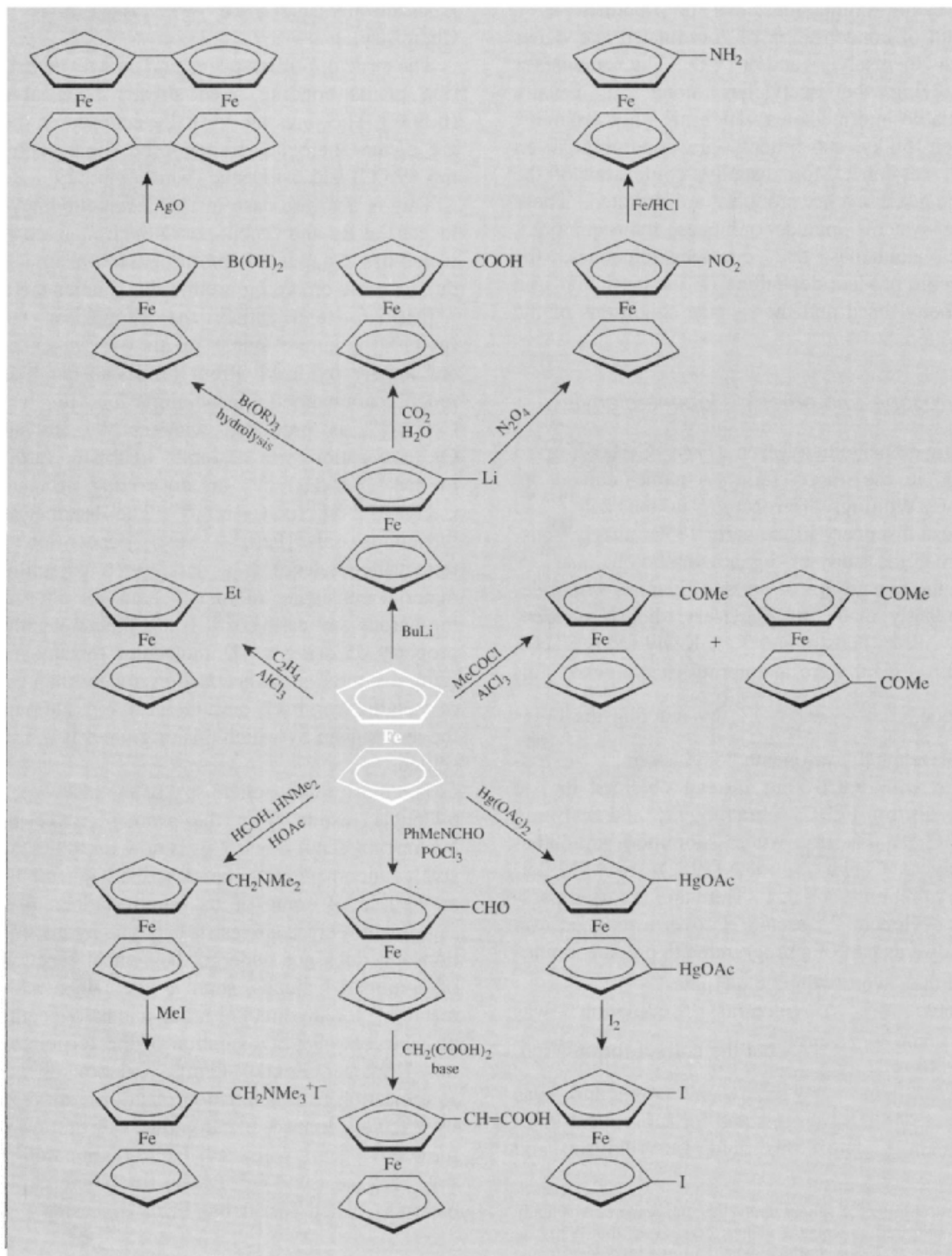
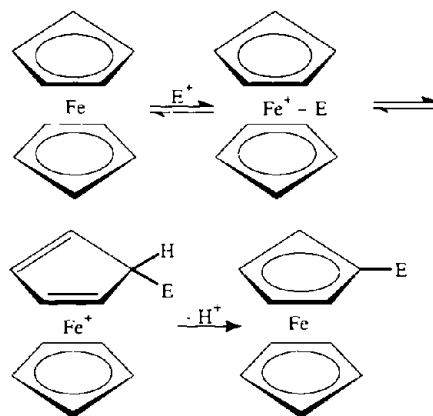


Figure 25.14 Some reactions of ferrocene.

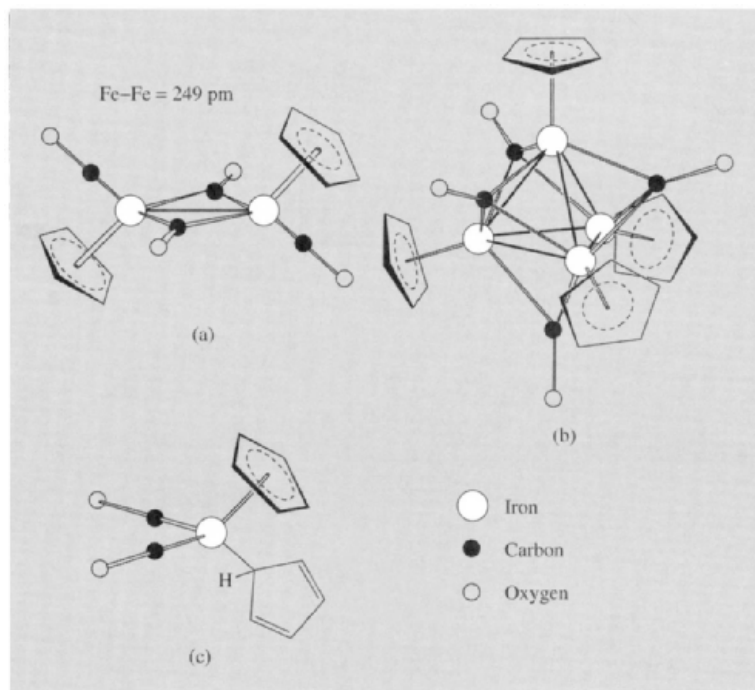
in general, electrophilic substituents ( $E^+$ ) interact with the metal atom and then transfer to the  $C_5H_5$  ring with proton elimination. Similar reactions are possible for ruthenocene and osmocene but usually occur less readily, and it appears that reactivity decreases with increasing size of the metal (see adjacent Scheme).

Many interesting cyclopentadienyl iron carbonyls have been prepared, the best known being the purple dimer,  $[Fe(\eta^5-C_5H_5)(CO)_2]_2$  (Fig. 25.15a), prepared by reacting  $Fe(CO)_5$  and dicyclopentadienyl at  $135^\circ C$  in an autoclave. Diamagnetism and an Fe-Fe distance of only 249 pm indicate the presence of an Fe-Fe bond. Prolonged reaction of the same reactants produces the very dark green, tetrameric cluster compound,  $[Fe(\eta^5-C_5H_5)(CO)]_4$  (Fig. 25.15b), which involves CO groups which are triply bridging and so give rise to an exceedingly low ( $1620\text{ cm}^{-1}$ )  $\nu_{CO}$  absorption.  $[Fe(\eta^1-C_5H_5)(\eta^5-C_5H_5)(CO)_2]$  (Fig. 25.15c) is also of note as



Scheme

an early example of a fluxional organometallic compound. The  $^1H$  nmr spectrum consists of only two sharp lines, one for each ring. A single line is expected for the pentahapto ring since all its protons are equivalent, but it is clear that some averaging process must be occurring for the



**Figure 25.15** Some cyclopentadienyl iron carbonyls: (a)  $[(\eta^5-C_5H_5)Fe(CO)_2]_2$ , (b)  $[(\eta^5-C_5H_5)Fe(CO)]_4$  and (c)  $[(\eta^1-C_5H_5)(\eta^5-C_5H_5)Fe(CO)_2]$ .

non-equivalent protons of the monohapto ring to produce just one line. It is concluded that the point of attachment of the monohapto ring to the metal must change repeatedly and rapidly ("ring whizzing") thus averaging the protons.

Although the cyclopentadienyls dominate the "aromatic" chemistry of this group, bis(arene) compounds are also well established. They are able to satisfy the 18-electron rule as the dications,  $[M(\text{arene})_2]^{2+}$  or by the two rings adopting different bonding modes; one  $\eta^6$  the other  $\eta^4$ .

Other aspects of the organometallic chemistry of this triad have been referred to in Chapter 19 but for fuller details more extensive reviews should be consulted.<sup>(50,59)</sup>

---

<sup>59</sup>G. WILKINSON, F. G. A. STONE and E. W. ABEL (eds.), *Comprehensive Organometallic Chemistry*, Vol. 4, Pergamon Press, Oxford, 1982, Iron, pp. 243–649, Ruthenium, pp. 650–965, Osmium, pp. 967–1064. E. W. ABEL, F. G. A. STONE and G. WILKINSON, (eds.), *Comprehensive Organometallic Chemistry II*, Vol. 7, Iron, Ruthenium and Osmium, 1995.

																1	2																														
																H	He																														
3	4																	5	6	7	8	9	10																								
Li	Be																	B	C	N	O	F	Ne																								
11	12																	13	14	15	16	17	18																								
Na	Mg																	Al	Si	P	S	Cl	Ar																								
19	20	21	22	23	24	25	26	27	28	29	30	31	32	33	34	35	36																														
K	Ca	Sc	Ti	V	Cr	Mn	Fe	Co	Ni	Cu	Zn	Ga	Ge	As	Se	Br	Kr																														
37	38	39	40	41	42	43	44	45	46	47	48	49	50	51	52	53	54																														
Rb	Sr	Y	Zr	Nb	Mo	Tc	Ru	Rh	Pd	Ag	Cd	In	Sn	Sb	Te	I	Xe																														
55	56	57	58	59	60	61	62	63	64	65	66	67	68	69	70	71	72																														
Cs	Ba	La	Hf	Ta	W	Re	Os	Ir	Pt	Au	Hg	Tl	Pb	Bi	Po	At	Rn																														
87	88	89	90	91	92	93	94	95	96	97	98	99	100	101	102	103	104																														
Fr	Ra	Ac	Rf	Db	Sg	Bh	Hs	Mt	Uun	Uuu	Uub																																				
																		105	106	107	108	109	110	111	112	113	114	115	116	117	118																
																		Ce	Pr	Nd	Pm	Sm	Eu	Gd	Th	Dy	Ho	Er	Tm	Yb	Lu																
																		Th	Pa	U	Np	Pu	Am	Cm	Bk	Cf	Es	Fm	Md	No	Lr																

# 26

## Cobalt, Rhodium and Iridium

### 26.1 Introduction

Although hardly any metallic cobalt was used until the twentieth century, its ores have been used for thousands of years to impart a blue colour to glass and pottery. It is present in Egyptian pottery dated at around 2600 BC and Iranian glass beads of 2250 BC.<sup>†</sup> The source of the blue colour was recognized in 1735 by the Swedish chemist G. Brandt, who isolated a very impure metal, or “regulus”, which he named “cobalt rex”. In 1780 T. O. Bergman showed this to be a new element. Its name has some resemblance to the Greek word for “mine” but is almost certainly derived from the German word *Kobold* for “goblin” or “evil spirit”. The miners of northern European countries thought that the spitefulness of such spirits was responsible for ores which, on smelting, not only failed

unexpectedly to yield the anticipated metal but also produced highly toxic fumes ( $\text{As}_4\text{O}_6$ ).

In 1803 both rhodium and iridium were discovered<sup>(1)</sup>, like their preceding neighbours in the periodic table, ruthenium and osmium, in the black residue left after crude platinum had been dissolved in aqua regia. W. H. Wollaston discovered rhodium, naming it after the Greek word  $\rho\acute{o}\delta\omicron\nu$  for “rose” because of the rose-colour commonly found in aqueous solutions of its salts. S. Tennant discovered iridium along with osmium, and named it after the Greek goddess Iris ( $\text{i}\rho\text{i}\varsigma, \text{i}\rho\text{i}\delta\text{-}$ ), whose sign was the rainbow, because of the variety of colours of its compounds.

### 26.2 The Elements

#### 26.2.1 Terrestrial abundance and distribution

Rhodium and iridium are exceedingly rare elements, comprising only 0.0001 and 0.001 ppm of the earth’s crust respectively, and even

<sup>†</sup> “Smalt”, produced by fusing potash, silica and cobalt oxide, can be used for colouring glass or for glazing pottery. The secret of making this brilliant blue pigment was apparently lost, to be rediscovered in the fifteenth century. Leonardo da Vinci was one of the first to use powdered smalt as a “new” pigment when painting his famous “The Madonna of the Rocks”.

<sup>1</sup> L. B. HUNT, *Platinum Metals Rev.* **31**, 32–41 (1987).

cobalt (29 ppm, i.e. 0.0029%), though widely distributed, stands only thirtieth in order of abundance and is less common than all other elements of the first transition series except scandium (25 ppm).

More than 200 ores are known to contain cobalt but only a few are of commercial value. The more important are arsenides and sulfides such as smaltite,  $\text{CoAs}_2$ , cobaltite (or cobalt glance),  $\text{CoAsS}$ , and linnaeite,  $\text{Co}_3\text{S}_4$ . These are invariably associated with nickel, and often also with copper and lead, and it is usually obtained as a byproduct or coproduct in the recovery of these metals. The world's major sources of cobalt are the African continent and Canada with smaller reserves in Australia and the former USSR. All the platinum metals are generally associated with each other and rhodium and iridium therefore occur wherever the other platinum metals are found. However, the relative proportions of the individual metals are by no means constant and the more important sources of rhodium are the nickel-copper-sulfide ores found in South Africa and in Sudbury, Canada, which contain about 0.1% Rh. Iridium is usually obtained from native osmiridium ( $\text{Ir} \sim 50\%$ ) or iridosmium ( $\text{Ir} \sim 70\%$ ) found chiefly in Alaska as well as South Africa.

### 26.2.2 Preparation and uses of the elements<sup>(2)</sup>

The production of cobalt<sup>(2,3)</sup> is usually subsidiary to that of copper and nickel and the methods employed differ widely, depending on which of these it is associated with. In general the ore is subjected to appropriate roasting treatment so as to remove gangue material as a slag and produce a "speiss" of mixed metal and oxides. In the case of arsenical ores,  $\text{As}_2\text{O}_6$  is condensed and provides a valuable byproduct. In the case of copper ores, the primary process

leaves a spent electrolyte from which iron is precipitated as the hydroxide by lime and the cobalt then separated by further electrolysis. Nickel ores yield acidic sulfate or chloride solutions and the methods used to separate the nickel and cobalt include: (a) precipitation of cobalt as the sulfide; (b) oxidation of cobalt and precipitation of  $\text{Co}(\text{OH})_3$ ; (c) making the solution alkaline with  $\text{NH}_3$  and removal of nickel either as the sparingly soluble  $(\text{NH}_4)_2\text{Ni}(\text{SO}_4)_2 \cdot 6\text{H}_2\text{O}$  or by selective reduction to the metal by  $\text{H}_2$  under pressure; (d) anion exchange, utilizing the preferential formation of  $[\text{CoCl}_4]^{2-}$ .

World production of cobalt in 1995 was about 20 000 tonnes, considerably below capacity. The major producing countries are Zaire, Zambia, Canada, Finland and the former Soviet Union.

The largest use of cobalt is in the production of chemicals for the ceramic and paint industries. In ceramics the main use now is not to provide a blue colour, but rather white by counterbalancing the yellow tint arising from iron impurities. Blue pigments are, however, used in paints and inks, and cobalt compounds are used to hasten the oxidation and hence the drying of oil-based paints. Cobalt compounds are also employed as catalysts in a range of organic reactions of which the "OXO" (or hydroformylation) reaction and hydrogenation and dehydrogenation reactions are the most important (pp. 1134–6).

Other uses include the manufacture of magnetic alloys. Of these the best known is "Alnico", a steel containing, as its name implies, aluminium and nickel, as well as cobalt. It is used for permanent magnets which are up to 25 times more powerful than ordinary steel magnets.

As already noted (p. 1073), the platinum metals are all isolated from concentrates obtained as "anode slimes" or "converter matte." In the classical process, after ruthenium and osmium have been removed, excess oxidants are removed by boiling, iridium is precipitated as  $(\text{NH}_4)_2\text{IrCl}_6$  and rhodium as  $[\text{Rh}(\text{NH}_3)_5\text{Cl}]\text{Cl}_2$ . In alternative solvent extraction processes (p. 1147)  $[\text{IrCl}_6]^{2-}$  is extracted in organic amines leaving rhodium in the aqueous phase to be precipitated, again, as  $[\text{Rh}(\text{NH}_3)_5\text{Cl}]\text{Cl}_2$ . In all cases ignition in  $\text{H}_2$

<sup>2</sup> J. HILL, Chap. 2 in D. THOMPSON (ed.), *Insights into Speciality Inorganic Chemicals*, pp. 5–34, R.S.C., Cambridge, 1995.

<sup>3</sup> *Kirk-Othmer Encyclopedia of Chemical Technology*, 4th edn., Vol. 6, pp. 760–77, Interscience New York, 1993.



yields the metals as powders or sponges which can be consolidated by the techniques of powder metallurgy.

In 1996, consumption in the western world was 14.2 tonnes of rhodium and 3.8 tonnes of iridium. Unquestionably the main uses of rhodium (over 90%) are now catalytic, e.g. for the control of exhaust emissions in the car (automobile) industry and, in the form of phosphine complexes, in hydrogenation and hydroformylation reactions where it is frequently more efficient than the more commonly used cobalt catalysts. Iridium is used in the coating of anodes in chloralkali plant and as a catalyst in the production of acetic acid. It also finds small-scale applications in specialist hard alloys.

### 26.2.3 Properties of the elements

Some of the important properties of these three elements are summarized in Table 26.1.

The metals are lustrous and silvery with, in the case of cobalt, a bluish tinge. Rhodium and iridium are both hard, cobalt less so but still appreciably harder than iron. Rhodium and Ir have fcc structures, the first elements in the transition series to do so; this is in keeping

with the view, based on band-theory calculations, that the fcc structure is more stable than either bcc or hcp when the outer d orbitals are nearly full. Cobalt, too, has an allotrope (the  $\beta$ -form) with this structure but this is only stable above 417°C; below this temperature the hcp  $\alpha$ -form is the more stable. However, the transformation between these allotropes is generally slow and the  $\beta$ -form, which can be stabilized by the addition of a few per cent of iron, is often present at room temperature. This, of course, has an effect on physical properties and is no doubt responsible for variations in reported values for some properties even in the case of very pure cobalt. By contrast the atomic weights of cobalt and rhodium at least are known with considerable precision, since these elements each have but one naturally occurring isotope. In the case of cobalt this is  $^{59}\text{Co}$ , but bombardment by thermal neutrons converts this to the radioactive  $^{60}\text{Co}$ . The latter has a half-life of 5.271 y and decays by means of  $\beta^-$  and  $\gamma$  emission to non-radioactive  $^{60}\text{Ni}$ . It is used in many fields of research as a concentrated source of  $\gamma$ -radiation, and also medically in the treatment of malignant growths. Iridium has two stable isotopes:  $^{191}\text{Ir}$  37.3% and  $^{193}\text{Ir}$  62.7%.

**Table 26.1** Some properties of the elements cobalt, rhodium and iridium

Property	Co	Rh	Ir
Atomic number	27	45	77
Number of naturally occurring isotopes	1	1	2
Atomic weight	58.933200(9)	102.90550(2)	192.217(3)
Electronic configuration	[Ar]3d <sup>7</sup> 4s <sup>2</sup>	[Kr]4d <sup>8</sup> 5s <sup>1</sup>	[Xe]4f <sup>14</sup> 5d <sup>7</sup> 6s <sup>2</sup>
Electronegativity	1.8	2.2	2.2
Metal radius (12-coordinate)/pm	125	134	135.5
Effective ionic radius (6-coordinate)/pm			
	V	55	57
	IV	60	62.5
	III	66.5	68
	II	—	—
MP/°C	1495	1960	2443
BP/°C	3100	3760	4550(±100)
$\Delta H_{\text{fus}}/\text{kJ mol}^{-1}$	16.3	21.6	26.4
$\Delta H_{\text{vap}}/\text{kJ mol}^{-1}$	382	494	612(±13)
$\Delta H_{\text{f}}(\text{monatomic gas})/\text{kJ mol}^{-1}$	425(±17)	556(±11)	669(±8)
Density (20°C)/g cm <sup>-3</sup>	8.90	12.39	22.56
Electrical resistivity (20°C)/ $\mu\text{ohm cm}$	6.24	4.33	4.71

The mps, bps and enthalpies of atomization are lower than for the preceding elements in the periodic tables, presumably because the  $(n - 1)d$  electrons are being drawn increasingly into the inert electron cores of the atoms. In the first series Co, like its neighbours Fe and Ni, is ferromagnetic (in both allotropic forms); while it does not attain the high saturation magnetization of iron, its Curie point ( $>1100^\circ\text{C}$ ) is much higher than that for Fe ( $768^\circ\text{C}$ ).

#### 26.2.4 Chemical reactivity and trends

Cobalt is appreciably less reactive than iron, and so contrasts less markedly with the two heavier members of its triad. It is stable to atmospheric oxygen unless heated, when it is oxidized first to  $\text{Co}_3\text{O}_4$ ; above  $900^\circ\text{C}$  the product is  $\text{CoO}$  which is also produced by the action of steam on the red-hot metal. It dissolves rather slowly in dil mineral acids giving salts of  $\text{Co}^{\text{II}}$ , and reacts on heating with the halogens and other non-metals such as B, C, P, As and S, but is unreactive to  $\text{H}_2$  and  $\text{N}_2$ .

Rhodium and iridium will also react with oxygen and halogens at red-heat, but only slowly, and these metals are especially notable for their extreme inertness to acids, even aqua regia. Dissolution of rhodium metal is best effected by fusion with  $\text{NaHSO}_4$ , a process used in its commercial separation. In the case of iridium, oxidizing molten alkalis such as  $\text{Na}_2\text{O}_2$  or  $\text{KOH} + \text{KNO}_3$  will produce  $\text{IrO}_2$  which can then be dissolved in aqua regia. Alternatively, a rather extreme measure which is efficacious with both metals, is to heat them with conc  $\text{HCl} + \text{NaClO}_3$  in a sealed tube at  $125\text{--}150^\circ\text{C}$ .

Table 26.2 is a list of examples of compounds of these elements in various oxidation states. The most striking feature of this, as compared to the corresponding lists for preceding triads, is that for the first time the range of oxidation states has diminished. This is a manifestation of the increasing stability of the  $(n - 1)d$  electrons, whose attraction to the atomic nucleus is now sufficient to prevent the elements attaining the highest oxidation states and so to render irrelevant the concept of a "group" oxidation

state. No oxidation states are found above  $+6$  for Rh and Ir, or above  $+5$  for Co. Indeed, examples of cobalt in  $+4$  and  $+5$  and of rhodium or iridium in  $+5$  and  $+6$  oxidation states are rare and sometimes poorly characterized.

The most common oxidation states of cobalt are  $+2$  and  $+3$ .  $[\text{Co}(\text{H}_2\text{O})_6]^{2+}$  and  $[\text{Co}(\text{H}_2\text{O})_6]^{3+}$  are both known but the latter is a strong oxidizing agent and in aqueous solution, unless it is acidic, it decomposes rapidly as the  $\text{Co}^{\text{III}}$  oxidizes the water with evolution of oxygen. Consequently, in contrast to  $\text{Co}^{\text{II}}$ ,  $\text{Co}^{\text{III}}$  provides few simple salts, and those which do occur are unstable. However,  $\text{Co}^{\text{III}}$  is unsurpassed in the number of coordination complexes which it forms, especially with  $N$ -donor ligands. Virtually all of these complexes are low-spin, the  $t_{2g}^6$  configuration producing a particularly high CFSE (p. 1131).

The effect of the CFSE is expected to be even more marked in the case of the heavier elements because for them the crystal field splittings are much greater. As a result the  $+3$  state is the most important one for both Rh and Ir and  $[\text{M}(\text{H}_2\text{O})_6]^{3+}$  are the only simple aquo ions formed by these elements. With  $\pi$ -acceptor ligands the  $+1$  oxidation state is also well known for Rh and Ir. It is noticeable, however, that the similarity of these two heavier elements is less than is the case earlier in the transition series and, although rhodium resembles iridium more than cobalt, nevertheless there are significant differences. One example is provided by the  $+4$  oxidation state which occurs to an appreciable extent in iridium but not in rhodium. (The ease with which  $\text{Ir}^{\text{IV}} \rightleftharpoons \text{Ir}^{\text{III}}$  sometimes occurs can be a source of annoyance to preparative chemists.)

Table 26.2 also reveals a diminished tendency on the part of these elements to form compounds of high coordination number when compared with the iron group and, apart from  $[\text{Co}(\text{NO}_3)_4]^{2-}$ , a coordination number of 6 is rarely exceeded. There is also a marked reluctance to form oxoanions (p. 1118). This is presumably because their formation requires the donation of  $\pi$  electrons from the oxygen atoms to the metal and the metals become progressively

Table 26.2 Oxidation states and stereochemistries of some compounds of cobalt, rhodium and iridium

Oxidation state	Coordination number	Stereochemistry	Co	Rh/Ir
-3	3		[Co(CO) <sub>3</sub> ] <sup>3-</sup>	[M(CO) <sub>3</sub> ] <sup>3-</sup>
-1 (d <sup>10</sup> )	4	Tetrahedral	[Co(CO) <sub>4</sub> ] <sup>-</sup>	[Rh(CO) <sub>4</sub> ] <sup>-</sup> , [Ir(CO) <sub>3</sub> (PPh <sub>3</sub> )] <sup>-</sup>
0 (d <sup>9</sup> )	4	Tetrahedral	[Co(PMe <sub>3</sub> ) <sub>4</sub> ]	
	6	Octahedral	[Co <sub>2</sub> (CO) <sub>8</sub> ]	[M <sub>4</sub> (CO) <sub>12</sub> ]
1 (d <sup>8</sup> )	2	Linear	[CoO <sub>2</sub> ] <sup>3-</sup>	
	3	Planar (?)		[RhCl(PCy <sub>3</sub> ) <sub>2</sub> ]
		T-shaped		[Rh(PPh <sub>3</sub> ) <sub>3</sub> ] <sup>+</sup>
	4	Square planar		[RhCl(PPh <sub>3</sub> ) <sub>3</sub> ] [Ir(CO)Cl(PPh <sub>3</sub> ) <sub>2</sub> ]
	5	Trigonal bipyramidal	[Co(NCMe) <sub>5</sub> ] <sup>+</sup>	[RhH(PF <sub>3</sub> ) <sub>4</sub> ], [Ir(CO)H(PPh <sub>3</sub> ) <sub>3</sub> ]
		Square pyramidal	[Co(NCPh) <sub>5</sub> ] <sup>+</sup>	
	6	Octahedral	[Co(bipy) <sub>3</sub> ] <sup>+</sup>	
2 (d <sup>7</sup> )	2	Linear	[Co{N(SiMe <sub>3</sub> ) <sub>2</sub> ] <sub>2</sub> ]	
	3	Planar	[Co{N(SiMe <sub>3</sub> ) <sub>2</sub> ] <sub>2</sub> (PPh <sub>3</sub> )]	
	4	Tetrahedral	[CoCl <sub>4</sub> ] <sup>2-</sup>	
		Square planar	[Co(phthalocyanine)]	[RhCl <sub>2</sub> {P( <i>o</i> -MeC <sub>6</sub> H <sub>4</sub> ) <sub>3</sub> ] <sub>2</sub> ]
	5	Trigonal bipyramidal	[CoBr{N(C <sub>2</sub> H <sub>4</sub> NMe <sub>2</sub> ) <sub>3</sub> }] <sup>+</sup>	
		Square pyramidal	[Co(CN) <sub>5</sub> ] <sup>3-</sup>	[Rh <sub>2</sub> (O <sub>2</sub> CMe) <sub>4</sub> ]
	6	Octahedral	[Co(H <sub>2</sub> O) <sub>6</sub> ] <sup>2+</sup>	[Rh <sub>2</sub> (O <sub>2</sub> CMe) <sub>4</sub> (H <sub>2</sub> O) <sub>2</sub> ]
	8	Dodecahedral	[Co(NO <sub>3</sub> ) <sub>4</sub> ] <sup>2-</sup>	
3 (d <sup>6</sup> )	4	Tetrahedral	[CoW <sub>12</sub> O <sub>40</sub> ] <sup>5-</sup>	
	5	Trigonal bipyramidal		[IrH <sub>3</sub> (PR <sub>3</sub> ) <sub>2</sub> ]
		Square pyramidal	[Co(corrole)(PPh <sub>3</sub> )] <sup>(a)</sup>	[RhI <sub>2</sub> Me(PPh <sub>3</sub> ) <sub>2</sub> ]
	6	Octahedral	[Co(NH <sub>3</sub> ) <sub>6</sub> ] <sup>3+</sup>	[MCl <sub>6</sub> ] <sup>3-</sup>
4 (d <sup>5</sup> )	4	Tetrahedral	[Co(1-norbornyl) <sub>4</sub> ] <sup>(b)</sup>	
	6	Octahedral	[CoF <sub>6</sub> ] <sup>2-</sup>	[MCl <sub>6</sub> ] <sup>2-</sup>
5 (d <sup>4</sup> )	6	Octahedral		[MF <sub>6</sub> ] <sup>-</sup>
	7	Pentagonal bipyramidal		[IrH <sub>5</sub> (PR <sub>3</sub> ) <sub>2</sub> ]
6 (d <sup>3</sup> )	6	Octahedral		[MF <sub>6</sub> ]

<sup>(a)</sup>Corrole is a tetrapyrrolic macrocycle

<sup>(b)</sup>1-Norbornyl is a bicyclo[2.2.1]hept-1-yl

less able to act as  $\pi$  acceptors as their d orbitals are filled.

Hydrido complexes of all three elements, and covering a range of formal oxidation states, are important because of their roles in homogeneous catalysis either as the catalysts themselves or as intermediates in the catalytic cycles.

## 26.3 Compounds of Cobalt, Rhodium and Iridium

Binary borides (p. 147) and carbides (p. 297) have been discussed already.

### 26.3.1 Oxides and sulfides

As a result of the diminution in the range of oxidation states which has already been mentioned, the number of oxides formed by these elements is less than in the preceding groups, being confined to two each for cobalt (CoO, Co<sub>3</sub>O<sub>4</sub>) and rhodium (Rh<sub>2</sub>O<sub>3</sub>, RhO<sub>2</sub>) and to just one for iridium (IrO<sub>2</sub>) (though an impure sesquioxide Ir<sub>2</sub>O<sub>3</sub> has been reported — see below). No trioxides are known.

The only oxide formed by any of these metals in the divalent state is CoO; this is prepared as an olive-green powder by strongly heating the metal in air or steam, or alternatively by heating

the hydroxide, carbonate or nitrate in the absence of air. It has the rock-salt structure and is anti-ferromagnetic below 289 K. By reacting it with silica and alumina, pigments are produced which are used in the ceramics industry. CoO is stable in air at ambient temperatures and above 900°C but if heated at, say, 600–700°C, it is converted into the black Co<sub>3</sub>O<sub>4</sub>. This is Co<sup>II</sup>Co<sup>III</sup><sub>2</sub>O<sub>4</sub> and has the normal spinel structure with Co<sup>II</sup> ions in tetrahedral and Co<sup>III</sup> in octahedral sites within the ccp lattice of oxide ions. This is to be expected (p. 1080) because of the dominating advantage of placing the d<sup>6</sup> ions in octahedral sites, where adoption of the low-spin configuration gives it a decisively favourable CFSE. The ability of Co<sub>3</sub>O<sub>4</sub> to absorb oxygen, and possibly also the retention of water in preparations from the hydroxide, have led to claims for the existence of Co<sub>2</sub>O<sub>3</sub>, but it is doubtful if these claims are valid. Oxidation of Co(OH)<sub>2</sub>, or addition of aqueous alkali to a cobalt(III) complex, produces a dark-brown material which on drying at 150°C in fact gives cobalt(III) oxide hydroxide, CoO(OH).

Heating rhodium metal or the trichloride in oxygen at 600°C, or simply heating the trinitrate, produces dark-grey Rh<sub>2</sub>O<sub>3</sub> which has the corundum structure (p. 242); it is the only stable oxide formed by this metal. The yellow precipitate formed by the addition of alkali to aqueous solutions of rhodium(III) is actually Rh<sub>2</sub>O<sub>3</sub>·5H<sub>2</sub>O rather than a genuine hydroxide. Electrolytic oxidation of Rh<sup>III</sup> solutions and addition of alkali gives a yellow precipitate of RhO<sub>2</sub>·2H<sub>2</sub>O, but attempts to dehydrate this produce Rh<sub>2</sub>O<sub>3</sub>. Black anhydrous RhO<sub>2</sub> is best obtained by heating Rh<sub>2</sub>O<sub>3</sub> in oxygen under pressure; it has the rutile structure, but it is not well characterized.

For iridium the position is reversed. This time it is the black dioxide, IrO<sub>2</sub>, with the rutile structure (p. 961), which is the only definitely established oxide. It is obtained by heating the metal in oxygen or by dehydrating the precipitate produced when alkali is added to an aqueous solution of [IrCl<sub>6</sub>]<sup>2-</sup>. Contamination either by unreacted metal or by alkali is, however, difficult to avoid. The other oxide, Ir<sub>2</sub>O<sub>3</sub>, is said to be

obtained by igniting K<sub>2</sub>IrCl<sub>6</sub> with NaCO<sub>3</sub> or, as its hydrate, by adding KOH to aqueous K<sub>3</sub>[IrCl<sub>6</sub>] under CO<sub>2</sub>. However, even if it is a true compound, it is always impure and is readily oxidized to IrO<sub>2</sub>.

Oxoanions are rare in this group; exceptions include the unstable [Co<sup>V</sup>O<sub>4</sub>]<sup>3-</sup> and [Co<sup>II</sup>O<sub>3</sub>]<sup>4-</sup>. Heating mixtures of the appropriate oxides in oxygen, or under pressure, produces materials with the stoichiometry, M<sub>3</sub>CoO<sub>4</sub>, which, together with their oxidizing properties, suggests the presence of Co<sup>V</sup>. When CoO is heated with 2.2 moles of Na<sub>2</sub>O at 550° in a sealed tube under argon, bright-red crystals of Na<sub>4</sub>Co<sup>II</sup>O<sub>3</sub> are formed. The compound hydrolyses immediately on contact with atmospheric moisture and is notable in containing discrete planar [CoO<sub>3</sub>]<sup>4-</sup> ions reminiscent of the carbonate ion (Co–O 186 ± 6 pm) and is similar to the red oxoferrate(II), Na<sub>4</sub>[FeO<sub>3</sub>]. The lustrous red tetracobaltate(II) Na<sub>10</sub>[Co<sub>4</sub><sup>II</sup>O<sub>9</sub>], with an anion analogous to the *catena*-tetracarbonate [C<sub>4</sub>O<sub>9</sub>]<sup>2-</sup>, is also known. For iridium, prolonged heating of IrO<sub>2</sub> and Li<sub>2</sub>O produces Li<sub>2</sub>IrO<sub>3</sub> which, when heated with 2.2 moles of Na<sub>2</sub>O at 800°C for 71 days, gives transparent red crystals of Na<sub>4</sub>IrO<sub>4</sub> in which the Ir(IV) is surrounded by four O<sup>2-</sup> in a square (Ir–O = 190.2 pm.)<sup>(4)</sup>

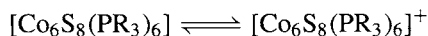
A larger number of sulfides have been reported but not all of them have been fully characterized. Cobalt gives rise to CoS<sub>2</sub> with the pyrites structure (p. 680), Co<sub>3</sub>S<sub>4</sub> with the spinel structure (p. 247), and Co<sub>1-x</sub>S which has the NiAs structure (p. 555) and is cobalt-deficient. All are metallic, as is Co<sub>9</sub>S<sub>8</sub> and the corresponding selenides and tellurides. The sulfides of rhodium and iridium are notable mainly for their inertness especially towards acids, and most of them are semiconductors. They are the disulfides MS<sub>2</sub>, obtained from the elements; the “sesquisulfides” M<sub>2</sub>S<sub>3</sub>, obtained by passing H<sub>2</sub>S through aqueous solutions of M<sup>III</sup>; and Rh<sub>2</sub>S<sub>5</sub> and IrS<sub>3</sub>, obtained by heating MCl<sub>3</sub> + S at 600°C. Numerous nonstoichiometric selenides and tellurides are also known.

<sup>4</sup> K. MADERAND and R. HOPPE, *Z. anorg. allg. Chem.* **619**, 1647–54 (1993).

Table 26.3 Halides of cobalt, rhodium and iridium (mp/°C)

Oxidation state	Fluorides	Chlorides	Bromides	Iodides
+6	RhF <sub>6</sub> black (70°) IrF <sub>6</sub> yellow (44°) bp 53°			
+5	[RhF <sub>5</sub> ] <sub>4</sub> dark red [IrF <sub>5</sub> ] <sub>4</sub> yellow (104°)			
+4	CoF <sub>4</sub> RhF <sub>4</sub> purple-red IrF <sub>4</sub> dark brown	IrCl <sub>4</sub> ?	IrBr <sub>4</sub> ?	IrI <sub>4</sub> ?
+3	CoF <sub>3</sub> light brown RhF <sub>3</sub> red IrF <sub>3</sub> black	RhCl <sub>3</sub> red IrCl <sub>3</sub> red	RhBr <sub>3</sub> red-brown IrBr <sub>3</sub> red-brown	RhI <sub>3</sub> black IrI <sub>3</sub> dark brown
+2	CoF <sub>2</sub> pink (1200°)	CoCl <sub>2</sub> blue (724°)	CoBr <sub>2</sub> green (678°)	CoI <sub>2</sub> a blue-black (515°)

Because of possible catalytic and biological relevance of metal–sulfur clusters, several such compounds of cobalt have been prepared. The action of H<sub>2</sub>S or M<sub>2</sub>S (M = alkali metal) on a non-aqueous solution of a convenient cobalt compound (often containing, or in the presence of, a phosphine) is a typical route. Diamagnetic [Co<sub>6</sub>S<sub>8</sub>(PR<sub>3</sub>)<sub>6</sub>] (R = Et, Ph) comprise an octahedral array of metal atoms (Co–Co in the range 281.7 to 289.4 pm), all faces capped by μ<sub>3</sub>-S atoms,<sup>(5)</sup> and show facile redox behaviour



An indication of the range of such clusters which might possibly be synthesized is given by the observation<sup>(6)</sup> that mass spectroscopic analysis of the products of laser-ablation of CoS

show no less than 83 gaseous ions ranging from [CoS<sub>2</sub>]<sup>-</sup> to [Co<sub>38</sub>S<sub>24</sub>]<sup>-</sup>.

### 26.3.2 Halides

The known halides of this triad are listed in Table 26.3. It can be seen that, apart from CoF<sub>3</sub>, CoF<sub>4</sub> and the doubtful iridium tetrahalides, they fall into three categories:

- higher fluorides of Ir and Rh;
- a full complement of trihalides of Ir and Rh;
- dihalides of cobalt

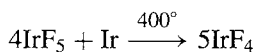
The octahedral hexafluorides are obtained directly from the elements and both are volatile, extremely reactive and corrosive solids, RhF<sub>6</sub> being the least stable of the platinum metal hexafluorides and reacting with glass even when carefully dried. They are thermally unstable and must be frozen out from the hot gaseous reaction mixtures, otherwise they dissociate.

<sup>5</sup> M. HONG, Z. HUANG, X. LEI, G. WEI, B. KANG and H. LIU, *Polyhedron*, **10**, 927–34 (1991).

<sup>6</sup> J. EL NAKAT, K. J. FISHER, I. G. DANCE and G. D. WILLET, *Inorg. Chem.* **32** 1931–40 (1993).

The pentafluorides of Rh and Ir may be prepared by the deliberate thermal dissociation of the hexafluorides. They also are highly reactive and are respectively dark-red and yellow solids, with the same tetrameric structure as  $[\text{RuF}_5]_4$  and  $[\text{OsF}_5]_4$  (p. 1083).

$\text{RhF}_4$  is a purple-red solid, usually prepared by the reaction of the strong fluorinating agent  $\text{BrF}_3$  on  $\text{RhBr}_3$ . The corresponding compound  $\text{IrF}_4$  has had an intriguing and instructive history.<sup>(7)</sup> It was first claimed in 1929 and again in 1956 but this material was shown in 1965 to be, in reality, the previously unknown  $\text{IrF}_5$ .  $\text{IrF}_4$  can now be made (1974) by reducing  $\text{IrF}_5$  with the stoichiometric amount of iridium-black:



The dark-brown product disproportionates above  $400^\circ$  into  $\text{IrF}_3$  and the volatile  $\text{IrF}_5$ . The structure features  $\{\text{IrF}_6\}$  octahedra which share 4 F atoms, each with one other  $\{\text{IrF}_6\}$  group, leaving a pair of *cis* vertices unshared: this is essentially a rutile type structure (p. 961) from which alternate metal atoms have been removed from each edge-sharing chain. It was the first 3D structure to have been found for a tetrafluoride.<sup>(7)</sup> Claims have been made for the isolation of all the other iridium tetrahalides, but there is some doubt as to whether these can be substantiated. This is an unexpected situation since +4 is one of iridium's common oxidation states and, indeed, the derived anions  $[\text{IrX}_6]^{2-}$  ( $X = \text{F}, \text{Cl}, \text{Br}$ ) are well known.

The most familiar and most stable of the halides of Rh and Ir, however, are the trihalides. Those of Rh range in colour from the red  $\text{RhF}_3$  to black  $\text{RhI}_3$  and, apart from the latter, which is obtained by the action of aqueous KI on the tribromide, they may be obtained in the anhydrous state directly from the elements.  $\text{RhF}_3$  has a structure similar to that of  $\text{ReO}_3$  (p. 1047), while  $\text{RhCl}_3$  is isomorphous with  $\text{AlCl}_3$  (p. 234). The anhydrous trihalides are generally unreactive and insoluble in water but, excepting the triiodide which is only known in this form,

water-soluble hydrates can be produced by wet methods.  $\text{RhF}_3 \cdot 6\text{H}_2\text{O}$  and  $\text{RhF}_3 \cdot 9\text{H}_2\text{O}$  can be isolated from aqueous solutions of  $\text{Rh}^{\text{III}}$  acidified with HF. Their aqueous solutions are yellow, possibly due to the presence of  $[\text{Rh}(\text{H}_2\text{O})_6]^{3+}$ . The dark-red deliquescent  $\text{RhCl}_3 \cdot 3\text{H}_2\text{O}$  is the most common compound of rhodium and the usual starting point for the preparation of other rhodium compounds, and is itself best prepared from the metal sponge. This is heated with KCl in a stream of  $\text{Cl}_2$  and the product extracted with water. The solution contains  $\text{K}_2[\text{Rh}(\text{H}_2\text{O})\text{Cl}_5]$  and treatment with KOH precipitates the hydrous  $\text{Rh}_2\text{O}_3$  which can be dissolved in hydrochloric acid and the solution evaporated to dryness.  $\text{RhBr}_3 \cdot 2\text{H}_2\text{O}$  also is formed from the metal by treating it with hydrochloric acid and bromine.

The iridium trihalides are rather similar to those of rhodium. Anhydrous  $\text{IrF}_3$  is obtained by reducing  $\text{IrF}_6$  with the metal,  $\text{IrCl}_3$  and  $\text{IrBr}_3$  by heating the elements, and  $\text{IrI}_3$  by heating its hydrate *in vacuo*. Water-soluble hydrates of the tri-chloride, -bromide, and -iodide are produced by dissolving hydrous  $\text{Ir}_2\text{O}_3$  in the appropriate acid and, like its rhodium analogue,  $\text{IrCl}_3 \cdot 3\text{H}_2\text{O}$  provides a convenient starting point in iridium chemistry.

Lower halides of Rh and Ir have been reported and, whilst their existence cannot be denied with certainty, further substantiation is needed. Unquestionably, the divalent state is the preserve of cobalt. Apart from the strongly oxidizing  $\text{CoF}_3$  (a light-brown powder isomorphous with  $\text{FeCl}_3$  and the product of the action of  $\text{F}_2$  on  $\text{CoCl}_2$  at  $250^\circ\text{C}$ ) and  $\text{CoF}_4$  (identified<sup>(8)</sup> in the gaseous phase by mass spectrometry, as the singly charged cation, when  $\text{CoF}_3$  and  $\text{TbF}_4$  are heated to 600–680 K), the only known halides of cobalt are the dihalides. In all of these the cobalt is octahedrally coordinated. The anhydrous compounds are prepared by dry methods:  $\text{CoF}_2$  (pink) by heating  $\text{CoCl}_2$  in HF;  $\text{CoCl}_2$  (blue) and  $\text{CoBr}_2$  (green) by the action of the halogens on the heated metal;  $\text{CoI}_2$  (blue-black) by the action

<sup>7</sup> N. BARTLETT and A. TRESSAUD, *Comptes Rendus* **278C**, 1501–4 (1974).

<sup>8</sup> M. V. KOBOROV, L. N. SAVINOVA and L. N. SIDEROV, *J. Chem. Thermodynam.* **25**, 1161–8 (1993).

of HI on the heated metal. The fluoride is only slightly soluble in water but the others dissolve readily to give solutions from which pink or red hexahydrates can be crystallized. These solutions can alternatively and more conveniently be made by dissolving the metal, oxide or carbonate in the appropriate hydrohalic acid. The chloride is widely used as an indicator in the desiccant, silica gel, since its blue anhydrous form turns pink as it hydrates (see p. 1131).

The disinclination of these metals to form oxoanions has already been remarked and the same is evidently true of oxohalides: none have been authenticated.

### 26.3.3 Complexes

The chemistry of oxidation states above IV is sparse. Apart from  $\text{RhF}_6$  and  $\text{IrF}_6$ , such chemistry as there is, is mainly confined to salts of  $[\text{RhF}_6]^-$  and  $[\text{IrF}_6]^-$ . These are prepared respectively by the action of  $\text{F}_2$  on  $\text{RhCl}_3$  and  $\text{KF}$  under pressure,<sup>(9)</sup> and by fluorinating a lower halide of iridium with  $\text{BrF}_3$  in the presence of a halide of the counter cation. Hydrido complexes of iridium in the formal oxidation state V are obtained by the action of  $\text{LiAlH}_4$  or  $\text{LiBH}_4$  on  $\text{Ir}^{\text{III}}$  compounds in the presence of phosphine or cyclopentadienyl ligands.  $[\text{IrH}_5(\text{PR}_3)_2]$ , in which the five hydrogens lie equatorially in a pentagonal bipyramid, and the "half sandwich",  $[(\eta^5\text{-C}_5\text{Me}_5)\text{IrH}_4]$ , are examples.

#### Oxidation state IV ( $d^5$ )

Cobalt provides only a few examples of this oxidation state, namely some fluoro compounds and mixed metal oxides, whose purity is questionable and, most notably, the thermally stable, brown, tetraalkyl,  $[\text{Co}(1\text{-norbornyl})_4]$ . Prepared by the reaction of  $\text{CoCl}_2$  and  $\text{Li}(1\text{-norbornyl})$ , it is the only one of a series of such compounds obtained for the first row transition

metals Ti to Co which has been structurally characterized.<sup>(10)</sup> It is tetrahedral and, with a  $d^5$  configuration, its room-temperature magnetic moment of 1.89 BM indicates that it is low-spin; the first example to be authenticated for a tetrahedral complex of a first row transition metal. Rhodium(IV) complexes are confined to salts of the oxidizing and readily hydrolysed  $[\text{RhX}_6]^{2-}$  ( $\text{X} = \text{F}, \text{Cl}$ ), the green solid  $\text{Cs}_2[\text{RhCl}_6]$  being one of the few to be confirmed.<sup>(11)</sup> Only iridium(IV) shows appreciable stability.

The salts of  $[\text{IrX}_6]^{2-}$  ( $\text{X} = \text{F}, \text{Cl}, \text{Br}$ ) are comparatively stable and their colour deepens from red, through reddish-black to bluish-black with increasing atomic weight of the halogen.  $[\text{IrF}_6]^{2-}$  is obtained by reduction of  $[\text{IrF}_6]^-$ ,  $[\text{IrCl}_6]^{2-}$  by oxidation of  $[\text{IrCl}_6]^{3-}$  with chlorine, and  $[\text{IrBr}_6]^{2-}$  by  $\text{Br}^-$  substitution of  $[\text{IrCl}_6]^{2-}$  in aqueous solution. The hexachloroiridates in particular have been the subject of many magnetic investigations. They have magnetic moments at room temperature somewhat below the spin-only value for the  $t_{2g}^5$  configuration (1.73 BM), and this falls with temperature. This has been interpreted as the result of antiferromagnetic interaction operating by a superexchange mechanism between adjacent  $\text{Ir}^{\text{IV}}$  ions via intervening chlorine atoms. More importantly, in 1953 in a short but classic paper,<sup>(12)</sup> J. Owen and K. W. H. Stevens reported the observation of hyperfine structure in the esr signal obtained from solid solutions of  $(\text{NH}_4)_2[\text{IrCl}_6]$  in the isomorphous, but diamagnetic,  $(\text{NH}_4)_2[\text{PtCl}_6]$ . This arises from the influence of the chlorine nuclei and, from the magnitude of the splitting, it was inferred that the single unpaired electron, which is ostensibly one of the metal  $d^5$  electrons, in fact spends only 80% of its time on the metal, the rest of the time being divided equally between the 6 chlorine ligands. This was the first unambiguous evidence that metal d electrons are able to move in molecular

<sup>10</sup> E. K. BYRNE, D. S. RICHESON and K. H. THEOPOLD, *J. Chem. Soc., Chem. Commun.*, 1491–2 (1986).

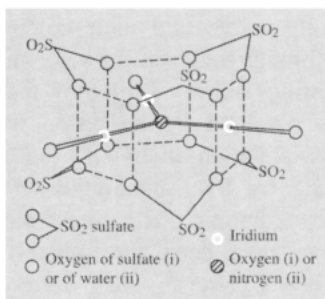
<sup>11</sup> I. J. ELLISON and R. D. GILLARD, *Polyhedron* **15**, 339–48 (1996).

<sup>12</sup> J. OWEN and K. W. H. STEVENS, *Nature* **171**, 836 (1953).

<sup>9</sup> A. K. BRIDSON, J. H. HOLLOWAY, E. G. HOPE and W. LEVASON, *Polyhedron* **11**, 7–11 (1992).

**Table 26.4**  $E^\circ$  for some  $\text{Co}^{\text{III}}/\text{Co}^{\text{II}}$  couples in acid solution

Couple	$E^\circ/V$
$[\text{Co}(\text{H}_2\text{O})_6]^{3+} + e^- \rightleftharpoons [\text{Co}(\text{H}_2\text{O})_6]^{2+}$	1.83
$[\text{Co}(\text{C}_2\text{O}_4)_3]^{3-} + e^- \rightleftharpoons [\text{Co}(\text{C}_2\text{O}_4)_3]^{4-}$	0.57
$[\text{Co}(\text{edta})]^- + e^- \rightleftharpoons [\text{Co}(\text{edta})]^{2-}$	0.37
$[\text{Co}(\text{bipy})_3]^{3+} + e^- \rightleftharpoons [\text{Co}(\text{bipy})_3]^{2+}$	0.31
$[\text{Co}(\text{en})_3]^{3+} + e^- \rightleftharpoons [\text{Co}(\text{en})_3]^{2+}$	0.18
$[\text{Co}(\text{NH}_3)_6]^{3+} + e^- \rightleftharpoons [\text{Co}(\text{NH}_3)_6]^{2+}$	0.108
$[\text{Co}(\text{CN})_6]^{3-} + \text{H}_2\text{O} + e^- \rightleftharpoons [\text{Co}(\text{CN})_5(\text{H}_2\text{O})]^{3-} + \text{CN}^-$	-0.8
$\frac{1}{2}\text{O}_2 + 2\text{H}^+ + 2e^- \rightleftharpoons \text{H}_2\text{O}$	1.229

**Figure 26.1** Trinuclear structure of  
(i)  $[\text{Ir}_3\text{O}(\text{SO}_4)_9]^{10-}$  and  
(ii)  $[\text{Ir}_3\text{N}(\text{SO}_4)_6(\text{H}_2\text{O})_3]^{4-}$ .

orbitals over the whole complex, and implies the presence of  $\pi$  as well as  $\sigma$  bonding.

In aqueous solution, the halide ions of  $[\text{IrX}_6]^{2-}$  may be replaced by solvent and a number of aquo substituted derivatives have been reported. Other  $\text{Ir}^{\text{IV}}$  complexes with  $O$ -donor ligands are  $[\text{IrCl}_4(\text{C}_2\text{O}_4)]^{2-}$ , obtained by oxidizing  $\text{Ir}^{\text{III}}$  oxalato complexes with chlorine, and  $\text{Na}_2\text{IrO}_3$ , obtained by fusing  $\text{Ir}$  and  $\text{Na}_2\text{CO}_3$ .

Two interesting trinuclear complexes must also be mentioned. They are  $\text{K}_{10}[\text{Ir}_3\text{O}(\text{SO}_4)_9] \cdot 3\text{H}_2\text{O}$ , obtained by boiling  $\text{Na}_2\text{IrCl}_6$  and  $\text{K}_2\text{SO}_4$  in conc sulfuric acid, and  $\text{K}_4[\text{Ir}_3\text{N}(\text{SO}_4)_6(\text{H}_2\text{O})_3]$ , obtained by boiling  $\text{Na}_3\text{IrCl}_6$  and  $(\text{NH}_4)_2\text{SO}_4$  in conc sulfuric acid. They have the structure shown in Fig. 26.1, analogous to that of the basic carboxylates,  $[\text{M}_3^{\text{III}}\text{O}(\text{O}_2\text{CR})_6\text{L}_3]^+$  (see Fig. 23.9). The oxo species formally contains 1  $\text{Ir}^{\text{IV}}$  and 2  $\text{Ir}^{\text{III}}$  ions and the nitride species 2  $\text{Ir}^{\text{IV}}$  ions and 1  $\text{Ir}^{\text{III}}$  ion, but in each case the charges are probably delocalized over the whole complex.

### Oxidation state III ( $d^6$ )

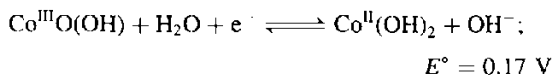
For all three elements this is the most prolific oxidation state, providing a wide variety of kinetically inert complexes. As has already been pointed out, these are virtually all low-spin and octahedral, a major stabilizing influence being the high CFSE associated with the  $t_{2g}^6$  configuration ( $\frac{12}{5}\Delta_o$ , the maximum possible for any  $d^x$  configuration). Even  $[\text{Co}(\text{H}_2\text{O})_6]^{3+}$  is low-spin but it is such a powerful oxidizing agent that it is unstable in aqueous solutions and only a few simple salt hydrates, such as the blue  $\text{Co}_2(\text{SO}_4)_3 \cdot 18\text{H}_2\text{O}$  and  $\text{MCo}(\text{SO}_4)_2 \cdot 12\text{H}_2\text{O}$  ( $\text{M} = \text{K}, \text{Rb}, \text{Cs}, \text{NH}_4$ ), which contain the hexaquo ion, and  $\text{CoF}_3 \cdot 3\frac{1}{2}\text{H}_2\text{O}$  can be isolated. This paucity of simple salts of cobalt(III) contrasts sharply with the great abundance of its complexes, especially with  $N$ -donor ligands<sup>(13)</sup>, and it is evident that the high CFSE is not the only factor affecting the stability of this oxidation state.

Table 26.4 illustrates the remarkable sensitivity of the reduction potential of the  $\text{Co}^{\text{III}}/\text{Co}^{\text{II}}$  couple to different ligands whose presence renders  $\text{Co}^{\text{II}}$  unstable to aerial oxidation. The extreme effect of  $\text{CN}^-$  can be thought of as being due, on the one hand, to the ability of its empty  $\pi^*$  orbitals to accept "back-donated" charge from the metal's filled  $t_{2g}$  orbitals and, on the other, to its effectiveness as a  $\sigma$  donor (enhanced partly by its negative charge). The magnitudes of the

<sup>13</sup> P. HENDRY and A. LUDI, *Adv. Inorg. Chem.* **35**, 117-98 (1990).



changes in  $E^\circ$  are even greater than those noted for the  $\text{Fe}^{\text{III}}/\text{Fe}^{\text{II}}$  couple (p. 1093), though if the two systems are compared it must be remembered that the oxidation state which can be stabilized by adoption of the low-spin  $t_{2g}^6$  configuration is +3 for cobalt but only +2 for iron. Nevertheless, the effect of increasing pH is closely similar, the  $\text{M}^{\text{III}}$  "hydroxide" of both metals being far less soluble than the  $\text{M}^{\text{II}}$  "hydroxide". In the case of cobalt this reduces  $E^\circ$  from 1.83 to 0.17 V:

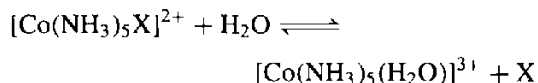


thereby facilitating oxidation to the +3 state.

Complexes of cobalt(III), like those of chromium(III) (p. 1027), are kinetically inert and so, again, indirect methods of preparation are to be preferred. Most commonly the ligand is added to an aqueous solution of an appropriate salt of cobalt(II), and the cobalt(II) complex thereby formed is oxidized by some convenient oxidant, frequently (if an *N*-donor ligand is involved) in the presence of a catalyst such as active charcoal. Molecular oxygen is often used as the oxidant simply by drawing a stream of air through the solution for a few hours, but the same result can, in many cases, be obtained more quickly by using aqueous solutions of  $\text{H}_2\text{O}_2$ .

The cobaltammines, whose number is legion, were amongst the first coordination compounds to be systematically studied<sup>†</sup> and are undoubtedly the most extensively investigated class of cobalt(III) complex. Oxidation of aqueous mixtures of  $\text{CoX}_2$ ,  $\text{NH}_4\text{X}$  and  $\text{NH}_3$  ( $\text{X} = \text{Cl}, \text{Br}, \text{NO}_3$ , etc.) can, by varying the conditions and particularly the relative proportions of the reactants, be used to prepare complexes of types such as  $[\text{Co}(\text{NH}_3)_6]^{3+}$ ,  $[\text{Co}(\text{NH}_3)_5\text{X}]^{2+}$  and  $[\text{Co}(\text{NH}_3)_4\text{X}_2]^+$ . The range of these compounds

is further extended by the replacement of X by other anionic or neutral ligands. The inertness of the compounds makes such substitution reactions slow (taking hours or days to attain equilibrium) and, being therefore amenable to examination by conventional analytical techniques, they have provided a continuing focus for kinetic studies. The forward (aquation) and backward (anation) reactions of the pentaammines:



must be the most thoroughly studied substitution reactions, certainly of octahedral compounds. Furthermore, the isolation of *cis* and *trans* isomers of the tetraammines (p. 914) was an important part of Werner's classical proof of the octahedral structure of 6-coordinate complexes. The kinetic inertness of cobalt(III) was also exploited by H. Taube to demonstrate the inner-sphere mechanism of electron transfer (see Panel on p. 1124).

Compounds analogous to the cobaltammines may be similarly obtained using chelating amines such as ethylenediamine or bipyridyl, and these too have played an important role in stereochemical studies. Thus *cis*- $[\text{Co}(\text{en})_2(\text{NH}_3)\text{Cl}]^{2+}$  was resolved into *d*(+) and *l*(-) optical isomers by Werner in 1911 thereby demonstrating, to all but the most determined doubters, its octahedral stereochemistry.<sup>‡</sup> More recently, the absolute configuration of one of the optical isomers of  $[\text{Co}(\text{en})_3]^{3+}$  was determined (see Panel on p. 1125).

Another *N*-donor ligand, which forms extremely stable complexes, is the  $\text{NO}_2^-$  ion: its best-known complex is the orange "sodium cobaltinitrite",  $\text{Na}_3[\text{Co}(\text{NO}_2)_6]$ , aqueous solutions of which were used for the quantitative precipitation of  $\text{K}^+$  as  $\text{K}_3[\text{Co}(\text{NO}_2)_6]$  in classical analysis. Treatment of this with fluorine yields

<sup>†</sup> The observation by B. M. Tassaert in 1798 that solutions of cobalt(II) chloride in aqueous ammonia gradually turn brown in air, and then wine-red on being boiled, is generally accepted as the first preparation of a cobalt(III) complex. It was realized later that more than one complex was involved and that, by varying the relative concentrations of ammonia and chloride ion, the complexes  $\text{CoCl}_3 \cdot x\text{NH}_3$  ( $x = 6, 5$  and  $4$ ) could be separated.

<sup>‡</sup> So deep-seated at that time was the conviction that optical activity could arise only from carbon atoms that it was argued that the ethylenediamine must be responsible, even though it is itself optically inactive. The opposition was only finally assuaged by Werner's subsequent resolution of an entirely inorganic material (p. 915).

### Electron Transfer (Redox) Reactions

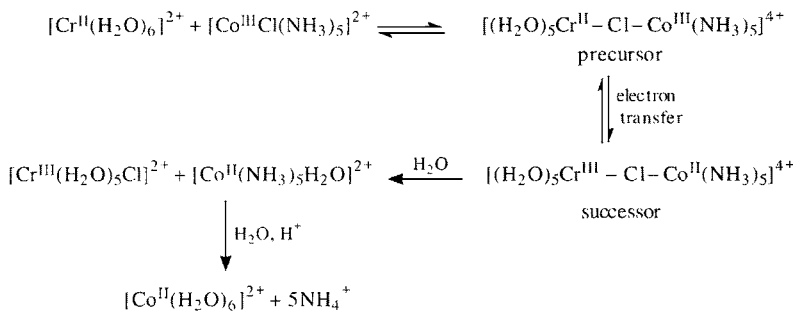
Two mechanisms exist for the transfer of charge from one species to another:

1. *Outer-sphere*. Here, electron transfer from one reactant to the other is effected without changing the coordination sphere of either. This is likely to be the case if both reactants are coordinatively saturated and can safely be assumed to be so if the rate of the redox process is faster than the rates observed for substitution (ligand transfer) reactions of the species in question. A good example is the reaction.



The observed rate law for this type of reaction is usually first order in each reactant. Extensive theoretical treatments have been performed, most notably by R. A. Marcus and N. S. Hush, details of which can be found in more specialized sources<sup>(14)</sup>

2. *Inner-sphere*. Here, the two reactants first form a bridged complex (*precursor*); intramolecular electron transfer then yields the *successor* which in turn dissociates to give the products. The first demonstration of this was provided by H. Taube. He examined the oxidation of  $[\text{Cr}(\text{H}_2\text{O})_6]^{2+}$  by  $[\text{CoCl}(\text{NH}_3)_5]^{2+}$  and postulated that it occurs as follows:



The superb elegance of this demonstration lies in the choice of reactants which permits no alternative mechanism.  $\text{Cr}^{\text{II}}$  ( $d^4$ ) and  $\text{Co}^{\text{II}}$  ( $d^7$ ) species are known to be substitutionally labile whereas  $\text{Cr}^{\text{III}}$  ( $d^3$ ) and  $\text{Co}^{\text{III}}$  (low-spin  $d^6$ ) are substitutionally inert. Only if electron transfer is preceded by the formation of a bridged intermediate can the inert cobalt reactant be persuaded to release a  $\text{Cl}^-$  ligand and so allow the quantitative formation of the (then inert) chromium product. Corroboration that electron transfer does not occur by an outer-sphere mechanism followed by loss of  $\text{Cl}^-$  from the chromium is provided by the fact that, if  $^{36}\text{Cl}^-$  is added to the solution, none of it finds its way into the chromium product.

Demonstration of ligand transfer is crucial to the proof that *this particular reaction* proceeds via an inner-sphere mechanism, and ligand transfer is indeed a usual feature of inner-sphere redox reactions, but it is not an *essential* feature of *all* such reactions.

The observed rate law for inner-sphere, as for outer-sphere, reactions is commonly first order in each reactant but this does not indicate which step is rate-determining. Again, details should be obtained from more extensive accounts.<sup>(14)</sup>

For their work in this field, Taube and Marcus were awarded Nobel Prizes for Chemistry in 1983 and 1992 respectively.

$\text{K}_3[\text{CoF}_6]$ , whose anion is notable not only as the only hexahalogeno complex of cobalt(III) but also for being high-spin and hence paramagnetic with a magnetic moment at room temperature of nearly 5.8 BM.

$[\text{Co}(\text{CN})_6]^{3-}$  has already been mentioned and is extremely stable, being inert to alkalis and, like  $[\text{Fe}(\text{CN})_6]^{4-}$ , which likewise involves the  $t_{2g}^6$  configuration, it is reportedly nontoxic.

Complexes of cobalt(III) with *O*-donor ligands are generally less stable than those with *N*-donors although the dark-green  $[\text{Co}(\text{acac})_3]$  and  $\text{M}_3[\text{Co}(\text{C}_2\text{O}_4)_3]$  complexes, formed from the chelating ligands acetylacetonate and oxalate, are stable. Other carboxylato complexes such as those of

<sup>14</sup> R. G. WILKINS, *Kinetics and Mechanism of Reactions of Transition Metal Complexes*, 2nd edn., VCH, Weinheim, 1991, 465 pp. T. J. MEYER and H. TAUBE, Chap. 9 in *Comprehensive Coordination Chemistry*, Vol. 1, pp. 331–84, Pergamon Press, Oxford, 1987.

### Determination of Absolute Configuration

Because they rotate the plane of polarized light in opposite directions (p. 919) it is a relatively simple matter to distinguish an optical isomer from its mirror image. But to establish their absolute configurations is a problem which for long defeated the ingenuity of chemists. Normal X-ray diffraction techniques do not distinguish between them, but J. M. Bijvoet developed the absorption edge, or anomalous, diffraction technique which does. In this method the wavelength of the X-rays is chosen so as to correspond to an electronic transition of the central metal atom, and under these circumstances phase changes are introduced into the diffracted radiation which are different for the two isomers. An understanding of the phenomenon not only allows the isomers to be distinguished but also their configurations to be identified. Once the absolute configuration of one complex has been determined in this way, it can then be used as a standard to determine the absolute configuration of other, similar, complexes by the relatively simpler method of comparing their *optical rotary dispersion* (ORD) and *circular dichroism* (CD) curves.<sup>(15)</sup>

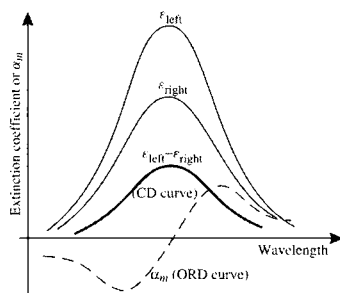
Normal measurements of optical activity are concerned with the ability of the optically active substance to rotate the plane of polarization of plane polarized light, its specific optical rotary power ( $\alpha_m$ ) being given by

$$\alpha_m = \frac{\alpha V}{m l} \text{ rad m}^2 \text{ kg}^{-1}$$

where  $\alpha$  is the observed angle of rotation,  $V$  is the volume,  $m$  is the mass, and  $l$  is the path length.

The reason why this phenomenon occurs is that plane polarized light can be considered to be made up of left- and of right-circularly polarized components, and the nature of an optically active substance is such that, in passing through it, one component passes through greater electron density than does the other. As a result, that component is slowed down relative to the other and the two components emerge somewhat out-of-phase, i.e. the plane of polarization of the light has been rotated. If the wavelength of the polarized light is varied, and  $\alpha_m$  then plotted against wavelength, the result is known as an *optical rotary dispersion* curve. For those wavelengths at which the substance is transparent,  $\alpha_m$  is virtually constant, which is to say the ORD curve is flat. But what happens when the wavelength of the light is such that it is absorbed by the substance in question?

In absorbing light the molecules of a substance undergo electronic excitations which involve displacement of electron charge. Because of their differing routes through the molecules, the two circularly polarized components of the light produce these excitations to different extents and are consequently absorbed to different extents. The difference in extinction coefficients,  $\epsilon_{\text{left}} - \epsilon_{\text{right}}$ , can be measured and is known as the *circular dichroism*. If the CD is plotted against wavelength it is therefore zero at wavelengths where there is no absorption but passes through a maximum, or a minimum, where absorption occurs. Accompanying these changes in CD it is found that the ORD curve is like a first derivative, passing through zero at the absorption maximum (Fig. A). Such a change in sign of  $\alpha_m$  highlights the importance of quoting the wavelength of the light used when classifying optical isomers as (+) or (-), since the classification could be reversed by simply using light of a different wavelength.<sup>†</sup>



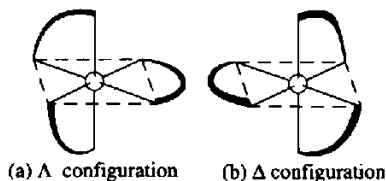
**Figure A** Diagrammatic representation of the Cotton effect (actually “positive” Cotton effect. The “negative” effect occurs when the CD curve shows a minimum and the ORD curve is the reverse of the above).

*Panel continues*

<sup>†</sup>The situation is perhaps not quite so bad as is implied here, since *single* measurements of  $\alpha_m$  are usually made at the sodium D line, 589.6nm. Nevertheless, it is clearly better to state the wavelength than to assume that this will be understood.

The behaviours of CD and ORD curves in the vicinity of an absorption band are collectively known as the *Cotton effect* after the French physicist A. Cotton who discovered them in 1895. Their importance in the present context is that molecules with the same absolute configuration will exhibit the same Cotton effect for the same d-d absorption and, if the configuration of one compound is known, that of *closely similar* ones can be established by comparison.

The optical isomer of  $[\text{Co}(\text{en})_3]^{3+}$  referred to in the main text is the (+)<sub>NAD</sub> isomer, which has a left-handed (*laevo*) screw axis as shown in Fig. Ba, and according to the convention recommended by IUPAC is given the symbol  $\Lambda$ . This is in contrast to its mirror image (Fig. Bb) which has a right-handed (*dextro*) screw axis and is given the symbol  $\Delta$ .

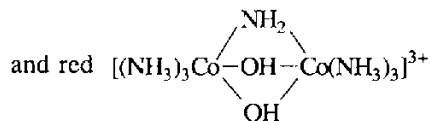
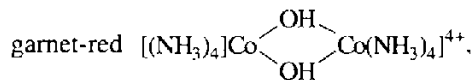


**Figure B** The absolute configuration of the optical isomers of a metal tris-chelates complex such as  $[\text{Co}(\text{en})_3]^{3+}$ . (a)  $\Lambda$  configuration and (b)  $\Delta$  configuration.

the acetate are, however, less stable but are involved in the catalysis of a number of oxidation reactions by  $\text{Co}^{\text{II}}$  carboxylates.

A noticeable difference between the chemistries of complexes of chromium(III) and cobalt(III) is the smaller susceptibility of the latter to hydrolysis, though limited hydrolysis, leading to polynuclear cobaltammines with bridging  $\text{OH}^-$  groups, is well known. Other commonly occurring bridging groups are  $\text{NH}_2^-$ ,  $\text{NH}_2^-$  and  $\text{NO}_2^-$ , and singly, doubly and triply bridged species are known such as

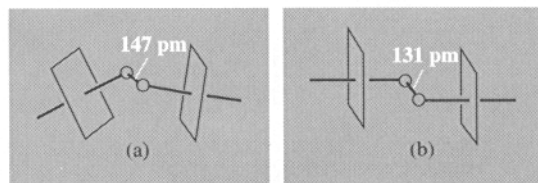
the bright-blue  $[(\text{NH}_3)_5\text{Co}-\text{NH}_2-\text{Co}(\text{NH}_3)_5]^{5+}$ ,



But probably the most interesting of the polynuclear complexes are those containing  $-\text{O}-\text{O}-$  bridges (see also p. 616).

In the preparation of cobalt(III) hexaammine salts by the aerial oxidation of cobalt(II) in aqueous ammonia it is possible, in the absence

of a catalyst, to isolate a brown intermediate,  $[(\text{NH}_3)_5\text{Co}-\text{O}_2-\text{Co}(\text{NH}_3)_5]^{4+}$ . This is moderately stable in conc aqueous ammonia and in the solid, but decomposes readily in acid solutions to  $\text{Co}^{\text{II}}$  and  $\text{O}_2$ , while oxidizing agents such as  $(\text{S}_2\text{O}_8)^{2-}$  convert it to the green, paramagnetic  $[(\text{NH}_3)_5\text{Co}-\text{O}_2-\text{Co}(\text{NH}_3)_5]^{5+}$  ( $\mu_{300} \sim 1.7 \text{ BM}$ ). The formulation of the brown compound poses no problems. The 2 cobalt atoms are in the +3 oxidation state and are joined by a peroxy group,  $\text{O}_2^{2-}$ , all of which accords with the observed diamagnetism; moreover, the stereochemistry of the central  $\text{Co}-\text{O}-\text{O}-\text{Co}$  group (Fig. 26.2a) is akin to that of  $\text{H}_2\text{O}_2$  (p. 634). The green compound is less straightforward. Werner thought that it too involved a peroxy group but in this instance bridging  $\text{Co}^{\text{III}}$  and  $\text{Co}^{\text{IV}}$  atoms.



**Figure 26.2**  $\text{O}_2$  bridges in dinuclear cobalt complexes: (a) peroxy ( $\text{O}_2^{2-}$ ) bridge, and (b) superoxo ( $\text{O}_2^-$ ) bridge.

Table 26.5 Spectra of octahedral low-spin complexes of cobalt(III)

Complex	Colour	$\nu_1/\text{cm}^{-1}$	$\nu_2/\text{cm}^{-1}$	$10Dq/\text{cm}^{-1}$	$B/\text{cm}^{-1}$
$[\text{Co}(\text{H}_2\text{O})_6]^{3+}$	Blue	16 600	24 800	18 200	670
$[\text{Co}(\text{NH}_3)_6]^{3+}$	Golden-brown	21 000	29 500	22 900	620
$[\text{Co}(\text{C}_2\text{O}_4)_3]^{3-}$	Dark green	16 600	23 800	18 000	540
$[\text{Co}(\text{en})_3]^{3+}$	Yellow	21 400	29 500	23 200	590
$[\text{Co}(\text{CN})_6]^{3-}$	Yellow	32 400	39 000	33 500	460

This could account for the paramagnetism, but esr evidence shows that the 2 cobalt atoms are actually equivalent, and X-ray evidence shows the central Co-O-O-Co group to be planar with an O-O distance of 131 pm, which is very close to the 128 pm of the superoxide,  $\text{O}_2^-$ , ion. A more satisfactory formulation therefore is that of 2  $\text{Co}^{\text{III}}$  atoms joined by a superoxide bridge. Molecular orbital theory predicts that the unpaired electron is situated in a  $\pi$  orbital extending over all 4 atoms. If this is the case, then the  $\pi$  orbital is evidently concentrated very largely on the bridging oxygen atoms.

If  $[(\text{NH}_3)_5\text{Co}-\text{O}_2-\text{Co}(\text{NH}_3)_5]^{4+}$  is treated with aqueous KOH another brown complex,  $[(\text{NH}_3)_4\text{Co}(\mu-\text{NH}_2)(\mu-\text{O}_2)\text{Co}(\text{NH}_3)_4]^{3+}$  is obtained and, again, a 1-electron oxidation yields a green superoxo species,  $[(\text{NH}_3)_4\text{Co}(\mu-\text{NH}_2)(\mu-\text{O}_2)\text{Co}(\text{NH}_3)_4]^{4+}$ . The sulfate of this latter is actually one component of Vortmann's sulfate — the other is the red  $[(\text{NH}_3)_4\text{Co}(\mu-\text{NH}_2)(\mu-\text{OH})\text{Co}(\text{NH}_3)_4](\text{SO}_4)_2$ . They are obtained by aerial oxidation of ammoniacal solutions of cobalt(II) nitrate followed by neutralization with  $\text{H}_2\text{SO}_4$ .

Apart from the above green superoxo-bridged complexes and the blue fluoro complexes,  $[\text{CoF}_6]^{3-}$  and  $[\text{CoF}_3(\text{H}_2\text{O})_3]$ , octahedral complexes of cobalt(III) (being low-spin) are diamagnetic. Their magnetic properties are therefore of little interest but, somewhat unusually for low-spin compounds, their electronic spectra have received a good deal of attention<sup>(16)</sup> (see Panel on p. 1128). Data for a representative sample of complexes are given in Table 26.5

Complexes of rhodium(III) are usually derived, directly or indirectly, from  $\text{RhCl}_3 \cdot 3\text{H}_2\text{O}$  and those of iridium(III) from  $(\text{NH}_4)_3[\text{IrCl}_6]$ . All the compounds of  $\text{Rh}^{\text{III}}$  and  $\text{Ir}^{\text{III}}$  are diamagnetic and low-spin, the vast majority of them being octahedral with the  $t_{2g}^6$  configuration. Their electronic spectra can be interpreted in the same way as the spectra of  $\text{Co}^{\text{III}}$  complexes, though the second d-d band, especially in the case of  $\text{Ir}^{\text{III}}$ , is frequently obscured by charge-transfer absorption. The d-d absorptions at the blue end of the visible region are responsible for the yellow to red colours which characterize  $\text{Rh}^{\text{III}}$  complexes.

Similarity with cobalt is also apparent in the affinity of  $\text{Rh}^{\text{III}}$  and  $\text{Ir}^{\text{III}}$  for ammonia and amines. The kinetic inertness of the amines of  $\text{Rh}^{\text{III}}$  has led to the use of several of them in studies of the *trans* effect (p. 1163) in octahedral complexes, while the amines of  $\text{Ir}^{\text{III}}$  are so stable as to withstand boiling in aqueous alkali. Stable complexes such as  $[\text{M}(\text{C}_2\text{O}_4)_3]^{3-}$ ,  $[\text{M}(\text{acac})_3]$  and  $[\text{M}(\text{CN})_6]^{3-}$  are formed by all three metals. Force constants obtained from the infrared spectra of the hexacyano complexes indicate that the M-C bond strength increases in the order  $\text{Co} < \text{Rh} < \text{Ir}$ . Like cobalt, rhodium too forms bridged superoxides such as the blue, paramagnetic,  $[\text{Cl}(\text{py})_4\text{Rh}-\text{O}_2-\text{Rh}(\text{py})_4\text{Cl}]^{5+}$  produced by aerial oxidation of aqueous ethanolic solutions of  $\text{RhCl}_3$  and pyridine.<sup>(17)</sup> In fact it seems likely that many of the species produced by oxidation of aqueous solutions of  $\text{Rh}^{\text{III}}$  and presumed to contain the metal in higher oxidation states, are actually superoxides of  $\text{Rh}^{\text{III}}$ .<sup>(18)</sup>

<sup>17</sup> N. S. A. EDWARDS, I. J. ELLISON, R. D. GILLARD and B. MILE, *Polyhedron* **12**, 371-4 (1993).

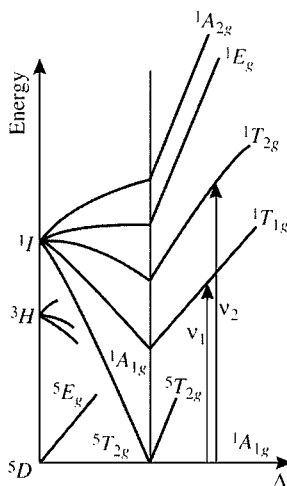
<sup>18</sup> I. J. ELLISON and R. D. GILLARD, *J. Chem. Soc., Chem. Commun.*, 851-3 (1992).

<sup>16</sup> A. B. P. LEVER, *Inorganic Electronic Spectroscopy*, 2nd edn., pp. 473-7, Elsevier, Amsterdam, 1984.

### Electronic Spectra of Octahedral Low-spin Complexes of Co(III)

It is possible to observe spin-allowed, d-d bands in the visible region of the spectra of low-spin cobalt(III) complexes because of the small value of  $10Dq$ , ( $\Delta$ ), which is required to induce spin-pairing in the cobalt(III) ion. This means that the low-spin configuration occurs in complexes with ligands which do not cause the low-energy charge transfer bands which so often dominate the spectra of low-spin complexes.

In practice two bands are generally observed and are assigned to the transitions:  $\nu_1 = {}^1T_{1g} \leftarrow {}^1A_{1g}$  and  $\nu_2 = {}^1T_{2g} \leftarrow {}^1A_{1g}$  (see Fig. A)



**Figure A** Simplified Energy Level diagram for  $d^6$  ions showing possible spin-allowed transitions in complexes of low-spin cobalt(III).

These transitions correspond to the electronic promotion  $t_{2g}^6 e_g^0 \rightarrow t_{2g}^5 e_g^1$  with the promoted electron maintaining its spin unaltered. The orbital multiplicity of the  $t_{2g}^5 e_g^1$  configuration is 6 and so corresponds to two orbital triplet terms  ${}^1T_{1g}$  and  ${}^1T_{2g}$ . If, on the other hand, the promoted electron changes its spin, the orbital multiplicity is again 6 but the two  $T$  terms are now spin triplets,  ${}^3T_{1g}$  and  ${}^3T_{2g}$ . A weak band attributable to the spin-forbidden  ${}^3T_{1g} \leftarrow {}^1A_{1g}$  transition is indeed observed in some cases in the region of  $11\,000$ – $14\,000\text{ cm}^{-1}$ .

Data for some typical complexes are given in Table 26.5. The assignments are made, producing values of the inter-electronic repulsion parameter  $B$  as well as of the crystal-field splitting,  $10Dq$ .

The colours of *cis* and *trans* isomers of complexes  $[\text{CoL}_4\text{X}_2]$  or  $[\text{Co}(\text{L-L})_2\text{X}_2]$  frequently differ and, although simple observation of colour will not alone suffice to establish a *cis* or *trans* geometry, an examination of the electronic spectra does have diagnostic value. Calculations of the effect of low-symmetry components in the crystal field show that the *trans* isomer will split the excited terms appreciably more than the *cis*, and the effect is most marked for  ${}^1T_{1g}$ , the lowest of the excited terms. In practice, if L-L and X are sufficiently far apart in the spectrochemical series (e.g. L-L = en and X = F which has been thoroughly examined), the  $\nu_1$  band splits completely, giving rise to three separate bands for the *trans* complex whereas the *cis* merely shows slight asymmetry in the lower energy band. Furthermore, because (like tetrahedral complexes) a *cis* isomer lacks a centre of symmetry, its spectrum is more intense than that of the centrosymmetric *trans* isomer.

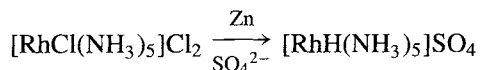
It is relevant to note at this point that, because the metal ions are isoelectronic, the spectra of low-spin  $\text{Fe}^{\text{II}}$  complexes might be expected to be similar to those of low-spin  $\text{Co}^{\text{III}}$ . However,  $\text{Fe}^{\text{II}}$  requires a much stronger crystal field to effect spin-pairing and the ligands which provide such a field also give rise to low-energy charge-transfer bands which almost always obscure the d-d bands. Nevertheless, the spectrum of the pale-yellow  $[\text{Fe}(\text{CN})_6]^{4-}$  shows a shoulder at  $31\,000\text{ cm}^{-1}$  on the side of a charge transfer absorption and this is attributed to the  ${}^1T_{1g} \leftarrow {}^1A_{1g}$  transition.

Despite the above similarities, many differences between the members of this triad are also to be noted. Reduction of a trivalent compound, which yields a divalent compound in the case of cobalt, rarely does so for the heavier elements where the metal, univalent compounds, or  $M^{II}$  hydrido complexes are the more usual products. Rhodium forms the quite stable, yellow  $[\text{Rh}(\text{H}_2\text{O})_6]^{3+}$  ion when hydrous  $\text{Rh}_2\text{O}_3$  is dissolved in mineral acid, and it occurs in the solid state in salts such as the perchlorate, sulfate and alums.  $[\text{Ir}(\text{H}_2\text{O})_6]^{3+}$  is less readily obtained but has been shown to occur in solutions of  $\text{Ir}^{III}$  in conc  $\text{HClO}_4$ .

There is also clear evidence of a change from predominantly class-a to class-b metal characteristics (p. 909) in passing down this group. Whereas cobalt(III) forms few complexes with the heavier donor atoms of Groups 15 and 16, rhodium(III), and more especially iridium(III), coordinate readily with *P*-, *As*- and *S*-donor ligands. Compounds with *Se*- and even *Te*- are also known.<sup>(19)</sup> Thus infrared, X-ray and  $^{14}\text{N}$  nmr studies show that, in complexes such as  $[\text{Co}(\text{NH}_3)_4(\text{NCS})_2]^+$ , the  $\text{NCS}^-$  acts as an *N*-donor ligand, whereas in  $[\text{M}(\text{SCN})_6]^{3-}$  ( $\text{M} = \text{Rh}, \text{Ir}$ ) it is an *S*-donor. Likewise in the hexahalogeno complex anions,  $[\text{MX}_6]^{3-}$ , cobalt forms only that with fluoride, whereas rhodium forms them with all the halides except iodide, and iridium forms them with all except fluoride.

Besides the thiocyanates, just mentioned, other *S*-donor complexes which are of interest are the dialkyl sulfides,  $[\text{MCl}_3(\text{SR}_2)_3]$ , produced by the action of  $\text{SR}_2$  on ethanolic  $\text{RhCl}_3$  or on  $[\text{IrCl}_6]^{3-}$ . Phosphorus and arsenic compounds are obtained in similar fashion, and the best known are the yellow to orange complexes,  $[\text{ML}_3\text{X}_3]$ , ( $\text{M} = \text{Rh}, \text{Ir}$ ;  $\text{X} = \text{Cl}, \text{Br}, \text{I}$ ;  $\text{L} =$  trialkyl or triaryl phosphine or arsine). These compounds may exist as either *mer* or *fac* isomers, and these are normally distinguished by their proton nmr spectra (a distinction previously made by the measurement of dipole moments). An especially

interesting feature of their chemistry is the ease with which they afford hydride and carbonyl derivatives. For instance, the colourless, air-stable  $[\text{RhH}(\text{NH}_3)_5]\text{SO}_4$  is produced by the action of Zn powder on ammoniacal  $\text{RhCl}_3$  in the presence of  $(\text{NH}_4)_2\text{SO}_4$ :



Ternary hydrides of Rh and Ir containing the octahedral  $[\text{MH}_6]^{3-}$  anions have been prepared<sup>(20)</sup> by the reaction of  $\text{LiH}$  and the metal under a high pressure of  $\text{H}_2$ . It is however unusual for hydrides of metals in such a high formal oxidation state as +3 to be stable in the absence of  $\pi$ -acceptor ligands and, indeed, in the presence of  $\pi$ -acceptor ligands such as tertiary phosphines and arsines, the stability of rhodium(III) hydrides is enhanced. Thus  $\text{H}_3\text{PO}_2$  reduces  $[\text{RhCl}_3\text{L}_3]$  to either  $[\text{RhHCl}_2\text{L}_3]$  or  $[\text{RhH}_2\text{CIL}_3]$ , depending on L; and the action of  $\text{H}_2$  on  $[\text{Rh}^I(\text{PPh}_3)_3\text{X}]$  ( $\text{X} = \text{Cl}, \text{Br}, \text{I}$ ) yields  $[\text{RhH}_2(\text{PPh}_3)_3\text{X}]$  which is, formally at least, an oxidation by molecular hydrogen. However, it is iridium(III) that forms more hydrido-phosphine and hydrido-arsine complexes than any other platinum metal. Using  $\text{NaBH}_4$ ,  $\text{LiAlH}_4$ ,  $\text{EtOH}$  or even  $\text{SnCl}_2 + \text{H}^+$  to provide the hydride ligand, complexes of the type  $[\text{MH}_n\text{L}_3\text{X}_{3-n}]$  can be formed for very many of the permutations which are possible from  $\text{L} =$  trialkyl or triaryl phosphine or arsine;  $\text{X} = \text{Cl}, \text{Br}$  or  $\text{I}$ . Many polynuclear hydride complexes are also known.<sup>(21)</sup>

### Oxidation state II ( $d^7$ )

There is a very marked contrast in this oxidation state between cobalt on the one hand, and the two heavier members of the group on the other. For cobalt it is one of the two most stable oxidation states, whereas for the others it is of only minor importance.

<sup>20</sup> W. BRONGER, M. GEHLEN and G. AUFFERMANN, *Z. anorg. allg. Chem.* **620**, 1983–5 (1994).

<sup>21</sup> T. M. G. CARNEIRO, D. MATT and P. BRAUNSTEIN, *Coord. Chem. Revs.* **96**, 49–88 (1989).

<sup>19</sup> A. Z. AL-RUBAIE, Y. N. AL-OBAIDI and L. Z. YOUSIF, *Polyhedron* **9**, 1141–6 (1990).

Many early reports of  $\text{Rh}^{\text{II}}$  and  $\text{Ir}^{\text{II}}$  complexes have not been verified and in some cases may have involved  $\text{M}^{\text{III}}$  hydrides. Monomeric compounds require stabilization by ligands such as phosphines or  $\text{C}_6\text{Cl}_5^-$ . Thus, the action of  $\text{LiC}_6\text{Cl}_5$  on  $[\text{L}_2\text{M}-\text{Cl}-\text{ML}_2]$ , where  $\text{L}_2 = 2[\text{P}(\text{OPh})_3]$ , cyclooctene or cycloocta-1,5-diene, affords *trans* square planar products of the type  $[\text{M}^{\text{I}}(\eta^1-\text{C}_6\text{Cl}_5)_2(\text{L}_2)]^-$ , oxidation of which yield monomeric paramagnetic compounds such as  $[\text{M}^{\text{II}}(\eta^1-\text{C}_6\text{Cl}_5)_2(\text{L}_2)]$  and, in the case of iridium, square planar  $[\text{Ir}^{\text{II}}(\eta^1-\text{C}_6\text{Cl}_5)_4]^{2-}$  isolated as its  $(\text{NBu}_4)^+$  salt.<sup>(22)</sup> Rhodium(II) is somewhat more common than iridium(II). Paramagnetic, *trans* square planar phosphines  $[\text{RhCl}_2\text{L}_2]$  and the alkyl  $(\text{RhR}_2(\text{tht})_2)$ , ( $\text{R} = 2,4,6\text{-Pr}_3\text{C}_6\text{H}_2$ ;  $\text{tht} = \text{tetrahydrothiophene}$ ) have been characterized.<sup>(23)</sup> Also, depending on temperature and relative concentrations, the reaction of  $\text{Rh}(\text{NO})\text{Cl}_2(\text{PPh}_3)_2$  and  $\text{Na}(\text{S}_2\text{CNR}_2)$  in benzene yields either  $\text{Rh}(\text{S}_2\text{CNR}_2)_2$  or  $\text{Rh}(\text{S}_2\text{CNR}_2)(\text{PPh}_3)$ , characterized by spectroscopic methods as square planar and square pyramidal respectively.<sup>(24)</sup>

Rhodium(II), however, is most familiar in a series of green dimeric diamagnetic compounds.<sup>(25)</sup> If hydrous  $\text{Rh}_2\text{O}_3$ , or better still  $\text{RhCl}_3 \cdot 3\text{H}_2\text{O}$  and sodium carboxylate, is refluxed with the appropriate acid and alcohol, green or blue solvated  $[\text{Rh}(\text{O}_2\text{CR})_2]_2$  is formed. Compounds of this type are generally air-stable and have the same bridged structure as the carboxylates of  $\text{Cr}^{\text{II}}$ ,  $\text{Mo}^{\text{II}}$  and  $\text{Cu}^{\text{II}}$ ; in the case of the acetate this involves a Rh–Rh distance of 239 pm which is consistent with a Rh–Rh bond. If rhodium acetate is treated with a strong acid such as  $\text{HBF}_4$ , whose anion has little tendency to coordinate, green solutions apparently containing the diamagnetic  $\text{Rh}_2^{4+}$  ion are obtained but

no solid salt of this has been isolated. Why no comparable  $\text{Ir}^{\text{II}}$  carboxylates, and very few other dimeric species stabilized by metal–metal bonding, have yet been prepared is not clear.

By contrast,  $\text{Co}^{\text{II}}$  carboxylates such as the red acetate,  $\text{Co}(\text{O}_2\text{CMe})_2 \cdot 4\text{H}_2\text{O}$ , are monomeric and in some cases the carboxylate ligands are unidentate. The acetate is employed in the production of catalysts used in certain organic oxidations, and also as a drying agent in oil-based paints and varnishes. Cobalt(II) gives rise to simple salts with all the common anions and they are readily obtained as hydrates from aqueous solutions. The parent hydroxide,  $\text{Co}(\text{OH})_2$ , can be precipitated from the aqueous solutions by the addition of alkali and is somewhat amphoteric, not only dissolving in acid but also redissolving in excess of conc alkali, in which case it gives a deep-blue solution containing  $[\text{Co}(\text{OH})_4]^{2-}$  ions. It is obtainable in both blue and pink varieties: the former is precipitated by slow addition of alkali at  $0^\circ\text{C}$ , but it is unstable and, in the absence of air, becomes pink on warming (cf. p. 1131).

Complexes of cobalt(II) are less numerous than those of cobalt(III) but, lacking any configuration comparable in stability with the  $t_{2g}^6$  of  $\text{Co}^{\text{III}}$ , they show a greater diversity of types and are more labile. The redox properties have already been referred to and the possibility of oxidation must always be considered when preparing  $\text{Co}^{\text{II}}$  complexes. However, providing solutions are not alkaline and the ligands not too high in the spectrochemical series, a large number of complexes can be isolated without special precautions. The most common type is high-spin octahedral, though spin-pairing can be achieved by ligands such as  $\text{CN}^-$  (p. 1133) which also favour the higher oxidation state. Appropriate choice of ligands can however lead to high-spin-low-spin equilibria as in  $[\text{Co}(\text{terpy})_2]\text{X}_2 \cdot n\text{H}_2\text{O}$  and some 5- and 6-coordinated complexes of Schiff bases and pyridines.<sup>(26)</sup>

Many of the hydrated salts and their aqueous solutions contain the octahedral, pink

<sup>22</sup> M. P. GARCIA, M. V. JIMENEZ, L. A. ORO and F. J. LAHOZ, *Organometallics* **12**, 4660–3 (1993).

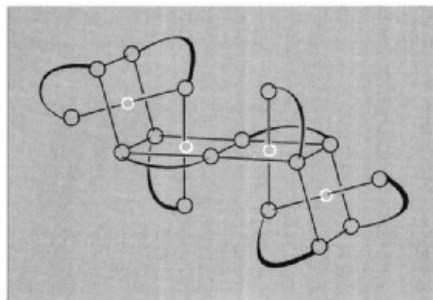
<sup>23</sup> R. S. HAY-MOTHERWELL, S. U. KOSCHMIEDER, G. WILKINSON, B. HUSSAIN-BATES and M. B. HURSTHOUSE, *J. Chem. Soc., Dalton Trans.*, 2821–30 (1991).

<sup>24</sup> K. K. PANDEY, D. T. NEHETE and R. B. SHARMA, *Polyhedron* **9**, 2013–18 (1990).

<sup>25</sup> F. A. COTTON and R. A. WALTON, *Multiple Bonds Between Metal Atoms*, Clarendon Press, Oxford, 1993, 787 pp.

<sup>26</sup> P. THUERY and J. ZARAMBOWITZ, *Inorg. Chem.* **25**, 2001–8 (1986).





**Figure 26.3** The tetrameric structure of  $[\text{Co}(\text{acac})_2]_4$ .

$[\text{Co}(\text{H}_2\text{O})_6]^{2+}$  ion, and bidentate *N*-donor ligands such as en, bipy and phen form octahedral cationic complexes  $[\text{Co}(\text{L-L})_3]^{3+}$ , which are much more stable to oxidation than is the hexaammine  $[\text{Co}(\text{NH}_3)_6]^{2+}$ . Acac yields the orange  $[\text{Co}(\text{acac})_2(\text{H}_2\text{O})_2]$  which has the *trans* octahedral structure and can be dehydrated to  $[\text{Co}(\text{acac})_2]$  which attains octahedral coordination by forming the tetrameric species shown in Fig. 26.3. This is comparable with the trimeric  $[\text{Ni}(\text{acac})_2]_3$  (p. 1157), like which it shows evidence of weak ferromagnetic interactions at very low temperatures.  $[\text{Co}(\text{edta})(\text{H}_2\text{O})]^{2+}$  is ostensibly analogous to the 7-coordinate  $\text{Mn}^{\text{II}}$  and  $\text{Fe}^{\text{II}}$  complexes with the same stoichiometry, but in fact the cobalt is only 6-coordinate, 1 of the oxygen atoms of the edta being too far away from the cobalt (272 compared to 223 pm for the other edta donor atoms) to be considered as coordinated.

Tetrahedral complexes are also common, being formed more readily with cobalt(II) than with the cation of any other truly transitional element (i.e. excluding  $\text{Zn}^{\text{II}}$ ). This is consistent with the CFSEs of the two stereochemistries (Table 26.6). Quantitative comparisons between the values given for CFSE(oct) and CFSE(tet) are not possible because of course the crystal field splittings,  $\Delta_o$  and  $\Delta_t$  differ. Nor is the CFSE by any means the most important factor in determining the stability of a complex. Nevertheless, where other factors are comparable, it can have a decisive effect and it is apparent that no configuration is more favourable than  $d^7$  to the adoption of a tetrahedral as opposed to

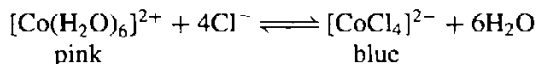
**Table 26.6** CFSE values<sup>†</sup> for high-spin complexes of  $d^0$  to  $d^{10}$  ions

No. of d electrons	0	1	2	3	4	5	6	7	8	9	10
CFSE(oct)/( $\Delta_o$ )	0	$\frac{2}{5}$	$\frac{4}{5}$	$\frac{6}{5}$	$\frac{3}{5}$	0	$\frac{2}{5}$	$\frac{4}{5}$	$\frac{6}{5}$	$\frac{3}{5}$	0
CFSE(tet)/( $\Delta_t$ )	0	$\frac{3}{5}$	$\frac{6}{5}$	$\frac{4}{5}$	$\frac{2}{5}$	0	$\frac{3}{5}$	$\frac{6}{5}$	$\frac{4}{5}$	$\frac{2}{5}$	0

<sup>†</sup>The Crystal Field Stabilization Energy (CFSE) is the additional stability which accrues to an ion in a complex, as compared to the free ion, because its d-orbitals are split. In an octahedral complex a  $t_{2g}$  electron increases the stability by  $2/5\Delta_o$  and an  $e_g$  electron decreases it by  $3/5\Delta_o$ . In a tetrahedral complex the orbital splitting is reversed and an *e* electron therefore increases the stability by  $3/5\Delta_t$ , whereas a  $t_2$  electron decreases it by  $2/5\Delta_t$ .

an octahedral stereochemistry. Thus, in aqueous solutions containing  $[\text{Co}(\text{H}_2\text{O})_6]^{2+}$  there are also present in equilibrium, small amounts of tetrahedral  $[\text{Co}(\text{H}_2\text{O})_4]^{2+}$ , and in acetic acid the tetrahedral  $[\text{Co}(\text{O}_2\text{CMe})_4]^{2-}$  occurs. The anionic complexes  $[\text{CoX}_4]^{2-}$  are formed with the unidentate ligands,  $\text{X} = \text{Cl}, \text{Br}, \text{I}, \text{SCN}$  and  $\text{OH}$ , and a whole series of complexes,  $[\text{CoL}_2\text{X}_2]$  ( $\text{L} =$  ligand with group 15 donor atom;  $\text{X} =$  halide, NCS), has been prepared in which both stereochemistries are found.  $[\text{CoCl}_2\text{py}_2]$  exists in two isomeric forms: a blue metastable variety which is monomeric and tetrahedral, and a violet, stable form which is polymeric and achieves octahedral coordination by means of chloride bridges. Ligand polarizability is an important factor determining which stereochemistry is adopted, the more polarizable ligands favouring the tetrahedral form since fewer of them are required to neutralize the metal's cationic charge. Thus, if  $\text{L} = \text{py}$ , replacement of  $\text{Cl}^-$  by  $\text{I}^-$  makes the stable form tetrahedral and if  $\text{L} =$  phosphine or arsine the tetrahedral form is favoured irrespective of  $\text{X}$ .

The most obvious distinction between the octahedral and tetrahedral compounds is that *in general* the former are pink to violet in colour whereas the latter are blue, as exemplified by the well-known equilibrium:



This is not an infallible distinction (as the blue but octahedral  $\text{CoCl}_2$  demonstrates) but is a useful

## Electronic Spectra and Magnetic Properties of High-spin Octahedral and Tetrahedral Complexes of Cobalt(II)

Cobalt(II) is the only common  $d^7$  ion and because of its stereochemical diversity its spectra have been widely studied. In a cubic field, three spin-allowed transitions are anticipated because of the splitting of the free-ion, ground  $^4F$  term, and the accompanying  $^4P$  term. In the octahedral case the splitting is the same as for the octahedral  $d^2$  ion and the spectra can therefore be interpreted in a semi-quantitative manner using the same energy level diagram as was used for  $V^{3+}$  (Fig. 22.9, p. 997). In the present case the spectra usually consist of a band in the near infrared, which may be assigned as  $\nu_1 = ^4T_{2g}(F) \leftarrow ^4T_{1g}(F)$ , and another in the visible, often with a shoulder on the low energy side. Since the transition  $^4A_{2g}(F) \leftarrow ^5T_{1g}(F)$  is essentially a 2-electron transition from  $t_{2g}^5 e_g^2$  to  $t_{2g}^3 e_g^4$  it is expected to be weak, and the usual assignment is

$$\begin{aligned}\nu_2(\text{shoulder}) &= ^4A_{2g}(F) \leftarrow ^4T_{1g}(F) \\ \nu_3 &= ^4T_{1g}(P) \leftarrow ^4T_{1g}(F)\end{aligned}$$

Indeed, in some cases it is probable that  $\nu_2$  is not observed at all, but that the fine structure arises from term splitting due to spin-orbit coupling or to distortions from regular octahedral symmetry.

In tetrahedral fields the splitting of the free ion ground term is the reverse of that in octahedral fields so that, for  $d^7$  ions in tetrahedral fields  $^2A_{2g}(F)$  lies lowest but three spin-allowed bands are still anticipated. In fact, the observed spectra usually consist of a broad, intense band in the visible region (responsible for the colour and often about 10 times as intense as in octahedral compounds) with a weaker one in the infrared. The only satisfactory interpretation is to assign these, respectively, as,  $\nu_3 = ^4T_1(P) \leftarrow ^4A_2(F)$  and  $\nu_2 = ^4T_1(F) \leftarrow ^4A_2(F)$  in which case  $\nu_1 = ^4T_2(F) \leftarrow ^4A_2(F)$  should be in the region  $3000\text{--}5000\text{ cm}^{-1}$ . Examination of this part of the infrared has sometimes indicated the presence of a band, though overlying vibrational bands make interpretation difficult.

Table 26.7 gives data for a number of octahedral and tetrahedral complexes, the values of  $10Dq$  and  $B$  having been derived by analysis of the spectra.<sup>(27)</sup> It is clear from these data that the "anomalous" blue colour of octahedral  $\text{CoCl}_2$  arises because 6  $\text{Cl}^-$  ions generate such a weak crystal field that the main band in its spectrum is at an unusually low energy, extending into the red region (hence giving a blue colour) rather than the green-blue region (which would give a red colour) more commonly observed for octahedral  $\text{Co}^{II}$  compounds.

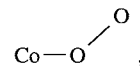
Magnetic properties provide a complementary means of distinguishing stereochemistry. The  $T$  ground term of the octahedral ion is expected to give rise to a temperature-dependent orbital contribution to the magnetic moment whereas the  $A$  ground term of the tetrahedral ion is not. As a matter of fact, in a tetrahedral field the excited  $^4T_2(F)$  term is "mixed into" the ground  $^4A_2$  term because of spin-orbit coupling and tetrahedral complexes of  $\text{Co}^{II}$  are expected to have magnetic moments given by  $\mu_e = \mu_{\text{spin-only}}(1 - 4\lambda/10Dq)$ , where  $\lambda = -170\text{ cm}^{-1}$  and  $\mu_{\text{spin-only}} = 3.87\text{ BM}$ .

Thus the magnetic moments of tetrahedral complexes lie in the range 4.4–4.8 BM, whereas those of octahedral complexes are around 4.8–5.2 BM at room temperature, falling off appreciably as the temperature is reduced.

empirical guide whose reliability is improved by a more careful analysis of the electronic spectra<sup>(27)</sup> (see Panel). Data for some octahedral and tetrahedral complexes are given in Table 26.7.

Square planar complexes are also well authenticated if not particularly numerous and include  $[\text{Co}(\text{phthalocyanine})]$  and  $[\text{Co}(\text{CN})_4]^-$  as well as  $[\text{Co}(\text{salen})]$  and complexes with other Schiff bases. These are invariably low-spin with magnetic moments at room temperature in the range 2.1–2.9 BM, indicating 1 unpaired electron. They are primarily of interest because

of their oxygen-carrying properties, discussed already in Chapter 14 where numerous reviews on the subject are cited. The uptake of dioxygen, which bonds in the bent configuration,



is accompanied by the attachment of a solvent molecule *trans* to the  $\text{O}_2$  and the retention of the single unpaired electron. There is fairly general agreement, based on esr evidence, that electron transfer from metal to  $\text{O}_2$  occurs just as in the bridged complexes referred to on

<sup>27</sup> pp. 480-504 of ref. 16.

Table 26.7 Electronic spectra of complexes of cobalt(II)

(a) Octahedral

Complex	$\nu_1/\text{cm}^{-1}$	$\nu_2/\text{cm}^{-1}$ (weak)	$\nu_3/\text{cm}^{-1}$ (main)	$10Dq/\text{cm}^{-1}$	$B/\text{cm}^{-1}$
[Co(bipy) <sub>3</sub> ] <sup>2+</sup>	11 300		22 000	12 670	791
[Co(NH <sub>3</sub> ) <sub>6</sub> ] <sup>2+</sup>	9000		21 100	10 200	885
[Co(H <sub>2</sub> O) <sub>6</sub> ] <sup>2+</sup>	8100	16 000	19 400	9200	825
CoCl <sub>2</sub>	6600	13 300	17 250	6900	780

(b) Tetrahedral

Complex	$\nu_2/\text{cm}^{-1}$	$\nu_3/\text{cm}^{-1}$ (main)	$10Dq/\text{cm}^{-1}$	$B/\text{cm}^{-1}$
[Co(NCS) <sub>4</sub> ] <sup>2-</sup>	7780	16 250	4550	691
[Co(N <sub>3</sub> ) <sub>4</sub> ] <sup>2-</sup>	6750	14 900	3920	658
[CoCl <sub>4</sub> ] <sup>2-</sup>	5460	14 700	3120	710
[CoI <sub>4</sub> ] <sup>2-</sup>	4600	13 250	2650	665

p. 1126, producing a situation close to the extreme represented by low-spin Co<sup>III</sup> attached to a superoxide ion, O<sub>2</sub><sup>-</sup>. (The opposite extreme, represented by Co<sup>II</sup>-O<sub>2</sub>, implies that the unpaired electron resides on the metal with the dioxygen being rendered diamagnetic by the loss of the degeneracy of its  $\pi^*$  orbitals with consequent spin pairing.) However, the precise extent of the electron transfer is probably determined by the nature of the ligand *trans* to the O<sub>2</sub>.

The difficulty of assigning a formal oxidation state is more acutely seen in the case of 5-coordinate NO adducts of the type [Co(NO)(salen)]. These are effectively diamagnetic and so have no unpaired electrons. They may therefore be formulated either as Co<sup>III</sup>-NO<sup>-</sup> or Co<sup>I</sup>-NO<sup>+</sup>. The infrared absorptions ascribed to the N-O stretch lie in the range 1624-1724 cm<sup>-1</sup>, which is at the lower end of the range said to be characteristic of NO<sup>+</sup>. But, as in all such cases which are really concerned with the differing polarities of covalent bonds, such formalism should not be taken literally.

Other 5-coordinate Co<sup>II</sup> compounds which have been characterized include [CoBr{N(C<sub>2</sub>H<sub>4</sub>NMe<sub>2</sub>)<sub>3</sub>}]<sup>+</sup>, which is high-spin with 3 unpaired electrons and is trigonal bipyramidal (imposed by the "tripod" ligand), and

[Co(CN)<sub>5</sub>]<sup>3-</sup>, which is low-spin with 1 unpaired electron and is square pyramidal. The latter complex is isolated from solutions of Co(CN)<sub>2</sub> and KCN as the yellow [NEt<sub>2</sub>Pr<sub>2</sub>]<sup>+</sup> salt, an extremely oxygen-sensitive and hygroscopic material. A further difficulty which hindered its isolation is its tendency to dimerize to the more familiar deep-violet, [(CN)<sub>5</sub>Co-Co(CN)<sub>5</sub>]<sup>6-</sup>. The absence of a simple hexacyano complex is significant as it seems to be generally the case that ligands such as CN<sup>-</sup>, which are expected to induce spin-pairing, favour a coordination number for Co<sup>II</sup> of 4 or 5 rather than 6; the planar [Co(diars)<sub>2</sub>](ClO<sub>4</sub>) is a further illustration of this. Presumably the Jahn-Teller distortion, which is anticipated for the low-spin  $t_{2g}^6 e_g^1$  configuration is largely responsible.

### Oxidation state I (d<sup>8</sup>)

Oxidation states lower than +2 normally require the stabilizing effect of  $\pi$ -acceptor ligands and some of these are appropriately considered along with organometallic compounds in Section 26.3.5. Exceptions are the square pyramidal anion of the black, Mg<sub>2</sub>[CoH<sub>5</sub>] (obtained by prolonged heating of the powdered metals under high

pressure of H<sub>2</sub>) and the linear anion of the garnet red CsK<sub>2</sub>[CoO<sub>2</sub>]<sup>(27a)</sup> (see p. 1166). However, although +1 is not a common oxidation state for cobalt, it is one of the two most common states for both rhodium and iridium and as such merits separate consideration.

Simple ligand-field arguments, which will be elaborated when M<sup>II</sup> ions of the Ni, Pd, Pt triad are discussed on p. 1157, indicate that the d<sup>8</sup> configuration favours a 4-coordinate, square-planar stereochemistry. In the present group, however, the configuration is associated with a lower oxidation state and the requirements of the 18-electron rule,<sup>†</sup> which favour 5-coordination, are also to be considered. The upshot is that most Co<sup>I</sup> complexes are 5-coordinate, like [Co(CNR)<sub>5</sub>]<sup>+</sup>, and square-planar Co<sup>I</sup> is apparently unknown. On the other hand, complexes of Rh<sup>I</sup> and Ir<sup>I</sup> are predominantly square planar, although 5-coordination does also occur.

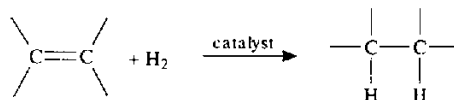
These complexes are usually prepared by the reduction of compounds such as RhCl<sub>3</sub>·3H<sub>2</sub>O and K<sub>2</sub>IrCl<sub>6</sub> in the presence of the desired ligand. It is often unnecessary to use a specific reductant, the ligand itself or alcoholic solvent being adequate, and not infrequently leading to the presence of CO or H in the product. A considerable proportion of the complexes of Rh<sup>I</sup> and Ir<sup>I</sup> are phosphines and of these, two in particular demand attention. They are Wilkinson's catalyst, [RhCl(PPh<sub>3</sub>)<sub>3</sub>], and Vaska's compound, *trans*-[IrCl(CO)(PPh<sub>3</sub>)<sub>2</sub>], both essentially square planar.

*Wilkinson's catalyst*, [RhCl(PPh<sub>3</sub>)<sub>3</sub>]. This red-violet compound<sup>(28)</sup>, which is readily obtained by refluxing ethanolic RhCl<sub>3</sub>·3H<sub>2</sub>O with an

<sup>†</sup> The filling-up of the bonding MOs of the molecule may be regarded, more simply, as the filling of the outer 9 orbitals of the metal ion with its own d electrons plus a pair of σ electrons from each ligand. A 4-coordinate d<sup>8</sup> ion is thus a "16-electron" species and is "coordinatively unsaturated". Saturation in this sense requires the addition of 10 electrons, i.e. 5 ligands, to the metal ion. By contrast rhodium(III) is a d<sup>6</sup> ion and so can expand its coordination sphere to accommodate 6 ligands with important consequences in catalysis which will be seen below.

<sup>27a</sup> F. BERNHARD and R. HOPPE. *Z. anorg. allg. Chem.* **620**, 187-91 (1994).

excess of PPh<sub>3</sub>, was discovered<sup>(29)</sup> in 1965. It undergoes a variety of reactions, most of which involve either replacement of a phosphine ligand (e.g. with CO, CS, C<sub>2</sub>H<sub>4</sub>, O<sub>2</sub> giving *trans* products) or oxidative addition (e.g. with H<sub>2</sub>, MeI) to form Rh<sup>III</sup>, but its importance arises from its effectiveness as a catalyst<sup>(30)</sup> for highly selective hydrogenations of complicated organic molecules which are of great importance in the pharmaceutical industry. Its use allowed, for the first time, rapid *homogeneous* hydrogenation at ambient temperatures and pressures:



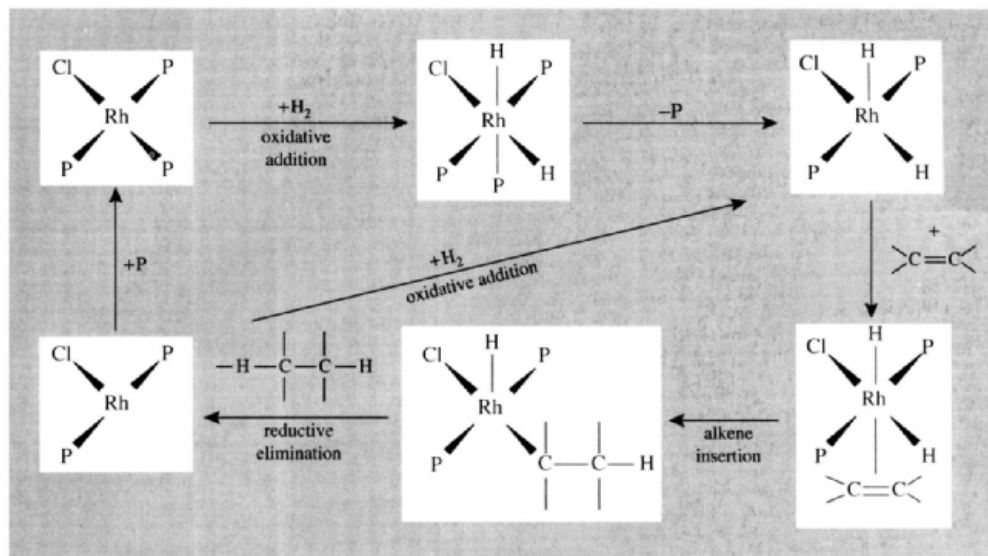
The precise mechanism is complicated and has been the subject of much speculation and controversy, but Fig. 26.4 shows a simplified but reasonable scheme. The essential steps in this are the oxidative addition of H<sub>2</sub> (if the hydrogen atoms are regarded as "hydridic", i.e. as H<sup>-</sup>, the metal's oxidation state increases from +1 to +3); the formation of an alkene complex; alkene insertion and, finally, the reductive elimination of the alkane (i.e. the metal's oxidation state reverting to +1). The rhodium catalyst is able to fulfil its role because the metal is capable of changing its coordination number (loss of phosphine from the dihydro complex being encouraged by the large size of the ligand) and it possesses oxidation states (+1 and +3) which differ by 2 and are of comparable stability.

The discovery of the catalytic properties of [RhCl(PPh<sub>3</sub>)<sub>3</sub>] naturally brought about a widespread search for other rhodium phosphines with catalytic activity. One of those which was found, also in Wilkinson's laboratory, was *trans*-[Rh(CO)H(PPh<sub>3</sub>)<sub>3</sub>] which can conveniently be

<sup>28</sup> The paramagnetic impurity which invariably accompanies Wilkinson's catalyst has proved difficult to identify. It is probably the air-stable, green, *trans*-[RhCl(CO)(PPh<sub>3</sub>)<sub>2</sub>]. see K. R. DUNBAR and S. C. HAEFFNER, *Inorg. Chem.* **31**, 3676-9 (1992).

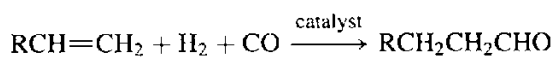
<sup>29</sup> J. F. YOUNG, J. A. OSBORN, F. H. JARDINE, and G. WILKINSON, *J. Chem. Soc., Chem. Commun.*, 131 2 (1965).

<sup>30</sup> R. S. DICKSON, *Homogeneous Catalysis with Compounds of Rhodium and Iridium*, D. Reidel, Dordrecht, 1985, 278 pp.



**Figure 26.4** The catalytic cycle for the hydrogenation of an alkene, catalysed by  $[\text{RhCl}(\text{PPh}_3)_3]$  in benzene; possible coordination of solvent molecules has been ignored and the ligand  $\text{PPh}_3$  has been represented as P throughout, for clarity.

dealt with here. It was found that, for steric reasons, it selectively catalyses the hydrogenation of alk-1-enes (i.e. terminal olefins) rather than alk-2-enes and it has been used in the *hydroformylation* of alkenes, (i.e. the addition of H and the formyl group, CHO) also known as the OXO process because it introduces oxygen into the hydrocarbon. This is a process of enormous industrial importance, being used to convert alk-1-enes into aldehydes which can then be converted to alcohols for the production of polyvinylchloride (PVC) and polyalkenes and, in the case of the long-chain alcohols, in the production of detergents:

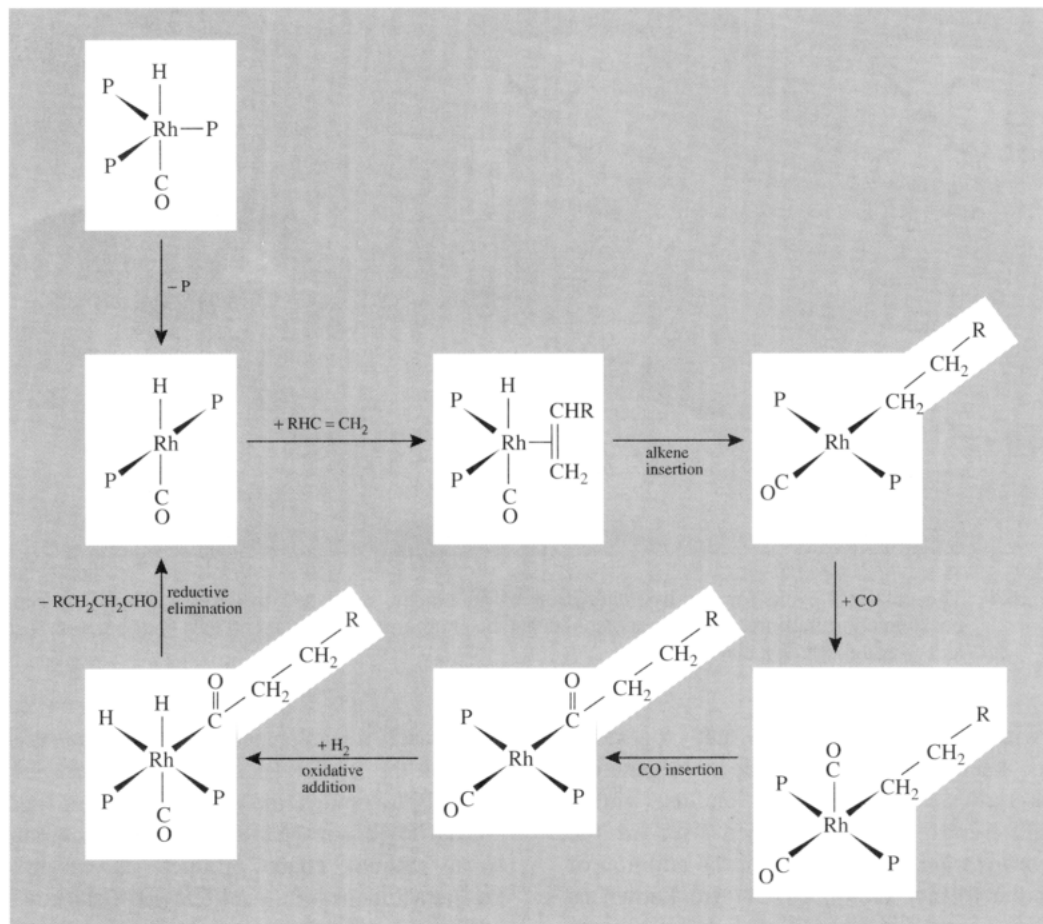


A simplified reaction scheme is shown in Fig. 26.5 Again, the ability of rhodium to change its coordination number and oxidation state is crucial, and this catalyst has the great advantage over the conventional cobalt carbonyl catalyst that it operates efficiently at much lower temperatures and pressures and produces straight-chain as opposed to branched-chain products.

The reason for its selectivity lies in the insertion step of the cycle. In the presence of the two bulky  $\text{PPh}_3$  groups, the attachment to the metal of  $-\text{CH}_2\text{CH}_2\text{R}$  (anti-Markovnikov addition, leading to a straight chain product) is easier than the attachment of  $-\text{CH}(\text{CH}_3)\text{R}$  (Markovnikov addition, leading to a branched-chain product).

*Vaska's compound*,  $\text{trans}[\text{IrCl}(\text{CO})(\text{PPh}_3)_2]$ . This yellow compound can be prepared by the reaction of triphenylphosphine and  $\text{IrCl}_3$  in a solvent such as 2-methoxyethanol which acts both as reducing agent and supplier of CO. It was discovered in 1961 by L. Vaska and J. W. di Luzio<sup>(31)</sup> and recognized as an ideal material for the study of oxidative addition reactions, since its products are generally stable and readily characterized. It is certainly the most thoroughly investigated compound of Ir<sup>I</sup>. It forms octahedral Ir<sup>III</sup> complexes in oxidative addition reactions with  $\text{H}_2$ ,  $\text{Cl}_2$ ,  $\text{HX}$ ,  $\text{MeI}$  and  $\text{RCO}_2\text{H}$ , and  $^1\text{H}$  nmr shows that in all cases the phosphine ligands are *trans* to each other. The 4 remaining ligands (Cl,

<sup>31</sup> L. VASKA and J. W. DI LUZIO, *J. Am. Chem. Soc.* **83**, 2784-5 (1961).



**Figure 26.5** The catalytic cycle for the hydroformylation of an alkene catalysed by *trans*-[Rh(CO)(PPh<sub>3</sub>)<sub>3</sub>]. The tertiary phosphine ligand has been represented as P throughout.

CO and two components of the reactant) therefore lie in a plane and 3 isomers are possible:



There is apparently no simple way of predicting which of these will be formed and each case must be examined individually. The situation is further complicated by the fact that, when the Cl of Vaska's compound is replaced by H, Me or Ph, addition of H<sub>2</sub> gives products in which the phosphines are now *cis*. Various

theoretical models have been suggested to account for this.<sup>(32)</sup>

Addition reactions with ligands such as CO and SO<sub>2</sub> (the addition of which as an uncharged ligand is unusual) differ in that no oxidation occurs and 5-coordinate 18-electron Ir<sup>I</sup> products are formed.

The facile absorption of O<sub>2</sub> by a solution of Vaska's compound is accompanied by a change in colour from yellow to orange which may be reversed by flushing with N<sub>2</sub>. This

<sup>32</sup> M. J. BURK, M. P. McGRATH, R. WHEELER and R. H. CRABTREE, *J. Am. Chem. Soc.* **110**, 5034-9 (1988).

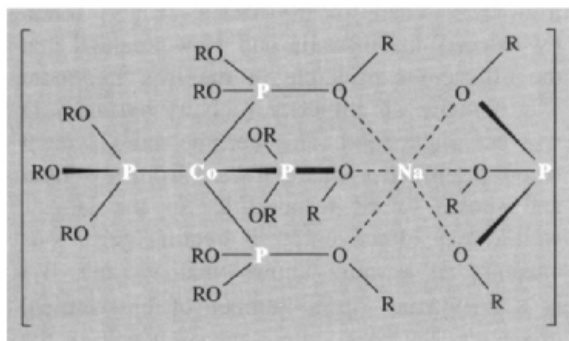
is one of the most widely studied synthetic oxygen-carrying systems and has been discussed earlier (p. 615). The O–O distance of 130 pm in the oxygenated product (see Fig. 14.5b, p. 617) is rather close to the 128 pm of the superoxide ion,  $O_2^-$ , but this would imply  $Ir^{II}$  which is paramagnetic whereas the compound is actually diamagnetic. The oxygenation is instead normally treated as an oxidative addition with the  $O_2$  acting as a bidentate peroxide ion,  $O_2^{2-}$ , to give a 6-coordinate  $Ir^{III}$  product. However, in view of the small “bite” of this ligand the alternative formulation in which the  $O_2$  acts as a neutral unidentate ligand giving a 5-coordinate  $Ir^I$  product has also been proposed.

Oxygen-carrying properties are evidently critically dependent on the precise charge distribution and steric factors within the molecule. Replacement of the Cl in Vaska's compound with I causes loss of oxygen-carrying ability, the oxygenation being irreversible. This can be rationalized by noting that the lower electronegativity of the iodine would allow a greater electron density on the metal, thus facilitating  $M \rightarrow O_2 \pi$  donation: this increases the strength of the  $M-O_2$  bond and, by placing charge in antibonding orbitals of the  $O_2$ , causes an increase in the O–O distance from 130 to 151 pm.

### Lower oxidation states

Numerous complexes of Co, Rh and Ir are known in which the formal oxidation state of the metal is zero,  $-1$ , or even lower. Many of these compounds contain CO,  $CN^-$  or RNC as ligands and so are more conveniently discussed under organometallic compounds (Section 26.3.5). However, other ligands such as tertiary phosphines also stabilize the lower oxidation states, as exemplified by the brown, tetrahedral, paramagnetic complex  $[Co^0(PMe_3)_4]$ : this is made by reducing an ethereal solution of  $CoCl_2$  with Mg or Na amalgam in the presence of  $PMe_3$ . Further treatment of the product with Mg/thf in the presence of  $N_2$  gives  $[Mg(thf)_4][Co^{-II}(N_2)(PMe_3)_4]$ . Similar

reactions with  $P(OMe)_3$  and  $P(OEt)_3$  give both paramagnetic monomers  $[Co^0\{P(OR)_3\}_4]$ , and diamagnetic dimers  $[Co_2^0\{P(OR)_3\}_8]$ , whereas the more bulky  $P(OPr^i)_3$  yields only the orange-red monomeric product. With an excess of sodium amalgam as reducing agent the product with this latter ligand is the white-crystalline  $Na[Co^{-I}\{P(OPr^i)_3\}_5]$ . In view of the ready solubility of this compound in pentane and the  $d^{10}$  configuration of  $Co^{-I}$  it may be that only 4 of the phosphite ligands are directly coordinated to the metal centre: one possible formulation would be



With the terdentate  $P$ -donor ligand,  $MeC(CH_2PPh_2)_3$ , (tppme) excess sodium amalgam and an atmosphere of  $N_2$  yields the deep-brown  $[(tppme)Co-N-N-Co(tppme)]$  which, unusually for a dimer, is paramagnetic.<sup>(33)</sup> The N–N distance in the linear bridge is 118 pm compared with 109.8 pm in  $N_2$  (p. 412).

Another technique for obtaining low oxidation states is by electrolytic reduction using cyclic voltametry. Some spectacular series can be achieved of which, perhaps, the most notable is based on  $[Ir^{III}(bipy)_3]^{3+}$ : this, when dissolved in MeCN, can be oxidized to  $[Ir^{IV}(bipy)_3]^{4+}$  and reduced in successive 1-electron steps to give every oxidation state down to  $[Ir^{-III}(bipy)_3]^{3-}$ , a total of 8 interconnected redox complexes. However, by no means all have been isolated as solid products from solution. Many other

<sup>33</sup> F. CECCONI, C. A. GHILARDI, S. MIDOLLINI, S. MONETI, A. ORLANDINI and M. BACCI, *J. Chem. Soc., Chem. Commun.*, 731–3 (1985).



such redox series are known for these and other elements.

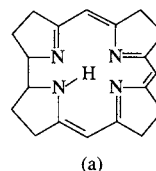
### 26.3.4 The biochemistry of cobalt<sup>(34)</sup>

The wasting disease in sheep and cattle known variously as “pine” (Britain), “bush sickness” (New Zealand), “coast disease” (Australia), and “salt sick” (Florida) has been recognized since the late eighteenth century. When it was realized to be an anaemic condition it was thought to be due to iron deficiency and was therefore treated, with mixed success, by administering iron salts. Then, in the 1930s, it was found by workers in Australia and New Zealand that the efficacious principle in the iron treatment was actually an impurity (cobalt) but its role was not understood. This became more evident when vitamin B<sub>12</sub> was extracted from raw liver and shown to be responsible for the latter’s well-known effectiveness in treating pernicious anaemia. It is now known that vitamin B<sub>12</sub> is a coenzyme<sup>†</sup> in a number of biochemical processes, the most important of which is the formation of erythrocytes (red blood-cells). It obviously functions extremely effectively, the human body for instance containing a mere 2–5 mg, concentrated in the liver.

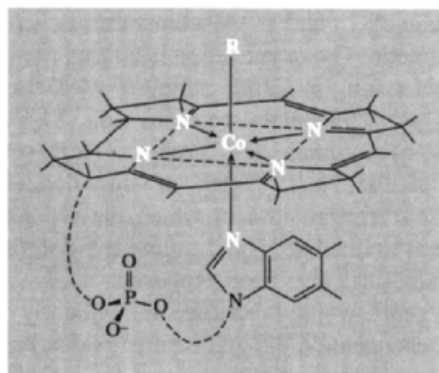
The structure of the diamagnetic, cherry-red vitamin B<sub>12</sub> is shown in Fig. 26.6 and it can be seen that the coordination sphere of the cobalt has many similarities with that of iron in haem (see Fig. 25.7). In both cases the metal is coordinated to 4 nitrogen atoms of an unsaturated macrocycle (in this case part of a “corrin” ring which is less symmetrical and not so unsaturated as the porphyrin in haem) with an imidazole nitrogen in the fifth position. A major

<sup>34</sup> W. KAIM and B. SCHWERDESKI, pp. 39–55 of *Bioinorganic Chemistry: Inorganic Elements in the Chemistry of Life*, Wiley, Chichester, 1994; L. R. MILGROM, *Chem. in Brit.* **31**, 923–7 (1994).

<sup>†</sup> Enzymes are proteins which act as very specific catalysts in biological systems. Their activity may depend on the presence of substances, often metal complexes, of much lower molecular weight. These activators are known as “coenzymes”.

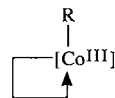


(a)



(b)

**Figure 26.6** Vitamin B<sub>12</sub>: (a) a corrin ring showing a square-planar set of N atoms and a replaceable H, and (b) simplified structure of B<sub>12</sub>. In view of the H displaced from the corrin ring, the Co–C bond, and the charge on the ribose phosphate, the cobalt is formally in the +3 oxidation state. This and related molecules are conveniently represented as:

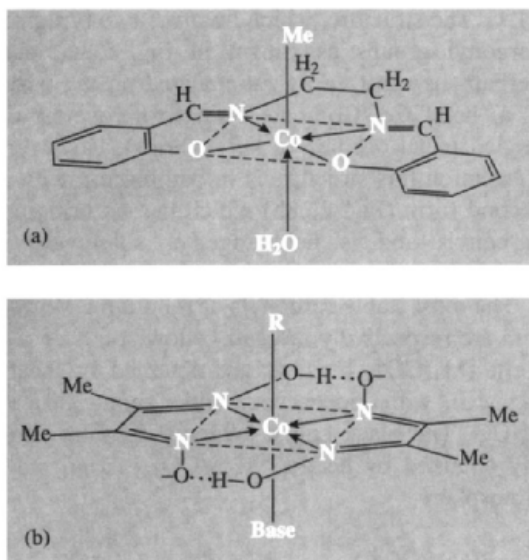


difference is apparent, however, in the sixth coordination position which, in haemoglobin, is either vacant or occupied by O<sub>2</sub>. Here it is filled by a  $\sigma$ -bonded carbon,<sup>(35)</sup> making vitamin B<sub>12</sub> the first, and so far the only, fully established naturally occurring organometallic compound. The usual methods of isolation lead to a product known as *cyanocobalamin*, which is the same as vitamin B<sub>12</sub> itself but with CN<sup>−</sup> instead of deoxyadenosine in the sixth coordination position. This is a labile site, and other derivatives such as *aquocobalamin* can be prepared.

Incorporation of cobalt into the corrin ring system modifies the reduction potentials of

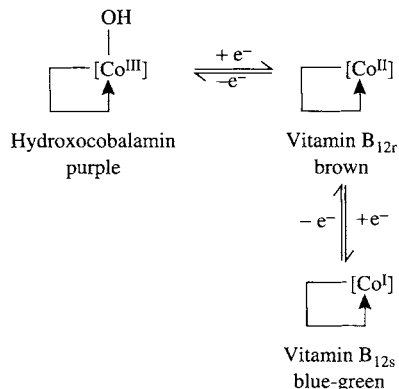
<sup>35</sup> D. C. HODGKIN, *Proc. Roy. Soc. A* **288**, 294–305 (1965).





**Figure 26.7** Model vitamin B<sub>12</sub> compounds: (a) a Schiff base derivative, and (b) a cobaloxime, in this case derived from dimethylglyoxime.

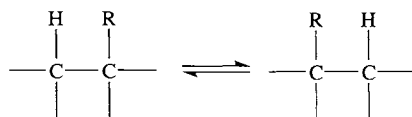
cobalt giving it three accessible and consecutive oxidation states:



The reductions are effected in nature by ferredoxin (p. 1102). This behaviour can be reproduced surprisingly well by simpler, model compounds. Some of the best known of these are obtained by the addition of axial groups to the square-planar complexes of Co<sup>II</sup> with Schiff bases, or substituted glyoximes (giving cobaloximes) as illustrated in Fig. 26.7. The reduced Co<sup>I</sup> species of these, along with vitamin

B<sub>12s</sub>, are amongst the most powerful nucleophiles known (hence, “supernucleophiles”), liberating H<sub>2</sub> from water.

Virtually all the biological processes, in which vitamin B<sub>12</sub> is active, involve substituent exchange of the type:



which, significantly, does not involve solvent protons. The precise mechanism of these reactions is not settled but all involve cleavage of the Co–C bond and it is evident from the study of model systems that the lack of complete planarity of the corrin ring is an important factor in controlling this.<sup>(36)</sup>

### 26.3.5 Organometallic compounds<sup>(37)</sup>

Many of the organometallic compounds of the elements of this group show valuable catalytic activity and, as discussed above, much of the chemistry of vitamin B<sub>12</sub> is the chemistry of the Co–Cσ bond. Simple homoleptic alkyls and aryls of cobalt, [CoR<sub>x</sub>], have not in fact been prepared, but this is evidently not due to thermodynamic instability of the Co–C bond. Compounds containing such bonds can be prepared in abundance, not only with (σ + π)-bonding ligands such as phosphines and CO but also with non-π-bonding ligands such as Schiff bases and glyoximes. These latter presumably owe their existence not to electronic but rather to steric factors, the additional ligands blocking what might otherwise be energetically favourable decomposition paths.

<sup>36</sup> M. RAVIKANTH and T. K. CHANRESHEKAR, *Structure and Bonding*, **82**, 105–88 (1995).

<sup>37</sup> R. S. DICKSON, *Organometallic Chemistry of Rhodium and Iridium*, Academic Press, New York, 1983, 432 pp.; C. WHITE, *Organometallic Compounds of Cobalt, Rhodium and Iridium*, Chapman & Hall, London 1985, 296 pp.

### Carbonyls (see p. 926)

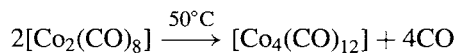
Because they possess an odd number of valence electrons the elements of this group can only satisfy the 18-electron rule in their carbonyls if M–M bonds are present. In accord with this, mononuclear carbonyls are not formed. Instead  $[M_2(CO)_8]$ ,  $[M_4(CO)_{12}]$  and  $[M_6(CO)_{16}]$  are the principal binary carbonyls of these elements. But reduction of  $[Co_2(CO)_8]$  with, for instance, sodium amalgam in benzene yields the monomeric and tetrahedral, 18-electron ion,  $[Co(CO)_4]^-$ , acidification of which gives the pale yellow hydride,  $[HCo(CO)_4]$ . Reductions employing Na metal in liquid  $NH_3$  yield the "super-reduced"  $[M(CO)_3]^{3-}$  (M = Co, Rh, Ir) containing these elements in their lowest formal oxidation state.<sup>(38)</sup>

The importance of cobalt carbonyls lies in their involvement in hydroformylation reactions discussed above. The original, and still widely used, process depends on the use of cobalt salts rather than the newer rhodium catalysts (pp. 1134–5). The mechanism of the cobalt cycle is more difficult to ascertain but it seems clear that the active agent is the hydride,  $[HCo(CO)_4]$ . It is, moreover, plausible that the cycle is basically the same as that outlined in Fig. 26.5 but starting with loss of CO from  $[HCo(CO)_4]$  rather than loss of phosphine from  $[Rh(CO)H(PPh_3)_3]$ , so producing a comparable coordinatively unsaturated intermediate to which the alkene can attach itself. The disadvantages of the system, as already mentioned, are its lack of specificity, leading to branched-chain products, and the necessity of high temperatures ( $>150^\circ C$ ) and pressure ( $\sim 200$  atm). In addition the volatility of  $[HCo(CO)_4]$  poses recovery problems.

The dinuclear octacarbonyls are obtained by heating the metal (or in the case of iridium,  $IrCl_3$  + copper metal) under a high pressure of CO (200–300 atm).  $Co_2(CO)_8$  is by far the best known, the other two being poorly characterized; it is an air-sensitive, orange-red solid melting at

$51^\circ C$ . The structure, which involves two bridging carbonyl groups as shown in Fig. 26.8a, can perhaps be most easily rationalized on the basis of a "bent" Co–Co bond arising from overlap of angled metal orbitals ( $d^2sp^3$  hybrids). However, in solution this structure is in equilibrium with a second form (Fig. 26.8b) which has no bridging carbonyls and is held together solely by a Co–Co bond.

The most stable carbonyls of rhodium and iridium are respectively red and yellow solids of the form  $[M_4(CO)_{12}]$  which are obtained by heating  $MCl_3$  with copper metal under about 200 atm of CO. The black cobalt analogue is more simply obtained by heating  $[Co_2(CO)_8]$  in an inert atmosphere

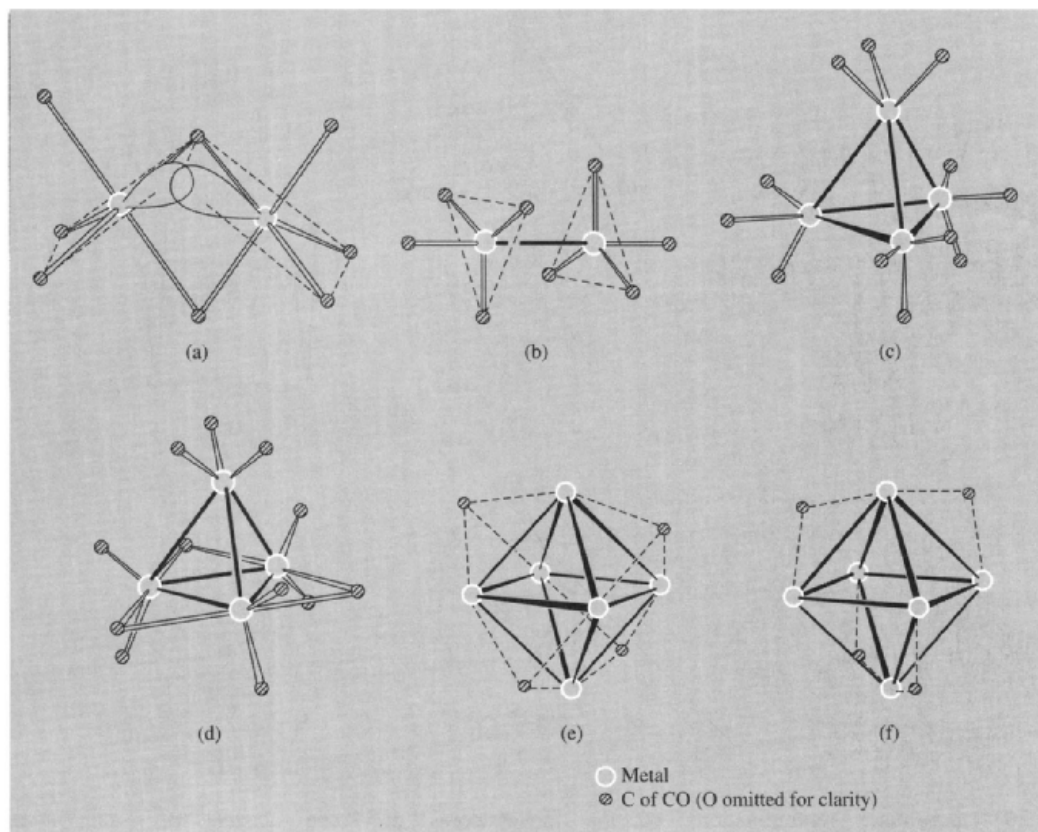


The structures are shown in Fig. 26.8c and d and differ in that, whereas the Ir compound consists of a tetrahedron of metal atoms held together solely by M–M bonds, the Rh and Co compounds each incorporate 3 bridging carbonyls. A similar difference was noted in the case of the trinuclear carbonyls of Fe, Ru and Os (p. 1104) and can be explained in a similar way.<sup>(39)</sup> The  $M_4$  tetrahedra of Co and Rh are small enough to be accommodated in an icosahedral array of CO ligands whereas the larger  $Ir_4$  tetrahedron forces the adoption of the less dense cube octahedral array of ligands.

Of the  $[M_6(CO)_{16}]$  carbonyls the very dark-brown Rh compound prepared simultaneously with and separated from  $[Rh_4(CO)_{12}]$  is the best known. In the solid its structure consists of an octahedral array of  $Rh(CO)_2$  units with the remaining 4 CO's bridging 4 faces of the octahedron (Fig. 26.8e). A black isomorphous, and presumably isostructural, Co analogue and an isostructural red Ir analogue are known. A second, black Ir isomer occurs which differs only in that it has 4 edge-bridging rather than face-bridging CO groups. Again rationalization is possible on the basis of the ligand polyhedral

<sup>38</sup> J. E. ELLIS, *Adv. Organometallic Chem.*, **31**, 1–52 (1990).

<sup>39</sup> B. F. G. JOHNSON and Y. V. ROBERTS, *Polyhedron*, **12**, 977–90 (1993).



**Figure 26.8** Molecular structures of some binary carbonyls of Co, Rh, and Ir. (a)  $\text{Co}_2(\text{CO})_8$  in solid state, showing the formation of a “bent” Co–Co bond. (b)  $\text{Co}_2(\text{CO})_8$  in solution. (c)  $\text{Ir}_4(\text{CO})_{12}$ . (d)  $\text{M}_4(\text{CO})_{12}$ ,  $\text{M} = \text{Co}, \text{Rh}$ . (e)  $\text{M}_6(\text{CO})_{16}$   $\text{M} = \text{Co}, \text{Rh}$  and  $\text{Ir}$  (for its red isomer). (f) black isomer of  $\text{Ir}_6(\text{CO})_{16}$ .

model. In *both* structures the ligands occupy the 16 vertices of a tetracapped truncated tetrahedron. In one case the 4 caps are the face-bridging ligands, in the other the edge-bridging ligands. The two structures are related by a simple rotation of the  $\text{M}_6$  octahedron about a  $\text{C}_4$  axis.<sup>(39)</sup>

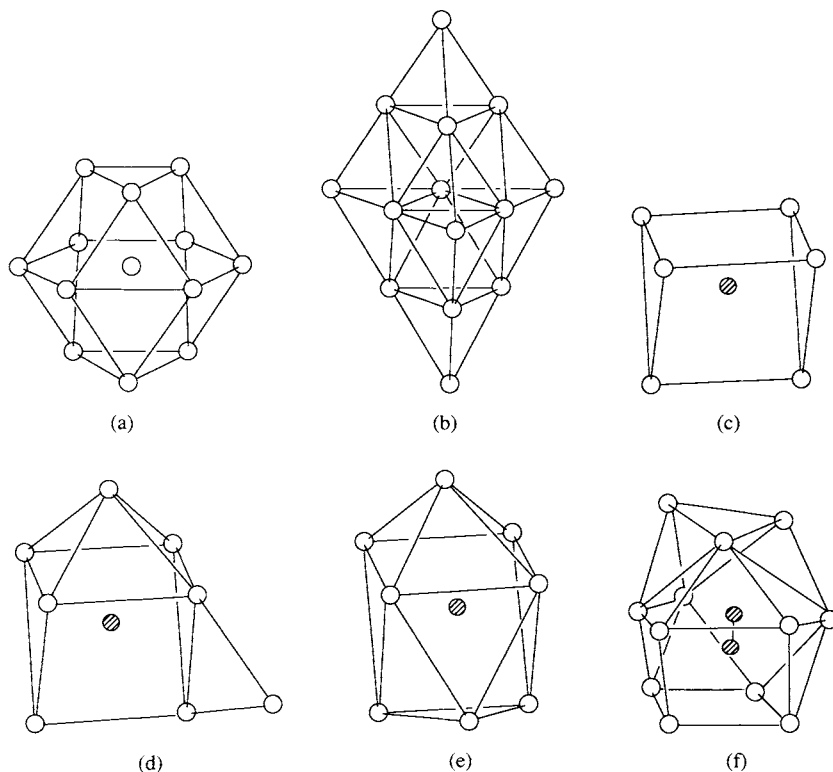
Carbonyl hydrides and carbonylate anions are obtained by reducing neutral carbonyls, as mentioned above, and in addition to mononuclear metal anions, anionic species of very high nuclearity have been obtained, often by thermolysis. These are especially numerous for Rh and in certain  $\text{Rh}_{13}$ ,  $\text{Rh}_{14}$  and  $\text{Rh}_{15}$  anions have structures conveniently visualized either as polyhedra encapsulating further metal atoms, or alternatively as arrays of metal atoms forming portions of hexagonal close packed or body

centred cubic lattices stabilized by CO ligands.  $[\text{Rh}_{13}\text{H}_3(\text{CO})_{24}]^{2-}$  (Fig 26.9a) is typical.

The anionic cluster  $[\text{Ir}_6(\text{CO})_{15}]^{2-}$  is octahedral and an increasing number of Ir clusters have been reported recently though their preparations are more difficult and yields usually smaller than for rhodium.  $[\text{Ir}_{14}(\text{CO})_{27}]^-$  has the highest nuclearity so far and is obtained as black crystals by oxidizing  $[\text{Ir}_6(\text{CO})_{15}]^{2-}$  with ferricinium ion<sup>(40)</sup> (Fig 26.9b).

The incorporation of interstitial or encapsulated heteroatoms is a common and stabilizing feature. Carbon is the most common and, as is the case in

<sup>40</sup> R. D. PERGOLA, L. GARLASCELLI, M. MANASSERO, N. MASCIOCCHI and P. ZANELLO, *Angew. Chem. Int. Edn. Engl.* **32**, 1347–9 (1993).



**Figure 26.9** Schematic representations of the metal cores of some clusters of group 9 metals. (a)  $[\text{Rh}_{13}\text{H}_3(\text{CO})_{24}]^{2-}$ ; the H atoms migrate within the cluster. (b)  $[\text{Ir}_{14}(\text{CO})_{27}]^-$ . (c)  $[\text{Rh}_6\text{C}(\text{CO})_{15}]^{2-}$ . (d)  $[\text{Rh}_8\text{C}(\text{CO})_{19}]$ ; a trigonal prism of 6 Rh atoms has one face capped by a seventh Rh atom and one edge bridged by the eighth Rh atom. (e)  $[\text{Co}_8\text{C}(\text{CO})_{18}]^{2-}$ ; the 8 Co atoms define a distorted bicapped trigonal prism which, alternatively, can be viewed as a distorted square antiprism. (f)  $[\text{Rh}_{12}(\text{C}_2)(\text{CO})_{25}]$ .

group 8 (p. 1107), may originate from the solvent or from cleavage of a CO ligand. The carbido C contributes 4 electrons to the cluster bonding and in the 90-electron species  $[\text{Rh}_6\text{C}(\text{CO})_{15}]^{2-}$  features trigonal prismatic coordination of  $\text{Rh}_6$  about the central C (Fig. 26.9c). More complex geometries are found for  $[\text{Rh}_8\text{C}(\text{CO})_{19}]$  (Fig. 26.9d) and  $[\text{Co}_8\text{C}(\text{CO})_{18}]^{2-}$  (Fig. 26.9e): these two iso-electronic clusters are not isostructural though a slight distortion would (hypothetically) transform one into the other. The central carbido C in the square antiprismatic  $[\text{Co}_8\text{C}(\text{CO})_{18}]^{2-}$  is formally 8-coordinate, the Co–C distances being in the range 195–220 pm with a mean value of 207 pm. Even more complicated structures are found for the large Rh clusters containing 2 carbido

C atoms:  $[\text{Rh}_{12}(\text{C}_2)(\text{CO})_{25}]$  (Fig. 26.9f has no symmetry elements but it is clear that the  $\text{Rh}_{12}$  cluster surrounds an ethanide unit  $\text{C}_2$  in which the C–C distance is only 147 pm); the cluster also has 14 pendant terminal CO groups, 10  $\mu$ -CO groups and one  $\mu_3$ -CO. In contrast,  $[\text{Rh}_{15}(\text{C})_2(\text{CO})_{28}]^-$  has individual 6-coordinate (octahedral) carbido C atoms symmetrically placed on each side of a central Rh which itself has 12 Rh nearest neighbours in addition to the 2 C atoms. Again, the approach to metal structures is notable and is one of the main interests in constructing large clusters and studying their chemical and catalytic activity.

H, P, As, S have also been encapsulated in ions such as  $[\text{Rh}_{13}(\text{H})_3(\text{CO})_{24}]^{2-}$ ,  $[\text{Rh}_9\text{P}(\text{CO})_{21}]^{2-}$ ,  $[\text{Rh}_{10}\text{As}(\text{CO})_{22}]^{3-}$  and  $[\text{Rh}_{17}(\text{S})_2(\text{CO})_{32}]^{3-}$ .

More recently N has been encapsulated<sup>(41)</sup> in  $[\text{Rh}_{14}(\text{N})_2(\text{CO})_{25}]^{2-}$  and  $[\text{Rh}_{23}(\text{N})_4(\text{CO})_{38}]^{3-}$ . The latter is the largest Rh cluster so far characterized. It consists of an irregular polyhedron of 21 Rh atoms encapsulating a pair of particularly close (257.1 pm) Rh atoms as well as 4 N atoms each of which is located in a semi octahedral site.

Other derivatives of the carbonyls are of course numerous; Ir forms many carbonyl halides of the types  $[\text{Ir}^{\text{I}}(\text{CO})_3\text{X}]$ ,  $[\text{Ir}^{\text{I}}(\text{CO})_2\text{X}_2]^-$ ,  $[\text{Ir}^{\text{III}}(\text{CO})_2\text{X}_4]^-$  and  $[\text{Ir}^{\text{III}}(\text{CO})\text{X}_5]^{2-}$ , but the stability of carbonyl halides falls off in the sequence  $\text{Ir} > \text{Rh} > \text{Co}$  and those of Co are only of the type  $[\text{Co}(\text{CO})_4\text{X}]$  and are very unstable.

The bulk of derivatives are obtained by the displacement of CO by other ligands. These include phosphines and other group 15 donors, NO, mercaptans and unsaturated organic molecules such as alkenes, alkynes and cyclopentadienyls.

### Cyclopentadienyls

Cobaltocene,  $[\text{Co}^{\text{II}}(\eta^5\text{-C}_5\text{H}_5)_2]$ , is a dark-purple air-sensitive material, prepared by the reactions of sodium cyclopentadiene and anhydrous  $\text{CoCl}_2$

in thf. Having 1 more electron than ferrocene, it is paramagnetic with a magnetic moment of 1.76 BM and, while it is thermally stable up to 250°C, its most obvious characteristic is its ready loss of this electron to form the yellow-green cobalticenium ion,  $[\text{Co}^{\text{III}}(\eta^5\text{-C}_5\text{H}_5)_2]^+$ . This resists further oxidation, being stable even in conc  $\text{HNO}_3$  but, like the isoelectronic ferrocene, is susceptible to nucleophilic attack on its rings.

Rhodocene,  $[\text{Rh}(\eta^5\text{-C}_5\text{H}_5)_2]$ , is also known but is unstable to oxidation and has a tendency to form dimeric species. Claims for the existence of iridocene probably refer to  $\text{Ir}^{\text{III}}$  complexes. However, the yellow rhodicenium and iridicenium cations are certainly known and are entirely analogous to the cobalticenium cation in their resistance to oxidation and susceptibility to nucleophilic attack.

Numerous “half-sandwich” compounds of the type  $[\text{M}(\eta^5\text{-C}_5\text{R}_5)\text{L}_2]$ ,  $\text{M} = \text{Rh}, \text{Ir}$ ;  $\text{R} = \text{H}, \text{Me}$ ;  $\text{L} = \text{CO}, \text{phosphine}$  etc.) are known and are useful reagents.  $[\text{Ir}(\eta^5\text{-C}_5\text{Me}_5)(\text{CO})_2]$  for instance is an excellent nucleophile and is also used in the photochemical activation of C–H in alkanes. It is particularly effective in the latter role when supercritical  $\text{CO}_2$  is the solvent.<sup>(42)</sup>

<sup>41</sup> S. MARTINENGO, G. CIANI and A. SIRONI, *J. Chem. Soc., Chem. Commun.*, 1405–6 (1992).

<sup>42</sup> M. JOBLING, S. M. HOWDLE, M. A. HEALY and M. POLIAKOFF, *J. Chem. Soc., Chem. Commun.*, 1287–90 (1990).

																1	2																
																H	He																
3	4															5	6	7	8	9	10												
Li	Be															B	C	N	O	F	Ne												
11	12															13	14	15	16	17	18												
Na	Mg															Al	Si	P	S	Cl	Ar												
19	20	21	22	23	24	25	26	27	28	29	30	31	32	33	34	35	36																
K	Ca	Sc	Ti	V	Cr	Mn	Fe	Co	Ni	Cu	Zn	Ga	Ge	As	Se	Br	Kr																
37	38	39	40	41	42	43	44	45	46	47	48	49	50	51	52	53	54																
Rb	Sr	Y	Zr	Nb	Mo	Tc	Ru	Rh	Pd	Ag	Cd	In	Sn	Sb	Te	I	Xe																
55	56	57	58	59	60	61	62	63	64	65	66	67	68	69	70	71	72																
Cs	Ba	La	Hf	Ta	W	Re	Os	Ir	Pt	Au	Hg	Tl	Pb	Bi	Po	At	Rn																
87	88	89	90	91	92	93	94	95	96	97	98	99	100	101	102																		
Fr	Ra	Ac	Rf	Db	Sg	Bh	Hs	Mt	Uun	Uuu	Uub																						
73	74	75	76	77	78	79	80	81	82	83	84	85	86	87	88	89	90																
Ce	Pr	Nd	Pm	Sm	Eu	Gd	Tb	Dy	Ho	Er	Tm	Yb	Lu																				
91	92	93	94	95	96	97	98	99	100	101	102	103	104	105	106	107	108																
Th	Pa	U	Np	Pu	Am	Cm	Bk	Cf	Es	Fm	Md	No	Lr																				

# 27

## Nickel, Palladium and Platinum

### 27.1 Introduction

An alloy of nickel was known in China over 2000 years ago, and Saxon miners were familiar with the reddish-coloured ore, NiAs, which superficially resembles Cu<sub>2</sub>O. These miners attributed their inability to extract copper from this source to the work of the devil and named the ore “Kupfernickel” (Old Nick’s copper). In 1751 A. F. Cronstedt isolated an impure metal from some Swedish ores and, identifying it with the metallic component of Kupfernickel, named the new metal “nickel”. In 1804 J. B. Richter produced a much purer sample and so was able to determine its physical properties more accurately.

Impure, native platinum seems to have been used unwittingly by ancient Egyptian craftsmen in place of silver, and was certainly used to make small items of jewellery by the Indians of Ecuador before the Spanish conquest. The introduction of the metal to Europe is a complex and intriguing story.<sup>(1)</sup> In 1736 A. de Ulloa, a Spanish astronomer and naval officer, observed an unworkable metal, *platina* (Spanish, little

silver), in the gold mines of what is now Colombia. Returning home in 1745 his ship was attacked by privateers and finally captured by the British navy. He was brought to London and his papers confiscated, but was fortunately befriended by members of the Royal Society and was indeed elected to that body in 1746 when his papers were returned. Meanwhile, in 1741, C. Wood brought to England the first samples of the metal and, following the eventual publication of de Ulloa’s report in 1748, investigation of its properties began in England and Sweden. It became known as “white gold” (a term now used to describe an Au/Pd alloy) and the “eighth metal” (the seven metals Au, Ag, Hg, Cu, Fe, Sn and Pb having been known since ancient times). Great difficulty was experienced in working it because of its high mp and brittle nature (due to impurities of Fe and Cu). Powder metallurgical techniques of fabrication were developed<sup>†</sup> in great secrecy in Spain by the

<sup>†</sup> Precedence must in fact be given to the South American Indians to whom platinum was available only in the form of fine, hand-separated grains which must have been fabricated by ingenious, if crude, powder metallurgy.

<sup>1</sup> L. B. HUNT, *Platinum Metals Rev.* **24**, 31–9 (1980).

Frenchman P. F. Chabeneau, and subsequently in London by W. H. Wollaston,<sup>(2)</sup> who in the years 1800–21 produced well over 1 tonne of malleable platinum. These techniques were developed because the chemical methods used to isolate the metal produced an easily powdered spongy precipitate. Not until the availability, half a century later, of furnaces capable of sustaining sufficiently high temperatures was easily workable, fused platinum commercially available.

In 1803, in the course of his study of platinum, Wollaston isolated and identified palladium from the mother liquor remaining after platinum had been precipitated as  $(\text{NH}_4)_2\text{PtCl}_6$  from its solution in aqua regia. He named it after the newly discovered asteroid, Pallas, itself named after the Greek goddess of wisdom ( $\pi\alpha\lambda\lambda\acute{\alpha}\delta\iota\omicron\nu$ , palladion, of Pallas).

## 27.2 The Elements

### 27.2.1 Terrestrial abundance and distribution

Nickel is the seventh most abundant transition metal and the twenty-second most abundant element in the earth's crust (99 ppm). Its commercially important ores are of two types:

- (1) *Laterites*, which are oxide/silicate ores such as garnierite,  $(\text{Ni,Mg})_6\text{Si}_4\text{O}_{10}(\text{OH})_8$ , and nickeliferous limonite,  $(\text{Fe,Ni})\text{O}(\text{OH})\cdot n\text{H}_2\text{O}$ , which have been concentrated by weathering in tropical rainbelt areas such as New Caledonia, Cuba and Queensland.
- (2) *Sulfides* such as pentlandite,  $(\text{Ni,Fe})_9\text{S}_8$ , associated with copper, cobalt and precious metals so that the ores typically contain about  $1\frac{1}{2}\%$  Ni. These are found in more temperate regions such as Canada, the former Soviet Union and South Africa.

Arsenide ores such as niccolite ( $\text{Kupfernickel}$  ( $\text{NiAs}$ ), smaltite  $((\text{Ni,Co,Fe})\text{As}_2)$  and nickel glance ( $\text{NiAsS}$ ) are no longer of importance.

The most important single deposit of nickel is at Sudbury Basin, Canada. It was discovered in 1883 during the building of the Canadian Pacific Railway and consists of sulfide outcrops situated around the rim of a huge basin 17 miles wide and 37 miles long (possibly a meteoritic crater). Fifteen elements are currently extracted from this region (Ni, Cu, Co, Fe, S, Te, Se, Au, Ag and the six platinum metals).

Although estimates of their abundances vary considerably, Pd and Pt (approximately 0.015 and 0.01 ppm respectively) are much rarer than Ni. They are generally associated with the other platinum metals and occur either native in placer (i.e. alluvial) deposits or as sulfides or arsenides in Ni, Cu and Fe sulfide ores. Until the 1820s all platinum metals came from South America, but in 1819 the first of a series of rich placer deposits which were to make Russia the chief source of the metals for the next century, was discovered in the Urals. More recently however, the copper-nickel ores in South Africa and Russia (where the Noril'sk-Talnakh deposits are well inside the Arctic Circle) have become the major sources, supplemented by supplies from Sudbury.

### 27.2.2 Preparation and uses of the elements<sup>(3,3a,4)</sup>

Production methods for all three elements are complicated and dependent on the particular ore involved; they will therefore only be sketched in outline. In the case of nickel the oxide ores are not generally amenable to concentration by normal physical separations and so the whole ore has to be treated. By contrast the sulfide ores

<sup>3</sup> J. HILL in D. THOMPSON (ed.), *Insights into Speciality Inorganic Chemicals*, pp. 5–34, R.S.C., Cambridge, 1995.

<sup>3a</sup> Kirk–Othmer *Encyclopedia of Chemical Technology*, 4th edn., Interscience, New York: Ni, 17, 1–47 (1996); Pt metals, 19, 347–407 (1996).

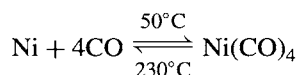
<sup>4</sup> F. R. HARTLEY (ed.) *Chemistry of the Platinum Group Metals*, Elsevier, Amsterdam, 1991, 642 pp.

<sup>2</sup> J. C. CHASTON, *Platinum Metals Rev.* 24, 70–9 (1980).

can be concentrated by flotation and magnetic separations, and for this reason they provide the major part of the world's nickel, though the use of laterite ores is appreciable.

A quarter of the world's nickel comes from Sudbury and there silica is added to the nickel/copper concentrates which are then subjected to a series of roasting and smelting operations. This reduces the sulfide and iron contents by converting the iron sulfide first to the oxide and then to the silicate which is removed as a slag. The resulting "matte" of nickel and copper sulfides is allowed to cool over a period of days, when  $\text{Ni}_3\text{S}_2$ ,  $\text{Cu}_2\text{S}$  and Ni/Cu metal<sup>†</sup> form distinct phases which can be mechanically separated. (In the older, Orford, process the matte was heated with  $\text{NaHSO}_4$  and coke, producing molten  $\text{Na}_2\text{S}$  which dissolved the copper sulfide and formed an upper layer, leaving the nickel sulfide below; on solidification the silvery upper layer was cut from the black lower layer — hence the process was commonly called the "tops and bottoms" process.) The matte may be cast directly as anode with pure nickel sheet as cathode and electrolysed using an aqueous  $\text{NiSO}_4$ ,  $\text{NiCl}_2$  electrolyte. Alternatively, the matte may be leached with hydrochloric acid, nickel chloride crystallized and converted to the oxide by high temperature oxidation with air, and finally the oxide reduced to the metal by  $\text{H}_2$  at  $600^\circ\text{C}$ .

The carbonyl process developed in 1899 by L. Mond is still used, though it is mainly of historic interest. In this the heated oxide is first reduced by the hydrogen in water gas ( $\text{H}_2 + \text{CO}$ ). At atmospheric pressure and a temperature around  $50^\circ\text{C}$ , the impure nickel is then reacted with the residual CO to give the volatile  $\text{Ni}(\text{CO})_4$ . This is passed over nucleating pellets of pure nickel at a temperature of  $230^\circ\text{C}$  when it decomposes, depositing nickel of 99.95% purity and leaving CO to be recycled.



<sup>†</sup> This metallic phase is worked for precious metals which are preferentially dissolved in it.

Somewhat higher pressures and temperatures (e.g. 20 atm and  $150^\circ\text{C}$ ) are used to form the carbonyl in modern Canadian plant, but the essential principle of the Mond process is retained.

Total world production of nickel is in the region of 1.0 million tonnes pa of which (1995) 25% comes from the former Soviet Union, 18% from Canada, 12% from New Caledonia and 10% from Australia. The bulk of this is used in the production of alloys both ferrous and non-ferrous. In 1889 J. Riley of Glasgow published a report on the effect of adding nickel to steel. This was noticed by the US Navy who initiated the use of nickel steels in armour plating. Stainless steels contain up to 8% Ni and the use of "Alnico" steel for permanent magnets has already been mentioned (p. 1114).

The non-ferrous alloys include the misleadingly named nickel silver (or German silver) which contains 10–30% Ni, 55–65% Cu and the rest Zn; when electroplated with silver (electroplated nickel silver) it is familiar as EPNS tableware. *Monel* (68% Ni, 32% Cu, traces of Mn and Fe) is used in apparatus for handling corrosive materials such as  $\text{F}_2$ ; cupro-nickels (up to 80% Cu) are used for "silver" coinage; *Nichrome* (60% Ni, 40% Cr), which has a very small temperature coefficient of electrical resistance, and *Invar*, which has a very small coefficient of expansion are other well-known Ni alloys. Electroplated nickel is an ideal undercoat for electroplated chromium, and smaller amounts of nickel are used as catalysts in the hydrogenation of unsaturated vegetable oils and in storage batteries such as the Ni/Fe batteries.

Ninety-eight per cent of the world's supply of platinum metals comes from three countries — the former Soviet Union (49%), the Republic of South Africa (43%), and Canada (6%). Because of the different proportions of Pt and Pd in their deposits, the Republic of South Africa is the major source of Pt and the former USSR of Pd. Only in the RSA (where the Bushveld complex contains over 70% of the world's reserves of the platinum metals at concentrations of 8–9 grams per tonne) are the



platinum metals the primary products. Elsewhere, with concentrations of a mere fraction of a gramme per tonne, millions of tonnes of ore must be mined, milled and smelted each year. Precious metal concentrates are obtained either from the metallic phase of the sulfide matte (see above) or as anode slimes in the electrolytic refinement of the baser metals. From these, all six platinum metals as well as Ag and Au are obtained by a composite process. Traditional methods were based on selective precipitation and developed to suit the composition of the

concentrate. Although these methods are still in use the efficiency of the separations is not high and costly recycling is required. Solvent extraction and ion exchange techniques offer superior efficiency and are increasingly replacing the classical processes. Fig. 27.1 outlines a typical solvent extraction process (see also p. 1073 and p. 1114).

Current annual world production of all platinum metals is around 380 tonnes of which perhaps 150 tonnes is platinum and 210 tonnes is palladium. 35 -40% of Pt and about half as

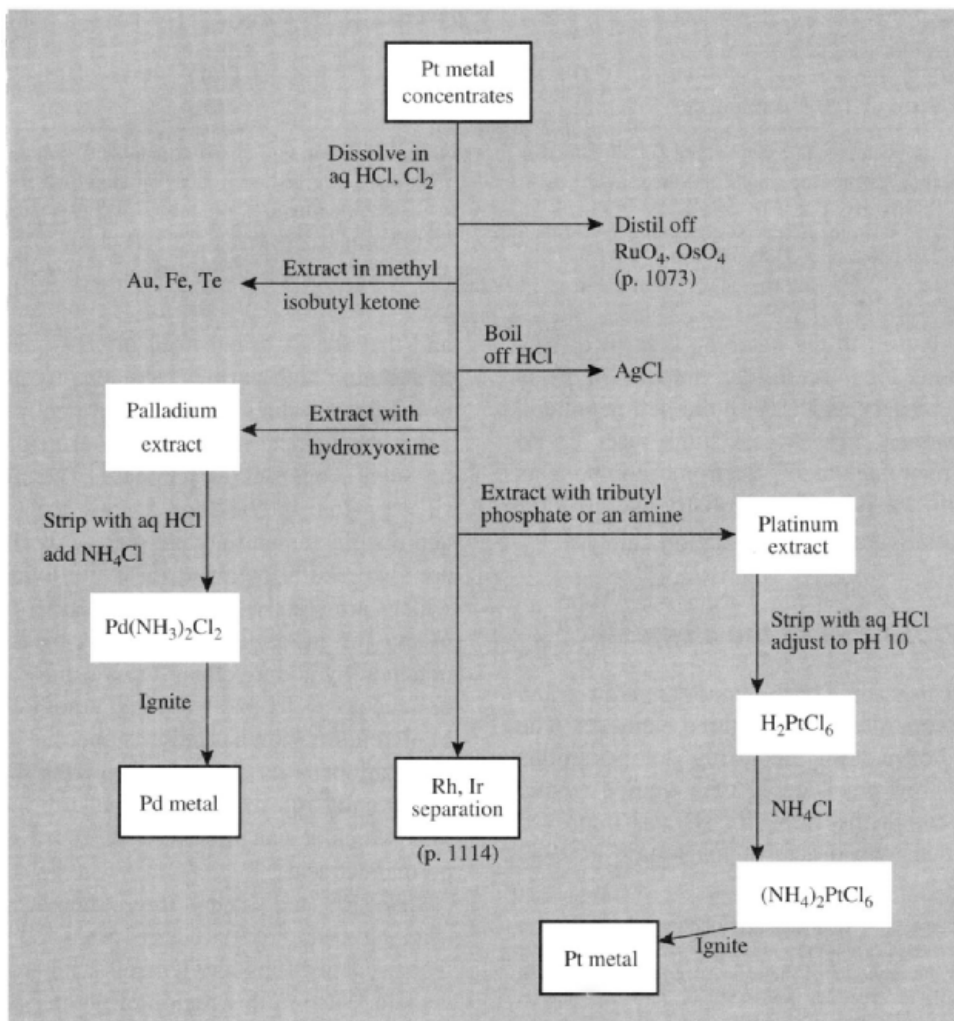


Figure 27.1 Flow diagram for refining palladium and platinum by solvent extraction.

Table 27.1 Some properties of the elements nickel, palladium and platinum

Property	Ni	Pd	Pt
Atomic number	28	46	78
Number of naturally occurring isotopes	5	6	6 <sup>(a)</sup>
Atomic weight	58.6934(2)	106.42(1)	195.078(2)
Electronic configuration	[Ar]3d <sup>8</sup> 4s <sup>2</sup>	[Kr]4d <sup>10</sup>	[Xe]4f <sup>14</sup> 5d <sup>9</sup> 6s <sup>1</sup>
Electronegativity	1.8	2.2	2.2
Metal radius (12-coordinate)/pm	124	137	138.5
Effective ionic radius (6-coordinate)/pm	—	—	57
	IV	61.5	62.5
	III	76	—
	II	86	80
MP/°C	1455	1552	1769
BP/°C	2920	2940	4170
$\Delta H_{\text{fus}}/\text{kJ mol}^{-1}$	17.2(±0.3)	17.6(±2.1)	19.7(±2.1)
$\Delta H_{\text{vap}}/\text{kJ mol}^{-1}$	375(±17)	362(±11)	469(±25)
$\Delta H_{\text{f}}(\text{monatomic gas})/\text{kJ mol}^{-1}$	429(±13)	377(±3)	545(±21)
Density (20°C)/g cm <sup>-3</sup>	8.908	11.99	21.45
Electrical resistivity (20°C)/μohm cm	6.84	9.93	9.85

<sup>(a)</sup>All have zero nuclear spin except <sup>195</sup>Pt (33.8% abundance) which has a nuclear spin quantum number  $\frac{1}{2}$ : this isotope finds much use in nmr spectroscopy both via direct observation of the <sup>195</sup>Pt resonance and even more by the observation of <sup>195</sup>Pt “satellites”. Thus, a given nucleus coupled to <sup>195</sup>Pt will be split into a doublet symmetrically placed about the central unsplit resonance arising from those species containing any of the other 5 isotopes of Pt. The relative intensity of the three resonances will be  $(\frac{1}{2} \times 33.8):66.2:(\frac{1}{2} \times 33.8)$ , i.e. 1:4:1.

much Pd is used in the catalytic control of car-exhaust emissions. A similar amount of Pt is used for jewellery and 18% in the petroleum and glass industries. The largest single use for Pd is in the manufacture of electronic components (46%), but 25% is used in dentistry and 10% for hydrogenation and dehydrogenation catalysis.<sup>†</sup>

### 27.2.3 Properties of the elements

Table 27.1 lists some of the important atomic and physical properties of these three elements. The prevalence of naturally occurring isotopes in this triad limits the precision of their quoted atomic weights, though the value for Ni was improved by more than two orders of magnitude in 1989

<sup>†</sup> It should not be overlooked that platinum has played a crucial role in the development of many branches of science even though the amounts of metal involved may have been small. Reliable Pt crucibles were vital in classical analysis on which the foundations of chemistry were laid. It was also widely used in the development of the electric telegraph, incandescent lamps, and thermionic valves.

and that for Pt fifteen fold in 1995. Difficulties in attaining high purities have also frequently led to disparate values for some physical properties, while mechanical history has considerable effect on such properties as hardness. The metals are silvery-white and lustrous, and are both malleable and ductile so that they are readily worked. They are also readily obtained in finely divided forms which are catalytically very active. *Platinum black*, for instance, is a velvety-black powder obtained by adding ethanol to a solution of PtCl<sub>2</sub> in aqueous KOH and warming. Another property of platinum which has led to numerous laboratory applications is its coefficient of expansion which is virtually the same as that of soda glass into which it can therefore be fused to give a permanent seal.

Like Rh and Ir, all three members of this triad have the fcc structure predicted by band theory calculations for elements with nearly filled d shells. Also in this region of the periodic table, densities and mps are decreasing with increase in Z across the table: thus, although by comparison

with the generality of members of the d block these elements are in each case to be considered as dense refractory metals, they are somewhat less so than their immediate predecessors, and palladium has the lowest density and melting point of any platinum metal.

Nickel is ferromagnetic, but less markedly so than either iron or cobalt and its Curie point (375°C) is also lower.

### 27.2.4 Chemical reactivity and trends

In the massive state none of these elements is particularly reactive and they are indeed very resistant to atmospheric corrosion at normal temperatures. However, nickel tarnishes when heated in air and is actually pyrophoric if very finely divided (finely divided Ni catalysts should therefore be handled with care). Palladium will also form a film of oxide if heated in air.

Nickel reacts on heating with B, Si, P, S and the halogens, though more slowly with F<sub>2</sub> than most metals do. It is oxidized at red heat by steam, and will dissolve in dilute mineral acids: slowly in most but quite rapidly in dil HNO<sub>3</sub>. Conc HNO<sub>3</sub>, on the other hand, renders it passive and dry hydrogen halides have little effect. It has a notable resistance to attack by aqueous caustic alkalis and therefore finds used in apparatus for producing NaOH.

Palladium is oxidized by O<sub>2</sub>, F<sub>2</sub> and Cl<sub>2</sub> at red heat and dissolves slowly in oxidizing acids. Platinum is generally more resistant to attack than Pd and is, for instance, barely affected by mineral acids except aqua regia. However, both metals dissolve in fused alkali metal oxides and peroxides. It is also wise to avoid heating compounds containing B, Si, Pb, P, As, Sb or Bi in platinum crucibles under reducing conditions (e.g. the blue flame of a bunsen burner) since these elements form low-melting eutectics with Pt which cause the metal to collapse. All three elements absorb molecular hydrogen to an extent which depends on their physical state, but palladium does so to an extent which is unequalled by any other metal (section 27.3.1).

A list of typical compounds of these elements is given in Table 27.2 and it is noticeable that the reduction in the range of oxidation states compared to that in previous groups is continuing and differences between the two heavier elements are becoming increasingly evident. The maximum oxidation state is +6 but this is attained only by the heaviest element, platinum, in PtF<sub>6</sub>; nickel and palladium only reach +4. At the other extreme, palladium and platinum provide no oxidation state below zero. The changes down the triad implied by these facts are also evidenced by those oxidation states which are the most stable for each element. For nickel, +2 is undoubtedly the most common and provides that element's most extensive aqueous chemistry. For palladium, +2 is again the most common, and [Pd(H<sub>2</sub>O)<sub>4</sub>]<sup>2+</sup> like [Pt(H<sub>2</sub>O)<sub>4</sub>]<sup>2+</sup> occurs in aqueous solutions from which potential ligands are excluded. For platinum, however, both +2 and +4 are prolific and form a vital part of early as well as more recent coordination chemistry.

Table 27.2 also reveals the reluctance of these elements to form compounds with high coordination numbers, a coordination number of 6 being rarely exceeded. In the divalent state nickel exhibits a wide and interesting variety of coordination numbers and stereochemistries which often exist simultaneously in equilibrium with each other, whereas palladium and platinum have a strong preference for the square planar geometry. The kinetic inertness of Pt<sup>II</sup> complexes has led to their extensive use in studies of geometrical isomerism and reaction mechanisms. As will be seen presently, these differences between the lightest and heaviest members of the triad can be largely rationalized by reference to their CFSEs.

Also in the divalent state, Pd and Pt show the class-b characteristic of preferring CN<sup>-</sup> and ligands with nitrogen or heavy donor atoms rather than oxygen or fluorine. Platinum(IV) by contrast is more nearly class-a in character and is frequently reduced to Pt<sup>II</sup> by *P*- and *As*-donor ligands. The organometallic chemistry of these metals is rich and varied and that involving unsaturated hydrocarbons is the most familiar of its type.

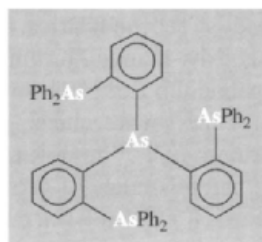
**Table 27.2** Oxidation states and stereochemistries of compounds of nickel, palladium and platinum

Oxidation state	Coordination number	Stereochemistry	Ni	Pd/Pt
-1	4	?	$[\text{Ni}_2(\text{CO})_6]^{2-}$	
0 ( $d^{10}$ )	3	Planar	$[\text{Ni}\{\text{P}(\text{OC}_6\text{H}_4\text{-2-Me})_3\}_3]$	$[\text{M}(\text{PPh}_3)_3]$
	4	Tetrahedral	$[\text{Ni}(\text{CO})_4]$	$[\text{M}(\text{PF}_3)_4]$
1 ( $d^9$ )	4	Tetrahedral	$[\text{NiBr}(\text{PPh}_3)_3]$	
	3	Trigonal planar	$[\text{Ni}(\text{NPh}_2)_3]^-$	
2 ( $d^8$ )	4	Tetrahedral	$[\text{NiCl}_4]^{2-}$	
		Square planar	$[\text{Ni}(\text{CN})_4]^{2-}$	$[\text{MCl}_4]^{2-}$
	5	Trigonal bipyramidal	$[\text{Ni}(\text{PPhMe}_2)_3(\text{CN})_2]$	$[\text{M}(\text{qas})\text{I}]^{+(a)}$
		Square pyramidal	$[\text{Ni}(\text{CN})_5]^{3-}$	$[\text{Pd}(\text{tpas})\text{Cl}]^{+(b)}$
	6	Octahedral	$[\text{Ni}(\text{H}_2\text{O})_6]^{2+}$	$[\text{Pd}(\text{diars})_2\text{I}_2]$
		Trigonal prismatic	NiAs	
	7	Pentagonal bipyramidal	$[\text{Ni}(\text{dapbH})_2(\text{H}_2\text{O})_2]^{2+(c)}$	
3 ( $d^7$ )	4	Square planar	—	$[\text{Pt}(\text{C}_6\text{Cl}_5)_4]^-$
	5	Trigonal bipyramidal	$[\text{NiBr}_3(\text{PET}_3)_2]$	
	6	Octahedral	$[\text{NiF}_6]^{3-}$	$[\text{PdF}_6]^{3-}$
4 ( $d^6$ )	6	Octahedral	$[\text{NiF}_6]^{2-}$	$[\text{MCl}_6]^{2-}$
	8	“Piano-stool”	—	$[\text{Pt}(\eta^5\text{-C}_5\text{H}_5)\text{Me}_3]$
5 ( $d^5$ )	6	Octahedral	—	$[\text{PtF}_6]^-$
6 ( $d^4$ )	6	Octahedral	—	$\text{PtF}_6$

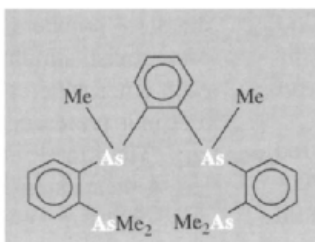
<sup>(a)</sup>qas, tris-(2-diphenylarsinophenyl)arsine,  $\text{As}(\text{C}_6\text{H}_4\text{-2-AsPh}_2)_3$ .

<sup>(b)</sup>tpas, 1,2-phenylenebis((2-dimethylarsinophenyl)-methylarsine).

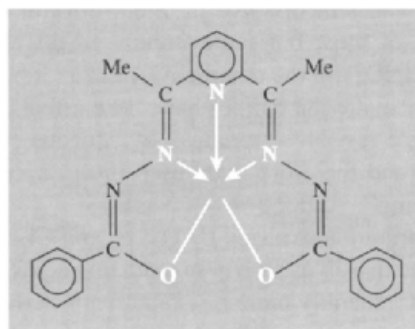
<sup>(c)</sup>dapbH, 2,6-diacetylpyridinebis(benzoic acid hydrazone).



(a)



(b)



(c)

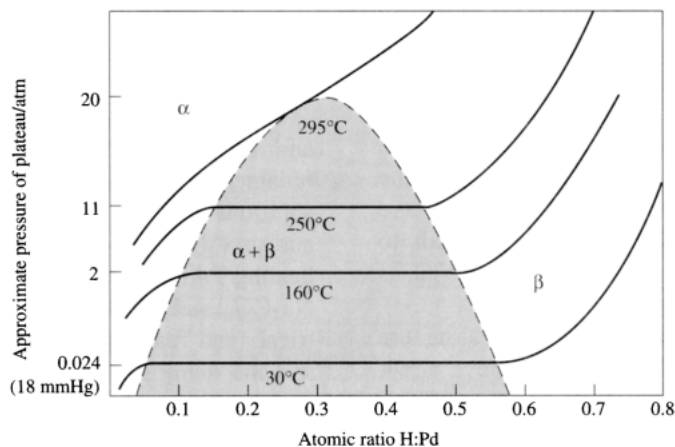
## 27.3 Compounds of Nickel, Palladium and Platinum

Such binary borides (p. 145), carbides (p. 297) and nitrides (p. 417) as are formed have been referred to already. The ability of the metals to absorb molecular hydrogen has also been alluded to above. While the existence of definite hydrides of nickel and platinum is in doubt the

existence of definite palladium hydride phases is not.

### 27.3.1 The Pd/H<sub>2</sub> system

The absorption of molecular hydrogen by metallic palladium has been the subject of theoretical and practical interest ever since 1866 when T. Graham reported that, on being cooled from red heat, Pd can absorb (or “occlude” as



**Figure 27.2** Pressure-concentration isotherms for the Pd/H<sub>2</sub> system: the biphasic region (in which the  $\alpha$ - and  $\beta$ -phases coexist) is shaded. (From A. G. Knapton, *Plat. Met. Revs.* **21**, 44 (1977). See also F. A. LEWIS, *ibid.* **38**, 112–18 (1994))

he called it) up to 935 times its own volume of H<sub>2</sub>.<sup>†</sup> The gas is given off again on heating and this provides a convenient means of weighing H<sub>2</sub> — a fact utilized by E. W. Morley in his classic work on the composition of water (1895).

As hydrogen is absorbed, the metallic conductivity falls until the material becomes a semiconductor at a composition of about PdH<sub>0.5</sub>. Palladium is unique in that it does not lose its ductility until large amounts of H<sub>2</sub> have been absorbed. The hydrogen is first chemisorbed at the surface of the metal but at increased pressures it enters the metal lattice and the so-called  $\alpha$ - and  $\beta$ -phase hydrides are formed (Fig. 27.2). The basic lattice structure is not altered but, whereas the  $\alpha$ -phase causes only a slight expansion, the  $\beta$ -phase causes an expansion of up to 10% by volume. The precise nature of the metal–hydrogen interaction is still unclear<sup>‡</sup> but the hydrogen has a high

mobility within the lattice and diffuses rapidly through the metal. This process is highly specific to H<sub>2</sub> and D<sub>2</sub>, palladium being virtually impervious to all other gases, even He, a fact which is utilized in the separation of hydrogen from mixed gases. Industrial installations with outputs of up to 9 million ft<sup>3</sup>/day (255 million litres/day) are operated and it is of great importance in these that formation of the  $\beta$ -phase hydride is avoided, since the gross distortions and hardening which accompany it may result in splitting of the diffusion membrane. This can be done by maintaining the temperature above 300°C (Fig. 27.2), or alternatively by alloying the Pd with about 20% Ag which has the additional advantage of actually increasing the permeability of the Pd to hydrogen (p. 39).

### 27.3.2 Oxides and chalcogenides

The elements of this group form only one reasonably well-characterized oxide each, namely NiO, PdO and PtO<sub>2</sub>, although claims for the existence of many others have been made. Formation of NiO by heating the metal in oxygen

<sup>†</sup> This approximates to a composition of Pd<sub>4</sub>H<sub>3</sub> and represents a concentration of hydrogen approaching that in liquid hydrogen!

<sup>‡</sup> In March 1989 S. Pons and M. Fleischmann reported the production of excess heat from heavy water electrolysis using Pd cathode and Pt anode, and postulated nuclear fusion (“cold fusion”) as the reason. In spite of widespread scepticism, work in many laboratories was quickly initiated and focused on: (a) measuring the excess heat effect, and (b) identifying any nuclear particles produced. Emissions of <sup>4</sup>He, <sup>3</sup>H and <sup>1</sup>n have been variously reported and it appears that production of

excess heat is associated with very heavy deuterium loading of Pd in the  $\beta$ -phase. Reproducibility is, however, poor and it seems probable that more than one effect is involved. The current consensus is against a “cold-fusion” explanation of the effects.

is difficult to achieve and incomplete conversion may well account for some of the claims for other nickel oxides, while grey to black colours probably arise from slight nonstoichiometry. It is best prepared as a green powder with the rock-salt structure (p. 242) by heating the hydroxide, carbonate or nitrate.  $\text{Ni}(\text{OH})_2$  is a green precipitate obtained by adding alkali to aqueous solutions of  $\text{Ni}^{\text{II}}$  salts and, like  $\text{NiO}$ , is entirely basic, dissolving easily in acids.

Black  $\text{PdO}$  can be produced by heating the metal in oxygen but it dissociates above about  $900^\circ\text{C}$ . It is insoluble in acids. However, addition of alkali to aqueous solutions of  $\text{Pd}(\text{NO}_3)_2$  produces a gelatinous dark-yellow precipitate of the hydrous oxide which is soluble in acids but cannot be fully dehydrated without loss of oxygen. No other palladium oxide has been characterized although the addition of alkali to aqueous solutions of  $\text{Pd}^{\text{IV}}$  produces a strongly oxidizing, dark-red precipitate which slowly loses oxygen and, at  $200^\circ\text{C}$ , forms  $\text{PdO}$ .

Addition of alkali to aqueous solutions of  $[\text{Pt}(\text{H}_2\text{O})_4](\text{ClO}_4)_2$  under an atmosphere of argon gives a white amphoteric hydroxide of  $\text{Pt}^{\text{II}}$  at pH 4 which redissolves at pH 10.<sup>(5)</sup> The precipitate slowly turns black at room temperature (more rapidly when dried at  $100^\circ\text{C}$ ) and has been formulated as  $\text{PtO}_x \cdot \text{H}_2\text{O}$ , but it is too unstable to be properly characterized. The stable oxide of platinum is found, instead, in the higher oxidation state. Addition of alkali to aqueous solutions of  $\text{PtCl}_4$  yields a yellow amphoteric precipitate of the hydrated dioxide which redissolves on being boiled with an excess of strong alkali to give solutions of  $[\text{Pt}(\text{OH})_6]^{2-}$ ; it also dissolves in acids. Dehydration by heating produces almost black  $\text{PtO}_2$  but this decomposes to the elements above  $650^\circ\text{C}$  and cannot be completely dehydrated without some loss of oxygen.

Nickel sulfides are very similar to those of cobalt, consisting of  $\text{NiS}_2$  (pyrites structure, p. 680),  $\text{Ni}_3\text{S}_4$  (spinel structure, p. 247), and the black, nickel-deficient  $\text{Ni}_{1-x}\text{S}$  (NiAs structure, p. 555), which is precipitated from aqueous

solutions of  $\text{Ni}^{\text{II}}$  by passing  $\text{H}_2\text{S}$ . There are also numerous metallic phases having compositions between  $\text{NiS}$  and  $\text{Ni}_3\text{S}_2$ .

Palladium and platinum both form a mono- and a di-sulfide. Brown  $\text{PdS}$  and black  $\text{PtS}_2$  are obtained when  $\text{H}_2\text{S}$  is passed through aqueous solutions of  $\text{Pd}^{\text{II}}$  and  $\text{Pt}^{\text{IV}}$  respectively. Grey  $\text{PdS}_2$  and green  $\text{PtS}$  are best obtained by respectively heating  $\text{PdS}$  with excess S and by heating  $\text{PtCl}_2$ ,  $\text{Na}_2\text{CO}_3$  and S. The crystal chemistry and electrical (and magnetic) properties of these phases and the many selenides and tellurides of Ni, Pd and Pt are complex.

### 27.3.3 Halides

The known halides of this group are listed in Table 27.3. This list differs from that of the halides of Co, Rh and Ir (Table 26.3) most obviously in that the +2 rather than the +3 oxidation state is now well represented for the heavier elements as well as for the lightest. The only hexa- and penta-halides are the dark-red  $\text{PtF}_6$  and  $(\text{PtF}_5)_4$  which are both obtained by controlled heating of Pt and  $\text{F}_2$ . The former is a volatile solid and, after  $\text{RhF}_6$ , is the least-stable platinum-metal hexafluoride. It is one of the strongest oxidizing agents known, oxidizing both  $\text{O}_2$  (to  $\text{O}_2^+[\text{PtF}_6]^-$ ) and Xe (to  $\text{XePtF}_6$ ) (p. 892). The pentafluoride is also very reactive and has the same tetrameric structure as the pentafluorides of Ru, Os, Rh and Ir (Fig. 25.3). It readily disproportionates into the hexa- and tetra-fluorides.

Platinum alone forms all 4 tetrahalides and these vary in colour from the light-brown  $\text{PtF}_4$  to the very dark-brown  $\text{PtI}_4$ .  $\text{PtF}_4$  is obtained by the action of  $\text{BrF}_3$  on  $\text{PtCl}_2$  at  $200^\circ\text{C}$  and is violently hydrolysed by water. The others are obtained directly from the elements, the chloride being recrystallizable from water but the bromide and iodide being more soluble in alcohol and in ether. The only other tetrahalide is the red  $\text{PdF}_4$  which is similar to its platinum analogue.

The most stable product of the action of fluorine on metallic palladium is actually  $\text{Pd}^{\text{II}}[\text{Pd}^{\text{IV}}\text{F}_6]$ , and true trihalides of Pd do not occur. Similarly, the diamagnetic "trichloride" and "tribromide" of Pt

<sup>5</sup> L. J. ELDING, *Inorg. Chim. Acta* **20**, 65-9 (1976).

Table 27.3 Halides of nickel, palladium and platinum (mp/°C)

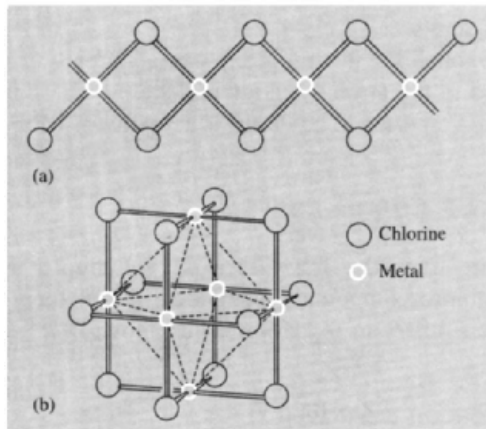
Oxidation State	Fluorides	Chlorides	Bromides	Iodides
+6	PtF <sub>6</sub> <sup>(a)</sup> dark red (61.3°)			
+5	[PtF <sub>5</sub> ] <sub>4</sub> deep red (80°)			
+4	PdF <sub>4</sub> brick-red	PtCl <sub>4</sub> red-brown (d 370°)	PtBr <sub>4</sub> brown-black (d 180°)	PtI <sub>4</sub> brown-black (d 130°)
+3	Pd[PdF <sub>6</sub> ] —	PtCl <sub>3</sub> green-black (d 400°)	PtBr <sub>3</sub> green-black (d 200°)	PtI <sub>3</sub> black (d 310°)
+2	NiF <sub>2</sub> yellow (1450°)	NiCl <sub>2</sub> yellow (1001°)	NiBr <sub>2</sub> yellow (965°)	NiI <sub>2</sub> black (780°)
	PdF <sub>2</sub> pale violet	$\alpha$ -PdCl <sub>2</sub> <sup>(b)</sup> dark red (d 600°)	PdBr <sub>2</sub> red-black	PdI <sub>2</sub> black
	—	$\beta$ -PdCl <sub>2</sub> <sup>(b)</sup> olive-green (d 581°)	PtBr <sub>2</sub> brown (d 250°)	PtI <sub>2</sub> black (d 360°)

<sup>(a)</sup>PtF<sub>6</sub> boils at 69.1°. <sup>(b)</sup> $\beta$ -PdCl<sub>2</sub> and  $\beta$ -PtCl<sub>2</sub> (reddish-black) contain M<sub>6</sub>Cl<sub>12</sub> clusters (Fig. 27.3b).

contain Pt<sup>II</sup> and Pt<sup>IV</sup> and the triiodide probably does also. Trihalides of nickel are confined to impure specimens of NiF<sub>3</sub>.

All the dihalides, except PtF<sub>2</sub>, are known, fluorine perhaps being too strongly oxidizing to be readily compatible with the metal in the lower of its two major oxidation states. Except for NiF<sub>2</sub>, the yellow to dark-brown dihalides of nickel can be obtained directly from the elements; they dissolve in water from which hexahydrates containing the [Ni(H<sub>2</sub>O)<sub>6</sub>]<sup>2+</sup> ion can be crystallized. These solutions may also be prepared more conveniently by dissolving Ni(OH)<sub>2</sub> in the appropriate hydrohalic acid. NiF<sub>2</sub> is best formed by the reaction of F<sub>2</sub> on NiCl<sub>2</sub> at 350°C and is only slightly soluble in water, from which the trihydrate crystallizes.

Violet, easily hydrolysed, PdF<sub>2</sub> is produced when Pd<sup>II</sup>[Pd<sup>IV</sup>F<sub>6</sub>] is refluxed with SeF<sub>4</sub> and is notable as one of the very few paramagnetic compounds of Pd<sup>II</sup>. The paramagnetism arises from the  $t_{2g}^6 e_g^2$  configuration of Pd<sup>II</sup> which is consequent on its octahedral coordination in the rutile-type structure (p. 961). The dichlorides of both Pd and Pt are obtained from the elements and exist in two isomeric forms: which form is produced depends on the exact experimental conditions used. The more usual  $\alpha$ -form of PdCl<sub>2</sub> is a red material with



**Figure 27.3** (a) The chain structure of  $\alpha$ -PdCl<sub>2</sub>, and (b) the M<sub>6</sub>Cl<sub>12</sub> structural unit of  $\beta$ -PdCl<sub>2</sub> and  $\beta$ -PtCl<sub>2</sub>. (Note its broad similarity with the [M<sub>6</sub>X<sub>12</sub>]<sup>n+</sup> unit of the lower halides of Nb and Ta shown in Fig. 22.6 and to the unit cell of the three-dimensional structure of NbO.)

a chain structure (Fig. 27.3a) in which each Pd has a square planar geometry. It is hygroscopic and its aqueous solution provides a useful starting point for studying the coordination chemistry of Pd<sup>II</sup>.  $\beta$ -PdCl<sub>2</sub> is also known and its structure is based on Pd<sub>6</sub>Cl<sub>12</sub> units in which, nevertheless, the preferred square-planar coordination of the Pd<sup>II</sup> is still

retained (Fig. 27.3b). Platinum dichlorides are less well-known. The high temperature modification,  $\alpha$ -PtCl<sub>2</sub> is insoluble in water but dissolves in hydrochloric acid forming [PtCl<sub>4</sub>]<sup>2-</sup> ions. It has been reported as both olive-green and black, the latter consisting of edge- and corner-sharing PtCl<sub>4</sub> units<sup>(6)</sup> (distinct from  $\alpha$ -PdCl<sub>2</sub>). The dark-red  $\beta$ -PtCl<sub>2</sub> is isomorphous with  $\beta$ -PdCl<sub>2</sub> and the Pt<sub>6</sub>Cl<sub>12</sub> unit is retained on dissolution in benzene. Red PdBr<sub>2</sub> and black PdI<sub>2</sub>, obtained respectively by the action of Br<sub>2</sub> on Pd and the addition of I<sup>-</sup> to aqueous solutions of PdCl<sub>2</sub>, are both insoluble in water but form [PdX<sub>4</sub>]<sup>2-</sup> ions on addition of HX (X = Br, I). PtBr<sub>2</sub> and  $\alpha$ -PtI<sub>2</sub> are obtained by thermal decomposition of the tetrahalides, the latter being accompanied by Pt<sub>3</sub>I<sub>8</sub> a mixed-valence (II, IV) iodide made up of octahedral PtI<sub>6</sub> and square planar PtI<sub>4</sub> units.<sup>(7)</sup>  $\beta$ -PtI<sub>2</sub> is prepared by hydrothermal synthesis from PtI<sub>4</sub>, KI and I<sub>2</sub> at 420°C and is made up of planar PtI<sub>4</sub> and planar Pt<sub>2</sub>I<sub>6</sub> units.<sup>(7)</sup>

Oxohalides in this group are apparently confined to the strongly oxidizing PtOF<sub>3</sub>. The compound reported to be PtOF<sub>4</sub> is actually O<sub>2</sub><sup>+</sup>[PtF<sub>6</sub>].

### 27.3.4 Complexes<sup>(8)</sup>

Apart from the few Pt<sup>VI</sup> and Pt<sup>V</sup> fluoro and oxofluoro compounds mentioned above, there is no chemistry in oxidation states above IV.

#### Oxidation state IV (d<sup>6</sup>)

All complexes in this oxidation state which have been characterized are octahedral and diamagnetic with the low-spin  $t_{2g}^6$  configuration.

<sup>6</sup> B. KREBS, C. BRENDEL and H. SCHÄFER, *Z. anorg. allg. Chem.* **561**, 119–31 (1988).

<sup>7</sup> G. THIELE, W. WEIGL and H. WOCHNER, *Z. anorg. allg. Chem.* **539**, 141–53 (1986).

<sup>8</sup> L. SACCONI, F. MANI and A. BENCINI, Ni, Chap. 50, pp. 1–347; M. J. RUSSELL and C. F. J. BARNARD, Pd, Chap. 51, pp. 1099–130; A. T. HUTTON, Pd(II)–S-donor Complexes, Chap. 51.8, pp. 1131–55; A. T. HUTTON and C. P. MORLEY, Pd(II)–P-donor Complexes, Chap. 51.9, pp. 1157–70; D. M. ROUNDHILL, Pt, Chap. 52, pp. 351–531 in *Comprehensive Coordination Chemistry*, Vol. 5, Pergamon Press, Oxford, 1987.

Fluorination of NiCl<sub>2</sub> + KCl produces red K<sub>2</sub>NiF<sub>6</sub> which is strongly oxidizing and will liberate O<sub>2</sub> from water. Dark red complexes of the type [Ni<sup>IV</sup>(L)](ClO<sub>4</sub>)<sub>2</sub> (H<sub>2</sub>L is a sixidentate oxime) have been obtained by the action of conc HNO<sub>3</sub> on [Ni<sup>II</sup>(H<sub>2</sub>L)](ClO<sub>4</sub>)<sub>2</sub> and are stable indefinitely under vacuum but are reduced in moist air.

Palladium(IV) complexes are rather sparse and much less stable than those of Pt<sup>IV</sup>. The best known are the hexahalogeno complexes [PdX<sub>6</sub>]<sup>2-</sup> (X = F, Cl, Br) of which [PdCl<sub>6</sub>]<sup>2-</sup>, formed when the metal is dissolved in aqua regia, is the most familiar. In all of these the Pd<sup>IV</sup> is readily reducible to Pd<sup>II</sup>. In water, [PdF<sub>6</sub>]<sup>2-</sup> hydrolyses immediately to PdO<sub>2</sub>.xH<sub>2</sub>O while the chloro and bromo complexes give [PdX<sub>4</sub>]<sup>2-</sup> plus X<sub>2</sub>. An organometallic chemistry of Pd<sup>IV</sup> is developing (p. 1167).

By contrast Pt<sup>IV</sup> complexes rival those of Pt<sup>II</sup> in number, and are both thermodynamically stable and kinetically inert. Those with halides, pseudo-halides, and N-donor ligands are especially numerous. Of the multitude of conceivable compounds ranging from [PtX<sub>6</sub>]<sup>2-</sup> through [PtX<sub>4</sub>L<sub>2</sub>] to [PtL<sub>6</sub>]<sup>4+</sup>, (X = F, Cl, Br, I, CN, SCN, SeCN; L = NH<sub>3</sub>, amines) a large number have been prepared and characterized though, curiously, they do not include the [Pt(CN)<sub>6</sub>]<sup>2-</sup> ion. K<sub>2</sub>PtCl<sub>6</sub> is commercially the most common compound of platinum and the brownish-red, “chloroplatinic acid”, H<sub>2</sub>[PtCl<sub>6</sub>](aq), is the usual starting material in Pt<sup>IV</sup> chemistry. It is prepared by dissolving platinum metal sponge in aqua regia, followed by one or more evaporations with hydrochloric acid. A route to Pt<sup>II</sup> chemistry also is provided by precipitation of the sparingly soluble K<sub>2</sub>PtCl<sub>6</sub> followed by its reduction with hydrazine to K<sub>2</sub>PtCl<sub>4</sub>. The chloroammines were extensively used by Werner and other early coordination chemists in their studies on the nature of the coordinate bond in general and on the octahedral geometry of Pt<sup>IV</sup> in particular.

O-donor ligands such as OH<sup>-</sup> and acac also coordinate to Pt<sup>IV</sup>, but S- and Se-, and more especially P- and As-donor ligands, tend to reduce it to Pt<sup>II</sup>.



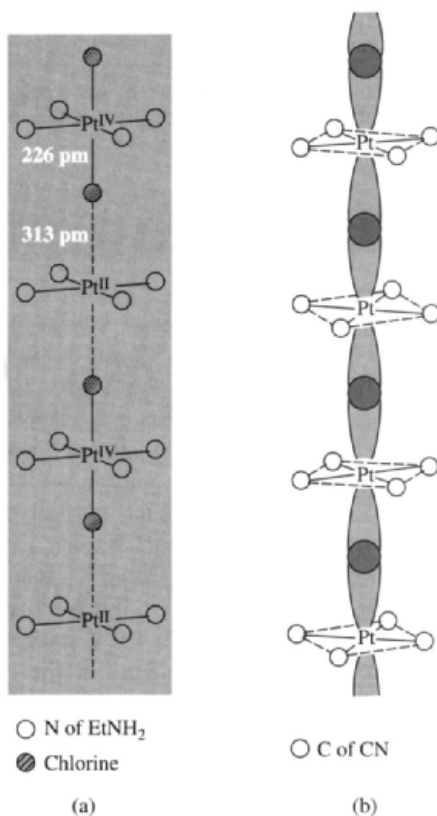
Oxidation state III ( $d^7$ )

Perhaps surprisingly, mononuclear  $M^{III}$  compounds are rather better represented by nickel than by either palladium or platinum.  $K_3NiF_6$  has been prepared by fluorinating  $KCl + NiCl_2$  at high temperatures and pressures. It is a violet crystalline material which is reduced by water with evolution of oxygen. The observed elongation of the  $[NiF_6]^{3-}$  octahedron has been ascribed to the Jahn–Teller effect (p. 1021) to be expected for a  $t_{2g}^6 e_g^1$  configuration although the reported magnetic moment of 2.5 BM at room temperature seems rather high for this configuration. Other examples include  $[Ni(bipy)_3]^{3+}$ , the black trigonal pyramidal  $[NiBr_3(PEt_3)_2]$  and a number of compounds with  $N$ -donor macrocyclic ligands. Among the very few monomeric trivalent compounds of Pd and Pt, the blue  $(NBu_4)[Pt(C_6Cl_5)_4]$  (obtained by oxidizing the  $Pt^{II}$  salt) and the red  $[Pd(1,4,7-trithiacyclononane)_2](ClO_4)_4 \cdot H_3O \cdot 3H_2O$  (obtained<sup>(9)</sup> by cyclovoltammetric oxidation in 70% aqueous  $HClO_4$ ) should be mentioned.

The most abundant examples of this oxidation state, however, are the dinuclear Pt compounds<sup>(10)</sup> of the type,  $[Pt_2(L-L)_4L_2]^{n-}$  with single Pt–Pt bonds and the same tetrabridged structure of  $Mo^{II}$  and  $Cr^{II}$  (p. 1032). The first of these was  $K_2[Pt_2(SO_4)_4(H_2O)_2]$ , prepared from  $[Pt(NO_2)_2(NH_3)_2]$  and sulfuric acid, but those with phosphate or  $P$ -donor, pyrophosphito,  $(P_2O_5H_2)^{2-}$ , bridges are more numerous. Pt–Pt distances range from 278.2(1) pm, found with pyrophosphito bridges, down to 245.1(1) pm in  $Cs_3[Pt_2(\mu-O_2CMe)_2(\mu-O_2CCH_2)_2]$ . This yellow complex is obtained by a complex procedure<sup>(11)</sup> from  $K_2PtCl_4$  and  $MeCOOAg$  and, besides a pair of  $O,O$ -donor acetate bridges, contains a pair of

unique  $C,O$ -donor,  $-O.CO.CH_2-$ , bridges. Stable tetraacetato bridged dimers are not found.

A number of compounds which have in the past been claimed to contain the trivalent metals have later turned out to contain them in more than one oxidation state. One such is H. Wolfram's red salt,  $Pt(EtNH_2)_4Cl_3 \cdot 2H_2O$ , which has a structure (Fig. 27.4a) consisting of alternate octahedral  $Pt^{IV}$  and square-planar  $Pt^{II}$  linked by Cl bridges, i.e.  $[Pt^{II}(EtNH_2)_4]^{2+} [trans-(\mu-Cl)_2-Pt^{IV}(EtNH_2)_4]^{2-} Cl^- \cdot 4H_2O$ . Other examples are



**Figure 27.4** Linear chain polymers of Pt. (a) The coordination of platinum in Wolfram's red salt,  $Pt(EtNH_2)_4Cl_3 \cdot 2H_2O$ , showing alternating  $Pt^{II}$  and  $Pt^{IV}$  linked by Cl bridges. Four remaining  $Cl^-$  ions and 4  $H_2O$  are situated within the lattice. (b) Stacking of square planar units in  $[Pt(CN)_4]^{n-}$  showing the possible overlap of  $d_{z^2}$  orbitals. (Note the successive  $45^\circ$  rotations, or "staircase staggering", of these units.)

<sup>9</sup> A. J. BLAKE, A. J. HOLDER, T. I. WHITE and M. SCHRÖDER, *J. Chem. Soc., Chem. Commun.*, 987–8 (1987).

<sup>10</sup> F. A. COTTON and R. A. WALTON, *Multiple Bonds between Atoms*, 2nd Edn., Oxford University Press, Oxford, pp. 508–32 (1993); K. UMAKOSHI and Y. SASAKI, *Adv. Inorg. Chem.* **40**, 187–239 (1994).

<sup>11</sup> T. YAMAGUCHI, Y. SASAKI and T. ITO, *J. Am. Chem. Soc.* **112**, 4038–40 (1990).

## Development of Ideas on the Stereochemistry of Nickel(II)

The way in which our present understanding of the stereochemical intricacies of  $Ni^{II}$  has evolved illustrates rather well the interplay of theory and experiment. On the basis of valence-bond theory, three types of complex of  $d^8$  ions were anticipated. These were:

- (i) *octahedral*, involving  $sp^3d_2$  hybridization and paramagnetism from 2 unpaired electrons;
- (ii) *tetrahedral*, involving  $sp^3$  hybridization and, again, paramagnetism from 2 unpaired electrons;
- (iii) *square planar*, involving  $d_{x^2-y^2}sp_3$  hybridization which implies the confinement of all 8 electrons in four  $d$  orbitals, so producing diamagnetism.

Since X-ray determinations of structure were too time-consuming to be widely used in the 1930s and 1940s and, in addition, square-planar geometry was a comparative rarity, any paramagnetic compound, which on the basis of stoichiometry appeared to be 4-coordinate, was presumed to be tetrahedral.

However, with the application in the 1950s of crystal field theory to transition-metal chemistry it was realized that CFSEs were unfavourable to the formation of tetrahedral  $d^8$  complexes, and previous assignments were re-examined. A typical case was  $[Ni(acac)_2]$ , which had often been cited as an example of a tetrahedral nickel complex, but which was shown<sup>(12)</sup> in 1956 to be trimeric and octahedral. The over-zealous were then inclined to regard tetrahedral  $d^8$  as non-existent until first L. M. Venanzi<sup>(13)</sup> and then N. S. Gill and R. S. Nyholm<sup>(14)</sup> demonstrated the existence of discrete tetrahedral species which in some cases were also rather easily prepared.

More comprehensive examination of spectroscopic and magnetic properties of  $d^8$  ions followed which provided an explanation for the different types of Lifschitz salts (p. 1160) and led to studies of systems exhibiting anomalous properties. Rational explanations of these properties were eventually forthcoming.

provided by the one-dimensional conductors of platinum,<sup>(14a)</sup> of which the cyano complexes are the best known. Thus  $K_2[Pt(CN)_4] \cdot 3H_2O$  is a very stable colourless solid, but by appropriate partial oxidation it is possible to obtain bronze-coloured, "cation deficient",  $K_{1.75}Pt(CN)_4 \cdot 1.5H_2O$ , and other partially oxidized compounds such as  $K_2Pt(CN)_4Cl_{0.3} \cdot 3H_2O$ . In these, square-planar  $[Pt(CN)_4]^{n-}$  ions are stacked (Fig. 27.4b) to give a linear chain of Pt atoms in which the Pt-Pt distances of 280–300 pm (compared to 348 pm in the original  $K_2[Pt(CN)_4] \cdot 3H_2O$  and 278 pm in the metal itself) allow strong overlap of the  $d_{z^2}$  orbitals. This accounts for the metallic conductance of these materials along the crystal axis. Indeed, there is considerable current interest in such "one-dimensional" electrical conductors.

Oxalato complexes [e.g.  $K_{1.6}Pt(C_2O_4)_2 \cdot 1.2H_2O$ ] originally prepared as long ago as 1888

by the German chemist H. G. Söderbaum, are also one-dimensional conductors with analogous structures.

### Oxidation state II ( $d^8$ )

This is undoubtedly the most prolific oxidation state for this group of elements. The stereochemistry of  $Ni^{II}$  has been a topic of continuing interest (see Panel), and kinetic and mechanistic studies on complexes of  $Pd^{II}$  and  $Pt^{II}$  have likewise been of major importance. It will be convenient to treat  $Ni^{II}$  complexes first and then those of  $Pd^{II}$  and  $Pt^{II}$  (p. 1161).

*Complexes of  $Ni^{II}$ .* The absence of any other oxidation state of comparable stability for nickel implies that compounds of  $Ni^{II}$  are largely immune to normal redox reactions.  $Ni^{II}$  forms salts with virtually every anion and has an extensive aqueous chemistry based on the green<sup>†</sup>  $[Ni(H_2O)_6]^{2+}$  ion which is always present in the absence of strongly complexing ligands.

<sup>12</sup> G. J. BULLEN, *Nature* **177**, 537–8 (1956).

<sup>13</sup> L. M. VENANZI, *J. Chem. Soc.* 719–24 (1958).

<sup>14</sup> N. S. GILL and R. S. NYHOLM, *J. Chem. Soc.* 3997–4007 (1959).

<sup>14a</sup> R. J. H. CLARK, *Chem. Soc. Rev.* **19**, 107–31 (1990).

<sup>†</sup> It was work on the absorption of light by solutions of nickel(II) which led A. Beer in 1852 to formulate the law which bears his name.

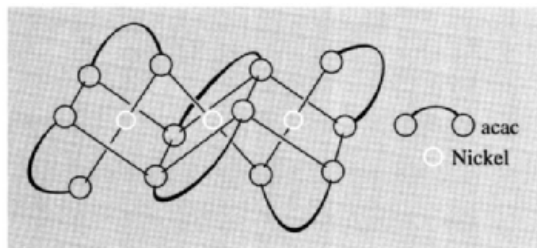


Figure 27.5 Trimeric structure of  $[\text{Ni}(\text{acac})_2]_3$ .

The coordination number of  $\text{Ni}^{\text{II}}$  rarely exceeds 6 and its principal stereochemistries are octahedral and square planar (4-coordinate) with rather fewer examples of trigonal bipyramidal (5), square pyramidal (5), and tetrahedral (4). Octahedral complexes of  $\text{Ni}^{\text{II}}$  are obtained (often from aqueous solution by replacement of coordinated water) especially with neutral *N*-donor ligands such as  $\text{NH}_3$ , en, bipy and phen, but also with  $\text{NCS}^-$ ,  $\text{NO}_2^-$  and the *O*-donor dimethylsulfoxide, dmsO ( $\text{Me}_2\text{SO}$ ).

The green trimer,  $[\text{Ni}(\text{acac})_2]_3$  (Fig 27.5), prepared by dehydrating the monomeric octahedral *trans*-dihydrate,  $[\text{Ni}(\text{acac})_2(\text{H}_2\text{O})_2]$  and mentioned in the Panel opposite, has interesting magnetic properties. Down to about 80 K it behaves as a normal paramagnet but below that the magnetic moment per nickel atom rises from about 3.2 BM (as expected for 2 unpaired electrons, i.e.  $S = 1$ ) to 4.1 BM at 4.3 K. This corresponds to the ferromagnetic coupling of all 6 unpaired electrons in the trimer (i.e.  $S' = 3$ ). Replacement of the  $-\text{CH}_3$  groups of acetylacetonate by the bulkier  $\text{C}(\text{CH}_3)_3$  apparently prevents the formation of

the trimer and leads instead to the red square-planar monomer (Fig. 27.6a).

Of the four-coordinate complexes of  $\text{Ni}^{\text{II}}$ , those with the square planar stereochemistry are the most numerous. They include the yellow  $[\text{Ni}(\text{CN})_4]^{2-}$ , the red bis(*N*-methylsalicylaldiminato)nickel(II) and the well-known bis(dimethylglyoximate)nickel(II) (Fig. 27.6b and c) obtained as a flocculent red precipitate in gravimetric determinations of nickel. Actually, in the solid state, this last compound consists of planar molecules stacked above each other so that Ni–Ni interactions occur (Ni–Ni 325 pm), and the nickel atoms should therefore be described as octahedrally coordinated. However, in non-coordinating solvents it dissociates into the square-planar monomer, while in bis(ethylmethylglyoximate)nickel(II) a much longer Ni–Ni separation (475 pm) indicates that even in the solid it must be regarded as square planar.

Although less numerous than the square-planar complexes, tetrahedral complexes of nickel(II) also occur. The simplest of these are the blue  $[\text{NiX}_4]^{2-}$  ( $\text{X} = \text{Cl}, \text{Br}, \text{I}$ ) ions, precipitated<sup>(14)</sup> from ethanolic solutions by large cations such as  $[\text{NR}_4]^+$ ,  $[\text{PR}_4]^+$  and  $[\text{AsR}_4]^+$ . Other examples include a number of those of the type  $[\text{NiL}_2\text{X}_2]$  ( $\text{L} = \text{PR}_3, \text{AsR}_3, \text{OPR}_3, \text{OAsR}_3$ ) amongst which were the first authenticated examples of tetrahedral nickel(II).<sup>(13)</sup>

A partial explanation, at least, can be provided for the relative abundances and ease of formation of the above stereochemical varieties of  $\text{Ni}^{\text{II}}$  complexes. It can be seen from Table 26.6 that the CFSEs of the  $d^8$  configuration, unlike those of the  $d^7$  configuration (e.g.  $\text{Co}^{\text{II}}$ ), favour an

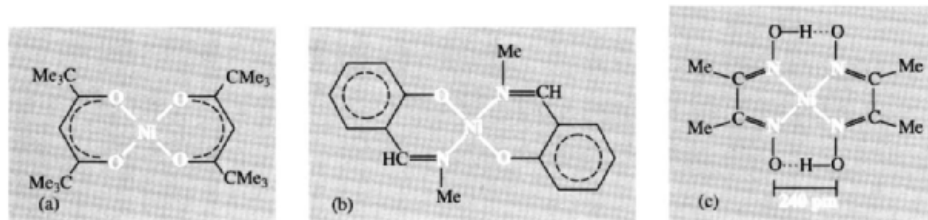


Figure 27.6 Some typical planar complexes of nickel(II): (a)  $[\text{Ni}(\text{Me}_6\text{-acac})_2]$ , (b)  $[\text{Ni}(\text{Me-sal})_2]$  and (c)  $[\text{Ni}(\text{dmgH})_2]$ . (Note the short O–O distance which is due to strong hydrogen bonding.)

### Electronic Spectra and Magnetic Properties of Complexes of Nickel(II)<sup>(15)</sup>

Nickel(II) is the only common  $d^8$  ion and its spectroscopic and magnetic properties have accordingly been extensively studied.

In a cubic field three spin-allowed transitions are expected because of the splitting of the free-ion, ground  $^3F$  term and the presence of the  $^3P$  term. In an octahedral field the splitting is the same as for the octahedral  $d^3$  ion and the same energy level diagram (p. 1029) can be used to interpret the spectra as was used for octahedral  $Cr^{III}$ . Spectra of octahedral  $Ni^{II}$  usually do consist of three bands which are accordingly assigned as:

$$\nu_1 = {}^3T_{2g}(F) \leftarrow {}^3A_{2g}(F) = 10Dq; \quad \nu_2 = {}^3T_{1g}(F) \leftarrow {}^3A_{2g}(F); \quad \nu_3 = {}^3T_{1g}(P) \leftarrow {}^3A_{2g}(F)$$

with  $\nu_1$  giving the value of  $\Delta$ , or  $10Dq$ , directly. Quite often there is also evidence of weak spin-forbidden (i.e. spin triplet  $\rightarrow$  singlet) absorptions and, in  $[Ni(H_2O)_6]^{2+}$  and  $[Ni(dmsO)_6]^{2+}$ , for instance, the  $\nu_2$  absorption has a strong shoulder on it. This is ascribed to a transition to the spin singlet  ${}^1E_g$  which occurs when the  ${}^1E_g$  and  ${}^3T_{1g}(F)$  terms are in close proximity.

For  $d^8$  ions in tetrahedral fields the splitting of the free-ion ground term is the inverse of its splitting in an octahedral field, so that  ${}^3T_{1g}(F)$  lies lowest. In this case three relatively intense bands are to be expected, arising from the transitions:

$$\nu_1 = {}^3T_2(F) \leftarrow {}^3T_1(F); \quad \nu_2 = {}^3A_2(F) \leftarrow {}^3T_1(F); \quad \nu_3 = {}^3T_1(P) \leftarrow {}^3T_1(F)$$

Table A gives data for a number of octahedral and tetrahedral complexes.

**Table A** Electronic spectra of some complexes of nickel(II)

Complex	$\nu_1/cm^{-1}$	$\nu_2/cm^{-1}$	$\nu_3/cm^{-1}$	$10Dq/cm^{-1}$
Octahedral				
$[Ni(dmsO)_6]^{2+}$	7 730	12 970	24 040	7 730
$[Ni(H_2O)_6]^{2+}$	8 500	13 800	25 300	8 500
$[Ni(NH_3)_6]^{2+}$	10 750	17 500	28 200	10 750
$[Ni(en)_3]^{2+}$	11 200	18 350	29 000	11 200
$[Ni(bipy)_3]^{2+}$	12 650	19 200	(a)	12 650
Tetrahedral				
$[NiI_4]^{2-}$		7 040	14 030	3 820
$[NiBr_4]^{2-}$		7 000	13 230, 14 140	3 790
$[NiCl_4]^{2-}$		7 549	14 250, 15 240	4 090
$[NiBr_2(OPPh_3)_2]$		7 250	15 580	3 950

<sup>(a)</sup>Obscured by intense charge-transfer absorptions.

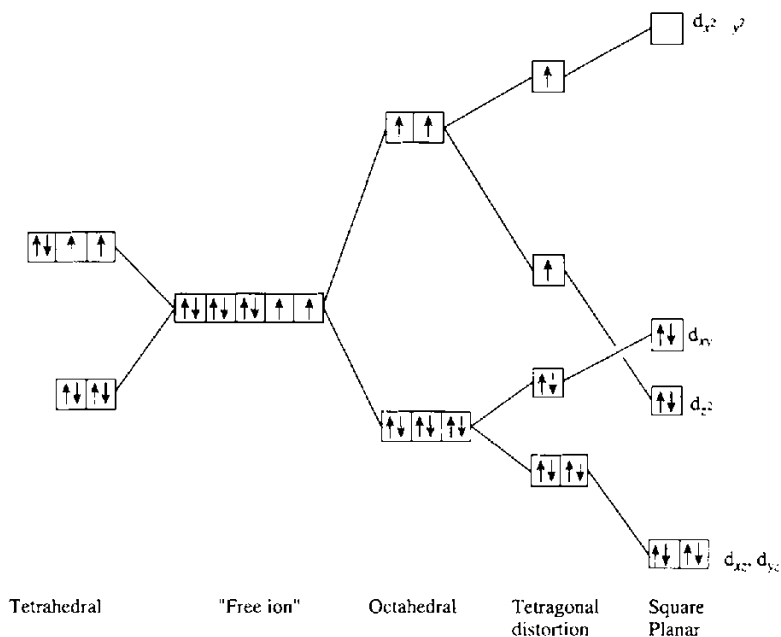
The  $T$  ground term of the tetrahedral ion is expected to lead to a temperature-dependent orbital contribution to the magnetic moment, whereas the  $A$  ground term of the octahedral ion is not, though "mixing" of the excited  ${}^3T_{2g}(F)$  term into the  ${}^3A_{2g}(F)$  ground term is expected to raise its moment to:

$$\mu_e = \mu_{\text{spin-only}}(1 - 4\lambda/10Dq)$$

where  $\lambda = -315 \text{ cm}^{-1}$  and  $\mu_{\text{spin-only}} = 2.83 \text{ BM}$ . (This is the exact reverse of the situations found for  $Co^{II}$ ; p. 1132.) The upshot is that the magnetic moments of tetrahedral compounds are found to lie in the range 3.2–4.1 BM (and are dependent on temperature, and are reduced towards  $\mu_{\text{spin-only}}$  by electron delocalization on to the ligands and by distortions from ideal tetrahedral symmetry) whereas those of octahedral compounds lie in the range 2.9–3.3 BM.

The spectra of square-planar  $d^8$  complexes are usually characterized by a fairly strong band in the yellow to blue region (i.e. about  $17\,000\text{--}22\,000 \text{ cm}^{-1}$  or  $600\text{--}450 \text{ nm}$ ) which is responsible for the reddish colour, and another band near the ultraviolet. The likelihood of  $\pi$ -bonding and attendant charge transfer makes a simple crystal-field treatment inappropriate, and unambiguous assignments are difficult.

<sup>15</sup>A. B. P. LEVER, *Inorganic Electronic Spectroscopy*, (2nd Edn.), pp. 507–611, Elsevier, Amsterdam, 1984.



**Figure 27.7** The splitting of d orbitals in fields of different symmetries, and the resulting electronic configurations of the  $\text{Ni}^{\text{II}}$   $d^8$  ion.

octahedral as opposed to a tetrahedral stereochemistry. It is also evident from Fig 27.7 that the square-planar geometry offers the possibility, not available in either the octahedral or tetrahedral cases, of accommodating all 8 d electrons in 4 lower orbitals, thus leaving the uppermost ( $d_{x^2-y^2}$ ) orbital empty. Providing therefore that the ligand field is of sufficiently low symmetry (or is sufficiently strong) to split the d orbitals enough to offset the energy required to pair-up 2 electrons, then the 4-coordinate, square-planar extreme can be energetically preferable not only to the tetrahedral but also to the 6-coordinate octahedral extreme. Thus, with the  $\text{CN}^-$  ligand which produces an exceptionally strong field, the square-planar  $[\text{Ni}(\text{CN})_4]^{2-}$  is formed rather than the tetrahedral isomer or the octahedral  $[\text{Ni}(\text{CN})_6]^{4-}$ . Also, many compounds of the type  $[\text{NiL}_2\text{X}_2]$ , in which low-symmetry crystal fields are clearly possible, are planar. However, this selfsame formulation was mentioned above as including examples of tetrahedral complexes: evidently the factors which determine the geometry of a particular complex are finely balanced.

This balance, which apparently involves both steric and electronic factors, is well illustrated by the series of complexes  $[\text{Ni}(\text{PR}_3)_2\text{X}_2]$  ( $\text{X} = \text{Cl}, \text{Br}, \text{I}$ ). The diamagnetic, planar forms are favoured by  $\text{R} = \text{alkyl}$ ,  $\text{X} = \text{I}$ , and the paramagnetic tetrahedral forms by  $\text{R} = \text{aryl}$ ,  $\text{X} = \text{Cl}$ . When mixed alkylarylphosphines are involved, conformational isomerism may occur. For example,  $[\text{NiBr}_2(\text{PEtPh}_2)_2]$  has been isolated in both a green, paramagnetic ( $\mu_{300} = 3.20 \text{ BM}$ ), tetrahedral form and a brown, diamagnetic, planar form.

These various stereochemistries are characterized by differing spectroscopic and magnetic properties (see Panel opposite). However, the crude traditional guidelines of colour and magnetism, namely that square planar compounds are red to yellow and diamagnetic whereas tetrahedral ones are green to blue and paramagnetic (due to the  $t_{2g}^6 e_g^2$  and  $e^4 t_2^4$  configurations respectively), cannot be regarded as rigorously diagnostic. The octahedral  $[\text{Ni}(\text{NO}_2)_6]^{4-}$  and square planar  $[\text{NiI}_2(\text{quinoline})_2]$  for instance, are respectively paramagnetic and diamagnetic (expected) but are

also brown-red and green (unexpected). Furthermore, the compounds,  $[\text{Bu}_2^i\text{P}(\mu\text{-O},\mu\text{-NR})\text{Ni}(\mu\text{-O},\mu\text{-NR})\text{P}(\text{Bu}_2^i)]$  ( $\text{R} = \text{Pr}^i$ , cyclohexyl) exist as both tetrahedral and square planar isomers of which not only the former but, uniquely, the latter also are paramagnetic.<sup>(16)</sup> Presumably the separation of  $d_{x^2-y^2}$  and  $d_{xy}$  orbitals (Fig 27.7) is sufficiently small to allow both to be singly occupied.

Many compounds, of which  $[\text{NiBr}_2(\text{PEtPh}_2)_2]$  mentioned above is one, exist in solution as mixtures of isomers giving rise to intermediate values of  $\mu_e$  (0–3.2 BM). Such behaviour, previously regarded as “anomalous” is due to one of three possible types of equilibria:

1. *Planar–tetrahedral equilibria.* Compounds such as  $[\text{NiBr}_2(\text{PEtPh}_2)_2]$  mentioned above as well as a number of *sec*-alkylsalicylaldiminato derivatives (i.e. Me in Fig. 27.6b replaced by a *sec*-alkyl group) dissolve in non-coordinating solvents such as chloroform or toluene to give solutions whose spectra and magnetic properties are temperature-dependent and indicate the presence of an equilibrium mixture of diamagnetic planar and paramagnetic tetrahedral molecules.

2. *Planar–octahedral equilibria.* Dissolution of planar  $\text{Ni}^{\text{II}}$  compounds in coordinating solvents such as water or pyridine frequently leads to the formation of octahedral complexes by the coordination of 2 solvent molecules. This can, on occasions, lead to solutions in which the  $\text{Ni}^{\text{II}}$  has an intermediate value of  $\mu_e$  indicating the presence of comparable amounts of planar and octahedral molecules varying with temperature and concentration; more commonly the conversion is complete and octahedral solvates can be crystallized out. Well-known examples of this behaviour are provided by the complexes  $[\text{Ni}(\text{L-L})_2\text{X}_2]$  ( $\text{L-L} =$  substituted ethylenediamine,  $\text{X} =$  variety of anions) generally known by the name of their discoverer I. Lifschitz. Some of these Lifschitz salts are yellow, diamagnetic and planar,  $[\text{Ni}(\text{L-L})_2]\text{X}_2$ , others are blue, paramagnetic, and octahedral,  $[\text{Ni}(\text{L-L})_2\text{X}_2]$  or

$[\text{Ni}(\text{L-L})_2(\text{solvent})_2]\text{X}_2$ . Which type is produced depends on the nature of L-L, X, and the solvent.

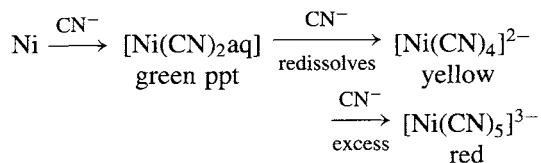
3. *Monomer–oligomer equilibria.*  $[\text{Ni}(\text{Me-sal})_2]$ , mentioned above as a typical planar complex, is a much studied compound. In pyridine it is converted to the octahedral bispyridine adduct ( $\mu_{300} = 3.1$  BM), while in chloroform or benzene the value of  $\mu_e$  is intermediate but increases with concentration. This is ascribed to an equilibrium between the diamagnetic monomer and a paramagnetic dimer, which must involve a coordination number of the nickel of at least 5; a similar explanation is acceptable also for the paramagnetism of the solid when heated above 180°C. The trimerization of  $\text{Ni}(\text{acac})_2$  to attain octahedral coordination has already been referred to but it may also be noted that it is reported to be monomeric and planar in dilute chloroform solutions.

Apart from the probably 5-coordinate  $\text{Ni}^{\text{II}}$  in the above oligomers, a number of well-characterized 5-coordinate complexes are known. These are either trigonal bipyramidal or square pyramidal, though the two forms are energetically similar and the stereochemistry is often imposed by the ligands. Thus the trigonal bipyramidal complexes, which are the more common, often involve tripod ligands (p. 907), while the quadri-dentate chain ligand,

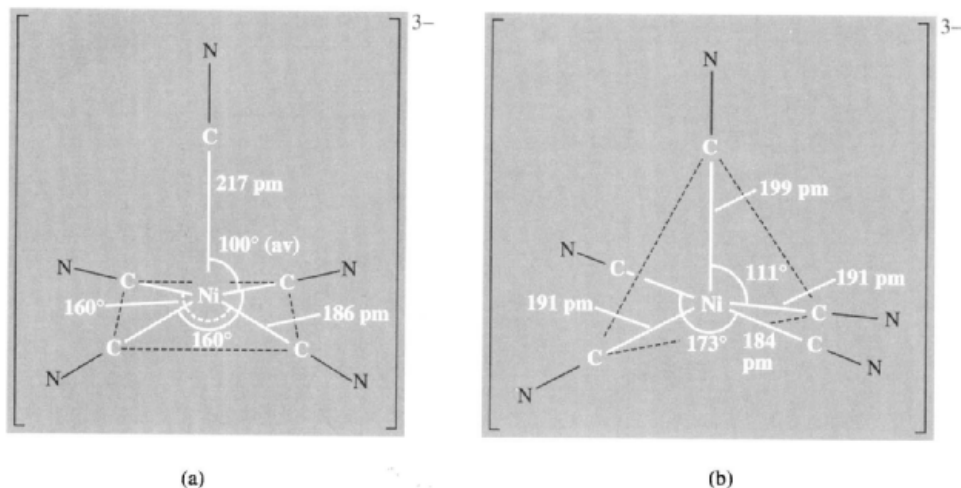


(tetars) produces square pyramidal complexes of the type  $[\text{Ni}(\text{tetars})\text{X}]^+$ . These 5-coordinate complexes can be of either high-spin or low-spin type. The former is found in  $[\text{NiBr}\{\text{N}(\text{C}_2\text{H}_4\text{NMe}_2)_3\}]^+$  but with *P*- or *As*-donor ligands low-spin configurations are found.

The  $\text{Ni}^{\text{II}}/\text{CN}^-$  system illustrates nicely the ease of conversion of the two stereochemistries. Although, as already pointed out, there is no evidence of a hexacyano complex, a square pyramidal pentacyano complex is known:



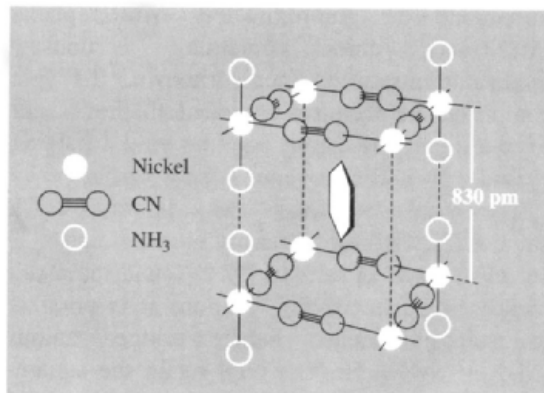
<sup>16</sup> T. FRÖMMELE, W. PETERS, H. WUNDERLICH and W. KUCHERN, *Angew. Chem. Int. Edn. Engl.* **31**, 612–13 (1992); *ibid.* **32**, 907–9 (1993).



**Figure 27.8** The structure of the distorted (a) square-pyramidal and (b) trigonal bipyramidal  $[\text{Ni}(\text{CN})_5]^{3-}$  ions in  $[\text{Cr}(\text{en})_3][\text{Ni}(\text{CN})_5] \cdot 1\frac{1}{2}\text{H}_2\text{O}$ .

The fascinating crystalline compound  $[\text{Cr}(\text{en})_3][\text{Ni}(\text{CN})_5] \cdot 1\frac{1}{2}\text{H}_2\text{O}$  contains both square pyramidal and trigonal bipyramidal anions though each is distorted from true  $C_{4v}$  or  $D_{3h}$  symmetry as shown in Fig. 27.8.

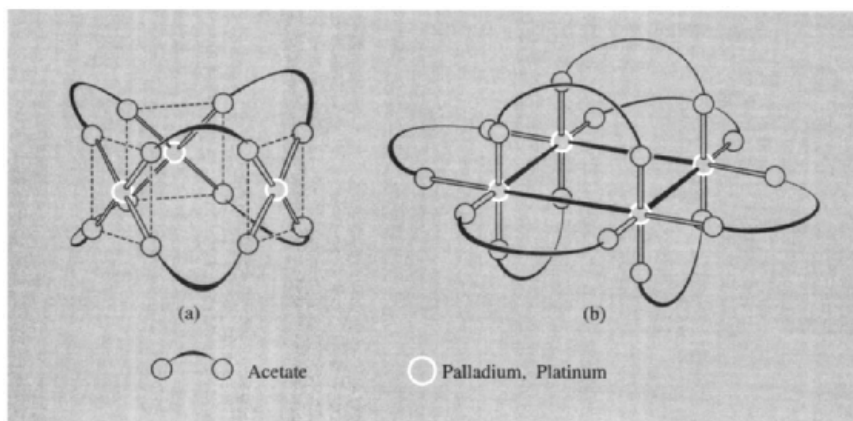
Another interesting cyano derivative of nickel(II)<sup>(16a)</sup> which may conveniently be mentioned here is the *clathrate* compound,  $[\text{Ni}(\text{CN})_2(\text{NH}_3)] \cdot x\text{C}_6\text{H}_6$  ( $x \leq 1$ ). If CN is added to the blue-violet solution obtained by mixing aqueous solutions of  $\text{Ni}^{\text{II}}$  and  $\text{NH}_3$ , and this is then shaken with benzene, a pale-violet precipitate is obtained. This precipitate is soluble in conc  $\text{NH}_3$ . The benzene and ammonia can be removed by heating it above  $150^\circ\text{C}$  but not by washing or by application of reduced pressure. The benzene molecule is, in fact, trapped inside a cage formed by the lattice in which the nickel ions are coordinated to 4 cyanides situated in a square plane, and half are additionally coordinated to 2 ammonias (Fig. 27.9). The observed magnetic moment per Ni atom of 2.2 BM is entirely consistent with this since this average moment arises solely from the octahedrally coordinated Ni atoms, the square-planar Ni being diamagnetic.



**Figure 27.9** A "cage" in the structure of  $[\text{Ni}(\text{CN})_2(\text{NH}_3)] \cdot x(\text{C}_6\text{H}_6)$ , showing a trapped benzene molecule.

*Complexes of Pd<sup>II</sup> and Pt<sup>II</sup>.* The effect of complexation on the splitting of d orbitals is much greater in the case of second- and third-row transition elements, and the associated effects already noted for  $\text{Ni}^{\text{II}}$  are even more marked for  $\text{Pd}^{\text{II}}$  and  $\text{Pt}^{\text{II}}$ , as a result, their complexes are, with rare exceptions, diamagnetic and the vast majority are planar also. Not many complexes are formed with *O*-donor ligands but, of the few that are,  $[\text{M}(\text{H}_2\text{O})_4]^{2+}$  ions, and the polymeric anhydrous acetates  $[\text{Pd}(\text{O}_2\text{CMe})_2]_3$  and  $[\text{Pt}(\text{O}_2\text{CMe})_2]_4$  (Fig. 27.10), are the most

<sup>16a</sup> K. R. DUNBAR and R. A. HEINTZ *Prog. Inorg. Chem.* **45**, 283-391 (1997).



**Figure 27.10** Anhydrous acetates of Pd<sup>II</sup> and Pt<sup>II</sup>: (a) trimeric  $[\text{Pd}(\text{O}_2\text{CMe})_2]_3$  involving square-planar coordinated Pd but no metal-metal bonding (average Pd-Pd = 315 pm), and (b) tetrameric  $[\text{Pt}(\text{O}_2\text{CMe})_2]_4$  involving octahedrally coordinated Pt and metal-metal bonds (average Pt-Pt = 249.5 pm). The four bridging ligands in the Pt<sub>4</sub> plane are much more labile than the others.

important.<sup>(17,18)</sup> Approximately square planar  $[\text{M}(\text{NO}_3)_4]^{2-}$  anions containing the unusual unidentate nitrate ion are also known.<sup>(19)</sup> Fluoro complexes are even less prevalent, the preference of these cations being for the other halides, cyanide, *N*- and heavy atom-donor ligands.

The complexes  $[\text{MX}_4]^{2-}$  (M = Pd, Pt; X = Cl, Br, I, SCN, CN) are all easily obtained and may be crystallized as salts of  $[\text{NH}_4]^+$  and the alkali metals. By using  $[\text{NR}_4]^+$  cations it is possible to isolate binuclear halogen-bridged anions  $[\text{M}_2\text{X}_6]^{2-}$  (X = Br, I) which retain the square-planar coordination of M. Aqueous solutions of yellowish-brown  $[\text{PdCl}_4]^{2-}$  and red  $[\text{PtCl}_4]^{2-}$  are common starting materials for the preparation of other Pd<sup>II</sup> and Pt<sup>II</sup> complexes by successive substitution of the chloride ligands. In both  $[\text{M}(\text{SCN})_4]^{2-}$  complexes the ligands bond through their  $\pi$ -acceptor (*S*) ends, though in the presence of stronger  $\pi$ -acceptor ligands such as  $\text{PR}_3$  and  $\text{AsR}_3$  they tend to bond through their *N* ends.<sup>†</sup> Not surprisingly, therefore, several

instances of linkage isomerism (p. 920) have been established in compounds of the type *trans*- $[\text{M}(\text{PR}_3)_2(\text{SCN})_2]$ .

Complexes with ammonia and amines, especially those of the types  $[\text{ML}_4]^{2+}$  and  $[\text{ML}_2\text{X}_2]$ , are numerous for Pd<sup>II</sup> and even more so for Pt<sup>II</sup>. Many of them were amongst the first complexes of these metals to be prepared and interest in them has continued since. For example, the colourless  $[\text{Pt}(\text{NH}_3)_4]\text{Cl}_2 \cdot \text{H}_2\text{O}$  can be obtained by adding  $\text{NH}_3$  to an aqueous solution of  $\text{PtCl}_2$  and, in 1828, was the first of the platinum amines to be discovered (by G. Magnus). Other salts of the  $[\text{Pt}(\text{NH}_3)_4]^{2+}$  ion are easily derived, the best known being Magnus's green salt  $[\text{Pt}(\text{NH}_3)_4][\text{PtCl}_4]$ . That a green salt should result from the union of a colourless cation and a red anion was unexpected and is a consequence of the crystal structure, which consists of the square-planar anions and cations stacked

<sup>17</sup> D. P. BANCROFT, F. A. COTTON, L. R. FALVELLO and W. SCHWOTZER, *Polyhedron* **7**, 615–21 (1988).

<sup>18</sup> T. YAMAGUCHI, T. UENO and T. ITO, *Inorg. Chem.* **32**, 4996–7 (1993).

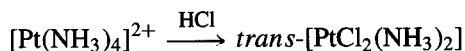
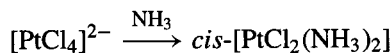
<sup>19</sup> L. I. ELDING, B. NORÉN and Å. OSKARSSON, *Inorg. Chim. Acta* **114**, 71–4 (1986).

<sup>†</sup> Steric, as well as electronic, effects are probably involved. When the ligand is *N*-bonded,  $\text{M} \leftarrow \text{N} \equiv \text{C} - \text{S}$  is linear and so sterically undemanding. However, when the ligand is *S*-bonded,  $\text{M} - \text{S} - \text{C}$  is nonlinear, the bonding and nonbonding electron pairs around the sulfur being more or less tetrahedrally disposed. On purely steric grounds, therefore, the latter type of bonding is expected to be less favoured than the former when bulky ligands such as  $\text{PR}_3$  and  $\text{AsR}_3$  are present.



alternately to produce a linear chain of Pt atoms only 325 pm apart. Interaction between these metal atoms shifts the d-d absorption of the  $[\text{PtCl}_4]^{2-}$  ion from the green region (whence the normal red colour) towards the red, so producing the green colour.

Magnus's salt is an electrolyte and non-ionized polymerization isomers (p. 921) of the stoichiometry  $\text{PtCl}_2(\text{NH}_3)_2$  are also known which can be prepared as monomeric *cis* and *trans* isomers:



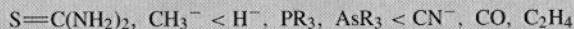
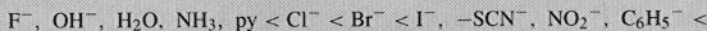
Their existence led Werner to infer a square-planar geometry for  $\text{Pt}^{\text{II}}$ .

Many substitution reactions are possible with these amines and were studied extensively in the 1920s by the Russian, I. I. Chernyaev (also transliterated from the Cyrillic as Tscherniaev, etc.). He noticed that when there are alternative positions at which an incoming ligand might effect a substitution; the position chosen depends not so much on the substituting or substituted ligand as on the nature of the ligand *trans* to that position. This became known as the “*trans*-effect” and has had a considerable influence on the synthetic coordination chemistry of  $\text{Pt}^{\text{II}}$  (see Panel).

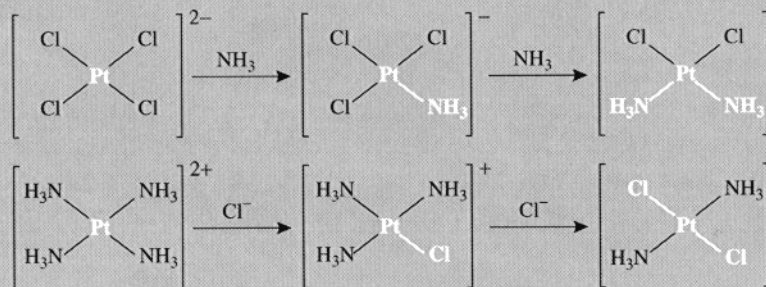
A resurgence of interest in these seemingly simple complexes of platinum started in 1969 when B. Rosenberg and co-workers discovered the anti-tumour activity of *cis*- $[\text{PtCl}_2(\text{NH}_3)_2]$

### The Trans Effect<sup>(20)</sup>

Because their rates of substitution are convenient for study, most work has been done with platinum complexes, and for these it is found that ligands can be arranged in a fairly consistent order indicating their relative abilities to labilize ligands *trans* to themselves:



The reason why the particular substitution reactions of  $[\text{PtCl}_4]^{2-}$  and  $[\text{Pt}(\text{NH}_3)_4]^{2+}$ , mentioned above, produce respectively *cis* and *trans* isomers is now evident. It is because, in both cases, in the second of the stepwise substitutions there is a choice of positions for the substitution and in each case it is a ligand *trans* to a  $\text{Cl}^-$  which is replaced in preference to a ligand *trans* to an  $\text{NH}_3$ :

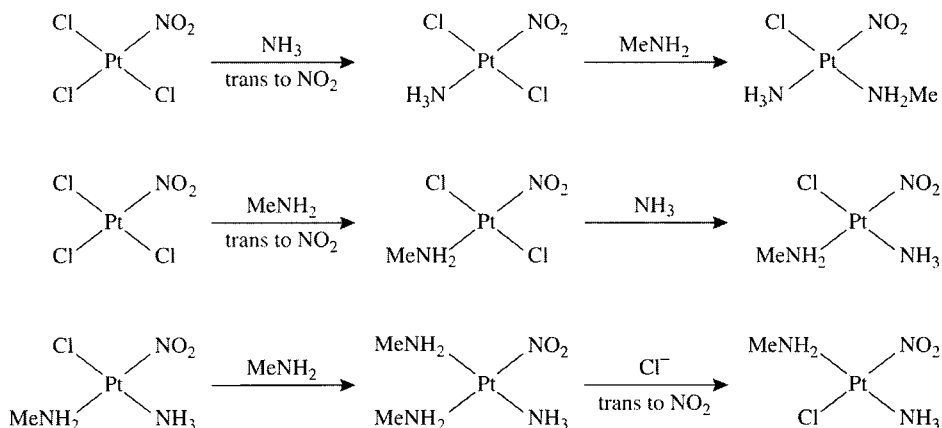


Similar considerations have been invaluable in devising synthetic routes to numerous other isomeric complexes of  $\text{Pt}^{\text{II}}$  but, as can be seen in Fig. A, other considerations such as the relative stabilities of the different Pt-ligand bonds are also involved.

Panel continues

<sup>20</sup>A. K. BABKOV, *Polyhedron* 7, 1203-6 (1988).

Explanations for the *trans*-effect abound and it seems that either  $\pi$  or  $\sigma$  effects, or both, are involved. The ligands exerting the strongest *trans*-effects are just those (e.g.  $C_2H_4$ , CO,  $PR_3$ , etc.) whose bonding to a metal is thought to have most  $\pi$ -acceptor character and which therefore remove most  $\pi$ -electron density from the metal. This reduces the electron density most at the coordination site directly opposite, i.e. *trans*, and it is there that nucleophilic attack is most likely. This interpretation is not directly concerned with stabilizing a particular ligand but rather with encouraging the attachment of a further ligand. It has consequently been applied most successfully to explaining kinetic phenomena such as reaction rates and the proportions of different isomers formed in a reaction (which depend on the rates of reaction), due to the stabilization of 5-coordinate reaction intermediates.



**Figure A** Preparation of the three isomers of  $[PtCl(NH_3)(NH_2Me)(NO_2)]$ . Where indicated these steps can be explained by the greater *trans*-effect of the  $NO_2^-$  ligand. Elsewhere the weakness of the Pt–Cl as compared to the Pt–N bond must be invoked.

On the other hand, a ligand which is a strong  $\sigma$ -donor is expected to produce an axial polarization of the metal, its lone-pair inducing a positive charge on the near side of the metal and a concomitant negative charge on the far side. This will weaken the attachment to the metal of the *trans* ligand. This interpretation has been most successfully used to explain thermodynamic, “ground state” properties such as the bond lengths and vibrational frequencies of the *trans* ligands and their nmr coupling constants with the metal.

In order to distinguish between kinetic and thermodynamic phenomena it is convenient to refer to the former as the “*trans*-effect” and the latter as the “*trans*-influence” or “static *trans*-effect”, though this nomenclature is by no means universally accepted. However, it appears that to account satisfactorily for the kinetic “*trans*-effect”, both  $\pi$  (kinetic) and  $\sigma$  (thermodynamic) effects must be invoked to greater or lesser extents. Thus, for ligands which are low in the *trans* series (e.g. halides), the order can be explained on the basis of a  $\sigma$  effect whereas for ligands which are high in the series the order is best interpreted on the basis of a  $\pi$  effect. Even so, the relatively high position of  $H^-$ , which can have no  $\pi$ -acceptor properties, seems to be a result of a  $\sigma$  mechanism or some other interaction.

(“cisplatin”). Binding of cisplatin to DNA appeared to be the central feature of the action and, since the *trans*-isomer is inactive, it was evident that chelation (or at least coordination to donor atoms in close proximity) is an essential part of the activity. Extensive studies, involving in particular proton nmr, suggested that Pt loses the  $Cl^-$  ligands and binds to N-7

atoms of a pair of guanine bases on adjacent strands of DNA.<sup>(21)</sup> Recent X-ray work<sup>(22)</sup> on a 12-base-pair fragment of double stranded DNA

<sup>21</sup> J. L. van der VEER and J. REEDIJK, *Chem. in Brit.* **20** 775–80 (1988).

<sup>22</sup> P. M. TAKAHARA, A. C. ROSENZWEIG, C. A. FREDERICK and S. J. LIPPARD, *Nature* **377**, 649–52 (1995).

confirms that the binding of Pt distorts the local DNA structure therefore inhibiting the cell division inherent in the proliferation of cancer cells.

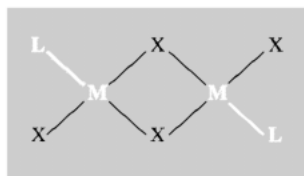
In order to avoid serious side effects of cisplatin (kidney- and neuro-toxicity) alternative Pt compounds have been developed. The most important of these is "carboplatin" in which the *cis*-chlorides are replaced by the *O*-chelate, cyclobutanedicarboxylate but all of them have ligands with NH groups which facilitate the hydrogen bonding thought to stabilize the distortions of the DNA structure.

Treatment of aqueous solutions of *cis*-[PtCl<sub>2</sub>(NH<sub>3</sub>)<sub>2</sub>] with a variety of pyrimidines yields blue, oligomeric (Pt<sub>4</sub>) compounds of the type known since the early 20th century as "platinum blues." They are mostly, mixed valence, paramagnetic compounds and although some have been characterized<sup>(23)</sup> others are less well-defined and include green and violet materials.

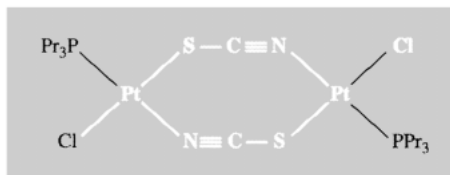
Stable complexes of Pd<sup>II</sup> and Pt<sup>II</sup> are formed with a variety of *S*-donor ligands which includes the inorganic sulfite (SO<sub>3</sub><sup>-</sup>) and thiosulfate (S<sub>2</sub>O<sub>3</sub><sup>2-</sup> apparently coordinating through 1 S and 1 O) but those with organo-sulfur ligands such as 1,2-dithiolenes are of more interest. The anions [M(mnt)<sub>2</sub>]<sup>2-</sup> (mnt = S<sub>2</sub>C<sub>2</sub>(CN)<sub>2</sub>, M = Ni, Pd, Pt) have a facile redox chemistry yielding products with unusual electrical properties. Most salts of the square planar [M(mnt)<sub>2</sub>]<sup>-</sup> crystallize in stacks, in which the anions associate in pairs, and are semiconductors but the nonstoichiometric (H<sub>3</sub>O)<sub>0.33</sub>Li<sub>0.8</sub>[Pt(mnt)<sub>2</sub>]1.67H<sub>2</sub>O is a linear conductor and Cs<sub>0.82</sub>[Pd(mnt)<sub>2</sub>]0.5H<sub>2</sub>O shows metallic conductance when subject to high pressure.<sup>(24)</sup>

The essentially class-b character of Pd<sup>II</sup> and Pt<sup>II</sup> is further indicated by the ready formation of complexes with phosphines and arsines. [M(PR<sub>3</sub>)<sub>2</sub>X<sub>2</sub>] and the arsine analogues are

particularly well known. Zero dipole moments indicate that the palladium complexes are invariably *trans*, whereas those of platinum may be either *cis* or *trans* the latter being much the more soluble and having lower mps. When these bisphosphines and bisarsines are boiled in alcohol, or alternatively when they are fused with MX<sub>2</sub>, the dimeric complexes [MLX<sub>2</sub>]<sub>2</sub> are frequently obtained. Again, zero dipole moments (in some cases confirmed by X-ray analysis) indicate that these are all of the symmetrical *trans* form (a).



(a)



(b)

By involving SCN<sup>-</sup> a novel 8-membered ring system has been produced (b).

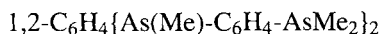
Nuclear magnetic resonance has proved to be a particularly useful tool in studying phosphines of platinum. The nuclear spins of <sup>31</sup>P and <sup>195</sup>Pt (both equal to 1/2) couple, and the strength of this coupling (as measured by the "coupling constant" *J*) is affected much more by ligands *trans* to the phosphine than by those which are *cis*. This has helped in determinations of structure and also in studies of the "*trans* influence". Platinum(II) also forms a number of quite stable monohydrido (H<sup>-</sup>) phosphines which have proved similarly interesting, the <sup>1</sup>H-<sup>195</sup>Pt coupling constants being likewise sensitive to the *trans* ligand.

It has already been pointed out that the overwhelming majority of complexes of Pd<sup>II</sup> and Pt<sup>II</sup> are square planar. However, 5-coordinate intermediates are almost certainly involved in many of the substitution reactions of these 4-coordinate complexes, and 5-coordinate trigonal

<sup>23</sup> see for instance, T. V. O'HALLORAN, P. K. MASCHARAK, I. D. WILLIAMS, M. M. ROBERTS and S. J. LIPPARD, *Inorg. Chem.* **26** 1261-70 (1987).

<sup>24</sup> M. B. HURSTHOUSE, R. L. SHORT, P. I. CLEMENSON and A. E. UNDERHILL, *J. Chem. Soc., Dalton Trans.*, 1101-4 (1989).

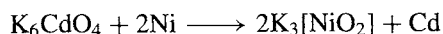
bipyramidal complexes with "tripod" ligands (p. 907) are well established. These ligands include the tetraarsine,  $\text{As}(\text{C}_6\text{H}_4\text{-2-AsPh}_2)_3$  (qas, p. 1150), its phosphine analogue and also  $\text{N}(\text{CH}_2\text{CH}_2\text{NMe}_2)_3$  i.e. ( $\text{Me}_6\text{tren}$ ). The somewhat less-rigid tetraarsine,



(tpas), however forms a red, square-pyramidal complex  $[\text{Pd}(\text{tpas})\text{Cl}]\text{ClO}_4$  with palladium.

### Oxidation state I ( $d^9$ )

Although nickel(I) is thought to be involved in some nickel-containing enzymes, this oxidation state is best represented by yellow to red, tetrahedral phosphines such as  $[\text{Ni}(\text{PPh}_3)_3\text{X}]$  ( $\text{X} = \text{Cl}, \text{Br}, \text{I}$ ) which are paramagnetic, as expected for a  $d^9$  configuration, and relatively stable.  $[\text{Ni}(\text{PMe}_3)_4][\text{BPh}_4]$  has also been structurally characterized. A more recent<sup>(25)</sup> example is  $\text{K}_3[\text{NiO}_2]$ . This dark red, air- and water-sensitive compound, like the  $\text{Fe}^{\text{I}}$  (p. 1082 footnote) and  $\text{Co}^{\text{I}}$  (p. 1134) analogues, is prepared by heating  $\text{K}_6\text{CdO}_4$  in a closed Ni cylinder at  $500^\circ\text{C}$  for 49 days when it reacts with the cylinder walls:

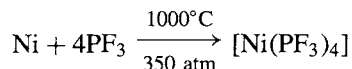


These anions are remarkable not only for the low coordination number but also for the low oxidation state of the metals in combination with oxygen which is more commonly to be found stabilizing *high* oxidation states.

### Oxidation state 0 ( $d^{10}$ )

Besides  $[\text{Ni}(\text{CO})_4]$  and organometallic compounds discussed in the next section, nickel is found in the formally zero oxidation state with ligands such as  $\text{CN}^-$  and phosphines. Reduction of  $\text{K}_2[\text{Ni}^{\text{II}}(\text{CN})_4]$  with potassium in liquid ammonia precipitates yellow  $\text{K}_4[\text{Ni}^0(\text{CN})_4]$ , which is sensitive to aerial oxidation. Being

isoelectronic with  $[\text{Ni}(\text{CO})_4]$  it is presumed to be tetrahedral. Similarity with the carbonyl is still more marked in the case of the gaseous and tetrahedral  $[\text{Ni}(\text{PF}_3)_4]$ , which also can be prepared directly from the metal and ligand:



The pale yellow  $[\text{Ni}(\text{PET}_3)_4]$  is also tetrahedral but with some distortion.<sup>(26)</sup> In sharp contrast to nickel, palladium forms no simple carbonyl,  $\text{Pt}(\text{CO})_4$  is prepared only by matrix isolation at very low temperatures and reports of  $\text{K}_4[\text{M}(\text{CN})_4]$  ( $\text{M} = \text{Pd}, \text{Pt}$ ) may well refer to hydrido complexes; in any event they are very unstable. The chemistry of these two metals in the zero oxidation state is in fact essentially that of their phosphine and arsine complexes and was initiated by L. Malatesta and his school in the 1950s. Compounds of the type  $[\text{M}(\text{PR}_3)_4]$ , of which  $[\text{Pt}(\text{PPh}_3)_4]$  has been most thoroughly studied, are in general yellow, air-stable solids or liquids obtained by reducing  $\text{M}^{\text{II}}$  complexes in  $\text{H}_2\text{O}$  or  $\text{H}_2\text{O}/\text{EtOH}$  solutions with hydrazine or sodium borohydride. They are tetrahedral molecules whose most important property is their readiness to dissociate in solution to form 3-coordinate, planar  $[\text{M}(\text{PR}_3)_3]$  and, in traces, probably also  $[\text{M}(\text{PR}_3)_2]$  species. The latter are intermediates in an extensive range of addition reactions (many of which may properly be regarded as *oxidative* additions) giving such products as  $[\text{Pt}^{\text{II}}(\text{PPh}_3)_2\text{L}_2]$ , ( $\text{L} = \text{O}, \text{CN}, \text{N}_3$ ) and  $[\text{Pt}^{\text{II}}(\text{PPh}_3)_2\text{LL}']$ , ( $\text{L}, \text{L}' = \text{H}, \text{Cl}; \text{R}, \text{I}$ ) as well as  $[\text{Pt}^0(\text{C}_2\text{H}_4)(\text{PPh}_3)_2]$  and  $[\text{Pt}^0(\text{CO})_2(\text{PPh}_3)_2]$ .

The mechanism by which this low oxidation state is stabilized for this triad has been the subject of some debate. That it is not straightforward is clear from the fact that, in contrast to nickel, palladium and platinum require the presence of phosphines for the formation of stable carbonyls. For most transition metals the  $\pi$ -acceptor properties of the ligand are thought to be of considerable importance and there is

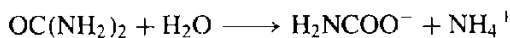
<sup>25</sup> A. MÖLLER, M. A. HITCHMAN, E. KRAUSZ and R. HOPPE, *Inorg. Chem.* **34**, 2684–91 (1995).

<sup>26</sup> M. HURSTHOUSE, K. J. IZOD, M. MOTEVALLI and P. THORNTON, *Polyhedron* **13**, 151–3 (1994).

no reason to doubt that this is true for  $\text{Ni}^0$ . For  $\text{Pd}^0$  and  $\text{Pt}^0$ , however, it appears that  $\sigma$ -bonding ability is also important, and the smaller importance of  $\pi$  backbonding which this implies is in accord with the higher ionization energies of Pd and Pt [804 and 865  $\text{kJ mol}^{-1}$  respectively] compared with that for Ni [737  $\text{kJ mol}^{-1}$ ].

### 27.3.5 The biochemistry of nickel<sup>(27)</sup>

Until the discovery in 1975 of nickel in jack bean urease (which, 50 years previously, had been the first enzyme to be isolated in crystalline form and was thought to be metal-free) no biological role for nickel was known. Ureases occur in a wide variety of bacteria and plants, catalyzing the hydrolysis of urea,



Results from an array of methods, including X-ray absorption, EXAFS, esr and magnetic circular dichroism, suggest that in all ureases the active sites are a pair of  $\text{Ni}^{\text{II}}$  atoms. In at least one urease,<sup>(27a)</sup> these are 350 pm apart and are bridged by a carboxylate group. One nickel is attached to 2 N atoms with a fourth site probably used for binding to urea. The second nickel has a trigonal bipyramidal coordination sphere.

Three other Ni-containing enzymes found in bacteria have now been identified:

*Hydrogenases*, most of which also contain Fe and catalyse the reaction,  $2\text{H}_2 + \text{O}_2 \longrightarrow 2\text{H}_2\text{O}$ . The Ni has a coordination sphere of 5 or 6 mixed S-, N-, O-donors and is believed to undergo redox cycling between III, II and I oxidation states.

*CO Dehydrogenase*, also incorporating Fe and catalysing the oxidation of CO to  $\text{CO}_2$ . The attachment of CO to a nickel centre coordinated to perhaps four S-donors is postulated.

*Methyl-coenzyme M reductase* participates in the conversion of  $\text{CO}_2$  to  $\text{CH}_4$  and contains 6-coordinate nickel(II) in a highly hydrogenated and highly flexible porphyrin system. This flexibility is believed to allow sufficient distortion of the octahedral ligand field to produce low-spin  $\text{Ni}^{\text{II}}$  (Fig. 27.7) which facilitates the formation of a  $\text{Ni}^{\text{I}}-\text{CH}_3$  intermediate.

### 27.3.6 Organometallic compounds<sup>(4,28)</sup>

All three of these metals have played major roles in the development of organometallic chemistry. The first compound containing an unsaturated hydrocarbon attached to a metal (and, indeed, the first organometallic compound if one excludes the cyanides) was  $[\text{Pt}(\text{C}_2\text{H}_4)\text{Cl}_2]_2$ , discovered by the Danish chemist W. C. Zeise as long ago as 1827 and followed 4 years later by the salt which bears his name,  $\text{K}[\text{Pt}(\text{C}_2\text{H}_4)\text{Cl}_3] \cdot \text{H}_2\text{O}$ .  $[\text{Ni}(\text{CO})_4]$  was the first metal carbonyl to be prepared when L. Mond and his co-workers discovered it in 1888. The platinum methyls, prepared in 1907 by W. J. Pope, were amongst the first-known transition metal alkyls, and the discovery by W. Reppe in 1940 that  $\text{Ni}^{\text{II}}$  complexes catalyse the cyclic oligomerization of acetylenes produced a surge of interest which was reinforced by the discovery in 1960 of the  $\pi$ -allylic complexes of which those of  $\text{Pd}^{\text{II}}$  are by far the most numerous.

#### $\sigma$ -Bonded compounds

These are of two main types: compounds of  $\text{M}^{\text{IV}}$ , which for platinum have been known since the beginning of this century and commonly involve the stable  $\{\text{PtMe}_3\}$  group; and compounds of the divalent metals, which were first studied by J. Chatt and co-workers in the late 1950's and are commonly of the type  $[\text{MR}_2\text{L}_2]$  (L = phosphine). In the  $\text{Pt}^{\text{IV}}$  compounds the metal is always octahedrally coordinated and this is frequently achieved in interesting ways. Thus the trimethyl halides, conveniently obtained

<sup>27</sup> A. F. KOŁODZIEJ, *Prog. Inorg. Chem.* **41**, 493–597 (1994); J. R. LANCASTER (ed.), *The Bioinorganic Chemistry of Nickel*, VCH, Weinheim, 1988, 337 pp.; H. SIGEL (ed.), *Metal Ions in Biological Systems*, Vol. 23, *Nickel and its Role in Biology*, Dekker, New York, 1988, 488 pp.

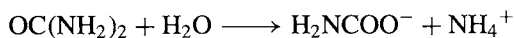
<sup>27a</sup> S. J. LIPPARD, *Science*, **268**, 996–7 (1995); E. JABRI, M. B. CARR, R. P. HAUSINGER and P. A. KARPLUS, *ibid.* pp. 998–1004.

<sup>28</sup> G. WILKE, *Angew. Chem. Int. Edn. Engl.* **27**, 185–206 (1988).

no reason to doubt that this is true for Ni<sup>0</sup>. For Pd<sup>0</sup> and Pt<sup>0</sup>, however, it appears that  $\sigma$ -bonding ability is also important, and the smaller importance of  $\pi$  backbonding which this implies is in accord with the higher ionization energies of Pd and Pt [804 and 865 kJ mol<sup>-1</sup> respectively] compared with that for Ni [737 kJ mol<sup>-1</sup>].

### 27.3.5 The biochemistry of nickel<sup>(27)</sup>

Until the discovery in 1975 of nickel in jack bean urease (which, 50 years previously, had been the first enzyme to be isolated in crystalline form and was thought to be metal-free) no biological role for nickel was known. Ureases occur in a wide variety of bacteria and plants, catalyzing the hydrolysis of urea,



Results from an array of methods, including X-ray absorption, EXAFS, esr and magnetic circular dichroism, suggest that in all ureases the active sites are a pair of Ni<sup>II</sup> atoms. In at least one urease,<sup>(27a)</sup> these are 350 pm apart and are bridged by a carboxylate group. One nickel is attached to 2 N atoms with a fourth site probably used for binding to urea. The second nickel has a trigonal bipyramidal coordination sphere.

Three other Ni-containing enzymes found in bacteria have now been identified:

*Hydrogenases*, most of which also contain Fe and catalyse the reaction,  $2\text{H}_2 + \text{O}_2 \longrightarrow 2\text{H}_2\text{O}$ . The Ni has a coordination sphere of 5 or 6 mixed S-, N-, O-donors and is believed to undergo redox cycling between III, II and I oxidation states.

*CO Dehydrogenase*, also incorporating Fe and catalysing the oxidation of CO to CO<sub>2</sub>. The attachment of CO to a nickel centre coordinated to perhaps four S-donors is postulated.

*Methyl-coenzyme M reductase* participates in the conversion of CO<sub>2</sub> to CH<sub>4</sub> and contains 6-coordinate nickel(II) in a highly hydrogenated and highly flexible porphyrin system. This flexibility is believed to allow sufficient distortion of the octahedral ligand field to produce low-spin Ni<sup>II</sup> (Fig. 27.7) which facilitates the formation of a Ni<sup>I</sup>-CH<sub>3</sub> intermediate.

### 27.3.6 Organometallic compounds<sup>(4,28)</sup>

All three of these metals have played major roles in the development of organometallic chemistry. The first compound containing an unsaturated hydrocarbon attached to a metal (and, indeed, the first organometallic compound if one excludes the cyanides) was [Pt(C<sub>2</sub>H<sub>4</sub>)Cl<sub>2</sub>]<sub>2</sub>, discovered by the Danish chemist W. C. Zeise as long ago as 1827 and followed 4 years later by the salt which bears his name, K[Pt(C<sub>2</sub>H<sub>4</sub>)Cl<sub>3</sub>].H<sub>2</sub>O. [Ni(CO)<sub>4</sub>] was the first metal carbonyl to be prepared when L. Mond and his co-workers discovered it in 1888. The platinum methyls, prepared in 1907 by W. J. Pope, were amongst the first-known transition metal alkyls, and the discovery by W. Reppe in 1940 that Ni<sup>II</sup> complexes catalyse the cyclic oligomerization of acetylenes produced a surge of interest which was reinforced by the discovery in 1960 of the  $\pi$ -allylic complexes of which those of Pd<sup>II</sup> are by far the most numerous.

#### $\sigma$ -Bonded compounds

These are of two main types: compounds of M<sup>IV</sup>, which for platinum have been known since the beginning of this century and commonly involve the stable {PtMe<sub>3</sub>} group; and compounds of the divalent metals, which were first studied by J. Chatt and co-workers in the late 1950's and are commonly of the type [MR<sub>2</sub>L<sub>2</sub>] (L = phosphine). In the Pt<sup>IV</sup> compounds the metal is always octahedrally coordinated and this is frequently achieved in interesting ways. Thus the trimethyl halides, conveniently obtained

<sup>27</sup> A. F. KOŁODZIEJ, *Prog. Inorg. Chem.* **41**, 493–597 (1994); J. R. LANCASTER (ed.), *The Bioinorganic Chemistry of Nickel*, VCH, Weinheim, 1988, 337 pp.; H. SIGEL (ed.), *Metal Ions in Biological Systems*, Vol. 23, *Nickel and its Role in Biology*, Dekker, New York, 1988, 488 pp.

<sup>27a</sup> S. J. LIPPARD, *Science*, **268**, 996–7 (1995); E. JABRI, M. B. CARR, R. P. HAUSINGER and P. A. KARPLUS, *ibid.* pp. 998–1004.

<sup>28</sup> G. WILKE, *Angew. Chem. Int. Edn. Engl.* **27**, 185–206 (1988).



by treating  $\text{PtCl}_4$  with  $\text{MeMgX}$  in benzene, are tetramers,  $[\text{PtMe}_3\text{X}]_4$ , in which the 4 Pt atoms form a cube involving triply-bridging halogen atoms<sup>†</sup> (Fig. 27.11a). The dimeric  $[\text{PtMe}_3(\text{acac})]_2$  is also unusual in that the acac is both *O*- and *C*-bonded (Fig. 27.11b), while in  $[\text{PtMe}_3(\text{acac})(\text{bipy})]$  7-coordination is avoided because the acac coordinates merely as a unidentate *C*-donor.  $\text{Pd}^{\text{IV}}$  compounds such as  $[\text{Pd}(\text{bipy})\text{Me}_3]$  are also octahedral but are limited in number and much less stable than those of  $\text{Pt}^{\text{IV}}$ , being susceptible to reductive elimination.<sup>(29)</sup>

<sup>†</sup> The chequered history of compounds of this type makes salutary reading. H. Gilman and M. Lichtenwalter (1938, 1953) reported the synthesis of  $\text{PtMe}_4$  in 46% yield by reacting  $\text{Me}_3\text{PtI}$  with  $\text{NaMe}$  in hexane. R. E. Rundle and J. H. Sturdivant determined the X-ray crystal structure of this product in 1947 and described it as a tetramer  $[(\text{PtMe}_4)_4]$ : this required the concept of a multicentred, 2-electron bond, and was one of the first attempts to interpret the bonding in a presumed electron-deficient cluster compound. In fact, tetramethylplatinum cannot be prepared in this way and is unknown; Gilman's compound was actually a hydrolysis product  $[(\text{PtMe}_3(\text{OH}))_4]$  and the mistaken identity of the crystal went undetected by the X-ray work because, at that time, the scattering curves for the 9-electron groups  $\text{CH}_3$  and  $\text{OH}$  were indistinguishable in the presence of Pt. Interestingly, the compound  $\text{PtMe}_3(\text{OH})$  had, in reality, already been synthesized by W. J. Pope and S. J. Peachey as long ago as 1909, and its tetrameric structure was confirmed by subsequent X-ray work.<sup>(30)</sup> In a parallel study,<sup>(31)</sup> the transparent tan-coloured tetramer  $[(\text{PtMe}_3\text{I})_4]$  has now been shown to be the same compound as was previously erroneously reported in 1938 as hexamethyldiplatinum,  $[\text{Me}_3\text{Pt}-\text{PtMe}_3]$ . This was equally erroneously described in 1949 on the basis of an incomplete X-ray structural study as a methyl-bridged oligomer  $[(\text{PtMe}_3)_{12}]$  or an infinite chain of methyl-bridged 6-coordinate  $\{\text{PtMe}_3\}$ -groups. A qualitative test for iodine would have revealed the error 30 years earlier.

Although  $\text{PtMe}_4$  remains unknown it has more recently been shown that reaction of  $[\text{PtMe}_2(\text{PPh}_3)_2]$  with  $\text{LiMe}$  yields the square-planar  $\text{Pt}^{\text{II}}$  complex  $\text{Li}_2[\text{PtMe}_4]$ , whereas reaction of  $[(\text{PtMe}_3\text{I})_4]$  with  $\text{LiMe}$  affords the octahedral  $\text{Pt}^{\text{IV}}$  complex  $\text{Li}_2[\text{PtMe}_6]$ .<sup>(32)</sup> The thermally stable, colourless, 8-coordinate complex  $[\text{PtMe}_3(\eta^5\text{-C}_5\text{H}_5)]$  is also known.<sup>(33)</sup>

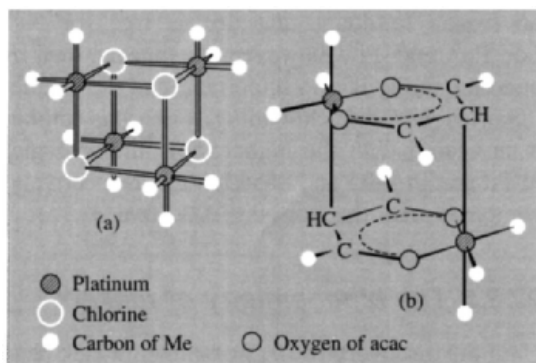
<sup>29</sup> A. J. CANTY, *Acc. Chem. Res.* **25**, 83–90 (1992); *Platinum Metals Rev.* **37**, 2–7 (1993).

<sup>30</sup> D. O. COWAN, N. G. KRIEGHOFF and G. DONNAY, *Acta Cryst.* **B24**, 287–8 (1968), and references therein.

<sup>31</sup> G. DONNAY, L. B. COLEMAN, N. G. KRIEGHOFF and D. O. COWAN, *Acta Cryst.* **B24**, 157–9 (1968), and references therein.

<sup>32</sup> G. W. RICE and R. S. TOBIAS, *J. Am. Chem. Soc.* **99**, 2141–9 (1977).

<sup>33</sup> O. HACKELBERG and A. WOJCIK, *Inorg. Chim. Acta* **44**, L63–L64 (1980).



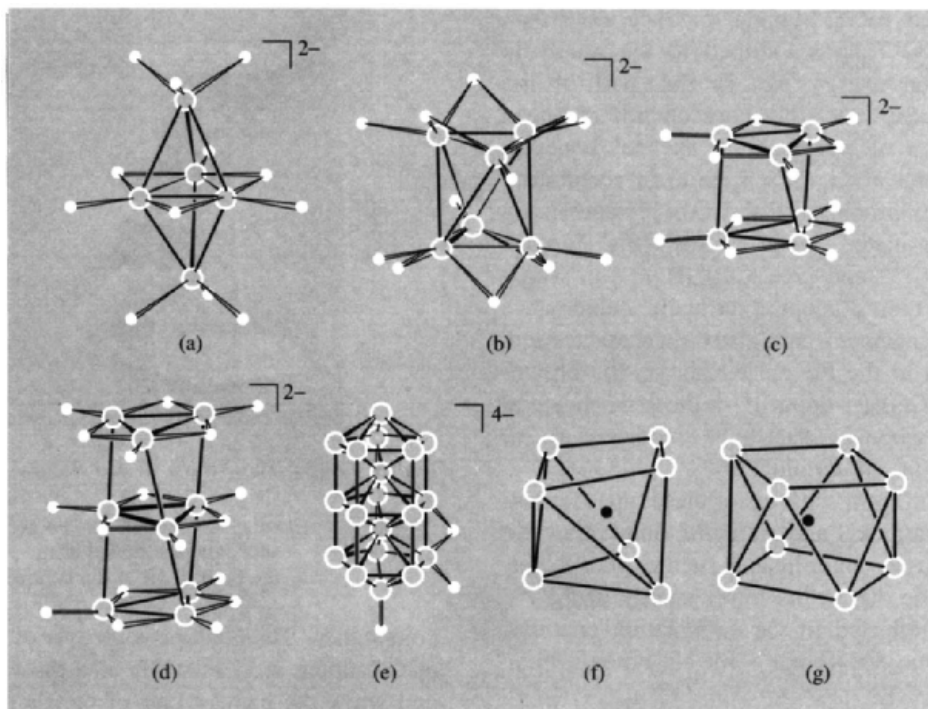
**Figure 27.11** Schematic representation of the structures of compounds containing octahedrally coordinated  $\text{Pt}^{\text{IV}}$ : (a) the tetramer,  $[\text{PtMe}_3\text{Cl}]_4$ , and (b) the dimer,  $[\text{PtMe}_3(\text{acac})]_2$ .

The stabilities of the  $[\text{ML}_2\text{R}_2]$  phosphines increase from  $\text{Ni}^{\text{II}}$  to  $\text{Pt}^{\text{II}}$  and for  $\text{Ni}^{\text{II}}$  they are only isolable when R is an *o*-substituted aryl. Those of  $\text{Pt}^{\text{II}}$ , on the other hand, are amongst the most stable  $\sigma$ -bonded organo-transition metal compounds while those of  $\text{Pd}^{\text{II}}$  occupy an intermediate position.

### Carbonyls (see p. 926)

On the basis of the 18-electron rule, the  $d^8s^2$  configuration is expected to lead to carbonyls of formula  $[\text{M}(\text{CO})_4]$  and this is found for nickel.  $[\text{Ni}(\text{CO})_4]$ , the first metal carbonyl to be discovered, is an extremely toxic, colourless liquid (mp  $-19.3^\circ$ , bp  $42.2^\circ$ ) which is tetrahedral in the vapour and in the solid (Ni–C 184 pm, C–O 115 pm). Its importance in the Mond process for manufacturing nickel metal has already been mentioned as has the absence of stable analogues of Pd and Pt. It may be germane to add that the introduction of halides (which are  $\sigma$ -bonded) reverses the situation:  $[\text{NiX}(\text{CO})_3]^-$  ( $\text{X} = \text{Cl}, \text{Br}, \text{I}$ ) are very unstable, the yellow  $[\text{Pd}^{\text{II}}(\text{CO})\text{Cl}_2]_n$  is somewhat less so, whereas the colourless  $[\text{Pt}^{\text{II}}(\text{CO})_2\text{Cl}_2]$  and  $[\text{PtX}_3(\text{CO})]^-$  are quite stable.

$[\text{Ni}(\text{CO})_4]$  is readily oxidized by air and can be reduced by alkali metals in liquid ammonia or thf to yield a series of polynuclear carbonylate anion



**Figure 27.12** Some carbonylate anion clusters of nickel and platinum: (a)  $[\text{Ni}_5(\text{CO})_{12}]^{2-}$ , (b)  $[\text{Ni}_6(\text{CO})_{12}]^{2-}$ , (c)  $[\text{Pt}_6(\text{CO})_{12}]^{2-}$ , (d)  $[\text{Pt}_9(\text{CO})_{18}]^{2-}$ , (e) the  $\text{Pt}_{19}$  core of  $[\text{Pt}_{19}(\text{CO})_{22}]^{4-}$  showing one of the 10 bridging COs and 2 of the 12 terminal COs (which are attached to each of the 6 metal atoms at each end of the ion), (f) the  $\text{Ni}_7\text{C}$  core of  $[\text{Ni}_7(\text{CO})_{12}\text{C}]^{2-}$ , (g) the  $\text{Ni}_8\text{C}$  core of  $[\text{Ni}_8(\text{CO})_{16}\text{C}]^{2-}$ . Clusters (c) and (d) are structural motifs found in Ni clusters of nuclearities up to 34 and 38<sup>(35)</sup>.

clusters but consisting mainly of  $[\text{Ni}_5(\text{CO})_{12}]^{2-}$  and  $[\text{Ni}_6(\text{CO})_{12}]^{2-}$ . The latter, being more stable and less toxic than the monomer, is a common starting material for the preparation of other clusters,<sup>(34)</sup> many of which are stabilized by encapsulated atoms of which carbon is especially efficacious. These clusters, which in general are intensely coloured and air-sensitive, have structures<sup>(35)</sup> based on the stacking of  $\text{Ni}_3$  triangles and  $\text{Ni}_4$  squares and, in carbon-centred clusters of higher nuclearities, based on  $\text{Ni}_7\text{C}$  and  $\text{Ni}_8\text{C}$  moieties (Fig. 27.12). Other clusters, derived from reactions of  $[\text{Ni}_6(\text{CO})_{12}]^{2-}$  and main group

reactants, have icosahedral frameworks<sup>(36)</sup> such as  $\text{Ni}_{10}\text{Se}_2$ ,  $\text{Ni}_9\text{Te}_3$  and  $\text{Ni}_{10}\text{Sb}$ . Some of these are centred with Ni, some centred with the main group element and others uncentred.

Reductions of  $[\text{PtCl}_6]^{2-}$  in an atmosphere of CO provide a series of clusters,  $[\text{Pt}_3(\text{CO})_6]_n^{2-}$  ( $n = 1-6, 10$ ) consisting of stacks of  $\text{Pt}_3$  triangles in slightly twisted columns; Pt–Pt = 266 pm in triangles, 303–309 pm between triangular planes (Fig. 27.12). A feature of these and other Pt clusters is that they mostly have electron counts lower than predicted by the usual electron counting rules. In the series just mentioned for instance,  $n = 1$  and  $n = 2$  have electron counts of 44 and 86 whereas 48 and 90 would

<sup>34</sup> J. K. BEATTIE, A. F. MASTERS and J. T. MEYER, *Polyhedron*, **14**, 829–68 (1995).

<sup>35</sup> A. F. MASTERS and J. T. MEYER, *Polyhedron* **14**, 339–65 (1995).

<sup>36</sup> A. J. KAHAIAN, J. B. THODEN and L. F. DAHL *J. Chem. Soc., Chem. Commun.*, 353–5 (1992).

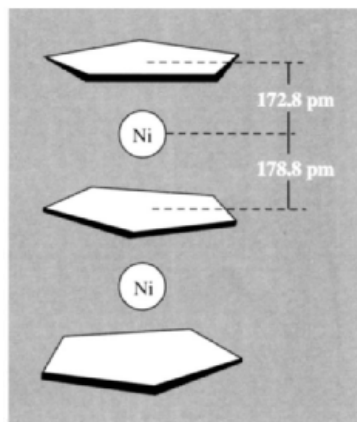


be expected for a triangle and trigonal prism respectively. This is ascribed to the relatively large 6s–6p energy gap in this part of the periodic table and the consequently reduced involvement of p-orbitals in skeletal bonding. Heating salts of the  $n = 3$  anion in acetonitrile under reflux produces  $[\text{Pt}_{19}(\text{CO})_{22}]^{4-}$  containing two encapsulated metal atoms (Fig. 27.12e).  $[\text{Pt}_{26}(\text{CO})_{32}]^{3-}$  and  $[\text{Pt}_{38}(\text{CO})_{44}\text{H}_x]^{2-}$ , in which the metal atoms adopt a virtually cubic close packed arrangement, have also been characterized. In contrast to the  $\text{Pt}_6$  cluster above, the brown-black  $[\text{Pt}_6(\text{CO})_6(\mu\text{-dppm})]^{2+}$  is the first octahedral platinum carbonyl cluster to be characterized. All its CO groups are terminal.<sup>(36a)</sup>

Palladium forms clusters of these types far less readily than nickel and platinum, unless they are stabilized by  $\sigma$ -donor ligands such as phosphines. This may be due to the lower energy of Pd–Pd bonds as reflected in the sublimation energies, 427, 354 and 565  $\text{kJ mol}^{-1}$  for Ni, Pd and Pt.

### Cyclopentadienyls

Nickelocene,  $[\text{Ni}^{\text{II}}(\eta^5\text{-C}_5\text{H}_5)_2]$ , is a bright green, reactive solid, conveniently prepared by adding a solution of  $\text{NiCl}_2$  in dimethylsulfoxide to a solution of  $\text{KC}_5\text{H}_5$  in 1,2-dimethoxyethane. It has the sandwich structure of ferrocene, and is similarly susceptible to ring-addition reactions, but its 2 extra electrons ( $\mu_e = 2.86 \text{ BM}$ ) must be accommodated in an antibonding orbital (p. 938). The orange-yellow,  $[\text{Ni}(\eta^5\text{-C}_5\text{H}_5)_2]^+$ , cation is therefore easily obtained by oxidation and the “triple-decker sandwich” cation,  $[\text{Ni}_2(\eta^5\text{-C}_5\text{H}_5)_3]^+$  (Fig. 27.13), is produced by reacting nickelocene with a Lewis acid such as  $\text{BF}_3$ . This latter cation is a 34 valence electron species [i.e.  $(2 \times 8) + (3 \times 6)$  for  $2\text{Ni}^{\text{II}}$  and  $3\text{C}_5\text{H}_5^-$ ] and there are theoretical grounds for supposing that this, and the 30-electron configuration, will offer the same sort of stability for binuclear sandwich compounds that the 18-electron configuration offers for mononuclear



**Figure 27.13** The “triple-decker sandwich” cation,  $[\text{Ni}_2(\eta^5\text{-C}_5\text{H}_5)_3]^+$ . Note that the  $\text{C}_5\text{H}_5$  rings are neither “staggered” nor “eclipsed”, and the nickel atoms are closer to the outer than to the central ring.

compounds. The cyclopentadienyls of palladium and platinum are less stable than those of nickel, and while the heavier pair of metals form some monocyclopentadienyl complexes, neither forms a metallocene.

### Alkene and alkyne complexes<sup>(37)</sup>

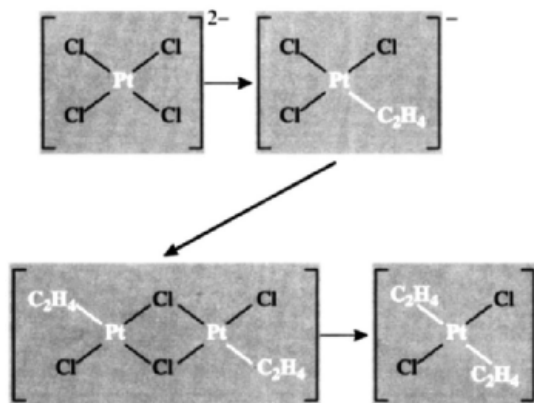
These are important not only for their part in stimulating the development of bonding theory (for a fuller discussion, see p. 931) but also for their catalytic role in some important industrial processes.

Apart from some  $\text{Pd}^0$  and  $\text{Pt}^0$  biphosphine complexes, the alkene and alkyne complexes involve the metals in the formally divalent state. Those of  $\text{Ni}^{\text{II}}$  are few in number compared to those of  $\text{Pd}^{\text{II}}$ , but it is  $\text{Pt}^{\text{II}}$  which provides the most numerous and stable compounds of this type. These are of the forms  $[\text{PtCl}_3\text{Alk}]^-$ ,  $[\text{PtCl}_2\text{Alk}]_2$  and  $[\text{PtCl}_2\text{Alk}_2]$ . They are generally prepared by treating an  $\text{M}^{\text{II}}$  salt with the hydrocarbon when a less strongly bonded anion is displaced. Thus, Zeise’s salt (p. 930) may be obtained by prolonged shaking of a solution of  $\text{K}_2\text{PtCl}_4$  in

<sup>36a</sup> L. HAO, G. J. SPIVAK, J. XIAO, J. J. VITTAL and R. J. PUDDEPHATT *J. Am. Chem. Soc.* **117**, 7011–12 (1995).

<sup>37</sup> V. G. ALBANO, G. NATILE and A. PANUNZI, *Coord. Chem. Revs.* **133**, 67–114 (1994).

dil HCl with  $C_2H_4$ , though the reaction can be speeded-up by the addition of a small amount of  $SnCl_2$ . Treatment of an ethanolic solution of the product with conc HCl then affords the orange dimer,  $[\{PtCl_2(C_2H_4)\}_2]$ . If this is then dissolved in acetone at  $-70^\circ C$  and further treated with  $C_2H_4$ , yellow, unstable crystals of the *trans*-bis(ethene) are formed:



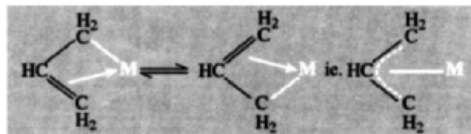
*cis*-Substituted dichloro complexes are obtained if chelating dialkenes such as *cis-cis*-cycloocta-1,5-diene (cod) are used (p. 932).

A common property of coordinated alkenes is their susceptibility to attack by nucleophiles such as  $OH^-$ ,  $OMe^-$ ,  $MeCO_2^-$ , and  $Cl^-$ , and it has long been known that Zeise's salt is slowly attacked by non-acidic water to give  $MeCHO$  and Pt metal, while corresponding Pd complexes are even more reactive.<sup>(38)</sup> This forms the basis of the Wacker process (developed by J. Smidt and his colleagues at Wacker Chemie, 1959–60) for converting ethene (ethylene) into ethanal (acetaldehyde) — see Panel overleaf.

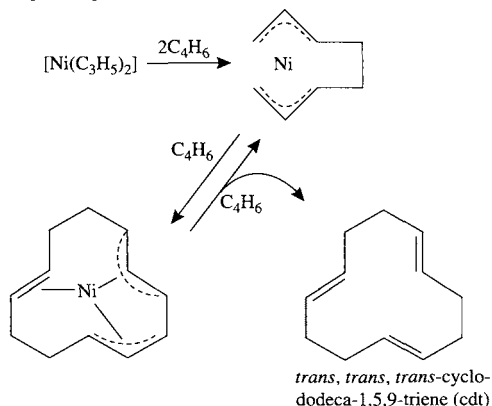
Alkyne complexes are essentially similar to the alkenes (p. 932) and those of  $Pt^{II}$ , particularly when the alkyne incorporates the *t*-butyl group, are the most stable.  $Ni^{II}$  alkyne complexes are less numerous and generally less stable but are of greater practical importance because of their role as intermediates in the cyclic oligomerization of alkynes, discovered by W. Reppe (see Panel).

### $\pi$ -Allylic complexes

The preparation and bonding of complexes of the  $\eta^3$ -allyl group,  $CH_2=CH-CH_2-$ , have already been discussed (p. 933). This group, and substituted derivatives of it, may act as  $\sigma$ -bonded ligands, but it is as 3-electron  $\pi$ -donor ligands that they are most important. Crudely:



The  $\pi$ -allyl complexes of  $Pd^{II}$ , e.g.  $[Pd(\eta^3-C_3H_5)X]_2$  ( $X = Cl, Br, I$ ), are very stable and more numerous than for any other metal, and neither Ni nor Pt form as many of these complexes. Indeed, the contrast between Pd and Pt is such that in reactions with alkenes, where a particular compound of Pt is likely to form an alkene complex, the corresponding compound of Pd is more likely to form a  $\pi$ -allyl complex. The role of the Pd and Ni complexes as intermediates in the oligomerization of conjugated dienes (of which 1,3-butadiene,  $C_4H_6$ , is the most familiar) have been extensively studied, particularly by G. Wilke and his group. For instance in the presence of  $[Ni(\eta^3-C_3H_5)_2]$  (or  $[Ni(acac)_2]_3 + Al_2Et_6$ ), butadiene trimerizes, probably via the catalytic cycle:



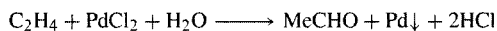
Other isomers of cdt are also obtained and, if a coordination site on the nickel is blocked by the addition of a ligand such as a tertiary phosphine, dimerization of the butadiene, rather than trimerization, occurs.

<sup>38</sup> A. HEUMANN, K.-J. JENS and M. REGLIER, *Prog. Inorg. Chem.* **42**, 483–576 (1994).

## Catalytic Applications of Alkene and Alkyne Complexes

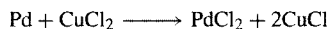
### The Wacker process

Ethanal is produced by the aerial oxidation of ethene in the presence of  $\text{PdCl}_2/\text{CuCl}_2$  in aqueous solution. The main reaction is the oxidative hydrolysis of ethene:

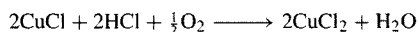


The mechanism of this reaction is not straightforward but the crucial step appears to be nucleophilic attack by water or  $\text{OH}^-$  on the coordinated ethene to give  $\sigma$ -bonded  $-\text{CH}_2\text{CH}_2\text{OH}$  which then rearranges and is eventually eliminated as  $\text{MeCHO}$  with loss of a proton.

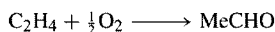
The commercial viability of the reaction depends on the formation of a catalytic cycle by reoxidizing the palladium metal *in situ*. This is achieved by the introduction of  $\text{CuCl}_2$ :



Because the solution is slightly acidic, the  $\text{CuCl}_2$  itself can be regenerated by passing in oxygen:

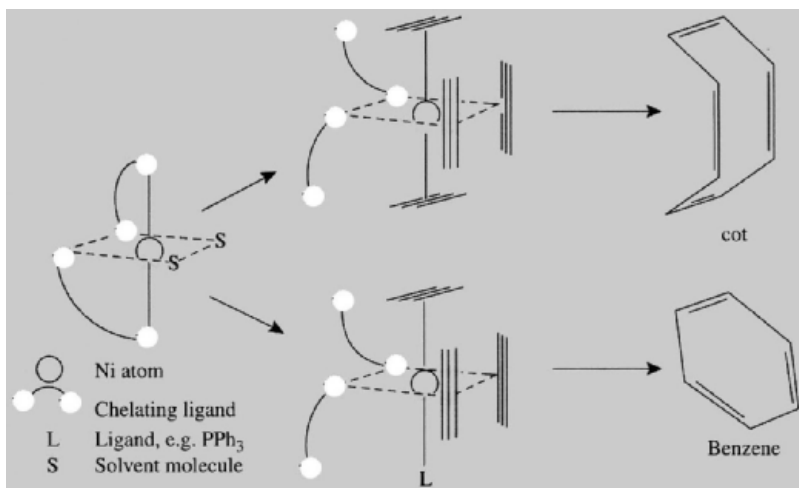


The overall reaction is thus:



### The Reppe Synthesis

Polymerization of alkynes by  $\text{Ni}^{\text{II}}$  complexes produces a variety of products which depend on conditions and especially on the particular nickel complex used. If, for instance, *O*-donor ligands such as acetylacetonate or salicylaldehyde are employed in a solvent such as tetrahydrofuran or dioxan, 4 coordination sites are available and cyclotetramerization occurs to give mainly cyclo-octatetraene (cot). If a less-labile ligand such as  $\text{PPh}_3$  is incorporated, the coordination sites required for tetramerization are not available and cyclic trimerization to benzene predominates (Fig. A). These syntheses are amenable to extensive variation and adaptation. Substituted ring systems can be obtained from the appropriately substituted alkynes while linear polymers can also be produced.



**Figure A** Cyclic oligomerizations of acetylene: tetramerization producing cyclooctatetraene (cot) and trimerization producing benzene.

1		2																																	
H		He																																	
3	4											5	6	7	8	9	10	11	12																
Li	Be											B	C	N	O	F	Ne																		
11	12											13	14	15	16	17	18																		
Na	Mg											Al	Si	P	S	Cl	Ar																		
19	20	21	22	23	24	25	26	27	28	29	30	31	32	33	34	35	36																		
K	Ca	Sc	Ti	V	Cr	Mn	Fe	Co	Ni	Cu	Zn	Ga	Ge	As	Se	Br	Kr																		
37	38	39	40	41	42	43	44	45	46	47	48	49	50	51	52	53	54																		
Rb	Sr	Y	Zr	Nb	Mo	Tc	Ru	Rh	Pd	Ag	Cd	In	Sn	Sb	Te	I	Xe																		
55	56	57	58	59	60	61	62	63	64	65	66	67	68	69	70	71	72																		
Cs	Ba	La	Hf	Ta	W	Re	Os	Ir	Pt	Au	Hg	Tl	Pb	Bi	Po	At	Rn																		
87	88	89	90	91	92	93	94	95	96	97	98	99	100	101	102	103	104																		
Fr	Ra	Ac	Rf	Db	Sg	Bh	Hs	Mt	Uun	Uun	Uun	Uun	Uun	Uun	Uun	Uun																			
																		58	59	60	61	62	63	64	65	66	67	68	69	70	71				
																		Ce	Pr	Nd	Pm	Sm	Eu	Gd	Tb	Dy	Ho	Er	Tm	Yb	Lu				
																		90	91	92	93	94	95	96	97	98	99	100	101	102	103	104			
																		Th	Pa	U	Np	Pu	Am	Cm	Bk	Cf	Es	Fm	Md	No	Lr				

# 28

## Copper, Silver and Gold

### 28.1 Introduction<sup>(1)</sup>

Collectively known as the “coinage metals” because of their former usage, these elements were almost certainly the first three metals known to man. All of them occur in the elemental, or “native”, form and must have been used as primitive money long before the introduction of gold coins in Egypt around 3400 BC.

Cold-hammering was used in the late Stone Age to produce plates of gold for ornamental purposes, and this metal has always been synonymous with beauty, wealth and power. Considerable quantities were accumulated by ancient peoples. The coffin of Tutankhamun (a minor Pharaoh who was only 18 when he died) contained no less than 112 kg of gold, and the legendary Aztec and Inca hoards in Mexico and Peru were a major reason for the Spanish conquests of Central and South America in the early sixteenth century. Today, the greatest hoard of gold is the 30 000 tonnes of bullion (i.e. bars) lying in the vaults of the US Federal Reserve Bank

in New York and belonging to eighty different nations.

Estimates of the earliest use of copper vary, but 5000 BC is not unreasonable. By about 3500 BC it was being obtained in the Middle East by charcoal reduction of its ores, and by 3000 BC the advantages of adding tin in order to produce the harder bronze was appreciated in India, Mesopotamia and Greece. This established the “Bronze Age”, and copper has continued to be one of man’s most important metals.

The monetary use of silver may well be as old as that of gold but the abundance of the native metal was probably far less, so that comparable supplies were not available until a method of winning the metal from its ores had been discovered. It appears, however, that by perhaps 3000 BC a form of cupellation<sup>†</sup> was in operation in Asia Minor and its use gradually

<sup>†</sup> Cupellation processes vary but consist essentially of heating a mixture of precious and base (usually lead) metals in a stream of air in a shallow hearth, when the base metal is oxidized and removed either by blowing away or by absorption into the furnace lining. In the early production of silver, the sulfide ores must have been used to give first a silver/lead alloy from which the lead was then removed.

<sup>1</sup> R. F. TYLECOTE, *History of Metallurgy*, The Metals Society, London, 1976, 182 pp.

spread, so that silver coinage was of crucial economic importance to all subsequent classical Mediterranean civilizations.

The name *copper* and the symbol Cu are derived from *aes cyprium* (later Cuprum), since it was from Cyprus that the Romans first obtained their copper metal. The words *silver* and *gold* are Anglo-Saxon in origin but the chemical symbols for these elements (Ag and Au) are derived from the Latin *argentum* (itself derived from the Greek ἀργός, *argos*, shiny or white) and *aurum*, gold.

## 28.2 The Elements

### 28.2.1 Terrestrial abundance and distribution

The relative abundances of these three metals in the earth's crust (Cu 68 ppm, Ag 0.08 ppm, Au 0.004 ppm) are comparable to those of the preceding triad — Ni, Pd and Pt. Copper is found mainly as the sulfide, oxide or carbonate, its major ores being copper pyrite (chalcopyrite),  $\text{CuFeS}_2$ , which is estimated to account for about 50% of all Cu deposits; copper glance (chalcocite),  $\text{Cu}_2\text{S}$ ; cuprite,  $\text{Cu}_2\text{O}$  and malachite,  $\text{Cu}_2\text{CO}_3(\text{OH})_2$ . Large deposits are found in various parts of North and South America, and in Africa and the former Soviet Union. The native copper found near Lake Superior is extremely pure but the vast majority of current supplies of copper are obtained from low-grade ores containing only about 1% Cu.

Silver is widely distributed in sulfide ores of which silver glance (argentite),  $\text{Ag}_2\text{S}$ , is the most important. Native silver is sometimes associated with these ores as a result of their chemical reduction, while the action of salt water is probably responsible for their conversion into "horn silver",  $\text{AgCl}$ , which is found in Chile and New South Wales. The Spanish Americas provided most of the world's silver for the three centuries after about 1520, to be succeeded in the nineteenth century by Russia. Appreciable quantities are now obtained as a byproduct in the production of other metals such as copper,

and the main producers are Mexico, the former Soviet Union, Peru, the USA and Australia.

Gold, too, is widely, if sparsely, distributed both native<sup>†</sup> and in tellurides, and is almost invariably associated with quartz or pyrite, both in veins and in alluvial or placer deposits laid down after the weathering of gold-bearing rocks. It is also present in sea water to the extent of around  $1 \times 10^{-3}$  ppm, depending on location, but no economical means of recovery has yet been devised. Prior to about 1830 a large proportion of the world's stock of gold was derived from ancient and South American civilizations (recycling is not a new idea), and the annual output of new gold was no more than 12 tonnes pa. This supply gradually increased with the discovery of gold in Siberia followed by "gold rushes" in 1849 (California: as a result of which the American West was settled), 1851 (New South Wales and Victoria: within 7 y the population of Australia doubled to 1 million), 1884 (Transvaal), 1896 (Klondike, North-west Canada) and, finally, 1900 (Nome area of Alaska) as a result of which by 1890 world production had risen to 150 tonnes pa. It is now 15 times that amount, ~2300 tonnes pa.

### 28.2.2 Preparation and uses of the elements<sup>(2,3)</sup>

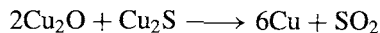
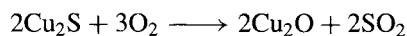
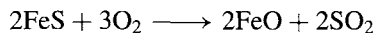
A few of the oxide ores of copper can be reduced directly to the metal by heating with coke, but the bulk of production is from sulfide ores containing iron, and they require more complicated treatment. These ores are comparatively lean (often ~0.5% Cu) and their exploitation requires economies of scale. They are therefore obtained in huge, open-pit operations employing shovels

<sup>†</sup> The "Welcome Stranger" nugget found in Victoria, Australia, in 1869 weighed over 71 kg and yielded nearly 65 kg of refined gold but was, unfortunately, exceptional.

<sup>2</sup> *Kirk-Othmer Encyclopedia of Chemical Technology*, 4th edn., Interscience, New York; for Cu see Vol. 7, 1993, pp. 505–20; for Ag, Vol. 22, 1997, pp. 163–95; for Au, Vol. 12, 1994, pp. 738–67.

<sup>3</sup> J. MARSDEN and I. HOUSE, *The Chemistry of Gold Extraction*, Ellis Horwood, Chichester, 1992, 597 pp.

of up to 25 m<sup>3</sup> (900 ft<sup>3</sup>) and trucks of up to 250 tonnes capacity, followed by crushing and concentration (up to 15–20% Cu) by froth-flotation. (The environmentally acceptable disposal of the many millions of tonnes of finely ground waste poses serious problems.) Silica is added to the concentrate which is then heated in a reverberatory furnace (blast furnaces are unsuitable for finely powdered ores) to about 1400°C when it melts. FeS is more readily converted to the oxide than is Cu<sub>2</sub>S and so, with the silica, forms an upper layer of iron silicate slag leaving a lower layer of copper matte which is largely Cu<sub>2</sub>S and FeS. The liquid matte is then placed in a converter (similar to the Bessemer converter, p. 1072) with more silica and a blast of air forced through it. This transforms the remaining FeS first to FeO and then to slag, while the Cu<sub>2</sub>S is partially converted to Cu<sub>2</sub>O and then to metallic copper:



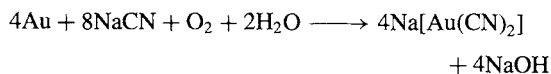
The major part of this “blister” copper is further purified electrolytically by casting into anodes which are suspended in acidified CuSO<sub>4</sub> solution along with cathodes of purified copper sheet. As electrolysis proceeds the pure copper is deposited on the cathodes while impurities collect below the anodes as “anode slime” which is a valuable source of Ag, Au and other precious metals.

About one-third of the copper used is secondary copper (i.e. scrap) but the annual production of new metal is nearly 8 million tonnes, the chief sources (1993) being Chile (22%), the USA (20%), the former Soviet Union (9%), Canada and China (7.5% each) and Zambia (5%). The major use is as an electrical conductor but it is also widely employed in coinage alloys as well as the traditional bronze (Cu plus 7–10% Sn), brass (Cu–Zn), and special alloys such as *Monel* (Ni–Cu).

Most silver is nowadays produced as a byproduct in the manufacture of non-ferrous metals such as copper, lead and zinc, when

the silver follows the base metal through the concentration and smelting processes. In the case of copper production, for instance, the anode slimes mentioned above are treated with hot, aerated dilute H<sub>2</sub>SO<sub>4</sub>, which dissolves some of the base metal content, then heated with a flux of lime or silica to slag-off most of the remaining base metals, and, finally, electrolysed in nitrate solution to give silver of better than 99.9% purity. As with copper, much of the metal used is salvage but over 10 000 tonnes of new metal were produced in 1993, mainly from Mexico (19%) the former Soviet Union, the USA and Peru (~13% each) and Australia (9%). Photography accounts for the use of about one-third of this and it is also used in silverware and jewellery, electrically, for silvering mirrors, and in the high-capacity Ag–Zn, Ag–Cd batteries. A minor though important use from 1826 until recent times was as dental amalgam (Hg/γ–Ag<sub>3</sub>Sn).

Traditionally, gold was recovered from river sands by methods such as “panning” which depend on the high density of gold (19.3 g cm<sup>-3</sup>) compared with sand (~2.5 g cm<sup>-3</sup>)<sup>†</sup> but as such sources are largely worked out, modern production depends on the mining of the gold-containing rock (typically, 5–15 ppm of Au). This is crushed to a fine powder (the consistency of talcum powder) to liberate the metallic grains and these are extracted either by the cyanide process or, after gravity concentration, by amalgamation with mercury (after which the Hg is distilled off). In the former the gold and any silver present is leached from the crushed rock with an aerated, dilute solution of cyanide:



It is then precipitated by adding Zn dust. Electrolytic refining may then be used to provide gold of 99.99% purity.<sup>‡</sup>

<sup>†</sup> In ancient times, gold-bearing river sands were washed over a sheep’s fleece which trapped the gold. It seems likely that this was the origin of the Golden Fleece of Greek mythology.

<sup>‡</sup> Gold is commonly alloyed with other metals in order to make it harder and cheaper. (An appropriate mixture of Au

Table 28.1 Some properties of the elements copper, silver and gold

Property		Cu	Ag	Au
Atomic number		29	47	79
Number of naturally occurring isotopes		2	2	1
Atomic weight		63.546(3)	107.8682(2)	196.96655(2)
Electronic configuration		[Ar]3d <sup>10</sup> 4s <sup>1</sup>	[Kr]4d <sup>10</sup> 5s <sup>1</sup>	[Xe]4f <sup>14</sup> 5d <sup>10</sup> 6s <sup>1</sup>
Electronegativity		1.9	1.9	2.4
Metal radius (12-coordinate)/pm		128	144	144
Effective ionic radius (6-coordinate)/pm	V	—	—	57
	III	54	75	85
	II	73	94	—
	I	77	115	137
Ionization energy/kJ mol <sup>-1</sup>	1st	745.3	730.8	889.9
	2nd	1957.3	2072.6	1973.3
	3rd	3577.6	3359.4	(2895)
MP/°C		1083	961	1064
BP/°C		2570	2155	2808
$\Delta H_{\text{fus}}/\text{kJ mol}^{-1}$		13.0	11.1	12.8
$\Delta H_{\text{vap}}/\text{kJ mol}^{-1}$		307(±6)	258(±6)	343(±11)
$\Delta H_{\text{(monatomic gas)}}/\text{kJ mol}^{-1}$		337(±6)	284(±4)	379(±8)
Density (20°C)/g cm <sup>-3</sup>		8.95	10.49	19.32
Electrical resistivity (20°C)/μohm cm		1.673	1.59	2.35

Total annual production of new gold is now about 2300 tonnes of which (1993) 27% comes from South Africa, 15% from the USA and 11% each from Australia and the former Soviet Union. The bulk of the gold from “Western” countries passes through the London Bullion Market which was established in 1666. Prices, which are quoted in troy oz,<sup>†</sup> are affected by speculative buying and can be subject to astonishing fluctuations.

The two main uses for gold are in settling international debts and in the manufacture of jewellery, but other important uses are in dentistry, the electronics industry (corrosion-free contacts), and the aerospace industry (brazing alloys and heat reflection), while in office buildings it has

and Cu will maintain the golden hue.) The proportion of gold is expressed in *carats*, a *carat* being a twenty-fourth part by weight of the metal so that pure gold is 24 *carats*. In the case of precious stones the *carat* expresses mass not purity and is then defined as 200 mg. The term is derived from the name of the small and very uniform seeds of the carob tree which in antiquity were used to weigh precious metals and stones (p. 272).

<sup>†</sup> 1 troy (or fine) oz = 31.1035 g as distinct from 1 oz avoirdupois = 28.3495 g.

been found that a mere 20 nm film on the inside face of windows cuts down heat losses in winter and reflects unwanted infrared radiation in summer.

### 28.2.3 Atomic and physical properties of the elements

Some important properties are listed in Table 28.1. As gold has only one naturally occurring isotope, its atomic weight is known with considerable accuracy; Cu and Ag each have 2 stable isotopes, and a slight variability of their abundance in the case of Cu prevents its atomic weight being quoted with greater precision. This is the first triad since Ti, Zr and Hf in which the ground-state electronic configuration of the free atoms is the same for the outer electrons of all three elements. Gold is the most electronegative of all metals: the value of 2.4 equals that for Se and approaches the value of 2.5 for S and I. Estimates of electron affinity vary considerably but typical values (kJ mol<sup>-1</sup>) are Cu 119.2, Ag 125.6 and Au 222.8. These may be compared with values for

H 72.8, O 141.0 and I 295.2 kJ mol<sup>-1</sup>. Consistent with this the compound CsAu has many salt-like rather than alloy-like properties and, when fused, behaves much like other molten salts. Similarly when Au is dissolved in solutions of Cs, Rb or K in liquid ammonia, the spectroscopic and other properties are best interpreted in terms of the solvated Au<sup>-</sup> ion (d<sup>10</sup>s<sup>2</sup>) analogous to a halide ion (s<sup>2</sup>p<sup>6</sup>).

The elements are obtainable in a state of very high purity but some of their physical properties are nonetheless variable because of their dependence on mechanical history. Their colours (Cu reddish, Ag white and Au yellow) and sheen are so characteristic that the names of the metals are used to describe them.<sup>†</sup> Gold can also be obtained in red, blue and violet colloidal forms by the addition of various reducing agents to very dilute aqueous solutions of gold(III) chloride. A remarkably stable example is the "Purple of Cassius", obtained by using SnCl<sub>2</sub> as reductant, which not only provides a sensitive test for Au<sup>III</sup> but is also used to colour glass and ceramics. Colloidal silver and copper are also obtainable but are less stable.

The solid metals all have the fcc structure, like their predecessors in the periodic table, Ni, Pd and Pt, and they continue the trend of diminishing mp and bp. They are soft, and extremely malleable and ductile, gold more so than any other metal. One gram of gold can be beaten out into a sheet of ~1.0 m<sup>2</sup> only 230 atoms thick (i.e. 1 cm<sup>3</sup> to 18 m<sup>2</sup>); likewise 1 g Au can be drawn into 165 m of wire of diameter 20 μm. The electrical and thermal conductances of the

three metals are also exceptional, pre-eminence in this case belonging to silver. All these properties can be directly related to the d<sup>10</sup>s<sup>1</sup> electronic configuration.

### 28.2.4 Chemical reactivity and trends

Because of the traditional designation of Cu, Ag and Au as a subdivision of the group containing the alkali metals (justified by their respective d<sup>10</sup>s<sup>1</sup> and p<sup>6</sup>s<sup>1</sup> electron configurations) some similarities in properties might be expected. Such similarities as do occur, however, are confined almost entirely to the stoichiometries (as distinct from the chemical properties) of the compounds of the +1 oxidation state. The reasons are not hard to find. A filled d shell is far less effective than a filled p shell in shielding an outer s electron from the attraction of the nucleus. As a result the first ionization energies of the coinage metals are much higher, and their ionic radii smaller than those of the corresponding alkali metals (Table 28.1 and p. 75). They consequently have higher mps, are harder, denser, less reactive, less soluble in liquid ammonia, and their compounds more covalent. Again, whereas the alkali metals stand at the top of the electrochemical series (with  $E^\circ$  between -3.045 and -2.714 V), the coinage metals are near the bottom: Cu<sup>+</sup>/Cu +0.521, Ag<sup>+</sup>/Ag +0.799, Au<sup>+</sup>/Au +1.691 V. On the other hand, a filled d shell is more easily disrupted than a filled p shell. The second and third ionization energies of the coinage metals are therefore *lower* than those of the alkali metals so that they are able to adopt oxidation states higher than +1. They also more readily form coordination complexes. In short, Cu, Ag and Au are transition metals whereas the alkali metals are not. Indeed, the somewhat salt-like character of CsAu and the formation of the solvated Au<sup>-</sup> ion in liquid ammonia, mentioned above, can be regarded as halogen-like behaviour arising because the d<sup>10</sup>s<sup>1</sup> configuration is 1 electron short of the closed configuration d<sup>10</sup>s<sup>2</sup> (cf hydrogen, p. 43).

<sup>†</sup> The colours arise from the presence of filled d bands near the electron energy surface of the s-p conduction band of the metals (Fermi surface). X-ray data indicate that the top of the d-band is ~220 kJ mol<sup>-1</sup> (2.3 eV/atom) below the Fermi surface for Cu so electrons can be excited from the d band to the s-p band by absorption of energy in the green and blue regions of the visible spectrum but not in the orange or red regions. For silver the excitation energy is rather larger (~385 kJ mol<sup>-1</sup>) corresponding to absorption in the ultraviolet region of the spectrum. Gold is intermediate but much closer to Cu, the absorption in the near ultraviolet and blue region of the spectrum giving rise to the characteristic golden yellow colour of the metal.



Copper, silver and gold are notable in forming an extensive series of alloys with many other metals and many of these have played an important part in the development of technology through the ages (p. 1173). In many cases the alloys can be thought of as nonstoichiometric intermetallic compounds of definite structural types and, despite the apparently bizarre formulae that emerge from the succession of phases, they can readily be classified by a set of rules first outlined by W. Hume-Rothery in 1926. The determining feature is the ratio of the number of electrons to the number of atoms ("electron concentration"), and because of this the phases are sometimes referred to as "electron compounds".

The fcc lattice of the coinage metals has 1 valency electron per atom ( $d^{10}s^1$ ). Admixture with metals further to the right of the periodic table (e.g. Zn) increases the electron concentration in the primary alloy ( $\alpha$ -phase) which can be described as an fcc solid solution

of M in Cu, Ag or Au. This continues until, as the electron concentration approaches 1.5 (i.e. 21/14), the fcc structure becomes less stable than a bcc arrangement which therefore crystallizes as the  $\beta$ -phase (e.g.  $\beta$ -brass, CuZn; see Fig. 28.1). Further increase in electron concentration results in formation of the more complex  $\gamma$ -brass phase of nominal formula  $\text{Cu}_5\text{Zn}_8$  and electron concentration of  $\{(5 \times 1) + (8 \times 2)\}/13 = 21/13 = 1.615$ . The phase is still cubic but has 52 atoms in the unit cell (i.e.  $4\text{Cu}_5\text{Zn}_8$ ). This  $\gamma$ -phase can itself take up more Zn until a third critical concentration is reached near 1.75 (i.e. 7/4 or 21/12) when the hcp  $\varepsilon$ -phase of  $\text{CuZn}_3$  is formed. Hume-Rothery showed that this succession of phases is quite general (and also holds for Groups 8, 9 and 10 to the left of the coinage metals if they are taken to contribute no electrons to the lattice).

The reactivity of Cu, Ag and Au decreases down the group, and in its inertness gold

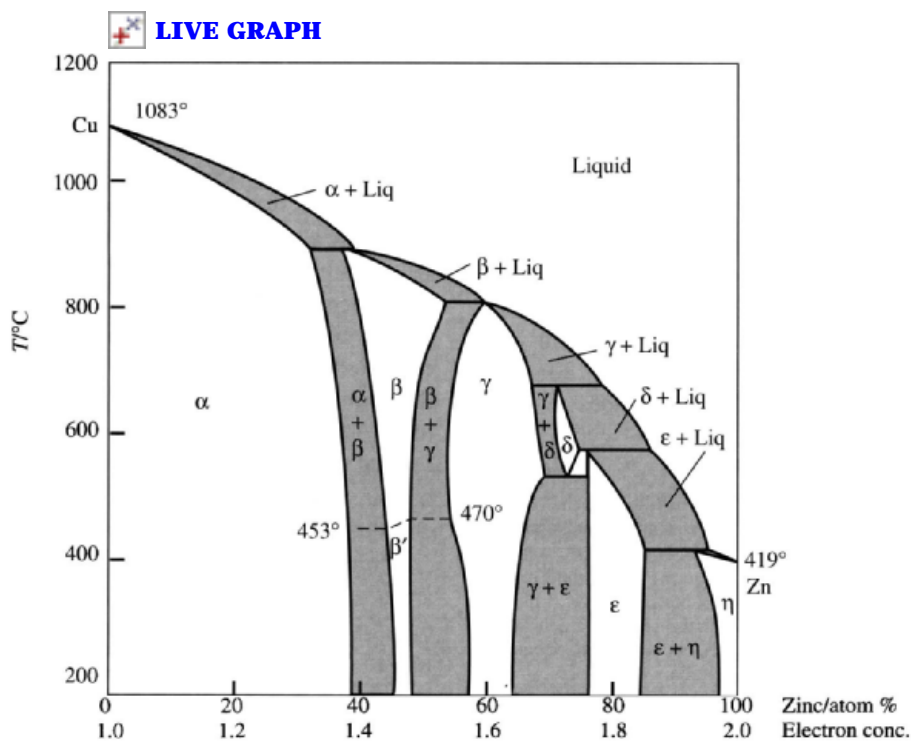


Figure 28.1 Phase diagram of the system Cu/Zn.

Table 28.2 Oxidation states and stereochemistries of copper, silver and gold

Oxidation state	Coordination number	Stereochemistry	Cu	Ag/Au
-1 ( $d^{10}s^2$ )	?	?		$[\text{Au}(\text{NH}_3)_n]^-$ (liq $\text{NH}_3$ )
0 ( $d^{10}s^1$ )	3	Planar	$[\text{Cu}(\text{CO})_3]$ (10 K)	$[\text{Ag}(\text{CO})_3]$ (10 K)
	4	—	$[(\text{CO})_3\text{CuCu}(\text{CO})_3]$ (30 K)	$[(\text{CO})_3\text{AgAg}(\text{CO})_3]$ (30 K)
< +1	8	See Fig. 28.10(a)		$[(\text{Ph}_3\text{P})\text{Au}\{\text{Au}(\text{PPh}_3)\}_7]^{2+}$
	10	See Fig. 28.10(c)		$[\text{Au}_{11}\text{I}_3\{\text{P}(\text{C}_6\text{H}_4-4-\text{F})_3\}_7]$
	12	Icosahedral		$[\text{Au}_{13}\text{Cl}_{12}(\text{PMe}_2\text{Ph})_{10}]^{3+}$
1 ( $d^{10}$ )	2	Linear	$[\text{CuCl}_2]^-$ , $\text{Cu}_2\text{O}$	$[\text{M}(\text{CN})_2]^-$
	3	Trigonal planar	$[\text{Cu}(\text{CN})_3]^{2-}$	$[\text{AgI}(\text{PEt}_2\text{Ar})_2]$ , $[\text{AuCl}(\text{PPh}_3)_2]$
	4	Tetrahedral	$[\text{Cu}(\text{py})_4]^+$	$[\text{M}(\text{diars})_2]^+$ , $[\text{Au}(\text{PMePh}_2)_4]^+$
		Square planar		$[\text{Au}\{\eta^2-\text{Os}_3(\text{CO})_{10}\text{H}\}_2]^-$
	6	Octahedral		$\text{AgX}$ (X = F, Cl, Br)
2 ( $d^9$ )	4	Tetrahedral	$\text{Cs}_2[\text{CuCl}_4]^{(a)}$	
		Square planar	$[\text{EtNH}_3]_2[\text{CuCl}_4]^{(a)}$	$[\text{Ag}(\text{py})_4]^{2+}$ $[\text{Au}\{\text{S}_2\text{C}_2(\text{CN})_2\}_2]^{2-}$
	5	Trigonal bipyramidal	$[\text{Cu}(\text{bipy})_2\text{I}]^+$	
		Square pyramidal	$[\{\text{Cu}(\text{dmgH})_2\}_2]^{(b)}$	
	6	Octahedral	$\text{K}_2\text{Pb}[\text{Cu}(\text{NO}_2)_6]$	
	7	Pentagonal bipyramidal	$[\text{Cu}(\text{H}_2\text{O})_2(\text{dps})]^{2+(c)}$	
	8	Dodecahedral (dist.)	$[\text{Cu}(\text{O}_2\text{CMe})_4]^{2+}$	
3 ( $d^8$ )	4	Square planar	$[\text{CuBr}_2(\text{S}_2\text{CNBu}'_2)]$	$[\text{AgF}_4]^-$ , $[\text{AuBr}_4]^-$
	5	Square pyramidal	$[\text{CuCl}(\text{PhCO}_2)_2(\text{py})_2]^{(d)}$	$[\text{Au}(\text{C}_6\text{H}_4\text{CH}_2\text{NMe}_2-2-\text{phen})(\text{PPh}_3)]^{2+}$
	6	Octahedral	$[\text{CuF}_6]^{3-}$	$[\text{AgF}_6]^{3-}$ , $[\text{AuI}_2(\text{diars})_2]^+$
4 ( $d^7$ )	6	?	$[\text{CuF}_6]^{2-}$	
5 ( $d^6$ )	6	Octahedral (?)		$[\text{AuF}_6]^-$

<sup>(a)</sup>See text, p. 1193. <sup>(b)</sup> $\text{dmgH}_2$  = dimethylglyoxime: see also Fig. 28.6

<sup>(c)</sup> $\text{dps}$  = 2,6-diacetylpyridine bissemicarbazone <sup>(d)</sup>G. SPEIER and V. FÜLÖP *J. Chem. Soc., Chem. Commun.*, 905–6 (1990).

resembles the platinum metals. All three metals are stable in pure dry air at room temperature but copper forms  $\text{Cu}_2\text{O}$  at red heat.<sup>†</sup> Copper is also attacked by sulfur and halogens, and the sensitivity of silver to sulfur and its compounds is responsible for the familiar tarnishing of the metal (black  $\text{Ag}_2\text{S}$ ) when exposed to air containing such substances. Under similar circumstances copper forms a green coating of a basic sulfate. In sharp contrast, gold is the only metal which will not react directly with sulfur. In general the reactions of the metals are assisted by the presence of oxidizing agents. Thus, in the absence of air, non-oxidizing acids have little effect, but

Cu and Ag dissolve in hot conc  $\text{H}_2\text{SO}_4$  and in both dil and conc  $\text{HNO}_3$ , while Au dissolves in conc HCl if a strong oxidizing agent is present. Thus *aqua regia*, a 3:1 mixture of conc HCl and conc  $\text{HNO}_3$ , was so named by alchemists because it dissolves gold, the king of metals. More recently, solutions of  $\text{Cl}_2$  and  $\text{Me}_3\text{NHCl}$  in MeCN have been shown<sup>(4)</sup> to be even better solvents of gold. In addition, the metals dissolve readily in aqueous cyanide solutions in the presence of air or, better still,  $\text{H}_2\text{O}_2$ .

Table 28.2 is a list of typical compounds of the elements, which reveals a further reduction in the range of oxidation states consequent on the stabilization of d orbitals at the end of the transition

<sup>†</sup> It was because of their resistance to attack by air, even when heated, that gold and silver were referred to as *noble* metals by the alchemists.

<sup>4</sup> Y. NAKAO, *J. Chem. Soc., Chem. Commun.*, 426–7 (1992).

series. Apart from a single  $\text{Cu}^{\text{IV}}$  fluoro-complex and possibly one or two  $\text{Cu}^{\text{IV}}$  oxo-species, neither Cu nor Ag is known to exceed the oxidation state +3 and even Au does so only in a few  $\text{Au}^{\text{V}}$  fluoro-compounds (see below): these may owe their existence at least in part to the stabilizing effect of the  $t_{2g}^6$  configuration. It is also significant that, in a number of instances, the +1 oxidation state no longer requires the presence of presumed  $\pi$ -acceptor ligands even though the  $\text{M}^{\text{I}}$  metals are to be regarded mainly as class b in character. Stable, zero-valent compounds are not found, but a number of cluster compounds with the metal in a fractional ( $<1$ ) oxidation state, especially of gold, are of interest. The only aquo ions of this group are those of  $\text{Cu}^{\text{I}}$  (unstable),  $\text{Cu}^{\text{II}}$ ,  $\text{Ag}^{\text{I}}$  and  $\text{Ag}^{\text{II}}$  (unstable). The best-known oxidation states, particularly in aqueous solution, are +2 for Cu, +1 for Ag, and +3 for Au. This accords with their ionization energies (Table 28.1) though, of course, few of the compounds are completely ionic. Silver has the lowest first ionization energy, while the sum of first and second is lowest for Cu and the sum of first, second, and third is lowest for Au. This is an erratic sequence and illustrates the most notable feature of the triad from a chemical point of view, namely that the elements are not well related either as three elements showing a monotonic gradation in properties or as a triad comprising a single lighter element together with a pair of closely similar heavier elements. "Horizontal" similarities with their neighbours in the periodic table are in fact more noticeable than "vertical" ones.

The reasons are by no means certain but no doubt involve several factors, of which size is probably a major one. Thus the  $\text{Cu}^{\text{II}}$  ion is smaller than  $\text{Cu}^{\text{I}}$  and, having twice the charge, interacts much more strongly with solvent water (heats of hydration are  $-2100$  and  $-580 \text{ kJ mol}^{-1}$  respectively). The difference is evidently sufficient to outweigh the second ionization energy of copper and to render  $\text{Cu}^{\text{II}}$  more stable in aqueous solution (and in ionic solids) than  $\text{Cu}^{\text{I}}$ , in spite of the stable  $d^{10}$  configuration of the latter. In the case of silver, however, the ionic radii are both much larger and

so the difference in hydration energies will be much smaller; in addition the second ionization energy is even greater than for copper. The +1 ion with its  $d^{10}$  configuration is therefore the more stable. For gold, the stability of the 6s orbital and instability of the 5d as compared to silver, and leading respectively to the possibility of  $\text{Au}^{\text{I}}$  and enhanced stability of  $\text{Au}^{\text{III}}$ , have been convincingly ascribed to relativistic effects operating on s and p electrons.<sup>(5)</sup> The high CFSE associated with square planar  $d^8$  ions (see p. 1131) is a further factor favouring the +3 oxidation state.

Coordination numbers in this triad are again rarely higher than 6, but the univalent metals provide examples of the coordination number 2 which tends to be uncommon in transition metals proper (i.e. excluding Zn, Cd and Hg).

Organometallic chemistry (see p. 1199) is not particularly extensive even though gold alkyls were amongst the first organo-transition metal compounds to be prepared. Those of  $\text{Au}^{\text{III}}$  are the most stable in this group, while  $\text{Cu}^{\text{I}}$  and  $\text{Ag}^{\text{I}}$  (but not  $\text{Au}^{\text{I}}$ ) form complexes, of lower stability, with unsaturated hydrocarbons.

## 28.3 Compounds of Copper, Silver and Gold

Binary carbides,  $\text{M}_2\text{C}_2$  (i.e. acetylides), are obtained by passing  $\text{C}_2\text{H}_2$  through ammoniacal solutions of  $\text{Cu}^+$  and  $\text{Ag}^+$ . Both are explosive when dry but regenerate acetylene if treated with a dilute acid. Copper and silver also form explosive azides while the even more dangerous "fulminating" silver and gold, which probably contain  $\text{M}_3\text{N}$ , are produced by the action of aqueous ammonia on the metal oxides. None of the metals reacts significantly with  $\text{H}_2$  but the reddish-brown precipitate, obtained when aqueous  $\text{CuSO}_4$  is reduced by hypophosphorous acid ( $\text{H}_3\text{PO}_2$ ), is largely  $\text{CuH}$ .

<sup>5</sup> P. PYYKKÖ and J.-P. DESCLAUX, *Acc. Chem. Res.* 12, 276-81 (1979).

### 28.3.1 Oxides and sulfides<sup>(6)</sup>

Two oxides of copper,  $\text{Cu}_2\text{O}$  (yellow or red) and  $\text{CuO}$  (black), are known, both with narrow ranges of homogeneity and both form when the metal is heated in air or  $\text{O}_2$ ,  $\text{Cu}_2\text{O}$  being favoured by high temperatures.  $\text{Cu}_2\text{O}$  (mp  $1230^\circ$ ) is conveniently prepared by the reduction in alkaline solution of a  $\text{Cu}^{\text{II}}$  salt using hydrazine or a sugar.<sup>†</sup>  $\text{CuO}$  is best obtained by igniting the nitrate or basic carbonate of  $\text{Cu}^{\text{II}}$ . Addition of alkali to aqueous solutions of  $\text{Cu}^{\text{II}}$  gives a pale-blue precipitate of  $\text{Cu}(\text{OH})_2$ . This will redissolve in acids and also in conc alkali (amphoteric) to give deep-blue solutions probably containing species of the type  $[\text{Cu}(\text{OH})_4]^{2-}$ .

The lower affinities of silver and gold for oxygen lead to oxides of lower thermal stabilities than those of copper.  $\text{Ag}_2\text{O}$  is a dark-brown precipitate produced by adding alkali to a soluble  $\text{Ag}^{\text{I}}$  salt;  $\text{AgOH}$  is probably present in solution but not in the solid. It is readily reduced to the metal, and decomposes to the elements if heated above  $160^\circ\text{C}$ . The action of the vigorous oxidizing agent,  $\text{S}_2\text{O}_8^{2-}$ , on  $\text{Ag}_2\text{O}$  or other  $\text{Ag}^{\text{I}}$  compounds, produces a black oxide of stoichiometry  $\text{AgO}$ . That this is not a compound of  $\text{Ag}^{\text{II}}$  is, however, evidenced by its diamagnetism and by diffraction studies which show it to contain two types of silver ion, one with 2 colinear oxygen neighbours ( $\text{Ag}^{\text{I}}-\text{O}$  218 pm) and the other with square-planar coordination ( $\text{Ag}^{\text{III}}-\text{O}$  205 pm). It is therefore formulated as  $\text{Ag}^{\text{I}}\text{Ag}^{\text{III}}\text{O}_2$ . Anodic oxidation of silver salts yields two further black oxides,  $\text{Ag}_2\text{O}_3$  ( $\text{Ag}^{\text{III}}-\text{O} = 202$  pm) and, at lower potentials,  $\text{Ag}_3\text{O}_4$ . In both of these the silver atoms are in a square planar oxygen environment. It is tempting to formulate  $\text{Ag}_3\text{O}_4$  as  $\text{Ag}^{\text{II}}\text{Ag}_2^{\text{III}}\text{O}_4$  but the average  $\text{Ag}-\text{O}$  distances of 203 pm and 207 pm respectively are the wrong

way round for this and instead imply non-integral oxidation states with the lower charge on the pair of silver atoms.<sup>(7)</sup> Hydrothermal treatment of  $\text{AgO}$  in a silver tube at  $80^\circ\text{C}$  and 4 kbar leads to an oxide which was originally (1963) incorrectly designated as  $\text{Ag}_2\text{O}(\text{II})$ . The compound has a metallic conductivity and the stoichiometry is, in fact,  $\text{Ag}_3\text{O}$ ; it can be described as an anti- $\text{BiI}_3$  structure (p. 559) in which oxide ions fill two-thirds of the octahedral sites in a hcp arrangement of  $\text{Ag}$  atoms ( $\text{Ag}-\text{O}$  229 pm;  $\text{Ag}-\text{Ag}$  276, 286, and 299 pm).

The action of alkali on aqueous  $\text{Au}^{\text{III}}$  solutions produces a precipitate, probably of  $\text{Au}_2\text{O}_3 \cdot x\text{H}_2\text{O}$ , which on dehydration yields brown  $\text{Au}_2\text{O}_3$ . This is the only confirmed oxide of gold. It decomposes if heated above about  $160^\circ\text{C}$  and, when hydrous, is weakly acidic, dissolving in conc alkali and probably forming salts of the  $[\text{Au}(\text{OH})_4]^-$  ion.

The sulfides are all black, or nearly so, and those with the metal in the +1 oxidation state are the more stable (p. 1174).  $\text{Cu}_2\text{S}$  (mp  $1130^\circ$ ) is formed when copper is heated strongly in sulfur vapour or  $\text{H}_2\text{S}$ , and  $\text{CuS}$  is formed as a colloidal precipitate when  $\text{H}_2\text{S}$  is passed through aqueous solutions of  $\text{Cu}^{2+}$ .  $\text{CuS}$ , however, is not a simple copper(II) compounds since it contains the  $\text{S}_2$  unit and is better formulated as  $\text{Cu}_2^{\text{I}}\text{Cu}^{\text{II}}(\text{S}_2)\text{S}$ .  $\text{Ag}_2\text{S}$  is very readily formed from the elements or by the action of  $\text{H}_2\text{S}$  on the metal or on aqueous  $\text{Ag}^{\text{I}}$ . The action of  $\text{H}_2\text{S}$  on aqueous  $\text{Au}^{\text{I}}$  precipitates  $\text{Au}_2\text{S}$  whereas passing  $\text{H}_2\text{S}$  through cold solutions of  $\text{AuCl}_3$  in dry ether yield  $\text{Au}_2\text{S}_3$ , which is rapidly reduced to  $\text{Au}^{\text{I}}$  or the metal on addition of water. The relationships between the crystal structures of the oxides and sulfides of  $\text{Cu}$ ,  $\text{Ag}$  and  $\text{Au}$  and the binding energies of the metals' d and p valence orbitals have been reviewed.<sup>(7a)</sup>

The selenides and tellurides of the coinage metals are all metallic and some, such as  $\text{CuSe}_2$ ,  $\text{CuTe}_2$ ,  $\text{AgTe}_{\sim 3}$  and  $\text{Au}_3\text{Te}_5$  are superconductors at low temperature (as also are  $\text{CuS}$  and  $\text{CuS}_2$ ).

<sup>6</sup> T. P. DIRKSE, *Copper, Silver, Gold and Zinc, Cadmium, Mercury Oxides and Hydroxides*, Pergamon, Oxford, 1986, 380 pp.

<sup>†</sup> This is the basis of the very sensitive Fehling's test for sugars and other reducing agents. A solution of a copper(II) salt dissolved in alkaline tartrate solution is added to the substance in question. If this is a reducing agent then a characteristic red precipitate is produced.

<sup>7</sup> B. STANDKE and M. JANSEN, *Angew. Chem. Int. Edn. Engl.* **25**, 77–8 (1986).

<sup>7a</sup> J. A. TOSSELL and D. J. VAUGHAN, *Inorg. Chem.* **20**, 3333–40 (1981).

Other phases are CuSe, CuTe;  $\text{Cu}_3\text{Se}_2$ ,  $\text{Cu}_3\text{Te}_2$ ; AgSe, AgTe;  $\text{Ag}_2\text{Se}_3$ ,  $\text{AgSe}_2$ ;  $\text{Ag}_5\text{Te}_3$ ;  $\text{Au}_2\text{Te}_3$  and  $\text{AuTe}_2$ . Most of these are nonstoichiometric.

### 28.3.2 High temperature superconductors<sup>(8-10)</sup>

Without doubt the main focus of interest in the field of copper oxide chemistry has, for the past decade, been on the production of high temperature superconductors of which  $\text{YBa}_2\text{Cu}_3\text{O}_7$  is the most familiar (see Panel). Like all “cuprate superconductors”, it is an oxygen deficient perovskite (if it were an “ideal” perovskite its six metal atoms would require the composition  $\text{YBa}_2\text{Cu}_3\text{O}_9$ . This massive oxygen deficiency results in a layered structure instead of the conventional 3-dimensional array — see p. 963). As shown in Fig. 28.2, the coordination of oxygen around copper is of two types, square planar for Cu(1) and square pyramidal for Cu(2). Due to the disparate effects of the large  $\text{Ba}^{2+}$  and the smaller more highly charged  $\text{Y}^{3+}$ , the Cu(2) are not situated at the centre of the square pyramid but only 30 pm above its base. They therefore lie in “puckered” or “dimpled”  $\text{CuO}_2$  planes connected by the apical oxygens to chains of square planar Cu(1).

Esr results indicate that both Cu(1) and Cu(2) sites have a mixture of  $\text{Cu}^{2+}$  and  $\text{Cu}^{3+}$  ions. It is generally believed that superconduction occurs via positive holes in the conduction band of the  $\text{CuO}_2$  planes and that the concentration of these holes is controlled, through the apical oxygens, by the non-conducting chains of Cu(1) which act as reservoirs of positive and negative charge. X-ray photoelectron spectroscopy shows that the conduction band has both copper (3d) and oxygen (2p) character, presumably as a result of  $\pi$

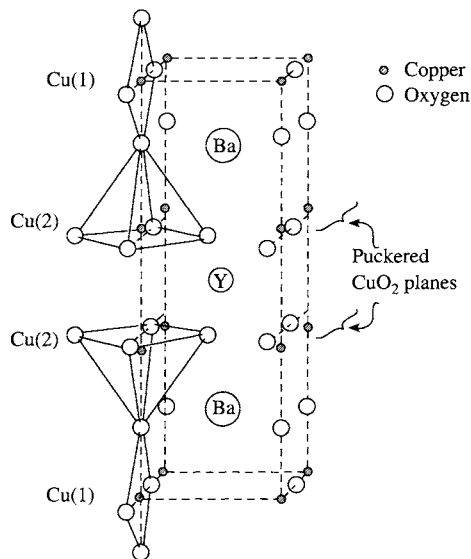


Figure 28.2 Structure of  $\text{YBa}_2\text{Cu}_3\text{O}_7$ .

interactions which would be at a maximum in the linear O–Cu–O bonds of perfect  $\text{CuO}_2$  planes. The extent of puckering of these planes, as well as the nature and composition of the charge reservoirs, are evidently crucial factors affecting the value of  $T_c$ . To obtain a proper understanding of these factors Y and Ba have been replaced by a range of other elements producing compounds with up to seven different elements as in  $\text{Tl}_{0.5}\text{Pb}_{0.5}\text{Sr}_2\text{Ca}_{1-x}\text{Y}_x\text{Cu}_2\text{O}_7$ .  $\text{La}_{2-x}\text{M}_x\text{CuO}_4$  ( $\text{M} = \text{Sr}, \text{Ba}$ ) and  $\text{HgBa}_2\text{Ca}_2\text{Cu}_3\text{O}_{8+\delta}$  are other examples where the oxidation state of  $\text{Cu} > (\text{II})$  and superconductivity occurs via positive holes, whereas in  $\text{Nd}_{2-x}\text{Ce}_x\text{CuO}_4$ , a so-called “electron superconductor”, the oxidation state of  $\text{Cu} < (\text{II})$  and excess electrons are the charge carriers. In each case, however, the path for conduction is provided by a  $\text{CuO}_2$  plane.

The properties of these brittle ceramics depend critically on the preparative conditions. Intimate mixtures of the oxides, carbonates or nitrates of the relevant metals in the required proportions are heated at temperatures of 900–1000°C. For  $\text{YBa}_2\text{Cu}_3\text{O}_{7-x}$ , all compositions in the range  $0 \leq x \leq 0.5$  superconduct and the highest  $T_c$  is found where  $x \sim 0$ . For others, the oxygen content must be stringently controlled. In all cases, the most

<sup>8</sup> C. N. R. RAO (Ed.), *Chemistry of High Temperature Superconductors*, World Scientific, Singapore, 1991, 520 pp.

<sup>9</sup> J. T. S. IRVINE, *Superconducting Materials*, Chap. 11, pp. 275–301 in D. THOMPSON (ed.), *Insights into Speciality Inorganic Chemicals*, R.S.C., Cambridge, 1995.

<sup>10</sup> A series of articles on Superconductivity, *Chem. in Brit.* **30**, 722–48 (1994).

## Superconductivity

H. Kammerling Onnes (Nobel Prize for Physics, 1913) discovered superconductivity in Leiden in 1911 when he cooled mercury to the temperature of liquid helium. Many other materials, mostly metals and alloys, were subsequently found to display superconductivity at very low temperatures.

Two properties characterize a superconductor:

1. It is perfectly conducting, i.e. it has zero resistance.
2. It is perfectly diamagnetic, i.e. it completely excludes applied magnetic fields. This is the Meissner effect and is the reason why a superconductor can levitate a magnet.

Superconductivity exists within the boundaries of three limiting parameters which must not be exceeded: the critical temperature ( $T_c$ ), the critical magnetic field ( $H_c$ ) and the critical current density ( $J_c$ ).

Until 1986 the highest recorded value of  $T_c$  was  $\sim 23$  K for  $\text{Nb}_3\text{Ge}$  but in that year Bednorz and Müller, in pioneering work for which they received the 1987 Nobel Prize for Physics, reported<sup>(11)</sup>  $T_c = 30$  K in an entirely new Ba-La-Cu-O ceramic system quickly identified as  $\text{La}_{2-x}\text{Ba}_x\text{CuO}_4$ . This prompted an examination of other Cu-O systems and the technologically important breakthrough in 1987 by the Houston and Alabama teams of C. W. Chu and M. K. Wu, of superconductivity at temperatures attainable in liquid nitrogen.<sup>(12)</sup>  $T_c = 95$  K in a material subsequently shown to be  $\text{YBa}_2\text{Cu}_3\text{O}_7$ , "YBCO". This, and other materials in which Y is replaced by a lanthanide, are referred to as "1,2,3" materials because of their stoichiometry. This produced a quite unprecedented explosion of activity amongst chemists, physicists and material scientists around the world. Though the highest  $T_c$  has been pushed up to 135 K (or 164 K under 350 kbar pressure) in  $\text{HgBa}_2\text{Ca}_2\text{Cu}_3\text{O}_8$ , YBCO is still the archetypal high temperature superconductor.

In spite of its long history, it was not until 1957 that Bardeen, Cooper and Schrieffer<sup>(13)</sup> provided a satisfactory explanation of superconductivity. This "BSC theory" suggests that pairs of electrons (Cooper pairs) move together through the lattice, the first electron polarizing the lattice in such a way that the second one can more easily follow it. The stronger the interaction of the two electrons the higher  $T_c$ , but it turns out as a consequence of this model that  $T_c$  should have an upper limit  $\sim 35$  K. The advent of high-temperature superconductors therefore necessitated a new, or at least modified, explanation for the pairing mechanism. Various suggestions have been made but none has yet gained universal acceptance.

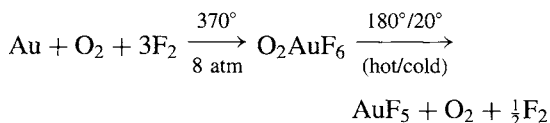
homogeneous products with the best grain alignment and the highest current density  $J_c$ , require the most careful control of sintering temperature, annealing and quenching rates. The major problems preventing large-scale practical applications therefore lie in the field of material processing. At present thin films of "YBCO" (see Panel), obtained for instance by its deposition on metal coated with  $\text{ZrO}_2$  to provide flexible tapes, appear to offer the most promising way forward.

### 28.3.3 Halides

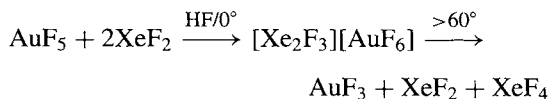
Table 28.3 is a list of the known halides: only gold forms a pentahalide and trihalides and, with

the exception of  $\text{AgF}_2$ , only copper (as yet) forms dihalides.

$\text{AuF}_5$  is an unstable, polymeric, diamagnetic, dark-red powder, produced by heating  $[\text{O}_2][\text{AuF}_6]$  under reduced pressure and condensing the product on to a "cold finger":



The compound tends to dissociate into  $\text{AuF}_3$  and, when treated with  $\text{XeF}_2$  in anhydrous HF solution below room temperature, yields yellow-orange crystals of the complex  $[\text{Xe}_2\text{F}_3][\text{AuF}_6]$ :



Again, in the +3 oxidation state, only gold is known to form binary halides, though  $\text{AuI}_3$  has not been isolated. The chloride and the

<sup>11</sup> J. G. BEDNORZ and K. A. MÜLLER, *Z. Phys. B* **64**, 189–93 (1986).

<sup>12</sup> M. K. WU, J. R. ASHBURN, C. J. TORNG, P. H. HOR, R. L. MENG, L. GAO, Z. J. HUANG, Y. Q. WANG and C. W. CHU, *Phys. Rev. Lett.* **58**, 908–10 (1987).

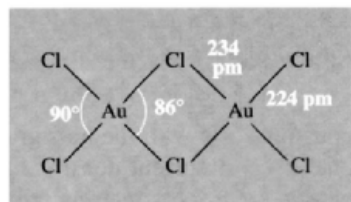
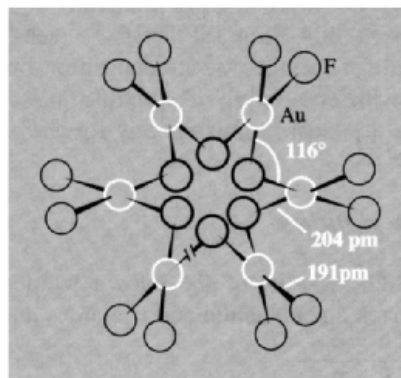
<sup>13</sup> J. BARDEEN, L. N. COOPER and J. R. SCHRIEFFER, *Phys. Rev.* **106**, 162–4 (1957).

Table 28.3 Halides of copper, silver and gold (mp/°C)

Oxidation state	Fluorides	Chlorides	Bromides	Iodides
+5	AuF <sub>5</sub> red (d > 60°)			
+3	AuF <sub>3</sub> orange-yellow (subl 300°)	AuCl <sub>3</sub> red (d > 160°)	AuBr <sub>3</sub> red-brown	
+2	CuF <sub>2</sub> white (785°) AgF <sub>2</sub> brown (690°)	CuCl <sub>2</sub> yellow-brown (630°)	CuBr <sub>2</sub> black (498°)	
+1	— AgF yellow (435°) —	CuCl white (422°) AgCl white (455°) AuCl yellow (d > 420°)	CuBr white (504°) AgBr pale yellow (430°) AuBr yellow	CuI white (606°) AgI yellow (556°) AuI yellow
+ $\frac{1}{2}$ (0,+1)	Ag <sub>2</sub> F yellow-green (d > 100°)			

bromide are red-brown solids prepared directly from the elements and have a planar dimeric structure in both the solid and vapour phases. Dimensions for the chloride are as shown in Structure (1). On being heated, both compounds lose halogen to form first the monohalide and finally metallic gold. Au<sub>2</sub>Cl<sub>6</sub> is one of the best-known compounds of gold and provides a convenient starting point for much coordination chemistry, dissolving in hydrochloric acid to give the stable [AuCl<sub>4</sub>]<sup>-</sup> ion. Treatment of Au<sub>2</sub>Cl<sub>6</sub> with F<sub>2</sub> or BrF<sub>3</sub> also affords a route to AuF<sub>3</sub>, a powerful fluorinating agent. This orange solid consists of square-planar AuF<sub>4</sub> units which share *cis*-fluorine atoms with 2 adjacent AuF<sub>4</sub> units so as to form a helical chain (Structure (2)).

No halides are known for gold in the +2 oxidation state and silver only forms the difluoride; this is obtained by direct heating of silver in a stream of fluorine. AgF<sub>2</sub> is thermally stable but is a vigorous fluorinating agent used especially to fluorinate hydrocarbons. For copper, on the other hand, 3 dihalides are stable and the anhydrous difluoride, dichloride and dibromide can all be obtained by heating the elements. The white ionic CuF<sub>2</sub> has a distorted rutile structure

(1) Au<sub>2</sub>Cl<sub>6</sub>(2) Unique helical chain structure of AuF<sub>3</sub>

(p. 961) with four shorter equatorial distances (Cu-F 193 pm) and two longer axial distances (Cu-F 227 pm). A similar distortion is found in

the  $d^4$  compound  $\text{CrF}_2$  (p. 1021). When prepared from aqueous solution by dissolving copper(II) carbonate or oxide in 40% hydrofluoric acid, blue crystals of the dihydrate are obtained; these are composed of puckered sheets of planar *trans*- $[\text{CuF}_2(\text{H}_2\text{O})_2]$  groups linked by strong H bonds to give distorted octahedral coordination about Cu with 2 Cu–O 194 pm, 2 Cu–F 190 pm, and 2 further Cu–F at 246.5 pm; the O–H...F distance is 271.5 pm. With anhydrous  $\text{CuCl}_2$  and  $\text{CuBr}_2$  their increasing covalency is reflected in their polymeric chain structure, consisting of planar  $\text{CuX}_4$  units with opposite edges shared, and by the deepening colours of brown and black respectively. The chloride and bromide are both very soluble in water, and various hydrates and complexes can be recrystallized. The solutions are more conveniently obtained by dissolution of the metal or  $\text{Cu}(\text{OH})_2$  in the relevant hydrohalic acid.

Iodide ions reduce  $\text{Cu}^{\text{II}}$  to  $\text{Cu}^{\text{I}}$ , and attempts to prepare copper(II) iodide therefore result in the formation of  $\text{CuI}$ . (In a quite analogous way attempts to prepare copper(II) cyanide yield  $\text{CuCN}$  instead.) In fact it is the electronegative fluorine which fails to form a salt with copper(I), the other 3 halides being white insoluble compounds precipitated from aqueous solutions by the reduction of the  $\text{Cu}^{\text{II}}$  halide. By contrast, silver(I) provides (for the only time in this triad) 4 well-characterized halides. All except  $\text{AgI}$  have the rock-salt structure (p. 242).<sup>†</sup> Increasing covalency from chloride to iodide is reflected in the deepening colour white  $\rightarrow$  yellow, as the

<sup>†</sup> At room temperature the stable form of silver iodide is  $\gamma$ - $\text{AgI}$  which has the cubic zinc blende structure (p. 1210).  $\beta$ - $\text{AgI}$ , which has the hexagonal  $\text{ZnO}$  (or wurtzite) structure (p. 1210), is the stable form between  $136^\circ$  and  $146^\circ$ . This structure is closely related to that of hexagonal ice (p. 624) and  $\text{AgI}$  has been found to be particularly effective in nucleating ice crystals in super cooled clouds, thereby inducing the precipitation of rain.  $\beta$ - $\text{AgI}$  has another remarkable property: at  $146^\circ$  it undergoes a phase change to cubic  $\alpha$ - $\text{AgI}$  in which the iodide sublattice is rigid but the silver sublattice “melts”. This has a dramatic effect on the (ionic) electrical conductivity of the solid which leaps from  $3.4 \times 10^{-4}$  to  $1.31 \text{ ohm}^{-1} \text{ cm}^2$ , a factor of nearly 4000. The iodide sublattice in  $\alpha$ - $\text{AgI}$  is bcc and this provides 42 possible sites for each  $2\text{Ag}^+$ , distributed as follows:

energy of the charge transfer ( $\text{X}^- \text{Ag}^+ \rightarrow \text{XAg}$ ) is lowered, and also in increasing insolubility. In the latter respect, however,  $\text{AgF}$  is quite anomalous in that it is one of the few silver(I) salts which form hydrates ( $2\text{H}_2\text{O}$  and  $4\text{H}_2\text{O}$ ). That it is soluble in water is understandable in view of its ionic character and the high solvation energy of the small fluoride ion, but the *extent* of its solubility (1800 g per litre of water at  $25^\circ\text{C}$ ) is astonishing. All 4  $\text{AgX}$  can be prepared directly from the elements but it is more convenient to prepare  $\text{AgF}$  by dissolving  $\text{AgO}$  in hydrofluoric acid and evaporating the solution until the solid crystallizes; the others can be made by adding  $\text{X}^-$  to a solution of  $\text{AgNO}_3$  or other soluble  $\text{Ag}^{\text{I}}$  compound, when  $\text{AgX}$  is precipitated. The most important property of these halides, particularly  $\text{AgBr}$ , is their sensitivity to light ( $\text{AgF}$  only to ultraviolet) which is the basis for their use in photography, discussed below.

All four monohalides of gold have been prepared but the fluoride only by mass spectrometric methods.<sup>(14)</sup>  $\text{AuCl}$  and  $\text{AuBr}$  are formed by heating the trihalides to no more than  $150^\circ\text{C}$  and  $\text{AuI}$  by heating the metal and iodine. At higher temperatures they dissociate into the elements.  $\text{AuI}$  is a chain polymer which features linear 2-coordinate Au with Au–I 262 pm and the angle Au–I–Au  $72^\circ$ .

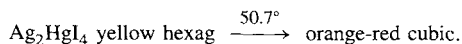
### 28.3.4 Photography

Photography is a good example of a technology which evolved well in advance of a proper understanding of the principles involved (see

---

6 sites having  $2\text{I}^-$  neighbours at 252 pm  
 12 sites having  $3\text{I}^-$  neighbours at 267 pm  
 24 sites having  $4\text{I}^-$  neighbours at 286 pm

The silver ions are almost randomly distributed on these sites, thus accounting for their high mobility. Many other fast ion conductors have subsequently been developed on this principle, e.g.



<sup>14</sup> D. SCHRODER, J. HRUŠAK, I. C. TORNIEPORTH-OETTING, T. M. KLAPOČKE and H. SCHWARTZ. *Angew. Chem. Int. Edn. Engl.* **33**, 212–4 (1994).



## History of Photography

In 1727 J. H. Schulze, a German physician, found that a paste of chalk and  $\text{AgNO}_3$  was blackened by sunlight and, using stencils, he produced black images. At the end of the eighteenth century Thomas Wedgwood (son of the potter Josiah) and Humphry Davy used a lens to form an image on paper and leather treated with  $\text{AgNO}_3$ , and produced pictures which unfortunately faded rather quickly.

The first permanent images were obtained by the French landowner J. N. Niépce using bitumen-coated pewter (bitumen hardens when exposed to light for *several hours* and the unexposed portions can then be dissolved away in oil of turpentine). He then helped the portrait painter, L. J. M. Daguerre, to perfect the “daguerreotype” process which utilized plates of copper coated with silver sensitized with iodine vapour. The announcement of this process in 1839 was greeted with enormous enthusiasm but it suffered from the critical drawback that each picture was unique and could not be duplicated.

Reproducibility was provided by the “calotype” process, patented in 1841 by the English landowner W. H. Fox Talbot, which used semi-transparent paper treated with  $\text{AgI}$  and a “developer”, gallic acid. This produced a “negative” from which any number of “positive” prints could subsequently be obtained. Furthermore it embodied the important discovery of the “latent image” which could be fully developed later. Even with Talbot’s very coarse papers, exposure times were reduced to a few minutes and portraits became feasible, even if uncomfortable for the subject.

Though Talbot’s pictures were undoubtedly much inferior in quality to Daguerre’s, the innovations of his process were the ones which facilitated further improvements and paved the way for photography as we now know it. Sir John Herschel, who first coined the terms “photography”, “negative” and “positive”, suggested the use of “hyposulphite” (sodium thiosulfate) for “fixing” the image, and later the use of glass instead of paper — hence, photographic “plates”. F. S. Archer’s “wet collodion” process (1851) reduced the exposure time to about 10 s and R. L. Maddox’s “dry gelatin” plates reduced it to only 0.5 s. In 1889 G. Eastman used a roll film of celluloid and founded the American Eastman Kodak Company.

Meanwhile the Scottish physicist, Clerk Maxwell (1861), recognizing that the sensitivities of the silver halides are not uniform across the spectrum, proposed a three-colour process in which separate negatives were exposed through red, green and blue filters, and thereby provided the basis for the later development of colour photography. Actually, the sensitivity is greatest at the blue end of the spectrum; a fact which seriously affected all early photographs. This problem was overcome when the German, H. W. Vogel, discovered that sensitivity could be extended by incorporating certain dyes into the photographic emulsion. “Spectral sensitization” at the present time is able to extend the sensitivity not only across the whole visible region but far into the infrared as well.

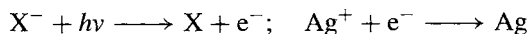
Panel). Most of the basic processes were established almost a century and a half ago, but a coherent theoretical explanation was not available until the publication in 1938 of the classic paper by R. W. Gurney and N. F. Mott. (*Proc. Roy. Soc. A* **164**, 151–67 (1938)). Since then the subject has stimulated a vast amount of fundamental research in wide areas of solid-state chemistry and physics.

A photograph is the permanent record of an image formed on a light-sensitive surface, and the essential steps in producing it are:

- (a) production of light-sensitive surface;
- (b) exposure to produce a “latent image”;
- (c) development of the image to produce a “negative”;
- (d) making the image permanent, i.e. “fixing” it;
- (e) making “positive” prints from the negative.

(a) In modern processes the light-sensitive surface is an “emulsion” of silver halide in gelatine, coated on to a suitable transparent film, or support. The halide is carefully precipitated so as to produce small uniform crystals, ( $<1 \mu\text{m}$  diameter, containing  $\sim 10^{12}$  Ag atoms), or “grains” as they are normally called. The particular halide used depends on the sensitivity required, but  $\text{AgBr}$  is most commonly used on films;  $\text{AgI}$  is used where especially fast film is required and  $\text{AgCl}$  and certain organic dyes are also incorporated in the emulsion.

(b) When, on exposure of the emulsion to light, a photon of energy  $h\nu$  impinges on a grain of  $\text{AgX}$ , a halide ion is excited and loses its electron to the conduction band, through which it passes rapidly to the surface of the grain where it is able to liberate an atom of silver:

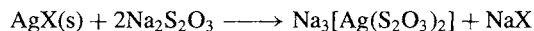


These steps are, in principle, reversible but in practice are not because the Ag is evidently liberated on a crystal dislocation, or defect, or at an impurity site such as may be provided by Ag<sub>2</sub>S, all of which allow the electron to reduce its energy and so become “trapped”. The function of the dye sensitizers is to extend the sensitivity of the emulsion across the whole visible spectrum, by absorbing light of characteristic frequency and providing a mechanism for transferring the energy to X<sup>-</sup> in order to excite its electron. As more photons are incident on the grain, so more electrons migrate and discharge Ag atoms at the same point. A collection of just a few silver atoms on a grain (in especially sensitive cases a mere 4–6 atoms but, more usually, perhaps 10 times that number) constitutes a “speck”, too small to be visible, but the concentration of grains possessing such specks varies across the film according to the varying intensity of the incident light thereby producing an invisible “latent image”. The parallel formation of X atoms leads to the formation of X<sub>2</sub> which is absorbed by the gelatine.

(c) The “development” or intensification of the latent image is brought about by the action of a mild reducing agent whose function is to selectively reduce those grains which possess a speck of silver, while leaving unaffected all unexposed grains. To this end, such factors as temperature and concentration must be carefully controlled and the reduction stopped before any unexposed grains are affected. Hydroquinone, 1,6-C<sub>6</sub>H<sub>4</sub>(OH)<sub>2</sub> is a common “developer” and the reduction is a good example of a catalysed solid-state reaction. Its mechanism is imperfectly understood but the complete reduction to metal of a grain (say 10<sup>12</sup> atoms of Ag), starting from a single speck (say 10 or 100 atoms of Ag), represents a remarkable intensification of the latent image of about 10<sup>11</sup> or 10<sup>10</sup> times, allowing vastly reduced exposure times; this is the real reason for the superiority of silver halides over all other photosensitive materials, though an intensive search for alternative systems still continues.

(d) After development, the image on the negative is “fixed” by dissolving away all

remaining silver salts to prevent their further reduction. This requires an appropriate complexing agent and sodium thiosulphate is the usual one since the reaction



goes essentially to completion and both products are water-soluble.

(e) A positive print is the reverse of the negative and is obtained by passing light through the negative and repeating the above steps using a printing paper instead of a transparent film.

### 28.3.5 Complexes<sup>(15,16)</sup>

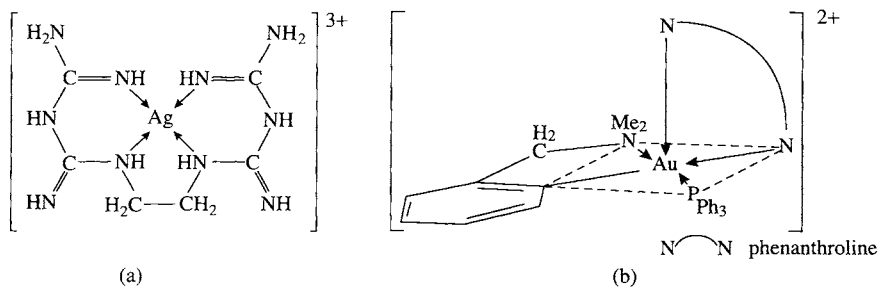
Oxidation states above +3 are attained only with difficulty and are confined mainly to AuF<sub>5</sub>, mentioned above, together with salts of the octahedral anion [AuF<sub>6</sub>]<sup>-</sup>, and to Cs<sub>2</sub>[Cu<sup>IV</sup>F<sub>6</sub>], prepared by fluorinating CsCuCl<sub>3</sub> at high temperature and pressure.

#### Oxidation state III (d<sup>8</sup>)

Copper(III) is generally regarded as uncommon, being very easily reduced, but because of its possible involvement in biological electron transfer reactions (p. 1199) a number of Cu<sup>III</sup> peptides have been prepared. The pale-green, paramagnetic (2 unpaired electrons), K<sub>3</sub>CuF<sub>6</sub>, is obtained by the reaction of F<sub>2</sub> on 3KCl + CuCl and is readily reduced. This is the only high-spin Cu<sup>III</sup> complex, the rest being low-spin, diamagnetic, and usually square planar, as is to be expected for a cation which, like Ni<sup>II</sup>, has a d<sup>8</sup> configuration and is more highly charged. Examples are violet [CuBr<sub>2</sub>(S<sub>2</sub>CNBU<sub>2</sub>)], obtained by reacting [Cu(S<sub>2</sub>CNBU<sub>2</sub>)] with Br<sub>2</sub>

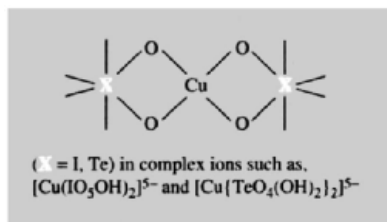
<sup>15</sup> B. J. HATHAWAY, *Copper*, Chap. 53, pp. 533–774; R. J. LANCASHIRE, *Silver*, Chap. 54, pp. 775–859; R. J. PUDDEPHATT, *Gold*, Chap. 55, pp. 861–923 in *Comprehensive Coordination Chemistry*, Vol. 5, Pergamon Press, Oxford, 1987.

<sup>16</sup> For gold in oxidation states other than III, see H. SCHMIDBAUR and K. C. DASH, *Adv. Inorg. Chem.* **25**, 239–66 (1982).



**Figure 28.3** (a) Silver(III) ethylenedibiguanide complex ion; the counter anion can be  $\text{HSO}_4^-$ ,  $\text{ClO}_4^-$ ,  $\text{NO}_3^-$  or  $\text{OH}^-$ . (b) Gold(III) (dimethylamino)phenyl complex ion; the counter anion can be  $\text{BF}_4^-$  or  $\text{ClO}_4^-$ .

in  $\text{CS}_2$ , and bluish  $\text{MCuO}_2$  ( $M = \text{alkali metal}$ ), obtained by heating  $\text{CuO}$  and  $\text{MO}_2$  in oxygen. The oxidation of  $\text{Cu}^{\text{II}}$  by alkaline  $\text{ClO}^-$  in the presence of periodate or tellurate ions yields salts in which chelated ligands apparently produce square-planar coordinated copper:



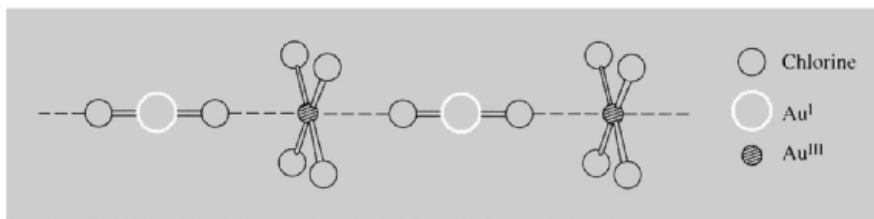
Silver(III) is quite similar to copper(III) and analogous, though more stable, periodate and tellurate complexes can be produced by the oxidation of  $\text{Ag}^{\text{I}}$  with alkaline  $\text{S}_2\text{O}_8^{2-}$ . The diamagnetic, red ethylenedibiguanide complex (Fig. 28.3a) is also obtained by peroxodisulfate oxidation and is again quite stable to reduction. However, yellow, diamagnetic, square-planar fluoro-complexes such as  $[\text{K}[\text{AgF}_4]]$ , obtained by fluorinating  $\text{AgNO}_3 + \text{KCl}$  at  $300^\circ\text{C}$ , are much less stable; they attack glass and fume in moist air.

For gold, by contrast, +3 is the element's best-known oxidation state and  $\text{Au}^{\text{III}}$  is often compared with the isoelectronic  $\text{Pt}^{\text{II}}$  (p. 1161). The usual route to gold(III) chemistry is by dissolving the metal in aqua regia, or the compound  $\text{Au}_2\text{Cl}_6$  in conc  $\text{HCl}$ , after which evaporation yields yellow chloroauric acid,  $\text{HAuCl}_4 \cdot 4\text{H}_2\text{O}$ , from which numerous salts of the square-planar ion  $[\text{AuCl}_4]^-$  can be obtained.

Other square-planar ions of the type  $[\text{AuX}_4]^-$  can then be derived in which  $\text{X} = \text{F, Br, I, CN, SCN}$  and  $\text{NO}_3$ , the last of these being of interest as one of the few authenticated examples of the unidentate nitrate ion (cf. p. 1162).  $[\text{Au}(\text{SCN})_4]^-$  contains  $S$ -bonded  $\text{SCN}^-$  but, as with  $\text{Pt}^{\text{II}}$  (p. 1162), this ligand also gives rise to linkage isomers, this time in the  $\text{K}^+$  and  $(\text{NEt}_4)^+$  salts of  $[\text{Au}(\text{CN})_2(\text{SCN})_2]^-$  and  $[\text{Au}(\text{CN})_2(\text{NCS})_2]^-$ . Numerous cationic complexes have been prepared with amines, both unidentate (e.g. py, quinoline, as well as  $\text{NH}_3$ ) and chelating (e.g. en, bipy, phen).  $[\text{Au}(\text{C}_6\text{H}_4\text{CH}_2\text{NMe}_2\text{-2})(\text{phen})(\text{PPh}_3)]^{2+}$  (Fig. 28.3b) is an example with the additional interest that its distorted square pyramidal structure<sup>(17)</sup> provides a rare example of  $\text{Au}^{\text{III}}$  with a coordination number in excess of 4. Octahedral  $[\text{Au}_2(\text{diars})_2]^+$  too has a "high" coordination number, though phosphine and arsine complexes are generally readily reduced to  $\text{Au}^{\text{I}}$  species. Reductions of  $\text{Au}^{\text{III}}$  to  $\text{Au}^{\text{I}}$  in aqueous solution by nucleophiles such as  $\text{I}^-$ ,  $\text{SCN}^-$  and other  $S$ -donor ligands have been studied. Most take place by rapid ligand substitution followed by the rate determining electron transfer, though some reductions by  $\text{I}^-$  take place without substitution. With  $\text{SCN}^-$  the rates of substitution and electron transfer are finely balanced.<sup>(18)</sup>

<sup>17</sup> J. VICENTE, M. T. CHICOTE, M. D. BERMUDEZ, P. G. JONES, C. FITTSCHEN and G. M. SHELDRIK, *J. Chem. Soc., Dalton Trans.*, 2361–6 (1986).

<sup>18</sup> S. ELMROTH, L. H. SKIBSTED and L. I. ELDING, *Inorg. Chem.* **28**, 2703–10 (1989).

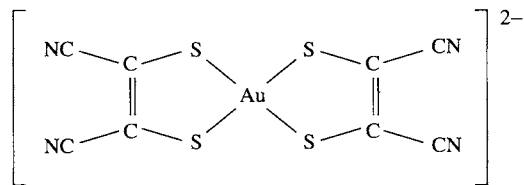


**Figure 28.4** The anions of the chlorocomplex of stoichiometry,  $\text{CsAuCl}_3$ , showing linearly coordinated  $\text{Au}^{\text{I}}$  and  $(4 + 2)$  tetragonally distorted, octahedral  $\text{Au}^{\text{III}}$ , i.e.  $\text{Cs}_2[\text{Au}^{\text{I}}\text{Cl}_2][\text{Au}^{\text{III}}\text{Cl}_4]$ .

In forming the fluoro complex  $[\text{AuF}_4]^-$  mentioned above, and indeed in forming the simple fluoride  $\text{AuF}_3$ ,  $\text{Au}^{\text{III}}$  differs from the isoelectronic  $\text{Pt}^{\text{II}}$  since the corresponding  $[\text{PtF}_4]^{2-}$  and  $\text{PtF}_2$  are unknown.

### Oxidation state II ( $d^9$ )

The importance of this oxidation state diminishes with increase in atomic number in the group, and most of the compounds ostensibly of  $\text{Au}^{\text{II}}$  are actually mixed valency  $\text{Au}^{\text{I}}/\text{Au}^{\text{III}}$  compounds. Examples include the sulfate  $\text{Au}^{\text{I}}\text{Au}^{\text{III}}(\text{SO}_4)_2$  and the chlorocomplex,  $\text{Cs}_2[\text{Au}^{\text{I}}\text{Cl}_2][\text{Au}^{\text{III}}\text{Cl}_4]$ , the anions of the latter being arranged so as to give linearly coordinated  $\text{Au}^{\text{I}}$  and tetragonally distorted, octahedral  $\text{Au}^{\text{III}}$  (Fig. 28.4). The analogous mixed-metal complex,  $\text{Cs}_2\text{AgAuCl}_6$ , has the same structure with  $\text{Ag}^{\text{I}}$  instead of  $\text{Au}^{\text{I}}$ . One of the few authenticated examples of  $\text{Au}^{\text{II}}$  is the maleonitriledithiolato complex



which has a magnetic moment at room temperature of 1.85 BM. Even here, however, esr evidence indicates appreciable delocalization of the unpaired electron on to the ligands and, in solution, the complex is readily oxidized to  $\text{Au}^{\text{III}}$ .

Compounds of  $\text{Ag}^{\text{II}}$  are more familiar and are, in general, square planar and paramagnetic ( $\mu_e \sim$

1.7–2.2 BM); this is as expected for an ion which is isoelectronic with  $\text{Cu}^{\text{II}}$  (see below), particularly in view of the greater crystal field splitting associated with 4d (as opposed to 3d) electrons. The  $\text{Ag}^{\text{II}}(\text{aq})$  ion has a transitory existence when  $\text{Ag}^{\text{I}}$  salts are oxidized by ozone in a strongly acid solution, but it is an appreciably stronger oxidizing agent than  $\text{MnO}_4^-$  [ $E^\circ(\text{Ag}^{2+}/\text{Ag}^+) = +1.980 \text{ V}$  in 4M  $\text{HClO}_4$ ;  $E^\circ(\text{MnO}_4^-/\text{Mn}^{2+}) = 1.507 \text{ V}$ ] and oxidizes water even when strongly acidic.<sup>†</sup> Of the acidic solutions the most stable is that in phosphoric acid, no doubt because of complex formation, and even  $\text{NO}_3^-$  and  $\text{ClO}_4^-$  ions appear to coordinate in solution since the colours of these solutions depend on their concentrations. A variety of complexes, particularly with heterocyclic amines, has been obtained by oxidation of  $\text{Ag}^{\text{I}}$  salts with  $[\text{S}_2\text{O}_8]^{2-}$  in aqueous solution in the presence of the ligand. They include  $[\text{Ag}(\text{py})_4]^{2+}$  and  $[\text{Ag}(\text{bipy})_2]^{2+}$  and are comparatively stable providing the counter-anion is a non-reducing ion such as  $\text{NO}_3^-$ ,  $\text{ClO}_4^-$  or  $\text{S}_2\text{O}_8^{2-}$ . Other complexes include some with *N*-, *O*-donor ligands such as pyridine carboxylates, and also the violet  $\text{Ba}[\text{AgF}_4]$ .

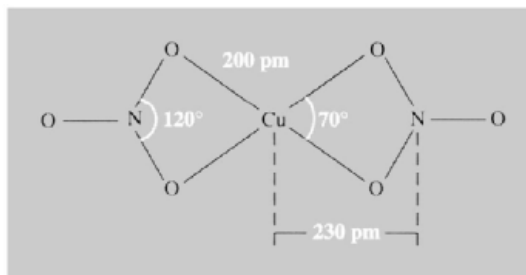
However, in this oxidation state it is copper which provides by far the most familiar and extensive chemistry. Simple salts are formed with most anions, except  $\text{CN}^-$  and  $\text{I}^-$ , which instead form covalent  $\text{Cu}^{\text{I}}$  compounds which are insoluble in water. The salts are predominantly water-soluble, the blue colour of their solutions

<sup>†</sup> Solutions of this type have potential use in the destruction of a variety of waste organic materials by electrochemical oxidation — see D. F. STEELE, *Chem. in Brit.* 27, 915–8 (1991).

arising from the  $[\text{Cu}(\text{H}_2\text{O})_6]^{2+}$  ion, and they frequently crystallize as hydrates. The aqueous solutions are prone to slight hydrolysis and, unless stabilized by a small amount of acid, are liable to deposit basic salts. Basic carbonates occur in nature (p. 1174), basic sulfates and chlorides are produced by atmospheric corrosion of copper, and basic acetates (verdigris) find use as pigments.

The best-known simple salt is the sulfate pentahydrate ("blue vitriol"),  $\text{CuSO}_4 \cdot 5\text{H}_2\text{O}$ , which is widely used in electroplating processes, as a fungicide (in Bordeaux mixture) to protect crops such as potatoes, and as an algicide in water purification. It is also the starting material in the production of most other copper compounds. It is significant, as will be seen presently, that in the crystalline salt 4 of the water molecules form a square plane around the  $\text{Cu}^{\text{II}}$  and 2, more remote, oxygen atoms from  $\text{SO}_4^{2-}$  ions complete an elongated octahedron. The fifth water is hydrogen-bonded between one of the coordinated waters and sulfate ions (p. 626). On being warmed, the pentahydrate loses water to give first the trihydrate, then the monohydrate; above about  $200^\circ\text{C}$  the virtually white anhydrous sulfate is obtained and this then forms  $\text{CuO}$  by loss of  $\text{SO}_3$  above about  $700^\circ\text{C}$ . Amongst the few salts of  $\text{Cu}^{\text{II}}$  which crystallize with 6 molecules of water and contain the  $[\text{Cu}(\text{H}_2\text{O})_6]^{2+}$  ion are the perchlorate, the nitrate (but the trihydrate is more easily produced) and Tutton salts.<sup>†</sup>

Attempts to prepare the anhydrous nitrate by dehydration always fail because of decomposition to a basic nitrate or to the oxide, and it was previously thought that  $\text{Cu}(\text{NO}_3)_2$  could not exist. In fact it can be obtained by dissolving copper metal in a solution of  $\text{N}_2\text{O}_4$  in ethyl acetate to produce  $\text{Cu}(\text{NO}_3)_2 \cdot \text{N}_2\text{O}_4$ , and then driving off the  $\text{N}_2\text{O}_4$  by heating this at  $85\text{--}100^\circ\text{C}$ . The observation by C. C. Addison



**Figure 28.5** The  $\text{Cu}(\text{NO}_3)_2$  molecule in the vapour phase (dimensions are approximate).

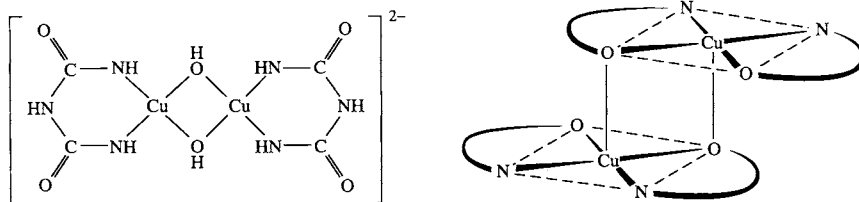
and B. J. Hathaway in 1958<sup>(19)</sup> that the blue  $\text{Cu}(\text{NO}_3)_2$  could be sublimed (at  $150\text{--}200^\circ\text{C}$  under vacuum) and must therefore involve covalently bonded  $\text{NO}_3^-$ , was completely counter to current views on the bonding of nitrates and initiated a spate of work on the coordination chemistry of the ion (p. 469). Solid  $\text{Cu}(\text{NO}_3)_2$  actually exists in two forms, both of which involve chains of copper atoms bridged by  $\text{NO}_3$  groups, but its vapour is monomeric (Fig. 28.5).

The most common coordination numbers of copper(II) are 4, 5 and 6, but regular geometries are rare and the distinction between square-planar and tetragonally distorted octahedral coordination is generally not easily made. The reason for this is ascribed to the Jahn–Teller effect (p. 1021) arising from the unequal occupation of the  $e_g$  pair of orbitals ( $d_{z^2}$  and  $d_{x^2-y^2}$ ) when a  $d^9$  ion is subjected to an octahedral crystal field. Occasionally, as in solid  $\text{KAlCuF}_6$  for instance, this results in a compression of the octahedron, i.e. “2 + 4” coordination (2 short and 4 long bonds).<sup>(20)</sup> The usual result, however, is an elongation of the octahedron, i.e. “4 + 2” coordination (4 short and 2 long bonds), as is expected if the metal’s  $d_{z^2}$  orbital is filled and its  $d_{x^2-y^2}$  half-filled. In its most extreme form this is equivalent to the complete loss of the axial ligands leaving a square-planar complex.

<sup>†</sup> Tutton salts are the double sulfates  $\text{M}_2\text{Cu}(\text{SO}_4)_2 \cdot 6\text{H}_2\text{O}$  which all contain  $[\text{Cu}(\text{H}_2\text{O})_6]^{2+}$  and belong to the more general class of double sulfates of  $\text{M}^{\text{I}}$  and  $\text{M}^{\text{II}}$  cations which are known as schönites after the naturally occurring  $\text{K}^{\text{I}}/\text{Mg}^{\text{II}}$  compound.

<sup>19</sup> C. C. ADDISON and B. J. HATHAWAY, *J. Chem. Soc.* 1958, 3099–106.

<sup>20</sup> M. ATANASOV, M. A. HITCHMAN, R. HOPPE, K. S. MURRAY, B. MOUBARAKI, D. REINEN and H. STRATEMEIER, *Inorg. Chem.* **32**, 3397–401 (1993).



**Figure 28.6** (a) Binuclear complex formed in biuret test (b) Schematic representation of square-pyramidal coordination of  $\text{Cu}^{\text{II}}$  in dimeric Schiff base complexes.

The effect of configurational mixing of higher-lying  $s$  orbitals into the ligand field  $d$ -orbital basis set is also likely to favour elongation rather than contraction.<sup>(21)</sup>

Elongation has the further consequence that the fifth and sixth stepwise stability constants (p. 908) are invariably much smaller than the first 4 for  $\text{Cu}^{\text{II}}$  complexes. This is clearly illustrated by the preparation of the amines. Tetraamines are easily isolated by adding ammonia to aqueous solutions of  $\text{Cu}^{\text{II}}$  until the initial precipitate of  $\text{Cu}(\text{OH})_2$  redissolves, and then adding ethanol to the deep blue solution,<sup>†</sup> when  $\text{Cu}(\text{NH}_3)_4\text{SO}_4 \cdot x\text{H}_2\text{O}$  slowly precipitates. Recrystallization of tetraamines from 0.880 ammonia yields violet-blue pentaamines, but the fifth  $\text{NH}_3$  is easily lost; hexaamines can only be obtained from liquid ammonia and must be stored in an atmosphere of ammonia. Pyridine and other monoamines are similar in behaviour to ammonia. Likewise, chelating  $N$ -donor ligands such as en, bipy and phen show a reluctance to form tris complexes (though these can be obtained if a high concentration of ligand is used) and a number of 5-coordinate complexes such as  $[\text{Cu}(\text{bipy})_2\text{I}]^+$  with a trigonal bipyramidal structure are known. The structure of  $[\text{Cu}(\text{bipy})_3]^{2+}$  in its perchlorate has been described<sup>(22)</sup> as square pyramidal (4 short bonds, av. 202.6 pm, and 1 long, 222.3 pm) but, since the sixth N atom only 246.9 pm from

the Cu, distorted octahedral is perhaps a better description. The macrocyclic  $N$ -donor, phthalocyanine, forms a square-planar complex and substituted derivatives are used to produce a range of blue to green pigments which are thermally stable to over  $500^\circ\text{C}$ , and are widely used in inks, paints and plastics.

In alkaline solution biuret,  $\text{HN}(\text{CONH}_2)_2$  reacts with copper(II) sulfate to give a characteristic violet colour due to the formation of the complexes  $[\text{Cu}_2(\mu\text{-OH})_2(\text{NHCONHCONH})_4]^{2-}$  (Fig. 28.6a) and  $[\text{Cu}(\text{NHCONHCONH})_2]^{2-}$ . This is the basis of the “biuret test” in which an excess of NaOH solution is added to the unknown material together with a little  $\text{CuSO}_4$  soln: a violet colour indicates the presence of a protein or other compound containing a peptide linkage.

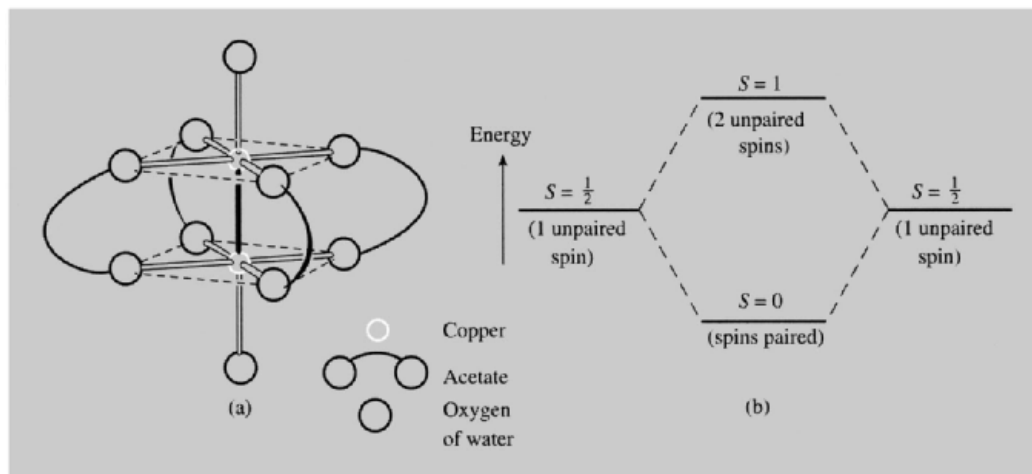
Copper(II) also forms stable complexes with  $O$ -donor ligands. In addition to the hexaaquo ion, the square planar  $\beta$ -diketonates such as  $[\text{Cu}(\text{acac})_2]$  (which can be precipitated from aqueous solution and recrystallized from non-aqueous solvents) are well known, and tartrate complexes are used in Fehling’s test (p. 1181).

Mixed  $O,N$ -donor ligands such as Schiff bases are of interest in that they provide examples not only of square-planar coordination but also, in the solid state, examples of square-pyramidal coordination by dimerization (Fig. 28.6(b)). A similar situation occurs in the bis-dimethylglyoximate complex, which dimerizes by sharing oxygen atoms, though the 4 coplanar donor atoms are all nitrogen atoms. Copper(II) carboxylates<sup>(15)</sup> are easily obtained by crystallization from aqueous solution or, in the case of the higher carboxylates, by precipitation with the appropriate acid from ethanolic solutions

<sup>21</sup> M. GERLOCH, *Inorg. Chem.* **20**, 638–40 (1981).

<sup>†</sup> This solution will dissolve cellulose which can be reprecipitated by acidification, a fact used in one of the processes for producing rayon.

<sup>22</sup> Z.-M. LIU, Z.-H. JIANG, D.-H. LIAO, G.-L. WANG, X.-K. YAO and H.-G. WANG, *Polyhedron* **10**, 101–2 (1991).



**Figure 28.7** (a) Dinuclear structure of copper(II) acetate, and (b) spin singlet ( $2S + 1 = 1$ ) and spin triplet ( $2S + 1 = 3$ ) energy levels in dinuclear  $\text{Cu}^{\text{II}}$  carboxylates.

of the acetate. In the early 1950s it was found that the magnetic moment of green copper(II) acetate monohydrate is lower than the spin-only value (1.4 BM at room temperature as opposed to 1.73 BM) and that, contrary to the Curie law, its susceptibility reaches a maximum around 270 K but falls rapidly at lower temperatures. Furthermore, the compound has a dimeric structure in which 2 copper atoms are held together by 4 acetate bridges (Fig. 28.7a). Clearly the single unpaired electrons on the copper atoms interact, or “couple”, antiferromagnetically to produce a low-lying singlet (diamagnetic) and an excited but thermally accessible triplet (paramagnetic) level (Fig. 28.7b). The separation is therefore only a few  $\text{kJ mol}^{-1}$  (at room temperature,  $RT$  the thermal energy available to populate the higher level  $\sim 2.5 \text{ kJ mol}^{-1}$ ) and as the temperature is reduced the population of the ground level increases and diamagnetism is eventually approached.

Similar behaviour is found in many other carboxylates of  $\text{Cu}^{\text{II}}$  as well as their adducts in which axial water is replaced by other *O*- or *N*-donor ligands. In spite of a continuous flow of work on these compounds there is still no general agreement as to the actual mechanism of the interaction nor on possible correlations of its magnitude with relevant

properties of the carboxylate and axial ligands.<sup>(23)</sup> The simplest interpretation is to assume that the singlet and triplet levels arise from a single interaction between the unpaired spins of the copper atoms and, with B. N. Figgis and R. L. Martin,<sup>(24)</sup> that this takes the form of “face-to-face” or  $\delta$  overlap of the copper  $d_{x^2-y^2}$  orbitals. However,  $\sigma$  overlap of  $d_{z^2}$  orbitals, or even a “superexchange” interaction transmitted via the  $\pi$  orbitals of the bridging carboxylates, are also feasible. It seems generally true that the magnetic interaction is greater for alkylcarboxylates than arylcarboxylates and for *N*-donor rather than *O*-donor axial ligands. More extensive correlations are unfortunately difficult to deduce from published results because of the existence of polymeric or other isomeric forms beside the dinuclear, and because of the possible presence of mononuclear impurities.

Mononuclear carboxylates such as  $\text{Ca}[\text{Cu}(\text{O}_2\text{-CMe})_4]$  and  $[\text{Cu}(\text{bet})_4](\text{NO}_3)_2$ , (bet =  $\text{N}^+\text{Me}_3\text{-CH}_2\text{COO}^-$ ) are also known.<sup>(25)</sup> In these

<sup>23</sup> M. KATO and Y. MUTO, *Coord. Chem. Revs.* **92**, 45–83 (1988).

<sup>24</sup> B. N. FIGGIS and R. L. MARTIN, *J. Chem. Soc.* 1956, 3837–46 (cf. quadruple bond in Cr(II) acetate (pp. 1032–4)).

<sup>25</sup> X.-M. CHEN and T. C. W. MAK, *Polyhedron* **10**, 273–6 (1991).

compounds each carboxylate ligand has one O close to the Cu (192–197 pm) and one much further away (277–307 pm) producing a distorted dodecahedral structure.

Other copper(II) complexes of stereochemical interests are the halogenocuprate(II) anions which can be crystallized from mixed solutions of the appropriate halides. The structures of the solids are markedly dependent on the counter cation. The compounds  $\text{MCuCl}_3$  ( $\text{M} = \text{Li}, \text{K}, \text{NH}_4$ ) contain red, planar  $[\text{Cu}_2\text{Cl}_6]^{2-}$  ions, and  $\text{CsCuCl}_3$  has a polymeric structure in which chains of  $\text{CuCl}_6$  octahedra (4 + 2 coordination) share opposite faces.<sup>(26)</sup> With larger counter cations such as  $[\text{PPh}_4]^+$ , discrete  $[\text{Cu}_2\text{Cl}_6]^{2-}$  ions are found which are distinctly non-planar, the coordination about each Cu being intermediate between square planar and tetrahedral.<sup>(27)</sup> The  $[\text{CuCl}_5]^-$  salts present an even greater variety which includes 5-coordinate trigonal bipyramidal and square-pyramidal coordination, as well as  $[\text{dienH}_3][\text{CuCl}_4]\text{Cl}$  which contains a square-planar anion and exhibits a curious mixture of ferro- and antiferro-magnetic properties. But it is the salts of  $[\text{CuX}_4]^{2-}$  which have received most attention<sup>(28)</sup>: e.g. depending on the cation,  $[\text{CuCl}_4]^{2-}$  displays structures ranging from square planar to almost tetrahedral (p. 913). The former is usually green and the latter orange in colour.  $(\text{NH}_4)_2[\text{CuCl}_4]$  is an oft-quoted example of planar geometry, but 2 long Cu–Cl distances of 279 pm (compared to 4 Cu–Cl distances of 230 pm) make 4 + 2 coordination a more reasonable description. In the  $[\text{EtNH}_3]^+$  salt the longer Cu–Cl distances increase still further to 298 pm, but the clearest example of square-planar  $[\text{CuCl}_4]^{2-}$  is the methadone salt in which the fifth and sixth Cl atoms are more than 600 pm from the  $\text{Cu}^{\text{II}}$ . At the other extreme,  $\text{Cs}[\text{CuX}_4]$  ( $\text{X} = \text{Cl}, \text{Br}$ ) and  $[\text{NMe}_4]_2[\text{CuCl}_4]$  approach a

tetrahedral geometry and it appears that this geometry is retained in aqueous solution since the electronic spectra in the two phases are the same. For  $[\text{CuCl}_4]^{2-}$  the Cu–Cl distance is close to 223 pm and the somewhat flattened (Jahn–Teller distorted) tetrahedron has four Cl–Cu–Cl angles in the range 100–103° and the other two enlarged to 124° and 130°. The angular distortions in  $[\text{CuBr}_4]^{2-}$  are almost identical: 4 at 100–102° and the others at 126° and 130°.

### *Electronic spectra and magnetic properties of copper(II)* <sup>(15,29)</sup>

Because the  $d^9$  configuration can be thought of as an inversion of  $d^1$ , relatively simple spectra might be expected, and it is indeed true that the great majority of  $\text{Cu}^{\text{II}}$  compounds are blue or green because of a single broad absorption band in the region 11 000–16 000  $\text{cm}^{-1}$ . However, as already noted, the  $d^9$  ion is characterized by large distortions from octahedral symmetry and the band is unsymmetrical, being the result of a number of transitions which are by no means easy to assign unambiguously. The free-ion  $^2D$  ground term is expected to split in a crystal field in the same way as the  $^5D$  term of the  $d^4$  ion (p. 1032) and a similar interpretation of the spectra is likewise expected. Unfortunately this is now more difficult because of the greater overlapping of bands which occurs in the case of  $\text{Cu}^{\text{II}}$ .

The  $T$  ground term of the tetrahedrally coordinated ion implies an orbital contribution to the magnetic moment, and therefore a value in excess of  $\mu_{\text{spin-only}}$  (1.73 BM). But the  $E$  ground term of the octahedrally coordinated ion is also expected to yield a moment  $[\mu_e = \mu_{\text{spin-only}}(1 - 2\lambda/10Dq)]$  in excess of 1.73 BM, because of “mixing” of the excited  $T$  term into the ground term, and the high value of  $\lambda$  ( $-850 \text{ cm}^{-1}$ ) makes the effect significant. In practice, moments of magnetically dilute compounds are in the range 1.9–2.2 BM, with compounds whose geometry approaches octahedral having moments

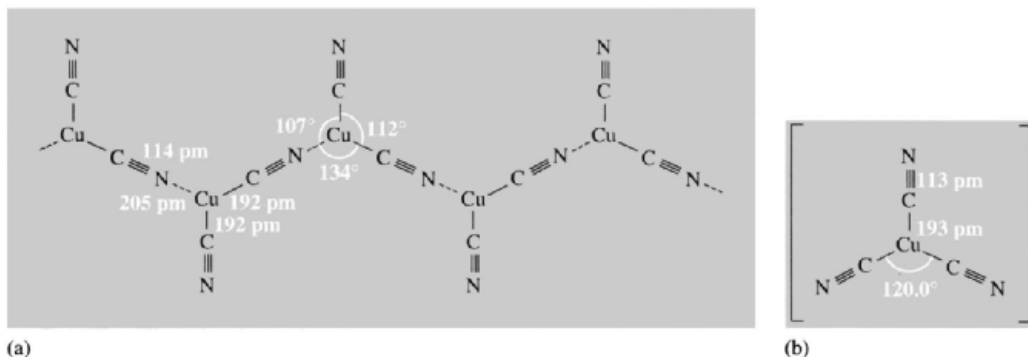
<sup>26</sup> W. J. A. MAASKANT, *Struct. & Bond.* **83**, 55–87 (1995).

<sup>27</sup> L. P. BATTAGLIA, A. B. CORRADI, U. GEISER, R. D. WILLETT, A. MOTORI, F. SANDROLINI, L. ANTOLINI, T. MANFREDINI, L. MENABUE and G. C. PELLACANI, *J. Chem. Soc., Dalton Trans.*, 265–71 (1988) and refs. therein.

<sup>28</sup> see for instance, C. L. BOUTCHARD, M. A. HITCHMAN, B. W. SKELTON and A. H. WHITE, *Aust. J. Chem.* **48**, 771–81 (1995).

<sup>29</sup> A. B. P. LEVER, *Inorganic Electronic Spectroscopy* 2nd edn., pp. 554–72, Elsevier, Amsterdam (1984).





**Figure 28.8** (a) Chain of  $\text{Cu}^{\text{I}}$  atoms linked by CN bridges to form the helical anion  $[\text{Cu}(\text{CN})_2]_{\infty}^{-}$  in  $\text{KCu}(\text{CN})_2$ , and (b) one of the two types of  $[\text{Cu}(\text{CN})_3]^{2-}$  ions in  $\text{Na}_2[\text{Cu}(\text{CN})_3] \cdot 3\text{H}_2\text{O}$  — the other set have Cu–C 195 pm and C–N 116 pm.

at the lower end, and those with geometries approaching tetrahedral having moments at the higher end, but their measurements cannot be used diagnostically with safety unless supported by other evidence.

### Oxidation state I ( $d^{10}$ )

All  $\text{M}^{\text{I}}$  cations of this triad are diamagnetic and, unless coordinated to easily polarized ligands, colourless too. In aqueous solution the  $\text{Cu}^{\text{I}}$  ion is very unstable with respect to disproportionation ( $2\text{Cu}^{\text{I}} \rightleftharpoons \text{Cu}^{\text{II}} + \text{Cu}(\text{s})$ ) largely because of the high heat of hydration of the divalent ion as already mentioned. At 25°C,  $K$  ( $= [\text{Cu}^{\text{II}}][\text{Cu}^{\text{I}}]^{-2}$ ) is large,  $(5.38 \pm 0.37) \times 10^5 \text{ l mol}^{-1}$ , and standard reduction potentials have been calculated<sup>(30)</sup> to be:

$$E^{\circ}(\text{Cu}^{\text{II}}/\text{Cu}) = +0.5072 \text{ V}$$

$$\text{and } E^{\circ}(\text{Cu}^{2+}/\text{Cu}^{\text{I}}) = +0.1682 \text{ V}$$

Nevertheless,  $\text{Cu}^{\text{I}}$  can be stabilized either in compounds of very low solubility or by complexing with ligands having  $\pi$ -acceptor character. Its solutions in MeCN are stable and electrochemical oxidation of the metal in this solvent provides a convenient preparative route. The usual stereochemistry is tetrahedral as in

complexes such as  $[\text{Cu}(\text{CN})_4]^{3-}$ ,  $[\text{Cu}(\text{py})_4]^+$ , and  $[\text{Cu}(\text{L-L})_2]^+$  (e.g. L-L = bipy, phen), but lower coordination numbers are possible such as 2, in linear  $[\text{CuCl}_2]^{-}$  formed when CuCl is dissolved in hydrochloric acid and 3, as in  $\text{K}[\text{Cu}(\text{CN})_2]$ , which in the solid contains trigonal, almost planar,  $\text{Cu}(\text{CN})_3$  units linked in a polymeric chain (Fig. 28.8). The discrete planar anion  $[\text{Cu}(\text{CN})_3]^{2-}$  is found in  $\text{Na}_2[\text{Cu}(\text{CN})_3] \cdot 3\text{H}_2\text{O}$ . In  $2[\text{Cu}(\text{C}_{25}\text{H}_{28}\text{N}_2\text{S}_2)\text{Cl}]^+[\text{Cu}_2\text{Cl}_4]^{2-}$  the bulky cation, consisting of an  $\text{N}_2\text{S}_2$  type macrocycle and a chloride ion coordinated to  $\text{Cu}^{\text{II}}$ , stabilizes the  $\text{Cu}^{\text{I}}$  anion in an unusual, non-planar form<sup>(31)</sup> (Fig. 28.9a).

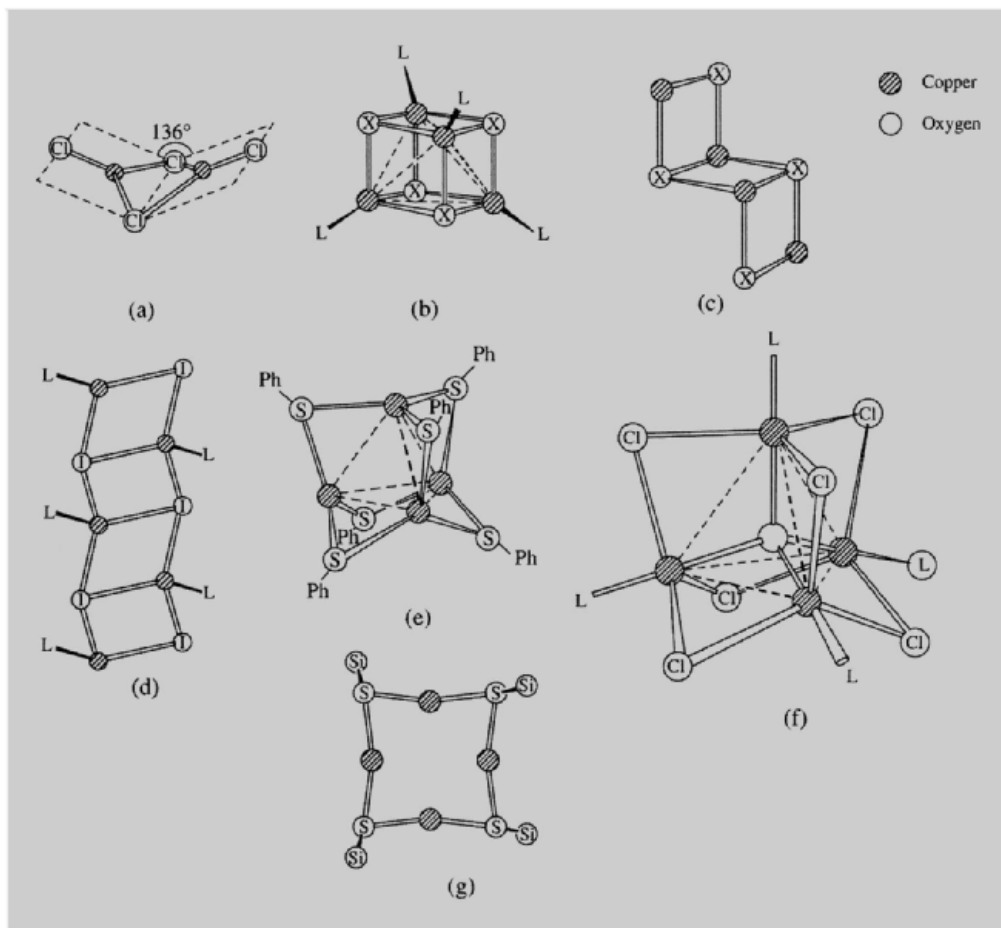
Polymers and oligomers form an expanding class of  $\text{Cu}^{\text{I}}$  complexes which,  $\text{Cu}^{\text{I}}$  being a  $d^{10}$  ion, are unlikely to involve M–M bonding. A wide range of structures, which frequently give rise to characteristic charge-transfer spectra,<sup>(32)</sup> is found. Stoichiometries of  $\text{CuXL}_n$  ( $n = 0.5, 1, 1.5$  and 2) are common and many different structures have been identified including “cubane”, open “step” (or “chair”) and “ladder” (Fig. 28.9b, c, d) depending on the nature of L and the particular halide involved as well as the stoichiometry.<sup>(33)</sup>

<sup>31</sup> L. ESCRICHE, N. LUCENA, J. CASABO, F. TEIXIDOR, R. KIV-  
EKÄS and R. SILLAPÄÄ, *Polyhedron* **14**, 649–54 (1995).

<sup>32</sup> M. MELNIK, L. MACASKOVA and C. E. HOLLOWAY, *Coord. Chem. Revs.* **126**, 71–92 (1993).

<sup>33</sup> B. SKELTON, A. F. WATERS and A. H. WHITE, *Aust. J. Chem.* **44**, 1207–15 (1991).

<sup>30</sup> L. CRAVATTA, D. FERRI and R. PALOMBARI, *J. Inorg. Nucl. Chem.* **42**, 593–8 (1980).



**Figure 28.9** Some polymers and oligomers of  $\text{Cu}^{\text{I}}$ : (a) non-planar  $[\text{Cu}_2\text{Cl}_4]^{2-}$ . (b) “cubane” complexes  $[\text{CuXL}]_4$ ; X = halide, L = phosphine or arsine. (c) “step” complexes  $[\text{CuXL}]_4$ ; X = halide, L = phosphine or arsine. (d) extended “ladder” of  $[\text{CuI}(\text{NC}_5\text{H}_4\text{-2-Me})]_x$ . (e)  $[\text{Cu}_4(\text{SPh})_6]^{2-}$ . (f)  $[\text{Cu}_4\text{OCl}_6\text{L}_4]$ , L =  $\text{OPPh}_3$ . (g) central portion of  $[(\text{Bu}^t\text{O})_3\text{SiSCu}]_4$ .

Iodocuprates(I) provide a series of polymeric anions made up of planar  $\{\text{CuI}_3\}$  or tetrahedral  $\{\text{CuI}_4\}$  units, culminating in  $(\text{pyH})_{24}[\text{Cu}_{36}\text{I}_{56}]\text{I}_4$ . The large anion in this consists of 36  $\{\text{CuI}_4\}$  tetrahedra joined by 2 or 3 edges, and may be visualized as a section of a c.c.p. lattice of iodides with  $\text{Cu}^{\text{I}}$  atoms occupying some of the tetrahedral interstices.<sup>(34)</sup>

S-donor ligands also contribute to this stereochemical diversity,  $\text{Cu}_4$  tetrahedra being found in

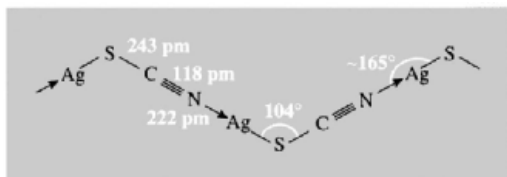
$[\text{Cu}_4(\text{SPh})_6]^{2-}$  and in  $[\text{Cu}_4\text{OCl}_6(\text{OPPh}_3)_4]$ , while  $[(\text{Bu}^t\text{O})_3\text{SiSCu}]_4$  provided<sup>(35)</sup> the first example of a square planar  $\text{Cu}_4\text{S}_4$  ring (Fig. 28.9e, f, g).

The +1 state is by far the best-known oxidation state of silver and salts with most anions are formed. These reveal the reluctance of  $\text{Ag}^{\text{I}}$  to coordinate to oxygen for, with the exceptions of the nitrate, perchlorate and fluoride, most are insoluble in water. The last two of these salts are also among the very few  $\text{Ag}^{\text{I}}$  salts which form

<sup>34</sup> H. HARTL and J. FUCHS, *Angew. Chem. Int. Edn. Engl.* **25**, 569–70 (1986).

<sup>35</sup> B. BECKER, W. WOJNOWSKI, K. PETERS, E.-M. PETERS and H. G. VON SCHNERING, *Polyhedron* **9**, 1659–66 (1990).

hydrates and, paradoxically, their solubilities are actually noted for their astonishingly high values (respectively 5570 and 1800 g l<sup>-1</sup> at 25°C). The hydrated ion is present in aqueous solution and a coordination number of 4 has been established.<sup>(36)</sup> Unlike Cu<sup>I</sup>, however, Ag<sup>I</sup> forms 4-coordinate tetrahedral complexes less readily than 2-coordinate linear ones. A wide variety of the latter are formed with *N*-, *P*- and *S*-donor ligands, some of them of great practical importance. The familiar dissolution of AgCl in aqueous ammonia is due to the formation of [Ag(NH<sub>3</sub>)<sub>2</sub>]<sup>+</sup>; the formation of [Ag(S<sub>2</sub>O<sub>3</sub>)<sub>2</sub>]<sup>3-</sup> in photographic "fixing" has already been mentioned (p. 1187), and the cyanide extraction process depends upon the formation of [M(CN)<sub>2</sub>]<sup>-</sup> (M = Ag, Au) (contrast polymeric [Cu(CN)<sub>2</sub>]<sup>-</sup>, Fig. 28.8). AgCN itself is a linear polymer, {Ag-C≡N→Ag-C≡N→} but AgSCN is non-linear mainly because the sp<sup>3</sup> hybridization of the sulfur forces a zigzag structure; there is also slight non-linearity at the Ag<sup>I</sup> atom.



Because of their inability to form linear complexes, chelating ligands tend instead to produce polymeric species, but compounds with coordination numbers higher than 2 can be produced, e.g. the almost tetrahedral diphosphine and diarsine complexes [Ag(L-L)<sub>2</sub>]<sup>+</sup> and the almost planar 5-coordinate [Ag(quinquepyridine)][PF<sub>6</sub>].<sup>(37)</sup> Four-coordination is also found in tetrameric phosphine and arsine halides [AgXL]<sub>4</sub> which occur in "cubane" and "step" (or "chair") forms like their copper analogues (Fig. 28.9). Indeed, [AgI(PPh<sub>3</sub>)<sub>4</sub>] exists in both forms. As with Cu<sup>I</sup>, sulfur and *S*-donor ligands yield many complexes

of high nuclearity. [Ag<sub>4</sub>(SCH<sub>2</sub>C<sub>6</sub>H<sub>4</sub>CH<sub>2</sub>S)<sub>3</sub>]<sup>2-</sup> contains the same tetrahedral {M<sub>4</sub>S<sub>6</sub>} centre<sup>(38)</sup> found in [Cu<sub>4</sub>(SPh)<sub>6</sub>]<sup>2-</sup> (Fig. 28.9e), while in the dark-red Na<sub>2</sub>[Ag<sub>6</sub>S<sub>4</sub>] the metal atoms are disposed octahedrally.<sup>(39)</sup> The cyclohexanethiolato complex [Ag(SC<sub>6</sub>H<sub>11</sub>)<sub>12</sub>] and (PPh<sub>3</sub>)<sub>4</sub>[AgSBU<sup>-</sup>]<sub>14</sub><sup>(40)</sup> consist respectively of 24- and 28-membered puckered rings of alternate Ag and S atoms.

Like Ag<sup>I</sup>, Au<sup>I</sup> also readily forms linear 2-coordinate complexes such as [AuX<sub>2</sub>]<sup>-</sup> (X = Cl, Br, I)<sup>(41)</sup> and also the technologically important [Au(CN)<sub>2</sub>]<sup>-</sup>. But it is much more susceptible to oxidation and to disproportionation into Au<sup>III</sup> and Au<sup>0</sup> which renders all its binary compounds, except AuCN, unstable to water. It is also more clearly a class b or "soft" metal with a preference for the heavier donor atoms P, As and S. Stable, linear complexes are obtained when tertiary phosphines reduce Au<sup>III</sup> in ethanol,



The Cl ligand can be replaced by other halides and pseudo-halides by metathetical reactions. Trigonal planar coordination is found in phosphine complexes of the stoichiometry [AuL<sub>2</sub>X] but 4-coordination, though possible, is less prevalent. Diarsine gives the almost tetrahedral complex [Au(diars)<sub>2</sub>]<sup>+</sup> but, for reasons which are not clear, the colourless complexes [AuL<sub>4</sub>]<sup>+</sup>[BPh<sub>4</sub>]<sup>-</sup> with monodentate phosphines fail to achieve a regular tetrahedral geometry.

Complexes with dithiocarbamates involve linear S-Au-S coordination but are dimeric and the Au-Au distance of 276 pm compared with 288 pm in the metal and 250 pm in gaseous Au<sub>2</sub> is indicative of metal-metal bonding.<sup>†</sup>

<sup>38</sup> G. HENKEL, P. BETZ and B. KREBS, *Angew. Chem. Int. Edn. Engl.* **26**, 145-6 (1987).

<sup>39</sup> J. HUSTER, B. BONSMANN and W. BRONGER, *Z. anorg. allg. Chem.* **619**, 70-2 (1993).

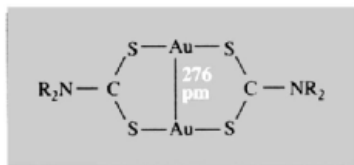
<sup>40</sup> I. DANCE, L. FITZPATRICK, M. SCUDDER and D. CRAIG, *J. Chem. Soc., Chem. Commun.*, 17-8 (1984).

<sup>41</sup> P. BRAUNSTEIN, A. MÜLLER and H. BÖGGE, *Inorg. Chem.* **25**, 2104-6 (1986).

<sup>†</sup> The stability of the 6s orbital in gold already referred to (p. 1180), allows it to participate in M-M interactions. This

<sup>36</sup> J. TEXTER, J. S. HASTRELTOR and J. L. HALL, *J. Phys. Chem.* **87**, 4690-3 (1983). See also *Acta Chem. Scand.* **A38**, 437-51 (1984).

<sup>37</sup> E. C. CONSTABLE, M. G. B. DREW, G. FORSYTH and M. D. WARD, *J. Chem. Soc., Chem. Commun.*, 1450-1 (1988).



In the thermal production of gold coatings on ceramics and glass, paints are used which comprise  $\text{Au}^{\text{III}}$  chloro-complexes and sulfur-containing resins dissolved in an organic solvent. It seems likely that polymeric species are responsible for rendering the gold soluble.

### Gold cluster compounds<sup>(42-44)</sup>

Polymeric complexes of the types formed by copper and silver are not found for gold but instead a range of variously coloured cluster compounds, with gold in an average oxidation state  $<1$  and involving M–M bonds, can be obtained by the general process of reducing a gold phosphine halide, usually with sodium borohydride. Yellow  $[\text{Au}_6\{\text{P}(\text{C}_6\text{H}_4\text{-4-Me})_3\}_6]^{2+}$  consists of an octahedron of 6 gold atoms with a phosphine attached to each. Red  $[\text{Au}_8(\text{PPh}_3)_8]^{2+}$  can be regarded as a chair-like, centred hexagon of gold atoms with an eighth gold situated above the chair, each gold atom having a phosphine attached to it (Fig. 28.10a). Clusters are known in which further gold atoms are added to the chair in a more or less spherical manner (e.g.  $[\text{Au}_{11}(\text{P}(\text{C}_6\text{H}_4\text{-4-F})_3)_7\text{I}_3]$  Fig. 28.10c in which the central gold has no attached ligand) and giving ultimately a centred icosahedron as found in the dark-red  $[\text{Au}_{13}\text{Cl}_2(\text{PMe}_2\text{Ph})_{10}]^{3+}$  (Fig. 28.10d). Another series of clusters can be distinguished with flatter, ring or torus shapes as in the red-brown  $[\text{Au}_8(\text{PPh}_3)_7]^{2+}$  and

facilitates M–M bonding in compounds of  $\text{Au}^{\text{I}}$ , which would otherwise not be expected for  $d^{10}$  ions, and considerably enhances the strength of this bonding when the oxidation state of Au  $< 1$ .

<sup>42</sup> D. M. P. MINGOS pp. 189–97 in A. J. WELCH and S. K. CHAPMAN (eds.), *The Chemistry of the Copper and Zinc Triads*, R. S. C., Cambridge, 1993.

<sup>43</sup> B. K. TEO, H. ZHANG and X. SHI *ibid.* pp. 211–34.

<sup>44</sup> D. M. P. MINGOS and M. J. WATSON, *Adv. Inorg. Chem.* **39**, 327–99 (1992).

green  $[\text{Au}_9\{\text{P}(\text{C}_6\text{H}_4\text{-4-Me})_3\}_8]^{3+}$  (Fig. 28.10b). This latter series is characterized by lower electron counts than the former, reflecting a lower involvement of p-orbitals in M–M bonding and therefore less tangential skeletal bonding (cf. p. 1170 for Pt). This accords with the observation that only clusters with an icosahedral structure (stabilized by both tangential *and* radial skeletal bonding) are stereochemically rigid on the nmr time scale at room temperature<sup>(42)</sup>.

Heteronuclear clusters<sup>(44)</sup> incorporating a range of other transition metals can be produced by the general method of reacting  $\text{AuPR}_3$  with a carbonyl anion of the appropriate metal. “Clusters of clusters” of Au–Ag have been synthesized with metal frameworks based on vertex sharing icosahedra, the basic unit being an Au-centred  $\{\text{Au}_7\text{Ag}_6\}$  icosahedron<sup>(43)</sup>. The largest of these is  $[\text{Au}_{22}\text{Ag}_{24}(\text{PPh}_3)_{12}\text{Cl}_{10}]$  consisting of four  $\{\text{Au}_7\text{Ag}_6\}$  icosahedra arranged tetrahedrally with six shared vertices. The spectacular, red-brown  $[\text{Au}_{55}(\text{PPh}_3)_{12}\text{Cl}_6]$  is prepared by reducing  $\text{Au}(\text{PPh}_3)\text{Cl}$  with  $\text{B}_2\text{H}_6$  and is probably best viewed as a cubo-octahedral fragment of close-packed Au atoms. From it, water soluble  $[\text{Au}_{55}(\text{Ph}_2\text{PC}_6\text{H}_4\text{SO}_3\text{Na}\cdot 2\text{H}_2\text{O})_{12}\text{Cl}_6]$  can be obtained by ligand exchange.<sup>(45)</sup>

### 28.3.6 Biochemistry of copper<sup>(46,47)</sup>

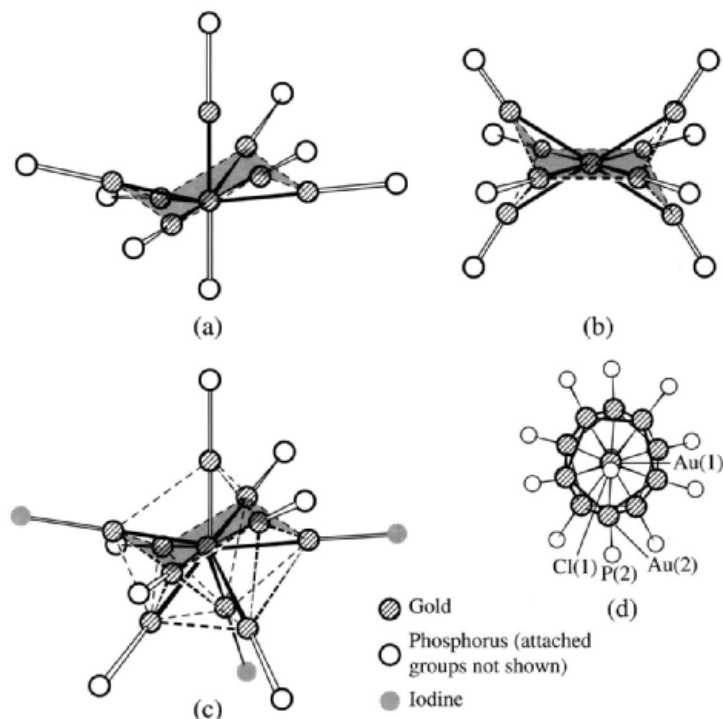
Metallic copper and silver both have antibacterial properties<sup>†</sup> and  $\text{Au}^{\text{I}}$  thiol complexes have found increasing use in the treatment of rheumatoid arthritis, but only copper of this group has a biological role in sustaining life. It is widely distributed in the plant and animal worlds, and its redox chemistry is involved in a variety of

<sup>45</sup> G. SCHMID, N. KLEIN, L. KORSTE, U. KREIBIG and D. SCHÖNAUER, *Polyhedron* **7**, 605–8 (1988).

<sup>46</sup> K. D. KARLIN and Z. TYEKLAR (eds.), *Bioinorganic Chemistry of Copper*, Chapman & Hall, New York, 1993, 506 pp.

<sup>47</sup> pp. 187–214 of W. KAIM and B. SCHWEDERSKI, *Bioinorganic Chemistry: Inorganic Elements in the Chemistry of Life*, Wiley, Chichester, 1994.

<sup>†</sup> This was unknowingly utilized in ancient Persia where, by law, drinking water had to be stored in bright copper vessels.



**Figure 28.10** Some gold cluster compounds. Note that a chair-like centred hexagon of gold atoms persists throughout these structures and is shaded in (a), (b), and (c): (a)  $[\text{Au}_8(\text{PPh}_3)_8]^{2+}$ , (b)  $\text{Au}_9\{\text{P}(\text{C}_6\text{H}_4\text{-4-Me})_3\}_8]^{3+}$ , (c)  $\text{Au}_{11}\text{I}_3\{\text{P}(\text{C}_6\text{H}_4\text{-4-F})_3\}_7]$ , and (d)  $[\text{Au}_{13}\text{Cl}_2(\text{PMe}_2\text{Ph})_{10}]^{3+}$ . In (d) the 12th icosahedral gold atom and the 13th (central) gold atom are obscured by Au(1).

oxidation processes. A human adult contains around 100 mg of copper, mostly attached to protein, an amount exceeded only by iron and zinc amongst transition metals, and requiring a daily intake of some 3–5 mg. Copper deficiency results in anaemia, and the congenital inability to excrete Cu, resulting in its accumulation, is Wilson's disease. The presence of copper, along with haem, in the electron transfer agent cytochrome c oxidase has already been mentioned (p. 1101).

Although complete structural details are rare, considerable progress has been made in understanding the mode of action of copper proteins, synthetic modelling being a major factor in this.<sup>(48)</sup> Biologically active copper centres can be divided into three main types:

*Type 1:* “blue” monomeric Cu with very distorted “3 + 1” coordination of 2N- and 2S-donors. This is apparently a compromise between the square planar 4N preferred by  $\text{Cu}^{\text{II}}$  and the tetrahedral 4S preferred by  $\text{Cu}^{\text{I}}$ , with a degree of flexibility facilitating a  $\text{Cu}^{\text{II}}/\text{Cu}^{\text{I}}$  couple. This type of centre is characterized by an intense blue colour because of a strong absorption at 600 nm arising from  $S \rightarrow \text{Cu}^{\text{II}}$  charge transfer.

*Type 2:* “normal” monomeric  $\text{Cu}^{\text{II}}$  in an essentially square planar environment with additional, very weak, tetragonal interactions and exhibiting normal esr.

*Type 3:* a pair of  $\text{Cu}^{\text{I}}$  atoms about 360 pm apart and attached to protein through histidine residues; these effect  $\text{O}_2$  transport by means of the reversible reaction  $2\text{Cu}^{\text{I}} \xrightleftharpoons{\text{O}_2} \text{Cu}^{\text{II}}(\mu\text{-O}_2)\text{Cu}^{\text{II}}$ . Whether the  $\text{O}_2$  is bonded as a  $\eta^1:\eta^1$  linear Cu–O–O–Cu bridge or  $\eta^2:\eta^2$  (i.e. O–O

<sup>48</sup> N. KITAJIMA, *Adv. Inorg. Chem.* **39**, 1–77 (1992).

perpendicular to the Cu–Cu axis) is still uncertain. The copper are esr inactive: Cu<sup>I</sup> because of its d<sup>10</sup> configuration and Cu<sup>II</sup> because strong antiferromagnetic interaction between the two atoms renders them diamagnetic.

A further class, *Type 4*, has been proposed. It is composed of three Cu<sup>II</sup> atoms two of which are strongly coupled, being only ~340 pm apart. The third Cu atom completes an isosceles triangle, being 390–400 pm from each of the first two, and is “normal”.

In a large number of molluscs the oxygen-carrying pigment is not haemoglobin but a haemocyanin. These proteins, with molecular weights of the order of 10<sup>6</sup>, are composed of differing numbers of subunits each containing a pair of type 3 copper centres. A limited cooperativity (p 1100) is displayed but its mechanism is not yet clear. The “blue proteins”<sup>(49)</sup> laccase and ascorbic oxidase are found in a variety of plants where they are involved in the oxidation of phenols, amines and ascorbate by O<sub>2</sub>. They contain a type 1 copper, responsible for their colour and name, along with a type 4 trimer which together form a very distorted 4Cu tetrahedron. One-electron transfers by means of Cu<sup>II</sup>/Cu<sup>I</sup> couples are involved but the mechanism by which O<sub>2</sub> is reduced is far from clear. Ceruloplasmin is also a blue protein which is found in all mammals: it participates in copper transport and storage as well as in oxidation processes. It is the deficiency of this protein which is responsible for Wilson’s disease.

Another oxidase, but non-blue, is galactose oxidase found in fungi where it catalyses the oxidation of –CH<sub>2</sub>OH in galactose to –CHO, simultaneously reducing O<sub>2</sub> to H<sub>2</sub>O<sub>2</sub>. With a molecular weight of 68 000 and containing a single type 2 Cu, it was thought likely that a Cu<sup>III</sup>/Cu<sup>I</sup> couple effected the 2-electron reduction of O<sub>2</sub>. However, spectroscopic evidence appears to refute this. The coordination of the Cu is square pyramidal with two histidine nitrogens, two tyrosine oxygens and an acetate oxygen. The currently favoured interpretation is that the more

tightly bound of the two tyrosines undergoes a 1-electron redox change which, together with a Cu<sup>II</sup>/Cu<sup>I</sup> couple, affords the required 2-electron transfer.

Cytochrome c oxidase contains two, or possibly three, copper atoms referred to as Cu<sub>A</sub> and Cu<sub>B</sub> since they do not fit into the usual classification. The former (possibly a dimer) is situated outside the mitochondrial membrane, whereas the latter is associated with an iron atom within the membrane. Both have electron transfer functions but details are as yet unclear.

### 28.3.7 Organometallic compounds<sup>(50)</sup>

Neutral binary carbonyls are not formed by these metals at normal temperatures<sup>†</sup> but copper and gold each form an unstable carbonyl halide, [M(CO)Cl]. These colourless compounds can be obtained by passing CO over MCl or, in the case of copper only (since the gold compound is very sensitive to moisture), by bubbling CO through a solution of CuCl in conc HCl or in aqueous NH<sub>3</sub>. The latter reactions can in fact be used for the quantitative estimation of the CO content of gases. A silver carbonyl [Ag(CO)][B(OTeF<sub>5</sub>)<sub>4</sub>] has also been prepared by mixing AgOTeF<sub>5</sub> and B(OTeF<sub>5</sub>)<sub>3</sub> under CO<sup>(51)</sup> but the weakness of the Ag–C bond is indicated by the fact that the CO stretching frequency (2204 cm<sup>-1</sup>) is the highest of any metal carbonyl. Complexes of the type [MLX], which are often polymeric, can be obtained for Cu<sup>I</sup> and Ag<sup>I</sup> with many olefins (alkenes) and acetylenes (alkynes) either by anhydrous methods or in solution. They are generally rather labile, often decomposing when

<sup>50</sup> F. P. PRUCHNIK, *Organometallic Chemistry of the Transition Elements*, Plenum Press, New York, 1990, 757 pp.

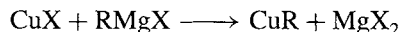
<sup>†</sup> Some have been synthesized by the condensation of Cu or Ag vapour and CO at temperatures of 6–15 K: e.g. M(CO)<sub>3</sub>, M<sub>2</sub>(CO)<sub>6</sub>, M(CO)<sub>2</sub> and M(CO). Thus [Ag(CO)<sub>3</sub>] is green, planar and paramagnetic; above 25–30 K it apparently dimerizes, perhaps by formation of an Ag–Ag bond (see D. McINTOSH and G. A. OZIN, *J. Am. Chem. Soc.* **98**, 3167–75 (1976), and references therein).

<sup>51</sup> P. K. HURLBURT, O. P. ANDERSON and S. H. STRAUSS, *J. Am. Chem. Soc.* **113**, 6277–8 (1991).

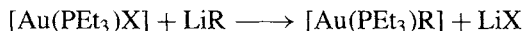
<sup>49</sup> A. G. SYKES, *Adv. Inorg. Chem.* **36**, 377–408 (1991).

isolated. The silver complexes have received most attention and the silver–olefin bonds are found to be thermodynamically weaker than, for instance, corresponding platinum–olefin bonds. Since the former bonds are also found to be somewhat unsymmetrical it seems likely that  $\pi$  bonding is weaker for the group 11 metals. Gold also forms olefin complexes, but not nearly so readily as silver and then only with high molecular weight olefins.

M–C $\sigma$  bonds can be formed by each of the M<sup>I</sup> metals. The simple alkyls and aryls of Ag<sup>I</sup> are less stable than those of Cu<sup>I</sup>, while those of Au<sup>I</sup> have not been isolated. Copper alkyls and aryls<sup>(52)</sup> are prepared by the action of LiR or a Grignard reagent on a Cu<sup>I</sup> halide:



CuMe is a yellow polymeric solid which explodes if allowed to dry in air, and CuPh, which is white and also polymeric, though more stable, is still sensitive to both air and water. Much greater stability is achieved by the  $\sigma$ -cyclopentadienyl complex [Cu( $\eta^1$ -C<sub>5</sub>H<sub>5</sub>)(PEt<sub>3</sub>)] prepared by the reaction of C<sub>5</sub>H<sub>6</sub>, CuO and PEt<sub>3</sub> in petroleum ether; a similar Au<sup>I</sup> compound, [Au( $\eta^1$ -C<sub>5</sub>H<sub>4</sub>Me)(PPh<sub>3</sub>)], is also known. Au<sup>I</sup> alkyls can be obtained like those of copper but only with an appropriate ligand present, e.g.:



The colourless solids are composed of linear monomers. A few anionic Au<sup>I</sup> alkyls are known of which [N(PPh<sub>3</sub>)<sub>2</sub>]<sup>+</sup>[Au(acac)<sub>2</sub>]<sup>-</sup> might be mentioned.<sup>(53)</sup> In this it is the central C of the ligand, HC(COMe)<sub>2</sub> which is attached to the metal.

The alkyl derivatives of Au<sup>III</sup> were discovered by W. J. Pope and C. S. Gibson in 1907; they include some of the most familiar and stable organo compounds of the group, and are notable for not requiring the stabilizing presence of  $\pi$ -bonding ligands. They are of three types:

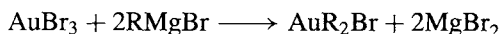
<sup>52</sup> P. P. POWER, *Prog. Inorg. Chem.* **39**, 75–112 (1991).

<sup>53</sup> J. VICENTE, M.-T. CHICOTE, I. SAURA-LLAMAS and M.-C. LAGUNAS, *J. Chem. Soc., Chem. Commun.*, 915–6 (1992).

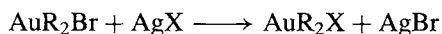
- AuR<sub>3</sub> (stable, when they occur at all, only in ether below –35°C);
- AuR<sub>2</sub>X (much the most stable); X = anionic ligand especially Br;
- AuRX<sub>2</sub> (unstable, only dibromides characterized).

Corresponding aryl derivatives are rare and unstable. Thus, while AuMe<sub>3</sub> decomposes above –35°C but is stabilized in [AuMe<sub>3</sub>(PPh<sub>3</sub>)], AuPh<sub>3</sub> is unknown.

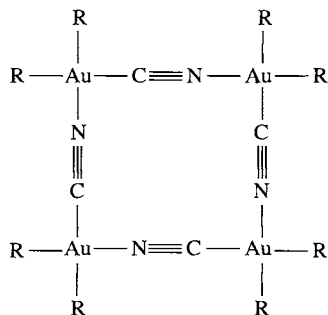
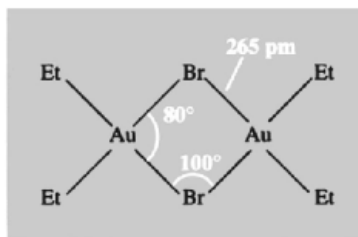
The dialkylgold(III) halides are generally prepared from the tribromide and a Grignard reagent:



Many other anions can then be introduced by metathetical reactions with the appropriate silver salt:



In all cases where the structure has been determined, the Au<sup>III</sup> attains planar four-fold coordination and polymerizes as appropriate to achieve this. The halides for instance are dimeric but with the cyanide, which forms linear rather than bent bridges, tetramers are produced:



		1		2													
				H	He												
3	4											5	6	7	8	9	10
Li	Be											B	C	N	O	F	Ne
11	12											13	14	15	16	17	18
Na	Mg											Al	Si	P	S	Cl	Ar
19	20	21	22	23	24	25	26	27	28	29	30	31	32	33	34	35	36
K	Ca	Sc	Ti	V	Cr	Mn	Fe	Co	Ni	Cu	Zn	Ga	Ge	As	Se	Br	Kr
37	38	39	40	41	42	43	44	45	46	47	48	49	50	51	52	53	54
Rb	Sr	Y	Zr	Nb	Mo	Tc	Ru	Rh	Pd	Ag	Cd	In	Sn	Sb	Te	I	Xe
55	56	57	58	59	60	61	62	63	64	65	66	67	68	69	70	71	72
Cs	Ba	La	Hf	Ta	W	Re	Os	Ir	Pt	Au	Hg	Tl	Pb	Bi	Po	At	Rn
87	88	89	90	91	92	93	94	95	96	97	98	99	100	101	102	103	104
Fr	Ra	Ac	Rf	Db	Sg	Bh	Hs	Mt	Uun	Uuu	Uub						
73	74	75	76	77	78	79	80	81	82	83	84	85	86	87	88	89	90
Ce	Pr	Nd	Pm	Sm	Eu	Gd	Tb	Dy	Ho	Er	Tm	Yb	La				
91	92	93	94	95	96	97	98	99	100	101	102	103	104				
Th	Pa	U	Np	Pu	Am	Cm	Bk	Cf	Es	Fm	Md	No	Lr				

# 29

## Zinc, Cadmium and Mercury

### 29.1 Introduction

The reduction of ZnO by charcoal requires a temperature of 1000°C or more and, because the metal is a vapour at that temperature and is liable to reoxidation, its collection requires some form of condenser and the exclusion of air. This was apparently first achieved in India in the thirteenth century. The art then passed to China where zinc coins were used in the Ming Dynasty (1368–1644). The preparation of alloyed zinc by smelting mixed ores does not require the isolation of zinc itself and is much more easily achieved. The small amounts of zinc present in samples of early Egyptian copper no doubt simply reflect the composition of local ores, but Palestinian brass dated 1400–1000 BC and containing about 23% Zn must have been produced by the deliberate mixing of copper and zinc ores. Brass was similarly produced by the Romans in Cyprus and later in the Cologne region of Germany.

Zinc was not intentionally made in medieval Europe, though small amounts were obtained by accidental condensation in the production of lead, silver and brass; it was imported from China by

the East India Company after about 1605. The English zinc industry started in the Bristol area in the early eighteenth century and production quickly followed in Silesia and Belgium. The origin of the name is obscure but may plausibly be thought to be derived from *Zinke* (German for spike, or tooth) because of the appearance of the metal.

Mercury is more easily isolated from its ore, cinnabar, and was used in the Mediterranean world for extracting metals by amalgamation as early as 500 BC, possibly even earlier. Cinnabar, HgS, was widely used in the ancient world as a pigment (vermilion). For over a thousand years, up to AD 1500, alchemists regarded the metal as a key to the transmutation of base metals to gold and employed amalgams both for gilding and for producing imitation gold and silver. Because of its mobility, mercury is named after the messenger of the gods in Roman mythology, and the symbol, Hg, is derived from *hydrargyrum* (Latin, liquid silver).

Cadmium made its appearance much later. In 1817 F. Stromeyer of Göttingen noticed that a sample of “cadmia” (now known as “calamine”), used in a nearby smelting works, was yellow



instead of white. The colour was not due to iron, which was shown to be absent, but arose instead from a new element which was named after the (zinc) ore in which it had been found (Greek *καδμεία*, cadmean earth, the ancient name of calamine).

## 29.2 The Elements

### 29.2.1 Terrestrial abundance and distribution

Zinc (76 ppm of the earth's crust) is about as abundant as rubidium (78 ppm) and slightly more abundant than copper (68 ppm). Cadmium (0.16 ppm) is similar to antimony (0.2 ppm); it is twice as abundant as mercury (0.08 ppm), which is itself as abundant as silver (0.08 ppm) and close to selenium (0.05 ppm). These elements are "chalcophiles" (p. 648) and so, in the reducing atmosphere prevailing when the earth's crust solidified, they separated out in the sulfide phase, and their most important ores are therefore sulfides. Subsequently, as rocks were weathered, zinc was leached out to be precipitated as carbonate, silicate or phosphate.

The major ores of zinc are ZnS (which is known as zinc blende in Europe and as sphalerite in the USA) and ZnCO<sub>3</sub> (calamine in Europe, smithsonite in the USA<sup>†</sup>). Large deposits are situated in Canada, the USA and Australia. Less important ores are hemimorphite, Zn<sub>4</sub>Si<sub>2</sub>O<sub>7</sub>(OH)<sub>2</sub>·H<sub>2</sub>O and franklinite, (Zn,Fe)O·Fe<sub>2</sub>O<sub>3</sub>. Cadmium is found as greenockite, CdS, but its only commercially important source is the 0.2–0.4% found in most zinc ores. Cinnabar, HgS, is the only important ore and source of mercury and is found along lines of previous volcanic activity. The most famous and extensive deposits are at Almaden in Spain; these contain up to 6–7% Hg and have been worked since Roman times. Other deposits, usually containing <1% Hg, are situated in the former Soviet Union, Algeria, Mexico, Yugoslavia and Italy.

<sup>†</sup> After James Smithson, founder of the Smithsonian Institution, Washington. The name calamine is applied in the USA to a basic carbonate.

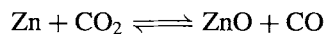
### 29.2.2 Preparation and uses of the elements<sup>(1)</sup>

The isolation of zinc, over 90% of which is from sulfide ores, depends on conventional physical concentration of the ore by sedimentation or flotation techniques. This is followed by roasting to produce the oxides; the SO<sub>2</sub> which is generated is used to produce sulfuric acid. The ZnO is then either treated electrolytically or smelted with coke. In the former case the zinc is leached from the crude ZnO with dil H<sub>2</sub>SO<sub>4</sub>, at which point cadmium is precipitated by the addition of zinc dust. The ZnSO<sub>4</sub> solution is then electrolysed and the metal deposited — in a state of 99.95% purity — on to aluminium cathodes.

A variety of smelting processes have been employed to effect the reduction of ZnO by coke:



These formerly involved the use of banks of externally heated, horizontal retorts, operated on a batch basis. They were replaced by continuously operated vertical retorts, in some cases electrically heated. Unfortunately none of these processes has the thermal efficiency of a blast furnace process (p. 1072) in which the combustion of the fuel for heating takes place in the same chamber as the reduction of the oxide. The inescapable problem posed by zinc is that the reduction of ZnO by carbon is not spontaneous below the boiling point of Zn (a problem not encountered in the smelting of Fe, Cu or Pb, for instance), and the subsequent cooling to condense the vapour is liable, in the presence of the combustion products, to result in the reoxidation of the metal:



The problem can be overcome by spraying the zinc vapour with lead as it leaves the top of the furnace. This chills and dissolves the zinc

<sup>1</sup> *Kirk-Othmer Encyclopedia of Chemical Technology*, 4th edn., Interscience, New York. For Zn, see Vol. 25, 1998, pp. 789–853. For Cd, see Vol. 4, 1992, pp. 748–60. For Hg, see Vol. 16, 1995, pp. 212–28.

so rapidly that reoxidation is minimal. The zinc then separates as a liquid of nearly 99% purity and is further refined by vacuum distillation to give a purity of 99.99%. Any cadmium present is recovered in the course of this distillation. The use of a blast furnace has the further advantage that the composition of the charge is not critical, and mixed Zn/Pb ores can be used (ZnS and PbS are commonly found together) to achieve the simultaneous production of both metals, the lead being tapped from the bottom of the furnace.

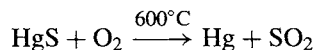
World production of zinc (1995) is about 7 million tonnes pa: of this, about 1 million tonnes pa is produced by each of Canada and Australia and 800 000 tonnes pa by China. Cadmium is produced in much smaller quantities (~20 000 tonnes pa) and these are dependent on the supply of zinc.

Zinc finds a wide range of uses. The most important, accounting for 40% of output, is as an anti-corrosion coating. The application of the coating takes various forms: immersion in molten zinc (hot-dip galvanizing), electrolytic deposition, spraying with liquid metal, heating with powdered zinc ("Sherardizing"), and applying paint containing zinc powder. In addition to brasses (Cu plus 20–50% Zn), a rapidly increasing number of special alloys, predominantly of zinc, are used for diecasting and, indeed, the vast majority of *pressure* diecastings are now made in these alloys. Zinc sheeting is used in roof cladding and the manufacture of dry batteries (see Panel, p. 1204) is a further use, though this has declined considerably in recent years.

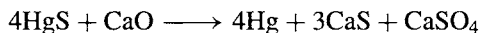
The major uses of cadmium are in batteries (67%) and coatings (7%). In the form of its compounds it is used in pigments (CdS –15%) and stabilizers, in PVC for instance, to prevent degradation by heat or ultraviolet radiation (10%).

The isolation of mercury is comparatively straightforward. The most primitive method consisted simply of heating cinnabar in a fire of brushwood. The latter acted as fuel and condenser, and metallic mercury collected in the ashes. Modern techniques are of course less crude than this but the basic principle is much the same. After being crushed and concentrated by

flotation, the ore is roasted in a current of air and the vapour condensed:



Alternatively, in the case of especially rich ores, roasting with scrap iron or quicklime is used:



Blowing air through the hot, crude, liquid metal oxidizes traces of metals such as Fe, Cu, Zn and Pb which form an easily removable scum. Further purification is by distillation under reduced pressure. About 4000 tonnes<sup>†</sup> of mercury are used annually but only half is from primary, mine production the other half being secondary production and sales from stockpiles. The main primary producer is now Spain, but several other countries, including the former Soviet Union, China and Algeria, have capacity for production.

The use of mercury for extracting precious metals by amalgamation has a long history and was extensively used by Spain in the sixteenth century when her fleet carried mercury from Almaden to Mexico and returned with silver. However, environmental concerns have resulted in falling demand and excess production capacity. It is still used in the extraction of gold and in the Castner–Kellner process for manufacturing chlorine and NaOH (p. 72), and a further major use is in the manufacture of batteries. It is also used in street lamps and AC rectifiers, while its small-scale use in thermometers, barometers and gauges of different kinds, are familiar in many laboratories.

### 29.2.3 Properties of the elements

A selection of some important properties of the elements is given in Table 29.1. Because the elements each have several naturally occurring isotopes their atomic weights cannot be quoted with great precision.

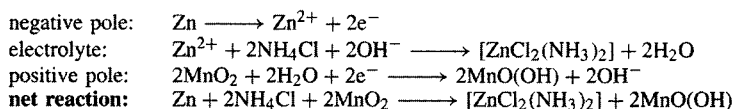
<sup>†</sup> Mercury is sold in iron *flasks* holding 76 lb of mercury and this is the unit in which output is normally measured.

### Dry Batteries

A portable source of electricity, if not a necessity, is certainly a great convenience in modern life and is dependent on compact, sealed, dry batteries. The main types are listed below and they incorporate the metals Zn, Ni, Hg and Cd as well as  $\text{MnO}_2$

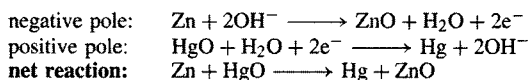
#### (a) Carbon-zinc cell

The first dry battery was that patented in 1866 by the young French engineer, G. Leclanché. The positive pole consisted of carbon surrounded by  $\text{MnO}_2$  (p. 1048) contained in a porous pot, and the negative pole was simply a rod of zinc. These were situated inside a glass jar containing the electrolyte, ammonium chloride solution thickened with sand or sawdust. This is still the basis of the most common type of modern dry cell in which a carbon rod is the positive pole, surrounded by a paste of  $\text{MnO}_2$ , carbon black, and  $\text{NH}_4\text{Cl}$ , inside a zinc can which is both container and negative pole. The reactions are:



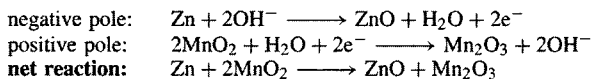
#### (b) Mercury cell

The negative pole of pressed amalgamated zinc powder and the positive pole of mercury(II) oxide and graphite are separated by an absorbent impregnated with the electrolyte, conc KOH:



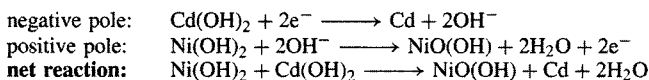
#### (c) Alkaline manganese cell

This is similar in principle to (a) but is contained in a manner akin to (b). The negative pole of powdered zinc, formed into a paste with the electrolyte KOH, and the positive pole of compressed graphite and  $\text{MnO}_2$  are separated by an absorbent impregnated with the electrolyte:



#### (d) Nickel-cadmium cell

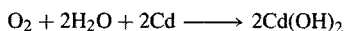
Unlike the cells above, which are all primary cells, this is a secondary (i.e. rechargeable) cell, and the two poles are composed in the uncharged condition of nickel and cadmium hydroxides respectively. These are each supported on microporous nickel, made by a sintering process, and separated by an absorbent impregnated with electrolyte. The charging reactions are:



During discharge these reactions are reversed. A crucial feature of the construction of this cell is that oxygen produced at the positive pole during charging by the side-reaction:



can migrate readily to the negative pole to be recombined in the reaction:



But for this rapid migration and recombination, the cell could not be sealed.

Table 29.1 Some properties of the elements zinc, cadmium and mercury

Property	Zn	Cd	Hg
Atomic number	30	48	80
Number of naturally occurring isotopes	5	8 <sup>(a)</sup>	7
Atomic weight	65.39(2)	112.411(8)	200.59(2)
Electronic configuration	[Ar]3d <sup>10</sup> 4s <sup>2</sup>	[Kr]4d <sup>10</sup> 5s <sup>2</sup>	[Xe]4f <sup>14</sup> 5d <sup>10</sup> 6s <sup>2</sup>
Electronegativity	1.6	1.7	1.9
Metal radius (12 coordinate)/pm	134	151	151
Effective ionic radius/pm	II	95	102
	I	—	119
Ionization energies/kJ mol <sup>-1</sup>	1st	906.1	876.5
	2nd	1733	1631
	3rd	3831	3644
$E^\circ(\text{M}^{2+}/\text{M})/\text{V}$	-0.7619	-0.4030	+0.8545
MP/°C	419.5	320.8	-38.9
BP/°C	907	765	357
$\Delta H_{\text{fus}}/\text{kJ mol}^{-1}$	7.28(±0.01)	6.4(±0.2)	2.30(±0.02)
$\Delta H_{\text{vap}}/\text{kJ mol}^{-1}$	114.2(±1.7)	100.0(±2.1)	59.1(±0.4)
$\Delta H_{(\text{monatomic gas})}/\text{kJ mol}^{-1}$	129.3(±2.9)	111.9(±2.1)	61.3
Density (25°C)/g cm <sup>-3</sup>	7.14	8.65	13.534(1)
Electrical resistivity (20°C)/μohm cm	5.8	7.5	95.8

<sup>(a)</sup>The half-life of  $9.3 \pm 1.9 \times 10^{15}$  y for <sup>113</sup>Cd is the longest known for any β-emitter; note that this is 2 million times the age of the earth ( $4.6 \times 10^9$  y).

Their most noticeable features compared with other metals are their low melting and boiling points, mercury being unique as a metal which is a liquid at room temperature. Zinc and cadmium are silvery solids with a bluish lustre when freshly formed. Mercury is also unusual in being the only element, apart from the noble gases, whose vapour is almost entirely monatomic, while its appreciable vapour pressure ( $1.9 \times 10^{-3}$  mmHg, i.e. 0.25 Pa, at 25°C), coupled with its toxicity, makes it necessary to handle it with care. The electrical resistivity of liquid mercury is exceptionally high for a metal, and this facilitates its use as an electrical standard (the international ohm is defined as the resistance of 14.4521 g of Hg in a column 106.300 cm long and 1 mm<sup>2</sup> cross-sectional area at 0°C and a pressure of 760 mmHg).

The structures of the solids, although based on the typically metallic hexagonal close-packing, are significantly distorted. In the case of Zn and Cd the distortion is such that, instead of having 12 equidistant neighbours, each atom has 6 nearest neighbours in the close-packed plane with the 3 neighbours in each of the adjacent planes

being about 10% more distant. In the case of (rhombohedral) Hg the distortion, again uniquely, is the reverse, with the coplanar atoms being the more widely separated (by some 16%). The consequence is that these elements are much less dense and have a lower tensile strength than their predecessors in Group 11. These facts have been ascribed to the stability of the d electrons which are now tightly bound to the nucleus: the metallic bonding therefore involves only the outer s electrons, and is correspondingly weakened.

### 29.2.4 Chemical reactivity and trends

Zinc and cadmium tarnish quickly in moist air and combine with oxygen, sulfur, phosphorus and the halogens on being heated. Mercury also reacts with these elements, except phosphorus and its reaction with oxygen was of considerable practical importance in the early work of J. Priestley and A. L. Lavoisier on oxygen (p. 601). The reaction only becomes appreciable at temperatures of about 350°C, but above about 400°C HgO decomposes back into the elements.

None of the three metals reacts with hydrogen, carbon or nitrogen.

Non-oxidizing acids dissolve both Zn and Cd with the evolution of hydrogen. With oxidizing acids the reactions are more complicated, nitric acid for instance producing a variety of oxides of nitrogen dependent on the concentration and temperature. Mercury is unreactive to non-oxidizing acids but dissolves in conc  $\text{HNO}_3$  and in hot conc  $\text{H}_2\text{SO}_4$  forming the  $\text{Hg}^{\text{II}}$  salts along with oxides of nitrogen and sulfur. Dilute  $\text{HNO}_3$  slowly produces  $\text{Hg}_2(\text{NO}_3)_2$ . Zinc is the only element in the group which dissolves in aqueous alkali to form ions such as aquated  $[\text{Zn}(\text{OH})_4]^{2-}$  (zincates).

All three elements form alloys with a variety of other metals. Those of zinc include the brasses (p. 1178) and, as mentioned above, are of considerable commercial importance. Those of mercury are known as amalgams and some, such as sodium and zinc amalgams, are valuable reducing agents: in a number of cases, high heats of formation and stoichiometric compositions suggest chemical combination.  $\text{Na}_5\text{Hg}_8$  and  $\text{Na}_3\text{Hg}$  for instance have been isolated and structurally characterized. They consist of "widespread" close-packed mercury ( $\text{Hg}-\text{Hg} > 500 \text{ pm}$ ) with respectively, all vacancies filled and all octahedral vacancies plus 5/6 tetrahedral vacancies filled with sodium atoms.<sup>(2)</sup> From caesium amalgams  $\text{CsHg}$  has been obtained and shown<sup>(3)</sup> to contain isolated square planar  $\text{Hg}_4$  clusters ( $\text{Hg}-\text{Hg} \sim 300 \text{ pm}$  whereas intercluster separation =  $419 \text{ pm}$ ). Amalgams are most readily formed by heavy metals, whereas the lighter metals of the first transition series (with the exception of manganese and copper) are insoluble in mercury. Hence iron flasks can be used for its storage.

Chemically, it is clear that Zn and Cd are rather similar and that Hg is somewhat distinct. The lighter pair are more electropositive, as indicated both by their electronegativity coefficients and electrode potentials (Table 29.1), while Hg has a

positive electrode potential and is comparatively inert. With the exception of the metallic radii, all the evidence indicates that the effects of the lanthanide contraction have died out by the time this group is reached. Compounds are characterized by the  $d^{10}$  configuration and, with the exception of derivatives of the  $\text{Hg}_2^{2+}$  ion, which formally involve  $\text{Hg}^{\text{I}}$ , they almost exclusively involve  $\text{M}^{\text{II}}$  (but see page 1213). The ease with which the  $s^2$  electrons are removed compared with the more firmly held d electrons is shown by the ionization energies. The sum of the first and second is in each case smaller than for the preceding element in Group 11, whereas the third is appreciably higher. Even so the first two ionization energies are high for mercury (as they are for gold) — perhaps reflecting the poor nuclear shielding afforded by the filled 4f shell — and this, coupled with the small hydration energy associated with the large  $\text{Hg}^{\text{II}}$  cation, accounts for the positive value of its electrode potential.

In view of the stability of the filled d shell, these elements show few of the characteristic properties of transition metals (p. 905) despite their position in the d block of the periodic table. Thus zinc shows similarities with the main-group metal magnesium, many of their compounds being isomorphous, and it displays the class-a characteristic of complexing readily with O-donor ligands. On the other hand, zinc has a much greater tendency than magnesium to form covalent compounds, and it resembles the transition elements in forming stable complexes not only with O-donor ligands but with N- and S-donor ligands and with halides and  $\text{CN}^-$  (see p. 1216) as well. As mentioned above, cadmium is rather similar to zinc and may be regarded as on the class-a/b borderline. However, mercury is undoubtedly class b: it has a much greater tendency to covalency and a preference for N-, P- and S-donor ligands, with which  $\text{Hg}^{\text{II}}$  forms complexes whose stability is rarely exceeded by those of any other divalent cation. Compounds of the  $\text{M}^{\text{II}}$  ions of this group are characteristically diamagnetic and those of  $\text{Zn}^{\text{II}}$ , like those of  $\text{Mg}^{\text{II}}$ , are colourless. By contrast, many compounds of

<sup>2</sup> H. J. DEISEROTH and D. TOELSTEDT, *Z. anorg. allg. Chem.* **615**, 43–8 (1992).

<sup>3</sup> H. J. DEISEROTH, A. STRUNK and W. BAUHOFFER, *Z. anorg. allg. Chem.* **575**, 31–8 (1989).

Table 29.2 Stereochemistries of compounds of Zn<sup>II</sup>, Cd<sup>II</sup> and Hg<sup>II</sup>

Coordination number	Stereochemistry	Zn	Cd	Hg
2	Linear	ZnEt <sub>2</sub>	CdEt <sub>2</sub>	[Hg(NH <sub>3</sub> ) <sub>2</sub> ] <sup>2+</sup>
3	Planar	[ZnMe(NPh <sub>3</sub> ) <sub>2</sub> ]		[HgI <sub>3</sub> ] <sup>-</sup>
	T-shaped			[Hg(SC <sub>6</sub> H <sub>2</sub> Bu <sup>t</sup> ) <sub>2</sub> (py)]
4	Tetrahedral	[Zn(H <sub>2</sub> O) <sub>4</sub> ] <sup>2+</sup> , [Zn(NH <sub>3</sub> ) <sub>4</sub> ] <sup>2+</sup>	[CdCl <sub>4</sub> ] <sup>2-</sup>	[Hg(SCN) <sub>4</sub> ] <sup>2-</sup>
	Planar	[Zn(glycyl) <sub>2</sub> ]		
5	Trigonal bipyramidal	[Zn(terpy)Cl <sub>2</sub> ]	[CdCl <sub>5</sub> ] <sup>3-</sup>	[Hg(terpy)Cl <sub>2</sub> ]
	Square pyramidal	[Zn(S <sub>2</sub> CNEt <sub>2</sub> ) <sub>2</sub> ] <sub>2</sub>	[Cd(S <sub>2</sub> CNEt <sub>2</sub> ) <sub>2</sub> ] <sub>2</sub>	[Hg(N(C <sub>2</sub> H <sub>4</sub> NMe <sub>2</sub> ) <sub>3</sub> )] <sup>+</sup>
6	Octahedral	[Zn(en) <sub>3</sub> ] <sup>2+</sup>	[Cd(NH <sub>3</sub> ) <sub>6</sub> ] <sup>2+</sup>	[Hg(C <sub>5</sub> H <sub>5</sub> NO) <sub>6</sub> ] <sup>2+</sup>
7	Pentagonal bipyramidal	[Zn(H <sub>2</sub> dapp)(H <sub>2</sub> O) <sub>2</sub> ] <sup>2+(a)</sup>	[Cd(quin) <sub>2</sub> (NO <sub>3</sub> ) <sub>2</sub> H <sub>2</sub> O] <sup>(b)</sup>	
8	Distorted dodecahedral	[Zn(NO <sub>3</sub> ) <sub>4</sub> ] <sup>2-(c)</sup>		[Hg(NO <sub>2</sub> ) <sub>4</sub> ] <sup>2-</sup>
	Distorted square antiprismatic			

<sup>(a)</sup>H<sub>2</sub>dapp = 2,6-diacetylpyridinebis(2'-pyridyl)hydrazone.

<sup>(b)</sup>The 2 nitrate ions are not equivalent (both are bidentate but one is coordinated symmetrically, the other asymmetrically) and the structure of the complex is by no means regular (p. 1217).

<sup>(c)</sup>The distortion arises because the bidentate nitrate ions are coordinated asymmetrically to such an extent that the stereochemistry may alternatively be regarded as approaching tetrahedral (p. 1217).

Hg<sup>II</sup>, and to a lesser extent those of Cd<sup>II</sup>, are highly coloured due to the greater ease of charge transfer from ligands to the more polarizing cations. The increasing polarizing power and covalency of their compounds in the sequence, Mg<sup>II</sup> < Zn<sup>II</sup> < Cd<sup>II</sup> < Hg<sup>II</sup>, is a reflection of the decreasing nuclear shielding and consequent increasing power of distortion in the sequence: filled p shell < filled d shell < filled f shell.

A further manifestation of these trends is the increasing stability of  $\sigma$ -bonded alkyls and aryls in passing down the group (p. 1221). Those of Zn and Cd are rather reactive and unstable to both air and water, whereas those of Hg are stable to both. (The Hg-C bond is not in fact strong but the competing Hg-O bond is weaker.) However, the M<sup>II</sup> ions do not form  $\pi$  complexes with CO, NO or olefins (alkenes), no doubt because of the stability of their d<sup>10</sup> configurations and their consequent inability to provide electrons for "back bonding". Likewise their cyanides presumably owe their stability primarily to  $\sigma$  rather than  $\pi$  bonding. The filled d shell also prevents  $\pi$  acceptance and complexes with cyclopentadienide ions (which are good  $\pi$  donors) are  $\sigma$ - rather than  $\pi$ -bonded.

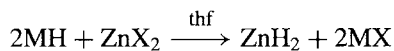
The range of stereochemistries found in compounds of the M<sup>II</sup> ions is illustrated in Table 29.2. Since the d<sup>10</sup> configuration affords no crystal field stabilization, the stereochemistry of a particular compound depends on the size and polarizing power of the M<sup>II</sup> cation and the steric requirements of the ligands. Thus both Zn<sup>II</sup> and Cd<sup>II</sup> favour 4-coordinate tetrahedral complexes though Cd<sup>II</sup>, being the larger, forms 6-coordinate octahedral complexes more readily than does Zn<sup>II</sup>. However, the still larger Hg<sup>II</sup> also commonly adopts a tetrahedral stereochemistry, and octahedral 6-coordination is less prevalent than for either of its congeners.<sup>†</sup> When it does occur it is usually highly distorted with 2 short and 4 long bonds, a distortion which in its extreme form produces the 2-coordinate, linear stereochemistry which is characteristic of

<sup>†</sup>An example of trigonal prismatic coordination has been reported for Hg in the green, zero-valent mixed-metal cluster [Hg{Pt(2,6-Me<sub>2</sub>C<sub>6</sub>H<sub>3</sub>NC)}<sub>6</sub>]; Y. YAMAMOTO, H. YAMAZAKI, and T. SAKURAI, *J. Am. Chem. Soc.* **104**, 2329-30 (1982). In [Hg(mac)<sub>2</sub>](HgBr<sub>4</sub>), (mac = 1-thia-4,7-diazacyclononane) the coordination in the cation is intermediate between octahedral and trigonal prismatic; U. HEINZEL and R. MATTES, *Polyhedron* **11**, 597-600 (1992).

$\text{Hg}^{\text{II}}$ . This is also found in organozinc and organocadmium compounds but only with  $\text{Hg}^{\text{II}}$  is it one of the predominant stereochemistries. Explanations of this fact have been given in terms of the promotional energies involved in various hybridization schemes, but it may be regarded pictorially as a consequence of the greater deformability of the  $d^{10}$  configuration of the large  $\text{Hg}^{\text{II}}$  ion. Thus, if 2 ligands are considered to approach the cation from opposite ends of the  $z$ -axis, the resulting deformation increases the electron density in the  $xy$ -plane and so discourages the close approach of other ligands. Coordination numbers greater than 6 are rare and generally involve bidentate,  $O$ -donor ligands with a small "bite", such as  $\text{NO}_3^-$  and  $\text{NO}_2^-$ .

## 29.3 Compounds of Zinc, Cadmium and Mercury<sup>(4-6)</sup>

Zinc hydride can be isolated from the reaction of  $\text{LiH}$  with  $\text{ZnBr}_2$  or  $\text{NaH}$  with  $\text{ZnI}_2$ :



The alkali metal halide remains in solution and  $\text{ZnH}_2$  is precipitated as a white solid of moderate stability at or below room temperature.<sup>(7)</sup>  $\text{CdH}_2$  and  $\text{HgH}_2$  are much less stable and decompose rapidly even below  $0^\circ$ . The complex metal hydrides  $\text{LiZnH}_3$ ,  $\text{Li}_2\text{ZnH}_4$  and  $\text{Li}_3\text{ZnH}_5$  have each been prepared as off-white powders by the reaction of  $\text{LiAlH}_4$  with the appropriate organometallic complex  $\text{Li}_n\text{ZnR}_{n+2}$ .

The carbides of these metals (which are actually acetylides,  $\text{MC}_2$ , p. 297) and also the

nitrides are unstable materials, those of mercury explosively so.

### 29.3.1 Oxides and chalcogenides

The principal compounds in this category are the monochalcogenides, which are formed by all three metals. It is a notable indication of the stability of tetrahedral coordination for the elements of Group 12 that, of the 12 compounds of this type, only  $\text{CdO}$ ,  $\text{HgO}$  and  $\text{HgS}$  adopt a structure other than wurtzite or zinc blende (both of which involve tetrahedral coordination of the cation — see below).  $\text{CdO}$  adopts the 6-coordinate rock-salt structure;  $\text{HgO}$  features zigzag chains of almost linear  $\text{O}-\text{Hg}-\text{O}$  units; and  $\text{HgS}$  exists in both a zinc-blende form and in a rock-salt form.

The normal oxide, formed by each of the elements of this group, is  $\text{MO}$ , and peroxides  $\text{MO}_2$  are known for  $\text{Zn}$  and  $\text{Cd}$ . Reported lower oxides,  $\text{M}_2\text{O}$ , are apparently mixtures of the metal and  $\text{MO}$ .

$\text{ZnO}$  is by far the most important manufactured compound of zinc<sup>(8)</sup> and, being an inevitable byproduct of primitive production of brass, has been known longer than the metal itself. It is manufactured by burning in air the zinc vapour obtained on smelting the ore or, for a purer and whiter product, the vapour obtained from previously refined zinc. It is normally a white, finely divided material with the wurtzite structure. On heating, the colour changes to yellow due to the evaporation of oxygen from the lattice to give a nonstoichiometric phase  $\text{Zn}_{1+x}\text{O}$  ( $x \leq 70$  ppm); the supernumerary  $\text{Zn}$  atoms produce lattice defects which trap electrons which can subsequently be excited by absorption of visible light.<sup>(9)</sup> Indeed, by "doping"  $\text{ZnO}$  with an excess of 0.02–0.03%  $\text{Zn}$  metal, a whole range of colours — yellow, green, brown, red — can be obtained. The reddish hues of the naturally

<sup>4</sup> M. FARNSWORTH, *Cadmium Chemicals*, International Lead Zinc Research Org. Inc., New York, 1980, 158 pp.

<sup>5</sup> C. A. MCAULIFFE (ed.), *The Chemistry of Mercury*, Macmillan, London, 1977, 288 pp.

<sup>6</sup> B. J. AYLETT, Group IIB, Chap. 30, pp. 187–328, in *Comprehensive Inorganic Chemistry*, Vol. 3, Pergamon Press, Oxford, 1973.

<sup>7</sup> J. J. WATKINS and E. C. ASHBY, *Inorg. Chem.* **13**, 2350–4 (1974).

<sup>8</sup> See pp. 530–2 of W. BÜCHNER, R. SCHLIEBS, G. WINTER and K. H. BÜCHEL, *Industrial Inorganic Chemistry*, VCH, Weinheim 1989.

<sup>9</sup> N. N. GREENWOOD, *Ionic Crystals, Lattice Defects and Nonstoichiometry*, Chaps. 6 and 7, pp. 111–81, Butterworths, London, 1968.

occurring form, zincite, arise, however, from the presence of Mn or Fe.

The major industrial use of ZnO is in the production of rubber where it shortens the time of vulcanization. As a pigment in the production of paints it has the advantage over the traditional "white lead" (basic lead carbonate) that it is non-toxic and is not discoloured by sulfur compounds, but it has the disadvantage compared to TiO<sub>2</sub> of a lower refractive index and so a reduced "hiding power" (p. 959). It improves the chemical durability of glass and so is used in the production of special glasses, enamels and glazes. Another important use is in antacid cosmetic pastes and pharmaceuticals. In the chemical industry it is the usual starting material for other zinc chemicals of which the soaps (i.e. salts of fatty acids, such as Zn stearate, palmitate, etc.) are the most important, being used as paint driers, stabilizers in plastics, and as fungicides. An important small scale use is in the production of "zinc ferrites". These are spinels of the type Zn<sub>x</sub><sup>II</sup>M<sub>1-x</sub><sup>II</sup>Fe<sub>2</sub><sup>III</sup>O<sub>4</sub> involving a second divalent cation (usually Mn<sup>II</sup> or Ni<sup>II</sup>). When  $x = 0$  the structure is that of an inverse spinel (i.e. half the Fe<sup>III</sup> ions occupy octahedral sites — see p. 1081). Where  $x = 1$ , the structure is that of a normal spinel (i.e. all the Fe<sup>III</sup> ions occupy octahedral sites), since Zn<sup>II</sup> displaces Fe<sup>III</sup> from the tetrahedral sites. Reducing the proportion of Fe<sup>III</sup> ions in tetrahedral sites lowers the Curie temperature. The magnetic properties of the ferrite can therefore be controlled by adjustment of the zinc content.

ZnO is amphoteric (p. 640), dissolving in acids to form salts and in alkalis to form zincates, such as [Zn(OH)<sub>3</sub>]<sup>-</sup> and [Zn(OH)<sub>4</sub>]<sup>2-</sup>. The gelatinous, white precipitate obtained by adding alkali to aqueous solutions of Zn<sup>II</sup> salts is Zn(OH)<sub>2</sub> which, like ZnO, is amphoteric.

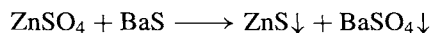
CdO is produced from the elements and, depending on its thermal history, may be greenish-yellow, brown, red or nearly black. This is partly due to particle size but more importantly, as with ZnO, is a result of lattice defects — this time in an NaCl lattice. It is more basic than ZnO, dissolving readily in acids but hardly at all in alkalis. White Cd(OH)<sub>2</sub> is precipitated from

aqueous solutions of Cd<sup>II</sup> salts by the addition of alkali and treatment with very concentrated alkali yields hydroxocadmiate such as Na<sub>2</sub>[Cd(OH)<sub>4</sub>]. Cadmium oxide and hydroxide find important applications in decorative glasses and enamels and in Ni–Cd storage cells. CdO also catalyses a number of hydrogenation and dehydrogenation reactions.

Treatment of the hydroxides of Zn and Cd with aqueous H<sub>2</sub>O<sub>2</sub> produces hydrated peroxides of rather variable composition. That of Zn has anti-septic properties and is widely used in cosmetics.

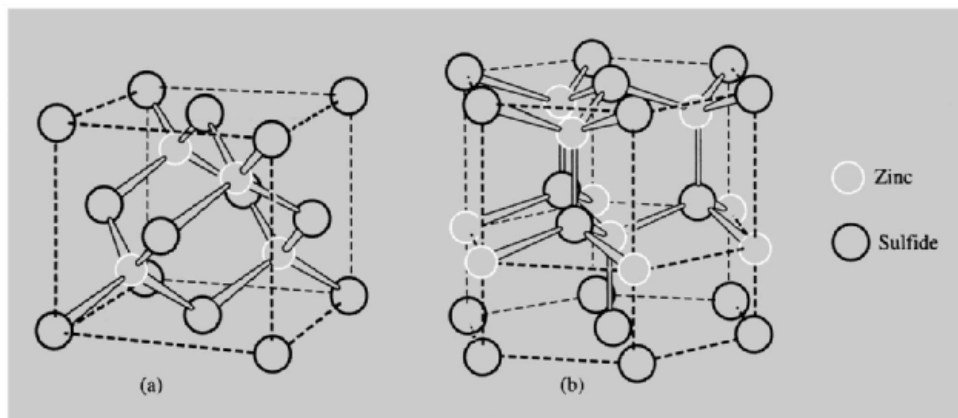
HgO exists in a red and a yellow variety. The former is obtained by pyrolysis of Hg(NO<sub>3</sub>)<sub>2</sub> or by heating the metal in O<sub>2</sub> at about 350°C; the latter by cold methods such as precipitation from aqueous solutions of Hg<sup>II</sup> by addition of alkali (Hg(OH)<sub>2</sub> is not known). The difference in colour is entirely due to particle size, both forms having the same structure which consists of zigzag chains of virtually linear O–Hg–O units with Hg–O 205 pm and angle Hg–O–Hg 107°. The shortest Hg···O distance between chains is 282 pm.

Zinc blende, ZnS, is the most widespread ore of zinc and the main source of the metal, but ZnS is also known in a second naturally occurring though much rarer form, wurtzite, which is the more stable at high temperatures. The names of these minerals are now also used as the names of their crystal structures which are important structure types found in many other AB compounds. In both structures each Zn is tetrahedrally coordinated by 4 S and each S is tetrahedrally coordinated by 4 Zn; the structures differ significantly only in the type of close-packing involved, being cubic in zinc-blende and hexagonal in wurtzite (Fig. 29.1). Pure ZnS is white and, like ZnO, finds use as a pigment for which purpose it is often obtained (as "lithopone") along with BaSO<sub>4</sub> from aqueous solution of ZnSO<sub>4</sub> and BaS:



Freshly precipitated ZnS dissolves readily in mineral acids with evolution of H<sub>2</sub>S, but roasting renders it far less reactive and it is then an acceptable pigment in paints for children's toys since it is harmless if ingested. ZnS also has





**Figure 29.1** Crystal structures of ZnS. (a) Zinc blende, consisting of two, interpenetrating, ccp lattices of Zn and S atoms displaced with respect to each other so that the atoms of each achieve 4-coordination ( $\text{Zn-S} = 235 \text{ pm}$ ) by occupying tetrahedral sites of the other lattice. The face-centred cube, characteristic of the ccp lattice, can be seen — in this case composed of S atoms, but an extended diagram would reveal the same arrangement of Zn atoms. Note that if all the atoms of this structure were C, the structure would be that of diamond (p. 275). (b) Wurtzite. As with zinc blende, tetrahedral coordination of both Zn and S is achieved ( $\text{Zn-S} = 236 \text{ pm}$ ) but this time the interpenetrating lattices are hexagonal, rather than cubic, close-packed.

interesting optical properties. It turns grey on exposure to ultraviolet light, probably due to dissociation to the elements, but the process can be inhibited by trace additives such as cobalt salts. Cathode rays, X-rays and radioactivity also produce fluorescence or luminescence in a variety of colours which can be extended by the addition of traces of various metals or the replacement of Zn by Cd and S by Se. It is widely used in the manufacture of cathode-ray tubes and radar screens.

Yellow ZnSe and brown ZnTe are structurally akin to the sulfide and the former especially is used mainly in conjunction with ZnS as a phosphor.

Chalcogenides of Cd are similar to those of Zn and display the same duality in their structures. The sulfide and selenide are more stable in the hexagonal form whereas the telluride is more stable in the cubic form. CdS is the most important compound of cadmium and, by addition of CdSe, ZnS, HgS, etc., it yields thermally stable pigments of brilliant colours from pale yellow to deep red, while colloidal dispersions are used to colour transparent glasses.

CdS and CdSe are also useful phosphors. CdTe is a semiconductor used as a detector for X-rays and  $\gamma$ -rays,<sup>(10)</sup> and mercury cadmium telluride<sup>(11)</sup> has found widespread (particularly military) use as an ir detector for thermal imaging.

HgS is polymorphic. The red  $\alpha$ -form is the mineral cinnabar, or vermilion, which has a distorted rock-salt structure and can be prepared from the elements.  $\beta$ -HgS is the rare, black, mineral metacinnabar which has the zinc-blende structure and is converted by heat to the stable  $\alpha$ -form. In the laboratory the most familiar form is the highly insoluble<sup>†</sup> black precipitate obtained by the action of  $\text{H}_2\text{S}$  on aqueous solutions of  $\text{Hg}^{\text{II}}$ . HgS is an unreactive substance, being attacked only by conc HBr, HI or aqua regia. HgSe and

<sup>10</sup> M. HAGE-ALI and P. SIFFERT, pp. 219–334 of *Semiconductors and Semimetals*, Vol. 43, Academic Press, San Diego, 1995.

<sup>11</sup> *ibid.* Vol. 18, 1981, 388 pp. devoted to mercury cadmium telluride.

<sup>†</sup> The solubility product,  $[\text{Hg}^{2+}][\text{S}^{2-}] = 10^{-52} \text{ mol}^2 \text{ dm}^{-6}$  but the actual solubility is greater than that calculated from this extremely low figure, since the mercury in solution is present not only as  $\text{Hg}^{2+}$  but also as complex species. In acid solution  $[\text{Hg}(\text{SH})_2]$  is probably formed and in alkaline

Table 29.3 Halides of zinc, cadmium and mercury (mp, bp, in parentheses)

Fluorides	Chlorides	Bromides	Iodides
ZnF <sub>2</sub> white (872°, 1500°)	ZnCl <sub>2</sub> white (275°, 756°)	ZnBr <sub>2</sub> white (394°, 702°)	ZnI <sub>2</sub> white (446°, d > 700°)
CdF <sub>2</sub> white (1049°, 1748°)	CdCl <sub>2</sub> white (568°, 980°)	CdBr <sub>2</sub> pale yellow (566°, 863°)	CdI <sub>2</sub> white (388°, 787°)
HgF <sub>2</sub> white (d > 645°)	HgCl <sub>2</sub> white (280°, 303°)	HgBr <sub>2</sub> white (238°, 318°)	HgI <sub>2</sub> α red, β yellow (257°, 351°)
Hg <sub>2</sub> F <sub>2</sub> yellow (d > 570°)	Hg <sub>2</sub> Cl <sub>2</sub> white (subl 383°)	Hg <sub>2</sub> Br <sub>2</sub> White (subl 345°)	Hg <sub>2</sub> I <sub>2</sub> yellow (subl 140°)

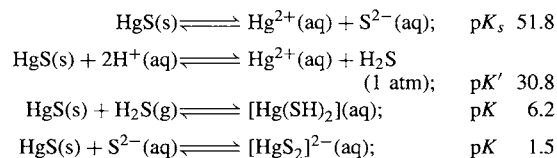
HgTe are easily obtained from the elements and have the zinc-blende structure.

### 29.3.2 Halides

The known halides are listed in Table 29.3. All 12 dihalides are known and in addition there are 4 halides of Hg<sub>2</sub><sup>2+</sup> which are conveniently considered separately. It is immediately obvious that the difluorides are distinct from the other dihalides, their mps and bps being much higher, suggesting a predominantly ionic character, as also indicated by their typically ionic three-dimensional structures (ZnF<sub>2</sub>, 6:3 rutile; CdF<sub>2</sub> and HgF<sub>2</sub>, 8:4 fluorite). ZnF<sub>2</sub> and CdF<sub>2</sub>, like the alkaline earth fluorides, have high lattice energies and are only sparingly soluble in water, while HgF<sub>2</sub> is hydrolysed to HgO and HF. The anhydrous difluorides can be prepared by the action of HF (in the case of Zn) or F<sub>2</sub> (Cd and Hg) on the metal.

The other halides of Zn<sup>II</sup> and Cd<sup>II</sup> are in general hygroscopic and very soluble in water (~400 g per 100 cm<sup>3</sup> for ZnX<sub>2</sub> and ~100 g per 100 cm<sup>3</sup> for CdX<sub>2</sub>). This is at least partly because of the formation of complex ions in solution, and the anhydrous forms are best prepared by

solution, [HgS<sub>2</sub>]<sup>2-</sup>: the relevant equilibria are:

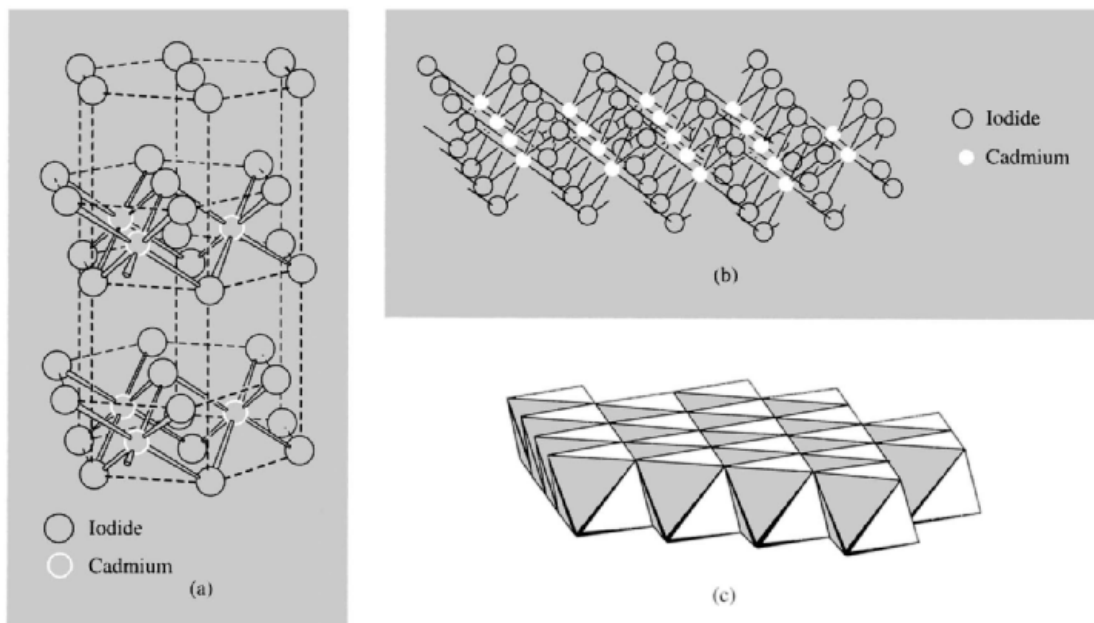


the dry methods of treating the heated metals with HCl, Br<sub>2</sub> or I<sub>2</sub> as appropriate. Aqueous preparative methods yield hydrates of which several are known. Significant covalent character is revealed by their comparatively low mps, their solubilities in ethanol, acetone and other organic solvents, and by their layer-lattice (2D) crystal structures. In all cases these may be regarded as close-packed lattices of halides ions in which the Zn<sup>II</sup> ions occupy tetrahedral, and the Cd<sup>II</sup> ions octahedral, sites. The structures of CdCl<sub>2</sub> (CdBr<sub>2</sub> is similar) and CdI<sub>2</sub> are of importance (Fig. 29.2) since they are typical of MX<sub>2</sub> compounds in which marked polarization effects are expected (see chap. 3, pp. 37–61 of ref. 9). Electron diffraction studies show that ZnX<sub>2</sub> (X = Cl, Br, I) have linear X–Zn–X structures in the gas phase.<sup>(12)</sup>

Concentrated, aqueous solutions of ZnCl<sub>2</sub> dissolve starch, cellulose (and therefore cannot be filtered through paper!), and silk. Commercially ZnCl<sub>2</sub> is one of the important compounds of zinc. It has applications in textile processing and, because when fused it readily dissolves other oxides, it is used in a number of metallurgical fluxes as well as in the manufacture of magnesia cements in dental fillings. Cadmium halides are used in the preparation of electroplating baths and in the production of pigments.

Covalency is still more pronounced in HgX<sub>2</sub> (X = Cl, Br, I) than in the corresponding

<sup>12</sup> M. HARGITTAL, J. TREMMEL and I. HARGITTAL, *Inorg. Chem.* **25**, 3163–6 (1986).



**Figure 29.2** The layer structure of crystalline CdI<sub>2</sub>: (a) Shows the hexagonal close-packing of I atoms with Cd atoms in alternate layers of octahedral sites sandwiched between layers of I atoms. In CdCl<sub>2</sub> the individual composite layers are identical with those in CdI<sub>2</sub>, but they are arranged so that the Cl atoms are ccp. (b) Shows a portion of an individual composite layer of CdI<sub>6</sub> (or CdCl<sub>6</sub>) octahedra. (c) Shows the same portion of a composite layer as in (b) and viewed from the same angle, but with CdI<sub>2</sub> (or CdCl<sub>2</sub>) units represented by solid, edge-sharing octahedra.

halides of Zn and Cd. These compounds are readily prepared from the elements and are low-melting volatile solids, soluble in many organic solvents. Their solubilities in water, where they exist almost entirely as HgX<sub>2</sub> molecules, decrease with increasing molecular weight, HgI<sub>2</sub> being only slightly soluble, and they may be precipitated anhydrous from aqueous solutions by metathetical reactions. Their crystalline structures reveal an interesting gradation. HgCl<sub>2</sub> is composed of linear Cl–Hg–Cl molecules (Hg–Cl = 225 pm and the next shortest Hg···Cl distance is 334 pm); HgBr<sub>2</sub> and HgI<sub>2</sub> have layer structures. However, in the bromide although the Hg<sup>II</sup> may be regarded as 6-coordinated, two Hg–Br distances are much shorter than the other four (248 pm compared to 323 pm). In the red variety of the iodide the Hg<sup>II</sup> is unambiguously tetrahedrally 4-coordinated (Hg–I = 278 pm). At temperatures above 126°C HgI<sub>2</sub> exists as a

less-dense, yellow form similar to HgBr<sub>2</sub>. In the gaseous phase all 3 of these Hg<sup>II</sup> halides exist as discrete linear HgX<sub>2</sub> molecules. Comparison of the Hg–X distances in these molecules (Hg–Cl = 228 pm, Hg–Br = 240 pm; Hg–I = 257 pm) with those given above, indicate an increasing departure from molecularity in passing from the solid chloride to the solid iodide.

HgCl<sub>2</sub> is the “corrosive sublimate” of antiquity, formerly obtained by sublimation from HgSO<sub>4</sub> and NaCl and used as an antiseptic. It is, however, a violent poison and was widely used as such in the Middle Ages.<sup>(5)</sup>

The halides are the most familiar compounds of mercury(I) and all contain the Hg<sub>2</sub><sup>2+</sup> ion (see below). Hg<sub>2</sub>F<sub>2</sub> is obtained by treating Hg<sub>2</sub>CO<sub>3</sub> (itself precipitated by NaHCO<sub>3</sub> from aqueous Hg<sub>2</sub>(NO<sub>3</sub>)<sub>2</sub> which in turn is obtained by the action of dil HNO<sub>3</sub> on an excess of metallic mercury) with aqueous HF. It dissolves in water

but is at once hydrolysed to the "black oxide" which is actually a mixture of Hg and HgO. On heating, it disproportionates to the metal and HgF<sub>2</sub>. The other halides are virtually insoluble in water and so, being free from the possibility of hydrolysis, may be precipitated from aqueous solutions of Hg<sub>2</sub>(NO<sub>3</sub>)<sub>2</sub> by addition of X<sup>-</sup>. Alternatively, they may be prepared by treatment of HgX<sub>2</sub> with the metal. Hg<sub>2</sub>Cl<sub>2</sub> and Hg<sub>2</sub>Br<sub>2</sub> are easily volatilized and their vapour densities correspond to "monomeric HgX". However, the diamagnetism of the vapour (Hg<sup>I</sup> in HgX would be paramagnetic) and the ultraviolet absorption at the wavelength (253.7 nm) characteristic of Hg vapour, make it clear that decomposition to Hg + HgX<sub>2</sub> is the real reason for the halved vapour density. Hg<sub>2</sub>I<sub>2</sub> decomposes similarly but even more readily, and the presence of finely divided metal is thought to be the cause of the greenish tints commonly found in samples of this otherwise yellow solid.

Calomel,<sup>†</sup> Hg<sub>2</sub>Cl<sub>2</sub>, has been widely used medicinally but possible contamination by the more soluble and poisonous HgCl<sub>2</sub> renders this a hazardous nostrum.

### 29.3.3 Mercury(I)

Raman spectra, indicative of [M–M]<sup>2+</sup> ions, are produced by the yellow glass obtained from the melt of Zn in ZnCl<sub>2</sub> and also by the colourless, very moisture sensitive crystals of Cd<sub>2</sub>Al<sub>2</sub>Cl<sub>8</sub> obtained from melts of Cd in CdCl<sub>2</sub> and AlCl<sub>3</sub>. X-ray studies show that the latter contains "ethane-like" [Cd<sub>2</sub>Cl<sub>6</sub>]<sup>4-</sup> groups with Cd–Cd reported as 257.6 pm<sup>(13)</sup> and 256.1 pm<sup>(14)</sup> (cf 302 pm in the metal itself). The <sup>113</sup>Cd nmr

spectrum<sup>(15)</sup> of [Cd{HB(3,5-Me<sub>2</sub>pz)<sub>3</sub>}]<sub>2</sub> (pz = polycyclic pyrazolyl ligand) yields a <sup>111</sup>Cd–<sup>113</sup>Cd coupling constant of 20 646 Hz, indicating a Cd–Cd bond; the first to be observed in a molecular complex of Cd. However, only for mercury is the formal oxidation state I of importance.

Mercury(I) compounds in general may be prepared, like the halides just discussed, by the reduction of the corresponding Hg<sup>II</sup> salt, often by the metal itself, or by precipitation from aqueous solutions of the nitrate. The nitrate is known as the dihydrate, Hg<sub>2</sub>(NO<sub>3</sub>)<sub>2</sub>·2H<sub>2</sub>O, and is stable in water if this is acidified, otherwise basic salts such as Hg(OH)(NO<sub>3</sub>) and Hg<sub>2</sub>(OH)(NO<sub>3</sub>) are precipitated. The perchlorate is the only other appreciably soluble salt, the rest being either insoluble or, like the sulfate, chlorate and salts of organic acids, only sparingly soluble. In all cases the dinuclear Hg<sub>2</sub><sup>2+</sup> ion is present rather than mononuclear Hg<sup>+</sup>. The evidence for this is overwhelming and includes the following:

- (1) In crystalline mercury(I) compounds, instead of the sequence of alternate M<sup>+</sup> and X<sup>-</sup> expected for MX compounds, Hg–Hg pairs are found in which the separation, though not constant, lies in the range 250–270 pm<sup>(5)</sup> which is shorter than the Hg–Hg separation of 300 pm found in the metal itself.
- (2) The Raman spectrum of aqueous mercury(I) nitrate has, in addition to lines characteristic of the NO<sub>3</sub><sup>-</sup> ion, a strong absorption at 171.7 cm<sup>-1</sup> which is not found in the spectra of other metal nitrates and is not active in the infrared; it is therefore diagnostic of the Hg–Hg stretching vibration since homonuclear diatomic vibrations are Raman active not infrared active.<sup>†</sup> Similar data have subsequently been produced for a number of other compounds in the solid state and in solution.

<sup>†</sup> Calomel, derived from the Greek words *καλός*-ς (beautiful) and *μέλας* (black), seems an odd name for a white solid. It might arise from the colour of the material obtained when Hg<sub>2</sub>Cl<sub>2</sub> is treated with ammonia; this is a product of variable composition (see below) which owes its colour to the presence of metallic mercury. Other more fanciful derivations are listed in the *Oxford English Dictionary* 2, 41 (1970).

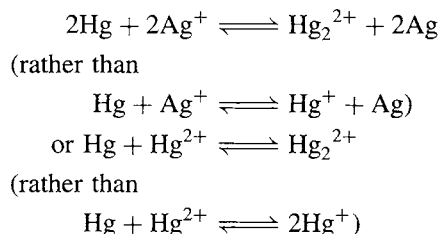
<sup>13</sup> R. FAGGIANI, R. J. GILLESPIE and J. E. VEKRIS, *J. Chem. Soc., Chem. Commun.*, 517–8 (1986).

<sup>14</sup> T. STAFFEL and G. MEYER, *Z. anorg. allg. Chem.* **548**, 45–54 (1987).

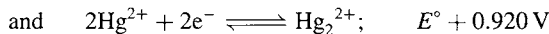
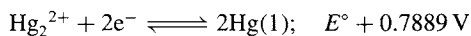
<sup>15</sup> D. L. REGER, S. S. MASON and A. L. RHEINGOLD, *J. Am. Chem. Soc.* **115**, 10406–7 (1993).

<sup>†</sup> Indeed, this is perhaps the earliest example of a new structural species to be established by Raman spectroscopy. (L. A. WOODWARD, *Phil. Mag.* **18**, 823–7 (1934).)

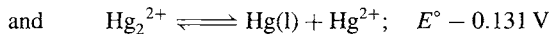
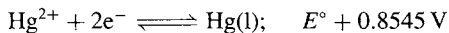
- (3) Mercury(I) compounds are diamagnetic, whereas the monatomic  $\text{Hg}^+$  ion would have a  $d^{10}s^1$  configuration and so be paramagnetic.
- (4) The measured emfs of concentration cells of mercury(I) salts are only explicable on the assumption that a 2-electron transfer is involved. This would not be the case if  $\text{Hg}^+$  were involved:  $[E = (2.303RT/nF) \log a_1/a_2]$  where  $n = 2$  for  $\text{Hg}_2^{2+}$  and  $n = 1$  for  $\text{Hg}^+$ .
- (5) It is found that "equilibrium constants" are in fact only constant if the concentration  $[\text{Hg}_2^{2+}]$  is employed rather than  $[\text{Hg}^+]^2$ , i.e. the equilibria must be of the type:



In order to understand the formation and stability of mercury(I) compounds it is helpful to consider the relevant reduction potentials:



From this it follows that



Now,  $E^\circ = (RT/nF) \ln K$ ,

$$\text{i.e. } E^\circ = (0.0591/n) \log_{10} K$$

$$\text{Hence, } \log_{10} K = -(0.131/0.0591) = -2.217,$$

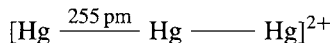
$$\text{i.e. } K = [\text{Hg}_2^{2+}]/[\text{Hg}_2^{2+}] = 0.0061$$

Thus, at equilibrium, aqueous solutions of mercury(I) salts will contain around 0.6% of mercury(II) and the rather finely balanced equilibrium is easily displaced. The presence of any reagent which reduces the activity (in effect the concentration) of  $\text{Hg}_2^{2+}$  more than that of  $\text{Hg}_2^{2+}$ , either by forming a less-soluble

salt or a more-stable complex of  $\text{Hg}_2^{2+}$  will displace the equilibrium to the right and cause the disproportionation of the  $\text{Hg}_2^{2+}$ . There are many such reagents, including  $\text{S}^{2-}$ ,  $\text{OH}^-$ ,  $\text{CN}^-$ ,  $\text{NH}_3$  and acetylacetonone. This is why the most stable  $\text{Hg}_2^{2+}$  salts are the insoluble ones and why there are few stable complexes. Those which are known all involve either *O*- or *N*-donor ligands,<sup>†</sup> the linear  $\text{O}-\text{Hg}-\text{Hg}-\text{O}$  group being a common feature of the former.

### Polycations of mercury

The  $\text{Hg}-\text{Hg}$  bond in  $\text{Hg}_2^{2+}$  may be ascribed to overlap of the 6s orbitals with little involvement of 6p orbitals or of the filled  $d^{10}$  shell of each atom. If this is regarded as the coordination of  $\text{Hg}$  to an  $\text{Hg}_2^{2+}$  cation, the coordination of a second  $\text{Hg}$  ligand is also feasible. Accordingly,  $\text{Hg}_3(\text{AlCl}_4)_2$  can be obtained from a molten mixture of  $\text{HgCl}_2$ ,  $\text{Hg}$  and  $\text{AlCl}_3$  and contains the discrete, virtually linear cation



in which the formal oxidation state of  $\text{Hg}$  is  $+\frac{2}{3}$ .

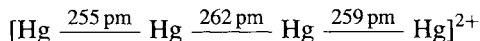
Still more interesting is the oxidation of  $\text{Hg}$  by  $\text{AsF}_5$  in liquid  $\text{SO}_2$ :<sup>(16,17)</sup> in this process the  $\text{AsF}_5$  serves both as an oxidant (being reduced to  $\text{AsF}_3$ ) and also as a fluoride-ion acceptor to give  $\text{AsF}_6^-$ . In a matter of minutes the colour of the solution becomes bright yellow then deepens to red as the  $\text{Hg}$  simultaneously turns to a shiny golden-yellow solid; the solid then begins to dissolve to give an orange and, finally, a colourless solution. By controlling the quantity of oxidant,  $\text{AsF}_5$ , and removing the solution at the appropriate stages, it is possible to crystallize a series of extremely moisture-sensitive materials:

<sup>†</sup> For this reason, although  $\text{Hg}_2^{2+}$  must be regarded as a class-b cation (e.g. the aqueous solubilities of its halides decrease in the order  $\text{F}^-$  to  $\text{I}^-$ ), it is evidently less so than  $\text{Hg}_2^{2+}$  which has a notable preference for *S* donors.

<sup>16</sup> I. D. BROWN, W. R. DATARS and R. J. GILLESPIE, pp. 1-41 in *Extended Linear Chain Compounds*, Plenum Press, New York, Vol. III (1982).

<sup>17</sup> R. J. GILLESPIE, P. GRANGER, K. R. MORGAN and G. J. SCHROBILGEN, *Inorg. Chem.* **23**, 887-91 (1984).

- (a) deep red-black  $\text{Hg}_4(\text{AsF}_6)_2$ , the cation of which is the almost linear



with Hg in the formal average oxidation state  $+\frac{1}{2}$ ;

- (b) orange  $\text{Hg}_3(\text{AsF}_6)_2$ , containing the trimeric cation mentioned above; and  
 (c) colourless  $\text{Hg}_2(\text{AsF}_6)_2$ , containing the dimeric  $\text{Hg}^{\text{I}}$  cation.

By working at lower temperatures ( $-20^\circ\text{C}$ ) to reduce the reaction rate, or by using specially designed apparatus which limits the access of  $\text{AsF}_5$  to the Hg, it has been possible to isolate large single crystals of the intermediate golden-yellow solid having dimensions up to  $35 \times 35 \times 2 \text{ mm}^3$ . X-ray analysis, supported by neutron diffraction, shows that it consists of a tetragonal lattice ( $a = b \neq c$ ) of octahedral  $\text{AsF}_6^-$  anions with two non-intersecting and mutually perpendicular chains of Hg atoms running through it in the  $a$  and  $b$  directions. Chemical analysis suggests the composition  $\text{Hg}_3(\text{AsF}_6)$  and a formal oxidation state of  $\text{Hg} = +\frac{1}{3}$ . However, the measured Hg–Hg separation of 264 pm along the chains is not commensurate with the parallel dimensions of the lattice unit cell,  $a = b = 754 \text{ pm}$  (cf.  $3 \times 264 \text{ pm} = 792 \text{ pm}$ ) and implies instead the nonstoichiometric composition  $\text{Hg}_{2.82}(\text{AsF}_6)$  or more generally  $\text{Hg}_{3-\delta}(\text{AsF}_6)$  since the composition apparently varies with temperature. Partially filled conduction bands formed by overlap of Hg orbitals produce a conductivity in the  $a$ – $b$  plane which approaches that of liquid mercury and the material becomes superconducting at 4 K.

Use of  $\text{SbF}_5$  instead of  $\text{AsF}_5$  produces a series of entirely analogous compounds including  $\text{Hg}_{3-\delta}(\text{SbF}_6)$  but because the unit cell of the  $(\text{SbF}_6)^-$  lattice is somewhat larger than that of  $(\text{AsF}_6)^-$ , it is formulated as  $\text{Hg}_{2.90}(\text{SbF}_6)$ . Oxidations of Hg by  $\text{Hg}(\text{MF}_6)_2$  ( $M = \text{Nb}, \text{Ta}$ ) in  $\text{SO}_2$  also yield  $\text{Hg}_{3-\delta}(\text{MF}_6)$  but, unlike the As and Sb compounds, these convert in a few hours into silver platelets of  $\text{Hg}_3\text{MF}_6$  which consist of two

sheets of F atoms separated by hexagonal sheets (rather than linear chains) of Hg atoms.<sup>(18)</sup>

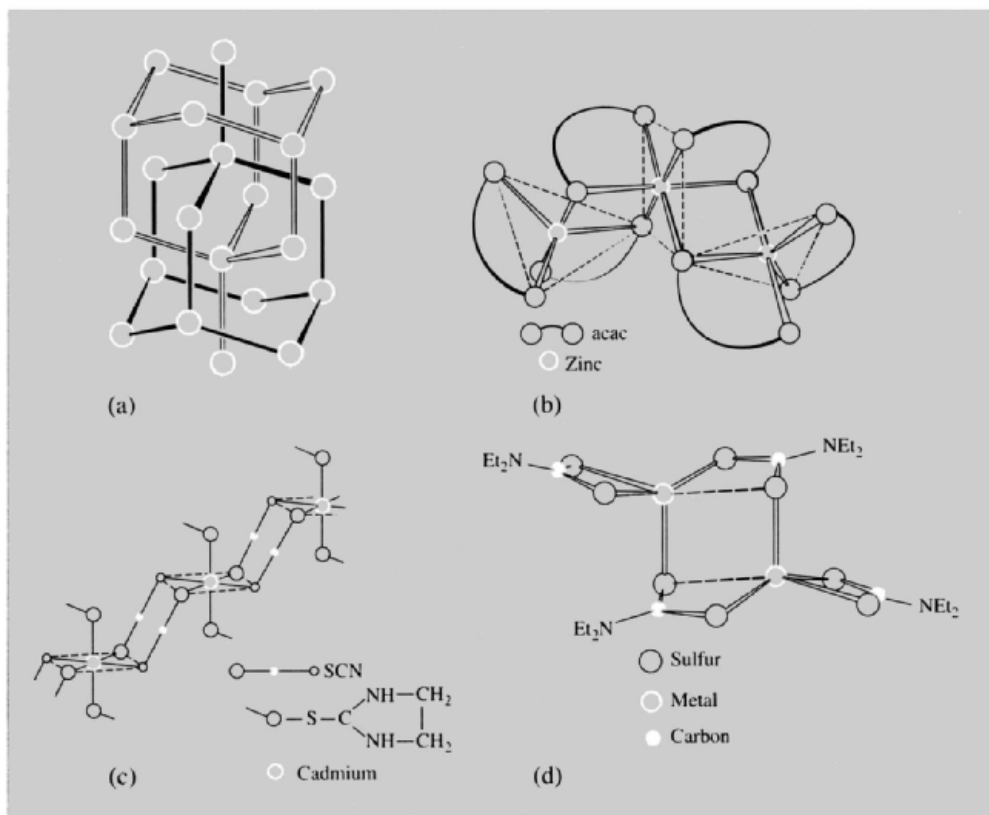
### 29.3.4 Zinc(II) and cadmium(II)<sup>(19)</sup>

The almost invariable oxidation state of these elements is +2 and, in addition to the oxides, chalcogenides and halides already discussed, salts of most anions are known. Oxo-salts are often isomorphous with those of  $\text{Mg}^{\text{II}}$  but with lower thermal stabilities. The carbonates, nitrates, and sulfates all decompose to the oxides on heating. Several, such as the nitrates, perchlorates and sulfates, are very soluble in water and form more than one hydrate.  $[\text{Zn}(\text{H}_2\text{O})_6]^{2+}$  is probably the predominant aquo species in solutions of  $\text{Zn}^{\text{II}}$  salts. Aqueous solutions are appreciably hydrolysed to species such as  $[\text{M}(\text{OH})(\text{H}_2\text{O})_x]^+$  and  $[\text{M}_2(\text{OH})(\text{H}_2\text{O})_x]^{3+}$  and a number of basic (i.e. hydroxo) salts such as  $\text{ZnCO}_3 \cdot 2\text{Zn}(\text{OH})_2 \cdot \text{H}_2\text{O}$  and  $\text{CdCl}_2 \cdot 4\text{Cd}(\text{OH})_2$  can be precipitated. Distillation of zinc acetate under reduced pressure yields a crystalline basic acetate,  $[\text{Zn}_4\text{O}(\text{OCOMe})_6]$ . The molecular structure of this consists of an oxygen atom surrounded by a tetrahedron of Zn atoms bridged across each edge by acetates. It is isomorphous with the basic acetate of beryllium (p. 122) but, in contrast, the  $\text{Zn}^{\text{II}}$  compound hydrolyses rapidly in water, no doubt because of the ability of  $\text{Zn}^{\text{II}}$  to increase its coordination number above 4.

The coordination chemistry of  $\text{Zn}^{\text{II}}$  and  $\text{Cd}^{\text{II}}$ , although much less extensive than for preceding transition metals, is still appreciable. Neither element forms stable fluoro complexes but, with the other halides, they form the complex anions  $[\text{MX}_3]^-$  and  $[\text{MX}_4]^{2-}$ , those of  $\text{Cd}^{\text{II}}$  being moderately stable in aqueous solution.<sup>(4)</sup> By using the large cation  $[\text{Co}(\text{NH}_3)_6]^{3+}$  it is also possible to isolate the trigonal bipyramidal  $[\text{CdCl}_5]^{2-}$

<sup>18</sup> I. D. BROWN, R. J. GILLESPIE, K. R. MORGAN, Z. TUN and P. K. UMMAT, *Inorg. Chem.* **23**, 4506–8 (1984).

<sup>19</sup> R. H. PRINCE, Zinc and Cadmium Chap. 56.1, pp. 925–1045, in *Comprehensive Coordination Chemistry*, Vol. 5, Pergamon Press, Oxford, 1987.



**Figure 29.3** Some polymeric complexes: (a) Interpenetrating “adamantine” frameworks in  $M(\text{CN})_2$ ,  $M = \text{Zn}, \text{Cd}$ . (Only  $M$  shown; straight lines are  $\text{CN}$  forming linear  $\text{MCNM}$  “rods”.) (b)  $[\text{Zn}(\text{acac})_2]_3$ , (c)  $[\text{Cd}\{\text{S}=\text{C}(\text{NHCH}_2)_2\}_2(\text{SCN})_2]$ , and (d)  $[\text{M}(\text{S}_2\text{CNEt}_2)_2]_2$ ,  $M = \text{Zn}, \text{Cd}, \text{Hg}$ . (Note that  $M$  is 5-coordinate but with one  $M\text{-S}$  distance appreciably greater than the other four.)

$[\text{MX}_3]^-$  and  $[\text{MX}_4]^{2-}$  are formed in  $\text{CH}_3\text{CN}$  solutions also.<sup>(20)</sup> Tetrahedral complexes are the most common type and are formed with a variety of  $O$ -donor ligands (more readily with  $\text{Zn}^{\text{II}}$  than  $\text{Cd}^{\text{II}}$ ), more stable ones with  $N$ -donor ligands such as  $\text{NH}_3$  and amines. Some of the apparently 3-coordinate complexes have a higher coordination number because of aquation or association but, no doubt because the ligand is bulky, 2-coordinated  $\text{Zn}$  occurs in  $[\text{Zn}\{\text{N}(\text{CMe}_3)(\text{SiMe}_3)\}_2]$ , the first homoleptic zinc amide to be structurally characterized.<sup>(21)</sup>

The ability of  $\text{CN}^-$  to co-ordinate through either  $\text{C}$  or  $\text{N}$  has interesting stereochemical consequences. Crystalline  $\text{M}(\text{CN})_2$  consist of linear  $\text{M}-\text{C}-\text{N}-\text{M}$  “rods” and tetrahedrally coordinated  $\text{M}^{\text{II}}$ , arranged so as to form interpenetrating “adamantine” frameworks (Fig. 29.3a). Each “rod” projects through a cyclohexane-like “window” of the other framework with the  $\text{M}$  atoms at each end occupying cavities of the other framework.<sup>(22)</sup> When aqueous solutions of  $\text{CdCl}_2 + \text{K}[\text{Cd}(\text{CN})_4]$  are left in contact with liquids such as  $\text{CCl}_4, \text{CMeCl}_3, \dots, \text{CMe}_4$ , crystals of the clathrates  $\text{Cd}(\text{CN})_2 \cdot \text{G}$  form at the interface

<sup>20</sup> D. P. GRADDON and C. S. KHOO, *Polyhedron* **7**, 2129–33 (1988).

<sup>21</sup> W. S. REES JR., D. M. GREEN and W. HESSE, *Polyhedron*, **11**, 1697–9 (1992).

<sup>22</sup> B. F. HOSKINS and R. ROBSON, *J. Am. Chem. Soc.* **112**, 1546–54 (1990).

of the immiscible liquids.<sup>(23)</sup> In these, the guest molecules G, occupy the cavities of a single adamantane framework.  $(\text{NMe}_4)[\text{Cu}^{\text{I}}\text{Zn}(\text{CN})_4]$  consists of a similar framework but this time half the cavities are occupied by  $\text{NMe}_4^+$  cations. Another type of framework is found in  $\text{Cd}(\text{CN})_2 \cdot \frac{2}{3}\text{H}_2\text{O} \cdot \text{Bu}'\text{OH}$  which crystallizes from 50% aqueous  $\text{Bu}'\text{OH}$  solutions of  $\text{Cd}(\text{CN})_2$ . It contains  $\text{CdCNCd}$  "rods" but this time they are bent,  $\frac{2}{3}$  of the Cd atoms are tetrahedrally co-ordinated by  $4\text{CN}^-$ , the other  $\frac{1}{3}$  being octahedrally co-ordinated by  $4\text{CN}^-$  and  $2\text{H}_2\text{O}$ . The result is a honeycomb framework with linear channels of hexagonal cross-section containing disordered  $\text{Bu}'\text{OH}$  molecules.<sup>(24)</sup> Linear channels are also found in  $\text{Cd}(\text{CN})_2 \cdot \text{G}$  ( $\text{G} = \text{dmf}, \text{dmsO}$ )<sup>(25)</sup> but the large cation in  $(\text{PPh}_4)_3[(\text{CN})_3\text{CdCNCd}(\text{CN})_3]$  apparently prevents the formation of a 3D framework and instead stabilizes the discrete anion.<sup>(26)</sup>

Complexes of higher coordination number are often in equilibrium with the tetrahedral form and may be isolated by increasing the ligand concentration or by adding large counter ions, e.g.  $[\text{M}(\text{NH}_3)_6]^{2+}$ ,  $[\text{M}(\text{en})_3]^{2+}$  or  $[\text{M}(\text{bipy})_3]^{2+}$ . With acetylacetonone, zinc achieves both 5- and 6-coordination by trimerizing to  $[\text{Zn}(\text{acac})_2]_3$  (Fig. 29.3b). Five-coordination is also found in adducts such as the distorted trigonal bipyramidal  $[\text{Zn}(\text{acac})_2(\text{H}_2\text{O})]$  and  $[\text{Zn}(\text{glycinate})_2(\text{H}_2\text{O})]$  while the hydrazinium sulfate  $(\text{N}_2\text{H}_5)_2\text{Zn}(\text{SO}_4)_2$  contains 6-coordinated zinc. This is isomorphous with the  $\text{Cr}^{\text{II}}$  compound (p. 1031) and in the crystalline form consists of chains of  $\text{Zn}^{\text{II}}$  bridged by  $\text{SO}_4^{2-}$  ions, with each  $\text{Zn}^{\text{II}}$  additionally coordinated to two *trans*- $\text{N}_2\text{H}_5^+$  ions. The zinc porphyrin complex,  $[\text{Zn}(\text{porph})(\text{thf})]$ , (porph = *meso*-tetraphenyltetrabenzoporphyrin)

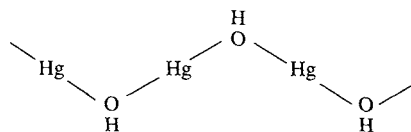
is approximately square pyramidal with thf at its apex. Being somewhat flexible the porphyrin is distorted into a saddle shape, 2 N being displaced above its mean plane and 2 N below it.<sup>(27)</sup>

Complexes with  $\text{SCN}^-$  throw light on the relative affinities of the two metals for *N*- and *S*-donors. In  $[\text{Zn}(\text{NCS})_4]^{2-}$  the ligand is *N*-bonded whereas in  $[\text{Cd}(\text{SCN})_4]^{2-}$  it is *S*-bonded.  $\text{SCN}^-$  can also act as a bridging group, as in  $[\text{Cd}\{\text{S}=\text{C}(\text{NHCH}_2)_2\}_2(\text{SCN})_2]$  when linear chains of octahedrally coordinated  $\text{Cd}^{\text{II}}$  are formed (Fig. 29.3c). A number of zinc-sulfur compounds are used as accelerators in the vulcanization of rubber. Among these are the dithiocarbamates, of which  $[\text{Zn}(\text{S}_2\text{CNET}_2)_2]_2$ , and the isostructural  $\text{Cd}^{\text{II}}$  and  $\text{Hg}^{\text{II}}$  compounds achieve 5-coordination by dimerizing (Fig. 29.3d).

Coordination numbers higher than 6 are rare and in some cases are known to involve chelating  $\text{NO}_3^-$  ions which not only have a small "bite" but, may also be coordinated asymmetrically so that the coordination number is not well defined.

### 29.3.5 Mercury(II)<sup>(28)</sup>

The oxide (p. 1209), chalcogenides (p. 1210) and halides (p. 1211) have already been described. Of them, the only ionic compound is  $\text{HgF}_2$  but other compounds in which there is appreciable charge separation are the hydrated salts of strong oxoacids, e.g. the nitrate, perchlorate, and sulfate. In aqueous solution such salts are extensively hydrolysed ( $\text{HgO}$  is only very weakly basic) and they require acidification to prevent the formation of polynuclear hydroxo-bridged species or the precipitation of basic salts such as  $\text{Hg}(\text{OH})(\text{NO}_3)$  which contains infinite zigzag chains:



<sup>23</sup> T. KITAZAWA, S. NISHIKIORI, A. YAMAGISHI, R. KURODA and T. IWAMOTO, *J. Chem. Soc., Chem. Commun.*, 413-5 (1992); T. KITAZAWA, T. KIKOYAMA, M. TAKEDA and T. IWAMOTO, *J. Chem. Soc., Dalton Trans.*, 3715-20 (1995).

<sup>24</sup> B. F. ABRAHAMS, B. F. HOSKINS and R. ROBSON, *J. Chem. Soc., Chem. Commun.*, 60-1 (1990).

<sup>25</sup> J. KIM, D. WHANG, Y.-S. KOH and K. KIM, *J. Chem. Soc., Chem. Commun.*, 637-8 (1994).

<sup>26</sup> T. KITAZAWA and M. TAKEDA, *J. Chem. Soc., Chem. Commun.*, 309-10 (1993).

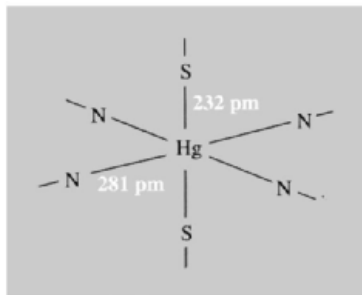
<sup>27</sup> R.-J. CHENG, Y.-R. CHEN, S. L. WANG and C. Y. CHENG, *Polyhedron*, **12**, 1353-60 (1993).

<sup>28</sup> K. BRODERSEN and H.-U. HUMMEL, *Mercury*, Chap. 56.2, pp. 1047-1130, in *Comprehensive Coordination Chemistry*, Vol. 5, Pergamon Press, Oxford, 1987.



Their ionic character is symptomatic of the marked reluctance of  $\text{Hg}^{\text{II}}$  to form covalent bonds to oxygen. In the presence of excess  $\text{NO}_3^-$  ions the aqueous nitrate forms the complex anion  $[\text{Hg}(\text{NO}_3)_4]^{2-}$  in which 8 oxygen atoms from the bidentate nitrate groups are equidistant from the mercury at 240 pm, which is almost precisely the sum of the ionic radii (140 + 102 pm). Also, the unusual regular octahedral coordination is found in complexes with *O*-donor ligands:  $[\text{Hg}(\text{C}_5\text{H}_5\text{NO})_6]^{2+}$  ( $\text{Hg}-\text{O} = 235$  pm),  $[\text{Hg}(\text{H}_2\text{O})_6]^{2+}$  ( $\text{Hg}-\text{O} = 234$  pm), and  $[\text{Hg}(\text{Me}_2\text{SO})_6]^{2+}$  ( $\text{Hg}-\text{O} = 234$  pm). In contrast, the more covalently bonding  $\beta$ -diketonates do not form complexes.

The most usual type of coordination in compounds of  $\text{Hg}^{\text{II}}$  with other donor atoms is a distorted octahedron with 2 bonds much shorter than the other 4. In the extreme, this results in linear 2-coordination in which case the bonds are largely covalent.  $\text{Hg}(\text{CN})_2$  is actually composed of discrete linear molecules (*C*-bonded  $\text{CN}^-$ ), whereas crystalline<sup>†</sup>  $\text{Hg}(\text{SCN})_2$  is built up of distorted octahedral units, all SCN groups being bridging:



With both these pseudo halides, an excess produces complex anions  $[\text{HgX}_3]^-$  and the tetrahedral  $[\text{HgX}_4]^{2-}$ .

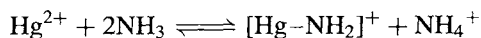
Similar halogeno complexes are produced in solution, and several salts of  $[\text{HgX}_3]^-$  have been isolated and characterized; they display a variety of stereochemistries. In  $[\text{HgCl}_3]^-$  the environment of the  $\text{Hg}^{\text{II}}$  is either distorted octahedral (with small cations such as  $\text{NH}_4^+$

or  $\text{Na}^+$ ) or distorted trigonal bipyramidal (with larger cations such as  $[\text{NEt}_4]^+$ ,  $[\text{SMe}_3]^+$  or  $[\text{NH}_2\{(\text{CH}_2)_2\text{NH}_3\}_2]^{3+}$ <sup>(29)</sup>), whereas in salts of  $[\text{HgBr}_3]^-$  and  $[\text{HgI}_3]^-$  the coordination is more commonly distorted tetrahedral. In  $[\text{NBu}_4][\text{HgI}_3]$  the anion is planar but, with one I-Hg-I angle  $115^\circ$ , its symmetry is  $C_{2v}$  rather than  $D_{3h}$ . In aqueous solution spectroscopic evidence suggests that  $[\text{HgCl}_3]^-$  is planar with  $2\text{H}_2\text{O}$  completing a trigonal bipyramidal coordination sphere;  $[\text{HgI}_3]^-$  is pyramidal with  $\text{H}_2\text{O}$  completing a tetrahedral coordination sphere, while  $[\text{HgBr}_3]^-$  shows features of both structures.<sup>(30)</sup>

In the presence of excess halide,  $[\text{HgX}_4]^{2-}$  complex ions are produced and in comparison with those of  $\text{Zn}^{\text{II}}$  and  $\text{Cd}^{\text{II}}$  it can be seen that their stabilities increase with the sizes of the anion and the cation so that  $[\text{HgI}_3]^{2-}$  is the most stable of all. Thus, the normally very insoluble  $\text{HgI}_2$  will dissolve in aqueous solutions of  $\text{I}^-$  which can then be made strongly alkaline without precipitation occurring. Such solutions are known as Nessler's reagent, which is used as a sensitive test for ammonia since this produces a yellow or brown coloration due to the formation of  $\text{Hg}_2\text{NI}\cdot\text{H}_2\text{O}$ , the iodo salt of Millon's base (see p. 1220). Adducts of the halides  $\text{HgX}_2$ , with *N*-, *S*-, and *P*-donor ligands are known, those with *N*-donors being especially numerous. Their stereochemistries are largely of the expected tetrahedral, or grossly distorted octahedral, types.

### $\text{Hg}^{\text{II}}$ -N compounds<sup>(5,28)</sup>

Mercury has a characteristic ability to form not only conventional ammine and amine complexes but also, by the displacement of hydrogen, direct covalent bonds to nitrogen, e.g.:



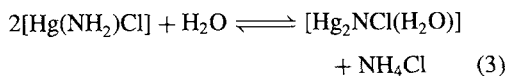
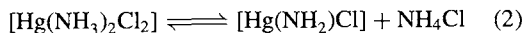
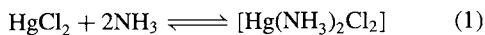
<sup>29</sup> The compound  $[\text{NH}_2\{(\text{CH}_2)_2\text{NH}_3\}_2]_2\text{HgCl}_8$  contains the trigonal bipyramidal anion  $[\text{HgCl}_5]^{3-}$ ; see L. P. BAITAGLIA, A. B. CORRADI, L. ANTOLINI, T. MANFREDINI, L. MENABUE, G. C. PELLACANI and G. PONTICELLI, *J. Chem. Soc., Dalton Trans.*, 2529-33 (1986).

<sup>30</sup> T. R. GRIFFITHS and R. A. ANDERSON, *J. Chem. Soc., Faraday*, **86**, 1425-35 (1990).

<sup>†</sup> Pellets of the dry powder, when ignited in air, form snake-like tubes of spongy ash of unknown composition — the so-called "Pharaoh's serpents".

Thus in the presence of an excess of  $\text{NH}_4^+$ , which suppresses this forward reaction, and counteranions such as  $\text{NO}_3^-$  and  $\text{ClO}_4^-$ , which have little tendency to coordinate, complexes such as  $[\text{Hg}(\text{NH}_3)_4]^{2+}$ ,  $[\text{Hg}(\text{L-L})_2]^{2+}$  and even  $[\text{Hg}(\text{L-L})_3]^{2+}$  (L-L = en, bipy, phen) can be prepared. But, in the absence of such precautions, amino, or imino-compounds are likely to be formed, often together. Because of this variety of simultaneous reactions and their dependence on the precise conditions, many reactions between  $\text{Hg}^{\text{II}}$  and amines, although first performed by alchemists in the Middle Ages, remained obscure until the application of X-ray crystallography and, still more recently, spectroscopic techniques such as nmr, infrared and Raman.

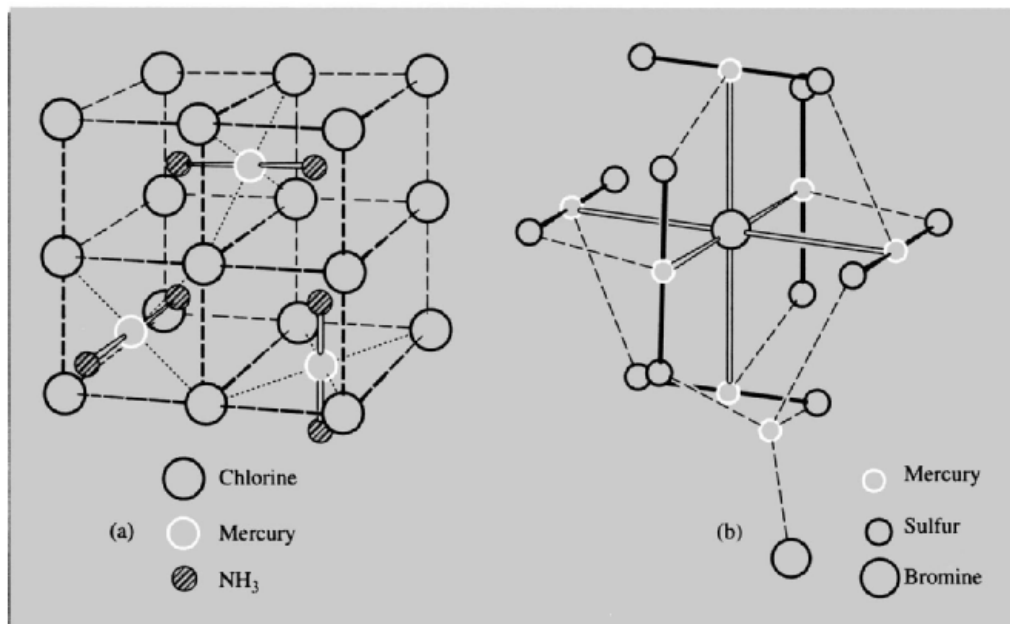
The action of aqueous ammonia on  $\text{HgCl}_2$ , for instance, may be described by the three reactions:



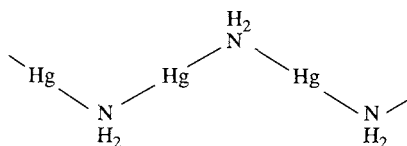
In general, all these products are obtained in proportions which depend on the concentrations of  $\text{NH}_3$  and  $\text{NH}_4^+$  and on the temperature, but more or less pure products can be prepared by suitably adjusting the conditions.

The diammine  $[\text{Hg}(\text{NH}_3)_2\text{Cl}_2]$ , descriptively known as “fusible white precipitate”, can be isolated by maintaining a high concentration of  $\text{NH}_4^+$ , since reactions (2) and (3) are thereby inhibited, or better still by using non-polar solvents. It is made up of a cubic lattice of  $\text{Cl}^-$  ions with linear  $\text{H}_3\text{N}-\text{Hg}-\text{NH}_3$  groups inserted so as to give the common, distorted octahedron coordination about  $\text{Hg}^{\text{II}}$  ( $\text{Hg}-\text{N} = 203$  pm,  $\text{Hg}-\text{Cl} = 287$  pm) (Fig. 29.4a).

By using a low concentration of  $\text{NH}_3$  and with no  $\text{NH}_4^+$  initially present, the amide  $[\text{Hg}(\text{NH}_2)\text{Cl}]$ , “infusible white precipitate” is



**Figure 29.4** (a) Crystal structure of  $\text{Hg}(\text{NH}_3)_2\text{Cl}_2$  showing linear  $\text{NH}_3-\text{Hg}-\text{NH}_3$  groups inside a lattice of chloride ions. (b) Central  $\text{Hg}_7\text{S}_{12}\text{Br}_2$  core of  $[\text{Hg}_7(\text{SC}_6\text{H}_{11})_{12}\text{Br}_2]$  showing, in an idealized manner, the octahedron of Hg atoms around a central Br. The tetrahedral coordination of the seventh Hg is completed with the second Br.



obtained. This consists of parallel chains of  $\{\text{Hg}(\text{NH}_2)\}_\infty$  as above, separated by  $\text{Cl}^-$  ions.

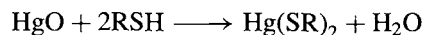
$[\text{Hg}_2\text{NCl}(\text{H}_2\text{O})]$  is the chloride of Millon's base,  $[\text{Hg}_2\text{N}(\text{OH})\cdot(\text{H}_2\text{O})_2]$ , and can be obtained either by heating the diammine, or amide with water or, better still, by the action of hydrochloric acid on Millon's base which is best prepared by the method, used in 1845 by its discoverer, of warming yellow  $\text{HgO}$  with aqueous  $\text{NH}_3$ . Replacement of the  $\text{OH}^-$  yields a series of salts,  $[\text{Hg}_2\text{NX}(\text{H}_2\text{O})]$ , the structures of which (and that of the base itself) consist, with only minor variations, of a network of  $\{\text{Hg}_2\text{N}\}^+$  units linked so that each N is tetrahedrally linked to 4 Hg and each Hg is linearly linked to 2 N ( $\text{Hg}-\text{N} = 204\text{--}209$  pm depending on X).<sup>(31)</sup> The  $\text{X}^-$  ions and water molecules are accommodated interstitially and these materials behave as anion exchangers.

When  $\text{Hg}_2\text{Cl}_2$  is treated with aqueous  $\text{NH}_3$  disproportionation occurs ( $\text{Hg}_2\text{Cl}_2 \longrightarrow \text{HgCl}_2 + \text{Hg}$ ); the  $\text{HgCl}_2$  then reacts as outlined above to give a precipitate of variable composition. The liberated mercury, however, renders the precipitate black, as previously mentioned, and so forms the basis of a distinctive qualitative test for  $\text{Hg}_2^{2+}$ .

### $\text{Hg}^{\text{II}}-\text{S}$ compounds<sup>(32)</sup>

As indicated by the insolubility and inertness of  $\text{HgS}$ ,  $\text{Hg}^{\text{II}}$  has a great affinity for sulfur.  $\text{HgO}$  reacts vigorously with mercaptans (which is why

RSH were given the name mercaptans<sup>†</sup>), displacing the H as with amines:



These mercaptides are low-melting solids, soluble in  $\text{CHCl}_3$  and  $\text{C}_6\text{H}_6$ . Though their structures depend on R and some, such as  $\text{Hg}(\text{SR})_2$ , ( $\text{R} = \text{Bu}^t, \text{Ph}$ ) are polymers containing tetrahedral  $\text{HgS}_4$  units, most contain linear (or nearly linear)  $\text{S}-\text{Hg}-\text{S}$ . Even in  $[\text{Hg}(\text{SC}_6\text{H}_2\text{Bu}_3)_2(\text{py})]$  where the Hg is 3-coordinate and T-shaped the  $\text{S}-\text{Hg}-\text{S}$  is still nearly linear ( $172^\circ$ ).<sup>(33)</sup> Most of the thioether ( $\text{SR}_2$ ) complexes which have been prepared are adducts of the  $\text{Hg}^{\text{II}}$  halides and include both monomeric and polymeric (i.e. X-bridged) species as is the case with mixed thiolate-halide complexes. In  $[\text{Hg}_7(\text{SC}_6\text{H}_{11})_{12}\text{Br}_2]$ , which is obtained as colourless crystals when methanolic solutions of  $\text{HgBr}_2$  and sodium cyclohexanethiolate are mixed, six Hg atoms are 4-coordinate but contain almost linear  $\text{S}-\text{Hg}-\text{S}$  (av. angle =  $159.3^\circ$ ) and the seventh Hg is tetrahedrally coordinated. The six Hg atoms form a distorted octahedron around a central Br (Fig. 29.4b).<sup>(34)</sup> The dithiocarbamate  $[\text{Hg}(\text{S}_2\text{CNET}_2)_2]$  exists in two forms, one of which has the same structure as the corresponding  $\text{Zn}^{\text{II}}$  and  $\text{Cd}^{\text{II}}$  compounds (Fig. 29.3d), while the other is polymeric.

### Cluster compounds involving mercury<sup>(35,36)</sup>

Mercury has a marked ability to bond to other metals. In addition to the amalgams already mentioned (p. 1206) it acts as a versatile structural building block by forming  $\text{Hg}-\text{M}$  bonds with cluster fragments of various types: e.g. reduction

<sup>†</sup> Mercaptans were discovered in 1834 by W. C. Zeise (pp. 930, 1167) who named them from the Latin *mercurium captans*, catching mercury.

<sup>33</sup> M. BOCHMANN, K. J. WEBB and A. K. POWELL, *Polyhedron* **11**, 513-6 (1992).

<sup>34</sup> T. ALSINA, W. CLEGG, K. A. FRASER and J. SOLA, *J. Chem. Soc., Chem. Commun.*, 1010-1 (1992).

<sup>35</sup> L. H. GADE, *Angew. Chem. Int. Edn. Engl.* **32**, 23-40 (1993).

<sup>36</sup> R. B. KING, *Polyhedron*, **7**, 1813-7 (1988).

<sup>31</sup> A. F. WELLS, *Structural Inorganic Chemistry*, 5th edn., Oxford University Press, Oxford, 1984: the structural chemistry of mercury is reviewed on pp. 1156-69.

<sup>32</sup> J. G. WRIGHT, M. J. NATAN, F. M. MACDONNELL, D. M. RALSTON and T. V. O'HALLORAN, *Prog. Inorg. Chem.* **38**, 323-412 (1990).

Table 29.4 Comparison of some typical organometallic compounds MR<sub>2</sub>

R	Zn		Cd		Hg	
	MP/°C	BP/°C	MP/°C	BP/°C	MP/°C	BP/°C
Me	-29.2	46	-4.5	105.5	—	92.5
Et	-28	117	-21	64 (19 mmHg)	—	159
Ph	107	d 280	173	—	121.8 (subl)	204 (10 mmHg)

of [RhCl(PMe<sub>3</sub>)<sub>3</sub>] with Na amalgams gives Hg<sub>6</sub>[Rh(PMe<sub>3</sub>)<sub>3</sub>]<sub>4</sub> which consists of an Hg<sub>6</sub> octahedron, four faces of which are capped by Rh(PMe<sub>3</sub>)<sub>3</sub> groups. Again, Hg<sup>II</sup> halides react with carbonylate anions yielding products such as [Os<sub>3</sub>(CO)<sub>11</sub>Hg]<sub>3</sub> comprising a most unusual "raft" structure in which three Os<sub>3</sub> triangles surround a central Hg<sub>3</sub> triangle in a planar array. From [Os<sub>10</sub>C(CO)<sub>24</sub>]<sup>2-</sup> it is possible to obtain [Os<sub>20</sub>Hg(C)<sub>2</sub>(CO)<sub>48</sub>]<sup>2-</sup> the central portion of which is an HgOs<sub>2</sub> triangle. Whereas the "raft" cluster has no redox chemistry, the {Os<sub>20</sub>Hg} cluster like the Os<sub>10</sub> cluster (p. 1108) from which it is formed, gives rise to five different redox states.

### 29.3.6 Organometallic compounds<sup>(37)</sup>

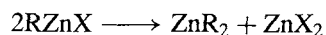
Although they were not the first organometallic compounds to be prepared (Zeise's salt was discovered in 1827) the discovery of zinc alkyls in 1849 by Sir Edward Frankland may be taken as the beginning of organometallic chemistry. Frankland's studies led to their employment as intermediates in organic synthesis, while the measurements of vapour densities led to his suggestion, crucial to the development of valency theory, that each element has a limited but definite combining capacity. After their discovery in 1900 Grignard reagents largely superseded the zinc alkyls in organic synthesis, but by then many of the reactions for which they are now used had already been worked out on the zinc compounds.

Alkyls of the types RZnX and ZnR<sub>2</sub> are both known and may be prepared by essentially the

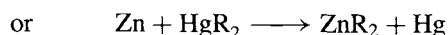
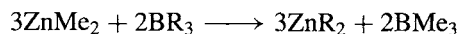
original method of heating Zn with boiling RX in an inert atmosphere (CO<sub>2</sub> or N<sub>2</sub>):



and then raising the temperature to distil the dialkyl:



These reactions work best with X = I but the less-expensive RBr can be used in conjunction with a Zn-Cu alloy instead of pure Zn. Diaryls are best obtained from appropriate organoboranes or organomercury compounds:

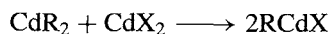


ZnR<sub>2</sub> are covalent, non-polar liquids or low-boiling solids (Table 29.4). They are invariably monomeric in solution with linear C-Zn-C coordination at the Zn atom. They are very susceptible to attack by air and those of low molecular weight are spontaneously flammable, producing a smoke of ZnO. Their reactions with water, alcohols and ammonia, etc., are generally similar to, but less vigorous than, those of Grignard reagents (p. 132) with the important difference that they are unaffected by CO<sub>2</sub>; indeed, they are often prepared under an atmosphere of this gas.

Organocadmium compounds are normally prepared from the appropriate Grignard reagents:



and then if desired:



They are thermally less stable than their Zn counterparts but generally less reactive (not normally

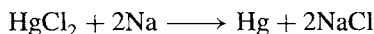
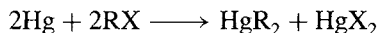
<sup>37</sup> J. L. WARDELL, *Organometallic Compounds of Zinc, Cadmium and Mercury*, Chapman & Hall, London, 1985, 220 pp.

catching fire in air), and so their most important use (but see also ref. 38) is to prepare ketones from acid chlorides:

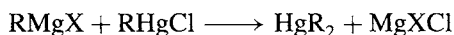
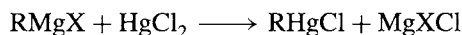


The use of Grignard reagents is impracticable here since they react further with the ketone.

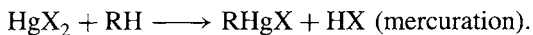
An enormous number of organomercury compounds are known. They are predominantly of the same stoichiometries as those of Zn and Cd, viz.  $RHgX$  and  $HgR_2$ , and may be prepared by the action of sodium amalgam on  $RX$ :



More usually they are made by the reaction of Grignard reagents on  $HgCl_2$  in thf:



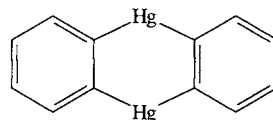
or simply by the action of  $HgX_2$  on a hydrocarbon:



$RHgX$  are crystalline solids, and  $HgR_2$  are extremely toxic liquids or low-melting solids (Table 29.4). They are essentially covalent materials except when  $X^- = F^-$ ,  $NO_3^-$  or  $SO_4^{2-}$ , in which cases the former are water-soluble and apparently ionic,  $[RHg]^+X^-$ . There are several reasons for the attention which these compounds have received. The search for pharmacologically valuable drugs has provided a continuing stimulus, and the existence of convenient preparative methods, coupled with their remarkable stability to air and water, has led to their extensive use in mechanistic studies. This stability sets them apart from the organic derivatives of Zn, Cd and Group 2 metals but arises from the extreme weakness of the  $Hg-O$  bond rather than an inherently strong  $Hg-C$  bond. In fact the latter is weak, being commonly only  $\sim 60 \text{ kJ mol}^{-1}$  and organomercury compounds are

thermally and photochemically unstable, in some cases requiring to be stored at low temperatures in the dark. Indeed, because of the weakness of the bond, Hg can be replaced by many metals which give stronger  $M-C$  bonds and the preparation of organo derivatives of other metals (e.g. of Zn and Cd as referred to above) is the most important application of these compounds.

It appears that all  $RHgX$  and  $HgR_2$  compounds are made up of linear  $R-Hg-X$  or  $R-Hg-R$  units, which could arise from  $sp$  hybridization of the metal.<sup>†</sup> In some cases polymerization is necessary to achieve this linearity. Thus, for instance, *o*-phenylene-mercury, which could conceivably be formulated as



is in fact a cyclic trimer (Fig. 29.5a).<sup>(39)</sup> Organomercury compounds generally have little tendency to coordinate to further ligands. Exceptions include irregularly 3-coordinated  $[HgMe(bipy)]NO_3$ <sup>(40)</sup> and  $[HgR(Hdz)]$ ,<sup>(41)</sup> T-shaped  $[Hg(2\text{-pyridylphenyl})Cl]$ <sup>(42)</sup> (Fig. 29.5b, c, d) and the tetrahedral  $[HgMe(np_3)]^+$  ( $np_3$  is the "tripod" phosphine  $N\{CH_2CH_2PPh_2\}_3$ ).<sup>(43)</sup>

Among the versatile and synthetically useful reactions are those typified by the absorption of alkenes (olefins) by methanolic solutions of salts, particularly, the acetate of  $Hg^{II}$ . The products are not  $\pi$  complexes, but  $\sigma$ -bonded addition

<sup>†</sup> Other possibilities which have been suggested include  $ds$  hybridization and minimization of interaction between metal  $d$  and non bonding ligand  $p$  orbitals — see pp. 351–2 of ref. 32.

<sup>39</sup> D. S. BROWN, A. G. MASSEY and D. A. WICKENS, *Acta Cryst.* **B34**, 1695–7 (1978).

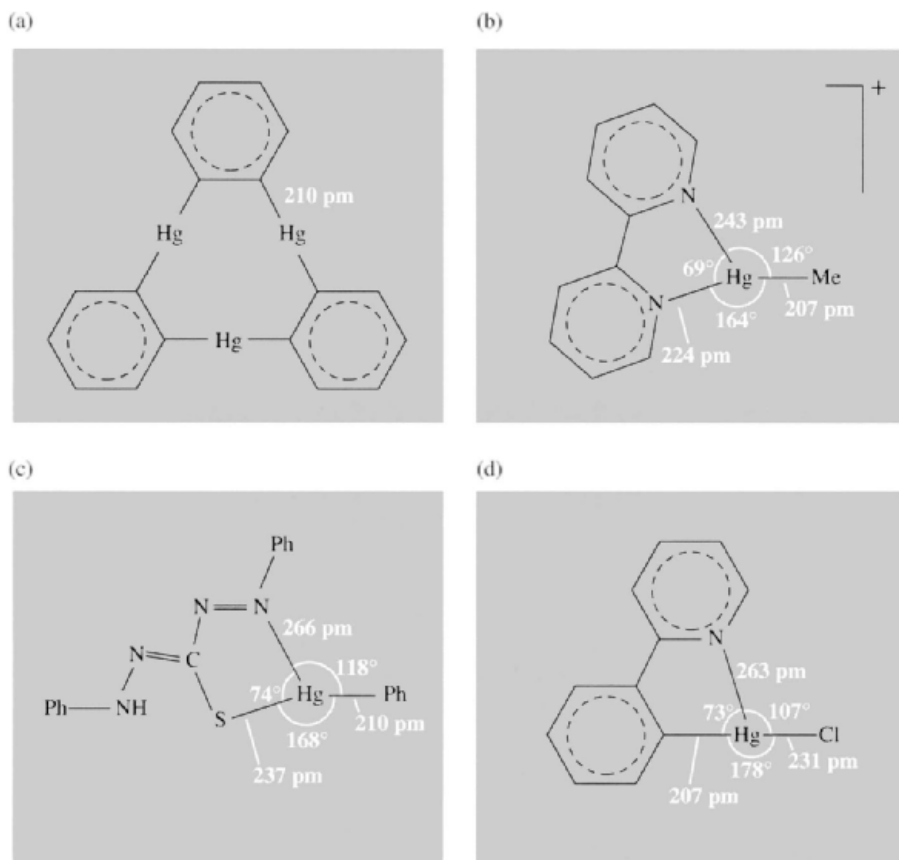
<sup>40</sup> A. J. CANTY and B. M. GATEHOUSE, *J. Chem. Soc., Dalton Trans.*, 2018–20 (1976).

<sup>41</sup> A. T. HUTTON and H. M. N. H. IRVING, *J. Chem. Soc., Chem. Commun.*, 1113–4 (1979).

<sup>42</sup> E. C. CONSTABLE, T. A. LEESE and D. A. TOCHER, *J. Chem. Soc., Chem. Commun.*, 570–1 (1989).

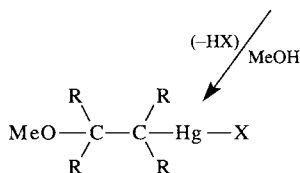
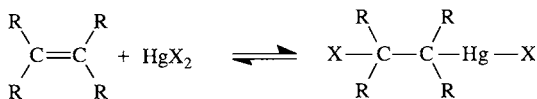
<sup>43</sup> C. A. GHILARDI, P. INNOCENTI, S. MIDOLLINI, A. ORLANDINI and A. VACCA, *J. Chem. Soc., Chem. Commun.*, 1691–3 (1992).

<sup>38</sup> P. R. JONES and P. J. DESIO, *Chem. Revs.* **78**, 491–516 (1978).

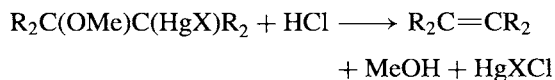


**Figure 29.5** (a) *o*-Phenylenemercury trimer, (b) the planar cation in  $[\text{HgMe}(\text{bipy})]\text{NO}_3$ , (c) phenylmercury(II)dithizonate, and (d) the approximately T-shaped  $[\text{Hg}(\text{2-pyridylphenyl})\text{Cl}]$ .

compounds, e.g.:

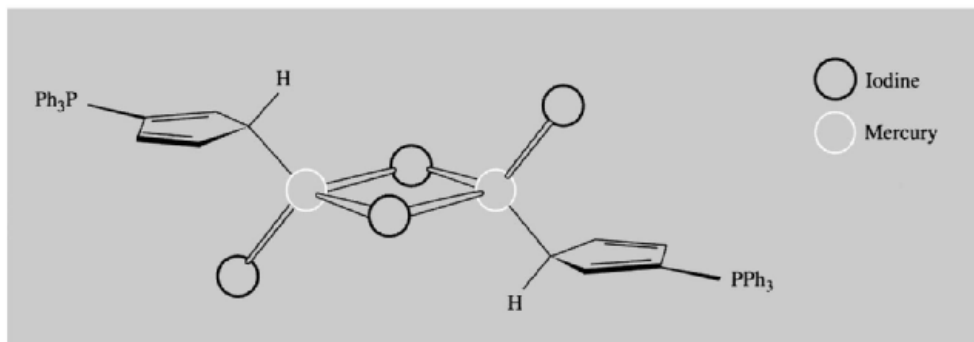


Regeneration of the alkene occurs on acidification, e.g. with HCl:



Methanolic solutions of  $\text{Hg}^{\text{II}}$  also absorb CO and the products, of the type  $\text{XHgC}(=\text{O})\text{OMe}$  are again  $\sigma$ -bonded.

A similar reluctance to form  $\pi$  bonds is seen in the cyclopentadienyls of mercury such as  $[\text{Hg}(\eta^1\text{-C}_5\text{H}_5)_2]$  and  $[\text{Hg}(\eta^1\text{-C}_5\text{H}_5)\text{X}]$ . As they are photosensitive and single crystals are very difficult to obtain, structural information has been derived mainly from infrared and nmr data. These show that the rings are monohapto and the compounds fluxional, i.e. the point of attachment of the Hg to the ring changes rapidly on the nmr time scale so that the 5 carbons are indistinguishable — the phenomenon of “ring whizzing”. In the case of  $[\text{Hg}(\eta^1\text{-C}_5\text{H}_4\text{PPh}_3)_2\text{I}_2]$  it has been possible to determine the structure by



**Figure 29.6** The structure of  $[\text{Hg}(\eta^1\text{-C}_5\text{H}_4\text{PPh}_3)\text{I}_2]_2$  showing the essentially tetrahedral coordination of the mercury atoms and of the carbon atoms attached to them.

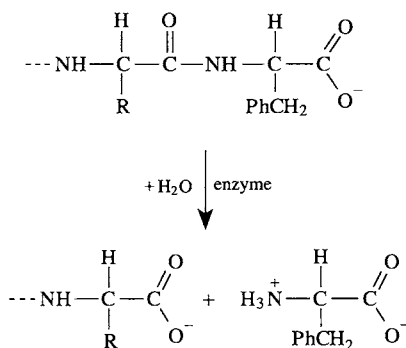
X-ray diffraction<sup>(44)</sup> which confirms the presence of an Hg–C  $\sigma$  bond (Fig. 29.6).

### 29.3.7 Biological and environmental importance<sup>(45,46,46a)</sup>

It is a remarkable contrast that, whereas Zn is biologically one of the most important metals and is apparently necessary to all forms of life,<sup>(47)</sup> Cd and Hg have no known beneficial biological role and are amongst the most toxic of elements.

The body of an adult human contains about 2 g of Zn but, as Zn enzymes are present in most body cells, its concentration is very low and realization of its importance was therefore delayed. The two Zn enzymes which have received most attention are carboxypeptidase A and carbonic anhydrase.

*Carboxypeptidase A* catalyses the hydrolysis of the terminal peptide bond in proteins during the process of digestion:



It has a molecular weight of about 34 000 and contains one Zn tetrahedrally coordinated to two histidine N atoms, a carboxyl O of a glutamate residue, and a water molecule. The precise mechanism of its action is not finally settled in spite of the intensive study of model systems,<sup>(48)</sup> but it is agreed that the first step is coordination of the terminal peptide to the Zn by its  $\text{C}=\text{O}$  group. This is thereby polarized, giving the C a positive charge and making it susceptible to nucleophilic attack. This attack is probably by the –OH of the attached water molecule, followed by proton-rearrangement and breaking of the C–N peptide bond,<sup>(49)</sup> though alternative possibilities,

<sup>44</sup> N. L. HOLY, N. C. BAENZIGER, R. M. FLYNN, and D. C. SWENSON, *J. Am. Chem. Soc.* **98**, 7823–4 (1976).

<sup>45</sup> W. KAIM and B. SCHWEDERSKI, *Bioinorganic Chemistry: Inorganic Elements in the Chemistry of Life*, Wiley, Chichester 1994; pp. 242–66 for Zn and pp. 335–43 for Cd, Hg.

<sup>46</sup> A. S. PRASAD, *Biochemistry of Zinc*, Plenum Press, New York, 1993, 303 pp.

<sup>46a</sup> A. SIGEL and H. SIGEL (eds.) *Metal Ions in Biological Systems*, Vol. 34, *Mercury and its Effects on the Environment and Biology*, Dekker, New York, 1997 604 pp.

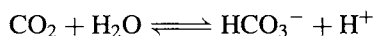
<sup>47</sup> D. BRYCE-SMITH, *Chem. Brit.* **25**, 783–6 (1989) but see also *ibid.* p. 1207.

<sup>48</sup> E. KIMURA, *Prog. Inorg. Chem.* **41**, 443–91 (1994); E. KIMURA and T. KOIKE, *Adv. Inorg. Chem.* **44**, 229–61 (1997).

<sup>49</sup> D. W. CHRISTIANSON and W. N. LIPSCOMB, *Acc. Chem. Res.* **22**, 62–9 (1989).

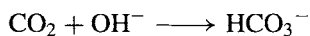
such as attack by the carboxyl group of a second glutamate residue in the enzyme have also been considered. In any event it is evident that the conformation of the enzyme provides a hydrophobic pocket, close to the Zn, which accommodates the non-polar side-chain of the protein being hydrolysed, and that this protein is, throughout, held in the correct position by H bonding to appropriate groups in the enzyme.

*Carbonic anhydrase* was the first Zn metallo-enzyme to be discovered (1940) and in its several forms is widely distributed in plants and animals. It catalyses the equilibrium reaction:



In mammalian erythrocytes (red blood-cells) the forward (hydration) reaction occurs during the uptake of  $\text{CO}_2$  by blood in tissue, while the backward (dehydration) reaction takes place when the  $\text{CO}_2$  is subsequently released in the lungs. The enzyme increases the rates of these reactions by a factor of about one million.

The molecular weight of the enzyme is about 30 000 and the roughly spherical molecule contains just one zinc atom situated in a deep protein pocket, which also contains a number of water molecules arranged in an ice-like order. This Zn is coordinated tetrahedrally to 3 imidazole nitrogen atoms of histidine residues and to a water molecule. Once again the precise details of the enzyme's action are not settled, but it seems probable that the coordinated  $\text{H}_2\text{O}$  ionizes to give  $\text{Zn-OH}^-$  and the nucleophilic  $\text{OH}^-$  then interacts with the C of  $\text{CO}_2$  (which may be held in the correct position by H bonds to its two oxygen atoms) to yield  $\text{HCO}_3^-$ . This is equivalent to replacing the slow hydration of  $\text{CO}_2$  with  $\text{H}_2\text{O}$ , by the fast reaction:



The latter would normally require a high pH and the contribution of the enzyme is therefore presumed to be the provision of a suitable environment, within the protein pocket, which allows the dissociation of the coordinated  $\text{H}_2\text{O}$  to occur in a medium of pH 7 which would otherwise be much too low.

A more recently established function of zinc is in proteins responsible for recognizing base-sequences in DNA and so regulating the transfer of genetic information during the replication of DNA. These so-called "zinc-finger" proteins contain 9 or 10  $\text{Zn}^{2+}$  ions each of which, by coordinating to 4 amino acids, stabilizes a protruding fold (finger) in the protein. The protein wraps around the double strand of DNA, each of the fingers binding to the DNA, their spacing matching the base sequence in the DNA and thus ensuring accurate recognition.<sup>(50)</sup>

Cadmium is extremely toxic and accumulates in humans mainly in the kidneys and liver; prolonged intake, even of very small amounts, leads to dysfunction of the kidneys. It acts by binding to the —SH group of cysteine residues in proteins and so inhibits SH enzymes. It can also inhibit the action of zinc enzymes by displacing the zinc.

The toxic effects of mercury have long been known,<sup>(51)</sup> and the use of  $\text{HgCl}_2$  as a poison has already been mentioned. The use of mercury salts in the production of felt<sup>†</sup> for hats and the dust generated in ill-ventilated workshops by the subsequent drying process, led to the nervous disorder known as "hatter's shakes" and possibly also to the expression "mad as a hatter".

The metal itself, having an appreciable vapour pressure, is also toxic, and produces headaches, tremors, inflammation of the bladder and loss of memory. The best documented case is that of Alfred Stock (p. 151) whose constant use of mercury in the vacuum lines employed in his studies of boron and silicon hydrides, caused him to suffer for many years. The cause was eventually recognized and it is largely due to Stock's publication in 1926 of details of his experiences that the need for care and adequate ventilation is now fully appreciated.

<sup>50</sup> N. P. PAVLETICH and C. O. PABO, *Science* **261**, 1701–7 (1993).

<sup>†</sup> It was apparently helpful to add  $\text{Hg}^{\text{II}}$  to the dil  $\text{HNO}_3$  used to roughen the surface of the animal hair employed in the making of felt which is a non-woven fabric of randomly oriented hairs.



Still more dangerous than metallic mercury or inorganic mercury compounds are organomercury compounds of which the methyl mercury ion  $\text{HgMe}^+$  is probably the most ubiquitous.<sup>(51)</sup> This and other organomercurials are more readily absorbed in the gastrointestinal tract than  $\text{Hg}^{\text{II}}$  salts because of their greater ability to permeate biomembranes. They concentrate in the blood and have a more immediate and permanent effect on the brain and central nervous system, no doubt acting by binding to the  $-\text{SH}$  groups in proteins. Naturally occurring anaerobic bacteria in the sediments of sea or lake floors are able to methylate inorganic mercury (Co-Me groups in vitamin  $\text{B}_{12}$  are able to transfer the Me to  $\text{Hg}^{\text{II}}$ ) which is then concentrated in plankton and so enters the fish food chain.

The Minamata disaster in Japan, when 52 people died in 1952, occurred because fish, which formed the staple diet of the small fishing community, contained abnormally high concentrations of mercury in the form of  $\text{MeHgSMe}$ . This was found to originate from a local chemical works where  $\text{Hg}^{\text{II}}$  salts were used (inefficiently) to catalyse the production of

acetylene from acetaldehyde, and the effluent then discharged into the shallow sea. Evidence of a similar bacterial production of organomercury is available from Sweden where methylation of  $\text{Hg}^{\text{II}}$  in the effluent from paper mills has been shown to occur. The use of organomercurials as fungicidal seed dressings has also resulted in fatalities in many parts of the world when the seed was subsequently eaten.

It is now apparent that bacteria have developed resistance to heavy metals and the detoxifying process is initiated and controlled by *metallo-regulatory* proteins which are able selectively to recognize metal ions. MerR is a small DNA-binding protein which displays a remarkable sensitivity to  $\text{Hg}^{2+}$ . The metal apparently binds to S atoms of cysteine and this has been a major incentive to recent work on Hg-S chemistry.<sup>(32)</sup>

Public concern about mercury poisoning has led to more stringent regulations for the use of mercury cells in the chlor-alkali industry (pp. 71-3, 798). The health record of this industry has, in fact, been excellent, but the added costs of conforming to still higher standards have led manufacturers to move from mercury cells to diaphragm cells, and this change has been made a legal requirement in Japan.

<sup>51</sup> S. KRISHNAMURTHY, *J. Chem. Ed.* **69**, 347-50 (1992).

																1	2																														
																		H	He																												
3	4																	5	6	7	8	9	10																								
Li	Be																	B	C	N	O	F	Ne																								
11	12																	13	14	15	16	17	18																								
Na	Mg																	Al	Si	P	S	Cl	Ar																								
19	20	21	22	23	24	25	26	27	28	29	30	31	32	33	34	35	36																														
K	Ca	Sc	Ti	V	Cr	Mn	Fe	Co	Ni	Cu	Zn	Ga	Ge	As	Se	Br	Kr																														
37	38	39	40	41	42	43	44	45	46	47	48	49	50	51	52	53	54																														
Rb	Sr	Y	Zr	Nb	Mo	Tc	Ru	Rh	Pd	Ag	Cd	In	Sn	Sb	Te	I	Xe																														
55	56	57	72	73	74	75	76	77	78	79	80	81	82	83	84	85	86																														
Cs	Ba	La	Hf	Ta	W	Re	Os	Ir	Pt	Au	Hg	Tl	Pb	Bi	Po	At	Rn																														
87	88	89	104	105	106	107	108	109	110	111	112																																				
Fr	Ra	Ac	Rf	Db	Sg	Bh	Hs	Mt	Uun	Uuu	Uub																																				
																		59	60	61	62	63	64	65	66	67	68	69	70	71																	
																		Ce	Pr	Nd	Pm	Sm	Eu	Gd	Tb	Dy	Ho	Er	Tm	Yb	Lu																
																		90	91	92	93	94	95	96	97	98	99	100	101	102	103																
																		Th	Pa	U	Np	Pu	Am	Cm	Bk	Cf	Es	Fm	Md	No	Lr																

# 30

## The Lanthanide Elements ( $Z = 58 - 71$ )

### 30.1 Introduction<sup>(1)</sup>

Not least of the confusions associated with this group of elements is that of terminology. The name “rare earth” was originally used to describe almost any naturally occurring but unfamiliar oxide and even until about 1920 generally included both  $\text{ThO}_2$  and  $\text{ZrO}_2$ . About that time the name began to be applied to the elements themselves rather than their oxides, and also to be restricted to that group of elements which could only be separated from each other with great difficulty. On the basis of their separability it was convenient to divide these elements into the “cerium group” or “light earths” (La to about Eu) and the “yttrium group” or “heavy earths” (Gd to Lu plus Y which, though much lighter than the others, has a comparable ionic radius and is

consequently found in the same ores, usually as the major component). It is now accepted that the “rare-earth elements” comprise the fourteen elements from  $_{58}\text{Ce}$  to  $_{71}\text{Lu}$ , but are commonly taken to include  $_{57}\text{La}$  and sometimes Sc and Y as well.

To avoid this confusion, and because many of the elements are actually far from rare, the terms “lanthanide”, “lanthanon” and “lanthanoid” have been introduced. Even now, however, there is no general agreement about the position of La, i.e. whether the group is made up of the elements La to Lu or Ce to Lu. Throughout this chapter the term “lanthanide” and the general symbol, Ln, will be used to refer to the fourteen elements cerium to lutetium inclusive, the Group 3 elements, scandium, yttrium and lanthanum having already been dealt with in Chapter 20.

The lanthanides comprise the largest naturally-occurring group in the periodic table. Their properties are so similar that from 1794, when J. Gadolin isolated “yttria” which he thought was the oxide of a single new element, until 1907, when lutetium was discovered, nearly a hundred claims were made for the discovery of elements

<sup>1</sup> K. A. Gschneider Jr. and L. Eyring (eds.), *Handbook on the Physics and Chemistry of Rare Earths*, North-Holland, Amsterdam, Vol. 1, (1978) to Vol. 21, (1995). An authoritative source of information on all topics associated with lanthanide elements.

### History of the Lanthanides<sup>(2-4)</sup>

In 1751 the Swedish mineralogist, A. F. Cronstedt, discovered a heavy mineral from which in 1803 M. H. Klaproth in Germany and, independently, J. J. Berzelius and W. Hisinger in Sweden, isolated what was thought to be a new oxide (or "earth") which was named *ceria* after the recently discovered asteroid, Ceres. Between 1839 and 1843 this earth, and the previously isolated *yttria* (p. 944), were shown by the Swedish surgeon C. G. Mosander to be mixtures from which, by 1907, the oxides of Sc, Y, La and the thirteen lanthanides other than Pm were to be isolated. The small village of Ytterby near Stockholm is celebrated in the names of no less than four of these elements (Table 30.1).

The classical methods used to separate the lanthanides from aqueous solutions depended on: (i) differences in basicity, the less-basic hydroxides of the heavy lanthanides precipitating before those of the lighter ones on gradual addition of alkali; (ii) differences in solubility of salts such as oxalates, double sulfates, and double nitrates; and (iii) conversion, if possible, to an oxidation state other than +3, e.g. Ce(IV), Eu(II). This latter process provided the cleanest method but was only occasionally applicable. Methods (i) and (ii) required much repetition to be effective, and fractional recrystallizations were sometimes repeated thousands of times. (In 1911 the American C. James performed 15 000 recrystallizations in order to obtain pure thulium bromate).

The minerals on which the work was performed during the nineteenth century were indeed rare, and the materials isolated were of no interest outside the laboratory. By 1891, however, the Austrian chemist C. A. von Welsbach had perfected the thoria gas "mantle" to improve the low luminosity of the coal-gas flames then used for lighting. Woven cotton or artificial silk of the required shape was soaked in an aqueous solution of the nitrates of appropriate metals and the fibre then burned off and the nitrates converted to oxides. A mixture of 99% ThO<sub>2</sub> and 1% CeO<sub>2</sub> was used and has not since been bettered. CeO<sub>2</sub> catalyses the combustion of the gas and apparently, because of the poor thermal conductivity of the ThO<sub>2</sub>, particles of CeO<sub>2</sub> become hotter and so brighter than would otherwise be possible. The commercial success of the gas mantle was immense and produced a worldwide search for thorium. Its major ore is monazite, which rarely contains more than 12% ThO<sub>2</sub> but about 45% Ln<sub>2</sub>O<sub>3</sub>. Not only did the search reveal that thorium, and hence the lanthanides, are more plentiful than had previously been thought, but the extraction of the thorium produced large amounts of lanthanides for which there was at first little use.

Applications were immediately sought and it was found that electrolysis of the fused chloride of the residue left after the removal of Th yielded the pyrophoric "mischmetall" (approximately 50% Ce, 25% La, 25% other light lanthanides) which, when alloyed with 30% Fe, is ideal as a lighter flint. Besides small amounts of lanthanides used in special glasses to control absorption at particular wavelengths, this was the pattern of usage until the 1940s. Before then there was little need for the pure metals and, because of the difficulty in obtaining them (high mps and very easily oxidized), such samples as were produced were usually impure. Attempts were also made to find element 61, which had not been found in the early studies, and in 1926 unconfirmed reports of its discovery from Illinois and Florence produced the temporary names *illinium* and *florentium*.

During the 1939–45 war, Mg-based alloys incorporating lanthanides were developed for aeronautical components and the addition of small amounts of mischmetall to cast-iron, by causing the separation of carbon in nodular rather than flake form, was found to improve the mechanical properties. But, more significantly from the chemical point of view, work on nuclear fission requiring the complete removal of the lanthanide elements from uranium and thorium ores, coupled with the fact that the lanthanides constitute a considerable proportion of the fission products, stimulated a great surge of interest. Solvent extraction and, more especially, ion-exchange techniques were developed, the work of F. H. Spedding and coworkers at Iowa State University being particularly notable.

As a result, in 1947, J. A. Marinsky, L. E. Glendenin, and C. D. Coryell at Oak Ridge, Tennessee, finally established the existence of element 61 in the fission products of <sup>235</sup>U and at the suggestion of Coryell's wife it was named *promethium* (later *promethium*) after Prometheus who, according to Greek mythology, stole fire from heaven for the use of mankind. Since about 1955, individual lanthanides have been obtainable in increasing amounts in elemental as well as combined forms.

belonging to this group. In view of the absence at that time of a conclusive test to determine whether or not a mixture was involved, this is not surprising. Indeed, there was a general lack of understanding of the large number of elements

involved since the periodic table of the time could accommodate only one element, namely La. Not until 1913, as a result of H. G. J. Moseley's work on atomic numbers, was it realized that there were just fourteen elements between La and Hf, and in 1918 Niels Bohr interpreted this as an expansion of the fourth quantum group from 18 to 32 electrons. More information is in the Panel above and in Table 30.1.

<sup>2</sup> F. SZABADVARY, pp. 33–80, Vol. 11 (1988) of ref. 1.

<sup>3</sup> C. K. JØRGENSEN, pp. 197–215, Vol. 11 (1988) of ref. 1.

<sup>4</sup> C. H. EVANS, *Chem. in Brit.* **25**, 880–2 (1989).

Table 30.1 The discovery of the oxides of Group 3 and the lanthanide elements<sup>(2,4)</sup>

Element	Discoverer	Date	Origin of name
<i>From ceria</i>			
Cerium, Ce	C. G. Mosander	1839	The asteroid, Ceres
Lanthanum, La	C. G. Mosander	1839	Greek <i>λανθάνειν</i> , <i>lanthanein</i> , to escape notice
Praseodymium, Pr	C. A. von Welsbach	1885	Greek <i>πρασιος</i> + <i>διδυμος</i> praseos + didymos, leek green + twin
Neodymium, Nd	C. A. von Welsbach	1885	Greek <i>νέος</i> + <i>διδυμος</i> , <i>neos</i> + <i>didymos</i> , new twin
Samarium, Sm	L. de Boisbaudran	1879	The mineral, samarskite
Europium, Eu	E. A. Demarcay	1901	Europe
<i>From yttria</i>			
Yttrium, Y	C. G. Mosander	1843	Ytterby
Terbium, Tb <sup>(a)</sup>	C. G. Mosander	1843	Ytterby
Erbium, Er <sup>(a)</sup>	C. G. Mosander	1843	Ytterby
Ytterbium, Yb	J. C. G. de Marignac	1878	Ytterby
Scandium, Sc	L. F. Nilson	1879	Scandinavia
Holmium, Ho	P. T. Cleve	1879	Latin <i>Holmia</i> : Stockholm
Thulium, Tm	P. T. Cleve	1879	Latin <i>Thule</i> , "most northerly land"
Gadolinium, Gd	J. C. G. de Marignac	1880	Finnish chemist, J. Gadolin
Dysprosium, Dy	L. de Boisbaudran	1886	Greek <i>δυσπροσιτος</i> , <i>dysprositos</i> , hard to get
Lutetium, Lu <sup>(b)</sup>	G. Urbain		
	C. A. von Welsbach	1907	Latin <i>Lutetia</i> : Paris
	C. James		

<sup>(a)</sup>Terbium and erbium were originally named in the reverse order.

<sup>(b)</sup>Originally spelled lutecium, but changed to lutetium in 1949.

## 30.2 The Elements

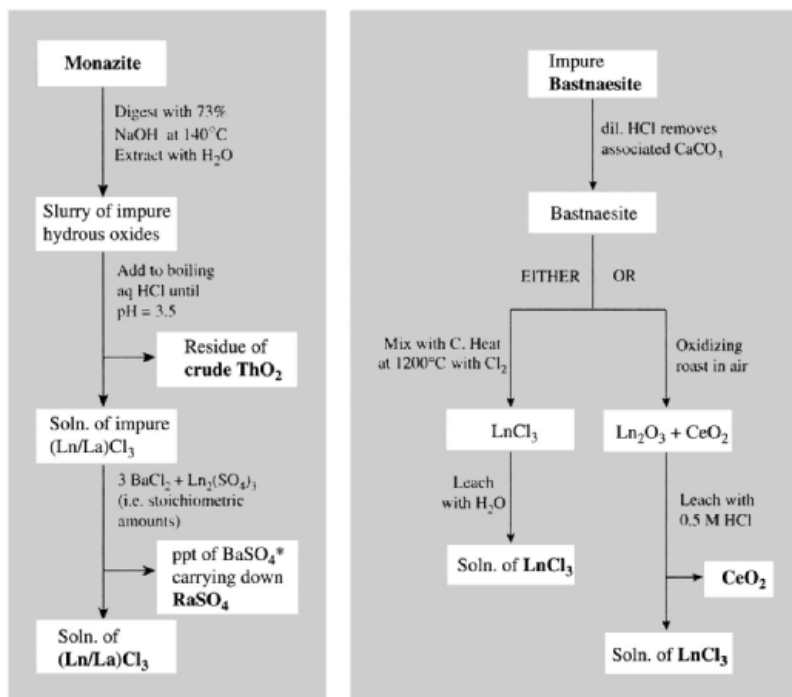
### 30.2.1 Terrestrial abundance and distribution

Apart from the unstable <sup>147</sup>Pm (half-life 2.623 y) of which traces occur in uranium ores, the lanthanides are actually not rare. Cerium (66 ppm in the earth's crust) is the twenty-sixth most abundant of all elements, being half as abundant as Cl and 5 times as abundant as Pb. Even Tm (0.5 ppm), the rarest after Pm, is rather more abundant in the earth's crust than is iodine.

There are over 100 minerals known to contain lanthanides but the only two of commercial importance are monazite, a mixed La, Th, Ln phosphate, and bastnaesite, an La, Ln fluorocarbonate (M<sup>III</sup>CO<sub>3</sub>F). Monazite is widely but sparsely distributed in many rocks but, because of its high density and inertness, it is concentrated by weathering into sands on beaches and river beds, often in the presence of other

similarly concentrated minerals such as ilmenite (FeTiO<sub>3</sub>) and cassiterite (SnO<sub>2</sub>). Deposits occur in southern India, South Africa, Brazil, Australia and Malaysia and, until the 1960s, these provided the bulk of the world's La, Ln and Th. Then, however, a vast deposit of bastnaesite, which had been discovered in 1949 in the Sierra Nevada Mountains in the USA, came into production. Bastnaesite is also now extracted in China in large quantities, and has become the most important single source of La and Ln.

The bulk of both monazite and bastnaesite is made up of Ce, La, Nd and Pr (in that order) but, whereas monazite typically contains around 5–10% ThO<sub>2</sub> and 3% yttrium earths, these and the heavy lanthanides are virtually absent in bastnaesite. Although thorium is only weakly radioactive it is contaminated with daughter elements such as <sup>228</sup>Ra which are more active and therefore require careful handling during the processing of monazite. This is a complication not encountered in the processing of bastnaesite.



\*These residues contain <sup>228</sup>Ra, a daughter element of Th and an active  $\gamma$ -emitter, and must therefore be handled with care

**Figure 30.1** Flow diagram for the extraction of the lanthanide elements.

### 30.2.2 Preparation and uses of the elements<sup>(5-8)</sup>

Conventional mineral dressing yields concentrates of the minerals of better than 90% purity. These can then be broken down (“opened”) by either acidic or alkaline attack, the latter being more usual nowadays. Details vary considerably since they depend on the ore being used and on the extent to which the metals are to be separated from each other, but the schemes

<sup>5</sup> Kirk-Othmer *Encyclopedia of Chemical Technology*, Vol. 14, pp. 1091-115 4th edn., Interscience, New York, 1995.

<sup>6</sup> B. JEZOWSKA-TRZEBIATOWSKA, S. KOPACZ and T. MIKULSKI, *The Rare Earth Elements, Occurrence and Technology*, Elsevier, Amsterdam, 1990, 540 pp.

<sup>7</sup> K. L. NASH and G. R. CHOPPIN (eds.), *Separations of Elements*, Plenum, New York, 1995, 286 pp.

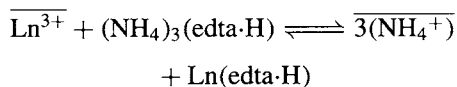
<sup>8</sup> R. G. BAUTISTA and N. JACKSON (eds.), *Rare Earths, Resources, Science Technology and Applications*, TMS, Warrendale USA, 1991, pp. 466.

outlined in Fig. 30.1 are typical of those used for monazite and bastnaesite to obtain solutions of the mixed chlorides. At this point the classical methods (see Panel, p. 1228) were formerly employed to separate the individual elements where this was required and, indeed the separation of lanthanum by the fractional crystallization of  $\text{La}(\text{NO}_3)_3 \cdot 2\text{NH}_4\text{NO}_3 \cdot 4\text{H}_2\text{O}$  is still used. However the separations can now be effected on a large scale by solvent extraction<sup>(7,9)</sup> using aqueous solutions of the nitrates and a solvent such as tri-*n*-butylphosphate,  $(\text{Bu}^n\text{O})_3\text{PO}$  (often with kerosene as an inert diluent), in which the solubility of  $\text{Ln}^{\text{III}}$  increases with its atomic weight. This type of process has the advantage of being continuous and is ideal where the product and feed are not to be changed.

Alternatively, for high-purity or smaller-scale production the more easily adapted ion-exchange

<sup>9</sup> R. G. BAUTISTA, pp. 1-28, Vol. 21 (1995) of ref 1.

techniques are ideal, the best of these being "displacement chromatography". Two separate columns of cation exchange resin are generally employed for this purpose. The first column is loaded with the  $\text{Ln}^{\text{III}}$  mixture and the second, or development, column is loaded with a so-called "retaining ion" such as  $\text{Cu}^{\text{II}}$  ( $\text{Zn}^{\text{II}}$  and  $\text{Fe}^{\text{III}}$  have also been used), and the two columns are coupled together. An aqueous solution (the "eluant") of a complexing agent, of which the triammonium salt of  $\text{edta}^{4-}$  is typical, is then passed through the columns, and  $\text{Ln}^{\text{III}}$  is displaced from the first column (barred species are bound to the resin):



The reaction at any point in the column becomes progressively displaced to the right as fresh complexing agent arrives and the reaction products are removed. The solution of  $\text{Ln}(\text{edta}\cdot\text{H})$  and  $(\text{NH}_4)_3(\text{edta}\cdot\text{H})$  then reaches the development column where  $\text{Cu}^{\text{II}}$  is displaced and  $\text{Ln}^{\text{III}}$  redeposited in a compact band at the top of the column:



This occurs because  $\text{Cu}^{\text{II}}$ , being smaller than  $\text{Ln}^{\text{III}}$ , is able to form in the solution phase, a complex with  $(\text{edta}\cdot\text{H})^{3-}$  of comparable stability, in spite of its lower charge. The  $\text{Cu}^{\text{II}}$  serves the additional purpose of keeping the complexing agent in a soluble form. If the resin were loaded instead with  $\text{H}^+$ ,  $\text{edta}\cdot\text{H}_4$  would be precipitated and would clog the resin. Even using  $\text{Cu}^{\text{II}}$  the composition of the eluant must be carefully controlled. The concentration of  $\text{edta}$  must not exceed 0.015 M, otherwise  $\text{Cu}_2(\text{edta})\cdot 5\text{H}_2\text{O}$  precipitates, and it is to encourage the formation of the more soluble salt of  $(\text{edta}\cdot\text{H})^{3-}$  that an acidic rather than neutral ammonium salt of  $\text{edta}^{4-}$  is used.

Once the  $\text{Ln}^{\text{III}}$  ions have been deposited on to the resin they are displaced yet again by the  $\text{NH}_4^+$  in the eluant. Now, the affinity of  $\text{Ln}^{\text{III}}$  ions for the resin decreases with increasing atomic weight, but so slightly that elution of the development column

with  $\text{NH}_4^+$  ions alone would not discriminate to an effective extent between the different lanthanides. However, the values of  $\Delta G^\circ$  (and therefore of  $\log K$ ) for the formation of  $\text{Ln}(\text{edta}\cdot\text{H})$  complexes, increase steadily along the series by a total of *ca.* 25% from  $\text{Ce}^{\text{III}}$  to  $\text{Lu}^{\text{III}}$ . Thus in the presence of the complexing agent, the tendency to leave the resin and go into solution is significantly greater for the heavy than for the light lanthanides. As a result, displacement of the  $\text{Ln}^{\text{III}}$  ions from the resin concentrates the heavier cations in the solution. The  $\text{Ln}^{\text{III}}$  ions therefore pass down the development column in a band, being repeatedly deposited and redissolved in what is effectively an automatic fractionation process, concentrating the heavier members in the solution phase. The result is that when all the copper has come off the column the lanthanides emerge in succession, heaviest first. They may then be precipitated from the eluant as insoluble oxalates and ignited to the oxides.

The production of mischmetal by the electrolysis of fused  $(\text{Ln},\text{La})\text{Cl}_3$ , and the difficulties in obtaining pure metals because of their high mps and ease of oxidation, have already been mentioned (Panel, p. 1228). Two methods are in fact available for producing the metals.

(i) *Electrolysis of fused salts.* A mixture of  $\text{LnCl}_3$  with either  $\text{NaCl}$  or  $\text{CaCl}_2$  is fused and electrolysed in a graphite or refractory-lined steel cell, which serves as the cathode, with a graphite rod as anode. This is used primarily for mischmetal, the lighter, lower-melting Ce, and for Sm, Eu and Yb for which method (ii) yields  $\text{Ln}^{\text{II}}$  ions.

(ii) *Metallothermic reduction.* This consists of the reduction of the anhydrous halides with calcium metal. Fluorides are preferred, since they are non-hygroscopic and the  $\text{CaF}_2$  produced is stable, unlike the other Ca halides which are liable to boil at the temperatures reached in the process.  $\text{LnF}_3 + \text{Ca}$  are heated in a tantalum crucible to a temperature  $50^\circ$  above the mp of Ln under an atmosphere of argon. After completion of the reaction, the charge is cooled and the slag and metal (of 97–99% purity) broken apart. The main impurity is Ca which is removed by melting

under vacuum. With the exceptions of Sm, Eu and Yb this method has general applicability.

In 1995 total world production of "rare earth oxides" was 68 000 tonnes of which China and the USA produced 30 000 and 29 000 tonnes of bastnaesite respectively with smaller quantities of monazite from Australia (as a by-product of  $\text{TiO}_2$  production) and India. The bulk of output is used without separation of individual lanthanides. Major uses are in the production of low alloy steels for plate and pipe where  $< 1\%$  Ln/La added in the form of mischmetall or silicides greatly improves strength and workability, and in petroleum "cracking" catalysis where various mixed metal oxides are employed. The walls of domestic "self-cleaning" ovens are treated with  $\text{CeO}_2$  which prevents the formation of tarry deposits, and  $\text{CeO}_2$  of varying purity is used to polish glass. Other small-scale uses include that of mischmetall in Mg-based alloys to produce lighter flints, while Ln/Co alloys are used for the construction of permanent magnets, and individual Ln oxides are used as phosphors in television screens and similar fluorescent surfaces.

Current availability of individual lanthanides (plus Y and La) in a state of high purity and relatively low cost has stimulated research into potential new applications. These are mainly in the field of solid state chemistry and include solid oxide fuel cells, new phosphors and perhaps most significantly high temperature superconductors (p. 1182.)

### 30.2.3 Properties of the elements

The metals are silvery in appearance (except for Eu and Yb which are pale yellow, see p. 112 and below) and are rather soft, but become harder across the series. Most of them exist in more than one crystallographic form, of which hcp is the most common; all are based on typically metallic close-packed arrangements, but their conductivities are appreciably lower than those of other close-packed metals.

The more important physical properties of the elements are summarized in Table 30.2. The alternation between several and few stable

isotopes for even and odd atomic number respectively, is mirrored by an even-odd variation in the natural abundances of the elements (see p. 4) and in the uncertainty of their atomic weights (see p. 17).

The electronic configurations of the free atoms are determined only with difficulty because of the complexity of their atomic spectra, but it is generally agreed that they are nearly all  $[\text{Xe}]4f^n 5d^0 6s^2$ . The exceptions are:

- (1) Cerium, for which the sudden contraction and reduction in energy of the 4f orbitals immediately after La is not yet sufficient to avoid occupancy of the 5d orbital.
- (2) Gd, which reflects the stability of the half-filled 4f shell;
- (3) Lu, at which point the shell has been filled.

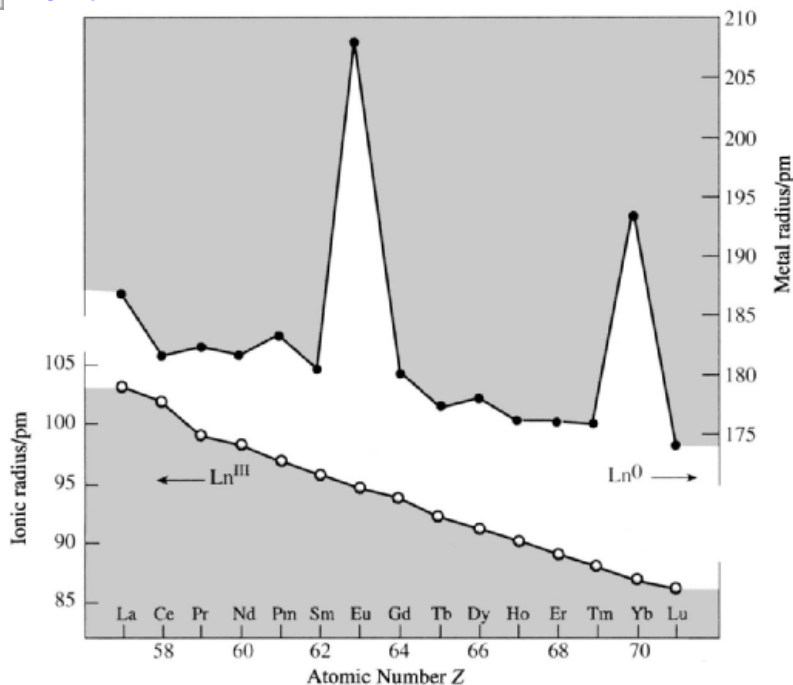
However, only in the case of cerium (see below) does this have any marked effect on the aqueous solution chemistry, which is otherwise dominated by the +3 oxidation state, for which the configuration varies regularly from  $4f^1$  ( $\text{Ce}^{\text{III}}$ ) to  $4f^{14}$  ( $\text{Lu}^{\text{III}}$ ). It is notable that a regular variation is found for any property for which this  $4f^n$  configuration is maintained across the series, whereas the variation in those properties for which this configuration is not maintained can be highly irregular. This is illustrated dramatically in size variations (Fig. 30.2). On the one hand, the radii of  $\text{Ln}^{\text{III}}$  ions decrease regularly from  $\text{La}^{\text{III}}$  (included for completeness) to  $\text{Lu}^{\text{III}}$ . This "lanthanide contraction" occurs because, although each increase in nuclear charge is exactly balanced by a simultaneous increase in electronic charge, the directional characteristics of the 4f orbitals cause the  $4f^n$  electrons to shield themselves and other electrons from the nuclear charge only imperfectly. Thus, each unit increase in nuclear charge produces a net increase in attraction for the whole extranuclear electron charge cloud and each ion shrinks slightly in comparison with its predecessor. On the other hand, although a similar overall reduction is seen in the metal radii, Eu and Yb are spectacularly irregular. The reason is that most of the metals are composed of a lattice of  $\text{Ln}^{\text{III}}$  ions with a  $4f^n$  configuration and 3 electrons in the

Table 30.2 Some properties of the lanthanide elements

Property	Ce	Pr	Nd	Pm	Sm	Eu	Gd	Tb	Dy	Ho	Er	Tm	Yb	Lu
Atomic number	58	59	60	61	62	63	64	65	66	67	68	69	70	71
Number of naturally occurring isotopes	4	1	7	—	7	2	7	1	7	1	6	1	7	2
Outer electron configuration	4f <sup>1</sup> 5d <sup>1</sup> 6s <sup>2</sup>	4f <sup>3</sup> 6s <sup>2</sup>	4f <sup>4</sup> 6s <sup>2</sup>	4f <sup>5</sup> 6s <sup>2</sup>	4f <sup>6</sup> 6s <sup>2</sup>	4f <sup>7</sup> 6s <sup>2</sup>	4f <sup>7</sup> 5d <sup>1</sup> 6s <sup>2</sup>	4f <sup>9</sup> 6s <sup>2</sup>	4f <sup>10</sup> 6s <sup>2</sup>	4f <sup>11</sup> 6s <sup>2</sup>	4f <sup>12</sup> 6s <sup>2</sup>	4f <sup>13</sup> 6s <sup>2</sup>	4f <sup>14</sup> 6s <sup>2</sup>	4f <sup>14</sup> 5d <sup>1</sup> 6s <sup>2</sup>
Atomic weight	140.116(1)	140.90765(2)	144.24(3)	—	150.36(3)	151.964(1)	157.25(3)	158.92534(2)	162.50(3)	164.93032(2)	167.26(3)	168.93421(2)	173.04(3)	174.967(1)
Metal radius (CN 6)/pm	181.8	182.4	181.4	183.4	180.4	208.4	180.4	177.3	178.1	176.2	176.1	175.9	193.3	173.8
Ionic radius (CN 6)/pm														
IV	87	85	—	—	—	—	—	76	—	—	—	—	—	—
III	102	99	98.3	97	95.8	94.7	93.8	92.3	91.2	90.1	89.0	88.0	86.8	86.1
II	—	—	129 <sup>(a)</sup>	—	122 <sup>(b)</sup>	117	—	—	107	—	—	103	102	—
$E^\circ(\text{M}^{4+}/\text{M}^{3+})/\text{V}$	1.72	3.2 <sup>(c)</sup>	4.9 <sup>(c)</sup>	—	—	—	—	3.1 <sup>(c)</sup>	5.4 <sup>(c)</sup>	—	—	—	—	—
$E^\circ(\text{M}^{3+}/\text{M}^{2+})/\text{V}$	—	—	−2.6	—	−1.55	−0.35	—	—	−2.5	—	—	−2.3	−1.05	—
$E^\circ(\text{M}^{3+}/\text{M})/\text{V}$	−2.34	−2.35	−2.32	−2.29	−2.30	−1.99	−2.28	−2.31	−2.29	−2.33	−2.32	−2.32	−2.22	−2.30
MP/°C	798	931	1021	1042	1074	822	1313	1365	1412	1474	1529	1545	819	1663
BP/°C	3433	3520	3074	(3000)	1794	1429	3273	3230	2567	2700	2868	1950	1196	3402
$\Delta H_{\text{fus}}/\text{kJ mol}^{-1}$	5.2(±1.2)	11.3(±2.1)	7.13	—	8.9(±0.4)	—	—	—	—	—	—	—	3.35	—
$\Delta H_{\text{vap}}/\text{kJ mol}^{-1}$	398	331	289	—	165(±17)	176	301	293	280	280	280	247	159	414
$\Delta H_f$ (monatomic gas)/kJ mol <sup>−1</sup>	419	356	328	301	207	178	398	389	291	301	317	232	152	—
Ionization energies/ kJ mol <sup>−1</sup>														
1st	541	522	530	536	542	547	595	569	567	574	581	589	603	513
2nd	1047	1018	1034	1052	1068	1085	1172	1112	1126	1139	1151	1163	1175	1341
3rd	1940	2090	2128	2140	2285	2425	1999	2122	2230	2221	2207	2305	2408	2054
$\Delta H$ (hydration Ln <sup>3+</sup> )/kJ mol <sup>−1</sup>	3370	3413	3442	3478	3515	3547	3571	3605	3637	3667	3691	3717	3739	3760
Density(25°C)/ g cm <sup>−3</sup>	6.770	6.773	7.007	—	7.520	5.234	7.900	8.229	8.550	8.795	9.066	9.321	6.965	9.840
Electrical resistivity (25°C)/μ ohm cm	73	68	64	(50)	88	90	134	114	57	87	87	79	29	79

<sup>(a)</sup>CN = 8.<sup>(b)</sup>CN = 7.<sup>(c)</sup>Estimated values since these M<sup>IV</sup> are not stable in aqueous solution.





**Figure 30.2** Variation of metal radius and 3+ ionic radius for La and the lanthanides. Other data for  $\text{Ln}^{\text{II}}$  and  $\text{Ln}^{\text{IV}}$  are in Table 30.2.

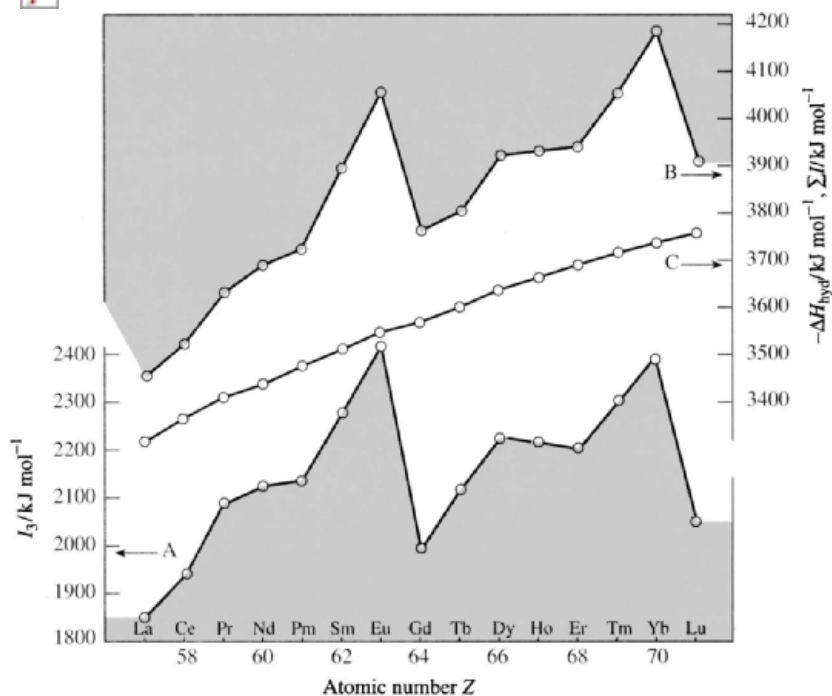
5d/6s conduction band. Metallic Eu and Yb, however, are composed predominantly of the larger  $\text{Ln}^{\text{II}}$  ions with  $4f^{n+1}$  configurations and only 2 electrons in the conduction band. The smaller and opposite irregularity for metallic Ce is due to the presence of ions in an oxidation state somewhat above +3. Similar discontinuities are found in other properties of the metals, particularly at Eu and Yb.

A contraction resulting from the filling of the 4f electron shell is of course not exceptional. Similar contractions occur in each row of the periodic table and, in the d block for instance, the ionic radii decrease by 20.5 pm from  $\text{Sc}^{\text{III}}$  to  $\text{Cu}^{\text{III}}$ , and by 15 pm from  $\text{Y}^{\text{III}}$  to  $\text{Ag}^{\text{III}}$ . The importance of the lanthanide contraction arises from its consequences:

- (1) The reduction in size from one  $\text{Ln}^{\text{III}}$  to the next makes their separation possible, but the smallness and regularity of the reduction makes the separation difficult.

- (2) By the time Ho is reached the  $\text{Ln}^{\text{III}}$  radius has been sufficiently reduced to be almost identical with that of  $\text{Y}^{\text{III}}$  which is why this much lighter element is invariably associated with the heavier lanthanides.
- (3) The total lanthanide contraction is of a similar magnitude to the expansion found in passing from the first to the second transition series, and which might therefore have been expected to occur also in passing from second to third. The interpolation of the lanthanides in fact almost exactly cancels this anticipated increase with the result, noted in preceding chapters, that in each group of transition elements the second and third members have very similar sizes and properties.

Redox processes, which of necessity entail a change in the occupancy of the 4f shell, vary in a very irregular manner across the series. Quantitative data from direct measurements are



**Figure 30.3** Variation with atomic number of some properties of La and the lanthanides: A, the third ionization energy ( $I_3$ ); B, the sum of the first three ionization energies ( $\Sigma I$ ); C, the enthalpy of hydration of the gaseous trivalent ions ( $-\Delta H_{\text{hyd}}$ ). The irregular variations in  $I_3$  and  $\Sigma I$ , which refer to redox processes, should be contrasted with the smooth variation in  $\Delta H_{\text{hyd}}$ , for which the  $4f^n$  configuration of  $\text{Ln}^{\text{III}}$  is unaltered.

far from complete for such processes, but the use of thermodynamic (Born–Haber) cycles<sup>(10)</sup> greatly improves the situation. Enthalpies of atomization ( $\Delta H_{\text{f}}$ ) and ionization energies are given in Table 30.2 and the variations of  $I_3$  and  $\Sigma I$  are shown in Fig. 30.3.  $I_3$  refers to the 1-electron change,  $4f^{n+1}(\text{Ln}^{2+}) \rightarrow 4f^n(\text{Ln}^{3+})$  and the close similarity of the two curves indicates that this change is the dominant factor in determining the shape of the  $\Sigma I$  curve. The variation of  $I_3$  across the series is in fact typical of the variation in energy of any process (e.g.  $-\Delta H_{\text{f}}$  which refers essentially to  $4f^{n+1}6s^2 \rightarrow 4f^n 5d^1 6s^2$ ) which involves the reduction of  $\text{Ln}^{3+}$  to  $\text{Ln}^{2+}$ . It is characterized by an increase in energy, first as each of the  $4f$  orbitals of the  $\text{Ln}^{\text{II}}$  ions are singly occupied and the stability of the  $4f$

shell steadily increases due to the corresponding increase in nuclear charge (La  $\rightarrow$  Eu); then again as each  $4f$  orbital is doubly occupied (Gd  $\rightarrow$  Lu). The sudden falls at Gd and Lu reflect the ease with which it is possible to remove the single electrons in excess of the stable  $4f^7$  and  $4f^{14}$  configurations. Explanations have been given for the smaller irregularities at the quarter- and three-quarter-shell stages, but require a careful consideration of interelectronic repulsion, as well as exchange energy, terms.<sup>(11)</sup>

### 30.2.4 Chemical reactivity and trends

The lanthanides are very electropositive and reactive metals. With the exception of Yb

<sup>10</sup> D. A. JOHNSON, *J. Chem. Ed.* **57**, 475–7 (1980).

<sup>11</sup> D. A. JOHNSON, *Adv. Inorg. Chem. Radiochem.* **20**, 1–132 (1977).

their reactivity apparently depends on size so that Eu which has the largest metal radius is much the most reactive. They tarnish in air and, if ignited in air or  $O_2$ , burn readily to give  $Ln_2O_3$  or, in the case of cerium,  $CeO_2$  (praseodymium and terbium yield nonstoichiometric products approximating to  $Pr_6O_{11}$  and  $Tb_4O_7$  respectively). When heated, they also burn in halogens producing  $LnX_3$ , and in hydrogen producing  $LnH_2$  and  $LnH_3$  (see below). They will, indeed, react, though usually less vigorously, with most non-metals if heated. Treatment with water yields hydrous oxides, and the metals dissolve rapidly in dilute acids, even in the cold, to give aqueous solutions of  $Ln^{III}$  salts.

The great bulk of lanthanide chemistry is of the +3 oxidation state where, because of the large sizes of the  $Ln^{III}$  ions, the bonding is predominantly ionic in character, and the cations display the typical class-a preference of  $O$ -donor ligands (p. 909). Three-dimensional lattices, characteristic of ionic character, are common and the coordination chemistry is quite different from, and less extensive than, that of the d-transition metals. Coordination numbers are generally high and stereochemistries, being determined largely by the requirements of the ligands and lacking the directional constraints of covalency, are frequently ill-defined, and the complexes distinctly labile. Thus, in spite of widespread opportunities for isomerism, there appears to be no confirmed example of a lanthanide complex existing in more than one molecular arrangement. Furthermore, only strongly complexing (i.e. usually chelating) ligands yield products which can be isolated from aqueous solution, and the comparative tenacity of the small  $H_2O$  molecule commonly leads to its inclusion, often with consequent uncertainty as to the coordination number involved. This is not to say that other types of complex cannot be obtained, but complexes with uncharged monodentate ligands, or ligands with donor atoms other than  $O$ , must usually be prepared in the absence of water.

Some typical compounds are listed in Table 30.3. Coordination numbers below 6 are found only with very bulky ligands and even

the coordination number of 6 itself is unusual, 7, 8 and 9 being more characteristic. Coordination numbers of 10 and over require chelating ligands with small "bites" (p. 917), such as  $NO_3^-$  or  $SO_4^{2-}$ , and are confined to compounds of the larger, lighter lanthanides. The stereochemistries quoted, especially for the high coordination numbers, are idealized and in most cases appreciable distortions are in fact found.

A number of trends connected with ionic radii are noticeable across the series. In keeping with Fajans' rules, salts become somewhat less ionic as the  $Ln^{III}$  radius decreases; reduced ionic character in the hydroxide implies a reduction in basic properties and, at the end of the series,  $Yb(OH)_3$  and  $Lu(OH)_3$ , though undoubtedly mainly basic, can with difficulty be made to dissolve in hot conc  $NaOH$ . Paralleling this change, the  $[Ln(H_2O)_x]^{3+}$  ions are subject to an increasing tendency to hydrolyse, and hydrolysis can only be prevented by use of increasingly acidic solutions.

However, solubility, depending as it does on the rather small difference between solvation energy and lattice energy (both large quantities which themselves increase as cation size decreases) and on entropy effects, cannot be simply related to cation radius. No consistent trends are apparent in aqueous, or for that matter nonaqueous, solutions but an empirical distinction can often be made between the lighter "cerium" lanthanides and the heavier "yttrium" lanthanides. Thus oxalates, double sulfates and double nitrates of the former are rather less soluble and basic nitrates more soluble than those of the latter. The differences are by no means sharp, but classical separation procedures depended on them.

Although lanthanide chemistry is dominated by the +3 oxidation state, and a number of binary compounds which ostensibly involve  $Ln^{II}$  are actually better formulated as involving  $Ln^{III}$  with an electron in a delocalized conduction band, genuine oxidation states of +2 and +4 can be obtained.  $Ce^{IV}$  and  $Eu^{II}$  are stable in water and, though they are respectively strongly oxidizing and strongly reducing, they have well-established

**Table 30.3** Oxidation states and stereochemistries of compounds of the lanthanides<sup>(a)</sup>

Oxidation state	Coordination number	Stereochemistry	Examples
2	6	Octahedral	$\text{LnZ}$ (Ln = Sm, Eu, Yb; Z = S, Se, Te)
	8	Cubic	$\text{LnF}_2$ (Ln = Sm, Eu, Yb)
3	3	Pyramidal	$[\text{Ln}\{\text{N}(\text{SiMe}_3)_2\}_3]$ (Ln = Nd, Eu, Yb)
	4	Tetrahedral	$[\text{Lu}(2,6\text{-dimethylphenyl})_4]^-$
		Distorted tetrahedral	$[\text{Ln}\{\text{N}(\text{SiMe}_3)_2\}_3(\text{OPPh}_3)]$ (Ln = Eu, Lu)
	6	Octahedral	$[\text{LnX}_6]^{3-}$ (X = Cl, Br); $\text{LnCl}_3$ (Ln = Dy–Lu)
	7	Capped trigonal prismatic	$[\text{Dy}(\text{dpm})_3(\text{H}_2\text{O})]^{(b)}$
		Capped octahedral	$[\text{Ho}\{\text{PhC}(\text{O})\text{CH}=\text{C}(\text{O})\text{Ph}_3\}(\text{H}_2\text{O})]$
	8	Dodecahedral	$[\text{Ho}(\text{tropolonate})_4]^-$
		Square antiprismatic	$[\text{Eu}(\text{acac})_3(\text{phen})]$
		Bicapped trigonal prismatic	$\text{LnF}_3$ (Ln = Sm–Lu)
	9	Tricapped trigonal prismatic	$[\text{Ln}(\text{H}_2\text{O})_9]^{3+}$ , $[\text{Eu}(\text{terpy})_3]^{3+}$
	Capped square antiprismatic	$[\text{Pr}(\text{terpy})\text{Cl}_3(\text{H}_2\text{O})_5] \cdot 3\text{H}_2\text{O}$	
	Bicapped dodecahedral	$[\text{Ln}(\text{NO}_3)_5]^{2-}$ (Ln = Ce, Eu)	
	12	Icosahedral	$[\text{Ce}(\text{NO}_3)_6]^{3-(c)}$
	15	See p. 1249	$[\text{Sm}(\eta^5\text{-C}_9\text{H}_7)_3]$
	16	See pp. 1248, 1249	$[\text{Nd}(\eta^5\text{-C}_5\text{H}_4\text{Me})_3]_4$ , $[\text{Ln}(\eta^8\text{-C}_8\text{H}_8)_2]^-$
4	6	Octahedral	$[\text{CeCl}_6]^{2-}$
	8	Cubic	$\text{LnO}_2$ (Ln = Ce, Pr, Tb)
		Square antiprismatic	$[\text{Ce}(\text{acac})_4]$ , $\text{LnF}_4$ (Ln = Ce, Pr, Tb)
	10	Complex	$[\text{Ce}(\text{NO}_3)_4(\text{OPPh}_3)_2]^{(c)}$
	12	Icosahedral	$[\text{Ce}(\text{NO}_3)_6]^{2-(c)}$

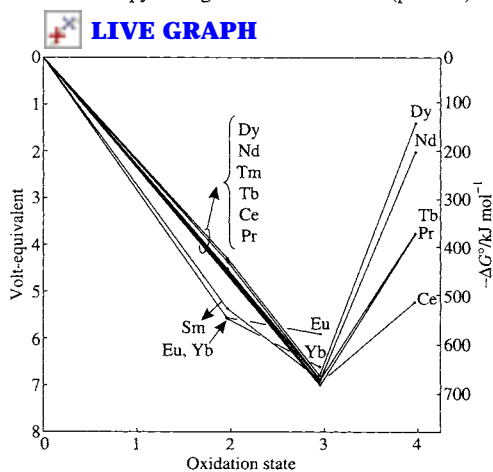
<sup>(a)</sup>Except where otherwise stated, Ln is used rather loosely to mean most of the lanthanides; the Pm compound, for instance, is usually missing simply because of the scarcity and consequent expense of Pm.

<sup>(b)</sup>dpm = dipivaloylmethane,  $\text{Me}_3\text{CC}(\text{O})\text{CH}=\text{C}(\text{O}^-)\text{CMe}_3$ .

<sup>(c)</sup>The structure can be visualized as octahedral if each  $\text{NO}_3^-$  is considered to occupy a single coordination site (p. 1245).

aqueous chemistries.  $\text{Ln}^{\text{IV}}$  (Ln = Pr, Nd, Tb, Dy) and  $\text{Ln}^{\text{II}}$  (Ln = Nd, Sm, Eu, Dy, Tm, Yb) also are known in the solid state but are unstable in water. The rather restricted aqueous redox chemistry which this implies is summarized in the oxidation state diagram (Fig. 30.4).

The prevalence of the +3 oxidation state is a result of the stabilizing effects exerted on different orbitals by increasing ionic charge. As successive electrons are removed from a neutral lanthanide atom, the stabilizing effect on the orbitals is in the order  $4f > 5d > 6s$ , this being the order in which the orbitals penetrate through the inert core of electrons towards the nucleus. By the time an ionic charge of +3 has been reached, the preferential stabilization of the 4f orbitals is such that in all cases the 6s and 5d orbitals have been emptied. Also, in most cases, the electrons remaining in the 4f orbitals are themselves so far



**Figure 30.4** Volt-equivalent versus oxidation state for lanthanides with more than one oxidation state.

embedded in the inert core as to be immovable by chemical means. Exceptions are Ce and, to

a lesser extent, Pr which are at the beginning of the series where, as already noted, the 4f orbitals are still at a comparatively high energy and can therefore lose a further electron. Tb<sup>IV</sup> presumably owes its existence to the stability of the 4f<sup>7</sup> configuration.

The stabilizing effects of half, and completely, filled shells can be similarly invoked to explain the occurrence of the divalent state in Eu<sup>II</sup>(4f<sup>7</sup>) and Yb<sup>II</sup>(4f<sup>14</sup>) while these, and the other known divalent ions are of just those elements which occupy elevated positions on the *I*<sub>3</sub> plot (Fig. 30.3).

The absence of 5d electrons and the inertness of the lanthanides' 4f shell makes  $\pi$  backbonding energetically unfavourable and simple carbonyls, for instance, have only been obtained in argon matrices at 8–12 K. On the other hand, essentially ionic cyclopentadienides are well known and an increasing number of  $\sigma$ -bonded Ln–C compounds have been produced (see section 30.3.5).

### 30.3 Compounds of the Lanthanides<sup>(12–15)</sup>

The reaction between H<sub>2</sub> and the gently heated (300–350°C) metals produces black, reactive and highly conducting solids, LnH<sub>2</sub>. These hydrides have the fcc fluorite structure (p. 118) and are evidently composed of Ln<sup>III</sup>, 2H<sup>-</sup>, e<sup>-</sup>, the electron being delocalized in a metallic conduction band. Further hydrogen can be accommodated in the interstices of the lattice and, with the exceptions of Eu and Yb, which are the two lanthanides

<sup>12</sup> S. COTTON, *Lanthanides and Actinides*, Macmillan, Basingstoke, 1991, 192 pp.

<sup>13</sup> G. MEYER and L. R. MORSS (eds.), *Synthesis of Lanthanide and Actinide Compounds*, Kluwer, Dordrecht, 1991, 367 pp.

<sup>14</sup> M. LESKALÄ and L. NIINISTÖ, pp. 203–334, Vol. 8 (1986) and pp. 91–320, Vol. 9 (1987) of ref. 1.

<sup>15</sup> T. MOELLER, The lanthanides, Chap. 44, pp. 1–101, in *Comprehensive Inorganic Chemistry*, Vol. 4, Pergamon Press, Oxford, 1973; Lanthanides and actinides, Vol. 7, *MTP International Review of Science, Inorganic Chemistry* (Series Two) (K. W. BAGNALL, ed.), Butterworths, London, 1975, 329 pp.

most favourably disposed to divalency, a limiting stoichiometry of LnH<sub>3</sub> can be achieved if high pressures are employed (p. 66). The composition of LnH<sub>3</sub> is Ln<sup>III</sup>, 3H<sup>-</sup> with conductivity correspondingly reduced as the additional H atom traps the previously delocalized electron (to form H<sup>-</sup>).

Metallic conductivity, arising from the presence of Ln<sup>III</sup> ions with the balance of electrons situated in a conduction band, is also found in some of the borides (p. 145) and carbides (p. 297).

#### 30.3.1 Oxides and chalcogenides<sup>(16,17)</sup>

Ln<sub>2</sub>O<sub>3</sub> are all well characterized. With three exceptions they are the final products of combustion of the metals or ignition of the hydroxides, carbonate, nitrate, etc. The exceptions are Ce, Pr and Tb, the most oxidized products of which are the dioxides, from which the sesquioxides can be obtained by controlled reduction with H<sub>2</sub>. Ln<sub>2</sub>O<sub>3</sub> adopt three structure types conventionally classified as:<sup>(18)</sup>

*A-type*, consisting of {LnO<sub>7</sub>} units which approximate to capped octahedral geometry, and favoured by the lightest lanthanides.

*B-type*, also consisting of {LnO<sub>7</sub>} units but now of three types, two are capped trigonal prisms and one is a capped octahedron; favoured by the middle lanthanides.

*C-type*, related to the fluorite structure but with one-quarter of the anions removed in such a way as to reduce the metal coordination number from 8 to 6 (but not octahedral); favoured by the middle and heavy lanthanides.

Ln<sub>2</sub>O<sub>3</sub> are strongly basic and the lighter, more basic, ones resemble the oxides of Group 2

<sup>16</sup> R. G. HAIRE and L. EYRING, pp. 413–506, Vol. 18 (1994) of ref. 1.

<sup>17</sup> L. EYRING, pp. 187–224 of ref. 13 for oxides; M. GUITTARD and J. FLAHAUT, pp. 321–52 of ref. 13 for sulfides.

<sup>18</sup> A. F. WELLS, *Structural Inorganic Chemistry*, 5th edn., pp. 544–7, Oxford University Press, Oxford, 1984.

in this respect. All are insoluble in water but absorb it to form hydroxides. They dissolve readily in aqueous acids to yield solutions which, providing they are kept on the acid side of pH 5 to avoid hydrolysis, contain the  $[\text{Ln}(\text{H}_2\text{O})_x]^{3+}$  ions. Hydrous hydroxides can be precipitated from these solutions by addition of ammonia or aqueous alkali. Crystalline  $\text{Ln}(\text{OH})_3$  have a 9-coordinate, tricapped, trigonal prismatic structure, and may be obtained by prolonged treatment of  $\text{Ln}_2\text{O}_3$  with conc NaOH at high temperature and pressure (hydrothermal ageing).

The pale-yellow  $\text{CeO}_2$  is a rather inert material when prepared by ignition, but in the hydrous, freshly precipitated form it redissolves quite easily in acids. The analogous dark-coloured  $\text{PrO}_2$  and  $\text{TbO}_2$  can be obtained by ignition but require more extreme conditions ( $\text{O}_2$  at 282 bar and  $400^\circ\text{C}$  for  $\text{PrO}_2$ , and atomic oxygen at  $450^\circ\text{C}$  for  $\text{TbO}_2$ ). All three dioxides have the fluorite structure. Since this is the structure on which C-type  $\text{Ln}_2\text{O}_3$  is based (by removing a quarter of the anions) it is not surprising that these three oxide systems involve a whole series of nonstoichiometric phases between the extremes represented by  $\text{LnO}_{1.5}$  and  $\text{LnO}_2$  (p. 643). The compositions and structures of these phases arise because the basic unit from which they are built is a so-called "coordination defect",  $[\text{M}_2^{\text{III}}\text{M}_{1.5}^{\text{IV}}\square\text{O}_6]^{(19)}$ .

Claims for the existence of several lower oxides,  $\text{LnO}$ , have been made but most have been rejected, and it seems that only  $\text{NdO}$ ,  $\text{SmO}$  (both lustrous golden yellow),  $\text{EuO}$  (dark red) and  $\text{YbO}$  (greyish-white) are genuine. They are obtained by reducing  $\text{Ln}_2\text{O}_3$  with the metal at high temperatures and, except for  $\text{EuO}$ , at high pressures. They have the NaCl structure but whereas  $\text{EuO}$  and  $\text{YbO}$  are composed of  $\text{Ln}^{\text{II}}$  and are insulators or semiconductors,  $\text{NdO}$  and  $\text{SmO}$  like the dihydrides consist essentially of  $\text{Ln}^{\text{III}}$  ions with the extra electrons forming a conduction band.  $\text{EuO}$  was unexpectedly found to be ferromagnetic at low temperatures. The

absence of conduction electrons, and the presence of 4f orbitals which are probably too contracted to allow overlap between adjacent cations, makes it difficult to explain the mechanism of the ferromagnetic interaction.  $\text{EuO}$  and the monochalcogenides have potential applications in memory devices.<sup>(20)</sup>

Chalcogenides of similar stoichiometry to the oxides, but for a wider range of metals, are known, though their characterization is made more difficult by the prevalence of nonstoichiometry and the occurrence of phase changes in several instances. In general the chalcogenides are stable in dry air but are hydrolysed if moisture is present. If heated in air they oxidize (sulfides especially) to basic salts of the corresponding oxo-anion and they show varying susceptibility to attack by acids with evolution of  $\text{H}_2\text{Z}$ .

Monochalcogenides,  $\text{LnZ}$  ( $\text{Z} = \text{S}, \text{Se}, \text{Te}$ ), have been prepared for all the lanthanides except Pm, mostly by direct combination.<sup>(17)</sup> They are almost black and, like the monoxides, have the NaCl structure. However, with the exceptions of  $\text{SmZ}$ ,  $\text{EuZ}$ ,  $\text{YbZ}$ ,  $\text{TmSe}$  and  $\text{TmTe}$ , they have metallic conductivity and evidently consist of  $\text{Ln}^{\text{III}} + \text{Z}^{2-}$  ions with 1 electron from each cation delocalized in a conduction band.  $\text{EuZ}$  and  $\text{YbZ}$ , by contrast, are semiconductors or insulators with genuinely divalent cations, but  $\text{SmZ}$  seem to be intermediate and may involve the equilibrium:



Trivalent chalcogenides,  $\text{Ln}_2\text{Z}_3$ , can be obtained by a variety of methods which include direct combination and, in the case of the sulfides, the action of  $\text{H}_2\text{S}$  on the chloride or oxide. As with  $\text{Ln}_2\text{O}_3$ , various crystalline modifications occur. When  $\text{Ln}_2\text{Z}_3$  are heated with an excess of chalcogen in a sealed tube at  $600^\circ\text{C}$ , products with compositions up to or nearing  $\text{LnZ}_2$  are obtained. They seem to be polychalcogenides, however, with the metal uniformly in the +3 state;  $\text{Ln}^{\text{IV}}$  chalcogenides are not known.

<sup>19</sup> B. F. HOSKINS and R. L. MARTIN, *Aust. J. Chem.* **48**, 709–39 (1995).

<sup>20</sup> Pages 23–41 of ref. 11.

### 30.3.2 Halides<sup>(12,13,21)</sup>

Halides of the lanthanides are listed in Table 30.4 and are of the types  $\text{LnX}_4$ ,  $\text{LnX}_3$  and  $\text{LnX}_2$ . Not surprisingly,  $\text{LnX}_4$  occur only as the fluorides of  $\text{Ce}^{\text{IV}}$ ,  $\text{Pr}^{\text{IV}}$  and  $\text{Tb}^{\text{IV}}$ .  $\text{CeF}_4$  is comparatively stable and can be prepared either directly from the elements or by the action of  $\text{F}^-$  on aqueous solutions of  $\text{Ce}^{\text{IV}}$  when it crystallizes as the monohydrate. The other tetrafluorides are thermally unstable and, as they oxidize water, can only be prepared dry;  $\text{TbF}_4$  from  $\text{TbF}_3 + \text{F}_2$  at  $320^\circ\text{C}$ , and  $\text{PrF}_4$  by the rather complex procedure of fluorinating a mixture of  $\text{NaF}$  and  $\text{PrF}_3$  with  $\text{F}_2$  ( $\rightarrow \text{Na}_2\text{PrF}_6$ ) and then extracting  $\text{NaF}$  from the reaction mixture with liquid  $\text{HF}$ .

Promethium apart, all possible trihalides (52) are known. The trifluorides, being very insoluble, can be precipitated as  $\text{LnF}_3 \cdot \frac{1}{2}\text{H}_2\text{O}$  by the action of  $\text{HF}$  on aqueous  $\text{Ln}(\text{NO}_3)_3$ . Aqueous solutions of the other trihalides are obtained by simply dissolving the oxides or carbonates in aqueous  $\text{HX}$ . Hydrated (6–8 $\text{H}_2\text{O}$ ) salts can be crystallized, though with difficulty because of their high solubilities. Preparation of the anhydrous trihalides by thermal dehydration of these hydrates is possible for fluorides and chlorides of the lighter lanthanides, and an atmosphere of  $\text{HX}$  extends the applicability of the method to heavier lanthanides. Because of the possible formation of oxohalides in preparations involving halides and oxygen-containing materials, direct combination, which is a completely general method, is often preferred for the anhydrous halides.

The anhydrous trihalides are ionic, high melting, crystalline substances which, apart from the trifluorides are extremely deliquescent. As can be seen from Table 30.4, the coordination number of the  $\text{Ln}^{\text{III}}$  changes with the radii of the ions, from 9 for the trifluorides of the large lanthanides to 6 for the triiodides of the smaller lanthanides. Their chief importance has been as materials from which the pure metals can be prepared.

The dihalides are obtained from the corresponding trihalides, most generally by reduction with the lanthanide metal itself<sup>(22)</sup> or with an alkali metal<sup>(23,24)</sup> and also, in the case of the more stable of the diiodides ( $\text{SmI}_2$ ,  $\text{EuI}_2$ ,  $\text{YbI}_2$ ), by thermal decomposition.<sup>†</sup>  $\text{SmI}_2$  and  $\text{YbI}_2$  can also be conveniently prepared in quantitative yield by reacting the metal with 1,2-diiodoethane in anhydrous tetrahydrofuran at room temperature:<sup>(25)</sup>  $\text{Ln} + \text{ICH}_2\text{CH}_2\text{I} \rightarrow \text{LnI}_2 + \text{CH}_2=\text{CH}_2$ . With the exception of  $\text{EuX}_2$ , all the dihalides are very easily oxidized and will liberate hydrogen from water. The occurrence of these dihalides parallels the occurrence of high values of the third ionization energy amongst the metals<sup>(10,11)</sup> (Fig. 30.3), with the reasonable qualification that, in this low oxidation state, iodides are more numerous than fluorides. The same types of structures are found as for the alkaline earth dihalides with the coordination number of the cation ranging from 9 to 6 and, like  $\text{CaI}_2$ , the diiodides of Dy, Tm and Yb form layer structures ( $\text{CdCl}_2$ ,  $\text{CdI}_2$ ; see Fig. 29.2) typical of compounds with large anions where marked polarization effects are expected.

The isomorphous diiodides of Ce, Pr and Gd stand apart from all the other, salt-like, dihalides. These three, like  $\text{LaI}_2$ , are notable for their metallic lustre and very high conductivities and are best formulated as  $\{\text{Ln}^{\text{III}}, 2\text{I}^-, e^-\}$ , the electron being in a delocalized conduction band. Besides the dihalides, other reduced species have been obtained such as  $\text{Ln}_5\text{Cl}_{11}$  ( $\text{Ln} = \text{Sm}, \text{Gd}, \text{Ho}$ ). They have fluorite-related structures (p. 118) in which the anionic sublattice is partially rearranged to accommodate additional anions,

<sup>22</sup> J. D. CORBETT, pp. 159–73 of ref. 13.

<sup>23</sup> G. MEYER, *Chem. Rev.* **88**, 93–107 (1988); G. MEYER, and T. SCHLEID, pp. 175–85 of ref. 13.

<sup>24</sup> A. SIMON, H. MATTAUSCH, G. J. MILLER, W. BAUHOFFER and R. K. KREMER, pp. 191–285, Vol. 15 (1991) of ref. 1.

<sup>†</sup> Dilute solid solutions of  $\text{Ln}^{\text{III}}$  ions in  $\text{CaF}_2$  may be reduced by Ca vapour to produce  $\text{Ln}^{\text{II}}$  ions trapped in the crystal lattice. By their use it has been possible to obtain the electronic spectra of  $\text{Ln}^{\text{II}}$  ions.

<sup>25</sup> P. GIRARD, J. L. NAMY and H. B. KAGAN, *J. Am. Chem. Soc.* **102**, 2693–8 (1980).

<sup>21</sup> H. A. EICK, pp. 365–412, Vol. 18 (1994) of ref. 1.

Table 30.4 Properties of lanthanide halides: colour, mp/°C and coordination<sup>(a)</sup>

	Ce	Pr	Nd	Sm	Eu	Gd	Tb	Dy	Ho	Er	Tm	Yb	Lu
LnF <sub>4</sub>	white 400 dec 8 sa	white dec 8 sa	--	--	--	--	white dec 8 sa	--	--	--	--	--	--
LnF <sub>3</sub>	white 1430 9 ttp	green 1395 9 ttp	violet 1374 9 ttp	white 1306 9 ttp	white 1276 9 ttp	white 1231 8 btp	white 1172 8 btp	green 1154 8 btp	pink 1143 8 btp	pink 1140 8 btp	white 1158 8 btp	white 1157 8 btp	white 1182 8 btp
LnCl <sub>3</sub>	white 817 9 ttp	green 786 9 ttp	mauve 758 9 ttp	yellow 682 9 ttp	yellow dec 9 ttp	white 602 9 ttp	white 582 8 btp	white 647 6 o	yellow 720 6 o	violet 776 6 o	yellow 824 6 o	white 865 6 o	white 925 6 o
LnBr <sub>3</sub>	white 733 9 ttp	green 691 9 ttp	violet 682 8 btp	yellow 640 8 btp	grey dec 8 btp	white 770 6 o	white 828 6 o	white 879 6 o	yellow 919 6 o	violet 923 6 o	white 954 6 o	white dec 6 o	white 1025 6 o
LnI <sub>3</sub>	yellow 766 8 btp	737 8btp	green 784 8 btp	orange 850 6 o	dec 6 o	yellow 925 6 o	957 6 o	green 978 6 o	yellow 994 6 o	violet 1015 6 o	yellow 1021 6 o	white dec 6 o	brown 1050 6 o
LnF <sub>2</sub>	--	--	--	purple 1417 8 c	yellow 1416 8 c	--	--	--	--	--	--	grey (1407) 8 c	--
LnCl <sub>2</sub>	--	--	green 841 9 ttp	brown 859 9 ttp	white 731 9 ttp	--	--	black 721 dec 8, 7	--	--	green 718 7 co	green 720 7 co	--
LnBr <sub>2</sub>	--	--	green 725 9 ttp	brown 669 8, 7	white 683 8, 7	--	--	black 7 co	--	--	green 7 co	yellow 673 6 o	--
LnI <sub>2</sub>	bronze 808	bronze 758	violet 562 8, 7	green 520 7 co	green 580 7 co	bronze 831	--	purple 721 dec 6 ol	--	--	black 756 6 ol	yellow 780 6 ol	--

<sup>(a)</sup>9 ttp = 9-coordinate tricapped trigonal prismatic; 8 sa = 8-coordinate square antiprismatic; 8 btp = 8-coordinate bicapped trigonal prismatic; 8 c = 8-coordinate cubic (fluorite); 8, 7 = mixed 8- and 7-coordinate (SrBr<sub>2</sub> structure); 7 co = 7-coordinate capped octahedral; 6 o = 6-coordinate octahedral; 6 ol = 6-coordinate octahedral layered.



**Table 30.5** Stoichiometries and structures of reduced halides ( $X/M < 2$ ) of scandium, yttrium, lanthanum and the lanthanides

Average oxidation state	Examples	Structural features
1.714	Sc <sub>7</sub> Cl <sub>12</sub> M <sub>7</sub> I <sub>12</sub> (La, Pr, Tb)	Discrete M <sub>6</sub> X <sub>12</sub> clusters
1.600	Sc <sub>5</sub> Cl <sub>8</sub>	Discrete M <sub>6</sub> X <sub>12</sub> clusters
1.500	M <sub>2</sub> Cl <sub>3</sub> (Y, Gd, Tb, Er, Lu) M <sub>2</sub> Br <sub>3</sub> (Y, Gd)	Single chains of edge-sharing metal octahedra with M <sub>6</sub> X <sub>12</sub> -type environment (edge-capped by X) along with parallel chains of edge-sharing MX <sub>6</sub> octahedra
1.429	Sc <sub>7</sub> Cl <sub>10</sub>	Single chains of edge-sharing metal octahedra with M <sub>6</sub> X <sub>8</sub> -type environment (face-capped by X)
1.000	MXH <sub>n</sub> (X = Cl, Br)(Sc, Y, Gd, Lu and probably other Ln)	Double chains of edge-sharing metal octahedra with M <sub>6</sub> X <sub>8</sub> -type environment with parallel chains of edge-sharing MCl <sub>6</sub> octahedra
		Double metal layers of edge-sharing metal octahedra, M <sub>6</sub> X <sub>8</sub> -type environment but with encapsulated H atoms

leading to irregular 7- and 8-coordination of the cations. In the case of Gd and Tb, further reduction gives rise to Ln<sub>2</sub>Cl<sub>3</sub> phases which are constructed from Ln<sub>6</sub> octahedra sharing *trans*-edges and sheathed with chlorine atoms which bridge adjacent chains. Gd<sub>2</sub>Cl<sub>3</sub> is a semiconductor and provided the first example of a lanthanide in an oxidation state < +2. Continued reduction finally produces “graphite-like” LnCl phases originally thought to be binary halides like ZrX (p. 966) but in fact, like ScCl (p. 950), requiring the presence of interstitial H atoms to stabilize the structure. They are therefore formulated as LnXH<sub>n</sub>. Structural characteristics are summarised in Table 30.5.<sup>(22,26–28)</sup>

Other interstitial atoms stabilizing such clusters are B, C, N and O.<sup>(22)</sup> Examples of carbon stabilized clusters include: isolated metal octahedra in Cs[Ln<sub>6</sub>I<sub>12</sub>C] (Ln = Er, Lu)<sup>(29)</sup> and Gd[Gd<sub>6</sub>Cl<sub>12</sub>C]; pairs of edge-sharing metal octahedra in Gd<sub>10</sub>Cl<sub>18</sub>(C<sub>2</sub>)<sub>2</sub>; and chains of edge-sharing metal octahedra in Gd<sub>4</sub>I<sub>5</sub>C.

### 30.3.3 Magnetic and spectroscopic properties<sup>(12)</sup>

The electronic configurations of the lanthanides are described by using the Russell–Saunders coupling scheme. Values of the quantum numbers *S* and *L* corresponding to the lowest energy are derived in the conventional manner.<sup>(12)</sup> These are then expressed for each ion in the form of a ground term with the symbolism that *S, P, D, F, G, H, I, ...* correspond to *L = 0, 1, 2, 3, 4, 5, 6, ...* in that order. The angular momentum vectors associated with *S* and *L* couple together (spin–orbit coupling) to produce a resultant angular momentum associated with an overall quantum number *J*. Because the 4f electrons of lanthanide ions are largely buried in the inner core, they are effectively shielded from their chemical environments. As a result, spin–orbit coupling is much larger than the crystal field (of the order of 2000 cm<sup>-1</sup> compared to 100 cm<sup>-1</sup>) and must be considered first. Note that this is precisely the reverse of the situation in the d-block elements where the d electrons are exposed directly to the influence of neighbouring groups and the crystal field is therefore much greater than the spin–orbit coupling.

*J* can take the values  $J = L + S, L + S - 1, \dots, L - S$  (or  $S - L$  if  $S > L$ ), each corresponding to a different energy, so that a “term” (defined

<sup>26</sup> A. SIMON, *Angew. Chem. Int. Edn. Engl.* **27**, 159–83 (1988).

<sup>27</sup> R. P. ZIEBARTH and J. CORBETT, *Acc. Chem. Res.* **22**, 256–62 (1989).

<sup>28</sup> H. MATTAUSCH, R. EGER, J. D. CORBETT and A. SIMON, *Z. anorg. allg. Chem.* **616**, 157–61 (1992).

<sup>29</sup> H. M. ARTELT, T. SCHLEID and G. MEYER, *Z. anorg. allg. Chem.* **618**, 18–25 (1992).

Table 30.6 Magnetic and spectroscopic properties of Ln<sup>III</sup> ions in hydrated salts

Ln	Unpaired electrons	Ground state	Colour	$\mu_e$ /BM	
				$g\sqrt{J(J+1)}$	Observed
Ce	1 (4f <sup>1</sup> )	<sup>2</sup> F <sub>5/2</sub>	Colourless	2.54	2.3–2.5
Pr	2 (4f <sup>2</sup> )	<sup>3</sup> H <sub>4</sub>	Green	3.58	3.4–3.6
Nd	3 (4f <sup>3</sup> )	<sup>4</sup> I <sub>9/2</sub>	Lilac	3.62	3.5–3.6
Pm	4 (4f <sup>4</sup> )	<sup>5</sup> I <sub>4</sub>	Pink	2.68	—
Sm	5 (4f <sup>5</sup> )	<sup>6</sup> H <sub>5/2</sub>	Yellow	0.85	1.4–1.7 <sup>(a)</sup>
Eu	6 (4f <sup>6</sup> )	<sup>7</sup> F <sub>0</sub>	Very pale pink	0	3.3–3.5 <sup>(a)</sup>
Gd	7 (4f <sup>7</sup> )	<sup>8</sup> S <sub>7/2</sub>	Colourless	7.94	7.9–8.0
Tb	6 (4f <sup>8</sup> )	<sup>7</sup> F <sub>6</sub>	Very pale pink	9.72	9.5–9.8
Dy	5 (4f <sup>9</sup> )	<sup>6</sup> H <sub>15/2</sub>	Yellow	10.65	10.4–10.6
Ho	4 (4f <sup>10</sup> )	<sup>5</sup> I <sub>8</sub>	Yellow	10.60	10.4–10.7
Er	3 (4f <sup>11</sup> )	<sup>4</sup> I <sub>15/2</sub>	Rose-pink	9.58	9.4–9.6
Tm	2 (4f <sup>12</sup> )	<sup>3</sup> H <sub>6</sub>	Pale green	7.56	7.1–7.5
Yb	1 (4f <sup>13</sup> )	<sup>2</sup> F <sub>7/2</sub>	Colourless	4.54	4.3–4.9
Lu	0 (4f <sup>14</sup> )	<sup>1</sup> S <sub>0</sub>	Colourless	0	0

<sup>(a)</sup>These are the values of  $\mu_e$  at room temperature. The values fall as the temperature is reduced (see text).

by a pair of  $S$  and  $L$  values) is said to split into a number of component “states” (each defined by the same  $S$  and  $L$  values plus a value of  $J$ ). The “ground state” of the ion is that with  $J = L - S$  (or  $S - L$ ) if the  $f$  shell is less than half-full, and that with  $J = L + S$  if the  $f$  shell is more than half-full. It is indicated simply by adding this value of  $J$  as a subscript to the symbol for the “ground term”.

The magnitude of the separation between the adjacent states of a term indicates the strength of the spin-orbit coupling, and in all but two cases (Sm<sup>III</sup> and Eu<sup>III</sup>) it is sufficient to render the first excited state of the Ln<sup>III</sup> ions thermally inaccessible, and so the magnetic properties are determined solely by the ground state. It can be shown that the magnetic moment expected for such a situation is given by:

$$\mu_e = g\sqrt{J(J+1)} \text{ BM},$$

$$\text{where } g = \frac{3}{2} + \frac{S(S+1) - L(L+1)}{2J(J+1)}$$

As can be seen in Table 30.6, this agrees very well with experimental values except for Sm<sup>III</sup> and Eu<sup>III</sup> and agreement is reasonable for these

also if allowance is made for the temperature-dependent population of excited states.

Electronic absorption spectra are produced when electromagnetic radiation promotes the ions from their ground state to excited states. For the lanthanides the most common of such transitions involve excited states which are either components of the ground term<sup>†</sup> or else belong to excited terms which arise from the same 4f<sup>*n*</sup> configuration as the ground term. In either case the transitions therefore involve only a redistribution of electrons within the 4f orbitals (i.e. f→f transitions) and so are orbitally forbidden just like d→d transitions. In the case of the latter the rule is partially relaxed by a mechanism which depends on the effect of the crystal field in distorting the symmetry of the metal ion. However, it has already been pointed out that crystal field effects are very much smaller in the case of Ln<sup>III</sup> ions and they

<sup>†</sup> The separation of these component states being, as pointed out above, of the order of a few thousand wavenumbers, such transitions produce absorptions in the infrared region of the spectrum. Ions which have no terms other than the ground term will therefore be colourless, having no transitions of sufficiently high energy to absorb in the visible region. This accounts for the colourless ions listed in Table 30.6.

cannot therefore produce the same relaxation of the selection rule. Consequently, the colours of  $\text{Ln}^{\text{III}}$  compounds are usually less intense. A further consequence of the relatively small effect of the crystal field is that the energies of the electronic states are only slightly affected by the nature of the ligands or by thermal vibrations, and so the absorption bands are very much sharper than those for  $d \rightarrow d$  transitions. Because of this they provide a useful means of characterizing, and quantitatively estimating,  $\text{Ln}^{\text{III}}$  ions.

Nevertheless, crystal fields cannot be completely ignored. The intensities of a number of bands ("hypersensitive" bands) show a distinct dependence on the actual ligands which are coordinated. Also, in the same way that crystal fields lift some of the orbital degeneracy ( $2L + 1$ ) of the terms of  $d^n$  ions, so they lift some of the  $2J + 1$  degeneracy of the states of  $f^n$  ions, though in this case only by the order of  $100 \text{ cm}^{-1}$ . This produces fine structure in some bands of  $\text{Ln}^{\text{III}}$  spectra.

$\text{Ce}^{\text{III}}$  and  $\text{Tb}^{\text{III}}$  are exceptional in providing (in the ultraviolet) bands of appreciably higher intensity than usual. The reason is that the particular transitions involved are of the type  $4f^n \rightarrow 4f^{n-1}5d^1$ , and so are not orbitally forbidden. These 2 ions have 1 electron more than an empty  $f$  shell and 1 electron more than a half-full  $f$  shell, respectively, and the promotion of this extra electron is thereby easier than for other ions.

Sm, Dy but more especially Eu and Tb have excited states which are only slightly lower in energy than excited states of typical ligands. If electrons on the ligand are excited, the possibility therefore exists that, instead of falling back to the ground state of the ligand, they may pass first to the excited state of the  $\text{Ln}^{\text{III}}$  and then fall to the metal ground state, emitting radiation of characteristic frequency in doing so (fluorescence or, more generally, luminescence). This is the basis of the commercial use of oxide phosphors of these elements on TV screens where the excitation is provided by electrical discharge. Excitation by uv light produces luminescence spectra

which yield information about the donor atoms and co-ordination symmetry.<sup>(30,31)</sup>

It has been possible, as already noted (footnote, p. 1240) to study the spectra of  $\text{Ln}^{\text{II}}$  ions stabilized in  $\text{CaF}_2$  crystals. It might be expected that these spectra would resemble those of the +3 ions of the next element in the series. However, because of the lower ionic charge of the  $\text{Ln}^{\text{II}}$  ions their  $4f$  orbitals have not been stabilized relative to the  $5d$  to the same extent as those of the  $\text{Ln}^{\text{III}}$  ions.  $\text{Ln}^{\text{II}}$  spectra therefore consist of rather broad, orbitally allowed,  $4f \rightarrow 5d$  bands overlaid with weaker and much sharper  $f \rightarrow f$  bands.

### 30.3.4 Complexes<sup>(12,14,32)</sup>

#### Oxidation state IV

The +4 oxidation state is found in  $\text{LnO}_2$ ,  $\text{LnF}_4$ , the ternary oxides  $\text{M}_2\text{LnO}_3$  and  $\text{Li}_8\text{LnO}_6$  ( $\text{Ln} = \text{Ce, Pr, Tb}$ ), and in the ternary fluorides  $\text{M}_3\text{LnF}_7$  ( $\text{Ln} = \text{Ce, Pr, Tb, Nd, Dy}$ ).  $\text{M}^{\text{IV}}\text{TbIO}_6 \cdot x\text{H}_2\text{O}$  has been obtained from aqueous alkaline solution<sup>(33)</sup> but Ce is the only lanthanide with a significant aqueous or co-ordination chemistry in this oxidation state. Fig. 30.4 shows that this situation is in no way surprising.

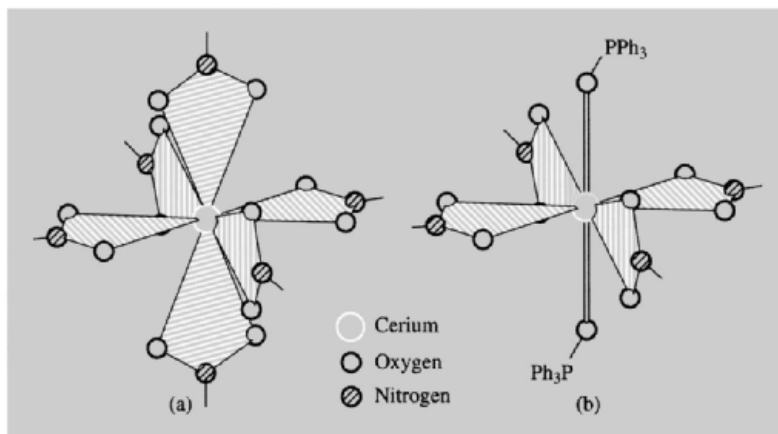
Aqueous "ceric" solutions are widely used as oxidants in quantitative analysis; they can be prepared by the oxidation of  $\text{Ce}^{\text{III}}$  ("cerous") solutions with strong oxidizing agents such as peroxodisulfate,  $\text{S}_2\text{O}_8^{2-}$ , or bismuthate,  $\text{BiO}_3^-$ . Complexation and hydrolysis combine to render  $E(\text{Ce}^{4+}/\text{Ce}^{3+})$  markedly dependent on anion and acid concentration. In relatively strong perchloric acid the aquo ion is present but in other acids coordination of the anion is likely. Also, if the pH is increased, hydrolysis to

<sup>30</sup> N. SABBATINI, M. GUARDIGOLI and J.-M. LEHN, *Coord. Chem. Revs.* **123**, 201–28 (1993).

<sup>31</sup> J. V. BEITZ, pp. 159–96, Vol. 18 (1994) of ref. 1.

<sup>32</sup> F. A. HART, Scandium, Yttrium and the Lanthanides, Chap. 39, pp. 1059–127, in *Comprehensive Coordination Chemistry*, Vol. 3, Pergamon Press, Oxford, 1987.

<sup>33</sup> Y. YING and Y. RU-DONG, *Polyhedron* **11**, 963–6 (1992).



**Figure 30.5** Nitrate complexes of  $\text{Ce}^{\text{IV}}$ . (a)  $[\text{Ce}(\text{NO}_3)_6]^{2-}$ : the  $\text{Ce}^{\text{IV}}$  is surrounded by 12 oxygen atoms from 6 bidentate nitrate ions in the form of an icosahedron (in each case the third oxygen is omitted for clarity). Note that this implies an octahedral disposition of the 6 nitrogen atoms. (b)  $[\text{Ce}(\text{NO}_3)_4(\text{OPPh}_3)_2]$ .

$\text{Ce}(\text{OH})^{3+}$  occurs followed by polymerization and finally, as the solution becomes alkaline, by precipitation of the yellow, gelatinous  $\text{CeO}_2 \cdot x\text{H}_2\text{O}$ .

Of the various salts which can be isolated from aqueous solution, probably the most important is the water-soluble double nitrate,  $(\text{NH}_4)_2[\text{Ce}(\text{NO}_3)_6]$ , which is the compound generally used in  $\text{Ce}^{\text{IV}}$  oxidations. The anion involves 12-coordinated Ce (Fig. 30.5a). Two *trans*-nitrates of this complex can be replaced by  $\text{Ph}_3\text{PO}$  to give the orange 10-coordinate neutral complex  $[\text{Ce}(\text{NO}_3)_4(\text{OPPh}_3)_2]$  (Fig. 30.5b). The sulfates  $\text{Ce}(\text{SO}_4)_2 \cdot n\text{H}_2\text{O}$  ( $n = 0, 4, 8, 12$ ) and  $(\text{NH}_4)_2\text{Ce}(\text{SO}_4)_3$ , and the iodate are also known. Also obtainable from aqueous solutions are complexes with other *O*-donor ligands such as  $\beta$ -diketonates, and fluoro complexes such as  $[\text{CeF}_8]^{4-}$  and  $[\text{CeF}_6]^{2-}$ . This last ion is not in fact 6-coordinated but achieves an 8-coordinate, square-antiprismatic geometry with the aid of fluoride bridges. In the orange  $[\text{CeCl}_6]^{2-}$  by contrast, the larger halide is able to stabilize a 6-coordinate, octahedral geometry. It is prepared by treatment of  $\text{CeO}_2$  with  $\text{HCl}$  but, because  $\text{Ce}^{\text{IV}}$  in aqueous solution oxidizes  $\text{HCl}$  to  $\text{Cl}_2$ , the reaction must be performed in a nonaqueous solvent such as pyridine or dioxan.

### Oxidation state III

The coordination chemistry of the large, electropositive  $\text{Ln}^{\text{III}}$  ions is complicated, especially in solution, by ill-defined stereochemistries and uncertain coordination numbers. This is well illustrated by the aquo ions themselves.<sup>(34)</sup> These are known for all the lanthanides, providing the solutions are moderately acidic to prevent hydrolysis, with hydration numbers probably about 8 or 9 but with reported values depending on the methods used to measure them. It is likely that the primary hydration number decreases as the cationic radius falls across the series. However, confusion arises because the polarization of the  $\text{H}_2\text{O}$  molecules attached directly to the cation facilitates hydrogen bonding to other  $\text{H}_2\text{O}$  molecules. As this tendency will be the greater, the smaller the cation, it is quite reasonable that the secondary hydration number increases across the series.

Hydrated salts with all the common anions can be crystallized from aqueous solutions and frequently, but by no means invariably, they contain the  $[\text{Ln}(\text{H}_2\text{O})_9]^{3+}$  ion. An enormous number of salts of organic acids such as oxalic, citric and

<sup>34</sup> E. N. RIZKALLA and G. R. CHOPPIN, pp. 529–58, Vol. 18 (1994) of ref. 1; T. KOWALL, F. FOGLIA, L. HELM and A. E. MERBACH, *J. Am. Chem. Soc.* **117**, 3790–9 (1995).

tartaric have been studied,<sup>(35)</sup> often for use in separation methods. These anions are, in fact, chelating *O* ligands which as a class provide the most extensive series of Ln<sup>III</sup> complexes. NO<sub>3</sub><sup>-</sup> is an inorganic counterpart and is notable for the high coordination numbers it yields, as in the 10-coordinate bicapped dodecahedral [Ce(NO<sub>3</sub>)<sub>5</sub>]<sup>2-</sup>, and in [Ce(NO<sub>3</sub>)<sub>6</sub>]<sup>3-</sup> which like its Ce<sup>IV</sup> analogue, has the 12-coordinate icosahedral geometry (Fig. 30.5a) (see also p. 469).

$\beta$ -diketonates (L-L) provide further important examples of this class of ligand, and yield complexes of the type [Ln(L-L)<sub>3</sub>L'] (L' = H<sub>2</sub>O, py, etc.) and [Ln(L-L)<sub>4</sub>]<sup>-</sup>, which are respectively 7- and 8-coordinate. Dehydration, under vacuum, of the hydrated tris-diketonates produces [Ln(L-L)<sub>3</sub>] complexes which probably increase their coordination by dimerizing or polymerizing. They may be sublimed, the most volatile and thermally stable being those with bulky alkyl groups R in [RC(O)CHC(O)R]<sup>-</sup>; they are soluble in non-polar solvents, and have received much attention as "nmr shift" reagents. Thus, in the case of organic molecules which are able to coordinate to Ln<sup>III</sup> (i.e. if they contain groups such as -OH or -COO<sup>-</sup>), the addition of one of these coordinatively unsaturated reagents produces a labile adduct; because this adduct is anisotropic the paramagnetic Ln<sup>III</sup> ion shifts the resonance line of each proton by an amount which is critically dependent on the spatial relationship of the Ln<sup>III</sup> and the proton. Greatly improved resolution is thereby obtained along with the possibility of distinguishing between alternative structures of the organic molecule.

Various crown ethers (p. 96) with differing cavity diameters provide a range of coordination numbers and stoichiometries, although crystallographic data are sparse. An interesting series, illustrating the dependence of coordination number on cationic radius and ligand cavity diameter, is provided by the complexes formed by the lanthanide nitrates and the 18-crown-6 ether (i.e. 1,4,7,10,13,16-

hexaoxacyclo-octadecane). For Ln = La–Gd the most thermally-stable product is that with a ratio of Ln:crown ether = 4:3, but the larger of these lanthanides (i.e. La, Ce, Pr and Nd) also form a 1:1 complex. This is [Ln(NO<sub>3</sub>)<sub>3</sub>L] in which the Ln<sup>III</sup> is 12-coordinate<sup>(36)</sup> (Fig. 30.6a). The 4:3 complex, on the other hand, is probably [Ln(NO<sub>3</sub>)<sub>2</sub>L]<sub>3</sub>[Ln(NO<sub>3</sub>)<sub>6</sub>] in which, compared to the 1:1 complex, the Ln<sup>III</sup> in the complex cation has lost one NO<sub>3</sub><sup>-</sup>, so reducing its coordination number to 10. The remaining, still smaller lanthanides (Tb–Lu) find the cavity of this ligand too large and form [Ln(NO<sub>3</sub>)<sub>3</sub>(H<sub>2</sub>O)<sub>3</sub>]L, in which the ligand is uncoordinated.

Unidentate *O* donors such as pyridine-*N*-oxide and triphenylphosphine oxide also form many complexes, as do alkoxides. This last group, like the alkoxides of Sc and Y (p. 951) is of special interest because of possible applications in the deposition of pure metal oxides by MOCVD techniques.<sup>(37)</sup> Attempts to prepare Ln(OR)<sub>3</sub> usually produce polynuclear clusters. Two examples will suffice: [Nd<sub>6</sub>(OPr<sup>*i*</sup>)<sub>17</sub>Cl], made up of 6 Nd atoms held together around a central Cl atom by means of bridging OCHMe<sub>2</sub> groups<sup>(38)</sup> (Fig. 30.6b). [Yb<sub>5</sub>O(OPr<sup>*i*</sup>)<sub>13</sub>] which consists of a square pyramid of Yb atoms containing a  $\mu_5$ -O. Four  $\mu_2$ -OPr<sup>*i*</sup> groups cap the faces of the square pyramid. A single terminal alkoxide completes a distorted octahedral coordination sphere for each metal atom.<sup>(39)</sup>

Complexes with *O*-donor ligands are more numerous than those with *N* donors, probably because the former ligands are more often negatively charged — a clear advantage when forming essentially ionic bonds. However, by using polar organic solvents such as ethanol, acetone or acetonitrile in order to avoid competitive coordination by water, complexes with

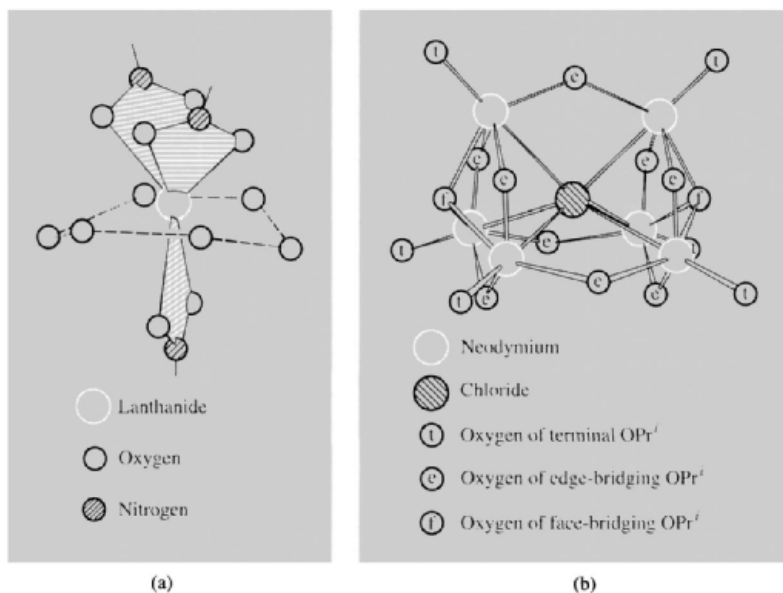
<sup>36</sup> J.-C. G. BÜNZLI, B. KLEIN and D. WESSNER, *Inorg. Chim. Acta* **44**, L147–9 (1980).

<sup>37</sup> D. C. BRADLEY, *Chem. Revs.* **89**, 1317–22 (1989).

<sup>38</sup> R. A. ANDERSEN, D. H. TEMPLETON and A. ZALKIN, *Inorg. Chem.* **17**, 1962–5 (1978).

<sup>39</sup> D. C. BRADLEY, H. CHUDZYNSKA, D. M. FRIGO, M. E. HAMMON, M. B. HURSTHOUSE and M. A. MAZID, *Polyhedron* **9**, 719–26 (1990).

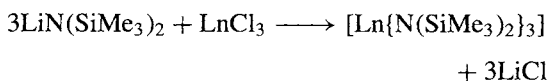
<sup>35</sup> A. OUCHI, Y. SUZUKI, Y. OHKI and Y. KOIZUMI, *Coord. Chem. Revs.* **92**, 29–43 (1988).



**Figure 30.6** (a)  $\text{Ln}(\text{NO}_3)_3$  (18-crown-6). For clarity only 2 of the oxygen atoms of each nitrate ion are shown, and only the 6 oxygen atoms of the crown ether. (Note the boat conformation of the crown ether which allows access to two  $\text{NO}_3^-$  on the open side and only one on the hindered side.) (b)  $[\text{Nd}_6(\text{OPr}^i)_{17}\text{Cl}]$ . Only the oxygens of the  $\text{OPr}^i$  groups are shown. Note that the 6 Nd atoms surrounding the Cl atom are situated at the corners of a trigonal prism, held together by 2 face-bridging and 9 edge-bridging alkoxides.

chelating ligands such as en, dien, bipy,<sup>(39a)</sup> and terpy can be prepared. Coordination numbers of 8, 9 and 10 as in  $[\text{Ln}(\text{en})_4]^{3+}$ ,  $[\text{Ln}(\text{terpy})_3]^{3+}$  and  $[\text{Ln}(\text{dien})_4(\text{NO}_3)_2]^{2+}$  are typical. Nor do complexes such as the well-known  $[\text{Ln}(\text{edta})(\text{H}_2\text{O})_3]^-$  show any destabilization because of the *N* donor atoms (edta has 4 oxygen and 2 nitrogen donor atoms). More pertinently, whereas the complexes of 18-crown-6-ethers mentioned above dissociate instantly in water, complexes of the *N*-donor analogues are sufficiently stable to remain unchanged.

As with other transition elements, the lanthanides can be induced to form complexes with exceptionally low coordination numbers by use of the very bulky ligand,  $\text{N}(\text{SiMe}_3)_2^-$ :



The volatile, but air-sensitive, and very easily hydrolysed products have a coordination number of 3, the lowest found for the lanthanides; they are apparently planar in solution (zero dipole moment) but pyramidal in the solid state. With  $\text{Ph}_3\text{PO}$  the 4-coordinate distorted tetrahedral adducts  $[\text{Ln}\{\text{N}(\text{SiMe}_3)_2\}_3(\text{OPPh}_3)]$  are obtained. So difficult is it to expand the coordination sphere that attempts to prepare bis- $(\text{Ph}_3\text{PO})$  adducts produce instead the dimeric peroxo bridged complex,  $[(\text{Ph}_3\text{PO})\{(\text{Me}_3\text{Si})_2\text{N}\}_2\text{LnO}_2\text{-Ln}\{\text{N}(\text{SiMe}_3)_2\}_2(\text{OPPh}_3)]$  (see p. 619).

Coordination by halide ions is rather weak, that of  $\text{I}^-$  especially so, but from non-aqueous solutions it is possible to isolate anionic complexes of the type  $[\text{LnX}_6]^{3-}$ . These are apparently, and unusually for  $\text{Ln}^{\text{III}}$ , 6-coordinate and octahedral. The heavier donor atoms S, Se,  $\text{P}^{(40)}$  and As form only a few

<sup>40</sup> M. D. FRYZUK, T. S. HADDAD and D. J. BERG, *Coord. Chem. Revs.* **99**, 137–212 (1990).

<sup>39a</sup> E. C. CONSTABLE, *Adv. Inorg. Chem.* **34**, 1–64 (1989).

compounds. Chelating dithiocarbamate ligands provide the best known examples such as  $[\text{Ln}(\text{S}_2\text{CNMe}_2)_3]$  and  $[\text{Ln}(\text{S}_2\text{CNMe}_2)_4]^-$ . Trigonal planar  $[\text{Sm}(\text{SAr})_3]$ , ( $\text{Ar} = \text{C}_6\text{H}_2\text{Bu}_3^{1-2,4,6}$ ) is a rare example of an Ln complex with a unidentate S-donor ligand and also an unusually low coordination number.<sup>(40)</sup>

### Oxidation state II<sup>(11)</sup>

The coordination chemistry in this oxidation state is essentially confined to the ions  $\text{Sm}^{\text{II}}$ ,  $\text{Eu}^{\text{II}}$  and  $\text{Yb}^{\text{II}}$ . These are the only ones with an aqueous chemistry and their solutions may be prepared by electrolytic reduction of the  $\text{Ln}^{\text{III}}$  solutions or, in the case of  $\text{Eu}^{\text{II}}$ , by reduction with amalgamated Zn. These solutions are blood-red for  $\text{Sm}^{\text{II}}$ , colourless or pale greenish-yellow for  $\text{Eu}^{\text{II}}$  and yellow for  $\text{Yb}^{\text{II}}$ , and presumably contain the aquo ions. All are rapidly oxidized by air, and  $\text{Sm}^{\text{II}}$  and  $\text{Yb}^{\text{II}}$  are also oxidized by water itself although aqueous  $\text{Eu}^{\text{II}}$  is relatively stable, especially in the dark.

A number of salts have been isolated but, especially those of  $\text{Sm}^{\text{II}}$  and  $\text{Yb}^{\text{II}}$ , are susceptible to oxidation even by their own water of crystallization. Carbonates and sulfates, however, have been characterized and shown to be isomorphous with those of  $\text{Sr}^{\text{II}}$  and  $\text{Ba}^{\text{II}}$ .

Europium and Yb display further similarity with the alkaline earth metals in dissolving in liquid ammonia to give intense blue solutions, characteristic of solvated electrons and presumably also containing  $[\text{Ln}(\text{NH}_3)_x]^{2+}$ . The solutions are strongly reducing and decompose on standing with the precipitation of orange  $\text{Eu}(\text{NH}_2)_2$  and brown  $\text{Yb}(\text{NH}_2)_2$  (always contaminated with  $\text{Yb}(\text{NH}_2)_3$ ) which are isostructural with the Ca and Sr amides.

### 30.3.5 Organometallic compounds<sup>(41)</sup>

The organometallic chemistry of lanthanides is far less extensive than that of transition elements

but, in spite of the lanthanides' inability to engage in  $\pi$  backbonding, it is one which has shown appreciable growth in the last quarter of a century. The compounds are of two main types: the predominantly ionic cyclopentadienides, and the  $\sigma$ -bonded alkyls and aryls. Organolanthanides of any type are usually thermally stable, but unstable with respect to water and air.

### Cyclopentadienides and related compounds

The series  $[\text{Ln}(\text{C}_5\text{H}_5)_3]$ ,  $[\text{Ln}(\text{C}_5\text{H}_5)_2\text{Cl}]$  and the less numerous  $[\text{Ln}(\text{C}_5\text{H}_5)\text{Cl}_2]$  are salts of the  $\text{C}_5\text{H}_5^-$  anion and their most general preparation is by the reaction of anhydrous  $\text{LnCl}_3$  and  $\text{NaC}_5\text{H}_5$  in appropriate molar ratios in thf. The metal atoms in these compounds display an apparent tendency to increase their coordination numbers: solvates and other adducts are readily formed. In polar solvents, where they are no doubt solvated, they are monomeric but, in non-polar solvents the  $\text{tris}(\text{C}_5\text{H}_5)$  compounds are insoluble, while the  $\text{bis}(\text{C}_5\text{H}_5)$  compounds dimerize. In the solid state the  $\text{tris}(\text{C}_5\text{H}_5)$  compounds show considerable structural diversity. Those of Er and Tm have  $\eta^5$  rings arranged in a trigonal plane around the metal and those of Lu and Pr are isostructural with the Sc and La analogues respectively (p. 953). In the Sm compound each  $\text{C}_5\text{H}_5^-$  ion is pentahapto towards 1 metal atom but some also act as bridges by presenting a ring vertex ( $\eta^1$ ) or edge ( $\eta^2$ ) towards an adjacent metal atom, so producing a chain structure.<sup>†</sup> In a less complicated way the blue  $[\text{Nd}(\text{C}_5\text{H}_4\text{Me})_3]$  is actually tetrameric, each Nd being attached to three rings in a pentahapto mode with one ring being further attached in a monohapto manner to an adjacent Nd. In spite of the steric bulk of the ligand,  $[\text{Sm}(\eta^5\text{-C}_5\text{Me}_5)_3]$  has been obtained.<sup>(42)</sup>  $[\text{Ln}(\text{C}_5\text{H}_5)_2\text{Cl}]$

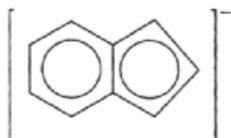
<sup>†</sup> Ring bridges of these types are found in alkaline earth cyclopentadienides such as  $[\text{Ca}(\text{C}_5\text{H}_5)_2]$  and are characteristic of the electrostatic nature of the bonding.

<sup>42</sup> W. J. EVANS, S. L. GONZALES and J. W. ZILLER, *J. Am. Chem. Soc.* **113**, 7423–4 (1991).

<sup>41</sup> C. J. SCHAEVERIEN, *Adv. Organometallic Chem.* **36**, 283–362 (1994).

are actually dimers  $[(\eta^5\text{-C}_5\text{H}_5)_2\text{Ln}(\mu\text{-Cl})_2\text{Ln}(\eta^5\text{-C}_5\text{H}_5)_2]$ . The Cl bridges can be replaced by, for instance, H, CN and OR and donor solvents will cleave the bridges. Most mono  $(\text{C}_5\text{H}_5)$  and  $(\text{C}_5\text{Me}_5)$  compounds are tris solvates such as  $[\text{Ln}(\eta^5\text{-C}_5\text{H}_5)_2(\text{thf})_3]$ .

Complexes with the two analogous ligands, indenide,  $\text{C}_9\text{H}_7^-$ ,

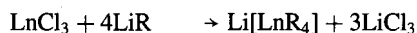


and cyclooctatetraenide,  $\text{cot}$ ,  $\text{C}_8\text{H}_8^{2-}$ , ions can be prepared by similar means. In solid  $[\text{Sm}(\text{C}_9\text{H}_7)_3]$  the 5-membered rings of the 3 ligands are bonded in a pentahapto manner and the compound shows little tendency to solvate, presumably because of the bulky nature of the  $\text{C}_9\text{H}_7^-$  ions. The lighter (and therefore larger)  $\text{Ln}^{\text{III}}$  ions form  $\text{K}[\text{Ln}(\eta^8\text{-C}_8\text{H}_8)_2]$ . The  $\text{Ce}^{\text{III}}$  member of the series has a similar “sandwich” structure to the so-called “uranocene” (p. 1279). The other members of the series have the same infrared spectrum and so also are presumed to have this structure.

Cyclopentadienyl derivatives of divalent lanthanides are also known<sup>(43)</sup>  $[\text{Ln}^{\text{II}}(\eta^5\text{-C}_5\text{H}_5)_2]$  ( $\text{Ln} = \text{Sm}, \text{Eu}, \text{Yb}$ ) might be expected to be isostructural with ferrocene but are “bent” i.e. rather than the two rings being parallel they are tilted relative to each other.

### Alkyls and aryls

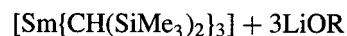
These are prepared by metathesis in thf or ether solutions:



<sup>43</sup> W. J. EVANS, *Polyhedron*, **6**, 803–35 (1987).

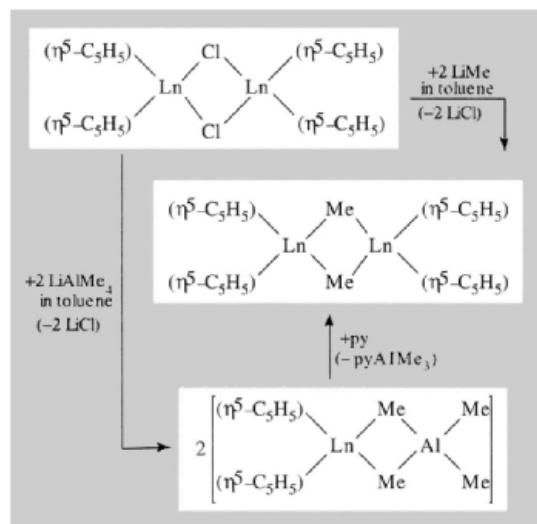
The triphenyls are probably polymeric and the first fully-characterized compound was  $[\text{Li}(\text{thf})_4][\text{Lu}(\text{C}_6\text{H}_3\text{Me}_2)_4]$  in which the Lu is tetrahedrally coordinated to four  $\sigma$ -aryl groups. More stable products, of the form  $[\text{LnR}_3(\text{thf})_2]$ , are obtained by the use of bulky alkyl groups such as  $-\text{CH}_2\text{CMe}_3$  and  $-\text{CH}_2\text{SiMe}_3$ .

Methyl derivatives, octahedral  $[\text{LnMe}_6]^{3-}$  species, are known for most of the lanthanides. The first homoleptic, neutral lanthanide alkyl<sup>(44)</sup> was obtained using the bulky alkyl  $\text{CH}(\text{SiMe}_3)_2$ :



Compounds containing lanthanide–carbon  $\sigma$ -bonds have recently been reviewed.<sup>(45)</sup>

Novel, mixed alkyl cyclopentadienides have also been prepared for the heavy lanthanides:<sup>(46)</sup>



<sup>44</sup> P. B. HITCHCOCK, M. F. LAPPERT, R. G. SMITH, R. A. BARTLETT and P. P. POWER, *J. Chem. Soc., Chem. Commun.*, 1007–9 (1988).

<sup>45</sup> S. A. COTTON, *Coord. Chem. Revs.* **160**, 93–127 (1997).

<sup>46</sup> J. HOLTON, M. F. LAPPERT, D. G. H. BALLARD, R. PEARCE, J. L. ATWOOD and W. E. HUNTER, *J. Chem. Soc., Dalton Trans.*, 45–61 (1979).



																1	2										
																H	He										
3	4											5	6	7	8	9	10										
Li	Be											B	C	N	O	F	Ne										
11	12											13	14	15	16	17	18										
Na	Mg											Al	Si	P	S	Cl	Ar										
19	20	21	22	23	24	25	26	27	28	29	30	31	32	33	34	35	36										
K	Ca	Sc	Ti	V	Cr	Mn	Fe	Co	Ni	Cu	Zn	Ga	Ge	As	Se	Br	Kr										
37	38	39	40	41	42	43	44	45	46	47	48	49	50	51	52	53	54										
Rb	Sr	Y	Zr	Nb	Mo	Tc	Ru	Rh	Pd	Ag	Cd	In	Sn	Sb	Te	I	Xe										
55	56	57	58	59	60	61	62	63	64	65	66	67	68	69	70	71	72										
Cs	Ba	La	Hf	Ta	W	Re	Os	Ir	Pt	Au	Hg	Tl	Pb	Bi	Po	At	Rn										
87	88	89	90	91	92	93	94	95	96	97	98	99	100	101	102	103	104										
Fr	Ra	Ac	Th	Pa	U	Np	Pu	Am	Cm	Bk	Cf	Es	Fm	Md	No	Lr											

# 31

## The Actinide and Transactinide Elements ( $Z = 90 - 103$ and $104 - 112$ )

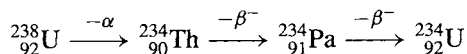
### 31.1 Introduction

The “actinides” (“actinons” or “actinoids”) are the fourteen elements from thorium to lawrencium inclusive, which follow actinium in the periodic table. They are analogous to the lanthanides and result from the filling of the 5f orbitals, as the lanthanides result from the filling of the 4f. The position of actinium, like that of lanthanum, is somewhat equivocal and, although not itself an actinide, it is often included with them for comparative purposes.

Prior to 1940 only the naturally occurring actinides (thorium, protactinium and uranium) were known; the remainder have been produced artificially since then. The “transactinides” are still being synthesized and so far the nine elements with atomic numbers 104–112 have been reliably established. Indeed, the 20 manmade transuranium elements together with technetium and promethium now constitute one-fifth of all the known chemical elements.

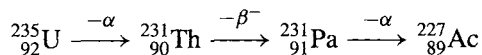
In 1789 M. H. Klaproth examined pitchblende, thought at the time to be a mixed oxide ore of zinc, iron and tungsten, and showed that it contained a new element which he named *uranium* after the recently discovered planet, Uranus. Then in 1828 J. J. Berzelius obtained an oxide, from a Norwegian ore now known as “thorite”; he named this *thoria* after the Scandinavian god of war and, by reduction of its tetrachloride with potassium, isolated the metal *thorium*. The same method was subsequently used in 1841 by B. Peligot to effect the first preparation of metallic uranium.

The much rarer element, protactinium, was not found until 1913 when K. Fajans and O. Göhring identified  $^{234}\text{Pa}$  as an unstable member of the  $^{238}\text{U}$  decay series:



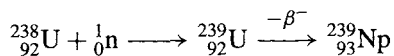
They named it brevium because of its short half-life (6.70 h). The more stable isotope  $^{231}\text{Pa}$

( $t_{\frac{1}{2}}$  32 760 y) was identified 3 years later by O. Hahn and L. Meitner and independently by F. Soddy and J. A. Cranston as a product of  $^{235}\text{U}$  decay:



As the parent of actinium in this series it was named protoactinium, shortened in 1949 to *protactinium*. Because of its low natural abundance its chemistry was obscure until 1960 when A. G. Maddock and co-workers at the UK Atomic Energy Authority worked up about 130 g from 60 tons of sludge which had accumulated during the extraction of uranium from  $\text{UO}_2$  ores. It is from this sample, distributed to numerous laboratories throughout the world, that the bulk of our knowledge of the element's chemistry was gleaned.

In the early years of this century the periodic table ended with element 92 but, with J. Chadwick's discovery of the neutron in 1932 and the realization that neutron-capture by a heavy atom is frequently followed by  $\beta^-$  emission yielding the next higher element, the synthesis of new elements became an exciting possibility. E. Fermi and others were quick to attempt the synthesis of element 93 by neutron bombardment of  $^{238}\text{U}$ , but it gradually became evident that the main result of the process was not the production of element 93 but nuclear fission, which produces lighter elements. However, in 1940, E. M. McMillan and P. H. Abelson in Berkeley, California, were able to identify, along with the fission products, a short-lived isotope of element 93 ( $t_{\frac{1}{2}}$  2.355 days):<sup>†</sup>



As it was the next element after uranium in the now extended periodic table it was named *neptunium* after Neptune, which is the next planet beyond Uranus.

<sup>†</sup>  $^{239}_{93}\text{Np}$  itself also decays by  $\beta^-$  emission to produce element 94 but this was not appreciated until after that element (plutonium) had been prepared from  $^{238}_{93}\text{Np}$ .

The remaining actinide elements were prepared<sup>(1-4)</sup> by various "bombardment" techniques fairly regularly over the next 25 years (Table 31.1) though, for reasons of national security, publication of the results was sometimes delayed. The dominant figure in this field has been G. T. Seaborg, of the University of California, Berkeley, in early recognition of which, he and E. M. McMillan were awarded the 1951 Nobel Prize for Chemistry.

The isolation and characterization of these elements, particularly the heavier ones, has posed enormous problems. Individual elements are not produced cleanly in isolation, but must be separated from other actinides as well as from lanthanides produced simultaneously by fission. In addition, all the actinides are radioactive, their stability decreasing with increasing atomic number, and this has two serious consequences. Firstly, it is necessary to employ elaborate radiation shielding and so, in many cases, operations must be carried out by remote control. Secondly, the heavier elements are produced only in the minutest amounts. Thus mendelevium was first prepared in almost unbelievably small yields of the order of 1 to 3 atoms per experiment! Paradoxically, however, the intense radioactivity also facilitated the detection of these minute amounts: first by the development and utilization of radioactive decay systematics, which enabled the detailed properties of the expected radiation to be predicted, and secondly, by using the radioactive decay itself to detect and count the individual atoms synthesized. Accordingly, the separations were effected by ion-exchange techniques, and the elements

<sup>1</sup> G. T. SEABORG (ed.), *Transuranium Elements; Products of Modern Alchemy*, Dowden, Hutchinson & Ross, Stroudsburg, 1978. This reproduces, in their original form, 122 key papers in the story of man-made elements.

<sup>2</sup> G. T. SEABORG and W. D. LOVELAND, *The Elements Beyond Uranium*, Wiley, New York, 1990, 359 pp.

<sup>3</sup> J. J. KATZ, L. R. MORSS and G. T. SEABORG (eds.) *The Chemistry of the Actinide Elements*, Chapman and Hall, London, 1986; Vol. 1, 1004 pp.; Vol 2, 912 pp.

<sup>4</sup> L. R. MORSS and J. FUGER (eds.), *Transuranium Elements: A Half Century*, Am. Chem. Soc., Washington, 1992, 700 pp.

Table 31.1 The discovery (synthesis) of the artificial actinides

Element	Discoverers	Date	Synthesis	Origin of name
93 Neptunium, Np	E. M. McMillan and P. Abelson	1940	Bombardment of $^{238}_{92}\text{U}$ with $^1_0\text{n}$	The planet Neptune
94 Plutonium, Pu	G. T. Seaborg, E. M. McMillan, J. W. Kennedy and A. Wahl	1940	Bombardment of $^{238}_{92}\text{U}$ with $^2_1\text{H}$	The planet Pluto (next planet beyond Neptune)
95 Americium, Am	G. T. Seaborg, R. A. James, L. O. Morgan and A. Ghiorso	1944	Bombardment of $^{239}_{94}\text{Pu}$ with $^1_0\text{n}$	America (by analogy with Eu, named after Europe)
96 Curium, Cm	G. T. Seaborg, R. A. James and A. Ghiorso	1944	Bombardment of $^{239}_{94}\text{Pu}$ with $^4_2\text{He}$	P. and M. Curie (by analogy with Gd, named after J. Gadolin)
97 Berkelium, Bk	S. G. Thompson, A. Ghiorso and G. T. Seaborg	1949	Bombardment of $^{241}_{95}\text{Am}$ with $^4_2\text{He}$	Berkeley (by analogy with Tb, named after the village of Ytterby)
98 Californium, Cf	S. G. Thompson, K. Street, A. Ghiorso and G. T. Seaborg	1950	Bombardment of $^{242}_{96}\text{Cm}$ with $^4_2\text{He}$	California (location of the laboratory)
99 Einsteinium, Es	Workers at Berkeley, Argonne and Los Alamos (USA)	1952	Found in debris of first thermonuclear explosion	Albert Einstein (relativistic relation between mass and energy)
100 Fermium, Fm	Workers at Berkeley, Argonne and Los Alamos (USA)	1952	Found in debris of first thermonuclear explosion	Enrico Fermi (construction of first self-sustaining nuclear reactor)
101 Mendelevium, Md	A. Ghiorso, B. H. Harvey, G. R. Choppin, S. G. Thompson and G. T. Seaborg	1955	Bombardment of $^{253}_{99}\text{Es}$ with $^4_2\text{He}$	Dimitri Mendeleev (periodic table of the elements)
102 Nobelium, No <sup>(a)</sup>	Workers at Dubna, USSR <sup>(b)</sup>	1965	Bombardment of $^{243}_{95}\text{Am}$ with $^{15}_7\text{N}$ (or $^{238}_{92}\text{U}$ with $^{22}_{10}\text{Ne}$ )	Alfred Nobel (benefactor of science) <sup>(a)</sup>
103 Lawrencium, Lr <sup>(c)</sup>	Workers at Berkeley and at Dubna <sup>(d)</sup>	1961–1971 <sup>(d)</sup>	Bombardment of mixed isotopes of $_{98}\text{Cf}$ with $^{10}_5\text{B}$ , $^{11}_5\text{B}$ ; and of $^{243}_{95}\text{Am}$ with $^{18}_8\text{O}$ , etc.	Ernest Lawrence (developer of the cyclotron)

<sup>(a)</sup>The first claim for element 102 was in 1957 by an international team working at the Nobel Institute for Physics in Stockholm. Their results could not be confirmed but their suggested name for the element was accepted.

<sup>(b)</sup>A full assessment of this work and that done at Berkeley and elsewhere has been carried out by the Transfermium Working Group, a neutral international group appointed jointly by IUPAC and IUPAP in 1987<sup>(5)</sup>.

<sup>(c)</sup>Formerly Lw; the present symbol was recommended by IUPAC in 1965.

<sup>(d)</sup>The Transfermium Working Group concluded that "In the complicated situation presented by element 103, with several papers of varying degrees of completeness and conviction, none conclusive, and referring to several isotopes, it is impossible to say other than that full confidence was built up over a decade with credit attaching to work in both Berkeley and Dubna". The detailed analysis of the many relevant publications is given in ref. 5.

<sup>5</sup>R. C. BARBER, N. N. GREENWOOD, A. Z. HRYNKIEWICZ, Y. P. JEANNIN, M. LEFORT, M. SAKAI, I. ULEHLA, A. H. WAPSTRA and D. H. WILKINSON, Discovery of the Transfermium Elements, *Prog. Particle Nucl. Phys.* **29**, 453–530 (1992). Also published, with comments in *Pure Appl. Chem.* **63**, 879–86 (1991) and **65**, 1757–814, 1815–24 (1993).

identified by chemical tracer methods and by their characteristic nuclear decay properties. In view of the quantities involved, especially of californium and later elements, it is clear that this would not have been feasible without accurate predictions of the chemical properties also. It was Seaborg's realization in 1944 that these elements should be regarded as a second f series akin to the lanthanides that made this possible. (Thorium, protactinium and uranium had previously been regarded as transition elements belonging to groups 4, 5 and 6, respectively.)

Elements beyond 103 are expected to be 6d elements forming a fourth transition series, and attempts to synthesize them have continued during the past thirty years. All 10 (including, of course, actinium) are now known and are discussed in the section on transactinide elements on p. 1280. The work has required the dedicated commitment of extensive national facilities and has been carried out at the Lawrence-Berkeley Laboratories, the Joint Institute for Nuclear Research at Dubna, and the Heavy-Ion Research Centre (GSI) at Darmstadt, Germany.

### Superheavy elements

Since the radioactive half-lives of the known transuranium elements and their resistance to spontaneous fission decrease with increase in atomic number, the outlook for the synthesis of further elements might appear increasingly bleak. However, theoretical calculations of nuclear stabilities, based on the concept of closed nucleon shells (p. 13) suggest the existence of an "island of stability" around  $Z = 114$  and  $N = 184$ .<sup>(6)</sup> Attention has therefore been directed towards the synthesis of element 114 (a congener of Pb in Group 14 and adjacent "superheavy" elements, by bombardment of heavy nuclides with a wide range of heavy ions, but so far without success.

Searches have been made for naturally occurring superheavies ( $Z = 112-15$ ) in ores of Hg,

Tl, Pb and Bi, on the assumption that they would follow their homologues in their geochemical evolution and could be recognized by the radiation damage caused over geological time by their very energetic decay. Early claims to have detected such superheavies in natural ores have been convincingly discounted.<sup>(7)</sup> More recent uncorroborated claims to success have been made but, even if confirmed, the concentrations found in the samples examined, are exceedingly small<sup>(8)</sup> (less than 1 in  $10^{13}$ ).

## 31.2 The Actinide Elements<sup>(2,3,9-12)</sup>

### 31.2.1 Terrestrial abundance and distribution

Every known isotope of the actinide elements is radioactive and the half-lives are such that only  $^{232}\text{Th}$ ,  $^{235}\text{U}$ ,  $^{238}\text{U}$  and possibly  $^{244}\text{Pu}$  could have survived since the formation of the solar system. In addition, continuing processes produce equilibrium traces of some isotopes of which the most prominent is  $^{234}\text{U}$  ( $t_{1/2}$   $2.45 \times 10^5$  y,

<sup>7</sup> F. BOSH, A. ELGORESY, W. KRÄTSCHMER, B. MARTIN, B. POVH, R. NOBILING, K. TRAXEL and D. SCHWALM, *Z. Physik A* **280**, 39-44 (1977); see also C. J. SPARKS, S. RAMAN, H. L. TAKEL, R. V. GENTRY and M. O. KRAUSE, *Phys. Rev. Letters* **38**, 205-8 (1977), for retraction of their earlier claim to have detected naturally occurring primordial superheavy elements.

<sup>8</sup> See, for instance, E. L. FIREMAN, B. H. KETELLE and R. W. STOUGHTON, *J. Inorg. Nucl. Chem.* **41**, 613-5 (1979).

<sup>9</sup> *Kirk-Othmer Encyclopedia of Chemical Technology*, 4th edn., Interscience, New York; for Actinides see Vol. 1, 1991, pp. 412-45; for Thorium see Vol. 24, 1997, pp. 68-88; for Uranium see Vol. 24, 1997, pp. 638-94; for Plutonium see Vol. 19, 1996, pp. 407-43.

<sup>10</sup> A. HARPER, Chap 17, pp. 435-56 in D. THOMPSON (ed.), *Insights into Speciality Inorganic Chemicals*, RSC, Cambridge, 1995.

<sup>11</sup> S. COTTON, *Lanthanides and Actinides*, Macmillan, Basingstoke, 1991, 192 pp.

<sup>12</sup> L. MANES (ed.) *Structure and Bonding*, Vol. 59/60, *Actinides - Chemistry and Physical Properties*, Springer, Berlin, 1985, 305 pp.

<sup>6</sup> B. FRICKE, *Struct. Bonding*, (Berlin), **21**, 89-144 (1975).

comprising 0.0054% of naturally occurring U isotopes).  $^{231}\text{Pa}$  (and therefore  $^{227}\text{Ac}$ ) is formed as a product of the decay of  $^{235}\text{U}$ , while  $^{237}\text{Np}$  and  $^{239}\text{Pu}$  are produced by the reactions of neutrons with, respectively,  $^{235}\text{U}$  and  $^{238}\text{U}$ . Traces of Pa, Np and Pu are consequently found, but only Th and U occur naturally to any useful extent. Indeed, these two elements are far from

rare: thorium comprises 8.1 ppm of the earth's crust, and is almost as abundant as boron, whilst uranium at 2.3 ppm is rather more abundant than tin. The radioactive decay schemes of the naturally occurring long-lived isotopes of  $^{232}\text{Th}$ ,  $^{235}\text{U}$  and  $^{238}\text{U}$ , together with the artificially generated series based on  $^{241}\text{Pu}$ , are summarized in Fig 31.1.

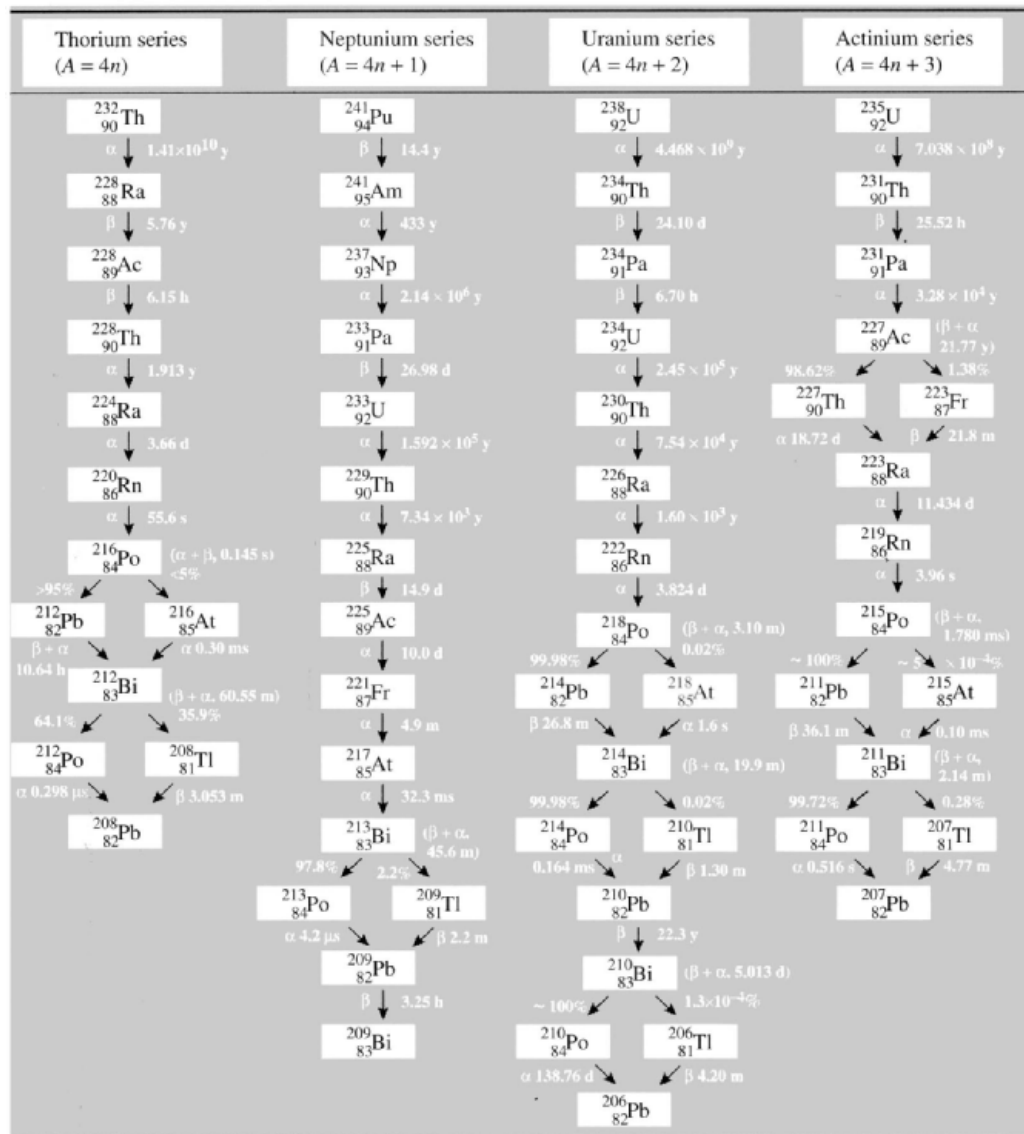


Figure 31.1 The radioactive decay series.

Thorium is widely but rather sparsely distributed and its only commercial sources are monazite sands (see p. 1229) and the mineral conglomerates of Ontario. The former are found in India, South Africa, Brazil, Australia and Malaysia, and in exceptional cases may contain up to 20% ThO<sub>2</sub> but more usually contain less than 10%. In the Canadian ores the thorium is present as uranothorite, a mixed Th,U silicate, which is accompanied by pitchblende. Even though present as only 0.4% ThO<sub>2</sub>, the recovery of Th, as a co-product of the recovery of uranium, is viable.

Uranium, too, is widely distributed and, since it probably crystallized late in the formation of igneous rocks, tends to be scattered in the faults of older rocks. Some concentration by leaching and subsequent re-precipitation has produced a large number of oxide minerals of which the most important are pitchblende or uraninite, U<sub>3</sub>O<sub>8</sub>, and carnotite, K<sub>2</sub>(UO<sub>2</sub>)<sub>2</sub>(VO<sub>4</sub>)<sub>2</sub>·3H<sub>2</sub>O. However, even these are usually dispersed so that typical ores contain only about 0.1% U, and many of the more readily exploited deposits are nearing exhaustion. The principal sources are Canada, Africa and countries of the former USSR.

The transuranium elements must all be prepared artificially. In the case of plutonium about 1200 tonnes have so far been produced worldwide, about three-quarters of it in civilian reactors.

### 31.2.2 Preparation and uses of the actinide elements<sup>(2,9)</sup>

The separation of basic precipitates of hydrous ThO<sub>2</sub> from the lanthanides in monazite sands has been outlined in Fig. 30.1 (p. 1230). These precipitates may then be dissolved in nitric acid and the thorium extracted into tributyl phosphate, (Bu<sup>n</sup>O)<sub>3</sub>PO, diluted with kerosene. In the case of Canadian production, the uranium ores are leached with sulfuric acid and the anionic sulfato complex of U preferentially absorbed onto an anion exchange resin. The Th is separated from Fe, Al and other metals in the liquor by solvent extraction.

Metallic thorium can be obtained by reduction of ThO<sub>2</sub> with Ca or by reduction of ThCl<sub>4</sub> with Ca or Mg under an atmosphere of Ar (like Ti, finely divided Th is extremely reactive when hot).

The uses of Th are at present limited and only a few hundred tonnes are produced annually, about half of this still being devoted to the production of gas mantles (p. 1228). In view of its availability as a by-product of lanthanide and uranium production, output could be increased easily if it were to be used on a large scale as a nuclear fuel (see below).

Uranium production depends in detail on the nature of the ore involved but, after crushing and concentrating by conventional physical means, the ore is usually roasted and leached with sulfuric acid in the presence of an oxidizing agent such as MnO<sub>2</sub> or NaClO<sub>3</sub> to ensure conversion of all uranium to UO<sub>2</sub><sup>2+</sup>. In a typical process the uranium is concentrated as a sulfato complex on an anion exchange resin from which it is eluted with strong HNO<sub>3</sub> and further purified by solvent extraction into tributyl phosphate (TBP) in either kerosene or hexane. The uranium is then stripped from the organic phase to give an aqueous sulfate solution from which so-called "yellow cake" is precipitated\* by addition of ammonia. This is converted to UO<sub>3</sub> by heating at 300°C, and then to UO<sub>2</sub> by reducing in H<sub>2</sub> at 700°C. Conversion to the metal is generally effected by reduction of UF<sub>4</sub> with Mg at 700°C.

Apart from its long-standing though small-scale use for colouring glass and ceramics, uranium's only significant use is as a nuclear fuel. The extent of this use depends on environmental and political considerations. In 1994 world production after nearly a decade of decline was 31 000 tonnes, 30% of which came from Canada and 23% each from the former Soviet Union and African countries (Niger, Namibia, the Republic of South Africa and Gabon). This, however, represented only half the reactor requirements. The rest came from recycling and stockpiles

---

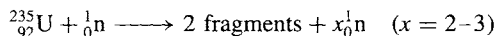
\* Yellow cake is a complicated mixture of salts and oxides, the composition of which approximates to (NH<sub>4</sub>)<sub>2</sub>U<sub>2</sub>O<sub>7</sub> but is dependent on the method by which it is produced (see p. 276 of ref. 2).

(which were expected to be exhausted within 4 or 5 years).

### Nuclear reactors and atomic energy<sup>(13–15)</sup>

In the process of nuclear fission a large nucleus splits into two highly energetic smaller nuclei and a number of neutrons; if there are sufficient neutrons and they have the correct energy, they can induce fission of further nuclei, so creating a self-propagating chain reaction. The kinetic energy of the main fragments is rapidly converted to heat as they collide with neighbouring atoms, the amount being of the order of  $10^6$  times that produced by chemically burning the same mass of combustible material such as coal.

In practical terms, the only naturally occurring fissile nucleus is  $^{235}_{92}\text{U}$  (0.72% abundant):



The so-called “fast” neutrons which this fission produces have energies of about 2 MeV ( $190 \times 10^6 \text{ kJ mol}^{-1}$ ) and are not very effective in producing fission of further  $^{235}_{92}\text{U}$  nuclei. Better in this respect are “slow” or “thermal” neutrons whose energies are of the order of 0.025 eV ( $2.4 \text{ kJ mol}^{-1}$ ), i.e. equivalent to the thermal energy available at ambient temperatures. In order to produce and sustain a chain reaction in uranium it is therefore necessary to counter the inefficiency of fast neutrons by either (a) increasing the proportion of  $^{235}_{92}\text{U}$  (i.e. fuel enrichment) or (b) slowing down (i.e. moderating) the fast neutrons. In addition, there must be sufficient uranium to prevent excessive loss of neutrons from the surface (i.e. a “critical mass” must be exceeded). If the reaction is not to run out of control, an adjustable neutron absorber is also required to ensure that the rate

of production of neutrons is balanced by the rate of their absorption.

The first manmade self-sustaining nuclear fission chain reaction was achieved on 2 December 1942 in a disused squash court at the University of Chicago by a team which included E. Fermi. This was before nuclear-fuel enrichment had been developed: alternate sections of natural-abundance  $\text{UO}_2$  and graphite moderator were piled on top of each other (hence, nuclear reactors were originally known as “atomic piles”) and the reaction was controlled by strips of cadmium which could be inserted or withdrawn as necessary. In this crude structure, 6 tonnes of uranium metal, 50 tonnes of uranium oxide and nearly 400 tonnes of graphite were required to achieve criticality. The dramatic success of Fermi’s team in achieving a self-sustaining nuclear reaction invited the speculation as to whether such a phenomenon could occur naturally.<sup>(16)</sup> In one of the most spectacular pieces of scientific detection work ever conducted, it has now unambiguously been established that such natural chain reactions have indeed occurred in the geological past when conditions were far more favourable than at present (see Panel).

If a chain reaction is to provide useful energy, the heat it generates must be extracted by means of a suitable coolant and converted, usually by steam turbines, into electrical energy. The high temperatures and the intense radioactivity generated within a reactor pose severe, and initially totally new, constraints on the design. The choices of fuel and its immediate container (cladding), of the moderator, coolant and controller involve problems in nuclear physics, chemistry, metallurgy and engineering. Nevertheless, the first commercial power station (as opposed to experimental reactors or those whose function was to produce plutonium for bomb manufacture) was commissioned in 1956 at Calder Hall in Cumberland, UK. Since then a variety of different types has been developed in several countries, as summarized in Fig. 31.2. At

<sup>13</sup> S. GLASSTONE and A. SESONSKE, *Nuclear Reactor Engineering*, 4th edn., Chapman and Hall, New York, 1994, 852 pp.

<sup>14</sup> R. L. MURRAY, *Nuclear Energy*, 4th edn., Pergamon, Oxford, 1993, 437 pp.

<sup>15</sup> Kirk–Othmer *Encyclopedia of Chemical Technology*, Vol. 17, 4th edn., 1996, pp. 369–465, Interscience, New York.

<sup>16</sup> P. K. KURODA, *Nature* **187**, 36–8 (1960).

### Natural Nuclear Reactors — The Oklo Phenomenon<sup>17)</sup>

Natural uranium consists almost entirely of the  $\alpha$  emitters  $^{235}\text{U}$  and  $^{238}\text{U}$ . As  $^{235}\text{U}$  decays more than six times faster than  $^{238}\text{U}$  (Fig. 31.1) the proportion of  $^{235}\text{U}$  is very slowly but inexorably decreasing with time. Prior to 1972, all analyses of naturally occurring uranium had shown this proportion to be notably constant at  $0.7202 \pm 0.0006\%$ .<sup>†</sup> In that year, however, workers at the French Atomic Energy laboratories in Pierrelatte performing routine mass spectrometric analyses recorded a value of 0.7171%. The difference was small but significant.

Contamination with commercially depleted U was immediately assumed, but it was gradually realized that the depletion was characteristic of the ore, which came from a mine at Oklo in Gabon, near the west coast ( $1^{\circ} 25'S$ ,  $13^{\circ} 10'W$ ). An intensive examination of the mine was quickly mounted and it was found that the depletion was not uniform but was greatest near those areas where the total U content was highest. The record depletion was an astonishingly low 0.296%  $^{235}\text{U}$  from an area where the total U content of the ore rose to around 60%. Incredible as it may appear in view of the diverse and exacting requirements for the construction of a manmade nuclear reactor, the only satisfactory explanation is that the Oklo mine is the site of a spent, prehistoric, natural nuclear reactor. There are now known to have been 14 such reactors in the Franceville basin at Oklo, all of which have been mined, plus a further one some 30 km to the southeast at Bangombé, which it is hoped to preserve essentially undisturbed.

The Oklo ore bed consists of sedimentary rocks believed to have been laid down about  $1.8 \times 10^9$  y ago.  $\text{U}^{\text{IV}}$  minerals in the igneous rocks, formed in the early history of the earth when the atmosphere was a reducing one, were converted to soluble  $\text{U}^{\text{VI}}$  salts by the atmosphere which had since become oxidizing. These were then re-precipitated as  $\text{U}^{\text{IV}}$  by bacterial reduction in the silt of a river delta and gradually buried under other sedimentary deposits. During this process the underlying granite rocks were tilted, the ores which contained about 0.5% U were fractured, and water percolating through the fissures created rich pockets of ore which in places consisted of almost pure  $\text{UO}_2$ . At that time the  $^{235}\text{U}$  content of the uranium was about 3%, which is the value to which the fuel used in most modern water-moderated reactors is now artificially enriched.

Under these circumstances the critical mass could be attained and a nuclear chain reaction initiated, with water as the necessary moderator. The 15% water of hydration contained in the clays associated with the ore would be ideal for this purpose. As the reaction proceeded, the consequent rise in temperature would have driven off water, so producing "undermoderation" and slowing the reaction, thereby avoiding a "run away" reaction. As a result, a particular reactor may have operated in a steady manner or perhaps in a slowly pulsating manner, as water was alternately driven off (causing loss of criticality and cooling) and re-absorbed (recovering criticality and again heating).

Further control of the reactions must have been effected by neutron-absorbing "poisons", such as lithium and boron, which are nearly always present in clays. That these are present in the Oklo clays in comparatively low concentrations is one of the factors which allowed the reactions to take place. As the nuclear fuel in the original, rich pockets was being used up, the poisons in the surrounding ore would be simultaneously "burned out" by escaping neutrons. Thus ore of only slightly poorer quality, which was initially prevented only by the poisons from being critical, would gradually become so and the chain reaction would be propagated further through the ore bed. It is thought that these reactors operated for about  $(0.2 - 1) \times 10^6$  y with output in the region of 10–100 kW, consuming altogether 4–6 tonnes of  $^{235}\text{U}$  from a total deposit of the order of 400 000 tonnes of uranium. Subsequent preservation of the fossil reactors is a result of continued burial which protected the uranium from redissolution.

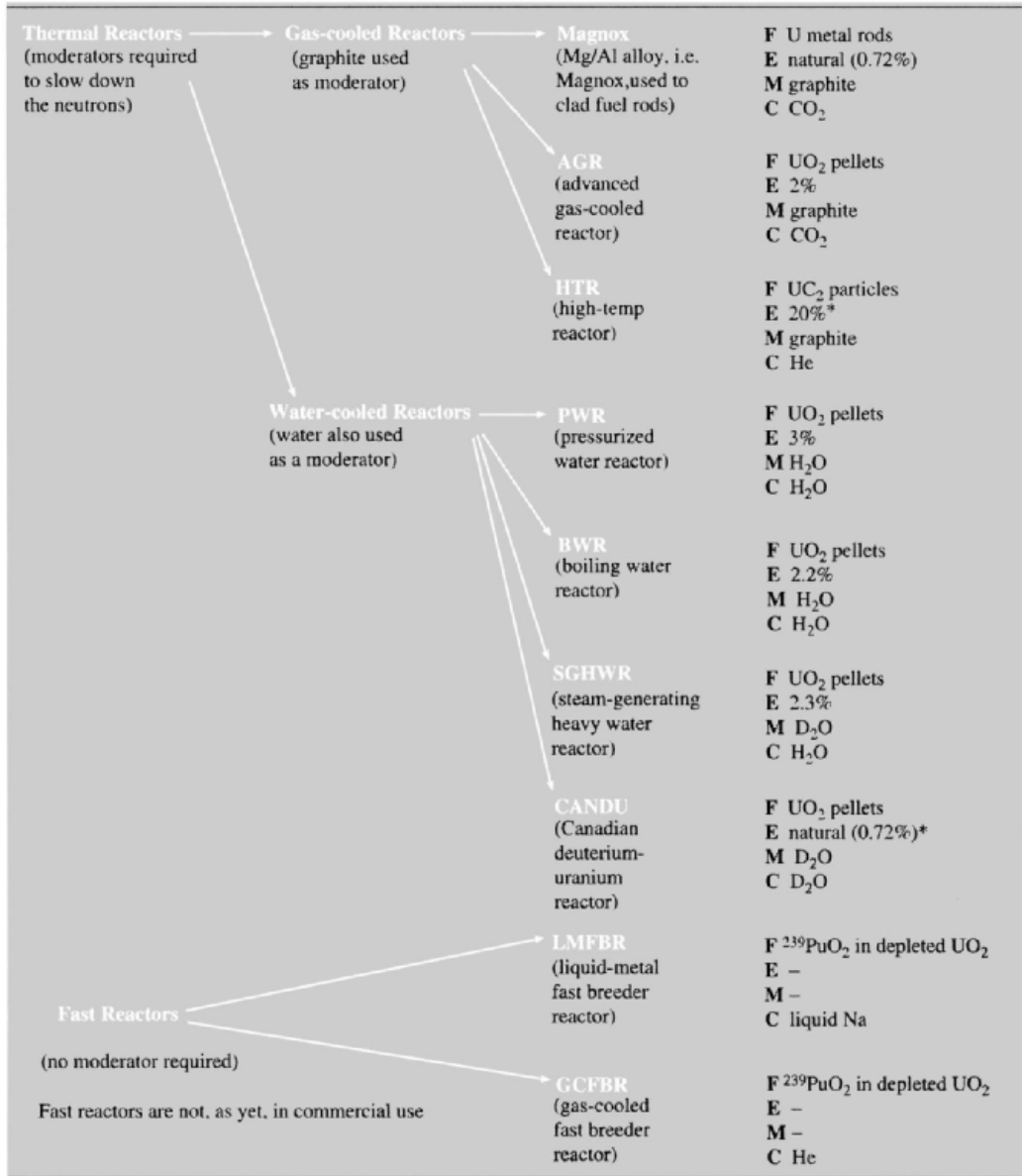
Confirmation of this explanation is unequivocally provided by the presence in the reactor zones of at least half of the more than 30 fission products of uranium. Although soluble salts, such as those of the alkali and alkaline earth metals, have been leached out, lanthanide and platinum metals remain along with traces of trapped krypton and xenon. Most decisively, the observed distribution of the various isotopes of these elements is that of fission products as opposed to the distribution normally found terrestrially. The reasons for the retention of these elements on this particular site is clearly germane to the problem of the long-term storage of nuclear wastes, and is therefore the subject of continuing study.

The circumstances which led to the Oklo phenomenon may well have occurred in other, as yet unidentified, places, but in view of the intervening natural depletion of  $^{235}\text{U}$ , the possibility of a natural chain reaction being initiated at the present time or in the future may be discounted.

<sup>17</sup>*Le Phenomene d'Oklo*, Proceedings of a Symposium on the Oklo Phenomenon, International Atomic Energy Agency, Vienna, Proceedings Series, 1975. *Natural Fission Reactions*, IAEA, Vienna, Panel Proceedings Series STI/PUB/475, 1978, 754 pp. R. WEST, Natural nuclear reactors. *J. Chem. Ed.* **53**, 336–40 (1976).

<sup>†</sup>If, as is believed (p. 13), the earth was formed about  $4.6 \times 10^9$  y ago it follows that the proportion of  $^{235}\text{U}$  at that time must have been about 25%.





\* HTR and CANDU could also possibly use <sup>232</sup>Th-<sup>233</sup>U fuel

**Figure 31.2** Various types of nuclear reactor currently in use or being developed (F fuel; E enrichment, expressed as %<sup>235</sup>U present; M moderator; C coolant).

the present time (1996) some 30 countries are operating nuclear power stations to supply energy.

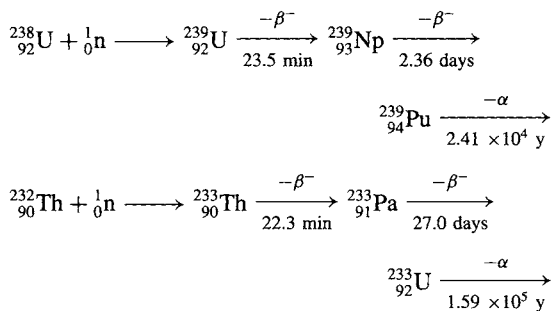
**Fuels.** Although the concentration of <sup>235</sup>U in natural uranium is sufficient to sustain a chain reaction, its effective dilution by the fuel

cladding and other materials used to construct the reactor make fuel enrichment advantageous. Indeed, if ordinary (light) water is used as moderator or coolant, a concentration of 2–3% <sup>235</sup>U is necessary to compensate for the inevitable

absorption of neutrons by the protons of the water. Enrichment also has the advantage of reducing the critical size of the reactor but this must be balanced against its enormous cost.

Early reactors used uranium in metallic form but this has been superseded by  $\text{UO}_2$  which is chemically less reactive and has a higher melting point.  $\text{UC}_2$  is also sometimes used but is reactive towards  $\text{O}_2$ .

In addition to  ${}^{235}_{92}\text{U}$ , which occurs naturally, two other fissile nuclei are available artificially. These are  ${}^{239}_{94}\text{Pu}$  and  ${}^{233}_{92}\text{U}$  which are obtained from  ${}^{238}_{92}\text{U}$  and  ${}^{232}_{90}\text{Th}$  respectively:



${}^{239}\text{Pu}$  is therefore produced to some extent in all currently operating reactors because they contain  ${}^{238}\text{U}$ , and this contributes to the reactor efficiency. More significantly, it offers the possibility of generating more fissile material than is consumed in producing it. Such "breeding" of  ${}^{239}\text{Pu}$  is not possible in thermal reactors because the net yield of neutrons from the fission of  ${}^{235}\text{U}$  is inadequate. But, if the moderator is dispensed with and the chain reaction sustained by using enriched fuel, then there are sufficient fast neutrons to "breed" new fissile material. Fast-breeder reactors are not yet in commercial use but prototypes are operating in France, the UK and Japan and use a core of  $\text{PuO}_2$  in "depleted"  $\text{UO}_2$  (i.e.  ${}^{238}\text{UO}_2$ ) surrounded by a blanket of more depleted  $\text{UO}_2$  in which the  ${}^{239}\text{Pu}$  is generated. By making use of the  ${}^{238}\text{U}$  as well as the  ${}^{235}\text{U}$ , such reactors can extract 50–60 times more energy from natural uranium, so using more efficiently the reserves of easily accessible ores. Sadly there are possible dangers associated with a "plutonium economy" which

have led to well-publicized objections, and future developments will be determined by social and political as well as by economic considerations.

The net yield of thermal neutrons from the fission of  ${}^{233}\text{U}$  is higher than from that of  ${}^{235}\text{U}$  and, furthermore,  ${}^{232}\text{Th}$  is a more effective neutron absorber than  ${}^{238}\text{U}$ . As a result, the breeding of  ${}^{233}\text{U}$  is feasible even in thermal reactors. Unfortunately the use of the  ${}^{232}\text{Th}/{}^{233}\text{U}$  cycle has been inhibited by reprocessing problems caused by the very high energy  $\gamma$ -radiation of some of the daughter products.

*Fuel enrichment.* All practicable enrichment processes require the uranium to be in the form of a gas.  $\text{UF}_6$ , which readily sublimates (p. 1269), is universally used and, because fluorine occurs in nature only as a single isotope, the compound has the advantage that separation depends solely on the isotopes of uranium. The first, and until recently the only, large-scale enrichment process was by gaseous diffusion which was originally developed in the "Manhattan Project" to produce nearly pure  ${}^{235}\text{U}$  for the first atomic bomb (exploded at Alamogordo, New Mexico, 5.30 a.m., 16 July 1945).  $\text{UF}_6$  is forced to diffuse through a porous membrane and becomes very slightly enriched in the lighter isotope. This operation is repeated thousands of times by pumping, in a kind of cascade process in which at each stage the lighter fraction is passed forward and the heavier fraction backwards. Unfortunately gaseous diffusion plants are large, very demanding in terms of membrane technology, and extremely expensive in energy: alternatives have therefore actively been sought.<sup>(18)</sup> So far the only viable alternative is the gas centrifuge process currently operating in the UK, The Netherlands, Germany, Japan and Russia. In a cylindrical centrifuge  ${}^{238}\text{UF}_6$  concentrates towards the walls and  ${}^{235}\text{UF}_6$  towards the centre. In practice the radial concentration gradient is transformed into an axial gradient by injecting the  $\text{UF}_6$  so as to set up an axial counter current so that both the enriched and depleted materials can be drawn off from

<sup>18</sup> C. WHITEHEAD, *Chem. Brit.* **26**, 1161–4 (1990).

peripheral positions where the pressure is higher. The centrifuges rotate at about 1000 revolutions per second and are arranged in a cascade system.

A promising alternative is provided by "Laser isotope separation". Because the ionization energies of  $^{235}\text{U}$  and  $^{238}\text{U}$  differ slightly, it is possible to ionize the former selectively by irradiating U vapour with laser beams precisely tuned to the appropriate wavelength. The ions can then be collected at a negative electrode.

*Cladding.* The Magnox reactors get their name from the magnesium-aluminium alloy used to clad the fuel elements, and stainless steels are used in other gas-cooled reactors. In water reactors zirconium alloys are the favoured cladding materials.

*Moderators.* Neutrons are most effectively slowed by collisions with nuclei of about the same mass. Thus the best moderators are those light atoms which do not capture neutrons. These are  $^2\text{H}$ ,  $^4\text{He}$ ,  $^9\text{Be}$  and  $^{12}\text{C}$ . Of these He, being a gas, is insufficiently dense and Be is expensive and toxic, so the common moderators are highly purified graphite or the more expensive heavy water. In spite of its neutron-absorbing properties, which as mentioned above must be offset by using enriched fuel, ordinary water is also used because of its cheapness and excellent neutron-moderating ability.

*Coolants.* Because they must be mobile, coolants are either gases or liquids.  $\text{CO}_2$  and He are appropriate gases and are used in conjunction with graphite moderators. The usual liquids are heavy and light water, with water also as moderator. In order to keep the water in the liquid phase it must be pressurized (PWR), otherwise it boils in the reactor core (BWR, etc.) in which case the coolant is actually steam. In the case of breeder reactors the higher temperatures of their more compact cores pose severe cooling problems and liquid Na (or Na/K alloy) is favoured, although highly compressed He is another possibility.

*Control rods.* These are usually made of boron steel or boron carbide (p. 149), but other good neutron absorbers which can be used are Cd and Hf.

### Nuclear fuel reprocessing<sup>(3,10)</sup>

Many of the fission products formed in a nuclear reactor are themselves strong neutron absorbers (i.e. "poisons") and so will stop the chain reaction before all the  $^{235}\text{U}$  (and  $^{239}\text{Pu}$  which has also been formed) has been consumed. If this wastage is to be avoided the irradiated fuel elements must be removed periodically and the fission products separated from the remaining uranium and the plutonium. Such reprocessing is of course inherent in the operation of fast-breeder reactors, but whether or not it is used for thermal reactors depends on economic and political factors. Reprocessing is currently undertaken in the UK, France and Russia but is not considered to be economic in the USA.

Irradiated nuclear fuel is one of the most complicated high-temperature systems found in modern industry, and it has the further disadvantage of being intensely radioactive so that it must be handled exclusively by remote control. The composition of the irradiated nuclear fuel depends on the particular reactor in question, but in general it consists of uranium, plutonium, neptunium, americium and various isotopes of over 30 fission-product elements. The distribution of fission products is such as to produce high concentrations of elements with mass numbers in the regions 90–100 (second transition series) and 130–145 ( $^{54}\text{Xe}$ ,  $^{55}\text{Cs}$ ,  $^{56}\text{Ba}$  and lanthanides). The more noble metals, such as  $^{44}\text{Ru}$ ,  $^{45}\text{Rh}$  and  $^{46}\text{Pd}$ , tend to form alloy pellets while class-a metals such as  $^{38}\text{Sr}$ ,  $^{56}\text{Ba}$ ,  $^{40}\text{Zr}$ ,  $^{41}\text{Nb}$  and the lanthanides are present in complex oxide phases.

The first step is to immerse the fuel elements in large "cooling ponds" of water for a hundred days or so, during which time the short-lived, intensely radioactive species such as  $^{131}_{53}\text{I}$  ( $t_{1/2} = 8.04$  days) lose most of their activity and the generation of heat subsides.

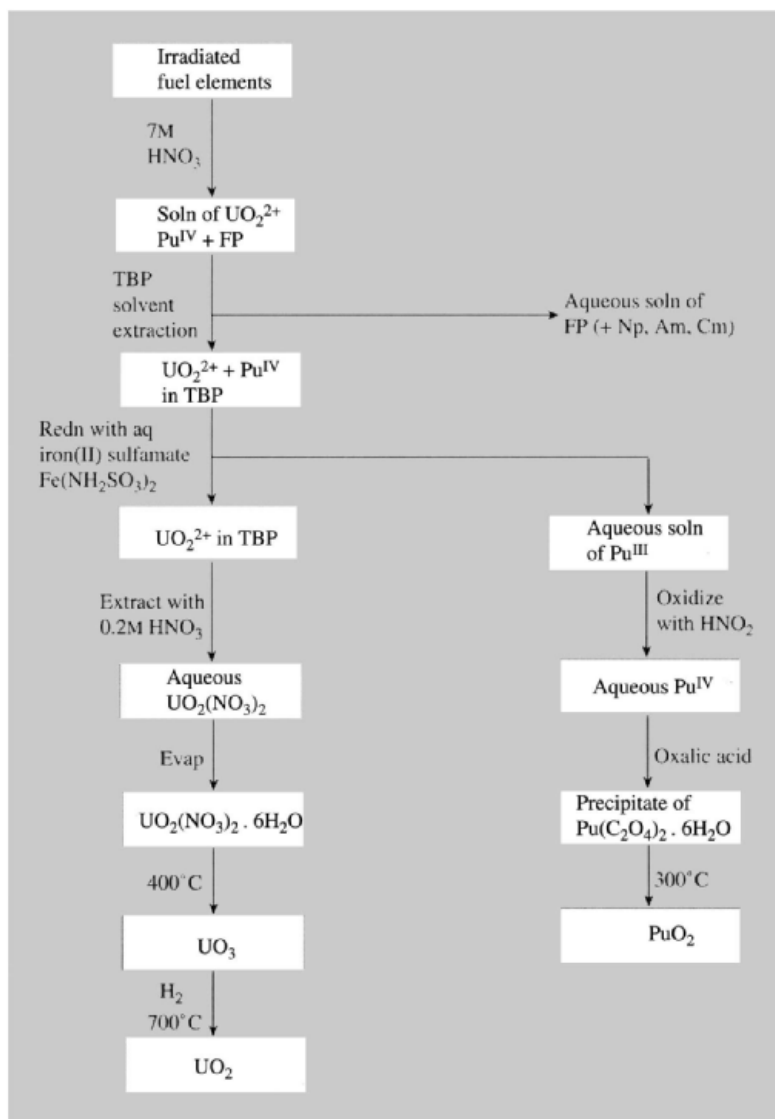
Then the fuel elements are dissolved in 7M  $\text{HNO}_3$  to give a solution containing  $\text{U}^{\text{VI}}$  and  $\text{Pu}^{\text{IV}}$  which, in the widely used plutonium-uranium-reduction, or Purex process, are extracted into 20% tributyl phosphate (TBP) in kerosene leaving most of the fission products

(FP) in the aqueous phase. Subsequent separation of U and Pu depends on their differing redox properties (Fig. 31.3). The separations are far from perfect (see p. 1097), and recycling or secondary purification by ion-exchange techniques is required to achieve the necessary overall separations.

This reprocessing requires the handling of kilogram quantities of Pu and must be adapted to

avoid a chain reaction (i.e. a criticality accident). The critical mass for an isolated sphere of Pu is about 10 kg, but in saturated aqueous solutions may be little more than 500 g. (Because of the large amounts of “inert”  $^{238}\text{U}$  present, U does not pose this problem.)

The solution of waste products is concentrated and stored in double-walled, stainless steel tanks shielded by a metre or more of concrete.



**Figure 31.3** Flow diagram for the reprocessing of nuclear fuel [FP = fission products; TBP =  $(\text{Bu}^n\text{O})_3\text{PO}$ ].

Vitrification processes are being developed in several countries in which the dried waste is calcined and heated with ground glass "frit" to produce a borosilicate glass which can be stored or disposed of more permanently if there is agreement on suitable sites.

$^{237}_{93}\text{Np}$ ,  $^{241}_{95}\text{Am}$  and  $^{243}_{95}\text{Am}$  can be extracted from reactor wastes and are available in kg quantities. Prolonged neutron irradiation of  $^{239}_{94}\text{Pu}$  is used at the Oak Ridge laboratories in Tennessee to produce:  $^{244}_{96}\text{Cm}$  on a 100-g scale;  $^{242}_{96}\text{Cm}$ ,  $^{249}_{97}\text{Bk}$ ,  $^{252}_{98}\text{Cf}$  and  $^{253}_{99}\text{Es}$  all on a mg scale; and  $^{257}_{100}\text{Fm}$  on a  $\mu\text{g}$  scale. For trace amounts of these mixtures, dissolution in nitric acid, absorption of the +3 ions on to a cation exchange resin and elution with ammonium  $\alpha$ -hydroxyisobutyrate provides an efficient separation of the elements from each other and from accompanying lanthanides, etc. The separation of macro amounts of these elements, however, is not feasible by this method because of radiolytic damage to the resin caused by their intense radioactivity. Much quicker solvent extraction processes similar to those used for reprocessing nuclear fuels are therefore used.

Because the sequence of neutron captures inevitably leads to  $^{258}_{100}\text{Fm}$  which has a fission half-life of only a few seconds, the remaining three actinides,  $^{101}\text{Md}$ ,  $^{102}\text{No}$  and  $^{103}\text{Lr}$ , can only be prepared by bombardment of heavy nuclei with the light atoms  $^4_2\text{He}$  to  $^{20}_{10}\text{Ne}$ . This raises the mass number in multiple units and allows the  $^{258}_{100}\text{Fm}$  barrier to be avoided; even so, yields are minute and are measured in terms of the number of individual atoms produced.

Apart from  $^{239}_{94}\text{Pu}$ , which is a nuclear fuel and explosive, the transuranium elements have in the past been produced mainly for research purposes. A number of specialized applications, however, have led to more widespread uses.  $^{238}_{94}\text{Pu}$  (produced by neutron bombardment of  $^{237}_{93}\text{Np}$  to form  $^{238}_{93}\text{Np}$  which decays by  $\beta$ -emission to  $^{238}_{94}\text{Pu}$ ) is a compact heat source ( $0.56\text{ W g}^{-1}$  as it decays by  $\alpha$ -emission) which, in conjunction with PbTe thermoelectric elements, for instance, provides a stable and totally reliable source of electricity with no moving parts. It has been

used in the form of  $\text{PuO}_2$  in kg quantities in the American Apollo and Galileo spacecraft. Since its  $\alpha$ -emission is harmless and is not accompanied by  $\gamma$ -radiation it is also used in heart pacemakers ( $\sim 160\text{ mg }^{238}_{94}\text{Pu}$ ) where it lasts about 5 times longer than conventional batteries before requiring replacements.  $^{241}_{95}\text{Am}$  is also widely used as an ionization source in smoke detectors and thickness gauges.

### 31.2.3 Properties of the actinide elements

The dominant feature of the actinides is their nuclear instability, as manifest in their radioactivity (mostly  $\alpha$ -decay) and tendency to spontaneous fission; both of these modes of decay become more pronounced (shorter half-lives) with the heavier elements. The radioactivity of Th and U is probably responsible for much of the earth's internal heat, but is of a sufficiently low level to allow their compounds to be handled and transported without major problems. By contrast, the instability of the heavier elements not only imposes most severe handling problems<sup>(19)</sup> but drastically limits their availability. Thus, for instance, the crystal structures of Cf and Es were determined on only microgram quantities,<sup>(1)</sup> while the concept of "bulk" properties is not applicable at all to elements such as Md, No and Lr which have never been seen and have only been produced in unweighably small amounts. Even where adequate amounts are available, the constant build-up of decay products and the associated generation of heat may seriously affect the measured properties (see also p. 753). An indication of the difficulties of working with these elements can be gained from the fact that two phases described in 1974 as two forms of Cf metal were subsequently shown, in fact, to be hexagonal  $\text{Cf}_2\text{O}_2\text{S}$  and fcc CfS.<sup>(20)</sup>

Some of the more important known properties of the actinides are summarized in Table 31.2.

<sup>19</sup> R. A. BULMAN, *Coord. Chem. Revs.* **31**, 221–50 (1980).

<sup>20</sup> W. H. ZACHARIASEN, *J. Inorg. Nucl. Chem.* **37**, 1441–2 (1975).

Table 31.2 Some properties of the actinide elements

Property	Th	Pa	U	Np	Pu	Am	Cm	Bk	Cf	Es	Fm	Md	No	Lr
Atomic number	90	91	92	93	94	95	96	97	98	99	100	101	102	103
Number of naturally occurring isotopes	1	—	3	—	—	—	—	—	—	—	—	—	—	—
Most common isotope:														
Mass number	232	231	238	237	239	241	244	249	252	252	257	256	259	262
Half-life <sup>(a)</sup>	$1.40 \times 10^{10}$ y ( $\alpha$ )	$3.25 \times 10^4$ y ( $\alpha$ )	$4.47 \times 10^9$ y ( $\alpha$ )	$2.14 \times 10^6$ y ( $\alpha$ )	$2.41 \times 10^4$ y ( $\alpha$ )	433 y ( $\alpha$ )	18.1 y ( $\alpha$ )	320 d ( $\beta^-$ )	2.64 y ( $\alpha$ )	472 d ( $\alpha$ )	100.5 d ( $\alpha$ )	78 min ( $\beta^+/\text{EC}$ )	58 min ( $\alpha$ , EC)	3.6 h ( $\alpha$ )
Relative nuclidic mass	232.0380	231.0359	238.0289 <sup>(b)</sup>	237.0482	239.0522	241.0568	244.0627	249.0750	252.0816	252.0830	257.0951	256.0941	259.1011	262.110
Electronic configuration, [Rn] plus	$6d^2 7s^2$	$5f^2 6d^1 7s^2$ or $5f^3 6d^2 7s^2$	$5f^3 6d^1 7s^2$	$5f^4 6d^1 7s^2$ or $5f^6 7s^2$	$5f^6 7s^2$	$5f^7 7s^2$	$5f^7 6d^1 7s^2$	$5f^9 7s^2$ or $5f^8 6d^1 7s^2$	$5f^{10} 7s^2$	$5f^{11} 7s^2$	$5f^{12} 7s^2$	$5f^{13} 7s^2$	$5f^{14} 7s^2$	$5f^{14} 6d^1 7s^2$
Metal radius (CN12) <sup>(c)</sup> /pm	179	163	156	155	159	173	174	170	$186 \pm 2$	$186 \pm 2$	—	—	—	—
Ionic radius (CN6)/pm	—	—	—	71	—	—	—	—	—	—	—	—	—	—
VI	—	—	73	72	71	—	—	—	—	—	—	—	—	—
V	—	78	76	75	74	—	—	—	—	—	—	—	—	—
IV	94	90	89	87	86	85	85	83	82.1	—	—	—	—	—
III	—	104	102.5	101	100	97.5	97	96	95	—	—	—	—	—
II	—	—	—	110	—	126 <sup>(d)</sup>	—	—	—	—	—	—	—	—
$E^\circ(\text{MO}_2^{2+}/\text{MO}_2^+)/\text{V}$	—	—	0.17	1.24	1.02	1.60	—	—	—	—	—	—	—	—
$E^\circ(\text{MO}_2^+/\text{M}^{4+})/\text{V}$	—	-0.05	0.38	0.64	1.04	0.82	—	—	—	—	—	—	—	—
$E^\circ(\text{M}^{3+}/\text{M}^{2+})/\text{V}$	-3.8	-1.4	-0.52	0.15	1.01	2.62	3.1	1.67	3.2	4.5	5.2	—	—	—
$E^\circ(\text{M}^{3+}/\text{M})/\text{V}$	-1.83	-1.47	-1.38	-1.30	-1.25	-0.90	—	—	—	—	—	—	—	—
$E^\circ(\text{M}^{2+}/\text{M})/\text{V}$	—	—	-1.66	-1.79	-2.00	-2.07	-2.06	-2.00	-1.91	-1.98	-2.07	-1.74	-1.26	-2.1
MP <sup>o</sup> /C	1750	1572	1135	644	640	1176	1345	1050	900	860	1527	827	827	1627
BP <sup>o</sup> /C	4788	(4722)	3818	(3902)	3228	(2607)	—	—	—	—	—	—	—	—
$\Delta H_{\text{fus}}/\text{kJ mol}^{-1}$	16.11	16.7	12.6	(9.46)	2.80	14.4	—	—	—	—	—	—	—	—
$\Delta H_{\text{vap}}/\text{kJ mol}^{-1}$	513.7	481	417	336	343.5	238.5	—	—	—	—	—	—	—	—
$\Delta H_f$ (monatomic gas)/ kJ mol <sup>-1</sup>	575	—	482	—	352	—	—	—	—	—	—	—	—	—
Density (25°C)/g cm <sup>-3(e)</sup>	11.72	15.37	19.05	20.45	19.86	13.67	13.51	14.78	—	—	—	—	—	—
Electrical resistivity (22°C)/ $\mu\text{ohm cm}$	15.4	19.1	30.8	122	150	71	—	—	—	—	—	—	—	—

<sup>(a)</sup>The rate of decay by spontaneous fission increases with atomic number and is an important additional cause of instability in the later actinides (*trans*-Np).<sup>(b)</sup>This value refers to the natural mixture of uranium isotopes, i.e. it is the atomic weight. Variations are possible because (i) some geological samples have anomalous isotopic compositions, and (ii) commercially available samples may have been depleted in <sup>235</sup>U. The value for <sup>238</sup>U itself is 238.0508.<sup>(c)</sup>For Pa, CN = 10 and for U, Np and Pu the structures are rather irregular so that the coordination number is not a precise concept.<sup>(d)</sup>For Am<sup>II</sup>, radius refers to CN = 8.<sup>(e)</sup>Polymorphism is common amongst the actinides and these data refer to the form most stable at room temperature.

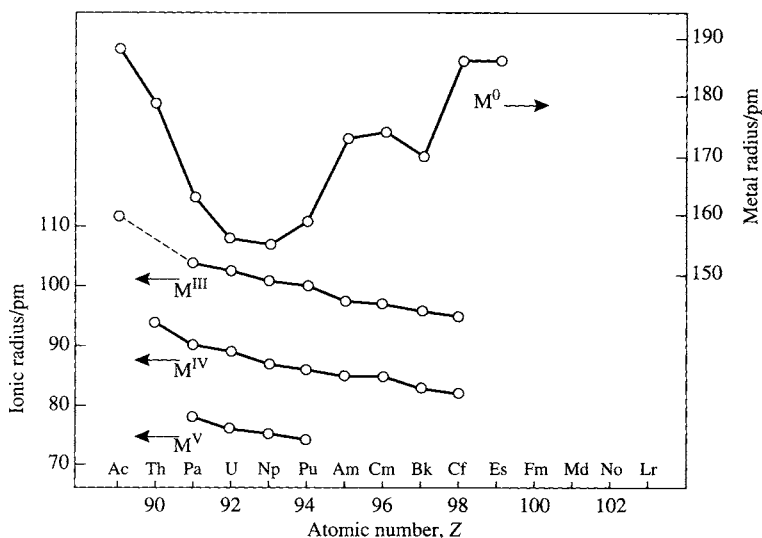


Figure 31.4 Metal and ionic radii of Ac and the actinides.

The metals are silvery in appearance but display a variety of structures. All except Cf have more than one crystalline form (Pu has six) but most of these are based on typically metallic close-packed arrangements. Structural variability is mirrored by irregularities in metal radii (Fig. 31.4) which are far greater than are found in lanthanides and probably arise from a variability in the number of electrons in the metallic bands of the actinide elements. From Ac to U, since the most stable oxidation state increases from +3 to +6, it seems likely that the sharp fall in metal radius is due to an increasing number of electrons being involved in metallic bonding. Neptunium and Pu are much the same as U but thereafter increasing metal radius is presumably a result of fewer electrons being involved in metallic bonding since it roughly parallels the reversion to a lanthanide-like preference for tervalency in the heavier actinides.

By contrast, the ionic radius in a given oxidation state falls steadily and, though the available data are less extensive, it is clear that an "actinide contraction" exists, especially for the +3 state, which is closely similar to the "lanthanide contraction" (see p. 1232).

### 31.2.4 Chemical reactivity and trends

The actinide metals are electropositive and reactive, apparently becoming increasingly so with atomic number. They tarnish rapidly in air, forming an oxide coating which is protective in the case of Th but less so for the other elements. Because of the self-heating associated with its radioactivity (100 g  $^{239}\text{Pu}$  generates  $\sim 0.2$  watts of heat) Pu is best stored in circulating dried air. All are pyrophoric when finely divided.

The metals react with most non-metals especially if heated, but resist alkali attack and are less reactive towards acids than might be expected. Concentrated HCl probably reacts most rapidly, but even here insoluble residues remain in the cases of Th (black), Pa (white) and U (black). Those of Th and U have the approximate compositions  $\text{HThO}(\text{OH})$  and  $\text{UH}(\text{OH})_2$ . Concentrated  $\text{HNO}_3$  passivates Th, U and Pu, but the addition of  $\text{F}^-$  ions avoids this and provides the best general method for dissolving these metals.

Reactions with water are complicated and are affected by the presence of oxygen. With boiling water or steam, oxide is formed on the surface of the metal and  $\text{H}_2$  is liberated. Since the metals react readily with the latter, hydrides are produced which themselves react rapidly with

**Table 31.3** Oxidation states of actinide elements

Oxidation states found only in solids are given in brackets; numbers in **bold** indicate the most stable oxidation states in aqueous solution. Colours refer to aqueous solutions<sup>(a)</sup>

Species present in H <sub>2</sub> O	Th	Pa	U	Np	Pu	Am	Cm	Bk	Cf	Es	Fm	Md	No	Lr
M <sup>II</sup>	—	—	—	—	—	(2)	—	—	(2)	(2)	2	2	<b>2</b>	—
M <sup>III</sup>	3	(3)	3	3	3	<b>3</b>	<b>3</b>	<b>3</b>	<b>3</b>	<b>3</b>	<b>3</b>	<b>3</b>	3	<b>3</b>
M <sup>IV</sup>	<b>4</b>	4	4	4	<b>4</b>	4	4	4	(4)	—	—	—	—	—
MO <sub>2</sub> <sup>+</sup>	c-less	c-less	g	y-g	br	pink	pale y	y	—	—	—	—	—	—
	—	<b>5</b>	5	<b>5</b>	5	5	—	—	—	—	—	—	—	—
MO <sub>2</sub> <sup>2+</sup>	—	c-less	unknown	g	purple <sup>(b)</sup>	y	—	—	—	—	—	—	—	—
	—	—	<b>6</b>	6	6	6	—	—	—	—	—	—	—	—
(MO <sub>5</sub> <sup>3-</sup> ) <sup>(c)</sup>	—	—	y	p	o	br	—	—	—	—	—	—	—	—
	—	—	—	7	7	—	—	—	—	—	—	—	—	—
	—	—	—	g	g	—	—	—	—	—	—	—	—	—

<sup>(a)</sup>bl = blue; br = brown; c-less = colourless; gr = green; o = orange; r = red; v = violet; y = yellow.

<sup>(b)</sup>Because of disproportionation, PuO<sub>2</sub><sup>+</sup> is never observed on its own and its colour must therefore be deduced from the spectrum of a mixture involving Pu in several oxidation states.

<sup>(c)</sup>This is probably too simple, hydroxo species such as [MO<sub>4</sub>(OH)<sub>2</sub>]<sup>3-</sup> being more likely.

water and so facilitate further attack on the metals.

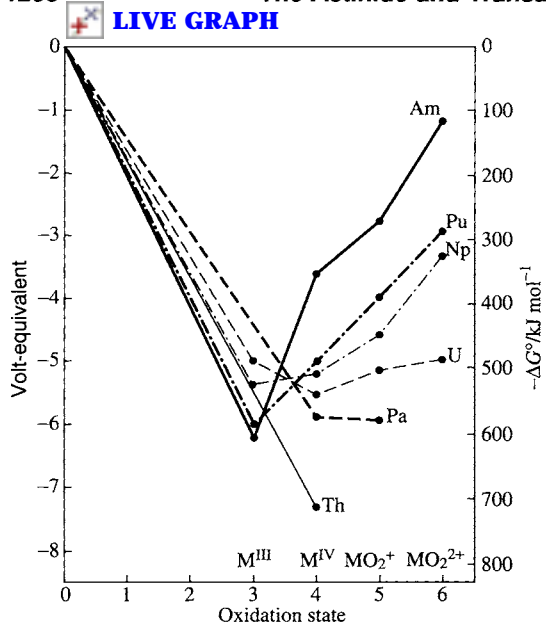
Knowledge of the detailed chemistry of the actinides is concentrated mainly on U and, to a lesser extent, Th and Pu.<sup>(21)</sup> Availability and safety are, of course, major problems for the remaining elements, but self-heating and radiolytic damage can be troublesome, the energy evolved in radioactive decay being far greater than that of chemical bonds. Thus in aqueous solutions of concentrations greater than 1 mg cm<sup>-3</sup> (i.e. 1 g l<sup>-1</sup>), isotopes with half-lives less than, say, 20 years, will produce sufficient H<sub>2</sub>O<sub>2</sub> to produce appreciable oxidation or reduction where the redox behaviour of the element allows this. Fortunately, the nuclear instability which produces these problems also assists in overcoming them: by performing chemical reactions with appropriate, non-radioactive, carrier elements containing only trace amounts of the actinide in question, it is possible to detect the presence of the latter, and hence explore its chemistry because of the extreme sensitivity of radiation detectors. Such “tracer” techniques have

provided remarkably extensive information particularly about the aqueous solution chemistry of the actinides.

Table 31.3 lists the known oxidation states. For the first three elements (Th, Pa and U) the most stable oxidation state is that involving all the valence electrons, but after this the most stable becomes progressively lower until, in the second half of the series, the +3 state becomes dominant. Appropriate quantitative data for elements up to Am are summarized in Fig. 31.5. The highest oxidation state attainable by Th, and the only one occurring in solution, is +4. Data for Pa are difficult to obtain because of its propensity for hydrolysis which results in the formation of colloidal precipitates, except in concentrated acids or in the presence of complexing anions such as F<sup>-</sup> or C<sub>2</sub>O<sub>4</sub><sup>2-</sup>. However, it is clear that +5 is its most stable oxidation state since its reduction to +4 requires rather strong reducing agents such as Zn/H<sup>+</sup>, Cr<sup>II</sup> or Ti<sup>III</sup> and the +4 state in solution is rapidly reoxidized to +5 by air. In the case of uranium the shape of the volt-equivalent versus oxidation state curve (pp. 435–8) reflects the ready disproportionation of UO<sub>2</sub><sup>+</sup> into the more stable U<sup>IV</sup> and UO<sub>2</sub><sup>2+</sup>; it should also be possible for atmospheric oxygen ( $\frac{1}{2}$ O<sub>2</sub> + 2H<sup>+</sup> +

<sup>21</sup> G. R. CHOPPIN and B. E. STOUT, *Chem. Brit.*, **27**, 1126–9 (1991).





**Figure 31.5** Volt-equivalent versus oxidation state for actinide ions.

$2e^- \rightleftharpoons H_2O$ ,  $E^\circ = 1.229 \text{ V}$ ) to oxidize  $U^{IV}$  to  $UO_2^{2+}$  though in practice this occurs only slowly. For the heavier elements the increasingly steep-sided trough indicates the increasing stability of the +3 state.

The redox behaviour of Th, Pa and U is of the kind expected for d-transition elements which is why, prior to the 1940s, these elements were commonly placed respectively in groups 4, 5 and 6 of the periodic table. Behaviour obviously like that of the lanthanides is not evident until the second half of the series. However, even the early actinides resemble the lanthanides in showing close similarities with each other and gradual variations in properties, providing comparisons are restricted to those properties which do not entail a change in oxidation state. The smooth variation with atomic number found for stability constants, for instance, is like that of the lanthanides rather than the d-transition elements, as is the smooth variation in ionic radii noted in Fig. 31.4. This last factor is responsible for the close similarity in the structures of many actinide and lanthanide compounds especially noticeable in the +3 oxidation state for which

a given actinide ion is only about 4 pm larger than the corresponding  $Ln^{3+}$ .

It is evident from the above behaviour that the ionization energies of the early actinides, though not accurately known, must be lower than for the early lanthanides. This is quite reasonable since it is to be expected that, when the 5f orbitals of the actinides are beginning to be occupied, they will penetrate less into the inner core of electrons, and the 5f electrons will therefore be more effectively shielded from the nuclear charge than are the 4f electrons of the corresponding lanthanides (i.e. the relationship between 4f and 5f series may be compared to that between 3d and 4d). Because the outer electrons are less firmly held, they are all available for bonding in the actinide series as far as Np (4th member), but only for Ce (1st member) in the lanthanides, and the onset of the dominance of the +3 state is accordingly delayed in the actinides. That the 5f and 6d orbitals of the early actinides are energetically closer than the 4f and 5d orbitals of the early lanthanides is evidenced by the more extensive occupation of the 6d orbitals in the neutral atoms of the former (compare the outer electron configuration in Tables 31.2 and 30.2). These 5f orbitals also extend spatially further than the 4f and are able to make a covalent contribution to the bonding which is much greater than that in lanthanide compounds. This leads to a more extensive actinide coordination chemistry and to crystal-field effects, especially with ions in oxidation states above +3, much larger than those found for lanthanide complexes. It is also important to remember that relativistic effects on the atomic properties and chemistry of these heavy elements cannot be safely ignored in attempts to explain or predict their behaviour.

Table 31.4 is a list of typical compounds of the actinides and demonstrates the wider range of oxidation states compared to lanthanide compounds. High coordination numbers are still evident, and distortions from the idealized stereochemistries which are quoted are again general. However, no doubt at least partly because the early actinides have received most attention, the widest range of stereochemistries is

**Table 31.4** Oxidation states and stereochemistries of compounds of the actinides  
 "An" is used as a general symbol for the actinide elements

Oxidation state	Coordination number	Stereochemistry	Examples
0	16	See Figs. 19.31 and 31.10	[An( $\eta^8$ -C <sub>8</sub> H <sub>8</sub> ) <sub>2</sub> ] (An = Th → Pu), [U( $\eta^8$ -C <sub>8</sub> H <sub>4</sub> Ph <sub>4</sub> ) <sub>2</sub> ]
3	6	Octahedral	[AnCl <sub>6</sub> ] <sup>3-</sup> (An = Np, Am, Bk)
	8	Bicapped trigonal prismatic	AnCl <sub>3</sub> (X = Br, An = Pu → Bk; X = I, An = Pa → Pu)
	9	Tricapped trigonal prismatic	AnCl <sub>3</sub> (An = U → Cm)
4	15	See p. 1278	[Th( $\eta^5$ -C <sub>5</sub> H <sub>3</sub> (SiMe <sub>3</sub> ) <sub>2</sub> ) <sub>3</sub> ]
	4	Complex	U(NPh <sub>2</sub> ) <sub>4</sub>
	5	Trigonal bipyramidal	U <sub>2</sub> (NEt <sub>2</sub> ) <sub>8</sub>
	6	Octahedral	[AnX <sub>6</sub> ] <sup>2-</sup> (An = U, Np, Pu; X = Cl, Br)
	7	Pentagonal bipyramidal	UBr <sub>4</sub>
	8	Cubic	[An(NCS) <sub>8</sub> ] <sup>4-</sup> (An = Th → Pu)
		Dodecahedral	[Th(C <sub>2</sub> O <sub>4</sub> ) <sub>4</sub> ] <sup>4-</sup> , [An(S <sub>2</sub> CNEt <sub>2</sub> ) <sub>4</sub> ] (An = Th, U, Np, Pu)
		Square antiprismatic	[An(acac) <sub>4</sub> ] (An = Th, U, Np, Pu)
	9	Tricapped trigonal prismatic	(NH <sub>4</sub> ) <sub>3</sub> [ThF <sub>7</sub> ]
		Capped square antiprismatic	[Th(tropolonate) <sub>4</sub> (H <sub>2</sub> O)]
10	Bicapped square antiprismatic	K <sub>4</sub> [Th(C <sub>2</sub> O <sub>4</sub> ) <sub>4</sub> ].4H <sub>2</sub> O	
	Complex	[Th(NO <sub>3</sub> ) <sub>4</sub> (OPPb <sub>3</sub> ) <sub>2</sub> ] <sup>(a)</sup>	
11	See Fig. 31.8a	[Th(NO <sub>3</sub> ) <sub>4</sub> (H <sub>2</sub> O) <sub>3</sub> ].2H <sub>2</sub> O	
12	Icosahedral	[Th(NO <sub>3</sub> ) <sub>6</sub> ] <sup>2-(a)</sup>	
14	Bicapped hexagonal antiprismatic	[U(BH <sub>4</sub> ) <sub>4</sub> ]	
20	See Fig. 31.9	[An( $\eta^5$ -C <sub>5</sub> H <sub>5</sub> ) <sub>4</sub> ] (An = Th, U)	
5	6	Octahedral	Cs[AnF <sub>6</sub> ] (An = U, Np, Pu)
	7	Pentagonal bipyramidal	PaCl <sub>5</sub>
	8	Cubic	Na <sub>3</sub> [AnF <sub>8</sub> ] (An = Pa, U, Np)
	9	Tricapped trigonal prismatic	M <sub>2</sub> [PaF <sub>7</sub> ] (M = NH <sub>4</sub> , K, Rb, Cs)
6	6	Octahedral	AnF <sub>6</sub> (An = U, Np, Pu), UCl <sub>6</sub> , Cs <sub>2</sub> [UO <sub>2</sub> X <sub>4</sub> ] <sup>(b)</sup> (X = Cl, Br)
	7	Pentagonal bipyramidal	[UO <sub>2</sub> (S <sub>2</sub> CNEt <sub>2</sub> ) <sub>2</sub> (ONMe <sub>3</sub> )] <sup>(b)</sup>
	8	Hexagonal bipyramidal	[UO <sub>2</sub> (NO <sub>3</sub> ) <sub>2</sub> (H <sub>2</sub> O) <sub>2</sub> ] <sup>(b)</sup>
7	Octahedral	Li <sub>5</sub> [AnO <sub>6</sub> ] (An = Np, Pu)	

<sup>(a)</sup>These compounds are isostructural with the corresponding compounds of Ce (see Fig. 30.5, p. 1245) and can be visualized as octahedral if each NO<sub>3</sub><sup>-</sup> is considered to occupy a single coordination site.

<sup>(b)</sup>The polyhedra of these complexes are actually flattened because the two *trans* U-O bonds of the UO<sub>2</sub><sup>2+</sup> group are shorter than the bonds to the remaining groups which form an equatorial plane.

now to be found in the +4 oxidation state rather than +3 as in the lanthanides.

### 31.3 Compounds of the Actinides<sup>(3,9,11,22-24)</sup>

Compounds with many non-metals are prepared, in principle simply, by heating the elements.

<sup>22</sup> G. MEYER and L. R. MORSS (eds.) *Synthesis of Lanthanide and Actinide Compounds*, Kluwer, Dordrecht, 1991, 367 pp.

<sup>23</sup> K. W. BAGNALL, Chap. 40, pp. 1129-228, in *Comprehensive Coordination Chemistry*, Vol. 3, Pergamon Press, Oxford, 1987.

<sup>24</sup> I. SANTOS, A. P. de MATOS and A. G. MADDOCK, *Adv. Inorg. Chem.* **34**, 65-144 (1989).

Hydrides of the types AnH<sub>2</sub> (An = Th, Np, Pu, Am, Cm) and AnH<sub>3</sub> (Pa → Am), as well as Th<sub>4</sub>H<sub>15</sub> (i.e. ThH<sub>3.75</sub>) have been so obtained but are not very stable thermally and are decidedly unstable with respect to air and moisture. Borides, carbides, silicides and nitrides (q.v.) are mostly less sensitive chemically and, being refractory materials, those of Th, U and Pu in particular have been studied extensively as possible nuclear fuels.<sup>(15,25)</sup> Their stoichiometries are very varied but the more important ones are the semi-metallic monocarbides, AnC, and mononitrides, AnN, all of which have the rock-salt structure: they are predominantly ionic

<sup>25</sup> K. NAITO and N. KAGEGASHIRA, *Adv. Nucl. Sci. Tech.* **9**, 99-180 (1976).

**Table 31.5** Oxides of the Actinide Elements<sup>(a)</sup>  
The most stable oxide of each element is printed in **bold**.

Formal oxidation state of metal	Th	Pa	U	Np	Pu	Am	Cm	Bk	Cf	Es
+6	—	—	UO <sub>3</sub>	—	—	—	—	—	—	—
	—	—	o-y <b>U<sub>3</sub>O<sub>8</sub></b> dark g	—	—	—	—	—	—	—
+5	—	<b>Pa<sub>2</sub>O<sub>5</sub></b> white	U <sub>2</sub> O <sub>5</sub> black	Np <sub>2</sub> O <sub>5</sub> dark br	—	—	—	—	—	—
+4	<b>ThO<sub>2</sub></b> white	PaO <sub>2</sub> black	UO <sub>2</sub> dark br	<b>NpO<sub>2</sub></b> br-g	<b>PuO<sub>2</sub></b> y-br	<b>AmO<sub>2</sub></b> black	<b>CmO<sub>2</sub></b> black	<b>BkO<sub>2</sub></b> br	CfO <sub>2</sub> black	—
+3	—	—	—	—	Pu <sub>2</sub> O <sub>3</sub> black	Am <sub>2</sub> O <sub>3</sub> r-br	<b>Cm<sub>2</sub>O<sub>3</sub></b> white	Bk <sub>2</sub> O <sub>3</sub> y-g	<b>Cf<sub>2</sub>O<sub>3</sub></b> pale g	<b>Es<sub>2</sub>O<sub>3</sub></b> <sup>(b)</sup> white

<sup>(a)</sup>br = brown; g = green; o = orange; r = red; y = yellow.

<sup>(b)</sup>This is the only known oxide of Es. It is expected to be the most stable for this actinide but investigation of the Es/O system is hampered not only by low availability but also by the high  $\alpha$ -activity ( $t_{1/2} = 20.5$  days) which causes crystals to disintegrate. Es<sub>2</sub>O<sub>3</sub> was characterized by electron diffraction using microgram samples measuring only about 0.03  $\mu\text{m}$  on edge.

but with supernumerary electrons in a delocalized conduction band.

### 31.3.1 Oxides and chalcogenides of the actinides<sup>(15,26)</sup>

Oxides of the actinides are refractory materials and, in fact, ThO<sub>2</sub> has the highest mp (3390°C) of any oxide. They have been extensively studied because of their importance as nuclear fuels.<sup>(25)</sup> However, they are exceedingly complicated because of the prevalence of polymorphism, nonstoichiometry and intermediate phases. The simple stoichiometries quoted in Table 31.5 should therefore be regarded as idealized compositions.

The only anhydrous trioxide is UO<sub>3</sub>, a common form of which ( $\gamma$ -UO<sub>3</sub>) is obtained by heating UO<sub>2</sub>(NO<sub>3</sub>) $\cdot$ 6H<sub>2</sub>O in air at 400°C; six other forms are also known.<sup>(27)</sup> Heating any of these, or indeed any other oxide of uranium, in air at 800–900°C yields U<sub>3</sub>O<sub>8</sub> which contains pentagonal bipyramidal UO<sub>7</sub> units and can be used in gravimetric determinations of uranium. Reduction with H<sub>2</sub> or H<sub>2</sub>S leads to a series of intermediate

nonstoichiometric phases (of which U<sub>2</sub>O<sub>5</sub> may be mentioned) and ending with UO<sub>2</sub>. Pentoxides are known also for Pa and Np. Pa<sub>2</sub>O<sub>5</sub> is prepared by igniting Pa<sup>V</sup> hydroxide in air, and the nonstoichiometric Np<sub>2</sub>O<sub>5</sub> by treating Np<sup>IV</sup> hydroxide with ozone and heating the resulting NpO<sub>3</sub> $\cdot$ H<sub>2</sub>O at 300°C under vacuum.

Dioxides are known for all the actinides as far as Cf. They have the fcc fluorite structure (p. 118) in which each metal atom has CN = 8; the most common preparative method is ignition of the appropriate oxalate or hydroxide in air. Exceptions are CmO<sub>2</sub> and CfO<sub>2</sub>, which require O<sub>2</sub> rather than air, and PaO<sub>2</sub> and UO<sub>2</sub>, which are obtained by reduction of higher oxides.

From Pu onwards, sesquioxides become increasingly stable with structures analogous to those of Ln<sub>2</sub>O<sub>3</sub> (p. 1238); BkO<sub>2</sub> is out-of-sequence but this is presumably due to the stability of the f<sup>7</sup> configuration in Bk<sup>IV</sup>. For each actinide the C-type M<sub>2</sub>O<sub>3</sub> structure (metal CN = 6) is the most common but A and B types (metal CN = 7) are often also obtainable.

Reports of monoxides formed as surface layers on the metals have not been substantiated although their existence in the vapour phase is not disputed (see pp. 237–8 of ref. 22).

The oxides are basic in character but their reactivity is usually strongly influenced by their thermal history, being much more inert if they have

<sup>26</sup> *J. Chem. Soc., Faraday Trans. II* **83**, 1065–285 (1987): a collection of papers on UO<sub>2</sub>.

<sup>27</sup> See for instance M. T. WELLER, P. G. DICKENS and D. J. PENNY, *Polyhedron* **7**, 243–4 (1988).

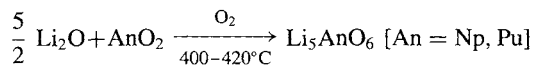
been ignited. Dioxides of Th, Np and Pu are best dissolved in conc HNO<sub>3</sub> with added F<sup>-</sup>, but all oxides of U dissolve readily in conc HNO<sub>3</sub> or conc HClO<sub>4</sub> to yield salts of UO<sub>2</sub><sup>2+</sup>.

Hydroxides are not well-characterized but gelatinous precipitates, which redissolve in acid, are produced by the addition of alkali to aqueous solutions of the actinides. Those of Th<sup>IV</sup>, Pa<sup>V</sup>, Np<sup>V</sup>, Pu<sup>IV</sup>, Am<sup>III</sup> and Cm<sup>III</sup> are stable to oxidation but lower oxidation states of these metals are rapidly oxidized. Aqueous solutions of hexavalent U, Np and Pu yield hydrous precipitates of AnO<sub>2</sub>(OH)<sub>2</sub>, which contain AnO<sub>2</sub><sup>2+</sup> units linked by OH bridges, but they are often formulated as hydrated trioxides AnO<sub>3</sub>·xH<sub>2</sub>O.

Actinide chalcogenides can be obtained for instance by reaction of the elements, and thermal stability decreases S > Se > Te. Those of a given actinide differ from those of another in much the same way as do the oxides. Nonstoichiometry is again prevalent and, where the actinide appears to have an uncharacteristically low oxidation state, semimetallic behaviour is usually observed.

### 31.3.2 Mixed metal oxides

Alkali and alkaline earth metallates are obtained by heating the appropriate oxides, in the presence of oxygen where necessary. For instance, the reaction



provides a means of stabilizing Np<sup>VII</sup> and Pu<sup>VII</sup> in the form of isolated [AnO<sub>6</sub>]<sup>5-</sup> octahedra.

By suitable adjustment of the proportions of the reactants, An<sup>VI</sup> species (An = U → Am) are obtained of which the "uranates" are the best known. These are of the types M<sub>2</sub><sup>I</sup>U<sub>2</sub>O<sub>7</sub>, M<sub>2</sub><sup>II</sup>UO<sub>4</sub>, M<sub>4</sub><sup>I</sup>UO<sub>5</sub> and M<sub>3</sub><sup>II</sup>UO<sub>6</sub> in each of which the U atoms are coordinated by 6 O atoms disposed octahedrally but distorted by the presence of 2 short *trans* U–O bonds, characteristic of the uranyl UO<sub>2</sub><sup>2+</sup> group. In view of the earlier inclusion of U in Group 6 it is interesting to note that, unlike Mo<sup>VI</sup> and W<sup>VI</sup>, U<sup>VI</sup> apparently does

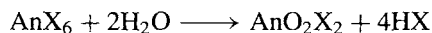
not show any tendency to form iso- or hetero-poly anions in aqueous solution.

M<sup>I</sup>An<sup>V</sup>O<sub>3</sub>, M<sub>3</sub><sup>I</sup>An<sup>V</sup>O<sub>4</sub> and M<sub>7</sub><sup>I</sup>An<sup>V</sup>O<sub>6</sub> have been characterized for An = Pa → Am. Compounds of the first of these types have the perovskite structure (p. 963), those of the second a defect-rock-salt structure (p. 242), and those of the third have structures based on hexagonally close-packed O atoms. In all cases, therefore, the actinide atom is octahedrally coordinated. It is also notable that magnetic and spectroscopic evidence shows that, for uranium, these compounds contain the usually unstable U<sup>V</sup> and not, as might have been supposed, a mixture of U<sup>IV</sup> and U<sup>VI</sup>.

BaAn<sup>IV</sup>O<sub>3</sub> (An = Th → Am) all have the perovskite structure and are obtained from the actinide dioxide. In accord with normal redox behaviour, the Pa and U compounds are only obtainable if O<sub>2</sub> is rigorously excluded, and the Am compound if O<sub>2</sub> is present. Actinide dioxides also yield an extensive series of nonstoichiometric, mixed oxide phases in which a second oxide is incorporated into the fluorite lattice of the AnO<sub>2</sub>. The UO<sub>2</sub>/PuO<sub>2</sub> system, for example, is of great importance in the fuel of fast-breeder reactors.

### 31.3.3 Halides of the actinide elements<sup>(28)</sup>

The known actinide halides are listed in Table 31.6. They range from AnX<sub>6</sub> to AnX<sub>2</sub> and their distribution follows much the same trends as have been seen already in Tables 31.3 and 31.5. Thus the hexahalides are confined to the hexafluorides of U, Np and Pu (which are volatile solids obtained by fluorinating AnF<sub>4</sub>) and the hexachloride of U, which is obtained by the reaction of AlCl<sub>3</sub> and UF<sub>6</sub>. All are powerful oxidizing agents and are extremely sensitive to moisture:



<sup>28</sup> J. C. TAYLOR, *Coord. Chem. Rev.* **20**, 197–273 (1976).

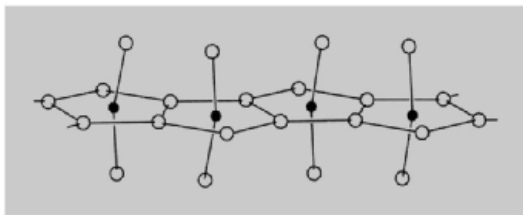
Table 31.6 Properties of actinide halides<sup>(a)</sup>

	Th	Pa	U	Np	Pu	Am	Cm	Bk	Cf	Es
AnF <sub>6</sub>			White 64° 6 o	Orange 54.7° 6 o	Brown 52° 6 o					
AnCl <sub>6</sub>			Dark green 177° 6 o							
AnF <sub>5</sub>		White na 7 pbp	Pale blue 348° 6 o	Pale blue na 7 pbp						
AnCl <sub>5</sub>		Yellow 306° 7 pbp	Brown na 6 o							
AnBr <sub>5</sub>		Dark red 6 o	Brown 6 o							
AnI <sub>5</sub>		Black								
An <sub>2</sub> F <sub>9</sub>		Black (9)	Black (9)							
An <sub>4</sub> F <sub>17</sub>			Black		Red					
AnF <sub>4</sub>	White 1068° 8 sa	Brown na 8 sa	Green 960° 8 sa	Green na 8 sa	Brown 1037° 8 sa	Tan na 8 sa	Brown na 8 sa	Yellow na 8 sa	Green na 8 sa	
AnCl <sub>4</sub>	White 770° 8 d	Green- yellow na 8 d	Green 590° 8 d	Red- brown 517° 8 d						
AnBr <sub>4</sub>	White 679° 8 d	Brown na 8 d	Brown 519° 7 pbp	Dark-red 464° 7 pbp						
AnI <sub>4</sub>	Yellow 556° 8 sa	Black na na	Black 506° 6 ol							
AnF <sub>3</sub>			Black decomp. 9 ttp	Purple na 9 ttp	Violet 1425° 9 ttp	Pink 1395° 9 ttp	White 1406° 9 ttp	Yellow na 9 ttp	Green na 8 btp	‡ na 8btp
AnCl <sub>3</sub>			Green 837° 9 ttp	Green 800° 9 ttp	Green 767° 9 ttp	Pink 715° 9 ttp	White 695° 9 ttp	Green 603° 9 ttp	Green 575° 9 ttp	White na 9 ttp
AnBr <sub>3</sub>			Red 727° 9 ttp	Green na 9 ttp	Green 681° 8 btp	White na 8 btp	White 625° 8 btp	Yellow- green na 8 btp	Pale- green na 6 o	Light-brown na 6 o
AnI <sub>3</sub>	Black na 8	Brown na 8 btp	Black 766° 8 btp	Purple 760° 8 btp	Green (777°) 8 btp	Yellow 950° 8 btp	White na 6 o	Yellow na 6 o	Yellow na 6 o	‡ na 6 ol
AnCl <sub>2</sub>						Black 9 ttp			Amber	‡
AnBr <sub>2</sub>						Black 8,7			Amber 8,7	‡
AnI <sub>2</sub>	Gold complex					Black 7 co			Violet	‡

<sup>(a)</sup>Key: Colour (‡ indicates preparation but no report of colour); mp/°C (na indicates value not reported); coordination 9 ttp = tricapped trigonal prismatic; 8 d = dodecahedral; 8 sa = square antiprismatic; 8 btp = bicapped trigonal prismatic; 8,7 = mixed 8- and 7-coordination (SrBr<sub>2</sub> structure); 7 cc = capped octahedral; 7 pbp = pentagonal bipyramidal; 6 o = octahedral; 6 och = octahedral chain, 6 ol = octahedral layered.

UF<sub>6</sub> is important in the separation of uranium isotopes by gaseous diffusion (p. 1259).

Pentahalides are, perhaps surprisingly, not found beyond Np (for which the pentafluoride alone is known) but all four are known for Pa. All the pentafluorides as well as PaCl<sub>5</sub> are polymeric and attain 7-coordination by means of double X-bridges between adjacent metal atoms (Fig. 31.6); by contrast UCl<sub>5</sub> and PaBr<sub>5</sub> consist of halogen-bridged dimeric An<sub>2</sub>X<sub>10</sub> units, e.g. Cl<sub>4</sub>U(μ-Cl)<sub>2</sub>UCl<sub>4</sub>. All are very sensitive to water, the hydrolysis of the U<sup>V</sup> halides being complicated by simultaneous disproportionation. Fluorides of intermediate compositions An<sub>2</sub>F<sub>9</sub> (An = Pa, U) and An<sub>4</sub>F<sub>17</sub> (An = U, Pu) have also been reported. U<sub>2</sub>F<sub>9</sub> is the best known; its black colour probably results from charge transfer between U<sup>IV</sup> and U<sup>V</sup>



**Figure 31.6** The polymeric structure of AnF<sub>5</sub> (An = Pa, U, Np) and PaCl<sub>5</sub>, showing the distorted pentagonal bipyramidal coordination of the metal.

A much more extensive series is formed by the tetrahalides of which the tetrafluorides are known as far as Cf. The early tetrafluorides ThF<sub>4</sub> → PuF<sub>4</sub> are produced by heating the dioxides in HF in the presence of H<sub>2</sub> for PaF<sub>4</sub> (in order to prevent oxidation) and in the presence of O<sub>2</sub> for NpF<sub>4</sub> and PuF<sub>4</sub> (in order to prevent reduction). The later tetrafluorides AmF<sub>4</sub> → CfF<sub>4</sub> are obtained by heating the corresponding trifluoride with F<sub>2</sub>. In all cases the metal is 8-coordinated, being surrounded by a slightly distorted square-antiprismatic array of F<sup>-</sup> ions. The tetrachlorides (Th → Np) are prepared by heating the dioxides in CCl<sub>4</sub> or a similar chlorinated hydrocarbon, whereas the tetrabromides (Th → Np) and tetraiodides (Th → U) are obtained from the elements. Eight-coordination is again common (this time

dodecahedral) but a reduction to 7-coordination occurs with UBr<sub>4</sub> and NpBr<sub>4</sub>, and to octahedral coordination for UI<sub>4</sub>. AnF<sub>4</sub> are insoluble in water and, for Th, U and Pu at least, are precipitated as the hydrate AnF<sub>4</sub>·2½H<sub>2</sub>O when F<sup>-</sup> is added to any aqueous solution of An<sup>IV</sup>. AnCl<sub>4</sub>, AnBr<sub>4</sub> and AnI<sub>4</sub> are rather hygroscopic, and dissolve readily in water and other polar solvents. An extensive coordination chemistry is based on the actinide tetrahalides, and UCl<sub>4</sub> is one of the best-known compounds of uranium, providing the usual starting point for most studies of U<sup>IV</sup> chemistry.

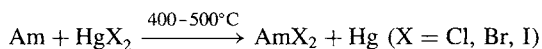
The trihalides are the most nearly complete series, all members having been obtained for the elements U → Es and the series could no doubt be extended. Preparative methods are varied and depend in particular on the actinide involved. For the heavier actinides (Am → Cf) heating the sesquioxide or dioxide in HX is generally applicable, but the lighter actinides require reducing conditions. For NpF<sub>3</sub> and PuF<sub>3</sub> the addition of H<sub>2</sub> to the reaction suffices, but UF<sub>3</sub> is best obtained by the reduction of UF<sub>4</sub> with metallic U or Al. Trichlorides and tribromides of these lighter actinides can be obtained by heating the actinide hydride with HX, and the triiodides by heating the metal with I<sub>2</sub> (U, Np) or HI (Pu). PaI<sub>3</sub> is said to be obtained by heating PaI<sub>5</sub> in a vacuum.

With the exception of their redox properties, the actinide trihalides form a homogeneous group showing strong similarities with the lanthanide trihalides. The ionic, high-melting trifluorides are insoluble in water, from which they can be precipitated as monohydrates; at Cf<sup>III</sup> (ionic radius = 95 pm) they show the same structural change from CN 9 to CN 8 as the lanthanides do at Gd<sup>III</sup> (ionic radius = 93.8 pm). The other trihalides are all hygroscopic, water-soluble solids, many of which crystallize as hexahydrates featuring 8-coordinate cations [AnX<sub>2</sub>(H<sub>2</sub>O)<sub>6</sub>]<sup>+</sup>. Reduction in coordination number as the cations get smaller, again parallels behaviour observed in the lanthanide trihalides but of course it occurs further along the series because of the larger size of the actinides.

Not surprisingly, in view of the stability of Th<sup>IV</sup>, ThI<sub>3</sub> is quite different from the above

trihalides. It is rapidly oxidized by air, reduces water with vigorous evolution of  $H_2$ , and is probably best regarded as  $[Th^{IV}, 3I^-, e^-]$ . The air-sensitive  $ThI_2$ , which is obtained by heating  $ThI_4$  with stoichiometric amounts of the metal, is similarly best formulated as  $[Th^{IV}, 2I^-, 2e^-]$ . It has a complicated layer structure and its lustre and high electrical conductivity indicate a close similarity with the diiodides of Ce, Pr and Gd.

Halides of truly divalent americium, however, can be prepared:



Like those of Eu with which they are structurally similar, these dihalides presumably owe their existence to their  $f^7$  configuration.  $CfBr_2$  and  $CfI_2$  are also known and it seems probable that actinide dihalides would be increasingly stable as far as No if the problems of availability, etc., were overcome.

Several oxohalides<sup>(3,22,23)</sup> are also known, mostly of the types  $An^{VI}O_2X_2$ ,  $An^VO_2X$ ,  $An^{IV}OX_2$  and  $An^{III}OX$ , but they have been less thoroughly studied than the halides. They are commonly prepared by oxygenation of the halide with  $O_2$  or  $Sb_2O_3$ , or in case of  $AnOX$  by hydrolysis (sometimes accidental) of  $AnX_3$ . As is to be expected, the higher oxidation states are formed more readily by the lighter actinides; thus  $AnO_2X_2$ , apart from the fluoro compounds, are confined to  $An = U$ . Conversely the lower oxidation states are favoured by the heavier actinides (from Am onwards).

### 31.3.4 Magnetic and spectroscopic properties<sup>(3,11)</sup>

As the actinides are a second f series it is natural to expect similarities with the lanthanides in their magnetic and spectroscopic properties. However, while previous treatments of the lanthanides (p. 1242) provide a useful starting point in discussing the actinides, important differences are to be noted. Spin-orbit coupling is again strong ( $2000-4000\text{ cm}^{-1}$ ) but, because of the greater exposure of the 5f

electrons, crystal-field splittings are now of comparable magnitude and  $J$  is no longer such a good quantum number. Furthermore, as already mentioned (p. 1266), the energy levels of the 5f and 6d orbitals are sufficiently close for the lighter actinides at least, to render the 6d orbitals accessible. As a result, rigorous treatments of electronic properties must consider each actinide compound individually. They must allow for the mixing of "J levels" obtained from Russell-Saunders coupling and for the population of thermally accessible excited levels. Accordingly, the expression  $\mu_e = g\sqrt{J(J+1)}$  is less applicable than for the lanthanides: the values of magnetic moment obtained at room temperature roughly parallel those obtained for compounds of corresponding lanthanides (see Table 30.6), but they are usually appreciably lower and are much more temperature-dependent.

The electronic spectra of actinide compounds arise from three types of electronic transition:

- (i)  $f \rightarrow f$  transitions (see p. 1243). These are orbitally forbidden, but the selection rule is partially relaxed by the action of the crystal field in distorting the symmetry of the metal ion. Because the field is stronger than for the lanthanides, the bands are more intense by about a factor of 10 and, though still narrow, are about twice as broad and are more complex than those of the lanthanides. They are observed in the visible and ultraviolet regions and produce the colours of aqueous solutions of simple actinide salts as given in Table 31.3.
- (ii)  $5f \rightarrow 6d$  transitions. These are orbitally allowed and give rise to bands which are therefore much more intense than those of type (i) and are usually rather broader. They occur at lower energies than do the  $4f \rightarrow 5d$  transitions of the lanthanides but are still normally confined to the ultraviolet region and do not affect the colour of the ion.
- (iii) *Metal*  $\rightarrow$  *ligand charge transfer*. These again are fully allowed transitions and

produce broad, intense absorptions usually found in the ultraviolet but sometimes trailing into the visible region. They produce the intense colours which characterize many actinide complexes, especially those involving the actinide in a high oxidation state with readily oxidizable ligands.

In view of the magnitude of crystal-field effects it is not surprising that the spectra of actinide ions are sensitive to the latter's environment and, in contrast to the lanthanides, may change drastically from one compound to another. Unfortunately, because of the complexity of the spectra and the low symmetry of many of the complexes, spectra are not easily used as a means of deducing stereochemistry except when used as "finger-prints" for comparison with spectra of previously characterized compounds. However, the dependence on ligand concentration of the positions and intensities, especially of the charge-transfer bands, can profitably be used to estimate stability constants.

### 31.3.5 Complexes of the actinide elements<sup>(3,11,23,29)</sup>

Because of the technical importance of solvent extraction, ion-exchange and precipitation processes for the actinides, a major part of their coordination chemistry has been concerned with aqueous solutions, particularly that involving uranium. It is, however, evident that the actinides as a whole have a much stronger tendency to form complexes than the lanthanides and, as a result of the wider range of available oxidation states, their coordination chemistry is more varied.

#### Oxidation state VII

This has been established only for Np and Pu, alkaline An<sup>VI</sup> solutions of which can

be electrolytically oxidized to give dark-green solutions probably containing species such as  $[\text{AnO}_4(\text{OH})_2]^{3-}$ . Similar strongly oxidizing solutions (the more so if made acidic) are obtained when the mixed oxides  $\text{Li}_5\text{AnO}_6$  are dissolved in water.

#### Oxidation state VI

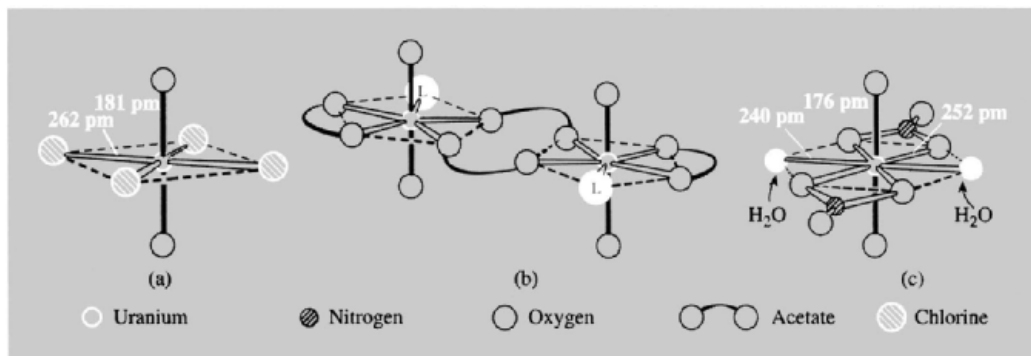
Fluorocomplexes of U<sup>VI</sup> are known of which  $(\text{NH}_4)_4\text{UF}_{10}$  with a probable coordination number of ten is notable.<sup>(30)</sup> Otherwise, apart from  $\text{UO}_3$  and the An<sup>VI</sup> halides already discussed, this oxidation state is dominated by the dioxo, or "actinyl"  $\text{AnO}_2^{2+}$  ions which are found both in aqueous solutions and in solid compounds of U, Np, Pu and Am. These dioxo ions retain their identity throughout a wide variety of reactions and are present, for instance, in the oxohalides  $\text{AnO}_2\text{X}_2$ . The An–O bond strength and the resistance of the group to reduction decreases in the order  $\text{U} > \text{Np} > \text{Pu} > \text{Am}$ . Thus yellow uranyl salts are the most common salts of uranium and are the final products when other compounds of the element are exposed to air and moisture. The nitrate is the most familiar and has the remarkable property, utilized in the extraction of U, of being soluble in nonaqueous solvents such as tributyl phosphate. On the other hand, the formation of  $\text{AmO}_2^{2+}$  requires the use of such strong oxidizing agents as peroxodisulfate,  $\text{S}_2\text{O}_8^{2-}$ . Similarly, whereas the oxofluorides  $\text{AnO}_2\text{F}_2$  are known for U, Np, Pu and Am, only U forms the corresponding oxochloride and oxobromide,  $\text{Cl}^-$  and  $\text{Br}^-$  reducing  $\text{AmO}_2^{2+}$  to  $\text{Am}^{\text{V}}$  species.

In aqueous solutions hydrolysis of the actinyl ions is important and such solutions are distinctly acidic. The reactions are complicated but, at least in the case of  $\text{UO}_2^{2+}$ , it appears that loss of  $\text{H}^+$  from coordinated  $\text{H}_2\text{O}$  is followed by polymerization involving –OH– bridges and yielding species such as  $[(\text{UO}_2)(\text{OH})]^+$ ,  $[(\text{UO}_2)_2(\text{OH})_2]^{2+}$  and  $[(\text{UO}_2)_3(\text{OH})_5]^+$ .

<sup>29</sup> N. B. MIKHEEV and A. N. KAMENSKAYA, *Coord. Chem. Revs.* **109**, 1–59 (1991).

<sup>30</sup> S. MILICEV and B. DRUZINA, *Polyhedron* **9**, 47–51 (1990).





**Figure 31.7** (a) The octahedral anion in  $\text{Cs}_2[\text{UO}_2\text{Cl}_4]$ . (b) Pentagonal bipyramidal coordination of U in dinuclear  $[\text{UO}_2(\text{O}_2\text{CMe})_2\text{L}]_2$  ( $\text{L} = \text{OPPh}_3, \text{OAsPh}_3$ ). (c) Hexagonal bipyramidal coordination of U in uranyl nitrate,  $\text{UO}_2(\text{NO}_3)_2 \cdot 6\text{H}_2\text{O}$ .

Actinyl ions seem to behave rather like divalent, class-a, metal ions of smaller size (or metal ions of the same size but higher charge) and, accordingly, they readily form complexes with  $\text{F}^-$  and  $O$ -donor ligands such as  $\text{OH}^-$ ,  $\text{SO}_4^{2-}$ ,  $\text{NO}_3^-$  and carboxylates.<sup>(31)</sup> The  $\text{O}=\text{An}=\text{O}$  groups are in all cases linear, and coordination of a further 4, 5 or 6 ligands is possible in the equatorial plane. Octahedral, pentagonal bipyramidal, and hexagonal bipyramidal geometries result;<sup>(32)</sup> some examples are shown in Fig. 31.7. These ligands lying in the plane may be neutral molecules such as  $\text{H}_2\text{O}$ ,  $\text{OPR}_3$ ,  $\text{OAsR}_3$ , py or the anions mentioned above, many of which are bidentate.

The axial  $\text{O}-\text{An}$  bonds are clearly very strong. They cannot be protonated and are nearly always shorter than the equatorial bonds. In the case of  $\text{UO}_2^{2+}$ , for instance, it is likely that the  $\text{U}-\text{O}$  bond order is even greater than 2, since the  $\text{U}-\text{O}$  distance is only about 180 pm; in spite of the difference in the ionic radii of the metal ions ( $\text{U}^{\text{VI}} = 73 \text{ pm}$ ,  $\text{Os}^{\text{VI}} = 54.5 \text{ pm}$ ), this is close to that of the  $\text{Os}=\text{O}$  double bond found in the isostructural, osmyl group (175 pm, see p. 1085). It is usually assumed that combinations

of appropriate metal 6d and 5f orbitals overlap with the three p orbitals (or two p and one sp hybrid) of each oxygen to produce one  $\sigma$  and two  $\pi$  bonds, i.e.  $\text{O} \equiv \text{U} \equiv \text{O}$ . This interpretation implies that the change from bent to linear geometries in comparing  $\text{MoO}_2^{2+}$  (p. 1024) and  $\text{UO}_2^{2+}$  is due to the involvement of empty f orbitals in the latter case. More pertinently, the unstable  $\text{ThO}_2$  which is isoelectronic with  $\text{UO}_2^{2+}$ , is bent (angle  $\text{O}-\text{Th}-\text{O}$   $122^\circ$ ) and the difference has been convincingly explained in a relativistic extended Hückel treatment, on the basis that d-orbitals favour bent and f-orbitals linear geometries; in  $\text{UO}_2^{2+}$  the 6d orbitals are lower in energy than the 5f whereas in  $\text{ThO}_2$  the order is reversed.<sup>(33)</sup>

### Oxidation state V

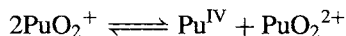
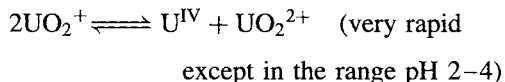
In aqueous solution the  $\text{AnO}_2^+$  ions ( $\text{An} = \text{Pa} \rightarrow \text{Am}$ ) may be formed, at least in the absence of strongly coordinating ligands. They are linear cations like  $\text{AnO}_2^{2+}$  but are less persistent and, indeed, it is probable that  $\text{PaO}_2^+$  should be formulated as  $[\text{PaO}(\text{OH})_2]^+$  and  $[\text{PaO}(\text{OH})]^{2+}$ . Hydrolysis is extensive in aqueous solutions of  $\text{Pa}^{\text{V}}$  and colloidal hydroxo species are formed which readily lead to precipitation of

<sup>31</sup> J. LECIEJEWICZ, N. W. ALCOCK and T. J. KEMP, *Structure and Bonding* **82**, 43–84 (1995).

<sup>32</sup> See pp. 1424–31 of ref. 3.

<sup>33</sup> P. PYYKKÖ, L. S. LAAKKONEN and K. TATSUMI, *Inorg. Chem.* **28**, 1801–5 (1989).

$\text{Pa}_2\text{O}_5 \cdot n\text{H}_2\text{O}$ .  $\text{NpO}_2^+$  in aqueous  $\text{HClO}_4$  is stable but  $\text{UO}_2^+$ ,  $\text{PuO}_2^+$  and  $\text{AmO}_2^+$  are unstable to disproportionation:



and then  $\text{PuO}_2^+ + \text{Pu}^{\text{IV}} \rightleftharpoons \text{Pu}^{\text{III}} + \text{PuO}_2^{2+}$ .<sup>†</sup>  
Likewise:

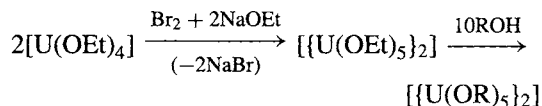


Though the low charge on  $\text{AnO}_2^+$  ions precludes the formation of very stable complexes, and disproportionation into  $\text{An}^{\text{IV}}$  and  $\text{An}^{\text{VI}}$  species is common, a number of complexes of  $\text{NpO}_2^+$  have been prepared,<sup>(34)</sup> several containing the pentagonal bipyramidal  $\{\text{NpO}_2(\text{SO}_4)_2\text{L}\}$  unit. In other cases, strongly coordinating ligands are able to replace the oxygen atoms of the  $\text{AnO}_2^+$  ions and so inhibit disproportionation where this might otherwise occur.  $\text{F}^-$  is notable in this respect and complex ions,  $\text{AnF}_6^-$  ( $\text{An} = \text{Pa}, \text{U}, \text{Np}, \text{Pu}$ ),  $\text{PaF}_7^{2-}$  and  $\text{PaF}_8^{3-}$  can be precipitated from aqueous HF solutions. However, in nonaqueous solvents, preparations such as the oxidation of  $\text{M}^{\text{I}}\text{F}$  and  $\text{AnF}_2$  by  $\text{F}_2$  are more common for U, Np and Pu and extend the range of complex ions to include  $\text{AnF}_7^{2-}$  ( $\text{An} = \text{U}, \text{Np}, \text{Pu}$ ) and  $\text{AnF}_8^{3-}$  ( $\text{An} = \text{U}, \text{Np}$ ). The stereochemistries of these anions are dependent on the particular counter cation as well as on An, and involve 6-, 7-, 8- and 9-coordination. The most remarkable of these complexes are the compounds  $\text{Na}_3\text{AnF}_8$  ( $\text{An} = \text{Pa}, \text{U}, \text{Np}$ ) in which the actinide ion is surrounded by 8  $\text{F}^-$  at the corners of a nearly perfect cube in spite of the large inter-ligand repulsions which this entails.

<sup>†</sup> In the diagram of volt-equivalent versus oxidation state of Pu (Fig. 31.5) the oxidation states III to VI inclusive lie virtually on a straight line. It follows that if either  $\text{Pu}^{\text{IV}}$  or  $\text{Pu}^{\text{V}}$  is dissolved in water, disproportionations are thermodynamically feasible, and within a matter of hours mixtures of Pu in all four oxidation states are obtained.

<sup>34</sup> M. S. GRIGOR'EV, I. A. CHARUSHNIKOV, N. N. KROT, A. I. YANOVSKII and Y. T. STRUCHNOV, *Russ. J. Inorg. Chem. (Engl. Trans.)* **39**, 1267–70 (1994).

Finally, the alkoxides  $\text{U}(\text{OR})_5$  must be mentioned.<sup>(35)</sup> Although easily hydrolysed, they are thermally stable and unusually resistant to disproportionation. They are usually dimeric,  $[(\text{RO})_4\text{U}(\mu\text{-OR})_2\text{U}(\text{OR})_4]$ , and are best obtained by the reactions:

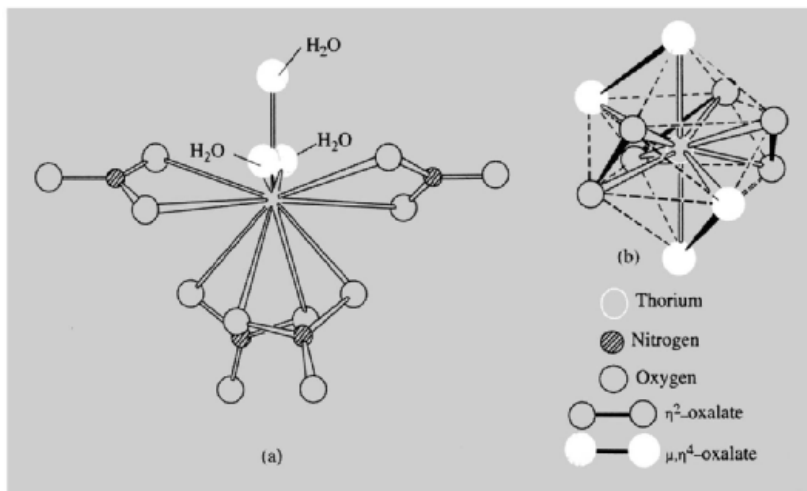


### Oxidation state IV

This is the only important oxidation state for Th, and is one of the two for which U is stable in aqueous solution; it is moderately stable for Pa and Np also. In water  $\text{Pu}^{\text{IV}}$ , like  $\text{Pu}^{\text{V}}$ , disproportionates into a mixture of oxidation states III, IV, V and VI, while  $\text{Am}^{\text{IV}}$  not only disproportionates into  $\text{Am}^{\text{III}} + \text{Am}^{\text{V}}\text{O}_2^+$  but also (like the strongly oxidizing  $\text{Cm}^{\text{IV}}$ ) undergoes rapid self-reduction due to its  $\alpha$ -radioactivity. As a result, aqueous  $\text{Am}^{\text{IV}}$  and  $\text{Cm}^{\text{IV}}$  require stabilization with high concentrations of  $\text{F}^-$  ion. Berkelium(IV), though easily reduced, clearly has an enhanced stability, presumably due to its  $f^7$  configuration, and the only other +4 ion is  $\text{Cf}^{\text{IV}}$ , found in the solids  $\text{CfF}_4$  and  $\text{CfO}_2$ .

In aqueous solutions the hydrated cations are probably 8- or even 9-coordinated and, because they are the most highly charged ions in the actinide series, they have the greatest tendency to split-off protons and so function as quite strong acids (slightly stronger in most cases than  $\text{H}_2\text{SO}_3$ ). This hydrolysis is followed by polymerization which has been most extensively studied in the case of Th. The aquated, dimeric ion,  $[\text{Th}_2(\text{OH})_2]^{6+}$ , which probably involves two OH bridges, seems to predominate even in quite acidic solutions, but in solutions more alkaline than pH 3 polymerization increases considerably and eventually yields an amorphous precipitate of the hydroxide. Just before precipitation it is noticeable that the polymerization process slows down and equilibrium may take weeks to attain.

<sup>35</sup> W. G. van der SLUYS and A. P. SATTELBERGER, *Chem. Revs.* **96**, 1027–40 (1990).



**Figure 31.8** (a) Eleven-coordinate Th in  $\text{Th}(\text{NO}_3)_4 \cdot 5\text{H}_2\text{O}$ : av. Th–O (of  $\text{NO}_3$ ) = 257 pm; av. Th–O (of  $\text{H}_2\text{O}$ ) = 246 pm. (b) The 10-coord. bicapped square antiprismatic anion in  $\text{K}_4[\text{Th}(\text{C}_2\text{O}_4)_4] \cdot 4\text{H}_2\text{O}$ . Note that two pyramidal (267 pm) and three equatorial edges (276 pm) are spanned by oxalate groups, but none of the longer edges of the squares (311 pm). The oxalate groups on the pyramidal edges are actually quadridentate, being coordinated also to adjacent Th atoms.

The same effect is found also with  $\text{Pu}^{\text{IV}}$  where the persistence of polymers, even at acidities which would prevent their formation, can cause serious problems in the reprocessing of nuclear fuels.

The isolation of  $\text{An}^{\text{IV}}$  salts with oxoanions is limited by hydrolysis and redox compatibility. Thus, with the possible exception of  $\text{Pu}(\text{CO}_3)_2$ , carbonate ions furnish only basic carbonates or carbonato complexes such as  $[\text{An}(\text{CO}_3)_5]^{6-}$  ( $\text{An} = \text{Th}, \text{U}, \text{Pu}$ ). Stable tetranitrates are isolable only for Th and Pu, but  $\text{Th}(\text{NO}_3)_4 \cdot 5\text{H}_2\text{O}$  is the most common salt of Th and is notable as the first confirmed example of 11-coordination (Fig. 31.8(a)).  $\text{Pu}(\text{NO}_3)_4 \cdot 5\text{H}_2\text{O}$  is isomorphous, and stabilization of  $\text{Pu}^{\text{IV}}$  by strong nitric acid solutions is crucial in the recovery of Pu by solvent extraction. *O*-donor ligands such as dmsO,  $\text{Ph}_3\text{PO}$  and  $\text{C}_5\text{H}_5\text{NO}$  form adducts, of which  $[\text{Th}(\text{NO}_3)_4(\text{OPPh}_3)_2]$  is known to have a 10-coordinate structure like its  $\text{Ce}^{\text{IV}}$  analogue (Fig. 30.5b, p. 1245) and  $[\text{Th}(\text{C}_5\text{H}_5\text{NO})_6(\text{NO}_3)_2]^{2+}$  has a 10-coordinate distorted bicapped antiprismatic structure.<sup>(36)</sup>

Anionic complexes  $[\text{An}(\text{NO}_3)_6]^{2-}$  ( $\text{An} = \text{Th}, \text{U}, \text{Np}, \text{Pu}$ ) are also obtained, that of Th, and probably the others, having bidentate  $\text{NO}_3^-$  ions forming a slightly distorted icosahedron similar to that of the  $\text{Ce}^{\text{IV}}$  analogue (see Fig. 30.5a).  $\text{Th}(\text{ClO}_4)_4 \cdot 4\text{H}_2\text{O}$  is readily obtained from aqueous solutions but attempts to prepare the  $\text{U}^{\text{IV}}$  salt have produced a green explosive solid of uncertain composition. Hydrated sulfates are known for Th, U, Np and Pu. That of Np is of uncertain hydration but the others can be prepared with both  $4\text{H}_2\text{O}$  and  $8\text{H}_2\text{O}$ ,  $\text{PuSO}_4 \cdot 4\text{H}_2\text{O}$  having possible use as an analytical standard.

The actinides provide a wider range of complexes in their +4 oxidation state than in any other, and these display the usual characteristics of actinide complexes, namely high coordination numbers and varied geometry. Complexes with halides and with *O*-donor chelating ligands are particularly numerous. The main fluoro-complexes are of the types  $[\text{AnF}_5]^-$ ,  $[\text{AnF}_6]^{2-}$ ,  $[\text{AnF}_7]^{3-}$ ,  $[\text{AnF}_8]^{4-}$  and  $[\text{An}_6\text{F}_{31}]^{7-}$  which are nearly all known for  $\text{An} = \text{Th} \rightarrow \text{Bk}$ . Their stoichiometries have not all been determined but, in some cases at least, are known

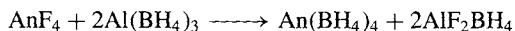
<sup>36</sup> D. M. L. GOODGAME, S. NEWNHAM, C. A. O'MAHONEY and D. J. WILLIAMS, *Polyhedron* **9**, 491–4 (1992).

to depend on the counter cation. For instance,  $[\text{UF}_6]^{2-}$  has a distorted cubic structure in its  $\text{K}^+$  salt and a distorted dodecahedral structure in its  $\text{Rb}^+$  salt.

Several carboxylates, both simple salts and complex anions, have been prepared often as a means of precipitating the  $\text{An}^{\text{IV}}$  ion from solution or, as in the case of simple oxalates, in order to prepare the dioxides by thermal decomposition. In  $\text{K}_4[\text{Th}(\text{C}_2\text{O}_4)_4] \cdot 4\text{H}_2\text{O}$  the anion is known to have a 10-coordinate, bicapped square antiprismatic structure (Fig. 31.8b).  $\beta$ -diketonates are precipitated from aqueous solutions of  $\text{An}^{\text{IV}}$  and the ligand by addition of alkali, and nearly all are sublimable under vacuum.  $[\text{An}(\text{acac})_4]$ , ( $\text{An} = \text{Th}, \text{U}, \text{Np}, \text{Pu}$ ) are apparently dimorphic but both structures are based on an 8-coordinate, distorted square antiprism.

Complexes with *S*-donor ligands are generally less stable and more liable to hydrolysis than those with *O*-donors but can be obtained if the ligand is anionic and chelating. Diethyldithiocarbamates  $[\text{An}(\text{S}_2\text{CNET}_2)_4]$  ( $\text{An} = \text{Th}, \text{U}, \text{Np}, \text{Pu}$ ) are the best known and possess an almost ideal dodecahedral structure.

Finally, the borohydrides  $\text{An}(\text{BH}_4)_4$  must be mentioned.<sup>(37)</sup> Those of Th and U were originally prepared as part of the Manhattan Project and those of Pa, Np and Pu have been prepared more recently, all by the general reaction



The compounds are isolated by sublimation from the reaction mixture. Perhaps surprisingly the compounds fall into two quite distinct classes. Those of Np and Pu are unstable, volatile, monomeric liquids which at low temperatures crystallize with the 12-coordinate structure of  $\text{Zr}(\text{BH}_4)_4$  (Fig. 21.7, p. 969). The borohydrides of Th, Pa and U, on the other hand, are thermally more stable and less reactive solids. They possess a curious helical polymeric structure in which each An is surrounded by 6  $\text{BH}_4^-$  ions, 4 being bridging groups attached by 2 H atoms and

2 being *cis* terminal groups attached by 3 H atoms. The coordination number of the actinide is therefore 14 and the stereochemistry may be described as bicapped hexagonal antiprismatic.

### Oxidation state III

This is the only oxidation state which, with the possible exception of Pa, is displayed by all actinides. From U onwards, its resistance to oxidation in aqueous solution increases progressively with increase in atomic number and it becomes the most stable oxidation state for Am and subsequent actinides (except No for which the  $f^{14}$  configuration confers greater stability on the +2 state).

Amber  $\text{Th}^{3+}(\text{aq})$  has recently been prepared from aqueous solutions of  $\text{ThCl}_4$  and  $\text{HN}_3$ , and is stable for over 1 h before being oxidized by water.<sup>(37a)</sup>  $\text{U}^{\text{III}}$  can be obtained by reduction of  $\text{UO}_2^{2+}$  or  $\text{U}^{\text{IV}}$ , either electrolytically or with Zn amalgam, but is thermodynamically unstable to oxidation not only by  $\text{O}_2$  and aqueous acids but by pure water also.<sup>†</sup> It is nevertheless possible to crystallize double sulfates or double chlorides from aqueous solution and these can then be used to prepare other  $\text{U}^{\text{III}}$  complexes in nonaqueous solvents. Crystallographic data are not plentiful but it has been shown that in  $(\text{NH}_4)\text{U}^{\text{III}}(\text{SO}_4)_2(\text{H}_2\text{O})_4$  each  $\text{SO}_4^{2-}$  is bidentate to one U and monodentate to a second. Three  $\text{H}_2\text{O}$  complete a coordination sphere of 9 oxygens for each uranium with a geometry intermediate between tricapped trigonal prismatic and monocapped square antiprismatic.<sup>(38)</sup> A number of cationic amide complexes are also known for which infrared evidence suggests<sup>(39)</sup>

<sup>†</sup> In pure water the activity of  $\text{H}^+$  is only  $10^{-7} \text{ mol dm}^{-3}$ , and  $E$  for the  $2\text{H}^+/\text{H}_2$  couple consequently falls to  $-0.414 \text{ V}$  compared to  $E^\circ = 0$ . However,  $E^\circ$  for  $\text{U}^{4+}/\text{U}^{3+}$  is even more negative ( $-0.607 \text{ V}$ ) and  $\text{U}^{\text{III}}$  will accordingly reduce water.

<sup>37a</sup> T. M. KLAPÖTKE and A. SCHULZ, *Polyhedron* **16**, 989–91 (1997).

<sup>38</sup> J. I. BULLOCK, M. F. C. LADD, D. C. POVEY and A. E. STOREY, *Inorg. Chim. Acta.* **43**, 101–8 (1980).

<sup>39</sup> J. I. BULLOCK, A. E. STOREY and P. THOMPSON, *J. Chem. Soc., Dalton Trans.*, 1040–4 (1979).

<sup>37</sup> R. H. BANKS and N. M. EDELSTEIN, *Lanthanide and Actinide Chemistry and Spectroscopy*, ACS Symposium, Series 131, Am. Chem. Soc., Washington, 1980, pp. 331–48.

the low symmetry coordination of 8 oxygen atoms to each uranium atom.

Instability also limits the number of complexes of  $\text{Np}^{\text{III}}$  and  $\text{Pu}^{\text{III}}$  but for  $\text{Am}^{\text{III}}$  the number so far prepared is apparently limited mainly by unavailability of the element. As has already been pointed out, the problem becomes still more acute as the series is traversed. While it is clear that lanthanide-like dominance by the trivalent state occurs with the actinides after Pu, the experimental evidence though compelling, is understandably sparse, being largely restricted to solvent extraction and ion-exchange behaviour.<sup>(40)</sup>

### Oxidation state II

This state is found for the six elements Am and Cf  $\rightarrow$  No, though in aqueous solution only for Fm, Md and No. However, for No, alone amongst all the f-series elements, it is the normal oxidation state in aqueous solution. The greater stabilization of the +2 state at the end of the actinides as compared to that at the end of the lanthanides which this implies, has been taken<sup>(40)</sup> to indicate a greater separation between the 5f and 6d than between the 4f and 5d orbitals at the ends of the two series. This is the reverse of the situation found at the beginnings of the series (p. 1266).

Reports of the observation of the +1 oxidation state in aqueous solutions of Md have not been substantiated despite attempts in several major laboratories, and it has been concluded that  $\text{Md}^{\text{I}}$  does not exist in either aqueous or ethanolic solutions.<sup>(41)</sup>

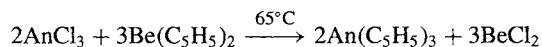
### 31.3.6 Organometallic compounds of the actinides<sup>(42)</sup>

The growth of organoactinide chemistry, like that of organolanthanide chemistry, is comparatively

recent. Attempts in the 1940s to prepare volatile carbonyls and alkyls of uranium for isotopic separations were unsuccessful though, as with the lanthanides, simple carbonyls of uranium have since been obtained in argon matrices quenched to 4 K. Subsequent work has mainly centred on cyclopentadienyls and, to a lesser extent, cyclooctatetraenyls;  $\sigma$ -bonded alkyl and aryl derivatives of the cyclopentadienyls have also been obtained. In general, these compounds are thermally stable, sublimable, but extremely air-sensitive solids which are sometimes water-sensitive also. Their bonding is evidently more covalent than that in organolanthanides, presumably because of the involvement of 5f orbitals, and relativistic effects.

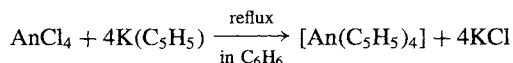
The cyclopentadienyls are of the three main types: (a)  $[\text{An}^{\text{III}}(\text{C}_5\text{H}_5)_3]$ , (b)  $[\text{An}^{\text{IV}}(\eta^5\text{-C}_5\text{H}_5)_4]$  and (c) derivatives of the type  $[\text{An}^{\text{IV}}(\eta^5\text{-C}_5\text{H}_5)_3\text{X}]$  where X is a halogen atom, an alkyl or alkoxy group, or  $\text{BH}_4$ .

(a)  $[\text{An}^{\text{III}}(\text{C}_5\text{H}_5)_3]$  ( $\text{An} = \text{Th} \rightarrow \text{Cf}$ ): the uranium compound is prepared directly from  $\text{UCl}_3$  and  $\text{K}(\text{C}_5\text{H}_5)$  but those of the heavier actinides are best made by the reaction:



Complete structural data are sparse but X-ray diffraction patterns suggest that both  $\eta^5$  and  $\eta^1$  bonding modes are involved (cf.  $\text{Sm}(\text{C}_5\text{H}_5)_3$  p. 1248). In  $[\text{Th}^{\text{III}}\{\eta^5\text{-C}_5\text{H}_5(\text{SiMe}_3)_2\}_3]$  the centres of three rings form a trigonal plane around the Th atom.<sup>(43)</sup> The spectroscopic properties of this blue paramagnetic compound imply a  $6d^1$  rather than  $5f^1$  configuration.<sup>(44)</sup>

(b)  $[\text{An}^{\text{IV}}(\text{C}_5\text{H}_5)_4]$  ( $\text{An} = \text{Th} \rightarrow \text{Np}$ ): the Pa compound is prepared by treating  $\text{PaCl}_4$  with  $\text{Be}(\text{C}_5\text{H}_5)_2$  but the general method of preparation is:



<sup>40</sup> See, for instance, E. K. HULET, ref. 37, pp. 239–63.

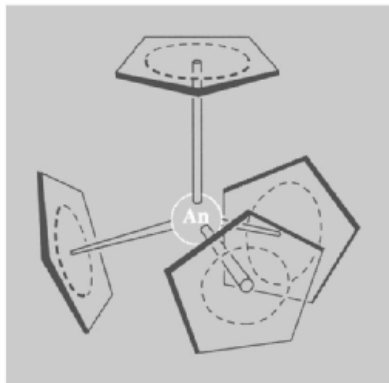
<sup>41</sup> K. HULET, P. A. BAISEN, R. DOUGAN, J. H. LANDRUM, R. W. LOUGHEED and J. F. WILD, *J. Inorg. Nucl. Chem.* **43**, 2941–5 (1981).

<sup>42</sup> T. J. MARKS and R. D. ERNST, pp. 211–70 of Chap. 21 in *Comprehensive Organometallic Chemistry*, Vol. 3, Pergamon Press, Oxford, 1982. See also Vol. 4 of *COMC II*, 1995.

<sup>43</sup> P. C. BLAKE, M. F. LAPPERT, J. L. ATWOOD and H. ZHANG, *J. Chem. Soc., Chem. Commun.*, 1148–9 (1986).

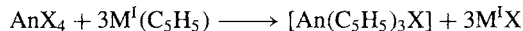
<sup>44</sup> W. K. KOT, G. V. SHALIMOFF and N. M. EDELSTEIN, *J. Am. Chem. Soc.* **110**, 986–7 (1988).

$[M(C_5H_5)_4]$  ( $M = Th, U$ ) contain four identical  $\eta^5$  rings arranged tetrahedrally around the metal atom (Fig. 31.9). The corresponding compounds of Pa and Np are probably the same since all four compounds have very similar nmr and ir spectra.



**Figure 31.9** Structure of  $[An(\eta^5-C_5H_5)_4]$  showing the tetrahedral arrangement of the four rings around the metal atom.

(c) Halide derivatives: the most plentiful are of the type  $[An^{IV}(C_5H_5)_3X]$  ( $An = Th, Pa, U, Np$ ); they can be prepared by the general reaction:



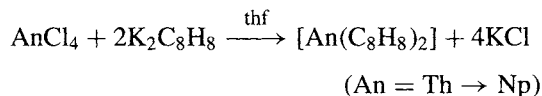
Indeed, the first report of an organoactinide was that of the pale brown  $[U(C_5H_5)_3Cl]$  by L. T. Reynolds and G. Wilkinson in 1956. They showed that, unlike  $Ln(C_6H_5)_3$ , this compound does not yield ferrocene on reaction with  $FeCl_2$ , suggesting greater covalency in the bonding of  $C_5H_5^-$  to  $U^{IV}$  than to  $Ln^{III}$ .

Replacement of Cl in  $[U(C_5H_5)_3Cl]$  and  $[Th(C_5H_5)_3Cl]$ , by other halogens or by alkoxy, alkyl, aryl or  $BH_4$  groups, provides the most extensive synthetic route in this field. An essentially tetrahedral disposition of three ( $\eta^5-C_5H_5$ ) rings and the fourth group around the metal appears to be general. The alkyl and aryl derivatives  $[An(\eta^5-C_5H_5)_3R]$  ( $An = Th, U$ ), are of interest as they provide a means of investigating the An–C  $\sigma$  bond, and mechanistic studies of their thermal decomposition (thermolysis) have been prominent. The precise mechanism is not yet certain but it is clearly not  $\beta$ -elimination

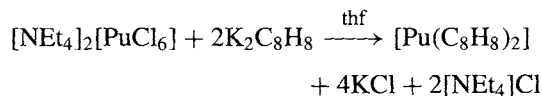
(of an olefin, see p. 926) since the eliminated molecule is RH, the H of which originates from a cyclopentadienyl ring. The decomposition of the Th compounds are cleaner than those of U and a crystalline product can be isolated from the thermolysis at  $170^\circ C$  of a solution of  $[Th(\eta^5-C_5H_5)_3Bu^n]$ . This product is a dimer with the 2 Th atoms bridged by a pair of ( $\eta^5, \eta^1-C_5H_5$ ) rings, i.e.  $[Th(\eta^5-C_5H_5)_2-\mu-(\eta^5, \eta^1-C_5H_5)]_2$ . This remarkable bridge system is like that in niobocene (Fig. 22.12a, p. 1001) but each Th has two additional ( $\eta^5-C_5H_5$ ) rings instead of one ( $\eta^5-C_5H_5$ ) and an H atom.

It has not so far been possible to obtain either  $An^{III}$  or  $An^{IV}$  compounds with three  $C_5Me_5$  rings around a single metal atom. However,  $[M(\eta^5-C_5Me_4H)_3Cl]^{(45)}$  ( $M = Th, U$ ) and  $[U(\eta^5-C_4Me_4P)_3Cl]^{(46)}$  have been prepared.

The complexes  $[An(\eta^8-C_8H_8)_2]$  of cyclooctatetraene (cot) have been prepared for  $An = Th \rightarrow Pu$  by the reactions:



and



followed by sublimation under vacuum. They are “sandwich” molecules with parallel and eclipsed rings (see Fig. 19.31, p. 942). This structure is strikingly similar to that of ferrocene (Fig. 19.27, p. 937), and extensive discussions on the nature of the metal-ring bonding suggests that this too is very similar.<sup>(3)</sup> In order to emphasise these resemblances with the d-series cyclopentadienyls, the names “uranocene”, etc., have been coined. Although thermally stable, these compounds are extremely sensitive to air and, except for uranocene, are also decomposed by water.

<sup>45</sup> F. G. N. CLOKE, S. A. HAWKES, P. B. HITCHCOCK and P. SCOTT, *Organometallics* **13**, 2895–7 (1994).

<sup>46</sup> P. GRADOZ, C. BOISSON, D. BAUDRY, M. LANCE, M. NIERLICH, J. VIGNER and M. EPHRITIKHINE, *J. Chem. Soc., Chem. Commun.*, 1720–1 (1992).

However, uranocene can be made more air-stable by use of sufficiently bulky substituents, and 1,3,5,7-tetraphenylcyclo-octatetraene yields the completely air-stable  $[U(\eta^8-C_8H_4Ph_4)_2]$ , in which the parallel ligands are virtually eclipsed but the phenyl substituents staggered and rotated on average  $42^\circ$  out of the  $C_8$  ring plane (Fig. 31.10).

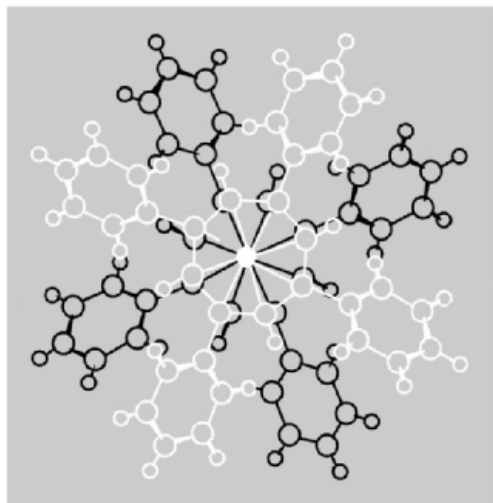


Figure 31.10 The structure of  $[U(\eta^8-C_8H_4Ph_4)_2]$ .

## 31.4 The Transactinide Elements ( $Z = 104-112$ )

### 31.4.1 Introduction

The addition of nine further elements ( $Z = 104-112$ ) to the Periodic Table during the past three decades has involved outstanding feats of intellectual and experimental virtuosity. Some of the discoveries have been widely accepted but others have been hotly contested and this has led to distressingly persistent disagreements concerning priority. For this reason IUPAC and IUPAP set up a neutral international group in 1987 to establish “the criteria that must be satisfied for the discovery of a new element to be recognised” and to apply these criteria to questions of priority in the discovery of the trans-fermium elements. Some of the conclusions of

this group have already been briefly mentioned (see Table 31.1). Their detailed Reports<sup>(5)</sup> were accepted by both IUPAC and IUPAP and the group’s final recommendations, which form the basis of this Section, have been very widely though not universally accepted by the scientific community. Many subtle and difficult points are involved and the full reports repay careful reading. It is also worth noting that the word *discovery* is something of a misnomer in this context: *synthesis and characterization* of new elements would perhaps be a better description.

The separate question of names and symbols for the new elements has, unfortunately, taken even longer to resolve, but definitive recommendations were ratified by IUPAC in August 1997 and have been generally accepted. It is clearly both unsatisfactory and confusing to have more than one name in current use for a given element and to have the same name being applied to two different elements. For this reason the present treatment refers to the individual elements by means of their atomic numbers. However, to help readers with the nomenclature used in the references cited, a list of the various names that are in use or that have been suggested from time to time is summarised in Table 31.7.

Two general types of nuclear reaction have been used to produce trans-fermium elements. The first type, hot fusion reactions, uses accelerated light particles with  $Z$  in the range 5–10 (typically  ${}^5B$ ,  ${}^6C$ ,  ${}^7N$ ,  ${}^8O$  or  ${}^{10}Ne$ ) to bombard targets with  $Z = 92-98$  (typically  ${}^{92}U$ ,  ${}^{94}Pu$ ,  ${}^{95}Am$ ,  ${}^{96}Cm$  or  ${}^{98}Cf$ ). This method can be used effectively up to about element 106 but, increasingly, the compound nucleus is formed with such high excitation energy that many particles, including charged ones, evaporate off before the desired product nucleus is reached. To solve this problem the group at Dubna suggested an ingenious alternative route, cold fusion, which exploits the fact that nuclei such as  ${}^{82}Pb$  or  ${}^{83}Bi$  have high binding energies due to closed nuclear shells. If these nuclei are bombarded with moderately heavy ions which are preferably also near closed nuclear shells (e.g.  ${}^{24}Cr$ ,  ${}^{26}Fe$  or  ${}^{28}Ni$ ) at energies just above the Coulomb

**Table 31.7** Names and symbols in current use (or proposed) for elements 104–112

Z	Systematic (1977) <sup>(a)</sup>	IUPAC (1997)	Other names suggested from time to time
104	Un-nil-quadium (Unq)	<b>Rutherfordium (Rf)</b>	Kurchatovium (Ku), Dubnium (Db)
105	Un-nil-pentium (Unp)	<b>Dubnium (Db)</b>	Nielsbohrium (Ns), Hahnium (Ha), Joliotium (Jl)
106	Un-nil-hexium (Unh)	<b>Seaborgium (Sg)</b>	Rutherfordium (Rf)
107	Un-nil-septium (Uns)	<b>Bohrium (Bh)</b>	Nielsbohrium (Ns)
108	Un-nil-octium (Uno)	<b>Hassium (Hs)</b>	Hahnium (Hn)
109	Un-nil-ennium (Une)	<b>Meitnerium (Mt)</b>	—
110	Un-un-nilium (Uun)	—	—
111	Un-un-unium (Uuu)	—	—
112	Un-un-bium (Uub)	—	—

<sup>(a)</sup>The hyphens in the systematic names have been inserted here to assist comprehension and pronunciation; they are not part of the names. The roots nil, un, bi, etc. were chosen to allow a unique set of three-letter symbols to be generated for any (atomic) number.

barrier, they produce compound product nuclei with much lower resultant excitation energies. As a result, the probability of (unwanted) fission is very much reduced and, under sufficiently fine-tuned conditions, neutron-only emission will dominate over all other light-particle emissions. This method has been outstandingly successful in producing elements with  $Z > 106$ .

### 31.4.2 Element 104

The first (inconclusive) work bearing on the synthesis of element 104 was published by the Dubna group in 1964. However, the crucial Dubna evidence (1969–70) for the production of element 104 by bombardment of  ${}_{94}\text{Pu}$  with  ${}_{10}\text{Ne}$  came after the development of a sophisticated method for rapid *in situ* chlorination of the product atoms followed by their gas-chromatographic separation on an atom-by-atom basis. This was a heroic enterprise which combined cyclotron nuclear physics and chemical separations. As we have seen, the actinide series of elements ends with  ${}_{103}\text{Lr}$ . The next element should be in Group 4 of the transition elements, i.e. a heavier congener of Ti, Zr and Hf.\* As such it would be expected to have a chloride

\* A happy consequence of nuclear systematics is that element 104 is in Group 4, element 105 is in Group 5, etc. This mnemonic holds to the end of the transition series at element 112 and presumably beyond; it can be compared with the similar relation between the group numbers of the post-transition main-group elements (13–18) and the group numbers of the preceding transition elements (3–8).

which is significantly more volatile than those of the actinide elements. After extensive preliminary work to develop and prove the method, the recoil products emitted from the target were chlorinated with a stream of gaseous  $\text{NbCl}_5$  or  $\text{ZrCl}_4$  within a fraction of a second from the instant of formation of the new atom, and then separated gas-chromatographically in a 4-metre-long quartz tube at either 250° or 300°C before being detected by spontaneous fission. When part of the tube was replaced by a KCl capillary the activity in the detection zone ceased, because of the formation of an involatile complex, presumably  $\text{K}_2[104]\text{Cl}_6$ . As no nucleus with  $Z > 104$  can be formed by bombarding  ${}_{94}\text{Pu}$  with  ${}_{10}\text{Ne}$ , and no spontaneously fissioning atom with  $Z < 104$  forms a volatile chloride, the new activity must be due to element 104. During the later stages of this work, and essentially contemporaneously with it, the Berkeley group established the reactions  ${}^{249}\text{Cf}({}^{12}\text{C}, 4n){}^{257}104$ ,  ${}^{249}\text{Cf}({}^{13}\text{C}, 3n){}^{259}104$  and  ${}^{248}\text{Cm}({}^{16}\text{O}, 6n){}^{258}104$  by elegant work which included the observation of generic parent–daughter  $\alpha$ -decays to the known isotopes  ${}^{253}102$  and  ${}^{255}102$ . It was concluded that credit for the discovery of element 104 should be shared between the groups at Dubna and Berkeley. Detailed references to the original papers, and an assessment of the many scientific points involved are in ref. 5. The name rutherfordium now recommended and adopted by IUPAC for element 104 was first suggested by the Berkeley group in 1969.



Nine isotopes of element 104 are now known with certainty in the mass range 255–264 and a tenth,  $^{254}\text{Rf}$ , is possible. They have half-lives in the range 7 ms–65 s and can only be produced slowly one atom at a time. This clearly restricts chemical studies, though ingenious techniques have been developed to overcome some of the problems.<sup>(47)</sup> It has been found that element 104 is indeed a Group 4 homologue and tends to resemble Zr and Hf rather than Th in its aqueous solution chemistry and extractability. The predominant oxidation state is +4 and complexes such as  $\text{RfCl}_6^{2-}$  have been confirmed. Distribution coefficients obtained for its extraction into thenoyltrifluoroacetone (TTA) lead to an ionic radius of 102 pm for 8-coordinated Rf, between those of Th and Pu. Gas-phase studies of element 104 by isothermal chromatography indicate that its bromides are more volatile than those of Hf, and that the chlorides of both Hf and Rf are more volatile than the bromides.<sup>(48,49)</sup>

### 31.4.3 Element 105

Attempts at the synthesis of element 105 were first reported from Dubna in 1968 but it was a further two years before cyclotron physics, combined with a thermal-gradient variant of gas-phase chromatography, plus parent–daughter  $\alpha$ -particle generic relations finally succeeded in convincingly establishing its formation. The main reactions studied were  $^{243}\text{Am}(^{22}\text{Ne},4n)^{261}105$  and  $^{243}\text{Am}(^{22}\text{Ne},5n)^{260}105$ . During the later stages of this work the Berkeley group published a convincing synthesis via  $^{249}\text{Cf}(^{15}\text{N},4n)^{260}105$  which was also secured, amongst much other evidence, by an  $\alpha$ -particle generic relation with  $^{256}103$ . The independent work from the two laboratories was essentially contemporaneous and

credit for the discovery of element 105 was shared.<sup>(5)</sup> The name now internationally accepted for element 105 is dubnium.

The pioneering gas thermochromatographic studies of I. Zvara and his group in the mid-1970s suggested that element 105 was a homologue of Nb and Ta. No further work on its chemistry was reported until 1988 when the first studies of aqueous solutions of element 105 were published.<sup>(50)</sup> Using the 35 s isotope formed by the reaction  $^{249}\text{Bk}(^{18}\text{O},5n)^{267}105$ , some 800 manual experiments (taking about 50 s each) were performed. It was found that, after fuming with concentrated nitric acid, atoms of element 105, dubnium, sorbed on glass surfaces just like the Group 5 elements Nb and Ta but unlike Zr and Hf in the preceding Group. Extraction studies also confirmed the affinity to Group 5, though dubnium appeared closer to Nb than to Ta, perhaps due to the influence of relativistic effects. Later work using computer-controlled procedures reduced the timescale to less than 40 s per experiment,<sup>(49)</sup> halide complexation and extraction behaviour showed element 105 to be most like Pa, a pseudo Group 5 element.

### 31.4.4 Element 106

Work at Berkeley-Livermore in 1974 first convincingly demonstrated the synthesis of this element via the reaction  $^{249}\text{Cf}(^{18}\text{O},4n)^{263}106$ . Contemporaneous work at Dubna applied their novel cold fusion method (p. 1280) to reactions such as  $^{82}\text{Pb} + ^{24}\text{Cr}$ : although this methodology was crucial to the synthesis of all later elements (107–112) it did not at that time demonstrate the formation of element 106 with adequate conviction. Very recently, element 106 was resynthesized by a new group at Berkeley using exactly the same reaction as employed in 1974.<sup>(51)</sup> The isotope  $^{263}106$  decays with a half-life of  $0.8 \pm 0.2$  s to  $^{259}104$  and then by a second

<sup>47</sup> D. C. HOFFMAN, *Proc. Robert A. Welch Foundation Conference XXXIV. Fifty Years with Transuranium Elements*, October 1990, pp. 255–76. D. C. HOFFMAN, *Chem. & Eng. News*, May 2, 24–34 (1994).

<sup>48</sup> B. KADKHODAYAN, A. TÜRLER, K. E. GREGORICH, M. J. NURMIA, D. M. LEE and D. C. HOFFMAN, *Nucl. Instr. and Methods in Phys. Res.* **A317**, 254–61 (1992).

<sup>49</sup> D. C. HOFFMAN, *Radiochim. Acta* **61**, 123–8 (1993).

<sup>50</sup> K. E. GREGORICH (and 11 others), *Radiochim. Acta* **43**, 223–31 (1988).

<sup>51</sup> K. E. GREGORICH, M. R. LANE, M. F. MOHAR, D. M. LEE, C. D. CACHER, E. R. SILWESTER and D. C. HOFFMAN, *Phys. Rev. Lett.* **72**, 1423–6 (1994).

$\alpha$ -particle emission to  $^{255}\text{No}$ , both of which were positively identified. The recommended name for element 106 is seaborgium, Sg.

Six isotopes of element 106 are now known (see Table 31.8) of which the most recent has a half-life in the range 10–30 s, encouraging the hope that some chemistry of this fugitive species might someday be revealed.<sup>†</sup> This heaviest isotope was synthesised by the reaction  $^{248}\text{Cm}(^{22}\text{Ne},4n)^{266}106$  and the present uncertainty in the half-life is due to the very few atoms which have so far been observed. Indeed, one of the fascinating aspects of work in this area is the development of philosophical and mathematical techniques to define and deal with the statistics of a small number of random events or even of a single event.<sup>(52)</sup>

### 31.4.5 Elements 107, 108 and 109

These three elements were all first synthesized by the cold fusion method at GSI, Darmstadt,<sup>(5)</sup> using a very sophisticated set of techniques. For element 107 (1981) an accelerated beam of ionized  $^{54}\text{Cr}$  atoms was made to impinge on a thin  $^{209}\text{Bi}$  foil; the reaction recoils were separated in flight from the incoming beam and from the unwanted products of transfer reactions by a velocity filter consisting of a combination of magnetic and electric fields. This facility is known by the acronym SHIP, i.e. separated heavy-ion reaction products. The product atoms were then implanted in position-sensitive solid-state detectors which recorded  $\alpha$ -particle decay energies or spontaneous fission events in position- and time-correlation with each other and with the time of implantation. Time-of-flight was also used to estimate the masses of these particles. Five atoms of  $^{262}107$  were detected and characterized in this way in the discovery experiments. Later work showed that

<sup>†</sup> The chemistry of 4 atoms of Sg in solution and of 3 atoms in the gas phase indicate that the element resembles its lighter homologues in Group 6, Mo and W; see M. SCHÄDEL and 17 others, *Nature* **388**, 55–7 (1997).

<sup>52</sup> K.-H. SCHMIDT, C.-C. SAHM, K. PIELENZ and H.-G. CLERC, *Z. Phys. A* **316**, 19–26 (1984).

the half-life was  $102 \pm 26$  ms and also established a second isotope,  $^{261}107$ , with  $t_{1/2}$  11.8 ms having an (unsymmetrical) uncertainty at the 68% level of (+5.3, –2.8). The recommended name for element 107 is bohrium, Bh.

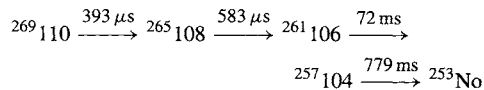
Element 108 was unequivocally established in 1984 using the SHIP facilities in Darmstadt to detect three atoms formed by the reaction  $^{208}\text{Pb}(^{58}\text{Fe},n)^{265}108$ . The half-life for  $\alpha$ -decay was 1.8 ms with an uncertainty of (+2.2, –0.7) ms, and both the daughter and granddaughter nuclides  $^{261}106$  and  $^{257}104$  were detected and characterized. Other isotopes of element 108 were in all probability obtained in Dubna at about the same time using reactions such as  $^{209}\text{Bi}(^{55}\text{Mn},n)^{263}108$ ,  $^{207}\text{Pb}(^{58}\text{Fe},n)^{264}108$  and  $^{208}\text{Pb}(^{58}\text{Fe},2n)^{264}108$ .<sup>(5)</sup> The recommended name for element 108 is hassium, Hs, after the latin name for Hesse, the region of Germany in which the GSI Laboratories are located.

Element 109 was also discovered by the Darmstadt GSI group in 1982 in an astonishingly virtuoso experiment which convincingly detected and unambiguously identified just *one atom* of  $^{266}109$  from the reaction  $^{209}\text{Bi}(^{58}\text{Fe},n)$ . A further two atoms were synthesized at GSI six years later in 1988. The isotope is an  $\alpha$ -emitter with a “half-life” of 3.4 ms (+1.6, –1.3 ms).<sup>(5)</sup> The recommended name for element 109 is meitnerium, Mt. It is salutary to contemplate the towering intellectual insights and prodigious technical achievements required to accomplish such experiments which can precisely identify a single atom amongst some  $10^{18}$  accompanying events.

### 31.4.6 Elements 110, 111 and 112

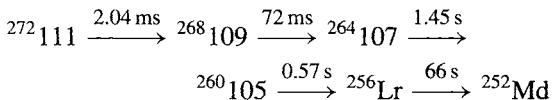
These three elements were first made during a 15-month period of intense activity from late 1994 to early 1996 at GSI, Darmstadt. They therefore post-date the deliberations of the IUPAC/IUPAP international working group,<sup>(5)</sup> but the publications convincingly meet the stringent criteria for discovery elaborated by that group and have been widely accepted by the scientific community. So far, no names have been officially proposed or recommended for elements 110–112.

Initially, one atom of  $^{269}110$  was detected on 9 November 1994 by the SHIP facilities at Darmstadt following the reaction  $^{208}\text{Pb}(^{62}\text{Ni},n)^{269}110$  and observation of the subsequent chain of four  $\alpha$ -decays:<sup>(53,54)</sup>



A further three atoms of  $^{269}110$  were observed during the next eight days leading to an average "half-life" of  $170\ \mu\text{s}$  (+160, -60  $\mu\text{s}$ ). [Note that the decay times listed for the above single-atom observations are not identical with the best values of the statistical half-lives for the species mentioned.] Subsequent work also identified a second isotope  $^{271}110$  with  $t_{1/2}$  623  $\mu\text{s}$ .

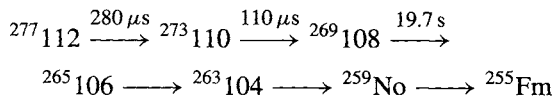
Element 111 was synthesized and characterized by the same group during the period 8–17 December 1994 using the analogous cold-fusion reaction,  $^{209}\text{Bi}(^{64}\text{Ni},n)^{272}111$ , followed by observation of up to five successive  $\alpha$ -emissions which could be assigned to the chain:<sup>(54,55)</sup>



Note also the production of new isotopes of elements 107 and 109 in this chain.

Element 112 emerged close to midnight on 9 February 1996 when the team at GSI unambiguously detected one atom of the new element after two weeks of bombarding a lead target with high-energy ionized atoms of zinc  $^{208}\text{Pb}(^{70}\text{Zn},n)^{277}112$ .<sup>(56)</sup> The new element emitted an  $\alpha$ -particle after 280  $\mu\text{s}$ , followed by several

others which formed a coherent decay scheme down to Fm:



This work is particularly significant for a number of reasons. Not only does  $^{277}112$  have the highest atomic number and the highest mass of any nuclide so far, but it is also expected to complete the 6d transition series of elements. Will the next elements 113, 114, etc. prove to be members of the boron and carbon groups or will relativistic effects supervene to stabilize other electronic configurations? Perhaps even more significantly, the new atomic species is approaching the "island of stability" which has been predicted on the basis of the expected nuclear closed shells of 114 protons and 184 or 178 neutrons, and it does indeed show clear signs of this increasing stability (decreasing instability). Moreover, the decay chain generates two new isotopes of elements 110 and 108 which themselves are the heaviest (and most stable) isotopes of these elements so far. Further increases in stability might well make chemical experimentation feasible. Clearly, exciting prospects lie ahead.

At present, some 36 isotopes of the transactinide elements have been characterized and these are summarized in Table 31.8.

**Table 31.8** Isotopes of the transactinide elements (1997)

Z (Discovered)	No. of isotopes	Mass range	$t_{1/2}$ range
<b>104</b> (1969)	9(?10)	253–262	7 ms–65 s
<b>105</b> (1970)	7	255–263	1.3 s–34 s
<b>106</b> (1974)	6	259–266	3.6 ms–30 s
<b>107</b> (1981)	3	261–264	12 ms–0.44 s
<b>108</b> (1984)	3	264, 265, 269	80 $\mu\text{s}$ –19.7 s
<b>109</b> (1982)	2	266, 268	3.4 ms–70 ms
<b>110</b> (1994)	3	269, 271, 273	0.1 ms–0.2 ms
<b>111</b> (1994)	1	272	1.5 ms
<b>112</b> (1996)	1	277	0.28 ms

<sup>53</sup> S. HOFMANN (and 11 others), *Z. Phys. A* **350**, 277–80 (1995).

<sup>54</sup> M. FREEMANTLE, *Chem. & Eng. News*, 13 March, 35–40 (1995).

<sup>55</sup> S. HOFMANN (and 11 others), *Z. Phys. A* **350**, 281–2 (1995).

<sup>56</sup> S. HOFMANN (and 11 others), *Z. Phys. A* **354**, 229–30 (1996).

# Appendix 1

## Atomic Orbitals

THE spacial distribution of electron density in an atom is described by means of atomic orbitals  $\psi(r, \theta, \phi)$  such that for a given orbital  $\psi$  the function  $\psi^2 dv$  gives the probability of finding the electron in an element of volume  $dv$  at a point having the polar coordinates  $r, \theta, \phi$ . Each orbital can be expressed as a product of two functions, i.e.  $\psi_{n,l,m}(r, \theta, \phi) = R_{n,l}(r)A_{l,m}(\theta, \phi)$ , where

(a)  $R_{n,l}(r)$  is a radial function which depends only on the distance  $r$  from the nucleus (independent of direction) and is defined by the two quantum numbers  $n, l$ ;

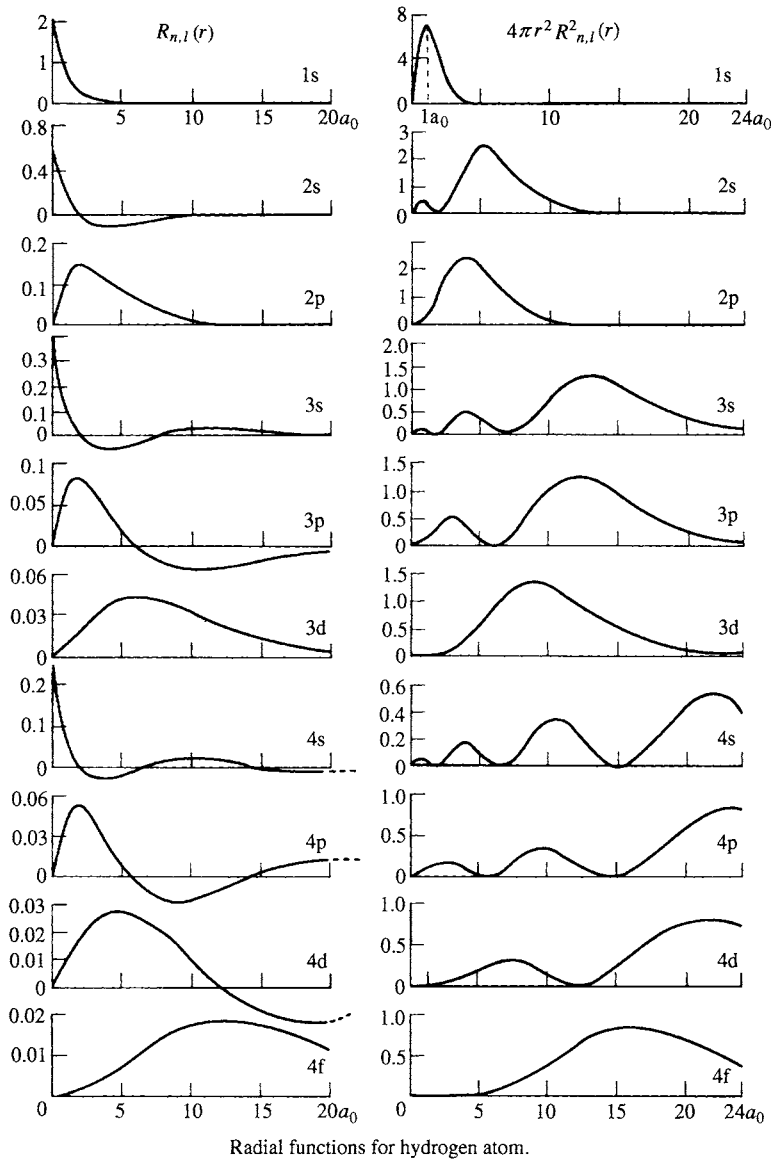
(b)  $A_{l,m}(\theta, \phi)$  is an angular function which is independent of distance but depends on the direction as given by the angles  $\theta, \phi$ ; it is defined by the two quantum numbers  $l, m$ .

Normalized radial functions for a hydrogen-like atom are given in Table A1.1 and plotted graphically in Fig. A1.1 for the first ten combinations of  $n$  and  $l$ . It will be seen that the radial functions for 1s, 2p, 3d, and 4f orbitals have no nodes and are everywhere of

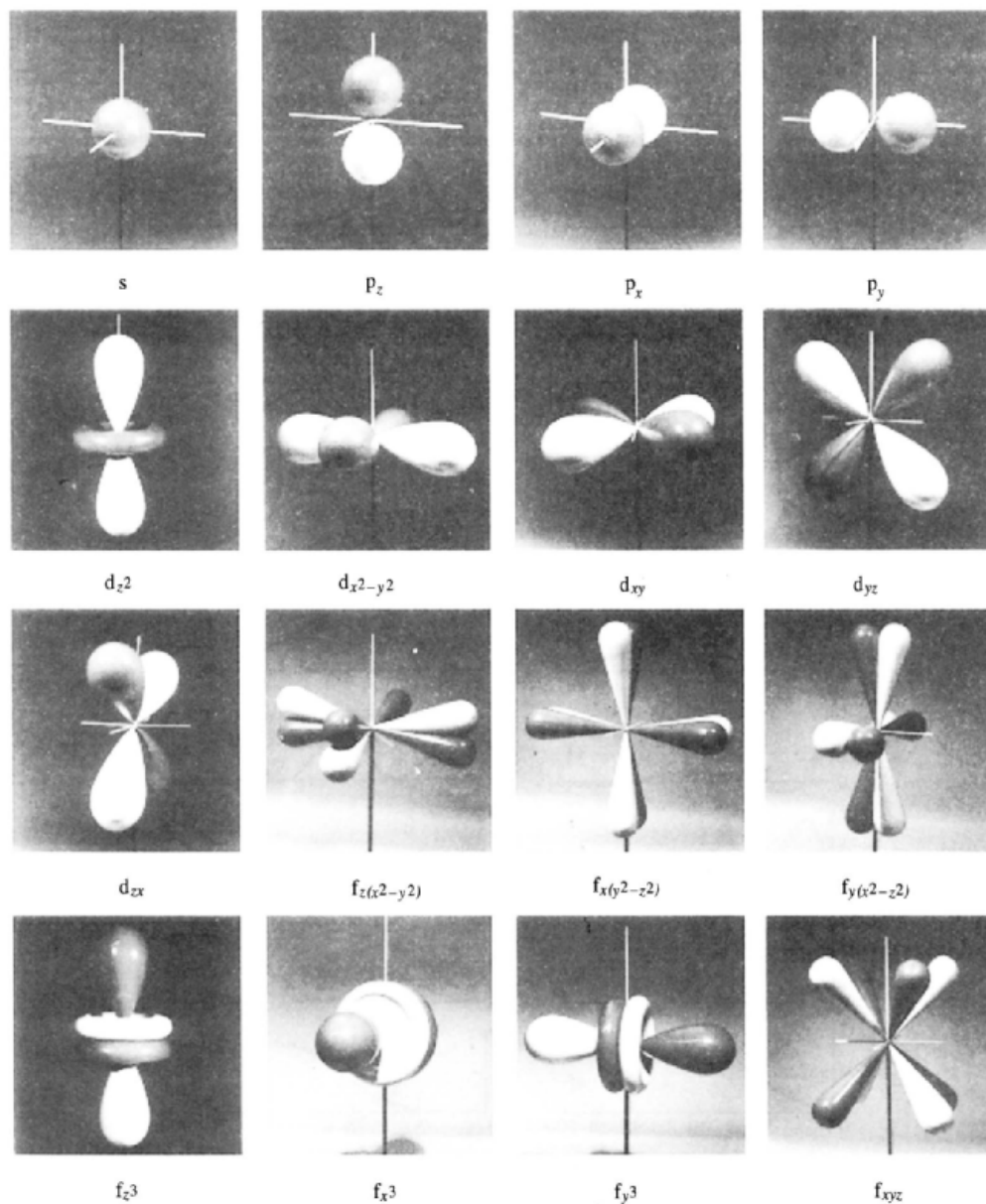
the same sign (e.g. positive). In general  $R_{n,l}(r)$  becomes zero ( $n - l - 1$ ) times between  $r$  equals 0 and  $\infty$ . The probability of finding an electron at a distance  $r$  from the nucleus is given by  $4\pi R_{n,l}^2(r)r^2 dr$ , and this is also plotted in Fig. A1.1. However, the probability of finding an electron frequently depends also on the direction chosen. The probability of finding an electron in a given direction, independently of distance from the nucleus, is given by the square of the angular dependence function  $A_{l,m}^2(\theta, \phi)$ . The normalized functions  $A_{l,m}(\theta, \phi)$  are listed in Table A1.2 and illustrated schematically by the models in Fig. A1.2. It will be seen that for s orbitals ( $l = 0$ ) the angular dependence function  $A$  is constant, independent of  $\theta$ , and  $\phi$ , i.e. the function is spherically symmetrical. For p orbitals ( $l = 1$ )  $A$  comprises two spheres in contact, one being positive and one negative, i.e. there is one planar node. The d and f functions ( $l = 2, 3$ ) have more complex angular dependence with 2 and 3 nodes respectively.

Table A1.1 Normalized radial functions  $R_{n,l}(r)$  for hydrogen-like atoms
$$R_{n,l}(r) = -\sqrt{\frac{4(n-l-1)!Z^3}{n^4[(n+l)!]^3a_0^3}} \times \left(\frac{2Zr}{a_0n}\right)^l L_{n+l}^{2l+1}\left(\frac{2Zr}{a_0n}\right) \times e^{-Zr/a_0n}$$

Orbital	$n$	$l$	$R_{n,l}$	=	Constant	×	Polynomial	×	Expon.
1s	1	0	$R_{1,0}$		$2(Z/a_0)^{3/2}$		1		$e^{-Zr/a_0}$
2s	2	0	$R_{2,0}$		$\frac{(Z/a_0)^{3/2}}{2\sqrt{2}}$		$\left(2 - \frac{Zr}{a_0}\right)$		$e^{-Zr/2a_0}$
2p	2	1	$R_{2,1}$		$\frac{(Z/a_0)^{3/2}}{2\sqrt{6}}$		$\frac{Zr}{a_0}$		$e^{-Zr/2a_0}$
3s	3	0	$R_{3,0}$		$\frac{2(Z/a_0)^{3/2}}{81\sqrt{3}}$		$\left(27 - 18\frac{Zr}{a_0} + 2\frac{Z^2r^2}{a_0^2}\right)$		$e^{-Zr/3a_0}$
3p	3	1	$R_{3,1}$		$\frac{4(Z/a_0)^{3/2}}{81\sqrt{6}}$		$\left(6\frac{Zr}{a_0} - \frac{Z^2r^2}{a_0^2}\right)$		$e^{-Zr/3a_0}$
3d	3	2	$R_{3,2}$		$\frac{4(Z/a_0)^{3/2}}{81\sqrt{30}}$		$\frac{Z^2r^2}{a_0^2}$		$e^{-Zr/3a_0}$
4s	4	0	$R_{4,0}$		$\frac{(Z/a_0)^{3/2}}{768}$		$\left(192 - 144\frac{Zr}{a_0} + 24\frac{Z^2r^2}{a_0^2} - \frac{Z^3r^3}{a_0^3}\right)$		$e^{-Zr/4a_0}$
4p	4	1	$R_{4,1}$		$\frac{(Z/a_0)^{3/2}}{265\sqrt{15}}$		$\left(80\frac{Zr}{a_0} - 20\frac{Z^2r^2}{a_0^2} + \frac{Z^3r^3}{a_0^3}\right)$		$e^{-Zr/4a_0}$
4d	4	2	$R_{4,2}$		$\frac{(Z/a_0)^{3/2}}{768\sqrt{5}}$		$\left(12\frac{Z^2r^2}{a_0^2} - \frac{Z^3r^3}{a_0^3}\right)$		$e^{-Zr/4a_0}$
4f	4	3	$R_{4,3}$		$\frac{(Z/a_0)^{3/2}}{768\sqrt{35}}$		$\frac{Z^3r^3}{a_0^3}$		$e^{-Zr/4a_0}$



**Figure A1.1** Radial functions for a hydrogen atom. (Note that the horizontal scale is the same in each graph but the vertical scale varies by as much as a factor of 100. The Bohr radius  $a_0 = 52.9$  pm.)



**Figure A1.2** Models schematically illustrating the angular dependence functions  $A_{l,m}(\theta, \phi)$ . There is no unique way of representing the angular dependence functions of all seven f orbitals. An alternative to the set shown is one  $f_{z^3}$ , three  $f_{xz^2}$ ,  $f_{yx^2}$ ,  $f_{zy^2}$ , and three  $f_{x(x^2-3y^2)}$ ,  $f_{y(y^2-3z^2)}$ , and  $f_{z(z^2-3x^2)}$ .

Table A1.2 Normalized angular dependence functions,  $A_{l,m}(\theta, \phi) = \Theta_{l,m}(\theta)\Phi_m(\phi)$ 

Orbital	Angular dependence function	Orbital	Angular dependence function
s	$\frac{1}{2\sqrt{\pi}}$		
p <sub>z</sub>	$\frac{\sqrt{3}}{2\sqrt{\pi}} \cos \theta$		
p <sub>x</sub>	$\frac{\sqrt{3}}{2\pi} \sin \theta \cos \phi$	f <sub>z<sup>3</sup></sub>	$\frac{\sqrt{7}}{4\sqrt{\pi}} (5 \cos^3 \theta - 3 \cos \theta)$
p <sub>y</sub>	$\frac{\sqrt{3}}{2\sqrt{\pi}} \sin \theta \sin \phi$	f <sub>z<sup>2</sup>x</sub>	$\frac{\sqrt{42}}{8\sqrt{\pi}} (5 \cos^2 \theta - 1) \sin \theta \cos \phi$
d <sub>z<sup>2</sup></sub>	$\frac{\sqrt{5}}{4\sqrt{\pi}} (3 \cos^2 \theta - 1)$	f <sub>z<sup>2</sup>y</sub>	$\frac{\sqrt{42}}{8\sqrt{\pi}} (5 \cos^2 \theta - 1) \sin \theta \sin \phi$
d <sub>x<sup>2</sup>-y<sup>2</sup></sub>	$\frac{\sqrt{15}}{4\sqrt{\pi}} \sin^2 \theta (2 \cos^2 \phi - 1)$	f <sub>z(x<sup>2</sup>-y<sup>2</sup>)</sub>	$\frac{\sqrt{105}}{4\sqrt{\pi}} \cos \theta \sin^2 \theta (2 \cos^2 \phi - 1)$
d <sub>zx</sub>	$\frac{\sqrt{15}}{2\sqrt{\pi}} \cos \theta \sin \theta \cos \phi$	f <sub>zxy</sub>	$\frac{\sqrt{105}}{2\sqrt{\pi}} \cos \theta \sin^2 \theta \cos \phi \sin \phi$
d <sub>zy</sub>	$\frac{\sqrt{15}}{2\sqrt{\pi}} \cos \theta \sin \theta \sin \phi$	f <sub>x<sup>3</sup></sub>	$\frac{\sqrt{70}}{8\sqrt{\pi}} \sin^3 \theta (4 \cos^3 \phi - 3 \cos \phi)$
d <sub>xy</sub>	$\frac{\sqrt{15}}{2\sqrt{\pi}} \sin^2 \theta \sin \phi \cos \phi$	f <sub>y<sup>3</sup></sub>	$\frac{\sqrt{70}}{8\sqrt{\pi}} \sin^3 \theta (3 \sin \phi - 4 \sin^3 \phi)$



# Appendix 2

## Symmetry Elements, Symmetry Operations and Point Groups

An object has *symmetry* when certain parts of it can be interchanged with others without altering either the identity or the apparent orientation of the object. For a discrete object such as a molecule 5 *elements of symmetry* can be envisaged:

*axis* of symmetry,  $C$ ;  
*plane* of symmetry,  $\sigma$ ;  
*centre of inversion*,  $i$ ;  
*improper axis* of symmetry,  $S$ ; and  
*identity*,  $E$ .

These elements of symmetry are best recognized by performing various *symmetry operations*, which are geometrically defined ways of exchanging equivalent parts of a molecule. The 5 symmetry operations are:

- $C_n$ , *rotation* of the molecule about a symmetry *axis* through an angle of  $360^\circ/n$ ;  $n$  is called the *order* of the rotation (twofold, threefold, etc.);
- $\sigma$  reflection of all atoms through a *plane* of the molecule;
- $i$ , inversion of all atoms through a *point* of the molecule;

- $S_n$ , *Rotation* of the molecule through an angle  $360^\circ/n$  followed by *reflection* of all atoms through a plane perpendicular to the axis of rotation; the combined operation (which may equally follow the sequence *reflection then rotation*) is called *improper rotation*;
- $E$ , the *identity* operation which leaves the molecule unchanged.

The rotation axis of highest order is called the *principal axis* of rotation; it is usually placed in the vertical direction and designated the  $z$ -axis of the molecule. Planes of reflection which are perpendicular to the principal axis are called *horizontal planes* ( $h$ ). Planes of reflection which contain the principal axis are called *vertical planes* ( $v$ ), or *dihedral planes* ( $d$ ) if they bisect 2 twofold axes.

The complete set of symmetry operations that can be performed on a molecule is called the *symmetry group* or *point group* of the molecule and the *order* of the point group is the number of symmetry operations it contains. Table A2.1 lists the various point groups, together with their elements of symmetry and with examples of each.

Table A2.1 Point groups

Point group	Elements of symmetry	Examples
$C_1$	$E$	CHFCIBr
$C_s$	$E, \sigma$	SO <sub>2</sub> FBr, HOCl, BFCIBr, SOCl <sub>2</sub> , SF <sub>5</sub> NF <sub>2</sub>
$C_i$	$E, i$	CHClBr-CHClBr (staggered)
$C_2$	$E, C_2$	H <sub>2</sub> O <sub>2</sub> , <i>cis</i> -[Co(en) <sub>2</sub> X <sub>2</sub> ]
$C_3$	$E, C_3$	PPH <sub>3</sub> (propeller)
$C_{2v}$	$E, C_2, 2\sigma_v$	H <sub>2</sub> O (V-shaped), H <sub>2</sub> CO (Y-shaped), ClF <sub>3</sub> (T-shaped), SF <sub>4</sub> (see-saw), SiH <sub>2</sub> Cl <sub>2</sub> , <i>cis</i> -[Pt(NH <sub>3</sub> ) <sub>2</sub> Cl <sub>2</sub> ], C <sub>6</sub> H <sub>5</sub> Cl
$C_{3v}$	$E, C_3, 3\sigma_v$	GeH <sub>3</sub> Cl, PCl <sub>3</sub> , O=PF <sub>3</sub>
$C_{4v}$	$E, C_4, 4\sigma_v$	SF <sub>5</sub> Cl, IF <sub>5</sub> , XeOF <sub>4</sub>
$C_{5v}$	$E, C_5, 5\sigma_v$	[Ni( $\eta^5$ -C <sub>5</sub> H <sub>5</sub> )(NO)]
$C_{6v}$	$E, C_6, 6\sigma_v$	[Cr( $\eta^6$ -C <sub>6</sub> H <sub>6</sub> )( $\eta^6$ -C <sub>6</sub> Me <sub>6</sub> )]
$C_{\infty v}$	$E, C_{\infty}, \infty\sigma_v$	NO, HCN, COS
$C_{2h}$	$E, C_2, \sigma_h, i$	<i>trans</i> -N <sub>2</sub> F <sub>4</sub>
$C_{3h}$	$E, C_3, \sigma_h, i$	B(OH) <sub>3</sub>
$C_{4h}$	$E, C_4, \sigma_h, i$	[Re <sub>2</sub> ( $\mu, \eta^2$ -SO <sub>4</sub> ) <sub>4</sub> ]
$D_3$	$E, C_3, 3C_2'$	trischelates [M(chel) <sub>3</sub> ], C <sub>2</sub> H <sub>6</sub> ( <i>gauche</i> )
$D_{2d}$	$E, C_2, 2C_2', 2\sigma_d, S_4$	B <sub>2</sub> Cl <sub>4</sub> (vapour, staggered), As <sub>4</sub> S <sub>4</sub>
$D_{3d}$	$E, C_3, 3C_2', 3\sigma_d, i, S_6$	R <sub>3</sub> W $\equiv$ WR <sub>3</sub> (staggered)
$D_{4d}$	$E, C_4, 4C_2', 4\sigma_d, S_8$	S <sub>8</sub> (crown), <i>closo</i> -B <sub>10</sub> H <sub>10</sub> <sup>2-</sup>
$D_{2h}$	$E, C_2, 2C_2', 2\sigma_v, \sigma_h, i$	B <sub>2</sub> Cl <sub>4</sub> (planar), B <sub>2</sub> H <sub>6</sub> , <i>trans</i> -[Pt(NH <sub>3</sub> ) <sub>2</sub> Cl <sub>2</sub> ], <i>trans</i> -[Co(NH <sub>3</sub> ) <sub>2</sub> Cl <sub>2</sub> Br <sub>2</sub> ] <sup>-</sup> , 1,4-C <sub>6</sub> H <sub>4</sub> Cl <sub>2</sub>
$D_{3h}$	$E, C_3, 3C_2', 3\sigma_v, \sigma_h, S_3$	BCl <sub>3</sub> , PF <sub>5</sub> , B <sub>3</sub> N <sub>3</sub> H <sub>6</sub> , [ReH <sub>9</sub> ] <sup>2-</sup>
$D_{4h}$	$E, C_4, 4C_2', 4\sigma_v, \sigma_h, i, S_4$	XeF <sub>4</sub> , PtCl <sub>4</sub> <sup>2-</sup> , <i>trans</i> -[Co(NH <sub>3</sub> ) <sub>4</sub> Cl <sub>2</sub> ] <sup>+</sup> , [Re <sub>2</sub> Cl <sub>8</sub> ] <sup>2-</sup> , <i>closo</i> -1,6-C <sub>2</sub> B <sub>4</sub> H <sub>6</sub>
$D_{5h}$	$E, C_5, 5C_2', 5\sigma_v, \sigma_h, S_5$	[Fe( $\eta^5$ -C <sub>5</sub> H <sub>5</sub> ) <sub>2</sub> ] eclipsed, B <sub>7</sub> H <sub>7</sub> <sup>2-</sup> , IF <sub>7</sub>
$D_{6h}$	$E, C_6, 6C_2', 6\sigma_v, \sigma_h, i, S_6$	C <sub>6</sub> H <sub>6</sub> , [Cr( $\eta^6$ -C <sub>6</sub> H <sub>6</sub> ) <sub>2</sub> ] (eclipsed)
$D_{\infty h}$	$E, C_{\infty}, \infty C_2', \infty\sigma_v, i$	Cl <sub>2</sub> , CO <sub>2</sub>
$S_4$	$E, S_4$	<i>cyclo</i> -Cl <sub>4</sub> B <sub>4</sub> N <sub>4</sub> R <sub>4</sub>
$T$	$E, 3C_2, 4C_3$	Si(SiMe <sub>3</sub> ) <sub>4</sub> , [Pt(PF <sub>3</sub> ) <sub>4</sub> ]
$T_d$	$E, 4C_3, 6\sigma_d, 3S_4$	SiF <sub>4</sub> , B <sub>4</sub> Cl <sub>4</sub> , [Ni(CO) <sub>4</sub> ], [Ir <sub>4</sub> (CO) <sub>12</sub> ]
$T_h$	$E, 4C_3, 3C_2, 3\sigma_h, i, 4S_6$	[Co(NO <sub>2</sub> ) <sub>6</sub> ] <sup>3-</sup> ( <i>trans</i> NO <sub>2</sub> groups eclipsed), [M( $\eta^2$ -NO <sub>3</sub> ) <sub>6</sub> ] <sup>n-</sup> , [W(NMe <sub>2</sub> ) <sub>6</sub> ]
$O_h$	$E, 3C_4, 4C_3, 6C_2', 3\sigma_h, 6\sigma_d, i, 3S_4, 4S_6$	SF <sub>6</sub> , B <sub>6</sub> H <sub>6</sub> <sup>2-</sup> (octahedron), C <sub>8</sub> H <sub>8</sub> (cubane)
$I_h$	$E, 6C_5, 10C_3, 15C_2, 15\sigma_v, i, 12S_{10}, 10S_6$	B <sub>12</sub> H <sub>12</sub> <sup>2-</sup> (icosahedron)

It is instructive to add to these examples from the numerous instances of point group symmetry mentioned throughout the text. In this way a facility will gradually be acquired in discerning the various elements of symmetry present in a molecule.

A convenient scheme for identifying the point group symmetry of any given species is set out in the flow chart.<sup>(1)</sup> Starting at the top of the chart

each vertical line asks a question: if the answer is "yes" then move to the right, if "no" then move to the left until the correct point group is arrived at. Other similar schemes have been devised.<sup>(2-5)</sup>

<sup>2</sup> R. L. CARTER, *J. Chem. Educ.* **45**, 44 (1968).

<sup>3</sup> F. A. COTTON, *Chemical Applications of Group Theory*, 2nd edn., pp. 45-7, Wiley-Interscience, New York, 1971.

<sup>4</sup> J. D. DONALDSON and S. D. ROSS, *Symmetry and Stereochemistry*, pp. 35-49, Intertext Books, London, 1972.

<sup>5</sup> J. A. SALTHOUSE and M. J. WARE, *Point Group Character Tables and Related Data*, p. 29, Cambridge University Press, 1972.

<sup>1</sup> J. DONOHUE, *Sov. Phys. Crystallogr.* **26**, 516 (1981); *Kristallografiya* **26**, 908-9 (1981).

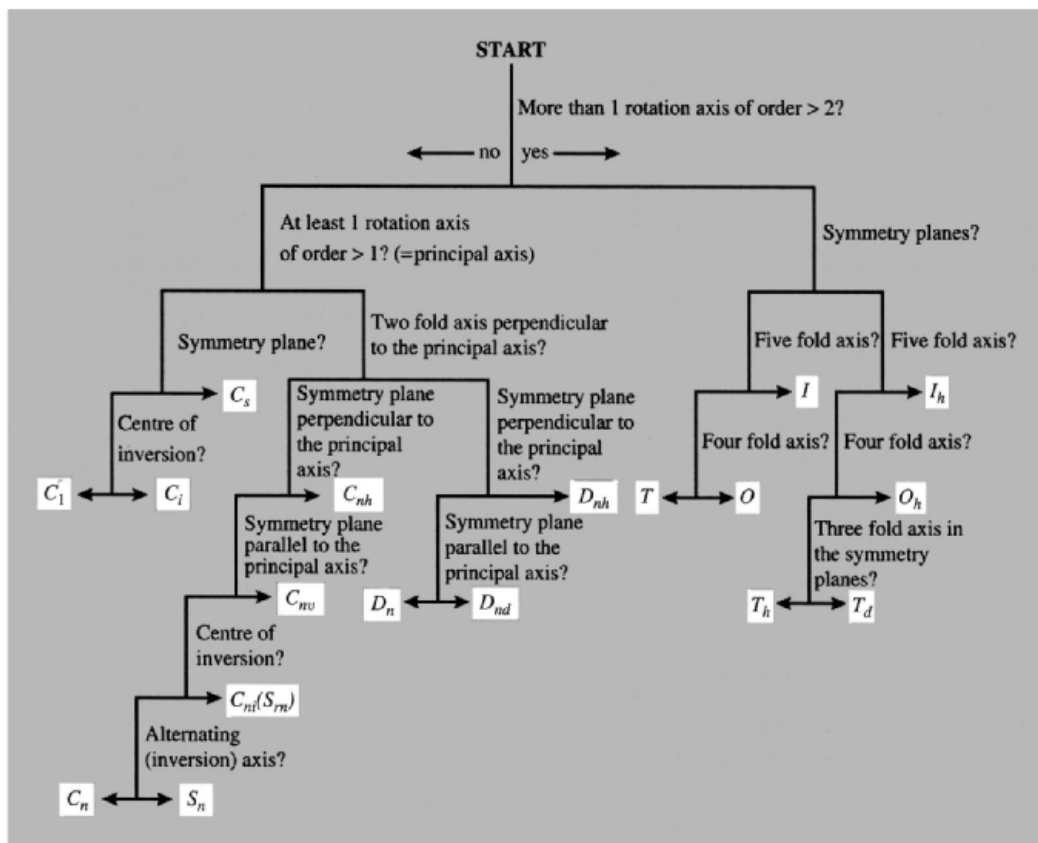


Figure A2.1 Point group symmetry flow chart.

# Appendix 3

## Some Non-SI Units<sup>†</sup>

Physical quantity	Name of unit	Symbol for unit	Definition of unit
Length	ångström	Å	$10^{-10}$ m (100 pm)
Time	minute	min	60 s
	hour	h	3600 s
	day	d	86 400 s
	erg	erg	$10^{-7}$ J
Energy	kilowatt hour	kWh	$3.6 \times 10^6$ J
	thermochemical calorie	cal <sub>th</sub>	4.184 J
Force	dyne	dyn	$10^{-5}$ N
Pressure	bar	bar	$10^5$ Pa
	atmosphere	atm	101 325 Pa
	conventional millimetre of mercury	mmHg	$13.5951 \times 9.806 65$ Pa i.e. 133.322 Pa
	torr	Torr	(101 325/760) Pa
Magnetic flux	maxwell	Mx	$10^{-8}$ Wb
Magnetic flux density (magnetic induction)	gauss	G, Gs	$10^{-4}$ T
Dynamic viscosity	poise	P	$10^{-1}$ Pa s
Concentration	—	M	mol dm <sup>-3</sup>
Radioactivity	curie	Ci	$3.7 \times 10^{10}$ s <sup>-1</sup>
Radioactive exposure	röntgen	R	$2.58 \times 10^{-4}$ C kg <sup>-1</sup>
Absorbed dose	rad	rad	$10^{-2}$ J kg <sup>-1</sup>
Angle	degree	°	$1^\circ = (\pi/180)$ radian

<sup>†</sup>The unit “degree Celsius” (°C) is identical with the kelvin (K). The Celsius temperature ( $t_C$ ) is related to the thermodynamic temperature  $T$  by the definition:  $t_C = T - 273.15$  K.

### Some useful conversion factors:

1 m = 3.280 839 9 ft = 39.370 079 inches  
 1 inch = 25.4 mm (defined)  
 1 statute mile = 1.609 344 km  
 1 light year =  $9.460 55 \times 10^{12}$  km  
 1 acre = 4046.8564 m<sup>2</sup>  
 1 gal (Imperial) = 1.200 949 gal (US) = 4.545 960 l  
 1 gal (US) = 0.832 674 7 gal (Imp.) = 3.785 411 8 l  
 1 lb (avoirdupois) = 0.453 592 37 kg  
 1 oz (avoirdupois) = 28.349 527 g  
 1 oz (troy, or apoth.) = 31.103 486 g  
 1 carat = 3.086 47 grains = 200 mg  
 1 tonne = 1000 kg = 2204.622 6 lb = 1.102 311 3 short tons  
 1 short ton = 907.184 74 kg = 2000 lb = 0.892 857 14 long tons  
 1 long ton = 1016.046 9 kg = 2240 lb = 1.120 short tons  
 1 atm = 101 325 Pa = 1.013 25 bar = 760 Torr = 14.695 95 lb/in<sup>2</sup>  
 1 Pa =  $10^{-5}$  bar  $\sim 1.019 716 \times 10^{-1}$  kg m<sup>-2</sup> =  $0.986 923 \times 10^{-5}$  atm  
 1 mdyn Å<sup>-1</sup> = 100 N m<sup>-1</sup>  
 1 calorie (thermochem) = 4.184 J (defined)  
 1 eV =  $1.602 19 \times 10^{-19}$  J  
 1 eV/molecule = 96.484 56 kJ mol<sup>-1</sup> = 23.060 36 kcal mol<sup>-1</sup>

# Appendix 4

## Abundance of Elements in Crustal Rocks/ppm (i.e. g/tonne)<sup>†</sup>

No.	Elt.	ppm	Σ%	No.	Elt.	ppm	No.	Elt.	ppm	No.	Elt.	ppm
1	O	455 000	45.50	20	Cl	126	39	Th	8.1	58	Tl	0.7
2	Si	272 000	72.70	21	Cr	122	40	Sm	7.0	59	Tm	0.5
3	Al	83 000	81.00	22	Ni	99	41	Gd	6.1	60	I	0.46
4	Fe	62 000	87.20	23	Rb	78	42	Er	3.5	61	In	0.24
5	Ca	46 600	91.86	24	Zn	76	43	Yb	3.1	62	Sb	0.2
6	Mg	27 640	94.62	25	Cu	68	44	Hf	2.8	63	Cd	0.16
7	Na	22 700	96.89	26	Ce	66	45	Cs	2.6	64	{Ag	0.08
8	K	18 400	98.73	27	Nd	40	46	Br	2.5		{Hg	0.08
9	Ti	6320	99.36	28	La	35	47	U	2.3	66	Se	0.05
10	H	1520	99.51	29	Y	31	48	{Sn	2.1	67	Pd	0.015
11	P	1120	99.63	30	Co	29		{Eu	2.1	68	Pt	0.01
12	Mn	1060	99.73	31	Sc	25	50	Be	2	69	Bi	0.008
13	F	544	99.79	32	Nb	20	51	As	1.8	70	Os	0.005
14	Ba	390	99.83	33	{N	19	52	Ta	1.7	71	Au	0.004
15	Sr	384	99.86		{Ga	19	53	Ge	1.5	72	{Ir	0.001
16	S	340	99.90	35	Li	18	54	Ho	1.3		{Te	0.001
17	C	180	99.92	36	Pb	13		{Mo	1.2	74	Re	0.0007
18	Zr	162	99.93	37	Pr	9.1	55	{W	1.2	75	{Ru	0.0001
19	V	136	99.95	38	B	9		{Tb	1.2		{Rh	0.0001

<sup>†</sup> Taken from W. S. Fyfe, *Geochemistry*, Oxford University Press, 1974, with some modifications and additions to incorporate later data. The detailed numbers are subject to various assumptions in the models of the global distribution of the various rock types within the crust, but they are broadly acceptable as an indication of elemental abundances. See also Table 1 in C. K. JØRGENSEN, *Comments Astrophys.* 17, 49–101 (1993).

# Appendix 5

## Effective Ionic Radii in pm for Various Oxidation States (in parentheses)<sup>†</sup>

s Block

<b>Li</b> (+1) 76	<b>Be</b> (+2) 45
<b>Na</b> (+1) 102	<b>Mg</b> (+2) 72.0
<b>K</b> (+1) 138	<b>Ca</b> (+2) 100
<b>Rb</b> (+1) 152	<b>Sr</b> (+2) 118
<b>Cs</b> (+1) 167	<b>Ba</b> (+2) 135
<b>Fr</b> (+1) 180	<b>Ra</b> (+2) <sup>III</sup> 148

p Block

<b>B</b> (+3) 27	<b>C</b> (+4) 16	<b>N</b> (-3) <sup>IV</sup> 146 (+3) 16 (+5) 13	<b>O</b> (-2) 140	<b>F</b> (-1) 133 (+7) 8	
<b>Al</b> (+3) 53.5	<b>Si</b> (+4) 40	<b>P</b> (+3) 44 (+5) 38	<b>S</b> (-2) 184 (+4) 37 (+6) 29	<b>Cl</b> (-1) 184 (+5) <sup>III</sup> 12 (+7) 27	
<b>Ga</b> (+3) 62.0	<b>Ge</b> (+2) 53.0 (+4) 46	<b>As</b> (+3) 58 (+5) 46	<b>Se</b> (-2) 198 (+4) 50 (+6) 42	<b>Br</b> (-1) 196 (+3) <sup>III</sup> 59 (+5) <sup>III</sup> 31 (+7) 39	
<b>In</b> (+3) 80.0	<b>Sn</b> (+2) 118 (+4) 69.0	<b>Sb</b> (+3) 76 (+5) 60	<b>Te</b> (-2) 221 (+4) 97 (+6) 56	<b>I</b> (-1) 220 (+5) 95 (+7) 53	<b>Xe</b> (+8) 48
<b>Tl</b> (+1) 150 (+3) 88.5	<b>Pb</b> (+2) 119 (+4) 77.5	<b>Bi</b> (+3) 103 (+5) 76	<b>Po</b> (+4) 94 (+6) 67	<b>At</b> (+7) 62	

d Block

(+1) (+2) (+3) (+4) (+5) (+6) (+7)	<b>Sc</b> 74.5	<b>Ti</b> 86 67.0 60.5	<b>V</b> 79 64.0 58 54	<b>Cr</b> { 73 ls 80 hs } 61.5 55 49 44	<b>Mn</b> 67 { 58 s ls 64.5 hs } 53.0 33 <sup>IV</sup> 25.5 <sup>IV</sup> 46	<b>Fe</b> { 61 ls 78.0 hs } { 53 s ls 64.5 hs } 58.5 - 25 <sup>IV</sup>	<b>Co</b> { 65 ls 74.5 hs } { 54.5 ls 61 hs } 53	<b>Ni</b> 69 { 56 ls 60 hs } 48 ls	<b>Cu</b> <sub>77</sub> 73 54 ls	<b>Zn</b> 74.0	(+1) (+2) (+3) (+4) (+5) (+6) (+7)
(+1) (+2) (+3) (+4) (+5) (+6) (+7) (+8)	<b>Y</b> 90.0	<b>Zr</b> 72	<b>Nb</b> 72 68 64	<b>Mo</b> 69 65 61 59	<b>Tc</b> 64.5 60 - 56	<b>Ru</b> 68 62.0 56.5 - 38 <sup>IV</sup> 36 <sup>IV</sup>	<b>Rh</b> 66.5 60 55	<b>Pd</b> <sub>59<sup>II</sup></sub> 86 76 61.5	<b>Ag</b> <sub>115</sub> 94 75	<b>Cd</b> 95	(+1) (+2) (+3) (+4) (+5) (+6) (+7) (+8)
(+1) (+2) (+3) (+4) (+5) (+6) (+7) (+8)	<b>La</b> 103.2	<b>Hf</b> 71	<b>Ta</b> 72 68 64	<b>W</b> 66 62 60	<b>Re</b> 63 58 55 53	<b>Os</b> 63.0 57.5 54.5 52.5 39 <sup>IV</sup>	<b>Ir</b> 68 62.5 57	<b>Pt</b> 86 - 62.5 57	<b>Au</b> <sub>137</sub> - 85 57	<b>Hg</b> <sub>119</sub> 102	(+1) (+2) (+3) (+4) (+5) (+6) (+7) (+8)
+3	<b>Ac</b> 112										

f Block

(+2) (+3) (+4)	<b>Ce</b> 102 87	<b>Pr</b> 99 85	<b>Nd</b> 129 <sup>III</sup> 98.3	<b>Pm</b> 97	<b>Sm</b> 122 <sup>III</sup> 95.8	<b>Eu</b> 117 94.7	<b>Gd</b> 93.8	<b>Tb</b> 92.3 76	<b>Dy</b> 107 91.2	<b>Ho</b> 90.1	<b>Er</b> 89.0	<b>Tm</b> 103 88.0	<b>Yb</b> 102 86.8	<b>Lu</b> 86.1	(+2) (+3) (+4)
(+2) (+3) (+4) (+5) (+6) (+7)	<b>Th</b> 94	<b>Pa</b> 104 90 78	<b>U</b> 102.5 89 78 73	<b>Np</b> 110 101 87 75 71	<b>Pu</b> 100 86 74 71	<b>Am</b> 126 <sup>VII</sup> 97.5 85	<b>Cm</b> 97 85	<b>Bk</b> 96 83	<b>Cf</b> 95 82.1	<b>Es</b>	<b>Fm</b>	<b>Md</b>	<b>No</b>	<b>Lr</b>	(+2) (+3) (+4) (+5) (+6) (+7)

<sup>†</sup>For coord. no. 6 unless indicated by superscript numerals<sup>III, IV</sup>, etc. (All data taken from R. D. Shannon, *Acta Cryst.* A32, 751-67 (1976).

# Appendix 6

## Nobel Prize for Chemistry

- 1901 **J. H. van't Hoff** (Berlin): discovery of the laws of chemical dynamics and osmotic pressure in solutions.
- 1902 **E. Fischer** (Berlin): sugar and purine syntheses.
- 1903 **S. Arrhenius** (Stockholm): electrolytic theory of dissociation.
- 1904 **W. Ramsay** (University College, London): discovery of the inert gaseous elements in air and their place in the periodic system.
- 1905 **A. von Baeyer** (Munich): advancement of organic chemistry and the chemical industry through work on organic dyes and hydroaromatic compounds.
- 1906 **H. Moissan** (Paris): isolation of the element fluorine and development of the electric furnace.
- 1907 **E. Buchner** (Berlin): biochemical researches and the discovery of cell-free fermentation.
- 1908 **E. Rutherford** (Manchester): investigations into the disintegration of the elements and the chemistry of radioactive substances.
- 1909 **W. Ostwald** (Gross-Bothen): work on catalysis and investigations into the fundamental principles governing chemical equilibria and rates of reaction.
- 1910 **O. Wallach** (Göttingen): pioneer work in the field of alicyclic compounds.
- 1911 **Marie Curie** (Paris): discovery of the elements radium and polonium, the isolation of radium, and the study of the nature and compounds of this remarkable element.
- 1912 **V. Grignard** (Nancy): discovery of the Grignard reagent.  
**P. Sabatier** (Toulouse): method of hydrogenating organic compounds in the presence of finely disintegrated metals.
- 1913 **A. Werner** (Zürich): work on the linkage of atoms in molecules which has thrown new light on earlier investigations and opened up new fields of research especially in inorganic chemistry.
- 1914 **T. W. Richards** (Harvard): accurate determination of the atomic weight of a large number of chemical elements.
- 1915 **R. Willstätter** (Munich): plant pigments, especially chlorophyll.
- 1916 Not awarded
- 1917 Not awarded
- 1918 **F. Haber** (Berlin–Dahlem): the synthesis of ammonia from its elements.

- 1919 Not awarded
- 1920 **W. Nernst** (Berlin): work in thermochemistry.
- 1921 **F. Soddy** (Oxford): contributions to knowledge of the chemistry of radioactive substances and investigations into the origin and nature of isotopes.
- 1922 **F. W. Aston** (Cambridge): discovery, by means of the mass spectrograph, of isotopes in a large number of non-radioactive elements and for enunciation of the whole-number rule.
- 1923 **F. Pregl** (Graz): invention of the method of microanalysis of organic substances.
- 1924 Not awarded
- 1925 **R. Zsigmondy** (Göttingen): demonstration of the heterogeneous nature of colloid solutions by methods which have since become fundamental in modern colloid chemistry.
- 1926 **T. Svedberg** (Uppsala): work on disperse systems.
- 1927 **H. Wieland** (Munich): constitution of the bile acids and related substances.
- 1928 **A. Windaus** (Göttingen): constitution of the sterols and their connection with the vitamins.
- 1929 **A. Harden** (London) and **H. von Euler-Chelpin** (Stockholm): investigations on the fermentation of sugars and fermentative enzymes.
- 1930 **H. Fischer** (Munich): the constitution of haemin and chlorophyll and especially for the synthesis of haemin.
- 1931 **C. Bosch** and **F. Bergius** (Heidelberg): the invention and development of chemical high pressure methods.
- 1932 **I. Langmuir** (Schenectady, New York): discoveries and investigations in surface chemistry.
- 1933 Not awarded
- 1934 **H. C. Urey** (Columbia, New York): discovery of heavy hydrogen.
- 1935 **F. Joliot** and **Irène Joliot-Curie** (Paris): synthesis of new radioactive elements.
- 1936 **P. Debye** (Berlin–Dahlem): contributions to knowledge of molecular structure through investigations on dipole moments and on the diffraction of X-rays and electrons in gases.
- 1937 **W. N. Haworth** (Birmingham): investigations on carbohydrates and vitamin C.  
**P. Karrer** (Zürich): investigations of carotenoids, flavins, and vitamins A and B<sub>2</sub>.
- 1938 **R. Kuhn** (Heidelberg): work on carotenoids and vitamins.
- 1939 **A. F. J. Butenandt** (Berlin): work on sex hormones.  
**L. Ruzicka** (Zürich): work on polymethylenes and higher terpenes.
- 1940 Not awarded.
- 1941 Not awarded.
- 1942 Not awarded.
- 1943 **G. Hevesy** (Stockholm): use of isotopes as tracers in the study of chemical processes.
- 1944 **O. Hahn** (Berlin–Dahlem): discovery of the fission of heavy nuclei.
- 1945 **A. J. Virtanen** (Helsingfors): research and inventions in agricultural and nutrition chemistry, especially fodder preservation.
- 1946 **J. B. Sumner** (Cornell): discovery that enzymes can be crystallized.  
**J. H. Northrop** and **W. M. Stanley** (Princeton): preparation of enzymes and virus proteins in a pure form.
- 1947 **R. Robinson** (Oxford): investigations on plant products of biological importance, especially the alkaloids.
- 1948 **A. W. K. Tiselius** (Uppsala): electrophoresis and adsorption analysis, especially for discoveries concerning the complex nature of the serum proteins.
- 1949 **W. F. Giauque** (Berkeley): contributions in the field of chemical thermodynamics, particularly concerning the behaviour of substances at extremely low temperatures.
- 1950 **O. Diels** (Kiel) and **K. Alder** (Cologne): discovery and development of the diene synthesis.
- 1951 **E. M. McMillan** and **G. T. Seaborg** (Berkeley): discoveries in the chemistry of the transuranium elements.



- 1952 **A. J. P. Martin** (London) and **R. L. M. Synge** (Bucksburn): invention of partition chromatography.
- 1953 **H. Staudinger** (Freiburg): discoveries in the field of macromolecular chemistry.
- 1954 **L. Pauling** (California Institute of Technology, Pasadena): research into the nature of the chemical bond and its application to the elucidation of the structure of complex substances.
- 1955 **V. du Vigneaud** (New York): biochemically important sulfur compounds, especially the first synthesis of a polypeptide hormone.
- 1956 **C. N. Hinshelwood** (Oxford) and **N. N. Semenov** (Moscow): the mechanism of chemical reactions.
- 1957 **A. Todd** (Cambridge): nucleotides and nucleotide co-enzymes.
- 1958 **F. Sanger** (Cambridge): the structure of proteins, especially that of insulin.
- 1959 **J. Heyrovský** (Prague): discovery and development of the polarographic method of analysis.
- 1960 **W. F. Libby** (Los Angeles): use of carbon-14 for age determination in archeology, geology, geophysics, and other branches of science.
- 1961 **M. Calvin** (Berkeley): research on the carbon dioxide assimilation in plants.
- 1962 **J. C. Kendrew** and **M. F. Perutz** (Cambridge): the structures of globular proteins.
- 1963 **K. Ziegler** (Mülheim/Ruhr) and **G. Natta** (Milan): the chemistry and technology of high polymers.
- 1964 **Dorothy Crowfoot Hodgkin** (Oxford): determinations by X-ray techniques of the structures of important biochemical substances.
- 1965 **R. B. Woodward** (Harvard): outstanding achievements in the art of organic synthesis.
- 1966 **R. S. Mulliken** (Chicago): fundamental work concerning chemical bonds and the electronic structure of molecules by the molecular orbital method.
- 1967 **M. Eigen** (Göttingen), **R. G. W. Norrish** (Cambridge) and **G. Porter** (London): studies of extremely fast chemical reactions, effected by disturbing the equilibrium by means of very short pulses of energy.
- 1968 **L. Onsager** (Yale): discovery of the reciprocity relations bearing his name, which are fundamental for the thermodynamics of irreversible processes.
- 1969 **D. H. R. Barton** (Imperial College, London) and **O. Hassel** (Oslo): development of the concept of conformation and its application in chemistry.
- 1970 **L. F. Leloir** (Buenos Aires): discovery of sugar nucleotides and their role in the biosynthesis of carbohydrates.
- 1971 **G. Herzberg** (Ottawa): contributions to the knowledge of electronic structure and geometry of molecules, particularly free radicals.
- 1972 **C. B. Anfinsen** (Bethesda): work on ribonuclease, especially concerning the connection between the amino-acid sequence and the biologically active conformation. **S. Moore** and **W. H. Stein** (Rockefeller, New York): contributions to the understanding of the connection between chemical structure and catalytic activity of the active centre of the ribonuclease molecule.
- 1973 **E. O. Fischer** (Munich) and **G. Wilkinson** (Imperial College, London): pioneering work, performed independently, on the chemistry of the organometallic so-called sandwich compounds.
- 1974 **P. J. Flory** (Stanford): fundamental achievements both theoretical and experimental in the physical chemistry of macromolecules.
- 1975 **J. W. Cornforth** (Sussex): stereochemistry of enzyme-catalysed reactions. **V. Prelog** (Zürich): the stereochemistry of organic molecules and reactions.
- 1976 **W. N. Lipscomb** (Harvard): studies on the structure of boranes illuminating problems of chemical bonding.

- 1977 **I. Prigogine** (Brussels): non-equilibrium thermodynamics, particularly the theory of dissipative structures.
- 1978 **P. Mitchell** (Bodmin, Cornwall): contributions to the understanding of biological energy transfer through the formulation of the chemiosmotic theory.
- 1979 **H. C. Brown** (Purdue) and **G. Wittig** (Heidelberg): for their development of boron and phosphorus compounds, respectively, into important reagents in organic synthesis.
- 1980 **P. Berg** (Stanford): the biochemistry of nucleic acids, with particular regard to recombinant-DNA.  
**W. Gilbert** (Harvard) and **F. Sanger** (Cambridge): the determination of base sequences in nucleic acids.
- 1981 **K. Fukui** (Kyoto) and **R. Hoffmann** (Cornell): quantum mechanical studies of chemical reactivity.
- 1982 **A. Klug** (Cambridge): development of crystallographic electron microscopy and the structural elucidation of biologically important nucleic acid-protein complexes.
- 1983 **H. Taube** (Stanford): mechanisms of electron transfer reactions of metal complexes.
- 1984 **R. B. Merrifield** (Rockefeller, New York): development of methodology for the synthesis of peptides on a solid matrix.
- 1985 **H. A. Hauptman** (Buffalo, NY) and **J. Karle** (Washington, DC): outstanding achievements in the development of direct methods for the determination of crystal structures.
- 1986 **D. R. Herschbach** (Harvard), **Y. T. Lee** (Berkeley) and **J. C. Polanyi** (Toronto): contributions concerning the dynamics of chemical elementary processes.
- 1987 **D. J. Cram** (Los Angeles), **J.-M. Lehn** (Strasbourg) and **C. J. Pedersen** (Wilmington, Delaware): development and use of molecules with structure specific interactions of high selectivity.
- 1988 **J. Deisenhofer** (Dallas, Texas), **R. Huber** (Martinsried) and **H. Michel** (Frankfurt am Main): determination of the three-dimensional structure of a photosynthetic reaction centre.
- 1989 **S. Altman** (Yale) and **T. Cech** (Boulder, Colorado): discovery of the catalytic properties of RNA.
- 1990 **E. J. Corey** (Harvard): development of the theory and methodology of organic synthesis.
- 1991 **R. R. Ernst** (Eidgenössische Technische Hochschule, Zürich): contributions to the development of the methodology of high resolution nmr spectroscopy.
- 1992 **R. A. Marcus** (California Institute of Technology): contributions to the theory of electron transfer reactions in chemical systems.
- 1993 **K. B. Mullis** (La Jolla, California): invention of the polymerase chain reaction.  
**M. Smith** (University of British Columbia): fundamental contributions to the establishment of oligonucleotide-based, site-directed mutagenesis and its development for protein studies.
- 1994 **G. A. Olah** (University of Southern California): contributions to carbocation chemistry.
- 1995 **P. Crutzen** (Max Planck Institute for Chemistry, Mainz), **M. Molina** (Massachusetts Institute of Technology) and **F. S. Rowland** (Irvine, California): work in atmospheric chemistry, particularly concerning the formation and decomposition of ozone.
- 1996 **R. F. Curl** (Rice University, Texas), **H. Kroto** (Sussex University) and **R. E. Smalley** (Rice University, Texas): discovery of a new form of carbon, the fullerenes.
- 1997 **P. D. Boyer** (Los Angeles) and **J. E. Walker** (Cambridge): pioneering work on enzymes that participate in the conversion of ATP.  
**J. C. Scou** (Aarhus): discovery of the first molecular pump, an ion-transporting enzyme  $\text{Na}^+\text{-K}^+$  ATPase.

# Appendix 7

## *Nobel Prize for Physics*

- 1901 **W. C. Röntgen** (Munich): discovery of the remarkable rays subsequently named after him.
- 1902 **H. A. Lorentz** (Leiden) and **P. Zeeman** (Amsterdam): influence of magnetism upon radiation phenomena.
- 1903 **H. A. Becquerel** (École Polytechnique, Paris): discovery of spontaneous radioactivity.  
**P. Curie** and **Marie Curie** (Paris): researches on the radiation phenomena discovered by H. Becquerel.
- 1904 **Lord Rayleigh** (Royal Institution, London): investigations of the densities of the most important gases and for the discovery of argon in connection with these studies.
- 1905 **P. Lenard** (Kiel): work on cathode rays.
- 1906 **J. J. Thomson** (Cambridge): theoretical and experimental investigations on the conduction of electricity by gases.
- 1907 **A. A. Michelson** (Chicago): optical precision instruments and the spectroscopic and metrological investigations carried out with their aid.
- 1908 **G. Lippmann** (Paris): method of reproducing colours photographically based on the phenomenon of interference.
- 1909 **G. Marconi** (London) and **F. Braun** (Strasbourg): the development of wireless telegraphy.
- 1910 **J. D. van der Waals** (Amsterdam): the equation of state for gases and liquids.
- 1911 **W. Wien** (Würzburg): the laws governing the radiation of heat.
- 1912 **G. Dalén** (Stockholm): invention of automatic regulators for use in conjunction with gas accumulators for illuminating lighthouses and buoys.
- 1913 **H. Kamerlingh Onnes** (Leiden): properties of matter at low temperatures and production of liquid helium.
- 1914 **M. von Laue** (Frankfurt): discovery of the diffraction of X-rays by crystals.
- 1915 **W. H. Bragg** (University College, London) and **W. L. Bragg** (Manchester): analysis of crystal structure by means of X-rays.
- 1916 Not awarded.
- 1917 **C. G. Barkla** (Edinburgh): discovery of the characteristic Röntgen radiation of the elements.
- 1918 **M. Planck** (Berlin): services rendered to the advancement of physics by discovery of energy quanta.

- 1919 **J. Stark** (Greifswald): discovery of the Doppler effect on canal rays and of the splitting of spectral lines in electric fields.
- 1920 **C. E. Guillaume** (Sèvres): service rendered to precise measurements in physics by discovery of anomalies in nickel steel alloys.
- 1921 **A. Einstein** (Berlin): services to theoretical physics, especially discovery of the law of the photoelectric effect.
- 1922 **N. Bohr** (Copenhagen): investigations of the structure of atoms, and of the radiation emanating from them.
- 1923 **R. A. Millikan** (California Institute of Technology, Pasadena): work on the elementary charge of electricity and on the photo-electric effect.
- 1924 **M. Siegbahn** (Uppsala): discoveries and researches in the field of X-ray spectroscopy.
- 1925 **J. Franck** (Göttingen) and **G. Hertz** (Halle): discovery of the laws governing the impact of an electron upon an atom.
- 1926 **J. Perrin** (Paris): the discontinuous structure of matter, and especially for the discovery of sedimentation equilibrium.
- 1927 **A. H. Compton** (Chicago): discovery of the effect named after him.  
**C. T. R. Wilson** (Cambridge): method of making the paths of electrically charged particles visible by condensation of vapour.
- 1928 **O. W. Richardson** (King's College, London): thermionic phenomenon and especially discovery of the law named after him.
- 1929 **L. V. de Broglie** (Paris): discovery of the wave nature of electrons.
- 1930 **V. Raman** (Calcutta): work on the scattering of light and discovery of the effect named after him.
- 1931 Not awarded.
- 1932 **W. Heisenberg** (Leipzig): the creation of quantum mechanics, the application of which has, inter alia, led to the discovery of the allotropic forms of hydrogen.
- 1933 **E. Schrödinger** (Berlin) and **P. A. M. Dirac** (Cambridge): discovery of new productive forms of atomic theory.
- 1934 Not awarded.
- 1935 **J. Chadwick** (Liverpool): discovery of the neutron.
- 1936 **V. F. Hess** (Innsbruck): discovery of cosmic radiation.  
**C. D. Anderson** (California Institute of Technology, Pasadena): discovery of the positron.
- 1937 **C. J. Davisson** (New York) and **G. P. Thomson** (London): experimental discovery of the diffraction of electrons by crystals.
- 1938 **E. Fermi** (Rome): demonstration of the existence of new radioactive elements produced by neutron irradiation and for the related discovery of nuclear reactions brought about by slow neutrons.
- 1939 **E. O. Lawrence** (Berkeley): invention and development of the cyclotron and for results obtained with it, especially with regard to artificial radioactive elements.
- 1940 Not awarded.
- 1941 Not awarded.
- 1942 Not awarded.
- 1943 **O. Stern** (Pittsburgh): development of the molecular ray method and discovery of the magnetic moment of the proton.
- 1944 **I. I. Rabi** (Columbia, New York): resonance method for recording the magnetic properties of atomic nuclei.
- 1945 **W. Pauli** (Zürich): discovery of the Exclusion Principle, also called the Pauli Principle.
- 1946 **P. W. Bridgman** (Harvard): invention of an apparatus to produce extremely high pressures and discoveries in the field of high-pressure physics.
- 1947 **E. V. Appleton** (London): physics of the upper atmosphere, especially the discovery of the so-called Appleton layer.
- 1948 **P. M. S. Blackett** (Manchester): development of the Wilson cloud chamber method and discoveries therewith in the field of nuclear physics and cosmic radiation.
- 1949 **H. Yukawa** (Kyoto): prediction of the existence of mesons on the basis of theoretical work on nuclear forces.

- 1950 **C. F. Powell** (Bristol): development of the photographic method of studying nuclear processes and discoveries regarding mesons made with this method.
- 1951 **J. D. Cockroft** (Harwell) and **E. T. S. Walton** (Dublin): pioneer work on the transmutation of atomic nuclei by artificially accelerated atomic particles.
- 1952 **F. Bloch** (Stanford) and **E. M. Purcell** (Harvard): development of new methods for nuclear magnetic precision measurements and discoveries in connection therewith.
- 1953 **F. Zernike** (Groningen): demonstration of the phase contrast method and invention of the phase contrast microscope.
- 1954 **M. Born** (Edinburgh): fundamental research in quantum mechanics, especially for the statistical interpretation of the wave function.  
**W. Bothe** (Heidelberg): the coincidence method and discoveries made therewith.
- 1955 **W. E. Lamb** (Stanford): the fine structure of the hydrogen spectrum.  
**P. Kusch** (Columbia, New York): precision determination of the magnetic moment of the electron.
- 1956 **W. Shockley** (Pasadena), **J. Bardeen** (Urbana) and **W. H. Brattain** (Murray Hill): investigations on semiconductors and discovery of the transistor effect.
- 1957 **T. Lee** (Columbia) and **C. Yang** (Princeton): penetrating investigation of the so-called parity laws, which has led to important discoveries regarding the elementary particles.
- 1958 **P. A. Cherenkov**, **I. M. Frank** and **I. E. Tamm** (Moscow): discovery and the interpretation of the Cherenkov effect.
- 1959 **E. Segrè** and **O. Chamberlain** (Berkeley): discovery of the antiproton.
- 1960 **D. A. Glaser** (Berkeley): invention of the bubble chamber.
- 1961 **R. Hofstadter** (Stanford): pioneering studies of electron scattering in atomic nuclei and discoveries concerning the structure of the nucleons.
- R. L. Mössbauer** (Munich): resonance absorption of gamma radiation and discovery of the effect which bears his name.
- 1962 **L. D. Landau** (Moscow): pioneering theories for condensed matter, especially liquid helium.
- 1963 **E. P. Wigner** (Princeton): the theory of the atomic nucleus and elementary particles, particularly through the discovery and application of fundamental symmetry principles.  
**Maria Goeppert-Mayer** (La Jolla) and **J. H. D. Jensen** (Heidelberg): discoveries concerning nuclear shell structure.
- 1964 **C. H. Townes** (Massachusetts Institute of Technology), and **N. G. Basov** and **A. M. Prokhorov** (Moscow): fundamental work in the field of quantum electronics, which led to the construction of oscillators and amplifiers based on the maser-laser-principle.
- 1965 **S. Tomonaga** (Tokyo), **J. Schwinger** (Cambridge, Mass.), and **R. P. Feynman** (California Institute of Technology, Pasadena): fundamental work in quantum electrodynamics, with deep-ploughing consequences for the physics of elementary particles.
- 1966 **A. Kastler** (Paris): discovery and development of optical methods for studying hertzian resonances in atoms.
- 1967 **H. A. Bethe** (Cornell): contributions to the theory of nuclear reactions, especially discoveries concerning the energy production in stars.
- 1968 **L. W. Alvarez** (Berkeley): decisive contributions to elementary particle physics, in particular the discovery of a large number of resonance states, made possible by the hydrogen bubble chamber technique and data analysis.
- 1969 **M. Gell-Mann** (California Institute of Technology, Pasadena): contributions and discoveries concerning the classification of elementary particles and their interactions.

- 1970 **H. Alfvén** (Stockholm): discoveries in magneto-hydrodynamics with fruitful applications in different parts of plasma physics. **L. Néel** (Grenoble): discoveries concerning antiferromagnetism and ferrimagnetism which have led to important applications in solid state physics.
- 1971 **D. Gabor** (Imperial College, London): invention and development of the holographic method.
- 1972 **J. Bardeen** (Urbana), **L. N. Cooper** (Providence) and **J. R. Schrieffer** (Philadelphia): theory of superconductivity, usually called the BCS theory.
- 1973 **L. Esaki** (Yorktown Heights) and **I. Giaever** (Schenectady): experimental discoveries regarding tunnelling phenomena in semiconductors and superconductors respectively. **B. D. Josephson** (Cambridge): theoretical predictions of the properties of a supercurrent through a tunnel barrier, in particular those phenomena which are generally known as the Josephson effects.
- 1974 **M. Ryle** and **A. Hewish** (Cambridge): pioneering research in radioastrophysics: Ryle for his observations and inventions, in particular of the aperture-synthesis technique, and Hewish for his decisive role in the discovery of pulsars.
- 1975 **A. Bohr** (Copenhagen), **B. Mottelson** (Copenhagen) and **J. Rainwater** (New York): discovery of the connection between collective motion and particle motion in atomic nuclei and the development of the theory of the structure of the atomic nucleus based on this connection.
- 1976 **B. Richter** (Stanford) and **S. C. C. Ting** (Massachusetts Institute of Technology): discovery of a heavy elementary particle of a new kind.
- 1977 **P. W. Anderson** (Murray Hill), **N. F. Mott** (Cambridge) and **J. H. van Vleck** (Harvard): fundamental theoretical investigations of the electronic structure of magnetic and disordered systems.
- 1978 **P. L. Kapitza** (Moscow): basic inventions and discoveries in the area of low-temperature physics. **A. A. Penzias** and **R. W. Wilson** (Holmdel): discovery of cosmic microwave background radiation.
- 1979 **S. L. Glashow** (Harvard), **A. Salam** (Imperial College, London) and **S. Weinberg** (Harvard): contributions to the theory of the unified weak and electromagnetic interaction between elementary particles, including, inter alia, the prediction of the weak neutral current.
- 1980 **J. W. Cronin** (Chicago) and **V. L. Fitch** (Princeton): discovery of violations of fundamental symmetry principles in the decay of neutral K-mesons.
- 1981 **K. M. Siegbahn** (Uppsala): development of high-resolution electron spectroscopy. **N. Bloembergen** (Harvard) and **A. L. Schawlow** (Stanford): development of laser spectroscopy.
- 1982 **K. G. Wilson** (Cornell): theory for critical phenomena in connection with phase transitions.
- 1983 **S. Chandrasekar** (Chicago): theoretical studies of the physical processes of importance to the structure and evolution of the stars. **W. A. Fowler** (California Institute of Technology, Pasadena): theoretical and experimental studies of the nuclear reactions of importance in the formation of the chemical elements in the universe.
- 1984 **C. Rubbia** and **S. Van der Meer** (CERN, Geneva): decisive contributions to the discovery of the field particles W and Z, communicators of weak interaction.
- 1985 **K. von Klitzing** (Stuttgart): discovery of the quantized Hall effect.
- 1986 **E. Ruska** (Berlin): fundamental work in electron optics and the design of the first electron microscope. **G. Binnig** and **H. Rohrer** (Zurich): design of the scanning tunneling microscope.

- 1987 **G. Bednorz** and **K. A. Müller** (Zürich): for their important breakthrough in the discovery of superconductivity in ceramic materials.
- 1988 **L. Lederman** (Batavia, Illinois), **M. Schwartz** (Mountain View, California) and **J. Steinberger** (Geneva): for the neutrino beam method and the demonstration of the doublet structure of the leptons through the discovery of the muon neutrino.
- 1989 **N. F. Ramsey** (Harvard): invention of the separated oscillatory fields method and its use in the hydrogen maser and other atomic clocks.  
**H. G. Dehmelt** (University of Washington, Seattle) and **W. Paul** (Bonn): development of the ion trap technique.
- 1990 **J. I. Friedman** and **H. W. Kendall** (Massachusetts Institute of Technology) and **R. E. Taylor** (Stanford): pioneering investigations concerning deep elastic scattering of electrons on protons and bound neutrons, of essential importance for the development of the quark model in particle physics.
- 1991 **P.-G. de Gennes** (Collège de France, Paris): discovery that methods developed for studying order phenomena in simple systems can be generalized to more complex forms of matter, in particular to liquid crystals and polymers.
- 1992 **G. Charpak** (École Supérieure de Physique et Chimie, Paris, and CERN Geneva): invention and development of particle detectors, in particular the multiwire proportional chamber.
- 1993 **R. A. Hulse** and **J. H. Taylor** (Princeton): discovery of a new type of pulsar, that has opened up new possibilities for the study of gravitation.
- 1994 **B. N. Brockhouse** (McMaster University) and **C. G. Schull** (Massachusetts Institute of Technology): pioneering contributions to neutron scattering techniques for studies of condensed matter (namely neutron spectroscopy and neutron diffraction techniques, respectively).
- 1995 **M. L. Perl** (Stanford) and **F. Reines** (Irvine, California): pioneering experimental contributions to lepton physics (discovery of the tau particle and detection of the neutrino, respectively).
- 1996 **D. M. Lee** (Cornell), **D. D. Osheroff** (Stanford) and **R. C. Richardson** (Cornell): discovery of the superfluid phase of helium-3.
- 1997 **S. Chu** (Stanford), **C. Cohen-Tannoudji** (École Normal Supérieure, Paris) and **W. D. Phillips** (NIST, Gaithersburg): development of methods to cool and trap neutral atoms with laser light.

Standard Atomic Weights of the Elements 1995

[Scaled to  $A_r(^{12}\text{C}) = 12$ , where  $^{12}\text{C}$  is a neutral atom in its nuclear and electronic ground state]

The atomic weights of many elements are not invariant but depend on the origin and treatment of the material. The standard values of  $A_r(\text{E})$  and the uncertainties (in parentheses, following the last significant figure to which they are attributed) apply to elements of natural terrestrial origin. The footnotes to this Table elaborate the types of variation which may occur for individual elements and which may be larger than the listed uncertainties of values of  $A_r(\text{E})$ . Names have not yet been assigned to elements with atomic numbers 110, 111 and 112 (see p. 1280).

Name	Symbol	Atomic Number	Atomic Weight	Footnotes	Name	Symbol	Atomic Number	Atomic Weight	Footnotes
Actinium*	Ac	89	(227)		Mercury	Hg	80	200.59(2)	
Aluminium	Al	13	26.981538(2)		Molybdenum	Mo	42	95.94(1)	g
Americium*	Am	95	(243)		Neodymium	Nd	60	144.24(3)	g
Antimony	Sb	51	121.760(1)	g	Neon	Ne	10	20.1797(6)	g m
Argon	Ar	18	39.948(1)	g r	Neptunium*	Np	93	(237)	
Arsenic	As	33	74.92160(2)		Nickel	Ni	28	58.6934(2)	
Astatine*	At	85	(210)		Niobium	Nb	41	92.90638(2)	
Barium	Ba	56	137.327(7)		Nitrogen	N	7	14.00674(7)	g r
Berkelium*	Bk	97	(247)		Nobelium*	No	102	(259)	
Beryllium	Be	4	9.012182(3)		Osmium	Os	76	190.23(3)	g
Bismuth	Bi	83	208.98038(2)		Oxygen	O	8	15.9994(3)	g r
Bohrium	Bh	107	(264)		Palladium	Pd	46	106.42(1)	g
Boron	B	5	10.811(7)	g m r	Phosphorus	P	15	30.973762(4)	
Bromine	Br	35	79.904(1)		Platinum	Pt	78	195.078(2)	
Cadmium	Cd	48	112.411(8)	g	Plutonium*	Pu	94	(244)	
Caesium	Cs	55	132.90545(2)		Polonium*	Po	84	(210)	
Calcium	Ca	20	40.078(4)	g	Potassium	K	19	39.0983(1)	
Californium*	Cf	98	(251)		Praseodymium	Pr	59	140.90765(2)	
Carbon	C	6	12.0107(8)	g r	Promethium*	Pm	61	(145)	
Cerium	Ce	58	140.116(1)	g	Protactinium*	Pa	91	231.03588(2)	
Chlorine	Cl	17	35.4527(9)	m	Radium*	Ra	88	(226)	
Chromium	Cr	24	51.9961(6)		Radon*	Rn	86	(222)	
Cobalt	Co	27	58.933200(9)		Rhenium	Re	75	186.207(1)	
Copper	Cu	29	63.546(3)	r	Rhodium	Rh	45	102.90550(2)	
Curium*	Cm	96	(247)		Rubidium	Rb	37	85.4678(3)	g
Dubnium	Db	105	(262)		Ruthenium	Ru	44	101.07(2)	g
Dysprosium	Dy	66	162.50(3)	g	Rutherfordium	Rf	104	(261)	
Einsteinium*	Es	99	(252)		Samarium	Sm	62	150.36(3)	g
Erbium	Er	68	167.26(3)	g	Scandium	Sc	21	44.955910(8)	
Europium	Eu	63	151.964(1)	g	Seaborgium	Sg	106	(266)	
Fermium*	Fm	100	(257)		Selenium	Se	34	78.96(3)	
Fluorine	F	9	18.9984032(5)		Silicon	Si	14	28.0855(3)	r
Francium*	Fr	87	(223)		Silver	Ag	47	107.8682(2)	g
Gadolinium	Gd	64	157.25(3)	g	Sodium	Na	11	22.989770(2)	
Gallium	Ga	31	69.723(1)		Strontium	Sr	38	87.62(1)	g r
Germanium	Ge	32	72.61(2)		Sulfur	S	16	32.066(6)	g r
Gold	Au	79	196.96655(2)		Tantalum	Ta	73	180.9479(1)	
Hafnium	Hf	72	178.49(2)		Technetium*	Tc	43	(98)	
Hassium	Hs	108	(269)		Tellurium	Te	52	127.60(3)	g
Helium	He	2	4.002602(2)	g r	Terbium	Tb	65	158.92534(2)	
Holmium	Ho	67	164.93032(2)		Thallium	Tl	81	204.3833(2)	
Hydrogen	H	1	1.00794(7)	g m r	Thorium*	Th	90	232.0381(1)	g
Indium	In	49	114.818(3)		Thulium	Tm	69	168.93421(2)	
Iodine	I	53	126.90447(3)		Tin	Sn	50	118.710(7)	g
Iridium	Ir	77	192.217(3)		Titanium	Ti	22	47.867(1)	
Iron	Fe	26	55.845(2)		Tungsten	W	74	183.84(1)	
Krypton	Kr	36	83.80(1)	g m	Ununbium	Uub	112	(277)	
Lanthanum	La	57	138.9055(2)	g	Ununnilium	Uun	110	(269)	
Lawrencium*	Lr	103	(262)		Ununium	Uuu	111	(272)	
Lead	Pb	82	207.2(1)	g m	Uranium*	U	92	238.0289(1)	g m
Lithium	Li	3	[6.941(2)] <sup>†</sup>	g m r	Vanadium	V	23	50.9415(1)	
Lutetium	Lu	71	174.967(1)	g	Xenon	Xe	54	131.29(2)	g m
Magnesium	Mg	12	24.3050(6)		Ytterbium	Yb	70	173.04(3)	g
Manganese	Mn	25	54.938049(9)		Yttrium	Y	39	88.90585(2)	
Meitnerium	Mt	109	(268)		Zinc	Zn	30	65.39(2)	
Mendelevium*	Md	101	(258)		Zirconium	Zr	40	91.224(2)	g

\*Element has no stable nuclides; the value given in parentheses is the atomic mass number of the isotope of longest known half-life. However, three such elements (Th, Pa and U) do have a characteristic terrestrial isotopic composition, and for these an atomic weight is tabulated.

<sup>†</sup>Commercially available Li materials have atomic weights that range between 6.939 and 6.996; if a more accurate value is required, it must be determined for the specific material.

g Geological specimens are known in which the element has an isotopic composition outside the limits for normal material. The difference between the atomic weight of the element in such specimens and that given in the Table may exceed the stated uncertainty.

m Modified isotopic compositions may be found in commercially available material because it has been subjected to an undisclosed or inadvertent isotopic fractionation. Substantial deviations in atomic weight of the element from that given in the Table can occur.

r Range in isotopic composition of normal terrestrial material prevents a more precise  $A_r(\text{E})$  being given; the tabulated  $A_r(\text{E})$  value should be applicable to any normal material.



## Recommended Consistent Values of Some Fundamental Physical Constants (1986)

(The numbers in parentheses are the standard deviation in the last digits of the quoted value.)

Quantity	Symbol	Value	Units	Uncertainty (ppm)
Permeability of vacuum	$\mu_0$	$4\pi \times 10^{-7}$ = 12.566 370 614 ...	$\text{N A}^{-2}$ $10^{-7} \text{N A}^{-2}$	(exact)
Speed of light in vacuum	$c$	299 792 458	$\text{m s}^{-1}$	(exact)
Permittivity of vacuum	$\epsilon_0$	8.854 187 817 ...	$10^{-12} \text{F m}^{-1}$	(exact)
Elementary charge	$e$	1.602 177 33(49)	$10^{-19} \text{C}$	0.30
Planck constant	$h$	6.626 0755(40)	$10^{-34} \text{J s}$	0.60
	$\hbar = h/2\pi$	1.054 572 66(63)	$10^{-34} \text{J s}$	0.60
Avogadro constant	$N_A$	6.022 136 7(38)	$10^{23} \text{mol}^{-1}$	0.59
(Unifed) atomic mass unit	$u$	1.660 540 2(10)	$10^{-27} \text{kg}$	0.59
$1u = m_u = \frac{1}{12} m(^{12}\text{C})$				
Electron mass	$m_e$	9.109 389 7(54)	$10^{-31} \text{kg}$	0.59
		0.510 999 06(15)	MeV	0.30
Proton mass	$m_p$	1.672 623 1(10)	$10^{-27} \text{kg}$	0.59
		938.272 31(28)	MeV	0.30
Neutron mass	$m_n$	1.674 928 6(10)	$10^{-27} \text{kg}$	0.59
		939.565 63(28)	MeV	0.30
Proton-electron mass ratio	$m_p/m_e$	1836.152 701(37)		0.020
Faraday constant $N_A e$	$F$	96 485.309(29)	$\text{C mol}^{-1}$	0.30
Rydberg constant	$R_\infty$	10 973 731.534(13)	$\text{m}^{-1}$	0.0012
Bohr radius	$a_0$	0.529 177 249(24)	$10^{-10} \text{m}$	0.045
Electron magnetic moment anomaly, $\mu_e/\mu_B - 1$	$a_e$	1.159 652 193(10)	$10^{-3}$	0.0086
Electron $g$ -factor, $2(1 + a_e)$	$g_e$	2.002 319 304 386(20)		$1 \times 10^{-5}$
Bohr magneton	$\mu_B$	9.274 0154(31)	$10^{-24} \text{J T}^{-1}$	0.34
Nuclear magneton	$\mu_N$	5.050 7866(17)	$10^{-27} \text{J T}^{-1}$	0.34
Electron magnetic moment	$\mu_e$	928.477 01(31)	$10^{-26} \text{J T}^{-1}$	0.34
Proton magnetic moment in Bohr magnetons	$\mu_p/\mu_B$	1.410 607 61(47)	$10^{-26} \text{J T}^{-1}$	0.34
Electron-proton magnetic moment ratio	$\mu_e/\mu_p$	1.521 032 202(15)	$10^{-3}$	0.010
Proton gyromagnetic ratio	$\gamma_p$	26 752.2128(81)	$10^4 \text{s}^{-1} \text{T}^{-1}$	0.30
Molar gas constant	$R$	8.314 510(70)	$\text{J mol}^{-1} \text{K}^{-1}$	8.4
Molar volume (ideal gas)	$V_m$	22.414 10(19)	L/mol	8.4
Boltzmann constant $R/N_A$	$k$	1.380 658(12)	$10^{-23} \text{J K}^{-1}$	8.5
Constant of gravitation	$G$	6.672 59(85)	$10^{-11} \text{m}^3 \text{kg}^{-1} \text{s}^{-2}$	128

### Greek Alphabet

$\alpha$ A Alpha	$\eta$ H Eta	$\nu$ N Nu	$\tau$ T Tau
$\beta$ B Beta	$\theta$ $\Theta$ Theta	$\xi$ $\Xi$ Xi	$\upsilon$ Y Upsilon
$\gamma$ $\Gamma$ Gamma	$\iota$ I Iota	$\omicron$ O Omicron	$\phi$ $\Phi$ Phi
$\delta$ $\Delta$ Delta	$\kappa$ K Kappa	$\pi$ $\Pi$ Pi	$\chi$ X Chi
$\epsilon$ E Epsilon	$\lambda$ $\Lambda$ Lambda	$\rho$ P Rho	$\psi$ $\Psi$ Psi
$\zeta$ Z Zeta	$\mu$ M Mu	$\sigma$ $\varsigma$ $\Sigma$ Sigma	$\omega$ $\Omega$ Omega

# Index

- $\alpha$ -Process in stars 11
- Absolute configuration, determination of 1125, 1126
- Abundance of elements, Tables of 1294
- Acetylides *see* Carbides
- Acidity function  $H_0$  (Hammett) 51, 52
- Acid strength of binary hydrides 49, 51  
of oxoacids (Pauling's rules) 50  
of HF 815
- Actinide contraction 1264
- Actinide elements  
abundance 1253  
alkyls and aryls 1278  
atomic and physical properties 1263  
carbonyls 1278  
chalcogenides 1471  
complexes  
+7 oxidation state 1273  
+6 oxidation state 1273  
+5 oxidation state 1274  
+4 oxidation state 1275  
+3 oxidation state 1277  
+2 oxidation state 1278  
+1 oxidation state 1278  
coordination numbers and stereochemistries 1267  
cyclopentadienyls 1278  
discovery 1252  
group trends 1264–1267  
halides 1269–1272  
hydrides 64, 1267  
lanthanide-like behaviour 1251, 1264, 1266  
magnetic properties 1272, 1273  
mixed metal oxides 1269  
organometallic compounds 1278–1280  
oxidation states 1268,  
oxides 1268–1269  
preparation of artificial elements 1252–1262  
problems of isolation and characterization 1251, 1260,  
1262, 1264  
redox behaviour 1265–1266  
separation from used nuclear fuels 1260–1262  
spectroscopic properties 1272–1273
- Actinium  
abundance 945  
discovery 944  
radioactive decay series 1254  
*see also* Actinide elements, Group 2 elements
- Actinoid *see* Actinide elements
- Actinon *see* Actinide elements
- Actinyl ions 1273, 1274
- Activated carbon 274  
*see also* Carbon
- Adenine 61, 62
- Adenosine triphosphate (ATP)  
discovery in muscle fibre 474  
in life processes 528, 1101  
in nitrogen fixation 1035, 1036  
in phosphorus cycle 476  
in photosynthesis 125
- Agate 342
- Air 411, 604, 889, 890
- Alane 227
- Albite 357
- Alkali metals (Li, Na, K, Rb, Cs, Fr)  
abundance 69  
alkoxides 87  
atomic properties 75  
biological systems containing 70, 71, 73, 97  
carbonates 59–90  
chelated complexes of  
chemical reactivity of 76  
complexes of 90  
crown-ether complexes of 90  
cryptates of 90  
cyanates 324  
cyanides 321  
discovery of 68, 69  
flame colours of 75  
halides  
imides, amides 99–102  
bonding in 80  
properties of 82–83  
hydrides  
reactions of 84  
hydroxides 86, 87  
hydrogen carbonates (bicarbonates) 88  
intercalation compounds with graphite 293, 294  
intermetallic compounds with As, Sb, Bi 554, 555  
isolation of 68, 69  
nitrates 89  
nitrites 90  
organometallic compounds 106  
oxoacid salts 87–90  
oxides 84  
ozonides 85

- Alkali metals — *contd*  
 peroxides 84, 85  
 physical properties 74, 75  
 polysulfides 677–679, 679, 681  
 reactions in liquid ammonia 78–79  
 sesquioxides 85  
 solubilities in liquid ammonia 78  
 solutions in amines 79  
 solutions in liquid ammonia 77–79  
 solutions in polyethers 79  
 suboxides 84, 85, 86  
 sulfides 679, 681, 682  
 superoxides 84, 85  
*see also* individual metals; Li, Na, K, Rb, Cs, Fr
- Alkaline earth metals (Be, Mg, Ca, Sr, Ba, Ra)  
 abundance 108–110  
 atomic properties 111  
 chemical reactivity of 112  
 complexes of 122–127  
 halides  
   crystal structures of 117–118  
   uses 118  
 hydride halides, MHX 119  
 hydrides 64, 115  
 hydroxides 119–122  
 intermetallic compounds with As, Sb, Bi 554, 555  
 organometallic compounds 127–138  
 oxides 119, 121  
 oxoacid salts 122  
 ozonides 119  
 peroxides 119  
 physical properties 112  
 stereochemistry of 114  
 sulfides 679  
 superoxides 121  
 thermal stability of oxoacid salts 113  
 univalent compounds of 113  
*see also* individual metals: Be, Mg, Ca, Sr, Ba, Ra
- Alkene insertion reactions (Ziegler) 259, 260  
 Alkene metathesis 1038  
   polymerization (Ziegler-Natta) 240, 241, 972  
 Allotelluric acid 782  
 Allotropy *see* individual elements: B, C, P, S etc.  
 Alnico steel 1114, 1146  
 Aluminium  
 abundance 217  
 alloys 220  
 borohydride 169, 228  
 chalcogenides 252  
 III-V compounds 255, 258  
 halide complexes 233–237  
 heterocyclic organo-AlN oligomers 265, 266  
 history of 216  
 hydrides 227  
 hydrido complexes 228–231  
 lower halides AlX, AlX<sub>2</sub> 233  
 organometallic compounds 257–266  
 orthophosphate AlPO<sub>4</sub> 526  
 production 216, 218–226  
 ternary oxide phases 247–252  
 trialkyls and triarylals 257, 258–260  
   dimeric structure of 253  
   preparation 259  
   in Ziegler-Natta catalysis 259–263, 972  
 trichloride 233  
   Friedel-Crafts activity of 234, 236  
   structure 234  
 trichloride adducts, structure of 234, 235, 672  
 trihalide complexes 233–237  
 uses 220  
*see also* Group 13 elements
- Aluminium hydroxide  
 bayerite and gibbsite 243, 245
- Aluminium ion  
 hydration number of 604
- Aluminium oxide hydroxide  
 diaspore and boehmite 243
- Aluminium oxides  
 catalytic activity 244  
 corundum 242, 243  
 “Saffil” fibres 244,  
 structural classification 242, 243  
*see also* Portland cement, High-alumina cement
- Aluminium trimethyl, Al<sub>2</sub>Me<sub>6</sub> 291, 258, 259  
 reactions with MgMe<sub>2</sub> 131
- Alumino-silicates *see* Silicate minerals
- Alumino-thermic process 1003
- Alums 216  
 chrome 1027  
 iron 1088  
 rhodium 1129  
 titanium 970  
 vanadium 993
- Amalgamation process 1175, 1201, 1203
- Americium 1252, 1262  
*see also* Actinide elements
- Amethyst 342
- Amidopolyphosphates 506
- Aminoboranes 209
- Ammonia  
 adduct with Ni<sub>3</sub> 441  
 chemical reactions 423, 424, 486  
 fertilizer applications 422  
 hydrazine, production from (Raschig synthesis) 427,  
 428  
 industrial production 408, 419  
 inversion frequency 423  
 inversion of, discovery 403  
 nitric acid production from 466, 467  
 odour 420  
 physical properties 422, 423  
 production statistics 420  
 synthesis of (Haber-Bosch) 408, 420  
 uses of 422
- Ammonia, liquid  
 acid-base reactions in 425  
 alkali metal solutions in 77–79, 392  
 ammonolysis of PCl<sub>5</sub> 535  
 amphoteric behaviour in 425  
 discovery of coloured metal solutions 408  
 H bonding in 52–55, 422  
 metathesis reactions in 425  
 redox reactions in 425  
 solubility of compounds in 424, 425  
 solvate formation in 425

- solvent properties of 77–79, 422, 424–426  
 syntheses in 426 and *passim*  
 synthesis of metal cluster ions in 392, 393  
 Ammonium nitrate  
   explosive decomposition of 466, 469  
   thermolysis of 443, 469  
 Ammonium nitrite, decomposition to N<sub>2</sub> 409  
 Ammonium phosphates 524  
 Ammonium salts 422  
 Amosites 351  
 Amphiboles 351  
 Amphoteric behaviour  
   definition 225  
   of Al and Ga 225  
   of SbCl<sub>5</sub> 697  
   of SF<sub>4</sub> (Lewis acid-base) 811  
   of V<sub>2</sub>O<sub>5</sub> 981  
   of ZnO 1209  
 Amphoteric cations 52  
 Anderson structure 1011  
 Andrieux's phosphide synthesis 489  
 Angeli's salt 459, 460  
 Angular functions 1285, 1288, 1289  
 Andrussow process for HCN 321  
 Anorthite 357, 358  
 Antiferroelectrics 58  
 Anti-knock additives 371, 799  
 Antimonates 577  
 Antimonides 554  
 Antimonious acid, H<sub>3</sub>SbO<sub>3</sub> 575, 578  
 Antimonite esters 561  
 Antimony  
   abundance and distribution 548–549  
   alloys 549, 554  
   allotropes 551–552  
   amino derivatives 561  
   atomic properties 550  
   catenation 583  
   chalcogenides 581, 582  
   chemical reactivity 552, 553, 577  
   cluster anions 553, 588  
   coordination geometries 554  
   encapsulated 554  
   extraction and production  
   halide complexes 564–570  
   halides 558–566  
     *see also* trihalides, pentahalides, oxide-halides, mixed  
       halides, halide complexes  
   halogeno-organic compounds 596, 598  
   history 547  
   hydride 551–558  
   intermetallic compounds *see* Antimonides  
   metal-metal bonded clusters 583, 588, 589  
   mixed halides 563, 562  
   organometallic compounds 592, 596–598  
   organometallic halides 596, 597  
   oxoacid salts of 591  
   oxidation state diagram 578  
   oxide Sb<sub>2</sub>O<sub>3</sub> 572–574  
   oxide halides 570–572  
   oxides and oxocompounds 572–578  
   pentahalides 561–562, 568–570, 785  
   pentaphenyl 545  
   physical properties 551, 552  
   selenium complex anions 581  
   sulfide, Sb<sub>2</sub>S<sub>3</sub> 547, 549, 580–581, 648  
   trichloride solvent system 560  
   trifluoride as fluorinating agent 560  
   trihalides 558–561, 564–566, 569  
   uses 549  
   volt-equivalent diagram 578  
 Anti-tumour activity of Pt<sup>II</sup> complexes 1163  
 Apatites 109, 475, 480, 525  
   reduction to phosphides 489  
 Aqua regia 790, 792, 1179  
 Aragonite 109  
 Arenes as η<sup>6</sup> ligands 940  
 Argentite (silver glance) 1174  
 Argon  
   atomic and physical properties 891  
   clathrates 893  
   discovery 889  
   production and uses 889  
   *see also* Noble gases  
 Arsenates 577  
 Arsenic  
   abundance and distribution 548, 549  
   allotropes 551  
   alloys 549, 554  
   amino derivatives 561  
   atomic properties 550  
   catenation 583–590  
   chalcogenide cluster cations 579  
   chalcogenides 578–583  
   chemical reactivity 552–554, 577  
   cluster anions 553, 588–591  
   coordination geometries 553  
   diiodide 564  
   encapsulated 554  
   extraction and production 548, 549  
   halide complexes 564–569  
   halides 558–566  
     *see also* trihalides, pentahalides, diiodide, oxide  
       halides, mixed halides, halide complexes  
   halogenoorganoarsenic compounds 593–596  
   history 547  
   hydrides 557, 558, 583, 679  
   intermetallic compounds *see* Arsenides  
   metal-metal bonded species 583–590  
   mixed halides 563  
   organoarsenic(I) compounds 597  
   organoarsenic(III) compounds 583–587, 592–594, 596  
     arsabenzene 593  
     arsanaphthalene 593  
     physiological activity 596  
     preparation of 593, 595  
     reactions of 593, 595  
   organoarsenic(V) compounds 594, 596  
   organic compounds 553  
   oxoacid salts of 591  
   oxidation state diagram 578  
   oxide As<sub>2</sub>O<sub>3</sub> 549, 572–575  
   reactions 574  
   structure and polymorphism 573  
   uses 549, 574  
   oxide halides 570–572

- Arsenic — *contd*  
 oxides and oxocompounds 570–578  
 pentahalides 561, 664  
 physical properties 551, 552  
 selenides 581  
 sulfide,  $As_2S_3$  547, 548, 578, 579, 648  
   chemical reactions 580, 581  
   structure 578, 579  
 sulfide,  $As_4S_4$  548, 578–581, 649  
 sulfides,  $As_4S_n$  578–580  
 triangular species 583, 586–589  
 trichloride solvent system 560  
 trihalides 558–561, 564, 566  
 uses 549  
 volt-equivalent diagram 578
- Arsenicals, therapeutic uses 593  
*see also* Organoarsenic(III) and Organoarsenic(V)  
 compounds
- Arsenides 554–558  
 stoichiometries 554  
 structures 554–557
- Arsenious acid  $As(OH)_3$  574
- Arsenite 575, 575, 577
- Arsenite esters 561
- Arsenopyrite 649
- Arsenidine complexes 597
- Arsine 558
- Arsinic acids  $R_2AsO(OH)$  594
- Arsinous acids  $R_2AsOH$  594
- Arsonic acids  $RAsO(OH)$  596
- Arsonous acids  $RAs(OH)_2$  594
- Asbestos 109, 351
- Asbestos minerals 349, 351
- Astatate ion,  $AtO_3^-$  886
- Astatide ion  $At^-$  886
- Astatine  
 abundance 796  
 atomic properties 800  
 chemistry 885, 886  
 nuclear synthesis 791, 795  
 radioactivity of isotopes 795, 885  
 redox systematics 885  
 trihalide ions 886  
*see also* Halogens
- Atactic polymer 972
- Atmophile elements 648
- Atmosphere  
 composition 409, 603  
 industrial production of gases from 409, 604  
 origin of  $O_2$  in 602
- Atom-at-a-time chemistry 1282
- Atomic energy 1256
- Atomic orbitals 1285–1289
- Atomic piles 1256  
*see also* Nuclear reactors
- Atomic properties, periodic trends in 23–27
- Atomic volume curve, periodicity of 23, 24
- Atomic weight, definition 15
- Atomic weights  
 history of 15, 601  
 precision of 15–19  
 relative uncertainty of
- Table of *see* front end paper  
 variability of 17–19, 368
- ATP *see* Adenosine triphosphate
- Austenite
- Autoprotolysis constants of anhydrous acids 710
- Azides 433
- Azoferradoxin 1036, 1098
- Azotobacter* 999, 1036
- Azotobacter vinelandii* 1036
- $\beta$ -alumina *see* Sodium  $\beta$ -alumina,  
 $\beta$ -elimination reactions 926
- Back ( $\pi$ ) bonding 923, 926, 927, 931, 1166
- Baddeleyite 955  
 structure of 955
- Baking powders 524, 525
- Barium  
 history of 108  
 organometallic compounds 136  
 polysulfides 681  
*see also* Alkaline earth metals
- Bart reaction 596
- Basic oxygen steel process 120, 1072
- Bastnaesite 945, 1229, 1232
- Batteries  
 dry 1204  
 lead 371, 549  
 sodium-sulfur 678
- Bauxite 243  
 production statistics 218  
 in Al production 219
- Bayer process 167
- Bayerite 243, 245
- Belousov-Zhabotinskii oscillating reactions 865
- Bentonite *see* Montmorillonite
- Benzene as  $\eta^6$  ligand 940–941
- Berkelium 1252, 1262  
*see also* Actinide elements
- Berry pseudorotation 474, 499, 914  
*see also* Stereochemical non-rigidity
- Beryl 107, 108, 349
- Beryllia *see* Beryllium oxide
- Beryllium  
 alkoxides etc 122, 129  
 alkyls 126–130  
 ‘anomalous’ properties of 114, 122  
 ‘basic acetate’ 122, 123  
 ‘basic nitrate’ 122  
 borohydride 115, 116  
 chloride 116, 117  
 complexes of 122–125  
 cyclopentadienyl complexes 130,  
 discovery 107, 108  
 fluoride 116  
 hydride 115, 115, 128  
 oxide 107, 119–120  
 salts, hydrolysis of 121  
 uses of metal and alloys 110  
*see also* Alkaline earth metals
- Beryllium compounds, toxicity of 107
- Beryllium ion, hydration number of 605
- Bessemer process 1072

- BHB bridge bond, comparison with H bond 64, 70  
*see also* Three-centre bonds
- “Big-bang” 1, 5, 10
- Biotite *see* Micas
- Bismuth  
 abundance and distribution 548, 549, 550  
 allotropes 551, 551  
 alloys 549, 554  
 atomic properties 550  
 Bi<sup>+</sup> cation 564, 591  
 catenation 582  
 chalcogenides 581, 582  
 chemical reactivity 552, 553, 577  
 cluster cations 564, 565, 583, 588–591  
 extraction and production 549, 550  
 halide complexes 564–567  
 halides 558–564  
*see also* trihalides, pentahalides, oxide halides, lower halides, mixed halides, halide complexes  
 history 547  
 hydride 557, 558  
 hydroxide, Bi(OH)<sub>3</sub> 575  
 hydroxo cluster cation, [Bi<sub>6</sub>(OH)<sub>12</sub>]<sup>6+</sup> 575, 591, 592  
 intermetallic compounds *see* Bismuthides  
 lower halides 564  
 metal-metal bonded clusters 583, 583–591  
 mixed halides 564  
 nitrate and related complexes 591, 592  
 organometallic compounds 592, 596, 599  
 oxidation state diagram 578  
 oxide, Bi<sub>2</sub>O<sub>3</sub> 573, 574  
 oxide halides 572, 572  
 oxides and oxo compounds 573–575  
 oxoacid salts of 591  
 pentafluoride 561  
 physical properties 550, 552  
 trihalides 558–561, 564, 566  
 uses 549  
 volt-equivalent diagram 578
- Bismuthates 577
- Bismuthides 554
- Bismuthine 557
- Biuret 305, 1191
- “Black oxide” of mercury 1213
- Blast furnace 1073
- Bleaching powder 790, 860
- “Blister” copper 1175
- “Blue proteins” 1198–1199
- Blue vitriol 1190
- Boehmite 243
- Bohrium 1281, 1283
- Boiling points, influence of H bonding 54
- Borane adducts, LBH<sub>3</sub> 165  
 amine-boranes 208–209
- Borane anions 151, 166, 178, 181, 590  
*see also* Boranes
- Boranes  
*arachno*-structures 152, 154, 159  
 bonding 157–162, 590  
 classification 151  
*closo*-structures 152, 153, 161  
*conjuncto*-structures 152, 155–157  
*hypho*-structures 152, 153, 172  
 as ligands 177  
*nido*-structures 152, 154, 161  
 nomenclature 157  
 optical resolution of *i*-B<sub>18</sub>H<sub>22</sub> 670  
 physical properties 162, 163  
 preparation 162  
 topology 158–160, 175  
*see also* Diborane, Petaborane, Decaborane, Metalloboranes, Carboranes, etc.
- Borate minerals  
 occurrence 140  
 production and uses 140  
*see also* Borates
- Borates 205–207  
 B–O distances in 206  
 industrial uses 207  
 structural principles 205
- Borax 139  
*see also* Borate minerals
- Borazanes 209
- Borazine 210, 408
- Bordeaux mixture (fungicide) 1190
- Boric acids  
 B(OH)<sub>3</sub> 203  
 HBO<sub>2</sub> 204
- Borides  
 bonding 151  
 catenation in 148  
 preparation 146  
 properties and uses 146  
 stoichiometry 145, 147  
 structure 147–151
- Born-Haber cycle 94–96, 79, 82–83
- Borohydrides *see* Borane anions, Tetrahydro-borates, etc.
- Boron 167  
 abundance 139  
 allotropes 141–144  
 atomic properties 144, 222  
 chemical properties 144, 145  
 crystal structures of allotropes 141  
 hydrides *see* Boranes  
 isolation 139–140, 144  
 neutron capture therapy using <sup>10</sup>B 179  
 nitride 208, 208  
 nuclear properties 144  
 oxide 203  
 physical properties 144, 222  
 sulfides 213–214  
 variables atomic weight of 17  
*see also* Group 13 elements
- Boron carbide  
 B<sub>4</sub>C 149  
 B<sub>13</sub>C<sub>2</sub> 149  
 B<sub>50</sub>C<sub>2</sub> 143
- Boron halides 195–202  
 B<sub>2</sub>X<sub>4</sub> 200  
 B<sub>*n*</sub>X<sub>*n*</sub> 200, 202  
 lower halides 199–202  
*see also* Boron trihalides
- Boron nitride, B<sub>50</sub>N<sub>2</sub> 143
- Boron-nitrogen compounds 207–211
- Boron-oxygen compounds 203–207  
 organic derivatives 207

- Boron trifluoride *see* Boron trihalides
- Boron trihalides  
 adducts 198–199  
 bonding 196  
 physical properties 196  
 preparation 196  
 scrambling reactions 197, 198
- Brass 1175, 1178, 1178, 1201, 1203, 1397
- Brimstone 645, 646
- Brønsted's acid-base theory 32, 48ff  
 in non-aqueous solutions 51  
 in aqueous solutions 628
- Bromates,  $\text{BrO}_3^-$  862–864  
 reaction scheme 866  
 redox systematics 853–856
- Bromic acid,  $\text{HBrO}_3$  863
- Bromides, synthesis of 821, 822  
*see also* individual elements
- Bromine  
 abundance and distribution 795  
 atomic and physical properties 800–804  
 cations  $\text{Br}_n^+$  842–844  
 history 790, 790, 792, 794, 925  
 monochloride 824–825, 833  
 monofluoride 825, 833  
 oxide fluorides 880–881  
 oxides 850, 851  
 nomenclature 853  
 redox properties 853–855  
*see also* individual compounds, bromic acid, bromates, perbromates, etc.  
 pentafluoride 832–834  
 production and uses 798, 800  
 radioactive isotopes 801, 802  
 reactivity 805  
 standard reduction potentials 854  
 stereochemistry 806  
 trifluoride 827–831, 832  
 volt-equivalent diagram 855  
*see also* Halogens
- Bronze 1173, 1175
- Bronzes  
 molybdenum 1016  
 titanium 964  
 tungsten 1016  
 vanadium 987
- “Brown-ring” complex 447, 1094
- Brucite 121, 352, 385
- Buffer solutions 48, 49, 521, 524
- Bulky tertiary phosphine ligands, special properties of 494
- Butadiene as a  $\eta^4$  ligand 935–936
- Cadmium  
 abundance 1204  
 chalcogenides 1208, 1210  
 coordination chemistry 1215–1217  
 discovery 1201  
 halides 1211–1212  
 organometallic compounds 1221  
 oxides 1211, 1212  
 production and uses 1202–120
- toxicity 1224  
*see also* Group 12 elements
- Cadmium chloride structure 1211
- Cadmium iodide structure type 556, 680, 680, 1211  
 relation to NiAs 556, 680, 680  
 nonstoichiometry in 679
- Caesium  
 abundance 70  
 compounds with oxygen 83–86  
 discovery 69
- Calamine (smithsonite) 1202
- Calcite 109
- Calcium  
 in biochemical processes 125  
 carbide 297, 298, 320  
 carbonate *see* limestone  
 cyclopentadienyl 136, 137  
 history of 108  
 organometallic compounds 136, 137  
 phosphates 524–526  
*see also* Alkaline earth metals, Lime, etc.
- Caliche (Chilean nitre) 796
- Californium 1252, 1262  
*see also* Actinide elements
- Calomel 1213
- Capped octahedral complexes 916
- Capped trigonal prismatic complex 916
- Caprolactam, for nylon-6 422
- Carat 272, 1176
- Carbaboranes *see* Carboranes
- Carbene ligands 929
- Carbides 297–301  
 silicon (SiC) 334
- Carbido complexes 927, 1107–1108
- Carbohydrates, photosyntheses of 125
- Carbon  
 abundance 270  
 allotropes 274–278, *see also* Fullerenes  
 atomic properties 276, 372–372  
 bond lengths (interatomic distances) 290, 292  
 chalcogenides 314–319  
 chemical properties 289  
 coordination numbers 290, 291, 292  
 cycle (global) 273  
 disulfide 313–318, 653  
 halides 301, 304  
 history of 268–270  
 hydrides of 301  
 interatomic distances in compounds 290–292  
 occurrence and distribution 270–274  
 oxides 305  
*see also* Carbon monoxide, Carbon dioxide  
 “monofluoride” 289  
 radioactive  $^{14}\text{C}$  276  
 suboxides 305
- Carbon dioxide 305, 314  
 aqueous solutions (acidity of) 309, 310  
 atmospheric 273–274  
 coordination chemistry 312  
 industrial importance 307, 308  
 insertion into M–C bonds 134, 312  
 as a ligand 312, 313  
 in photosynthesis 125

- physical properties 305  
 production and uses of 311  
 use in  $^{14}\text{C}$  syntheses 310
- Carbon monoxide 305–310  
 bonding in 926, 927  
 chemical reactions 306, 308  
 industrial importance 307  
 as a ligand 926–929  
 physical properties 306  
 poisoning effect of 306, 1101  
 preparation of pure 306  
 similarity to  $\text{PF}_3$  as a ligand 496
- Carbonates, terrestrial distribution 274, 273
- Carbonic acid 310
- Carbonic anhydrase 1225
- Carbonyl fluoride, reaction with  $\text{OF}_2$  640
- Carbonyl halides *see* Carbon oxohalides
- Carbonyls *see* Carbon monoxide as a ligand  
*see also* individual elements
- Carboplatin 1165
- Carboranes 161, 181ff  
 bonding 181  
 chemical reactions 186, 189  
 isomerization 185–187  
 preparation 181–185  
 structures 181, 185
- Carborundum *see* Silicon carbide
- Carbosilanes 362
- Carboxypeptidase A 1224
- Carbyne ligands 928–930
- Carnotite 977
- Caro's acid *see* Peroxomonosulfuric acid
- Cast-iron 1071
- Cassiterite *see* Tin dioxide
- Castner-Kellner process (chlor-alkali) 790, 1203
- Catalysis  
 ammonia, oxidation to  $\text{NO}$ ,  $\text{NO}_2$  423, 465, 466  
 synthesis (Haber–Bosch) 43, 421–422  
 ammonia(l)/metal solutions, effects of impurities 78  
*conjuncto* boranes, preparation of 162  
 $\text{C}_{60}$ , hydroxylation by base 284  
 carbonylation of  $\text{B}_{12}\text{H}_{12}^{2-}$  180  
 C–H bonds, homogeneous catalytic activity of 494  
 chlorination of organic compounds by  $\text{CuCl}$  798  
 $\text{S}_2\text{Cl}_2$  to  $\text{SCl}_2$  by  $\text{FeCl}_3$  689  
 $\text{SiC}$  to  $\text{SiCl}_4$  by  $\text{NiCl}_2$  811  
 $\text{SO}_2$  to  $\text{O}_2\text{SCl}_2$  by  $\text{C}$  or  $\text{FeCl}_3$  694  
 Claus process for recovery of  $\text{S}$  from  $\text{H}_2\text{S}$  651, 699  
 “clock” reactions, autocatalysis 864  
 C–N–O cycle in stars 9  
 contact process for  $\text{H}_2\text{SO}_4$  646, 700, 708, 981  
 CO, organic reactions of 309  
 $\text{CS}_2$ , chlorination by  $\text{Fe}/\text{FeCl}_3$  and by  $\text{I}_2$  317  
 synthesis by  $\text{SiO}_2$  or  $\text{Al}_2\text{O}_3$  317  
 Fischer–Tropsch process 309, 1106  
 fluorination of ammonia by  $\text{Cu}$  439  
 graphite by acid 289  
 $\text{SOF}_2$  by  $\text{CsF}$  685  
 $\text{SO}_3$  by  $\text{AgF}$  640  
 graphite  $\rightarrow$  diamond transition by molten metals 278  
 $\text{H}_2$ , *ortho-para* conversion by paramagnetic species 35  
 HCN, production of 321  
 hydrazine, decomposition by heavy metals 428  
 hydrodesulfurization (HDS) by  $\text{Mo}$  compounds 1005  
 hydroformylation of alkenes 309, 593, 1135, 1140  
 hydrogen peroxide, decomposition of 635  
 production of 634  
 hydrogenation by metal hydrides 47  
 hydrogenation of alkenes 1134–1135  
 NO by  $\text{Pt}/\text{charcoal}$  431  
 unsaturated organic compounds 38, 43, 1146  
 hypohalous acids, decomposition of 858  
 hyponitrous acid (HONNOH), base decomposition of 460  
 nitramide ( $\text{H}_2\text{NNO}_2$ ), base decomposition of 459  
 $\text{O}_2$ , preparation from  $\text{H}_2\text{O}_2$  603  
 organotin compounds, synthesis of 399  
 oxidation of  $\text{SF}_4$  by  $\text{O}_2/\text{NO}_2$  687  
 $\text{SO}_2$  700, 708  
 phase transfer catalysis by Br-containing compounds 794  
 cryptands 97  
 Reppe synthesis by  $\text{Ni}^{\text{II}}$  complexes 309, 1167, 1172  
 propene, dimerization by  $\text{AlPr}_3^t$  260  
 $\text{S}_4\text{N}_4$ , depolymerization to  $2\text{S}_2\text{N}_2$  by  $\text{Ag}_2\text{S}$  725  
 silanes, formation by  $\text{Cu}$  338, 363  
 hydrolysis by base 339  
 silicone polymers, cross linking of 365  
 steam-hydrocarbon reforming process 39, 421  
 Wacker process by  $\text{PdCl}_2/\text{CuCl}_2$  1172  
 water-gas shift reaction 38–39, 311, 421, 1106  
*see also* Catalysts
- Catalysts  
 alumina (activated) 243, 245  
 $\text{BF}_3$  199, 200, 686  
 carbon (activated) 274, 305, 321, 694  
 carbonyl complexes of metals 309, 593, 1106, 1135, 1142  
 crown ethers in synthesis of organoantimony compounds 596  
 dithiolato complexes in polymerizations and oxidations 674  
 Friedel Crafts 171, 176, 186, 199, 235–6, 338, 385  
 HBr 812  
 HCl in hydrolysis of glucose 812  
 heteropolymetalates in petrochemical industry 1014  
 HF 200, 810  
 $\text{I}_2$  317, 508, 800  
 Ir 321, 1115  
 lanthanide oxides 1232  
 “magic acid” in organic catalytic processes 570  
 metalloenzymes in biological systems 1138  
 $\text{MoS}_2$  in hydrogenations 1018  
 $\text{NEt}_3$  in malathion production 509  
 Ni, Pd, Pt 43, 321, 421, 431, 603, 634, 646, 810, 1148  
 NO complexes in homogeneous catalysis 450, 452  
 $\text{N}_2\text{O}_5$  in decomposition of ozone 458  
 nonstoichiometric oxides in heterogeneous catalysis 644  
 organotin compounds for polyurethanes 400  
 $\text{Ph}_3\text{PO}$  as an O atom transfer catalyst 504  
 polymerization catalysts 105, 200, 229  
 polyphosphoric acid in petrochemical processes 520  
 Pt/Re for lead-free petroleum products 1043  
 Rh 321, 1115  
 $\text{SbFCl}_4$  in fluorinations 304



- Catalysts — *contd*  
 tin oxide systems 385  
 Vaska's compound 615, 1135–1136  
 $V_2O_5$  708, 981  
 Wilkinson's catalyst 43, 1134–1135  
 zeolites 309, 359  
 Ziegler–Natta catalysts 260–261, 972  
*see also* Catalysis
- Catenation in Group 14 elements 374, 402  
*Catena*-polyarsanes 584–587  
*Catena*- $S_8$  diradical 660, 662  
*Catena*- $S_x$  656, 659  
 formation at  $\lambda$  point 660
- Caustic soda *see* Sodium hydroxide
- Cellophane 317
- Cement 251, 252
- Cementite 1075
- Cerium 1229  
 diiodide 1240  
 +4 oxidation state 1236, 1239, 1244  
 production 1230  
*see also* Lanthanide elements
- Chabazite *see* Zeolites
- Chain polyphosphates 526–529  
 diphosphates 526  
 tripolyphosphates 528, 528  
*see also* Adenosine triphosphate, Sodium  
 tripolyphosphate, Graham's salt, Kurrol's salt,  
 Maddrell's salt
- Chain reactions, nuclear 1256, 1261
- Chalcocite (copper glance) 1174
- Chalcogens, group trends 754–759  
*see also* S, Se, Te, Po
- Chalcophile elements 646, 648
- Chalcopyrite (copper pyrite)  $CuFeS_2$  649, 1174, 1365
- Chaoite 275, 276
- Chelate effect 910–911
- Chelation 906, 910
- Chemical periodicity 20ff
- Chemical properties of the elements, periodic trends in 23
- Chemical shear structures 644  
*see also* oxides of Ti, Mo, W, Re, etc.
- Chemiluminescence of phosphorus 483
- Chernobyl, nuclear reactor disaster 146
- Chevreton phases 1018, 1031
- Chile saltpetre 407  
*see also* Sodium nitrate
- Chlorates,  $ClO_3^-$  862–865  
 redox properties 1001, 1002
- Chloric acid,  $HClO_3$  863
- Chlorides, synthesis of 821, 822  
*see also* individual elements
- Chlorin 126
- Chlorine  
 abundance and distribution 795  
 atomic and physical properties 800–804  
 bleaching power 790, 793  
 cations  $Cl_2^+$ ,  $Cl_3^+$  842, 843  
 dioxide,  $ClO_2$  844, 845, 846–848  
 history 790–793  
 hydrate 790  
 monofluorides 824–827, 832  
 oxide fluorides 875–880  
 oxides 844–850  
 oxoacids and oxoacid salts 853ff  
 nomenclature 853  
 redox properties 853–855  
*see* individual compounds, Hypochlorous acid,  
 Hypochlorites, Chlorous acid, etc.  
 pentafluoride 832–834  
 production and uses 797–798  
 radioactive isotopes 801, 802  
 reactivity 805  
 standard reduction potentials 850  
 stereochemistry 806  
 toxicity 793  
 trifluoride 827–830, 852  
 volt equivalent diagram 855  
*see also* Halogens
- Chlorite 355, 357, 413
- Chlorites,  $ClO_2^-$  854, 855, 859–862, 1002, 1007–1009
- Chlorofluorocarbons 608, 793, 848
- Chlorophylls 109, 125–127
- Chloroplatinic acid 1154
- Chlorosulfanes *see* Sulfur chlorides
- Chlorous acid,  $HClO_2$  854, 855, 859, 861
- Chromate ion 1009, 1024, 1193
- Chromate alum 1028
- Chrome ochre 1003
- Chromic acid 1007
- Chromite 1003
- Chromium  
 abundance 1003  
 bis(cyclopentadienyl) 939, 1038  
 borazine complex 210  
 carbonyls 928–929, 1037  
 carbyne complexes 929  
 chalcogenides 680, 1017, 1018  
 complexes  
 +6 oxidation state 1023–1024  
 +5 oxidation state 1024–1025  
 +4 oxidation state 1025–1027  
 +3 oxidation state 1027–1031  
 +2 oxidation state 1031–1035  
 with S 666  
 compounds with quadruple metal-metal bonds  
 1032–1034  
 cyclooctatetraene complex 943  
 cyclopentadienyls 939, 1037  
 dibenzene “sandwich” compound 940, 1039  
 discovery 1002  
 dithiolene complex redox series 675  
 halides and oxohalides 1019–1023  
 hexacarbonyl 928, 1037  
 importance of  $Cr^{III}$  in early coordination  
 chemistry 914, 1027  
 organometallic compounds 371, 373–375, 1207–1210  
 oxides 1007–1009  
 peroxo complexes 636, 637  
 polynuclear complexes in dyeing and tanning 1030  
 “polyphenyl” compounds 940  
 production and uses 1003  
 sulfides, nonstoichiometry in 679  
*see also* Group 6 elements
- Chromocene 1038
- Chrysotile 351, 352, 357

- Cinnabar (vermillion), HgS 649, 1202, 1210  
 Circular dichroism (CD) 1125  
 Cisplatin 1164  
 Class-a and class-b metal ions 909  
*see also* Ligands  
 Clathrate compounds 893, 1161  
 Claus process (S from H<sub>2</sub>S) 651, 652, 699  
 uses of 356  
 Clock reaction (H. Landolt) 864  
 Cluster compounds  
   boranes incorporating P, As or Sb 212  
   boron carbide 149  
   boron hydrides 151–180  
   carbido metal carbonyls 1107–1108  
   carboranes 181–189  
   cobalt, rhodium and iridium carbonyls 928ff,  
     1140–1143  
   cobalt–sulfur complexes 1119  
   of germanium, tin and lead 383, 392–396, 455–458  
   of indium 256–7  
   gold phosphines 1197  
   iron, ruthenium and osmium carbonyls 928ff,  
     1104–1108  
   lanthanide halides 1242  
   lithium alkyls 103–105  
   lithium imides 100  
   mercury-containing 1120  
   metal borides 148, 149–151  
   metalloboranes 171–173, 178  
   metallocarboranes 189–195  
   molybdenum and tungsten dihalides 1022  
   nickel, palladium and platinum carbonyls 1168–71  
   niobium and tantalum halides 991  
   of phosphorus, arsenic, antimony and bismuth 563,  
     588–591  
   rhenium alkyls 1068, 1069  
   rhenium carbidocarbonyls 1065  
   scandium halides 950  
   stabilization by encapsulated heteroatoms 950, 966,  
     992, 1065, 1107, 1141, 1169, 1242  
   of tellurium 761, 764  
   Te<sub>6</sub><sup>4+</sup> 161, 761  
   technetium and rhenium chalcogenides 1049  
   tungsten and molybdenum halides 1021–1022  
   zirconium halides 965  
 Cluster and cage structure 918  
*see also* Cluster compounds  
 Cobalt  
   abundance 1113  
   allyl complexes 933  
   arsenide 555, 556  
   atomic and physical properties 1115–1116  
   biochemistry of 1138, 1139, 1322  
   carbido carbonyls 1141–1142  
   carbonyls 928, 929, 1140–1143  
   complexes  
     +5 oxidation state 1121  
     +4 oxidation state 1121  
     +3 oxidation state 1122–1129  
     +2 oxidation state 1129–1133  
     +1 oxidation state 1133  
     lower oxidation states 1137  
     with S 666–669  
     with SO<sub>2</sub> 701  
   coordination numbers and stereochemistries 1117  
   cyclobutadiene complex 936  
   cyclooctatetraene complexes 942  
   cyclopentadienyls 1143  
   dithiolene complexes, redox series 676  
   halides 1119–1121  
   importance of Co<sup>III</sup> in early coordination chemistry  
     914, 1122, 1123, 1302  
   nitrate (anhydrous) 469  
   nitrate complexes 469, 470, 543  
   optical resolution of [Co{(μ-OH)<sub>2</sub>Co(NH<sub>3</sub>)<sub>4</sub>]<sub>3</sub> 670, 915  
   organometallic compounds 1139–1143  
   oxidation states 1117  
   oxides 1117–1119  
   oxoanions 1120, 1121  
   production and uses 1114, 1115  
   reactivity of element 1116  
   relationship with other transition elements 1116–1117  
   standard reduction potentials 1122  
   sulfides 1118  
 Cobaltite (cobalt glance) 1114  
 Cobaltocene 939, 1143  
 Coesite 342, 343  
 Coinage metals (Cu, Ag, Au) 1173  
*see also* Group 11 elements and individual element  
 Coke 274  
   historical importance is steel making 1070, 1072  
*see also* Carbon  
 “Cold fusion” 1151  
 Cold fusion (nuclear) 1280, 1283–4  
 Columbite 977  
 Columbium 976  
*see also* Niobium  
 Combustion 600–602, 612  
 Complexometric titration of Bi<sup>III</sup> with EDTA 577  
 Contact process *see* Sulfuric acid manufacture  
 Cooperativity 1100, 1199  
 Cooper pairs 1183  
 Coordinate bond 198, 921  
*see also* Donor-acceptor complexes  
 Coordination number 912  
   two 945  
   three 913  
   four 913  
   five 914  
   six 916  
   seven 916  
   eight 916  
   nine 917  
   above nine 917  
 Copper  
   abundance 1174  
   acetylide 1180  
   alkenes and alkynes 1199  
   alkyls and aryls 1200  
   biochemistry of 1197  
   carboxylates 1192–1193  
   chalcogenides 1181–1182  
   complexes  
     +3 oxidation state 1187  
     +2 oxidation state 1189–1194

- Copper — *contd*  
 +1 oxidation state 1194–1197  
 Cu–S–O system 677  
 halides 1183–1185  
 history 1173  
 nitrate, structure of 471, 1190  
 nitrate complexes 469, 470, 471, 544  
 organometallic compounds 925, 1199, 1200  
 oxides 1181  
 production and uses 1174, 1175  
*see also* Group 11 elements
- Copper oxide  $\text{Cu}_{2-x}\text{O}$ , nonstoichiometry in 642  
 “Corrosive sublimate” 1212
- Corundum *see* Aluminium oxides
- Cosmic black-body radiation 2
- Cossee mechanism 261
- Cotton effect 1125
- Creutz-Taube anion 1097
- Cristobalite 343, 344
- Critical mass 1256, 1257, 1261
- Crocidolite 351
- Crocoite 1003
- Crown ethers 96, 97  
 complexes with alkali metals 95, 97  
 complexes with alkaline earth metals 124  
 “hole sizes” of 96  
 “triple-decker” complex
- Cryolite 219
- Crypt, molecular structure of 98  
 complexes with alkali metals 97, 393, 394  
 complexes with alkaline earth metals 125
- Crystal field  
 octahedral 922  
 strong 923  
 weak 922
- Crystal field splittings 922–923
- Crystal field stabilization energy 1131
- Crystal field theory 922
- Cubic, eight coordination 916, 1275, 1480
- Cupellation 1173
- Cuprite 1174
- Curium 1252, 1262  
*see also* Actinide elements
- Cyanamide 319  
 industrial production 324
- Cyanates 320, 324  
 as ligands 325
- Cyanide ion as ligand 322, 926
- Cyanide process 1175, 1196
- Cyanogen 319–321  
 halides 320, 323, 340
- Cyanuric acid 305
- Cyanuric compounds 320, 323
- Cyclobutadiene as  $\eta^4$  ligand 935–938
- Cycloheptatrienyl as  $\eta^7$  ligand 941
- Cyclometaphosphimic acids 541, 542
- Cyclometaphosphoric acids  $(\text{HPO}_3)_n$  512  
*see also* *Cyclo*-polyphosphoric acid, *Cyclo*-poly-phosphates
- Cycloocta-1,5-diene (cod) as ligand 932
- Cyclooctatetraene as  $\eta^8$  ligand 942  
 as  $\eta^2$ ,  $\eta^4$ ,  $\eta^6$ , etc., ligand 943
- Cyclopentadienyl  
 as  $\eta^5$  ligand 937–940  
 as  $\eta^1$  ligand 940  
*see also* Ferrocene, individual metals
- Cyclo*-polyarsanes 584–586
- Cyclo*-polyphosphates 529–531
- Cyclophosphazanes 533, 534
- Cyclo* polyphosphoric acids 529  
*see also* *Cyclo*-metaphosphoric acids
- Cyclo*- $\text{S}_6$  ( $\epsilon$ -sulfur) 656
- Cyclo*- $\text{S}_7$  656–657
- Cyclo*- $\text{S}_8$  ( $\alpha$ )  
 crystal and molecular structure 654  
 physical properties 654–656  
 polymerization at  $\lambda$  point 660  
 solubility 654  
 transition  $\alpha$ - $\text{S}_8 \rightleftharpoons \beta$ - $\text{S}_8$  654  
 vapour pressure 660
- Cyclo*- $\text{S}_9$  657
- Cyclo*- $\text{S}_{10}$  656–657
- Cyclo*- $\text{S}_{11}$  657
- Cyclo*- $\text{S}_{12}$  656–658
- Cyclo*- $\text{S}_{18}$  656, 658, 778
- Cyclo*- $\text{S}_{20}$  656, 659
- Cyclo*-silicates 347, 349
- Cytochromes 1095, 1101, 1198, 1279
- Cytosine 61, 62
- d-block contraction 27, 222, 251, 561, 655, 1234
- d orbitals 922–923, 1285–1289  
 splitting by crystal fields 922–923
- Dalton’s atomic theory 509
- Dalton’s law of multiple proportions 509
- Dawson structure 1015
- Decaborane,  $\text{B}_{10}\text{H}_{14}$  159, 163  
 adduct formation 176  
 Brønsted acidity 175  
 chemical reactions 175–177  
 preparations 187  
 structure 175
- Degussa process for HCN 321
- Density of the elements  
 periodic trends in 24
- Denticity 906
- Deoxyribonucleic acids 476
- Detergents  
 polyphosphates in 474, 477  
 sodium tripolyphosphate in 528
- Deuterium  
 atomic properties 34  
 discovery 32  
*ortho*- and *para*- 36  
 physical properties 35  
 preparation 39
- Dewar-Chatte-Duncanson theory 931
- Diagonal relationship 27  
 B and Si 202, 347  
 Be and Al 107  
 Li and Mg 76, 102, 1113  
 N and S 722
- Diamond  
 chemical properties 278  
 occurrence and distribution 271, 272

- physical properties 278  
production and uses 272
- Diarsane,  $\text{As}_2\text{H}_4$  583  
*see also* Arsenic hydrides
- Diaspore 243
- Diatomaceous earth 342
- Diatomic molecules (homonuclear), bond dissociation energies of 584
- Diazotization of aromatic amines 463
- Dibenzenechromium 940, 1039  
*see also* Benzene as  $\eta^6$  ligand
- Diborane,  $\text{B}_2\text{H}_6$  154, 159  
chemical reactions 163–170  
cleavage reactions 165  
hydroboration reactions 166, 183  
preparation 164  
pyrolysis 164
- Dibromonium cation  $\text{Br}_2^+$ , compound with  $\text{Sb}_3\text{F}_{16}^-$  569
- Dicacodyl,  $\text{As}_2\text{Me}_4$  583–585
- Dichlorine hexoxide,  $\text{Cl}_2\text{O}_6$  844, 845, 849, 850
- Dichlorine monoxide,  $\text{Cl}_2\text{O}$  844–847
- Dichromate ion,  $\text{Cr}_2\text{O}_7^{2-}$  1009
- Dicyandiamide 320, 324
- Dielectric constant, influence of H bonding 55
- Dihydrogen 34  
coordination chemistry of 44–7
- Dimethylaminophosphorus dihalides 533
- Dimethyl sulfoxide as ionizing solvent 694
- Dinitrogen  
complexes, synthesis of 413, 414  
coordination modes 415  
discovery of donor properties 414, 1097  
isoelectronic with  $\text{CO}$ ,  $\text{C}_2\text{H}_4$  416  
as ligand 408, 413–416
- Dinitrogen monoxide *see* Nitrous oxide
- Dinitrogen pentoxide  $\text{N}_2\text{O}_5$  444, 458
- Dinitrogen tetroxide 444, 454–458  
chemical reactions 456–458  
nonaqueous solvent properties 456–458  
physical properties 456, 457  
preparation 456  
structure 455  
*see also* Nitrogen dioxide
- Dinitrogen trioxide,  $\text{N}_2\text{O}_3$  444
- Diopside 349
- Dioxygen  
bonding in metal complexes 619–620  
chemical properties 612, 613  
coordination chemistry of 615  
difluoride 639  
molecular-orbital diagram 606  
paramagnetic behaviour 601  
reactions of coordinated  $\text{O}_2$  619–620  
reaction with haemoglobin 614, 1099–1101  
singlet state 607, 614, 716  
singlet-triplet transitions 606  
superoxo and peroxo complexes 615, 616  
Vaska's discovery of reversible coordination 615, 1135  
*see also* Oxygen, Oxygen carriers, Singlet
- Diphosphazenes 535
- Diphosphonic acid *see* Diphosphorous acid
- Diphosphoric acid,  $\text{H}_4\text{P}_2\text{O}_7$  510, 516, 518
- Diphosphorous acid,  $\text{H}_4\text{P}_2\text{O}_5$  512
- Diphosphorus tetrahalides 497
- Disilenes 362
- Disulfates,  $\text{S}_2\text{O}_7^{2-}$  705, 712  
imido derivatives 743  
preparation in liquid  $\text{SO}_2$  700
- Disulfites,  $\text{S}_2\text{O}_5^-$  705, 720
- Disulfuric acid,  $\text{H}_2\text{S}_2\text{O}_7$  705, 711
- Disulfurous acid,  $\text{H}_2\text{S}_2\text{O}_5$  853, 705, 720
- Dithiocarbamates 317  
as ligands 665, 673, 674, 796
- Dithiolenes as ligands 665, 674–676
- Dithionates,  $\text{S}_2\text{O}_6^{2-}$  705, 715
- Dithionic acid,  $\text{H}_2\text{S}_2\text{O}_6$  705, 715
- Dithionites,  $\text{S}_2\text{O}_4^{2-}$  705, 720
- Dithionous acid,  $\text{H}_2\text{S}_2\text{O}_4$  705, 720
- DNA *see* Deoxyribonucleic acids
- Döbereiner's triads 21
- Dodecahedral complexes 916
- Dolomite 109, 272
- Donor-acceptor complexes  
of  $\text{AlX}_3$  235–237  
of  $\text{AsX}_3$  552, 564  
of  $\text{CN}^-$  321, 322  
of  $\text{CO}$  *see* Carbonyls  
of *cyclo*-polyarsanes 584–586  
of *cyclo*-polyphosphazenes 540  
of dithiocarbamates and xanthates 673, 674, 1080  
of dithiolenes 674  
first ( $\text{H}_3\text{NBF}_3$ ) 408  
of  $\text{GaH}_3$  232  
of Group 13 halides 237–239  
of  $\text{H}_2\text{S}$  673, 673, 714  
of  $\text{N}_2$  414–416, 1097  
of  $\text{NO}$  *see* Nitrosyls  
of  $\text{O}_2$  615–620  
of  $\text{PH}_3$  and tertiary phosphines 493–495  
of  $\text{PX}_3$  495, 497  
of  $\text{S}_n$  665–672  
of  $\text{SbF}_5$  561, 569, 570, 702  
of  $\text{SCN}^-$  324–327, 345  
of  $\text{SF}_4$  686  
of  $\text{S}_4\text{N}_4$  723  
of  $\text{SO}$ ,  $\text{S}_2\text{O}_2$ ,  $\text{SO}_2$  700–703  
of  $\text{SO}_3$  703, 704  
stability of 198  
*see also* Class-a and class-b metal ions, Coordinate bond, Ligands, individual elements
- Double-helix structure of nucleic acids 474
- Downs cell 72, 73
- Dry batteries 1204
- Dubnium 1281–2
- Dysprosium 1229  
+4 oxidation state 1244  
*see also* Lanthanide elements
- e-Process in stars 8
- Effective atomic number (EAN) rule 921  
*see also* Eighteen electron rule
- Effective ionic radii, Table of 1295
- Eighteen electron rule 1037, 1104, 1109, 1112, 1134
- Einsteinium 1252, 1262  
*see also* Actinide elements

- Eka-silicon, Mendeleev's predictions 29
- Electrical properties, influence of H bonding 53
- Electric arc process of steelmaking 1072
- Electrofluorination 821
- Electron affinity 75, 82, 800
- Electron-counting rules  
for boranes 161  
for carbonyl clusters 1107, 1142, 1169  
for carboranes 181  
for gold-phosphine clusters 1197  
for metal-halide clusters 966, 1018, 1022  
for metallocarboranes 194
- Electron transfer reactions, mechanisms of 1124
- Electronegativity  
definition of 26  
periodic trends in 26
- Electronic structure and chemical periodicity 21–23
- Electronic structure of atoms 21–23
- Elements  
abundance in crustal rocks 1294  
bond dissociation energies of gaseous diatomic 584  
cosmic abundance 3ff, 12ff  
isotopic composition of 47  
table of atomic weights *see* inside back cover  
origin of 1, 5, 9ff, 12ff  
periodic table of *see* inside front cover  
periodicity in properties 20–31  
 $Z = 104$ –112, *see* Transactinide
- Ellingham diagram 308, 307, 369
- Emerald 107, 1003
- Enstatite 349
- Entropy and the chelate effect 910
- Equilibrium process in stars (e-process) 8
- Erbium 1229  
*see also* Lanthanide elements
- Ethene (ethylene) as a ligand 930, 931
- Eutrophication 478, 528
- Europium 1229  
+2 oxidation state 1239, 1240, 1241, 1248  
magnetic properties of 1243  
*see also* Lanthanide elements
- Exclusion principle (Pauli) 22
- Extended X-ray absorption fine structure (EXAFS) 1036
- f-block contraction 562, 1234
- Faraday's phosphide synthesis 489
- Faujasite 358
- Fehling's test 1181
- Feldspars 354, 358, 414
- Fenton's reagent 636
- Fermium 1252, 1262  
*see also* Actinide elements
- Fermi level, definition of 332
- Ferredoxins 1035, 1036, 1098, 1101–1103
- Ferricinium ion 1109
- Ferrites 1081, 1209
- Ferritin 1098, 1104
- Ferrocene  
bonding 938–939  
historical importance of 924, 1070, 1109  
physical properties 937  
reactions 1109–1112  
structure 937  
synthesis 938, 1109
- Ferrochrome 1003
- Ferroelectricity 57–58, 386, 571
- Ferromanganese 1041
- Ferromolybdenum 1003
- Ferrophosphorus 480, 492, 525
- Ferrosilicon alloys 330
- "Ferrous oxide",  $Fe_{1-x}O$ , nonstoichiometry in 643, 644
- Ferrovandium 977
- First short period, "anomalous" properties of 27
- Fischer (Karl) reagent 628
- Fischer-Tropsch process 309, 1106
- Fish population, relation to phosphate-rich waters 479
- Flint 328, 342
- Fluorapatite *see* Apatites
- Fluoridation and dental caries 447, 525, 791, 792
- Fluorides 820–821  
solubility in HF 817  
synthesis 820–821
- Fluorinated peroxo compounds 639, 640
- Fluorinating agents 820–821  
 $AsF_3$ ,  $SbF_3$  560  
 $AsF_5$ ,  $BiF_5$ ,  $SbF_5$  562, 563
- Fluorine  
abundance and distribution 795  
atomic and physical properties 800–804  
chemical synthesis of 821  
history 789–792  
isolation 789, 791  
oxides *see* Oxygen fluorides  
oxoacid, HOF 789, 853, 856  
preparation of fluorides using 820  
production and uses 796–798  
radioactive isotopes 801, 802, 936  
reactivity 804–806  
stereochemistry 806  
toxicity 792, 810  
*see also* Halogens
- Fluorite,  $CaF_2$  109  
crystal structure of 117
- Fluorspar 789, 790  
fluorescence 789, 790  
*see also* Fluorite
- Fluorosulfuric acid 689
- Fluxional behaviour *see* Stereochemical non-rigidity
- Francium  
abundance 68  
discovery 68  
*see also* Alkali metals
- Frasch process for sulfur 646
- Freons (eg  $CCl_2F_2$ ) 304, 791
- Friedel-Crafts catalysis  
 $AlX_3$  complexes 171, 176, 186, 235, 236, 338  
 $BF_3$  complexes 199  
 $SnCl_4$  385
- Fullerenes  
chemical properties 282–7  
discovery 279  
incorporation of heteroatoms 287–9  
structure 280
- Fullerides 285
- Fullerols 284

- Fuller's earth *see* Montmorillonite  
 "Fulminating" silver and gold 1180  
 Fulminate ion 319, 433  
 Fundamental physical constants, Table of values back end paper  
 "Fusible white precipitate" 1219
- g (gerade), definition 938  
 Gabbro rock 358  
 Gadolinium 1229  
   diiodide 1242  
   *see also* Lanthanide elements  
 Galena (Pb glance) 649  
   roasting reactions 677  
   *see also* Lead sulfide  
 Gallane 231  
 Gallium  
   abundance 218  
   arsenide, semiconductor 221  
   chalcogenides 252, 253  
   III-V compounds 256  
   discovery 216  
   as eka-aluminium 216  
   hydride 231  
   hydride halides 232  
   lower halides 240  
   organometallic compounds 262-266  
   oxides 246  
   production and uses 219  
   sulfides 285, 286  
   trihalides 237  
   *see also* Group 13 elements  
 Gallium, ion, hydration number of 605  
 Garnets 348  
   magnetic properties of 946, 1081  
 Garnierite 1145  
 Germanes *see* Germanium hydrides  
 Germanium  
   abundance 368  
   atomic properties 371, 372  
   chalcogenides 389, 390  
   chemical reactivity and group trends 373, 375  
   cluster anions 393  
   dihalides 376  
   dihydroxide 382  
   dioxide 383  
   discovery 367  
   halogeno complexes 376  
   hydrides 374, 373  
   hydrohalides 375  
   isolation from flue dust 369  
   monomeric Ge(OAr)<sub>2</sub> 390  
   monoxide 376, 382  
   organo compounds 376, 396, 404  
   physical properties 371, 372  
   silicate analogues 383  
   sulfate 387  
   tetraacetate 387  
   tetrahalides 375, 377  
   uses 369  
 Germanocene 398  
 German silver 1146  
 Germenes 397  
 Germylenes 397  
 Gibbs' phase rule 676  
 Gibbsite 243, 245, 352  
 Girbotol process 311  
 Glassmaker's soap 1048  
 Gold  
   abundance 1174  
   alkyls 1180, 1200  
   chalcogenides 1181-1182  
   cluster compounds 1197, 1198  
   complexes  
     +3 oxidation state 1188-1189  
     +2 oxidation state 1189  
     +1 oxidation state 1196  
     lower oxidation states 1197  
     with S 666  
   halides 1183-1184  
   history 1173  
   nitrate complexes 469, 471  
   organometallic compounds 925, 1199-1200  
   oxide 1181  
   production and uses 1367, 1174,  
   *see also* Group 11 elements  
 Goldschmidt's geochemical classification  
 Graham's salt 528-531  
 Graphite  
   alkali metal intercalates 293  
   chemical properties 289-292  
   halide intercalates 295, 295  
   intercalation compounds 293-294  
   monofluoride 289  
   occurrence and distribution 270  
   oxide 289, 290  
   oxide intercalates 296  
   physical properties 278  
   production and uses 271  
   structure 275  
   subfluoride 289-290  
 Greek alphabet *see* back end paper  
 Greenhouse effect 273, 687  
 Grignard reagents 131-136  
   allyl 933  
   constitution of 131, 132  
   crystalline adducts of 133  
   preparation of 132  
   Schlenk equilibrium 131, 132  
   synthetic uses of 134, 135, 151  
 Group 0 elements *see* Noble gases  
 Group 1 elements *see* Alkali metals  
 Group 2 elements *see* Alkaline earth metals  
 Group 3 elements (Sc, Y, La; Ac)  
   atomic and physical properties 946, 947  
   chemical reactivity 948-949  
   group trends 948-949  
   high coordination, numbers 952  
   oxidation states lower than +3 949, 950  
   *see also* individual elements and Lanthanide elements  
 Group 4 elements (Ti, Zr, Hf)  
   atomic and physical properties 957-958  
   coordination numbers and stereochemistries 960  
   group trends 957-960

- Group 4 elements (Ti, Zr, Hf) — *contd*  
 oxidation states 960  
*see also* Titanium, Zirconium, Hafnium, Rutherfordium
- Group 5 elements (V, Nb, Ta)  
 atomic and physical properties 978  
 coordination numbers and stereochemistries 980  
 group trends 979, 980  
 oxidation states 980  
*see also* Vanadium Niobium, Tantalum, Dubnium
- Group 6 elements (Cr, Mo, W)  
 atomic and physical properties 1004, 1008  
 coordination numbers and stereochemistries 1006  
 group trends 1005  
 oxidation states 1006  
*see also* Chromium, Molybdenum, Tungsten
- Group 7 elements (Mn, Tc, Re)  
 atomic and physical properties 1043  
 coordination numbers and stereochemistries 1046  
 group trends 1044, 1045  
 oxidation states 1046  
 oxoanions 1049, 1050  
 redox properties 1044, 1045  
*see also* Manganese, Technetium, Rhenium
- Group 8 elements *see* Iron, Ruthenium, Osmium
- Group 9 elements *see* Cobalt, Rhodium, Iridium
- Group 10 elements *see* Nickel, Palladium, Platinum
- Group 11 elements (Cu, Ag, Au)  
 atomic and physical properties 1176, 1177  
 coordination numbers and stereochemistries 1179, 1180  
 group trends 1177–1180  
 oxidation states 1179  
*see also* Copper, Silver, Gold
- Group 12 elements (Zn, Cd, Hg)  
 atomic and physical properties 1203, 1205  
 coordination numbers and stereochemistries 1207  
 group trends 1205–1208  
*see also* Zinc, Cadmium, Mercury, Element 112
- Group 13 elements (B, Al, Ga, In, Tl)  
 amphoteric behaviour of Al, Ga 225  
 atomic properties 222  
 chemical reactivity 224–227  
 group trends 223–227, 237  
 +1 oxidation state 224, 227  
 physical properties 222, 224  
 trihalide complexes, stability of 237–239  
 unusual stereochemistries 256  
*see also* individual elements
- Group 14 elements *see* Carbon, Silicon, Germanium, Tin, Lead
- Group 15 elements  
*see* Nitrogen, Phosphorus, Arsenic, Antimony, Bismuth
- Group 16 elements *see* Oxygen, Sulfur, Selenium, Tellurium, Polonium
- Group 17 elements *see* Halogens
- Guanidine 305
- Guanine 61, 62
- Guano 408
- Gunpowder 645, 646
- Gypsum 109, 122  
 diluent in superphosphate fertilizer 525  
 occurrence in evaporites 647  
 process for H<sub>3</sub>PO<sub>4</sub> manufacture 521, 522  
 S recovery from 651, 652
- H bridge-bond in boranes and carboranes 154
- Haber–Bosch ammonia synthesis 408, 409,  
 historical development 421  
 production statistics 421  
 technical details 421
- Haem 126, 1099
- Haematin 1099
- Haematite 1071
- Haemocyanin 1199
- Haemoglobin 1098–1101
- Hafnates 964
- Hafnium  
 abundance 955  
 alkyls and aryls 973  
 carbonyls 973  
 complexes  
   +4 oxidation state 967–969  
   +3 oxidation state 969  
   lower oxidation states 971  
 compounds with oxoanions 966, 967  
 cyclopentadienyls 973–975  
 dioxide 962  
 discovery 954  
 halides 964–966  
 neutron absorber 965, 1258  
 organometallic compounds 973–975  
 production and uses 956  
 sulfides 962  
*see also* Group 4 elements
- Hahnium, *see* Dubnium
- Halates, XO<sub>3</sub><sup>−</sup> 862–866  
 astatate 885  
 disproportionation 855
- Halic acids, HOXO<sub>2</sub> 862–863
- Halides 819–824  
 astatide 886  
 intercalation into graphite 294, 295  
 synthesis of 819–823  
 trends in properties 823  
*see also* individual elements: Al, As, Be, B, etc. *and*  
 individual halides: Br<sup>−</sup>, Cl<sup>−</sup>, etc.
- Halites, XO<sub>2</sub><sup>−</sup> 859–862
- Hall effect 258, 549, 552, 1017
- Halogen cations, X<sub>n</sub><sup>+</sup> 842–844  
*see also* Polyhalonium cations
- Halogen(I) fluorosulfates, XO<sub>2</sub>F 883–885
- Halogen(I) nitrates XONO 883, 884
- Halogen(I) perchlorates, XOClO<sub>3</sub> 883, 884
- Halogens (F, Cl, Br, I, At) 784–887  
 abundance and distribution 795, 796  
 atomic and physical properties 800–804  
 charge-transfer complexes 806–809  
 history (time charts) 790, 791  
 origin of name 789, 790  
 production and uses 796, 800  
 reactivity towards graphite 296  
 stereochemistry 806  
*see also* individual elements, Interhalogen compounds
- Halous acids, HOXO 859, 861
- Hammett acidity function *H*<sub>0</sub> 51, 52
- Hapticity  
 classification of organometallic compounds 925  
 distinction from connectivity 925, 928

- Hassium 1281, 1283  
Hausmannite 1041, 1049  
Heat of vaporization, influence of H bonding 54  
Heavy water 39  
Helium  
  abundance in universe 3  
  atomic and physical properties 891, 890  
  discovery 888  
  production and uses 889, 890  
  thermonuclear reactions in stars 10  
  *see also* Noble gases  
Hemimorphite 348  
Hertzprung–Russell diagrams 6  
Heteropoly blues 1015  
Heteropolymolybdates 1013, 1015  
Heteropolytungstates 1013, 1015  
Heteropolyvanadates  
Hexamethylphosphoramide 532  
Hexathionates,  $S_6O_6^{2-}$ , preparation and structure 717, 718, 851  
High temperature superconductivity 945, 1183–3, 1232  
High–alumina cement 251  
High-spin complexes 923  
Hittorf's allotrope of phosphorus 482  
Holmium 1229  
  *see also* Lanthanide elements  
"Horn silver" 1174  
Hume–Rothery rules 1178  
Hydrargillite 243, 245  
Hydrazido complexes with metals 430  
  *see also* Dinitrogen as a ligand  
Hydrazine 408, 422, 427–431  
  acid-base properties 428  
  as a bridging ligand 431  
  hydrate 429, 430  
  industrial production 429  
  methyl derivatives as fuels 429  
  molecular structure and conformation 427, 428  
  oxidation of 434  
  preparation 427  
  properties of 427  
  reaction with nitrous acid 432  
  reducing properties 430  
  uses 429  
  water treatment using 429  
Hydrides, binary 64–67  
  acid strength of 48  
  bonding in 64  
  of boron *see* Boranes  
  classification of 64  
  complex 67  
  covalent 64, 67  
  interstitial 67  
  ionic 64, 65  
  nonstoichiometric 66, 67  
  and periodic table 65  
  of sulfur *see* Sulfanes  
  *see also* individual elements  
Hydroboration *see* Diborane  
Hydrochloric acid, HCl(aq) 790, 792, 809, 812  
  azeotrope 815  
Hydrofluoric acid, HF(aq) 790  
  acid strength of 814  
  azeotrope 815  
  preparation of fluorides using 820–821  
Hydroformylation of alkenes 309, 1135, 1140  
Hydrogen  
  abundance (terrestrial) 32  
  abundance in universe 2  
  atomic properties 34  
  chemical properties 43  
  cyanide, H bonding in 55  
  as the essential element in acids 32  
  history of 32, 33  
  industrial production 38  
  ionized forms of 36  
  isotopes of 34  
  *see also* Deuterium, Tritium  
  *ortho*- and *para*- 32, 35  
  physical properties of 34  
  portable generator for 39  
  preparation 38  
  stereochemistry of 44  
  *see also* Dihydrogen  
  thermonuclear reactions in stars 9  
  variable atomic weight of 17  
Hydrogen azide,  $HN_3$  432, 433  
Hydrogen bond 33, 52–64  
  in ammonia 423  
  in aquo complexes 625  
  bond lengths (table) 60  
  comparison with BHB bonds 64  
  in DNA 61, 62  
  and ferroelectricity 57  
  in HF 812, 813  
  influence on properties 53  
  influence on structure 59  
  in proteins and nucleic acids 61, 62  
  and proton nmr 56  
  strength of X-ray and neutron diffraction 56  
  theory of 63  
  and vibrational spectroscopy 56  
  in water 623  
Hydrogen bromide, HBr  
  azeotrope 815  
  hydrates 815  
  physical properties 813  
  production and uses 811, 812  
Hydrogen chloride, HCl  
  hydrates 813, 814  
  nonaqueous solvent properties 813  
  physical properties 813  
  production and uses 811–812  
  *see also* Hydrochloric acid  
Hydrogen dinitrate ion,  $[H(NO_3)_2]^-$  468  
"Hydrogen economy" 39, 39  
Hydrogen fluoride, HF 809–810  
  H bonding in 52–53, 812  
  hydrates 814  
  nonaqueous solvent properties 816–818  
  physical properties 812, 813  
  preparation of fluorides using 820  
  production and uses 809–811  
  skin burns, treatment of 810  
  *see also* Hydrofluoric acid



- Hydrogen halides, HX 809–819  
 chemical reactivity 813–816  
 nonaqueous solvent properties 816–819  
 physical properties 812, 813  
 preparation and uses 809–812
- Hydrogen iodide, HI  
 azeotrope 815  
 hydrates 815  
 physical properties 812  
 production and uses 811, 812
- Hydrogen-ion concentration *see* pH scale
- Hydrogen peroxide 633  
 acid-base properties 636–638  
 chemical properties 634, 638  
 physical properties 633, 634, 635  
 preparation 633  
 production statistics 634  
 redox properties 634–637  
 structure 635  
 uses of 633–634
- Hydrogen sulfate ion,  $\text{HSO}_4^-$  705, 706, 711–713
- Hydrogen sulfide,  $\text{H}_2\text{S}$   
 chemistry 682  
 as ligand 665, 673  
 molecular properties 682, 767  
 occurrence in nature 646–648, 651, 771  
 physical properties 682, 767  
 preparation (laboratory) 682  
 protonated  $[\text{SH}_3]^+$  683  
*see also* Sulfanes, Wackenroder's solution
- Hydrogen sulfite ion,  $\text{HSO}_3^-$  705, 719
- Hydrometalation 926
- Hydronitrous acid *see* Nitroxyl acid
- Hydroperoxides 636
- Hydroxonium ion,  $\text{H}_3\text{O}^+$  628–631, 814, 815
- Hydroxyl ion, hydration of 630, 632
- Hydroxylamine 422, 431–432  
 configurational isomers 432, 432  
 hydroxylamides of sulfuric acid 744–746  
 preparation 495, 431, 432  
 properties 495, 431, 432
- Hypersensitive bands in spectra of lanthanides 1244
- Hypobromous acid,  $\text{HOBr}$  853, 855, 857, 858
- Hypochlorite,  $\text{OCl}^-$  854, 855, 857–859  
 molecular hypochlorites 859
- Hypochlorous acid,  $\text{HOCl}$  853–859  
 preparation 857  
 reactions 858–859  
 uses 860
- Hypofluorites (covalent) 639, 688
- Hypofluorous acid,  $\text{HOF}$  638, 639  
 preparation 791, 853, 856
- Hypohalates,  $\text{OX}^-$  853–859
- Hypohalous acids,  $\text{HOX}$  853–859
- Hypoiodous acid,  $\text{HOI}$  853–859
- Hyponitric acid,  $\text{H}_2\text{N}_2\text{O}_3$  530, 459
- Hyponitrites 459–461
- Hyponitrous acid,  $\text{H}_2\text{N}_2\text{O}_2$  459–459
- Hypophosphoric acid (diphosphoric(IV) acid),  $\text{H}_4\text{P}_2\text{O}_6$   
 512, 515–516  
 isomerism to isohypophosphoric acid 515
- Hypophosphorous acid,  $\text{H}_3\text{PO}_2$  512, 513
- Hypophosphites 513, 516  
 “Hyposulphite” used in photography 1186, 1196
- Icosagens 227
- Icosahedron, symmetry elements of 141
- Ilmenite 955, 960, 963
- Inclusion compounds 985  
*see also* Clathrate compounds
- Indium  
 abundance 218  
 chalcogenides 252–254  
 III–V compounds 255–258  
 discovery 216  
 lower halides 240  
 organometallic compounds 262,  
 oxide 247  
 production and uses 219  
 trihalides 237, 238  
*see also* Group 13 elements
- Industrial chemicals, production statistics 407  
*see also* individual elements
- Industrial Revolution 1070, 1072
- Inert-pair effect 27  
 in Al, Ga, In, Tl 226  
 in Ge, Sn, Pb 374  
 in P, As, Sb, Bi 553, 566, 568
- “Infusible white precipitate” 1219
- Inner-sphere reactions 1124
- Ino-silicates 347, 349–351
- Interelectronic repulsion parameter  
 for hexaquo chromium(III) 1029  
 for hexaquo vanadium(III) 996  
 for high-spin complexes of cobalt(III) 1127  
 for high-spin complexes of cobalt(II) 1132
- Interhalogen compounds 824–828  
 diatomic, XY 824–828, 833  
 first preparation 790, 791  
 hexa-atomic,  $\text{XF}_5$  832–835  
 octa-atomic,  $\text{IF}_7$  832–835  
 tetra-atomic,  $\text{XY}_3$  828–831, 833  
*see also* Polyhalide anions, Polyhalonium cations
- Invar 1146
- Iodates,  $\text{IO}_3^-$  862, 863  
 reaction scheme 866  
 redox systematics 854–856
- Iodic acid,  $\text{HIO}_3$  863, 864, 866
- Iodides, synthesis of 822  
*see also* individual elements
- Iodine  
 abundance and distribution 795  
 atomic and physical properties 800–804  
 cations  $\text{I}_n^+$  842–844  
 charge-transfer complexes 806–809  
 colour of solutions 806–809  
 crystal structure 803  
 goitre treatment 790, 794  
 heptafluoride 832–835  
 history 790, 791, 793  
 Karl Fischer reagent for  $\text{H}_2\text{O}$  627  
 monohalides 824–828, 833  
 oxoacids and oxoacid salts 853  
 nomenclature 853

- redox properties 854–856  
*see also* individual compounds, Iodic acid, Iodates,  
 Periodic acids, Periodates, etc.  
 oxide fluorides 881–883  
 oxides 851–853  
 pentafluoride 832–834  
 “pentoxide”,  $I_2O_5$  851–853  
 production and uses 799, 800  
 radioactive isotopes 801, 802  
 reactivity 805  
 standard reduction potentials 854  
 stereochemistry 806  
 trichloride 828–829, 831, 833  
 trifluoride 828, 830, 831, 833  
 volt equivalent diagram 855  
*see also* Halogens  
 Iodine trichloride, complex and  $SbCl_5$  568  
 Iodyl fluorosulfate,  $IO_2SO_2F$  882  
 Ionic-bond model 79–81, 963  
 deviations from 81  
 Ionic radii 80, 81  
 table of 1295  
 Ionization energy, periodicity of 24  
 Iridium  
 abundance 1113  
 atomic and physical properties 1115–1116  
 carbonyls 928, 1140–1143  
 complexes  
   +5 oxidation state 1121  
   +4 oxidation state 1121–1122  
   +3 oxidation state 1121, 1127, 1129  
   +2 oxidation state 1129–1130  
   +1 oxidation state 1133–1137  
   lower oxidation states 1137  
   with  $SO_2$  702  
 coordination numbers and stereochemistries 1117  
 cyclopentadienyls 1143  
 discovery 1113  
 halides 1119–1121  
 organometallic compounds 1139–1143  
 oxidation states 1117  
 oxides 1117, 1118  
 production and uses 1114  
 reactivity of element 1116  
 relationship with other transition elements 1116–1117  
 sulfides 1117  
 Iron  
 abundance 1071  
 allyls 933  
 alums 1088  
 atomic and physical properties 1074  
 biochemistry of 1098  
 bis (cyclopentadienyl) *see* Ferrocene  
 carbidocarbonyls 1107–1108  
 carbonyl halides 1108  
 carbonyl hydrides and carbonylate 1107  
 carbonyls 928, 1071, 1104  
 chalcogenides 1080, 1081  
 complexes  
   +3 oxidation state 1088–1091  
   +2 oxidation state 1091–1095  
   lower oxidation states 1098  
   with S 666, 671  
   with SO 696  
   with  $SO_2$  702  
 coordination numbers and stereochemistries  
 cyclooctatetraene complexes 945  
 cyclopentadienyls 1109–1112  
   *see also* Ferrocene  
 dithiocarbamate complexes 673, 1090  
 electronic spin states 1079  
 halides 1083–1085  
 history 1070, 1072  
 mixed metal oxides (ferrites) 1081  
 organometallic compounds 937, 1104–1112  
 oxidation states 1077, 1078  
 oxides 1079, 1080  
 oxoanions 1081, 1121  
 production and uses 1071–1072  
 proteins 1098–1104  
 reactivity of element 1075  
 relationship with other transition elements 1077  
 standard reduction potentials 1077, 1093, 1101  
 Iron age 1070  
 Iron pyrites  
   reserves of 651  
   source of S 759–649  
   structure 555, 557, 680  
 Iron-sulfur proteins 1102–1104  
 Irving-Williams order 909,  
 Isocyanates 319, 322  
   as polyurethane intermediates 305  
 Isohyphosphoric acid [diphosphoric (III,  $H_4P_2O_6$ )] 512,  
   515, 516  
 Isomerism 918  
   *cis-trans* 919, 1128  
   ‘classical-nonclassical’ in organoboron structures 186  
   conformational 918  
   coordination 920  
   *fac-mer* 919  
   geometrical 919  
   ionization 920  
   ligand 921  
   linkage 920  
   optical 919  
   polymerization 921  
   polytopal 918  
   *syn-anti* 935  
 Isopolymolybdates 1175–1183  
 Isopolyniobates 987  
 Isopolytantalates 987  
 Isopolytungstates 1175–1183  
 Isopolyvanadates 1146–1150  
 Isotopes, definition of 22  
  
 Jahn-Teller effect 1021  
   in  $Cu^{II}$  1190  
   in high-spin  $Cr^{II}$  1021, 1032  
   in high-spin  $Mn^{II}$  1049, 1057  
   in low-spin  $Co^{II}$  1133  
   in  $Ti^{III}$  970  
 Jasper 342  
 Joliotium, *see* Dubnium

- Kaolinite 349, 352–354, 357  
 Karl Fischer reagent 627  
 Keatite 342, 343  
 Keggin structure 1014, 1015  
 Keiselguhr 342  
 Kinetic inertness  
   of chromium(III) complexes 1027  
   of cobalt(III) complexes 1123  
 Kirsanov reactions 535  
 Kraft cheese process 524  
 Kraft paper process 89  
 Kroll process 955, 956  
 Krypton  
   atomic and physical properties 801, 890  
   clathrates 893  
   compounds of 903  
   discovery 889  
   *see also* Noble gases  
 Kupfernickel 1144, 1145  
 Kurchatovium *see* Rutherfordium  
 Kurrol's salt 528–531
- Landolt's chemical clock 864  
 Lanthanide contraction 27, 1232, 1234  
 Lanthanide elements  
   abundance 1229  
   alkyls and aryls 249  
   aquo ions 1245  
   arsenides 555  
   atomic and physical properties 1232–1235  
   carbonyls 1238  
   chalcogenides 679, 1238, 1239  
   complexes 1244–1248  
   coordination numbers and stereochemistries 1236, 1237  
   cyclopentadienides 1238  
   group trends 1232–1237  
   halides 1240–1242  
   history 1228, 1228  
   magnetic properties 1242–1244  
   organometallic compounds 1248, 1249  
   +2 oxidation state 1240, 1248  
   +4 oxidation state 1240, 1244  
   oxides 1238, 1239  
   production and uses 1230–1232  
   as products of nuclear fission 1228, 1251, 1260  
   separation of individual elements 1424, 1426–1428  
   spectroscopic properties 1242–1244  
   *see also* individual elements and Group 3 elements  
 Lanthanoid *see* Lanthanide elements  
 Lanthanon *see* Lanthanide elements  
 Lanthanum  
   abundance 945  
   complexes 950–953  
   discovery 944, 1228  
   halides 949–950  
   organometallic compounds 953  
   oxide 949  
   production and uses 945–946  
   salts with oxoanions 949  
   *see also* Group 3 elements, Lanthanide elements  
 Lapis lazuli 359  
 Laser, ruby 1029
- Lattice defects, nonstoichiometry 643  
   *see also* Spinel (inverse) and individual elements  
 Lattice energy  
   calculation of 82  
   of hypothetical compounds 83  
   Lawrencium 1252, 1262  
   *see also* Actinide elements  
 Lead  
   abundance 368  
   alloys 371  
   in antiquity 367  
   atomic properties 371  
   atomic weight variability 368  
   benzene complex with Pb<sup>II</sup> 405  
   bis(cyclopentadienyl) 395, 404  
   chalcogenides 389  
   chemical reactivity and group trends 435, 373,  
   cluster anions 374, 393  
   cluster complexes 387, 395  
   dihalides 375, 381, 382  
   dinitrate 388  
   halogeno complexes 382  
   hydride 375  
   hydroxo cluster cation 395  
   isolation and purification 369–371  
   metal–metal bonded compounds 392  
   mixed dihalides 382  
   monomeric Pb(OAr)<sub>2</sub> 390  
   monoxide 383, 384, 386, 395  
   nitrate, thermolysis of 456, 469  
   nonstoichiometric oxides 385–387  
   organohydrides 375  
   organometallic compounds 402–405  
   oxides, nonstoichiometric 384–387  
   oxides, uses of 386  
   oxoacid salts 388  
   Pb–S–O system 677  
   physical properties 371, 372  
   pigments 386, 388  
   production statistics 369, 370, 371  
   pseudohalogen derivatives 389  
   radiogenic origin 368  
   sulfate 388  
   tetraacetate 388  
   tetrafluoride 388  
   tetrahalides 375, 381  
   toxicity 367, 368  
   uses 371, 386  
 Lead chamber process for H<sub>2</sub>SO<sub>4</sub> 646  
 Leblanc process for NaOH 71, 790  
 Lewis acid (acceptor) 905  
   *see also* Donor-acceptor complexes, Class-a and class-b  
   metals  
 Lewis base (donor) 198, 905  
   *see also* Donor-acceptor complexes, Ligands  
 Lifschitz salts 1156, 1160  
 Ligand field theory 922  
 Ligands  
   ambidentate 907, 920  
   chelating 906  
   classification as “hard” and “soft” 326, 909  
   classification by number of donor atoms 906–907  
   macrocylic 907

- non-innocent 1055  
 "octopus" 99  
 tripod 907  
*see also* Class-a and class-b metals, Hapticity, Linkage isomerism, Synergic bonding
- Ligand polyhedral model 1105, 1140–1  
 Lime, production and uses of 119–121  
 Limestone, occurrence and uses 109, 120–121, 274  
 Limonite 1071, 1146  
 Linde synthetic zeolites 358, 359  
 Linkage isomerism  
   of nitrite ion 463, 464, 920  
   of SO<sub>2</sub> 702  
   of thiocyanate ion 326, 920
- Litharge *see* Lead monoxide
- Lithium  
   abundance 69  
   acetylide, synthetic use of 103  
   alkyls and aryls 102–106  
   aluminium hydride 228–9  
   "anomalous" properties of 75–76  
   compounds with oxygen 84, 85  
   coordination chemistry of 90–4  
   diagonal relationship with Mg 76, 102  
   discovery of 68  
   methyl, bonding in 103  
   methyl, structure of tetrameric cluster 103, 104, 113  
   organometallic compounds 102–106  
   production of metal 71, 73  
   reduction potential of 75, 76  
   stereochemistry of 91  
   terrestrial distribution of 69  
   variable atomic weight of 18  
*see also* Alkali metals
- Lithium compounds  
   industrial uses of 70  
   organometallics, synthesis of 102, 103  
   organometallics, synthetic uses of 105–106
- Lithium tetrahydroaluminate  
   synthetic reactions of 229
- Lithophile elements 648
- Lodestone 1080
- Loellingite structure 557
- Lone pair, stereochemical influence 377, 772, 775–777
- Lonsdaleite 274, 276
- Low-spin complexes  
   of cobalt(III), electronic spectra  
   of octahedral, d<sup>4</sup> ions, 1087
- Lutetium 1228  
*see also* Lanthanide elements
- Macrocyclic effect 911
- Macrocyclic polyethers *see* Crown ethers
- Maddrell's salt 528–531
- Madelung constant 83
- "Magic acid" 570
- "Magic numbers" in nuclear structure 3, 13
- Magma, crystallization of silicates from 329
- Magnéli-type phases  
   of molybdenum and tungsten oxides  
   of titanium oxides 959  
   of vanadium oxides 952
- Magnesium  
   alkyl alkoxides 133, 136  
   in biochemical processes 125  
   complexes of 123–126  
   cyclopentadienyl 136  
   diagonal relationship with Li 76, 102  
   dialkyls and diaryls 131–133  
   history of 108  
   organometallic compounds 131  
     *see also* Grignard reagents  
   porphyrin complexes of *see* Chlorophyll  
   production and uses of 110, 111  
*see also* Alkaline earth metals
- Magnetic moment  
   of low-spin, octahedral, d<sup>4</sup> ions 1087  
   orbital contribution to 1132, 1158  
*see also* individual transition elements, Spin equilibria
- Magnetic quantum number *m* 22
- Magnetite, Fe<sub>3</sub>O<sub>4</sub> 1071  
   inverse spinel structure 249, 1080
- Magnus's salt 1163
- Malachite 1174
- Malathion 509
- Manganates 1050, 1051, 1222
- Manganese  
   abundance 1040  
   allyl complexes 934  
   biochemistry of 1061–2  
   carbonyls 928, 1062–1064  
   chalcocogenides 1049  
   complexes  
     +4 oxidation state 1056  
     +3 oxidation state 1057–1058  
     +2 oxidation state 1058–1061  
     lower oxidation states 1061  
     with S 667–669  
     with SO<sub>2</sub> 702  
   cyclooctatetraene complex 943  
   cyclopentadienyls 1065–1067  
   dioxides 1045–1048  
     uses of 1048  
   halides and oxohalides 1051  
   nodules 1041  
   organometallic compounds 935, 943, 1062–1069  
   oxides 1045  
   production and uses 1041–1043  
*see also* Group 7 elements
- Manganin 1042
- Manganocene
- Marcasite structure 555–557, 680  
   mineral FeS<sub>2</sub> 648
- Marine acid 793
- Marsh's test for As 558
- Martensite 1075
- Masurium 1040  
*see also* Technetium
- Mass number of atom 22
- Matches 474, 509
- Meitnerium 1281, 1283
- Melamine 323
- Mellitic acid 289
- Melting points, influence of H bonding 54
- Mendeleev's periodic table 20

- Mendeleev, prediction of new elements 29, 217  
 Mendeleevium 1252, 1262  
*see also* Actinide elements  
 Mercaptans, origin of name 1220  
 Mercuration 1222  
 Mercury  
 abundance 1202  
 alkyls and aryls 1222  
 chalcogenides 1208, 1211  
 cyclopentadienyls 1223  
 halides 1211–1213  
 history 1173  
 organometallic compounds 926, 1222–1224  
 +1 oxidation state 1213–1215  
 +2 oxidation state 1413–1416  
 oxide 1208–1209  
 polycations 1214, 1215  
 production and uses 1203  
 sulfide, solubility of 638, 679  
 toxicity 1225  
 Mesoperiodic acid *see* Periodic acids  
 Metal cations  
 amphoteric 52  
 hydrolysis of 51  
 Metallocarbohedrenes (met-cars) 300  
 Metalloboranes 172–174, 178  
 Metallocarboranes 189–195  
 bonding 188, 190, 194  
 chemical reactions 195  
 structures 188  
 synthesis 189–191  
 Metallocenes *see* Ferrocene, individual metals  
 Metalloregulatory proteins 1226  
 Metaperiodic acid *see* Periodic acids  
 Metaphosphates *see* Chain polyphosphates,  
 Cyclo-polyphosphates  
 Metaphosphimic acid tautomers 541  
*see also* Tetrametaphosphimates  
 Metatelluric acid ( $H_2TeO_4$ )<sub>n</sub> 781  
 Methane 300  
 as greenhouse gas 274, 302  
 in Haber-Bosch  $NH_3$  synthesis 420  
 Methanides *see* Carbides  
 Methyl bridges  
 in  $Al_2Me_6$  258, 259  
 in  $BeMe_2$  127  
 in  $MgMe_2$  and  $Mg(AlMe_3)_2$  131  
 Methyl methacrylate 321  
 Methylene complexes *see* Carbene ligands  
 Methylparathion 509  
 Meyer's periodic table 21, 23  
 Meyer reaction 596  
 Mica 109, 349, 356–413  
 Millon's base 1218, 1220  
 Mischmetall 946, 1228  
 Mohorovicic discontinuity 358  
 Mohr's salt 1092  
 Molecular orbital theory of coordination compounds  
 922–924  
 Molecular sieves *see* Zeolites  
 Molybdates 1008–1016  
 Molybdenite,  $MoS_2$  649, 1003  
 Molybdenum  
 abundance 1002  
 benzene tricarbonyl 941  
 biological activity 1035–7  
 blues 1008  
 bronzes 1016  
 carbonyls 928, 1037, 1038  
 carbyne complexes 929  
 chalcogenides 1017–1018  
 complexes  
 +6 oxidation state 1023–1024  
 +5 oxidation state 1024–1025  
 +4 oxidation state 1025–1027  
 +3 oxidation state 1027–1031  
 +2 oxidation state 1031–1035  
 with S 666–669, 672  
 with  $SO_2$  702  
 compounds with quadruple metal–metal bonds  
 1032–1034  
 cyclopentadienyl compounds 933, 1038  
 discovery 1002  
 halides and oxohalides 1019  
 heteropolyacids and salts 1014–1016  
 isopolyacids and salts 1009–1014  
 nitrogen fixation, role in 1035–1037  
 nonstoichiometric oxides 1008  
 organometallic compounds 1037–1039  
 oxides 1007–1009  
 production and uses 1003, 1004  
*see also* Group 6 elements  
 Molybdic acid 1010  
 Molybdocene 1038  
 Molybdoferredoxin 1035, 1098  
 Monactin 96  
 Monazite 945, 1230, 1232, 1254  
 Mond process 1146,  
 Monel 1146  
 $\gamma$ -Monoclinic sulfur 655  
 Montmorillonite 349, 353, 356  
 Mössbauer spectroscopy  
 with  $^{57}Fe$  1094, 1095, 1096, 1101  
 with  $^{127}I$ ,  $^{129}I$  802, 838, 841  
 of nonstoichiometric oxides 642  
 with  $^{99}Ru$  1062  
 with  $^{119}Sn$  371  
 with  $^{125}Te$  753  
 with  $^{129}Xe$  898  
 Mother-of-pearl 122  
 Muriatic acid 792  
 Muscovite *see* Mica  
 Myoglobin 1098–1101  
 n–p–n junction *see* Transistor  
 n-type semiconductor *see* Semiconductor, Transistor  
 Nacreous sulfur 655  
 NADP 125  
 Names of elements having  $Z > 100$  30, 1252, 1280–1283  
 $NbS_2Cl_2$  structure 671  
 $NbS_2X_2$  667  
 Neodymium 1228  
 +2 oxidation state 1237, 1239, 1241

- +4 oxidation state 1244  
*see also* Lanthanide elements
- Neon  
 atomic and physical properties 891, 892  
 discovery 889  
*see also* Noble gases
- Neptunium 1252, 1262  
 bis(cyclooctatetraene) 942  
 radioactive decay series 1254  
*see also* Actinide elements
- Nernst equation (for electrode potentials) 435
- Neso-silicates 347, 348
- Nessler's reagent 1218
- Neutrons  
 fast 1256  
 slow, thermal 1256
- Newnham process for roasting PbS 677
- Nicolite (Kupfernickel) 1145
- Nichrome 1146
- Nickel  
 abundance 1145  
 alkene and alkyne complexes 1170–1172  
 $\pi$ -allylic complexes 933, 1172  
 "anomalous" behaviour of Ni<sup>II</sup> 1160, 1159  
 aryls 1168  
 atomic and physical properties 1148–1150  
 biochemistry of 1167  
 carbonyls 928, 929, 1168–1170  
 chalcogenides 1152  
 complexes  
   +4 oxidation state 1154  
   +3 oxidation state 1155  
   +2 oxidation state 1156–1162  
   +1 oxidation state 1166  
   zero oxidation state 1166, 1167  
   with SO<sub>2</sub> 702  
 coordination numbers and stereochemistries 1150  
 cyclobutadiene complexes 936  
 cyclopentadienyls 1170  
 dithiolene complexes, redox series 675  
 halides 1152, 1153  
 organometallic compounds 1167–1172  
 oxidation states 1150  
 oxides 1151, 1152  
 phosphides 489  
 production and uses 1145–1148  
 reactivity of elements 1149  
 tetracarbonyl 928, 929, 1168
- Nickel arsenide 555, 556, 649  
 relation to CdI<sub>2</sub> 556, 697  
 structure type 555, 556,
- Nickelocene 939, 1170,
- Nickel silver 1146
- Nielsbohrium, *see* Bohrium
- Niobates 987
- Niobium  
 abundance 977  
 alkyls and aryls 999  
 bronzes 987  
 carbonylate anions 980, 1000  
 chalcogenides 988  
 complexes  
   +5 oxidation state 994  
   +4 oxidation state 994–995  
   compounds with oxoanions 993  
   cyclopentadienyls 940, 1000–1001  
   discovery 976  
   halides and oxohalides 988  
   nonstoichiometric oxides 982  
   organometallic compounds 999–1001  
   oxides 982, 983  
   production and uses 977  
   *see also* Group 5 elements
- Nitramide, H<sub>2</sub>NNO<sub>2</sub> 459
- Nitrates 465, 467–472, 539–545  
 coordination modes 469–471  
 thermal stability 469  
*see also* individual elements
- Nitric acid 422, 456, 457, 459, 465–468  
 anhydrous 465, 467  
 hydrates 469, 468  
 industrial production 466, 467  
 industrial uses 467  
 ionization in H<sub>2</sub>SO<sub>4</sub> 711  
 self-ionic dissociation
- Nitric oxide, NO 422, 442  
 bonding in paramagnetic molecule 446  
 catalytic production from NH<sub>3</sub> 466  
 chemical reactions 446  
 colourless, not blue 446  
 complexes with transition metals *see* Nitrosyl complexes  
 crystal structure 446  
 dimeric 446  
 physical properties 446  
 preparation 445  
 reaction with atomic N 413
- Nitride ion, N<sup>3-</sup> 417  
 as ligand 418–419
- Nitrides 417–419
- Nitrido complexes *see* Nitride ion as ligand, also individual elements
- Nitriles *see* Cyanides
- Nitrite ion, NO<sub>2</sub><sup>-</sup>  
 coordination modes 463  
 nitro-nitrito isomerism 463, 464, 920
- Nitrites 422, 461–465  
*see also* Nitro-nitrito isomerism
- Nitrogen  
 abundance in atmosphere 406, 407–409  
 abundance in crustal rocks 407  
 active *see* atomic  
 atomic, production and reactivity of 412, 413  
 atomic properties 411, 412, 550  
 atypical group properties 416, 550  
 chemical reactivity 412–416  
 comparison with C and O 416  
 comparison with heavier Group 15 elements 416, 551, 577  
 cycle in nature 406, 408, 410  
 dinitrogen tetrafluoride 439, 440  
 dioxide 444, 455, 612  
*see also* Dinitrogen tetroxide  
 discovery 406

- Nitrogen — *contd*  
 fixation, industrial 466  
   *see also* Haber-Bosch ammonia synthesis  
 fixation, natural 999, 1035–1037, 1098, 1102  
 halides 438–441  
 history 407, 408  
 hydrides of 426–433  
   *see also* Ammonia, Hydrazine, Hydroxylamine  
 industrial uses 409  
   isotopes, discovery of 408  
 isotopes, separation of 142  
 ligand 408  
 monoxide *see* Nitric oxide  
 multiple bond formation 416, 417  
 oxidation states 434, 437  
 oxides 443–458  
   *see also* individual oxides  
 oxoacids 459–466  
   *see also* individual oxoanions  
 oxoanion salts *see* Nitrosyl halides, Nitryl halides  
 physical properties 412  
 production 411  
 standard reduction potential for N species 434  
 stereochemistry 413  
 synthesis of pure 409  
 tribromide 441  
 trichloride 441  
 trifluoride 438–439  
 triiodide, ammonia adduct 441  
 trioxide 444, 458  
   *see also* Dinitrogen  
 Nitrogenase 1035, 1098  
 Nitro-nitrito isomerism 463, 464, 920  
 Nitronium ion 458, 712  
 Nitroprusside ion 1094, 1095  
 Nitrosyl azide 433, 443  
 Nitrosyl trifluoride, ONF<sub>3</sub> 438, 439  
 Nitrosyl halides 441, 442  
 Nitrosyl complexes 447–453  
   coordination modes 450, 450–452  
   electronic structure of 450, 451  
   preparation 448, 449  
   *see also* individual elements  
 Nitrous acid 459, 461–462  
   reaction with hydrazine 432  
 Nitrous oxide, N<sub>2</sub>O 443–445  
   chemical reactions 443, 445  
   isotopically labelled 443  
   physical properties 442, 445  
   preparation 443  
   use in “whipped” ice cream 445  
 Nitroxyl 459, 461  
 Nitroxyl acid 459  
 Nitryl halides, XNO<sub>2</sub> 441  
 Nmr spectroscopy with:  
   <sup>10</sup>B 144  
   <sup>11</sup>B 144, 197  
   <sup>79,81</sup>Br 802, 803  
   <sup>13</sup>C 276, 326, 914, 995, 1104, 1105  
   <sup>35,37</sup>Cl 791, 802, 803  
   <sup>19</sup>F 197, 499, 562, 563, 684, 739, 791, 802–803, 817,  
   841, 904, 1022  
   <sup>1</sup>H 34, 56, 230, 532, 933, 935, 940, 973, 1111, 1129,  
   1135, 1165, 1223  
   <sup>2,3</sup>H 34  
   <sup>127</sup>I 802, 803  
   <sup>95</sup>Mo 1025  
   <sup>14</sup>N 326, 408, 411, 1025  
   <sup>15</sup>N 408, 411  
   <sup>17</sup>O 601, 604, 605, 630, 984, 1012  
   <sup>31</sup>P 474, 482, 516, 1165  
   <sup>195</sup>Pt 1165  
   <sup>33</sup>S 662  
   <sup>77</sup>Se 762, 769  
   <sup>29</sup>Si 330  
   <sup>119</sup>Sn 371  
   <sup>125</sup>Te 762  
   <sup>51</sup>V 985  
   <sup>183</sup>W 1012  
 NO *see* Nitric oxide  
 Nobel prize for Chemistry, list of laureates 1296–1299  
 Nobel prize for Physics, list of laureates 1300–1304  
 Nobelium 1252, 1463  
   *see also* Actinide elements  
 Noble gases (He, Ne, Ar, Kr, Xe, Rn) 888–904  
   atomic and physical properties 890–891  
   bonding in compounds of 897  
   chemical properties 892–904  
   clathrates 893  
   discovery 888, 889  
   production and uses 889, 890, 1044  
   *see also* individual elements  
 Nomenclature of elements having Z > 100 30, 1252,  
 1280–1283  
 Nonactin 96  
 Nonaqueous solvent systems  
   AsCl<sub>3</sub> 561  
   BrF<sub>3</sub> 820, 821  
   ClF<sub>3</sub> 829  
   HCl 819  
   HF 570, 816–819  
   H<sub>2</sub>SO<sub>4</sub> 710–712, 759  
   ICl 827  
   IF<sub>5</sub> 834  
   NH<sub>3</sub> 77–79, 424–426  
   SbCl<sub>3</sub> 561, 655  
   SO<sub>2</sub> 664, 700, 759  
   superacids 570  
 Non-haem iron proteins (NHIP) 1102, 1103  
 Nonstoichiometry  
   in chalcogenides 765, 766  
   in oxides 642–644  
   in sulfides 679  
   *see also* individual compounds  
 Nuclear fission 1256  
   products 1257, 1260  
   spontaneous 1253, 1262  
 Nuclear fuels 1257–1262  
   breeding 1259  
   enrichment 1259  
   reprocessing 1097, 1260–1262  
 Nuclear reactions in stars 7–13  
 Nuclear reactors 1256–1260  
   different types 1258  
   natural 1257

- Nuclear structure of atoms 22  
 Nuclear waste, storage 1257, 1261  
 Nucleic acid  
   definition  
   double helix structure of 474  
   and H bonding 60, 62  
 Nucleogenesis 2ff  
 Nylon-6 and -66, 422
- Obsidian 342  
 Octahedral complexes 914–916, 922–923  
   distortions in 915–916 *see also* Jahn–Teller effect  
 “Octopus” ligands 99  
 Oddo’s rule 3  
 Oklo phenomenon 1257  
 Oligomerization of acetylene 1172  
 Olivine 109, 347  
 One-dimensional conductors 1156, 1165  
 Onyx 342  
 Opal 342  
 Open-hearth process 1072  
 Optical activity 919, 1125  
 Optical isomers 915, 919, 1125  
 Optically active metal cluster compound 667  
 Optical rotatory dispersion (ORD) 1125  
 Orbital contribution to magnetic moment  
   of high-spin complexes of  $\text{Co}^{\text{II}}$  1132  
   of octahedral  $d^2$  ions 996  
   of octahedral  $d^4$  ions 1089  
   of tetrahedral complexes of  $\text{Ni}^{\text{II}}$  1158  
 Orbital degeneracy 1244  
 Orbital quantum number,  $l$  26,  
 Orford process 1146  
 Organometallic compounds 924–943  
   classification 924–925  
   definition 924  
   dihapto ligands 930–933  
   heptahapto ligands 941  
   hexahapto ligands 940–941  
   monohapto ligands 925–930  
   octahapto ligands 941–943  
   pentahapto ligands 937–940  
   tetrahapto ligands 935–937  
   trihapto ligands 933–935  
   *see also* individual elements and ligands  
 Orpiment *see* Arsenic sulfide,  $\text{As}_2\text{S}_3$   
 Orthonitrate ion,  $\text{NO}_4^{3-}$  472  
 Orthoperiodic acid *see* Periodic acids  
 Orthophosphates 523–526  
    $\text{AlPO}_4$ , structural analogy with  $\text{SiO}_2$  526  
   uses of 524–525  
   *see also* individual metals  
 Orthophosphoric acid *see* Phosphoric acid  
 Osmates 1082  
 Osmiamates 1085  
 Osmium  
   abundance 1071  
   anomalous atomic weight of in Re ores 19  
   atomic and physical properties 1074–1075  
   carbido-carbonyls 1107–1108  
   carbonyl halides 1108  
   carbonyl hydrides and carbonylate anions 1105–1108  
   carbonyls 928, 929, 1104–1105  
   chalcogenides 1081  
   complexes  
     +8 oxidation state 1085  
     +7 oxidation state 1085  
     +6 oxidation state 1085–1086  
     +5 oxidation state 1086  
     +4 oxidation state 1086–1088  
     +3 oxidation state 1088–1089  
     +2 oxidation state 1091–1098  
     with  $\text{SO}_2$  702  
   coordination numbers and stereochemistries 1078  
   cyclooctatetraene complex 943  
   discovery 1070  
   halides and oxohalides 1082–1083  
   organometallic compounds 1104–1112  
   oxidation states 1077, 1079  
   oxides 1079, 1081  
   oxoanions 1082  
   production and uses 1072–1074  
   reactivity of element 1075  
   relationship with other transition elements 1075–1079  
   standard reduction potentials 1077  
 Osmocene 937, 1111  
 Osmyl complexes 1085, 1086  
 Outer-sphere reactions 1124  
 Oxidation state  
   periodic trends in 27–28  
   variability of 27, 905  
 Oxides 640–644  
   acid-base properties 628, 640, 641  
   classification 640–642  
   nonstoichiometry in 642–644  
   structure types 641, 753  
   *see also* individual elements  
 Oxonium ion 48  
 OXO process (hydroformylation) 309, 1135, 1140  
 Oxovanadium (vanadyl) ion 982, 995  
 Oxygen  
   abundance 600, 602  
   allotropes 607  
   atomic 611, 612  
   atomic properties 604, 605  
   chemical properties 612–615  
   coordination geometries 613–615  
   crown ether compounds 95–97, 124, 601  
   difluoride 638  
   fluoride 638–640  
   history 600, 601, 604  
   industrial production 604  
   industrial uses 604  
   isotopes, separation of 604  
   liquefaction 601, 604  
   liquid 601, 603–604, 606  
   occurrence in atmosphere, hydrosphere and lithosphere  
     600, 602, 605  
   origin of, in atmosphere 602  
   origin of blue colour in liquid 607  
   oxidation states 613  
   physical properties 605  
   preparation 603, 604  
   radioactive isotopes 605  
   reduction potential, pH dependence 628–629



- Oxygen — *contd*  
 roasting of metal sulfides 676–678  
 standard reduction potentials 628, 629, 737  
*see also* Dioxygen, Ozone
- Oxygen carriers  
 complexes of cobalt 1132  
 haemocyanin 1199  
 haemoglobin and synthetic models 1098–1101  
 Vaska's compound 615, 617, 1136, 1137  
*see also* Dioxygen
- Oxyhyponitrous acid *see* Hyponitric acid
- Ozone, O<sub>3</sub>  
 bonding 607, 608  
 chemical reactions 609–611, 848, 849  
 discovery 607  
 environmental implications 608, 848  
 hole 608  
*see also* Chlorofluorocarbons  
 molecular structure 607, 608, 708  
 physical properties 607, 608  
 preparation 609, 611
- Ozonide ion, O<sub>3</sub><sup>−</sup> 610
- Ozonides (organic) 610, 611
- Ozonolysis 610, 611, 849
- p-Process in stars 13
- p-type semiconductors *see* Semiconductor, Transistor
- Palladium  
 absorption of hydrogen 1150, 1151  
 abundance 1145  
 alkene and alkyne complexes 1170–1172  
 alkyls and aryls 1167, 1168  
 π-allylic complexes 953, 1172, 1172  
 atomic and physical properties 1148–1149  
 carbonyl chloride 1168  
 chalcogenides 1152  
 complexes  
   +4 oxidation state 1154  
   +3 oxidation state 1154, 1156  
   +2 oxidation state 1156–1166  
   zero oxidation state 1166–1167  
 coordination numbers and stereochemistries 1150  
 discovery 1144  
 halides 1152–1154  
 organometallic compounds 1167–1172  
 oxidation states 1150  
 oxides 1151, 1152  
 production and uses 1146, 1147  
 reactivity of element 1149
- Paraperiodic acid *see* Periodic acids
- Parathion 509
- Patronite 977
- Pauli exclusion principle 22
- Pearlite 1075
- Pentaborane, B<sub>5</sub>H<sub>9</sub> 154, 159, 163  
 Brønsted acidity 171, 172  
 chemical reactivity 171  
 metalloborane derivatives 171–173  
 preparation 165  
 properties 170  
 structure 171
- Pentagonal bipyramidal complexes 916
- Pentathionates, S<sub>5</sub>O<sub>6</sub><sup>2−</sup>, preparation and structure 717, 718, 851
- Pentlandite 1145
- Perbromates, BrO<sub>4</sub><sup>−</sup> 871–872  
 discovery 789, 871  
 radiochemical synthesis 871  
 redox systematics 854, 855, 872  
 structure 871
- Perbromic acid, HBrO<sub>4</sub> 871
- Perbromyl fluoride, FBrO<sub>3</sub> 881
- Perchlorates, ClO<sub>4</sub><sup>−</sup> 865–871  
 bridging ligand 791, 868–871  
 chelating ligand 868–871  
 coordinating ability 791, 868–871, 1020  
 monodentate ligand 791, 868–871  
 production and uses 865, 867  
 redox systematics 854, 855  
 structure 868
- Perchloric acid, HClO<sub>4</sub> 865–868  
 chemical reactions 867, 868  
 hydrates 867  
 physical properties 865, 866  
 preparation 865, 866  
 structure 868
- Perchloryl fluoride, FClO<sub>3</sub> 876, 879, 880
- Perhalates, XO<sub>4</sub><sup>−</sup> 854, 855, 865–875
- Perhalic acids, HOXO<sub>3</sub> 865–875
- Periodates 872–875  
 redox systematics 854, 855  
 reaction schemes 874  
 structural relations 873  
 synthesis 872, 873  
 transition metal complexes 875
- Periodic acids 872–875  
 acid-base systematics 874  
 nomenclature 872  
 preparation 873  
 redox systematics 854, 855  
 structural relations 873
- Periodic reactions  
 Belousov-Zhabotinskii reactions 865, 865  
 Bray's reaction 865
- Periodic table *see* inside front cover  
 and atomic structure 20–23  
 history of 20, 21  
 and predictions of new elements 29–31
- Permanganates 1050, 1051
- Perosmate 1082, 1085
- Perovskite structure 963  
 in ternary sulfides 681
- Peroxo anions 638
- Peroxodisulfates, S<sub>2</sub>O<sub>8</sub><sup>2−</sup> 713
- Peroxodisulfuric acid, H<sub>2</sub>S<sub>2</sub>O<sub>8</sub> 713
- Peroxo complexes of O<sub>2</sub> 616
- Peroxo compounds, fluorinated 639, 640
- Peroxo-chromium complexes 637, 1024
- Peroxodiphosphoric acid, H<sub>4</sub>P<sub>2</sub>O<sub>8</sub> 512
- Peroxomonophosphoric acid, H<sub>3</sub>PO<sub>5</sub> 512
- Peroxomonosulfuric acid, H<sub>2</sub>SO<sub>5</sub> 705, 712
- Peroxonitric acid, HOONO<sub>2</sub> 458
- Peroxonitrous acid, HOONO 459
- Peroxoselenous acid 783
- Peroxtellurates 783

- Perrhenates 1050  
 Perruthenates 1082  
 Pertechnetate ion 1050  
 Perxenates,  $\text{XeO}_6^{4-}$  901  
 pH scale 32, 49  
 "Pharaoh's serpents" 1218  
 Phase rule 676  
 Phase-transfer catalysis 97  
 Phenacite 347  
 Phlogiston theory 30, 600, 601, 793  
 Phlogopite *see* Micas  
 Phosgene 305  
 Phospha-alkenes 545  
 Phospha-alkynes 545  
 Phosphate cycles in nature 475–479  
 Phosphate rock  
   occurrence and reserves 476  
   phosphorus production from 480, 520, 525  
   statistics of uses 525  
 Phosphates *see* Chain phosphates, Cyclophosphates,  
   Orthophosphates, Superphosphates, Tripolyphosphates  
 Phosphatic fertilizers 474, 477–479, 520, 524–526  
 Phosphazenes 534–536  
 Phosphides 489–492  
 Phosphine,  $\text{PH}_3$   
   chemical reactions 492, 493  
   comparison with  $\text{NH}_3$ ,  $\text{AsH}_3$ ,  $\text{SbH}_3$ ,  $\text{BiH}_3$  557  
   inversion frequency 493  
   Lewis base activity 493–495  
   molecular structure 492, 493  
   preparation 492  
   tertiary phosphine ligands 494  
 Phosphinic acid *see* Hypophosphorous acid  
 Phosphinoboranes 211  
 Phosphites 513, 514  
 Phosphonic acid *see* Phosphorous acid  
 Phosphonitrilic chloride ( $\text{NPCl}_2$ )<sub>x</sub> 408  
   *see also* Polyphosphazenes  
 Phosphoramidic acid 532  
 Phosphorescence  
   of arsenic 550  
   of phosphorus 474, 485  
 Phosphoric acid,  $\text{H}_3\text{PO}_4$  516, 517, 518–522  
   autoprotolysis 518  
   in colas and soft drinks 520  
   hemihydrate 518–521  
   industrial production 521–522  
   industrial uses 520  
   polyphosphoric acids in 522  
   proton-switch conduction in 518, 598  
   self-dehydration to diphosphoric acid 518  
   self-ionization 518  
   structure 518  
   successive replacement of H in 519, 521  
   "thermal" process 521, 522  
   trideutero 518  
   "wet" process 520, 521  
 Phosphoric triamide 532  
 Phosphorus acid,  $\text{H}_3\text{PO}_3$  512, 514  
 Phosphorus  
   abundance and distribution 475  
   allotropes 473, 474, 479–483  
   alloys 492  
   atomic properties 482–483  
   black allotropes 481–483, 551  
   bond energies 483  
   catenation 473, 483, 485  
   chemical reactivity 483, 578  
   cluster anions 491, 588  
   coordination geometries 483  
   disproportionation in aqueous solutions 511–513  
   encapsulated 554  
   fertilizers 474, 477–479, 520, 604  
   halides 495  
     *see also* individual triahalides and pentahalides  
   history 473, 474  
   Hittorf's violet allotrope 481  
   hydrides 492–495  
     *see also* Phosphine  
   mixed halides 495  
   multiple bond formation 473  
   organic compounds 542–546  
   oxides 503–506  
     *see also* "Phosphorus trioxide", "Phosphorus  
       pentoxide"  
   oxohalides 501, 502  
   oxosulfides 507, 510  
   pentaphenyl 545  
   peroxide,  $\text{P}_2\text{O}_6$  506  
   production and uses 479, 480, 520, 525  
   pseudohalides 495, 501  
   radioactive  $^{32}\text{P}$  482  
   red, amorphous 481, 482, 483  
   stereochemistry 485–486  
   sulfides 506–509  
     industrial uses of 509  
     organic derivatives 509  
     physical properties 507  
     stoichiometry 506  
     structures 507  
     synthesis 506, 508  
   thiohalides 498, 501–503, 508  
   triangulo- $\mu_3$ - $\text{P}_3$  species 587, 588  
   white,  $\alpha$ - $\text{P}_4$  480–481, 483, 551  
   ylides 545  
 Phosphorus oxoacids 510–531  
   lower oxoacids 516–517  
   nomenclature 511–512, 517  
   standard reduction potentials 513  
   structural principles 510–512, 517  
   volt-equivalent diagram 513  
   *see also* individual acids and their salts, e.g. Phosphoric  
     acid, Phosphates, etc.  
 Phosphorus pentahalides 495, 498–501  
   ammonolysis of  $\text{PCl}_5$  with liquid  $\text{NH}_3$  535  
   fluxionality of  $\text{PF}_5$  498  
   industrial production of  $\text{PCl}_5$  500  
   ionic and covalent forms 498–501, 537  
   mixed pentahalides 499  
   organo derivatives 499–501  
   reactions of  $\text{PCl}_5$  with  $\text{NH}_4\text{Cl}$ -diphosphazenes 535  
   structural isomerism 499, 500  
   "Phosphorus pentoxide",  $\text{P}_4\text{O}_{10}$  504–506  
   chemical reactions 505  
   *cyclo*-phosphates, relation to 530  
   hydrolysis 505, 520

- "Phosphorus pentoxide",  $P_4O_{10}$  — *contd*  
   polymorphism 504, 505  
   preparation 504  
   structure 504  
 Phosphorus tribromide 496, 497, 500  
 Phosphorus trichloride  
   chemical reactions 497  
   hydrolysis to phosphates 514  
   industrial production 496  
   organophosphorus derivatives 496, 497, 514  
 Phosphorus trifluoride 495, 496  
   as a poison 1101  
   similarity to CO as ligand 496  
 Phosphorus triiodide 495, 497  
 "Phosphorus trioxide",  $P_4O_6$   
   disproportionation to  $P_4O_n$  504  
   hydrolysis 504  
   preparation 503, 504  
   structure 504  
 Phosphoryl  
   halides,  $POX_3$  502  
   pseudohalides 501  
 Photographic image intensification with  $^{35}S$  662  
 Photographic process 790, 794, 1185–1187  
 Photosynthesis  
   manganese in 1061  
   NADP in 125  
    $^{18}O$  tracer experiments 601, 602  
   as origin of atmospheric  $O_2$  602  
   *see also* Chlorophylls  
 Photosystem II 1056, 1061  
 Phyllo-silicates 347, 349–354  
 Physical constants, table of consistent values: end paper  
 Physical properties, periodic trends in 23  
   *see also* individual elements  
 Piezoelectricity 58, 345  
 Pig-iron 1072  
 Pitchblende 1250, 1255  
 Plagioclase *see* Feldspars  
 Plaster of Paris 122  
 Platinum  
   abundance 1145  
   alkene and alkyne complexes 1170–1172  
   alkyls and aryls 1167–1168  
    $\pi$ -allylic complexes 934, 1172  
   anti-tumour compounds 1163  
   atomic and physical properties 1148–1149  
   blues 1165  
    $\beta$ -elimination in alkyls and aryls 926  
   black 1148  
   carbonylate anions 1169  
   catalytic uses 466, 467, 1145  
   chalcogenides 1152  
   complexes  
     +6 and +5 oxidation states 1154  
     +4 oxidation state 1154–1155  
     +3 oxidation state 1155–1156  
     +2 oxidation state 1156–1166  
     zero oxidation state 1166–1167  
     with S 666  
     with  $SO_2$  702  
   coordination numbers and stereochemistries 1150  
   halides 1152–1154  
   optical resolution of  $[Pt(S_5)_3]^{2-}$  670  
   organometallic compounds 931, 932, 1167–1172  
     *see also* Zeise's salt  
   oxidation states 1150  
   oxides 1151, 1152  
   production and uses 1146, 1147  
   reactivity of element 1149  
   sulfide, structure 679  
 Platinum metals, definition 1070  
 Plutonium  
   "breeding" 1259  
   bis(cyclooctatetraene) 942  
   critical mass 1261  
   discovery 1252  
   extraction from irradiated nuclear fuel 1260, 1261  
   natural abundance 1253  
   redox behaviour 1265–1267  
   self-heating 1264  
   *see also* Actinide elements  
 Plutonium economy 1259  
 P–N compounds 531–542  
 Point groups 1290–1292  
 Pollution, atmospheric by  $SO_2$  646, 698–699, 710  
   *see also* Eutrophication, Water  
 Polonium  
   abundance 747  
   allotropy 751  
   atomic and physical properties 753, 754, 890  
   chemical reactivity 754–759  
   coordination geometries 756  
   dioxide 780  
   discovery 747  
   halides 767, 768, 769, 770  
   hydride,  $H_2Po$  766, 767  
   hydroxide 781  
   nitrate 786  
   oxides 779–780  
   polonides 765, 766  
   production and uses 750  
   radioactivity 748, 750  
   redox properties 755  
   selenate 786  
   sulfate 786  
   toxicity 757–759  
 Polyethene (polythene) 261, 262, 972  
 Polyhalide anions 827, 829–831, 834–839  
   bonding 838, 839  
   containing astatine 887  
   structural data 836–839  
 Polyhalonium cations 827, 829–831, 833–835  
   stoichiometries 839  
   structures 840  
 Polyiodides 806, 835–839  
 Polypeptide chains 61, 62  
 Polymetaphosphoric acid 512  
 Polyphosphates, factors affecting rate of degradation 523  
   *see also* Chain polyphosphates, *Cyclo*-polyphosphates  
 Polyphosphazenes 536  
   analogy with silicones 536  
   applications 542–543  
   basicities 540  
   bonding in 537–540  
   hydrolysis 541

- melting points of  $(\text{NPX}_2)_n$  538  
 pentameric  $(\text{NPCl}_2)_5$  538  
 preparation 536, 537  
 reactions 540–542  
 structure 536–538  
 tetrameric  $(\text{NPCl}_2)_4$  537, 538  
 trimeric  $(\text{NPX}_2)_3$  537  
 Polyphosphoric acid 511  
   catalyst for petrochemical processes 52  
 Polysulfanes *see* Sulfanes  
 Polysulfates,  $\text{S}_n\text{O}_{3n+1}^{2-}$  712  
 Polysulfides  
   of chlorine *see* Sulfur chlorides  
   of hydrogen *see* Sulfanes  
   use in Na/S batteries 678  
 Polythiazyl *see*  $(\text{SN})_x$   
 Polythionates,  $\text{S}_n\text{O}_6^{2-}$  705, 714, 716–718  
   seleno- and telluro- derivatives 717, 782  
 Polythionic acids,  $\text{H}_2\text{S}_n\text{O}_6$  705, 716  
 Polyurethane 305, 422  
 Polywater 632, 633  
 Porphin 126  
 Porphyrin complexes of Mg *see* Chlorophylls  
 Portland cement  
   constitution of 252  
   manufacture of 252  
   *see also* High-alumina cement  
 Potassium  
   abundance 69  
   compounds with oxygen 84–85  
   discovery 68  
   graphite intercalates 293–295  
   nitrate, thermolysis of 468, 469, 541  
   orthonitrate 474  
   phosphates 524  
   polysulfides 681, 682  
   polythionates, preparation and structure 717  
   production of metal 73, 74  
   silyl 339, 340  
   terrestrial distribution of 70  
   *see also* Alkali metals  
 Potassium chlorate, thermal decomposition to give  $\text{O}_2$  603  
 Potassium compounds  
   as fertilizers 73  
   production and uses of 73, 74  
 Potassium permanganate, thermal decomposition to give  $\text{O}_2$  603  
 Powder metallurgy 1005, 1144  
 Praseodymium 1229  
   diiodide 1441  
   +4 oxidation state 1237, 1239, 1244  
   *see also* Lanthanide elements  
 Praseodymium-oxygen system  
   ordered defects and nonstoichiometry in 643–644  
 Principal quantum number  $n$  22  
 Promethium 1228  
   *see also* Lanthanide elements  
 Protactinium  
   abundance 1253  
   bis(cyclooctatetraene) 942  
   discovery 1250  
   redox behaviour 1265–67  
   *see also* Actinide elements 628–631, 814, 815  
   Proton, hydration of 951, 952  
     *see also* Hydrogen, ionized forms, and pH  
   Proton-switch conduction  
     in  $\text{H}_2\text{O}$  623  
     in  $\text{H}_3\text{PO}_4$  518  
     in  $\text{H}_2\text{SO}_4$  843  
   Protoporphyrin IX (PIX) 1099  
   Prout's hypothesis 888  
   Prussian blue 1094  
   Pseudohalogen concept 319, 324  
     *see also* individual elements for pseudohalo derivatives  
   PTFE *see* Teflon  
   Purex process 1261  
   Purple of Cassius 1177  
   PVC plastics, organotin stabilizers for 409  
   Pyrite structure 555, 557, 680  
     *see also* Iron pyrites  
   Pyrochlore 977  
   Pyrophosphoric acid *see* Diphosphoric acid  
   Pyrophosphoryl halides 502, 503, 506  
   Pyrophyllite 352–355, 413  
   Pyrrhotite  $\text{Fe}_{1-x}\text{S}$  649  
  
 Quadruple metal-metal bonds 1031–1035  
 Quantum numbers 22  
 Quartz 342–344  
   enantiomorphism 342  
   uses 346  
 Quaternary arsonium compounds 594  
 Quaternary bismuth cations,  $\text{BiR}_4^+$  599  
 Quaternary phosphonium cations 485, 495, 498–501, 545, 546  
  
 r-Process in stars 12  
 Racah parameter *see* Interelectronic repulsion parameter  
 Radial functions 1285–1287  
 Radioactive decay series 1254  
 Radioactive elements  
   discovery 21  
   varying atomic weights of 18  
 Radiocarbon dating 277  
 Radium, history of 108  
   *see also* Alkaline earth elements  
 Radius ratio rules 80  
 Radon  
   atomic and physical properties 890, 891  
   difluoride 903  
   discovery 889  
   fluoro complexes 903  
   *see also* Noble gases  
 Rare earths *see* Lanthanide elements  
 Raschig synthesis of hydrazine 427, 428  
 Rayon 317, 422, 653  
 Realgar *see* Arsenic sulfide,  $\text{As}_4\text{S}_4$   
 Red cake 977  
 Red lead,  $\text{Pb}_3\text{O}_4$  385, 388  
 Reduction potentials *see* Standard reduction potentials  
 Reinecke's salt 1028  
 Relativistic effects 599, 1180  
 Reppe synthesis 309, 1167, 1172  
 Rhenates 1051

- Rhenium  
 abundance 1041  
 alkyls 1062, 1068–1069  
 carbidocarbonyls 1065–1066  
 carbonyls 928, 1062–1064  
 chalcogenides 1049  
 complexes  
   +7 oxidation state 1054  
   +6 oxidation state 1055  
   +5 oxidation state 1055  
   +4 oxidation state 1056  
   +3 oxidation state 1057–1058  
   +2 oxidation state 1058  
   lower oxidation states 1061  
 compounds with metal-metal multiple bonds 1057, 1058, 1230  
 cyclopentadienyls 1067–1068  
 discovery 1040  
 halides and oxohalides 1051–1054  
 nine-coordinate hydrido complex 1046, 1054  
 organometallic compounds 1062–1068  
 oxides 1045–1049  
 production and uses 1041  
 trioxide 1047  
   structure of 1047
- Rhodium  
 abundance 1113  
 atomic and physical properties 1114–1115  
 carbidocarbonyls 1141–1142  
 carbonyls 928, 1140–1143  
 complexes  
   +4 oxidation state 1121  
   +3 oxidation state 1122–1129  
   +2 oxidation state 1129  
   +1 oxidation states 1133–1136  
   lower oxidation states 1137  
   with SO<sub>2</sub> 702  
 coordination numbers and stereochemistries 1117  
 cyclopentadienyls 1143  
 discovery 1113  
 halides 1119–1121  
 optical resolution of  
   *cis*-[Rh{η<sup>2</sup>-(NH)<sub>2</sub>SO<sub>2</sub>}<sub>2</sub>(OH)<sub>2</sub>]<sub>2</sub><sup>-</sup> 670  
 organometallic compounds 1139–1143  
 oxidation states 1117  
 oxides 1117, 1118  
 production and uses 1114  
 reactivity of element 1116  
 relationship with other transition elements 1119, 1295  
 sulfides 1118
- Rhodocene 1143
- Ribonucleic acids 476
- Ring-laddering 99
- Ring-stacking 99
- “Ring whizzing” 1112, 1223
- RNA 476
- Rochelle salt, discovery of ferroelectricity in 57, 963
- Roussin’s salts 447, 1094
- Rubidium  
 abundance 70  
 compounds with oxygen 70–71  
 discovery 69  
*see also* Alkali metals
- Rubridoxins 1098, 1101, 1102
- Ruby 242, 1003  
   laser 1029
- Russell-Saunders coupling 1242
- Rusting of iron 1076, 1076
- Ruthenates 1082
- Ruthenium  
 abundance 1071  
 atomic and physical properties 1074–1076  
 bipyridyl complexes and solar energy conversion 1096  
 blue 1097  
 carbidocarbonyls 1107–1108  
 carbonyl halides 1108  
 carbonyl hydrides and carbonylate anions 1105–1108  
 carbonyl 928, 1104–1105  
 chalcogenides 1081  
 complexes  
   +8 oxidation state 1085  
   +7 oxidation state 1085  
   +6 oxidation state 1085  
   +5 oxidation state 1086  
   +4 oxidation state 1086–1088  
   +3 oxidation state 1088, 1091  
   +2 oxidation state 1091–1097  
   with S 668–670  
   with SO<sub>2</sub> 702  
 coordination numbers and stereochemistries 1078  
 discovery 1070  
 halides 1082–1084  
 mixed valence compounds of 1097  
 nitrosyl complexes 1097  
 organometallic compounds 1104–1287  
 oxidation states 1077, 1078  
 oxides 1079, 1080, 1255  
 oxoanions 1081  
 production and uses 1073  
 reactivity of element 1075  
 relationship to other transition elements 1075–1079  
 standard reduction potentials 1077
- Ruthenium red 1091
- Ruthenocene 937, 1111
- Rutherfordium 1281–2
- Rutile 955, 961, 1119  
   structure type 962
- s-Process in stars 12
- “Saffil” fibres 244
- Salt (NaCl)  
   history 790, 792  
   location of deposits 793, 795  
   uses in chemical industry 71, 72  
   world production statistics
- “Salt cake” 89, 810
- Saltpetre 407  
   *see also* Potassium nitrate
- Samarium 1228  
 magnetic properties 1243  
 +2 oxidation state 1239, 1240, 1241, 1248  
*see also* Lanthanide elements
- “Sandwich” molecules 189, 264, 924, 1109  
*see also* Ferrocene, cyclopentadienyls of individual elements, Dibenzenechromium, Uranocene

- Scandium  
 abundance 945  
 complexes 950–953  
 discovery 944, 1228  
 as eka-boron 944  
 halides 949, 950  
 organometallic compounds 953  
 oxide 949  
 production 945  
 salts with oxoanions 949  
*see also* Group 3 elements
- Scheelite 1003, 1004, 1169  
 Schönites 1190  
 SCOPE 273  
 Scotch hearth process for roasting PbS 677  
 Seaborgium 1281–3  
 Se<sub>2</sub> as ligand 758, 759  
 Secondary valency 912  
 Selenates 781  
 Selenic acid, H<sub>2</sub>SeO<sub>4</sub> 782  
 Selenides 765, 766  
 Selenites and diselenites 781  
 Selenium  
 abundance 748  
 allotropy 761–753  
 atomic and physical properties 753, 754  
 chemical reactivity 754–759  
 coordination geometries 756–757  
 dioxide 779, 780  
 discovery 747  
 halide complexes 776  
 halides 767, 768, 772  
 hydride, H<sub>2</sub>Se 759, 766–767  
 nitride, Se<sub>4</sub>N<sub>4</sub> 783  
 organocompounds 759, 786, 787  
 oxides 779–780  
 oxoacids 781–783  
 oxohalides 777, 910  
 polyatomic anions 762–5  
 polyatomic cations, Se<sub>n</sub><sup>2+</sup>, [Te<sub>n</sub>Se<sub>4–n</sub>]<sup>2+</sup> 759–761  
 production and uses 748, 749  
 pseudohalides 778, 779, 911  
 redox properties 755  
 sulfate 786  
 sulfides 783  
 toxicity 759  
 trioxide 780
- Selenocyanate ion 329, 324–325  
 ambidentate properties 757, 778  
 Selenopolythionates 783  
 Selenosulfates 783  
 Selenous acid, H<sub>2</sub>SeO<sub>3</sub> 781  
 Semiconductors  
 II–VI 255  
 III–V 221, 255, 258, 549  
 As, Sb and Bi chalcogenides 581, 679  
 nonstoichiometric oxides 644
- Shear plane  
 SHIP technique 1283  
 SI prefixes, origin of inside back cover  
 SI units inside back cover  
 conversion to non SI units 1293  
 Siderite 1071  
 Siderophile elements 648  
 Silaethenes 362  
 Silaneimines 361  
 Silanethiones 360  
 Silanes  
 chemical reaction 338–339  
 homocyclic polysilanes 763  
 physical properties 337  
 silyl halides 339, 340  
 silyl potassium 339, 340  
 synthesis 337  
 Silenes 362  
 Silica  
 fumed 345  
 gel 345  
 historical importance 328  
 hydrated 346  
 phase diagram 344  
 polymorphism 342–346  
 in transistor technology 383  
 uses 345, 346  
 vitreous 344  
*see also* Quartz, Tridymite, Cristobalite, Coesite, Stishovite
- Silicate minerals 347–359  
 comparison with silicones 364  
 Silicates 328–330, 347–359  
 with chain structures (metasilicates) 349, 350  
 with discrete units 347–348  
 disilicates 348  
 with framework structures 354–359  
 with layer structures 349–357  
 metasilicates 348, 350  
 orthosilicates 347, 348  
 soluble (Na, K) 344, 346  
 Silicides 336–337  
 preparation 336  
 structural units in 337  
 Silicomanganese 1041  
 Silicon  
 abundance and distribution 329  
 atomic properties 330, 371  
 carbide 334  
 chemical properties of 328, 331, 372  
 coordination numbers 335  
 dioxide *see* Silica  
 double bonds to 362  
 halides 340–342  
 history 328  
 hydrides *see* Silanes  
 isolation 329, 330  
 nitride 360  
 organic compounds 361–366  
 physical properties 330, 371, 372  
 purification 330  
 sulfide 359  
 Silicones 364–366  
 comparison with mineral silicates 364  
 elastomers 365  
 oils 365  
 organotin, curing agents for 400  
 resins 365

- Silicones — *contd*  
 synthesis 364, 365  
 uses 365
- Siloxanes 364, 366
- Silylamides 360, 361
- Silver  
 abundance 1174  
 acetylide 1180  
 alkenes and alkynes 1199  
 chalcogenides 1181–1182  
 complexes  
   +3 oxidation state 1187, 1188  
   +2 oxidation state 1189  
   +1 oxidation state 1195, 1196  
 halides 1183–1185  
 history 1173  
 nitrate, thermolysis of 469  
 organometallic compounds 1199–1200  
 oxides 1181  
 production and uses 1174
- Silver halides in photographic emulsions 1186
- Singlet oxygen 607  
 generation of 614  
 reactions of 615
- Skutterudite *see* Cobalt arsenide
- Smalt 1113
- Smaltite 1114, 1145
- S–N heterocycles incorporating a third element 736, 737
- (SN)<sub>x</sub> polymer  
 partially halogenated derivatives 728  
 structure 727, 728  
 superconducting properties of 408, 646, 722, 727, 728  
 synthesis 726, 728
- S<sub>2</sub>N<sub>2</sub> 725, 726  
 polymerization to (SN)<sub>x</sub> *qv* 726–727  
 preparation 727  
 structure and bonding 726
- S<sub>4</sub>N<sub>2</sub> 727, 728
- S<sub>4</sub>N<sub>4</sub> 408, 646, 722–725  
 preparation 722  
 reactions 725, 730, 734, 736  
 structure and bonding 856, 857
- S<sub>5</sub>N<sub>6</sub> 729
- S<sub>11</sub>N<sub>2</sub> 728–729
- S<sub>14+x</sub>N<sub>2</sub> 728–729
- Soapstone *see* Talc
- Sodalite *see* Ultramarines
- Sodanitre *see* Chile saltpetre
- Sodide anion, Na<sup>−</sup> 99
- Sodium  
 abundance 69  
 β-alumina  
   structure and properties 249, 250  
   use in Na/S batteries 678  
 arsenide 554  
 azide 409, 453, 440  
 bismuthate 554  
 carbonate  
   hydrates of 88, 89, 104  
   production and uses of 89  
 chlorate 862  
 compounds with oxygen 84–86  
 diphosphates 526, 527  
 discovery 68  
 distribution 69, 70  
 dithionite 721, 722  
 hydroxide, production and uses of 72, 89  
 hypophosphite 513  
 nitrate, thermolysis of 468, 469  
 nitroprusside 447  
 nitroxylate 459  
 orthonirate 471  
 phosphates 512, 521, 523, 524–525  
 polysulfides 677–679, 681, 688  
 polythionates, preparation and structure 717–718  
 production of metal 71  
 silicates, soluble 343, 346  
 solutions in liquid ammonia 77–79, 393  
 sulfate, production and uses of 89  
 sulfide batteries 678, 679  
 thiosulfate, in photography 714, 1186, 1187  
 tripolyphosphate 527, 528  
*see also* Alkali metals
- Sodium chloride structure 80, 242, 983  
*see also* Salt
- Sodium hypochlorite  
 industrial uses 860  
 Raschig synthesis of hydrazine using 427, 428
- Solar energy conversion 1096
- Solvo-acids and bases  
 in anhydrous H<sub>2</sub>SO<sub>4</sub> 711  
 in liquid AsCl<sub>3</sub>, SbCl<sub>3</sub> 560  
 in liquid BrF<sub>3</sub> 831  
 in liquid NH<sub>3</sub> 425  
 in liquid N<sub>2</sub>O<sub>4</sub> 457  
 in water 628
- Soro-silicates 347–349
- Solvay process 71  
 byproduct Ca from 112
- Spallation 14
- Spectral sensitization of photographic emulsions 1186
- Spectroscopic terms 1242
- Sphalerite (Zinc blende) 649, 1202  
 structure of 679, 1209
- Spiegeleisen 1041
- Spin crossover *see* Spin equilibria
- Spin equilibria  
 in Cr<sup>II</sup> and Mo<sup>II</sup> compounds 1034  
 in Fe<sup>II</sup> compounds 1095  
 in Fe<sup>III</sup> compounds 1096  
 in Mn<sup>II</sup> compounds 1066–1067  
 in niobium halides 992
- Spinel 109
- Spinel structure  
 in Co<sub>3</sub>O<sub>4</sub> 1118  
 defect structure of γ-Al<sub>2</sub>O<sub>3</sub> 243  
 in Fe<sub>3</sub>O<sub>4</sub> (inverse) 1079  
 in ferrites and garnets 1081  
 in Mn<sub>3</sub>O<sub>4</sub> 1048  
 normal and inverse 247–249, 1080  
 in ternary sulfides 681  
 valence disordered types 249
- Spin-forbidden bands  
 in compounds of Fe<sup>III</sup> 1089

- in compounds of  $\text{Mn}^{\text{II}}$  1060
- in compounds of  $\text{Ni}^{\text{II}}$  1158
- Spin-orbit coupling
  - in actinide ions 1271
  - in  $d^4$  ions 1087
  - in octahedral  $\text{Ni}^{\text{II}}$  1158
  - in lanthanide ions 1242
  - in tetrahedral  $\text{Co}^{\text{II}}$  1132
- Spin quantum number  $m_s$  22
- Spodumene 69, 349
- Square antiprismatic complexes 916
- Square planar complexes 913
- Square pyramidal complexes 914
- Stability constants of coordination compound
  - factors affecting 908–911
  - overall 908
  - stepwise 908
- Staging *see* Graphite intercalation compound
- Standard reduction potentials 434
  - IUPAC sign convention 436
  - see also* individual elements
- Stannates 354
- Stannocene 402
- Starch/iodine reaction 790, 864
- Stars
  - spectral classification of 5
  - temperatures of 5
- Steel 1072–1075
- Stellar evolution 5
- Stereochemical non-rigidity (fluxional behaviour)
  - $\text{Al}(\text{BH}_4)_3$ ,  $\{\text{Al}(\text{BH}_4)_2\text{H}_\mu\}_2$  230
  - allyl complexes 934
  - Berry pseudorotation mechanism 474, 499
  - 5-coordinate compounds 914
  - 8-coordinate compounds 995
  - $\text{Fe}(\text{CO})_5$  914, 1104
  - iron cyclopentadienyl complexes 1111
  - $\text{PF}_5$  498
  - $\text{SF}_4$  684
  - titanium cyclopentadienyl 974
- Stibine
- Stibinidene complexes 597
- Stibnite *see* Antimony sulfide,  $\text{Sb}_2\text{S}_3$
- Stishovite 342
- Strength of oxoacids, Pauling's rules 50
- Strontium
  - history 108
  - organometallic compounds 136
  - polysulfides 681
  - see also* Alkaline earth metals
- stylx numbers *see* Boranes, topology
- Sulfamic acid,  $\text{H}[\text{H}_2\text{NSO}_3]$  408, 741, 742
- Sulfamide  $(\text{H}_2\text{N})_2\text{SO}_2$  742, 743
- Sulfanes 682–683
  - nonexistence of  $\text{SH}_4$  and  $\text{SH}_6$  685
  - physical properties 683
  - preparation 682
  - synthesis of polythionic acids from 716
  - see also* Hydrogen sulfide
- Sulfate ion as ligand ( $\eta^1$ ,  $\eta^2$ ,  $\mu$ ) 712
- Sulfates 711, 712
  - see also* individual elements
- Sulfide minerals
  - geochemical classification 648
  - names and formulae 649
- Sulfides
  - anionic polysulfides 678, 681, 682
  - applications and uses 677–679
  - electrical properties 681
  - hydrolysis 678, 679, 682
  - industrial production 678
  - magnetic properties 681
  - preparation (laboratory) 677
  - roasting in air 676–678
  - solubility in water 678, 679
  - $\text{S}_n^{2-}$  structures 631, 681
  - structural chemistry 679–681
  - see also* individual elements
- Sulfates 703
- Sulfites,  $\text{SO}_3^{2-}$  705, 719
  - in paper manufacture 652
  - protonation to  $\text{HSO}_3^-$  719
- Sulfoxylates,  $\text{MS}(\text{O})\text{OR}$  703
- Sulfur
  - abundance 647
  - allotropes 646, 652–661
    - see also* individual allotropes, e.g. *Cyclo-S<sub>n</sub>*, *Catena-S<sub>n</sub>* etc.
  - atomic properties 661
  - atomic S 664
  - atomic weight, variability of 18, 661, 662
  - in biological complexes 667
  - bromides  $\text{S}_n\text{Br}_2$  691
  - catenation 652, 656ff, 681–683, 689, 690, 716–718
  - chemical reactivity 662–664
  - chiral helices 660
  - chlorides 689–692, 716
    - industrial applications of  $\text{SCl}_2$  and  $\text{S}_2\text{Cl}_2$  690
    - preparation 690, 691
    - properties of  $\text{S}_n\text{Cl}_2$  690, 691
    - $[\text{SCl}_3]^+$  691, 693
    - $\text{SCl}_7\text{I}$  693
  - chlorofluorides 640, 686–689
  - conformations (c, dt, lt) 656, 659, 665
  - conversion to  $\text{SO}_2/\text{SO}_3$  for  $\text{H}_2\text{SO}_4$  *see* Sulfuric acid
  - coordination geometries 663
  - Crystex 659
  - dihedral angles in  $\text{S}_n$  654, 655
  - fibrous ( $\psi$ ,  $\phi$ ) 659–660
  - fluorides 683–689
    - chemical reactions 685–689
    - fluxionality of  $\text{SF}_4$  685
    - isomeric  $\text{S}_2\text{F}_2$  684
    - physical properties 685, 687
    - stoichiometries 684
    - structures 684–685
    - synthesis 685–688
  - gaseous species 661
  - halides 683–693
    - see also* individual halides
  - hexafluoride 685, 687
    - applications as a dielectric gas 687
    - reaction with  $\text{SO}_3$  695
  - history 645, 646
  - iodides 691–693



- Sulfur — *contd*
- bond energy relations in 691
  - SCl<sub>7</sub>I 693
  - [S<sub>2</sub>L<sub>4</sub>]<sup>2+</sup> 692, 693
  - [S<sub>7</sub>I]<sup>+</sup> 692
  - [S<sub>14</sub>I<sub>3</sub>]<sup>3+</sup> 692
  - λ point 660
  - as ligands 701–703
  - ligand properties of chelating –S<sub>n</sub>– 665, 670, 672
  - ligand properties of S atom 665–666
  - ligand properties of S<sub>2</sub><sup>2-</sup> 665–669, 668, 671
  - liquid 654, 660
  - monoxide 698
  - nitrides 722–729
  - organic thio ligands 673
  - origin in caprock of salt domes 647
  - oxidation states 664
  - oxidation state diagram of species 706
  - oxides 695–704
    - higher, SO<sub>3+x</sub>, SO<sub>4</sub> 704,
    - lower dioxides 695–698
    - lower oxides S<sub>n</sub>O 695–698
    - see also* Sulfur dioxide, Sulfur trioxide
  - oxoacids 706–721
    - schematic classification 707
    - table of 705
    - thermodynamic interrelations 706
    - see also* individual oxoacids and oxoacid anion
  - oxofluorides 688
    - see also* Thionyl fluorides, Sulfuryl fluorides
  - peroxofluorides 689
  - plastic (χ) 659
  - polyatomic cations 664, 665
  - polymeric (μ) 659
  - production 649–652
    - Frasch process 649–650
    - from pyrite 651
    - from sour gas and crude oil 651
    - statistics 762, 768
  - radioactive isotopes 661
  - reserves 651
  - rhombohedral *see* Cyclo-α-S<sub>8</sub>
  - rubbery S 659
  - S–S bonds 652, 654, 662, 667, 681–683, 716–718
  - S<sub>2</sub> 656, 661
  - S<sub>3</sub> 656, 661
  - S<sub>4</sub> 661
  - S<sub>4</sub><sup>2+</sup> *see* polyatomic cations
  - S<sub>8</sub> *see* Cyclo-S<sub>8</sub>
  - S<sub>8</sub><sup>2+</sup> *see* polyatomic cations
  - S<sub>n</sub> *see* Cyclo-S<sub>n</sub>
  - S<sub>19</sub><sup>2+</sup> *see* polyatomic cations
  - SN compounds 686, 721–746
    - see also* S<sub>4</sub>N<sub>4</sub>, S<sub>2</sub>N<sub>2</sub>, (SN)<sub>x</sub>, S–N–X compounds,
    - Sulfur imides, S–N–O compounds, Sulfur-nitrogen anions, Sulfur-nitrogen cations
  - singlet state S<sub>2</sub> 661
  - standard reduction potentials of S species 706
  - terrestrial distribution 647
  - triplet state S<sub>2</sub> 661
  - uses 651, 653
  - uses of radioactive <sup>35</sup>S 661, 714
  - volt-equivalent diagram of S species 706
  - see also* Chalcogenides
  - Sulfur chloride pentafluoride SF<sub>5</sub>Cl
    - photolytic reduction to S<sub>2</sub>F<sub>10</sub> 687
    - reaction with O<sub>2</sub> 640
    - synthetically useful reactions of 688, 689
  - Sulfur dioxide 698–701
    - atmospheric pollution by 646, 698–700, 699
    - chemical reactions 700
    - clathrate hydrate 700
    - industrial production 698, 708
    - insertion into M–C bonds 702, 703
    - as ligand 701–703
    - molecular and physical properties 700, 780
    - in M–S–O phase diagrams 677
    - solvent for chemical reactions 662, 701
    - toxicity 700
    - uses 700
    - see also* Wackenroder's solution, Sulfuric acid production
  - Sulfur imides, S<sub>8–n</sub>(NH)<sub>n</sub> 735–735
  - Sulfur-nitrogen anions, S<sub>x</sub>N<sub>y</sub><sup>-</sup> 733–734
  - Sulfur-nitrogen cations, S<sub>x</sub>N<sub>y</sub><sup>+</sup> 730–733
  - Sulfur-nitrogen-halogen compounds 736–740
    - cyclo-(NSF)<sub>n</sub> 736–738
    - N<sub>3</sub>S<sub>3</sub>Cl<sub>3</sub> 738
    - N<sub>3</sub>S<sub>3</sub>X<sub>3</sub>O<sub>3</sub> 738
    - S<sub>4</sub>N<sub>3</sub>Cl and S<sub>4</sub>N<sub>4</sub>Cl<sub>2</sub> 739
    - thiazyl halides NSX 736–738
  - Sulfur-nitrogen-oxygen compounds 740
    - amides of H<sub>2</sub>SO<sub>4</sub> 741
    - see also* Sulfamic acid, Sulfamide
    - hydrazine derivatives of H<sub>2</sub>SO<sub>4</sub> 743
    - hydroxylamine derivatives of H<sub>2</sub>SO<sub>4</sub> 743–746
    - imido and nitrido derivatives of H<sub>2</sub>SO<sub>4</sub> 743
    - sulfur-nitrogen oxides 740, 741
  - Sulfur trioxide
    - chemical reactions 703, 704
    - molecular and physical properties 703, 704
    - monomeric 703, 704
    - polymeric 703, 704
    - polymorphism 703, 704
    - preparation by catalytic oxidation of SO<sub>2</sub> 700, 708
    - reaction with F<sub>2</sub> 640
    - reaction with SF<sub>6</sub> 695
    - trimeric 703, 704
    - see also* Sulfuric acid production
  - Sulfuric acid 706, 712
    - amides of 741–743
    - autoprotolysis in anhydrous 710
    - contact process 646, 700, 708–710, 981
    - D<sub>2</sub>SO<sub>4</sub> 710, 711
    - history 646, 708
    - hydrates 710
    - hydrazine derivatives of 744
    - hydroxylamine derivatives of 744–746
    - imido derivatives of 743, 744
    - ionic dissociation equilibria in anhydrous 711
    - lead chamber process 646, 708
    - nitrido derivatives of 743, 744
    - physical properties
    - physical properties of D<sub>2</sub>SO<sub>4</sub>
    - production from sulfide ores 708
    - production from sulfur 652–652, 708

- production statistics 407, 708, 710  
 solvent system 711  
 uses 710  
 Sulfurous acid,  $\text{H}_2\text{SO}_3$  652, 700, 705, 717, 718  
 Sulfuryl chloride 694, 695  
 Sulfuryl fluoride 688, 694  
 mixed fluoride halides 694  
 Super acids  
    $\text{HF}/\text{SO}_3/\text{SbF}_5$   
    $\text{HSO}_3\text{F}/\text{SbF}_5$   
 Superconductivity  
   in Chevrel phases 1018, 1031  
   high temperature 945, 1182–3, 1232  
   of metal sulfides 680  
   use of Nb/Zr in magnets 978  
 Superheavy elements 30, 1253  
 Supernucleophiles 1139  
 Superoxo complexes of  $\text{O}_2$  616, 1127  
 Superphosphate fertilizer 474, 525  
 Swarts reaction 560  
 Symmetry elements 1290–1292  
 Symmetry operations 1290–1292  
 Synergic bonding  
   in alkene complexes 926, 927  
   in CO and  $\text{CN}^-$  complexes 931  
   in cobalt cyanides 1122  
   *see also* Back ( $\pi$ ) bonding  
 Synthesis gas 1106
- Talc 109  
 Tanabe-Sugano diagrams  
   for  $d^2$  ions 997  
   for  $d^3$  ions 1029  
   for  $d^6$  ions 1096, 1128  
   for  $d^8$  ions 1156  
   for  $\text{Mn}^{\text{II}}$  1156  
 Tantalates 987  
 Tantalite 977  
 Tantalum  
   abundance 977  
   alkyls and aryls 999  
   carbene complex 926  
   carbonylate anions 999–1000  
   chalcogenides 987  
   complexes  
     +5 oxidation state 994  
     +4 oxidation state 944–996  
   compounds with oxoanions 993  
   cyclopentadienyls 1000–1001  
   discovery 976  
   halides and oxohalides 988–999  
   organometallic compounds  
   oxides 929, 982, 983, 999–1000  
   production and uses 977  
   *see also* Group 5 elements  
 Technetates 1050  
 Technetium  
   abundance 1041  
   carbonyls 928, 1062–1063  
   chalcogenides 1049  
   complexes  
     +7 oxidation state 1054  
     +6 oxidation state 1055  
     +5 oxidation state 1055  
     +4 oxidation state 1056  
     +3 oxidation state 1057–1058  
     +2 oxidation state 1058  
     lower oxidation states 1061  
   cyclopentadienyls 1067–1068  
   discovery 1040  
   halides and oxohalides 1051–1054  
   nuclear medicine, role in 1042  
   organometallic compounds 1062–1067  
   oxides 1045  
   production and uses 1041  
   *see also* Group 7 elements  
 Tectites 394  
 Tecto-silicates 414–416, 347  
 Teflon (PTFE) 304, 791  
 Tellurates 782  
 Telluric acid,  $\text{Te}(\text{OH})_6$  782  
 Tellurides 765, 766  
 Tellurites 781  
 Tellurium  
   abundance 748  
   allotropy 751  
   atomic and physical properties 753, 754  
   chemical reactivity 754–759  
   coordination geometries 756–757  
   dioxide 779, 780  
   discovery 747  
   halide complexes 776  
   halides 767–776  
   hydride,  $\text{H}_2\text{Te}$  759, 766  
   nitrate 786  
   nitride,  $\text{Te}_3\text{N}_4$  783  
   organo compounds 786–788  
   oxides 779–780  
   oxoacids 781–783  
   oxohalides 777  
   polyatomic anions 762–5  
   polyatomic cations  
      $\text{Te}_n^{m+}$  759, 761  
      $[\text{Te}_n\text{Se}_{4-n}]^{2+}$  761  
   production and uses 748, 749  
   redox properties 755–756  
   sulfide,  $\text{TeS}_7$  783  
   toxicity 759  
   trioxide 780  
 Tellurocyanate ion,  $\text{TeCN}^-$  779  
 Telluropolythionates 783  
 Tellurous acid 781  
 Terbium 1229  
   +4 oxidation state 1237, 1239  
   *see also* Lanthanide elements  
 Tetracyanoethylene complexes, bonding in 931  
 Tetrafluoroethylene complexes, bonding in 932  
 Tetrafluoronitronium cation  $\text{NF}_4^+$  439  
 Tetrahalogenophosphonium cations  $\text{PX}_4^+$  499–500  
 Tetrahedral complexes 914  
 Tetrahydroaluminate ion, as ligand 231

- Tetrahydroborates  
 of Al 260, 228, 229  
 of Ga 231  
 of Zr and Hf 969  
 use in synthesis 166–168
- Tetrametaphosphimate conformers 542
- Tetrathionates,  $S_4O_6^{2-}$ , preparation and structure 717, 718
- Thallium  
 abundance 217  
 chalcogenides 252–254  
 III–V compounds 255–258  
 discovery 217  
 halide complexes 240  
 lower halides 241  
 monohalides 241, 242  
 organometallic compounds 261, 265  
 oxides 246  
 production 221  
 similarity of  $Tl^I$  to alkali metals 226  
 trihalides 239  
 triiodide  $Tl^I[I_3]^-$  239, 240  
*see also* Group 13 elements
- Thiazyl halides NSX 736–738
- Thioarsenites 580
- Thiocarbonyl (CS) complexes 319
- Thiocyanates 320, 324  
 as ambidentate ligands 326–327, 907, 920
- Thioethers as ligands 673
- Thionitrosyl (NS) complexes 453, 454
- Thionyl bromide 694
- Thionyl chloride 693, 694  
 relation to  $SO_2$  and  $Me_2SO$  as ionizing solvent 694
- Thionyl fluoride 688, 693, 694  
 mixed fluoride chloride 694
- Thiophosphoryl  
 halides,  $PSX_3$  500, 502  
 pseudohalides 501
- Thioselenates 783
- Thiosulfates,  $S_2O_3^{2-}$  705, 714, 715  
 as ligands 714, 715  
 redox reactions in analysis 714, 715  
 structure 714, 715  
 use in photography 714, 1186, 1187
- Thiosulfuric acid,  $H_2S_2O_3$  705, 714  
 isomeric  $H_2S.SO_3$  714  
 redox interconversions in water 714
- Thio-urea 317
- Thiovanadyl ion
- Thixotropy 356, 968
- Thorium  
 abundance 1253  
 bis(cyclooctatetraene) 942  
 production and uses 1255  
 radioactive decay series 1254  
 redox behaviour 1265–1267  
 use as a nuclear fuel 1258, 1259  
*see also* Actinide elements
- Thortveitite 348
- Three-centre bonds  
 in Al trialkyls and triaryls 258  
 in beryllium alkyls 127  
 BHB bond 64, 151ff  
 BBB bond 158
- BHM bond 177  
 $H_3^+$  ion 37  
 in magnesium alkyls 127
- Thulium 1228  
*see also* Lanthanide elements
- Thymine 61, 62
- Thyroxine 794, 795
- Tin  
 abundance 368  
 allotropes 373  
 alloys 370  
 in antiquity 367, 368  
 atomic properties 371–372  
 bis(cyclopentadienyl) 402  
 chalcogenides 389  
 chemical reactivity and group trends 373  
 cluster anions 374, 393  
 cluster complexes 383, 395  
 compounds, use of 385, 400  
 dibromide 380  
 dichloride 379, 380  
 difluoride 379  
 dihalides 375, 377–381  
 diiodide 380  
 dioxide 384, 386, 387, 388, 400  
 halogeno complexes 377–381, 399  
 hydrides 375  
 hydroxo species 383, 395  
 isolation and purification 369  
 metal-metal bonded compounds 391, 396, 399–404  
 monomeric  $Sn(OAr)_2$  391  
 monoxide 377, 383, 387, 388  
 nitrates 387  
 organometallic compounds 396–403  
   oligomerization 396  
   production statistics 400  
   toxic action 400  
   uses of 400  
 oxoacid salts 387, 388  
 physical properties 371, 373  
 production statistics 368, 379  
 pseudohalogen derivatives 389  
 sulfide 389  
 tetrahalides 375, 381, 385  
 uses 370, 385
- Titanates 963–964  
 ferroelectric properties 963
- Titanium  
 abundance 955  
 alkoxides 967  
 alkyls and aryls 973  
 alum 970  
 bronzes 964  
 carbonyls 973  
 complexes  
   +4 oxidation state 967–969  
   +3 oxidation state 969–971  
   lower oxidation states 971–975  
   with S 670, 672  
 compounds with oxoanions 966  
 cyclooctatetraene complex 943  
 cyclopentadienyls 973–975  
 dioxide 959

- discovery 954  
 estimation using  $\text{H}_2\text{O}_2$  968  
 halides 964–966  
 mixed metal oxides (titanates) 963–964  
 nonstoichiometric oxide phases 642, 961  
 organometallic compounds 972–975  
 production and uses 955–956  
 “sponge” 956  
 sulfides 962  
*see also* Group 4 elements  
 “Titanocene” 973  
 Tobermorite gel 252  
 Tolman’s cone angle 494  
 Tooth enamel 477  
 Toothpastes, calcium compounds in 528  
 “Tops and bottoms” process 1146  
*Trans*-effect 1164  
   in  $[\text{OsNCl}_5]^{2-}$  1085  
   in  $\text{Pt}^{\text{II}}$  complexes 1163, 1164  
   in  $\text{Rh}^{\text{III}}$  complexes 1127  
*Trans*-influence 1164, 1165  
   in  $[\text{OsNCl}_5]^{2-}$  1085  
   in  $\text{Pt}^{\text{II}}$  complexes 1165  
 Transactinide elements 1280–4  
 Transferrin 1103  
 Transistor action 331, 332  
   chemistry of manufacture 332  
   discovery 331  
 Transition element ions  
   coordination chemistry 905–943  
   *see also* individual elements  
 Transition elements  
   definition of 905  
   characteristic properties 905  
   *see also* Transition element ions and individual elements  
 Transuranium elements  
   discovery of 21, 29, 1252  
   extraction from reactor wastes 1262  
   *see also* Actinide elements  
 Tricalcium aluminate,  $\text{Ca}_3\text{Al}_2\text{O}_6$ , structure 251  
   *see also* Portland cement  
 Tricalcium phosphate  $[\text{Ca}_5(\text{PO}_4)_3\text{OH}]$  524  
 Tri-capped trigonal prismatic complexes 917  
 Tridymite 343  
 Trigonal bipyramidal complexes 914  
 Trigonal prismatic complexes 915  
 Triperiodic acid *see* Periodic acids  
 Triphosphoric acid  $\text{H}_5\text{P}_3\text{O}_{10}$  512  
 “Triple-decker” complexes 1170  
 Tris(dimethylamino)phosphine 533  
 Trithiocarbonates 317  
 Trithionates,  $\text{S}_3\text{O}_6^{2-}$ , preparation and structure 717, 718  
 Tritium  
   atomic properties 34  
   discovery 33  
   physical properties 35  
   preparation of tritiated compounds 42  
   radioactivity of 42  
   synthesis 41  
   uses as a tracer 42  
 Tropylium (cycloheptatrienyl) 942  
 Tungstates 1009–1016  
 Tungsten  
   abundance 1003  
   benzene tricarbonyl 941  
   blues 1008  
   bronzes 1016  
   carbonyls 928, 1037–1038  
   carbyne complexes 929  
   chalcogenides 1017–1018  
   complexes  
     +6 oxidation state 1023–1024  
     +5 oxidation state 1024, 1025  
     +4 oxidation state 1025–1027  
     +3 oxidation state 1027–1031  
     +2 oxidation state 1031–1034  
     with S 670  
   cyclopentadienyl derivatives 1039  
   discovery 1002  
   halides and oxohalides 1019–1023  
   hexacarbonyl 928, 1038  
   heteropolyacids and salts 1014–1016  
   isopolyacids and salts 1009–1014  
   nonstoichiometric oxides 1008  
   organometallic compounds 829, 940, 941, 1037–1039  
   oxides 1007–1009  
   production and uses 1003  
   *see also* Group 6 elements  
 Tungstic acid 1010  
 Tungstocene 1038  
 Turnbull’s blue 1094  
 Tutton salts  
   of copper 1190  
   of vanadium 993  
 Type metal 547, 549  
 Tyrian purple 790, 791, 793  
*u* (ungerade), definition of 938  
 Ultramarines 354, 359  
 Units  
   conversion factors 1293  
   non-SI 1293  
   SI, definitions *see* inside back cover  
   SI, derived *see* inside back cover  
 Universe  
   expansion of 2, 5  
   origin of 1, 2  
 Uranium  
   abundance 1253  
   bis(cyclooctatetraene) 942  
   isotopic enrichment 1259  
   production 1255  
   radioactive decay series 1254  
   redox behaviour 1265–1267  
   variable atomic weight 17  
   *see also* Actinide elements  
 Uranium hexafluoride 1259, 1269–1271  
 Uranium oxides, nonstoichiometry in 643  
 “Uranocene” 1279  
 Uranyl ion 1266, 1269, 1273–1274  
 Urea 305, 311, 323, 422  
   hydrazine production from 429  
   phosphate 524  
   Wöhler’s synthesis 408

- Valence, periodic trends in 27  
 Valence bond theory of transition metal complexes 921–924  
 Valinomycin 96  
 Vanadates 981, 983–987  
 Vanadium  
 abundance 977  
 accumulation in blood of invertebrates 999  
 alkyls and aryls 999  
 biochemistry of 999  
 bronzes 987  
 carbonyl 928, 1000  
 chalcogenides 988  
 complexes  
 +5 oxidation state 994  
 +4 oxidation state 994–996  
 +3 oxidation state 996–998  
 +2 oxidation state 998  
 compounds with oxoanions 993  
 cyclopentadienyls 939, 1000  
 discovery 976  
 dithiolene complexes 674, 675  
 halides and oxohalides 988–993  
 hexacarbonyl 828, 928,  
 isopolyacids and salts 983–987  
 nonstoichiometric oxides 982  
 organometallic compounds 927, 939, 941, 942,  
 997–1001  
 oxides 981–983  
 production and uses 977  
*see also* Group 5 elements  
 Vanadocene 1000  
 Vanadyl compounds 982, 995, 996  
 Van Arkel-de Boer process 956  
 Vaska's compound 615, 616, 1135–1137  
 Venus, atmosphere of 645, 646  
 Vermiculite 349, 357  
 Viscose rayon 317  
 Vitamin B<sub>12</sub> 1138, 1139, 1226  
 Volt equivalent  
 definition 434  
 diagrams 436–438  
*see also* individual elements for volt equivalent diagrams  
 Vortmann's sulfate 1127  
 Vulcanization of rubber 646  
 Wackenroder's solution 717, 719  
 Wacker process 1172  
 Wade's rules 161, 162, 181, 553, 590, 591  
 Water  
 acid-base behaviour 48, 628  
 aquo complexes 625  
 autoprotolysis constant 48  
 chemical properties 627  
 clathrate hydrates 626, 627  
 distribution and availability 621–623  
 H bonding in 52–55  
 heavy (D<sub>2</sub>O) 623  
 history 620  
 hydrates 625–627  
 hydrolysis reactions 627  
 ice, polymorphism 624  
 ionic product of 48  
 Karl Fischer reagent for 627  
 lattice water 625  
 physical properties 623–625, 754  
 pollution of 622  
 polywater 632, 633  
 purification and recycling 622, 623  
 self ionic dissociation of 48  
 tritiated (T<sub>2</sub>O) 623  
 zeolitic water 625  
 Water-gas shift reaction 38, 311, 421, 1106  
 in Haber-Bosch NH<sub>3</sub> synthesis 421  
 Water supplies, treatment of 120  
 White arsenic *see* Arsenic oxide, As<sub>2</sub>O<sub>3</sub>  
 "White gold" 1144  
 "White lead" 388, 1209  
 Wilkinson's catalyst 43, 1134–1135  
 Wilson's disease 1198  
 Wittig reaction 474, 475, 545  
 with arsenic ylides 594  
 Wolfram's red salt 1135  
 Wolfram 1002  
*see also* Tungsten  
 Wolframite 1003, 1004  
 Wrought-iron 1073  
 Wurtzite structure (ZnS) 679, 1209  
 x-Process in stars 13  
 X-ray absorption spectroscopy 1036  
 Xanthates 317, 646  
 γ-S<sub>8</sub> from Cu<sup>I</sup> ethyl xanthate 655  
 as ligands 693  
 XeF<sub>2</sub> 894–894  
 bonding 897, 898  
 bonding compared with H bond 64  
 XeF<sub>4</sub> 894–896  
 XeF<sub>6</sub> 894, 895, 896, 898, 900, 901  
 Xenate ion, HXeO<sub>4</sub><sup>-</sup> 901  
 Xenon  
 atomic and physical properties 890, 891  
 carbon bonds 902–903  
 chemical reactivity discovered 893  
 chloride 896  
 clathrates 893  
 discovery 889  
 fluorides 893–903  
 fluorocomplexes 898, 901  
 fluorosulfate 899, 900  
 nitrogen bonds 902  
 oxidation states 894  
 oxides 894–896  
 oxoanions (xenate, perxenate) 901  
 oxofluorides 900  
 perchlorate 899  
 stereochemistry 894, 895  
 trifluoromethyl compounds  
 Xerography 750  
 Xerox process (xerography) 750  
 "Yellow cake" 1255  
 Ylides 545  
 arsonium 594

- Ytterbium 1228  
+2 oxidation state 1237, 1239, 1240, 1241, 1248  
*see also* Lanthanide elements
- Yttrium  
abundance 945  
complexes 950–953  
discovery 944, 1228  
halides 949–950  
organometallic compounds 953  
oxide 949  
oxo salts 949  
production and uses 945, 946  
*see also* Group 3 elements, Lanthanide elements
- Zeise's salt 930, 931, 1167, 1170
- Zeolite 354–359
- Ziegler-Natta catalysis 260, 261, 972
- Zinc  
abundance 1202  
alkyls and aryls 1221  
biochemistry 1224  
chalcogenides 1208, 1209, 1210  
coordination chemistry 1215–1217  
ferrites 1209  
halides 1211–1213  
history 1201  
organometallic compounds 1221  
+2 oxidation state 1215–1217  
oxides 1202, 1208  
  nonstoichiometry in 642, 1208  
production and uses 1202–1203  
*see also* Group 12 elements
- Zinc blende (sphalerite) 1202  
  structure 679, 1209
- Zinc-finger proteins 1225
- Zintl phases 78, 257, 393, 553, 762
- Zircon 347, 955
- Zirconates 964
- Zirconium dioxide 244, 955, 967  
  “Saffil” fibres 244
- Zirconium  
abundance 955  
alkyls and aryls 973  
borohydride 969  
carbonyls 974  
complexes  
  +4 oxidation state 967–969  
  +3 oxidation state 969  
  lower oxidation states 971  
compounds with oxoanions 966, 1226  
cyclopentadienyls 974–975  
dioxide (baddeleyite) 275, 955, 961  
discovery 954  
disulfide 962  
halides 964, 966  
in nuclear reactors 956, 1461  
organometallic compounds 973  
production and uses 955  
tetrahydroborate 166